Scientific and Technical Aerospace Reports

STAR

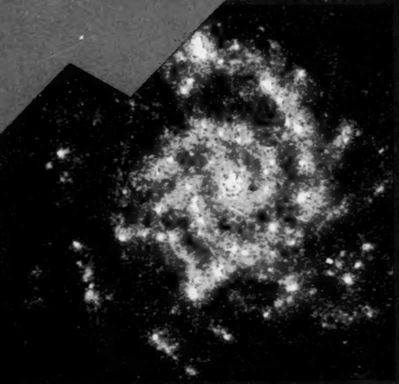

An Abstract Journal

Volume 31, Number 2
February 1993
N93-10961 to N93-12543

Scientific and Technical Aerospace Reports

STAR

Scientific and Technical Aerospace Reports (STAR) is an abstract journal that provides comprehensive coverage of worldwide aerospace-related reports. It is a major product of the International Aerospace Database managed by the NASA Scientific and Technical Information (STI) Program. The coverage includes reports on aeronautics, space, and supporting disciplines. *STAR* lists current, publicly available reports entered into the NASA STI Database during the 4-week period preceding publication. A typical citation and abstract appear on page viii. They explain how to read the items that are announced in this journal.

NASA sponsors a companion journal, *International Aerospace Abstracts (IAA)* (*NOVA* for internal NASA use) that lists abstracts of the open literature on aerospace subjects available worldwide. *IAA* is available for sale through the AIAA.

Entries found in *STAR* and *IAA* are available through NASA's online service, RECON, as the International Aerospace Database and through DIALOG as the Aerospace Database.

Information on aerospace and related subjects is gathered by the NASA STI Program through national and international agreements and exchanges and is made available to the NASA community as well as to the public in many forms through various outlets. The section on NASA STI Program Products and Services contains additional information.

For further information please contact:
NASA Center for AeroSpace Information (CASI)
P.O. Box 8757
Baltimore, Maryland 21240-0757
(301) 621-0390

US ISSN 0036-8741

Volume 31 Number 2 / February 1993

TABLE OF CONTENTS

AERONAUTICS For related information see also *Astronautics.*

01 AERONAUTICS (GENERAL) .... N.A.

02 AERODYNAMICS 195
Includes aerodynamics of bodies, combinations, wings, rotors, and control surfaces; and internal flow in ducts and turbomachinery. For related information see also *34 Fluid Mechanics and Heat Transfer.*

03 AIR TRANSPORTATION AND SAFETY 203
Includes passenger and cargo air transport operations; and aircraft accidents. For related information see also *16 Space Transportation* and *85 Urban Technology and Transportation.*

04 AIRCRAFT COMMUNICATIONS AND NAVIGATION 204
Includes digital and voice communication with aircraft; air navigation systems (satellite and ground based); and air traffic control. For related information see also *17 Space Communications, Spacecraft Communications, Command and Tracking* and *32 Communications and Radar.*

05 AIRCRAFT DESIGN, TESTING AND PERFORMANCE 206
Includes aircraft simulation technology. For related information see also *18 Spacecraft Design, Testing and Performance* and *39 Structural Mechanics.* For land transportation vehicles see *85 Urban Technology and Transportation.*

06 AIRCRAFT INSTRUMENTATION 209
Includes cockpit and cabin display devices; and flight instruments. For related information see also *19 Spacecraft Instrumentation* and *35 Instrumentation and Photography.*

07 AIRCRAFT PROPULSION AND POWER 209
Includes prime propulsion systems and systems components, e.g., gas turbine engines and compressors; and onboard auxiliary power plants for aircraft. For related information see also *20 Spacecraft Propulsion and Power, 28 Propellants and Fuels,* and *44 Energy Production and Conversion.*

08 AIRCRAFT STABILITY AND CONTROL 214
Includes aircraft handling qualities; piloting; flight controls; and autopilots. For related information see also *05 Aircraft Design, Testing and Performance.*

09 RESEARCH AND SUPPORT FACILITIES (AIR) 216
Includes airports, hangars and runways; aircraft repair and overhaul facilities; wind tunnels; shock tubes; and aircraft engine test stands. For related information see also *14 Ground Support Systems and Facilities (Space).*

ASTRONAUTICS For related information see also *Aeronautics.*

12 ASTRONAUTICS (GENERAL) 219
For extraterrestrial exploration see *91 Lunar and Planetary Exploration.*

13 ASTRODYNAMICS 220
Includes powered and free-flight trajectories; and orbital and launching dynamics.

14 GROUND SUPPORT SYSTEMS AND FACILITIES (SPACE) 221
Includes launch complexes, research and production facilities; ground support equipment, e.g., mobile transporters; and simulators. For related information see also *09 Research and Support Facilities (Air).*

15 LAUNCH VEHICLES AND SPACE VEHICLES 222
Includes boosters; operating problems of launch/space vehicle systems; and reusable vehicles. For related information see also *20 Spacecraft Propulsion and Power.*

16 SPACE TRANSPORTATION 223
Includes passenger and cargo space transportation, e.g., shuttle operations; and space rescue techniques. For related information see also *03 Air Transportation and Safety* and *18 Spacecraft Design, Testing and Performance.* For space suits see *54 Man/System Technology and Life Support.*

17 SPACE COMMUNICATIONS, SPACECRAFT COMMUNICATIONS, COMMAND AND TRACKING . 224
Includes telemetry; space communications networks; astronavigation and guidance; and radio blackout. For related information see also *04 Aircraft Communications and Navigation* and *32 Communications and Radar.*

N.A.—no abstracts were assigned to this category for this issue.

18 SPACECRAFT DESIGN, TESTING AND PERFORMANCE **224**
Includes satellites; space platforms; space stations; spacecraft systems and components such as thermal and environmental controls; and attitude controls. For life support systems see *54 Man/System Technology and Life Support*. For related information see also *05 Aircraft Design, Testing and Performance, 39 Structural Mechanics*, and *16 Space Transportation*.

19 SPACECRAFT INSTRUMENTATION .... **N.A.**
For related information see also *06 Aircraft Instrumentation* and *35 Instrumentation and Photography*.

20 SPACECRAFT PROPULSION AND POWER **230**
Includes main propulsion systems and components, e.g., rocket engines; and spacecraft auxiliary power sources. For related information see also *07 Aircraft Propulsion and Power, 28 Propellants and Fuels, 44 Energy Production and Conversion*, and *15 Launch Vehicles and Space Vehicles*.

CHEMISTRY AND MATERIALS

23 CHEMISTRY AND MATERIALS (GENERAL) **236**

24 COMPOSITE MATERIALS **236**
Includes physical, chemical, and mechanical properties of laminates and other composite materials. For ceramic materials see *27 Nonmetallic Materials*.

25 INORGANIC AND PHYSICAL CHEMISTRY **244**
Includes chemical analysis, e.g., chromatography; combustion theory; electrochemistry; and photochemistry. For related information see also *77 Thermodynamics and Statistical Physics*.

26 METALLIC MATERIALS **254**
Includes physical, chemical, and mechanical properties of metals, e.g., corrosion; and metallurgy.

27 NONMETALLIC MATERIALS **263**
Includes physical, chemical, and mechanical properties of plastics, elastomers, lubricants, polymers, textiles, adhesives, and ceramic materials. For composite materials see *24 Composite Materials*.

28 PROPELLANTS AND FUELS **273**
Includes rocket propellants, igniters and oxidizers; their storage and handling procedures; and aircraft fuels. For related information see also *07 Aircraft Propulsion and Power, 20 Spacecraft Propulsion and Power*, and *44 Energy Production and Conversion*.

29 MATERIALS PROCESSING **276**
Includes space-based development of products and processes for commercial application. For biological materials see *55 Space Biology*.

ENGINEERING For related information see also *Physics*.

31 ENGINEERING (GENERAL) **276**
Includes vacuum technology; control engineering; display engineering; cryogenics; and fire prevention.

32 COMMUNICATIONS AND RADAR **277**
Includes radar; land and global communications; communications theory; and optical communications. For related information see also *04 Aircraft Communications and Navigation* and *17 Space Communications, Spacecraft Communications, Command and Tracking*. For search and rescue see *03 Air Transportation and Safety*, and *16 Space Transportation*.

33 ELECTRONICS AND ELECTRICAL ENGINEERING **288**
Includes test equipment and maintainability; components, e.g., tunnel diodes and transistors; microminiaturization; and integrated circuitry. For related information see also *60 Computer Operations and Hardware* and *76 Solid-State Physics*.

34 FLUID MECHANICS AND HEAT TRANSFER **296**
Includes boundary layers; hydrodynamics; fluidics; mass transfer and ablation cooling. For related information see also *02 Aerodynamics* and *77 Thermodynamics and Statistical Physics*.

35 INSTRUMENTATION AND PHOTOGRAPHY **309**
Includes remote sensors; measuring instruments and gauges; detectors; cameras and photographic supplies; and holography. For aerial photography see *43 Earth Resources and Remote Sensing*. For related information see also *06 Aircraft Instrumentation* and *19 Spacecraft Instrumentation*.

36 LASERS AND MASERS **314**
Includes parametric amplifiers. For related information see also *76 Solid-State Physics*.

37 MECHANICAL ENGINEERING 323
Includes auxiliary systems (nonpower); machine elements and processes; and mechanical equipment.

38 QUALITY ASSURANCE AND RELIABILITY 331
Includes product sampling procedures and techniques; and quality control.

39 STRUCTURAL MECHANICS 333
Includes structural element design and weight analysis; fatigue; and thermal stress. For applications see *05 Aircraft Design, Testing and Performance* and *18 Spacecraft Design, Testing and Performance.*

GEOSCIENCES For related information see also *Space Sciences.*

42 GEOSCIENCES (GENERAL) .... N.A.

43 EARTH RESOURCES AND REMOTE SENSING 342
Includes remote sensing of earth resources by aircraft and spacecraft; photogrammetry; and aerial photography. For instrumentation see *35 Instrumentation and Photography.*

44 ENERGY PRODUCTION AND CONVERSION 344
Includes specific energy conversion systems, e.g., fuel cells; global sources of energy; geophysical conversion; and windpower. For related information see also *07 Aircraft Propulsion and Power, 20 Spacecraft Propulsion and Power,* and *28 Propellants and Fuels.*

45 ENVIRONMENT POLLUTION 349
Includes atmospheric, noise, thermal, and water pollution.

46 GEOPHYSICS 357
Includes aeronomy; upper and lower atmosphere studies; ionospheric and magnetospheric physics; and geomagnetism. For space radiation see *93 Space Radiation.*

47 METEOROLOGY AND CLIMATOLOGY 366
Includes weather forecasting and modification.

48 OCEANOGRAPHY 372
Includes biological, dynamic, and physical oceanography; and marine resources. For related information see also *43 Earth Resources and Remote Sensing.*

LIFE SCIENCES

51 LIFE SCIENCES (GENERAL) 374

52 AEROSPACE MEDICINE 375
Includes physiological factors; biological effects of radiation; and effects of weightlessness on man and animals.

53 BEHAVIORAL SCIENCES 385
Includes psychological factors; individual and group behavior; crew training and evaluation; and psychiatric research.

54 MAN/SYSTEM TECHNOLOGY AND LIFE SUPPORT 387
Includes human engineering; biotechnology; and space suits and protective clothing. For related information see also *16 Space Transportation.*

55 SPACE BIOLOGY 391
Includes exobiology; planetary biology; and extraterrestrial life.

MATHEMATICAL AND COMPUTER SCIENCES

59 MATHEMATICAL AND COMPUTER SCIENCES (GENERAL) 391

60 COMPUTER OPERATIONS AND HARDWARE 404
Includes hardware for computer graphics, firmware, and data processing. For components see *33 Electronics and Electrical Engineering.*

61 COMPUTER PROGRAMMING AND SOFTWARE 406
Includes computer programs, routines, algorithms, and specific applications, e.g., CAD/CAM.

62 COMPUTER SYSTEMS 417
Includes computer networks and special application computer systems.

63 CYBERNETICS 420
Includes feedback and control theory, artificial intelligence, robotics and expert systems. For related information see also *54 Man/System Technology and Life Support.*

64 NUMERICAL ANALYSIS 423
Includes iteration, difference equations, and numerical approximation.

65 STATISTICS AND PROBABILITY 428
Includes data sampling and smoothing; Monte Carlo method; and stochastic processes.

66 SYSTEMS ANALYSIS 430
Includes mathematical modeling; network analysis; and operations research.

67 THEORETICAL MATHEMATICS 430
Includes topology and number theory.

PHYSICS For related information see also *Engineering.*

70 PHYSICS (GENERAL) 430
For precision time and time interval (PTTI) see *35 Instrumentation and Photography;* for geophysics, astrophysics or solar physics see *46 Geophysics, 90 Astrophysics,* or *92 Solar Physics.*

71 ACOUSTICS 432
Includes sound generation, transmission, and attenuation. For noise pollution see *45 Environment Pollution.*

72 ATOMIC AND MOLECULAR PHYSICS 435
8Includes atomic structure, electron properties, and molecular spectra.

73 NUCLEAR AND HIGH-ENERGY PHYSICS 442
Includes elementary and nuclear particles; and reactor theory. For space radiation see *93 Space Radiation.*

74 OPTICS 446
Includes light phenomena and optical devices. For lasers see *36 Lasers and Masers.*

75 PLASMA PHYSICS 449
Includes magnetohydrodynamics and plasma fusion. For ionospheric plasmas see *46 Geophysics.* For space plasmas see *90 Astrophysics.*

76 SOLID-STATE PHYSICS 458
Includes superconductivity. For related information see also *33 Electronics and Electrical Engineering* and *36 Lasers and Masers.*

77 THERMODYNAMICS AND STATISTICAL PHYSICS 470
Includes quantum mechanics; theoretical physics; and Bose and Fermi statistics. For related information see also *25 Inorganic and Physical Chemistry* and *34 Fluid Mechanics and Heat Transfer.*

SOCIAL SCIENCES

80 SOCIAL SCIENCES (GENERAL) .... N.A.
Includes educational matters.

81 ADMINISTRATION AND MANAGEMENT 472
Includes management planning and research.

82 DOCUMENTATION AND INFORMATION SCIENCE 473
Includes information management; information storage and retrieval technology; technical writing; graphic arts; and micrography. For computer documentation see *61 Computer Programming and Software.*

83 ECONOMICS AND COST ANALYSIS 480
Includes cost effectiveness studies.

84 LAW, POLITICAL SCIENCE AND SPACE POLICY .... N.A.
Includes NASA appropriation hearings; aviation law; space law and policy; international law; international cooperation; and patent policy.

85 URBAN TECHNOLOGY AND TRANSPORTATION 481
Includes applications of space technology to urban problems; technology transfer; technology assessment; and surface and mass transportation. For related information see *03 Air Transportation and Safety, 16 Space Transportation,* and *44 Energy Production and Conversion.*

SPACE SCIENCES For related information see also *Geosciences.*

88 SPACE SCIENCES (GENERAL) .... **N.A.**

89 ASTRONOMY **481**
Includes radio, gamma-ray, and infrared astronomy; and astrometry.

90 ASTROPHYSICS **483**
Includes cosmology; celestial mechanics; space plasmas; and interstellar and interplanetary gases and dust. For related information see also *75 Plasma Physics.*

91 LUNAR AND PLANETARY EXPLORATION **486**
Includes planetology; and manned and unmanned flights. For spacecraft design or space stations see *18 Spacecraft Design, Testing and Performance.*

92 SOLAR PHYSICS **487**
Includes solar activity, solar flares, solar radiation and sunspots. For related information see *93 Space Radiation.*

93 SPACE RADIATION **489**
Includes cosmic radiation; and inner and outer earth's radiation belts. For biological effects of radiation see *52 Aerospace Medicine.* For theory see *73 Nuclear and High-Energy Physics.*

GENERAL

Includes aeronautical, astronautical, and space science related histories, biographies, and pertinent reports too broad for categorization; histories or broad overviews of NASA programs.

99 GENERAL **489**

SUBJECT INDEX **I-1**

PERSONAL AUTHOR INDEX **I-119**

CORPORATE SOURCE INDEX **I-133**

CONTRACT NUMBER INDEX **I-153**

REPORT NUMBER INDEX **I-157**

APPENDIX **A-1**

TYPICAL CITATION AND ABSTRACT

NASA SPONSORED
ON MICROFICHE

ACCESSION NUMBER → **N93-10068*#** Washington Univ., Seattle. Dept. of Atmospheric Sciences. ← **CORPORATE SOURCE**

TITLE → **AIR-SEA INTERACTION AND REMOTE SENSING Status Report, 1 Dec. 1991 - 30 Nov. 1992**

AUTHORS → Kristina B. Katsaros and Serhad S. Ataktuerk 1992 12 p

Original contains color illustrations ← **PUBLICATION DATE**

CONTRACT OR GRANT → (Grant NAGw-1322)

REPORT NUMBERS → (NASA-CR-190913; NAS 1.26:190913) Avail: CASI HC ← **AVAILABILITY SOURCE**

PRICE CODE → A03/MF A01; 2 functional color pages

The first part of the proposed research was a joint effort between our group and the Applied Physics Laboratory (APL), University of Washington. Our own research goal is to investigate the relation between the air-sea exchange processes and the sea state over the open ocean and to compare these findings with our previous results obtained over a small body of water namely, Lake Washington. The goals of the APL researchers are to study (1) the infrared sea surface temperature (SST) signature of breaking waves and surface slicks, and (2) microwave and acoustic scattering from water surface. The task of our group in this joint effort is to conduct measurements of surface fluxes (of momentum, sensible heat, and water vapor) and atmospheric radiation (longwave and shortwave) to achieve our research goal as well as to provide crucial complementary data for the APL studies. The progress of the project is summarized. Author

VOLUME 31 NUMBER 2 / FEBRUARY 1993

Scientific and Technical Aerospace Reports

A Monthly Publication of the National Aeronautics and Space Administration

01 AERONAUTICS (GENERAL)

No abstracts in this category.

02 AERODYNAMICS

Includes aerodynamics of bodies, combinations, wings, rotors, and control surfaces; and internal flow in ducts and turbomachinery.

For related information see also *34 Fluid Mechanics and Heat Transfer.*

N93-11008# Messerschmitt-Boelkow-Blohm G.m.b.H., Munich (Germany). Space Group.
FLOW FIELD CALCULATIONS AROUND THE HERMES SPACEPLANE DURING REENTRY PHASE [STROEMUNGSFELDBERECHNUNGEN UM DEN HERMES RAUMGLETTER WAEHREND DER WIEDEREINTRITTSPHASE]
Gerhard Hartmann and Claus Weiland 1991 11 p In GERMAN Presented at the DGLR-Jahrestagung 1991 and DLR Kongress 1991, Berlin, Fed. Republic of Germany, 10-13 Sep. 1991 Submitted for publication
(MBB-UK-0148-91-PUB; ETN-92-92113) Avail: CASI HC A03/MF A01

A calculation process to obtain the friction free flow with real gas in equilibrium around a reentry body is presented. The characteristics of the solution method are shown. The technique of net generation is addressed. The general procedure of net generation and the necessary adjustments of network configuration to body forms is explained. The flow field around Hermes using solutions of numerical flow simulation is reported, and is analyzed with regard to flow mechanical characteristics. Two results are presented for chemical nonequilibrium and compared with the corresponding solutions for chemical equilibrium. ESA

N93-11020# Rolls-Royce Ltd., Derby (England).
APPLICATION OF LAMINAR FLOW TO AERO ENGINE NACELLES
A. J. Mullender, A. L. Bergin (Manchester Univ., England), and D. I. A. Poll (Manchester Univ., England) 1 May 1991 9 p Presented at the Royal Aeronautical Society Boundary Layer Transition and Control, Cambridge, England, 8-12 Apr. 1991 Sponsored by Ministry of Defence and RAE
(PNR-90916; ETN-92-92205) Avail: CASI HC A02/MF A01

In the search for methods of reducing aircraft drag, the engine nacelle is considered as a candidate for laminar flow control. Preliminary results from wind tunnel tests on a two dimensional model of Laminar Flow Control (LFC) by suction nacelles, are presented. An approach to transition prediction using stability theory is outlined. The experimental results demonstrated the achievement of laminar flow by suction to a length Reynolds number of 4,600,000, in a two dimensional model with a pressure distribution similar to that found on a conventional aero engine nacelle. The theoretical results obtained to date are not inconsistent with the experimental results. The theoretically predicted separation bubble is located above the first suction compartment of the laminar flow central model and would be removed with the application of suction. ESA

N93-11050 Department of the Navy, Washington, DC.
RIBLESS RAM AIR PARACHUTE Patent
James A. Buckley, inventor (to Navy) 7 Jan. 1992 9 p Filed 7 May 1990
(AD-D015351; US-Patent-5,078,344; US-Patent-Appl-SN-519626; US-Patent-Class-244-145) Avail: US Patent and Trademark Office

The upper and lower panel of a ram air inflated parachute canopy are connected on the interior of the canopy by lines extending between the panels at points spaced chordwise and spanwise of the panels so that airflow is unrestricted within the canopy and the weight and bulk of chordwise ribs is eliminated. The parachute suspension lines have connections to the lower panel at points where the interior lines connect to the lower panel and these connections may be made by loops incorporated in the lower panel. The interior line lengths and the proportions of spanwise end panels of the canopy may correspond to a triangular chordwise cross sectional shape of the canopy. The upper panel may have an extension in front of the lower panel with lines extending between the extension and the suspension lines to downwardly curve the extension and partially close the open forward end of the canopy. GRA

N93-11070# Rolls-Royce Ltd., Derby (England).
A COMBINED EXPERIMENTAL AND THEORETICAL STUDY OF LAMINAR FLOW CONTROL WITH PARTICULAR RELEVANCE TO AERO ENGINE NACELLES
A. J. Mullender and D. I. A. Poll (Manchester Univ., England) 30 Apr. 1992 5 p Presented at the 1st European Forum on Laminar Flow Technology, Hamburg, Fed. Republic of Germany, 16-18 Mar. 1992 Sponsored by Ministry of Defence and Ministry of Trade and Industry
(PNR-90991; ETN-92-92247) Copyright Avail: CASI HC A01/MF A01

A two dimensional model having a datum pressure distribution representative of that found on a typical nacelle was tested in the 2.7 by 2.1 m low turbulence, low speed, closed circuit wind tunnel. The model features full chord suction through a continuous laser drilled surface mounted on 13 independently controlled plenum chambers. Boundary layer state is determined by the use of 48 microphones mounted beneath the surface and an array of hot films. Incidence is variable over the range -5 to +5 deg, which enables a wide range of surface pressure distributions representative of a spectrum of designs applicable to aeroengine nacelles, from natural laminar flow through hybrid laminar flow control to laminar flow control by boundary layer suction. Theoretical methods, being developed and validated in a parallel study for both the determination of the mean compressible boundary layer development with suction, using a finite difference scheme and stability analysis of the resultant boundary layer profiles are also considered. These codes are to be used to determine a method for boundary layer prediction which can be applied to the design of optimized nacelles. ESA

N93-11113# Rolls-Royce Ltd., Derby (England).
A EUROPEAN COLLABORATIVE NLF NACELLE FLIGHT DEMONSTRATOR
P. P. Shipley, N. T. Birch, H. Riedel (Deutsche Forschungsanstalt fuer Luft- und Raumfahrt, Brunswick, Germany), K. H. Horstmann (Deutsche Forschungsanstalt fuer Luft- und Raumfahrt, Brunswick, Germany), and P. Luecking (Motoren- und Turbinen-Union Muenchen G.m.b.H., Germany) 7 Apr. 1992 10 p
(PNR-90992; ETN-92-92248) Copyright Avail: CASI HC A02/MF A01

Progress made to date on the collaborative Natural Laminar Flow (NLF) nacelle flight demonstrator program is described. The aerodynamic concept of the NLF nacelle is described in terms of the expected drag benefits, the required design methodology, and the requirements for flight testing. The nacelle aerodynamic design is considered, including the effects of installation, using a three dimensional Euler method. Forthcoming flight program and overall objectives of the flight testing are also described. ESA

N93-11141# Deutsche Forschungsanstalt fuer Luft- und Raumfahrt, Goettingen (Germany). Abt. Instabilitaeten und Abloesung.
ON THE INSTABILITY OF HYPERSONIC FLOW PAST A POINTED CONE: COMPARISON OF THEORETICAL AND EXPERIMENTAL RESULTS OF MACH 18 [UEBER DIE INSTABILITAET DER HYPERSONISCHEN KEGELUMSTROEMUNG: VERGLEICH THEORETISCHER UND EXPERIMENTELLER ERGEBNISSE BEI MACH 8]
Martin Simen (Dornier Luftfahrt G.m.b.H., Friedrichshafen, Germany) and Uwe Dallmann Aug. 1991 75 p
(DLR-FB-92-02; ETN-92-92400) Avail: CASI HC A04/MF A01; DLR, Wissenshaftliches Berichtswesen, VB-PL-DO, Postfach 90 60 58, 5000 Cologne, Fed. Republic of Germeny, HC

In view of the prevailing discrepancies between experiment and theory with regard to instabilities in hypersonic flow, an extended theoretical approach was studied. For hypersonic flow past a pointed cone thin layer Navier-Stokes solutions were compared to similarity solutions with different modeling of viscosity temperature laws. The formulation of the stability equations in curvilinear coordinates allows a discussion of various representations of the local body metric. A systematic sensitivity study of basic state profiles and spatial amplification rates was performed. It was found that the improved agreement with the experiment in the viscous first mode region is equally due to the extended stability analysis, where cone metric is specified, and the extended mean flow solution as well. In the second mode region, the major improvement results from the more complete basic state formulation, however, the close agreement with measured growth rate was only achieved when the stability analysis was based on a conical metric. ESA

N93-11157# Centro Italiano Ricerche Aerospaziali, Naples.
THERMOKINETIC MODELLING AND HYPERSONIC FLOW
Salvatore Borrelli, Giuseppe Leone, and Antonio Schettino 9 Oct. 1991 25 p Presented at the 11th AIDAA Congress, Forli, Italy, 14-18 Oct. 1991 Sponsored in part by Italian Space Agency
(DILC-EST-TN-218; ETN-92-92410) Avail: CASI HC A03/MF A01

The influence of chemical modeling on the computation of high enthalpy flows is considered. Some classical thermokinetic models are used to point out the differences in flow field characteristics due to the use of such different models (Park '85, Rachich, Evans Huber, Kang Dunn and Monti-Napolitano). The differences obtained are evidenced, and an attempt to explain them is made by analyzing their modeling significance. From the computational point of view, the approach is based on Euler boundary layer equation coupling. The inviscid flow field is calculated with an upwind flux difference splitting formulation. The viscous part is based on boundary layer equation written in difference form and for reactive gas. ESA

N93-11221*# National Aeronautics and Space Administration. Hugh L. Dryden Flight Research Facility, Edwards, CA.
OVERVIEW OF SUPERSONIC LAMINAR FLOW CONTROL RESEARCH ON THE F-16XL SHIPS 1 AND 2
Bianca T. Anderson and Marta Bohn-Meyer Oct. 1992 15 p Presented at the 1992 Aerotech Conference, Anaheim, CA, 5-8 Oct. 1992
(RTOP 533-02-39)
(NASA-TM-104257; H-1858; NAS 1.15:104257; SAE Paper 92-1994) Avail: CASI HC A03/MF A01

NASA is directing research to develop technology for a high-speed civil transport. Supersonic laminar flow control has been identified as a program element, since it offers significant drag-reduction benefits and is one of the more promising technologies for producing an economically viable aircraft design. NASA is using two prototype F-16XL aircraft to research supersonic laminar flow control. The F-16XL planform is similar to design planforms of high-speed civil transports. The planform makes the aircraft ideally suited for developing technology pertinent to high-speed transports. The supersonic laminar flow control research programs for both aircraft are described. Some general results of the ship-1 program demonstrate that significant laminar flow was obtained using laminar flow control on a highly swept wing at supersonic speeds. Author

N93-11223*# National Aeronautics and Space Administration. Lewis Research Center, Cleveland, OH.
THE ENGINE DESIGN ENGINE. A CLUSTERED COMPUTER PLATFORM FOR THE AERODYNAMIC INVERSE DESIGN AND ANALYSIS OF A FULL ENGINE
J. Sanz, K. Pischel, and D. Hubler 1992 10 p Presented at the Grand Challenges, Washington, DC, 20-22 Sep. 1992, sponsored by NRL
(RTOP 505-62-52)
(NASA-TM-105838; E-7278; NAS 1.15:105838) Avail: CASI HC A02/MF A01

An application for parallel computation on a combined cluster of powerful workstations and supercomputers was developed. A Parallel Virtual Machine (PVM) is used as message passage language on a macro-tasking parallelization of the Aerodynamic Inverse Design and Analysis for a Full Engine computer code. The heterogeneous nature of the cluster is perfectly handled by the controlling host machine. Communication is established via Ethernet with the TCP/IP protocol over an open network. A reasonable overhead is imposed for internode communication, rendering an efficient utilization of the engaged processors. Perhaps one of the most interesting features of the system is its versatile nature, that permits the usage of the computational resources available that are experiencing less use at a given point in time. Author

N93-11250 Virginia Polytechnic Inst. and State Univ., Blacksburg.
THE HEMISPHERE-CYLINDER AT AN ANGLE OF ATTACK Ph.D. Thesis
Ngoc Thai Hoang 1991 318 p
Avail: Univ. Microfilms Order No. DA9220636

An experimental investigation was carried out of the flow over a hemisphere-cylinder at angles of attack alpha = 0 deg to 90 deg. Visualizations of skin-friction lines were conducted and were focused mainly on the development of the laminar separation bubble as a function of angle of attack, the conditions under which open and closed separation exist, and the interaction between the separation bubble and the leeward vortices. A digital processing method was developed to convert flow visualizations to numerical data. Static pressure measurements over a large range of Reynolds numbers were obtained for two models with different sizes and the same length-to-diameter ratios. Detailed velocity fields, mapped out by a seven hole probe and a laser-Doppler velocimeter (LDV) probe, were carefully examined to provide information on the development of vortical structures on the surfaces of the model. Comparisons were made of the results obtained using these two instruments. The flow field in the

wake of the hemisphere-cylinder was also examined at an angle of attack alpha = 30 deg. A small bead was strategically placed near the nose to force vortex asymmetry. Different sizes of beads were also tested to investigate the effectiveness on the asymmetric pattern. Hot-wire anemometers and a dynamic signal analyzer were employed to study the unsteady motion of leeward vortices.
Dissert. Abstr.

N93-11365# Admiralty Research Establishment, Gosport (England).
EXPERIMENTS ON LOW ASPECT RATIO HYDROPLANES TO MEASURE LIFT UNDER STATIC AND DYNAMIC CONDITIONS
A. R. J. M. Lloyd and B. Ward Mar. 1990 41 p Original contains color illustrations
(ARE-TM(UHR)-90306; BR114028; ETN-92-92296) Copyright
Avail: CASI HC A03/MF A01

Experiments in the circulating water channel to measure lift forces on low aspect ratio hydroplanes under static and dynamic conditions are described. The dynamic conditions consisted of oscillating runs and ramping motions. Empirical equations to represent the results are given. The results showed the dynamic effects on oscillating hydroplanes were small but worth noting. The most interesting aspect of the experiment was the delayed stall noted during the ramping motion experiments. ESA

N93-11377# Admiralty Research Establishment, Gosport (England). Maritime Div.
LIFT COEFFICIENT OF A RANDOMLY OSCILLATING HYDROPLANE
M. J. Smith Aug. 1991 46 p Original contains color illustrations
(DRA/Mar-TM(MTH)-91320; BR305563; ETN-92-92294)
Copyright Avail: CASI HC A03/MF A01

The measurement of lift on a randomly oscillating hydroplane is described. A comparison is made between oscillating the hydroplane randomly or with regular sinusoidal signals together with the different methods of analysis. In the 'regular' experiments three different aspect ratio hydroplanes were tested in several different flow speeds and a number of different oscillation frequencies. As the 'random' tests were performed when the regular experiments allowed, only one hydroplane aspect ratio (1.5), was tested in one flow speed (2.5 m/s nominal). For the random experiments two spectra were used, one narrow band and one broadband. Spectrum 1 was a 5 second period ITTC spectrum covering frequencies from 0.12 to 0.44 Hz. Spectrum 2 was a constant energy density spectrum covering frequencies from zero to 1.2 Hz. It was found that measurement of lift coefficient and other similar quantities on constrained models can be conducted more quickly and efficiently using random signals. Explanations are given. ESA

N93-11464# Glasgow Univ. (Scotland). Dept. of Aerospace Engineering.
THE CONVECTION SPEED OF THE DYNAMIC STALL VORTEX Final Report, 1 Nov. 1989 - 31 Oct. 1991
R. B. Green, R. A. Galbraith, and A. J. Niven 1 Jan. 1992 125 p
(Grant AF-AFOSR-0397-89)
(AD-A247258; GU-AERO-9202) Avail: CASI HC A06/MF A02

This report describes measurements of the convection speed of the dynamic stall vortex. A survey reveals a disharmony between the various researchers as to the dependency of the convection speed upon the aerofoil motion. A preliminary analysis of pressure data from aerofoil models tested at Reynolds and Mach numbers of 1.5 million and 0.11 respectively showed that the convection speed was independent of aerofoil motion and model type to a first order. Testing a high aspect ratio NACA 0015 showed that wind tunnel constraint was not a significant factor. An enhanced analysis technique produced results which, in spite of their poor accuracy, suggest that at low pitch rates the convection speed falls with increasing reduced pitch rate to a constant value for the NACA 0015 and 0018 models. The effect of a leading edge trip was to significantly alter the details of the dynamic stall and to change the vortex convection speed. Although the convection speed/aerofoil motion dependency anomaly has not been not fully solved, it is suggested that leading edge effects influence the convection speed, and the aerofoil leading edge geometry, Reynolds and Mach numbers are highlighted. GRA

N93-11532*# National Aeronautics and Space Administration. Hugh L. Dryden Flight Research Facility, Edwards, CA.
CORRELATION OF FOREBODY PRESSURES AND AIRCRAFT YAWING MOMENTS ON THE X-29A AIRCRAFT AT HIGH ANGLES OF ATTACK
David F. Fisher, David M. Richwine (PRC Kentron, Inc., Edwards, CA.), and Stephen Landers (PRC Kentron, Inc., Edwards, CA.) Nov. 1992 17 p Presented at the AIAA Flight Test Conference, Hilton Head, SC, 24-26 Aug. 1992
(RTOP 533-02-38)
(NASA-TM-4417; H-1851; NAS 1.15:4417; AIAA Paper 92-4105)
Copyright Avail: CASI HC A03/MF A01

In-flight pressure distributions at four fuselage stations on the forebody of the X-29A aircraft have been reported at angles of attack from 15 to 66 deg and at Mach numbers from 0.22 to 0.60. At angles of attack of 20 deg and higher, vortices shed from the nose strake caused suction peaks in the pressure distributions that generally increased in magnitude with angle of attack. Above 30 deg-angle of attack, the forebody pressure distributions became asymmetrical at the most forward station, while they remained nearly symmetrical until 50 to 55 deg-angle of attack for the aft stations. Between 59 to 66 deg-angle of attack, the asymmetry of the pressure distributions changed direction. Yawing moments for the forebody alone were obtained by integrating the forebody pressure distributions. At 45 deg-angle of attack, the aircraft yaws to the right and at 50 deg and higher, the aircraft yaws to the left. The forebody yawing moments correlated well with the aircraft left yawing moment at an angle of attack of 50 deg or higher. At a 45 deg-angle of attack, the forebody yawing moments did not correlate well with the aircraft yawing moment, but it is suggested that this was due to asymmetric pressures on the cockpit region of the fuselage which was not instrumented. The forebody was also shown to provide a positive component of directional stability of the aircraft at angles of attack of 25 deg or higher. A Mach number effect was noted at angles of attack of 30 deg or higher at the station where the nose strake was present. At this station, the suction peaks in the pressure distributions at the highest Mach number were reduced and much more symmetrical as compared to the lower Mach number pressure distributions. Author

N93-11605*# North Carolina State Univ., Raleigh.
EXPERIMENTAL INVESTIGATION OF THE EFFECTS OF AFT BLOWING WITH VARIOUS NOZZLE EXIT GEOMETRIES ON A 3.0 CALIBER TANGENT OGIVE AT HIGH ANGLES OF ATTACK: FOREBODY PRESSURE DISTRIBUTIONS Final Technical Report
Ndaona Chokani and N. M. Gittner 1 May 1992 93 p
(Contract NCC1-46)
(NASA-CR-190935; NAS 1.26:190935) Avail: CASI HC A05/MF A01

An experimental study of the effects of aft blowing on the asymmetric vortex flow of a slender, axisymmetric body at high angles of attack was conducted. A 3.0 caliber tangent ogive body fitted with a cylindrical afterbody was tested in a wind tunnel under subsonic, laminar flow test conditions. Asymmetric blowing from both a single nozzle and a double nozzle configuration, positioned near the body apex, was studied. Aft blowing was observed to alter the vortex asymmetry by moving the blowing-side vortex closer to the body surface while moving the non-blowing-side vortex further away from the body. The effect of increasing the blowing coefficient was to move the blowing-side vortex closer to the body surface at a more upstream location. The data also showed that blowing was more effective in altering the initial vortex asymmetry at the higher angles of attack than at the lower. The effects of changing the nozzle exit geometry were studied and it was observed that blowing from a nozzle with a low, broad exit geometry was more effective in reducing the vortex asymmetry than blowing from a high, narrow exit geometry. Author

N93-11607*# Institute for Computer Applications in Science and Engineering, Hampton, VA.
REVIEW OF PRECONDITIONING METHODS FOR FLUID DYNAMICS Final Report
Eli Turkel (Tel-Aviv Univ., Israel) Sep. 1992 36 p Submitted for publication
(Contract NAS1-19480; RTOP 505-90-52-01)
(NASA-CR-189712; NAS 1.26:189712; ICASE-92-47) Avail: CASI HC A03/MF A01

We consider the use of preconditioning methods to accelerate the convergence to a steady state for both the incompressible and compressible fluid dynamic equations. Most of the analysis relies on the inviscid equations though some applications for viscous flow are considered. The preconditioning can consist of either a matrix or a differential operator acting on the time derivatives. Hence, in the steady state the original steady solution is obtained. For finite difference methods the preconditioning can change and improve the steady state solutions. Several preconditioners previously discussed are reviewed and some new approaches are presented. Author

N93-11610*# National Aeronautics and Space Administration. Langley Research Center, Hampton, VA.
FURTHER BUFFETING TESTS IN A CRYOGENIC WIND TUNNEL
D. G. Mabey (Royal Aircraft Establishment, Bedford, England), R. P. Boyden, and W. G. Johnson, Jr. Sep. 1992 55 p Previously announced as X92-71521
(RTOP 505-59-30-01)
(NASA-TM-107621; NAS 1.15:107621; RAE-TM-Aero-2231)
Avail: CASI HC A04/MF A01

Further measurements of buffeting, using wing-root strain gauges, were made in the NASA Langley 0.3 m Cryogenic Wind Tunnel to refine techniques which will be used in larger cryogenic facilities such as the United States National Transonic Facility (NTF) and European Transonic Wind Tunnel (ETW). The questions addressed included the relative importance of variations in frequency parameter and Reynolds number, the choice of model material (considering both stiffness and damping) and the effects of static aeroelastic distortion. The main series of tests was made on half models of slender 65 deg delta wings with a sharp leading edge. The three delta wings had the same planform but widely different bending stiffness and frequencies (obtained by varying both the material and the thickness of the wings). It was known that the flow on this configuration would be insensitive to variations in Reynold number. Additional tests were made on one unswept half-wing of aspect ratio 1.5 with an NPL 9510 aerofoil section, known to be sensitive to variations in Reynolds number at transonic speeds. For brevity the test Mach numbers were restricted to $M = 0.21$ and 0.35 for the delta wings and to $M = 0.30$ for the unswept wing. Author

N93-11622*# National Aeronautics and Space Administration. Langley Research Center, Hampton, VA.
LOW-SPEED LONGITUDINAL AND LATERAL-DIRECTIONAL AERODYNAMIC CHARACTERISTICS OF THE X-31 CONFIGURATION
Daniel W. Banks, Gregory M. Gatlin, and John W. Paulson, Jr. Oct. 1992 340 p
(RTOP 505-68-30-04)
(NASA-TM-4351; L-16921; NAS 1.15:4351) Avail: CASI HC A15/MF A03

An experimental investigation of a 19 pct. scale model of the X-31 configuration was completed in the Langley 14 x 22 Foot Subsonic Tunnel. This study was performed to determine the static low speed aerodynamic characteristics of the basic configuration over a large range of angle of attack and sideslip and to study the effects of strakes, leading-edge extensions (wing-body strakes), nose booms, speed-brake deployment, and inlet configurations. The ultimate purpose was to optimize the configuration for high angle of attack and maneuvering-flight conditions. The model was tested at angles of attack from -5 to 67 deg and at sideslip angles from -16 to 16 deg for speeds up to 190 knots (dynamic pressure of 120 psf). Author

N93-11686# Von Karman Inst. for Fluid Dynamics, Rhode-Saint-Genese (Belgium).
A THREE DIMENSIONAL HIGH RESOLUTION UPWIND FINITE VOLUME EULER SOLVER
M. Manna Apr. 1992 126 p
(VKI-TN-180; ETN-92-92363) Avail: CASI HC A07/MF A02

A general three dimensional single block Euler solver was developed and validated for a large number of test cases. The evaluation of the residuals via sophisticated upwind techniques was shown to represent a reliable and valuable alternative to classical central schemes. The high resolution schemes, although computationally expensive, can therefore be recognized as a good starting point for the construction of a Navier-Stokes solver. No major differences, especially for high order schemes, were found between the approximate Rieman solver of Roe and the flux vector splitting method of Van Leer, in terms of capabilities of accurately resolving shock waves and contact discontinuities. However, the Van Leer scheme, which is certainly less expensive and more robust than Roe's one, has a worse resolution for grid aligned shear flows, and therefore its use for viscous computations should probably not be encouraged. The modified version proposed by Hanel, which seems to have overcome the misinterpretation of the shear phenomena, is worth implementation and further investigation. ESA

N93-11742# Texas Univ., Austin. Dept. of Aerospace Engineering and Engineering Mechanics.
EFFECTS OF SWEEP ON THE PHYSICS OF UNSTEADY SHOCK-INDUCED TURBULENT SEPARATED FLOWS Final Report, 1 Mar. 1989 - 30 Jun. 1991
David S. Dolling 10 Jan. 1992 43 p
(Grant AF-AFOSR-0112-86)
(AD-A247035; AFOSR-92-0154TR) Avail: CASI HC A03/MF A01

To examine the effects of sweepback on the unsteady separation in Mach 5 compression ramp interactions, fluctuating wall pressure measurements have been made upstream of the corner line in interactions generated by unswept, and 10, 20, 25, 30, 40, and 50 deg. swept models. The streamwise ramp angle was 28 deg. in all cases. The data were analyzed using standard time series analysis techniques and condition all sampling algorithms. The results show that in highly swept interactions (i.e., corner line sweeps greater than 25 deg.), the rms distributions of pressure fluctuations as well as the mean distributions are quasi-conically symmetric. Rms levels decrease globally with increasing sweep as does the maximum rms generated by the translating separation shock. The length of the intermittent region, over which the separation shock foot translates, decreases with increasing sweep. In a given interaction, the length of the intermittent region grows spanwise. Dominant separation shock frequencies, observed in both surface pressure fluctuations and separation shock foot histories, increase from about 0.3 to 0.5 kHz for unswept flow to about 2-7 kHz in highly swept flows. In a given interaction, shock frequencies decrease spanwise. Separation shock dynamics defined in terms of the shock foot history and its statistics are essentially the same in all interactions. The separation shock foot position is normally distributed, and the mean shock velocities are essentially equal. The only difference is in the length of the region in which the separation shock moves. Higher frequencies are a direct result of the decrease in the length scale of the separation shock motion. GRA

N93-11874 Saint Andrew's Univ. (Scotland).
NONLINEAR STABILITY OF FLOWS OVER RIGID AND FLEXIBLE BOUNDARIES Ph.D. Thesis
Michael Dominic Thomas 1990 212 p
Avail: Univ. Microfilms Order No. BRDX93484

The importance of nonlinearity in the stability of flows over compliant and rigid walls is discussed in three parts. The first part considers inviscid flow with a free surface over a flexibility boundary. The dispersion relation is obtained, and the conditions for linear instability investigated. The linear dispersion relation is then used to show that the conditions for nonlinear three-wave resonance are often met. In some circumstances, the resonance may be of 'explosive' sort, involving waves of opposite energy sign; but non-explosive resonant configurations are most common. Next, the wave-amplitude evolution equations for three-wave resonance are derived, firstly by a 'direct' approach, and then via a variational (averaged Lagrangian) method. Results agree with those of Case and Chiu for capillary-gravity waves, and Craik and Adam, for three-layer fluid flow, on taking the appropriate limits. We also consider a nonlinear model for the flexible boundary. In the second part, stability of Blasius flow over a compliant surface is studied. This extension of the rigid-wall work of Craik and Hendriks determines the quadratic interaction coefficients of three-wave resonance, and complements the linear analysis of Carpenter and Garrad and others. First, the linear eigenvalue spectrum is investigated for various values of the wall parameters. Then, resonant triads are located and the quadratic interaction coefficients determined numerically. By way of introduction some rigid-wall results are also presented, extending those of Hendriks. Author

N93-11876*# National Aeronautics and Space Administration. Langley Research Center, Hampton, VA.
BOUNDARY LAYER RELAMINARIZATION DEVICE Patent Application
Theodore R. Creel, inventor (to NASA) 7 Jan. 1992 13 p
(NASA-Case-LAR-14470-1; NAS 1.71:LAR-14470-1; US-Patent-Appl-SN-823809) Avail: CASI HC A03/MF A01

Relamination of a boundary layer formed in supersonic flow over the leading edge of a swept airfoil is accomplished by means of at least one band, especially a quadrangular band, and most preferably a square band. Each band conforms to the leading edge and the upper and lower surfaces of the airfoil as an integral part thereof and extends perpendicularly from the leading edge. Each band has a height of about two times the thickness of the maximum expected boundary layer. NASA

N93-11882# Royal Aerospace Establishment, Bedford (England). Aerospace Div.
INTRODUCTION OF ELECTRONIC PRESSURE SCANNING AT THE ROYAL AEROSPACE ESTABLISHMENT
J. W. Holmes Oct. 1991 28 p Presented at the 37th Instrument Society of America International Instrumentation Symposium, San Diego, CA, 5-9 May 1991
(RAE-TM-Aero-2222; BR305818; ETN-92-92304) Copyright Avail: CASI HC A03/MF A01

An electronic pressure scanning system was installed at the Royal Aerospace Establishment (England), and used to provide pressure data in wind tunnel tests in aircraft models. The results and conclusions from the laboratory experiments that were undertaken to assess the effectiveness of the system in the wind tunnel environment are presented. The system's performance during model tests in the first six months of tunnel running is discussed. It is shown that the system offers considerable savings in pressure data gathering times over mechanical pressure switches previously in use. Error analysis of the data from the system indicated that existing high measurement accuracy was retained. The advantages and disadvantages of using such a system are highlighted. ESA

N93-11883# Royal Aerospace Establishment, Bedford (England). Aerospace Div.
THE 13 FT BY 9 FT LOW SPEED WIND TUNNEL FACILITY AT DRA (AEROSPACE DIVISION) BEDFORD (ENGLAND)
M. N. Cripps 4 Dec. 1991 24 p Original contains color illustrations
(RAE-TM-Aero-2228; BR308896; ETN-92-92305) Copyright Avail: CASI HC A03/MF A01

The Defence Research Agency (DRA) 13 ft by 9 ft low speed tunnel at the Royal Aerospace Establishment, Bedford (England), is described. The facility was commissioned in 1954 to provide low turbulence tests, concerning speeds up to 90 m/s at atmospheric pressure. The tunnel provides an ideal low speed research facility for both full and half models, with a range of support options for sting and strut mounted full models or floor mounted half models. Static and dynamic measurements can be made, along with a variety of flow visualization techniques, such as liquid crystals, laser illuminated smoke screen, and microtufts. The tunnel has a fast start up and shut down time, requires minimal supervision by the user and has relatively low operating costs. ESA

N93-11886 Texas A&M Univ., College Station.
LEADING EDGE FILM COOKING HEAT TRANSFER INCLUDING THE EFFECT OF MAINSTREAM TURBULENCE Ph.D. Thesis
Shichuan Ou 1991 278 p
Avail: Univ. Microfilms Order No. DA9216993

The influence of high mainstream turbulence on the leading edge heat transfer coefficient and film effectiveness for film slots and film holes with three injection configurations (i.e., one row at plus or minus 15 deg, one row at plus or minus 40 deg, and two rows at plus or minus 15 deg and plus or minus 40 deg from the stagnation line) were studied experimentally for flow across a blunt body with a semi-cylinder leading edge and a flat afterbody. The cross sectional slot length-to-width ratio was equal to two. Adjacent slots in each row were spaced three cross-sectional slot lengths aparts (p = 3l); however, adjacent holes in each row were spaced four hole-diameters apart (P = 4d). Each slot had the same cross-sectional area as each hole. All slots and holes were inclined at 30 deg and 90 deg to the surface in the spanwise and streamwise directions, respectively. The spanwise and streamwise distributions of heat transfer coefficient and film effectiveness were obtained under various conditions of the blowing ratio (B = 0.4, 0.8, 1.2), the mainstream turbulence levels (Tu = 3.31-5.07 percent generated by a bar grid and 7.59-9.67 percent generated by a passive grid), and the Reynolds numbers (Re(sub D) = 25,000, 40,000, 100,000). The results show that, for one row injection, the heat transfer coefficient increases and the film effectiveness decreases with increasing blowing ratio. The film effectiveness reaches its maximum at blowing ratio of B = 0.8 for two row injection. The heat transfer coefficient increases and the film effectiveness decreases with increasing mainstream turbulence level at low blowing ratio. However, the mainstream turbulence effect decreases at high blowing ratio. Both the heat transfer coefficient and the film effectiveness increase with increasing mainstream Reynolds number. For one row injection, the film cooling performance decreases with increasing blowing ratio regardless of the mainstream turbulence level and the Reynolds number. For two row injection, the blowing ratio B = 0.8 provides the best film cooling performance, but the difference between B = 0.8 and B = 0.4 is small. Two row injection usually provides better performance than corresponding one row injection. The film cooling performance between two rows of slots (P = 3l) and two rows of holes (P = 4d) is comparable. The former performs slightly better that the latter at low mainstream turbulence, but the reverse is true at high mainstream turbulence. The blowing ratio B = 0.8 performs the best for both geometries at both low and high mainstream turbulence levels. The liquid crystal thermal visualization technique reveals that a blowing ratio of 0.8 or less is recommended for leading edge film cooling with two row injection. Dissert. Abstr.

N93-11899 Arizona State Univ., Tempe.
NUMERICAL STUDY OF ADVANCED ROTOR BLADES Ph.D. Thesis
Ghasem L. Abdy 1992 161 p
Avail: Univ. Microfilms Order No. DA9223078

In this study, the effect of rigid body motion on the aerodynamics of a blade in the context of computational fluid dynamics is investigated. Specifically, the feathering and flapping motion of a rigid blade is studied. The three dimensional

Navier-Stokes equations are solved using an implicit, time-accurate, lower-upper decomposition method. The implicit method provides higher stability time limits with the additional advantage of time accurate analysis for unsteady flow problems. The inviscid part of the equations is cast into diagonal form using the characteristics of Euler equations. Only the convection terms are treated implicitly. The explicit treatment of viscous terms offers simpler finite difference equations suitable for analytic matrix inversion than time consuming numerical matrix inversion. The method benefits from a small computational work load and small computer memory requirements, and it is easily adapted for vectorization on vector machines. The computer code is used to investigate the flow over helicopter blades in hover and forward flight up to high angles of attack. The blade dynamics for a blade known as British Experimental Rotor Program (BERP) is computed in forward flight. Results show that the blade tip acts as an effective stall barrier and improves blade performance over the conventional blades.
Dissert. Abstr.

N93-12001 Virginia Univ., Charlottesville.
FLOW VISUALIZATION OF SUPERSONIC FLOW THROUGH A COMBUSTOR SECTION Ph.D. Thesis
John David Abbitt, III 1991 135 p
Avail: Univ. Microfilms Order No. DA9217327

An experimental investigation of flow characteristics in a supersonic combustor was performed covering both non-reacting and reacting flows. The first phase of the investigation included a spatially resolved, three-dimensional characterization of mixing properties of air injected sonically into a ducted, non-reacting, supersonic (Mach 2) air freestream. Laser-induced iodine fluorescence was used to generate images that were processed to yield planar injectant mole fraction distributions throughout the flowfield. Cross-sectional images of the duct show the evolution of the supersonic mixing of the injectant and main flow as the mixture passes through the duct. This data was used to generate one-dimensional mixing schedules. The study suggests that the dominant mixing mechanism of the injectant gas with the main flow is large-scale streamwise vorticity generated in the flow, rather than fine scale turbulence. In the second phase of this study, three methods of flow visualization (shadowgraphs, broadband emission, and planar laser-induced fluorescence of OH) were used to investigate effects of a hydrogen-air-reaction in the supersonic flowfield. Shadowgraphs of the flow, both non-reacting and reacting, were used to ascertain flow quality, to locate flow features such as shocks and boundary layers, and to evaluate effects of heat release on these features. The spatial distribution of broadband chemiluminescence emission from the flame was examined as a function of temperature. OH produced by the H2-O2 reaction was imaged using planar laser-induced fluorescence. By translating the laser sheet across the entire duct cross-section, a three-dimensional description of the location of OH was obtained and used to map out reaction zones, flame fronts, and flame boundaries. The study showed a strong dependence of the injectant penetration and OH distribution on the air stagnation temperature. Penetration of the injectant jets into the duct, and the size of the zones containing OH both increased as the main flow stagnation temperature was decreased. Reaction zones were found away from regions containing fuel in the non-reacting study indicating that the pressure rise associated with the reaction forced a large redistribution of the regions containing fuel. Dissert. Abstr.

N93-12004*# North Carolina State Univ., Raleigh. Dept. of Mechanical and Aerospace Engineering.
AN INVESTIGATION OF THE EFFECTS OF AFT BLOWING ON A 3.0 CALIBER TANGENT OGIVE BODY AT HIGH ANGLES OF ATTACK M.S. Thesis
Nathan M. Gittner 1992 100 p
(Contract NCC1-46)
(NASA-CR-190934; NAS 1.26:190934) Avail: CASI HC A05/MF A02

An experimental investigation of the effects of aft blowing on the asymmetric vortex flow of a slender, axisymmetric body at high angles of attack was conducted. A 3.0 caliber tangent ogive body fitted with a cylindrical afterbody was tested in a wind tunnel under subsonic, laminar flow test conditions. Asymmetric blowing from both a single nozzle and a double nozzle configuration, positioned near the body apex, was investigated. Aft blowing was observed to alter the vortex asymmetry by moving the blowing-side vortex closer to the body surface while moving the non-blowing-side vortex further away from the body. The effect of increasing the blowing coefficient was to move the blowing-side vortex closer to the body surface at a more upstream location. The data also showed that blowing was more effective in altering the initial vortex asymmetry at the higher angles of attack than at the lower. The effects of changing the nozzle exit geometry were investigated and it was observed that blowing from a nozzle with a low, broad exit geometry was more effective in reducing the vortex asymmetry than blowing from a high, narrow exit geometry. Author

N93-12063# Calspan-Buffalo Univ. Research Center, NY.
A PRELIMINARY STUDY ASSOCIATED WITH THE EXPERIMENTAL MEASUREMENT OF THE AERO-OPTIC CHARACTERISTICS OF HYPERSONIC CONFIGURATIONS Final Report, 10 Feb. 1991 - 9 Feb. 1992
Michael S. Holden Jun. 1992 158 p
(Contract F49620-91-C-0026)
(AD-A253792; AFOSR-92-0692TR) Avail: CASI HC A08/MF A02

A program of fundamental, experimental research and analysis has been conducted to design additional components necessary to modify, assemble and develop a ground-based facility (LENS) to duplicate flowfield environment around a hypersonic endo-atmospheric interceptor to evaluate optical seeker performance. Aero-optic instrumentation, used to measure the aero-optical characteristics of the viscous and shock layer over transpiration-and-filmed cooled nosetips at hypersonic speeds were also investigated. In the design of the facility, particular care was taken in designing the systems for a contamination-free hypersonic flow and in isolating the loads associated with the operation of the shock tunnel from the model support system and the aero-optic instrumentation. Five instrumentation systems, including holography, imagery, boresight/jitter, radiometry, and spectrometry were evaluated to provide consistent evaluation in ENDO-LEAP mission environments. State-of-the-art CFD codes with capabilities determining the inherent salient flowfield features such as turbulence and reacting chemistry were investigated and the GASP code was selected as the basic computational method. The stress levels and motion of shock tunnels were studied and analyzed using two approaches, a numeric marching code and a numeric solution to the wave equation. A flight test program based on existing sounding rocket technology was examined in order to design a high confidence flight test to validate the LENS ground test results. GRA

N93-12179# Army Natick Research and Development Command, MA.
THE DEGRADATION OF PARACHUTES: AGE AND MECHANICAL WEAR Final Report, Oct. 1988 - Sep. 1990
Ronald A. Segars May 1992 56 p
(DA Proj. 1L1-62786-D-283)
(AD-A252243; NATICK/TR-92/035) Avail: CASI HC A04/MF A01

New and previously published data involving the strength of parachute suspension cord are consolidated and critically analyzed for the purpose of extracting the effect of age (storage life) from the combined effect of age use (number of jumps). Test results from both new and used parachutes (some as old as 23 years) show that a 35 percent decrease is the tensile strength of parachute suspension cord (usually occurring within the first five year of service) can be attributed to use. Fluorescence measurements and mass spectral data obtained on samples selected from the previous in-house studies show no correlation between the strength of the parachute suspension cord and any of the fluorescence or mass spectral. This lack of correlation indicates that breakdown of nylon 66 is negligible in normally aged parachutes. This is consistent with the analysis of the strength data which shows a degradation rate of approximately 0.5 percent per year for unused parachutes under normal storage conditions. GRA

N93-12190 Purdue Univ., West Lafayette, IN.
UNSTEADY PROPELLER/WING AERODYNAMIC INTERACTIONS Ph.D. Thesis
Robert Thomas Johnston 1991 212 p
Avail: Univ. Microfilms Order No. DA9215573

The unsteady nature of the propeller slipstream interacting with a wing was studied by flow visualization and unsteady wing surface pressure measurements. This work has yielded information on the motion of the propeller wake as it passes over the wing. The flow field encountered in a propeller swirl recovery vane combination was investigated using a stator mounted downstream of a propeller. Flow visualization was done on the motion of the propeller helical vortex as it passes over the center of a 9.0 aspect ratio wing. Viscous dissipation at the leading edge causes the vortex to be severed, with the filaments ending on the upper and lower wing surface. The propeller tip vortex was found to experience significant spanwise displacements when passing across a lifting wing. An image vortex effect which deformed the propeller tip vortex was observed at the wing leading edge. Unsteady wing surface pressures in the propeller wake were measured by traversing a pressure instrumented wing section in a spanwise direction through the propeller wake. Inexpensive microphones proved to be suitable for pressure measurements of this type and were successfully utilized in this experiment. The propeller tip vortex was identifiable as a small region of low pressure relative to the rest of the wake. Vortex position on the wing was evident from contour plots of the pressures. Spanwise motions of the tip vortex were plotted and found to support an image vortex model proposed after the flow visualization tests. Chordwise motion of the tip vortex showed that for a lifting wing condition the upper surface vortex had a higher velocity than the lower surface. This observation of the chordwise speed agrees with what is expected for flow over lifting wing. Viscous action on the surface of the wing was attributed with decreasing the magnitude of the wing surface pressure fluctuations as the wake progressed along the wing surface. The vortex interaction encountered in the flow field of a propeller and a stator was investigated using smoke flow visualization. A stator at angle of attack was used to generate a line vortex which interacted with the helical vortex filaments generated by a propeller. Changes in the relative vortex strengths and vortex rotational directons yielded several distinct vortex structures. Axial flow in the vortex cores is determined to influence the development of the vortex interaction. Dissert. Abstr.

N93-12208 Illinois Univ. at Urbana-Champaign, Savoy.
A TRAINABLE IMAGE PATTERN CLASSIFICATION SYSTEM FOR DETECTION OF DAMAGED SOYBEAN SEEDS Ph.D. Thesis
William Walter Casady 1991 147 p
Avail: Univ. Microfilms Order No. DA9210758

Optical properties of asymptomatic soybean seeds, green seeds, and four classes of soybean seeds discolored by fungi were determined using a spectroradiometer. Knowledge of the optical properties of soybean seeds provided a means of identifying that differences in spectral reflectance existed which could be used for discriminating among asymptomatic soybean seeds and seeds discolored by a pathogen. This knowledge also aided in identifying the feasibility of using color filters as a means for separation of soybean seed classes. Electromagnetic radiation between 436 and 724 nm provided the most information for linear separation of soybean seeds which was useful for identifying differences. Dissert. Abstr.

N93-12321*# National Aeronautics and Space Administration. Langley Research Center, Hampton, VA.
AN APPROACH TO CONSTRAINED AERODYNAMIC DESIGN WITH APPLICATION TO AIRFOILS
Richard L. Campbell Nov. 1992 24 p
(RTOP 505-59-10-03)
(NASA-TP-3260; L-17108; NAS 1.60:3260) Avail: CASI HC A03/MF A01

An approach was developed for incorporating flow and geometric constraints into the Direct Iterative Surface Curvature (DISC) design method. In this approach, an initial target pressure distribution is developed using a set of control points. The chordwise locations and pressure levels of these points are initially estimated either from empirical relationships and observed characteristics of pressure distributions for a given class of airfoils or by fitting the points to an existing pressure distribution. These values are then automatically adjusted during the design process to satisfy the flow and geometric constraints. The flow constraints currently available are lift, wave drag, pitching moment, pressure gradient, and local pressure levels. The geometric constraint options include maximum thickness, local thickness, leading-edge radius, and a 'glove' constraint involving inner and outer bounding surfaces. This design method was also extended to include the successive constraint release (SCR) approach to constrained minimization. Author

N93-12343*# Princeton Univ., NJ. Dept. of Mechanical and Aerospace Engineering.
STUDIES OF A FLAT WAKE ROTOR THEORY Final Report
H. C. Curtiss, Jr. and R. M. McKillip, Jr. Oct. 1992 35 p
(Grant NAG1-1038)
(NASA-CR-190936; NAS 1.26:190936; MAE-T1960) Avail: CASI HC A03/MF A01

A computer code was developed at Princeton University to calculate the velocity components in the flow field near a lifting rotor. The induced velocity components in the rotor flow field predicted by this theory are compared with experiment. It appears that on balance, this relatively simple theory gives a reasonable prediction of the average induced velocities in a rotor flow and is quite suitable for such applications as estimating the influence of the rotor wake on the tail surfaces of rotorcraft. The theory predicts that significant induced velocity components are present in all three flow directions in the wake at a lifting rotor. It should be noted , however, that there are a few experimental measurements of the longitudinal and lateral induced velocity components in the rotor wake. This theory, known as the flat wake theory, is essentially the rotary wing analog of Prandtl's lifting line theory. The theory is described in this report. Calculations based on the theory are presented and compared with a modern free wake theory. Author

N93-12344 Missouri Univ., Rolla.
NEW ACCELERATION POTENTIAL METHOD FOR SUPERSONIC UNSTEADY AERODYNAMICS OF LIFTING SURFACES, FURTHER EXTENSION OF THE NONPLANAR SUPERSONIC DOUBLET POINT METHOD, AND NONLINEAR, NONGRADIENT OPTIMIZED RATIONAL FUNCTION APPROXIMATIONS FOR SUPERSONIC, TRANSIENT RESPONSE UNSTEADY AERODYNAMICS Ph.D. Thesis
Ashish Tewari 1992 170 p
Avail: Univ. Microfilms Order No. DA9224685

A new method is devised for the calculation of pressure and aerodynamic influence coefficients on lifting-surface configurations oscillating in supersonic flow. The scheme is based upon the concept of the acceleration potential doublet and provides a simpler alternative to the Doublet Point method. The kernel function is expressed in a form analytic on the Mach boundary, and the nonplanar interference is treated by a finite-difference approximation. The normalwash is averaged over a trapezoidal averaging region instead of the rectangular region of the Doublet Point method. The concept of kernel separation into steady and unsteady parts is reserved for averaging regions lying directly downstream of the sending point. Good comparisons are observed with other methods. The nonplanar, supersonic Doublet-Point method is further extended to the treatment of surfaces with non-zerodihedral angle. Rational-function approximation in the Laplace domain with consistently optimized lag-states is presented for supersonic unsteady aerodynamics. The new approximation provides the capability to predict the transient response of lifting-surfaces in supersonic flow by using an analytic continuation from pure oscillatory motion to a general motion. The lag-states in the resulting unsteady aerodynamic state-space form are determined through a nonlinear, nongradient optimization procedure. Repeated optimized lag-state values are replaced by a higher order pole in the rational unsteady aerodynamic transfer-function. Although the multiple-pole arises out of a repeated lag-state, its use in a non-repeated case drastically reduces the cost of optimization while retaining a fit accuracy as well as the total number of augmented states in the formulation. The rational function approximations are inadequate for transonic regime. Dissert. Abstr.

N93-12352# National Aerospace Lab., Tokyo (Japan). Aeroengine Div.

AIR EJECTOR EXPERIMENTS USING THE TWO-DIMENSIONAL SUPERSONIC CASCADE TUNNEL: RELATIONSHIP BETWEEN EJECTOR PERFORMANCE AND THROAT AREA RATIO, PART 1 Report No. 2 [CHOUONSOKU NIJIGEN YORURETSU FUUDOU YOU KUUKI EZEKUTA NO JIKKEN. DAI 2 HOU: EZEKUTA SEINOU TO MENSEKIHI NO KANKEI, 1]

Susumu Takamori and Hajime Sakaguchi Dec. 1991 34 p In JAPANESE

(NAL-TM-642-Pt-1; JTN-92-80411) Avail: CASI HC A03/MF A01

To determine the feasibility of using an ejector as a suction pump for boundary layer air removal in the two dimensional supersonic cascade tunnel, especially when a portion of the tunnel's air supply is used for its primary flow, both subsonic and supersonic air ejector tests were conducted. The tested ejector was axially symmetrical and a center jet type, with its geometrical configuration being varied, i.e. the primary nozzle to mixing tube throat area ratio, and the straight mixing space (mixing tube) and diverging passage section (diffuser) lengths. These configuration changes enabled geometrical effects on ejector performance to be obtained. The experimental results on the air ejector's zero secondary flow performance were discussed in the first report, whereas this report presents the experimental results concerning the relationship between subsonic ejector performance and throat area ratio, i.e., the effects of the primary nozzle to mixing tube throat area ratio on the secondary flow rate of a subsonic ejector. Author (NASDA)

N93-12353*# National Aeronautics and Space Administration. Hugh L. Dryden Flight Research Facility, Edwards, CA.

A SUMMARY OF THE FOREBODY HIGH-ANGLE-OF-ATTACK AERODYNAMICS RESEARCH ON THE F-18 AND THE X-29A AIRCRAFT

Lisa J. Bjarke, John H. DelFrate, and David F. Fisher Nov. 1992 20 p Presented at the SAE Aerotech 1992 Conference, Anaheim, CA, 5-8 Oct. 1992

(RTOP 505-68-71; RTOP 533-02-38)

(NASA-TM-104261; H-1862; NAS 1.15:104261; SAE-92-1996) Avail: CASI HC A03/MF A01

High-angle-of-attack aerodynamic studies have been conducted on both the F18 High Alpha Research Vehicle (HARV) and the X-29A aircraft. Data obtained include on- and off-surface flow visualization and static pressure measurements on the forebody. Comparisons of similar results are made between the two aircraft where possible. The forebody shapes of the two aircraft are different and the X-29A forebody flow is affected by the addition of nose strakes and a flight test noseboom. The forebody flow field of the F-18 HARV is fairly symmetric at zero sideslip and has distinct, well-defined vortices. The X-29A forebody vortices are more diffuse and are sometimes asymmetric at zero sideslip. These asymmetries correlate with observed zero-sideslip aircraft yawing moments. Author

N93-12369# National Aerospace Lab., Kakuda (Japan).

MACH 4 TESTING OF SCRAMJET INLET MODELS Report No. 1 [MAHHA 4 NI OKERU SUKURAMUJETTO KUUKI TORIIREGUCHI NO JIKKEN, SONO 1]

Takeshi Kanda, Tomoyuki Komuro, Goro Masuya, Kenji Kudo, Atsuo Murakami, Kouichiro Tani, Yoshio Wakamatsu, and Nobuo Chinzei Dec. 1991 57 p In JAPANESE

(NAL-TR-1137; JTN-92-80405) Avail: CASI HC A04/MF A01

A parametric study of several scramjet inlet models was conducted in a Mach 4 wind tunnel. The investigated parameters were side plate sweep angle, contraction ratio, and cowl geometry. Wall and pitot pressures were measured and schlieren photographs were taken. A schlieren photograph of the shock pattern inside one of the models correlated well with calculation results. Both the mass capture ratio and total pressure recovery were found to be between 50 to 80 percent. Within the range of the present study, an optimum sweep angle and a cowl length which maximized total pressure recovery were obtained. Author (NASDA)

N93-12399*# Analytical Services and Materials, Inc., Hampton, VA.

PROBABILITY DENSITY FUNCTIONS IN TURBULENT CHANNEL FLOW

Surya P. G. Dinavahi Oct. 1992 23 p

(Contract NAS1-18599; RTOP 763-23-35-19)

(NASA-CR-4454; NAS 1.26:4454) Avail: CASI HC A03/MF A01

The probability density functions (pdf's) of the fluctuating velocity components, as well as their first and second derivatives, are calculated using data from the direct numerical simulations (DNS) of fully developed turbulent channel flow. It is observed that, beyond the buffer region, the pdf of each of these quantities is independent of the distance from the channel wall. It is further observed that, beyond the buffer region, the pdf's for all the first derivatives collapse onto a single universal curve and those of the second derivatives also collapse onto another universal curve, irrespective of the distance from the wall. The kinetic-energy dissipation rate exhibits log normal behavior. Author

N93-12414# Helsinki Univ. of Technology, Otaniemi (Finland). Lab. of Aerodynamics.

NUMERICAL INVESTIGATIONS INTO THE BASE DRAG OF VARIOUS WEDGES USING THE BASE FLOW MODEL DEVELOPED BY MAURI TANNER

Esa Salminen and Seppo Laine 12 Jun. 1992 51 p

(Rept-B-36; ISBN-951-22-1042-8) Avail: CASI HC A04/MF A01

The base flow model of Tanner for two-dimensional wedges is studied. The separation region is modeled to form a closed body behind the wedge. The flow past the wedge and the separation region, the form of which is systematically varied, is calculated using potential flow theory. Three wedges are studied: 5, 30, and 60 degrees. The potential flow is calculated using a low-order panel method. For the 60 degree-wedge, results are compared with experiments. Author

N93-12466# Deacon Research, Palo Alto, CA.

HYPERSONIC FLOW DIAGNOSTIC DEVELOPMENT Final Report, 3 Mar. 1990 - 30 Sep. 1991

Anthony OKeefe May 1992 88 p

(Contract F33615-90-C-3000)

(AD-A255045; WL-TR-92-3034) Avail: CASI HC A05/MF A01

We have developed and demonstrated in our labs two techniques which can be used for the non-intrusive sensing of air flows in a wide range of temperature and pressures. The single levels realized in the laser induced fluorescence sensing of molecular oxygen are approximately 5 to 7 times weaker than the predicted levels, due to errors in either the published absorption cross section, the published predissociation rates, or both. The reduced signal levels will increase the difficulty in system integration into the wind tunnel environment, but do not preclude it. The much greater signals realized using the Rayleigh scatter analysis of gas density have been demonstrated in our labs and have been shown to be ideal for this type of remote analysis. We have been able to make the first remote density measurements in the Mach 6 facility at WPAFB in both static, free stream, and across shocks near test models. Work is continuing to improve the systems. GRA

N93-12503# National Aerospace Lab., Tokyo (Japan). Advanced Aircraft Research Group.
WIND TUNNEL INVESTIGATION OF A TWIN-ENGINE JET TRANSPORT SEMI-SPAN MODEL WITH UPPER SURFACE BLOWN JET FLAP [SOUHATSU USB HANSAI MOKEI FUUDOU SHIKEN]
Hitoshi Takahashi, Hirotoshi Fujieda, Akihito Iwasaki, Toshimi Fujita, and Masaki Saito (Kawasaki Heavy Industries Ltd., Kobe, Japan) Dec. 1991 46 p In JAPANESE
(NAL-TR-1134; JTN-92-80402) Avail: CASI HC A03/MF A01

In parallel with the research and development conducted by the National Aerospace Laboratory (NAL) on the experimental aircraft 'ASKA', a Short TakeOff and Landing (STOL) Computer Aided Design (CAD) program for four engine Upper Surface Blowing (USB) aircraft was developed and refined. To apply this CAD program to twin and three engine USB aircraft, aerodynamic data must be acquired for twin engine USB aircraft. This led to the present study which modified the existing four engine USB semispan model into a twin engine model and subsequently conducted low speed wind tunnel tests. Resultant aerodynamic characteristics of the numerous aerodynamic elements included in this model are described. Author (NASDA)

N93-12529 North Carolina State Univ., Raleigh.
AN ENGINEERING METHOD FOR INTERACTIVE INVISCID-BOUNDARY LAYERS IN THREE-DIMENSIONAL HYPERSONIC FLOWS Ph.D. Thesis
Christopher J. Riley 1992 137 p
Avail: Univ. Microfilms Order No. DA9221522

An engineering method has been developed that couples an approximate three-dimensional inviscid technique with the axisymmetric analog and a set of approximate convective-heating equations. The displacement effect of the boundary layer on the outer inviscid flow is calculated and included as a boundary condition in the inviscid technique. This accounts for the viscous interaction present at lower Reynolds numbers. The method is applied to blunted axisymmetric and three dimensional elliptic cones at angle of attack for the laminar hypersonic flow of a perfect gas. The method is also applied to turbulent and equilibrium-air conditions. The present technique predicts surface heating rates, pressures, and shock shapes that compare favorably with experimental (ground-test and flight) data and numerical solutions of the Navier-Stokes and viscous shock-layer equations. In addition, the inclusion of the viscous interaction significantly improves results obtained at lower Reynolds numbers. The new technique represents a major improvement over current engineering aerothermal methods with only a modest increase in computational effort. Dissert. Abstr.

03 AIR TRANSPORTATION AND SAFETY

Includes passenger and cargo air transport operations; and aircraft accidents.

For related information see also *16 Space Transportation* and *85 Urban Technology and Transportation.*

N93-11319# Deutsche Lufthansa A.G., Cologne (Germany).
[ACTIVITIES REPORT OF LUFTHANSA] Annual Report, 1990 [LUFTHANSA DAS JAHR 1990]
Rolf-Dieter Grass, ed. 1990 72 p In GERMAN
(ETN-92-92100) Avail: CASI HC A04/MF A01

The following are reported: an 8.4 percent turnover increase in 1990; an important investment program in order to increase and renew the fleet; prospects in international competition for Europe, North America, South America, Asia, Africa, the Near East, and Germany following German reunification; a new freightage strategy; the personnel education program; Lufthansa commercial plane characteristics; the development of an environmental program, with a view to reducing pollution and fuel consumption; the construction of a new aircraft enameling hall for 'aquastripping', a newly patented process for taking enamel off the plane surfaces; and the use of solid enamel containing less solvent, to drastically reduce noxious solvent vapor emissions. ESA

N93-11357 Civil Aviation Authority, London (England).
UK AIRMISSES INVOLVING COMMERCIAL AIR TRANSPORT, MAY-AUGUST 1991
1992 34 p
(ETN-92-92260) Copyright Avail: Civil Aviation Authority, Greville House, 37 Gratton Road, Cheltenham, England

In the introduction the following are briefly discussed: origination of an airmiss; purpose of airmiss reports; investigation of airmiss reports; categorization of airmisses; involvement of commercial air transport aircraft; airmisses related to flying hours. Tabulated statistics of the following are presented: the number of incidents of commercial air transport airmisses; commercial air transport aircraft involved in airmisses; commercial air transport airmisses related to flying hours. Reports in the commercial air transport airmisses from May - Aug. 1991 are presented. These contain summaries of: pilot reports, transcripts of relevant RT frequencies, radar video recordings, and reports from appropriate air traffic control and operating authorities. The working groups discussion is summarized, and the risk and cause assessed. ESA

N93-11375 Bundesanstalt fuer Flugsicherung, Frankfurt am Main (Germany).
[ACTIVITIES REPORT OF THE GERMAN INSTITUTE FOR FLIGHT SAFETY] Annual Report, 1990 [JAHRESBERICHT DER BUNDESANSALT FUER FLUGSICHERUNG 1990]
1990 49 p In GERMAN
(ETN-92-92272) Copyright Avail: Fachinformationszentrum Karlsruhe, 7514 Eggenstein-Leopoldschafen 2, Germany

Subjects reported cover: execution of air traffic services, operative control home record tape printing system maintenance, flight data processing in aeronautical telecommunication service, measures taken for increasing safety and regularity during flight operations, air traffic accidents in German air space, faults against air traffic rules, description of the Cooperative Air Traffic Management Concept (CATMAC), air traffic development statistics, navigation and radiotelephony techniques, information communication techniques, radar techniques, the Coordination Center for Military Aerospace Utilization (COMIL), simulation techniques, testing, investments, personnel, regional stations. ESA

N93-11471# National Transportation Safety Board, Washington, DC.
AIRCRAFT ACCIDENT REPORT: ATLANTIC SOUTHEAST AIRLINES, INC. FLIGHT 2311, UNCONTROLLED COLLISION WITH TERRAIN, AN EMBRAER EMB-120, N270AS, BRUNSWICK, GEORGIA, 5 APRIL 1991
28 Apr. 1992 51 p
(PB92-910403; NTSB/AAR-92/03) Avail: CASI HC A04/MF A01

This report explains the loss of control, in flight, and crash of Atlantic Southeast Airlines, Inc., Flight 2311, while the airplane was conducting a landing approach to runway 07 at the Glynco Jetport, Brunswick, Georgia. The safety issues discussed in the report include the certification and inspection requirements for the Hamilton Standard model 14RF and other model propeller systems, and the scheduling of reduced flightcrew rest periods that are beyond the intent of Federal regulations. Safety recommendations concerning these issues were made to the Federal Aviation Administration, Atlantic Southeast Airlines, Inc., and the Regional Airline Association. GRA

N93-12193# National Transportation Safety Board, Washington, DC.

AIRCRAFT ACCIDENT REPORT: EXPLOSIVE DECOMPRESSION-LOSS OF CARGO DOOR IN FLIGHT, UNITED AIRLINES FLIGHT 811, BOEING 747-122, N4713U, HONOLULU, HI, 24 FEBRUARY 1989

18 Mar. 1992 116 p Supersedes PB90-910401
(PB92-910402; NTSB/AAR-92/02) Avail: CASI HC A06/MF A02

The report explains the explosive decompression resulting from the loss of a cargo door inflight on United Airlines flight 811, a Boeing 747-122, near Honolulu, Hawaii, on 24 Feb. 1989. The safety issues discussed in the report are the design and certification of the B-747 cargo doors, the operation and maintenance to assure the continuing airworthiness of the doors, and emergency response. Recommendations concerning these issues were made to the Federal Aviation Administration, the State of Hawaii, and the U.S. Department of Defense. GRA

N93-12489# Air Force Systems Command, Wright-Patterson AFB, OH.

EVALUATION OF CKU-5/A EJECTION SEAT CATAPULTS UNDER VARIED ACCELERATION LEVELS Final Report, Aug. 1987 - Mar. 1991

James W. Brinkley and Carl G. Toler May 1991 134 p
(AF Proj. 7231)
(AD-A248021; AL-TR-1991-0111) Avail: CASI HC A07/MF A02

Post accident investigations of high performance aircraft, such as the F-16, led to the concern about the performance of the ACES 2 ejection seat catapult (CKU-5/A) loaded by an impressed acceleration. In response to this concern, eight catapults were tested using a horizontal deceleration facility in cooperation with the F-16 System Program Office, the Life Support System Program Office, and the Naval Ordnance Station at Indian Head, Maryland. The objective of the tests was to evaluate the performance of the ACES 2 CKU-5/A catapult operating at impressed acceleration levels of 0, 3.5, and 7 G in the +Z axis. Analysis of the test results indicates that, although the velocity at separation was not significantly affected, significant delays in time to first motion and time to catapult strip-off occurred. Furthermore, critically high accelerations will be imparted to the ejection seat and crewmember. The Dynamic Response Index Modeling Technique was used to estimate the probability of injury from the catapult acceleration data. The probability of spinal injury increases from less than 1 percent at the 0-G level to greater than 99 percent at the 7-G level. GRA

04 AIRCRAFT COMMUNICATIONS AND NAVIGATION

Includes digital and voice communication with aircraft; air navigation systems (satellite and ground based); and air traffic control.

For related information see also *17 Space Communications, Spacecraft Communications, Command and Tracking* and *Communications and Radar.*

N93-10961*# State Univ. of New York, Buffalo. Dept. of Industrial Engineering.

METHODS AND PRINCIPLES FOR DETERMINING TASK DEPENDENT INTERFACE CONTENT Semiannual Progress Report

Valerie L. Shalin, Norman D. Geddes (Applied Systems Intelligence, Inc., Gainesville, GA.), and Brian G. Mikesell Aug. 1992 46 p
(Grant NAG1-1342)
(NASA-CR-190837; NAS 1.26:190837) Avail: CASI HC A03/MF A01

Computer generated information displays provide a promising technology for offsetting the increasing complexity of the National Airspace System. To realize this promise, however, we must extend and adapt the domain-dependent knowledge that informally guides the design of traditional dedicated displays. In our view, the successful exploitation of computer generated displays revolves around the idea of information management, that is, the identification, organization, and presentation of relevant and timely information in a complex task environment. The program of research that is described leads to methods and principles for information management in the domain of commercial aviation. The multi-year objective of the proposed program of research is to develop methods and principles for determining task dependent interface content. Author

N93-11139*# University of Central Florida, Orlando. Dept. of Industrial Engineering and Management Systems.

DESIGN OF AN AIR TRAFFIC COMPUTER SIMULATION SYSTEM TO SUPPORT INVESTIGATION OF CIVIL TILTROTOR AIRCRAFT OPERATIONS Annual Report

Ralph V. Rogers 15 Aug. 1992 17 p
(Grant NAG2-625)
(NASA-CR-190811; NAS 1.26:190811) Avail: CASI HC A03/MF A01

This research project addresses the need to provide an efficient and safe mechanism to investigate the effects and requirements of the tiltrotor aircraft's commercial operations on air transportation infrastructures, particularly air traffic control. The mechanism of choice is computer simulation. Unfortunately, the fundamental paradigms of the current air traffic control simulation models do not directly support the broad range of operational options and environments necessary to study tiltrotor operations. Modification of current air traffic simulation models to meet these requirements does not appear viable given the range and complexity of issues needing resolution. As a result, the investigation of systemic, infrastructure issues surrounding the effects of tiltrotor commercial operations requires new approaches to simulation modeling. These models should be based on perspectives and ideas closer to those associated with tiltrotor air traffic operations. Author

N93-11152# Sandia National Labs., Albuquerque, NM.

DEVELOPMENT OF A GPS-AIDED MOTION MEASUREMENT, POINTING, AND STABILIZATION SYSTEM FOR A SYNTHETIC APERTURE RADAR

J. R. Fellerhoff and S. M. Kohler 1991 6 p Presented at the 48th Annual Meeting of the Institute of Navigation Conference, Washington, DC, 29 Jun. - 1 Jul. 1992
(Contract DE-AC04-76DP-00789)
(DE92-017053; SAND-91-2303C; CONF-9206212-1) Avail: CASI HC A02/MF A01

An advanced Synthetic Aperture Radar Motion Compensation System has been developed by Sandia National Laboratories (SNL). The system includes a miniaturized high accuracy ring laser gyro inertial measurement unit, a three axis gimbal pointing and stabilization assembly, a differential Global Positioning System (GPS) navigation aiding system, and a pilot guidance system. The system provides several improvements over previous SNL motion compensation systems and is capable of antenna stabilization to less than 0.01 degrees RMS and absolute position measurement to less than 5.0 meters RMS. These accuracies have been demonstrated in recent flight testing aboard a DHC-6-300 'Twin Otter' aircraft. DOE

N93-11252# Federal Aviation Administration, Cambridge, MA. Operator Performance and Safety Analysis Div.

DESIGN OF INSTRUMENT APPROACH PROCEDURE CHARTS: COMPREHENSION SPEED OF MISSED APPROACH INSTRUCTIONS CODED IN TEXT OR ICONS Final Report, Jul. - Dec. 1991

David W. Osborne (Dynatrend, Inc., Woburn, MA.) and M. Stephen Huntley Feb. 1992 62 p
(PB92-205673; DOT-VNTSC-FAA-92-3; DOT/FAA/RD-92/3)
Avail: CASI HC A04/MF A01

Instrument approach procedure (IAP) charts are often cluttered and confusing. The quantified effects of chart design changes on information transfer are needed by chart manufacturers to make changes which will enhance information transfer and human performance. The present study was conducted as part of a continuing effort at the Volpe National Transportation Systems Center Human Performance Laboratory to develop human performance-based design guidelines for IAP charts. The objectives of the experiment were to determine whether encoding missed approach instructions in text or icons would result in more efficient information transfer, and if the information transfer efficiency for either coding technique was dependent upon the level of information content. Twelve pilots currently licensed for instrument (IFR) flight participated as subjects. Text instructions were either taken directly or developed from instructions found on National Ocean Service (NOS) IAP charts. Because of formatting inconsistencies in current NOS missed approach instructions, a standard format was developed. In order to approximate the range of information content found in current NOS missed approach instructions, these instructions possessed one of three levels of information content: low, medium, and high. Comprehension speed was measured by counting the number of one second presentations (glances) subjects required to view the instructions in order to verbally report them. Report accuracy was also measured. Subjects completed questionnaires concerning their flight experience, preferences for IAP chart manufacturers, and preference for text or iconic coding of the instructions. GRA

N93-11344 Deutsche Geodaetische Kommission, Munich (Germany).
CONSTRUCTION OF A GEODESIC STRAPDOWN INERTIAL NAVIGATION SYSTEM FOR POINT DETERMINATION Ph.D. Thesis - Technische Hochschule [AUFBAU EINES GEODAETISCHEN STRAPDOWN INERTIALSYSTEMS ZUR PUNKTBESTIMMUNG]
Dieter Keller 1991 123 p In GERMAN
(Ser-C-367; ISBN-3-7696-9415-5; ETN-92-92273) Copyright Avail: Deutsche Geodaetische Kommission, Marstallplatz 8, D-8000 Munich 22, Germany

The point determination is to be realized with accuracies of some decimeters. Prior to reaching the ultimate limit of power for strapdown inertial systems, a point accuracy determination of more than one meter is an important intermediate objective. The results obtained in the point determination show accuracies less than ten meters for about 35 minute measuring runs. Strong residual systems are to be recognized in the point determination errors, which can be reduced in different ways. One possibility of reduction of residual systems is the improvement of the state space model by extension of the state vector for the modelization of further dominant sensor errors, e.g., the gyroscope random walk errors. All dominant acceleration errors depend strongly on temperature. The temperature behavior is obtained in stationary long time labor tests. ESA

N93-11419# New Brunswick Univ., Fredericton.
DREDGING RESEARCH PROGRAM: FEASIBILITY OF A KINEMATIC DIFFERENTIAL GLOBAL POSITIONING SYSTEM Final Report
David E. Wells and Alfred Kleusberg Mar. 1992 42 p
(Contract DAAL03-86-D-0001)
(AD-A248953; WES/TR/DRP-92-1) Avail: CASI HC A03/MF A01

This report considers the feasibility of using the Global Positioning System (GPS) to obtain three-dimensional positions, at decimeter (or better) accuracies, in real time for hydrographic survey vessels, dredges, and offshore tide gage buoys. The various technical constraints associated with using GPS to obtain high-accuracy positions of a moving platform are discussed. Real-time, decimeter-level kinematic differential GPS positioning can only be obtained if GPS carrier beat phase ambiguities can be resolved on the fly. Resolution of carrier beat phase ambiguities on the fly can only be achieved (if at all) with improved P-code pseudoranging. Dual-frequency receivers will be required. Codeless techniques for tracking the P-code may be almost as useful as code-correlation techniques in providing pseudorange measurements for carrier beat phase ambiguity resolution. Problems in four areas remain to be solved if decimeter-level systems are to be feasible: reducing pseudorange noise, avoiding multipath, overcoming possible adverse effects of selective availability, and overcoming the effects of vessel dynamics. GRA

N93-11472# Coast Guard Academy, New London, CT. Center for Advanced Studies.
LORAN AND THE EFFECTS OF TERRESTRIAL PROPAGATION
Benjamin B. Peterson and Kevin Dewalt May 1992 44 p
(PB92-197219; USCGA-07-92) Avail: CASI HC A03/MF A01

Since the LORAN electronic navigation system has recently become available in Central United States, the Federal Aviation Administration has expressed an interest in learning more about the propagation of LORAN over land. LORAN receivers are experiencing interference effects from the atmosphere which are creating more inaccuracies than predicted by theoretical models. The study focuses on two phenomena which reduce the accuracy of LORAN: Envelope-to-Cycle Difference (ECD) and skywave interference. Why and how these effects reduce LORAN accuracy and how we have developed models to predict them are explained. ECD is predicted as a function of ground conductivity and ECD biases can be predicted for various skywave delays on the Austron 5000 receiver. With these models LORAN receiver manufacturers will be able to predict the inaccuracies caused by ECD and skywave interference and avoid them. GRA

N93-11704# Federal Aviation Administration, Atlantic City, NJ.
CONTROLLER EVALUATION OF INITIAL DATA LINK TERMINAL AIR TRAFFIC CONTROL SERVICES: MINI STUDY 2, VOLUME 1 Final Report
Nicholas J. Talotta Apr. 1992 97 p
(Contract FAA-T2001-B)
(DOT/FAA/CT-92/2-Vol-1) Avail: CASI HC A05/MF A02

This document details the results of the second mini-study of the Federal Aviation Administration (FAA) Technical Center investigation and development of initial terminal air traffic control (ATC) services for transmission using data link technology. Initial data link services were evaluated under part task simulation conditions in order to identify service delivery methods which optimize controller acceptance, performance, and workload, and to study the effects of various potential data link message response delays. Author

N93-11705# Federal Aviation Administration, Atlantic City, NJ.
CONTROLLER EVALUATION OF INITIAL DATA LINK TERMINAL AIR TRAFFIC CONTROL SERVICES: MINI STUDY 2, VOLUME 2 Final Report
Nicholas J. Talotta Apr. 1992 123 p
(Contract FAA-T2001-B)
(DOT/FAA/CT-92/2-Vol-2) Avail: CASI HC A06/MF A02

This document details the results of the second mini-study of the Federal Aviation Administration (FAA) Technical center investigation and development of initial terminal air traffic control (ATC) services for transmission using data link technology. Initial data link services were evaluated under part task simulation conditions in order to identify service delivery methods which optimize controller acceptance, performance, and workload, and to study the effects of various potential data link message response delays. Author

N93-12320*# National Aeronautics and Space Administration. Ames Research Center, Moffett Field, CA.
INTEGRATION OF RADAR ALTIMETER, PRECISION NAVIGATION, AND DIGITAL TERRAIN DATA FOR LOW-ALTITUDE FLIGHT
Richard E. Zelenka Aug. 1992 11 p
(RTOP 505-64-13)
(NASA-TM-103958; A-92158; NAS 1.15:103958) Avail: CASI HC A03/MF A01

Avionic systems that depend on digitized terrain elevation data for guidance generation or navigational reference require accurate absolute and relative distance measurements to the terrain, especially as they approach lower altitudes. This is particularly exacting in low-altitude helicopter missions, where aggressive terrain hugging maneuvers create minimal horizontal and vertical clearances and demand precise terrain positioning. Sole reliance on airborne precision navigation and stored terrain elevation data for above-ground-level (AGL) positioning severely limits the operational altitude of such systems. A Kalman filter is presented which blends radar altimeter returns, precision navigation, and stored terrain elevation data for AGL positioning. The filter is evaluated using low-altitude helicopter flight test data acquired over moderately rugged terrain. The proposed Kalman filter is found to remove large disparities in predicted AGL altitude (i.e., from airborne navigation and terrain elevation data) in the presence of measurement anomalies and dropouts. Previous work suggested a minimum clearance altitude of 220 ft AGL for a near-terrain guidance system; integration of a radar altimeter allows for operation of that system below 50 ft, subject to obstacle-avoidance limitations. Author

05 AIRCRAFT DESIGN, TESTING AND PERFORMANCE

Includes aircraft simulation technology.

For related information see also *18 Spacecraft Design, Testing and Performance* and *39 Structural Mechanics*.For land transportation vehicles see *85 Urban Technology and Transportation.*

N93-10968*# National Aeronautics and Space Administration. Langley Research Center, Hampton, VA.
RECENT ADVANCES IN MULTIDISCIPLINARY OPTIMIZATION OF ROTORCRAFT
Howard M. Adelman, Joanne L. Walsh, and Jocelyn I. Pritchard Sep. 1992 14 p Presented at the Fourth AIAA/USAF/NASA/OAI Symposium on Multidisciplinary Analysis and Optimization, Independence, OH, 21-23 Sep. 1992
(DA Proj. 1L1-62211-A-47-A; RTOP 505-63-36-06)
(NASA-TM-107665; NAS 1.15:107665; AVSCOM-TR-92-B-012; AIAA Paper 92-4777) Avail: CASI HC A03/MF A01

A joint activity involving NASA and Army researchers at NASA LaRC to develop optimization procedures to improve the rotor blade design process by integrating appropriate disciplines and accounting for all of the important interactions among the disciplines is described. The disciplines involved include rotor aerodynamics, rotor dynamics, rotor structures, airframe dynamics, and acoustics. The work is focused on combining these five key disciplines in an optimization procedure capable of designing a rotor system to satisfy multidisciplinary design requirements. Fundamental to the plan is a three-phased approach. In phase 1, the disciplines of blade dynamics, blade aerodynamics, and blade structure are closely coupled while acoustics and airframe dynamics are decoupled and are accounted for as effective constraints on the design for the first three disciplines. In phase 2, acoustics is integrated with the first three disciplines. Finally, in phase 3, airframe dynamics is integrated with the other four disciplines. Representative results from work performed to date are described. These include optimal placement of tuning masses for reduction of blade vibratory shear forces, integrated aerodynamic/dynamic optimization, and integrated aerodynamic/dynamic/structural optimization. Examples of validating procedures are described. Author

N93-11161# Centro Italiano Ricerche Aerospaziali, Naples.
ARTIFICIAL INTELLIGENCE AND CFD: EXPERT SYSTEMS FOR THE DESIGN OF AIRFOILS AND FOR GRID GENERATION
Domenico Quagliarella 29 Jan. 1992 14 p
(DIGE-EST-TN-016; ETN-92-92413) Avail: CASI HC A03/MF A01

The potential application of Artificial Intelligence (AI) and of Expert Systems (ES) to Computational Fluid Dynamics (CFD) is shown. The application of such techniques to the design of aerodynamic shapes is discussed. The expert system IDEA (Intelligence Design of Airfoils) is presented. The problems connected to the acquisition and codification of aerodynamic design expertise are shown. Application of AI techniques to the problem of the positioning/decomposition of a computational domain is outlined. The solution of such problems is important to facilitate the generation of three dimensional grids and to create better data structures for massively parallel computing. ESA

N93-11170*# National Aeronautics and Space Administration. Langley Research Center, Hampton, VA.
CORRECTION TECHNIQUES FOR DEPTH ERRORS WITH STEREO THREE-DIMENSIONAL GRAPHIC DISPLAYS
Russell V. Parrish, Anthony Holden, and Steven P. Williams Oct. 1992 19 p
(DA Proj. 1L1-61102-AH-45; RTOP 505-64-13-32)
(NASA-TP-3244; L-17045; NAS 1.60:3244; ATCOM-TR-92-B-011)
Avail: CASI HC A03/MF A01

Three-dimensional (3-D), 'real-world' pictorial displays that incorporate 'true' depth cues via stereopsis techniques have proved effective for displaying complex information in a natural way to enhance situational awareness and to improve pilot/vehicle performance. In such displays, the display designer must map the depths in the real world to the depths available with the stereo display system. However, empirical data have shown that the human subject does not perceive the information at exactly the depth at which it is mathematically placed. Head movements can also seriously distort the depth information that is embedded in stereo 3-D displays because the transformations used in mapping the visual scene to the depth-viewing volume (DVV) depend intrinsically on the viewer location. The goal of this research was to provide two correction techniques; the first technique corrects the original visual scene to the DVV mapping based on human perception errors, and the second (which is based on head-positioning sensor input data) corrects for errors induced by head movements. Empirical data are presented to validate both correction techniques. A combination of the two correction techniques effectively eliminates the distortions of depth information embedded in stereo 3-D displays. Author

N93-11334# Rolls-Royce Ltd., Derby (England).
THE CHANGING NATURE OF DESIGN
D. A. Ford 7 Mar. 1992 3 p Presented at the Rapid Prototyping Conference, Cheltenham, England, 6-7 Feb. 1992
(PNR-91011; ETN-92-92253) Avail: CASI HC A01/MF A01

The changing nature of design in the aerospace industry away from traditional drafting and design methods towards electronic design data and concurrent engineering is discussed. The new methods show an improved time base from component design to test. Some of the technologies which have contributed to the development of rapid development manufacture are the following: computer aided design fully integrated with analysis; computer aided drafting; simultaneous engineering between design and manufacture; multi-axis machine capability; process modeling of manufacturing processes; automated coordinate measurement machines; and rapid prototyping. The importance of rapid prototyping for commercial benefit is discussed, noting the Japanese experience and philosophy towards marketing: it is concluded that there is some way to go to satisfy the many demands on rapid prototyping, particularly speed of processing, cost of equipment, finished part definition, and materials. ESA

N93-11461# Systems Control Technology, Inc., Arlington, VA.
ROTORCRAFT HEALTH AND USAGE MONITORING SYSTEMS: A LITERATURE SURVEY Final Report
Larry Miller, Barbara McQuiston, Jeff Frenster, and Diane Wohler May 1991 71 p
(Contract DTFA01-87-C-00014)
(DOT/FAA/RD-91/6; SCR-91RR-5) Avail: CASI HC A04/MF A01

The rotorcraft industry is developing a number of techniques, methodologies, and associated equipment for monitoring health and usage of critical rotorcraft flight components. Industry is planning to incorporate this technology on a number of new aircraft. The Federal Aviation Administration (FAA) has the responsibility for certification of these aircraft and the equipment they contain. This effort is concerned with the health and usage equipment. To best accomplish the certification of these equipment, the FAA expects to develop detailed certification criteria addressing specific issues of concern. In the near-term, the FAA objective is to develop a better understanding of what is being developed by industry (with emphasis on United States industry), what firms are involved, who are the key people involved, what parts of this technology are mature to the point that some airworthiness credit may be appropriate, and what parts of this technology are not yet mature. With information such as this, the issues that need to be addressed via certification criteria can be determined quickly. This effort is principally intended to provide support in reaching the FAA's near-term objectives. This report describes the results of an extensive literature search of health and usage monitoring technology. Over 1,000 abstracts were reviewed and analyzed. The report contains a description of 20 systems and abstracts of 90 papers pertinent to health and usage monitoring. Author

N93-11485# Royal Aerospace Establishment, Farnborough (England). Propulsion Dept.

DEVELOPMENTS IN ICING TEST TECHNIQUES FOR AEROSPACE APPLICATIONS IN THE RAE PYESTOCK (ENGLAND) ALTITUDE TEST FACILITY

A. R. Osborn, V. E. W. Garratt, and R. G. T. Drage 25 Sep. 1990 15 p Presented at the Tenth International Symposium on Air Breathing Engines, Nottingham, England, 1-6 Sep. 1991 Previously announced in IAA as A91-56223
(RAE-TM-P-1214; P305695-04; ETN-92-92300) Copyright
Avail: CASI HC A03/MF A01

The development of cloud simulation and the icing certification regulations are reviewed. Royal Aerospace Establishment (RAE) test facilities and their capability for monitoring voice formation and shedding are described. The development of water spray rakes is discussed. The use of the calibration facility in exploring these variables and the development of special measurement equipment is explained. The altitude test facilities at Pyestock are used in support of clearance of aeroengines, intakes, and helicopter rotors to operate under severe icing conditions. An important aspect of the work is the simulation of the wet icing cloud in terms of water concentration, mean droplet size, and spectrum. Water spray rakes or booms were developed and individual nozzles were calibrated in a wind tunnel using a laser particle sizer. In future work, the main objectives are to satisfy the customer requirements and the evolving demands of international regulatory authorities. ESA

N93-11719 Wichita State Univ., KS.

A SIMPLIFIED NUMERICAL PROCEDURE TO COMPUTE THE OPTIMAL TRAJECTORY OF AN AIRCRAFT Ph.D. Thesis

Bijan Rashidian 1991 122 p
Avail: Univ. Microfilms Order No. DA9221971

A simplified numerical method to obtain the optimal flight path trajectory for an aircraft flying in the presence of proximate aircrafts (commonly called intruders) or the presence of the restricted airspace zones is presented. Singular perturbation method along with Energy state approximation is used to formulate the mathematical model. The Pontryagin's Minimum Principle along with an efficient and realistic method of modeling the control time history is then used to calculate the optimal trajectory flight path. Several flight path and cost scenarios involving multiple intruders and risk airspaces, and some correlation with published data are presented. With the proper scaling of the weighting parameters the method generates trajectories with different end conditions and trajectory objectives. Dissert. Abstr.

N93-11725 Georgia Inst. of Tech., Atlanta.

A THEORY FOR THE ANALYSIS OF ROTORCRAFT OPERATING IN ATMOSPHERIC TURBULENCE Ph.D. Thesis

Mark Francis Costello 1992 170 p
Avail: Univ. Microfilms Order No. DA9223775

A frequency domain model describing the atmospheric turbulence velocity field which is experienced by rotorcraft components is developed. Atmospheric turbulence over any particular rotor blade is approximated radially and azimuthally. With this expansion, a stochastic model is formed. The model is cast in the frequency domain. Example results are given for the CH-47D Tandem Rotor Helicopter. The model developed is drastically different from standard conventional rotorcraft atmospheric turbulence models owing to the fact that the statistics of atmospheric turbulence, which determine the stochastic model, are sampled at points on the rotating blade elements as opposed to the conventional rotorcraft atmospheric turbulence models which compute the statistics of atmospheric turbulence at the center of gravity of the aircraft. Dissert. Abstr.

N93-11838# Naval Oceanographic and Atmospheric Research Lab., Bay Saint Louis, MS.

EMBEDDED TRAINING CAPABILITIES FOR THE LAMPS MK 3 SYSTEM Final Report

Robert S. Romalewski and James H. Hammond Jan. 1992 11 p
(AD-A250697; NOARL-PR-92-020-252) Avail: CASI HC A03/MF A01

An SH-60 helicopter incorporation the Light Airborne MultiPurpose System (LAMPS) MK 3 was tested using the AN/SRO-4 UHF secure data link to AN/SQQ-28 Sonobuoy Processor at the Naval Air Test Center (NATC) Patuxent River, MD. During the time the helicopter was on the simulated mission, it 'dropped' sonobuoys and received normal mission feedback. This was done during testing of a potential wide-area network, with the acoustic stimulation for the LAMPS MK 3 accomplished by passing control and acoustic information from an ANN/SQQ-89 On-Board Trained (OBT) at Patuxent River via an on-site data link network. A master control unit was used to drive NATC's OBT from Fleet ASW Training Center, Norfolk, over normal telephone lines. Multiple OBT connections from the master control unit are possible and will further team training by combining expertise located at another training center with all other connected assets. Other additions to the OBT interface will provide additional aircrew radar training via the AN/ APS-124 Remote Radar Operator (REMRO) system and EW software upgrades. The OBT is used at NATC in evaluation of helicopter ASW subsystems as well as for training. GRA

N93-11863*# National Aeronautics and Space Administration. Hugh L. Dryden Flight Research Facility, Edwards, CA.

FLIGHT TEST RESULTS FROM A SUPERCRITICAL MISSION ADAPTIVE WING WITH SMOOTH VARIABLE CAMBER

Sheryll Goecke Powers, Lannie D. Webb, Edward L. Friend, and William A. Lokos Nov. 1992 31 p Presented at the AIAA 6th Biennial Flight Test Conference, Hilton Head, SC, 24-26 Aug. 1992
(RTOP 533-02-11)
(NASA-TM-4415; H-1855; NAS 1.15:4415; AIAA Paper 92-4101)
Copyright Avail: CASI HC A03/MF A01

The mission adaptive wing (MAW) consisted of leading- and trailing-edge variable-camber surfaces that could be deflected in flight to provide a near-ideal wing camber shape for any flight condition. These surfaces featured smooth, flexible upper surfaces and fully enclosed lower surfaces, distinguishing them from conventional flaps that have discontinuous surfaces and exposed or semiexposed mechanisms. Camber shape was controlled by either a manual or automatic flight control system. The wing and aircraft were extensively instrumented to evaluate the local flow characteristics and the total aircraft performance. This paper discusses the interrelationships between the wing pressure, buffet, boundary-layer and flight deflection measurement system analyses and describes the flight maneuvers used to obtain the data. The results are for a wing sweep of 26 deg, a Mach number of 0.85, leading and trailing-edge cambers (delta(sub LE/TE)) of 0/2 and 5/10, and angles of attack from 3.0 deg to 14.0 deg. For the well-behaved flow of the delta(sub LE/TE) = 0/2 camber, a typical cruise camber shape, the local and global data are in good agreement with respect to the flow properties of the wing. For the delta(sub LE/TE) = 5/10 camber, a maneuvering camber shape, the local and global data have similar trends and conclusions, but not the clear-cut agreement observed for cruise camber. Author

N93-12053# Naval Postgraduate School, Monterey, CA.
DEVELOPMENT OF A 1/7-SCALE F/A-18 UAV FOR SUPERMANEUVERABILITY RESEARCH M.S. Thesis
Michael S. Shelton Sep. 1991 128 p
(AD-A247261) Avail: CASI HC A07/MF A02

A 1/7-scale F/A-18 Hornet UAV was constructed for use in generic fighter high-angle-of-attack research. The aircraft, purchased as a kit, has been extensively modified to incorporate rudders and trailing edge flaps. In addition, an emergency parachute recovery system (EPRS) was installed for use in the event of departure from controlled flight, loss of radio signal, structural failure or any other anomally that would preclude a normal landing recovery. Parachute performance data and design considerations are discussed. Aerodynamic and dynamic data have been determined, such as cg, moments of inertia, full and empty weights, surface areas, aspect ratio and wing loading. Preliminary performance estimations have been determined and the aircraft has been flown. Future research to include the employment of nonconventional yaw control methods using forebody strakes and possibly pneumatic blowing is discussed. The need to pursue cooperative thesis research in the investigation of a Digital Flight Control System (DFCS), utilizing fly-by-wire active flight controls, is discussed. This UAV generic fighter program is planned as a multi-thesis student project, and this thesis documents the research and work of the second student involved with the project. GRA

N93-12206 Illinois Univ. at Urbana-Champaign, Savoy.
AN EXPERIMENTAL STUDY OF THE RELATIONSHIP BETWEEN FORCES AND MOMENTS AND VORTEX BREAKDOWN ON A PITCHING DELTA WING Ph.D. Thesis
Mohammad Reza Soltani 1992 265 p
Avail. Univ. Microfilms Order No. DA9215885

Wind-tunnel experiments were performed to study the complex flow mechanisms on a 70 deg sharp leading-edge delta wing model at both static and dynamic conditions at a Reynolds number of 1.43 x 10(exp 6). Large amplitude oscillatory motions were produced by sinusoidally pitching the model over a range of reduced frequencies. Ramp motions were obtained using an initial sinusoidal increase in angle of attack and hold. Aerodynamic forces and moments were obtained from a six component internal strain-gauge balance. In addition, smoke flow visualization was conducted to study the development and breakdown of the leading-edge vortices under static, dynamic, and ramp conditions. The visualization experiment was performed at a Reynolds number of 0.16 x 10(exp 6). Static forces compared well with previously published data. The non-linear vortex lift and the movement of the burst point over the wing surface were related to changes in the measured lift-curve slope. Asymmetrical bursting produced by testing the model at nonzero sideslip angle had a significant influence on the magnitude of the measured forces and moments. Dynamic data varied substantially with reduced frequency. Large forces and moments overshoots, a delay in dynamic stall, and a hysteresis loop between the values of aerodynamic loads in upstroke and downstroke motion were observed. The dynamic vortex breakdown point was seen to reach the trailing-edge at a smaller angle of attack than it did when in the static case. However, at large angles of attack, its position lagged that of the static model. The magnitude of the rolling moment coefficient was strongly influenced by the reduced frequency. For the ramp motion case, aerodynamic forces and moments closely followed those of the oscillatory case during the pitch-up motion. However, upon cessation of the motion, the persistence of the dynamic effects was a strong function of the pitch rate. Terminating the motion at 24 deg angle of attack produced lower lift and normal force values when the data were compared to their static values. This was caused by the early bursting phenomenon observed during the dynamic motion, thus reducing dynamic lift and normal force coefficients.
Dissert. Abstr.

N93-12354# National Aerospace Lab., Tokyo (Japan). Management Team Flight Test Section.
FLIGHT TEST PROGRESS OF THE STOL RESEARCH AIRCRAFT ASKA [STOL JIKKENKI ASUKA NO HIKOU SHIKEN KIROKU SHASHIN TO SHIKEN KEIKA]
Eiichi Abo Dec. 1991 28 p In JAPANESE Original contains color illustrations
(NAL-TM-643; JTN-92-80412) Avail: CASI HC A03/MF A01

Flight tests of the STOL research aircraft 'ASKA' were conducted during the period of about three and a half years from Oct. 1985 to Mar. 1989 and provided many productive results. The resultant progress of these flight tests are subsequently described using applicable photographs. Author (NASDA)

N93-12485# Maryland Univ., College Park. Dept. of Aerospace Engineering.
THE FOURTH WORKSHOP ON DYNAMICS AND AEROELASTIC STABILITY MODELING OF ROTORCRAFT SYSTEMS Final Report, 1 May 1991 - 30 Apr. 1992
Inderjit Chopra Nov. 1991 821 p Workshop held in College Park, MD, 19-21 Nov. 1991
(Contract DAAL03-91-G-0159)
(AD-A255065; ARO-28860.1-EG-CF) Avail: CASI HC A99/MF A10

The workshop was held as scheduled. An assessment of the state-of-the-art of predictive capability for rotorcraft dynamics problems was made. GRA

N93-12488# Dayton Univ., OH.
EVALUATION OF ALTERNATIVES FOR INCREASING A-7D REARWARD VISIBILITY Interim Report, Aug. 1988 - May 1990
G. J. Frank and G. J. Stenger Apr. 1992 154 p
(Contract F33615-84-C-3404)
(AD-A255071; UDR-TR-90-121; WL-TR-92-3009) Avail: CASI HC A08/MF A02

Experience has shown that the present A-7D canopy provides poor rearward visibility for defensive maneuvering against an adversary behind the A-7. Alternatives were identified and evaluated for increasing rearward visibility, including: increasing the length of the canopy transparency; adding external mirrors; modifying the existing internal mirrors; using a refractive lens; and altering the canopy profile. This evaluation showed that increasing the transparency length would provide the greatest increase in rearward visibility with the least distortion. The feasibility of extending the transparency was analyzed using a finite element model which showed that the transparency could be extended without increasing the maximum stress levels. Advanced composites were used to design an alternate canopy frame to allow the transparency to be extended by five inches. This frame was designed to be as stiff and strong as the current aft frame. The design required no modification to the surrounding fuselage and did not change the overall canopy weight. GRA

N93-12458*# National Aeronautics and Space Administration. Langley Research Center, Hampton, VA.
ACTIVE COOLING FROM THE SIXTIES TO NASP
H. Neale Kelly and Max L. Blosser *In its* Current Technology for Thermal Protection Systems Oct. 1992 p 189-249 (For primary document see N93-12447 02-18)
Avail: CASI HC A04/MF A03

06 AIRCRAFT INSTRUMENTATION

Includes cockpit and cabin display devices; and flight instruments.

For related information see also *19 Spacecraft Instrumentation* and *35 Instrumentation and Photography.*

N93-12367# National Aerospace Lab., Tokyo (Japan). Control Systems Div.
FLIGHT SIMULATOR EVALUATION OF D-SIZE LIQUID CRYSTAL FLAT PANEL DISPLAYS Report No. 2 [EKISHOUGATA FURATTO PANERU DESIPUREI NO SHIMYURETA HYOUKA SHIKEN. SONO 2: D SAIZU GATA PFD, DMD]
Hiroyasu Kawahara, Kaoru Wakairo, and Akira Watanabe Dec. 1991 27 p In JAPANESE Original contains color illustrations
(NAL-TR-1136; JTN-92-80404) Avail: CASI HC A03/MF A01

The so-called 'glass cockpit' has been introduced in recent years into commercial aircraft, where large color Cathode Ray Tubes (CRT's) are used as the primary flight instruments. In the near future, cockpit instruments using various types of flat panel displays such as a Liquid Crystal Flat Display (LCD), Light Emission Diode (LED), or plasma displays will be put into practical use, thereby superseding CRT's. Among these displays, the LCD seems to have the most superior advantages. The National Aerospace Laboratory (NAL) and Japan Aviation Electronics Industry, Ltd. (JAE) jointly conducted flight simulations to evaluate basic functions, performance, and display formats of D-size LCD displays using an NAL flight simulator. Two types of displays, a Primary Flight Display (PFD) and a Digital Map Display (DMD), were evaluated. Simulation results indicate that both LCD's have sufficient functions and performance necessary for actual use in commercial aircraft. The general outline and results from these simulator evaluation tests are described. Author (NASDA)

N93-12370# National Aerospace Lab., Tokyo (Japan). Control Systems Div.
AN OPTICAL FIBER MULTI-TERMINAL DATA BUS SYSTEM FOR AIRCRAFT [KOUKUUKI YOU MARUCHITAMINARU HIKARI DETABASU NO KENKYUU]
Mitsuyoshi Mayanagi, Minoru Takizawa, Akira Watanabe, and Kaoru Wakairo Oct. 1991 103 p In JAPANESE
(NAL-TR-1125; JTN-92-80393) Avail: CASI HC A06/MF A02

An optical fiber multiterminal data bus system was constructed and tested so as to provide the necessary technology bases for use on a Fly-By-Light (FBL) control system which will be required on future aircraft. The data bus system, designed and built in accordance with the protocol and system organization requirements set forth in MIL-STD-1553B (United States Air Force (USAF)), is a breadboard model comprised of a bus control unit, five remote terminal units, an 8:8 star coupler, and 12 fiber optic cables. This system improved the data transmission rate to 2 M bit/sec. Single fiber optic cable was utilized as the data transmission medium, with an electrically passive and transmitting 8:8 star coupler being newly developed for optical coupling. Serial bus control and message handling techniques were also developed for the data bus. The adaptability of this newly developed data bus to the FBL control system was verified by flight simulator tests. Author (NASDA)

N93-12383# National Aerospace Lab., Tokyo (Japan). Control Systems Div.
LIQUID CRYSTAL FLAT PANEL DISPLAY EVALUATION TESTS USING A FLIGHT SIMULATOR Report No. 1 [EKISHOU GATA FURATTO PANERU DESUPUREI NO SHIMYURETA HYOUKA SHIKEN. SONO 1: 5 INCHI GATA EADI]
Hiroyasu Kawahara, Kaoru Wakairo, and Akira Watanabe Sep. 1991 32 p In JAPANESE Original contains color illustrations
(NAL-TR-1122; JTN-92-80409) Avail: CASI HC A03/MF A01

Color Liquid Crystal Display (LCD) are currently being developed as next generation flight instrument indicators. The National Aerospace Laboratory (NAL) and Yokogawa Electric Corporation performed evaluation tests on function, performance and display formats of a 5 x 5 inch flat panel LCD display. In these tests, twenty-three pilots evaluated the LCD using a flight simulator. It was confirmed that this display is an effective indicator for flight instruments. The results of these evaluation tests are discussed. Author (NASDA)

07 AIRCRAFT PROPULSION AND POWER

Includes prime propulsion systems and systems components, e.g., gas turbine engines and compressors; and onboard auxilliary power plants for aircraft.

For related information see also *20 Spacecraft Propulsion and Power, 28 Propellants and Fuels,* and *44 Energy Production and Conversion.*

N93-10983*# National Aeronautics and Space Administration. Lewis Research Center, Cleveland, OH.
AN INTERACTIVE PREPROCESSOR FOR THE NASA ENGINE PERFORMANCE PROGRAM
Jeffrey J. Berton and Robert M. Plencner Aug. 1992 28 p
(RTOP 505-69-50)
(NASA-TM-105786; E-7216; NAS 1.15:105786) Avail: CASI HC A03/MF A01

The Simplified NEPP Automated Preprocessor (SNAP), which is written to aid in the preparation of input data files for the NASA Engine Performance Program (NEPP), is described. Specifically, SNAP is a software package on the Virtual Machine operating system that prompts the NEPP user for input information via a series of menus. The data collected from these menus are assimilated into an input file suitable for the running of NEPP. SNAP acts as a user-friendly preprocessing interface for NEPP. This serves as an introduction to the SNAP software, a user's manual, a description of the program logic, and a maintenance manual for future modifications to the software. Author

N93-11019# Rolls-Royce Ltd., Derby (England).
MATERIALS: TOWARD THE NON-METALLIC ENGINE
P. J. Postans 1 Jan. 1992 5 p
(PNR-90915; ETN-92-92204) Copyright Avail: CASI HC A01/MF A01

The constraints that are put on the aeroengine by the limited strength and temperature capability of available materials are considered. The trends in engine materials from steel and aluminum to titanium and nickel are discussed. The present requirement for new materials to be lighter, stiffer, have predictable behavior at high stress levels, and operate well above today's temperatures, is stressed. The role of fiber reinforced metals and ceramics, the most promising successors to today's metals, is discussed. The eventual aim, to use ceramic composites for turbine aerofoils and discs, is also discussed. ESA

N93-11023# Rolls-Royce Ltd., Derby (England).
AN EXPERIMENTAL EVALUATION OF PREDICTION METHODS FOR CONTRAFANS
David Geoffrey Henshaw 15 Nov. 1991 10 p Presented at the European Propulsion Forum 1991, Paris, France, 13-15 Nov. 1991
(PNR-90924; ETN-92-92209) Copyright Avail: CASI HC A02/MF A01

The testing of a contrafan rig in an anechoic wind tunnel at tunnel speeds up to Mach 0.22 is described. The rig is a one-sixth scale model of the fans and bypass duct of the RB529 contrafan engine, and was tested to assess the noise and performance of this configuration at off design conditions. In duct and far field noise levels were measured for a number of different model geometries, demonstrating the effects of changing the rotor-rotor spacing, of changing the rear rotor-rear strut separation, and of removing the front inlet structs. The effects of incidence and forward speed on noise levels were also measured. ESA

N93-11024# Rolls-Royce Ltd., Derby (England). Mechanical Test Engineering Dept.
TESTING FOR INTEGRITY
J. Horsley 18 Oct. 1991 14 p Presented at RAeS/IMechE Aeroengine Reliability, Integrity and Safety, Bristol, England, 17-18 Oct. 1991
(PNR-90927; ETN-92-92210) Copyright Avail: CASI HC A03/MF A01

Principal tests involved and techniques and facilities used to carry out tests of stresses and strains induced in gas turbine engine components during service are described. Focus is on civil engines. Three categories of tests are outlined: engine tests, component tests, and specimen tests. Lubrication and transmission testing is also considered. ESA

N93-11036# Rolls-Royce Ltd., Derby (England).
ROLLS-ROYCE CIVIL ENGINE TECHNOLOGY
C. Hornblower 5 Dec. 1991 10 p Presented at the Avia India 1991 Conference, New Dehli, India, 5 Dec. 1991
(PNR-90936; ETN-92-92216) Copyright Avail: CASI HC A02/MF A01

The Trent engine and the technology that produces it are described. Details of the following are given: design philosophy, Trent family, engine configuration, nacelle, wide chord fan, structure, high pressure system, low pressure turbine, FADEC control system, operational considerations, and development program. ESA

N93-11037# Rolls-Royce Ltd., Derby (England).
THE TRENT: TOWARDS GREATER THRUST
C. Hornblower 11 Oct. 1991 8 p Presented at the International Pacific Air and Space Technology Conference, Gifu, Tokyo, 7-11 Oct. 1991
(PNR-90937; ETN-92-92217) Copyright Avail: CASI HC A02/MF A01

The Trent engine and the technology that produces it are described. Details of the following are given: design philosophy, Trent family, engine configuration, nacelle, wide chord fan, structure, high pressure system, low pressure turbine, FADEC control system, operational considerations, and development program. ESA

N93-11038# Rolls-Royce Ltd., Derby (England).
FROM RB211 TO TRENT: AN ONGOING DEVELOPMENT STRATEGY
C. Hornblower 6 Sep. 1991 9 p Presented at the 10th International Society of AirBreathing Engines, Nottingham, England, 1-6 Sep. 1991 Previously announced in IAA as A91-56246
(PNR-90938; ETN-92-92218) Copyright Avail: CASI HC A02/MF A01

An overview of the development and present state of the art of the RB211 (RB211-22, RB211-524, and RB211-535) and the Trent engines is given. The three shaft configuration of the RB211, designed in 1967, has stood the test of time well in operational service. The concept produced a truly modular engine which was exploited by progressive development and technology read across as the family of engines increased. The engine has accumulated over 40 million service hours, and it powers variants of the Lockheed Tristar and Boeing 747, 757, and 767 in 66 customer airlines. The market demands for further improvements in wide body aircraft capacity and operating costs now call for engines in the 70,000 to 80,000 lb thrust class with growth requirements to 95,000 lb and possibly more. The Rolls-Royce contender in this arena is the Trent engine, the latest development of the RB211 and one which takes the first fundamental steps to modify the architecture of the engine in terms of both the mounting arrangement and the number of aerodynamic stages employed, to deliver thrust levels twice those of the original RB211 first tested twenty two years ago. ESA

N93-11039# Rolls-Royce Ltd., Derby (England).
INTRODUCTION TO THE ROLLS-ROYCE DESIGN PROCESS
A. J. B. Jackson 15 Apr. 1991 102 p Presented at the Integrated Manager Development Scheme Product Evaluation (IMDS) Course, Coventry, England, Apr. 1991
(PNR-90939; ETN-92-92219) Copyright Avail: CASI HC A06/MF A02

A set of graphics for a lecture on an integrated manager development scheme, given as part of a product evaluation course, is presented. The important selling points of Rolls-Royce, safety, thrust, and competitiveness are discussed. These take into account such factors as fuel and thermal efficiency. The Trent engine is considered with respect to the following: powerplant, sales, performance, materials, weight, and cost. Under design engineering the following are presented: design, performance, compressor technology, turbine technology, powerplant and noise technologies, mechanical and material technologies, and the detail drawing offices. The experimental manufacture and development process, the production, and 'after sales' are also discussed. ESA

N93-11040# Rolls-Royce Ltd., Derby (England).
THE ROLE OF TURBOMACHINERY TESTING FOR STABILITY IN DISTORTED FLOW
T. P. Hynes (Cambridge Univ., England) and D. D. Williams (Rolls-Royce Ltd., Bristol, England) 15 Nov. 1991 17 p Presented at the RAeS Conference, Paris, France, Nov. 1991
(PNR-90943; ETN-92-92220) Copyright Avail: CASI HC A03/MF A01

Reasons for turbomachinery testing are discussed: performance verification, problem diagnosis, part of technology development. The task of stability assessment for realistic problems is of such difficulty that no theory or calculation method that exists presently is able to make reliable predictions without some empirical input. The combination of theory and empiricism represents a great challenge to those who work in the particular field. Some of the ways in which work has contributed to understanding in this area are reviewed. Progress to date is summarized and the role that testing plays in future areas of development is discussed. The importance of taking account of the environment in which a compressor is operating when making a stability assessment for a distorted inlet flow is stressed. Measures of the strength of flow field coupling, compressor testing for inlet distortion, total temperature, distortion, and coupling in turbofan geometries are discussed. ESA

N93-11055# Rolls-Royce Ltd., Derby (England).
EXPERIMENTAL HEAT TRANSFER RESULTS IN TURBINE STATORS AND ROTORS AND A COMPARISON WITH THEORY
R. W. Ainsworth (Oxford Univ., England), W. D. E. Allan (Oxford Univ., England), T. V. Jones (Oxford Univ., England), T. Garside (Oxford Univ., England), N. W. Harvey, and R. C. Kingcombe (Defence Research Agency, Farnborough, England) 15 Nov. 1991 35 p Presented at the 3rd European Propulsion Forum, Paris, France, 13-15 Nov. 1991 Sponsored by Ministry of Defence and Science Research Council
(PNR-90945; ETN-92-92222) Copyright Avail: CASI HC A03/MF A01

Detailed heat transfer distributions of heat transfer to both turbine stators and rotors was measured under simulated full scale turbine conditions of Reynolds number and Mach number. Transient techniques were used to perform both these measurements and in particular the isentropic light piston tunnel and thin film heat transfer gauge instrumentation were employed. The results presented are mean heat transfer values and these compared satisfactorily with values found from available methods of boundary layer analysis. Stator endwall measurements were similarly satisfactorily predicted. Therefore, it is clear that both stator and rotor mean heat transfer may be estimated in the regions considered using available methods when boundary layer transition can be defined. ESA

N93-11061# Rolls-Royce Ltd., Derby (England).
CONCORDE PROPULSION: DID WE GET IT RIGHT? THE ROLLS-ROYCE/SNECMA OLYMPUS 593 ENGINE REVIEWED
G. A. Ganley (Rolls-Royce Ltd., Bristol, England) 1 Oct. 1991

11 p Presented at the SAE Aerotech 1991, CA, 23-26 Sep. 1991
(PNR-90970; ETN-92-92237) Copyright Avail: CASI HC A03/MF A01

The adopted control philosophy is considered. The engine and its reheat and secondary nozzle systems are considered from a mechanical point of view, and the mechanical performance is evaluated as a function of the special aspects of supersonic flight. How the long hot soak at cruise, which sets the Olympus apart from all other engines, was obtained is considered by giving an overview of the engine on a modular and system basis that includes the following: compressor intake module, low pressure compressor module, intermediate casing and gear box modules, high pressure (HP) compressor module Olympus 593 stage 6 HP compressor peak temperature and stress range, combustion module, turbine modules, reheat system, secondary nozzle assemby, engine electrical system. It is concluded that the 600,000 hours of operational experience, over half at Mach 2.0, have shown that the adopted control philosophies were correct and are showing that the most significant difference between civil subsonic and supersonic engines is the cruise at high inlet air temperatures which has produced some unexpected mechanical affects. ESA

N93-11062# Rolls-Royce Ltd., Derby (England).
SIMULTANEOUS ENGINEERING IN THE DESIGN OF AERO ENGINES
R. J. Hill 1 Nov. 1991 16 p Presented at the BUAA Inst./Northwest Polytechnical/Nanjing Aeronautic Inst./Zhuzhou Inst. Lectures, China, 6-20 Oct. 1991
(PNR-90973; ETN-92-92238) Copyright Avail: CASI HC A03/MF A01

Simultaneous engineering, a way of managing the design of aero-engines to reduce the risk, cost, and time required to launch an aero-engine and to ensure that it can be made at the most economical cost possible is defined and discussed. It is receiving increasing attention as the costs of launching a major engine increase and the market becomes more competitive. A typical product launch cycle and cost base are illustrated and the organizational structure of simultaneous engineering is considered. The help brought to this process by computer aided engineering is shown. Applications to the production of compressor blades, combustors, and the Trent wide chord fan blades are illustrated. The balancing of technology acqusition to manufacturing and engineering is considered. The application of simultaneous engineering in aero-gas turbine design and manufacture summarizes the whole process. ESA

N93-11063# Rolls-Royce Ltd., Derby (England).
THE TRENT FAMILY OF ENGINES
R. J. Hill 13 Nov. 1991 16 p Presented at the BUAA Inst./Northwest Polytechnical/Nanjing Aeronautic Inst./Zhuzhou Inst. Lectures,China, 6-20 Oct. 1991
(PNR-90974; ETN-92-92239) Copyright Avail: CASI HC A03/MF A01

The concept of a 'family' of engines is introduced. The evolution of the Trent family from the RB211 is outlined giving attention to the development of the different engine components: the fan, compressors, combustor, and turbines. The engine's full authority digital electronic system is discussed. ESA

N93-11068# Rolls-Royce Ltd., Derby (England). Aerospace Group.
ADVANCED THREE-SHAFT ENGINES: CONFIGURED FOR RELIABILITY, EFFICIENCY, AND GROWTH
H. M. Baseley 5 Mar. 1991 12 p Presented at the 43rd AGM of the Aeronautical Society of India, 7-8 Feb. 1992
(PNR-90986; ETN-92-92245) Copyright Avail: CASI HC A03/MF A01

The family of Rolls-Royce RB211 3 shaft engines is examined and the series of unique benefits which are enjoyed by operators because of the 3 shaft concept are outlined. The benefits are addressed under three main headings: fundamental design features; in service reliability and efficiency; and future growth capability. The Trent engine, which represents the advanced three shaft growth engine family, is considered. ESA

N93-11069# Rolls-Royce Ltd., Derby (England). Aerospace Group.
MAINTAINABILITY OF LARGE GAS TURBINE AERO ENGINES
John G. Chambers 30 Apr. 1992 7 p Presented at the I Mech E Conference on Maintenance, Birmingham, England, Jun. 1992
(PNR-90987; ETN-92-92246) Copyright Avail: CASI HC A02/MF A01

The approach to maintainability on the RB211 engine series is outlined with the aim of transferring ideas elsewhere. History has shown its original revolutionary concepts to be excellent, and experience has dictated needs, and found ways and means of further enhancement. The influences of engine size increases and the advent of the electronic revolution are touched upon. It is considered that maintainability needs to be thought about very carefully, both at the conceptual and the detailed design stage. Whether the machine can be easily and conveniently broken down into subassemblies must be considered. It must be ensured that those items which need to be maintained on a relatively regular basis are positioned for easy access, with due regard for adverse environment conditions, such as temperature, and intrusion of the elements. If the opportunity arises whereby a significant design change occurs, the maximum advantage should be taken of this opportunity by the process of consultation with people who have had to use the machine for real in its true environment. It should be noted however that this consultation process should in any case be going on continuously as a catalyst to any product improvement process. ESA

N93-11085# Rolls-Royce Ltd., Derby (England).
CIVIL AIRCRAFT ENGINES: THE NEXT GENERATION
R. P. Arthey 14 Oct. 1991 5 p Presented at the 9th World Airports Conference, London, England, 10-13 Sep. 1991
(PNR-90962; ETN-92-92235) Copyright Avail: CASI HC A01/MF A01

Some commercial pressures and trends that define the direction in which the aircraft engine industry is going are discussed: more power, more fuel efficient, more reliable, quieter, and cleaner engines are required. The way in which engine manufacturers are responding is discussed. The critical importance of close cooperation between airframe constructors and engine manufacturers is stressed. It is concluded that in order to achieve the required goals in supersonic transport without putting engine manufacturers at unacceptable business risk, international collaboration will be necessary. ESA

N93-11105# Rolls-Royce, Inc., Atlanta, GA.
ADVANCED MATERIALS IN GAS TURBINE ENGINES: AN ASSESSMENT
S. Gupta and M. Goulette (Rolls-Royce Ltd., Derby, England) Nov. 1991 7 p Presented at the 1991 Yokohama International Gas Turbine Congress, Yokohama, Japan, 27 Oct. - 1 Nov. 1991
(PNR-90946; ETN-92-92223) Copyright Avail: CASI HC A02/MF A01

The following requirements for advanced materials are considered: low density, high temperature capability, high specific strength and stiffness, low expansion coefficients, reliable and predictable behavior, and low cost. The large number of potential material options are discussed: high temperature polymers, titanium aluminides, metal matrix composites, glass composites, ceramic composites, carbon/carbon composites, and carbon ceramic composites. The application development of these advanced materials is considered. ESA

N93-11106# Rolls-Royce, Inc., Atlanta, GA.
DEVELOPMENT OF ADVANCED CARBON-CARBON ANNULAR FLAMEHOLDERS FOR GAS TURBINES
S. Gupta, W. Westphal, A. F. Jarvis (Rolls-Royce Ltd., Bristol, England), and R. Dirling (Science Applications International Corp.,

Santa Ana, CA.) Nov. 1991 5 p Presented at the 1991 Yokohama International Gas Turbine Congress, Yokohama, Japan, 27 Oct. - 1 Nov. 1991
(PNR-90947; ETN-92-92224) Copyright Avail: CASI HC A01/MF A01

A program to assess the potential of using carbon-carbon composites in aero gas turbine engines is discussed: a set of annular flameholders was the chosen component system. These were designed, fabricated, coated, and successfully engine tested. The viability of using an integrated approach to the material system, design, and fabication was clearly demonstrated. The critical areas identified were the low interlaminar strength of the material, difficulties of obtaining an acceptable coating on complex parts, lack of reliability and repeatability in the coating and fabrication processes, and susceptibility of the coatings to such environmental factors as humidity. The program, as a whole, was a success.
ESA

N93-11108# Rolls-Royce Ltd., Derby (England).
THE DEVELOPMENT OF THE ROLLS-ROYCE TRENT AERO GAS TURBINE
M. A. Spencer 8 Apr. 1991 28 p Presented at the Inst. of Mechanical Engineers' North Eastern Branch, 8 Apr. 1991
(PNR-90949; ETN-92-92226) Copyright Avail: CASI HC A03/MF A01

A lecture given to mechanical engineers, which was backed up by a set of figures that are listed but not given, is presented. Reasons why the Trent was launched are given together with a brief description of the configuration of the engine. Explanations for some of the major decisions taken to date are given, and the aircaft market is discussed. The status of the test program is covered and some of the significant test results obtained to date are discussed. The Trent, the largest member of the RB211 family, recently commenced its development test program which will lead to engine certification in the middle of 1992 and entry into service in 1993.
ESA

N93-11112# Rolls-Royce Ltd., Derby (England).
DEVELOPMENT OF THE NEUTRON DIFFRACTION TECHNIQUE FOR THE DETERMINATION OF NEAR SURFACE RESIDUAL STRESSES IN CRITICAL GAS TURBINE COMPONENTS
A. N. Ezeilo (Imperial Coll. of Science and Technology, London, England), P. S. Webster, G. A. Webster (Imperial Coll. of Science and Technology, London, England), and P. J. Webster (Salford Univ., England) 1 Apr. 1991 7 p Presented at the NATO Advanced Research Workshop on Measurement of Residual and Applied Stress Using Neutron Diffraction, Oxford, England, Mar. 1991 Submitted for publication
(PNR-90984; ETN-92-92243) Copyright Avail: CASI HC A02/MF A01

The role of residual stress in improving the fatigue performance of a compressor assembly is outlined. One method of producing compressive residual stresses in the surface region of components to give improved resistance to fatigue fracture is shot peening. Neutron diffraction methods are successfully being used to determine through thickness engineering strains in polycrystalline materials. Results of measurements that were made on shot peened samples of a nickel superalloy are given. Good instrumental characteristics, sample positioning in the beam and the correction of near surface data resulted in the accurate determinations of the residual stress fields. It is observed that the stress profile has a characteristic shape irrespective of material or of the peening intensity employed, and also that the distribution of stresses balancing the surface compressive field results in a peak tension of approximately one third of the maximum surface compression.
ESA

N93-11114# Rolls-Royce Ltd., Derby (England).
A KNOWLEDGE-BASED BLACKBOARD SYSTEM TO INTERPRET GRAPHICAL DATA FROM VIBRATION TESTS OF GAS TURBINES
R. J. Allwood (Loughborough Univ. of Technology, England), S. P. King (Loughborough Univ. of Technology, England), and N. J. Pitts (Rolls-Royce Ltd., Bristol, England) 13 Apr. 1992 19 p Presented at AI Eng 1992, Waterloo, Ontario, 1992
(PNR-90993; ETN-92-92249) Copyright Avail: CASI HC A03/MF A01

The second phase of a research project to develop an automatic vibration data analysis system is described. The normal graphical presentation of the data is retained and image processing methods are applied to it, coupled with knowledge about the response of an engineering system to excitation to locate the features an experienced engineer would find. Further knowledge coded for an expert system is used to identify and interpret the features found. In particular a 'blackboard' approach is used to enable a comparison to be made between the results from several blades in one stage of the engine and therefore expected to respond in a similar way. Several factors, particularly the effect of gauge position, make this comparison a difficult and challenging task, but it is essential if the system's report to an engineer is to be made in engineering units.
ESA

N93-11206# Rolls-Royce Ltd., Derby (England).
THE USE OF SIMULTANEOUS ENGINEERING FOR THE DESIGN AND MANUFACTURE OF THE LOW PRESSURE TURBINE FOR THE ROLLS-ROYCE TRENT ENGINE
A. G. Dodd and M. C. Butcher 1 Oct. 1991 24 p
(PNR-90887; ETN-92-92191) Copyright Avail: CASI HC A03/MF A01

The activities needed to devise and then produce a new low pressure turbine for an engine, are outlined. If done in sequence these would take an unacceptable seven years. Hence, to create the design, the activities of the technical specialists and data transfer between the analysis tools, were integrated. The means by which early activities were arranged in parallel, using a 'hierarchy of iteration,' are outlined. Problems of working in parallel are also addressed, together with changes to traditional work methods and the lessons that were learned. The reduction in elapsed manufacturing timescales are stressed. It is shown how during this simultaneous engineering, the integration of all the design and technology specialities, together with the manufacturing suppliers, occurred at a very early stage in the design. Work proceeded in parallel, and the parts were delivered ahead of the competition. The low pressure turbine achieved its efficiency targets, hence the quality of the product was not compromised.
ESA

N93-11207# Rolls-Royce Ltd., Derby (England). Aerospace Group.
INNOVATION IN ENGINEERING
T. Broughton 8 Apr. 1992 14 p
(PNR-90889; ETN-92-92192) Copyright Avail: CASI HC A03/MF A01

Graphics on the subject of how to achieve the world beating competitive design and manufacture of very complex products, such as the Trent engine, through integrated engineering are presented. It is concluded that since there are large gains in the aerospace industry for those who provide the right product at right cost, the following must be performed: improvement of the product in terms of performance, lower costs, and shorter lead times. This requires the following: product innovation for the metal engine and process innovation for the business engine; continued investment in people to operate these processes and provide an environment in which they can realize their full potential; and continued investment in advanced computing systems for predictive modeling, computer aided engineering, and advanced technology acquisition programs.
ESA

N93-11208# Rolls-Royce Ltd., Derby (England). Aerospace Group.
SIMULTANEOUS ENGINEERING IN AERO GAS TURBINE DESIGN AND MANUFACTURE
T. Broughton 8 Apr. 1992 10 p
(PNR-90890; ETN-92-92193) Copyright Avail: CASI HC A02/MF A01

An analysis of the engineering process of aero gas turbine design and manufacture is carried out. In an attempt to optimize this process to the needs of business, the philosophies of simultaneous engineering are explored and are applied to it. The management of people is discussed in this highly integrated environment, and the impact of computer aided engineering is examined as an enabling device for simultaneous engineering. Examples of the successful implementation of simultaneous engineering are given, including the process of acquiring new design and manufacturing technologies. ESA

N93-11339 Motoren- und Turbinen-Union Muenchen G.m.b.H. (Germany).
INCREASE OF ENERGY USE ON COOLED HIGH TEMPERATURE TURBINE, PHASE 3 Final Report [STEIGERUNG DER ENERGIEAUSNUTZUNG IN GEKUEHLTEN HOCHTEMPERATURTURBINEN PHASE 3. ABSCHLUSSBERICHT]
Hans-Juergen Dietrichs and Bertram Stubert 19 Jul. 1991 59 p In GEORGIAN
(Contract BMFT-LVT-8701-1)
(MTUM-B91EW-0029-Phase-3; ETN-92-92291) Copyright Avail: Fachinformationszentrum Karslruhe, 7514 Eggenstein-Leopoldshafen 2, Germany

Detailed investigations of the shock boundary layer interaction in transonic turbine cascades were carried out. Theoretical investigations were concentrated on the improvement of advanced computational fluid dynamic codes, e.g., three dimensional Euler, and three dimensional Navier-Stokes, and the comprehension of secondary flow phenomena. The theoretical and experimental results were the basis for the aerodynamic design of a highly loaded transonic high power turbine. The analysis of cold flow rig and of engine tests showed a 2 percent increase of turbine efficiency and an extension of the operating range towards stage pressure ratios of 4.0. ESA

N93-11530*# National Aeronautics and Space Administration. Lewis Research Center, Cleveland, OH.
OVERVIEW OF HIGH PERFORMANCE AIRCRAFT PROPULSION RESEARCH
Thomas J. Biesiadny Oct. 1992 17 p Presented at the Aerotech 1992 Conference, Anaheim, CA, 5-8 Oct. 1992
(RTOP 505-68-32)
(NASA-TM-105839; E-7280; NAS 1.15:105839) Avail: CASI HC A03/MF A01

The overall scope of the NASA Lewis High Performance Aircraft Propulsion Research Program is presented. High performance fighter aircraft of interest include supersonic flights with such capabilities as short take off and vertical landing (STOVL) and/or high maneuverability. The NASA Lewis effort involving STOVL propulsion systems is focused primarily on component-level experimental and analytical research. The high-maneuverability portion of this effort, called the High Alpha Technology Program (HATP), is part of a cooperative program among NASA's Lewis, Langley, Ames, and Dryden facilities. The overall objective of the NASA Inlet Experiments portion of the HATP, which NASA Lewis leads, is to develop and enhance inlet technology that will ensure high performance and stability of the propulsion system during aircraft maneuvers at high angles of attack. To accomplish this objective, both wind-tunnel and flight experiments are used to obtain steady-state and dynamic data, and computational fluid dynamics (CFD) codes are used for analyses. This overview of the High Performance Aircraft Propulsion Research Program includes a sampling of the results obtained thus far and plans for the future. Author

N93-12077*# National Aeronautics and Space Administration. Lewis Research Center, Cleveland, OH.
AN EXPERIMENTAL INVESTIGATION OF THE FLOW IN A DIFFUSING S-DUCT
Steven R. Wellborn (Iowa State Univ. of Science and Technology, Ames.), Bruce A. Reichert, and Theodore H. Okiishi (Iowa State Univ. of Science and Technology, Ames.) Aug. 1992 13 p Presented at the 28th Joint Propulsion Conference and Exhibit, Nashville, TN, 6-8 Jul. 1992; sponsored by AIAA, SAE, ASME, and ASEE Previously announced in IAA as A92-54090
(RTOP 505-62-52)
(NASA-TM-105809; E-7240; NAS 1.15:105809; AIAA Paper 92-3622) Copyright Avail: CASI HC A03/MF A01

Compressible, subsonic flow through a diffusing S-duct has been experimentally investigated. Benchmark aerodynamic data are presented for flow through a representative S-duct configuration. The collected data would be beneficial to aircraft inlet designers and is suitable for the validation of computational codes. Measurements of the 3D velocity field and total and static pressures were obtained at five cross-sectional planes. Surface static pressures and flow visualization also helped to reveal flow field characteristics. All reported tests were conducted with an inlet centerline Mach number of 0.6 and a Reynolds number, based on the inlet centerline velocity and duct inlet diameter, of 2.6 x 10(exp 6). The results show that a larger region of streamwise flow separation occurred within the duct. Details about the separated flow region, including mechanisms which drive this complicated flow phenomenon, are discussed. Transverse velocity components indicate that the duct curvature induces strong pressure driven secondary flows, which evolve into a large pair of counter-rotating vortices. These vortices convect the low momentum fluid of the boundary layer towards the center of the duct, degrading both the uniformity and magnitude of the total pressure profile. Author

N93-12214*# Purdue Univ., West Lafayette, IN. School of Mechanical Engineering.
HYPERVELOCITY SCRAMJET COMBUSTOR-NOZZLE ANALYSIS AND DESIGN Final Technical Report, 15 Feb. 1988 - 31 Dec. 1991
H. Doyle Thompson and Joe D. Hoffman Nov. 1992 6 p
(Grant NAG1-854)
(NASA-CR-190965; NAS 1.26:190965) Avail: CASI HC A02/MF A01

The progress report for the grant entitled 'Hypervelocity of Scramjet Combustor-Nozzle Analysis and Design' is presented. The three main tasks in the program are combustor modeling study, development of anaylsis capabilities for hypersonic scramjet nozzles, and development of optimum design methods for hypersonic scramjet nozzles. The research performed was documented in a series of technical publications and presentations at various conferences. A brief description of the research in each of the above three areas and a list of the resulting technical publications are included. L.R.R.

N93-12402*# National Aeronautics and Space Administration. Lewis Research Center, Cleveland, OH.
CONCURRENT OPTIMIZATION OF AIRFRAME AND ENGINE DESIGN PARAMETERS
Thomas M. Lavelle, Robert M. Plencner, and Jonathan A. Seidel Oct. 1991 17 p Presented at the Fourth Symposium on Multidisciplinary Analysis and Optimization, Cleveland, OH, 21-23 Sep. 1992; sponsored by AIAA, USAF, and OAI
(RTOP 505-69-50)
(NASA-TM-105908; E-7382; NAS 1.15:105908; AIAA Paper 92-4713) Avail: CASI HC A03/MF A01

An integrated system for the multidisciplinary analysis and optimization of airframe and propulsion design parameters is being developed. This system is known as IPAS, the Integrated Propulsion/Airframe Analysis System. The traditional method of analysis is one in which the propulsion system analysis is loosely coupled to the overall mission performance analysis. This results in a time consuming iterative process. First, the engine is designed and analyzed. Then, the results from this analysis are used in a mission analysis to determine the overall aircraft performance. The results from the mission analysis are used as a guide as the engine is redesigned and the entire process repeated. In IPAS, the propulsion system, airframe, and mission are closely coupled. The propulsion system analysis code is directly integrated into the mission analysis code. This allows the propulsion design parameters to be optimized along with the airframe and mission design parameters, significantly reducing the time required to obtain an optimized solution. Author

N93-12418*# National Aeronautics and Space Administration. Lewis Research Center, Cleveland, OH.

AN IMPROVED NUMERICAL MODEL FOR WAVE ROTOR DESIGN AND ANALYSIS

Daniel E. Paxson and Jack Wilson (Sverdrup Technology, Inc., Brook Park, OH.) Oct. 1992 12 p Proposed for presentation at the 31st Aerospace Sciences Meeting, Reno, NV, 11-14 Jan. 1993; sponsored by AIAA
(RTOP 505-62-10)
(NASA-TM-105915; E-7398; NAS 1.15:105915; AIAA Paper 93-0482) Avail: CASI HC A03/MF A01

A numerical model has been developed which can predict both the unsteady flows within a wave rotor and the steady averaged flows in the ports. The model is based on the assumptions of one-dimensional, unsteady, and perfect gas flow. Besides the dominant wave behavior, it is also capable of predicting the effects of finite tube opening time, leakage from the tube ends, and viscosity. The relative simplicity of the model makes it useful for design, optimization, and analysis of wave rotor cycles for any application. This paper discusses some details of the model and presents comparisons between the model and two laboratory wave rotor experiments. Author

08 AIRCRAFT STABILITY AND CONTROL

Includes aircraft handling qualities; piloting; flight controls; and autopilots.

For related information see also *05 Aircraft Design, Testing and Performance.*

N93-11046 Department of the Navy, Washington, DC.

DROPPABLE JET VANE TVC Patent

Michael D. Jacobson, inventor (to Navy) 21 Jan. 1992 6 p Filed 6 Jan. 1975
(AD-D015341; US-Patent-5,082,202; US-Patent-Appl-SN-537640; US-Patent-Class-244-322) Avail: US Patent and Trademark Office

A jet vane thrust vector control unit is provided to pitch a missile over into a generally horizontal path after the missile has been vertically launched. A collar affixed to the base of the missile by explosive bolts is utilized to mount the unit so that the unit can be jettisoned after it has done its job. GRA

N93-11160# Centro Italiano Ricerche Aerospaziali, Naples.

AUTOMATIC CONTROL LAWS FOR AIRCRAFT IN PARABOLIC FLIGHT [LEGGI DI CONTROLLO AUTOMATICO PER VELIVOLI IN VOLO PARABOLICO]

E. Filippone and L. Verde 15 Oct. 1991 56 p In ITALIAN
(DILC-EST-TR-211; ETN-92-92412) Avail: CASI HC A04/MF A01

Experimental results from tests conducted in microgravity are reported. The dynamic model used is presented. Open and closed loop control for parabolic flight are described. The results for the numerical simulation relating to the presented control laws are shown, in particular the temporal sequence being shown for each simulation. ESA

N93-11176*# National Aeronautics and Space Administration. Langley Research Center, Hampton, VA.

A PROBLEM FORMULATION FOR GLIDESLOPE TRACKING IN WIND SHEAR USING ADVANCED ROBUST CONTROL TECHNIQUES

Christine M. Belcastro, B.-C. Chang (Drexel Univ., Philadelphia, PA.), and Robert Fischl (Drexel Univ., Philadelphia, PA.) Aug. 1992 21 p
(RTOP 505-64-52-01)
(NASA-TM-104164; NAS 1.15:104164) Avail: CASI HC A03/MF A01

A formulation of the longitudinal glideslope tracking of a transport-class aircraft in severe wind shear and turbulence for application to robust control system design is presented. Mathematical wind shear models are incorporated into the vehicle mathematical model, and wind turbulence is modeled as an input disturbance signal. For this problem formulation, the horizontal and vertical wind shear gradients are treated as real uncertain parameters that vary over an entire wind shear profile. The primary objective is to examine the formulation of this problem into an appropriate design format for use in m-synthesis control system design. Author

N93-11178*# National Aeronautics and Space Administration. Hugh L. Dryden Flight Research Facility, Edwards, CA.

FLIGHT-DETERMINED STABILITY ANALYSIS OF MULTIPLE-INPUT-MULTIPLE-OUTPUT CONTROL SYSTEMS

John J. Burken Nov. 1992 19 p Presented at the AIAA Guidance, Navigation, and Control Conference, Hilton Head, SC, 10-12 Aug. 1992 Previously announced in IAA as A92-55196
(RTOP 533-02-38)
(NASA-TM-4416; H-1837; NAS 1.15:4416; AIAA Paper 92-4396) Copyright Avail: CASI HC A03/MF A01

Singular value analysis can give conservative stability margin results. Applying structure to the uncertainty can reduce this conservatism. This paper presents flight-determined stability margins for the X-29A lateral-directional, multiloop control system. These margins are compared with the predicted unscaled singular values and scaled structured singular values. The algorithm was further evaluated with flight data by changing the roll-rate-to-aileron command-feedback gain by +/- 20 percent. Minimum eigenvalues of the return difference matrix which bound the singular values are also presented. Extracting multiloop singular values from flight data and analyzing the feedback gain variations validates this technique as a measure of robustness. This analysis can be used for near-real-time flight monitoring and safety testing. Author

N93-11459*# National Aeronautics and Space Administration. Langley Research Center, Hampton, VA.

MODIFIED OPTIMAL CONTROL PILOT MODEL FOR COMPUTER-AIDED DESIGN AND ANALYSIS

John B. Davidson and David K. Schmidt (Arizona State Univ., Tempe.) Oct. 1992 29 p
(RTOP 505-64-30-01)
(NASA-TM-4384; L-16979; NAS 1.15:4384) Avail: CASI HC A03/MF A01

This paper presents the theoretical development of a modified optimal control pilot model based upon the optimal control model (OCM) of the human operator developed by Kleinman, Baron, and Levison. This model is input compatible with the OCM and retains other key aspects of the OCM, such as a linear quadratic solution for the pilot gains with inclusion of control rate in the cost function, a Kalman estimator, and the ability to account for attention allocation and perception threshold effects. An algorithm designed for each implementation in current dynamic systems analysis and design software is presented. Example results based upon the analysis of a tracking task using three basic dynamic systems are compared with measured results and with similar analyses performed with the OCM and two previously proposed simplified optimal pilot models. The pilot frequency responses and error statistics obtained with this modified optimal control model are shown to compare more favorably to the measured experimental results than the other previously proposed simplified models evaluated. Author

N93-11576# Ecole Centrale de Lyon (France). Lab. de Mecanique des Fluides.

ACTIVE CONTROL OF AEROACOUSTIC COUPLINGS BY MEANS OF ADAPTIVE SYSTEMS Ph.D. Thesis [CONTROLE ACTIF DES COUPLAGES AEROACOUSTIQUES A L'AIDE DE SYSTEMES AUROADAPTATIFS]

Mohammed Sebbani 1991 183 p In FRENCH
(ECL-91-18; ETN-92-92337) Avail: CASI HC A09/MF A02

The active control of aerodynamic instabilities is investigated. Instead of using a standard feedback loop the experiments are carried out with a new real time adaptive control system. Two experiments are performed: one to control flow excited instabilities occurring in a cavity, the other to suppress surge in a compressor reservoir system. In both cases, the sensor signal is simultaneously used as the reference signal and as the signal to be minimized. The controller suppresses both the closed loop and the natural instability. The controller modifies the system response. Theoretical and experimental results are in agreement. The results lead to the conclusion that the adaptive method is well suited for active control of instabilities: the controller automatically finds its optical parameters, avoids closed loop instabilities, and adapts to evolution of the system operating conditions. ESA

N93-11585# Aerospatiale, Chatillon (France). Div. des Engins Tactiques.
ADVANCED CONTROL FOR THE DESIGN OF STT MISSILE AUTOPILOT
P. Bendotti and M. MSaad (Ecole Nationale Superieure d'Ingenieuers Electriciens de Grenoble, Saint-Martin-d'Heres, France) 1992 20 p
(Rept-921-320-102; ETN-92-92348) Avail: CASI HC A03/MF A01

An autopilot design for a Skid-To-Turn (STT) missile is described. Its stability robustness and performances in the presence of large aerodynamic variations and modeling errors are discussed. The stability robustness is investigated using the singular value approach. The autopilot is obtained by combining a multivariable linear quadratic control design with a robust parameter estimator to deal with the missile model parameter uncertainties. The underlying linear quadratic control design is mainly motivated by its stability margins. The control design and the parameter estimation are derived in the discrete time domain using the delta operator. The latter is motivated by the required fast sampling and the convergence of the discrete time results to their continuous time counterpart. ESA

N93-11871 Southampton Univ. (England).
APPLICATION OF EIGENSTRUCTURE ASSIGNMENT TO THE CONTROL OF POWERED LIFT COMBAT AIRCRAFT Ph.D. Thesis
Phillip Raymond Smith 1990 311 p
Avail: Univ. Microfilms Order No. BRDX93358

An examination of the Eigenstructure Assignment control law design technique and its application to both a vectored thrust aircraft and a helicopter example are presented. In reviewing the design method new insight is shed upon the role of the left eigenvectors, which are shown to determine the nature of the input coupling into a dynamic system. It is concluded that selection of the right eigenvectors alone, as is often shown in the literature is insufficient to ensure decoupling in the system response. In each of the application studies, a non-linear aircraft mathematical model is examined in a number of different parts of the flight envelope. They are linearized to provide a state space representation of the aircraft and fixed gain controllers are designed using the method of Eigenstructure Assignment. These controllers are then implemented in the non-linear models and their behavior examined. It is seen that some classes of nonlinearity cause degradation of the closed-loop performance, whereas others result in instability or limit cycles. Examination of the frequency domain characteristics of a helicopter example are considered. This allows the controlled aircraft handling qualities to be determined. It is shown that simple dynamic elements in the command path can be used to tune the response when problems in obtaining a sufficiently high bandwidth are encountered. It is finally concluded that the method provides a viable approach to aircraft control law design, a chief attraction being the very simple structure of the resulting control laws. Author

N93-12216*# National Aeronautics and Space Administration. Langley Research Center, Hampton, VA.
MODELING AND MODEL SIMPLIFICATION OF AEROELASTIC VEHICLES: AN OVERVIEW
Martin R. Waszak, Carey S. Buttrill, and David K. Schmidt (Arizona State Univ., Tempe.) Sep. 1992 20 p
(RTOP 505-64-52-03)
(NASA-TM-107691; NAS 1.15:107691) Avail: CASI HC A03/MF A01

The rigid-body degrees of freedom and elastic degrees of freedom of aeroelastic vehicles are typically treated separately in dynamic analysis. Such a decoupling, however, is not always justified and modeling assumptions that imply decoupling must be used with caution. The frequency separation between the rigid-body and elastic degrees of freedom for advanced aircraft may no longer be sufficient to permit the typical treatment of the vehicle dynamics. Integrated, elastic vehicle models must be developed initially and simplified in a manner appropriate to and consistent with the intended application. This paper summarizes key results from past research aimed at developing and implementing integrated aeroelastic vehicle models for flight controls analysis and design. Three major areas will be addressed: (1) the accurate representation of the dynamics of aeroelastic vehicles, (2) properties of several model simplification methods, and (3) the importance of understanding the physics of the system being modeled and of having a model which exposes the underlying physical causes for critical dynamic characteristics. Author

N93-12304*# National Aeronautics and Space Administration. Langley Research Center, Hampton, VA.
A MONITOR FOR THE LABORATORY EVALUATION OF CONTROL INTEGRITY IN DIGITAL CONTROL SYSTEMS OPERATING IN HARSH ELECTROMAGNETIC ENVIRONMENTS
Celeste M. Belcastro, Robert Fischl (Drexel Univ., Philadelphia, PA.), and Moshe Kam (Drexel Univ., Philadelphia, PA.) Oct. 1992 23 p
(RTOP 505-64-10-10)
(NASA-TM-4402; L-17057; NAS 1.15:4402) Avail: CASI HC A03/MF A01

This paper presents a strategy for dynamically monitoring digital controllers in the laboratory for susceptibility to electromagnetic disturbances that compromise control integrity. The integrity of digital control systems operating in harsh electromagnetic environments can be compromised by upsets caused by induced transient electrical signals. Digital system upset is a functional error mode that involves no component damage, can occur simultaneously in all channels of a redundant control computer, and is software dependent. The motivation for this work is the need to develop tools and techniques that can be used in the laboratory to validate and/or certify critical aircraft controllers operating in electromagnetically adverse environments that result from lightning, high-intensity radiated fields (HIRF), and nuclear electromagnetic pulses (NEMP). The detection strategy presented in this paper provides dynamic monitoring of a given control computer for degraded functional integrity resulting from redundancy management errors, control calculation errors, and control correctness/effectiveness errors. In particular, this paper discusses the use of Kalman filtering, data fusion, and statistical decision theory in monitoring a given digital controller for control calculation errors. Author

N93-12305*# National Aeronautics and Space Administration. Lewis Research Center, Cleveland, OH.
ANALYSIS OF FAULT-TOLERANT NEUROCONTROL ARCHITECTURES
T. Troudet (Sverdrup Technology, Inc., Brook Park, OH.) and W. Merrill 1992 12 p Proposed for presentation at the 31st Conference on Decision and Control, Tucson, AZ, 16-18 Dec. 1992; sponsored by IEEE
(RTOP 505-62-50)
(NASA-TM-105898; E-7210; NAS 1.15:105898) Avail: CASI HC A03/MF A01

The fault-tolerance of analog parallel distributed implementations of a multivariable aircraft neurocontroller is analyzed by simulating weight and neuron failures in a simplified scheme of analog processing based on the functional architecture of the ETANN chip (Electrically Trainable Artificial Neural Network). The neural information processing is found to be only partially distributed throughout the set of weights of the neurocontroller synthesized with the backpropagation algorithm. Although the degree of distribution of the neural processing, and consequently the fault-tolerance of the neurocontroller, could be enhanced using Locally Distributed Weight and Neuron Approaches, a satisfactory level of fault-tolerance could only be obtained by retraining the degrated VLSI neurocontroller. The possibility of maintaining neurocontrol performance and stability in the presence of single weight of neuron failures was demonstrated through an automated retraining procedure of the neurocontroller based on a pre-programmed choice and sequence of the training parameters. Author

N93-12361# National Aerospace Lab., Tokyo (Japan).
ON STABILITY AND CONTROL OF SSTO SPACEPLANE IN SUPER- AND HYPERSONIC ASCENDING PHASE
Andreas Diekmann and Koichi Matsushima Nov. 1991 38 p
Sponsored by Commission of the European Communities
(NAL-TR-1128T; JTN-92-80396) Avail: CASI HC A03/MF A01

The natural dynamic stability of a Single Stage To Orbit (SSTO) National Aerospace Laboratory spaceplane configuration is evaluated at seven reference points on a super to hypersonic and constant dynamic pressure ascent trajectory. It is shown that dynamic instability occurs in the longitudinal and lateral motion during wide parts of the regarded trajectory. To counteract these instabilities a simple output feedback control is introduced to achieve a pole assignment of the dominant modes according to handling quality criteria commonly used for conventional aircraft. The sensitivity of augmented stability parameters to deviations in the feedback gain constants is evaluated. The dynamic behavior of stability augmented spaceplane is investigated by numerical simulation of its longitudinal motion during an ascent in standard clear air turbulence. Results indicate the sufficient performance of the control design. The controlled elevator deflection angles remain small despite the severe natural instability which occurred during wide parts of the ascent trajectory. Author (NASDA)

N93-12362# National Aerospace Lab., Tokyo (Japan). Advanced Aircraft Research Group.
A WIND TUNNEL INVESTIGATION TO DETERMINE BUFFET COUNTERMEASURES FOR STOL AIRCRAFT ALPHA-SWEEP FLIGHT TESTING [STOL ZENKI MOKEI BAFETTO TAISAKU FUUDOU SHIKEN]
Hitoshi Takahashi, Teruomi Nakaya, Yoshio Hayashi, Shigeo Kayaba, Masayoshi Noguchi, Isamu Nonaka, Masataka Hashidate, Hideo Hoshino, Shigeru Baba, and Takashi Inoue (Kawasaki Heavy Industries Ltd., Kobe, Japan) Nov. 1991 48 p In JAPANESE
(NAL-TR-1129; JTN-92-80397) Avail: CASI HC A03/MF A01

During alpha sweep flight testing of the Short TakeOff and Landing (STOL) experimental aircraft 'ASKA', a buffet occurred earlier than expected, as well as large airframe vibrations, both of which contributed to preventing the high angle of attack portion of alpha sweep testing from being conducted. Wind tunnel tests were subsequently performed in order to delay the onset of the wind buffet that prevented the performance of this flight test and also to determine effective aerodynamic means to alleviate the buffet's strength. Results confirmed that both triangular fences fitted to the side of the nacelle and a drooped nose on the leading edge between the nacelles were most effective. These buffet countermeasures were then applied on 'ASKA' and flight tests were conducted. It was found that the onset of a buffet was delayed and the vibration frequency of the airframe was reduced. This allowed the alpha sweep testing to be safely carried out at higher angles of attack; hence enabling the initial objective to be achieved. Author (NASDA)

N93-12413*# Draper (Charles Stark) Lab., Inc., Cambridge, MA.
AIR-BREATHING HYPERSONIC VEHICLE GUIDANCE AND CONTROL STUDIES: AN INTEGRATED TRAJECTORY/CONTROL ANALYSIS METHODOLOGY, PHASE 2 Final Report
Philip D. Hattis and Harvey L. Malchow Oct. 1992 86 p
(Contract NAS1-18565; RTOP 505-70-64-01)
(NASA-CR-189703; NAS 1.26:189703) Avail: CASI HC A05/MF A01

An integrated trajectory/control analysis algorithm has been used to generate trajectories and desired control strategies for two different hypersonic air-breathing vehicle models and orbit targets. Both models used cubic spline curve fit tabulated winged-cone accelerator vehicle representations. Near-fuel-optimal, horizontal takeoff trajectories, imposing a dynamic pressure limit of 1000 psf, were developed. The first model analysis case involved a polar orbit and included the dynamic effects of using elevons to maintain longitudinal trim. Analysis results indicated problems with the adequacy of the propulsion model and highlighted dynamic pressure/altitude instabilities when using vehicle angle of attack as a control variable. Also, the magnitude of computed elevon deflections to maintain trim suggested a need for alternative pitch moment management strategies. The second analysis case was reformulated to use vehicle pitch attitude relative to the local vertical as the control variable. A new, more realistic, air-breathing propulsion model was incorporated. Pitch trim calculations were dropped and an equatorial orbit was specified. Changes in flight characteristics due to the new propulsion model have been identified. Flight regimes demanding rapid attitude changes have been noted. Also, some issues that would affect design of closed-loop controllers were ascertained. Author

N93-12415# Helsinki Univ. of Technology, Otaniemi (Finland). Lab. of Aerodynamics.
DYNAC: A COMPUTER PROGRAM FOR ANALYZING THE DYNAMICAL STABILITY OF AIRCRAFT
Kari Renko 1 Feb. 1991 56 p
(Rept-B-31; ISBN-951-22-0519-X) Avail: CASI HC A04/MF A01

A macro-package for the Mathematica computer program is developed for analyzing aircraft as a part of a linear time-continuous control system. The package includes the classical small disturbance stability theory, linearized aircraft transfer functions, root locus method, and several frequency domain methods like Nyquist plots and Bode plots. Test cases are presented to demonstrate the use of the package. Author

09 RESEARCH AND SUPPORT FACILITIES (AIR)

Includes airports, hangars and runways; aircraft repair and overhaul facilities; wind tunnels; shock tubes; and aircraft engine test stands.

For related information see also *14 Ground Support Systems and Facilities (Space).*

N93-11057* National Aeronautics and Space Administration. Langley Research Center, Hampton, VA.
METHOD OF REMOTELY CHARACTERIZING THERMAL PROPERTIES OF A SAMPLE Patent
Joseph S. Heyman, inventor (to NASA), D. Michele Heath, inventor (to NASA), Christopher Welch, inventor (to NASA), William P. Winfree, inventor (to NASA), and William E. Miller, inventor (to NASA) 21 Jul. 1992 5 p Filed 30 Sep. 1991 Continuation of US-Patent-Appl-SN-524108, filed 16 May 1990 which is a continuation of US-Patent-Appl-SN-146939, filed 22 Jan. 1988
(NASA-Case-LAR-13508-3-CU; US-Patent-5,131,758; US-Patent-Appl-SN-768094; US-Patent-Appl-SN-524108; US-Patent-Appl-SN-146939; US-Patent-Class-374-5; US-Patent-Class-374-4; US-Patent-Class-374-57; US-Patent-Class-73-147; Int-Patent-Class-G01N-25/72) Avail: US Patent and Trademark Office

A sample in a wind tunnel is radiated from a thermal energy source outside of the wind tunnel. A thermal imager system, also located outside of the wind tunnel, reads surface radiations from the sample as a function of time. The produced thermal images are characteristic of the heat transferred from the sample to the flow across the sample. In turn, the measured rates of heat loss of the sample are characteristic of the flow and the sample.
Official Gazette of the U.S. Patent and Trademark Office

N93-11224# Loughborough Univ. of Technology (England). Dept. of Transport Technology.
AN INVESTIGATION OF GROUND ACCESS MODE CHOICE FOR DEPARTING PASSENGERS
Sara Louise Bolland, Patrick N. Ndoh, and Norman Ashford Apr. 1992 110 p
(TT-9201; ISBN-0-904747-36-X; ETN-92-92379) Copyright
Avail: CASI HC A06/MF A02

Some aspects of ground access airports were investigated. The term ground access covers the total spectrum of transportation which services an airport, both on and off the airfield. London's major airport, Heathrow (England), was chosen as a base for the investigation. From the data collected the following were analyzed: the different modes and combinations of modes used to access the airport; any patterns that may be found among different groupings of passengers and the choice of modes they used; the passengers' evaluation of the level of service experiences in relation to their chosen mode(s); other modes considered or which they would have liked to see available. The development of mode choice models was investigated using the findings of the study. Background information on the topic is reviewed and methodology and analytical procedures used are discussed. The data and results are reviewed. Findings are summarized and some useful conclusions, both for London Heathrow and airports in general, are drawn. ESA

N93-11225# Centro Italiano Ricerche Aerospaziali, Naples.
WIND TUNNEL OPERATOR AIMED COMPARISON BETWEEN TWO ELECTRONIC PRESSURE SCANNER SYSTEMS
F. Nitti (Italian Aerospace Research Center, Capua.) and F. Fusco (Italian Aerospace Research Center, Capua.) 28 Feb. 1992 8 p Repr. from ISA, 1992, Paper 92-0197
(DLAS-EST-TR-040; ETN-92-92414) Avail: CASI HC A02/MF A01

A comparison made between two different electronic pressure scanner systems is outlined. This comparison was done from the wind tunnel user point of view and covered the following topics: software and hardware setting up for a test configuration; calibration procedure; versatile and user friendly features of the software packages managing the systems; and response stability measurement. Differences and similarities of the systems are outlined. ESA

N93-11367# Sandia National Labs., Albuquerque, NM.
GROUND TEST FACILITY FOR SEI NUCLEAR ROCKET ENGINES
C. D. Harmon, C. A. Ottinger, L. C. Sanchez, and L. R. Shipers 1992 13 p Presented at the 28th Joint Propulsion Conference, Nashville, TN, 6-8 Jul. 1992 Previously announced in IAA as A92-48860
(Contract DE-AC04-76DP-00789)
(DE92-017418; SAND-92-1566C; CONF-920747-8) Avail: CASI HC A03/MF A01

Nuclear Thermal Propulsion (NTP) has been identified as a critical technology in support of the NASA Space Exploration Initiative (SEI). In order to safely develop a reliable, reusable, long-lived flight engine, facilities are required that will support ground tests to qualify the nuclear rocket engine design. Initial nuclear fuel element testing will need to be performed in a facility that supports a realistic thermal and neutronic environment in which the fuel elements will operate at a fraction of the power of a flight weight reactor/engine. Ground testing of nuclear rocket engines is not new. New restrictions mandated by the National Environmental Protection Act of 1970, however, now require major changes to be made in the manner in which reactor engines are now tested. These new restrictions now preclude the types of nuclear rocket engine tests that were performed in the past from being done today. A major attribute of a safely operating ground test facility is its ability to prevent fission products from being released in appreciable amounts to the environment. Details of the intricacies and complications involved with the design of a fuel element ground test facility are presented in this report with a strong emphasis on safety and economy. DOE

N93-11435# Royal Aerospace Establishment, Farnborough (England).
THE MEASUREMENT OF THE VELOCITY FIELD INDUCED BY A GUST GENERATOR IN A CLOSED-CIRCUIT SUBSONIC WIND-TUNNEL
R. T. Jones 23 Feb. 1988 28 p
(RAE-TM-Mat-Str-1102; BR106727; ETN-92-92299) Copyright
Avail: CASI HC A03/MF A01

The design, installation and testing of a moving vane gust generating system and the equipment used to measure its effect in a 4 by 3 ft closed circuit subsonic wind tunnel are described. The downstream effect of oscillating the vanes of this gust generator at an amplitude of 3 deg, using sinusoidal frequency sweeps, was measured at 90 different positions in the tunnel working section for each of four airstream velocities, 30, 35, 40 and 45 m/s. The results are presented in the form of 'carpet' plots showing the magnitude of the transfer functions of gust velocity at the measurement points to the generator motion. These plots of the gust as its travels down the tunnel clearly show the decay and the effects of the tunnel wall boundary layer. Further selected tests were made at gust vane ampitudes of 1 and 5 deg to investigate the linearity of the system. The results show no significant difference from the transfer functions obtained for a gust vane amplitude of 3 deg. ESA

N93-11447# Lawrence Livermore National Lab., CA.
OPERATING CHARACTERISTICS OF A 7.6 mm (0.30 INCH) DIAMETER TWO-STAGE LIGHT-GAS GUN
A. R. Susoeff, R. S. Hawke, P. R. Bowen, D. W. Greenwood, and F. R. Marshall Jul. 1992 17 p
(Contract W-7405-eng-48)
(DE92-018783; UCRL-ID-111473) Avail: CASI HC A03/MF A01

A series of tests was conducted to determine the operating requirements needed to obtain maximum projectile velocity within the engineering design limits of a two-stage light-gas gun with a 7.6 mm (0.30 inch) diameter bore launch tube. The tests were conducted in a medium vacuum flight range. Previous experience with the gun was used to establish the minimum requirements for optimum efficiency. Two operating parameters, propellant load and drive gas pressure, were varied in order to find an initial optimum operating condition at a conservative propellant load. Propellant load and driver gas pressure were then incrementally increased. This procedure was methodically applied until significant mechanical deformation of a critical gun component took place. This report presents the results of these tests. Projectile velocity was measured to better than 3 percent accuracy using a magnetic induction technique. A 0.485 gram polycarbonate projectile was launched to a velocity of 7.77 km/s during the tests. DOE

N93-11616# Federal Aviation Administration, Atlantic City, NJ.
UPGRADE PRECISION RUNWAY MONITOR (PRM) OPERATIONAL TEST AND EVALUATION (OT/E) TEST PLAN
Ricardo Astillero, Thomas Bratton, Charles Dudas, and Jeffrey Livings Oct. 1992 42 p
(DOT/FAA/CT-TN92/13) Avail: CASI HC A03/MF A01

The Upgrade Precision Runway Monitor (Upgrade PRM) Operational and Integration tests are defined that will be conducted at the Federal Aviation Administration (FAA) Operational facilities. These tests will be executed at Raleigh-Durham Airport (RDU) following the Contractor Site Acceptance Test. The Upgrade PRM test configuration is addressed in conjunction with the associated interfaces which will be required to perform the testing in as near an operational environment as possible. The Air Traffic (AT) Operational requirements and test objectives are contained in this test plan. In addition to providing requirements traceability, this plan contains a description of the tests which will be executed, associated success criteria, roles and responsibilities of test personnel, and the overall flow of activities required for a successful test program. Author

N93-11728# Loughborough Univ. of Technology (England). Dept. of Transport Technology.

AIRPORT STAND ASSIGNMENT MODEL Final Report

A. Marawa and N. J. Ashford Jul. 1991 185 p
(TT-9104; ISBN-0-904947-31-9; ETN-92-92378) Copyright
Avail: CASI HC A09/MF A02

Work carried out in a contract, to develop an airport stand assignment simulation model, is summarized. The objectives are: to provide an interactive airport stand assignment model suitable for microcomputers for use at medium sized regional airports in both operations and planning; to provide an assignment model which will enable regional airport planners to determine current and future capacity according to the parameters by which regional airport operators decide to define capacity. Sufficient information is provided to understand and trace the logic and methodology that went into the development of the model. Guidance is also given on how to use the simulation model. ESA

N93-11751# Army Engineer Topographic Labs., Fort Belvoir, VA.

AUTOMATED EXTRACTION OF AIRCRAFT RUNWAY PATTERNS FROM RADAR IMAGERY

Richard A. Hevenor and Pi-Fuay Chen 5 May 1992 6 p
(AD-A254258; TEC-R-168) Avail: CASI HC A02/MF A01

A method is presented to extract linear terrain features from synthetic radar imagery. An input radar image is smoothed with an edge preserving smoothing operation. Edge detection is performed using a Sobel operator, and both the magnitude and the directional images are computed. The edges are strengthened using several iterations of a relaxation operation in which both the magnitude image and the directional image are updated with each iteration. The output of the relaxation operation is a binary edge image, which is thinned. A connected components routine is run in which two passes through the image are used to provide a unique label for each connected component. The connected components related only to the runway pattern are extracted by computing certain properties of each component. A border-following algorithm is used to follow only the outermost borders and give each of the pixels on an outermost border a maximum brightness value. GRA

N93-11906# Royal Aerospace Establishment, Bedford (England). Aerospace Div.

STRAIN-GAUGE BALANCE PERFORMANCE AND INTERNAL TEMPERATURE GRADIENTS MEASURED IN A CRYOGENIC ENVIRONMENT

R. D. Law 29 Jan. 1992 36 p Presented at the Second European Wind Tunnel Cryogenic Technology Review Meeting, Cologne, Germany, Jun. 1988
(RAE-TM-Aero-2232; BR309937; ETN-92-92306) Copyright
Avail: CASI HC A03/MF A01

Tests in which strain gauged balances and a simple axisymmetric dummy balance were subjected to temperature gradients are described. An external body of revolution was fitted over each balance to provide shielding from gas flows of 16 m/s at temperatures between ambient and 90 K. Convection around the balances could be controlled, and by extending the body of revolution the direction of temperature gradients was changed. A beam analysis is used to demonstrate that thermally induced axial force readings from the balance can be predicted from temperatures measured at the flexure roots. An axial force calibration was carried out in the balance at ambient and cryogenic temperatures to quantify sensitivity changes. To measure changes in interactions at low temperatures, pitching moment or normal force were also applied simultaneously with axial force. The results highlight the mechanism by which temperature gradients affect the outputs of strain gauged balances during temperature transients. During coding axial force, errors of up to 50 percent of full scale occur in individual flexures due to differential contraction within the balance. ESA

N93-11910*# Tennessee Univ. Space Inst., Tullahoma.

A WALL INTERFERENCE ASSESSMENT/CORRECTION SYSTEM Semiannual Report No. 2, Jan. - Jun. 1992

Ching F. Lo, N. Ulbrich, W. L. Sickles (Calspan Corp., Arnold AFS, TN.), and Cathy X. Qian 1992 40 p
(Grant NAG2-733)
(NASA-CR-190617; NAS 1.26:190617) Avail: CASI HC A03/MF A01

A Wall Signature method, the Hackett method, has been selected to be adapted for the 12-ft Wind Tunnel wall interference assessment/correction (WIAC) system in the present phase. This method uses limited measurements of the static pressure at the wall, in conjunction with the solid wall boundary condition, to determine the strength and distribution of singularities representing the test article. The singularities are used in turn for estimating wall interferences at the model location. The Wall Signature method will be formulated for application to the unique geometry of the 12-ft Tunnel. The development and implementation of a working prototype will be completed, delivered and documented with a software manual. The WIAC code will be validated by conducting numerically simulated experiments rather than actual wind tunnel experiments. The simulations will be used to generate both free-air and confined wind-tunnel flow fields for each of the test articles over a range of test configurations. Specifically, the pressure signature at the test section wall will be computed for the tunnel case to provide the simulated 'measured' data. These data will serve as the input for the WIAC method-Wall Signature method. The performance of the WIAC method then may be evaluated by comparing the corrected parameters with those for the free-air simulation. Each set of wind tunnel/test article numerical simulations provides data to validate the WIAC method. A numerical wind tunnel test simulation is initiated to validate the WIAC methods developed in the project. In the present reported period, the blockage correction has been developed and implemented for a rectangular tunnel as well as the 12-ft Pressure Tunnel. An improved wall interference assessment and correction method for three-dimensional wind tunnel testing is presented in the appendix. L.R.R.

N93-12016*# National Aeronautics and Space Administration. Lewis Research Center, Cleveland, OH.

ACOUSTICAL EVALUATION OF THE NASA LEWIS 9 BY 15 FOOT LOW SPEED WIND TUNNEL

Milo D. Dahl and Richard P. Woodward Nov. 1992 64 p
(RTOP 505-62-21)
(NASA-TP-3274; E-6137; NAS 1.60:3274) Avail: CASI HC A04/MF A01

The test section of the NASA Lewis 9- by 15-Foot Low Speed Wind Tunnel was acoustically treated to allow the measurement of acoustic sources located within the tunnel test section under simulated free field conditions. The treatment was designed for high sound absorption at frequencies above 250 Hz and to withstand tunnel airflow velocities up to 0.2 Mach. Evaluation tests with no tunnel airflow were conducted in the test section to assess the performance of the installed treatment. This performance would not be significantly affected by low speed airflow. Time delay spectrometry tests showed that interference ripples in the incident signal resulting from reflections occurring within the test section average from 1.7 dB to 3.2 dB wide over a 500 to 5150 Hz frequency range. Late reflections, from upstream and downstream of the test section, were found to be insignificant at the microphone measuring points. For acoustic sources with low directivity characteristics, decay with distance measurements in the test section showed that incident free field behavior can be measured on average with an accuracy of +/- 1.5 dB or better at source frequencies from 400 Hz to 10 kHz. The free field variations are typically much smaller with an omnidirectional source. Author

N93-12268# Sandia National Labs., Albuquerque, NM.
SYSTEM DESIGN AND RADIATION FIELD CHARACTERISTICS OF THE HIGH FLUX NEUTRON RADIOGRAPHY FACILITY (HFNRF) AT SANDIA NATIONAL LABORATORIES
J. G. Kelly, F. M. McCrory, and P. J. Cooper (Science and Engineering Associates, Inc., Albuquerque, NM.) 1992 10 p
Presented at the 4th World Conference on Neutron Radiography, San Francisco, CA, 11-14 May 1992
(Contract DE-AC04-76DP-00789)
(DE92-013984; SAND-91-2689C; CONF-9205157-1) Avail: CASI HC A02/MF A01

The High Flux Neutron Radiography Facility (HFNRF) has been fabricated, tested, and used successfully. This paper describes the final design features and presents the results of the radiation measurements made during the characterization tests. A complete neutron spectrum (from 10(exp -8) to 15 MeV) has been measured with the aid of activation foils. Gold foils were used to determine a thermal neutron flux of 9.4 x 10(exp 7) n/sq cm at the image plane in the Sandia Annular Core Research Reactor (ACRR) operating at 1.0 MW. The reactor can be operated at 20 MW for 10-second periods with the radiography tube in the central cavity. In pulse mode with peak power of 24,000 MW and a 7.6 ms FWHM approximately 1.9 x 10(exp 10) n/sq cm will be generated with a peak flux of 2.3 x 10(exp 12) n/sq cm(sec).
DOE

N93-12349*# MCAT Inst., San Jose, CA.
STUDY OF OPTICAL TECHNIQUES FOR THE AMES UNITARY WIND TUNNELS. PART 4: MODEL DEFORMATION Progress Report
George Lee Aug. 1992 41 p
(Contract NCC2-716)
(NASA-CR-190980; NAS 1.26:190980; MCAT-92-016) Avail: CASI HC A03/MF A01

A survey of systems capable of model deformation measurements was conducted. The survey included stereo-cameras, scanners, and digitizers. Moire, holographic, and heterodyne interferometry techniques were also looked at. Stereo-cameras with passive or active targets are currently being deployed for model deformation measurements at NASA Ames and LaRC, Boeing, and ONERA. Scanners and digitizers are widely used in robotics, motion analysis, medicine, etc., and some of the scanner and digitizers can meet the model deformation requirements. Commercial stereo-cameras, scanners, and digitizers are being improved in accuracy, reliability, and ease of operation. A number of new systems are coming onto the market. Author

N93-12359# National Aerospace Lab., Tokyo (Japan). Control Systems Div.
SIMULATION ANALYSIS OF A CABLE-MOUNT SYSTEM USED FOR DYNAMIC WIND TUNNEL TESTS [KEBURU SHIJI DOUTEKI FUUDOU SHIKEN MOKEI NO SUUGAKU MODERU NI YORU UNDOU TOKUSEI KAISEKI]
Masaaki Yanagihara, Masahiko Nagayasu, Shuichi Sasa, and Takashi Shimomura Oct. 1991 53 p In JAPANESE
(NAL-TR-1127; JTN-92-80395) Avail: CASI HC A04/MF A01

Dynamic wind tunnel tests using a cable mounted aircraft model were conducted in the National Aerospace Laboratory (NAL) large-scale, low speed wind tunnel to identify the aerodynamic characteristics of the NAL spaceplane. The model was suspended by two cables and had freedom of motion. Motion characteristics of the model were investigated using a mathematical simulation model. Results showed both the longitudinal and lateral motions consist of three oscillational modes, where one of the longitudinal modes displayed several characteristics very similar to the short period mode of a free flight model. The other two modes were strongly affected by cable forces and moments, with one of these being significantly low damped and having high frequency translational oscillation caused by cable force. This mode approached the phugoid mode when a spring was added to the front cable and its spring constant was decreased. One lateral motion mode was found to have similar characteristics to the dutch roll mode, whereas one of the other two modes was unstable when the model was located near the center height of the wind tunnel and the cable tension was low. Author (NASDA)

12 ASTRONAUTICS (GENERAL)

For extraterrestrial exploration see *91 Lunar and Planetary Exploration.*

N93-11216# Research Inst. of National Defence, Linkoeping (Sweden). Huvudavdelning foer Informationsteknologi.
CONTRIBUTIONS TO CD SPACE COMMITTEE, 1991: SUMMARY AND ANALYSIS [CD RYMDKOMMITTEARBETE 1991: SAMMANFATTNING OCH ANALYS]
U. Ekblad and T. Orhaug Feb. 1992 47 p In SWAHILI
Sponsored by Royal Ministry for Foreign Affairs, Stockholm, Sweden
(PB92-195312; FOA-A-30061-9.4) Avail: CASI HC A03/MF A01

A summary of the contributions to CD and its space committee during the 1991 sessions is given. A synthesis of these is made. In conclusion, proposals for problems and areas where further work may be carried out in the future are given. GRA

N93-11528*# National Aeronautics and Space Administration, Washington, DC.
PAYLOAD ADVISORY PANEL RECOMMENDATIONS
Berrien Moore, III 8 Nov. 1991 18 p
(NASA-TM-108012; NAS 1.15:108012) Avail: CASI HC A03/MF A01

The Payload Advisory Panel proposes a restructured Earth Observing System (EOS) mission to address high-priority science and environmental policy issues in Earth System Science. These issues have been identified through studies conducted by the Intergovernmental Panel on Climate Change (IPCC), the United States Environmental Protection Agency (EPA), and the Committee on Earth and Environmental Sciences (CEES). The restructured EOS defers efforts to improve the understanding of the middle and upper stratosphere and solid earth geophysics. The strategy of the mission combines high priority new measurements with continuation of critical data sets begun by missions which precede EOS. Collaborative arrangements with international partners are an essential part of the program and additional arrangements are posed. The need for continuity in Earth observations and the urgency of environmental questions require launch of some EOS elements as soon as possible. They further require maintenance of the EOS objective of obtaining consistent 15-year measurement records. Author

N93-11754*# Advisory Committee on the Future of the US Space Program, Washington, DC.
THE FIRST MEETING OF THE ADVISORY COMMITTEE ON THE FUTURE OF THE US SPACE PROGRAM (C-FUSSP)
1990 43 p Meeting held in Washington, DC, 13-15 Sep. 1990
(NASA-CR-190995; NAS 1.26:190995) Avail: CASI HC A03/MF A01

These are minutes of the Advisory Committee on the Future of the U.S. Space Program (C-FUSSP). From September 13-15, 1990, presentations were made by the major leaders at NASA as well as industry leaders. The presentations draw on previous studies of the future of NASA space programs. Allowance was made for plenty of questions. The minutes reflect the views of governmental units such as the National Space Council, the NASA Administrators Office, Office of Space Science and Applications, Office of Space Flight, Office of Space Operations, Office of Aeronautics, Exploration, and Technology as well as other pertinent units and outside organizations. Members of the committee are listed at the conclusion of the minutes. R.L.B.

N93-11904 Texas Univ., Austin.
DYNAMICS OF SPACE DEBRIS Ph.D. Thesis

Joshua Ashenberg 1992 192 p
Avail: Univ. Microfilms Order No. DA9225508

The problem of space debris under the perturbations of the earth oblateness and the atmosphere is investigated. Analytical and computational tools for dealing with the short and long term are developed. The short-term is modeled by applying the equations for the general relative motion. The equations for the volume as well as the propagations of the uncertainty in the breakup are derived and solved. The long-term is modeled as the differential changes in the secular orbital elements due to the oblateness and the atmospheric forces. The latter are derived by averaging the effects of the general atmospheric perturbations. Any expansion in small eccentricity leads to an approximate solution for the envelope of the debris cloud. A statistical model for the propagation of uncertainties under the atmospheric forces, is derived as well. In addition to these models, some handy formulas and procedures for the purpose of preliminary investigation, are developed. Most of the suggested models in this work are in a good agreement with the precise numerical solutions. Dissert. Abstr.

N93-12213*# Alabama Univ., Huntsville.
CONTROLS ASTROPHYSICS AND STRUCTURES EXPERIMENT IN SPACE (CASES) ADVANCED STUDIES AND PLANNING Final Report
S. T. Wu 1989 52 p
(Contract NAS8-36955)
(NASA-CR-184410; NAS 1.26:184410) Avail: CASI HC A04/MF A01

The CASES (Controls, Astrophysics, and Structures Experiment in Space) program consists of a flight demonstration of CSI (Controls-Structures Interactions) technology on the Space Shuttle. The basis structure consists of a 32 m deployable boom with actuators and sensors distributed along its length. Upon deployment from the Orbiter bay, the CASES structure will be characterized dynamically and its deformations controlled by a series of experimental control laws; and cold gas thrusters at its tip will be used to orient the Orbiter to a fixed celestial reference. The scientific observations will consist of hard x-ray imaging, at high resolution, of the Sun and the Galactic center. The hard x-ray observations require stable (few arc min) pointing at these targets for one or more position-sensitive proportional counters in the Orbiter bay, which view the object to be imaged through an aperture-encoding mask at the boom tip. This report gives the concensus developed at the second CASES Science Working Group meeting, which took place at NASA Marshall Space Flight Center May 16-17, 1990. An earlier paper and scientific summaries are available and form the basis for the present discussion. L.R.R.

13 ASTRODYNAMICS

Includes powered and free-flight trajectories; and orbital and launching dynamics.

N93-11169# Joint Publications Research Service, Arlington, VA.
JPRS REPORT: SCIENCE AND TECHNOLOGY. CENTRAL EURASIA: ENGINEERING AND EQUIPMENT
5 Aug. 1992 28 p Transl. into ENGLISH from various Russian articles
(JPRS-UEQ-92-009) Avail: CASI HC A03/MF A01

Abstracts of publications in science and technology with respect to engineering and equipment in Central Eurasia are presented. The following topics are discussed: aviation and space technology; nuclear energy; non-nuclear energy; and mechanics of gases, liquids, and solids. Author

N93-11335 Deutsche Geodaetische Kommission, Munich (Germany).
EPHEMERIS CALCULATION AND ORBIT DETERMINATION OF GEOSTATIONARY SATELLITES, USING TAYLOR SERIES INTEGRATION Ph.D. Thesis - Technische Univ. [EPHEMERIDENRECHNUNG UND BAHNBESTIMMUNG GEOSTATIONAERER SATELLITEN MIT HILFE DER TAYLORREIHENINTEGRATION]
Oliver Montenbruck 1991 99 p In GERMAN
(Ser-C-384; ISBN-3-7696-9430-9; ETN-92-92279) Copyright
Avail: Deutsche Geodaetische Kommission, Marstallplatz 8, D-8000 Munich 22, Germany

It is shown that Taylor series integration allows problems of celestial mechanics for interplanetary orbits to be solved with relatively simple orbit models. The method is adapted to the computation of satellite orbits. A new implementation concept is included, which allows a programmation of the equations of motion. It offers simultaneously extension possibilities, which are necessary for the computation of special terms of the power function. The linking of Sun and Moon ephemeris for the treatment of gavitational disturbances of the satellite orbit is used as an example. This concept is represented with the principles of Taylor series integration, and compared with variants of the process. The power spectrum of the method is examined for disturbed and undisturbed Kepler orbits. ESA

N93-11348 GKSS-Forschungszentrum Geesthacht (Germany).
ORBITAL PERTURBATIONS DUE TO THE ALBEDO EFFECT
L. Sehnal (Ceskoslovenska Akademie Ved, Ondrejov.), D. Vokrouhlicky (Karlova Univ., Prague, Czechoslovakia), and J. Straka 1991 6 p Presented at the 3rd International Symposium on Spacecraft Flight Dynamics, Darmstadt, Germany, 30 Sep. - 4 Oct. 1991
(GKSS-91/E/59; ETN-92-92280) Copyright Avail: Fachinformationszentrum Karlsruhe, 7514 Eggenstein-Leopoldshafen 2, Germany

Some aspects of the perturbative influence of the radiation reflected from the Earth surface on the motion of an artificial satellite are discussed. The model taken into account uses the development of the albedo distribution into a series of spherical harmonics. The dependence of the albedo inverse square root of the solar zenith angle is taken into account. Joint consideration of the diffusive and specular reflection results in a narrow peak of the radiative pressure near the borders of the Earth shadow. The role of scattering of the radiation in the Earth atmosphere is estimated using a simple model of cloudiness distribution. The radial component of the disturbing acceleration is the most conspicuous one; the effect due to the accentuated specular reflection at the Earth's shadow borders is perceptible on the 10 exp - 9 power m/sq s for ERS-1 satellite. ESA

N93-11486# Royal Aerospace Establishment, Farnborough (England). Aerospace Div.
ORBIT PERTURBATIONS DUE TO AN AXI-SYMMETRIC GRAVITATIONAL FIELD, ANALYZED OVER EXTENDED PERIODS OF TIME
R. H. Gooding 31 Jan. 1992 27 p Presented at the 1991 AAS/AIAA Astrodynamics Specialist Conference, Durango, CO, 20 Aug. 1991 Previously announced in IAA as A92-43382 Submitted for publication
(RAE-TM-Space-386; BR309781; ETN-92-92302) Copyright
Avail: CASI HC A03/MF A01

The untruncated orbital theory for perturbations due to the Earth's zonal harmonics, previously developed to cover all terms associated with (J sub 2) squared and (J sub l), is extended to cover the secular and long periodic effects associated with (J sub 2) cubed and (J sub 2)(J sub l). If (J sub 2) and J(sub l) (for l less than 2) are regarded as first order and second order respectively, this means that formal third order errors will no longer build up to second order over a timescale of order up to 1/J(sub 2) in angular measure. The extended theory was partially checked out for an Earth model involving just J(sub 2) and J(sub 3). The main feature of the approach is the way in which delta zeta, the short period perturbation in the oscillating element zeta, is separated from the mean element zeta. The present work is concerned with the variation of the mean element zeta. ESA

14 GROUND SUPPORT SYSTEMS AND FACILITIES (SPACE)

Includes launch complexes, research and production facilities; ground support equipment, e.g., mobile transporters; and simulators.

For related information see also *09 Research and Support Facilities (Air).*

N93-11398*# National Aeronautics and Space Administration. Lewis Research Center, Cleveland, OH.
THE NASA CSTI HIGH CAPACITY POWER PROJECT
J. Winter, J. Dudenhoefer, A. Juhasz, G. Schwarze, R. Patterson, D. Ferguson, R. Titran, P. Schmitz (Sverdrup Technology, Inc., Brook Park, OH.), and J. Vandersande (Jet Propulsion Lab., California Inst. of Tech., Pasadena.) Aug. 1992 9 p Presented at the 27th Intersociety Energy Conversion Engineering Conference, San Diego, CA, 3-7 Aug. 1992; sponsored by SAE, ACS, AIAA, ASME, IEEE, AIChE, and ANS
(RTOP 590-13-00)
(NASA-TM-105813; E-7244; NAS 1.15:105813) Avail: CASI HC A02/MF A01

The SP-100 Space Nuclear Power Program was established in 1983 by DOD, DOE, and NASA as a joint program to develop technology for military and civil applications. Starting in 1986, NASA has funded a technology program to maintain the momentum of promising aerospace technology advancement started during Phase 1 of SP-100 and to strengthen, in key areas, the chances for successful development and growth capability of space nuclear reactor power systems for a wide range of future space applications. The elements of the Civilian Space Technology Initiative (CSTI) High Capacity Power Project include Systems Analysis, Stirling Power Conversion, Thermoelectric Power Conversion, Thermal Management, Power Management, Systems Diagnostics, Environmental Interactions, and Material/Structural Development. Technology advancement in all elements is required to provide the growth capability, high reliability and 7 to 10 year lifetime demanded for future space nuclear power systems. The overall project will develop and demonstrate the technology base required to provide a wide range of modular power systems compatible with the SP-100 reactor which facilitates operation during lunar and planetary day/night cycles as well as allowing spacecraft operation at any attitude or distance from the sun. Significant accomplishments in all of the project elements will be presented, along with revised goals and project timelines recently developed. Author

N93-11401*# National Aeronautics and Space Administration. Lewis Research Center, Cleveland, OH.
IMPLEMENTATION OF A MODEL BASED FAULT DETECTION AND DIAGNOSIS FOR ACTUATION FAULTS OF THE SPACE SHUTTLE MAIN ENGINE
A. Duyar (Florida Atlantic Univ., Boca Raton.), T.-H. Guo, W. Merrill, and J. Musgrave Jul. 1992 15 p Presented at the Third Annual Conference on Health Monitoring for Space Propulsion Systems, Cincinnati, OH, 13-14 Nov. 1991; sponsored by Cincinnati Univ.
(RTOP 582-01-41)
(NASA-TM-105781; E-7208; NAS 1.15:105781) Avail: CASI HC A03/MF A01

In a previous study, Guo, Merrill and Duyar, 1990, reported a conceptual development of a fault detection and diagnosis system for actuation faults of the space shuttle main engine. This study, which is a continuation of the previous work, implements the developed fault detection and diagnosis scheme for the real time actuation fault diagnosis of the space shuttle main engine. The scheme will be used as an integral part of an intelligent control system demonstration experiment at NASA Lewis. The diagnosis system utilizes a model based method with real time identification and hypothesis testing for actuation, sensor, and performance degradation faults. Author

N93-11428 Department of the Navy, Washington, DC.
BOOSTER ROCKET RANGE SAFETY SYSTEM Patent
John R. Renzi, inventor (to Navy) (Courtney and Co., Philadelphia, PA.) 2 Jun. 1992 7 p Filed 25 Sep. 1991
(AD-D015363; US-Patent-5,117,758; US-Patent-Appl-SN-765618; US-Patent-Class-102-378) Avail: US Patent and Trademark Office

In response to an abort command, fragmentation of a propellant booster rocket carried on a missile is limited by positioning of annular shaped charges at axially spaced locations on the outer shell of the booster rocket. Detonation of the charges thereby severs an intermediate section of the rocket from forward and aft sections which remain attached to the missile. The intermediate section is separated from the missile by such severing action to prevent further fragmenting forces from being imparted thereto. GRA

N93-11631# Sandia National Labs., Albuquerque, NM.
LIGHTNING THREAT WARNING SYSTEM AT THE TONOPAH TEST RANGE
R. Smith Jul. 1992 21 p
(Contract DE-AC04-76DP-00789)
(DE92-040444; SAND-90-0351) Avail: CASI HC A03/MF A01

This report documents the lightning threat warning system at the Tonopah Test Range and the technology it uses. The report outlines each of the system's individual components and the information each contributes. DOE

N93-12317# Lawrence Livermore National Lab., CA.
INERT GAS ELECTRIC HEATER FOR ELEVATED TEMPERATURE TESTING OF SMALL PROPULSION COMPONENTS
J. C. Whitehead, R. K. Lanning, M. C. Evans, and N. J. Barabas 25 Jun. 1992 8 p Presented at the 28th Joint Propulsion Conference, Nashville, TN, 6-8 Jul. 1992 Previously announced in IAA as A92-48946
(Contract W-7405-eng-48)
(DE92-017434; UCRL-JC-110950; CONF-920747-5) Avail: CASI HC A02/MF A01

An electric heater for inert gas has been developed to enable safe, nontoxic, indoor, low cost testing of miniature propulsion components which operate on warm gas. High pressure helium regulated to 7 MPa (1000 psi) is passed through in 8-kW electric heating element to raise its temperature to 700 C (1300 F) at mass flow rates up to 2 grams/sec. The pressure and temperature are independently adjustable to lower values, and the temperature controller rapidly varies the electric power in response to changes in flow rate, so that pulsed-flow as well as continuous-flow components can be tested. The heating element is a 3.2 mm (1/8 inch) diameter nickel alloy tube, which carries the helium internally and up to 80 amperes of electric current in its wall. A transparent polycarbonate safety shield ensures personnel safety while permitting direct visual and auditory observations. Digital displays of time, pressure, and temperatures are adjacent to the test hardware, to facilitate realtime interpretation of test results and video documentation. Equations for pressure drop, heat transfer, electrical resistance, stress, and thermal response time are presented to facilitate designing similar systems. DOE

15 LAUNCH VEHICLES AND SPACE VEHICLES

Includes boosters; operating problems of launch/space vehicle systems; and reusable vehicles.

For related information see also *20 Spacecraft Propulsion and Power.*

N93-11002*# National Aeronautics and Space Administration. Marshall Space Flight Center, Huntsville, AL.
SPACECRAFT FLIGHT CONTROL SYSTEM DESIGN SELECTION PROCESS FOR A GEOSTATIONARY COMMUNICATION SATELLITE
C. Barret Sep. 1992 20 p
(NASA-TP-3289; M-700; NAS 1.60:3289) Avail: CASI HC A03/MF A01

The Earth's first artificial satellite, Sputnik 1, slowly tumbled in orbit. The first U.S. satellite, Explorer 1, also tumbled out of control. Now, as we launch the Mars observer and the Cassini spacecraft, stability and control have become higher priorities. The flight control system design selection process is reviewed using as an example a geostationary communication satellite which is to have a life expectancy of 10 to 14 years. Disturbance torques including aerodynamic, magnetic, gravity gradient, solar, micrometeorite, debris, collision, and internal torques are assessed to quantify the disturbance environment so that the required compensating torque can be determined. Then control torque options, including passive versus active, momentum control, bias momentum, spin stabilization, dual spin, gravity gradient, magnetic, reaction wheels, control moment gyros, nutation dampers, inertia augmentation techniques, three-axis control, reactions control system (RCS), and RCS sizing, are considered. A flight control system design is then selected and preliminary stability criteria are met by the control gains selection. Author

N93-11726 Texas Univ., Austin.
NUMERICAL SIMULATION FOR THE COAXIAL ELECTROMAGNETIC LAUNCHER USING HYBRID POTENTIALS WITH FE-BE METHOD Ph.D. Thesis
Jui-Hung Chang 1992 122 p
Avail: Univ. Microfilms Order No. DA9225543

A hybrid scheme combining finite and boundary elements is applied to analyze the transient behavior of a conducting coaxial rigid projectile accelerating in electromagnetic field produced by the field coils with some prescribed current inputs. The problem geometry is assumed to be axisymmetric and the forcing currents are circumferential. The corresponding initial/boundary value problem associated with certain assumptions is derived from Maxwell's field equations in terms of electric and magnetic potentials. A formulation which mixes the vector and scalar magnetic potentials is considered to be suitable for this specific problem. Due to the axisymmetric assumption, the problem reduces to a simplified one with only one component of the vector potential involved. Thermal effects due to ohmic losses are considered during the launching process. Dissert. Abstr.

N93-12130# Wright Lab., Wright-Patterson AFB, OH.
AN INVESTIGATION OF ELECTROMAGNETIC LAUNCHER REPEATABILITY Final Report, Mar. 1991 - Apr. 1992
Mark W. Heyse, James B. Cornette, and Jere L. Brown Jul. 1992 13 p
(AF Proj. 1203)
(AD-A254339; WL-TP-92-009) Avail: CASI HC A03/MF A01

Electromagnetic launcher (EML) performance repeatability has been identified as a potential development issue for several years. Investigation of this issue has been difficult because an EML that is powered on a relatively continuous basis to provide long duration operation has not been available. A battery charged capacitor power system has enabled long duration, 6 to 7 seconds, EML experiments. This paper provides a summary of an experiment to investigate EML launch to launch performance consistency. A series of 8 ten-shot bursts, each separated by 15 to 30 minutes, performed in a single day using a single set of bore materials is the subject of this paper. GRA

N93-12161# Wright Lab., Eglin AFB, FL. Armament Directorate.
ELECTROMAGNETIC LAUNCHER CONTROL USING FINITE STATE MACHINES Final Report, Mar. 1991 - Apr. 1992
Jeffrey M. Gay, James B. Cornette, and Mark W. Heyse Jul. 1992 11 p
(AD-A254433; WL/MN-TR-92-008) Avail: CASI HC A03/MF A01

This paper shows the continued viability of sequential Finite State Machines (FSM's) as a means to control the sequencing of Electromagnetic Launcher (EWL) systems. While computer controlled sequencing is an attractive alternative, FSM's are easy to design, inexpensive, and reliable. Several FSM controllers are currently in use for the long duration EML experiments at the Hypervelocity Research Facility, Eglin AFB, FL. This paper discusses the basic system design with reference to design procedure and systems interfacing. Flexibility, and the fail-safe nature of the FSM (i.e., system interrupt capability) are also discussed. Where requirements include repeatability, reliability, ease of operation, relative low cost, and flexibility, the FSM is presented as a reasonable alternative to more expensive computer-based systems. GRA

N93-12505# IAP Research, Inc., Dayton, OH.
RAILGUN ARMATURE VELOCITY IMPROVEMENT, SBIR PHASE 2 Technical Report, 1 Mar. 1990 - 31 Dec. 1991
Leo E. Thurmond and David P. Bauer Aug. 1992 71 p
(Contract DNA001-90-C-0024)
(AD-A254749; IAP-TR-91-09; DNA-TR-92-10) Avail: CASI HC A04/MF A01

Railgun hypervelocity performance has not been repeatably demonstrated at velocities over 6 km/s. A significant performance limiting phenomena is the formation of secondary current paths in parallel with the main projectile accelerating plasma. A confined plasma armature technique was developed to prevent secondary armature formation. Confinement prevents loss of ionized material from the plasma armature and thereby prevents formation of a low rail-to-rail conductance. We controlled pressure in the confined armature via controlled venting through ports in the rails. Railgun tests with the confined armature show that sealing at the rail-confinement vessel interface is critical and difficult to achieve. Our tests show that during low seal leakage operation secondaries are prevented. However, maintaining good seal for the entire launch is very difficult. GRA

N93-12543*# National Aeronautics and Space Administration. Langley Research Center, Hampton, VA.
DEPLOYABLE REFLECTOR ANTENNA PERFORMANCE OPTIMIZATION USING AUTOMATED SURFACE CORRECTION AND ARRAY-FEED COMPENSATION
Lyle C. Schroeder, M. C. Bailey, and John L. Mitchell Oct. 1992 70 p Original contains color illustrations
(RTOP 590-14-41-03)
(NASA-TP-3228; L-17065; NAS 1.60:3228) Avail: CASI HC A04/MF A01; 11 functional color pages

Methods for increasing the electromagnetic (EM) performance of reflectors with rough surfaces were tested and evaluated. First, one quadrant of the 15-meter hoop-column antenna was retrofitted with computer-driven and controlled motors to allow automated adjustment of the reflector surface. The surface errors, measured with metric photogrammetry, were used in a previously verified computer code to calculate control motor adjustments. With this system, a rough antenna surface (rms of approximately 0.180 inch) was corrected in two iterations to approximately the structural surface smoothness limit of 0.060 inch rms. The antenna pattern and gain improved significantly as a result of these surface adjustments. The EM performance was evaluated with a computer program for distorted reflector antennas which had been previously verified with experimental data. Next, the effects of the surface distortions were compensated for in computer simulations by superimposing excitation from an array feed to maximize antenna performance relative to an undistorted reflector. Results showed that a 61-element array could produce EM performance improvements equal to surface adjustments. When both mechanical surface adjustment and feed compensation techniques were applied, the equivalent operating frequency increased from approximately 6 to 18 GHz. Author

16 SPACE TRANSPORTATION

Includes passenger and cargo space transportation, e.g., shuttle operations; and space rescue techniques.

For related information see also *03 Air Transportation and Safety* and *18 Spacecraft Design, Testing and Performance.* For space suits see *54 Man/System Technology and Life Support.*

N93-11007# Messerschmitt-Boelkow-Blohm G.m.b.H., Ottobrunn (Germany).

DEVELOPMENT TRENDS IN SPACE TRANSPORTATION SYSTEMS: FROM HERMES TO SAENGER [ENTWICKLUNGSTENDENZEN BEI RAUMTRANSPORT-SYSTEMEN - VON HERMES ZU SAENGER]

Volker vonTein and Dietrich E. Koelle 1991 9 p In GERMAN Presented at the DGLR-Jahrestagung 1991 and DLR Koegress 1991, Berlin, Fed. Republic of Germany, 10-13 Sep. 1991 Submitted for publication
(MBB-UK-0146-91-PUB; ETN-92-92112) Avail: CASI HC A02/MF A01

The criteria for the development of future space transportation systems are given. A trend in reducing transportation costs by reutilizing transportation systems is outlined. The European Hermes project represents a first step towards reutilization and manned winged apparatus. The technological and organizational requirements and the German participation in this project are described. The Saenger concept is shown as a logical advancement of this project, and of the corresponding technology. It consists of a two stage winged space tug with horizontal launch. A space transportation system with low launching costs, higher safety, and mission flexibility is expected. It should complete cargo rocket Ariane 5. ESA

N93-11101*# Alabama Univ., Huntsville. Center for Microgravity and Materials Research.

RESIDUAL ACCELERATION DATA ON IML-1: DEVELOPMENT OF A DATA REDUCTION AND DISSEMINATION PLAN

Semiannual Report No. 7, 1 Mar. - 30 Sep. 1992

Melissa J. B. Rogers, J. Iwan D. Alexander, and Randy Wolf 30 Sep. 1992 34 p
(Grant NAG8-759)
(NASA-CR-190807; NAS 1.26:190807) Avail: CASI HC A03/MF A01

The need to record some measure of the low-gravity environment of an orbiting space vehicle was recognized at an early stage of the U.S. Space Program. Such information was considered important for both the assessment of an astronaut's physical condition during and after space missions and the analysis of the fluid physics, materials processing, and biological sciences experiments run in space. Various measurement systems were developed and flown on space platforms beginning in the early 1970's. Similar in concept to land based seismometers that measure vibrations caused by earthquakes and explosions, accelerometers mounted on orbiting space vehicles measure vibrations in and of the vehicle due to internal and external sources, as well as vibrations in a sensor's relative acceleration with respect to the vehicle to which it is attached. The data collected over the years have helped to alter the perception of gravity on-board a space vehicle from the public's early concept of zero-gravity to the science community's evolution of thought from microgravity to milligravity to g-jitter or vibrational environment. Since the advent of the Shuttle Orbiter Program, especially since the start of Spacelab flights dedicated to scientific investigations, the interest in measuring the low-gravity environment in which experiments are run has increased. This interest led to the development and flight of numerous accelerometer systems dedicated to specific experiments. It also prompted the development of the NASA MSAD-sponsored Space Acceleration Measurement System (SAMS). The first SAMS units flew in the Spacelab on STS-40 in June 1991 in support of the first Spacelab Life Sciences mission (SLS-1). SAMS is currently manifested to fly on all future Spacelab missions. Author

N93-11685# European Space Agency, Paris (France).

EVALUATION OF TRANSPORTATION SYSTEMS FOR ADVANCED SPACE FLIGHT MISSIONS [BEWERTUNG VON TRANSPORTSYSTEMEN FUER FORTSCHRITTLICHE RAUMFLUGMISSIONEN]

Juergen P. Schleinitz (Deutsche Forschungsanstalt fuer Luft- und Raumfahrt, Lampoldshausen, Germany) Apr. 1992 264 p Transl. into ENGLISH of Bewertung von Transportsystemen fuer fortschrittliche Raumflugmissionen (Lampoldshausen, Germany, DLR), Jul. 1990 187 p Original language document was announced as N91-21181
(ESA-TT-1256; DLR-FB-90-39; ETN-92-92346) Avail: CASI HC A12/MF A03; Original German version available from DLR, Wissenschaftliches Berichtswesen, VB-PL-DO, Postfach 90 60 58, 5000 Cologne, Germany, HC

The purpose of the analysis reported was to compile as much as possible by way of characteristic data (theoretical/hardware) concerning the 9 listed propulsion concepts, to include these in mass and cost models, in conjunction with a generally applicable transfer vehicle architecture. In order to perform a system analysis employing three completely different mission scenarios, propulsion system mass and cost models were gathered and determined. Concepts like liquid oxygen/liquid hydrogen electrostatic and magnetoplasma propulsion, nuclear thermal, solar thermal, laser thermal, and mass driver reaction engine propulsion, as well as solar sails and aerobraking were considered. Considerations with regard to service life and reliability were taken into account. Clear advantages, especially the lowering of transport costs in near Earth and cis-lunar orbits, are expected with the implementation of solar thermal propulsion. Electric propulsion systems promise advantages in the transfer of large payloads, especially in interplanetary operations. The utilization of laser thermal propulsion between lower Earth orbit and lunar orbit is preferred only when the existing laser stations can be used for additional applications. ESA

N93-12151*# National Aeronautics and Space Administration. John F. Kennedy Space Center, Cocoa Beach, FL.

DEBRIS/ICE/TPS ASSESSMENT AND INTEGRATED PHOTOGRAPHIC ANALYSIS FOR SHUTTLE MISSION STS-46

Gregory N. Katnik, Scott A. Higginbotham, and J. Bradley Davis Sep. 1992 112 p Original contains color illustrations
(NASA-TM-107552; NAS 1.15:107552) Avail: CASI HC A06/MF A02; 40 functional color pages

A Debris/Ice/TPS assessment and integrated photographic analysis was conducted for Shuttle Mission STS-46. Debris inspections of the flight elements and launch pad were performed before and after launch. Ice/frost conditions on the External Tank were assessed by the use of computer programs, nomographs, and infrared scanner data during cryogenic loading of the vehicle followed by on-pad visual inspection. High speed photography was analyzed after launch to identify ice/debris sources and evaluate potential vehicle damage and/or in-flight anomalies. This report documents the debris/ice/TPS conditions and integrated photographic analysis of Shuttle Mission STS-46, and the resulting effect on the Space Shuttle Program. Author

17 SPACE COMM., SPACECRAFT COMM., COMMAND & TRACKING

Includes telemetry; space communications networks; astronavigation and guidance; and radio blackout.

For related information see also *04 Aircraft Communications and Navigation* and *32 Communications and Radar.*

N93-11430*# National Aeronautics and Space Administration. Lewis Research Center, Cleveland, OH.
DIRECT BROADCAST SATELLITE: RADIO PROGRAM
James E. Hollansworth Oct. 1992 11 p
(RTOP 144-10-2A)
(NASA-TM-105910; E-7355; NAS 1.15:105910) Avail: CASI HC A03/MF A01

NASA is committed to providing technology development that leads to the introduction of new commercial applications for communications satellites. The Direct Broadcast Satellite-Radio (DBS-R) Program is a joint effort between The National Aeronautics and Space Administration (NASA) and The United States Information Agency/Voice of America (USIA/VOA) directed at this objective. The purpose of this program is to define the service and develop the technology for a direct-to-listener satellite sound broadcasting system. The DBS-R Program, as structured by NASA and VOA, is now a three-phase program designed to help the U.S. commercial communications satellite and receiver industry bring about this new communications service. Major efforts are being directed towards frequency planning hardware and service development, service demonstration, and experimentation with new satellite and receiver technology. Author

18 SPACECRAFT DESIGN, TESTING AND PERFORMANCE

Includes satellites; space platforms; space stations; spacecraft systems and components such as thermal and environmental controls; and attitude controls.

For life support systems see *54 Man/System Technology and Life Support.* For related information see also *05 Aircraft Design, Testing and Performance, 39 Structural Mechanics,* and *16 Space Transportation.*

N93-10970*# National Aeronautics and Space Administration. Langley Research Center, Hampton, VA.
TESTS OF AN ALTERNATE MOBILE TRANSPORTER AND EXTRAVEHICULAR ACTIVITY ASSEMBLY PROCEDURE FOR THE SPACE STATION FREEDOM TRUSS
Walter L. Heard, Jr., Judith J. Watson, Mark S. Lake, Harold G. Bush, J. Kermit Jensen (Lockheed Engineering and Sciences Co., Hampton, VA.), Richard E. Wallsom (Lockheed Engineering and Sciences Co., Hampton, VA.), and James E. Phelps (Lockheed Engineering and Sciences Co., Hampton, VA.) Oct. 1992 34 p
(RTOP 506-43-41-02)
(NASA-TP-3245; L-17051; NAS 1.60:3245) Avail: CASI HC A03/MF A01

Results are presented from a ground test program of an alternate mobile transporter (MT) concept and extravehicular activity (EVA) assembly procedure for the Space Station Freedom (SSF) truss keel. A three-bay orthogonal tetrahedral truss beam consisting of 44 2-in-diameter struts and 16 nodes was assembled repeatedly in neutral buoyancy by pairs of pressure-suited test subjects working from astronaut positioning devices (APD's) on the MT. The truss bays were cubic with edges 15 ft long. All the truss joint hardware was found to be EVA compatible. The average unit assembly time for a single pair of experienced test subjects was 27.6 sec/strut, which is about half the time derived from other SSF truss assembly tests. A concept for integration of utility trays during truss assembly is introduced and demonstrated in the assembly tests. The concept, which requires minimal EVA handling of the trays, is shown to have little impact on overall assembly time. The results of these tests indicate that by using an MT equipped with APD's, rapid EVA assembly of a space station-size truss structure can be expected. Author

N93-11001*# National Aeronautics and Space Administration. Lewis Research Center, Cleveland, OH.
SITE PROJECT. PHASE 1: CONTINUOUS DATA BIT-ERROR-RATE TESTING Final Report
Gene Fujikawa and Robert J. Kerczewski Sep. 1992 90 p
(RTOP 650-60-23)
(NASA-TP-3279; E-6513; NAS 1.60:3279) Avail: CASI HC A05/MF A01

The Systems Integration, Test, and Evaluation (SITE) Project at NASA LeRC encompasses a number of research and technology areas of satellite communications systems. Phase 1 of this project established a complete satellite link simulator system. The evaluation of proof-of-concept microwave devices, radiofrequency (RF) and bit-error-rate (BER) testing of hardware, testing of remote airlinks, and other tests were performed as part of this first testing phase. This final report covers the test results produced in phase 1 of the SITE Project. The data presented include 20-GHz high-power-amplifier testing, 30-GHz low-noise-receiver testing, amplitude equalization, transponder baseline testing, switch matrix tests, and continuous-wave and modulated interference tests. The report also presents the methods used to measure the RF and BER performance of the complete system. Correlations of the RF and BER data are summarized to note the effects of the RF responses on the BER. Author

N93-11162# Joint Publications Research Service, Arlington, VA.
JPRS REPORT: SCIENCE AND TECHNOLOGY. CENTRAL EURASIA: SPACE. DEVELOPMENT OF SOVIET SPACECRAFT FOR MANNED MISSIONS
27 May 1992 29 p Transl. into ENGLISH of various Russian articles
(JPRS-USP-92-003) Avail: CASI HC A03/MF A01

A number of designs involving manned spacecraft developed in the Soviet Union in 1960-1980 are described. The features of the design of the individual vehicles are presented. In addition, the outcome of the programs are discussed and points of information about the little-known vehicles that were referred to in the press are clarified. L.R.R.

N93-11736# California Univ., Los Angeles. Inst. of Geophysics and Planetary Physics.
BEAM-PLASMA INTERACTIONS AND RADIATION GENERATION DURING THE EJECTION OF ELECTRON AND ION BEAMS IN SPACE Final Report, Mar. 1988 - Nov. 1991
M. Ashour-Abdalla, H. Okuda, P. L. Pritchett, and D. Schriver Feb. 1992 68 p
(Contract F19628-88-K-0022)
(AD-A253993; RL-TR-92-23) Avail: CASI HC A04/MF A01

Multi-dimensional electrostatic and electromagnetic particle simulations are used to investigate the nature of beam-plasma interactions and radiation generation during the injection of dense electron beams into the ionosphere from spacecraft. The nature of the injection process is determined primarily by the relative value of two characteristic time scales: the beam stagnation time t(sub s) and the plasma response time t(sub rp). When t(sub s) is less than t(sub rp), spacecraft charging is significant and most of the beam electrons are drawn back into the spacecraft. When t(sub s) is greater than t(sub rp), vehicle charging is reduced and the beam propagates away from the source. In this latter case there is strong beam-plasma turbulence which destroys the coherence of the beam within one or two gyroperiods. The spatial distribution of the beam has the form of a hollow cylinder near the source. As the beam propagates away from the source, the cylinder becomes increasingly filled. Return currents are associated with the field-aligned flow of ambient electrons, while current closure is provided primarily by the cross-field motion of the ions. The beam-plasma interaction leads to the formation of coherent current structures. Whistler waves with a peak in the frequency range 0.5 to 0.7 Omega(sub e) are produced by these structures via a coherent Cerenkov interaction. The Whistler waves propagate at angles substantially away from the resonance cone and are predominantly electromagnetic in nature. GRA

N93-11798# Air Force Inst. of Tech., Wright-Patterson AFB, OH. Foreign Aerospace Science and Technology Center.
HYBRID GUIDANCE FOR MANEUVERING FLIGHT VEHICLES
Dehai Ling 4 Feb. 1992 22 p Transl. into ENGLISH from Yuhang Xuebao (China), no. 2, 1987 p 44-52
(AD-A254110; FASTC-ID(RS)T-0787-91) Avail: CASI HC A03/MF A01

This article puts forward one type of guidance option related to the maneuver programming of reentering flight vehicles. The option in question makes use of a radiation sensing system, precisely determining the location of the starting point of the reentering flight vehicle. Use is also made of strap-on type inertial guidance systems to control the impact points of flight vehicles. Maneuvering flight is an important direction in the development of the technology of strategic flight vehicles. It is possible to use it in sudden defense, adding programming, raising precision, and recovery. Maneuvering flight tests are capable of giving complete checks in all such areas as flight vehicle propulsion systems, materials structure, heat resistance systems, stability, guidance circuits, and attitude control systems. It is capable of carrying out experiments on different technological levels. Options which are relatively simple and easy to carry out are to make the reentering flight vehicle, within the longitudinal plane, fly maneuvers according to preset programs. Going through precise inertial guidance or celestial-inertial guidance systems, guidance is carried out on the flight vehicle in the main power stage, with controls and corrections to the free section flight orbital plane, such that the trajectory is capable of entering into the predicted reentry corridor. As far as initial flight tests are concerned, it is possible to make use of inertial guidance systems which already exist, relaxing the requirements for launch plane controls and lateral impact point deviations. GRA

N93-11836 Polytechnic Univ., Brooklyn, NY.
STRUCTURAL DYNAMICS OF LARGE SPACE STRUCTURES HAVING PARAMETRIC UNCERTAINTIES Ph.D. Thesis
Robert Michael Koch 1991 126 p
Avail: Univ. Microfilms Order No. DA9129343

Deployable periodic large space structures have been shown to exhibit high dynamic sensitivity to period-breaking imperfections and uncertainties. These can be brought on by manufacturing or assembly errors, structural imperfections, as well as nonlinear and/or nonconservative joint behavior. In addition, the necessity of precise pointing and position capability requires the consideration of these usually negligible and unknown parametric uncertainties and their effect on the overall dynamic response of large periodic space structures. This work describes a new approach for the global dynamic solution of beam-like periodic space structures possessing parametric uncertainties. Specifically, the effect of randomly flexible joints is considered on both the free and nonsteady forced vibration of simply-supported periodic large space trusses. The formulation is a hybrid approach in terms of an extended Timoshenko beam continuum model, Monte Carlo simulation scheme, and first-order perturbation methods. The mean and mean-square response statistics for both the free and forced random vibration problems are derived for various input random joint stiffness probability distributions. The solutions to the following numerical examples are performed: (1) the global free vibration of a simply-supported ten-bay periodic truss structure with both uniform and truncated-Gaussian joint stiffness probability densities; and (2) the transient global random response of a simply-supported viscously-damped ten-bay periodic truss structure with spatially-independent random joint stiffnesses to a nonsteady half-sine wave support displacement. Presently, the method was applied to simply-supported, beam-like periodic truss structures with randomly flexible joints. However, it is directly extendable to both beam and plate continuum models possessing other end conditions and random parametric uncertainties. Author

N93-11885 Howard Univ., Washington, DC.
RAPID MANEUVERING OF LARGE FLEXIBLE ORBITING SYSTEMS Ph.D. Thesis
Feiyue Li 1991 209 p
Avail: Univ. Microfilms Order No. DA9217244

Some future space missions will require rapid, large angle, 3-D maneuvering of large flexible spacecraft in target acquisition, target tracking, and surveying multi targets, etc. The optimal control problem is studied for the 2-D and 3-D maneuvering (slewing) and vibrational control of large flexible orbiting systems, with the orbiting Spacecraft Control Laboratory Experiment (SCOLE) model as an example. The controls of the system are provided by bounded torques and forces. The optimal control problem is formulaed by applying Pontryagin's Maximum Principle to the system equations derived by using Lagrange's equations. The resulting nonlinear two point boundary value problem (TPBVP) is solved numerically by using the quasilinearization technique, a proposed time shortening strategy, as well as the shooting method. According to the order of the chapter, the research work covers minimum time maneuvers of rigid spacecraft; rapid maneuvers of 2-D and then 3-D flexible spacecraft; the effects of structural offset, axial shortening, and gravitational torque on the slewing of the flexible spacecraft; and a combined technique for solving the minimum time maneuver problems. A useful solution procedure, based on the quasilinearization algorithm, was developed and tested for solving the nonlinear TPBVP. This program could also be easily modified to solve the slewing maneuvers of other flexible systems. Also, another combined technique was proposed for solving the minimum slewing control problem of rigid spacecraft. It is shown that one of the four initial costates associated with the quaternions can be arbitrarily selected without affecting the optimal controls and thus simplifying the computation. The Euler rotation theorem has been found quite useful in the estimation of the unknown initial costate and minimum slewing time. The results of a tradeoff analysis indicate that a compromise may be researched to solve the conflict between the rapid slew and the small flexible amplitude requirements for multi-input control system. The numerical responses indicate the large differences between the linearized and nonlinear systems. The linearized system can represent the nonlinear system adequately for predicting the major motions but not as well for the secondary motions. The structural offset (if any) results in a first order nonlinear effects. Dissert. Abstr.

N93-11908# Committee on Commerce, Science, and Transportation (U.S. Senate).
THE SPACE STATION FREEDOM AND SPACE LAUNCH ISSUES
Washington GPO 1992 48 p Hearing before the Committee on Commerce, Science, and Transportation, 102d Congress, 2d Session, 18 Mar. 1992
(S-Hrg-102-762; GPO-57-213cc; ISBN-0-16-039175-X) Avail: CASI HC A03/MF A01; Subcommittee on Science, Technology, and Space, Senate, Washington, DC 20515 HC; SOD

Opening statements are given by Senator Gore and two other senators. Two witnesses, the Associate Administrator of NASA Office of Space Systems Development, and the Associate Administrator of NASA Office of Space Flight, presented prepared statements, the latter's concluding remarks speak of the Space Station Freedom as the next vital step toward evolving mankind's capabilities to live and work in space and to explore and benefit from this new frontier. Additional comments from the American Space Transportation Association are found in the appendix. These comments, in the main touch on both the Space Station Freedom and commercial space launch vehicles as well as the Advanced Solid Rocket Motor. R.L.B.

N93-11999 Stanford Univ., CA.
THE ORDER n SIMULATION OF TETHER MOTIONS BASED ON A RIGID BODY TETHER MODEL Ph.D. Thesis
Gregory Scott Woodward 1992 183 p
Avail: Univ. Microfilms Order No. DA9221688

NASA is currently planning several missions involving the use of tethers in space; therefore, there exists a need for a simulation

tool that can be used to predict the motion of long tethers with a high degree of fidelity. In the past, researchers have used analysis based on a 'lumped mass' model; that is, the mass of the tether was represented by spring-connected particles. A shortcoming of a model of this type is that it cannot simulate bending and torsional stiffnesses. To overcome this limitation, a new model which uses rigid bodies rather than particles to represent the mass of the tether, which enables one to simulate bending and torsional stiffnesses, and to more closely approximate the inertia of the actual tether, is developed. In order to approximate the motion of a continuous tether as closely as possible, one must work with a large number of rigid bodies (or particles), which leads to large values of n, the number of degrees of freedom. Simulations performed by most dynamical codes require a number of mathematical operations proportional to n(exp 3), and are prohibitively slow for large values of n. The order (n) algorithm, which requires a number of operations proportional to n rather than n(exp 3), was used as a basis for this dynamical analysis. Extensions to the theory of the order (n) algorithm developed in this thesis resulted in full utilization of the advantages of the chain structure of the system, and were implemented in a computer program called DYNAMO, which is capable of simulating recursive dynamical systems, such as the tether model, very efficiently. DYNAMO was extensively verified by numerous test cases, and has been used to study the deployment and retrieval of a tethered satellite. Post-processing and animation programs were also developed as aids to interpretation of the simulation output data.
Dissert. Abstr.

N93-12064# Aerospace Corp., El Segundo, CA. Technology Operations.

FORECASTING THE RELATIVISTIC ELECTRON FLUX AT GEOSYNCHRONOUS ORBIT

David J. Gorney and Harry C. Koons 15 Apr. 1992 33 p
(Contract F04701-88-C-0089)
(AD-A254016; TR-92(2508)-1; SSD-TR-92-29) Avail: CASI HC A03/MF A01

A neural network, developed to model the temporal variations of relativistic (greater than 3 MeV) electrons at geosynchronous orbit, has been used to make reasonably accurate day-ahead forecasts of the relativistic electron flux at geosynchronous orbit. This model can be used to forecast days when internal discharges might occur on geosynchronous satellites or satellites operating within the outer Van Allen radiation belt. The neural network (in essence, a nonlinear prediction filter) consists of three layers of neurons, containing 10 neurons in the input layer, 6 neurons in a hidden layer, and 1 output neuron. The network inputs consist of ten consecutive days of the daily sum of the planetary magnetic index, Sigma Kp. The output is a prediction of the daily averaged electron flux for the tenth day. The neural network model, together with projections of Sigma Kp based on its historical behavior, can be used to make the day-ahead forecasts of the relativistic electron flux at geosynchronous orbit. A significantly better forecast is obtained by modifying the network to include one additional input, the measured daily averaged electron flux for the day prior to the forecast day, and one more neuron in the hidden layer. Both models are described in this report. GRA

N93-12152*# Sverdrup Technology, Inc., Brook Park, OH.

EFFECT OF INERT PROPELLANT INJECTION ON MARS ASCENT VEHICLE PERFORMANCE Final Report

James E. Colvin (Arizona Univ., Tucson.) and Geoffrey A. Landis Sep. 1992 30 p Presented at the 28th Joint Propulsion Conference and Exhibit, Nashville, TN, 6-8 Jul. 1992; sponsored by AIAA, SAE, ASME, and ASEE Sponsored by NASA. Lewis Research Center
(RTOP 506-41-11)
(NASA-CR-189238; E-7312; NAS 1.26:189238; AIAA Paper 92-3447) Avail: CASI HC A03/MF A01

A Mars ascent vehicle is limited in performance by the propellant which can be brought from Earth. In some cases the vehicle performance can be improved by injecting inert gas into the engine, if the inert gas is available as an in-situ resource and does not have to be brought from Earth. Carbon dioxide, nitrogen, and argon are constituents of the Martian atmosphere which could be separated by compressing the atmosphere, without any chemical processing step. The effect of inert gas injection on rocket engine performance was analyzed with a numerical combustion code that calculated chemical equilibrium for engines of varying combustion chamber pressure, expansion ratio, oxidizer/fuel ratio, and inert injection fraction. Results of this analysis were applied to several candidate missions to determine how the required mass of return propellant needed in low Earth orbit could be decreased using inert propellant injection. Author

N93-12185 North Carolina State Univ., Raleigh.

PHYSIOLOGICALLY CONSTRAINED AEROCAPTURE FOR MANNED MARS MISSIONS Ph.D. Thesis

James Evans Lyne 1992 221 p
Avail: Univ. Microfilms Order No. DA9221274

Aerobraking has been proposed as a critical technology for manned missions to Mars. The variety of mission architectures currently under consideration presents aerobrake designers with an enormous range of potential entry scenarios. Two of the most important considerations in the design of an aerobrake are the required control authority (lift-to-drag ratio, L/D) and the aerothermal environment which the vehicle will encounter. Therefore, this study examined the entry corridor width and stagnation-point heating rate and load for the entire range of probable entry velocities, lift-to-drag ratios, and ballistic coefficients for capture at both Earth and Mars. To accomplish this, a peak deceleration limit for the aerocapture maneuvers had to be established. Previous studies had used a variety of load limits without adequate proof of their validity. Existing physiological and space flight data were examined, and it was concluded that a deceleration limit of 5 G was appropriate. When this load limit was applied, numerical studies showed that an aerobrake with an L/D of 0.3 could provide an entry corridor width of at least 1 degree for all Mars aerocaptures considered with entry velocities up to 9 km/s. If 10 km/s entries are required, an L/D of 0.4 to 0.5 would be necessary to maintain a corridor width of at least 1 degree. For Earth return aerocapture, a vehicle with an L/D of 0.4 to 0.5 was found to provide a corridor width of 0.7 degree or more for all entry velocities up to 14.5 km/s. Aerodynamic convective heating calculations were performed assuming a fully catalytic, 'cold' wall; radiative heating was calculated assuming that the shock layer was in thermochemical equilibrium. Heating rates were low enough for selected entries at Mars that a radiatively cooled thermal protection system might be feasible, although an ablative material would be required for most scenarios. Earth return heating rates were generally more severe than those encountered by the Apollo vehicles, and would require ablative heat shields in all cases. Dissert. Abstr.

N93-12379# Aerospace Corp., El Segundo, CA. Technology Operations.

THE RELATIONSHIP BETWEEN ELECTROSTATIC DISCHARGES ON SPACECRAFT P78-2 AND THE ELECTRON ENVIRONMENT

H. C. Koons and D. J. Gorney 15 Mar. 1992 29 p
(Contract F04701-88-C-0089)
(AD-A255179; TR-0091(6940-06)-2; SMC-TR-92-35) Avail: CASI HC A03/MF A01

The relationship between the energetic electron environment and electrostatic discharges on the P78-2 (SCATHA) spacecraft has been examined. Internal discharges occur near perigee while surface discharges occur about uniformly over the radial range covered by SCATHA, 5.5 to 8 Re. The surface discharges peak at local midnight and decrease toward local morning, while the internal discharges have a broad occurrence maximum centered on local noon. Both types are far more likely to occur when the Earth's magnetic field is disturbed. Although few surface discharges occur when the Planetary Magnetic Index, Kp, is less than 4, a modest number of internal discharges occur under these quiet to normal conditions. In all cases where internal discharges occurred under quiet to normal conditions, a period of very disturbed conditions had occurred a few days earlier. Surface discharges have a strong tendency to occur when the flux of electrons with energies of 10's of keV is high, while internal discharges occur when the flux of electrons with energies of 100's of keV is high and the flux of 10's of keV electrons is low. A significant correlation has been found between the occurrence of discharges on SCATHA and an estimate of the energetic electron fluence at geosynchronous orbit obtained from a neural network model of the relativistic electron flux at geosynchronous orbit. At predicted daily fluences greater than 1010 elec/sq cm almost all discharges result from internal charging. The incidence of internal discharges at predicted daily fluences above 1010 elec/sq cm is sufficiently high to warrant the use of this predictor to issue warnings for real time satellite operations. GRA

N93-12408# Naval Postgraduate School, Monterey, CA.

DESIGN AND EVALUATION OF ION SOURCE FOR SATELLITE CHARGE CONTROL M.S. Thesis

Michael E. Melvin Jun. 1992 118 p
(AD-A255172) Avail: CASI HC A06/MF A02

This thesis describes the design of a new spacecraft charge control device that incorporates a solid ion source made of Lithium or Potassium salt impregnated into a porous tungsten plug. The ion source was configured with a re-entrant thin-wall heat shield to reduce heat loss and an experimental thermocouple imbedded in the plug to accurately measure emission temperature. The initial design of the charge control device included an extraction grid, deceleration grid, and an electron filament source. Experiments were conducted on the charge control device and results were used to modify the design for optimization of current out of the device versus power used. Incremental testing and modifications resulted in the deceleration grid being removed and the extraction plate's wire mesh being removed to allow a clear path for the ions. With these changes the requirement of 10 microamps was achieved at 13 watts with the Potassium ion source. GRA

N93-12442*# Martin Marietta Space Systems, Inc., Denver, CO. Astronautics Group.

MANNED MARS SYSTEM STUDY (MMSS): MARS TRANSPORTATION AND FACILITY STUDY. VOLUME 1: EXECUTIVE SUMMARY Final Report

Jul. 1990 30 p
(Contract NAS8-37126)
(NASA-CR-184473; NAS 1.26:184473; MCR-90-537-Vol-1) Avail: CASI HC A03/MF A01

The purpose of the study was to design and analyze systems for conducting human missions to Mars and the moon, with special emphasis on the transportation and facility infrastructure. This study was conducted by Martin Marietta Astronautics Group, with an important teaming role by Science Applications International Corporation (SAIC). This work included the studies and separate reports of the FY-1988 and 1989 case studies as well as special analyses and parametric studies. Author

N93-12443*# Martin Marietta Space Systems, Inc., Denver, CO. Astronautics Group.

MANNED MARS SYSTEM STUDY (MMSS): MARS TRANSPORTATION AND FACILITY INFRASTRUCTURE STUDY. VOLUME 2: TECHNICAL REPORT Final Report

Jul. 1990 390 p
(Contract NAS8-37126)
(NASA-CR-184474; NAS 1.26:184474; MCR-90-537-Vol-2) Avail: CASI HC A17/MF A04

The Manned Mars System Study (MMSS) was conducted for the Marshall Space Flight Center (MSFC) over the 35 month period between May 15, 1987 and April 30, 1990. During the course of the study, the NASA Office of Exploration (OEXP; Code Z) was created and MSFC was subsequently designated the Transportation Integration Agent (TIA) for support of the OEXP Mission Analysis and Systems Engineering (MASE) team. As a result of this action, modifications to the contract redirected the efforts to be consistent with NASA's overall objectives, including lunar transportation system design. A large number of written submittals were required in order to provide TIA support to MASE. A list summarizing the documents which have been prepared and delivered by Martin Marietta under this contract during the course of this work is presented. In nearly all cases, full sets of view-graphs were also provided to the MSFC COTR, and in several cases magnetic media were provided as well. To incorporate all of these materials (more than 2,000 pages) into the present report would obviously produce an extremely unwieldy and confusing document. Therefore, a summary of key findings are presented in this final report, supplemented by other material produced under this contract but not already available in the widespread literature. Author

N93-12447*# National Aeronautics and Space Administration. Langley Research Center, Hampton, VA.

CURRENT TECHNOLOGY FOR THERMAL PROTECTION SYSTEMS

Stephen J. Scotti, comp. Washington Oct. 1992 321 p
Workshop held in Hampton, VA, 11-12 Feb. 1992
(RTOP 506-43-31-04)
(NASA-CP-3157; L-17118; NAS 1.55:3157) Avail: CASI HC A14/MF A03

Interest in thermal protection systems for high-speed vehicles is increasing because of the stringent requirements of such new projects as the Space Exploration Initiative, the National Aero-Space Plane, and the High-Speed Civil Transport, as well as the needs for improved capabilities in existing thermal protection systems in the Space Shuttle and in turbojet engines. This selection of 13 papers from NASA and industry summarizes the history and operational experience of thermal protection systems utilized in the national space program to date, and also covers recent development efforts in thermal insulation, refractory materials and coatings, actively cooled structures, and two-phase thermal control systems. For individual titles, see N93-12448 through N93-12460.

N93-12448*# National Aeronautics and Space Administration. Ames Research Center, Moffett Field, CA.

REUSABLE THERMAL PROTECTION SYSTEM DEVELOPMENT: A PROSPECTIVE

Howard Goldstein *In* NASA. Langley Research Center, Current Technology for Thermal Protection Systems Oct. 1992 p 1-18 (For primary document see N93-12447 02-18)
Avail: CASI HC A03/MF A03

The state of the art in passive reusable thermal protection system materials is described. Development of the Space Shuttle Orbiter, which was the first reusable vehicle, is discussed. The thermal protection materials and given concepts and some of the shuttle development and manufacturing problems are described. Evolution of a family of grid and flexible ceramic external insulation materials from the initial shuttle concept in the early 1970's to the present time is described. The important properties and their evolution are documented. Application of these materials to vehicles currently being developed and plans for research to meet the space programs future needs are summarized. Author

N93-12449*# National Aeronautics and Space Administration. Lyndon B. Johnson Space Center, Houston, TX.

THERMAL PROTECTION SYSTEMS MANNED SPACECRAFT FLIGHT EXPERIENCE

Donald M. Curry *In* NASA. Langley Research Center, Current Technology for Thermal Protection Systems Oct. 1992 p 19-41 (For primary document see N93-12447 02-18)
Avail: CASI HC A03/MF A03

Since the first U.S. manned entry, Mercury (May 5, 1961), seventy-five manned entries have been made resulting in significant progress in the understanding and development of Thermal Protection Systems (TPS) for manned rated spacecraft. The TPS materials and systems installed on these spacecraft are compared. The first three vehicles (Mercury, Gemini, Apollo) used ablative (single-use) systems while the Space Shuttle Orbiter TPS is a multimission system. A TPS figure of merit, unit weight lb/sq ft, illustrates the advances in TPS material performance from Mercury (10.2 lb/sq ft) to the Space Shuttle (1.7 lb/sq ft). Significant advances have been made in the design, fabrication, and certification of TPS on manned entry vehicles (Mercury through Shuttle Orbiter). Shuttle experience has identified some key design and operational issues. State-of-the-art ceramic insulation materials developed in the 1970's for the Space Shuttle Orbiter have been used in the initial designs of aerobrakes. This TPS material experience has identified the need to develop a technology base from which a new class of higher temperature materials will emerge for advanced space transportation vehicles. Author

N93-12450*# National Aeronautics and Space Administration. Ames Research Center, Moffett Field, CA.
ADVANCED CERAMIC MATRIX COMPOSITES FOR TPS c24
Daniel J. Rasky *In* NASA. Langley Research Center, Current Technology for Thermal Protection Systems Oct. 1992 p 43-61 (For primary document see N93-12447 02-18)
Avail: CASI HC A03/MF A03

Recent advances in ceramic matrix composite (CMC) technology provide considerable opportunity for application to future aircraft thermal protection system (TPS), providing materials with higher temperature capability, lower weight, and higher strength and stiffness than traditional materials. The Thermal Protection Material Branch at NASA Ames Research Center has been making significant progress in the development, characterization, and entry simulation (arc-jet) testing of new CMC's. This protection gives a general overview of the Ames Thermal Protection Materials Branch research activities, followed by more detailed descriptions of recent advances in very-high temperature Zr and Hf based ceramics, high temperature, high strength SiC matrix composites, and some activities in polymer precursors and ceramic coating processing. The presentation closes with a brief comparison of maximum heat flux capabilities of advanced TPS materials. Author

N93-12451*# Supermaterials Research and Development Corp., Cleveland, OH.
THERMAL PROTECTION USING VERY HIGH TEMPERATURE CERAMICS c27
George R. Adamczyk *In* NASA. Langley Research Center, Current Technology for Thermal Protection Systems Oct. 1992 p 63-76 (For primary document see N93-12447 02-18)
Avail: CASI HC A03/MF A03

The purpose of the paper is to expose the reader to a technology that may solve some of the toughest materials problems facing thermal protection for use in aerospace. Supermaterials has created a system capable of producing unique material properties. Over 10 years and many man-hours have been invested in the development of this technology. Applications range from the food industry to the rigors of outer space. The flexibility of the system allows for customization not found in many other processes and at a reasonable cost. The ranges of materials and alloys that can be created are endless. Many cases with unique characteristics have been identified and we can expect even more with further development. Author

N93-12452*# Lockheed Missiles and Space Co., Palo Alto, CA.
SUPERPLASTIC FORMING OF CERAMIC INSULATION c27
T. G. Nieh, J. P. Wittenauer, and J. Wadsworth *In* NASA. Langley Research Center, Current Technology for Thermal Protection Systems Oct. 1992 p 77-87 (For primary document see N93-12447 02-18)
(Contract DAAL03-89-C-0028)
Avail: CASI HC A03/MF A03

Superplasticity has been demonstrated in many fine-grained structural ceramics and ceramic composites, including yttria-stabilized tetragonal zirconia polycrystal (YTZP), alumina, and Al2O3-reinforced zirconia (Al2O3/YTZ) duplex composites and SiC-reinforced Si3N4. These superplastic ceramics obviously offer the potential benefit of forming net shape or near net shape parts. This could be particularly useful for forming complicated shapes that are difficult to achieve using conventional forming techniques, or require elaborate, subsequent machining. In the present study, we successfully demonstrated the following: (1) superplastic 3Y-TXP and 20 percent Al2O3/YTZ composite have for the first time been successfully deformed into hemispherical caps via a biaxial gas-pressure forming technique; (2) no experimental difficulty was encountered in applying the required gas pressures and temperatures to achieve the results, thus, it is certain that higher rates of deformation than those presented in this study will be possible by using the current test apparatus at higher temperatures and pressures; and (3) an analytical model incorporating material parameters, such as variations during forming in the strain rate sensitivity exponent and grain growth-induced strain hardening, is needed to model accurately and therefore precisely control the biaxial gas-pressure forming of superplastic ceramics. Based on the results of this study, we propose to fabricate zirconia insulation tubes by superplastic extrusion of zirconia polycrystal. This would not only reduce the cost, but also improve the reliability of the tube products. Author

N93-12453*# Technetics, Inc., DeLand, FL.
CERAMIC TBS/POROUS METAL COMPLIANT LAYER c27
Robert P. Tolokan and G. P. Jarrabet *In* NASA. Langley Research Center, Current Technology for Thermal Protection Systems Oct. 1992 p 89-96 (For primary document see N93-12447 02-18)
Avail: CASI HC A02/MF A03

Technetics Corporation manufactures metal fiber materials and components used in aerospace applications. Our technology base is fiber metal porous sheet material made from sinter bonded metal fibers. Fiber metals have percent densities (metal content by volume) from 10 to 65 percent. Various topics are covered and include the following: fiber metal materials, compliant layer thermal bayer coatings (TBC's), pad properties, ceramic/pad TBC design, thermal shock rig, fabrication, and applications. Author

N93-12454*# National Aeronautics and Space Administration. Langley Research Center, Hampton, VA.
PREDICTED AND TESTED PERFORMANCE OF DURABLE TPS c24
John L. Shideler *In its* Current Technology for Thermal Protection Systems Oct. 1992 p 97-129 (For primary document see N93-12447 02-18)
Avail: CASI HC A03/MF A03

The development of thermal protection systems (TPS) for aerospace vehicles involves combining material selection, concept design, and verification tests to evaluate the effectiveness of the system. The present paper reviews verification tests of two metallic and one carbon-carbon thermal protection system. The test conditions are, in general, representative of Space Shuttle design flight conditions which may be more or less severe than conditions required for future space transportation systems. The results of this study are intended to help establish a preliminary data base from which the designers of future entry vehicles can evaluate the applicability of future concepts to their vehicles. Author

N93-12455*# National Aeronautics and Space Administration. Langley Research Center, Hampton, VA.
RECENT ADVANCES IN CARBON-CARBON SUBSTRATE TECHNOLOGY AT NASA. LANGLEY RESEARCH CENTER c24
Philip O. Ransone, Y. Robert Yamaki (Lockheed Engineering and Sciences Co., Hampton, VA.), and Howard G. Maahs *In its* Current Technology for Thermal Protection Systems Oct. 1992 p 131-148 (For primary document see N93-12447 02-18)
Avail: CASI HC A03/MF A03

A comparison of specific strengths of candidate high-temperature materials as a function of temperature is shown. From this comparison, it is apparent why there is an interest in carbon-carbon composites for applications as a strong, light-weight thermal protection system (TPS), or as hot structure, for applications above 2500 F. The lower bound of the carbon-carbon band is representative of the tensile strength of cross-ply Advanced Carbon-Carbon (ACC). The upper bound represents capabilities of various experimental carbon-carbon composites. Thin carbon-carbon composites, such as would be used as TPS panels or hot aero-structure, are usually constructed of layups of 2-D fabrics of carbon-fiber yarns (tows). Although the in-plane strengths of these composites can be very attractive, a major problem area is low interlaminar strength. The low interlaminar strength is the result of a relatively weak carbon matrix and poor interaction between the fibers and matrix. The purpose of this paper is to discuss strategies being employed to improve the interlaminar strengths of the materials at the upper bound of the carbon-carbon band, and to present some recent encouraging results. The emphasis of these strategies is to improve interlaminar shear and tensile strengths while maintaining, or even improving, the inplane properties. Author

N93-12456*# National Aeronautics and Space Administration. Langley Research Center, Hampton, VA.
CURRENT RESEARCH IN OXIDATION-RESISTANT CARBON-CARBON COMPOSITES AT NASA. LANGLEY RESEARCH CENTER **c24**
Craig W. Ohlhorst, Wallace L. Vaughn, and David M. Barrett *In its* Current Technology for Thermal Protection Systems Oct. 1992 p 149-168 (For primary document see N93-12447 02-18)
Avail: CASI HC A03/MF A03

The significant potential of carbon-carbon composites for high-temperature structural applications is well established. For hypersonic vehicle applications, desirable properties include low density, high specific strength and stiffness, low coefficients of thermal expansion, and retention of mechanical properties above 3000 F. A significant problem associated with carbon materials, however, is that they oxidize rapidly in air at temperatures above about 800 F, and therefore must be protected from oxidation. Successful development of effective methods of oxidation protection is key to the eventual utilization of carbon-carbon composites on hypersonic vehicles such as NASP. In this presentation, the basic elements of an oxidation-protection system are described. Results from oxidation-performance evaluations of state-of-the-art ACC-4 type material in simulated airframe vehicle environments (temperature, pressure, and time) conducted at NASA Langley are also presented. NASA Langley has an active research effort to improve the oxidation resistance of carbon-carbon materials for airframe structural and vehicle thermal protection applications. Conversion coating and sealant development research is highlighted. Author

N93-12457*# National Aeronautics and Space Administration. Langley Research Center, Hampton, VA.
THERMAL CONTROL/OXIDATION RESISTANT COATINGS FOR TITANIUM-BASED ALLOYS **c24**
Ronald K. Clark, Terryl A. Wallace, George R. Cunnington (Lockheed Missiles and Space Co., Palo Alto, CA.), and Karl E. Wiedemann (Analytical Services and Materials, Inc., Hampton, VA.) *In its* Current Technology for Thermal Protection Systems Oct. 1992 p 169-188 (For primary document see N93-12447 02-18)
Avail: CASI HC A03/MF A03

Extensive research and development efforts have been expended toward development of thermal control and environmental protection coatings for NASP and generic hypersonic vehicle applications. The objective of the coatings development activities summarized here was to develop light-weight coatings for protecting advanced titanium alloys from oxidation in hypersonic vehicle applications. A number of new coating concepts have been evaluated. Coated samples were exposed to static oxidation tests at temperatures up to 1000 C using a thermogravimetric apparatus. Samples were also exposed to simulated hypersonic flight conditions for up to 10 hr to determine their thermal and chemical stability and catalytic efficiency. The emittance of samples was determined before and after exposure to simulated hypersonic flight conditions. Author

N93-12458*# National Aeronautics and Space Administration. Langley Research Center, Hampton, VA.
ACTIVE COOLING FROM THE SIXTIES TO NASP **c05**
H. Neale Kelly and Max L. Blosser *In its* Current Technology for Thermal Protection Systems Oct. 1992 p 189-249 (For primary document see N93-12447 02-18)
Avail: CASI HC A04/MF A03

Vehicles, such as the X-15 or National Aero-Space Plane, traveling at hypersonic speeds through the earth's atmosphere experience aerodynamic heating. The heating can be severe enough that a thermal protection system is required to limit the temperature of the vehicle structure. Although several categories of thermal protection systems are mentioned briefly, the majority of this paper describes convectively cooled structures for large areas. Convective cooling is a method of limiting structural temperatures by circulating a coolant through the vehicle structure. Efforts to develop convectively cooled structures during the past 30 years--from early engine structures, which were intended to be tested on the X-15, to structural--are described. Many of the lessons learned from these research efforts are presented. Author

N93-12459*# National Aeronautics and Space Administration. Goddard Space Flight Center, Greenbelt, MD.
ADVANCED TWO-PHASE HEAT TRANSFER SYSTEMS **c34**
Theodore D. Swanson *In* NASA. Langley Research Center, Current Technology for Thermal Protection Systems Oct. 1992 p 251-290 (For primary document see N93-12447 02-18)
Avail: CASI HC A03/MF A03

Future large spacecraft, such as the Earth Observing System (EOS) platforms, will require a significantly more capable thermal control system than is possible with current 'passive' technology. Temperatures must be controlled much more tightly over a larger surface area. Numerous heat load sources will often be located inside the body of the spacecraft without a good view to space. Power levels and flux densities may be higher than can be accommodated with traditional technology. Integration and ground testing will almost certainly be much more difficult with such larger, more complex spacecraft. For these and similar reasons, the Goddard Space Flight Center (GSFC) has been developing a new, more capable thermal control technology called capillary pumped loops (CPL's). CPL's represent an evolutionary improvement over heat pipes; they can transport much greater quantities of heat over much longer distances and can serve numerous heat load sources. In addition, CPL's can be fabricated into large cold plates that can be held to tight thermal gradients. Development of this technology began in the early 1980's and is now reaching maturity. CPL's have recently been baselined for the EOS-AM platform (1997 launch) and the COMET spacecraft (1992 launch). This presentation describes this new technology and its applications. Most of the viewgraphs are self descriptive. For those that are less clear additional comments are provided. Author

N93-12460*# National Aeronautics and Space Administration. Langley Research Center, Hampton, VA.
THERMOSTRUCTURAL APPLICATIONS OF HEAT PIPES FOR COOLING LEADING EDGES OF HIGH-SPEED AEROSPACE VEHICLES **c34**
Charles J. Camarda and David E. Glass (Analytical Services and Materials, Inc., Hampton, VA.) *In its* Current Technology for Thermal Protection Systems Oct. 1992 p 291-318 (For primary document see N93-12447 02-18)
Avail: CASI HC A03/MF A03

Heat pipes have been considered for use on wing leading edge for over 20 years. Early concepts envisioned metal heat pipes cooling a metallic leading edge. Several superalloy/sodium heat pipes were fabricated and successfully tested for wing leading edge cooling. Results of radiant heat and aerothermal testing indicate the feasibility of using heat pipes to cool the stagnation region of shuttle-type space transportation systems. The test model withstood a total seven radiant heating tests, eight aerothermal tests, and twenty-seven supplemental radiant heating tests. Cold-wall heating rates ranged from 21 to 57 Btu/sq ft-s and maximum operating temperatures ranged from 1090 to 1520 F. Follow-on studies investigated the application of heat pipes to cool the stagnation regions of single-stage-to-orbit and advanced shuttle vehicles. Results of those studies indicate that a 'D-shaped' structural design can reduce the mass of the heat-pipe concept by over 44 percent compared to a circular heat-pipe geometry.

Simple analytical models for heat-pipe startup from the frozen state (working fluid initially frozen) were adequate to approximate transient, startup, and steady-state heat-pipe performance. Improvement in analysis methods has resulted in the development of a finite-element analysis technique to predict heat-pipe startup from the frozen state. However, current requirements of light-weight design and reliability suggest that metallic heat pipes embedded in a refractory composite material should be used. This concept is the concept presently being evaluated for NASP. A refractory-composite/heat-pipe-cooled wing leading edge is currently being considered for the National Aero-Space Plane (NASP). This concept uses high-temperature refractory-metal/lithium heat pipes embedded within a refractory-composite structure and is significantly lighter than an actively cooled wing leading edge because it eliminates the need for active cooling during ascent and descent. Since the NASP vehicle uses cryogenic hydrogen to cool structural components and then burns this fuel in the combustor, hydrogen necessary for descent cooling only, when the vehicle is unpowered, is considered to be a weight penalty. Details of the design of the refractory-composite/heat-pipe-cooled wing leading edge are currently being investigated. Issues such as thermal contact resistance and thermal stress are also being investigated.

Author

N93-11925*# Honeywell, Inc., Minneapolis, MN. Systems and Research Center.
A STATE-BASED APPROACH TO TREND RECOGNITION AND FAILURE PREDICTION FOR THE SPACE STATION FREEDOM
Kyle S. Nelson and George D. Hadden *In* NASA. Lyndon B. Johnson Space Center, Fifth Annual Workshop on Space Operations Applications and Research (SOAR 1991), Volume 1 Jan. 1992 p 27-32 (For primary document see N93-11921 02-59)
Avail: CASI HC A02/MF A04

N93-11926*# Aerospace Corp., Albuquerque, NM.
REQUIREMENTS AND OPPORTUNITIES FOR SATELLITE AUTONOMY Abstract Only
W. Spencer Campbell and Chris Gdanski (Phillips Lab., Kirtland AFB, NM.) *In* NASA. Lyndon B. Johnson Space Center, Fifth Annual Workshop on Space Operations Applications and Research (SOAR 1991), Volume 1 Jan. 1992 p 33 (For primary document see N93-11921 02-59)
Avail: CASI HC A01/MF A04

N93-11927*# National Aeronautics and Space Administration. Goddard Space Flight Center, Greenbelt, MD.
AN EXPERT SYSTEM FOR DIAGNOSING ENVIRONMENTALLY INDUCED SPACECRAFT ANOMALIES
Mark Rolincik (University Research Foundation, Greenbelt, MD.), Michael Lauriente, Harry C. Koons (Aerospace Corp., Los Angeles, CA.), and David Gorney (Aerospace Corp., Los Angeles, CA.) *In* NASA. Lyndon B. Johnson Space Center, Fifth Annual Workshop on Space Operations Applications and Research (SOAR 1991), Volume 1 Jan. 1992 p 36-44 Sponsored by NASA, Washington and AFGL (For primary document see N93-11921 02-59)
(Contract F04701-88-C-0089)
Avail: CASI HC A02/MF A04

N93-11932*# Interface and Control Systems, West Melbourne, FL.
SPACECRAFT ATTITUDE CONTROL USING A SMART CONTROL SYSTEM
Brian Buckley and Louis Wheatcraft (Barrios Technology, Inc., Houston, TX.) *In* NASA. Lyndon B. Johnson Space Center, Fifth Annual Workshop on Space Operations Applications and Research (SOAR 1991), Volume 1 Jan. 1992 p 70-79 (For primary document see N93-11921 02-59)
Avail: CASI HC A02/MF A04

N93-11953*# Planning Research Corp., El Segundo, CA.
REQUIREMENTS AND APPLICATIONS FOR ROBOTIC SERVICING OF MILITARY SPACE SYSTEMS
Otto C. Ledford, Jr. and Rodney G. Bennett (Air Force Space Div., El Segundo, CA.) *In* NASA. Lyndon B. Johnson Space Center, Fifth Annual Workshop on Space Operations Applications and Research (SOAR 1991), Volume 1 Jan. 1992 p 206-212 (For primary document see N93-11921 02-59)
Avail: CASI HC A02/MF A04

N93-11977*# National Aeronautics and Space Administration. Lyndon B. Johnson Space Center, Houston, TX.
ROLE OF AUTOMATION IN THE ACRV OPERATIONS Abstract Only
S. F. Sepahban *In its* Fifth Annual Workshop on Space Operations Applications and Research (SOAR 1991), Volume 1 Jan. 1992 p 399 (For primary document see N93-11921 02-59)
Avail: CASI HC A01/MF A04

N93-11982*# National Aeronautics and Space Administration. Langley Research Center, Hampton, VA.
A SMART END-EFFECTOR FOR ASSEMBLY OF SPACE TRUSS STRUCTURES
William R. Doggett, Marvin D. Rhodes, Marion A. Wise (Lockheed Engineering and Sciences Co., Hampton, VA.), and Maurice F. Armistead (Planning Research Corp., Hampton, VA.) *In* NASA. Lyndon B. Johnson Space Center, Fifth Annual Workshop on Space Operations Applications and Research (SOAR 1991), Volume 1 Jan. 1992 p 422-431 (For primary document see N93-11921 02-59)
Avail: CASI HC A02/MF A04

19 SPACECRAFT INSTRUMENTATION

For related information see also *06 Aircraft Instrumentation* and *35 Instrumentation and Photography.*

N93-11954*# National Aeronautics and Space Administration. Marshall Space Flight Center, Huntsville, AL.
AUTOGUIDANCE VIDEO SENSOR FOR DOCKING
Michael L. Book, Thomas C. Bryan, Richard T. Howard, and Richard W. Dabney *In* NASA. Lyndon B. Johnson Space Center, Fifth Annual Workshop on Space Operations Applications and Research (SOAR 1991), Volume 1 Jan. 1992 p 214-219 (For primary document see N93-11921 02-59)
Avail: CASI HC A02/MF A04

20 SPACECRAFT PROPULSION AND POWER

Includes main propulsion systems and components, e.g., rocket engines; and spacecraft auxilliary power sources.

For related information see also *07 Aircraft Propulsion and Power, 28 Propellants and Fuels, 44 Energy Production and Conversion,* and *15 Launch Vehicles and Space Vehicles.*

N93-10965*# National Aeronautics and Space Administration. Lewis Research Center, Cleveland, OH.
LUNAR AND MARTIAN ENVIRONMENTAL INTERACTIONS WITH NUCLEAR POWER SYSTEM RADIATORS
Marla E. Perez-Davis, James R. Gaier, and Cynthia M. Katzan (Sverdrup Technology, Inc., Brook Park, OH.) Aug. 1992 10 p Presented at the Nuclear Technologies Space Exploration, Jackson Hole, WY, 16-19 Aug. 1992; sponsored by ANS
(RTOP 506-41-41)
(NASA-TM-105747; E-7045-1; NAS 1.15:105747) Avail: CASI HC A02/MF A01

Future NASA space missions include a permanent manned presence on the moon and an expedition to the planet Mars. Such steps will require careful consideration of environmental interactions in the selection and design of required power systems. Several environmental constituents may be hazardous to performance integrity. Potential threats common to both the moon and Mars are low ambient temperatures, wide daily temperature swings, solar flux, and large quantities of dust. The surface of Mars provides the additional challenges of dust storms, winds, and a carbon dioxide atmosphere. In this review, the anticipated environmental interactions with surface power system radiators are described, as well as the impacts of these interactions on radiator durability, which were identified at NASA Lewis Research Center. Author

N93-10973# Sandia National Labs., Albuquerque, NM.
GROUND TEST FACILITIES FOR EVALUATING NUCLEAR THERMAL PROPULSION ENGINES AND FUEL ELEMENTS
G. C. Allen, D. F. Beck, C. D. Harmon, and L. R. Shipers 1992 12 p Presented at the Nuclear Technologies for Space Exploration, Jackson, WY, 16-19 Aug. 1992
(Contract DE-AC04-76DP-00789)
(DE92-017039; SAND-92-1099C; CONF-920803-14) Avail: CASI HC A03/MF A01

Interagency panels evaluating nuclear thermal propulsion development options have consistently recognized the need for constructing a major new ground test facility to support fuel element and engine testing. This paper summarizes the requirements, configuration, and design issues of a proposed ground test complex for evaluating nuclear thermal propulsion engines and fuel elements being developed for the Space Nuclear Thermal Propulsion (SNTP) program. DOE

N93-10998# Strategic Defense Initiative Organization, Washington, DC.
LIGHTWEIGHT EXOATMOSPHERIC PROJECTILE (LEAP) TEST PROGRAM. SUPPLEMENTAL ENVIRONMENTAL ASSESSMENT
Jun. 1992 94 p
(AD-A252286) Avail: CASI HC A05/MF A01

The proposed action is to modify previously planned Lightweight Exoatmospheric Projectile (LEAP) Test Program activities (LEAP EA, July 1991, Ref 32) at White Sands Missile Range (WSMR), New Mexico; Kwajalein Missile Range (KMR), U.S. Army Kwajalein Atoll (USAKA); and Wake Island. The proposed action includes modifications of flight trajectories for LEAP flights 3, 5, and 6. Two additional flights, LEAP-X and LEAP-7 have been added to the program. LEAP-X is a single rocket test flight from KMR and LEAP-7 is a two-rocket test flight from KMR and Wake Island. Component/assembly ground tests will take place at Orbital Sciences Corporation (OSC), Space Data Division (SDD), Chandler, Arizona; Phillips Laboratory, Edwards Air Force Base, California; Rocketdyne Division of Rockwell International; Boeing Aerospace and Electronics, Kent, Washington; Hughes Aircraft Corporation, Missile Systems Group, Canoga Park California; Aerojet, Sacramento, California; and Thiokol Corporation, Elkton, Maryland. GRA

N93-11042*# Alabama Univ., Huntsville. Propulsion Research Center.
ROCKET BASED COMBINED CYCLE (RBCC) PROPULSION TECHNOLOGY WORKSHOP. VOLUME 1: EXECUTIVE SUMMARY
Kent T. Chojnacki 28 Aug. 1992 18 p
(Contract NAS8-38609)
(NASA-CR-184382; NAS 1.26:184382; UAH-TR-92/001-Vol-1)
Avail: CASI HC A03/MF A01

The goal of the Rocket-Based Combined Cycle (RBCC) Propulsion Technology Workshop was to assess the RBCC propulsion system's viability for Earth-to-Orbit (ETO) transportation systems. This was accomplished by creating a forum (workshop) in which past work in the field of RBCC propulsion systems was reviewed, current technology status was evaluated, and future technology programs in the field of RBCC propulsion systems were postulated, discussed, and recommended. Author

N93-11043*# Alabama Univ., Huntsville. Propulsion Research Center.
ROCKET BASED COMBINED CYCLE (RBCC) PROPULSION WORKSHOP, VOLUME 2 Final Report
Kent T. Chojnacki 28 Aug. 1992 72 p
(Contract NAS8-38609)
(NASA-CR-184383; NAS 1.26:184383; UAH-TR-91/001-Vol-2)
Avail: CASI HC A04/MF A01

The goal of the Rocket Based Combined Cycle (RBCC) Propulsion Technology Workshop, was to impart technology information to the propulsion community with respect to hypersonic combined cycle propulsion capabilities. The major recommendation resulting from this technology workshop was as follows: conduct a systems-level applications study to define the desired propulsion system and vehicle technology requirements for LEO launch vehicles. All SSTO and TSTO options using the various propulsion systems (airbreathing combined cycle, rocket-based combined cycle, and all rocket) must be considered. Such a study should be accomplished as soon as possible. It must be conducted with a consistent set of ground rules and assumptions. Additionally, the study should be conducted before any major expenditures on a RBCC technology development program occur. Author

N93-11173*# N Ray Engineering Co., Inc., San Diego, CA.
FEASIBILITY OF USING NEUTRON RADIOGRAPHY TO INSPECT THE SPACE SHUTTLE SOLID ROCKET BOOSTER AFT SKIRT, FORWARD SKIRT AND FRUSTUM. PART 1: SUMMARY REPORT Final Report
J. P. Barton, J. W. Bader, J. S. Brenizer (Virginia Univ., Charlottesville.), and B. Hosticka (Virginia Univ., Charlottesville.) May 1992 12 p Presented at the Fourth World Conference on Neutron Radiography, San Francisco, CA, 10-14 May 1992
(Contract NAS8-38681)
(NASA-CR-184357; NAS 1.26:184357; NRE-052992; JPB-014NA)
Avail: CASI HC A03/MF A01

The space shuttle's solid rocket boosters (SRB) include components made primarily of aluminum that are parachuted back for retrieval from the ocean and refurbished for repeated usage. Nondestructive inspection methods used on these aging parts to reduce the risk of unforeseen problems include x-ray, ultrasonics, and eddy current. Neutron radiography tests on segments of an SRB component show that entrapped moisture and naturally occurring aluminum corrosion can be revealed by neutron radiography even if present in only small amounts. Voids in sealant can also be evaluated. Three alternatives are suggested to follow-up this study: (1) take an SRB component to an existing neutron radiography system; (2) take an existing mobile neutron radiography system to the NASA site; or (3) plan a dedicated system custom designed for NASA applications. Author

N93-11402*# National Aeronautics and Space Administration. Lewis Research Center, Cleveland, OH.
PRELIMINARY CHARACTERIZATION OF A WATER VAPORIZER FOR RESISTOJET APPLICATIONS
W. Earl Morren Sep. 1992 17 p Presented at the 28th Joint Propulsion Conference and Exhibit, Nashville, TN, 6-8 Jul. 1992; sponsored by AIAA, SAE, ASME, and ASEE Previously announced in IAA as A92-54041
(RTOP 506-42-31)
(NASA-TM-105877; E-7342; NAS 1.15:105877; AIAA Paper 92-3533) Avail: CASI HC A03/MF A01

A series of tests was conducted to explore the characteristics of a water vaporizer intended for application to resistojet propulsion systems. The objectives of these tests were to (1) observe the effect of orientation with respect to gravity on vaporizer stability, (2) characterize vaporizer efficiency and outlet conditions over a range of flow rates, and (3) measure the thrust performance of a vaporizer/resistojet thruster assembly. A laboratory model of a forced-flow, once-through water vaporizer employing a porous heat exchange medium was built and characterized over a range of flow rates and power levels of interest for application to water resistojets. In a test during which the vaporizer was rotated about a horizontal axis normal to its own axis, the outlet temperature and mass flow rate through the vaporizer remained steady. Throttlability to 30 percent of the maximum flow rate tested was demonstrated. The measured thermal efficiency of the vaporizer was near 0.9 for all tests. The water vaporizer was integrated with an engineering model multipropellant resistojet. Performance of the vaporizer/thruster assembly was measured over a narrow range of operating conditions. The maximum specific impulse measured was 234 s at a mass flow rate and specific power level (vaporizer and thruster combined) of 154 x 10(exp-6)kg/s and 6.8 MJ/kg, respectively. Author

N93-11424 Department of the Navy, Washington, DC.
INFLATABLE DEVICE FOR EXCLUDING SEA WATER FROM A ROCKET MOTOR Patent
Michael J. Purser, inventor (to Navy) (Courtney and Co., Philadelphia, PA.) 30 Jun. 1992 10 p Filed 18 Dec. 1991
(AD-D015365; US-Patent-5,125,318; US-Patent-Appl-SN-805594; US-Patent-Class-89-109) Avail: US Patent and Trademark Office

An inflatable water exclusion device for protecting the rocket motor of a solid-propellant-powered missile, launched from below the surface of the sea by means of launching gas, from being damaged by a spout of water spurting up into the atmosphere. The device consists of a round base plate that attaches to an expellable baffle assembly located within the throat of the rocket motor nozzle, and an inflatable elastomer-coated cloth bag that is attached to the rim of the base plate. As the missile ascends toward the surface of the sea, launching gas that was originally contained within the voids of the rocket motor expands and streams out through the nozzle thereby causing the bag to inflate. After the missile has breached the surface of the sea the rocket motor ignites, thereby causing the baffle assembly and the inflatable water exclusion device attached thereto to be expelled from the nozzle and fall back into the sea. GRA

N93-11596# Edgerton, Germeshausen and Grier, Inc., Idaho Falls, ID.
A DEVELOPMENT APPROACH FOR NUCLEAR THERMAL PROPULSION
D. Buden 1992 11 p Presented at the American Nuclear Society Meeting, Jackson Hole, WY, 16-19 Aug. 1992
(Contract DE-AC07-76ID-01570)
(DE92-018020; EGG-M-92359; CONF-9208114-1) Avail: CASI HC A03/MF A01

The cost and time to develop nuclear thermal propulsion systems are very approach dependent. The objectives addressed are the development of an 'acceptable' nuclear thermal propulsion system that can be used as part of the transportation system for people to explore Mars and to enhance the performance of other missions within highly constrained budgets and schedules. To accomplish this, it was necessary to identify the cost drivers considering mission parameters, safety of the crew, mission success, facility availability and time and cost to construct new facilities, qualification criteria, status of technologies, management structure, and use of such system engineering techniques as concurrent engineering. DOE

N93-11608*# Colorado State Univ., Fort Collins. Dept. of Mechanical Engineering.
ADVANCED ELECTRIC PROPULSION RESEARCH, 1991
Annual Report, 1 Jan. - 31 Dec. 1991
Jeffery M. Monheiser Oct. 1992 74 p
(Grant NGR-06-002-112)
(NASA-CR-190761; NAS 1.26:190761) Avail: CASI HC A04/MF A01

A simple model for the production of ions that impinge on and sputter erode the accelerator grid of an ion thruster is presented. Charge-exchange and electron-impact ion production processes are considered, but initial experimental results suggest the charge-exchange process dominates. Additional experimental results show the effects of changes in thruster operating conditions on the length of the region from which these ions are drawn upstream into the grid. Results which show erosion patterns and indicate molybdenum accelerator grids erode more rapidly than graphite ones are also presented. Author

N93-11614*# National Aeronautics and Space Administration. Lewis Research Center, Cleveland, OH.
HOT FIRE TEST RESULTS OF SUBSCALE TUBULAR COMBUSTION CHAMBERS
John M. Kazaroff, Robert S. Jankovsky, and Albert J. Pavli (Sverdrup Technology, Inc., Brook Park, OH.) Nov. 1992 12 p
Previously announced as N93-10020
(RTOP 593-12-21)
(NASA-TP-3222; E-6849; NAS 1.60:3222) Avail: CASI HC A03/MF A01

Advanced, subscale, tubular combustion chambers were built and test fired with hydrogen-oxygen propellants to assess the increase in fatigue life that can be obtained with this type of construction. Two chambers were tested: one ran for 637 cycles without failing, compared to a predicted life of 200 cycles for a comparable smooth-wall milled-channel liner configuration. The other chamber failed at 256 cycles, compared to a predicted life of 118 cycles for a comparable smooth-wall milled-channel liner configuration. Posttest metallographic analysis determined that the strain-relieving design (structural compliance) of the tubular configuration was the cause of this increase in life. Author

N93-11766# Sandia National Labs., Albuquerque, NM.
CLOSED FORM LOW-THRUST TRAJECTORIES FOR MARS MISSIONS
J. W. Purvis 1992 4 p Presented at the 28th Joint Propulsion Converence, Nashville, TN, 6-8 Jul. 1992
(Contract DE-AC04-76DP-00789)
(DE92-017431; SAND-92-1598C; CONF-920747-6) Avail: CASI HC A01/MF A01

Several closed form trajectory solutions have been developed for low-thrust interplanetary flight and used with patched conics for analysis of combined propulsion systems. The solutions provide insight into alternative types of Mars missions and show considerable mass savings for fast crewed missions with outbound trip times on the order of 90-100 days. DOE

N93-11824# Sandia National Labs., Albuquerque, NM.
STRUCTURAL INTEGRITY OF A CONFINEMENT VESSEL FOR TESTING NUCLEAR FUELS FOR SPACE PROPULSION
V. L. Bergmann 1992 19 p Presented at the Society of Women Engineers' National Convention, Orlando, FL, 22-29 Jun. 1992
(Contract DE-AC04-76DP-00789)
(DE92-016796; SAND-92-0315C; CONF-9206206-1) Avail: CASI HC A03/MF A01

Nuclear propulsion systems for rockets could significantly reduce the travel time to distant destinations in space. However, long before such a concept can become reality, a significant effort must be invested in analysis and ground testing to guide the development of nuclear fuels. Any testing in support of development of nuclear fuels for space propulsion must be safely contained to prevent the release of radioactive materials. This paper describes analyses performed to assess the structural integrity of a test confinement vessel. The confinement structure, a stainless steel pressure vessel with bolted flanges, was designed for operating static pressures in accordance with the ASME Boiler and Pressure Vessel Code. In addition to the static operating pressures, the confinement barrier must withstand static overpressures from off-normal conditions without releasing radioactive material. Results from axisymmetric finite element analyses are used to evaluate the response of the confinement structure under design and accident conditions. For the static design conditions, the stresses computed from the ASME code are compared with the stresses computed by the finite element method. DOE

N93-11889 Toledo Univ., OH.
NUMERICAL MODELING OF A VORTEX STABILIZED ARCJET
Ph.D. Thesis

Gary Edward Pawlas 1991 167 p
Avail: Univ. Microfilms Order No. DA9216431

Arcjet thrusters are being actively considered for use in Earth orbit maneuvering applications. Satellite station-keeping is an example of a maneuvering application requiring the low thrust, high specific impulse of an arcjet. Experimental studies are currently the chief means of determining an optimal thruster configuration. Earlier numerical studies have failed to include all of the effects found in typical arcjets including complex geometries, viscosity and swirling flow. Arcjet geometries are large area ratio converging-diverging nozzles with centerbodies in the subsonic portion of the nozzle. The nozzle walls serve as the anode while the centerbody functions as the cathode. Viscous effects are important because the Reynolds number, based on the throat radius, is typically less than 1,000. Experimental studies have shown a swirl or circumferential velocity component stabilizes a constricted arc. The equations are described which governs the flow through a constricted arcjet thruster. An assumption that the flowfield is in local thermodynamic equilibrium leads to a single fluid plasma temperature model. An order of magnitude analysis reveals the governing fluid mechanics equations are uncoupled from the electromagnetic field equations. A numerical method is developed to solve the governing fluid mechanics equations, the Thin Layer Navier-Stokes equations. A coordinate transformation is used in deriving the governing equations to simplify the application of boundary conditions in complex geometries. An axisymmetric formulation is employed to include the swirl velocity component as well as the axial and redial velocity components. The numerical method is an implicit finite-volume technique and allows for large time steps to reach a converged steady-state solution. The inviscid fluxes are flux-split and Gauss-Seidel line relaxation is used to accelerate convergence. 'Converging diverging' nozzles with exit-to-throat area ratios up to 100:1 and annual nozzles were examined. Comparisons with experimental data and previous numerical results were in excellent agreement. Quantities examined included Mach number and static wall pressure distributions, and oblique shock structures. As the level of swirl and viscosity in the flowfield increased the mass flow rate and thrust decreased. The technique was used to predict the flow through a typical arcjet thruster geometry. Results indicate swirl and viscosity play an important role in the complex geometry of an arcjet by shifting the Mach contours upstream and reducing the mass flow rate and thrust. Dissert. Abstr.

N93-12009*# Alabama Univ., Huntsville.
EXAMINATION OF VARIOUS TURBULENCE MODELS FOR APPLICATION IN LIQUID ROCKET THRUST CHAMBERS Final Report
R. J. Hung 30 Apr. 1991 56 p
(Contract NAS8-36955)
(NASA-CR-184406; NAS 1.26:184406) Avail: CASI HC A04/MF A01

There is a large variety of turbulence models available. These models include direct numerical simulation, large eddy simulation, Reynolds stress/flux model, zero equation model, one equation model, two equation k-epsilon model, multiple-scale model, etc. Each turbulence model contains different physical assumptions and requirements. The natures of turbulence are randomness, irregularity, diffusivity and dissipation. The capabilities of the turbulence models, including physical strength, weakness, limitations, as well as numerical and computational considerations, are reviewed. Recommendations are made for the potential application of a turbulence model in thrust chamber and performance prediction programs. The full Reynolds stress model is recommended. In a workshop, specifically called for the assessment of turbulence models for applications in liquid rocket thrust chambers, most of the experts present were also in favor of the recommendation of the Reynolds stress model. Author

N93-12013*# Alabama Univ., Huntsville.
SUPERCONDUCTING APPLICATIONS IN PROPULSION SYSTEMS. MAGNETIC INSULATION FOR PLASMA PROPULSION DEVICES Final Report
Dora E. Gonzalez and Gerald R. Karr Jun. 1990 18 p
(Contract NAS8-36955)
(NASA-CR-184401; NAS 1.26:184401) Avail: CASI HC A03/MF A01

The purpose of this paper is to review the status of knowledge of the basic concepts needed to establish design parameters for effective magnetic insulation. The objective is to estimate the effectiveness of the magnetic field in insulating the plasma, to calculate the magnitude of the magnetic field necessary to reduce the heat transfer to the walls sufficiently enough to demonstrate the potential of magnetically driven plasma rockets. Author

N93-12056# EG and G Energy Measurements, Inc., Idaho Falls.
TUTORIAL ON NUCLEAR THERMAL PROPULSION SAFETY FOR MARS
D. Buden 1992 15 p Presented at the 28th Joint Propulsion Conference, Nashville, TN, 6-8 Jul. 1992 Previously announced in IAA as A92-49091
(Contract DE-AC07-76ID-01570)
(DE92-017946; EGG-M-92274; AIAA Paper 92-3696; CONF-920747-9) Avail: CASI HC A03/MF A01

Safety is the prime design requirement for nuclear thermal propulsion (NTP). It must be built in at the initiation of the design process. An understanding of safety concerns is fundamental to the development of nuclear rockets for manned missions to Mars and many other applications that will be enabled or greatly enhanced by the use of nuclear propulsion. To provide an understanding of the basic issues, a tutorial has been prepared. This tutorial covers a range of topics including safety requirements and approaches to meet these requirements, risk and safety analysis methodology, NERVA reliability and safety approach, and life cycle risk assessments. DOE

N93-12088*# Pratt and Whitney Aircraft, West Palm Beach, FL. Government Engine Business.
SPACE TRANSPORTATION BOOSTER ENGINE CONFIGURATION STUDY. VOLUME 3: PROGRAM COST ESTIMATES AND WORK BREAKDOWN STRUCTURE AND WBS DICTIONARY Final Report, Mar. 1986 - Mar. 1989
1 Dec. 1989 160 p
(Contract NAS8-36857)
(NASA-CR-184458; NAS 1.26:184458; FR-19691-4-Vol-3) Avail: CASI HC A08/MF A02

The objective of the Space Transportation Booster Engine Configuration Study is to contribute to the ALS development effort by providing highly reliable, low cost booster engine concepts for both expendable and reusable rocket engines. The objectives of the Space Transportation Booster Engine (STBE) Configuration Study were: (1) to identify engine development configurations which enhance vehicle performance and provide operational flexibility at low cost; and (2) to explore innovative approaches to the follow-on Full-Scale Development (FSD) phase for the STBE. Author

N93-12148*# National Aeronautics and Space Administration. Marshall Space Flight Center, Huntsville, AL.
A COMPARISON OF HIGH CYCLE FATIGUE METHODOLOGIES
D. A. Herda Aug. 1992 19 p
(NASA-TM-103601; NAS 1.15:103601) Avail: CASI HC A03/MF A01

To evaluate alternate turbopump development (ATD) high cycle fatigue (HCF) methodology, a comparison was made with the space shuttle main engine (SSME) methodology. This report documents the comparison and evaluates ATD's HCF system. Author

N93-12363*# National Aeronautics and Space Administration. Lewis Research Center, Cleveland, OH.
NUCLEAR THERMAL PROPULSION TRANSPORTATION SYSTEMS FOR LUNAR/MARS EXPLORATION
John S. Clark, Stanley K. Borowski, Melvin C. McIlwain (GenCorp Aerojet, Sacramento, CA.), and Dennis G. Pellaccio (Science Applications International Corp., Albuquerque, NM.) Sep. 1992 13 p Presented at the Nuclear Power Engineering in Space

Nuclear Rocket Engines Conference, Kazakhstan, Russia, 22-26 Sep. 1992; sponsored by the Research and Production Association LUCH Semipalatinsk
(RTOP 593-71-00)
(NASA-TM-105870; E-7334; NAS 1.15:105870) Avail: CASI HC A03/MF A01

Nuclear thermal propulsion technology development is underway at NASA and DoE for Space Exploration Initiative (SEI) missions to Mars, with initial near-earth flights to validate flight readiness. Several reactor concepts are being considered for these missions, and important selection criteria will be evaluated before final selection of a system. These criteria include: safety and reliability, technical risk, cost, and performance, in that order. Of the concepts evaluated to date, the Nuclear Engine for Rocket Vehicle Applications (NERVA) derivative (NDR) is the only concept that has demonstrated full power, life, and performance in actual reactor tests. Other concepts will require significant design work and must demonstrate proof-of-concept. Technical risk, and hence, development cost should therefore be lowest for the concept, and the NDR concept is currently being considered for the initial SEI missions. As lighter weight, higher performance systems are developed and validated, including appropriate safety and astronaut-rating requirements, they will be considered to support future SEI application. A space transportation system using a modular nuclear thermal rocket (NTR) system for lunar and Mars missions is expected to result in significant life cycle cost savings. Finally, several key issues remain for NTR's, including public acceptance and operational issues. Nonetheless, NTR's are believed to be the 'next generation' of space propulsion systems - the key to space exploration. Author

N93-12368# National Aerospace Lab., Kakuda (Japan).
COMBUSTION CHARACTERISTICS OF THE LO2/GCH4 FUEL-RICH PREBURNERS FOR STAGED COMBUSTION CYCLE ROCKET ENGINES [SANSO-METAN NENRYOU RICCHI PURIBANA NO NENSHOU TOKUSEI]
Fumiei Ono, Hiroshi Tamura, Hiroshi Sakamoto, and Masaki Sasaki Sep. 1991 25 p In JAPANESE
(NAL-TR-1124; JTN-92-80392) Avail: CASI HC A03/MF A01

The combustion characteristics of Liquid Oxygen (LO2)/Gaseous Methane (GCH4) fuel rich preburners were experimentally studied using subscale hardware. Three types of preburners with coaxial type propellant injection elements were designed and fabricated, and were used for hot fire testing. LO2 was used as oxidizer, and GCH4 at room temperature was used as fuel. The tests were conducted at chamber pressures ranging from 6.7 to 11.9 M Pa, and oxidizer to fuel ratios ranged from 0.16 to 0.42. The test results, which include combustion gas temperature T(sub c), characteristic velocity C(sup *) and soot adhesion data, are presented. The T(sub c) efficiency and the C(sup *) efficiency were found to be a function of oxidizer to fuel ratio and chamber pressure. These efficiencies are correlated by an empirical correlation parameter which accounts for the effects of oxidizer to fuel ratio and chamber pressure. The exhaust plumes were colorless and transparent under all tests conditions. There was some soot adhesion to the chamber wall, but no soot adhesion was observed on the main injector simulator orifices. Higher temperature igniter gas was required to ignite the main propellants of the preburner compared with that of the LO2/Gaseous Hydrogen (GH2) propellants combination. Author (NASDA)

N93-12372# National Aerospace Lab., Kakuda (Japan).
CHARACTERISTICS OF HEAT TRANSFER TO NICKEL PLATED CHAMBER WALLS OF HIGH PRESSURE ROCKET COMBUSTORS
Akinaga Kumakawa, Masaki Sasaki, Kazuo Sato, Fumiei Ono, Hiroshi Sakamoto, and Nobuyuki Yatsuyanagi Oct. 1991 17 p
(NAL-TR-1126T; JTN-92-80394) Avail: CASI HC A03/MF A01

The chamber walls of two water cooled calorimetric combustors of different chamber lengths were electroplated with nickel of different thickness to investigate decreasing the temperature of the substrate copper wall and prolonging thrust chamber life. Combustion tests were conducted using Liquid OXygen (LOX)/gaseous hydrogen, LOX/gaseous methane, and LOX/Ram Jet 1J (RJ-1J) propellants. The maximum chamber pressure was 12 M Pa and the maximum heat flux reached 120 M W/sq m. For both the LOX/hydrogen and LOX/methane propellants, heat flux values measured at the throat section of the nickel plated chambers were 20 to 30 percent less than those measured for the bare copper chamber walls. This infers that subcritical microcracks observed within the nickel layer functioned to relax the layer's thermal stress and to cause a higher thermal resistance than expected. On the other hand, the test results of the LOX/RJ-1J propellant showed that the wall material and/or temperature, the presence of hydrogen, and the injection pattern of propellants all affected the characteristics of carbon deposition on the chamber wall. The heat flux values were lowered by 50 percent compared to those without carbon deposition. Both nickel layers survived approximately 30 firing tests having a total duration of 600 sec. The durability and reliability of the nickel plating were verified, there by showing that a thin layer of nickel plating is useful for decreasing the heat load of high pressure thrust chambers. Author (NASDA)

N93-12409*# Sverdrup Technology, Inc., Brook Park, OH.
EXTENDED-TESTING OF XENON ION THRUSTER HOLLOW CATHODES Final Report
Timothy R. Sarver-Verhey Jul. 1992 26 p Presented at the 28th Joint Propulsion Conference and Exhibit, Nashville, TN, 6-8 Jul. 1992; sponsored by AIAA, SAE, ASME, and ASEE Previously announced in IAA as A92-48811
(Contract NAS3-25266; RTOP 506-42-31)
(NASA-CR-189227; E-7279; NAS 1.26:189227; AIAA Paper 92-3204) Avail: CASI HC A03/MF A01

A hollow cathode wear-test of 508 hours was successfully completed at an emission current of 23.0 A and a xenon flow rate of 10 Pa-L/s. This test was the continuation of a hollow cathode contamination investigation. Discharge voltage was stable at 16.7 V. The cathode temperature averaged 1050 C with a 7 percent drop during the wear-test. Discharge ignition voltage was found to be approximately 20 V and was repeatable over four starts. Post-test analyses of the hollow cathode found a much improved internal cathode condition with respect to earlier wear-test cathodes. Negligible tungsten movement occurred and no formation of mono-barium tungsten was observed. These results correlated with an order-of-magnitude reduction in propellant feed-system leakage rate. Ba2CaWO6 and extensive calcium crystal formation occurred on the upstream end of the insert. Ba-Ca compound depositions were found on the Mo insert collar, on the Re electrical leads, and in the gap between the insert and cathode wall. This wear-test cathode was found to be in the best internal condition and had the most stable operating performance of any hollow cathode tested during this contamination investigation. Author

N93-12441*# Pratt and Whitney Aircraft, West Palm Beach, FL. Government Engine Business.
SPACE TRANSPORTATION BOOSTER ENGINE CONFIGURATION STUDY. VOLUME 2: DESIGN DEFINITION DOCUMENT AND ENVIRONMENTAL ANALYSIS Final Report, Mar. 1986 - Mar. 1989
1 Dec. 1989 388 p
(Contract NAS8-36857)
(NASA-CR-184459; NAS 1.26:184459; FR-19691-4-Vol-2) Avail: CASI HC A17/MF A04

The objective of the Space Transportation Booster Engine (STBE) Configuration Study is to contribute to the Advanced Launch System (ALS) development effort by providing highly reliable, low cost booster engine concepts for both expendable and reusable rocket engines. The objectives of the space Transportation Booster Engine (STBE) Configuration Study were: (1) to identify engine configurations which enhance vehicle performance and provide operational flexibility at low cost, and (2) to explore innovative approaches to the follow-on Full-Scale Development (FSD) phase for the STBE. Author

N93-12484*# National Aeronautics and Space Administration. Lewis Research Center, Cleveland, OH.
THE 10 kW POWER ELECTRONICS FOR HYDROGEN ARCJETS
John A. Hamley, Luis R. Pinero, and Gerald M. Hill 1992 22 p
Presented at the 1992 JANNAF Propulsion Meeting, Indianapolis, IN, 24-28 Feb. 1992 Previously announced as N93-10033
(RTOP 506-42-31)
(NASA-TM-105614; E-6951; NAS 1.15:105614) Avail: CASI HC A03/MF A01

A combination of emerging mission considerations such as 'launch on schedule', resource limitations, and the development of higher power spacecraft busses has resulted in renewed interest in high power hydrogen arcjet systems with specific impulses greater than 1000 s for Earth-space orbit transfer and maneuver applications. Solar electric propulsion systems with about 10 kW of power appear to offer payload benefits at acceptable trip times. This work outlines the design and development of 10 kW hydrogen arcjet power electronics and results of arcjet integration testing. The power electronics incorporated a full bridge switching topology similar to that employed in state of the art 5 kW power electronics, and the output filter included an output current averaging inductor with an integral pulse generation winding for arcjet ignition. Phase shifted, pulse width modulation with current mode control was used to regulate the current delivered to arcjet, and a low inductance power stage minimized switching transients. Hybrid power Metal Oxide Semiconductor Field Effect Transistors were used to minimize conduction losses. Switching losses were minimized using a fast response, optically isolated, totem-pole gate drive circuit. The input bus voltage for the unit was 150 V, with a maximum output voltage of 225 V. The switching frequency of 20 kHz was a compromise between mass savings and higher efficiency. Power conversion efficiencies in excess of 0.94 were demonstrated, along with steady state load current regulation of 1 percent. The power electronics were successfully integrated with a 10 kW laboratory hydrogen arcjet, and reliable, nondestructive starts and transitions to steady state operation were demonstrated. The estimated specific mass for a flight packaged unit was 2 kg/kW. Author

N93-12522*# Alabama Univ., Huntsville.
USERS MANUAL FOR PROGRAM NYQUIST: LIQUID ROCKET NYQUIST PLOTS DEVELOPED FOR USE ON A PC COMPUTER
Wilbur C. Armstrong Jun. 1992 124 p
(Contract NAS8-36955)
(NASA-CR-184451; NAS 1.26:184451) Avail: CASI HC A06/MF A02

The piping in a liquid rocket can assume complex configurations due to multiple tanks, multiple engines, and structures that must be piped around. The capability to handle some of these complex configurations have been incorporated into the NYQUIST code. The capability to modify the input on line has been implemented. The configurations allowed include multiple tanks, multiple engines, and the splitting of a pipe into unequal segments going to different (or the same) engines. This program will handle the following type elements: straight pipes, bends, inline accumulators, tuned stub accumulators, Helmholtz resonators, parallel resonators, pumps, split pipes, multiple tanks, and multiple engines. The code is too large to compile as one program using Microsoft FORTRAN 5; therefore, the code was broken into two segments: NYQUIST1.FOR and NYQUIST2.FOR. These are compiled separately and then linked together. The final run code is not too large (approximately equals 344,000 bytes). Author

N93-12523*# Pratt and Whitney Aircraft, West Palm Beach, FL. Government Engine Business.
SPACE TRANSPORTATION BOOSTER ENGINE CONFIGURATION STUDY. VOLUME 1: EXECUTIVE SUMMARY Final Report, Mar. 1986 - Mar. 1989
1 Dec. 1989 118 p
(Contract NAS8-36857)
(NASA-CR-184457; NAS 1.26:184457; FR-19691-4-Vol-1) Avail: CASI HC A06/MF A02

The objective of the Space Transportation Booster Engine (STBE) Configuration Study is to contribute to the Advanced Launch System (ALS) development effort by providing highly reliable, low cost booster engine concepts for both expendable and reusable rocket engines. The objectives of the Space Transportation Booster Engine (STBE) Configuration Study were to identify engine configurations which enhance vehicle performance and provide operational flexibility at low cost, and to explore innovative approaches to the follow-on full-scale development (FSD) phase for the STBE. Author

N93-12537 Maryland Univ., College Park.
EXPERIMENTS AND ANALYSIS CONCERNING THE USE OF EXTERNAL BURNING TO REDUCE AEROSPACE VEHICLE TRANSONIC DRAG Ph.D. Thesis
Charles Joseph Trefny 1991 297 p
Avail: Univ. Microfilms Order No. DA9222775

The external combustion of hydrogen to reduce transonic drag was studied. A control volume analysis is developed and indicates that the specific impulse performance of external burning is competitive with other forms of airbreathing propulsion and depends on the fuel-air ratio, freestream Mach number, and the severity of the base drag. A method is presented for sizing fuel injectors for a desired fuel-air ratio in the unconfined stream. A two-dimensional Euler analysis is also presented which indicates that the total axial force generated by external burning depends on the total amount of energy input and is independent of the transverse and streamwise distribution of heat addition. Good agreement between the Euler and control volume analysis is demonstrated. Features of the inviscid external burning flowfield are discussed. Most notably, a strong compression forms at the sonic line within the burning stream which may induce separation of the plume and prevent realization of the full performance potential. An experimental program was conducted in a Mach 1.26 free-jet to demonstrate drag reduction on a simple expansion ramp geometry, and verify hydrogen-air stability limits at external burning conditions. Stable combustion appears feasible to Mach numbers of between 1.4 and 2 depending on the vehicle flight trajectory. Drag reduction is demonstrated on the expansion ramp at Mach 1.26, however force levels showed little dependence on fuel pressure or altitude in contrast to control volume analysis predictions. Various facility interference mechanisms and scaling issues were studied and are discussed. Dissert. Abstr.

N93-11133 Alabama Univ., Huntsville. Dept. of Mechanical Engineering.
EFFECTS OF REACTING FLOWS WITH TURBULENCE AND SHOCK WAVES ON EFFICIENCY OF SCRAMJET COMBUSTORS
T. J. Chung and W. S. Yoon *In* JHU, The 28th JANNAF Combustion Subcommittee Meeting, Volume 1 Oct. 1991 p 1-14 (For primary document see N93-11132 02-25)
Avail: CPIA, 10630 Little Patuxent Pkwy., Suite 202, Columbia, MD 21044-3200 HC

N93-11449*# National Aeronautics and Space Administration. Marshall Space Flight Center, Huntsville, AL.
SOLUTION OF TWO-PHASE REACTING FLOW IN LIQUID THRUST CHAMBERS
Anthony Dang (Physical Research, Inc., Irvine, CA.), Homayun K. Navaz (Physical Research, Inc., Irvine, CA.), and Klaus W. Gross *In* JHU, The 28th JANNAF Combustion Subcommittee Meeting, Volume 2 Oct. 1991 p 9-18 (For primary document see N93-11448 02-25)
(Contract NAS8-38798)
Avail: CPIA, 10630 Little Patuxent Pkwy., Suite 202, Columbia, MD 21044-3200 HC

N93-11948*# Sverdrup Technology, Inc., Brook Park, OH.
AUTONOMOUS POWER SYSTEM: INTEGRATED SCHEDULING
Mark J. Ringer *In* NASA. Lyndon B. Johnson Space Center,

Fifth Annual Workshop on Space Operations Applications and Research (SOAR 1991), Volume 1 Jan. 1992 p 180-188 (For primary document see N93-11921 02-59)
(Contract NAS3-25266)
Avail: CASI HC A02/MF A04

23 CHEMISTRY AND MATERIALS (GENERAL)

N93-10978*# National Aeronautics and Space Administration. Lewis Research Center, Cleveland, OH.
RELATIVE SLIDING DURABILITY OF CANDIDATE HIGH TEMPERATURE FIBER SEAL MATERIALS
Christopher DellaCorte and Bruce M. Steinetz Aug. 1992 21 p
(RTOP 505-63-1A; RTOP 763-22-28)
(NASA-TM-105806; E-7236; NAS 1.15:105806) Avail: CASI HC A03/MF A01

The relative sliding durability behavior of six candidate ceramic fibers for high temperature sliding seal applications is reviewed and compared. Pin on disk tests were used to evaluate potential seal materials by sliding a tow or bundle of the candidate ceramic fiber against a superalloy test disk. Tests were conducted in air under a 2.65 N load, at a sliding velocity of 0.025 m/sec and at temperatures from 25 to 900 C. Friction was measured during the tests and fiber wear, indicated by the extent of fibers broken in the tow or bundle, was measured at the end of each test. For most of the fibers, friction and wear increase with test temperature. The relative fiber durability ranking correlates with tensile strength, indicating that tensile data, which is more readily available than sliding durability data, may be useful in predicting fiber wear behavior under various conditions. A dimensional analysis of the wear data shows that the fiber durability is related to a dimensionless durability ratio which represents the ratio of the fiber strength to the fiber stresses imposed by sliding. The analysis is applicable to fibers with similar diameters and elastic moduli. Based upon the results of the research program, three fiber candidates are recommended for further study as potential seal materials. They are a silicon based complex carbide-oxide fiber, an alumina-boria-silica and an aluminosilicate fiber. Author

N93-12177# State Univ. of New York, Buffalo. Dept. of Chemistry.
POSITIVE ION CHEMISTRY OF ACETYLENE AND METHYLACETYLENE CLUSTERS. FORMATION OF BENZENE AND C(SUB 2n)H(SUB 2n)(+) IONS VIA INTRACLUSTER POLYMERIZATION REACTIONS
M. T. Coolbaugh, Stephanie Gumina, Gopal Vaidyanathan, and James F. Garvey 1 Jun. 1992 22 p
(Contract N00014-88-K-0483)
(AD-A250931; TR-30) Avail: CASI HC A03/MF A01

We report the observation of large (n up to approximately 25) acetylene and methylacetylene cluster ions--the largest yet reported from ionization of neutral (C2H2)(n) or (CH3CCH)(n) clusters. The cluster ion intensity distributions of both systems display prominent magic numbers at n = 3. This finding is indicative of intra-cluster ion-molecule reactions giving rise to what are most likely benzene and trimethylbenzene ions from (C2H2)(n)(+) and (CH3CCH)(n)(+) cluster ions, respectively. The n acetylene cluster ion intensity distributions observed under efficient clustering conditions are further characterized by unexpected features, most notably a sharp break at n = 7 and a strong magic number at n = 14. The mass spectra of methyl-acetylene display a less dramatic break at n = 7 and a weak magic number around n = 10. These surprising structures may arise as a result of the formation of particularly stable covalently bonded molecule ions. In view of the unique properties of carbon it is possible that these ions possess spherical cage geometries reminiscent of the fullerenes. GRA

24 COMPOSITE MATERIALS

Includes physical, chemical, and mechanical properties of laminates and other composite materials.
For ceramic materials see *27 Nonmetallic Materials.*

N93-11065# Rolls-Royce Ltd., Derby (England).
GENERATION OF THERMAL STRAINS IN CARBON FIBRE-REINFORCED BISMALEIMIDE (PMR-15) COMPOSITES, PART 1, 2 AND 3
M. Simpson (Sheffield Univ., England), P. M. Jacobs (Sheffield Univ., England), and F. R. Jones (Sheffield Univ., England) 1 Apr. 1991 25 p Repr. from Composites, v. 22, no. 2, Mar. 1991 p 89-112 Previously announced in IAA as A91-39531
Sponsored by Ministry of Defence
(PNR-90976-Pt-1-2-3; ETN-92-92241) Copyright Avail: CASI HC A03/MF A01

The level of residual thermal strain which develops on PMR-15 crossply laminates was determined from the curvature of unbalanced 0/90 deg. beams. The hysteresis in the temperature dependence of the beam deflection was attributed to the plasticizing effect of entrapped curing volatiles (mainly water and methanol). Vacuum drying was shown to remove the hysteresis but increase the magnitude of the residual thermal strain. The latter appears to result from a complex interaction between the enhancement in matrix expansion coefficient, a reduction in transverse modulus, and the strain free temperature. Since the strain free temperature is in the region of 300 C, it was not proved possible to demonstrate its reduction directly. These values of thermal strain were compared with predictions obtained from measured transverse and matrix expansion coefficients. The presence of residual volatiles also appears to be responsible for some variability in the temperature dependence of the matrix dominated expansion coefficients. Post curing at higher temperatures gives rise to better reproducibility in the values of transverse and matrix expansion. ESA

N93-11072*# National Aeronautics and Space Administration. Langley Research Center, Hampton, VA.
THERMAL RESIDUAL STRESSES IN SILICON-CARBIDE/TITANIUM (0/90) LAMINATE
C. A. Bigelow Jul. 1992 28 p
(RTOP 763-23-41-85)
(NASA-TM-107649; NAS 1.15:107649) Avail: CASI HC A03/MF A01

The current work formulated a micromechanical analysis of a cross-ply laminate and calculated the thermal residual stress in a very thick (0/90)(sub 2n) silicon-carbide/titanium laminate. Results were also shown for a unidirectional laminate of the same material. Discrete fiber-matrix models assuming a rectangular array of fibers with a fiber volume fraction of 32.5 percent and a three-dimensional, finite-element analysis were used. Significant differences in the trends and magnitudes for the fiber, matrix, and interface stresses were calculated for unidirectional and (0/90) models. Larger hoop stresses calculated for the (0/90) model indicate that it may be more susceptible to radial cracking when subjected to mechanical loading than the unidirectional model. The axial stresses in the matrix were calculated to be slightly larger for the (0/90) model. The compressive axial stresses in the fiber were significantly larger in the (0/90) model. The presence of the cross-ply in the (0/90) model reduced the constraint on the fiber, producing radial interface stresses that were less compressive, which could lead to earlier failure of the fiber-matrix interface. Author

N93-11107# Rolls-Royce, Inc., Atlanta, GA.
SMALL PARTICLE IMPACT DAMAGE IN CARBON-CARBON COMPOSITES
S. Gupta and W. Westphal 1 Nov. 1991 6 p Presented at the 1991 Yokohama International Gas Turbine Congress, Yokohama, Japan, 27 Oct. - 1 Nov. 1991
(PNR-90948; ETN-92-92225) Copyright Avail: CASI HC A02/MF A01

Carbon-carbon composites, an important member of the fast emerging families of advanced material systems, which are making it feasible to achieve large advances in aero gas turbines of the future, are considered. In spite of a combination of outstanding properties, carbon-carbon composites do have serious oxidation problems. Oxidation protection technologies, essentially a barrier coating, become essential. Such coating systems, in addition to providing oxidation protection, must also accommodate environmental conditions in the engine. Small particle impact damage was one of the concerns. An experiment to investigate this, in which alumina grit was impacted on the surface of test specimens in a vertical erosion wind tunnel, is outlined. It was found that small particle impacts could indeed cause physical damage to the coating and consequently reduce its effectiveness, and as such must be considered in developing component applications for carbon-carbon composites. ESA

N93-11128# Aeronautical Research Inst. of Sweden, Stockholm. Composite Mechanics Section.
MIXED MODE BENDING TEST OF THE INTERLAMINAR FRACTURE TOUGHNESS OF CARBON/EPOXY M.S. Thesis - Royal Inst. of Technology
Kaare Ljung May 1992 68 p Sponsored by Defence Material Administration
(FFA-TN-1992-04; ETN-92-92391) Avail: CASI HC A04/MF A01

The Mixed Mode Bending (MMB) test for evaluation of the laminate interlaminar fracture toughness under various mixed mode loading conditions is described. The tests were performed on unidirectional carbon/epoxy HTA7-6376C split beam specimens. The MMB fixture is slightly modified to fit the tension machine. The test rig, specimen preparation, and test procedure are described. Both analytical and empirical evaluation methods were used. No significant difference due to evaluation technique was seen in G(sub 1C) for pure mode 1 loading condition but the empirical evaluation of G(sub C) became more unreliable with increasing portion of G(sub 2). Both the single mode values G(sub 1C) and G(sub 2C) were found to be lower than reported by the manufacturer. ESA

N93-11143# Deutsche Forschungsanstalt fuer Luft- und Raumfahrt, Cologne (Germany). Inst. fuer Werkstoff-Forschung.
CURING AND MECHANICAL PROPERTIES OF T800-V398 GRAPHITE/BISMALEIMIDE AT DIFFERENT TEMPERATURES
Shuzhen Bai (Beijing Inst. of Aeronautics and Astronautics, China) and Piet W. M. Peters Feb. 1992 46 p
(DLR-FB-92-02; ETN-92-92404) Avail: CASI HC A03/MF A01; DLR, Wissenshaftliches Berichtswesen, VB-PL-DO, Postfach 90 60 58, 5000 Cologne, Fed. Republic of Germany, HC

The cure of T800-V398 graphite/bismaleimide was investigated by dynamic and isothermal differential scanning calorimeter experiments and described by analytical expressions. Laminates were produced from the prepreg according to different cure cycles. The influence of these cure cycles on the mechanical properties at different temperatures was investigated. At increasing test temperatures, the strain at interphase failure passes through a minimum before increasing again on approaching glass transition temperature. Experiments up to temperatures of 250 to 300 C showed that matrix properties and matrix and interface dominated properties change considerably. From the Weibull distributions for the flexural fracture strain and using a model for transverse cracking, it can be concluded that the decrease in fracture strain is caused by a reduction in interface strength. A post cure improves the tranverse properties in terms of fracture strain and strength and the improvement sustains in the range of temperatures investigated. ESA

N93-11229 Michigan State Univ., East Lansing.
AN INTERLAYER SHEAR SLIP THEORY FOR COMPOSITE LAMINATES WITH NONRIGID BONDING Ph.D. Thesis
Xianqiang Lu 1991 120 p
Avail: Univ. Microfilms Order No. DA9216328

An interlayer shear slip theory (ISST) is presented to study composite laminates with different kinds of interfacial bonding conditions. It is a displacement-based multiple-layer technique which satisfies the continuity requirements for the interlaminar shear stresses across the composite interfaces. By allowing the discontinuity of the displacements on the composite interfaces, the mechanical behavior of nonrigid interface is simulated by a linear shear slip law. The governing equations and associated boundary conditions for composite laminates with nonrigid bonding are derived from the principle of virtual displacement. In assessing the ISST, some numerical results from ISST are compared with those from elasticity analysis and embedded-layer technique. Excellent agreements are concluded. In addition, the comparison between the results from experiments and ISST analysis is performed. A reasonable agreement is achieved. A comprehensive application of ISST in the analysis of composite laminates with delaminations of different kinds of size, location and position is performed. It is concluded that the transverse shear effect should be considered in the delamination analysis. In addition, with the use of finite element technique, some cases of static and vibration analysis are examined. The effect of delamination on the transverse deflection, natural frequencies, and vibration mode shapes is investigated. The results from these studies further verify the feasibility of using ISST in studying the composite laminates with nonrigid bonding. Dissert. Abstr.

N93-11247 Akron Univ., OH.
FRACTURE MECHANICS OF MODEL FIBER COMPOSITES Ph.D. Thesis
Chi Wang 1992 140 p
Avail: Univ. Microfilms Order No. DA9220656

Fracture of matrix material caused by a tensile break in a fiber was investigated. A model was constructed, consisting of two inextensible fibers touching end-to-end and embedded in an elastic block. Energy release rates were calculated by finite element analysis (FEA) for a circular crack growing outwards from the point where the fiber ends separated as they were pulled apart. The results are compared with experimental observations on steel rod/silicone resin systems. It is found that, when a fiber breaks, a circular crack grows outwards in a stable way under increasing load. After the crack reaches a certain size, approximately half way to the edge of the resin block, the strain energy release reaches a minimum value and then increases, and the crack accelerates. The force required to propagate a crack is predicted successfully by linear elastic fracture mechanics at all stages of crack growth. In particular, good agreement was obtained with the maximum force that the system could support--the breaking load. When the sample was surrounded by a rigid tube, representing neighboring fibers surrounding the broken one, growth of a crack required an increasing load at all stages. The sample finally fractured when the broken fiber was pulled out with resin still attached to it. Many inclined cracks initiated at the rod/matrix interface were observed. This is attributed to shear deformation in the matrix. Fracture of fiber composites under shear deformation was simulated by applying a tension to the rod in a bush mounting. A bush mounting consists of a cylindrical rubber tube bonded on its inner and outer curved surfaces to a rigid rod and cylindrical tube, respectively. FEA results reveal that tri-axial tension occurs in the matrix at the rod/matrix interface corner although the bonded rubber matrix is mainly in shear deformation. Therefore, cavitation is expected to take place at that corner. After a crack is initiated at this interface corner, a constant force is predicted to propagate the interfacial crack. Dissert. Abstr.

N93-11262 Purdue Univ., West Lafayette, IN.
METHODS OF ANALYSIS FOR THICK-SECTION COMPOSITE STRUCTURES Ph.D. Thesis
Jiayi Luo 1991 141 p
Avail: Univ. Microfilms Order No. DA9215605

Based on classical anisotropic theory, analytical solutions for composite tubes and curved beams are developed by using multilayer conditions and effective properties, respectively. For the thermal stress analysis of tubes, several global-local techniques are developed and tested numerically. The Refined Global-Local method gives the best results with saving much computing costs of multilayer analyses. For curved beams, the multilayer solution considers effects of rigid-body-motion terms and substantially

improves stress evaluation given by previous solutions. The global-local solution using effective moduli gives global agreements with the modified multilayer solution for thick curved beams of multiple repeating sublaminates. In order to estimate the applicability of effective moduli in composite dynamics, a series-expansion solution for plane harmonic wave propagation in the layer direction is developed and used for the dispersion analysis of laminated plates in multilayer and effective formulations, respectively. Also, for cases normal to the layer direction, the results from using effective moduli and using the multilayer solution are calculated and compared. The limitation of effective moduli for wave analysis of composite laminates is discussed.
Dissert. Abstr.

N93-11281# Colorado State Univ., Fort Collins. Dept. of Chemistry.

OPTICAL PROPERTIES OF COMPOSITE MEMBRANES CONTAINING ARRAYS OF NANOSCOPIC GOLD CYLINDERS
Interim Report
Colby A. Foss, Jr., Gabor L. Hornyak, Jon A. Stockert, and Charles R. Martin 20 Jul. 1992 15 p
(Contract N00014-82-K-0612)
(AD-A253659; TR-74-ONR) Avail: CASI HC A02/MF A01

Nano-chemistry, physics and materials are important and evolving fields in modern science. One of the most interesting aspects of nanomaterials concerns the optical properties of nanoscopic metal particles. While bulk metals are optically opaque, effective medium theory (EMT) predicts that collections of small metal particles can be transparent, provided that the wavelength of light employed is much greater than a characteristic dimension of the particle. Hence, EMT can be used as a guide to prepare metal-containing composites that are both electronically conductive and optically transparent. We have recently shown that composites of this type can be prepared by electrochemical deposition of metals within the pores of a microporous template membrane. In this report we show for the first time that composite membranes prepared via this template route can be optically transparent throughout the near infrared (NIR) and into the visible region of the electromagnetic spectrum. Furthermore, we show that by changing the shapes of the particles prepared, the color of the composite membrane can be reproducibly and predictably varied. Finally we show that these results are in general agreement with the predictions of the appropriate formulation of EMT. GRA

N93-11399*# National Aeronautics and Space Administration. Lewis Research Center, Cleveland, OH.

THERMOMECHANICAL FATIGUE BEHAVIOR OF SiC/Ti-24Al-11Nb IN AIR AND ARGON ENVIRONMENTS
Paul A. Bartolotta and Michael J. Verrilli Aug. 1992 16 p
Presented at the 11th Symposium on Composite Materials: Testing and Design, Pittsburgh, PA, 4-5 May 1992; sponsored by the American Society for Testing and Materials
(RTOP 510-01-50)
(NASA-TM-105723; E-7122; NAS 1.15:105723) Avail: CASI HC A03/MF A01

A series of tension-tension, load-controlled thermomechanical fatigue (TMF) tests were conducted on a titanium aluminide composite in both laboratory air and a flowing argon environment. Results from these tests show that the environment plays an increasingly important role as applied stress levels are decreased. Differences in damage mechanisms between the two environments were observed which corresponds to observed variations in TMF lives. Author

N93-11409 National Physical Lab., Teddington (England). Div. of Materials Metrology.

ANALYTICAL METHOD OF CALCULATING THE THERMOELASTIC CONSTANTS OF A MULTI-PHASE UNIDIRECTIONAL COMPOSITE
L. N. McCartney Mar. 1992 56 p Original contains color illustrations
(Grant IED-RA-6/25/01)
(NPL-DMM(A)-57; ETN-92-92371) Copyright Avail: National Physical Lab., Teddington, Middlesex, TW11 0LW, England

A multiple concentric cylinder model of a unidirectional composite was analyzed under three different loading cases, namely, biaxial tension, longitudinal shear, and tranverse shear. The model assures that the concentric cylinders are made of different transverse isotropic materials, that they are perfectly bonded together, and that the cylinder assembly is embedded in a surrounding transverse isotropic medium which has the same thermoelastic constants as the composite. The solution technique develops sets of recurrence relations avoiding the need to solve sets of linear algebraic equations. The model was used to predict values for the seven independent thermoelastic constants of the composite, and to calculate the displacement and stress distributions throughout the cylinder assembly. Predictions were made showing the dependence of the thermoelastic constants on the volume fraction for the case of a two cylinder model. Example stress and displacement distributions in both two and four cylinder models are presented to demonstrate that the appropriate continuity conditions are satisfied. A technique is described, using multiple cylinders, which enables the transverse shear modulus to be calculated, avoiding the stress concentrations which are encountered in the surrounding effective composite medium if only two cylinders are used to represent the composite. ESA

N93-11422# Naval Research Lab., Washington, DC. Condensed Matter Div.

MATERIALS SCIENCE AND ENGINEERING AT THE NAVAL RESEARCH LABORATORY: RESEARCH PROGRAMS AND 1990 PUBLICATIONS
Robert A. Gray, ed. and Maureen Long, ed. Nov. 1991 126 p
(PB92-199488; NRL-Pub-183-6000) Avail: CASI HC A07/MF A02

Programs in materials science and engineering that are conducted at the Naval Research Laboratory are described. It also lists the publications resulting from the research that appeared in the open literature during 1990. The research was generally conducted within the Materials Science and Component Technology Directorate. However, research at NRL has a multidisciplinary approach; strong collaborative efforts are conducted with other organizational components of the Laboratory. For the publications noted here, joint research was conducted with the Condensed Matter and Radiation Sciences Division.
GRA

N93-11470# Federal Coordinating Council for Science, Engineering and Technology, Washington, DC. Committee on Industry and Technology.

ADVANCED MATERIALS AND PROCESSING: THE FEDERAL PROGRAM IN MATERIALS SCIENCE AND TECHNOLOGY. A REPORT BY THE FCCSET COMMITTEE ON INDUSTRY AND TECHNOLOGY TO SUPPLEMENT THE PRESIDENT'S FISCAL YEAR 1993 BUDGET
1992 69 p
(PB92-199108) Avail: CASI HC A04/MF A01

The goal of the advanced materials and processing program (AMPP) is to improve the manufacture and performance of materials to enhance the nation's quality of life, security, industrial productivity, and economic growth. The AMPP will focus special attention on the interfaces between universities, government laboratories and industry and on the process of technology transfer from basic research to application. Continuing input from all parties will be sought and collaboration will be fostered through mechanisms such as consortia and cooperative research and development agreements. The President's Fiscal Year (FY) 1993 budget includes $1821.4 million for materials Research & Development (R&D) representing an increase of 10 percent over the FY 1992 base. Special emphasis is placed on synthesis and processing, those areas critical to the development of new materials, and to the improvement of reliability, cost, and quality of all materials. The budget also increases emphasis on those programs which are aimed at bridging the gap between the innovation of new materials and their application. GRA

N93-11543*# National Aeronautics and Space Administration. Lewis Research Center, Cleveland, OH.
SILICON CARBIDE FIBER REINFORCED STRONTIUM ALUMINOSILICATE GLASS-CERAMIC MATRIX COMPOSITE Patent Application
Narottam Bansal, inventor (to NASA) 4 Jun. 1992 7 p
(NASA-Case-LEW-15263-1; NAS 1.71:LEW-15263-1; US-Patent-Appl-SN-892054) Avail: CASI HC A02/MF A01

A SrO-Al2O3 - 2SrO2 (SAS) glass ceramic matrix is reinforced with CVD SiC continuous fibers. This material is prepared by casting a slurry of SAS glass powder into tapes. Mats of continuous CVD-SiC fibers are alternately stacked with the matrix tapes. This tape-mat stack is warm-pressed to produce a 'green' composite. Organic constituents are burned out of the 'green' composite, and the remaining interim material is hot pressed. NASA

N93-11586# Aerospatiale Aquitaine, Saint-Medard en Jalles (France).
TOUGHNESS OF SI3N4-SiC WHISKER COMPOSITES
E. Champion (Limoges Univ., France), P. Goursat (Limoges Univ., France), J. L. Besson (Limoges Univ., France), V. Madigou (Pau Univ., France), M. Monthioux (Pau Univ., France), and P. Lespade 1992 9 p
(Rept-921-430-101; ETN-92-92349) Avail: CASI HC A02/MF A01

The effects of a second phase in a silicon nitride matrix ceramic material is investigated. The presence of silicon carbide whiskers improves the mechanical properties of the composite and offers potentialities for high temperature applications. Different techniques of sintering and shaping were applied. The microstructure, the modulus of rupture, and the toughness of the composite were investigated. The microstructural study of the SiC-Si3N4 composites shows that neither the aspect ratio of the whiskers nor the processing route have any influence on the matrix grain size distribution. The composites exhibit a higher toughness than the monolithic ceramic. Increase in both crack initiation and crack propagation resistances is observed. The R-curve effect suggests that to be efficient the whiskers diamater must exceed a critical size. ESA

N93-11588# Aerospatiale Aquitaine, Saint-Medard en Jalles (France). Lab. Materiaux et Structure Composites.
SILICON CARBIDE MATRIX COMPOSITES
P. Pernot, P. Lespade, and M. Parlier (Office National d'Etudes et de Recherches Aerospatiales, Paris, France) 1992 4 p
(Rept-921-430-103; ETN-92-92351) Avail: CASI HC A01/MF A01

The latest development for silicon carbide/silicon carbide and carbon/silicon carbide composites are presented. These composites are obtained by processes based on infiltration, and pyrolysis of organometallic materials. Ceramic matrix composites are promising materials for thermostructural applications in the field of aerospace industry where there is a need for low density, damage tolerant materials, able to operate at high temperature under high stresses. The latest developments concern: a polyvinylsilane precursor, a two step infiltration process. This approach allows the achievement of a composite with residual porosity ranging between 10 and 20 depending on fiber architecture. The microstructures of the green bodies and of the pyrolysed matrices were investigated. ESA

N93-11589# Aerospatiale Aquitaine, Saint-Medard en Jalles (France). Lab. Materiaux et Structures Composites.
HIGH TEMPERATURE OXIDATION PROTECTION OF CARBON/CARBON COMPOSITES
G. Rousseau, F. Saugnac, and F. Bourserau 1992 8 p
(Rept-921-430-105; ETN-92-92353) Avail: CASI HC A02/MF A01

A new concept for providing oxidation resistance to high temperature is presented. Carbon/carbon composites are very good candidates for all the thermostructural needs in the future. Nevertheless, their weak resistance against oxygen implies an oxidation protection coating. Up to 1600 C protection based on silicon carbide and silica glass presents very good results. Above this temperature the SiO/SiC reaction occurs and protection decreases. Long term oxidation protection of carbon/carbon composites above 1600 C is a challenging problem. On the basis of the SiC/SiO2 behavior, a new concept which uses aluminum nitride and alumina successive coatings over SiC is developed. ESA

N93-11590# Aerospatiale Aquitaine, Saint-Medard en Jalles (France). Strategic and Space Div.
AEROSPATIALE PROCESSES FOR THREE DIMENSIONAL PREFORMS
Georges Cahuzac 1992 8 p Presented at the ECCM-5, Bordeaux, France, 7-10 Apr. 1992
(Rept-921-430-147; ETN-92-92354) Avail: CASI HC A02/MF A01

Aerospatiale patented processes to manufacture composite parts free of delamination risk composite parts are summarized. To achieve free delamination risk parts, very particular processes were developed. They are able to weave a great number of shapes: blocks, plates, profiles, thick or thin cylinders, cones and complex shapes. Weaving machines are fully automated. Their applications are presently for carbon-carbon and other thermostructural materials, but they are also suitable for any kind of thick resin impregnated composite parts. One of the processes consists of a network of rods used to hold yarns then replaced. Many types of machines are used depending on parts. Another process uses computer aided design and computer aided manufacturing methods. The process begins by machining a foamy mandrel, inserting pins at suitable positions, deposing dry yarns, then stitching them from outside. A manufacture method for thick fabric with different layers of yarns interlocked is presented. ESA

N93-11611*# Lockheed Engineering and Sciences Co., Hampton, VA.
TENSION AND COMPRESSION FATIGUE RESPONSE OF UNNOTCHED 3D BRAIDED COMPOSITES
M. A. Portanova Aug. 1992 20 p
(Contract NAS1-19000; RTOP 505-63-50-04)
(NASA-CR-189678; NAS 1.26:189678) Avail: CASI HC A03/MF A01

The unnotched compression and tension fatigue response of a 3-D braided composite was measured. Both gross compressive stress and tensile stress were plotted against cycles to failure to evaluate the fatigue life of these materials. Damage initiation and growth was monitored visually and by tracking compliance change during cycle loading. The intent was to establish by what means the strength of a 3-D architecture will start to degrade, at what point will it degrade beyond an acceptable level, and how this material will typically fail. Author

N93-11623*# National Aeronautics and Space Administration. Langley Research Center, Hampton, VA.
STUDY OF COMPRESSION-LOADED AND IMPACT-DAMAGED STRUCTURALLY EFFICIENT GRAPHITE-THERMOPLASTIC TRAPEZOIDAL-CORRUGATION SANDWICH AND SEMISANDWICH PANELS
Dawn C. Jegley Nov. 1992 31 p
(RTOP 505-63-50-08)
(NASA-TP-3264; L-17129; NAS 1.60:3264) Avail: CASI HC A03/MF A01

The structural efficiency of compression-loaded trapezoidal-corrugation sandwich and semisandwich composite panels is studied to determine their weight savings potential. Sandwich panels with two identical face sheets and a trapezoidal corrugated core between them and semisandwich panels with a corrugation attached to a single skin are considered. An optimization code is used to find the minimum weight designs for critical compressive load levels ranging from 3000 to 24,000 lb/in. Graphite-thermoplastic panels based on the optimal minimum weight designs were fabricated and tested. A finite element analysis of several test specimens was also conducted. The results of the optimization study, the finite element analysis, and the experiments are presented. The results of testing impact damage panels are also discussed. Author

N93-11658# Pacific Northwest Lab., Richland, WA.
GLOBAL-LOCAL FINITE ELEMENT ANALYSIS OF COMPOSITE STRUCTURES
J. E. Deibler Jun. 1992 6 p Presented at the Swanson Analysis Systems Technology Conference, Pittsburg, PA, 8-11 Jun. 1992
(Contract DE-AC06-76RL-01830)
(DE92-019138; PNL-SA-21006; CONF-9206253-1) Avail: CASI HC A02/MF A01

The development of layered finite elements has facilitated analysis of laminated composite structures. However, the analysis of a structure containing both isotropic and composite materials remains a difficult problem. A methodology has been developed to conduct a 'global-local' finite element analysis. A 'global' analysis of the entire structure is conducted at the appropriate loads with the composite portions replaced with an orthotropic material of equivalent materials properties. A 'local' layered composite analysis is then conducted on the region of interest. The displacement results from the 'global' analysis are used as loads to the 'local' analysis. The laminate stresses and strains can then be examined and failure criteria evaluated. DOE

N93-11708# Societe Nationale d'Etude et de Construction de Moteurs d'Aviation, Paris (France).
STUDY OF THE BEHAVIOR OF TITANIUM AND CERAMIC FIBER MATRIX COMPOSITE ALLOY Final Report [ETUDE DU COMPORTEMENT D'ALLIAGES COMPOSITES A MATRICES DE TITANE ET FIBRES CERAMIQUES. RAPPORT FINAL]
G. Lamanthe 20 Oct. 1991 45 p In FRENCH
(Contract DRET/DS/SR-90150)
(ETN-92-92087) Avail: CASI HC A03/MF A01

An investigation on the fiber/matrix interface of the Ti/SiC model metal matrix composite in terms of shear resistances, using a push-out indentation experiment, in consideration of heat treatment during manufacturing, is presented. A bibliographic study on the nature of the fiber/matrix interface and the push-out method is given, and experimental work and results analyses are presented. Japanese research experiences are described. ESA

N93-11739# Naval Surface Warfare Center, Bethesda, MD. Carderock Div.
EFFECT OF ASSEMBLY ANOMALIES ON THE STRAIN RESPONSE OF COMPOSITES IN THE SPHERE JOINT REGION OF THE DARPA MAN-RATED DEMONSTRATION ARTICLE
E. T. Camponeschi, Jr., R. E. Bohlmann, J. Hall, and T. T. Carr Apr. 1992 72 p
(AD-A254204; CARDEROCKDIV-SME-92/22) Avail: CASI HC A04/MF A01

The compressive response of thick, quasi-isotropic, AS4/3501-6 laminates with geometric anomalies were investigated theoretically and experimentally. The specimens considered were rectilinear with nominal dimensions of 10 inches long, by 4 inches wide, by 0.78 inches thick. The anomalies were designed to simulate expected fit-up clearance conditions resulting from normal manufacturing tolerances in the sphere joint regions of the DARPA Man Rated Demonstration Article. Tests were conducted both with unfilled fit-up gaps and with fit-up gaps filled with a polymer shimming material (Hysol EA9394). Strains were monitored in the specimen gage sections and in regions of high strain concentration resulting from the manufacturing anomalies. Measured strains correlated well with predicted strains from an ABAQUS Finite Element Analysis. For all test cases the specimens were able to withstand strains due to the anomalies when gage section strain reached 7000 microstrain. One specimen with no anomalies was tested to failure in uniaxial compression and failed in the gage section at 89,000 psi and 13,500 microstrain, which is equivalent to thin-section composite failure strains. GRA

N93-11795# Colorado School of Mines, Golden. Center for Welding and Joining Research.
INFILTRATION KINETICS AND INTERFACIAL BOND STRENGTH OF METAL MATRIX COMPOSITES Final Report
Glen R. Edwards and David L. Olson Jul. 1992 86 p
(Contracts MT-CWR-092-028; N00014-88-K-0500)
(AD-A254002) Avail: CASI HC A05/MF A01

The research accomplishments for this three-year metal matrix composite research program centered upon three areas: infiltration kinetics, wettability studies and predictions of interfacial properties. A pre-conditioning reaction model was hypothesized to explain the incubation period observed to precede the liquid metal infiltration of SiC particulate, and a rate equation for pre-conditioning was experimentally established for the infiltration of SiC particulate by liquid aluminum. Experimental wettability studies were completed for aluminum-silicon, aluminum-magnesium, and aluminum-lithium alloys in contact with SiC by utilizing a capillary rise apparatus. The oxide layers on the ceramic substrate and on the molten metal surface were observed to strongly influence wetting behavior. Differential optical reflectance was used to measure the optical transitions in aluminum and its alloys. Interfacial bond energies were estimated using a work of decohesion model. Punch shear tests then provided relative estimates of bond strengths for several aluminum alloys in contact with silicon carbide. Concepts from surface science and thermodynamics were coupled to theoretically predict wettability. Wetting was treated as a surface phenomenon, in which a surface reaction monolayer was sufficient to cause wetting. Aluminum matrix composite processing using the liquid metal route is complicated by the oxide barrier formed on the liquid metal. A transport model was used to explain the observed interfacial reaction behavior. GRA

N93-11835# Dayton Univ. Research Inst., OH.
PENETRATION MECHANICS OF COMPOSITES Report, Jan. 1990 - Mar. 1991
N. S. Brar and B. Azzi Apr. 1992 70 p
(Contract DAAL03-89-K-0031)
(AD-A249230; UDR-TR-92-45; ARO-24102.3-MS) Avail: CASI HC A04/MF A01

This report contains 3 sections: (1) The tensile strength of roving bundles of S-2 Glass fibers (quasistatic strength of 535 plus or minus 16 ksi) is measured using a modified split Hopkinson bar with two specimen designs at strain rates 10(exp 3)/S. The mean tensile strength measured from one sample design is approximately 700 plus or minus 150 ksi at a strain rate 600 s(exp -1), approximately 500 plus or minus 120 ksi at a strain rate of approximately 1200 s(exp -1) from the other. There is a very good agreement on the monofilament strength derived from the statistical analysis of the stress-strain data obtained from the two sample designs. (2) A reverse impact technique to measure the force on projectile noses penetrating fiber reinforced plastic target panels is presented. Fifty mm diameter GRP and KRP flyers are impacted against different nose-shaped steel bar targets instrumented with manganin gauges. The penetration into the 12.7 mm thick GRP is steady for the flat nose bar, but transient for the conical and hemispherical nose shapes. The penetration into the 37.4 mm thick KRP is steady for the conical and hemispherical nose shapes. (3) Five modes of failure (shock, double shear, single shear, cavity expansion, tensile stretching) of S-2 Glass composites during penetration with different nose-shaped projectiles are identified. The shock stage is especially dominant in flat nose-shape projectiles and a simple model is presented. GRA

N93-11905# Royal Aerospace Establishment, Farnborough (England). Aerospace Div.
SCANNING ELECTRON MICROSCOPY OF THE EFFECTS OF MOISTURE AND ELEVATED TEMPERATURE ON THE FIBRE/MATRIX BOND IN CFRP
G. D. Howard 9 Aug. 1991 20 p
(RAE-TM-Mat-Str-1183; BR305095-16; ETN-92-92303) Copyright Avail: CASI HC A03/MF A01

The mechanical behavior of Carbon Fiber Reinforced Plastics (CFRP) is studied. The fiber/matrix is investigated, using scanning electron microscopy, to determine signs of degradation due to prolonged exposure to high humidity and thermal spiking. There is evidence that degradation of the fiber/matrix interface occurs, not only as a result of the thermal spiking of environmentally conditioned carbon fiber/epoxy resin systems but also as a result of their prolonged exposure to high humidity environments. The results of the study show that spiking of a carbon fiber reinforced epoxy resins causes degradation of the fiber/matrix bond, which could account for the extra 70 percent by weight of moisture absorbed with no corresponding drop in modulus. It was also observed that if the relative humidity of the conditioning is high, the fiber/matrix interface is subjected to attack by absorbed moisture alone. ESA

N93-11998 Michigan State Univ., East Lansing.
THE USE OF HIGH-FREQUENCY DYNAMIC INFORMATION FOR THE EVALUATION OF DAMAGE IN FIBER REINFORCED COMPOSITE MATERIALS Ph.D. Thesis
James Phillip Nokes 1992 153 p
Avail: Univ. Microfilms Order No. DA9223231

The details of a dynamic nondestructive inspection (NDI) technique with improved sensitivity to localized damage in fiber reinforced composite materials is presented. The extent of the internal damage was determined using measured changes in the dynamic properties of the system (damping, dynamic stiffness, and mode shape). A modal analysis system was developed incorporating both a Laser Doppler Vibrometer (LDV) and an Electronic Speckle Pattern Interferometer (ESPI) to obtain the response information at higher frequencies. The LDV system was used to measure the dynamic characteristics of composite beams over a frequency range extending to approximately 12Khz. ESPI provided a technique for acquiring whole field displacement maps of the various mode shapes. The potential of this system to detect delaminations in fiber reinforced epoxy beams was investigated. As part of the investigation the relationships between the dynamic characteristics and internal damage was examined. A modified data analysis approach was developed to analyze the extended dynamic information. The approach utilized the three dynamic parameters to form a set of linear functions that approximated the relationship between the loss factors and the resonant frequencies. The slopes of these curves were shown to be sensitive to localized damage in composite materials. Experimental verification of the system was done using delaminated cross-ply composites in a cantilever beam configuration. The results of these experiments showed that the best sensitivity to delamination damage is found from changes in the dynamic characteristics of torsional modes of vibration. Dissert. Abstr.

N93-12015*# National Aeronautics and Space Administration. Lewis Research Center, Cleveland, OH.
ICAN/DAMP-INTEGRATED COMPOSITE ANALYZER WITH DAMPING ANALYSIS CAPABILITIES: USER'S MANUAL
Dimitrious A. Saravanos (Ohio Aerospace Inst., Brook Park.) and Jose G. Sanfeliz Nov. 1992 39 p
(RTOP 505-63-53)
(NASA-TP-3292; E-6898; NAS 1.60:3292) Avail: CASI HC A03/MF A01

This manual describes the use of the computer code ICAN/DAMP (Integrated Composite Analyzer with Damping Analysis Capabilities) for the prediction of damping in polymer-matrix composites. The code is written in FORTRAN 77 and is a version of the ICAN (Integrated Composite ANalyzer) computer program. The code incorporates a new module for synthesizing the material damping from micromechanics to laminate level. Explicit micromechanics equations based on hysteretic damping are programmed relating the on-axis damping capacities to the fiber and matrix properties and fiber volume ratio. The damping capacities of unidirectional composites subjected to off-axis loading are synthesized from on-axis damping values. The hygrothermal effect on the damping performance of unidirectional composites caused by temperature and moisture variation is modeled along with the damping contributions from interfacial friction between broken fibers and matrix. The temperature rise is continuously vibrating composite plies and composite laminates is also estimated. The ICAN/DAMP user's manual provides descriptions of the damping analysis module's functions, structure, input requirements, output interpretation, and execution requirements. It only addresses the changes required to conduct the damping analysis and is used in conjunction with the 'Second Generation Integrated Composite Analyzer (ICAN) Computer Code' user's manual (NASA TP-3290). Author

N93-12054# Northrop Corp., Hawthorne, CA. Aircraft Div.
COMPOSITE FAILURE ANALYSIS HANDBOOK. VOLUME 2: TECHNICAL HANDBOOK. PART 3: CASE HISTORIES Final Report, Jan. 1987 - Oct. 1990
R. J. Kar Feb. 1992 129 p
(Contract F33616-87-C-5212)
(AD-A249131; WL-TR-91-4032-Vol-2-Pt-3; DOT/FAA/CT-91-23-Vol-2-Pt-3) Avail: CASI HC A07/MF A02

The objective of this program was to create a comprehensive handbook for use in conducting failure analysis investigations on failed composite structure. This program builds upon previous efforts as documented in the Compendium of Post-Failure Analysis Techniques for Composite Materials, AFWAL-TR-86-4137. The purpose of creating this handbook was to document the techniques, the fractographic and material property data and case history studies currently being utilized in the analysis of failed composite structure. The major tasks on this program included: (1) procedural guidelines for field investigation techniques; (2) an expanded fractographic data base for carbon/epoxy materials tested under known conditions; (3) a fractographic data base for resin based composite materials other than carbon/epoxy; (4) fractographic documentation of composite material and processing defects; (5) documentation of fracture characteristics in adhesive and mechanical joint failures; (6) compilation of material property data for composite materials; and (7) documentation of case histories recently conducted on failed composite structures. GRA

N93-12076*# National Aeronautics and Space Administration. Lewis Research Center, Cleveland, OH.
THE EFFECT OF CONTACT STRESSES IN FOUR-POINT BEND TESTING OF GRAPHITE/EPOXY AND GRAPHITE/PMR-15 COMPOSITE BEAMS
Wieslaw K. Binienda (Akron Univ., OH.), Gary D. Roberts, and Demetrios S. Papadopoulos (Case Western Reserve Univ., Cleveland, OH.) Oct. 1992 24 p Previously announced in IAA as A92-33589
(RTOP 505-63-5A)
(NASA-TM-105891; E-7358; NAS 1.15:105891) Avail: CASI HC A03/MF A01

The results of in-plane four-point bend experiments on unidirectionally reinforced composite beams are presented for graphite/epoxy (T300/934) and graphite/polyimide (G30-500/PMR-15) composites. The maximum load and the location of cracks formed during failure were measured for testpieces with fibers oriented at various angles to the beam axis. Since most of the beams failed near one or more of the load points, the strength of the beams was evaluated in terms of a proposed model, for the local stress distribution. In this model, an exact solution to the problem of a localized contact force acting on a unidirectionally reinforced half plane is used to describe the local stress field. The stress singularity at the load points is treated in a manner similar to the stress singularity at a crack tip in fracture mechanisms problems. Using this approach, the effect of fiber angle and elastic material properties on the strength of the beam is described in terms of a load intensity factor. For fiber angles less than 45 deg from the beam axis, a single crack is initiated near one of the load points at a critical value of the load intensity factor. The critical load intensity factor decreases with the increasing fiber angle. For larger fiber angles, multiple cracks occur at locations both near and away from the load points, and the load intensity factor at failure increases sharply with increasing fiber angle. Author

N93-12078*# National Aeronautics and Space Administration. Lewis Research Center, Cleveland, OH.
THERMOSTRUCTURAL TAILORING OF FIBER COMPOSITE STRUCTURES
Thomas H. Acquaviva Oct. 1992 116 p
(RTOP 505-90-52)
(NASA-TM-105882; E-7349; NAS 1.15:105882) Avail: CASI HC A06/MF A02

A significant area of interest in design of complex structures involves the study of multidisciplined problems. The coordination of several different intricate areas of study to obtain a particular design of a structure is a new and pressing area of research. In the past, each discipline would perform its task consecutively using the appropriate inputs from the other disciplines. This process usually required several time-consuming iterations to obtain a satisfactory design. The alternative pursued here is combining various participating disciplines and specified design requirements into a formal structural computer code. The main focus of this research is to develop a multidiscipline structural tailoring method for select composite structures and to demonstrate its application to specific areas. The development of an integrated computer program involves the coupling of three independent computer programs using an excutive module. This module will be the foundation for integrating a structural optimizer, a composites analyzer and a thermal analyzer. With the completion of the executive module, the first step was taken toward the evolution of multidiscipline software in the field of composite mechanics. Through the use of an array of cases involving a variety of objective functions/constraints and thermal-mechanical load conditions, it became evident that simple composite structures can be designed to a combined loads environment. Author

N93-12181# Dayton Univ., OH. Research Inst.
MECHANICAL PROPERTIES FOR ADVANCED ENGINE MATERIALS Final Report, 27 Aug. 1987 - 17 May 1991
N. E. Ashbaugh, M. Khobaib, G. A. Hartman, D. Coker, and J. L. Kroupa Apr. 1992 167 p
(Contract F33615-87-C-5243)
(AD-A252632; UDR-TR-91-149; WL-TR-91-4149) Avail: CASI HC A08/MF A02

The experimental evaluation of advanced mechanical properties that characteize the behavior of emerging materials for aerospace structures under a broad range of conditions representative of those encountered in service was emphasized in this investigation. The information guided the development of life prediction methodologies which are based on the concept of damage tolerance as a design philosophy. The research effort was subdivided into four interrelated tasks: (1) material characterization tests; (2) experimental procedure and test developments; (3) analytical and modeling developments; and (4) test support activities and data archival. Material characterization tests for fatigue, creep, and crack growth responses were conducted on a titanium matrix composite reinforced with continuous SiC fibers and fabricated from a foil-fiber-foil layup. The molybdenum wire used in the weaving of the fiber mats was a major factor in the development of damage under fatigue and creep test conditions. A model ceramic matrix composite composed of an aluminosilicate glass matrix and SiC fiber tows provided some interesting fatigue and fracture toughness responses. Behavior of monolithic materials were evaluated under creep, creep crack growth, fatigue crack growth, and oxidation conditions. Significant developments in test procedures and systems have been accomplished with emphasis on conducting thermomechanical fatigue (TMF) tests. GRA

N93-12235# Air Force Inst. of Tech., Wright-Patterson AFB, OH. Foreign Technology Div.
CARBON/CARBON COMPOSITION ABLATION EFFECTS ON IONIZED BOUNDARY LAYERS
Wei Shuru, Wang Ce, and Wang Fuhan 13 Jan. 1992 10 p
Transl. into ENGLISH from Kongqidonglixue Xuebao (China), v. 7, no. 4, 1989 p 413-416
(AD-A254465; FTD-ID(RS)T-0785-91; FASTC-ID(RS)T-0785-91) Avail: CASI HC A02/MF A01

A calculation method for carbon/carbon composition thermochemical ablation effects on ionized laminar and turbulent boundary layers is given. In the boundary layers, 20 gas species are considered and all chemical reactions which occurred in them are assumed to be at equilibrium. The new solving method for boundary layer equations and simple disposal for transport properties are applied. The calculation examples indicate that ablation has great effects on ionization properties of the boundary layers and that ionizations of the alkaline metals are not always dominant. GRA

N93-12292# National Materials Advisory Board, Washington, DC.
HIGH-PERFORMANCE SYNTHETIC FIBERS FOR COMPOSITES
Apr. 1992 141 p
(Contracts MDA903-89-K-0078; MDA972-92-C-0028)
(AD-A252645; NMAB-458) Avail: CASI HC A07/MF A02

This report describes the properties of the principal classes of high-performance synthetic fibers, as well as several current and potential methods of synthesis and processing to attain desirable properties. Various promising classes of materials and methods of fiber synthesis are suggested for farther investigation. Successful fiber reinforcement of a matrix is heavily dependent on the interfact between the two components. The report emphasizes our relatively poor fundamental understanding of fiber-matrix reactions and this 'interphase' region. Research directed at improving our understanding of the properties and behavior of the boundary region is identified as a prime need if advances are to be made in fiber and composite performance. The report emphasizes the complex interdisciplinary nature of fiber science and makes strong policy recommendations for long-range continuity of fiber research and for increased support of education in fiber science. Because of the highly international scope of the commercial fiber and composites industries and the critical importance of fibers for military and space applications, the report considers the consequences of government policy affecting these industries. Attention is called to the need for improving procedures leading to governmental decisions affecting the fiber industry. The need for a policy to provide support for development and production of small quantities of specialty fibers for strategic military applications is also emphasized. GRA

N93-12296# Stanford Univ., CA.
ADVANCED MODELING AND OPTIMIZATION OF PIEZOELECTRIC COMPOSITES Final Technical Report, 1 Jun. 1990 - 31 May 1992
John A. Hossack and Bert A. Auld Jul. 1992 119 p
(Contract N00014-90-J-1924)
(AD-A253800) Avail: CASI HC A06/MF A02

The aim of this project was to obtain a more complete understanding of the physical phenomena occurring in piezoelectric transducers, with the aim of obtaining optimal designs and improved manufacturability. Of key importance in design are conversion efficiency, bandwidth, and control of spurious modes. The transducer structures considered are 1:3, 0:3, 2:2, and 1:3:1. Contributions to the advancement of 1:3 modeling and fabrication are: (1) finite element modeling of composite lattices with complex unit cells, (2) transmission line and reciprocity modeling of distributed period composites, (3) fabrication of test transducers for verification of the modeling principles. New modeling theory for 0:3 composites aims at replacing the empirical cubes model with a model consisting of nearly close-packed spherical particles. This approach estimates more closely the performance of 0:3 composites and points the way for further studies. The 2:2 structures considered are, in fact, multilayered electroded transducers with a single piezoelectric material. But multiple piezoelectrics and alternating piezo and nonpiezo layers may also be considered. A procedure has been developed, and confirmed experimentally, for tailoring the transducer time-domain response by applying multiple excitations. Finally, 1:3:1 transducers with a periodic addition of empty voids have been developed. This version produces a more uniform thickness mode displacement and improved coupling, predicted from finite element modeling and confirmed experimentally. GRA

N93-12302*# National Aeronautics and Space Administration. Lewis Research Center, Cleveland, OH.
FRACTURE TOUGHNESS TESTING OF POLYMER MATRIX COMPOSITES
Joseph E. Grady Nov. 1992 39 p
(RTOP 505-63-1B)
(NASA-TP-3199; E-6455; NAS 1.60:3199) Avail: CASI HC A03/MF A01

A review of the interlaminar fracture indicates that a standard specimen geometry is needed to obtain consistent fracture toughness measurements in polymer matrix composites. In general, the variability of measured toughness values increases as the toughness of the material increases. This variability could be caused by incorrect sizing of test specimens and/or inconsistent data reduction procedures. A standard data reduction procedure is therefore needed as well, particularly for the tougher materials. Little work has been reported on the effects of fiber orientation, fiber architecture, fiber surface treatment or interlaminar fracture toughness, and the mechanisms by which the fibers increase fracture toughness are not well understood. The little data that is available indicates that woven fiber reinforcement and fiber sizings can significantly increase interlaminar fracture toughness. Author

N93-12306*# Analytical Services and Materials, Inc., Hampton, VA.
MICROMECHANICAL COMBINED STRESS ANALYSIS: MICSTRAN, A USER MANUAL
R. A. Naik Oct. 1992 27 p
(Contract NAS1-19399; RTOP 505-63-50-04)
(NASA-CR-189694; NAS 1.26:189694) Avail: CASI HC A03/MF A01

Composite materials are currently being used in aerospace and other applications. The ability to tailor the composite properties by the appropriate selection of its constituents, the fiber and matrix, is a major advantage of composite materials. The Micromechanical Combined Stress Analysis (MICSTRAN) code provides the materials engineer with a user-friendly personal computer (PC) based tool to calculate overall composite properties given the constituent fiber and matrix properties. To assess the ability of the composite to carry structural loads, the materials engineer also needs to calculate the internal stresses in the composite material. MICSTRAN is a simple tool to calculate such internal stresses with a composite ply under combined thermomechanical loading. It assumes that the fibers have a circular cross-section and are arranged either in a repeating square or diamond array pattern within a ply. It uses a classical elasticity solution technique that has been demonstrated to calculate accurate stress results. Input to the program consists of transversely isotropic fiber properties and isotropic matrix properties such as moduli, Poisson's ratios, coefficients of thermal expansion, and volume fraction. Output consists of overall thermoelastic constants and stresses. Stresses can be computed under the combined action of thermal, transverse, longitudinal, transverse shear, and longitudinal shear loadings. Stress output can be requested along the fiber-matrix interface, the model boundaries, circular arcs, or at user-specified points located anywhere in the model. The MICSTRAN program is Windows compatible and takes advantage of the Microsoft Windows graphical user interface which facilitates multitasking and extends memory access far beyond the limits imposed by the DOS operating system. Author

N93-12371# National Aerospace Lab., Tokyo (Japan). Aeroengine Div.
IMPACT TEST OF CARBON, KEVLAR, AND GLASS FIBRE HYBRID FRP PLATES [KABON, KEBURA, GARASU KEI HAIBURIDDO FUKUGOUZAI HEIBAN NO SHOUGEKI SHIKEN]
Ryosaku Hashimoto, Akinori Ogawa, Kunihiko Ohotake, and Tadasi Natumura (Ishikawajima-Harima Heavy Industries Co. Ltd., Tokyo, Japan) Apr. 1991 32 p In JAPANESE
(NAL-TR-1100; JTN-92-80406) Avail: CASI HC A03/MF A01

The high velocity impact response of hybrid Fiber Reinforced Plastic (FRP) plates (carbon, Kevlar and glass fiber) was experimentally studied to determine the influence of laminate structures. Impact velocities from 80 to 280 m/sec were obtained using a high pressure nitrogen gas gun, with all the tested target specimens being mounted in a frame type fixture. The impact and residual velocities were measured by electronic counters connected to a system composed of two photocells and two infrared Light Emission Diodes (LED's) and the tangential and radial direction dynamic strains were directly recorded. The delaminated area was subsequently measured by ultrasonic C-scanning, with the damage being characterized by this delaminated area and the energy absorbing capacity. Author (NASDA)

N93-12483# Naval Command, Control and Ocean Surveillance Center, San Diego, CA. Research, Development, Test and Evaluation Div.
MECHANICAL PROPERTIES OF CENTRIFUGALLY CAST METAL MATRIX COMPOSITES Final Technical Report
J. D. Maltby Jul. 1992 24 p
(AD-A254321; NRAD-TR-1517) Avail: CASI HC A03/MF A01

The objective of this report was to determine the tensile and compressive mechanical properties for two metal matrix composite (MMC) aluminum cylinders. The cylinders were manufactured through use of a centrifugal casting process. GRA

N93-12532 Purdue Univ., West Lafayette, IN.
ANALYSIS OF DELAMINATION IN COMPOSITE LAMINATES UNDER LOW-VELOCITY IMPACT Ph.D. Thesis
Chan-Jiun Jih 1991 155 p
Avail: Univ. Microfilms Order No. DA9215571

Composite laminates subjected to foreign object impact often experience extreme damage that may not be visible on the impacted surface. This damage in the form of delamination may lead to significant reduction in compressive strength of the laminate. In this study, the fracture mechanics approach is employed to predict the extent of delamination for a given impact condition. Static linear beam models for two types of specimens are developed and verified by 2-D plane strain finite element methods. Thermal residual stresses are also considered in the analysis. Then, static three-point bending tests are performed on four different lay-ups of laminates to determine interlaminar fracture toughness. A drop-weight impact tower is constructed to perform the dynamic impact test. The validity of the quasi-static assumption for the drop-weight impact is examined. A simple spring-mass model is used to predict the peak load of the drop-weight impact. Also, the methodology of the prediction of impact-induced delamination under drop-weight impact is proposed and verified by the test results. Dissert. Abstr.

N93-12450*# National Aeronautics and Space Administration. Ames Research Center, Moffett Field, CA.
ADVANCED CERAMIC MATRIX COMPOSITES FOR TPS
Daniel J. Rasky *In* NASA. Langley Research Center, Current Technology for Thermal Protection Systems Oct. 1992 p 43-61 (For primary document see N93-12447 02-18)
Avail: CASI HC A03/MF A03

N93-12454*# National Aeronautics and Space Administration. Langley Research Center, Hampton, VA.
PREDICTED AND TESTED PERFORMANCE OF DURABLE TPS
John L. Shideler *In its* Current Technology for Thermal Protection Systems Oct. 1992 p 97-129 (For primary document see N93-12447 02-18)
Avail: CASI HC A03/MF A03

N93-12455*# National Aeronautics and Space Administration. Langley Research Center, Hampton, VA.
RECENT ADVANCES IN CARBON-CARBON SUBSTRATE TECHNOLOGY AT NASA. LANGLEY RESEARCH CENTER
Philip O. Ransone, Y. Robert Yamaki (Lockheed Engineering and Sciences Co., Hampton, VA.), and Howard G. Maahs *In its*

Current Technology for Thermal Protection Systems Oct. 1992 p 131-148 (For primary document see N93-12447 02-18)
Avail: CASI HC A03/MF A03

N93-12456*# National Aeronautics and Space Administration. Langley Research Center, Hampton, VA.
CURRENT RESEARCH IN OXIDATION-RESISTANT CARBON-CARBON COMPOSITES AT NASA. LANGLEY RESEARCH CENTER
Craig W. Ohlhorst, Wallace L. Vaughn, and David M. Barrett *In its* Current Technology for Thermal Protection Systems Oct. 1992 p 149-168 (For primary document see N93-12447 02-18)
Avail: CASI HC A03/MF A03

N93-12457*# National Aeronautics and Space Administration. Langley Research Center, Hampton, VA.
THERMAL CONTROL/OXIDATION RESISTANT COATINGS FOR TITANIUM-BASED ALLOYS
Ronald K. Clark, Terryl A. Wallace, George R. Cunnington (Lockheed Missiles and Space Co., Palo Alto, CA.), and Karl E. Wiedemann (Analytical Services and Materials, Inc., Hampton, VA.) *In its* Current Technology for Thermal Protection Systems Oct. 1992 p 169-188 (For primary document see N93-12447 02-18)
Avail: CASI HC A03/MF A03

25 INORGANIC AND PHYSICAL CHEMISTRY

Includes chemical analysis, e.g., chromatography; combustion theory; electrochemistry; and photochemistry.

For related information see also *77 Thermodynamics and Statistical Physics.*.

N93-10986# Purdue Univ., West Lafayette, IN. Dept. of Chemistry.
PRECONVERSION CATALYTIC DEOXYGENATION OF PHENOLIC FUNCTIONAL GROUPS Quarterly Technical Progress Report, 1 Jan. - 31 Mar. 1992
Clifford P. Kubiak 1992 9 p
(Contract DE-FG22-89PC-89770)
(DE92-018304; DOE/PC-89770/T12) Avail: CASI HC A02/MF A01

The deoxygenation of phenols is a conceptually simple, but unusually difficult chemical transformation to achieve. The phenolic C-O bond energy of 103 kcal/mol is as strong as a benzene C-H bond and over 10 kcal/mol stronger than the C-O bonds of methanol and ethanol. The consequence of this is that the hydrogenation/deoxygenation methods in current use require severe conditions and give low selectivities. The ongoing research described herein is based on the unprecedented, but thermodynamically promising, use of carbon monoxide as the oxygen atom acceptor for the catalytic deoxygenation of phenols. DOE

N93-11035# Rolls-Royce Ltd., Derby (England). Company Applied Science Lab.
ROTATIONAL CARS MEASUREMENTS IN A ROTATING CAVITY WITH AXIAL THROUGHFLOW OF COOLING AIR: OXYGEN CONCENTRATION MEASUREMENTS
John D. Black and Christopher A. Long (Sussex Univ., Brighton, England) 15 Dec. 1991 28 p Submitted for publication Sponsored in part by Defence Research Agency
(PNR-90935; ETN-92-92215) Copyright Avail: CASI HC A03/MF A01

In a rotating cavity rig, which models cooling air flow in the spaces between discs of a gas turbine compressor, the build up of oxygen concentration after the cooling gas was changed from nitrogen to air was monitored using rotational Coherent AntiStokes Raman Spectroscopy (CARS). From this information an estimate of the fraction of the throughflow entering the rotating cavity was obtained. This demonstrated that rotational CARS can be applied as a nonintrusive concentration measurement technique in a rotating engineering test rig. ESA

N93-11132 Johns Hopkins Univ., Columbia, MD. Chemical Propulsion Information Agency.
THE 28TH JANNAF COMBUSTION SUBCOMMITTEE MEETING, VOLUME 1
Mary T. Gannaway, ed. Oct. 1991 531 p Meeting held in San Antonio, TX, 28 Oct. - 1 Nov. 1991; sponsored by the Joint NASA, Army, Navy, Air Force Interagency Propulsion Committee
(Contract N00014-91-C-0001)
(CPIA-Publ-573-Vol-1) Avail: CPIA, 10630 Little Patuxent Pkwy., Suite 202, Columbia, MD 21044-3200 HC

The volume, the first of four volumes, is a collection of 42 unclassified/unlimited papers which were presented at the 28th Joint Army-Navy-NASA-Air Force (JANNAF) Combustion Subcommittee Meeting, 28 Oct. - 1 Nov. 1991, at Brooks Air Force Base, San Antonio, Texas. Specific subjects discussed include the following: electrothermal-chemical gun technology, laser ignition of gun propellants, interior ballistic modeling, ram accelerators, cartridge cases, and liquid propellant guns. For individual titles, see N93-11133 through N93-11138.

N93-11133 Alabama Univ., Huntsville. Dept. of Mechanical Engineering.
EFFECTS OF REACTING FLOWS WITH TURBULENCE AND SHOCK WAVES ON EFFICIENCY OF SCRAMJET COMBUSTORS c20
T. J. Chung and W. S. Yoon *In* JHU, The 28th JANNAF Combustion Subcommittee Meeting, Volume 1 Oct. 1991 p 1-14 (For primary document see N93-11132 02-25)
Avail: CPIA, 10630 Little Patuxent Pkwy., Suite 202, Columbia, MD 21044-3200 HC

The mutual effects of chemical reactions, shock waves, and turbulence on the flowfield and the resulting efficiency of scramjet combustors are examined. Calculations are carried out using the Taylor-Galerkin finite elements. Example problems include scramjet flame holders and supersonic diffusers in which finite rate chemistry (hydrogen-oxygen reactions) is incorporated in turbulence interacting with shock waves. In general, chemical reactions are triggered by shock waves and they in turn disperse the shock discontinuities. For the scramjet flame holder with larger ramp angles, combustion appears to have been completed upstream of the flame holder. For the supersonic diffuser, turbulence causes the shock discontinuities to be further dispersed. Contour lines for all chemical species change in directions parallel to the wall and toward the center line (circulations and mixing), but other flow variables do not show such trends as distinctively as chemical species. Author

N93-11134*# National Aeronautics and Space Administration. Langley Research Center, Hampton, VA.
IGNITION DELAYS, HEATS OF COMBUSTION, AND REACTION RATES OF ALUMINUM ALKYL DERIVATIVES AS USED AS IGNITION AND COMBUSTION ENHANCERS FOR SUPERSONIC COMBUSTORS
T. W. Ryan, III (Southwest Research Inst., San Antonio, TX.), Stuart T. Schwab (Southwest Research Inst., San Antonio, TX.), W. W. Harlowe (Southwest Research Inst., San Antonio, TX.), and G. L. Pellett *In* JHU, The 28th JANNAF Combustion Subcommittee Meeting, Volume 1 Oct. 1991 p 15-24 (For primary document see N93-11132 02-25)
Avail: CPIA, 10630 Little Patuxent Pkwy., Suite 202, Columbia, MD 21044-3200 HC

The use of hydrocarbon fuels in supersonic combustors is limited by the fact that these types of fuels typically do not ignite and burn fast enough to complete combustion in a reasonably sized combustor. Changing to an alternative type of fuel, such as hydrogen, is one approach to this problem. Another more attractive approach is the use of additives in hydrocarbon fuels. If this problem is to be addressed using a fuel additive approach, the additive must act to reduce the ignition delay time and increase the overall reaction rate. It is also desirable that the additive have the highest volumetric energy density. The aluminum alkyls meet all these requirements. The disadvantage of these materials is the fact that they are very unstable and are therefore difficult to store and handle. The use of more stable adducts of these alkyls may mitigate the handling problems, but they may also reduce the reactivity and energy density benefits. There are currently no data available on the ignition quality, reaction rates, or the heats of combustion of these types of materials. The work in this paper was based on adapting an apparatus and procedure developed at Southwest Research Institute (SwRI) for rating the ignition quality of fuels for diesel engines, for use with the alkyls. The alkyls and various adducts of these materials were injected into the bomb using a high-pressure injection system. The bomb was pre-charged with air that was set at various initial temperatures and pressures. The ignition delay times were determined for several different test materials at these different initial conditions. The data are presented in absolute terms as well as comparisons with the parent alkyls. The heats of reaction of the various test materials were estimated based on a computation of the heat release using the pressure data recorded during combustion in the bomb. In addition, the global reaction rates for each material were compared at a selected temperature and pressure. Author

N93-11135*# National Aeronautics and Space Administration. Ames Research Center, Moffett Field, CA.

EMPLOYMENT OF RADICALS AND EXCITED STATE SPECIES FOR SUPERSONIC COMBUSTION PHOTOCHEMICAL IGNITION OF PREMIXED HYDROGEN/OXYGEN MIXTURES WITH ArF LASER

Yehuda Nachshon (Energia, Inc., Princeton, NJ.), Suresh K. Gulati (Energia, Inc., Princeton, NJ.), John G. Stevens (Energia, Inc., Princeton, NJ.), Moshe Lavid (Energia, Inc., Princeton, NJ.), and Richard Jaffe *In* JHU, The 28th JANNAF Combustion Subcommittee Meeting, Volume 1 Oct. 1991 p 25-35 (For primary document see N93-11132 02-25)
(Contract NAS2-13187)
Avail: CPIA, 10630 Little Patuxent Pkwy., Suite 202, Columbia, MD 21044-3200 HC

The success of the new generation of hypersonic flight vehicles depends on the attainment of a true breakthrough in combustion technology. Conventional combustion processes are currently hindered by constraints imposed by severe conditions associated with the harsh hypersonic flow field. This is a research effort to determine the feasibility of using radicals and excited state species to improve the combustion of reactive systems fueled by hydrogen. These species have lower energy barriers than their ground state counterparts. Hence, they are capable of very high reaction rates, which can result in quantum enhancement in various combustion characteristics relevant to supersonic flows, such as ignition delay time, autoignition temperature, minimum ignition energy, combustion residence time, and overall combustion efficiency. The effect of in-situ production of atomic oxygen O(P-3) on hydrogen combustion is examined. The experimental test conditions are similar to those anticipated for supersonic combustion, i.e., $M = 6\text{-}10$, $P = 0.5$ atm, ER (equivalence ratio) = 1, and the temperature range is 500-750 K. Atomic oxygen at the ground level O(P-3) is produced by photodissociating molecular oxygen with ArF excimer laser line (193 nm). Experimental results are very promising. Successful ignitions were obtained outside the explosion peninsula (above the second limit). Minimum laser ignition energies are given for various equivalence ratios at different temperatures. A detailed computer program is presented for calculating the rate of molecular oxygen photo-dissociation at the ignition site. It includes laser propagation through a non-uniform temperature absorbing medium, non-linear absorption 'hole drilling' in the output laser, and bleaching of the absorbers at the excited levels of the ground electronic state. Combination of measured laser energies and calculated dissociation rates of molecular oxygen yields the minimum required concentration of atomic oxygen for photo-chemical ignition. Results are presented for fuel-lean (0.2 - 1.0) and fuel-rich (1.0 - 2.0) hydrogen/oxygen mixtures at different temperatures (up to 800 K). Author

N93-11136 Naval Postgraduate School, Monterey, CA. Dept. of Aeronautics and Astronautics.

THE EFFECTS OF BYPASS AIR ON BORON CARBIDE COMBUSTION IN A SOLID FUEL RAMJET

Benveniste Natan and David W. Netzer *In* JHU, The 28th JANNAF Combustion Subcommittee Meeting, Volume 1 Oct. 1991 p 37-43 Sponsored by NWC and NAS-NRC (For primary document see N93-11132 02-25)
Avail: CPIA, 10630 Little Patuxent Pkwy., Suite 202, Columbia, MD 21044-3200 HC

The effects of bypass air on the combustion of highly loaded boron carbide fuel grains in a solid fuel ramjet (SFRJ) motor were investigated experimentally. It was found that combustion efficiency can be significantly increased by employing high bypass ratios with low dump momentum, the results of good mixing of bypass air with the boron carbide particles which are ignited within the port of the upstream fuel grain. Increasing pressure increased efficiency, apparently through the resulting increased residence time. Increased overall equivalence ratio (grain length) was found to be beneficial, the result of a smaller percentage of larger particles which are generated in the recirculation zone. Some of the reduction in combustion efficiency was determined to be due to incomplete combustion of the hydroxy-terminated polybutadiene (HTPB) rather than just to the incomplete burning of the particulates. Author

N93-11137 California State Univ., Sacramento.

THE COMBUSTION TIME LAG AND ITS ROLE IN RAMJET COMBUSTION INSTABILITY

Frederick H. Reardon *In* JHU, The 28th JANNAF Combustion Subcommittee Meeting, Volume 1 Oct. 1991 p 45-63 (For primary document see N93-11132 02-25)
Avail: CPIA, 10630 Little Patuxent Pkwy., Suite 202, Columbia, MD 21044-3200 HC

The concept of a combustion time lag has proven useful in the study of combustion instability in both liquid propellant rockets and liquid-fueled ramjets. Direct measurement of the time lag is not feasible; for liquid propellant rockets, the time lag has been calculated from knowledge of the axial distribution of energy release in the combustion chamber. The same approach was applied in this study to ramjet combustors. A computational fluid dynamics code was used to calculate the axial distribution of the mean gas temperature and axial velocity in a coaxial-dump ramjet combustor. The dependence of the combustion time lag on several combustor design parameters was investigated for two modes of fuel injection. For fuel injection from the wall of the air inlet duct just upstream of the dump plane, the time lag increased with increasing fuel drop diameter and with increasing jet penetration distance (for most cases), and decreased with increasing air velocity and increasing fuel/air ratio. When the fuel was injected uniformly across the air inlet duct well upstream of the dump plane, the time lag was larger for longer combustors, was relatively insensitive to drop size and inlet/combustor diameter ratio, and decreased with increasing air velocity and fuel/air ratio. These results were used in a previously developed combustion instability model. Unfortunately, the combustion time lag values calculated appear to be too small by about a factor of two. The major reason for the disagreement appears to be the method of determining the time lag from the CFD results. Author

N93-11138 California Univ., Irvine. Dept. of Mechanical and Aerospace Engineering.

METAL SLURRY DROPLET AND SPRAY COMBUSTION

W. A. Sirignano and R. Bhatia *In* JHU, The 28th JANNAF Combustion Subcommittee Meeting, Volume 1 Oct. 1991 p 65-74 (For primary document see N93-11132 02-25)
(Contract N00014-89-J-1135)
Avail: CPIA, 10630 Little Patuxent Pkwy., Suite 202, Columbia, MD 21044-3200 HC

Analytical and numerical studies on the problem of vaporization of liquid fuel and ignition of the metal from the slurry droplets are presented. Two limiting cases, one consisting of a single metal particle enveloped by a liquid hydrocarbon, and another consisting of many fine metal particles inside a liquid hydrocarbon carrier droplet, are analyzed. A three part analysis is presented. In the first part, the governing spherically symmetric, unsteady conservation equations are simplified using the Schvab-Zel'dovich and von Mises transformations. Forced convection is considered in the second part and the gas-phase includes the effects of variable thermophysical properties and non-unitary Lewis number. The liquid-phase analysis addresses the effects of transient heating and circulation. Calculations are made for both liquid vaporization without combustion and vaporization followed by combustion. The third part analyzes a fine-metal slurry droplet. Here, the gasification stages consist of a surface regression period which terminates upon the formation of a solid shell on the droplet surface. Depending on the shell characteristics, different modes of liquid vaporization from the droplet are shown to occur. Bubble formation and growth is considered in the analysis. Effects of particle size and solid loading ratio are determined. Author

N93-11218# Wisconsin Univ., Madison. Dept. of Chemistry.

CHEMICAL REACTIONS AND PROPERTIES OF ORGANOSILICON COMPOUNDS RELATED TO NEW MATERIALS Final Technical Report, 1 Oct. 1988 - 30 Sep. 1991

Robert West 29 May 1992 11 p
(Grant AF-AFOSR-0004-89)
(AD-A253233; AFOSR-92-0698TR) Avail: CASI HC A03/MF A01

A completely ordered polysilane polymer has been prepared. The surface tension of polysilane polymers has been investigated, and found to span a large range from 20 to 52 mdyne/cm. The polymer poly(n-butyl-n-hexylsilylene) was found to have a hexaponal columnar structure, at all temperatures from -80 to +200 C. Many polysilane copolymers were also observed to have columnar liquid crystalline structures. Several linear polysilane oligomers were synthesized as model compounds for the study of high polymers. New types of alpha-pi conjugated polymers were synthesized and studied, based on alternating polysilane and acetylene groups. New disilenes were synthesized, including the first example of a disilene with a silyl substituent. The oxidation of disilenes by oxygen was investigated and found to produce 1,2-disilaoxetanes which rearrange intramolecularly to 1,3-cyclodisiloxanes. Disilenes were found to react with aldehydes, ketones and thioketones by 2+2 cycloaddition to produce four-membered ring compounds. Reactions of disilenes with ketenes and acid chlorides were also investigated. With white phosphorus, disilenes react to produce nobel bicyclobutane molecules which may be further converted to tricyclic asterane structures. The first platinum derivatives of disilenes were synthesized. The first siladiimides have been synthesized. These are salts of anions containing partial double bounds between silicon and each of two nitrogen atoms. The chemical reactions, spectroscopy and structure of siladiimides has been investigated. GRA

N93-11259 Yale Univ., New Haven, CT.

NUMERICAL CALCULATIONS OF AN AXISYMMETRIC LAMINAR DIFFUSION FLAME WITH DETAILED AND REDUCED REACTION MECHANISMS Ph.D. Thesis

Yuenong Xu 1991 180 p
Avail: Univ. Microfilms Order No. DA9221460

Newton's method is applied in the primitive variable formulation to solve the system of fully elliptic equations governing two-dimensional chemically reacting flows. This new numerical approach is compared to Newton's method in the stream function-vorticity formulation and the SIMPLER algorithm in the calculations of an axisymmetric laminar diffusion flame in a confined coflowing jet using a flame sheet model. The results indicate that Newton's method in the primitive variable formulation gives a better performance in terms of accuracy and computing time. The proposed numerical approach is also employed to solve the same diffusion flame using a reduced mechanism, a skeletal mechanism, a C(sub 1)-chain mechanism, and a C(sub 2)-chain mechanism. The grid points are globally adapted by equidistributing the mesh. The numerical results of the different chemical mechanisms are discussed and compared to experimental data. The agreement is generally quite good. The present reduced four step mechanism shows better numerical stability than the previous reduced mechanisms. The solution of the reduced mechanism is very close to those of the C(sub 1) and C(sub 2) mechanisms. The comparisons also indicate that the C(sub 2)-chain reactions have little effect on the aerodynamic and thermal solution fields. Dissert. Abstr.

N93-11280# Colorado State Univ., Fort Collins. Dept. of Chemistry.

NEAR-IR ABSORPTION SPECTRA FOR THE C70 FULLERENE ANIONS Interim Report

Del R. Lawson, Daniel L. Feldheim, Colby A. Foss, Peter K. Dorhout, and C. M. Elliott 20 Jul. 1992 19 p
(Contract N00014-82-K-0612)
(AD-A253658; TR-75-ONR) Avail: CASI HC A02/MF A01

C70, like C60, can exist in a number of oxidation states including C70(1-), C70(2-), C70(3-) and C70(4-). We have discovered unique visible and near-IR absorption transitions which appear upon reduction of C70. These transitions are observed upon one, two, three and four-electron electrochemical reductions of C70. In contrast to C60, however, the electronic properties of C70 are less well understood. In particular, previous theoretical studies of C70(1-) failed to predict the existence of the near-IR transition we observe in the spectrum of C70(1-). In this paper, in addition to presenting the heretofore unreported spectra of the various C70 anions, we attempt a first-order explanation of the energies and intensities of the various spectral absorptions; this explanation is based on the published molecular orbital diagram for neutral C70 and a structural distortion that we suggest occurs upon reduction of C70. GRA

N93-11361# Bertin et Cie, Tarnos (France). Div. Genie Chimique et Combustion.

SIMPLIFIED MODELLING OF SOOT INCEPTION AND GROWTH

Christophe Belot, Denis Rebuffat, Alain Jaffre, Dominique Goffe, and Didier Grouset 1991 28 p Submitted for publication Sponsored by Direction des Recherches, Etudes et Techniques
(ETN-92-92266) Avail: CASI HC A03/MF A01

A simplified model was developed for soot inception and growth calculations suited to implementation in turbulent combustion modeling. For this purpose, emphasis was put on the choice of a reduced number of variables in order to restrict the additional balance equations to be considered in an overall fluid dynamics computation. Care was taken to describe as accurately as possible the various processes governing soot inception and growth. The model simulates the population of the polycyclic aromatic hydrocarbons with two variables characterizing two classes of light and heavy precursors. The evolution of the soot particles is described with three variables providing their total amount, mean diameter and size distribution width. The model main simplifying assumptions consist in presumed forms of the precursors mass distribution and of the soot particles size distribution. Another basic feature of the model is a semi global expression used as a substitute for the first aromatic rings formation chemistry. Several laminar premixed hydrocarbon flames were simulated, the corresponding experimental conditions ranging from low pressure to atmospheric, nearly to heavily sooting flames. The computed precursors and soot concentration profiles were compared with measured values. Satisfactory agreement is obtained between calculated and measured profiles in a rather wide range of conditions. The model reproduces the essential features of soot inception and shows the important parts played by the various processes involved in the polycyclic aromatic hydrocarbon evolution. ESA

N93-11396 National Physical Lab., Teddington (England). Div. of Materials Metrology.

SIGNAL-TO-NOISE ASSESSMENT AND MEASUREMENT IN SPECTROSCOPIES WITH PARTICULAR REFERENCE TO AUGER AND X RAY PHOTOELECTRON SPECTROSCOPIES

M. P. Seah and P. J. Cumpson Jan. 1992 18 p Sponsored by Dept. of Trade and Industry
(NPL-DMM(A)-45; ETN-92-92368) Copyright Avail: National Physical Lab., Teddington, Middlesex, TW11 0LW, England

An analysis of some of the problems associated with the measurement of signal to noise ratios in electron spectroscopy was made. The assessment of the signal to noise ratio for counting systems, in particular, where the statistics are Poissonian, is developed. In order to measure the noise statistics accurately, it is shown that at least 135 measures of the counts at a given setting are required. These may be used to confirm or disprove the Poissonian nature of the count. At high counting rates, the counting system dead time causes deviations form the Poisson character. However, if the counting system gives Poissonian statistics, simple equations may be used to give the signal to noise figures from spectral measurements. In systems with more than one detector, the allocation of the data from the different detectors to different energy channels may provide some effective smoothing so that the noise appearing in the spectrum may be up to 25 percent too low compared with a Poissonian estimate. In this case the true signal to noise ratio may only be observed from the detector outputs directly, prior to data reduction by the computer. In practical situations, the dominance of the Poissonian counting statistics should be exhibited over most of the effective measurement range. However, when searching at the limits of spatial resolution in Auger Electron Spectrometry (AES) (very low beam currents) or the highest sensitivity (small signals in a large background) in AES or X-ray Photoelectron Spectroscopy (XPS), other noise sources become important and should be considered. ESA

N93-11439# Illinois Univ., Urbana.

SELECTIVE CARBON OXYGEN BOND SCISSION DURING REACTIONS OF OXYGENATES ON SINGLE CRYSTAL CATALYSTS

1992 2 p
(Contract DE-FG02-91ER-14178)
(DE92-018687; DOE/ER-14178/T1) Avail: CASI HC A01/MF A01

We have discovered that the carbon-oxygen bond in methanol can be selectively broken if the surface structure of the platinum catalyst is appropriately tailored. The objective of this project is to determine if variations in surface structure allow one to selectively break C-O and C-H bonds. The decomposition of a wide range of oxygenates on several carefully chosen faces of group VIII metals will be examined to see when C-O bond scission occurs and what new chemistry we can find on stepped surfaces. DOE

N93-11444# Massachusetts Inst. of Tech., Cambridge. Dept. of Chemical Engineering.

DIRECT CATALYTIC DECOMPOSITION OF NITRIC OXIDE

M. Flytzani-Stephanopoulos, A. F. Sarofim, and Y. Zhang 1992 12 p
(Contract DE-FG22-91PC-91293)
(DE92-018759; DOE/PC-91293/2) Avail: CASI HC A03/MF A01

This project will investigate a suitable catalyst system for the direct NO decomposition, for post-combustion NO(x) control. The proposed process will not use a reductant, such as ammonia in case of Selective Catalytic Reduction (SCR) process for catalytic reduction of NO(x) to nitrogen. This is a simplified process basically involving passing the flue gas through a catalytic converter, thus avoiding problems generally associated with the commercial Selective Catalytic Reduction (SCR) process, namely high operating cost, ammonia slip, and potential N2O emissions. A brief description of the proposed work is as follows: Catalysts will be prepared by incorporating metal cations into zeolite supports according to ion exchange procedures widely used in preparation of metal/zeolite catalysts. Zeolites will be modified to improve catalytic activity, by blocking ion exchange sites in the small pores of zeolites with promoter cations of high valence. The catalysts of primary interest include copper (Cu), palladium (Pd), platinum (Pt), silver (Ag), and nickel (Ni) exchanged zeolites. DOE

N93-11448 Johns Hopkins Univ., Columbia, MD. Chemical Propulsion Information Agency.

THE 28TH JANNAF COMBUSTION SUBCOMMITTEE MEETING, VOLUME 2

Mary T. Gannaway, ed. Oct. 1991 595 p Meeting held in San Antonio, TX, 28 Oct. - 1 Nov. 1991; sponsored by Joint NASA, Army, Navy, Air Force Interagency Propulsion Committee
(Contract N00014-91-C-0001)
(CPIA-Publ-573-Vol-2) Avail: CPIA, 10630 Little Patuxent Pkwy., Suite 202, Columbia, MD 21044-3200 HC

This volume, the second of four volumes, is a collection of 50 unclassified/unlimited papers which were presented at the 28th Joint Army-Navy-NASA-Air Force (JANNAF) Combustion Subcommittee Meeting, 28 October - 1 November 1991, at Brooks Air Force Base, San Antonio, Texas. Specific subjects discussed include combustion instability in liquid and solid rockets, nitramines, propellant kinetics, and propellant flame diagnostics. For individual titles, see N93-11449 through N93-11455.

N93-11449*# National Aeronautics and Space Administration. Marshall Space Flight Center, Huntsville, AL.

SOLUTION OF TWO-PHASE REACTING FLOW IN LIQUID THRUST CHAMBERS c20

Anthony Dang (Physical Research, Inc., Irvine, CA.), Homayun K. Navaz (Physical Research, Inc., Irvine, CA.), and Klaus W. Gross *In* JHU, The 28th JANNAF Combustion Subcommittee Meeting, Volume 2 Oct. 1991 p 9-18 (For primary document see N93-11448 02-25)
(Contract NAS8-38798)
Avail: CPIA, 10630 Little Patuxent Pkwy., Suite 202, Columbia, MD 21044-3200 HC

A comprehensive Navier-Stokes code was developed for liquid rocket engine thrust chamber performance prediction. The code features multiple phases for liquid fuel and oxidizer droplets, group combustion effects, atomization models, full finite rate chemistry and the Chien low Reynolds number turbulence model. The multiple phase equations were cast in an Eulerian-Eulerian framework, which is essential for the treatment of dense spray. The discretization scheme is fully implicit and is based on the Lax-Friedrichs Total Variation Diminishing (TVD) scheme, which is accurate, very efficient and capable of handling steep gradients and stiff chemistry. The efficiency of the numerical scheme is essential for this application since the set of governing equations can be quite large (typically about forty in number). Preliminary results were obtained for the Space Shuttle Main Engine (SSME) and compared favorably with existing codes such as TDK and VIPER. Author

N93-11450*# National Aeronautics and Space Administration. Lewis Research Center, Cleveland, OH.

TEST PROGRAM TO PROVIDE VALIDATION DATA FOR THE ROCKET COMBUSTOR INTERACTIVE DESIGN (ROCCID) CODE

Thong V. Nguyen (Aerojet-General Corp., Sacramento, CA.), R. E. Walker (Aerojet-General Corp., Sacramento, CA.), and Mark D. Klem *In* JHU, The 28th JANNAF Combustion Subcommittee Meeting, Volume 2 Oct. 1991 p 31-50 (For primary document see N93-11448 02-25)
(Contract NAS3-25556)
Avail: CPIA, 10630 Little Patuxent Pkwy., Suite 202, Columbia, MD 21044-3200 HC

A description of the hardware design and test philosophy leading to the successful testing of a LOX/RP-1 engine designed using the ROCCID interactive methodology is provided. The specific test logic that guided this test program as well as the results containing both performance and stability data are provided. All testing was conducted with a single chamber design (diameter = 19.5 cm, contraction ratio = 2.0, length = 35.6 cm) and one 105 element O-F-O injector. The mixture ratio, O/F, was varied from 1.13 to 6.74:1 and chamber pressure ranged from 800 to 1750 psia, exclusive of chug stability tests which were conducted with chamber pressures as low as 250 psia. The testing, which was performed with and without acoustic cavities, included both stable and high frequency combustion instability results. All combustion instabilities were spontaneous. Although combustion perturbation bombs were used and generated over-pressures in the range of approximately 5 to 62 percent of the mean chamber pressure, no tests were driven unstable by the bombs. A comparison between the predicted and actual performance and stability is also provided. The measured performance was lower than the predicted values by approximately 5 percent, probably the result of poorer than predicted propellant mixing. The agreement of the predicted stability trends with the measured trends is reasonable; however, improvements to the component models are needed to increase the accuracy of the methodology. Author

N93-11451*# Pennsylvania State Univ., University Park. Propulsion Engineering Research Center.

A SUMMARY OF THE JANNAF WORKSHOP ON DIAGNOSTICS

Robert J. Santoro *In* JHU, The 28th JANNAF Combustion Subcommittee Meeting, Volume 2 Oct. 1991 p 143-149 (For primary document see N93-11448 02-25)
(Grant NAGw-1356)
Avail: CPIA, 10630 Little Patuxent Pkwy., Suite 202, Columbia, MD 21044-3200 HC

A JANNAF sponsored workshop on diagnostics oriented towards problems associated with liquid rocket engine combustion driven instability identified measurement capabilities and needs in three areas: (1) spray atomization, vaporization and mixing; (2) test stand diagnostics; and (3) measurement needs for rocket code validation. The workshop recommended that diagnostics are presently at an appropriate point to allow direct application to a benchmark problem. Although many suitable techniques are available to address needed measurements, the workshop did identify dense sprays to be an area requiring further work. The requirements for test stand diagnostics emphasized tailoring the diagnostics to the appropriate level of the test activity (e.g., subscale, development engine, etc.). Furthermore, the need for rugged, remote techniques with specified spatial and temporal resolution were identified. The workshop also recognized that rocket code validation requires extensive measurement capabilities for the development of validation data bases. Critical measurements and required accuracies were specifically cited. Author

N93-11452*# National Aeronautics and Space Administration. Lewis Research Center, Cleveland, OH.

COAXIAL INJECTOR SPRAY CHARACTERIZATION USING WATER/AIR AS SIMULANTS

Michelle M. Zaller (Sverdrup Technology, Inc., Brook Park, OH.) and Mark D. Klem *In* JHU, The 28th JANNAF Combustion Subcommittee Meeting, Volume 2 Oct. 1991 p 151-160 Previously announced as N92-14112 (For primary document see N93-11448 02-25)
(Contract NAS3-25266)
Avail: CPIA, 10630 Little Patuxent Pkwy., Suite 202, Columbia, MD 21044-3200 HC

Quantitative information about the atomization of injector sprays is required to improve the accuracy of computational models that predict the performance and stability of liquid propellant rocket engines. An experimental program is being conducted at NASA-Lewis to measure the drop size and velocity distributions in shear coaxial injector sprays. A phase/Doppler interferometer is used to obtain drop size data in water air shear coaxial injector sprays. Droplet sizes and axial component of droplet velocities are measured at different radii for various combinations of water flow rate, air flow rate, injector liquid jet diameter, injector annular gap, and liquid post recess. Sauter mean diameters measured in the spray center 52 mm downstream of the liquid post tip range from 28 to 68 microns, and mean axial drop velocities at the same location range from 37 to 120 m/s. The shear coaxial injector sprays show a high degree of symmetry; the mean drop size and velocity profiles vary with liquid flow rate, post recess, and distance from the injector face. The drop size data can be used to estimate liquid oxygen/hydrogen spray drop sizes by correcting property differences between water-air and liquid oxygen/hydrogen. Author

N93-11453*# Carnegie-Mellon Univ., Pittsburgh, PA. Dept. of Mechanical Engineering.

PHYSICAL PROCESSES INVOLVED IN INJECTION AND ATOMIZATION OF LIQUID PROPELLANTS

Norman Chigier, H. Eroglu, U. Shavit, and M. Xu *In* JHU, The 28th JANNAF Combustion Subcommittee Meeting, Volume 2 Oct. 1991 p 175-185 (For primary document see N93-11448 02-25)
(Grant NAG8-126)
Avail: CPIA, 10630 Little Patuxent Pkwy., Suite 202, Columbia, MD 21044-3200 HC

Under contract to NASA Marshall Space Center, a series of experiments were conducted to determine the fundamental physical processes of injection and atomization of liquid propellants for rocket combustion chambers. For co-axial injectors, liquid and gas flow rates were progressively changed. Microphotography was used to obtain details of wave disturbances on liquid surfaces. Direct measurements were made of wavelength and frequency of wave propagation on liquid surfaces. Linear increases of wavelength was found along the length of the liquid surface while frequency remained constant. Measured frequencies were in the range of those measured in combustion instability experiments. Final disintegration of liquid jets occurred in a sudden disruption, producing a shower of droplets with a wide range of drop sizes and velocities. Detailed measurements were made in the sprays using the phase Doppler particle analyzer (PDPA). Measurements of drop size, velocity, and number density are related to the disintegration process. Initiation of disturbances occurs in the injector or by interaction with the surrounding gas stream. The gas stream drives the waves and accelerates the liquid surface. Increasing turbulence intensity in the gas stream is a very effective means of reducing drop size. Large eddies from the gas stream penetrate into the liquid stream causing disruption. Author

N93-11454*# Aerometrics, Inc., Sunnyvale, CA.

EXPERIMENTAL INVESTIGATION OF ROCKET INJECTOR ATOMIZATION

Subra V. Sankar, A. BrenadelaRosa, A. Isakovic, and W. D. Bachalo *In* JHU, The 28th JANNAF Combustion Subcommittee Meeting, Volume 2 Oct. 1991 p 187-198 (For primary document see N93-11448 02-25)
(Contract NAS8-37403)
Avail: CPIA, 10630 Little Patuxent Pkwy., Suite 202, Columbia, MD 21044-3200 HC

The atomization characteristics of scaled-down versions of a coaxial rocket injector and a quadruplet rocket injector was investigated using a phase Doppler particle analyzer. The coaxial rocket injector was operated in the conventional mode with liquid nitrogen being injected through its inner orifice and gaseous nitrogen being injected through its outer annulus. The shearing action occurring at the liquid-gas interface causes the liquid jet to atomize. The performance characteristics of the coaxial injector under different flow and geometric conditions are discussed. Specifically, the effects of the gas pressure and the injector recess size on flow variables such as the mean particle diameter, the Sauter mean diameter, number density, volume flux, and droplet velocity are presented. In the case of the quadruplet injector, liquid nitrogen was injected through the four orifices of the injector and the impaction of the four liquid jet streams causes liquid atomization. A simple spray characterization for the quadruplet injector is also presented. Author

N93-11455*# Pennsylvania State Univ., University Park.

AN EXPERIMENTAL STUDY OF DROPLET DISPERSION IN TURBULENT FLOWS

Y.-H. Song and D. A. Santavicca *In* JHU, The 28th JANNAF

Combustion Subcommittee Meeting, Volume 2 Oct. 1991 p 199-203 (For primary document see N93-11448 02-25)
(Contract NAG8-160; DAAL03-91-G-0137)
Avail: CPIA, 10630 Little Patuxent Pkwy., Suite 202, Columbia, MD 21044-3200 HC

An experimental apparatus and measurement technique for the study of droplet dispersion under high pressure, high temperature, evaporating conditions are presented. Preliminary results for two turbulent flow conditions are presented and different methods for analyzing the droplet trajectory measurements are discussed. The preliminary results clearly show that significant droplet dispersion can be achieved with this system over times typical of droplet lifetimes in actual spray. Analysis of these results shows that droplet dispersion increases with turbulence intensity and as a square function of time. Author

N93-11490# Cambridge Univ. (England).
IMPACT IGNITION OF LIQUID PROPELLANTS Annual Report, Jan. 1991 - Jan. 1992
J. E. Field, N. K. Bourne, and S. M. Walley 30 Apr. 1992 31 p
(Contract DAJA45-91-M-0061; DA Proj. 1L1-61102-BH-57)
(AD-A252299; R/D-6541-AN-09) Avail: CASI HC A03/MF A01

The report describes a preliminary study of the impact ignition of liquid propellants. In one experimental set up, two dimensional cavities were shocked and the cavity collapse studied by both high-speed framing and streak photography. Cavities in water and liquid propellant (LCP 1846) were studied. Cavity sizes were in the range 1 - 7 mm and shock strengths in the range up to 1.5 GPa were used. The cavities were observed to involute and produce a high speed jet which crossed the cavity and impacted the downstream wall sending a shock into the surrounding material. The gas in the cavity was heated by rapid compression achieving temperatures sufficient to cause gas luminescence. Finally, the jet penetrated the downstream wall of the cavity to form a pair of vortices which travelled downstream with the flow. Jet velocities up to ca. 500 m/s were observed. A more general discussion of cavity collapse and the initiation of explosion is presented in Appendix 1 (Bourne and Field 1991, Proc.Roy.Soc. 435, 423-435). In the second series of experiments, drop-weight impacts were performed on layers of propellant of various geometries using a transparent anvil apparatus. This experimental set-up allows high-speed photographic recording of the event. The drop weight had a mass of 5 kg and was dropped from a height of 1.3 m. No ignition events were observed. Flow velocities of up to about 200 m/s were observed. Of particular interest was the production of filaments of cavities in the impacted layers. GRA

N93-11545*# National Aeronautics and Space Administration. Lewis Research Center, Cleveland, OH.
CHRONOPOTENTIOMETRY OF REFRACTORY METALS, ACTINIDES AND OXYANIONS IN MOLTEN SALTS: A REVIEW
Narottam P. Bansal Sep. 1992 41 p
(RTOP 505-01-50)
(NASA-TM-105862; E-7322; NAS 1.15:105862) Avail: CASI HC A03/MF A01

The applications of chronopotentiometry to the study of electrochemical behavior of three technologically important areas of refractory metals, actinides, and oxyanions in molten salts are critically reviewed. Chronopotentiometry is a very versatile diagnostic tool to understand the reaction mechanism of the electrode processes for the electrochemical reduction/oxidation of these electroactive species in molten salt solutions. Well adherent, compact, and uniformly thick coatings of refractory metals may be electrodeposited from their solutions in molten salts. Author

N93-11551# Sandia National Labs., Albuquerque, NM.
LOADS FROM THE DETONATION OF HYDROGEN-AIR-STEAM MIXTURES
K. W. Boyack, S. R. Tieszen, and D. W. Stamps Jul. 1992 141 p
(Contract DE-AC04-76DP-00789)
(DE92-019318; SAND-92-0541) Avail: CASI HC A07/MF A02

The purpose of this study is to investigate transient pressure loads from hydrogen combustion. Specifically, this study relates pressure loads to variations in mixture and initial conditions, mixture heterogeneities, ignition location, and variations in geometry. This study has shown that initial conditions and variations in mixture have a large effect upon the adiabatic isochoric complete combustion, detonation, and reflected detonation pressures. An inert gas layer between a detonable gas mixture and surface can give rise to reflected pressures higher than in the homogeneous case. A deflagration-to-detonation transition (DDT) event near a surface gives rise to higher reflected pressures, and lower impulses, than if the DDT occurred far from the surface. Edges and corners focus detonation waves, which increases both pressures and impulses over those seen from a normally reflected detonation. The loads at points behind an obstacle is less than the load that would be seen if the obstacle were not there. DOE

N93-11644# Allied-Signal Aerospace Co., Kansas City, MO.
ACID COPPER SULFATE PLATING BATH: CONTROL OF CHLORIDE AND COPPER
K. J. Borhani Aug. 1992 36 p
(Contract DE-AC04-76DP-00613)
(DE92-019473; BDX-613-3417) Avail: CASI HC A03/MF A01

Plated-through holes in high-reliability printed wiring boards require a ductile copper plate of uniform consistency. The level of control of the chemical constituents in the electroplating solutions dictates the physical properties of the copper plate. To improve the control of the chemical bath constituents, in-situ methods for electrochemically determining copper and chloride in acid copper sulfate baths were developed. A solid-state ion-selective electrode was used for the chloride ion and proved to be more reproducible than conventional silver chloride turbidimetric methods. The use of a copper solid-state ion-selective electrode in-situ was also successful in this application. DOE

N93-11755# California Univ., Los Angeles. Dept. of Chemistry and Biochemistry.
OXIDATION, NITRIDATION, AND FLUORINE ETCHING OF Si Final Report, 1 Nov. 1988 - 30 Apr. 1992
Emily A. Carter 29 Jun. 1992 18 p
(Grant AF-AFOSR-0108-89)
(AD-A253559; AFOSR-92-0717TR) Avail: CASI HC A03/MF A01

Studies of the structure and dynamics of Si, Ge, and SiGe surfaces and interfaces were carried out using isothermal molecular dynamics and isobaric-isothermal Monte Carlo techniques. Concomitantly, we calculated the fundamental interactions of fluorine atoms with silicon using ab initio quantum mechanics, in order to understand the mechanism of etching silicon by fluorine. Fundamental results from those studies suggest that the surface is highly disordered during etching and that this disorder is produced from the energy released during the extremely exothermic reaction of F atoms with silicon. In order to understand oxidation and nitridation of silicon by, H2O and NH3, we must begin by determining the nature of the interaction of H atoms with Si, since they are generated during these reactions and desorption of H atoms can be rate-limiting. We completed studies of H atom adsorption, diffusion, and desorption, learning about the complicated nature of diffusion and desorption on the Si(100) surface. We also developed two new ab initio electronic structure tools: (1) pseudospectral full configuration interaction, a method for treating electron correlation numerically; and (2) a reaction barrier following method for finding transition states for chemical reactions. GRA

N93-11801# EG and G Rocky Flats, Inc., Golden, CO.
CALCULATION OF BINARY PHASE DIAGRAMS BETWEEN THE ACTINIDE ELEMENTS, RARE EARTH ELEMENTS, AND TRANSITION METAL ELEMENTS
J. E. Selle 26 Jun. 1992 100 p
(Contract DE-AC34-90DP-62349)
(DE92-019119; RFP-4450) Avail: CASI HC A05/MF A02

Attempts were made to apply the Kaufman method of calculating binary phase diagrams to the calculation of binary phase diagrams between the rare earths, actinides, and the refractory transition metals. Difficulties were encountered in applying the method to the rare earths and actinides, and modifications were necessary to provide accurate representation of known diagrams. To calculate the interaction parameters for rare earth-rare earth diagrams, it was necessary to use the atomic volumes for each of the phases: liquid, body-centered cubic, hexagonal close-packed, and face-centered cubic. Determination of the atomic volumes of each of these phases for each element is discussed in detail. In some cases, empirical means were necessary. Results are presented on the calculation of rare earth-rare earth, rare earth-actinide, and actinide-actinide diagrams. For rare earth-refractory transition metal diagrams and actinide-refractory transition metal diagrams, empirical means were required to develop values for the enthalpy of vaporization for rare earth elements and values for the constant (C) required when intermediate phases are present. Results of using the values determined for each element are presented. DOE

N93-11808# Purdue Univ., West Lafayette, IN. Dept. of Chemistry.

EXPLORATION OF THE IONIZABLE METAL CLUSTER-ELECTRODE SURFACE ANALOGY: INFRARED SPECTROELECTROCHEMISTRY OF (Pt24(CO)30)(SUP n), (Pt26(CO)32)(SUP n), AND (Pt38(CO)44)(SUP n) (n = 0 TO -10), AND COMPARISONS WITH POTENTIAL-DEPENDENT SPECTRA OF CO ADLAYERS ON PLATINUM SURFACES

J. D. Roth, G. J. Lewis, L. K. Safford, X. Jiang, and L. F. Dahl May 1992 49 p
(Contract N00014-91-J-1409)
(AD-A252544; TR-123) Avail: CASI HC A03/MF A01

Infrared spectroelectrochemistry has been utilized to explore the vibrational properties of the high-nuclearity platinum carbonyl clusters (Pt24(CO)30)n, etc. as a function of the charge n in dichloromethane, acetonitrile, acetone, tetrahydrofuran, and methanol. The clusters exhibit unusually reversible voltammetric and spectroelectrochemical behavior, with a sequence of redox steps spanning n = 0 to (in one case) -10, having formal potentials, Ef, between ca 0.5 and -2.5 V vs ferrocenium-ferrocene. Largely two-electron steps are observed for (Pt26(CO)32)n, involving even-charge states (n = -2, -4, -6, -8, -10). Sequential one-electron steps are found for (Pt24(CO)30)n and (Pt38(CO)44)n, although the regions of electrode potential over which odd-charge states (n = -1, -3, -5, -7) are stable (i.e., the spacings between Ef values) are markedly smaller than for the even-charge states. The C-O stretching frequencies for the bridging (nu(b)(co)) and especially the terminal (nu(t)(co)) coordinated CO ligands decrease systematically as n becomes more negative. Author (GRA)

N93-11847# Kentucky Univ., Lexington. Center for Applied Energy Research.

SYNTHESIS OF SINGLE PHASE (ALPHA)-Fe, Fe3C AND Fe7C3 NANO-PARTICLES BY CO2 LASER PYROLYSIS TECHNIQUE

P. C. Eklund and X. X. Bi 1992 29 p
(Contract DE-AC22-91PC-90056)
(DE92-015654; DOE/PC-90056/T4) Avail: CASI HC A03/MF A01

Iron-containing catalysts have been known to be useful in assisting the Fischer-Tropsch (FT) reaction for synthesizing hydrocarbons. However, it has been well recognized that iron catalyst are not stable during the reaction but converted into iron carbides. It is thus important to understand the role of the iron carbides in the catalytic reaction of the FT-synthesis. It has been found difficult to produce iron carbide nano-particles as a single phase, because iron carbide phases are only metastable under 1 atm pressure. Iron carbide bulk particles prepared so far are often contaminated with metallic iron, iron oxides and free carbon. In this study, we investigate the synthesis of iron carbide nano-particles using CO2 laser pyrolysis technique. We show that this technique is successful in synthesizing alpha-Fe, Fe3C and Fe7C3 nano-particles in their single phase with sizes in the range of 5 to 20 nm. In particular, we have produced for the first time the Fe7C3 which has been known to exist but unable to be produced as a single phase. Furthermore, it is interesting that Fe5C2 which has carbon and iron ratio between Fe3C and Fe7C3, is not seen in any run of our synthesis. DOE

N93-11866# Combustion Inst., Pittsburgh, PA.

THE TWENTY-THIRD INTERNATIONAL SYMPOSIUM ON COMBUSTION Final Report, 15 Sep. 1990 - 1991

1991 1965 p Proceedings held in Orleans, France, 22-27 Jul. 1990
(Contract MIPR-FQ8671-9001535; AF-AFOSR-0332-90)
(AD-A250377) Avail: CASI HC A99/MF A10

One of the important activities of The Combustion Institute during the period of Grant AFOSR-90-0332 DEF, effective September 15, 1990, was the Twenty-Third International Symposium on Combustion. The proceedings were published in a volume as a permanent record. It includes the Hottel Lecture, four invited papers, three invited mini-reviews, and 230 contributed papers, all refereed by the Program Subcommittee. Peter P. Gray, Master of Gonville and Caius College, Cambridge University gave the Hottel Lecture on The Non-linear Role of Chemistry in Combustion. Papers were organized in five Colloquia: Reaction Kinetics in Combustion; Laminar Flames; Turbulent Combustion; Combustion in Practical Systems; Combustion of Solid Fuels. Topical sessions included Detonations, Diagnostic Methods, Fire, High Temperature Synthesis, Ignition, Microgravity Combustion, Non-Steady Flames, Propellents, Soot, and Spray and Droplet Combustion. There were 307 poster presentations of work-in-progress presented at the conference. Over 1,000 scientists from 25 countries attended the symposium. Research papers were also presented at our Section Meetings during this period on various subjects of combustion. We publish our journal, 'Combustion and Flame,' monthly. GRA

N93-11918# Los Alamos National Lab., NM.

HIGH-PRECISION THORIUM RIMS FOR GEOCHEMISTRY

B. L. Fearey, B. M. Tissue, J. A. Olivares, G. W. Loge, M. T. Murrell, and C. M. Miller 1992 5 p Presented at the 6th International Symposium on Resonance Ionization Spectroscopy and its Applications, Santa Fe, NM, 24-29 May 1992
(Contract W-7405-eng-36)
(DE92-017405; LA-UR-92-1841; CONF-920574-14) Avail: CASI HC A01/MF A01

We present our latest results in the development of resonance ionization mass spectrometry (RIMS) using cw lasers to measure isotope ratios of importance in geochemistry and geochronology. The RIMS method provides a higher ionization efficiency than thermal ionization allowing analysis of smaller sample sizes, while maintaining equivalent internal precision. The bias introduced in the Th-230/Th-232 ratio measurements by the RIMS method when using narrow-band and broad-band lasers is discussed. Spectra of Th-239, which can be used as an internal standard, are also presented. DOE

N93-12062# Pittsburgh Univ., PA. Dept. of Chemistry.

THE ROLE OF BACKBOND STRAIN IN SILICON SURFACES ON THE DECOMPOSITION OF NH3 AND PH3

M. L. Colaianni, P. J. Chen, and J. T. Yates, Jr. 23 Jun. 1992 14 p
(Contract N00014-82-C-0280)
(AD-A253771; TR-49) Avail: CASI HC A03/MF A01

Silicon adatoms on the Si(111)-(7x7) surface form strained Si-Si backbonds with underlying silicon atoms. The strain at adatom sites causes both NH2(a) and PH2(a) to be thermally unstable compared to the same species on the Si(100)-(2x1) surfaces which contains less-strained silicon surface atoms. The surface strain induces enhanced NH2(a) and PH2(a) dissociation on Si(111)-(7x7) adatom sites compared to Si(100)-(2x1). Thus both NH2(a) and PH2(a) can participate in recombination reactions on Si(100) to produce major amounts of NH3(g) and PH3(g) above 600 K; such reactions are absent on Si(111)-(7x7) surfaces. GRA

N93-12091# Kentucky Univ., Lexington. Dept. of Chemistry.
LASER SPECTROSCOPY AND DYNAMICS OF TRANSIENT SPECIES FORMED IN PYROLYSIS REACTIONS
D. J. Clouthier Nov. 1991 15 p
(Contract DE-FG05-86ER-13544)
(DE92-016206; DOE/ER-13544/5) Avail: CASI HC A03/MF A01

This research concerns the study of the spectroscopy and excited state dynamics of a number of transient molecules containing either sulfur or oxygen. The identification and study of sulfur species which are analogs of important oxygen-containing combustion intermediates is important to our understanding of reactive intermediates. The oxygen-containing species chosen for study are new systems whose electronic spectra have not previously been identified. The major experimental technique used in this work was pyrolysis jet spectroscopy. Since many of the species have not been previously studied by laser techniques, much effort was devoted to determining methods for producing and observing them. We have been very successful in a number of cases and have developed some further experimental techniques. DOE

N93-12105# SRI International Corp., Menlo Park, CA. Materials Research and Chemical Engineering Lab.
CHEMISTRY OF LOWER VALENT ACTINIDE HALIDES
K. H. Lau and D. L. Hildenbrand Jan. 1992 11 p
(Contract DE-FG03-89ER-13986)
(DE92-017031; DOE/ER-13986/T1) Avail: CASI HC A03/MF A01

This research effort was concerned almost entirely with the first two members of the actinide series, thorium and uranium, although the work was later extended to some aspects of the neptunium-fluorine system in a collaborative program with Los Alamos National Laboratory. Detailed information about the lighter actinides will be helpful in modeling the properties of the heavier actinide compounds, which will be much more difficult to study experimentally. In this program, thermochemical information was obtained from high temperature equilibrium measurements made by effusion-beam mass spectrometry and by effusion-pressure techniques. Data were derived primarily from second-law analysis so as to avoid potential errors in third-law calculations resulting from uncertainties in spectroscopic and molecular constants. This approach has the additional advantage of yielding reaction entropies that can be checked for consistency with various molecular constant assignments for the species involved. In the U-F, U-Cl, and U-Br systems, all of the gaseous species UX, UX(sub 2), UX(sub 3), UX(sub 4), and UX(sub 5), where X represents the halogen, were identified and characterized; the corresponding species ThX, ThX(sub 2), ThX(sub 3), and ThX(sub 4) were studied in the Th-F, Th-Cl, and Tn-Br systems. A number of oxyhalide species in the systems U-0-F, U-0-Cl, Th-0-F, and Th-O-Cl were studied thermochemically. Additionally, the sublimation thermodynamics of NpF4(s) and NpO2F2(s) were studied by mass spectrometry. DOE

N93-12112# California Univ., Berkeley. Lawrence Berkeley Lab.
FREELY PROPAGATING OPEN PREMIXED TURBULENT FLAMES STABILIZED BY SWIRL
C. K. Chan (Hong Kong Polytechnic, Kowloon.), K. S. Lau (Hong Kong Polytechnic, Kowloon.), W. K. Chin (Hong Kong Polytechnic, Kowloon.), and R. K. Cheng Dec. 1991 17 p Presented at the 1992 Spring Meeting of the Western States Section of the Combustion Institute, Corvallis, OR, 23-24 Mar. 1992
(Contract DE-AC03-76SF-00098)
(DE92-017116; LBL-31581; CONF-9203140-3) Avail: CASI HC A03/MF A01

A novel means has been developed for using weak swirl to stabilize freely propagating open premixed turbulent flames (swirl numbers between 0.05 to 0.3). By injecting a small amount of air tangentially into the co-flow of a concentric burner, stationary flames can be maintained above the burner exit for a large range of mixture, turbulence and flow conditions. The absence of physical surfaces in the vicinity of the flame provides free access to laser diagnostics. Laser Doppler anemometry and laser Mie scattering measurements of four flames with and without incident turbulence show that their features are typical of wrinkled laminar flames. The most distinct characteristics is that flame stabilization does not rely on flow recirculation. Centrifugal force induced by swirl causes flow divergence, and the flame is maintained at where the local mass flux balances the burning rate. The flame speeds can be estimated based on the centerline velocity vector, which is locally normal to the flame brush. This flame geometry is the closest approximation to the 1-D planar flame for determining fundamental properties to advance turbulent combustion theories. DOE

N93-12119# Massachusetts Univ., Amherst. Dept. of Chemical Engineering.
PROBING FLAME CHEMISTRY WITH MBMS, THEORY, AND MODELING
P. R. Westmoreland Mar. 1992 30 p
(Contract DE-FG02-91ER-14192)
(DE92-011433; DOE/ER-14192/1) Avail: CASI HC A03/MF A01

The program objective is to establish kinetics of combustion and molecular weight growth in C3 hydrocarbon flames as part of an ongoing study of flame chemistry. Specific reactions to be studied are as follows: the oxidation reactions of O and OH with C3's; and (2) the growth reactions of C3H5 and C3H3 with themselves and with unsaturated hydrocarbons. Our approach combines molecular-beam mass spectroscopy (MBMS) experiments which give the following: concentrations of stable species and free radicals in low-pressure flat flames; theoretical predictions of rate constants by thermochemical kinetics, Biomedical Quantum-RRK, RRKM, and master-equation theory; and whole-flame modeling using full mechanisms of elementary reactions. Detailed MBMS flame data are the principal results of the first nine months of the grant. Spatial profiles of temperature, area expansion ratio, and mole fraction have been mapped in two low-pressure flat flames, one fuel-lean (phi = 0.229) and the other fuel-rich (phi = 1.64) in propene/oxygen/argon. Species identities and trends suggest certain chemical pathways, but reaction theory and flame modeling are beginning to provide specific, quantitative insights into oxidation and growth chemistry. DOE

N93-12135# Department of Energy, Oak Ridge, TN. Office of Scientific and Technical Information.
SUMMARIES OF FY 1991 RESEARCH IN THE CHEMICAL SCIENCES
Aug. 1992 145 p
(DE92-011920; DOE/ER-0144-10) Avail: CASI HC A07/MF A02

Paragraph summaries are presented of 431 research projects at national laboratories, offsite institutions, and small businesses in the fields of photochemical and radiation sciences, chemical physics, atomic physics, chemical energy, separations and analysis, heavy element chemistry, and chemical engineering. An addendum of late grants is included. Special facilities are described. Indexes of topics, institutions, and investigators are also included. DOE

N93-12172# North Carolina State Univ., Raleigh. Dept. of Physics.
RESEARCH AT AND OPERATION OF THE MATERIAL SCIENCE X RAY ABSORPTION BEAMLINE (X-11) AT THE NATIONAL SYNCHROTRON LIGHT SOURCE
1992 15 p
(Contract DE-FG05-89ER-45384)
(DE92-018598; DOE/ER-45384/T1) Avail: CASI HC A03/MF A01

This report discusses three projects at the Material Science X-Ray Absorption Beamline. The following topics are discussed: XAFS study of some titanium silicon and germanium compounds; initial XAS results of zirconium/silicon reactions; and low angle electron yield detector. DOE

N93-12186# Etalon, Inc., Boston, MA.
RESONANT MEMBRANE SPATIAL LIGHT MODULATORS Final Report, 1 Jul. 1991 - 31 Mar. 1992
Mark W. Miles 1 Jun. 1992 3 p
(Contract DAAL03-91-C-0028)
(AD-A253893; ARO-29024.1-EL-SBI) Avail: CASI HC A01/MF A01

Incorporating an aluminum layer to allow for contacting the arrays resulted in the generation of residual materials which compromised structures. Attempts to resolve the problem using alternate etch chemistries and protective layers were unsuccessful. A previously discarded wet etch approach was revisited and has produced structures. First attempts at driving the devices revealed shorts apparently due to sidewall deposition of aluminium during the primary deposition. This can be overcome by optimizing position during the evaporation, and adding an oxygen plasma step to insulate any exposed aluminum. GRA

N93-12215*# Alabama Univ., Huntsville. Center for Applied Optics.
ANALYSIS OF MATERIALS FROM MSFC LDEF EXPERIMENTS Final Report, Feb. 1990 - Jul. 1991
R. Barry Johnson 31 Jul. 1991 5 p
(Contract NAS8-36955)
(NASA-CR-184425; NAS 1.26:184425; UAH-5-32354) Avail: CASI HC A01/MF A01

In preparation for the arrival of the Long Duration Exposure Facility (LDEF) samples, a material testing and handling approach was developed for the evaluation of the materials. A configured lab was made ready for the de-integration of the LDEF experiments. The lab was prepared to clean room specifications and arranged with the appropriate clean benches, tables, lab benches, clean room tools, particulate counter, and calibrated and characterized analytical instrumentation. Clean room procedures were followed. Clean room attire and shoe cleaning equipment were selected and installed for those entering. Upon arrival of the shipping crates they were taken to the lab, logged in, and opened for examination. The sample trays were then opened for inspection and test measurements. The control sample measurements were made prior to placement into handling and transport containers for the flight sample measurements and analysis. Both LDEF flight samples and LDEF type materials were analyzed and tested for future flight candidate material evaluation. Both existing and newly purchased equipment was used for the testing and evaluation. Existing Space Simulation Systems had to be upgraded to incorporate revised test objectives and approaches. Fixtures such as special configured sample holders, water, power and LN2 feed-throughs, temperature measurement and control, front surface mirrors for reflectance and deposition, and UV grade windows had to be designed, fabricated, and installed into systems to achieve the revised requirements. New equipment purchased for LDEF analysis was incorporated into and/or used with existing components and systems. A partial list of this equipment includes a portable monochromator, enhanced UV System, portable helium leak detector for porosity and leak measurements, new turbo pumping system, vacuum coaster assembly, cryopumps, and analytical and data acquisition equipment. A list of materials tested, equipment designed, fabricated and installed, systems used, and analytical research accomplished on both LDEF flight samples and on similar materials which were lab tested for a comparative analysis to the LDEF flight samples is presented. Author

N93-12219# Oak Ridge National Lab., TN.
A CRYOGENIC ENRICHMENT TECHNIQUE FOR GAS CHROMATOGRAPHIC DETECTION OF S2F10 IN SF6 DISCHARGES
I. Sauers and R. A. Cacheiro 1992 5 p Presented at the Institute of Electrical and Electronics Engineers (IEEE) Symposium on Electrical Insulation, Baltimore, MD, 6-11 Jun. 1992
(Contract DE-AC05-84OR-21400)
(DE92-011045; CONF-9206140-1) Avail: CASI HC A01/MF A01

In conventional gas chromatography (GC), S2F10, in the presence of SF6, is only detectable down to a concentration of approximately 50 ppm (parts-per-million). This limit is largely due to the interference of the SF6 peak with S2F10. The detection limit can be reduced by employing an enrichment procedure similar to the on-line procedure employed by KEMA whereby S2F10 is selectively trapped, increasing the S2F10 concentration relative to SF6, followed by subsequent GC analysis. Using commercially available components we have set up a similar system and have evaluated some of the parameters influencing peak resolution and detectability of S2F10 in SF6, such as trapping temperature, desorption rates, and carrier gas flow. In addition to S2F10, other compounds relevant to SF6 decomposition were examined using this system. These compounds include SOF4, SO2F2, SOF2, SF4, SO2, SiF4, and S2OF10. Contrary to the KEMA results, S2OF10 was found to have a lower retention time than S2F10 in both the cryogenic enrichment system and in conventional GC. Finally we report on the first analyses of corona-discharged SF6 using this technique, which has at least a 1000-fold improvement in sensitivity over the conventional GC technique. DOE

N93-12254# University of Southern California, Los Angeles. Dept. of Chemistry.
GAS-SURFACE INTERACTIONS NEAR DISSOCIATION THRESHOLD Final Report, Nov. 1988 - Oct. 1991
Hanna Reisler and Curt Wittig 26 Mar. 1992 12 p
(Grant AF-AFOSR-0057-89)
(AD-A250205; AFOSR-92-0306TR) Avail: CASI HC A03/MF A01

The main thrust of our program was directed towards the study collision-induced dissociation (CID) of hyperthermal molecules on insulators (MgO), semiconductors (GaAs), and metals (Ag). Supersonic beams of nitroso compounds entered the UHV chamber with kinetic energies variable between 0.5 and 7 eV. NO products were detected state-selectively using two-frequency laser ionization. CID yields were measured as a function of surface temperature and incident kinetic energy, and complete energy deposition in the NO product was determined in each case. CID yields rise sharply with incident kinetic energy, with non-vanishing values even slightly below dissociation threshold at high surface temperature. The yield depends on the stiffness of the surface. The NO distributions are similar to those obtained in the gas-phase unimolecular decomposition of these molecules and indicate a broad distribution of internal energies. In the newest phase of this program, the photodissociation of ClNO adsorbed on a rough MgO surface is studied at 365 nm. The NO state distributions differ greatly from those obtained in gas-phase photodissociation and suggest that ClNO aggregates as islands on the surface and the NO and Cl undergo multiple collisions before desorption. GRA

N93-12255# Sandia National Labs., Livermore, CA.
OH ROTATIONAL TEMPERATURE AND CONCENTRATION MEASUREMENTS IN A SUPERSONIC JET
T. G. Mataga and R. J. Cattolica 1991 14 p Presented at the 24th International Symposium on Combustion, Sydney (Australia), 5-10 Jul. 1992
(Contract DE-AC04-76DR-00789)
(DE92-006700; SAND-91-8733; CONF-920707-10) Avail: CASI HC A03/MF A01

Axial and radial profiles of the rotational temperature and concentration of the OH molecule in an axisymmetric combustion-driven supersonic free jet were measured over a Mach number range from M = 1.5 - 7.5 and number density from 10(exp 12) to 10(exp 14) cm(exp -3). The free jet was produced from the combustion products of a low-pressure (51.8-torr) H2/O2/Ar flame (Phi = 1.09) expanded from a converging quartz nozzle into a vacuum. The temperature and concentration of the OH molecule were measured via laser-induced fluorescence (LIF) from the R(sub 1)(3), R(sub 1)(4), and R(sub 1)(7) lines in the (1.0) band of the A (sup 2)Sigma - Chi (sup 2)Pi transition with detection in the (1, 1) band. The temperature was measured using a two-line technique. An empirical model of the fluorescence yield was developed using time-resolved fluorescence quenching rates measured on the jet axis to correct the fluorescence signals for quenching effects.

The predicted fluorescence yield increased by a factor of 23 along the jet axis as the temperature decreased from 772 K to 100 K, primarily due to the corresponding decrease in number density for this isentropic expansion. The increase in fluorescence yield due to the density decrease was reduced due to an increase in the collisional cross-section following a T(exp -0.5) temperature dependence. The fluorescence yield increased with increasing rotational quantum number. At a temperature of 400 K, the fluorescence yield increased by 30-percent from $N' = 5$ to $N' = 8$. The measured OH rotational temperature and concentration profiles were in good agreement with the predictions of a method of characteristics solution for the behavior of the supersonic free jet. DOE

N93-12257# Princeton Univ., NJ. Dept. of Mechanical and Aerospace Engineering.

INHIBITION OF MOIST CARBON MONOXIDE OXIDATION BY TRACE AMOUNTS OF HYDROCARBONS

R. A. Yetter and F. L. Dryer 1992 21 p Presented at the 24th International Symposium on Combustion, Sydney (Australia), 5-10 Jul. 1992
(Contract DE-FG02-86ER-13503)
(DE92-008736; CONF-920707-21) Avail: CASI HC A03/MF A01

The moist carbon monoxide oxidation reaction perturbed by small quantities of hydrocarbons is studied over the temperature range 1026 - 1140 K at 1 atm to yield information on the reactions of OH, H, and O radicals with hydrocarbons (RH) and on general mechanistic inhibition behavior. The inhibiting action of hydrocarbons below the second explosion limit of $CO/H_2O/O_2$ mixtures is used for obtaining rate parameters for RH + OH in the case of methane and propane. Considering all the hydrocarbons studied, the general ranking of effectiveness as an inhibitor was found to follow the order: propene, propane, methane, ethane, ethene, and acetylene. In fact, acetylene was observed to always promote the oxidation of moist CO, thus emphasizing the importance of O-atom radical attack rather than OH attack on acetylene. The kinetics of these mixtures are shown to complement mechanistic studies on RH/O_2 mixtures for the development and validation of hierarchical hydrocarbon oxidation reaction mechanisms. DOE

N93-12267# Georgia Inst. of Tech., Atlanta. School of Civil Engineering.

FORMIC ACID: DEVELOPMENT OF AN ANALYTICAL METHOD AND USE AS PROCESS INDICATOR IN ANAEROBIC SYSTEMS M.S. Thesis

Sharon L. Perkins Mar. 1992 152 p
(Contract N00123-89-G-0573)
(AD-A250668) Avail: CASI HC A08/MF A02

An analytical method which could be routinely used for determining formic acid was developed. This procedure was utilized to examine the fluctuation of formic acid concentration in anaerobic batch reactors which were fed substrates containing various amounts of substances known to induce stress in these systems. The results were examined to determine possible correlation between these fluctuations and system performance; however, the health or inhibition of the experimental systems was not conclusively established. Also, several full scale and pilot systems were analyzed for the presence of formic acid. Based on the results of this research, it was concluded that formic acid concentrations in a system that was not subjected to stressful substances are very low. There was correlation between system stress and formic acid accumulation in systems exposed to toxic levels of ammonia. There was an indication that formic acid increases were dependent on the type of toxicity induced. Finally, when the system was stressed, the concentration of formic acid increased an order of magnitude over unstressed systems. GRA

N93-12282# Wisconsin Univ., Madison.

SYSTEMS OF EVOLUTION EQUATIONS IN THERMOCHEMICAL EQUATIONS Final Report, 1 Sep. 1988 - 29 Feb. 1992

Athanassios Tzavaras 29 Apr. 1992 9 p
(Contract DAAL03-88-K-0185)
(AD-A254891; ARO-26218.6-MA) Avail: CASI HC A02/MF A01

In the framework of continuum mechanics the motion of deforming bodies is described by systems of nonlinear evolution equations, that arise by combining balance laws with constitutive relations characterizing the material response. The nonlinear character of the material response often induces a destabilizing mechanism that competes with dissipative mechanisms, such as viscosity or thermal diffusion. As a result of the competition coherent structures may appear, which at some level of modeling manifest themselves as singularities in the solutions of the corresponding model. These structures are diverse in nature, ranging from shock waves to shear bands to propagating phase boundaries, and no common theory can encompass all of them at present. Various instances of such phenomena were studied as part of the project. Specifically (a) a class of test problems intended to test a thermoplastic instability mechanism for shear band formation at high strain rates; (b) dynamics of spurt phenomena in viscoelastic flows; and (c) self-similar viscous and hydrodynamic limits for the equations of isentropic gas dynamics and the Broadwell system. GRA

N93-12311# Tennessee Univ., Knoxville. Measurement and Control Engineering Center.

ON-LINE ANALYSIS OF CHEMICAL COMPOSITION USING AN FT-RAMAN SPECTROMETER IN THE NEAR-IR

A. A. Garrison 1992 3 p Presented at the Society of Photo-Optical Instrumentation Engineers (SPIE) Conference on Optically Based Methods for Process Analysis, Somerset, NJ, 23-26 Mar. 1992
(Contract DE-FC07-88ID-12691)
(DE92-016503; CONF-9203165-1) Avail: CASI HC A01/MF A01

Newly commercialized Fourier transform Raman spectroscopic instrumentation provides a simpler alternative for vibrational spectroscopic analysis. Instrument vendors currently design for laboratory use, but there are many potential process applications of these stable, easy to use instruments. Raman spectroscopy is highly suited to analysis of aqueous samples. Near infrared excitation minimized fluorescence interference and allows for remote operation via fiber optic probes. The Department of Energy has funded research at the Measurement and Control Center to establish the utility of this method for on-line composition analysis in distillation columns. Laboratory evaluation and instrument employs an air-cooled laser and a thermoelectrically cooled detector. The device is mounted on a three by three foot cart for convenient location in control rooms. Current fiber optic extension cables allow for analysis in a cell thirty five meters from the instrument. Application of the device to an acid recovery column at Tennessee Eastman Corporation in Kingsport, Tennessee will be discussed. Sensor placement is critical to optimal application of any on-line device. Potential energy savings and product throughput increase will be detailed. DOE

N93-12428# Pennsylvania Univ., Philadelphia. Dept. of Chemistry.

CATALYTIC HYDROGENATION OF CARBON MONOXIDE

B. B. Wayland 1992 14 p
(Contract DE-FG02-86ER-13615)
(DE92-014729; DOE/ER-13615/6) Avail: CASI HC A03/MF A01

Developing strategies to accomplish the reduction and hydrogenation of carbon monoxide to produce organic oxygenates at mild conditions is addressed. Our approaches to this issue are based on the recognition that rhodium macrocycles have unusually favorable thermodynamic values for producing a series of intermediates implicated in the catalytic hydrogenation of CO. Observations of metalloformyl complexes produced by reactions of H_2 and CO, and reductive coupling of CO to form metallo alpha-diketone species have suggested a multiplicity of routes to organic oxygenates that utilize these species as intermediates.

Thermodynamic and kinetic-mechanistic studies are used in constructing energy profiles for a variety of potential pathways, and these schemes are used in guiding the design of new metallospecies to improve the thermodynamic and kinetic factors for individual steps in the overall process. Variation of the electronic and steric effects associated with the ligand arrays along with the influences of the reaction medium provide the chemical tools for tuning these factors. Emerging knowledge of the factors that contribute to M-H, M-C, and M-O bond enthalpies is directing the search for ligand arrays that will expand the range of metal species that have favorable thermodynamic parameters to produce the primary intermediates for CO hydrogenation. Studies of rhodium complexes are being extended to non-macrocyclic ligand complexes that emulate the favorable thermodynamic features associated with rhodium macrocycles, but that also manifest improved reaction kinetics. Multifunctional catalyst systems designed to couple the ability of rhodium complexes to produce formyl and diketone intermediates with a second catalyst that hydrogenates these imtermediates are promising approaches to accomplish CO hydrogenation at mild conditions. DOE

N93-12478# City Coll. of the City Univ. of New York, NY. Inst. for Physicochemical Hydrodynamics.
STUDIES IN PREMIXED COMBUSTION
G. I. Sivashinsky 1992 13 p
(Contract DE-FG02-88ER-13822)
(DE92-018646; DOE/ER-13822/5) Avail: CASI HC A03/MF A01

This report discusses the following topics on premixed combustion: theory of turbulent flame propagation; pattern formation in premixed flames and related problems; and pattern formation in extended systems. DOE

N93-12518# Howard Univ., Washington, DC. Dept. of Electrical Engineering.
GROWTH OF SOLID SOLUTIONS OF ALUMINUM NITRIDE AND SILICON CARBIDE BY METALORGANIC CHEMICAL VAPOR DEPOSITION Semiannual Report, 25 Nov. 1991 - 1 Jul. 1992
I. Jenkins, K. G. Irvine, M. G. Spencer, V. Dmitriev, and N. Chen 27 Aug. 1992 14 p
(Contract N00014-92-J-1136)
(AD-A255000) Avail: CASI HC A03/MF A01

We report the growth of solid solutions of (AlN)(x)(SiC)(1-x) over the entire composition range from x = 0.1 to X = 0.9. We believe this is the first report of a solid solution of (AlN)(x)(SiC)(1-x) produced by metal organic vapor deposition. Growth was performed in a low pressure vertical reactor using the silane-propane-ammonia-trimethylaluminium-hydrogen gas system on both silicon and silicon carbide substrates. Growth temperatures were between 1200 - 1250 C and growth pressures varied between 10 and 76 Torr. The composition of the solid solutions were strongly dependent on system pressure. GRA

N93-12042# Ecole Polytechnique, Palaiseau (France). Lab. de Physique des Milieux Ionises.
SATURATION EFFECTS IN ABSORPTION SPECTROSCOPY OF THE K(ALPHA) RAYS OF ALUMINUM [EFFETS DE SATURATION EN SPECTROSCOPIE D'ABSORPTION DES RAIES K ALPHA DE L'ALUMINIUM]
Claude Chenais-Popovics, Christian Fievet, Jean-Paul Geindre, Isao Matsushima (Tsukuba Univ., Japan), and Jean-Claude Gauthier *In its* The 1989 Scientific Report of the Laboratory for the Use of High Power Lasers Apr. 1990 p 119-124 In FRENCH (For primary document see N93-12023 02-36)
Avail: CASI HC A02/MF A03

N93-12050# Ecole Polytechnique, Palaiseau (France). Lab. de Physique des Milieux Ionises.
HYDRODYNAMIC STUDY OF MULTILAYER TARGETS BY SPATIAL AND TEMPORAL RESOLUTION SHADOW SPECTROSCOPY [ETUDE DE L'HYDRODYNAMIQUE DE CIBLES MULTICOUCHES PAR OMBROSCOPIE RESOLUE SPATIALEMENT SPECTRALEMENT]
Jean-Paul Geindre, Claude Chenais-Popovics, Patrick Audebert, Isao Matsushima (Tsukuba Univ., Japan), and Jean-Claude Gauthier *In its* The 1989 Scientific Report of the Laboratory for the Use of High Power Lasers Apr. 1990 p 161-165 In FRENCH (For primary document see N93-12023 02-36)
Avail: CASI HC A01/MF A03

26 METALLIC MATERIALS

Includes physical, chemical, and mechanical properties of metals, e.g., corrosion; and metallurgy.

N93-10984# Sandia National Labs., Albuquerque, NM.
HEAT-AFFECTED ZONE CRACKING OF NITRONIC 60 STAINLESS STEEL
M. C. Maguire, C. V. Robino, B. K. Damkroger, and T. J. Lienert (Edison Welding Inst., Columbus, OH.) 1992 3 p Presented at the American Welding Society Annual Conference, Houston, TX, 25-30 Apr. 1992
(Contract DE-AC04-76DP-00789)
(DE92-018286; SAND-92-1803C; CONF-9204174-1) Avail: CASI HC A01/MF A01

Nitronic 60 is a nitrogen-strengthened austenitic stainless steel used for applications where metal-to-metal wear and galling resistance are required. In addition, it does not transfer to martensite with strain or upon cooling to cryogenic temperatures. In comparison to type 304 stainless steel, the nickel content is similar, chromium content is slightly reduced, and manganese, silicon, and nitrogen are all increased in Nitronic 60. Although studies have shown that it can be joined with arc welding, its fabrication weldability is limited by heat-affected zone (HAZ) cracking. The HAZ cracking behavior of this alloy is investigated during autogenous gas tungsten arc welding and pulsed autogenous Nd:YAG welding. DOE

N93-10995# Ames Lab., IA.
INTERNAL FRICTION PEAKS DUE TO OXYGEN, NITROGEN, AND HYDROGEN IN V-Nb ALLOYS
O. Buck, O. N. Carlson, H. Indrawirawan, L. J. H. Brasche, and D. T. Peterson 1991 35 p Presented at the American Society for Testing and Materials (ASTM) Symposium on Mechanics and Mechanisms of Material Damping, Baltimore, MD, 13-15 Mar. 1991
(Contract W-7405-eng-82)
(DE92-012155; IS-M-683; CONF-910374-2) Avail: CASI HC A03/MF A01

Richter's and Snoek's original works established the existence of an anelastic relaxation produced by a stress-induced interstitial reorientation in bcc metals. This anelastic relaxation, now referred to as a Snoek peak, has been studied extensively and well characterized in the past for the interstitials carbon, nitrogen, and oxygen. The existence of a hydrogen Snoek peak in bcc metals has been a matter of some controversy, however. We have studied relaxation peaks in V, Nb, and V-Nb alloys recently. The alloys have complete mutual solubility and are of interest since they have an extremely high room temperature solid solubility for hydrogen. They also have, over a certain composition range, not shown any hydride phase precipitation at temperatures as low as 4 K. Thus, if a hydrogen Snoek peak does exist, it should be found in such alloys. Indeed there is evidence now of a spectrum of hydrogen relaxation peaks below room temperature. Furthermore, due to the difference in the atomic radii of V and Nb there is a large misfit in dilute alloys of these elements. This and possibly some chemical interaction can cause trapping (or antitrapping) of the interstitials at the substitutional sites, causing solute-interstitial peaks. The present paper provides an overview of our observations regarding: (1) the effect of hydrogen on the oxygen and nitrogen Snoek peaks in pure V and Nb, (2) the oxygen relaxation peaks in V-Nb alloys, (3) the hydrogen relaxation spectrum in V-Nb alloys, and (4) the effect of oxygen on the hydrogen relaxation spectrum in V-Nb alloys. DOE

N93-11026# Messerschmitt-Boelkow-Blohm G.m.b.H., Munich (Germany).

CORROSION PROTECTION OF MATERIALS FOR AIRCRAFT USING ION BEAM PROCESSES. CORROSION AND BONDING STRENGTH EXAMINATIONS. PHYSICAL ANALYSIS OF LASER COMPOSITION [KORROSIONSSCHUTZ VON LUFTFAHRTRELEVANTEN WERKSTOFFEN DURCH IONENSTRAHLVERFAHREN - KORROSIONS- UND HAFTFESTIGKEITSUNTERSUCHINGEN/PHYSIKALISCHE ANALYTIK DER SCHICHTZUSAMMENSETZUNG]

Ursula Koch, Heike Roland, and Meinhard Meyer 1991 7 p In GERMAN Submitted for publication
(MBB-Z-0405-91-PUB; ETN-92-92122) Avail: CASI HC A02/MF A01

The corrosion behavior of corrosion susceptible aluminum alloys, which were treated against corrosion using Physical Vapor Deposition (PVD) and Ion Beam Assisted Deposition (IBAD), is examined. The corrosion behavior of PVD and IBAD coatings is shown to be good. The stability against corrosion of clad layers was not obtained, on account of low layer thickness and higher microporosity. It was demonstrated that the corrosion behavior of aluminum alloys could be highly improved by physical coating. ESA

N93-11027# Messerschmitt-Boelkow-Blohm G.m.b.H., Munich (Germany). Zentrallabor.

SURFACE PROTECTION IN THE AIRCRAFT INDUSTRY [OBERFLAECHENSCHUTZ IN DER LUFTFAHRTINDUSTRIE]

Franz Josef Gammel 1992 12 p In GERMAN Presented at the Jahrestagung Verschleiss- und Korrosionsfeste Oberflaechen fuer Hochfeste Bauteile, Bad Nauheim, 9-10 Mar. 1992, Fed. Republic of Germany
(MBB-Z-0432-92-PUB; ETN-92-92126) Avail: CASI HC A03/MF A01

Among a number of surface protection techniques used in the aircraft industry, three methods pertaining to the electroplating field are presented: aluminum adhesive bonding preparatory treatment, steel chemical nickel plating, and titanium metallization. These processes are discussed using utilization examples such as the realization of clean surfaces for aircraft fuselage. It is shown that galvanic processes are in the foreground. ESA

N93-11031# Rolls-Royce Ltd., Derby (England).

SHORT FATIGUE CRACK GROWTH IN A NICKEL-BASE SUPERALLOY AT ROOM AND ELEVATED TEMPERATURE Final Report

J. C. Healy (Birmingham Univ., England), L. Grabowski, and C. J. Beevers (Birmingham Univ., England) 10 Aug. 1990 12 p
(PNR-90892; ETN-92-92194) Copyright Avail: CASI HC A03/MF A01

The fatigue behavior of Waspaloy was studied using an optical system developed to monitor short crack growth at elevated temperatures. Tests conducted at 19 and 500 C revealed the dominant mechanism of crack formation was slip band cracking. Crack formation was also associated with coarse carbide particles within the matrix. The dominant failure mechanism at 19 and 500 C was one of mixed mode 1 and 2 fractures, with mode 2 shear displacements giving rise to surface roughness induced non-closure. Oxide and plasticity induced non-closure processes made only a minor contribution to the overall growth process. Short fatigue crack growth measured at R 0.1 was faster at 500 C than at 19 C at an equivalent value of Delta-K(sub 1). This was attributed to a change in slip character from highly planar to one involving increasing amounts of cross slip at 19 and 500 C respectively. ESA

N93-11033# Rolls-Royce Ltd., Derby (England).

MODELLING SHORT CRACK GROWTH BEHAVIOUR IN NICKEL-BASE SUPERALLOYS

L. Grabowski and J. E. King (Cambridge Univ., England) 1 Mar. 1991 18 p Submitted for publication Sponsored in part by British Gas Corp. and Fellowship of Engineering
(PNR-90912; ETN-92-92201) Copyright Avail: CASI HC A03/MF A01

A description of the features and mechanisms of facetted short crack growth in Ni base superalloys is presented, and existing short crack growth models are reviewed in terms of their application to Ni base alloys. A new two phase model for local microstructural effects on short crack growth in Waspaloy is presented which is derived from detailed observations of crack growth through individual grains. It differs from all previous models in highlighting the importance of crack path perturbations within grains. Potential applications of the model in alloy development are discussed. ESA

N93-11109# Rolls-Royce Ltd., Derby (England).

SIGMA PHASE IN NICKEL BASED SUPERALLOYS

C. Small and K. Clay 27 Mar. 1991 19 p Presented at the British Crystallographic Association Spring Meeting, Sheffield, England, 27 Mar. 1991
(PNR-90950; ETN-92-92227) Copyright Avail: CASI HC A03/MF A01

A set of graphics that discuss nickel-based superalloys as possible materials for withstanding high pressure turbine operating conditions is presented. The composition, microstructure, and phase behavior of these alloys are summarized. Identification of phases through metallography, transmission electron microscopy, and X-ray diffraction is discussed. The experimental technique of X-ray diffraction is presented together with an example. Integration of X-ray diffraction into alloy development programs is illustrated. ESA

N93-11111# Rolls-Royce Ltd., Derby (England).

PRESENT AND FUTURE TRENDS IN TURBINE BLADE MATERIAL AND MANUFACTURE TECHNOLOGY

G. J. S. Higginbotham and D. A. Ford (Rolls-Royce Ltd., Bristol, England) 2 Apr. 1991 22 p Presented at the 2nd British/Italian Workshop, Bath, England, 11 Mar. 1991
(PNR-90960; ETN-92-92233) Copyright Avail: CASI HC A03/MF A01

Single crystal superalloys with high temperature strengths suitable for turbine blading are introduced. Special attention is given to nickel based alloys and their casting techniques. Development trends in the furnaces used in this casting are considered. The advantages, potential practical problems, and remedies are discussed. Quality assurance and wall section measurement though ultrasonics are also discussed. Single crystal inspection requirements and techniques, notably back reflection X-ray diffraction techniques, are outlined. Consequential problems from exploiting single crystal alloys in more demanding applications are discussed, and a case history showing how the new material was first used for the potentially higher stressed second stage blade in two stage turbines, is outlined. Future trends, including 3rd generation single crystal alloys which require the addition of yttrium to maintain environmental resistance, are considered. ESA

N93-11115# Rolls-Royce Ltd., Derby (England).

ELEVATED TEMPERATURE FATIGUE CRACK GROWTH IN A NICKEL BASE SUPERALLOY UNDER DWELL CONDITIONS

J. Byrne (Portsmouth Polytechnic, England), R. Hall (Portsmouth Polytechnic, England), M. Alabraba (Portsmouth Polytechnic, England), L. Grabowski, and I. W. Hussey 2 Aug. 1992 8 p Presented at the 6th International Conference on Mechanical Behavior of Materials, 29 Jul. - 2 Aug. 1991 Sponsored by Science Research Council
(PNR-90997; ETN-92-92251) Copyright Avail: CASI HC A02/MF A01

Corner crack growth was studied in Waspaloy at 550 to 650 C under cyclic (0.25 Hz) and 5 minute dwell at peak load conditions, both at R = 0.1. No significant effect of dwell in fatigue crack growth rate was found at 550 C, where predominantly transgranular cracking occurred. At 600 and 650 C, under dwell cycling a transition to entirely intergranular cracking was accompanied by a severe increase in crack growth rate. Using the change in temperature as a correlating parameter, dwell cycling behavior at 650 C is successfully predicted using a linear summation model based on static load and fatigue data. ESA

N93-11240# Stanford Univ., CA. Lab. of Physics.
THEORY OF SMALL METAL CLUSTERS, FILMS, AND WIRES
Final Report, 1 Mar. 1990 - 31 Dec. 1991
Walter A. Harrison Jun. 1992 8 p
(Contract N00014-90-J-1670)
(AD-A253120) Avail: CASI HC A02/MF A01

The work for this period was directed at the analysis of the effective Coulomb U* for metal clusters and the generalization of our theory of Coulomb effects in f-shell metals to transition-metal systems. The study of U* for clusters was completed, and pursuit of the problem did not seem further warranted. The initial generalization of the theory of Coulomb effects was also completed and applied to the experiments by Ulrich Gradmann and coworkers in Clausthal, Germany. That theory is being published together with the experiment. These calculations explain an increase in moment for atoms at surfaces, steps, or kinks in steps on metal surfaces. The theory was then generalized, with the inclusion of exchange as well as the Coulomb repulsion, and the evaluation of the total energy. The aim was determination of the nature of the ground state localization or nonlocalizion and the number of occupied resonances if localized. The corresponding electronic structure provides the basis for the understanding of virtually all of the properties of these systems, including the spin-dependent scattering which presumably gives rise to giant magnetoresistance. This analysis was essentially complete at the end of the tenure of the grant and preliminary application was made to transition-metal impurities in copper. GRA

N93-11244# Helsinki Univ. of Technology, Espoo (Finland). Lab. of Foundry Engineering.
INTERNATIONAL ADI-SEMINAR: AUSTEMPERED DUCTILE IRON
1991 215 p Seminar held in Espoo, Finland, 6-8 Nov. 1991
(PB92-180660; VAL-7/1991; ISBN-951-22-0920-9) Avail: CASI HC A10/MF A03

The contents are as follows: Opening Lecture; What is ADI - History and State of the Art; Microstructure and Mechanical Properties of ADI - Constitution of ADI, Kinetics of Austempering, Future Prospects; Thermal Stability of ADI; Alloying Elements in ADI - Heat Treatment of ADI, Theory and Practice, Future Prospects; ADI-Applications in Car Components, Future Prospects; Case-Studies on ADI Applications in USA; Kymenite--Applications Since 1973; Kymenite--Industrial Gear Units; and Kymenite in Railway Applications. GRA

N93-11336 GKSS-Forschungszentrum Geesthacht (Germany).
MICROSTRUCTURE AND MECHANICAL PROPERTIES OF REACTIVE HOT ISOSTATIC PRESSED TIAl POWDER MATERIAL
W. G. Smarsly (Motoren- und Turbinen-Union Muenchen G.m.b.H., Germany) and M. Dahms 1991 8 p Presented at the International Symposium on Intermetallic Compounds: Structure and Mechanical Properties, Sendai, Japan, 17-20 Jun. 1991
(GKSS-91/E/60; ETN-92-92281) Copyright Avail: Fachinformationszentrum Karslruhe, 7514 Eggenstein-Leopoldshafen 2, Germany

A powder metallurgical process developed to produce TiAl components for aerospace application is outlined. Elemental titanium and aluminum powders are randomly mixed and precompacted by cold pressing and deformed by extrusion at room temperature. The precompacted elemental powder blend is Hot Isostatically Pressed (HIP) to form intermetallic phases. HIP of the green compacts results in a fully dense material. Subsequent heat treatments were applied to achieve chemical homogenity and microstructures with different Ti3Al and TiAl phase morphology. Mechanical properties of the HIP and heat treated intermetallic material were investigated by hardness testing, bending, and tensile tests. Microstructures and properties are discussed as a result of the processing parameters. ESA

N93-11337 GKSS-Forschungszentrum Geesthacht (Germany).
TITANIUM-ALUMINIDES BY HOT ISOSTATIC PRESSING OF COLD EXTRUDED TITANIUM-ALUMINIUM POWDER MIXTURES
M. Dahms (Technische Univ., Hamburg, Germany), J. Seeger (Technische Univ., Hamburg, Germany), W. Smarsly (Motoren- und Turbinen-Union Muenchen G.m.b.H., Germany), and B. Wildhagen 1991 11 p Repr. from ISIJ International, v. 31, no. 10, 1991 p 1093-1099
(GKSS-91/E/67; ETN-92-92282) Copyright Avail: Fachinformationszentrum Karlsruhe, 7514 Eggenstein-Leopoldshafen 2, Germany

The production of gamma base titanium aluminides by Reactive Hot Isostatic Pressing (RHIP) of cold extruded titanium aluminum elemental powder mixtures is reported. Various RHIP temperatures as well as additional heat treatments were applied in order to obtain different microstructures. Compression samples were tested between room temperature and 900 C. Changes in microstructures during compression such as microcracking, inhomogeneous deformation, and dynamic recrystallization were investigated. The measured properties are discussed with respect to microstructure. ESA

N93-11519# Lawrence Livermore National Lab., CA.
REVIEW OF PHONON BEHAVIOR AND MICROSTRUCTURAL DEVELOPMENT LEADING TO MARTENSITIC TRANSFORMATIONS IN Ni(x)Al(100-x) ALLOYS
L. E. Tanner, S. M. Shapiro (Brookhaven National Lab., Upton, NY.), D. Schryvers (Antwerp Univ., Belgium), and Y. Noda (Chiba Univ., Japan) 1 Apr. 1992 14 p Presented at the Annual Fall Meeting of the Materials Research Society, Boston, MA, 2-6 Dec. 1991
(Contracts W-7405-eng-48; DE-AC02-76CH-00016)
(DE92-014782; UCRL-JC-107924; CONF-911202-80) Avail: CASI HC A03/MF A01

Elastic and inelastic neutron-scattering and high-resolution electron-microscopy examinations of the beta(sub 2)(B2) phase of Ni(x)Al(100-x) alloys show a direct relationship between the anomalous changes in lattice dynamical behavior and the evolution of static premartensitic structural configurations as the (beta)(sub 2) cools toward its martensitic transformation temperature, M(sub s). The resulting microstructure is fine-scale mosaic assembly of nonuniformly distorted and modulated domains, in which (110) zone axes (1 -1 0) shear-plus shuffle displacements give rise to the (110)B2 micromodulations of approximately 1.3 nm wavelength. These displacements are derived from the unusually low energy of the Sigma(sub 4) group axes (zeta zeta 0)-Ta(2) phonon mode and its anomalous temperature dependent incomplete softening at zeta = 0 (viz., the elastic constant C') and at zeta approx. = 0.16. These inhomogeneously strained domains (ISD's) are believed to be centered on low strain-amplitude defects. The are viewed as strain embryos of the product 7M(5, bar-2) martensite but are generally too weak to act as potent nucleation centers. Similar ISD configurations develop at defects with higher strain amplitudes (e.g., dislocations, grain boundaries) and these are the most likely sites for heterogeneous nucleation to occur. DOE

N93-11524# Michigan Technological Univ., Houghton. Dept. of Metallurgical and Materials Engineering.
ENVIRONMENT-INDUCED EMBRITTLEMENT: STRESS CORROSION CRACKING AND METAL-INDUCED EMBRITTLEMENT; ENVIRONMENTAL EMBRITTLEMENT OF IRON ALUMINIDE ALLOYS
L. A. Heldt, W. W. Milligan, and C. L. White 1991 8 p
(Contract DE-FG02-86ER-45255)

(DE92-018714; DOE/ER-45255/4) Avail: CASI HC A02/MF A01

This research program has included two thrusts. The first addressed environment-induced embrittlement in a parallel study of stress corrosion cracking and metal-induced embrittlement. This work has examined (1) mechanical properties as influenced by embrittling environments, (2) fractography and crystallography or transgranular cracking, (3) the mechanics of cracking, (4) the extent and role of local plastic flow, and (5) local chemistry within stress corrosion and metal-induced cracks. The embrittlement of iron aluminide alloys by air was addressed by determining the effect of water and hydrogen upon the mechanical properties. Slow strain rate testing in aqueous environments was carried out at controlled anodic and cathodic potentials. The effect of cathodically charged hydrogen and the effect of subsequent baking were measured. Environmental susceptibility was measured as affected by alloy composition, microstructure and degree of ordering. DOE

N93-11557# Pacific Northwest Lab., Richland, WA.

ISOTOPIC TAILORING WITH 59-Ni TO STUDY THE EFFECT OF HELIUM ON MICROSTRUCTURAL EVOLUTION AND MECHANICAL PROPERTIES OF NEUTRON-IRRADIATED Fe-Cr-Ni ALLOYS

F. A. Garner, M. L. Hamilton, L. R. Greenwood, J. F. Stubbins, and B. M. Oliver Mar. 1992 29 p Presented at the 16th Annual Symposium of American Society of Testing and Materials, Denver, CO, 21-22 Jun. 1992
(Contract DE-AC06-76RL-01830)
(DE92-019372; PNL-SA-19945; CONF-920673-10) Avail: CASI HC A03/MF A01

Tensile testing on three model Fe-Cr-Ni alloys removed from four discharges of the Ni-59 isotopic doping experiment in FFTF-MOTA indicates that helium/dpa ratios typical of fusion reactors do not produce changes in the yield strength or elongation that are significantly different from those at much lower helium generation rates. It also appears that tensile properties approach a saturation level that is dependent only on the final irradiation temperature, but not prior temperature history or thermomechanical starting condition. The saturation in mechanical properties reflects a similar saturation in microstructure that is independent of starting condition. The successful conduct of an isotopic doping experiment was found to require post-irradiation measurement of the helium levels in order to compensate for uncertainties in the cross sections for burn-out and burn-in of Ni-59 and for uncertainties in neutron flux and spectra in the vicinity of the edge of the core. DOE

N93-11572# Ames Lab., IA.

DEVELOPMENT OF STRENGTH AND CONDUCTIVITY IN DEFORMATION PROCESSED COPPER BASE ALLOYS Ph.D. Thesis

M. Insoo 20 Jul. 1992 67 p
(Contract W-7405-eng-82)
(DE92-018807; IS-T-1576) Avail: CASI HC A04/MF A01

Deformation processed copper based composite alloys have been recently investigated. In these composite alloys, copper, a matrix material, contributes to a high thermal and electrical conductivity, and a second phase material such as Fe, Nb, Cr, Mo, Ta, and W acts as a reinforcement of the strength of the composites. Tungsten was chosen as the bcc phase in the first experiment because W has a high melting temperature which is expected to reduce the decrease in high temperature strength resulting from coarsening of fibers. However, brittleness of tungsten may bring crack problems. Because the matrix is ductile but the second phase is hard enough to resist the external forces, cracks may occur at the interfaces between deformed matrix and undeformed second phase. The purpose of the first experiment is to investigate the possibility of deformation of Cu-W compacts. DOE

N93-11578# Ecole Centrale de Lyon (France). Lab. de Technologie des Surfaces.

POLYETHYLENE-TEREPHTHALATE/ALUMINUM ADHESION Ph.D. Thesis [ADHESION POLYETHYLENE-TEREPHTALATE/ALUMINIUM]

Madeleine Bou 1991 167 p In FRENCH
(ECL-91-33; ETN-92-92339) Avail: CASI HC A08/MF A02

The adhesion and adherence properties of an aluminum coating, obtained by vapor phase deposition in a polyethylene-terephthalate film is investigated. The metallized film is a barrier for oxygen and water vapor. A better knowledge of the chemical bonds between the aluminum and the polymer atoms at the film surface is required. The results are compared to those obtained from adhesion mechanical tests, in order to correlate macroscopic and microscopic properties. The surface is analyzed by x-ray photoelectron spectroscopy, and by transmission electron microscopy. At the Al/polyethylene-terephthalate interface, new compounds are identified and their formation process is modeled. The physical chemical characteristics of the Au/polythylene-terephthalate interface was also studied. From the adhesion test results, it was demonstrated that the mechanical properties are functions of the film microstructure and of the nature of the interface. ESA

N93-11595# Edgerton, Germeshausen and Grier, Inc., Idaho Falls, ID.

THE INFLUENCE OF PROCESSING ATMOSPHERE ON TWIN-ROLL MELT-SPINNING OF ALUMINUM ALLOYS

C. H. Sellers, K. S. Aldrich, M. M. Cortez, and R. N. Wright 1992 11 p Presented at the Minerals, Metals, and Materials Society (TMS) Annual Meeting and Exhibition, San Diego, CA, 1-5 Mar. 1992
(Contract DE-AC07-76ID-01570)
(DE92-017895; EGG-M-91349; CONF-920305-13) Avail: CASI HC A03/MF A01

Melt-spun samples of Al-2 percent Fe have been produced in two different processing atmospheres, ambient pressure argon, and a high vacuum. High speed video photography and microstructural analysis of the ribbons indicate that the processing pressure influences the interaction of the melt with the copper rolls and thus the thermal history. This results in significant differences in ribbon microstructure. DOE

N93-11600# Sandia National Labs., Albuquerque, NM.

LOW ENERGY HELIUM IMPLANTATION IN EVAPORATED NICKEL SURFACES

R. E. Nygren, B. L. Doyle, D. S. Walsh, W. Ottenberger (Max-Planck-Inst. fuer Plasmaphysik, Garching, Germany), J. N. Brooks, and A. Krauss 1992 16 p Presented at the 10th International Converence on Plasma-Surface Interactions in Controlled Fusion Devices, Monterey, CA, 30 Mar. - 3 Apr. 1992
(Contract DE-AC04-76DP-00789)
(DE92-019297; SAND-92-0370C; CONF-920311-23) Avail: CASI HC A03/MF A01

This paper reports data on helium (He) implantation at low energy (100-200 eV) in nickel (Ni) that support a concept for He self-pumping in tokamaks, and specifically an experiment in TEXTOR. These data indicate trapping saturates at about 4 x 10(exp 19) He/m(exp 2) areal density for He implanted at 100 eV He in Ni at 500 C. Neither prior implantation of deuterium (D) nor D bombardment of Ni surfaces already containing implanted He significantly changed the He saturation value. A model for trapping capacity and these data were used to predict He self pumping in TEXTOR. DOE

N93-11609*# National Aeronautics and Space Administration. Lewis Research Center, Cleveland, OH.

DETERMINATION OF PARAMETERS OF A NEW METHOD FOR PREDICTING ALLOY PROPERTIES

Guillermo Bozzolo (Analex Corp., Brook Park, OH.) and John Ferrante Oct. 1992 11 p
(RTOP 505-90-53)

(NASA-TM-105895; E-7361; NAS 1.15:105895) Avail: CASI HC A03/MF A01

Recently, a semiempirical method for alloys based on equivalent crystal theory was introduced. The method successfully predicts the concentration dependence of the heat of formation and lattice parameter of binary alloys. A study of the parameters of the method is presented, along with new results for (gamma)Fe-Pd and (gamma)Fe-Ni alloys. Author

N93-11621*# National Aeronautics and Space Administration. Goddard Space Flight Center, Greenbelt, MD.

EDDY CURRENT CHARACTERIZATION OF MAGNETIC TREATMENT OF MATERIALS

E. James Chern Oct. 1992 12 p
(NASA-TM-104573; NAS 1.15:104573; Rept-92E02736) Avail: CASI HC A03/MF A01

Eddy current impedance measuring methods have been applied to study the effect that magnetically treated materials have on service life extension. Eddy current impedance measurements have been performed on Nickel 200 specimens that have been subjected to many mechanical and magnetic engineering processes: annealing, applied strain, magnetic field, shot peening, and magnetic field after peening. Experimental results have demonstrated a functional relationship between coil impedance, resistance and reactance, and specimens subjected to various engineering processes. It has shown that magnetic treatment does induce changes in a material's electromagnetic properties and does exhibit evidence of stress relief. However, further fundamental studies are necessary for a thorough understanding of the exact mechanism of the magnetic-field processing effect on machine tool service life. Author

N93-11635*# National Aeronautics and Space Administration. Lewis Research Center, Cleveland, OH.

REVIEW OF THE PHYSICAL AND MECHANICAL PROPERTIES AND POTENTIAL APPLICATIONS OF THE B2 COMPOUND NiAl: UNABRIDGED VERSION OF A PAPER PUBLISHED IN INTERNATIONAL MATERIALS REVIEW

Ronald D. Noebe, Randy R. Bowman, and Michael V. Nathal Apr. 1992 124 p
(RTOP 505-63-5A)
(NASA-TM-105598; E-6925; NAS 1.15:105598) Avail: CASI HC A06/MF A02

Considerable work has been performed on NiAl over the last three decades, with an extremely rapid growth in research on this intermetallic occurring in the last few years due to recent interest in this material for electronic and high temperature structural applications. However, many physical properties and the controlling fracture and deformation mechanisms over certain temperature regimes are still in question. Part of this problem lies in the incomplete characterization of many of the alloys previously investigated. Fragmentary data on processing conditions, chemistry, microstructure and the apparent difficulty in accurately measuring composition has made direct comparison between individual studies sometimes tenuous. Therefore, the purpose of this review is to summarize all available mechanical and pertinent physical properties on NiAl, stressing the most recent investigations, in an attempt to understand the behavior of NiAl and its alloys over a broad temperature range. Author

N93-11762# Arizona State Univ., Tempe.

ELECTRONIC STRUCTURE AND REACTIVITIES OF TRANSITION METAL CLUSTERS

1992 83 p
(Contract DE-FG02-86ER-13558)
(DE92-016623; DOE/ER-13558/6) Avail: CASI HC A05/MF A01

The following are reported: theoretical calculations (configuration interaction, relativistic effective core potentials, polyatomics, and CASSCF); proposed theoretical studies (clusters of Cu, Ag, Au, Ni, Pt, Pd, Rh, Ir, Os, and Ru); transition metal cluster ions; transition metal carbide clusters; bimetallic mixed transition metal clusters); reactivity studies on transition metal clusters (reactivity with H(sub 2), C(sub 2)H(sub 4), hydrocarbons; and NO and CO chemisorption on surfaces). Computer facilities and codes to be used, are described. DOE

N93-11773# Oak Ridge National Lab., TN.

RELATIONSHIP OF BAINITIC MICROSTRUCTURE TO IMPACT TOUGHNESS IN Cr-Mo AND Cr-W STEELS

R. L. Klueh and D. J. Alexander 1992 7 p Presented at the International Conference on Martensitic Transformations, Monterey, CA, 20-24 Jul. 1992
(Contract DE-AC05-84OR-21400)
(DE92-017828; CONF-920722-3) Avail: CASI HC A02/MF A01

Non-classical bainite microstructures can develop during continuous cooling of low-carbon alloy steels. These differ from classical upper and lower bainite developed by isothermal transformation. Two non-classical bainite microstructures were produced in a 3Cr-1.5Mo-0.25V-0.1C steel using different cooling rates after austenitizing--water quenching and air cooling. The carbide-free acicular bainite formed in the quenched steel had a lower ductile-brittle transition temperature (DBTT) than the granular bainite formed in the air-cooled steel. With increasing tempering parameter (defined by tempering time and temperature), the DBTT of both decreased and approached a common value, although the final value occurred at a much lower tempering parameter for the quenched steel than for the air-cooled steel. The upper-shelf enery was similarly affected by microstructure. These observations along with similar observations in two Cr-W steels indicate that control of the bainite microstructure can be used to optimize strength and toughness. DOE

N93-11782# California Inst. of Tech., Pasadena. Graduate Aeronautical Labs.

THE CONVERSION OF PLASTIC WORK TO HEAT AROUND A DYNAMICALLY PROPAGATING CRACK IN METALS

A. J. Rosakis, J. J. Mason, and G. Ravichandran 1991 12 p
(Contract N00014-90-J-1340)
(AD-A253801; GALCIT-SM-92-17) Avail: CASI HC A03/MF A01

Investigations of the temperature rise at a dynamically propagating crack tip using an infrared detector array are reported. Also, a measurement of the fraction of plastic work converted to heat using a split hopkinson bar apparatus in conjunction with an infrared detector array is summarized. For 4340 steel it is seen that approximately 85 percent of the plastic work is converted to heat leading to a temperature rise of 300 C at a crack tip propagating 600 m/s in steel. This result is compared to earlier studies that report a 450 C temperature rise at a crack tip propagating 900 m/s in steel. In a titanium alloy the temperature rise is higher than that in steel for equal plastic work rate densities. The conditions at the crack tip are shown to be adiabatic, and, as a result, this effect is due to the difference in density, heat capacity, and crack tip speed. Thermal conductivity has no effect. GRA

N93-11787# Air Force Inst. of Tech., Wright-Patterson AFB, OH. Foreign Technology Div.

THE EFFECT OF SILICON, TIN, AND CHROMIUM ON THE CORROSION AND MECHANICAL PROPERTIES OF ZIRCONIUM - MOLYBDENUM - NIOBIUM

N. M. Gruzdeva and A. S. Adamova 3 Dec. 1991 21 p Transl. into ENGLISH from Fiziko-Khimiya Splavov Tsirkoniya (USSR), 1968 p 208-215
(AD-A254102; FTD-ID(RS)T-0921-91) Avail: CASI HC A03/MF A01

This investigation had as its goal the explanation of the effect of tin, chromium, and silicon on the corrosion and mechanical properties of the indicated ternary alloys. Tin and chromium were selected as the alloying additives, since their favorable effect on the corrosion and strength properties of zirconium is well known. The selection of silicon was based on the fact that its addition to titanium strongly increases the heat resistance of titanium at 800 and 1000 deg. The alloying additions of tin, chromium, and silicon were introduced to the ternary alloys in small quantities. GRA

N93-11830# Oak Ridge National Lab., TN.
OXIDATION-SULFIDATION BEHAVIOR OF IRON ALLOYS CONTAINING 16 TO 40 ATOMIC PERCENT ALUMINUM
J. H. DeVan and P. F. Tortorelli 1992 13 p Presented at the International Conference on Advances in Corrosion and Protection, Manchester, England, 28 Jun. 1992
(Contract DE-AC05-84OR-21400)
(DE92-017824; CONF-9206234-1) Avail: CASI HC A03/MF A01

Iron aluminide alloys containing 16-40 at. percent aluminum and 0-5 at. percent chromium were tested in H2S-H2-H20 gas mixtures at 800 C and in air at 800-1000 C. Results were compared with those for developmental Fe-Cr-Al alloys. Alloys containing 18 percent or more aluminum were highly resistant to H2S-H2-H2O gas mixtures, and the corrosion behavior did not change significantly with aluminum concentrations above 18 percent. A 20 at. percent Al level was found to be critical for sustained oxidation resistance of binary Fe-Al alloys in air at 900 C and above. However, the addition of 5 at. percent Cr at the 16 at. percent Al level reduced the oxidation rate in air to that of alloys containing (ge) 20 percent Al. Corrosion rates of iron aluminides were comparable to Fe-Cr-Al alloys in air but were significantly lower than Cr-containing alloys in H2S-H2-H2O. The respective corrosion processes operative for iron aluminides in mixed gas and air are discussed in terms of the observed alloying effects.
DOE

N93-11850# Case Western Reserve Univ., Cleveland, OH. Dept. of Materials Science and Engineering.
MICROMECHANISMS OF DEFORMATION AND FRACTURE IN ALUMINUM BASED MMC'S: INTERFACE EFFECTS Final Report, 1 Feb. 1989 - 28 Feb. 1992
John J. Lewandowski 27 Apr. 1992 40 p
(Contract DAAL03-89-K-0068)
(AD-A253560; ARO-25390.9-MS) Avail: CASI HC A03/MF A01

Microstructural effects on the deformation and fracture of Aluminum-based metal matrix composites were determined. Microstructural variables investigated included the reinforcement size, volume fraction, and matrix microstructure. Reinforcement sizes studied included 5 and 13 micrometer SiC particulates at both the 15 and 20 volume percent levels. Matrix microstructures were systematically varied via heat treatment and were quantified using transmission electron microscopy. Fracture toughness was evaluated using J-integral test techniques and utilized in-situ monitoring of fracture inside a Scanning Electron Microscope. Mixed mode fracture toughness tests were also conducted. In addition to the fracture toughness tests, additional tests were conducted on specimens deformed under high pressure. The composites exhibited high ductility under pressure (e.g., ef = 80 percent). Laminated composites were additionally processed and exhibited significant improvements in both bend ductility and fracture toughness.
GRA

N93-11857# Oak Ridge National Lab., TN.
THE MECHANICAL AND MICROSTRUCTURAL STABILITY OF AUSTENITIC STAINLESS STEELS STRENGTHENED BY MC-FORMING ELEMENTS
R. W. Swindeman and P. J. Maziasz 1992 5 p Presented at the International Conference on Creep of Materials, Orlando, FL, 17-21 May 1992
(Contract DE-AC05-84OR-21400)
(DE91-015314; CONF-920505-3) Avail: CASI HC A01/MF A01

Creep-resistant austenitic stainless steels have been developed that owe their strengths to the addition of MC-forming techniques. Examples are Esshete 1250, 17-14CuMo, Sumitomo ST3Cu(reg sign), Nippon Kokan Tempaloy Al(reg sign), and the HT-UPS steels designed by Maziasz. The HT-UPS steels, basically Cr(14)-Ni(16)-Mo(2 percent)-Fe with V, Ti, and Nb additions, were found to have higher creep strengths than the other steels due to the formation of an ultrafine precipitate distribution on dislocations produced by warm or cold work prior to service. Under constant-load creep conditions, the microstructure of the HT-UPS steel was found to be stable for long periods of time, and creep rates changed very little over thousands of hours. Studies were made to determine if the strength of the HT-UPS alloys would be degraded by variable temperatures and stresses that could disturb the precipitate-stabilized dislocation microstructure. Experiments included variable stress creep testing, repetitious and combined creep-relaxation testing, and creep-fatigue testing. Temperatures were in the range 600 to 800 C. Times extended to beyond 20,000 h in some cases. Recovery creep strains were measured and used as an indicator of microstructural changes during creep.
DOE

N93-11895 Virginia Univ., Charlottesville.
MECHANISMS OF LOCALIZED AQUEOUS CORROSION IN ALUMINUM-LITHIUM-COPPER ALLOYS Ph.D. Thesis
Rudolph G. Buchheit, Jr. 1991 301 p
Univ. Microfilms Order No. DA9218039

The objective of this dissertation was to determine the role of microstructural heterogeneity, the localized environment chemistry and surface films in localized corrosion and stress corrosion cracking of an Al-3Cu-2Li alloy 2090. The influence of microstructural heterogeneity was studied by identifying the phases important to local corrosion and preparing these in bulk form for characterization of their corrosion behavior by standard electrochemical techniques. Based on this characterization, preferential boundary attack was determined to occur via selective dissolution of the T1 (Al2CuLi) intermetallic phase on subgrain boundries. A gross form of pitting associated with impurity Al-Cu-Fe particles was shown to initiate by the local galvanic attack of the matrix by the noble particles. The short-transverse stress corrosion cracking (SCC) behavior of the alloy was studied using a static load, smooth bar SCC technique in Cl-,Cl-/CrO4(sup 2-) and Cl-/CO3(sup 2-) environments. Results showed that anodic dissolution SCC subgrain boundaries was to be expected when applied potentials were more positive than the breakaway potential (E sub br) of T sub 1 but were less positive than E sub br of alpha-Al. It was shown that this criterion was not satisfied in aerated Cl(-) solutions and S-T SCC resistance was good. This criterion was satisfied in Cl(-)/CO 3(sup 2-) environments and in alkaline isolated fissures exposed to a CO2(-) containing atmosphere. Anodic polarization showed that the corrosion behavior of T sub 1 was unaffected in alkaline CO3(sup 2-) environments but the alpha-Al phase was passivated. X ray diffraction of crevice walls from artificial crevices suggested that passivation of alpha-Al occurred by the formation of Li2(Al2(OH)6)2(+)-Co3(sup 2-)-nH2o. Simulated crevice experiments were performed with various model alloys to determine the effects of Al(3+),Li(+) and Cu(2+) hydrolysis on steady state crevice pH. The effect of an external cathode on crevice chemistry was also studied by changing bulk solution aeration and specimen potential. Results showed that for 2090, crevice acidification occurred when the bulk solution was aerated. When the crevice was coupled to a deaerated solution, subjected to a net cathodic polarization or isolated from a bulk solution, an alkaline crevice developed. Based on predictions from hydrolysis product distribution diagrams, this chemistry evolves due to lithium dissolution combined with hydrogen reduction.
Dissert. Abstr.

N93-12107# Westinghouse Savannah River Co., Aiken, SC.
MECHANICAL PROPERTIES OF 1950'S VINTAGE 304 STAINLESS STEEL WELDMENT COMPONENTS AFTER LOW TEMPERATURE NEUTRON IRRADIATION
R. L. Sindelar, G. R. Caskey, Jr., J. K. Thomas, J. R. Hawthorne (Materials Engineering Associates, Inc., Lanham, MD.), A. L. Hiser (Materials Engineering Associates, Inc., Lanham, MD.), R. A. Lott (Westinghouse Science and Technology Center, Pittsburgh, PA.), J. A. Begley (Westinghouse Science and Technology Center, Pittsburgh, PA.), and R. P. Shogan (Westinghouse Science and Technology Center, Pittsburgh, PA.) 1991 53 p Presented at the 16th Annual Symposium of American Society of Testing and Materials (ASTM), Denver, CO, 21-22 Jun. 1992
(Contract DE-AC09-89SR-18035)

(DE92-017059; WSRC-MS-91-293; CONF-920673-7) Avail: CASI HC A04/MF A01

The reactor vessels of the nuclear production reactors at the Savannah River Site (SRS) were constructed in the 1950's from Type 304 stainless steel plates welded with Type 308 stainless steel filler using the multipass metal inert gas process. An irradiated mechanical properties database has been developed for the vessel with materials from archival primary coolant system piping irradiated at low temperatures (75 to 150 C) in the State University of New York at Buffalo reactor (UBR) and the High Flux Isotope Reactor (HFIR) to doses of 0.065 to 2.1 dpa. Fracture toughness, tensile, and Charpy-V impact properties of the weldment components (base, weld, and weld heat-affected-zone (HAZ)) have been measured at temperatures of 25(degrees)C and 125 C in the L-C and C-L orientations for materials in both the irradiated and unirradiated conditions for companion specimens. Fracture toughness and tensile properties of specimens cut from an SRS reactor vessel sidewall with doses of 0.1 and 0.5 dpa were also measured at temperatures of 25 and 125 C. The irradiated materials exhibit hardening with loss of work hardenability and a reduction in toughness relative to the unirradiated materials. The HFIR-irradiated materials show an increase in yield strength between about 20 and 190 percent with a concomitant tensile strength increase between about 15 to 30 percent. The elastic-plastic fracture toughness parameters and Charpy-V energy absorption both decrease and show only a slight sensitivity to dose. The irradiation-induced decrease in the elastic-plastic fracture toughness (J(sub def) at 1 mm crack extension) is between 20 to 65 percent; the range of J(sub IC) values are 72.8 to 366 kJ/m(sup 2) for the irradiated materials. Similarly, Charpy V-notch results show a 40 to 60 percent decrease in impact energies. DOE

N93-12118# Johns Hopkins Univ., Baltimore, MD. School of Engineering.
EFFECT OF MICROSTRUCTURE ON PASSIVE FILM FORMATION AND BREAKDOWN ON Al ALLOYS Annual Report, 15 Dec. 1990 - 14 Dec. 1991
J. Kruger, J. W. Wagner, R. S. Lillard, C. C. Streinz, and P. J. Moran 27 Jan. 1992 73 p
(Contract N00014-89-J-1180)
(AD-A245863) Avail: CASI HC A04/MF A01

Dynamic imaging microellipsometry (DIM) has been utilized to examine the passive film growth on a dynamically compacted Al-1 percent Ta alloy. SEM observation revealed Al3Ta precipitates up to 20 microns in diameter. These precipitates were identified ellipsometrically demonstrating in-situ spatial resolution of at least 20 microns. In addition, it was observed that a thinner passive film formed over the precipitates than over the matrix material. This may result in an incompatibility between the two films that results in local strains or flaws, such as dislocations, that promote (Cl-) ingress and degrade the protective nature of the passive film. Ellipsometric analysis of the passivation of Al(8 at. percent)Ta and Al(11 at. percent)W has demonstrated that the passive films formed on the alloys are thinner than on pure aluminum. To a first approximation, the film thickness on both alloys is half that of pure aluminum at a given applied potential. It has also been observed that the index of the passive film on the Al-W alloy increases at an applied overpotential of approximately 1 volt. The scanning electrochemical impedance spectroscopy (EIS) technique developed during the first two years has been improved and quantitatively demonstrated. This was accomplished by examining two electrochemical systems. The first was a homogeneous 99.999 percent aluminum electrode. GRA

N93-12158# Westinghouse Savannah River Co., Aiken, SC.
REACTOR MATERIALS PROGRAM: MECHANICAL PROPERTIES OF IRRADIATED TYPES 304 AND 304L STAINLESS STEEL WELDMENT COMPONENTS
R. L. Sindelar and G. R. Caskey, Jr. Dec. 1991 120 p
(Contract DE-AC09-89SR-18035)
(DE92-018105; WSRC-TR-91-11) Avail: CASI HC A06/MF A02

The vessels (reactor tanks) of the Savannah River Site nuclear production reactors constructed in the 1950's are comprised of Type 304 stainless steel with Type 308 stainless steel weld filler. Irradiation exposure to the reactor tank sidewalls through reactor operation has caused a change in the mechanical properties of these materials. A database of as-irradiated mechanical properties for site-specific materials and irradiation conditions has been produced for reactor tank structural analyses and to quantify the effects of radiation-induced materials degradation for evaluating reactor service life. The data has been collected from the SRL Reactor Materials Program (RMP) irradiations and testing of archival stainless steel weldment components and from previous SRL programs to measure properties of irradiated reactor Thermal Shield weldments and reactor tank (R-tank) sidewall material. Irradiation programs of the RMP are designed to quantify mechanical properties at tank operating temperatures following irradiation to present and future tank wall maximum exposure conditions. The exposure conditions are characterized in terms of fast neutron fluence (E(sub n) greater than 0.1 MeV) and displacements per atom (dpa)(sup 3). Tensile properties, Charpy-V notch toughness, and elastic-plastic fracture toughness were measured for base, weld, and weld heat-affected zone (HAZ) weldment components from archival piping specimens following a Screening Irradiation in the University of Buffalo Reactor (UBR) and following a Full-Term Irradiation in the High Flux Isotope Reactor (HFIR). DOE

N93-12232# Sandia National Labs., Albuquerque, NM.
THE EFFECT OF TEMPERATURE DEPENDENT THERMAL PROPERTIES ON PARAMETRIC WELD SIZE PREDICTIONS
G. A. Knorovsky 1992 2 p Presented at the American Welding Society Annual Conference, Houston, TX, 25-30 Apr. 1992
(Contract DE-AC04-76DP-00789)
(DE92-018816; SAND-92-1799C; CONF-9204174-2-Extd-Abst)
Avail: CASI HC A01/MF A01

Parametric weld size predictions, in which weld size and shape are predicted given a knowledge of material and process parameters, offer a great deal of benefit to the welding engineer. This is so because the technique promises to replace expensive and time-consuming lab or shop activity followed by destructive examination with simple numeric or nomographic calculations. The work to be presented here uses a simple two-dimensional axisymmetric spot-on-plate computer simulation in which thermal diffusivity vs. temperature is varied. DOE

N93-12237# Pratt and Whitney Aircraft, West Palm Beach, FL. Government Engines and Space Propulsion.
FATIGUE IN SINGLE CRYSTAL NICKEL SUPERALLOYS Technical Progress Report, 16 Sep. 1991 - 15 Aug. 1992
Daniel P. DeLuca and Charles Annis 15 Aug. 1992 9 p
(Contract N00014-91-C-0124)
(AD-A254603; PW-FR-21998-10) Avail: CASI HC A02/MF A01

This program investigates the seemingly unusual behavior of single crystal airfoil materials. The fatigue initiation processes in single crystal (SC) materials are significantly more complicated and involved than fatigue initiation and subsequent behavior of a (single) macrocrack in conventional, isotropic materials. To understand these differences is the major goal of this project. GRA

N93-12241# Southwest Research Inst., San Antonio, TX.
MICROSTRUCTURE-BASED FATIGUE LIFE PREDICTION METHODS FOR NAVAL STEEL STRUCTURES Annual Report No. 1, 15 Jul. 1991 - 15 Jul. 1992
K. S. Chan, D. L. Davidson, and R. C. McClung 15 Jul. 1992 53 p
(Contract N00014-91-C-0214)
(AD-A254628) Avail: CASI HC A04/MF A01

The goal of the subject program is to develop fundamental understandings of the relationships between microstructure and fatigue damage in structural steels of interest to naval applications. Quantitative descriptions of these relationships will be incorporated within practical engineering models for the prediction of S-N fatigue life. The focus of the first year of the program has been on experimental observations of fatigue damage in different microstructures for HSLA steels. Experimental methods were developed to study microcrack nucleation and growth with S-N fatigue specimens. Microstructures were modified with various heat treatments and characterized with appropriate optical and electron microscopy. The basic framework of potential microstructure-fatigue damage relationships has been sketched. GRA

N93-12248# Naval Air Development Center, Warminster, PA. Aircraft and Crew Systems Technology Directorate.
FATIGUE CRACK GROWTH IN AERMET 100 STEEL
Eun U. Lee 18 Oct. 1991 25 p
(AD-A249068; NADC-91111-60) Avail: CASI HC A03/MF A01

The fatigue behavior of a newly developed landing gear steel, AerMet 100, was studied. In this study, the fatigue tests were performed under constant amplitude loading for stress ratios R = 0.1, 0.5, and 0.8 in dry nitrogen gas and a 3.5 percent NaCl solution at room temperature. The fatigue crack growth resistance of the AerMet 100 steel is superior to that of the 300M steel, which has been widely used for aircraft landing gears. Within the employed range of stress ratios, the greater the stress ratio, the smaller is the threshold stress intensity range for fatigue crack growth delta(K(sub th)) and the greater is the fatigue crack growth rate da/dN for lower delta(K). For higher delta(K), however, the da/dN values of different stress ratios are similar in both environments. The delta(K(sub th)) is greater and da/dN is smaller for lower delta(K) in a 3.5 percent NaCl solution than in dry nitrogen gas, whereas the da/dN values are quite close for higher delta(K) in both environments. This feature is attributable to corrosion-product-induced crack closure. GRA

N93-12256# Los Alamos National Lab., NM.
INFLUENCE OF STRAIN RATE ON THE STRUCTURE/PROPERTY BEHAVIOR OF THE ALPHA-2 ALLOY Ti-24.5Al-10.5Nb-1.5Mo
G. T. Gray, III, Sun Ig Hong, and B. J. Marquardt 1992 9 p
Presented at the 7th World Conference and Exhibition on Titanium, San Diego, CA, 28 Jun. - 2 Jul. 1992
(Contract W-7405-eng-36)
(DE92-008490; LA-UR-92-659; CONF-920604-1) Avail: CASI HC A02/MF A01

Preliminary dislocation g (dot) b analysis revealed that following room temperature deformation at low strain rate the majority of the dislocations are a-dislocations lying on basal planes, 2nd order pyramidal (a/2 + c) slip on (1211), and 1st order pyramidal a-slip on (1011). Increasing the rate of deformation at room temperature to 6000 s(exp -1) is seen to result in increased a-slip on prism planes and a decreased amount of basal slip. At high-strain-rates and elevated temperatures the substructure was seen to be generally similar to that observed following high-rate deformation at room temperature except for an increased amount of basal slip and a somewhat higher incidence of 2nd order pyramidal slip. The defect generation and the rate sensitivity of Ti-24.5Al-10.5Nb-1.5Mo are discussed as a function of strain rate and temperature and contrasted to that observed in conventional titanium alloys and TiAl. DOE

N93-12261# Ames Lab., IA.
STRESS DEPENDENCE OF THE MAGNETIC PROPERTIES OF STEELS Ph.D. Thesis
M. K. Devine Jun. 1992 100 p
(Contract W-7405-eng-82)
(DE92-018804; IS-T-1539) Avail: CASI HC A05/MF A02

The purpose of this work was to develop an in situ magnetic hysteresis measurement technique for monitoring applied stresses in structural components. Stress measurements were first made by wrapping samples with a flux coil and magnetizing with a solenoid. Next, stress measurements were made using an in situ measurement technique under laboratory conditions. Then structural components of similar metallurgy to the laboratory specimens were measured to confirm that laboratory measurements correspond to field measurements. Finally, stress tests were performed on industrial components. DOE

N93-12269# Air Force Inst. of Tech., Wright-Patterson AFB, OH. Foreign Technology Div.
NATURE OF THE BETA-PHASE OF NICKEL-ALUMINUM SYSTEM
L. N. Guseva 2 Jan. 1992 9 p Transl. into ENGLISH from Akad Nauk SSSR Doklady (USSR), v. 77, no. 3, 1951 p 415-418
(AD-A254101; FTD-ID(RS)T-1199-91) Avail: CASI HC A02/MF A01

During the detailed study of system nickel-aluminum in the field of Beta-phase with x-ray method (1) it was established that at room temperature the Beta-phase preserves uniformity from 45.25 to 60 at. percent Ni. Later than (2) during the determination of the boundary of Beta-phase from the nickel side were obtained the same results. Data with respect to a change in lattice constant and density of alloys with composition change allowed Bradley and Taylor to establish that the solid solutions in the region of the uniformity of Beta-phase have uncommon structure. Alloys with 50 at. percent Ni have the body-centered cubic structure of the type CsCl with a regulated atomic arrangement. With an increase in the content of nickel are formed solid solutions by the statistical substitution of aluminum atoms in crystal lattice by nickel atoms. The substitution, however, of nickel atoms by aluminum atoms is observed only to 51 at. percent Al; with further increase in the content of aluminum solid solutions have defective structure, since part of the positions in the lattice, occupied earlier by nickel, remains free. This leads to the change of the number of atoms in the unit cell, which on the boundary of phase reaches value of 1.84. GRA

N93-12322# National Research Inst. for Metals, Tokyo (Japan).
DESIGN AND DEVELOPMENT OF Ni-BASE SUPERALLOY AND Ti ALLOYS
Michio Yamazaki 1992 28 p Sponsored by Ministry of International Trade and Industry
(NRIM-SR-92-01) Avail: CASI HC A03/MF A01

This overview article describes what has been done in NRIM for design and development of Ni base superalloys and Ti alloys of high temperature use. Most of those works were performed in two national projects. For Ni base alloys we have developed alloy design programs in which compositions of two phases, gamma and gamma prime, can be estimated and properties of alloys are described and predicted as functions of the phase compositions and the phase volume fraction. For Ti alloys similar design programs were studied for alpha and beta phases, and later for alpha and alpha(2) phases. For Ni-base alloys, after developing the first version of the design program, we applied this to develop conventionally cast alloys, directionally solidified columnar alloys, single crystal alloys, superplastically workable alloys, and oxide dispersion strengthened alloys. The second version of alloy design program for Ni-base alloys was then developed and was chiefly applied to single crystal alloys. For the above alloy development projects we have proposed a number of new alloys. By using the alloys proposed, process studies were done mainly by companies participating in the projects. Author

N93-12445# Oak Ridge National Lab., TN.
PROCESSING AND PROPERTIES OF NbTi BASED ALLOYS
Vinod K. Sikka, Srinath Viswanathan, and Edward A. Loria (Niobium Products Co., Inc., Coraopolis, PA.) 1992 9 p Presented at the 7th International Symposium on Superalloys, Champion, PA, 20-24 Sep. 1992
(Contract DE-AC05-84OR-21400)
(DE92-016692; CONF-920932-1) Avail: CASI HC A02/MF A01

The processing characteristics, tensile properties, and oxidation response of two Nb-Ti-Al-Cr alloys were investigated. One creep test at 650 C and 172 MPa was conducted on the base alloy which contained 40Nb-40-Ti-10Al-10Cr. A second alloy was modified with 0.11 at. percent carbon and 0.07 at. percent yttrium. Alloys were arc melted in a chamber backfilled with argon, drop cast into a water-cooled copper mold, and cold rolled to obtain a 0.8-mm sheet. The sheet was annealed at 1100 C for 0.5 h. Longitudinal tensile specimens and oxidation specimens were obtained for both the base alloy and the modified alloy. Tensile properties were obtained for the base alloy at room temperature, 400, 600, 700, 800, 900, and 1000 C, and for the modified alloy at room temperature, 400, 600, 700, and 800 C. Oxidation tests on the base alloy and modified alloy, as measured by weight change, were carried out at 600, 700, 800, and 900 C. Both the base alloy and the modified alloy were extremely ductile and were cold rolled to the final sheet thickness of 0.8 mm without an intermediate anneal. The modified alloy exhibited some edge cracking during cold rolling. Both alloys recrystallized at the end of a 0.5-h annealing treatment. The alloys exhibited moderate strength and oxidation resistance below 600 C, similar to the results of alloys reported in the literature. The addition of carbon produced almost no charge in either the yield strength or ductility as measured by total elongation. A small increase in the ultimate tensile strength and a corresponding decrease in the reduction of area below 600 C were observed. Carbon addition also served to marginally refine the grain size after annealing. The results of this study and those of similar alloys reported in the literature suggest that 40Nb-40Ti-10Al-10Cr forms a good base alloy suitable for alloying for improvement in its oxidation and high-temperature strength properties. DOE

N93-12468# Northrop Corp., Hawthorne, CA. Aircraft Div.
SPECTRUM FATIGUE BEHAVIOUR OF POWDER METALLURGY ALUMINUM ALLOYS Final Report, Sep. 1985 - Mar. 1991
G. V. Searich and M. T. Hahn Oct. 1991 275 p
(Contract F33615-C-5041)
(AD-A255060; NOR-91-49; WL-TR-91-4064) Avail: CASI HC A12/MF A03

The fatigue crack growth behavior of three aluminum alloys was examined under constant amplitude and spectrum loading. The fatigue behavior of extrusions and hand forgings of second-generation powder metallurgy (PM) alloy CW67 (X7093) was compared to the fatigue behavior of extrusions of 7091 (a first-generation PM alloy) and 7075 (an ingot metallurgy alloy). Spectrum fatigue crack growth tests were performed using the FALSTAFF fighter spectrum as well as an actual fighter aircraft spectrum. Additionally, overload/underload fatigue crack growth tests were performed to correlate the constant amplitude and spectrum fatigue behaviors. For these tests, overload-induced crack jumps and crack growth retardation were measured. Tensile properties, fracture toughness, stress-life fatigue, and stress corrosion cracking were also evaluated. For the spectrum fatigue tests in particular, the crack growth behavior was correlated to the microstructure and fractography. In summary, the fine-grained PM alloys exhibited significantly higher strengths, toughness, and stress-life fatigue resistance than 7075, but markedly lower constant amplitude fatigue crack growth resistance. Under a tension-dominated FALSTAFF spectrum, PM alloys were generally inferior in crack growth resistance compared to IM alloys, which is consistent with constant amplitude fatigue behavior. However, in spectrums having more compressive loads, the spectrum fatigue life of CW67 was equal to or better than IM7075. GRA

N93-12476# Oak Ridge National Lab., TN.
THEORY OF NORMAL METALS
G. D. Mahan (Tennessee Univ., Knoxville.) Jun. 1992 43 p Presented at the International Center for Theoretical Physics (ICTP) Spring College on Superconductivity, Trieste (Italy), 27 Apr. - 30 Jun. 1992
(Contract DE-AC05-84OR-21400)
(DE92-016828; CONF-9204167-1) Avail: CASI HC A03/MF A01

The organizers requested that I give eight lectures on the theory of normal metals, 'with an eye on superconductivity.' My job was to cover the general properties of metals. The topics were selected according to what the students would need to known for the following lectures on superconductivity. My role was to prepare the ground work for the later lectures. The problem is that there is not yet a widely accepted theory for the mechanism which pairs the electrons. Many mechanisms have been proposed, with those of phonons and spin fluctuations having the most followers. So I tried to discuss both topics. I also introduced the tight-binding model for metals, which forms the basis for most of the work on the cuprate superconductors. DOE

N93-12480# Utah Univ., Salt Lake City. Dept. of Chemistry.
THERMOCHEMISTRY OF TRANSITION METAL CLUSTERS
P. B. Armentrout 1992 3 p
(Contract DE-FG02-91ER-14193)
(DE92-018713; DOE/ER-14193/1) Avail: CASI HC A01/MF A01

Collision-induced dissociation studies show that Ti, Fe, Co, and Ni cluster ions dissociate primarily by sequential atom loss, with exceptions. Studies of V and Cr clusters are being analyzed. A cluster ion photodissociation spectrometer is being constructed and tested. DOE

N93-12487# Westinghouse Idaho Nuclear Co., Inc., Idaho Falls.
IMPROVED CORROSION RESISTANCE OF HASTELLOY G-30 IN NITRIC/HYDROFLUORIC ACID SOLUTIONS BY WELDING WITH INCONEL 72 WELD WIRE
B. C. Norby 3 Mar. 1992 15 p Presented at the Corrosion 1992 Conference and Exhibition, Nashville, TN, 27 Apr. - 1 May 1992
(Contract DE-AC07-84ID-12435)
(DE92-017233; WINCO-11787; CONF-920458-10) Avail: CASI HC A03/MF A01

When welding Hastelloy G-30, secondary phases form in the weld metal. These phases cause the weld metal to be preferentially attacked in nitric acid (HNO3) solutions contaminated with minor amounts of hydrofluoric acid (HF). A post weld solution anneal and water quench is necessary to assure that these phases redissolve into the solid. When a post weld solution anneal and water quench is not feasible, improved corrosion resistance can be obtained by welding with INCO 72 weld wire. When welding Hastelloy G-30 with INCO 72, there can be a region at the weldmetal/base-metal interface that does not benefit from the INCO 72 weld wire. This region consists of melted and resolidified Hastelloy G-30. This unmixed zone can be preferentially attacked in HNO3 solutions contaminated with minor amounts of HF. Long term corrosion immersion tests have shown that the rate of attack at the weld-metal/base-metal interface can be as high as 50 mpy. Welding techniques that increase the mixing of the melted Hastelloy G-30 with the INCO 72 weld wire can reduce the interface corrosion rate. DOE

N93-12494# EG and G Energy Measurements, Inc., Idaho Falls.
A TAGUCHI EXPERIMENTAL DESIGN STUDY OF TWIN-WIRE ELECTRIC ARC SPRAYED ALUMINUM COATINGS
T. J. Steeper (Westinghouse Savannah River Co., Aiken, SC.), D. J. Varacalle, Jr. (Westinghouse Savannah River Co., Aiken, SC.), G. C. Wilson (Westinghouse Savannah River Co., Aiken, SC.), R. W. Johnson, G. Irons, W. R. Kratochvil (Hobart-Tafa Corp., Concord, NH.), and W. L. II Riggs 1992 7 p Presented at the 1992 International Thermal Spray Conference, Orlando, FL, 1-5 Jun. 1992
(Contract DE-AC07-76ID-01570)
(DE92-018022; EGG-M-91298; CONF-9206135-4) Avail: CASI HC A02/MF A01

An experimental study was conducted on the twin-wire electric arc spraying of aluminum coatings. This aluminum wire system is being used to fabricate heater tubes that emulate nuclear fuel tubes for use in thermal-hydraulic experiments. Experiments were conducted using a Taguchi fractional-factorial design parametric study. Operating parameters were varied around the typical process parameters in a systematic design of experiments in order to display the range of processing conditions and their effect on the resultant coating. The coatings were characterized by hardness tests, optical metallography, and image analysis. The paper discusses coating qualities with respect to hardness, roughness, deposition efficiency, and microstructure. The study attempts to correlate the features of the coatings with the changes in operating parameters. A numerical model of the process is presented including gas, droplet, and coating dynamics. DOE

27 NONMETALLIC MATERIALS

Includes physical, chemical, and mechanical properties of plastics, elastomers, lubricants, polymers, textiles, adhesives, and ceramic materials.

For composite materials see *24 Composite Materials.*

N93-10962*# National Aeronautics and Space Administration. Lewis Research Center, Cleveland, OH.

ANALYSIS OF PRECRACKING PARAMETERS AND FRACTURE TOUGHNESS FOR CERAMIC SINGLE-EDGE-PRECRACKED-BEAM SPECIMENS

Sung R. Choi (Cleveland State Univ., OH.), Abhisak Chulya (Cleveland State Univ., OH.), and Jonathan A. Salem Aug. 1992 25 p

(Contract DE-AI05-87OR-21749; RTOP 505-63-M)

(NASA-TM-105568; E-6893; NAS 1.15:105568) Avail: CASI HC A03/MF A01

The single-edge-precracked-beam (SEPB) method involves creation of a straight-through crack from an indentation crack. The straight-through crack is developed by applying a controlled bending load to a specimen via a precracking fixture. The fixture induces the following sequence: (1) stable growth of the indentation crack; (2) pop-in; and finally, (3) arrest-thereby forming a straight-through precrack. The effects of indentation load on precracking load as well as precrack size were studied for experimental variables such as specimen width, fixture span, and material. Finite element analysis was used to obtain the stress distribution and stress intensity factor, thus providing a quantitative prediction of the precracking load and precrack size for silicon nitride, alumina, silicon cabide, and two SiC whisker-reinforced silicon nitrides. Fracture toughness values obtained from the SEPB method were compared with those obtained from other methods.

Author

N93-10972# California Univ., Berkeley. Lawrence Berkeley Lab.

LIQUID-LIQUID EQUILIBRIA IN BINARY SYSTEMS: MONTE-CARLO SIMULATION FOR CALCULATING THE EFFECT OF NONRANDOM MIXING

S. M. Lambert, D. S. Soane, and J. M. Prausnitz Apr. 1992 9 p Presented at the 6th International Conference on Fluid Properties and Phase Equilibria for Chemical Process Design, Cortina d'Ampezzo (Italy), 19-24 Jul. 1992

(Contract DE-AC03-76SF-00098)

(DE92-017020; LBL-32295; CONF-9207105-2) Avail: CASI HC A02/MF A01

Monte-Carlo simulations of a lattice model for incompressible monomer/r-mer mixtures are used to obtain accurate results for the configurational energy of mixing. Based on simulation results, the energy of mixing is correlated as a function of temperature and composition using an empirical expression. The configurational Helmholtz energy is obtained upon using the Gibbs-Helmholtz equation with Guggenheim's athermal entropy of mixing as boundary condition. Since Monte-Carlo simulations give essentially exact results for the lattice model, the effects of nonrandom mixing on the configurational thermodynamic properties of a binary mixture can be determined. The expression generated here produces coexistence curves that are more accurate than those from other models, especially near the critical region.

DOE

N93-11010# Messerschmitt-Boelkow-Blohm G.m.b.H., Ottobrunn (Germany). Zentrallabor.

A CONTRIBUTION TO FATIGUE FAILURE MORPHOLOGIES IN FIBER REINFORCED PLASTICS [BEITRAG ZU SCHWINGBRUCHMORPHOLOGIEN IN FASERVERSTAERKTEN KUNSTSTOFFEN]

Horst E. Franz 1991 24 p In GERMAN Submitted for publication

(MBB-Z-0212-91-PUB; ETN-92-92116) Avail: CASI HC A03/MF A01

Tests carried out at different frequencies showing that vibratory band formation is independent from frequency are reported. Tests were carried out with constant amplitudes and with increase of amplitude during vibratory stresses. Vibratory band was observed for both types of stresses. It was clearly demonstrated that vibratory bands are not only produced during quick failure progress. Vibratory type failure morphologies of 6 mm thick samples showed in which measure the local stress intensity is determined for the formation of vibratory type bands. No humidity influence on failure morphology could be determined.

ESA

N93-11011# Messerschmitt-Boelkow-Blohm G.m.b.H., Munich (Germany).

EROSION MECHANISMS IN CERAMIC STRUCTURES [EROSIONSMECHANISMEN AN KERAMIKSTRUKTUREN]

S. Foeckersperger (European Space Agency. European Space Research and Technology Center, ESTEC, Noordwijk, Netherlands), Michael Elsner, W. Zoerner (Technische Univ., Munich, Germany), and J. Blumenberg (Technische Univ., Munich, Germany) 1992 7 p Repr. from Zeitschrift fuer Flugwissenschaften und Weltraumforschun, v. 16, 1992 p 28-33 In GEORGIAN Previously announced in IAA as A92-30686

(MBB-UK-0171-92-PUB; ETN-92-92115) Avail: CASI HC A02/MF A01

Erosion processes to which the highly thermal ceramic components of a spacecraft are submitted during reentry, are described. The effects of mechanical erosion, chemical reaction, and sublimation are analyzed. Analytical models are developed. The material loss caused by erosion mechanisms is estimated.

ESA

N93-11018# Rolls-Royce Ltd., Derby (England). Advanced Ceramics Centre.

PROCESSING OF CERAMIC MATRIX COMPOSITES

David A. Clarke (Warwick Univ., Coventry, England) 1 Dec. 1991 18 p Presented at Conference, Birmingham, England, 7 Nov. 1991

(PNR-90914; ETN-92-92203) Copyright Avail: CASI HC A03/MF A01

The term 'Ceramic Matrix Composites' (CMC's) can be used to cover a wide range of materials depending on the bounds used to define 'composite.' In this paper CMC's are taken to mean those materials where a discontinuous or continuous reinforcing phase is introduced as a key unit in its own right early in the manufacturing process. CMC's based around microstructural toughening (e.g., zirconia toughened alumina) are not covered. A summary of the benefits and applications of particulate, whisker, chopped fiber, and continuous fiber reinforced materials is presented. Methods for handling and preforming these materials are covered together with the suitability of each for various applications. The manufacturing methods, based on solid, liquid, and gas phase infiltration of these structures with ceramic matrices are discussed, and the benefits and limitations of each approach outlined.

ESA

N93-11032# Rolls-Royce Ltd., Derby (England).

A TEST FACILITY FOR THE THERMOFLUID-DYNAMICS OF GAS BEARING LUBRICATION FILMS

S. I. Hogg (Oxford Univ., England), S. J. Hughes (Oxford Univ., England), and T. V. Jones (Oxford Univ., England) 8 Apr. 1992 10 p Sponsored by Science Research Council

(PNR-90897; ETN-92-92196) Copyright Avail: CASI HC A02/MF A01

A novel test facility for making fundamental investigations of hydrodynamic gas bearing lubrication films is described. The work forms part of a wider research effort aimed towards the introduction of gas lubricated bearings in future gas turbine designs. The need for this experiment is discussed in the context of previous studies, and the design and manufacture of the facility is described. Some interesting test results for a hydrostatic thrust bearing are described. The results were obtained whilst commissioning the facility. These results are compared with numerical simulations obtained by solving Reynolds equation.

ESA

N93-11059* National Aeronautics and Space Administration. Langley Research Center, Hampton, VA.

SEMI-INTERPENETRATING POLYMER NETWORK FOR TOUGHER AND MORE MICROCRACKING RESISTANT HIGH TEMPERATURE POLYMERS Patent

Ruth H. Pater, inventor (to NASA) 22 Sep. 1992 11 p Filed 6 Mar. 1991 Division of US-Patent-Appl-SN-301925, filed 26 Jan. 1989
(NASA-Case-LAR-13925-2; US-Patent-5,149,746; US-Patent-Appl-SN-665371; US-Patent-Appl-SN-301925; US-Patent-Class-525-422; US-Patent-Class-525-432; US-Patent-Class-525-903; Int-Patent-Class-C08L-79/08) Avail: US Patent and Trademark Office

A process for making a semi-interpenetrating polymer network which includes a high performance thermosetting polyimide having a nadic end group acting as a crosslinking site and a high performance linear thermoplastic polyimide is disclosed. Provided is an improved high temperature matrix resin which is capable of performing at 316 C in air for several hundreds of hours. This resin has significantly improved toughness and microcracking resistance, excellent processability and mechanical performance, and cost effectiveness.
Official Gazette of the U.S. Patent and Trademark Office

N93-11066# Rolls-Royce Ltd., Derby (England). Advanced Ceramics Centre.

AERO ENGINE CERAMICS: THE VISION, THE REALITY, AND THE PROGRESS

James P. Angus 18 Feb. 1992 22 p Presented at Aerotech 1992, Birmingham, England, 16 Jan. 1992
(PNR-90983; ETN-92-92242) Copyright Avail: CASI HC A03/MF A01

In order to provide an understanding of what Rolls-Royce are trying to achieve with ceramics, three areas are covered: the vision, the reality, and the progress. The 'vision' is described in terms of the benefit to engines and the potential cost savings to customers; the advantages of the high thrust to weight ratio offered by ceramics are discussed. For the 'reality' of trying to achieve this vision, some of the key technical issues to be addressed are described. These are discussed with reference to a component well suited to composite ceramics, the exhaust diffuser. Responses to the challenge these issues create are explained. Under 'progress' some of the real achievements made are discussed. The full range of ceramics being considered for aeroengines are discussed with a focus on one of the most promising groups of ceramics, the fiber reinforced ceramic composites. ESA

N93-11079# California Inst. of Tech., Pasadena. Dept. of Electrical Engineering.

DEVELOPMENT OF STABLE METALLIZATION SYSTEMS Final Report, 15 Mar. 1989 - 14 Mar. 1992

Marc-A. Nicolet 29 Apr. 1992 10 p
(Contract DAAL03-89-K-0049)
(AD-A253569; ARO-26287.29-MS) Avail: CASI HC A02/MF A01

Shallow Si n(+)p junctions equipped with a reactively sputtered Ta36Si14N50 amorphous metallic diffusion barrier of about 100 nm thickness have survived, without a detectable degradation of their reverse current, a 30 min long vacuum annealing test of 700 C with Al (Al melts at 660 C), 750 C with Au, and 950 C with Cu. For all three metallizations, these temperatures are records that much surpass any previously known results. This same Ta-Si-N film also acts as an excellent conducting annealing cap for GaAs. Implications of these findings are briefly discussed. A list of collaborators and of papers acknowledging the support of this contract are given. GRA

N93-11084# Rolls-Royce Ltd., Derby (England).

MODELLING THE BEHAVIOUR OF GAS BUBBLES IN EPOXY RESIN

Jonathan R. Wood (Surrey Univ., Guildford, England) and Michael G. Bader (Surrey Univ., Guildford, England) 1 Aug. 1991 11 p Presented at the ICCM-VIII, HI, 15-19 Jul. 1991 Previously announced in IAA as A92-32610
(PNR-90961; ETN-92-92234) Copyright Avail: CASI HC A03/MF A01

The behavior of bubbles containing a noncondensable gas in an uncured unmodified bisphenol-A resin was studied. The investigation involved the monitoring of bubbles and the subsequent modeling of their behavior utilizing mass diffusion equations. A novel method of measuring the diffusion coefficient of gases in epoxy resin was employed based on the observation of bubble dissolution rates. The effect of temperature, concentration of gas in solution, and initial bubble size was shown to affect the time to complete solution of gas bubbles. ESA

N93-11086# Rolls-Royce Ltd., Derby (England).

THE DRESSING OF RESIN BONDED DIAMOND GRINDING WHEELS

J. A. Scott, T. M. A. Maksoud (Wales Polytechnic, Pontypridd.), and J. E. Morgan (Bristol Univ., England) 1 Oct. 1991 14 p
(PNR-90965; ETN-92-92236) Copyright Avail: CASI HC A03/MF A01

The effect of a driven rotary steel dressing device on the subsequent performance of a resin bonded diamond grinding wheel, used to grind silicon nitride ceramics, is described. The influence of increasing dressing parameters such as speed ratio and dresser depth of cut are shown to cause an increase in dressing forces, consistent with the size of chip produced in a dressing operation. However, only the total number of dressing cuts taken in a dressing operation influences the grinding forces generated in a subsequent ceramic grinding operation to any statistically significant level. Replication of the dressing technique showed that the system can dictate the peripheral condition of a grinding wheel and that this condition can be reproduced. This is important if a ceramic grinding operation is to be effectively controlled. The grinding forces generated when grinding silicon nitride components are reduced as the number of dressing passes increases due to blunted or glazed grits being replaced by smaller number of sharp grits. This effect also causes an increase in the level of compressive residual stresses produced. ESA

N93-11149# Michigan Univ., Ann Arbor. Dept. of Materials Science and Engineering.

WORKSHOP ON SURFACE SCIENCE AND TECHNOLOGY Final Report

John C. Bilello and Robert R. Reeber Mar. 1992 96 p Workshop held in Ann Arbor, MI, 7-9 Nov. 1990
(Contract DAAL03-90-G-0135)
(AD-A253566; ARO-28216.1-MS-CF) Avail: CASI HC A05/MF A01

The objective of this workshop was to review and assess the state of the art of surface science and technology as well as to identify new research opportunities essential for the understanding and control of surface degradation, adhesion, corrosion and wear. A cross-section of Academic, Army and NASA professionals contributed their talents. It is anticipated that the knowledge gained through programs focussing on the Army and national needs will result in new materials coating systems that have novel properties, increased durability and reliability and the potential for significantly lowering the Army's maintenance and logistics costs. GRA

N93-11150# Massachusetts Inst. of Tech., Cambridge. Dept. of Chemistry.

SYNTHESIS AND SIDE CHAIN LIQUID CRYSTAL POLYMERS BY LIVING RING OPENING METATHESIS POLYMERIZATION. 5: INFLUENCE OF MESOGENIC GROUP AND INTERCONNECTING GROUP ON THE THERMOTROPIC BEHAVIOR OF THE RESULTING POLYMERS

Zen Komiya and Richard R. Schrock 22 Jul. 1992 38 p
(Contract N00014-92-J-1433)
(AD-A253568; TR-18) Avail: CASI HC A03/MF A01

Norbornene derivatives containing 4'-cyano-4-biphenyloxy mesogens linked to the norbornene through methylene groups (n = 3 to 7, 9 to 12) and an ester were polymerized by Mo(CHR)(NAr)(O-t-Bu)2 (Ar = 2, 6-C6H3-i-Pr2, R = t-Bu) in a living manner. Polymers in which n = 3 were amorphous, whereas all other polymers (n = 4 to 7, 9 to 12) displayed enantiotropic nematic mesophases that were independent of the molecular weight. Polymers having 9 to 12 methylene spacers did not undergo side chain crystallization and did not show an odd-even effect, in contrast to analogous polymers containing 4'-methoxy-4-biphenyloxy mesogens, which exhibited side chain crystallization when n greater than 8 and an odd-even effect when n less than 7. The lower tendency to form a more ordered phase and the absence of an odd-even effect are attributed to dipole-dipole repulsions between 4'-cyano-4-biphenyloxy mesogens. Polymers containing 4'methoxy-4-biphenyloxy mesogens attached through ether linkages gave highly crystalline SCLPCs, even with relatively few spacers (n = 4 to 6). GRA

N93-11187# Massachusetts Inst. of Tech., Cambridge. Dept. of Chemistry.

SYNTHESIS OF SIDE CHAIN LIQUID CRYSTAL POLYMERS BY LIVING RING OPENING METATHESIS POLYMERIZATION. REPORT 3: INFLUENCE OF MOLECULAR WEIGHT, INTERCONNECTING UNIT AND SUBSTITUENT ON THE MESOMORPHIC BEHAVIOR OF POLYMERS WITH LATERALLY ATTACHED MESOGENS

Coleen Pugh and Richard R. Schrock 8 Apr. 1992 50 p
(Contract N00014-89-J-1542)
(AD-A248698; TR-15-Rept-3) Avail: CASI HC A03/MF A01

Norbornene derivatives containing laterally attached 2,5-bis(4'-n-alkoxybenzoyloxy) mesogens were polymerized by controlled ring opening metathesis polymerization to provide polymers in high yield with 5-100 repeat units and narrow molecular weight distributions. Monomers with n greater than 1 displayed monotropic or enantiotropic nematic mesophases. All polymers displayed enantiotropic nematic mesophases regardless of the spacer, molecular weight or length or the n-alkoxy substituent. Constitutional isomers of poly(5-carbo(2',5'-bis-(4"-methoxybenzoyloxy)benzyloxy) bicyclo(2.2.1)hept-2-ene)s containing laterally attached mixed phenylester/benzylester units are amorphous. GRA

N93-11188# Massachusetts Inst. of Tech., Cambridge. Dept. of Chemistry.

SYNTHESIS OF SIDE CHAIN LIQUID CRYSTAL POLYMERS BY LIVING RING OPENING METATHESIS POLYMERIZATION. REPORT 2: INFLUENCE OF MOLECULAR WEIGHT, POLYDISPERSITY, AND FLEXIBLE SPACER LENGTH (N=9-12) ON THE THERMOTROPIC BEHAVIOR OF THE RESULTING PLYMERS

Zen Komiya, Coleen Pugh, and Richard R. Schrock 31 Mar. 1992 27 p
(Contract N00014-89-J-1542)
(AD-A248700; TR-14-Rept-2) Avail: CASI HC A03/MF A01

The living ring opening metathesis polymerization of 5-carbon(n-((4'-methoxy-4 biphenylyl)oxy)alkyl) bicyclo 2.2.1hept-2-ene (1-n, n = 9 to 12) with Mo(CH-t-Bu)(NAr) (0-t-Bu)2 (Ar = 2,6-C6H3-i-Pr2) is described. Polymers with degrees of polymerization from 5 to 100 and narrow molecular weight distributions (M(sub w)/M(sub n) = 1.07 to 1.28) were obtained in high yield. All polymers exhibit side chain crystallization along with a nematic mesophase. Isotropization temperatures increase with increasing molecular weight and then become independent of molecular weight at approximately 30 to 50 repeat units. Side chain crystallization is suppressed as molecular weight increases. GRA

N93-11192# Utah State Univ., Logan. Dept. of Chemistry and Biochemistry.

ORGANOMETALLIC NLO POLYMERS. 3. COPOLYMERIZATION OF BRIDGED BIS(FERROCENYL) AND BIS(CYANOACETATE) MONOMERS VIA THE KNOEVENAGEL CONDENSATION Technical Report No. 8, 15 Apr. 1991 - 15 Apr. 1992

Michael E. Wright and Matthew S. Sigman 10 May 1992 23 p
(Contract N00014-91-J-1625)
(AD-A250214) Avail: CASI HC A03/MF A01

The bridged bis(ferrocenyl) monomer ((eta(sup 5)-C5H4-CHO)Fe(eta(sup 5)-C5H4))2SiMe2 (1) was prepared in two steps from (eta(sup 5)-C5H4SnBu3)2Fe. The bis(cyanoacetate) monomers, CNCH2CO2(CH2)(n)O2CCH2CN (2) (where n = 4, 6, and 8) where prepared in high yield by reacting ethyl cyanoacetate with the appropriate diol in the presence of Ti(OC4H9)4. Knoevenagel polycondensation K2CO3, THF, 40 C of 1 and 2 afforded a new class of organometallic accordion copolymers. Average molecular weights for the accordion copolymers ranged from 9100 to 26,600 with polydispersities of approximately 2.1. The Knoevenagel polycondensation reaction appeared to produce a mixture of E- and Z-isomers (9/1, respectively); however, isomerically enriched polymer (i.e., 98 percent E-isomer) was obtained through selective precipitation. GRA

N93-11194# Missouri Univ., Rolla. Dept. of Chemistry.

MOLECULAR MOBILITY OF THE INTERFACE IN A MODEL COMPOSITE: A NMR STUDY Interim Report, Aug. 1990 - Jul. 1992

Joan E. Gambogi and Frank D. Blum 15 Jul. 1992 35 p
(Contract N00014-91-J-1274)
(AD-A253311; UMR-FDB-26) Avail: CASI HC A03/MF A01

The interface of a model polymer composite has been probed using solid-state NMR techniques. The adsorption of aminoalkylsilane coupling agents onto silica surfaces and the interaction of these functional silanes with a bismaleimide resin was studied. Carbon-13 CP/MAS NMR was used to confirm the bonding between the silane and bismaleimide (BMI) resin and elucidate the nature of the crosslinking reaction of BMI. Deuterated coupling agents were synthesized, adsorbed, and reacted on silica surfaces. The deuterium labels on the coupling agents allowed their dynamics to be probed independently of the other organic materials present through the use of 2-H solid-echo NMR. The experimental results were consistent with motions where the alkyl portion of the coupling agent undergoes gauche migration (gtt - ttg) and pair gauche production (ttt - gtg) conformational isomerizations plus slow anisotropic rotation. The room temperature spectra were simulated with a model that included hopping between two discrete sites on the tetrahedral lattice with a jump rate of 8 x 10(exp 5) sec(exp -1) and plus rotational diffusional constants of R(parallel) = 7 x 10(exp 4) and R(perpendicular) = 1 x 10(exp 4) cm(exp -1). Polymerizing BMI resin over the chemisorbed coupling agent resulted in a line shape that could be modelled as a simple two site jump with occupational probabilities of 0.7 and 0.3 and a jump frequency of 1.7 x 10(exp 5) sec(exp -1). The anisotropic rotation was no longer required to simulate these spectra. The types of motions of the coupling agent were not affected significantly over the temperature range -100 C to 85 C, although the exchange rate was changed. GRA

N93-11203# Kernforschungszentrum G.m.b.H., Karlsruhe (Germany). Inst. fuer Materialforschung.

FRACTURE BEHAVIOR OF POLYMERS AT CRYOGENIC TEMPERATURES Thesis - Karlsruhe Univ. [BRUCHVERHALTEN VON POLYMEREN BEI KRYOGENEN TEMPERATUREN]

Thomas Saatkamp Dec. 1991 83 p In GEORGIAN
(KfK-4969; ETN-92-92158) Copyright Avail: CASI HC A05/MF A01

The crack propagation behavior of polymers at cryogenic temperatures is determined by the physical processes taking place at the crack tip. It is shown that stable or unstable crack growth does not depend on the experimental set up, but on the properties of the polymers. Plastification processes at the crack tip are temperature and time dependent. During unstable crack growth, a crack arrest behavior caused by adiabatic heating and plastification at the crack tip is observed in most of the polymers. Under certain conditions, the increase in temperature is sufficient to attain the dispersion range of the second glass transition, as a result of which plastification is intensified. ESA

N93-11205# Rolls-Royce Ltd., Derby (England). Advanced Ceramics Centre.
INDUSTRIAL APPLICATIONS AND MARKETS FOR CERAMIC MATRIX COMPOSITES
David A. Clarke (Warwick Univ., Coventry, England) 20 Aug. 1991 34 p
(PNR-90884; ETN-92-92189) Copyright Avail: CASI HC A03/MF A01

An assessment of the annual world market for Ceramic Matrix Composites (CMC), which is expected to expand by about 300 percent to nearly a thousand million pounds (monetary) by the year 2000, is presented. Focus is on the use of particulate and fiber reinforced ceramics in applications such as cutting tools, space structures, heat engines, optical/electronic units, and armors. The types of materials in use and the reasons for their selection are discussed together with an assessment of what industry must now do to realize the full potential of CMC materials in a wide range of market roles. ESA

N93-11397 National Physical Lab., Teddington (England). Div. of Materials Metrology.
VAMAS ROUND ROBIN PROJECT ON POLYMER COMPOSITE DELAMINATION IN MODE 1 AND MODE 2: CYCLIC LOADING
W. R. Broughton Mar. 1992 58 p Sponsored by Dept. of Industry and Trade
(NPL-DMM(A)-47; ETN-92-92369) Copyright Avail: National Physical Lab., Teddington, Middlesex, TW11 0LW, England

A VAMAS (Versailles Project on Advanced Materials and Standards) round robin program was set up in two stages to study delamination behavior of polymer composite materials under both static (stage 1) and cyclic (stage 2) mode 1 and mode 2 loading conditions. Experimental results from cyclic loading tests carried out for stage 2 of the program are presented. This stage is concerned with modeling and evaluating delimination growth under mode 1 and mode 2 fatigue loadings. For the characterization of delamination behavior under cyclic loading, aligned carbon fiber/epoxy, aligned glass fiber/epoxy, and woven glass fiber/epoxy composite materials were studied. Two specimen types were tested: a double cantilever beam specimen for mode 1I loading and an end notched flexure specimen for mode 2 loading. The results from these tests showed that cyclic delamination is governed by the total strain energy release rate. ESA

N93-11400 Department of the Navy, Washington, DC.
SILVER LINED CERAMIC VESSEL AND METHOD OF PREPARATION Patent
William A. Ferrando, inventor (to Navy) (Courtney and Co., Philadelphia, PA.), Amarnath P. Divecha, inventor (to Navy) (Courtney and Co., Philadelphia, PA.), and James Kerr, inventor (to Navy) (Courtney and Co., Philadelphia, PA.) 9 Jun. 1992 3 p Filed 10 May 1991
(AD-D015360; US-Patent-5,120,575; US-Patent-Appl-SN-700375; US-Patent-Class-427-229) Avail: US Patent and Trademark Office

A reaction vessel comprising (1) a porous ceramic structure having interconnecting open pores, and (2) a silver metal coating the inner ceramic surfaces of the reaction vessel and filling the interconnecting open pores to form a strong bond between the porous ceramic structure and the silver coating. The reaction vessel can be produced by (1) coating the inner surface and infiltrating the continuous open pores of an unglazed porous ceramic structure (or vessel) with molten AgNO3, (2) decomposing the AgNO3 to silver metal, and then (3) repeating steps (1) and (2) until all the pores are filled with silver metal. GRA

N93-11413# Rensselaer Polytechnic Inst., Troy, NY. Dept. of Chemistry.
CVD OF AlN AND SiC USING CYCLIC ORGANOMETALLIC PRECURSORS
L. V. Interrante, C. Amato, and D. J. Larkin Dec. 1991 10 p
(Contract N00014-91-J-1917)
(AD-A246910) Avail: CASI HC A02/MF A01

The use of cyclic organometallic molecules as single-source MOCVD precursors is illustrated by means of examples taken from our recent work on AlN and SiC deposition, with particular focus on SiC. Molecules containing (AlN)3 and (SiC)2 rings as the 'core structure' were employed as the source materials for these studies. The organoaluminum amide, (Me2AlNH2)3, was used as the AlN source and has been studied in a molecular beam sampling apparatus in order to determine the gas phase species present in a hot-wall CVD reactor environment. In the case of SiC CVD, a series of disilacyclobutanes (Si(XX')CH2)2 (with X and X' = H, CH3, and CH2SiH2CH3), were examined in a cold-wall, hot-stage CVD reactor in order to compare their relative reactivities and prospective utility as single-source CVD precursors. The parent compound, disilacyclobutane, (SiH2CH2)2, was found to exhibit the lowest deposition temperature (ca. 670 C) and to yield the highest purity SiC films. This precursor gave a highly textured, polycrystalline film on the Si(100) substrates. GRA

N93-11425 Department of the Navy, Washington, DC.
CORROSION RESISTANT CHROMATE CONVERSION COATINGS FOR HEAT-TREATED ALUMINUM ALLOYS Patent
Lionel J. Balin, inventor (to Navy) (Courtney and Co., Philadelphia, PA.) and Wash Kostinko, inventor (to Navy) (Courtney and Co., Philadelphia, PA.) 23 Jun. 1992 4 p Filed 19 Mar. 1991
(AD-D015366; US-Patent-5,123,978; US-Patent-Appl-SN-671592; US-Patent-Class-148-247) Avail: US Patent and Trademark Office

An improved method of coating 7000 series aluminum alloys, which are difficult to coat uniformly, with a coating resistant to long term corrosion in a salt spray environment is disclosed. By using a chromate solution of very low pH and applying that solution first as a cleaner, followed by brush application to form the final coating, an extended resistance to corrosion at least 2 to 3 times the usual duration is achieved readily. GRA

N93-11442# Oak Ridge National Lab., TN.
CERAMIC TECHNOLOGY PROJECT
Mar. 1992 504 p
(Contract DE-AC05-84OR-21400)
(DE92-018748; ORNL/TM-11984) Avail: CASI HC A22/MF A04

The Ceramic Technology Project was developed by the USDOE Office of Transportation Systems (OTS) in Conservation and Renewable Energy. This project, part of the OTS's Materials Development Program, was developed to meet the ceramic technology requirements of the OTS's automotive technology programs. Significant accomplishments in fabricating ceramic components for the USDOE and NASA advanced heat engine programs have provided evidence that the operation of ceramic parts in high-temperature engine environments is feasible. These programs have also demonstrated that additional research is needed in materials and processing development, design methodology, and data base and life prediction before industry will have a sufficient technology base from which to produce reliable cost-effective ceramic engine components commercially. A five-year project plan was developed with extensive input from private industry. In July 1990 the original plan was updated through the estimated completion of development in 1993. The objective is to develop the industrial technology base required for reliable ceramics for application in advanced automotive heat engines. The project approach includes determining the mechanisms controlling reliability, improving processes for fabricating existing ceramics, developing new materials with increased reliability, and testing these materials in simulated engine environments to confirm reliability. Although this is a generic materials project, the focus is on the structural ceramics for advanced gas turbine and diesel engines, ceramic bearings and attachments, and ceramic coatings for thermal barrier and wear applications in these engines. To facilitate the rapid transfer of this technology to US industry, the major portion of the work is being done in the ceramic industry, with technological support from government laboratories, other industrial laboratories, and universities. DOE

N93-11497# Allied-Signal Aerospace Co., Kansas City, MO.
AN EVALUATION OF FIELD-FLOW FRACTIONATION FOR MOLECULAR WEIGHT CHARACTERIZATION OF POLYMERIC MATERIALS
E. N. Fuller Aug. 1992 31 p
(Contract DE-AC04-76DP-00613)
(DE92-019192; KCP-613-4802) Avail: CASI HC A03/MF A01

An evaluation has been made of field-flow fractionation for potential polymer molecular weight characterization applications at Allied-Signal Inc., Kansas City Division. The obtained data show that the technique can provide useful information regarding polymer molecular weights which are analogous to those obtained by gel permeation chromatography. DOE

N93-11549# Lawrence Livermore National Lab., CA.
LASER GLASSES
M. J. Weber May 1992 22 p Presented at the 1992 Optics International Conference, Padova, Italy, 8-13 Jun. 1992
(Contract W-7405-eng-48)
(DE92-018061; UCRL-JC-109922; CONF-9206141-2) Avail: CASI HC A03/MF A01

The chemical composition of a glass affects its range of transparency, linear and nonlinear refractive indices, absorption and emission transition probabilities and cross sections, rates of nonradiative decay of excited ions by multiphonon processes, and physical and chemical durability; all of which are important for laser action. Because of the compositional versatility of glass, it is possible to tailor the chemical composition of glasses to optimize various physical and spectroscopic properties of interest for specific laser applications. In the past 30 years many different oxide and halide glasses and dopant ions have been investigated. This has resulted in glass lasers operating in the visible and near infrared either continuously or in ultrashort (ps) pulses. The forms of glass amplifying media have ranged from micron-diameter optical fibers for communications to rods and disks with dimensions up to one meter for inertial confinement fusion lasers. The physical processes involved in obtaining stimulated emission in glass are generally understood and the glass compositional space has been explored extensively. Nevertheless, further advances in the properties and characteristics of glass lasers are anticipated by the development of additional host glass compositions, novel methods of preparing glass, and new laser operating techniques. DOE

N93-11552# Sandia National Labs., Albuquerque, NM.
EVALUATION OF EPOXY CURED WITH ETHACURE 100 CURING AGENT FOR USE IN HEADERS FOR THERMAL BATTERIES
R. A. Guidotti and B. J. Wells Jul. 1992 15 p
(Contract DE-AC04-76DP-00789)
(DE92-019326; SAND-92-0763) Avail: CASI HC A03/MF A01

Diethyltoluenediamine (DETDA) (Ethyl Corp.'s Ethacure 100) was evaluated as a curing agent to replace methylenedianiline (MDA) (Shell's Agent Z), which is a suspected carcinogen. Shell Z and Ethacure 100 are used to cure Epon 828 epoxy resin for encapsulation of headers for thermal batteries at Sandia. The physical properties of the alumina-filled epoxies cured with Shell Z and Ethacure 100 were characterized to determine if the material strengths were comparable. The study also included epoxies that were aged at 130 C for one month, to simulate storage at 40 C for 25 years. Properties that were measured included tensile strength, elastic modulus, shear strength, butt tensile strength, and elongation. The specific heats of the alumina-filled epoxies were measured for use in thermal-modeling programs for thermal batteries. Batteries built with the Ethacure 100-cured epoxy encapsulation were aged for up to one year at 74 C and were subjected to severe (1,800 g/50 ms) lateral shock to test the adhesion to the stainless steel header. DOE

N93-11570# Martin Marietta Energy Systems, Inc., Oak Ridge, TN.
MICROWAVE SINTERING OF MULTILAYER CERAMIC CAPACITORS
R. J. Lauf, C. E. Holcombe, and C. Hamby 1992 7 p Presented at the Material Research Society Spring Meeting, San Francisco, CA, 27 Apr. - 2 May 1992
(Contract DE-AC05-84OR-21400)
(DE92-018772; CONF-920402-49) Avail: CASI HC A02/MF A01

Multilayer ceramic capacitors of several compositions (both Z5U and NPO types) were sintered in air in both conventional and microwave furnaces. Several casketing and insulation techniques were used to improve temperature uniformity and minimize dopant losses. Zirconia and yttria are suitable packing materials as either powders or fibers. After sintering, the packing material remains friable and can be recycled. The presence of metallization layers did not interfere with the microwave process and no arcing was observed at surfaces where the internal electrodes emerged. In some runs, however, local thermal runaway was observed, which could severely decrease process yields and must be eliminated in a commercial process. DOE

N93-11577# Ecole Centrale de Lyon (France). Lab. de Materiaux-Mecanique Physique.
STUDY AND CHARACTERIZATION OF CERAMIC-METAL BONDS MANUFACTURED BY SOLID STATE BONDING TECHNIQUES. APPLICATION TO Ag/Al2O3 Ph.D. Thesis [ETUDE ET CARACTERISATION DES LIAISONS CERAMIQUE-METAL ELABOREES PAR THERMOCOMPRESSION. APPLICATION AU COUPLE AG/AL2O3]
Boualem Serier 1991 168 p In FRENCH
(ECL-91-19; ETN-92-92338) Avail: CASI HC A08/MF A02

The ceramic-metal bonds obtained from nonreactive systems often show improved mechanical and sealing properties when compared to those from reactive systems. The reason is the presence of intermediate phases which form from reactive systems. The Ag/Al2O3 system was chosen because of the large difference between thin thermal expansion coefficient. The specimens were obtained by solid state bonding and submitted to mechanical tests. The role of the oxygen content and the strain percent of the metal are highlighted. High quality interfaces were obtained from fabrication processes involving low temperatures, low applied stress, and a simple temperature cycle consisting of a temperature increase followed by a temperature decrease. The effect of oxygen at the Ag/Al2O3 interface is discussed and the diffusion coefficients and the toughness are studied. ESA

N93-11580# Ecole Centrale de Lyon (France). Lab. des Materiaux Mecanique-Physique.
STUDY OF METAL-CERAMIC INTERFACES OF Co-Cr-Mo ALLOYS: ROLE OF TUNGSTEN (W) AND MANGANESE (Mn) ADDITIONS Ph.D. Thesis [ETUDE DES INTERFACES METAL-CERAMIQUE SUR DES ALLIAGES CO-CR-MO: ROLE D'UNE ADDITION DE TUNGSTENE (W) ET DE MANGANESE (MN)]
Bambang Soegijono 1992 164 p In FRENCH
(ECL-92-01; ETN-92-92341) Avail: CASI HC A08/MF A02

The micromechanical properties of the metal-ceramic bondings of a cobalt alloy used in odontological applications are investigated. Mechanical adhesion tests, surface analysis, and the characterization of the material's structure were performed. The effects of the metal surface composition and of the characteristics of the ceramic surface (before sintering) on the metal-ceramic interface adhesion are studied. The role taken by processes such as diffusion, oxidation, and chemical bonding on the interface properties are considered. The choice of the materials and the heat treatments are explained. The possible correlation between chemical composition, the mechanical properties, and the diffusion kinetics of some typical elements are analyzed. The results showed that the adhesion characteristics of the interface depend on the chemical composition of the alloy chosen. ESA

N93-11628# Pittsburgh Univ., PA. Dept. of Materials Science and Engineering.
COMPUTER SIMULATIONS FOR THE ADSORPTION OF POLYMERS ONTO SURFACES

A. C. Balazs 1992 11 p
(Contract DE-FG02-90ER-45438)
(DE92-018942; DOE/ER-45438/2) Avail: CASI HC A03/MF A01

The objective is to develop theoretical models and computer simulations to examine the adsorption of polymers onto a variety of surfaces, and to understand how the chain architecture and conditions such as the surface or solvent affect the extent of adsorption and the morphology of the interfacial layers. Results obtained last year are summarized under the following headings: behavior of copolymers at a liquid-liquid interface, grafted homopolymer chains in a poor solvent, amphiphilic comb copolymers in oil/water solutions, modeling polymer adsorption onto influenza virus, and behavior of polymers in concentrated surfactant solutions. Plans for future work are also given. DOE

N93-11654# Oak Ridge National Lab., TN.
DEVELOPMENT OF WEAR RESISTANT CERAMIC COATINGS FOR DIESEL ENGINE COMPONENTS
M. H. Haselkorn Apr. 1992 111 p Prepared in cooperation with Caterpillar Tractor Co., Peoria, IL
(Contract DE-AC05-84OR-21400)
(DE92-019068; ORNL/Sub-87-SA582/1) Avail: CASI HC A06/MF A02

Improved fuel economy and a reduction of emissions can be achieved by insulation of the combustion chamber components to reduce heat rejection. However, insulating the combustion chamber components will also increase the operating temperature of the piston ring/cylinder liner interface from approximately 150 C to over 300 C. Existing ring/liner materials can not withstand these higher operating temperatures and for this reason, new materials need to be developed for this critical tribological interface. The overall goal of this program is the development of piston ring/cylinder liner material pairs which would be able to provide the required friction and wear properties at these more severe operating conditions. More specifically, this program first selected, and then evaluated, potential wear resistant coatings which could be applied to either piston rings an or cylinder liners and provide, at 350 C under lubricated conditions, coefficients of friction below 0.1 and wear rates of less than 25 x 10(exp -6) mm/hour. The processes selected for applying the candidate wear resistant coatings to piston rings and/or cylinder liners were plasma spraying, chemical vapor, physical vapor and low temperature arc vapor deposition techniques as well as enameling techniques. DOE

N93-11735# Oak Ridge National Lab., TN.
ENGINE TESTING OF CERAMIC CAM-ROLLER FOLLOWERS
Y. Kalish Apr. 1992 98 p Prepared in cooperation with Detroit Diesel Allison, MI
(Contract DE-AC05-84OR-21400)
(DE92-019188; ORNL/Sub-90-SF985/1) Avail: CASI HC A05/MF A02

For several years, DDC has been developing monolithic ceramic heat engine components. One of the components, developed for an application in our state-of-the-art on-highway, heavy-duty diesel engine, the Series 60, is a silicon nitride cam-roller follower. Prior to starting this program, each valve train component in the Series 60 was considered for conversion to a ceramic material. Many advantages and disadvantages (benefits and risks) were considered. From this effort, one component was selected, the cam-roller follower. Using a system design approach, a ceramic cam-roller follower offered functional improvement at a reasonable cost. The purpose of the project was to inspect and test 100 domestically produced silicon nitride cam-roller followers built to the requirements of the DDC series 60 engine. DOE

N93-11793# Cortana Corp., Falls Church, VA.
COMPARATIVE EFFECTS OF DRAG-REDUCING POLYMERS. AN EXPERIMENTAL REPORT Final Report, Aug. 1988 - Dec. 1991
G. Murphree 9 Jul. 1992 27 p
(Contract MDA972-88-C-0064)
(AD-A254001) Avail: CASI HC A03/MF A01

The experiments described in this report were performed within the framework of the overall ASTI Team effort in polymer science. The underlying predicate of this program has been to achieve a basis for understanding the shear viscosity of dilute polymer solutions through a detailed description of the molecular interactions. Interaction descriptions must include water/polymer, water/surface and polymer/surface contributions to provide understanding of the mechanisms determining the shear viscosity and related noise and drag reduction effects. Although certain anionic polymeric drag reduction effects observed herein are not dramatic compared to those achieved with the standard polyethylene-oxide, these types of polymers offer the potential for drastically altering the interaction between the surface and adjacent layers of water molecules. It can be assumed that the water layer/surface interaction is dependent on the nature of the surface potential and the presence of strongly interacting species in that region. Thus, any mechanism reducing the concentration of such active species near the surface should reduce the overall strength of the interaction. However, drag reduction actually increased for polyacrylamide changing from deionized water to 'instant ocean' (salt water environment). This suggests the role of ions in determining polymer effectiveness may be complex. GRA

N93-11861# Los Alamos National Lab., NM.
SYNTHESIS OF NANOCRYSTALLINE POWDERS FOR OXIDE CERAMICS BY MICROWAVE PLASMA PYROLYSIS
D. Vollath, R. Varma, and K. E. Sickafus 1992 7 p Presented at the Material Research Society Spring Meeting, San Francisco, CA, 27 Apr. - 2 May 1992
(Contract W-7405-eng-36)
(DE92-017410; LA-UR-92-1779; CONF-920402-43) Avail: CASI HC A02/MF A01

Pyrolytically prepared ceramic powders usually exhibit excellent homogeneity and small grain sizes. The energy efficiency of those methods for synthesis is, particularly in systems heated electrically, very poor. The situation can be improved dramatically using a microwave plasma as a source of energy. This has been confirmed by the synthesis of alumina- and zirconia-based ceramic powders for which an efficiency of more than 80 percent was found. Aqueous solutions of nitrates of zirconium, yttrium, and aluminum were used as starting materials. Electron microscopy revealed that, through proper selection of the experimental conditions, it is possible to obtain nanocrystalline powders with cubic structure. Because of the extreme conditions during synthesis, it is possible to prepare solid solutions in systems without diminishing equilibrium solubility. DOE

N93-11862# Army Natick Labs., MA.
PROGRESS ON POLYMER DEGRADATION BY PHOTOELECTRON TRANSFER Final Report, May 1990 - Aug. 1991
John W. Cullen, Stephen J. Weininger, and David E. Remy Dec. 1991 15 p
(DA Proj. 1L1-61102-AH-52)
(AD-A246276; Natick/TR-92/010) Avail: CASI HC A03/MF A01

1,5-Bis(3-hydroxypropoxy)-9,10-dimethoxyanthracene has been prepared and incorporated into poly (2-butynediyl oxalate). The photolysis results of the copolymer are described. Progress toward the preparation of 2-(4-carboxyphthalimoyl)-9, 10- dimethoxyanthracene from 2-amino-9, 10-anthraquinone and mellitic anhydride is described. Synthetic intermediates have been characterized by ultraviolet visible, infrared and proton nuclear magnetic resonance spectroscopy. For some time this laboratory has been interested in energy absorptive materials, specifically polymers which could decompose cleanly to gaseous products on thermal or photic excitation. We recently reported the synthesis of some unsaturated polyoxalates according to the following equation and their characterization. The thermal decomposition of these polymers was studied by thermogravimetric analysis (TGA), differential scanning calorimetry (DSC) and mass spectroscopy. The polymers were characterized by 1H-NMR spectra run in DMSO-d6. Since the chemical shifts of the end groups were sufficiently different from those of the internal groups, it is possible to determine molecular weights and degree of polymerization (DP) values by NMR end group analysis. GRA

N93-11912*# National Aeronautics and Space Administration. Langley Research Center, Hampton, VA.
MULTI-LAYER LIGHT-WEIGHT PROTECTIVE COATING AND METHOD FOR APPLICATION Patent Application
Karl E. Wiedemann, inventor (to NASA) (AS&M, Inc., Hampton, VA.), Ronald K. Clark, inventor (to NASA), and Patrick J. Taylor, inventor (to NASA) (AS&M, Inc., Hampton, VA.) 10 Jul. 1992 17 p
(NASA-Case-LAR-14448-1; NAS 1.71:LAR-14448-1; US-Patent-Appl-SN-912960) Avail: CASI HC A03/MF A01

A thin, light-weight, multi-layer coating is provided for protecting metals and their alloys from environmental attack at high temperatures. A reaction barrier is applied to the metal substrate and a diffusion barrier is then applied to the reaction barrier. A sealant layer may also be applied to the diffusion barrier if desired. The reaction barrier is either non-reactive or passivating with respect to the metal substrate and the diffusion barrier. The diffusion barrier is either non-reactive or passivating with respect to the reaction barrier and the sealant layer. The sealant layer is immiscible with the diffusion barrier and has a softening point below the expected use temperature of the metal. NASA

N93-11983# Technische Univ., Eindhoven (Netherlands).
ORIENTATION, STRESS, AND DENSITY DISTRIBUTIONS IN INJECTION-MOULDED AMORPHOUS POLYMERS DETERMINED BY OPTICAL TECHNIQUES Ph.D. Thesis
Reinhold Wimberger-Friedl 1991 241 p
(ETN-92-92271) Avail: CASI HC A11/MF A03

Papers concerning the following are presented: stress optical behavior of polycarbonate and polymethyl methacrylate; birefringence in quenched and injection molded polycarbonate; density distributions in amorphous polymers; and injection molded optical components. It is concluded that the state of an injection molded amorphous polymer can be quantified in terms of molecular orientation, residual stress, and density distribution by optical measurements. For individual titles, see N93-11984 through N93-11991.

N93-11984# Technische Univ., Eindhoven (Netherlands).
THE PECULIAR RHEO-OPTICAL BEHAVIOUR OF BISPHENOL-A-POLYCARBONATE AND POLYMETHYLMETHACRYLATE
Reinhold Wimberger-Friedl *In its* Orientation, Stress, and Density Distributions in Injection-Moulded Amorphous Polymers Determined by Optical Techniques 1991 p 13-39 Repr. from Rheol. Acta, v. 30, 1991 p 329 (For primary document see N93-11983 02-27)
Avail: CASI HC A03/MF A03

Investigation of the rheological and stress optical behavior of the melts of several grades of bisphenol A polycarbonate and polymethyl methacrylate (PMMA) is reported. Pertinent flow birefringence measurements were carried out in a remodeled cone-plate apparatus. The shear stress in the polymer melt was calculated from the dynamic moduli, which was determined separately. It was shown that the linear stress optical rule is obeyed. In this way the stress optical coefficient C of the melt can be determined. The low molecular weight polycarbonates all behaved as Maxwellian fluids. The main stress direction did not deviate significantly from 45 deg. In the temperature range from 160 to 260 C, the stress optical coefficients of the different grades lay between 3 and 4 x 10 -9/Pa and showed a weak temperature dependence. The stress optical coefficient of PMMA was about a factor of 100 lower and showed a peculiar temperature dependence, changing its sign at 144 C. The results are discussed in terms of the anisotropy of the polarizability of the polymer chain. ESA

N93-11985# Technische Univ., Eindhoven (Netherlands).
THE TIME-DEPENDENT STRESS-OPTICAL BEHAVIOUR OF POLYCARBONATE IN THE GLASS TRANSITION REGION
Reinhold Wimberger-Friedl *In its* Orientation, Stress, and Density Distributions in Injection-Moulded Amorphous Polymers Determined by Optical Techniques 1991 p 41-65 Submitted for publication (For primary document see N93-11983 02-27)
Avail: CASI HC A03/MF A03

The mechanical and stress optical behavior of bisphenol A polycarbonate was investigated in the glass transition region. For this purpose, optical creep experiments were carried out in shear and elongation on a tensile tester specially designed for use on a microscope stage. A Kohlrausch Williams Watts (KWW) equation with a temperature independent parameter beta could successfully be applied to the curves describing the time dependent values of the stress optical coefficient for several temperatures. The temperature dependence of the corresponding retardation time could be established and described by the WLF (Williams, Landel, and Ferry) equation. For variable stresses, the time dependent birefringence is obtained from a generalized linear stress optical rule as modeled according to linear superposition. The time temperature superposition principle was applied to all measurements. With the dynamic moduli, some deviations were observed at the transition from the rubbery plateau to the alpha relaxation. The stain optical coefficient was found to decrease with increasing time and strain. The strain dependence was found to be independent of temperature at constant stress. ESA

N93-11986# Technische Univ., Eindhoven (Netherlands).
THE MEASUREMENT AND CALCULATION OF BIREFRINGENCE IN QUENCHED POLYCARBONATE SPECIMENS
Reinhold Wimberger-Friedl *In its* Orientation, Stress, and Density Distributions in Injection-Moulded Amorphous Polymers Determined by Optical Techniques 1991 p 69-88 Repr. from Polymer, v. 30, 1989 p 1143 (For primary document see N93-11983 02-27)
Avail: CASI HC A03/MF A03

Stress induced birefringence in quenched polycarbonate disks was calculated with a numerical program and compared with birefringence measurements. Use was made of a thermoviscoelastic material model with a discontinuous change of the properties at the glass transition temperature, Tg. Birefringence was calculated with the aid of the stress optical rule using the measured stress optical coefficients in the molten and the glass state, respectively. The birefringence present at the moment of glass transition is 'frozen in' and added to the birefringence, which builds up below Tg. The calculated birefringence distributions fit the distributions measured in the cross sections of the samples. The birefringence distributions are unbalanced because of the contribution of frozen-in orientation, induced by the cooling stresses above Tg. In constrained quenching the contact with the wall leads to high tensile stresses in the melt, which induce, depending on the adhesion of the polymer to the wall, unexpected birefringence distributions. ESA

N93-11987# Technische Univ., Eindhoven (Netherlands).
MOLECULAR ORIENTATION INDUCED BY COOLING STRESSES IN POLYCARBONATE. 1: FREE QUENCHING
Reinhold Wimberger-Friedl *In its* Orientation, Stress, and Density Distributions in Injection-Moulded Amorphous Polymers Determined by Optical Techniques 1991 p 89-122 Submitted for publication (For primary document see N93-11983 02-27)
Avail: CASI HC A03/MF A03

The residual birefringence distributions in quenched polycarbonate disks was determined in cross sections. Unbalanced distributions of approximately parabolic shape were obtained in general. The systematic variation of the birefringence distribution with quench conditions was interpreted in terms of a stress and an orientation contribution. The distributions were predicted by a numerical program making use of the linear stress optical rule with a different stress optical coefficient above and below the glass transition. The contribution of molecular orientation was distinguished experimentally from the stress contribution by annealing experiments, layer removal, and sectioning. The influence of sectioning on birefringence was investigated with the numerical program, measurements in oblique incidence, rod quenching, and layer removal. ESA

N93-11988# Technische Univ., Eindhoven (Netherlands).
MOLECULAR ORIENTATION INDUCED BY COOLING STRESSES IN POLYCARBONATE. 2: CONSTRAINED QUENCH AND INJECTION MOULDING
Reinhold Wimberger-Friedl *In its* Orientation, Stress, and Density Distributions in Injection-Moulded Amorphous Polymers Determined by Optical Techniques 1991 p 123-148 Submitted for publication (For primary document see N93-11983 02-27)
Avail: CASI HC A03/MF A03

An experiment to determine residual birefringence distributions in polycarbonate samples, obtained by quenching in a specially designed apparatus and by injection modeling, is presented. The birefringence in the quenched samples is positive and almost constant, independent of the quench temperature, but varies strongly with initial temperature between 150 and 180 C. The residual stress level, as determined by layer removal and sectioning, is very low. The birefringence distribution is due to a tensile equibiaxial orientation which is induced by cooling stresses built up above Tg (glass transition temperature). The samples which were injection molded with a high injection speed and without packing pressure display the same birefringence distribution as the quenched samples apart from a local maximum beneath the surface due to the shear flow during filling. The birefringence plateau in the core hardly depends on the mould temperature, as it is mainly determined by a tensile orientation induced by cooling stresses above Tg. The residual stress level is in the order of only 1 MPa. The application of a packing pressure leads to a compressive stress maximum beneath the surface and tensile stresses at the surface. ESA

N93-11989# Technische Univ., Eindhoven (Netherlands).
MEASUREMENT OF THE DENSITY DISTRIBUTIONS IN QUENCHED POLYCARBONATE SPECIMENS BY A QUANTITATIVE SCHLIEREN-OPTICAL TECHNIQUE
Reinhold Wimberger-Friedl, G. Prast, A. V. Kurstjens, and J. G. deBruin *In its* Orientation, Stress, and Density Distributions in Injection-Moulded Amorphous Polymers Determined by Optical Techniques 1991 p 151-168 Submitted for publication (For primary document see N93-11983 02-27)
Avail: CASI HC A03/MF A03

A new technique for the determination of spatial density distributions is described. The density is derived from the refractive index gradient as determined with a quantitative Schlieren optical technique. The advantages of this technique are a high spatial resolution and sensitivity. Gapwise profiles can be measured without slicing the sample so that more reliable data are obtained quickly. This is demonstrated for the gapwise density distributions in quenched polycarbonate specimens. It is shown that the density distribution is determined by a competition between the local cooling rate variation and the cooling stress distribution. The residual density is predominantly determined by the coolant temperatures, whereas for low coolant temperatures the density in the core is lower than at the surface. The observed effects are explained semiquantitatively by a simple model using calculated cooling stresses and cooling rates. Author (ESA)

N93-11990# Technische Univ., Eindhoven (Netherlands).
GAPWISE DENSITY DISTRIBUTIONS IN INJECTION-MOULDED POLYMETHYLMETHACRYLATE
Reinhold Wimberger-Friedl and J. G. DeBruin *In its* Orientation, Stress, and Density Distributions in Injection-Moulded Amorphous Polymers Determined by Optical Techniques 1991 p 169-192 Submitted for publication (For primary document see N93-11983 02-27)
Avail: CASI HC A03/MF A03

An experiment to determine residual polymethylmethacrylate density distributions in injection molded polymethylmethacrylate, with the aid of a quantitative Schlieren optical technique, is presented. The gapwise distributions typically show a maximum beneath the surface. The height of the maximum as well as the level in the core vary with distance from the gate of the mold. The density distributions and the influence of the molding parameters are explained by the pressure course measured in the cavity and the process of vitrification of the sample during molding. The magnitudes of the variations of the gapwise distributions agree with the average density variations measured in a density gradient column. Residual stresses do not contribute significantly to the determined distributions. The density maximum is found closer to the surface than the maximum in birefringence which is induced by the shear flow during filling. The magnitude of the density variations is less than predicted by the pseudocompressibility as determined in samples vitrified under constant pressure. Author (ESA)

N93-11991# Technische Univ., Eindhoven (Netherlands).
ANALYSIS OF THE BIREFRINGENCE DISTRIBUTIONS IN COMPACT DISCS OF POLYCARBONATE
Reinhold Wimberger-Friedl *In its* Orientation, Stress, and Density Distributions in Injection-Moulded Amorphous Polymers Determined by Optical Techniques 1991 p 195-215 Repr. from Polym. Eng. Sci., v. 30, 1990 p 813 (For primary document see N93-11983 02-27)
Avail: CASI HC A03/MF A03

Birefringence distributions in injection molded compact disks were determined in radial and tangential cross sections and interpreted in terms of the process. The influence of processing conditions is discussed in several examples. It is shown that despite the high birefringence level the retardation of a beam of normal incidence is almost zero due to several compensation mechanisms. One optical axis is almost perpendicular to the surface. The medium, however, is biaxial with the preferential directions depending on the distance from the surface and the radial position. In contrast to a parallel beam zero retardation cannot be achieved with a convergent beam in injection molded polycarbonate disks for that reason. Author (ESA)

N93-11993*# Alabama Univ., Huntsville. Dept. of Chemistry.
ANALYSIS OF SURFACES FROM THE LDEF A0114, PHASE 2 Semiannual Report, 1 Sep. 1991 - 29 Feb. 1992
John C. Gregory 29 Feb. 1992 49 p
(Grant NAG1-1228)
(NASA-CR-190596; NAS 1.26:190596) Avail: CASI HC A03/MF A01

Analysis of surfaces from the Long Duration Exposure Facility (LDEF) continued during the reporting period. Work has continued on profilometry measurements of eroded and corroded sample surfaces, optical transmission measurements, analysis of the pinhole camera, and x-ray photoelectron spectroscopy (XPS) analysis of some samples. Papers that have appeared or have been accepted for publications are listed. Several of these papers and an abstact are included. For individual titles, see N93-11994 through N93-11994.

N93-11994*# Alabama Univ., Huntsville. Dept. of Chemistry.
EROSION RATES FOR POLYMERS MEASURED ON LDEF
John C. Gregory *In its* Analysis of Surfaces from the LDEF A0114, Phase 2 29 Feb. 1992 22 p Presented at the LDEF Workshop, Hampton, VA, 19-22 Nov. 1991 (For primary document see N93-11993 02-27)
Avail: CASI HC A03/MF A01

The summary and viewgraphs of work presented at the Long Duration Exposure Facility (LDEF) materials workshop are given. Experimental data for erosion depths and rates for polymers measured on LDEF are given. In general, agreement is reasonably good between erosion rates from the University of Alabama in Huntsville (UAH) LDEF experiment and prior data obtained at much lower mission fluences. Agreement is particularly satisfying in the case of Kapton where the prior data base is large. In spite of the known presence of siliceous contamination on LDEF surfaces, the erosion rates of the highly erodible materials are hardly affected, if at all. Graphs showing changes in optical properties (reflectance and transmittance) of metal films are included. L.R.R.

N93-12086# National Inst. of Standards and Technology, Gaithersburg, MD. Materials Science and Engineering Lab.

WORKSHOP ON CHARACTERIZING DIAMOND FILMS

Albert Feldman, Charles P. Beetz (Advanced Technology Materials, Inc., Danbury, CT.), Michael Drory (Crystallume, Menlo Park, CA.), and Sandor Holly (Rockwell International Corp., Canoga Park, CA.) Jun. 1992 96 p Workshop held in Gaithersburg, MD, 27-28 Feb. 1992

(PB92-205426; NISTIR-4849) Avail: CASI HC A05/MF A01

A workshop was held at NIST on February 27th and 28th to discuss specific topics deemed important to the characterization of diamond films made by chemical vapor deposition and to address the need for standards in diamond technology. The workshop was held in response to a recommendation in a recent report assessing diamond technology in Japan. The audience targeted for the workshop were the producers and potential users of CVD diamond technology in the United States. University scientists were invited as experts in property measurements. There were 35 attenders at the workshop. The workshop consisted of presentations in the areas of thermal conductivity measurement, mechanical properties measurement, and the need for standards. Author

N93-12123# Argonne National Lab., IL.

DEVELOPMENT OF NONDESTRUCTIVE EVALUATION METHODS AND PREDICTION OF EFFECTS OF FLAWS ON THE FRACTURE BEHAVIOR OF STRUCTURAL CERAMICS

W. A. Ellingson, J. P. Singh, D. L. Holloway, S. L. Dieckman, D. Singh, E. A. Sivers, S. H. Sheen, and M. J. Wheeler May 1992 13 p Presented at the 6th Annual Fossil Energy Materials Conference, Oak Ridge, TN, 12-14 May 1992

(Contract W-31-109-eng-38)

(DE92-016395; ANL/CP-72465; CONF-9205123-10) Avail: CASI HC A03/MF A01

Characterization of ceramic matrix composites (continuous and whisker-type) by nondestructive evaluation (NDE) methods and an understanding of fracture behavior, together with correlation of fracture and NDE data, may provide insight into the prediction of component performance and the development of process technology. Knowledge of the degradation extent of fiber tows or monofilament degradation after processing, extent of open porosity before densification, and filament/fiber alignments before and after processing are also examples of important variables to be measured. Work in this program has emphasized continuous fiber ceramic matrix composites (CFCCs) that use chemical vapor infiltration (CVI)-infiltrated SiC/SiC materials, primarily those made of Nicalon satin or plain weave with 16 x 16 tows/in. in 2-D layups. All studied samples were provided by Oak Ridge National Laboratory and were made using 100 layers per inch. CVI specimens with 0/30/60, 0/90, and 0/45 were examined by 3-D X-ray microtomography to characterize in-plane fiber orientations. Current information suggests that for Nicalon-type fiber architecture, a +/- 2 1/2 deg misalignment may not affect mechanical properties. Thus the near-term goal has been to establish a detection capability for angular orientation. By using 512 x 512 images from 3-D X-ray CT data with pixel sizes of less than 140 microns and a special 2-D fast-Fourier transform image processing analysis, we have shown that fiber orientations to +/- 2 1/2 deg with SiC/SiC CVI type 2-D weave architecture can be measured. DOE

N93-12165# Massachusetts Inst. of Tech., Cambridge. Dept. of Chemistry.

CONTROLLED SYNTHESIS OF POLYENES BY CATALYTIC METHODS

R. R. Schrock 1992 14 p

(Contract DE-FG02-86ER-13564)

(DE92-015286; DOE/ER-13564/11) Avail: CASI HC A03/MF A01

A more direct approach to polyenes by the direct polymerization of acetylenes has been achieved. We were able to show that polymerization of acetylene itself can be controlled with a well-characterized alkylidene catalyst, but only if a base such as quinuclidine is present in order to slow down the rate of propagation relative to initiation. (Quinuclidine may also stabilize vinylalkylidene intermediates formed in the reaction). Unfortunately, 'living polyenes' were no more stable than isolated polyenes, and so this approach had its limitations. Direct polymerization of acetylene by Mo(CH-t-Bu)(NAr)(O-t-Bu)2 was more successful, but inherent polyene instability was still a problem. The most important result of the past grant period is the finding that dipropargyl derivatives (HC=CCH2XCH2C(triple bond)CH; X = CH2, C(CO2R)2, SiR2, etc.), which have been reported to be cyclopolymerized by various classical catalysts by as yet unknown mechanisms, are polymerized by Mo(CH-t-Bu)(NAr)(OCMe(CF3)2)2 in dimethoxyethane. We speculate that intramolecular formation of a five-membered ring in the product of alpha addition is fast enough to yield another terminal alkylidene on the time scale of the polymerization reaction, while a six-membered ring is formed in a reaction involving a more reaction terminal alkylidene. Either intermediate alkylidene, but most likely the terminal alkylidene, could react with additional monomer to lead to growth of a chain having 'dangling' triple bonds that eventually could be employed to form crosslinks. DOE

N93-12168# EG and G Energy Measurements, Inc., Idaho Falls.

A DESIGN OF EXPERIMENT STUDY OF PLASMA SPRAYED ALUMINA-TITANIA COATINGS

T. J. Steeper, D. J. Varacalle, Jr., G. C. Wilson, and W. L. Riggs, II (TubalCain Co., Loveland, OH.) 1992 7 p Presented at the 1992 International Thermal Spray Conference, Orlando, FL, 1-5 Jun. 1992

(Contract DE-AC07-76ID-01570)

(DE92-017877; EGG-M-92006; CONF-9206135-5) Avail: CASI HC A02/MF A01

An experimental study of the plasma spraying of alumina-titania powder is presented. This powder system is being used to fabricate heater tubes that emulate nuclear fuel tubes for use in thermal-hydraulic testing. Coating experiments were conducted using a Taguchi fractional-factorial design parametric study. Operating parameters were varied around the typical spray parameters in a systematic design of experiments in order to display the range of plasma processing conditions and their effect on the resultant coating. The coatings were characterized by hardness and electrical tests, image analysis, and optical metallography. Coating qualities are discussed with respect to dielectric strength, hardness, porosity, surface roughness, deposition efficiency, and microstructure. The attributes of the coatings are correlated with the changes in operating parameters. DOE

N93-12184# North Carolina State Univ., Raleigh.

GROWTH, CHARACTERIZATION, AND DEVICE DEVELOPMENT IN MONOCRYSTALLINE DIAMOND FILMS Report, 1 Apr. - 30 Jun. 1992

Robert F. Davis Jun. 1992 15 p

(Contract N00014-90-J-1604)

(AD-A252648) Avail: CASI HC A03/MF A01

Initial bias-enhanced heteroepitaxial nucleation on single crystal SiC has proven to be successful. Transmission electron microscopy (TEM) showed that approximately half of the diamond nuclei were in epitaxial alignment with the SiC substrate. Further TEM both confirmed this epitaxy and also clearly indicated that the nuclei were tilted by several degrees. This tilting was determined to be a result of the high density of inefficient misfit dislocations at the interface. It was found that the tilt component of the misfit dislocations could account for the misorientation in the crystals. It was also suggested that by attempting to grow diamond (114) on SiC(221) the interfacial strain energy and resulting misorientation could be significantly reduced. Photoemission spectroscopy was used to compare the effect of plasma cleaning procedures, and high temperature annealing procedures, on natural type 2B diamond (111) surface. The hydrogen on the diamond surface was desorbed by annealing the diamond to approximately 950 C, and the sharp peak in the photoemission spectra, observed prior to annealing and indicative of a negative electron affinity surface, disappeared.

The peak could be recovered by exposing the surface to either plasma generated or hot filament excited mono-atomic hydrogen. GRA

N93-12189 Cincinnati Univ., OH.
EROSION PREDICTIONS AND MEASUREMENTS OF HIGH-TEMPERATURE COATINGS AND SUPERALLOYS USED IN TURBOMACHINES Ph.D. Thesis
Metwally Anwar Metwally 1992 221 p
Avail: Univ. Microfilms Order No. DA9223986

Nickel and cobalt superalloys are widely used in the hot section of gas turbines. Protective coatings are used to enhance superalloy erosion-corrosion at elevated temperatures. This investigation is devoted to wind tunnel measurements and analytical prediction of erosion rates and particle rebound characteristics of some newly developed coatings and superalloys. Both erosion rates and particle rebound characteristics are necessary for accurate prediction of erosion in turbomachines. The abrasive particles used in the measurements were coal ash with a weight average diameter of 15 microns. A three components laser Doppler velocimetry system was used to measure both particle impact and rebound velocities over a wide range of impingement angle. Empirical correlations have been developed for the restitution coefficients of both coated and uncoated surfaces. A high temperature erosion test facility was used to measure the erosion rates for the coatings and superalloys. The data was accumulated for wide ranges of the erosion parameters, namely, impingement angle, impact velocity, material temperature, and mass of particles which have the main effects on the material erosion behaviors. Erosion models have been developed to predict the erosion rates of materials whose behavior are ductile. The developed rebound and erosion models were used to predict the particle dynamics and resulting blade surfaces erosion of coal ash particles in a power turbine of an automotive gas turbine engine for both coated and uncoated blade surfaces. The results show the three dimensional particle trajectories through the turbine flow passages and the particle impact locations over the blade surfaces. The predicted counters of erosion rate and its related parameters over the blade surfaces are presented for coated and uncoated blades. In addition an experimental study was conducted which confirmed the locations of the blade surface impacts predicted by the theoretical analysis. Also, an attempt was made to estimate coating lives based on the erosion models. Dissert. Abstr.

N93-12246# Illinois Univ., Urbana.
NANOPHASE CERAMICS Final Report, 15 Jul. 1988 - 24 Jan. 1992
Robert S. Averback 21 May 1992 9 p
(Contract DAAL03-88-K-0094)
(AD-A254661; ARO-25526.10-MS) Avail: CASI HC A02/MF A01

At the time of initiation of this research, the materials community was just becoming aware of the pioneering work on nanophase materials by Prof. Gleiter, in Germany, and the forecasts of new materials with highly desirable properties were being offered. For ceramic materials, the potential for low temperature sintering and superplastic deformation were very exciting possibilities while the effect of nanoscale grain structures on other properties were also of interest. This research, therefore, was initiated to evaluate the properties of monolithic nanophase ceramic materials. GRA

N93-12276# Naval Research Lab., Washington, DC.
WORKSHOP ON ADHESION AND INTERMOLECULAR FORCES
J. W. Mintmire, R. J. Colton, P. P. Schmidt, and R. G. Brandt 18 Sep. 1992 103 p Workshop held in Alexandria, VA, 18-19 Jun. 1992
(AD-A255191; NRL/MR/6179-92-7143) Avail: CASI HC A06/MF A02

This report provides an overview of a workshop on adhesion and intermolecular forces organized by the Surface Chemistry Branch of NRL and supported by the Office of Naval Research. The workshop was held 18-19 June 1992 in Alexandria, Virginia. A summary of the panel discussion is presented, as well as extended abstracts of most of the presentations. GRA

N93-12289# Pennsylvania Univ., Philadelphia. Dept. of Chemistry.
THE PEIERLS GROUND STATE, SOLITONS AND POLARONS IN RING-CONTAINING POLYMERS Technical Report, 3 Mar. 1991 - 30 Jun. 1992
A. J. Epstein 5 Jun. 1992 11 p
(Contract N00014-90-J-1559)
(AD-A254914; TR-1992-13) Avail: CASI HC A03/MF A01

The report of doping of polyacetylene to form a highly conducting polymer opened the question concerning the nature of the electronic states of the polymer backbone that are formed upon charge transfer between the polymer and dopant backbone. Extensive study of polyacetylene has demonstrated that this system is a degenerate Peierls semiconductor with a bandgap introduced through bond alternation. Pernigraniline is a semiconductor analogous to trans-polyacetylene. However, it differs from polyacetylene in that the overlap between adjacent sites can be modulated by both changes in bond length and changes in ring torsion angle. It is shown that as a result of these two independent order parameters there are differing types of charge excitation possible on pernigraniline backbone, with both bond order excitations such as bond order solitons and ring torsion excitations such as ring torsion polarons possible. Recent photoexcitation spectroscopy studies have confirmed the presence of both bond order solitons and ring rotation polarons. GRA

N93-12297# Connecticut Univ., Storrs. Inst. of Materials Science.
MODIFIED EPOXY ADHESIVES AND PRIMERS Final Report
Andrew Garton 30 Jun. 1992 29 p
(Contract DAAL03-88-K-0090)
(AD-A253857; ARO-25760.6-MS) Avail: CASI HC A03/MF A01

A range of monoepoxy additives for epoxy resins, and non-reactive additives for polyimides, have been examined with a view to understanding the mechanism of their 'fortifying action, and to examine their usefulness in adhesive applications. An increase in strength of 50 percent and an increase in modulus of 40 percent is achievable by this method, along with a decrease in water uptake, decreased expansion coefficient, and a modified failure mechanism. These properties of the bulk resin translate into modest improvements in adhesive bond performance, particularly for low temperature cured systems, and in humid environments. It should be cautioned, however, that the effect of the additives will vary with the geometry of the joint and the test procedure. The mechanism of property modification is explained on a quantitative basis using the concept of free volume. The contributions of molecular interactions and of the depression in glass transition temperature are separated. The monoepoxy additive are shown to function more efficiently than unreactive additives in epoxy systems. A synergism between these additives and CTBM rubber modifiers is also reported. GRA

N93-12337# Dexter Corp., Pittsburgh, CA. Aerospace Div.
PHASE TRANSFER CATALYTIC NUCLEOPHILIC ADDITION REACTIONS: SYNTHESIS OF POLYMERS AND ACETYLENIC TERMINATED RESINS Final Technical Report, Jun. 1991 - 15 Aug. 1992
David K. Klapprott and Ray Kellman 15 Aug. 1992 30 p
(Contract F49620-91-C-0052)
(AD-A254717; AFOSR-92-0825TR) Avail: CASI HC A03/MF A01

Solid-liquid phase transfer catalysis (SLPTC) was studied to facilitate the preparation of acetylene-terminated (AT) resins. 3-Ethylphenol, as a model system, was found to react with p,p' - difluorobenzophenone and p,p' - difluorodiphenylsulfone in refluxing pyridine using SLPTC to give high yields of the corresponding disubstitution products. However, the p,p'-dichloro derivatives afforded a mixture consisting predominantly of monosubstituted product. 3-Ethynylphenol was reacted under similar conditions to afford AT resins which were compared with AT resins made by conventional synthesis methods. High molecular weight, soluble polyetherether ketones and polysulfones were made by reacting bisphenols and appropriate difluoroaromatic compounds in refluxing pyridine using SLPTC. GRA

N93-12398*# National Aeronautics and Space Administration. Lewis Research Center, Cleveland, OH.
STUDIES ON THE REACTIVE MELT INFILTRATION OF SILICON AND SILICON-MOLYBDENUM ALLOYS IN POROUS CARBON
M. Singh and D. R. Behrendt Sep. 1992 11 p Presented at the 94th Annual Meeting of the American Ceramic Society, Minneapolis, MN, 12-16 Apr. 1992
(RTOP 537-04-10)
(NASA-TM-105860; E-7320; NAS 1.15:105860) Avail: CASI HC A03/MF A01

Investigations on the reactive melt infiltration of silicon and silicon-1.7 and 3.2 at percent molybdenum alloys into porous carbon preforms have been carried out by process modeling, differential thermal analysis (DTA) and melt infiltration experiments. These results indicate that the initial pore volume fraction of the porous carbon preform is a critical parameter in determining the final composition of the raction-formed silicon carbide and other residual phases. The pore size of the carbon preform is very detrimental to the exotherm temperatures due to liquid silicon-carbon reactions encountered during the reactive melt infiltration process. A possible mechanism for the liquid silicon-porous (glassy) carbon reaction has been proposed. The composition and microstructure of the reaction-formed silicon carbide has been discussed in terms of carbon preform microstructures, infiltration materials, and temperatures. Author

N93-12440# Pennsylvania Univ., Philadelphia. Dept. of Chemistry.
SYNTHESIS AND CONDUCTIVITY OF COPOLYMER OF 4,4'-DIAMINODIPHENYLAMINE AND TEREPHTHALOYL CHLORIDE Technical Report, 31 May 1992 - 30 Jun. 1992
G. Gordon, J. Yue, and A. J. Epstein 5 Jun. 1992 7 p
(Contract N00014-90-J-1559)
(AD-A254880; Rept-1992-12) Avail: CASI HC A02/MF A01

The synthesis of the copolymer of 4-4'-diaminodiphenylamine sulfate with terephthaloyl chloride, (a copolymer of polyamide and polyaniline), is reported. After doping With S03 the conductivity of this copolymer approaches that of salts of polyaniline derivatives. GRA

N93-12479# Pennsylvania Univ., Philadelphia. Dept. of Materials Science and Engineering.
ATOMIC BONDING AT CERAMIC INTERFACES USING SCANNING TUNNELING MICROSCOPY
D. A. Bonnell Feb. 1992 11 p
(Contract DE-FG02-90ER-45428)
(DE92-018706; DOE/ER-45428/1) Avail: CASI HC A03/MF A01

Progress made during space charge calculations are given for pure $SrTiO_3$. The first two years of the above listed grant can be considered in terms of three approaches which converge in the third year. Specifically, results in STM analyses of oxide grain boundaries, in design and construction of a new microscope, and in theoretical calculations of space charge are summarized. For clarity, calculation methodology is detailed. Publications, presentations, and supported students are also listed. DOE

N93-12500# Northwestern Univ., Evanston, IL.
MIXED IONIC AND ELECTRONIC CONDUCTIVITY IN POLYMERS
M. A. Ratner and D. F. Shriver Jul. 1992 7 p
(Contract DE-FG02-85ER-45220)
(DE92-018723; DOE/ER-45220/7) Avail: CASI HC A02/MF A01

In the past year, we have made progress in the theory of mixed ionic and electronic conductivity in polymers. On the experimental side, we have prepared polypyrroles with pendant polyethers and studied their conductivity in the reduced state. Theoretical progress was made in the application of Monte Carlo methods to ion motion in polymers. DOE

N93-12451*# Supermaterials Research and Development Corp., Cleveland, OH.
THERMAL PROTECTION USING VERY HIGH TEMPERATURE CERAMICS
George R. Adamczyk *In* NASA. Langley Research Center, Current Technology for Thermal Protection Systems Oct. 1992 p 63-76 (For primary document see N93-12447 02-18)
Avail: CASI HC A03/MF A03

N93-12452*# Lockheed Missiles and Space Co., Palo Alto, CA.
SUPERPLASTIC FORMING OF CERAMIC INSULATION
T. G. Nieh, J. P. Wittenauer, and J. Wadsworth *In* NASA. Langley Research Center, Current Technology for Thermal Protection Systems Oct. 1992 p 77-87 (For primary document see N93-12447 02-18)
(Contract DAAL03-89-C-0028)
Avail: CASI HC A03/MF A03

N93-12453*# Technetics, Inc., DeLand, FL.
CERAMIC TBS/POROUS METAL COMPLIANT LAYER
Robert P. Tolokan and G. P. Jarrabet *In* NASA. Langley Research Center, Current Technology for Thermal Protection Systems Oct. 1992 p 89-96 (For primary document see N93-12447 02-18)
Avail: CASI HC A02/MF A03

28 PROPELLANTS AND FUELS

Includes rocket propellants, igniters, and oxidizers; their storage and handling procedures; and aircraft fuels.

For related information see also *07 Aircraft Propulsion and Power, 20 Spacecraft Propulsion and Power,* and *44 Energy Production and Conversion.*

N93-11045 Department of the Navy, Washington, DC.
HIGH ENERGY CAST EXPLOSIVES BASED ON DINITROPROPYLACRYLATE Patent
Barbara A. Scott, inventor (to Navy) and Lily E. Koch, inventor (to Navy) 3 Mar. 1992 4 p Filed 7 May 1976
(AD-D015340; US-Patent-5,092,944; US-Patent-Appl-SN-682937; US-Patent-Class-149-19.3) Avail: US Patent and Trademark Office

A castable explosive composition of 80 to 87 percent cyclo-1,3,5,7- tetramethylene-2,4,6,8- tetra nitramine (HMX) in dinitropropyl acrylate binder is obtained through careful choice of particle sizes. Up to 92 percent solids loading, without loss of castability, is obtained when spherical aluminum is incorporated into the mix. Other comonomers may be used in the binder and other solids added. GRA

N93-11376# Royal Armament Research and Development Establishment, Fort Halstead (England). Military Div.
A PRELIMINARY INVESTIGATION OF THE DEGRADATION AND STABILISATION OF THE ENERGETIC OXETANE BINDER POLYNIMMO
P. Bunyan, A. V. Cunliffe, A. Davis, and F. A. Kirby Dec. 1991 14 p
(RARDE-7/91; BR308904; ETN-92-92293) Copyright Avail: CASI HC A03/MF A01

Information on the structure and functionality of poly(3-Nitratomethyl-3-methyloxetrane), polyNIMMO, is presented and the properties of binders cured with the isocyanate Desmodur N-100 are considered. Results from the ageing of crosslinked polyNIMMO are presented and the effects of adding the stabilizer 2 nitrodiphenylamine, (2NDPA), are demonstrated. It is shown that decomposition of the nitrate ester groups of unstabilized polyNIMMO is a major process but the rate of this process is much lower than that observed for nitroglycerin. Decomposition of the nitrate ester groups in polyNIMMO is accompanied by chain scission of the polyether backbone. Two effects were observed as a result of adding 1 percent of 2NDPA: the rate of nitrate ester breakdown was significantly reduced, and the rate of polymer chain scission was greatly retarded. Results indicate that chain scission only becomes significant when the stabilizer has been consumed. Current results show that the stabilized binder still retains its network structure after one year at 60 C. ESA

N93-11380# Los Alamos National Lab., NM.

DESTRUCTION OF EXPLOSIVES AND ROCKET FUELS BY SUPERCRITICAL WATER OXIDATION

R. B. Dyer, S. J. Buelow, D. M. Harradine, J. M. Robinson, B. R. Foy, J. H. Atencio, P. C. DellOrco, K. A. Funk, R. E. McInroy, and C. K. Rofer et al 1992 10 p Presented at the 16th Annual Army Environmental R/D Symposium, Williamsburg, VA, 23-25 Jun. 1992
(Contract W-7405-eng-36)
(DE92-018874; LA-UR-92-2378; CONF-9206231-1) Avail: CASI HC A02/MF A01

Traditional methods for disposing of PEP's have been open burning or open detonation (OB/OD); however, regulatory agencies are likely to prohibit OB/OD because of the uncontrolled air emissions and soil contaminations. Likewise, controlled incineration carries a liability for air pollution because large quantities of NO(x) are produced in the conventional combustion chemistry of PEP's. Soil and ground water have already been contaminated with PEP's through normal operations at manufacturing plants and military bases. Incineration can be used for decontamination of these soils, with the associated liability for air pollution, but few satisfactory and economic methods exist for ground water decontamination. A clear need exists for improved disposal and destruction methods. The destruction of energetic materials, including propellants, explosives and pyrotechnics (PEP's) by oxidation in supercritical water is described. The focus is on the chemistry of the process. The destruction efficiencies and products of reaction contained in the aqueous and gaseous effluents of several representative PEP's are reported. DOE

N93-11550# Argonne National Lab., IL.

REFORMERS FOR THE PRODUCTION OF HYDROGEN FROM METHANOL AND ALTERNATIVE FUELS FOR FUEL CELL POWERED VEHICLES

R. Kumar, S. Ahmed, M. Krumpelt, and K. M. Myles Aug. 1992 26 p
(Contract W-31-109-eng-38)
(DE92-019300; ANL-92/31) Avail: CASI HC A03/MF A01

The objective was to assess the present state of technology of reformers that convert methanol (or other alternative fuels) to a hydrogen-rich gas mixture for use in a fuel cell, and to identify the R&D needs for developing reformers for transportation applications. Steam reforming and partial oxidation are the two basic types of fuel reforming processes. The former is endothermic while the latter is exothermic. Reformers are therefore typically designed as heat exchange systems, and the variety of designs used includes shell-and-tube, packed bed, annular, plate, and cyclic bed types. Catalysts used include noble metals and oxides of Cu, Zn, Cr, Al, Ni, and La. For transportation applications a reformer must be compact, lightweight, and rugged. It must also be capable of rapid start-up and good dynamic performance responsive to fluctuating loads. A partial oxidation reformer is likely to be better than a steam reformer based on these considerations, although its fuel conversion efficiency is expected to be lower than that of a steam reformer. A steam reformer better lends itself to thermal integration with the fuel cell system; however, the thermal independence of the reformer from the fuel cell stack is likely to yield much better dynamic performance of the reformer and the fuel cell propulsion power system. For both steam reforming and partial oxidation reforming, research is needed to develop compact, fast start-up, and dynamically responsive reformers. For transportation applications, steam reformers are likely to prove best for fuel cell/battery hybrid power systems, and partial oxidation reformers are likely to be the choice for stand-alone fuel cell power systems. DOE

N93-11566# Los Alamos National Lab., NM.

DETONATION REACTIONS FROZEN BY FREE EXPANSION AND ANALYZED BY MASS SPECTROMETRY

N. R. Greiner, H. A. Fry, and N. C. Blais 1992 24 p Presented at the 11th Annual Working Group Institute on Synthesis of High Energy Density Materials, Monticello, NY, 8-11 Jun. 1992
(Contract W-7405-eng-36)
(DE92-018605; LA-UR-92-2388; CONF-9206226-1) Avail: CASI HC A03/MF A01

The molecular design of new more powerful and less sensitive explosives requires detailed knowledge of reaction mechanisms and compositions of molecular products from explosives having a variety of molecular structures and performance parameters. We describe a new apparatus and method for analyzing detonation reactions using 30-250 mg charges. The apparatus consists of a TOF mass spectrometer interfaced to a high-vacuum firing chamber through a skimmer and a laser-schlieren optical system. The fireball normally produced by a detonation is frozen sequentially from the outside inward in a continuum of stages by free adiabatic expansion into the vacuum. Expansion of a given volume element begins when the rarefaction wave arrives from the free surface of the charge, and we find that no significant mixing occurs during the expansion. In this way, the chemical history of the detonation is frozen in time and imprinted on the structure of the expanding frozen fireball. Our apparatus isolates a core sample from the expanding fireball as an undisturbed molecular beam and provides a series of mass spectra derived from successive segments of the core. The assembled data set from each pellet fired is a sequence of 95 mass spectra that characterizes the molecules resistant to change at a succession of times separated by a few (ns) in the detonation reaction. These molecules are associated with the slower (rate-determining) steps or stable products in the reaction sequence and give valuable clues to reaction mechanisms. Our mass spectrometer automatically records expansion velocities of the core segments, and an electronic framing camera concurrently records a sequences of laser-schlieren images of the detonation and expansion. The number of spectra over which a change is observed can be related, through the hydrodynamics of the detonation and expansion, to the rate of that change in the detonating sample. DOE

N93-11665 Department of the Navy, Washington, DC.

ENERGETIC COMPOSITES OF CYCLODEXTRIN NITRATE ESTERS AND NITRATE ESTER PLASTICIZERS Patent

John P. Consaga, inventor (to Navy) (Courtney and Co., Philadelphia, PA.) and Steven L. Collignon, inventor (to Navy) (Courtney and Co., Philadelphia, PA.) 19 May 1992 4 p Filed 8 Jul. 1991
(AD-D015364; US-Patent-5,114,506; US-Patent-Appl-SN-728918; US-Patent-Class-149-88) Avail: US Patent and Trademark Office

This invention relates to an energetic composite made of a mixture of (1) a solid nitrate ester of a cyclodextrin or a mixture of cyclodextrins; and (2) an energetic organic nitrate ester plasticizer. GRA

N93-11794# Department of Energy, Washington, DC. Office of Transportation Technologies.

FEDERAL ALTERNATIVE FUEL PROGRAM LIGHT DUTY VEHICLE OPERATION

Mar. 1992 96 p
(DE92-018124; DOE/CE-0351) Avail: CASI HC A05/MF A01

This annual report to Congress details the first year of the Federal light duty vehicle operations as required by Section 400AA(b)(1)(B) of the Energy Policy and Conservation Act (EPCA). Alternative Motors Fuels Act (AMFA) encourages the use and production of AFV's that use methanol, ethanol, and natural gas. The Congress has recognized that displacement of energy derived from imported oil with alternative fuels will help to achieve energy security and improve air quality. In passing this Act, the Federal Government is assisting clean-burning, non-petroleum

transportation fuels to reach a threshold level of commercial application and consumer acceptability at which they can successfully compete with petroleum-base transportation fuels. The objectives of the program are to demonstrate the environmental, economic, and performance characteristics of alternative fuel fleet vehicles and to provide information on engine/vehicle manufacturers as well as the general public. This report details the first year of the Federal light duty vehicle operations, from Jan. - Sep. 1991. The Federal test vehicles are composed of 65 M85 fuel and 16 conventional gasoline fuel vehicles. The following sections discuss the vehicle operation and performance characteristics of the AMFA test vehicles in a fleet environment.
DOE

N93-12085*# National Aeronautics and Space Administration. Lewis Research Center, Cleveland, OH.

DESIGN OF SMALL STIRLING DYNAMIC ISOTOPE POWER SYSTEM FOR ROBOTIC SPACE MISSIONS

D. J. Bents, J. G. Schreiber, C. A. Withrow, B. I. McKissock, and P. C. Schmitz (Sverdrup Technology, Inc., Brook Park, OH.) Oct. 1992 11 p Presented at the Tenth Symposium on Space Nuclear Power and Propulsion, Albuquerque, NM, 10-14 Jan. 1992; sponsored by Inst. for Space Nuclear Power Studies
(RTOP 590-13-11)
(NASA-TM-105919; E-7395; NAS 1.15:105919) Avail: CASI HC A03/MF A01

Design of a multihundred-watt Dynamic Isotope Power System (DIPS) based on the U.S. Department of Energy (DOE) General Purpose Heat Source (GPHS) and small (multihundred-watt) free-piston Stirling engine (FPSE) technology is being pursued as a potential lower cost alternative to radioisotope thermoelectric generators (RTG's). The design is targeted at the power needs of future unmanned deep space and planetary surface exploration missions ranging from scientific probes to Space Exploration Initiative precursor missions. Power level for these missions is less than a kilowatt. Unlike previous DIPS designs which were based on turbomachinery conversion (e.g. Brayton), this small Stirling DIPS can be advantageously scaled down to multihundred-watt unit size while preserving size and mass competitiveness with RTG's. Preliminary characterization of units in the output power ranges 200-600 We indicate that on an electrical watt basis the GPHS/small Stirling DIPS will be roughly equivalent to an advanced RTG in size and mass but require less than a third of the isotope inventory.
Author

N93-12147# Science Applications International Corp., San Diego, CA. Foreign Applied Sciences Assessment Center.

SOVIET CHEMICAL PROPELLANT RESEARCH AND DEVELOPMENT

Edward H. deButts, Kurt Baum (Fluorochem, Inc., Azusa, CA.), Merrill W. Beckstead (Brigham Young Univ., Provo, UT.), Karl O. Christe (Rockwell International Corp., Canoga Park, CA.), Kenneth O. Hartman (Hercules, Inc., Cumberland, MD.), and William A. Jeffrey (Grumman Aerospace Corp., Bethpage, NY.) Dec. 1991 170 p
(PB92-195577) Avail: CASI HC A08/MF A02

In the second half of the 1980s, the Soviet Union had a strong and continuing research effort devoted to understanding the behavior of chemical propellants suitable to support development of advanced propellants for practical applications. Recent soviet work concentrated on solid propellants, through liquid propellants powered the largest and most advanced deployed Soviet rockets. The assessment summarizes the Soviet state of the art in chemical propellants in the late 1980s and projects the trends of that period into the next decade. It is based on a broad and deep review of Soviet literature published in 1985-1991 and is presented in an unclassified report. The extent and quality of Soviet efforts in propellant-related areas vary widely. Significant work is reported on solid propellants, combustion, advanced ingredients, and plume modeling. Very little material is published on actual propellants or propellant behavior or on rocket motors, possibly for security reasons. Likewise, very little Soviet liquid propellant research is reported, but here the reason is probably the maturity of the technology involved.
GRA

N93-12171# Midwest Research Inst., Golden, CO.

ALTERNATIVE FUEL EVALUATION PROGRAM: ALTERNATIVE FUEL LIGHT DUTY VEHICLE PROJECT. DATA COLLECTION RESPONSIBILITIES, TECHNIQUES, AND TEST PROCEDURES

Jul. 1992 31 p
(Contract DE-AC02-83CH-10093)
(DE92-010598; NREL/TP-420-4894) Avail: CASI HC A03/MF A01

This report describes the data gathering and analysis procedures that support the US Department of Energy's implementation of the Alternative Motor Fuels Act (AMFA) of 1988. Specifically, test procedures, analytical methods, and data protocols are covered. The aim of these collection and analysis efforts, as mandated by AMFA, is to demonstrate the environmental, economic, and performance characteristics of alternative transportation fuels.
DOE

N93-12236# Princeton Univ., NJ. Dept. of Mathematics.

ASYMPTOTIC ANALYSIS OF REACTING MATERIALS WITH SATURATED EXPLOSION. 2: HIGH-FREQUENCY WAVES Report, 1 Jan. 1989 - 31 Dec. 1991

Robert F. Almgren, Andrew Majda, and Rodolfo R. Rosales 1991 47 p Repr. from Studies in Applied Mathematics, v. 84, 1991 p 315-360
(Contract DAAL03-89-K-0013)
(AD-A254473; ARO-26113.15-MA) Avail: CASI HC A03/MF A01

The interaction of small-scale material inhomogeneities with high-frequency acoustic waves is known to have a prominent role in accelerating the heat-release rate in liquid and solid explosive materials. In the present paper, simplified asymptotic equations are studied which incorporate the above interaction, and which include reactant depletion at leading order. Because fuel may be completely exhausted, singularities do not always form in the model equations; it is conjectured that when a singularity does form, the material has initiated. The detailed mechanisms by which shock formation and resonant wave interaction can either enhance or retard reaction are explored. In a realistic model for inhomogeneous condensed-phase reaction, with pressure-dependent reaction rate and nonconstant initial fuel concentration, initiation of the material depends on correct placement of the fuel relative to the acoustic waves.
GRA

N93-12265# Sandia National Labs., Livermore, CA.

PROPELLANT REMOVAL FROM ROCKET MOTORS CONTAINING DOUBLE-BASE COMPOSITIONS

L. Whinnery, S. Griffiths, J. Hruby, R. Larson, J. Lipkin, B. Long, and C. Schoenfelder 1992 10 p Presented at the 23rd International Annual Conference of Fraunhofer-Institut fuer Chemische Technologie: Waste Management of Energetic Materials and Polymers and Exhibition, Karlsruhe (Germany), 30 Jun. - 3 Jul. 1992
(Contract DE-AC04-76DR-00789)
(DE92-013567; SAND-92-8503C; CONF-920647-1) Avail: CASI HC A02/MF A01

The uncertain environmental consequences and regulations associated with using open burning/open detonation for the disposal of energetic materials are forcing both manufacturers and users to examine alternative disposal technologies. In general, these alternatives involve a material removal operation followed by processing steps that lead to reuse of valuable constituents and/or disposal of waste. While a number of post-removal processing options appear to be viable, the initial step of removing an energetic material, such as a solid rocket motor propellant, from its container remains a significant technological challenge. Large rocket motors containing highly energetic propellant, hazard class 1.1, are of particular concern because of their inherent handling hazards. We describe the results of a study using thermal cycling to increase the surface area of inert propellant formulations. The propellant removal method studied employs thermal cycling

to cryogenic temperatures (cryocycling). Using inert propellants and liquid nitrogen we have demonstrated that this process produces multiple cracks throughout the bulk of the grain. The properties of the actual and inert propellants are being measured, and a model is being developed to relate experiments on inert material to actual propellant. Possible methods to increase thermal gradients, crack propagation, and initiation are also presented.
DOE

N93-12281# Naval Surface Warfare Center, Crane, IN.
SIMULATOR, TACTICAL USE, FLARE (STUF) PROJECT REPORT Final Report, 2 Jul. 1989 - 30 Sep. 1990
Paul R. Brown, Tommy J. Sanders, and Russell J. Huxhold 11 Mar. 1992 28 p
(AD-A254890; NSWCCR/RDTR-92/0006) Avail: CASI HC A03/MF A01

A large number of infrared (IR) decoy flares, which are used to counter IR missile threats, have been expended during past training exercises of Naval combat pilots. In an effort to maintain a current level of training using the most cost-effective manner, a low cost training simulator was desired. The deployment of relatively low cost simulators in place of decoy flares during training exercises will be a savings of nearly 50 percent of the cost of the expendable used. Simulator, Tactical Use, Flare (STUF) has been developed by Crane Division, Naval Surface Warfare Center (NAVSURFWARCENDIV Crane) for use as a training substitution for decoy flares. The purpose of this round is complete visual simulation of an expendable decoy flare. A complete review of the design phase, design optimization, and engineering tests of the STUF round at NAVSURFWARCENDIV Crane will be presented.
GRA

N93-12285# Delaware Univ., Newark. Dept. of Chemistry.
ENERGETICS SOLIDS DEGRADATION IN HIGH TEMPERATURE WATER Final Report, 1 Jul. 1989 - 30 Jun. 1992
Thomas B. Brill 1 Jun. 1992 27 p
(Contract DAAL03-89-K-0096)
(AD-A254900; ARO-26887.1-CH) Avail: CASI HC A03/MF A01

Strategies have been developed to determine the kinetics and mechanisms of degradation of energetic molecules in water up to 500 deg C. FTIR and Fr-Raman spectroscopy enable studies to be made and provide a wide spectral window in which many species can be followed simultaneously. Numerous spectroscopic and cell design hurdles have been encountered and surmounted so far. Cell designs and a process flow system that should provide clean kinetic studies are nearly completed at this time.
GRA

N93-11951*# Aerospace Medical Research Labs., Wright-Patterson AFB, OH. Toxicology Div.
OCCUPATIONAL SAFETY CONSIDERATIONS WITH HYDRAZINE FUELS
H. J. Clewell, T. S. Haddad, M. E. George, J. N. McDougal, and M. E. Andersen *In* NASA. Lyndon B. Johnson Space Center, Fifth Annual Workshop on Space Operations Applications and Research (SOAR 1991), Volume 1 Jan. 1992 p 199-202 (For primary document see N93-11921 02-59)
Avail: CASI HC A01/MF A04

29 MATERIALS PROCESSING

Includes space-based development of products and processes for commercial applications.
For biological materials see *55 Space Biology.*

N93-12197*# National Aeronautics and Space Administration. Lewis Research Center, Cleveland, OH.
DYNAMIC ANALYSIS OF A PRE-AND-POST ICE IMPACTED BLADE
G. H. Abumeri (Sverdrup Technology, Inc., Brook Park, OH.), E. S. Reddy (Sverdrup Technology, Inc., Brook Park, OH.), P. L. N. Murthy, and C. C. Chamis Oct. 1992 20 p Presented at the Aircraft Design Systems Meeting, Hilton Head, SC, 24-26 Aug. 1992; sponsored by AIAA
(RTOP 505-68-1C)
(NASA-TM-105829; E-7264; NAS 1.15:105829) Avail: CASI HC A03/MF A01

The dynamic characteristics of an engine blade are evaluated under pre-and-post ice impact conditions using the NASA in-house computer code BLASIM. The ice impacts the leading edge of the blade causing severe local damage. The local structural response of the blade due to the ice impact is predicted via a transient response analysis by modeling only a local patch around the impact region. After ice impact, the global geometry of the blade is updated using deformations of the local patch and a free vibration analysis is performed. The effects of ice impact location, size and ice velocity on the blade mode shapes and natural frequencies are investigated. The results indicate that basic nature of the mode shapes remains unchanged after impact and that the maximum variation in natural frequencies occurs for the twisting mode of the blade.
Author

N93-12401*# Alabama Univ., Huntsville. Materials Processing Lab.
MATERIALS PROCESSING IN LOW GRAVITY Final Report
Gary L. Workman 28 Nov. 1990 23 p
(Contract NAS8-36955)
(NASA-CR-184421; NAS 1.26:184421) Avail: CASI HC A03/MF A01

The final report of the Materials Processing in Low Gravity Program in which The University of Alabama in Huntsville designed, fabricated and performed various low gravity experiments in materials processing from November 7, 1989 through November 6, 1990 is presented. The facilities used in these short duration low gravity experiments include the Drop Tube and Drop Tower at Marshall Space Flight Center (MSFC), and the KC-135 aircraft at Ellington Field. During the performance of this contract, the utilization of these ground-based low gravity facilities for materials processing experiments have been instrumental in providing the opportunity to determine the feasibility of performing a number of experiments in the microgravity of Space, without the expense of a space-based experiment. Since the KC-135 was out for repairs during the latter part of the reporting period, a number of the KC-135 activities concentrated on repair and maintenance of the equipment that normally is flown on the aircraft. A number of periodic reports were given to the TCOR during the course of this contract, hence this final report is meant only to summarize the many activities performed and not redundantly cover materials already submitted.
L.R.R.

31 ENGINEERING (GENERAL)

Includes vacuum technology; control engineering; display engineering; cryogenics; and fire prevention.

N93-11494# Sandia National Labs., Albuquerque, NM.
ROBUST SOLDER JOINT ATTACHMENT OF COAXIAL CABLE LEADS TO PIEZOELECTRIC CERAMIC ELECTRODES
P. T. Vianco 1992 9 p Presented at the 46th Annual Frequency Control Symposium, Hershey, PA, 28 May 1992
(Contract DE-AC04-76DP-00789)
(DE92-017042; SAND-92-0003C; CONF-9205222-1) Avail: CASI HC A02/MF A01

A technique was developed for the solder attachment of coaxial cable leads to the silver-bearing thick film electrodes on piezoelectric ceramics. Soldering the cable leads directly to the thick film caused bonds with low mechanical strength due to poor solder joint geometry. A barrier coating of 1.5 micron Cu/1.5 micron Ni/1.0 micron Sn deposited on the thick film layer improved the strength of the solder joints by eliminating the absorption of Ag from the thick film which was responsible for the improper solder joint geometry. The procedure does not require special preparation of the electrode surface and is cost effective due to the use of non-precious metal films and the batch processing capabilities of the electron beam deposition technique. DOE

N93-11613*# National Aeronautics and Space Administration. Langley Research Center, Hampton, VA.
OPEN-LOOP CHARACTERISTICS OF MAGNETIC SUSPENSION SYSTEMS USING ELECTROMAGNETS MOUNTED IN A PLANAR ARRAY
Nelson J. Groom and Colin P. Britcher (Old Dominion Univ., Norfolk, VA.) Nov. 1992 34 p
(RTOP 590-14-11-02)
(NASA-TP-3229; L-17055; NAS 1.60:3229) Avail: CASI HC A03/MF A01

The open-loop characteristics of a Large-Gap Magnetic Suspension System (LGMSS) were studied and numerical results are presented. The LGMSS considered provides five-degree-of-freedom control. The suspended element is a cylinder that contains a core composed of permanent magnet material. The magnetic actuators are air core electromagnets mounted in a planar array. Configurations utilizing five, six, seven, and eight electromagnets were investigated and all configurations were found to be controllable from coil currents and observable from suspended element positions. Results indicate that increasing the number of coils has an insignificant effect on mode shapes and frequencies. Author

N93-11619*# National Aeronautics and Space Administration. Hugh L. Dryden Flight Research Facility, Edwards, CA.
A RULE-BASED SYSTEM FOR REAL-TIME ANALYSIS OF CONTROL SYSTEMS
Richard R. Larson and D. Edward Millard (Computer Sciences Corp., Edwards AFB, CA.) Oct. 1992 15 p Presented at the IEEE/AIAA 11th Digital Avionics Systems Conference, Seattle, WA, 5-8 Oct. 1992
(RTOP 505-64-30)
(NASA-TM-104258; H-1859; NAS 1.15:104258) Avail: CASI HC A03/MF A01

An approach to automate the real-time analysis of flight critical health monitoring and system status is being developed and evaluated at the NASA Dryden Flight Research Facility. A software package was developed in-house and installed as part of the extended aircraft interrogation and display system. This design features a knowledge-base structure in the form of rules to formulate interpretation and decision logic of real-time data. This technique has been applied for ground verification and validation testing and flight testing monitoring where quick, real-time, safety-of-flight decisions can be very critical. In many cases post processing and manual analysis of flight system data are not required. The processing is described of real-time data for analysis along with the output format which features a message stack display. The development, construction, and testing of the rule-driven knowledge base, along with an application using the X-31A flight test program, are presented. Author

N93-11672# Sandia National Labs., Albuquerque, NM.
INTERFACIAL MICROCHEMICAL CHARACTERIZATION NEEDS IN SURFACE PROCESSING
S. W. Gaarenstroom (General Motors Research Labs., Warren, MI.), R. J. Anderson (Sandia National Labs., Livermore, CA.), G. C. Nelson, R. J. Baird (Ford Motor Co., Detroit, MI.), M. J. Zaluzec (Ford Motor Co., Detroit, MI.), P. L. Coduti (Inland Steel Co., Chicago, IL.), and Michael Liehr (International Business Machines Corp., Yorktown Heights, NY.) 1992 19 p Presented at the Workshop on Surface Processing, Dearborn, MI, 10-12 Dec. 1991
(Contract DE-AC04-76DP-00789)
(DE92-018269; SAND-92-1518C; GMR-7661; CONF-911281-2)
Avail: CASI HC A03/MF A01

Interfacial microchemical characterization is required in all aspects of surface processing as applied to transportation and utility technologies. Corrosion protection, fuel cells and batteries, wear surfaces, polymers and polymer-oxide interfaces, thin film multilayers, photoelectrochemical systems, and organized molecular assemblies are just a few examples of interfacial systems of interest to these industries. A number of materials and processing problems, both related to fundamental understanding and to monitoring manufacturing operations, have been identified where our microchemical characterization abilities need improving. Over twenty areas for research are identified where progress will contribute to improved understanding of materials and processes, improved problem solving abilities, improved manufacturing consistency, and lower costs. Some of the highest priority areas for research include (1) developing techniques and methods with improved chemical specificity at interfaces, (2) developing fast, real-time surface and interface probes and (3) improving the cost and reliability of manufacturing monitors. Increased collaboration among University, Industry, and Government laboratories will be a prerequisite to making the required progress in a timely fashion. DOE

N93-11901# National Inst. of Standards and Technology, Gaithersburg, MD. Metric Program.
RECOMMENDED AGENCY PROCEDURES FOR IMPLEMENTING FEDERAL METRIC POLICY Final Report
James B. McCracken and Gary P. Carver Jun. 1992 18 p
(PB92-205467; NISTIR-4855) Avail: CASI HC A03/MF A01

Recommendations to assist Federal Agencies in the transition to use of metric units in regulations, data requests, recordkeeping, and reporting requirements are presented. Although intended for Federal Agency use, the recommendations may be useful to state and local government agencies and other organizations. Author

N93-11902# National Inst. of Standards and Technology, Gaithersburg, MD. Metric Program.
A METRIC AMERICA: A DECISION WHOSE TIME HAS COME - FOR REAL
Gary P. Carver Jun. 1992 14 p
(PB92-205459; NISTIR-4858) Avail: CASI HC A03/MF A01

The Metric Conversion Act of 1975 (amended in 1988) and a 1991 Presidential Executive Order provide both the rationale and the mandate for transition to the use of metric units. Federal agencies are developing and implementing metric transition plans, cooperating on mutual concerns, and working with industry and user groups to establish realistic schedules for change. GRA

N93-12072# Texas Univ., Austin. Center for Transportation Research.
AN EVALUATION OF REPAIR TECHNIQUES USED FOR UNCONTROLLED LONGITUDINAL CRACKING AND FAILED LONGITUDINAL JOINTS Interim Report
Brock E. Hoskins, David W. Fowler, and B. Frank McCullough Jan. 1991 29 p Sponsored by Federal Highway Administration Prepared for Texas State Dept. of Highways and Public Transportation
(PB92-205616; CTR-3-12D-84-920-4; RR-920-4; FHWA/TX-91/920-4) Avail: CASI HC A03/MF A01

Uncontrolled longitudinal cracking was a commonly observed distress in continuously reinforced concrete pavements in the Houston, Texas, area in the 1970's. In the early 1980's, the cracks were repaired by grooving the pavement surface along the crack line and then filling the groove and underlying crack with a polymer mortar. In 1989-90, the pavement was reconstructed using a 4-inch bonded concrete overlay. Prior to the overlay, a condition survey was made and the performance and effectiveness of the crack repair treatment were analyzed and included in the report. The concrete overlay project also included the restoration of a few hundred feet of longitudinal joints where the steel tie bars appeared to have failed. The load transfer was reestablished using a stitching process where 3-inch deep slots were cut transversely across the joint into the slabs on both sides of the joint. A steel bar was placed in the slot and the slot filled with epoxy. Measurements and discussions of the effectiveness are included in the report. Author

N93-12106# Sandia National Labs., Albuquerque, NM.
AN EVALUATION OF THE BLIND LAP JOINT FOR THE SURFACE MOUNT ATTACHMENT OF CHIP COMPONENTS

P. T. Vianco and J. F. DalPorto 1992 24 p Presented at the Surface Mount International Conference, San Jose, CA, 30 Aug. - 3 Sep. 1992
(Contract DE-AC04-76DP-00789)
(DE92-017045; SAND-92-0212C; CONF-9208104-1) Avail: CASI HC A03/MF A01

Blind lap solder joints were used to attach leadless ceramic chip resistors to polyimidequartz circuit boards. Hand soldering and vapor phase reflow techniques were evaluated. The solder was 62Sn-36Pb-2Ag (wt. percent). The integrity of the solder joints was assessed by microstructural examination and room temperature shear tests. These analyses were performed on as-fabricated circuit boards as well as an those samples exposed to thermal cycling (308 cycles; -55 to 125 C; 6 C/min ramps; 120 min hold periods;) or thermal shock (100 cycles, -55 C to 125 C; liquid-to-liquid transfer; 10 min hold periods). In all cases, microscopy revealed no cracks within the solder joints. The shear strengths of the joints were 13.4 lb (59 N), as-fabricated; 10.5 lb (47 N), 308 thermal cycles; and 14.0 lb (62 N), 100 thermal shock cycles. All values were well within acceptability limits for the particular application. Measurements of the intermetallic compound thicknesses at the copper land/solder interface indicated that the additional heating cycle of the hand soldering step decreased the layer thickness as compared to non-hand soldered joints. The successful implementation of the blind lap joint can provide increased device densities on circuit boards by reducing bonding pad extension beyond the ceramic chip foot print. DOE

N93-12202*# National Aeronautics and Space Administration. Pasadena Office, CA.
BACKWARD ASSEMBLY PLANNING WITH DFA ANALYSIS Patent Application
Sukhan Lee, inventor (to NASA) (Jet Propulsion Lab., California Inst. of Tech., Pasadena.) 28 Aug. 1992 42 p
(Contract NAS7-918)
(NASA-Case-NPO-18817-1-CU; NAS 1.71:NPO-18817-1-CU; US-Patent-Appl-SN-942499) Avail: CASI HC A03/MF A01

An assembly planning system that operates based on a recursive decomposition of assembly into subassemblies is presented. The planning system analyzes assembly cost in terms of stability, directionality, and manipulability to guide the generation of preferred assembly plans. The planning in this system incorporates the special processes, such as cleaning, testing, labeling, etc., that must occur during the assembly. Additionally, the planning handles nonreversible, as well as reversible, assembly tasks through backward assembly planning. In order to decrease the planning efficiency, the system avoids the analysis of decompositions that do not correspond to feasible assembly tasks. This is achieved by grouping and merging those parts that can not be decomposable at the current stage of backward assembly planning due to the requirement of special processes and the constraint of interconnection feasibility. The invention includes methods of evaluating assembly cost in terms of the number of fixtures (or holding devices) and reorientations required for assembly, through the analysis of stability, directionality, and manipulability. All these factors are used in defining cost and heuristic functions for an AO* search for an optimal plan. NASA

32 COMMUNICATIONS AND RADAR

Includes radar; land and global communications; communications theory; and optical communications.

For related information see also *04 Aircraft Communications and Navigation* and *17 Space Communications, Spacecraft Communications, Command and Tracking.* For search and rescue see *03 Air Transportation and Safety,* and *16 Space Transportation.*

N93-10977# Royal Signals and Radar Establishment, Malvern (England).
ON UNDERSTANDING IN COMMUNICATING SYSTEMS AND THE ERROR IN THE CHINESE ROOM THOUGHT-EXPERIMENT
T. A. D. White and S. C. Giess Nov. 1990 26 p
(RSRE-Memo-4391; BR115853) Copyright Avail: CASI HC A03/MF A01

John Searle has proposed the Chinese Room thought-experiment to refute the notion of what he calls strong AI (Artificial Intelligence): thinking is merely the manipulation of formal symbols. We discuss the Chinese Room thought-experiment, and show that Searle's argument is in error. We show, therefore, that the Chinese Room thought-experiment provides no grounds for the conclusion that computer hardware, solely on the basis of running computer software, can never be regarded as intelligent. Author

N93-11009# Messerschmitt-Boelkow-Blohm G.m.b.H., Munich (Germany). Kommunikationssyteme und Antriebe.
PROJECT AND TEST OF A RECONFIGURABLE MULTIPLE FEED SYSTEM IN C-BAND [ENTWURF UND TEST EINES REKONFIGURIERBAREN MEHRFACHERREGERSYSTEMS IM C-BAND]
Helmut Wolf, Ernst Sommer, Norbert Nathrath, and Herbert Rosseg 1992 6 p In GERMAN Presented at the ITG Diskussionssitzung ueber Mehrelemente Antennen, Bad Duerkheim/Weinstrasse, Fed. Republic of Germany, 1-2 Apr. 1992
(MBB-UK-0162-92-PUB; ETN-92-92114) Avail: CASI HC A02/MF A01

The optimization, building, and space qualification of demonstration model of a multiple feed system with reconfigurable supply network for the feeding of a reflector antenna with contoured radiation diagram are reported. The model project is based on Intelsat 7 satellites. The contour of the illuminated zone was reconfigurated for various satellite positions over the Atlantic Ocean. The construction of the demonstration model is described. Test results are given, and measured data of the reconfigured radiation diagram are presented. A very good agreement is obtained with the theoretical project results. ESA

N93-11044 Department of the Navy, Washington, DC.
SHORT-RANGE RADAR SYSTEM Patent
Bennie E. Macomber, inventor (to Navy) and Daniel A. Goss, inventor (to Navy) 29 Oct. 1991 6 p Filed 13 Apr. 1976
(AD-D015339; US-Patent-5,061,933; US-Patent-Appl-SN-677193; US-Patent-Class-342-128) Avail: US Patent and Trademark Office

This document describes a short-range radar system having a unique method of processing a linear FM/CW signal so as to provide target range information at the time of target detection. The linear FW/CW signal is mixed with a portion of the transmitted signal and with an intermediate frequency ramp signal to produce a difference frequency signal in the form of a frequency ramp which is a function of the range to the target. The ramp signal is then converted to a pulse which is determinative of the range to the target. GRA

N93-11047# Department of the Navy, Washington, DC.
NON-LINEAR DATA CONVERSION SYSTEM FOR DYNAMIC RANGE DIGITAL SIGNAL PROCESSING Patent
Steve J. Koerner, inventor (to Navy) 19 Nov. 1991 6 p Filed 25 Sep. 1989

(AD-D015347; US-Patent-5,066,952; US-Patent-Appl-SN-412248; US-Patent-Class-341-138) Avail: US Patent and Trademark Office

The data acquisition portion of a data signal processing system has a nonlinear data compression and conversion arrangement and a data decompression and scaling arrangement. The nonlinear data compression and conversion arrangement employs graduated reference voltage levels provided by resistors having graduated, unequal values, such as values being related as a geometric progression. The graduated form of the reference voltage levels provide a form of data compression wherein large value and small value measurements will have essentially the same fractional resolution. The data decompression and scaling arrangement can decompress previously compressed digital signals and limit the digital data width of such signals in systems which have input dynamic range requirements greater than their output resolution requirements. GRA

N93-11116*# Old Dominion Univ., Norfolk, VA. Dept. of Computer Science.

PHOTONICS AND OTHER APPROACHES TO HIGH SPEED COMMUNICATIONS Progress Report, period ending 29 Feb. 1992

Kurt Maly Jun. 1992 61 p
(Grant NAG1-908)
(NASA-CR-190362; NAS 1.26:190362) Avail: CASI HC A04/MF A01

Our research group of 4 faculty and about 10-15 graduate students was actively involved (as a group) in the development of computer communication networks for the last five years. Many of its individuals have been involved in related research for a much longer period. The overall research goal is to extend network performance to higher data rates, to improve protocol performance at most ISO layers and to improve network operational performance. We briefly state our research goals, then discuss the research accomplishments and direct your attention to attached and/or published papers which cover the following topics: scalable parallel communications; high performance interconnection between high data rate networks; and a simple, effective media access protocol system for integrated, high data rate networks. For individual titles, see N93-11117 through N93-11119.

N93-11117*# Old Dominion Univ., Norfolk, VA. Dept. of Computer Science.

SCALABLE PARALLEL COMMUNICATIONS

K. Maly, S. Khanna, C. M. Overstreet, R. Mukkamala, M. Zubair, Y. S. Sekhar, and E. C. Foudriat *In its* Photonics and Other Approaches to High Speed Communications Jun. 1992 29 p
(For primary document see N93-11116 02-32)
(Contracts NAG1-87263; CIT-596045; N00174-C-91-0119; SUN-596044)
Avail: CASI HC A03/MF A01

Coarse-grain parallelism in networking (that is, the use of multiple protocol processors running replicated software sending over several physical channels) can be used to provide gigabit communications for a single application. Since parallel network performance is highly dependent on real issues such as hardware properties (e.g., memory speeds and cache hit rates), operating system overhead (e.g., interrupt handling), and protocol performance (e.g., effect of timeouts), we have performed detailed simulations studies of both a bus-based multiprocessor workstation node (based on the Sun Galaxy MP multiprocessor) and a distributed-memory parallel computer node (based on the Touchstone DELTA) to evaluate the behavior of coarse-grain parallelism. Our results indicate: (1) coarse-grain parallelism can deliver multiple 100 Mbps with currently available hardware platforms and existing networking protocols (such as Transmission Control Protocol/Internet Protocol (TCP/IP) and parallel Fiber Distributed Data Interface (FDDI) rings); (2) scale-up is near linear in n, the number of protocol processors, and channels (for small n and up to a few hundred Mbps); and (3) since these results are based on existing hardware without specialized devices (except perhaps for some simple modifications of the FDDI boards), this is a low cost solution to providing multiple 100 Mbps on current machines. In addition, from both the performance analysis and the properties of these architectures, we conclude: (1) multiple processors providing identical services and the use of space division multiplexing for the physical channels can provide better reliability than monolithic approaches (it also provides graceful degradation and low-cost load balancing); (2) coarse-grain parallelism supports running several transport protocols in parallel to provide different types of service (for example, one TCP handles small messages for many users, other TCP's running in parallel provide high bandwidth service to a single application); and (3) coarse grain parallelism will be able to incorporate many future improvements from related work (e.g., reduced data movement, fast TCP, fine-grain parallelism) also with near linear speed-ups. Author

N93-11118*# Old Dominion Univ., Norfolk, VA. Dept. of Computer Science.

HIGH PERFORMANCE INTERCONNECTION BETWEEN HIGH DATA RATE NETWORKS

E. C. Foudriat, K. Maly, C. M. Overstreet, L. Zhang, and W. Sun *In its* Photonics and Other Approaches to High Speed Communications Jun. 1992 9 p Presented at the International Workshop on Advanced Communications and Applications for High Speed Networks, Munich, Fed. Republic of Germany, 16-19 Mar. 1992 (For primary document see N93-11116 02-32)
(Contract NAG1-908; RF-596044; INF-89-002-01)
Avail: CASI HC A02/MF A01

The bridge/gateway system needed to interconnect a wide range of computer networks to support a wide range of user quality-of-service requirements is discussed. The bridge/gateway must handle a wide range of message types including synchronous and asynchronous traffic, large, bursty messages, short, self-contained messages, time critical messages, etc. It is shown that messages can be classified into three basic classes, synchronous and large and small asynchronous messages. The first two require call setup so that packet identification, buffer handling, etc. can be supported in the bridge/gateway. Identification enables resequences in packet size. The third class is for messages which do not require call setup. Resequencing hardware based to handle two types of resequencing problems is presented. The first is for a virtual parallel circuit which can scramble channel bytes. The second system is effective in handling both synchronous and asynchronous traffic between networks with highly differing packet sizes and data rates. The two other major needs for the bridge/gateway are congestion and error control. A dynamic, lossless congestion control scheme which can easily support effective error correction is presented. Results indicate that the congestion control scheme provides close to optimal capacity under congested conditions. Under conditions where error may develop due to intervening networks which are not lossless, intermediate error recovery and correction takes 1/3 less time than equivalent end-to-end error correction under similar conditions. Author

N93-11119*# Old Dominion Univ., Norfolk, VA. Dept. of Computer Science.

A SIMPLE, EFFECTIVE MEDIA ACCESS PROTOCOL SYSTEM FOR INTEGRATED, HIGH DATA RATE NETWORKS

E. C. Foudriat, K. Maly, C. M. Overstreet, S. Khanna, and L. Zhang *In its* Photonics and Other Approaches to High Speed Communications Jun. 1992 13 p Submitted for publication
(For primary document see N93-11116 02-32)
(Contract NAG1-87263; N00174-C-91-0119; CIT-596045)
Avail: CASI HC A03/MF A01

The operation and performance of a dual media access protocol for integrated, gigabit networks are described. Unlike other dual protocols, each protocol supports a different class of traffic. The Carrier Sensed Multiple Access-Ring Network (CSMA/RN) protocol and the Circulating Reservation Packet (CRP) protocol support asynchronous and synchronous traffic, respectively. The two protocols operate with minimal impact upon each other. Performance information demonstrates that they support a complete range of integrated traffic loads, do not require call setup/termination or a special node for synchronous traffic control, and provide effective pre-use and recovery. The CRP also provides guaranteed access and fairness control for the asynchronous system. The paper demonstrates that the CSMA-CRP system fulfills many of the requirements for gigabit LAN-MAN networks most effectively and simply. To accomplish this, CSMA-CRP features are compared against similar ring and bus systems, such as Cambridge Fast Ring, Metaring, Cyclic Reservation Multiple Access, and Distributed Dual Queue Data Bus (DQDB). Author

N93-11234# Sandia National Labs., Albuquerque, NM.
THE TOMOGRAPHIC FORMULATION OF SPOTLIGHT MODE SYNTHETIC APERTURE RADAR EXTENDED TO THREE DIMENSIONAL TARGETS
C. V. Jakowatz, Jr. and P. A. Thompson 1992 3 p Presented at the Digital Signal Processing Workshop, Starved Rock, IL, 15 Sep. 1992
(Contract DE-AC04-76DP-00789)
(DE92-013666; SAND-92-1045C; CONF-9209114-1) Avail: CASI HC A01/MF A01

In this paper we take a new look at the tomographic formulation of spotlight mode synthetic aperture radar (SAR), so as to include the case of targets having three-dimensional structure. This bridges the work of David C. Munson and his colleagues, who first described SAR in terms of two-dimensional tomography, with Jack Walker's original derivation of spotlight mode SAR imaging via Doppler analysis. The main result is to demonstrate that the demodulated radar return data from a spotlight mode collection represent a certain set of samples of the three-dimensional Fourier transform of the target reflectivity function, and to do so using tomographic principles instead of traditional Doppler arguments. We then show that the tomographic approach is useful in interpreting the two-dimensional SAR image of a three-dimensional scene. In particular, the well-known SAR imaging phenomenon commonly referred to as layover is easily explained in terms of tomographic projection. DOE

N93-11354# Department of the Navy, Washington, DC.
ARBITRARY WAVEFORM GENERATOR Patent Application
Fletcher A. Blackmon, inventor (to Navy) 13 Apr. 1992 14 p
(AD-D015346; US-Patent-Appl-SN-807577; Navy-Case-73624)
Avail: CASI HC A03/MF A01

It is a general purpose and object of the present invention to provide an arbitrary waveform generator. It is a further object that the generator has the ability to produce both pulse waveforms and continuous waveforms. Other objects are that the generator be compact and only require low power for lending itself to battery powered operation. These objects are accomplished with the present invention by providing a system in which digital waveforms are created using a software package such as DADiSP. The software package forms signals that are then transferred to an EPROM. Each signal type occupies a certain block of address space within the EPROM. A great number of signals may be digitally stored in this way. The operator then constructs simple microprocessor computer codes to access any signal, any combination of signals, or all signals to form a unique waveform generation sequence. Therefore the operator selects arbitrarily which of the previously stored signals to generate. Key features include the EPROM storing a single pulse for pulse waveforms and a single period of waveform for continuous waveforms. Other key features are the ability to control the sequence of generation, the number of times each signal is generated, the time between pulses, and the time between the generation of different signal types. These features are controlled by the microprocessor codes residing in a microprocessor. GRA

N93-11366# Royal Military Coll. of Science, Shrivenham (England).
SPEECH RECOGNITION SYSTEMS AND THEIR MILITARY APPLICATIONS
R. E. Coueffin and H. A. R. Hancock 1983 86 p
(BR91882; ETN-92-92297) Copyright Avail: CASI HC A05/MF A01

The ways of assessing Automatic Speech Recognition (ASR) system performance is discussed. The major speech recognition technologies available now and under development are considered. Trends of likely future developments and likely future capabilities are examined. The project investigates the scope of applications of ASR to machine control, data entry, communications and security, with special emphasis on military applications. A time scale of probable future developments is included. It is recommended that ASR should only be used, at present, where: the resulting action is not critical to the mission; there is a limited number of operators; the vocabulary is limited; an alternative control system is available; training of the system is possible. The areas in ASR systems where further development is required are suggested. ESA

N93-11383# Royal Signals and Radar Establishment, Malvern (England). Speech Research Unit.
THE DEVELOPMENT OF THE SPEAKER INDEPENDENT ARM CONTINUOUS SPEECH RECOGNITION SYSTEM
M. J. Russell 15 Jan. 1992 30 p
(RSRE-Memo-4473; BR308890; ETN-92-92316) Copyright
Avail: CASI HC A03/MF A01

The development of a speaker dependent continuous speech recognition system based on phoneme level hidden Markov models is described. The system is part of the Airborne Reconnaissance Mission (ARM) project, that aims at reaching the accurate recognition of continuously spoken airborne reconnaissance reports using a speech recognition system and Markov models. The system is configured to recognize continuously spoken airborne reconnaissance reports, a task which involves a vocabulary of approximately 500 words. On a test set of speech from 80 male subjects, the final system achieves a word accuracy of 74.1 percent with no explicit syntactic constraints. The evolution of the speaker independent ARM system, in terms of the performance of its various versions of the evaluation set, is summarized. Comparison of the final versions of the speaker dependent and speaker independent ARM systems shows that many of the empirically derived parameters are similar on both systems. ESA

N93-11384# Royal Signals and Radar Establishment, Malvern (England). Speech Research Unit.
PRELIMINARY RESULTS ON THE USE OF LINEAR DISCRIMINANT ANALYSIS IN THE ARM CONTINUOUS SPEECH RECOGNITION SYSTEM
S. M. Peeling and K. M. Ponting 16 Dec. 1991 26 p Sponsored in part by IED
(RSRE-Memo-4511; BR308899; ETN-92-92318) Copyright
Avail: CASI HC A03/MF A01

Linear discriminant analysis is used to generate speech data transformations. This transformed data is then used within the Airborne Reconnaissance Mission (ARM) continuous speech recognition system. The aim of the ARM project is accurate recognition of continuously spoken airborne reconnaissance reports using a speech recognition system based on phoneme level hidden Markov models. A fuller description of a linear discriminant analysis, which is applied to speaker dependent data in the ARM system, is given. Preliminary results are presented from experiments using transformed data alone and also in conjunction with one, or both, of the word transition penalties and variable frame rate analysis. Speaker dependent results are reported which are significantly better then the best obtained previously. ESA

N93-11385# Royal Signals and Radar Establishment, Malvern (England). Speech Research Unit.
THE USE OF LINEAR DISCRIMINANT ANALYSIS IN THE ARM CONTINUOUS SPEECH RECOGNITION SYSTEM
S. M. Peeling and K. M. Ponting 9 Jan. 1992 31 p Sponsored in part by IED
(RSRE-Memo-4512; BR308900; ETN-92-92319) Copyright
Avail: CASI HC A03/MF A01

Linear discriminant analysis is used to generate speech data transformations. This transformed data is then used within the Airborne Reconnaissance Mission (ARM) continuous speech recognition system. The aim of the ARM project is accurate recognition of continuously spoken airborne reconnaissance reports using a speech recognition system based on phoneme level hidden Markov models. A short description of a linear discriminant analysis, which is applied to speaker dependent data in the ARM system, is given. Experiments are described using transformed data in conjunction with variable frame rate analysis and word transition penalties. Speaker independent results are reported which are as good as the best obtained previously using cosine transformations and variable frame rate analysis. The two sets of results are compared. ESA

N93-11387# Royal Signals and Radar Establishment, Malvern (England).

ON THE DEFINITION AND CALCULATION OF EFFECTIVE IMPEDANCES AND AVERAGED BOUNDARY CONDITIONS WITH APPLICATION TO THE ANALYSIS OF HIGH COMPLEXITY FREQUENCY SELECTIVE SURFACES

A. J. Mackay and J. G. Gallagher Jul. 1991 27 p
(RSRE-Memo-4518; P304769-42; ETN-92-92321) Copyright
Avail: CASI HC A03/MF A01

The use of averaged boundary conditions is studied as a method of analysis for electrical scattering from large structures which are geometrically complex on a scale much smaller than a wavelength. The emphasis is placed on how they may be used for the study of Frequency Selective Surfaces (FSS) and an example concerning a sparse array of small thin dipoles is given. FSS have a large number of applications. Examples include the design and construction of radomes and antennas and the construction of passive microwave and millimeter wave filters. With the improvements in computer technology, numerical methods become ever more important in FSS design. However, it still remains the case that FSS with highly complex patterns are not amenable to modal analysis methods in a realistic period of time. ESA

N93-11391# Royal Signals and Radar Establishment, Malvern (England).

A COMPARISON OF FEED-FORWARD NETWORKS AND MAXIMUM LIKELIHOOD ON A POINT-SOURCE LOCATION PROBLEM

Andrew R. Webb 17 Apr. 1991 34 p
(RSRE-Memo-4567; BR308887; ETN-92-92332) Copyright
Avail: CASI HC A03/MF A01

The problem of point source location using a multibeam focal plane staring array radar is considered. It is viewed as one in functional approximation in which the position of the source is regarded as a nonlinear function of the sampled radar image. An approximant is constructed, using a training set, which minimizes the mean square error in the position estimate. The problem of generalization is discussed. Two feed forward network architectures are considered: a particular radial basis function network which arises as a consequence of the minimum mean square error solution and is appropriate when the signal to noise ratio is 'small', and a multilayer perceptron, chosen for high signal to noise ratio approximation. The errors in the position estimates for each of these approaches are compared with a maximum likelihood position estimation method. The maximum likelihood method gives better overall performance and has the advantage that it is not dependent on the signal to noise ratio. ESA

N93-11395 National Physical Lab., Teddington (England). Div. of Electrical Science.

AN UNCERTAINTY BUDGET FOR VHF AND UHF REFLECTOMETERS

N. M. Ridler and C. J. Medley May 1992 34 p
(NPL-DES-120; ETN-92-92367) Copyright Avail: National Physical Lab., Teddington, Middlesex, TW11 0LW, England

Details of the derivation of an uncertainty budget for one port immittance or complex voltage reflection coefficient measuring instruments, operating at VHF and UHF in the 14 mm 50 ohm coaxial line size, are reported. The principles of the uncertainty budget are given along with experimental results obtained using six ports and a network analyzer as the measuring instruments. Details of the types of calibration for which the uncertainty budget is suitable are reported. Various aspects of the uncertainty budget are considered and general principles and treatment of the type A and type B contributions are discussed. Experimental results obtained using the uncertainty budget are given. A summary of uncertainties for the six ports and HP8753B automatic network analyzer are also given. ESA

N93-11426 Department of the Navy, Washington, DC.

METHOD OF STEERING THE GAIN OF A MULTIPLE ANTENNA GLOBAL POSITIONING SYSTEM RECEIVER Patent

Alan G. Evans, inventor (to Navy) (Courtney and Co., Philadelphia, PA.) and Bruce R. Hermann, inventor (to Navy) (Courtney and Co., Philadelphia, PA.) 2 Jun. 1992 7 p Filed 16 Nov. 1990
(AD-D015367; US-Patent-5,119,103; US-Patent-Appl-SN-621685; US-Patent-Class-342-423) Avail: US Patent and Trademark Office

A method for steering the gain of a multiple antenna Global Positioning System (GPS) receiver toward a plurality of a GPS satellites simultaneously is provided. The GPS signals of a known wavelength are processed digitally for a particular instant in time. A range difference or propagation delay between each antenna for GPS signals received from each satellite is first resolved. The range difference consists of a fractional wavelength difference and an integer wavelength difference. The fractional wavelength difference is determined by each antenna's tracking loop. The integer wavelength difference is based upon the known wavelength and separation between each antenna with respect to each satellite position. The range difference is then used to digitally delay the GPS signals at each antenna with respect to a reference antenna. The signal at the reference antenna is then summed with the digitally delayed signals to generate a composite antenna gain. The method searches for the correct number of integer wavelengths to maximize the composite gain. The range differences are also used to determine the attitude of the array. GRA

N93-11487# Royal Signals and Radar Establishment, Malvern (England).

DIAGNOSTIC RHYME TEST STATISTICAL ANALYSIS PROGRAMS

A. Sim (Atomic Weapons Research Establishment, Aldermaston, England), R. Bain, A. J. Belyavin (Royal Air Force Inst. of Aviation Medicine, Farnborough, England), and R. L. Pratt Aug. 1991 64 p
(RSRE-91026; BR305835; ETN-92-92310) Copyright Avail: CASI HC A04/MF A01

The statistical techniques and associated computer programs used to analyze data from Diagnostic Rhyme Test (DRT) are described. The DRT is used extensively for assessing the intelligibility of military communications systems and became an accepted NATO standard for testing linear predictive coders. The DRT vocabulary comprises ninety six minimally contrasting rhyming word pairs, the initial consonants of which differ only by a single acoustic feature, or attribute. There are six such attributes: voicing, nasality, sustention, silibation, graveness, and compactness. The attribute voicing is present when the vocal cords are excited: in the word pair 'veal-feel', the consonant 'v' is voiced, but the constant 'f' is unvoiced. The procedure for the implementation of the DRT is presented. To ensure the stability of the results, tests using not less than eight talkers and eight listeners are conducted. ESA

N93-11509# Air Force Inst. of Tech., Wright-Patterson AFB, OH. Foreign Aerospace Science and Technology Center.

MICROWAVE GUIDANCE TECHNOLOGY AND ITS APPLICATIONS

Lu Liu 4 Feb. 1992 23 p Transl. into ENGLISH from Shijie Daodan Yu Hangtian (China), no. 1, 1991 p 42-47
(AD-A254107; FASTC-ID(RS)T-1064-91) Avail: CASI HC A03/MF A01

This article provides the basic features of millimeter wave guidance technology as well as the primary millimeter wave guidance systems and their characteristics. It also analyzes current levels of technology inside and outside China and discusses future prospects of millimeter wave technology and its applications. Millimeter waves revere to the frequency spectrum of operational wave lengths from one to ten millimeters. This corresponds to operational frequencies between 300 and 30 GHz. The position on the electromagnetic frequency spectrum of millimeter waves is between microwave and infrared waves. This determines that millimeter waves have both microwave and optical characteristics. Millimeter waves are weakened by the atmosphere to a much greater extent than are microwaves. There are marked changes in the amount of loss as the frequencies are changed. In general, the higher the frequency the greater the attenuation. However, due to absorption effect of vapors and oxygen, peaks appear at certain frequencies, resulting in especially great attenuation rises around 35, 94, 140, and 220 GHz. Another way of putting this is that the areas where there is slight attenuation are called transmission windows. GRA

N93-11515# Pacific Northwest Lab., Richland, WA.
CELLULAR AND MOLECULAR PATHWAYS OF EXTREMELY-LOW-FREQUENCY ELECTROMAGNETIC FIELD INTERACTIONS WITH LIVING SYSTEMS
T. S. Tenforde Jun. 1992 16 p Presented at the 1st World Congress for Electricity and Magnetism in Biology and Medicine, Orlando, FL, 14-29 Jun. 1992
(Contract DE-AC06-76RL-01830)
(DE92-019084; PNL-SA-20368; CONF-920630-1) Avail: CASI HC A03/MF A01

There is growing evidence that environmental electric and magnetic fields in the extremely-low-frequency (ELF) band below 300 Hz can influence biological functions by mechanisms that are only poorly understood at the present time. The primary objectives of this paper are to review the physical properties of ELF fields, their interactions with living systems at the tissue, cellular, and subcellular levels, and the key role of cell membranes in the transduction of signals from imposed ELF fields. Topics of discussion include signal-to-noise ratios for single cells and cell aggregates, resonance phenomena involving a combination of static and ELF magnetic fields, and the possible influence of ELF fields on molecular signaling pathways that involve membrane receptors and cytoplasmic second messengers. DOE

N93-11591# Aerospatiale, Cannes (France).
LESSONS DRAWN FROM 2 EXISTING SATELLITE NETWORKS: ARABSAT AND EUTELSAT. APPLICATION TO THE PACIFIC BASIN PROJECTS
Jean-Jacques Bloch 1992 7 p Presented at Conference BTC 1992, Jan. 1992
(Rept-921-440-101; ETN-92-92355) Avail: CASI HC A02/MF A01

The Arabsat and Eutelsat systems are described. The Arabsat belongs to an organization which includes 20 countries of the Arab League. The Eutelsat belongs to the European telecommunication system which includes 29 countries, and is based op the Intelsat model. The current use of their payload is reviewed and compared with their respective planning stage predictions. From this perspective, some teachings are drawn which could be profitable for emerging region Pacific basin networks, now in the planning stage. In the Pacific basin several private and governmental regional satellite networks either newly existing or in the design phase are vying to deliver services to potential customers. These services include national television, commercial television, VSAT (Very Small Aperture Terminal) networks, and regional or domestic telephony. ESA

N93-11632# Lawrence Livermore National Lab., CA.
TEMPORAL SCATTERING AND RESPONSE SOFTWARE USERS' MANUAL, VERSION 2 AND 3
R. R. McLeod Jun. 1992 48 p
(Contract W-7405-eng-48)
(DE92-040934; UCRL-MA-104861-Ver-2-3) Avail: CASI HC A03/MF A01

This manual gives complete information on how to use the TSAR electromagnetic analysis software. Included are descriptions of input files, the details of how these files affect the problem, and output data specifications. What is not included is the theory of the finite-difference time-domain (FDTD) algorithm or details of the TSAR implementation of it. This manual assumes that readers are sufficiently familiar with FDTD that they only need the 'how to' knowledge presented here. This is a reference manual rather than a tutorial manual. To help new users become familiar with the TSAR software, a set of example problems is included with the TSAR distribution. DOE

N93-11661# Lawrence Livermore National Lab., CA.
RADIO PILL ANTENNA RANGE TEST
W. F. Cummins and R. J. Kane May 1992 26 p
(Contract W-7405-eng-48)
(DE92-019903; UCRL-ID-110629) Avail: CASI HC A03/MF A01

In order to investigate the potential of a proposed 'radio pill' beacon transmitter, a range test experiment was devised and carried out in the VHF frequency range. Calculations and previous work indicated that optimum sensitivity and, thus, distance would be obtained in this frequency range provided body radio-frequency (RF) absorption was not too great. A ferrite-core loop antenna is compatible with a pill geometry and has better radiation efficiency than an air core loop. The ferrite core may be a hollow cylinder with the electronics and batteries placed inside. However, this range test was only concerned with experimentally developing test range data on the ferrite core antenna itself. A one turn strap loop was placed around a 9.5 mm diameter by 18.3 mm long stack of ferrite cores. This was coupled to a 50 Omega transmission line by 76 mm of twisted pair line and a capacitive matching section. This assembly was excited by a signal generator at output levels of -10 to +10 dBm. Signals were received on a VHF receiver and tape recorder coupled to a 14 element, circularly polarized Yagi antenna at a height of 2.5 m. Field strength measurements taken at ranges of 440, 1100, and 1714 m. Maximum field strengths referenced to 0 dBm transmitter level were -107 to -110 dB at 440 m, -124 to -127 dBm at 1100 m, and -116 to -119 dBm at 1714 m when the antenna cylinder was horizontal. Field strengths with a vertical antenna were about 6 dB below these values. The latter transmit site was elevated and had a clear line-of-site path to the receiving site. The performance of this test antenna was better than that expected from method-of-moment field calculations. When this performance data is scaled to a narrow bandwidth receiving system, ground level receiving ranges of a few to 10 km can be expected. Clear line-of-sight ranges where either or both the transmitter and receiver are elevated could vary from several km to 100 km. DOE

N93-11675# Lawrence Livermore National Lab., CA.
PREDICTION OF ELECTROMAGNETIC PULSE GENERATION BY PICOSECOND AVALANCHES IN HIGH-PRESSURE AIR
D. J. Mayhall and J. H. Yee May 1992 7 p Presented at the 9th International Conference on High Power Particle Beams, Washington, DC, 25-29 May 1992
(Contract W-7405-eng-48)
(DE92-019382; UCRL-JC-108748; CONF-920515-32) Avail: CASI HC A02/MF A01

The gas avalanche switch is a laser-activated, high voltage switch, consisting of a set of pulse charged electrodes in a high pressure gas. Induced electrons from a picosecond scale laser pulse initiate an avalanche discharge between high voltage and grounded electrodes. If the voltage, pressure, and dimensions are correct, the rapid avalanche, fueled by the immense number of electrons available in the gas, collapses the applied voltage in picoseconds and generates electromagnetic pulses with widths as short as 1 to 10 ps and 3 dB bandwidths of 20 to 120 GHz. With proper voltage or pressure detuning, wider pulses and lower bandwidths occur. A number of versions of the switch are possible. The simplest is a parallel plate capacitor, consisting of a gas between two parallel plate conductors. High voltage is applied across the two plates. A parallel plate, Blumlein geometry features a center electrode between two grounded parallel plates. This geometry emits a single pulse in each direction along the parallel plates. A frozen wave geometry with multiple, oppositely charged center electrodes will emit AC pulses. Series switches consisting of gas gaps between two electrodes are also possible. A recent investigation with an overvolted series gap reported voltage switching times as short as 50 ps. For investigation of these switches, we have developed a 2-D, electromagnetic, finite difference, electron fluid computer code for ionization in high pressure gases. This code simultaneously, self consistently, and implicitly solves Maxwell's curl equations for transverse magnetic modes between perfectly conducting parallel plates. It solves electron fluid conservation equations for density, momentum, and energy. The coordinates are presently rectangular. Multiple charged, rectilinear, perfect conductors may be situated between the plates. DOE

N93-11716*# University of Central Florida, Orlando. Dept. of Industrial Engineering and Management System.
IMPLEMENTING SYSTEM SIMULATION OF C3 SYSTEMS USING AUTONOMOUS OBJECTS
Ralph V. Rogers 1987 6 p Sponsored in part by FAA
(Grant NAG2-625)
(NASA-CR-190845; NAS 1.26:190845) Avail: CASI HC A02/MF A01

The basis of all conflict recognition in simulation is a common frame of reference. Synchronous discrete-event simulation relies on the fixed points in time as the basic frame of reference. Asynchronous discrete-event simulation relies on fixed-points in the model space as the basic frame of reference. Neither approach provides sufficient support for autonomous objects. The use of a spatial template as a frame of reference is proposed to address these insufficiencies. The concept of a spatial template is defined and an implementation approach offered. Discussed are the uses of this approach to analyze the integration of sensor data associated with Command, Control, and Communication systems. Author

N93-11760# Federal Aviation Administration, Washington, DC.
FUTURE FAA TELECOMMUNICATIONS PLAN
Aug. 1991 677 p
(AD-A249133) Avail: CASI HC A99/MF A06

The FDIO system is a subelement of the En Route Air Traffic Control Systems element of the NAS communications system. FDIO provides terminal and en route air traffic controllers with direct user input/output of flight plan and flight movement information and updates. FDIO replaces existing Flight Data Entry and Printout (FDEP) and Flight Strip Printer (FSP) systems, and also extends flight data services to terminal locations not presently served by FDEP. The FDIO system concept evolved from the need to increase the reliability and maintainability of the present system. Increases in flight traffic and resultant data loads have caused delays in the processing of data sent to and from FDEP sites, and to FSP's. FDIO will duplicate all of the functions of the FDEP and FSP system while providing extended capabilities. Flight strips will be displayed, as they are in the current system, by printing on the FAA flight strip forms. A CRT capability will be included as a function in all sites. Where no CRT is used, the display for message composition will be Remote Flight Strip Printers (Terminal) (RFSP(T)). A keyboard will provide for data entry and error display as in the current system. Two central control units will be used at each Central Computer Complex (CCC) and one remote control unit at each FDEP site. GRA

N93-11764# Army Electronic Proving Ground, Fort Huachuca, AZ.
ANTENNA PATTERN MEASUREMENT FACILITIES Final Report
15 Apr. 1992 48 p Supersedes AD-A248964 dated 16 May 1991
(AD-A250219; TOP-6-2-604) Avail: CASI HC A03/MF A01

The test operations procedure (TOP) is an overview of procedures for testing antennas using the Automated Data Acquisition and Analysis System (ADAAS) at the Antenna Test Facility (ATF), U.S. Army Electronic Proving Ground, Fort Huachuca, Arizona. The ATF has two test ranges: an outdoor compact range and an arc range. The Compact Range uses a parabolic reflector to collimate radio frequency energy in order to simulate far-field testing. A large hydraulic positioner moves the test antenna through azimuth and elevation arcs to allow testing of an entire hemisphere of coverage. The Arc Range operates in the near field using uncollimated RF. It uses a turntable to rotate the test item through the desired range of azimuth; a probe antenna moving along the vertical arc structure provides elevation coverage. The combination provides full hemispherical coverage. The TOP describes procedures for measuring antenna gain; locations of beams, lobes, and nulls; and other antenna characteristics. It contrasts the capabilities of the two ranges and provides guidelines to help the user select the right range for a particular test. GRA

N93-11800# Sandia National Labs., Albuquerque, NM.
EXCITON KINETICS IN POLY(DI-N-HEXYLSILANE)
R. G. Kepler, Z. G. Soos (Princeton Univ., NJ.), and J. R. G. Thorne (Pennsylvania Univ., Philadelphia.) 1992 10 p Presented at the Spring Meeting of the European Materials Research Society: International Conference on Electronic Materials, Strasbourg, France, 2-5 Jun. 1992
(Contract DE-AC04-76DP-00789)
(DE92-018278; SAND-92-1357C; CONF-920694-1) Avail: CASI HC A02/MF A01

We have previously shown that large charge carriers are generated by exciton-exciton annihilation in solid films of poly(di-n-hexylsilane). Using the phenomenon we show that the exciton-exciton annihilation rate constant (gamma) at ambient temperature is not a function of the photon energy used to create the excitons even at energies well out into the long wavelength tail of the exciton absorption band. We also show that the excitons remain highly mobile throughout their 600 ps lifetime and that they diffuse distances comparable to the crystallite size in the film. The value of (gamma) obtained in these studies is in excellent agreement with those obtained previously in fluorescence intensity studies. DOE

N93-11811# Illinois Univ., Urbana. Dept. of Electrical and Computer Engineering.
PUBLICATION OF PAPERS PRESENTED AT URSI 23RD GENERAL ASSEMBLY AS A SPECIAL SECTION OF RADIO SCIENCE Final Report, 1 Feb. 1991 - 31 Jan. 1992
K. C. Yeh 15 May 1992 129 p General Assembly held in Prague, Czechoslovakia, 28 Aug. - 5 Sep. 1990
(Contract DAAL03-91-M-0149)
(AD-A253561; ARO-28787.1-GS) Avail: CASI HC A07/MF A02

A symposium entitled Radio Propagation in the Ionosphere and Magnetosphere: Theory and Application was convened at the 23rd General Assembly of URSI, August 28 through September 5, 1990. Of-the 49 papers presented at this symposium, 13 were selected for publication in Radio Science, Volume 27, Number 2, March-April 1992. These papers cover a broad field of ionospheric and magnetospheric propagation of both experimental and theoretical nature. GRA

N93-11913 Cranfield Inst. of Tech., Bedford (England).
THE DESIGN AND IMPLEMENTATION OF RADAR CLUTTER MODELLING AND ADAPTIVE TARGET DETECTION TECHNIQUES Ph.D. Thesis
Mohammed Hussain Ali 1990 242 p
Avail: Univ. Microfilms Order No. BRDX92918

The analysis and reduction of radar clutter is investigated. Clutter is the term applied to unwanted radar reflections from land, sea, precipitation, and/or man-made objects. A great deal of useful information regarding the characteristics of clutter can be obtained by the application of frequency domain analytical methods. Thus, some considerable time was spent assessing the various techniques available and their possible application to radar clutter. In order to better understand clutter, use of a clutter model was considered desirable. There are many techniques which will enable a target to be detected in the presence of clutter. One of the most flexible of these is that of adaptive filtering. This technique was thoroughly investigated and a method for improving its efficacy was devised. The modified adaptive filter employed differential adaption times to enhance detectability. Adaptation time as a factor relating to target detectability is a new concept and was investigated in some detail. It was considered desirable to implement the theoretical work in dedicated hardware to confirm that the modified clutter model and the adaptive filter technique actually performed as predicted. The equipment produced is capable of operation in real time and provides an insight into real time DSP applications. This equipment is sufficiently rapid to produce a real time display on the actual PPI system. Finally a software package was also produced which would simulate the operation of a PPI display and thus ease the interpretation of the filter outputs. Dissert. Abstr.

N93-11917# Sandia National Labs., Albuquerque, NM.
AUTOMATIC ATTENUATION/PHASE CALIBRATION SYSTEM (AAPCS)
C. J. Still Jun. 1992 70 p
(Contract DE-AC04-76DP-00789)
(DE92-017354; SAND-91-1743) Avail: CASI HC A04/MF A01

An automatic attenuation/phase calibration system which simultaneously certifies attenuation and transmission angle through up to 100 dB of loss has been developed at Sandia National Laboratories. System hardware is commercially available while the software and the certification techniques constitute the development effort. The system is computer controlled and intended primarily for standards type measurements. DOE

N93-12083# Iowa Univ., Iowa City. Dept. of Physics and Astronomy.
FINAL TECHNICAL REPORT
D. H. Berman 1992 2 p
(Contract N00014-89-J-2042)
(AD-A253529) Avail: CASI HC A01/MF A01

The final technical report for NRL Grant No. N00014-89-J-42 is presented. The report consists of the following papers: (1) Simulations of rough interface scattering; (2) Boundary effects in Quantum Mechanics; (3) Rough interface scattering without plane waves; (4) The small-slope approximation for monostatic scattering; (5) Renormalization of propagation in a waveguide with rough boundaries; and (6) Completeness of scattering states for rough interfaces. GRA

N93-12095# Northwest Research Associates, Inc., Bellevue, WA.
NEW METHODS FOR NONLINEAR TRACKING AND NONLINEAR CHAOTIC SIGNAL PROCESSING Progress Report No. 1, 1 Jun. - 25 Jul. 1992
Jon A. Wright 5 Aug. 1992 2 p
(Contract N00014-92-C-0043)
(AD-A254320) Avail: CASI HC A01/MF A01

We have tested a program on some examples. The simplest algorithm already works to identify signals when there are roughly equal amounts of two different signals or one signal and an approximately equal amount of noise. That version of the algorithm doesn't work satisfactorily when the ratio of strengths is 10 to 1, i.e., if the noise is ten times the signal. We expect that the refinements that are not yet tested will extend the range. We are also developing the tools to decide when one has successfully identified a signal. We expect soon to test the algorithms on a variety of combinations of unknown signals and unknown relative strengths. We will begin work shortly on the tracking algorithms. GRA

N93-12101# Sandia National Labs., Albuquerque, NM.
LIMITATIONS OF MULTIPLE FEEDS IN A POLARIMETRIC-RADAR COMPACT RANGE
K. W. Sorensen, W. H. Schaedla, and B. C. Brock 1991 18 p Presented at the IEEE-American Physical Society International Symposium, Chicago, IL, 18-25 Jul. 1992
(Contract DE-AC04-76DP-00789)
(DE92-017526; SAND-91-2899C; CONF-920750-6) Avail: CASI HC A03/MF A01

The compact range has become widely used as a means of simulating far-field free-space conditions for RCS measurements. The most obvious way to illuminate such a range is to place a single feed at the focus of the lens or reflector system which collimates the field. However, in order to achieve greater isolation between the radar transmitter and receiver over wide bandwidths, two feeds are often used. Recently, interest has increased in the use of the compact range for performing complete polarimetric measurements, and the idea of similarly achieving greater polarization isolation through the use of multiple feeds is enticing. However, when the system is intended to measure the coherent polarization scattering matrix, the use of multiple feeds can lead to serious errors if the feed system is not carefully considered. It is well known that the use of a separate transmit and receive feed will result in a small bi-static angle for the RCS measurement. Often, this is considered acceptable and of no consequence to the validity of the data. As will be shown, the use of separate transmit and receive feeds can cause phase errors between the elements of the polarization scattering matrix. The situation is made worse by the fact that the magnitude of these errors depends on the location of the scatterer with respect to the range axis. This position dependence makes post-measurement correction of the data difficult if not impractical. DOE

N93-12132# Brookhaven National Lab., Upton, NY.
PROPOSAL FOR THE EXPERIMENTAL DEMONSTRATION OF THE COHERENT RADIATION
A. G. Ruggiero 1992 7 p Presented at the Advanced Accelerator Concepts Workshop, Port Jefferson, NY, 14-20 Jun. 1992
(Contract DE-AC02-76CH-00016)
(DE92-017695; BNL-47599; CONF-9206193-2) Avail: CASI HC A02/MF A01

It is of great importance to provide an experimental demonstration of the coherence of the radiation of electromagnetic waves from a short bunch of electrons performing oscillations in a direction transverse to the main direction of motion. It is known that electrons circulating in a storage ring lose energy to synchrotron radiation. Another method to stimulate radiation is to let an electron bunch travel through a wiggler or an ondulator device. In either case the spectrum usually peaks in correspondence of wavelengths considerably smaller than the length of the electron bunch, in this situation the power radiated is then linearly proportional to the number N of electrons in the bunch, as it is customarily observed. Nevertheless, it may be possible conceiving a situation where the bunch length is considerably smaller or at least comparable to the wavelength of the peak of the radiation spectrum. If this is the case, it is then speculated that the power radiated is proportional to the square N(sup 2) of the number of particles in the bunch. This effect, which we can call a coherent effect, is of course very important since it would help to enhance the amount of the power radiated with a lower electron intensity. Unfortunately, the coherent effect is difficult to observe since it is not easy to create beam and trajectory parameters which yield a bunch of length smaller than the radiation wavelength. We thus propose here an experiment which has two goals: (1) to generate an experimental situation where electrons in a bunch of length (ell) radiate electromagnetic power at a variable wavelength (lambda), and (2) to observe with measurements the total amount of radiation versus lambda and the beam intensity N. This experiment can be executed at the Accelerator Test Facility either at Brookhaven or at Argonne National Laboratory. DOE

N93-12160# Phillips Lab., Kirtland AFB, NM.
BROADBAND EMP TRANSIENT MEASUREMENT PREEMPHASIS FILTER Final Report, Jan. 1989 - Nov. 1991
Jonathan P. Hull Feb. 1992 14 p
(AF Proj. 1209)
(AD-A254414; AD-E201120; PL-TR-91-1083) Avail: CASI HC A03/MF A01

The broadband electromagnetic pulse (EMP) transient measurement preemphasis filter ('Filter') was developed to improve the signal-to-noise ratio in the high-frequency portion of single-pass EMP transient response measurements. Improvements of 12 dB and more have been observed at frequencies above 80 MHz with no loss of dynamic range in frequency components below that point. GRA

N93-12207 Surrey Univ., London (England).
ALL-DIGITAL MULTICARRIER DEMODULATORS FOR ON-BOARD PROCESSING SATELLITES IN MOBILE COMMUNICATION SYSTEMS Ph.D. Thesis
Wan Hung Yim 1991 230 p
Avail: Univ. Microfilms Order No. BRDX94966

Economical operation of future satellite systems for mobile communications can only be fulfilled by using dedicated on-board processing satellites, which would allow both cheap earth terminals and lower space segment costs. With on-board modems and codecs, the up-link and down-link can be optimized separately. An attractive scheme is to use frequency-division multiple access/single chanel per carrier (FDMA/SCPC) on the up-link and time division multiplexing (TDM) on the down-link. This scheme allows mobile terminals to transmit a narrow band, low power signal, resulting in smaller dishes and high power amplifiers (HPA's) with lower output power. On the up-link, there are hundreds to thousands of FDM channels to be demodulated on-board. The most promising approach is the use of all-digital multicarrier demodulators (MCD's), where analog and digital hardware are efficiently shared among channels, and digital signal processing (DSP) is used at an early stage to take advantage of very large scale integration (VLSI) implementation. A MCD consists of a channellizer for separation of frequency division multiplexing (FDM) channels, followed by individual modulators for each channel. Major research areas in MCD's are in multirate DSP, and the optimal estimation for synchronization, which form the basis of the thesis. Complex signal theories are central to the development of structured approaches for the sampling and processing of bandpass signals, which are the foundations in both channellizer and demodulator design. In multirate DSP, polyphase theories replace many ad-hoc, tedious and error-prone design procedures. For example, a polyphase-matrix deep space network frequency and timing system (DFT) channellizer includes all efficient filter bank techniques as special cases. Also, a polyphase-lattice filter is derived, not only for sampling rate conversion, but also capable of sampling phase variation, which is required for symbol timing adjustment in all-digital demodulators. In modulation schemes, a systematic survey is reported, based on two expressions that includes all formats in linear and constant envelope modulation. In synchronization techniques, classifications according to the criterion of statistical optimization, the data dependecy, and the method of parameter extraction, reflect the inherent complexity and performance of numerous existing algorithms. The designs of two new algorithms are presented: a differential decision frequency error detector that is simple and fast; a dual-comb-filter frequency/timing error detector that is targeted at VLSI implementation. The real-time implementation of a complete 4 x 16 kb/s MCD for the T-SAT project is described in detail, which proved many of the structured design concepts developed in this thesis. The requirements of software tools for various levels of simulation in multirate DSP and communications are analyzed. This led to the implementation of a data-flow oriented simulation system, which was used in all research work in the thesis.
Dissert. Abstr.

N93-12230# Massachusetts Univ., Amherst. Dept. of Electrical and Computer Engineering.
OPTICAL GENERATION, CONTROL AND SENSING OF MILLIMETER WAVES Final Technical Report, 1 Jan. 1988 - 31 Aug. 1991
Alfred P. DeFonzo Jul. 1992 9 p
(Grant AF-AFOSR-0106-88)
(AD-A254700; AFOSR-92-0781TR) Avail: CASI HC A02/MF A01

An optically excited, frequency invariant, coplanar stripline antenna that we developed is presented. A comprehensive full wave analysis of optically excited coplanar striplines developed by us is also briefly reviewed. The work confirms the earlier hypothesis regarding the existence of new mechanisms. The reported findings imply the existence of a deeper and more fundamental physics underlying the optical generation, sensing, and control of electromagnetic radiation. An extensive bibliography is provided. As of August 1991, the following characteristics have been achieved: Center frequency - N/A* Bandwidth greater than 1 THz (3 dB received power); Beam quality greater than 99 percent TEBoo Gaussian; SNR greater than 105; Energy output 25 femtojoules per pulse; and Energy efficiency 0.003 percent (optical to electromagnetic). GRA

N93-12240# Range Commanders Council, White Sands Missile Range, NM.
GUIDE TO SYNCHRONIZATION OF VIDEO SYSTEMS TO IRIG TIMING
Jul. 1992 76 p
(AD-A254626; RCC-456-92) Avail: CASI HC A05/MF A01

This document addresses a broad field of video synchronization to IRIG timing with emphasis on color synchronization. This document deals with fundamental synchronization principles, numerical relationships, and the basis of implementation techniques. Chapters are devoted to synchronization principles, RS-170 monochrome, NTSC color methods, high-speed monochrome, and high-speed color synchronization. GRA

N93-12331# Federal Aviation Administration, Atlantic City, NJ.
LOW DENSITY RADIO COMMUNICATIONS LINK (LDRCL) OPERATIONAL TEST AND EVALUATION (OT/E) INTEGRATION AND OPERATION TEST PLAN
Wayne E. Bell, Michael R. Melillo, Tuan A. Tran, and John Warren Oct. 1992 88 p
(DOT/FAA/CT-TN92/4) Avail: CASI HC A05/MF A01

This plan addresses the Operational Test and Evaluation (OT&E) Integration testing of the Low Density Radio Communications Link (LDRCL) equipment in the current National Airspace System (NAS) environment. The approach and concept were to conduct integration tests with appropriate NAS systems to verify that NAS requirements and LDRCL specifications requirements were satisfied. This will be accomplished by conducting factor acceptance and site acceptance tests at the contractor's facility in Richardson, Texas, and extensive integration tests at the following key sites: San Antonio, Texas; Scurry, Texas; and Mina, Nevada. Author

N93-12332# Naval Surface Weapons Center, Dahlgren, VA.
NONLINEAR RESISTIVE GRID WAVELET TRANSFORMATIONS FOR TEXTURE FEATURE EXTRACTION
George W. Rogers, Carey E. Priebe, and Jeffrey L. Solka Jun. 1992 32 p
(AD-A254705; NSWCDD-TR-92/237) Avail: CASI HC A03/MF A01

This report describes an analog method to extract gray-scale texture features. This method uses a nonlinear resistive grid to perform a two-dimensional pseudowavelet transform of the initial input image. Texture features are computed using first- and second-order variance estimates of the transform coefficients. Some preliminary results are presented indicating the natural segmentation that the nonlinearity provides at the boundary of two dissimilar textures. GRA

N93-12356# Naval Research Lab., Washington, DC.
EXTENSION OF FRESNEL NEAR-FIELD REGION BY SINGLE-CYCLE SINUSOIDAL PULSES Interim Report
S. N. Samaddar 21 Aug. 1992 56 p
(AD-A254736; NRL/MR/5313-92-7111) Avail: CASI HC A04/MF A01

A circular conducting disk antenna is excited by three uniform current waveforms namely, a very high frequency CW sin omega(sub 0)t, a single-cycle sin omega(sub 0)t, and a single-cycle cos omega(sub 0)t. The energy per cycle associated with each of these waveforms is taken to be the uM. From the behavior of the radiated energy densities along the axis of the disk, it is found that if the CW waveform extends the near field to unit distance, then the corresponding distances are 1.375 and 3.75 for the single-cycle sin omega(sub 0)t and the single-cycle cos omega(sub 0)t respectively. These results show that the method of energy transfer to a large distance along the axis of an aperture (or disk) becomes more efficient when a short pulse, instead of a CW source, is applied. This will have applications wherever a transmission of high intensity beam of energy far away from a radiating device is needed. GRA

N93-12366*# National Aeronautics and Space Administration. Lewis Research Center, Cleveland, OH.

DAMPING AND SCATTERING OF ELECTROMAGNETIC WAVES BY SMALL FERRITE SPHERES SUSPENDED IN AN INSULATOR

Gerald W. Englert Aug. 1992 12 p
(RTOP 505-62-52)
(NASA-TM-105837; E-6363-1; NAS 1.15:105837) Avail: CASI HC A03/MF A01

The intentional degradation of electromagnetic waves by their penetration into a media comprised of somewhat sparsely distributed energy absorbing ferrite spheres suspended in an electrical insulator is investigated. Results are presented in terms of generalized parameters involving wave length and sphere size, sphere resistivity, permeability, and spacing; their influence on dissipation of wave power by eddy currents, magnetic hysteresis, and scattering is shown. Author

N93-12377# Naval Postgraduate School, Monterey, CA.

COMPUTER MODELING OF TACTICAL HIGH FREQUENCY ANTENNAS M.S. Thesis

Bobby G. Gregory, Jr. Jun. 1992 111 p
(AD-A255176) Avail: CASI HC A06/MF A02

The purpose of this thesis was to compare the performance of three tactical high frequency antennas to be used as possible replacement for the Tactical Data Communications Central (TDCC) antennas. The antennas were modeled using the Numerical Electromagnetics Code, Version 3 (NEC3), and the Eyring Low Profile and Buried Antenna Modeling Program (PAT7) for several different frequencies and ground conditions. The performance was evaluated by comparing gain at the desired takeoff angles, the voltage standing wave ratio of each antenna, and its omni-directional capability. The buried antenna models, the ELPA-302 and horizontal dipole, were most effective when employed over poor ground conditions. The best performance under all conditions tested was demonstrated by the HT-20T. Each of these antennas have tactical advantages and disadvantages and can optimize communications under certain conditions. The selection of the best antenna is situation dependent. An experimental test of these models is recommended to verify the modeling results. GRA

N93-12407# Naval Postgraduate School, Monterey, CA.

METHOD OF MOMENTS ANALYSIS OF SYMMETRIC DUAL REFLECTOR ANTENNAS WITH FEEDS M.S. Thesis

Manuel V. Ordonez Jun. 1992 83 p
(AD-A255171) Avail: CASI HC A05/MF A01

Small symmetric dual reflector antennas have low efficiencies because of conflicting requirements for the subreflector and feed. Low efficiency is more pronounced for antenna configurations with main reflector diameters less than 50 times its operating wavelength. The subreflector and feed geometry must be small to reduce blockage but yet large enough to be an efficient scatterer. It may be possible to compensate for this by tuning the feed and subreflector. That is, by proper choice of the antenna geometry and dimensions and by using low-blockage feeds, the efficiency may be enhanced. Existing computer codes have been modified in this thesis to reflect these changes in antenna feeds in order to optimize the antenna efficiency. A feed system consisting of a feed dipole in the presence of parasitic elements has resulted in an efficiency by 55 percent. Other untested feed configurations may produce even higher efficiencies. GRA

N93-12417# EG and G Energy Measurements, Inc., Las Vegas, NV.

CURVE FITTING AND ERROR MODELING FOR THE DIGITIZATION PROCESS NEAR THE NYQUIST RATE

C. W. Baumgart, M. E. Dunham, and J. D. Moses (Los Alamos National Lab., NM.) Mar. 1992 35 p
(Contract DE-AC08-88NV-10617)
(DE92-018189; EGG-10617-5101) Avail: CASI HC A03/MF A01

The Nyquist and Shannon theorems originated the concept of sampling a band-limited signal at a minimum rate. By sampling at this minimum rate, enough information is gathered to allow an accurate reconstruction of the original analog signal. These theorems were derived for time-quantized signals and did not include simultaneous amplitude quantization. In addition, the underlying assumptions on which these theorems were based are violated in typical use. Therefore, actual practice in data acquisition has been to oversample signal bandwidth by two to three times to conserve accuracy. We report a new numerical investigation of digitization process accuracy, with respect to sample rate, sample amplitude resolution, and record length. This investigation is based on the use of a computer algorithm that reconstructs original analog test signals from their ideally digitized representations. A Monte Carlo technique is used to simulate simultaneous time and amplitude quantization of the test signals, followed by an optimal least-squares curvefit routine which reconstructs the input signal from the digitized data.In this way, we examine the error sensitivity to the digitization process in each reconstructed signal parameter. We find that although no specific Nyquist limit exists for a known wave shape, the parameter errors vary continuously with respect to the aforementioned variables, and critical sample densities of two to four sample periods per risetime are seen. Plots of curve-fitted parameter error versus fundamental digitization variables are useful in specifying experimental tasks and indicate further directions for reconstruction algorithm development. DOE

N93-12422# Michigan State Univ., East Lansing. Dept. of Materials Science and Mechanics.

STOCHASTIC MODELS OF WAVEFRONT PROPAGATION IN RANDOM GRANULAR MEDIA Final Report

Martin Ostoja-Starzewski Aug. 1992 39 p
(Contract DACA39-90-M-2528)
(AD-A255127; WES/CR/SL-92-5) Avail: CASI HC A03/MF A01

Determination of the effects of material microscale randomness on wavefront propagation is the focus of this report. The study is set in the context of one-dimensional microstructures with material randomness, of high signal-to-noise ratio, being present in constitutive moduli and grain lengths. Two different, but related, categories of problems - transient waves in granular microstructures and acceleration wavefronts in nonlinear elastic/dissipative continua - are discussed. In the first category, special focus is placed on microstructures with nonlinear elastic grains and an extension to two- and three-dimensional wave propagation. In the second category, particular attention is given to the phenomenon of stochastic competition between dissipation and elastic nonlinearity in formation of a shock from an acceleration wave. Explicit formulas for critical inverse amplitudes are obtained and illustrated graphically for different cases of correlatedness between dissipation and elastic nonlinearity. Additionally, the problem of determination of random time to form a shock is discussed. The common thread of both problem categories studied here is the use of Markov diffusion processes in description of wave evolutions in one as well as two and three dimensions. GRA

N93-12433# Mitre Corp., Bedford, MA.

REAL-TIME ADAPTIVE SIDELOBE CANCELLER ARCHITECTURES AND IMPLEMENTATIONS

Terry L. Rorabaugh, John J. Vaccaro, Kevin H. Grace, Richard A.

Games, and Willard L. Eastman Jul. 1992 22 p
(Contract F19628-89-C-0001)
(AD-A254842; M91-60) Avail: CASI HC A03/MF A01

A programmable, reconfigurable digital signal processing (DSP) array has been designed in response to the need for a real-time adaptive sidelobe canceller to support wide-bandwidth high-frequency (HF) radar concepts. These concepts incorporate multiple (up to 128) main beams and many degrees of freedom by using many auxiliary antenna elements, and employ frequency sub-banding to partition a 1 MHz instantaneous bandwidth. The real-time sidelobe canceller is based on the Gram-Schmidt orthogonalization procedure and uses concurrent block adaptation to derive an optimal solution for the available data. The sidelobe canceller implementation configures the modular DSP array into a two-dimensional Gram-Schmidt processor. A proof-of-concept sidelobe canceller implementation will be able to perform sidelobe cancellation on two simultaneous main beams using eight auxiliary channels. The DSP array sidelobe canceller can be expanded to use over 40 auxiliary channels to support over 128 main beams. The array consists of TMS32OC30-based processing nodes that provide four independent data ports (two inputs and two outputs) connected via high-speed serial data links that support 2-megaword-per-second sustained throughput rates (8-megaword-per-second burst rates). These manually configured data connections are separated from the control structure, allowing a variety of interconnection strategies (one-dimensional, two-dimensional, ring, etc.). A host processor is used to download application code and control the system. This programmable, reconfigurable array processor can also be used for a variety of other applications, including the singular value decomposition matrix-matrix multipliers, and frequency and transforms. GRA

N93-12436# Princeton Univ., NJ. Dept. of Electrical Engineering and Computer Science.
DIGITAL SIGNAL PROCESSING Final Report, 1 Mar. 1989 - 29 Feb. 1992
Ken Steiglitz and Bede Liu May 1992 7 p
(Contract DAAL03-89-K-0074)
(AD-A254870; ARO-26118.1-EL) Avail: CASI HC A02/MF A01

A wide variety of problems in digital signal processing were studied, with emphasis on the scalability of architectures for large array processors, timing and reliability limits in large arrays, delay performance of statistical multiplexers, robust signal processing, and digital image coding and processing. Results in the study of array processors include the development of a particular architecture that scales very well for iterative computations on a regular lattice, and a testing method particularly suited to lattice-gas computations. Related work describes design methods for redundant arrays, and arrays that incorporate error detection and correction. In the study of the delay performance of statistical multiplexers, a method is given for computation of the queue-length probability distribution function in the presence of voice traffic. The work in robust signal processing studies the effect of incomplete information on the performance of matched filters. An approach is presented for the compression of color images with limited palette size that does not require color quantization of the decoded image. For comparable quality and bit rates, the proposed technique significantly reduces the decoder computational complexity. Finally, different approaches are compared for block motion compensation coding of interlaced sequences. It is shown that proper use of that redundancy can significantly improve the coding efficiency. GRA

N93-12461# Electro-Optical Sciences, Inc., Irvington, NY.
LASER DOPPLER EXPERIMENTS Final Report
Thomas Shultz, Douglas Brenner, Marek Elbaum, Michael Greenebaum, and George Lind 19 Jun. 1992 70 p
(Contract N00014-90-C-0215)
(AD-A252883; EOS/FR-0214) Avail: CASI HC A04/MF A01

This document constitutes the Final Report on Contract N00014-90-C-0214/P00001, Relative Merits of Innovative Imaging Sensor Systems, and covers the period 18 January 1991 through 12 April 1992. The purpose of the work was to conduct research and assist efforts in ground-based optical identification and tracking at the Innovative Science and Technology Experimental Facility (ISTEF) in Florida. The technology areas covered included signal processing, the collection of target signature data, and proof-of-concept field demonstrations of sensor systems. A major portion of the work centered on the design of a laser Doppler field experiment which would be suitable for deployment at ISTEF, a site which is uniquely well suited for obtaining signature data relevant to the rocket lift-off episode. In the present report, we discuss the methods used in the underlying analysis and recapitulate the key results and recommendations obtained. GRA

N93-12481*# National Aeronautics and Space Administration. Lewis Research Center, Cleveland, OH.
DATA DISTRIBUTION SATELLITE
Grady H. Stevens Feb. 1992 17 p Presented at the International Space Year Conference on Earth and Space Science Information Systems, Pasadena, CA, 10-13 Feb. 1992; sponsored by California Inst. of Tech. Previously announced in IAA as A92-48224
(RTOP 144-50-50)
(NASA-TM-105778; E-7205; NAS 1.15:105778) Avail: CASI HC A03/MF A01

The Data Distribution Satellite (DDS), operating in conjunction with the planned space network, the National Research and Education Network and its commercial derivatives, would play a key role in networking the emerging supercomputing facilities, national archives, academic, industrial, and government institutions. Centrally located over the United States in geostationary orbit, DDS would carry sophisticated on-board switching and make use of advanced antennas to provide an array of special services. Institutions needing continuous high data rate service would be networked together by use of a microwave switching matrix and electronically steered hopping beams. Simultaneously, DDS would use other beams and on board processing to interconnect other institutions with lesser, low rate, intermittent needs. Dedicated links to White Sands and other facilities would enable direct access to space payloads and sensor data. Intersatellite links to a second generation ATDRS, called Advanced Space Data Acquisition and Communications System (ASDACS), would eliminate one satellite hop and enhance controllability of experimental payloads by reducing path delay. Similarly, direct access would be available to the supercomputing facilities and national data archives. Economies with DDS would be derived from its ability to switch high rate facilities amongst users needed. At the same time, having a CONUS view, DDS would interconnect with any institution regardless of how remote. Whether one needed high rate service or low rate service would be immaterial. With the capability to assign resources on demand, DDS will need only carry a portion of the resources needed if dedicated facilities were used. Efficiently switching resources to users as needed, DDS would become a very feasible spacecraft, even though it would tie together the space network, the terrestrial network, remote sites, 1000's of small users, and those few who need very large data links intermittently. Author

N93-12512# Cornell Univ., Ithaca, NY. School of Electrical Engineering.
COMPOSITE TASKING FOR SENSOR ARRAYS Final Report, 1 Jun. 1990 - 31 May 1992
A. Steinhardt and A. Bojanczyk 7 Aug. 1992 6 p
(Contract DAAL03-90-G-0092)
(AD-A254997; ARO-26945.8-MA-SDI) Avail: CASI HC A02/MF A01

We explored a number of issues regarding efficient updating in adaptive array signal processing. Our focus was on techniques for efficient and paralyzable deletion of data as arises in excising obsolete data in recursive least squares, noise suppression via covariance differencing, etc. Our key result was the development of hyperbolic singular value decomposition, a new canonic matrix factorization. GRA

N93-12519*# LinCom Corp., Los Angeles, CA.
SPACE STATION COMMUNICATIONS AND TRACKING SYSTEMS MODELING AND RF LINK SIMULATION Final Report
Chit-Sang Tsang, Chak M. Chie, and William C. Lindsey Jul. 1986 111 p
(Contract NAS9-17332)
(NASA-CR-185684; NAS 1.26:185684; TR-8513-03) Avail: CASI HC A06/MF A02

In this final report, the effort spent on Space Station Communications and Tracking System Modeling and RF Link Simulation is described in detail. The effort is mainly divided into three parts: frequency division multiple access (FDMA) system simulation modeling and software implementation; a study on design and evaluation of a functional computerized RF link simulation/analysis system for Space Station; and a study on design and evaluation of simulation system architecture. This report documents the results of these studies. In addition, a separate User's Manual on Space Communications Simulation System (SCSS) (Version 1) documents the software developed for the Space Station FDMA communications system simulation. The final report, SCSS user's manual, and the software located in the NASA JSC system analysis division's VAX 750 computer together serve as the deliverables from LinCom for this project effort. Author

N93-11939*# Jet Propulsion Lab., California Inst. of Tech., Pasadena.
OPERATOR ASSISTANT TO SUPPORT DEEP SPACE NETWORK LINK MONITOR AND CONTROL
Lynne P. Cooper, Rajiv Desai, and Elmain Martinez *In* NASA. Lyndon B. Johnson Space Center, Fifth Annual Workshop on Space Operations Applications and Research (SOAR 1991), Volume 1 Jan. 1992 p 122-128 Sponsored by NASA, Washington (For primary document see N93-11921 02-59)
Avail: CASI HC A02/MF A04

33 ELECTRONICS AND ELECTRICAL ENGINEERING

Includes test equipment and maintainability; components, e.g., tunnel diodes and transistors; microminiaturization; and integrated circuitry.

For related information see also *60 Computer Operations and Hardware* and *76 Solid-State Physics.*

N93-11051 Department of the Navy, Washington, DC.
UNEQUAL STUB LENGTH DIPLEXING MICROWAVE FREQUENCY DISCRIMINATOR CIRCUIT Patent
Carl P. Tresselt, inventor (to Navy) 14 Jan. 1992 5 p Filed 18 Jan. 1991
(AD-D015352; US-Patent-5,081,424; US-Patent-Appl-SN-644363; US-Patent-Class-329-322) Avail: US Patent and Trademark Office

A microwave frequency discriminator circuit useful as a frequency linearization device includes a microstrip input conductor and a pair of microstrip output conductors, a pair of resistors, a pair of microstrip transmission line diplexer stubs of unequal lengths, a pair of detector diodes, and a quad of microstrip filter stubs. Each resistor is connected at one end to the same end of the input conductor and in parallel relation to one another. Each diplexer stub is connected at one end to an opposite end of one resistor and in parallel relation to one another. Each diplexer stub is open-circuited at an opposite end. Each detector diode is connected at one end to the one end of one stub and at an opposite end to one output conductor. The filter stubs are interposed in spaced pairs in one output conductor. GRA

N93-11053 Department of the Navy, Washington, DC.
HIGH SPEED PARALLEL BACKPLANE Patent
Albert J. Corda, inventor (to Navy) 2 Jun. 1992 6 p Filed 29 Jan. 1990
(AD-D015372; US-Patent-5,119,273; US-Patent-Appl-SN-471314; US-Patent-Class-361-413) Avail: US Patent and Trademark Office

A cylindrical high speed parallel backplane for electrically interconnecting a plurality of printed circuit boards in a data processing system is presented. A plurality of cylindrical plate conductor structures are arranged parallel to one another. A plurality of circuit board connectors are disposed radially about the perimeter of the plate conductor structures to electrically connect the printed circuit board to the plate conductors structures. This cylindrical design of the backplane provides a short signal path length between the printed circuit boards connected to the backplane, thereby, providing for broad bandwidth capability. GRA

N93-11239# Space Systems/Loral, Palo Alto, CA.
HIGH TEMPERATURE SUPERCONDUCTIVITY SPACE EXPERIMENT (HTSSE) Final Report, Dec. 1990 - Nov. 1991
J. Fiedziusko and J. Curtis 2 Apr. 1992 27 p
(Contract N00014-91-C-2056)
(AD-A253119) Avail: CASI HC A03/MF A01

Novel filter configurations utilizing dielectric resonators in combination with high temperature superconductors (HTS) were successfully developed and flight qualified for the High Temperature Superconductivity Space Experiment (HTSSE). All program goals were met and the developed filters exhibit the best electrical performance (extremely low insertion loss) reported to this date. Filters and resonator configurations developed on this problem have the potential for extremely high Q factors (in the the order of tens of millions) when very low loss, high dielectric constant materials such as sapphire (or similar compounds) are used. Higher power handling and precise tuning of the filters is also possible. GRA

N93-11257# Columbia Univ., New York, NY. Microelectronics Science Lab.
INTERFACIAL AND THIN FILM CHEMISTRY IN ELECTRON DEVICE FABRICATION Final Report, 15 Sep. 1986 - 31 Dec. 1991
D. Auston, G. Flynn, I. Herman, R. Osgood, and N. Turro Jan. 1992 69 p
(Contract N00014-86-K-0694)
(AD-A253579) Avail: CASI HC A04/MF A01

Progress on the Columbia URI program on 'Interfacial and Thin Film Chemistry in Electron Device Fabrication' is reported for the 1986-1991 period. Three broad areas of research included MBE Growth and Devices, Laser Surface Interactions, and Fundamentals of Processing Gas/Surface Interactions. Research in the area of MBE Growth and Devices included Heterostructures Grown by Molecular Beam Epitaxy by Professor Wen Wang and Interface Chemical Modification of Metal on Superconductor-Semiconductor Systems by Professor Ed Yang. Research in the area of Laser Surface Interactions included Laser-Surface Interactions and In Situ Diagnostics of Surface Chemistry During Electronic Processing by Professor Richard Osgood, Jr.; In Situ Optical Diagnostics of Semiconductors Prepared by Laser Chemical Processing and Other Novel Methods by Professor Irving Herman; and Ultrafast Optoelectronic Measurements of Surfaces and Interfaces by Professor David Auston. Research in Fundamentals of Processing Gas/Surface Interactions included Quantum State-Resolved Studies of Gas/Surface Chemical Reactions by Professor George Flynn and Photochemical and Photophysical Probes of Interfaces by Professor Nicholas Turro. Research results of Columbia's Principal Investigators supported by ONR/URI were published in nearly 200 scholarly articles which are listed in this report. GRA

N93-11364# Rex, Thompson and Partners, Farnham (England).
A COMPARISON OF THE ACHIEVED AND PREDICTED DEFECT RATES OF SOME CONTINUOUSLY OPERATING ELECTRONIC EQUIPMENT
B. H. Goodsell and J. Rex Jun. 1977 16 p

(Contract K/MGW11a/334)
(RTP/909/10-Issue-2; BR86833; ETN-92-92295) Copyright
Avail: CASI HC A03/MF A01

In-service defect rates achieved by items of continuously running electronic equipment wered studied. These were compared with the defect rates predicted for the items using the guided weapon system reliability prediction manual. They were also related to complexity as measured by 'total population of components'. To preserve manufacturers' confidentiality equipment is identified only by a code letter. Twelve of the items in the survey were ground based radar equipment and two were large ground based assemblies of electronic equipment operating at low-medium power. ESA

N93-11393 National Physical Lab., Teddington (England). Div. of Electrical Science.
A MUTUAL INDUCTANCE TECHNIQUE FOR CONTACT-FREE T(SUB c) MEASUREMENT OF HIGH TEMPERATURE SUPERCONDUCTORS
P. G. Quincey, M. Phillipson, and S. Martinez (Toulouse Univ., France) Nov. 1991 21 p
(NPL-DES-116; ETN-92-92365) Copyright Avail: National Physical Lab., Teddington, Middlesex, TW11 0LW, England

A mutual inductance instrument, set up as part of a thin film devices program for measurement at frequencies above 100 GHz section, is described. The mutual inductance technique operates by measuring the induced voltage on a pickup coil which lies on top of a second coil, driven at about 2 kHz, while the thin film acts as a screen between two coaxial voils. Further details on the principle of operation are given. The basic design is outlined. The electrical properties of metals and superconductors at kHz frequencies are outlined, and hence the expected form and size of changes in signal as a sample passes through the superconducting transition are also included. Experimental details and typical results are given. It is concluded that the mutual inductance rig described provides a useful contact free transition temperature (Tc) measurement facility for thin films. Sensitivity is more than adequate for small samples giving a clear value for the onset Tc with an uncertainty of around 0.5 K. The width of the transition is also indicated, though this is most useful as a comparative value between in-house samples rather than an objective figure. The measurement would also provide information about the penetration depth and internal (rather than transport) critical current density of samples. ESA

N93-11414# Lehigh Univ., Bethlehem, PA. Center for Solid State Studies.
RELIABILITY OF SMALL GEOMETRY VLSI DEVICES FOR MICROELECTRONICS Final Report
Marvin H. White 15 Feb. 1992 48 p
(Contract N00014-86-K-0411)
(AD-A247355) Avail: CASI HC A03/MF A01

This proposal is a continuation of a project which began in August 1986. The goal of the project, in a broad sense, is to perform exploratory research into the physics of carriers in silicon inversion layers with a focus on the issues which affect the reliability of small geometry VLSI devices. This project permits us to study the physical electronics of silicon surfaces and the overlying insulators. In the proposed project we stress the application of this research to the area of Wafer Scale Integration where reliability and fault tolerance are key issues for the SDI program. The extensive signal processing and data storage required to implement high-resolution, sensor-based systems demands that consideration be given to the area of system and component reliability. At the component level the issues revolve around the reliability of the scaled MOS Transistor with nanometric feature sizes. One important area is the susceptibility of the gate insulator to (1) hot electron trapping, (2) premature dielectric breakdown, and (3) space radiation environment considerations which can limit the MTTF of the SDIO mission. A second issue at the component level is the SDI need for low-power, high-density, nonvolatile data storage with nondestructive readout (NDRO), radiation tolerance and immunity to single event upsets (SEU's). GRA

N93-11432# Argonne National Lab., IL.
RESULTS OF ADVANCED BATTERY TECHNOLOGY EVALUATIONS FOR ELECTRIC VEHICLE APPLICATIONS
W. H. DeLuca, K. R. Gillie, J. E. Kulaga, J. A. Smaga, A. F. Tummillo, and C. E. Webster 1992 11 p Presented at the 1992 Society of Automotive Engineers (SAE) Future Transportation Technology Conference, Costa Mesa, CA, 10-13 Aug. 1992
(Contract W-31-109-eng-38)
(DE92-018766; ANL/CP-76687; CONF-9208113-1) Avail: CASI HC A03/MF A01

Advanced battery technology evaluations are performed under simulated electric-vehicle operating conditions at the Analysis and Diagnostic Laboratory (ADL) of Argonne National Laboratory. The ADL results provide insight into those factors that limit battery performance and life. The ADL facilities include a test laboratory to conduct battery experimental evaluations under simulated application conditions and a post-test analysis laboratory to determine, in a protected atmosphere if needed, component compositional changes and failure mechanisms. This paper summarizes the performance characterizations and life evaluations conducted during 1991-1992 on both single cells and multi-cell modules that encompass eight battery technologies (Na/S, Li/MS (M=metal), Ni/MH, Ni/Cd, Ni/Zn, Ni/Fe, Zn/Br, and Pb-acid). These evaluations were performed for the Department of Energy, Office of Transportation Technologies, Electric and Hybrid Propulsion Division, and the Electric Power Research Institute. The ADL provides a common basis for battery performance characterization and life evaluations with unbiased application of tests and analyses. The results help identify the most-promising R&D approaches for overcoming battery limitations, and provide battery users, developers, and program managers with a measure of the progress being made in battery R&D programs, a comparison of battery technologies, and basic data for modeling. DOE

N93-11434# Royal Aerospace Establishment, Farnborough (England). Radio and Navigation Dept.
A THEORETICAL STUDY OF THE PERFORMANCE OF A SMALL PERMANENT MAGNET, THREE-PHASE ALTERNATOR WHEN DRIVING A PURELY RESISTIVE LOAD VIA A FULL-WAVE RECTIFICATION CIRCUIT
J. W. R. Cox 18 Jan. 1984 121 p
(RAE-TR-84009; RAE-Rad-Nav-130; BR92327; ETN-92-92298) Copyright Avail: CASI HC A06/MF A02

The output characteristics of a small, three phase permanent magnet alternator connected to a three phase full wave rectifier having a pure resistive load are explained. The machine equations, though simplified to preserve mathematical tractability, are derived from first principles, whilst those of the bridge are exact, save for the assumption of constant voltage drop across the diodes when conducting. Agreement between the measured and calculated output characteristic is good in view of the assumptions made. In the short circuit region of the output characteristic, theory and experiment diverge due to the fact that short circuit current depends principally on the output inductance of the machine. A description of a simple method used for measuring the permanence of a small sample of rare Earth cobalt permanent magnet material is also presented. ESA

N93-11438# California Inst. of Tech., Pasadena. Div. of Chemistry and Chemical Engineering.
ELECTRON TRANSFER RATES AT SEMICONDUCTOR/LIQUID INTERFACES
N. S. Lewis 1992 12 p
(Contract DE-FG03-88ER-13932)
(DE92-018559; DOE/ER-13932/T2) Avail: CASI HC A03/MF A01

Work has focused on several aspects of the fundamental chemistry and physics semiconductor/liquid junction behavior. These projects have been directed primarily towards GaAs/liquid contacts, because GaAs/liquid systems provide high energy conversion efficiencies and offer an opportunity to gain mechanistic understanding of the factors that are important to control in an efficient photoelectrochemical energy conversion system. DOE

N93-11456*# National Aeronautics and Space Administration. Pasadena Office, CA.
OVERCHARGE AND OVERDISCHARGE PROTECTION OF AMBIENT TEMPERATURE SECONDARY LITHIUM CELLS Patent Application
Chen-Kuo Huang, inventor (to NASA) (Jet Propulsion Lab., California Inst. of Tech., Pasadena.), Subbarao Surampudi, inventor (to NASA) (Jet Propulsion Lab., California Inst. of Tech., Pasadena.), Alan I. Attia, inventor (to NASA) (Jet Propulsion Lab., California Inst. of Tech., Pasadena.), and Gerald Halpert, inventor (to NASA) (Jet Propulsion Lab., California Inst. of Tech., Pasadena.) 2 Sep. 1992 14 p
(Contract NAS7-918)
(NASA-Case-NPO-18343-1-CU; NAS 1.71:NPO-18343-1-CU; US-Patent-Appl-SN-942491) Avail: CASI HC A03/MF A01

A cathode additive is provided for protecting an ambient temperature secondary lithium cell from overcharging or overdischarging. The cathode additive is chosen to create an upper voltage plateau which is slightly higher than a characteristic charge cutoff voltage of the cathode of the cell. The cathode additive additionally creates a lower voltage plateau which is slightly lower than the characteristic discharge cutoff voltage of the cell. Preferably, the cathode additive is a transition metal oxide or a sulfide and may, for example, include a mixture of Li2Mn2O4 and Li(0.1)MoO2. NASA

N93-11491# Raytheon Co., Lexington, MA.
RF VACUUM MICROELECTRONICS Quarterly Progress Report, 25 May - 28 Jun. 1992
24 Jul. 1992 10 p
(Contract MDA972-91-C-0032; ARPA Order 81-62)
(AD-A253910) Avail: CASI HC A02/MF A01

VHF micro-triode (cylindrical) wafers were started. Design for planar triode was completed, and masks were received. Planar triode wafers were started. VHF test parts for planar diode were designed and ordered. New evaporator parts were received and final assembly started. Moly tips were improved with 'double evaporation'. A 25 microA/tip emission from 100 tip array was achieved. Control and yield on silicon tips was improved. Work function was lowered by 'metalization of tips'. Mask was designed to be compatible with Raytheon test stand. GRA

N93-11492# Lockheed Missiles and Space Co., Palo Alto, CA. Research Lab.
AN ACCURATE AND EFFICIENT METHOD TO CALCULATE THE RATE OF SINGLE EVENT UPSETS FROM THE LET SPECTRUM AND SEU CROSS SECTION TEST RESULTS Report No. 1
D. L. Chenette, T. L. Schumaker, and A. E. Williamson 20 Mar. 1992 42 p
(Contract F19628-90-C-0101)
(AD-A253917; PL-TR-92-2084; AD-E201115) Avail: CASI HC A03/MF A01

A specific implementation is presented for calculating the rate of single event upsets in microelectronic devices. The implementation is based on the method of Pickel and Blandford (1980), who combined device test results, the flux distribution of particles in the space environment, and a model for the geometry of the device. The device test data are summarized as an upset cross section expressed as a function of the linear energy transfer (LET). The flux distribution of particles in the environment is described by an integral LET spectrum. The device geometry model is that of a solid rectangular prism. A numerical integration of the LET spectrum and path length distribution in the solid over the upset cross section is performed to obtain the resultant upset rate. GRA

N93-11504# Varian Associates, Palo Alto, CA.
10 kW L-BAND AMPLIFIER TUBES FOR EFFICIENT AND RELIABLE TROPOSCATTER COMMUNICATION TRANSMITTER SYSTEMS Final Report, Apr. 1983 - Mar. 1987
Edward L. Eisen, Mike Chase, Merrald Schrader, and Don Priest Dec. 1991 110 p
(Contract F30602-83-C-0149)
(AD-A253246; RL-TR-92-5) Avail: CASI HC A06/MF A02

The purpose of this program was to develop two advanced development model high power amplifier tubes specifically for troposcatter communication application. Varian Associates was awarded a single contract to develop a klystron model tube and a klystrode model tube. Critical elements of the specification for the two tubes were (1) power output 10xw, (2) 10 MHz electronics bandwidth, (3) 750-980 MHz tuning range, and (4) efficiency 50 percent. The challenge for the klystron design was to be able to maintain efficiency in excess of 50 percent over the full 10 MHz bandwidth. This was accomplished with an eight cavity design. The klystrode challenge required designing a new grid shape that integrates a converging electron beam with a cavity with a minimal magnetic field focusing. Results of the program were that basically most of the performance specifications were demonstrated. However, the klystron showed a sharp drop-off in power at 840 MHz due to a second harmonic cavity mode. The klystrode has considerably less gain than the existing klystron and thus additional RF drive is required. GRA

N93-11507# University of Southern California, Los Angeles.
CONTACTLESS OPTOELECTRONIC INTEGRATED CIRCUITS FOR REMOTE FIBER OPTIC COMMUNICATION AND SENSING APPLICATIONS Final Report, 1 Jun. 1989 - 31 Dec. 1991
Stephen R. Forrest 5 May 1992 58 p
(Contract DAAL03-89-K-0021)
(AD-A253573; ARO-26147.3-EL) Avail: CASI HC A04/MF A01

In this program, we introduced several new concepts which are directed at considerably reducing the complexity of existing optoelectronic integrated circuits (OEICs) and their associated systems by providing 100 percent of the power requirements of the circuits located at the remote node from the near-end terminal using optical means. In particular, remote powering via the use of monolithically integrated photovoltaic (PV) cells associated with each circuit was demonstrated in the In(0.53)Ga(0.47)As/InP materials system. A novel optical logic circuit which could be optically configured to operate variously as an amplifier, bistable switch, latching switch, S-R flip flop or an inverter was used as the focus of this demonstration. Furthermore, very high sensitivity, novel heterojunction phototransistors were demonstrated for use in high sensitivity, low power applications which typify optically powered circuits. It is expected that providing local, contactless power using PV cells monolithically integrated onto the functional OEIC chip can be used to advantage in highly complex, high density optical interconnect and optical computing systems. The study of these latter applications was a central feature of a broader program which we are now pursuing at Princeton University. GRA

N93-11514# Tennessee Valley Authority, Chattanooga.
ENERGY EFFICIENT MOTORS REFERENCE GUIDE
N. D. Sadanandan and A. H. Eltom Mar. 1992 97 p
(DE92-019073; TVA-92019073) Avail: CASI HC A05/MF A02

The motor reference guide is the result of data and information collected and organized by the Industrial and Large Commercial staff of the Tennessee Valley Authority. The information was collected over several months from motor manufacturers, technical papers, textbooks, and files of former TVA engineers. Additionally, computer simulations were performed to develop data not currently available in literature. The guide is not intended to be a textbook on motors, but a quick and ready reference for the TVA field staff to assist in the technical and economic evaluation of energy-efficient motors versus standard motors. However, chapters on motor related topics such as rotating fields, power factor correction, and impact of power quality on motor performances have also been included to complement the text. DOE

N93-11553# Sandia National Labs., Albuquerque, NM.
EVALUATION OF FLOTATION FOR PURIFICATION OF PYRITE FOR USE IN THERMAL BATTERIES

R. A. Guidotti and F. W. Reinhardt Jul. 1992 35 p
(Contract DE-AC04-76DP-00789)
(DE92-019330; SAND-92-0874) Avail: CASI HC A03/MF A01

The purification of pyrite (FeS2) used in Li-alloy/FeS2 thermal batteries by the physical process of flotation was evaluated for reduction of the quartz impurity. The process was compared to the standard process of leaching with concentrated hydrofluoric acid. Flotation was an attractive alternative because it avoided many of the safety and environmental concerns posed by the use of concentrated HF. The effects of particle size and initial purity of the pyrite feed material upon the final purity and yield of the product concentrate were examined for batch sizes from 3.5 to 921 kg. Feed materials as coarse as 8 mm and as fine as -325 mesh were treated; the coarse pyrite was ground wet in a rod mill or dry in a vibratory mill to -230 mesh prior to flotation. Both the HF-leached and the flotation-treated pyrite were leached with HCl (1:1 v/v) to remove acid-soluble impurities. The flotation-purified pyrite concentrates were formulated into catholytes; their electrochemical performance was evaluated in both single cells and 5-cell batteries for comparison to data generated under the same discharge conditions for catholytes formulated with HF/HCl purified pyrite. DOE

N93-11574# Ecole Centrale de Lyon (France).
PREPARATION OF SILICON OXYNITRIDE THIN FILMS BY PLASMA CHEMICAL VAPOR DEPOSITION FOR CHEMICAL IMPLANTATION. APPLICATION TO A pH ISFET Ph.D. Thesis [PREPARATION DE COUCHES MINCES D'OXYNITRURE DE SILICIUM PAR PECVD EN VUE DE GREFFAGE CHIMIQUE. APPLICATION A UN ISFET PH]
Jean-Marc Chovelon 1991 118 p In FRENCH
(ECL-91-12; ETN-92-92335) Avail: CASI HC A06/MF A02

Some of the characteristics of Ion Sensitive Field Effect Transistors (ISFET) are investigated. The purpose of the study is to investigate problems concerning the choice of a dielectric film that reacts to pH changes and can be used either as a reference field effect transistor or an ion sensitive sensor. Common electrodes and ISFET's are compared. The silicon, oxynitride films, obtained by the plasma chemical vapor deposition, were analyzed by infrared spectroscopy. Electric measures and chemical implantations were performed. The results show that the composition of silicon oxynitrides at the surface can be controlled for pH ISFET uses. A fabrication process of ISFET's, presenting a particular geometry, is proposed. By applying the ISFET's, pH and either ion chemical sensors can be obtained, either by chemical implantation on a thermal silicon substrate, or by introducing ion sensitive molecules in a lattice of alkyl chains already implanted in silicon oxynitride. ESA

N93-11604*# EIC, Inc., Norwood, MA.
LONG CYCLE LIFE RECHARGEABLE LITHIUM BATTERIES Final Report, 23 Apr. 1990 - 20 Oct. 1992
D. M. Pasquariello, E. B. Willstaedt, and K. M. Abraham 19 Oct. 1992 69 p
(Contract NAS7-1100)
(NASA-CR-190937; NAS 1.26:190937; Rept-89063) Avail: CASI HC A04/MF A01

Cycle life and safety of delta-LiAl/TiS2 cells were evaluated using laboratory and AA-size cells. Analysis of the alloys (which contained 60, 70, 80, or 85 wt-pct. lithium and are designated 60 LiAl etc.) showed them to contain a mixture of elemental Li and Al4Li9. Cycling efficiencies correlated with the amount of free lithium in the anode. Using an electrolyte with the composition 48 v/o THF:48 v/o 2-MeTHF:4 v/o 2-MeF/LiAsF6(1.5M), a 70 LiAl/TiS2 laboratory cell yielded a cycling efficiency of 96.4 pct. when cycled at a 100 pct. discharge depth which compares well with Li anode cycling efficiencies of 96 to 97.5 pct. obtained previously in this electrolyte. The highest cycling efficiency of any delta-LiAl/TiS2 laboratory cell was 96.7 pct. when the 60 LiAl alloy was used with the 35 v/o PC:35 v/o EC:30 v/o triglyme/LiAsF6(1.0M) electrolyte. The 70 LiAl alloy was selected for further testing in AA cells since it was malleable for the fabrication of spirally wound electrodes, and its overall cycling performance was sufficiently good. AA-size 70 LiAl/TiS2 cells appear to have capacity/rate properties similar to those for identical Li/TiS2 cells. The use of the delta-LiAl alloy anodes does not appear to offer any safety advantage when cycled cells are shorted or heated. Author

N93-11639# Sandia National Labs., Albuquerque, NM.
AN ANALOG MACROMODEL OF THE SG1525A PWM FOR USE WITH SPICE2G.6 SIMULATORS
C. W. Raney 1992 15 p Presented at the 35th Midwest Symposium on Circuits and Systems, Washington, DC, 12 Aug. 1992
(Contract DE-AC04-76DP-00789)
(DE92-019423; SAND-92-0660C; CONF-9208119-2) Avail: CASI HC A03/MF A01

An analog macromodel for the SG1525A PWM (pulse width modulator) that is compatible with SPICE2G.6 and PSPICE analog simulators has been developed. It exhibits no convergence problems; simulates realistic line and load responses, frequency response, and output voltage levels; and has time domain capability. Model development and a comparison of macromodel performance with actual measurements are discussed. DOE

N93-11643# Allied-Signal Aerospace Co., Kansas City, MO.
ANALYSIS OF PLASMA-TREATED WIRE INSULATION
M. Hester Jul. 1992 19 p
(Contract DE-AC04-76DP-00613)
(DE92-019471; KCP-613-4810) Avail: CASI HC A03/MF A01

A method was developed, and fixtures were built to test the bond strength of wire insulation. Bond strength comparisons were made between dissimilar insulation types to determine how they would respond to potting materials or adhesives after plasma treatment. Five different types of insulation were tested for bondability. These wire insulation types were being considered for substitution to improve manufacturability. The results show that all the insulation types responded to the plasma treatment but that polyolefin had higher bonding strength. DOE

N93-11693# Sandia National Labs., Albuquerque, NM.
CHARACTERISTICS OF CURRENT FILAMENTATION IN HIGH GAIN PHOTOCONDUCTIVE SEMICONDUCTOR SWITCHING
F. J. Zutavern, G. M. Loubriel, M. W. OMalley, W. D. Helgeson, D. L. McLaughlin, and G. J. Denison 1992 26 p Presented at the 20th International Power Modulator Symposium, Myrtle Beach, SC, 23-25 Jun. 1992
(Contract DE-AC04-76DP-00789)
(DE92-018277; SAND-92-0254C; CONF-920671-7) Avail: CASI HC A03/MF A01

Characteristics of current filamentation are reported for high gain photoconductive semiconductor switches (PCSS). Infrared photoluminescence is used to monitor carrier recombination radiation during fast initiation of high gain switching in large (1.5 cm gap) lateral GaAs PCSS. Spatial modulation of the optical trigger, a 200 to 300 ps pulse width laser, is examined. Effects on the location and number of current filaments, rise time, and delay to high gain switching, minimum trigger energy, and degradation of switch contacts are presented. Implications of these measurements for the theoretical understanding and practical development of these switches are discussed. Efforts to increase current density and reduce switch size and optical trigger energy requirements are described. Results from contact development and device lifetime testing are presented and the impact of these results on practical device applications is discussed. DOE

N93-11758# Illinois Univ., Urbana. Dept. of Electrical and Computer Engineering.
VUV AND UV SOURCES AND SPECTROSCOPIC APPLICATIONS Final Technical Report, 1 Nov. 1989 - 31 Oct. 1991
J. G. Eden Dec. 1991 145 p
(Grant AF-AFOSR-0038-89)
(AD-A247293; AFOSR-92-0114TR) Avail: CASI HC A07/MF A02

Extensive experimental studies of small molecules as potential 'hosts' for short wavelength (lambda less than 200 nm) energy-storage lasers have been conducted. Laser spectroscopy of the rare gas dimers and Group IIB dimers have yielded structural constants for a significant number of previously unobserved states. Also, Fano 'windows' have been observed in Ne2 in the energy region lying between v(+) = 0 and v(+) = 3 of the Ne2(+) ground state X(sup 2)sigma. Bound free emission studies of Cd2 and Zn2 have been carried out and the structural constants for the sigma-1 upper states have been determined. The growth of GaAs and GaN by photo-assisted MOCVD has also been demonstrated. Gallium arsenide has been grown epitaxially at temperatures as low as 450 C by illuminating the surface with ArF (193 nm) radiation. Also, polycrystalline GaN (preferentially oriented (100)) has been grown on GaAs and sapphire at temperatures as low as 700 C and at growth rates exceeding 2 micrometers/hour. GRA

N93-11781# Illinois Univ., Urbana. Coordinated Science Lab.
VLSI DESIGN FOR RELIABILITY Final Report, Jan. 1989 - Jan. 1990
Ibrahim N. Hajj, Vasant B. Rao, Ping Yang, Richard Burch, and Hungse Cha Dec. 1991 60 p
(Contract F30602-88-D-0028)
(AD-A253207; RL-TR-91-429) Avail: CASI HC A04/MF A01

This report describes the work accomplished during the period Jan. 1989 to Jan. 1990 on reliability analysis of VLSI CMOS circuits for electromigration prevention. The work involved three subtasks: (1) development of probabilistic simulation techniques to replace expensive exhaustive circuit simulation, (2) extraction and modeling of transistor circuit description and parasitics from layout, and (3) extraction of metal bus and line models from layout, and calculation of the current densities. In probabilistic simulation, new techniques for computing expected and variance current and voltage waveforms in CMOS circuits are developed and implemented in the program CREST. A proof that electromigration median-time-to-failure predictions are mathematically related to expected and variance current density waveforms in the busses is also given. For very large designs, transistor level probabilistic simulation, although significantly faster than exhaustive deterministic circuit simulation, is still not cost-effective. Thus the development of probabilistic macromodeling simulation technique is initiated. Initial results show that such an approach is feasible. This will make it possible to include other technologies, such as BiCMOS. GRA

N93-11833 California Univ., Berkeley.
THEORETICAL STUDIES OF HIGH-TEMPERATURE SUPERCONDUCTORS AND HIGHLY COMPRESSED HYDROGEN Ph.D. Thesis
Troy Walter Barbee, III 1990 132 p
Avail: Univ. Microfilms Order No. DA9126475

Studies of the structural, electronic, and superconducting properties of hydrogen under high pressure and of constraints on mechanisms for high temperature superconductivity from experimental data are presented. The objective of the hydrogen studies was to understand the complex behavior of the simplest element in the periodic table under pressure. The studies of high temperature oxide superconductors seek to constrain or exclude classes of proposed mechanisms based on experimental data and standard theoretical models. The structural and electronic properties of hydrogen under pressure are studied via a first-principles total-energy method. An oriented molecular hexagonal close-packed (m-hcp) structure is found to be the most stable molecular phase, and metallization is predicted to occur via band overlap in this structure at a pressure near 200 GPa. At pressures near 400 GPa, the molecules dissociate and hydrogen undergoes a transition to a simple hexagonal atomic structure. At even higher pressures, a transition into the body-centered cubic structure is predicted to occur. The superconducting properties of atomic metallic hydrogen are calculated within a first-principles approach for three candidate structures: the simple hexagonal structures: the simple hexagonal (sh), distorted simple hexagonal (dsh), and rhombohedral (9R) structures. In all three cases, high temperature superconductivity with a transition temperature between 100 and 200 K is predicted to occur. The applicability of the standard phonon-based mechanism to high temperature superconductivity in the oxides is analyzed in light of isotope effect experiments. We find that for the highest T(sub c) oxides, phonons cannot account for the high T(sub c) and small isotope effect observed. Some proposed modifications of the usual phono-based model are discussed. Estimates of the phonon coupling strength in the oxides are used together with the isotope effect results and other experimental data to constrain combined phonon-nonphonon mechanisms. We conclude that within our three dimensional isotropic Fermi liquid model, such a combined mechanism cannot explain superconductivity in Y-Ba-Cu-O and comment on other calculations using a combined phonon-nonphonon. Author

N93-11916# Allied-Signal Aerospace Co., Kansas City, MO.
HIGH-FREQUENCY LSI CONTACTOR
T. F. Boehm and R. D. Reinholdt Jul. 1992 78 p
(Contract DE-AC04-76DP-00613)
(DE92-017285; KCP-613-4800) Avail: CASI HC A05/MF A01

Tests were conducted and results reported on design parameters for physical and electrical characteristics of test fixtures for testing digital integrated circuits at frequencies up to 200 MHz. Fixture design characteristics included investigation of 50-ohm signal paths, input and output connections, resistor termination and loads, printed circuit board layout, and device interface. The test fixtures designed provide good performance at the 200-MHz design goal with minimal distortion and noise and no signal attenuation. DOE

N93-12057# EG and G Energy Measurements, Inc., Idaho Falls.
LABORATORY TESTING OF THE ELECTROSOURCE TRACTION BATTERY
J. E. Hardin Mar. 1992 19 p
(Contract DE-AC07-76ID-01570)
(DE92-017993; EGG-EP-9701) Avail: CASI HC A03/MF A01

This report is to describe the testing performed on the electrosource lead acid modules. They use composite lead wire, paste processing which bypasses the hydroset process, and a side-by-side bipolar plate design. These concepts improved the energy density and cost as compared to the present product. The Idaho National Engineering Laboratory's interest lies in evaluating these new ideas and comparing the modules made with this technology to other commercially available lead-acid products. DOE

N93-12071# Ecole Centrale de Lyon (France).
PROGRAMME AND ABSTRACTS. WORKSHOP ON EXPERT EVALUATION AND CONTROL OF COMPOUND SEMICONDUCTOR MATERIALS AND TECHNOLOGIES NO. 1: (EXAMTEC 199)
22 May 1992 122 p Workshop held in Ecole Centrale de Lyon, France, 19-22 May 1992
(Contract DAJS45-92-M-0190)
(AD-A254023; R/D-6901-EE-03) Avail: CASI HC A06/MF A02

This workshop included the following topics: Performance and Reliability of Micro-Optoelectronic Devices in Connection with Material Properties and Process Conditions; Material Related Issues and their Characterization in View of III-V Heterojunction Device Optimization; Material Problems for the Development of InGaAs/InAlAs HEMT's Technology; Theoretical and Experimental Study of Failure Mechanisms in RF Reliability Life Tested HEMT's; A Study of Detrimental Transient Effects in GaAs HEMT's; Relating Micron Wave Mapped Data to Physical Parameters for MODFET's; Performance and Reliability of Micro-Optoelectronic Devices in Connection with Material Properties and Process Conditions; Material Related Reliability Aspects of III-V Optical Devices; A Possible Origin of Degradation Mechanisms in AlGaAs/GaAs Laser-Like Structures; Thermal Stability of Pseudomorphic HEMT's; Detailed Process Analysis for Controlling the Yield of GaAs MMIC's Technology; Spatially Resolved Photoluminescence Techniques Applied to the Control of InGaAsP/InP Laser Processing; Growth and Characterization of Epitaxial Structures; Atomic Ordering and Phase Separations in Compound Semiconductors and their Effect on Device Behavior; Improved Device Quality by Strained Layer Epitaxy; II-VI Semiconductor Strained Heterostructures: A Structural Review; and Interface Properties of Strained InGaAs/InP Quantum Wells Grown by LP-MOVPE. GRA

N93-12084# National Inst. of Standards and Technology, Boulder, CO. Electronics and Electrical Engineering Lab.
TRANSMISSION/REFLECTION AND SHORT-CIRCUIT LINE METHODS FOR MEASURING PERMITTIVITY AND PERMEABILITY
James Baker-Jarvis, Michael D. Janezic, John H Grosvenor, Jr., and Richard G. Geyer May 1992 121 p
(PB92-205376; NIST/TN-1355) Avail: CASI HC A06/MF A02; SOD HC

The transmission/reflection and short-circuit line methods for measuring complex permittivity and permeability of materials in waveguides and coaxial lines are examined. Equations for complex permittivity and permeability are developed from first principles. In addition, new formulations for the determination of complex permittivity and permeability independent of reference plane position are derived. For the one-sample transmission/reflection method and two-position short-circuit line measurements, the solutions are stable for frequencies corresponding to integral multiples of one-half wavelength in the sample. For two-sample methods, the solutions are unstable for frequencies where both samples resonate simultaneously. Criteria are given for sample lengths to maintain stability. An optimized solution is also presented for the scattering parameters. The solution is stable over all frequencies and is capable of reducing scattering parameter data on materials with higher dielectric constants. An uncertainty analysis for the various techniques is developed and the results are compared. The errors incurred due to the uncertainty in scattering parameters, length measurement, and reference plane position are used as inputs to the uncertainty models. Author

N93-12089# Los Alamos National Lab., NM.
THE DEVELOPMENT OF A ONE MICROSECOND PULSE LENGTH, REPETITIVELY PULSED, HIGH POWER MODULATOR, AND A LONG-PULSE ELECTRON BEAM DIODE FOR THE PRODUCTION OF INTENSE MICROWAVES
R. M. Stringfield, R. J. Faehl, M. V. Fazio, R. F. Hoeberling, T. J. T. Kwan, D. G. Rickel, F. VanHaaften, R. F. Wasierski, A. Erickson (Mission Research Corp., Los Alamos, NM.), and K. Rust (Superconducting Super Collider Lab., Dallas, TX.) 1992 7 p Presented at the 9th International Conference on High Power Particle Beams, Washington, DC, 25-29 May 1992
(Contract W-7405-eng-36)
(DE92-015974; LA-UR-92-1695; CONF-920515-18) Avail: CASI HC A02/MF A01

This paper discusses the pulse power and explosive emission electron beam diode development effort we have undertaken to power a relativistic klystron amplifier (RKA) microwave source. The pulsed power and electron beam must enable the RKA to Produce one kilojoule of 13 GHz radiation per pulse at a 5 Hz repetition frequency. These efforts include tests and improvements of a 1 (mu)s pulse length thyratron switched modulator, and the computational and experimental design of a 1-(mu)s-pulse-length explosive emission electron gun. The one microsecond pulse length is almost an order of magnitude beyond what has been achieved heretofore with an RKA. Achieving a peak power approaching 1 GW for 1 (mu)s requires a well behaved electron beam on that time scale. An electron beam diode has been developed that delivers a peak current of 4 to 5 kA for a pulse duration exceeding 1 (mu)s, at a beam kinetic energy above 600 keV. BANSHEE is the high voltage modulator designed for use as an electron beam driver for high power microwave tube development. The BANSHEE output pulse design parameters are 1 MV and 10 kA, with a 1 (mu)s pulse width at a repetition rate of 3-5 Hz, driving a load of impedance of 100 ohms. BANSHEE is a thyratron-switched line-type modular with a pulse transformer output stage. The modulator design is pushing the state of the art in thyratron technology and capacitor lifetime. The results of the BANSHEE modulator testing are described. DOE

N93-12113# Lawrence Livermore National Lab., CA.
ULTRA-WIDEBAND GENERATORS
P. A. Pincosy, P. Poulsen, and J. J. Morrison 20 Dec. 1991 6 p Presented at the Society of Photo-Optical Instrumentation Engineers Symposium on Laser and Radiation Los Angeles, CA, 19-24 Jan. 1992
(Contract W-7405-eng-48)
(DE92-018026; UCRL-JC-107579; CONF-920124-25) Avail: CASI HC A02/MF A01

High-power ultra-wideband pulses with equivalent center frequences of 10 GHz require picosecond switching times of high electric fields. We are developing a high-pressure gas switch that is designed to store several joules of energy. The switch has an overvoltaged gap that is pulse charged to operating voltages before the electron avalanche causes the voltage to collapse. Depending on the gas pressure (designed for up to 100 atm) and the electric field, the voltage collapse time can be hundreds of picoseconds down to a few picoseconds. Uniform development of the avalanche is initiated by photoionization from a bare spark or an ultraviolet laser. The pulse-power charging system is designed to charge the transmission line in a few nanoseconds. The stored energy that would flow as a post-pulse component is to be minimized. Tests of the repetition rate for the switch are part of the development. Data in this paper indicate the achieved gap electric field, the voltage collapse time, and the launched pulse power and energy down transmission line. DOE

N93-12121# Lawrence Livermore National Lab., CA.
REFLECTION MASKS FOR SOFT X RAY PROJECTION LITHOGRAPHY
A. M. Hawryluk, N. M. Ceglio, D. W. Phillion, D. P. Gaines (Brigham Young Univ., Provo, UT.), R. Browning (Stanford Univ., CA.), R. F. Pease (Stanford Univ., CA.), D. Stewart (Micrion Corp., Peabody, MA.), and N. Economou (Micrion Corp., Peabody, MA.) Jul. 1991 9 p Presented at the Society of Photo-Optical Instrumentation Engineers (SPIE) Meeting, San Diego, CA, 21-26 Jul. 1991
(Contract W-7405-eng-48)
(DE92-014779; UCRL-JC-108669; CONF-9107115-76) Avail: CASI HC A02/MF A01

Soft X-ray Project Lithography (SXPL) may be used to fabricate high resolution structures for future integrated circuits. This technique will use a reflection mask which is a substrate coated with an x-ray multilayer mirror and patterned with a thin (approximately 50 nm) layer of x-ray absorber. Mask patterning processes must not degrade the reflectivity of the x-ray mirror and mask repair techniques must be developed. The technical challenges of conventional reflecting optical imaging system designs are severe and mask technology can have a significant impact on this issue. Specifically, innovative mask designs can reduce the complexity of the optical system by decreasing the number of mirrors and replacing aspheric optical surfaces with spherical surfaces. We have developed a technique, called Encoded Mask Lithography, with which we have designed an optical system which uses only two (spherical) imaging mirrors and has less than 100 nm spatial resolution, negligible distortion and greater than 30 mm diameter field of view. DOE

N93-12133# Department of the Navy, Washington, DC.
TRANSLATING WEDGE HEAT SINK Patent Application
Mark W. Sewell, inventor (to Navy) (Courtney and Co., Philadelphia, PA.) 18 May 1992 14 p
(AD-D015357; US-Patent-Appl-SN-884976; Navy-Case-74029) Avail: CASI HC A03/MF A01

This patent application discloses a device for dissipating heat from cased electronics where optimum heat transfer is required, and easy removability is desired. The device finds utility in sonobuoys, buoys, missiles and mines, as well as cabling electronics such as transoceanic communications equipment. The device contains a translating wedge which is drawn into a forced fit between the heat generating module and a conducting wedge which contacts the electronics case, resulting in a high efficiency conducting thermal path from the electronics to the equipment case. The device is particularly efficacious in circular cased electronics. GRA

N93-12156# Los Alamos National Lab., NM.
MILLIWATT GENERATOR PROJECT
T. W. Latimer and G. H. Rinehart May 1992 20 p
(Contract W-7405-eng-36)
(DE92-015348; LA-12236-PR) Avail: CASI HC A03/MF A01

This report covers progress on the Milliwatt Generator Project from April 1986 through March 1988. Activities included fuel processing and characterization, production of heat sources, fabrication of pressure-burst test units, compatibility studies, impact testing, and examination of surveillance units. The major task of the Los Alamos Milliwatt Generator Project is to fabricate MC2893A heat sources (4.0 W) for MC2730A radioisotope thermoelectric generators (RTG's) and MC3599 heat sources (4.5 W) for MC3500 RTG's. The MWG Project interfaces with the following contractors: Sandia National Laboratories, Albuquerque (designer); E.I. du Pont de Nemours and Co. (Inc.), Savannah River Plant (fuel); Monsanto Research Corporation, Mound Facility (metal hardware); and General Electric Company, Neutron Devices Department (RTG's). In addition to MWG fabrication activities, Los Alamos is involved in (1) fabrication of pressure-burst test units, (2) compatibility testing and evaluation, (3) examination of surveillance units, and (4) impact testing and subsequent examination of compatibility and surveillance units. DOE

N93-12191# Wyoming Univ., Laramie. Dept. of Electrical Engineering.
ENERGY EFFICIENT DRIVEPOWER: AN OVERVIEW
Sadrul Ula, Larry E. Birnbaum, and Don Jordan 1992 52 p
Sponsored by DOE
(PB92-199173) Avail: CASI HC A04/MF A01

Energy efficiency is a major concern to industry for a variety of reasons. Operating expenses and public relations are just two of these. While a lot of effort has been expended in the area of electrical energy efficiency, the area of concern in the report, most papers use a limited approach when examining the opportunities for efficiency improvement. However, use of a systems approach--examining the entire power train system from when electrical power first enters a facility to the final output is presented. This type of approach to electrical energy efficiency can improve the overall efficiency by a significant amount. There are many methods of driving mechanical loads such as waste steam (steam turbine), centralized hydraulic systems, and compressed air. Only electric-drive systems were analyzed. Depending on the application and facilities, these other methods may be a viable alternative to electric drivepower systems. The document assumes that the reader has an understanding of the basic concepts, practices, and terminology used in electrical and mechanical engineering. The reader should be familiar with terms such as voltage, current, dc power, ac power, power factor, horse power, torque, angular velocity, kilowatt-hours, efficiency, harmonics, and gear ratio. GRA

N93-12192# Wyoming Univ., Laramie. Dept. of Electrical Engineering.
ENERGY EFFICIENT DRIVEPOWER: LITERATURE REFERENCE LIST: CULLED REFERENCES
1992 52 p Sponsored by DOE
(PB92-199181) Avail: CASI HC A04/MF A01

A listing of the references which have been culled from the main reference lists in order to reduce the bulk of these documents is presented. They are listed here by their general format and subject area for the convenience of the oversight committee. GRA

N93-12198 North Carolina State Univ., Raleigh.
MECHANISMS ASSOCIATED WITH ELECTRORHEOLOGY
Ph.D. Thesis
Ying Chen 1992 158 p
Avail: Univ. Microfilms Order No. DA9219660

To develop an understanding of the mechanisms associated with electrorheology, a theoretical model for the electrostatic interaction force between particles in a chain is developed and compared with the measured force between particles in a single chain of a model ER fluid. The calculations show that electric field concentrations are about an order of magnitude higher near the particle contacts. The force between particles predicted by this model is in reasonable agreement with that measured experimentally. Studies on the behavior of zeolite-based ER fluids indicate that the strength of ER fluids is determined by: (1) the force of interaction between particles in a single-row chain and (2) an enhancement of the force due to the observed clustering of particles into multi-row chains. The force enhancement factor (structure parameter) varied with the shear rate and the concentration of particles, but was relatively independent of the electric field, temperature and host fluid. When the appropriate structure parameter was taken into account, reasonable agreement existed between the predicted and the measured shear stress-shear strain curves and the concentration dependence of the yield stress. The present theoretical and experimental considerations thus indicate that the electrostatic polarization force between the particles is a major factor in determining the shear strength of ER fluids under static shear conditions. The mechanical and electrical properties of ER fluids can thus be determined from the physical properties of the phases that are present. Finally, an estimate of the maximum attainable yield strength of ER fluids is given.
Dissert. Abstr.

N93-12290# Stanford Univ., CA. Lab. of Physics.
NONLINEAR DELAY LINE PHASE SHIFTERS FOR TERAHERTZ SUPERCONDUCTIVE ELECTRONIC CIRCUITS
Final Report, Sep. 1987 - Jul. 1991
Malcom R. Beasley and Howard J. Snortland Jun. 1992 63 p
(Contract F19628-87-K-0050)
(AD-A255119; RL-TR-92-156) Avail: CASI HC A04/MF A01

We report on the development of an electrically controllable superconducting phase shifter suitable for operation in a terahertz heterodyne receiver. The key physical principle of operation, and that of nonlinear kinetic inductance, is developed into a device theory and also appropriate design rules. Critical figures of merit are then identified and optimized designs presented. Experimental tests of prototypes are described. The tests were used to help further refine the design rules. Although a practical phase shifter was not produced, the prospects for the device concept appear good. GRA

N93-12294# Wyoming Univ., Laramie. Dept. of Electrical Engineering.
ENERGY EFFICIENT DRIVEPOWER: LITERATURE REFERENCE LIST. VOLUME 1: GENERAL USER'S SUPPLEMENT
Sadrul Ula, Don L. Jordan, and Larry E. Birnbaum 1992 85 p
(PB92-199157) Avail: CASI HC A05/MF A01

A large number of information sources in the area of the efficient use of drivepower are listed. This is a broad area, covering not jet electric motors but all the parts of a system which transport power from where it enters a facility to where the load is driven and controlled. It was determined during the course of the research, that the information was written for all types of audiences. This was realized when the researchers, all with advanced degrees in Electrical Engineering, encountered an article on motors which would require about a week's worth of study just to understand the jargon. As a result, the references are rated as to expected knowledge base of the reader. GRA

N93-12295# Wyoming Univ., Laramie. Dept. of Electrical Engineering.
ENERGY EFFICIENT DRIVEPOWER: LITERATURE REFERENCE LIST. VOLUME 2: DESIGN ENGINEER'S SUPPLEMENT
Sadrul Ula, Don L. Jordan, and Larry E. Birnbaum 1992 49 p
(PB92-199165) Avail: CASI HC A03/MF A01

A large number of information sources in the area of the efficient use of drivepower are listed. This is a broad area, covering not just electrical motors, but all the parts of a system which transport power from where it enters a facility to where the load is driven and controlled. It was determined during the course of the research, that the information was written for all types of audiences. This was realized when the researchers, all with advanced degrees in Electrical Engineering, encountered an article on motors which would require about a week's worth of study just to understand the jargon. As a result, the references are rated as to expected knowledge base of the reader. GRA

N93-12301*# National Aeronautics and Space Administration. Lewis Research Center, Cleveland, OH.
PARAMETERIZATION OF SOLAR CELLS
J. Appelbaum, A. Chait, and D. Thompson Oct. 1992 23 p
(RTOP 506-41-11)
(NASA-TM-105885; E-7188; NAS 1.15:105885) Avail: CASI HC A03/MF A01

The aggregation (sorting) of the individual solar cells into an array is commonly based on a single operating point on the current-voltage (I-V) characteristic curve. An alternative approach for cell performance prediction and cell screening is provided by modeling the cell using an equivalent electrical circuit, in which the parameters involved are related to the physical phenomena in the device. These analytical models may be represented by a double exponential I-V characteristic with seven parameters, by a double exponential model with five parameters, or by a single exponential equation with four or five parameters. In this article we address issues concerning methodologies for the determination of solar cell parameters based on measured data points of the I-V characteristic, and introduce a procedure for screening of solar cells for arrays. We show that common curve fitting techniques, e.g., least squares, may produce many combinations of parameter values while maintaining a good fit between the fitted and measured I-V characteristics of the cell. Therefore, techniques relying on curve fitting criteria alone cannot be directly used for cell parameterization. We propose a consistent procedure which takes into account the entire set of parameter values for a batch of cells. This procedure is based on a definition of a mean cell representing the batch, and takes into account the relative contribution of each parameter to the overall goodness of fit. The procedure is demonstrated on a batch of 50 silicon cells for Space Station Freedom. Author

N93-12340# Cree Research, Inc., Durham, NC.
HIGH TEMPERATURE RECTIFIERS AND MOS DEVICES IN 6H-SILICON CARBIDE Final Report, 1 Jul. 1991 - 31 Jan. 1992
J. W. Palmour, J. A. Edmond, and C. H. Carter, Jr. 27 Apr. 1992 34 p
(Contract DAAL03-91-C-0046)
(AD-A254725) Avail: CASI HC A03/MF A01

A major emphasis in the aerospace industry has been to increase the performance and efficiency of aircraft engines (including helicopters). Most of the improvements require the engine to run hotter, be more compact and more precisely controlled. All of these requirements increase the temperature of an increasing number of electronic components on the engine. This contract involved the development of two types of solid state devices for use in various engine applications using silicon carbide which is the premiere semiconductor material for high temperature (and other) applications. One device is a high voltage, low current rectifier which can operate to at least 350 deg C for use in an igniter circuit. The developments required involved decreasing the doping level of the background layer in epitaxial growth, improving the passivation and packaging to withstand the high voltage and high temperature. The other is a 350 deg C small signal MOSFET which can be used as an amplifier for a variety of sensors. For this portion of the research, the major focus was on characterization of the thermal oxide and the oxide interface through fabrication and characterization of MOS capacitors and various MOSFET designs. GRA

N93-12360# California Univ., Berkeley. Dept. of Electrical Engineering and Computer Science.
VLSI RELIABILITY RESEARCH Final Report
Chenming Hu 6 Aug. 1992 7 p
(Contract N00014-85-K-0603)
(AD-A254883) Avail: CASI HC A02/MF A01

Aggressive scaling toward submicron VLSI technologies has greatly heightened the need for a better basic understanding of the reliability failure mechanisms and the need for better testing methods and technological solutions. This project researched these issues for the four leading failure models of VLSI systems: oxide wearout, radiation effects, hot-electron induced degradation, and interconnect and contact electromigration. We have developed quantitative physical (not simply empirical) models for the failure mechanisms, more accurate methods for testing, screening and reliability prediction, and explored promising new technologies for improved VLSI reliability. Many of the research results have already been accepted and used by the semiconductor industry. GRA

N93-12421# Interuniversity Micro-Electronics Center, Leuven (Belgium).
BACK-GATE BIAS GENERATOR Final Technical Report, 5 Jul. 1991 - 4 Jul. 1992
P. Smeys and J. P. Colinge 4 Sep. 1992 31 p
(Grant AF-AFOSR-0360-90)
(AD-A255126; RHD-03) Avail: CASI HC A03/MF A01

The back-gate generator is a small circuit element which allows for the compensation of the threshold voltage shift generated in silicon-on-insulator MOS transistors by ionizing radiations. This device is integrated on a regular SOI chip. It senses the threshold shifts and applies a back-gate voltage designed to nullify this shift induced by the external harsh environment. GRA

N93-12437# New Mexico Univ., Albuquerque.
THE 44TH ANNUAL GASEOUS ELECTRONICS CONFERENCE Final Report, 1 Sep. 1991 - 31 Aug. 1992
Harold M. Anderson May 1992 229 p Conference held in Albuquerque, NM, 22-25 Oct. 1991
(Contract DAAL03-91-G-0326)
(AD-A254872; ARO-28901.1-PH-CF) Avail: CASI HC A11/MF A03

The decade of the 1990's is opening for the Gaseous Electronics Conference with precedent setting growth. The technical program comprises 110 oral presentations and 191 poster presentations for a total of 301 papers. The total number of authors are 582. Two timely workshops will be held dealing with the following: GEC Reference Cell Issues and Comparison Session on High Density Plasma Processing. Other arranged sessions deal with the following: Particulates in RF Discharges; Cathodes in Discharges; Electron and Atom Collision Related Phenomena; New and Alternative Applications for Plasma Processing; and Ionized Gas Physics in Pulsed Power Applications. GRA

N93-12502# Cincinnati Univ., OH. Dept. of Physics.
MESOSCOPIC EFFECTS IN ELECTRONIC MICROSTRUCTURES Final Report, Jun. 1989 - Jun. 1992
Rostislav Serota 12 Aug. 1992 4 p
(Contract DAAL03-89-K-0108)
(AD-A254889; ARO-26941.7-EL) Avail: CASI HC A01/MF A01

In the course of the reported project we studied transport and thermodynamic properties of ultra-small electronic microstructures, known as mesoscopic, using various theoretical approaches and techniques. The main goal of this research is the improved characterization of and understanding of limitations on quantum electronic devices. We obtained several important results and breakthroughs in our analysis of hopping conduction in

Si-MOSFETs, far infra-red absorption in metal-insulator composites, and orbital magnetism of metals and quantum dots in semiconductor heterostructures. GRA

34 FLUID MECHANICS AND HEAT TRANSFER

Includes boundary layers; hydrodynamics; fluidics; mass transfer; and ablation cooling.

For related information see also *02 Aerodynamics* and *77 Thermodynamics and Statistical Physics.*

N93-10969*# National Aeronautics and Space Administration. Hugh L. Dryden Flight Research Facility, Edwards, CA.

AEROTHERMAL TEST RESULTS FROM THE SECOND FLIGHT OF THE PEGASUS BOOSTER

Gregory K. Noffz, Timothy R. Moes, Edward A. Haering, Jr., and Paul Kolodziej (National Aeronautics and Space Administration. Ames Research Center, Moffett Field, CA.) Oct. 1992 44 p
(RTOP 505-59-40)
(NASA-TM-4391; H-1827; NAS 1.15:4391) Avail: CASI HC A03/MF A01

A survey of temperature, heat-flux, and pressure measurements was obtained at speeds through Mach 8.0 on the second flight of the Pegasus air-launched space booster system. All sensors were distributed on the wing-body fairing or fillet. Sensors included thin foil-gauge thermocouples installed near the surface within the thermal protection system. Thermocouples were also installed on the surface of nonablating plugs. The resulting temperature time history allowed derivation of convective heat flux. In addition, commercially available calorimeters were installed on the fillet at selected locations. Calorimeters exhibited a larger change in measured heat flux than collocated nonablating plugs in response to particular events. Similar proportional variations in heat flux across different regions of the fillet were detected by both the calorimeters and nonablating plugs. Pressure ports were installed on some nonablating plugs to explore the effects of port protrusion and high-frequency noise on pressure requirements. The effect of port protrusion on static-pressure measurements was found to decrease with increasing Mach number. High-frequency noise suppression was found to be desirable but not required on any future flight. Author

N93-10981*# National Aeronautics and Space Administration. Lewis Research Center, Cleveland, OH.

SMALL EXPERIMENTS FOR THE MATURATION OF ORBITAL CRYOGENIC TRANSFER TECHNOLOGIES

David J. Chato and William J. Taylor Sep. 1992 11 p Presented at the 1992 World Space Congress, Washington, DC, 28 Aug. - 5 Sep. 1992; sponsored by the International Astronautical Federation
(RTOP 506-42-73)
(NASA-TM-105849; E-7295; NAS 1.15:105849) Avail: CASI HC A03/MF A01

The no-vent method is a promising approach to handling the problems of low-g venting during propellant transfer. A receiver tank is first cooled to remove thermal energy from the tank wall and the resultant vapor vented overboard. The nozzles mix the incoming liquid and residual vapor in the tank maintaining a thermodynamic state which allows the tank to fill with liquid without venting. Ground based testing at NASA Lewis Research Center (LeRC) has demonstrated the no-vent fill process and attempted to bound its low-gravity performance. But, low-gravity testing is required to validate the method. As an alternative to using a dedicated spacecraft for validation, several small scale experiments to study no-vent fill in low-g were formulated. Cost goals quickly limited the search to two possibilities: a secondary payload on the space shuttle, or a small scale sounding rocket experiment. The key issues of small scale experimentation are discussed, and a conceptual design of a sounding rocket experiment with liquid hydrogen for studying the fill process is presented. Author

N93-11017# Rolls-Royce Ltd., Derby (England).

AN ADVANCED COMBUSTION RESEARCH FACILITY FOR VALIDATING COMPUTATIONAL FLUID DYNAMICS CODES

J. B. Bullard (Defence Research Agency, Farnborough, England), C. D. Hurley (Defence Research Agency, Farnborough, England), and N. C. Eccles 1 Dec. 1991 13 p Presented at the European Propulsion Forum, Paris, France, 13-15 Nov. 1991
(PNR-90913; ETN-92-92202) Copyright Avail: CASI HC A03/MF A01

The Sector Combustion Rig (SCR), built to obtain experimental data which could be used to verify computational fluid dynamic programs and to investigate the formation and consumption of combustion products through a combustor, is described. This rig was designed to accommodate sectors of full size engine combustion chambers and to test them at real or simulated engine operating conditions. Changes made to improve the operating, measurement, and data handling capabilities of the rig as a result of experience from several years of operations are described together with some of the features which contribute to the uniqueness of the SCR. The SCR gas analysis system and instrumentation are described. Extracts from some results obtained during a recent program of tests on a Rolls-Royce RB211 combustor are given. ESA

N93-11025# Rolls-Royce Ltd., Derby (England).

THE PREDICTION OF CONVECTIVE HEAT TRANSFER IN ROTATING SQUARE DUCTS

T. Bo (Manchester Univ., England), H. Iacovides (Manchester Univ., England), and B. E. Launder (Manchester Univ., England) 30 Sep. 1991 7 p Presented at the 8th International Turbulence Shear Flows Symposium, Fed. Republic of Germany, 1 Sep. 1991 Previously announced in IAA as A92-40146 Sponsored by RAE
(PNR-90929; ETN-92-92211) Copyright Avail: CASI HC A02/MF A01

A numerical study of developing flow through a heated duct of square cross section rotating in an orthogonal mode is presented. Two different turbulence models were employed. An Effective Viscosity Model (EVM) and an Algebraic Stress Model (ASM). In both cases simplified nearwall models were employed in which the solution of the epsilon transport equation was not carried out. At moderate rotational speeds the EVM heat transfer predictions are found to be in close agreement with existing measurements. At high rotational rates rotational buoyancy effects are shown to become important. EVM predicted heat transfer behavior, while still reasonable, begins to deviate from the experimental one. The ASM model with a simplified nearwall extension was found to be even less appropriate when rotational buyancy is significant. ESA

N93-11067# Rolls-Royce Ltd., Derby (England).

THE PREDICTION OF CONVECTIVE HEAT TRANSFER IN ROTATING SQUARE DUCTS

T. Bo (Manchester Univ., England), H. Lacovides (Manchester Univ., England), and B. E. Launder (Manchester Univ., England) 12 Oct. 1991 7 p Presented at the 8th Symposium on Turbulent Shear Flows, Munich, Fed. Republic of Germany, 9-11 Sep. 1991 Sponsored RAE
(PNR-90985; ETN-92-92244) Copyright Avail: CASI HC A02/MF A01

A numerical study of developing flow through a heated duct of square cross section rotating in orthogonal mode is presented. Two different turbulence models were employed: an Effective Viscosity Model (EVM) and an Algebraic Stress Model (ASM). In both cases, instead of solving the epsilon equation across the near wall sublayer, the length scale distribution was prescribed. At a rotation number Ro of 0.12, Coriolis induced secondary motions produce a mean heat transfer coefficient on the pressure surface that is more than twice that in the suction surface: a behavior that is accurately captured by both EVM and ASM schemes. For the test case at Ro = 0.24, experiments suggest that this ratio exceeds 4:1 in places though the predicted ratios are closer to 3:1. Curiously, the apparent contribution of buoyancy forces to the resultant Nusselt number depends greatly on whether the ASM or EVM closure is adopted. ESA

N93-11074*# Georgia Tech Research Inst., Atlanta. Signature Technology Lab.
LV SOFTWARE SUPPORT FOR SUPERSONIC FLOW ANALYSIS Semiannual Technical Report, 15 Oct. 1991 - 14 Apr. 1992
William A. Bell 16 Apr. 1992 12 p
(Grant NAG3-1215)
(NASA-CR-190209; NAS 1.26:190209) Avail: CASI HC A03/MF A01

The software for configuring a Laser Velocimeter (LV) counter processor system was developed using structured design. The LV system includes up to three counter processors and a rotary encoder. The software for configuring and testing the LV system was developed, tested, and included in an overall software package for data acquisition, analysis, and reduction. Error handling routines respond to both operator and instrument errors which often arise in the course of measuring complex, high-speed flows. The use of networking capabilities greatly facilitates the software development process by allowing software development and testing from a remote site. In addition, high-speed transfers allow graphics files or commands to provide viewing of the data from a remote site. Further advances in data analysis require corresponding advances in procedures for statistical and time series analysis of nonuniformly sampled data. Author

N93-11142*# Alabama Univ., Huntsville. College of Science.
KINETICS OF DIFFUSIONAL DROPLET GROWTH IN A LIQUID/LIQUID TWO-PHASE SYSTEM Semiannual Progress Report, period ending 15 Sep. 1992
James K. Baird 15 Sep. 1992 13 p
(Grant NAG8-816)
(NASA-CR-190805; NAS 1.26:190805) Avail: CASI HC A03/MF A01

In the case of the diaphragm cell transport equation where the interdiffusion coefficient is a function of concentration, we have derived an integral of the form, t = B(sub 0) + B(sub L)ln(delta(c)) + B(sub 1)(delta(c)) + B(sub 2)(delta(c))(exp 2) +... where t is the time and (delta(c)) is the concentration difference across the frit. The coefficient, B(sub 0), is a constant of integration, while the coefficient, B(sub L), B(sub 1), B(sub 2), ..., depend in general upon the cell constant, the compartment volumes, the interdiffusion coefficient, and various of its concentration derivatives evaluated at the mean concentration for the cell. Explicit formulae for B(sub L), B(sub 1), B(sub 2), ... are given. Author

N93-11148# State Univ. of New York, Stony Brook.
FRONT TRACKING AND THE INTERACTION OF NONLINEAR WAVES Final Report, 15 Feb. 1989 - 14 Feb. 1992
James Glimm and John W. Grove May 1992 15 p
(Contract DAAL03-89-K-0017)
(AD-A253544; ARO-26616.26-MA) Avail: CASI HC A03/MF A01

The research program has emphasized innovative computations and theory. The computations and theory support and enhance each other. A coherent approach was used which depends upon abstracting important mathematical concepts and computational methods from individual applications to a wide range of applications involving complex continua, including wave refractions, flows in elastic and plastic media, and complex fluid mixing. Adaptive computational methods were developed for flows with discontinuities and implemented on modern parallel computers. GRA

N93-11171*# SECA, Inc., Huntsville, AL.
CFD MODELING OF TURBULENT FLOWS AROUND THE SSME MAIN INJECTOR ASSEMBLY USING POROSITY FORMULATION Final Report
Gary C. Cheng, Y. S. Chen, and Richard C. Farmer May 1992 57 p Original contains color illustrations
(Contract NAS8-38871)
(NASA-CR-184359; NAS 1.26:184359) Avail: CASI HC A04/MF A01; 5 functional color pages

Hot gas turbulent flow distribution around the main injector assembly of the Space Shuttle Main Engine (SSME) and LOX flow distribution through the LOX posts have a great effect on the combustion phenomena inside the main combustion chamber. In order to design a CFD model to be an effective engineering analysis tool with good computational turn-around time (especially for 3-D flow problems) and still maintain good accuracy in describing the flow features, the concept of porosity was employed to describe the effects of blockage and drag force due to the presence of the LOX posts in the turbulent flow field around the main injector assembly of the SSME. Two-dimensional numerical studies were conducted to identify the drag coefficients of the flows, both through tube banks and round the shielded posts, over a wide range of Reynolds numbers. Empirical, analytical expressions of the drag coefficients as a function of local flow Reynolds number were then deduced. The porosity model was applied to the turbulent flow around the main injector assembly of the SSME, and analyses were performed. The 3-D CFD analysis was divided into three parts: LOX dome, hot gas injector assembly, and hydrogen cavity. The numerical results indicate that the mixture ratio at the downstream of injector face was close to stoichiometric around baffle elements. Author

N93-11172*# National Aeronautics and Space Administration. Lewis Research Center, Cleveland, OH.
SYSTEM AND METHOD FOR CANCELLING EXPANSION WAVES IN A WAVE ROTOR Patent Application
Daniel E. Paxson, inventor (to NASA) 26 May 1992 17 p
(NASA-Case-LEW-15218-1; NAS 1.71:LEW-15218-1; US-Patent-Appl-SN-889003) Avail: CASI HC A03/MF A01

A wave rotor system that is comprised of a wave rotor coupled to first and second plates is described. Special ports are provided, one in each of the first and second end plates, to cancel expansion waves generated by the release of working fluid from the wave rotor. One of the expansion waves is reflected in the wave rotor from a reflecting portion and provided to the special port in the second end plate. Fluid present at the special port in the second end plate has a stagnation pressure and mass flow which is the same as that of the cells of the wave rotor communicating with such special port. This allows for cancellation of the expansion wave generated by the release of working fluid from the wave rotor. The special port in the second end plate has a first end corresponding to the head of the expansion wave and a second end corresponding to the tail of the expansion wave. Also, the special port is configured to continually change along the circumference of the second end plate to affect expansion wave cancellation. An expansion wave generated by a second release of working fluid from the wave rotor is cancelled in a similar manner to that described above using a special port in the first end plate. The cycle of operation of the wave rotor system is designed so that the stagnation pressure and mass flow of the fluid present at the special ports is the same so that the special ports may be connected by a common duct. NASA

N93-11197 Louisiana State Univ., Baton Rouge.
AN ADAPTIVE DIFFERENCING SCHEME FOR ELLIPTIC FLOWS Ph.D. Thesis
Therese Estelle Rhodes 1991 216 p
Avail: Univ. Microfilms Order No. DA9207526

The formulation of a computationally efficient multiple-grid adaptive differencing (MAD) scheme for two-dimensional elliptic flow and heat transfer problems is discussed. This algorithm equi-distributes a measure of the error by using higher order differencing schemes locally in adaptively determined high error-estimate regions. The third-order accurate QUICK scheme is used in regions of high error estimate which are dynamically flagged on the basis of a preliminary first order upwind solution. Boundary conditions for the flagged region are taken from the preliminary upwind solution. Multigrid type calculations are performed. Three multiple-grid schemes are developed. In the first scheme,

MAD1-WFDS, the entire domain and flagged subdomains are solved at each multiple-grid iteration. The second scheme, MAD2-WDS, solves the entire domain at each iteration, employing the QUICK forms of the discretized equations in the flagged regions and the original upwind formulation elsewhere. The third algorithm, MAD3-FDS, is similar to the first, except the entire domain is not solved after the subdomain solution. Instead, only the unflagged portion of the problem domain is solved, using the improved values obtained in the flagged regions as boundary conditions. The three MAD algorithms are applied to two convection-diffusion and two flow problems. MAD1-WFDS shows the best improvement to the upwind scheme but requires the most additional computing time. MAD2-WDS requires the least additional computing time, but shows the least improvement over the upwind solution. The code for MAD1-WFDS is parallelized to reduce the real computation time required for problem solutions. The upwind and QUICK schemes are also parallelized for comparison. Several program levels or granularities were parallelized to determine an optimal level of parallelization. A real time savings of 26.4 percent was achieved in one case (in spite of the fact that the solution was not computed on a dedicated machine) at a cost of a 7.8 percent increase in cpu time required by the parallel run over the serial run.
Dissert. Abstr.

N93-11217 State Univ. of New York at Buffalo, Amherst.
FUNDAMENTAL SOLUTIONS AND BOUNDARY ELEMENT FORMULATIONS FOR CONVECTIVE FLUID FLOW Ph.D. Thesis
Yifei Shi 1992 215 p
Avail: Univ. Microfilms Order No. DA9222106

The primary aim of this dissertation is to develop the fundamental solutions and boundary element (BEM) formulations for general convective thermoviscous flow problems including both incompressible and compressible flow. The fluid is idealized as being a homogeneous isotropic Newtonian fluid. The BEM formulations use the governing equations for the idealized convective viscous and inviscid fluid, to derive the necessary fundamental solutions and integral formulations. A number of enhancements have been incorporated in the existing work to make the numerical implementation more efficient, more accurate and therefore increase its applicability. These advances permit the solution of a wide variety of problems involving viscous, inviscid as well as thermoviscous fluids for a range of Reynolds numbers. The fundamental solutions and BEM formulations discussed in this dissertation include problems of convective heat transfer, convective potential flow, convective incompressible thermoviscous fluid flow as well as compressible thermoviscous fluid flow. All of the formulations (except for viscous compressible flow) mentioned above have been implemented in a series of boundary element solution technique computer programs. Several relevant problems of varied interest in thermoviscous fluid mechanics are included to illustrate the applicability and accuracy of the method.
Dissert. Abstr.

N93-11241 University of Western Ontario, London.
BOUNDARY CONDITION METHODS IN THE NUMERICAL SOLUTION OF THE NAVIER-STOKES EQUATIONS WITH THE APPLICATION TO FREE SURFACE PROBLEMS Ph.D. Thesis
Hua Yang 1991 185 p
(ISBN-0-315-64278-5) Avail: Univ. Microfilms Order No. DANN64278

The numerical simulation of fluid flows is discussed in two parts. The first part is concerned with the treatment of pressure or vorticity boundary conditions in the numerical solution of the Navier-Stokes equations. The second part is concerned with the numerical algorithm for simulating the dynamics of capillary surface. In Part 1, two new accurate finite-difference algorithms are described. They can be easily adapted on a uniform grid for solving general flows. The first approach, designated as Zero Perturbation Method, uses the combination of the momentum and divergence equations at the boundary to provide the implicit pressure boundary conditions. The second approach, designated as Computational Boundary Condition Method, utilizes a computational solution domain to avoid the problems of no explicit boundary conditions for pressure or vorticity in the Navier-Stokes equations. Numerical experiments were carried out by second-order finite difference approach and alternating direction implicit (ADI) solution procedure. All tests were performed on uniform grids by means of Zero Perturbation Method and Computational Boundary Condition Method. The computed convergence rates for all variables are in excellent agreement with the theoretical prediction. Results for the classical driven cavity problem are found to be very accurate in comparison to previous investigators. In Part 2, the analysis was made on the dynamics of liquids in a low gravity environment which is essentially dominated by its capillary effects. There are two major difficulties in numerical simulation: (1) accurate tracking of the curvature of an interface undergoing large deformations; and (2) diagnosing the initiation break-up of an interface, i.e. break-up of a liquid drop. A successful resolution of these difficulties requires an algorithm capable of accurate determination of pressure and velocities along the deformed interface. The required algorithms are described in Part 2.
Dissert. Abstr.

N93-11251# Vermont Univ., Burlington. Coll. of Engineering and Mathematics.
A NEW TWO-PHASE FLOW AND TRANSPORT MODEL WITH INTERPHASE MASS EXCHANGE
J. F. Guarnaccia and G. F. Pinder 1992 11 p Repr. from Mathematical Modeling in Water Resources (Southhampton, England, Computational Mechanics Publications), v. 2, Jun. 1992 p 281-288
(Contract EPA-R-818955)
(PB92-206564; EPA/600/A-92/156) Avail: CASI HC A03/MF A01

The focus of the numerical investigation is on modelling the emplacement and subsequent removal through dissolution of a Denser-than-water Non-Aqueous Phase Liquid (DNAPL) in a saturated ground-water system. Specifically the model must address two flow and transport regimes. First is the emplacement of DNAPL in the subsurface. Here two-phase flow dominates as the DNAPL displaces the water. The second flow and transport regime involves the dissolution of the immobile residual through interphase mass exchange and transport of the dissolved contaminant in the water phase. Numerical simulation of the problem is computationally intensive involving the iterative simultaneous solution of coupled nonlinear partial differential equations over fine time and space discretizations. The paper presents an overview of the equation development including the constitutive relations necessary to describe DNAPL emplacement (hysteresis) and dissolution (kinetic mass exchange), and describes an efficient collocation based parallel algorithm to solve the governing equations. In addition, model results are reported.
GRA

N93-11358 Civil Aviation Authority, London (England).
UK AIRMISSES INVOLVING COMMERCIAL AIR TRANSPORT, JANUARY-APRIL 1991
1991 33 p
(ETN-92-92261) Copyright Avail: Civil Aviation Authority, Greville House, 37 Gratton Road, Cheltenham, England

In the introduction the following are briefly discussed: origination of an airmiss; purpose of airmiss reports; investigation of airmiss reports; categorization of airmisses; involvement of commercial air transport aircraft; airmisses related to flying hours. Tabulated statistics of the following are presented: the number of incidents of commercial air transport airmisses; commercial air transport aircraft involved in airmisses; commercial air transport airmisses related to flying hours. Reports on the commercial air transport airmisses from Jan. - Apr. 1991 are presented. These contain summaries of: pilot reports, transcripts of relevant RT frequencies; radar video recordings, and reports from appropriate air traffic control and operating authorities. The working groups discussion is summarized, and the risk and cause assessed.
ESA

N93-11359# Technical Research Centre of Finland, Espoo. Reactor Lab.

MEASURING AND MODELLING OF PARTICLE-FLUID FLOW IN A RISER REACTOR

Pekka Viitanen Feb. 1992 76 p Sponsored by Finnish Ministry of Trade and Industry; Technical Research Centre of Finland; Neste Oy; and A. Ahlstroem Oy
(VTT-Pubs-88; ISBN-951-38-4066-2; ETN-92-92262) Copyright
Avail: CASI HC A05/MF A01

An introduction to the basics of fluidization techniques and especially the principle of a Fluidized Catalyst Cracking (FCC) plant is given. The flow in the riser reactor of an FCC plant is essentially a two phase flow with gaseous fluid flow and particulate flow consisting of the cracking catalyst. Experimental results obtained from tracer measurements done in an FCC plant are presented. Measurements indicate that a dilute phase flow is dominating the flow structure of the catalyst in the riser. Different approaches to model two phase flow are reviewed. Axial dispersion model fit is done and a simulation model is constructed in order to calculate the radial distribution of the cracking catalyst on the FCC riser. A satisfactory agreement with the experiments and the model is achieved when the slip velocity between discrete particles and the fluid is described using the Newtonian drag force. The Newtonian drag is argued to be due to turbulent fluid flow. ESA

N93-11360# Technical Research Centre of Finland, Espoo. Ship Lab.

PRESSURE AND NOISE INDUCED BY A CAVITATING MARINE SCREW PROPELLER Ph.D. Thesis - Helsinki Univ. of Technology

Jerzy Matusiak Jan. 1992 102 p Sponsored by Merenkulun Saeaetioe
(VTT-Pubs-87; ISBN-951-38-4065-4; ETN-92-92263) Copyright
Avail: CASI HC A06/MF A02

A method of evaluating the intermittent propeller blade fixed cavitation and shedding of free cavitation bubbles is presented. The number and size of free cavitation bubbles are related to the variation of propeller blade attached cavitation. The beta type probability density distribution of the initial bubble size is proposed. This distribution is normalized with respect to the sheet cavitation thickness. The effect of the simplications in the dynamic model of the cavitation bubbles on their collapse downstream of partially and fully cavitating hydrofoils is discussed. The method of calculating the low frequency pressures induced by fixed blade cavitation and high frequency broadband noise caused by the collapse of free bubbles in propeller flows is presented. The method yields noise spectra in the frequency range from the blade passing frequency to tens of kiloHertz. Computed pressure and noise induced by the cavitating propellers are compared to the values measured in model and full scale experiments. The fractal structure of the bubble cloud and the proposed method of evaluating the collapse of the bubble cloud downstream of the fixed cavities yield noise spectra which correlate well with the experimental results of full and model scale measurements. ESA

N93-11362# Ecole Centrale de Lyon (France). Lab. de Mecanique des Fluides et d'Acoustique.

SIMULATION OF COMPRESSIBLE TURBULENT FLOWS BY A MIXED FINITE ELEMENT/FINITE VOLUME METHOD Ph.D. Thesis [SIMULATION DES ECOULEMENTS TURBULENTS COMPRESSIBLES PAR UNE METHODE MIXTE ELEMENTS FINIS-VOLUMES FINIS]

Catherine LeRibault 1991 119 p In FRENCH
(ETN-92-92267) Avail: CASI HC A06/MF A02

Since compressible turbulent flows are a subject of considerable importance in aeronautics, a code to compute compressible turbulent flows in complex geometries, was developed. The classical k-epsilon model was used to describe the turbulent flow. In the vicinity of the solid boundaries, wall laws are used to impose the boundary conditions at a small distance from the wall. The k-epsilon modelization was introduced in a mixed finite element/finite volume method developed to compute compressible flows. In order to compute the flow in complex geometries, unstructured meshes are used. The time derivative and the advection terms are integrated by finite volumes, whereas the source and the viscous terms are interpolated with a classical finite element formulation. The stabilization of both acoustic and convective waves is realized by applying flux splitting techniques. The wall laws are imposed within the variational formulation. This method was first validated for low Mach number flows; comparisons with both experiments and numerical simulations were performed. This method was applied to simulate higher Mach number flows, (supersonic mixing layers, compression corners and a transonic flow over bump). ESA

N93-11363# Ecole Centrale de Lyon (France). Lab. de Mecanique des Fluides et d'Acoustique.

A STUDY OF THE WALL-PRESSURE FLUCTUATIONS DOWNSTREAM OF A BLADE-WALL JUNCTION Ph.D. Thesis [ETUDE DES FLUCTUATIONS DE PRESSION PARIETALE EN AVAL D'UNE JONCTION AUBE/PAROI]

Mohammed Garoum 1991 109 p In FRENCH
(ECL-91-07; ETN-92-92268) Avail: CASI HC A06/MF A02

The three dimensional flow that develops downstream of a blade wall junction was studied. A five hole Pitot probe was used to measure the three components of the mean velocity and to estimate the longitudinal component of the mean vorticity. The shape, the location and the strength of the horseshoe vortex was quantified. It was found that a very energetic vortex sheet exists behind the trailing edge, between the wake and the horseshoe vortex. It was shown that, within the investigated range of velocity, the geometrical characteristics of the flow are not modified by the free stream velocity. However, the strength of the horseshoe vortex is proportional to this velocity. Wall pressure spectra were measured at different locations and compared with spectra measured under a boundary layer without the blade. This comparison showed that the contribution of the wake and the horseshoe vortex to the spectra is less than six decibels. Nevertheless, each of these contributions affects a well defined frequency domain: the horseshoe vortex at low frequencies and the wake at high frequencies. The contributions change with a Strouhal scaling law when the free stream velocity is changed. ESA

N93-11416# University of Southern California, Los Angeles. Dept. of Aerospace Engineering.

DYNAMICAL EFFECTS OF SUCTION/HEATING ON TURBULENT BOUNDARY LAYERS Quarterly Report, 1 Oct. 1991 - 1 Jan. 1992

Ron Blackwelder 1 Jan. 1992 13 p
(Contract N00014-92-J-1062)
(AD-A248459) Avail: CASI HC A03/MF A01

The main emphasis of this quarter has been to test the effects of suction in a controlled environment with the emulated wall eddy structure. A study of the curved working wall of the test section in the Goertler Wind Tunnel showed that there were sufficient stresses within the plexiglas that cutting elongated slits for suction would probably cause the surface to develop step-type roughnesses. Thus several individual holes were initially drilled along the streamline direction in a spanwise region between two vortices. Air was withdrawn through this series of holes to provide a semi-continuous region of suction. Differing rates of suction through these holes were used to explore the effects upon the eddy structure. These preliminary results were obtained using visualization; i.e., smoke as introduced via a smoke wire into the boundary layer. Images were captured using a video camera and analyzed to determine the best suction rates. The preliminary results showed that suction has a large effect upon individual streaks of low speed fluid. Without the suction, the low speed region lying in the upwelling zone between two streamwise vortices was broken down by a secondary instability. This instability typically caused the low speed fluid marked with the smoke to oscillate from side to side in a manifestation of an inflectional instability in the spanwise direction as found and reported earlier in this research. With increasing distance downstream, the oscillation amplitude grew very rapidly until it broke down into complete turbulence. GRA

N93-11440# Doty Scientific, Inc., Columbia, SC.
MICROTUBE STRIP HEAT EXCHANGER
F. D. Doty Jul. 1992 10 p
(Contract DE-FG01-90CE-15440)
(DE92-018709; DOE/CE-15440/T5) Avail: CASI HC A02/MF A01

The purpose of this contract has been to explore the limits of miniaturization of heat exchangers with the goals of (1) improving the theoretical understanding of laminar heat exchangers, (2) evaluating various manufacturing difficulties, and (3) identifying major applications for the technology. A low-cost, ultra-compact heat exchanger could have an enormous impact on industry in the areas of cryocoolers and energy conversion. Compact cryocoolers based on the reverse Brayton cycle (RBC) would become practical with the availability of compact heat exchangers. Many experts believe that hardware advances in personal computer technology will rapidly slow down in four to six years unless lowcost, portable cryocoolers suitable for the desktop supercomputer can be developed. Compact refrigeration systems would permit dramatic advances in high-performance computer work stations with 'conventional' microprocessors operating at 150 K, and especially with low-cost cryocoolers below 77 K. NASA has also expressed strong interest in our MTS exchanger for space-based RBC cryocoolers for sensor cooling. We have demonstrated feasibility of higher specific conductance by a factor of five than any other work in high-temperature gas-to-gas exchangers. These laminar-flow, microtube exchangers exhibit extremely low pressure drop compared to alternative compact designs under similar conditions because of their much shorter flow length and larger total flow area for lower flow velocities. The design appears to be amenable to mass production techniques, but considerable process development remains. The reduction in materials usage and the improved heat exchanger performance promise to be of enormous significance in advanced engine designs and in cryogenics. DOE

N93-11529*# National Aeronautics and Space Administration. Lewis Research Center, Cleveland, OH.
DIRECT NUMERICAL SIMULATION OF INSTABILITIES IN PARALLEL FLOW WITH SPHERICAL ROUGHNESS ELEMENTS
R. G. DeAnna Aug. 1992 36 p
(DA Proj. 1L1-61102-AH-45; RTOP 505-62-OK)
(NASA-TM-105847; E-7291; NAS 1.15:105847; AVSCOM-TR-92-C-023) Avail: CASI HC A03/MF A01

Results from a direct numerical simulation of laminar flow over a flat surface with spherical roughness elements using a spectral-element method are given. The numerical simulation approximates roughness as a cellular pattern of identical spheres protruding from a smooth wall. Periodic boundary conditions on the domain's horizontal faces simulate an infinite array of roughness elements extending in the streamwise and spanwise directions, which implies the parallel-flow assumption, and results in a closed domain. A body force, designed to yield the horizontal Blasius velocity in the absence of roughness, sustains the flow. Instabilities above a critical Reynolds number reveal negligible oscillations in the recirculation regions behind each sphere and in the free stream, high-amplitude oscillations in the layer directly above the spheres, and a mean profile with an inflection point near the sphere's crest. The inflection point yields an unstable layer above the roughness (where U''(y) is less than 0) and a stable region within the roughness (where U''(y) is greater than 0). Evidently, the instability begins when the low-momentum or wake region behind an element, being the region most affected by disturbances (purely numerical in this case), goes unstable and moves. In compressible flow with periodic boundaries, this motion sends disturbances to all regions of the domain. In the unstable layer just above the inflection point, the disturbances grow while being carried downstream with a propagation speed equal to the local mean velocity; they do not grow amid the low energy region near the roughness patch. The most amplified disturbance eventually arrives at the next roughness element downstream, perturbing its wake and inducing a global response at a frequency governed by the streamwise spacing between spheres and the mean velocity of the most amplified layer. Author

N93-11537# Sandia National Labs., Albuquerque, NM.
SIMULATION OF LIQUID DROP BREAKUP BEHAVIOR IN A FLOW FIELD USING DISCRETE ELEMENT TECHNIQUES
F. T. Harper, E. D. Gorham, and M. S. El-Genk 1992 24 p
Presented at the International Topical Meeting on Reactor Thermal Hydraulics: Towards the Next Generation of Nuclear Power Plants, Salt Lake City, UT, 20-24 Sep. 1992
(Contract DE-AC04-76DP-00789)
(DE92-019435; SAND-92-1795C; CONF-920903-11) Avail: CASI HC A03/MF A01

In this study, a discrete element technique was used to simulate drop breakup in two dimensions. A series of simulations in which the drop breakup occurred in the presence of a flow field was performed. The density ratio of the flow field to the drop in the simulations was comparable to many of the isothermal liquid/liquid drop breakup experiments performed to investigate hydrodynamic breakup during Fuel Coolant Interactions (FCI's). The randomly directed internal kinetic energy of the drop increased rapidly at the beginning of the interaction between the drop and the flow field due to momentum transfer from the flow field to the drop. After the initial increase in internal energy of the drop, the momentum transferred from the flow field to the drop in the form of translational kinetic energy of the center of mass of the drop. It was also observed that the drops simulated in the presence of a flow field required higher internal kinetic energies to fragment than did the drops observed in the simulations performed in the absence of a flow field. DOE

N93-11538# Purdue Univ., West Lafayette, IN. School of Nuclear Engineering.
INTERFACIAL AREA AND TWO-PHASE FLOW STRUCTURE DEVELOPMENT MEASURED BY A DOUBLE-SENSOR PROBE
Waihung Leung, S. T. Revankar, Yoshihiko Ishii, and Mamoru Ishii Jun. 1992 126 p
(Contract DE-FG02-90ER-14147)
(DE92-019459; DOE/ER-14147/2; PU-NE-92/1) Avail: CASI HC A07/MF A02

In this report, we studied the local phasic characters of dispersed flow regime both at the entrance and at the fully developed regions. Since the dispersed phase is distributed randomly in the medium and enclosed in relatively small interfaces, the phasic measurement becomes difficult to obtain. Local probe must be made with a miniaturized sensor in order to reduce the interface distortion. The double-sensor resistivity probe has been widely used in local void fraction and interface velocity measurements because they are small in comparison with the interfaces. It has been tested and proved to be an accurate local phasic measurement tool. In these experiments, a double-sensor probe was employed to measure the local void fraction and interface velocity in an air-water system. The test section was flow regime can be determined by visualization. Furthermore, local phasic measurements can be verified by photographic studies. We concentrated our study on the bubbly flow regime only. The local measurements were conducted at two axial locations, L/D = 8 and 60, in which the first measurement represents the entrance region where the flow develops, and the second measurement represents the fully developed flow region where the radial profile does not change as the flow moves along the axial direction. Four liquid flow rates were chosen in combination with four different gas injection rates. The superficial liquid velocities were j sub t = 1.0, 0.6, 0.4, and 0.1 m/s and superficial gas velocities were j sub g = 0.0965, 0.0696, 0.0384, and 0.0192 m/s. These combinations put the two-phase flow well in the bubbly flow regime. In this sequence of phenomenological studies, the local void fraction, interface area concentration, sauter mean diameter, bubble velocity and bubble frequency were measured. DOE

N93-11575# Ecole Centrale de Lyon (France). Lab. de Mecanique et d'Acoustique.

RESOLUTION OF THE PRESSURE EQUATION BY THE BOUNDARY ELEMENT METHOD. APPLICATION TO MULTISTAGE TURBOMACHINES Ph.D. Thesis [RESOLUTION DE L'EQUATION DE PRESSION PAR LA METHODE DES ELEMENTS FRONTIERES. APPLICATION AUX TURBOMACHINES MULTIETAGEES]

Eric Larrey 1991 197 p In FRENCH
(ECL-91-16; ETN-92-92336) Avail: CASI HC A09/MF A03

The purpose of the study is to develop a method to predict the internal flow of turbomachines during a fast transient operation phase. The available methods to represent transient phenomena can not be applied to fast transient phenomena. The available three dimensional computer codes can predict the flow in only one isolated wheel. The calculation method developed is based on an original meridian method: the pressure's force is calculated by solving the pressure equation, at both the machine walls, using the boundary element technique. The pressure's force obtained is applied to calculate the flow velocity fields and the enthalpy by the finite volume method. Concerning the influence of the choice of the boundary conditions in the pressure evaluation, the following conclusions can be drawn: Neumann conditions enlarge the correction zone, while Dirichlet conditions tend to reduce it. ESA

N93-11606*# Princeton Univ., NJ. Gas Dynamics Lab.

TURBULENCE MODELING IN SHOCK WAVE/TURBULENT BOUNDARY LAYER INTERACTIONS Final Technical Report, 5 Apr. 1989 - 4 Apr. 1992

A. J. Smits Oct. 1992 20 p
(Grant NAG3-1032)
(NASA-CR-190933; NAS 1.26:190933) Avail: CASI HC A03/MF A01

The research performed was an experimental program to help develop turbulence models for shock wave boundary layer interactions. The measurements were taken in a Mach 3, 16 deg compression corner interaction, at a unit Reynolds number of 63 x 10(exp 6)/m. The data consisted of heat transfer data taken upstream and downstream of the interaction, hot wire measurements of the instantaneous temperature and velocity fluctuations to verify the Strong Reynolds Analogy, and single- and double-pulsed Rayleigh scattering images to study the development of the instantaneous shock/turbulence interaction. Author

N93-11615# DCW Industries, La Canada, CA.

PROGRESS IN DEVELOPING A TRANSITION MODEL FOR HIGH-SPEED FLOWS

David C. Wilcox 20 Oct. 1992 48 p
Avail: CASI HC A03/MF A01

Research is summarized which was conducted during the past year whose aim is to develop and test an accurate and efficient method for describing boundary-layer development in the transition region. A low Reynolds number version of the Wilcox k-epsilon model was postulated and tested against experimental data for 10 fully turbulent boundary layers and for more than 20 transitional cases. Overall discrepancies between theory and experiment are smaller than those for simpler correlations designed for use with algebraic turbulence models. Singular perturbation analysis of the compressible viscous sublayer and defect layer was initiated with some interesting preliminary results. Some progress was made toward eliminating the k-epsilon model's sensitivity to the freestream boundary condition on epsilon. Author

N93-11633*# Institute for Computer Applications in Science and Engineering, Hampton, VA.

FULLY NONLINEAR DEVELOPMENT OF THE MOST UNSTABLE GOERTLER VORTEX IN A THREE DIMENSIONAL BOUNDARY LAYER Final Report

S. R. Otto and Andrew P. Bassom (Exeter Univ., England) Sep. 1992 25 p Submitted for publication
(Contracts NAS1-18605; NAS1-19480; RTOP 505-90-52-01)
(NASA-CR-189710; NAS 1.26:189710; ICASE-92-45) Avail: CASI HC A03/MF A01

The nonlinear development is studied of the most unstable Gortler mode within a general 3-D boundary layer upon a suitably concave surface. The structure of this mode was first identified by Denier, Hall and Seddougui (1991) who demonstrated that the growth rate of this instability is O(G sup 3/5) where G is the Gortler number (taken to be large here), which is effectively a measure of the curvature of the surface. Previous researchers have described the fate of the most unstable mode within a 2-D boundary layer. Denier and Hall (1992) discussed the fully nonlinear development of the vortex in this case and showed that the nonlinearity causes a breakdown of the flow structure. The effect of crossflow and unsteadiness upon an infinitesimal unstable mode was elucidated by Bassom and Hall (1991). They demonstrated that crossflow tends to stabilize the most unstable Gortler mode, and for certain crossflow/frequency combinations the Gortler mode may be made neutrally stable. These vortex configurations naturally lend themselves to a weakly nonlinear stability analysis; work which is described in a previous article by the present author. Here we extend the ideas of Denier and Hall (1992) to the three-dimensional boundary layer problem. It is found that the numerical solution of the fully nonlinear equations is best conducted using a method which is essentially an adaption of that utilized by Denier and Hall (1992). The influence of crossflow and unsteadiness upon the breakdown of the flow is described. Author

N93-11637# Edgerton, Germeshausen and Grier, Inc., Idaho Falls, ID.

PARTICLE-FLUID TWO-PHASE FLOW MODELING

G. A. Mortensen and J. A. Trapp (Colorado Univ., Denver.) 1992 18 p Presented at the Japan-US Seminar on Two-phase Flow Dynamics, San Francisco, CA, 6-10 Jul. 1992
(Contract DE-AC07-76ID-01570)
(DE92-017847; EGG-M-92378; CONF-9207115-1) Avail: CASI HC A03/MF A01

This paper describes a numerical scheme and computer program, DISCON, for the calculation of two-phase flows that does not require the use of flow regime maps. This model is intermediate between-thermal instantaneous and the averaged two-fluid model. It solves the Eulerian continuity, momentum, and energy equations for each liquid control volume, and the Lagrangian mass, momentum, energy, and position equations for each bubble. The bubbles are modeled individually using a large representative number of bubbles, thus, avoiding the numerical diffusion associated with Eulerian models. DISCON has been used to calculate the bubbling of air through a column of water and the subcooled boiling of water in a flow channel. The results of these calculations are presented. DOE

N93-11638# Oak Ridge National Lab., TN.

EFFECTS OF PHYSICAL PROPERTIES AND GEOMETRY ON SHAPES AND STABILITY OF POLARIZABLE DROPS IN EXTERNAL FIELDS

F. K. Wohlhuter (Tennessee Univ., Knoxville.) and O. A. Basaran Jul. 1992 14 p Presented at the 6th International Conference on Magnetic Fluids, Paris, France, 20-24 Jul. 1992
(Contract DE-AC05-84OR-21400)
(DE92-018865; CONF-9207117-1) Avail: CASI HC A03/MF A01

Equilibrium shapes and stability of linearly and nonlinearly polarizable drops floating freely between the two faces of a parallel-plate capacitor and subjected to an electric (magnetic) field are found by solving the Young-Laplace equation for surface shape and the Maxwell equations for field distribution. Accounting for nonlinear polarization at last brings theory and experiment into accord. Finite plate separation - as in any real experiment - is also found to play a big role. DOE

N93-11670# Utah Univ., Salt Lake City. Dept. of Chemical Engineering.

3-D TURBULENT PARTICLE DISPERSION SUBMODEL DEVELOPMENT

J. P. Smith 1991 40 p
(Contract DE-FG22-90PC-90094)
(DE92-018212; DOE/PC-90094/T2) Avail: CASI HC A03/MF A01

The lack of a mathematical description of the interactions of fluid turbulence with other physics-chemical processes is a major obstacle in modeling many industrial program. Turbulent two-phase flow is a phenomenon that is of significant practical importance to coal combustion as well as other disciplines. The interactions of fluid turbulence with the particulate phase has yet to be accurately and efficiently modeled for these industrial applications. On 15 May 1991 work was initiated to cover four major tasks toward the development of a computational submodel for turbulent particle dispersion that would be applicable to coal combustion simulations. Those four tasks are: (1) A critical evaluation of the 2-D Lagrangian particle dispersion submodel; (2) Development of a 3-D submodel for turbulent particle dispersion; (3) Evaluation of the 3-D submodel for turbulent particle dispersion; and (4) Exploration of extensions of the Lagrangian dispersion theory to other applications including chemistry-turbulence interactions. DOE

N93-11671# Utah Univ., Salt Lake City. Dept. of Chemical Engineering.
3-D TURBULENT PARTICLE DISPERSION SUBMODEL DEVELOPMENT
P. J. Smith 1991 34 p
(Contract DE-FG22-90PC-90094)
(DE92-018228; DOE/PC-90094/T1) Avail: CASI HC A03/MF A01

The lack of a mathematical description of the interactions of fluid turbulence with other physicochemical processes is a major obstacle in modeling many industrial program. Turbulent two phase flow is a phenomenon that is of significant practical importance to coal combustion as well as other disciplines. The interactions of fluid turbulence with the particulate phase has yet to be accurately and efficiently modeled for these industrial applications. Four major tasks were started toward the development of a computational submodel for turbulent particle dispersion that would be applicable to coal combustion simulations. Those four tasks are: (1) A critical evaluation of the 2-D Lagrangian particle dispersion submodel; (2) Development of a 3-D submodel for turbulent particle dispersion; (3) Evaluation of the 3-D submodel for turbulent particle dispersion; and (4) Exploration of extensions of the Lagrangian dispersion theory to other applications including chemistry-turbulence interactions. DOE

N93-11698 Clarkson Univ., Potsdam, NY.
AN EXPERIMENTAL STUDY OF FLOW PATTERNS AND ENDWALL HEAT TRANSFER UPSTREAM OF A SURFACE-MOUNTED RECTANGULAR OBSTRUCTION IN A TURBULENT BOUNDARY LAYER Ph.D. Thesis
Quan Chen 1991 215 p
Avail: Univ. Microfilms Order No. DA9201045

A seven-phase experimental investigation documented the three-dimensional separation region in front of a surface-mounted rectangular obstruction. The obstruction was centered between sidewalls of a wind tunnel in a turbulent approaching boundary layer. The major feature of this flow was a horseshoe vortex system near the junction. Real-time vortex structures were visualized with a laser sheet. Interior velocity, turbulence intensity and velocity power spectrum measurements were obtained with a Laser Doppler Anemometer (LDA) and a hot-wire anemometer. Ink dot surface flow visualizations and pressure measurements were acquired on the endwall under the vortex system. Endwall heat transfer coefficients were nonintrusively measured by an infrared imaging system. Laser sheet flow visualizations indicated a vortex system with randon oscillations. In the time-averaged sense, ink-dot flow visualizations, LDA measurements and endwall pressure measurements indicated a well defined primary vortex. The separation region was 70 percent larger, in the streamwise direction, than that in front of a cylinder with a diameter the same as the obstruction width. The time-averaged primary vortex center, where maximum values of turbulence intensity were measured, was located farther away from the obstruction leading edge at higher freestream velocities. Endwall heat transfer coefficient distribution measurements on the endwall surface revealed that the obstruction established a complex heat transfer pattern. Local heat transfer rates as much as 80 percent greater than the undisturbed two-dimensional level were recorded upstream of the obstruction along the test section centerline. A local heat transfer coefficient peak was associated with the local maximum turbulence intensity measured near the endwall by LDA. Dissert. Abstr.

N93-11722 Purdue Univ., Indianapolis, IN.
CALCULATION OF NOZZLE/AFTBODY FLOWFIELD INTERACTIONS Ph.D. Thesis
David Infante Driscoll 1991 214 p
Avail: Univ. Microfilms Order No. DA9215542

A numerical technique is presented to analyze the influence of two-demensional and axisymmetric aftbody flowfields on the performance of propulsive nozzles. The analysis employs a numerical technique based on the strong conservation law form of the governing equations for fluid flow (i.e., the Navier-Stokes equations), and uses an implicit Beam-Warming algorithm to obtain the steady state solution as the asymptotic solution in time. Characteristic boundary point unit processes are utilized, and a comparison is made between extrapolated boundary point unit processes and numerical method of characteristics boundary point unit processes. Two-equation turbulence models are investigated and a comparison is made between zero- and two-equation turbulence models for several representative flow cases.
Dissert. Abstr.

N93-11756# Naval Research Lab., Washington, DC.
MIXING REGIMES IN A SPATIALLY CONFINED, TWO-DIMENSIONAL, SUPERSONIC SHEAR LAYER Interim Report
P. Vuillermoz and E. S. Oran 31 Jul. 1992 40 p
(AD-A254302; NRL/MR/4404-92-7106) Avail: CASI HC A03/MF A01

The evolution of a high-speed, compressible, confined, temporally evolving supersonic mixing layer between hydrogen and oxygen gas streams is examined using time-dependent, two-dimensional, numerical simulations that include the effects of viscosity, molecular diffusion, and thermal conduction. The flow shows three distinct mixing regimes: an apparently ordered, laminar stage in which the structures grow due to the initial perturbation; a convective-mixing regimes in which vortices begin to interact and structures grow; and a diffusive-mixing regime in which vortical structures break down and diffusive mixing dominates. Varying the strength of the diffusion terms shows that these effects are important in the laminar and diffusive-mixing stages, but not in the convective mixing stage. Varying the convective Mach shows that compressibility does not change the general structural features of the mixing process, although higher compressibility results in a slower transition between the various flow regimes. Increasing the size of the computational domain increases the absolute time of transition from convective to diffusive mixing, but does not affect the dimensionless time normalized to the system size. GRA

N93-11767# Los Alamos National Lab., NM.
NUMERICAL ANALYSIS OF THE FLOW FIELDS IN A RQL GAS TURBINE COMBUSTOR
Michael C. Cline, Gerald J. Micklow (Florida Univ., Gainesville.), S. L. Yang (Michigan Technological Univ., Houghton.), and H. L. Nguyen (National Aeronautics and Space Administration. Lewis Research Center, Cleveland, OH.) 1992 21 p Presented at the 28th Joint Propulsion Conference, Nashville, TN, 6-8 Jul. 1992
(Contract W-7405-eng-36)
(DE92-017509; LA-UR-92-1964; CONF-920747-7) Avail: CASI HC A03/MF A01

The KIVA-2 code was modified to allow calculation of the flow field in a Richburn/Quick quench/Lean burn (RQL) staged gas turbine combustor including the airblast fuel nozzle. The results illustrate the complicated flow field present in RQL combustors.

In particular the thermal protection requirements of the quick-quench mixer used in this study may be similar to those of the rich-burn combustor despite the presence of the cool dilution jet. Variation of the mass flow split between the fuel nozzle air passages has a significant effect on the flow as well as the level of the NO emissions. In addition, the slanted dilution slots form a counter-rotating flow field. From the results obtained to date, it appears that the modified KIVA-2 code can be used to study the effects of various RQL combustor design and operating conditions. DOE

N93-11774# Minnesota Mining and Mfg. Co., Saint Paul. Corporate Research Labs.
ADVANCED HEAT PUMP FOR THE RECOVERY OF VOLATILE ORGANIC COMPOUNDS
Mar. 1992 97 p
(Contract DE-FC07-88ID-12707)
(DE92-011592; DOE/ID-12707/T1) Avail: CASI HC A05/MF A02

Emissions of Volatile Organic Compounds (VOC) from stationary industrial and commercial sources represent a substantial portion of the total U.S. VOC emissions. The 'Toxic-Release Inventory' of the U.S. Environmental Protection Agency estimates this to be at about 3 billion pounds per year (1987 estimates). The majority of these VOC emissions are from coating processes, cleaning processes, polymer production, fuel production and distribution, foam blowing, refrigerant production, and wood products production. The U.S. Department of Energy's (DOE) interest in the recovery of VOC stems from the energy embodied in the recovered solvents and the energy required to dispose of them in an environmentally acceptable manner. This Phase 1 report documents 3M's work in close working relationship with its subcontractor Nuclear Consulting Services (Nucon) for the preliminary conceptual design of an advanced Brayton cycle heat pump for the recovery of VOC. The Nucon designed Brayton cycle heat pump for the recovery of methyl ethyl ketone and toluene from coating operations at 3M Weatherford, OK, was used as a base line for the work under cooperative agreement between 3M and ODE. See appendix A and reference (4) by Kovach of Nucon. This cooperative agreement report evaluates and compares an advanced Brayton cycle heat pump for solvent recovery with other competing technologies for solvent recovery and reuse. This advanced Brayton cycle heat pump is simple (very few components), highly reliable (off the shelf components), energy efficient, and economically priced. DOE

N93-11799# Sandia National Labs., Albuquerque, NM.
USING NEKTON TO SOLVE SYSTEMS OF DISCRETE BOLTZMANN EQUATIONS
J. R. Torczynski 1992 17 p Presented at the 1992 Fluent Incorporated Software Users Group Meeting, Burlington, VT, 13-15 Oct. 1992
(Contract DE-AC04-76DP-00789)
(DE92-018272; SAND-92-0777C; CONF-9210135-1) Avail: CASI HC A03/MF A01

A discrete-velocity-gas (DVG) model of the Boltzmann equation, that employs four velocity states, was implemented numerically by using the computational fluid dynamics code NEKTON to solve the DVG species-transport (discrete Boltzmann) equations. The model is applicable to rarefied two-dimensional isothermal flow and is used to simulate flow through a channel. As expected, the velocity profile is found to be uniform for large Knudsen numbers (free molecular flow) and parabolic for small Knudsen numbers (near continuum flow). Since there are no conceptual differences between the four-state model and models employing more velocity states to better represent the Boltzmann equation, implementation of models with more velocity states appear to be straightforward. DOE

N93-11843# Los Alamos National Lab., NM.
HYDRODYNAMIC PARTICLE MIGRATION IN SMALL-AMPLITUDE, OSCILLATORY, CIRCULAR COUETTE FLOW: THE LIMITS OF REVERSIBILITY
H. Brenner (Massachusetts Inst. of Tech., Cambridge.), S. A. Altobelli (Lovelace Foundation for Medical Education and Research, Albuquerque, NM.), A. L. Graham, and J. R. Abbott 1992 4 p Presented at the 11th International Congress of Rheology, Brussels, Belgium, 17-21 Aug. 1992
(Contracts W-7405-eng-36; DE-AC04-76DP-00789)
(DE92-008480; LA-UR-92-633; CONF-920852-1; SAND-91-2273C)
Avail: CASI HC A01/MF A01

Initially well-mixed suspensions of large spherical particles in viscous Newtonian fluids subjected to continuous nonhomogeneous shear flows demix and establish large concentration gradients. A number of experimental studies have determined that the particles migrate to the low shear-rate region in one-dimensional flow fields. Other investigators have proposed mechanisms to model the migration caused by the presence of nonuniform shear gradients. Here, we report on the shear-induced migration of particles in the annular space between two coaxial cylinders (a wide-gap Couette), with the inner cylinder oscillating and the outer cylinder fixed. In these experiments, the conditions are such that colloidal and inertial forces do not exert an appreciable effect on the suspensions of neutrally bouyant spherical particles in Newtonian liquids. Nuclear magnetic resonance (NMR) imaging is used to measure the concentration profile during the demixing of the initially well-mixed suspensions. DOE

N93-11856 City Univ. of New York, NY.
MODE INTERACTION MODELS IN NEAR-WALL TURBULENCE Ph.D. Thesis
Sanjeev Sanghi 1992 154 p
Avail: Univ. Microfilms Order No. DA9218266

The dynamics of near wall turbulence is characterized by intermittent bursts during which fine scale turbulence is produced. Bursting events have been observed in low dimensional dynamical models built from empirical eigenfunctions of the proper orthogonal decomposition (POD). Severly truncated models, which did not account for streamwise variations in an explicit way, have been derived and studied by Aubry et al. (1988). In the present work, the persistency of intermittent behavior in higher dimensional models is investigated. First, the new truncations account for streamwise variations. Intermittent behavior persists in all the models, but exhibits additional complexities. In particular, the non zero streamwise modes become excited during the bursts so that the infinitely long streamwise rolls burst in the streamwise direction into smaller scales. In all cases, intermittency seems to be due to homoclinic cycles connecting hyperbolic fixed points or complicated limit sets. The triggering of the higher order streamwise modes by nonlinear interactions is also analyzed. The influence of another proper orthogonal mode (i.e. smaller structures in the normal direction) is also investigated: bursts still occur in the same way, the second mode participating along with the first. A coherent structure study is performed in these models in order to connect the findings of this investigation to those of the other researchers. Most experimentally observed structures, i.e. streaks, streamwise rolls, horseshoe vortical structures, and shear layers, are clearly identified and it is proposed that they are a part of the same structure. The POD technique is used to expand the vorticity field into 'coherent vortical structures'. To calculate the POD modes for any vector, its autocorrelation tensor is needed. It is, however, shown in this work that the POD modes and eigenvalues of the vorticity vector can be calculated from the POD modes and the eigenvalues of the velocity vector. This method is applied to the turbulent wall layer and the spectrum of eigenvalues of the vorticity modes is compared with the vorticity modes. As expected, the peak shifts toward the right for the vorticity spectrum. As a trial case the first two vortical structures are evaluated for one realization. Finally, a dynamic eddy viscosity model based on the application of the approximate inertial manifold technique to the POD modes is proposed. Dissert. Abstr.

N93-11870 Brown Univ., Providence, RI.
NUMERICAL INVESTIGATION OF THREE-DIMENSIONALLY EVOLVING JETS Ph.D. Thesis

James E. Martin 1991 258 p
Avail: Univ. Microfilms Order No. DA9204916

The inviscid mechanisms governing the three-dimensional evolution of ring- and helix-dominated jets by means of vortex filament simulations are studied. The spatially periodic calculations provide a detailed picture of the processes leading to the concentration, reorientation, and stretching of the vorticity. In the purely axisymmetric case, a wavy perturbation in the streamwise direction leads to the formation of vortex rings connected by braid regions, which become depleted of vorticity. The curvature of the jet shear layer leads to a loss of symmetry and the position of the free stagnation point is shifted toward the jet axis. As a result, the upstream neighborhood of a vortex ring is depleted of vorticity at a faster rate than the downstream side. When the ring-dominated jet is also subjected to a sinusoidal perturbation in the azimuthal direction, it develops regions of counterrotating streamwise vorticity, whose sign is determined by a competition between local and global induction effects. In a manner similar to plane shear layers, the streamwise braid vorticity collapses into counterrotating round vortex tubes. In addition, the cores of the vortex rings develop a wavy dislocation. A jet corresponding to R/theta = 22.6 develops rings that slowly rotate preventing their instability. For R/theta = 11.3, on the other hand, we observe a Widnall-type instability of the rings. The growth of the momentum thickness is more dramatic. For the case of a helical perturbation only, we observe the emergence of a helical vortex. The streamwide braid vorticity and that due to the helix are of single opposite signs. The streamwise braid vorticity is of infinite aspect ratio and in sheet-like form. If the helical symmetry is broken by introducing an additional azimuthal wave, a Kelvin-Helmholtz instability leads to single-signed streamwise vortices, in contrast to the counterrotating vortices of the ring-dominated jet. For R/theta = 11.3, we observe vortex helix instability. Following a scenario first proposed by Browand and Laufer, the inclusion of a subharmonic axisymmetric perturbation leads to helical pairing. We also consider helical perturbations of azimuthal wavenumber two plus simulations with helical waves of opposite-signed azimuthal wavenumber.
Dissert. Abstr.

N93-11881 Durham Univ. (England).
THE AERODYNAMICS OF CURVED JETS AND BREAKAWAY IN COANDA FLARES, VOLUMES 1 AND 2 Ph.D. Thesis
Peter Senior 1991 446 p
Avail: Univ. Microfilms Order No. BRD-96044

An investigation was carried out into external-Coanda Effect flares designed by British Petroleum International plc. The phenomenon of interest was breakaway of an underexpanded axisymmetric curved wall jet from the guiding surface due to high blowing pressure. A survey of investigations of similar flows suggested very complex jet fluid dynamics. Strong cell structure including shock waves was present giving buok and discrete compression and bulk dilatation. More expansion was imposed by the radial velocity components. Wall curvature and a rear-facing step added further significant influences. The combination of these factors is known to produce highly non-linear turbulence, and this constitutes a major difficulty for the application of computational methods to the flare. In view of the amount of resources required to eliminate the problems of using a Navier-Stokes code, an economical approach was adopted, matching the Method of Characteristics to various simplified models and an integral boundary layer. In this experimental work, a planar model of the flare was constructed and studied using a wide range of methods in order to achieve accuracy and provide comparability with other work. An axisymmetric model was designed and investigated in a similar manner, so that the influence of this geometry could be clearly distinguished. A full-scale flare was subjected to a restricted range of tests to compare the laboratory results with the industrial application. The results from all the experiments demonstrated good correspondence. The main conclusion was that amalgamation of separation bubbles is crucial for breakaway. These are present long before breakaway, and are strongly reduced by decreasing the cell scale, adding a rear-facing step and axisymmetry, which leads to improved breakaway performance. Although the computational methods did not prove robust enough for all design purposes, they did permit significant insights into the mechanisms of breakaway.
Dissert. Abstr.

N93-11995# Mississippi State Univ., Mississippi State. Diagnostic Instrumentation and Analysis Lab.
A COMPARISON OF VELOCITY PROFILE MEASUREMENTS IN THE CDIF DIFFUSER WITH FLOW FIELD MODEL CALCULATIONS
O. P. Norton, W. W. Wilson, and R. L. Cook 1992 9 p Presented at the 30th Symposium on Engineering Aspects of Magnetohydrodynamics, Baltimore, MD, 29 Jun. - 2 Jul. 1992
(Contract DE-AC02-80ET-15601)
(DE92-015367; CONF-920677-11) Avail: CASI HC A02/MF A01

A series of test runs were made at the Component Development and Integration Facility (CDIF) facility in April and May of 1991. During this test series, the magnet was not energized and thus no power was produced. A commercial computational fluid dynamics program was used to predict the flow in the channel and diffuser. The results of these calculations are compared to velocity measurements made with a laser Doppler velocimeter (LDV) during the tests. The numerical calculations were made using PHOENICS, a commercial program for computing fluid flows. The calculations predict that the flow will still be supersonic as it exits the constant area section of the diffuser, and will thus continue to accelerate in the diverging section which follows. Then, a strong shock is predicted in the diverging section of the diffuser which decelerates the flow to subsonic conditions. Downstream of this shock, the calculation predicts a skewed velocity profile, with the main flow adhering to one wall and a recirculation region against the opposite wall. Laser Doppler velocity (LDV) measurements were made in the diffuser to CDIF. These measurements indicate that, near the center of the diffuser, the velocity distribution histogram may be bimodal, with one peak at about 600-700 meters/second, and the second peak at about 1400-1600 meters/second. In these combustion gases, the sonic velocity is 800-850 meters per second. Thus, one peak in the velocity histogram is subsonic and the other is supersonic. This suggests that the bimodal distribution might be due to an oscillating strong shock wave. This bimodal distribution is not always present. Other measurements, made under what appear to be identical operating conditions, show only a unimodal subsonic velocity histogram. These measurements also show a region of reverse flow near one wall.
DOE

N93-12003 Purdue Univ., West Lafayette, IN.
TURBULENCE STRUCTURE AND POLYMER DRAG REDUCTION IN ADVERSE PRESSURE GRADIENT BOUNDARY LAYERS Ph.D. Thesis
John Edward Koskie 1991 219 p
Avail: Univ. Microfilms Order No. DA9215585

One zero pressure gradient Newtonian boundary layer and two adverse pressure gradient equilibrium boundary layers in a water channel were examined. The momentum thickness Reynolds numbers, Re(sub theta), were in the range 1360 to 4980. The adverse pressure gradient boundary layers were characterized by equilibrium parameters, beta of 1.8 and 2.4. These boundary layers were modified by injecting a drag reducing polymer solution at 2.6 and 5.1 times the flow rate of the undisturbed flows inside of y(+) = 5. The sum of the viscous and Reynolds shear stresses was sometimes less than the total shear stress in the drag reduced boundary layer and in these cases the production of Reynolds shear and normal stresses was virtually eliminated. The mean streamwise velocity measurements in the drag reduced boundary layers showed that both parameters, kappa and B, of the logarithmic velocity profile changed. The slope parameter, kappa, varied directly with the percent drag reduction. The peak in the root-mean-square streamwise velocities remained essentially unchanged in the presence of polymer but its location moved away from the wall. The root-mean-square normal velocities and the Reynolds shear stress were reduced in the inner region of the boundary layer during drag reduction. The adverse pressure gradient boundary layers did not separate during drag reduction even when large amounts of polymer were injected. The influence of the polymer on the turbulent boundary layer structure was greatly reduced, but the effects of polymer were consistent with those in the zero pressure gradient boundary layer. The hypothesis that the extensional motions in the flow must be strong enough to stretch the polymer molecules so that stretched molecules will form an anisotropic viscosity that damps the small scales of the turbulence (Hinch, 1977) was supported by the present data. Walker's (1985) modified mixing length model correctly predicted the wall shear stress coefficient, c(sub f), in all the drag reduced boundary layers as long as the measured polymer concentration in the linear sublayer was within the range of concentrations for which the model was derived and the non-Newtonian shear stresses in the boundary layer were small. Mixed scaling of the average time between bursts best scaled the present zero and adverse pressure gradient Newtonian boundary layer data. The data was consistent with the hypothesis that the method of tripping the boundary layer affects the average burst period at very low Reynolds numbers. Dissert. Abstr.

N93-12010# General Atomic Co., San Diego, CA.

A MODEL FOR ANALYTICAL PERFORMANCE PREDICTION OF HYPERVAPOTRON

C. B. Baxi and H. Falter (Joint European Torus Project, Abingdon, England) Jul. 1992 6 p Presented at the International Topical Meeting on Reactor Thermal Hydraulics: Towards the Next Generation of Nuclear Power Plants, Salt Lake City, UT, 20-24 Sep. 1992
(Contract DE-AC03-89ER-51114)
(DE92-018885; GA-A-20959; CONF-920903-10) Avail: CASI HC A02/MF A01

A hypervapotron is a water-cooled device which combines the advantages of finned surfaces with the large heat transfer rates possible during boiling heat transfer. Hypervapotrons have been used as beam dumps in the past and plans are under way to use them for divertor cooling in the Joint European Torus (JET). Experiments at JET have showed that a surface heat flux of 25 MW/sq m can be achieved in hypervapotrons. This performance makes such a device very attractive for cooling of divertor of the International Thermonuclear Experimental Reactor (ITER). This paper presents an analytical method to predict the thermal performance of the hypervapotrons. Preliminary results show an excellent agreement between experimental results and analytical prediction over a wide range of flow velocities, pressures, subcooling temperatures and heat fluxes. This paper also presents the predicted performance of hypervapotrons made of materials other than copper. After further development and verification, the analytical method could be used for optimizing designs and performance prediction. DOE

N93-12070# Energetics, Inc., Columbia, MD.

PROCEEDINGS OF THE DOE/ADVANCED HEAT EXCHANGERS PROGRAM REVIEW

Feb. 1992 365 p Review held in Herndon, VA, 13 Feb. 1992 Sponsored by DOE
(DE92-014385; CONF-9202108-Summ) Avail: CASI HC A16/MF A03

Semiannual review meetings of the USDOE's Advanced Heat Exchanger Program with the objective of reviewing ongoing and recently completed project activities. Personnel from industrial contractors and National Laboratories present technical aspects of their projects. The projects deal with high temperature heat exchangers for waste heat recuperation and process heat exchange and other areas such as materials performance and heat transfer enhancement. Topics presented are high pressure heat exchangers, ceramic heat exchangers, enhanced tubes, and materials studies to include silicon carbide whiskers and alumina. DOE

N93-12082*# Alabama Univ., Huntsville.

APPLICATION OF A TWO-LAYER NEAR WALL MODEL TO FULLY DEVELOPED AND ROTATING CHANNEL TURBULENT FLOWS Final Report

C. P. Chen and K. L. Guo Nov. 1991 49 p
(Contract NAS8-36955)
(NASA-CR-184441; NAS 1.26:184441) Avail: CASI HC A03/MF A01

The two-layer near wall approach in combination with the k-epsilon model was applied to rotating flows. Validation studies show that the conventional length scales have to be modified to account for rotating effects. Guided by the Lam and Bremhorst's low Reynolds number model with the rotation-corrected k-epsilon model, a new set of length scales formulation is proposed. The developments and validations of the current model are reported. A fully elliptic numerical method developed to solve the two-dimensional Reynolds-averaged Navier-Stokes equations is employed for the computational study. Author

N93-12128# Argonne National Lab., IL.

DISRUPTION SHAPE EFFECTS ON THE PERFORMANCE OF ENHANCED TUBES WITH THE SEPARATION AND REATTACHMENT MECHANISM

B. Arman and T. J. Rabas 1992 10 p Presented at the ASME National Heat Transfer Conference and Exposition, San Diego, CA, 9-12 Aug. 1992
(Contract W-31-109-eng-38)
(DE92-016602; ANL/CP-75351; CONF-920804-16) Avail: CASI HC A02/MF A01

A non-orthogonal, body-fitted numerical code is used to determine the thermo-hydraulic performance of enhanced tubes with transverse periodic sine-, semicircle-, arc-, and trapezoid-shaped disruptions. The turbulence closure was achieved with a two-layer turbulence model. It is shown that there is a tradeoff of the heat-transfer and pressure-drop performances when the disruption shape becomes more contoured; that is, both the heat transfer and the pressure drop increase. The local heat transfer is strongly dependent on the shape in the vicinity of the disruption but it is less dependent in the downstream recirculation region and in the boundary layer development zone. With increasing pitch, effect of the shape on the heat-transfer performance becomes less important. The pressure drop is more dependent on the disruption shape and it continues to decrease when the disruptions become less contoured because of the reduced form drag which is by far the major contribution to the total pressure drop. DOE

N93-12157 Massachusetts Univ., Amherst.

REGULAR AND CHAOTIC MIXING OF VISCOUS FLUIDS IN ECCENTRIC ROTATING CYLINDERS Ph.D. Thesis

Paul David Swanson 1991 152 p
Avail: Univ. Microfilms Order No. DA9132920

In this research we study the mixing of viscous fluids in a model flow, the eccentric cylinder system. The flow between eccentric rotating cylinders is used because an analytic expression for the stream function exists and we have fabricated an apparatus to experimentally generate the flow. We use the flow to determine the extent to which several computational methods are able to predict the experimental mixing in the flow. We have found that Poincare sections give a good indication of the maximum extent of mixing in the experiments but they give no information on the rate of mixing. The locations of elliptic periodic points give an indication of where 'islands' of regular behavior will occur in the flow. The manifolds of the hyperbolic periodic point with the largest eigenvalue give a template of the striation pattern which forms in the experiments. Finally, stretching plots appear to match the experiments quite well. We have found that co-rotation of the cylinders leads to mixing over a larger region of the flow domain than the equivalent counter-rotating motion of the cylinders. Driving the cylinders with different waveforms appears to produce little or no difference in the mixing. The Melnikov method has been adapted to adjust the waveforms such that the resultant mixing is in even closer agreement. In addition, we have determined that the points which stretch the most start on the stable manifold of a hyperbolic periodic point and end up on the unstable manifold. This results in the stretching plots assuming the shape of the manifolds and consequently matching the striation patterns of the experiments. Finally, we have determined that the methods of analysis presented here can be applied to flows where only a discretized representation of the velocity field exists. This means that our methods of analysis will be effective even when the flow field must be determined numerically. Dissert. Abstr.

N93-12162# Virginia Polytechnic Inst. and State Univ., Blacksburg. Dept. of Engineering Science and Mechanics.
LAMINAR BOUNDARY-LAYER BREAKDOWN Final Report, 1 Oct. 1990 - 30 Sep. 1991
Ali H. Nayfeh 7 Jul. 1992 9 p
(Contract N00014-91-J-1309)
(AD-A254489) Avail: CASI HC A02/MF A01

The objective of the work is to use dynamical system theory to determine the mechanisms that are responsible for the breakdown of laminar flows and to investigate the possibility of modifying the transition process to affect the subsequent well-developed turbulence structure. Experiments performed in low-disturbance wind-tunnels established two scenarios for the laminar-boundary-layer breakdown: the fundamental- and subharmonic-modes of breakdown. The experimental observations of the subharmonic breakdown are very similar to our observations of the breakdown of regular motions in metallic and composite structural systems into chaotic motions. Therefore, we used dynamical system theory to conduct an analysis for the subharmonic breakdown in boundary layers similar to the one we successfully used to explain the breakdown in the response of the structural systems. The results can be used to modify the breakdown process and hence the resulting turbulent motion. GRA

N93-12173*# Institute for Computer Applications in Science and Engineering, Hampton, VA.
SINGULARITIES OF THE EULER EQUATION AND HYDRODYNAMIC STABILITY Final Report
S. Tanveer and Charles G. Speziale Oct. 1992 23 p Submitted for publication
(Contracts NAS1-18605; NAS1-19480; DE-FG02-92ER-14270; NSF DMS-91-07608; RTOP 505-90-52-01)
(NASA-CR-189720; NAS 1.26:189720; ICASE-92-54) Avail: CASI HC A03/MF A01

Equations governing the motion of a specific class of singularities of the Euler equation in the extended complex spatial domain are derived. Under some assumptions, it is shown how this motion is dictated by the smooth part of the complex velocity at a singular point in the unphysical domain. These results are used to relate the motion of complex singularities to the stability of steady solutions of the Euler equation. A sufficient condition for instability is conjectured. Several examples are presented to demonstrate the efficacy of this sufficient condition which include the class of elliptical flows and the Kelvin-Stuart Cat's Eye. Author

N93-12221# Brookhaven National Lab., Upton, NY.
ENHANCED CONVECTIVE AND FILM BOILING HEAT TRANSFER BY SURFACE GAS INJECTION
M. R. Duignan, G. A. Greene, and T. F. Irvine, Jr. Apr. 1992 107 p
(Contract DE-AC02-76CH-00016)
(DE92-016755; BNL-52326) Avail: CASI HC A06/MF A02

Heat transfer measurements were made for stable film boiling of water over a horizontal, flat stainless steel plate from the minimum film boiling point temperature, T(sub SURFACE) approximately 500 K, to T(sub SURFACE) approximately 950 K. The pressure at the plate was approximately 1 atmosphere and the temperature of the water pool was maintained at saturation. The data were compared to the Berenson film-boiling model, which was developed for minimum film-boiling-point conditions. The model accurately represented the data near the minimum film-boiling point and at the highest temperatures measured, as long as it was corrected for the heat transferred by radiation. On the average, the experimental data lay within plus or minus 7 percent of the model. Measurements of heat transfer were made without film boiling for nitrogen jetting into an overlying pool of water from nine 1-mm-diameter holes, drilled in the heat transfer plate. The heat flux was maintained constant at approximately 26.4 kW/sq m. For water-pool heights of less than 6 cm the heat transfer coefficient decreased linearly with a decrease in heights. Above 6 cm the heat transfer coefficient was unaffected. For the entire range of gas velocities which measured (0 to 8.5 cm/s), the magnitude of the heat transfer coefficient only changed by approximately 20 percent. The heat transfer data bound the Konsetov model for turbulent pool heat transfer which was developed for vertical heat transfer surfaces. This agreement suggests that surface orientation may not be important when the gas jets do not locally affect the surface heat transfer. Finally, a database was developed for heat transfer from the plate with both film boiling and gas jetting occurring simultaneously, in a pool of water maintained at its saturation temperature. The effect of passing nitrogen through established film boiling is to increase the heat transfer from that surface. DOE

N93-12245# Iowa Univ., Iowa City. Inst. of Hydraulic Research.
FLOW IN CURVED DUCTS OF VARYING CROSS-SECTION
F. Sotiropoulos and V. C. Patel Jul. 1992 205 p
(AD-A254660; IIHR-358) Avail: CASI HC A10/MF A03

Two numerical methods for solving the incompressible Navier-Stokes equations are compared with each other by applying them to calculate laminar and turbulent flows through curved ducts of regular cross-section. Detailed comparisons, between the computed solutions and experimental data, are carried out in order to validate the two methods and to identify their relative merits and disadvantages. Based on the conclusions of this comparative study a numerical method is developed for simulating viscous flows through curved ducts of varying cross-sections. The proposed method is capable of simulating the near-wall turbulence using fine computational meshes across the sublayer in conjunction with a two-layer k-epsilon model. Numerical solutions are obtained for: (1) a straight transition duct geometry, and (2) a hydroturbine draft-tube configuration at model scale Reynolds number for various inlet swirl intensities. The report also provides a detailed literature survey that summarizes all the experimental and computational work in the area of duct flows. GRA

N93-12313# Argonne National Lab., IL.
THE INFLUENCE OF THE PRANDTL NUMBER ON THE THERMAL PERFORMANCE OF TUBES WITH THE SEPARATION AND REATTACHMENT ENHANCEMENT MECHANISM
T. J. Rabas and B. Arman 1992 12 p Presented at the American Society of Mechanical Engineers National Heat Transfer Conference and Exposition, San Diego, CA, 9-12 Aug. 1992
(Contract W-31-109-eng-38)
(DE92-016601; ANL/CP-76052; CONF-920804-15) Avail: CASI HC A03/MF A01

This paper demonstrates that the heat-transfer performance of an enhanced tube with transverse, rectangular disruptions can be predicted with a numerical modeling method, an accomplishment not previously achieved. This computer code is then used to determine the influence of the Prandtl number. The numerical simulation demonstrated that six distinct regions exist: the three rib surfaces, the upstream and downstream recirculation regions, and the boundary-layer development zone. Three zones dominate the thermal performance: the rib top and downstream faces and the downstream recirculation zone. The thermal performance at the rib region begins to dominate tile overall performance as the Prandtl number becomes large. The contribution from the downstream recirculation zone becomes more important and dominates for low Prandtl number fluids such as air. The Reynolds number dependence at the rib region and the downstream recirculation zone is similar to that for reattaching flows with exponents in the 0.65 to 0.75 range. The location of the maximum in the recirculation moves closer to the rib with increasing Reynolds and Prandtl numbers and is bounded upstream by the location of the maximum wall shear stress and downstream by the reattachment length. The high turbulence level near the surface in this region is responsible for the heat-transfer enhancement. DOE

N93-12329*# Eloret Corp., Palo Alto, CA.
SOLUTION OF NONLINEAR FLOW EQUATIONS FOR COMPLEX AERODYNAMIC SHAPES Final Technical Report, 1 Sep. 1990 - 30 Sep. 1992
M. Jahed Djomehri 4 Nov. 1992 10 p
(Contract NCC2-689)
(NASA-CR-190979; NAS 1.26:190979) Avail: CASI HC A02/MF A01

Solution-adaptive CFD codes based on unstructured methods for 3-D complex geometries in subsonic to supersonic regimes were investigated, and the computed solution data were analyzed in conjunction with experimental data obtained from wind tunnel measurements in order to assess and validate the predictability of the code. Specifically, the FELISA code was assessed and improved in cooperation with NASA Langley and Imperial College, Swansea, U.K. Author

N93-12333# California Univ., Berkeley.
OSCILLATIONS AND CONCENTRATIONS IN COMPRESSIBLE AND INCOMPRESSIBLE FLUIDS Final Report, 1 Jan. 1989 - 31 Dec. 1991
Phillip Colella Jun. 1992 5 p
(Contract DAAL03-88-K-0197)
(AD-A254706; ARO-26272.8-MA) Avail: CASI HC A01/MF A01

A fast vortex method was developed for solving the incompressible Euler equations in three dimensions. It is based on a combination of Anderson's Method of Local Corrections, which uses a hybrid of a finite difference representation and a particle representation to compute the velocity field induced on the vortices, and of adaptive mesh refinement for the finite difference calculation. The resulting algorithm is faster than any other existing finite difference or multipole-based algorithm for this problem and is 10-20 times faster than the direct N-body method for problems of current research interest. In addition, a good deal of technology was developed for finite-difference Poisson solvers of independent interest and usefulness, such as a multigrid-based local refinement algorithm for Mehrstellen discretizations of Poisson's equation in three dimensions, and efficient treatment of boundary conditions for boundaries that have infinite extent in one or more of the coordinate directions. GRA

N93-12355# Naval Research Lab., Washington, DC.
FLUID-STRUCTURE INTERACTION USING RETARDED POTENTIAL AND ABAQUS Interim Report
C. T. Dyka and M. A. Tamm 19 Aug. 1992 17 p
(AD-A254735; NRL/MR/6386-92-7104) Avail: CASI HC A03/MF A01

The transient analysis of coupled fluid-structure systems is a very challenging and important area of particular concern to the naval community. However, the general state of affairs in this class of problems is far from fully satisfactory. In this paper, a brief discussion concerning first transient structural analysis and then fluid-structure interaction is undertaken. Following this, the nonlinear finite element method (FEM) program ABAQUS is used to model the structure, while the fluid realm is discretized with boundary elements (BEM) employing the retarded potential (RP) formulation. The RP method has not been extensively applied in the past to such classes of problems due primarily to storage requirements. However, the RP approach does offer important advantages over both the use of FEM for the fluid or the-widely used Doubly Asymptotic Approximation (DAA), which is also a boundary element method. Discussion concerning time stepping (including automatic considerations), modeling and applications, accuracy, storage, stability, and the overall efficiency of this coupled technique in a MICRO-VAX environment is included. We conclude that the RP method is quite viable for the fluid and that the coupling to ABAQUS to form ABAQUS-RP is a very promising tool for transient, nonlinear, fluid-structure interaction. GRA

N93-12374# National Aerospace Lab., Tokyo (Japan). Aircraft Aerodynamics Div.
ON THE GOERTLER INSTABILITY OF BOUNDARY LAYERS
J. M. Floryan (University of Western Ontario, London.) Jul. 1991 48 p Sponsored by Natural Sciences and Engineering Research Council and Science and Technology Agency
(NAL-TR-1120T; JTN-92-80407) Avail: CASI HC A03/MF A01

Goertler instability occurs due to the action of centrifugal forces in boundary layers over curved surfaces, where it most commonly results in the generation of steady streamwise vortices. This study provides a summary of the current knowledge of this phenomenon. All existing experimental evidence is discussed. Experimental facts that bear on the theoretical modeling of the instability are pointed out. Linear theory is discussed in detail and compared critically with available experiments. Understanding of the nonlinear evolution of the vortices and their effect on the laminar to turbulent transition process are reviewed. The available nonlinear theories and direct numerical simulations are critically compared with the experiments. Centrifugal instability of turbulent boundary layers is discussed in detail. Effects of the instability on heat transfer and the associated buoyancy forces on the instability are discussed. A summary of the open questions is given. Author (NASDA)

N93-12382# National Aerospace Lab., Tokyo (Japan). Aeroengine Div.
EFFECTS OF COOLING-AIR INJECTION ON SECONDARY FLOWS AND LOSSES IN A TURBINE CASCADE
Atsumasa Yamamoto, Yasuhiro Kondo (Aoyamagakuin Univ., Tokyo, Japan), and Rinichi Murao (Aoyamagakuin Univ., Tokyo, Japan) Sep. 1991 20 p
(NAL-TR-1121T; JTN-92-80408) Avail: CASI HC A03/MF A01

In order to investigate the overall performance and internal flows of air cooled turbine blade rows, flows in a linear cascade model were examined using secondary air injections originating from various points located along the blade surfaces. This secondary air interacted with the cascade passage vortices and significantly changed the loss distribution. The cascade overall energy loss decreased when the air was injected along the mainstream whereas it increased when the air was injected against the mainstream flow from several points on the blade leading edge. Effects on the overall kinetic energy of the secondary flows and on the cascade outlet flow angle are also discussed. Author (NASDA)

N93-12397*# Alabama Univ., Huntsville.
FNAS COMPUTATIONAL FLUID DYNAMICS Final Report, 20 Mar. 1989 - 19 Dec. 1990
John P. Ziebarth 19 Dec. 1990 57 p
(Contract NAS8-36955)
(NASA-CR-184394; NAS 1.26:184394) Avail: CASI HC A04/MF A01

This work involves the coordination of necessary resources, facilities, and special personnel to provide a workshop to promote the exchange of CFD technology between industry, universities, and government. Critical flow problems have been isolated and simulation of these is being done. Author

N93-12406# Naval Postgraduate School, Monterey, CA.
NUMERICAL ANALYSIS OF OSCILLATING FLOW ABOUT A CIRCULAR CYLINDER M.S. Thesis
John E. Lotshaw Jun. 1992 79 p
(AD-A255164) Avail: CASI HC A05/MF A01

The numerical experiments, carried out through the use of the vorticity-stream function equations and their finite difference form, on sinusoidally-oscillating as well as coexisting flows (sinusoidal oscillation plus steady mean flow) at low and intermediate Keulegan-Carpenter numbers are described. A third-order in time, second-order in space, three-level predictor-corrector finite-difference scheme has been used. The

Poisson equation for the stream function was solved by a Fast Poisson Solver based on the High Order Difference Approximation with Identity Expansion (HODIE) and the Fast Fourier Transform (FFT) methods provided by the National Center for Atmospheric Research for the solution of separable elliptic partial differential equations with a non-square grid. The analysis has produced force-transfer and fluid-damping coefficients comparable to those obtained experimentally for both types of flows (i.e., with and without current) and to those obtained with a square grid through the use of the IMSL library. GRA

N93-12435# Ohio State Univ., Columbus. Dept. of Mechanical Engineering.
COMPRESSIBLE MIXING LAYERS WITH AND WITHOUT PARTICLES
M. Samimy, G. S. Elliott, D. D. Glawe, M. F. Reeder, and S. A. Arnefte Aug. 1992 91 p
(Contracts N00014-87-K-0169; N00014-90-J-1730)
(AD-A254854; TR-MEMS-92-101) Avail: CASI HC A05/MF A01

An extensive experimental research program has been carried out to explore the effects of compressibility in high Reynolds number turbulent free mixing layers. Three mixing layers with convective Mach numbers of 0.51 (Case 1), 0.64 (Case 3), and 0.86 (Case 2) were investigated. While Case 1 marks the onset of the compressibility effect on the mixing layer growth rate, the vorticity growth rate of Case 3 is approximately 50 percent less than that of an incompressible mixing layer with the same velocity ratio. Various experimental techniques such as laser Doppler velocimetry, two-point space-time correlations, filtered Rayleigh scattering based flow visualizations, and conventional laser sheet lighting have been utilized. GRA

N93-12462# Naval Surface Warfare Center, Bethesda, MD. Ship Hydromechanics Dept.
BUBBLE DISSOLVING IN TURBULENT PIPE FLOW Final Report
Scott Gowing Apr. 1992 45 p
(AD-A252927; CDNSWC/SHD-1348-01) Avail: CASI HC A03/MF A01

Measurements are presented of bubble dissolving in turbulent pipe flow at pipe Reynolds numbers of 2 x 10 exp 4, 1 x 10 exp 5, and 2 x 10 exp 5 based on pipe diameter. The mass transfer coefficient is determined and it increases with Reynolds number. The coefficient appears to be independent of bubble size for the diameter range of 20-170 microns. The mass transfer Nusselt number is determined and depends approximately on the bubbles' Peclet number to the one half power. The values of the mass transfer coefficients are similar to those for the same size bubbles rising buoyantly in still water. Suppression of dissolving by bubble rotation is hypothesized to prevent a significant increase in dissolving for the turbulent flow regime compared to the rising bubble regime. Surfactants in the water are also suspected of slowing the dissolving rates. GRA

N93-12475# National Inst. of Standards and Technology, Gaithersburg, MD. Polymers Div.
TWO-FLUID MEASUREMENTS ON THIN FILMS
Frederick I. Mopsik May 1992 26 p Sponsored by DNA
(PB92-205350; NIST/TN-1294) Avail: CASI HC A03/MF A01; SOD HC

The two-fluid technique to measure the dielectric constant and thickness of a thin polymeric film is discussed. The advantages include the ability to make a non-contacting measurement both of the effective electrical thickness of the film as well as the dielectric constant. The requirements for an accurate measurement are examined and the error as a function of the cell spacing, sample thickness, and dielectric constant of the second fluid are evaluated. The specifications of both the cell and the second fluid are examined. For the cell, it must be stable to good accuracy with handling, settable to small gaps, and have a well-defined electrode area through the use of a guard ring with a narrow guard gap. A design of a holder that is suitable for films from 6 micrometers to 50 micrometers is illustrated. GRA

N93-12492# Pittsburgh Energy Technology Center, PA.
DRAG ON AN OSCILLATING ROD IN A NON-NEWTONIAN FLUID
C. E. Maneschy (Pittsburgh Univ., PA.) and M. Massoudi May 1992 26 p
(DE92-014746; DOE/PETC-TR/92/8) Avail: CASI HC A03/MF A01

In recent years there has been some interest in the calculation of the wall shear stress and drag for the flow of non-Newtonian fluids (such as coal-slurries) past solid surfaces. Stokes obtained an exact solution for the rotational oscillations of an infinite cylindrical rod in a Newtonian fluid. Casarella and Laura considered the problem when the rod is undergoing both torsional and longitudinal oscillations. This type of flow has relevance to several important technical applications, such as off-shore drilling and the sea-state excitation of rods and cables. Rajagopal studied the problem of an infinite rod undergoing both torsional and longitudinal oscillations in an incompressible second grade fluid. In this work, we continue his work to calculate the drag force on an oscillating rod. The shear stresses at the surface of the oscillating cylinder are calculated for different values of the non-Newtonian parameter '(cflx a)'. The results are compared with the analytical results available in literature for the case of Newtonian fluid and the agreement is very good. Furthermore, the values for the work done in a complete cycle of motion are presented in a table for different values of '(cflx a)'. DOE

N93-12539*# Pratt and Whitney Aircraft, East Hartford, CT. Commercial Engineering.
THREE-DIMENSIONAL TURBOPUMP FLOWFIELD ANALYSIS Final Report, Feb. 1988 - Apr. 1992
O. P. Sharma, K. A. Belford, and R. H. Ni 27 Apr. 1992 181 p
(Contract NAS8-36950)
(NASA-CR-190978; NAS 1.26:190978; PWA-6142-43) Avail: CASI HC A09/MF A02

A program was conducted to develop a flow prediction method applicable to rocket turbopumps. The complex nature of a flowfield in turbopumps is described and examples of flowfields are discussed to illustrate that physics based models and analytical calculation procedures based on computational fluid dynamics (CFD) are needed to develop reliable design procedures for turbopumps. A CFD code developed at NASA ARC was used as the base code. The turbulence model and boundary conditions in the base code were modified, respectively, to: (1) compute transitional flows and account for extra rates of strain, e.g., rotation; and (2) compute surface heat transfer coefficients and allow computation through multistage turbomachines. Benchmark quality data from two and three-dimensional cascades were used to verify the code. The predictive capabilities of the present CFD code were demonstrated by computing the flow through a radial impeller and a multistage axial flow turbine. Results of the program indicate that the present code operated in a two-dimensional mode is a cost effective alternative to full three-dimensional calculations, and that it permits realistic predictions of unsteady loadings and losses for multistage machines. Author

N93-12030# Ecole Polytechnique, Palaiseau (France). Lab. pour l'Utilisation des Lasers Intenses.
HYDRODYNAMIC EFFICIENCIES IN IMPLOSION EXPERIMENTS [RENDEMENTS HYDRODYNAMIQUES DANS LES EXPERIENCES D'IMPLOSION]
Michel Koenig, Edouard Fabre, Jean-Michel Boudenne, Alain Michard, and P. Fews (Bristol Univ., England) *In its* The 1989 Scientific Report of the Laboratory for the Use of High Power Lasers Apr. 1990 p 55-59 In FRENCH (For primary document see N93-12023 02-36)
Avail: CASI HC A01/MF A03

N93-12039# Ecole Nationale Superieure de Mecanique et d'Aerotechnique, Poitiers (France). Lab. d'Energetique et de Detonique.
NUMERICAL SIMULATION OF A PRESSURE GRADIENT IN A MULTILAYER TARGET: TEMPERATURE EVOLUTION [SIMULATION NUMERIQUE D'UNE RAMPE DE PRESSION DANS UNE CIBLE MULTICOUCHES. EVOLUTION DE LA TEMPERATURE]
Jean-Pierre Romain *In* Ecole Polytechnique, The 1989 Scientific Report of the Laboratory for the Use of High Power Lasers Apr. 1990 p 100-105 In FRENCH (For primary document see N93-12023 02-36)
Avail: CASI HC A02/MF A03

N93-12459*# National Aeronautics and Space Administration. Goddard Space Flight Center, Greenbelt, MD.
ADVANCED TWO-PHASE HEAT TRANSFER SYSTEMS
Theodore D. Swanson *In* NASA. Langley Research Center, Current Technology for Thermal Protection Systems Oct. 1992 p 251-290 (For primary document see N93-12447 02-18)
Avail: CASI HC A03/MF A03

N93-12460*# National Aeronautics and Space Administration. Langley Research Center, Hampton, VA.
THERMOSTRUCTURAL APPLICATIONS OF HEAT PIPES FOR COOLING LEADING EDGES OF HIGH-SPEED AEROSPACE VEHICLES
Charles J. Camarda and David E. Glass (Analytical Services and Materials, Inc., Hampton, VA.) *In its* Current Technology for Thermal Protection Systems Oct. 1992 p 291-318 (For primary document see N93-12447 02-18)
Avail: CASI HC A03/MF A03

35 INSTRUMENTATION AND PHOTOGRAPHY

Includes remote sensors; measuring instruments and gages; detectors; cameras and photographic supplies; and holography.

For aerial photography see *43 Earth Resources and Remote Sensing.* For related information see also *06 Aircraft Instrumentation,* and *19 Spacecraft Instrumentation.*

N93-11048 Department of the Navy, Washington, DC.
FIBER PEEL FORCE MEASURING APPARATUS Patent
Josephine Covino-Hrbacek, inventor (to Navy), Albert H. Lepie, inventor (to Navy), and Thomas S. Stephens, inventor (to Navy) 14 Apr. 1992 5 p Filed 6 May 1991
(AD-D015349; US-Patent-5,103,678; US-Patent-Appl-SN-697351; US-Patent-Class-73-828) Avail: US Patent and Trademark Office

An apparatus for measuring peel force exerted on optical fiber being pulled from a bobbin upon which it is wound, with the pull being in the direction of the longitudinal axis of the truncated-conically-shaped bobbin, is presented. One end of an elongaged lever arm holds the bobbin cantilevered from the bobbin end opposite that from which the optical fiber is pulled so that the bobbin is positioned generally horizontally over a horizontal base to which the opposite end of the lever arm is pivotally attached. An intermediate point on the arm beneath the bobbin is in contact with a load measuring device so that as the fiber is pulled any reaction by the arm upon the device provides a measure of the peel force upon the fiber. GRA

N93-11049 Department of the Navy, Washington, DC.
SHUTTER APPARATUS Patent
John G. Dibble, inventor (to Navy) 5 May 1992 7 p Filed 4 Mar. 1991
(AD-D015350; US-Patent-5,111,036; US-Patent-Appl-SN-664897; US-Patent-Class-250-214) Avail: US Patent and Trademark Office

An apparatus for protecting the image recording media in a tracking camera from destructive illumination is presented. The apparatus includes a shutter assembly mounted between the lens and the camera and a sensor assembly mounted in juxtaposition with the camera so that a sensor at one end of the tube in the sensor assembly detects destructive illumination before it impinges on the lens. The sensor causes a signal to be passed through circuitry connecting to the shutter assembly, activating a rotary solenoid which moves a blade to an interrupting position between the lens and the camera until no further destructive illumination impinges on the sensor. The shutter blade return to a non-interrupting position when the sensor no longer receives destructive illumination. GRA

N93-11320# Rolls-Royce Ltd., Derby (England).
IN-PLANE ESPI MEASUREMENTS IN HOSTILE ENVIRONMENTS
Richard W. T. Preater (City Univ., London, England) and Robin C. Swain (City Univ., London, England) 1 Aug. 1991 13 p Presented at the Optical Applied Science and Engineering Conference, San Diego, CA, 21-26 Jul. 1991 Sponsored by Science Research Council
(PNR-90919; ETN-92-92207) Copyright Avail: CASI HC A03/MF A01

Solutions used to take reliable Electronic Speckle Pattern Interferometry (ESPI) in-plane measurements in a high speed rotating specimen in an environment consisting of severe turbulence, electromagnetic interference, and vibrations are detailed. The experimental set up and techniques are described and the following are discussed: electromagnetic interference, carrier fringe shapes, component windage, alignment, and speed variations. Some of the problems encountered when using ESPI in a hostile environment were overcome and repeatable fringe patterns obtained from a high speed rotating specimen with a maximum tip speed of 200 m/s. Small modifications prevented the severe turbulence and electromagnetic interference from disrupting the experiments. ESA

N93-11330 Deutsche Geodaetische Kommission, Munich (Germany).
OBJECT BASED MULTI-IMAGE MATCHING Ph.D. Thesis - Technische Univ. [OBJEKTGESTUETZTE MEHRBILDZUORDNUNG]
Carl-Thomas Schneider 1991 65 p In GEORGIAN
(Ser-C-375; ISBN-3-7696-9422-8; ETN-92-92276) Copyright
Avail: Deutsche Geodaetische Kommission, Marstallplatz 8, D-8000 Munich 22, Germany

The object based multi-image matching is an algorithm that allows the equivalent processing of an arbitrary number of images, at least two, with simultaneous object reconstruction. This algorithm presents the possibility to measure nonsignalized surfaces and signalized points. This method is implemented in a photogrammetric measurement system, which allows a highly automated photogrammetric processing. Examples of practical applications in automobile, medicine, and aerospace industries are given. ESA

N93-11346 Deutsche Geodaetische Kommission, Munich (Germany).
PHOTOGRAMMETRIC POINT DETERMINATION USING DIGITAL IMAGERY OF THREE-LINE SCANNER SYSTEMS Ph.D. Thesis - Technische Univ. [PHOTOGRAMMETRISCHE PUNKTBESTIMMUNG MIT BILDDATEN DIGITALER DREIZEILENKAMERAS]
Franz Mueller 1991 82 p In GEORGIAN
(Ser-C-372; ISBN-3-7696-9419-7; ETN-92-92275) Copyright
Avail: Deutsche Geodaetische Kommission, MarstallPlatz 8, D-8000 Munich 22, Germany

Geometrical aspects of object point determination and reconstruction of the exterior orientation with digital imagery of three line scanner systems are investigated. The accuracy potential of three line image data is outlined. The mathematical model is interpreted as a special case of generalized combined point determination, which is able to process both image coordinates of frame photographs and linear array imagery. Optical imaging sensors used in aerial photogrammetry and remote sensing are summarized. Digital three line scanners and related projects and missions are described. The mathematical model of point determination is explained. The dependence of the accuracy of point determination in photogrammetric and nonphotogrammetric parameters is outlined. ESA

N93-11410 National Physical Lab., Teddington (England). Div. of Radiation Science and Acoustics.
THE ELECTRON-BEAM WATER CALORIMETER PROJECT AT THE NATIONAL PHYSICAL LABORATORY
M. R. McEwen Feb. 1992 21 p
(NPL-RSA(EXT)-30; ETN-92-92372) Copyright Avail: National Physical Lab., Teddington, Middlesex, TW11 0LW, England

A water calorimeter was designed and constructed for use in high energy electron beams to obtain absorbed dose to water directly eliminating the need to use stopping powers. The construction and testing of the calorimeter are described and the results of a comparison with the primary standard graphite calorimeter are given. The difference in the graphite and water calorimeters was immediately noticeable. The graphite shows an almost flat post irradiation cooling curve allowing an accurate extrapolation to calculate the absorbed dose to graphite. On the other hand, the cooling curve for the water calorimeter is anything but flat. There is a large post irradiation 'spike' that lasts for approximately 80 seconds. Only after this does the temperature trace begin to resemble that of the graphite calorimeter. This means that the extrapolations are very long, introducing a (possibly) large uncertainty in the determination of absorbed dose to water. Conclusions are drawn and given. ESA

N93-11460# Federal Aviation Administration, Atlantic City, NJ.
HIGH CAPACITY VOICE RECORDER (HCVR) OPERATIONAL TEST AND EVALUATION (OT/E) INTEGRATION TEST REPORT
Wayne Bell, Andy Colon, and Edward Lind Oct. 1992 42 p
(DOT/FAA/CT-TN92/30) Avail: CASI HC A03/MF A01

This report describes the Operational Test and Evaluation OT&E) Integration tests performed by ACW-400A on the High Capacity Voice Recorder (HCVR) equipment. This Commercial Off-The-Shelf (COTS) equipment is being acquired to replace existing 152-channel voice recorders currently in use at Air Route Traffic Control Centers (ARTCC's) and the New York Terminal Radar Approach Control (TRACON) Facility. Tests to verify FAA-P-2878 (Purchase Description) requirements were performed at the Federal Aviation Administration (FAA) Technical Center. Tests to verify NAS-SS-1000, Volume 1, System Level Requirements, and Volume 4, Subsystem Level Requirements were performed at the Seattle ARTCC (the designated key test site). This equipment did not meet all FAA-P-2879 or NASA-SS-1000 requirements, primarily because it is COTS equipment and was not specifically designed to meet FAA requirements. The advantages of this equipment, however, outweigh the disadvantages, in the opinion of ACW-400A. The HCVR equipment is, therefore, recommended for deployment under the conditions cited in this report. Author

N93-11542# Lawrence Livermore National Lab., CA.
HIGH FRAME-RATE, LARGE FIELD WAVEFRONT SENSOR
K. Avicola, J. T. Salmon, J. Brase, K. Waltjen, R. Presta, and K. S. Balch Mar. 1992 19 p Presented at the Laser Guide Star Adaptive Optics Workshop, Albuquerque, NM, 10-12 Mar. 1992
(Contract W-7405-eng-48)
(DE92-019547; UCRL-JC-109552; CONF-9203139-2) Avail: CASI HC A03/MF A01

A two-stage intensified 192 x 239 pixel imager developed by Eastman Kodak for motion analysis was used to construct a 1 kHz frame-rate Hartmann wavefront sensor. The sensor uses a monolithic array of lenslets with a focal length that is adjusted by an index fluid between the convex surface and an optical flat. The accuracy of the calculated centroid position, which is related to wavefront measurement accuracy, was obtained as a function of spot power and spot size. The sensor was then dynamically tested at a 1 kHz frame-rate with a 9 x 9 lenslet array and a fast steering mirror, which swept a plane wavefront across the wavefront sensor. An 8 cm diameter subaperture will provide a return signal (589 nm) level of about 1000 photons/ms using the AVLIS 1 kW laser (stretched pulse) as guide star source, which is sufficient to yield a wavefront measurement of better than gamma/10 rms. If an area of 6 x 6 pixels per Hartmann spot were allocated, this wavefront sensor could support a 32 x 32, or 1024, element deformable mirror. DOE

N93-11554# Mound Lab., Miamisburg, OH.
HOT-WIRE VS LASER, IS THERE A DIFFERENCE?
A. C. Munger, T. M. Beckman, and D. P. Kramer 1992 11 p Presented at the 18th International Pyrotechnics Seminar, Breckenridge, CO, 13-17 Jul. 1992
(Contract DE-AC04-88DP-43495)
(DE92-019337; MLM-3758(OP); CONF-920796-8) Avail: CASI HC A03/MF A01

When a design for an ordnance device utilizing new technology begins to take shape, all of the various design elements are approached individually and then ultimately tested as a single system. This approach allows the various elements to float within an overall design envelope. The embracing of laser technology for the ignition system of various ordnance designs should ideally take this path. The reality for many of us is that the total system will not be completely re-engineered. The laser ignition system will need to be integrated into existing systems. This will require innovative electrical to laser interfaces and also require that the physical output of the new device duplicate that of the replaced electrical devices. This seems like a given when the technology is examined; after all, both hot-wire technology and laser technology provide energy to effect ignition of the energetic material and should have no influence on the burning characteristics. This statement appears to be the 'truth' but when asked to produce any evidence to support the contention, we at Mound had none. This paper will report on some experiments that were conducted to begin building the data base that supports this hypothesis. DOE

N93-11562# Massachusetts Inst. of Tech., Cambridge. Research Lab. of Electronics.
INVESTIGATION OF A CESIUM RAMAN TIME/FREQUENCY STANDARD Final Report, Mar. 1986 - Jun. 1989
Shaoul Ezekiel Dec. 1991 70 p
(Contract F19628-86-K-0002)
(AD-A252677; RL-TR-91-413) Avail: CASI HC A04/MF A01

The objective of this program was to determine the feasibility of developing an improved portable cesium clock using a semiconductor laser excited resonance Raman interaction. Such a clock has the potential to be smaller, lighter, less expensive, and more accurate than conventional cesium clocks because it does not require a microwave cavity or state selection magnets. To demonstrate this, an experimental Raman cesium clock was constructed. To excite the Raman transition in this beam, a semiconductor laser was amplitude modulated at 4.6 GHz (half of the 9.2 GHz cesium hyperfine transition frequency) so that the two modulation sidebands were tuned to the resonance Raman transition frequency. The observed signal to noise ratio of about 1800 for a 2 second averaging time was detector noise limited, but only a factor of two smaller than the shot noise limit. For a 15 cm interaction zone separation, such as in the experimental Raman clock, this signal to noise ratio corresponds to a fractional frequency stability of 6x10(exp -12) (for a 100 second averaging time). This compares favorably with commercial cesium clocks. Once detector noise is eliminated, the shot noise limited fractional stability would be 2.7x10(exp -12) (for 100 sec.). GRA

N93-11612*# Georgia Inst. of Tech., Atlanta.
FREQUENCY RESPONSE IN SHORT THERMOCOUPLE WIRES Final Report, Apr. 1989 - Jun. 1992
L. J. Forney, E. L. Meeks, J. Ma, and G. C. Fralick (National Aeronautics and Space Administration. Lewis Research Center, Cleveland, OH.) Oct. 1992 119 p

(Contract NCC3-135)
(NASA-CR-190943; NAS 1.26:190943; E19-666-4) Avail: CASI HC A06/MF A02

Theoretical expressions are derived for the steady state frequency response of a thermocouple wire. In particular, the effects of axial heat conduction are demonstrated for a nonuniform wire with unequal material properties and wire diameters across the junction. The amplitude ratio at low frequency omega approaches 0 agrees with the results of Scadron and Warshawsky (1952) for a steady state temperature distribution. Moreover, the frequency response for a nonuniform wire in the limit of infinite length l approaches infinity is shown to reduce to a simple expression that is analogous to the classic first order solution for a thermocouple wire with uniform properties. Theoretical expressions are also derived for the steady state frequency response of a supported thermocouple wire. In particular, the effects of axial heat conduction are demonstrated for both a supported one material wire and a two material wire with unequal material properties across the junction. For the case of a one material supported wire, an exact solution is derived which compares favorably with an approximate expression that only matches temperatures at the support junction. Moreover, for the case of a two material supported wire, an analytical expression is derived that closely correlates numerical results. Experimental measurements are made for the steady state frequency response of a supported thermocouple wire. In particular, the effects of axial heat conduction are demonstrated for both a supported one material wire (type K) and a two material wire (type T) with unequal material properties across the junction. The data for the amplitude ratio and phase angle are correlated to within 10 pct. with the theoretical predictions of Forney and Fralick (1991). This is accomplished by choosing a natural frequency omega sub n for the wire data to correlate the first order response at large gas temperature frequencies. It is found that a large bead size, however, will increase the amplitude ratio at low frequencies but decrease the natural frequency of the wire. The phase angle data are also distorted for imperfect junctions. Author

N93-11648# Materials Research Labs., Melbourne (Australia).
CHARACTERIZATION OF DEFLAGRATING MUNITIONS BY ROTATING PRISM HIGH SPEED PHOTOGRAPHY
Trevor J. Kinsey, Tim J. Bussell, and Michael C. Chick Victoria, Australia Aug. 1992 23 p
(MRL-TR-91-43; AR-006-842) Copyright Avail: CASI HC A03/MF A01

We report on the use of a rotating prism high speed camera for determining the characteristics of a munition undergoing rapid deflagration in field experiments. The technique has been applied to study the controlled deflagration of Composition B filled 105 mm shell and 81 mm mortar bombs as representative thick and thin cased munitions respectively; however the report is mostly illustrated with results from the study on 105 mm shell. The deflagration event has been characterized in terms of case expansion rate, initial fragment velocity, time to case burst, time to reaction from the nose end and the deflagration rate of the filling. Products escaping from the fracturing case eventually obscured the image which limited the extent of the measurement. Author

N93-11662*# Alabama Univ., Huntsville. Cosmic Ray Lab.
DEVELOPMENT OF A SCINTILLATING OPTICAL FIBER IONIZATION CALORIMETER Final Report
Y. Takahashi 1 Oct. 1990 35 p
(Contract NAS8-36955)
(NASA-CR-184415; NAS 1.26:184415; UAH-5-32274) Avail: CASI HC A03/MF A01

A design study of a scintillation fiber (SF) calorimeter for a cosmic ray observation is made. An evaluation of various fibers and design configuration was made. The proposed design has a dimension of 1 m (W) x 1 m (L) x 16 cm (H) contains 1000 fibers at each of 40 x- or 40 y-layers interleaved with 1mm thick leadplates. Two or four CCD Particle Track Imaging Systems are connected to a bundle of SF edges at x- and y-ends. The overall weight of a calorimeter is 1,200 kg including read-out systems and supporting boards. The designed calorimeter can measure cosmic ray nuclei and gamma-rays with position, angles and energy information suitable for detailed spectrum analysis. The system is particularly beneficial at very high energies where the flux is extremely low and it requires a very long exposure over many years in space. Emulsion chambers have an advantage for cosmic ray measurements if the exposure is limited to several months in space. In fact, the most important energy region for the current cosmic ray studies is at around 1,000 TeV where a drastic change of elemental composition is indicated by various indirect observations. A detector whose size is in the order of 1 m(sup 2) requires several years of exposure in space accumulate sufficient statistics near 1,000 TeV. Emulsions will be strongly contaminated by background radiation for such a long duration flight, while SF calorimeter is totally immune from this concern. This is particularly important for long-duration experiments. The SF calorimeter also allows time-tagging of individual events, extending the experimental capability in various ways. Author

N93-11673# Sandia National Labs., Albuquerque, NM.
INITIAL LABORATORY EVALUATION OF COLOR VIDEO CAMERAS
P. L. Terry 1991 11 p Presented at the Institute of Nuclear Materials Management (INMM) Annual Meeting, Orlando, FL, 19-22 Jul. 1992
(Contract DE-AC04-76DP-00789)
(DE92-018274; SAND-91-2579C; CONF-9207102-8) Avail: CASI HC A03/MF A01

Sandia National Laboratories has considerable experience with monochrome video cameras used in alarm assessment video systems. Most of these systems, used for perimeter protection, were designed to classify rather than identify an intruder. Monochrome cameras are adequate for that application and were selected over color cameras because of their greater sensitivity and resolution. There is a growing interest in the identification function of security video systems for both access control and insider protection. Color information is useful for identification purposes, and color camera technology is rapidly changing. Thus, Sandia National Laboratories established an ongoing program to evaluate color solid-state cameras. Phase one resulted in the publishing of a report titled, 'Initial Laboratory Evaluation of Color Video Cameras (SAND--91-2579).' It gave a brief discussion of imager chips and color cameras and monitors, described the camera selection, detailed traditional test parameters and procedures, and gave the results of the evaluation of twelve cameras. In phase two, six additional cameras were tested by the traditional methods and all eighteen cameras were tested by newly developed methods. This report details both the traditional and newly developed test parameters and procedures, and gives the results of both evaluations. DOE

N93-11723 Brunel Univ., Uxbridge (England).
THREE-DIMENSIONAL IMAGE STRUCTURE IN IN-LINE FRAUNHOFER HOLOGRAPHY Ph.D. Thesis
Abdul Raouf 1991 213 p
Avail: Univ. Microfilms Order No. BRDX95449

A new theoretical model for the three dimensional images from a finite aperture in-line Fraunhofer hologram is presented. Existing work only deals with the case of single object, this work has been extended to the case of two identical coplanar discs. The resulting image equation is solved numerically for several different limiting apertures and their results are compared with the image intensity data from the holograms recorded on Agfa 8E 75HD film. Excellent quantitative agreement is found, verifying the theoretical predictions. Three different criteria for determining the disc diameter and disc separation describing their errors are discussed for both numerical and experimental data. A data acquisition system based upon a digital interfaced with a PC, and high resolution video camera is described. Dissert. Abstr.

N93-11757# Eaton Corp., Milwaukee, WI. Corporate Research and Development Center.
LOW COST HUMIDITY SENSOR Final Report, Sep. 1987 - Oct. 1991
Selami Y. Pusatcioglu and Joe C. Zuercher Apr. 1992 100 p
(Contract GRI-5087-245-1518)
(PB92-205772; GRI-92/0142) Avail: CASI HC A05/MF A02

The objective of the project was to develop a low-cost, high accuracy humidity sensor having good stability that is suitable for use in residential and commercial HVAC controls applications. Ionic polymer materials using advanced micro-electronics fabrication and design techniques were evaluated to develop a low-cost humidity sensor. The approach of using the Langmuir-Blodgett Films proved unsuccessful due to need for additional basic research in this field. Thus, the project concentrated on 'thicker' films using a spin coating approach. Based on the characterization of the sorption behavior of candidate polymer materials, the sulfonated tetrafluoroethylene perfluoroether (commercially sold by DuPont under the trademark 'Nafion') was selected as the most desirable ionic polymer material. A proprietary sensor design and fabrication process was developed using an interdigitated electrode configuration on a silicon substrate overcoated with the Nafion polymer. A number of sensors were fabricated and tested for drift, accuracy, and chemical immunity. Author

N93-11768# Los Alamos National Lab., NM.
CALIBRATION TECHNIQUES FOR HIGH FLUX X RAY DETECTORS
G. C. Idzorek and R. G. Hockaday 1992 11 p Presented at the SPIE International Symposium on Optical Applied Science and Engineering, San Diego, CA, 19-24 Jul. 1992
(Contract W-7405-eng-36)
(DE92-017513; LA-UR-92-1942; CONF-920792-14) Avail: CASI HC A03/MF A01

A system is described for calibrating high flux (10(exp 11) W) x-ray detectors using moderate flux (10(exp -4) W) synchrotron and low flux (10(exp -7) W) conventional x-ray producing machines. The detectors have been designed for output currents of one milliampere to 100 amperes which results in output currents during calibration of approximately 10(exp -16) to 10(exp -12) amperes. The small calibration output currents led to the development of statistical methods to reduce the calibration measurement errors to acceptable levels. A personal computer is used to acquire, analyze, store, and display the calibration data in real time to allow the scientist to explore and correct the calibration technique or eliminate external noise sources. DOE

N93-11802# Pacific Northwest Lab., Richland, WA.
ULTRA WIDE BAND 3-D CROSS SECTION (RCS) HOLOGRAPHY
H. D. Collins and T. E. Hall Jul. 1992 25 p Presented at the Review of Progress in Quantitative Non Destructive Evaluation, La Jolla, CA, 19-24 Jul. 1992
(Contract DE-AC06-76RL-01830)
(DE92-019133; PNL-SA-20954; CONF-920799-1) Avail: CASI HC A03/MF A01

Ultra wide band impulse holography is an exciting new concept for predictive radar cross section (RCS) evaluation employing near-field measurements. Reconstruction of the near-field hologram data maps the target's scattering areas, and uniquely identifies the 'hot spot' locations on the target. In addition, the target and calibration sphere's plane wave angular spectrums are computed (via digital algorithm) and used to generate the target's far-field RCS values in three dimensions for each frequency component in the impulse. Thin and thick targets are defined in terms of their near-field amplitude variations in range. Range gating and computer holographic techniques are applied to correct these variations. Preliminary experimental results on various targets verify the concept of RCS holography. The unique 3-D presentation (i.e., typically containing 524,288 RCS values for a 1024 (times) 512 sampled aperture for every frequency component) illustrates the efficacy of target recognition in terms of its far-field plane wave angular spectrum image. RCS images can then be viewed at different angles for target recognition, etc. DOE

N93-11806# Oak Ridge National Lab., TN.
EVALUATION OF ADVANCED PRESSURE SENSOR TECHNOLOGY
J. M. Weiss (Electric Power Research Inst., Palo Alto, CA.) and R. L. Shepard 1992 10 p Presented at the 8th Power Plant Dynamics, Control and Testing Symposium, Knoxville, TN, 27-29 May 1992
(Contract DE-AC05-84OR-21400)
(DE92-011004; CONF-920538-6) Avail: CASI HC A02/MF A01

New pressure sensing technology is being evaluated to improve pressure sensor performance for utility applications. Existing pressure sensors do not have accuracies required to be compatible with distributed control systems (DCS). The most common type of pressure sensor utilizes a fluid fill to couple the process pressure to the measuring device. This coupling can lead to significant sensor performance degradation during a transient with no prior warning to the operator and cannot be detected by the usual signal validation techniques. Additionally, rising maintenance costs to assure calibration and response compliance of pressure sensors have become a significant factor in power plant operation. These costs and accuracy limitations define the need for new pressure sensing methods. Since there are no other known programs to develop improved pressure sensors for the utility industry, EPRI has initiated the R & D process to develop and commercialize high accuracy, essentially maintenance-free pressure sensors. Alternative concepts being investigated include fiber optic, silicon integrated circuit, resonant mechanical structures, ultrasonic, and fluorescent technologies. This paper outlines the initial steps taken thus far to identify the appropriate technology(s) for future R & D effort. DOE

N93-11822# Los Alamos National Lab., NM.
HIGH-SPEED TEST STATION FOR SOLID-STATE IMAGERS
G. J. Yates, K. L. Albright, and B. T. Turko (California Univ., Berkeley. Lawrence Berkeley Lab.) 1992 13 p Presented at the SPIE International Symposium on Optical Applied Science and Engineering, San Diego, CA, 19-24 Jul. 1992
(Contracts W-7405-eng-36; DE-AC03-76SF-00098)
(DE92-018990; LA-UR-92-2352; CONF-920792-19) Avail: CASI HC A03/MF A01

A PC-based programmable solid-state imager test station has been designed and is in final development phases. It is designed to provide a flexible universal high-speed platform for evaluation of different imager designs and formats including various multiport configurations. The system provides drive and acquisition circuitry and components to allow electro-optic characterization of imagers as a function of pixel readout rate. The data are scan-converted to RS- 170 format for analysis. The system's functional capabilities and performance are presented. Examples of program code to generate three phase clocks for an 8-port Frame Transfer EEV CCD are included. A sampling of preliminary results obtained from variable rate clocking of this imager will be discussed. DOE

N93-11827# Mississippi State Univ., Mississippi State. Diagnostic Instrumentation and Analysis Lab.
A DISTRIBUTED DATA ACQUISITION AND CENTRALIZED DATA REDUCTION SYSTEM FOR FLEXIBLE AND EFFICIENT MEASUREMENTS
T. Phillip, Ping-Rey Jang, and R. D. Benton 1991 4 p Presented at the International Society Symposium on Mini and Microcomputers, Long Beach, CA, 11-13 Dec. 1991
(Contract DE-AC02-80ET-15601)
(DE92-019021; CONF-9112129-1) Avail: CASI HC A01/MF A01

The Diagnostic Instrumentation and Analysis Laboratory (DIAL) at Mississippi State University (MSU) is developing nonintrusive optical diagnostic instrumentation to characterize a magnetohydrodynamic (MHD) gas stream. The optical instrumentation systems are being developed, as part of the US Department of Energy (DOE) development program for the MHD power process, to measure gas temperature profiles, gas velocity and turbulence intensity profiles, and average particle size and particle size distribution, etc. since these instruments are primarily intended for field use, most of them have been developed as stand-alone systems, providing for ease of operation. Each stand-alone system, also called a target system, has the capability to acquire data, do a preliminary analysis, and display the result. The data from various instrumentation systems are logged to a central computer for detailed analysis, and to trace the history of instrument operation through an IEEE 488 based network. This system has been used with success for over five years in our field measurements at different locations in the US. Although the implementation presented here is based on a particular environment, the principles described are applicable in a variety of situations. DOE

N93-11828# Massachusetts General Hospital, Boston. Physics Research Lab.
HIGH RESOLUTION TOMOGRAPHIC INSTRUMENT DEVELOPMENT
1992 130 p
(Contract DE-FG02-87ER-60519)
(DE92-017314; DOE/ER-60519/T4) Avail: CASI HC A07/MF A02

Our recent work has concentrated on the development of high-resolution PET instrumentation reflecting in part the growing importance of PET in nuclear medicine imaging. We have developed a number of positron imaging instruments and have the distinction that every instrument has been placed in operation and has had an extensive history of application for basic research and clinical study. The present program is a logical continuation of these earlier successes. PCR-I, a single ring positron tomograph was the first demonstration of analog coding using BGO. It employed 4 mm detectors and is currently being used for a wide range of biological studies. These are of immense importance in guiding the direction for future instruments. In particular, PCR-II, a volume sensitive positron tomograph with 3 mm spatial resolution has benefitted greatly from the studies using PCR-I. PCR-II is currently in the final stages of assembly and testing and will shortly be placed in operation for imaging phantoms, animals and ultimately humans. Perhaps the most important finding resulting from our previous study is that resolution and sensitivity must be carefully balanced to achieve a practical high resolution system. PCR-II has been designed to have the detection characteristics required to achieve 3 mm resolution in human brain under practical imaging situations. The development of algorithms by the group headed by Dr. Chesler is based on a long history of prior study including his joint work with Drs. Pelc and Reiderer and Stearns. This body of expertise will be applied to the processing of data from PCR-II when it becomes operational. DOE

N93-11907 Illinois Univ. at Urbana-Champaign, Savoy.
NUCLEAR MAGNETIC RESONANCE MICROSCOPY: NEW THEORETICAL AND TECHNICAL DEVELOPMENTS Ph.D. Thesis
Xiaohong Zhou 1992 207 p
Avail: Univ. Microfilms Order No. DA9215920

Some new developments are described in the theory, instrumentation and applications of nuclear magnetic resonance (NMR) microscopy. The purpose is to theoretically analyze resolution limits in NMR microscopy and develop experimental techniques to achieve the highest possible spatial resolution for a variety of biomedical applications. In the theoretical analysis, resolution limits due to linewidth broadening, unbounded diffusion and signal to noise ratio (SNR) were evaluated for both projection reconstruction and Fourier transform imaging techniques. The results indicate that projection reconstruction gives a higher SNR and requires a smaller magnetic field gradient to overcome the resolution limit due to linewidth broadening. Experimentally, 3-D projection reconstruction techniques were employed to achieve the optimal spatial resolution with isotropic voxels. Using a custom-built NMR microscope, isotropic voxels as small as (6.4 microns)(sup 3) were achieved on phantoms and tissue specimens. With this resolution, the natural contrast phenomenon was studied in fixed human brain tissue from the putamen and the microscopic NMR images were correlated with endogenous T sub 2 contrast. Correlation between the microscopic NMR images and optical micrographs greatly assisted in the interpretations of the complicated tissue structures. The effect was also studied of a contrast agent (dextran magnetite) on microscopic NMR images of fresh rat liver and spleen tissues and the importance is shown of contrast agents in detecting microscopic tissue structures. To extend NMR microscopy to in vivo studies, an instrument using surface RF coils was developed. Performance of a set of surface coils spanning from 6 to 43mm were theoretically evaluated and experimentally verified on phantoms with the same sample-loss as tissues. Both theoretical and experimental results indicate that isotropic resolution of the order of (50 micron)(sup 3) is possible in the regions close to the surface (approx. 2 cm) of an object under in vivo conditions. Several technical problems in the NMR microscopy, including gradient induced vibrations, slow motion, magnetic susceptibility artifacts, and extra echoes, are also discussed and solutions to minimize these problems are proposed and tested. Dissert. Abstr.

N93-12069# Los Alamos National Lab., NM.
HIGH-SPEED FPS VIDICON CAMERA
George J. Yates, Robert A. Gallegos, Michael H. Barron, and Hans Bucher 1992 13 p Presented at the SPIE International Symposium on Optical Applied Science and Engineering, San Diego, CA, 19-24 Jul. 1992
(Contract W-7405-eng-36)
(DE92-018989; LA-UR-92-2351; CONF-920792-20) Avail: CASI HC A03/MF A01

A new high-speed, high-resolution electrostatic deflection vidicon camera for use with high-definition diode electron gun Focus Projection and Scan (FPS) vidicons has been designed and partially developed. It is asynchronously resettable to permit time-phased synchronization with randomly occurring transient optical events. Programmable rasters allows selection of nonstandard variable size and speed formats for specific imaging aspect ratios and readout requirements. Readout rates as high as 625 Hz (1.6 ms field period) with 256 scan lines per field with limiting resolution greater than or = 20 lp/mm and dynamic range greater than or = 200:1 from Plumbicon (PbO) and Saticon (Se-As-Te) targets are presented. Charge equilibrium problems resulting in superlinear transfer characteristics from transient low intensity pulsed illumination are discussed. Camera circuitry and potential scientific and medical applications are included. DOE

N93-12140# Brookhaven National Lab., Upton, NY.
OPERATING EXPERIENCE USING VENTURI FLOW METERS AT LIQUID HELIUM TEMPERATURE
K. C. Wu 1992 9 p Presented at the Instrument Society of America Conference, Houston, TX, 18-23 Oct. 1992
(Contract DE-AC02-76CH-00016)
(DE92-014693; BNL-47507; CONF-921055-2) Avail: CASI HC A02/MF A01

Experiences using a commercial venturi to measure single phase helium flow near 4 K (degree Kelvin) for cooling superconducting magnets have been presented. The mass flow rate was calculated from the differential pressure and the helium density evaluated from measured pressure and temperature. The venturi flow meter, with a full range of 290 g/s (0.29 Kg/s) at design conditions, has been found to be reliable and accurate. The flow measurements have been used, with great success, for evaluating the performance of a cold centrifugal compressor, the thermal acoustic heat load of a cryogenic system, and the cooling of a superconducting magnet after quench. DOE

N93-12205*# National Aeronautics and Space Administration. Langley Research Center, Hampton, VA.
COMPENSATED HIGH TEMPERATURE STRAIN GAGE Patent Application
Thomas C. Moore, Sr., inventor (to NASA) 12 Aug. 1992 10 p

(NASA-Case-LAR-14776-1; NAS 1.71:LAR-14776-1; US-Patent-Appl-SN-928865) Avail: CASI HC A02/MF A01

A device for measuring strain in substrates at high temperatures, in which the thermally induced apparent strain is nulled, is presented. Two gages are used: one active gage and one compensating gage. Both gages are placed on the substrate to be gaged; the active gage is attached such that it responds to mechanical and thermally induced apparent strain while the compensating gage is attached such that it does not respond to mechanical strain and measures only thermally induced apparent strain. A thermal blanket is placed over the two gages to maintain the gages at the same temperature. The two gages are wired as adjacent arms of a Wheatstone bridge which nulls the thermally induced apparent strain giving a true reading of the mechanical strain in the substrate. NASA

N93-12279*# Sverdrup Technology, Inc., Brook Park, OH.
ADVANCED ONE-DIMENSIONAL OPTICAL STRAIN MEASUREMENT SYSTEM, PHASE 4 Final Report
Christian T. Lant Oct. 1992 12 p
(RTOP 590-21-11)
(NASA-CR-190760; E-7390; NAS 1.26:190760) Avail: CASI HC A03/MF A01

An improved version of the speckle-shift strain measurement system was developed. The system uses a two-dimensional sensor array to maintain speckle correlation in the presence of large off-axis rigid body motions. A digital signal processor (DSP) is used to calculate strains at a rate near the RS-170 camera frame rate. Strain measurements were demonstrated on small diameter wires and fibers used in composite materials research. Accurate values of Young's modulus were measured on tungsten wires, and silicon carbide and sapphire fibers. This optical technique has measured surface strains at specimen temperatures above 750 C and has shown the potential for measurements at much higher temperatures. Author

N93-12365# National Aerospace Lab., Tokyo (Japan). Control Systems Div.
ACCURACY IMPROVEMENT OF LINEAR ESTIMATED MOTION USING DIFFERENTIAL TYPE SENSORS [BIBUNGATA SENSA DOUNYUU NI YORU UNDOU SUITEI SEIDO NO KOUJOU]
Shuichi Sasa, Masahiko Nagayasu, Masaaki Yanagihara, and Takashi Shimomura Dec. 1991 19 p In JAPANESE
(NAL-TR-1135; JTN-92-80403) Avail: CASI HC A03/MF A01

Linear motion estimation was performed by application of a Kalman filter in conjunction with position, velocity, and acceleration sensors. The relationship between the sensor accuracy and the accuracy of the estimated motion was investigated. Motion estimation accuracy was evaluated using the Riccati equation covariance matrix obtained from the Kalman filter. The relation between the accuracy of the velocity and acceleration sensors and the motion estimation accuracy was subsequently derived numerically. The problem was analyzed for both discrete and continuous time systems with the sensor accuracy that is necessary to attain the specified motion estimation accuracy then being derived. Author (NASDA)

N93-12373# National Aerospace Lab., Tokyo (Japan). Computational Sciences Div.
VIDEO CAMERA AS A VISUAL SENSOR [SHIKAKU SENSA TOSHITE NO BIDEO KAMERA]
Hiromi Gomi Nov. 1991 26 p In JAPANESE
(NAL-TR-1132; JTN-92-80400) Avail: CASI HC A03/MF A01

A literature search was performed to investigate the human eyes and video cameras as visual sensors for pattern recognition, with measurements being subsequently taken on the characteristics of image data, i.e., Y-signal stability, gamma characteristic, the relative illuminance of the image plane due to lens, space resolution, and automatic focusing precision. Results are used to develop a visual sensor system having higher space and luminance resolutions than the human eye; thereby enabling pattern recognition to be easily performed. The presented system controls the camera iris and orientation using a long focal length lens under sufficient lighting conditions. Author (NASDA)

N93-12517# Air Force Inst. of Tech., Wright-Patterson AFB, OH. Foreign Aerospace Science and Technology Center.
BIONICS AND PROBLEMS OF INSTRUMENT MANUFACTURE
V. Y. Manoylov 18 Mar. 1992 9 p Transl. into ENGLISH from Izvestiya Vysshikh Uchebnikh Zavedeniy (Kronika, USSR, Priborostroveniye), v. 9, no. 4, 1966 p 139-141
(AD-A254461; FASTC-ID(RS)T-1237-91) Avail: CASI HC A02/MF A01

A conference was organized by the following groups: The Academy of Sciences of the USSR, the Scientific Council for Complex Problem 'Cybernetics', the Ministry of Higher and Secondary Special Education of the USSR, the Ministry of the Radio Industry of the USSR, the Academy of Medical Science, and the All-Union Scientific and Technical Society. The main topic of the conference was instrumentation in the context of bionics. Author

N93-11934*# McDonnell-Douglas Space Systems Co., Houston, TX.
FUZZY CONTROL SYSTEM FOR A REMOTE FOCUSING MICROSCOPE
Jonathan J. Weiss and Luc P. Tran *In* NASA. Lyndon B. Johnson Space Center, Fifth Annual Workshop on Space Operations Applications and Research (SOAR 1991), Volume 1 Jan. 1992 p 87-93 (For primary document see N93-11921 02-59)
Avail: CASI HC A02/MF A04

N93-11935*# National Aeronautics and Space Administration. Lyndon B. Johnson Space Center, Houston, TX.
FUZZY LOGIC CONTROL FOR CAMERA TRACKING SYSTEM
Robert N. Lea, R. H. Fritz (Link Flight Simulation Corp., Binghamton, NY.), J. Giarratano (Houston Univ., TX.), and Yashvant Jani (LinCom Corp., Houston, TX.) *In its* Fifth Annual Workshop on Space Operations Applications and Research (SOAR 1991), Volume 1 Jan. 1992 p 94-99 (For primary document see N93-11921 02-59)
Avail: CASI HC A02/MF A04

36 LASERS AND MASERS

Includes parametric amplifiers.
For related information see also *76 Solid-State Physics.*

N93-10997# Textron Defense Systems, Everett, MA.
CO2 LASER FREQUENCY DOUBLING Final Report, 24 Sep. 1991 - 24 Apr. 1992
24 Apr. 1992 64 p
(Contract N00014-91-C-2279)
(AD-A251060) Avail: CASI HC A04/MF A01

This work addresses the possibility of a high average power coherent light source in the mid-infrared, specifically in the 4.8 micrometers atmospheric window. The approach is to frequency-double the 9.55 micrometers CO2 laser line, yielding 4.775 micrometers. In order to achieve efficient conversion, the intensity of the laser is increased by intracavity resonant modulation, or modelocking. The intensity for efficient conversion in typical available lengths of doubling material is at a minimum 20 MW sq cm. However, the most efficient CO2 lasers operate with a pulse duration of at least 1 microsec, the characteristic time for energy transfer from N2 to CO2 at 1 atmosphere. Without modulation a fluence of at least 20 J sq cm would therefore be needed for high overall system efficiency. With modulation at a 1:10 or better mark-to-space ratio, this fluence is reduced to the 2 J sq cm range that typifies the surface damage threshold of available materials. One important unknown was the effect on damage threshold of a modulated versus an unmodulated pulse. Was the threshold dependent on peak intensity, or fluence? Other questions related to the specific material AgGaSe2, silver gallium selenide, chosen for this work. What was the quality of the second harmonic beam; what was the effective nonlinear coefficient; what was the temperature dependence of the phase-matching; and what was its thermal conductivity (to remove absorbed heat in an average power situation)? GRA

N93-11064# Rolls-Royce Ltd., Derby (England).
IN-PLANE STRAIN MEASUREMENT ON HIGH SPEED ROTATING COMPONENTS USING PULSED LASER ESPI
Richard W. T. Preater (City Univ., London, England) and Robin C. Swain (City Univ., London, England) 1 Dec. 1991 10 p Presented at the SEM Fall Conference, Baltimore, MD, 5-8 Nov. 1991 Sponsored by Science Research Council
(PNR-90975; ETN-92-92240) Copyright Avail: CASI HC A02/MF A01

The use of pulsed laser Electronic Speckle Pattern Interferometry (ESPI) for the measurement of in plane displacements and strain in rotating component is demonstrated. Differing component configurations over a very wide range of rotational speed produce clear high contrast interference fringe patterns. For regions of limited optical access the use of fiber optics in conjunction with infrared diode lasers may provide a suitable alternative. The noncontact approach and the freezing of the component notion lends itself to the use of this technique in an industrial environment. Conventional plane mirror optics and twin cylindrical mirror optics are also illustrated and discussed. ESA

N93-11155# Lawrence Livermore National Lab., CA.
A SYNOPSIS OF RESISTIVE WALL EFFECTS IN VERY SHORT WAVELENGTH FREE ELECTRON LASERS
W. A. Barletta Apr. 1992 6 p Presented at the 4th Generation Light Sources Workshop, Stanford, CA, 24-27 Feb. 1992
(Contract W-7405-eng-48)
(DE92-018065; UCRL-JC-110298; CONF-9202111-5) Avail: CASI HC A02/MF A01

The finite resistivity of the beam tube in the wiggler of a free electron laser (FEL) can give rise to longitudinal and transverse effects that may limit the performance of the FEL amplifiers and oscillators. Potential limiting effects may be (1) longitudinal-head-to-tail energy sweep or modulation in a beam pulse train, or (2) a transverse-coherent transverse oscillation of the beam pulse of a pulse train growing from head to tail in a pulse or pulse train. This brief synopsis outlines the constraints placed on FEL design by the wall effects. DOE

N93-11195# Naval Research Lab., Washington, DC.
TUNABLE, SHORT PULSE HARD X RAYS FROM A COMPACT LASER SYNCHROTRON SOURCE Interim Report
Phillip Sprangle, Antonio Ting, Eric Esarey, and Amnon Fisher 16 Jul. 1992 28 p
(AD-A254288; NRL/MR/4790-92-6973) Avail: CASI HC A03/MF A01

The development of a compact, tunable, near monochromatic hard x-ray source would have profound and wide ranging applications in a number of areas. These areas include x ray diagnostics, medical imaging, microscopy, nuclear resonance absorption, solid-state physics and material sciences. The properties of the x-ray beam which are important for these applications include spectral width, spectral brightness, photon flux, pulse configuration and polarization. Presently, third generation synchrotron sources are being pursued which are based on high energy electron storage rings and undulator magnetic fields. In the following, a laser synchrotron source (LSS) is proposed in which the magnetic undulator is replaced by ultra-high intensity laser pulses, e.g., from a Nd:YAG/Nd:glass laser, and the electron storage ring is replaced by an electron beam of substantially lower energy, e.g., from an RF linac or a high current betatron. Recent advances in compact, short pulse, high intensity laser technology make the LSS a potentially attractive compact source, particularly at high x-ray energies. GRA

N93-11278# Massachusetts Inst. of Tech., Cambridge. Plasma Fusion Center.
EXPERIMENTAL AND THEORETICAL INVESTIGATION OF HIGH GRADIENT ACCELERATION
G. Bekefi, C. Chen, S. Chen, B. Danly, R. J. Temkin, and J. S. Wurtele Feb. 1992 109 p
(Contract DE-FG02-91ER-40648)
(DE92-015299; DOE/ER-40648/1) Avail: CASI HC A06/MF A02

This report contains a technical progress summary of the research conducted under the auspices of DOE Grant No. DE-FG0291ER-40648, 'Experimental and Theoretical Investigations of High Gradient Acceleration'. This grant supports three research tasks: Task A consists of the design and fabrication of a 17 GHz of photocathode gun, Task B supports the testing of high gradient acceleration using a 33 GHz structure, and Task C comprises theoretical investigations, both in support of the experimental tasks and on critical physics issues for the development of high energy linear colliders. This report is organized as follows. The development of an rf gun design and research progress on the picosecond laser system is summarized in Section 2, the status of the studies of the LBL/Haimson high gradient structure using a 50 MW free-electron laser is summarized in Section 3, and theoretical research progress is described in Section 4. Supporting material is contained in Appendices A-G. DOE

N93-11332 Deutsche Geodaetische Kommission, Munich (Germany).
ANALYSIS OF LUNAR LASER RANGING IN THE FRAMEWORK OF A POST-NEWTONIAN THEORY Ph.D. Thesis - Technische Univ. [ANALYSE VON LASERMESSUNGEN ZUM MOND IM RAHMEN EINER POST-NEWTON'SCHEN THEORIE]
Juergen Mueller 1991 132 p In GEORGIAN Sponsored by DFG and Technische Univ.
(Ser-C-383; ISBN-3-7696-9429-5; ETN-92-92278) Copyright
Avail: Deutsche Geodaetische Kommission, Marstallplatz 8, D-8000 Munich 22, Germany

It is shown that the analysis of Lunar Laser Ranging (LLR) data provides an excellent tool for the determination of parameters concerning the Earth-Moon system and the test of Einstein's theory of gravity in the first Post Newtonian (PN) approximation. All equations of the LLR model are to be formulated at the first PN level, and their influences on the analysis of the LLR data are to be estimated. Based on these results, the existing programs are to be changed and new determinations of the parameters are to be performed. The equations for the analysis of Very Long Baseline Interferometry (VLBI) are derived to the LLR equations, to be used for a later combination of both observation data. ESA

N93-11388# Royal Signals and Radar Establishment, Malvern (England). Electronics Div.
CO2 LASER FREQUENCY DOUBLING USING AgGaSe2
E. K. Gorton and P. D. Mason Sep. 1991 26 p
(RSRE-Memo-4528; BR308891; ETN-92-92322) Copyright
Avail: CASI HC A03/MF A01

AgGaSe2 samples are examined using a CO2 laser for the frequency doubling application. AgGaSe2 is an optical material which demonstrates a high figure of merit for nonlinear optics in the infrared. It transmits between 0.7 and 19 micrometers, has a refractive index around 2.6, a band gap of approximately 1.82 eV, and is a negative birefringent material. This material can be phase matched for frequency doubling of CO2 laser radiation and has shown up to 60 percent conversion efficiency under best conditions. The results are compared with a coupled wave equation model which includes absorption. Good agreement between the results and the model is obtained. Best energy conversion efficiency obtained under experimental conditions was 7 percent with an antireflection coated 2 cm long sample. ESA

N93-11411 National Physical Lab., Teddington (England). Div. of Radiation Science and Acoustics.
USE OF THE PROGRAM ANISN TO CALCULATE RESPONSE FUNCTIONS FOR A BONNER SPHERE SET WITH A He-3 DETECTOR
D. J. Thomas Mar. 1992 44 p Sponsored in part by EURADOS
(Contract CEC-B16-003-UK)
(NPL-RSA(EXT)-31; ETN-92-92373) Copyright Avail: National Physical Lab., Teddington, Middlesex, TW11 0LW, England

The use of the one dimensional discrete ordinates neutron transport code ANISN, to perform calculations of response functions for a particular type of Bonner sphere set, is reported. This set is based on a 32 mm diameter spherical He-3 proportional counter as a central thermal neutron detector which is placed inside polyethylene moderating spheres with diameters ranging from 7.6 to 45.7 cm (3 to 15 inches). Calculations were also made of the sensitivity of the response functions to polyethylene density and to the pressure of He-3 in the central detector. The results are compared with experimental measurements of the sphere responses. ESA

N93-11418# California Univ., Santa Barbara.
UCSB FEL USER MODE ADAPTION PROJECT Final Report, 1 Jan. 1986 - 31 Dec. 1990
Vincent Jaccarino 14 Apr. 1992 13 p
(Contract N00014-86-K-0110)
(AD-A248734) Avail: CASI HC A03/MF A01

This research sponsored by the SDIO Biomedical and Materials Sciences FEL Program held the following objectives: Provide a facility in which in-house and outside user research in the materials and biological sciences can be carried out in the Far Infrared using-the unique properties of the UCSB electrostatic accelerator-driven FEL; Develop and implement new FEL concepts and FIR technology and encourage the transfer and application of this research; Train graduate students, post doctoral researchers and technical personnel in varied aspects of scientific user disciplines, FEL science and FIR technology in a cooperative, interdisciplinary environment. In summary, a free electron laser facility has been developed which is operational from 200 GHz, (6.6 cm exp -1), to 4.8 THz, (160 cm exp -1) tunable under computer control and able to deliver kilowatts of millimeter wave and far-infrared power. This facility has a well equipped user lab that has been used to perform ground breaking experiments in scientific areas as diverse as bio-physics. Nine graduate students and post doctoral researchers have been trained in the operation, use and application of these free-electron lasers. GRA

N93-11500# Brookhaven National Lab., Upton, NY.
SCALING OF GAIN WITH ENERGY SPREAD AND ENERGY IN THE PEP FEL
A. S. Fisher 13 Jul. 1992 8 p
(Contract DE-AC02-76CH-00016)
(DE92-019248; BNL-47803; CAP-85-92R) Avail: CASI HC A02/MF A01

The Sag Harbor paper on the PEP FEL discusses the scaling of various FEL parameters with energy spread (sigma)(sub (var epsilon)). Some of this material is repeated here, and the benefit of increasing the energy spread is examined. How much energy spread can be achieved with damping wigglers is the next topic. Finally, the dependence of gain and saturation length on beam energy and undulator field is considered. DOE

N93-11659# Lawrence Livermore National Lab., CA.
EXPERIMENTAL STUDIES OF X RAY LASER SPECTRAL PROFILES: OBSERVATION OF GAIN NARROWING AND SATURATION BEHAVIOR
J. A. Koch, B. J. MacGowan, L. B. DaSilva, D. L. Matthews, S. Mrowka, J. H. Underwood, and P. J. Batson 17 Jul. 1992 15 p Presented at the 11th International Conference on Spectra Line Shapes, Carry Le Rouet, France, 8-12 Jun. 1992
(Contracts W-7405-eng-48; DE-AC03-76SF-00098)
(DE92-019603; UCRL-JC-110209; CONF-9206255-1) Avail: CASI HC A03/MF A01

We discuss our recent measurements of the spectral width of the 206.38 Angstrom x-ray laser transition in Ne-like Se. These measurements used a high-resolution grating spectrometer and were performed over a wide range of laser amplifier lengths. The data have enabled us to extrapolate the intrinsic line width and to observe the effects of gain-narrowing and saturation on the line profile. We find an intrinsic width which is 1.4 times the Doppler width, we observe gain-narrowing in intermediate length amplifiers, and we observe no re-broadening in long, saturated amplifiers. These results suggest that collisional line-broadening has a significant effect on the line profile and saturation behavior of this laser. We discuss modeling we have performed in order to simulate the experimental data, and we discuss future experimental and theoretical efforts we believe are necessary in order to understand line broadening and line transfer issues in x-ray laser plasmas. DOE

N93-11691# Stanford Linear Accelerator Center, CA.
A SINGLE BEAM LASER TRACKER AS AN ALIGNMENT TOOL
B. T. Wand, C. LeCocq, M. Gaydosh, and R. E. Ruland Jul. 1992 66 p Presented at the 1992 American Society for Photogrammetry and Remote Sensing/American Congress on Surveying and Mapping/Resource Technology (ASPRS/ACSM/RT) Convention on Monitoring and Mapping Global Change, Washington, DC, 3-8 Aug. 1992
(Contract DE-AC03-76SF-00515)
(DE92-017746; SU-SLAC-PUB-5847; CONF-920892-2) Avail: CASI HC A04/MF A01

In December 1991 the Survey and Alignment team of the Stanford Liner Accelerator Center (SLAC) purchased a Chesapeake single beam laser tracker. This paper will discuss first experiences and applications with this new type of an alignment instrument. DOE

N93-11720 Drexel Univ., Philadelphia, PA.
A STUDY OF THE CO2 LASER NEAR THRESHOLD Ph.D. Thesis
David Wilson Bromley 1991 147 p
Avail: Univ. Microfilms Order No. DA9213862

When the cavity losses of a laser are varied across threshold there is a delay in its bifurcation. We studied the effects of sweeping the cavity losses with an Acousto-Optic Modulator. For very high frequencies, Q-Switching occurs and the delay is dependent upon the depth of modulation. For medium frequencies, the delay is dependent upon the frequency. For lower frequencies, the delay turns into an apparent anticipation, which also depends upon frequency. We studied these effects experimentally and show the existence of scaling relations. We also studied the effects using the rate equations and show that the anticipation is still a delay but the bifurcation is affected as it is swept across threshold in either direction. Dissert. Abstr.

N93-11737# Oregon State Univ., Corvallis. Dept. of Physics.
MATTER-WAVE INTERFEROMETRY WITH LASER COOLED ATOMS Summary Report
David McIntyre 1 Jun. 1992 3 p
(Contract N00014-91-J-1198)
(AD-A253999) Avail: CASI HC A02/MF A01

This program is investigating matter wave interferometry with laser cooled atoms. A slow beam of laser cooled rubidium atoms will be used as the matter wave source. The atom optical elements are microfabricated amplitude transmission gratings which will be used in a three-grating interferometer to split and recombine the rubidium beam. The interferometer will be a useful new tool for precision atomic physics and a sensitive inertial sensor. The principal tasks in this research program are production of a laser cooled rubidium atomic beam, fabrication of submicron amplitude transmission gratings, and construction and testing of the atomic interferometer. Several technical issues must be addressed in each task. The atomic beam must have high brightness to ensure adequate signal to noise ratio and a low temperature to ensure a long coherence length. The gratings must be phase coherent over their area so that the interferometer fringes are not washed out. The interferometer must be vibration isolated so that the fringes do not move appreciably during the signal integration time. GRA

N93-11765# Lawrence Livermore National Lab., CA.

PROGRESS TOWARD X RAY LASING BETWEEN AUTOIONIZING TRANSITIONS

S. B. Libby, A. L. Osterheld, A. Szoke, R. S. Walling, and B. K. F. Young 25 Jun. 1992 4 p Presented at the 3rd International Colloquium on X Ray Lasers, Schliersee, Germany, 18-22 May 1992
(Contract W-7405-eng-48)
(DE92-017428; UCRL-JC-109842; CONF-920523-1) Avail: CASI HC A01/MF A01

We report progress on a Delta(n) = 1 laser scheme between autoionizing states. Such a scheme has high quantum efficiency, and it does not suffer from trapping of the resonance transition draining the lower laser level. The upper laser level is optically pumped, and its Auger decay rate is slower than that of the lower laser level. We report on a study of pumping of the 1s2s3p manifold of Li-like Al, using the 1825.6 eV transition of Ne-like Rb. DOE

N93-11786# Air Force Inst. of Tech., Wright-Patterson AFB, OH. Foreign Technology Div.

CHINESE JOURNAL OF LASERS (SELECTED ARTICLES)

10 Dec. 1991 16 p Transl. into ENGLISH from Zhongguo Jiguang (China), v. 17, no. 1, 1990 p 1-4 and 39
(AD-A254100; FTD-ID(RS)T-1474-90) Avail: CASI HC A03/MF A01

In the oscillation-amplification system of copper vapor laser devices, we opted for the use of stretched or widened pulse width input amplification as well as double pass amplification technology. The output power is capable, as compared to the unwidened or unstretched and travelling wave amplification output powers, of being higher by 7 percent and 8 percent respectively. The amount of fluctuation or jitter of the output optical waveform of copper vapor laser devices relative to input optical waveforms was +/- 4.0 ns, while the amount of fluctuation or jitter between the two oscillators was +/- 9.0 ns. GRA

N93-11805# Visidyne, Inc., Burlington, MA.

THE DESIGN, DEVELOPMENT, AND TEST OF BALLOONBORNE AND GROUNDBASED LIDAR SYSTEMS. VOLUME 3: GROUNDBASED LIDAR SYSTEMS Final Report, 30 May 1986 - 31 Dec. 1990

O. Shepherd, G. Aurilio, R. D. Bucknam, A. G. Hurd, and N. F. Robertie 1 Jun. 1991 56 p
(Contract F19628-86-C-0105)
(AD-A247552; VI-1707-C-Vol-3; PL-TR-91-2191-Vol-3; AD-E200874) Avail: CASI HC A04/MF A01

This is Volume 3 of a three volume final report on the design, development and test of balloonborne and groundbased lidar systems. Volume 1 describes the design and fabrication of a balloonborne CO2 coherent payload to measure the 10.6 micrometers backscatter from atmospheric aerosols as a function of altitude. Volume 2 describes the August 1987 flight test of Atmospheric Balloonborne Lidar Experiment, ABLE 2. In this volume we describe groundbased lidar development and measurements. A design was developed for installation of the ABLE lidar in the GL rooftop dome. A transportable shed was designed to house the ABLE lidar at the various remote measurement sites. Refurbishment and modification of the ABLE lidar were completed to permit groundbased lidar measurements of clouds and aerosols. Lidar field measurements were made at Ascension Island during SABLE 89. Lidar field measurements were made at Terciera, Azores during GABLE 90. These tasks have been successfully completed, and recommendations for further lidar measurements and data analysis have been made. GRA

N93-12011# OPTRA, Inc., Beverly, MA.

LASER SURFACE PROFILOMETER WITH SUB-ANGSTROM RESOLUTION

D. J. Mansur, D. W. Voorhes, and G. Wyntjes 1992 11 p Presented at the 1992 Conference on Microlithography, San Jose, CA, 8-13 Mar. 1992
(Contract DE-AC02-88ER-80585)
(DE92-018926; CONF-9203173-1) Avail: CASI HC A03/MF A01

Single point diamond turning technology, has allowed the manufacture of highly aspheric optics that were unimaginable just a few years ago. Testing these optics is typically either expensive (i.e. null lens systems), destructive (contacting stylus profilers), or slow (existing optical profilers). We describe a noncontacting surface profilometer with 5 micron lateral spatial resolution and sub-Angstrom height resolution. The instrument is configured as a polarizing interferometer that operates at near zero path difference and uses a visible laser diode as a light source. The instrument incorporates an autofocussing mechanism that allows high resolution profilometry over a vertical range of plus or minus 1 mm. The system bandwidth of 200 kHz allows for very fast profiling (87 cm/sec) without loss of resolution. The sensor head is very compact (6 x 6 x 10 cm) and all the processing electronics are contained on a single PC-compatible card. The instrument's autofocussing feature, high speed capability and compact size make it ideally suited for inprocess and final acceptance testing of steep aspheric optics. We will present data that demonstrates our ability to accurately measure the macroscopic and microscopic features of single point diamond turned aspheric optics typically used in high resolution x-ray lithography systems. DOE

N93-12023# Ecole Polytechnique, Palaiseau (France). Lab. pour l'Utilisation des Lasers Intenses.

THE 1989 SCIENTIFIC REPORT OF THE LABORATORY FOR THE USE OF HIGH POWER LASERS [LABORATOIRE POUR L'UTILISATION DES LASERS INTENSES: RAPPORT SCIENTIFIC 1989]

Christine Labaune, ed. and Danielle Smadja, ed. Apr. 1990 210 p In FRENCH
(ETN-92-92175) Avail: CASI HC A10/MF A03

Reports from the laboratory concerning the use of high power lasers are presented. The reports principally cover research on laser plasma physics and laser plasma interactions. The reports are listed under the following headings: interaction, transport, compression, hydrodynamics; atomic physics; instrumentation, lasers, diagnostics. For individual titles, see N93-12024 through N93-12052.

N93-12024# Ecole Polytechnique, Palaiseau (France). Centre de Physique Theorique.

STIMULATED BRILLOUIN BACKSCATTERING INSTABILITY IN THE CASE OF A HIGH POWER LASER: APPLICATION TO WAVE PULSATION PARTICLE ACCELERATION EXPERIMENTS [L'INSTABILITE DE RETRODIFFUSION BRILLOUIN STIMULEE DANS LE CAS D'UNE ONDE LASER INTENSE. APPLICATION AUX EXPERIENCES D'ACCELERATION DE PARTICULES PAR BATTEMENT D'ONDES]

Philippe Mounaix, Guy Laval, and Denis Pesme *In its* The 1989 Scientific Report of the Laboratory for the Use of High Power Lasers Apr. 1990 p 1-10 In FRENCH (For primary document see N93-12023 02-36)
Avail: CASI HC A02/MF A03

The growth rate of Brillouin instability in a subdense plasma is calculated for high power laser flux (but less than the field corresponding to that of laser wave propagation in the relativistic state). The anti-Stokes component is shown to be ignorable. Temporal and spatial growth rates are calculated. In acceleration experiments where the effective length of the pulse is less than the plasma length, it is shown that in the nonrelativistic states the Brillouin instability cannot be ignored, but that its role becomes less important as the flux and the electron temperature rise. ESA

N93-12025# Ecole Polytechnique, Palaiseau (France). Lab. pour l'Utilisation des Lasers Intenses.
OBSERVATION AND ANALYSIS OF THE STOKES AND ANTI-STOKES COMPONENTS OF STIMULATED RAMAN BACKSCATTERING [OBSERVATION ET ANALYSE DES COMPOSANTES STOKES ET ANTI-STOKES DE LA RETRODIFFUSION RAMAN STIMULEE]
Christine Labaune, Sophie Baton, Denis Pesme, and H. A. Baldis (National Research Council of Canada, Ottawa, Ontario) *In its* The 1989 Scientific Report of the Laboratory for the Use of High Power Lasers Apr. 1990 p 11-34 In FRENCH (For primary document see N93-12023 02-36)
Avail: CASI HC A03/MF A03

An experiment to observe the backward emitted anti-Stokes component in two types of plasma is described: (1) in subcritical homogenous plasma, preformed by explosion of thin films irradiated by a laser beam focused along a line; and (2) in plasma produced by the irradiation of thin targets in a monobeam experiment. The temporal evolutions of the Raman anti-Stokes components for both plasmas are shown. The theoretical prediction of isolated Raman instability, Raman instability in presence of plasma wave, and Raman instability when the plasma wave is strongly turbulent, is shown. ESA

N93-12026# Ecole Polytechnique, Palaiseau (France). Lab. pour l'Utilisation des Lasers Intenses.
STUDY OF FILAMENTATION IN SUBDENSE PLASMA INTERACTION EXPERIMENTS [ETUDE DE LA FILAMENTATION DANS DES EXPERIENCES D'INTERACTION EN PLASMA SOUS-DENSE]
Sophie Baton, Christine Labaune, H. A. Baldis (National Research Council of Canada, Ottawa, Ontario), D. Giulietti (Consiglio Nazionale delle Ricerche, Pisa, Italy), and E. Schifano (Consiglio Nazionale delle Ricerche, Pisa, Italy) *In its* The 1989 Scientific Report of the Laboratory for the Use of High Power Lasers Apr. 1990 p 35-40 In FRENCH (For primary document see N93-12023 02-36)
Avail: CASI HC A02/MF A03

Experiments in preformed homogenous plasmas of density lower than the critical density necessary to fundamentally study filamentation and autofocalization are described. Schlieren image diagnostics are discussed, and refraction diagnostics are compared with simulations. The essentially qualitative results observe, on the one hand, filamentary structures whose dimensions are in agreement with those of ponderomotive filamentation, and, on the other hand, angular diagrams whose interpretation brings in a density hollow on the axis of the plasma related to autofocalization. ESA

N93-12027# Toulouse Univ. (France). Interaction Laser-Matiere.
X PULSE RADIATION AROUND THE CRITICAL SURFACE [RAYONNEMENT X PULSE AUX ENVIRONS DE LA SURFACE CRITIQUE]
Cecile Arnas, Jacques Briand, M. Armengaud, Alain Gomes, and Yves Quemener *In* Ecole Polytechnique, The 1989 Scientific Report of the Laboratory for the Use of High Power Lasers Apr. 1990 p 41-44 In FRENCH (For primary document see N93-12023 02-36)
Avail: CASI HC A01/MF A03

Preliminary results of experiments studying X-ray emission around critical density, to better understand laser wave parametric instabilities and resonant absorption mechanism, processes at the origin of locally intense energy buildups, are presented. During the interaction period, the plasma is shown to be the seat of a pulsed X-ray emission. The characteristic time interval separating these 'structures' varies in relation with the power and wavelength of the laser. ESA

N93-12028# Ecole Polytechnique, Palaiseau (France). Lab. pour l'Utilisation des Lasers Intenses.
X-UV SPECTROSCOPY TEMPORAL RESOLUTION [SPECTROSCOPIE X-UV RESOLUE TEMPORELLEMENT]
Rene Benattar and Aybars Sezen *In its* The 1989 Scientific Report of the Laboratory for the Use of High Power Lasers Apr. 1990 p 45-49 In FRENCH (For primary document see N93-12023 02-36)
Avail: CASI HC A01/MF A03

A study to characterize the transport region of a laser plasma, where electron density is greater than critical density and density and temperature gradients are very steep, is presented. The supercritical medium was considered by measurement of the refraction index and its spatial distribution. A spectrograph operating in the X-UV range, corresponding, during the laser pulse, to the most important part of the transport region radiation, detects the spectrum of a material through the plasma to be sensed. The modification of the spectrum of the emitter to the plasma traverse gives information on the refractive index of the medium. Results showing the spectra of Al, Mg/Al, and Teflon/Al, are given. ESA

N93-12029# Ecole Polytechnique, Palaiseau (France). Lab. pour l'Utilisation des Lasers Intenses.
INTERPRETATION OF EXPERIMENTS MEASURING THE BACK FACE OF THIN ALUMINUM STRIPS BY COMPARISON WITH NUMERICAL SIMULATIONS [INTERPRETATION DES EXPERIENCES DE MESURE DE TEMPERATURE DE FACE ARRIERE DE FEUILLES MINCES D'ALUMINIUM PAR COMPARAISON AVEC LES SIMULATIONS NUMERIQUES]
Rene Benattar and Victor Malka *In its* The 1989 Scientific Report of the Laboratory for the Use of High Power Lasers Apr. 1990 p 50-54 In FRENCH (For primary document see N93-12023 02-36)
Avail: CASI HC A01/MF A03

Experiments using X-UV imagery which show the importance of radiative transfer during ablation of Z weak material, such as aluminum, by a high power ultraviolet laser are described. Measurements are compared with two mumerical simulation programs (MULTI and FILM). Shock propagation shows a correct dependence in relation to the thickness of the film. The back face temperatures are perfectly reproduced by the MULTI simulations, including the radiative transfer. The agreement between experiment and MULTI shows the importance of radiation transfer in this type of interaction. The temperature of the back face is determined more by radiative heating than by shock wave heating, in particular for the thinnest films (5 micrometers). ESA

N93-12030# Ecole Polytechnique, Palaiseau (France). Lab. pour l'Utilisation des Lasers Intenses.
HYDRODYNAMIC EFFICIENCIES IN IMPLOSION EXPERIMENTS [RENDEMENTS HYDRODYNAMIQUES DANS LES EXPERIENCES D'IMPLOSION] c34
Michel Koenig, Edouard Fabre, Jean-Michel Boudenne, Alain Michard, and P. Fews (Bristol Univ., England) *In its* The 1989 Scientific Report of the Laboratory for the Use of High Power Lasers Apr. 1990 p 55-59 In FRENCH (For primary document see N93-12023 02-36)
Avail: CASI HC A01/MF A03

Experiments on the implosion of high aspect ratio glass microballoons, filled with an equimolar mixture of 10 atmosphere D-T gas, aimed at determining hydrodynamic efficiencies, the characteristics (density and temperature) of the wall, are described. Experimental results for kinetic and thermal variations, obtained for 350 and 450 micrometer targets, at an absorbed laser power of about 120 J, are compared with values given by simulations with the FILM code. The comparison is made at the time of shock reflection on the internal wall of the shell. The use of X spectroscopy in such experiments is discussed. ESA

N93-12031# Toulouse Univ. (France). Interaction Laser-Matiere.
DEVELOPMENT OF A HYDRODYNAMIC CODE: MINNIE [MISE AU POINT D'UN CODE HYDRODYNAMIQUE LAGRANGIEN DIDIMENSIONNEL: MINNIE]
Pascal Marcerou and Jean-Pierre Dinguirard *In* Ecole Polytechnique, The 1989 Scientific Report of the Laboratory for

the Use of High Power Lasers Apr. 1990 p 60-63 In FRENCH (For primary document see N93-12023 02-36)
Avail: CASI HC A01/MF A03

The development of hydrodynamic two dimensional Lagrangian code (Minnie) adapted to the study of plasmas created by laser-material interaction is outlined. The geometry of the plasma and the mesh are described and the steps for the simulation are explained. The code is principally intended for the study of the radiative transfer of an X-ray using hydrodynamic results obtained at different times. Steps to position at one point in space, and study, in a certain direction and for a given angular aperture, the luminous spectrum coming from the plasma, are given. ESA

N93-12032# Paris XI Univ., Orsay (France). Lab. de Physique des Gaz et des Plasmas.
NONLINEAR BEHAVIOR OF RESONANT ABSORPTION IN A PLASMA AT MICROWAVE FREQUENCY [COMPORTEMENT NON-LINEAIRE DE L'ABSORPTION RESONANTE DANS UN PLASMA AUX FREQUENCES MICRO-ONDES]
Brigitte Cros, Arnaud Chiron, Gilles Matthieussent, Jacques Godiot, and Anne Heron (Ecole Polytechnique, Palaiseau, France) *In* Ecole Polytechnique, The 1989 Scientific Report of the Laboratory for the Use of High Power Lasers Apr. 1990 p 64-68 In FRENCH (For primary document see N93-12023 02-36)
Avail: CASI HC A01/MF A03

An experimental device which creates an argon plasma without magnetic field in a multipolar discharge is described. Theoretical models of the parabolic density profile and resonant absorption of an electromagnetic wave are given. Experiment results showing the plasma wave excitations in the neighborhood of the parabolic density profile summit are given. ESA

N93-12033# Ecole Polytechnique, Palaiseau (France). Centre de Physique Theorique.
ELECTRON ACCELERATION IN A RELATIVISTIC ELECTRON PLASMA WAVE [ACCELERATION D'ELECTRONS DANS UNE ONDE PLASMA ELECTRONIQUE RELATIVISTE] c75
Patrick Mora *In its* The 1989 Scientific Report of the Laboratory for the Use of High Power Lasers Apr. 1990 p 69-72 In FRENCH (For primary document see N93-12023 02-36)
Avail: CASI HC A01/MF A03

The development of a three dimensional code calculating the electron beam trajectory in accelerating structure is reported. An electron plasma wave excited to a known amplitude is supposed and the electron acceleration in the field of this wave is analytically and numerically studied. Account is taken of the Lorentzian envelope of the field. The results of the code are not detailed but correspond to a degradation of acceleration performances with relation to one dimensional calculation. The code allows optimization of electron beam parameters, in particular, focalization conditions. Results related to diagnostics including the following can be predicted: global accelerated electron energy spectrum; spectrum for different angles; and deflection in relation to final energy. ESA

N93-12034# Ecole Polytechnique, Palaiseau (France). Lab. pour l'Utilisation des Lasers Intenses.
LOW PRESSURE GAS MULTIPHOTOIONIZATION FOR WAVE PACKET EXPERIMENTS [MULTIPHOTOIONISATION DES GAZ A BASSE PRESSION POUR LES EXPERIENCES DE BATTEMENT D'ONDES] c75
Francois Amiranoff, Anthony Dyson, Jean-Raphael Marques, Christian Stenz, P. Benkheiri, C. Gregory, F. Jacquet, P. Mine, B. Montes, and P. Poilleux et al *In its* The 1989 Scientific Report of the Laboratory for the Use of High Power Lasers Apr. 1990 p 73-76 In FRENCH (For primary document see N93-12023 02-36)
Avail: CASI HC A01/MF A03

Experiments to create and diagnose a plasma, from laser wavelength 1.064 and 1.053 micrometers injected into a plasma of about 5 mm and of density 1.078 times 10 to the 17th power e(-)/cu cm +/- 0.5 , are described. The plasma is produced by multiphotoionization of hydrogen or deuterium at 2 mbar pressure. The density of the plasma obtained near the laser lens focusing corresponds to the initial atom density in the vessel. The density is measured by mass Thomson diffusion. Results and numerical simulation show that sufficiently wide and homogenous laser spots must be obtained, even for relatively short pulses (100 ps). ESA

N93-12035# Ecole Polytechnique, Palaiseau (France). Lab. pour l'Utilisation des Lasers Intenses.
LASER MATERIAL INTERACTION IN CONFINED MEDIUM [DE L'INTERACTION LASER-MATIERE EN MILIEU CONFINE] c75
David Devaux (Etablissement Technique Central de l'Armement, Arcueil, France), Remy Fabbro (Etablissement Technique Central de l'Armement, Arcueil, France), Jean Virmont, Patrick Ballard (Peugeot S.A., Velizy, France), and Jean Fournier (Peugeot S.A., Velizy, France) *In its* The 1989 Scientific Report of the Laboratory for the Use of High Power Lasers Apr. 1990 p 77-82 In FRENCH (For primary document see N93-12023 02-36)
Avail: CASI HC A02/MF A03

The technique of dielectric metallic target confinement is discussed. Improvements in experimental measurements by piezodielectric sensor are described. Laser material interaction by the hydrodynamic code FILM is described. The formed plasma is visualized using a streak camera. ESA

N93-12036# Peugeot S.A., Velizy (France). Etudes et Recherches.
STUDY OF THE EFFECTS OF A PLASTIC WAVE INDUCED BY LASER PULSE IN A METALLIC MATERIAL. APPLICATION TO THE IMPROVEMENT OF FATIGUE STRENGTH [ETUDE DES EFFETS D'UNE ONDE PLASTIQUE INDUITE PAR PULSE LASER DANS UN MATERIAU METALLIQUE. APPLICATION A L'AMELIORATION DE LA TENUE EN FATIQUE] c75
Patrick Ballard, Jean Fournier, David Devaux (Ecole Polytechnique, Palaiseau, France), and Remy Fabbro (Etablissement Technique Central de l'Armement, Arcueil, France) *In* Ecole Polytechnique, The 1989 Scientific Report of the Laboratory for the Use of High Power Lasers Apr. 1990 p 83-87 In FRENCH (For primary document see N93-12023 02-36)
Avail: CASI HC A01/MF A03

The prediction of the surface stress of the plastic field of a wave induced by confined irradiation of a metallic target by a laser pulse is addressed. The theoretical model is calculated using the plasma pressure. The gain in fatigue strength is calculated. ESA

N93-12037# Ecole Nationale Superieure de Mecanique et d'Aerotechnique, Poitiers (France). Lab. d'Energetique et de Detonique.
STUDY OF THE DYNAMIC DEGRADATION UNDER THE ACTION OF A SHOCK WAVE INDUCED BY PULSED LASER [ETUDE DE L'ENDOMMAGEMENT DYNAMIQUE SOUS L'ACTION D'UNE ONDE DE CHOC INDUITE PAR UNE IMPULSION LASER]
Francois Cottet and Michel Boustie *In* Ecole Polytechnique, The 1989 Scientific Report of the Laboratory for the Use of High Power Lasers Apr. 1990 p 88-93 In FRENCH (For primary document see N93-12023 02-36)
Avail: CASI HC A02/MF A03

A numerical study of dynamic degradation under shock wave spalling, which lead to the development of a code to carry out simulations after the appearance of the first crack in the material, is presented. Experiments confirming the validation of the degradation model for aluminum and determining the parameters for copper are reported. ESA

N93-12038# Ecole Nationale Superieure de Mecanique et d'Aerotechnique, Poitiers (France). Lab. d'Energetique et de Detonique.
SHOCK WAVES INDUCED BY PULSED LASER IN CONFINED INTERACTION: NUMERICAL SIMULATION [ONDES DE CHOC INDUITES PAR IMPULSION LASER EN INTERACTION CONFINEE. SIMULATIONS NUMERIQUES]
Jean-Pierre Romain and Patrick Darquey *In* Ecole Polytechnique,

The 1989 Scientific Report of the Laboratory for the Use of High Power Lasers Apr. 1990 p 94-99 In FRENCH (For primary document see N93-12023 02-36)
Avail: CASI HC A02/MF A03

Experimental results obtained by different authors on pressure measurements, shock damping measurements, confinement thickness effects, and different acceleration measurements are compared to simulations of the SHYLAC code in order to validate the code in different target configurations. Analysis of the experiments, results in the determination of the interaction performance in relation to irradiation conditions. ESA

N93-12039# Ecole Nationale Superieure de Mecanique et d'Aerotechnique, Poitiers (France). Lab. d'Energetique et de Detonique.

NUMERICAL SIMULATION OF A PRESSURE GRADIENT IN A MULTILAYER TARGET: TEMPERATURE EVOLUTION [SIMULATION NUMERIQUE D'UNE RAMPE DE PRESSION DANS UNE CIBLE MULTICOUCHES. EVOLUTION DE LA TEMPERATURE] **c34**

Jean-Pierre Romain *In* Ecole Polytechnique, The 1989 Scientific Report of the Laboratory for the Use of High Power Lasers Apr. 1990 p 100-105 In FRENCH (For primary document see N93-12023 02-36)
Avail: CASI HC A02/MF A03

The one dimensional hydrodynamic Lagrangian code Shylac was used to simulate the temperature evolution of pressure gradients produced by successive shocks and by direct shock. In relation to a moderate pressure (1 Mbar) direct shock, compression by a successive levels has little influence on the final density (the gain is about 2 percent); however, it does have a strong influence on the final temperature, which is reduced by half. At every high pressure (30 Mbar), the decrease in temperature remains relatively the same, while the gain in density becomes even more sensitive (about 13 percent rather than 2 percent). ESA

N93-12040# Nice Univ. (France). Lab. de Physique de la Matiere Condensee.

OBSERVATION OF PULSES PROPAGATING AT SUPRALUMINOUS SPEED IN AN OPTICAL FIBER [OBSERVATION D'IMPULSIONS SE PROPAGEANT A VITESSE SUPRALUMINIQUE DANS UNE FIBRE OPTIQUE]

Jean Botineau, Olivier Legrand, Claude Leycuras, Carlos Montes, and Eric Picholle *In* Ecole Polytechnique, The 1989 Scientific Report of the Laboratory for the Use of High Power Lasers Apr. 1990 p 106-109 In FRENCH (For primary document see N93-12023 02-36)
Avail: CASI HC A01/MF A03

The theory of relativity that forbids any transmission of information at a speed greater than that of light is discussed. An experiment with a luminous pulse propagating along an optical fiber faster than the 'normal' speed of light in the fiber is described. Although the experiment shows the propagation of a luminous pulse less than the speed of light, no theoretical limit appears in explaining the propagation, so that such a pulse apparently propagates faster than any signal. ESA

N93-12041# Ecole Polytechnique, Palaiseau (France). Lab. de Physique des Milieux Ionises.

ABSORPTION SPECTROSCOPY OF L(ALPHA, BETA) TRANSITIONS IN A LASER GERMANIUM PLASMA [SPECTROSCOPIE D'ABSORPTION DES TRANSITIONS L (ALPHA, BETA) DANS UN PLASMA DE GERMANIUM CREE PAR LASER]

Claude Chenais-Popovics, Jean-Paul Geindre, Jean-Claude Gauthier, M. Klapisch (Lawrence Livermore National Lab., CA.), C. Bauche-Arnoult (Paris-Sud Univ., Orsay, France), J. Bauche (Paris-Sud Univ., Orsay, France), J. Bruneau (Centre d'Etudes de Limeil-Valenton, Villeneuve Saint-Georges, France), D. Desenne (Centre d'Etudes de Limeil-Valenton, Villeneuve Saint-Georges, France), M. Louis-Jacquet (Centre d'Etudes de Limeil-Valenton, Villeneuve Saint-Georges, France), and D. Naccache *In its* The 1989 Scientific Report of the Laboratory for the Use of High Power Lasers Apr. 1990 p 111-118 In FRENCH (For primary document see N93-12023 02-36)
Avail: CASI HC A02/MF A03

A spectroscopic study of the 2p-3d absorption transitions in germanium is reported. Radiative transition and autoionization probabilities were calculated by a simulation code, as well as the wavelengths of the transitions. The absorption coefficients as a function of wavelength are given. Good agreement is found between measurement and simulation. ESA

N93-12042# Ecole Polytechnique, Palaiseau (France). Lab. de Physique des Milieux Ionises.

SATURATION EFFECTS IN ABSORPTION SPECTROSCOPY OF THE K(ALPHA) RAYS OF ALUMINUM [EFFETS DE SATURATION EN SPECTROSCOPIE D'ABSORPTION DES RAIES K ALPHA DE L'ALUMINIUM] **c25**

Claude Chenais-Popovics, Christian Fievet, Jean-Paul Geindre, Isao Matsushima (Tsukuba Univ., Japan), and Jean-Claude Gauthier *In its* The 1989 Scientific Report of the Laboratory for the Use of High Power Lasers Apr. 1990 p 119-124 In FRENCH (For primary document see N93-12023 02-36)
Avail: CASI HC A02/MF A03

The evolution of the optical depth and its deduced density when the thickness of the absorbent layer increases are studied. A saturation effect of the apparent optical depth of the K(alpha) transitions is shown to possibly perturb the integrated density measurement of this layer. The correct description of this effect depends a lot on the relation between the instrumental width and the intrinsic width of the observed spectra. ESA

N93-12043# Paris-Sud Univ., Orsay (France). Lab. de Spectroscopie Atomique et Ionique.

GAIN IN A CONFINED ALUMINUM PLASMA [GAIN DANS UN PLASMA D'ALUMINIUM CONFINE] **c75**

Pierre Jaegle, Antoine Carillon, Bernard Gauthe, Gerard Jamelot, and Jean-Pierre Raucourt *In* Ecole Polytechnique, The 1989 Scientific Report of the Laboratory for the Use of High Power Lasers Apr. 1990 p 125-127 In FRENCH (For primary document see N93-12023 02-36)
Avail: CASI HC A01/MF A03

A confinement by a target with a form which retards the lateral expansion of a plasma is shown and discussed. The spatial distributions of the lithiumoid aluminum beam at 105.7 A and the neighboring beams are shown. These curves were obtained during a five beam experiment. The presence of an emission region apparently inside the target is explained by the width of the slot used. The emission is seen to stop at a target distance less than 800 micro. The gain production region, with planar targets and a 600 ps pulse, is found at 200 to 300 micro from the target. Thus the form is proved to allow a plasma confinement and the confined plasma is proved to be amplificatory. ESA

N93-12044# Paris-Sud Univ., Orsay (France). Lab. de Spectroscopie Atomique et Ionique.

PRELIMINARY STUDY OF THE HOMOGENEITY OF THE DENSITY AND TEMPERATURE OF LONG PLASMAS USED FOR X LASER STUDIES [ETUDE PRELIMINAIRE DE L'HOMOGENEITE DE LA DENSITE ET DE LA TEMPERATURE DES PLASMAS LONGS EMPLOYES POUR LES ETUDES SUR LE LASER X] **c75**

Gailila Abdelatif, M. Berland, Antoine Carillon, P. Dhez, and Jean-Pierre Raucourt *In* Ecole Polytechnique, The 1989 Scientific Report of the Laboratory for the Use of High Power Lasers Apr. 1990 p 128-129 In FRENCH (For primary document see N93-12023 02-36)
Avail: CASI HC A01/MF A03

Experimental tests of the homogeneity of long plasmas are described. The X-UV fluxes are evaluated using a charged coupled device with pinhole to detect the photons from an aluminum plasma. Although the results are preliminary, it appears that the plasma emission is not homogeneous along its axis ESA

N93-12045# Paris-Sud Univ., Orsay (France). Lab. de Spectroscopie Atomique et Ionique.
EXPERIMENTAL STUDY OF X RAY LASER IN LITHUMOID ALUMINUM [ETUDE EXPERIMENTALES DU LASER A RAYONS X DANS L'ALUMINIUM LITHIUMOIDE]
Antoine Carillon, Pierre Jaegle, Annie Klisnick, Jean-Pierre Raucourt, C. Lewis (Queens Univ., Belfast, Northern Ireland), D. Neely (Queens Univ., Belfast, Northern Ireland), J. Uhomoibhi (Queens Univ., Belfast, Northern Ireland), M. Key (Rutherford Appleton Lab., Chilton, England), S. Ramsden (Hull Univ., England), and G. Jamelot *In* Ecole Polytechnique, The 1989 Scientific Report of the Laboratory for the Use of High Power Lasers Apr. 1990 p 130-131 In FRENCH (For primary document see N93-12023 02-36)
Avail: CASI HC A01/MF A03

Experiments where a streak camera was placed behind a plane field array following the plasma axis are reported. The images obtained were digitized by two dimensional microdensitometry and processed. The time evolutions of the gain for 3d-5f, 3d-4f, transitions are shown. The gains obtained are less than those measured with lower length targets. This may be caused by radiative trapping due to reabsorption in the regions where the population inversion is maximal of resonance beams emitted by the dense zones of the plasma. Contrary to previous findings, the gain appears to be greater for the 3d-5f beam than 3d-4f. ESA

N93-12046# Paris-Sud Univ., Orsay (France). Lab. de Spectroscopie Atomique et Ionique.
MODELING FOR THE STUDY OF AN X LASER IN A RECOMBINATION PLASMA; GAIN CALCULATIONS AT 105.7 AND 154.6 A [MODELISATION POUR L'ETUDE D'UN LASER X DANS UN PLASMA EN RECOMBINAISON; CALCULS DE GAIN A 105,7 ET 154,6 A]
Annie Klisnick, Alain Sureau, Helene Guennou, C. Moller, and Jean Virmont *In* Ecole Polytechnique, The 1989 Scientific Report of the Laboratory for the Use of High Power Lasers Apr. 1990 p 132-137 In FRENCH Prepared in cooperation with Ecole Polytechnique, Palaiseau, France (For primary document see N93-12023 02-36)
Avail: CASI HC A02/MF A03

The modeling of the production and evolution of a laser plasma in order to study the operating conditions of an X laser in such medium is addressed. The principle scheme studied concerns the population inversions between the excited levels of lithiumoid ions which produce at the recombination time of heliumoid ions in lithiumoid ions during the plasma recooling phase. The modeling of the hydrodynamic and atomic physics mechanisms is described. Results concerning the hydrodynamic evolution and the gain over the emitted beams at 105.7 and 154.6 A of an aluminum plasma are discussed. ESA

N93-12047# Lawrence Livermore National Lab., CA.
BREMSSTRAHLUNG ABSORPTION IN PLASMAS [ABSORPTION DE BREMSSTRAHLUNG DANS LES PLASMAS] c75
B. Rozsnyai and Michele Lamoureux (Paris-Sud Univ., Orsay, France) *In* Ecole Polytechnique, The 1989 Scientific Report of the Laboratory for the Use of High Power Lasers Apr. 1990 p 138-141 In FRENCH (For primary document see N93-12023 02-36)
Avail: CASI HC A01/MF A03

Low energy photon absorption and the Gaunt factor of Bremsstrahlung are discussed. Physical hypothesis chosen to take account of the strong electron density of certain plasmas which greatly influence predictions relating to the emission or absorption of Bremsstahlung are discussed. Figures illustrating that the choice of model adopted to describe the atomic ions of the dense plasma has a great influence on the theoretical evaluations used to deduce Bremsstrahlung are given. ESA

N93-12048# Ecole Polytechnique, Palaiseau (France). Lab. pour l'Utilisation des Lasers Intenses.
DIRECT RADIATIVE RECOMBINATION OF ATOMIC IONS [RECOMBINAISON RADIATIVE DIRECTE DES IONS ATOMIQUES] c75
Alain Poquerusse *In its* The 1989 Scientific Report of the Laboratory for the Use of High Power Lasers Apr. 1990 p 142-147 In FRENCH (For primary document see N93-12023 02-36)
Avail: CASI HC A02/MF A03

Direct radiative recombination as an elementary process governing plasma evolution is addressed. Mathematical models for this and other isoelectronic sequences are shown and discussed. ESA

N93-12049# Paris VI Univ. (France). Lab. de Spectroscopie.
ATOMIC STRUCTURE AND SPECTRAL PERTURBATIONS IN DENSE AND HOT PLASMAS [STRUCTURE ATOMIQUE ET PERTURBATIONS SPECTRALES DANS LES PLASMAS DENSES ET CHAUDS] c75
Hoe Nguyen, Claire Bousquet, Zoubeida Dhaouadi, Brigitte dEtat, Jeanne Grumberg, Elisabeth Leboucher-Dalimier, M. Brisard, Philippe Malnoult, and Jean-Pierre Arranz *In* Ecole Polytechnique, The 1989 Scientific Report of the Laboratory for the Use of High Power Lasers Apr. 1990 p 148-160 In FRENCH (For primary document see N93-12023 02-36)
Avail: CASI HC A03/MF A03

A theoretical study on the related electronic states in ultradense plasmas is given. The principal experimental results relating to high density effects and to the combined effects of radiative transfer and transverse inhomogeneity are presented. ESA

N93-12050# Ecole Polytechnique, Palaiseau (France). Lab. de Physique des Milieux Ionises.
HYDRODYNAMIC STUDY OF MULTILAYER TARGETS BY SPATIAL AND TEMPORAL RESOLUTION SHADOW SPECTROSCOPY [ETUDE DE L'HYDRODYNAMIQUE DE CIBLES MULTICOUCHES PAR OMBROSCOPIE RESOLUE SPATIALEMENT SPECTRALEMENT] c25
Jean-Paul Geindre, Claude Chenais-Popovics, Patrick Audebert, Isao Matsushima (Tsukuba Univ., Japan), and Jean-Claude Gauthier *In its* The 1989 Scientific Report of the Laboratory for the Use of High Power Lasers Apr. 1990 p 161-165 In FRENCH (For primary document see N93-12023 02-36)
Avail: CASI HC A01/MF A03

An experiment to study the absorption and emission of a multilayer target composed of a layer of high Z (samarium) covering a light material (chorinated plastic) is described. The experiment device is described and results are compared to numerical simulations. The measurements allow detailed study of the radiative heating of a laser target. ESA

N93-12051# Paris-Sud Univ., Orsay (France). Lab. de Spectroscopie Atomique et Ionique.
ANALYSIS OF THE INSTRUMENT OPERATION OF A FOCAL CIRCLE SPECTROGRAPH AND NUMERICAL RECONSTITUTION OF THE SPECTRUM EMITTED BY A PLASMA COLUMN [ANALYSE DE LA FONCTION D'INSTRUMENT D'UN SPECTROGRAPHE A CERCLE FOCAL ET RECONSTITUTION NUMERIQUE DU SPECTRE EMIS PAR UNE COLONNE DE PLASMA]
Jean-Pierre Raucourt, Gerard Jamelot, Antoine Carillon, and Pierre Jaegle *In* Ecole Polytechnique, The 1989 Scientific Report of the Laboratory for the Use of High Power Lasers Apr. 1990 p 166-169 In FRENCH (For primary document see N93-12023 02-36)
Avail: CASI HC A01/MF A03

A study aimed at the numerical reconstitution of the X-UV emission spectrum of a plasma column is presented. The operation of spectrograph camera using the focal circle is described. The application of the method to the analysis of the directivity of a lithumoid aluminum spectrum is described. ESA

N93-12052# Ecole Polytechnique, Palaiseau (France).
ACTIVITY OF THE TECHNICAL GROUPS (LULI PALAISEAU, FRANCE) [ACTIVITE DES GROUPES TECHNIQUES (LULI, PALAISEAU)]
In its The 1989 Scientific Report of the Laboratory for the Use of High Power Lasers Apr. 1990 p 170-173 In FRENCH (For primary document see N93-12023 02-36)
Avail: CASI HC A01/MF A03

Technical group activities of the laboratory for high power lasers (LULI) are reported: for the laser group, maintenance and development of lasers; for the electronic group, a 20 input acquisition system for experiments, and a new energy measurement system; for the experimental group, charge transfer detectors in the X field, and spectrography in the 40 to 200 A field. ESA

N93-12163 Maryland Univ., College Park.
RESEARCH ON STIMULATED RAMAN SCATTERING WITH APPLICATIONS TO ATMOSPHERIC LIDAR Ph.D. Thesis
Zhiping Chu 1991 171 p
Avail: Univ. Microfilms Order No. DA9133049

Research has been conducted on stimulated Raman scattering (SRS) to extend conventional lasers into the infrared where lidar systems can make important contributions to observations of the atmosphere. An efficient 'Raman shifted' dye laser system was used to generate tunable and narrow band radiation at 760 and 940 nm for differential absorption lidar applications. The requisite tunability and spectral purity of the output is derived from the dye laser input by controlling the Raman cell at pressure below 14 atm. The converted radiation is optimized for different pump focusing geometries. Energy conversion efficiencies of 45 percent and 37 percent at 765 and 940 nm, respectively, were obtained. Optical depth measurements and calculations were made at the centers of 25 lines in the P branch of the oxygen A-band in air. The data and theoretical calculations agree, indicating a high spectral purity of the light source. High resolution parameters of water vapor at 940 nm were obtained using this narrow linewidth Raman-shifted dye laser in conjunction with a multi-pass optical absorption call. Optical strengths and Lorentz widths were reduced from the data using a Voigt line profile to numerically correct for finite laser linewidth. Some lines are compared with prior measurements by Giver et al. that used a wholly different method. Some lines, which were not covered in Giver's experiments, were compared with Hitran database. The simultaneous generation of several Stokes orders was investigated in H2, D2, and CH4, for the purpose of multiple wavelength lidar. The study was focused on the redistribution of the pump energy into the different SRS components. Optimal experimental conditions were investigated and calculated. Eye-safe radiation at 1.54 micrometers was generated for lidar applications, by Raman shifting Nd:YAG laser light (1.06 micrometers) in methane. To increase conversion efficiency, a novel self-seeding oscillator and amplifier system was designed and used. Backward first Stokes radiation was separated and used as seed by being refocussed into the Raman cell and amplified by the rest of the pump pulse. A maximum conversion efficiency of 18 percent was obtained. Dissert. Abstr.

N93-12238# University of Central Florida, Orlando. Center for Research in Electro-Optics and Lasers.
OPTICAL LIMITING Final Report
Eric W. VanStryland 22 May 1992 32 p
(Contract DAAL03-90-G-0089)
(AD-A254620; ARO-27838.4-PH) Avail: CASI HC A03/MF A01

We have been performing careful measurements of the nonlinear optical properties of some organic dyes to determine their suitability for use in devices that can protect sensors against damage from high intensity laser radiation. Dyes that show large excited state absorption with small linear absorption are suitable for such devices. We investigated the nonlinearities for pulses from picoseconds to nanoseconds and find that, since the excited state absorption is cumulative, the dyes can limit well for nanosecond pulses but not for picoseconds. However, when used in tandem with a second passive nonlinear optical material, we find that we can significantly increase the temporal range over which the device limits. In addition, we find that the dynamic range of limiting devices can be substantially increased using two elements without a significant increase in the optical limiting threshold. GRA

N93-12250# Los Alamos National Lab., NM.
LASER-ABLATION PROCESSES
R. S. Dingus 1992 8 p Presented at the Society of Photo-Optical Instrumentation Engineers' International Symposium on Laser Spectroscopy as Part of SPIE's Symposium on Optics, Electro-Optics and Laser Applications in Science and Engineering, Los Angeles, CA, 19-24 Jan. 1992
(Contract W-7405-eng-36)
(DE92-011226; LA-UR-92-989; CONF-920124-19) Avail: CASI HC A02/MF A01

The various mechanisms by which ablation of materials can be induced with lasers are discussed. The various ablation processes and potential applications are reviewed from the threshold for ablation up to fluxes of about 10(exp 13) W/sq cm, with emphasis on three particular processes; namely, front-surface spallation, two-dimensional blowoff, and contained vaporization. DOE

N93-12262# Visidyne, Inc., Burlington, MA.
THE DESIGN, DEVELOPMENT, AND TEST OF BALLOONBORNE AND GROUNDBASED LIDAR SYSTEMS. VOLUME 1: BALLOONBORNE COHERENT CO2 LIDAR SYSTEM Final Report, 30 May 1986 - 31 Dec. 1990
O. Shepherd, G. Aurilio, R. D. Bucknam, A. G. Hurd, and S. A. Rappaport 1 Jun. 1991 118 p
(Contract F19628-86-C-0105)
(AD-A247551; VI-1707-A-Vol-1; PL-TR-91-2191-Vol-1; AD-E200880) Avail: CASI HC A06/MF A02

This is Volume 1 of a three volume final report on the design, development, and test of balloonborne and groundbased lidar systems. Volume 2 describes the flight test of Atmospheric Balloonborne Lidar Experiment, ABLE 2, which successfully made atmospheric density backscatter measurements during a flight over White Sands Missile Range. Volume 3 describes groundbased lidar development and measurements, including the design of a telescope dome lidar installation, the design of a transportable lidar shed for remote field sites, and field measurements of atmospheric and cloud backscatter from Ascension Island during SABLE 89 and Terciera, Azores during GABLE 90. In this volume, Volume 1, the design and fabrication of a balloonborne CO2 coherent lidar payload are described. The purpose of this payload is to measure, from altitudes greater than 20 km, the 10.6 micrometers backscatter from atmospheric aerosols as a function of altitude. Minor modifications to the lidar would provide for aerosol velocity measurements to be made. The lidar and payload system design was completed, and major components were fabricated and assembled. These tasks have been successfully completed, and recommendations for further lidar measurements and data analysis have been made. GRA

N93-12275# Naval Research Lab., Washington, DC.
X RAY LASER PROGRAM, FY 1991 Final Report, 1 Oct. 1990 - 30 Sep. 1991
16 Sep. 1992 141 p
(AD-A255190; NRL/MR/4721-92-6980) Avail: CASI HC A07/MF A02

This report details the progress achieved by the Radiation Hydrodynamics Branch in X-Ray Laser experiments and modeling during FY-91. Some of the experimental work discussed was carried out at Sandia National Laboratories in a cooperative program with NRL. It is divided into sections whose authors are separately identified. Topics presented in detail include the first demonstration of a soft x-ray inversion by resonant photopumping, detailed analysis of other photopumped x-ray laser scheme, feasibility of population inversions in fluorine driven by ultra short pulse lasers, fully time dependent radiation transport modeling, and analysis of pumping mechanisms in neonlike lasers. GRA

N93-12335# SRI International Corp., Menlo Park, CA. Molecular Physics Lab.

NOVEL NONLINEAR LASER DIAGNOSTIC TECHNIQUES Annual Report, 6 Jun. 1991 - 31 May 1992

Gregory W. Faris, Jay B. Jeffries, and David L. Huestis 10 Jul. 1992 28 p
(Contract F49620-90-C-0044)
(AD-A254709; MP-92-142) Avail: CASI HC A03/MF A01

Research on novel laser-based diagnostic techniques was performed in two areas: (1) extension of laser-based diagnostics to shorter wavelengths for two-phonon detection of atomic ions and for other detection techniques requiring high powers in the vuv, and (2) investigation of the feasibility of quantitative concentration, temperature, and velocity measurements using two-phonon-excited amplified spontaneous emission of atomic oxygen and hydrogen. For the first task, the two-photon-resonant difference-frequency mixing process was extended to higher powers and shorter wavelengths. This radiation was used to perform multiphoton spectroscopy at shorter wavelengths in the vuv, including two-phonon-excited fluorescence in neon at 133 nm. On the second task, laser-induced fluorescence measurements of atomic hydrogen in a variety of low-pressure flames were compared with simultaneous ASE observations. The bandwidth of H atom ASE at 1200 and 1800 K was measured. Simultaneous O atom ASE and LIF in an H2/O2 low-pressure flame have been demonstrated, and a model to calculate the intensity variation for laser gain measurements on a diode probe laser for atomic oxygen was assembled. GRA

N93-12405# Naval Postgraduate School, Monterey, CA.

THEORY FOR A HIGH POWER FREE ELECTRON LASER AND TACTICAL APPLICATIONS M.S. Thesis

David J. Frost Jun. 1992 78 p
(AD-A255161) Avail: CASI HC A05/MF A01

The free electron laser (FEL) shows potential as a source of coherent, high average power radiation. The achievement of high average power is one of the main topics of current FEL research. This thesis examines the Boeing Average Power Laser Experiment (APLE), whose main goal is to demonstrate the FEL's high average power capability for the first time. The experiment is in the design stage, with completion scheduled for 1996. The first part of this thesis presents a version of a conventional Theater Ballistic Missile Defense (TBMD) system. The advantages of directed energy weapons, specifically the FEL, are also discussed. The remainder of this thesis examines APLE. Chapter 5 presents research on the oscillator, and Chapter 6 deals with the amplifier. Research indicates the current APLE design is feasible and can meet its design goal. Suggestions are presented for optimizing the performance of the oscillator/amplifier system. GRA

N93-12514# Oak Ridge National Lab., TN.

CHARACTERIZATION OF UNDERIVATIZED PTERINS BY LASER DESORPTION FOURIER TRANSFORM MASS SPECTROMETRY

K. B. Jacobson and R. L. Hettich 1992 15 p Presented at the 6th International Conference on Pteridines, Seoul, Republic of Korea, 6-13 Jun. 1992
(Contract DE-AC05-84OR-21400)
(DE92-016785; CONF-9206207-1) Avail: CASI HC A03/MF A01

Laser desorption FTMS provides a soft ionization technique for non-volatile pterins and generates characteristic positive and negative ions. The positive ion spectra usually consist of (M+Na)(sup +) and (M+K)(sup +) ions, whereas the negative ion spectra reveal (M-H)(sup -) ions as well as fragment ions. Collision-induced dissociation experiments were used to probe the fragmentation pathways of these negative ions. The fragmentation observed for negative ions is influenced by the exact structure and oxidation state of the pterin and provides detailed structural information which can be used to differentiate isomeric forms. This report describes the detailed examination of the fragmentation of 6-methylpterin that is obtained by using laser desorption Fourier transform mass spectrometry (LDFTMS). In particular, deuterium exchange reactions were used to locate acidic hydrogens and to probe rearrangement processes. DOE

N93-12516*# Alabama Univ., Huntsville. Center for Applied Optics.

DEVELOPMENT SUMMARY OF A SYMPATHETIC DISCHARGE CO2 LASER FOR LIDAR USE Final Report

Holger M. Jaenisch and R. Barry Johnson 5 Aug. 1991 105 p
(Contract NAS8-36955)
(NASA-CR-184433; NAS 1.26:184433; UAH-5-32439) Avail: CASI HC A06/MF A02

A commercial pulsed sympathetic discharge laser has been characterized and modified for use as a potential lidar. This report summarizes the initial findings and modifications made to the baseline system. The new laser performance is then checked with theory and operational results are presented. The laser has inherent mode instability and high chirp. Several solutions were tried and their results are presented. Author

37 MECHANICAL ENGINEERING

Includes auxiliary systems (nonpower); machine elements and processes; and mechanical equipment.

N93-10966*# National Aeronautics and Space Administration. Lewis Research Center, Cleveland, OH.

EXPERIMENTAL VALIDATION OF BOUNDARY ELEMENT METHODS FOR NOISE PREDICTION

A. F. Seybert (Kentucky Univ., Lexington.) and Fred B. Oswald Jul. 1992 8 p Presented at the Inter-Noise 1992, Toronto, Ontario, 20-22 Jul. 1992; sponsored by the International Inst. of Noise Control Engineering
(DA Proj. 1L1-62211-A-47-A; RTOP 505-63-36)
(NASA-TM-105729; E-7132; NAS 1.15:105729; AVSCOM-TR-92-C-013) Avail: CASI HC A02/MF A01

Experimental validation of methods to predict radiated noise is presented. A combined finite element and boundary element model was used to predict the vibration and noise of a rectangular box excited by a mechanical shaker. The predicted noise was compared to sound power measured by the acoustic intensity method. Inaccuracies in the finite element model shifted the resonance frequencies by about 5 percent. The predicted and measured sound power levels agree within about 2.5 dB. In a second experiment, measured vibration data was used with a boundary element model to predict noise radiation from the top of an operating gearbox. The predicted and measured sound power for the gearbox agree within about 3 dB. Author

N93-10982*# National Aeronautics and Space Administration. Lewis Research Center, Cleveland, OH.

MAXIMUM LIFE SPIRAL BEVEL REDUCTION DESIGN

M. Savage (Akron Univ., OH.), M. G. Prasanna (Akron Univ., OH.), and H. H. Coe Jul. 1992 17 p Presented at the 28th Joint Propulsion Conference and Exhibit, Huntsville, TN, 6-8 Jul. 1992; sponsored by AIAA, SAE, ASME, and ASEE Previously announced in IAA as A92-49030
(DA Proj. 1L1-62211-A-47-A; RTOP 505-63-36)
(NASA-TM-105790; E-7220; NAS 1.15:105790; AVSCOM-TR-92-C-004) Avail: CASI HC A03/MF A01

Optimization is applied to the design of a spiral bevel gear reduction for maximum life at a given size. A modified feasible directions search algorithm permits a wide variety of inequality constraints and exact design requirements to be met with low sensitivity to initial values. Gear tooth bending strength and minimum contact ratio under load are included in the active constraints. The optimal design of the spiral bevel gear reduction includes the selection of bearing and shaft proportions in addition to gear mesh parameters. System life is maximized subject to a fixed back-cone distance of the spiral bevel gear set for a specified speed ratio, shaft angle, input torque, and power. Significant parameters in the design are: the spiral angle, the pressure angle, the numbers of teeth on the pinion and gear, and the location and size of the four support bearings. Interpolated polynomials expand the discrete bearing properties and proportions into continuous variables for gradient optimization. After finding the continuous optimum, a designer can analyze near optimal designs for comparison and selection. Design examples show the influence of the bearing lives on the gear parameters in the optimal configurations. For a fixed back-cone distance, optimal designs with larger shaft angles have larger service lives. Author

N93-11054# Rolls-Royce Ltd., Derby (England). Manufacturing Engineering Gear Section.

THE APPLICATION OF MANUFACTURING SYSTEMS ENGINEERING FOR AERO ENGINE GEARS

Stephen M. S. Pewsey (Rolls-Royce Ltd., Bristol, England) 31 Oct. 1991 9 p Presented at the Gear Manufacture and Quality Control Seminar, Bristol, England, 31 Oct. 1991

(PNR-90944; ETN-92-92221) Copyright Avail: CASI HC A02/MF A01

The adoption of manufacturing systems engineering principles in order to improve cost effectiveness of manufacturing operations is considered. The introduction of cells where families of parts are made from raw material to finished product using a team approach has been initiated. The benefits to date are significant in terms of lead time reductions, inventory, and nonconformance savings as well as improvements in work force motivation and morale. The overall corporate manufacturing strategy of gears is explained. Some of the problems encountered with the transfer of gear production from one site to another with minimum disruption are described. Some of the radical changes being made in the manufacture of gears in line with the strategy of making Rolls-Royce a total quality organization are also described. ESA

N93-11177*# National Aeronautics and Space Administration. Pasadena Office, CA.

TERMINAL SLIDER CONTROL OF NONLINEAR ROBOTIC SYSTEMS Patent Application

Subaramanian T. Venkataraman, inventor (to NASA) (Jet Propulsion Lab., California Inst. of Tech., Pasadena.) and Sandeep Gulati, inventor (to NASA) (Jet Propulsion Lab., California Inst. of Tech., Pasadena.) 18 Jun. 1992 36 p

(Contract NAS7-918)

(NASA-Case-NPO-18584-1-CU; NAS 1.71:NPO-18584-1-CU; US-Patent-Appl-SN-921192) Avail: CASI HC A03/MF A01

This invention provides robust nonlinear controllers for robotic operations in unstructured environments based upon a new class of sliding modes denoted terminal sliders that enforce closed loop system convergence to equilibrium in finite time. Improved performance results from the elimination of high frequency control switching previously employed for robustness to parametric uncertainties. Improved performance also results from the dependence of terminal slider stability upon the rate of change of uncertainties over the sliding surface rather than the magnitude of the uncertainty itself for robust control. Terminal sliding mode control also yields improved convergence where convergence time is finite and is to be controlled. This invention also applies terminal sliders to robot manipulator control and benchmark performance with the traditional computed torque control method and provides for design of control parameters. NASA

N93-11220 Arizona State Univ., Tempe.

OPTIMAL OUTPUT FEEDBACK VIBRATION CONTROL OF ROTOR-BEARING SYSTEMS Ph.D. Thesis

Guangwuu William Fan 1991 140 p

Avail: Univ. Microfilms Order No. DA9210373

A procedure for the lateral vibration control of general high-order asymmetric discrete rotor-bearing systems is presented. It is found that the complex mode and balanced realization methods can be successively applied to a general linear high-order asymmetric system to obtain a further reduced-order model without loss of model accuracy. However, the balanced realization method, by itself, is not a good choice for such systems. The matrix transformations between the original high-order system and the reduced-order system are derived for the design of the Linear Quadratic Regulator (LQR). An LQR-based least-squares output feedback control procedure is introduced for the LQR control of high-order asymmetric discrete systems, and takes advantage of the fact that an 'almost' LQR control is possible without using an observer. Furthermore, the number of measured states can be much less than the number of eigenvectors retained in the reduced-order model while acceptable performance and robustness of the controller are still maintained. The simulation result on a 52-degree-of-freedom rotor model shows that the lateral vibration can be effectively reduced by monitoring a single location along the shaft with the control inputs at horizontal and vertical directions at a single location for a certain spin speed. The spill-over problem of the LQR control system is also investigated for both collocated and non-collocated cases based on the same reduced-order model. Furthermore, the discussion of the robustness of the closed-loop control system against system parameters when including the actuator dynamics is also addressed by means of root-locus plots. The application of the well-known Linear Quadratic Gaussian (LQG) and LQG with Loop Transfer Recovery (LQC/LTR) techniques on two typical low-order rotor dynamic systems is discussed so that a comparison with an LQR-based least-squares output feedback controller can be made. Dissert. Abstr.

N93-11261 Virginia Polytechnic Inst. and State Univ., Blacksburg.

MODELING AND IDENTIFICATION OF FLEXIBLE JOINTS IN VEHICLE STRUCTURES Ph.D. Thesis

Kwangju Lee 1992 189 p

Avail: Univ. Microfilms Order No. DA9218022

A simple, design-oriented model of joints in vehicle structures is developed. This model accounts for the flexibility, the offsets of rotation centers of joint branches, and the coupling between rotations of a joint branch in different planes. The model parameters consist of torsional spring rates, the coordinates of the flexible hinges, and the orientations of planes in which the torsional springs are located. The model parameters are selected to be physically meaningful. In some cases, the behavior of joints can be accurately represented by using simpler models. The conditions under which the joint model can be simplified are discussed. A family of joint models with different levels of complexity are also defined. A probabilistic system identification is used to estimate the joint parameters by using the measured displacements. The parameters are estimated by minimizing the discrepancies between the measured and predicted displacements. Statistical tests which identify important parameters are also presented. These tests can be used to simplify the joint models without significantly reducing the accuracy in predicting structural responses. The identification methodology is applied to automotive structures with joints and also to isolated subassemblies consisting of joints and attached branches. Dissert. Abstr.

N93-11263 Illinois Univ. at Urbana-Champaign, Savoy.

THERMAL NON-NEWTONIAN ELASTOHYDRODYNAMIC LUBRICATION OF LINE CONTACTS UNDER SLIDING-ROLLING AND SIMPLE SLIDING CONDITIONS Ph.D. Thesis

Shao Wang 1991 203 p

Avail: Univ. Microfilms Order No. DA9211026

A thermal Reynolds-Erying equation is derived to study the elastohydrodynamic lubrication of line contacts. This lubrication condition is usually found in spur gears, roller bearings, and cams. The inlet region with back-flow is treated with a control volume scheme to obtain the temperature solution. A computationally-simple formulation for the stationary surface temperature is developed for simple sliding conditions. The most influential dimensionless groups are identified from the complete sets of dimensionless groups. Numerical results obtained for sliding and rolling and for simple sliding conditions are used to develop formulas for the thermal and non-Newtonian (Ree-Eyring) film thickness reduction factor. Even when thermal effects are small, these formulas can still give a film thickness reduction due to the non-Newtonian effects. Results for the maximum temperatures and traction coefficient are also presented. The pressure dependence of lubricant thermal conductivity is found to significantly affect the maximum lubricant temperature. The thermal effects on film thickness and traction are found to be more pronounced for simple sliding than for combined sliding and rolling conditions. Under simple sliding, the heat transferred to the stationary surface is found to be very small compared to that transferred to the moving surface and lubricating fluid. Dissert. Abstr.

N93-11324 National Physical Lab., Teddington (England). Div. of Materials Metrology.
THE THEORETICAL BACKGROUND TO BS7167: 1990 - SPECIFICATION FOR BORDEAUX CONNECTIONS
T. A. E. Gorley Mar. 1992 11 p
(Contract HSE-1533)
(NPL-DMM(A)-50; ETN-92-92255) Copyright Avail: National Physical Lab., Teddington, Middlesex, TW11 0LW, England

The theoretical background to the specification of Bordeaux connections (components of lifting gear used to join together wire rope and a chain, or two lengths of wire rope, where the joined lengths have to run over a sheave as in the case of grabbing cranes) is documented. Decisions taken in the drafting of earlier specifications are not documented. The design criteria for BS7167:1990 are addressed. The various parts of the Bordeaux connection specified in the standard are discussed in turn: the link portion, the rope portion, and the grab shackle. Some tests on the new design undertaken by the Health and Safety Executive confirm the new design criteria to be adequate for the strengths of rope to be used with this component. ESA

N93-11325 National Physical Lab., Teddington (England). Div. of Materials Metrology.
THE TECHNICAL BACKGROUND TO STANDARDS FOR SHACKLES
T. A. E. Gorley and G. T. Anthony Mar. 1992 27 p
(Contract HSE-1533)
(NPL-DMM(A)-51; ETN-92-92256) Copyright Avail: National Physical Lab., Teddington, Middlesex, TW11 0LW, England

The technical background to British and international standards for shackles is documented in order to provide a reference for future drafting and revisions of standards. The following are discussed: the stress analysis of shackles, a test program for shackles, the work performed by a working group set up to rationalize the design of cage suspension gear, shackle design formula, the development of International Standards Organization (ISO) standards for shackles, and the development of revised British standards. Under the technical background to the revision of BS3032, the following are considered: marking, material and heat treatment, hardness, mechanical properties, form and dimensions, tolerances, and screw threads. The decisions upon which the revision of the BS3551 were based are described. ESA

N93-11326 National Physical Lab., Teddington (England). Div. of Materials Metrology.
A STUDY OF THE EFFECTS OF TOLERANCES ON RIGGING SCREWS, TURNBUCKLES, AND ASSOCIATED COMPONENTS IN BS4429: 1987
T. A. E. Gorley Mar. 1992 12 p
(Contract HSE-1533)
(NPL-DMM(A)-53; ETN-92-92257) Copyright Avail: National Physical Lab., Teddington, Middlesex, TW11 0LW, England

The failure modes already examined in a previous paper are reanalyzed to include the worst effects of tolerances. The previous paper, entitled 'the technical background to the revision of BS4429:1969, specification for rigging screws and turnbuckle', should be read in conjunction with this paper. The following are discussed: estimation of stress in the rigging screw body; the failure load at the cross section through the Tommy bar hole in the rigging screw body; thread stripping load in the rigging screw body; failure of the core area of the thread of the rigging screw body; tensile failure of the turnbuckle arms; stripping of the thread in the 'nuts' at the ends of the turnbuckle body; the parting of the arms from the nut in the turnbuckle; failure of the screw threads of the accessories; the maximum stress on the eye of the elongated eye; screwed forks; screwed trapezoidal hooks; and locknuts. It is concluded that effect of tolerances is acceptable but the analysis reinforces the concern regarding the screwed end of the rigging screw body. The screwed end must be fully engaged in use and the manufacturer must take special care that the dimensions of this part of the rigging screw are adequate. A recommendation is made for amending the dimensional criteria for this part of the rigging screw body. ESA

N93-11327 National Physical Lab., Teddington (England). Div. of Materials Metrology.
THE TECHNICAL BACKGROUND TO STANDARDS FOR EYEBOLTS
T. A. E. Gorley Mar. 1992 41 p
(Contract HSE-1533)
(NPL-DMM(A)-52; ETN-92-92258) Copyright Avail: National Physical Lab., Teddington, Middlesex, TW11 0LW, England

Background to the drafting of a revised British standard, BS 4278:1984 and new International Organization Standard, ISO 3266, for eyebolts for general lifting processes is detailed. For the British standard, the following are considered: the alignment of the eye and the effects of inclined loads, the strength of eyebolts and the withdrawal of BS 529, mismatch of threads, and material selection. For the international standard, the following are considered: the recessing of the eyebolt into the load, inclined loading, and the joint between the shank and the eyebolt collar. Arguments are based upon experience obtained in using and manufacturing eyebolts to earlier standards. Theory is only used where it was considered necessary to confirm matters. Experience shows that eyebolts made properly in compliance with the standards will be sufficiently strong. A paper on the British test results of nonaxial loading of eyebolts is presented in the appendix. ESA

N93-11423 Department of the Navy, Washington, DC.
PAYOUT TENSION CONTROL SYSTEM FOR REEL MOUNTED CABLE Patent
Gerhard B. Winkler, inventor (to Navy) (Courtney and Co., Philadelphia, PA.) 9 Jun. 1992 5 p Filed 29 May 1990
(AD-D015362; US-Patent-5,120,024; US-Patent-Appl-SN-529294; US-Patent-Class-254-391) Avail: US Patent and Trademark Office

A payout control arm is angularly displaceable about a brake shaft during payout of a cable from a storage reel in response to tensioning forces transmitted through the cable from a payout load with the cable being entrained about a pulley rotatably carried on the control arm in spaced relation to the brake shaft. Gearing drivingly connects the pulley to the brake shaft to stop payout and cause the cable to frictionally grip the pulley in response to brake engagement thereby preventing continued transmittal of tensioning forces to the reel. GRA

N93-11427# Texas A&M Univ., College Station. Transportation Inst.
AN AUTONOMOUS VEHICLE: CONSTRAINED TEST AND EVALUATION
Norman C. Griswold Nov. 1991 42 p Sponsored by Texas Dept. of Transportation
(PB92-205608; TTI-2-1-90/1-1245; RR-1245-1; FHWA/TX-92/1245-1) Avail: CASI HC A03/MF A01

The objective of the research is to develop an autonomous vehicle which utilizes stereo camera sensors (using ambient light) to follow complex paths at speeds up to 35 mph with consideration of moving vehicles within the path. The task is intended to demonstrate the contribution to safety of a vehicle under automatic control. All of the long-term scenarios investigating future reduction in congestion involve an automatic system taking control, or partial control, of the vehicle. A vehicle which includes a collision avoidance system is a prerequisite to an automatic control system. The report outlines the results of a constrained test of a vision controlled vehicle. In order to demonstrate its ability to perform on the current street system the vehicle was constrained to recognize, approach, and stop at an ordinary roadside stop sign. GRA

N93-11540# Lawrence Livermore National Lab., CA.
THE INTENSITY OF KNOCK IN AN INTERNAL COMBUSTION ENGINE: AN EXPERIMENTAL AND MODELING STUDY
J. S. Cowart, M. Haghgooie, C. E. Newman, G. C. Davis, W. J. Pitz, and C. K. Westbrook Jun. 1992 20 p Presented at the 1992 SAE International Fuels and Lubricants Meeting and Exposition, San Francisco, CA, 19-22 Oct. 1992
(Contract W-7405-eng-48)
(DE92-019504; UCRL-JC-110069; CONF-9210152-1) Avail: CASI HC A03/MF A01

From this knock intensity modeling study important initial results were obtained, as well as direction for future work. The detailed model study showed that knock intensity can be correlated to knock model results, thus future use of knock occurrence and intensity modeling for engine development appears viable. The detailed model's predicted rate of carbon monoxide concentration change (at 1100 K) with time revealed that a linear correlation existed with the percent cycles knocking, while the rate of end-gas temperature change (at 1000 K) correlated approximately linearly with the fraction of cycles knocking. The reduced model shows a similar linear correlation of dT/dt with percent cycles knocking, but the correlation is much weaker than that observed with the detailed model. These results indicate that reactions which lead to products formation and the accompanying heat release must be taken into account in the reduced model. These reactions are of the type which consume aldehydes and olefins to produce carbon monoxide and thereby carbon dioxide. DOE

N93-11548# Edgerton, Germeshausen and Grier, Inc., Idaho Falls, ID.
DEVELOPMENT OF AN INTELLIGENT SYSTEM FOR COOLING RATE AND FILL CONTROL IN GMAW
C. J. Einerson, H. B. Smartt, J. A. Johnson, P. L. Taylor, and K. L. Moore (Idaho State Univ., Pocatello.) 1992 5 p Presented at the 3rd International Conference on Trends in Welding Research, Gatlinburg, TN, 1-5 Jun. 1992
(Contract DE-AC07-76ID-01570)
(DE92-017849; EGG-M-92381; CONF-9206173-6) Avail: CASI HC A01/MF A01

A control strategy for gas metal arc welding (GMAW) is developed in which the welding system detects certain existing conditions and adjusts the process in accordance to pre-specified rules. This strategy is used to control the reinforcement and weld bead centerline cooling rate during welding. Relationships between heat and mass transfer rates to the base metal and the required electrode speed and welding speed for specific open circuit voltages are taught to a artificial neural network. Control rules are programmed into a fuzzy logic system. Traditional control of the GMAW process is based on the use of explicit welding procedures detailing allowable parameter ranges on a pass by pass basis for a given weld. The present work is an exploration of a completely different approach to welding control. In this work the objectives are to produce welds having desired weld bead reinforcements while maintaining the weld bead centerline cooling rate at preselected values. The need for this specific control is related to fabrication requirements for specific types of pressure vessels. The control strategy involves measuring weld joint transverse cross-sectional area ahead of the welding torch and the weld bead centerline cooling rate behind the weld pool, both by means of video, calculating the required process parameters necessary to obtain the needed heat and mass transfer rates (in appropriate dimensions) by means of an artificial neural network, and controlling the heat transfer rate by means of a fuzzy logic controller. The result is a welding machine that senses the welding conditions and responds to those conditions on the basis of logical rules, as opposed to producing a weld based on a specific procedure. DOE

N93-11556# EG and G Rocky Flats, Inc., Golden, CO.
THERMAL STRESS AND STRAIN ANALYSIS IN TRAVELING AUTOGENOUS WELDS
J. R. Roper, J. Vossler, and D. Osborn 1992 21 p Presented at the Methods and Applications of Radioanalytical Chemistry Users Conference, Monterey, CA, 5 Sep. 1992
(Contract DE-AC34-90DP-62349)
(DE92-019363; RFP-4608; CONF-9209170-1) Avail: CASI HC A03/MF A01

This paper reports on the progress of a project to develop models for welding transient thermal stresses and strains, and post weld residual stresses and distortion. The type of welding considered is a traveling autogenous weld, with penetration by thermal conduction only. This type of welding correlates most closely with conduction mode gas tungsten arc welding or defocused electron beam or laser welding processes (without filler metal additions). The material which is modeled is type 304 stainless steel, using a mesh which simulates a small coupon of sheet material. The analyses are three dimensional. Details of application of the MARC data structure and subroutine usage in a way which is suitable for the analysis of coupled thermal-mechanical problems under boundary conditions typical of welding processes are emphasized. Special considerations involve locally intense heat input, steep temperature gradients, high temperature thermophysical and mechanical properties (including material models which account for dynamic recovery), high velocity weld pool convection, radiative and convective heat losses, and the necessity of working with large 3-D meshes with many degrees of freedom. The primary problems are availability of high temperature time dependant mechanical data, numerical stability, computational time and diskspace, and verification of results. Calculated results are qualitatively consistent with generally accepted welding stresses and postweld distortion of a welded plate. DOE

N93-11650*# Ball Corp., Boulder, CO. Aerospace Systems Group.
TEST PROGRAM, HELIUM II ORBITAL RESUPPLY COUPLING Final Report
William S. Hyatt 20 Dec. 1991 43 p
(Contract NAS9-18021)
(NASA-CR-185681; NAS 1.26:185681) Avail: CASI HC A03/MF A01

The full scope of this program was to have included development tests, design and production of custom test equipment and acceptance and qualification testing of prototype and protoflight coupling hardware. This program was performed by Ball Aerospace Systems Division, Boulder, Colorado until its premature termination in May 1991. Development tests were performed on cryogenic face seals and flow control devices at superfluid helium (He II) conditions. Special equipment was developed to allow quantified leak detection at large leak rates up to 8.4 x 10(exp -4) SCCS. Two major fixtures were developed and characterized: The Cryogenic Test Fixture (CTF) and the Thermal Mismatch Fixture (Glovebox). The CTF allows the coupling hardware to be filled with liquid nitrogen (LN2), liquid helium (LHe) or sub-cooled liquid helium when hardware flow control valves are either open or closed. Heat leak measurements, internal and external helium leakage measurements, cryogenic proof pressure tests and external load applications are performed in this fixture. Special reusable MLI closures were developed to provide repeatable installations in the CTF. The Thermal Mismatch Fixture allows all design configurations of coupling hardware to be engaged and disengaged while measuring applied forces and torques. Any two hardware components may be individually thermally preconditioned within the range of 117 deg K to 350 deg K prior to engage/disengage cycling. This verifies dimensional compatibility and operation when thermally mismatched. A clean, dry GN2 atmosphere is maintained in the fixture at all times. The first shipset of hardware was received, inspected and cycled at room temperature just prior to program termination. Author

N93-11653# Argonne National Lab., IL.
VEHICLE/GUIDEWAY INTERACTION IN MAGLEV SYSTEMS

Y. Cai, S. S. Chen, and D. M. Rote Mar. 1992 50 p
(Contract W-31-109-eng-38)
(DE92-019051; ANL-92/19) Avail: CASI HC A03/MF A01

Dynamic interactions between the vehicle and guideway in a high-speed ground transportation system based on magnetically levitated (maglev) vehicles were studied, with an emphasis on the effects of vehicle and guideway parameters. Two dynamic models for the vehicle are presented. In one model, the vehicle is considered to be a moving force traveling at various speeds on a simply supported single- or two-span beam. In the second model, the vehicle is considered to be one-dimensional and has two degrees of freedom; this model consists of the primary and secondary suspensions of the vehicle, with lumped masses, linear springs, and dampings. The Bernoulli-Euler beam equation is used to model the characteristics of a flexible guideway, and the guideway synthesis is based on modal analysis. Analyses were performed to gain an understanding of response characteristics under various loading conditions and to provide benchmark data for verification of existing comprehensive computer programs and some basic design guidelines for maglev systems. Finally, the German Transrapid maglev system was evaluated. DOE

N93-11679# EG and G Rocky Flats, Inc., Golden, CO.
THE EFFECTS OF CHEMISTRY ON WELD PROFILES IN PARTIAL AND FULL PENETRATION WELDS
P. Burgardt and R. D. Campbell 1992 21 p Presented at the 3rd International Conference on Trends in Welding Research, Gatlinburg, TN, 1-5 Jun. 1992
(Contract DE-AC34-90DP-62349)
(DE92-016865; RFP-4522; CONF-9206173-5) Avail: CASI HC A03/MF A01

This paper presents information on the differences in chemistry effects between partial and full penetration welds. Partial penetration welds accurately and repeatably illustrate the results of surface tension-driven fluid flow. Fluid flow and weld shape in partial penetration welds depend on the surface tension-temperature coefficient in the weld pool. The partial penetration concepts apply to single pass, full penetration welds which have nearly 3-dimensional heat flow. When the full penetration weld has 2-dimensional heat flow, material chemistry establishes the tendency of the weld to assume a particular shape, but the resultant weld and underbead shape cannot be predicted by the partial penetration d/w ratios. The full penetration underbead root reinforcement depends on the magnitude of surface tension rather than on the slope of the surface tension-temperature gradient. DOE

N93-11832# Westinghouse Electric Corp., Orlando, FL.
ADVANCED COAL-FUELED GAS TURBINE SYSTEMS
24 Apr. 1992 8 p
(Contract DE-AC21-86MC-23167)
(DE92-018939; DOE/MC-23167/3099) Avail: CASI HC A02/MF A01

No combustion tests for this program were conducted during this reporting period of January 1 to March 31, 1992. DOE-sponsored slogging combustor tests have been suspended since December 1991 in order to perform combustion tests on Northern States Power Company (NSP) coals. The NSP coal tests were conducted to evaluate combustor performance when burning western sub bituminous coals. The results of these tests will guide commercialization efforts, which are being promoted by NSP, Westinghouse Electric, and Textron Defense Systems. The NSP testing has been completed and preparation of the final report for that effort is underway. Although the NSP testing program has been completed, the Westinghouse/DOE program will not be resumed immediately. The reason for this is that Textron Defense Systems (TDS) has embarked on an internally funded program requiring installation of a new liquid fuel combustor system at the Haverhill site. The facility modifications for this new system are significant and it is not possible to continue the Westinghouse/DOE testing while these modifications are being made. These facility modifications are being performed during the period February 15, 1992 through May 31, 1992. The Westinghouse/DOE program can be resumed upon completion of this work. DOE

N93-11865# Carnegie-Mellon Univ., Pittsburgh, PA. Dept. of Electrical and Computer Engineering.
RESEARCH ON A RECONFIGURABLE MODULAR MANIPULATOR SYSTEM
P. K. Khosla and T. Kanade 1992 9 p
(Contract DE-FG02-89ER-14042)
(DE92-018943; DOE/ER-14042/3) Avail: CASI HC A02/MF A01

Research has been conducted on developing the theoretical basis and the technology for a Reconfigurable Modular Manipulation System (RMMS). Unlike a conventional manipulator which has a fixed configuration, the RMMS consists of a set of interchangeable modules that can be rapidly assembled into a system of manipulators with appropriate configurations depending on the specific task requirement. For effective development and use of such a versatile and flexible system a program of theoretical and experimental research has been pursued aimed at developing the basis for next generation of autonomous manipulator systems. The RMMS concept extends the idea of autonomy from sensor-based to configuration based autonomy. One of the important components is the development of design methodologies for mapping tasks into manipulator configurations and for automatic generation of manipulator specific algorithms (e.g., kinematics and dynamics) in order to make the hardware transparent to the user. DOE

N93-11887 Texas A&M Univ., College Station.
DETERMINATION OF LOOSE SPLINE COUPLING COEFFICIENTS OF ROTOR BEARING SYSTEMS IN TURBOMACHINERY Ph.D. Thesis
Sang Kyu Park 1991 248 p
Avail: Univ. Microfilms Order No. DA9216995

Analytical and experimental studies have been carried out to determine the stiffness and damping coefficients of loose spline couplings used in high speed rotating machinery from which a realistic assessment of rotor stability can be made at the turbomachinery design stage. This is believed to be the first attempt ever to determine these coefficients experimentally. Experimental modal parameters of the rotor bearing system with a spline coupling are found using modal testing for given spline geometry, misalignment, lubrication condition, torque, and rotational speeds. A dual rotor computer algorithm which contains a spline coupling model is developed in order to calculate the analytical modal parameters. Support bearing coefficients are obtained using a pressure dam bearing computer code which employs lubrication theory. Spline coupling coefficients are determined by adjusting the model until the analytical modal parameters match the experimental modal parameters. Both computer simulations and impact testing show that shaft speed and torque are the most important parameters which affect the system natural frequency and logarithmic decrement. However, the modal parameters are not very sensitive to the spine coupling coefficients. Only the second natural frequency shows any sensitivity to the spline angular stiffness. The lateral stiffness coefficient of the spline coupling decreases as rotational speed increases. Lateral and angular damping do not influence the modal parameter until unreasonably large values are considered. This is due to the large value of damping in the pressure dam bearings. Since the modal parameters are insensitive to the spline coefficients, a set of error bounds for the experimental values are chosen to determine the ranges of the loose spline coupling coefficients. The results show that the value of the spline lateral stiffness is between 2.0 x10(exp 7) and 8.0 x 10(exp 8) N/m and the spline angular stiffness is between 2.0 x 10(exp 5) and 8.0 x 10(exp 8) N/m, and the spline angular stiffness is between 2.0 x 10(exp 6) Nm/rad. However, it is impossible to identify the spline damping coefficients because the effect of the support bearing damping coefficients suppress the nonsynchronous whirling motion due to the spline friction even at speeds above the first critical speed. Dissert. Abstr.

N93-11992*# Alabama Univ., Huntsville.
KC-135 MATERIALS HANDLING ROBOTICS Final Report, 9 Feb. 1990 - 1 Feb. 1991
Gary L. Workman 23 Apr. 1991 25 p
(Contract NAS8-36955)
(NASA-CR-184430; NAS 1.26:184430) Avail: CASI HC A03/MF A01

Robot dynamics and control will become an important issue for implementing productive platforms in space. Robotic operations will become necessary for man-tended stations and for efficient performance of routine operations in a manned platform. The current constraints on the use of robotic devices in a microgravity environment appears to be due to an anticipated increase in acceleration levels due to manipulator motion and for safety concerns. The objective of this study will be to provide baseline data to meet that need. Most texts and papers dealing with the kinematics and dynamics of robots assume that the manipulator is composed of joints separated by rigid links. However, in recent years several groups have begun to study the dynamics of flexible manipulators, primarily for applying robots in space and for improving the efficiency and precision of robotic systems. Robotic systems which are being planned for implementation in space have a number of constraints to overcome. Additional concepts which have to be worked out in any robotic implementation for a space platform include teleoperation and degree of autonomous control. Some significant results in developing a robotic workcell for performing robotics research on the KC-135 aircraft in preperation for space-based robotics applications in the future were generated. In addition, it was shown that TREETOPS can be used to simulate the dynamics of robot manipulators for both space and ground-based applications. L.R.R.

N93-12114# EG and G Energy Measurements, Inc., Idaho Falls.
ELECTRIC AND HYBRID VEHICLE PROGRAM, SITE OPERATOR PROGRAM
J. F. Warren Jan. 1992 35 p
(Contract DE-AC07-76ID-01570)
(DE92-018055; EGG-EP-10152) Avail: CASI HC A03/MF A01

Activities during the first quarter centered around integrating the new participants into the program. A meeting of the Site Operators, in conjunction with the first meeting of the Electric Vehicle Users Task Force, was held in October. A second meeting of the Task Force was held in December. During these meetings the new contractual requirements were explained to the participants. The Site Operator Data Base was distributed and explained. The Site Operators will begin using the data base in December 1991 and will supply the operating and maintenance data to the INEL on a monthly basis. The Operators requested that they be able to have access to the data of the other Operators and it was agreed that they would be provided this on floppy disk monthly from the INEL. Presentations were made to the DOE sponsored Automotive Technology Development-Contractors Coordination Meeting in October. An overview of the program was given by EG&G. Representatives from Arizona Public Service, Texas A&M University, and York Technical College provided details of their programs and the results and future goals. Work was begun on commercializing the Versatile Data Acquisition System (VDAS). A Scope of Work has been written for a Cooperative Research and Development Agreement (CRADA) to be submitted to the USABC. If implemented, the CRADA will provide funds for the development and commercialization of the VDAS. Participants in the Site Operator Program will test prototypes of the system within their fleets, making the data available to the USABC and other interested organizations. The USABC will provide recommendations on the data to be collected. Major activities by the majority of the Operators were involved with the continued operation and demonstration of existing vehicles. In addition, several of the operators were involved in identifying and locating vehicles to be added to their fleets. A list of the vehicles in each Site Operator fleet is included as Appendix A to this report. DOE

N93-12122# Universal Energy Systems, Inc., Dayton, OH.
FRICTION OF SELF-LUBRICATING SURFACES BY ION BEAM TECHNIQUES
R. S. Bhattacharya and A. K. Rai May 1992 82 p
(Contract DE-AC02-88CE-90026)
(DE92-016069; DOE/CE-90026/3) Avail: CASI HC A05/MF A01

UES, Inc. conducted a research and development program designed to establish conditions for ion implantation/mixing of suitable additives into the surfaces of bulk ceramics and metals for obtaining self-lubricating low friction and wear characteristics. The substrates considered were ZrO2, Al2O3, Si3N4, steel, and Ni-base superalloy. The lubricant additives chosen were BaF2/CaF2Ag, MoS2, WS2, and B2O3. The initial tasks of the program were to synthesis these lubricant compounds by co-implantation of constituent elements if sufficient beams of desired elements were obtained. The final tasks were to investigate high energy (MeV) ion mixing of deposited coatings as well as to investigate ion beam assisted deposition using low energy ion beams. It was shown that MoS2 can be synthesized by co-implantation of Mo(+) and S(+) in ceramic materials with appropriate choice of energies to obtain nearly overlapping depth profiles. The sliding life of DC magnetron sputtered MoS(2) films of thicknesses approximately 7500 A on ceramic materials such as sapphire, Si3N4 and ZrO3 were improved by ten to thousand fold after 2 Mev Ag(+) ion mixing. Ion beam assisted deposition (IBAD) and ion beam mixing were utilized to fabricate self-lubricating coatings of CaF2/Ag and BaF/CaF2/Ag composites. DOE

N93-12149*# National Aeronautics and Space Administration. Marshall Space Flight Center, Huntsville, AL.
SPACE STATION FREEDOM SEAL LEAKAGE RATE ANALYSIS AND TESTING SUMMARY: AIR LEAKS IN AMBIENT VERSUS VACUUM EXIT CONDITIONS
P. I. Rodriguez and R. Markovitch (Sverdrup Technology, Inc., Huntsville, AL.) Aug. 1992 22 p
(NASA-TM-103604; NAS 1.15:103604) Avail: CASI HC A03/MF A01

This report is intended to reveal the apparent relationship of air seal leakage rates between 2 atmospheres (atm) to 1 atm and 1 atm to vacuum conditions. Gas dynamics analysis is provided as well as data summarizing the MSFC test report, 'Space Station Freedom (S.S. Freedom) Seal Flaw Study With Delta Pressure Leak Rate Comparison Test Report'. Author

N93-12196*# Alabama Univ., Huntsville. Dept. of Chemical and Materials Engineering.
VACUUM CHAMBER TRANSLATION/POSITIONING MECHANISM AND WELDING POWER SUPPLY CONTROLLER Final Report
James E. Smith, Jr. and John L. Cashon Aug. 1992 26 p
(Contract NAS8-36955)
(NASA-CR-184465; NAS 1.26:184465) Avail: CASI HC A03/MF A01

Welding in the vacuum of space represents an important and fundamental problem for space exploration. Repairs or connection of metal components on orbit or during travel to the moon or distant planets may be required. Cracks or holes in spacecraft skin or supporting structures external to the pressurized section will require some type of repair that must be permanently made to the skin or support by welding. The development of a translation/positioning system that will permit research into welding of metal samples in a small vacuum chamber located at Marshall Space Flight Center (MSFC) is addressed. The system and associated software was tested to the extent possible without the availability of the welder power supply or control computer that must be supplied by MSFC. Software has been developed for straight line welding. More extensive and varied translations are possible with simple alterations to the operating software to use the full capabilities of this three axes system. The source code 'VW.BAS' has been provided to serve as an example for further development of the vacuum welder translation system. L.R.R.

N93-12203*# National Aeronautics and Space Administration. Lewis Research Center, Cleveland, OH.
AUTOMATIC SYSTEM FOR INSTALLATION AND REPLACEMENT OF SPACE STATION COMPONENTS Patent Application
Andrew L. Gordan, inventor (to NASA) and James L. Dolce, inventor (to NASA) 28 May 1992 19 p
(NASA-Case-LEW-14906-1; NAS 1.71:LEW-14906-1; US-Patent-Appl-SN-889572) Avail: CASI HC A03/MF A01

Service equipment for use in hostile environments is presented. The equipment includes a detachable service unit secured to a stationary service unit. The detachable service unit includes a housing with an exterior plate, a power control interface for connection to an exterior power source, locating pins located in said exterior plate, an electrical connector in the exterior plate electrically coupled to said power control interface, and a pair of clamping receptacles formed in the exterior plate and located on adjacent opposite edges of the exterior plate. The stationary unit includes an electrical connector for connection to the electrical connector of the detachable service unit, a clamping apparatus for clamping and unclamping the detachable service unit from the stationary unit, a base clamp assembly for mounting the clamping apparatus onto the stationary unit, and locating pin holes for receiving the locating pins and aligning the detachable service unit onto the stationary unit. The detachable service unit have mating scalloped faces which aid in alignment and provide a mechanism for heat dissipation. NASA

N93-12220# Sandia National Labs., Livermore, CA.
SOME CONSISTENCY REQUIREMENTS ON HARDENING-RECOVERY EVOLUTION EQUATIONS FOR WELDING, PART 1
L. A. Bertram May 1992 46 p
(Contract DE-AC04-76DP-00789)
(DE92-015992; SAND-92-8447-Pt-1) Avail: CASI HC A03/MF A01

Welding residual stresses and distortions arise from complex thermomechanical processes driven by the room temperature to melt temperature changes imposed on the metals. These changes also cause many order of magnitude changes in some mechanical properties of the metal in and near the fusion zone, where the principal distortions arise. Thus while stresses are low there at the time of peak temperature, the deformations are large and important. Simulation, to be useful, should treat this zone with a consistent accuracy near the fusion zone and in cooler metal further away. Calculations should also make the maximum possible use of thermophysical property data available for commercially interesting alloys. Heuristic viscoplastic equations of the Armstrong-Frederick type are considered here, and analytical solutions for some nonisothermal processes are employed to restrict the values of hardening-recovery parameters applied to welding processes. Results indicate that use of Ashby and Frost's deformation mechanism maps as templates organizes this analysis, and puts the need for additional data into a clear context for the example of 304L Stainless Steel. DOE

N93-12274# Massachusetts Inst. of Tech., Cambridge.
THE EFFECTS OF ALUMINUM OXIDE ON INERTIAL WELDING OF ALUMINUM IN SPACE APPLICATIONS M.S. Thesis
Michael H. Smith May 1992 135 p
(AD-A255100) Avail: CASI HC A07/MF A02

Inertial friction welding of 2219 aluminum alloy studs to 2219 aluminum alloy plates is investigated in air and in an argon atmosphere to determine the effects of an intact oxide layer on weld quality. Scratch-brushing of plates and studs was performed in an argon atmosphere to break up the oxide layer and prevent reformation prior to testing. Argon was used to simulate the near-oxygen free space environment. Weld quality was determined by a bend test and by measurement of the fraction of the weld surface area that was dimpled in appearance following fracture of the weld. The fundamental theories of friction and wear that are applicable to friction welding are reviewed. A brief survey of current welding methods that may have application in space is presented, as well as a discussion of their feasibility and limitations. Characteristics of the space station are discussed as well as their consequences on welding in space. A qualitative model of the process of inertial friction welding based on the theories of friction and observations of welds and weld fractures is developed and presented. GRA

N93-12327*# National Aeronautics and Space Administration. Lewis Research Center, Cleveland, OH.
METHOD AND APPARATUS FOR GRIPPING TEST SPECIMENS Patent Application
Rebecca A. MacKay, inventor (to NASA) and Michael V. Nathal, inventor (to NASA) 18 May 1992 12 p
(NASA-Case-LEW-15345-1; NAS 1.71:LEW-15345-1; US-Patent-Appl-SN-884980) Avail: CASI HC A03/MF A01

A pair of solid-teeth wedges are employed in an improved gripping system. The wedges fit inside a pair of plates having an angled cavity to accommodate them. As stress is applied to the specimen, the wedges are urged toward the specimen by the angled cavity to increase the gripping force. An alignment fixturing device is used to properly position the grips on the test specimen. This device not only axially aligns the grips but also locates them at the proper spacing. NASA

N93-12364# National Aerospace Lab., Kakuda (Japan).
SEALING CHARACTERISTICS OF A CARBON SEGMENTED CIRCUMFERENTIAL SEAL FOR A LIQUID OXYGEN TURBOPUMP [EKITAI SANSO TABOPONPU YOU SEGUMENTOSHIRU NO MIPPUU TOKUSEI]
Mamoru Oike, Yoshiaki Watanabe, Masataka Kikucti, and Masataka Nosaka (National Space Development Agency, Tokyo, Japan) Nov. 1991 19 p In JAPANESE
(NAL-TR-1130; JTN-92-80398) Avail: CASI HC A03/MF A01

The liquid oxygen turbopump for the LE-7 rocket engine is driven by fuel enriched hot gas and has a helium purge seal placed between the pump and the turbine to separate the turbine drive gas from the oxygen. An experimental study on a carbon segmented circumferential seal with Rayleigh steps was conducted in order to develop a helium purge seal with low leakage and high durability. The experimental and analytical results concerning the sealing characteristics of this carbon segmented seal are described. A comparison between the results shows that the effects of both the seal pressure and rotational speed on the leakage rate are fairly dependent on the opening force induced by the Rayleigh steps. Since the carbon sealing surface was worn in conformity with the profile of the deformed runner sealing surface, the time dependent relationships which exist between the static and dynamic leakage rates and the sealed pressure, which are caused by progression of carbon wear, were clarified. Author (NASDA)

N93-12434# Naval Postgraduate School, Monterey, CA. Dept. of Mechanical Engineering.
A SURFACE INTEGRAL APPROACH TO THE MOTION PLANNING OF NONHOLONOMIC SYSTEMS
Ranjan Mukherjee 6 Aug. 1992 35 p
(AD-A254844; NPS-ME-92-003) Avail: CASI HC A03/MF A01

Nonholonomic mechanical systems are governed by constraints of motion that are nonintegrable differential expressions. Unlike holonomic constraints, these differential constraints do not reduce the number of dimensions of the configuration space of a system. Therefore, a nonholonomic system can access a configuration space of dimension higher than the number of degrees of freedom of the system. In this paper, we develop an algorithm for planning admissible trajectories for nonholonomic systems that will take the system from one point in its configuration space to another. In our algorithm we first converge the independent variables to their desired values and then use closed trajectories of the independent variables to converge the dependent variables. We use Stokes's theorem in our algorithm to convert the problem of finding a closed path into that of finding a surface area in the space of the independent variables, such that the dependent variables converge to their desired values as the independent variables traverse along the boundary of this surface area. The use of Stokes's theorem simplifies the motion planning problem and also imparts global characteristics. The salient features of our algorithm are apparent in the two examples that we discuss: a planar space robot and a disk rolling without slipping on a flat surface. GRA

N93-12463# National Aerospace Lab., Kakuda (Japan).
AN EXPERIMENTAL STUDY OF A SMALL HIGH SPEED LH2 ROCKET PUMP: FUNDAMENTAL MECHANICAL DESIGN Report No. 2 [ROKETTO YOU KOGATA LH2 PONPU NO KENKYUU SHISAKU. SONO 2: KOUZOU KIHON SEKKEI]
Masataka Kikuchi, Mineo Suzuki (National Aerospace Lab., Tokyo, Japan), Takashi Shimura, Mitsuo Watanabe, Kenjiro Kamijo, Masataka Nosaka (National Space Development Agency, Tokyo, Japan), and Shougo Warashina (Ishikawajima-Harima Heavy Industries Co. Ltd., Tokyo, Japan) Sep. 1991 27 p In JAPANESE
(NAL-TR-1123; JTN-92-80410) Avail: CASI HC A03/MF A01

A small high speed Liquid Hydrogen (LH2) pump was designed, fabricated, and tested in order to obtain technical data necessary for the development of upper stage rocket engines, e.g., the LE-5 and Orbiter Transfer Vehicle (OTV) engines. The pump's basic mechanical design is described, as well as its mechanical performance during tests using LH2 (both at nominal operating and rapid start and stop conditions). It was confirmed that the same materials employed for liquid oxygen pump components can be used, except for the impeller. An impeller made of titanium alloy (Ti-5Al-2.5Sn) was machined and then diffusion bonded, and subsequently withstood a high speed operating condition (50,000 rpm) for 350 sec. A balance piston configuration was selected for axial thrust control, where the impeller acts as a balance disk. The piston's performance was satisfactory, although the impeller's balance position during the tests was different from design calculations. Post-test examinations revealed light rubbing traces on the impeller and casing at the balance piston orifice. This positional discrepancy was caused by an inaccurate estimate of the orifice flow coefficients and leakage flow rate. Stress analysis on other components and machine specifications for critical mating parts were also verified as satisfactory. Self lubricated ball bearings and rotating shaft seals showed adequate performance. Results indicate that smooth operation was achieved, thus confirming the soundness of the pump's mechanical design. Author (NASDA)

N93-12521*# Georgia Inst. of Tech., Atlanta. School of Mechanical Engineering.
A VISION-BASED END-POINT CONTROL FOR A TWO-LINK FLEXIBLE MANIPULATOR M.S. Thesis
Klaus Obergfell 23 Aug. 1991 158 p
(Grant NAG1-623)
(NASA-CR-190967; NAS 1.26:190967) Avail: CASI HC A08/MF A02

The measurement and control of the end-effector position of a large two-link flexible manipulator are investigated. The system implementation is described and an initial algorithm for static end-point positioning is discussed. Most existing robots are controlled through independent joint controllers, while the end-effector position is estimated from the joint positions using a kinematic relation. End-point position feedback can be used to compensate for uncertainty and structural deflections. Such feedback is especially important for flexible robots. Computer vision is utilized to obtain end-point position measurements. A look-and-move control structure alleviates the disadvantages of the slow and variable computer vision sampling frequency. This control structure consists of an inner joint-based loop and an outer vision-based loop. A static positioning algorithm was implemented and experimentally verified. This algorithm utilizes the manipulator Jacobian to transform a tip position error to a joint error. The joint error is then used to give a new reference input to the joint controller. The convergence of the algorithm is demonstrated experimentally under payload variation. A Landmark Tracking System (Dickerson, et al 1990) is used for vision-based end-point measurements. This system was modified and tested. A real-time control system was implemented on a PC and interfaced with the vision system and the robot. Author

N93-11961*# Rice Univ., Houston, TX. Dept. of Electrical and Computer Engineering.
FAULT DETECTION AND FAULT TOLERANCE IN ROBOTICS
Monica Visinsky, Ian D. Walker, and Joseph R. Cavallaro *In* NASA. Lyndon B. Johnson Space Center, Fifth Annual Workshop on Space Operations Applications and Research (SOAR 1991), Volume 1 Jan. 1992 p 262-271 Sponsored in part by Mitre Corp. (For primary document see N93-11921 02-59)
(Grants NSF MIP-89-09498; NSF MSS-90-24391)
Avail: CASI HC A02/MF A04

N93-11967*# Wisconsin Univ., Madison. Center for Space Automation and Robotics.
IMPORTANCE OF NUMEROSITY AND DISTRIBUTION OF ARTICULATIONS WITHIN THE DIGITS, WRISTS, AND ARMS OF TELEMANIPULATORS CONFRONTED WITH DEXTROUS ASSEMBLY TASKS Abstract Only
Steven F. Wiker, Nell Duffie, and Thomas Yen *In* NASA. Lyndon B. Johnson Space Center, Fifth Annual Workshop on Space Operations Applications and Research (SOAR 1991), Volume 1 Jan. 1992 p 310 (For primary document see N93-11921 02-59)
Avail: CASI HC A01/MF A04

N93-11968*# Aerospace Medical Research Labs., Wright-Patterson AFB, OH.
THE DEVELOPMENT OF SYSTEM COMPONENTS TO PROVIDE PROPRIOCEPTIVE AND TACTILE INFORMATION TO THE HUMAN FOR FUTURE TELEPRESENCE SYSTEMS Abstract Only
Ammon K. Wright *In* NASA. Lyndon B. Johnson Space Center, Fifth Annual Workshop on Space Operations Applications and Research (SOAR 1991), Volume 1 Jan. 1992 p 311 (For primary document see N93-11921 02-59)
Avail: CASI HC A01/MF A04

N93-11969*# National Aeronautics and Space Administration. Goddard Space Flight Center, Greenbelt, MD.
ADVANCED MECHANISMS FOR ROBOTICS
John M. Vranish *In* NASA. Lyndon B. Johnson Space Center, Fifth Annual Workshop on Space Operations Applications and Research (SOAR 1991), Volume 1 Jan. 1992 p 314-320 (For primary document see N93-11921 02-59)
Avail: CASI HC A02/MF A04

N93-11970*# Odetics, Inc., Anaheim, CA. AIM Div.
EXOSKELETON MASTER CONTROLLER WITH FORCE-REFLECTING TELEPRESENCE
James B. Burke, Stephen J. Bartholet, and David K. Nelson (Aerospace Medical Research Labs., Wright-Patterson AFB, OH.) *In* NASA. Lyndon B. Johnson Space Center, Fifth Annual Workshop on Space Operations Applications and Research (SOAR 1991), Volume 1 Jan. 1992 p 321-330 (For primary document see N93-11921 02-59)
Avail: CASI HC A02/MF A04

N93-11971*# Grumman Aerospace Corp., Bethpage, NY. Space and Electronics Div.
REMOTE SYSTEMS DEVELOPMENT
R. Olsen, O. Schaefer, and J. Hussey *In* NASA. Lyndon B. Johnson Space Center, Fifth Annual Workshop on Space Operations Applications and Research (SOAR 1991), Volume 1 Jan. 1992 p 331-347 (For primary document see N93-11921 02-59)
Avail: CASI HC A03/MF A04

N93-11972*# National Aeronautics and Space Administration. Lyndon B. Johnson Space Center, Houston, TX.
AN INTEGRATED DEXTEROUS ROBOTIC TESTBED FOR SPACE APPLICATIONS

Larry C. Li, Hai Nguyen, and Edward Sauer (Lockheed Engineering and Sciences Co., Houston, TX.) *In its* Fifth Annual Workshop on Space Operations Applications and Research (SOAR 1991), Volume 1 Jan. 1992 p 348-361 (For primary document see N93-11921 02-59)
Avail: CASI HC A03/MF A04

N93-11973*# Carnegie-Mellon Univ., Pittsburgh, PA. Robotics Inst.
SELF MOBILE SPACE MANIPULATOR PROJECT Abstract Only
H. Ben Brown, Mark Friedman, Yangsheng Xu, and Takeo Kanade *In* NASA. Lyndon B. Johnson Space Center, Fifth Annual Workshop on Space Operations Applications and Research (SOAR 1991), Volume 1 Jan. 1992 p 362 (For primary document see N93-11921 02-59)
Avail: CASI HC A01/MF A04

N93-11974*# Deutsche Agentur fuer Raumfahrtangelegenheiten G.m.b.H., Bonn (Germany).
AUTOMATION AND ROBOTICS FOR COLUMBUS: AN IMPLEMENTATION CONCEPT FOR THE FREE FLYING LABORATORY (MTFF)
G. Goelz and B. Sommer *In* NASA. Lyndon B. Johnson Space Center, Fifth Annual Workshop on Space Operations Applications and Research (SOAR 1991), Volume 1 Jan. 1992 p 364-381 (For primary document see N93-11921 02-59)
Avail: CASI HC A03/MF A04

N93-11975*# Barrios Technology, Inc., Houston, TX. Mission Operations Directorate.
SPACE STATION ROBOTICS PLANNING TOOLS
Bridget Mintz Testa *In* NASA. Lyndon B. Johnson Space Center, Fifth Annual Workshop on Space Operations Applications and Research (SOAR 1991), Volume 1 Jan. 1992 p 382-390 (For primary document see N93-11921 02-59)
Avail: CASI HC A02/MF A04

N93-11979*# Oak Ridge National Lab., TN. Center for Engineering Systems Advanced Research.
RESEARCH AND DEVELOPMENT AT ORNL/CESAR TOWARDS COOPERATING ROBOTIC SYSTEMS FOR HAZARDOUS ENVIRONMENTS
R. C. Mann, K. Fujimura, and M. A. Unseren *In* NASA. Lyndon B. Johnson Space Center, Fifth Annual Workshop on Space Operations Applications and Research (SOAR 1991), Volume 1 Jan. 1992 p 402-406 (For primary document see N93-11921 02-59)
Avail: CASI HC A01/MF A04

38 QUALITY ASSURANCE AND RELIABILITY

Includes product sampling procedures and techniques; and quality control.

N93-10963*# National Aeronautics and Space Administration. Lewis Research Center, Cleveland, OH.
NONDESTRUCTIVE EVALUATION OF CERAMIC AND METAL MATRIX COMPOSITES FOR NASA'S HITEMP AND ENABLING PROPULSION MATERIALS PROGRAMS
Edward R. Generazio Aug. 1992 27 p Presented at the 16th Annual Conference on Composites, Materials, and Structures, Cocoa Beach, FL, 12-15 Jan. 1992
(RTOP 510-01-50)
(NASA-TM-105807; E-7238; NAS 1.15:105807) Avail: CASI HC A03/MF A01

In a preliminary study, ultrasonic, x-ray opaque, and fluorescent dye penetrants techniques were used to evaluate and characterize ceramic and metal matrix composites. Techniques are highlighted for identifying porosity, fiber alignment, fiber uniformity, matrix cracks, fiber fractures, unbonds or disbonds between laminae, and fiber-to-matrix bond variations. The nondestructive evaluations (NDE) were performed during processing and after thermomechanical testing. Specific examples are given for Si3N4/SiC (SCS-6 fiber), FeCrAlY/Al2O3 fibers, Ti-15-3/SiC (SCS-6 fiber) materials, and Si3N4/SiC (SCS-6 fiber) actively cooled panel components. Results of this study indicate that the choice of the NDE tools to be used can be optimized to yield a faithful and accurate evaluation of advanced composites. Author

N93-11015# Rolls-Royce Ltd., Derby (England).
JAPANESE STYLE TOTAL QUALITY CONTROL: A FIRST HAND EXPERIENCE
S. C. Cook 20 Nov. 1991 33 p
(PNR-90909; ETN-92-92199) Copyright Avail: CASI HC A03/MF A01

The scope, concepts and practices of Total Quality Control (TQC) as operated in Japan today are described. The following mechanisms and elements are introduced: policy deployment, cross functional management, small group activities, suggestion systems, standardization, the TQC promotion department, and TQC education. It is shown on a practical level, how TQC operates in the research and engineering divisions of the aeroengine and space operation at Ishikawajima Harima Industries in Japan. Japanese style TQC is a well developed, well promoted, well structured, common approach to achieving customer satisfaction through continuous improvements. Furthermore, TQC itself is being continuously improved with the Japanese still refining, extending, and developing TQC. ESA

N93-11016# Rolls-Royce Ltd., Derby (England).
NONDESTRUCTIVE INSPECTION AND LIFE DETERMINATION OF DISC MATERIAL
Hugh K. Craig 5 Dec. 1991 17 p Presented at the International Conference on Non-Destructive Inspection, Paris, France, 4-5 Dec. 1991
(PNR-90911; ETN-92-92200) Copyright Avail: CASI HC A03/MF A01

The prime role of nondestructive evaluation is to support development and validation of the two main processes: the materials and manufacturing method design and engineering design of the engine. The second role of nondestructive evaluation is to monitor, on a routine basis, these design processes during the manufacture and service operations. Shortcomings in the method which link the manufacturing inspection capability to the initial design life of parts are discussed. A methodology which establishes the imperfection size frequency distribution for disc materials is outlined. The data validates the disc material manufacturing process and is also used with the probabilistic lifing methods. The development of DRACULA, a program for the detection of radial-axial subsurface cracks which was brought to a generic state of service readiness and is used for disc life management, is addressed. The major points of subsurface radial-axial fatigue crack work are discussed: ultrasonic detection methods, potential sensitivity, mathematical modeling, and inspection experience. ESA

N93-11034# Rolls-Royce Ltd., Derby (England).
ON THE BASIS OF EXPERIENCE: BUILT IN PRODUCT RELIABILITY
9 Feb. 1991 17 p Presented at the Reliability and Maintainability Symposium, Orlando, FL, 29-31 Jan. 1991
(PNR-90932; ETN-92-92212) Copyright Avail: CASI HC A03/MF A01

Rolls Royce product reliability is considered based on experience in supporting commercial gas turbine engines and airline customers during the years of its existence. Reliability on return on investment is addressed. The meaning of 'reliability' and 'return on investment' is discussed. ESA

N93-11110# Rolls-Royce Ltd., Derby (England).
QUALITY MANAGEMENT OF FINITE ELEMENT ANALYSIS
John Barlow 13 Sep. 1991 19 p Presented at the 3rd

NAFEMS International Conference, 9-13 Sep. 1991
(PNR-90951; ETN-92-92228) Copyright Avail: CASI HC A03/MF A01

A quality management system covering the use of finite element analysis is described. The main topics are as follows: acquisition, development and verification of software (including the software suppliers software quality control system), support, documentation, error control, internal software, software acceptance and release; development and qualification of analysis methods, including software evaluation, analysis procedure qualification and documentation, procedure quality checks, control of analysis procedure errors; product design and integrity analysis, including project quality assurance and analysis planning, task specification and allocation, analysis, execution, results checking and analysis records. Other issues include the commercial and business advantages of quality systems, project and technical management and the training and experience of personnel. The items are correlated with the requirements of International Standard Organization 9001. ESA

N93-11154# EG and G Energy Measurements, Inc., Idaho Falls.
SURFACE RECONSTRUCTION OF A THREE-DIMENSIONAL ULTRASONIC FLAW
Lat S. Koo 1992 10 p Presented at the International Union of Theoretical and Applied Mechanics Symposium on Inverse Problems in Engineering Mechanics, Tokyo, Japan, 11-15 May 1992
(Contracts DE-AC07-76ID-01570; W-7405-eng-82)
(DE92-018029; EGG-M-91631; CONF-920550-1) Avail: CASI HC A02/MF A01

In three-dimensional inverse scattering problems, the reconstruction of a solid scatterer is often difficult, if not impossible, and computationally expensive due to the dimensionality. To obtain only the geometrical information, a surface reconstruction algorithm is naturally more desirable since no additional knowledge can be gained from doing the solid reconstruction, and the computation is reduced to two dimensions. With the application of the first Born approximation, a simple surfaces reconstruction technique for a three-dimensional target is proposed. In general, this method is ill-posed. However, the numerical instability part of the ill-posedness is removable when the surface has a two-fold symmetry with respect to a plane. To demonstrate this approach, three analytical examples are shown. DOE

N93-11209 Iowa State Univ. of Science and Technology, Ames.
APPLICATION OF THE BOUNDARY ELEMENT METHOD TO ELASTIC WAVE SCATTERING PROBLEMS IN ULTRASONIC NONDESTRUCTIVE EVALUATION Ph.D. Thesis
Paul Jay Schafbuch 1991 249 p
Avail: Univ. Microfilms Order No. DA9126246

The boundary element method (BEM) is used to numerically simulate the interaction of ultrasonic waves with material defects such as voids, inclusions, and open cracks. The time harmonic formulation is in 3D and therefore allows flaws of arbitrary shape to be modeled. The BEM makes such problems feasible because the underlying boundary integral equation only requires a surface (2D) integration and difficulties associated with the seemingly infinite extent of the host domain are not encountered. The computer code utilized in this work is built upon recent advances in elastodynamic boundary element theory such as a scheme for self adjusting integration order and singular integration regularization. Incident fields may be taken as compressional or shear plane waves or predicted by an approximate Gauss-Hermite beam model. The code is highly optimized for voids and has been coupled with computer aided engineering packages for automated flaw shape definition and mesh generation. Subsequent graphical display of intermediate results supports model refinement and physical interpretation. Final results are typically cast in a nondestructive evaluation (NDE) context as either scattering amplitudes or flaw signals (via a measurement model based on a reciprocity integral). The near field is also predicted which allows for improved physical insight into the scattering process and the evaluation of certain modeling approximations. The accuracy of the BEM approach is first examined by comparing its predictions to those of other models for single, isolated scatters. The comparisons are with the predictions of analytical solutions for spherical defects and with MOOT and T-matrix calculations for axisymmetric flaws. Experimental comparisons are also made for volumetric shapes with different characteristic dimensions in all three directions, since no other numerical approach has yet produced results of this type. Theoretical findings regarding the fictitious eigenfrequency difficulty are substantiated through the analytical solution of a fundamental elastodynamics problem and corresponding BEM studies. Given the confidence in the BEM technique engendered by these comparisons, it is then used to investigate the modeling of 'open', cracklike defects amenable to a volumetric formulation. The limits of applicability of approximate theories (e.g., quasistatic, Kirchhoff, and geometric theory of diffraction) are explored for elliptical cracks, from this basis. The problem of two interacting scatterers is then considered. Results from a fully implicit approach and from a more efficient hybrid scheme are compared with generalized Born and farfield approximate interaction theories. Dissert. Abstr.

N93-11587# Aerospatiale Aquitaine, Saint-Medard en Jalles (France).
USING NDT TECHNIQUES IN THE MAINTENANCE OF AERONAUTICAL PRODUCTS
Pierre Barbier and Pascal Blondet 1992 40 p Presented at the Symposium on Aeronautical Maintenance and Logistics, Bordeaux, France, 13-17 Jan. 1992; sponsored by Association Aeronautique et Astronautique de France and Sogerma Socea
(Rept-921-430-102; ETN-92-92350) Avail: CASI HC A03/MF A01

The use of nondestructive test (NDT) concepts in the maintenance and safety of aircraft and other aeronautical engines is discussed. Maintenance lies in the concept of damage tolerance, a concept introduced within the framework of the aeronautical regulation by the Federal Aviation Regulation and Jet Airworthiness Requirements. This concept lies in the fact that certain damages can evolve and must be detected by NDT before they reach a critical size beyond which the structure would not bear the applied critical loads. In this context, NDT plays a key role. Different NDT techniques used in aeronautical maintenance are presented, and the concept of reliability of NDT's, in terms of detection probability, is discussed. The automation of the NDT techniques applied to high performance turbine engine components is considered. The state of the art of the up to date solutions used for this kind of application is given. Information about the last developments of NDT techniques concerning the fields of computer tomography and holography are included. ESA

N93-11601# Pacific Northwest Lab., Richland, WA.
ACOUSTIC EMISSION MONITORING OF HFIR VESSEL DURING HYDROSTATIC TESTING
M. A. Friesel and J. F. Dawson Aug. 1992 52 p
(Contract DE-AC06-76RL-01830)
(DE92-019316; PNL-8277) Avail: CASI HC A04/MF A01

This report discusses the results and conclusions reached from applying acoustic emission monitoring to surveillance of the High Flux Isotope Reactor vessel during pressure testing. The objective of the monitoring was to detect crack growth and/or fluid leakage should it occur during the pressure test. The report addresses the approach, acoustic emission instrumentation, installation, calibration, and test results. DOE

N93-11617# Federal Aviation Administration, Cambridge, MA.
MAGNETO-OPTIC IMAGING INSPECTION OF SELECTED CORROSION SPECIMENS
Stephen N. Bobo Jul. 1992 23 p
(DOT/FAA/CT-TN92/20; DOT-VNTSC-FA1H2-92) Avail: CASI HC A03/MF A01

A feasibility demonstration was conducted at the facilities of Physical Research Instrumentation Company (PRI) in Redmond, Washington. The purpose of the demonstration was to compare the effectiveness of the PRI Model 301-1 magneto-optic imaging

(MOI) system with conventional eddy current methods of detecting corrosion in aircraft test panels, previously identified by eddy current scanning. The study indicated that MOI may not be able to detect gradual differences in thinning that are less than 10 percent of base metal thickness. Also, with MOI, it appears to be more difficult to provide quantitative estimates of residual thickness than is the case with eddy current scanning. On the other hand, MOI visualization of the extent of corrosion is simple and free of the labor intensive point-by-point mapping, which is required by eddy current scanning. Author

N93-12055# EG and G Energy Measurements, Inc., Idaho Falls.
ULTRASONIC SENSING OF GMAW: LASER/EMAT DEFECT DETECTION SYSTEM
N. M. Carlson, J. A. Johnson, E. D. Larsen, A. VanClark, Jr., S. R. Schaps, and C. M. Fortunko 1992 5 p Presented at the 3rd International Conference on Trends in Welding Research, Gatlinburg, TN, 1-5 Jun. 1992
(Contract DE-AC07-76ID-01570)
(DE92-017916; EGG-M-92287; CONF-9206173-8) Avail: CASI HC A01/MF A01

In-process ultrasonic sensing of welding allows detection of weld defects in real time. A noncontacting ultrasonic system is being developed to operate in a production environment. The principal components are a pulsed laser for ultrasound generation and an electromagnetic acoustic transducer (EMAT) for ultrasound reception. A PC-based data acquisition system determines the quality of the weld on a pass-by-pass basis. The laser/EMAT system interrogates the area in the weld volume where defects are most likely to occur. This area of interest is identified by computer calculations on a pass-by-pass basis using weld planning information provided by the off-line programmer. The absence of a signal above the threshold level in the computer-calculated time interval indicates a disruption of the sound path by a defect. The ultrasonic sensor system then provides an input signal to the weld controller about the defect condition. DOE

N93-12204*# National Aeronautics and Space Administration. Langley Research Center, Hampton, VA.
METHOD AND APPARATUS FOR EVALUATING MULTILAYER OBJECTS FOR IMPERFECTIONS Patent Application
Joseph S. Heyman, inventor (to NASA) and M. N. Abedin, inventor (to NASA) (AS&M, Inc., Hampton, VA.) 15 Apr. 1992 15 p
(NASA-Case-LAR-14581-1-SB; NAS 1.71:LAR-14581-1-SB; US-Patent-Appl-SN-873407) Avail: CASI HC A03/MF A01

A multilayer object where the layers are arranged in a stacking direction is evaluated for imperfections such as voids, delaminations, and microcracks. First, an acoustic wave is transmitted into the object in the stacking direction via an appropriate transducer/waveguide combination. The wave propagates through the multilayer object and is received by another transducer/waveguide combination preferably located on the same surface as the transmitting combination. The received acoustic wave is correlated with the presence or absence of imperfections by generating pulse echo signals indicative of the received acoustic wave, wherein the successive signals form distinct groups over time. The respective peak amplitudes of each group are sampled and fitted to an exponential curve, wherein a substantial fit of approximately 80-90 percent indicates the absence of imperfections. Alternatively, the time interval between distinct groups can be measured, wherein equal intervals indicate the absence of imperfections and unequal intervals indicate the presence of imperfections. NASA

N93-12510# Army Materiel Systems Analysis Activity, Aberdeen Proving Ground, MD.
OPERATING CHARACTERISTIC ANALYSIS FOR RELIABILITY GROWTH PROGRAMS Final Report
Paul M. Ellner and Robert E. Mioduski Aug. 1992 76 p
(AD-A254993; AMSAA-TR-524) Avail: CASI HC A05/MF A01

Operating characteristic (OC) analysis concepts are extended to the reliability growth setting. Consumer (Government) and producer (contractor) statistical risks are expressed in terms of the reliability growth curve parameters, test duration, and reliability requirement. For a given confidence level, these risks are shown to depend solely on the expected number of failures during the growth test and the ratio of the MTBF to be achieved at the end of the growth program to the MTBF technical requirement to be demonstrated with confidence. Formulas are developed for computing these risks as a function of the test duration and growth curve planning parameters. GRA

N93-12533 Iowa State Univ. of Science and Technology, Ames.
ULTRASONIC FLAW CLASSIFICATION AND SIZING Ph.D. Thesis
Sung-Jin Song 1991 199 p
Avail: Univ. Microfilms Order No. DA9212192

Flaw classification (determination of the flaw type) and flaw sizing (prediction of the flaw shape, orientation and sizing parameters) are very important issues in ultrasonic nondestructive evaluation of materials. In this work, new techniques for both classification and sizing are described. In the area of flaw classification, a methodology is developed which can solve classification problems in weldments using probabilistic neural networks. In the area of flaw sizing, four new approaches are presented including (1) the determination of distance-gain-size (DGS) curves and frequency response curves for flat-bottom holes based on a theoretical ultrasonic scattering model, (2) a time-of-flight equivalent (TOFE) sizing method for relatively large (greater than 1 mm) flaws in materials, (3) an amplitude-based equivalent (ABE) sizing method, and (4) a first moment (FM) sizing method. Both the third and fourth methods are shown to be new viable techniques for sizing relatively small (less than 1 mm) flaws in materials. Dissert. Abstr.

39 STRUCTURAL MECHANICS

Includes structural element design and weight analysis; fatigue; and thermal stress.

For applications see *05 Aircraft Design, Testing and Performance* and *18 Spacecraft Design, Testing and Performance.*

N93-10967*# National Aeronautics and Space Administration. Lewis Research Center, Cleveland, OH.
A CREEP CAVITY GROWTH MODEL FOR CREEP-FATIGUE LIFE PREDICTION OF A UNIDIRECTIONAL W/Cu COMPOSITE
Young-Suk Kim (Research Inst. of Industrial Science and Technology, Pohang, Republic of Korea), Michael J. Verrilli, and Gary R. Halford May 1992 19 p Presented at the Second Symposium on Advances in Fatigue Lifetime Predictive Techniques, Pittsburgh, PA, 4-5 May 1992; sponsored by the American Society for Testing and Materials
(RTOP 510-01-50)
(NASA-TM-105780; E-7207; NAS 1.15:105780) Avail: CASI HC A03/MF A01

A microstructural model was developed to predict creep-fatigue life in a (0)(sub 4), 9 volume percent tungsten fiber-reinforced copper matrix composite at the temperature of 833 K. The mechanism of failure of the composite is assumed to be governed by the growth of quasi-equilibrium cavities in the copper matrix of the composite, based on the microscopically observed failure mechanisms. The methodology uses a cavity growth model developed for prediction of creep fracture. Instantaneous values of strain rate and stress in the copper matrix during fatigue cycles were calculated and incorporated in the model to predict cyclic life. The stress in the copper matrix was determined by use of a simple two-bar model for the fiber and matrix during cyclic loading. The model successfully predicted the composite creep-fatigue life under tension-tension cyclic loading through the use of this instantaneous matrix stress level. Inclusion of additional mechanisms such as cavity nucleation, grain boundary sliding, and the effect of fibers on matrix-stress level would result in more generalized predictions of creep-fatigue life. Author

N93-11004*# National Aeronautics and Space Administration. Lewis Research Center, Cleveland, OH.
CERAMIC COMPONENT RELIABILITY WITH THE RESTRUCTURED NASA/CARES COMPUTER PROGRAM
Lynn M. Powers, Alois Starlinger, and John P. Gyekenyesi Sep. 1992 22 p Presented at the 37th International Gas Turbine and Aeroengine Congress, Cologne, Germany, 1-4 Jun. 1992; sponsored by ASME
(RTOP 505-63-5B)
(NASA-TM-105856; E-6797; NAS 1.15:105856) Avail: CASI HC A03/MF A01

The Ceramics Analysis and Reliability Evaluation of Structures (CARES) integrated design program on statistical fast fracture reliability and monolithic ceramic components is enhanced to include the use of a neutral data base, two-dimensional modeling, and variable problem size. The data base allows for the efficient transfer of element stresses, temperatures, and volumes/areas from the finite element output to the reliability analysis program. Elements are divided to insure a direct correspondence between the subelements and the Gaussian integration points. Two-dimensional modeling is accomplished by assessing the volume flaw reliability with shell elements. To demonstrate the improvements in the algorithm, example problems are selected from a round-robin conducted by WELFEP (WEakest Link failure probability prediction by Finite Element Postprocessors). Author

N93-11013# Rolls-Royce Ltd., Derby (England).
APPLICATION OF POLYIMIDES TO AEROENGINE COMPONENTS
D. J. Lind and S. W. Hill 20 Oct. 1991 21 p Presented at the Polymide Conference and Loughborough Symposium, Loughborough, England, 26 Sep. 1991
(PNR-90907; ETN-92-92197) Copyright Avail: CASI HC A03/MF A01

The application of polymeric composites near the core of the large RB-211 civil engines and current military engines is considered. This requires 250 C continuous operating temperatures and hence the use of the high temperature polyimide systems such as PMR-15 (Polymerization of Monomer Reactants). The use of these high temperature PMR-15/carbon fiber reinforced plastic composites has been restricted due to problems associated with microcracks, formed in particular during thermal cycling. Factors influencing microcrack formation and the control of these factors are considered. Analytical techniques, developed to observe the chemical and physical changes that occur during manufacture, storage, and processing of PMR-15 materials, are described: high performance liquid chromatography, gel permeation chromatography, Fourier transform infrared spectroscopy, differential scanning calorimetry, dynamic mechanical analysis, and simultaneous thermal analysis mass spectrometry. The current status and future trends for PMR-15 composites are outlined. Rigorous control over source materials and processes has resulted in significant improvements which allow the engineering programs to be pursued. ESA

N93-11014# Rolls-Royce Ltd., Derby (England). Materials Analysis Lab.
NEUTRON DIFFRACTION RESIDUAL STRESS STUDIES FOR AERO-ENGINE COMPONENT APPLICATIONS
K. Clay and C. Small 5 Dec. 1991 30 p Presented at the British Crystallographic Association Industrial Group Meeting, Farnborough, England, 7 Nov. 1991
(PNR-90908; ETN-92-92198) Copyright Avail: CASI HC A03/MF A01

Computer graphics for a presentation describing how Rolls-Royce is refining the method of residual stress measurement by neutron diffraction to suit the characteristic stress fields of components are presented. Results to date are given. An outline of how this residual stress data is to be used in developing stress models for critical rotating components is given. ESA

N93-11021# Rolls-Royce Ltd., Derby (England).
AUTOMATED FRINGE ANALYSIS FOR MOIRE INTERFEROMETRY
John B. Brownell and Ric J. Parker 1 Aug. 1991 13 p Presented at the Optical Applied Science and Engineering Conference, San Diego, CA, 21-26 Jul. 1991 Sponsored by Ministry of Defence
(PNR-90918; ETN-92-92206) Copyright Avail: CASI HC A03/MF A01

Data extraction from high resolution moire interferometry was automated using the technique of phase stepping fringe analysis. The hardware and software systems of phase stepping moire interferometry are described. Test measurements are gathered expediently and with high accuracy so that detailed distortion and strain distributions can be determined. Illustrative examples that demonstrate the techniques accuracy for both displacement and strain are given: numerical super moire; tensile loaded specimen; and composite plate with a 'hole'. It is shown that the combination of moire interferometry and phase stepping fringe analysis gives accurate and detailed data from experimental studies. The displacement maps are of high spatial resolution and low enough noise to enable direct numerical differentiation in order to determine the surface in plane strain components. ESA

N93-11022# Rolls-Royce Ltd., Derby (England).
FRINGE ANALYSIS OF IN-PLANE DISPLACEMENTS ON HIGH SPEED ROTATING COMPONENTS
Richard W. T. Preater and Robin C. Swain 1 Aug. 1991 13 p Presented at the Optical Applied Science and Engineering Conference, San Diego, CA, 21-26 Jul. 1991 Sponsored by Science Research Council
(PNR-90920; ETN-92-92208) Copyright Avail: CASI HC A03/MF A01

Application of the two dimensional Fourier transform method of fringe analysis to electronic speckle pattern interferometric fringes produced from a specimen in high speed rotation is presented. In order to obtain correlated speckle patterns from the specimen in high speed rotation, a Q switched pulsed laser was used and the illumination delivered precisely so that the same portion of the component was illuminated each time the laser was fired. Some of the problems arising from the shape of the fringes and method of analysis are disussed. The removal of tilt from the phase, windowing, and phase unwrapping are addressed. The resulting phasemaps are relatively smooth due to the use of compact windows when filtering. ESA

N93-11080# General Physics Corp., Cape Canaveral AFS, FL.
PRESSURE VESSEL BURST TEST PROGRAM Progress Report No. 3
Maurice R. Cain, Douglas E. Sharp, and Michael D. Coleman 25 Jul. 1992 12 p Presented at the 28th AIAA/SAE/ASME/ASEE Joint Propulsion Conference and Exhibit, Nashville, TN, 6-8 Jul. 1992 LIMITED REPRODUCIBILITY: Availability: Document partially illegible
(AD-A253708; Rept-45SPW-TR-92-1; AIAA Paper 92-3608)
Avail: CASI HC A03/MF A01

Since the initial paper, additional pressure vessels have been burst using pneumatic pressure. Tests were designed to explore burst characteristics and used a well-instrumentated arena. Data trends for current experiments are presented. This paper is the third progress report on the program and addresses: (1) a brief review of current methods for assessing vessel safety and burst parameters; (2) a review of pneumatic burst testing operations and testing results, including a comparison to current methods for burst assessment; and (3) a review of the basis for the current test program including planned testing. GRA

N93-11158# Centro Italiano Ricerche Aerospaziali, Naples.
NUMERICAL AND EXPERIMENTAL RESULTS IN VIBROACOUSTICAL ACTIVE CONTROL OF STRUCTURAL ELEMENTS WITH PIEZOELECTRIC MATERIALS
Leonardo Lecce (Naples Univ., Italy), Antonio Concilio, and Saverio F. DelGatto 8 Nov. 1991 13 p Presented at the Workshop on Smart Materials and Structures, Aachen, Fed. Republic of

Germany, 3-6 Jun. 1991
(DILC-EST-TN-224; ETN-92-92411) Avail: CASI HC A03/MF A01

Results of an ongoing research on the noise and vibration control inside an aircraft cabin, with active control systems using piezoelectric sensors and actuators, are presented. Available analytical models, able to predict the piezoelectric actuators action upon simple structural elements, were extended to typical structures of the fuselage, like panels and frames. Some numerical models (finite element method) were developed where it was possible to treat the vibration and vibroacoustic phenomena of the complete structure control system. Experimental results are reported, in order to validate the numerical and analytical models and to obtain an evaluation of the capability of this approach. The results are encouraging and show an increasing interest for the development of such systems. ESA

N93-11175*# Virginia Univ., Charlottesville.
MICROMECHANICS OF METAL MATRIX COMPOSITES USING THE GENERALIZED METHOD OF CELLS MODEL (GMC) USER'S GUIDE Final Report
Jacob Aboudi and Marek-Jerzy Pindera Oct. 1992 46 p
(RTOP 510-01-50)
(NASA-CR-190756; E-7354; NAS 1.26:190756) Avail: CASI HC A03/MF A01

A user's guide for the program gmc.f is presented. The program is based on the generalized method of cells model (GMC) which is capable via a micromechanical analysis, of predicting the overall, inelastic behavior of unidirectional, multi-phase composites from the knowledge of the properties of the viscoplastic constituents. In particular, the program is sufficiently general to predict the response of unidirectional composites having variable fiber shapes and arrays. Author

N93-11200 Maine Univ., Orono.
NONLINEAR RESPONSE OF THIN STEEL PLATE STRUCTURES SUBJECTED TO STATIC, CYCLIC, AND DYNAMIC LOADS Ph.D. Thesis
Changqing Du 1991 325 p
Avail: Univ. Microfilms Order No. DA9128624

In steel plate structures where the plate panels are supported along their boundaries, the plate exhibits post-buckling strength. There is a need to investigate the post-buckling behavior of thin steel plate panels subjected to monotonic and cyclic loads. Following previous research in this field and recent experimental work, the study reported herein presents a theoretical approach to the problem, which gives a better understanding of the post-buckling behavior of steel plate shear walls under monotonic and cyclic loads. A nonlinear finite element program was developed to predict the post-buckling behavior and ultimate strength of steel plate structures subjected to in-plane loads. Using the nonlinear program, several problems dealing with the post-buckling strength of thin plates subjected to in-plane loads were analyzed. The results from the finite element analysis and the results from tests and/or semi-empirical formulas were compared. A truss member with tri-linear stress-strain relationship to be used in an analytical model for thin steel plate shear walls was developed. Using this model, parametric studies were undertaken for thin steel plate shear walls. Another analytical model was developed to predict the hysteretic behavior of the steel plate shear wall under cyclic loads. Good agreement was obtained between the results from the analytical model and tests conducted at the University of Maine. The hysteretic analytical model was applied to analyze a steel plate shear wall building subjected to static wind loads and earthquake ground acceleration. A ten story building with steel plate shear walls located at the core of the building was considered. This application of the analytical strip model demonstrated that this model makes the computation of the earthquake nonlinear response of a complex steel plate shear wall building possible. More studies on the behavior of buildings with thin steel plate walls subjected to earthquakes are required. Dissert. Abstr.

N93-11202 Texas Univ., Austin.
ON THE STABILITY OF CONFINED SHELLS UNDER EXTERNAL PRESSURE Ph.D. Thesis
Fengshou Li 1991 173 p
Avail: Univ. Microfilms Order No. DA9128287

In a number of practical problems, long cylindrical shells are lined with a thin, contacting inner liner shell. For example, many pipelines are lined with a stainless steel liner to protect them from caustic contents. Many tunnels and ducts are lined with a steel liner to seal them. In many cases such structures must withstand significant external pressure. Pressurizing fluid often penetrates the outer shell and collapses the liner. Under some circumstances the collapse, which is initially confined to a short length of the structure, can propagate with much more catastrophic consequences. This dissertation addresses the conditions under which collapse can occur and the condition under which a buckle will propagate. Of particular interest is the influence of the outer shell on both collapse phenomena. The approach followed involves the numerical solution of the response of two concentric, smoothly contacting rings (long shells) under external pressure. The inner ring is assumed to have a small initial geometric imperfection which is also loaded with external pressure. As the pressure is increased, the two rings deform and detach from each other over a varying length. The prebuckling and large deflection postbuckling equilibrium states are obtained through a specially developed numerical solution procedure. Linearly elastic and elastic-plastic material models are considered. The composite structure was found to exhibit a limit load instability. The sensitivity of this limit load was studied parametrically. The complete response of this two-dimensional problem is used in an energy balance type of analysis to obtain the confined buckle propagation pressure in confined elastic shells. The predicted results are in good agreement with the experiment. The cross-over pressure of the slip-on buckle arrestor is studied through an idealized model based on the two-dimensional solution. The results are in reasonably good agreement with experiment for relatively longer arrestors. Dissert. Abstr.

N93-11219# California Inst. of Tech., Pasadena. Graduate Aeronautical Labs.
ON THE DEPENDENCE OF THE DYNAMIC CRACK TIP TEMPERATURE FIELDS IN METAL UPON CRACK TIP VELOCITY AND MATERIAL PARAMETERS
James J. Mason and Ares J. Rosakis 1992 29 p
(Contract N00014-90-J-1340)
(AD-A253657; GALCIT-SM-92-3) Avail: CASI HC A03/MF A01

Although various approximations have been used to analytically predict the temperature rise at a dynamic crack tip and its relation to the crack tip velocity or the material properties, few experimental investigations of these effects exist. Here, the method of using a high speed infrared detector array to measure the temperature distribution at the tip of a dynamically propagating crack tip is outlined, and the results from a number of experiments on different metal alloys are reviewed. First the effect of crack tip velocity is reviewed, and it is seen that the maximum temperature increases with increasing velocity and that a significant change in the geometry of the temperature distribution occurs at higher velocities in steel due to the opening of the crack faces behind the crack tip. Next, the effect of thermal properties is examined, and it is seen that, due to adiabatic conditions at the crack tip, changes in thermal conductivity do not significantly affect the temperature field. Changes in density and heat capacity are more likely to produce significant differences in temperature than changes in thermal conductivity. Finally, the effect of heat upon the crack tip deformation is reviewed, and it is seen that the generation of heat at the crack tip in steel leads to the formation of a shear band at 45 deg to the surface of the specimen. In titanium, no conclusive evidence of shear band formation is seen. GRA

N93-11369# Royal Aircraft Establishment, Farnborough (England).
FATIGUE CRACK CLOSURE: A REVIEW

R. M. J. Kemp 25 Sep. 1990 68 p
(RAE-TR-90046; ICAF-1776; BR300216) Copyright Avail: CASI HC A04/MF A01

The phenomenon of fatigue crack closure is now recognized as one of the most influential mechanisms operating during fatigue. This literature survey traces the development of research into fatigue crack closure and has been divided to present the two major approaches. The first part covers early work carried out between 1970 to 1980 which, broadly speaking, adopted a 'continuum' approach. The second part covers the period 1980 to 1988 when a mechanistic approach was widely adopted. The survey has highlighted, firstly, the critical nature of experimental technique in the achievement of a meaningful measurement of crack closure load and secondly, that a diversity of mechanisms may operate to produce closure. Particular attention has been given to crack closure in aluminum alloys and also to work relating crack closure to the corrosion fatigue situation. Author

N93-11372 Cincinnati Univ., OH.

COMPUTATION OF SINGLE SOLID PARTICLE IMPACT ON THE TARGET OF DUCTILE MATERIAL TO STUDY THE REBOUND CHARACTERISTICS OF PARTICLE Ph.D. Thesis

Jian Jong Yeuan 1992 181 p
Avail: Univ. Microfilms Order No. DA9223999

The objective of this research work is to simulate a single solid particle impact on a solid target using elastic-plastic theory. The entire impact process involves the adhesion, deformation and rebound process interacting between the solid particle and the target. The governing equations for two dimensional elastic-plastic flow are formulated in Lagrangian coordinates. The equation of state in the elastic region is the time rate of change of Hooke's law. In the plastic region, the experimental Hugoniot equation of state and the yield condition of R. von Mises are used. The effect of strain rate on the material strength is considered using a semi-empirical formulation. The developed computer program employs a finite volume numerical technique and two step explicit MacCormack scheme, which is second order accurate in time, allowing finer resolution of the transient phenomena of impact. Results are presented for a hard tool steel particle impacting on a mild steel target at impact angles of 20 to 90 degrees. The computational results are compared with experimental data for a range of impacting velocities up to 350 m/sec. The effect of particle in the particle rebound characteristics are also investigated. In the previous research, the particle rebound characteristics obtained from experiments were correlated and used in the calculation of particle trajectories in turbomachinery flows. Here, the computational results are applied to predict solid particle trajectories in a highly loaded axial flow turbine. Dissert. Abstr.

N93-11403*# National Aeronautics and Space Administration. Lewis Research Center, Cleveland, OH.

APPLICATION OF ARTIFICIAL NEURAL NETWORKS IN NONLINEAR ANALYSIS OF TRUSSES

J. Alam (Youngstown State Univ., OH.) and L. Berke Nov. 1991 37 p
(RTOP 307-50-00)
(NASA-TM-105319; E-6676; NAS 1.15:105319) Avail: CASI HC A03/MF A01

A method is developed to incorporate neural network model based upon the Backpropagation algorithm for material response into nonlinear elastic truss analysis using the initial stiffness method. Different network configurations are developed to assess the accuracy of neural network modeling of nonlinear material response. In addition to this, a scheme based upon linear interpolation for material data, is also implemented for comparison purposes. It is found that neural network approach can yield very accurate results if used with care. For the type of problems under consideration, it offers a viable alternative to other material modeling methods. Author

N93-11544*# National Aeronautics and Space Administration. Langley Research Center, Hampton, VA.

RIGID BODY MODE IDENTIFICATION OF THE PAH-2 HELICOPTER USING THE EIGENSYSTEM REALIZATION ALGORITHM

Axel Schenk (Deutsche Forschungsanstalt fuer Luft- und Raumfahrt, Goettingen, Germany) and Richard S. Pappa Oct. 1992 52 p
(RTOP 590-14-61-01)
(NASA-TM-107690; NAS 1.15:107690; DLR-IB-232-91/J07)
Avail: CASI HC A04/MF A01

The rigid body modes of the PAH-2 'Tiger' helicopter were identified using the Eigensystem Realization Algorithm (ERA). This work complements ground vibration tests performed using DLR's traditional phase resonance technique and the ISSPA (Identification of Structural System Parameters) method. Rigid body modal parameters are important for ground resonance prediction. Time-domain data for ERA were obtained by inverse Fourier transformation of frequency response functions measured with stepped-sine excitation. Mode purity (based on the Phase Resonance Criterion) was generally equal to or greater than corresponding results obtained in the ground vibration tests. All identified natural frequencies and mode shapes correlate well with corresponding ground vibration test results. The modal identification approach discussed in this report has become increasingly attractive in recent years due to the steadily declining cost and increased performance of scientific computers. As illustrated in this application, modern time-domain methods can be successfully applied to data acquired using DLR's existing test equipment. Some suggestions are made for future applications of time domain modal identification in this manner. Author

N93-11579# Ecole Centrale de Lyon (France). Lab. de Mecanique des Solides.

CRUSHING BEHAVIOR OF TUBULAR STRUCTURES IN MULTI-MATERIALS Ph.D. Thesis [COMPORTEMENT A L'ECRASEMENT DE STRUCTURES TUBULAIRES EN MULTI-MATERIAUX]

Xuguang Wang 1991 143 p In FRENCH
(ECL-91-37; ETN-92-92340) Avail: CASI HC A07/MF A02

Work to improve the crushing behavior of tubular structures in order to optimize a structure to absorb the impact energy is presented. The influence of external reinforcement by a composite material on the crushing behavior of metallic tubular structures is studied. It is shown that external reinforcement improves their crush strength. The major role of composite reinforcement is to guide and to constrain the metal tubes to deform in a manner favorable for dissipating energy. The problem of plastic deformation of circular tubes subjected to axial compressive loads is examined. For axisymmetric mode, a realistic model is proposed, which takes into account the extensibility of the shell in both axial and circumferential directions, and also the internal flexion of the wall. For nonaxisymmetric mode, a model with moving hinges is studied. It is shown that the 'minimum principle' can generally result in good estimates of mean crushing force. However, in some cases it can result in poor estimation of the geometrical parameters which describe the deformation process. Only the quasi-static crushing behavior of multi-material tubular structures is examined. ESA

N93-11582# Ecole Centrale de Lyon (France). Lab. de Mecanique des Solides.

DESCRIPTION OF THE STRUCTURAL RESPONSES IN THE MEDIUM-FREQUENCY RANGE BY AN ENERGETIC FORMULATION Ph.D. Thesis [DESCRIPTION DES REPONSES STRUCTURALES DANS LE DOMAINE DES MOYENNES FREQUENCES A L'AIDE D'UNE FORMULATION ENERGETIQUE]

Yuskar Lase 1992 216 p In FRENCH
(ECL-92-16; ETN-92-92343) Avail: CASI HC A10/MF A03

A method based on an energetic formulation of the dynamical behavior of structure in the medium frequency range, at which the finite element method is no longer practical, is presented.

The spatial variation of energy within each subsystem is analyzed. By introducing active and reactive power flows, and the total energy and Lagrangian densities, the modal and propagation characteristics of a structure are obtained. The energetic formulation is derived from an equation of motion of second order, and a system of differential equations governing the spatial evolution of the total energy and Lagrangian densities is obtained. In the case of flexural vibrations, the equations describe progressive waves, evanescent waves, and coupling terms. By applying a spatial average over a wave length and using the far field hypothesis, this system of equations is simplified to a differential equation of second order. A procedure using a simplified energetic formulation is presented to estimate the transfer functions. The rod, beam, membrane and plate are considered. Examples to illustrate the efficiency and advantages of the present method are presented. ESA

N93-11624*# National Aeronautics and Space Administration. Lewis Research Center, Cleveland, OH.

DESIGN OF A HIGH-TEMPERATURE EXPERIMENT FOR EVALUATING ADVANCED STRUCTURAL MATERIALS

Theodore T. Mockler, Mario Castro-Cedeno, Herbert J. Gladden, and Albert Kaufman (Analex Corp., Brook Park, OH.) Aug. 1992 35 p Original contains color illustrations
(RTOP 510-01-50)
(NASA-TM-105833; E-6287; NAS 1.15:105833) Avail: CASI HC A03/MF A01; 16 functional color pages

This report describes the design of an experiment for evaluating monolithic and composite material specimens in a high-temperature environment and subject to big thermal gradients. The material specimens will be exposed to aerothermal loads that correspond to thermally similar engine operating conditions. Materials evaluated in this study were monolithic nickel alloys and silicon carbide. In addition, composites such as tungsten/copper were evaluated. A facility to provide the test environment has been assembled in the Engine Research Building at the Lewis Research Center. The test section of the facility will permit both regular and Schlieren photography, thermal imaging, and laser Doppler anemometry. The test environment will be products of hydrogen-air combustion at temperatures from about 1200 F to as high as 4000 F. The test chamber pressure will vary up to 60 psia, and the free-stream flow velocity can reach Mach 0.9. The data collected will be used to validate thermal and stress analysis models of the specimen. This process of modeling, testing, and validation is expected to yield enhancements to existing analysis tools and techniques. Author

N93-11707# Oxford Univ. (England). Dept. of Engineering Science.

TIME-FREQUENCY DOMAIN ANALYSIS OF VIBRATION SIGNALS FOR MACHINERY DIAGNOSTICS. 3: THE PRESENT POWER SPECTRAL DENSITY

W. J. Wang and P. D. McFadden 1992 41 p Sponsored by Science Research Council
(OUEL-1911/92; ETN-92-92063) Avail: CASI HC A03/MF A01

The Present Power Spectral Density (PPSD), also referred to as the local power spectral density, is defined and its application to the calculation of the time frequency distribution of a nonstationary signal is examined. The PPSD distribution represents the energy distribution of the signal over the frequency domain at every instant of time. It can correctly reveal the presence of local changes in the signal, and avoids the disadvantages arising from the nonlinearity which is inherent in the Wigner-Ville distribution. The selection of the local emphasizing function is discussed, and it is shown that the Gaussian function is well suited to the calculation of the PPSD, giving a distribution which is free from ripple and easy to interpret. The application of the PPSD is demonstrated using numerically generated test signals and experimentally measured time domain averages of the gear meshing vibration from industrial and helicopter gearboxes. The results show that the PPSD provides a powerful tool for the early detection of local gear damage. ESA

N93-11713 California Univ., Berkeley.

SOME EXACT SOLUTIONS OF THE EQUATIONS OF FINITE ELASTICITY Ph.D. Thesis

Jeremiah Gerard Murphy 1990 150 p
Avail: Univ. Microfilms Order No. DA9126716

Finite deformations of special, compressible, elastic materials are considered. Attention is restricted to elastic materials having the following separable form of the strain energy function: W = f(i(sub 1)) + g(i(sub 2)) + h(i(sub 3)), where f, g, and h are twice continuously differentiable functions of the appropriate principal invariant of the stretch tensor. Three special cases are then considered; for each class, two of the functions f, g, and h are linear functions and the third is an arbitrary function. The effect of several constitutive restrictions on the form of the strain energy functions of the materials will be examined. Controllable deformations have a form which is independent of the specific form of the strain energy function. Necessary and sufficient conditions for a deformation to be controllable for each of the materials described above will be obtained and then used to show that azimuthal shearing deformation is controllable for these materials. Qualitative features of such azimuthal shearing are then studied. Spherical and cylindrical expansion deformations are also controllable for the materials of interest and the qualitative features of these deformations for the so-called materials of type 2 will be considered. The steady rotation of a cylinder or tube and the eversion of both cylindrical and spherical shells are not controllable deformations for all three types of elastic material. However, for some of the representative materials chosen, a number of closed form solutions to the equations of equilibrium or motion, as the case may be, will be obtained which describe the above-mentioned deformations. These solutions provide the basis for the discussion of the qualitative features of such deformations for compressible materials. Dissert. Abstr.

N93-11721 Michigan Technological Univ., Houghton.

CRASHWORTHY CHARACTERISTICS OF CIRCULAR TUBES IN AXISYMMETRIC BUCKLING Ph.D. Thesis

Yong-Bin Yuan 1991 244 p
Avail: Univ. Microfilms Order No. DA9220733

The crashworthy behavior of circular tubes in axisymmetric buckling is examined. After a literature review, the problems with the previous work in this area are identified. DOM steel tubes with various thickness to diameter ratios are tested to deepen the understanding of their crushing behavior. Based on experimental observations, kinematic models are established for the first and subsequent cycles of axisymmetric collapse. The models are more general and realistic than the models previously proposed by several other authors. The models are theoretically analyzed and half buckling wave length is determined by minimizing the initial buckling load, instead of mean crush load. Various characteristics associated with the crushing process are studied such as the ultimate crush load, peak crust load, crush load fluctuation, effective crushing distance, and specific energy. The predicted results for these parameters are compared with experimental data, and other authors' predictions. The effect of friction between the tube and the supporting platens on the crushing behavior is theoretically studied. It is found that the end-condition influence the folding configuration and crush load history. Dissert. Abstr.

N93-11775# Lawrence Livermore National Lab., CA.

SOME REMARKS ON SHELL ELEMENT ANALYSIS WITH DYNA3D AND NIKE3D

R. G. Whirley, B. E. Engelmann, B. N. Maker, and T. E. Spelce 24 Mar. 1992 27 p
(Contract W-7405-eng-48)
(DE92-018784; UCRL-ID-110111) Avail: CASI HC A03/MF A01

There has been some confusion in the user community recently regarding the various shell element formulations now available in DYNA3D (Whirley and Hallquist, 1991) and NIKE3D (Maker, Ferencz, and Hallquist, 1991). In particular, questions have been raised about the behavior of these elements under large strain, and the display of meaningful results from such problems using

TAURUS (Spelce and Hallquist, 1991). This brief report is intended to aid the DYNA/NIKE user community by elaborating on the formulation of the DYNA3D/NIKE3D shell elements and on the display of shell data using TAURUS. In the following discussion no attempt is made to give a complete description of the theoretical development or implementation of any of the elements. Readers interested in a more complete discussion of the shell elements in DYNA3D and NIKE3D are directed to the published papers cited in the code User Manuals. DOE

N93-11792# Oak Ridge National Lab., TN.
REPEATABLE SENSITIVITY OF OPTICAL-TIME-DOMAIN-REFLECTOMETRY-BASED STRAIN MEASUREMENT
S. W. Kercel and J. D. Muhs 1992 15 p Presented at the SPIE International Symposium on Optical Applied Science and Engineering, San Diego, CA, 19-24 Jul. 1992
(Contract DE-AC05-84OR-21400)
(DE92-016910; CONF-920792-6) Avail: CASI HC A03/MF A01

Optical time-domain reflectometry (OTDR) is a simple and rugged technique for measuring quantities, such as strain, that affect the propagation of light in an optical fiber. For engineering applications of OTDR, it is important to know the repeatable limits of its performance. The authors constructed an OTDR-based, submillimeter resolution, strain measurement system from off-the-shelf components. The system repeatably resolves changes in time of flight to within +/- 2 ps. Using a 1 m, single-mode fiber as a gauge and observing the time of flight between Fresnel reflections, we observed a repeatable sensitivity of 400 microstrains. Using the same fiber to connect the legs of a 3 dB directional coupler to form a loop, we observed a repeatable sensitivity of 200 microstrains. Realizable changes to the system that should improve the repeatable sensitivity to 20 microstrains or less are discussed. DOE

N93-11890 Polytechnic Univ., Brooklyn, NY.
ELASTIC STRESSES, TWIN BOUNDARIES, AND FATIGUE CRACKING Ph.D. Thesis
Periya Gopalan 1991 254 p
Avail: Univ. Microfilms Order No. DA9129366

Prior finite element method (FEM) calculations had shown that high cycle fatigue cracks would start at twin boundaries, when the stress axis made an angle other than 90 deg to the twin boundaries, because elastic interactions would produce highest stresses there. This investigation was undertaken to test this idea. Finite element method analysis was carried out for twin orientations of 70-30 alpha-brass to determine the stress distribution in the vicinity of the boundary. The stresses were resolved onto twelve possible slip systems. From these data the orientations which develop highest stresses at the boundary, due to elastic interaction, on slip systems parallel to the twin boundary were determined. Three diffusion bonded bicrystals of 70-30 alpha-brass, having a boundary plane at 45 deg to the loading axis, were fatigued at low strain amplitudes. The component crystals were so oriented that Bicrystal 1 produced low elastic interaction stresses and Bicrystal 2 and 3 were of matrix/twin orientations, with highest total stresses on slip systems nearly parallel to the twin boundary. Only for the initial few cycles did Bicrystal 1 reveal no slip bands near the boundary, whereas Bicrystals 2 and 3 produced significant slip bands nearly parallel to the twin boundary at the outset. With repeated cycling, the matrix of Bicrystal 2 also showed a secondary slip band at the boundary where it produced large incompatibility strains and subsequent cracking. Fatigue cracks were initiated along slip band extrusions away from the bicrystal boundary in Bicrystal 1 and along the twin boundary in Bicrystal 2 and 3. For all three bicrystals cracking commenced where the stresses and therefore the strains were highest. Dissert. Abstr.

N93-11891 Iowa Univ., Iowa City.
COMPUTATIONAL DYNAMICS OF HIGH-SPEED FLEXIBLE MULTIBODY SYSTEMS Ph.D. Thesis
Jeha Ryu 1991 168 p
Avail: Univ. Microfilms Order No. DA9217202

Computational methods are developed for dynamic analysis of high speed flexible multibody systems with stress stiffening effects. By adding the nonlinear terms of the strain-displacement relationship to the strain energy of a flexible body, a general method is presented to compute the stress stiffness matrix of an arbitrary flexible body undergoing large gross motion accompanied by small elastic deformations. The theory indentifies stress stiffness resulting from applied and constraint reaction loads as well as from a system of 12 inertial loads distributed throughout the flexible body. This stress stiffness can be preprocessed by a readily available finite element analysis program for general structures. System equations of motion that include the stress stiffening terms are derived by a recursive algorithm without elimination. Relative joint and deformation modal coordinates are used to describe gross body motion and elastic deformation, respectively. An iterative method is represented to solve the resultant system equations of motion. Numerical results show that stress stiffening effects are important in mechanical systems with high flexibility and/or with high speed operation. In order to determine whether a flexible multibody system reveals stress stiffening effects or not in a given operational evironment, a direct and practical criterion based on the examination of the variation of the first eigenvalue of the total modal stiffness matrix is also presented. An efficient hybrid method is presented for more accurate prediction of dynamic solutions. The hybrid method employs stress and elastic displacement superposition as a function of inertial and constraint reaction loads predicted by flexible body dynamic simulations. In the hybrid method, the quasi-static equilibrium equations are solved efficiently by an integrated form of distribution of the inertial loads arising gross body motion and elastic deformation of a flexible body. Also, the hybrid method is extended to handle the system in which stress stiffening effects are important. A theoretical explanation is made for the hybrid method in terms of the mode-acceleration method. Numerical examples are presented in order to show the computational procedure. Dissert. Abstr.

N93-11903# Massachusetts Inst. of Tech., Cambridge. Sea Grant Coll. Program.
DEEP PENETRATION INTO FRICTIONAL DUCTILE AND BRITTLE MATERIALS
Fu Shu Jeng, H. H. Einstein, A. J. Whittle, and J. T. Germaine 1992 350 p
(Grant NA86AA-D-SG089; NOAA Project RO-33)
(PB92-205566; MITSG-92-7) Avail: CASI HC A15/MF A03

The mooring of offshore platforms and tension piles may involve deep penetration into rocks. There is, however, a significant lack of the knowledge regarding deep penetration into a rock mass. The research, therefore, was intended to study the phenomena and mechanisms of deep penetration, first through experimentation and then, based on the experimental results, by developing models for frictional, ductile/brittle materials. In the experimental study, rapid and slow penetration tests and pullout tests were performed which involved a systematic variation of the testing conditions including brittleness of the material confining conditions, joint conditions (orientation and spacing), nose shape of penetrator, and penetration velocity. It was found that the brittle material was fractured due to penetration. A crushed zone near the penetrator, chipping at top surface and radial cracking were observed. By measuring the acceleration history in rapid penetration tests, the energy required to achieve a particular penetration depth was obtained. Through comparison with the results of slow penetration tests, it was also possible to assess the effect of penetration rate. GRA

N93-11909 Pennsylvania State Univ., University Park.
SLOW CRACK GROWTH IN VACUUM Ph.D. Thesis
Armando Carlos Gonzalez 1991 135 p
Avail: Univ. Microfilms Order No. DA9127332

The slow crack growth behavior of various glasses and single crystals was examined using a double cantilever beam (DCB) fracture specimen in the absence of environmental effects. Crack growth tests were conducted within a steel vacuum chamber, at total pressures below 3(10)(exp 7) Torr. Crack velocities ranged between 10(exp -9) m/s and 10(exp -3) m/s and were controlled by adjusting the load on the specimen through a micrometer drive. No correlation was found between crystal structure, bonding or any other material property, and crack growth behavior. In general, glasses were more susceptible to crack growth than single crystals, and in calcium fluoride, crack growth susceptibility was linked to the presence of a particular point defect. In soda-lime glass specimens, charged particle and photon emission was monitored during slow crack growth in vacuum using an electron multiplier and photomultiplier. Below a crack velocity of 10(exp -3) m/s no signals were detected. Transient acceleration above this 'threshold' velocity did produce detectable charged particle and photon emission. Overall, signal levels were considerably lower than for fast fracture experiments. These differences are explained in terms of the minimum energy requirements necessary to form a new surface. Electric potentials ranging between 1kV and 2.9kV were applied across cracks in calcium fluoride and soda-lime glass DCB specimens in vacuum. This potential significantly increased the work of fracture by generating an attractive interfacial force across the crack. As this force changes with time, cracks can advance or retreat at a constant applied stress. These results are used to create a model that describes vacuum slow crack growth in terms of a decaying interfacial energy. It is proposed that in some crystals this can occur by point defect motion behind the crack tip, and in glasses through surface reconstructions. It is concluded that for materials which are susceptible to vacuum slow crack growth, K(sub IC), the critical fracture toughness, is not unique but must be defined in terms of the secondary processes that accompany fracture. Dissert. Abstr.

N93-12000 Washington Univ., Seattle.
A CONSISTENT CRACKED BAR VIBRATION THEORY Ph.D. Thesis
Jonathan Yi Yao 1991 197 p
Avail: Univ. Microfilms Order No. DA9223581

The development of a consistent one-dimensional vibration theory of cracked bar and its several applications are presented. Moreover, analytical solutions for the vibration of bars with a bilinear type of breathing crack are presented. A variational theorem is used to derive the governing equations of the longitudinal vibration of cracked bars, the lateral vibration of cracked beams, and the torsional vibration of cracked shafts. To account for the effect of a crack, displacement, strain, and stress disturbance functions are introduced. Results from fracture mechanics are used to determine these disturbance functions. Analytical solutions for longitudinal vibration of bars and lateral vibration of beams with an open crack are obtained. The Rayleigh's quotient method is employed to solve the problem of the torsional vibration of shafts with a circular crack. For the longitudinal vibration bars and the lateral vibration of beams with a breathing crack, the bilinear character of the system and the appropriate initial and continuity conditions are utilized. The dynamic response of the bilinear system is found by using the solutions of the linear system with open crack and of those without crack and imposing appropriate continuity conditions for the transition from open to closed crack. The results found for open crack and breathing crack are compared with the experimental results and the various numerical and analytic results available. The results obtained are in better agreement with the experimental results than those of previous work, especially for large crack depths and higher vibration modes. Dissert. Abstr.

N93-12005*# National Aeronautics and Space Administration. Langley Research Center, Hampton, VA.
STRUCTURAL DESIGN USING EQUILIBRIUM PROGRAMMING
Stephen J. Scotti Oct. 1992 20 p Presented at the 33rd AIAA/ASME/ASCE/AHS/ASC Structures, Structural Dynamics, and Materials Conference, Dallas, TX, 13-15 Apr. 1992
(RTOP 506-43-71-04)
(NASA-TM-107593; NAS 1.15:107593) Avail: CASI HC A03/MF A01

Multiple nonlinear programming methods are combined in the method of equilibrium programming. Equilibrium programming theory has been appied to problems in operations research, and in the present study it is investigated as a framework to solve structural design problems. Several existing formal methods for structural optimization are shown to actually be equilibrium programming methods. Additionally, the equilibrium programming framework is utilized to develop a new structural design method. Selected computational results are presented to demonstrate the methods. Author

N93-12008 Virginia Polytechnic Inst. and State Univ., Blacksburg.
THERMAL FRACTURE SERVICE LIFE ANALYSIS OF A CASE BONDED VISCO-ELASTIC CYLINDER Ph.D. Thesis
Hossein Rahemi 1992 182 p
Avail: Univ. Microfilms Order No. DA9223464

Environmental temperature changes produce cyclic thermal stresses in structures. Because temperature and hence thermal stresses are random and mechanical properties such as strength, relaxation, modulus, and fracture toughness are time and temperature dependent as well as statistically variable quantities in rocket motor grains, crack growth will also be random. To include all these effects, the Forman crack growth rate relation will be used. The probability of failure, defined as the change that a crack growing under the influence of such stresses exceeds the critical crack length, is calculated. A hazard function will be defined as the probability of failure during a single cycle after the cylinder has survived N previous cycles. The hazard function will then be integrated to yield the progressively increasing probability of fracture. The stress distribution through the cylindrical wall is not uniform; as a result, a step by step finite element analysis will be carried out to determine stress intensity and critical crack size as the crack travels through the varying stress field. The probability of failure is conditioned on the chance that a crack exists. Dissert. Abstr.

N93-12020*# National Aeronautics and Space Administration. Langley Research Center, Hampton, VA.
DECENTRALIZED CONTROL OF LARGE FLEXIBLE STRUCTURES BY JOINT DECOUPLING
Tzu-Jeng Su and Jer-Nan Juang Oct. 1992 31 p
(RTOP 469-01-11-02)
(NASA-TM-107694; NAS 1.15:107694) Avail: CASI HC A03/MF A01

A decentralized control design method is presented for large complex flexible structures by using the idea of joint decoupling. The derivation is based on a coupled substructure state-space model, which is obtained from enforcing conditions of interface compatibility and equilibrium to the substructure state-space models. It is shown that by restricting the control law to be localized state feedback and by setting the joint actuator input commands to decouple joint 'degrees of freedom' (dof) from interior dof, the global structure control design problem can be decomposed into several substructure control design problems. The substructure control gains and substructure observers are designed based on modified substructure state-space models. The controllers produced by the proposed method can operate successfully at the individual substructure level as well as at the global structure level. Therefore, not only control design but also control implementation is decentralized. Stability and performance requirement of the closed-loop system can be achieved by using any existing state feedback control design method. A two-component mass-spring damper system and a three-truss structure are used as examples to demonstrate the proposed method. Author

N93-12194 Kansas Univ., Lawrence.
LINEAR AND GEOMETRICALLY NONLINEAR p-VERSION THREE DIMENSIONAL CURVED SHELL ELEMENT FOR ISOTROPIC, GENERALLY ORTHOTROPIC AND LAMINATED COMPOSITE MATERIALS Ph.D. Thesis
Robert Michael Sorem 1991 301 p
Avail: Univ. Microfilms Order No. DA9210119

A completely hierarchical p-version nine-node curved shell element is developed for isotropic, orthotropic, and laminated composite material behavior for both linear static and geometrically nonlinear analysis. The element approximation functions and the corresponding nodal variables are derived directly from the Lagrange family of three dimensional solid elements. This is accomplished by first establishing one dimensional hierarchical approximations and the corresponding nodal variable operators in the xi, eta, and zeta directions (xi, eta, and zeta are between -1 and 1) for p(xi) + 1, p(eta) + 1, and p(zeta) + 1 equally spaced nodes using Lagrange interpolation functions and then taking their products (also known as tensor product). The resulting element displacement approximation is completely hierarchical and is of arbitrary polynomial order p(xi), p(eta), and p(zeta) in the xi, eta , and zeta directions. The element geometry is described by the coordinates of the nodes located at the middle surface (zeta = 0) of the element and the nodal vectors. Retaining true derivatives of phi (i.e., derivatives with respect to gamma instead of zeta) enables modeling of junctions that may exhibit step changes in the shell thickness without loss of C(exp 0) continuity. The element provides variable higher-order transverse shear effects which can be controlled through the p-level. Since the nodal vectors do not necessarily have to be normal to the middle surface of the shell, the element formulation permits non-differentiable geometries (sharp junctions) in modeling. The simplicity of the p-version models and therefore, economy in modeling resulting from the use of these elements when compared with h-models is quite obvious even from the relatively simple geometries used in this study. All numerical examples presented show good convergence of the quadratic functional, displacements, and stresses as the p-level is increased. The quadratic functional converges monotonically; whereas, the convergence of the displacements and the stresses is not necessarily monotonic. The hierarchical nature of the formulation yields a computationally efficient system at the element level as well as assembly and solution level. Computational effort devoted to lower p-levels need not be repeated when computations are performed for higher p-levels. Dissert. Abstr.

N93-12199 Illinois Univ., Chicago.

THE GENERALIZED GOURSAT-RIEMANN PROBLEM FOR PLANE WAVES IN ISOTROPIC ELASTIC SOLIDS Ph.D. Thesis

Tankin Wang 1992 111 p
Avail: Univ. Microfilms Order No. DA9226277

The generalized Goursat-Riemann problem for plane waves propagating in an isotropic elastic half space with constant initial and non-constant boundary conditions (which is distinct from the Goursat-Riemann problem for which the initial and boundary conditions are constant) is investigated. Since both the generalized and the basic Goursat-Riemann problems possess an essential singularity from applying different initial and boundary conditions, we restrict our solution of the generalized Goursat-Riemann problem to an infinitesimal time span near t = 0 and analyze it by a temporal perturbation method. By the temporal perturbation of the solutions to the generalized Goursat-Riemann problem near t = 0, we are able to evaluate the deviation of the wave curves from the solution of the Goursat-Riemann problem as well as the curvature of the wave fronts in various wave patterns. Four basic wave patterns were found to be of importance for which the initial and final stress states are on (1) the fast simple wave curve, (2) the slow simple wave curve, (3) the fast shock wave curve, and on (4) the slow shock wave curve. Our analysis shows that the geometry of the stress path and the curvilinear wave fronts depend on the impact at the boundary and the partition of the stress space. In particular, the wave fronts are straight lines and the stress in a region between the wave fronts is constant if the impact at the boundary is pointed in either the fixed direction or clockwise in the theta* direction from the eigenvector of the fast simple wave; otherwise the wave front is curvilinear. We have shown that the simple waves, the shock waves, and the interaction of non-linear waves are basic wave structures in the generalized Goursat-Riemann problem subject to constant initial and non-constant boundary conditions. We elaborated on the behavior of these wave structures in our solution and paved the way toward solving a more general set of combined non-constant initial and boundary value problems for non-linear wave propagation in an isotropic elastic medium. Dissert. Abstr.

N93-12200 Texas Univ., Austin.

A GAME THEORETIC APPROACH TO LINEAR DYNAMIC ESTIMATION Ph.D. Thesis

Ravi N. Banavar 1992 114 p
Avail: Univ. Microfilms Order No. DA9225515

The state estimation problem of a linear dynamic system, in a deterministic as well as a stochastic framework, is addressed. In the deterministic scenario, the disturbances are assumed as finite energy processes of an unknown spectrum. The measure of performance is in the form of a disturbance attenuation function and resembles an induced norm. An optimal estimate bounds the attenuation function from above. The disturbance attenuation function is converted to a performance measure for a zero-sum linear-quadratic (LQ) game and the exogenous inputs--the disturbances and the initial state--are viewed as adversaries to the estimator. Adopting a variational procedure, optimal strategies of each player in the game are determined. These optimal strategies are shown to satisfy a saddle point condition. Satisfaction of the saddle inequality helps establish the bound on the disturbance attenuation function. The optimal estimator, restricted to a class of functions of the measurement alone, is both unbiased and linear in structure. With a few mild assumptions, the results are extended to a linear time-invariant system on an infinite horizon and the optimal estimator obtained is shown to impose an upper bound on the H-infinity norm. The discrete time version of the problem follows in a similar vein as the continuous case. In the stochastic framework, the disturbances are assumed to be white Gaussian processes and the measure of performance chosen is the expected value of an exponential function of the estimation error. If the statistical parameters are viewed as deterministic weighting functions in the attenuation function, the optimal statistical estimator obtained by minimizing the exponential cost is identical to the deterministic estimator. The worst-case (H-infinity) deterministic design is thus lent a stochastic interpretation. Further, the structure of the optimal stochastic estimator is shown to be non-unique. This non-uniqueness also helps to establish the Kalman filter (H2) and the Worst-case (H-infinity) filter as two optimal filter structures for the same LQ game problem that result in identical saddle values. Dissert. Abstr.

N93-12210 Texas A&M Univ., College Station.

FOURIER CONTINUUM FINITE ELEMENTS FOR NONLINEAR STRUCTURAL ANALYSIS Ph.D. Thesis

Kent Thomas Danielson 1991 130 p
Avail: Univ. Microfilms Order No. DA9216914

The effectiveness of using Fourier series for the continuum analysis of axisymmetric structures undergoing large nonaxisymmetric deformation is evaluated. The plane of axisymmetry is modeled by isoparametric quadrilateral finite elements with the dependence in the circumferential direction determined by a Fourier series. The mathematical equations to perform this procedure were developed and a complete computer program was written to implement the technique. The computer code was used to analyze several structures subjected to different loadings and exhibiting various amounts of geometric nonlinearity. The nonlinearity produces a coupling between harmonics which complicates the technique and increases the computational expense when compared to linear Fourier series analysis. The harmonic coupling was shown to be more pronounced for continuum analyses than seen in previous shell analyses. In addition, a single harmonic load component can significantly stimulate a response for many harmonics. For analyses involving only a few harmonics, the size of the resulting model can be much smaller than it would be if brick elements were to be used. This model reduction can significantly reduce the amount of computational effort needed for analyzing this class of problems. Several different preconditioned indirect solution techniques were also compared to direct solution of the simultaneous equations occurring at each Newton-Raphson iteration. The inverted uncoupled stiffness matrices was used as a preconditioner for various Gauss-Seidel and conjugate gradient iterative techniques. The indirect solvers were shown to be robust and quite efficient when compared to direct inversion of the stiffness matrix. The effectiveness of the indirect solvers are more efficient for analyses involving larger numbers of harmonics. Furthermore, the Fourier series approach provides a very simple and efficient way to conduct adaptive refinement in the circumferential direction. First, an inexpensive nonlinear analysis can be performed using only a few harmonics. Another analysis involving more harmonics can then be performed using the results from the first analysis as a starting point for Newton-Raphson iteration. Since most of the deformation usually occurs in the lower modes, this adaptive technique generally required only a few of the expensive Newton-Raphson iterations involving the larger number of harmonics. However, the nonlinear Fourier series method is still only effective for a moderate number of harmonics. The computer code was also used in an unsuccessful attempt to model solid body contact (e.g., a tire in contact with the road). Futher work is needed to address the mixed boundary condition in the circumferential direction resulting from the contact conditions. Dissert. Abstr.

N93-12253# Air Force Inst. of Tech., Wright-Patterson AFB, OH.

STUDIES IN CONTROL FOR VIBRATION SUPPRESSION OF THE UWAA 20-BAY PLANAR TRUSS M.S. Thesis

Michael J. Shepherd 1991 113 p
(AD-A250193; AFIT/CI/CIA-91-133) Avail: CASI HC A06/MF A02

This thesis is based on research conducted at the newly constructed Aeronautics and Astronautics Control Sciences Laboratory at the University of Washington. The set up of the UWAA 20-bay planar truss is described, and is based upon a similar experimental test bed at the United States Air Force Academy. Validation of existing open loop finite element models of the truss in the cantilevered configuration was conducted for this research. The formulation of non-linear and approximate linear models for the two primary means of structurally-borne actuation, the air jet thrusters and the reaction mass actuators, is also explored. Computer non-linear simulation and experimental testing of classical analog controllers to actively suppress vibration of the planar bending modes of the truss using the air jet thruster and reaction mass actuators independently and jointly for hybrid linear/non-linear actuation is reported in this thesis. The design of an optimal controller for the reaction mass actuators utilizing linear quadratic Gaussian techniques is reported, and includes non-linear simulation of hybrid actuation utilizing the optimal reaction mass actuator controllers and the classical air jet thruster controllers. Recommendations for future study based upon both the hardware implementation and the computer simulation are suggested in the conclusions section of this thesis. GRA

N93-12277*# National Aeronautics and Space Administration. Lewis Research Center, Cleveland, OH.

STOCHASTIC SENSITIVITY MEASURE FOR MISTUNED HIGH-PERFORMANCE TURBINES

Durbha V. Murthy (Toledo Univ., OH.) and Christophe Pierre (Michigan Univ., Ann Arbor.) Aug. 1992 21 p Presented at the Fourth International Symposium on Transport Phenomena and Dynamics of Rotating Machinery, Honolulu, HI, 5-9 Apr. 1992
(Grants NAG3-742; NAG3-1163; RTOP 505-62-21)
(NASA-TM-105821; ICOMP-92-13; E-7252; NAS 1.15:105821)
Avail: CASI HC A03/MF A01

A stochastic measure of sensitivity is developed in order to predict the effects of small random blade mistuning on the dynamic aeroelastic response of turbomachinery blade assemblies. This sensitivity measure is based solely on the nominal system design (i.e., on tuned system information), which makes it extremely easy and inexpensive to calculate. The measure has the potential to become a valuable design tool that will enable designers to evaluate mistuning effects at a preliminary design stage and thus assess the need for a full mistuned rotor analysis. The predictive capability of the sensitivity measure is illustrated by examining the effects of mistuning on the aeroelastic modes of the first stage of the oxidizer turbopump in the Space Shuttle Main Engine. Results from a full analysis mistuned systems confirm that the simple stochastic sensitivity measure predicts consistently the drastic changes due to misturning and the localization of aeroelastic vibration to a few blades. Author

N93-12300*# National Aeronautics and Space Administration. Langley Research Center, Hampton, VA.

DYNAMIC TEST/ANALYSIS CORRELATION USING REDUCED ANALYTICAL MODELS

Paul E. McGowan, A. Filippo Angelucci, and Mehzad Javeed (Lockheed Engineering and Sciences Co., Hampton, VA.) Sep. 1992 13 p Presented at the 33d Structures, Structural Dynamics, and Materials Conference, Dallas, TX, 13-17 Apr. 1992 Previously announced in IAA as A92-34448
(RTOP 590-14-21-01)
(NASA-TM-107671; NAS 1.15:107671) Avail: CASI HC A03/MF A01

Test/analysis correlation is an important aspect of the verification of analysis models which are used to predict on-orbit response characteristics of large space structures. This paper presents results of a study using reduced analysis models for performing dynamic test/analysis correlation. The reduced test-analysis model (TAM) has the same number and orientation of DOF as the test measurements. Two reduction methods, static (Guyan) reduction and the Improved Reduced System (IRS) reduction, are applied to the test/analysis correlation of a laboratory truss structure. Simulated test results and modal test data are used to examine the performance of each method. It is shown that selection of DOF to be retained in the TAM is critical when large structural masses are involved. In addition, the use of modal test results may provide difficulties in TAM accuracy even if a large number of DOF are retained in the TAM. Author

N93-12376# Naval Postgraduate School, Monterey, CA.

NATURAL CONVECTION HEAT TRANSFER STUDIES OF SIMULATED AND ACTUAL ELECTRONIC COMPONENTS USING DIELECTRIC LIQUIDS FOR IMMERSION COOLING M.S. Thesis

Ronald G. Thompson, Jr Jun. 1992 119 p
(AD-A255173) Avail: CASI HC A06/MF A02

Two experimental studies of the natural convection characteristics of heated protrusions immersed in dielectric liquids were conducted. The first study used a three by three array of simulated 20 pin dual-in-line chips which were made from aluminum blocks with foil heaters. The second set of experiments used a three by three array of thermal evaluation devices mounted on an alumina substrate. The devices were 8.9 mm square chips which contained resistors and a type of temperature sensing transistor. Both studies used an insulated Plexiglas enclosure with a top mounted heat exchanger maintained at a constant 10 C. Each array was mounted on a Plexiglas substrate, and spacers were used to vary the horizontal distance from the components to the enclosure wall. Five separate enclosure widths were used, with a maximum spacing of 40 mm. The vertically oriented aluminum blocks were tested with FC-71 and power levels ranging from 0.115 W/chip to 2.9 W/chip. The non-dimensional data obtained was used to develop an empirical correlation which predicts Nusselt number as a function of Rayleigh number and enclosure width. The correlation was accurate to within 4 percent of the array averaged data, and the maximum uncertainty in the Nusselt number was 7.4 percent. GRA

N93-12411*# Virginia Polytechnic Inst. and State Univ., Blacksburg. Engineering Science and Mechanics.

VERIFICATION OF RAIN-FLOW RECONSTRUCTIONS OF A VARIABLE AMPLITUDE LOAD HISTORY M.S. Thesis, 1990 Final Report

John D. Clothiaux and Norman E. Dowling Oct. 1992 107 p
(Grant NAG1-822; RTOP 505-63-50-04)
(NASA-CR-189670; NAS 1.26:189670) Avail: CASI HC A06/MF A02

The suitability of using rain-flow reconstructions as an alternative to an original loading spectrum for component fatigue life testing is investigated. A modified helicopter maneuver history is used for the rain-flow cycle counting and history regenerations. Experimental testing on a notched test specimen over a wide range of loads produces similar lives for the original history and the reconstructions. The test lives also agree with a simplified local strain analysis performed on the specimen utilizing the rain-flow cycle count. The rain-flow reconstruction technique is shown to be a viable test spectrum alternative to storing the complete original load history, especially in saving computer storage space and processing time. A description of the regeneration method, the simplified life prediction analysis, and the experimental methods are included in the investigation. Author

N93-12412*# National Aeronautics and Space Administration. Marshall Space Flight Center, Huntsville, AL.
THE MECHANISM OF BOLT LOADING
H. M. Lee Oct. 1992 14 p
(NASA-TM-108377; NAS 1.15:108377) Avail: CASI HC A03/MF A01

It is shown that the mechanism of bolt loading for preloaded fasteners can be effectively portrayed through simple spring models and some algebraic manipulations. Understanding schematically what is involved in such joints provides insight into the distribution of loads. The developed equations confirm that for both symmetric and nonsymmetric joints the loading plane factor and the stiffness factor directly affect the load seen in preloaded fasteners. The manner in which an external loading is transferred through the joint can be explained as energy dissipated in the various springs of both the abutment and the bolt itself. Author

N93-12419*# National Aeronautics and Space Administration. Marshall Space Flight Center, Huntsville, AL.
SHEAR JOINT CAPABILITY VERSUS BOLT CLEARANCE
H. M. Lee Oct. 1992 22 p
(NASA-TM-108378; NAS 1.15:108378) Avail: CASI HC A03/MF A01

The results of a conservative analysis approach into the determination of shear joint strength capability for typical space-flight hardware as a function of the bolt-hole clearance specified in the design are presented. These joints are comprised of high-strength steel fasteners and abutments constructed of aluminum alloys familiar to the aerospace industry. A general analytical expression was first arrived at which relates bolt-hole clearance to the bolt shear load required to place all joint fasteners into a shear transferring position. Extension of this work allowed the analytical development of joint load capability as a function of the number of fasteners, shear strength of the bolt, bolt-hole clearance, and the desired factor of safety. Analysis results clearly indicate that a typical space-flight hardware joint can withstand significant loading when less than ideal bolt hole clearances are used in the design. Author

N93-12467# Massachusetts Inst. of Tech., Cambridge.
STUDY OF RESIDUAL STRESSES AND MICROCRACKS IN HIGH STRENGTH STEEL WELDMENTS: AN INVESTIGATION OF MICROCRACK FORMATION AND STRESSED GROWTH USING LASER MICROSCOPY M.S. Thesis
Stephen Edward Iwanowicz Jun. 1992 294 p
(AD-A255059) Avail: CASI HC A13/MF A03

The confocal scanning laser microscope (CSLM) allows viewing welds with a resolution to 0.25 microns. The image processor of the CSLM provides effectively infinite depth of field by superposing the in-focus parts of images. Slopes of more than 30 deg do degrade the image, however. Four-point bend tests of bead-on-plate welds on 1 1 mm thick mild steel, HY-100, HSLA-100, and HY-130 were performed to strains of 0 to 0.02 parallel to the weld bead. A longitudinal, single-pass weld bead of E7014 was manually applied to one specimen of each material with shielded metal arc welding. Displacement-load and moment-curvature results were as expected. Images from gold-shadowed replicas studied using the CSLM were recorded both on video tape and photographically. Initial microcracks 1-200 microns long were observed in the weld metal. No microcracks were observed in the HAZ of any material. Slag and oxide layers sometimes interfered with observing the weld metal and adjacent baseplate. Under monotonic loading, cracks widened with little growth and Widmanstatten structures appeared unchanged. Crack-like features, 1.5 microns long were present on the weld and on the HAZ. These features are probably oxide cracks and did not appear to grow when stressed. GRA

N93-12536 Wisconsin Univ., Milwaukee.
CREEP FAILURE IN LINEAR AND NONLINEAR VISCOELASTIC MATERIALS Ph.D. Thesis
Khaled Mahmoud El-Balawy 1992 149 p
Avail: Univ. Microfilms Order No. DA9225205

For high reliability structures and structural components the residual strength must be estimated on the basis of Theoretical Fracture Mechanics. This evaluation procedure, coupled with the NDE, i.e., nondestructive evaluation techniques such as X rays, neutron diffraction and acoustic emission (AE), and other nondestructive methods of inspection, allows one to avoid catastrophic failures due to the metal fatigue, stress corrosion or other time dependent mechanisms leading to deterioration of strength and other pertinent mechanical properties which influence delayed fracture of structural components. Examples of integration of the equation of motion of a preexisting crack contained either in a linear or nonlinear viscoelastic polymer are provided for several crack and load configurations. The double logarithmic representation of the creep compliance function is used for both linear and nonlinear range of material behavior. The influence of stress level on such a log-log representation in the nonlinear range is accounted for through a modified power law of Gordon Williams. Finally, the approach of continuum mechanics is combined with certain micro-structural considerations and used to derive the fundamental relationships between the rate of fracture growth, geometry of the component and the material characteristics of the solid. Dissert. Abstr.

42 GEOSCIENCES (GENERAL)

No abstracts in this category.

43 EARTH RESOURCES AND REMOTE SENSING

Includes remote sensing of earth resources by aircraft and spacecraft; photogrammetry; and aerial photography.

For instrumentation see *35 Instrumentation and Photography.*

N93-11140# Deutsche Forschungsanstalt fuer Luft- und Raumfahrt, Oberpfaffenhofen (Germany). Abt. Fernerkungsanwendungen.
AN EVIDENTIAL REASONING APPROACH TO THE CLASSIFICATION OF SATELLITE IMAGES Thesis - Technische Univ. [EVIDENZBASIERTE KLASSIFIZIERUNG VON SATELLITENBILDDATEN]
Gabriele Lohmann Aug. 1991 107 p
(DLR-FB-91-29; ETN-92-92398) Avail: CASI HC A06/MF A02; DLR, Wissenshaftliches Berichtswesen, VB-PL-DO, Postfach 90 60 58, 5000 Cologne, Fed. Republic of Germany, HC

The state of the art in classification is reviewed. Basic notational conventions from Shafer's theory of evidence are introduced. The concept of sources of evidence is related to the concept of feature spaces. How belief functions can be derived from parametric models is described. The problem of combining evidence via

Dempster's rule and by addition of weights of evidence is addressed. A new algorithm for classifying satellite images is presented. The new algorithm, called EBIS (Evidence Based Interpretation of Satellite Images), is used for ecological mappings. Several parametric models and their corresponding weight functions are described. Some worked examples are presented. The EBIS algorithm does not impose the constraints of traditional classification algorithms and is therefore applicable to a wider range of image data and object classes. In EBIS, a feature space is regarded as a source of evidence in the sense of the Dempster Shafer theory, and methods of evidential reasoning are used for combining evidence stemming from several disparate sources. This makes EBIS particularly useful for integrating different data sources such as various sensors, digital elevation models, or other types of ancillary data. ESA

N93-11213 Open Univ., Oxford (England).

VOLCANOLOGY FROM SPACE: APPLICATIONS OF INFRARED REMOTE SENSING Ph.D. Thesis

Clive Oppenheimer 1991 255 p

Avail: Univ. Microfilms Order No. BRDX96410

Remote sensing techniques are being used increasingly to address volcanological problems. This thesis is concerned with the interpretation of multispectral infrared data of volcanic thermal features. Data from the two short wavelength infrared (SWIR) bands of the Landsat Thematic Mapper (TM) are used to constrain sizes and temperatures of subpixel resolution hot spots. Analysis of a 1989 TM scene of Lonquimay volcano suggests a cooling from 250 to 170 degrees C of the crust of an active lava flow down 1.5 km of its length. Estimates of the summed radiative and convective heat losses from the flow top fall from 6 to 3 MW per 30 x 30 m pixel downflow. Thermal data were collected at volcanoes in Chile, Nicaragua and Italy to test assumptions explicit in such calculations. These surveys suggest that SWIR emission from fumarole fields is dominated by that from the interior walls of vents, and that surface temperatures around fumarole vents are lower than those of typical active lava bodies. The relative response of the two SWIR sensors of the TM is sensitive to such differences and therefore provides a basis for the interpretation of thermal anomalies known only from satellite data. Comparison of measurements in the two SWIR bands is performed with fourteen TM scenes recorded between 1984 and 1991, of a persistent hot spot at Lascar volcano, Chile. Evolution of the thermal source is charted by comparing the summed spectral radiance in each of the SWIR bands. Thus it appears that Lascar has experienced at least two periods of lava dome growth punctuated by the explosive eruptions of 1986 and 1990. Infrared sensors to be deployed on forthcoming remote sensing platforms, including the Japanese Earth Resources Satellite and NASA's Earth Observing System, promise to constrain thermal emissions from volcanoes more effectively than possible with existing orbital systems. These investigations will improve understanding of the physical processes that influence the emplacement of lavas, as well as the potential for detecting eruption precursors and evaluating volcanic hazards. Dissert. Abstr.

N93-11663*# National Aeronautics and Space Administration. Goddard Space Flight Center, Greenbelt, MD.

THE EARLY EARTH OBSERVING SYSTEM REFERENCE HANDBOOK: EARTH SCIENCE AND APPLICATIONS DIVISION MISSIONS, 1990-1997

1990 83 p

(NASA-TM-107963; NAS 1.15:107963) Avail: CASI HC A05/MF A01

Prior to the launch of the Earth Observing System (EOS) series, NASA will launch and operate a wide variety of new earth science satellites and instruments, as well as undertake several efforts collecting and using the data from existing and planned satellites from other agencies and nations. These initiatives will augment the knowledge base gained from ongoing Earth Science and Applications Division (ESAD) programs. This volume describes three sets of ESAD activities -- ongoing exploitation of operational satellite data, research missions with upcoming launches between now and the first launch of EOS, and candidate earth probes. Author

N93-11701# Florida Univ., Gainesville. Dept. of Civil Engineering.

LAND USE/LAND COVER CLASSIFICATION USING DIGITALLY MERGED SPOT PANCHROMATIC AND LANDSAT THEMATIC MAPPER IMAGERY Final Report

Scot E. Smith and Clare Brown 1992 91 p

(Contract NA90AA-H-CZ-809)

(PB92-188416; CM-303) Avail: CASI HC A05/MF A01

The classification and mapping of land-use/land-cover and transportation networks through manual interpretation of digital satellite data are described. The interpretation and mapping were achieved through integration of a raster-based image processing system and a vector-based geographic information system (GIS). The primary hypothesis of the study was that manual interpretation of digitally merged SPOT 2 panchromatic and Landsat 5 Thematic Mapper (TM) data for land-use/land-cover mapping can produce classification accuracies comparable to those acquired through the interpretation of 1:24,000 infrared photography. A secondary hypothesis was that road networks can be accurately digitized from the merged product. The land use/land cover classification system used in the study was the Florida Land Use, Cover and Forms Classification scheme (FLUCCS). The study demonstrates that manual interpretation of merged satellite data can produce classification accuracies for land-use/land-cover of 94.5 percent for Level 1 and 92.0 percent for Level 2. The results are comparable to accuracies achieved through manual interpretation of color infrared aerial photography. With regard to the secondary hypothesis, the study showed that the precision of digitization was on the order of 6 to 8 meters. However, overall accuracy could not be reasonably assessed due to unidentified systematic error. Author

N93-11878*# National Aeronautics and Space Administration, Washington, DC.

A COMPREHENSIVE MISSION TO PLANET EARTH: WOODS HOLE SPACE SCIENCE AND APPLICATIONS ADVISORY COMMITTEE PLANNING WORKSHOP

29 Jul. 1991 74 p

(NASA-TM-108011; NAS 1.15:108011) Avail: CASI HC A04/MF A01

The NASA program Mission to Planet Earth (MTPE) is described in this set of visuals presented in Massachusetts on July 29, 1991. The problem presented in this document is that the earth system is changing and that human activity accelerates the rate of change resulting in increased greenhouse gases, decreasing levels of stratospheric ozone, acid rain, deforestation, decreasing biodiversity, and overpopulation. Various national and international organizations are coordinating global change research. The complementary space observations for this activity are sun-synchronous polar orbits, low-inclination, low altitude orbits, geostationary orbits, and ground measurements. The Geostationary Earth Observatory is the major proposed mission of MTPE. Other proposed missions are EOS Synthetic Aperture Radar, ARISTOTELES Magnetic Field Experiment, and the Global Topography Mission. Use of the NASA DC-8 aircraft is outlined as carrying out the Airborne Science and Applications Program. Approved Earth Probes Program include the Total Ozone Mapping Spectrometer (TOMS). Other packages for earth observation are described. R.L.B.

N93-12006*# Massachusetts Inst. of Tech., Cambridge. Research Lab. of Electronics.

EXPERIMENTAL MEASUREMENT AND THEORETICAL MODELING OF MICROWAVE SCATTERING AND THE STRUCTURE OF THE SEA SURFACE INFLUENCING RADAR OBSERVATIONS FROM SPACE Final Report, 1 Mar. 1988 - 30 Sep. 1992

David Arnold and J. A. Kong 30 Sep. 1992 25 p

(Grant NAGw-1272)
(NASA-CR-190998; NAS 1.26:190998) Avail: CASI HC A03/MF A01

The electromagnetic (EM) bias 'epsilon' is an error present in radar altimetry of the ocean due to the nonuniform reflection from wave troughs and crests. The EM bias is defined as the difference between the mean reflecting surface and the mean sea surface. A knowledge of the EM bias is necessary to permit error reduction in mean sea level measurements by satellite radar altimeters. Direct measurements of the EM bias were made from a Shell Offshore oil production platform in the Gulf of Mexico for a six month period during 1989 and 1990. Measurements of the EM bias were made at 5 and 14 Ghz. During the EM bias experiments by Melville et al., a wire wave gauge was used to obtain the modulation of the high frequency waves by the low frequency waves. It became apparent that the EM bias was primarily caused by the modulation of the short waves. This was reported by Arnold et al. The EM bias is explained using physical optics scattering and an empirical model for the short wave modulation. Measurements of the short wave modulation using a wire wave gauge demonstrated a linear dependence of the normalized bias on the short wave modulation strength, M. The theory accurately predicts this dependence by the relation epsilon = -alphaMH sub 1/3. The wind speed dependence of the normalized bias is explained by the dependence of the short wave modulation strength on the wind speed. While other effects such as long wave tilt and curvature will have an effect on the bias, the primary cause of the bias is shown to be due to the short wave modulation. This report will present a theory using physical optics scattering and an empirical model of the short wave modulation to estimate the EM bias. The estimated EM bias will be compared to measurements at C and Ku bands. Author

N93-12280# European Space Agency. ESRIN, Frascati (Italy).
ERS-1 USER HANDBOOK
Lois Proud, ed. (Eurimage, France) and Bruce Battrick, ed. Netherlands May 1992 160 p
(ESA-SP-1148; ISBN-92-9092-029-7; ETN-92-92345) Copyright Avail: CASI HC A08/MF A02

The document was designed to assist ERS-1 users in assessing ERS-1 services and in ordering products. The mission of the successfully commissioned ERS-1 satellite, is summarized. The range of ERS-1 products available to users are specified. The network access to ERS-1 can be performed by online interactive VT2000 compatible terminals. In case of users without network access, the ERS-1 Help Desk can be contacted to perform the required direct network access catalog functions. A guide through the ERS-1 order form is provided. A user's product requirements can be satisfied either with data already acquired by the satellite or with data from future data acquisitions. Several ground coverage maps are presented. The imagery is only available for areas within the reception zones of the ERS-1 ground stations. When placing an order for ERS-1 products, the user specifies the area for which they require coverage by delineating the area of interest using latitude and longitude coordinates. The user's guide appendices provide the user with additional information. ESA

N93-12351*# National Aeronautics and Space Administration. Ames Research Center, Moffett Field, CA.
ESTIMATION OF PHOTOSYNTHETIC CAPACITY USING MODIS POLARIZATION: 1988 PROPOSAL TO NASA HEADQUARTERS
Vern C. Vanderbilt Aug. 1992 11 p
(RTOP 462-61-04-10)
(NASA-TM-103945; A-92145; NAS 1.15:103945) Avail: CASI HC A03/MF A01

The remote sensing community has clearly identified the utility of NDVI (normalized difference vegetation index) and SR (simple ratio) and other vegetation indices for estimating such metrics of landscape ecology as green foliar biomass, photosynthetic capacity, and net primary production. Both theoretical and empirical investigations have established cause and effect relationships between the photosynthetic process in plant canopies and these combinations of remotely sensed data. Yet it has also been established that the relationships exhibit considerable variability that appears to be ecosystem-dependent and may represent a source of ecologically important information. The overall hypothesis of this proposal is that the ecosystem-dependent variability in the various vegetation indices is in part attributable to the effects of specular reflection. The polarization channels on MODIS provide the potential to estimate this specularly reflected light and allow the modification of the vegetation indices to better measure the photosynthetic process in plant canopies. In addition, these polarization channels potentially provide additional ecologically important information about the plant canopy. Author

N93-12357# Army Chemical Research and Development Center, Aberdeen Proving Ground, MD.
FIXED POINTS OF EXPANSIVE ANALYTIC MAPS (2) Final Report, Oct. 1990 - Jun. 1992
Walter O. Egerland and Charles E. Hansen Sep. 1992 23 p
(AD-A254737; BRL-TR-3394) Avail: CASI HC A03/MF A01

The main result of this note, the 'Encircling Theorem,' states conditions that assure that an analytic function is expansive in the closed unit disk D and has a fixed point in D. A corollary describes in detail the case of a conformal sap. From a new covering lemma for polynomials further sufficient conditions are deduced that guarantee that a polynomial of degree n, n - 1,2,..., is expansive and has a fixed point in D. On the other hand, an important example shows that for each n greater than 3 polynomials of degree n exist that cover D but do not have a fixed point in D. Finally, the distribution of the fixed points of any finite Blaschke - product is established. GRA

44 ENERGY PRODUCTION AND CONVERSION

Includes specific energy conversion systems, e.g., fuel cells; global sources of energy; geophysical conversion; and windpower.

For related information see also *07 Aircraft Propulsion and Power, 20 Spacecraft Propulsion and Power,* and *28 Propellants and Fuels.*

N93-10989# Sandia National Labs., Albuquerque, NM.
THE 1992 DOE/SANDIA CRYSTALLINE PHOTOVOLTAIC TECHNOLOGY PROJECT REVIEW MEETING
Alexander Maish, ed. Jul. 1992 177 p Meeting held in Albuquerque, NM, 14-15 Jul. 1992
(Contract DE-AC04-76DP-00789)
(DE92-018544; SAND-92-1454; CONF-9207110) Avail: CASI HC A09/MF A02

The proceedings for the annual project review meeting held by Sandia National Laboratories' Photovoltaic Technology and Photovoltaic Evaluation Departments are presented. Overview sessions covered the following: Department of Energy (DOE) programs, including those at Sandia and the National Renewable Energy Laboratory (NREL); and non-DOE programs, including the EPRI concentrator collector program, the Japanese crystalline silicon program, and some concentrating photovoltaic activities in Europe. Additional sessions included papers on Sandia's Photovoltaic Device Fabrication Laboratory's collaborative research, cell processing research, the activities of the participants in the Concentrator Initiative Program, and photovoltaic technology evaluation at Sandia and NREL. DOE

N93-11214 Stanford Univ., CA.
ADMITTANCE SPECTROSCOPY OF COPPER INDIUM DISELENIDE/CADMIUM SULFIDE SOLAR CELLS Ph.D. Thesis
Walter A. Strifler 1992 164 p
Avail: Univ. Microfilms Order No. DA9221672

This dissertation concentrates on admittance spectroscopy of CuInSe2/CdS heterojunction solar cells prepared by chemical spray pyrolysis (CSP) and by multiple-source evaporation (MSE). The primary goal is to examine some of the more important electrical characteristics of these heterojunctions and determine if the spray-pyrolyzed cells behave similar, albeit at a lower efficiency, to higher quality cells prepared by other techniques. The primary analytical tool used in this study is admittance spectroscopy. The theory of admittance spectroscopy is developed using the concept of equivalent circuits. The traditional temperature-swept technique for admittance spectroscopy is shown to be inadequate for measuring most heterojunction samples examined in this study because of the large parallel leakage conductance found in these devices. Instead, a frequency-swept admittance technique is developed and employed to correct for the parallel conductance effect and reveal the true nature of slow charge in the depletion layer. In addition to admittance spectroscopy, the two sets of solar cell diodes are characterized using a variety of measurement techniques including capacitance-voltage, current-voltage over spectral response, capacitance dispersion over wavelength, and solar efficiency. The different pieces of experimental data are discussed to form a self-consistent physical model of the polycrystalline solar cells. Charge transport across the diode junction is dominated by recombination processes within the CuInSe2 depletion layer for both sets of diodes although the large parallel conductance in the CSP diodes often masks this characteristic. The CSP solar cells exhibit a pronounced blue peak in the spectral response indicating that electron collection is the limiting factor in the overall short-circuit quantum efficiency. A large degree of capacitance dispersion is found in both sets of diodes. Supporting measurements indicate that the majority of this dispersion is due to interface traps in the MSE diodes and bulk acceptor traps in the CSP diodes. The high density of bulk acceptor traps in the CuInSe2 are located approximately 0.30 eV above the valence band and exhibit a capture cross section of approximately 5 x 10(exp -18)/sq cm. The dissertation concludes with a summary of the important mechanisms that presently dominate the efficiency of the CuInSe2/CdS solar cells prepared by CSP. Dissert. Abstr.

N93-11381# Los Alamos National Lab., NM.
STATUS AND PROSPECTS FOR HOT DRY ROCK (HDR) IN THE US
D. Brown and D. Duchane 1992 8 p Presented at the Geothermal Resources Council Meeting, San Diego, CA, 4-7 Oct. 1992
(Contract W-7405-eng-36)
(DE92-018876; LA-UR-92-2189; CONF-921083-6) Avail: CASI HC A02/MF A01

The vast majority of accessible geothermal energy exists in the form of heat stored in dry rock at depth. For nearly the last two decades, the Los Alamos National Laboratory has been engaged in a program to develop the technology to mine the thermal energy in this hot dry rock (HDR). The world's first heat mine was developed and operated at Fenton Hill, NM in the 1970's by using drilling and hydraulic fracturing techniques to create an artificial reservoir in hot rock and subsequently circulating water through this reservoir to mine the heat from the rock. Over the last ten years, a much larger, deeper, and hotter heat mine has been constructed at Fenton Hill and a permanent energy extraction plant has been built on the surface. A long-term testing program has recently begun to evaluate the potential for sustained energy extraction from the large Fenton Hill heat mine. This paper summarizes the history of HDR research and development at Los Alamos, reports the initial results of the long-term testing program at Fenton Hill, and discusses the possible future course of HDR technology. DOE

N93-11513# Argonne National Lab., IL.
SEALANT RESEARCH FOR SOLID OXIDE FUEL CELLS
S. E. Dorris, I. Bloom, M. C. Hash, and M. Krumpelt Jun. 1992 6 p Presented at the US DOE Contractors Review Meeting on Fuel Cells, Morgantown, WV, 14-15 Jul. 1992
(Contract W-31-109-eng-38)
(DE92-019044; ANL/CP-76387; CONF-920748-3) Avail: CASI HC A02/MF A01

The objective of this work is to develop sealing materials for solid oxide fuels cells (SOFC's). A suitable sealant must form strong, dense bonds with SOFC components, be chemically and mechanically compatible with the components, be stable at 1000 C in the operating environment of the SOFC (H2 and H2O on the anode side, O2 on the cathode side), and must be nonconductive. DOE

N93-11571# Argonne National Lab., IL.
INTERMEDIATE TEMPERATURE ELECTROLYTES FOR SOFC
I. Bloom, M. Krumpelt, M. C. Hash, J. P. Zebrowski, and D. Zurawski 1992 6 p Presented at the US Department of Energy Contractors Review Meeting on Fuel Cells, Morgantown, WV, 14-15 Jul. 1992
(Contract W-31-109-eng-38)
(DE92-018786; ANL/CP-76343; CONF-920748-2) Avail: CASI HC A02/MF A01

The objective of this work is to identify a new set of materials that would allow the operation of the solid oxide fuel cell in the 600-800 C temperature range. The approach that is being used is to start with a systematic evaluation of new electrolyte materials and then to develop compatible electrode and interconnect materials. DOE

N93-11626# Los Alamos National Lab., NM.
REACTANT GAS FLOW FIELDS IN ADVANCED PEM (PROTON EXCHANGE MEMBRANE) FUEL CELL DESIGNS
M. C. Kimble and N. E. Vanderborgh 1992 6 p Presented at the 27th Intersociety Energy Conversion Engineering Conference, San Diego, CA, 3-7 Aug. 1992
(Contract W-7405-eng-36)
(DE92-018897; LA-UR-92-2155; CONF-920801-20) Avail: CASI HC A02/MF A01

A mathematical model of the two-phase flow in a fuel cell gas channel is developed and used to predict the mass, momentum, and thermal distributions of a multi-component gas and liquid water mixture on the cathode side. Regions where flooding may occur are demonstrated by using the model evaluated with various operating conditions typical of fuel cell operations. Conditions where dry, saturated, and two-phase flows are introduced into the channel are demonstrated and the results compared. These results show the distribution of water and heat in the channel which may be used to design better flow channels. DOE

N93-11733# Northwestern Univ., Evanston, IL.
STUDIES IN NONLINEAR PROBLEMS OF ENERGY
B. J. Matkowsky Jul. 1992 55 p
(Contract DE-FG02-87ER-25027)
(DE92-018551; DOE/ER-25027/6) Avail: CASI HC A04/MF A01

Emphasis has been on combustion and flame propagation. The research program was on modeling, analysis and computation of combustion phenomena, with emphasis on transition from laminar to turbulent combustion. Nonlinear dynamics and pattern formation were investigated in the transition. Stability of combustion waves, and transitions to complex waves are described. Combustion waves possess large activation energies, so that chemical reactions are significant only in thin layers, or reaction zones. In limit of infinite activation energy, the zones shrink to moving surfaces, termed fronts which must be found during the analysis, so that the problems are moving free boundary problems. The studies are carried out for limiting case with fronts, while the numerical studies are carried out for finite, though large, activation energy. Accurate resolution of the solution in the reaction zones is essential, otherwise false predictions of dynamics are possible. Since the the reaction zones move, adaptive pseudo-spectral methods were developed. The approach is based on a synergism of analytical and computational methods. The numerical computations build on and extend the analytical information. Furthermore, analytical solutions serve as benchmarks for testing the accuracy of the computation. Finally, ideas from analysis (singular perturbation theory) have induced new approaches to computations. The computational results suggest new analysis to be considered. Among the recent interesting results, was spatio-temporal chaos in combustion. One goal is extension of the adaptive pseudo-spectral methods to adaptive domain decomposition methods. Efforts have begun to develop such methods for problems with multiple reaction zones, corresponding to problems with more complex, and more realistic chemistry. Other topics included stochastics, oscillators, Rysteretic Josephson junctions, DC SQUID, Markov jumps, laser with saturable absorber, chemical physics, Brownian movement, combustion synthesis, etc. DOE

N93-11771# Sandia National Labs., Albuquerque, NM.
EVALUATION TESTS FOR PHOTOVOLTAIC CONCENTRATOR RECEIVER SECTIONS AND MODULES
J. R. Woodworth and M. L. Whipple Jun. 1992 44 p
(Contract DE-AC04-76DP-00789)
(DE92-017745; SAND-92-0958) Avail: CASI HC A03/MF A01

Sandia has developed a third-generation set of specifications for performance and reliability testing of photovoltaic concentrator modules. Several new requirements have been defined. The primary purpose of the tests is to screen new concentrator designs and new production runs for susceptibility to known failure mechanisms. Ultraviolet radiation testing of materials precedes receiver section and module performance and environmental tests. The specifications include the purpose, procedure, and requirements for each test. Recommendations for future improvements are presented. DOE

N93-11777# New Energy Development Organization, Tokyo (Japan).
NEDO FUEL/STORAGE TECHNOLOGY SUBCOMMITTEE
Oct. 1991 86 p In JAPANESE Presented at the 11th New Energy Development Organization Meeting, Tokyo, Japan, Oct. 1991
(DE92-526262; ETDE/JP-MF-92526262) Avail: CASI HC A05/MF A01

The integrated activity in 1990 and the plan in 1991 of the Fuel/Storage Technology Subcommittee were reported in the 11th research report meeting (held in October, 1991) of NEDO. Five projects as to the technical development, such as power generation using fuel cells, power storage system using new type battery, super heat pump/energy accumulating system, ceramic gas turbine, and application of superconductivity power, were promoted in 1990 like the previous year. As the representative cases, the operating researches of 1000 kW class system of phosphoric acid fuel cells and of 200 kW class system for an isolated island were finished because the expected results could be obtained, and the development is to be forwarded to make this technique practical in 1991. Other examples are as follows: the completion of 1000 kW class pilot plants of Na-S cells and Zn-Br cells; the design and fabrication of 1000 kW class pilot system of super heat pump; and the experimental manufacturing and evaluation of characteristics of superconductive wire. DOE

N93-11814# Midwest Research Inst., Golden, CO.
ELECTRICITY FROM BIOMASS: A DEVELOPMENT STRATEGY
Apr. 1992 114 p
(Contract DE-AC02-83CH-10093)
(DE92-010590; DOE/CH-10093/152) Avail: CASI HC A06/MF A02

The purpose of this document is to review the current status of biomass power technology and to evaluate the future directions for development that could significantly enhance the contribution of biomass power to U.S. production of electricity. This document reviews the basic principles of biomass electric systems, the previous contributions of industry and the National Biomass Energy Programs to technology development, and the options for future technology development. It discusses the market for biomass electric technology and future needs for electric power production to help establish a market-oriented development strategy. It projects trends in the performance and cost of the technology and examines the changing dynamics of the power generation market place to evaluate specific opportunities for biomass power development. In a separate document, the Biomass Power Program Five Year R&D Plan, the details of schedules, funding, and roles of participating R&D organizations within the R&D program funded by the U.S. Department of Energy (DOE) are presented. In evaluating the future directions for research and development, two cases are examined. DOE

N93-11823# Chicago Univ., IL. Inst. for Nuclear Studies.
PARTICIPATION IN MULTILATERAL EFFORT TO DEVELOP HIGH PERFORMANCE INTEGRATED CPC EVACUATED COLLECTORS
R. Winston and J. J. OGallagher 31 May 1992 21 p
(Contract DE-FG03-86SF-16592)
(DE92-015946; DOE/SF-16592/T1) Avail: CASI HC A03/MF A01

The University of Chicago Solar Energy Group has had a continuing program and commitment to develop an advanced evacuated solar collector integrating nonimaging concentration into its design. During the period from 1985-1987, some of our efforts were directed toward designing and prototyping a manufacturable version of an Integrated Compound Parabolic Concentrator (ICPC) evacuated collector tube as part of an international cooperative effort involving six organizations in four different countries. This 'multilateral' project made considerable progress towards a commercially practical collector. One of two basic designs considered employed a heat pipe and an internal metal reflector CPC. We fabricated and tested two large diameter (125 mm) borosilicate glass collector tubes to explore this concept. The other design also used a large diameter (125 mm) glass tube but with a specially configured internal shaped mirror CPC coupled to a U-tube absorber. Performance projections in a variety of systems applications using the computer design tools developed by the International Energy Agency (IEA) task on evacuated collectors were used to optimize the optical and thermal design. The long-term goal of this work continues to be the development of a high efficiency, low cost solar collector to supply solar thermal energy at temperatures up to 250 C. Some experience and perspectives based on our work are presented and reviewed. Despite substantial progress, the stability of research support and the market for commercial solar thermal collectors were such that the project could not be continued. A cooperative path involving university, government, and industrial collaboration remains the most attractive near term option for developing a commercial ICPC. DOE

N93-11825# Los Alamos National Lab., NM.
PROSPECTS FOR THE COMMERCIAL DEVELOPMENT OF HOT DRY ROCK GEOTHERMAL ENERGY IN NEW MEXICO
D. V. Duchane and F. Goff 1992 10 p Presented at the New Mexico Conference on the Environment: Toward A Sustainable Environment, Albuquerque, NM, 13-15 Sep. 1992
(Contract W-7405-eng-36)
(DE92-018999; LA-UR-92-2489; CONF-9209164-3) Avail: CASI HC A02/MF A01

A vast store of energy is available to the world in the form of hot dry rock (HDR) which exists almost everywhere beneath the surface of the earth. The Los Alamos National Laboratory has developed technology to mine the heat from HDR by using techniques developed in the petroleum industry. In practice, an artificial reservoir is created in the hot rock and water is circulated through the reservoir to extract the thermal energy and bring it to the surface. There are virtually no adverse environmental effects from an HDR plant when the system is operated in a closed-loop mode with the process water continually recirculated. An experimental plant at Fenton Hill, NM is now undergoing long-term testing to demonstrate that energy can be obtained from HDR on a sustained basis with operational procedures which are readily adaptable to industry. Significant HDR resources exist in the state of New Mexico. Resources in the Valles Caldera, Zuni Uplift, and Rio Grande Rift have been evaluated in detail. Studies indicate that it should be possible to economically develop high grade HDR resources with technology available today. As advanced concepts for developing and operating HDR systems are investigated, even more widespread utilization of the technology will be commercially feasible. DOE

N93-11845# New Energy Development Organization, Tokyo (Japan).

NEDO SOLAR TECHNOLOGY SUBCOMMITTEE

Oct. 1991 75 p In JAPANESE Presented at the 11th New Energy Development Organization Meeting, Tokyo, Japan, Oct. 1991
(DE92-526256; ETDE/JP-MF-92526256) Avail: CASI HC A04/MF A01

Five papers were reported in the 11th research report meeting held in October, 1991 in the Solar Technology Subcommittee of NEDO. Several themes as to development of the solar technology and development of commercialization technology of the industrial solar system which were forwarded in 1990 were explained including themes presented in these 5 papers. For example, the following items were developed for the photovoltaic power generation of the solar technology development: new type solar cells, practical use of amorphous solar cells, development of ultra-highly efficient solar cells, research and development of independent dispersion type as the utilization system, hybrid type photovoltaic power generation using solar light and heat, and the manufacturing equipment of compound type semi-conductors for solar cells, etc. As for the technical development to make the industrial solar system practical use, the following techniques such as the research of elementary techniques including the solar energy collector, the advanced heat process using new metal hydrides for refrigerating heat generation and chemical energy conversion technique are researched. In addition, the development of an MW class large wind power generation system is also advanced as a research object of this Subcommittee. DOE

N93-12012# Sandia National Labs., Albuquerque, NM.

SODIUM REFLUX POOL-BOILER SOLAR RECEIVER ON-SUN TEST RESULTS

C. E. Andraka, J. B. Moreno, R. B. Diver, and T. A. Moss (Oak Ridge National Lab., TN.) Jun. 1992 320 p
(Contract DE-AC04-76DP-00789)
(DE92-018932; SAND-89-2773) Avail: CASI HC A14/MF A03

The efficient operation of a Stirling engine requires the application of a high heat flux to the relatively small area occupied by the heater head tubes. Previous attempts to couple solar energy to Stirling engines generally involved directly illuminating the heater head tubes with concentrated sunlight. In this study, operation of a 75-kW(sub t) sodium reflux pool-boiler solar receiver has been demonstrated and its performance characterized on Sandia's nominal 75-kW(sub t) parabolic-dish concentrator, using a cold-water gas-gap calorimeter to simulate Stirling engine operation. The pool boiler (and more generally liquid-metal reflux receivers) supplies heat to the engine in the form of latent heat released from condensation of the metal vapor on the heater head tubes. The advantages of the pool boiler include uniform tube temperature, leading to longer life and higher temperature available to the engine, and decoupling of the design of the solar absorber from the engine heater head. The two-phase system allows high input thermal flux, reducing the receiver size and losses, therefore improving system efficiency. The receiver thermal efficiency was about 90 percent when operated at full power and 800 C. Stable sodium boiling was promoted by the addition of 35 equally spaced artificial cavities in the wetted absorber surface. High incipient boiling superheats following cloud transients were suppressed passively by the addition of small amounts of xenon gas to the receiver volume. Stable boiling without excessive incipient boiling superheats was observed under all operating conditions. The receiver developed a leak during performance evaluation, terminating the testing after accumulating about 50 hours on sun. The receiver design is reported here along with test results including transient operations, steady-state performance evaluation, operation at various temperatures, infrared thermography, x-ray studies of the boiling behavior, and a postmortem analysis. DOE

N93-12017*# Rockwell International Corp., Canoga Park, CA. Rocketdyne Div.

LUNAR PMAD TECHNOLOGY ASSESSMENT Final Report

Kenneth J. Metcalf Feb. 1992 217 p
(Contract NAS3-25808)
(NASA-CR-189225; NAS 1.26:189225) Avail: CASI HC A10/MF A03

This report documents an initial set of power conditioning models created to generate 'ballpark' power management and distribution (PMAD) component mass and size estimates. It contains converter, rectifier, inverter, transformer, remote bus isolator (RBI), and remote power controller (RPC) models. These models allow certain studies to be performed; however, additional models are required to assess a full range of PMAD alternatives. The intent is to eventually form a library of PMAD models that will allow system designers to evaluate various power system architectures and distribution techniques quickly and consistently. The models in this report are designed primarily for space exploration initiative (SEI) missions requiring continuous power and supporting manned operations. The mass estimates were developed by identifying the stages in a component and obtaining mass breakdowns for these stages from near term electronic hardware elements. Technology advances were then incorporated to generate hardware masses consistent with the 2000 to 2010 time period. The mass of a complete component is computed by algorithms that calculate the masses of the component stages, control and monitoring, enclosure, and thermal management subsystem. Author

N93-12019*# Rockwell International Corp., Canoga Park, CA. Rocketdyne Div.

POWER SYSTEM COMMONALITY STUDY Final Report

Franklin D. Littman Jul. 1992 45 p
(Contract NAS3-25808)
(NASA-CR-190765; NAS 1.26:190765) Avail: CASI HC A03/MF A01

A limited top level study was completed to determine the commonality of power system/subsystem concepts within potential lunar and Mars surface power system architectures. A list of power system concepts with high commonality was developed which can be used to synthesize power system architectures which minimize development cost. Examples of potential high commonality power system architectures are given in this report along with a mass comparison. Other criteria such as life cycle cost (which includes transportation cost), reliability, safety, risk, and operability should be used in future, more detailed studies to select optimum power system architectures. Nineteen potential power system concepts were identified and evaluated for planetary surface applications including photovoltaic arrays with energy storage, isotope, and nuclear power systems. A top level environmental factors study was completed to assess environmental impacts on the identified power system concepts for both lunar and Mars applications. Potential power system design solutions for commonality between Mars and lunar applications were identified. Isotope, photovoltaic array (PVA), regenerative fuel cell (RFC), stainless steel liquid-metal cooled reactors (less than 1033 K maximum) with dynamic converters, and in-core thermionic reactor systems were found suitable for both lunar and Mars environments. The use of SP-100 thermoelectric (TE) and SP-100 dynamic power systems in a vacuum enclosure may also be possible for Mars applications although several issues need to be investigated further (potential single point failure of enclosure, mass penalty of enclosure and active pumping system, additional installation time and complexity). There are also technical issues involved with development of thermionic reactors (life, serviceability, and adaptability to other power conversion units). Additional studies are required to determine the optimum reactor concept for Mars applications. Various screening criteria (availability, environmental compatibility, mass competitiveness of energy storage, safety, and practicality for the application) were used to define concept applicability for each lunar and Mars application. A screening study resulted in 13 power systems for lunar applications and 15 for Mars applications. A commonality analysis showed several power systems with potentially high commonality (across both lunar and Mars applications). These high commonality systems include d PVA/RFC, dynamic isotope (1033 K Stirling, 1133 K Brayton, and 1300 K Brayton PCU's), SP-100 TE and dynamic derivatives (Mars systems required vacuum enclosure), in-core thermionic reactor, and liquid metal cooled reactor/Stirling cycle (1033 K). The generic commonality results were used to synthesize 3 high commonality power system architectures: (1) predominantly PV (limited nuclear and isotope), (2) predominantly in-core thermionic reactor/DIPS, and (3) predominantly SP-100 reactor/DIPS. The in-core thermionic reactor/DIPS power system architecture had the lowest total mass. Specific outputs from this study included lists of power system requirements, power system candidates, a power system application matrix, power system characteristics (mass), power system commonality ratings, example high commonality power system architectures, architecture masses, and issues/design solutions for lunar/Mars commonality. Author

N93-12074# Sandia National Labs., Albuquerque, NM.
MIRROR ALIGNMENT TECHNIQUES FOR POINT-FOCUS SOLAR CONCENTRATORS
R. B. Diver Jun. 1992 43 p
(Contract DE-AC04-76DP-00789)
(DE92-019643; SAND-92-0668) Avail: CASI HC A03/MF A01

Accurate alignment and focus of mirror facets are critical for the integration of concentrators and receivers in many of the low-cost stretched-membrane concentrators currently under development. In this report, the theoretical development of computer software that traces light rays from a source to a facet of a point-focusing solar concentrator and then to a target is given. Examples of approaches for the alignment of faceted point-focusing solar concentrators, which make use of targets generated by this computer program, are also presented. DOE

N93-12075# Sandia National Labs., Albuquerque, NM.
MEASURED DATA FOR THE SANDIA 34-METER VERTICAL AXIS WIND TURBINE
T. D. Ashwill Jul. 1992 119 p
(Contract DE-AC04-76DP-00789)
(DE92-019807; SAND-91-2228) Avail: CASI HC A06/MF A02

The 34-meter Test Bed is a research-oriented, variable-speed vertical-axis wind turbine located at the USDA Agricultural Research Station in Bushland, Texas. Sandia National Laboratories designed and built this machine to perform research in structural dynamics, aerodynamics, and fatigue. Testing to determine its performance in various wind conditions and rotation rates has been ongoing for over three years. This report documents a broad range of test data and includes comparisons to analytical results. DOE

N93-12144# Washington Univ., Seattle.
INVESTIGATION OF HIGH EFFICIENCY MONOLITHIC MULTIBANDGAP SOLAR CELLS Final Report, 15 Nov. 1990 - 15 Nov. 1991
Larry Olsen 15 Nov. 1991 26 p
(Grant AF-AFOSR-0095-91)
(AD-A254326; AFOSR-92-0784TR) Avail: CASI HC A03/MF A01

This program involved investigations of AlGaAs/GaAs multijunction solar cells. Most of the low level effort was devoted to studies of the electronic properties of AlGaAs films. Finite diffusion lengths could only be obtained for Al(x)Ga(1-x)As films with the aluminum concentration in the range from 0 to 0.1. Photoresponse of Al/AlGaAs Schottky barriers were analyzed to measure minority carrier diffusion length (L). Values of L for p-type AlGaAs with $x = 0$ were typically in the range of 0 to 0.5 micron. It is clear that much more effort must be made to reduce oxygen and water impurity levels in the WSU barrel-type reactor before improved AlGaAs could be grown. An apparent bandgap shift implied by photoresponse data for Al/AlGaAs Schottky barriers is explained as being due to improper mixing of Al and Ga precursors. Results are discussed for films grown with improved mixing which do not exhibit the apparent bandgap shift. Estimated performance for a two-cell, AlGaAs/GaAs structure is given based on characteristics of Al(.37)Ga(.63)As cells fabricated from wafers obtained from Varian, and GaAs cells fabricated for epi wafers grown with the WSU reactor. GRA

N93-12166# Northeast Photosciences, Hollis, NH.
PHOTOVOLTAIC SYSTEMS BASED ON SPECTRALLY SELECTIVE HOLOGRAPHIC CONCENTRATORS, PHASE 1 Final Report, May - Dec. 1991
Jacques E. Ludman Nov. 1991 55 p
(Contract F33615-91-C-2136)
(AD-A252811; FY1455-91-08827-Rpt-1-Phase 1; WL-TR-92-2041-Phase-1) Avail: CASI HC A04/MF A01

The feasibility of a new holographic technique for concentrating solar energy and splitting its spectrum with a single hologram to generate power, using two or more solar cells optimized at different portion of the solar spectrum, is demonstrated. Various holographic materials, techniques for making holograms, and combinations of solar cells of different materials were investigated. Techniques were developed for testing system efficiencies. A number of potential problems and difficulties were successfully addressed. Holograms and solar cell systems were fabricated and tested, and demonstration units were fabricated. GRA

N93-12222# Sandia National Labs., Albuquerque, NM.
DEVELOPMENT OF CONTRACTOR CELLS, PHASE 1
Jun. 1992 42 p Prepared in cooperation with Applied Solar Energy Corp., City of Industry, CA
(Contract DE-AC04-76DP-00789)
(DE92-017343; SAND-92-7006) Avail: CASI HC A03/MF A01

The microgrooved passivated emitter solar cell approach combines a thin diffused top junction layer of approximately 0.2 micron depth and 120-180 Omega/square sheet resistance with a thin (100-200 A) silicon dioxide surface passivation layer. The front gridlines sit on top of a heavily diffused N++ region to reduce contact resistance between front gridlines and the N surface. High-quality float zone silicon with nominal resistivity of 0.20 Omega-cm or 0.15 Omega-cm is used for this work. To achieve the highest possible concentration performance and lower system cost, the cell area was reduced to 1 square centimeter from 1.58 square centimeters used at the University of New South Wales. The gridlines spacing is 127 microns designed to match the available prismatic cover. The baseline process requires four lithographic masking steps. A single lift-off process for evaporated gridlines is used to provide 8-microns-thick metallization to avoid the non-uniform metal plating and disposal of hazardous plating solutions. The front and back contact materials are space-qualified, vacuum-deposited layers of titanium-palladium and silver. A double-layer antireflection coating of TiO(x) and Al2O3 is used to reduce surface reflection from the cells; this antireflection coating is designed to match with the SiO2 passivation layer. Four different gridline widths (20, 16, 8, and 2 microns) were tested and evaluated for the best performance at high intensities. A three-level lithographic masking process was evaluated for reduced costs and a five-level lithographic masking process was evaluated for increased yield. DOE

N93-12312# Sandia National Labs., Albuquerque, NM.
RELIABILITY ANALYSIS OF A UTILITY-SCALE SOLAR POWER PLANT
G. J. Kolb 1992 9 p Presented at the INTER-RAMQ Conference for Electric Power Industry, Philadelphia, PA, 25-28 Aug. 1992
(Contract DE-AC04-76DP-00789)
(DE92-016550; SAND-92-1252C; CONF-9208103-1) Avail: CASI HC A02/MF A01

This paper presents the results of a reliability analysis for a solar central receiver power plant that employs a salt-in-tube receiver. Because reliability data for a number of critical plant components have only recently been collected, this is the first time a credible analysis can be performed. This type of power plant will be built by a consortium of western US utilities led by the Southern California Edison Company. The 10 MW plant is known as Solar Two and is scheduled to be on-line in 1994. It is a prototype which should lead to the construction of 100 MW commercial-scale plants by the year 2000. The availability calculation was performed with the UNIRAM computer code. The analysis predicted a forced outage rate of 5.4 percent and an overall plant availability, including scheduled outages, of 91 percent.

The code also identified the most important contributors to plant unavailability. Control system failures were identified as the most important cause of forced outages. Receiver problems were rated second with turbine outages third. The overall plant availability of 91 percent exceeds the goal identified by the US utility study. This paper discuses the availability calculation and presents evidence why the 91 percent availability is a credible estimate.
DOE

N93-12394*# National Hydrogen Association, Washington, DC.
THE HYDROGEN TECHNOLOGY ASSESSMENT, PHASE 1
Addison Bain 1991 128 p
(Contract NCC10-0006)
(NASA-CR-190969; NAS 1.26:190969) Avail: CASI HC A07/MF A02

The purpose of this phase 1 report is to begin to form the information base of the economics and energy uses of hydrogen-related technologies on which the members of the National Hydrogen Association (NHA) can build a hydrogen vision of the future. The secondary goal of this report is the development of NHA positions on national research, development, and demonstration opportunities. The third goal, with the aid of the established hydrogen vision and NHA positions, is to evaluate ongoing federal research goals and activities. The evaluations will be performed in a manner that compares the costs associated with using systems that achieve those goals against the cost of performing those tasks today with fossil fuels. From this ongoing activity should emerge an NHA information base, one or more hydrogen visions of the future, and cost and performance targets for hydrogen applications to complete in the market place.
Author

N93-12446# Kauppa-ja Teollisuusministerio, Helsinki (Finland). Energy Dept.
LIEKKI AND JALO: COMBUSTION AND FUEL CONVERSION
Thomas M. Grace (Grace, T. M. Co., Inc., Appleton, WI), Ulrich Renz (Technische Hochschule, Aachen, Germany), and Adel F. Sarofim (Massachusetts Inst. of Tech., Cambridge.) 1992 38 p
(DE92-540921; KTM/E-B-106; ISBN-951-47-4473-X) Avail: CASI HC A03/MF A01

LIEKKI and JALO are well conceived and structured programs designed to strengthen Finland's special needs in combustion and gasification to utilize a diversity of fuels, increase the ratio of electrical to heat output, and to support the export market. Started in 1988, these two programs provide models of how universities, Technical research center's laboratories (VTT's), and industry can collaborate successfully in order to achieve national goals. The research is focused on long term goals in certain targeted niche areas. This is an effective way to use limited resources. The niche areas were chosen in a rational manner and appear to be appropriate for Finland. The LIEKKI and JALO programs have helped pull together research efforts that were previously more fragmented. For example, the combustion modeling area still appears fragmented. Individual project objectives should be tied to program goals at a very early stage to provide sharper focusing to the research. Both the LIEKKI and JALO programs appear to be strongly endorsed by industry. Industrial members of the Executive Committees were very supportive of these programs. There are good mechanisms for technology transfer in place, and the programs provide opportunities to establish good interfaces between industrial people and the individual researchers. The interest of industry is shown by the large number of applied projects that are supported by industry. This demonstrates the relevancy of the programs. There is a strong interaction between the JALO program and industry in black liquor gasification. DOE

N93-12498# Oak Ridge National Lab., TN.
STIRLING HEAT PUMP EXTERNAL HEAT SYSTEMS: AN APPLIANCE PERSPECTIVE
A. D. Vasilakis (Advanced Mechanical Technology, Inc., Newton, MA.) and J. F. Thomas 1992 8 p Presented at the 27th Intersociety Energy Conversion Engineering Conference, San Diego, CA, 3-7 Aug. 1991
(Contract DE-AC05-84OR-21400)
(DE92-018251; CONF-920801-19) Avail: CASI HC A02/MF A01

A major issue facing the Stirling Engine Heat Pump is system cost, and, in particular, the cost of the External Heat System (EHS). The need for high temperature at the heater head (600 C to 700 C) results in low combustion system efficiencies unless efficient heat recovery is employed. The balance between energy efficiency and use of costly high temperature materials is critical to design and cost optimization. Blower power consumption and NO(x) emissions are also important. A new approach to the design and cost optimization of the EHS system was taken by viewing the system from a natural gas-fired appliance perspective. To develop a design acceptable to gas industry requirements, American National Standards Institute (ANSI) code considerations were incorporated into the design process and material selections. A parametric engineering design and cost model was developed to perform the analysis, including the impact of design on NO(x) emissions. Analysis results and recommended EHS design and material choices are given. DOE

45 ENVIRONMENT POLLUTION

Includes atmospheric, noise, thermal, and water pollution.

N93-11003*# National Aeronautics and Space Administration. Goddard Space Flight Center, Greenbelt, MD.
THE NASA/NATIONAL SPACE SCIENCE DATA CENTER TRAPPED RADIATION ENVIRONMENT MODEL PROGRAM, 1964 - 1991
James I. Vette Nov. 1991 47 p
(NASA-TM-107993; NAS 1.15:107993; NSSDC/WDC-A-R/S-91-29) Avail: CASI HC A03/MF A01

The major effort that NASA, initially with the help of the United States Air Force (USAF), carried out for 27 years to synthesize the experimental and theoretical results of space research related to energetic charged particles into a quantitative description of the terrestrial trapped radiation environment in the form of model environments is detailed. The effort is called the Trapped Radiation Environment Modeling Program (TREMP). In chapter 2 the historical background leading to the establishment of this program is given. Also, the purpose of this modeling program as established by the founders of the program is discussed. This is followed in chapter 3 by the philosophy and approach that was applied in this program throughout its lifetime. As will be seen, this philosophy led to the continuation of the program long after it would have expired. The highlights of the accomplishments are presented in chapter 4. A view to future possible efforts in this arena is given in chapter 5, mainly to pass on to future workers the differences that are perceived from these many years of experience. Chapter 6 is an appendix that details the chronology of the development of TREMP. Finally, the references, which document the work accomplished over these years, are presented in chapter 7. Author

N93-11082# Bundesministerium fuer Forschung und Technologie, Bonn (Germany).
THE TRANSALL CAMPAIGN. A CONTRIBUTION TO THE GERMAN OZONE RESEARCH PROGRAM [DIE TRANSALL-KAMPAGNE EIN BEITRAG ZUM DEUTSCHEN OZONFORSCHUNGSPROGRAMM]
3 Dec. 1991 27 p In GERMAN
(Rept-37/91; ETN-92-92101) Avail: CASI HC A03/MF A01

The advantage of an airborne instrument carrier for ozone research is demonstrated. The measuring location can follow the development of stratospheric dynamics. The status of the stratosphere can be explored with good horizontal resolution. The vertical resolution of remote sensors is improved. The Transall C 160 allows vision in all directions for remote sensing. It also allows measurement flight during eight hours up to 9000 m high. The objective and the scientifc surrounding fields are described. The scientific experiments are presented: lidar, Differential Optical

Absorption Spectroscopy (DOAS), Michelson Interferometer for Passive Atmospheric Sounding (MIPAS), the characterization of aerosols, and the tritium experiment. ESA

N93-11087*# National Aeronautics and Space Administration, Washington, DC.

SCIENTIFIC ASSESSMENT OF OZONE DEPLETION: 1991

1991 326 p Prepared in cooperation with Dept. of the Environment, London, England, NOAA, Washington, DC, UN Environment Programme, Nairobi, Kenya, and WMO, Geneva, Switzerland Original contains color illustrations
(NASA-TM-107976; NAS 1.15:107976; GORMP-25) Avail: CASI MF A03; print copy available at WMO, Geneva, Switzerland; 1 functional color page

Over the past few years, there have been highly significant advances in the understanding of the impact of human activities on the Earth's stratospheric ozone layer and the influence of changes in chemical composition of the radiative balance of the climate system. Specifically, since the last international scientific review (1989), there have been five major advances: (1) global ozone decreases; (2) polar ozone; (3) ozone and industrial halocarbons; (4) ozone and climate relations; and (5) ozone depletion potentials (ODP's) and global warming potentials (GWP's). These topics and others are discussed. For individual titles, see N93-11088 through N93-11098.

N93-11088*# National Aeronautics and Space Administration. Langley Research Center, Hampton, VA.

SOURCE GASES: CONCENTRATIONS, EMISSIONS, AND TRENDS

Paul J. Fraser (Commonwealth Scientific and Industrial Research Organization, Aspendale, Australia), Robert Harriss, Stuart A. Penkett (East Anglia Univ., Norwich, England), Yoshihiro Makide (Tokyo Univ., Japan), Eugenio Sanhueza (Instituto Venezolano de Investigaciones Cientificas, Caracas.), Fred N. Alyea (Georgia Inst. of Tech., Atlanta.), F. Sherwood Rowland (California Univ., Irvine.), Don Blake (California Univ., Irvine.), Toru Sasaki (Meteorological Research Inst., Tokyo, Japan), and Derek M. Cunnold (Georgia Inst. of Tech., Atlanta.) et al *In* NASA, Washington, Scientific Assessment of Ozone Depletion: 1991 1991 41 p (For primary document see N93-11087 02-45)
Avail: CASI MF A03; print copy available at WMO, Geneva, Switzerland; 1 functional color page

Source gases are defined as those gases that influence levels of stratospheric ozone (O3) by transporting species containing halogen, hydrogen, and nitrogen to the stratosphere. Examples are the CFC's, methane (CH4), and nitrous oxide (N2O). Other source gases that also come under consideration in an atmospheric O3 context are those that are involved in the O3 or hydroxyl (OH) radical chemistry of the troposphere. Examples are CH4, carbon monoxide (CO), and nonmethane hydrocarbons (NMHC's). Most of the source gases, along with carbon dioxide (CO2) and water vapor (H2O), are climatically significant and thus affect stratospheric O3 levels by their influence on stratospheric temperatures. Carbonyl sulphide (COS) could affect stratospheric O3 through maintenance of the stratospheric sulphate aerosol layer, which may be involved in heterogeneous chlorine-catalyzed O3 destruction. The previous reviews of trends and emissions of source gases, either from the context of their influence on atmospheric O3 or global climate change, are updated. The current global abundances and concentration trends of the trace gases are given in tabular format. Author

N93-11089*# National Aeronautics and Space Administration. Goddard Space Flight Center, Greenbelt, MD.

OZONE AND TEMPERATURE TRENDS

Richard S. Stolarski, Vitali Fioletov (Central Aerological Observatory, Moscow, USSR), Lane Bishop (Allied Signal Corp., Buffalo, NY.), Sophie Godin (Centre National de la Recherche Scientifique, Paris, France), Rumen D. Bojkov (World Meteorological Organization, Geneva, Switzerland), Volker Kirchhoff (Instituto de Pesquisas Espaciais, Sao Jose dos Campos, Brazil), Marie-Lise Chanin (Centre National de la Recherche Scientifique, Paris, France), Joseph M. Zawodny (National Aeronautics and Space Administration. Langley Research Center, Hampton, VA.), Christos S. Zerefos (Aristotle Univ. of Thessaloniki, Greece), and William Chu (National Aeronautics and Space Administration. Langley Research Center, Hampton, VA.) *In* NASA, Washington, Scientific Assessment of Ozone Depletion: 1991 1991 34 p (For primary document see N93-11087 02-45)
Avail: CASI MF A03; print copy available at WMO, Geneva, Switzerland; 1 functional color page

An update of the extensive reviews of the state of knowledge of measured ozone trends published in the Report of the International Ozone Trends Panel is presented. The update contains a review of progress since these reports, including reviewing of the ozone records, in most cases through March 1991. Also included are some new, unpublished reanalyses of these records including a complete reevaluation of 29 stations located in the former Soviet Union. The major new advance in knowledge of the measured ozone trend is the existence of independently calibrated satellite data records from the Total Ozone Mapping Spectrometer (TOMS) and Stratospheric Aerosol and Gas Experiment (SAG) instruments. These confirm many of the findings, originally derived from the Dobson record, concerning northern mid-latitude changes in ozone. We now have results from several instruments, whereas the previously reported changes were dependent on the calibration of a single instrument. This update will compare the ozone records from many different instruments to determine whether or not they provide a consistent picture of the ozone change that has occurred in the atmosphere. The update also briefly considers the problem of stratospheric temperature change. As in previous reports, this problem received significantly less attention, and the report is not nearly as complete. This area needs more attention in the future. Author

N93-11090*# National Aeronautics and Space Administration. Langley Research Center, Hampton, VA.

HETEROGENEOUS PROCESSES: LABORATORY, FIELD, AND MODELING STUDIES

Lamont R. Poole, Michael J. Kurylo (National Aeronautics and Space Administration, Washington, DC.), Rod L. Jones (Cambridge Univ., England), Andreas Wahner (Kernforschungsanlage, Juelich, Germany), Jack G. Calvert (National Center for Atmospheric Research, Boulder, CO.), M.-T. Leu (Jet Propulsion Lab., California Inst. of Tech., Pasadena.), A. Fried (National Center for Atmospheric Research, Boulder, CO.), Mario J. Molina (Massachusetts Inst. of Tech., Cambridge.), Robert F. Hampson (National Inst. of Standards and Technology, Gaithersburg, MD.), and M. C. Pitts (Hughes STX, Inc., Greenbelt, MD.) et al *In* NASA, Washington, Scientific Assessment of Ozone Depletion: 1991 1991 18 p (For primary document see N93-11087 02-45)
Avail: CASI MF A03; print copy available at WMO, Geneva, Switzerland; 1 functional color page

The efficiencies of chemical families such as ClO(x) and NO(x) for altering the total abundance and distribution of stratospheric ozone are controlled by a partitioning between reactive (active) and nonreactive (reservoir) compounds within each family. Gas phase thermodynamics, photochemistry, and kinetics would dictate, for example, that only about 1 percent of the chlorine resident in the lower stratosphere would be in the form of active Cl or ClO, the remainder existing in the reservoir compounds HCl and ClONO2. The consistency of this picture was recently challenged by the recognition that important chemical transformations take place on polar regions: the Airborne Antarctic Ozone Experiment (AAOE) and the Airborne Arctic Stratospheric Expedition (AASA). Following the discovery of the Antarctic ozone hole, Solomon et al. suggested that the heterogeneous chemical reaction: ClONO2(g)+HCl(s) yields Cl2(g)+HNO3(s) could play a key role in converting chlorine from inactive forms into a species (Cl2) that would rapidly dissociate in sunlight to liberate atomic chlorine and initiate ozone depletion. The symbols (s) and (g) denote solid phase, or adsorbed onto a solid surface, and gas phase, respectively, and represent the approach by which such a reaction is modeled rather than the microscopic details of the reaction.

The reaction was expected to be most important at altitudes where PSC's were most prevalent (10 to 25 km), thereby extending the altitude range over which chlorine compounds can efficiently destroy ozone from the 35 to 45 km region (where concentrations of active chlorine are usually highest) to lower altitudes where the ozone concentration is at its peak. This chapter will briefly review the current state of knowledge of heterogeneous processes in the stratosphere, emphasizing those results obtained since the World Meteorological Organization (WMO) conference. Sections are included on laboratory investigations of heterogeneous reactions, the characteristics and climatology of PSC's, stratospheric sulfate aerosols, and evidence of heterogeneous chemical processing. Author

N93-11091*# National Aeronautics and Space Administration. Goddard Space Flight Center, Greenbelt, MD.

STRATOSPHERIC PROCESSES: OBSERVATIONS AND INTERPRETATION

William H. Brune (Pennsylvania State Univ., University Park.), R. Anthony Cox (National Environmental Research Council, Reading, England), Richard Turco (California Univ., Los Angeles.), Guy P. Brasseur (National Center for Atmospheric Research, Boulder, CO.), W. Andrew Matthews (Department of Scientific and Industrial Research, Lauder, New Zealand), Xiuji Zhou (State Meteorological Inst., Beijing, China), Anne Douglass, Rudi J. Zander (Liege Univ., Belgium), Margarita Prendez (Chile Univ., Santiago.), and Jose M. Rodriguez (Atmospheric and Environmental Research, Inc., Cambridge, MA.) et al *In* NASA, Washington, Scientific Assessment of Ozone Depletion: 1991 1991 21 p (For primary document see N93-11087 02-45)

Avail: CASI MF A03; print copy available at WMO, Geneva, Switzerland; 1 functional color page

Explaining the observed ozone trends discussed in an earlier update and predicting future trends requires an understanding of the stratospheric processes that affect ozone. Stratospheric processes occur on both large and small spatial scales and over both long and short periods of time. Because these diverse processes interact with each other, only in rare cases can individual processes be studied by direct observation. Generally the cause and effect relationships for ozone changes were established by comparisons between observations and model simulations. Increasingly, these comparisons rely on the developing, observed relationships among trace gases and dynamical quantities to initialize and constrain the simulations. The goal of this discussion of stratospheric processes is to describe the causes for the observed ozone trends as they are currently understood. At present, we understand with considerable confidence the stratospheric processes responsible for the Antarctic ozone hole but are only beginning to understand the causes of the ozone trends at middle latitudes. Even though the causes of the ozone trends at middle latitudes were not clearly determined, it is likely that they, just as those over Antarctica, involved chlorine and bromine chemistry that was enhanced by heterogeneous processes. This discussion generally presents only an update of the observations that have occurred for stratospheric processes since the last assessment (World Meteorological Organization (WMO), 1990), and is not a complete review of all the new information about stratospheric processes. It begins with an update of the previous assessment of polar stratospheres (WMO, 1990), followed by a discussion on the possible causes for the ozone trends at middle latitudes and on the effects of bromine and of volcanoes. Author

N93-11092*# National Aeronautics and Space Administration. Goddard Space Flight Center, Greenbelt, MD.

TROPOSPHERIC PROCESSES: OBSERVATIONS AND INTERPRETATION

Ivar S. A. Isaksen (Oslo Univ., Norway), J. A. Fuglestvedt (Oslo Univ., Norway), Yuan-Pern Lee (National Tsing Hua Univ., Hsinchu, Taiwan), Colin Johnson (United Kingdom Atomic Energy Authority, Harwell, England), Roger Atkinson (Statewide Air Pollution Research Center, Riverside, CA.), Joseph Lelieveld (Max-Planck-Inst. fuer Chemie, Mainz, Germany), Howard Sidebottom (Dublin Inst. for Advanced Studies, Ireland), Anne Thompson, William H. Brune (Pennsylvania State Univ., University Park.), and Michael Oppenheimer (Environmental Defense Fund, Inc., New York, NY.) et al *In* NASA, Washington, Scientific Assessment of Ozone Depletion: 1991 1991 26 p (For primary document see N93-11087 02-45)

Avail: CASI MF A03; print copy available at WMO, Geneva, Switzerland; 1 functional color page

Three aspects of tropospheric chemical processes imposed by manmade emission of source gases will be discussed. First, the implications for the OH distribution and thereby for the lifetime of source gases which are controlled by reactions with OH in the troposphere (e.g., CH4 and HCFC) are investigated. This is of importance for stratosphere ozone and climate. Second, we will study the impact of source gas emission on tropospheric ozone and discuss the possibility to estimate indirect climate effects from the changes in ozone and other climate gases. Finally, the degradation of HFC and HCFC's is discussed. Author

N93-11093*# Cambridge Univ. (England).

OZONE DEPLETION AND CHLORINE LOADING POTENTIALS

John A. Pyle, Donald J. Wuebbles (Lawrence Livermore National Lab., CA.), Susan Solomon (National Oceanic and Atmospheric Administration, Rockville, MD.), Sergei Zvenigorodsky (Academy of Sciences, USSR, Moscow), Peter Connell (Lawrence Livermore National Lab., CA.), Malcolm K. W. Ko (Atmospheric and Environmental Research, Inc., Cambridge, MA.), Donald A. Fisher (Du Pont de Nemours, E. I. and Co., Wilmington, DE), Frode Stordal (Norwegian Inst. for Air Research, Lillestrom.), and Debra Weisenstein (Atmospheric and Environmental Research, Inc., Cambridge, MA.) *In* NASA, Washington, Scientific Assessment of Ozone Depletion: 1991 1991 20 p (For primary document see N93-11087 02-45)

Avail: CASI MF A03; print copy available at WMO, Geneva, Switzerland; 1 functional color page

The recognition of the roles of chlorine and bromine compounds in ozone depletion has led to the regulation or their source gases. Some source gases are expected to be more damaging to the ozone layer than others, so that scientific guidance regarding their relative impacts is needed for regulatory purposes. Parameters used for this purpose include the steady-state and time-dependent chlorine loading potential (CLP) and the ozone depletion potential (ODP). Chlorine loading potentials depend upon the estimated value and accuracy of atmospheric lifetimes and are subject to significant (approximately 20-50 percent) uncertainties for many gases. Ozone depletion potentials depend on the same factors, as well as the evaluation of the release of reactive chlorine and bromine from each source gas and corresponding ozone destruction within the stratosphere. Author

N93-11094*# National Aeronautics and Space Administration. Langley Research Center, Hampton, VA.

RADIATIVE FORCING OF CLIMATE

V. Ramanswamy (Princeton Univ., NJ.), Keith Shine (Reading Univ., England), Conway Leovy (Washington Univ., Seattle.), Wei-Chyung Wang (State Univ. of New York, Albany.), Henning Rodhe (Stockholm Univ., Sweden), Donald J. Wuebbles (Lawrence Livermore National Lab., CA.), M. Ding (Stockholm Univ., Sweden), Joseph Lelieveld (Max-Planck-Inst. fuer Chemie, Mainz, Germany), Jae A. Edmonds (Department of Energy, Washington, DC.), and M. Patrick McCormick et al *In* NASA, Washington, Scientific Assessment of Ozone Depletion: 1991 1991 30 p (For primary document see N93-11087 02-45)

Avail: CASI MF A03; print copy available at WMO, Geneva, Switzerland; 1 functional color page

An update of the scientific discussions presented in Chapter 2 of the Intergovernmental Panel on Climate Change (IPCC) report is presented. The update discusses the atmospheric radiative and chemical species of significance for climate change. There are two major objectives of the present update. The first is an extension of the discussion on the Global Warming Potentials (GWP's), including a reevaluation in view of the updates in the lifetimes of the radiatively active species. The second important objective is to underscore major developments in the radiative forcing of climate due to the observed stratospheric ozone losses occurring between 1979 and 1990. Author

N93-11095*# National Aeronautics and Space Administration. Goddard Space Flight Center, Greenbelt, MD.

FUTURE CHLORINE-BROMINE LOADING AND OZONE DEPLETION

Michael J. Prather, Abdel Moneim Ibrahim (Egyptian Meteorological Authority, Cairo.), Toru Sasaki (Meteorological Research Inst., Tokyo, Japan), Frode Stordal (Norwegian Inst. for Air Research, Lillestrom.), and Guido Visconti (Aquila Univ., Italy) *In* NASA, Washington, Scientific Assessment of Ozone Depletion: 1991 1991 49 p (For primary document see N93-11087 02-45)
Avail: CASI MF A03; print copy available at WMO, Geneva, Switzerland; 1 functional color page

The prediction of future ozone requires three elements: (1) a scenario for the net emissions of chemically and radiatively active trace gases from the land and oceans; (2) a global atmospheric model that projects the accumulation of these gases; and (3) a chemical transport model that describes the distribution of ozone for a prescribed atmospheric composition and climate. This chapter, of necessity, presents models for all three elements and focuses on the following: (1) atmospheric abundance of chlorine and bromine in the form of halocarbons; and (2) the associated perturbations to stratospheric ozone. Author

N93-11096*# National Aeronautics and Space Administration. Goddard Space Flight Center, Greenbelt, MD.

PREDICTED AIRCRAFT EFFECTS ON STRATOSPHERIC OZONE

Malcolm K. W. Ko (Atmospheric and Environmental Research, Inc., Cambridge, MA.), Steve Wofsy (Harvard Univ., Cambridge, MA.), Dieter Kley (Kernforschungsanlage, Juelich, Germany), Evgeny A. Zhadin (Central Aerological Observatory, Dolgoprudnyi, USSR), Colin Johnson (United Kingdom Atomic Energy Authority, Harwell, England), Debra Weisenstein (Atmospheric and Environmental Research, Inc., Cambridge, MA.), Michael J. Prather (National Aeronautics and Space Administration. Goddard Inst. for Space Studies, New York, NY.), and Donald J. Wuebbles (Lawrence Livermore National Lab., CA.) *In* NASA, Washington, Scientific Assessment of Ozone Depletion: 1991 1991 18 p (For primary document see N93-11087 02-45)
Avail: CASI MF A03; print copy available at WMO, Geneva, Switzerland; 1 functional color page

The possibility that the current fleet of subsonic aircraft may already have caused detectable changes in both the troposphere and stratosphere has raised concerns about the impact of such operations on stratospheric ozone and climate. Recent interest in the operation of supersonic aircraft in the lower stratosphere has heightened such concerns. Previous assessments of impacts from proposed supersonic aircraft were based mostly on one-dimensional model results although a limited number of multidimensional models were used. In the past 15 years, our understanding of the processes that control the atmospheric concentrations of trace gases has changed dramatically. This better understanding was achieved through accumulation of kinetic data and field observations as well as development of new models. It would be beneficial to start examining the impact of subsonic aircraft to identify opportunities to study and validate the mechanisms that were proposed to explain the ozone responses. The two major concerns are the potential for a decrease in the column abundance of ozone leading to an increase in ultraviolet radiation at the ground, and redistribution of ozone in the lower stratosphere and upper troposphere leading to changes in the Earth's climate. Two-dimensional models were used extensively for ozone assessment studies, with a focus on responses to chlorine perturbations. There are problems specific to the aircraft issues that are not adequately addressed by the current models. This chapter reviews the current status of the research on aircraft impact on ozone with emphasis on immediate model improvements necessary for extending our understanding. The discussion will be limited to current and projected commercial aircraft that are equipped with air-breathing engines using conventional jet fuel. The impacts are discussed in terms of the anticipated fuel use at cruise altitude. Author

N93-11097*# National Aeronautics and Space Administration. Goddard Space Flight Center, Greenbelt, MD.

PREDICTED ROCKET AND SHUTTLE EFFECTS ON STRATOSPHERIC OZONE

Robert S. Harwood (Edinburgh Univ., Scotland), Igor L. Karol (Main Geophysical Observatory, Leningrad, USSR), Charles H. Jackman, Lian-Xiong Qiu (Academia Sinica, Beijing, China), Michael J. Prather (National Aeronautics and Space Administration. Goddard Inst. for Space Studies, New York, NY.), and John A. Pyle (Cambridge Univ., England) *In* NASA, Washington, Scientific Assessment of Ozone Depletion: 1991 1991 13 p (For primary document see N93-11087 02-45)
Avail: CASI MF A03; print copy available at WMO, Geneva, Switzerland; 1 functional color page

The major chemical effluents of either solid- or liquid-fueled rockets that can potentially perturb stratospheric ozone include chlorine compounds (HCl), nitrogen compounds (NO(x)), and hydrogen compounds (H2 and H2O). Radicals (Cl, ClO, H, OH, HO2, NO, and NO2) formed directly or indirectly from rocket exhaust can cause the catalytic destruction of ozone. Other exhaust compounds that could presumably lead to ozone destruction either by direct reaction with ozone or by providing a surface for heterogeneous processes include the particulates Al2O3, ice, and soot. These topics are discussed in terms of the possible effects of rocket exhausts on stratospheric ozone. Author

N93-11098*# Department of Scientific and Industrial Research, Lauder (New Zealand).

ULTRAVIOLET RADIATION CHANGES

Richard L. McKenzie, John E. Frederick (Illinois Univ., Chicago.), Mohammad Ilyas (Sains Malaysia Univ., Penang.), V. Filyushkin (Central Aerological Observatory, Dolgoprudnyi, USSR), Andreas Wahner (Kernforschungsanlage, Juelich, Germany), K. Stamnes (Alaska Univ., Fairbanks.), P. Muthusubramanian (Madurai-Kamaraj Univ., Madurai, India), M. Blumthaler (Innsbruck Univ., Austria), Colin E. Roy (Australian Radiation Lab., Melbourne.), and Sasha Madronich (National Center for Atmospheric Research, Boulder, CO.) *In* NASA, Washington, Scientific Assessment of Ozone Depletion: 1991 1991 16 p (For primary document see N93-11087 02-45)
Avail: CASI MF A03; print copy available at WMO, Geneva, Switzerland; 1 functional color page

A major consequence of ozone depletion is an increase in solar ultraviolet (UV) radiation received at the Earth's surface. This chapter discusses advances that were made since the previous assessment (World Meteorological Organization (WMO)) to our understanding of UV radiation. The impacts of these changes in UV on the biosphere are not included, because they are discussed in the effects assessment. Author

N93-11127 Institut d'Aeronomie Spatiale de Belgique, Brussels.

REINTERPRETATION OF OZONE DATA FROM BASE ROI BAUDOUIN (ANTARCTICA)

H. Kelder (Royal Netherlands Meteorological Inst., De Bilt.) and C. Muller 1992 24 p Submitted for publication Sponsored in part by Commission of the European Communities
(Aeronomica-Acta-A-365; ETN-92-92390) Copyright Avail: Institut d'Aeronomie Spatiale de Belgique, 3 Avenue Circulaire, B-1180 Brussels, Belgium

The ozone Dobson measurements obtained in Antarctica at the Belgian 'Base Roi Baudouin' (70 deg 26 minutes south, 24 deg 19 minutes east) in 1965 and 1966 were retrieved from archives and a study of the original observers notes was made in order to check possible seasonal ozone phenomena. No systematic anomaly in the first analysis was found; meteorological data from the site together with Brewer-Mast ozone soundings concur that the conditions did not correspond either in 1965 nor 1966 to the current ozone hole situation. However, the data yields excellent correlation with stratospheric temperature and shows in 1966 a clear November maximum of 474 Dobson units in opposition to an October average value of 344 Dobson units. ESA

N93-11232# Alaska Univ., Fairbanks.

INTERNATIONAL CONFERENCE ON THE ROLE OF THE POLAR REGIONS IN GLOBAL CHANGE: PROCEEDINGS, VOLUME 1

G. Weller, ed., C. L. Wilson, ed., and B. A. B. Severin, ed. Dec. 1991 362 p Conference held in Fairbanks, AK, 11-15 Jun. 1990
(Contract DE-FG06-90ER-60949)
(DE92-013652; CONF-9006128-Vol-1) Avail: CASI HC A16/MF A03

The International Conference on the Role of the Polar Regions in Global Change took place on the campus of the University of Alaska Fairbanks on 11-15 Jun. 1990. The goal of the conference was to define and summarize the state of knowledge on the role of the polar regions in global change, and to identify gaps in knowledge. To this purpose experts in a wide variety of relevant disciplines were invited to present papers and hold panel discussions. While there are numerous conferences on global change, this conference dealt specifically with polar regions which occupy key positions in the global system. These two volumes of conference proceedings include papers on the following topics: (1) detection and monitoring of change; (2) climate variability and climate forcing; (3) ocean, sea ice, and atmosphere interactions and processes; (4) effects on biota and biological feedbacks; (5) ice sheet, glacier and permafrost responses and feedbacks; (6) paleoenvironmental studies; and, (7) aerosols and trace gases. DOE

N93-11233# Alaska Univ., Fairbanks.

INTERNATIONAL CONFERENCE ON THE ROLE OF THE POLAR REGIONS IN GLOBAL CHANGE: PROCEEDINGS, VOLUME 2

G. Weller, ed., C. L. Wilson, ed., and B. A. B. Severin, ed. Dec. 1991 404 p Conference held in Fairbanks, AK, 11-15 Jun. 1990
(Contract DE-FG06-90ER-60949)
(DE92-013653; CONF-9006128-Vol-2) Avail: CASI HC A18/MF A04

The International Conference on the Role of the Polar Regions in Global Change took place on the campus of the University of Alaska Fairbanks on 11-15 Jun. 1990. The goal of the conference was to define and summarize the state of knowledge on the role of the polar regions in global change, and to identify gaps in knowledge. To this purpose experts in a wide variety of relevant disciplines were invited to present papers and hold panel discussions. While there are numerous conferences on global change, this conference dealt specifically with the polar regions which occupy key positions in the global system. These two volumes of conference proceedings include papers on the following topics: (1) detection and monitoring of change; (2) climate variability and climate forcing; (3) ocean, sea ice, and atmosphere interactions and processes; and (4) effects on biota and biological feedbacks; (5) ice sheet, glacier and permafrost responses and feedbacks, (6) paleoenvironmental studies; and, (7) aerosol and trace gases. DOE

N93-11466# Army Engineer Topographic Labs., Fort Belvoir, VA.

GLOBAL CLIMATE CHANGE (GCC) ISSUES AND THEIR IMPACTS ON THE US ARMY CORPS OF ENGINEERS

Jack E. Huntley and John E. Neander Nov. 1991 136 p
(AD-A247279; TEC-SR-1) Avail: CASI HC A07/MF A02

This report is a survey of recent findings and arguments within the scientific arena on the subject of global climate change. The focus of this report looks at global, continental, and regional issues, as well as surface and upper atmospheric effects. Potential responses by the biosphere as well as the impacts on Army operations by global climate change are examined. The geologic past provides a detailed record of Earth's climate system. It also reveals changes that took place in the concentration of atmospheric gasses as Earth's climate switched from glacial to interglacial periods. The secular record of temperature shows that Earth's climate has warmed from 0.5 C to 0.7 C this past century. The world's populace is injecting tremendous amounts of greenhouse gasses into the atmosphere at a rate where the effective doubling of pre-industrial carbon dioxide (CO2) concentration could occur between the years 2035 to 2050. Clouds have been found to have a net cooling effect on the global average temperature. Anthropogenic pollutants and gasses produced from biological sources may increase the amount of clouds around the world, thus adding to the cooling effect. Aftereffects of volcanic eruption, and gasses emitted by phytoplankton that lead to cloud formation retard global warming. Weapon and support systems may require upgraded data bases to match vegetation changes due to evolving climate patterns. GRA

N93-11569# Colorado State Univ., Fort Collins. Dept. of Atmospheric Science.

STUDIES OF THE ROLE OF CLOUDS IN CO2-INDUCED CLIMATE CHANGE

D. A. Randall Jul. 1992 13 p
(Contract DE-FG02-89ER-69027)
(DE92-018648; DOE/ER-69027/3) Avail: CASI HC A03/MF A01

Predictions of global change based on climate models are influencing both national and international policies on energy and the environment. Existing climate models show some skill in simulating the present climate, but suffer from many widely acknowledged deficiencies. Among the most serious problems is the need to apply 'flux corrections' to prevent the models from drifting away from the observed climate in control runs that do not include external perturbing influences such as increased carbon dioxide (CO2) concentrations. The flux corrections required to prevent climate drift are typically comparable in magnitude to the observed fluxes themselves. During the past three years, we have conducted a research program designed to investigate global air-sea interaction as it relates to the global warming problem, with special emphasizing the role of clouds. Our research includes model development efforts; application of models to simulation of present and future climates, with comparison to observations wherever possible; and vigorous participation in ongoing efforts to compare the present generation of atmospheric general circulation models. DOE

N93-11655# Oak Ridge National Lab., TN. Carbon Dioxide Information Analysis Center.

CLIMATE CHANGE AND WATER SUPPLY, MANAGEMENT AND USE: A LITERATURE REVIEW

L. H. Chang, J. D. Draves, and C. T. Hunsaker May 1992 91 p
(Contract DE-AC05-84OR-21400)
(DE92-019069; ORNL/CDIAC-52) Avail: CASI HC A05/MF A01

There is evidence that atmospheric concentrations of CO2, tropospheric O3, and CH4, among other gases that contribute to the greenhouse effect, have increased in recent decades, and that these changes may induce changes in global air temperatures and regional climate features in coming years. A literature review was conducted to sample the literature base on which our understanding of the water resource impacts of climate change rests. Water resource issues likely to be important include hydrologic response to climate change, the resilience of water supply systems to changing climatic and hydrologic conditions, and the effects of climate change on water quality and water uses (such as navigation and energy generation). A computer-assisted search of literature on the effects of climate change on these subjects was conducted. All studies were classified by type of paper (e.g., review, discussion, case study), region, water resource variable studied, and source of climate scenario. The resulting bibliography containing more than 200 references was largely annotated. Case studies of potential hydrologic impacts have been more common than studies of impacts on water management or water use, but this apparent research gap is decreasing. Case studies demonstrating methods of incorporating potential risks of climate change into water project planning and management have been performed. Considerable variability in regional coverage exists; the Great Lakes basin and California receive relatively more attention than such regions as New England and the Missouri River basin. General circulation model-based and hypothetical climate scenarios have been the dominant sources of climate scenarios used in case studies, although a variety of other methods for developing climate scenarios have been developed. DOE

N93-11676# Lawrence Livermore National Lab., CA.

MODELING THE DISPERSION OF TRACER PLUMES IN THE COLORADO FRONT RANGE BOUNDARY LAYER DURING NIGHT- AND DAY-TIME CONDITIONS

R. Lange 17 Jul. 1992 6 p Presented at the 10th Symposium on Turbulence and Diffusion, Portland, OR, 29 Sep. - 2 Oct. 1992
(Contract W-7405-eng-48)
(DE92-019384; UCRL-JC-110559; CONF-9209158-4) Avail: CASI HC A02/MF A01

The 1991 ASCOT (Atmospheric Studies in Complex Terrain) field study in the vicinity of the Department of Energy's Rocky Flats Plant, CO, was conducted to study the local and regional circulations and their interactions with synoptic flows over the complex terrain of the Rocky Mountains Colorado Front range. The ASCOT study focused on nocturnal flows from canyons and off slopes along the Front Range and their effect on transport and diffusion in the area. The study was combined with the Rocky Flats Winter validation Study (WVS) which had similar objectives but included a number of transition- and daytime experiments. Tracer plumes were released as part of this combined field campaign over the period of February 3 to 19, 1991 from the Rocky Flats Plant. Twelve intensive experiments, centered around eleven-hour long surface releases of sulfur hexafluoride (SF6) tracer material, were conducted by teams of personnel from a number of national laboratories, government agencies and private contractors. The concentration patterns resulting from the transport and turbulent diffusion of the SF6 traces plumes within the atmospheric boundary layer during two night, one morning transition, and one day time period were simulated. The model used for these simulations was the Lawrence Livermore National Laboratory (LLNL) 3-D, diagnostic MATHEW/ADPIC atmospheric dispersion model for complex terrain and flow conditions. The model, the selected experiments, and the results of the comparison of predicted with observed tracer concentrations are presented. DOE

N93-11677# Lawrence Livermore National Lab., CA.

THE ROLE OF REFRIGERANTS IN CLIMATE CHANGE

D. J. Wuebbles Jun. 1992 21 p Presented at the International Institute of Refrigeration Meeting on Refrigeration, Energy and Environment, Trondheim, Norway, 22-24 Jun. 1992
(Contract W-7405-eng-48)
(DE92-019385; UCRL-JC-110859; CONF-9206130-2) Avail: CASI HC A03/MF A01

The primary chemicals used as refrigerants, chlorofluorocarbons (CFC's), and the compounds being considered as their replacements (HCFC's and HFC's) have been intensely studied because of concerns about chlorine chemistry effects on stratospheric ozone. Increasing attention is being given to the potential effects of these compounds in concerns about global warming. CFC's, HCFC's, and HFC's absorb infrared radiation and thus are greenhouse gases that can influence radiative forcing on climate. The purpose of this paper is to describe the current understanding of the role of refrigerants in affecting climate. Increasing atmospheric concentrations of CFC's have accounted for about 24 pct. of the direct increase in radiative forcing from greenhouse gases over the last decade. However, observed decreases in stratospheric ozone, thought to be connected to increasing stratospheric chlorine from CFC's, suggests a cooling tendency over the last decade. This cooling tendency has strong latitudinal gradients, but is, when globally averaged, about comparable in magnitude and opposite in sign to the radiative forcing from CFC's over this period. Because of their shorter atmospheric lifetimes, the direct radiative influence on climate from the replacement compounds should generally be much smaller than the CFC's. DOE

N93-11680# Oak Ridge National Lab., TN.

THE RELATIVE IMPORTANCE OF SULFUR AND NITROGEN COMPOUNDS IN THE ACIDIFICATION OF FRESHWATER

H. VanMiegroet 1992 33 p Presented at the Dahlem Workshop on Acidification of Freshwater Ecosystems, Berlin (Germany), 27 Sep. - 2 Oct. 1992
(Contract DE-AC05-84OR-21400)
(DE92-016899; CONF-9209156-1) Avail: CASI HC A03/MF A01

The acid-base chemistry of streams and lakes is regulated by the amount and composition of atmospheric deposition and by biogeochemical processes in the catchment and within streams and lakes. In this paper the influence of nitrogen (N) and sulfur (S) compounds will be discussed for the following reasons: (1) because they are major constituents of atmospheric deposition that have recently become the focus of critical loads assessments in Europe and North America; and (2) because they are essential nutrients for most biota and cycle naturally through terrestrial and aquatic ecosystems. In order to evaluate the relative impact of atmospheric inputs on freshwater acidity, it is necessary to clearly define 'acidification' and to understand the mechanisms of change caused or mediated by natural and anthropogenic processes. DOE

N93-11702# Florida Univ., Gainesville. Dept. of Coastal and Oceanographic Engineering.

PHYSICAL EFFECTS OF VEGETATION ON WIND-BLOWN SAND IN THE COASTAL ENVIRONMENTS OF FLORIDA Final Report

D. M. Sheppard and A. W. Niedoroda Feb. 1992 52 p Prepared in cooperation with Environmental Science and Engineering, Inc., Gainesville, FL
(UF Proj. 4910451123312)
(PB92-188424; UPN-90100411) Avail: CASI HC A04/MF A01

One and two-dimensional, second order turbulence plant canopy flow models were developed for the purpose of estimating the effect of coastal vegetation on wind blown sand transport. The computer program that solves the governing differential equations uses measured leaf area density profiles and drag coefficients for crop plants similar in shape and size to the more common coastal vegetation in Florida. Author

N93-11744# Lawrence Livermore National Lab., CA.

ATMOSPHERIC REACTIVE NITROGEN: A MODEL STUDY OF NATURAL AND ANTHROPOGENIC SOURCES AND THE ROLE OF MICROBIAL SOIL EMISSIONS

J. Dignon, J. E. Penner, C. S. Atherton, and J. J. Walton Feb. 1992 12 p Presented at the 7th World Conference on the Chemistry of the Atmosphere: Its Impact on Global Changes, Baltimore, MD, 2-6 Dec. 1991
(Contract W-7405-eng-48)
(DE92-010717; UCRL-JC-107393; CONF-911212-1) Avail: CASI HC A03/MF A01

Nitrogen oxides (NO(x) = NO + NO2) are primary pollutants which react in the atmosphere to form nitric acid (HNO3). Nitric acid is a major contributor to acid wet and dry deposition and can also affect the reactive nitrogen nutrients in soil and ocean ecosystems. In addition, NO(x) takes part in the photochemical cycle of ozone (O3). Tropospheric O3 is important from both an atmospheric and a biological perspective. It acts as a greenhouse gas warming the earth's surface and as a chemical oxidant which can cause injury to humans, plants, and animals. Anthropogenic sources including 22 Tg N from fossil fuel burning and 5 to 13 Tg N from biomass burning constitute the largest contribution (Tg = 10(exp 12) g). Less is understood about the natural sources of NO(x) andin particular the emissions from microbial activity in soils. Here we present a model calculated, seasonally and spatially resolved (1x1 degree), inventory of the annual soil emissions of NO(x) from microbial activity from natural vegetation ecosystems. The soil emissions model addresses the emissions of soils from the natural vegetation types. Emissions from soil microbial activity have been shown to be temperature and moisture dependent.

DOE

N93-11846# Institute of Energy Economics of Japan.
ENVIRONMENTAL PROBLEMS AND TRENDS OF INTERNATIONAL RESPONSES, 2
25 Nov. 1991 294 p In JAPANESE
(DE92-531118; IEE-SR-228) Avail: CASI HC A13/MF A03

This is a report 'Survey for impacts of global environmental issues on utilization of alternative energies for oil' conducted for NEDO. Based mainly on field surveys in the U.S. and European developed countries and developing countries, stated are each country's opinions and concrete measures against the global warming. The paper describes trends in international meetings and the attitudes of different countries in Chap. 1, domestic and international policy responses in Chap. 2, feasibility of technological options and responses of each country in Chap. 3, and international and technological cooperations with the East (USSR and East Europe) and the South (LDCs) in Chap. 4. Each country, especially in West Europe, starts to have their own targets for stabilization of CO2 emissions and agrees with each other in a general course of actions to be taken. A further step of framework is targeted at a meeting scheduled for June 1992 in Brazil. It is indispensable to establish conditions under which USSR, East European, and developing countries can participate in international tackling with the global warming problem. DOE

N93-11864# Rensselaer Polytechnic Inst., Troy, NY. Dept. of Biology.
TENTH INTERNATIONAL SYMPOSIUM ON ENVIRONMENTAL BIOGEOCHEMISTRY Abstracts Only
H. L. Ehrlich Jan. 1992 92 p Presented at the 10th International Symposium on Environmental Biogeochemistry, San Francisco, CA, 19-23 Aug. 1991
(Contract DE-FG05-91ER-61105)
(DE92-016200; CONF-9108209-Absts) Avail: CASI HC A05/MF A01

The primary task of this Symposium on Environmental Biogeochemistry was to examine our current understanding of Global Change and the Biogeochemistry of Radiative Trace Gases. The symposium was divided into 12 non-overlapping sessions: Paleoatmospheres and paleoclimates; Global distributions and atmospheric reactions; Poster presentations on the topics of sessions 1, 2, 4, 5, and 7; Terrestrial systems and land use change - 1; Terrestrial and land use change - 11; Fluxes and cycling in aquatic systems; Metals, organics, and depositional environments; Poster presentations on the topics of sessions 6, 9, 10 and 12; Biological Mechanisms of formation and destruction - 1; Biological mechanisms of formation and destruction - 11; High latitude systems; and Global sources, sinks, and feedbacks. DOE

N93-11920 Washington State Univ., Pullman.
ATMOSPHERIC DISPERSION IN MOUNTAIN VALLEYS AND BASINS Ph.D. Thesis
K. Jerry Allwine 1991 195 p
Avail. Univ. Microfilms Order No. DA9226129

The primary goal of this research is to further characterize and understand dispersion in valley and basin atmospheres. A secondary, and related goal, is to identify and understand the dominant physical processes governing this dispersion. This has been accomplished through a review of the current literature, and analyses of recently collected data from two field experiments. This work should contribute to an improved understanding of material transport in the atmospheric boundary layer. It was found that dispersion in a freely draining valley (Brush Creek valley, CO) atmosphere is much greater than in an enclosed basin (Roanoke, VA) atmosphere primarily because of the greater wind speeds moving past the release point and the greater turbulence levels. The development of a cold air pool in the Roanoke basin is the domanant process governing nighttime dispersion in the basin, while the nighttime dispersion in the Brush Creek valley is dominated by turbulent diffusion and plume confinement between the valley sidewalls. The interaction between valley flows and above ridgetops flows is investigated. A 'ventilation rate' of material transport between the valley and above ridgetop flows is determined. This is important in regional air pollution modeling and global climate modeling. A simple model of dispersion in valleys, applicable through a diurnal cycle, is proposed.

Dissert. Abstr.

N93-12098# Argonne National Lab., IL.
COMPARISON OF PASSIVE-REMOTE AND CONVENTIONAL FOURIER TRANSFORM INFRARED SYSTEMS FOR CONTINUOUSLY MONITORING INCINERATOR EMISSIONS
J. C. Demirgian, C. L. Hammer, and R. T. Kroutil (Army Chemical Research and Development Center, Aberdeen Proving Ground, MD.) 1992 10 p Presented at the 1992 Incineration Conference, Albuquerque, NM, 11-14 May 1992
(Contract W-31-109-eng-38)
(DE92-015225; ANL/CP-74716; CONF-920527-7) Avail: CASI HC A02/MF A01

Significant improvements in detection technology are needed to comply with the requirements in the Clean Air Act of 1990, Title 3, which requires the monitoring of air toxics. Fourier transform infrared (FTIR) spectroscopy can satisfy these requirements in two different modes. Conventional FTIR spectrometers can be installed on-stream so that a vapor stream enters an infrared cell for analysis. Other types of FTIR spectrometers can detect chemical plumes remotely, measure the natural emissions of the molecules in the plume. The samples do not come to the instrument, and the instrument has neither source nor reflector mirrors. We will discuss the applications of FTIR spectrometry for both conventional and passive-remote FTIR spectroscopy. Some applications of conventional FTIR include a continuous emission monitor for measuring incinerator emissions and determining indoor air quality. Passive-remote FTIR spectroscopy can be used to identify and track a chemical plume. It can also be used to detect fugitive emissions. Hence, it can be used as an independent means to assure compliance with environmental regulations in real-time. Because of the relatively simple instrumentation, passive-remote instruments can be helicopter- or vehicle-mounted for mobile detection of plumes. DOE

N93-12104# California Univ., Berkeley. Lawrence Berkeley Lab.
STRATOSPHERIC AIRCRAFT: IMPACT ON THE STRATOSPHERE?
H. Johnston Feb. 1992 28 p Presented at the CHEMRAWN 7: World Conference on the Chemistry of the Atmosphere: Its Impact on Global Changes, Baltimore, MD, 2-6 Dec. 1991
(Contract DE-AC03-76SF-00098)
(DE92-016997; LBL-31884; CONF-911212-2) Avail: CASI HC A03/MF A01

The steady-state distribution of natural stratospheric ozone is primarily maintained through production by ultraviolet photolysis of molecular oxygen, destruction by a catalytic cycle involving nitrogen oxides (NO(sub x)), and relocation by air motions within the stratosphere. Nitrogen oxides from the exhausts of a commercially viable fleet of supersonic transports would exceed the natural source of stratospheric nitrogen oxides if the t should be equipped with 1990 technology jet engines. This model-free comparison between a vital natural global ingredient and a proposed new industrial product shows that building a large fleet of passenger stratospheric aircraft poses a significant global problem. NASA and aircraft industries have recognized this problem and are studying the redesign of jet aircraft engines in order to reduce the nitrogen oxides emissions. In 1989 atmospheric models identified two other paths by which the ozone destroying effects of stratospheric aircraft might be reduced or eliminated: (1) Use relatively low supersonic Mach numbers and flight altitudes. For a given rate of nitrogen oxides injection into the stratosphere, the calculated reduction of total ozone is a strong function of altitude, and flight altitudes well below 20 kilometers give relatively low calculated ozone reductions. (2) Include heterogeneous chemistry in the two-dimensional model calculations. Necessary conditions for answering the question on the title above are to improve the quality of our understanding of the lower stratosphere and to broaden our knowledge of hetergeneous stratospheric chemistry. This article reviews recently proposed new mechanisms for heterogeneous reactions on the global stratospheric sulfate aerosols. DOE

N93-12314# Argonne National Lab., IL.

REDUCTION IN GLOBAL WARMING DUE TO FUEL ECONOMY IMPROVEMENTS AND EMISSIONS CONTROL OF CRITERIA POLLUTANTS: NEW US LIGHT-DUTY VEHICLES (1968-1991)

M. E. Pitstick, D. J. Santini, and H. Chauhan (Delaware Univ., Newark.) 1992 7 p Presented at the 27th Intersociety Energy Conversion Engineering Conference, San Diego, CA, 3-7 Aug. 1992
(Contract W-31-109-eng-38)
(DE92-016636; ANL/CP-75268; CONF-920801-11) Avail: CASI HC A02/MF A01

This paper explores the impact of US emission controls and fuel economy improvements on the global warming potential (GWP) of new light-duty vehicles. Fuel economy improvements have reduced the GWP of both passenger cars and light-duty trucks by lowering the per mile emissions of carbon dioxide (CO2). Further GWP reductions have been achieved by emission standards for criteria pollutants: carbon monoxide (CO), hydrocarbons (HC), and nitrogen oxides (NO(sub x)). The GWP of a criteria pollutant was calculated by multiplying the emission rate by a relative global warming factor to obtain a CO2 equivalent emission rate. Both CO2 and criteria pollutant emission rates per vehicle have decreased substantially for new light-duty vehicles over the period from 1968 to 1991. Over that period, the GWP from CO2 was reduced by almost 50 percent in new vehicles by improving fuel economy. In that same time period, the GWP from criteria pollutants from new vehicles was reduced with emission controls by from 80 to 90 percent depending on the global warming time frame of interest. Consequently, total reductions in the GWP of new passenger cars and light-duty trucks have been on the order of 55 to 75 percent compared to precontrol (before 1968) new vehicles. However, the reduction in GWP caused by emission control of criteria pollutants has been larger than the reduction caused by improved fuel economy (i.e., reduced CO2). The contribution of criteria pollutants to the GWP of precontrol new vehicles was substantial, but their contribution has been reduced significantly due to US emission controls. As a result, the contribution of criteria pollutants to global warming is now much less than the contribution of CO2 from fuel consumption. DOE

N93-12474# Alliance to Save Energy, Washington, DC.

THE USES AND LIMITS OF ECONOMIC MODELS AS A CLIMATE CHANGE POLICY TOOL Summary Report

M. B. Zimmerman and W. A. Nitze 1991 7 p Presented at the Workshop on the Uses and Limits of Economic Models as a Climate Change Policy Tool, Washington, DC, 1-2 Feb. 1991
(Contract DE-FG01-91PE-10015)
(DE92-015792; CONF-9102177-Summ) Avail: CASI HC A02/MF A01

The Alliance to Save Energy initiated this workshop as a means of bringing climate change policy makers and economists together on the eve of the opening negotiating session for a climate change convention. The one and one-half day workshop was attended by 16 analysts who provided presentations on modeling approaches. There is a need for policy makers to be better able to evaluate the growing literature estimating the potential cost of policy options. Our hope is that this report, to be presented at the conclusion of the negotiations on the framework convention on climate change at the Earth Summit in Brazil, will help policy makers in the US and elsewhere evaluate the costs and benefits of national climate change mitigation policies. Although it is still unclear how far the convention will go in requiring emissions reductions, many countries are proceeding with detailed plans to reduce domestic carbon dioxide (CO(sub 2)) emissions. Our goal in holding the workshop and writing this report is to spark a new level of dialogue between the producers and users of information on the costs and benefits of climate mitigation policies leading to the development of more cost-effective policy solutions at the national and international levels. DOE

N93-12496# Westinghouse Idaho Nuclear Co., Inc., Idaho Falls.

ENVIRONMENTAL RESTORATION PROJECT CONFIGURATION CONTROL

L. L. Hutterman 19 Aug. 1991 9 p Presented at the Environmental Remediation 1991 Conference, Pasco, WA, 8-11 Sep. 1991
(Contract DE-AC07-84ID-12435)
(DE92-017223; WINCO-11735; CONF-910981-66) Avail: CASI HC A02/MF A01

Projecting budget requirements for performing environmental restoration activities in a manner consistent with the regulatory agencies requires long-term planning, scheduling, and budget forecasting. The Westinghouse Idaho Nuclear Company, Inc. (WINCO) Environmental Restoration Program is responsible for 14 operable units at the Idaho Chemical Processing Plant (ICPP) at the Idaho National Engineering Laboratory (INEL). To facilitate response to US Department of Energy (DOE) requirements, a baseline document has been established, and activities for each of the environmental release sites have been developed. The baseline document is based primarily on the activities identified in the Interagency Agreement (IAG) for operable unit scoping and investigation. In addition, the schedule for some sites reflects fiscal year 1991 Consent Order Compliance Agreement requirements. Planning has been conducted through completion of the Record of Decision. The baseline document provides management with a defensible basis to project and control costs. Work that requires modification in scope, changes to applicable DOE or regulatory orders/guidance, or identification of additional release sites will normally impact costs and schedule. The impact of these changes will be evaluated and the baseline revised to reflect the changes. Management can use the baseline to evaluate potential cost impacts and assist with decision making when resources are limited to select the optimal technical strategy and minimize the impact to cost and schedule for other projects. DOE

N93-12524# Environmental Protection Agency, Washington, DC. Air and Radiation Div.

ALLOWANCE SYSTEM: PROPOSED ACID RAIN RULE

Dec. 1991 8 p
(PB92-226174; EPA/400/1-91/034) Avail: CASI HC A02/MF A01

The U.S. Environmental Protection Agency (EPA) has proposed four rules containing the core acid rain requirements: the Permits Rule (40 CFR Part 72), the Allowance System Rule (40 CFR Part 73), the Continuous Emission Monitoring Rule (40 CFR Part 75), and the Excess Emissions Rule (40 CFR Part 77). The EPA will also propose additional rules at a future date. These rules will include requirements for facilities that elect to opt into the Acid Rain program (40 CFR Part 74) and for the nitrogen oxide (NO(x)) control program (40 CFR Part 76). The fact sheet summarizes the key components of EPA's proposed Allowance System. GRA

N93-12525# Environmental Protection Agency, Washington, DC. Office of Air and Radiation.

UNITED STATES/CANADA AIR QUALITY AGREEMENT Progress Report

Mar. 1992 80 p
(PB92-228030; EPA/400/1-92/002) Avail: CASI HC A05/MF A01

The Canada-United States Air Quality Agreement, signed 13 Mar. 1991, marked a new era of cooperation aimed at helping to guarantee cleaner air and a healthier environment for millions of Canadians and Americans. Now, one year later, progress was made by each country, individually and together. A forum for discussion was established; programs to resolve domestic and transboundary air quality issues are being shared; lessons learned from existing and past programs also are being shared; and the pursuit of data compatibility between countries is under way. GRA

46 GEOPHYSICS

Includes aeronomy; upper and lower atmosphere studies; ionospheric and magnetospheric physics; and geomagnetism.

For space radiation see *93 Space Radiation.*

N93-10964*# Southwest Research Inst., San Antonio, TX. Instrumentation and Space Research Div.
STUDIES OF INTERACTIVE PLASMA PROCESSES IN THE POLAR CUSP Final Report
J. Hunter Waite, Jr. 1 Sep. 1992 34 p Original contains color illustrations
(Grant NAGw-1657; SwRI Proj. 15-2783)
(NASA-CR-190892; NAS 1.26:190892) Avail: CASI HC A03/MF A01; 4 functional color pages

The final report for NAGW-1657 (SwRI Project 15-2783) is presented. Several distinctly different areas of research are discussed: (1) studies of the thermal structure of polar outflows; (2) Prognoz-8 data analysis; and (3) the Ulysses Jupiter encounter. Author

N93-10985# Los Alamos National Lab., NM.
DIFFUSION OF ECHO 7 ELECTRON BEAMS DURING BOUNCE MOTION
R. J. Nemzek 1992 33 p Presented at the Chapman Conference on Auroral Plasma Dynamics, Minneapolis, MN, 21-25 Oct. 1991
(Contract W-7405-eng-36)
(DE92-018288; LA-UR-92-2284; CONF-9110188-1) Avail: CASI HC A03/MF A01

The Echo 7 sounding rocket experiment injected electron beams into the magnetosphere and detected them after one or more bounces along field lines near L = 6.5. Waves with equatorial amplitudes of a few mV/m diffused the beams so that only approximately 20 percent of the initial current returned to the rocket altitude in the Northern Hemisphere. On successive bounces the electron flux continued to drop at the same rate. These results imply a lifetime of approximately 1.7 for 20 kev electrons just outside of the loss cone. Comparison with other Echo flights shows that the beam return is dependent upon geomagnetic conditions: low activity causes there to be less scattering and high activity can actually prevent detection of the returning beam. DOE

N93-11006# Bonn Univ. (Germany). Inst. fuer Physik.
SODIUM-LIDAR MESOSPHERE EXAMINATIONS: SELECTED ELEMENTS OF THE EXPERIMENTAL CONSTRUCTION OF A MOBILE INSTRUMENT AND EVALUATION OF THE DATA ACQUIRED WITH A STATIONARY Na-LIDAR DURING THE DYANA CAMPAIGN Thesis [NATRIUM-LIDAR UNTERSUCHUNGEN DER MESOSPHAERE: AUSGEWAEHLTE ELEMENTE DES EXPERIMENTELLEN AUFBAUS EINES MOBILEN INSTRUMENTES UND AUSWERTUNG DER MIT EINEM STATIONAEREN NA-LIDAR WAEHREND DER DYANA-KAMPAGNE GEWONNENEN DATEN]
Stefan Schmitz Jul. 1991 154 p In GEORGIAN
(Bonn-IR-91-78; ETN-92-92107) Avail: CASI HC A08/MF A02

A new mobile sodium lidar instrument in construction for the measurement of the temperature and sodium density profiles in the mesosphere is presented. The specifications of the lidar container are outlined. A newly developed counting electronics which yields higher count rates and raises the sensitivity of the optical detection branch is described. The synchronization electronics allow coordination of the simultaneous measurements of four lidar instruments, necessary during the Latitudinal Distribution of Middle Atmosphere Structure (LADIMAS) campaign. The results of measurements during the Dynamics Adapted Network for the Atmosphere (DYANA) campaign with the stationary sodium lidar are presented. ESA

N93-11083# Bonn Univ. (Germany). Inst. fuer Physik.
COMPUTER SIMULATION AND EXPERIMENTAL INVESTIGATION OF THE ABSORPTION CELL FOR THE ROCKETBORNE DIODE-LASER EXPERIMENT MASERATI Thesis [COMPUTERSIMULATION IND EXPERIMENTELLE UNTERSUCHUNG UEBER ABOSRPTIONSZELLEN FUER DAS RAKETENGETRAGENE DIODEN-LASER-EXPERIMENT MASERATI]
Dorothee Rebscher Nov. 1991 77 p In GEORGIAN
(Bonn-IR-91-62; ETN-92-92106) Avail: CASI HC A05/MF A01

The Middle Atmosphere Spectroscopic Experiment on Rockets for Analysis of Trace Gas Influences (MASERATI) Rocketborne Experiment measures altitude profiles of water vapor and carbon dioxide in the middle atmosphere. The second derivative absorption technique, based on wavelength tunable lead salt diode lasers, is used. The white cell is analyzed by computer simulator and in experiment, with regard to the special requirements of a rocket flight. The results are compared with simulations of the Herriott cell. It is shown that the three mirror white cell is a possible configuration for monitoring trace gases in the middle atmosphere. The possibility of an astigmatism compensated system is verified. ESA

N93-11120# Loughborough Univ. of Technology (England). Dept. of Mathematical Sciences.
COLLIDING PLANE GRAVITATIONAL WAVES WITH COLINEAR POLARIZATION
J. B. Griffths, C. A. Hoenselaers, and P. C. Ashby May 1992 8 p Sponsored in part by Science Research Council
(Maths-Rept-A-160; ETN-92-92383) Avail: CASI HC A02/MF A01

The colliding plane wave problem is considered using an unconventional coordinate system. This permits a complete solution to be explicitly stated for the general case of arbitrary approaching waves with constant and aligned polarization. The starting point is a sufficiently general solution of the main equation, and the subsidiary equations to obtain an explicit expression for M. This is achieved by adopting a new coordinate system. In some ways, these new coordinates are not as well suited to the colliding plane wave situation as those more commonly used. However, the disadvantages of the coordinate system are compensated for by the fact that equations can be explicitly integrated to give the metric function M. ESA

N93-11129# Norwegian Defence Research Establishment, Kjeller.
INTERPRETATION OF MEASUREMENTS FROM THE SUPRATHERMAL ELECTRON SPECTROMETER ON THE NEED-2 ROCKET
Knut Svenes and Jan Troeim 23 Mar. 1992 26 p
(FFI-92/7009; ETN-92-9239337) Avail: CASI HC A03/MF A01

The data acquired by the suprathermal electron spectrometer, during the NEED (NonMaxwellian Electron Energy Distribution) campaign, is analyzed. The entire NEED campaign involved two ionospheric sounding rockets and incoherent scatter radar facilities. The purpose of this arrangement was for the radar to monitor the ionosphere prior to and during the flight to obtain a large scale picture of the ionospheric background dynamics. The rocket was able to obtain in situ plasma measurements to illuminate the various small scale processes prevailing in the F region at the time. The results show the customary electron temperature increase from the E layer into the F layer on the upleg. Moreover, the electron temperatures were strongly spin modulated with significantly enhanced temperatures in the wake region. ESA

N93-11183 Utah State Univ., Logan.
NEW SINGULARITY AND EXISTENCE OF SOLUTIONS IN ANISOTROPIC, TIME-DEPENDENT, MAXIMALLY GAUSS-BONNET EXTENDED GRAVITY Ph.D. Thesis

Takayuki Kitaura 1991 119 p
Avail: Univ. Microfilms Order No. DA9222279

Some unification theories, including superstring theories, suggest spacetimes of higher dimensions than four. We consider the maximally Gauss-Bonnet extended Einstein Lagrangian, commonly known as the Lovelock Lagrangian, as a viable candidate for a gravitational Lagrangian that generalizes Einstein's theory in such higher dimensional spacetimes. In this dissertation, motivated by the success of the Kasner cosmology, we study the diagonal metric, time-dependent, homogeneous cosmology based on the Lovelock Lagrangian. We use the Palatini variation to obtain the field equations from the Lagrangian. The field equations are then integrated to obtain the most general diagonal metric, time-dependent, anisotropic solution. The solutions obtained are not in a desirable form; they are algebraic expressions of a time variable in terms of metric variables whereas we would like to have expressions of the metric variables as functions of a time variable. We prove the theorems regarding the conditions under which this inversion is possible. It is shown that, for certain solutions we found, the second time derivatives of the metric components of the solution, rather than the metric components, diverge, and this forces a certain curvature invariant to diverge. Thus, the singularity behavior of these solutions we found differs from the classical Kasner solution. Perturbative solutions both emerging from and evolving toward a singularity are obtained. The equation of geodesic deviation is solved perturbatively to show that the co-moving coordinates do not break down at a singularity.
Dissert. Abstr.

N93-11184 Wisconsin Univ., Madison.

THE FORCING OF A MID-LATITUDE UPPER-TROPOSPHERIC JET STREAK BY A SIMULATED MESOSCALE CONVECTIVE SYSTEM Ph.D. Thesis

Bart Joseph Wolf 1991 248 p
Avail: Univ. Microfilms Order No. DA9209344

The forcing of a jet streak aloft by organized diabatic processes within a simulated mid-latitude mesoscale convective system (MCS) is investigated. Using isentropic diagnostics, a series of numerical simulations are examined to study the interaction between adiabatic processes and latent heat release in relation to the isallobaric flow field, ageostrophic motion, and stability changes. The dominant ageostrophic modes and their relative impact on the generation of kinetic energy are determined, along with the relative influence of Kinetic Energy (KE) generation by the rotational and irrotational mass transport. The sensitivity of the numerical forecasts of MCS development to resolution is examined. The MCS develops a vigorous mass circulation characterized by relatively weak low level inflow and mass gains aloft very early in its life cycle. By the mature stage, intense vertical mass flux links a vigorous inflow branch with an impressive, relatively shallow pattern of mass divergence aloft, above the level of maximum diabatic heating at 325 K. As the MCS decays, significant divergence persists aloft for several hours. Results indicate that this mass circulation develops primarily due to isallobaric ageostrophic motion, with the divergent outflow aloft being forced by the diabatic component resulting from latent heat release. As part of this coupling, mass convergence into the MCS by the adiabatic component dominates at low levels. The inertial advection of the ageostrophic wind (IADVA) is the dominant component of ageostrophic motion aloft. The inertial diabatic terms are largest near the level of maximum heating, and are responsible for the development of inertial instability to the north of the MCS, resulting in this quadrant being preferred for outflow. The local wind tendency components tend to dominate at low levels. The upper level production of specific KE is also predominantly due to the IADVA component, and represents the mechanism through which the acceleration of the up-stream jet streak occurs. Partitioning the KE generation into its rotational and irrotational components shows the latter to be the key source of the positive generation of the diabatically forced jet streak.
Dissert. Abstr.

N93-11222 Illinois Univ. at Urbana-Champaign, Savoy.

LIDAR STUDIES OF GRAVITY WAVES IN THE MESOPAUSE REGION Ph.D. Thesis

Daniel Charles Senft 1991 160 p
Avail: Univ. Microfilms Order No. DA9210985

Nightly and seasonal variations in gravity wave activity in the mesopause region are examined by analyzing 60 nights of Na lidar observations obtained during a five-year period at Urbana, Illinois. The lidar data were used to calculate atmospheric density perturbations and their spectra. The atmospheric density variances, density vertical shear variances, vertical wind variances, omega-spectra magnitudes, and m-spectra magnitudes all exhibit considerable nightly variability as well as strong annual and semi-annual variations with the largest values in summer. The annual mean value of the root mean square (rms) density perturbations is 5.6 percent, with a mid-summer value that is 2 to 3 times larger. The Richardson number (Ri) for the wave field varies between 1/2 and 2 for most of the year, although Ri sometimes falls well below 1/4 during the summer. The omega-spectra exhibit power-law shapes with slopes varying between -1.28 and -2.45, with an annual mean of -1.82. The m-spectra also exhibit power-law shapes with slopes varying between -2.20, and -3.55, with a mean of -2.90. The magnitudes of both the omega-spectra and m-spectra vary by more than a factor of 10 throughout the year, with the largest values in summer. The variability of the m-spectra slopes and magnitudes is not consistent with linear instability theory and the concept of a universal vertical wave number spectrum. The characteristic periods (T(sub *) = 2(pi)/omega(sub *) vary between 3 and 50 h with an annual mean of 9.7 h. The characteristic vertical wavelengths (lambda(sub *) = 2(pi)/m(sub *) vary between 8.9 and 27 km with an annual mean of 14.1 km. The rms bandwidths of the wave field have mean values of bar-omega(sub rms) = 2(pi)/(44 min) and bar-m(sub rms) = 2(pi)/(6.2 km).
Dissert. Abstr.

N93-11226 Harvard Univ., Cambridge, MA.

QUASIGEOSTROPHIC VORTICES IN ZONAL SHEAR Ph.D. Thesis

Robert Daniel VanBuskirk 1991 186 p
Avail: Univ. Microfilms Order No. DA9211757

We analyze piece-wise uniform distributions of quasigeostrophic potential vorticity and their dynamics in uniform potential vorticity background zonal flows bar-v = (bar-v(sub x)(y))(bar-x). We develop a spectrally accurate boundary integral method for both solving the initial-value problem and calculating families steady-state vortices and their linear stability. We apply these methods to vortices in zonal velocity profiles which have a linear, quadratic, or cubic dependence on the latitudinal variable y. When we have a variable shear zonal profile with a nearby region of adverse (opposite sign) vorticity there is a limit to the size steady vortices can attain. The limiting vortex has a stagnation point on its boundary that mediates the filamentation of vorticity and provides a mechanism for dynamically limiting the vortex size. We also examine vortices in zonal flows, for the case of finite Rossby deformation radius L(sub R). Steady vortices in a same-signed (prograde) background shear of a given strength, have a limit to their latitudinal height but no limit to their longitudinal length, and are always linearly stable. Steady finite L(sub R) vortices of fixed strength in an adverse shear background have a maximum area that they can attain. If a finite L(sub R) vortex in adverse shear initially has an area slightly larger than this maximum, it fissions into two smaller vortices. With a fixed cubic zonal profile and a fixed vortex strength and L(sub R), there exists two types of steady vortex families. For weak vortices or small L(sub R), the limiting zone-like vortex has a maximum latitudinal height, but is infinitely long. While for strong vortices or large L(sub R) there exists a maximum area vortex. Finally we show that the velocity field of the Great Red Spot of Jupiter is not consistent with a quasigeostrophic uniform potential vortex embedded in an average zonal flow that also has uniform potential vorticity.
Dissert. Abstr.

N93-11228# Scripps Institution of Oceanography, La Jolla, CA.
PROPAGATION OF REGIONAL PHASES: OBSERVATIONS AND THEORY Final Report, 6 Apr. 1989 - 1 Jul. 1991
J. A. Orcutt and M. A. Hedlin 30 Sep. 1991 103 p
(Contract F19628-89-K-0018)
(AD-A246891; AD-E200865; PL-TR-91-2160) Avail: CASI HC A06/MF A02

In this study we present the results of investigations dealing with three topics. (1) We have continued our investigation of the influence the regular repetition of features in seismograms, introduced at the source and/or during propagation by layer resonance, has on the spectrum of the recorded coda. We have developed an automatic algorithm that discriminates mining explosions from nuclear explosions and earthquakes. (2) We consider the influence large crustal inhomogeneities, or topographic undulations, in the vicinity of receivers can have on the character of the recorded seismic coda. Specifically, we have developed a migration technique that scans the recorded coda for phases generated by local scattering interactions. (3) We have developed a regularized approach to seismic deconvolution that allows the introduction of a priori information, such as that describing the statistical nature of the additive noise and the underlying model, into the inversion process. We investigate how this algorithm can enhance the images produced by the migration algorithm developed in the previous section. GRA

N93-11235# Oak Ridge National Lab., TN.
HIGH RESOLUTION IMAGE PROCESSING OF GEOPHYSICAL DATA WITH DIFFRACTION TOMOGRAPHY
A. J. Witten, W. C. King (Military Academy, West Point, NY.), and J. R. Ursic (Environmental Protection Agency, Chicago, IL.) 1992 16 p Presented at the Army Science Conference, Orlando, FL, 22-25 Jun. 1992
(Contract DE-AC05-84OR-21400)
(DE92-014134; CONF-9206171-1) Avail: CASI HC A03/MF A01

This paper presents a method of detection and imaging that has as its input the data collected from the most commonly employed geophysical tools. The method makes use of the Generalized Projection Slice Theorem (GPST) in the analysis of these data to yield results ranging from greatly improved detection to high resolution images of subsurface features and buried objects. Detection capability can be greatly enhanced by incorporating this more rigorous signal processing procedure into the statistically based maximum likelihood estimator. The paper includes a theoretical development of the new signal processing procedures, results from the implementation of the theory with a number of commonly used geophysical tools, including a presentation of the improved capability for tunnel detection and location estimation and detection of buried ordnance. High resolution imaging of a variety of buried wastes was achieved through the application of geophysical diffraction tomography, a method that fully exploits the principles of the GPST. DOE

N93-11249 California Univ., Los Angeles.
THE KALMAN FILTER FOR TWO-DIMENSIONAL STABLE AND UNSTABLE ATMOSPHERES Ph.D. Thesis
Ricardo Todling 1992 194 p
Avail: Univ. Microfilms Order No. DA9221036

The NASA Earth Observing System project will represent a 100-fold increase in the amount of data available to be used in conjunction with numerical weather and climate prediction models. As a consequence, better data assimilation schemes than the current, widely used Optimal Interpolation (OI), or modified versions of it, are required. The two most promising methods for data assimilation are the adjoint method and the extended, nonlinear Kalman filter (KF). Routine implementation of the KF would require computational resources much beyond the ones available at present, and consequently, seeking approximations to this method is an active area of research. Related to the need of finding streamlined, efficient algorithms for the KF are questions about the filter's performance in the presence of strong nonlinear instabilities. We study these problems in the linear context by implementing a KF for two simple two-dimensional (2-D) systems. A linear shallow-water model is used to simulate a one-layer, barotropic atmosphere, and a two-layer, linear shallow-water model is used to simulate a baroclinic atmosphere. Under certain conditions both systems develop instabilities resembling their nonlinear equivalent as observed in the real atmosphere. In the presence of such barotropic and baroclinic linear instabilities, forecast errors grow exponentially for cases where no update with observations is made. When the model is updated by using the KF for data assimilation, results show that the filter is able to keep the errors bounded, even when only a very small number of observations are available. Sequential estimation theory gives a way of comparing the KF with OI. A comparison of these data assimilation methods, for the one-layer barotropically unstable problem, shows that, for some observational patterns, OI fails to keep the errors from growing exponentially, whereas the KF keeps the errors bounded. One approach to obtain a KF algorithm for routine applications is the banded approximation for the forecast error covariance matrix. We implement this approximation for our 2-D shallow-water models and results show that the banded approximation is a reasonably good approximation only when the model error covariance matrix is assumed to be diagonal. Dissert. Abstr.

N93-11265# Swedish Inst. of Space Physics, Uppsala.
IONOSPHERIC RESPONSE TO PARTICLE PRECIPITATION WITHIN AURORA Ph.D. Thesis - Uppsala Univ.
Jan-Erik Wahlund Mar. 1992 168 p
(IRF-SR-208; ETN-92-92170) Copyright Avail: CASI HC A08/MF A02

Based on measurements using the EISCAT incoherent scatter radar system in northern Scandinavia, a thesis discussing ionospheric response processes, and in particular a mechanism leading to atmospheric gas escape from a planet, is presented. From the observations, it is suggested that the energy dissipation into the background plasma through Joule heating, the production of a few hundred eV energetic runaway electrons, and strong ion outflows, are partly produced by the simultaneous presence of ion acoustic turbulence and field aligned currents above auroral arcs. The thesis includes the following studies: thin auroral ionization layers in connection with pulsating aurora; strong ion outflows from the F region ionosphere during auroral activity; topside ionospheric ion outflows during auroral activity; and electron energization in the topside auroral ionosphere. For individual titles, see N93-11266 through N93-11273.

N93-11266# Swedish Inst. of Space Physics, Uppsala.
OBSERVATIONS OF THIN AURORAL IONIZATION LAYERS BY EISCAT IN CONNECTION WITH PULSATING AURORA
Jan-Erik Wahlund, H. J. Opgenoorth, and P. Rothwell (Sussex Univ., Brighton, England) *In its* Ionospheric Response to Particle Precipitation Within Aurora Mar. 1992 11 p Repr. from Journal of Geophysical Research, v. 94, no. A12, 1 Dec. 1989 p 17,223-17,233 Previously announced as A90-20755 Sponsored by Swedish Natural Science Research Council and Science Research Council (For primary document see N93-11265 02-46)
Copyright Avail: CASI HC A03/MF A02

Very thin auroral ionization layers of less than 4.5 km extent were identified in high resolution EISCAT data during an event of pulsating aurora on 3 Dec. 1986. The auroral forms were recorded by a monostatic television camera system at the EISCAT site. The structures in the altitude profiles of electron density were found to be thinner than would be expected from collisional energy deposition of a monoenergetic and monodirectional precipitation of electrons. These ionization layers are shown to be probably associated with enhanced aurora. The measurements suggest that the precipitating electrons lose some of their energy by wave-particle interaction with large amplitude plasma waves in a confined ionospheric altitude region situated at altitudes around 100 to 120 km. The ionospheric plasma waves in the electron plasma frequency range might then accelerate ambient ionospheric electrons above the ionization threshold of the neutral gas, leading to enhanced secondary ionization. Such a process would involve high electric field amplitudes. ESA

N93-11267# Swedish Inst. of Space Physics, Uppsala.

EISCAT OBSERVATIONS OF STRONG ION OUTFLOWS FROM THE F-REGION IONOSPHERE DURING AURORAL ACTIVITY: PRELIMINARY RESULTS

Jan-Erik Wahlund and H. J. Opgenoorth *In its* Ionospheric Response to Particle Precipitation Within Aurora Mar. 1992 4 p Repr. from Geophysical Research Letters, v. 16, no. 7, Jul. 1989 p 727-730 Previously announced as A89-47397 Sponsored by Swedish Natural Science Research Council (For primary document see N93-11265 02-46)

Copyright Avail: CASI HC A01/MF A02

EISCAT observations of large outward field aligned flows of the bulk ion population in the F region during auroral activity are presented. These ion outflows are most commonly observed within auroral arcs, and are not well correlated with diffuse aurora. The ions (mainly O(+)) may reach field aligned outward velocities of more than 500 m/s and the calculated ion fluxes usually reach 10 exp 13 m(exp -2)(s exp -1). Strong electron temperature enhancements in the F region are observed in connection with almost all ion outflow events. However, high electron temperatures are not always an indicator for these strong ion outflow events. The exact mechanisms causing the ion outflow is not yet understood, but several possible mechanisms are discussed. ESA

N93-11268# Swedish Inst. of Space Physics, Uppsala.

EISCAT OBSERVATIONS OF TOPSIDE IONOSPHERIC ION OUTFLOWS DURING AURORAL ACTIVITY: REVISITED

Jan-Erik Wahlund, H. J. Opgenoorth, I. Haeggstroem (Swedish Inst. of Space Physics, Kiruna.), K. J. Winser (Royal Coll. of Surgeons, Dublin, Ireland), and G. O. L. Jones (University Coll. of Wales, Aberystwyth.) *In its* Ionospheric Response to Particle Precipitation Within Aurora Mar. 1992 39 p Sponsored by Swedish Natural Science Research Council and Science Research Council (For primary document see N93-11265 02-46)

Copyright Avail: CASI HC A03/MF A02

EISCAT observations of large field aligned bulk ion outflows from the topside ionosphere during auroral activity are presented. The ions (mainly O(+)) start their outflows from a variable altitude and may reach field aligned outward velocities of up to 1500 m/s in the altitude region 900 to 1500 km. The observed ion fluxes are about a factor of 10 larger than previously observed reaching 2 x 10 exp 14 m(exp -2)(s exp -1), and in some cases is nonconstant with altitude. Two different types of ion outflows were identified. The first type is related to periods of strong perpendicular electric fields, enhanced and anisotropic ion temperatures, and low electron densities below 300 km, indicating small amounts of auroral precipitation. The second type is related to auroral arcs and enhanced electron temperatures. The exact mechanisms causing the ion outflows is still not yet understood, but additional mechanisms other than thermal expansion are required to explain the observations presented. ESA

N93-11269# Swedish Inst. of Space Physics, Uppsala.

ELECTRON ENERGIZATION IN THE TOPSIDE AURORAL IONOSPHERE: ON THE IMPORTANCE OF ION-ACOUSTIC TURBULENCE

Jan-Erik Wahlund, H. J. Opgenoorth, F. R. E. Forme, M. A. L. Persson, I. Haeggstroem (Swedish Inst. of Space Physics, Kiruna.), and J. Lilensten (Grenoble-1 Univ., Saint Martin d'Heres, France) *In its* Ionospheric Response to Particle Precipitation Within Aurora Mar. 1992 33 p Sponsored by Swedish Natural Science Research Council; CEDAR; Swedish Inst. of Space Physics, Uppsala; Uppsala Univ.; and French Embassy (For primary document see N93-11265 02-46)

Copyright Avail: CASI HC A03/MF A02

EISCAT observations show enhancements of electron temperatures up to 8000 K in the topside ionosphere during active auroral conditions. These temperature enhancements correlate with electron density enhancements in the altitude region 170 to 230 km, which indicate that auroral electron precipitation in the 100 to 500 eV range is associated with the electron heating. Electron densities in other altitude intervals show no such correlation, thereby, indicating that auroral particles outside the energy range 100 to 500 eV are not the major regular cause for this bulk electron heating. Observations of ion acoustic turbulence in connection with the bulk electron heating events are also presented. Such turbulence will give a greatly enhanced Joule heating in the presence of field aligned currents because of the resulting anomalous resistivity by the turbulently fluctuating electric fields. This heating will occur in addition to the classical collisional heating by precipitating particles, and is probably a major heat source for the topside ionospheric electrons. In fact, the precipitating electrons in the 100 to 500 eV range may themselves be runaway suprathermal electrons produced by the ion-acoustic turbulence. An ion-ion two stream instability is suggested to be the cause of the observed enhanced ion acoustic fluctuations. ESA

N93-11270# Swedish Inst. of Space Physics, Uppsala.

EFFECTS OF CURRENT DRIVEN INSTABILITIES ON THE ION AND ELECTRON TEMPERATURES IN THE TOPSIDE IONOSPHERE

F. R. E. Forme (Centre National d'Etudes des Telecommunications, Issy-les-Moulineaux, France), Jan-Erik Wahlund, H. J. Opgenoorth, M. A. L. Persson, and E. V. Mishin (Academy of Sciences, USSR, Troitsk) *In its* Ionospheric Response to Particle Precipitation Within Aurora Mar. 1992 28 p Sponsored by Swedish Natural Science Research Council; Swedish Inst. of Space Physics, Uppsala; Uppsala Univ.; and French Embassy (For primary document see N93-11265 02-46)

Copyright Avail: CASI HC A03/MF A02

One dimensional time dependent model calculations of the effects of low frequency turbulence, due to three different current driven instabilities, on the ion and electron temperatures in the topside ionosphere were performed. For field aligned current strengths of a few tens, the ion acoustic, the ion cyclotron, and the Buneman instabilites are found to affect the behavior of the transport coefficients and in turn produce greatly enhanced plasma temperatures. The effects of these instabilities are compared with each other and for normally observed plasma parameters it is found that these instabilities appear at high altitudes above 2000 km. Different characteristic time evolutions for the three instabilities are investigated and the instabilities are found to be short lived and disappear after a few seconds due to the action for both ion and electron heating. The electron heat conduction is found to be inhibited when ion-acoustic or Buneman turbulence are presented. The calculations are compared with recent EISCAT observations of simultaneous enhanced electron temperatures and ion-acoustic turbulence in the topside ionosphere. Calculations indicate that low frequency turbulence is a major contributor in the energy balance of the topside ionospheric thermal plasma. ESA

N93-11271# Swedish Inst. of Space Physics, Uppsala.

COMMENT ON 'EISCAT RADAR OBSERVATIONS OF ENHANCED INCOHERENT SCATTER SPECTRA AND THEIR RELATION TO AURORAL LUMINOSITY AND FIELD-ALIGNED CURRENTS' BY P. N. COLLIS ET AL.

Jan-Erik Wahlund, H. J. Opgenoorth, and E. V. Mishin (Academy of Sciences, USSR, Troitsk) *In its* Ionospheric Response to Particle Precipitation Within Aurora Mar. 1992 4 p (For primary document see N93-11265 02-46)

Copyright Avail: CASI HC A01/MF A02

The validity of results concerning the existence of field aligned currents of several mA/sq m and higher in the auroral zone are questioned. Major arguments why such large field aligned current densities could not possibly exist in the auroral zone are presented. The conclusion that the electron-ion current driven instability cannot be responsible for the strongly asymmetric spectra observed (unless the plasma density is depleted below about 1000/cu cm), but by another referenced mechanism, is made. ESA

N93-11272# Swedish Inst. of Space Physics, Uppsala.
SCATTERING OF ELECTROMAGNETIC WAVES FROM A PLASMA: ENHANCED ION ACOUSTIC FLUCTUATIONS DUE TO ION-ION TWO-STREAM INSTABILITIES
Jan-Erik Wahlund, F. R. E. Forme, H. J. Opgenoorth, M. A. L. Persson, E. V. Mishin (Academy of Sciences, USSR, Troitsk), and A. S. Volokitin (Academy of Sciences, USSR, Troitsk) *In its* Ionospheric Response to Particle Precipitation Within Aurora Mar. 1992 10 p Sponsored by Swedish Natural Science Research Council; Uppsala Univ.; and French Embassy (For primary document see N93-11265 02-46)
Copyright Avail: CASI HC A02/MF A02

Observations by the EISCAT and Millstone Hill radars of strongly enhanced, often asymmetric, ion acoustic line spectra in the topside auroral ionosphere are studied. Such strongly enhanced ion acoustic spectra are shown to arise naturally in a plasma unstable to the ion two stream instability. A linear theory of density fluctuations is used for the calculations, which should be applicable to weakly unstable nonmagnetized plasmas near the onset threshold of the instability. ESA

N93-11273# Swedish Inst. of Space Physics, Uppsala.
ON THE ORIGIN OF ION ACOUSTIC TURBULENCE IN THE AURORAL TOPSIDE IONOSPHERE
Jan-Erik Wahlund, M. A. L. Persson, F. R. E. Forme, H. J. Opgenoorth, K. Stasiewicz, and I. Haeggstroem (Swedish Inst. of Space Physics, Kiruna.) *In its* Ionospheric Response to Particle Precipitation Within Aurora Mar. 1992 23 p Sponsored by Swedish Natural Science Research Council; Swedish Inst. of Physics, Uppsala; Uppsala Univ.; and French Embassy (For primary document see N93-11265 02-46)
Copyright Avail: CASI HC A03/MF A02

EISCAT observations of naturally enhanced ion lines from the topside ionosphere, which can be interpreted in terms of enhanced ion acoustic fluctuations above a multiple auroral arc structure, are presented. These fluctuations, sometimes reaching a turbulent level, are shown to be most likely produced by a H(+)-O(+) two stream instability that is active in the topside auroral ionosphere. The existence of field aligned currents in the range of 5 to 60 micro-A/sq m are inferred from the data, which are preferably upward directed during the occurrence of enhanced ion lines. These upward field aligned currents are shown to be the probable cause for the observed ionospheric ion outflows, which create the H(+)-O(+) instability higher up. An enhanced parallel electric field, due to the effective resistivity associated with the ion acoustic turbulence, can accelerate the ions to large velocities and create elevated ion conics and beams higher up. ESA

N93-11282# Boston Univ., MA. Center for Space Physics.
THE EFFECTS OF MAGNETIC STORM PHASES ON F-LAYER IRREGULARITIES FROM AURORAL TO EQUATORIAL LATITUDES Quarterly Report, 1 Apr. - 30 Jun. 1992
Jules Aarons and Michael Mendillo 30 Jun. 1992 7 p
(Contract N00014-89-J-1754)
(AD-A253905) Avail: CASI HC A02/MF A01

The review of equatorial data relative to F-layer irregularities continued during this period with an emphasis in this quarter on the results of a long series of optical measurements. The study uses the largest optical data base yet obtained of equatorial airglow depletions to describe such observational features of irregularity plume onset and development under different seasonal and geomagnetic conditions. We are most interested in the data showing the extreme altitudes/latitudes reached by such effects. GRA

N93-11331 Deutsche Geodaetische Kommission, Munich (Germany).
AN APPROXIMATE SOLUTION OF THE FIXED GRAVIMETRIC BOUNDARY VALUE PROBLEM IN THE INTERIOR AND THE EXTERIOR OF THE EARTH'S BODY Ph.D. Thesis - Stuttgart Univ. [EINE APPROXIMATIVE LOESUNG DER FIXEN GRAVIMETRISCHEN RANDWERTAUFGABE IM INNEN- UND AUSSENRAUM DER ERDE]
Johannes Engels 1991 117 p In GEORGIAN
(Ser-C-379; ISBN-3-7696-9425-2; ETN-92-92277) Copyright
Avail: Deutsche Geodaetische Kommission, Marstallplatz 8, D-8000 Munich 22, Germany

The geoid is constructed after the solution of an exterior and an interior boundary value problem. It does not use reductions. The gravitational part of the potential fulfills the Laplacian differential equation on mass free points. In the interior, the potential obeys the Poisson differential equation. It is verified that the mass density function is compatible with the boundary function, as prescribed by the Newtonian gravitational law. A correction function is added to the model density and to the model potential. A correction potential function is chosen which fulfills the bipotential equation. Gravity values at the Earth's surface are taken to be boundary values. The geometry of the surface is considered as known. ESA

N93-11352 Max-Planck-Inst. fuer Physik und Astrophysik, Garching (Germany). Inst. fuer Extraterrestrische Physik.
PLASMA MEASUREMENTS IN MAGNETOSPHERIC TAIL Thesis - Ludwig-Maximilian-Univ. [PLASMAMESSUNGEN IM MAGNETOSPHAERENSCHWEIF]
Wolfgang Baumjohann Jan. 1992 32 p In GERMAN
(MPE-233; ETN-92-92290) Copyright Avail: Fachinformationszentrum Karlsruhe, 7514 Eggenstein-Leopoldshafen 2, Germany

Precise values were given for numerous tail parameters, e.g., thickness, temperature, and geometry. Theoretical predictions were verified, using observations in numerous fields, e.g., pressure equilibrium and adiabatic convection. It was possible to detect the quick but continuous plasma flow in the vicinity of the neutral layer, on account of high time resolution. The constancy of the relationship between electron and ion temperature over a broad temperature field was outlined. The investigations showed clearly that the essential modification in the plasma layer during a substorm occurred in the central plasma layer, and not in the plasma boundary layer. ESA

N93-11421# California Inst. of Tech., Pasadena. Seismological Lab.
MODELING REGIONAL SEISMIC WAVES Final Report, 24 Mar. 1989 - 31 Jul. 1991
Donald V. Helmberger and David G. Harkrider 31 Jul. 1991 109 p
(Contract F19628-89-K-0028)
(AD-A246894; AD-E200867; PL-TR-91-2192) Avail: CASI HC A06/MF A02

This study can be divided into three main topics: modeling regional broad-band seismograms from the Imperial Valley to Pasadena; determining surface wave magnitudes for NTS events using regional data, and waveform modeling to determine depth of earthquakes in Tibet leading to new origin times and a better estimation of P(sub n) and S(sub n) velocities. In section 1, broad-band wave propagation along a corridor from Imperial Valley to Pasadena, California is addressed. The path consists of 50 km of slow basin structure with a shallow moho followed by 250 km of relatively normal Southern California structure approaching Pasadena. In section 2, surface wave magnitudes for 112 Nevada Test Site (NTS) explosions from a data set of regional long-period seismograms from North American stations are calculated. In order to utilize the newer regional stations (Delta less than 25 deg), a new method for determining M(sub s) has been developed which employs synthetic seismograms to establish a relationship between the amplitude of the regional Airy phase, or Rayleigh pulse, of the data and an associated surface wave magnitude, based on conventional M(sub s) determinations, calculated from a synthetic seismogram propagated to 40 deg. In section 3, a note on the relocation of the Tibetan earthquake is presented. Present ISC locations for earthquakes beneath Tibet indicates a random distribution of events down to a depth of about 50 km. GRA

N93-11535# Los Alamos National Lab., NM.

GEOSTATIONARY-SATELLITE BEACON-RECEIVER ARRAY FOR STUDIES OF IONOSPHERIC IRREGULARITIES

R. C. Carlos, A. R. Jacobson, and Guanghui Wu 1992 12 p Presented at the Beacon Satellite Symposium, Boston, MA, 5-12 Jul. 1992
(Contract W-7405-eng-36)
(DE92-018979; LA-UR-92-2125; CONF-9207118-1) Avail: CASI HC A03/MF A01

Ionospheric irregularities can be studied by various techniques. These include widely spaced Doppler sounders or ionosondes, Faraday rotation polarimetry, and two-frequency differential Doppler, and radio interferometry. With geostationary satellites, one usually uses Faraday rotation of the beacon signal to measure the ionospheric TEC (total electron content). With a network of polarimeters, the horizontal wave parameters of Traveling Ionospheric Disturbances (TIDS) can be deduced, but the shortcoming of this technique is its poor sensitivity. This paper describes a geostationary-satellite beacon-receiver array at Los Alamos, New Mexico, which will be employed for the studying of ionospheric irregularities, especially the fine-scale TIDS. DOE

N93-11564# Sandia National Labs., Albuquerque, NM.

PROPAGATION OF RELATIVISTIC HIGH CURRENT ELECTRON BEAMS ACROSS THE GEOMAGNETIC FIELD

J. S. Wagner 1991 7 p Presented at the NATO Advanced Study Institute Program on the Behavior of Systems in the Space Environment, Pitlochry, England, 6-21 Jul. 1991
(Contract DE-AC04-76DP-00789)
(DE92-018276; SAND-91-1492C; CONF-9107232-1) Avail: CASI HC A02/MF A01

Relativistic high current electron beams can be transported long distances across the geomagnetic field using the IFR (ion focused regime) technique. IFR is a method of providing strong electrostatic focusing and guiding of the beam. The guiding is sufficiently strong to allow the beam to transport any angle with respect to geomagnetic field. In the IFR method, first an ionizing laser (or any ionizing method) is used to create a preionized cylindrical channel. DOE

N93-11669# Westinghouse Savannah River Co., Aiken, SC.

STRUCTURE OF THE NOCTURNAL BOUNDARY LAYER OVER A COMPLEX TERRAIN

M. J. Parker and S. Raman (North Carolina State Univ., Raleigh.) 1992 7 p Presented at the 10th Symposium on Turbulence and Diffusion, Portland, OR, 29 Sep. - 2 Oct. 1992
(Contract DE-AC09-89SR-18035)
(DE92-018141; WSRC-MS-92-236; CONF-9209158-1) Avail: CASI HC A02/MF A01

The complex nature of the nocturnal boundary layer (NBL) has been shown extensively in the literature Project STABLE was conducted in 1988 to study NBL turbulence and diffusion over the complex terrain of the Savannah River Site (SRS) near Augusta, Georgia. The third night of the study was particularly interesting because of the unusual phenomena observed in the structure of the NBL. Further analyses of microscale and mesoscale data from this night are presented using data from SRS network of eight 61 m towers over 900 sq km, from six launches of an instrumented tethersonde, from permanent SRL meteorological instrumentation at seven levels of the 304 m (1,000 ft) WJBF-TV tower near SRS, and additional data collected at 36 m (CC) by North Carolina State University (NCSU) including a one dimensional sonic anemometer, fine wire thermocouple, and a three dimensional propeller anemometer. Also, data from the nearby Plant Vogtle nuclear power plant observation tower and the National Weather Service at Augusta's Bush Field (AGS) are presented. The passage of a mesoscale phenomenon, defined as a microfront (with an explanation of the nomenclature used), and a vertical composite schematic of the NBL which shows dual low level wind maxima, dual inversions, and a persistent, elevated turbulent layer over a complex terrain are described. DOE

N93-11692# Edgerton, Germeshausen and Grier, Inc., Idaho Falls, ID.

QUATERNARY VOLCANISM, TECTONICS, AND SEDIMENTATION IN THE IDAHO NATIONAL ENGINEERING LABORATORY AREA

W. R. Hackett and R. P. Smith 1992 18 p Presented at the Utah Geology and Mineral Field Excursion Meeting, Ogden, UT, May 1992
(Contract DE-AC07-76ID-01570)
(DE92-017851; EGG-M-92071; CONF-9205227-1) Avail: CASI HC A03/MF A01

In this article, we discuss the regional context and describe localities for a two-day field excursion in the vicinity of the Idaho National Engineering Laboratory (INEL). We address several geologic themes: (1) Late Cenozoic, bimodal volcanism of the Eastern Snake River Plain (ESRP); (2) the regional tectonics and structural geology of the basin and range province to the northwest of the ESRP; (3) fluvial, lacustrine, and aeolian sedimentation in the INEL area; and (4) the influence of quaternary volcanism and tectonics on sedimentation near the INEL. DOE

N93-11699# Danish Meteorological Inst., Copenhagen. Div. of Research and Development.

DATA REPORT 92-1. BRORFELDE GEOMAGNETIC OBSERVATORY MAGNETIC RESULTS, 1990

1992 26 p
Avail: CASI HC A03/MF A01

Brorfelde geomagnetic observatory was established in 1978 by the Danish Meteorological Institute as a successor to the observatory at Rude Skov which suffered from disturbances from electric trains. A description of the background for the removal of the observatory and of buildings and instrumentation is given. Author

N93-11740# Connecticut Univ., Storrs. Dept. of Geology and Geophysics.

CRUSTAL AND UPPER MANTLE VELOCITY GRADIENTS IN THE VICINITY OF THE EAST KAZAKH TEST SITE

Vernon F. Cormier and Michael D. Kalmbach 9 Sep. 1991 45 p
(Contract F19628-90-K-0043)
(AD-A246889; PL-TR-91-2215; AD-E200868; SR-1) Avail: CASI HC A03/MF A01

The Lg wave is simulated three dimensionally by ray methods, in homogeneous models of the crust with smooth variations in thickness. Variations typical of mountainous regions are utilized, and the effect of these variations is examined in detail. Ray modeling shows that Lg is strongly attenuated by propagation across the thickened crustal root found beneath mountain ranges. While variations in the width of the mountain root are found to be unimportant, variations in the width of transition between thick and thin crust strongly influence attenuation. Propagation paths across transition regions 100 km wide result in weak Lg while 200 km transitions cause very little Lg attenuation. Lg is found to propagate very efficiently within a mountain root, with amplitude increased slightly by lateral reflections. Propagation across mountain belts at angles from 90 to 20 degrees (relative to strike) is shown to cause strong attenuation at all angles, with no identifiable optimal path. The technique is applied to a rough thickness model of the Central Asian crust and although attenuation is predicted, close comparison of the synthetics with earthquake recordings reveals discrepancies that can not be entirely explained by ray methods in a homogeneous crust. This suggests that a more accurate model of the crust is required. Including variations in crustal Q, surface sedimentary layers in the basin regions and the large scale 3-D heterogeneities associated with the uplifted regions. GRA

N93-11785# Army Lab. Command, White Sands Missile Range, NM. Atmospheric Sciences Lab.

THE SENSITIVITY OF THE RECEIVER COHERENCE DIAMETER AND MODULATION TRANSFER FUNCTION TO VARIATIONS OF A DAMP UNSTABLE ATMOSPHERE Final Report

Henry Rachele and Arnold Tunick Jul. 1992 45 p
(AD-A253269; ASL-TR-0314) Avail: CASI HC A03/MF A01

The purpose of this study was to examine the sensitivity of the receiver coherence diameter, r(sub 0), and the modulation transfer function (MTF) to variations of the natural atmosphere from an assumed ideal average state and from misrepresentation of the atmospheric effects due to errors in measurement and processing of the basic meteorological parameters. The concept was simplified by assuming that all natural variations and errors due to sensor performance and positioning can be lumped and that collectively are normally distributed, even though the natural variations are known not to be normal. For this study, the authors selected two sets of data to analyze. The data from Davis, California, were collected during unstable conditions with clear skies. Bar graphs were used to show distributions resulting from total errors. They include the friction velocity u*; windspeed V(sub r); temperature scaling parameter T*; specific humidity scaling parameter q*; Obukhov scaling length L; structure parameter C(sup 2)(sub n); and receiver coherence diameter r(sub 0). Additionally, the authors take the minimum, maximum, and mean r(sub 0) for each case and plot the resulting near and far-field slow MTF.
GRA

N93-11788# California Univ., Santa Cruz.

APPLICATION OF THE THEORY OF WAVE PROPAGATION THROUGH RANDOM MEDIA TO PHASE AND AMPLITUDE FLUCTUATIONS OF SEISMIC P-WAVES Final Report, 1 Jun. 1989 - 31 Mar. 1992

Stanley M. Flatte 10 Jan. 1992 26 p
(Contract F19628-89-K-0027)
(AD-A253274; UCSC-1992001; PL-TR-92-2036; AD-E201028)
Avail: CASI HC A03/MF A01

Statistical descriptions of variations in seismic-wave velocity in the Earth are related to observations in phase, travel-time, and amplitude fluctuations of seismic-wave signals received at teleseismic and regional distances. Results were obtained by analysis of NORESS and NORSAR data, by stochastic tomography techniques and by numerical simulation. Combination of NORESS and NORSAR data has led to a more highly resolved Transverse Coherence Function of travel time, confirming the Flatte-Wu (FW) model of heterogeneities under NORSAR. Nonlinear inversion applied to NORSAR data has also verified the FW model parameters. Work to compare the FW stochastic model with deterministic heterogeneity models is in progress. Attempts to understand regional propagation by the same techniques have been unsuccessfully due to inability to identify high-frequency crustal propagation paths for regional ranges. Numerical simulation of fluctuations from a point source have verified models of turbulence (applied to the atmosphere). GRA

N93-11791# Colorado School of Mines, Golden. Center for Wave Phenomena.

DIFFERENTIAL EQUATION-BASED SEISMIC DATA FILTERING

Jianchao Li and K. Larner May 1992 27 p
(Contract DE-FG02-89ER-14079)
(DE92-016282; CWP-124; DOE/ER-14079/14) Avail: CASI HC A03/MF A01

Suppressing noise and enhancing useful seismic signal by filtering is one of the important tasks of seismic data processing. Conventional filtering methods are implemented through either the convolution operation or various mathematical transforms. In this paper, we describe a methodology for studying and implementing filters, which, unlike those conventional filtering methods, is based on solving differential equations in the time and space domain. We call this kind of filtering, differential equation-based filtering (DEBF). DEBF does not require that the seismic data be stationary, so filtering parameters can vary with every time and space point. Also, in 2-D and 3-D, DEBF has higher computational efficiency than do conventional multiple-trace filtering methods. Examples with synthetic and field seismic data show the DEBF methods presented here to be efficient and effective. DOE

N93-11810# Panametrics, Inc., Waltham, MA.

DEVELOPMENT AND USE OF DATA ANALYSIS PROCEDURES FOR THE CRRES PAYLOADS AFGL-701-2/DOSIMETER AND AFGL-701-4/FLUXMETER AND APPLICATION OF THE DATA ANALYSIS RESULTS TO IMPROVE THE STATIC AND DYNAMIC MODELS OF THE EARTH'S RADIATION BELTS

Bronislaw K. Dichter and Frederick A. Hanser 4 Mar. 1992 17 p
(Contract F19628-87-C-0169)
(AD-A253287; PL-TR-92-2066; AD-E201097; SR-4) Avail: CASI HC A03/MF A01

Response of the AFGL-701-4/Dosimeter instrument, flown on the CRRES spacecraft, to electrons with energies between 1 and 10 MeV is described. GRA

N93-11846# Hawaii Univ., Honolulu. Dept. of Geology and Geophysics.

PHYSICAL CHARACTERIZATION OF MAGMATIC LIQUIDS

M. H. Manghnani 1991 12 p
(Contract DE-FG03-85ER-13418)
(DE92-015931; DOE/ER-13418/T2) Avail: CASI HC A03/MF A01

Long-range goals of this research project are: (1) Characterization of seismic velocity and attenuation (V(sub P), V(sub S), Q(sub P)(sup -1), Q(sup S)(sup -1)) and electrical properties of selected Hawaiian and related rocks under appropriate controlled environments of pressure, temperature, and volatile/fluid content; and (2) Characterization of the elastic, viscoelastic, and thermodynamic properties (V(sub P), V(sub S), Q(sub P)(sup -1), Q(sub S)(sup -1), viscosity and compressibility) of molten basalts, picrites and komatites, and related silicate melts to approximately 1600 C using the ultrasonic interferometry method. In addition, the pressure dependences of V(sub P), (sub S) and bulk modulus will be determined using the Brillouin scattering and diamond-anvil cell techniques. DOE

N93-11898 Illinois Univ. at Urbana-Champaign, Savoy.

DYNAMICS OF PLANETARY WAVES IN THE ATMOSPHERE Ph.D. Thesis

Ping Chen 1992 157 p
Avail: Univ. Microfilms Order No. DA9215788

The following problems are investigated in this thesis: (1) the effects of wave transience on the propagation of planetary waves in the stratosphere; (2) the coupling of the equatorial and extratropical quasi-biennial oscillations; and (3) the propagation of planetary waves between the troposphere and stratosphere. Two distinct maxima in the EP-flux convergence, one below the stratospheric polar jet and the other north of the zero wind line in the tropics, are found for steady and transient waves in a variety of realistic zonal flows in the Northern Hemisphere winter stratosphere, suggesting that the bimodal structure in the EP-flux convergence in observations (e.g., Randel and Held 1991) is a general feature of the winter stratosphere. The maximum in the tropics is due to the linear critical line absorption of meridionally propagating waves (e.g., Dickinson 1970), and the maximum in high latitudes is caused by the dissipation of highly non-WKBJ waves at local maximum of the refractive index at a jet. The existence and location of the maximum in the EP-flux convergence in high latitudes are insensitive to transience. Its strength, however, is very sensitive to transcience, and the sensitivity is much larger for wave 2. The equatorial wing QBO affects strongly the propagation of planetary waves, and produces a significant QBO in the EP-flux divergence in high latitudes. The QBO in high latitudes reveals a layered structure in the vertical, and its vertical patterns agree well with the vertical shears of the wind QBO at the equator. The QBO in the EP-Flux divergence in high latitudes is primarily due to the change of the refractive index there. The change of the refractive index in high latitudes is mainly caused by the change of the zonal-mean thermal anomalies there, which, in turn, are induced by the changes of the equatorial winds through the thermal wind balance. There is also a maximum in the EP-flux convergence in the upper troposphere in high and middle latitudes. The formation of this maximum is due to the dissipation of non-WKBJ waves near a local maximum of the refractive index at the tropopause. The local maximum in refractive index at the tropopause is caused by the vertical gradient of the buoyancy frequency and the vertical shear of the zonal flow there. The tropopause acts like a valve for the upward propagation of planetary waves. The key controlling parameters are the vertical gradient of the buoyancy frequency and the vertical shear of the zonal winds at the tropopause. A smaller vertical gradient of the buoyancy frequency and a smaller vertical shear of the zonal flow at the tropopause enhance the upward propagation of planetary waves. Dissert. Abstr.

N93-11900 Johns Hopkins Univ., Baltimore, MD.

LABORATORY AND NUMERICAL STUDIES OF DYNAMICAL PROCESSES RELATED TO THERMAL CONVECTION IN THE EARTH'S MANTLE Ph.D. Thesis

Stuart Alan Weinstein 1992 241 p
Avail: Univ. Microfilms Order No. DA9216649

The results are presented of both numerical simulations and laboratory experiments designed to study various problems related to the structure of mantle convection. The effects were studied of internal heat generation, variable viscosity and plates on the structure of thermal convection. Numerical and laboratory studies of time-dependent thermal convection in a fluid with constant properties were performed in large aspect-ratio configurations in which the fluid is heated from below as well as internally. These studies show that the structure of convection changes dramatically as the amount of internal heating is increased from zero. In situations where most of the heat is supplied internally, instabilities of the cold, upper boundary layer become the prominent features of the flow. In the absence of internal heating the convection planforms are the symmetric spoke pattern in which connected spokes of ascending and descending flow have, on average, equal strength. However, with large amounts of internal heat production, the planform becomes asymmetric with buoyancy concentrated in isolated descending acurate sheets and cylindrical plumes. With the exception of the plumes, the planform resemble the manner in which the mid-ocean ridges and subduction zones are distributed. The planform of convection in a Boussinesq fluid with a temperature-dependent viscosity is also investigated with laboratory and numerical experiments. When the fluid is bounded above and below by rigid boundaries the planforms obtained are spoke patterns. However, when a stress-free condition is applied to the upper boundary the descending flows form a dendritic network of descending sheets and upwellings occur in the form of plumes as well as sheets. The coupling between plate motions and mantle convection is studied using a numerical model consisting of a thin non-Newtonian layer atop a thick Newtonian viscous fluid layer. The non-Newtonian layer has a simple power law rheology characterized by a power law index n and stiffness constant mu sub p. A systematic study of steady, single cell configurations shows that under certain conditions the non-Newtonian layer behaves like a mobile tectonic plate. Time dependent calculations indicate that the geometry and number of plates does not necessarily resemble the planform of convection below.
Dissert. Abstr.

N93-12136# Los Alamos National Lab., NM.

MODELS OF VOLCANIC ERUPTION HAZARDS

K. H. Wohletz 1992 5 p Presented at the Geothermal Resources Council Meeting, San Diego, CA, 4-7 Oct. 1992
(Contract W-7405-eng-36)
(DE92-013432; LA-UR-92-1372; CONF-921083-2) Avail: CASI HC A01/MF A01

Volcanic eruptions pose an ever present but poorly constrained hazard to life and property for geothermal installations in volcanic areas. Because eruptions occur sporadically and may limit field access, quantitative and systematic field studies of eruptions are difficult to complete. Circumventing this difficulty, laboratory models and numerical simulations are pivotal in building our understanding of eruptions. For example, the results of fuel-coolant interaction experiments show that magma-water interaction controls many eruption styles. Applying these results, increasing numbers of field studies now document and interpret the role of external water eruptions. Similarly, numerical simulations solve the fundamental physics of high-speed fluid flow and give quantitative predictions that elucidate the complexities of pyroclastic flows and surges. A primary goal of these models is to guide geologists in searching for critical field relationships and making their interpretations. Coupled with field work, modeling is beginning to allow more quantitative and predictive volcanic hazard assessments. DOE

N93-12142# Colorado School of Mines, Golden. Center for Wave Phenomena.

SEISMIC WAVE PROPAGATION IN THINLY-LAYERED MEDIA WITH STEEP REFLECTORS Ph.D. Thesis

H. L. Deng May 1992 45 p
(Contract DE-FG02-89ER-14079)
(DE92-015619; CWP-114; DOE/ER-14079/12) Avail: CASI HC A03/MF A01

Seismic waves reflected from steep reflectors in the earth's subsurface spend a significant amount of time travelling more or less horizontally. Therefore, accurate imaging of steep geologic structure requires knowledge of the behavior of these horizontally propagating waves. In particular, the effect of tunneling on seismic waves propagating in thinly-layered media must be understood. I describe a method for modeling seismic waves traveling in thinly-layered media. This method, a frequency-wavenumber finite-difference scheme coupled with the Born approximation, is useful in studying seismic waves reflected from steep geologic structures. DOE

N93-12155# Lawrence Livermore National Lab., CA.

REAL-TIME CLASSIFICATION OF SIGNALS FROM THREE-COMPONENT SEISMIC SENSORS USING NEURAL NETS

B. C. Bowman and F. Dowla May 1992 12 p Presented at the IEEE Transactions on Instrumentation and Measurement and 4th Institut Industriel De Transfert De Technologie (IITT) International Conference on Artificial Intelligence and Expert Systems, Paris (France), 21-22 Oct. 1992
(Contract W-7405-eng-48)
(DE92-014886; UCRL-JC-109410; CONF-921098-1) Avail: CASI HC A03/MF A01

Adaptive seismic data acquisition systems with capabilities of signal discrimination and event classification are important in treaty monitoring, proliferation, and earthquake early detection systems. Potential applications include monitoring underground chemical explosions, as well as other military, cultural, and natural activities where characteristics of signals change rapidly and without warning. In these applications, the ability to detect and interpret events rapidly without falling behind the influx of the data is critical. We developed a system for real-time data acquisition, analysis, learning, and classification of recorded events employing some of the latest technology in computer hardware, software, and artificial neural networks methods. The system is able to train dynamically, and updates its knowledge based on new data. The software is modular and hardware-independent; i.e., the front-end instrumentation is transparent to the analysis system. The software is designed to take advantage of the multiprocessing environment of the Unix operating system. The Unix System V shared memory and static RAM protocols for data access and the semaphore mechanism for interprocess communications were used. As the three-component sensor detects a seismic signal, it is displayed graphically on a color monitor using X11/Xlib graphics with interactive screening capabilities. For interesting events, the triaxial signal polarization is computed, a fast Fourier Transform (FFT) algorithm is applied, and the normalized power spectrum is transmitted to a backpropagation neural network for event classification. The system is currently capable of handling three data channels with a sampling rate of 500 Hz, which covers the bandwidth of most seismic events. The system has been tested in laboratory setting with artificial events generated in the vicinity of a three-component sensor. DOE

N93-12182 Florida State Univ., Tallahassee.

ANALYSIS OF AIR AND SEA PHYSICAL PROPERTIES AND SURFACE FLUXES USING A COMBINATION OF IN SITU AND SEASAT DATA Ph.D. Thesis

David M. Legler 1992 149 p

Avail: Univ. Microfilms Order No. DA9222396

An objective technique which produces regularly spaced fields of winds, temperatures, humidity, wind stress and sensible and latent heat fluxes is developed. It combines in-situ Volunteer Observing Ship (VOS) data and remotely sensed data from SEASAT during the analysis period, July 7 - October 10, 1978 for the north Atlantic. The objective technique is a variational method which reduces a set of several constraints expressing closeness to input data, climatology and kinematics. Analysis results are presented for monthly and 5-day periods during the analysis period. Seasonal (3 month) means of temperature, humidity, and flux determined by the monthly and 5-day results are comparable. However, 5-day wind results had much smaller errors than the monthly mean winds averaged over the 3-month period. Variability of the 5-day results indicates high variability of temperatures, humidity, and heat fluxes in the vicinity of the Gulf Stream. Sea surface temperature (SST) variability is high in the eastern Atlantic and is coupled to wind driven ocean variability in the region. Heat fluxes are coupled to and determined by various parameters. The variations for both sensible and latent heat fluxes in the extratropics are determined by the position and strength of the circulation of the semi-permanent high pressure system. Some evidence is also found to indicate dependence of SST on latent heat. In the tropics, the heat fluxes are determined by a combination of factors, including zonal wind and SST. Estimates of errors due to insufficient sampling and random data are presented for the monthly results. The sampling and random errors in wind stress are in the range of 10-20 percent of the mean values. For the sensible and latent heat fluxes, the sampling errors are about half of those attributable to random errors. Because of the difference operator used in diagnosing heat fluxes, these are found to be more sensitive to the accuracies of temperatures and humidity than accuracies of winds.

Dissert. Abstr.

N93-12209 Illinois Univ. at Urbana-Champaign, Savoy.

FUNDAMENTAL ANALYSIS OF THE TOMOGRAPHIC IMAGING SYSTEM FOR RECONSTRUCTING IONOSPHERIC DISTRIBUTIONS Ph.D. Thesis

Helen Ru-Lin Na 1991 151 p

Avail: Univ. Microfilms Order No. DA9210932

Ionospheric tomography has generated great interest due to the possibility of two-dimensional imaging of electron density profiles. Traditional methods have, thus far, been capable of only one-dimensional imaging. Tomographic reconstructions are possible from existing one dimensional data and can be enhanced by knowledge gained through traditional imaging methods. In this thesis, a complete ionospheric imaging system is presented. The ionosphere is a plasma of ionized gas formed by ionization of the upper atmosphere by solar radiation and high-energy particles from the sun. Regions of irregular electron concentration exist within this layer of plasma, which interfere with the propagation of radio signals as they are reflected around the earth's surface by the ionosphere. Although there are well-accepted theories on the formation of the ionosphere, there are no corresponding theories for the formation of these irregularities. As a result, imaging the electron density is the best method of determining the location and nature of these irregularities. In this thesis, the ionospheric system was analyzed and modeled as a tomographic imaging system. The complete ionospheric imaging system was formulated in three segments: the ionospheric data acquisition system, the system model, and a reconstruction algorithm. The fundamental resolution limits of this system were then analyzed in several ways. The resolution of the imaging system based upon controllable parameters was examined followed by a quantitative measure of the complete imaging system's resolving capability. The effect of the various resolution degradation factors was then isolated and methods of compensation were investigated. Once the resolving capabilities of the system have been thoroughly determined, a variety of methods for enhancing the reconstruction algorithm will be developed. These methods will take advantage of existing knowledge of the ionosphere. A new Orthogonal Decomposition Algorithm was then developed. This algorithm removes some of the resolution degradation factors found in the original reconstruction algorithm by using orthogonal decomposition. A generalized development is given, and an interesting example of choosing Fourier kernels as the set of basis functions is presented. Finally, the future of ionospheric imaging will be discussed.

Dissert. Abstr.

N93-12263# Los Alamos National Lab., NM.

FOIL OPTIMIZATION FOR LOW ENERGY NEUTRAL ATOM IMAGING

H. O. Funsten, D. J. McComas, and B. L. Barraclough 1992 17 p Presented at the SPIE Symposium on Instrumentation for Magnetospheric Imagery, San Diego, CA, 19-24 Jul. 1992

(Contract W-7405-eng-36)

(DE92-013435; LA-UR-92-1360; CONF-920793-1) Avail: CASI HC A03/MF A01

Magnetospheric imaging has been proposed using remote detection of low energy neutral atoms (LENA's) of magnetospheric origin. In the detector, LENA's can be removed from the immense ambient EUV by charge modification (ionization) using a carbon stripping foil and can be subsequently deflected into an E/q analysis section. The detector sensitivity efficiency of LENA's is highly dependent on the ionization probability of neutrals as they transit the carbon foil. In this study, we present equilibrium charge state distributions and scatter distributions for 1-30 keV atomic hydrogen and oxygen transitting 0.5 micrograms/sq cm carbon foils. The fraction of hydrogen exiting a foil as H(+) ranges from approximately 5 percent at 1 keV to 41 percent at 30 keV. The fraction of oxygen exiting the foil as O(+) ranges from 2 percent at 10 keV to 8 percent at 30 keV. Results obtained after coating the exit surface of foils with either aluminum (which forms aluminum oxide when exposed to air) or gold suggests that the exit surface chemistry has no effect on the charge state distributions due to foil contamination from exposure to air. Scattering resulting from the atom-foil interaction is shown to be independent of the charge state distribution, suggesting that the interaction mechanisms resulting in charge exchange and scattering are distinctly different. DOE

N93-12264# Los Alamos National Lab., NM.

LOW ENERGY NEUTRAL ATOM IMAGING

D. J. McComas, H. O. Funsten, J. T. Gosling, K. R. Moore, and M. F. Thomsen 1992 15 p Presented at the 1992 SPIE International Symposium on Optical Applied Science and Engineering, San Diego, CA, 19-24 Jul. 1992

(Contract W-7405-eng-36)

(DE92-013531; LA-UR-92-1329; CONF-920792-2) Avail: CASI HC A03/MF A01

Energetic neutral atom (ENA) and low energy neutral atom (LENA) imaging of space plasmas are emerging as a new technology which promises to revolutionize the way we view and understand large scale space plasma phenomena and dynamics. ENA's and LENA's are produced in the magnetosphere by charge exchange between energetic and plasma ions and cold geocoronal neutrals. While imaging techniques have been previously developed for observing ENA's, with energies above several tens of keV, most of the ions found in the terrestrial magnetosphere have lower energies. We recently suggested that LENA's could be imaged by first converting the neutrals to ions and then electrostatically analyzing them to reject the UV background. In this paper, we extend this work to examine in detail the sensor elements needed to make a LENA imager. These elements are (1) a biased collimator to remove the ambient plasma ions and electrons and set the azimuthal field-of-view; (2) a charge modifier to convert a portion of the incident LENA's to ions; (3) an electrostatic analyzer to reject UV light and set the energy passband; and (4) a coincidence detector to measure converted LENA's while rejecting noise and penetrating radiation. We also examine the issue of LENA imager sensitivity and describe ways of optimizing sensitivity in the various sensor components. Finally, we demonstrate in detail how these general considerations are implemented by describing one relatively straightforward design based on a hemispherical electrostatic analyzer. DOE

N93-12270# California Univ., Santa Cruz.
STUDY OF SEISMIC CODA GENERATION IN CRUST WITH NON-UNIFORM SCATTERING AND ANELASTIC PROPERTIES Final Report, 14 Sep. 1989 - 14 Dec. 1991
John E. Vidale 18 Jun. 1992 40 p
(Contract F19628-89-K-0048)
(AD-A254350; UCSC-1992002; PL-TR-92-2038; AD-E201132)
Avail: CASI HC A03/MF A01

A series of investigations to determine which structures affect the amplitude, duration, frequency content, and directional properties of ground motion response to explosions and earthquakes was conducted. Investigations have shown that the shallowest tens of meters are crucial to the properties of the seismic wavefield. The shallow layers are marked by great lateral heterogeneity in velocity and attenuation, and consequently we observe both vertical and lateral resonances. The scrambling of the wavefield each time it reflects from the free surface is undoubtedly very important for seismic propagation to regional distances, but we are only beginning to understand the details of this interaction. GRA

N93-12299*# Aerodyne Research, Inc., Billerica, MA.
STRATOSPHERIC AIRCRAFT EXHAUST PLUME AND WAKE CHEMISTRY STUDIES
R. C. Miake-Lye, M. Martinez-Sanchez, R. C. Brown, C. E. Kolb, D. R. Worsnop, M. S. Zahniser, G. N. Robinson, J. M. Rodriguez, M. K. W. Ko, and R-L. Shia et al Oct. 1992 109 p
(Contract NAS1-19161; RTOP 537-01-20-01)
(NASA-CR-189688; NAS 1.26:189688; ARI-RR-902) Avail: CASI HC A06/MF A02

This report documents progress to date in an ongoing study to analyze and model emissions leaving a proposed High Speed Civil Transport (HSCT) from when the exhaust gases leave the engine until they are deposited at atmospheric scales in the stratosphere. Estimates are given for the emissions, summarizing relevant earlier work (CIAP) and reviewing current propulsion research efforts. The chemical evolution and the mixing and vortical motion of the exhaust are analyzed to track the exhaust and its speciation as the emissions are mixed to atmospheric scales. The species tracked include those that could be heterogeneously reactive on the surfaces of the condensed solid water (ice) particles and on exhaust soot particle surfaces. Dispersion and reaction of chemical constituents in the far wake are studied with a Lagrangian air parcel model, in conjunction with a radiation code to calculate the net heating/cooling. Laboratory measurements of heterogeneous chemistry of aqueous sulfuric acid and nitric acid hydrates are also described. Results include the solubility of HCl in sulfuric acid which is a key parameter for modeling stratospheric processing. We also report initial results for condensation of nitric acid trihydrate from gas phase H2O and HNO3. Author

N93-12308# Colorado School of Mines, Golden. Center for Wave Phenomena.
A DIP-DEPENDENT DIVERGENCE CORRECTION Ph.D. Thesis
F. Fazzari 1992 46 p
(Contract DE-FG02-89ER-14079)
(DE92-016283; CWP-116; DOE/ER-14079/15) Avail: CASI HC A03/MF A01

A divergence correction is conventionally applied to zero-offset data in an effort to preserve amplitude information. The conventional divergence correction compensates for the geometrical spreading of a point source in a horizontally layered medium where velocity varies with depth only. The dip-dependent divergence correction extends the conventional correction for improved amplitude processing of dipping beds. The dip-dependent divergence correction is computed by dynamic ray tracing, and applied to stacked data using a dip decomposition technique. This correction decreases amplitudes relative to the conventional correction for steep dips and late times. In a data example from the Gulf of Mexico, the conventional correction over-amplified the reflection off a salt dome flank by a factor of 1.6. High amplitudes near salt flanks are also associated with the presence of hydrocarbons. Applying the dip-dependent divergence correction ensures that 'bright spots' are not due to over-amplification of steep dips by the conventional correction. In areas like the Gulf of Mexico, where the velocity function varies primarily with depth, and steep beds are commonplace, the dip-dependent divergence correction is an inexpensive way to improve the amplitude information in seismic images. DOE

N93-12318# Colorado School of Mines, Golden. Center for Wave Phenomena.
MIGRATION BY THE KIRCHHOFF, SLANT STACK, AND GAUSSIAN BEAM METHODS
Dave Hale 1992 18 p
(Contract DE-FG02-89ER-14079)
(DE92-018640; DOE/ER-14079/16; CWP-126) Avail: CASI HC A03/MF A01

Gaussian beam migration offers features that are unmatched by any other single depth migration method. Unfortunately, computer algorithms for Gaussian beam migration are more complicated and difficult to understand that those for most other methods. One way to simplify Gaussian beam migration is to understand how it is related to other methods that may be more familiar. In particular, Gaussian beam migration is similar to Kirchhoff integral migration. It is also similar to the phase-shift (or slant stack) migration method. In a sense, the Gaussian beam approach to depth migration is to combine the best of these more familiar methods to obtain an efficient, robust, and flexible method for seismic imaging. DOE

N93-12378# Aerospace Corp., El Segundo, CA. Technology Operations.
THE EXTREMELY LOW FREQUENCY WAVE ANALYZER
H. C. Koons, J. L. Roeder, and W. B. Harbridge 15 Mar. 1992 15 p
(Contract F04701-88-C-0089)
(AD-A255178; TR-0091(6940-06)-6; SSD-TR-92-XX) Avail: CASI HC A03/MF A01

This report describes the Extremely Low Frequency Wave Analyzer flown as part of the LASSII (Low Altitude Satellite Studies of Ionospheric Irregularities) experiment aboard the CRRES (Chemical Release and Radiation Effects Satellite). This instrument measures electrostatic and electromagnetic waves in the ambient ionosphere and during the CRRES chemical releases. GRA

47 METEOROLOGY AND CLIMATOLOGY

Includes weather forecasting and modification.

N93-10971# Massachusetts Univ., Amherst. Microwave Remote Sensing Lab.
THE MILLIMETER WAVE CLOUD PROFILING RADAR SYSTEM (CPRS) Annual Progress Report No. 2
A. L. Pazmany, S. M. Sekelsky, and R. E. McIntosh Jun. 1992 13 p
(Contract DE-FG02-90ER-61060)
(DE92-016970; DOE/ER-61060/2) Avail: CASI HC A03/MF A01

The Cloud Profiling Radar System (CPRS) is a single antenna, two frequency (33 GHz and 95 GHz) polarimetric radar which is currently under the development at the University of Massachusetts (UMASS). This system will be capable of making four dimensional Doppler and polarimetric measurements of clouds. This report gives details about the status of the various subsystems under development and discusses current research activities. DOE

N93-11144# Federal Aviation Administration, Washington, DC. Surveillance Office.
SUMMARY OF FINDINGS FROM THE PIREP-BASED ANALYSES CONDUCTED DURING THE 1988 TO 1990 EVALUATIONS OF TDWR-BASED AND TDWR/LLWAS-BASED ALERT SERVICES PROVIDED TO LANDING/DEPARTING PILOTS Final Report, Mar. 1988 - Aug. 1991
Lloyd Stevenson Jul. 1992 59 p
(AD-A253859; DOT-VNTSC-FAA-91-15; DOT/FAA/NR/92-6)
Avail: CASI HC A04/MF A01

The Federal Aviation Administration (FAA) is developing the Terminal Doppler Weather Radar (TDWR). Starting in 1988 the TDWR Program conducted a series of evaluations of a TDWR-based alert service to provide wind shear and microburst alerts to landing and departing pilots. Starting in 1989, a second series of evaluations was initiated involving an integrated alert service consisting of TDWR and the Phase 3 Low Level Wind Shear Alert System (LLWAS). Evaluations are expected to continue through 1992. The radio communications between local control and landing and departing pilots were analyzed for 224 of the 323 alert periods that occurred during 1989 through 1990 and represents one component of the overall investigation that took place. A key element of the communications were the pilot reports (PIREP's) of weather-related encounters and observations made during the alert periods. PIREP's were used to evaluate the accuracy of the issued alerts from the pilot's viewpoint as to the location and intensity of the wind-related encounters, and to identify situations in which pilots reported wind-related encounters that were not provided alert coverage. GRA

N93-11159 Colorado State Univ., Fort Collins.
NUMERICAL AND OBSERVATIONAL INVESTIGATIONS OF LONG-LIVED, MCS-INDUCED, SEVERE SURFACE WIND EVENTS: THE DERECHO Ph.D. Thesis
Jerome Michael Schmidt 1991 209 p
Avail: Univ. Microfilms Order No. DA9134475

This study addresses the production of sustained, straight-line, severe surface winds associated with mesoscale convection systems (MCS's) of extratropical origin otherwise known as derechos. The physical processes which govern the observed derecho characteristics are identified and their possible forcing mechanisms are determined. Detailed observations of two derechos are presented along with simulations using the Colorado State University Regional Atmospheric Modeling System (CSU-RAMS). The observations revealed a derecho environment characterized by strong vertical wind shear through the depth of the troposphere and large values of convective available potential energy (CAPE). The thermodynamic environment of the troposphere in each case had a distinct three-layer structure consisting of: (1) a surface-based stable layer of 1-to-2 km in depth, (2) an elevated well-mixed layer of 2-4 km in depth, and (3) an upper tropospheric layer of intermediate stability that extended to the tropopause. Two primary sets of simulations were performed to assess the impact of the observed environmental profiles on the derecho structure, propagation, and longevity. The first set consisted of nested-grid regional-scale simulations initialized from the standard NMC analyses on a domain having relatively coarse horizontal resolution (75 km). The second set of simulations consisted of two and three-dimensional experiments initialized in a horizontally homogeneous environment having a relatively fine horizontal resolution (2 km) and explicit micro-physics. The results from these experiments indicate the importance of convectively-induced gravity waves on the MCS structure, propagation, longevity, and severe surface wind development. The sensitivity of the simulated convection and gravity waves to variations in the vertical wind shear and moisture profiles are described. Detailed Doppler radar analyses and 3-D simulations of a severe, bow echo squall line are presented which reveal the unique 3-D circulation features which accompany these mesoscale convective systems. We illustrate how the mesoscale and convective-scale flow fields within the bow echo establish the severe surface wind maximum. Dissert. Abstr.

N93-11168*# National Aeronautics and Space Administration. Langley Research Center, Hampton, VA.
ATLAS OF ALBEDO AND ABSORBED SOLAR RADIATION DERIVED FROM NIMBUS 7 EARTH RADIATION BUDGET DATA SET, NOVEMBER 1985 TO OCTOBER 1987
G. Louis Smith, David Rutan (Lockheed Engineering and Sciences Co., Hampton, VA.), and T. Dale Bess Oct. 1992 57 p
(RTOP 578-12-26-70)
(NASA-RP-1281; L-17107; NAS 1.61:1281) Avail: CASI HC A04/MF A01

An atlas of monthly mean global contour maps of albedo and absorbed solar radiation is presented for 21 months from Nov. 1985 to Oct. 1987. These data were retrieved from measurements made by the shortwave wide-field-of-view radiometer of the Earth Radiation Budget (ERB) instrument aboard the Nimbus 7 spacecraft. Profiles of zonal mean albedos and absorbed solar radiation were tabulated. These geographical distributions are provided as a resource for researchers studying the radiation budget of the Earth. The El Nino/Southern Oscillation event of 1986-1987 is included in this data set. This atlas of albedo and absorbed solar radiation extends to 12 years the period covered by two similar atlases: NASA RP-1230 (Jul. 1975 - Oct. 1978) and NASA RP-1231 (Nov. 1978 - Oct. 1985). These three compilations complement the atlases of outgoing longwave radiation by Bess and Smith in NASA RP-1185, RP-1186, and RP-1261, which were also based on the Nimbus 6 and 7 ERB data. Author

N93-11236# Sandia National Labs., Albuquerque, NM.
NUMERICAL COMPUTATION OF THE LIGHTNING RESPONSE OF AN EARTH-COVERED MUNITIONS STORAGE BUNKER AND COMPARISON WITH EXPERIMENTS
K. O. Merewether and M. E. Morris 1992 5 p Presented at the 21st International Conference on Lightning Protection, Berlin (Germany), 22-25 Sep. 1992
(Contract DE-AC04-76DP-00789)
(DE92-014268; SAND-92-1009C; CONF-9209107-3) Avail: CASI HC A01/MF A01

This paper presents recent progress in using finite-difference analysis codes to simulate the responses of complex structures due to direct lightning. Significant advances were made in interfacing a finite-difference code with commercial computer aided design tools, in suppressing a pervasive instability associated with the thin-wire algorithm for modeling conductors much smaller than a cell size, and in visualizing the results with color movies. Preliminary comparisons between the results of the finite-difference code and the results obtained during a recent rocket-triggered lightning test are also presented. DOE

N93-11237# Colorado State Univ., Fort Collins. Dept. of Atmospheric Science.
THE USE OF ARM DATA TO TEST AN IMPROVED PARAMETERIZATION OF UPPER TROPOSPHERIC CLOUDS FOR USE IN CLIMATE MODELS
D. A. Randall May 1992 4 p
(Contract DE-FG02-92ER-61363)
(DE92-014353; DOE/ER-61363/T1) Avail: CASI HC A01/MF A01

We have proposed to provide and further develop an advanced finite-difference climate model for use in CHAMMP. The model includes advanced parameterizations of cumulus convection, boundary-layer processes, cloud formation, and land-surface vegetation, as well as parameterizations of radiative transfer and gravity wave drag. Postprocessing codes and a user's guide will also be provided. DOE

N93-11242# National Oceanic and Atmospheric Administration, Miami, FL. Atlantic Oceanographic and Meteorological Labs.
HURRICANE RESEARCH DIVISION FISCAL YEAR 1991 PROGRAMS: FISCAL YEAR 1992 PROJECTIONS
Jan. 1992 63 p
(PB92-138320) Avail: CASI HC A04/MF A01

The contents are as follows: Introduction; FY-91 Programs -

FY-92 Projections; Laboratory Research; Observational Hurricane Studies; Spectral Modeling of a Hurricane with Full Physics; Development of a Nested Spectral Barotropic Hurricane Track Prediction Model; Initialization of Tropical Cyclone Models; Asymmetric Evolution of the Hurricane; Objective Analysis of the Hurricane and its Environment; Atlantic Tropical Climate and Hurricane Cycles; Large-Scale Influences on Tropical Cyclone Intensity Change; Tropical Cyclone Awareness Research; Storm Surge; GALE; EMEX; TOGA COARE; Observational Studies of the South Florida Sea Breeze; Ground Truth for Rainfall Estimates in Hurricanes; Cooperative Research Projects; and Appendix A: Publications. GRA

N93-11256# National Oceanographic Data Center, Washington, DC.

MARINERS WEATHER LOG, VOLUME 36, NUMBER 1, WINTER 1992 Quarterly Report

Richard M. DeAngelis, ed. 1992 96 p

(PB92-161025) Avail: CASI HC A05/MF A01; SOD HC

The contents are as follows: Rating northeasters; What about (Hurricane) Bob; A Titanic memorial; Ice patrol; Departments--Whale Oil and Wicks, Ocean Queries, editor's desk, sea photography, PMO report, Mailbag, Marine observation program, Radio officer tips, Hurricane alley; and Marine Weather Review--July, August and September 1991--North Atlantic Ocean, North Pacific Ocean, Pressure and track charts, Tables. GRA

N93-11329 Royal Netherlands Meteorological Inst., De Bilt. Div. of Oceanographic Research.

LAM AND NEDWAM STATISTICS OVER THE PERIOD OCTOBER 1990 - APRIL 1991

R. A. vanMoerkerken 1991 80 p

(KNMI-TR-137; ISBN-90-369-2004-3; ETN-92-92270) Copyright Avail: Royal Netherlands Meteorological Inst., P.O. Box 201, 3730 AE De Bilt, Netherlands

Wind fields from an atmospheric fine mesh Limited Area Model (LAM) and wave heights predicted, on the basis of these wind fields, by a shallow-water third generation wave model (NEDWAM) were compared with observations. The comparison is made for the following elements: wind direction, wind speed, wave height, low frequency wave height, and wave period for the period Oct. 1990 - Apr. 1991 inclusive for the following locations: EPF and K-13 in the southern North Sea and AUK in the central North Sea. A comparison between GONO (wind and wave model) and LAM/NEDWAM was also made. ESA

N93-11340# Stockholm Univ. (Sweden). Dept. of Meteorology.

TIME SCALES CHARACTERIZING THE PROCESSING OF WATER AND CLOUD CONDENSATION NUCLEI BY CLOUDS

Henning Rodhe Mar. 1992 15 p

(CM-80; ETN-92-92292) Avail: CASI HC A03/MF A01

Various definitions were formulated of time scales characterizing the processing of water and cloud condensation nuclei by clouds. Rough attempts were made to quantify these time scales using available data on cloud occurrence and cloud properties. The average atmospheric lifetime of water molecules was found to be about two days. The water molecules that are eventually removed by precipitation have a lifetime of about ten days. The average number of cloud encounters of an airparcel in the lower troposphere in between two encounters of a precipitating cloud is of the order of 10. The average number of condensation/evaporation cycles experienced by a water molecule during its atmopsheric residence time is about 2. ESA

N93-11349 GKSS-Forschungszentrum Geesthacht (Germany). Inst. fuer Physik.

DETECTION OF CLOUD-TOP HEIGHT FROM BACKSCATTERED RADIANCES WITHIN THE OXYGEN A BAND. PART 1: THEORETICAL STUDY

J. Fischer and H. Grassl (Max-Planck-Inst. fuer Meteorologie, Hamburg, Germany) 1991 17 p Repr. from Journal of Applied Meteorology, v. 30, no. 9, Sep. 1991 p 1245-1259 Previously announced in IAA as A91-51701

(GKSS-91/E/76-Pt-1; ETN-92-92283) Copyright Avail: Fachinformationszentrum Karlsruhe, 7514 Eggenstein-Leopoldshafen 2, Germany

A series of radiative transfer calculations were performed to study the possibility of determining cloud top pressure (height) from backscattered solar radiances within the oxygen A band absorption. For the development of a cloud top pressure algorithm, the impact of perturbing effects, such as varying cloud properties, Sun elevation, and surface albedo are taken into account. The most important quantities are total cloud optical thickness delta C and the vertical profile of liquid water content. The effects of cloud optical thickness, if delta C is greater than 1, are already taken into account by a cloud top algorithm, which only considers two radiances inside and outside the oxygen absorption band. For one layer clouds, the cloud top heights may be derived to within an accuracy of 200 m. Multilayer clouds or varying liquid water content profiles can only be matched with an inverse technique using radiances at up to 16 wavelengths, which, however, give cloud top height estimates to within an error of only 50 m for all 900 cloud cases considered. ESA

N93-11350 GKSS-Forschungszentrum Geesthacht (Germany). Inst. fuer Physik.

DETECTION OF CLOUD-TOP HEIGHT FROM BACKSCATTERED RADIANCES WITHIN THE OXYGEN A BAND. PART 2: MEASUREMENTS

J. Fischer, W. Cordes, A. Schmitz-Pfeiffer (Deutsche Forschungsanstalt fuer Luft- und Raumfahrt, Wessling, Germany), W. Renger (Deutsche Forschungsanstalt fuer Luft- und Raumfahrt, Wessling, Germany), and P. Moerl (Deutsche Forschungsanstalt fuer Luft- und Raumfahrt, Wessling, Germany) 1991 10 p Repr. from Journal of Applied Meteorology, v. 30, no 9, Sep. 1991 p 1260-1267 Previously announced in IAA as A91-51702

(GKSS-91/E/77-Pt-2; ETN-92-92284) Copyright Avail: Fachinformationszentrum Karlsruhe, 7514 Eggenstein-Leopoldshafen 2, Germany

Detection of cloud top heights from reflected solar radiation measurements within the oxygen A band absorption is reported. A description of both instruments and algorithms used for retrieval of cloud top height and cloud optical thickness is given. This included the optical multichannel analyzer which measured multispectral radiances, and the backscatter lidar system ALEX-F which performed lidar measurements. The accuracy of the estimated cloud top heights was to within 40 m over stratus clouds when compared with simultaneously taken lidar measurements. Estimations of the cloud optical thickness from reflected radiances at lambda = 755 nm are reasonable. Between both cloud optical thickness and cloud top height, a positive cross correlation was found to be significant at scales up to 5 km, which confirms a relationship between cloud top height and cloud optical thickness. These experimental results show the potential of multichannel radiance measurements for the detection of physical cloud properties. ESA

N93-11505# Army Lab. Command, White Sands Missile Range, NM. Atmospheric Sciences Lab.

SURFACE WIND SPEED DISTRIBUTIONS Final Report

Elton P. Avara and Bruce T. Miers Jun. 1992 73 p

(AD-A253268; ASL-TR-0313) Avail: CASI HC A04/MF A01

Some weapon systems are sensitive to winds in the lowest layers of the atmosphere. Wind speed distributions and random wind speeds derived from the distributions are often required to help determine the operational capabilities of these systems. A literature survey revealed investigators usually used either a log-normal or a Weibull distribution as the model for the distribution of wind speeds independent of direction. In addition to these two distributions, a gamma distribution is also evaluated in this report. Wind speeds observed in three different geographical regions during nine selected meteorological conditions (weather classes), three diurnal time periods, and five seasonal time periods were evaluated. This report contains the results of the wind speed analysis for some of the combinations of weather classes, diurnal time periods, and seasonal time periods for each of the three geographical regions--European Lowlands, European Highlands, and Mideast Desert. The observed wind speed distributions were adequately presented by the analytical distributions except in a few cases. For those exceptions, the observed empirical wind speed distributions should be used rather than the analytical distributions to generate random wind speeds in simulation studies. GRA

N93-11657# Pacific Northwest Lab., Richland, WA.
KEY WINTERTIME METEOROLOGICAL FEATURES OF THE GRAND CANYON AND THE COLORADO PLATEAUS BASIN
C. D. Whiteman and K. J. Allwine Jun. 1992 3 p Presented at the 4th Arizona Weather Symposium, Scottsdale, AZ, 10-12 Jun. 1992
(Contract DE-AC06-76RL-01830)
(DE92-019134; PNL-SA-20809; CONF-9206256-1) Avail: CASI HC A01/MF A01

In the winter of 1989-1990 a major meteorological and air pollution experiment was conducted in the Colorado Plateaus Basin (Richards et al., 1991). The focus of the experiment, conducted by Arizona's Soft River Project, was to investigate the influence of three 750-MW coal-fired power plant units at the Navajo Generating Station near Page, Arizona, on visibility at Grand Canyon National Park. As part of the meteorological experiment, surface and upper air data were collected from multiple sites within the basin. This data set is the most comprehensive meteorological data set ever collected within the region, and the purpose of this paper is to briefly summarize the key wintertime meteorological features of the Colorado Plateaus Basin and the Grand Canyon, through which the basin drains, using analyses of the Winter Visibility Study data. Our analyses focused primarily on thermally driven circulations within the basin and the Grand Canyon, but we also investigated the surface energy budget that drives these circulations and the interactions between the thermal circulations and the overlying synoptic-scale flows. DOE

N93-11678# Sandia National Labs., Albuquerque, NM.
ROCKET-TRIGGERED LIGHTNING TEST OF AN EARTH-COVERED MUNITIONS STORAGE BUNKER
G. H. Schnetzer and R. J. Fisher 1992 10 p Presented at the 1992 International Conference on Lightning and Static Electricity, Atlantic City, NJ, 6-8 Oct. 1992
(Contract DE-AC04-76DP-00789)
(DE92-016790; SAND-91-2654C; CONF-9210113-1) Avail: CASI HC A02/MF A01

During the summer of 1991, nine negative cloud-to-ground lightning flashes, comprising a total of 38 individual return strokes, were triggered to designated attachment points on a munitions storage bunker. Measurements were simultaneously made of the incident flash currents, both return-stroke and continuing current components, and of response at 24 test points located throughout the bunker. The recorded responses included currents, voltages, and electric and magnetic fields throughout the structure and its lightning protection system. The maximum responses observed at each test point, as directly measured and a linearly scaled to median and severe return-stroke incident current amplitudes, are presented and discussed. DOE

N93-11803# National Weather Service, Kansas City, MO.
PROCEEDINGS OF THE NATIONAL WEATHER SERVICE AVIATION WORKSHOP: POSTPRINT VOLUME
B. Lambert Mar. 1992 430 p Workshop held in Kansas City, MO, 10-13 Dec. 1991
(PB92-176148; NOAA-TM-NWS-CR-102) Avail: CASI HC A19/MF A04

Papers presented at the National Weather Service Aviation Workshop (Dec. 10-13, 1991) are provided. The topics covered by these papers include aviation user requirements; fog and stratus forecasting; forecasting mesoscale en-route weather; special aviation related services; present terminal forecast procedures; Doppler radar and downbursts; profilers, Meteorological Data Collection and Reporting System (MDCRS), and LDS; Automated Surface Observations (ASOS); using computer generated products and satellite data; and the future of aviation weather. GRA

N93-11817# Air Force Inst. of Tech., Wright-Patterson AFB, OH.
A COMPARISON OF RADAR RAINFALL ESTIMATES AND RAIN GAGE MEASUREMENTS DURING TWO DENVER THUNDERSTORMS M.S. Thesis
David J. Speltz 1992 92 p
(AD-A254267; AFIT/CI/CIA-92-070) Avail: CASI HC A05/MF A01

It has long been hoped that rainfall measurements made with weather radars would be able to supplement or even replace rain gage networks. During the summer of 1991 Colorado State University's (CSU) Department of Atmospheric Science participated in an experiment which was intended, in part, to determine how useful radar measurements are in helping to estimate heavy rainfall from thunderstorms. A dense array of 41 automatic rain gages operated by the Denver Urban Drainage and Flood Control District (UDFCD) provided precipitation measurements to compare with the radar results. Two thunderstorms were observed: the first occurred on June 6 and produced up to 43.7 mm (1.72 in) of rain in 85 minutes, while the August 5 storm resulted in peak rainfall amounts of 37.8 mm (1.49 in) in 60 minutes. Unfortunately, estimates of rainfall made by using a relation between the radar measured reflectivity (Z) and the rain rate (R) are frequently in error by large amounts. The radar estimate over gage 540 during the June 6 storm was 58.8 mm (2.31 in) higher than the gage amount, an error of 201 percent. During the August 5 event gage 1720 recorded 37.8 mm, while the radar estimate was 27.8 mm (1.09 in) lower. Such large errors are unacceptable for most meteorological or hydrological purposes. The use of different Z-R relations provided overall improvement during both storms, while reflectivity thresholds resulted in better estimates during the June 6 storm, in which hail was present. GRA

N93-11819# Air Force Inst. of Tech., Wright-Patterson AFB, OH.
A COMPOSITE STUDY OF THE MADDEN-JULIAN OSCILLATION M.S. Thesis
Robert J. Falvey 1992 153 p
(AD-A254269; AFIT/CI/CIA-92-068) Avail: CASI HC A08/MF A02

A composite based on the phase of the 30-60 day oscillation (referred to here as the Madden-Julian Oscillation or MJO) is used to examine kinematic and thermodynamic fields over the equatorial western Pacific Ocean for three Northern Hemisphere winter seasons (1986-89). The composite is based on Outgoing Longwave Radiation (OLR) data from NOAA polar-orbiting satellites plotted in time versus longitude diagrams. Eastward propagation of low OLR (inferred deep convection) values associated with the trough of the MJO wave was clearly visible in these Hovmoller diagrams. These diagrams were used to construct a four convective phase composite. The composite is then applied to the OLR and model analysis data from the European Center for Medium Range Weather Forecasts (ECMWF) and the National Meteorological Center (NMC). Large scale heat and moisture budgets are calculated and compared to other tropical budget studies. Emphasis is placed on inter-phase variability and the role of El Nino-Southern Oscillation (ENSO) as a modulator of convective activity. The OLR composite reveals that during the two warm years (1986-87 and 1987-88) the main convective activity was centered between the 2.5 deg S and 5.0 deg S. It shifted to between 10.0 deg S and 15.0 deg S during the cold year (1988-89). The OLR data also indicated that the convection was stronger in the warm years than in the cold year. The eastward propagation of the convection was also evident. GRA

N93-11839 Michigan Univ., Ann Arbor.
AN INVERSION TECHNIQUE TO RECOVER LOWER THERMOSPHERIC WINDS FROM SPACE-BORNE REMOTE

MEASUREMENTS OF (OI) 5577 A Ph.D. Thesis
Bruno Nardi 1991 276 p
Avail: Univ. Microfilms Order No. DA9135658

A new wind inversion technique that was developed to obtain neutral wind profiles from space-borne Fabry-Perot Interferometer (FPI) measurements of atmospheric airglow is presented. This generalized numerical technique is applied to (OI) 5577 A measurements taken with the FPI on board NASA's Dynamics Explorer-2 (DE-2) satellite to obtain wind profiles in the lower thermosphere (altitude range: 90 km to 150 km). DE2-FPI was the first satellite-borne instrument with sufficient spectral resolution to recover wind (and temperature) information from atmospheric emissions. An inversion technique must be applied to retrieve true wind profiles from space-borne (OI) 5577 A measurements because the non-local nature of this emission causes information to be averaged over altitude. As a precursory step to the wind inversion, two brightness inversion techniques to recover the (OI) 5577 A volume emission rate profiles were developed. Both the wind and the brightness inversion techniques were assessed for statistical and systematic errors using a DE2-FPI numerical simulator, also developed here. With this inversion method, it was possible to retrieve lower thermospheric winds with an accuracy of up to approximately +/- 10 m/s. It was also shown that 5577 A volume emission rate profiles for both night-glow and day-glow can be successfully retrieved if constrained to Chapman layers. A preliminary study of the polar E-region wind field was conducted; inverted, binned, and averaged polar DE2-FPI data was compared with the wind fields predicted by the National Center for Atmospheric Research - Thermospheric General Circulation Model (NCAR-TGCM) and the Univeristy College London - Thermospheric General Circulation Model (UCL-TGCM). The measured lower thermospheric wind field showed significantly stronger winds than model predictions, with less of an inclination toward the classic polar two cell pattern. Finally, an experiment was conducted to compare ground-based measurements of lower thermospheric winds made with an FPI and an incoherent scatter radar at the Sondre Stromfjord, Greenland facility. It was found that the ideal geophysical conditions required by the two instruments were almost mutually exclusive for this particular measurement. The necessary conditions for making simultaneous measurements were identified and confirmed by obtaining several hours of observations during a period exhibiting such conditions. Author

N93-11880*# National Oceanic and Atmospheric Administration, Boulder, CO. Office for Interdisciplinary Earth Studies.
REPORTS TO THE NATION ON OUR CHANGING PLANET. WINTER 1991 NO. 1: THE CLIMATE SYSTEM Semiannual Report, Apr. - Sep. 1992
1991 23 p LIMITED REPRODUCIBILITY: More than 20% of this document may be affected by color photographs Original contains color illustrations
(Contract NCC5-42)
(NASA-CR-190954; NAS 1.26:190954) Avail: CASI HC A03/MF A01; 18 functional color pages

This pamphlet is a semi-annual report for the period April 1992 through September 1992 dealing with the study of climatology. This introductory pamphlet treats in the simplest of terms such topics as climate change, the greenhouse effect, the global heat engine, hydrology, oceanography, computers and climatology, ice ages, and global warming. Informative charts are included.
R.L.B.

N93-11888# National Hurricane Center, Coral Gables, FL.
DIAGNOSTIC REPORT OF THE NATIONAL HURRICANE CENTER: OCTOBER AND NOVEMBER 1990, VOLUME 3, NUMBER 3
C. J. McAdie and E. N. Rappaport 1990 86 p
(PB91-242297) Avail: CASI HC A05/MF A01

Contents: 1: Overview of Tropical Activity for October and November 1990 -- (1) Mean flow patterns for the Atlantic and Eastern Pacific Basins; Month of October 1990; Month of November 1990; (2) Tropical wave and topical cyclone summary; 2: Topical Cyclone Activity in the Atlantic Basis -- (1) Overview; (2) Preliminary reports; Hurricane Joseophine (21 September-6 October 1990), Hurricane Klaus (3-9 October 1990), Hurricane Lili (6-15 Ocober 1990), Tropical Storm Marco (9-13 October 1990), Hurricane Nana (16-21 October 1990), (3) Official Forecast and Tracking Model Performance; 3: Tropical Cyclone Activity in the Eastern Pacific Basin -- (1) Overview; (2) Preliminary reports; Hurricane Odile (23 September-2 October 1990), Hurricane Polo (28 September-1 October 1990), Tropical Storm Rachel (27 September-3 October 1990), Tropical Storm Simon (9-14 October 1990), Hurricane Trudy (16 October-1 November 1990), Hurricane Vance (21-31 October 1990); (3) Offical Forecast and Tracking Model Performance.
GRA

N93-11896# Climate Analysis Center, Washington, DC.
PROCEEDINGS OF THE SIXTEENTH ANNUAL CLIMATE DIAGNOSTICS WORKSHOP
Mar. 1992 477 p Workshop held in Los Angeles, CA, 28 Oct. - 1 Nov. 1991
(PB92-198803) Avail: CASI HC A21/MF A04

The Sixteenth Annual Climate Diagnostics Workshop was hosted by the Department of Atmospheric Sciences at the University of California in Los Angeles. These Proceedings provide a published record of the presentations made at the Workshop. Sessions were conducted on the following topics: ENSO, Low-Frequency Variability, Stratosphere, Ocean Circulation, Ocean-Atmosphere Interaction, Contemporary Climate Variations and Issues, Global Climate Change, Hydrology and Precipitation, ENSO and Seasonal Forecasts, and Climate Prediction. GRA

N93-11897# World Meteorological Organization, Geneva (Switzerland). World Climate Data and Monitoring Programme.
CCL WORKING GROUP ON CLIMATE DATA
Nov. 1991 146 p Meeting held 11-15 Nov. 1991 Original contains color illustrations
(WCDMP-18; WMO/TD-488) Avail: CASI HC A07/MF A02

This working group report on climate data presents the proceedings of the World Meteorological Organization's Commission for Climatology (CCL) meeting of November 11-15, 1991. The majority of the report consists of 15 annexes dealing with reports of various subgroups and includes a list of participants. The initial 6 chapters include topics such as the Global Climate Observing System (GCOS) and a guide to climatological practices. R.L.B.

N93-11997 Kent Univ., Canterbury (England).
STATISTICAL METHODS FOR THE COMPARISON OF SPATIAL PATTERNS IN METEOROLOGICAL VARIABLES Ph.D. Thesis
Jacqueline Mary Potts 1991 285 p
Avail: Univ. Microfilms Order No. BRDX96436

Methods are considered for comparing spatial patterns in meteorological variables such as mean sea level pressure. Values of the variable are assumed to be available at a set of grid points. Meteorologists need to do this in order to assess the accuracy of weather forecasts. A multivariate normal model is proposed and methods for modeling spatial correlation as a parametric function of distance are examined. The properties of some univariate measures of similarity currently used by meteorologists are investigated, looking in particular at those based on mean squared error and correlation. A method which compares the gradients of the patterns rather than the actual data values is also discussed. The relationship between the mean squared error and correlation is considered. The effect of spatial autocorrelation on the distribution of the mean squared error and the correlation coefficient is examined and methods for estimating the effective sample size are given. Existing measures which compare the cumulative distribution function of the values of a variable at a point are considered and a new score of this type is derived. The distribution of two such measures is obtained and the combination of measures from a set of grid points is discussed. The use of multivariate techniques in which the measures are applied to principal components rather than to values at grid points is suggested as a means of allowing for spatial correlation and of identifying the nature of the differences between patterns. Dissert. Abstr.

N93-12154# Lawrence Livermore National Lab., CA.

VISUALIZING WIND VELOCITIES BY ADVECTING CLOUD TEXTURES

N. Max, R. Crawfis, and D. Williams Apr. 1992 10 p Presented at the Visualization 1992, Boston, MA, 19-23 Oct. 1992
(Contract W-7405-eng-48)
(DE92-014717; UCRL-JC-110242; CONF-921079-2) Avail: CASI HC A02/MF A01

In order to visualize both clouds and wind in climate simulations, we have rendered clouds using a 3-D texture which is advected by the wind flow. Clouds have a significant influence on global temperatures, because they reflect the short wave radiation from the sun, and also absorb and reflect the longer wave radiation re-emitted by the earth. It is not certain which of these effects is larger, so the influence of clouds is an open research problem. Clouds are the least understood aspect of climate models; it is not even known whether global warming will cause an increase in cloudiness. Cloud response to climate perturbations has the capability to magnify the climate change or to reduce its severity. Visualization is an important tool for analyzing and understanding climate simulation output, and we have developed algorithms for visualizing scalar climate data, including cloud density. It is also important to visualize wind velocity, which is a vector field. When a time sequence of cloud data is viewed in animation, motion of the cloud density gives information about the prevailing winds. We have added texture to the clouds, and advected the texture with the wind. We used a 3-D volume texture, evaluated at a contour surface of cloud density, and advected the three texture coordinates. In addition to helping visualize the wind, the resulting realistic cloud textures will portray climate modeling research results easily to the general public. DOE

N93-12167# Electro-Optical Sciences, Inc., Irvington, NY.

MULTIANGLE LIDAR PERFORMANCE IN THE PRESENCE OF HORIZONTAL INHOMOGENEITIES IN ATMOSPHERIC EXTINCTION AND SCATTERING Final Report

Dina Gutkowicz-Krusin 11 Jun. 1992 24 p
(Contract N00014-90-C-0215)
(AD-A252882; EOS/FR-0215) Avail: CASI HC A03/MF A01

The performance of the single-ended multiangle lidar for measurements of atmospheric extinction and backscattering is analyzed in the presence of signal-induced shot noise. An algorithm for determining the transmission coefficient in the presence of horizontal inhomogeneities is described. The analysis indicates that real-time measurements of atmospheric properties with the multiangle lidar may be feasible even in inhomogeneous regions. GRA

N93-12170# Weather Squadron (45th), Patrick AFB, FL.

WEATHER IMPACTS ON SPACE OPERATIONS Final Report

J. T. Madura, Billie F. Boyd, and W. H. Bauman 25 Jul. 1992 14 p
(AD-A253720; Rept-45SPW-TR-92-2) Avail: CASI HC A03/MF A01

Although launch (and landing for space shuttle) are the most visible space launch operations, there is much weather sensitive work to be accomplished between flights, such as moving vehicles, moving/stacking solid rocket boosters (SRB's), fueling, etc. The major weather item of concern in the Cape Canaveral area is lightning, since the KSC/CCAF's area is near the area of maximum thunderstorm occurrence in the United States. Weather support at KSC/CCAF includes weather Observations, forecasts, climatological studies, and consultant services to a wide variety of Range Users. GRA

N93-12180# Air Force Inst. of Tech., Wright-Patterson AFB, OH.

TEMPORAL MONITORING OF VHF AND LF ATMOSPHERICS AND THEIR RELATION TO LIGHTNING M.S. Thesis

Arthur E. Zemke 30 Mar. 1992 181 p
(AD-A252617; AFIT/CI/CIA-92-026) Avail: CASI HC A09/MF A02

Atmospheric discharges of various types emit electromagnetic radiation over a wide range of frequencies. VHF transients are associated with the discharges that occur during the preliminary charge separation and breakdown processes of lightning. Correlated VHF-LF activity emitted at relatively high magnitudes are normally attributed to lightning's powerful return stroke and recoil streamer discharges. This research hypothesized that VHF atmospherics (precursors) exist at least 1 minute or more before correlated VHF-LF transient activity (return strokes or recoil streamers) is detected during known lightning and thunderstorm periods. For 56 days, high-sampling-rate digitizers continuously monitored atmospheric conditions in VHF and LF bandwidths and measured the peak magnitude of transients as they occurred. The data was recorded in a computer file and used to characterize transient activity during various weather periods. The experimental results collected throughout confirmed lightning and thunderstorm intervals showed a significant increase in transient activity and that VHF atmospherics were detected on the average at least 3 minutes before any correlated VHF-LF transient activity was measured. In a few cases, the lead time was even greater when the initial VHF existed an average of at least 11 minutes before the onset of correlated VHF-LF. GRA

N93-12251# Air Force Inst. of Tech., Wright-Patterson AFB, OH.

AN OBSERVATIONAL STUDY OF A PREFRONTAL CONVECTIVE RAINBAND USING TAMEX SINGLE- AND DUAL-DOPPLER DATA M.S. Thesis

Michael R. Beeson 1991 115 p
(AD-A249839; AFIT/CI/CIA-91-122) Avail: CASI HC A06/MF A02

The kinematic structure of a prefrontal rainband that caused heavy rainfall over Northern and Central Taiwan on 25 Jun. 1987 was investigated using TAMEX single- and dual-Doppler data. Fields of winds and reflectivity were derived in a 50 km by 50 km grid using an objective analysis scheme with 1 km grid spacing in three directions. Vertical velocities were computed from the analastic continuity equation by integrating downward with variational adjustment. Results showed that the convective activity in the prefrontal region was deep with moderate intensity and heavy rainfall. The convective activity over the front was weak and confined to the lower layers, and rainfall decreased dramatically after the frontal passage. Vertical motions below 2 km were weak and were mostly caused by lifting along the frontal slope. In the prefrontal area the vertical motions were stronger and extended to higher levels. The eastern part of the frontal system lagged behind due to the influence of the Central Mountain Range, causing a curved front. The flow was from rear-to-front at all levels, except for the part near the coastline, where front-to-rear flow was seen at lower levels. In the lower levels a strong southwesterly Monsoon flow supplied the inflow of moist air, and strong veering with height was seen. The slow movement of the system, the orientation of the rainbands, and the terrain effects combined to produce periods of very heavy rainfall on the west coast of Central Taiwan. GRA

N93-12293# National Oceanographic Data Center, Washington, DC.

MARINERS WEATHER LOG, VOLUME 36, NUMBER 2, SPRING 1992

Richard M. DeAngelis, ed. 1992 104 p
(PB92-204213) Avail: CASI HC A06/MF A02; SOD HC

Contents: Oceanos' heroes; Where have all the data gone--Merchant ship observations from WW 2 remain a mystery; North Atlantic hurricanes--1991; Eastern North hurricanes--1992; and Central North Pacific hurricanes--1991. GRA

N93-12339# Naval Postgraduate School, Monterey, CA. Meteorology Dept.
OPERATIONS PLAN FOR THE TROPICAL CYCLONE MOTION (TCM-92) MINI-FIELD EXPERIMENT Interim Report, Oct. 1991 - Sep. 1992
Russell L. Elsberry, George M. Dunnavan, and Eric J. McKinley
May 1992 51 p
(NR Proj. RR0-330)
(AD-A254723; NPS-MR-92-002) Avail: CASI HC A04/MF A01

A WC-130 instrumented aircraft will be deployed in the Western North Pacific region near Guam during 21 July-18 August 1992 to obtain in situ measurements in Mesoscale Convective Systems embedded in tropical cyclones. Four hypotheses related to different tropical cyclone track modification or genesis mechanisms will be tested. The scientific basis for these hypotheses is described and observations and models of midlatitude mesoscale convective systems are reviewed to provide a basis for planning the WC-130 missions. Aircraft operations and the Experiment Operations Center are described, along with tentative flight tracks. Descriptions of the real-time observations and the data to be archived for post-experiment analyses are provided. GRA

N93-12420# California State Univ., San Diego. Computer Systems Lab.
AUTOMATIC CLOUD CLASSIFICATION FROM MULTI-SPECTRAL SATELLITE DATA Final Report, 1 May 1990 - 30 Sep. 1991
Catherine Gautier, D. Lavallee, P. Peterson, and D. Schweizer
30 Sep. 1991 170 p
(Grant AF-AFOSR-0209-90)
(AD-A255125; AFOSR-92-0727TR) Avail: CASI HC A08/MF A02

This project was aimed at developing an operational 'expert' system to perform the classification of satellite images into cloud types. The approach we have used is based on a number of assumptions. The first one is that such a classification is possible with satellite images of 1 km (or more) resolution. A second assumption, which lays the foundations for all classifications, is that there exists a parameter space wherein some clustering of the data occurs, so the task is to identify this parameter space from the data. An additional assumption necessary to physically interpret the results, but not necessary for the classification itself, is that the clusters found in this parameter space can be related to cloud types or physical features. We chose a Bayesian classifier for our classification. We believe that this type of classifier is best suited for the task because clouds are fuzzy objects which have overlapping characteristics. Also, with a Bayesian classifier, each point in the parameter space has a probability to belong to each class, although this probability may be anywhere between zero and one. GRA

N93-12424# Naval Postgraduate School, Monterey, CA.
A REAL TIME SHARPENING OF NOGAPS PREDICTIONS OF MID-LATITUDE CENTRAL PACIFIC CYCLONES M.S. Thesis
Edward J. Harrington Jun. 1992 68 p
(AD-A255157) Avail: CASI HC A04/MF A01

A Modifying Model is developed which sharpens the 24 hour position forecast issued by the Navy Operational Global Atmospheric Prediction model (NOGAPS) 24 hours into a selected, mid-latitude, Central Pacific cyclone. The technique measuring cyclone characteristics within the first 24 hours and using these values in regression equations to provide improved forecasts for the next 24 hour position forecast. Generally, the modified position forecasts are to the left and ahead of the NOGAPS position forecasts along the anticipated track of the cyclone. Probability ellipses about the Modifying Model estimates cover about 50 to 60 percent of the area of the corresponding NOGAPS probability ellipses. Only cyclones in the deepening phase (central pressure decreasing) or forecast to be in the deepening phase are utilized in the data base. The Modifying Model is sufficiently simple that shipboard personnel can make the computations in real time. GRA

N93-12507# Pennsylvania State Univ., University Park. Dept. of Meteorology.
THE VERTICAL DISTRIBUTION OF HEATING IN THE TROPICAL ATMOSPHERE Annual Report No. 1
William M. Frank 15 Aug. 1992 5 p
(Contract N00014-92-J-1069)
(AD-A254982) Avail: CASI HC A01/MF A01

The project is designed to achieve three major goals: (1) assist the planning of TOGA COARE to optimize experimental design and measurement strategy, focussing on the larger scale arrays but paying particular attention to the problem of integrating the measurements from the arrays; (2) participate in the TOGA COARE field program during the IOP; and (3) carry out a research program examining the mean properties and vertical heating profiles of mesoscale through synoptic-scale circulation systems in the COARE region, exploring the relationships between these systems and larger scale forcing, and determining the processes that determine the vertical structure of the atmosphere during COARE. GRA

N93-12534 Maryland Univ., College Park.
INTERANNUAL VARIABILITIES OF THE EAST ASIAN SUMMER MONSOON AND TROPICAL SEA SURFACE TEMPERATURES Ph.D. Thesis
Suhung Shen 1991 186 p
Avail: Univ. Microfilms Order No. DA9222761

The interannual variabilities of the summer rainfall over China, the tropical sea surface temperature (SST) as well as their relationships have been studied. It is found that the rainfall over the study domain is not coherent and can be divided into south and north climate regimes. The dominant period of the SST is 3-6 years over the eastern Pacific but decadal over the Indian to western Pacific oceans. However, the biennial variability is shown to be a fundamental variability in both the rainfall and the tropical SST. The significant correlations have been shown between the SST and the rainfall over both the tropical Pacific and Indian Oceans. This relationship also is biennial and is more significant when the SST's lag the rainfall by 3-6 months. The westerlies over the tropical western Pacific influence the SST strongly over the eastern Pacific. It is found in this study that the variations of the westerlies over the western Pacific, to a great extent, are associated with that of the East Asian summer monsoon. In summary, the East Asian summer monsoon plays an active role in the interactions between the atmosphere and the ocean over the tropics. It may be important for the biennial variability of the tropical system. Dissert. Abstr.

48 OCEANOGRAPHY

Includes biological, dynamic, and physical oceanography; and marine resources.

For related information see also *43 Earth Resources and Remote Sensing.*

N93-11253# Texas A&M Univ., Galveston. Sea Grant Coll. Program.
BIBLIOGRAPHY OF PUBLICATIONS FROM THE TEXAS A AND M SEA GRANT COLLEGE PROGRAM, 1968-1992
May 1992 107 p
(Grant NA16RG0457-01)
(PB92-205517; TAMU-SG-92-603) Avail: CASI HC A06/MF A02

The bibliography includes all publications produced by the Texas A&M University Sea Grant College Program from its inception in 1968 through May 1992. The citations are listed by topics in chronological order, so more recent works are found toward the end of each section. A brief abstract describes each publication, with the exception of subsequently replaced publications, annual reports and directories. GRA

N93-11642# California Univ., San Diego, La Jolla.
STUDIES OF OCEAN PREDICTABILITY AT DECADE TO CENTURY TIME SCALES USING A GLOBAL OCEAN GENERAL CIRCULATION MODEL IN A PARALLEL COMPETING ENVIRONMENT
10 Mar. 1992 6 p
(Contract DE-FG03-91ER-61215)
(DE92-019457; DOE/ER-61215/1) Avail: CASI HC A02/MF A01

The first phase of the proposed work was almost completed on schedule. Scientists at the San Diego Supercomputer Center (SDSC) succeeded in putting a version of the Hamburg Isopycnal Coordinate Ocean Model (OPYC) onto the INTEL parallel computer. Due to the slow run speeds of the OPYC on the parallel machine, another ocean model is being used during the first part of phase 2. The model chosen is the Large Scale Geostrophic (LSG) model from the Max Planck Institute. DOE

N93-11718*# National Aeronautics and Space Administration. Goddard Space Flight Center, Greenbelt, MD.
NIMBUS-7 SCANNING MULTICHANNEL MICROWAVE RADIOMETER (SMMR) PARM TAPE USER'S GUIDE
D. Han, P. Gloersen, S. T. Kim (Computer Sciences Corp., Rockville, MD.), C. C. Fu (Computer Sciences Corp., Rockville, MD.), R. P. Cebula (Hughes STX, Inc., Lanham, MD.), and D. MacMillan (Interferometrics, Inc., Vienna, VA.) Aug. 1992 146 p
(Contract NAS5-29386)
(NASA-RP-1284; NAS 1.61:1284; Rept-92B00104) Avail: CASI HC A07/MF A02

The Scanning Multichannel Microwave Radiometer (SMMR) instrument, onboard the Nimbus-7 spacecraft, collected data from Oct. 1978 until Jun. 1986. The data were processed to physical parameter level products. Geophysical parameters retrieved include the following: sea-surface temperatures, sea-surface windspeed, total column water vapor, and sea-ice parameters. These products are stored on PARM-LO, PARM-SS, and PARM-30 tapes. The geophysical parameter retrieval algorithms and the quality of these products are described for the period between Nov. 1978 and Oct 1985. Additionally, data formats and data availability are included. Author

N93-11734# Skidaway Inst. of Oceanography, Savannah, GA.
THE FLUX AND RECYCLING OF BIOACTIVE SUBSTANCES IN THE SURFACE SEDIMENTS OF THE DEEP BASINS OFF SOUTHERN CALIFORNIA
R. A. Jahnke 18 Mar. 1992 4 p
(Contract DE-FG09-88ER-60627)
(DE92-019172; DOE/ER-60627/4) Avail: CASI HC A01/MF A01

We have used pore water gradients and in situ benthic flux chamber measurements to assess the total and down-core variations in the organic carbon remineralization rate. To augment standard pore water extractions, we developed techniques to extract pore water samples at 2-mm sampling intervals, greatly improving our assessment of near- surface vertical gradients. In addition, much emphasis was placed on directly measuring the exchange of chemicals between the bottom waters and sediment pore waters via in situ benthic flux chamber incubations. The latter were performed with the MANOP bottom lander, and in later expeditions, the Benthic Experimental chamber Instrument (BECI). Results from these measurements were used to assess the several aspects of seafloor organic matter diagenesis. DOE

N93-11821# Naval Oceanographic and Atmospheric Research Lab., Bay Saint Louis, MS.
VALIDATION TEST REPORT FOR THE FIRST-GENERATION DART GULF STREAM FORECASTING SYSTEM Final Report
Theodore J. Bennett, Jr. and Robert C. Rhodes Apr. 1992 47 p
(AD-A254286; NOARL-20) Avail: CASI HC A03/MF A01

Acoustic propagation within the Northwest Atlantic is highly dependent on the meandering Gulf Stream front and it's associated drifting rings, the so called mesoscale structure of the ocean. Considerable variability in space and time characterize this structure. This report documents the validation of a system that makes nowcasts and forecasts of the Gulf Stream frontal path. The validation was done as part of the transition of the first-generation Data Assimilation Research and Transition (DART) model to operational environment are the crux of the validation. In one set of experiments, operational front and ring maps are used to initialize and verify 1- and 2-week forecast experiments. In the other set of experiments, the value the DART model adds to the present operational capability is estimated. The proposed operational use of the model is simulated by setting up a simple data assimilation system that uses a 1-week forecast to interporate across long data gaps that arise during the mapping of front and ring positions. The gappy paths are constructed by superimposing observed data gaps on complete frontal paths. This report also provides guidance to an operator on how to use a model forecast to fill in the data gaps. Both sets of experiments show the system to be a statistically significant improvement over an assumption of persistence, i.e., no change over time. GRA

N93-12002 Ohio State Univ., Columbus.
ORTHOGONAL FUNCTIONS OVER THE OCEANS AND APPLICATIONS TO THE DETERMINATION OF ORBIT ERROR, GEOID AND SEA SURFACE TOPOGRAPHY FROM SATELLITE ALTIMETRY Ph.D. Thesis
Cheinway Hwang 1991 299 p
Avail: Univ. Microfilms Order No. DA9211149

A set of orthogonal functions over the oceans are determined and then applied to the expansions of oceanic signals. Ultimately, these functions are incorporated in the parameter estimation problem using a model that simultaneously reduces satellite radial orbit errors, improves the geoid, and estimates the sea surface topography. To construct a possible set of orthogonal functions (over the oceans), three methods were studied. In one method, an attempt was made to solve the spherical Helmholtz equation over the oceans with either the Dirichlet boundary condition or the Newmann boundary condition or the mixed boundary condition. This method leads to successful developments of the spherical cap harmonics and generalized Fourier-Bessel series for some regularized oceanic domains. The other study employs the Shwarz-Christoffel conformal mapping, as well as an auxiliary mapping, to transform the irregular domain (the oceans) onto the interior of a unit disk where a set of orthogonal functions are easy to find. The set of orthogonal functions over the oceans are then found through the relationship between the two domains implied by the mappings. The third method involves the Gram-Schmidt process for which a new technique for computing the integrals of the products of two associated Legendre functions is developed and a fast Fourier transform (FFT) method is used to compute the inner products of spherical harmonics over the oceans. Also, for the entire unit sphere, the generalized 2-D Fourier series and the generalized Fourier-Tschebycheff series are proposed as alternatives for the spherical harmonics. The expansions of the Levitus SST into the orthonormal functions constructed by the Gram-Schmidt process show that 98.5 percent of the energy of that signal is contained within degree 10 of the orthonormal functions. Such expansions also render regular spectral behavior of oceanic signal as compared to that from spherical harmonic expansions. A method of detecting band limited oceanic signal is also developed using these orthonormal functions. The applications of these functions to the simultaneous model yield lower correlations between expansion coefficients and show that the cut-off frequency (the highest degree determinable) of the SST from the Geosat data is in the vicinity of degree 15 of the functions. Some other improved simultaneous models have also been tested in an attempt to better separate the geoid and the SST signal. This study concludes that the orthonormal functions are suitable for representing oceanic signal with excellent spectral behavior and can be applied to a future altimetric mission such as TOPEX/POSEIDON. Dissert. Abstr.

N93-12094# Coastal Engineering Research Center, Vicksburg, MS.
THE WAVE INFORMATION STUDIES (WIS) WAVE MODEL, VERSION 2.0 (USER'S GUIDE) Final Report
J. M. Hubertz Jun. 1992 43 p
(AD-A254313; CERC-WIS-27) Avail: CASI HC A03/MF A01

This report provides guidance on application of the Wave Information Studies Wave Model, Version 2.0 (WISWAVE 2.0), and a description of the upgrades from Version 1.0. The present version operates in all water depths, while the previous version operated only in depths sufficient not to affect wave propagation. The present version also allows for changing water depths during a simulation as would be the case in storm surge applications or regions of large tidal amplitude. The structure and operation of the model are described. Input necessary to operate the model is described and an example input data set is provided. The theory, equations, and solution techniques contained within the model are described in the references provided. The theory, equations, and solution techniques associated with the upgrade to include shallow-water effects are described in Appendix A. Documented subroutines associated with the upgrade are provided in Appendix B. GRA

N93-12247# Woods Hole Oceanographic Inst., MA.
THE STRUCTURE AND TRANSPORT OF THE BRAZIL CURRENT BETWEEN 27 DEG AND 36 DEG SOUTH Ph.D. Thesis
Jan C. Zemba Jun. 1991 163 p
(Contract N00014-82-C-0019; NSF OCE-86-14486)
(AD-A247635; WHOI-91-37) Avail: CASI HC A08/MF A02

An analysis of four hydrographic sections from the Thomas Washington marathon cruises--27, 31, 34 and 36 deg S--identifies downstream changes in the Brazil Current. They detail the current's change from a relatively small (12 Sv), near surface feature to a large (80 Sv), deep current. Growth comes from a recirculation cell, deepening shear and a deeper zero velocity surface (required if NADW is to flow south). A four layer, basinwide model at 31 deg S ties the size of the Brazil Current and recirculation to various limits on layer-to-layer exchanges south of the section. The resulting flow pattern is consistent with equatorward meridional heat flux in the South Atlantic. Qualitative downstream changes in the total potential vorticity illuminate the presence of both frictional and inertial flow regimes. The presence of a frictional regime at the inshore edge suggests that care should be taken in assuming that potential vorticity is conserved in western boundary currents. The final picture which emerges is not of a small, surface-trapped Brazil Current; rather, it is that of a classic western, boundary current, increasing in strength and depth before turning east into the interior ocean. GRA

N93-12288# Naval Oceanographic and Atmospheric Research Lab., Bay Saint Louis, MS.
OCEANOGRAPHIC EXPERT SYSTEM: POTENTIAL FOR TESS(3) APPLICATIONS Final Report
M. Lybanon Jul. 1992 13 p
(AD-A254908; NOARL-TN-286) Avail: CASI HC A03/MF A01

The Naval Research Laboratory (NRL-SSC) has developed an expert system with a rule base that 'knows' about the evolution of mesoscale features in the Gulf Stream region of the North Atlantic. The expert system uses rules that describe the 'features' kinematics to evolve an earlier 'state' to a later time. The NRL-SSC expert system has the potential to be useful in an operational environment. Hence, it is proposed as a candidate for implementation on the Tactical Environmental Support System, third generation (TESS (3)). GRA

N93-12431# Johns Hopkins Univ., Baltimore, MD.
PARAMETERS FOR PREDICTING RED TIDES OF BIOLUMINESCENT DINOFLAGELLATES: METEOROLOGICAL EVENTS AND FRONTAL WATER CIRCULATION PATTERNS Annual Report
Howard H. Seliger 1992 11 p
(Contract N00014-92-J-1094)
(AD-A254835) Avail: CASI HC A03/MF A01

Climatic events and bio-physical sequences involved in red tide formation have been characterized by mnemonic symbols and applied to geographical regions with spatial scales from meters to hundreds of kilometers and temporal scales ranging from daily to annual. Red tides may represent selections for optimization for sexual mating and for delivery of sexual or overwintering benthic cysts to 'seed bed' areas. A frontal convergence zone at the seaward edge of upwelling regions can exist and be a source of dinoflagellates transported into nearshore waters below a pycnocline. The physical hydrographic integrity of red tide surface patches enhances transport within geostrophic surface current jets with minimal dilution losses. Stepwise emigration and colonization are fortuitous consequences of red tide formation. Anthropogenic hypereutrophication along coastlines may have enhanced the efficiencies of stepwise emigrations, permitting colonization of areas not previously accessible. GRA

51 LIFE SCIENCES (GENERAL)

N93-10974# Lawrence Livermore National Lab., CA.
MOLECULAR CYTOGENETICS: A NOVEL APPROACH FOR MEASURING CHROMOSOME TRANSLOCATIONS IN INDIVIDUALS YEARS AFTER EXPOSURE TO LOW LEVELS OF IONIZING RADIATION
Joe Nathan Lucas and Tore Straume Apr. 1992 5 p Presented at the 2nd International Conference on Effects of Low-Dose Ionizing Radiation, Bournemouth, United Kingdon, 18-20 May 1992
(Contract W-7405-eng-48)
(DE92-018066; UCRL-JC-109874; CONF-9205118-1) Avail: CASI HC A01/MF A01

Chromosome painting was developed in our laboratory to facilitate rapid and accurate detection of chromosome translocations in human cells. Chromosome painting is the selective staining of one or more chromosomes by fluorescence in situ hybridization (FISH) using whole chromosome probes. This method permits essentially uniform hybridization and staining along the entire lengths of targeted chromosomes. Staining all other chromosomes a different color makes interchromosomal exchange aberrations readily apparent as bicolored chromosomes. Here we present a brief discussion of this methodology and recent results from studies in our laboratory. DOE

N93-11630# Brookhaven National Lab., Upton, NY.
THE POTENTIAL EFFECTS OF CONCURRENT INCREASES IN TEMPERATURE, CO2 AND O3 ON NET PHOTOSYNTHESIS, AS MEDIATED BY RUBISCO
S. Long Jul. 1992 26 p Presented at the Air Pollutants and Plant Metabolism Conference, Blacksburg, VA, 13-16 Jun. 1992
(Contract DE-AC02-76CH-00016)
(DE92-019411; BNL-47624; CONF-9206254-1) Avail: CASI HC A03/MF A01

At the leaf level, under light saturating and light limiting conditions, it is shown that elevated atmospheric CO2 concentration not only alters the scale of the response of carbon gain to rising temperature, but can alter the direction of response. These points bring into serious question the value of any predictions of plant production which ignore not only the direct effect of CO2 on carbon gain, but also the basic interactions of temperature, CO2, and O3. While many factors may potentially diminish the enhancement of light saturated leaf photosynthetic rates with increase in atmospheric CO2 concentrations, no mechanism has so far been identified which could remove the parallel stimulation of light-limited photosynthesis. DOE

N93-12014*# National Aeronautics and Space Administration. Ames Research Center, Moffett Field, CA.
EFFECT OF HEMORRHAGE ON CARDIAC OUTPUT, VASOPRESSIN, ALDOSTERONE, AND DIURESIS DURING IMMERSION IN MEN
J. E. Greenleaf, K. Simanonok (California Univ., Davis.), E. M.

Bernauer (California Univ., Davis.), C. E. Wade, and L. C. Keil
Sep. 1992 13 p
(RTOP 199-18-12-07)
(NASA-TM-103949; A-92141; NAS 1.15:103949) Avail: CASI
HC A03/MF A01

The purpose of this research was to test the hypotesis that a reduction in blood volume would attenuate or eliminate immersion-induced increases in cardiac output (Q(sub co)) and urine excretion, and to investigate accompanying vasoactive and fluid-electrolyte hormonal responses. Eight men (19-23 yr) were supine during a 2-hr control period in air, and then sat for 5-hr test periods in air at 20 C (dry control, DC); water at 34.5 C (wet control, WC); and water (34.5 C) after hemorrhage (WH) of 14.8 plus or minus 0.3 percent of their blood volume. Blood volume was -11.6 plus or minus 0.6 percent at immersion (time 0). Mean (bar-X hrs 1-5) Q(sub co) was unchanged in WC (5.3 plus or minus 0.01 l/min) and in WH (4.5 plus or minus 0.1 l/min), but decreased (P less than 0.05) in DC to 3.6 plus or minus 0.1 l/min. Mean urine excretion rates were 1.0 plus or minus 0.2 ml/min for DC and 1.1 plus or minus 0.2 ml/min for WH; both were lower (P less than 0.05) than that for WC of 2.0 plus or minus 0.4 ml/min. Plasma (Na+) and (Osm) were unchanged in all experiments. Mean plasma vasopressin (PVP) (bar-X hrs 1-5) was 1.1 plus or minus 0.1 pg/ml in WC, and higher (P less than 0.05) in DC (2.1 plus or minus 0.2 pg/ml)and WH (2.1 plus or minus 0.1 pg/ml); it was unchanged during air and water test periods. Thus, hemorrhage attenuated the immersion-induced increase in Q(sub co), eliminated the WC diuresis, maintained plasma renin activity and PVP at DC levels and did not change immersion-induced aldosterone suppression; the osmotic diuresis during control immersion is apparently not due to either aldosterone suppression or vasopressin suppression. Author

N93-12174*# National Aeronautics and Space Administration. Marshall Space Flight Center, Huntsville, AL.
MICROBIOLOGICAL ANALYSIS OF DEBRIS FROM STS-42 IML-1 BY DIRECT PLATING OF RINSE WATERS
G. A. Smithers Oct. 1992 20 p
(NASA-TM-108375; NAS 1.15:108375) Avail: CASI HC
A03/MF A01

Microbial analysis of air filter debris from the Spacelab International Microgravity Laboratory-1 (IML-1) mission was performed via direct plating of rinse waters on a battery of selective and nonselective nutrient agars. Microbial isolates were identified using Minitek and Biolog technologies. Twenty-four types of bacteria were recovered and classified; a similar number of fungal types was observed, but these were not identified. This procedure can provide information about the proportions of organism types present at the time of debris collection. Author

N93-12266# Columbia Univ., New York, NY. Center for Radiological Research.
RADIATION PHYSICS, BIOPHYSICS, AND RADIATION BIOLOGY
E. J. Hall May 1992 60 p
(Contract DE-FG02-88ER-60631)
(DE92-013673; DOE/ER-60631/10) Avail: CASI HC A04/MF
A01

The following research programs from the Center for Radiological Research of Columbia University are described: design and development of a new wall-less ultra miniature proportional counter for nanodosimetry; some recent measurements of ionization distributions for heavy ions at nanometer site sizes with a wall-less proportional counter; a calculation of exciton energies in periodic systems with helical symmetry -- application to a hydrogen fluoride chain; electron energy-loss function in polynucleotide and the question of plasmon excitation; a non-parametric, microdosimetric-based approach to the evaluation of the biological effects of low doses of ionizing radiation; high-LET radiation risk assessment at medium doses; high-LET radiobiological effects -- increased lesion severity or increased lesion proximity; photoneutrons generated by high energy medical linacs; the biological effectiveness of neutrons; implications for radiation protection; molecular characterization of oncogenes induced by neutrons; and the inverse dose-rate effect for oncogenic transformation by charged particles is LET dependent. DOE

N93-12315# Oak Ridge National Lab., TN.
SCALING ISSUES FOR BIODIVERSITY PROTECTION
S. M. Pearson, M. G. Turner, R. H. Gardner, and R. V. ONeill
1992 33 p Presented at the United States Department of Agriculture (USDA) Forest Service Symposium on Biodiversity in Managed Landscapes: Theory and Practice, Sacramento, CA, 12-15 Jul. 1992
(Contract DE-AC05-84OR-21400)
(DE92-016689; CONF-9207106-1) Avail: CASI HC A03/MF
A01

Environmental heterogeneity, in both space and time, has been important in the evolution and maintenance of biodiversity. Moreover, this heterogeneity is hierarchical in nature. Differences occur between biomes, between landscapes. Thus, hierarchical patterns of heterogeneity are a consequence of the complexity within ecological communities, and the maintenance of biodiversity means the preservation of this complexity. Natural landscapes are dynamic systems that exhibit temporal and spatial heterogeneity. However, the exploitative nature of human activity tends to simplify landscapes (Krummel et al. 1987). The challenge of preserving biodiversity in managed landscapes is to incorporate natural levels of spatial and temporal heterogeneity into management schemes. The concept of scale has emerged as an important topic among ecologists that recognize the role of heterogeneity in natural ecosystems. Subjects related to scale such as grain (level of detail) and extent (size of area or duration of time) are frequently used to determine the appropriate interpretation of ecological data. Likewise, scale is important when applying ecological principles to biodiversity protection and conservation. The scale of a conservation endeavor affects the strategy involved, realistic goals, and probability of success. For instance, the spatial extent of a reserve system may be determined, for better or worse, by biogeography, distribution of surviving populations, political boundaries, or fiscal constraints. Our objectives are to: emphasize the importance of natural patterns of spatial and temporal heterogeneity, encourage a broader-scale perspective for conservation efforts, and illustrate the interaction between landscape-level heterogeneity and organism-based scales of resource utilization with a simulation experiment. DOE

N93-12482# Arkansas Univ., Fayetteville. Dept. of Chemical Engineering.
BIOLOGICAL CONVERSION OF SYNTHESIS GAS CULTURE DEVELOPMENT
K. T. Klasson, R. Basu, E. R. Johnson, E. C. Clausen, and J. L. Gaddy Mar. 1992 55 p
(Contract DE-FG21-90MC-27225)
(DE92-001279; DOE/MC-27225/3091) Avail: CASI HC
A04/MF A01

Research continues on the conversion of synthesis by shift reactions involving bacteria. Topics discussed here include: biological water gas shift, sulfur gas utilization, experimental screening procedures, water gas shift studies, H2S removal studies, COS degradation by selected CO-utilizing bacteria, and indirect COS utilization by Chlorobia. DOE

52 AEROSPACE MEDICINE

Includes physiological factors; biological effects of radiation; and effects of weightlessness on man and animals.

N93-11146# Princeton Univ., NJ.
PHYSIOLOGICAL ANALYSES OF THE AFFERENTS CONTROLLING BRAIN NEUROCHEMICAL SYSTEMS Annual Report, 1 Jun. 1991 - 31 May 1992
Barry L. Jacobs 30 Jun. 1992 3 p
(Grant AF-AFOSR-0294-90)

(AD-A253185; AFOSR-92-0734TR) Avail: CASI HC A01/MF A01

Two types of experiments are described. The first was directed at the neurochemical systems that control the activity of brain serotonergic (dorsal raphe nucleus) neurons. The second examines the effects of serotonin and norepinephrine on the activity of target neurons carrying out sensory information processing or motor function. Both sets of studies utilize single unit activity in combination with multibarrel microiontophoresis in awake animals. This research program provides critical links for understanding both the control of brain neurochemical systems and the control exerted by them. This will help to elucidate, more broadly, the role of these modulatory brainstem neurochemical systems in processes such as state-dependent changes in physiology and behavior, and arousal and attention. GRA

N93-11193# Cryopharm Corp., Pasadena, CA.
FREEZE-DRIED HUMAN RED BLOOD CELLS Progress Report
15 Jul. 1992 49 p
(Contract N00014-90-C-0053)
(AD-A253295) Avail: CASI HC A03/MF A01

A preliminary clinical evaluation of in vivo circulation of autologous, lyophilized and reconstituted human red blood cells was undertaken to establish a baseline level of in vivo performance of lyophilized red blood cells from both human volunteers and cynomolgus monkeys. The cell survival results demonstrated that reconstituted, lyophilized red cells remained in circulation in vivo for the same period as normal non-lyophilized red blood cells. Since our last progress report we have obtained additional in vivo survival data from a total of four healthy volunteers. The design of the clinical study protocol followed accepted procedures for red cell in vivo survival studies. In all of the four volunteers, no changes in vital signs occurred after an infusion of a small dose of the autologous lyophilized red blood cells and no associated adverse side effects were observed during the study and through the final follow-up examination conducted one week post infusion. In all four volunteers, peripheral blood samples were collected in citrate-phosphate-dextrose and adenine-1 (CPDA-1) for up to 6 days post infusion to measure the level of circulating chromium labeled red cells and to allow accurate estimation of the circulating half lives of the cells. Urine sample collection was also carried out during the first 24 hours post infusion for measurement of the levels of chromium clearance by the kidneys. Each volunteer was subjected to gamma imaging and external probe counts over the heart, spleen and liver at 4 hours and 24 hours post-infusion to determine the organ distribution of the radiolabeled reconstituted red blood cells. GRA

N93-11283# Advisory Group for Aerospace Research and Development, Neuilly-Sur-Seine (France). Aerospace Medical Panel.
ALLERGIC, IMMUNOLOGICAL AND INFECTIOUS DISEASE PROBLEMS IN AEROSPACE MEDICINE [LES PROBLEMES CAUSES PAR LES MALADIES ALLERGIQUES, IMMUNOLOGIQUES ET CONTAGIEUSES EN MEDECINE AEROSPATIALE]
Apr. 1992 211 p In ENGLISH and FRENCH Symposium held in Rome, Italy, 21-25 Oct. 1991
(AGARD-CP-518; ISBN-92-835-0664-2) Copyright Avail: CASI HC A10/MF A03

These proceedings include the technical evaluation report, the opening address, and 36 papers of the symposium. The theme of the symposium was the fight against infectious diseases, mainly the vaccine-preventable ones, and the study of inhalent allergic diseases. Enormous development in the last few years has allowed us to understand and prevent many pathological conditions, whereas the setting up of laboratory tests has allowed us to monitor with great precision the immune function which may be depressed by the environmental stimuli to space or military flight. Lastly, the development of military and civilian air travel, which favors the spreading of infectious and parasitic diseases, requires the setting up of correct prophylactic measures. For individual titles, see N93-11284 through N93-11318.

N93-11284# Eidgenoessische Technische Hochschule, Zurich (Switzerland). Space Biology Group.
SPACE FLIGHT AND IMMUNE SYSTEM
A. Cogoli *In* AGARD, Allergic, Immunological and Infectious Disease Problems in Aerospace Medicine Apr. 1992 10 p (For primary document see N93-11283 02-52)
Copyright Avail: CASI HC A02/MF A03

Depression of lymphocyte response to mitogens in cosmonauts after spaceflight was reported for the first time in the early seventies by Soviet immunologists. Today we know that depression of lymphocyte function affects at least 50 percent of space crew members. Investigations on the ground on subjects undergoing physical and psychological stress indicate that stress is a major factor immune depression of astronauts. This despite the fact that weightlessness per-se has a strong inhibitory effect of lymphocyte activation in-vitro. Although the changes observed never harmed the health of astronauts, immunological changes must be seriously investigated and understood in view of long duration flights on space stations in an Earth orbit and to other planets like Mars and the Moon. Author

N93-11285# Defence and Civil Inst. of Environmental Medicine, North York (Ontario).
MECHANISMS OF IMMUNE FAILURE IN BURN INJURY
Brian G. Sparkes *In* AGARD, Allergic, Immunological and Infectious Disease Problems in Aerospace Medicine Apr. 1992 12 p (For primary document see N93-11283 02-52)
Copyright Avail: CASI HC A03/MF A03

The burden on military medical services in handling burn casualties is daunting as all physiological systems will become affected. Severe burns in a battlefield setting have a very low salvage rate, to a great degree because of the immune failure which invariably develops. Evaluations of responses of lymphocytes taken from burn patients over several weeks following the burn (greater than 30 percent TBSA), have revealed that the immune failure which follows thermal injury involves T cell activation events. Interleukin 2, which is normally produced by activated T lymphocytes, is very poorly produced by cells cultivated in vitro taken from non-surviving patients, whereas some production continues, although at below normal levels, in patients who ultimately survive their injury. IL2 exogenously added to lymphocyte cultures enhances the proliferation of cells from surviving patients but gives no such help to cells from nonsurvivors. The TAC portion of the IL2 receptor (IL2R alpha), expressed on the T cell surface, appears to be responsible for this difference, as the number of lymphocytes able to express ILR2 alpha falls post-burn. A lipid protein complex (LPC) produced in skin by burning has been shown to inhibit the immune response in vivo and the growth of IL2-dependent lymphocytes in culture. Cerium nitrate, applied topically to the burn patient, is thought to fix the LPC in the burn eschar and prevents its entry into the circulation. In a study of 10 patients, bathed in cerium nitrate, some T lymphocyte activities were found to be in the normal range rather than suppressed. Such a treatment promises to be useful in improving chances of survival in severe burn injury. Author

N93-11286# Turin Univ. (Italy).
CLINICAL TYPES OF HEPATITIS B
Mario Rizzetto and Roberto Nisini (Divisione Aerea Studi Ricerche e Sperimentazioni, Pratica di Mare, Italy) *In* AGARD, Allergic, Immunological and Infectious Disease Problems in Aerospace Medicine Apr. 1992 7 p (For primary document see N93-11283 02-52)
Copyright Avail: CASI HC A02/MF A03

Hepatitis B is a parenterally and sexually transmitted disease of global importance. The disease runs more frequently a subclinical and anicteric course, with a significative rate of cases that become chronic. Chronic hepatitis may progress to cirrhosis or cancer. The strategies by which Hepatitis B can be diminished and eventually eliminated are: immunization, measures to prevent exposure to infective blood or blood derivatives, and education (in particular awareness that hepatitis B is a sexually transmitted disease). Author

N93-11287# Aerospace Medical Research Labs., Brooks AFB, TX. Epidemiologic Research Div.

VIRAL HEPATITIS IN THE US AIR FORCE, 1980 - 1989

M. D. Parkinson, R. W. Stout, D. R. Mahon, W. F. Clardy, R. W. Warner, M. E. Weston, and W. H. Wolfe *In* AGARD, Allergic, Immunological and Infectious Disease Problems in Aerospace Medicine Apr. 1992 2 p (For primary document see N93-11283 02-52)

Copyright Avail: CASI HC A01/MF A03

Viral hepatitis and its acute and chronic complications continue to pose significant threats to the readiness of military personnel. Knowledge about the specific viral agents and their routes of transmission are important in developing prevention strategies. A recent analysis of hepatitis in the U.S. Navy for the period 1975-1984 is reviewed. In order to better characterize the risk of viral hepatitis among Air Force personnel, a comprehensive review of inpatient and quarters data for hepatitis A, B and 'non-A, non-B' were reviewed from Air Force medical treatment facilities worldwide for the period 1980-1989. Following a discussion of the study methodology, preliminary data and hepatitis type-specific demographic risk variables are discussed. Preliminary results from a hepatitis serosurvey (A, B, and C antibody with use of a supplemental validating assay) of the subset of the study cohort who are currently on active duty are briefly reviewed. Author

N93-11288# Zurich Univ. (Switzerland). Div. of Epidemiology and Prevention of Communicable Diseases.

HEPATITIS A AND HEPATITIS B: RISKS COMPARED TO OTHER VACCINE PREVENTABLE DISEASES AND IMMUNIZATION RECOMMENDATIONS

R. Steffen *In* AGARD, Allergic, Immunological and Infectious Disease Problems in Aerospace Medicine Apr. 1992 4 p (For primary document see N93-11283 02-52)

Copyright Avail: CASI HC A01/MF A03

The incidence rate of hepatitis A is 3(-6)/1000 per month of stay in a developing country in unprotected travelers. Trampers and other persons feeding themselves under bad hygienic conditions have a rate of 20/1000. In many industrialized countries, persons below the age of 50 years have a seroprevalence rate of anti-HAV less than 20 percent. Hepatitis A morbidity and mortality in travelers is far greater than the one of any other vaccine preventable infection in travelers, with the exception that hepatitis B shows a slightly greater mortality in expatriates. Future studies will determine the role of hepatitis C and E. Typhoid fever shows an incidence rate of 0.3/1000 in foreigners on the Indian subcontinent, and in many parts of North and West Africa, excluding Tunisia, in other parts of the third world it is tenfold lower. In poliomyelitis, tetanus, diphtheria, cholera, rabies, and Japanese encephalitis, the incidence rate is greater than or equal to 0.002/1000. Author

N93-11289# Camerino Univ. (Italy). Dept. of Hygiene.

VACCINATION AGAINST HEPATITIS B: THE ITALIAN STRATEGY

A. R. Zanetti, J. Grappasonni, E. Tanzi (Milan Univ., Italy), and L. Romano (Milan Univ., Italy) *In* AGARD, Allergic, Immunological and Infectious Disease Problems in Aerospace Medicine Apr. 1992 3 p (For primary document see N93-11283 02-52)

Copyright Avail: CASI HC A01/MF A03

Viral hepatitis type B is a major worldwide public health problem. Infection with the hepatitis B virus (HBV) may progress to chronic liver disease including chronic active hepatitis, cirrhosis, and hepatocellular carcinoma. Moreover, it has been estimated that between 200 and 300 million individuals in the world are chronic carriers of HBV. The availability of safe and effective vaccines allows the establishment of immunization programs aimed at the elimination of hepatitis B and the reduction of morbidity and mortality due to its sequelae. The topics covered include the following: (1) vaccines against hepatitis type B; (2) safety, immunogenicity, and efficacy of hepatitis B vaccines; (3) strategies for control of hepatitis B by immunization; and (4) hepatitis B vaccination in Italy. Author

N93-11290# World Health Organization, Geneva (Switzerland). Global Programme on AIDS.

HIV INFECTION IN THE NINETIES

Lars O. Kallings *In* AGARD, Allergic, Immunological and Infectious Disease Problems in Aerospace Medicine Apr. 1992 5 p (For primary document see N93-11283 02-52)

Copyright Avail: CASI HC A01/MF A03

By the year 2000, a cumulative global total of 30 to 40 million men, women, and children are projected to have been infected with HIV. This will present a 3 to 4 times increase of the present total. Currently, it is estimated that about 5000 persons are newly infected daily. Worldwide, the predominant and increasing mode for transmission is by heterosexual intercourse. Therefore, the number of infected women will equal that of men. Consequently, more infants will be infected by their mothers and more infants will be orphaned as their parents die of AIDS. By the end of the 1990's, over one million adults, most of them in developing countries. Although the majority of HIV infections are currently occurring in Sub-Saharan Africa, the annual number of HIV infections in Asia is projected to exceed that in Africa during the 1990's. Also in industrialized countries, the proportion of heterosexual transmission is increasing, and AIDS is becoming one of the predominant causes of death in young men and women. In spite of promising scientific progress, vaccines and therapeutic drugs are not expected to have any major impact on the global development of the pandemic during the 1990's. The World Health Organization (WHO) is promoting behavioral changes, condom use, and control of other sexually transmitted diseases as the most important preventive measures. Insight into the dynamics of the HIV/AIDS pandemic and into the growing understanding of the main factors which are fuelling the continued and increasing HIV transmission is given. A short survey of the epidemiological background, the current trends, and the forecasts of the directions of the epidemic during the next decade are presented. Author

N93-11291# Walter Reed Army Medical Center, Washington, DC. Div. of Retrovirology.

AIDS/HIV IN THE US MILITARY

Donald S. Burke and Edmund C. Tramont *In* AGARD, Allergic, Immunological and Infectious Disease Problems in Aerospace Medicine Apr. 1992 6 p (For primary document see N93-11283 02-52)

Copyright Avail: CASI HC A02/MF A03

HIV infection (AIDS) burst upon the scene a decade ago. Because it is a sexually transmitted disease that infects blood and kills its victim, it is military relevant and will impact on all aspects of the military. The USAMRDC as Lead Agent for Infectious Disease Research in the DoD has developed a comprehensive approach to address military concerns: surveillance of infection rates (intelligence) around the world and in the military; behavioral research to develop more effective means of education to change behavior; and biological research to develop a quick and easy field test, and a vaccine or drug to prevent the disease from occurring despite exposure. Its success will influence the success of the Army in the future. Author

N93-11292# Aerospace Medical Research Labs., Brooks AFB, TX. Epidemiologic Research Div.

ESTIMATES OF HUMAN IMMUNODEFICIENCY VIRUS (HIV) INCIDENCE AND TRENDS IN THE US AIR FORCE

Ronald D. Warner, Robert E. Mathis, Mary E. Weston, Larry R. Bigbee (Defense Manpower Data Center, Monterey, CA.), Craig W. Hendrix (Air Force Medical Center, Lackland AFB, TX.), and Daniel R. Lucey (Air Force Medical Center, Lackland AFB, TX.) *In* AGARD, Allergic, Immunological and Infectious Disease Problems in Aerospace Medicine Apr. 1992 5 p (For primary document see N93-11283 02-52)

Copyright Avail: CASI HC A01/MF A03

Between early 1986 and February 1991, over 700,000 United States Air Force (USAF) active duty personnel had been screened for antibodies to the Human Immunodeficiency Virus (HIV). All HIV-infected patients are evaluated at Wilford Hall USAF Medical Center, and staged using the Walter Reed scheme. Two total-force screenings were conducted prior to October 1990. The USAF case registry is maintained by the Epidemiological Research Division. Computer support for incidence calculations is provided by the Defense Manpower Data Center. During the first screening (February 1986-September 1988), 721 HIV-positive personnel were detected from a USAF population of approximately 607,000. The estimated seroprevalence was 1.2/1000. From the second screening 206 positive individuals were detected among approximately 571,000 personnel. As of January 1991, among the total 942 HIV-positives, only 29 were female. Three hundred and fifty-one (37.3 percent) remained on active duty in the US; 296 (31.5 percent) were on temporary disability retirement lists; 193 (20.5 percent) had separated or retired; and 101 (10.7 percent) had died. From June 1987 through June 1990, the estimated incidence of HIV infection in USAF personnel declined from 0.19 to 0.17/1000 person-years. The rate for males in June 1987 was estimated at 0.21/1000 person years. In all, the highest rate was among black males. In October 1985, the US Department of Defense (DOD) mandated that all applicants for military service be tested for evidence of antibodies to the human immunodeficiency virus (HIV). This testing continues, and if they test-positive, applicants are denied entry. Testing of those already in the US military services began soon afterward. Between early 1986 and February 1991, over 700,000 active-duty US Air Force (USAF) personnel were tested for the presence of HIV antibodies. In addition to two total-force (USAF, USAF Reserves, and Air National Guard) screenings prior to October 1990, USAF personnel have been tested in conjunction with: evaluation and treatment for other sexually transmitted diseases, routine and periodic physical examinations, enrollment in drug or alcohol rehabilitation programs, orders to permanent overseas assigments, and clinically-indicated medical reasons. The 1987-1990 HIV incidence estimates are discussed in a relatively young, mobile male population by age, ethnicity/race, sex, and occupational category at time of positive HIV antibody test. Author

N93-11293# Rome Univ. (Italy). Dept. of Allergy and Clinical Immunology.

SILENT HIV INFECTION

Fernando Aiuti, Fabrizio Ensoli, Valeria Fiorelli, Ivano Mezzaroma, Elena Pinter, Emma Guerra, and Giuseppe Luzi *In* AGARD, Allergic, Immunological and Infectious Disease Problems in Aerospace Medicine Apr. 1992 4 p (For primary document see N93-11283 02-52)

Copyright Avail: CASI HC A01/MF A03

The period of latency between infection by the human immunodeficiency virus type-1 (HIV-1) and the production of specific antibodies to viral antigens may be prolonged and, occasionally, may last for years. This condition of seronegative infection could represent a serious risk of viral transmission from subjects who are unaware of their status. However, whether these individuals are actually infectious, especially through body fluids, has not been clarified. We have performed a prospective study in 65 high risk individuals seronegative for HIV-1 antibodies for a prolonged period of time. Twelve of them (18 percent) were shown to be carriers of HIV-1 proviral sequences by the polymerase chain reaction (PCR). The virus was isolated from nitrogen-stimulated peripheral blood lymphocytes (PBMC) in five out of ten subjects tested since the first positive PCR. In two of them, virus could also be isolated from cell free plasma, subsequently they remained seronegative during 10 months of follow-up. These data indicate that delayed seroconversions may be associated with productive infection, suggesting that mechanism(s) other than viral latency may be responsible for the absence of antibody responses to HIV-1 proteins. Furthermore our findings suggest that prolonged seronegative individuals can transmit HIV-infection through their body fluids. Author

N93-11294# Istituto Superiore di Sanita, Rome (Italy). Lab. of Virology.

HIV VARIABILITY AND PERSPECTIVES OF A VACCINE

P. Verani, S. Butto, B. Taddeo, M. Federico, and G. B. Rossi *In* AGARD, Allergic, Immunological and Infectious Disease Problems in Aerospace Medicine Apr. 1992 5 p (For primary document see N93-11283 02-52)

Copyright Avail: CASI HC A01/MF A03

Since Human Immunodeficiency Virus (HIV) was identified as the causative agent of Acquired Immunodeficiency Syndrome (AIDS) the pressing challenge that researchers are facing is the development of a vaccine against this disease. Although progress has been made in the study of the biology of HIV faster than for any other virus, the development of an effective vaccine has been slowed by the peculiar features of HIV. The difficulties standing before a rationale approach to vaccine design are: (1) the ability of the virus to rapidly change its genome sequency; (2) its spreading from cell to cell; (3) its ability to establish latent infection integrating its genome into that of the target cell without expressing any viral genes and, thus remaining hidden inside the infected cell; and (4) its insidious attack on the immune system upon which a vaccine depends in order to be effective. The design of a rationale approach to a vaccine is discussed. Author

N93-11295# Aerospace Medical Research Labs., Brooks AFB, TX. Epidemiologic Research Div.

IMMUNOLOGICAL PARAMETERS IN CURRENT AND FORMER US AIR FORCE PERSONNEL

William H. Wolfe, Judson C. Miner, and Joel E. Michalek *In* AGARD, Allergic, Immunological and Infectious Disease Problems in Aerospace Medicine Apr. 1992 5 p (For primary document see N93-11283 02-52)

Copyright Avail: CASI HC A01/MF A03

Major advancements have been made in the laboratory assessment of the immune system over the past decade. There has been a proliferation of sophisticated techniques to measure the number and functional capacity of subsets of lymphocytes and other cellular elements of the immune system. Unfortunately, the space of this technology has made it difficult for many practicing physicians to develop and maintain an understanding of these new tests. Additionally, appropriate reference values for these tests in 'normal' populations are unclear and little has been done to assess the effects of factors such as age, race, and lifestyle on these measures of immunity. Laboratory assays are available to assess both the counts of the various cellular elements of immunity in the peripheral blood as well as the functional capacity of many of these cells. Tests of delayed cutaneous hypersensitivity are based on techniques used in allergy testing and tuberculosis control. After antigens such as Trichophyton or Candida are injected intradermally, the skin's reactivity correlates with the recall sensitivity of the T cells to each antigen used. Counts of total T lymphocytes (CD2 cells) and B lymphocytes (CD20 cells) are decreased in immune deficiency conditions and are elevated with lymphoproliferative diseases. The helper/inducer T lymphocytes (CD4 cells) are commonly decreased in progressive HIV infection and are increased in autoimmune disorders. The suppressor T cells (CD8) are increased in some viral infections and immunodeficiency states. The CD4/CD8 ratio is a commonly used measure of immune system capability. Tests of activated T lymphocytes (CD25 cells) assess the presence of stimulated T lymphocytes. Unstimulated T cells do not react to this test. This is a useful test in identifying the presence of lymphoproliferative disorders. Count of total lymphocytes is also made. Tests of the functional status of the cellular components of the immune system assess the response of the cells in the peripheral blood to stimulation with various mitogens such as phytohemagglutinin. These test measure the cells' capability to become activated by external stimuli. The natural killer cell assay measures the body's lytic response to foreign tissue cells both before and after stimulation with interlukin. This response is decreased with impaired natural immunity. Standard quantitative measurements of immune globulins (IgA, IgG, and IgM) are also useful in the assessment of immune functions. They measure the ability of specific B lymphocytes to secrete specific classes of antibody. A useful approach to the categorization of several of the quantitative and functional tests of immunity is shown. The tests provide a comprehensive assessment. As part of a comprehensive epidemiologic study of current and former Air Force personnel, an extensive assessment of the immune system was conducted by a single immunology reference laboratory using stringent quality control standards. All of the tests described above were used in this study. The demographic characteristics of these study subjects are displayed. All of the subjects were middle-aged males, most of whom did not currently smoke tobacco. Nearly 80 percent of them currently drink alcoholic beverages. Author

N93-11296# Air Force Medical Center, Lackland AFB, TX. Dept. of Infectious Diseases.

EARLY MARKERS OF HIV INFECTION AND SUBCLINICAL DISEASE PROGRESSION

M. J. Dolan, D. R. Lucey, C. W. Hendrix, G. P. Melcher, G. A. Spencer, and R. N. Boswell *In* AGARD, Allergic, Immunological and Infectious Disease Problems in Aerospace Medicine Apr. 1992 6 p (For primary document see N93-11283 02-52)
Copyright Avail: CASI HC A02/MF A03

Human Immunodeficiency Virus (HIV) infection in U.S. Air Force personnel between 1985 and 1989 was examined through a mandatory serologic survey, and through annual examination of infected patients. CD4+ cell counts were determined by flow cytometry; Beta 2 microglobulin and neopterin were measured by immunoassay. During this period, 933 cases were found, of which 161 were documented seroconversions, giving an incidence rate of 15.6/100,000 person-years. For patients with greater than 400 CD4 cells/microliter, the rate of initial occurrence of opportunistic infection was 1 percent and 4 percent at 1 and 2 years, respectively. HIV infected persons with less than 400 CD4+ cell/microliter, in contrast, had rates of 21 percent at 1 year and 36 percent at 2 years. In a cross-sectional study, Beta 2 microglobulin concentration was shown to increase in both the serum and spinal fluid of patients infected with HIV as their blood CD4 numbers declined. Neopterin levels in serum and spinal fluid showed a similar trend, with significantly lower neopterin concentrations in the group that had greater than 1000 CD4+ T cells compared to the 0-600 CD4+ cell group. Longitudinal studies included correlation of HIV p24 antigen with CD4 counts over a one year period. The p24 antigen-positive group has a 21 percent decline in CD4+ T cells, while the antigen negative group has a 14 percent decline. Specific helper T-cell subsets were also examined over a 6 month period. A significant decline was seen in the CD4+/DC29+, CD4+/DC45R+, and overall CD4+ subsets which were not seen in AZT treated patients. A significant increase in the CD4+/CD29+ memory T-cell subset, which is responsible for response to recall antigens and is capable of Upsilon interferon secretion, was noted in the AZT-treated group. Author

N93-11297# Harvard School of Public Health, Boston, MA. Dept. of Biostatistics.

ANALYSIS OF DISEASE PROGRESSION FROM CLINICAL OBSERVATIONS OF US AIR FORCE ACTIVE DUTY MEMBERS INFECTED WITH THE HUMAN IMMUNODEFICIENCY VIRUS: DISTRIBUTION OF AIDS SURVIVAL TIME FROM INTERVAL CENSORED OBSERVATIONS

Jorge Aragon, Mary Weston (Aerospace Medical Research Labs., Brooks AFB, TX.), and Ronald Warner (Aerospace Medical Research Labs., Brooks AFB, TX.) *In* AGARD, Allergic, Immunological and Infectious Disease Problems in Aerospace Medicine Apr. 1992 3 p (For primary document see N93-11283 02-52)
Copyright Avail: CASI HC A01/MF A03

A nonparametric estimator of the Acquired Immunodeficiency Syndrome (AIDS) survival time (after developing AIDS) is computed for the AIDS data set from the US Air Force (USAF). Survival times are unobservable. They are censored by the screening mechanism. The Armstrong Laboratory's Epidemiologic Research Division maintains data on over 940 active duty US Air Force (USAF) individuals who tested positive for Human Immunodeficiency Virus (HIV) antibodies. Many have been clinically evaluated six times since 1986. The HIV-positive individual is classified in seven stages of the disease complex as time progresses. Exact times of transition from one stage to the next are unknown. It is known that transition occurred between two consecutive evaluations. The aim of this study is to analyze distributions of the times that individuals spend in each stage of the HIV disease complex. We discuss methods used to obtain nonparametric estimators of the distributions of times that individuals spend in stage 6. Finally, we hope to model the median time spent in each stage of the disease. This, along with incidence and separation data, will allow us to predict the impact of HIV disease on USAF individual and medical care systems. Author

N93-11298# Jackson (Henry M.) Foundation, Washington, DC.

RELATING COGNITIVE FUNCTION TO MILITARY AVIATOR PERFORMANCE IN EARLY HIV INFECTION

R. L. Mapou, James R. Rundell (Uniformed Services Univ. of the Health Sciences, Bethesda, MD.), G. G. Kay (Georgetown Univ., Washington, DC.), and E. C. Tramont (Walter Reed Army Medical Center, Washington, DC.) *In* AGARD, Allergic, Immunological and Infectious Disease Problems in Aerospace Medicine Apr. 1992 6 p (For primary document see N93-11283 02-52)
Copyright Avail: CASI HC A02/MF A03

There has been controversy about whether cognitive changes occur in early human immunodeficiency virus (HIV) disease. In those studies reporting cognitive changes, findings are typically subclinical, and their relationship to daily and/or occupational functioning has not been addressed. The potential effects of changes may vary as a function of occupational demands. This is germane to military performance, where occupational demands cover a wide spectrum of complexity. In particular, such effects are important to consider in the many cognitively-demanding specialties associated aviation. Ways in which possible HIV-related military performance decrements in aviators may be measured empirically are explored. First, studies from Walter Reed Army Medical Center (WRAMC), which have shown cognitive changes in early HIV disease, are described. This is followed by a summary of presentations and discussions at a November, 1990 conference, entitled, HIV and Military Performance: Assessment Methodologies, held at WRAMC. The third section describes a program of research, which is developing measures to detect cognitive difficulties in civilian aviators. The application of measures from this research to research on HIV is discussed. Finally, a research program being developed to examine the possible impact of HIV-related cognitive changes on military aviator performance is presented. Author

N93-11299# Air Force Medical Center, Lackland AFB, TX.

NEUROPSYCHIATRIC MORBIDITY IN EARLY HIV DISEASE: IMPLICATIONS FOR MILITARY OCCUPATIONAL FUNCTION

George R. Brown, James R. Rundell (Walter Reed Army Medical Center, Washington, DC.), Susan E. McManis (Air Force Medical Center, Lackland AFB, TX.), Sarah N. Kendall, and Richard A. Jenkins (Walter Reed Army Medical Center, Washington, DC.) *In* AGARD, Allergic, Immunological and Infectious Disease Problems in Aerospace Medicine Apr. 1992 14 p (For primary document see N93-11283 02-52)
Copyright Avail: CASI HC A03/MF A03

The Military Medical Consortium for Applied Retroviral Research's (MMCARR) Behavioral Medicine Human Immunodeficiency Virus (HIV) Research component is conducting a tri-service, comprehensive, and longitudinal research study in military HIV-infected personnel at all stages of infection. Identification of neuropsychiatric and psychosocial outcomes and their determinants will help the military minimize the impact of the HIV epidemic on military readiness and function. Neuropsychiatric and psychosocial findings are among the most common complications seen in early HIV Disease and among the most likely to have an adverse impact on military readiness and function. The study has demonstrated that the average HIV-infected service-person experiences at least transient military occupational difficulty following notification of HIV status. More than 15 percent at any given time have levels of clinical or subclinical anxiety or depression that are referrable for mental health intervention. Ten percent of study subjects have a current major mood disorder and 5 percent have a psychoactive substance use disorder. Finally, 17 percent of study subjects have experienced serious suicidal ideation or behaviors at least once since notificaiton of seropositivity. Fortunately, however, data also indicate at least partial effectiveness of current primary, secondary, and tertiary preventive efforts. Only about 1 percent of Air Force HIV-infected persons are discharged for psychiatric reasons prior to eventual medical discharge. Further, a large majority of active-duty patients demonstrate solid military occupational and social performance. Though military HIV neurobehavioral research is still in progress, preliminary data identify social support and pre-HIV psychiatric predisposition as important factors associated with current neuropsychiatric status. Author

N93-11300# World Health Organization, Geneva (Switzerland). Div. of Communicable Disease.

COMMUNICABLE DISEASES: A MAJOR BURDEN OF MORBIDITY AND MORTALITY

G. Torrigiani *In* AGARD, Allergic, Immunological and Infectious Disease Problems in Aerospace Medicine Apr. 1992 3 p (For primary document see N93-11283 02-52)

Copyright Avail: CASI HC A01/MF A03

Communicable diseases, complicated by malnutrition and other adverse socioeconomic factors, continue in the present decade to contribute greatly to the unacceptably high levels of morbidity, mortality, and disability, particularly in the under-five age group, in all developing countries. It is estimated that five million deaths occur per year from diseases which can be prevented by vaccines available today, and that another five million people are being crippled, blinded, or mentally retarded as a result of the same diseases. Some of the most important communicable diseases, with their mortality rate, are reported. Some of the topics discussed include sexually transmitted diseases, disease control, chemotherapy, and environment management. Author

N93-11301# Aerospace Medical Research Labs., Brooks AFB, TX. Epidemiology Div.

SUSCEPTIBILITY IN USAF RECRUITS TO VACCINE PREVENTABLE DISEASES

William F. Clardy *In* AGARD, Allergic, Immunological and Infectious Disease Problems in Aerospace Medicine Apr. 1992 3 p (For primary document see N93-11283 02-52)

Copyright Avail: CASI HC A01/MF A03

Because of increasing incidence of mumps in a cohort of under immunized young adults and the concern about the impact of this disease on the USAF recruit population, two studies were undertaken. These studies took a retrospective look at the following: mumps in the active duty population; a cost analysis of immunizing all or only susceptible individuals; the actual antibody response in a group of two hundred and seventy-six recruits in basic training; the demographic patterns of susceptibility; and the types of previous immunication documentation. The conclusions were that the numbers of new mumps cases per year did not justify immunizing all recruits or screening for mumps antibodies. Author

N93-11302# Sclavo Research Center, Rome (Italy). Office of the Surgeon General of the Army.

ABSENCE OF PROTECTIVE IMMUNITY AGAINST DIPHTHERIA IN A LARGE PROPORTION OF YOUNG ADULTS

R. Rappuoli, A. Podda, F. Giovannoni, L. Nencioni, M. Peragallo, and P. Francolini *In* AGARD, Allergic, Immunological and Infectious Disease Problems in Aerospace Medicine Apr. 1992 2 p (For primary document see N93-11283 02-52)

Copyright Avail: CASI HC A01/MF A03

The schedule of vaccination which is recommended worldwide for diphtheria, tetanus, and other diseases provides good immunity during childhood. However, little attention has been paid to keep an effective immunity in adults. We have collected sera from 334 recruits of the Italian Army and tested them for the presence of protective immunity against diphtheria and tetanus. In vivo neutralization assays were performed on rabbits and mice and the values below 1/100 IU/ml were considered negative. Of the recruits, 22.9 percent were negative for diphtheria, while only 5.3 percent of them did not have protective immunity against tetanus. This finding shows that a large proportion of the Italian young adults are susceptible to diphtheria, and this could be dangerous if they travel to sites where this disease is still endemic, or if they come into contact with people coming from such areas. A booster vaccination of young adults against diphtheria should enter in the common practice in order to avoid this risk. In order to reduce the side effects which are often associated with diphtheria vaccination in adults, we have developed a vaccine which contains a highly purified nontoxic mutant of diphtheria toxin. This vaccine is combined with tetanus toxoid and can be routinely used as a booster in adults. Author

N93-11303# Divisione Aerea Studi Ricerche e Sperimentazioni, Pratica di Mare (Italy).

DRAMATIC REDUCTION OF MENINGOCOCCAL MENINGITIS AMONG MILITARY RECRUITS IN ITALY AFTER INTRODUCTION OF SPECIFIC VACCINATION

R. Biselli, A. Fattorossi, P. M. Matricardi, R. Nisini, T. Stroffolini, and R. DAmelio (Istituto Superiore di Sanita, Rome, Italy) *In* AGARD, Allergic, Immunological and Infectious Disease Problems in Aerospace Medicine Apr. 1992 5 p (For primary document see N93-11283 02-52)

Copyright Avail: CASI HC A01/MF A03

Meningococcal meningitis still represents a serious infectious disease with a mortality rate that can be as high as 10 percent even in developed countries. Military recruits are generally a high risk group for meningococcal disease, with a reported incidence of 4 to 10 times greater than that of the general population. In Italy the results of the National Meningitis Surveillance Program showed a high attack rate of the disease among recruits in 1985 as well as in 1986, with 92 and 95 percent of the cases, respectively, caused by serogroup C and thus preventable. These findings constituted the motivating factors leading to the authorities' decision to make vaccination against meningococcal disease mandatory for recruits starting from January 1987. After almost 5 years from the introduction of meningococcal vaccination, we present a summary of the epidemiological and immunological effects of the vaccination. From the epidemiological point of view we have observed a dramatic reduction of the prevalence of the disease. In 1987, that is the year in which we had 150,000 unvaccinated and 150,000 vaccinated recruits, the protective efficacy was 91.2 percent. From the immunological point of view, vaccination is highly effective, as seroconversion against polysaccharide (PS) A and C is 84 and 91 percent, respectively. The spectrotypic analysis of the sera before and after vaccination shows that the type of response is mainly oligoclonal, like the majority of the responses to PS's, and the antibodies induced by sole PS are not qualitatively different from the antibodies induced by natural immunization. In addition, the efficacy is not modified by environmental factors like hypoxia, as demonstrated during permanence at 16,174 feet for 20 days. In conclusion, the anti-meningococcal PSA and PSC vaccine can be looked at as a very safe and effective method in controlling the spread of the disease in military recruits since: (1) its efficacy is very high, considering approximately 90 percent of the subjects develop a protective response; (2) it is safe; and (3) it has proven to provide satisfactory immunological response even under unfavorable conditions, like hypobaric hypoxia. Author

N93-11304# Hopital d'Instruction des Armees, Paris (France).

IMMUNIZATION OF PERSONNEL TRAVELING TO A DESTINATION IN TROPICAL COUNTRIES: FRENCH POSITION [IMMUNISATION DU PERSONNEL NAVIGANT A DESTINATION DES PAYS TROPICAUX: POSITION FRANCAISE]

F. Didelot, C. P. Giudicelli, J. P. Gourbat, J. P. Burlaton, G. Nedelec, and A. Seigneuric *In* AGARD, Allergic, Immunological and Infectious Disease Problems in Aerospace Medicine Apr. 1992 3 p In FRENCH (For primary document see N93-11283 02-52)

Copyright Avail: CASI HC A01/MF A03

The possibility of infectious risks incurred during sojourns in tropical zones justifies preliminary prevention. Aside from obligatory measures, it is important to discern recommended and other desirable actions. The obligatory measures essentially concern antimalarial vaccination for those personnel whose travel brings them into the intertropical zones of Africa and America. The partial and limited efficacity of the anticholera vaccination has practically justified its abandonment. The recommended measures include vaccinations against tetanus, diphtheria, poliomyelitis, (BCG) and typhoid. Obligatory in France for all children, except for the latter, these vaccinations must be replaced by boosters for all adults. Well tolerated, the new vaccine against typhoid (polyosidic, purified Vi antigen) merits being systematically employed. Other immunizations are desirable: vaccinations against meningococcic meningitis (serogroups A and C) in the young adult and against viral hepatitis B and injection of gammaglobulins for the prevention of hepatitis A virus. Finally, the high tolerance for anti-rabies vaccine leads to counseling the generalization of its use, due to the possible risk of a supply default at an opportune moment. Contradictions are restated and a vaccinal calendar is proposed. Aside from oral forms of vaccines against cholera and against typhoid, future perspectives concern vaccines against viral hepatitis A and against Japanese encephalitis. These are directed against the major risks, those such as malaria and AIDS unfortunately appear, even today, to be aleatory. Author

N93-11305# Divisione Aerea Studi Ricerche e Sperimentazioni, Pratica di Mare (Italy).

CLINICAL AND IMMUNOLOGICAL RESPONSE TO VACCINATION WITH PARENTERAL OR ORAL VACCINES IN TWO GROUPS OF 30 RECRUITS

Roberto Nisini, Roberto Biselli, Paolo M. Matricardi, Andrea Fattorossi, and Raffaele DAmelio *In* AGARD, Allergic, Immunological and Infectious Disease Problems in Aerospace Medicine Apr. 1992 4 p (For primary document see N93-11283 02-52)

Copyright Avail: CASI HC A01/MF A03

The clinical and immunological responses to typhoid vaccination with parenteral and oral vaccines in two groups of 30 adult male subjects were studied. Specific anti-Salmonella typhi cell-mediated immunity and total or specific anti-lipopolysaccharide fecal immunoglobulin (Ig) A titers in vaccinated subjects were monitored. Cellular antibacterial activity was significantly increased only in orally vaccinated subjects. Serum arming activity and inhibition experiments suggested an IgA-dependent cellular cytotoxicity in those orally vaccinated. In these subjects, a total and anti-lipopolysaccharide fecal IgA increase was observed lasting up to 8 months after completion of vaccination schedule. In parenteral vaccinated subjects, an early onset transitory increase of IgM rheumatoid factor was observed. Oral vaccine was well tolerated and free of side effects, whereas 65 percent of parenterally vaccinated subjects reported side effects such as fever, headache, malaise, and local tenderness in the injection site. Author

N93-11306# Georgetown Univ., Washington, DC. Dept. of Pediatrics.

STUDIES OF SAFETY, INFECTIVITY, AND IMMUNOGENICITY OF A NEW TEMPERATURE SENSITIVE (TS) 51-1 STRAIN OF S. TYPHI AS A NEW LIVE ORAL TYPHOID FEVER VACCINE CANDIDATE

J. A. Bellanti, B. J. Zeligs, S. Vetro, Y.-H. Pung, S. Luccioli, M. J. Malavasic, A. M. Hooke, T. R. Ubertini, R. Vanni, and L. Nencioni *In* AGARD, Allergic, Immunological and Infectious Disease Problems in Aerospace Medicine Apr. 1992 6 p Prepared in cooperation with Sclavo S.p.A., Sienna, Italy (For primary document see N93-11283 02-52)

Copyright Avail: CASI HC A02/MF A03

This report describes the results of a phase 1 study evaluating the safety, infectivity, and immunogenicity of a new live oral S. typhi ts 51-1 typhoid fever vaccine in the human. Three normal males subjects ranging in age from 20 to 40 years received 3 oral doses of S. typhi ts 51-1, each dose containing 10(exp 9) organisms. Prior to and following immunization each subject was carefully monitored by clinical and laboratory parameters over a two week period during which serial specimens of blood and stool were analyzed for the presence of the organism. Blood specimens were also obtained for the determination of serum antibody and cell-mediated immune responses and stool filtrates were analyzed for the development of coproantibody. The results of these studies indicate that: (1) the vaccine is well tolerated with no clinical or laboratory evidence of adverse reactions; (2) ts 51-1 was detected in only one stool specimen from one volunteer; the organism recovered displayed characteristics of the ts 51-1 vaccine strain; (3) although no significant humoral or cell-mediated lymphocytotoxic immune responses were detected in the blood, coproantibody was detected in stool specimens from all of the 3 immunized subjects and IgA-armed ADCC activity was detected in 2 of 3 subjects. These studies indicate that S. typhi ts 51-1 may be a suitable strain for the development of an improved oral typhoid fever vaccine. Studies are in progress to determine optimal methods of vaccine delivery preparatory to larger phase 2 studies of efficacy. Author

N93-11307# Zurich Univ. (Switzerland). Div. of Epidemiology and Prevention of Communicable Diseases.

RECENT LESSONS ON THE SAFETY AND EFFECTIVENESS OF MALARIA CHEMOPROPHYLAXIS IN A NON-IMMUNE POPULATION

R. Steffen *In* AGARD, Allergic, Immunological and Infectious Disease Problems in Aerospace Medicine Apr. 1992 4 p (For primary document see N93-11283 02-52)

Copyright Avail: CASI HC A01/MF A03

To assess adverse events (AE) and the effectiveness of malaria chemoprophylaxis in short term travelers to East Africa, two similar follow-up studies were conducted, the second of which is on-going. Pooled data of both studies are presented, in which all passengers returning from Kenya by British, German, or Swiss charter flights were distributed a questionnaire aboard and a second one three months later. Any report of documented malaria or of a hospitalization for adverse events was investigated with the physician. So far, 98,650 travelers have completed at least one questionnaire. AE were reported by 22.3 percent of 30,871 having used mefloquine (MQ), by 19.9 percent of 5,342 having used chloroquine (CQ) 300 mg base/week, by 22.2 percent of 7,930 having used Q 600 mg base/week, by 29.4 percent of 1,114 having used amodiaquine (AQ), by 1.63 percent of 24,532 having used sulfadoxine/pyrimethamine (SP), and by 26.1 percent of 6,851 having used CQ plus proguanil (PG). Dizziness was more frequent with MQ than with other agents. Twenty hospitalizations were attributed to AE: seven occurred after prophylaxis with CQ (including 2 cases of psychosis), four were attributed to SP (2 fatal), and five to AC (2 fatal). Just two were attributed to MQ: one each for psychosis and one for seizures in a known epileptic, one additional case with seizures was not hospitalized. Prophylactic effectiveness was 94 percent (95 percent C.I. 85-96) for MQ, 84 percent (77-90) for SP, 74 percent (48-88) for CQ+PG, and 30-54 percent for CQ in various dosages. In conclusion, mefloquine appears to be highly efficacious for malaria prophylaxis in areas with widely distributed chloroquine resistant P. falciparum. Tolerance seems to be comparable to the one of chloroquine; thus, the contra-indication of the use of mefloquine in pilots will have to be reconsidered. Author

N93-11308# Walter Reed Army Medical Center, Washington, DC. Dept. of Immunology.

USE OF NOVEL ADJUVANTS AND DELIVERY SYSTEMS TO IMPROVE THE HUMORAL AND CELLULAR IMMUNE RESPONSE TO MALARIA VACCINE CANDIDATE ANTIGENS

D. M. Gordon *In* AGARD, Allergic, Immunological and Infectious Disease Problems in Aerospace Medicine Apr. 1992 4 p (For primary document see N93-11283 02-52)

Copyright Avail: CASI HC A01/MF A03

The immune effector mechanisms responsible for the solid protection against malaria, as demonstrated by immunization with radiation attenuated sporozoites, are poorly understood. An effective malaria vaccine must induce a well orchestrated combination of humoral and cellular immune responses directed against critical parasite antigens/epitopes expressed during different stages of the parasites complicated life-cycle. Currently, licensed human vaccine adjuvants, such as alum, may improve antibody production but are poor stimulators of cellular effector mechanisms, while potent cellular stimulants such as Freund's adjuvant are too reactogenic for human use. Over the last five years, we have systematically evaluated several methods of antigen presentation to include chemical conjugation to bacterial carrier proteins, emulsification in 'Freund's-like' preparations, and incorporation into liposomes. This work has resulted in the production of safe, potent vaccine delivery systems capable of targeting multiple antigenic determinants to the host's immune system. Further advances in malaria vaccine development now depends on the identification of appropriate parasite epitopes for inclusion in a multicomponent-multistage vaccine. Author

N93-11309# DOMPE S.p.A., L'Aquila (Italy). Biotechnology Dept.

CYTOKINES AS VACCINE ADJUVANTS: INTERLEUKIN 1 AND ITS SYNTHETIC PEPTIDE 163-171

Aldo Tagliabue *In* AGARD, Allergic, Immunological and Infectious Disease Problems in Aerospace Medicine Apr. 1992 5 p (For primary document see N93-11283 02-52)
Copyright Avail: CASI HC A01/MF A03

The possibility of preventing infectious diseases by employing efficacious vaccine is rapidly growing as the consequence of the new technologies in recombinant DNA and protein chemistry. However, the increasing number of synthetic and recombinant antigens further stresses the importance of the role of appropriate adjuvants to ensure the maximal vaccine activity and the protection of all vaccines. Several approaches can be applied to develop safe and effective agents capable of enhancing specific immune responses which can then protect the host from the pathogen. Among others, the direct use as adjuvant of those cytokines which are induced in animals by the classical Freund adjuvants has recently become a matter of investigation. In particular, interleukin 1 (IL-1) has been shown to possess adjuvant activity for a variety of infectious and tumor antigens. However, the numerous side effects associated to the proinflammatory action of IL-1 represent a serious disadvantage for its use as a vaccine adjuvant. Therefore, it was of great interest that the observation of a nonapeptide contained in the IL-1beta sequence (residues 163-171 corresponding to the sequence VQGEESNDK) is devoid of all the proinflammatory activities but maintains the immunostimulating activity of the whole IL-1beta. Thus, 163-171 peptide was successfully employed in animals to potentiate the specific immune response against T helper-dependent cellular antigens, T helper-independent polysaccharidic antigens and recombinant, as well as synthetic antigenic preparations derived from human pathogens. Furthermore, IL-1 and 163-171 peptide were successfully used in tumor vaccines in experimental systems. Therefore, it can be concluded that 163-171 peptide is potentially a good candidate as vaccine adjuvant for human use. Author

N93-11310# World Health Organization, Geneva (Switzerland). Microbiology and Immunology Support Services.

FUTURE APPROACHES TO VACCINE DEVELOPMENT SINGLE-DOSE VACCINES USING CONTROLLED-RELEASE DELIVERY SYSTEMS

M. T. Aguado *In* AGARD, Allergic, Immunological and Infectious Disease Problems in Aerospace Medicine Apr. 1992 4 p (For primary document see N93-11283 02-52)
Copyright Avail: CASI HC A01/MF A03

The development of new vaccines, both more efficacious and easier to deliver, has become an area of research that can certainly benefit from recent technical developments. In particular, the conversion of multiple-dose vaccines into single-dose vaccines may represent an important advance which should lead to improved vaccination coverage, as well as to a reduction in vaccination costs. Taking these considerations into account, one of the main goals of our program has become the development of a strategy to convert multiple dose vaccines to single-dose vaccines with the same or increased effectiveness. The initial priority of this project was to develop a single-dose tetanus vaccine, as one of the most urgent needs of the Expanded Program on Immunization to control neonatal tetanus. The use of controlled-release systems, already applied to deliver a whole array of drugs and hormones both in cattle and man, appears to be one way of accomplishing our goal. Among these systems, polymeric particles have been widely used for injectables. They can be classified into two main groups: the reservoir type, with material in solution in the cavity formed by a polymeric membrane; and the monolithic type, with materials evenly dispersed throughout the polymeric matrix. Indeed, the first type is usually known as microcapsules and the second as microspheres. Microspheres seems to be preferred to microcapsules because of the better control of drug or vaccine liberation. At present, the pre-clinical results obtained seem to point in the direction of the successful development of single-dose controlled-release vaccines. Author

N93-11311# Georgetown Univ., Washington, DC. Dept. of Pediatrics.

EPIDEMIOLOGIC VIEW OF ALLERGIC DISEASES IN NORTH AMERICA: IMPLICATIONS FOR AEROSPACE MEDICINE

J. A. Bellanti *In* AGARD, Allergic, Immunological and Infectious Disease Problems in Aerospace Medicine Apr. 1992 3 p (For primary document see N93-11283 02-52)
Copyright Avail: CASI HC A01/MF A03

The allergic disorders comprise a heterogeneous group of diseases which involve the respiratory tract (e.g., allergic rhinitis and asthma), the skin (e.g., atopic eczema), and the gastrointestinal tract (e.g., allergic gastroenteritis, food allergy) and which afflict 50 million Americans. The respiratory allergic diseases affect major segments of the population (15 to 17 percent) who may be recruited as aircraft personnel; therefore, these diseases pose particular risk to flying safety or personnel either directly, or indirectly as a consequence of their disease or of the adverse effects of medications now used in the treatment of these disorders. Moreover, recent evidence is now accumulating to suggest that other environmental factors encountered in aerospace operations, e.g., gravity, oxygen, and stress, may also contribute to the immunologic responses involved in and responsible for clinical manifestations of these allergic disorders. A thorough knowledge of these allergic diseases and reactions associated with therapy are, therefore, essential for proper screening of personnel prior to entry into the aerospace field. Moreover, principles of allergic therapy should be applied to existing trained personnel and combined with a knowledge of careful use of medications which are least likely to be associated with performance decrement. The availability of new medications which have minimal adverse effects, e.g., non-sedating antihistaminic drugs, are addressing some of the problems associated with these issues. Author

N93-11312# Divisione Aerea Studi Ricerche e Sperimentazioni, Pratica di Mare (Italy).

THE SCREENING OF INHALANT ALLERGIC DISEASES IN THE SELECTION OF CANDIDATES FOR AIRCRAFT PILOTING

P. M. Matricardi, R. Nisini, R. Biselli, L. Urbani, C. DeAngelis, G. Petrelli, and R. DAmelio *In* AGARD, Allergic, Immunological and Infectious Disease Problems in Aerospace Medicine Apr. 1992 5 p (For primary document see N93-11283 02-52)
Copyright Avail: CASI HC A01/MF A03

The validity of Phadiatop CAP as a tool in the mass screening for inhalant allergies was investigated. Two-hundred and seventy of 1815 Italian recruits were classified as allergics to inhalant allergens on the basis of history, physical examination, SPT for inhalants, and/or RAST for the seven most common aeroallergens in Italy. Phadiatop was positive in six-hundred and twenty-three (34.3 percent) subjects: in 265/270 allergics and in 357 subjects which had never experienced allergic symptoms; the vast majority of these subjects were also positive to STP and/or RAST. The level of Phadiatop reactivity was lower in this group with respect to the allergic one. In a subgroup of 98 subjects, bronchial hyperresponsiveness was also examined. A very high percentage (85 percent) of the subjects with bronchial hyperresponsiveness were also positive to Phadiatop, suggesting that atopy is one of the major etiologic factors of bronchial hyperreactivity in our population sample. We conclude that Phadiatop CAP is extremely useful in the screening of inhalant allergies in candidates to aircraft piloting. Author

N93-11313# Red Cross Hospital, The Hague (Netherlands) Dept. of Respiratory Medicine.

PHADIATOP: A SCREENING TEST FOR INHALANT ALLERGY

A. M. J. Wever *In* AGARD, Allergic, Immunological and Infectious Disease Problems in Aerospace Medicine Apr. 1992 3 p (For primary document see N93-11283 02-52)
Copyright Avail: CASI HC A01/MF A03

The Phadiatop test, a new in vitro test for inhalant allergy, was evaluated in relation to a panel of seven RAST tests with the common inhalant allergens in the Netherlands, and in comparison with the PRIST for total immunoglobulin E (IgE) determinations, in two populations: one in which the prevalence of inhalant allergy was expected to be high and one in which it was expected to be low. The Phadiatop was classified positive or negative according to percentage binding, total IgE was considered elevated at values greater than or equal to 200, greater than or equal to 150, and greater than or equal to 100 kU/l at ages 12-14, 15-16, and 17 years and over respectively. The RAST panel as reference was considered positive when at least on RAST result was class 2 or more. From the predictive values (which depend on the prevalence of the disease in the population) and the accuracies of the Phadiatop and the PRIST for the RAST, it can be concluded that the Phadiatop is a highly efficient test, much more so that the PRIST, in correctly classifying atopic and non-atopic subjects as judged by the reference RAST panel. Author

N93-11314# Navy Hospital, La Spezia (Italy).

IN VIVO AND IN VITRO DIAGNOSIS OF ALLERGIC RESPIRATORY DISEASE DURING SCREENING PROCEDURES IN THE ITALIAN NAVY: COMPARATIVE EVALUATION OF A RECENT QUANTITATIVE AUTOMATIZED ENZYME IMMUNOASSAY METHOD TO DOSE SPECIFIC IgE

G. Anzalone, M. DelTrecco, A. Vizzaccaro, and A. Corsico *In* AGARD, Allergic, Immunological and Infectious Disease Problems in Aerospace Medicine Apr. 1992 7 p (For primary document see N93-11283 02-52)
Copyright Avail: CASI HC A02/MF A03

The observation of a large number of young allergic patients gave us the possibility to acquire crucial information on the epidemiology, the aetiology, and the pathogenesis of respiratory allergies and particularly that of bronchial asthma. The diagnostic protocol used accomplished in a satisfactory way the proposed tasks to screen allergic conscripts and to clinically study already in service patients. Our evaluation of the recently introduced immunoassay ABBOTT-MATRIX confirmed its characteristics of specificity and reproducibility. It also demonstrated to be an easy to use 'in vitro' system with very poor requirements of intervention by the operator. We emphasize the need to routinarly introduce 'in vitro' research of allergies for the preliminary screening of the candidates to the Military Academies, the schools for P. Officers, and to special categories with an expensive training and high risk, like pilots or divers. Author

N93-11315# Defence and Civil Inst. of Environmental Medicine, North York (Ontario). Central Medical Board.

ASTHMA IN AIRCREW: ASSESSMENT, TREATMENT AND DISPOSITION

Gary W. Gray *In* AGARD, Allergic, Immunological and Infectious Disease Problems in Aerospace Medicine Apr. 1992 4 p (For primary document see N93-11283 02-52)
Copyright Avail: CASI HC A01/MF A03

Asthma represents a spectrum of increased airway reactivity from mildly increased responsiveness through to severe life-threatening bronchospasm. Rational recommendations for treatment and aeromedical disposition require a careful assessment of bronchial reactivity through correlation of the clinical findings with results of pulmonary function testing including an objective measure of airway reactivity. Airway challenge testing with methacholine allows a safe, objective assessment of airway reactivity. In the Canadian Forces, aircrew candidates with a history of wheezing, recurrent cough or bronchitis in childhood, or abnormal screening PFT's are further screened with an airway challenge test. Applicants with a PC20 less than 4 mg/ml are disqualified from pilot selection, and less than 2 mg/ml from other aircrew. Trained aircrew who develop wheezing are assessed with full pulmonary function testing including a methacholine challenge test. Those with objectively confirmed mild bronchial hyper-reactivity requiring no treatment or controlled by inhaled anti-inflammatory agents (corticosteroids, sodium cromoglycate, nedocromial sodium) are returned to flying in other than fast jets where even minor small airway instability may worsen ventilation-perfusion mismatch caused by +Gz. Author

N93-11316# Belgian Air Force, Brussels. Medical Centre of Aerospace Medicine.

ALLERGY SCREENING AND FOLLOW-UP IN STUDENT PILOTS OF THE BELGIAN AIR FORCE (BAF)

N. Mortier, P. Vandenbosch, and C. Vancutsem *In* AGARD, Allergic, Immunological and Infectious Disease Problems in Aerospace Medicine Apr. 1992 3 p (For primary document see N93-11283 02-52)
Copyright Avail: CASI HC A01/MF A03

The different methods used in the Medical Center of Aerospace Medicine, Brussels (Med C Aerospace) to detect allergy in pilot applicants, are discussed. During the period 1987 through 1989, the Total immunoglobuline E (IgE) levels were also determined at the start of pilot training. The aim was to assess if Total IgE could be used as an additional selection criterion. We conclude that it is not useful to determine the total IgE in the selection of pilot candidates. The existing investigations and examination methods are sufficient to detect allergy. Author

N93-11317# Hellenic Air Force General Hospital, Athens (Greece). Div. of Allergy.

ALLERGIC AND NONALLERGIC RHINITIS IN GREEK PILOTS

C. Grigoreas, D. Pappas, A. Agelidis, and E. Chimonas *In* AGARD, Allergic, Immunological and Infectious Disease Problems in Aerospace Medicine Apr. 1992 3 p (For primary document see N93-11283 02-52)
Copyright Avail: CASI HC A01/MF A03

In order to study the Allergic Rhinitis (AR) and Nonallergic Rhinitis (NAR) in Greek pilots, we examined 144 Greek male pilots, aged from 23 to 50 years, with symptoms of chronic rhinitis. The diagnosis was based on: (1) detailed history; (2) physical examination; (3) Skin Prick Tests (SPT) on common aeroallergens (positive SPT greater than 3 mm wheal); and (4) nasal secretions for assessment of eosinophilia (positive eosinophilia 20 percent eosinophils in nasal smears). Also, we measured serum total immunoglobuline E (IgE) (IV/ml) by the Paper-Radioimmunosorbent Test (PRIST) method and expressed as geometric mean value. We excluded patients suffering from chronic rhinitis (infections, mechanical-anatomic, drug-induced, sinusitis, and metabolic states) and bronchial asthma. Eighty-six patients (59.7 percent) had Seasonal Allergic Rhinitis (SAR), 30 patients (20.8 percent) had Perennial Allergic Rhinitis (PAR), 22 patients (15.3 percent) had Vasomotor Rhinitis (VR), and 6 patients (4.2 percent) had Nonallergic Rhinitis with Eosinophilia (NARE). One patient with PAR and 2 patients with NARE possessed nasal polyps. The frequency of major positive SPT in the SAR group was: (1) grasses (80.2 percent), (2) olive (69.7 percent), (3) parietaria (50 percent); and in the PAR group was: (1) House dust (100 percent), (2) mite D. Farinae (93.3 percent), (3) mite D. Pteronyssinus (90 percent). The levels of IgE among the four groups were 174.6 IV/ml in the VR group and 39.2 IV/ml in the NARE group. It is concluded, that in Greek pilots: (1) AR (SAR and PAR) was more frequent than NAR (VR and NARE); (2) the major aeroallergens responsible were different in patients with AR, since pollens predominated in the SAR group and house dust-mites in the PAR group; (3) patients with NARE had a high prevalence of nasal polyps; and (4) IgE levels were higher in patients with AR (SAR and PAR) than in patients with NAR (VR and NARE). Author

N93-11318# Hellenic Air Force General Hospital, Athens (Greece). Center of Aviation Medicine.
CORRELATION OF SERUM ALPHA SUB 1 ANTITRYPSIN WITH CIGARETTE SMOKING AND PULMONARY FUNCTION STATUS IN GREEK PILOTS, FOR A TEN YEAR PERIOD
J. Palermos, K. Kyriakos, S. Michalopoulou, Ch. Daskalopoulos, and A. Bitsaktsis *In* AGARD, Allergic, Immunological and Infectious Disease Problems in Aerospace Medicine Apr. 1992 3 p (For primary document see N93-11283 02-52)
Copyright Avail: CASI HC A01/MF A03

Quantitative and mainly qualitative aberration of the alpha sub 1 Antitrypsin (a sub 1 AT) a major constituent of the human antielastase screen, is strictly associated with the development of lung emphysema. Certain factors like cigarette smoking and environmental pollution may contribute to that. In this study, we have correlated cigarette smoking with the serum a sub 1 AT concentration as well with the trend of predicted values of Forced Vital Capacity (FVC) and 1st Second Forced Expiratory Volume (FEV sub 1) over a ten year period. The study population consisted of 113 randomly selected male pilots, of the Greek Airforce, being in flight duties grouped into nonsmokers (n = 49, age x = 36.3) and effective smokers (n = 64, age x = 38.4) smoking for more than ten years. Serum a sub 1 AT level was 176 plus or minus 36 md/gl (mean plus or minus SD) and 199 plus or minus 32 mg/dl for nonsmokers and smokers, respectively (p less than 0.001). Serum a sub 1 AT level for Greek male population was 190 plus or minus 35 mg/dl and the frequency of individuals with intermediate serum a sub 1 AT level was 2.7 percent. Recent and past (ten years ago recorded) FVC and FEV sub 1 predicted values were measured. This data suggest that: (1) cigarette smoking affects serum a sub 1 AT level; (2) intermediate serum a sub 1 AT level cannot be employed as a predictive criterion for flight personnel's pulmonary status; (3) ten years of cigarette smoking worsens the pulmonary function status significantly; and (4) extra physical exercise improves it. Author

N93-11445# Massachusetts General Hospital, Boston. Labs. of Photomedicine.
CENTER OF EXCELLENCE IN LASER MEDICINE
J. A. Parrish 1992 6 p
(Contract DE-FG02-91ER-61228)
(DE92-018760; DOE/ER-61228/3) Avail: CASI HC A02/MF A01

Achievements during the first six months of funding to prepare for a Center of Excellence in biomedical laser development include limited specific research projects within the Center's three broad interest areas, and program development to establish the Center and its activities. Progress in the three interest areas -- new medical laser systems development, optical diagnostics, and photosensitization, is reported. Feasibility studies and prototype development were emphasized, to enhance establishing a substantial Center through future support. Specific projects are an optimized laser-catheter system for reversal of vasospasm; optical detection of major skin burn depth and cancers using fluorescent drugs, and photosensitization of vascular tissues. In addition, an interdepartmental Laser Center was established at MGH to enhance collaborations and institutional committment to the Center of Excellence. Competitive postdoctoral research fellowships, with provision for matching funds from other departments, have been announced. DOE

N93-11561# Rockefeller Univ., New York, NY.
CARBOXYALKYLATED HEMOGLOBIN AS A POTENTIAL BLOOD SUBSTITUTE Final Annual Report, 1 Sep. 1988 - 31 Oct. 1991
James M. Manning 19 Nov. 1991 25 p
(Contract DAMD17-88-C-8169)
(AD-A252329) Avail: CASI HC A03/MF A01

The major focus has been on the preparation and full characterization of a new hemoglobin crosslinker - 2,5-diisothiocyanatobenzene sulfonic acid. Collaborative studies with investigators at the Letterman Army Institute of Research indicated that carboxymethylated hemoglobin was cleared from the circulation of rats with a half time of 42 minutes. The pseudo-first order plot indicates that a homogeneous population of molecules was present. In addition, there was no adverse pathological findings. The plasma retention time of the DIBS-crosslinked material that we prepared was also determined at Letterman to be 3-4 times longer than that of carboxymethylated hemoglobin. Cross-linking agents to produce derivatives of molecular weight 128,000 were also evaluated during this period. Other carboxyalkylating agents such as succinic semialdehyde in the presence of sodium cyanoborohydride have begun to be evaluated and compared with the carboxymethylated derivative. GRA

N93-11841# Harvard Univ., Cambridge, MA. Div. of Applied Sciences.
THE EFFECTS OF LUMINANCE BOUNDARIES ON COLOR PERCEPTION Annual Report, 15 Mar. 1991 - 14 Mar. 1992
R. E. Kronauer, C. F. Stromeyer, III, A. Chaparro, and R. T. Eskew, Jr. 30 Apr. 1992 12 p
(Grant AF-AFOSR-0304-89)
(AD-A250705; AFOSR-92-0375TR) Avail: CASI HC A03/MF A01

Extensive measurements were made for detecting luminance and red-green flashes in the center of a bright yellow field. Thresholds, plotted in L- and M-cone contrast coordinates, indicate that chromatic flashes are more visible than luminance flashes even at very small size (2 inch diameter). Over a wide range of flash diameters and durations the chromatic flashes are detected with considerably higher efficiency (in units of cone contrast energy) than the most detectable luminance stimuli (small drifting gratings). The higher gain of the chromatic mechanisms has important physiological implications and is potentially useful in display technology. Detailed studies with luminance and chromatic stimuli suggest that the chromatic mechanisms have a constant spectral tuning, even for spots as small as 2 inches: the chromatic response is determined by a constant, equally weighted difference of L and M cone contrast. A suprathreshold luminance flash (a pedestal) facilitates detection of a coincident chromatic flash. Earlier studies suggested that the facilitation will grow strongly when the stimuli were decreased in size. In contrast, we find that facilitation is constant (2-3x) for stimuli from 2 inches to 2 deg diameter. GRA

N93-11873# Michigan Univ., Ann Arbor. Div. of Nuclear Medicine.
NEW TECHNIQUES FOR POSITRON EMISSION TOMOGRAPHY IN THE STUDY OF HUMAN NEUROLOGICAL DISORDERS
D. E. Kuhl 1992 11 p
(Contract DE-FG02-87ER-60561)
(DE92-015353; DOE/ER-60561/6) Avail: CASI HC A03/MF A01

The general goals of the physics and kinetic modeling projects are to: (1) improve the quantitative information extractable from PET images, and (2) develop, implement and optimize tracer kinetic models for new PET neurotransmitter/receptor ligands aided by computer simulations. Work towards improving PET quantification has included projects evaluating: (1) iterative reconstruction algorithms using supplemental boundary information, (2) automated registration of dynamic PET emission and transmission data using sinogram edge detection, and (3) automated registration of multiple subjects to a common coordinate system, including the use of non-linear warping methods. Simulation routines have been developed providing more accurate representation of data generated from neurotransmitter/receptor studies. Routines consider data generated from complex compartmental models, high or low specific activity administrations, non-specific binding, pre- or post-injection of cold or competing ligands, temporal resolution of the data, and radiolabeled metabolites. Computer simulations and human PET studies have been performed to optimize kinetic models for four new neurotransmitter/receptor ligands, (C-11)TRB (muscarinic), (C-11)flumazenil (benzodiazepine), (F-18)GBR12909, (dopamine), and (C-11)NMPB (muscarinic). DOE

N93-11893# Naval Health Research Center, San Diego, CA.
SMOKING STATUS AND BODY COMPOSITION, EXERCISE, DIETARY INTAKE, AND ALCOHOL/CAFFEINE CONSUMPTION Interim Report
Doris A. Abood and Terry L. Conway Dec. 1991 34 p
(AD-A250648; NHRC-91-22) Avail: CASI HC A03/MF A01

Although research on smoking status and body composition reveals conflicting results, extant literature indicates that dietary intake, alcohol consumption, exercise, light/moderate versus heavy smoking, and the recency of smoking cessation are important variables to investigate. This study examined these variables in 1,820 Navy men. Of five body composition variables, only lean body mass was significantly (p less than .05) related to smoking status. However, heavy smokers exercised the least and never smokers exercised the most. Heavy smokers also tended to eat high-fat meat more often, and eat lean meat, leafy vegetables, fruit, and fiber less often than all other groups. Long-term quitters were more similar to never smokers and short-term quitters more similar to light/moderate smokers in eating patterns and consumption of low-fat foods. Heavy smokers drank twice as much alcohol and caffeine as never smokers and former smokers. In summary, smoking was associated with very low levels of exercise, a high-fat diet, and heavy consumption of alcohol-all of which are associated with the leading causes of death and disability in the United States. Navy health promotion efforts should continue to encourage smokers to quit as well as to modify other negative health behaviors that may accompany addiction to nicotine. GRA

N93-12145# Army Research Inst. of Environmental Medicine, Natick, MA.
SUSTAINING HEALTH AND PERFORMANCE IN THE COLD: ENVIRONMENTAL MEDICINE GUIDANCE FOR COLD-WEATHER OPERATION
A. J. Young, D. E. Roberts, D. P. Scott, J. E. Cook, and M. Z. Mays Jul. 1992 64 p
(AD-A254328; USARIEM-TN-92-2) Avail: CASI HC A04/MF A01

This Technical Note reviews how the environment can impact on soldier health and performance during cold-weather operations. In addition, ways of coping with these environmental stresses are presented. GRA

N93-12427*# Alabama Univ., Huntsville. Environmental Lab. Section.
ECLSS MEDICAL SUPPORT ACTIVITIES Final Report, 10 Apr. 1990 - 9 Apr. 1991
William J. Crump and Melvin V. Kilgore, Jr. 30 Apr. 1991 368 p
(Contract NAS8-36955)
(NASA-CR-184429; NAS 1.26:184429) Avail: CASI HC A16/MF A03

During the period from April 10, 1990 to April 9, 1991, the Consortium for the Space Life Sciences provided technical assistance to the NASA/MSFC water recovery efforts. This assistance was in the form of literature reviews, technical recommendations, and presentations. This final report summarizes the activities completed during this period and identifies those areas requiring additional efforts. The tasks which the University of Alabama in Huntsville (UAH) water recovery team addressed were either identified by MSFC technical representatives or chosen from those outlined in the subject statement of work. Author

N93-12469# Connecticut Univ., Storrs. Dept. of Communication Sciences.
AUDITORY PERCEPTION Final Report, 1 Nov. 1989 - 31 Oct. 1990
Marion F. Cohen 28 Aug. 1992 9 p
(Grant AF-AFOSR-0008-89)
(AD-A255061; AFOSR-92-0850TR) Avail: CASI HC A02/MF A01

During the past year we have continued our experiments designed to study the role of cross-spectrum coherent frequency change on signal detection. We have studied the effects of frequency glides and frequency jitter on cross-spectrum fusion, specifically addressing the issues of maximum spectral distance and harmonic relationship between signal and masker, and we have found that the improved detection which we reported last year cannot be solely attributed to either. We have spent considerable time developing two experimental paradigms to be used in our future studies of signal separation as it relates to separation of a direct sound from its echo. The results of initial experiments using these paradigms indicate that a signal following an identical waveform is considerably more difficult to detect than when it is leading that waveform. These results cannot be accounted for by traditional temporal masking. We have also continued our experiments using 'noise-problem people' as subjects in an effort to determine if their ability to perform these tasks is related to their difficulty listening in background noise. GRA

53 BEHAVIORAL SCIENCES

Includes psychological factors; individual and group behavior; crew training and evaluation; and psychiatric research.

N93-10979# Royal Signals and Radar Establishment, Malvern (England).
AN INTRODUCTION TO THE INFORMATION PROCESSING COMPONENTS OF THE BRAIN
S. Collins 12 Jan. 1990 24 p
(RSRE-Memo-4350; BR113301) Copyright Avail: CASI HC A03/MF A01

Over the past decade there has been increasing interest in neurologically inspired computational techniques. This interest arises from the concurrence of two factors: (1) a growing list of interesting tasks for which serial digital computers are unsuitable; and (2) information gained from the application of new techniques in neurobiology. This text is intended to provide an introduction to neurobiological terms for physical scientists and engineers, with some pointers to further reading. As an introduction, little prior knowledge is assumed and the text begins with a short description of a generic neuron. This description is followed by more detailed discussions of those aspects of neurobiology of particular importance in information processing. The topics covered include the following. The electrical signals used to represent information. The ion conduction mechanisms employed by cells to support these signals. The behavior of cell and membranes and intercellular junctions. Finally, a few commennets on the immediate implications of even a superficial understanding of neurobiology are included. Author

N93-11081# Aerospace Medical Research Labs., Wright-Patterson AFB, OH.
DEVELOPMENT OF A TACTILE PERCEIVED ATTITUDE TRANSDUCER Final Report, Oct. 1989 - Dec. 1991
Tamara L. Chelette Dec. 1991 21 p
(AD-A253724; AL-SR-91-0002) Avail: CASI HC A03/MF A01

The objective of this effort was to design, build, and test a research device for measuring a research subject's perceived spatial orientation without the use of vision. The device consists of a multi-gimbaled structure that supports the dominant hand. A restraint system prevents slippage and shear movement. The subject indicates the perceived horizontal plane by placing his or her hand parallel to that perceived plane. This report contains a complete description of the device as well as the results of some fundamental testing on human performance with the device. In addition, the use of the device in spatial orientation research on the Dynamic Environment Simulator, a multiaxial human centrifuge, is described. The Tactile Perceived Attitude Transducer (TPAT) described herein is a simple and effective technique for reporting perceived attitude. Its accuracy, precision, and discrimination characteristics match those of more constrained or more complex devices. GRA

N93-11212 Politecnico di Milano (Italy). Dipartimento di Elettronica.
ONTOLOGY OF MIND, SUBJECTIVE ONTOLOGY, AND THE EXAMPLE OF TEMPORAL EXPRESSIONS
Gabriella Airenti (Turin Univ., Italy) and Marco Colombetti Mar. 1992 30 p
(Rept-92-018; ETN-92-92419) Avail: Politecnico di Milano, Piazza Leonardo da Vinci 32, 20133 Milan, Italy

A methodology for cognitive science is discussed. Some important aspects of the ontology of mind, with the purpose of identifying the features that a sound theory of mental processes should have are considered. Relationships between theories of the mind and computational models are analyzed, and it is argued that no existing computational approach alone is able to account for all functionalities of a cognitive system. In the constructive part, it is argued that human representations embed a subjective ontology of the world, which can be studied systematically. How this study could be carried on is discussed, and the theory for a fragment of the subjective ontology of time is derived from linguistic data. ESA

N93-11415# Memphis State Univ., TN. Dept. of Psychology.
QUESTIONING MECHANISMS DURING COMPLEX LEARNING Final Report, Jan. 1990 - Jan. 1992
Arthur C. Graesser 11 Mar. 1992 66 p
(Contract N00014-90-J-1492)
(AD-A247382; TR-92-1-ONR) Avail: CASI HC A04/MF A01

This research investigated human question asking and answering during comprehension and complex learning. The primary studies investigated questioning during tutoring. We collected and analyzed transcripts of tutoring sessions on research methods (college students) and basic algebra (7th graders). Student questions were 100 times as frequent in tutoring sessions as classroom settings, which might partially explain why learning is substantially better in tutoring. We analyzed the knowledge states, properties of questions, strategies, and interaction patterns of students and tutors. Students did attempt to self-regulate their knowledge by identifying knowledge deficits and asking questions that repair such deficits, but they need substantial training in improving question asking skills. Students' answers to deep questions (e.g., why, why-not, how, what-if) were poor in quality, so the tutor helped answer these questions in a collaborative process that took several conversational turns. In one auxiliary study, we designed a human-computer interface that facilitates the speed and quality of questioning, called the Point and Query (P and Q) interface. The frequency of student questions on the P and Q software was approximately 800 times that in a classroom setting. In a second auxiliary project, we investigated the stimulus conditions that trigger questions when students comprehend text and attempt to solve mathematics problems. GRA

N93-11488# Purdue Univ., West Lafayette, IN. Jet Propulsion Center.
VISUAL PSYCHOPHYSICS OF EGOMOTION Annual Report, 1 Dec. 1990 - 30 Nov. 1991
Kathleen Turano 24 Feb. 1992 11 p
(Grant AF-AFOSR-0154-91)
(AD-A248349; AFOSR-92-0202TR) Avail: CASI HC A03/MF A01

Two psychophysical studies investigated an observer's ability to perceive self motion. In both studies, the stimuli were computer-generated images simulating an observer moving relative to a volume of randomly-positioned dots. The first study investigated an observer's ability to determine whether s/he was moving forward along a straight or curved path as forward speed was varied. The results showed that with eye movements, the deviation required to detect a departure from a straight path increased with forward speed. When eye movements were restricted, the required deviation remained constant across forward speeds. A second study investigated the effectiveness of various sizes and retinal locations of the stimulus in determining the direction of a curved path. The results showed an increasing linear relationship between optimal size and retinal eccentricity. Given optimally-scaled stimuli, the central and peripheral retinal locations yielded equivalent performance. Finally, a computational model has been developed to emulate a human observer's ability to detect a curved path of motion. Computer simulations of the model have been run on a task to discriminate between a curved and straight path of motion. The simulation results closely match psychophysical data. GRA

N93-11503# Boston Univ., MA. Center for Adaptive Systems.
VISUAL PERCEPTION OF STRUCTURE FROM MOTION Final Report, 1 Nov. 1988 - 30 Apr. 1992
James T. Todd 30 Apr. 1992 7 p
(Grant AF-AFOSR-0016-89)
(AD-A253235; AFOSR-92-0703TR) Avail: CASI HC A02/MF A01

The research performed in this project has examined the abilities of human observers to perceive 3D form from different types of optical structure within moving or stationary visual images. The research has been organized into four general problem areas, including the low level detection of coherent, motion, the analysis of 3D form from motion, the analysis of image shading and texture, and the identification of image contours. Our basic strategy in all of these areas has been to identify the key assumptions of current computational models; to test the psychological validity of those assumptions using appropriate psychophysical procedures; and, based on the results of those experiments, to develop alternative models that more closely match the perceptual capabilities of actual human observers. In contrast to most common methods of 3D image analysis, which are designed to compute precise metrical descriptions, our results have shown that human perception is primarily concerned with more abstract aspects of object structure, such as affine or ordinal properties, which are easier to computer and are more robust to uncontrolled changes in viewing conditions. GRA

N93-11779# Dynamics Research Corp., Wilmington, MA. Systems Div.
DEVELOPMENT OF THE PERSONNEL-BASED SYSTEM EVALUATION AID (PER-SEVAL) PERFORMANCE SHAPING FUNCTIONS Final Report, Nov. 1986 - Aug. 1990
Lawrence H. OBrien, Robert Simon, and Hariharan Swaminathan Jun. 1992 122 p
(Contract MDA903-86-C-0412; DA Proj. 2Q1-62785-A-791)
(AD-A252820; ARI-RN-92-50) Avail: CASI HC A06/MF A02

This report describes how the Personnel-Based System Evaluation Aid (PER-SEVAL) performance shaping functions were developed. It describes how PER-SEVAL will use these functions to identify minimum levels of personnel characteristics for a particular contractor's design. Finally, procedures for future validation of the functions are outlined. The PER-SEVAL performance shaping functions were developed by conducting regression analyses of data obtained from the U.S. Army Research Institute for the Behavioral and Social Sciences' Project A database. They predict task performance as a function of personnel characteristics and training. Separate functions are provided for different types of tasks. Two types of training variables are used in the performance shaping functions--frequency and recency of practice. GRA

N93-12225# Iowa Univ., Iowa City.
META-ANALYSIS OF INTEGRITY TESTS: A CRITICAL EXAMINATION OF VALIDITY GENERALIZATION AND MODERATOR VARIABLES Final Report, 28 Sep. 1991 - 30 Jun. 1992
D. S. Ones, C. Viswesvarn, and F. Schmidt Jun. 1992 99 p
(Contract N00014-91-J-4168)
(AD-A254681) Avail: CASI HC A05/MF A02

A comprehensive meta-analysis was conducted to investigate whether integrity test validities are generalizable and to estimate differences in validity due to potential moderating influences. The database included 665 validity coefficients across 576,464 data points. Results indicate that integrity test validities are positive and in many cases substantial for predicting both job performance and counterproductive behaviors on the job such as theft, disciplinary problems, and absenteeism. Validities were found to be generalizable. The estimated mean operational predictive validity of integrity tests for supervisory ratings of job performance is .41. For the criterion of counterproductive behaviors, results indicate that use of concurrent validation study designs may overestimate the predictive criterion-related validity applicable in selection situations. Our results based on external criterion measures (i.e., excluding self reports) and predictive validity studies using applicants indicate that integrity tests predict the broad criterion of organizationally disruptive behaviors better than they predict the narrower criterion of employee theft alone. Our results also indicated substantial evidence for the construct validity of integrity tests. Perhaps the most important conclusion of this research is that despite the influence of moderators, integrity test validities are positive across situations and settings. GRA

N93-12252# Air Force Systems Command, Brooks AFB, TX.
INTRODUCTION TO TRAINING DECISIONS MODELING TECHNOLOGIES: THE TRAINING DECISIONS SYSTEM Final Report, Jan. 1990 - Apr. 1990
Keric B. O. Chin, Theodore A. Lamb, Winston R. Bennett, and David S. Vaughan (McDonnell-Douglas Missile Systems Co., Saint Louis, MO.) Apr. 1992 27 p
(AF Proj. 1121)
(AD-A249862; AL-TP-1992-0014) Avail: CASI HC A03/MF A01

This paper is an introduction to the Training Decisions Modeling Technologies under development at the Armstrong Laboratory. These technologies are intended to support Air Force Training Managers by providing them with cost and resource information about the impact of their decisions on the AF training system. The Training Decisions System (TDS), which forms the baseline technologies for the research program, uses information about jobs performed by airmen, personnel assignment flows, course training content, and training resources to determine training capacities and the most cost-effective training options available. The TDS develops a model of a job specialty's Utilization and Training (U and T) pattern according to data collection results and simulates the flow of airmen through it. Based on this simulation, TDS tabulates the costs associated with training and evaluates the training capacity of the training system (i.e., the ability of the training system to provide training to a given number of airmen). GRA

N93-12432# Naval Aerospace Medical Research Lab., Pensacola, FL.
THE OMPAT LEVEL 1 NEUROPHYSIOLOGICAL PERFORMANCE ASSESSMENT BATTERY: NPPAB Interim Report, Oct. 1989 - Oct. 1991
D. L. Reeves, R. R. Stanny, G. F. Wilson, R. I. Herning, and W. Pickworth Dec. 1991 32 p
(AD-A254840; NAMRL-Mono-43) Avail: CASI HC A03/MF A01

This report presents specifications and methodology for the tests of the Tri-service Neurophysiological Performance Assessment Battery (NPPAB). The NPPAB is designed to evaluate the effects of medical pharmaceuticals on military-relevant human performance. It is intended to serve as an initial screening tool that will identify neurological systems and functions adversely affected by chemical agents. The tests of the NPPAB comprise seven electrophysiological procedures designed to assess the functioning of the visual, auditory, and somatosensory systems, as well as the higher-order processes of selective attention and short-term memory. GRA

54 MAN/SYSTEM TECHNOLOGY AND LIFE SUPPORT

Includes human engineering; biotechnology; and space suits and protective clothing.

For related information see also *16 Space Transportation.*

N93-10994# Maryland Univ., College Park. Office of Research Administration and Advancement.
COORDINATED ACTION IN 3-D SPACE Annual Interim Report, 15 Dec. 1990 - 14 Jan. 1992
Robert M. Stinman 12 Mar. 1992 4 p
(Grant AF-AFOSR-0124-91)
(AD-A249830; AFOSR-92-0233TR) Avail: CASI HC A01/MF A01

This grant tests alternative hypotheses about mechanisms controlling gaze-shifts while manipulating nearby objects, viz., on-line feedback vs. learned, preplanned coordinated movements; and studies speed and accuracy of visually-guided arm movements. Work this year concentrated primarily on instrumentation: i.e., (1) a SUN workstation was procured and configured; (2) an interface between the Maryland RFM and a PC was constructed (this allowed old DEC computers to be retired); (3) a hands-on, calibrated workspace was constructed; and (4) software for data acquisition and analysis was developed. Progress was made with more intellectual activities while this new instrumentation was developed, viz., (1) a behavioral trigonometric technique was worked out for estimating the eyes's centers of rotation with the head free to move, (2) slow control was shown to be sensitive only to velocity and not to position (contrary to prior claims), (3) Pizlo completed a Ph.D thesis on shape constancy by human beings and computers, and (4) it was shown that unspaced word-texts could be read out-loud easily. This provocative finding makes great difficulties for all contemporary theories of reading because they assume that spaces in texts are required to parse words effectively. GRA

N93-11279# Federal Aviation Administration, Washington, DC. Office of Aviation Medicine.
COMPARISONS OF MOLECULAR SIEVE OXYGEN CONCENTRATORS FOR POTENTIAL MEDICAL USE ABOARD COMMERCIAL AIRCRAFT Final Report
Harvey M. England, Jr., Bruce C. Wilcox, Jr., and Garnet A. McLean Jun. 1992 10 p
(AD-A253648; DOT/FAA/AM-92/22) Avail: CASI HC A02/MF A01

Medically-impaired air travelers requiring supplemental oxygen must depend on airlines to provide oxygen cylinders. Performance, space, and cost are considerations in providing this service. Tests were conducted in an altitude chamber to assess the viability of Molecular Sieve Oxygen Concentrators (MSOC's) as an alternative. Five different MSOC's were placed in the altitude chamber, and connected to a mass spectrometer outside. Gas concentration was digitized at one sample-per-second and stored on line via a microcomputer. Tests at ground level showed four of the five MSOC produced oxygen at 95 percent purity at 2 liters per minute flow, which was maintained until 13,000 feet. Increasing altitude resulted in graded reductions of oxygen levels. At 25,000 feet, only two MSOC withstood sudden decompression. Results of this study indicate that some MSOC indeed have the potential to provide oxygen for the medically-impaired air traveler. GRA

N93-11559# Aerospace Medical Research Labs., Wright-Patterson AFB, OH.
THE EFFECT OF VARIABLE SEAT BACK ANGLES ON HUMAN RESPONSE TO +Gz IMPACT ACCELERATIONS Interim Report, Jul. 1986 - Apr. 1991
Chris E. Perry, Dena M. Bonetti, and James W. Brinkley May 1991 137 p
(AF Proj. 7231)
(AD-A250673; AL-TR-1991-0110) Avail: CASI HC A07/MF A02

During 1986-1987, eighty-two human impact experiments were accomplished on a vertical deceleration tower to determine the influence of variable seat back angles on human dynamic response to short-duration acceleration applied in the +x axis. Subjects were exposed to acceleration at a level of 10 G using a vertical deceleration tower. The seat back angle varied as follows: (1) +5 deg (5 deg aft of vertical), (2) 0 deg (vertical), (3) -5 deg (5 deg forward of vertical), and (4) -10 deg (10 deg forward of vertical). The resultant seat loads in the z-axis did not show statistically significant differences as the seat back angle was varied. Data showed a trend for head acceleration in the -x axis to increase and for head acceleration in the +x axis to decrease as the seat back angle became more negative. This implies that cervical spine flexion increases as the seat back angle becomes more negative. This is supported by motion analysis using high-speed photography which indicated a trend for increased forward rotation of the head as the seat back angle became more negative. These experimental data will be used in the formulation of biodynamic models. GRA

N93-11649*# National Aeronautics and Space Administration. Lyndon B. Johnson Space Center, Houston, TX.
THE LOCATOR SYSTEM FOR WANDERING INDIVIDUALS
Shayla Davidson Aug. 1992 21 p Original contains color illustrations
(NASA-TM-104754; S-688; NAS 1.15:104754) Avail: CASI HC A03/MF A01; 2 functional color pages

Configurations and operation strategies are described for a wanderer locator system based on wireless radio frequency communication designed to monitor elderly patients who may wander beyond safe perimeters in the home or in an institutional setting. The modular components of this wandering notification system are (1) portable transmitter/receivers to be worn or carried by the patient and the caretaker, (2) detectors to be mounted in doorways or other perimeters of a safe area, (3) programmable central processing units to control, communicate with, and/or trace the portable and remote devices, and (4) a cathode ray tube that can display information on patient location or system status. Photographs of all system components and illustrations of operations concepts are included. Author

N93-11743# Human Engineering Labs., Aberdeen Proving Ground, MD.
SYSTEM FOR GENERATING DYNAMIC VIDEO IMAGERY FOR HUMAN FACTORS RESEARCH Final Report
D. R. Shires, F. F. Holly, C. A. Chang, J. Mazurczak, and S. P. Schipani Feb. 1992 78 p
(AD-A248675; HEL-TN-3-92) Avail: CASI HC A05/MF A01

A computer-controlled system was developed which provides the capability to generate processed dynamic imagery for human factors research. Processing of the video may involve any operation such as enhancing, degrading, or adding overlays. This system may also be used during experimental trials to perform data collection and score subject responses. The system is comprised of several components: a computer, an image processor, two lapse video cassette recorders, and a custom built VCR control circuit. When possible, processing is performed as the video is being displayed to a subject. When processing complexity is too great, the video is processed before experimentation. The input to the system is imagery on a video tape. The imagery is processed frame by frame and the results are stored on the output video tape. Processing appears to be performed in real time when this resultant tape is played at the regular speed. The flexibility and cost effectiveness of the system make it an ideal developmental tool, test-bed, and simulator for the processing of dynamic visual imagery. The hardware and software for implementing the system are discussed in detail. GRA

N93-11783# North Carolina Univ., Chapel Hill. Dept. of Computer Science.
ADVANCED TECHNOLOGY FOR PORTABLE PERSONAL VISUALIZATION Progress Report, Jan. - Jun. 1992
Frederick P. Brooks, Jr. and Henry Fuchs Jun. 1992 119 p
(Contract DAEA18-90-C-0044)
(AD-A253808) Avail: CASI HC A06/MF A02

Despite the recent avalanche of publicity on virtual reality, the state of the art in head-mounted displays is still at the 'toy' stage. Although extravagant claims are made almost daily on television and in the popular press, there is very little that can be usefully accomplished today with virtual reality technologies. We at UNC have been working since the early 1970s on aspects of these technologies and have been advancing the state of the art by a 'driving problem' approach; we let the needs of selected applications stimulate the direction of the technological developments and then test new results by their impact on solving the original application. We have been working on three application areas: molecular modeling, 3D medical imaging, and modeling of architectural interiors. GRA

N93-11784# Naval Research Lab., Washington, DC.
DIRECT MANIPULATION AND INTERMITTENT AUTOMATION IN ADVANCED COCKPITS Final Report
James A. Ballas, Constance L. Heitmeyer, and Manuel A. Perez 21 Jul. 1992 52 p
(AD-A253814; NRL/FR/5534-92-9375) Avail: CASI HC A04/MF A01

Increasing use of automation in computer systems, such as advanced cockpits, present special challenges in the design of user interfaces. The challenge is particularly difficult when automation is intermittent because the interface must support smooth transitions from automated to manual mode. A theory of direct manipulation predicts that this interface style will smooth the transition. Interfaces were designed to test the prediction and to evaluate two aspects of direct manipulation: semantic distance and engagement. Empirical results supported the theoretical prediction and also showed that direct engagement can have some adverse effects on another concurrent manual task. Generalizations of our results to other complex systems are presented. GRA

N93-11812# Hamilton Standard Div., United Aircraft Corp., Windsor Locks, CT.
SUBMARINE ADVANCED INTEGRATED LIFE SUPPORT SYSTEM (SAILS) PROGRAM Final Report, 1 Oct. 1990 - 1 Oct. 1991
1 Oct. 1991 43 p
(Contract N00014-87-C-0790)
(AD-A253564; BD-92-02) Avail: CASI HC A03/MF A01

Next generation submarines will require more sophisticated ship systems as component volume, weight, reliability and acoustic signatures become critical tradeoff parameters. System effectiveness becomes particularly important as acquisition cost drives the selection of advanced technologies. General Electric exhibited foresight in the early 1980's by initiating IR and D efforts targeted at developing a modified electrolysis cell which simultaneously converts carbon dioxide to liquid organics and water to pure oxygen without the presence of gaseous hydrogen. This effort was augmented by contracts from the Naval Research Laboratory shortly thereafter. Although some progress was made towards the goal, significant, consistent improvements in cathode performance were not realized until organometallic electrode structures were implemented in 1986 by Hamilton Standard. Research efforts were initiated under a contract with the Office of Naval Research in 1987, but the program was put on hold shortly thereafter due to naval funding limitations. GRA

N93-12018*# National Aeronautics and Space Administration. Ames Research Center, Moffett Field, CA.
TECHNIQUES FOR OPTIMAL CROP SELECTION IN A CONTROLLED ECOLOGICAL LIFE SUPPORT SYSTEM
Ann McCormack, Cory Finn, and Betsy Dunsky Aug. 1992 16 p
(RTOP 199-61-12-42)
(NASA-TM-103950; A-92142; NAS 1.15:103950) Avail: CASI HC A03/MF A01

A Controlled Ecological Life Support System (CELSS) utilizes a plant's natural ability to regenerate air and water while being grown as a food source in a closed life support system. Current plant research is directed toward obtaining quantitative empirical data on the regenerative ability of each species of plant and the system volume and power requirements. Two techniques were adapted to optimize crop species selection while at the same time minimizing the system volume and power requirements. Each allows the level of life support supplied by the plants to be selected, as well as other system parameters. The first technique uses decision analysis in the form of a spreadsheet. The second method, which is used as a comparison with and validation of the first, utilizes standard design optimization techniques. Simple models of plant processes are used in the development of these methods. Author

N93-12079# Battelle Columbus Labs., OH.
EVALUATION OF MULTILAYER MASK CONCEPT FOR RESPO 21 Final Report
T. A. Pettenski Dec. 1991 148 p
(Contract DLA900-86-C-2045)
(AD-A253392) Avail: CASI HC A07/MF A02

The RESPO 21 multilayer mask is discussed. The following topics are covered: background, design goals, previous work, functional characteristics, design, prototype fabrication, and testing. GRA

N93-12195*# Lockheed Engineering and Sciences Co., Houston, TX.
ASTRONAUT CANDIDATE STRENGTH MEASUREMENT USING THE CYBEX 2 AND THE LIDO MULTI-JOINT 2 DYNAMOMETERS Final Report
Amy E. Carroll and Robert P. Wilmington May 1992 28 p
(Contract NAS9-17900)
(NASA-CR-185679; NAS 1.26:185679; LESC-30277) Avail: CASI HC A03/MF A01

The Anthropometry and Biomechanics Laboratory in the man-Systems division at NASA's Johnson Space Center has as one of its responsibilities the anthropometry and strength measurement data collection of astronaut candidates. The anthropometry data is used to ensure that the astronaut candidates are within the height restrictions for space vehicle and space suit design requirements, for example. The strength data is used to help detect abnormalities or isolate injuries to muscle groups that could jeopardize the astronauts safety. The Cybex II Dynamometer has been used for strength measurements from 1985 through 1991. The Cybex II was one of the first instruments of its kind to measure strength and similarity of muscle groups by isolating the specific joint of interest. In November 1991, a LIDO Multi-Joint II Dynamometer was purchased to upgrade the strength measurement data collection capability of the Anthropometry and Biomechanics Laboratory. The LIDO Multi-Joint II Dynamometer design offers several advantages over the Cybex II Dynamometer including a more sophisticated method of joint isolation and a more accurate and efficient computer based data collection system. Author

N93-12211*# Lockheed Engineering and Sciences Co., Houston, TX.
METHODOLOGY ISSUES CONCERNING THE ACCURACY OF KINEMATIC DATA COLLECTION AND ANALYSIS USING THE ARIEL PERFORMANCE ANALYSIS SYSTEM Final Report
R. P. Wilmington, Glenn K. Klute, ed., Amy E. Carroll, ed., Mark A. Stuart, ed., Jeff Poliner, ed., Sudhakar Rajulu, ed., and Julie Stanush, ed. Jun. 1992 63 p
(Contract NAS9-17900)
(NASA-CR-185689; NAS 1.26:185689; LESC-30302) Avail: CASI HC A04/MF A01

Kinematics, the study of motion exclusive of the influences of mass and force, is one of the primary methods used for the analysis of human biomechanical systems as well as other types of mechanical systems. The Anthropometry and Biomechanics Laboratory (ABL) in the Crew Interface Analysis section of the Man-Systems Division performs both human body kinematics as well as mechanical system kinematics using the Ariel Performance Analysis System (APAS). The APAS supports both analysis of analog signals (e.g. force plate data collection) as well as digitization and analysis of video data. The current evaluations address several methodology issues concerning the accuracy of the kinematic data collection and analysis used in the ABL. This document describes a series of evaluations performed to gain quantitative data pertaining to position and constant angular velocity movements under several operating conditions. Two-dimensional as well as three-dimensional data collection and analyses were completed in a controlled laboratory environment using typical hardware setups. In addition, an evaluation was performed to evaluate the accuracy impact due to a single axis camera offset. Segment length and positional data exhibited errors within 3 percent when using three-dimensional analysis and yielded errors within 8 percent through two-dimensional analysis (Direct Linear Software). Peak angular velocities displayed errors within 6 percent through three-dimensional analyses and exhibited errors of 12 percent when using two-dimensional analysis (Direct Linear Software). The specific results from this series of evaluations and their impacts on the methodology issues of kinematic data collection and analyses are presented in detail. The accuracy levels observed in these evaluations are also presented. Author

N93-12229# Massachusetts Inst. of Tech., Cambridge. Research Lab. of Electronics.
SUPER AUDITORY LOCALIZATION FOR IMPROVED HUMAN-MACHINE INTERFACES Annual Technical Report, 1 Mar. 1991 - 29 Feb. 1992
Nathaniel Durlach 7 Jan. 1992 9 p
(Grant AF-AFOSR-0200-90)
(AD-A254699; AFOSR-92-0762TR) Avail: CASI HC A02/MF A01

Work during the period 3/1/91 - 2/29/92 has continued on the development of a hybrid stimulation system in which a virtual auditory environment is combined with a real visual environment. This system has been developed to help explore the effects of various transformations of auditory-localization cues on both resolution and response bias. Initial research has focused on the effects of altering the cues available to the listener for determining sound source direction in the horizontal plane. Of particular interest are alterations that magnify these cues and thus lead to supernormal performance. Although these experiments have not yet been completed, results to date indicate that current models of auditory behavior are adequate for predicting the observed changes in resolution but inadequate for predicting the observed change in response bias. GRA

N93-12291# Naval Air Warfare Center, Warminster, PA. Aircraft Div.
EFFECTIVENESS OF NASA 1032 AND 1035 AND AIR FORCE 1030 AND 1034 UNITS IN PROTECTION AGAINST COLD WATER HYPOTHERMIA Final Report, 7 Feb. - 28 Mar. 1991
Annette C. Drew, Jonathan W. Kaufman, and Gregory K. Askew 16 Aug. 1991 34 p
(AD-A255120; NAWCADWAR-92056-60) Avail: CASI HC A03/MF A01

Our lab examined the relative cold exposure protection afforded by two sets of clothing ensembles. One set consisted of National Aeronautics and Space Administration suits (NASA1032 and NASA1035) and the other consisted of Air Force suits (AF1030 and AF1034). Eight healthy male subjects wearing these ensembles were exposed on four separate occasions to cold water (T(sub water) - 4.4 C) in an environmentally controlled chamber with cold ambient air temperature (T(sub air) - 5.6 C). Each subject tested either a NASA or an Air Force set of clothing ensembles for the ability to keep body core temperature (T(sub re)) above 35 C (onset of hypothermia) in both head-out immersion and enclosed within a raft. Subjects in the NASA suits were given up to 6 hours for the immersion trials and 24 hours for the raft trials, although none of the subjects in either suit were able to endure the entire duration of the experiments due to a variety of reasons. The NASA1032 appeared to perform better than the NASA1035 in both immersion and raft trials as none of the NASA1032 subjects'

T(sub re) fell to 35 C and the mean change in T(sub re) (delta-T(sub re)) was somewhat smaller in the NASA1032 (p less than 0.06). Both NASA1032 and NASA1035 subjects showed comparable mean exposure duration times. GRA

N93-12423# Florida Inst. of Tech., Melbourne. Dept. of Mechanical and Aerospace Engineering.
STUDIES OF A LASER/NUCLEAR THERMAL HARDENED BODY ARMOR Final Report, 31 Jan. - 30 Sep. 1991
N. Y. Misconi, Gerald J. Caldarella, and Joseph F. Roach Aug. 1992 53 p
(DA Proj. 1L1-62786-AH-98)
(AD-A255128; NATICK-TR-92/130) Avail: CASI HC A04/MF A01

The problem of laser/nuclear hardening of body armors and other applications, such as rigid walls, etc., has been investigated in this study. Earlier results from studies of hardening against space systems, which were supported by the Air Force Office of Scientific Research (AFOSR) and carried out by the Principal Investigator during 1984 to 1989 are summarized. The concepts of particle layer and photon multiple scattering inside the layers were utilized in developing a laser shield to protect against laser weapons in the 0.22 to 2.4 micrometer region of the spectrum. Protection against the threats from CO2 laser weapons are addressed, and the development of a protective shield is detailed. It is now possible to apply a coating that will protect against laser/nuclear threats and reduction of solar loads for 0.22 to 16 micrometers of the spectrum. Applications are expected for rigid walls (Army containers), human body armor, thermal jackets for military hardware, etc. Finally, a mathematical model was created to help predict how the laser hardening material will behave under specific constraints that have not yet been tested in the laboratory. Also, this model can be used to extrapolate the performance of similar materials/coatings in the mid- to far-infrared wavelengths and also predict the broadband performance. GRA

N93-12486# Naval Air Warfare Center, Warminster, PA. Aircraft Div.
HUMAN PERFORMANCE IN COMPLEX TASK ENVIRONMENTS: A BASIS FOR THE APPLICATION OF ADAPTIVE AUTOMATION Final Report
Jeffrey G. Morrison, Jonathan P. Gluckman, and John E. Deaton 1 Mar. 1992 11 p
(AD-A255067; NAWCADWAR-92032-60) Avail: CASI HC A03/MF A01

There are a number of human performance issues that are highlighted by the application of adaptive automation technology to complex task environments. Few of these issues have received empirical human performance research. This paper describes those issues that have arisen with the Naval Air Warfare Center's Adaptive Allocation for Intelligent Cockpits (AFAIC) program. GRA

N93-12491# Institute for Defense Analyses, Alexandria, VA.
THE EFFECTS OF WEARING PROTECTIVE CHEMICAL WARFARE COMBAT CLOTHING ON HUMAN PERFORMANCE Final Report, Sep. 1989 - Aug. 1991
Henry L. Taylor and Jesse Orlansky Aug. 1991 203 p
(Contract MDA903-89-C-0003)
(AD-A250716; IDA-P-2433; IDA/HQ-90-36732; AD-E501518)
Avail: CASI HC A10/MF A03

U.S. Department of Defense studies to measure performance decrements associated with wearing chemical warfare (CW) protective combat clothing indicate that heat stress produced seriously degraded human performance. Even when heat stress is not a significant factor, performance of many combat, combat support, and combat service support tasks is degraded. In most field studies, many crews of combat units became operationally ineffective due to voluntary withdrawal of individual crew members. Many combined arms, field studies, and laboratory studies indicate that when CW-protective combat clothing is worn performance is seriously degraded in the following areas: (1) the detection of targets, engagement time, and accuracy of fire; (2) manual dexterity tasks; and (3) psychological effects. Further, the degree of performance degradation varied with the tasks performed. Training in CW-protective combat clothing permits learning to modify procedures and consequently reduce negative effects, provided heat stress is not a significant factor. A growing body of evidence indicates there is inadequate training in the use of CW-protective combat clothing. A critical need exists for more and better training of skills needed under CW conditions. GRA

N93-12508# Anacapa Sciences, Inc., Fort Rucker, AL.
SELECTIVE FACTORS AFFECTING ROTARY WING AVIATOR PERFORMANCE WITH SYMBOLOGY SUPERIMPOSED ON NIGHT VISION GOGGLES
John W. Ruffner, Monty G. Grubb, and David B. Hamilton Jul. 1992 69 p
(Contract MDA903-87-C-0523)
(AD-A254983; ASI690-349-91; ARI-RR-1622) Avail: CASI HC A04/MF A01

This report presents the findings of a review of the literature on night vision goggles (NVG's), head-up displays (HUD's), and helmet-mounted displays (HMD's). The review was conducted to identify factors affecting the performance of pilots using the NVG-HMD system that superimposes symbology on the NVG image. The perceptual and attentional problems associated with using NVG's, HUD's, and HMD's are well documented in the literature, but they are not well understood. The literature suggests that use of the NVG-HMD system is likely to result in several perceptual and attentional problems, most notably errors in distance estimation, inappropriate division of attention, and spatial disorientation. A coordinated program of research on the NVG-HMD system should be undertaken using laboratory simulation devices, flight simulators, and operational aircraft. Priority should be given to investigating the effects of variables that are identified as important in the literature review, and of practical significance to the Army and that have not been determined by design decisions. GRA

N93-12509# Anacapa Sciences, Inc., Fort Rucker, AL.
AN EVALUATION OF CREW COORDINATION AND PERFORMANCE DURING A SIMULATED UH-60 HELICOPTER MISSION Interim Report, Jan. 1990 - Jun. 1991
R. C. Thornton, George L Kaempf, Joseph L. Zeller, Jr., and D. M. McAnualty Jul. 1992 75 p
(Contract MDA903-87-C-0523)
(AD-A254984; ASI690-344-91; ARI-RN-92-63) Avail: CASI HC A04/MF A01

This research was designed to develop measures of aircrew coordination and mission effectiveness and to identify crew coordination training requirements for U.S. Army rotary-wing flight. Twenty crews planned and conducted a three-segment mission scenario in the UH-60 Flight Simulator that exposed crews to situations requiring coordination. Crew performance and communications were recorded during the final two scenario segments, and three mission effectiveness measures were developed from the records: navigational accuracy, threat avoidance and evasion, and instrument approach. Communication rate, topics, functions, and content areas were analyzed as indexes of crew coordination. The results indicate that substantial differences in performance and communication profiles exist between crewmembers and across mission segments. There were significant relationships between crew coordination levels and performance on the three mission tasks. The results also indicate the need for aircrew coordination training for Army helicopter pilots. Five recommendations are made for an Army aircrew coordination training program. GRA

N93-11922*# Defense Advanced Research Projects Agency, Arlington, VA. Advanced Systems Technology Office.
FROM PILOT'S ASSOCIATE TO SATELLITE CONTROLLER'S ASSOCIATE
David L. Neyland, Carl Lizza (Wright Lab., Wright-Patterson AFB, OH.), and Philip A. Merkel (BDM International, Inc., Arlington, VA.) *In* NASA. Lyndon B. Johnson Space Center, Fifth Annual Workshop on Space Operations Applications and Research (SOAR 1991),

Volume 1 Jan. 1992 p 2-8 (For primary document see N93-11921 02-59)
Avail: CASI HC A02/MF A04

N93-11924*# McDonnell-Douglas Space Systems Co., Huntington Beach, CA. Space Station Div.
DISTRIBUTED ENVIRONMENTAL CONTROL
Gary A. Cleveland *In* NASA. Lyndon B. Johnson Space Center, Fifth Annual Workshop on Space Operations Applications and Research (SOAR 1991), Volume 1 Jan. 1992 p 19-26 (For primary document see N93-11921 02-59)
Avail: CASI HC A02/MF A04

N93-11930*# McDonnell-Douglas Space Systems Co., Houston, TX. Space Station Div.
INTELLIGENT FAULT MANAGEMENT FOR THE SPACE STATION ACTIVE THERMAL CONTROL SYSTEM
Tim Hill and Robert M. Faltisco *In* NASA. Lyndon B. Johnson Space Center, Fifth Annual Workshop on Space Operations Applications and Research (SOAR 1991), Volume 1 Jan. 1992 p 60-66 (For primary document see N93-11921 02-59)
Avail: CASI HC A02/MF A04

N93-11941*# Aerospace Corp., Los Angeles, CA.
ADVANCED SATELLITE WORKSTATION: AN INTEGRATED WORKSTATION ENVIRONMENT FOR OPERATIONAL SUPPORT OF SATELLITE SYSTEM PLANNING AND ANALYSIS
Stewart A. Sutton *In* NASA. Lyndon B. Johnson Space Center, Fifth Annual Workshop on Space Operations Applications and Research (SOAR 1991), Volume 1 Jan. 1992 p 133-141 (For primary document see N93-11921 02-59)
Avail: CASI HC A02/MF A04

N93-11976*# National Aeronautics and Space Administration. Ames Research Center, Moffett Field, CA.
HABITAT AUTOMATION
Rodney E. Swab *In* NASA. Lyndon B. Johnson Space Center, Fifth Annual Workshop on Space Operations Applications and Research (SOAR 1991), Volume 1 Jan. 1992 p 391-398 (For primary document see N93-11921 02-59)
Avail: CASI HC A02/MF A04

N93-11981*# ST Systems Corp., Lanham, MD.
OPERATOR VISION AIDS FOR SPACE TELEOPERATION ASSEMBLY AND SERVICING
Thurston L. Brooks, Ilhan Ince, and Greg Lee *In* NASA. Lyndon B. Johnson Space Center, Fifth Annual Workshop on Space Operations Applications and Research (SOAR 1991), Volume 1 Jan. 1992 p 412-421 (For primary document see N93-11921 02-59)
Avail: CASI HC A02/MF A04

55 SPACE BIOLOGY

Includes exobiology; planetary biology; and extraterrestrial life.

N93-12319*# National Aeronautics and Space Administration. Ames Research Center, Moffett Field, CA.
AN OVERVIEW OF GRAVITATIONAL PHYSIOLOGY
Jaime Miquel and Kenneth A. Souza Oct. 1991 59 p
(RTOP 107-30-31)
(NASA-TM-102849; A-90237; NAS 1.15:102849) Avail: CASI HC A04/MF A01

The focus of this review is on the response of humans and animals to the effects of the near weightless condition occurring aboard orbiting spacecraft. Gravity is an omnipresent force that has been a constant part of our lives and of the evolution of all living species. Emphasis is placed on the general mechanisms of adaptation to altered gravitational fields and vectors, i.e., both hypo- and hypergravity. A broad literature review of gravitational biology was conducted and the general state of our knowledge in this area is discussed. The review is specifically targeted at newcomers to the exciting and relatively new area of space and gravitational biology. Author

59 MATHEMATICAL AND COMPUTER SCIENCES (GENERAL)

N93-11921*# National Aeronautics and Space Administration. Lyndon B. Johnson Space Center, Houston, TX.
FIFTH ANNUAL WORKSHOP ON SPACE OPERATIONS APPLICATIONS AND RESEARCH (SOAR 1991), VOLUME 1
Kumar Krishen, ed. Washington Jan. 1992 454 p Symposium held in Houston, TX, 9-11 Jul. 1991; sponsored by NASA. Johnson Space Center, AF Phillips Lab., and Houston Univ.
(NASA-CP-3127-Vol-1; S-650-Vol-1; NAS 1.55:3127-Vol-1) Avail: CASI HC A20/MF A04

More than 110 papers were presented at this Symposium, sponsored by the U.S. Air Force Phillips Laboratory, the University of Houston-Clear Lake, and NASA JSC. The technical areas covered were Intelligent Systems, Automation and Robotics, Human Factors and Life Sciences, and Environmental Interactions. The U.S. Air Force and NASA programmatic overviews and panel discussions were also held in each technical area. These proceedings, along with the comments and suggestions made by the panelists and keynote speakers, will be used in assessing the progress made in joint USAF/NASA projects and activities. Furthermore, future collaborative/joint programs will also be identified. The symposium proceedings includes papers covering various disciplines presented by experts from NASA, the Air Force, universities, and industry. For individual titles, see N93-11922 through N93-11982.

N93-11922*# Defense Advanced Research Projects Agency, Arlington, VA. Advanced Systems Technology Office.
FROM PILOT'S ASSOCIATE TO SATELLITE CONTROLLER'S ASSOCIATE c54
David L. Neyland, Carl Lizza (Wright Lab., Wright-Patterson AFB, OH.), and Philip A. Merkel (BDM International, Inc., Arlington, VA.) *In* NASA. Lyndon B. Johnson Space Center, Fifth Annual Workshop on Space Operations Applications and Research (SOAR 1991), Volume 1 Jan. 1992 p 2-8 (For primary document see N93-11921 02-59)
Avail: CASI HC A02/MF A04

Associate technology is an emerging engineering discipline wherein intelligent automation can significantly augment the performance of man-machine systems. An associate system is one that monitors operator activity and adapts its operational behavior accordingly. Associate technology is most effectively applied when mapped into management of the human-machine interface and display-control loop in typical manned systems. This paper addresses the potential for application of associate technology into the arena of intelligent command and control of satellite systems, from diagnosis of onboard and onground of satellite systems fault conditions, to execution of nominal satellite control functions. Rather than specifying a specific solution, this paper draws parallels between the Pilot's Associate concept and the domain of satellite control. Author

N93-11923*# Jet Propulsion Lab., California Inst. of Tech., Pasadena.
A MODEL-BASED REASONING APPROACH TO SENSOR PLACEMENT FOR MONITORABILITY c65
Steve Chien, Richard Doyle, and Luiz HomemdeMello *In* NASA. Lyndon B. Johnson Space Center, Fifth Annual Workshop on Space Operations Applications and Research (SOAR 1991), Volume 1 Jan. 1992 p 9-18 Sponsored by NASA, Washington (For primary document see N93-11921 02-59)
Avail: CASI HC A02/MF A04

An approach is presented to evaluating sensor placements to maximize monitorability of the target system while minimizing the number of sensors. The approach uses a model of the monitored system to score potential sensor placements on the basis of four monitorability criteria. The scores can then be analyzed to produce a recommended sensor set. An example from our NASA application domain is used to illustrate our model-based approach to sensor placement. Author

N93-11924*# McDonnell-Douglas Space Systems Co., Huntington Beach, CA. Space Station Div.
DISTRIBUTED ENVIRONMENTAL CONTROL **c54**
Gary A. Cleveland *In* NASA. Lyndon B. Johnson Space Center, Fifth Annual Workshop on Space Operations Applications and Research (SOAR 1991), Volume 1 Jan. 1992 p 19-26 (For primary document see N93-11921 02-59)
Avail: CASI HC A02/MF A04

We present an architecture of distributed, independent control agents designed to work with the Computer Aided System Engineering and Analysis (CASE/A) simulation tool. CASE/A simulates behavior of Environmental Control and Life Support Systems (ECLSS). We describe a lattice of agents capable of distributed sensing and overcoming certain sensor and effector failures. We address how the architecture can achieve the coordinating functions of a hierarchical command structure while maintaining the robustness and flexibility of independent agents. These agents work between the time steps of the CASE/A simulation tool to arrive at command decisions based on the state variables maintained by CASE/A. Control is evaluated according to both effectiveness (e.g., how well temperature was maintained) and resource utilization (the amount of power and materials used). Author

N93-11925*# Honeywell, Inc., Minneapolis, MN. Systems and Research Center.
A STATE-BASED APPROACH TO TREND RECOGNITION AND FAILURE PREDICTION FOR THE SPACE STATION FREEDOM **c18**
Kyle S. Nelson and George D. Hadden *In* NASA. Lyndon B. Johnson Space Center, Fifth Annual Workshop on Space Operations Applications and Research (SOAR 1991), Volume 1 Jan. 1992 p 27-32 (For primary document see N93-11921 02-59)
Avail: CASI HC A02/MF A04

A state-based reasoning approach to trend recognition and failure prediction for the Altitude Determination, and Control System (ADCS) of the Space Station Freedom (SSF) is described. The problem domain is characterized by features (e.g., trends and impending failures) that develop over a variety of time spans, anywhere from several minutes to several years. Our state-based reasoning approach, coupled with intelligent data screening, allows features to be tracked as they develop in a time-dependent manner. That is, each state machine has the ability to encode a time frame for the feature it detects. As features are detected, they are recorded and can be used as input to other state machines, creating a hierarchical feature recognition scheme. Furthermore, each machine can operate independently of the others, allowing simultaneous tracking of features. State-based reasoning was implemented in the trend recognition and the prognostic modules of a prototype Space Station Freedom Maintenance and Diagnostic System (SSFMDS) developed at Honeywell's Systems and Research Center. Author

N93-11926*# Aerospace Corp., Albuquerque, NM.
REQUIREMENTS AND OPPORTUNITIES FOR SATELLITE AUTONOMY Abstract Only **c18**
W. Spencer Campbell and Chris Gdanski (Phillips Lab., Kirtland AFB, NM.) *In* NASA. Lyndon B. Johnson Space Center, Fifth Annual Workshop on Space Operations Applications and Research (SOAR 1991), Volume 1 Jan. 1992 p 33 (For primary document see N93-11921 02-59)
Avail: CASI HC A01/MF A04

The requirements for autonomous control of spacecraft functions have been well articulated by a wide selection of US Air Force mission analyses and architecture studies. The opportunities however, to implement these autonomy functions have been limited. An overview of documented requirements is presented to demonstrate the scope of autonomous functions needed, and potential time frames for implementation is derived. The missed opportunities are analyzed to provide lessons learned, and near term opportunities will be reviewed. The current initiatives at the Phillips Laboratory are described in terms of the requirements addressed and the proposed approaches will show program risk reduction for satellite autonomy technology insertion into space operations. Author

N93-11927*# National Aeronautics and Space Administration. Goddard Space Flight Center, Greenbelt, MD.
AN EXPERT SYSTEM FOR DIAGNOSING ENVIRONMENTALLY INDUCED SPACECRAFT ANOMALIES **c18**
Mark Rolincik (University Research Foundation, Greenbelt, MD.), Michael Lauriente, Harry C. Koons (Aerospace Corp., Los Angeles, CA.), and David Gorney (Aerospace Corp., Los Angeles, CA.) *In* NASA. Lyndon B. Johnson Space Center, Fifth Annual Workshop on Space Operations Applications and Research (SOAR 1991), Volume 1 Jan. 1992 p 36-44 Sponsored by NASA, Washington and AFGL (For primary document see N93-11921 02-59)
(Contract F04701-88-C-0089)
Avail: CASI HC A02/MF A04

A new rule-based, machine independent analytical tool was designed for diagnosing spacecraft anomalies using an expert system. Expert systems provide an effective method for saving knowledge, allow computers to sift through large amounts of data pinpointing significant parts, and most importantly, use heuristics in addition to algorithms, which allow approximate reasoning and inference and the ability to attack problems not rigidly defined. The knowledge base consists of over two-hundred (200) rules and provides links to historical and environmental databases. The environmental causes considered are bulk charging, single event upsets (SEU), surface charging, and total radiation dose. The system's driver translates forward chaining rules into a backward chaining sequence, prompting the user for information pertinent to the causes considered. The use of heuristics frees the user from searching through large amounts of irrelevant information and allows the user to input partial information (varying degrees of confidence in an answer) or 'unknown' to any question. The modularity of the expert system allows for easy updates and modifications. It not only provides scientists with needed risk analysis and confidence not found in algorithmic programs, but is also an effective learning tool, and the window implementation makes it very easy to use. The system currently runs on a Micro VAX II at Goddard Space Flight Center (GSFC). The inference engine used is NASA's C Language Integrated Production System (CLIPS). Author

N93-11928*# National Aeronautics and Space Administration. Lewis Research Center, Cleveland, OH.
AN EMBEDDED RULE-BASED DIAGNOSTIC EXPERT SYSTEM IN Ada **c61**
Robert E. Jones and Eugene M. Liberman (Sverdrup Technology, Inc., Brook Park, OH.) *In* NASA. Lyndon B. Johnson Space Center, Fifth Annual Workshop on Space Operations Applications and Research (SOAR 1991), Volume 1 Jan. 1992 p 45-51 (For primary document see N93-11921 02-59)
Avail: CASI HC A02/MF A04

Ada is becoming an increasingly popular programming language for large Government-funded software projects. Ada with it portability, transportability, and maintainability lends itself well to today's complex programming environment. In addition, expert systems have also assumed a growing role in providing human-like reasoning capability expertise for computer systems. The integration is discussed of expert system technology with Ada programming language, especially a rule-based expert system using an ART-Ada (Automated Reasoning Tool for Ada) system shell. NASA Lewis was chosen as a beta test site for ART-Ada. The test was conducted by implementing the existing Autonomous Power EXpert System (APEX), a Lisp-based power expert system, in ART-Ada. Three components, the rule-based expert systems, a graphics user interface, and communications software make up SMART-Ada (Systems fault Management with ART-Ada). The rules were written in the ART-Ada development environment and converted to Ada source code. The graphics interface was developed with the Transportable Application Environment (TAE) Plus, which generates Ada source code to control graphics images. SMART-Ada communicates with a remote host to obtain either simulated or real data. The Ada source code generated with ART-Ada, TAE Plus, and communications code was incorporated into an Ada expert system that reads the data from a power distribution test bed, applies the rule to determine a fault, if one exists, and graphically displays it on the screen. The main objective, to conduct a beta test on the ART-Ada rule-based expert system shell, was achieved. The system is operational. New Ada tools will assist in future successful projects. ART-Ada is one such tool and is a viable alternative to the straight Ada code when an application requires a rule-based or knowledge-based approach. Author

N93-11929*# UFA, Inc., Newton, MA.
INTEGRATION OF TASK LEVEL PLANNING AND DIAGNOSIS FOR AN INTELLIGENT ROBOT **c63**
Amy W. Chan *In* NASA. Lyndon B. Johnson Space Center, Fifth Annual Workshop on Space Operations Applications and Research (SOAR 1991), Volume 1 Jan. 1992 p 52-59 (For primary document see N93-11921 02-59)
(Contract NAS8-38420)
Avail: CASI HC A02/MF A04

A satellite floating space is diagnosed with a telerobot attached performing maintenance or replacement tasks. This research included three objectives. The first objective was to generate intelligent path planning for a robot to move around a satellite. The second objective was to diagnose possible faulty scenarios in the satellite. The third objective included two tasks. The first task was to combine intelligent path planning with diagnosis. The second task was to build an interface between the combined intelligent system with Robosim. The ability of a robot to deal with unexpected scenarios is particularly important in space since the situation could be different from time to time so that the telerobot must be capable of detecting that the situation has changed and the necessity may exist to alter its behavior based on the new situation. The feature of allowing human-in-the-loop is also very important in space. In some extreme cases, the situation is beyond the capability of a robot so our research project allows the human to override the decision of a robot. Author

N93-11930*# McDonnell-Douglas Space Systems Co., Houston, TX. Space Station Div.
INTELLIGENT FAULT MANAGEMENT FOR THE SPACE STATION ACTIVE THERMAL CONTROL SYSTEM **c54**
Tim Hill and Robert M. Faltisco *In* NASA. Lyndon B. Johnson Space Center, Fifth Annual Workshop on Space Operations Applications and Research (SOAR 1991), Volume 1 Jan. 1992 p 60-66 (For primary document see N93-11921 02-59)
Avail: CASI HC A02/MF A04

The Thermal Advanced Automation Project (TAAP) approach and architecture is described for automating the Space Station Freedom (SSF) Active Thermal Control System (ATCS). The baseline functionally and advanced automation techniques for Fault Detection, Isolation, and Recovery (FDIR) will be compared and contrasted. Advanced automation techniques such as rule-based systems and model-based reasoning should be utilized to efficiently control, monitor, and diagnose this extremely complex physical system. TAAP is developing advanced FDIR software for use on the SSF thermal control system. The goal of TAAP is to join Knowledge-Based System (KBS) technology, using a combination of rules and model-based reasoning, with conventional monitoring and control software in order to maximize autonomy of the ATCS. TAAP's predecessor was NASA's Thermal Expert System (TEXSYS) project which was the first large real-time expert system to use both extensive rules and model-based reasoning to control and perform FDIR on a large, complex physical system. TEXSYS showed that a method is needed for safely and inexpensively testing all possible faults of the ATCS, particularly those potentially damaging to the hardware, in order to develop a fully capable FDIR system. TAAP therefore includes the development of a high-fidelity simulation of the thermal control system. The simulation provides realistic, dynamic ATCS behavior and fault insertion capability for software testing without hardware related risks or expense. In addition, thermal engineers will gain greater confidence in the KBS FDIR software than was possible prior to this kind of simulation testing. The TAAP KBS will initially be a ground-based extension of the baseline ATCS monitoring and control software and could be migrated on-board as additional computation resources are made available. Author

N93-11931*# Systems Control Technology, Inc., Palo Alto, CA.
INTELLIGENT DIAGNOSTICS SYSTEMS Abstract Only **c63**
Barbara M. McQuiston and Ronald L. DeHoff *In* NASA. Lyndon B. Johnson Space Center, Fifth Annual Workshop on Space Operations Applications and Research (SOAR 1991), Volume 1 Jan. 1992 p 67 (For primary document see N93-11921 02-59)
Avail: CASI HC A01/MF A04

Intelligent systems have been applied to today's problems and could also be applied to space operations integrity. One of these systems is the XMAN tool designed for 'troubleshooting' jet engines. XMAN is the eXpert MAiNtenance tool developed to be an expert information analysis tool which stores trending and diagnostic data on Air Force engines. XMAN operates with a 'network topology' which follows a flow chart containing engine management information reports required by the governments technical order procedures. With XMAN technology, the user is able to identify engine problems by presenting the assertions of the fault isolation logic and attempting to satisfy individual assertions by referring to the databases created by an engine monitoring system. The troubleshooting process requires interaction between the technician and the computer to acquire new evidence form auxiliary maintenance tests corroboration of analytical results to accurately diagnose equipment malfunctions. This same technology will be required for systems which are functioning in space either with an onboard crew, or with an unmanned system. The technology and lessons learned developing this technology while suggesting definite applications for its use with developing space systems are addressed. Author

N93-11932*# Interface and Control Systems, West Melbourne, FL.
SPACECRAFT ATTITUDE CONTROL USING A SMART CONTROL SYSTEM **c18**
Brian Buckley and Louis Wheatcraft (Barrios Technology, Inc., Houston, TX.) *In* NASA. Lyndon B. Johnson Space Center, Fifth Annual Workshop on Space Operations Applications and Research (SOAR 1991), Volume 1 Jan. 1992 p 70-79 (For primary document see N93-11921 02-59)
Avail: CASI HC A02/MF A04

Traditionally, spacecraft attitude control has been implemented using control loops written in native code for a space hardened processor. The Naval Research Lab has taken this approach during the development of the Attitude Control Electronics (ACE) package. After the system was developed and delivered, NRL decided to explore alternate technologies to accomplish this same task more efficiently. The approach taken by NRL was to implement the ACE control loops using systems technologies. The purpose of this effort was to: (1) research capabilities required of an expert system in processing a classic closed-loop control algorithm; (2) research the development environment required to design and test an embedded expert systems environment; (3) research the complexity of design and development of expert systems versus a conventional approach; and (4) test the resulting systems against the flight acceptance test software for both response and accuracy. Two expert systems were selected to implement the control loops. Criteria used for the selection of the expert systems included that they had to run in both embedded systems and ground based environments. Using two different expert systems allowed a comparison of the real-time capabilities, inferencing capabilities, and the ground-based development environment. The two expert systems chosen for the evaluation were Spacecraft Command Language (SCL), and NEXTPERT Object. SCL is a smart control system produced for the NRL by Interface and Control Systems (ICS). SCL was developed to be used for real-time command, control, and monitoring of a new generation of spacecraft. NEXPERT Object is a commercially available product developed by Neuron Data. Results of the effort were evaluated using the ACE test bed. The ACE test bed had been developed and used to test the original flight hardware and software using simulators and flight-like interfaces. The test bed was used for testing the expert systems in a 'near-flight' environment. The technical approach, the system architecture, the development environments, knowledge base development, and results of this effort are detailed. Author

N93-11933*# Space Industries, Inc., Webster, TX.
DESIGN DEVELOPMENT OF A NEURAL NETWORK-BASED TELEMETRY MONITOR **c63**
Michael F. Lembeck *In* NASA. Lyndon B. Johnson Space Center, Fifth Annual Workshop on Space Operations Applications and Research (SOAR 1991), Volume 1 Jan. 1992 p 80-86 (For primary document see N93-11921 02-59)
Avail: CASI HC A02/MF A04

This paper identifies the requirements and describes an architectural framework for an artificial neural network-based system that is capable of fulfilling monitoring and control requirements of future aerospace missions. Incorporated into this framework are a newly developed training algorithm and the concept of cooperative network architectures. The feasibility of such an approach is demonstrated for its ability to identify faults in low frequency waveforms. Author

N93-11934*# McDonnell-Douglas Space Systems Co., Houston, TX.
FUZZY CONTROL SYSTEM FOR A REMOTE FOCUSING MICROSCOPE **c35**
Jonathan J. Weiss and Luc P. Tran *In* NASA. Lyndon B. Johnson Space Center, Fifth Annual Workshop on Space Operations Applications and Research (SOAR 1991), Volume 1 Jan. 1992 p 87-93 (For primary document see N93-11921 02-59)
Avail: CASI HC A02/MF A04

Space Station Crew Health Care System procedures require the use of an on-board microscope whose slide images will be transmitted for analysis by ground-based microbiologists. Focusing of microscope slides is low on the list of crew priorities, so NASA is investigating the option of telerobotic focusing controlled by the microbiologist on the ground, using continuous video feedback. However, even at Space Station distances, the transmission time lag may disrupt the focusing process, severely limiting the number of slides that can be analyzed within a given bandwidth allocation. Substantial time could be saved if on-board automation could pre-focus each slide before transmission. The authors demonstrate the feasibility of on-board automatic focusing using a fuzzy logic ruled-based system to bring the slide image into focus. The original prototype system was produced in under two months and at low cost. Slide images are captured by a video camera, then digitized by gray-scale value. A software function calculates an index of 'sharpness' based on gray-scale contrasts. The fuzzy logic rule-based system uses feedback to set the microscope's focusing control in an attempt to maximize sharpness. The systems as currently implemented performs satisfactorily in focusing a variety of slide types at magnification levels ranging from 10 to 1000x. Although feasibility has been demonstrated, the system's performance and usability could be improved substantially in four ways: by upgrading the quality and resolution of the video imaging system (including the use of full color); by empirically defining and calibrating the index of image sharpness; by letting the overall focusing strategy vary depending on user-specified parameters; and by fine-tuning the fuzzy rules, set definitions, and procedures used. Author

N93-11935*# National Aeronautics and Space Administration. Lyndon B. Johnson Space Center, Houston, TX.
FUZZY LOGIC CONTROL FOR CAMERA TRACKING SYSTEM **c35**
Robert N. Lea, R. H. Fritz (Link Flight Simulation Corp., Binghamton, NY.), J. Giarratano (Houston Univ., TX.), and Yashvant Jani (LinCom Corp., Houston, TX.) *In its* Fifth Annual Workshop on Space Operations Applications and Research (SOAR 1991), Volume 1 Jan. 1992 p 94-99 (For primary document see N93-11921 02-59)
Avail: CASI HC A02/MF A04

A concept utilizing fuzzy theory has been developed for a camera tracking system to provide support for proximity operations and traffic management around the Space Station Freedom. Fuzzy sets and fuzzy logic based reasoning are used in a control system which utilizes images from a camera and generates required pan and tilt commands to track and maintain a moving target in the camera's field of view. This control system can be implemented on a fuzzy chip to provide an intelligent sensor for autonomous operations. Capabilities of the control system can be expanded to include approach, handover to other sensors, caution and warning messages. Author

N93-11936*# Jet Propulsion Lab., California Inst. of Tech., Pasadena.
INTELLIGENT DATA MANAGEMENT FOR REAL-TIME SPACECRAFT MONITORING **c63**
Ursula M. Schwuttke, Les Gasser (University of Southern California, Los Angeles.), and Bruce Abramson (University of Southern California, Los Angeles.) *In* NASA. Lyndon B. Johnson Space Center, Fifth Annual Workshop on Space Operations Applications and Research (SOAR 1991), Volume 1 Jan. 1992 p 100-106 Sponsored by NASA, Washington (For primary document see N93-11921 02-59)
Avail: CASI HC A02/MF A04

Real-time AI systems have begun to address the challenge of restructuring problem solving to meet real-time constraints by making key trade-offs that pursue less than optimal strategies with minimal impact on system goals. Several approaches for adapting to dynamic changes in system operating conditions are known. However, simultaneously adapting system decision criteria in a principled way has been difficult. Towards this end, a general technique for dynamically making such trade-offs using a combination of decision theory and domain knowledge has been developed. Multi-attribute utility theory (MAUT), a decision theoretic approach for making one-time decisions is discussed and dynamic trade-off evaluation is described as a knowledge-based extension of MAUT that is suitable for highly dynamic real-time environments, and provides an example of dynamic trade-off evaluation applied to a specific data management trade-off in a real-world spacecraft monitoring application. Author

N93-11937*# National Aeronautics and Space Administration. Lyndon B. Johnson Space Center, Houston, TX.
ON THE ACQUISITION AND REPRESENTATION OF PROCEDURAL KNOWLEDGE **c61**
T. Saito (Computer Sciences Corp., Houston, TX.), C. Ortiz, and R. B. Loftin (Houston Univ., TX.) *In its* Fifth Annual Workshop on Space Operations Applications and Research (SOAR 1991), Volume 1 Jan. 1992 p 108-117 (For primary document see N93-11921 02-59)
Avail: CASI HC A02/MF A04

Historically knowledge acquisition has proven to be one of the greatest barriers to the development of intelligent systems. Current practice generally requires lengthy interactions between the expert whose knowledge is to be captured and the knowledge engineer whose responsibility is to acquire and represent knowledge in a useful form. Although much research has been devoted to the development of methodologies and computer software to aid in the capture and representation of some of some types of knowledge, little attention has been devoted to procedural knowledge. NASA personnel frequently perform tasks that are primarily procedural in nature. Previous work is reviewed in the field of knowledge acquisition and then focus on knowledge acquisition for procedural tasks with special attention devoted to the Navy's VISTA tool. The design and development is described of a system for the acquisition and representation of procedural knowledge-TARGET (Task Analysis and Rule Generation Tool). TARGET is intended as a tool that permits experts to visually describe procedural tasks and as a common medium for knowledge refinement by the expert and knowledge engineer. The system is designed to represent the acquired knowledge in the form of production rules. Systems such as TARGET have the potential to profoundly reduce the time, difficulties, and costs of developing knowledge-based systems for the performance of procedural tasks. Author

N93-11938*# Astronautics Corp. of America, Milwaukee, WI.
A METHODOLOGY TO EMULATE AND EVALUATE A PRODUCTIVE VIRTUAL WORKSTATION Abstract Only c61
David Krubsack and David Haberman *In* NASA. Lyndon B. Johnson Space Center, Fifth Annual Workshop on Space Operations Applications and Research (SOAR 1991), Volume 1 Jan. 1992 p 118 Prepared in cooperation with Marquette Univ., Milwaukee, WI (For primary document see N93-11921 02-59)
Avail: CASI HC A01/MF A04

The Advanced Display and Computer Augmented Control (ADCACS) Program at ACT is sponsored by NASA Ames to investigate the broad field of technologies which must be combined to design a 'virtual' workstation for the Space Station Freedom. This program is progressing in several areas and resulted in the definition of requirements for a workstation. A unique combination of technologies at the ACT Laboratory have been networked to effectively create an experimental environment. This experimental environment allows the integration of nonconventional input devices with a high power graphics engine within the framework of an expert system shell which coordinates the heterogeneous inputs with the 'virtual' presentation. The flexibility of the workstation is evolved as experiments are designed and conducted to evaluate the condition descriptions and rule sets of the expert system shell and its effectiveness in driving the graphics engine. Workstation productivity has been defined by the achievable performance in the emulator of the calibrated 'sensitivity' of input devices, the graphics presentation, the possible optical enhancements to achieve a wide field of view color image and the flexibility of conditional descriptions in the expert system shell in adapting to prototype problems. Author

N93-11939*# Jet Propulsion Lab., California Inst. of Tech., Pasadena.
OPERATOR ASSISTANT TO SUPPORT DEEP SPACE NETWORK LINK MONITOR AND CONTROL c32
Lynne P. Cooper, Rajiv Desai, and Elmain Martinez *In* NASA. Lyndon B. Johnson Space Center, Fifth Annual Workshop on Space Operations Applications and Research (SOAR 1991), Volume 1 Jan. 1992 p 122-128 Sponsored by NASA, Washington (For primary document see N93-11921 02-59)
Avail: CASI HC A02/MF A04

Preparing the Deep Space Network (DSN) stations to support spacecraft missions (referred to as pre-cal, for pre-calibration) is currently an operator and time intensive activity. Operators are responsible for sending and monitoring several hundred operator directivities, messages, and warnings. Operator directives are used to configure and calibrate the various subsystems (antenna, receiver, etc.) necessary to establish a spacecraft link. Messages and warnings are issued by the subsystems upon completion of an operation, changes of status, or an anomalous condition. Some points of pre-cal are logically parallel. Significant time savings could be realized if the existing Link Monitor and Control system (LMC) could support the operator in exploiting the parallelism inherent in pre-cal activities. Currently, operators may work on the individual subsystems in parallel, however, the burden of monitoring these parallel operations resides solely with the operator. Messages, warnings, and directives are all presented as they are received; without being correlated to the event that triggered them. Pre-cal is essentially an overhead activity. During pre-cal, no mission is supported, and no other activity can be performed using the equipment in the link. Therefore, it is highly desirable to reduce pre-cal time as much as possible. One approach to do this, as well as to increase efficiency and reduce errors, is the LMC Operator Assistant (OA). The LMC OA prototype demonstrates an architecture which can be used in concert with the existing LMC to exploit parallelism in pre-cal operations while providing the operators with a true monitoring capability, situational awareness and positive control. This paper presents an overview of the LMC OA architecture and the results from initial prototyping and test activities. Author

N93-11940*# National Aeronautics and Space Administration. Lewis Research Center, Cleveland, OH.
SPACE COMMUNICATION ARTIFICIAL INTELLIGENCE FOR LINK EVALUATION TERMINAL (SCAILET) c63
Anoosh K. Shahidi (Sverdrup Technology, Inc., Brook Park, OH.), Richard F. Schlegelmilch (Akron Univ., OH.), Edward J. Petrik, and Jerry L. Walters *In* NASA. Lyndon B. Johnson Space Center, Fifth Annual Workshop on Space Operations Applications and Research (SOAR 1991), Volume 1 Jan. 1992 p 130-132 (For primary document see N93-11921 02-59)
Avail: CASI HC A01/MF A04

A software application to assist end-users of the high burst rate (HBR) link evaluation terminal (LET) for satellite communications is being developed. The HBR LET system developed at NASA Lewis Research Center is an element of the Advanced Communications Technology Satellite (ACTS) Project. The HBR LET is divided into seven major subsystems, each with its own expert. Programming scripts, test procedures defined by design engineers, set up the HBR LET system. These programming scripts are cryptic, hard to maintain and require a steep learning curve. These scripts were developed by the system engineers who will not be available for the end-users of the system. To increase end-user productivity a friendly interface needs to be added to the system. One possible solution is to provide the user with adequate documentation to perform the needed tasks. With the complexity of this system the vast amount of documentation needed would be overwhelming and the information would be hard to retrieve. With limited resources, maintenance is another reason for not using this form of documentation. An advanced form of interaction is being explored using current computer techniques. This application, which incorporates a combination of multimedia and artificial intelligence (AI) techniques to provided end-users with an intelligent interface to the HBR LET system, is comprised of an intelligent assistant, intelligent tutoring, and hypermedia documentation. The intelligent assistant and tutoring systems address the critical programming needs of the end-user. Author

N93-11941*# Aerospace Corp., Los Angeles, CA.
ADVANCED SATELLITE WORKSTATION: AN INTEGRATED WORKSTATION ENVIRONMENT FOR OPERATIONAL SUPPORT OF SATELLITE SYSTEM PLANNING AND ANALYSIS c54
Stewart A. Sutton *In* NASA. Lyndon B. Johnson Space Center, Fifth Annual Workshop on Space Operations Applications and Research (SOAR 1991), Volume 1 Jan. 1992 p 133-141 (For primary document see N93-11921 02-59)
Avail: CASI HC A02/MF A04

A prototype integrated environment, the Advanced Satellite Workstation (ASW), is described that has been developed and delivered for evaluation and operator feedback in an operational satellite control center. The current ASW hardware consists of a Sun Workstation and Macintosh II Workstation connected via an ethernet Network Hardware and Software, Laser Disk System, Optical Storage System, and Telemetry Data File Interface. The central mission of ASW is to provide an intelligent decision support and training environment for operator/analysts of complex systems such as satellites. There have been many workstation implementations recently which incorporate graphical telemetry displays and expert systems. ASW is a considerably broader look at intelligent, integrated environments for decision support, based upon the premise that the central features of such an environment are intelligent data access and integrated toolsets. A variety of tools have been constructed in support of this prototype environment including: an automated pass planner for scheduling vehicle support activities, architectural modeler for hierarchical simulation and analysis of satellite vehicle subsystems, multimedia-based information systems that provide an intuitive and easily accessible interface to Orbit Operations Handbook and other relevant support documentation, and a data analysis architecture that integrates user modifiable telemetry display systems, expert systems for background data analysis, and interfaces to the multimedia system via inter-process communication. Author

N93-11942*# Loral Space and Range Systems, Sunnyvale, CA. Artificial Intelligence Group.

MISSION CONTROL CENTER ENHANCEMENT OPPORTUNITIES IN THE 1990'S **c81**

Wayne Hartman *In* NASA. Lyndon B. Johnson Space Center, Fifth Annual Workshop on Space Operations Applications and Research (SOAR 1991), Volume 1 Jan. 1992 p 142-149 (For primary document see N93-11921 02-59)

Avail: CASI HC A02/MF A04

The purpose of this paper is to present a framework for understanding the major enhancement opportunities for Air Force Mission Control Center/Test Support Centers (MCC's/TSC's) in the 1990's. Much of this paper is based on the findings of Study 232 and work currently underway in Study 2-6 for the Air Force Systems Command, Space System Division, Network Program Office. In this paper, we will address MCC/TSC enhancement needs primarily from the operator perspective, in terms of the increased capabilities required to improve space operations task performance. Author

N93-11943*# National Aeronautics and Space Administration. Lyndon B. Johnson Space Center, Houston, TX.

THE DEVELOPMENT AND TECHNOLOGY TRANSFER OF SOFTWARE ENGINEERING TECHNOLOGY AT NASA. JOHNSON SPACE CENTER **c61**

C. L. Pitman, D. M. Erb (Mitre Corp., Houston, TX.), M. E. Izygon (National Academy of Sciences - National Research Council, Houston, TX.), E. M. Fridge, III, G. B. Roush, D. M. Braley, and R. T. Savely *In its* Fifth Annual Workshop on Space Operations Applications and Research (SOAR 1991), Volume 1 Jan. 1992 p 152-162 Sponsored in part by NAC-NRC (For primary document see N93-11921 02-59)

Avail: CASI HC A03/MF A04

The United State's big space projects of the next decades, such as Space Station and the Human Exploration Initiative, will need the development of many millions of lines of mission critical software. NASA-Johnson (JSC) is identifying and developing some of the Computer Aided Software Engineering (CASE) technology that NASA will need to build these future software systems. The goal is to improve the quality and the productivity of large software development projects. New trends are outlined in CASE technology and how the Software Technology Branch (STB) at JSC is endeavoring to provide some of these CASE solutions for NASA is described. Key software technology components include knowledge-based systems, software reusability, user interface technology, reengineering environments, management systems for the software development process, software cost models, repository technology, and open, integrated CASE environment frameworks. The paper presents the status and long-term expectations for CASE products. The STB's Reengineering Application Project (REAP), Advanced Software Development Workstation (ASDW) project, and software development cost model (COSTMODL) project are then discussed. Some of the general difficulties of technology transfer are introduced, and a process developed by STB for CASE technology insertion is described. Author

N93-11944*# National Aeronautics and Space Administration. Lyndon B. Johnson Space Center, Houston, TX.

SYSTEM DIAGNOSTIC BUILDER **c61**

Joseph L. Nieten (GHG Corp., Houston, TX.) and Roger Burke *In its* Fifth Annual Workshop on Space Operations Applications and Research (SOAR 1991), Volume 1 Jan. 1992 p 163-167 (For primary document see N93-11921 02-59)

Avail: CASI HC A01/MF A04

The System Diagnostic Builder (SDB) is an automated software verification and validation tool using state-of-the-art Artificial Intelligence (AI) technologies. The SDB is used extensively by project BURKE at NASA-JSC as one component of a software re-engineering toolkit. The SDB is applicable to any government or commercial organization which performs verification and validation tasks. The SDB has an X-window interface, which allows the user to 'train' a set of rules for use in a rule-based evaluator. The interface has a window that allows the user to plot up to five data parameters (attributes) at a time. Using these plots and a mouse, the user can identify and classify a particular behavior of the subject software. Once the user has identified the general behavior patterns of the software, he can train a set of rules to represent his knowledge of that behavior. The training process builds rules and fuzzy sets to use in the evaluator. The fuzzy sets classify those data points not clearly identified as a particular classification. Once an initial set of rules is trained, each additional data set given to the SDB will be used by a machine learning mechanism to refine the rules and fuzzy sets. This is a passive process and, therefore, it does not require any additional operator time. The evaluation component of the SDB can be used to validate a single software system using some number of different data sets, such as a simulator. Moreover, it can be used to validate software systems which have been re-engineered from one language and design methodology to a totally new implementation. Author

N93-11945*# National Aeronautics and Space Administration. Lyndon B. Johnson Space Center, Houston, TX.

KNOWLEDGE-BASED SYSTEM V AND V IN THE SPACE STATION FREEDOM PROGRAM **c61**

Keith Kelley (IBM Federal Systems Div., Houston, TX.), David Hamilton (IBM Federal Systems Div., Houston, TX.), and Chris Culbert *In its* Fifth Annual Workshop on Space Operations Applications and Research (SOAR 1991), Volume 1 Jan. 1992 p 168-173 (For primary document see N93-11921 02-59)

Avail: CASI HC A02/MF A04

Knowledge Based Systems (KBS's) are expected to be heavily used in the Space Station Freedom Program (SSFP). Although SSFP Verification and Validation (V&V) requirements are based on the latest state-of-the-practice in software engineering technology, they may be insufficient for Knowledge Based Systems (KBS's); it is widely stated that there are differences in both approach and execution between KBS V&V and conventional software V&V. In order to better understand this issue, we have surveyed and/or interviewed developers from sixty expert system projects in order to understand the differences and difficulties in KBS V&V. We have used this survey results to analyze the SSFP V&V requirements for conventional software in order to determine which specific requirements are inappropriate for KBS V&V and why they are inappropriate. Further work will result in a set of recommendations that can be used either as guidelines for applying conventional software V&V requirements to KBS's or as modifications to extend the existing SSFP conventional software V&V requirements to include KBS requirements. The results of this work are significant to many projects, in addition to SSFP, which will involve KBS's. Author

N93-11946*# Aerospace Corp., El Segundo, CA. Computer Science and Technology Subdivision.

AN APPROACH TO INTEGRATING AND CREATING FLEXIBLE SOFTWARE ENVIRONMENTS **c61**

Kirstie L. Bellman *In* NASA. Lyndon B. Johnson Space Center, Fifth Annual Workshop on Space Operations Applications and Research (SOAR 1991), Volume 1 Jan. 1992 p 174-177 (For primary document see N93-11921 02-59)

Avail: CASI HC A01/MF A04

Engineers and scientists are attempting to represent, analyze, and reason about increasingly complex systems. Many researchers have been developing new ways of creating increasingly open environments. In this research on VEHICLES, a conceptual design environment for space systems, an approach was developed, called 'wrapping', to flexibility and integration based on the collection and then processing of explicit qualitative descriptions of all the software resources in the environment. Currently, a simulation is available, VSIM, used to study both the types of wrapping descriptions and the processes necessary to use the metaknowledge to combine, select, adapt, and explain some of the software resources used in VEHICLES. What was learned about the types of knowledge necessary for the wrapping approach is described along with the implications of wrapping for several key software engineering issues. E.R.

N93-11947*# Air Force Inst. of Tech., Wright-Patterson AFB, OH.

DESIGN OF AN Ada EXPERT SYSTEM SHELL FOR THE VHSIC AVIONIC MODULAR FLIGHT PROCESSOR Abstract Only **c61**

F. Jesse Fanning *In* NASA. Lyndon B. Johnson Space Center, Fifth Annual Workshop on Space Operations Applications and Research (SOAR 1991), Volume 1 Jan. 1992 p 178 (For primary document see N93-11921 02-59)

Avail: CASI HC A01/MF A04

The Embedded Computer System Expert System Shell (ES Shell) is an Ada-based expert system shell developed at the Avionics Laboratory for use on the VHSIC Avionic Modular Processor (VAMP) running under the Ada Avionics Real-Time Software (AARTS) Operating System. The ES Shell provides the interface between the expert system and the avionics environment, and controls execution of the expert system. Testing of the ES Shell in the Avionics Laboratory's Integrated Test Bed (ITB) has demonstrated its ability to control a non-deterministic software application executing on the VAMP's which can control the ITB's real-time closed-loop aircraft simulation. The results of these tests and the conclusions reached in the design and development of the ES Shell have played an important role in the formulation of the requirements for a production-quality expert system inference engine, an ingredient necessary for the successful use of expert systems on the VAMP embedded avionic flight processor. Author

N93-11948*# Sverdrup Technology, Inc., Brook Park, OH.

AUTONOMOUS POWER SYSTEM: INTEGRATED SCHEDULING **c20**

Mark J. Ringer *In* NASA. Lyndon B. Johnson Space Center, Fifth Annual Workshop on Space Operations Applications and Research (SOAR 1991), Volume 1 Jan. 1992 p 180-188 (For primary document see N93-11921 02-59)

(Contract NAS3-25266)

Avail: CASI HC A02/MF A04

The Autonomous Power System (APS) project at NASA Lewis Research Center is designed to demonstrate the abilities of integrated intelligent diagnosis, control and scheduling techniques to space power distribution hardware. The project consists of three elements: the Autonomous Power Expert System (APEX) for fault diagnosis, isolation, and recovery (FDIR), the Autonomous Intelligent Power Scheduler (AIPS) to determine system configuration, and power hardware (Brassboard) to simulate a space-based power system. Faults can be introduced into the Brassboard and in turn, be diagnosed and corrected by APEX and AIPS. The Autonomous Intelligent Power Scheduler controls the execution of loads attached to the Brassboard. Each load must be executed in a manner that efficiently utilizes available power and satisfies all load, resource, and temporal constraints. In the case of a fault situation on the Brassboard, AIPS dynamically modifies the existing schedule in order to resume efficient operation conditions. A database is kept of the power demand, temporal modifiers, priority of each load, and the power level of each source. AIPS uses a set of heuristic rules to assign start times and resources to each load based on load and resource constraints. A simple improvement engine based upon these heuristics is also available to improve the schedule efficiency. This paper describes the operation of the Autonomous Intelligent Power Scheduler as a single entity, as well as its integration with APEX and the Brassboard. Future plans are discussed for the growth of the Autonomous Intelligent Power Scheduler. Author

N93-11949*# McDonnell-Douglas Space Systems Co., Houston, TX.

METHODOLOGIES FOR BUILDING ROBUST SCHEDULES **c61**

John H. Dean *In* NASA. Lyndon B. Johnson Space Center, Fifth Annual Workshop on Space Operations Applications and Research (SOAR 1991), Volume 1 Jan. 1992 p 189-193 (For primary document see N93-11921 02-59)

(Contract NAS9-17885)

Avail: CASI HC A01/MF A04

COMPASS is the name of a Computer Aided Scheduling System designed and built for NASA. COMPASS can be used to develop schedule of activities based upon the temporal relationships of the activities and their resource requirements. COMPASS uses this information, and guided by the user, develops precise start and stop times for the activities. In actual practice however, it is impossible to know with complete certainty what the actual durations of the scheduled activities will really be. The best that one can hope for is knowledge of the probability distribution for the durations. This paper investigates methodologies for using a scheduling tool like COMPASS that is based upon definite values for the resource requirements, while building schedules that remain valid in the face of the schedule execution perturbations. Representations for the schedules developed by these methodologies are presented, along with a discussion of the algorithm that could be used by a computer onboard a spacecraft to efficiently monitor and execute these schedules. Author

N93-11950*# National Aeronautics and Space Administration. Lyndon B. Johnson Space Center, Houston, TX.

COMPASS: AN Ada BASED SCHEDULER **c61**

Mary Beth McMahon (McDonnell-Douglas Space Systems Co., Houston, TX.) and Chris Culbert *In its* Fifth Annual Workshop on Space Operations Applications and Research (SOAR 1991), Volume 1 Jan. 1992 p 194-198 (For primary document see N93-11921 02-59)

(Contract NAS9-17885)

Avail: CASI HC A01/MF A04

COMPASS is a generic scheduling system developed by McDonnell Douglas and funded by the Software Technology Branch of NASA Johnson Space Center. The motivation behind COMPASS is to illustrate scheduling technology and provide a basis from which custom scheduling systems can be built. COMPASS was written in Ada to promote readability and to conform to DOD standards. COMPASS has some unique characteristics that distinguishes it from commercial products. This paper discusses these characteristics and uses them to illustrate some differences between scheduling tools. Author

N93-11951*# Aerospace Medical Research Labs., Wright-Patterson AFB, OH. Toxicology Div.

OCCUPATIONAL SAFETY CONSIDERATIONS WITH HYDRAZINE FUELS **c28**

H. J. Clewell, T. S. Haddad, M. E. George, J. N. McDougal, and M. E. Andersen *In* NASA. Lyndon B. Johnson Space Center, Fifth Annual Workshop on Space Operations Applications and Research (SOAR 1991), Volume 1 Jan. 1992 p 199-202 (For primary document see N93-11921 02-59)

Avail: CASI HC A01/MF A04

A simple pharmacokinetic model and a specially designed dermal vapor exposure chamber which provides respiratory protection were used to determine the rate of penetration of hydrazine and 1,1-dimethylhydrazine (UDMH) vapor through the skin of rats. Parameters for the pharmacokinetic model were determined from intravenous and inhalation exposure data. The model was then used to estimate the skin permeation coefficient for hydrazine or UDMH vapor from the dermal-vapor exposure

data. This analysis indicates that UDMH vapor has a relatively high permeability through skin (0.7 cm/hr), a value somewhat higher than was obtained for hydrazine by the same procedure (0.09 cm/hr). Based on these skin permeability results, a skin-only vapor exposure limit giving protection equivalent to the inhalation Threshold Limit Value (TLV) could be calculated. The current TLV's for UDMH and hydrazine are 0.5 and 0.1 ppm, respectively. The corresponding skin-only TLV equivalents, for personnel wearing respiratory protection, are 32 ppm for UDMH and 48 ppm for hydrazine. Should the proposed lowering to the TLV's for these compounds to 0.01 ppm be adopted, the equivalent skin-only TLV's would become 0.64 ppm for UDMH and 4.8 for hydrazine.
Author

N93-11952*# ISX Corp., Westlake Village, CA.
MANAGER'S ASSISTANT SYSTEMS FOR SPACE SYSTEM PLANNING Abstract Only **c61**
William L. Bewley, Robert Burnard, Gary E. Edwards, and James Shoop *In* NASA. Lyndon B. Johnson Space Center, Fifth Annual Workshop on Space Operations Applications and Research (SOAR 1991), Volume 1 Jan. 1992 p 203 (For primary document see N93-11921 02-59)
Avail: CASI HC A01/MF A04

This paper describes a class of knowledge-based 'assistant' systems for space system planning. Derived from technology produced for the DARPA/USAF Pilot's Associate program, these assistant systems help the human planner by doing the bookkeeping to maintain plan data and executing the procedures and heuristics currently used by the human planner to define, assess, diagnose, and revise plans. Intelligent systems for Space Station Freedom assembly sequence planning and Advanced Launch System modeling will be presented as examples. Ongoing NASA-funded work on a framework supporting the development of such tools will also be described. Author

N93-11953*# Planning Research Corp., El Segundo, CA.
REQUIREMENTS AND APPLICATIONS FOR ROBOTIC SERVICING OF MILITARY SPACE SYSTEMS **c18**
Otto C. Ledford, Jr. and Rodney G. Bennett (Air Force Space Div., El Segundo, CA.) *In* NASA. Lyndon B. Johnson Space Center, Fifth Annual Workshop on Space Operations Applications and Research (SOAR 1991), Volume 1 Jan. 1992 p 206-212 (For primary document see N93-11921 02-59)
Avail: CASI HC A02/MF A04

The utility of on-orbit servicing of spacecraft has been demonstrated by NASA several times using shuttle-based astronaut EVA. There has been interest in utilizing on-orbit servicing for military space systems as well. This interest has been driven by the increasing reliance of all branches of the military upon space-based assets, the growing numbers, complexity, and cost of those assets, and a desire to normalize support policies for space-based operations. Many military satellites are placed in orbits which are unduly hostile for astronaut operations and/or cannot be reached by the shuttle. In addition, some of the projected tasks may involve hazardous operations. This has led to a focus on robotic systems, instead of astronauts, for the basis of projected servicing systems. This paper describes studies and activities which will hopefully lead to on-orbit servicing being one of the tools available to military space systems designers and operators. The utility of various forms of servicing has been evaluated for present and projected systems, critical technologies have been identified, and strategies for the development and insertion of this technology into operational systems have been developed. Many of the projected plans have been adversely affected by budgetary restrictions and evolving architectures, but the fundamental benefits and requirements are well understood. A method of introducing servicing capabilities in a manner which has a low impact on the system designer and does not require the prior development of an expensive infrastructure is discussed. This can potentially lead to an evolutionary implementation of the full technology. Author

N93-11954*# National Aeronautics and Space Administration. Marshall Space Flight Center, Huntsville, AL.
AUTOGUIDANCE VIDEO SENSOR FOR DOCKING **c19**
Michael L. Book, Thomas C. Bryan, Richard T. Howard, and Richard W. Dabney *In* NASA. Lyndon B. Johnson Space Center, Fifth Annual Workshop on Space Operations Applications and Research (SOAR 1991), Volume 1 Jan. 1992 p 214-219 (For primary document see N93-11921 02-59)
Avail: CASI HC A02/MF A04

The Automated Rendezvous and Docking system (ARAD) is composed of two parts. The first part is the sensor which consists of a video camera ringed with two wavelengths of laser diode. The second part is a standard Remote Manipulator System (RMS) target used on the Orbiter that has been modified with three circular pieces of retro-reflective tape covered by optical filters which correspond to one of the wavelengths of laser diode. The sensor is on the chase vehicle and the target is on the target vehicle. The ARAD system works by pulsing one wavelength laser diodes and taking a picture. Then the second wavelength laser diodes are pulsed and a second picture is taken. One picture is subtracted from the other and the resultant picture is thresholded. All adjacent pixels above threshold are blobbed together (X and Y centroids calculated). All blob centroids are checked to recognize the target out of noise. Then the three target spots are windowed and tracked. The three target spot centroids are used to evaluate the roll, yaw, pitch, range, azimuth, and elevation. From that a guidance routine can guide the chase vehicle to dock with the target vehicle with the correct orientation. Author

N93-11955*# National Inst. of Standards and Technology, Gaithersburg, MD. Robot Systems Div.
MODEL-BASED VISION FOR SPACE APPLICATIONS **c61**
Karen Chaconas, Marilyn Nashman, and Ronald Lumia *In* NASA. Lyndon B. Johnson Space Center, Fifth Annual Workshop on Space Operations Applications and Research (SOAR 1991), Volume 1 Jan. 1992 p 220-229 (For primary document see N93-11921 02-59)
Avail: CASI HC A02/MF A04

This paper describes a method for tracking moving image features by combining spatial and temporal edge information with model based feature information. The algorithm updates the two-dimensional position of object features by correlating predicted model features with current image data. The results of the correlation process are used to compute an updated model. The algorithm makes use of a high temporal sampling rate with respect to spatial changes of the image features and operates in a real-time multiprocessing environment. Preliminary results demonstrate successful tracking for image feature velocities between 1.1 and 4.5 pixels every image frame. This work has applications for docking, assembly, retrieval of floating objects and a host of other space-related tasks. Author

N93-11956*# North Carolina Univ., Charlotte. Dept. of Computer Science.
CONTACT DETECTION AND CONTACT MOTION FOR ERROR RECOVERY IN THE PRESENCE OF UNCERTAINTIES **c61**
Jing Xiao *In* NASA. Lyndon B. Johnson Space Center, Fifth Annual Workshop on Space Operations Applications and Research (SOAR 1991), Volume 1 Jan. 1992 p 230-237 (For primary document see N93-11921 02-59)
Avail: CASI HC A02/MF A04

Due to various kinds of uncertainties, a robot motion may fail and result in some unintended contact between the object held by the robot and the environment, which greatly hampers robotics applications on tasks with high-precision requirements, such as assembly tasks. Aiming at automatically recovering a robotic task from such a failure, this paper discusses, in the presence of uncertainties, contact detection based on contact motion for recovery. It presents a framework for on-line recognizing contacts using multiple sensor modalities in the presence of sensing uncertainties and means for ensuring successful compliant motions in the presence of sensing and control uncertainties. Author

N93-11957*# EXOS, Inc., Burlington, MA.
EXOS RESEARCH ON MASTER CONTROLLERS FOR ROBOTIC DEVICES **c63**
Beth A. Marcus, Ben An, and Brian Eberman (Massachusetts Inst. of Tech., Cambridge.) *In* NASA. Lyndon B. Johnson Space Center, Fifth Annual Workshop on Space Operations Applications and Research (SOAR 1991), Volume 1 Jan. 1992 p 238-245 (For primary document see N93-11921 02-59)
(Contracts NAS8-38910; NAS9-18452)
Avail: CASI HC A02/MF A04

Two projects are currently being conducted by EXOS under the Small Business Innovation Research (SBIR) program with NASA. One project will develop a force feedback device for controlling robot hands, the other will develop an elbow and shoulder exoskeleton which can be integrated with other EXOS devices to provide whole robot arm and hand control. Aspects covered are the project objectives, important research issues which have arisen during the developments, and interim results of the projects. The Phase 1 projects currently underway will result in hardware prototypes and identification of research issues required for complete system development and/or integration. Author

N93-11958*# Oak Ridge National Lab., TN.
GENERATION OF 3-D SURFACE MAPS IN WASTE STORAGE SILOS USING A STRUCTURED LIGHT SOURCE Abstract Only **c61**
B. L. Burks, J. C. Rowe, M. A. Dinkins, B. Christensen (Sandia National Labs., Albuquerque, NM.), C. Selleck (Sandia National Labs., Albuquerque, NM.), D. Jacoboski (Westinghouse Materials Co. of Ohio, Cincinnati.), and R. Markus (Westinghouse Materials Co. of Ohio, Cincinnati.) *In* NASA. Lyndon B. Johnson Space Center, Fifth Annual Workshop on Space Operations Applications and Research (SOAR 1991), Volume 1 Jan. 1992 p 246 (For primary document see N93-11921 02-59)
(Contract DE-AC05-84OR-21400)
Avail: CASI HC A01/MF A04

Surface contours inside the large waste storage tanks typical of the Department of Energy (DOE) complex are, in general, highly irregular. In addition to pipes and other pieces of equipment in the tanks, the surfaces may have features such as mounds, fissures, crystalline structures, and mixed solid and liquid forms. Prior to remediation activities, it will be necessary to characterize the waste to determine the most effective remediation approaches. Surface contour data will be required both prior to and during remediation. The use is described of a structured light source to generate 3-D surface contour maps of the interior of waste storage silos at the Feed Materials Production Center at Fernald, OH. The landscape inside these large waste storage tanks bears a strong resemblance to some of the landscapes that might be encountered during lunar or planetary exploration. Hence, these terrestrial 3-D mapping techniques may be directly applicable to extraterrestrial exploration. In further development, it will be demonstrated that these 3-D data can be used for robotic task planning just as 3-D surface contour data of a satellite could be used to plan maintenance tasks for a space-based servicing robot. Author

N93-11959*# Southwest Research Inst., San Antonio, TX. Robotics and Automation Dept.
FUZZY LOGIC CONTROL OF TELEROBOT MANIPULATORS **c63**
Ernest A. Franke and Ashok Nedungadi *In* NASA. Lyndon B. Johnson Space Center, Fifth Annual Workshop on Space Operations Applications and Research (SOAR 1991), Volume 1 Jan. 1992 p 248-253 (For primary document see N93-11921 02-59)
Avail: CASI HC A02/MF A04

Telerobot systems for advanced applications will require manipulators with redundant 'degrees of freedom' (DOF) that are capable of adapting manipulator configurations to avoid obstacles while achieving the user specified goal. Conventional methods for control of manipulators (based on solution of the inverse kinematics) cannot be easily extended to these situations. Fuzzy logic control offers a possible solution to these needs. A current research program at SRI developed a fuzzy logic controller for a redundant, 4 DOF, planar manipulator. The manipulator end point trajectory can be specified by either a computer program (robot mode) or by manual input (teleoperator). The approach used expresses end-point error and the location of manipulator joints as fuzzy variables. Joint motions are determined by a fuzzy rule set without requiring solution of the inverse kinematics. Additional rules for sensor data, obstacle avoidance and preferred manipulator configuration, e.g., 'righty' or 'lefty', are easily accommodated. The procedure used to generate the fuzzy rules can be extended to higher DOF systems. Author

N93-11960*# Jet Propulsion Lab., California Inst. of Tech., Pasadena.
A NEW SCHEME OF FORCE REFLECTING CONTROL **c63**
Won S. Kim *In* NASA. Lyndon B. Johnson Space Center, Fifth Annual Workshop on Space Operations Applications and Research (SOAR 1991), Volume 1 Jan. 1992 p 254-261 Sponsored by NASA, Washington (For primary document see N93-11921 02-59)
Avail: CASI HC A02/MF A04

A new scheme of force reflecting control has been developed that incorporates position-error-based force reflection and robot compliance control. The operator is provided with a kinesthetic force feedback which is proportional to the position error between the operator-commanded and the actual position of the robot arm. Robot compliance control, which increases the effective compliance of the robot, is implemented by low pass filtering the outputs of the force/torque sensor mounted on the base of robot hand and using these signals to alter the operator's position command. This position-error-based force reflection scheme combined with shared compliance control has been implemented successfully to the Advanced Teleoperation system consisting of dissimilar master-slave arms. Stability measurements have demonstrated unprecedentedly high force reflection gains of up to 2 or 3, even though the slave arm is much stiffer than operator's hand holding the force reflecting hand controller. Peg-in-hole experiments were performed with eight different operating modes to evaluate the new force-reflecting control scheme. Best task performance resulted with this new control scheme. Author

N93-11961*# Rice Univ., Houston, TX. Dept. of Electrical and Computer Engineering.
FAULT DETECTION AND FAULT TOLERANCE IN ROBOTICS **c37**
Monica Visinsky, Ian D. Walker, and Joseph R. Cavallaro *In* NASA. Lyndon B. Johnson Space Center, Fifth Annual Workshop on Space Operations Applications and Research (SOAR 1991), Volume 1 Jan. 1992 p 262-271 Sponsored in part by Mitre Corp. (For primary document see N93-11921 02-59)
(Grants NSF MIP-89-09498; NSF MSS-90-24391)
Avail: CASI HC A02/MF A04

Robots are used in inaccessible or hazardous environments in order to alleviate some of the time, cost and risk involved in preparing men to endure these conditions. In order to perform their expected tasks, the robots are often quite complex, thus increasing their potential for failures. If men must be sent into these environments to repair each component failure in the robot, the advantages of using the robot are quickly lost. Fault tolerant robots are needed which can effectively cope with failures and continue their tasks until repairs can be realistically scheduled. Before fault tolerant capabilities can be created, methods of detecting and pinpointing failures must be perfected. This paper develops a basic fault tree analysis of a robot in order to obtain a better understanding of where failures can occur and how they contribute to other failures in the robot. The resulting failure flow chart can also be used to analyze the resiliency of the robot in the presence of specific faults. By simulating robot failures and fault detection schemes, the problems involved in detecting failures for robots are explored in more depth. Author

N93-11962*# Texas A&I Univ., Kingsville. Dept. of Electrical Engineering and Computer Science.

A NEURO-COLLISION AVOIDANCE STRATEGY FOR ROBOT MANIPULATORS **c63**

Joel P. Onema and Robert A. Maclaunchlan *In* NASA. Lyndon B. Johnson Space Center, Fifth Annual Workshop on Space Operations Applications and Research (SOAR 1991), Volume 1 Jan. 1992 p 272-279 (For primary document see N93-11921 02-59)

Avail: CASI HC A02/MF A04

The area of collision avoidance and path planning in robotics has received much attention in the research community. Our study centers on a combination of an artificial neural network paradigm with a motion planning strategy that insures safe motion of the Articulated Two-Link Arm with Scissor Hand System relative to an object. Whenever an obstacle is encountered, the arm attempts to slide along the obstacle surface, thereby avoiding collision by means of the local tangent strategy and its artificial neural network implementation. This combination compensates the inverse kinematics of a robot manipulator. Simulation results indicate that a neuro-collision avoidance strategy can be achieved by means of a learning local tangent method. Author

---

N93-11963*# Barrios Technology, Inc., Houston, TX.

INTERACTIVE COLLISION DETECTION Abstract Only **c63**

Brad Bell *In* NASA. Lyndon B. Johnson Space Center, Fifth Annual Workshop on Space Operations Applications and Research (SOAR 1991), Volume 1 Jan. 1992 p 280 (For primary document see N93-11921 02-59)

Avail: CASI HC A01/MF A04

The assembly of Space Station Freedom will require operations where large bodies are manipulated in close proximity to one other. A fast and reliable method for performing collision detection would greatly benefit the development and verification of such operations. The Interactive Graphics and Operations Analysis Laboratory (IGOAL) has developed an algorithm for performing collision detection which provides accurate results at interactive speeds. This algorithm uses a highly-optimized ray tracer for performing the analysis. The purpose of this presentation is to describe the algorithm and demonstrate its capabilities. Author

---

N93-11964*# Jet Propulsion Lab., California Inst. of Tech., Pasadena.

AN 8-DOF DUAL-ARM SYSTEM FOR ADVANCED TELEOPERATION PERFORMANCE EXPERIMENTS **c63**

Antal K. Bejczy and Zoltan F. Szakaly *In* NASA. Lyndon B. Johnson Space Center, Fifth Annual Workshop on Space Operations Applications and Research (SOAR 1991), Volume 1 Jan. 1992 p 282-293 Sponsored by NASA, Washington (For primary document see N93-11921 02-59)

Avail: CASI HC A03/MF A04

This paper describes the electro-mechanical and control features of an 8-DOF manipulator manufactured by AAI Corporation and installed at the Jet Propulsion Lab. (JPL) in a dual-arm setting. The 8-DOF arm incorporates a variety of features not found in other lab or industrial manipulators. Some of the unique features are: 8-DOF revolute configuration with no lateral offsets at joint axes; 1 to 5 payload to weight ratio with 20 kg (44 lb) payload at a 1.75 m (68.5 in.) reach; joint position measurement with dual relative encoders and potentiometer; infinite roll of joint 8 with electrical and fiber optic slip rings; internal fiber optic link of 'smart' end effectors; four-axis wrist; graphite epoxy links; high link and joint stiffness; use of an upgraded JPL Universal Motor Controller (UMC) capable of driving up to 16 joints. The 8-DOF arm is equipped with a 'smart' end effector which incorporates a 6-DOF forcemoment sensor at the end effector base and grasp force sensors at the base of the parallel jaws. The 8-DOF arm is interfaced to a 6 DOF force reflecting hand controller. The same system is duplicated for and installed at NASA-Langley. Author

---

N93-11965*# Jet Propulsion Lab., California Inst. of Tech., Pasadena.

PERFORMANCE EXPERIMENTS WITH ALTERNATIVE ADVANCED TELEOPERATOR CONTROL MODES FOR A SIMULATED SOLAR MAXIMUM SATELLITE REPAIR **c63**

H. Das, H. Zak, W. S. Kim, A. K. Bejczy, and P. S. Schenker *In* NASA. Lyndon B. Johnson Space Center, Fifth Annual Workshop on Space Operations Applications and Research (SOAR 1991), Volume 1 Jan. 1992 p 294-301 Sponsored by NASA, Washington (For primary document see N93-11921 02-59)

Avail: CASI HC A02/MF A04

Experiments are described which were conducted at the JPL Advanced Teleoperator Lab to demonstrate and evaluate the effectiveness of various teleoperator control modes in the performance of a simulated Solar Max Satellite Repair (SMSR) task. THe SMSR was selected as a test because it is very rich in performance capability requirements and it actually has been performed by two EVA astronauts in the Space Shuttle Bay in 1984. The main subtasks are: thermal blanket removal; installation of a hinge attachment for electrical panel opening; opening of electrical panel; removal of electrical connectors; relining of cable bundles; replacement of electrical panel; securing parts and cables; re-mate electrical connectors; closing of electrical panel; and reinstating thermal blanket. The current performance experiments are limited to thermal blanket cutting, electrical panel unbolting and handling electrical bundles and connectors. In one formal experiment even different control modes were applied to the unbolting and reinsertion of electrical panel screws subtasks. The seven control modes are alternative combinations of manual position and rate control with force feedback and remote compliance referenced to force-torque sensor information. Force-torque sensor and end effector position data and task completion times were recorded for analysis and quantification of operator performance. Author

---

N93-11966*# National Aeronautics and Space Administration. Lyndon B. Johnson Space Center, Houston, TX.

EFFECTS OF SPATIALLY DISPLACED FEEDBACK ON REMOTE MANIPULATION TASKS **c63**

Meera K. Manahan (Lockheed Engineering and Sciences Co., Houston, TX.), Mark A. Stuart (Lockheed Engineering and Sciences Co., Houston, TX.), John M. Bierschwale (Lockheed Engineering and Sciences Co., Houston, TX.), Ellen Y. Hwang (Lockheed Engineering and Sciences Co., Houston, TX.), and A. J. Legendre *In its* Fifth Annual Workshop on Space Operations Applications and Research (SOAR 1991), Volume 1 Jan. 1992 p 302-309 (For primary document see N93-11921 02-59)

Avail: CASI HC A02/MF A04

Several studies have been performed to determine the effects on computer and direct manipulation task performance when viewing conditions are spatially displaced. Whether results from these studies can be directly applied to remote manipulation tasks is questionable. The objective of this evaluation was to determine the effects of reversed, inverted, and inverted/reversed views on remote manipulation task performance using two 3-Degree of Freedom (DOF) hand controllers and a replica position hand controller. Results showed that trials using the inverted viewing condition showed the worst performance, followed by the inverted/reversed view and the reversed view when using the 2x3 DOF. However, these differences were not significant. The inverted and inverted/reversed viewing conditions were significantly worse than the normal and reversed viewing conditions when using the Kraft Replica. A second evaluation was conducted in which additional trials were performed with each viewing condition to determine the long term effects of spatially displaced views on task performance for the hand controllers. Results of the second evaluation indicated that there was more of a difference in performance between the perturbed viewing conditions and the normal viewing condition with the Kraft Replica than with the 2x3 DOF. Author

N93-11967*# Wisconsin Univ., Madison. Center for Space Automation and Robotics.
IMPORTANCE OF NUMEROSITY AND DISTRIBUTION OF ARTICULATIONS WITHIN THE DIGITS, WRISTS, AND ARMS OF TELEMANIPULATORS CONFRONTED WITH DEXTROUS ASSEMBLY TASKS Abstract Only **c37**
Steven F. Wiker, Neil Duffie, and Thomas Yen *In* NASA. Lyndon B. Johnson Space Center, Fifth Annual Workshop on Space Operations Applications and Research (SOAR 1991), Volume 1 Jan. 1992 p 310 (For primary document see N93-11921 02-59)
Avail: CASI HC A01/MF A04

This study was conducted to evaluate the impact of successive exclusion of degrees-of-freedom within digits (thumb and index finger) and wrist when performing tasks demanding varying degrees of end effector kinematic complexity. The analysis was performed by successive constraining articulations in the fingers (thumb and index) and wrists or human subjects via splints, and then timing performance of part movement, positioning, and assembly operations requiring different levels of kinematic freedom. Analysis of performance times showed that transferring degrees-of-freedom, or articulations, from the digits to the wrist and arm had little or no material affect upon manipulation performance times if wrist and arm kinematics were unrestricted. If wrist and arm kinematics are not constrained and are of high-quality, our findings show that transferring kinematic freedom from the digits to the wrist and arms or remote end effectors offers limited or no consequence in terms of remote assembly operations. The importance of such findings, in terms of development and implementation of commercially attractive telemanipulators, is discussed. Author

N93-11968*# Aerospace Medical Research Labs., Wright-Patterson AFB, OH.
THE DEVELOPMENT OF SYSTEM COMPONENTS TO PROVIDE PROPRIOCEPTIVE AND TACTILE INFORMATION TO THE HUMAN FOR FUTURE TELEPRESENCE SYSTEMS Abstract Only **c37**
Ammon K. Wright *In* NASA. Lyndon B. Johnson Space Center, Fifth Annual Workshop on Space Operations Applications and Research (SOAR 1991), Volume 1 Jan. 1992 p 311 (For primary document see N93-11921 02-59)
Avail: CASI HC A01/MF A04

System components are presented that are being implemented to augment teleoperated systems by providing both force and tactile information to the human operator. The concept proposed is the control of a manipulator to perform tasks; i.e., flight line maintenance and repair of combat aircraft or satellites while under the control of a human operator at a remote location to maintain mission effectiveness in a hostile environment. The human would control the motion of the manipulator via a master system with information from the remote site being fed back by direct stimulation of the humans sensory mechanisms or by graphic interpretation of displays. We are interested in providing the operator feedback of position, force, auditory, vision, and tactile information to aide in the human's cognitive ability to control the manipulator. This sensory information from the remote site would then be presented to the operator in such a manner as to enhance his performance while providing him a sense of being present at the remote location, this is known as telepresence. Also discussed is the research done by the Human Sensory Feedback (HSF) facility at the Armstrong Laboratory to provide tactile and proprioceptive feedback to the operator. The system components of this system includes tactile sensor and stimulators, dexterous robotic hands, and the control of positioning and operating industrial robots with exoskeletal mechanisms. Author

N93-11969*# National Aeronautics and Space Administration. Goddard Space Flight Center, Greenbelt, MD.
ADVANCED MECHANISMS FOR ROBOTICS **c37**
John M. Vranish *In* NASA. Lyndon B. Johnson Space Center, Fifth Annual Workshop on Space Operations Applications and Research (SOAR 1991), Volume 1 Jan. 1992 p 314-320 (For primary document see N93-11921 02-59)
Avail: CASI HC A02/MF A04

An overview of applied research and development at NASA-Goddard (GSFC) on mechanisms and the collision avoidance skin for robots is presented. First the work on robot end effectors is outlined, followed by a brief discussion on robot-friendly payload latching mechanisms and compliant joints. This, in turn, is followed by the collision avoidance/management skin and the GSFC research on magnetostrictive direct drive motors. Finally, a new project, the artificial muscle, is introduced. Each of the devices is described in sufficient detail to permit a basic understanding of its purpose, fundamental principles of operation, and capabilities. In addition, the development status of each is reported along with descriptions of breadboards and prototypes and their test results. In each case, the implications of the research for commercialization is discussed. The chronology of the presentation will give a clear idea of both the evolution of the R&D in recent years and its likely direction in the future. Author

N93-11970*# Odetics, Inc., Anaheim, CA. AIM Div.
EXOSKELETON MASTER CONTROLLER WITH FORCE-REFLECTING TELEPRESENCE **c37**
James B. Burke, Stephen J. Bartholet, and David K. Nelson (Aerospace Medical Research Labs., Wright-Patterson AFB, OH.) *In* NASA. Lyndon B. Johnson Space Center, Fifth Annual Workshop on Space Operations Applications and Research (SOAR 1991), Volume 1 Jan. 1992 p 321-330 (For primary document see N93-11921 02-59)
Avail: CASI HC A02/MF A04

A thorough understanding of the requirements for successful master-slave robotic systems is becoming increasingly desirable. Such systems can aid in the accomplishment of tasks that are hazardous or inaccessible to humans. Although a history of use has proven master-slave systems to be viable, system requirements and the impact of specifications on the human factors side of system performance are not well known. In support of the next phase of teleoperation research being conducted at the Armstrong Research Laboratory, a force-reflecting, seven degree of freedom exoskeleton for master-slave teleoperation has been concepted, and is presently being developed. The exoskeleton has a unique kinematic structure that complements the structure of the human arm. It provides a natural means for teleoperating a dexterous, possibly redundant manipulator. It allows ease of use without operator fatigue and faithfully follows human arm and wrist motions. Reflected forces and moments are remotely transmitted to the operator hand grip using a cable transmission scheme. This paper presents the exoskeleton concept and development results to date. Conceptual design, hardware, algorithms, computer architecture, and software are covered. Author

N93-11971*# Grumman Aerospace Corp., Bethpage, NY. Space and Electronics Div.
REMOTE SYSTEMS DEVELOPMENT **c37**
R. Olsen, O. Schaefer, and J. Hussey *In* NASA. Lyndon B. Johnson Space Center, Fifth Annual Workshop on Space Operations Applications and Research (SOAR 1991), Volume 1 Jan. 1992 p 331-347 (For primary document see N93-11921 02-59)
Avail: CASI HC A03/MF A04

Potential space missions of the nineties and the next century require that we look at the broad category of remote systems as an important means to achieve cost-effective operations, exploration and colonization objectives. This paper addresses such missions, which can use remote systems technology as the basis for identifying required capabilities which must be provided. The relationship of the space-based tasks to similar tasks required for terrestrial applications is discussed. The development status of the required technology is assessed and major issues which must be addressed to meet future requirements are identified. This includes the proper mix of humans and machines, from pure teleoperation to full autonomy; the degree of worksite compatibility for a robotic system; and the required design parameters, such as degrees-of-freedom. Methods for resolution are discussed including analysis, graphical simulation and the use of laboratory test beds. Grumman experience in the application of these techniques to a variety of design issues are presented utilizing the Telerobotics Development Laboratory which includes a 17-DOF robot system, a variety of sensing elements, Deneb/IRIS graphics workstations and control stations. The use of task/worksite mockups, remote system development test beds and graphical analysis are discussed with examples of typical results such as estimates of task times, task feasibility and resulting recommendations for design changes. The relationship of this experience and lessons-learned to future development of remote systems is also discussed. Author

N93-11972*# National Aeronautics and Space Administration. Lyndon B. Johnson Space Center, Houston, TX.

AN INTEGRATED DEXTEROUS ROBOTIC TESTBED FOR SPACE APPLICATIONS **c37**

Larry C. Li, Hai Nguyen, and Edward Sauer (Lockheed Engineering and Sciences Co., Houston, TX.) *In its* Fifth Annual Workshop on Space Operations Applications and Research (SOAR 1991), Volume 1 Jan. 1992 p 348-361 (For primary document see N93-11921 02-59)

Avail: CASI HC A03/MF A04

An integrated dexterous robotic system was developed as a testbed to evaluate various robotics technologies for advanced space applications. The system configuration consisted of a Utah/MIT Dexterous Hand, a PUMA 562 arm, a stereo vision system, and a multiprocessing computer control system. In addition to these major subsystems, a proximity sensing system was integrated with the Utah/MIT Hand to provide capability for non-contact sensing of a nearby object. A high-speed fiber-optic link was used to transmit digitized proximity sensor signals back to the multiprocessing control system. The hardware system was designed to satisfy the requirements for both teleoperated and autonomous operations. The software system was designed to exploit parallel processing capability, pursue functional modularity, incorporate artificial intelligence for robot control, allow high-level symbolic robot commands, maximize reusable code, minimize compilation requirements, and provide an interactive application development and debugging environment for the end users. An overview is presented of the system hardware and software configurations, and implementation is discussed of subsystem functions. Author

N93-11973*# Carnegie-Mellon Univ., Pittsburgh, PA. Robotics Inst.

SELF MOBILE SPACE MANIPULATOR PROJECT Abstract Only **c37**

H. Ben Brown, Mark Friedman, Yangsheng Xu, and Takeo Kanade *In* NASA. Lyndon B. Johnson Space Center, Fifth Annual Workshop on Space Operations Applications and Research (SOAR 1991), Volume 1 Jan. 1992 p 362 (For primary document see N93-11921 02-59)

Avail: CASI HC A01/MF A04

A relatively simple, modular, low mass, low cost robot is being developed for space EVA that is large enough to be independently mobile on a space station or platform exterior, yet versatile enough to accomplish many vital tasks. The robot comprises two long flexible links connected by a rotary joint, with 2-DOF 'wrist' joints and grippers at each end. It walks by gripping pre-positioned attachment points, such as trusswork nodes, and alternately shifting its base of support from one foot (gripper) to the other. The robot can perform useful tasks such as visual inspection, material transport, and light assembly by manipulating objects with one gripper, while stabilizing itself with the other. At SOAR '90, we reported development of 1/3 scale robot hardware, modular trusswork to serve as a locomotion substrate, and a gravity compensation system to allow laboratory tests of locomotion strategies on the horizontal face of the trusswork. In this paper, we report on project progress including the development of: (1) adaptive control for automatic adjustment to loads; (2) enhanced manipulation capabilities; (3) machine vision, including the use of neural nets, to guide autonomous locomotion; (4) locomotion between orthogonal trusswork faces; and (5) improved facilities for gravity compensation and telerobotic control. Author

N93-11974*# Deutsche Agentur fuer Raumfahrtangelegenheiten G.m.b.H., Bonn (Germany).

AUTOMATION AND ROBOTICS FOR COLUMBUS: AN IMPLEMENTATION CONCEPT FOR THE FREE FLYING LABORATORY (MTFF) **c37**

G. Goelz and B. Sommer *In* NASA. Lyndon B. Johnson Space Center, Fifth Annual Workshop on Space Operations Applications and Research (SOAR 1991), Volume 1 Jan. 1992 p 364-381 (For primary document see N93-11921 02-59)

Avail: CASI HC A03/MF A04

With nearly forty percent of the funding, Germany is the main contributor to the European COLUMBUS Programme, followed by Italy, France and further ESA member states. The COLUMBUS elements are the Attached Laboratory (APM) to be permanently attached to the Space Station FREEDOM, the polar platform (PPF) and the Man Tended Free Flyer (MTFF). The latter element is regarded to be of special interest for the German micro-g community. Until now the implementation of A&R Technologies has not been included as part of the system concept for the COLUMBUS laboratory modules. Yet especially for the Free Flyer, a high degree of A&R will be indispensible. An A&R system concept and implementation options for A&R are given to make the COLUMBUS labs 'intelligent' laboratories in orbit. Author

N93-11975*# Barrios Technology, Inc., Houston, TX. Mission Operations Directorate.

SPACE STATION ROBOTICS PLANNING TOOLS **c37**

Bridget Mintz Testa *In* NASA. Lyndon B. Johnson Space Center, Fifth Annual Workshop on Space Operations Applications and Research (SOAR 1991), Volume 1 Jan. 1992 p 382-390 (For primary document see N93-11921 02-59)

Avail: CASI HC A02/MF A04

The concepts are described for the set of advanced Space Station Freedom (SSF) robotics planning tools for use in the Space Station Control Center (SSCC). It is also shown how planning for SSF robotics operations is an international process, and baseline concepts are indicated for that process. Current SRMS methods provide the backdrop for this SSF theater of multiple robots, long operating time-space, advanced tools, and international cooperation. Author

N93-11976*# National Aeronautics and Space Administration. Ames Research Center, Moffett Field, CA.

HABITAT AUTOMATION **c54**

Rodney E. Swab *In* NASA. Lyndon B. Johnson Space Center, Fifth Annual Workshop on Space Operations Applications and Research (SOAR 1991), Volume 1 Jan. 1992 p 391-398 (For primary document see N93-11921 02-59)

Avail: CASI HC A02/MF A04

A habitat, on either the surface of the Moon or Mars, will be designed and built with the proven technologies of that day. These technologies will be mature and readily available to the habitat designer. We believe an acceleration of the normal pace of automation would allow a habitat to be safer and more easily maintained than would be the case otherwise. This document examines the operation of a habitat and describes elements of that operation which may benefit from an increased use of automation. Research topics within the automation realm are then defined and discussed with respect to the role they can have in the design of the habitat. Problems associated with the integration of advanced technologies into real-world projects at NASA are also addressed. Author

N93-11977*# National Aeronautics and Space Administration. Lyndon B. Johnson Space Center, Houston, TX.

ROLE OF AUTOMATION IN THE ACRV OPERATIONS Abstract Only **c18**

S. F. Sepahban *In its* Fifth Annual Workshop on Space Operations

Applications and Research (SOAR 1991), Volume 1 Jan. 1992 p 399 (For primary document see N93-11921 02-59)
Avail: CASI HC A01/MF A04

The Assured Crew Return Vehicle (ACRV) will provide the Space Station Freedom with contingency means of return to earth (1) of one disabled crew member during medical emergencies, (2) of all crew members in case of accidents or failures of SSF systems, and (3) in case of interruption of the Space Shuttle flights. A wide range of vehicle configurations and system approaches are currently under study. The Program requirements focus on minimizing life cycle costs by ensuring simple operations, built-in reliability and maintainability. The ACRV philosophy of embedded operations is based on maximum use of existing facilities, resources and processes, while minimizing the interfaces and impacts to the Space Shuttle and Freedom programs. A preliminary integrated operations concept based on this philosophy and covering the ground, flight, mission support, and landing and recovery operations has been produced. To implement the ACRV operations concept, the underlying approach has been to rely on vehicle autonomy and automation, to the extent possible. Candidate functions and processes which may benefit from current or near-term automation and robotics technologies are identified. These include, but are not limited to, built-in automated ground tests and checkouts; use of the Freedom and the Orbiter remote manipulator systems, for ACRV berthing; automated passive monitoring and performance trend analysis, and periodic active checkouts during dormant periods. The major ACRV operations concept issues as they relate to the use of automation are discussed. Author

N93-11978*# Jet Propulsion Lab., California Inst. of Tech., Pasadena.
DECISION RULES FOR SPACEBORNE OPERATIONS PLANNING Abstract Only **c66**
Jeffrey H. Smith *In* NASA. Lyndon B. Johnson Space Center, Fifth Annual Workshop on Space Operations Applications and Research (SOAR 1991), Volume 1 Jan. 1992 p 400 (For primary document see N93-11921 02-59)
Avail: CASI HC A01/MF A04

Recent study of Space Station Freedom requirements for extravehicular activity (EVA) to perform external maintenance tasks emphasize an oversubscription of resources for performing on-orbit tasks. Extravehicular robotics (EVR) and cooperative EVA combined with EVR (using crew and robots synergistically to perform tasks) have been suggested as a part of the solution to reduce EVA. The question remains however, 'Under what conditions is it cost-effective to use the EVA and/or EVR resource.' The answer to such a question also has implications for the Space Station Freedom and its external maintenance as well as the Space Exploration Initiative (SEI) where the issue of work-system allocation is magnified by the long distances and scope of EVA work. This paper describes a simple technique of interest to operational planners and robot technology planners for determining in an economic context whether to use EVA alone, EVR alone, or Cooperative EVA. It is also shown that given: (1) the task times for these alternatives; and (2) the marginal costs of EVA, EVR, and IVA, the appropriate work system for performing the task can be identified. The paper illustrates how the work system choice is based on the ratio of costs. An example using Space Station Freedom data is presented to illustrate the trade-offs among alternative work-systems. Author

N93-11979*# Oak Ridge National Lab., TN. Center for Engineering Systems Advanced Research.
RESEARCH AND DEVELOPMENT AT ORNL/CESAR TOWARDS COOPERATING ROBOTIC SYSTEMS FOR HAZARDOUS ENVIRONMENTS **c37**
R. C. Mann, K. Fujimura, and M. A. Unseren *In* NASA. Lyndon B. Johnson Space Center, Fifth Annual Workshop on Space Operations Applications and Research (SOAR 1991), Volume 1 Jan. 1992 p 402-406 (For primary document see N93-11921 02-59)
Avail: CASI HC A01/MF A04

One of the frontiers in intelligent machine research is the understanding of how constructive cooperation among multiple autonomous agents can be effected. The effort at the Center for Engineering Systems Advanced Research (CESAR) at the Oak Ridge National Laboratory (ORNL) focuses on two problem areas: (1) cooperation by multiple mobile robots in dynamic, incompletely known environments; and (2) cooperating robotic manipulators. Particular emphasis is placed on experimental evaluation of research and developments using the CESAR robot system testbeds, including three mobile robots, and a seven-axis, kinematically redundant mobile manipulator. This paper summarizes initial results of research addressing the decoupling of position and force control for two manipulators holding a common object, and the path planning for multiple robots in a common workspace. Author

N93-11980*# Rockwell International Corp., Downey, CA.
AUTOMATED RESUPPLY OF CONSUMABLES: ENHANCEMENT OF SPACE COMMERCIALIZATION OPPORTUNITIES **c66**
Davoud Manouchehri and A. J. Mauceri *In* NASA. Lyndon B. Johnson Space Center, Fifth Annual Workshop on Space Operations Applications and Research (SOAR 1991), Volume 1 Jan. 1992 p 407-411 (For primary document see N93-11921 02-59)
Avail: CASI HC A01/MF A04

This paper addresses work performed at Rockwell International's Space Systems Division to investigate the feasibility of, and develop concepts for, automated and/or robotic resupply of consumables on orbit. The work focuses on the resupply of satellites and is described in five sections. First, the various problems relating the resupply on orbit are discussed: for example, economic concerns, fuel handling problems, and safety issues. Next major methods of effecting fuel transfer on orbit are summarized, together with their advantages and disadvantages. Direct fuel exchange is emphasized as the most feasible technique. Third, guidelines are developed for automated/robotic refueling mechanisms to accomplish on-orbit consumable resupply. For example, the guidelines cover safety, reliability, maintainability, alignment, induced loads, thermal protection, leaks, extravehicular activity (EVA) interface, and so on. The fourth part of the paper covers the development of design concepts for satellite resupply robotic interfaces that comply with the guidelines. Concepts include servicer fluid transfer system and satellite propulsion system, and a combined docking/umbilical device. Last, future technical development in these areas are discussed. Author

N93-11981*# ST Systems Corp., Lanham, MD.
OPERATOR VISION AIDS FOR SPACE TELEOPERATION ASSEMBLY AND SERVICING **c54**
Thurston L. Brooks, Ilhan Ince, and Greg Lee *In* NASA. Lyndon B. Johnson Space Center, Fifth Annual Workshop on Space Operations Applications and Research (SOAR 1991), Volume 1 Jan. 1992 p 412-421 (For primary document see N93-11921 02-59)
Avail: CASI HC A02/MF A04

This paper investigates concepts for visual operator aids required for effective telerobotic control. Operator visual aids, as defined here, mean any operational enhancement that improves man-machine control through the visual system. These concepts were derived as part of a study of vision issues for space teleoperation. Extensive literature on teleoperation, robotics, and human factors was surveyed to definitively specify appropriate requirements. This paper presents these visual aids in three general categories of camera/lighting functions, display enhancements, and operator cues. In the area of camera/lighting functions concepts are discussed for: (1) automatic end effector or task tracking; (2) novel camera designs; (3) computer-generated virtual camera views; (4) computer assisted camera/lighting placement; and (5) voice control. In the technology area of display aids, concepts are presented for: (1) zone displays, such as imminent collision or indexing limits; (2) predictive displays for temporal and spatial location; (3) stimulus-response reconciliation displays; (4) graphical display of depth cues such as 2-D symbolic depth, virtual views, and perspective depth; and (5) view enhancements through image processing and symbolic representations. Finally, operator visual cues (e.g., targets) that help identify size, distance, shape, orientation and location are discussed. Author

N93-11982*# National Aeronautics and Space Administration. Langley Research Center, Hampton, VA.
A SMART END-EFFECTOR FOR ASSEMBLY OF SPACE TRUSS STRUCTURES **c18**
William R. Doggett, Marvin D. Rhodes, Marion A. Wise (Lockheed Engineering and Sciences Co., Hampton, VA.), and Maurice F. Armistead (Planning Research Corp., Hampton, VA.) *In* NASA. Lyndon B. Johnson Space Center, Fifth Annual Workshop on Space Operations Applications and Research (SOAR 1991), Volume 1 Jan. 1992 p 422-431 (For primary document see N93-11921 02-59)
Avail: CASI HC A02/MF A04

A unique facility, the Automated Structures Research Laboratory, is being used to investigate robotic assembly of truss structures. A special-purpose end-effector is used to assemble structural elements into an eight meter diameter structure. To expand the capabilities of the facility to include construction of structures with curved surfaces from straight structural elements of different lengths, a new end-effector has been designed and fabricated. This end-effector contains an integrated microprocessor to monitor actuator operations through sensor feedback. This paper provides an overview of the automated assembly tasks required by this end-effector and a description of the new end-effector's hardware and control software. Author

60 COMPUTER OPERATIONS AND HARDWARE

Includes hardware for computer graphics, firmware, and data processing.

For components see *33 Electronics and Electrical Engineering.*

N93-11258# National Inst. of Standards and Technology, Gaithersburg, MD.
COMPUTER SECURITY TRAINING AND AWARENESS COURSE COMPENDIUM
Kathie Everhart, ed. May 1992 230 p
(PB92-205442; NISTIR-4846) Avail: CASI HC A11/MF A03

The training and awareness courses in the compendium implement Public Law 100-235, the Computer Security Act of 1987, which requires training for all employees responsible for the management and use of federal computer systems that process sensitive information. The publication is divided into five audience categories: (1) Executives, (2) Program/Functional Managers, (3) IRM, Security, and Audit Personnel, (4) ADP Management, Operations, and Programming Staff, and (5) End Users. In addition to the five audience categories, there are five training content areas for each audience category: (1) Computer Security Basics, (2) Security Planning and Management, (3) Computer Security Policy and Procedures, (4) Contingency Planning, and (5) Systems Life Cycle Management. The level of training required in each area will vary from general awareness to specific training courses depending on the training objectives established by each agency. GRA

N93-11462*# Illinois Univ., Urbana-Champaign. Coordinated Science Lab.
A REAL-TIME DIAGNOSTIC AND PERFORMANCE MONITOR FOR UNIX M.S. Thesis
Hongchao Dong Sep. 1992 57 p
(Grant NAG1-613)
(NASA-CR-190975; NAS 1.26:190975; UILU-ENG-92-2232; CRHC-92-17) Avail: CASI HC A04/MF A01

There are now over one million UNIX sites and the pace at which new installations are added is steadily increasing. Along with this increase, comes a need to develop simple efficient, effective and adaptable ways of simultaneously collecting real-time diagnostic and performance data. This need exists because distributed systems can give rise to complex failure situations that are often un-identifiable with single-machine diagnostic software. The simultaneous collection of error and performance data is also important for research in failure prediction and error/performance studies. This paper introduces a portable method to concurrently collect real-time diagnostic and performance data on a distributed UNIX system. The combined diagnostic/performance data collection is implemented on a distributed multi-computer system using SUN4's as servers. The approach uses existing UNIX system facilities to gather system dependability information such as error and crash reports. In addition, performance data such as CPU utilization, disk usage, I/O transfer rate and network contention is also collected. In the future, the collected data will be used to identify dependability bottlenecks and to analyze the impact of failures on system performance. Author

N93-11539# Allied-Signal Aerospace Co., Kansas City, MO.
DESIGN OF A PCM DATA COMPRESSOR
T. A. Navickas Aug. 1992 73 p
(Contract DE-AC04-76DP-00613)
(DE92-019469; KCP-613-4972) Avail: CASI HC A04/MF A01

Development of automated test equipment for an advanced telemetry system requires continuous monitoring of PCM data while exercising telemetry inputs. This requirements leads to a large amount of data that needs to be stored and later analyzed. For example, a data stream of 4 Mb/s and a test time of 30 min. would yield 900 Mb of raw data. Information must be stored to correlate the raw data to the test stimulus. This leads to a total of 1.8 Gb of data to be stored and analyzed. There is no method to analyze this amount of data in a reasonable time. A data compression method is needed to reduce the amount of data collected to a reasonable amount The solution to the problem was data reduction. Data reduction was accomplished by real time limit checking, time stamping, and smart software. Limit checking was accomplished by an eight-state finite-state machine and four compression algorithms. Time stamping was needed to correlate stimulus to the appropriate output for data reconstruction. The software was written in the C programming language with a DOS extender used to allow it to run in extended mode. A 94 to 98 percent compression in the amount of data gathered was accomplished using this method. DOE

N93-11761# National Academy of Sciences - National Research Council, Washington, DC.
COMPUTER SCIENCE AND TELECOMMUNICATIONS BOARD SUMMARY OF ACTIVITIES
M. S. Blumenthal 27 Mar. 1992 6 p
(Contract DE-FG05-87ER-25029)
(DE92-016467; DOE/ER-25029/3) Avail: CASI HC A02/MF A01

The Computer Science and Telecommunications Board (CSTB) considers technical and policy issues pertaining to computer science, telecommunications, and associated technologies. CSTB actively disseminates the results of its completed projects to those in a position to help implement their recommendations or otherwise use their insights. It provides a forum for the exchange of information on computer science, computing technology, and telecommunications. This report discusses the major accomplishments of CSTB. DOE

N93-11809# Institute for Defense Analyses, Alexandria, VA.
INTEGRITY-ORIENTED CONTROL OBJECTIVES: PROPOSED REVISIONS TO THE TRUSTED COMPUTER SYSTEM EVALUATION CRITERIA (TCSEC), DOD 5200.28-STD Final Report
Terry Mayfield, John M. Boone, and Stephen R. Welke Oct. 1991 150 p
(Contract MDA903-89-C-0003)
(AD-A253989; IDA-D-967; IDA/HQ-91-038812; AD-E501549)
Avail: CASI HC A07/MF A02

Control objectives, as they apply to automated information systems, express fundamental computer security requirements and serve as guidance to the development of more specific systems evaluation criteria. Within the DoD, the control objectives contained in the Trusted Computer System Evaluation Criteria (TCSEC), DoD 5200.28-STD, are of primary concern to the development of product evaluation criteria. The TCSEC's scope is currently confined to address only confidentiality protection of information. This document is intended to extend the scope of the TCSEC so that the control objectives, contained therein, will also address the protection of information and computing resource integrity. The document provides new and modified statements of control objectives along with discussion and rationale for their inclusion or revision. The revisions were initially determined as a result of an examination of various mechanisms and policy abstractions that seemed focused on integrity. The revisions were further reinforced by an examination of Federal law and policy. The basis in Federal law and policy for the revised control objectives is discussed. A summary, key text, cross-references, and commentary notes of each law and policy used in the derivation of the revisions are provided. The document is intended to be used as a strawman to foster further debate and research leading to a new standard for evaluation criteria that encompasses both integrity and confidentiality. GRA

N93-12345*# Boeing Co., Seattle, WA. Defense and Space Group.

REQUIREMENTS SPECIFICATION LANGUAGE (RSL) AND SUPPORTING TOOLS

Deborah Frincke (California Polytechnic State Univ., San Luis Obispo.), Dave Wolber (California Polytechnic State Univ., San Luis Obispo.), Gene Fisher (California Polytechnic State Univ., San Luis Obispo.), and Gerald C. Cohen 1 Nov. 1992 73 p
(Contract NAS1-18586; RTOP 505-64-10-06)
(NASA-CR-189700; NAS 1.26:189700) Avail: CASI HC A04/MF A01

This document describes a general purpose Requirement Specification Language (RSL). RSL is a hybrid of features found in several popular requirement specification languages. The purpose of RSL is to describe precisely the external structure of a system comprised of hardware, software, and human processing elements. To overcome the deficiencies of informal specification languages, RSL includes facilities for mathematical specification. Two RSL interface tools are described. The Browser view contains a complete document with all details of the objects and operations. The Dataflow view is a specialized, operation-centered depiction of a specification that shows how specified operations relate in terms of inputs and outputs. Author

N93-12346*# Boeing Co., Seattle, WA. Defense and Space Group.

FORMAL REPRESENTATION OF THE REQUIREMENTS FOR AN ADVANCED SUBSONIC CIVIL TRANSPORT (ASCT) FLIGHT CONTROL SYSTEM

Deborah Frincke (California Polytechnic State Univ., San Luis Obispo.), Dave Wolber (California Polytechnic State Univ., San Luis Obispo.), Gene Fisher (California Polytechnic State Univ., San Luis Obispo.), Gerald C. Cohen, and R. E. McLees 1 Nov. 1992 46 p
(Contract NAS1-18586; RTOP 505-64-10-07)
(NASA-CR-189699; NAS 1.26:189699) Avail: CASI HC A03/MF A01

A partial requirement specification for an Advanced Subsonic Civil Transport (ASCT) Flight Control System is described. The example was adopted from requirements given in a NASA Contractor report. The language used to describe the requirements, Requirements Specification Language (RSL), is described in a companion document. Author

N93-12347*# Boeing Military Airplane Development, Seattle, WA.

FORMAL MECHANIZATION OF DEVICE INTERACTIONS WITH A PROCESS ALGEBRA

E. Thomas Schubert (California Univ., Davis.), Karl Levitt (California Univ., Davis.), and Gerald C. Cohen (Boeing Co., Seattle, WA.) 1 Nov. 1992 58 p
(Contract NAS1-18586; RTOP 505-64-10-07)
(NASA-CR-189644; NAS 1.26:189644) Avail: CASI HC A04/MF A01

The principle emphasis is to develop a methodology to formally verify correct synchronization communication of devices in a composed hardware system. Previous system integration efforts have focused on vertical integration of one layer on top of another. This task examines 'horizontal' integration of peer devices. To formally reason about communication, we mechanize a process algebra in the Higher Order Logic (HOL) theorem proving system. Using this formalization we show how four types of device interactions can be represented and verified to behave as specified. The report also describes the specification of a system consisting of an AVM-1 microprocessor and a memory management unit which were verified in previous work. A proof of correct communication is presented, and the extensions to the system specification to add a direct memory device are discussed. Author

N93-12425# Naval Postgraduate School, Monterey, CA.

FERROELECTRIC MEMORY DEVICES AND A PROPOSED STANDARDIZED TEST SYSTEM DESIGN M.S. Thesis

Javier M. Covelli Jun. 1992 135 p
(AD-A255159) Avail: CASI HC A07/MF A02

Ferroelectric bulk material devices have been in existence for over 20 years. Not until recently have there been fabrication techniques that consistently and feasibly produce thin film ferroelectric materials. The physical characteristics of thin film ferroelectric capacitors and their subsequent integration into memory design may prove ferroelectric memory devices to be the ultimate in design for nonvolatile, radiation hard computer memory. This thesis describes current memory systems, some of the recent achievements in ferroelectrics and the prospects for further application of ferroelectrics as an alternative for current memory design. It explores the different testing methodologies being implemented to test ferroelectric devices and suggests a flexible, fully programmable and autonomous new test system design that allows high speed aging and fatigue testing of on-chip ferroelectric capacitors for memory applications. GRA

N93-12430# Royal Signals and Radar Establishment, Malvern (England).

FORMAL SPECIFICATION OF THE VIPER MICROPROCESSOR IN HOL

C. H. Pygott Jun. 1990 34 p
(RSRE-90009; BR304494-5; ETN-92-92308; AD-A242147)
Copyright Avail: CASI HC A03/MF A01

A mathematically rigorous specification of the required behavior of the VIPER microprocessor in the HOL (Higher Order Logic) notation is presented. This specification is used as the starting point for a chain of proofs in an attempt to show that a number of implementations of this specification are indeed correct. The VIPER microprocessor was invented to satisfy the need for a highly trusted 32 bit computer used in safety critical applications. The need for such a chip arises in areas such as the arming and fuzing of weapons, fly by wire control systems in high performance military and civil aircraft, and in the instrumentation of nuclear reactors. The study demonstrates that it is possible to write a specification for the functions of a powerful microprocessors, using simple concepts in first order logic. The experience shows that HOL is a satisfactory basis for the formal specification of VIPER. ESA

N93-12520*# Nonvolatile Electronics, Inc., Plymouth, MN.

ULTRA-DENSE MAGNETORESISTIVE MASS MEMORY Quarterly Report No. 5, 15 Jul. - 15 Oct. 1992

J. M. Daughton, R. Sinclair, T. Dupuis, and J. Brown 30 Oct. 1992 114 p
(Contract NAS7-1152)
(NASA-CR-190955; NAS 1.26:190955) Avail: CASI HC A06/MF A02

This report details the progress and accomplishments of Nonvolatile Electronics (NVE), Inc., on the design of the wafer scale MRAM mass memory system during the fifth quarter of the project. NVE has made significant progress this quarter on the one megabit design in several different areas. A test chip, which will verify a working GMR bit with the dimensions required by the 1 Meg chip, has been designed, laid out, and is currently being processed in the NVE labs. This test chip will allow electrical specifications, tolerances, and processing issues to be finalized before construction of the actual chip, thus providing a greater assurance of success of the final 1 Meg design. A model has been developed to accurately simulate the parasitic effects of unselected sense lines. This model gives NVE the ability to perform accurate simulations of the array electronic and test different design concepts. Much of the circuit design for the 1 Meg chip has been completed and simulated and these designs are included. Progress has been made in the wafer scale design area to verify the reliable operation of the 16 K macrocell. This is currently being accomplished with the design and construction of two stand alone test systems which will perform life tests and gather data on reliabiliy and wearout mechanisms for analysis. Author

N93-12538*# Boeing Military Airplane Development, Seattle, WA.

FORMAL DESIGN SPECIFICATION OF A PROCESSOR INTERFACE UNIT

David A. Fura, Phillip J. Windley (Idaho Univ., Moscow.), and Gerald C. Cohen 1 Nov. 1992 253 p
(Contract NAS1-18586; RTOP 505-64-10-07)
(NASA-CR-189698; NAS 1.26:189698) Avail: CASI HC A12/MF A03

This report describes work to formally specify the requirements and design of a processor interface unit (PIU), a single-chip subsystem providing memory-interface bus-interface, and additional support services for a commercial microprocessor within a fault-tolerant computer system. This system, the Fault-Tolerant Embedded Processor (FTEP), is targeted towards applications in avionics and space requiring extremely high levels of mission reliability, extended maintenance-free operation, or both. The need for high-quality design assurance in such applications is an undisputed fact, given the disastrous consequences that even a single design flaw can produce. Thus, the further development and application of formal methods to fault-tolerant systems is of critical importance as these systems see increasing use in modern society. Author

N93-12540*# Illinois Univ., Urbana-Champaign. Coordinated Science Lab.

MEASUREMENT AND ANALYSIS OF OPERATING SYSTEM FAULT TOLERANCE

I. Lee, D. Tang, and R. K. Iyer Oct. 1992 38 p
(Contract NAG1-613; N00014-91-J-1116)
(NASA-CR-190973; NAS 1.26:190973; UILU-ENG-92-2240; CRHC-92-22) Avail: CASI HC A03/MF A01

This paper demonstrates a methodology to model and evaluate the fault tolerance characteristics of operational software. The methodology is illustrated through case studies on three different operating systems: the Tandem GUARDIAN fault-tolerant system, the VAX/VMS distributed system, and the IBM/MVS system. Measurements are made on these systems for substantial periods to collect software error and recovery data. In addition to investigating basic dependability characteristics such as major software problems and error distributions, we develop two levels of models to describe error and recovery processes inside an operating system and on multiple instances of an operating system running in a distributed environment. Based on the models, reward analysis is conducted to evaluate the loss of service due to software errors and the effect of the fault-tolerance techniques implemented in the systems. Software error correlation in multicomputer systems is also investigated. Author

N93-12541*# Illinois Univ., Urbana-Champaign. Coordinated Science Lab.

SIMULATION AND ANALYSIS OF SUPPORT HARDWARE FOR MULTIPLE INSTRUCTION ROLLBACK

Neil J. Alewine 10 Oct. 1992 54 p
(Grant NAG1-613)
(NASA-CR-190972; NAS 1.26:190972; UILU-ENG-92-2239; CRHC-92-21) Avail: CASI HC A04/MF A01

Recently, a compiler-assisted approach to multiple instruction retry was developed. In this scheme, a read buffer of size 2N, where N represents the maximum instruction rollback distance, is used to resolve one type of data hazard. This hardware support helps to reduce code growth, compilation time, and some of the performance impacts associated with hazard resolution. The 2N read buffer size requirement of the compiler-assisted approach is worst case, assuring data redundancy for all data required but also providing some unnecessary redundancy. By adding extra bits in the operand field for source 1 and source 2 it becomes possible to design the read buffer to save only those values required, thus reducing the read buffer size requirement. This study measures the effect on performance of a DECstation 3100 running 10 application programs using 6 read buffer configurations at varying read buffer sizes. Author

61 COMPUTER PROGRAMMING AND SOFTWARE

Includes computer programs, routines, alogorithms, and specific applications, e.g., CAD/CAM.

N93-11145# Carnegie-Mellon Univ., Pittsburgh, PA. Dept. of Computer Science.

DERIVING AND MANIPULATING MODULE INTERFACES Ph.D. Thesis

Robert L. Nord May 1992 174 p
(Contract N00014-84-K-0415; ARPA Order 5404)
(AD-A253869; CMS-CS-92-126) Avail: CASI HC A08/MF A02

A formal method for systematically integrating general-purpose software modules into efficient systems is presented. The integration is accomplished through adjustment of abstract interfaces and transformation of the underlying data representations. The method provides the software designer with the ability to delay or revise design decisions in cases where it is difficult to reach an a priori agreement on interfaces and/or data representations. To demonstrate the method, the development of a text buffer for a simple interactive text editor is given. For each basic operation on the text buffer, a natural and efficient choice of data representation is made. This organizes the operations into several components, with each component containing those operations using the same data representation. The components are then combined using formal program-manipulation methods to obtain an efficient composite representation that supports all of the operations. This approach provides meaningful support for later adaptation. Should a new editing operation be added at a later time, the initial components can be reused in another combining process, thereby obtaining a new composite representation that works for all of the operations including the new one. There are also ramifications for the application of formal methods to larger-scale systems, as this method can be applied to the manipulation of the interfaces between modules in larger software systems. GRA

N93-11210# Loughborough Univ. of Technology (England). Dept. of Mathematical Sciences.

OPTIMIZED SOFTWARE FOR A GENERALIZED POLAK-RIBIERE ALGORITHM IN UNCONSTRAINED OPTIMIZATION

K. M. Khoda, Y. Liu, and C. Storey Apr. 1992 16 p
(Maths-Rept-A-156; ETN-92-92380) Avail: CASI HC A03/MF A01

A Generalized Polak-Ribiere (GPR) algorithm for unconstrained nonlinear optimization, which takes the effects of inexact line searches into account, is developed. Based on various implementations of the new algorithm, an optimized software routine, the GPR routine, is proposed for general purpose use. Selected aspects of this routine are discussed. The new routine proved to be considerably more efficient than a number of comparable routines currently available. ESA

N93-11231# Los Alamos National Lab., NM.
EVALUATION OF A CRAY PERFORMANCE TOOL USING A LARGE HYDRODYNAMICS CODE
Kenneth M. Lord (Cray Research, Inc., Eagan, MN.) and Margaret L. Simmons 1992 11 p Presented at the 6th International Conference on Modelling Techniques and Tools for Performance Evaluation, Edinburgh, Scotland, 16-18 Sep. 1992
(Contract W-7405-eng-36)
(DE92-013239; LA-UR-92-1453; CONF-9209109-1) Avail: CASI HC A03/MF A01

This paper will discuss an automatic tool that was recently developed by Cray Research, Inc. for use on its parallel supercomputer. The tool is called ATEXPERT; when used in conjunction with the Cray Fortran compiling system, CF77, it produces a parallelized version of a code based on loop-level parallelism, plus information to enable the programmer to optimize the parallelized code and improve performance. The information obtained through the use of the tool is presented in an easy-to-read graphical format, making the digestion of such a large quantity of data relatively easy and thus, improving programmer productivity. In this paper we address the issues that we found when we took a large Los Alamos hydrodynamics code, PUEBLO, that was highly vectorizable, but not parallelized, and using ATEXPERT proceeded to parallelize it. We show that through the advice of ATEXPERT, bottlenecks in the code can be found, leading to improved performance. We also show the dependence of performance on problem size, and finally, we contrast the speedup predicted by ATEXPERT with that measured on a dedicated eight-processor Y-MP. DOE

N93-11341# Royal Signals and Radar Establishment, Malvern (England).
THE VISTA STRUCTURED ASSEMBLER
J. Kershaw Jan. 1992 35 p
(RSRE-91034; BR308889; ETN-92-92312) Copyright Avail: CASI HC A03/MF A01

The VISTA is a structured assembly language for the VIPER microprocessor chip. The VISTA language is described by means of an annotated example. Instructions for using the VISTA translator are given. A formal grammar of VISTA, and descriptions of VIPER and the VIPER object program format, are included. Though the syntax of VISTA and the appearance of VISTA programs are reminiscent of a high level language, the actual statements are VIPER machine instructions. VISTA provides the clarity and much of the convenience of a true high level language without the need for a complex and possibly in a trustworthy compiling program. The advantage of a relatively simple language like VISTA is that it does not need a complex compiler. Not only is the VISTA translator very much smaller than a typical compiler, but its outputs are also similar enough to the inputs to be checked easily. The outputs are printable, and annotated in such a way that mechanical checking is possible. ESA

N93-11345 Deutsche Geodaetische Kommission, Munich (Germany).
STATISTICAL PROCESS FOR THE AUTOMATIC IMAGE ANALYSIS AND ITS EVALUATION FOR OBJECT RECOGNITION AND MEASUREMENTS Ph.D. Thesis - Stuttgart Univ. [STATISTISCHE VERFAHREN FUER DIE AUTOMATISCHE BILDANALYSE UND IHRE BEWERTUNG BEI DER OBJEKTERKENNUNG UND -VERMESSUNG]
Wolfgang Foerstner 1991 110 p In GERMAN
(Ser-C-370; ISBN-3-7696-9417-1; ETN-92-92274) Copyright Avail: Deutsche Geodaetische Kommission, Marstallplatz 8, D-8000 Munich 22, Germany

A possible structure for the description of the analysis process is represented. Three levels are distinguished. In the low level vision, the preprocessing of image takes place, with a view to extracting the essential image characteristics. In the second level, the extraction of image structures takes place, e.g., data reduction. In high level vision, the importance of the extracted structures is outlined, e.g., the interpretation of image content. The theoretical principles for the design and analysis of the methods are developed. The linear structure of the evaluation process is criticized. It is shown that a frame is missing for the linking of the processes and for the determination of the step by step progress, with regard to the quality of interpretation results. ESA

N93-11356# EG and G Energy Measurements, Inc., Idaho Falls.
OPERATOR'S GUIDE FOR VAXGAP, A GAMMA-RAY SPECTRUM ANALYSIS PACKAGE
E. W. Killian and D. A. Femec Aug. 1992 87 p
(Contract DE-AC07-76ID-01570)
(DE92-019096; EGG-2672) Avail: CASI HC A05/MF A01

This report describes the gamma-ray analysis program VAXGAP, which has continually evolved at the Idaho National Engineering Laboratory over a period of several years. It is an integrated suite of computer programs for performing analyses of pulse-height spectra from high-resolution gamma-ray spectrometers and assorted support functions. VAXGAP programs operate on Digital Equipment Corporation (DEC) VAX computers running the VMS operating system, and were written in VAX FORTRAN and DEC Digital Command Language (DCL). These programs make use of DEC GKS and ReGIS for graphical output on standard terminals and printers, and DEC windows for graphics on workstations and terminals that support the X Window System protocol. This report addresses the use of VAXGAP for data acquisition and control, energy scale calibration, and real-time analyses of background and sample pulse-height spectra. Also addressed are the creation and use efficiency tables and isotope libraries, manipulation of spectrum files and their contents, and graphical display of on-going acquisitions, saved spectra, and mathematical fits to spectral peaks. DOE

N93-11368* Research Inst. for Computing and Information Systems, Houston, TX.
ANALYSIS OF METHODS Final Technical Report
Richard J. Mayer, ed. (Texas A&M Univ., College Station.), Keith A. Ackley (Texas A&M Univ., College Station.), M. Sue Wells (Texas A&M Univ., College Station.), Paula S. D. Mayer (Texas A&M Univ., College Station.), Thomas M. Blinn (Texas A&M Univ., College Station.), Louis P. Decker (Texas A&M Univ., College Station.), Joel A. Toland (Texas A&M Univ., College Station.), J. Wesley Crump (Texas A&M Univ., College Station.), Christopher P. Menzel (Texas A&M Univ., College Station.), and Charles A. Bodenmiller (Texas A&M Univ., College Station.) et al 8 Mar. 1991 134 p
(Contract NCC9-16; RICIS Proj. IM-06)
(NASA-CR-190278; NAS 1.26:190278; KBSL-89-1001) Copyright Avail: CASI HC A07/MF A02

Information is one of an organization's most important assets. For this reason the development and maintenance of an integrated information system environment is one of the most important functions within a large organization. The Integrated Information Systems Evolution Environment (IISEE) project has as one of its primary goals a computerized solution to the difficulties involved in the development of integrated information systems. To develop such an environment a thorough understanding of the enterprise's information needs and requirements is of paramount importance. This document is the current release of the research performed by the Integrated Development Support Environment (IDSE) Research Team in support of the IISEE project. Research indicates that an integral part of any information system environment would be multiple modeling methods to support the management of the organization's information. Automated tool support for these methods is necessary to facilitate their use in an integrated environment. An integrated environment makes it necessary to maintain an integrated database which contains the different kinds of models developed under the various methodologies. In addition, to speed the process of development of models, a procedure or technique is needed to allow automatic translation from one methodology's representation to another while maintaining the integrity of both. The purpose for the analysis of the modeling methods included in this document is to examine these methods with the goal being to include them in an integrated development support environment. To accomplish this and to develop a method for allowing intra-methodology and inter-methodology model element reuse, a thorough understanding of multiple modeling methodologies is necessary. Currently the IDSE Research Team is investigating the family of Integrated Computer Aided Manufacturing (ICAM) DEFinition (IDEF) languages IDEF(0), IDEF(1), and IDEF(1x), as well as ENALIM, Entity Relationship, Data Flow Diagrams, and Structure Charts, for inclusion in an integrated development support environment. M.G.

N93-11371# Rochester Inst. of Tech., NY.
SOFTWARE QUALITY METHODOLOGY INTEGRATION STUDY RESULTS Final Report, Sep. 1987 - Jul. 1990
Jeffrey A. Lasky and Michael J. Lutz May 1992 112 p
(Contract F30602-88-D-0026)
(AD-A253891; RL-TR-92-79) Avail: CASI HC A06/MF A02

The thrust of this effort was to examine the software quality methodology and determine what improvements were necessary to improve utility of this technology. Rome Laboratory has been working in the area of software quality since the earlier 70's. The goal of the framework was to provide program managers a quantitative method for gaining insight into the quality of their software products (i.e., software requirements specification, preliminary design, detailed design, coding). This effort identified short falls in the methodology due to technology advances and the need to make enhancements. Safety is one area the software quality framework does not support or address. This effort identified new quality factors that would be needed to address safety and software quality issues. Factors, criteria definitions, and metric element questions from the software quality model were reviewed within the context of defining safety. Object oriented technology (OOT) was also examined to determine what should be added to the framework. New software developments are using object oriented design and to take advantage of this technology the framework needs to be updated. Seven software quality factors and ten software criteria were identified as being impacted by the use of object oriented technology. GRA

N93-11378# Sandia National Labs., Albuquerque, NM.
AUTHENTICATION ALGORITHM FOR THE UNIVERSAL AUTHENTICATED ITEM MONITORING SYSTEMS (AIMS)
L. Fox, J. Davis, C. Jenkins, and L. Schoeneman 1992 4 p
Presented at the Institute of Nuclear Materials Management Annual Meeting, Orlando, FL, 19-22 Jul. 1992
(Contract DE-AC04-76DP-00789)
(DE92-018826; SAND-92-1646C; CONF-9207102-39) Avail: CASI HC A01/MF A01

The authentication algorithm for the AIMS system (1) provides for a method of insuring transmitted data validity. An AIMS sensor transmitter (ASTX) and Receiver Processing Unit (RPU) contain unique and identical thirty-two byte authentication keys. The ASTX'S use the authentication algorithm to generate unique authentication bytes that resultant processing of the authentication algorithm. Each message contains the transmitted data with the authentication bytes appended to it. Algorithm processing depends upon internal ASTX counters, identification bytes, data, and the authentication key. Using the data transmitted, an RPU can compute a result and compare it with the transmitted authentication bytes. Comparison of data generates a result determining validity of data. The data entering the algorithm represents a very large range of numbers, which provides a greater level of difficulty for predication of future results. Structure of the algorithm provides a method to alter the format of messages, which allows for integration into systems other than AIMS with the same effectiveness. DOE

N93-11386# Royal Signals and Radar Establishment, Malvern (England).
USING ELLA FOR HIGH LEVEL DESIGN: MODELLING THE MOTOROLA 6800 MICROPROCESSOR
A. R. Huggett 5 Sep. 1991 55 p
(RSRE-Memo-4515; BR305232; ETN-92-92320) Copyright
Avail: CASI HC A04/MF A01

The design and development of an abstract high level ELLA model of a Motorola 6800 microprocessor, including all of the 197 codes which make up the 6800 instruction set, is described. An overview of the ELLA language is given. ELLA is a textual language for describing digital hardware designs. The language is designed so that ELLA circuit descriptions are always realizable in hardware. The components of a circuit are described in ELLA by functions. A function definition declares the number and types of inputs and outputs. The function body is composed of a number of constructs, which describe how the inputs map to the outputs. Before any functions may be written in ELLA it is necessary to define the variable types which they will use. This is achieved by means of the TYPE statement. The Motorola 6800 is a simple 8 bit von Neumann microprocessor which has two 8 bit accumulators, an index register, a stack pointer, and a condition codes register. It also has a program counter. In addition, an address buffer was created. ESA

N93-11389# Royal Signals and Radar Establishment, Malvern (England). Electronics Div.
A PROCESS MONITOR FOR THE TRANSPUTER
K. R. Milner and L. Choda Nov. 1991 14 p Sponsored in part by Commission of the European Communities and Ministry of Defence
(RSRE-Memo-4554; BR308893; ETN-92-92328) Copyright
Avail: CASI HC A03/MF A01

A survey of performance monitoring tools for parallel machines is given. The particular problems of designing a performance monitor for the transputer is given. A monitor process which outputs data such as process active time and communication waiting time for each process being monitored is described. The objective was to produce a software monitor which runs in parallel with the application code to be monitored. Such a software monitor will necessarily be intrusive to some extent, but this is the price to be paid for the collection of performance data. The application is found to be rarely significantly perturbed and the information provided by a good monitoring tool is found to be possibly invaluable. ESA

N93-11390# Royal Signals and Radar Establishment, Malvern (England).
QR DECOMPOSITION BASED ALGORITHMS AND ARCHITECTURES FOR LEAST-SQUARES ADAPTIVE FILTERING
I. K. Proudler and J. G. McWhirter Jan. 1992 72 p
(RSRE-Memo-4562; BR308888; ETN-92-92330) Copyright
Avail: CASI HC A04/MF A01

The application of the method QR Deomposition (QRD) to adaptive filtering and beamforming problems is demonstrated. QR decomposition is a form of orthogonal triangularization which is particularly useful in least squares computations and forms the basis of some very stable numerical algorithms. The problem of an adaptive time series filter is also considered. Here, the data vectors exhibit a simple time shift invariance and the corresponding data matrix is of Toeplitz structure. The resulting orthogonal least squares lattice and 'fast Kalman' algorithms may be implemented using far fewer processing elements. These 'fast' QRD algorithms are very similar to the more conventional ones but, in general, are found to have superior numerical properties. The problem of multichannel adaptive filtering which arises, for example, in broadband adaptive beamforming is discussed. In this case, the data matrix has a block Toeplitz structure which may be exploited to generate an efficient multichannel fast Kalman or least squares lattice algorithm. ESA

N93-11392# Royal Signals and Radar Establishment, Malvern (England).
APPLYING ALGEBRAIC TECHNIQUES TO MICROCODE COMPILATION
C. J. Cant Jan. 1992 22 p
(RSRE-Memo-4568; BR309561; ETN-92-92333) Copyright
Avail: CASI HC A03/MF A01

The effectiveness of using algebraic techniques in the compilation of microcode is assessed. As an example system of microcode, the SMITE secure processor is considered. The SMITE research program is directed towards producing secure computing solutions, and a processor for a secure workstation was built. The instruction set of this workstation is high level language orientated and is based on that of the FLEX instruction set. The advantage of this architecture is that it uses capability addressing and this can be used as the basis of a scheme for fine grained protection of data. The firmware which supports the instruction set of SMITE/FLEX is implemented in microcode. The components of the SMAC (SMITE Microcode, Analysers, and Compilers) System, which was developed to aid the 'correct' implementation of this microcode, are described. The report also explains how an algebraic approach was used to ensure that the objectives were satisfied in the SMAC system. ESA

N93-11405# Royal Signals and Radar Establishment, Malvern (England). Electronics Div.
THE EVOLUTION OF TEN15
D. J. Tombs and D. I. Bruce 11 Nov. 1991 18 p
(RSRE-Memo-4543; BR308892; ETN-92-92325) Copyright
Avail: CASI HC A03/MF A01

Areas for study and potential evolution for the intermediate language Ten15 are described. Ten15 is a machine independent intermediate language developed to meet a wide variety of programming requirements; in particular, it offers a high degree of integrity. The design goals of Ten15 and its relationship with TDF (an intermediate format for distributing software applications) are described. The state of Ten15 at the point of its abandonment is outlined, and a detailed discussion on a number of aspects of Ten15, to highlight perceived deficiencies and possible paths of progress, is given. ESA

N93-11406# Royal Signals and Radar Establishment, Malvern (England). Electronics Div.
TEN15 DEVELOPMENTS TO SUPPORT PARALLELISM
P. W. Edwards, D. J. Tombs, and D. I. Bruce Nov. 1991 14 p
(RSRE-Memo-4545; BR307617; ETN-92-92326) Copyright
Avail: CASI HC A03/MF A01

The work done towards developing the Ten15 abstract machine to include facilities required for the expression of parallelism and techniques for implementation on parallel machines is described. The reasons for noncompletion of the development are given. Ten15 is an abstract machine founded on the use of strong typing for efficient integrity enforcement, intended to support the implementation of complete systems. The type system extends beyond the requirements of typical programming languages to support functions appropriate to operating systems. The unified type system ensures consistency both within and between separately compliled program modules, and between both static and dynamic program constructions. ESA

N93-11407# Royal Signals and Radar Establishment, Malvern (England). Electronics Div.
THE WEB APPROACH TO ELLA
H. S. Field-Richards Nov. 1991 27 p
(RSRE-Memo-4549; BR307520; ETN-92-92327) Copyright
Avail: CASI HC A03/MF A01

The literate programming approach to ELLA using Donald Knuth's WEB system is described. The system enables the ELLA program and its documentation to be bound together in one file. The memo was produced directly from a WEB file. This WEB file was also used to produce the program which was run on the ELLA system. An example of a complete and runnable piece of ELLA is given. The WEB system itself is relatively easy to learn and requires only a few rules to be used. Since, however, it is not pure ELLA there is the second disadvantage that it requires some preprocessing to produce the ELLA required for the compiler. The programming style that WEB engenders is very natural and far more obvious than a pure ELLA program. There are several advantages that WEB has over pure ELLA: WEB extends the ELLA by introducing macros; it is much easier to write structured programs, putting off low level code until it is needed, by allowing code to be defined after it has been used elsewhere; and it provides a table of contents and a full index which references program variables, macros, and functions. ESA

N93-11436# Royal Signals and Radar Establishment, Malvern (England).
A FORMAL DEFINITION OF THE STATIC SEMANTICS OF ELLA'S CORE
J. D. Morison and M. G. Hill Aug. 1991 102 p Sponsored by IED
(RSRE-91024; BR305233; ETN-92-92309) Copyright Avail: CASI HC A06/MF A02

A formal definition of the static semantics of ELLA core constructs is given. The ELLA system is an integrated hardware design toolset, which comprises the ELLA language compiler, the ELLA Applications Support Environment (EASE), the ELLA simulator and the ELLANET procedural interface. ELLA described a circuit as a hierarchy of interconnected nodes of networks. At the heart of the full ELLA language are a set of core constructs into which any ELLA description can be transformed. A set of formal transformation rules which map these core constructs into a set of data structures is described. These transformation rules define the static semantics of the language. Examples are given of circuits which are translated from the full language into ELLA's core and of core circuits which are translated via the formal transformation system into a set of data structures. ESA

N93-11458*# Research Inst. for Advanced Computer Science, Moffett Field, CA.
KRYLOV SUBSPACE METHODS FOR COMPLEX NON-HERMITIAN LINEAR SYSTEMS Thesis
Roland W. Freund May 1991 98 p
(Contract NCC2-387; NSF DCR-84-12314)
(NASA-CR-190931; NAS 1.26:190931; RIACS-TR-91.11) Avail: CASI HC A05/MF A02

We consider Krylov subspace methods for the solution of large sparse linear systems $Ax = b$ with complex non-Hermitian coefficient matrices. Such linear systems arise in important applications, such as inverse scattering, numerical solution of time-dependent Schrodinger equations, underwater acoustics, eddy current computations, numerical computations in quantum chromodynamics, and numerical conformal mapping. Typically, the resulting coefficient matrices A exhibit special structures, such as complex symmetry, or they are shifted Hermitian matrices. In this paper, we first describe a Krylov subspace approach with iterates defined by a quasi-minimal residual property, the QMR method, for solving general complex non-Hermitian linear systems. Then, we study special Krylov subspace methods designed for the two families of complex symmetric respectively shifted Hermitian linear systems. We also include some results concerning the obvious approach to general complex linear systems by solving equivalent real linear systems for the real and imaginary parts of x. Finally, numerical experiments for linear systems arising from the complex Helmholtz equation are reported. Author

N93-11478# Institut National Polytechnique, Grenoble (France).
DYNAMIC PROGRAMMING AND IMAGE PROCESSING ON DISTRIBUTED MEMORY PARALLEL MACHINES Ph.D. Thesis [PROGRAMMATION DYNAMIQUE ET TRAITEMENT D'IMAGES SUR MACHINES PARALLELES A MEMOIRE DISTRIBUEE]
Serge Miguet 1990 158 p In ENGLISH and FRENCH
(ETN-92-92174) Avail: CASI HC A08/MF A02

A thesis on the implementation of parallel algorithms on distributed memory computers is presented. By taking into account several examples from dynamic programming, linear algebra, and image processing, the specific problems that occur when programming these machines are exposed: interconnection topologies, data allocation strategies, workload balancing, and interprocessor communication. The examples studied are computer intensive and memory consuming algorithms for which an efficient parallelization is very interesting. They are difficult to parallelize because of the great interdependency between the tasks composing the algorithms. Research articles are reprinted. For individual titles, see N93-11479 through N93-11484.

N93-11479# Ecole Normale Superieure, Lyon (France). Lab. de l'Informatique du Parallelisme.
DYNAMIC PROGRAMMING ON A RING OF PROCESSORS
Serge Miguet and Yves Robert *In* Inst. National Polytechnique de Grenoble, Dynamic Programming and Image Processing on Distributed Memory Parallel Machines 1990 p 55-69 Repr. from Hypercubes and Distributed Computers (North-Holland, Netherlands, Elseiver Science Publisher B.V.), 1989 p 19-33 Sponsored by CNRS (For primary document see N93-11478 02-61)
Avail: CASI HC A03/MF A02

Various data allocation strategies for the parallel implementation of some dynamic programming problems in a ring of processors are discussed. Column oriented schemes are considered and blocks of r consecutive columns of the cost matrix are allocated to the processors in a wraparound fashion. It is shown that the smaller the r, the better balanced the arithmetic, but also the more costly the communications. The optical value of r, which minimizes the parallel execution time as a function of the ratio of the number of processors over the problem size, and the ratio of the elemental communication time over the elemental arithmetic time are analytically determined. These theoretical results are corroborated by numerical experiments on a ring of transputers. ESA

N93-11480# Ecole Normale Superieure, Lyon (France). Lab. de l'Informatique du Parallelisme.
PATH PLANNING ON A RING OF PROCESSORS
Serge Miguet and Yves Robert *In* Inst. National Polytechnique de Grenoble, Dynamic Programming and Image Processing on Distributed Memory Parallel Machines 1990 p 73-86 Repr. from Intern. J. Computer Math. (England, Gordon and Breach, Science Publishers, Inc.), v. 32, 1990 p 61-74 Sponsored by CNRS (For primary document see N93-11478 02-61)
Avail: CASI HC A03/MF A02

The implementation of Bitz and Kung's path planning algorithm on a ring of general purpose processors is discussed. Bitz and Kung's algorithm, originally designed for the Warp machine, is shown to be efficient in this context, due to the intensive interprocessor communications required. A modified more performing version which updates a segment of k positions within the step and allocates blocks of r consecutive rows of the map to the processors in a wraparound fashion is designed. Bitz and Kung's algorithm corresponds to the situation (K, r) = (1, 1). The optical values of the parameters (k, r), which minimize the parallel execution time as a function of the problem size and the number of processors, are analytically determined. The theoretical results are corroborated by numerical experiments on a ring of 32 transputers. ESA

N93-11481# Ecole Normale Superieure, Lyon (France). Lab. de l'Informatique du Parallelisme.
SYMMETRIC MATRIX-VECTOR PRODUCT ON A RING OF PROCESSORS
Ken Grigg (Carleton Univ., Ottawa, Ontario), Serge Miguet, and Yves Robert *In* Inst. National Polytechnique de Grenoble, Dynamic Programming and Image Processing on Distributed Memory Parallel Machines 1990 p 89-98 Repr. from Information Processing Letters (North-Holland, Netherlands, Elsevier Science Publishers B.V.), v. 35, 1990 p 239-248 Revised Sponsored by CNRS and Natural Sciences and Engine ering Research Council (For primary document see N93-11478 02-61)
Avail: CASI HC A02/MF A02

The implementation of the product of a symmetric matrix by a vector on a unidirectional ring of general pupose processors is discussed. One of these kernels, issuing from control systems, is discussed. The difficulty comes from the fact that only one half of the matrix is stored (in a distributed way) in the processor memories. An efficient algorithm is derived and its performance as a function of the problem size and of the number of processors is analytically determined. The algorithm is shown to be optimal, both with or without the assumption that arithmetic and communications can overlap. The theoretical results are corroborated by numerical experiments in a ring of 32 transputers. ESA

N93-11482# Ecole Normale Superieure, Lyon (France). Lab. de l'Informatique du Parallelisme.
SCATTERING ON A RING OF PROCESSORS
Pierre Fraigniaud, Serge Miguet, and Yves Robert *In* Inst. National Polytechnique de Grenoble, Dynamic Programming and Image Processing on Distributed Memory Parallel Machines 1990 p 101-107 Repr. from Parallel Computing (North-Holland, Netherlands, Elsevier Science Publishers B.V.), v. 13, 1990 p 377-383 Sponsored in part by CNRS and Direction des Recherches et Etudes Techniques (For primary document see N93-11478 02-61)
Avail: CASI HC A02/MF A02

The scattering operation in a ring architecture is addressed. A proof that the complexity of scattering on an oriented ring of p processors is (p - 1) (beta + L(tau)), where L = the length of the messages, beta = the communication startup, andtau = the elemental propagation time is presented. ESA

N93-11483# Ecole Normale Superieure, Lyon (France). Lab. de l'Informatique du Parallelisme.
Z-BUFFER ON A TRANSPUTER-BASED MACHINE
Jian-Jin Li and Serge Miguet *In* Inst. National Polytechnique de Grenoble, Dynamic Programming and Image Processing on Distributed Memory Parallel Machines 1990 p 111-127 Sponsored by CNRS, and Institut de Mathematiques Appliquees de Grenoble (For primary document see N93-11478 02-61)
Avail: CASI HC A03/MF A02

The parallel implementation of the Z buffer algorithm on a distributed memory machine is described. The Z buffer is one of of the most popular techniques used to generate a representation of a scene consisting of objects in a three dimensional world. Two different parallel implementations on a network of transputers are proposed and compared. In the first approach, the description of the scene is distributed among the processors configured as a tree. The picture is processed in a pipelined fashion, in order to output parts of the image during the computation of the remainder. The influence of the degree and the height of the tree on the global performance of the algorithm is shown. In a second approach, a ring network is used to interconnect the processors. In this version, both the picture and the scene description are distributed to the processors. The tiles are therefore redistributed dynamically among the processors at the beginning of the computation. The two approaches are shown to be complementary: for stall pictures or large scenes, a tree based algorithm performs better than a ring based algorithm, but vice versa for large pictures or smaller scenes. Substantial speedups are obtained over the sequential implementation with up to 32 processors. ESA

N93-11484# Ecole Normale Superieure, Lyon (France). Lab. de l'Informatique du Parallelisme.
REDUCTION OPERATIONS ON A DISTRIBUTED MEMORY MACHINE WITH A RECONFIGURABLE INTERCONNECTION NETWORK
Serge Miguet and Yves Robert *In* Inst. National Polytechnique de Grenoble, Dynamic Programming and Image Processing on Distributed Memory Parallel Machines 1990 p 131-151 Sponsored by CNRS; Institut de Mathematiques Appliquee de Grenoble; and Commission of the European Communities (For primary document see N93-11478 02-61)
Avail: CASI HC A03/MF A02

Reduction operations with distributed memory machines whose interconnection networks are reconfigurable are addressed. More precisely, focus is on machines whose interconnection graph can be configured as any graph of maximum degree d. The best way of interconnecting the p processors as a function of p, d, and some problem and machine dependent parameters that characterize the ratio communication/arithmetic for the reduction operation are given. Experiments on transputer based networks are in good accordance with the theoretical results. ESA

N93-11536# Sandia National Labs., Albuquerque, NM.
OPTIMIZATION OF EXPRESSIONS INVOLVING ARRAY CLASSES
K. G. Budge 1992 8 p Presented at the American National Standards Institute X3J16/ISO WG21 Meeting, Toronto, Ontario, 12-18 Jul. 1992
(Contract DE-AC04-76DP-00789)
(DE92-019421; SAND-92-1655C; CONF-9207136-1) Avail: CASI HC A02/MF A01

C++ is rapidly gaining in popularity as a scientific programming language. The data encapsulation inherent in the class concept and the availability of operator overloading for compact representation of operations make it an ideal language for translating concepts in mathematical physics into computer code. Furthermore, its strong type checking and memory management features facilitate correct coding of algorithms. Unfortunately, C++ code which is written in the true spirit of the language is often very inefficient under current compiler implementations. Many of the inefficiency issues, such as unnecessary copy operations or proliferation of temporaries, have been well-characterized. Some may be alleviated by clever C++ coding, but others cannot be alleviated except by writing C-like code that sacrifices one or more of the best features of the language. This document describes a major source of efficiency problems in expressions using overloaded operators on array classes, and proposes certain minor modifications to the C++ language standard which will facilitate optimization of these expressions. DOE

N93-11555# Fermi National Accelerator Lab., Batavia, IL.
A COMPUTER ALGORITHM FOR AUTOMATIC BEAM STEERING
E. Drennan Jun. 1992 10 p
(Contract DE-AC02-76CH-03000)
(DE92-019338; FNAL-TM-1787) Avail: CASI HC A02/MF A01

Beam steering is done by modifying the current in a trim or bending magnet. If the current change is the right amount, the beam can be made to bend in such a manner that it will hit a swic or BPM downstream from the magnet at a predetermined set point. Although both bending magnets and trim magnets can be used to modify beam angle, beam steering is usually done with trim magnets. This is so because, during beam steering the beam angle is usually modified only by a small amount which can be easily achieved with a trim magnet. Thus in this note, all steering magnets will be assumed to be trim magnets. There are two ways of monitoring beam position. One way is done using a BPM and the other is done using a swic. For simplicity, beam position monitoring in this paper will be referred to being done with a swic. Beam steering can be done manually by changing the current through a trim magnet and monitoring the position of the beam downstream from the magnet with a swic. Alternatively the beam can be positioned automatically using a computer which periodically updates the current through a specific number of trim magnets. The purpose of this note is to describe the steps involved in coming up with such a computer program. There are two main aspects to automatic beam steering. First a relationship between the beam position and the bending magnet is needed. Secondly a beamline setup of swics and trim magnets has to be chosen that will position the beam according to the desired specifications. A simple example will be looked at that will show that once a mathematical relationship between the needed change of the beam position on a swic and the change in trim currents is established, a computer could be programmed to calculate and update the trim currents. DOE

N93-11592 Politecnico di Milano (Italy). Dipartimento di Elettronica.
GEOMETRICAL CONCEPTS ABOUT LEARNING RULES IN NETWORKS WITH BINARY AND TERNARY OUTPUT FUNCTIONS
F. Carlucci and G. StortiGajani Mar. 1992 27 p
(Rept-92-020; ETN-92-92421) Avail: Politecnico di Milano, Piazza Leonardo da Vinci 32, 20133 Milan, Italy

A study aimed at posing the backgrounds, in particular from a geometrical point of view, for a learning procedure for mixed binary and ternary output units, is presented. To achieve this result, the examination of the geometrical properties of a single neuron as related to its activation function was chosen. The case of linear and single step (thus binary) output functions is considered: with the preliminary analysis (that gives the geometrical interpretation of the neuron's output and weights) it is possible to obtain the best weight correction to apply in these two cases. The three step (ternary) output function is studied: a geometrical introduction is followed by the ternary unit convergence theorem. This theorem is an extension of the well known 'perceptron convergence theorem': if a solution exists, it will be reached in finite time. ESA

N93-11594 Politecnico di Milano (Italy). Dipartimento di Elettronica.
A FAST PIPELINED INNER PRODUCT UNIT
Luigi Dadda Apr. 1992 22 p
(Rept-92-025; ETN-92-92423) Avail: Politecnico di Milano, Piazza Leonardo da Vinci 32, 20133 Milan, Italy

In the processing chain of samples generated in a group of channels in the Fermi project for the design of a calorimeter to be used for high energy particle experiments, a weighted sum of the samples of specified time windows, that is, an inner product of a weighed and of a samples vector, is required. A scheme of a unit performing such operation is described. The window is determined by the unit controller, and the n = 15 bits N samples are supplied in parallel form by a buffer memory at the basic clock rate of 67 Msample/sec. The weights are stored in a memory and read out in synchronism with the samples in skew form. The inner product unit is composed by a pipelined multiplier generating the products in skew form and by a skew input accumulator. The skew form allows the additions to be performed at high speed, the carries propagation being obtained as in a serial adder. This at the expense of a latency of n + (log(sub 2)N) clock periods. The implementation of fault detection is also discussed. ESA

N93-11599# Sandia National Labs., Albuquerque, NM.
TEMPERATURE TRACKING SPICE MACRO-MODEL FOR LASER AND LED DRIVEN OPTO-COUPLER ASSEMBLIES
M. F. Deveney 1992 7 p Presented at the 35th Midwest Symposium on Circuits and Systems, Washington, DC, 12 Aug. 1992
(Contract DE-AC04-76DP-00789)
(DE92-019296; SAND-92-0661C; CONF-9208119-1) Avail: CASI HC A02/MF A01

SPICE 2G.6 compatible models were required for two opto-coupler assemblies in order to perform simulations to assess the design margins of the circuits in which they are used. Both of these assemblies are made up of discrete components, with one employing a laser diode as the light source, while the second uses a LED. Although, in use, these assemblies couple digital-like pulse trains, they are analog devices capable of operating over wider ranges of voltage than digital devices. Robust models which accurately simulate over these voltage ranges were desired. Also for ease of use, models that would track the operation of each of the assemblies over the entire specified temperature range were preferred. In addition to simulating the assembles in their intended mode of operation, it was necessary to reproduce an unwanted noise signal transfer that was observed in an early prototype circuit. DOE

N93-11618*# Institute for Computer Applications in Science and Engineering, Hampton, VA.

CONCURRENT FILE OPERATIONS IN A HIGH PERFORMANCE FORTRAN Final Report

Peter Brezany (Wien Univ., Austria), Michael Gerndt (Forschungszentrum Juelich G.m.b.H., Germany), Piyush Mehrotra, and Hans Zima (Wien Univ., Austria) Sep. 1992 18 p Submitted for publication
(Contracts NAS1-18605; NAS1-19480; RTOP 505-90-52-01)
(NASA-CR-189711; NAS 1.26:189711; ICASE-92-46) Avail: CASI HC A03/MF A01

Distributed memory multiprocessor systems can provide the computing power necessary for large scale scientific applications. A critical performance issue for a number of these applications is the efficient transfer of data to secondary storage. Recently several research groups have proposed FORTRAN language extensions for exploiting the data parallelism of such scientific codes on distributed memory architectures. However, few of these high performance FORTRAN's provide appropriate constructs for controlling the use of the parallel I/O capabilities of modern multiprocessing machines. In this paper, we propose constructs to specify I/O operations for distributed data structures in the context of Vienna Fortran. These operations can be used by the programmer to provide information which can help the compiler and runtime environment make the most efficient use of the I/O subsystem. Author

N93-11664*# National Aeronautics and Space Administration. Pasadena Office, CA.

MAPPINGS BETWEEN CODEWORDS OF TWO DISTINCT (N,K) REED-SOLOMON CODES OVER GF(2 SUP J) Patent Application

Marvin Perlman, inventor (to NASA) (Jet Propulsion Lab., California Inst. of Tech., Pasadena.) 3 Sep. 1992 98 p
(Contract NAS7-918)
(NASA-Case-NPO-18771-1-CU; NAS 1.71:NPO-18771-1-CU; US-Patent-Appl-SN-942500) Avail: CASI HC A05/MF A02

A process for realizing mappings between code-words of two distinct (N,K) Reed-Solomon (RS) codes over GF(2 sup J) having selected two independent parameters: J, specifying the number of bits per symbol; and E(sub 1), the symbol error correction capability of the code, wherein said independent parameters J and E yield the following: N = 2(sup J)-1 total number of symbols per codeword; 2E, the number of symbols assigned a role of check symbols; and K-N-2E, the number of code symbols representing information, all within a codeword of an (N,K) RS code over GF(2 sup J), and having selected said parameters for encoding, the implementation of a decoder are governed by: 2(sup J) field elements defined by a degree J primitive polynomial over GF(2) denoted by F(x); a code generator polynomial of degree 2E containing 2E consecutive roots of a primitive element defined by F(x); and, in a Berlekamp RS code, the basis in which the RS information and check symbols are represented. The process includes separate transformation steps for symbol-by-symbol conversion for a first RS code to ultimately a second conventional RS code capable of being corrected by a conventional RS decoder, followed by a reverse sequence of the inverse of the first set of steps to arrive at codewords having connected information symbols, at which time check symbols of the RS code may be discarded. NASA

N93-11688 National Physical Lab., Teddington (England). Div. of Information Technology and Computing.

INTERFACING MATLAB AND SOFTWARE WRITTEN IN OTHER LANGUAGES

B. P. Butler May 1992 25 p
(NPL-DITC-200/92; ETN-92-92377) Copyright Avail: National Physical Lab., Teddington, Middlesex, TW11 0LW, England

Issues involved in calling object code routines from the Matlab environment are discussed. The use of compiled FORTRAN subprograms, is focused upon, although some consideration is given to other high level languages. Special reference is made to the use of gateways under VAX/VMS systems. Methods are proposed for overcoming particular difficulties and conclusions are presented which are derived from practical experience of writing interface software. The ability to harness the power of reliable mathematical software systems such as the NAG library is highlighted. ESA

N93-11712# Royal Signals and Radar Establishment, Malvern (England).

COMPUTING OPTIMUM ROUTES ACROSS TERRAIN USING DAP

R. Haynes, C. Packer, J. B. G. Roberts, and P. Simpson Jul. 1989 35 p Original contains color illustrations
(RSRE-Memo-4299; BR111965) Copyright Avail: CASI HC A03/MF A01

Dynamic programming techniques provide quantitative ways for determining optimum routes across complex terrain for various assumed categories of vehicle, taking account of gradients, the presence of absence of roads, and obstacles such as rivers, urban areas, woods, etc. We have investigated the effectiveness of a highly parallel SIMD computer (Mil-DAP) to this problem. We conclude that, although impressive computation speeds can be obtained on high resolution digital maps with Mil-DAP, the conflict between exploiting high order SIMD parallelism and minimizing the number of necessary computation operations is such that in this case Mil-DAP does not command a dominating advantage over a conventional uniprocessor. Author

N93-11717*# Research Inst. for Computing and Information Systems, Houston, TX.

AN EVACS SIMULATION WITH NESTED TRANSACTIONS

David Auty (Softech, Inc., Houston, TX.), Collin Atkinson (Houston Univ., Clear Lake, TX.), and Charlie Randall (GHG Corp., Houston, TX.) 30 Jun. 1992 36 p
(Contracts NCC9-16; UHCL-102; RICIS Proj. SE-16)
(NASA-CR-190636; NAS 1.26:190636) Avail: CASI HC A03/MF A01

Documented here is the recent effort of the MISSION Kernel Team on an Extra-Vehicular Activity Control System (EVACS) simulation with nested transactions. The team has implemented the EVACS simulation along with a design for nested transactions. The EVACS simulation is a project wide aid to exploring Mission and Safety Critical (MASC) applications and their support software. For this effort it served as a trial scenario for demonstrating nested transactions and exercising the transaction support design. The EVACS simulation is a simulation of some aspects of the Extra-Vehicular Activity Control System, in particular, just the selection of communication frequencies. Its current definition is quite narrow, serving only as a starting point for prototyping purposes. (EVACS itself may be supplanted in a larger scenario of a lunar outpost with astronauts and a lunar rover.) Initially the simulation of frequency selection was written without consideration of nested transactions. This scenario was then modified to embed its processing in nested transactions. To simplify the prototyping effort, only two aspects of the general design for transaction support have been implemented: the basic architecture and state recovery. The simulation has been implemented in the programming language Smalltalk. It consists of three components: (1) a simulation support code which provides the framework for initiating, interacting and tracing the system; (2) the EVACS application code itself, including its calls upon nested transaction support; and (3) a transaction support code which implements the logic necessary for nested transactions. Each of these components deserves further description, but for now only the transaction support is discussed. Author

N93-11859# Naval Postgraduate School, Monterey, CA.

THE EFFECT OF TASK COMPLEXITY ON USER INTERFACES: A COMPARISON OF COMMAND LANGUAGE INTERFACE AND DIRECT MANIPULATION INTERFACE M.S. Thesis

Nancy A. Reinhard Mar. 1991 135 p
(AD-A246061) Avail: CASI HC A07/MF A02

A computer-user interface is the software that communicates the user's inputs to the computer and returns information from the computer back to the user. A variety of user interfaces have been developed, including command language interfaces, direct manipulation interfaces, and menus. This research explored the relative benefits of command language interfaces (CLI) and direct manipulation interfaces (DMI) for performance of simple and complex tasks by novices. Two levels of task complexity were used, one requiring five inputs (simple) and one requiring 24 inputs (complex). Dependent variables were (1) time to complete each task set, (2) number of errors, and (3) number of references to online help. Results indicate that learning to use a DMI takes longer than learning to use a CLI. No significant difference was observed in time to complete the simple task. However, once a novice learns to use a DMI, a complex task requires less time, fewer errors are made, and references to help screens are required less often. With complex tasks, direct manipulation interfaces appear to help novices to be more productive than do command language interfaces. GRA

N93-12022*# National Aeronautics and Space Administration. Lewis Research Center, Cleveland, OH.

COMPUTER AIDED DESIGN AND MANUFACTURING OF COMPOSITE PROPFAN BLADES FOR A CRUISE MISSILE WIND TUNNEL MODEL

Scott A. Thorp and Kevin M. Downey (Sverdrup Technology, Inc., Brook Park, OH.) Sep. 1992 66 p
(RTOP 535-03-0B)
(NASA-TM-105269; E-6497; NAS 1.15:105269) Avail: CASI HC A04/MF A01

One of the propulsion concepts being investigated for future cruise missiles is advanced unducted propfans. To support the evaluation of this technology applied to the cruise missile, a joint DOD and NASA test project was conducted to design and then test the characteristics of the propfans on a 0.55-scale, cruise missile model in a NASA wind tunnel. The configuration selected for study is a counterrotating rearward swept propfan. The forward blade row, having six blades, rotates in a counterclockwise direction, and the aft blade row, having six blades, rotates in a clockwise direction, as viewed from aft of the test model. Figures show the overall cruise missile and propfan blade configurations. The objective of this test was to evaluate propfan performance and suitability as a viable propulsion option for next generation of cruise missiles. This paper details the concurrent computer aided design, engineering, and manufacturing of the carbon fiber/epoxy propfan blades as the NASA Lewis Research Center. Author

N93-12110# California Univ., Berkeley. Lawrence Berkeley Lab.

DENSITY EQUALIZING MAP PROJECTIONS: A NEW ALGORITHM

D. W. Merrill, S. Selvin, and M. S. Mohr Feb. 1992 3 p Presented at the Distancia 1992: International Meeting on Distance Analysis, Rennes (France), 22-26 Jun. 1992
(Contract DE-AC03-76SF-00098)
(DE92-017088; LBL-31984; CONF-9206213-1) Avail: CASI HC A01/MF A01

In the study of geographic disease clusters, an alternative to traditional methods based on rates is to analyze case locations on a transformed map in which population density is everywhere equal. Although the analyst's task is thereby simplified, the specification of the density equalizing map projection (DEMP) itself is not simple and continues to be the subject of considerable research. Here a new DEMP algorithm is described, which avoids some of the difficulties of earlier approaches. The new algorithm avoids illegal overlapping of transformed polygons; finds the unique solution that minimizes map distortion; provides constant magnification over each map polygon; defines a continuous transformation over the entire map domain; defines an inverse transformation; can accept optional constraints such as fixed boundaries; and can use commercially supported minimization software. Work is continuing to improve computing efficiency and improve the algorithm. DOE

N93-12131# Stanford Univ., CA. Dept. of Computer Science.

POLYNOMIAL DUAL NETWORK SIMPLEX ALGORITHMS

James B. Orlin, Serge A. Plotkin, and Eva Tardos Aug. 1991 25 p
(Contract N00014-88-K-0166; NSF CCR-90-08226)
(AD-A254340; SU-STAN-CS-91-1374) Avail: CASI HC A03/MF A01

We show how to use polynomial and strongly polynomial capacity scaling algorithms for the transshipment problem to design a polynomial dual network simplex pivot rule. Our best pivoting strategy leads to an O(m(sub2) log n) bound on the number of pivots, where n and m denotes the number of nodes and arcs in the input network. If the demands are integral and at most B, we also give an O(m(m + n log n) min(log(nB), m log n))-time implementation of a strategy that requires somewhat more pivots. GRA

N93-12137# Lawrence Livermore National Lab., CA.

HIGHER-ORDER GENERIC FUNCTIONS FOR CLOS

J. E. Hernandez Mar. 1992 9 p Presented at the Conference on Object-Oriented Programming Systems, Languages, and Applications, Vancouver (Canada), 18-22 Oct. 1992
(Contract W-7405-eng-48)
(DE92-013447; UCRL-JC-109776; CONF-921084-1) Avail: CASI HC A02/MF A01

This paper presents a framework for developing higher-order generic functions within the Common Lisp Object System similar to the ones in Common Lisp for processing sequences. The framework consist of several CLOS classes which define a protocol that allows other classes to inherit default methods for many higher-order generic functions. These generic functions provide an elegant and uniform framework for processing CLOS objects that primarily represent collections of other objects. DOE

N93-12146# Raytheon Co., Marlborough, MA. Equipment Div.

TESTABILITY DESIGN RATING SYSTEM. VOLUME 2: ANALYTICAL PROCEDURE Final Report, Jun. 1989 - Feb. 1991

Ronald E. Press, Michael E. Keller, and Gregory J. Maguire Feb. 1992 486 p
(Contract F30602-89-C-0121)
(AD-A254333; RL-TR-92-12-Vol-2) Avail: CASI HC A21/MF A04

This effort provides a means of rating the testability of an electronic design at any stage in the design life. Volume 1, Testability Handbook, discusses the particulars of the circuit design and how they relate to testability. It also discusses the software developed in this program and how to obtain the software. The software, which will run on any IBM compatible PC having 512 k of available memory and a hard disk, asks a number of questions, and based on the answers, will provide a testability rating and a credibility rating. Volume 2 provides means of doing the testability analysis without the computer. GRA

N93-12159# Army Armament Research, Development and Engineering Center, Watervliet, NY. Benet Lab.

MULTIFRACTAL ANALYSIS AT NEGATIVE q Final Report

Mark Johnson and L. V. Meisel Aug. 1992 13 p
(AD-A254370; ARCCB-TR-92037) Avail: CASI HC A03/MF A01

A box-based correlation integral algorithm for the determination of generalized fractal dimensions is described. The algorithm has been tested for Euclidean curves, Koch symmetric, and asymmetric triadic split snowflake halls, and the multifractal construction based on Mandelbrot's 13-element generator is well-suited to the analysis of experimental data with inherent uncertainty, it is efficient, and it converges to analysis results for the model point sets at all q values. GRA

N93-12187# Argonne National Lab., IL. Environmental Assessment and Information Sciences Div.

PROGRAM FOR IMPLEMENTING SOFTWARE QUALITY METRICS

H. P. Yule and C. A. Riemer Apr. 1992 27 p
(Contract W-31-109-eng-38)
(DE92-018617; ANL/EAIS/TM-71) Avail: CASI HC A03/MF A01

This report describes a program by which the Veterans Benefit Administration (VBA) can implement metrics to measure the performance of automated data systems and demonstrate that they are improving over time. It provides a definition of quality, particularly with regard to software. Requirements for management and staff to achieve a successful metrics program are discussed. It lists the attributes of high-quality software, then describes the metrics or calculations that can be used to measure these attributes in a particular system. Case studies of some successful metrics programs used by business are presented. The report ends with suggestions on which metrics the VBA should use and the order in which they should be implemented. DOE

N93-12234# Lawrence Livermore National Lab., CA.
DYNAMIC MULTIMODAL FUNCTION OPTIMIZATION USING GENETIC ALGORITHMS
W. Cedeno and V. Vemuri 20 Jul. 1992 13 p Presented at the 18th Conference Latin American of Information, Las Palmas de Gran, Spain, 31 Aug. - 4 Sept. 1992
(Contract W-7405-eng-48)
(DE92-019602; UCRL-JC-111089; CONF-9208118-1) Avail: CASI HC A03/MF A01

Many optimization techniques work well for unimodal functions. If applied to multimodal functions, they tend to converge to only one of the many peaks. Optimization of multimodal functions becomes even more difficult if the function parameters change dynamically. Genetic algorithms have been successfully applied by several investigators for static optimization of multimodal functions. This modest success is primarily due to the ability of genetic algorithms to locate more than one peak. In this paper, we introduce a combination of selection and replacement operators that is suitable for multimodal function optimization in a dynamic environment using various test functions; performance of this new operator is studied. Utility of this new operator to multimodal function optimization in a dynamic environment is described. DOE

N93-12242# Kaman Sciences Corp., Colorado Springs, CO.
ALGORITHMS FOR SENSOR FUSION: DECENTRALIZED BAYESIAN HYPOTHESIS TESTING WITH FEEDBACK, VOLUME 1 Final Report, Oct. 1990 - May 1991
Pramod K. Varshney and Samawal Al-Hakeem Dec. 1991 152 p
(Contract F30602-89-C-0082)
(AD-A254633; RL-TR-91-423-Vol-1) Avail: CASI HC A08/MF A02

Classical signal detection involved centralized signal processing. A single sensor was employed for making observations which were processed centrally. The need for increased reliability and survivability of communication systems has led to the deployment of multiple sensors for signal detection. Various types of sensors are utilized to observe the environment. The collected data is sent to a central processor where classical hypothesis testing procedures are employed for signal processing. GRA

N93-12278*# National Aeronautics and Space Administration. Langley Research Center, Hampton, VA.
CURRENT STATE AND FUTURE DIRECTION OF COMPUTER SYSTEMS AT NASA LANGLEY RESEARCH CENTER
James L. Rogers, ed. and Jerry H. Tucker, ed. Sep. 1992 34 p
(RTOP 509-10-11-04)
(NASA-TM-107685; NAS 1.15:107685) Avail: CASI HC A03/MF A01

Computer systems have advanced at a rate unmatched by any other area of technology. As performance has dramatically increased there has been an equally dramatic reduction in cost. This constant cost performance improvement has precipitated the pervasiveness of computer systems into virtually all areas of technology. This improvement is due primarily to advances in microelectronics. Most people are now convinced that the new generation of supercomputers will be built using a large number (possibly thousands) of high performance microprocessors. Although the spectacular improvements in computer systems have come about because of these hardware advances, there has also been a steady improvement in software techniques. In an effort to understand how these hardware and software advances will effect research at NASA LaRC, the Computer Systems Technical Committee drafted this white paper to examine the current state and possible future directions of computer systems at the Center. This paper discusses selected important areas of computer systems including real-time systems, embedded systems, high performance computing, distributed computing networks, data acquisition systems, artificial intelligence, and visualization. Author

N93-12284# Mitre Corp., Bedford, MA.
A GENETIC ALGORITHM FOR SEARCH ROUTE PLANNING Final Report
James R. VanZandt Jul. 1992 49 p
(Contract F19628-89-C-0001)
(AD-A254894; MTR-11177; ESD-TR-92-262) Avail: CASI HC A03/MF A01

Planning an airborne search for a relocatable target involves minimizing the risk to the crew while maximizing the estimated likelihood of finding targets. When the number of potential sites is small, the problem reduces to finding the best (usually the shortest) route connecting them. When the number of sites is larger, however, the planner must also decide which of them are to be visited. This report presents a genetic algorithm for selecting both an appropriate set of sites to visit and an appropriate routing pattern. The procedure also accounts for the finite turning radius of the aircraft. GRA

N93-12326# Royal Signals and Radar Establishment, Malvern (England).
SYNTAX AND LEXIS OF THE SPECIFICATION LANGUAGE Z
C. T. Sennett Feb. 1990 25 p
(RSRE-Memo-4367; BR113378) Copyright Avail: CASI HC A03/MF A01

A contribution to the standardization of the specification language Z is presented. It deals with the presentation issues which need to be settled in the definition of the Z language from the viewpoint of users and tool makers. These include lexical matters, the representation of Z in ASCII symbols, overall questions of syntax and usage, detailed areas of syntactic divergence, and some unresolved issues in the type-checking system. Author

N93-12341# Naval Surface Warfare Center, Silver Spring, MD.
REENGINEERING USING A DATA ABSTRACTION BASED SPECIFICATION LANGUAGE Final Report
Randall E. Duran 27 Sep. 1991 71 p
(AD-A254726; NAVSWC-TR-91-388) Avail: CASI HC A04/MF A01

This report describes how a reengineering methodology was developed and applied to convert part of a system implemented in CMS-2 to a new C implementation. In particular, this methodology used Larch specifications as an intermediate design representation that was obtained through reverse engineering. The benefits of using this methodology and ways of improving it, primarily through automation, are suggested. GRA

N93-12384*# Research Inst. for Computing and Information Systems, Houston, TX.
THE SoRReL PAPERS: RECENT PUBLICATIONS OF THE SOFTWARE REUSE REPOSITORY LAB
David A. Eichmann, ed. (West Virginia Univ., Morgantown.) 20 May 1992 125 p
(Contract NCC9-16; RICIS Proj. SE-43)
(NASA-CR-190894; NAS 1.26:190894) Avail: CASI HC A06/MF A02

The entire publication is presented of some of the papers recently published by the SoRReL. Some typical titles are as follows: Design of a Lattice-Based Faceted Classification System; A Hybrid Approach to Software Reuse Repository Retrieval; Selecting Reusable Components Using Algebraic Specifications; Neural Network-Based Retrieval from Reuse Repositories; and A Neural Net-Based Approach to Software Metrics. For individual titles, see N93-12385 through N93-12393.

N93-12385*# West Virginia Univ., Morgantown. Software Reuse Repository Lab.

DESIGN OF A LATTICE-BASED FACETED CLASSIFICATION SYSTEM

David A. Eichmann and John Atkins *In* Research Inst. for Computing and Information Systems, The SoRReL Papers: Recent Publications of the Software Reuse Repository Lab 20 May 1992 8 p Presented at the Second International Conference on Software Engineering and Knowledge Engineering, Skokie, IL, 21-23 Jun. 1990 Sponsored in part by MountainNet (For primary document see N93-12384 02-61)
Avail: CASI HC A02/MF A02

We describe a software reuse architecture supporting component retrieval by facet classes. The facets are organized into a lattice of facet sets and facet n-tuples. The query mechanism supports precise retrieval and flexible browsing. Author

N93-12386*# West Virginia Univ., Morgantown. Software Reuse Repository Lab.

A HYBRID APPROACH TO SOFTWARE REPOSITORY RETRIEVAL: BLENDING FACETED CLASSIFICATION AND TYPE SIGNATURES

David A. Eichmann *In* Research Inst. for Computing and Information Systems, The SoRReL Papers: Recent Publications of the Software Reuse Repository Lab 20 May 1992 6 p Presented at the Third International Conference on Software Engineering and Knowledge Engineering, Skokie, IL, 27-29 Jun. 1991 (For primary document see N93-12384 02-61)
Avail: CASI HC A02/MF A02

We present a user interface for software reuse repository that relies both on the informal semantics of faceted classification and the formal semantics of type signatures for abstract data types. The result is an interface providing both structural and qualitative feedback to a software reuser. Author

N93-12387*# West Virginia Univ., Morgantown. Software Reuse Repository Lab.

SELECTING REUSABLE COMPONENTS USING ALGEBRAIC SPECIFICATIONS

David A. Eichmann *In* Research Inst. for Computing and Information Systems, The SoRReL Papers: Recent Publications of the Software Reuse Repository Lab 20 May 1992 11 p Submitted for publication (For primary document see N93-12384 02-61)
Avail: CASI HC A03/MF A02

A significant hurdle confronts the software reuser attempting to select candidate components from a software repository - discriminating between those components without resorting to inspection of the implementation(s). We outline a mixed classification/axiomatic approach to this problem based upon our lattice-based faceted classification technique and Guttag and Horning's algebraic specification techniques. This approach selects candidates by natural language-derived classification, by their interfaces, using signatures, and by their behavior, using axioms. We briefly outline our problem domain and related work. Lattice-based faceted classifications are described; the reader is referred to surveys of the extensive literature for algebraic specification techniques. Behavioral support for reuse queries is presented, followed by the conclusions. Author

N93-12388*# West Virginia Univ., Morgantown. Software Reuse Repository Lab.

NEURAL NETWORK-BASED RETRIEVAL FROM SOFTWARE REUSE REPOSITORIES

David A. Eichmann and Kankanahalli Srinivas *In* Research Inst. for Computing and Information Systems, The SoRReL Papers: Recent Publications of the Software Reuse Repository Lab 20 May 1992 14 p Submitted for publication (For primary document see N93-12384 02-61)
Avail: CASI HC A03/MF A02

A significant hurdle confronts the software reuser attempting to select candidate components from a software repository - discriminating between those components without resorting to inspection of the implementation(s). We outline an approach to this problem based upon neural networks which avoids requiring the repository administrators to define a conceptual closeness graph for the classification vocabulary. Author

N93-12389*# West Virginia Univ., Morgantown. Software Reuse Repository Lab.

INHERITANCE FOR SOFTWARE REUSE: THE GOOD, THE BAD, AND THE UGLY

Murali Sitaraman and David A. Eichmann *In* Research Inst. for Computing and Information Systems, The SoRReL Papers: Recent Publications of the Software Reuse Repository Lab 20 May 1992 8 p (For primary document see N93-12384 02-61)
Avail: CASI HC A02/MF A02

Inheritance is a powerful mechanism supported by object-oriented programming languages to facilitate modifications and extensions of reusable software components. This paper presents a taxonomy of the various purposes for which an inheritance mechanism can be used. While some uses of inheritance significantly enhance software reuse, some others are not as useful and in fact, may even be detrimental to reuse. The paper discusses several examples, and argues for a programming language design that is selective in its support for inheritance. Author

N93-12390*# West Virginia Univ., Morgantown. Software Reuse Repository Lab.

SUPPORTING MULTIPLE DOMAINS IN A SINGLE REUSE REPOSITORY

David A. Eichmann *In* Research Inst. for Computing and Information Systems, The SoRReL Papers: Recent Publications of the Software Reuse Repository Lab 20 May 1992 14 p Previously announced as N92-32654 Sponsored in part by MountainNet (For primary document see N93-12384 02-61)
Avail: CASI HC A03/MF A02

Domain analysis typically results in the construction of a domain-specific repository. Such a repository imposes artificial boundaries on the sharing of similar assets between related domains. A lattice-based approach to repository modeling can preserve a reuser's domain specific view of the repository, while avoiding replication of commonly used assets and supporting a more general perspective on domain interrelationships. Author

N93-12391*# West Virginia Univ., Morgantown. Software Reuse Repository Lab.

ASSESSING REPOSITORY TECHNOLOGY: WHERE DO WE GO FROM HERE?

David A. Eichmann *In* Research Inst. for Computing and Information Systems, The SoRReL Papers: Recent Publications of the Software Reuse Repository Lab 20 May 1992 18 p Previously announced as N92-31272 Submitted for publication Sponsored in part by MountainNet (For primary document see N93-12384 02-61)
Avail: CASI HC A03/MF A02

Three sample information retrieval systems, archie, autoLib, and Wide Area Information Service (WAIS), are compared with regard to their expressiveness and usefulness, first in the general context of information retrieval, and then as perspective software reuse repositories. While the representational capabilities of these systems are limited, they provide a useful foundation for future repository efforts, particularly from the perspective of repository distribution and coherent user interface design. Author

N93-12392*# West Virginia Univ., Morgantown. Software Reuse Repository Lab.

A NEURAL NET-BASED APPROACH TO SOFTWARE METRICS

G. Boetticher, Kankanahalli Srinivas, and David A. Eichmann *In* Research Inst. for Computing and Information Systems, The SoRReL Papers: Recent Publications of the Software Reuse Repository Lab 20 May 1992 16 p Submitted for publication (For primary document see N93-12384 02-61)
Avail: CASI HC A03/MF A02

Software metrics provide an effective method for characterizing software. Metrics have traditionally been composed through the definition of an equation. This approach is limited by the fact that all the interrelationships among all the parameters be fully understood. This paper explores an alternative, neural network approach to modeling metrics. Experiments performed on two widely accepted metrics, McCabe and Halstead, indicate that the approach is sound, thus serving as the groundwork for further exploration into the analysis and design of software metrics.
Author

N93-12393*# West Virginia Univ., Morgantown. Software Reuse Repository Lab.
BALANCING GENERALITY AND SPECIFICITY IN COMPONENT-BASED REUSE
David A. Eichmann and Jon Beck *In* Research Inst. for Computing and Information Systems, The SoRReL Papers: Recent Publications of the Software Reuse Repository Lab 20 May 1992 25 p Submitted for publication Sponsored in part by MountainNet (For primary document see N93-12384 02-61)
Avail: CASI HC A03/MF A02

For a component industry to be successful, we must move beyond the current techniques of black box reuse and genericity to a more flexible framework supporting customization of components as well as instantiation and composition of components. Customization of components strikes a balanced between creating dozens of variations of a base component and requiring the overhead of unnecessary features of an 'everything but the kitchen sink' component. We argue that design and instantiation of reusable components have competing criteria - design-for-use strives for generality, design-with-reuse strives for specificity - and that providing mechanisms for each can be complementary rather than antagonistic. In particular, we demonstrate how program slicing techniques can be applied to customization of reusable components.
Author

N93-12400*# Institute for Computer Applications in Science and Engineering, Hampton, VA.
AN ADVANCING FRONT DELAUNAY TRIANGULATION ALGORITHM DESIGNED FOR ROBUSTNESS Final Report
D. J. Mavriplis Oct. 1992 33 p Submitted for publication
(Contracts NAS1-18605; NAS1-19480; RTOP 505-90-52-01)
(NASA-CR-189719; NAS 1.26:189719; ICASE-92-49) Avail: CASI HC A03/MF A01

A new algorithm is described for generating an unstructured mesh about an arbitrary two-dimensional configuration. Mesh points are generated automatically by the algorithm in a manner which ensures a smooth variation of elements, and the resulting triangulation constitutes the Delaunay triangulation of these points. The algorithm combines the mathematical elegance and efficiency of Delaunay triangulation algorithms with the desirable point placement features, boundary integrity, and robustness traditionally associated with advancing-front-type mesh generation strategies. The method offers increased robustness over previous algorithms in that it cannot fail regardless of the initial boundary point distribution and the prescribed cell size distribution throughout the flow-field.
Author

N93-12403*# Institute for Computer Applications in Science and Engineering, Hampton, VA.
STATIC ASSIGNMENT OF COMPLEX STOCHASTIC TASKS USING STOCHASTIC MAJORIZATION Final Report
David Nicol (College of William and Mary, Williamsburg, VA.), Rahul Simha (College of William and Mary, Williamsburg, VA.), and Don Towsley (Massachusetts Univ., Amherst.) Oct. 1992 25 p Submitted for publication
(Contracts NAS1-18605; NAS1-19480; NSF ASC-88-19393; NSF NCR-89-07909)
(NASA-CR-189716; NAS 1.26:189716; ICASE-92-51) Avail: CASI HC A03/MF A01

We consider the problem of statically assigning many tasks to a (smaller) system of homogeneous processors, where a task's structure is modeled as a branching process, and all tasks are assumed to have identical behavior. We show how the theory of majorization can be used to obtain a partial order among possible task assignments. Our results show that if the vector of numbers of tasks assigned to each processor under one mapping is majorized by that of another mapping, then the former mapping is better than the latter with respect to a large number of objective functions. In particular, we show how measurements of finishing time, resource utilization, and reliability are all captured by the theory. We also show how the theory may be applied to the problem of partitioning a pool of processors for distribution among parallelizable tasks.
Author

N93-12515*# Mississippi State Univ., Mississippi State.
AN INVESTIGATION OF ERROR CORRECTING TECHNIQUES FOR OMV AND AXAF Quarterly Report, 16 Aug. - 16 Nov. 1991
Frank Ingels and John Fryer 16 Nov. 1991 100 p
(Grant NAG8-104)
(NASA-CR-190950; NAS 1.26:190950) Avail: CASI HC A05/MF A02

The original objectives of this project were to build a test system for the NASA 255/223 Reed/Solomon encoding/decoding chip set and circuit board. This test system was then to be interfaced with a convolutional system at MSFC to examine the performance of the concantinated codes. After considerable work, it was discovered that the convolutional system could not function as needed. This report documents the design, construction, and testing of the test apparatus for the R/S chip set. The approach taken was to verify the error correcting behavior of the chip set by injecting known error patterns onto data and observing the results. Error sequences were generated using pseudo-random number generator programs, with Poisson time distribution between errors and Gaussian burst lengths. Sample means, variances, and number of un-correctable errors were calculated for each data set before testing.
Dissert. Abstr.

N93-11928*# National Aeronautics and Space Administration. Lewis Research Center, Cleveland, OH.
AN EMBEDDED RULE-BASED DIAGNOSTIC EXPERT SYSTEM IN Ada
Robert E. Jones and Eugene M. Liberman (Sverdrup Technology, Inc., Brook Park, OH.) *In* NASA. Lyndon B. Johnson Space Center, Fifth Annual Workshop on Space Operations Applications and Research (SOAR 1991), Volume 1 Jan. 1992 p 45-51 (For primary document see N93-11921 02-59)
Avail: CASI HC A02/MF A04

N93-11937*# National Aeronautics and Space Administration. Lyndon B. Johnson Space Center, Houston, TX.
ON THE ACQUISITION AND REPRESENTATION OF PROCEDURAL KNOWLEDGE
T. Saito (Computer Sciences Corp., Houston, TX.), C. Ortiz, and R. B. Loftin (Houston Univ., TX.) *In its* Fifth Annual Workshop on Space Operations Applications and Research (SOAR 1991), Volume 1 Jan. 1992 p 108-117 (For primary document see N93-11921 02-59)
Avail: CASI HC A02/MF A04

N93-11938*# Astronautics Corp. of America, Milwaukee, WI.
A METHODOLOGY TO EMULATE AND EVALUATE A PRODUCTIVE VIRTUAL WORKSTATION Abstract Only
David Krubsack and David Haberman *In* NASA. Lyndon B. Johnson Space Center, Fifth Annual Workshop on Space Operations Applications and Research (SOAR 1991), Volume 1 Jan. 1992 p 118 Prepared in cooperation with Marquette Univ., Milwaukee, WI (For primary document see N93-11921

02-59)
Avail: CASI HC A01/MF A04

N93-11943*# National Aeronautics and Space Administration. Lyndon B. Johnson Space Center, Houston, TX.
THE DEVELOPMENT AND TECHNOLOGY TRANSFER OF SOFTWARE ENGINEERING TECHNOLOGY AT NASA. JOHNSON SPACE CENTER
C. L. Pitman, D. M. Erb (Mitre Corp., Houston, TX.), M. E. Izygon (National Academy of Sciences - National Research Council, Houston, TX.), E. M. Fridge, III, G. B. Roush, D. M. Braley, and R. T. Savely *In its* Fifth Annual Workshop on Space Operations Applications and Research (SOAR 1991), Volume 1 Jan. 1992 p 152-162 Sponsored in part by NAC-NRC (For primary document see N93-11921 02-59)
Avail: CASI HC A03/MF A04

N93-11944*# National Aeronautics and Space Administration. Lyndon B. Johnson Space Center, Houston, TX.
SYSTEM DIAGNOSTIC BUILDER
Joseph L. Nieten (GHG Corp., Houston, TX.) and Roger Burke *In its* Fifth Annual Workshop on Space Operations Applications and Research (SOAR 1991), Volume 1 Jan. 1992 p 163-167 (For primary document see N93-11921 02-59)
Avail: CASI HC A01/MF A04

N93-11945*# National Aeronautics and Space Administration. Lyndon B. Johnson Space Center, Houston, TX.
KNOWLEDGE-BASED SYSTEM V AND V IN THE SPACE STATION FREEDOM PROGRAM
Keith Kelley (IBM Federal Systems Div., Houston, TX.), David Hamilton (IBM Federal Systems Div., Houston, TX.), and Chris Culbert *In its* Fifth Annual Workshop on Space Operations Applications and Research (SOAR 1991), Volume 1 Jan. 1992 p 168-173 (For primary document see N93-11921 02-59)
Avail: CASI HC A02/MF A04

N93-11946*# Aerospace Corp., El Segundo, CA. Computer Science and Technology Subdivision.
AN APPROACH TO INTEGRATING AND CREATING FLEXIBLE SOFTWARE ENVIRONMENTS
Kirstie L. Bellman *In* NASA. Lyndon B. Johnson Space Center, Fifth Annual Workshop on Space Operations Applications and Research (SOAR 1991), Volume 1 Jan. 1992 p 174-177 (For primary document see N93-11921 02-59)
Avail: CASI HC A01/MF A04

N93-11947*# Air Force Inst. of Tech., Wright-Patterson AFB, OH.
DESIGN OF AN Ada EXPERT SYSTEM SHELL FOR THE VHSIC AVIONIC MODULAR FLIGHT PROCESSOR Abstract Only
F. Jesse Fanning *In* NASA. Lyndon B. Johnson Space Center, Fifth Annual Workshop on Space Operations Applications and Research (SOAR 1991), Volume 1 Jan. 1992 p 178 (For primary document see N93-11921 02-59)
Avail: CASI HC A01/MF A04

N93-11949*# McDonnell-Douglas Space Systems Co., Houston, TX.
METHODOLOGIES FOR BUILDING ROBUST SCHEDULES
John H. Dean *In* NASA. Lyndon B. Johnson Space Center, Fifth Annual Workshop on Space Operations Applications and Research (SOAR 1991), Volume 1 Jan. 1992 p 189-193 (For primary document see N93-11921 02-59)
(Contract NAS9-17885)
Avail: CASI HC A01/MF A04

N93-11950*# National Aeronautics and Space Administration. Lyndon B. Johnson Space Center, Houston, TX.
COMPASS: AN Ada BASED SCHEDULER
Mary Beth McMahon (McDonnell-Douglas Space Systems Co., Houston, TX.) and Chris Culbert *In its* Fifth Annual Workshop on Space Operations Applications and Research (SOAR 1991), Volume 1 Jan. 1992 p 194-198 (For primary document see N93-11921 02-59)
(Contract NAS9-17885)
Avail: CASI HC A01/MF A04

N93-11952*# ISX Corp., Westlake Village, CA.
MANAGER'S ASSISTANT SYSTEMS FOR SPACE SYSTEM PLANNING Abstract Only
William L. Bewley, Robert Burnard, Gary E. Edwards, and James Shoop *In* NASA. Lyndon B. Johnson Space Center, Fifth Annual Workshop on Space Operations Applications and Research (SOAR 1991), Volume 1 Jan. 1992 p 203 (For primary document see N93-11921 02-59)
Avail: CASI HC A01/MF A04

N93-11955*# National Inst. of Standards and Technology, Gaithersburg, MD. Robot Systems Div.
MODEL-BASED VISION FOR SPACE APPLICATIONS
Karen Chaconas, Marilyn Nashman, and Ronald Lumia *In* NASA. Lyndon B. Johnson Space Center, Fifth Annual Workshop on Space Operations Applications and Research (SOAR 1991), Volume 1 Jan. 1992 p 220-229 (For primary document see N93-11921 02-59)
Avail: CASI HC A02/MF A04

N93-11956*# North Carolina Univ., Charlotte. Dept. of Computer Science.
CONTACT DETECTION AND CONTACT MOTION FOR ERROR RECOVERY IN THE PRESENCE OF UNCERTAINTIES
Jing Xiao *In* NASA. Lyndon B. Johnson Space Center, Fifth Annual Workshop on Space Operations Applications and Research (SOAR 1991), Volume 1 Jan. 1992 p 230-237 (For primary document see N93-11921 02-59)
Avail: CASI HC A02/MF A04

N93-11958*# Oak Ridge National Lab., TN.
GENERATION OF 3-D SURFACE MAPS IN WASTE STORAGE SILOS USING A STRUCTURED LIGHT SOURCE Abstract Only
B. L. Burks, J. C. Rowe, M. A. Dinkins, B. Christensen (Sandia National Labs., Albuquerque, NM.), C. Selleck (Sandia National Labs., Albuquerque, NM.), D. Jacoboski (Westinghouse Materials Co. of Ohio, Cincinnati.), and R. Markus (Westinghouse Materials Co. of Ohio, Cincinnati.) *In* NASA. Lyndon B. Johnson Space Center, Fifth Annual Workshop on Space Operations Applications and Research (SOAR 1991), Volume 1 Jan. 1992 p 246 (For primary document see N93-11921 02-59)
(Contract DE-AC05-84OR-21400)
Avail: CASI HC A01/MF A04

62 COMPUTER SYSTEMS

Includes computer networks and special application computer systems.

N93-11005*# National Aeronautics and Space Administration. Lewis Research Center, Cleveland, OH.
DESCRIPTION OF THE SSF PMAD DC TESTBED CONTROL SYSTEM DATA ACQUISITION FUNCTION
Anastacio N. Baez, Michael Mackin, and Theodore Wright Aug. 1992 8 p Presented at the 27th Intersociety Energy Conversion Engineering Conference, San Diego, CA, 3-7 Aug. 1992; sponsored by ANS, SAE, ACS, AIAA, ASME, and IEEE
(RTOP 474-42-10)
(NASA-TM-105843; E-7286; NAS 1.15:105843) Avail: CASI HC A02/MF A01

The NASA LeRC in Cleveland, Ohio has completed the development and integration of a Power Management and Distribution (PMAD) DC Testbed. This testbed is a reduced scale representation of the end to end, sources to loads, Space Station Freedom Electrical Power System (SSF EPS). This unique facility is being used to demonstrate DC power generation and distribution, power management and control, and system operation techniques considered to be prime candidates for the Space Station Freedom.

A key capability of the testbed is its ability to be configured to address system level issues in support of critical SSF program design milestones. Electrical power system control and operation issues like source control, source regulation, system fault protection, end-to-end system stability, health monitoring, resource allocation, and resource management are being evaluated in the testbed. The SSF EPS control functional allocation between on-board computers and ground based systems is evolving. Initially, ground based systems will perform the bulk of power system control and operation. The EPS control system is required to continuously monitor and determine the current state of the power system. The DC Testbed Control System consists of standard controllers arranged in a hierarchical and distributed architecture. These controllers provide all the monitoring and control functions for the DC Testbed Electrical Power System. Higher level controllers include the Power Management Controller, Load Management Controller, Operator Interface System, and a network of computer systems that perform some of the SSF Ground based Control Center Operation. The lower level controllers include Main Bus Switch Controllers and Photovoltaic Controllers. Power system status information is periodically provided to the higher level controllers to perform system control and operation. The data acquisition function of the control system is distributed among the various levels of the hierarchy. Data requirements are dictated by the control system algorithms being implemented at each level. A functional description of the various levels of the testbed control system architecture, the data acquisition function, and the status of its implementationis presented. Author

N93-11180 Politecnico di Milano (Italy). Dipartimento di Elettronica.
IMPLICIT PARALLELISM IN GENETIC ALGORITHMS
Alberto Bertoni (Milan Univ., Italy) and Marco Dorigo Apr. 1992 10 p
(Rept-92-012; ETN-92-92416) Avail: Politecnico di Milano, Piazza Leonardo da Vinci 32, 20133 Milan, Italy

Holland's theorem in impliclit parallelism is addressed. Holland demonstrated an omega(n(exp 3)/c(sub 1)) lower bound to the number of schemata usefully processed by the genetic algorithm on a population of n = c(sub 1)2(sup l) binary strings, with c(sub 1) a small integer. Holland's result is shown to be probabilistic in nature, and similar results in the case of arbitrary c(sub 1) are given. ESA

N93-11181 Politecnico di Milano (Italy). Dipartimento di Elettronica.
PARALLEL GENETIC ALGORITHMS: INTRODUCTION AND OVERVIEW OF CURRENT RESEARCH
Marco Dorigo and Vittorio Maniezzo Feb. 1992 41 p
(Rept-92-015; ETN-92-92417) Avail: Politecnico di Milano, Piazza Leonardo da Vinci 32, 20133 Milan, Italy

An overview of sequential and parallel genetic algorithms is presented. Genetic algorithms are good candidates for implementation in parallel hardware, given some minor adjustments of their basic paradigm aimed at eliminating sequential blocks. The standard genetic algorithm is outlined, and its most promising distributed versions are introduced. Several systems using a distributed genetic algorithm on parallel hardware are presented. Special attention is devoted to learning classifier systems, which are systems using genetic algorithms as a rule discovery mechanism, and to their implementation on parallel machines. ESA

N93-11584# Aerospatiale, Chatillon (France). Div. des Engins Tactiques.
PARALLEL ARCHITECTURE FOR IMAGE PROCESSING WITH OPTIC FIBER GUIDED MISSILE
B. Longuet 30 Oct. 1991 9 p
(Rept-921-320-101; ETN-92-92347) Avail: CASI HC A02/MF A01

The choices concerning the architecture of the image processor for target recognition and terminal guidance with fiber optic guided missile are summarized. This missile carries an infrared imager whose image is transmitted through an optical fiber to the control station where it is processed for use by the operator. In the missile control station, the image processing assembly provides a decision aid to the operator who only intervenes, in the new concept, for high level actions. The splitting-up of the processing to be performed by the processor shows the specificity of the architecture of the real time processings. Mission control is achieved through high level processings and artificial intelligence techniques are used to complement the conventional algorithms. The goals, the processing to be produced, and constraints of the project for the image processors are presented. ESA

N93-11651*# Illinois Univ., Urbana-Champaign. Coordinated Science Lab.
AUTOMATIC DATA PARTITIONING ON DISTRIBUTED MEMORY MULTICOMPUTERS Ph.D. Thesis
Manish Gupta 25 Sep. 1992 162 p
(Contract NAG1-613; N00014-90-J-1270; NSF MIP-86-57563)
(NASA-CR-190976; NAS 1.26:190976; UILU-ENG-92-2237; CRHC-92-19) Copyright Avail: CASI HC A08/MF A02

Distributed-memory parallel computers are increasingly being used to provide high levels of performance for scientific applications. Unfortunately, such machines are not very easy to program. A number of research efforts seek to alleviate this problem by developing compilers that take over the task of generating communication. The communication overheads and the extent of parallelism exploited in the resulting target program are determined largely by the manner in which data is partitioned across different processors of the machine. Most of the compilers provide no assistance to the programmer in the crucial task of determining a good data partitioning scheme. A novel approach is presented, the constraints-based approach, to the problem of automatic data partitioning for numeric programs. In this approach, the compiler identifies some desirable requirements on the distribution of various arrays being referenced in each statement, based on performance considerations. These desirable requirements are referred to as constraints. For each constraint, the compiler determines a quality measure that captures its importance with respect to the performance of the program. The quality measure is obtained through static performance estimation, without actually generating the target data-parallel program with explicit communication. Each data distribution decision is taken by combining all the relevant constraints. The compiler attempts to resolve any conflicts between constraints such that the overall execution time of the parallel program is minimized. This approach has been implemented as part of a compiler called Paradigm, that accepts Fortran 77 programs, and specifies the partitioning scheme to be used for each array in the program. We have obtained results on some programs taken from the Linpack and Eispack libraries, and the Perfect Benchmarks. These results are quite promising, and demonstrate the feasibility of automatic data partitioning for a significant class of scientific application programs with regular computations. Author

N93-11714# National Inst. of Standards and Technology, Gaithersburg, MD. Advanced Systems Div.
INTEGRATED SERVICES DIGITAL NETWORK CONFORMANCE TESTING. LAYER 1, PHYSICAL LAYER. PART 2: BASIC RATE U INTERFACE, USER SIDE Final Report
D. P. Stokesberry and K. M. Roberts Mar. 1992 97 p
(PB92-181114; NIST/SP-823/2) Avail: CASI HC A05/MF A02

The American National Standard for Telecommunications (ANS) T1.601-1988 specifies the minimal set of requirements to provide for satisfactory transmission between the network and the Network Termination (NT). It describes both the physical interface and the electrical characteristics of the signals appearing at the network side of the NT, commonly called the U interface point, or U reference point. Equipment designed to operate on the North American Integrated Services Digital Network (ISDN) Basic Access U Interface must conform with the set of minimal requirements. The document describes a set of conformance test specifications for all NTs connected to the Basic Rate ISDN user-network interface. These tests were developed and approved by the members of the North American ISDN Users' Forum. GRA

N93-11860# Sandia National Labs., Albuquerque, NM.
THE NETWORK DESTRUCTION PROBLEM (EXTENDED ABSTRACT)
C. A. Phillips 27 Apr. 1992 27 p Presented at the 33rd Annual Symposium on Foundations of Computer Science, Pittsburgh, PA, 25-27 Oct. 1992
(Contract DE-AC04-76DP-00789)
(DE92-016171; SAND-92-0186C; CONF-9210128-1-Extd-Abst)
Avail: CASI HC A03/MF A01

In the network destruction problem, we wish to find the most cost effective way to reduce the ability of a network to transport a commodity. Potential applications include disabling of military supply lines, communication networks, national energy systems, and illicit drug networks. Given a network represented as a graph, we wish to compute a fixed-budget attack strategy which will maximally inhibit the network's capability. In this paper we introduce the network destruction problem and prove several complexity results. We prove the problem is strongly NP-complete for general graphs, even of bounded degree, and weakly NP-complete for series-parallel graphs, grid graphs, bandwidth-k graphs with k greater than or = 3, and Halin graphs (and thus for k-outerplaner graphs with k greater than or = 2). We describe three pseudopolynomial-time approximation schemes. Finally, we describe a polynomial-time algorithm for outerplanar graphs. Thus, network destruction separates outerplanar graphs from series-parallel graphs, separates 1-outerplanar from 2-outerplanar graphs, and separates bandwidth-2 graphs from bandwidth-3 graphs. DOE

N93-12233# Oak Ridge National Lab., TN.
AN IMPLEMENTATION OF A PARALLEL MOL SOLVER ON THE INTEL GAMMA PARALLEL COMPUTER
W. F. Lawkins and J. S. Payne 17 Jun. 1992 7 p Presented at the 7th International Association of Mathematics and Computer Simulation Conference on Computer Methods for Partial Differential Equations, New Brunswick, NJ, 22-24 Jun. 1992
(Contract DE-AC05-84OR-21400)
(DE92-018947; CONF-9206185-8) Avail: CASI HC A02/MF A01

An implicit parallel method-of-lines solver that has been implemented on the MIMD Intel Gamma prototype supercomputer is discussed. The strategy for implementation is to execute the ODE solver sequentially and to do the numerical linear algebra in parallel. Performance studies for this implementation are presented. DOE

N93-12239# Stanford Univ., CA. Dept. of Computer Science.
ASSEMBLING POLYHEDRA WITH SINGLE TRANSLATIONS
Randall H. Wilson and Achim Schweikard Oct. 1991 16 p
(Contract N00014-88-K-0620)
(AD-A254623; SU-STAN-CS-91-1387) Avail: CASI HC A03/MF A01

The problem of partitioning an assembly of polyhedral objects into two subassemblies that can be separated arises in assembly planning. We describe an algorithm to compute the set of all translations separating two polyhedra with n vertices in 0(n) steps and show that this is optimal. Given an assembly of k polyhedra with a total of n vertices, an extension of this algorithm identifies a valid translation and removable subassembly in 0(k2n4) steps if one exists. Based on the second algorithm, a polynomial time method for finding a complete assembly sequence consisting of single translations is derived. An implementation incorporates several changes to achieve better average-case performance; experimental results obtained for composite objects consisting of isothetic polyhedra are described. GRA

N93-12358# Naval Surface Warfare Center, Silver Spring, MD.
A METHODOLOGY FOR SYSTEMS REQUIREMENTS SPECIFICATION AND TRACEABILITY FOR LARGE REAL TIME COMPLEX SYSTEMS
Michael Edwards and Steven L. Howell 27 Sep. 1991 62 p
(AD-A254738; NAVSWC-TR-91-584) Avail: CASI HC A04/MF A01

This document describes the beginnings of a methodology for requirements specification and traceability of real-time, large-scale, complex computer-intensive systems. The method is aimed at better understanding, the top-level system requirements and how they relate to the system under design. The methodology will cover the requirements aspects of system development over the entire system development life cycle, beginning with the specification of the requirements and tracing those requirements to the design and final implementation. GRA

N93-12395*# Illinois Univ., Urbana-Champaign. Coordinated Science Lab.
PERFORMANCE EVALUATION AND MODELING TECHNIQUES FOR PARALLEL PROCESSORS Ph.D. Thesis
Robert Tod Dimpsey Sep. 1992 158 p
(Contract NAG1-613; N00014-91-J-1116)
(NASA-CR-190974; NAS 1.26:190974; UILU-ENG-92-2234; CRHC-92-18) Avail: CASI HC A08/MF A02

In practice, the performance evaluation of supercomputers is still substantially driven by singlepoint estimates of metrics (e.g., MFLOPS) obtained by running characteristic benchmarks or workloads. With the rapid increase in the use of time-shared multiprogramming in these systems, such measurements are clearly inadequate. This is because multiprogramming and system overhead, as well as other degradations in performance due to time varying characteristics of workloads, are not taken into account. In multiprogrammed environments, multiple jobs and users can dramatically increase the amount of system overhead and degrade the performance of the machine. Performance techniques, such as benchmarking, which characterize performance on a dedicated machine ignore this major component of true computer performance. Due to the complexity of analysis, there has been little work done in analyzing, modeling, and predicting the performance of applications in multiprogrammed environments. This is especially true for parallel processors, where the costs and benefits of multi-user workloads are exacerbated. While some may claim that the issue of multiprogramming is not a viable one in the supercomputer market, experience shows otherwise. Even in recent massively parallel machines, multiprogramming is a key component. It has even been claimed that a partial cause of the demise of the CM2 was the fact that it did not efficiently support time-sharing. In the same paper, Gordon Bell postulates that, multicomputers will evolve to multiprocessors in order to support efficient multiprogramming. Therefore, it is clear that parallel processors of the future will be required to offer the user a time-shared environment with reasonable response times for the applications. In this type of environment, the most important performance metric is the completion of response time of a given application. However, there are a few evaluation efforts addressing this issue. Author

N93-12410*# National Aeronautics and Space Administration. Lewis Research Center, Cleveland, OH.
ISDN AT NASA LEWIS RESEARCH CENTER
Catherine Murphy Bakes (Kent State Univ., OH.), Fredric Goldberg, and Steven W. Eubanks Oct. 1992 38 p
(NASA-TM-105911; E-7388; NAS 1.15:105911) Avail: CASI HC A03/MF A01

An expository investigation of the potential impact of the Integrated Services Digital Network (ISDN) at NASA Lewis Research Center is described. To properly frame the subject, the paper contains a detailed survey of the components of Narrowband ISDN. The principles and objectives are presented as decreed by the Consultative Committee for International Telephone and Telegraph (CCITT). The various channel types are delineated and their associated service combinations are described. The subscriber-access network functions are explained pictorially via the ISDN reference configuration. A section on switching techniques is presented to enable the reader to understand the emergence of the concept of fast packet switching. This new technology is designed to operate over the high bandwidth, low error rate transmission media that characterizes the LeRC environment. A brief introduction to the next generation of networks is covered with sections on Broadband ISDM (B-ISDN), Asynchronous Transfer Mode (ATM), and Synchronous Optical Networks (SONET). Applications at LeRC are presented, first in terms of targets of opportunity, then in light of compatibility constraints. In-place pilot projects and testing are described that demonstrate actual usage at LeRC. Author

63 CYBERNETICS

Includes feedback and control theory, artificial intelligence, robotics and expert systems.

For related information see also *54 Man/System Technology and Life Support.*

N93-11000# Stottler Henke Associates, Inc., Belmont, CA.
INTELLIGENT TDA SYSTEMS USING NEURAL NETWORKS, PHASE 1 Final Technical Report, Oct. 1991 - May 1992
Richard H. Stottler and Andrea L. Henke May 1992 74 p
(Contract DACA76-91-C-0026)
(AD-A252556; TEC-0007) Avail: CASI HC A04/MF A01

The overall objective of Phase 1 was to develop a prototype intelligent Tactical Decision Aids (IDA) neural network system through the use of an expert system to neural network translator. From the resulting prototype network, the performance of the complete TDA system could be determined. The Phase 1 results absolutely demonstrated the feasibility of this concept and cleared the way for development of a complete system in Phase 2. Current TDA systems require too much expertise from the user and run too slowly for use in tactical situations, when time is in short supply. In tactical situations, terrain is an extremely important factor and represents one of the main inputs to these systems. The Airborne Avenues of Approach (AAA) Planning problem was chosen. While initial route planning is performed prior to the start of the mission, a need exists to automate and speed the process. Additionally, a system which could meet the rigorous real-time requirements of an on-board AAA re-planner would prove enormously beneficial in many time-critical tactical situations. GRA

N93-11147# Brown Univ., Providence, RI. Div. of Applied Mathematics.
STOCHASTIC CONTROL AND NONLINEAR ESTIMATION Final Technical Report, 1 Oct. 1988 - 31 Mar. 1992
Wendell H. Fleming and Harold J. Kushner 7 Jul. 1992 7 p
(Grant AF-AFOSR-0015-89)
(AD-A253543; AFOSR-92-0715TR) Avail: CASI HC A02/MF A01

In stochastic control, a major focus of this research was numerical methods for finding approximately optimal control laws. Dynamic programming and Monte Carlo optimization algorithms were followed. Both probabilistic methods, based on weak convergence ideas, and analytical methods were used to prove convergence of algorithms. The latter were based on viscosity solution methods for nonlinear partial differential equations. In nonlinear estimation, low dimensional approximate nonlinear filters were found for cases when a piecewise one-to-one function of a system state plus low intensity observation noise was observed. GRA

N93-11174*# National Aeronautics and Space Administration. Pasadena Office, CA.
THE ADAPTIVE NEURON MODEL: AN ARCHITECTURE FOR THE RAPID LEARNING OF NONLINEAR TOPOLOGICAL TRANSFORMATIONS Patent Application
Raoul Tawel, inventor (to NASA) (Jet Propulsion Lab., California Inst. of Tech., Pasadena.) 28 Aug. 1992 34 p
(Contract NAS7-918)
(NASA-Case-NPO-18579-1-CU; NAS 1.71:NPO-18579-1-CU; US-Patent-Appl-SN-937335) Avail: CASI HC A03/MF A01

A method for the rapid learning of nonlinear mappings and topological transformations using a dynamically reconfigurable artificial neural network is presented. This fully-recurrent Adaptive Neuron Model (ANM) network was applied to the highly degenerate inverse kinematics problem in robotics, and its performance evaluation is bench-marked. Once trained, the resulting neuromorphic architecture was implemented in custom analog neural network hardware and the parameters capturing the functional transformation downloaded onto the system. This neuroprocessor, capable of 10(exp 9) ops/sec, was interfaced directly to a three degree of freedom Heathkit robotic manipulator. Calculation of the hardware feed-forward pass for this mapping was benchmarked at approximately 10 microsec. NASA

N93-11227 Politecnico di Milano (Italy). Dipartimento di Elettronica.
ALECSYS AND THE AUTONOMOUSE: LEARNING TO CONTROL A REAL ROBOT BY DISTRIBUTED CLASSIFIER SYSTEMS
Marco Dorigo Apr. 1992 36 p
(Rept-92-011; ETN-92-92415) Avail: Politecnico di Milano, Piazza Leonardo da Vinci 32, 20133 Milan, Italy

ALECSYS (A LEarning Classifier SYStem), is a parallel distributed learning classifier system that provides the learning system designer with two basic tools. The first tool, low level parallelism, allows him to use the desired computational power by parallelization of a single learning Classifier System (CS); the second tool, high level parallelism, gives him the possibility to connect, with great flexibility, many cooperating CS's. AutonoMouse, a little autonomous robot, shaped like a mouse, that gives ALECSYS a body, is discussed. The design of autonomous mouse sized robots (AutonoMouses) with the capacity of surviving in a real environment is focused upon. The overall goal is very ambitious and cannot be solved by any existing computational paradigm. Results obtained using ALECSYS as learning software, the transputer as computing hardware, and a home made AutonoMouse as robot, are reported. ALECSYS is illustrated and experiments, both in a simulated environment and in the real world, are reported. ESA

N93-11343# Royal Signals and Radar Establishment, Malvern (England). Imaging Processing Research Section.
SELF-SUPERVISION IN MULTILAYER ADAPTIVE NETWORKS
Stephen P. Luttrell 6 Dec. 1991 32 p
(RSRE-Memo-4467; BR308061; ETN-92-92315) Copyright
Avail: CASI HC A03/MF A01

The theoretical derivation and the numerical simulation of the phenomenon of self-supervision are presented. The problem of a pair of communication channels that cause mutual distortion is considered. In the numerical simulations, a simple demonstration of the improvement in performance is presented. In order to make contact with the theory of unsupervised adaptive networks, the communication channel problem is derived as a nested Vector Quantizer (VQ). The effect of the inner VQ models the mutual channel distortion and influences the way in which the outer VQ's must be optimized. This is the phenomenon of self-supervision, where one part of an overall unsupervised network supervises the optimization of another part of the network. The principle may be generalized to a multilayer unsupervised network. Self supervision is a very convenient hybrid which combines the best properties of unsupervised and supervised network training algorithms. ESA

N93-11457 Columbia Univ., New York, NY.
OBJECT RECOGNITION WITH A ROBOT HAND Ph.D. Thesis
Kenneth Stanley Roberts 1991 192 p
Avail: Univ. Microfilms Order No. DA9209885

People are good at identifying a physical object, even if they cannot see it, just by feeling around on it with their fingers. This way of acquiring knowledge about the world by active touch exploration is called 'haptic' perception. Our robot haptic object recognition task is to take data from the haptic exploration of a physical object, identify the object as one from a given set, and compute its position and orientation. We present a new scheme for a robot hand-arm system to do haptic perception. It uses a segmentation algorithm to extract multiple types of features. Then it analyzes the attributes of each feature, and the geometric and adjacency relations with other features - to eliminate impossible interpretations and correctly identify the object. Our segmentation algorithm is the first one designed for the special characteristics of data from haptic exploration: fully 3-D, sparse and acquired incrementally over time by multiple sensors. Our matching algorithm uses a new geometric constraint for pairs of line segments. We have implemented the scheme on our Utah/MIT multi-finger robot hand system. Dissert. Abstr.

N93-11593 Politecnico di Milano (Italy). Dipartimento di Elettronica.
SELF-TUNING PI-PID REGULATORS FOR STABLE SYSTEMS WITH VARYING DELAY
A. Leva, C. Maffezzoni, and R. Scattolini 1992 31 p Sponsored in part by Italian Ministry of University and Scientific and Technological Research and CNR
(Rept-92-023; ETN-92-92422) Avail: Politecnico di Milano, Piazza Leonardo da Vinci 32, 20133 Milan, Italy

A self tuning PI-PID regulator based on a fixed structure simplified model of the process is presented. To cope with the majority of real sized applications, the simplified model is assumed to incorporate a variable or unknown time delay. Therefore, the core of the PI-PID regulator is an effective identification algorithm suitable for the online estimation of the unknown time delay in sampled systems. In the development, particular emphasis is given to all those aspects which make an algorithm really applicable in an industrial environment, such as startup and initial tuning phase, choice of the sampling period, ease of the control synthesis criterion. Simulation experiments demonstrate the potential of the new regulator. ESA

N93-11667 Politecnico di Milano (Italy). Dipartimento di Elettronica.
A PID AUTO-TUNING ALGORITHM BASED ON RELAY FEEDBACK
Alberto Leva 1992 31 p
(Rept-92-019; ETN-92-92420) Avail: Politecnico di Milano, Piazza Leonardo da Vinci 32, 20133 Milan, Italy

A PID autotuning algorithm based on relay feedback is presented. Its main feature is the capability of exploring different points of the process frequency response before performing the actual tuning procedure. In addition, the algorithm minimizes the a priori amount of information required on the process; in fact, the use is only asked to specify the minimum phase margin required for the closed loop system. The algorithm was ported into an industrial DCS environment. Some experimental results, obtained by simulation, are presented. ESA

N93-12096# New Mexico State Univ., Las Cruces.
NEURAL NETWORK MODELS OF AIR COMBAT MANEUVERING Final Technical Report, Sep. 1988 - Dec. 1991
Roger W. Schvaneveldt, Timothy E. Goldsmith, Alan E. Benson, and Wayne L. Waag Jul. 1992 53 p
(Contract F33615-88-C-0010)
(AD-A254653; AL-TR-1992-0037) Avail: CASI HC A04/MF A01

The primary goal of this project was to explore the applicability of artificial neural network (NN) models in the domain of air combat maneuvering (ACM). The work investigated several models: (1) NN models that select ACM on the basis of training with the production rules of a model, Air Combat Expert Simulation (ACES); (2) NN models that mimic the action selections of the Automated Maneuvering Logic (AML) System; (3) NN models that predict the outcome of engagements flown in the Simulator for Air-to-Air Combat (SAAC) given summary measures of various parameters measured during the engagements; and (4) NN models that predict future aircraft control inputs in SAAC engagements given the values of flight parameters at particular points in time. These various models incorporate knowledge about air combat maneuvers and components of maneuvers as well as rudimentary knowledge about maneuver planning and situational awareness. For most of the models, validation tests were conducted using data different from that used in training the models. The authors provide details on each of these efforts as well as a review of the ACES model, a presentation of the basics of NNs, and an overview of a software system developed for the implementation and testing of the NN models. GRA

N93-12138# Sandia National Labs., Albuquerque, NM.
A VMEBUS ULTRASONIC SENSOR CONTROLLER FOR MAPPING AND SERVO CONTROL IN ROBOTIC SYSTEMS
W. D. Drotning and P. Garcia 1992 9 p Presented at the Sensors Expo, Chicago, IL, 29 Sep. - 1 Oct. 1992
(Contract DE-AC04-76DP-00789)
(DE92-013661; SAND-92-0374C; CONF-9209113-1) Avail: CASI HC A02/MF A01

An ultrasonic sensor controller has been developed and applied in a variety of robotic systems for operation in hazardous and remote environments. The controller consists of hardware and software that control multiple ultrasonic range sensors and provide workspace information to robot controllers for rapid, safe, and reliable operation. The programmable multichannel controller resides on a VMEbus for high speed communication to a multiprocessor architecture. The sensor controller has been used in a number of applications, which include providing high precision range information for proximity servocontrol of robots, and performing surface and obstacle mapping functions for safe path planning of robots in unstructured environments. DOE

N93-12153# Sandia National Labs., Livermore, CA.
TRANSIENT REDUCTION ANALYSIS USING NEURAL NETWORKS (TRANN)
P. T. Larson and D. A. Sheaffer 1992 5 p Presented at the International Telemetering Conference, San Diego, CA, 26-29 Oct. 1992
(Contract DE-AC04-76DR-00789)
(DE92-012150; SAND-92-8494C; CONF-921065-1) Avail: CASI HC A01/MF A01

Our telemetry department has an application for a data categorization/compression of a high speed transient signal in a short period of time. Categorization of the signal reveals important system performance and compression is required because of the terminal nature of our telemetry testing. Until recently, the hardware for the system of this type did not exist. A new exploratory device from Intel has the capability to meet these extreme requirements. This integrated circuit is an analog neural network capable of performing 2 billion connections per second. The two main advantages of this chip over traditional hardware are the obvious computation speed of the device and the ability to compute a three layer feed-forward neural network classifier. The initial investigative development work using the Intel chip has been completed. The results from this proof of concept will show data categorization/compression performed on the neural network integrated circuit in real time. We will propose a preliminary design for a transient measurement system employing the Intel integrated circuit. DOE

N93-12226# Maryland Univ., College Park. Lab. for Plasma Research.
ADAPTIVE NEURAL NETWORK MODELS FOR INTELLIGENT COMPUTATIONS Final Report, 1 Sep. 1989 - 31 Dec. 1991
H. H. Chen, Y. C. Lee, and G. Z. Sun 31 Dec. 1991 9 p
(Grant AF-AFOSR-0492-89)
(AD-A254689; AFOSR-92-0826TR) Avail: CASI HC A02/MF A01

By looking closely at the dynamics of learning, it was discovered that for different input the states of network tended to cluster around three values plus the initial state. These four states can be considered as possible states of an actual finite state machine and the movement between these states as a function of input can be interpreted as the state transition of a state machine. This four state machine constructed is a perfect state machine that recognize the dual parity grammar. It recognizes dual parity strings with arbitrary length. This rule extraction generalization power is qualitatively different from that of the 'data interpolation' paradigm which is usually true for a feedforward neural net. GRA

N93-12258# California Univ., Davis.
COMPUTATIONAL NONLINEAR CONTROL Annual Technical Report No. 1
A. J. Krener 31 May 1992 8 p
(Grant AF-AFOSR-0228-91)
(AD-A253547; Rept-3-448724-22529; AFOSR-92-0728TR) Avail: CASI HC A02/MF A01

The goal of this research is to develop a computationally feasible approach to the design of compensators for nonlinear plants such as high performance aircraft and robots. The basic approach is to take parts of the current theory of nonlinear control, and extend and modify them as needed so as to develop numerical algorithms. To date the emphasis has been on a perturbational approach developed from well-established linear methodologies. We have written a MATLAB based set of algorithms which accomplish feedback linearization, input-output injection linearization and nonlinear regulation. These are incorporated into a Nonlinear-System-Toolbox which is available via telnet. GRA

N93-12259# New Mexico State Univ., Las Cruces. Computing Research Lab.
COMPLEX COGNITIVE INFORMATION PROCESSING: A COMPUTATIONAL ARCHITECTURE WITH A CONNECTIONIST IMPLEMENTATION Final Report, 15 May 1988 - 14 Jan. 1992
John A. Barnden 24 Jul. 1992 23 p
(Grant AF-AFOSR-0215-88)
(AD-A254041; AFOSR-92-0795TR) Avail: CASI HC A02/MF A01

We developed several novel representational and processing techniques for use in connectionist systems designed for high-level AI-like applications such as common-sense reasoning and natural language understanding. The techniques were used, for instance, in a connectionist system (Conposit/SYLL) that implements Johnson-Laird's mental-model theory of human syllogistic reasoning. This theory was chosen as a case study for verifying the power of the techniques, because it was developed independently of the project, contains complex symbolic structures of various types, and requires complex sequences of operations. The resulting connectionist system is probably the most advanced, complex, and complete connectionist rule-based system in existence. It has a more complete scheme for binding rule-variables and for role binding than any other connectionist system. The representational techniques developed in the project were Relative-Position Encoding (RPE) and Pattern-Similarity Association (PSA). RPE allows structure to be encoded by the relative positioning of connectionist activation patterns within a subnetwork. PSA allows structure to be encoded by having different substructures include similar activation subpatterns. These techniques are similar to data structuring techniques used in computer memory (in particular, PSA is similar to associative addressing), but they had not previously been used in any non-trivial way in connectionism. The most distinctive processing technique developed in the project was the Temporal-Winner-Take-All (TWTA) method for selection in connectionist networks. This is more convenient and efficient for some purposes than conventional WTA methods. GRA

N93-12439# Barron Associates, Inc., Standardsville, VA.
ACTIVE CONTROL OF COMPLEX SYSTEMS VIA DYNAMIC (RECURRENT) NEURAL NETWORKS Final Report, 15 Apr. 1989 - 30 May 1992
David G. Ward, B. E. Parker, Jr., and Roger L. Barron 30 May 1992 219 p
(Contract N00014-89-C-0137)
(AD-A254878; Rept-141-02/03-F) Avail: CASI HC A10/MF A03

In this work the synthesis of artificial neural networks is examined from the perspective of statistical estimation of functions, and the development of synthesis algorithms is centered on new tools for building dynamic (recurrent) neural networks that incorporate internal feedbacks and time delays. The DynNet algorithm is described; it learns the feedforward and feedback structure of a nonlinear dynamic neural network and optimizes the coefficients therein. Applications of the algorithm are presented for the following areas: time-series predictions related to an advanced turbopropulsion combustion process; rapid predictions of the responses of a synchronous generator to changes in its input and load conditions; predictions of the behavior of a deterministic chaotic process; and on-line, real-time, optimal two-point boundary-value guidance of an air-to-air missile. The report outlines the advantages of dynamic neural networks and probes the issues related to their synthesis and use. GRA

N93-11929*# UFA, Inc., Newton, MA.
INTEGRATION OF TASK LEVEL PLANNING AND DIAGNOSIS FOR AN INTELLIGENT ROBOT
Amy W. Chan *In* NASA. Lyndon B. Johnson Space Center, Fifth Annual Workshop on Space Operations Applications and Research (SOAR 1991), Volume 1 Jan. 1992 p 52-59 (For primary document see N93-11921 02-59)
(Contract NAS8-38420)
Avail: CASI HC A02/MF A04

N93-11931*# Systems Control Technology, Inc., Palo Alto, CA.
INTELLIGENT DIAGNOSTICS SYSTEMS Abstract Only
Barbara M. McQuiston and Ronald L. DeHoff *In* NASA. Lyndon B. Johnson Space Center, Fifth Annual Workshop on Space Operations Applications and Research (SOAR 1991), Volume 1 Jan. 1992 p 67 (For primary document see N93-11921 02-59)
Avail: CASI HC A01/MF A04

N93-11933*# Space Industries, Inc., Webster, TX.
DESIGN DEVELOPMENT OF A NEURAL NETWORK-BASED TELEMETRY MONITOR
Michael F. Lembeck *In* NASA. Lyndon B. Johnson Space Center, Fifth Annual Workshop on Space Operations Applications and Research (SOAR 1991), Volume 1 Jan. 1992 p 80-86 (For primary document see N93-11921 02-59)
Avail: CASI HC A02/MF A04

N93-11936*# Jet Propulsion Lab., California Inst. of Tech., Pasadena.
INTELLIGENT DATA MANAGEMENT FOR REAL-TIME SPACECRAFT MONITORING
Ursula M. Schwuttke, Les Gasser (University of Southern California, Los Angeles.), and Bruce Abramson (University of Southern California, Los Angeles.) *In* NASA. Lyndon B. Johnson Space Center, Fifth Annual Workshop on Space Operations Applications and Research (SOAR 1991), Volume 1 Jan. 1992 p 100-106 Sponsored by NASA, Washington (For primary document see N93-11921 02-59)
Avail: CASI HC A02/MF A04

N93-11940*# National Aeronautics and Space Administration. Lewis Research Center, Cleveland, OH.
SPACE COMMUNICATION ARTIFICIAL INTELLIGENCE FOR LINK EVALUATION TERMINAL (SCAILET)
Anoosh K. Shahidi (Sverdrup Technology, Inc., Brook Park, OH.), Richard F. Schlegelmilch (Akron Univ., OH.), Edward J. Petrik, and Jerry L. Walters *In* NASA. Lyndon B. Johnson Space Center, Fifth Annual Workshop on Space Operations Applications and Research (SOAR 1991), Volume 1 Jan. 1992 p 130-132 (For primary document see N93-11921 02-59)
Avail: CASI HC A01/MF A04

N93-11957*# EXOS, Inc., Burlington, MA.
EXOS RESEARCH ON MASTER CONTROLLERS FOR ROBOTIC DEVICES
Beth A. Marcus, Ben An, and Brian Eberman (Massachusetts Inst. of Tech., Cambridge.) *In* NASA. Lyndon B. Johnson Space Center, Fifth Annual Workshop on Space Operations Applications

and Research (SOAR 1991), Volume 1 Jan. 1992 p 238-245 (For primary document see N93-11921 02-59)
(Contracts NAS8-38910; NAS9-18452)
Avail: CASI HC A02/MF A04

N93-11959*# Southwest Research Inst., San Antonio, TX. Robotics and Automation Dept.
FUZZY LOGIC CONTROL OF TELEROBOT MANIPULATORS
Ernest A. Franke and Ashok Nedungadi *In* NASA. Lyndon B. Johnson Space Center, Fifth Annual Workshop on Space Operations Applications and Research (SOAR 1991), Volume 1 Jan. 1992 p 248-253 (For primary document see N93-11921 02-59)
Avail: CASI HC A02/MF A04

N93-11960*# Jet Propulsion Lab., California Inst. of Tech., Pasadena.
A NEW SCHEME OF FORCE REFLECTING CONTROL
Won S. Kim *In* NASA. Lyndon B. Johnson Space Center, Fifth Annual Workshop on Space Operations Applications and Research (SOAR 1991), Volume 1 Jan. 1992 p 254-261 Sponsored by NASA, Washington (For primary document see N93-11921 02-59)
Avail: CASI HC A02/MF A04

N93-11962*# Texas A&I Univ., Kingsville. Dept. of Electrical Engineering and Computer Science.
A NEURO-COLLISION AVOIDANCE STRATEGY FOR ROBOT MANIPULATORS
Joel P. Onema and Robert A. Maclaunchlan *In* NASA. Lyndon B. Johnson Space Center, Fifth Annual Workshop on Space Operations Applications and Research (SOAR 1991), Volume 1 Jan. 1992 p 272-279 (For primary document see N93-11921 02-59)
Avail: CASI HC A02/MF A04

N93-11963*# Barrios Technology, Inc., Houston, TX.
INTERACTIVE COLLISION DETECTION Abstract Only
Brad Bell *In* NASA. Lyndon B. Johnson Space Center, Fifth Annual Workshop on Space Operations Applications and Research (SOAR 1991), Volume 1 Jan. 1992 p 280 (For primary document see N93-11921 02-59)
Avail: CASI HC A01/MF A04

N93-11964*# Jet Propulsion Lab., California Inst. of Tech., Pasadena.
AN 8-DOF DUAL-ARM SYSTEM FOR ADVANCED TELEOPERATION PERFORMANCE EXPERIMENTS
Antal K. Bejczy and Zoltan F. Szakaly *In* NASA. Lyndon B. Johnson Space Center, Fifth Annual Workshop on Space Operations Applications and Research (SOAR 1991), Volume 1 Jan. 1992 p 282-293 Sponsored by NASA, Washington (For primary document see N93-11921 02-59)
Avail: CASI HC A03/MF A04

N93-11965*# Jet Propulsion Lab., California Inst. of Tech., Pasadena.
PERFORMANCE EXPERIMENTS WITH ALTERNATIVE ADVANCED TELEOPERATOR CONTROL MODES FOR A SIMULATED SOLAR MAXIMUM SATELLITE REPAIR
H. Das, H. Zak, W. S. Kim, A. K. Bejczy, and P. S. Schenker *In* NASA. Lyndon B. Johnson Space Center, Fifth Annual Workshop on Space Operations Applications and Research (SOAR 1991), Volume 1 Jan. 1992 p 294-301 Sponsored by NASA, Washington (For primary document see N93-11921 02-59)
Avail: CASI HC A02/MF A04

N93-11966*# National Aeronautics and Space Administration. Lyndon B. Johnson Space Center, Houston, TX.
EFFECTS OF SPATIALLY DISPLACED FEEDBACK ON REMOTE MANIPULATION TASKS
Meera K. Manahan (Lockheed Engineering and Sciences Co., Houston, TX.), Mark A. Stuart (Lockheed Engineering and Sciences Co., Houston, TX.), John M. Bierschwale (Lockheed Engineering and Sciences Co., Houston, TX.), Ellen Y. Hwang (Lockheed Engineering and Sciences Co., Houston, TX.), and A. J. Legendre *In its* Fifth Annual Workshop on Space Operations Applications and Research (SOAR 1991), Volume 1 Jan. 1992 p 302-309 (For primary document see N93-11921 02-59)
Avail: CASI HC A02/MF A04

64 NUMERICAL ANALYSIS

Includes iteration, difference equations, and numerical approximation.

N93-10991# Vanderbilt Univ., Nashville, TN. Dept. of Mathematics.
MATCHING AND VERTEX PACKING: HOW HARD ARE THEY?
Michael D. Plummer 1991 52 p
(Contracts N00014-85-K-0488; N00014-91-J-1142)
(AD-A245928) Avail: CASI HC A04/MF A01

Two of the most well-known problems in graph theory are: find a maximum matching (or perfect matching, if one exists); and find a maximum independent set of vertices. The first problem - usually called the matching problem - is known to have a polynomial algorithm; the second - often called the vertex packing problem - is known to be NP-complete. However, many graph theorists, especially those who do not deal much with complexity of algorithms, know little more about the complexity issues associated with these two problems than these two basic facts. What is not so widely known within the graph theory community is that these two problems have motivated a great deal of recent activity in the area of algorithms and their complexity. Of course it is not known whether or not P = NP, but most workers in the area currently believe that equality is unlikely to hold. Motivated by this belief, a number of people have studied variations of both matching and vertex packing with the general theme being two-fold. On the one hand, one can add various side conditions to the matching problem and study the complexity, both sequential and parallel, of the resulting problems. On the other hand, one can investigate certain large and interesting classes of graphs trying to prove that for these classes the vertex packing problem has a polynomial solution. GRA

N93-11121# Loughborough Univ. of Technology (England). Dept. of Mathematical Sciences.
EQUIVALENCE TRANSFORMATIONS OF RATIONAL MATRICES
N. P. Karampetakis (Aristotle Univ. of Thessaloniki, Greece), A. C. Pugh, and A. I. G. Vardulakis (Aristotle Univ. of Thessaloniki, Greece) Jun. 1992 14 p
(Maths-Rept-A-163; ETN-92-92384) Avail: CASI HC A03/MF A01

The known theories of transformations between polynomial matrices are extended to the case of rational matrices. Specifically, Omega equivalence of rational matrices with possibly different dimensions is defined, which has the property of preserving the zero structure of rational matrices in the region (Omega is contained in C union the set infinity). ESA

N93-11122# Loughborough Univ. of Technology (England). Dept. of Mathematical Sciences.
REMARKS ON THE ROBINSON-TRAUTMAN SOLUTIONS
C. Hoenselaers and Z. Perjes (Central Research Inst. for Physics, Budapest, Hungary) Jun. 1992 12 p
(Maths-Rept-A-167; ETN-92-92385) Avail: CASI HC A03/MF A01

Robinson-Trautman (RT) space-times with a spacelike Killing vector are considered. RT solutions are algebrically special gravitational vacuum fields with an expanding but not twisting null eigenvector of the Weyl tensor. Special initial values are shown for which the solution does not exist for all future times. In general, however, the solution will asymptotically go over into the C metric. Perturbations of the C metric are discussed. The results of numerical calculations are shown. ESA

N93-11123# Loughborough Univ. of Technology (England). Dept. of Mathematical Sciences.
CONSTRAINED KP HIERARCHY AND BI-HAMILTONIAN STRUCTURES
W. Oevel and W. Strampp (Kassel Univ., Germany) Jun. 1992 30 p
(Maths-Rept-A-168; ETN-92-92386) Avail: CASI HC A03/MF A01

The Kadomtsev-Petviashvili (KP) hierarchy is considered together with the evolutions of eigenfunctions and adjoint eigenfunctions. By constraining the KP flows in terms of squared eigenfunctions, 1 + 1 dimensional integrable equations with scattering problems given by pseudodifferential Lax operators are obtained. The bi-Hamiltonian nature of these systems is shown by a systematic construction of two general Poisson brackets in the algebra of associated Lax operators. Gauge transformations provide Miura links to modified equations. These systems are constrained flows of the modified KP hierarchy, for which again a general description of their bi-Hamiltonian nature is given. The gauge transformations are shown to be Poisson maps relating the bi-Hamiltonian structures of the constrained KP hierarchy and the modified KP hierarchy. The simplest realization of this scheme yields the AKNS hierarchy and its Miura link to the Kaup-Broer hierarchy. ESA

N93-11124# Loughborough Univ. of Technology (England). Dept. of Mathematical Sciences.
EQUIVALENCE TRANSFORMATIONS OF RATIONAL MATRICES AND APPLICATIONS
N. P. Karampetakis (Aristotle Univ. of Thessaloniki, Greece), A. C. Pugh, and A. I. Vardulakis (Aristotle Univ. of Thessaloniki, Greece) Jun. 1992 31 p Sponsored by Greek National Foundation
(Maths-Rept-A-169; ETN-92-92387) Avail: CASI HC A03/MF A01

The known theories of transformations between polynomial matrices are extended to the case of rational matrices. Specifically, Omega equivalence between rational matrices having possibly different dimensions is defined, which has the property of preserving the zero structure of rational matrices on the region (Omega is contained in C union the set of infinity). Some implications of this new equivalence transformation for linear system theory are provided. ESA

N93-11125# Loughborough Univ. of Technology (England). Dept. of Mathematical Sciences.
ON A CERTAIN MCMILLAN DEGREE CONDITION APPEARING IN CONTROL
A. C. Pugh, N. P. Karampetakis (Aristotle Univ. of Thessaloniki, Greece), G. E. Hayton (Hull Univ., England), and A. I. G. Vardulakis (Aristotle Univ. of Thessaloniki, Greece) Jun. 1992 22 p Submitted for publication Sponsored by Greek National Foundation
(Maths-Rept-A-170; ETN-92-92388) Avail: CASI HC A03/MF A01

A number of interpretations of the McMillan degree conditions appearing in the transformation of full equivalence are presented. The most satisfactory explanation seems to be that of guaranteeing the existence of a linear map between the solution sets of the ordinary differential equations which underly the matrices involved in the transformation. The explanations appear to highlight the role that the conditions play in proof of invariance of the zero structure of two matrices related by the transformation. In this sense the explanations serve to underline the conditions as a device rather than a fundamental requirement of the theory. However, a complete explanation emerges in terms of maps between the solution spaces of the associated dynamical systems; thus, it is apparent that the McMillan degree conditions are of fundamental importance on the study of equivalence of linear systems. ESA

N93-11126# Loughborough Univ. of Technology (England). Dept. of Mathematical Sciences.
DARBOUX THEOREMS AND WRONSKIAN FORMULAS FOR INTEGRABLE SYSTEMS. 1: CONSTRAINED KP FLOWS
W. Oevel Jul. 1992 38 p
(Maths-Rept-A-172; ETN-92-92389) Avail: CASI HC A03/MF A01

Generalizations of the classical Darboux theorem are established for pseudodifferential scattering operators. Iteration of the Darboux transformation leads to a gauge transformed operator with coefficients given by Wronskian formulas involving a set of eigenfunctions of the scattering operators. Nonlinear integrable partial differential equations are associated with the scattering operators which arise as a symmetry reduction of the multicomponent Kadomtsev-Petviashvili (KP) hierarchy. With a suitable linear time evolution for the eigenfunctions, the Darboux transformation is used to obtain solutions of the integrable equations in terms of Wronskian determinants. ESA

N93-11182 Politecnico di Milano (Italy). Dipartimento di Elettronica.
THE COMPLEXITY OF SOME MULTICRITERIA ARBORESCENCE PROBLEMS
Francesco Maffioli 1992 19 p Sponsored in part by Italian Ministry of University and Scientific and Technological Research
(Rept-92-016; ETN-92-92418) Avail: Politecnico di Milano, Piazza Leonardo da Vinci 32, 20133 Milan, Italy

The complexity of the problem of finding an optimum arborescence (treelike form and appearance) of a given digraph with a request to an objective function obtained combining linearly two (or more) objective functions of various kinds is studied. Problems which are solvable in polynomial time and NP completeness results are presented. ESA

N93-11199 Iowa State Univ. of Science and Technology, Ames.
NUMERICAL SOLUTION OF INVERSE PROBLEMS IN MECHANICS USING THE BOUNDARY ELEMENT METHOD Ph.D. Thesis
Shuvra Das 1991 120 p
Avail: Univ. Microfilms Order No. DA9126186

Due to the ill-posed nature of inverse problems, it is difficult to obtain solutions using well known analytical and numerical techniques. The use of boundary element method as a numerical technique to solve inverse problems is quite new. In this work, the algorithms for the solution of two kinds of inverse problems are examined in detail. For the first kind, the shape and location of a part of the boundary is unknown; and for the second kind, the boundary condition is not specified on a part of the boundary. Boundary value problems with partially unknown boundary are ill-posed. To solve these problems additional information is necessary. Over-specified boundary data in the form of experimentally measured quantities can be used as additional information for solving the problem. An algorithm, based on the boundary element method and nonlinear optimization techniques, is proposed to solve this inverse problem. Using the overspecified boundary data, a functional is formed which involves parameters describing the unknown boundary. Minimization of this functional with respect to these parameters determines the unknown boundary. The performance of this scheme is examined through two problems. It is shown that the algorithm performs well even for complex shapes of the unknown boundary. For the problems in which the specified boundary conditions are insufficient, experimentally obtained data at some internal points are used as additional conditions. The boundary is divided into straight boundary elements and the unknown boundary conditions are represented as unknowns at the nodes of the boundary elements. It is shown that, for practical reasons, the number of nodes where the boundary condition is not specified is usually larger than the number of probes used for obtaining interior data. This results in an under-determined system of linear equations. A regularization method is used to solve these equations. The scheme, when applied to several example problems showed satisfactory performance. Few guidelines for the placement of the temperature probes in the interior of the domain are developed through numerical experiments. Dissert. Abstr.

N93-11211# Loughborough Univ. of Technology (England). Dept. of Mathematical Sciences.

PRECONDITIONED LOW-ORDER NEWTON METHODS

Y. F. Hu and C. Storey May 1992 24 p
(Maths-Rept-A-159; ETN-92-92382) Avail: CASI HC A03/MF A01

Low order Newton methods that make use of previously obtained second derivative information by suitable preconditioning are proposed. When applied to a particular two dimensional Newton method (the 'LS (Line Search) method'), a member of the Broyden family of quasi-Newton methods is obtained. Algorithms based on this preconditioned LS model are tested against some variations of the BFGS method and shown to be superior in terms of number of iterations and functions evaluations, but not so effective in terms of number of gradient evaluations. ESA

N93-11246*# Institute for Computer Applications in Science and Engineering, Hampton, VA.

DOMAIN DECOMPOSITION: A BRIDGE BETWEEN NATURE AND PARALLEL COMPUTERS Final Support

David E. Keyes (Yale Univ., New Haven, CT.) Sep. 1992 44 p Submitted for publication
(Contracts NAS1-18605; NAS1-19480; NSF ECS-89-57475; RTOP 505-90-52-01)
(NASA-CR-189709; NAS 1.26:189709; ICASE-92-44) Avail: CASI HC A03/MF A01

Domain decomposition is an intuitive organizing principle for a partial differential equation (PDE) computation, both physically and architecturally. However, its significance extends beyond the readily apparent issues of geometry and discretization, on one hand, and of modular software and distributed hardware, on the other. Engineering and computer science aspects are bridged by an old but recently enriched mathematical theory that offers the subject not only unity, but also tools for analysis and generalization. Domain decomposition induces function-space and operator decompositions with valuable properties. Function-space bases and operator splittings that are not derived from domain decompositions generally lack one or more of these properties. The evolution of domain decomposition methods for elliptically dominated problems has linked two major algorithmic developments of the last 15 years: multilevel and Krylov methods. Domain decomposition methods may be considered descendants of both classes with an inheritance from each: they are nearly optimal and at the same time efficiently parallelizable. Many computationally driven application areas are ripe for these developments. A progression is made from a mathematically informal motivation for domain decomposition methods to a specific focus on fluid dynamics applications. To be introductory rather than comprehensive, simple examples are provided while convergence proofs and algorithmic details are left to the original references; however, an attempt is made to convey their most salient features, especially where this leads to algorithmic insight. Author

N93-11254*# National Aeronautics and Space Administration. Lewis Research Center, Cleveland, OH.

ON AN ORIGIN OF NUMERICAL DIFFUSION: VIOLATION OF INVARIANCE UNDER SPACE-TIME INVERSION

Sin-Chung Chang Jul. 1992 14 p Presented at the 23rd Modeling and Simulation Conference, Pittsburgh, PA, 30 Apr. - 1 May 1992
(RTOP 505-62-52)
(NASA-TM-105776; E-7066; NAS 1.15:105776) Avail: CASI HC A03/MF A01

The invariant properties of the convection equation $du/dt + adu/dx = 0$ (where d is the partial differential operator) with respect to spatial reflection, time reversal, and space-time inversion are studied. Generally, a finite-difference analog of this equation may possess some or none of these properties. It is shown that, under certain conditions, the von Neumann amplification factor of an analog satisfies a special relation for each invariant property this analog possesses. Particularly, an analog is neutrally stable and thus free of numerical diffusion if it possesses the invariant property related to space-time inversion. It is also explained why generally (1) an upwind scheme possesses neither the invariant property related to spatial reflection nor that related to space-time inversion, and (2) an explicit scheme possesses neither the invariant property related to time reversal nor that related to space-time inversion. Extension to the viscous case and a remarkable connection between the current work and a new numerical framework for solving conservation laws are also discussed. Author

N93-11323# Loughborough Univ. of Technology (England). Dept. of Mathematical Sciences.

INVERSE SPECTRAL TRANSFORM FOR THE 2 + 1-DIMENSIONAL GARDNER EQUATION

B. G. Konopelchenko (Institute of Nuclear Physics, Novosibirsk, USSR) Jan. 1991 18 p
(Maths-Rept-A-138; ETN-92-92254) Avail: CASI HC A03/MF A01

The 2 + 1-dimensional integrable generalization of the Gardner equation is solved by the inverse spectral transform method. Wide classes of exact solutions are constructed explicitly by the delta bar dressing method. They are the rational solutions, including the decaying and plane lumps solutions, with functional parameters and plane solitons. ESA

N93-11431# Texas A&M Univ., College Station.

STATIONARY TIME SERIES ANALYSIS USING INFORMATION AND SPECTRAL ANALYSIS Technical Report No. 187

Emanuel Parzen Sep. 1992 15 p
(Contract DAAL03-90-G-0069; Proj. 6547)
Avail: CASI HC A03/MF A01

The technical aims of this paper are: to discuss some roles of information ideas and spectral analysis in time series analysis; to extend spectral estimation by exponential models and extend (to time series) goodness of fit tests by components. The practice of statistics and time series analysis can 'stand on the shoulders of giants' if we develop a framework which unifies diverse methods. Information ideas are central to a unified framework since they clarify and extend methods by providing many levels of relationship between time series analysis, classical statistical methods for independent samples, and signal processing problems called inverse problems with positivity constraints. Author

N93-11437# Royal Signals and Radar Establishment, Malvern (England).

ON RECURSIVE FREE TYPES IN Z

A. Smith Aug. 1991 40 p
(RSRE-91028; P304797-47; ETN-92-92311) Copyright Avail: CASI HC A03/MF A01

Inconsistent specifications may give rise to false conclusions in reasoning, thus destroying the point of having a specification. In ordinary mathematics, an equation can be written down which is syntactically correct, but for which no solution exists: the equation $x = x + 1$, defined over the real numbers, has no value of x which satisfies it. Similarly it is possible to specify objects using the formal specification language Z, which can not possibly exist. Such specifications are called inconsistent and can arise in a number of ways. The inconsistent specifications which may arise when using the formal specification language Z are discussed. The report is concerned with inconsistencies that can arise when using recursive free types, and recursive functions defined over recursive free types. The intended audience of the report consists of Z practitioners who wish to avoid writing meaningless specifications. ESA

N93-11446# Argonne National Lab., IL.

THE EFFICIENT PARALLEL ITERATIVE SOLUTION OF LARGE SPARSE LINEAR SYSTEMS

M. T. Jones and P. E. Plassmann Jun. 1992 16 p Presented at the IMA Workshop on Sparse Matrix Computations: Graph Theory Issues and Algorithms, Minneapolis, MN, 14-18 Oct. 1991

(Contract W-31-109-eng-38)
(DE92-018769; ANL/CP-76726; CONF-9110404-1) Avail: CASI HC A03/MF A01

The development of efficient, general-purpose software for the iterative solution of sparse linear systems on a parallel MIMD computer requires an interesting combination of expertise. Parallel graph heuristics, convergence analysis, and basic linear algebra implementation issues must all be considered. In this paper, we discuss how we have incorporated recent results in these areas into a general-purpose iterative solver. First, we consider two recently developed parallel graph coloring heuristics. We show how the method proposed by Luby, based on determining maximal independent sets, can be modified to run in an asynchronous manner and give an expected running time bound for this modified heuristic. In addition, a number of graph reduction heuristics are described that are used in our implementation to improve the individual processor performance. The effect of these various graph reductions on the solution of sparse triangular systems is categorized. Finally, we discuss the performance of this solver from the perspective of two large-scale applications: a piezoelectric crystal finite-element modeling problem, and a nonlinear optimization problem to determine the minimum energy configuration of a three-dimensional, layered superconductor model. DOE

N93-11463# Naval Air Development Center, Warminster, PA.
A PRIMER ON POLYNOMIAL RESULTANTS Final Report, Mar. - Dec. 1991
Ronald F. Gleeson and Robert M. Williams 5 Dec. 1991 27 p
(AD-A246883; NADC-91112-50) Avail: CASI HC A03/MF A01

Nonlinearity is one of the most stubborn difficulties of contemporary engineering and science. In this paper we are concerned with a broadly useful tool, the resultant, for manipulating polynomial nonlinearities, and we review several techniques for solving systems of nonlinear polynomial equations. The resultant, a classical algebraic tool, has become much more practical recently with the advent of symbolic software (such as Mathematics and Maple) which can evaluate 10x10 symbolic determinants in a matter of minutes on a desktop computer. While much of this paper is concerned with applying resultants to systems of univariate equations, the last section considers the generalization to the multivariate situation. Nonlinear multivariate applications appear in various areas of engineering such as chaos, signal processing, circuit theory, robotics and control theory. Two illustrations of the power of the resultant formalism are provided. First, the problem of finding the coordinates on the Earth's surface viewed by each pixel of a reconnaissance aircraft camera is discussed. Second, the Lorenz model of chaos theory is considered. GRA

N93-11520# Argonne National Lab., IL.
SOME NUMERICAL RESULTS ON BEST UNIFORM POLYNOMIAL APPROXIMATION OF CHI(SUP ALPHA) ON INTERVAL (0,1)
A. J. Carpenter and R. S. Varga 1992 35 p Presented at the USSR-US Leningrad Conference on Approximation Theory, Leningrad (USSR), 13-26 May 1991
(Contract W-31-109-eng-38)
(DE92-014859; ANL/CP-75917; CONF-9105344-1) Avail: CASI HC A03/MF A01

Let alpha be a positive number, and let E(sub n)(chi(sup alpha);interval (0,1)) denote the error of best uniform approximation to chi(sup alpha), by polynomials of degree at most n, on the interval (0,1). The Russian mathematician S.N. Bernstein established the existence of a nonnegative constant Beta(alpha) such that Beta(alpha): = lim(n approaches infinity) 2n(sup 2 alpha) E(sub n)(chi(sup alpha);interval (0.1). In addition, Bernstein showed that Beta(alpha) less than (Gamma(2 alpha) absolute value sin(pi alpha)) / pi (alpha greater than 0) and that (Gamma(2 alpha) absolute value sin(pi alpha)) / pi (1 - 1 / 2(alpha) - 1)) less than Beta(alpha) where alpha is greater than 1/2, so that the asymptotic behavior of Beta(alpha) is known when alpha approaches infinity. Still, the problem of trying to determine Beta(alpha) more precisely, for all alpha greater than 0, is intriguing. To this end, we have rigorously determined the numbers for thirteen values of alpha, where these numbers were calculated with a precision of at least 200 significant digits. For each of these thirteen values of alpha, Richardson's extrapolation was applied to the products to obtain estimates of Beta(alpha) to approximately 40 decimal places. Included are graphs of the points (alpha, Beta(alpha)) for the thirteen values of alpha that we considered. DOE

N93-11531*# National Aeronautics and Space Administration. Lewis Research Center, Cleveland, OH.
COMPARISON OF TRUNCATION ERROR OF FINITE-DIFFERENCE AND FINITE-VOLUME FORMULATIONS OF CONVECTION TERMS
B. P. Leonard (Akron Univ., OH.) Sep. 1992 15 p
(Contract NCC3-233; RTOP 505-62-21)
(NASA-TM-105861; ICOMP-92-19; E-7321; NAS 1.15:105861)
Avail: CASI HC A03/MF A01

Judging by errors in the computational-fluid-dynamics literature in recent years, it is not generally well understood that (above first-order) there are significant differences in spatial truncation error between formulations of convection involving a finite-difference approximation of the first derivative, on the one hand, and a finite-volume model of flux differences across a control-volume cell, on the other. The difference between the two formulations involves a second-order truncation-error term (proportional to the third-derivative of the convected variable). Hence, for example, a third (or higher) order finite-difference approximation for the first-derivative convection term is only second-order accurate when written in conservative control-volume form as a finite-volume formulation, and vice versa. Author

N93-11547*# Georgia Inst. of Tech., Atlanta.
NUMERICAL ANALYSIS OF RIGHT-HALF PLANE ZEROS FOR A SINGLE-LINK MANIPULATOR M.S. Thesis
Douglas Lynn Girvin 3 Mar. 1992 100 p
(Grant NAG1-623)
(NASA-CR-190966; NAS 1.26:190966) Avail: CASI HC A05/MF A02

The purpose of this research is to further develop an understanding of how nonminimum phase zero location is affected by structural link design. As the demand for light-weight robots that can operate in a large workspace increases, the structural flexibility of the links become more of an issue in controls problems. When the objective is to accurately position the tip while the robot is actuated at the base, the system is nonminimum phase. One important characteristic of nonminimum phase systems is system zeros in the right half of the Laplace plane. The ability to pick the location of these nonminimum phase zeros would give the designer a new freedom similar to pole placement. The research targets a single-link manipulator operating in the horizontal plane and modeled as a Euler-Bernoulli beam with pinned-free end conditions. Using transfer matrix theory, one can consider link designs that have variable cross-sections along the length of the beam. A FORTRAN program was developed to determine the location of poles and zeros given the system model. The program was used to confirm previous research on nonminimum phase systems, and develop a relationship for designing linearly tapered links. The method allows the designer to choose the location of the first pole and zero and then defines the appropriate taper to match the desired locations. With the pole and zero location fixes, the designer can independently change the link's moment of inertia about its axis of rotation by adjusting the height of the beam. These results can be applied to inverse dynamic algorithms currently under development at Georgia Tech. Author

N93-11636# Oak Ridge National Lab., TN.
SCALAPACK: A SCALABLE LINEAR ALGEBRA LIBRARY FOR DISTRIBUTED MEMORY CONCURRENT COMPUTERS
Jaeyoung Choi, D. W. Walker, J. J. Dongarra, and R. Pozo (Tennessee Univ., Knoxville.) 1992 9 p Presented at the 4th Symposium on Frontiers of Massively Parallel Computing, McLean, VA, 19-21 Oct. 1992

(Contract DE-AC05-84OR-21400)
(DE92-017823; CONF-9210148-1) Avail: CASI HC A02/MF A01

This paper describes ScaLAPACK, a distributed memory version of the LAPACK software package for dense and banded matrix computations. Key resign features are the use of distributed versions of the Level 3 BLAS as building blocks, and an object-based interface to the library routines. The square block scattered decomposition is described. The implementation of a distributed memory version of the right-looking LU factorization algorithm on the Intel Delta multicomputer is discussed, and performance results are presented that demonstrate the scalability of the algorithm. DOE

N93-11837# Maryland Univ., College Park.
PERFORMANCE OF THE h-p VERSION OF THE FINITE ELEMENT METHOD WITH VARIOUS ELEMENTS
I. Babuska and H. C. Elman Sep. 1991 32 p
(Contract N00014-90-J-1030; NSF CCR-88-20279)
(AD-A250689; BN-1128; MD91-33-IBHR; TR91-33) Avail: CASI HC A03/MF A01

The paper addresses the performance of square elements of type Q(p) and Q'(p). (The Q(p) resp. Q'(p) are elements of degree p analogous to the well known 9 and 8 noded elements for p = 2.) The performance is analyzed theoretically for the class of analytic functions. Numerical experiments confirm the conclusions drawn from the theory. The computational complexity of a solution algorithm is studied using timings of the computation on an Alliant FX/8 computer. The data show that high order elements are preferable. GRA

N93-12061# District of Columbia Univ., Washington, DC.
A SUMMER PROGRAM IN MATHEMATICS AND COMPUTER SCIENCE FOR ACADEMICALLY ORIENTED STUDENTS, JUNE 24 - JULY 26, 1991, WASHINGTON, DC Final Report
Bernis Barnes 26 Jul. 1991 148 p Sponsored by ONR
(AD-A249139) Avail: CASI HC A07/MF A02

The 1991 summer intervention program in mathematics and computer science for academic oriented students was one of our most successful. The five-week program provided intensive and rigorous study for thirty-six mainly ninth and tenth grade students from the D.C. area. As in the previous nine years of the program, addressing the problems of the under-representation of minorities, especially Blacks and Hispanics in engineering, natural science, and other mathematics-based fields, was given a high priority. During the summer, the students most of whom are from the under-represented groups were encouraged to strengthen their background in mathematics and to pursue careers in mathematics-based fields. They were also exposed to career opportunities in mathematics-based fields, and to how they should prepare themselves in high school to increase their career options by the time they reach college. The program faculty which has years of experience in teaching local minority students provided the encouragement and motivation, as well as a carrying and supportive environment. The purpose of this project is to implement an intensive pre-college intervention program for academically talented students, mainly ninth and tenth grade students from the District of Columbia area, that is designed to increase their representation in mathematics-based careers. By offering the program at this grade level, the students are able to take more rigorous math courses while in high school. GRA

N93-12176# International Centre for Theoretical Physics, Trieste (Italy).
AN ISOMORPHISM FOR ALGEBRA OF DISTRIBUTIONS WITH COMPACT SUPPORT ON LIE GROUPS
K. El-Hussein Aug. 1991 21 p
(DE92-603605; IC-91/235) Avail: CASI HC A03/MF A01

Let H, H(sub 0),...,H(sub L), L is an element of IN) be a finite sequence of abelian connected Lie Groups, G(sub L) = H, G(sub 1) = G(sub i+1)(chi)(sub (rho)i+1)H(sub i+1) (0 is less than or equal to i is less than or equal to L - 1) and G = G(sub 0)(chi)(sub (rho)o)H(sub 0) the Lie groups which are the semi-direct product of G(sub i) by H(sub i) (0 is less than or equal to i is less than or equal to L), where (rho)(sub i) : H(sub i) approaches Aut(G(sub i)) is a group homomorphism (0 is less than or equal to i is less than or equal to L). Let G-tilde = H x H(sub L) x...x H(sub 0) be the Lie group of the direct product of H, H(sub L),..., and H(sub 0) and let epsilon'(G-tilde) the Topological vector space of all distributions with compact support on G-tilde. In this paper, we prove that there is a structure of algebra on epsilon'(G-tilde) such that the algebra (convolution) of all distributions with compact support on G is isomorphic onto epsilon'(G-tilde). DOE

N93-12243# Vanderbilt Univ., Nashville, TN. Dept. of Mathematics.
TWO EXTENDABILITY IN TWO CLASSES OF CLAW-FREE GRAPHS
Michael D. Plummer 1992 20 p
(Contract N00014-91-J-1142)
(AD-A254639) Avail: CASI HC A03/MF A01

A graph, G, is 2-extendable if it has at least six vertices and every pair of independent edges extends to (i.e., is a subset of) a perfect matching. In this paper, two classes of claw-free graphs are discussed: those which are 3-regular and 3-connected and those which are 4-regular and 4-connected (as well as even). None of the first class is 2-extendable, whereas those of the second class which are 2-extendable are determined. More particularly in the graphs belonging to these classes, those pairs of independent edges which extend to a perfect matching are determined. GRA

N93-12298*# Institute for Computer Applications in Science and Engineering, Hampton, VA.
SPURIOUS MODES IN SPECTRAL COLLOCATION METHODS WITH TWO NON-PERIODIC DIRECTIONS Final Report
S. Balachandar (Illinois Univ., Urbana.) and Ravi K. Madabhushi (Illinois Univ., Urbana.) Sep. 1992 12 p Submitted for publication
(Contract NAS1-19480; RTOP 505-90-52-01)
(NASA-CR-189713; NAS 1.26:189713; ICASE-92-48) Avail: CASI HC A03/MF A01

Collocation implementation of the Kleiser-Schumann's method in geometries with two non-periodic directions is shown to suffer from three spurious modes - line, column and checkerboard - contaminating the computed pressure field. The corner spurious modes are also present but they do not affect evaluation of pressure related quantities. A simple methodology in the inversion of the influence matrix will efficiently filter out these spurious modes. Author

N93-12328# Texas A&M Univ., College Station.
LIMIT THEOREMS FOR FISHER-SCORE CHANGE PROCESSES Technical Report No. 186
Lajos Horvath (Utah Univ., Salt Lake City.) and Emanuel Parzen Sep. 1992 16 p
(Contract DAAL03-90-G-0069; Proj. 6547)
Avail: CASI HC A03/MF A01

Change analysis is concerned with 'fluctuation' of the data (in accordance with probability distributions fitted to a whole sample) from 'non-stationarity' (changes in the parameters of probability distributions). To detect change over time in a sequence of observations one forms for various transformations of the data sample change processes on (0,1); the transformations are called 'data score functions'. One can choose non-parametric score functions which detect changes of location, scale, skewness, etc. in the probability distribution of the observations. When a parametric model is available for the distribution of each observation one can detect changes in the parameter values by transforming the data by parametric score functions which we call Fisher-score functions. This paper studies the asymptotic distributions (under the null hypothesis of no change) of Fisher-score change processes which are cusums of scored data. They are related to cuscore processes or cumulative score processes. Author

N93-12350# National Aerospace Lab., Tokyo (Japan). Computational Sciences Div.
DIFFERENCE APPROXIMATIONS FOR HYPERBOLIC CONSERVATION LAWS AND CONSISTENCY WITH CHARACTERISTICS
Hideaki Aiso Feb. 1991 22 p
(NAL-TR-1098T; JTN-92-80391) Avail: CASI HC A03/MF A01

In the theory of conservation laws, characteristics may be considered as paths along which infinitesimal perturbations propagate. The concept of characteristics can not be directly applied to difference approximations for conservation laws, but it is possible to discuss difference approximations from the viewpoint of the discrete propagation of infinitesimal perturbations. In this report, a new concept, 'the consistency with characteristics', is proposed for difference approximations for scalar conservation laws and a sufficient condition under which the consistency with characteristics is satisfied is given. The difference approximations of conservation form for scalar conservation laws are discussed from the viewpoint of the consistency with characteristics. Furthermore, a straightforward extension of the concept to difference approximations is considered for systems of conservation laws. Author (NASDA)

N93-12465# Stanford Univ., CA. Dept. of Operations Research.
MATHEMATICAL METHODS IN OPERATIONS RESEARCH AND COMPUTER SCIENCE Final Report, 1 Jan. 1989 - 31 Dec. 1991
George B. Dantzig and Richard W. Cottle Jun. 1992 14 p
(Contract N00014-89-J-1659)
(AD-A254782) Avail: CASI HC A03/MF A01

Our progress on the fundamental problem of decision science, solving large-scale optimization problems whose parameters are subject to uncertainty, has been so rapid during the past year that we are now in a position to tackle the most general type of stochastic models one is likely to encounter in practice. It is particularly relevant to the Navy during this critical period of deciding how best to down-size the military and yet maintain a force robust and ready to handle any combination of contingencies that might arise in the future with high probability. A major breakthrough in this area has the potential of profoundly affecting the quality of planning, the reduction of cycle time to improve products, the reduction of time to militarily deploy in crisis, and generally improve the industrial competitiveness of U.S. until the time that other countries catch on. By way of background, our approach uses a combination of decomposition methods (D-W and Benders), importance sampling, and (if necessary) parallel processors. GRA

N93-12511# Yale Univ., New Haven, CT. Dept. of Computer Science.
PERTURBATION THEORY FOR THE SOLUTION OF SYSTEMS OF LINEAR EQUATIONS
Shivkumar Chandrasekaran and Ilse Ipsen Oct. 1991 47 p
(Contract N00014-88-K-0573; NSF CCR-91-02853)
(AD-A254994; YaleU/DCS/RR-866) Avail: CASI HC A03/MF A01

We present expressions for absolute and relative errors in individual components of the solution to systems of linear equations. We consider three kinds of linear systems: non-singular, underdetermined of full row rank, and least squares of full column rank. No assumptions regarding the structure or distribution of the perturbations are required. Our expressions for component-wise relative errors allow the following conclusions: for any linear system there is at least one solution component whose sensitivity to perturbations is proportional to the condition number of the matrix, but--depending on the relation between right-hand side and matrix--there may exist components that are much better conditioned. For a least squares problem, the sensitivity of the components also depends on the right-hand side and may be as high as the square of the condition number. Least squares problems are therefore always more receptive to ill-conditioning than linear systems. In addition, we show that the component-wise relative errors for linear systems are reduced by column scaling only if column scaling manages to reduce the perturbations. Regarding underdetermined linear systems of full column rank, the problem of finding the minimal-norm solution can be formulated so that the same analysis as for least squares problems is applicable here as well. Finally, we define component-wise condition numbers that measure the sensitivity of the solution components to perturbations. They have simple geometric interpretations and can be computed and estimated as efficiently as the conventional condition numbers. GRA

65 STATISTICS AND PROBABILITY

Includes data sampling and smoothing; Monte Carlo method; and stochastic processes.

N93-10980# Royal Signals and Radar Establishment, Malvern (England).
INCORPORATING PRIOR PROBABILITIES AND MISCLASSIFICATION COSTS INTO NETWORK TRAINING: AN EXAMPLE FROM MEDICAL PROGNOSIS
David Lowe and Andrew R. Webb 1 Nov. 1989 38 p
(RSRE-Memo-4343; BR113093) Copyright Avail: CASI HC A03/MF A01

Feed-forward layered networks trained on a pattern classification task in which the number of training patterns in each class is non-uniform, bias strongly in favor of those classes with the largest membership. This is an unfortunate property of networks when the relative importance of classes with smaller membership is much greater than that of classes with many training patterns. In addition, there are many pattern classification tasks where different penalties are associated with misclassifying a pattern belonging to one class as another class. It is not generally known how to compensate for such effects in network training. An analytical regularization scheme is discussed, whereby prior expectations of class importance occurring in the generalization data and misclassification costs may be incorporated into the training phase (these compensating for the uneven and unfair class distributions occurring in the training set). The effects of the proposed scheme on the feature extraction criterion employed in the hidden layer of the network is discussed. An illustration of the results is presented by considering a real medical prognosis problem concerning data collected from head-injured coma patients. Relationships between least mean square error minimization and Bayesian minimum risk estimation is mentioned and the importance and relevance of input/output coding schemes for network performance is considered. Author

N93-11417# Naval Postgraduate School, Monterey, CA.
THE USE OF STATISTICAL MEASURES TO VALIDATE SYSTEM DYNAMICS MODELS M.S. Thesis
Todd D. Stephan Mar. 1992 75 p
(AD-A248569) Avail: CASI HC A04/MF A01

System dynamics modelers have often been criticized for their informal methods of model validation and for not using more formal, quantifiable measures to lend confidence to the validation process. Numerous proponents of the system dynamics approach have highlighted this shortcoming, however, and have suggested a variety of appropriate statistical measures which could be used in the model validation process. The objective of this thesis is to complement earlier validation efforts of the Abdel-Hamid and Madnick System Dynamics Model of Software Development by submitting the model to a battery of appropriate statistical measures. The model is evaluated with statistics which have been used by others in the system dynamics field. The evaluation makes two different comparisons. First, an evaluative comparison is made between data generated by the model and actual data of two real software projects. Then, an evaluative comparison is made between model generated data and data obtained by direct experimentation for two different experiments, using the model's gaming interface. The two evaluations serve to promote confidence in the model. GRA

N93-11820# Los Alamos National Lab., NM.
IDENTIFICATION AND ESTIMATION OF SOURCES OF TRANSMITTED VARIATION
J. R. Wendelberger and G. E. P. Box (Wisconsin Univ., Madison.) 1992 37 p Presented at the Joint Statistical Meetings of the American Statistical Association, the Biometric Society and the Institute of Mathematical Statistics, Boston, MA, 9-13 Aug. 1992
(Contract W-7405-eng-36)
(DE92-015246; LA-UR-92-1707; CONF-920893-1) Avail: CASI HC A03/MF A01

Errors in the settings of experimental variables are transmitted, via a response function, to a measured response. For nonlinear response functions, variation in a response can be studied to analyze variation transmitted from experimental variables. A new indirect method for identifying sources of transmitted variation is proposed. Using a first-order approximation for transmitted error, the log of the sample variances obtained from replicate measurements can be modeled as a loglinear function of the components of the vector of squared gradients of the response function. After selection of a particular model using the identification method, parameter values may be estimated. A formal procedure for estimating the variances of the errors in experimental variables is developed using maximum likelihood theory. Approximate standard errors of these estimates are obtained from asymptotic theory. DOE

N93-12081# Texas A&M Univ., College Station. Research Foundation.
HISTORY OF STATISTICS IN REAL TIME: HAMMERS AND NAILS
Emanuel Parzen May 1992 8 p
(Contract DAAL03-90-G-0069)
(AD-A253521; TR-170; ARO-27574.6-MA) Avail: CASI HC A02/MF A01

Contents: (1) Is what statisticians do fun?; (2) Statistical hammers and nails can help guide what statisticians do; (3) Hammers that make statisticians dull; (4) History of Statistics in Real Time and Stigler's Book; (5) Esoteric research should provide esoteric hammers; and (6) Quality control of the art of statistical science. GRA

N93-12334# Texas A&M Univ., College Station. Dept. of Statistics.
CHANGE ANALYSIS AND FISHER-SCORE CHANGE PROCESSES
Emanuel Parzen May 1992 18 p
(Contract DAAL03-90-G-0069)
(AD-A254707; TR-171; ARO-27574.7-MA) Avail: CASI HC A03/MF A01

This paper aims to synthesize classical statistical methods and changepoint hypothesis testing and to contribute to solutions of the historical basic applied problem of statistics: distinguish change (of the model) from fluctuation (within the model), the variability expected under homogeneity. Contents are: (0) Goals; (1) Comparison, change analysis as probability study of (X,Y); (2) Asymptotic distributions of sample change processes; (3) One way analysis of variance (AOV); (4) Change analysis approach to AOV; (5) Components of change analysis; (6) Four phases of change analysis (7) Nonparametric statistics from multisample analysis; (8) Fisher-Score change processes. GRA

N93-12426# Naval Postgraduate School, Monterey, CA. Dept. of Operations Research.
INTERACTIVE ANALYSIS OF GAPPY BIVARIATE TIME SERIES USING AGSS Final Report, Sep. 1991 - May 1992
Peter A. Lewis and Bonnie Ray Jun. 1992 11 p
(AD-A255160; NPSOR-92-013) Avail: CASI HC A03/MF A01

Bivariate time series which display nonstationary behavior, such as cycles or long-term trends, are common in fields such as oceanography and meteorology. These are usually very large-scale data sets and often may contain long gaps of missing values in one or both series, with the gaps perhaps occurring at different time periods in the two series. We present a simplified but effective method of interactively examining and filling in the missing values in such series using extensions of the methods available in AGSS, an APL2-based statistical software package. Our method allows for possible detrending and removal of seasonal components before automatically estimating arbitrary patterns of missing values for each series. Interactive bivariate spectral analysis can then be performed on the detrended and deseasonalized interpolated data if desired. We illustrate our results using a bivariate time series of ocean current velocities measured off the California coast. GRA

N93-12429# Texas A&M Univ., College Station. Dept. of Statistics.
RESEARCH IN STATISTICAL INFERENCE Final Report, 1 Jan. 1989 - 31 Aug. 1991
Raymond J. Carroll 31 Aug. 1991 3 p
(Grant AF-AFOSR-0240-89)
(AD-A252928; AFOSR-92-0680TR) Avail: CASI HC A01/MF A01

During this period of research a substantial research program continued in statistical inference, one that has seen the publication of nearly 100 papers and a book since the initiation of support. The papers written or revised in 1991-1992 are as follows: (1) An Asymptotic Theory for Sliced Inverse Regression, T. Hsing and R. J. Carroll; (2) Measurement Error Regression with Unknown Link: Dimension Reduction and Data Visualization, Raymond Carroll and Ker-Chau Li; (3) Further Remarks on Robustness in the Logistic Regression Model, R. J. Carroll and Shane Pederson; (4) Semiparametric Comparison of Regression Curves Via Normal Likelihoods, R. J. Carroll and Peter Hall; and (5) Theoreticas Aspects of Ill-Posed Problems in Statistics, A. C. M. Van Rooij, F. H. Ruymgaart and R. J. Carroll. GRA

N93-12513# Stanford Univ., CA. Dept. of Statistics.
NONNORMAL MULTIVARIATE DISTRIBUTIONS: INFERENCE BASED ON ELLIPTICALLY CONTOURED DISTRIBUTIONS
T. W. Anderson Jul. 1992 30 p
(Contract DAAL03-89-K-0033)
(AD-A254999; SU-TR-28) Avail: CASI HC A03/MF A01

The class of elliptically contoured distributions, which includes multivariate t-distributions and contaminated normal distributions, serves as a useful generalization of the class of normal multivariate distributions. The density, marginal and conditional densities, and moments of an elliptically contoured distribution are related in a simple fashion to those of a normal distribution. The asymptotic normal distributions of the sample mean and covariance matrix are developed and are compared with the asymptotic distributions of the maximum likelihood estimators of the parameters of an elliptically contoured distribution. The class of elliptically contoured distributions serves as a model for evaluating other robust estimators. Many test procedures for normal distributions are easily modified for the elliptically contoured distributions. Further generalizations are discussed. GRA

N93-11923*# Jet Propulsion Lab., California Inst. of Tech., Pasadena.
A MODEL-BASED REASONING APPROACH TO SENSOR PLACEMENT FOR MONITORABILITY
Steve Chien, Richard Doyle, and Luiz HomemdeMello *In* NASA. Lyndon B. Johnson Space Center, Fifth Annual Workshop on Space Operations Applications and Research (SOAR 1991), Volume 1 Jan. 1992 p 9-18 Sponsored by NASA, Washington (For primary document see N93-11921 02-59)
Avail: CASI HC A02/MF A04

66 SYSTEMS ANALYSIS

Includes mathematical modeling; network analysis; and operations research.

N93-11711# Advisory Group for Aerospace Research and Development, Neuilly-Sur-Seine (France). Flight Mechanics Panel.
AGARD FLIGHT TEST TECHNIQUES SERIES. VOLUME 10: WEAPON DELIVERY ANALYSIS AND BALLISTIC FLIGHT TESTING [L'ANALYSE DU LARGAGE D'ARMES ET LES ESSAIS EN VOL BALISTIQUE]
R. J. Arnold (Air Force Systems Command, Eglin AFB, FL.) and J. B. Knight (Air Force Systems Command, Eglin AFB, FL.) Jul. 1992 170 p
(AGARD-AG-300-Vol-10; ISBN-92-835-0677-4) Copyright Avail: CASI HC A08/MF A02

This volume in the AGARD Flight Test Techniques series treats stores ballistic modeling/testing from the overall system standpoint. All aspects of the ballistic testing design, data collection techniques, data reduction, analysis techniques, and finally the Operational Flight Program modeling techniques are addressed. Considerable effort has been expended to keep this report straightforward so that it can be understood by management as well as engineering personnel, but with sufficient engineering principles addressed so that a true ballistician could use it from an application perspective. This AGARDograph has been sponsored by the Flight Mechanics Panel of AGARD. Author

N93-12260# Naval War Coll., Newport, RI.
THE FUTURE OF CARRIER AVIATION Final Report
Thomas W. Trotter May 1992 119 p
(AD-A254043) Avail: CASI HC A06/MF A01

Over the last 45 years the U.S. Navy has generally maintained a fleet of 15 aircraft carriers and almost as many carrier air wings. During this time frame, carrier air power was designed with a strong Soviet maritime threat in mind, but used against a myriad of third world nations. With missions ranging from crisis-response to sustained combat operations, aircraft carriers have continually been one of the United States' most visible forms of forward-deployed defense. Like the other branches of defense, the Navy is scaling back active forces. With fewer deployable carriers and a marked decrease in funding, the Navy must reevaluate carrier aviation's role in a markedly changed world. This study investigates future requirements for carrier aviation by critically evaluating: (1) the historical application of carrier air power across a broad spectrum of past scenarios; (2) carrier air power's applicability in light of the increased emphasis on regional threats; (3) variants of forward-defense to counter the changed threat; (4) future carrier aviation requirements; and (5) historical and alternative modes in the deployment of carriers. Additionally, this study addresses the variety of forces at work, which interact and impact upon the size and composition of the Navy's current and future carrier and air wing structure. Specifically, the Navy's two future strike aircraft programs, the AX and the FA-18 E/F, are investigated for their future application. Finally, a series of detailed recommendations are provided as measures to best preserve the future of carrier aviation. GRA

N93-11978*# Jet Propulsion Lab., California Inst. of Tech., Pasadena.
DECISION RULES FOR SPACEBORNE OPERATIONS PLANNING Abstract Only
Jeffrey H. Smith *In* NASA. Lyndon B. Johnson Space Center, Fifth Annual Workshop on Space Operations Applications and Research (SOAR 1991), Volume 1 Jan. 1992 p 400 (For primary document see N93-11921 02-59)
Avail: CASI HC A01/MF A04

N93-11980*# Rockwell International Corp., Downey, CA.
AUTOMATED RESUPPLY OF CONSUMABLES: ENHANCEMENT OF SPACE COMMERCIALIZATION OPPORTUNITIES
Davoud Manouchehri and A. J. Mauceri *In* NASA. Lyndon B. Johnson Space Center, Fifth Annual Workshop on Space Operations Applications and Research (SOAR 1991), Volume 1 Jan. 1992 p 407-411 (For primary document see N93-11921 02-59)
Avail: CASI HC A01/MF A04

67 THEORETICAL MATHEMATICS

Includes topology and number theory.

N93-12217# Carnegie-Mellon Univ., Pittsburgh, PA. Graduate School of Industrial Administration.
DECOMPOSITION OF BALANCED MATRICES. PART 5: GOGGLES
Michele Conforti, Gerard Cornuejols, and M. R. Rao Oct. 1991 42 p
(Grants NSF DDM-88-00281; NSF DDM-89-01495; NSF DDM-90-01705)
(AD-A247462; MSRR-573) Avail: CASI HC A03/MF A01

It is assumed that G is a bipartite graph that is signable to be balanced and contains goggles. The following theorom is proved. At least one of the following alternatives occurs for a bipartite graph G: (1) the graph G has no cycle of length 4k + 2, (2) the graph G has a chordless cycle of length 4k + 2, (3) there exist two complete bipartite graphs K1,K2 in G having disjoint node sets, with the property that the removal of the edges in K1,K2 disconnects G, and (4) there exists a subset S of the nodes of G with the property that the removal of S disconnects G, where S can be partitioned into three disjoint sets T,A, and N, such that T does not equal the null set, some node x is a member of T is adjacent to every node in the union of A and N, and if the cardinal of set T is greater than or equal to 2, then the cardinal of set A is greater than or equal to 2 and every node of T is adjacent to every node of A. A 0,1 matrix is balanced if it does not contain a square submatrix of odd order with two ones per row and per column. Balanced matrices are important in integer programming and combinatorial optimization since the associated set packing and set covering polytopes have integral vertices. To a 0,1 matrix A we associate a bipartite graph G(V(sup T), V(sup C), E) as follows: the node nets V(sup T) and V(sup C) represent the row set and the column set of A and edge ij belongs to E if and only if a(sub ij) = 1. Since a 0,1 matrix is balanced if and only if the associated bipartite graph does not contain a chordless cycle of length 4k + 2, the above theorom provides a decomposition of balanced matrices into elementary matrices whose associated bipartite graphs have no cycle of length 4k + 2. GRA

70 PHYSICS (GENERAL)

For precision time and time interval (PTTI) see *35 Instrumentation and Photography;* for geophysics, astrophysics or solar physics see *46 Geophysics, 90 Astrophysics,* or *92 Solar Physics.*

N93-11420# Clarkson Univ., Potsdam, NY. Dept. of Mathematics and Computer Science.
THE THIRD POTSDAM-5 KIEV INTERNATIONAL WORKSHOP ON NONLINEAR PROCESSES IN PHYSICS
A. S. Fokas, D. J. Kaup, A. C. Newell, and V. E. Zakharov Aug. 1991 10 p Workshop held in Potsdam, NY, 1-11 Aug. 1991 Sponsored in part by NSF; DOE; AFOSR; ONR; and Sloan Foundation
(AD-A249140) Avail: CASI HC A02/MF A01

The Third Potsdam-5 Kiev Workshop on Nonlinear Processes in Physics was held at Clarkson University, Potsdam, NY from August 1-11, 1991. It was sponsored by the Clarkson School of Science and was funded by the National Science Foundation, the Department of Energy, the US Air Force of Scientific Research, the US Office of Naval Research, the Sloan Foundation and the School of Science of Clarkson University. The organizing committee was A.S. Fokas, D.J. Kaup, A.C. Newell and V.E. Zakharov. This was the first major scientific workshop in the USA where the Soviet scientists formed a major contingent of the participants. There were 31 USSR participants out of a total of 106 participants. The emphasis of the workshop was on the interaction between mathematical techniques and problems of physical interest. It was particularly successful in mixing plasma physicists, fluid physicists and soliton theorists. The exchanges between these groups, particularly with the participation of the Soviet delegation, were quite stimulating. The most difficult part of the organization of this conference was the travel arrangements of the Soviet participants. We appreciate the efforts of Ildar Gabitov in this direction. However, in spite of our efforts several invited Soviet scientists were not able to attend, mainly because of difficulties in arranging their travel to the USA. GRA

N93-11468# Lehigh Univ., Bethlehem, PA. Materials Research Center.
NANOSTRUCTURE, DEFECT CHEMISTRY AND PROPERTIES OF RELAXOR FERROELECTRICS Final Report, 1 Jan. 1982 - 31 Jan. 1990
M. P. Harmer and D. M. Smyth 1 Feb. 1992 182 p
(Contract N00014-82-K-0190)
(AD-A247294; Rept-533614) Avail: CASI HC A09/MF A02

This research focused on cation ordering, defect chemistry, and dielectric properties of the BaTiO3-Ba(Zn(1/3)Nb(2/3))O3 (BZN) system. The latter compound was chosen as an analog of the PbO-based relaxor ferroelectrics to avoid the severe experimental restrictions caused by the volatility and reducibility of PbO. Two types of ordering of the Zn and Nb content of BZN were observed: a 1:1 (alternate layer) type that represents a local compositional change and charge imbalance that restricts the size of ordered domains, and a 1:2 type that is consistent with the composition of BZN. The effects of the Zn/Nb ratio and doping on the type and extent of ordering were determined. The defect chemistry of BZN is closely related to that of BaTiO3, which has been well-characterized. The material usually contains a large concentration of extrinsic oxygen vacancies because of compositional variations and ZnO loss. Mass-action expressions and thermodynamic parameters of the oxidation and reduction reactions, and of the band gap were determined. The proposed defect model is in excellent quantitative agreement with the experimental observations. The evolution of dielectric properties was studied as the Ti content of BaTiO3 was gradually replaced by Zn(1/3)Nb(2/3). GRA

N93-11511# Argonne National Lab., IL.
ALTERNATING-PHASE FOCUSING: A MODEL TO STUDY NONLINEAR DYNAMICS
L. Sagalovsky and J. R. Delayen 1992 9 p Presented at the International Workshop on Nonlinear Problems in Accelerator Physics, Berlin, Germany, 30 Mar. - 2 Apr. 1992
(Contract W-31-109-eng-38)
(DE92-019027; ANL/CP-76665; CONF-9203174-1) Avail: CASI HC A02/MF A01

We discuss a new model to study alternating-phase focusing (APF). Our approach is based on representing the accelerating electric field with a continuous phase modulated traveling wave. The resulting nonlinear equations of motion can be solved analytically to predict the regions of stable APF motion. We also identify the key parameters which adequately describe the physics of APF. The model is believed to be applicable to low-(beta) ion linacs with short independently-controlled superconducting cavities being developed at ANL. DOE

N93-11567# Colorado School of Mines, Golden. Center for Wave Phenomena.
COMPUTATIONAL ASPECTS OF GAUSSIAN BEAM MIGRATION
D. Hale 1992 16 p
(Contract DE-FG02-89ER-14079)
(DE92-018641; DOE/ER-14079/17; CWP-127) Avail: CASI HC A03/MF A01

The computational efficiency of Gaussian beam migration depends on the solution of two problems: (1) computation of complex-valued beam times and amplitudes in Cartesian (x,z) coordinates; and (2) limiting computations to only those (x,z) coordinates within a region where beam amplitudes are significant. The first problem can be reduced to a particular instance of a class of closest-point problems in computational geometry, for which efficient solutions, such as the Delaunay triangulation, are well known. Delaunay triangulation of sampled points along a ray enables the efficient location of that point on the raypath that is closest to any point (x,z) at which beam times and amplitudes are required. Although Delaunay triangulation provides an efficient solution to this closest point problem, a simpler solution, also presented in this paper, may be sufficient and more easily extended for use in 3-D Gaussian beam migration. The second problem is easily solved by decomposing the subsurface image into a coarse grid of square cells. Within each cell, simple and efficient loops over (x,z) coordinates may be used. Because the region in which beam amplitudes are significant may be difficult to represent with simple loops over (x,z) coordinates, I use recursion to move from cell to cell, until entire region defined by the beam has been covered. Benchmark tests of a computer program implementing these solutions suggest that the cost of Gaussian hewn migration is comparable to that of migration via explicit depth extrapolation in the frequency-space domain. For the data sizes and computer programs tested here, the explicit method was faster. However, as data size was increased, the computation time for Gaussian beam migration grew more slowly than that for the explicit method. DOE

N93-11598# Argonne National Lab., IL.
CRYOSTABILIZATION OF HIGH-TEMPERATURE SUPERCONDUCTING MAGNETS WITH SUBCOOLED FLOW IN MICROCHANNELS
Y. S. Cha, J. R. Hull, and U. S. Choi Jul. 1992 19 p Presented at the Applied Superconductivity Conference, Chicago, IL, 23-28 Aug. 1992
(Contract W-31-109-eng-38)
(DE92-018174; ANL/CP-75523; CONF-920802-1) Avail: CASI HC A03/MF A01

Subcooled flow of liquid nitrogen in microchannels is proposed as a means to enhance the stability of a superconducting magnet. Analysis shows high current density or a low stabilizer fraction is obtainable in a cryostable magnet. Increase in stability (using the Stekley criterion) is directly related to coolant velocity and coolant channel aspect ratio, however, there is a corresponding increase in pressure drop of the system. Another constraint is the coolant temperature rise, which is found to be a function of coolant residence time and the coolant to conductor ratio. DOE

N93-11625# Los Alamos National Lab., NM.
MEASUREMENT OF AC ELECTRICAL CHARACTERISTICS OF SSC SUPERCONDUCTING DIPOLE MAGNETS
K. M. Smedley (Superconducting Super Collider Lab., Dallas, TX.) and R. E. Shafer 1992 4 p Presented at the 15th International Conference on High Energy Accelerators, Hamburg, Germany, 20-24 Jul. 1992
(Contract W-7405-eng-36)
(DE92-018888; LA-UR-92-2179; CONF-920706-10) Avail: CASI HC A01/MF A01

Experiments were conducted to measure the AC electrical characteristics of SSC superconducting dipole magnets over the frequency range of 0.1 Hz to 10 kHz. A magnet equivalent circuit representing the magnet DC inductance, eddy current losses, coil-to-ground, and turn-to-turn capacitance was synthesized from the experimental data. This magnet equivalent circuit can be used to predict the current ripple distribution along the superconducting magnet string and can provide dynamic information for the design of the collider current regulation loop. DOE

N93-11666 National Physical Lab., Teddington (England). Div. of Mechanical and Optical Metrology.
EUROMET PROJECT NO. 231: UNCERTAINTIES IN MASS MEASUREMENT. NPL'S ANALYSIS OF DATA FROM THE CALIBRATION OF WEIGHT SET NPLW43
Stuart Davidson and Sylvia Lewis Jan. 1992 29 p
(NPL-MOM-107; ETN-92-92375) Copyright Avail: National Physical Lab., Teddington, Middlesex, TW11 0LW, England

A previous project on the comparison of small mass standards highlighted some differences of approach in the statistical analysis and calculation of uncertainties of measurement when calibrating mass standards. In a subsequent project, a common set of weighting data was analyzed in order to facilitate a direct comparison between their analysis methods. The National Physical Laboratory (NPL) analysis of the data is reported. ESA

N93-11759# Florida Univ., Gainesville. Dept. of Physics.
AN ANALYTIC DESCRIPTION OF THICK-WALL BUBBLES
Jooyoo Hong 1992 12 p
(Contract DE-FG05-86ER-40272)
(DE92-016465; UFIFT-HEP-92-15; DOE/ER-40272/161) Avail: CASI HC A03/MF A01

A new approximation scheme to the false-vacuum decay is suggested. In this scheme the bounce solutions can be obtained in an explicit and analytic way even for thick-wall bubbles. The result is compared with Coleman's thin-wall description, which shows that it nicely comprises the result of the latter prescription. Some applications are also discussed. DOE

N93-12116# Queens Coll., Flushing, NY. Dept. of Physics.
OPTIMIZATION OF FILM SYNTHESIZED RARE EARTH TRANSITION METAL PERMANENT MAGNET SYSTEMS
F. J. Cadieu 1992 20 p
(Contract DE-FG02-86ER-45265)
(DE92-018726; DOE/ER-45265/6) Avail: CASI HC A03/MF A01

Progress is reported in three areas: high coercivity Sm-Fe-Ti-V, Sm-Fe-Zr, and two element Sm-Fe Sm(sub 5)(Fe,T)(sub 17) type crystalline phases; ThMn(sub 12) type pseudobinary SmFe(12-x)T(x)(0 less than x less than 1.5); and sputter process control for the synthesis of precisely textured rare earth-transition metal magnetic films. DOE

71 ACOUSTICS

Includes sound generation, transmission and attenuation. For noise pollution see *45 Environmental Pollution.*

N93-10999# Miami Univ., FL. Div. of Applied Marine Physics.
FEASIBILITY ASSESSMENT OF A TRANSIENT SOUND SENSOR BASED ON THE SILICON RETINA ARCHITECTURE Progress Report
Jorge F. Willemsen 23 Jun. 1992 14 p
(Contract N00014-92-J-1192)
(AD-A252288) Avail: CASI HC A03/MF A01

In the Background section of the proposal I described the basic conceptual elements which underlie the Silicon Retina (SR) and those which underlie passive mammalian hearing. My original intention was to utilize the frequency discrimination capability manifested in mammalian hearing as the mechanism on which to base an acoustic analogue to the SR concept. Specifically, mammals have sophisticated frequency dependent sensors which transmit responses to discrete and well-resolved frequencies upward to higher processing levels. Each intermediate processor transmits the precise frequency information upstream. Thus one may think of acoustic frequencies as being analogous to visual positional information, since in the ray limit of optics there is a one to one correspondence between the relative locations of external objects and the retinal sensors which are stimulated at any given time. The SR mechanism was to be implemented by comparing individual frequencies with running averages over groups of nearby frequencies, eliciting a response when the intensities of these differed by a prescribed amount. The next step in the program was to remain open-minded regarding the implementation of directional acoustic arrays, with the idea pf steering an array making use of the 'alert' response created by the introduction of a non-background signal. In this way it was envisioned that the 'cocktail party effect' would be achieved. GRA

N93-11156# Centro Italiano Ricerche Aerospaziali, Naples.
NUMERICAL STUDY FOR THE STUDY OF MEDIUM SPEED INTERNAL NOISE PROBLEMS [METODI NUMERICI PER LO STUDIO DELLE PROBLEMATICHE DI RUMPRE INTERNO NEI MEZZI VELOCI]
L. Lecce (Naples Univ., Italy), F. Marulo (Naples Univ., Italy), S. DeRosa, G. Pezzullo, and A. Paonessa (Alenia Spazio S.p.A., Naples, Italy) 31 Jul. 1991 23 p In ITALIAN Presented at the Symposium on High Speed Marine Vehicles
(DILC-EST-TN-200; ETN-92-92409) Avail: CASI HC A03/MF A01

Specific problems of marine vehicle internal noise are summarized and a review of some numerical techniques available for vibroacoustic transport vehicle analysis is given: FEM/BEM (Finite/Boundary Element Method), and SEA (Statistical Energy Analysis). The more significant FEM is described in detail and with reference to aerospace vehicles. Practical examples of this technique are given with numerical/experimental comparison results, showing the usefulness of this technique at least for the medium to low frequency range (0 to 500 Hz). Active control of internal noise is discussed along with significant noise reduction results. ESA

N93-11179 Open Univ., Oxford (England).
SOUND PROPAGATION OVER RIGID POROUS LAYERS Ph.D. Thesis
Craig Howorth 1991 556 p
Avail: Univ. Microfilms Order No. BRDX95967

Two related topics are discussed: (1) the measurement of the acoustical characteristics of rigid porous materials, that is the impedance and propagation constant; and (2) the propagation of sound over the surface of a hard backed layer of such a material. A review of impedance measurement leads to the selection of an indirect method which is employed successfully on a wide range of surfaces. A numerical comparison of impedance models follows including a one-parameter semi-empirical model, a phenomenological model, and a microstructural model which relates several physical parameters of a material to the acoustical properties of a surface. The models differ in their prediction of the acoustical properties of a low porosity material. A numerical comparison of the solutions of point source propagation in the presence of a porous media indicates that the 'extended' Weyl van der Pol approximation is reliable over short source receiver distances. The study is extended to examine the phenomenon of the acoustical surface wave. Three experimental techniques are used to produce new evidence for the existence of such a wave which shows good agreement with the theoretical predictions. The indirect method is used to obtain impedances and model parameters for a wide variety of surfaces varying from soils to fiberglass and which are compared with the results of an impedance technique and with standing wave tube measurements. The indirect method of impedance is employed together with the microstructural model and the propagation model examined earlier in studies of the acoustical properties of porous road surfaces. It proves possible to use the indirect method both to determine the microstructural parameters and to classify the acoustical properties of such a previous surface when the sound source is either a loudspeaker point source or a vehicle. The results of the parameter determination are validated by a series of non-acoustical measurements. With regard only to the excess attenuation provided by these surfaces, optimum combinations of material parameters are suggested which should lead to the production of a low noise road surface for many types of vehicle and tire tread patterns. Dissert. Abstr.

N93-11204# Rolls-Royce Ltd., Derby (England). Noise Research Group.
THE DESIGN AND COMMISSIONING OF AN ACOUSTIC LINER FOR PROPELLER NOISE TESTING IN THE ARA TRANSONIC WIND TUNNEL
M. E. Wood (Aircraft Research Association Ltd., Bedford, England) and D. A. Neuman 1 Dec. 1991 40 p
(PNR-90880; ETN-92-92188) Copyright Avail: CASI HC A03/MF A01

An acoustic liner was designed and manufactured for use in a transonic wind tunnel to provide an acoustically acceptable environment for propeller noise testing up to high subsonic Mach number. Details of the aerodynamic design and development are presented and calibration of the liner with propeller model support systems is included. It is shown how the design of the acoustic treatment was aided by the use of a theoretical model for the tunnel reverberant field. An acoustic development program was undertaken involving horn tests to improve the quality of the liner. The success of this is demonstrated by propeller noise results. These results also provided the basis for definition of the practical acoustic regime of a lined tunnel suitable for the accurate measurement of propeller noise. ESA

N93-11321# Rolls-Royce Ltd., Derby (England).
THE EFFECTS OF PLATE SPACING AND DOWNSTREAM PLATE LENGTH ON THE ACOUSTIC RESONANCE EXCITED BY FLOW PAST TWO PLATES IN TANDEM IN A DUCT
M. L. Legerton (University Coll. of Swansea, Wales), S. A. T. Stoneman (University Coll. of Swansea, Wales), and R. Parker (University Coll. of Swansea, Wales) 19 Jul. 1991 14 p
Presented at the 2nd World Conference on Experimental Heat Transfer, Fluid Mechanics and Thermodynamics, Dubrovnik, Yugoslavia, 23-28 Jun. 1991
(PNR-90958; ETN-92-92231) Copyright Avail: CASI HC A03/MF A01

The effects of plate spacing and downstream plate chord on the acoustic resonance generated by vortex shedding from tandem plates in a duct were investigated. The resonant sound amplitude and frequency were measured for various combinations of plate spacing and downstream plate chord. The test rig, a blow down open circuit wind tunnel specifically designed for the study of flow induced acoustic resonances, is described, together with the experimental procedure. Results are given and discussed. It is found that the plate spacing affected both the amplitude of the sound produced, and the velocity range over which the resonance was excited. The plate chord affected only the amplitude of the sound produced. The models of other investigators, developed to explain the effects of place spacing, are shown to have shortcomings. A hypothesis is proposed which is consistent with the observed variation with plate spacing in the velocity range over which the resonance occurred. ESA

N93-11322# Rolls-Royce Ltd., Derby (England).
AN EXPERIMENTAL INVESTIGATION INTO FLOW INDUCED ACOUSTIC RESONANCES IN AN ANNULAR CASCADE
M. L. Legerton (University Coll. of Swansea, Wales), S. A. T. Stoneman (University Coll. of Swansea, Wales), and R. Parker (University Coll. of Swansea, Wales) 21 Jun. 1991 10 p
Presented at the 5th International Conference on Flow Induced Vibrations, Brighton, England, 20-22 May 1991
(PNR-90959; ETN-92-92232) Copyright Avail: CASI HC A02/MF A01

The effects of plate spacing on the acoustic resonances generated by vortex shedding from annular cascades of plates in tandem in a duct were investigated. The experimental apparatus, a blow down, open circuit annular wind tunnel, the experimental procedure, and data processing are described. Results are given and discussed. It was found that the plate spacing affected both the amplitude of the sound produced and the velocity range over which each mode was excited. The velocity range over which each mode was excited is thought to be influenced by both the natural shedding frequency and the interaction with the downstream plate. ESA

N93-11328 National Physical Lab., Teddington (England). Div. of Radiation Science and Acoustics.
A SURVEY OF EUROPEAN CALIBRATION FACILITIES FOR UNDERWATER ACOUSTICS Final Report
Stephen P. Robinson and Roy C. Preston Apr. 1992 76 p
(NPL-RSA(EXT)-32; ETN-92-92259) Copyright Avail: National Physical Lab., Teddington, Middlesex, TW11 0LW, England

The final report of a survey of underwater acoustical calibration facilities in Europe, whose aim was to collect information on such facilities and foster links between organizations active in the field, is presented. To achieve this aim, a contact person of each participating country was asked to carry out a survey of the activity in his country and report back to the coordination laboratory. To help this task, each contact person was provided with a questionnaire to be mailed to each establishment active in the field. The questionnaire is included in the appendix together with the names and addresses of the contact people and a list of the establishments within each country contributing information to the project. The 64 organizations which provided information for the survey are listed and the facilities existing in each of the 127 participating countries are described. A summary of the replies is included. It is apparent that although there is a considerable amount of activity in Europe in this field, there are no established standards of calibration. Nor are there any systems of traceable measurements through accredited calibration laboratories. However, there is willingness to collaborate across national boundaries and to make calibration facilities available to organizations in other countries. ESA

N93-11370*# National Aeronautics and Space Administration. Lewis Research Center, Cleveland, OH.
A CONCEPT FOR A COUNTERROTATING FAN WITH REDUCED TONE NOISE
James H. Dittmar Aug. 1992 11 p
(RTOP 535-03-10)
(NASA-TM-105736; E-7138; NAS 1.15:105736) Avail: CASI HC A03/MF A01

As subsonic jet engine designs incorporate higher bypass ratios to reduce jet noise and increase engine cycle efficiency, the fan noise becomes a significant part of the perceived total noise. The conventional method of reducing fan tone noise is to design a low tip-speed device. An alternative approach of using a counterrotating fan with a high number of rotor blades is investigated in this report. The source of noise at the blade passing frequency of this device is the rotor-only mechanism, which is cut off for a subsonic tip speed rotor. The interaction noise occurs at twice the blade passing frequency, which, for this fan, was shifted high enough in frequency to be above the perceived noise rating range. The result was a counterrotating fan which had more potential for tone noise reduction than does the conventional fan. A potential broadband noise reduction was also indicated. Author

N93-11523# Sandia National Labs., Albuquerque, NM.
DYNAMICS AND RESPONSE OF POLYMER-COATED ACOUSTIC DEVICES
S. J. Martin and G. C. Frye 1992 5 p Presented at the Solid State Sensor and Actuator Workshop, Hilton Head Island, SC, 21-25 Jun. 1992
(Contract DE-AC04-76DP-00789)
(DE92-014289; SAND-92-0102C; CONF-9206172-1) Avail: CASI HC A01/MF A01

In this paper we consider the dynamic behavior and the electrical response of a thickness-shear mode resonator with a polymer film coating one face. With glassy polymers (shear stiffness G' approx. 10(exp 10) dyne/cm(exp 2)), this film tends to move synchronously with the oscillating resonator surface, while with rubbery polymers (G' approx. 10(exp 7) dyne/cm(exp 2)), the upper portions of the film lag behind the driven resonator/film interface, causing shear deformation of the film. As polymer properties change, interesting dynamic film behavior results, notably a film resonance when the acoustic phase shift across the film is an odd multiple of pi/2. This dynamic behavior influences the electrical response of the resonator due to the coupling between shear displacement and electric field in the piezoelectric quartz. Utilizing the fact that the polymer shear modulus changes rapidly as a function of temperature, these film behavior trends were demonstrated by measuring the electrical characteristics of a polyisobutylene-coated resonator as a function of frequency and at several temperatures. We show how these changing film dynamics can be correlated with changes in the measured electrical response. DOE

N93-11526# Yale Univ., New Haven, CT. Dept. of Computer Science.

ON THE INVERSE SCATTERING PROBLEM FOR THE HELMHOLTZ EQUATION IN ONE DIMENSION

Yu Chen 22 Jun. 1992 79 p
(Contract N00014-89-J-1527; NSF DMS-90-12751)
(AD-A253130) Avail: CASI HC A05/MF A01

Interest in the numerical solution of acoustic inverse scattering problems arises in a number of areas. Examples include medical diagnostics, nondestructive industrial testing, geophysical prospecting for petroleum and minerals, and detection of earthquakes. The highly nonlinear and oscillatory nature of the problem is one of the major difficulties one encounters in the construction of effective inversion algorithms. Schemes based on global or local linearization methods, or nonlinear optimization techniques, tend to work only when the index of refraction is almost constant. They develop serious convergence problems whenever the perturbation of the index of refraction increases. Limited successes in the solution of the inverse problems have been achieved only in one dimensional cases (Gelfand-Levitan and layer stripping methods are among the most notable). These methods are generally numerically unstable since the procedures used to calculate the index of refraction are ill-conditioned. We present a method for the solution of inverse problems for the one dimensional Helmholtz equation. The scheme is based on a combination of the standard Riccati equation for the impedance function with a new trace formula for the derivative of the index of refraction, and can be viewed as a frequency domain version of the layer-stripping approach. GRA

N93-11620*# National Aeronautics and Space Administration. Langley Research Center, Hampton, VA.

LABORATORY STUDY OF EFFECTS OF SONIC BOOM SHAPING ON SUBJECTIVE LOUDNESS AND ACCEPTABILITY

Jack D. Leatherwood and Brenda M. Sullivan (Lockheed Engineering and Sciences Co., Hampton, VA.) Oct. 1992 28 p
(RTOP 537-03-21-03)
(NASA-TP-3269; L-17050; NAS 1.60:3269) Avail: CASI HC A03/MF A01

A laboratory study was conducted to determine the effects of sonic boom signature shaping on subjective loudness and acceptability. The study utilized the sonic boom simulator at the Langley Research Center. A wide range of symmetrical, front-shock-minimized signature shapes were investigated together with a limited number of asymmetrical signatures. Subjective loudness judgments were obtained from 60 test subjects by using an 11-point numerical category scale. Acceptability judgments were obtained using the method of constant stimuli. Results were used to assess the relative predictive ability of several noise metrics, determine the loudness benefits of detailed boom shaping, and derive laboratory sonic boom acceptability criteria. These results indicated that the A-weighted sound exposure level, the Stevens Mark 7 Perceived Level, and the Zwicker Loudness Level metrics all performed well. Significant reductions in loudness were obtained by increasing front-shock rise time and/or decreasing front-shock overpressure of the front-shock minimized signatures. In addition, the asymmetrical signatures were rated to be slightly quieter than the symmetrical front-shock-minimized signatures of equal A-weighted sound exposure level. However, this result was based on a limited number of asymmetric signatures. The comparison of laboratory acceptability results with acceptability data obtained in more realistic situations also indicated good agreement. Author

N93-11634*# Lockheed Missiles and Space Co., Sunnyvale, CA.

ACOUSTIC FILL FACTORS FOR A 120 INCH DIAMETER FAIRING

Y. Albert Lee Sep. 1992 24 p Prepared in cooperation with Swales and Associates, Beltsville, MD
(Contract NAS5-30375)
(NASA-CR-189284; NAS 1.26:189284; SSV-2197; SS-1666-7750)
Avail: CASI HC A03/MF A01

Data from the acoustic test of a 120-inch diameter payload fairing were collected and an analysis of acoustic fill factors were performed. Correction factors for obtaining a weighted spatial average of the interior sound pressure level (SPL) were derived based on this database and a normalized 200-inch diameter fairing database. The weighted fill factors were determined and compared with statistical energy analysis (VAPEPS code) derived fill factors. The comparison is found to be reasonable. Author

N93-11752# Aerospace Corp., El Segundo, CA. Technology Operations.

ACOUSTIC MEASUREMENT OF THE MECHANICAL PROPERTIES OF THIN MATERIAL SPECIMENS

E. C. Johnson, J. D. Pollchik, and J. N. Schurr 15 May 1992 22 p
(Contract F04701-88-C-0089)
(AD-A253538; TR-0091(6935-08)-1; SSD-TR-92-17) Avail: CASI HC A03/MF A01

An acoustic technique is presented which permits accurate measurement of the dynamic Poisson's ratio, and the Young's, shear, and bulk moduli for a specimen which exists as a thin (less than 10 mil) layer. This technique should prove especially useful in situations where a bulk specimen is either not readily available or would not properly reflect the properties of the material when configured as a thin layer. The report includes a detailed discussion of the theory underlying the technique. As a test, three materials which could be easily formed into both a thin specimen and a thick specimen were selected. The technique was then used to determine the Poisson's ratio and acoustic velocities of the material constituting each thin specimen. These values were then contrasted to those of the bulk specimens obtained in a more conventional manner. The technique, as presented, could be extended for a number of applications, including the cure monitoring of adhesives. GRA

N93-11884 North Carolina State Univ., Raleigh.

NEAR-FIELD AND FAR-FIELD SOUND RADIATION FROM A LINE-DRIVEN FLUID-LOADED INFINITE FLAT PLATE HAVING PERIODIC AND NON-PERIODIC ATTACHED RIB STIFFENERS Ph.D. Thesis

Benjamin Adams Cray 1992 134 p
Avail: Univ. Microfilms Order No. DA9220188

The far-field and near-field solutions for the radiated acoustic pressure from a line-driven fluid-loaded, rib-stiffened thin elastic plate was obtained. The plate has been configured to have two sets of rib stiffeners, though the formulation given may be extended to include additional rib-stiffener sets. The stiffeners composing a given set are identical and are spaced periodically with distance l. However, one set of stiffeners is shifted by an amount delta from the other set. In this manner, portions of the plate may be configured with repeating sections having non-periodic rib spacing. The stiffeners exert reactive forces upon the plate, but not angular moments. Fluid loading is included on the upper surface of the plate while the lower surface is unloaded, except for a time harmonic line force applied normal to the lower surface. The far-field radiated pressure has been obtained using the method of stationary phase. Numerical integration techniques were necessary to obtain the near-field acoustic pressure. Numerical calculations are presented for the radiated near-field and far-field sound pressure level, at a fixed observation position, for changes in frequency. For the far-field region, the sound pressure level is obtained for changes in offset at a fixed frequency. The directional radiation characteristics of the stiffened plate are also presented. The near-field variation of acoustic pressure along the horizontal surface of the plate at a fixed frequency is given. At certain frequencies the investigation revealed that the wavelength of the stiffened plate's near-field acoustic oscillations--due to the propagating flexural wave-- was much greater than that given by the unstiffened plate's bending wavelength. The effect may be due to the stiffened plate's flexural response being split into two components that are close together in wavenumber. The wavelength of acoustic oscillation appears to result from taking the difference of the two spectral components. Dissert. Abstr.

N93-12021*# Institute for Computer Applications in Science and Engineering, Hampton, VA.

A GENERAL INTRODUCTION TO AEROACOUSTICS AND ATMOSPHERIC SOUND Final Report

James Lighthill (University Coll., London, England) Oct. 1992 35 p Presented at the ICASE/NASA Langley Research Center Workshop on Aeroacoustics, 6-9 Apr. 1992
(Contract NAS1-18605; RTOP 505-90-52-01)
(NASA-CR-189717; NAS 1.26:189717; ICASE-92-52) Avail: CASI HC A03/MF A01

A single unifying principle (based upon the nonlinear 'momentum-flux' effects produced when different components of a motion transport different components of its momentum) is used to give a broad scientific background to several aspects of the interaction between airflows and atmospheric sound. First, it treats the generation of sound by airflows of many different types. These include, for example, jet-like flows involving convected turbulent motions (with the resulting aeroacoustic radiation sensitively dependent on the Mach number of convection) and they include, as an extreme case, the supersonic 'boom' (shock waves generated by a supersonically convected flow pattern). Next, an analysis is given of sound propagation through nonuniformly moving airflows, and the exchange is quantified of energy between flow and sound; while, finally, problems are examined of how sound waves 'on their own' may generate the airflows known as acoustic streaming. Author

N93-12080*# National Aeronautics and Space Administration. Langley Research Center, Hampton, VA.

PUBLICATIONS ON ACOUSTICS RESEARCH AT THE LANGLEY RESEARCH CENTER, JANUARY 1987 - SEPTEMBER 1992

Linda W. Sutherland, comp. Sep. 1992 70 p
(RTOP 535-03-11-03)
(NASA-TM-107674; NAS 1.15:107674) Avail: CASI HC A04/MF A01

This report is a compilation of publications from acoustics research at the Langley Research Center. The reports listed are in chronological order and summarize the research output of the Acoustics Division for the period January 1987 - September 1992. Author

N93-12097# Washington State Univ., Pullman. Dept. of Physics.

INTERACTION OF SOUND WITH SOUND BY NOVEL MECHANISMS: ULTRASONIC FOUR-WAVE MIXING MEDIATED BY A SUSPENSION AND ULTRASONIC THREE-WAVE MIXING AT A FREE SURFACE Ph.D. Thesis

Harry J. Simpson 7 Aug. 1992 319 p
(Contract N00014-89-J-3800)
(AD-A254657) Avail: CASI HC A14/MF A03

Two mechanisms of sound interacting with sound are experimentally and theoretically investigated. Ultrasonic four-wave mixing in a dilute particle suspension, analogous to optical four-wave mixing in photorefractive materials, involves the interaction of three ultrasonic wavefields that produces a fourth scattered wavefield. The experimental configuration consists of two ultrasonic (800 kHz) pump waves that are used to produce a grating in a suspension of 25 mm diameter polymer particles in salt water. The pump waves are counter-propagating, and form a standing wavefield in the suspension. The less compressible particles are attracted to the pressure nodes in response to the time averaged radiation pressure. A higher frequency (2-10 MHz) ultrasonic wavefield is used to probe the resulting grating. The ultrasonic Bragg scattering is then measured. The scattering depends strongly on the response to the pump wave and is an unusual class of acoustical nonlinearity. Ultrasonic three-wave mixing at a free surface uses a high amplitude 400 kHz plane wavefield incident at 33 deg on a water-air interface to interact with a normally incident high frequency (4.6 MHz) focused probe wavefield. The 400 kHz pump wavefield reflects from the surface and produces oscillating surface displacements that form a traveling phase grating. GRA

N93-12324 Institute of Sound and Vibration Research, Southampton (England). Fluid Dynamics and Acoustics Group.

WAVEFRONT RECONSTRUCTION USING A LEAST SQUARES APPROACH

O. Kirkeby and P. A. Nelson Jul. 1992 30 p
(ISVR-TR-203) Copyright Avail: Issuing Activity

This work investigates a very basic problem in sound field reproduction: the reproduction of a two-dimensional plane wave in a free field using monopole sources. We derive the least squares solution for the sound pressure as a function of frequency, and some computer calculations illustrate the typical behavior of the error and the reproduced sound field. The results suggest that the model can be improved by including the sound pressure gradient in the objective function because the sound pressure itself does not strongly indicate in which direction the sound is travelling. Author

N93-12375# National Aerospace Lab., Tokyo (Japan). Thermofluid Dynamics Div.

EVALUATION OF ACOUSTIC IMPEDANCE MODELS FOR A PERFORATED PLATE [TAKOUBAN NI TAISURU ONKYOU INPIDANSU MODERU NO HYOUKA]

Minoru Watanabe Dec. 1991 38 p In JAPANESE
(NAL-TR-1133; JTN-92-80401) Avail: CASI HC A03/MF A01

The construction formed by bonding a perforated plate to honeycomb backed by an impervious plate has been widely used to acoustically line aircraft engine ducts. Several semiempirical models have been proposed to predict the acoustic impedance of perforated plates. In this study, the impedance models were used to theoretically estimate the sound attenuations in a two dimensional duct with sheared flow. A reasonable impedance model was recommended by comparing the estimated and the experimental attenuation observed using a flow duct facility. A practical calculation method of acoustic impedance is also described. Author (NASDA)

N93-12471# Naval Postgraduate School, Monterey, CA.

STUDY OF SOUND PROPAGATION IN A WEDGE-SHAPED OCEAN AND COMPARISON WITH OTHER METHODS M.S. Thesis

George Nassaopoulos Jun. 1992 88 p
(AD-A255165) Avail: CASI HC A05/MF A01

After several years of research, the image theory has been found acceptable to solve the sound propagation problem within a wedge-shaped fluid overlying either a slow or a fast bottom. Some further observations where done in this research. The primary purpose was the development and computer application of a new analysis, the doublet analysis, based on the image theory. In this analysis, the features of the image theory are studied from another point of view, based on a collection of acoustic doublets. GRA

72 ATOMIC AND MOLECULAR PHYSICS

Includes atomic structure, electron properties, and molecular spectra.

N93-11189# Iowa Univ., Iowa City.

DETERMINATION OF STEPSIZE PARAMETERS FOR INTERMOLECULAR VIBRATIONAL ENERGY TRANSFER

D. C. Tardy Mar. 1992 38 p

(Contract DE-FG02-87ER-13700)
(DE92-010770; DOE/ER-13700/T2) Avail: CASI HC A03/MF A01

Intermolecular energy transfer of highly excited polyatomic molecules plays an important role in many complex chemical systems: combustion, high temperature, and atmospheric chemistry. By monitoring the relaxation of internal energy, we have observed trends in the collisional efficiency (beta) for energy transfer as a function of the substrate's excitation energy and the complexities of substrate and deactivator. For a given substrate beta increases as the deactivator's mass increase to approx 30 amu and then exhibits a nearly constant value; this is due to a mass mismatch between the atoms of the colliders. In a homologous series of substrate molecules (C3 to C8) beta decreases as the number of atoms in the substrate increases; replacing F with H increases beta. All substrates, except for CF2Cl2 and CF2HCl below 10,000 cm(exp -1), exhibited that beta is independent of energy, i.e., (Delta E)(sub all) is linear with energy. The results are interpreted with a simple model which considers that beta is a function of the ocillators energy and its vibrational frequency. Limitations of current approximations used in high temperature unimolecular reactions were evaluated and better approximations were developed. The importance of energy transfer in product yields was observed for the photoactivation of perfluorocyclopropene and the photoproduction of difluoroethyne. DOE

N93-11196# Stanford Univ., CA. Dept. of Chemistry.
STATE-RESOLVED REACTION DYNAMICS Final Technical Report, 1 Dec. 1988 - 30 Nov. 1991
Richard N. Zare 27 Jul. 1992 23 p
(Grant AF-AFOSR-0264-89)
(AD-A254291; Rept-6871; AFOSR-92-0792TR) Avail: CASI HC A03/MF A01

This research effort is comprised of two groups of experiments. The first group measures and characterizes the electron ejected in a photoionization event. The second group is concerned with understanding the role of energy in affecting the outcome of ion-molecule reactions. High resolution, angle-resolved photoelectron spectroscopy was carried out following resonance enhanced multiphoton ionization (REMPI) of nitric oxide. These measurements have led to a complete description of this photoionization event. Photoelectron spectroscopy was also used to measure the degree of vibrational state-selectivity resulting from REMPI of NH3 and HBr/DBr. Additionally, the rotational state distributions resulting from HBr/DBr/HCl REMPI were measured using LIF. These state distributions were used in the study of the near resonant charge transfer reaction of DBr(+) + HBr, where the reagent ion was state-selectively prepared with REMPI and the product state distributions were monitored with LIF. Vibrationally state-selected ammonia ions generated by REMPI were used to investigate the effect of kinetic and vibrational energy in determining the product formation tendencies of the reaction NH3(+) + ND3. Measurement of the product cross sections has shown the differing effects of vibrational and translational excitation on dynamics of this ion-molecule system. GRA

N93-11412 National Physical Lab., Teddington (England). Div. of Radiation Science and Acoustics.
MEASUREMENT OF ABSORBED DOSE TO WATER FOR MEDIUM ENERGY X RAYS
K. E. Rosser Jun. 1992 24 p
(NPL-RSA(EXT)-33; ETN-92-92374) Copyright Avail: National Physical Lab., Teddington, Middlesex, TW11 0LW, England

Various types of ionization chambers suitable for the measurement of absorbed dose to water for medium energy x-rays were investigated with the aim of finding a chamber with all recommended characteristics. The chamber correction factors to be applied to an ionization chamber calibrated in terms of air kerma when used to measure absorbed dose to water were investigated and the ratios of mean mass energy absorption coefficients of water to air were calculated. Four types of parallel plate and four types of cylindrical ionization chambers were calibrated in air over the medium energy x-ray range. It was found that the energy response of a Grenz chamber with 1 mm perspex plate over its front window, a Farmer type 2505/3, a Farmer type 2515/1, and a type NE2561 did not vary by more than 4. The chamber correction factor for each of these chambers was compared with that for a Farmer type 2505/3 chamber. A method of determining the chamber by comparison with a chamber with a known chamber correction factor is outlined. The stem correction was measured for a NE2561 ionization chamber and is expected to be the largest constituent of the chamber correction factor. The values of the ratios of mean mass energy absorption coefficients of water to air were calculated for the geometry of the prototype water calorimeter and were found to be greater than those given in a referenced study by a maximum of 0.74 percent at 180 kV generating potential due to differences in phantom size, field size, incident spectrum, and source to surface distance. ESA

N93-11443# Tennessee Technological Univ., Cookeville. Dept. of Physics.
NUCLEAR STRUCTURE MODELS: APPLICATIONS AND DEVELOPMENT
P. B. Semmes Jul. 1992 13 p
(Contract DE-FG05-92ER-40694)
(DE92-018758; DOE/ER-40694/1) Avail: CASI HC A03/MF A01

This report discusses the following topics: Studies of Superdeformed States; Signature Inversion in Odd-Odd Nuclei - A fingerprint of Triaxiality; Signature Inversion in Cs-120 - Evidence for a Residual p-n Interaction; Signatures of Gamma Deformation in Nuclei and an Application to Xe-125; Nuclear Spins and Moments - Fundamental Structural Information; and Electromagnetic Properties of Ir-181 - Evidence of Beta Stretching. DOE

N93-11467# Joint Inst. for Lab. Astrophysics, Boulder, CO.
STATE-RESOLVED DYNAMICS OF ION-MOLECULE COLLISIONS IN A FLOWING AFTERGLOW Final Report, 1 Nov. 1988 - 31 Oct. 1991
Stephen R. Leone and Veronica M. Bierbaum 16 Dec. 1991 33 p
(Grant AF-AFOSR-0783-89)
(AD-A247288; AFOSR-92-0151TR) Avail: CASI HC A03/MF A01

The dynamics of ion-molecule collision processes have been explored in flowing afterglow-drift and single collision instruments using laser-induced fluorescence and Doppler resolved laser probing. The velocity distributions of Ba(+) drifted in both helium and argon buffer gases have been determined and compared with theoretical predictions. Ion mobilities and parallel and perpendicular temperatures have been measured as a function of field strength; in addition, the first experimental determination of skewness parameters has been made for Ba(+) in argon. Small but definitive differences in the mobility and temperature of CO(+) in helium have been observed for different rotational states of CO(+); moreover, in contrast to results for atomic systems, the parallel and perpendicular temperatures have been determined to be nearly identical. Preliminary studies of the rotational alignment of the 1,3,5-trifluorobenzene cation have been carried out; in some spectral regions, substantial polarized laser-induced fluorescence was observed. Product vibrational excitation for the proton transfer reaction O(-) + HF was measured as a function of enhanced collision energy; in contrast to results for neutral systems, the fraction of total energy entering vibration was found to increase slightly as the reagent collision energy is increased. Rotationally state-resolved product state distributions have been obtained for the charge transfer reaction Ar(+) + N2 using jet cooled N2 reagent; substantial bimodal charater was observed, implicating two dynamically distinct pathways for conversion of reactants to products. GRA

N93-11541# Cornell Univ., Ithaca, NY.
EXPERIMENTAL STUDY OF INTERACTIONS OF HIGHLY CHARGED IONS WITH ATOMS AT keV ENERGIES
V. O. Kostroun Jul. 1992 11 p

(Contract DE-FG02-86ER-13519)
(DE92-019512; DOE/ER-13519/6) Avail: CASI HC A03/MF A01

This Progress Report describes the experimental work carried out, and the work in progress, at the Cornell EBIS Laboratory during the period 7/1/1991 to 6/30/1992. During this period, a number of experiments were carried out. The absolute values of the total, one, two and three electron transfer cross sections for highly charged argon ions (8 less than or = q less to or = 16) colliding with argon at 2.3 qkev laboratory energy were measured. The distribution of recoil ions and molecular fragments formed in highly charged ion atom and molecule collisions was measured in order to help the interpretation of electron spectra in the 40 to 320 eV energy range emitted in Ar(exp q+)+Ar (8 less than or = q less than or = 16) collisions at 2.3 qkeV that were measured in our laboratory. The interpretation of the electron spectra is still under way. A new collision chamber was built which contains an ion decelerating lens system and a high resolution monochromator-analyzer combination. Ions extracted from the Cornell Electron Beam Ion Source were successfully decelerated from 2.3 qkeV down to 30 qeV Preliminary 0 deg translational energy spectra for Ar(exp 12+) on Ar at a collision energy of 38.6 qeV show a 0.56 qeV resolution. Work is in progress to extend measurements of cross sections and recoil ion charge state distributions down to collision energies in the 10 eV/amu range. DOE

N93-11560# California Univ., Santa Barbara. Dept. of Chemistry.

TETRAHEDRAL ATOM ZINCOPHOSPHATE STRUCTURES: SYNTHESIS, CRYSTAL STRUCTURE, AND SPECTROSCOPIC STUDIES OF (Zn(PO2(OC2H5)2)2)x, A ONE-DIMENSIONAL INORGANIC POLYMER Technical Report No. 22, 1 Jun. 1991 - 31 May 1992

William T. Harrison, Tina M. Nenoff, Thurman E. Gier, and Galen D. Stucky 15 May 1992 32 p
(Contract N00014-90-J-1159)
(AD-A251051) Avail: CASI HC A03/MF A01

The synthesis, structure and some properties of a new, anhydrous, zinc ethyl phosphate are described. Zn(O2P(OC2H5)2)2 (ZnPOEt) crystallizes in the monoclinic space group C2/c(No. 15) with a = 22.176(6), b = 8.042(2), c = 9.0883(3) A, beta = 96.553 (8) deg, V = 1610 A(exp 3), rho(sub calc) = 1.533 g/cm(exp 3), mu = 17.8 cm(exp -1) and Z = 4, with R(F(sub 0)) = 6.94 percent for 658 observed reflections (I greater than 3 sigma(I)). The novel structure consists of infinite 1-dimensional chains of vertex-linked zinc-oxygen and phosphorous-oxygen tetrahedra forming 4-rings: two of the phosphate P-0 vertices are coordinated to ethyl (-C2H5) groups, and the herringbone crystal packing is determined by van der Waals' forces between these terminal organic groups. Physical (TGA, DSC) and spectroscopic data (IR, H-1 and P-31 NMR) are presented. The physical data show a melting, followed by a decomposition reaction, eventually resulting in Zn(PO3)2. ZnPOEt is soluble in and recrystallizable from several polar and non-polar solvents: the NMR data suggest that ZnPOEt maintains a polymeric state in solution. ZnPOEt is contrasted with its sulphur-containing analogue, Zn(S2P(OC2H5)2)2. GRA

N93-11597# Westinghouse Savannah River Co., Aiken, SC.

TRIP REPORT: MARSHALL SPACE CENTER COMPUTED TOMOGRAPHY

J. R. Harbour and M. K. Andrews 1991 4 p
(Contract DE-AC09-89SR-18035)
(DE92-018139; WSRC-RD-91-25) Avail: CASI HC A01/MF A01

BIR Inc. is a small company out of the Chicago area which sells equipment for producing images by tomography. They have built a relatively large instrument, called ACTIS, for NASA at the Marshall Space Center in Huntsville, Alabama and still gave access to this instrument. BIR has a grant from the Department of Energy (DOE) to determine the utility of computed tomography (CT) for characterization of nuclear and hazardous waste within the DOE complex. As part of this effort, the potential of this technique for obtaining images of canistered waste forms has been investigated. Funding for data acquisition was provided through this grant. DOE

N93-11640# Sandia National Labs., Albuquerque, NM.

AN NMR STUDY OF THE OCCUPATION OF C(SUB 60) INTERSTITIAL SITES BY OXYGEN MOLECULES

R. A. Assink, D. A. Loy, J. E. Schirber, and B. Morosin 1991 6 p Presented at the Material Research Society Spring Meeting, San Francisco, CA, 27 Apr. - 2 May 1992
(Contract DE-AC04-76DP-00789)
(DE92-019436; SAND-91-2592C; CONF-920402-50) Avail: CASI HC A02/MF A01

The C-13 NMR of FCC C(sub 60) under magic angle spinning (MAS) conditions yields linewidths on the order of 1 Hz at fields of 4.7 T. The spectrum consists of a primary resonance at 143.7 ppm and a minor peak shifted 0.7 ppm downfield. The intensity of the minor resonance relative to the primary resonance was found to vary from 0.6 to 5.5 percent depending on the sample history. The downfield shift obeys Curie's law and is attributed to the Fermi contact coupling interaction between paramagnetic oxygen molecules and all 60 carbon atoms of rapidly rotating adjacent C(sub 60) molecules. Exposure of the sample to 1 kbar oxygen for 1 3/4 hours resulted in a spectrum of 7 evenly spaced resonances corresponding with 0 to 6 of the adjacent octahedral interstitial sites being filled with oxygen molecules. At ambient pressure, the oxygen diffused out of the lattice on time scales ranging from hours to days. DOE

N93-11681# Yale Univ., New Haven, CT. Dept. of Physics.

RESEARCH IN ELEMENTARY PARTICLES AND INTERACTIONS

R. Adair, J. Sandweiss, and M. Schmidt May 1992 148 p
(Contract DE-FG02-92ER-40704)
(DE92-018089; DOE/ER-40704/1) Avail: CASI HC A07/MF A02

Research of the Yale University groups in the areas of elementary particles and their interactions are outlined. Work on the following topics is reported: development of CDF trigger system; SSC detector development; study of heavy flavors at TPL; search for composite objects produced in relativistic heavy-ion collisions; high-energy polarized lepton-nucleon scattering; rare K(+) decays; unpolarized high-energy muon scattering; muon anomalous magnetic moment; theoretical high-energy physics including gauge theories, symmetry breaking, string theory, and gravitation theory; study of e(+)e(-) interactions with the SLD detector at SLAC; and the production and decay of particles containing charm and beauty quarks. DOE

N93-11709# Washington Univ., Seattle. Dept. of Chemistry.

MAGNETIC RESONANCE ELUCIDATION OF MOLECULE/MACROMOLECULE INTERACTION STEREOCHEMISTRY Final Report, Feb. 1991 - Mar. 1992

Niels H. Andersen 9 Jul. 1992 8 p
(Contracts N00014-91-J-1393; N00014-88-K-0202; RRO-4106)
(AD-A253030) Avail: CASI HC A02/MF A01

Our primary accomplishments were the development of software for the computer-aided structure elucidation of structural features of biological systems based on NOESY data: (1) simulating accurate theoretical NOESY spectra based on structural models, motional assumptions and NMR experiment parameters; and (2) the automated extraction of modeling constraints directly from raw NOESY data. The most recent software developments are the incorporation of model-free order parameters into NOESY simulations and the addition of routines for comparing computer-extracted distances (or cross-rates) with the expectation ranges based on the full spectrum of torsional freedom so as to generate precision estimates for NOE-distances from a single NOESY spectrum. These methods have been used to define the conformational states of a variety of polypeptide and drug molecule systems including: prostaglandin and steroid analogs, peptide hormones such as dynorphin-related peptides and GNRH analogs, rigid and flexible endothelin analogs, and a small protein allergen. The methods have also been applied to receptor-bound peptides. GRA

N93-11715# National Inst. of Standards and Technology, Gaithersburg, MD. Ionizing Radiation Div.

MASS ENERGY-TRANSFER AND MASS ENERGY-ABSORPTION COEFFICIENTS, INCLUDING IN-FLIGHT POSITRON ANNIHILATION FOR PHOTON ENERGIES 1 keV TO 100 MeV, 1992

P. D. Higgins, F. H. Attix, J. H. Hubbell, S. M. Seltzer, and M. J. Berger Mar. 1992 70 p Prepared in cooperation with Cleveland Clinic Foundation, OH; and Wisconsin Univ., Madison
(PB92-181106; NISTIR-4812) Avail: CASI HC A04/MF A01

Mass energy-transfer and mass energy-absorption coefficients are tabulated in units of sq cm/g for photon energies between 1 keV and 100 MeV for 29 elements (Z = 1-92), and 14 mixtures and compounds of general desimetric interest. Cross sections for photo-effects, incoherent scattering, and pair and triplet production are those compiled or generated by the National Institute of Standards and Technology (NIST) (formerly the National Bureau of Standards). Corrections are included for in-flight positron annihilation, previously not applied in NIST calculations for energies above 10 MeV. Agreement with recently published data is good for energies above 1 MeV, but the authors find differences in mass energy-absorption coefficients in the low energy region of as much as 4 percent compared with the last NIST compilation, and as much as 9 percent when compared with other recent compilations. Author

N93-11746# Brookhaven National Lab., Upton, NY.

STRANGE QUARK MATTER

C. B. Dover Jun. 1992 12 p Presented at the International Conference on the Structure of Baryons and Related Mesons, New Haven, CT, 1-4 Jun. 1992
(Contract DE-AC02-76CH-00016)
(DE92-016949; BNL-47670; CONF-920637-1) Avail: CASI HC A03/MF A01

We investigate the properties of multi-strange baryonic systems, comparing conventional many-Lambda hypernuclei, where the strange quarks are localized in individual hyperons, to 'strangelets' or chunks of strange matter, which involves delocalized quarks which roam in a single large bag. Mass formulae and strong/weak decay modes for such objects are discussed, as well as the prospects for producing multi-strange systems in relativistic heavy ion collisions. For production, we consider two extremes, one based on the coalescence model and another which assumes the formation of quark-gluon-plasma. We mention the experimental searches which are underway or planned, using heavy ion beams. DOE

N93-11778# National Inst. of Standards and Technology, Gaithersburg, MD.

ATOMIC STRUCTURE OF Ni-LIKE SOFT X RAY LASING IONS

J. Reader 1992 4 p
(Contract DE-FG03-91SF-18865)
(DE92-019273; DOE/SF-18865/T1) Avail: CASI HC A01/MF A01

The object of this research was to use the GDL laser at the Laboratory for Laser Energetics (LLE) at the University of Rochester to determine the atomic structure of ions of nickel isoelectronic sequence for which lasing in the soft x-ray region has been observed. To accomplish this goal, two experiments were carried out at the LLE. Excellent spectra were photographed for Ni-like ions of the following atoms: Gd, Tb, Dy, Er, Yb, Lu, and Hf. Thousands of spectral lines were observed in these exposures. The plates are now in the process of being measured and analyzed at NIST. In the second experiment, spectra of the following atoms were photographed with a laser energy of about 45 J in green light: Fe, Cd, Ce, Sn, Mo, and Rh. The spectrum of Fe was particularly excellent, evidencing several strong, previously unobserved transitions at about 32 angstroms for the Li-like ion Fe-23. These transitions are of the type n=3-4, which will be important for determining an accurate ionization energy for this ion. The measurements of the wavelengths for these transitions are being completed at the present time. They will eventually be combined with new measurements of the n=2-2 resonance lines obtained from tokamak observations to produce an improved set of energy levels for Fe-23. DOE

N93-11804# United Technologies Research Center, East Hartford, CT.

THEORETICAL STUDY OF THE RADIATIVE AND KINETIC PROPERTIES OF SELECTED METAL OXIDES AND AIR MOLECULES Technical Report, 15 Apr. 1988 - 30 Sep. 1991

H. H. Michels 1 May 1992 114 p
(Contract DNA001-88-C-0032)
(AD-A251090; R91-927893; DNA-TR-91-189) Avail: CASI HC A06/MF A02

A theoretical research program directed toward the study of the energetics and LWIR radiative properties of selected uranium/oxygen band systems has been undertaken. Included in this research program was the investigation of the strongest electronic and vibrational bands in the LWIR region for the species UO, UO(+), UO2, UO2(+), and UO2(++). The program for accomplishing this research effort was formulated into three separate tasks: (1) adaptation of our electronic structure codes to the DNA CRAY X-MP computer, (2) calculation of pertinent electronic wavefunctions and energies, as a function of internuclear separation and within a relativistic framework, for selected species of the uranium/oxygen system which may be important in the LWIR region, and (3) calculation of electronic transition moments and transition probabilities between specific vibrational levels of the electronic states corresponding to the strongest radiating band systems belonging to the uranium/oxygen system and prediction of IR and possible optical oscillator strengths. The results obtained to date for the uranium/oxygen system indicate that both UO(+) and UO2(+) are very strong LWIR radiators in the 10-14 micrometer region. In addition, UO(+), which is a potential late time radiator, exhibits strong visible bands and should be efficiently solar pumped. A careful evaluation of the low-lying excited states of UO2(+), particularly those charge transfer states that arise by promotion of an electron from (mainly) ligand MO's to a central uranium atom MO, indicates that such transitions lie well outside of the region for efficient solar pumping of UO2(+). GRA

N93-11829# Argonne National Lab., IL.

MULTIPHOTON IONIZATION AND ION-PAIR FORMATION IN MOLECULAR HYDROGEN

S. T. Pratt, E. F. McCormack, J. L. Dehmer, and P. M. Dehmer 1992 11 p Presented at the 10th International Conference on Vacuum Ultraviolet Radiation Physics, Paris, France, 27-31 Jul. 1992
(Contract W-31-109-eng-38)
(DE92-019026; ANL/CP-76280; CONF-920735-2) Avail: CASI HC A03/MF A01

We have investigated both photoionization and ion-pair formation in molecular hydrogen by using double-resonance excitation via the E,F (sup 1)Sigma(sub g)(sup +), v=6 level. The energetic threshold for ion-pair formation occurs just below the H(sub 2)(sup +) X (sup 2)Sigma(sub g)(sup +), v(sup +)=9 ionization threshold. The spectrum in this region was studied by using both conventional and constant-ionic-state photoelectron spectroscopy, as well as by monitoring the H(sup -) production. The decay dynamics in this region are extremely rich, because excited levels may decay by rotational and vibrational autoionization, by predissociation to neutral H + H* (n=2,3,4), by predissociation to the ion pair H(sup +) + H(sup -), and by fluorescence. In addition, the dissociative potential curve of the 2p(sigma)(sub u)3s(sigma)(sub g) (sup 1)Sigma(sub u)(sup +) doubly excited electronic state crosses the H(sub 2)(sup +) X (sup 2)Sigma(sub u)(sup +) potential curve in the same energy region, and the electronic autoionization of this state is found to significantly influence these decay processes. DOE

N93-11844# Washington Univ., Seattle.

NUCLEON AXIAL COUPLING CONSTANTS AND QCD SUM RULES

E. M. Henley, W. Y. P. Hwang (National Taiwan Univ., Taipei.), and L. S. Kisslinger (Carnegie-Mellon Univ., Pittsburgh, PA.) 1991 9 p Presented at the Symposium on Contemporary Physics, Philadelphia, PA, 31 Oct. - 1 Nov. 1991
(Contract DE-FG06-88ER-40427)
(DE92-014227; DOE/ER-40427/35-N91; CONF-9110382-1)
Avail: CASI HC A02/MF A01

QCD sum rules are used to obtain the isovector and 'isoscalar' axial vector coupling constants, g(sub A) and g(sub A)(sup S). We find g(sub A) = 1.26 plus or minus 0.08, g(sub A)(sup S) = 0.13 plus or minus 0.08 with sum results for g(sub A) - 1 and g(sub A) + g(sub A)(sup S). These sum rules also show that in the limit of chiral symmetry restoration, g(sub A) approaches 1 and g(sub A)(sup S) approaches -1. DOE

N93-11849# Oak Ridge National Lab., TN.

ELECTRON EMISSION DURING MULTICHARGED ION-METAL SURFACE INTERACTIONS

P. A. Zeijlmans vanEmmichoven, C. C. Havener, I. G. Hughes, S. H. Overbury, M. T. Robinson, D. M. Zehner, and F. W. Meyer 1992 9 p Presented at the 14th Werner Brandt Workshop on Charged Particle Penetration Phenomena, Oak Ridge, TN, 30 Apr. - 1 May 1992
(Contract DE-AC05-84OR-21400)
(DE92-017134; CONF-9204144-3) Avail: CASI HC A02/MF A01

The electron emission during multicharged ion-metal surface interactions will be discussed. The interactions lead to the emission of a significant number of electrons. Most of these electrons have energies below 30 eV. For incident ions with innershell vacancies, the emission of Auger electrons that fill these vacancies has been found to occur mainly below the surface. We present recently measured electron energy distributions which are used to discuss the mechanisms that lead to the emission of Auger and of low-energy electrons. DOE

N93-11851*# Eloret Corp., Sunnyvale, CA.

THEORETICAL RESEARCH PROGRAM TO STUDY CHEMICAL REACTIONS IN AOTV BOW SHOCK TUBES Periodic Research Report, 1 Apr. - 31 Dec. 1991

Peter Taylor 7 May 1992 79 p
(Contract NCC2-371)
(NASA-CR-188927; NAS 1.26:188927) Avail: CASI HC A05/MF A01

Effort continued through this period to refine and expand the SIRIUS/ABACUS program package for CASSCF and RASSCF second derivatives. A new approach to computing the Gaussian integral derivatives that require much of the time in gradient and Hessian calculations was devised. Several different studies were undertaken in the area of application calculations. These include a study of proton transfer in the HF trimer, which provides an analog of rearrangement reactions, and the extension of our previous work on Be and Mg clusters to Ca clusters. In addition, a very accurate investigation of the lowest-lying potential curves of the O2 molecule was completed. These curves are essential for evaluating different models of the terrestrial atmosphere nightglow. The most effort this year was devoted to a large scale investigation of stationary points on the C4H4 surface, and the thermochemistry of acetylene/acetylene reaction. For individual titles, see N93-11852 through N93-11855.

N93-11852*# National Aeronautics and Space Administration. Ames Research Center, Moffett Field, CA.

THE STRUCTURES, BINDING ENERGIES AND VIBRATIONAL FREQUENCIES OF Ca3 AND Ca4: AN APPLICATION OF THE CCSD(T) METHOD

Timothy J. Lee, Alistair P. Rendell, and Peter R. Taylor (Eloret Corp., Palo Alto, CA.) *In* Eloret Corp., Theoretical Research Program to Study Chemical Reactions in AOTV Bow Shock Tubes 7 May 1992 22 p Sponsored in part by NRC (For primary document see N93-11851 02-72)
(Contract NCC2-371)
Avail: CASI HC A03/MF A01

The Ca3 and Ca4 metallic clusters have been investigated using state-of-the-art ab initio quantum mechanical methods. Large atomic natural orbital basis sets have been used in conjunction with the singles and doubles coupled-cluster (CCSD) method, a coupled-cluster method that includes a perturbational estimate of connected triple excitations, denoted CCSD(T), and the multireference configuration interaction (MRCI) method. The equilibrium geometries, binding energies and harmonic vibrational frequencies have been determined with each of the methods so that the accuracy of the coupled-cluster methods may be assessed. Since the CCSD(T) method reproduces the MRCI results very well, cubic and quartic force fields of Ca3 and Ca4 have been determined using this approach and used to evaluate the fundamental vibrational frequencies. The infrared intensities of both the e' mode of Ca3 and the t2 mode of Ca4 are found to be small. The results obtained in this study are compared and contrasted with those from our earlier studies on small Be and Mg clusters. Author

N93-11853*# Oslo Univ. (Norway). Dept. of Chemistry.

ON THE EVALUATION OF DERIVATIVES OF GAUSSIAN INTEGRALS

Trygve Helgaker and Peter R. Taylor (Eloret Corp., Palo Alto, CA.) *In* Eloret Corp., Theoretical Research Program to Study Chemical Reactions in AOTV Bow Shock Tubes 7 May 1992 11 p (For primary document see N93-11851 02-72)
(Contract NCC2-371)
Avail: CASI HC A03/MF A01

We show that by a suitable change of variables, the derivatives of molecular integrals over Gaussian-type functions required for analytic energy derivatives can be evaluated with significantly less computational effort than current formulations. The reduction in effort increases with the order of differentiation. Author

N93-11854*# National Aeronautics and Space Administration. Ames Research Center, Moffett Field, CA.

CONNECTED TRIPLE EXCITATIONS IN COUPLED-CLUSTER CALCULATIONS OF HYPERPOLARIZABILITIES: NEON

Julia E. Rice (IBM Research Lab., San Jose, CA.), Gustavo E. Scuseria (Rice Univ., Houston, TX.), Timothy J. Lee, Peter R. Taylor (Eloret Corp., Palo Alto, CA.), and Jan Almloef (Minnesota Univ., Minneapolis.) *In* Eloret Corp., Theoretical Research Program to Study Chemical Reactions in AOTV Bow Shock Tubes 7 May 1992 12 p (For primary document see N93-11851 02-72)
Avail: CASI HC A03/MF A01

We have calculated the second hyperpolarizability gamma of neon using the CCSD(T) method. The accuracy of the CCSD(T) approach has been established by explicit comparison with the single, double and triple excitation coupled-cluster (CCSDT) method using extended basis sets that are known to be adequate for the description of gamma. Our best estimate for gamma(sub 0) of 110 +/- 3 a.u. is in good agreement with other recent theoretical values and with Shelton's recent experimental estimate of 108 +/- 2 a.u. Comparison of the MP2 and CCSD(T) hyperpolarizability values indicates that MP2 gives a very good description of the electron correlation contribution to gamma(sub 0). We have combined MP2 frequency-dependent corrections with the CCSD(T) gamma(sub 0) to yield values of gamma(-2 omega;omega,omega,0) and gamma(exp K)(-omega;omega,0,0). Author

N93-11855*# Polyatomics Research, Inc., Mountain View, CA.

CONCERTED HYDROGEN ATOM EXCHANGE BETWEEN THREE HF MOLECULES

Andrew Komornicki, David A. Dixon (Du Pont de Nemours, E. I. and Co., Wilmington, DE), and Peter R. Taylor (Eloret Corp., Palo Alto, CA.) *In* Eloret Corp., Theoretical Research Program to Study Chemical Reactions in AOTV Bow Shock Tubes 7 May 1992 13 p Previously announced in IAA as A92-26468 (For primary document see N93-11851 02-72)
Avail: CASI HC A03/MF A01

We have investigated the termolecular reaction involving concerted hydrogen exchange between three HF molecules, with particular emphasis on the effects of correlation at the various stationary points along the reaction. Using an extended basis, we have located the geometries of the stable hydrogen-bonded trimer, which is of C(sub 3h) symmetry, and the transition state for hydrogen exchange, which is of D(sub 3h) symmetry. The energies of the exchange reation were then evaluated at the correlated level, using a large atomic natural orbital basis and correlating all valence electrons. Several correlation treatments were used, namely, configration interaction with single and double excitations, coupled-pair functional, and coupled-cluster methods. We are thus able to measure the effect of accounting for size-extensivity. Zero-point corrections to the correlated level energetics were determined using analytic second derivative techniques at the SCF level. Our best calculations, which include the effects of connected triple excitations in the coupled-cluster procedure, indicate that the trimer is bound by 9 +/- 1 kcal/mol relative to three separate monomers, in excellent agreement with previous estimates. The barrier to concerted hydrogen exchange is 15 kcal/mol above the trimer, or only 4.7 kcal/mol above three separated monomers. Thus the barrier to hydrogen exchange between HF molecules via this termolecular process is very low. Author

N93-11867# Ecole Polytechnique, Palaiseau (France). Des Milieux Ionises.
DIAGNOSTICS AND MODELING OF H(-) ION SOURCES Final Report, 1 Sep. 1989 - 31 Dec. 1991
Marthe Bacal 24 Feb. 1992 37 p
(Grant AF-AFOSR-0538-89)
(AD-A250664; AFOSR-92-0273TR) Avail: CASI HC A03/MF A01

The negative ion temperature has been measured in hydrogen and deuterium, using the laser photodetachment technique. The negative ion temperature is strongly dependent on the neutral gas pressure, the discharge current and the electron temperature. It was inferred that many-body processes (fields, turbulence or collisions in fields) cause an increase in the negative ion temperature and adversely affect extracted beam quality. The deuterium negative ion temperature is significantly lower, compared to that found in hydrogen. The modeling of surface effects has been initiated by varying the surface/volume ratio in a pure volume negative ion source. It was found that the increase of this ratio was only effective for enhancing the negative ion density when the power density was high enough, so that the volume destruction processes should control the production of vibrationally excited molecules. The modeling of a volume source with some amount of surface negative ion production due to positive ion and atom impact has shown that increasing the surface/volume ratio leads to a significant increase in negative ion density. GRA

N93-11872# Wisconsin Univ., Madison. Dept. of Chemistry.
DESIGN AND SYNTHESIS OF MOLECULAR SYSTEMS CAPABLE OF SUPPORTING INTRACAVITY CHEMICAL REACTIONS Final Report
Howard W. Whitlock, Jr. 13 May 1992 3 p
(Contract N00014-88-K-0358)
(AD-A251024) Avail: CASI HC A01/MF A01

This project involves the synthesis of molecules containing concave functional groups capable of supporting chemical reactions. Salient sub-problems have to do with the distinction between steric encumbrance and steric hindrance, and with development of well documented intracavity covalent bond-forming reactions. Host molecules bearing functional groups capable of hydrogen bond formation, metal ion complexation, and aldimine condensation are of primary interest, their functional groups being in a sterically encumbered but not hindered environment. The structural motif involves construction of cyclophanes bearing the desired reactive group oriented in an inward-pointing manner, in combination (optionally) with structural features that enhance binding of the external co-reactor. GRA

N93-11875# California Univ., Berkeley. Lawrence Berkeley Lab.
STUDIES OF TRANSITION STATES AND RADICALS BY NEGATIVE ION PHOTODETACHMENT Ph.D. Thesis
R. B. Metz Dec. 1991 504 p
(Contract DE-AC03-76SF-00098)
(DE92-017011; LBL-31878) Avail: CASI HC A22/MF A04

Negative ion photodetachment is a versatile tool for the production and study of transient neutral species such as reaction intermediates and free radicals. Photodetachment of the stable XHY(-) anion provides a direct spectroscopic probe of the transition state region of the potential energy surface for the neutral hydrogen transfer reaction X + HY yields XH + Y, where X and Y are halogen atoms. The technique is especially sensitive to resonances, which occur at a specific energy, but the spectra also show features due to direct scattering. We have used collinear adiabatic simulations of the photoelectron spectra to evaluate trail potential energy surfaces for the biomolecular reactions and have extended the adiabatic approach to three dimensions and used it to evaluate empirical potential energy surfaces for the I + HI and Br + HI reactions. In addition, we have derived an empirical, collinear potential energy surface for the Br + HBr reaction that reproduces our experimental results and have extended this surface to three dimensions. Photodetachment of a negative ion can be also used to study neutral free radicals. We have studied the vibrational and electronic spectroscopy of CH2NO2 by photoelectron spectroscopy of CH2NO2(-), determining the electron affinity of CH2NO2, gaining insight on the bonding of the (sup 2)B(sub 1) ground state and observing the (sup 2)A(sub 2) excited state for the first time. Negative ion photodetachment also provides a novel and versatile source of mass-selected, jet-cooled free radicals. We have studied the photodissociation of CH2NO2 at 270, 235, and 208 nm, obtaining information on the dissociation products by measuring the kinetic energy release in the photodissociation. DOE

N93-11914# Academy of Sciences of the Ukrainian SSR, Kiev. Inst. Teoreticheskoj Fiziki.
SCATTERING OF POLARIZED ELECTRONS BY ORIENTED DEUTERONS [RASSEYANIE POLYARIZOVANNYKH EHLEKTRONOV NA ORIENTIROVANNYKH DEJTRONAKH]
V. K. Tartakovskij, Lyong Zuen Fu, and A. V. Fursaev 1991 12 p In RUSSIAN
(DE92-624834; ITF-91-2) Avail: CASI HC A03/MF A01

The differential cross section of elastic scattering of polarized ultrarelativistic electrons by oriented deuterons is calculated. The contributions of different type orientations to the cross section are investigated. The new information, which can be determined in experiments with the oriented particles is discussed. The polarization of the scattered electrons in the case of the unpolarizated incident electron beam is calculated. DOE

N93-12100# California Univ., Berkeley. Lawrence Berkeley Lab.
THRESHOLD PHOTODETACHMENT SPECTROSCOPY OF NEGATIVE IONS Ph.D. Thesis
T. N. Kitsopoulos Dec. 1991 187 p
(Contract DE-AC03-76SF-00098)
(DE92-017090; LBL-31876) Avail: CASI HC A09/MF A02

This thesis is concerned with the development and application of high resolution threshold photodetachment spectroscopy of negative ions. Chapter 1 deals with the principles of our photodetachment technique, and in chapter 2 a detailed description of the apparatus is presented. The threshold photodetachment spectra of I(-), and SH(-), presented in the last sections of chapter 2, indicated that a resolution of 3 cm(exp -1) can be achieved using our technique. In chapter 3 the threshold photodetachment spectroscopy study of the transition state region of I + HI and I + Di reactions is discussed. Our technique probes the transition state region directly, and the results of our study are the first unambiguous observations of reactive resonances in a chemical reaction. Chapters 4, 5, and 6 are concerned with the spectroscopy of small silicon and carbon clusters. From our spectra we were able to assign electronic state energies and vibrational frequencies for the low lying electronics states of Si(n) (n=2,3,4), C5 and their corresponding anions. DOE

N93-12111# California Univ., Berkeley. Lawrence Berkeley Lab.
SURVEY OF COMPOSITE PARTICLE MODELS OF ELECTROWEAK INTERACTION
Mahiko Suzuki May 1992 25 p Presented at the International Symposium on Bound Systems and Extended Objects, Karuizawa (Japan), 19-21 Mar. 1992
(Contract DE-AC03-76SF-00098)
(DE92-017110; LBL-32363; UCB-PTH-92/17; CONF-9203168-1)
Avail: CASI HC A03/MF A01

Models of composite weak bosons, the top-condensate model of electroweak interaction and related models we surveyed. Composite weak bosons must be tightly bound with a high compositeness scale in order to generate approximate puge symmetry dynamically. However, naturalness argument suggests that the compositeness scale is low at least in toy models. In the top-condensate model, where a composite Higgs doublet is formed with a very high scale, the prediction of the model is insensitive to details of the model and almost model-independent Actually, the numerical prediction of the t-quark and Higgs boson masses does not test compositeness of the Higgs boson nor condensation of the t-quark field. To illustrate the point, a composite t(sub R)-quark model is discussed which leads to the same numerical prediction as the top-condensate model. However, different constraints an imposed on the structure of the Higgs sector, depending on which particles are composite. The attempt to account the large t-b mass splitting by the high compositeness scale of the top-condensate model is reinterpreted in terms of fine tuning of more than one vacuum expectation value. It is difficult to lower, without a fourth generation, the t-quark mass in the composite particle models in general because the Yukawa coupling of the i-quark to the Higgs boson, f(sub t)(sup 2)/4(pi) = 0.1 for m(sub t) = 200 GeV, is too small for a coupling of a composite particle. DOE

N93-12115# City Coll. of the City Univ. of New York, NY. Dept. of Physics.
ELECTRONIC TRANSPORT AND LASING IN MICROSTRUCTURES
M. Lax 1992 14 p
(Contract DE-FG02-84ER-45058)
(DE92-018725; DOE/ER-45058/8) Avail: CASI HC A03/MF A01

We consider the interaction of hot carriers with hot phonons in a quantum well. Transport is considered in the transverse direction and tunneling through the well barriers. Time-dependent transport effects down to the femto-second regime are included, as are strong and/or microwave fields, with negative resistance effects. Resonant tunneling assisted by phonon relaxation and infra-red radiation are explored. The limitations on transmission of information due to partition noise, as influenced by the design of semiconductor feedback lasers are considered. The use of light scattering and decision theory to detect shell-like aerosols is examined. DOE

N93-12117# Pacific Northwest Lab., Richland, WA.
ADVANCED METHODS FOR STRUCTURAL CHARACTERIZATION OF LARGE MULTIPLY CHARGED IONS: OBTAINING CHARGE STATE DETERMINATION AND IMPROVED SENSITIVITY
R. D. Smith, A. L. Rockwood, and H. R. Udseth Jun. 1991 3 p Presented at the American Society for Mass Spectrometry (ASMS) Meeting, Nashville, TN, 19-24 May 1991
(Contract DE-AC06-76RL-01830)
(DE91-015264; PNL-SA-19123; CONF-9105181-30) Avail: CASI HC A01/MF A01

There is growing interest in obtaining structural information for large molecules by the methods of tandem mass spectrometry. Electrospray ionization (ESI) now allows the efficient production of high molecular weight ions having high charge states. The application of existing instrumental methods for this purpose encounters several problems. One is that the primary ion beam flux is, to a crude approximation, inversely related to the square of molecular weight for large molecules due to the number of charges on each ion, the width of th charge state distribution, are the limitations upon electrospray ion currents. Since the number of 'useful' and desired fragmentation pathways increase approximately linearly with molecular weight, the sensitivity demands increase approximately with the inverse third power of molecular weight. A second problem for methods utilizing a multiply charged parent ion is the necessity of determining the charge states of product ions from tandem experiments. The combination of these problems will grow dramatically with molecular weight, currently limits the application to high molecular weight biomolecules. A solution to these problems is investigated. DOE

N93-12224# Georgia Univ., Athens. Dept. of Physics and Astronomy.
HIGH ENERGY HADRON-HADRON COLLISIONS
T. T. Chou Dec. 1991 16 p
(Contract DE-FG09-84ER-40160)
(DE92-018253; DOE/ER-40160/8) Avail: CASI HC A03/MF A01

Results of a study on high energy collision with the geometrical model are summarized in three parts: (1) the elastic hadron-hadron collision, (2) the inelastic hadron-hadron collision, and (3) the e(+)e(-) annihilation. More recent studies are highlighted below. For elastic scattering, a modified form for the hadronic matter form factor of the proton was proposed which remains to be dipole in form but contains an energy-dependent range parameter. This new expression of the opacity function fits the elastic (bar-p)p scattering very well from the ISR to S(bar-p)pS energies. Extrapolation of this theory also yielded results in good agreement with the (bar-p)p differential cross section measured at the Tevatron. For inelastic hadron-hadron collisions, we have made a systematic investigation of the single-particle momentum spectra in the entire S(bar-p)pS energy region. Results are useful for the extrapolation of angular distribution to the higher SSC energies. In e(+)e(-) annihilation, a detailed analysis of all available experimental multiplicity data from PETRA to LEP energies has been performed. We discovered that the cluster size of emitted hadrons increases steadily with energy and is close to 2 as we predicted. DOE

N93-12323# Wisconsin Univ., Madison.
STATE-RESOLVED COLLISIONAL ENERGY TRANSFER IN HIGHLY VIBRATIONALLY EXCITED POLYATOMIC MOLECULES Final Report, 1 Nov. 1988 - 31 Oct. 1991
F. F. Crim 11 Jun. 1992 17 p
(Grant AF-AFOSR-0028-89)
(AD-A253299; AFOSR-92-0679TR) Avail: CASI HC A03/MF A01

The transfer of energy in isolated or colliding molecules is a fundamental process with practical consequences for complex phenomena occurring in atmospheric chemistry, combustion, molecular lasers, plasmas, and a host of other environments containing energetic species. We have developed a technique that combines vibrational overtone excitation, to prepare highly vibrationally excited initial states, and time-resolved spectroscopic detection, to probe the evolution of the prepared state, for studying energy transfer in vibrationally energized molecules. We have used this approach to determine directly, for the first time, the frequencies of the three ungerade vibrations in the first electronically excited state of acetylene. Using this information we have characterized highly vibrationally excited states of acetylene and directly the frequencies and rotational constants of the perturbing vibrational states at these energies. Combining these spectroscopic insights on the vibrationally and electronically excited states of acetylene has allowed us to determine the energy transfer rates and pathways in the collisional relaxation of a polyatomic molecule containing 10,000 cm(exp -1) of vibrational energy. Rotational energy transfer is very rapid, occurring on about every other collision, but is essentially unaffected by the identity of the vibrational state in which the rotational relaxation occurs. GRA

N93-12444# Massachusetts Univ., Amherst. Dept. of Physics and Astronomy.
MEDIUM ENERGY NUCLEAR PHYSICS RESEARCH
G. A. Peterson, J. F. Dubach, R. S. Hicks, and R. A. Miskimen
Jun. 1992 44 p
(Contract DE-FG02-88ER-40415)
(DE92-016972; DOE/ER-40415/19) Avail: CASI HC A03/MF A01

This paper covers the following topics: Experiment 87-02 --Threshold Electrodisintegration of the Deuteron at High Q(sup 2); Measurement of the 5th Structure Function in Deuterium and C-12; Single-Particle Densities of sd-Shell Nuclei; Experiment 84-28 --Transverse Form Factors of Sn-117; Experiment 82-11 --Elastic Magnetic Electron Scattering from C-13; Experiment 89-09 --Measurement of the Elastic Magnetic Form Factor of He-3 at High Momentum Transfer; Experiment 89-15 --Coincidence Measurement of the D(e,e'p) Cross-Section at Low Excitation Energy and High Momentum Transfer; Experiment 87-09 --Measurement of the Quadrupole Contribution to the N yields delta Excitation; Experiment E-140 --Measurement of the x-, Q(sup 2) and A-Dependence of R = sigma(sub L)/sigma(sub T); PEP Beam-Gas Event Analysis --Physics with the SLAC TPC/2(gamma) Detector; Drift Chamber Tests at Brookhaven National Laboratory; Experiment PR-89-031 --Multi-nucleon Knockout Using the CLAS Detector; Electronics Design for the CLAS Region 1 Drift Chamber; Color Transparencies in the Electroproduction of Nucleon Resonances; and Experiment PR-89-015 --Study of Coincidence Reactions in the Dip and Delta-Resonance Regions. DOE

73 NUCLEAR AND HIGH-ENERGY PHYSICS

Includes elementary and nuclear particles; and reactor theory.

For space radiation see *93 Space Radiation.*

N93-11028# Hahn-Meitner-Inst. fuer Kernforschung, Berlin (Germany). Bereich Datenverarbeitung und Elektronik.
RADIATION DAMAGE BY HIGH ENERGY ELECTRONS IN GaAs: A DLTS (DEEP LEVEL TRANSIENT SPECTROSCOPY) EXAMINATION Ph.D. Thesis - Technische Univ. [STRAHLENSCHAEDIGUNG DURCH HOCHENERGIEELEKTRONEN IN GAAS: EINE DLTS-UNTERSUCHUNG]
Bertel Lehmann Oct. 1991 155 p In GEORGIAN
(HMI-B-494; ETN-92-92146) Copyright Avail: CASI HC A08/MF A02

An isothermal variation of the DLTS (Deep Level Transient Spectroscopy) technique is developed and applied to the study of displacement damage in GaAs, through the determination of threshold energies and displacement cross sections. Results correspond to those of a light emitting diode based method. A pronounced anisotropy is found for the threshold energy. A linearly increasing displacement probability function is shown to model the displacement cross section in 100 angular brackets direction, as compared with the 111 angular brackets direction, which requires only a single step function. Differences in the damage between these two directions are as large as a factor of two. ESA

N93-11060 Department of the Navy, Washington, DC.
EMITTANCE MEASURING DEVICE FOR CHARGED PARTICLE BEAMS Patent
Ralph B. Fiorito, inventor (to Navy) and Donald W. Rule, inventor (to Navy) 9 Jun. 1992 5 p Filed 5 Jul. 1990
(AD-D015371; US-Patent-5,120,968; US-Patent-Appl-SN-548652)
Avail: US Patent and Trademark Office

The invention is a device to measure the emittance of a charged particle beam. The device is capable of providing precise time resolution limited only, by the chosen detector. The device allows a complete emittance determination as a function of time. The preferred embodiment of the invention comprises a plurality of thin foils which generate an optical transition radiation (OTR) pattern: a lens system to collect the OTR pattern from the said foils; an optical mask to allow passage of the OTR pattern; and a detector array or similar device placed behind the mask which intercepts, senses, and measures the point source OTR pattern for each perforation in the mask. GRA

N93-11077# Continuous Electron Beam Accelerator Facility, Newport New, VA.
HIGHER-ORDER-MODE DAMPING AND MICROWAVE ABSORPTION AT 2 K
I. E. Campisi, K. E. Finger, L. K. Summers, and A. M. Johnson
Mar. 1992 5 p Presented at the 3rd European Particle Accelerator Conference, Berlin (Germany), 24-28 Mar. 1992
(Contract DE-AC05-84ER-40150)
(DE92-016960; DOE/ER-40150/188; CEBAF-PR-92-010; CONF-920315-41) Avail: CASI HC A01/MF A01

A special ceramic material for microwave absorption at low temperature has been developed at CEBAF to manufacture the 676 Higher-Order-Mode (HOM) loads for the machine. The accelerator includes 338 5-cell niobium cavities, resonating in the fundamental TM(sub 010) pi mode at 1497 MHs, in two antiparallel linacs (160 cavities each) and an injector (18 cavities). Higher-Order-Mode (HOM) power generation in the machine is expected to be in the tens of milliwatts per cavity at the nominal beam current of 200 micro-A. This amount of power constitutes a small fraction of the power dissipated by the superconducting cavities at the operating gradient of 5 MV/m (typically less than 5 W per cavity) and the HOM power is more efficiently absorbed at the bath temperature of 2 K than at room temperature. The HOM extraction is done via two S-band waveguides located orthogonally to each other at one end of the cavities and a load is placed at the end of each waveguide. This HOM damping scheme is characteristic of CEBAF alone; the low operating temperature and the vacuum in common with the superconducting cavities prevent the use of standard absorbers. Totally new materials and a novel absorber shape were developed for this application. DOE

N93-11130# Nationaal Inst. voor Kernfysica en Hoge Energiefysica, Amsterdam (Netherlands).
NUCLEON STRUCTURE FUNCTIONS FROM DEEP INELASTIC MUON SCATTERING
M. A. J. Botje 1992 9 p Presented at the 27th Rencontres de Moriond, Les Arcs, France, 22-28 Mar. 1992
(NIKHEF-H+K/92-01; ETN-92-92395) Avail: CASI HC A02/MF A01

Deep inelastic muon scattering was measured, at the New Muon Collaboration (NMC), simultaneously on hydrogen and deuterium at incident muon energies of 90 and 280 GeV. The data cover a wide kinematic range. Preliminary results are presented on the nucleon structure functions (F sub 2)(sup p) and (F sub 2)(sup d). In the region of kinematic overlap the data are in good agreement with previous results from SLAC and BCDMS (x greater than 0.07) but disagree with those obtained from a recent analysis of the EMC apparatus (x greater than 0.03). A next-to-leading order quantum chromodynamics analysis of the NMC data is presented. Good agreement is found between theory and data. The flavor non-singlet and singlet quark distributions and the gluon distribution are extracted with good precision down to low values of x(0.008). These results and low x extrapolations, based on recent parton distribution fits, are compared. A preliminary result on the strong coupling constant alpha (sub s) is given. ESA

N93-11131# Nationaal Inst. voor Kernfysica en Hoge Energiefysica, Amsterdam (Netherlands).
USING THE 16 VIEWSCREENS DURING COMMISSIONING OF AmPS
R. Maas Feb. 1992 10 p

(NIKHEF-K/AmPS/92-01; ETN-92-92396) Avail: CASI HC A02/MF A01

The Amsterdam Pulse Stretcher (AmPS) was equipped with 16 viewscreens, which interfere strongly with the beam. In order to reach the stage where an attempt can be made to correct the machine closed orbit, the beam should travel for at least one turn around the machine. To do so, AmPS is considered as a beamline. The beam is transported from one viewscreen to the next one, corrected each time by a preceding orbit corrector. Simulations show that this procedure improves the root mean square value of the observed orbit deviations at the viewscreens, and reduces the value of the maximum beam excursions. Extending the number of monitors by 16 'q-monitors', thus enables the use of all 32 available orbit correctors and improves the root mean square value by another factor 3: the average reduction of x sub(root mean square) in this case becomes about a factor 10. ESA

N93-11429# Brookhaven National Lab., Upton, NY.

THE FOXHOLE ACCELERATING STRUCTURE

R. C. Fernow and J. Claus 17 Jul. 1992 46 p
(Contract DE-AC02-76CH-00016)
(DE92-019052; BNL-52336; CAP-86-92R) Avail: CASI HC A03/MF A01

This report examines some properties of a new type of open accelerating structure. It consists of a series of rectangular cavities, which we call foxholes, joined by a beam channel. The power for accelerating the particles comes from an external radiation source and enters the cavities through their open upper surfaces. Analytic and computer calculations are presented showing that the foxhole is a suitable structure for accelerating relativistic electrons. DOE

N93-11433# EG and G Energy Measurements, Inc., Idaho Falls.

A GAS-COOLED CERMET REACTOR SYSTEM FOR PLANETARY BASE POWER

Salim N. Jahshan and Jeffrey A. Borkowski 1992 13 p Presented at the Nuclear Technologies for Space Exploration, Jackson, WY, 16-19 Aug. 1992
(Contract DE-AC07-76ID-01570)
(DE92-018017; EGG-M-91626; CONF-920803-16) Avail: CASI HC A03/MF A01

Fission nuclear power is foreseen as the source for electricity in colonization exploration. A gas-cooled, cermet-fueled reactor is proposed that can meet many of the design objectives. The highly enriched core is compact and can operate at high temperature for a long life. The helium coolant powers a Brayton cycle that compares well with the SP-100-based Brayton cycle. The power cycle can be upgraded further under certain siting-related conditions by the addition of a low temperature Rankine cycle. DOE

N93-11493# California Univ., Berkeley. Lawrence Berkeley Lab.

APPLICATION OF THE MOYER METHOD TO TRANSVERSE SHIELDING OF LINEAR BREMSSTRAHLUNG SOURCES

W. P. Swanson, R. K. Sun, and R. H. Thomas Dec. 1991 13 p Presented at the Annual Meeting of the Health Physics Society, Columbus, OH, 21-25 Jun. 1992
(Contract DE-AC03-76SF-00098)
(DE92-017027; LBL-31653; CONF-920617-7) Avail: CASI HC A03/MF A01

The Moyer method is applied to the design of transverse shielding for an electron linear accelerator, assuming uniform beam power loss along the accelerator structure. Parameters for this application are given and sample calculations are shown. For a beam power loss uniformly distributed with distance along a straight line of 0.5W/m, it is predicted that 1.2 m of concrete are needed to reduce the dose equivalent rate to 1.39 x 10(exp -8) Sv/s, (5 mrem/hour) at a transverse distance of 3.5 m from the source. DOE

N93-11498# Brookhaven National Lab., Upton, NY.

TOPICS ON RF BEAM CONTROL OF A SYNCHROTRON

S. Y. Zhang and W. T. Weng 13 Jul. 1992 27 p
(Contract DE-AC02-76CH-00016)
(DE92-019217; BNL-47813; AGS/AD-92-3) Avail: CASI HC A03/MF A01

In this paper, several typical situations of longitudinal motion in synchrotron design and operation are studied. The study is based on a unified beam dynamic model of synchrotron oscillation under phase and radial feedbacks. Cases studied include frequency error, lock-in range, bunch excursion, phase manipulation, injection, and field errors. DOE

N93-11499# Brookhaven National Lab., Upton, NY.

ANALYSIS OF PERIODIC TRANSIENT BEAM LOADING OF THE AGS

S. Y. Zhang and W. T. Weng 13 Jul. 1992 20 p
(Contract DE-AC02-76CH-00016)
(DE92-019243; BNL-47771; AGS/AD-92-2) Avail: CASI HC A03/MF A01

In this note, we discuss the multi-batch bunched beam loading during the injection from the Booster to the AGS. The full intensity beam injection to the upgraded AGS RF system with beam phase and radial feedbacks is studied. It is shown that a beam phase feed-back is necessary in order to guarantee a predictable beam behavior after the first batch injection, otherwise the initial phase deviation for the following batch injections cannot be controlled. However, the effectiveness of the phase feedback control of the transient beam loading is limited by the associated emittance blow-up in the process. It is shown that a fast power amplifier feedback with a moderate gain can significantly reduce the transient effect of the bunched beam injection. DOE

N93-11510# Los Alamos National Lab., NM.

BEAM-LOADING STABILITY IN SYNCHROTRONS WITH A HIGHER RF HARMONIC

Tai-Sen F. Wang 1992 4 p Presented at the 15th International Conference on High Energy Accelerators, Hamburg, Germany, 20-24 Jul. 1992
(Contract W-7405-eng-36)
(DE92-018982; LA-UR-92-2086; CONF-920706-11) Avail: CASI HC A01/MF A01

This work is an attempt to extend Robinson's stability studies to include a higher RF harmonic. Using an equivalent circuit model, the stability of the '0-mode' coherent dipole oscillation of bunched beams is studied for synchrotrons or storage rings, with RF systems operated at the fundamental and a higher harmonic, i.e., a 2nd and 3rd harmonic. Analytical expressions of the stability criteria are derived from the linearized equations. Numerical examples of stability are given for fully nonlinear cases. DOE

N93-11517# Oak Ridge National Lab., TN.

NORTH AMERICAN RADIOACTIVE BEAM INITIATIVES

J. D. Garrett 1992 15 p Presented at the International Workshop on the Physics and Techniques of Secondary Nuclear Beams, Dourdan, France, 23-25 Mar. 1992
(Contract DE-AC05-84OR-21400)
(DE92-019185; CONF-9203164-2) Avail: CASI HC A03/MF A01

After a brief review of existing radioactive beam facilities in North America, two new initiative (the Oak Ridge Radioactive Ion Beam Facility and the IsoSpin Laboratory) are described in some detail. An evaluation of which nuclei these facilities will be able to study, which cannot be studied with stable targets and beams, is also presented. DOE

N93-11521# Kansas Univ., Lawrence. Dept. of Physics and Astronomy.

RESEARCH IN HEAVY-ION NUCLEAR PHYSICS

S. J. Sanders and F. W. Prosser Jan. 1992 18 p
(Contract DE-FG02-89ER-40506)
(DE92-015099; DOE/ER-40506/5) Avail: CASI HC A03/MF A01

This report discusses the following topics: Fusion-fission in light nuclear systems; High-resolution Q-value measurement for the

Mg-24 + Mg-24 reaction; Heavy-ion reactions and limits to fusion; and Hybrid MWPC-Bragg curve detector development. DOE

N93-11525# National Lab. for High Energy Physics, Tsukuba (Japan).

ANALYSIS OF THE PREBUNCHER FOR THE KEK 40-MeV PROTON LINAC

Takao Kato Dec. 1991 27 p
(DE92-514988; KEK-91-10) Avail: CASI HC A03/MF A01

The electromagnetic fields of the prebuncher for the KEK 40-MeV proton linac have been studied using the code MAFIA. Part of the calculated results were compared with the experimental results. A beam simulation of the beam transport line between the prebuncher and the linac was performed using code LEBT; it runs on a supercomputer in order to calculate beam dynamics, including space-charge effects. The capture efficiency of the linac and the emittance growth in the beam line are discussed in connection with the space-charge effects. DOE

N93-11641# Brookhaven National Lab., Upton, NY.

RF BEAM LOADING IN THE BROOKHAVEN AGS WITH BOOSTER INJECTION

S. Y. Zhang, E. Raka, and W. T. Weng 1992 4 p Presented at the 15th International Conference on High Energy Accelerators, Hamburg, Germany, 20-24 Jul. 1992
(Contract DE-AC02-76CH-00016)
(DE92-019452; BNL-47149; CONF-920706-24) Avail: CASI HC A01/MF A01

Multi-batch bunched beam loading during injection from the Booster to the AGS is discussed. The full intensity beam injection to the upgraded AGS rf system with beam phase and radial feedbacks is studied. It is shown that a beam phase feedback is necessary in order to guarantee a predictable hewn behavior after the first batch injection, otherwise the initial phase deviation for the following batch injections cannot be controlled. However, the effectiveness of the phase feedback control of the transient beam loading may be limited by an emittance blow up in the process. It is shown that a fast power amplifier feedback with a moderate gain can significantly reduce the transient effect of the bunched beam injection. DOE

N93-11652# Argonne National Lab., IL.

RESEARCH AND DEVELOPMENT OF SUPERCONDUCTING LINEAR ACCELERATORS FOR NEUTRAL PARTICLE BEAM APPLICATIONS

J. R. Delayen, C. L. Bohn, W. L. Kennedy, G. L. Nicholls, C. T. Roche, and L. Sagalovsky 1992 11 p Presented at the Neutral Particle Beam Technical Symposium and Scientific Exchange, Argonne, IL, 28 Apr. - 1 May 1992
(Contract W-31-109-eng-38)
(DE92-019043; ANL/CP-76578; CONF-9204170-3) Avail: CASI HC A03/MF A01

Experiments with superconducting cavities designed for applications in continuous-wave, high-current ion linear accelerators have resulted in very high CW accelerating gradients, up to 18 MV/m, with only a few watts of power dissipation in the cavity walls. These results make the prospects for compact, lightweight Neutral Particle Beam accelerators very attractive, and they compel further work to develop RF superconductivity for this application. Accordingly, we have completed two designs of experiments for testing superconducting resonators with high-current ion beams. The first is the preliminary design of a superconducting linac section to be tested at the end of the Continuous-Wave Deuterium Demonstrator (CWDD), and the second is the conceptual design of a superconducting cavity test using the beam from Chalk River Nuclear Laboratory's RFQ-1250. In addition, a theoretical investigation of cumulative beam breakup has led to a classification of transient beam breakup in beams consisting of delta-function bunches, and the formalism was extended to include distributions of deflecting-mode frequencies in the accelerating structures. An analytic model of the transverse dynamics of space-charge-dominated beams in a continuous linear focusing channel was also formulated based on the Fokker-Planck equation and used in a first calculation of emittance growth and halo formation. In addition, a method for radio-frequency control of superconducting cavities with beam loading has been devised. DOE

N93-11668# Tufts Univ., Medford, MA. Dept. of Physics and Astronomy.

HIGH ENERGY PHYSICS AT TUFTS UNIVERSITY

15 Jul. 1992 98 p
(Contract DE-FG02-92ER-40702)
(DE92-018081; DOE/ER-40702/2) Avail: CASI HC A05/MF A02

This report discusses the following topics: Neutrino Interactions in the 15-foot Bubble Chamber; Pion and Kaon Production of Charm and Charm-Strange States; Study of Heavy Flavors at the Tagged Particle Spectrometer; Neutrino Oscillations at the Fermilab Main Injector; Soudan II Nucleon Decay Project; Physics at the Antiproton-Proton Collider at s = 1.8 TeV; Designing the Solenoidal Detector for the Supercollider; Neutrino Telescope Proposal; Polarization in Inclusive Hyperon Production and QCD Subprocesses; Production and Decay Characteristics of Top Quarks; Scattering in Extended Skyrmion Models and Spin Dependence; Search for Top Quark Production at the Tevatron; Polarization Correlations in Hadronic Production of Top Quarks; and Computation and Networking. DOE

N93-11687# Rutherford Appleton Lab., Chilton (England).

PARTICLE PHYSICS EXPERIMENTS, 1991

B. A. Roberts, comp. Jan. 1992 204 p
(RAL-92-001; ETN-92-92364) Avail: CASI HC A10/MF A03

A compilation of the experiments performed in the field of particle physics, is given. The following contributions are presented: study of neutrino and antineutrino interactions with protons using BEBC bubble chamber; search for the neutron electric dipole moment using ultracold neutrons; a 4 pi solid angle detector for the CERN proton-antiproton collider; an experiment on photoproduction at high energy; measurement of the nucleon structure function; a nucleon lifetime experiment; measurements of proton-antiproton interactions; photoproduction in the range of 70 to 180 GeV; the Soudan-2 proton decay experiment; neutrino physics; the search of gluonium states; the hadron production of charm using silicon detectors; measurement of the decay of two neutral pions into two charged pions; the search for direct production of meson states; study of a neodymium/hydrogen bubble chamber exposed to a 800 GeV/c beam; studies of electron-position interactions and annihilation; study of lepton production in hadronic collisions; search for dibaryons; progress on the VA2 experiment; CP violation study in neutral kaon system; radiative decay of hyperons and radiative kaon structure; meson spectroscopy with a 4 pi neutral and charged detector; dark matter experiments; development of an optical fiber microvertex detector; study of heavy ion collisions; study of high energy nucleus-nucleus interactions; Sudbury neutrino observatory; search for the H-particle; radiative weak decays; the Omni-purpose apparatus experiment; the detector with lepton, photon and hadron identification and other detectors. ESA

N93-11763# Los Alamos National Lab., NM.

BANSHEE: HIGH-VOLTAGE REPETITIVELY PULSED ELECTRON-BEAM DRIVER

F. VanHaaften 1992 4 p Presented at the 20th International Power Modulator Symposium, Myrtle Beach, SC, 23-25 Jun. 1992
(Contract W-7405-eng-36)
(DE92-017413; LA-UR-92-1716; CONF-920671-3) Avail: CASI HC A01/MF A01

BANSHEE (Beam Accelerator for a New Source of High-Energy Electrons) this is a high-voltage modulator that is used to produce a high-current relativistic electron beam for high-power microwave tube development. The goal of the BANSHEE research is first to achieve a voltage pulse of 700 - 750 kV with a 1 micro-s pulse widthdriving a load of approximately 100 Omega, the pulse repetition frequency (PRF) of a few hertz. The ensuing goal is to increase the pulse amplitude to a level approaching 1 MV. We conducted tests using half the modulator with an output load of 200 Omega, up to a level of approximately 650 kV at a PRF of 1 Hz and 525 kV at a PRF of 5 Hz. We then conducted additional testing using the complete system driving a load of approximately 100 Omega. DOE

N93-11776# Brookhaven National Lab., Upton, NY.

STATIC AND TRANSIENT BEAM LOADING OF A SYNCHROTRON

S. Y. Zhang and W. T. Weng 13 Jul. 1992 27 p
(Contract DE-AC02-76CH-00016)
(DE92-019244; BNL-47773; AGS/AD-92-1) Avail: CASI HC A03/MF A01

In a synchrotron, when the beam induced current is comparable to the driver current, the RF cavity is subjected to beam loading perturbation and corrective steps have to be implemented to regain beam stability. In this paper, the static and transient beam loading will be studied. We first discuss the static beam loading, which includes the cavity detuning condition, the stability condition, and the generator power dissipation. The beam current induced beam phase deviation is used as criterion to study the transient beam loading. The upgraded and the old AGS RF system parameters are used as an example to demonstrate how to choose cavity and generator parameters to satisfy the stability requirements under the beam loading. The dynamic models for the beam loading with beam control, and the beam loading with fast power amplifier feedback are presented and analyzed. It is shown that the beam phase and radial feedbacks alone are insufficient for the transient beam loading compensation, but the fast power amplifier feedback can provide effective correction on the beam loading. The limitation of the fast feedback and the beam loading with tuning and AVC loops are also discussed. DOE

N93-11831# Argonne National Lab., IL.

DYNAMIC VACUUM ANALYSIS FOR APS HIGH HEAT FLUX BEAMLINE FRONT ENDS USING OPTICAL RAY-TRACING SIMULATION METHODS

S. Xu and R. W. Nielsen 1992 11 p Presented at the Conference on Physics and Engineering of Advanced Detectors and Collection/Focusing Systems, San Diego, CA, 19-24 Jul. 1992
(Contract W-31-109-eng-38)
(DE92-019032; ANL/CP-76700; CONF-920768-5) Avail: CASI HC A03/MF A01

The high-power and high-flux x-ray beams produced by third generation synchrotron radiation sources such as the Advanced Photon Source (APS) can cause significantly high gas desorption rates on beamline front-end components if beam missteering occurs. The effect of this gas desorption needs to be understood for dynamic vacuum analysis. To simulate beam missteering conditions, optical ray-tracing methods have been employed. The results of the ray-tracing analysis have been entered into a system-oriented vacuum program to provide dynamic vacuum calculations for determination of pumping requirements for the beamline front-ends. The APS will provide several types of synchrotron radiation sources, for example, undulators, wigglers, and bending magnets. For the purpose of this study, the wiggler source was chosen as a 'worst case' scenario due to its high photon flux, high beam power, and relatively large beam cross section. DOE

N93-11919# Los Alamos National Lab., NM.

ON SOME PRACTICAL CONSIDERATION OF THE ELECTRON BEAM BREAKUP TRANSIT TIME OSCILLATOR

T. J. T. Kwan 1992 7 p Presented at the 9th International Conference on High Power Particle Beams, Washington, DC, 25-29 May 1992
(Contract W-7405-eng-36)
(DE92-017406; LA-UR-92-1828; CONF-920515-29) Avail: CASI HC A02/MF A01

The electron beam breakup transit time oscillator (BTO) makes use of the interaction between an electron beam and the azimuthally asymmetric transverse magnetic mode (TM(sub 110)) of a cavity to facilitate the exchange of energy between them. Linear theory has shown a large growth rate in the regime where space-charge effects can be ignored. In this study, we have investigated the non-ideal elements in the BTO and evaluated their effects accordingly. The practical issues under consideration are electron beam quality, energy, and space-charge potential. Our calculations indicate only modestly unfavorable scalings with respect to these parameters. DOE

N93-12103# Sandia National Labs., Albuquerque, NM.

DIVERGENCE IN INTENSE ION BEAMS CAUSED BY INCOMPLETE CHARGE NEUTRALIZATION

C. L. Olson and J. W. Poukey 1992 7 p Presented at the 9th International Conference on High Power Particle Beams, Washington, DC, 25-29 May 1992
(Contract DE-AC04-76DP-00789)
(DE92-016891; SAND-91-2744C; CONF-920515-27) Avail: CASI HC A02/MF A01

Space charge neutralization for light ion fusion (LIF) ion beam transport is usually assumed to be perfect in the 'charge-neutral' region of the diode and in the gas transport cell. However, small charge clumps in the beam will not be totally charge-neutralized, and the residual net space charge may contribute to the beam microdivergence theta(sub mu). If the net potential of the clump is limited only by electron trapping, the minimum potential will be e(phi) approximately 1/2 m(sub e)v(sub i)(sup 2) where m(sub e) is the electron mass and v(sub i) is the ion velocity. For proton beams this leads to theta(sub mu) approximately (m(sub e)/M(sub p))sup 1/2 approximately 23 mrad, where M(sub p) is the proton rest mass. For non-protonic beams, different results occur. The mechanism predicts no dependence of theta(sub mu) on diode voltage, non-protonic theta(sub mu) greater than proton theta(sub mu) for proton-contaminated beams, and axial energy spread Delta epsilon(sub parallel) / epsilon(sub parallel) is approximately +/- 2 theta(sub mu), which are all consistent with present data. Results of analytic studies and computer simulations of this mechanism are presented. Plasma shielding reduces the effects of this mechanism but collisions and magnetic fields reduce the plasma shielding effects. 2-D PIC MAGIC simulations show that this mechanism contributes to theta(sub mu) both in the 'charge-neutral' region and in the gas transport region. It is concluded that this mechanism is especially important in the 'charge-neutral' region. DOE

N93-12108# Argonne National Lab., IL.

PHOTODISINTEGRATION OF THE DEUTERON AT HIGH ENERGY

R. J. Holt 1992 9 p Presented at the International Conference on the Structure of Baryons and Related Mesons, New Haven, CT, 1-4 Jun. 1992
(Contract W-31-109-eng-38)
(DE92-017066; ANL/CP-76530; CONF-920637-2) Avail: CASI HC A02/MF A01

Measurements of the angular distribution for the gamma d yields pn reaction were performed at SLAC for photon energies between 0.7 and 1.8 GeV (experiment NE8) and between 1.6 and 4.4. GeV (experiment NE17). The final results for experiment NE8 will be presented, but only preliminary results for NE17 will be discussed. The data at theta(sub cm) = 90 degrees appear to follow the constituent counting rules. The angular distribution at high photon energies exhibit large values of the cross section at forward angles. There is evidence that the cross section may also be large at backward angles and high energies. DOE

N93-12126# California Univ., Berkeley. Lawrence Berkeley Lab.

THE DIAGNOSTICS SYSTEM FOR THE MULTIPLE HEAVY ION BEAMS INDUCTION LINAC EXPERIMENT, MBE-4

S. Eylon Sep. 1991 10 p Presented at the Accelerator Instrumentation Workshop, Newport News, VA, 28-31 Oct. 1991
(Contract DE-AC03-76SF-00098)
(DE92-017109; LBL-31427; CONF-9110118-7) Avail: CASI HC A02/MF A01

MBE-4 is a four beam current amplifying induction linac experiment conducted at LBL as a part of the Heavy Ion Fusion Accelerator Research (HIFAR) program for studying accelerator physics issues of a heavy ion driver for inertial fusion. The four ion beams (Cs(+), 10 mA) are focused by electrostatic quadrupoles and accelerated from about 200 keV to 900 keV through 24 induction gaps. Current amplification of up to nine times is achieved while the beam pulse duration is compressed from about 3 to 0.5 micro-s. The diagnostic system enables the complete time-resolved 2-D transverse phase space distribution of the beam to be measured. Reduction of the raw data yields the beam current, current profile, emittance, centroid position, and angle as well as the beam envelope parameters. In addition, the longitudinal energy distribution is obtained from measurements using a calibrated electrostatic spectrometer. The diagnostic system hardware, as well as the data acquisition and reduction routines, are controlled by an IBM pc-XT. We shall describe the diagnostic system and discuss its performance in view of the specific issues which result from the acceleration and amplification of multiple beams of heavy ions. DOE

N93-12129# EG and G Energy Measurements, Inc., Idaho Falls.
NUCLEAR FUELS FOR VERY HIGH TEMPERATURE APPLICATIONS
L. B. Lundberg and R. R. Hobbins 1992 7 p Presented at the 27th Intersociety Energy Conversion Engineering Conference, San Diego, CA, 3-7 Aug. 1992
(Contract DE-AC07-76ID-01570)
(DE92-018021; EGG-M-92067; CONF-920801-18) Avail: CASI HC A02/MF A01

The success of the development of nuclear thermal propulsion devices and thermionic space nuclear power generation systems depends on the successful utilization of nuclear fuel materials at temperatures in the range 2000 to 3500 K. Problems associated with the utilization of uranium bearing fuel materials at these very high temperatures while maintaining them in the solid state for the required operating times are addressed. The critical issues addressed include evaporation, melting, reactor neutron spectrum, high temperature chemical stability, fabrication, fission induced swelling, fission product release, high temperature creep, thermal shock resistance, and fuel density, both mass and fissile atom. Candidate fuel materials for this temperature range are based on UO2 or uranium carbides. Evaporation suppression, such as a sealed cladding, is required for either fuel base. Nuclear performance data needed for design are sparse for all candidate fuel forms in this temperature range, especially at the higher temperatures. DOE

N93-12497# Stanford Linear Accelerator Center, CA.
PRE-COMPRESSION OF BUNCH LENGTH IN THE SLC DAMPING RINGS
F. J. Decker, T. Limberg, and J. Turner Jul. 1992 3 p Presented at the 15th International Conference on High Energy Accelerators, Hamburg (Germany), 20-24 Jul. 1992
(Contract DE-AC03-76SF-00515)
(DE92-018154; SU-SLAC-PUB-5871; CONF-920706-7) Avail: CASI HC A01/MF A01

After extraction, the damping ring (DR) bunch length is compressed in the RTL (Ring-To-Linac) transport line to achieve the desired linac bunch length. For this, an energy spread is induced proportional to the DR bunch length, producing large, aperture filling, horizontal beam sizes in the dispersive regions of the RTL. There, nonlinear magnetic fields and wakefields cause higher order dispersion at the beginning of the linac, which increases the effective beam emittance. More important, in the presence of DR extraction jitter this causes linac launch jitter which makes linac operation unstable at high currents. A precompression of the DR bunch length would reduce the horizontal beam size in the RTL and thus relieve the problems mentioned above. It can be achieved by a modulation of the damping ring RF amplitude with a so-called 'bunch muncher' shortly before extraction. A principle limitation is the inevitable increase in energy spread of the extracted bunch which sets the lower limit for the achievable bunch length in the linac. For SLC parameters the possible reduction in DR bunch length is about 35 percent. The routinely operation of the 'bunch muncher' consists of two 'munches', cancelling the effect of the beam loading and keeping the extraction phase unchanged. DOE

74 OPTICS

Includes light phenomena; and optical devices.
For lasers see *36 Lasers and Masers.*

N93-11052# Department of the Navy, Washington, DC.
FIBER OPTIC POLISHING SYSTEM Patent
Michael Bramson, inventor (to Navy) 21 Apr. 1992 6 p Filed 1 Oct. 1990
(AD-D015353; US-Patent-5,106,394; US-Patent-Appl-SN-591208; US-Patent-Class-51-309) Avail: US Patent and Trademark Office

An optical glass fiber polishing apparatus and a method utilizing a slurry comprised of water, CeO, glycerin, and, where needed, a base such as NaOH to realize transmission loss in the fiber as it is polished towards the fiber core are presented. The intensity of light introduced at one end of the fiber is measured at the opposite end, continuously and without interruption of the polishing, to determine polishing progress through the cladding towards the core. GRA

N93-11058* National Aeronautics and Space Administration. Lewis Research Center, Cleveland, OH.
PHASE-STEPPING FIBER-OPTIC PROJECTED FRINGE SYSTEM FOR SURFACE TOPOGRAPHY MEASUREMENTS Patent
Carolyn R. Mercer, Inventor (to NASA) and Glenn Beheim, inventor (to NASA) 8 Sep. 1992 6 p Filed 13 May 1991
(NASA-Case-LEW-14996-1; US-Patent-5,146,293; US-Patent-Appl-SN-703435; US-Patent-Class-356-356; US-Patent-Class-356-360; US-Patent-Class-356-376; US-Patent-Class-382-26; US-Patent-Class-364-575; Int-Patent-Class-G01B-11/02) Avail: US Patent and Trademark Office

A projected fringe interferometer for measuring the topography of an object is presented. The interferometer periodically steps the phase angle between a pair of light beams emanating from a common source. The steps are pi/2 radians (90 deg) apart, and at each step a video image of the fringes is recorded and stored. Photodetectors measure either the phase and theta of the beams or 2(theta). Either of the measures can be used to control one of the light beams so that the 90 deg theta is accurately maintained. A camera, a computer, a phase controller, and a phase modulator established closed-loop control of theta. Measuring the phase map of a flat surface establishes a calibration reference.
Official Gazette of the U.S. Patent and Trademark Office

N93-11071# Optical Society of America, Washington, DC.
ORGANIZATION OF THE OPTICAL SOCIETY OF AMERICA PHOTONIC SCIENCE TOPICAL MEETING SERIES. VOLUME 14: PHOTOREFRACTIVE MATERIALS EFFECTS, AND DEVICES Final Report, 1 Jan. - 31 Dec. 1991
Jarus W. Quinn 22 May 1992 484 p Meeting held in Beverly, MA, 29-31 Jul. 1991
(Grant AF-AFOSR-0176-91)
(AD-A253001; AFOSR-92-0511TR-Vol-14) Avail: CASI HC A21/MF A04

Attached is a list of reports supported by the Optical Society of America: Photorefractive Materials, Effects, and Devices; Integrated Photonics Research; Nonlinear Guided Wave Phenomena; Optical Amplifiers and Their Applications; Optical Computing; Picosecond Electronics and Optoelectronics; Quantum Optoelectronics; Photonic Switching; Microphysics of Surfaces: Beam Induced Processes; Soft X-ray Projection Lithography; Short Wavelength Coherent Radiation, Generation and Applications; and, Presistent Spectral Hole-Burning: Science and Applications. GRA

N93-11099# Optical Society of America, Washington, DC.
THE FOURTH OSA TOPICAL MEETING PROCEEDINGS ON PICOSECOND ELECTRONICS AND OPTOELECTRONICS, VOLUME 9 Final Report, 1 Jan. - 31 Dec. 1991
Jarus W. Quinn 22 May 1992 287 p Meeting held in Salt Lake City, UT, 13-15 Mar. 1991
(Grant AF-AFOSR-0176-91)
(AD-A253472; AFOSR-92-0520TR-Vol-9) Avail: CASI HC A13/MF A03

Contents: Terahertz Sources and Spectroscopy; Ultrafast Optoelectronics; Electro-Optic Sampling; Ultrafast Photodetectors; High-Speed Transistors and Electronics; Millimeter-Wave Circuits; Ultrafast Lasers; Tunneling; Materials; Picosecond Superconductive Electronics; High-Capacity Lightwave Transmission: Ultra-High Speed or Wavelength Multiplexing; and Photon-Assisted Resonant Tunneling Through a GaAs/A1GaAs Multiple Quantum Well Structure. GRA

N93-11186# EIC, Inc., Norwood, MA.
FAST ELECTROCHROMIC SWITCHING FOR OPTICAL HARDENING APPLICATIONS Technical Report, 5 Aug. 1988 - 5 Dec. 1990
Stuart F. Cogan, R. D. Rauh, Trung H. Nguyen, Rochelle B. Jones, and John D. Westwood 1 Apr. 1992 53 p
(Contract DNA001-88-C-0102)
(AD-A248174; C946F; DNA-TR-91-99) Avail: CASI HC A04/MF A01

Infrared optical switching devices based on closed-tube-vapor-transport grown single crystals of group IV metal dichalcogenides were investigated. Reversible infrared reflectance modulation was identified in alkali metal intercalated HfS2 and ZrS2. A reflectance driven transmittance modulation of 0.01 to 50 percent from 2-16 microns was observed with Li(x)HfS2 single crystals chemically lithiated and delithiated. Similar, although less dramatic, modulation was obtained with Ag(x)HfS2 crystals. Efforts to develop practical optical switching devices based on this IR modulation focused on the incorporation of electroactive and photoactive electron donor-acceptor complexes in the van der Waals' gaps of the crystals. Electron donor (e.g., Li or Ag) intercalation is readily achieved because of coulombic stabilization of the intercalated crystal through intercalation of the chalcogens (e.g., S) and the donor cation. Intercalation of electron acceptors (e.g., I and Br) into reduced (donor intercalated) dichalcogenides was found energetically unfavorable and resulted in deintercalation of the donor. Mixed-metal (group IV and V) dichalcogenide crystals, that are intrinsically n-type, were also used as hosts for acceptor intercalation. The as-grown mixed-metal crystals had higher electrical conductivities and were more IR reflective than pure HfS2 or ZrS2. Attempts to intercalate I and Br into the mixed-metal crystals resulted in extensive exfoliation. The use of metallocenes, principally chromcene and HfS2 remains unknown. Electrically driven optical switching in the 700-1100 nm wavelength range was observed in HfS2 crystals that had been lithiated and treated in iodine. A sharp increase in electrical conductivity and decrease in transmittance was observed at electrical field strength of 0.7 V/micrometer in the c-axis direction. The switching was reversible with applied electric field and independent of polarity. GRA

N93-11342# Royal Signals and Radar Establishment, Malvern (England).
EXTRACTION OF SHAPE INFORMATION FROM PREDICTED IRRADIANCE PROFILES IN INFRARED IMAGES
P. W. Foulkes 5 Mar. 1992 17 p
(RSRE-Memo-4464; BR301923; ETN-92-92314) Copyright Avail: CASI HC A03/MF A01

The problem of infrared image formation is addressed and an irradiance equation for simple infrared scenes is derived. The difficulties caused by mutual illumination of one or more bodies are considered and it is shown how the infrared irradiance equation can also be specified for more complex scenes. The infrared irradiance equation derived is solved in closed form for some simple geometries for both Lambertian and non-Lambertian surfaces. Experimental results from a variety of scene geometries are in agreement with the theoretically derived equations, indicating the validity of the theoretical analysis. The use of a knowledge of the formation of infrared images to predict the image irradiance pattern of a particular object is demonstrated. It is shown that with a knowledge of the radiance properties and surface geometry of the object, it is possible to detect instances of that object in a scene. Examples of successful object detection based on an understanding of the image irradiance are presented. ESA

N93-11408 National Physical Lab., Teddington (England). Div. of Materials Metrology.
BASICITY AND OPTICAL BASICITIES OF SLAGS
K. C. Mills Feb. 1992 35 p
(NPL-DMM(A)-48; ETN-92-92370) Copyright Avail: National Physical Lab., Teddington, Middlesex, TW11 0LW, England

Various terms used to define basicity are outlined. The concept of optical basicity is discussed and its relationships with the following are discussed: elemental partition between slag and metal phases for example S, P, and O; solubility of oxides in the slag phase; thermodynamic properties; and structure and certain physical properties of the slag. ESA

N93-11489# Tennessee State Univ., Nashville. Dept. of Physics, Mathematics, and Computer Science.
EVALUATION OF AN ANALYTICAL MODEL FOR PREDICTING LIGHT SCATTERING FROM CYLINDRICALLY-SHAPED OBJECTS IN THE OCEAN Final Report
Patricia G. Hull 5 Mar. 1992 11 p
(Contract N00014-90-J-1588)
(AD-A248414) Avail: CASI HC A03/MF A01

The polarization state of light in the ocean can be used to enhance visibility. We are investigating the consequences of scattering from non-spherically-symmetric particles on light propagation and visibility in the ocean. To calculate scattering from non-spherical marine micro-organisms, it is usually necessary to resort to approximate methods. One promising approximation is the coupled-dipole approach in which an arbitrarily-shaped object is divided into a number of identical elements arranged on a cubic lattice. Each element is treated as a spherical, dipolar oscillator with its polarizability specified by the real and imaginary parts of the index of refraction. Interactions between dipoles are included by determining the field at a particular dipole due to the incident field and the fields induced by the other dipole oscillators. The scattered field is then the sum of the fields due to each oscillator. The coupled-dipole method is promising because, in principle, an organism of any shape can be modelled, and all sixteen elements of the scattering matrix calculated. We have applied this approach to calculate scattering from spherical particles to verify the limits of the approximation, and from other shapes to investigate the effects of non-'sphericity and chirality on scattering. In particular, we calculated all 16 Mueller matrix elements for the scattering from a finite cylinder, a single-s=d helix, 14-strand helix, and ensembles of these particles. The effects of pitch, size, wavelength, and complex index of refraction were investigated. GRA

N93-11527# New Mexico Univ., Albuquerque. Center for High Technology Materials.
OPTOELECTRONICS RESEARCH CENTER Final Report, 1 Feb. 1991 - 31 Jan. 1992
S. R. Brueck 16 May 1992 437 p
(Contract F49620-89-C-0028)
(AD-A253132; AFOSR-92-0672TR) Avail: CASI HC A19/MF A04

The AFOSR Optoelectronics Research Center (OERC) at the Center for High Technology Materials of the University of New Mexico has become a leading university optoelectronics program. Novel InGaAs and AlGaAs device structures have been pioneered. Exciting recent results include demonstration of large second-order nonlinearities in SiO2 and extensive development of PLZT. Processing advances include investigation of 3-5 regrowth over patterned wafers and the extension of interferometric lithography techniques. External cavity operation of diode lasers has provided a wealth of information about internal device physics and the fundamental limits of laser spectral and temporal characteristics. Single element and array geometries modeling has led to greater understanding and device performance. The OSR OERC has pioneered development of surface-emitting lasers. Since the first demonstration of the resonant-periodic gain concept was reported several years ago, advances have been made in device and mirror design, optical pumping with record output powers, in ultrafast gain switched operation, in record low series resistance, and overall and slope efficiencies for electrical operation. A recent advance in integrated structures is the coupling of phototransistors with surface-emitting lasers to make smart pixels that can operate in parallel on an array of optical signals. GRA

N93-11627# Lawrence Livermore National Lab., CA.
COMPUTATION OF SMALL SCALE VELOCITY TURBULENCE AND ITS EFFECT ON OPTICAL SCINTILLATIONS AND STIMULATED THERMAL RAYLEIGH SCATTERING
J. A. Viecelli, D. H. Chambers, and T. J. Karr 23 Sep. 1991 37 p Previously announced in IAA as A92-35489
(Contract W-7405-eng-48)
(DE92-018934; UCID-21771-Rev-1) Avail: CASI HC A03/MF A01

Coherent high-power light beams propagating long distances through turbulent fluids are subject to many kinds of scattering effects; among these are small-scale thermal index instabilities, in which the fluid is heated by the small fraction of light absorbed, amplifying the pre-existing index fluctuations and producing stimulated small-angle Rayleigh scattering. Turbulent velocity fluctuations can inhibit the rate of growth of these instabilities by dispersing the thermal perturbations created by the beam. Methods for computing the turbulent diffusion of the heating perturbations, compatible with fast Fourier transform beam propagation computations, are presented. Propagation calculations of scintillation coherence times and small-scale velocity turbulence thresholds for stimulated thermal Rayleigh scattering are included. DOE

N93-11892# State Univ. of New York, Buffalo. Dept. of Electrical and Computer Engineering.
IMPACT OF FINITE FREQUENCY DEVIATION ON THE PERFORMANCE OF DUAL-FILTER HETERODYNE FSK LIGHTWAVE SYSTEMS
Ozan K. Tonguz, M. O. Tanrikulu, and Leonid G. Kazovsky (Stanford Univ., CA.) 1991 44 p
(Contract N00014-91-J-1857)
(AD-A247611) Avail: CASI HC A03/MF A01

A detailed theoretical analysis is given for the impact of finite frequency deviation on the sensitivity of dual-filter heterodyne Frequency Shift Keying (FSK) lightwave systems. Our analysis provides closed-form signal-to-noise ratio (SNR) results for estimating the bit-error-ratio (BER) performance of the system. These closed-form results provide an insight into the impact of finite frequency deviation 2 Delta fd, laser linewidth Delta v, bit rate Rb, and IF filter bandwidths on the system performance. It is shown that there is a well-defined relationship between the choice of frequency deviation and the tolerable amount of laser phase noise. When there is no phase noise, a frequency deviation of 2 Delta fd = 0.72 Rb, is sufficient for 1 dB sensitivity penalty with respect to infinite frequency deviation case; whereas for a linewidth of Delta v = 0.50 Rb the required frequency deviation increases to 2 Delta fd = 3.42 Rb for the same sensitivity penalty. The sensitivity degradation can be very severe for a fixed linewidth as the frequency deviation gets smaller: for a linewidth of 20 percent the sensitivity penalty is only 0.54 dB when the frequency deviation is infinite whereas it is 3.48 dB when the frequency deviation is 2 Delta fd = Rb. We also quantify the impact of finite frequency deviation on optimum IF filter bandwidths. For a fixed linewidth, the optimum IF filter bandwidth decreases as frequency deviation becomes smaller: for Delta v = 0.5 Rb the optimum IF filter bandwidth GRA

N93-12201*# Alabama Univ., Huntsville. Center for Applied Optics.
ANALYSIS OF ADVANCED OPTICAL GLASS AND SYSTEMS Final Report
R. Barry Johnson and Chen Feng 9 Aug. 1991 58 p
(Contract NAS8-36955)
(NASA-CR-184434; NAS 1.26:184434; UAH-5-32389) Avail: CASI HC A04/MF A01

Optical lens systems performance utilizing optical materials comprising reluctant glass forming compositions was studied. Such special glasses are being explored by NASA/Marshall Space Flight Center (MSFC) researchers utilizing techniques such as containerless processing in space on the MSFC Acoustic Levitation Furnace and on the High Temperature Acoustic Levitation Furnace in the conceptual design phase for the United States Microgravity Laboratory (USML) series of shuttle flights. The application of high refractive index and low dispersive power glasses in optical lens design was investigated. The potential benefits and the impacts to the optical lens design performance were evaluated. The results of the studies revealed that the use of these extraordinary glasses can result in significant optical performance improvements. Recommendations of proposed optical properties for potential new glasses were also made. Applications of these new glasses are discussed, including the impact of high refractive index and low dispersive power, improvements of the system performance by using glasses which are located outside of traditional glass map, and considerations in establishing glass properties beyond conventional glass map limits. L.R.R.

N93-12227# Texas A&M Univ., College Station. Dept. of Electrical Engineering.
FIBER OPTIC DELAY LINE SIGNAL PROCESSORS Final Technical Report, Sep. 1988 - Sep. 1991
Henry F. Taylor Jun. 1992 39 p
(Contract F19628-88-K-0053)
(AD-A254691; RL-TR-92-135) Avail: CASI HC A03/MF A01

The objective of this program was to develop new techniques for the processing of wideband analog signals based upon the use of optical fiber delay lines. During the course of the research, new concepts in optical processing have been developed and demonstrated. A new type of reflective tap was studied in which an internal mirror is fabricated in a continuous length of fiber. Operation of a reflectively tapped transversal filter with a bandwidth of 10 GHz was demonstrated, the highest bandwidth reported to date for any signal processor. This device has performed 1011 analog multiplications per second in a relatively simple processor design. It is also possible to perform optical simulation of radar targets using the reflectively tapped fiber. GRA

N93-12272# Rome Lab., Griffiss AFB, NY.
OPTICAL BEAMFORMER Report, Jan. 1987 - Jan. 1992
Anthony M. Greci, Richard N. Smith, and Salvatore L. Carollo Apr. 1992 17 p
(AF Proj. 4519)
(AD-A254354; RL-TR-92-74) Avail: CASI HC A03/MF A01

This report describes research on optical beamforming performed in-house at Rome Laboratory. An optically linked antenna array was beamformed using an optical star coupler. Beamforming and nulling were performed using grin lenses as phase elements. The work was performed at an RF of 8 GHz. GRA

N93-12531 Arizona Univ., Tucson.
LIGHT SCATTERING FROM A SPHERE ON OR NEAR AN INTERFACE Ph.D. Thesis
Gorden Wayne Videen 1992 130 p
Avail: Univ. Microfilms Order No. DA9220701

The light scattering problem of a sphere on or near a plane surface is solved using an extension of Mie theory. The approach taken is to solve the boundary conditions at the sphere and at the surface simultaneously and develop the scattering amplitude and Mueller scattering matrices. This is performed by projecting the fields in the half space region not including the sphere multiplied by an appropriate Fresnel reflection coefficient onto the half space region including the sphere. An assumption is made that the scattered fields from the sphere, reflecting off the surface and interacting with the sphere, are incident on the surface at near-normal incidence. The exact solution is asymptotically approached when either the sphere is a large distance from the surface of the conductivity of the medium behind the surface approaches infinity. The solution is greatly simplified in the asymptotic limit when the sphere is small compared with the wavelength. Comparisons are made between the experimental Mueller matrices of a contaminated surface and matrices predicted using this simplified system. Comparisons are also made between experimental BRDF's and those predicted using the sphere-surface scattering theory. Dissert. Abstr.

75 PLASMA PHYSICS

Includes magnetohydrodynamics and plasma fusion.
For ionospheric plasmas see *46 Geophysics*. For space plasmas see *90 Astrophysics*.

N93-10975# Lawrence Livermore National Lab., CA.
X RAY DIAGNOSTIC TECHNIQUES IN ICF
J. D. Kilkenny Feb. 1992 33 p Presented at the Inertial Confinement Fusion Course, Princeton, NJ, 2 Feb. 1991
(Contract W-7405-eng-48)
(DE92-018069; UCRL-JC-107332; CONF-9202120-1) Avail: CASI HC A03/MF A01

In a large ICF facility, there are usually tens of diagnostics based on optical, x-ray, and neutron instruments. X-ray diagnostic techniques are the subject of this article. Thermonuclear products are used in a complementary manner to diagnose the parameters of imploded fuel and are also the subject of the subsequent article. There are two different techniques for x-ray diagnostics, those relying on self-emission and those relying on backlighting. We examine four representative x-ray diagnostics, two relying on self-emission and two relying on backlighting. DOE

N93-10988# General Atomic Co., San Diego, CA.
SCALING OF LOWER HYBRID CURRENT DRIVE WITH TEMPERATURE
R. W. Harvey, M. G. McCoy (Lawrence Livermore National Lab., CA.), A. K. Ram, A. Bers (Massachusetts Inst. of Tech., Cambridge.), and V. Fuchs (Case Western Reserve Univ., Cleveland, OH.) Jun. 1992 5 p Presented at the Topical Conference Meeting on Radio Frequency Heating and Current Drive of Fusion Devices, Brussels, Belgium, 7-10 Jul. 1992
(Contracts DE-AC03-89ER-51114; W-7405-eng-48; DE-FG02-90ER-54084)
(DE92-018541; GA-A-20945; CONF-920717-4) Avail: CASI HC A01/MF A01

The 3-D Fokker-Planck/quasilinear code (CQL3D) is used to study the temperature scaling of lower hybrid current drive (LHCD) in the JET and JT-60 experiments. An offset-linear increase of current drive efficiency is obtained as a function of volume average temperature (T(sub e)) up to approximately 2.5, and reduced rate of efficiency increase is found at higher temperatures. The LHCD results indicate some fast wave/LH current drive synergy in the JET LH/FW experiments; however, code results discussed here show that synergy is not due to TTMP damping of the fast wave. DOE

N93-11029# Stuttgart Univ. (Germany). Inst. fuer Plasmaforschung.
CURRENT SCALING OF PLASMA FOCUS DEVICES [STROMSKALIERUNG VON PLASMAFOKUSANLAGEN]
C. Schiuma, H. Herold, H. J. Kaeppeler, M. Shakhatre, and S. K. H. Auluck (Bhabha Atomic Research Centre, Bombay, India) Mar. 1990 17 p In GEORGIAN Presented at the DPG Fuehjahrstagung, Munich, Fed. Republic of Germany, 13 Mar. 1990
(IPF-90-1; ETN-92-92148) Avail: CASI HC A03/MF A01

An analytical solution for the circuit equation with resistance R equal to zero in the compression phase is derived. It was shown that it was possible to discuss the influence of finite resistance in current variation and scaling parameters. The model solutions were checked out by numerical integrations of the current equation. Whereas the ohmic resistance cannot be neglected at the beginning of the rundown phase, its influence is negligible at the end of the rundown phase and in the compression phase. The theoretically determined values were compared with the results of numerous probe measurements. ESA

N93-11030# Stuttgart Univ. (Germany). Inst. fuer Plasmaforschung.
INSTABILITIES IN THE RUNDOWN PHASE OF THE PLASMA FOCUS [INSTABILITAETEN IN DER LAUFPHASE DES PLASMAFOKUS]
H. J. Kaeppeler Jul. 1990 31 p In GEORGIAN Presented at the Plasmakolloquium, 5 Jul. 1990
(IPF-90-3; ETN-92-92149) Avail: CASI HC A03/MF A01

The linear dispersion relation was derived from a three fluid theory (electrons, ions, and neutrals) with the aid of the Computer Algebra (CA) code MACSYMA. Four instabilities appeared in the rundown phase of the plasma focus, two of them gradient driven. The first two were unstable electrostatic waves with very high phase velocities. They did not contribute to anomalous dissipation. The third was identified as a gradient driven space charge instability, which might lead to current chopping. The fourth was the gradient driven electron acoustic wave instability. ESA

N93-11041# General Atomic Co., San Diego, CA.
DIRECT ELECTRON ABSORPTION OF FAST WAVES ON THE D3-D TOKAMAK
C. C. Petty, R. I. Pinsker, S. C. Chiu, J. S. deGrassie, J. Lohr, T. C. Luce, M. J. Mayberry, R. Prater, M. Porkolab (Massachusetts Inst. of Tech., Cambridge.), and P. T. Bonoli (Massachusetts Inst. of Tech., Cambridge.) Jun. 1992 4 p Presented at the Topical Conference Meeting on Radio Frequency Heating and Current Drive of Fusion Devices, Brussels (Belgium), 7-10 Jul. 1992
(Contracts DE-AC03-89ER-51114; DE-AC02-78ET-51013; DE-AC02-76CH-03073; DE-AC05-84OR-21400)
(DE92-016254; GA-A-20934; CONF-920717-2) Avail: CASI HC A01/MF A01

The fast Alfven wave (FW) was previously used to heat tokamak plasmas via ion cyclotron resonance heating (ICRH); however, FW can also be absorbed directly by electrons when the resonance condition omega - kappa(nu(sub e)) = 0 is satisfied. The direct electron absorption of FW is due to electron Landau damping and transit-time magnetic pumping. For a Maxwellian electron distribution, the e-folding damping length for FW in the ICRF is given by the following: lambda(sub e)(exp -1) = kappa(sub perpendicular)(R(sub e))((the square root of pi)/2)(beta(sub e))(xi(sub e))(exp(sup -xi(sub e)(exp 2)))(1 + 1/(alpha(exp 2))). The RW absorption is maximized when xi(sub e) = 1/(the square root of 2). The FW absorption also decreases rapidly with increasing magnetic field since (lambda(sub e)(exp -1)) is proportional to B(exp -3). The experiments of D3-D were aimed at characterizing the direct electron absorption of FW as xi(sub e) and B were varied. DOE

N93-11102# Stuttgart Univ. (Germany). Inst. fuer Plasmaforschung.
THE BASIC EQUATIONS FOR A FOUR COMPONENT MAGNETOPLASMA FLOW WITH NON EQUILIBRIUM IONIZATION [DIE GRUNDGLEICHUNGEN FUER EINE VIERKOMPONENTIGE MAGNETOPLASMA-STROEMUNG MIT NICHTGLEICHGEWICHTSIONISATION]
H. J. Kaeppeler Jan. 1991 37 p In GEORGIAN
(IPF-91-1; ETN-92-92151) Avail: CASI HC A03/MF A01

It is shown that the basic equations for a four fluid theory consisting of singly and doubly charged ions, electrons and neutrals, or of a singly charged ionic component with neutrals and electrons and a nonreacting impurity component, are derived from the main conservation laws. The linerarized and Fourier transformed equations are also given. The Quasi Analytical Method (QAM) for solving systems of nonlinear differential equations is used as a referrence. Equilibrium solutions and linearization are dealt with, in order to show how QAM is connected to previously used methods of linerarization and to establish linear dispersion relations. ESA

N93-11103# Stuttgart Univ. (Germany). Inst. fuer Plasmaforschung.

ANALYTICAL AND NUMERICAL PRINCIPLES FOR THE SCALING OF PLASMA FOCUS EXPERIMENTS, WITH REGARD TO ELECTRICAL RESISTANCE [ANALYTISCHE UND NUMERISCHE GRUNDLAGEN FUER DIE SKALIERUNG VON PLASMAFOKUSEXPERIMENTEN MIT BERUECKSICHTIGUNG DES ELEKTRISCHEN WIDERSTANDES]

Carlo Schiuma, H. J. Kaeppeler, and H. Herold Feb. 1991 124 p In GEORGIAN

(IPF-91-2; ETN-92-92152) Avail: CASI HC A06/MF A02

Analytical solutions for the circuit equation with finite resistance R not equal to zero in the run down phase, and with R equal to zero in the compression phase, are derived. An analytical scaling theory is established for maximum pinch currents under influence of finite resistance. The two dimensional three fluid magnetohydrodynamic code is extended to the determination of the resistance. Using a magnetohydrodynamic calculation, the conditions imposed on the model solutions, (constant axial velocity and constant resistance in the run down phase) are found to be acceptable. The analytically determined values for discharge current are compared with magnetohydrodynamic calculations and experiment. ESA

N93-11153# Lawrence Livermore National Lab., CA.

DEVELOPMENT OF A GEOMETRY-COMPENSATED NEUTRON TIME-OF-FLIGHT DETECTOR FOR ICF APPLICATIONS WITH APPROXIMATELY 200 ps TIME RESPONSE

T. J. Murphy and R. A. Lerche 11 May 1992 15 p Presented at the 9th Topical Conference on High-Temperature Plasma Diagnostics, Santa Fe, NM, 15-19 Mar. 1992

(Contract W-7405-eng-48)

(DE92-018024; UCRL-JC-109356; CONF-920362-39) Avail: CASI HC A03/MF A01

Current mode neutron time-of-flight detectors are used on Nova for neutron yield, ion temperature, and neutron emission time measurements. Currently used detectors are limited by the time response of the microchannel plate photomultiplier tubes (MCP-PMT's) used with the scintillators, scintillator decay time, scintillator thickness, and oscilloscope response time. A change in the geometry of the scintillator allows one to take advantage of the increased time resolution made possible by more advanced transient recorders and microchannel plate photomultiplier tubes. A prototype detector has been designed to incorporate these changes, and could potentially yield time resolution of less than 150 ps. Experimental results are presented demonstrating an ion temperature measurement of a direct-drive DT implosion on Nova. DOE

N93-11185 Wisconsin Univ., Madison.

A NEW PITCH ANGLE DIAGNOSTIC FOR ELECTRON CYCLOTRON RESONANCE PLASMA Ph.D. Thesis

Shu Wai Lam 1991 137 p

Avail: Univ. Microfilms Order No. DA9211624

In electron cyclotron resonance (ECR) plasma etching, it is important to know the ratio of the perpendicular to parallel ion energy because it determines the angle of incidence at the etching surface, which in turn determines the limit of the etch anisotropy. A novel instrument, a Pitch-Angle Diagnostic (PAD), which is capable of directly measuring T(sub i perpendicular)/E(sub z), the ratio of the perpendicular ion temperature to the parallel ion energy in a magnetized plasma, is described. The fact that the PAD results compared well at pressures above 1 mTorr with the LIF results obtained by the other investigators constituted a simple validation of this diagnostic. As the pressure is reduced from 4 to 1 mTorr, T(sub i perpendicular)/E(sub z) decreases monotonically. The increases of T(sub i perpendicular)/E(sub z) measured by PAD at pressures below 1 mTorr indicates the presence of an energy distribution with several components irrespective of the type of gases and the net input power. The ratio of T(sub i perpendicular)/E(sub z) always decreases with the increase of power. The choice of the radial boundary surface in the source chamber is shown to play an important role in the determination of T(sub i perpendicular)/E(sub z) in the downstream chamber. A distinct decrease in T(sub i perpendicular)/E (sub z) in the downstream region was observed when the inner wall of the source chamber was covered by an insulating anodized aluminum liner. Throttling the system while maintaining the same pressure has a negligible effect on the ratio of T(sub i perpendicular)/E(sub z). Only the pressure of the system, the net input microwave power, and the boundary of the system matter. The ratio of T(sub i perpendicular)/E(sub z) always decreases towards the chamber wall. Dissert. Abstr.

N93-11191 California Univ., Los Angeles.

TOPICS IN HIGH-INTENSITY LASER PLASMA INTERACTION Ph.D. Thesis

Wim Pieter Leemans 1991 153 p

Avail: Univ. Microfilms Order No. DA9205964

The interaction of high intensity laser pulses with pre-formed and laser-produced plasmas is studied. Through experiments and simulations we have investigated stimulated Compton scattering in preformed plasmas and the plasma physics aspects of tunnel-ionized gases. A theoretical study is presented on the nonlinear dynamics of relativistic plasma waves driven by colinear optical mixing. The electron density-fluctuation spectra induced by stimulated Compton scattering have been directly observed for the first time. A CO2 laser was focused into pre-formed plasmas with densities n(e) varied from 0.4-6 x 10(exp 16) cu cm. The fluctuations corresponding to backscatter were probed using Thomson scattering. At low n(e), the scattered spectra peak at a frequency shift Delta omega is approximately kv(sub e) and appears to be in a linear regime. At the highest n(e), a nonlinear saturation of the SCS instability is observed due to a self-induced perturbation of the electron distribution function. Tunnel-ionized plasmas have been studied through experiments and particle simulations. Experimentally, qualitative evidence for plasma temperature control by varying the laser polarization was obtained by the measurement of stimulated Compton scattering fluctuation spectra and x-ray emission from such plasmas. A higher parallel temperature than expected from the single-particle tunneling model was observed. Simulations indicate that stochastic heating and the Weibel instability play an important role in plasma heating in all directions and isotropization. The non-linear dynamics associated with beatwave (Delta omega, Delta k) excited long wavelength plasma waves in the presence of strong, short wavelength density ripple have been examined, using the relativistic Lagrangian oscillator model. This model shows period doubling that roughly follows Feigenbaum scaling, and a transition to chaos. However, wavebreaking is found to occur after the first bifurcation, thereby limiting the applicability of the Lagrangian model. It is found that the origin of this bifurcation is linked to the stability of an equivalent Mathieu equation to 1/2 subharmonic resonances. Finally, a PIC-code simulation shows spatial wavenumber peaks displaced (Delta k)/2 on both sides of the driver frequencies, giving support to the idea that the bifurcation behavior may be experimentally observable. Dissert. Abstr.

N93-11201# Stuttgart Univ. (Germany). Inst. fuer Plasmaforschung.

CONTRIBUTIONS TO PLASMA FOCUS PHYSICS SINCE 1970 FROM THE INSTITUTE OF PLASMA RESEARCH, STUTTGART (FED. REPUBLIC OF GERMANY) [BEITRAEGE ZUR PHYSIK DES PLASMAFOKUS AUS DEM IPF STUTTGART SEIT 1970]

H. J. Kaeppeler Mar. 1991 37 p In GEORGIAN Presented at the Festkolloquium, Stuttgart, Fed. Republic of Germany, 26 Mar. 1991

(IPF-91-4; ETN-92-92154) Avail: CASI HC A03/MF A01

Works on the physics of dense plasma focus are summarized.

Various short time diagnostic methods are developed and applied to the determination of plasma parameters in the plasma focus experiment: time resolved neutron spectroscopy, shadowgraphy, Mach Zehnder interferometry, holographic interferometry, and Thomson spectrometry. Overall, dynamical phenomena of the plasma focus are well understood. The phenomena during breakdown, spoke formation, electrode phenomena, filamentation in the pinch phase, and saturation of neutron production are shown to need clarification. ESA

N93-11245# Utrecht State Univ. (Netherlands).
ION TEMPERATURE MEASUREMENTS IN TOKAMAK PLASMAS BY RUTHERFORD SCATTERING Ph.D. Thesis
A. A. E. vanBlokland 9 Oct. 1991 166 p Sponsored in part by Stichting voor Fundamenteel Onderzoek der Materie, Utrecht (Netherlands), Nederlandse Organisatie voor Wetenschappelijk Onderzoek, The Hague, and Euratom, Brussels (Belgium)
(PB92-184738) Avail: CASI HC A08/MF A02

The contents are as follows: Small angle Rutherford scattering theory; Atomic physics aspects; Experimental set-up of the Rutherford scattering system; Measurements with the Rutherford scattering diagnostic at TEXTOR; and ion heat conduction in ohmic plasmas at TEXTOR. GRA

N93-11275# Naval Research Lab., Washington, DC.
PROCEEDINGS OF THE 14TH INTERNATIONAL CONFERENCE ON THE NUMERICAL SIMULATION OF PLASMAS
1991 83 p Conference held in Annapolis, MD, 3-6 Sep. 1991
(AD-A249095) Avail: CASI HC A05/MF A01

Partial Contents are as follows: Numerical Simulations of the Vlasov-Maxwell Equations by Coupled Particle-Finite Element Methods on Unstructured Meshes; Electromagnetic PIC Simulations Using Finite Elements on Unstructured Grids; Modelling Travelling Wave Output Structures with the Particle-in-Cell Code CONDOR; SST--A Single-Slice Particle Simulation Code; Graphical Display and Animation of Data Produced by Electromagnetic, Particle-in-Cell Codes; A Post-Processor for the PEST Code; Gray Scale Rendering of Beam Profile Data; A 2D Electromagnetic PIC Code for Distributed Memory Parallel Computers; 3-D Electromagnetic PIC Simulation on the NRL Connection Machine; Plasma PIC Simulations on MIMD Computers; Vlasov-Maxwell Algorithm for Electromagnetic Plasma Simulation on Distributed Architectures; MHD Boundary Layer Calculation Using the Vortex Method; and Eulerian Codes for Plasma Simulations. GRA

N93-11277# National Inst. for Fusion Science, Nagoya (Japan).
SHAFRANOV SHIFT IN LOW-ASPECT-RATIO HELIOTRON/TORSATRON CHS
H. Yamada, K. Ida, and H. Iguchi Sep. 1991 32 p
(DE92-782100; NIFS-110) Avail: CASI HC A03/MF A01

The MHD equilibrium properties of neutral-beam-heated plasmas have been experimentally investigated in the Compact Helical System (CHS), a low-aspect-ratio (A(sub p) approx. 5) heliotron/torsatron. This configuration is characterized by a strong breaking of helical symmetry. The radial profiles measured by various diagnostics have shown significant Shafranov shift due to plasma pressure. The deviation of the magnetic axis from its vacuum position has reached 50 percent of the minor radius. When the three-dimensional equilibrium code VMEC is used to reconstruct the equilibrium from the experimental data, the result is in good agreement with the experimentally observed Shafranov shift as well as the diamagnetic pressure in plasmas with beta less than or equal to 1.2 percent and beta(sub 0) less than or equal to 3.3 percent. This beta value corresponds to half of the conventional equilibrium beta limit defined by the Shafranov shift reaching a value of half the minor radius. Although tangential neutral beam injection has caused pressure anisotropies (p parallel)/(p perpendicular) less than or equal to 3, the description of the equilibrium assuming isotropic pressure is consistent with the experiment. DOE

N93-11382# General Atomic Co., San Diego, CA.
THERMAL ANALYSIS AND DESIGN OF POLARIZER MIRRORS FOR WAVEGUIDES IN THE D3-D TOKAMAK
C. B. Baxi, J. L. Doane, and D. L. Sevier Jul. 1992 9 p Presented at the SPIE International Symposium on Optical Applied Science and Engineering, San Diego, CA, 19-24 Jul. 1992
(Contract DE-AC03-89ER-51114)
(DE92-018884; GA-A-20972; CONF-920792-21) Avail: CASI HC A02/MF A01

A new high power electron cyclotron heating (ECH) system designed to operate at 110 GHz with a power output of 2 MW has been introduced on DIII-D. All components of the system are capable of handling a 10 second pulse at an interval of 10 minutes. Transmission of ECH power from the the source (a millimeter-wave gyrotron) to the plasma through waveguide miter bends may change the polarization and rotate the polarization major axis. Polarizing elements are therefore required to correct for the effect of transmission lines and also to generate proper polarization for coupling into the plasma. Rotating mirrors with different rectangular grooved gratings in two successive miter bends can generate the required wide range of elliptical polarizations. Peak heat fluxes due to ohmic losses in these mirrors are several MW/m(sup 2) for a 0.5 MW gyrotron power. The complex distribution of losses in the grooves requires a detailed thermal stress analysis to ensure that temperature and stress limits are not exceeded. The desired pulse length is 10 sec, with a cooling time of 10 min between pulses. The temperature rise in the polarizing mirrors must be limited to less than 300 C to prevent thermal fatigue and outgassing in the vacuum lines. This paper presents an analysis for the polarizing mirrors for the DIII-D ECH system. DOE

N93-11495# Lawrence Livermore National Lab., CA.
HIGH ENERGY X RAY IMAGING DIAGNOSTIC ON NOVA
B. A. Hammel, O. L. Landen, B. A. Remington, and R. A. Pasha 11 May 1992 14 p Presented at the 9th Topical Conference on High-Temperature Plasma Diagnostics, Santa Fe, NM, 15-19 Mar. 1992
(Contract W-7405-eng-48)
(DE92-018067; UCRL-JC-109473; CONF-920362-38) Avail: CASI HC A03/MF A01

We have developed a diagnostic suitable for high photon energy (approximately 7 kev) time resolved one dimensional x-ray imaging on Nova. This diagnostic uses a 15 micron wide, 750 micron long imaging slit mounted on a 20X magnification snout which is coupled to an x-ray streak camera of variable streak speed. This diagnostic fits into retractable manipulators on the 10-beam chamber at Nova. In situ backlit grid experiments using a large-area backlighter give a spatial resolution FWHM of about 17 micron with high brightness. DOE

N93-11516# Lawrence Livermore National Lab., CA.
THREE DIMENSIONAL AND 2D SIMULATION OF AN EXPANDING PLASMA USING A DARWIN HYBRID PARTICLE CODE
D. E. Shumaker, D. V. Anderson, and G. F. Simonson 2 Mar. 1992 50 p
(Contract W-7405-eng-48)
(DE92-019095; UCRL-ID-109852) Avail: CASI HC A03/MF A01

We present some initial results using our 3D hybrid particle code, QN3D, to simulate the expansion of a high energy plasma into a lower density plasma. These simulations give good agreement with expected properties of the diamagnetic void produced by the high energy ions. In order to study the longer time behavior of this system, we use a 2D version of the same code. In these 2D simulations we observe the formation of fluted plasma boundary which occurs during the collapse of the plasma. DOE

N93-11534# Lawrence Livermore National Lab., CA.
NOVA UPGRADE: A PROPOSED ICF FACILITY TO DEMONSTRATE IGNITION AND GAIN, REVISION 1
Jul. 1992 19 p

(Contract W-7405-eng-48)
(DE92-018960; UCRL-LR-106736-Rev-1) Avail: CASI HC A03/MF A01

The present objective of the national Inertial Confinement Fusion (ICF) Program is to determine the scientific feasibility of compressing and heating a small mass of mixed deuterium and tritium (DT) to conditions at which fusion occurs and significant energy is released. The potential applications of ICF will be determined by the resulting fusion energy yield (amount of energy produced) and gain (ratio of energy released to energy required to heat and compress the DT fuel). Important defense and civilian applications, including weapons physics, weapons effects simulation, and ultimately the generation of electric power will become possible if yields of 100 to 1,000 MJ and gains exceeding approximately 50 can be achieved. Once ignition and propagating burn producing modest gain (2 to 10) at moderate drive energy (1 to 2 MJ) has been achieved, the extension to high gain (greater than 50) is straightforward. Therefore, the demonstration of ignition and modest gain is the final step in establishing the scientific feasibility of ICF. Lawrence Livermore National Laboratory (LLNL) proposes the Nova Upgrade Facility to achieve this demonstration by the end of the decade. This facility would be constructed within the existing Nova building at LLNL for a total cost of approximately $400 M over the proposed FY 1995-1999 construction period. This report discusses this facility. DOE

N93-11565# California Univ., Berkeley. Electronics Research Lab.
SELF-GENERATED STOCHASTIC HEATING IN AN RF DISCHARGE
A. Lichtenberg 1992 10 p
(Contract DE-FG03-87ER-13727)
(DE92-018558; DOE/ER-13727/T2) Avail: CASI HC A02/MF A01

We have studied the nonlinear dynamics of stochastic heating arising from the reflection of electrons from moving sheaths as an underlying mechanism for electron power deposition in RF discharges. We examined the dynamics of the electron collision with the sheaths in the regime in which the sheath motion is small compared to the average electron velocity to derive a mop that describes the electron motion. We have shown that for a high frequency, (omega/2(pi) approximately = 50MHz), the electrons will strike the moving wall with random phase. At low pressures, this stochasticity is an intrinsic property of the dynamics. The stochastic electron heating leads to a power law electron distribution. The stochastic heating was determined in both the slow sheath and fast sheath velocity regimes assuming an incident Maxwellian distribution. DOE

N93-11568# Columbia Univ., New York, NY.
HIGH BETA AND CONFINEMENT STUDIES ON TFTR
G. A. Navratil, A. Bhattacharjee, R. Iacono, M. E. Mauel, S. A. Sabbagh, and J. Kesner (Massachusetts Inst. of Tech., Cambridge.) 1992 55 p
(Contract DE-FG02-89ER-53297)
(DE92-018647; DOE/ER-53297/4) Avail: CASI HC A04/MF A01

A new regime of high poloidal beta operation in TFTR was developed in the course of the first two years of this project (9/25/89 to 9/24/91). Our proposal to continue this successful collaboration between Columbia University and the Massachusetts Institute of Technology with the Princeton Plasma Physics Laboratory for a three year period (9/25/91 to 9/24/94) to investigate improved confinement and tokamak performance in high poloidal beta plasmas in TFTR through the DT phase of operation was approved by the DOE. This is a report of our progress during the first 9 month budget period of the three year grant (9/25/91 to 6/24/92). During the approved three year project period we plan to (1) extend and apply the low current, high QDD discharges to the operation of TFTR using Deuterium and Tritium plasma; (2) continue the analysis and plan experiments on high poloidal beta phenomena in TFTR including stability properties, enhanced global confinement, local transport, bootstrap current, and divertor formation; (3) design and carry out experiments on TFTR which attempt to elevate the central q to values greater than 2 where entry to the second stability regime is predicted to occur; and (4) collaborate on high beta experiments using bean-shaped plasmas with a stabilizing conducting shell in PBX-M. In the seven month period covered by this report, we havemade progress in each of these four areas through the submission of 4 TFTR Experimental Proposals and the partial execution of 3 of these using a total of 4.5 run days during the August 1991 to February 1992 run. DOE

N93-11645# Lawrence Livermore National Lab., CA.
HIGH BANDWIDTH SECOND-HARMONIC GENERATION IN PARTIALLY DEUTERATED KDP
M. S. Webb, D. Eimerl, and S. P. Velsko 30 Jan. 1992 18 p
Presented at the Soc. of Photo-Optical Instrumentation Engineers' International Symposium on Laser Spectroscopy as part of SPIE's Symposium on Optics, Electro-Optics and Laser Applications in Science and Engineering, Los Angeles, CA, 19-25 Jan. 1992
(Contract W-7405-eng-48)
(DE92-019505; UCRL-JC-109555; CONF-920124-26) Avail: CASI HC A03/MF A01

We have experimentally determined the spectrally noncritical phasematching behavior of type 1 frequency doubling in KDP and its dependence on deuteration level in partially deuterated KDP. The first order wavelength sensitivity parameter, the partial derivative of delta k/partial derivative of gamma, for type 1 doubling of 1.053 micron light vanishes for a KD*P crystal with a deuteration level between 10 and 14 percent. Very high bandwidth frequency doubling of Nd:glass lasers is possible with such a crystal. DOE

N93-11660# General Atomic Co., San Diego, CA.
FUSION PROGRAMS IN APPLIED PLASMA PHYSICS
Jul. 1992 12 p
(Contract DE-AC03-89ER-53277)
(DE92-019639; GA-A-21007) Avail: CASI HC A03/MF A01

The Applied Plasma Physics (APP) program at General Atomics (GA) described here includes four major elements: (1) Applied Plasma Physics Theory Program, (2) Alpha Particle Diagnostic, (3) Edge and Current Density Diagnostic, and (4) Fusion User Service Center (USC). The objective of the APP theoretical plasma physics research at GA is to support the DIII-D and other tokamak experiments and to significantly advance our ability to design a commercially-attractive fusion reactor. We categorize our efforts in three areas: magnetohydrodynamic (MHD) equilibria and stability; plasma transport with emphasis on H-mode, divertor, and boundary physics; and radio frequency (RF). The objective of the APP alpha particle diagnostic is to develop diagnostics of fast confined alpha particles using the interactions with the ablation cloud surrounding injected pellets and to develop diagnostic systems for reacting and ignited plasmas. The objective of the APP edge and current density diagnostic is to first develop a lithium beam diagnostic system for edge fluctuation studies on the Texas Experimental Tokamak (TEXT). The objective of the Fusion USC is to continue to provide maintenance and programming support to computer users in the GA fusion community. The detailed progress of each separate program covered in this report period is described. DOE

N93-11674# Sandia National Labs., Albuquerque, NM.
HEAT LOAD MATERIAL STUDIES: SIMULATED TOKAMAK DISRUPTIONS
J. M. Gahl (New Mexico Univ., Albuquerque.), J. M. McDonald, A. Zakharov (Academy of Sciences, USSR, Moscow), and S. Tserevitinov (Kurchatov, I. V. Inst. of Atomic Energy, Moscow, USSR) 1991 19 p Presented at the International Conference on Fusion Reactor Materials, Clearwater, FL, 17-22 Nov. 1991
(Contract DE-AC04-76DP-00789)
(DE92-018275; SAND-91-1613C; CONF-911111-41) Avail: CASI HC A03/MF A01

It is clear that an improved understanding of the effects of tokamak disruptions on plasma facing component materials is needed for the ITER program. Very large energy fluxes are predicted to be deposited in ITER and could be very damaging to the machine. During 1991, Sandia National Laboratories and the University of New Mexico conducted cooperative tokamak disruption simulation experiments at several Soviet facilities. These facilities were located at the Efremov Institute in Leningrad, the Kurchatov Atomic Energy Institute (Troisk and Moscow) and the Institute for Physical Chemistry of the Soviet Adademy of Sciences in Moscow. Erosion of graphite from plasma stream impact is seen to be much less than that observed with laser or electron beams with similar energy fluxes. This, along with other data obtained, seem to suggest that the 'vapor shielding' effect is a very important phenomenon in the study of graphite erosion during tokamak disruption. DOE

N93-11694# Sandia National Labs., Albuquerque, NM.
RESULTS FROM THE US/USSR EXCHANGE FOR HEAT LOAD MATERIAL STUDIES OF SIMULATED TOKAMAK DISRUPTIONS
J. M. Gahl (New Mexico Univ., Albuquerque.), J. F. Crawford (New Mexico Univ., Albuquerque.), J. M. McDonald, R. T. McGrath, and A. Zakharov (Academy of Sciences, USSR, Moscow) 1992 13 p Presented at the 10th International Conference on Plasma-Surface Interactions in Controlled Fusion Devices, Monterey, CA, 30 Mar. - 3 Apr. 1992
(Contract DE-AC04-76DP-00789)
(DE92-018285; SAND-92-0797C; CONF-920311-22) Avail: CASI HC A03/MF A01

This paper presents recent results from exchange I.2 of the US/USSR Exchange Program of Cooperation for Magnetic Confinement Fusion. Previous results from this exchange demonstrated much lower than expected ablation of graphites when the graphites were exposed to disruption like heat fluxes delivered by plasma gun sources. This lower than expected ablation has been accounted for by the 'vapor shielding' effect. Vapor shielding occurs when material is ablated from the surface of the graphite target early in the plasma pulse. This ablated material then shields the surface of the target from the rest of the incoming plasma pulse. Vapor shielding has been inferred from diagnostics and ablation data at all participating laboratories, and clear evidence of the effect has been found by laser interferometry at Kurchatov (Troitsk) in the 2MK-200 machine. Recent results from Kurchatov on the 2MK-200 and MKT experiments continue to indicate that the erosion of graphite exposed to disruption like heat fluxes is much lower than expected. Work from the University of New Mexico on the PLAIDS experiment confirms earlier important work conducted on the VIKA experiment at Efremov. This is particularly interesting in that PLAIDS and VIA have very similar plasma pulse characteristics. DOE

N93-11729# Science Applications International Corp., San Diego, CA.
NONLINEAR EFFECTS OF ICRF POWER ON DRIFT WAVE STABILITY AND TRANSPORT IN TOKAMAKS, TASK 1
J. B. McBride Jul. 1992 36 p
(Contract DE-AC03-88ER-53270)
(DE92-018488; DOE/ER-53270/T2; SAIC-92/1160) Avail: CASI HC A03/MF A01

In a previous report we summarized the results obtained for Task 1 of Contract Number AC03-88ER53270 for the two-year period of performance of the work supported by the contract. That report constituted the final report for Task 1. Since then, the contract was extended and the funding for Task 1 was incremented with $35 K of new funds. The purpose for incrementing the contract was to begin a collaboration with the PBX-M group at Princeton Plasma Physics Laboratory (PPPL) in the area of ion Bernstein wave (IBW) effects in the PBX-M experiment. This report summarizes the initial results of that collaboration obtained under the incremental continuation funding. In the intervening period, experimental and theoretical program directions changed so that no further funds were committed to Task 1. DOE

N93-11730# California Univ., Davis.
DEVELOPMENT OF A NEW PLASMA DIAGNOSTIC OF THE CRITICAL SURFACE AND STUDIES OF THE ION ACOUSTIC DECAY INSTABILITY USING COLLECTIVE THOMSON SCATTERING
K. Mizuno, J. S. DeGroot, and W. Seka (Rochester Univ., NY.) 1991 30 p
(Contract DE-FG03-91SF-18861)
(DE92-018508; DOE/SF-18861/T1) Avail: CASI HC A03/MF A01

We have developed 5-channel collective Thomson scattering system to measure the ion acoustic wave excited by the ion acoustic wave decay instabilities. The multichannel collective Thomson scattering technique was established with 4 omega probe laser beam using GDL laser system at LLE, Univ. of Rochester. We have obtained the ionic charge state Z by measuring the second harmonic emission from the ion acoustic decay instability. The LASNEX computer simulation calculations have been carried out. The experimental results agree very well with the LASNEX computer simulation results with the flux number $f = 0.1$. In high power laser regime, the spectrum become broad, and the alpha-gamma decreases indicating that the turbulent like spectrum is observed. In order to understand the experimental results, we have developed a theory to study absorption of laser and heat transport. This new theory includes the temporal evolution of the heat conduction region. The results agree with flux-limited hydrodynamic simulations. DOE

N93-11731# California Univ., Davis.
DEVELOPMENT OF A NEW PLASMA DIAGNOSTIC OF THE CRITICAL SURFACE AND STUDIES OF THE ION ACOUSTIC DECAY INSTABILITY USING COLLECTIVE THOMSON SCATTERING
K. Mizuno, J. S. DeGroot, W. Seka (Rochester Univ., NY.), and R. P. Drake (Lawrence Livermore National Lab., CA.) 1992 30 p
(Contract DE-FG03-91SF-18861)
(DE92-018526; DOE/SF-18861/T2) Avail: CASI HC A03/MF A01

We have developed 5-channel collective Thomson scattering system to measure the ion acoustic wave excited by the ion acoustic wave decay instabilities. The multichannel collective Thomson scattering technique was established with 4 omega probe laser beam using GDL laser system at LLE, Univ. of Rochester. We have obtained the ionic charge state Z by measuring the second harmonic emission from the ion acoustic decay instability. The LASNEX computer simulation calculations have been carried out. The experimental results agree very well with the LASNEX computer simulation results with the flux number $f = 0.l$. In high power laser regime, the spectrum become broad, and the Delta-gamma decreases indicating that the turbulent like spectrum is observed. In order to understand the experimental results, we have developed a theory to study absorption of laser and heat transport. This new theory includes the temporal evolution of the heat conduction region. The results agree with flux-limited hydrodynamic simulations. DOE

N93-11745# Texas Univ., Austin. Inst. for Fusion Studies.
NONLINEAR EVOLUTION OF RESISTIVE TEARING MODE INSTABILITY WITH SHEAR FLOW AND VISCOSITY
L. Ofman, P. J. Morrison, and R. S. Steinolfson (Southwest Research Inst., San Antonio, TX.) Dec. 1991 41 p
(Contract DE-FG05-80ET-53088)
(DE92-012138; DOE/ET-53088/530; IFSR-530) Avail: CASI HC A03/MF A01

The nonlinear evolution of the tearing mode instability with equilibrium shear flow is investigated via numerical solutions of the resistive magnetohydrodynamic equations. The two-dimensional simulations are in slab geometry, are periodic in the x-direction, and are initiated with solutions of the linearized MHD equations. The magnetic Reynolds number S was varied from 10(sup 2) to 10(sup 5), a parameter V that measures the strength of the flow in units of the average Alfven speed was varied, and the viscosity as measured by the Reynolds number of S(sub nu) satisfied S(sub nu) greater than 10(sup 3). When the shear flow is small (V less than 0.3) the tearing mode saturates within one resistive time, while for larger flows the nonlinear saturation develops on a longer time scale. The two-dimensional spatial structure of both the flux function and the steam function distort in the direction of the equilibrium flow. The magnetic energy release decreased and the saturation time increased with V, for both small and large resistivity. The validity of the numerical solutions was tested by verifying that the total energy and the magnetic helicity were conserved. Total energy dissipation rate dE/dt decreases as the tearing mode approached its saturated state. DOE

N93-11826# Mississippi State Univ., Mississippi State.
POTASSIUM D-LINE FITTING FOR INVESTIGATION OF MHD BOUNDARY LAYERS
L. E. Bauman 1992 8 p Presented at the 23rd AIAA Plasma Dynamics and Lasers Conference, Nashville, TN, 6-8 Jul. 1992
(Contract DE-AC02-80ET-15601)
(DE92-019020; CONF-9207111-2) Avail: CASI HC A02/MF A01

Vitally important for accurate heat transfer and conductivity models is knowledge of the profiles of temperature and seed atom density in the thermal boundary layers of the flow. Recent work by Vasileva, et al. applied a technique to the potassium emission from the U25BM facility, comparing model calculations of temperature profiles to an inverse solution for potassium D-line emission on the U25BM facility. The character of their solution differed from that for a model turbulent boundary layer, which they suggested may be explained by a non-axisymmetric flow structure. With the availability of potassium D-line spectra from many tests on the component Development and Integration Facility (CDIF) and the Coal fired Flow Facility (CFFF), an effort was begun to solve for the seed atom density profile as well as the temperature profile at the measurement points in these facilities. The preliminary results are reported here. DOE

N93-11834# National Inst. for Fusion Science, Nagoya (Japan).
FAST COOLING PHENOMENA WITH ICE PELLET INJECTION IN THE JIPP T-IIU TOKAMAK
M. Sakamoto, K. N. Sato, and Y. Ogawa Oct. 1991 32 p
(DE92-782105; NIFS-116) Avail: CASI HC A03/MF A01

Ice pellet injection experiments were carried out in the JIPP T-IIU tokamak in order to study thermal (cooling) transport just after injection. The cut-off problem of electron cyclotron emission (ECE) signals due to the rise in density has been resolved by careful measurements of temperature profile at a high time resolution (Delta t = 2ms) during its decay phase. The phenomenon of ultra-fast cooling (so-called pre-cooling) has been identified using the two different methods of ECE and soft X-ray (SXR) measurements. In the outer region (r greater than r(sub inv)) of the plasma the cooling propagation velocity is comparable to or slightly greater than the pellet velocity, while in the central region (r less than r(sub inv)) the propagation velocity is significantly greater than the pellet velocity. Ice pellet were injected into various kinds of JIPP T-IIU plasmas, the current and sawtooth phase of which had different values, including a no-sawtooth plasma. The existence of the sawtooth oscillation and arrival of a pellet near the inversion radius r(sub inv) of the sawtooth oscillations have turned out to be necessary conditions for the pre-cooling, and even just after the sawtooth crash the pre-cooling may start around the q = 1 surface, not at the plasma center. Simultaneous measurements of electron temperature and density profiles indicate that the central temperature always decreases before the central density increases. Some anomalous transport might be induced by pellet injection at the central region. DOE

N93-12059# Lawrence Livermore National Lab., CA.
A RING CODED-APERTURE MICROSCOPE FOR HIGH-RESOLUTION IMAGING OF HIGH-ENERGY X RAYS
D. Ress, D. R. Ciarlo, J. E. Stewart, P. M. Bell, and D. R. Kania 11 May 1992 15 p Presented at the 9th Topical Conference on High-Temperature Plasma Diagnostics, Santa Fe, NM, 15-19 Mar. 1992
(Contract W-7405-eng-48)
(DE92-018004; UCRL-JC-109368; CONF-920362-37) Avail: CASI HC A03/MF A01

We use annular apertures to produce coded images of inertialconfinement fusion targets. The images are formed with 4-9 keV x rays; they are unfolded to obtain high-quality estimates of the source spatial distribution. Excellent time-integrated images have been obtained using x-ray film as a detector, and we are working to obtain time-resolved images using a gated microchannel-plate x-ray detector. Preliminary resolution-grid experiments show that the spatial resolution is less than or = 5 microns, and further experiments are planned to confirm a predicted resolution of less than or = 3 microns. We discuss the apertures, x-ray detectors, and image-processing software that forms this novel x-ray microscope. DOE

N93-12060# Lawrence Livermore National Lab., CA.
PLASMA TEMPERATURES FROM FIRST-HIT NEUTRON TIME-OF-FLIGHT SPECTRA
R. A. Lerche, S. P. Hatchett, M. D. Cable, M. B. Nelson, and T. J. Murphy 11 May 1992 16 p Presented at the 9th Topical Conference on High-Temperature Plasma Diagnostics, Santa Fe, NM, 15-19 Mar. 1992
(Contract W-7405-eng-48)
(DE92-018006; UCRL-JC-109357; CONF-920362-35) Avail: CASI HC A03/MF A01

We describe a new technique for determining an ICF plasma temperature from a neutron time-of-flight spectrum recorded with a multi-element detector array -- even when each array element becomes fully saturated. A temperature uncertainty less than 20 percent is achieved over a yield range greater than 10,000 using a 960-element array. Analysis of a spectrum formed by the first detected neutron (first hit) in each array element is used to determine the full spectrum's temporal width. Temperatures for deuterium filled capsules have been determined from spectra recorded with the 20-meter, 960-element LaNSA detector. A temperature of 0.88 +/- 0.09 keV was determined for a capsule producing only 1.4 x 10(exp 6) neutrons. Temperatures determined for capsules yielding more than 2 x 10(exp 9) neutrons are consistent with those determined with a 20-meter current-mode time-of-flight detector. DOE

N93-12066# EG and G Energy Measurements, Inc., Idaho Falls.
COMPREHENSIVE COMPUTATIONAL MODEL FOR THERMAL PLASMA PROCESSING
C. H. Chang 1992 8 p Presented at the 10th Symposium on Energy Engineerning Sciences, Argonne, IL, 11-13 May 1992
(Contract DE-AC07-76ID-01570)
(DE92-018015; EGG-M-92264; CONF-9205147-2) Avail: CASI HC A02/MF A01

A new numerical model is described for simulating thermal plasmas containing entrained particles, with emphasis on plasma spraying applications. The plasma is represented as a continuum multicomponent chemically reacting ideal gas, while the particles are tracked as discrete Lagrangian entities coupled to the plasma. The overall computational model is embodied in a new computer code called LAVA. Computational results are presented from a transient simulation of alumina spraying in a turbulent argon-helium plasma jet in air environment, including torch geometry, substrate, and multiple species with chemical reactions. Plasma-particle interactions including turbulent dispersion have been modeled in a fully self-consistent manner. DOE

N93-12087# Mississippi State Univ., Mississippi State. Diagnostic Instrumentation and Analysis Lab.
OVERVIEW OF RECENT DIAGNOSTIC MEASUREMENTS AT THE USA MHD FACILITIES
R. L. Cook, R. D. Benton, W. S. Shepard, J. S. Lindner, O. P. Norton, W. W. Wilson, L. E. Bauman, J. P. Singh, F. Y. Yueh, and D. L. Monts et al 1992 12 p Presented at the 11th International Conference on Magnetohydrodynamics (MHD) Electrical Power Generation, Beijing (China), 12-16 Oct. 1992

(Contract DE-AC02-80ET-15601)
(DE92-015365; CONF-921038-2) Avail: CASI HC A03/MF A01

The DOE development program for MHD is a multiyear program employing two major test facilities and having as a goal the demonstration of the practicality and commercial viability of MHD for electric power generation. This method of direct energy conversion will use our vast coal resources to generate electricity at highly attractive efficiencies in an environmentally acceptable manner. As part of this program, the Diagnostic Instrumentation and Analysis Laboratory (DIAL) at Mississippi State University is developing and applying advanced optical diagnostic measurement techniques and instrumentation systems to provide nonintrusive, remote, real-time measurements on large-scale MHD facilities. The main program objectives of DIAL are to: (1) Develop and apply spectroscopic diagnostic techniques for flow-field measurements. (2) Help characterize and evaluate various gas stream components of an MHD power plant. (3) Provide field measurements for support of MHD engineering development test facilities. (4) Provide necessary data to validate and further develop relevant analytical models. (5) Evaluate optical systems for application as performance monitors and control instruments. DOE

N93-12092# EG and G Energy Measurements, Inc., Idaho Falls.
NUMERICAL SIMULATION OF ALUMINA SPRAYING IN ARGON-HELIUM PLASMA JET
C. H. Chang 1992 7 p Presented at the 1992 International Thermal Spray Conference, Orlando, FL, 1-5 Jun. 1992
(Contract DE-AC07-76ID-01570)
(DE92-017859; EGG-M-91307; CONF-9206135-3) Avail: CASI HC A02/MF A01

A numerical model is described for simulating thermal plasmas containing entrained particles, with emphasis on plasma spraying applications. The plasma is represented as a continuum multicomponent chemically reacting ideal gas, while the particles are tracked as discrete Lagrangian entities coupled to the plasma. Computational results are presented from a transient simulation of alumina spraying in a turbulent argon-helium plasma jet in air environment, including torch geometry, substrate, and multiple species with chemical reactions. Particle-plasma interactions including turbulent dispersion have been modeled in a fully self-consistent manner. Interactions between the plasma and the torch and substrate walls are modeled using wall functions. DOE

N93-12139# Tennessee Univ., Tullahoma. Space Inst.
TRANSIENT PHENOMENA IN MHD EXPERIMENTS
B. C. Winkleman and J. T. Lineberry 1992 8 p Presented at the 11th International Conference on Magnetohydrodynamics (MHD) Electrical Power Generation, Beijing (China), 12-16 Oct. 1992
(Contract DE-AC02-79ET-10815)
(DE92-014496; DOE/ET-10815/192; CONF-921038-1) Avail: CASI HC A02/MF A01

Wideband data from combustion driven MHD experiments are presented and discussed. These data were acquired in past research conducted on several MHD test trains of varying size and interaction. The signal characteristics of the high frequency data are reviewed and notable couplings between the plasmadynamics and electrical output are derived. Observations from these analyses that are of interest to MHD power and MHD system design are noted. The importance of wideband data and its analysis for a more complete interpretation of the MHD process is emphasized. DOE

N93-12141# Mississippi State Univ., Mississippi State. Diagnostic Instrumentation and Analysis Lab.
THE ROLE OF ADVANCED OPTICAL DIAGNOSTICS IN MONITORING AND CONTROLLING AN MHD POWER PLANT. PART 2: 50 MW(t), POC TOPPING CYCLE
R. A. Kumar and R. L. Cook 1992 12 p Presented at the 11th International Conference on Magnetohydrodynamics (MHD) Electrical Power Generation, Beijing (China), 12-16 Oct. 1992
(Contract DE-AC02-80ET-15601)
(DE92-015368; CONF-921038-3-Pt-2) Avail: CASI HC A03/MF A01

To properly characterize and control a complex MHD power conversion system, the direct measurement of various gas stream performance parameters is required. Model calculations have been carried out for the expected variation of various performance parameters that can be tracked using nonintrusive optical diagnostic techniques. Appropriate measurement systems are summarized and some control strategies are discussed. This latter discussion can form the basis for the integration of standard measurement parameters with the gas stream performance/control parameters to optimize the performance and safety of an MHD power plant. DOE

N93-12188# New York Univ., New York. Magneto-Fluid Dynamics Div.
PLASMA PROPERTIES Annual Report, 1 Jan. - 31 Dec. 1991
Harold Weitzner Jun. 1992 47 p
(Contract DE-FG02-86ER-53223)
(DE92-018635; DOE/ER-53223/178) Avail: CASI HC A03/MF A01

The Magneto-Fluid Dynamics Division works on a wide range of problems originating in plasma physics, with the primary focus being on problems from magnetic fusion plasma physics. This report discusses the following topics: MHD equilibrium and stability; MHD transport; statistical analysis; edge physics studies; wave propagation; basic plasma physics; and space plasma physics. DOE

N93-12307# General Atomic Co., San Diego, CA.
HELIUM TRANSPORT STUDIES ON D3-D
D. F. Finkenthal (California Univ., Berkeley.), D. L. Hillis (Oak Ridge National Lab., TN.), M. R. Wade (Oak Ridge National Lab., TN.), J. T. Hogan (Oak Ridge National Lab., TN.), C. C. Klepper (Oak Ridge National Lab., TN.), P. K. Mioduszewski (Oak Ridge National Lab., TN.), W. P. West, K. H. Burrell, and R. P. Seraydarian May 1992 4 p Presented at the 14th International Conference on Plasma and 19th EPS Conference on Controlled Fusion and Plasma Physics, Innsbruck (Austria), 29 Jun. - 3 Jul. 1992
(Contracts DE-AC03-89ER-51114; DE-FG03-89ER-51116)
(DE92-016251; GA-A-20933; CONF-920610-9) Avail: CASI HC A01/MF A01

The measurement of Helium density profiles in tokamak plasmas is necessary for helium transport studies. These studies are important in predicting the helium ash transport properties for ITER and will have important implications for the design. Poor helium transport in reactors could lead to a buildup of fusion ash, causing fuel dilution and increased radiation that will result in degraded fusion power and possibly quench ignition altogether. Present estimates indicate that He concentrations in the core must be kept below 10 percent in order to maintain continuous reactor operation. Helium transport studies have begun on the DM-D tokamak using charge exchange recombination (CER) spectroscopy for helium density measurements. Helium transport behavior has been observed by injecting helium gas puffs into DM-D plasmas and measuring the He density profile evolution. The profiles are used to calculate the relevant helium transport properties. This paper covers the results obtained from puffing He gas into L-mode plasmas of various electron densities. The results obtained in DIII-D L-mode plasmas are similar to measurements made at TEXTOR and JT-60. DOE

N93-12309# Argonne National Lab., IL.
PARTICLE-JET INTERACTIONS IN AN MHD SECOND STAGE COMBUSTOR
S. A. Lottes and S. L. Chang 1992 13 p Presented at the 30th Symposium on Engineering Aspects of Magnetohydrodynamics, Baltimore, MD, 29 Jun. - 2 Jul. 1992
(Contract W-31-109-eng-38)
(DE92-016390; ANL/CP-75446; CONF-920677-14) Avail: CASI HC A03/MF A01

An Argonne two-phase combustion flow computer code is used to simulate reacting flows to aid in the development of an advanced combustor for magnetohydrodynamic power generation. The combustion code is a general hydrodynamics computer code for two-phase, two-dimensional, steady state, turbulent, and reacting flows, based on mass, momentum, and energy conservation laws for multiple gas species and particles. The combustion code includes turbulence, integral combustion, and particle evaporation submodels. A recently developed integral combustion submodel makes calculations more efficient and more stable while still preserving the major physical effects of the complex combustion processes. The combustor under investigation is a magnetohydrodynamic second stage combustor in which opposed jets of oxidizer are injected into a confined cross-stream of hot coal gas flow following a first stage swirl combustor. The simulation is intended to enhance the understanding of the seed particle evaporation in the combustor and evaluate the effects of combustor operating conditions on seed particle evaporation and vapor dispersion, which directly affect overall magnetohydrodynamic power generation. Computation results show that oxidizer jet angle and particle size may greatly affect particle evaporation and vapor dispersion. At a jet angle about 130 degrees, particle evaporation rate is the highest because of the highest average gas temperature. As particle size increases beyond 10 microns in diameter, the effects of particle size on wall deposition rate, evaporation delay, and downstream seed vapor dispersion become more pronounced. DOE

N93-12416# Argonne National Lab., IL.
RESULTS FROM A LARGE-SCALE MHD PROPULSION EXPERIMENT
M. Petrick, J. Libera, J. X. Bouillard, E. S. Pierson, and D. Hill 1992 28 p Presented at the 30th Symposium on Engineering Aspects of Magnetohydrodynamics, Baltimore, MD, 29 Jun. - 2 Jul. 1992
(Contract W-31-109-eng-38)
(DE92-018177; ANL/CP-76633; CONF-920677-16) Avail: CASI HC A03/MF A01

Magnetohydrodynamic (MHD) thrusters have long been recognized as potentially attractive candidates for ship propulsion because such systems eliminate the conventional rotating drive components. The MHD thruster is essentially an electromagnetic (EM) pump operating in seawater. An electrical current is passed directly through the seawater and interacts with an applied magnetic field; the interaction of the magnetic field and the electrode current in the seawater results in a Lorentz force acting on the water, and the reaction to this force propels the vessel forward. The concept of EM propulsion has been examined periodically during the past 35 years as an alternative method of propulsion for surface ships and submersibles. The conclusions reached in early studies were that MHD thrusters restricted to fields of 2 T (the state-of-the-art at that time) were impractical and very inefficient. With the evolution of superconducting magnet technology, later studies investigated the performance of MHD thrusters with much higher magnetic field strengths and concluded that at higher fields (greater than 6-T) practical MHD propulsion systems appear possible. The feasibility of attaining the requisite higher magnetic fields has increased markedly because of rapid advances in building high-field superconducting magnets and the recent evolution of high-temperature superconductors. DOE

N93-12493# Texas Univ., Austin. Inst. for Fusion Studies.
ANOMALOUS ION THERMAL TRANSPORT IN HOT ION PLASMAS BY THE ION TEMPERATURE GRADIENT MODE
J. Y. Kim, W. Horton, and B. Coppi 1992 22 p
(Contract DE-FG05-80ET-53088)
(DE92-016686; DOE/ET-53088/553; IFSR-553) Avail: CASI HC A03/MF A01

Experiments show that the observed radial profiles of the ion thermal conductivity chi(sub i) have the opposite shapes with those obtained from the ion temperature gradient mode (eta(sub i) mode) turbulence model by the traditional mixing length estimate. In this work, this radial profile problem is reconsidered with an electromagnetic study of the linear stability of the toroidal eta(sub i) mode and a new rule for choosing the mixing length. It is first shown that the electromagnetic effect gives a significant stabilizing effect on the toroidal eta(sub i) mode, and that the observed reduction of chi(sub i)(r) in the core region can be explained by this electromagnetic effect. Secondly, in view of earlier numerical simulations showing the transfer of fluctuation energy to larger scales than those for the fastest growth rate, as well as fluctuation measurements indicating longer radial correlation lengths, a new mixing length formula is proposed to explain the radial increase of the chi(sub i). It is shown the new formula fits well the observed chi(sub i)(r) profiles in two TFTR supershot discharges and also gives the scaling law in the current and the magnetic field which agrees better with experiment than the conventional formula. DOE

N93-12501# Oak Ridge National Lab., TN.
TRANSPORT MECHANISMS ACTING IN TOROIDAL DEVICES: A THEORETICIAN'S VIEW
B. A. Carreras 1992 24 p Presented at the 14th International Conference on Plasma and 19th EPS Conference on Controlled Fusion and Plasma Physics, Innsbruck, Austria, 29 Jun. - 3 Jul. 1992
(Contract DE-AC05-84OR-21400)
(DE92-018738; CONF-920610-13) Avail: CASI HC A03/MF A01

Understanding the basic mechanisms of transport in toroidal confinement devices remains one of the more challenging scientific issues in magnetic confinement. At the same time, it is a critical issue for the magnetic fusion program. Recent progress in understanding fluctuations and transport has been fostered by the development and use of new diagnostics, bringing new perspectives on these studies. This has stimulated new theoretical developments. In this paper, a view of the most recent issues and progress in this area is given. The role of long wavelengths in core transport and the relation between shear flows and turbulence at the plasma edge are the primary topics considered. DOE

N93-12504# TRW Space Technology Labs., Redondo Beach, CA. Applied Technology Div.
MHD INTEGRATED TOPPING CYCLE PROJECT
Jan. 1992 116 p
(Contract DE-AC22-87PC-90274)
(DE92-018087; DOE/PC-90274/T18; MHD-ITC-92-001) Avail: CASI HC A06/MF A02

The overall objective of the project is to design and construct prototypical hardware for an integrated MHD topping cycle, and conduct long duration proof-of-concept tests of integrated system at the US DOE Component Development and Integration Facility in Butte, Montana. The results of the long duration tests will augment the existing engineering design data base on MHD power train reliability, availability, maintainability, and performance, and will serve as a basis for scaling up the topping cycle design to the next level of development, an early commercial scale power plant retrofit. The components of the MHD power train to be designed, fabricated, and tested include: A slagging coal combustor with a rated capacity of 50 MW thermal input, capable of operation with an Eastern (Illinois no. 6) or Western (Montana Rosebud) coal, a segmented supersonic nozzle, a supersonic MHD channel capable of generating at least 1.5 MW of electrical power, a segmented supersonic diffuser section to interface the channel with existing facility quench and exhaust systems, a complete set of current control circuits for local diagonal current control along the channel, and a set of current consolidation circuits to interface the channel with the existing facility inverter. DOE

N93-12526# Science Applications International Corp., San Diego, CA.
TECHNOLOGY EVALUATION REPORT OF RETECH, INC., PLASMA CENTRIFUGAL FURNACE, VOLUME 1
Jul. 1992 190 p
(Contract EPA-68-CO-0048)

(PB92-216035; EPA/540/5-91/007A-Vol-1) Avail: CASI HC A09/MF A02

A demonstration of the Retech, Inc. Plasma Centrifugal Furnace (PCF) was conducted under the Superfund Innovative Technology Evaluation (SITE) Program at the Department of Energy's (DOE's) Component Development and Integration Facility in Butte, Montana. The furnace uses heat generated from a plasma arc to melt and vitrify solid feed material. The feed soil was a mixture of Silver Bow Creek soil and 10 percent by weight No. 2 diesel oil, spiked to provide 28,000 ppm zinc oxide and 1000 ppm hexichlorobenzene in the soil/oil mixture. Pre-treatment soil and scrubber liquor/makeup sampling was performed to characterize the material inputs to the process. Following treatment, the vitrified soil, scrubber liquor, and stack gas were sampled to determine the technology's suitability for use in destroying and immobilizing contaminants in the test soil. The results from the test were used to draw conclusions on the technology. The conclusions derived from the test results are presented. GRA

N93-12527# Science Applications International Corp., San Diego, CA.

TECHNOLOGY EVALUATION REPORT OF RETECH, INC., PLASMA CENTRIFUGAL FURNACE, VOLUME 2

Jul. 1992 331 p
(Contract EPA-68-CO-0048)
(PB92-216043; EPA/540/5-91/007B-Vol-2) Avail: CASI HC A15/MF A03

A demonstration of the Retech, Inc. Plasma Centrifugal Furnace (PCF) was conducted under the Superfund Innovative Technology Evaluation (SITE) Program at the Department of Energy's (DOE's) Component Development and Integration Facility in Butte, Montana. The following conclusions were derived from the test results: (1) the treated soil did not leach any metals at levels above the regulatory limits; (2) the process achieved a Destruction and Removal Efficiency (DRE) of greater than 99.99 percent for the Principal Organic Hazardous Constituent (POHC); (3) the air pollution control system did not reduce the level of particulate emissions to below the RCRA limit; (4) a high percentage of the metals fed to the furnace are encapsulated in the treated soil; (5) the PCF is advantageous over other incinerator technologies in that is can successfully immobolize heavy metals in the slag; however, this treatment option can be more expensive than conventional incineration. The report is the second volume of the two-volume series. This volume contains the appendixes for the demonstration of the plasma centrifugal furnace. GRA

N93-12535 Auburn Univ., AL.

ION TEMPERATURE MEASUREMENTS ON FIELD REVERSED CONFIGURATION PLASMAS Ph.D. Thesis

Miles Hunt Baron 1991 184 p
Avail: Univ. Microfilms Order No. DA9224034

The experimental methods are examined which were used on field reversed configuration (FRC) plasmas, specifically FRX-C/LSM, to obtain ion temperature measurements and to explain their results. Field reversed configuration plasmas have been studied for about three decades and over these years no single reliable diagnostic has been developed to directly obtain the deuterium temperature. An attempt is made to explain the discrepancies which arise among the deuterium temperatures derived from neutron rate, impurity Doppler broadening and subtraction of the electron temperature from the total temperature obtained from pressure balance. Additionally, a new method of obtaining the deuterium temperature is proposed and attempted. This new method involves the injection of frozen deuterium pellets into an FRC. By spectroscopically observing the Doppler broadening of the D light emitted from the charge-exchange neutrals surrounding the ablating pellet it is predicted that a deuterium temperature can be obtained. The modeling, experimental set-up, and experimental results of the pellet injection experiment are explained. Spectroscopic measurements of the normal oxygen and carbon impurity concentrations, rotation velocity, and translation velocity of field reversed configuration plasmas in FRX-C/LSM are also presented. Dissert. Abstr.

N93-12033# Ecole Polytechnique, Palaiseau (France). Centre de Physique Theorique.

ELECTRON ACCELERATION IN A RELATIVISTIC ELECTRON PLASMA WAVE [ACCELERATION D'ELECTRONS DANS UNE ONDE PLASMA ELECTRONIQUE RELATIVISTE]

Patrick Mora *In its* The 1989 Scientific Report of the Laboratory for the Use of High Power Lasers Apr. 1990 p 69-72 In FRENCH (For primary document see N93-12023 02-36)
Avail: CASI HC A01/MF A03

N93-12034# Ecole Polytechnique, Palaiseau (France). Lab. pour l'Utilisation des Lasers Intenses.

LOW PRESSURE GAS MULTIPHOTOIONIZATION FOR WAVE PACKET EXPERIMENTS [MULTIPHOTOIONISATION DES GAZ A BASSE PRESSION POUR LES EXPERIENCES DE BATTEMENT D'ONDES]

Francois Amiranoff, Anthony Dyson, Jean-Raphael Marques, Christian Stenz, P. Benkheiri, C. Gregory, F. Jacquet, P. Mine, B. Montes, and P. Poilleux et al *In its* The 1989 Scientific Report of the Laboratory for the Use of High Power Lasers Apr. 1990 p 73-76 In FRENCH (For primary document see N93-12023 02-36)
Avail: CASI HC A01/MF A03

N93-12035# Ecole Polytechnique, Palaiseau (France). Lab. pour l'Utilisation des Lasers Intenses.

LASER MATERIAL INTERACTION IN CONFINED MEDIUM [DE L'INTERACTION LASER-MATIERE EN MILIEU CONFINE]

David Devaux (Etablissement Technique Central de l'Armement, Arcueil, France), Remy Fabbro (Etablissement Technique Central de l'Armement, Arcueil, France), Jean Virmont, Patrick Ballard (Peugeot S.A., Velizy, France), and Jean Fournier (Peugeot S.A., Velizy, France) *In its* The 1989 Scientific Report of the Laboratory for the Use of High Power Lasers Apr. 1990 p 77-82 In FRENCH (For primary document see N93-12023 02-36)
Avail: CASI HC A02/MF A03

N93-12036# Peugeot S.A., Velizy (France). Etudes et Recherches.

STUDY OF THE EFFECTS OF A PLASTIC WAVE INDUCED BY LASER PULSE IN A METALLIC MATERIAL. APPLICATION TO THE IMPROVEMENT OF FATIGUE STRENGTH [ETUDE DES EFFETS D'UNE ONDE PLASTIQUE INDUITE PAR PULSE LASER DANS UN MATERIAU METALLIQUE. APPLICATION A L'AMELIORATION DE LA TENUE EN FATIQUE]

Patrick Ballard, Jean Fournier, David Devaux (Ecole Polytechnique, Palaiseau, France), and Remy Fabbro (Etablissement Technique Central de l'Armement, Arcueil, France) *In* Ecole Polytechnique, The 1989 Scientific Report of the Laboratory for the Use of High Power Lasers Apr. 1990 p 83-87 In FRENCH (For primary document see N93-12023 02-36)
Avail: CASI HC A01/MF A03

N93-12043# Paris-Sud Univ., Orsay (France). Lab. de Spectroscopie Atomique et Ionique.

GAIN IN A CONFINED ALUMINUM PLASMA [GAIN DANS UN PLASMA D'ALUMINIUM CONFINE]

Pierre Jaegle, Antoine Carillon, Bernard Gauthe, Gerard Jamelot, and Jean-Pierre Raucourt *In* Ecole Polytechnique, The 1989 Scientific Report of the Laboratory for the Use of High Power Lasers Apr. 1990 p 125-127 In FRENCH (For primary document see N93-12023 02-36)
Avail: CASI HC A01/MF A03

N93-12044# Paris-Sud Univ., Orsay (France). Lab. de Spectroscopie Atomique et Ionique.

PRELIMINARY STUDY OF THE HOMOGENEITY OF THE DENSITY AND TEMPERATURE OF LONG PLASMAS USED FOR X LASER STUDIES [ETUDE PRELIMINAIRE DE L'HOMOGENEITE DE LA DENSITE ET DE LA TEMPERATURE DES PLASMAS LONGS EMPLOYES POUR LES ETUDES SUR LE LASER X]

Gailila Abdelatif, M. Berland, Antoine Carillon, P. Dhez, and

Jean-Pierre Raucourt *In* Ecole Polytechnique, The 1989 Scientific Report of the Laboratory for the Use of High Power Lasers Apr. 1990 p 128-129 In FRENCH (For primary document see N93-12023 02-36)
Avail: CASI HC A01/MF A03

N93-12047# Lawrence Livermore National Lab., CA.
BREMSSTRAHLUNG ABSORPTION IN PLASMAS [ABSORPTION DE BREMSSTRAHLUNG DANS LES PLASMAS]
B. Rozsnyai and Michele Lamoureux (Paris-Sud Univ., Orsay, France) *In* Ecole Polytechnique, The 1989 Scientific Report of the Laboratory for the Use of High Power Lasers Apr. 1990 p 138-141 In FRENCH (For primary document see N93-12023 02-36)
Avail: CASI HC A01/MF A03

N93-12048# Ecole Polytechnique, Palaiseau (France). Lab. pour l'Utilisation des Lasers Intenses.
DIRECT RADIATIVE RECOMBINATION OF ATOMIC IONS [RECOMBINAISON RADIATIVE DIRECTE DES IONS ATOMIQUES]
Alain Poquerusse *In its* The 1989 Scientific Report of the Laboratory for the Use of High Power Lasers Apr. 1990 p 142-147 In FRENCH (For primary document see N93-12023 02-36)
Avail: CASI HC A02/MF A03

N93-12049# Paris VI Univ. (France). Lab. de Spectroscopie.
ATOMIC STRUCTURE AND SPECTRAL PERTURBATIONS IN DENSE AND HOT PLASMAS [STRUCTURE ATOMIQUE ET PERTURBATIONS SPECTRALES DANS LES PLASMAS DENSES ET CHAUDS]
Hoe Nguyen, Claire Bousquet, Zoubeida Dhaouadi, Brigitte dEtat, Jeanne Grumberg, Elisabeth Leboucher-Dalimier, M. Brisard, Philippe Malnoult, and Jean-Pierre Arranz *In* Ecole Polytechnique, The 1989 Scientific Report of the Laboratory for the Use of High Power Lasers Apr. 1990 p 148-160 In FRENCH (For primary document see N93-12023 02-36)
Avail: CASI HC A03/MF A03

76 SOLID-STATE PHYSICS

Includes superconductivity.
For related information, see also *33 Electronics and Electrical Engineering* and *36 Lasers and Masers.*

N93-10987# Oak Ridge National Lab., TN.
GROWTH MECHANISMS OF LAYERED SUPERCONDUCTORS
S. J. Pennycook, M. F. Chisholm, D. E. Jesson, R. Feenstra, S. Zhu, and D. H. Lowndes Jun. 1992 13 p Presented at the Material Research Society Spring Meeting, San Francisco, CA, 27 Apr. - 2 May 1992
(Contract DE-AC05-84OR-21400)
(DE92-018492; CONF-920402-48) Avail: CASI HC A03/MF A01

Using a combination of Z-contrast imaging, scanning tunneling microscopy, and plan view diffraction contrast imaging, we have studied the growth and relaxation mechanisms of YBa2Cu3O(7-x) deposited on MgO and SrTiO3 substrates. Two-dimensional island growth occurs on SrTiO3 substrates, with relaxation through the nucleation of dislocation half-loops. Then the threading dislocation segments with a screw component can lead to kinetic roughening through the development of growth pyramids. In contrast, growth on MgO occurs by true one-dimensional island growth (with no wetting layer), most of the interface being incommensurate with the substrate (although crystallographically aligned). Dislocations with both edge and screw components are generated on island coalescence. A highly anisotropic surface energy is shown to be responsible for cell-by-cell c(perpendicular) growth being thermodynamically preferred, although at high supersaturations a transition a(perpendicular) growth occurs. DOE

N93-10992# International Centre for Theoretical Physics, Trieste (Italy).
HYDRODYNAMIC FLUCTUATIONS AND LIGHT SCATTERING IN HOT ELECTRON GAS OF SEMICONDUCTORS
N. A. Zakhleniuk and V. A. Kochelap Oct. 1991 32 p
(DE92-622800; IC-91/301) Avail: CASI HC A03/MF A01

Hydrodynamical fluctuations of the electron gas are the low-frequency and long-range stochastic excitations over steady state of the system. These fluctuations are responsible for the set of the physical phenomena which occur for both equilibrium and nonequilibrium conditions (for example, the current noises, the light scattering, etc.). We investigate the hot electron plasma that can be characterized by two time parameters - the electric charge decay time tau(sub M) and the electron energy relaxation time tau(sub T). Our consideration is based on the Boltzmann-Langevin kinetic equation for the fluctuations of the electron distribution function delta-F. The solution of this equation is found under typical criteria for the hot electron plasma: tau(sub p) much less than tau(sub ee) much less than tau(sub e), where tau(sub p), tau(sub e) are the times of relaxation of the momentum and energy of the electrons, tau(sub ee) is the electron-electron scattering time. It is shown that the fluctuation delta F can be expressed via the two fluctuating parameters: delta-n(omega, q), delta-T(omega, q) and via the initial steady state distribution function. For them the hydrodynamic equations are deduced and as a result, the following correlation functions are calculated: (delta-n delta-n)(sub omega,q), (delta-T delta-T)(sub omega,q), (delta-n delta-T)(sub omega,q). The analysis of these correlators shows the next features of the general results which are not restricted by above criteria: (1) There are cross-over correlations of delta-n and delta-T, that mean the mutual influence of the electron density fluctuations and their temperature. (2) The time and space dependences of the fluctuations strongly differ from that under the above mentioned limits. (3) It is important that these features are characteristic, as well, for the equilibrium electron plasma under arbitarary relation between tau(sub M) and tau(sub T). DOE

N93-10996# California Univ., Santa Barbara. Dept. of Chemistry.
THE SYNTHESIS AND CRYSTAL STRUCTURE OF LaHSe2O6, A LAYERED, ANHYDROUS SELENITE Technical Report No. 1, 1 Jun. 1991 - 31 May 1992
Russell E. Morris, William T. Harrison, Galen D. Stucky, and Anthony K. Cheetham 15 May 1992 17 p
(Contract N00014-90-J-1159)
(AD-A251050) Avail: CASI HC A03/MF A01

Lanthanum hydrogen selenite, LaHSe2O6, M(sub r), = 393.83, orthorhombic, P(sub c)2(sub 1)b (No. 29), a = 7.139(6) A, b = 19.008(9) A, c = 8.469(9) A, (alpha = 90 deg, beta = 90 deg, gamma = 90 deg, V = 1149.24 cu A, Z = 8, D(sub x) = 4.55 g cu cm, mu = 199.7 cm(-1), lambda (Mo Ka, graphite monochromator) = 0.71073 A, F(000) = 1392, room temperature 298(2) K. Final R = 3.61 percent, wR = 4.21 percent for 1701 observed reflections with I greater than 3 sigma(I)). LaHSe2O6 has been prepared using hydrothermal synthetic techniques and its crystal structure elucidated by single crystal X-ray diffraction. This new structure consists of layers of LaO10, HSeO3 and SeO3 polyhedra parallel to the ac-place; the layers are interconnected by Se-OH...O-(Se,La) hydrogen bonds. GRA

N93-11056* National Aeronautics and Space Administration. Pasadena Office, CA.
INAS HOLE-IMMOBILIZED DOPING SUPERLATTICE LONG-WAVE-INFRARED DETECTOR Patent
Joseph Maserjian, inventor (to NASA) (Jet Propulsion Lab., California Inst. of Tech., Pasadena.) 21 Jul. 1992 11 p Filed 7 Feb. 1991
(NASA-Case-NPO-17880-1-CU; US-Patent-5,132,763; US-Patent-Appl-SN-651882; US-Patent-Class-357-30; US-Patent-Class-357-4; US-Patent-Class-357-16; Int-Patent-Class-H01L-29/205; Int-Patent-Class-H01L-31/10)
Avail: US Patent and Trademark Office

An approach to long-wave-infrared (LWIR) technology is discussed. The approach is based on molecular beam epitaxy (MBE) growth of hole immobilized doping superlattices in narrow band gap 3-5 semiconductors, specifically, InAs and InSb. Such superlattices are incorporated into detector structures suitable for focal plane arrays. An LWIR detector that has high detectivity performance to wavelengths of about 16 microns at operating temperatures of 65K, where long-duration space refrigeration is plausible, is presented.
Official Gazette of the U.S. Patent and Trademark Office

N93-11076# International Centre for Theoretical Physics, Trieste (Italy).
CRITICAL CURRENTS IN POLYCRYSTALLINE YBa2Cu3O(7-x): SELF-FIELD AND GRAIN SIZE DEPENDENCE
E. Babic (Zagreb Univ., Yugoslavia), M. Prester (Zagreb Univ., Yugoslavia), D. Dobrac (Zagreb Univ., Yugoslavia), Z. Marohnic (Zagreb Univ., Yugoslavia), S. Bernik, P. Nazar, P. Stastny, and F. C. Matacotta Oct. 1991 31 p
(DE92-617540; IC-91/345) Avail: CASI HC A03/MF A01

The variation of critical currents (I(sub c)) and their distributions (CCD) with thickness (t) has been investigated for two high quality YBa2Cu3O(7-x) samples with different average grain size (AGS approx equal 10 and 30 micrometer for samples S(sub 1) and S(sub 2) respectively) in the temperature range 78 to 90 K and in the applied magnetic field H less than 50 0e. The critical current density (J(sub c)) for S(sub 1) initially increased but later on leveled off on reducing the thickness, whereas for S(sub 2) remained essentially unchanged even after three-fold reduction in thickness. Since the other parameters related to macroscopic homogeneity have not changed on reducing the thickness of the samples, the variations of J(sub c) are interpreted in terms of thickness and grain size dependent self-field effects. The same model explains well the changes of CCD curves with thickness and may also explain the variation of J(sub c) with the grain size, as reported recently for ceramic YBaCuO samples. DOE

N93-11190# Argonne National Lab., IL.
THE DOMAIN STRUCTURE FEATURES OF EPITAXIAL PbTiO3 THIN FILMS PREPARED BY MOCVD
G. R. Bai, H. L. M. Chang, C. M. Foster, and D. J. Lam Mar. 1992 5 p Presented at the 8th International Conference on Advanced Science and Technology, Argonne, IL, 28 Mar. 1992
(Contract W-31-109-eng-38)
(DE92-010907; ANL/CP-75722; CONF-9203110-3) Avail: CASI HC A01/MF A01

Ferroelectric oxide thin films have attracted great interest in recent years because of their potential applications in numerous electro-optic, pyroelectric, acousto-optical, and nonvolatile memory devices, and a variety of methods such as sputtering, laser ablation, and MOCVD has been used for preparation of the films. Among these ferroelectric materials, the PbTiO3 thin film has been extensively studied because of its small dielectric constant, large spontaneous polarization, small coercive field, and high Curie temperature of approx 500 C. However, very little work has dealt with the detailed structural properties of the films. In this work, we have prepared epitaxial PbTiO3 thin films by MOCVD and performed some detailed studies on the structure of the films, particularly those related to the twin domain structure, using X-ray diffraction technique. Based on the comparison of the domain structure features of the films grown at above Curie temperature with those of the films grown at below Curie temperature as well as of bulk PbTiO3 single crystal, a model is proposed to explain our experimental results. DOE

N93-11238# Ames Lab., IA.
PULSED-FIELD-GRADIENT NMR INVESTIGATIONS OF HYDROGEN DIFFUSION IN ZrH(x)
G. Majer (Max-Planck-Inst. fuer Metallforschung, Stuttgart Germany), W. Renz (Max-Planck-Inst. fuer Metallforschung, Stuttgart, Germany), A. Seeger (Max-Planck-Inst. fuer Metallforschung, Stuttgart, Germany), and R. G. Barnes 10 Apr. 1992 12 p Presented at the Interaction Symposium on Metal-Hydrogen Systems, Uppsala (Sweden), Jun. 1992
(Contract W-7405-eng-82)
(DE92-014393; IS-M-712; CONF-9206175-1) Avail: CASI HC A03/MF A01

The macroscopic diffusivities of protons in zirconium dihydrides, ZrH(x) (1.58 less than or equal to x less than or equal to 1.93), were investigated by means of pulsed-field-gradient NMR at temperatures up to 900 K. The diffusion coefficients follow normal Arrhenius behavior, D = D(sub 0) (dot) exp(-H(sub a)/k(sub B)T), with activation energies between E(sub a) = 614 meV (x = 1.58) and E(sub a) = 760 meV (x = 1.93). The E(sub a) values, which increase sharply as x approaches the limiting value 2, agree satisfactorily with data based on the spin-lattice relaxation rate, Gamma(sub 1), measured on the same samples. A combined analysis of both Gamma(sub 1) and D measurements provides useful information about the underlying diffusion mechanism. It is shown that the diffusing H atoms jump between nearest neighbor tetrahedral sites. The attempt frequency nu(sup a) is approximately 10(exp 13) s(sup -1) is in accordance with neutron scattering data. The experimental results on the hydrogen diffusivity are compatible with the so-called adiabatic mechanism of diffusion. DOE

N93-11394 National Physical Lab., Teddington (England). Div. of Electrical Science.
HIGH FREQUENCY RESPONSE FROM YBa2Cu3O(7-x) JOSEPHSON DEVICES ON SrTiO3 BICRYSTAL SUBSTRATES
P. G. Quincey, M. Stewart, M. C. Wicks, and J. R. Birch Mar. 1992 16 p Sponsored by National Measurement System Policy Unit Optoelectronics Programme
(NPL-DES-118; ETN-92-92366) Copyright Avail: National Physical Lab., Teddington, Middlesex, TW11 0LW, England

The production of thin film Josephson devices responding to microwave radiation from 10 to 109 GHz is described. A bicrystal substrated approach was used which fused polished single crystals of strontium titanate, and deposited YBa2Cu3O(7-x) thin film by inverted cylindrical magnetron sputtering. The preliminary devices use substrates and film on the (110) orientation. Patterning by wet etching to produce a narrow strip of film across the bicrystal boundary created a device with Josephson response to microwave radiation although so far only below 77K. The high frequency limit for this response was explored by illuminating the junction with 1 W source at 11.8 GHz, with voltage steps observed up to the 210th harmonic. ESA

N93-11496# Oak Ridge National Lab., TN.
ATOMISTIC PROCESSES OF SURFACE SEGREGATION DURING Si-Ge MBE GROWTH
D. E. Jesson, S. J. Pennycook, J. M. Baribeau, and D. C. Houghton 1992 20 p Presented at the Spring Meeting of the European Materials Research Society: International Conference on Electronic Materials, Strasbourg, France, 2-5 Jun. 1992
(Contract DE-AC05-84OR-21400)
(DE92-019180; CONF-920694-2) Avail: CASI HC A03/MF A01

Atomic-scale segregation at step edges during growth is proposed as the origin of ordering in the Si-Ge system. Cross-sectional Z-contrast imaging of as-grown structures reveals that a variety of ordered phase variants can exist at Si on Ge interfaces as a result of vertical segregation during superlattice growth. Long-range ordering in alloys is predicted to arise due to segregation at monolayer or bilayer steps depending on the evolving surface morphology. DOE

N93-11501# Brookhaven National Lab., Upton, NY.
FRUSTRATED PHASE SEPARATION AND HIGH TEMPERATURE SUPERCONDUCTIVITY
V. J. Emery and S. A. Kivelson 1992 16 p Presented at the Conference on Phase Separation in Cuprate Superconductors, Sicily, Italy, 6-12 May 1992
(Contract DE-AC02-76CH-00016)
(DE92-019249; BNL-47796; CONF-9205236-1) Avail: CASI HC A03/MF A01

A dilute system of neutral holes in an antiferromagnet separates into a hole-rich and a hole-poor phase. The phase separation is frustrated by long-range Coulomb interactions but, provided the dielectric constant is sufficiently large, there remain large-amplitude low-energy fluctuations in the hole density at intermediate length scales. The extensive experimental evidence showing that this behavior gives a reasonable picture of high temperature superconductors is surveyed. Further, it is shown that the scattering of mobile holes from the local density fluctuations may account for the anomalous normal-state properties of high temperature superconductors and also provide the mechanism of pairing. DOE

N93-11512# Argonne National Lab., IL.
LANDAU LEVEL QUANTIZATION AND SUPERCONDUCTIVITY
H. Akera (Hokkaido Univ., Sapporo, Japan), A. H. MacDonald (Indiana Univ., Bloomington.), and M. R. Norman Jul. 1992 10 p Presented at the 33rd Yamada Conference on the Application of High Magnetic Fields in Semiconductor Physics, Chiba, Japan, 3-7 Aug. 1992
(Contracts W-31-109-eng-38; DE-FG02-86ER-45247)
(DE92-019028; ANL/CP-76653; CONF-9208110-1) Avail: CASI HC A02/MF A01

A microscopic calculation of vortex-lattice states in two-dimensional electron systems at strong magnetic fields is made taking fully the Landau level quantization into account within the mean field scheme. Results of the order parameter and the local density of states are presented both in the limit of pairing in a single Landau level and in the semiclassical regime of weaker fields and differences from the Abrikosov vortex state are discussed. DOE

N93-11522# Argonne National Lab., IL.
PROPERTIES OF HOT ISOSTATICALLY PRESSED Bi(2)Sr(1.7)CaCu(2)O(x)
S. Nash (Marquette Univ., Milwaukee, WI.), K. C. Goretta, D. J. Miller, A. C. Biondo, D. Shi, S. Sengupta, and R. B. Poeppel Apr. 1992 6 p Presented at the Material Research Society Spring Meeting, San Francisco, CA, 27 Apr. - 2 May 1992
(Contract W-31-109-eng-38)
(DE92-016394; ANL/CP-74842; CONF-920402-35) Avail: CASI HC A02/MF A01

Dense Bi(2)Sr(1.7)CaCu(2)O(x) (2212) superconductor pellets were made by hot isostatic pressing in an inert atmosphere. The pellets exhibited a small amount of preferred orientation of the grains. The transport critical current density (J(sub c)) values were very low for all specimens. Dislocations, planar faults, and intergrowths of the Bi(2)Sr(2)CuO(x) phase, which were produced during the pressing, caused the intragranular J(sub c) to increase substantially. DOE

N93-11533# Ames Lab., IA.
MAGNETIC PROPERTIES OF HIGH-T(c) SUPERCONDUCTORS Ph.D. Thesis
Junho Gohng 20 Jul. 1992 125 p
(Contract W-7405-eng-82)
(DE92-018809; IS-T-1625) Avail: CASI HC A06/MF A02

Magnetic properties of high-Tc superconductors have been studied in order to determine the free energy surface, the characteristic critical fields, order parameter structure, and the grain size effect on magnetization. Studies of the thermodynamic reversibility for YBa2Cu3O(7-delta) show the rounding in magnetization vs. temperature curves is a reflection of thermodynamic fluctuations near (Tc). Specific heat jump C(O)-C(H) values that have been calculated from the free energy surfaces show good agreement with the direct calorimetric measurements. Comparative studies of the free energy surfaces, flux creep and critical currents for both melt-textured and grain-aligned YBa2Cu3O(7-delta) samples have been undertaken in order to evaluate the difference caused by different microstructures in these samples. Magnetic field and temperature dependence of the average Ginzburg-Landau order parameter 'f' is evaluated by fitting the magnetization data of grain-aligned YBa2Cu3O(7-delta) to the Hao-Clem model in the region of thermodynamic reversibility. H sub c(T) and H sub c2(T) were also determined from the fitting along with the K sub c(T) values. Lastly, studies on the grain size effect on free energy and specific heat jump in grain aligned YBa2Cu3O(7-delta) samples show that the free energy is reduced by about 15 pct. as the average grain size changes from 37.5 to 12.7 microns. DOE

N93-11558# Utah Univ., Salt Lake City. Dept. of Materials Science and Engineering.
TRIISOPROPYLINDIUM: A NEW PRECURSOR FOR OMVPE GROWTH
C. H. Chen, C. T. Chiu, and G. B. Stringfellow 22 May 1992 31 p
(Contract N00014-91-J-1447)
(AD-A250672; TR-19) Avail: CASI HC A03/MF A01

The organometallic vapor phase epitaxial (OMVPE) growth of In-containing III-V semiconductors typically uses trimethylindium (TMIn). However, TMIn suffers from several problems. First, it is well known that the effective vapor pressure of solid TMIn changes with time because of changes in the surface area. Secondly, TMIn decomposes slowly for temperatures lower than 400 C in an atmospheric pressure OMVPE reactor; it is too stable for some low-temperature applications. In addition, it causes carbon contamination, especially at low temperatures, due to the CH3 radicals. Thus, there is a need for new In precursors that are liquids at room temperature and do not contain CH3 radicals. This work reports the first decomposition and OMVPE growth studies for a newly developed indium source, triisopropylindium (TIPIn). The decomposition was carried out in an isothermal flow tube reactor with the reaction products analyzed using a mass spectrometer. The temperature for 50 percent decomposition is approximately 110 C for TIPIn in a He ambient. This is about 200 C lower than that for TMIn under similar conditions. The mass spectroscopic peaks occur at m/e = 39, 42, 43, 71, and 86, indicating that the major product for TIPIn decomposition is C6H14. GRA

N93-11563# Argonne National Lab., IL.
STRUCTURE AND PROPERTY OF HETEROEPITAXIAL TiO2/VO2 MULTILAYERS
H. L. M. Chang, Y. Gao, T. J. Zhang, and D. J. Lam Jun. 1992 21 p Presented at the 6th International Conference on Slid Films and Furfaces (ICSFS-6), Paris, France, 29 Jun. - 3 Jul. 1992
(Contract W-31-109-eng-38)
(DE92-018181; ANL/CP-75751; CONF-9206221-1) Avail: CASI HC A03/MF A01

Various types of TiO2/VO2 multilayer structures have been prepared on sapphire substrates by a low-pressure metal-organic chemical vapor deposition process. X-ray diffraction and transmission electron microscopy techniques were used to study the crystallinity and epitaxial relationships of the deposited films. High resolution electron microscopy was used to examine the microstructure of the overlayers and interfaces. Electrical resistivity measurements were performed to investigate the metal-semiconductor phase transition of VO2 layers in multilayer structures. DOE

N93-11573# Ecole Centrale de Lyon (France). Lab. de Mecanique des Solides.
CONTRIBUTION TO THE STUDY OF THE ANISOTROPIC VISCOELASTICITY OF LARGE STRAINS: THE CASE OF THE MONOCRYSTAL Ph.D. Thesis [CONTRIBUTION A L'ETUDE DE LA VISCOPLASTICITE ANISOTROPE EN GRANDES DEFORMATIONS. LE CAS DU MONOCRISTAL]
Joseph Aime Michel Boukadia 1990 169 p In FRENCH
(ECL-90-29; ETN-92-92334) Avail: CASI HC A08/MF A02

The anisotropic viscoelasticity of large strains and torsion are investigated. In a phenomenologic approach, it is shown that the problem of applying the concepts of plasticity is the choice of the Torsion's referent system. The viscoplasticity in single crystals is also investigated. A rotating reference system is applied to describe kinetic phenomena of single crystals. The mechanical behavior of a face centered cubic single crystal, concerning viscosity, plasticity, and viscoplasticity, are analyzed by simple shear and failure mechanisms. The Bingham and Norton-Hoff methods are applied. The elastic phenomena can be taken into account without difficulties. The approach is constrained by the hypothesis that symmetric systems are symmetrically activated. However, by the hypothesis a two dimensional response was obtained. The model can be applied to the analysis of polycrystals. ESA

N93-11581# Ecole Centrale de Lyon (France). Lab. de Mecanique des Solides.

CONTRIBUTION TO THE MONOCRYSTAL BEHAVIOR STUDY DURING LARGE PLASTIC STRAINS Ph.D. Thesis [CONTRIBUTION A L'ETUDE DU COMPORTEMENT DU MONOCRISTAL EN GRANDES DEFORMATIONS PLASTIQUES]

Ahmed Chenaoui 1992 213 p In FRENCH
(ECL-92-13; ETN-92-92342) Avail: CASI HC A10/MF A03

The plastic or viscoplastic behavior of a face centered cubic monocrystal under shear stress is investigated. The results obtained by applying the plastic model, which is velocity independent, were not accurate and lead to an indetermination involving the lattice rotation. By applying the viscoplastic model those inaccuracies are removed. In a second step of the study, the plastic deformation and the elasticity are taken into account, and the results are similar to those obtained for a rigid crystal. The results obtained for a two dimensional monocrystal were proved to be true for a three dimensional crystal. The model was applied to a body centered cubic crystal structure and some difficulties, due to an increase of the number of parameters, were found. ESA

N93-11602# Lawrence Livermore National Lab., CA.

PREPARATION, OPTICAL AND LASER PROPERTIES OF Nd-DOPED SOL-GEL SILICA

I. M. Thomas, S. A. Payne, and G. D. Wilke 1 Jul. 1992 10 p Presented at the SPIE International Symposium on Optical Applied Science and Engineering, San Diego, CA, 19-24 Jul. 1992
(Contract W-7405-eng-48)
(DE92-019378; UCRL-JC-109256; CONF-920792-25) Avail: CASI HC A02/MF A01

A sol-gel process has been used to prepare homogeneous, fully dense, cylindrical samples of neodymium-doped silica and neodymium-aluminum-doped silica. The absorption and emission spectra, fluorescent lifetimes and quantum yields of all samples were measured. The quantum yields of Nd2O3-SiO2 samples were very low due to clustering of the Nd in the silica matrix. The incorporation of alumina eliminated the clustering and quantum yields up to 55 percent were obtained. We showed that these quantum yields of less than unity were caused by residual OH quenching of the Nd fluorescence. The fluorescent properties were unchanged when the OH was replaced with OD. One sample was demonstrated to lase under laser pumping. DOE

N93-11629# City Coll. of the City Univ. of New York, NY. Dept. of Physics.

MAGNETIC PROPERTIES AND CRITICAL BEHAVIOR OF THE CONDUCTIVITY NEAR THE M-I TRANSITION

M. Sarachik Jul. 1992 8 p
(Contract DE-FG02-84ER-45153)
(DE92-018948; DOE/ER-45153/9) Avail: CASI HC A02/MF A01

This report summarizes work on the metal-insulator transition. The report is divided into two sections. Section one contains brief descriptions of work on the metallic phase, while section two presents work on the insulator phase. DOE

N93-11646# Cornell Univ., Ithaca, NY.

STUDIES OF THE 3 TO 5 COMPOUNDS IN THE MEGABAR REGIME

A. L. Ruoff 1992 15 p
(Contract DE-FG02-87ER-45320)
(DE92-019517; DOE/ER-45320/5) Avail: CASI HC A03/MF A01

We developed techniques for making high pressure measurements (x-ray diffraction and optical measurements) on samples in the multimegabar regime and we made systematic studies of the crystal structure of 3-4 compounds and other materials as a function of pressure with the broad objective of providing experimental data over a broad range of coordination number and interatomic spacing which can play a leading role in the testing and development of theoretical models of binding. DOE

N93-11647# Lawrence Livermore National Lab., CA.

FLUX PINNING IN OXYGEN-DEPLETED YBa2Cu3O(7-y) SINGLE CRYSTALS

M. D. Lan, J. Z. Liu, R. N. Shelton, H. B. Radousky, B. W. Veal, and J. W. Downey Apr. 1992 8 p Presented at the Material Research Society Spring Meeting, San Francisco, CA, 27 Apr. - 2 May 1992
(Contract W-7405-eng-48)
(DE92-019548; UCRL-JC-110481; CONF-920402-51) Avail: CASI HC A02/MF A01

Magnetic properties and flux pinning of oxygen-deficient YBa2Cu3O(7-y) single crystals have been studied. The superconducting transition temperature and inductive critical current density decrease as the level of oxygen depletion increases. No obvious enhancement in the pinning strength was found in the oxygen-depleted YBa2Cu3O(7-y) system for the applied field along the c-axis. We attribute this absence of enhanced pinning to the mismatch of the oxygen vacancy size with the superconducting coherence length over our temperature regime. DOE

N93-11682# Brown Univ., Providence, RI. Dept. of Geological Sciences.

GRAIN BOUNDARY TRANSPORT AND RELATED PROCESSES IN NATURAL FINE GRAINED AGGREGATES

R. A. Yund and J. R. Farver Jul. 1992 5 p
(Contract DE-FG02-90ER-14144)
(DE92-018239; DOE/ER-14144/3) Avail: CASI HC A01/MF A01

A new technique for measuring grain boundary diffusion rates in polycrystalline aggregates was developed. The technique was successfully employed to determine oxygen grain boundary diffusion rates in natural fine-grained quartz aggregates (novaculites) over a wide range of temperatures. In addition, we have demonstrated the major role of fluid composition on the microstructure and oxygen bulk diffusivity in a novaculite sample. Most recently, we have successfully produced hot-pressed fine-grained monomineralic quartz and feldspar aggregates and have measured oxygen grain boundary diffusion rates in these aggregates for comparison to the natural novaculite samples. DOE

N93-11683*# National Aeronautics and Space Administration, Washington, DC.

ICCG-10: TENTH INTERNATIONAL CONFERENCE ON CRYSTAL GROWTH. POSTER PRESENTATION ABSTRACTS

1992 228 p Conference held in San Diego, CA, 16-21 Aug. 1992
(Grant NAGw-3079)
(NASA-CR-190920; NAS 1.26:190920) Avail: CASI HC A11/MF A03

Poster presentation abstracts from the tenth International Conference on Crystal Growth (ICCG) (Aug. 16-21, 1992) are provided. Topics discussed at the conference include crystal growth mechanisms, superconductors, semiconductors, laser materials, optical materials, and biomaterials. Organizing committees, ICCG advisory board and officers, and sponsors of the conference are also included. L.R.R.

N93-11684*# National Aeronautics and Space Administration, Washington, DC.

ICCG-10: TENTH INTERNATIONAL CONFERENCE ON CRYSTAL GROWTH. ORAL PRESENTATION ABSTRACTS

1992 206 p Conference held in San Diego, CA, 16-21 Aug. 1992

(Grant NAGw-3079)
(NASA-CR-190919; NAS 1.26:190919) Avail: CASI HC A10/MF A03

Oral presentation abstracts from the tenth International Conference on Crystal Growth (ICCG) (Aug. 16-21, 1992) are provided. Topics discussed at the conference include superconductors, semiconductors, nucleation, crystal growth mechanisms, and laser materials. Organizing committees, ICCG advisory board and officers, and sponsors of the conference are also included. L.R.R.

N93-11703# Argonne National Lab., IL.

A STUDY OF PARAMETERS THAT INFLUENCE GROWTH AND STABILITY OF THE (Bi(1-x)Pb(x))2 Sr2Ca2Cu3O(y) PHASE

J. S. Luo, N. Merchant, V. A. Maroni, D. M. Gruen, B. S. Tani, W. L. Carter, G. N. Riley, Jr., and K. H. Sandhage (American Superconductor Corp., Watertown, MA.) Apr. 1992 8 p Presented at the Material Research Society Spring Meeting, San Francisco, CA, 27 Apr. - 2 May 1992
(Contract W-31-109-eng-38)
(DE92-015187; ANL/CP-73655; CONF-920402-23) Avail: CASI HC A02/MF A01

The growth and stability of the (Bi(1-x)Pb(x))2 Sr2Ca2Cu3O(y) (Bi-2223) phase contained in silver-sheathed wires has been investigated by a combination of x-ray diffraction, scanning electron microscopy, energy dispersive x-ray analysis, and transmission electron microscopy. Silver tubes loaded with Bi-2223 precursor powders were processed into filaments using established metallurgical techniques. The filaments were then heat-treated at selected temperatures (800 to 845 C) for a range of times (10 to 6000 min) in a 7.5 percent oxygen atmosphere. From these studies it has been possible to investigate the time-temperature-oxygen pressure domains wherein Bi2Sr2CaCu2O8 (Bi-2212) + second phases transform to Bi-2223. Fractional conversion (Bi-2212) to (Bi-2223) versus time data show good conformance to the kinetic model for a diffusion-controlled reaction at the interface between thin sheets and a fine powder or a fluid. Quenching experiments also reveal that the Bi-2223 phase is stable in a limited temperature interval between 810 and 830 C. DOE

N93-11706# Ames Lab., IA.

RECRYSTALLIZATION OF AMORPHOUS OR NANOCRYSTALLINE NdBa2Cu3O(7-x) AND GdBa2Cu3O(7-x)

T. J. Folkerts, S. I. Yoo, Youwen Xu, M. J. Kramer, K. W. Dennis, and R. W. McCallum 1992 6 p Presented at the Material Research Society Spring Meeting, San Francisco, CA, 27 Apr. - 2 May 1992
(Contracts W-7405-eng-82; DE-FG02-90ER-45427)
(DE92-016302; IS-M-716; CONF-920402-33) Avail: CASI HC A02/MF A01

Using a novel melt-spinning technique, we have produced highly disordered NdBa2Cu3O(7-x) and GdBa2Cu3O(7-x) materials. Samples which were melt-spun in an O2 environment consist of nanocrystals with the tetragonal REBa2Cu3O(7-x) structure; samples which were processed in an N2 environment consist of an amorphous matrix with small amounts of crystalline BaCu2O2, as shown by x-ray diffraction and electron microscopy. High temperature XRD studies indicate that the BaCu2O2 is eliminated during heating to 500 C in O2 and that the REBa2Cu3O(7-x) phase recrystallizes directly from the amorphous matrix at temperatures below 800 C. Preliminary magnetization measurements show that higher temperature heat treatments are needed to restore superconductivity. DOE

N93-11724# Duke Univ., Durham, NC. Dept. of Chemistry.

SYNTHESIS AND CHARACTERIZATION OF NOVEL ORGANOGALLIUM-PHOSPHORUS COMPOUNDS: X RAY CRYSTAL STRUCTURES OF Ph2GaP (SiMe3)2Ga (Ph2Cl, Ph2 (Cl)Ga.P (SiMe3)3, AND Ph3Ga.P (SiMe3)3

Richard L. Wells, Steven R. Aubuchon, Mark F. Self, Jerry P. Jasinski, and Richard C. Woudenberg 17 Jul. 1992 36 p
(Contract N00014-89-J-1545)
(AD-A253841; DU/DC/TR-28) Avail: CASI HC A03/MF A01

A Ga-P-Ga-Cl ring containing the compound, Ph2GaP(SiMe3)2Ga(Ph)2Cl (1), is reported. Compound 1 is an example of a four-membered ring system with mixed bridging of the two gallium centers and was prepared via the reaction of Ph2GaCl with P(SiMe3)3 in a 2:1 mole ratio in either toluene or pentane. Curiously, 1 was originally isolated as a minor product (ca 5 percent yield) from the reaction of LiP(SiMe3)2 with Ph2GaCl in a 1:1 mole ratio. X-ray crystallographic analyses shows the Ga-P-Ga-Cl ring of 1 to be non-planar. The reaction of Ph2GaCl and P(SiMe3)3 in a 1:1 mole ratio in either toluene or pentane yields Ph2(Cl)Ga.P(SiMe3)3 (2). Compound 3, Ph3Ga.P(SiMe3)3, was also originally isolated as a minor product (ca. 10 percent) from the reaction of LiP(SiMe3)2 with Ph2GaCl in a 1:1 mole ratio and is an additional reported example of an adduct formed through ligand redistribution involving LiE(SiMe3)2 (E = P or As) as a reactant. The straightforward synthesis of 3 can be accomplished by the 1:1 mole reaction of Ph3Ga and P(SiMe3)3 in pentane. Both 2 and 3 are structural examples of adducts containing a Ga-P bond with aryl ligands on the gallium center. Compound 1 belongs to the monoclinic system, space group P2(sub 1)/c, with z = 4, a = 10.579(2) A, b = 15.653(5) A, c = 20.428(4) A, and beta = 91.80(2) deg. Compound 2 crystallizes in an orthorhombic system, space group P2(sub 1)2(sub 1)2(sub 1) with z = 4, a = 9.3320(10) A, b = 9.768(2) A, and c = 30.581(6) A. Compound 3 belongs to the monoclinic system, space group P2(sub 1)/n, with z = 4, a = 18.81(3) A, b = 19.25(2) A, c = 18.93(2) A, and beta = 112.8(1) deg. GRA

N93-11727# SRI International Corp., Menlo Park, CA.

MECHANICAL PROPERTIES OF SEMICONDUCTORS AND THEIR ALLOYS Final Report, 1 Sep. 1988 - 13 Jan. 1992

A. Sher, M. A. Berding, A. T. Paxton, S. Krishnamurthy, and A.-B. Chen Feb. 1992 330 p
(Contract F49620-88-K-0009)
(AD-A253908; AFOSR-92-0690TR) Avail: CASI HC A15/MF A01

A wide range of subjects have been treated in this contract. We have devoted time to the development and applications of two first principles computational methods: one, the full-potential linear muffin tin orbital (FP-LMTO) method is somewhat mature and highly accurate, while the other, linear combination of atomic orbitals (LCAO), is less accurate but more flexible and is easily incorporated into the other calculations we have in place, e.g., surface Green's function methods and CPA. Tight binding has also been used. These methods have been applied to solve a host of mechanical-property problems including elastic constants, cleavage energies, sublimation energies, interactions between surface atoms relating to their surface order-disorder state and growth theory, surface segregation, bulk order-disorder theory and phase stability, the effect of dislocations on electronic transport and electro-optic properties of semiconductors, the Ni-Al intermetallic phase diagram, planar fault energies in L12 alloys, high-performance structural metal alloy design, and a contribution to understanding the Jones theory of metal alloying. Many of these subjects have been brought to publishable conclusions. Whenever possible, we have presented our detailed results in the form of preprints and reprints, with only brief summaries of the work given here. In instances where the research is incomplete, we have given somewhat longer expositions. GRA

N93-11747# Pittsburgh Univ., PA. Dept. of Physics and Astronomy.

THE PHYSICS OF PATTERN FORMATION AT LIQUID INTERFACES

J. V. Maher Jun. 1992 9 p
(Contract DE-FG02-84ER-45131)
(DE92-016971; DOE/ER-45131/10) Avail: CASI HC A02/MF A01

During the past year we have submitted six papers for publication, three related to the dynamics of macroscopic interfaces, and ultimately all related to solidification, and three related to the internal structure of disorderly materials, with possible applications to the processing of composite materials. In addition to completing all these projects during the past year, we have begun two new projects, one on pattern formation and one on aggregation within a composite system. A brief description is given of this research in this paper. DOE

N93-11753# National Academy of Sciences - National Research Council, Washington, DC.
SOLID STATE SCIENCES COMMITTEE FORUM Final Report, 1 Mar. 1991 - 29 Feb. 1992
Philip Smith May 1992 21 p
(Grant AF-AFOSR-0185-91)
(AD-A253556; AFOSR-92-0723TR) Avail: CASI HC A03/MF A01

The 1991 SSSC Forum was conducted under the auspices of the Board on Physics and Astronomy's Solid State Sciences Committee (SSSC) and cosponsored with the National Materials Advisory Board (NMAB). The Forum was the culmination of a year-long dissemination effort following up the NCR study Materials Science and Engineering for the 1990s that was released in September of 1989 and successfully brought together experts and policy makers in the field of advanced materials processing to discuss issues pertinent to the field. Support for the Forum was provided by the Air Force office of Scientific Research (AFOSR), the Department of Energy (DOE), the National Science Foundation (NSF), and the office of Naval Research (ONR). GRA

N93-11772# Oak Ridge National Lab., TN.
STEP-DRIVEN SURFACE SEGREGATION AND ORDERING DURING Si-Ge MBE GROWTH
D. E. Jesson, S. J. Pennycook, J. M. Baribeau, and D. C. Houghton Jun. 1992 9 p Presented at the Material Research Society Spring Meeting, San Francisco, CA, 27 Apr. - 2 May 1992
(Contract DE-AC05-84OR-21400)
(DE92-017827; CONF-920402-44) Avail: CASI HC A02/MF A01

An important role of type S(sub B) step edges in determining the as-grown microstructure of Si-Ge superlattices and alloys is implicated from direct Z-contrast images of as-grown structures. A variety of different ordered phase variants can arise at each Si on Ge interface as a result of vertical segregation during superlattice growth. A new monoclinic-ordered structure is predicted to arise as a result of lateral segregation during alloy growth. DOE

N93-11790# Booz-Allen and Hamilton, Inc., Arlington, VA.
SYSTEMS ENGINEERING AND TECHNICAL ASSISTANCE IN SUPPORT OF DIGITAL GALLIUM ARSENIDE INSERTION PROJECTS Final Report, 8 Nov. 1988 - 29 Feb. 1992
Daniel H. Butler 30 Apr. 1992 99 p
(Contract MDA972-89-C-0035)
(AD-A253751) Avail: CASI HC A05/MF A02

Booz-Allen provided a high level of support, including systems engineering analyses and technical assistance for systems insertion efforts using digital Gallium Arsenide (GaAs). Once insertion candidates were chosen, Booz-Allen supported the insertion efforts by acting as a liaison between the government and GaAs contractors, attending and arranging contractor reviews, providing meeting facilities, and producing presentation materials. A major accomplishment under this contract was the development of a methodology for appraising the likelihood of a successful technology insertion. This methodology is described in detail. Systems analyses and other work performed according to the terms of the statement of work is described as well. The conclusion discusses accomplishments under this project and of the DARPA digital GaAs insertion program generally. GRA

N93-11797# Sandia National Labs., Albuquerque, NM.
THE CHEMISTRY OF Si3N4 AND Si DEPOSITION STUDIED USING MOLECULAR BEAM TECHNIQUES
R. J. Buss, P. Ho, and W. G. Breiland 1992 10 p Presented at the 182d Meeting of the Electrochemical Society, Toronto, Ontario, 11-16 Oct. 1992
(Contract DE-AC04-76DP-00789)
(DE92-018268; SAND-92-0722C; CONF-921036-4) Avail: CASI HC A02/MF A01

Molecular beam techniques can be used to obtain valuable kinetic information for the chemistry of high temperature deposition processes. Molecular beam measurements of Si3N4 deposited from SiF4 and NH3 have shown that the CVD reactor chemistry is dominated by surface reactions of the starting gases. Using a beam of heated silane, it is shown that the translational and internal energy of the gas does not influence its surface reactivity in silicon CVD. The IRIS (Imaging of Radicals Interacting with Surfaces) technique for measuring the surface reactivity of radicals during deposition is also discussed with examples (SiH, SiO, and NH). DOE

N93-11813# Midwest Research Inst., Golden, CO.
MICROSCOPIC ORIGINS OF METASTABLE EFFECTS IN a-Si:H AND DEEP DEFECT CHARACTERIZATION IN a-Si,Ge:H ALLOYS
J. D. Cohen (Oregon Univ., Eugene.) Jul. 1992 22 p
(Contract DE-AC02-83CH-10093)
(DE92-010588; NREL/TP-451-4938) Avail: CASI HC A03/MF A01

This report describes works to use transient photocapacitance and photocurrent measurements to determine the deep defect distribution and processes in low-band-gap a-Si, Ge:H alloys. Samples for these studies were produced by the photochemical vapor deposition (photo-CVD) growth method and were obtained through a collaboration with researchers at the University of Delaware. This report discusses how a detailed comparison between the photocapacitance and photocurrent spectra can be used to separately examine the majority and minority carrier processes. The results are as follows: (1) The midgap defect densities in the alloy regime near 1.3 eV can be as low as 5 x 10(exp 16) cm(exp -3) in such photo-CVD samples. (2) There exists a second defect band roughly 0.4 eV below E(sub C) of a similar magnitude to the midgap defect density that exhibits significant lattice relaxation behavior in its electron trapping dynamics. (3) The hole (mu)(tau) products determined for the lowest defect sample are roughly 5 x 10(exp -10) sq cm/V, comparable with the highest hole (mu)(tau) products reported in sandwich geometry measurements for alloys in this composition range. (4) The hole (mu)(tau) is found to be roughly inversely proportional to the midgap defect density for the samples studied. This is consistent with the fact that the effective minority carrier lifetime for such measurements is limited by the deep state trapping time. DOE

N93-11816# Midwest Research Inst., Golden, CO.
RECOMBINATION AND METASTABILITY IN AMORPHOUS SILICON AND SILICON GERMANIUM ALLOYS
M. Silver (North Carolina Univ., Chapel Hill.) Jul. 1992 14 p
(Contract DE-AC02-83CH-10093)
(DE92-010593; NREL/TP-451-4962) Avail: CASI HC A03/MF A01

This report describes the first year of a continuing research study to understand how recombination, trapping, and band-mobility modification affecting the electronic properties of amorphous semiconductors can be measured, characterized, and described by an appropriate spectrum of defect states, and how light-induced defects in a-Si:H and native defects in a-SiGe:H affect transport properties in these materials. The objective was to determine how the Staebler-Wronski defects affect the electronic processes in a-Si:H and a-SiGe:H films. To do this, electroluminescence (EL) and forward bias current in p-i-n devices (i-layer thicknesses greater than 2 micron) were studied both experimentally and theoretically before and after light soaking. A simple picture was developed to compare forward bias current to the EL signal. The result was unexpected: the product of the final current times the rise time was not constant before and after light soaking as expected from the concept of gain band width, but instead changed radically. The rise time t(sub x) increased by more than one order of magnitude while the final current I(sub f) did not change significantly with light soaking. On the other hand the I(sub f)t(sub x) product did hold close to a constant when only the applied voltage changed. DOE

N93-11818# Midwest Research Inst., Golden, CO.
RESEARCH ON STABLE, HIGH-EFFICIENCY, AMORPHOUS SILICON MULTIJUNCTION MODULES
A. Catalano (Solarex Corp., Newtown, PA.), M. Bennett (Solarex Corp., Newtown, PA.), L. Chen (Solarex Corp., Newtown, PA.), R. DAiello (Solarex Corp., Newtown, PA.), B. Fieselmann (Solarex Corp., Newtown, PA.), Y. Li (Solarex Corp., Newtown, PA.), J. Newton (Solarex Corp., Newtown, PA.), R. Podlesny (Solarex Corp., Newtown, PA.), and L. Yang (Solarex Corp., Newtown, PA.) Aug. 1992 47 p
(Contract DE-AC02-83CH-10093)
(DE92-010599; NREL/TP-411-4995) Avail: CASI HC A03/MF A01

This report describes work to demonstrate a multijunction module with a 'stabilized' efficiency (600 h, 50 C, AM1.5) of 10.5 percent. Triple-junction devices and modules using a-Si:H alloys with carbon and germanium were developed to meet program goals. ZnO was used to provide a high optical transmission front contact. Proof of concept was obtained for several important advances deemed to be important for obtaining high (12.5 percent) stabilized efficiency. They were (1) stable, high-quality a-SiC:H devices and (2) high-transmission, textured ZnO. Although these developments were not scaled up and included in modules, triple-junction module efficiencies as high as 10.85 percent were demonstrated. NREL measured 9.62 and 9.00 percent indoors and outdoors, respectively. The modules are expected to lose no more than 20 percent of their initial performance. DOE

N93-11842# Sandia National Labs., Albuquerque, NM.
IMPLANTED He RETENTION AND RELEASE FROM BORONIZED LAYERS
B. L. Doyle, D. S. Walsh, and W. R. Wampler 1991 17 p
Presented at the 10th International Conference on Plasma-Surface Interactions in Controlled Fusion Devices, Monterey, CA, 30 Mar. - 3 Apr. 1992
(Contract DE-AC04-76DP-00789)
(DE92-013983; SAND-91-2484C; CONF-920311-9) Avail: CASI HC A03/MF A01

He-3 has been implanted at an energy of 3 keV into amorphous hydrogenated boron-carbon (a-BC) films deposited by RF sputtering onto single crystal Si substrates. The initial composition of the films was analyzed by nuclear-enhanced backscattering spectrometry to be B2C with approximately 20 percent H and approximately 10 percent O. The areal density of the implanted and retained He-3 was measured in situ by a new ion beam analysis technique using the He-3 (He-3,pp) three-body nuclear reaction. The He trapping or pumping efficiency at room temperature is only 3.4 percent for low fluence implants and the a-BC layer saturates with He at a fluence of 5 x 10(exp 17) He/cm(exp 2). At this saturation fluence, only 3.1 x 10(exp 15) He/cm(exp 2) is retained in the film. Isochronal annealing of the implanted samples reveals a distributed release of implanted He at approximately 200 C which corresponds to a trap activation energy of 1.65 plus or minus 0.25 eV. He-3 was trapped less efficiently at 250 C than at room temperature and exhibited a saturated retention of 8.6 x 10(exp 14) He/cm(exp 2). These results indicate that wall pumping should play only a minor role in the interpretation of the Textor He-pump experiment carried out earlier this year. The results also show that the unintentional deposition of a-BC, onto He pumping plates could adversely affect the operation of such devices, and should therefore be avoided. DOE

N93-11868# Utah Univ., Salt Lake City. Dept. of Materials Science and Engineering.
BASIC PRINCIPLES OF ORGANOMETALLIC VAPOR PHASE EPITAXY
G. B. Stringfellow 22 May 1992 22 p
(Contract N00014-91-J-1447)
(AD-A250665; TR-33) Avail: CASI HC A03/MF A01

Crystal growth processes in general and epitaxy in particular are often discussed in terms three disciplines: thermodynamics, mass transport and hydrodynamics, and chemical reaction kinetics. This paper will concentrate on two of these, the thermodynamic and kinetic aspects of organometallic vapor phase epitaxy (OMVPE). Three major influences of thermodynamics will be discussed: (1) Thermodynamics defines the driving force and hence the upper limit of growth rate. This occurs only when all reactants in the system are allowed to equilibrate with the substrate. (2) Thermodynamics often controls stoichiometry and the solid composition of alloys. An understanding of thermodynamic and kinetic constraints leads to the ability to grow metastable alloys. (3) The driving force for phase separation and/or ordering into natural superlattice structures during growth is also governed by thermodynamics. The actual ordered structures observed are dependent on the surface kinetics. This aspect of kinetics will be addressed in addition to the kinetics of both homogeneous and heterogeneous chemical reactions occurring for a variety of precursor molecules. Each of these topics is addressed in terms of fundamental concepts, with examples from recent research on the OMVPE growth of III/V semiconductor compounds and alloys. GRA

N93-11869# Utah Univ., Salt Lake City. Dept. of Materials Science and Engineering.
TRIISOPROPYLINDIUM: DECOMPOSITION STUDY AND USE FOR LOW TEMPERATURE GROWTH
C. H. Chen and G. B. Stringfellow 22 May 1992 26 p
(Contract N00014-91-J-1447)
(AD-A250666; TR-20) Avail: CASI HC A03/MF A01

The organometallic vapor phase epitaxial (OMVPE) growth of In-containing III-V semiconductors typically uses trimethylindium (TMIn). However, TMIn suffers from several problems. First, it is well known that the effective vapor pressure of solid TMIn changes with time because of changes in the surface area. Secondly, TMIn decomposes slowly for temperatures lower than 400 C in an atmospheric pressure OMVPE reactor; it is too stable for some low temperature applications. In addition, it causes carbon contamination, especially at low temperatures, due to the CH3 radicals. Thus, there is a need for new In precursors that are liquids at room temperature and do not contain CH3 radicals. This work reports the first decomposition and OMVPE growth studies for a newly developed indium source, triisopropylindium (TIPIn). The decomposition study was carried out in an isothermal flow tube reactor with the reaction products analyzed using a mass spectrometer. The temperature for 50 percent decomposition is approximately 110 C for TIPIn in a He ambient. This is about 2OO C lower than that for TMIn under similar conditions. GRA

N93-11894# Dartmouth Coll., Hanover, NH. Dept. of Physics.
EXCITONS IN SEMICONDUCTING SUPERLATTICES, QUANTUM WELLS, AND TERNARY ALLOYS
M. D. Sturge, R. E. Nahory, and M. C. Tamargo (Bell Communications Research, Inc., Red Bank, NJ.) Jun. 1992 10 p
(Contract DE-FG02-87ER-45330)
(DE92-015178; DOE/ER-45330/5) Avail: CASI HC A02/MF A01

Semiconducting layered structures can now be fabricated with precisely defined layer thicknesses down to one monolayer. An example is the 'superlattice' (SL) structure, in which to semiconductors with different band gaps are interleaved. The electronic and optical properties of the SL are quite different from those of the constitutents and offer interesting new possibilities both in device design and in basic physics. This proposal aims to improve our understanding of optically excited states in SL's, particularly in the so-called 'Type 2 indirect' SL's in which in electron and hole created by optical excitation are separated both in real and in momentum space. We study these structures by time-resolved tunable laser spectroscopy, with and without external perturbations such as magnetic field, electric field, and uniaxial stress. In SL's with only a few atomic layers per period the familiar 'effective mass model' of semiconductor states breaks down. We have made precise optical experiments on well-characterized material to test current 'first principles' calculations of the band structure. Our work under this grant has shown that the material we are using is of sufficiently high quality to test the theoretical predictions. Comparison of theory and experiment provides a new and sensitive probe of the interface quality on a fine scale. Statistical analysis of the temperature dependence of the exciton decay dynamics provides complementary information. From a careful study of the exciton spectra of the recently discovered mixed type 1- type 2 CdTe/CdZnTe SL's we have obtained the band offset at the CdTe/CdZnTe interface to unprecedented accuracy. DOE

N93-11915# California Univ., Berkeley. Lawrence Berkeley Lab.
SILICON ON INSULATOR STRUCTURES IN SELECTIVE EPITAXIAL GROWTH
Z. Weng, R. Gronsky, J. Lou, and W. Oldham Nov. 1991 8 p Presented at the Annual Fall Meeting of the Materials Research Society, Boston, MA, 2-6 Dec. 1991
(Contract DE-AC03-76SF-00098)
(DE92-017118; LBL-31609; CONF-911202-83) Avail: CASI HC A02/MF A01

Silicon-on-insulator structures were formed by the selective epitaxial growth (SEG) of silicon and the epitaxial lateral overgrowth (ELO) of oxide shapes using an LPCVD hot-walled reactor at 850 C. The homoepitaxial interface changed character with modifications of the gas composition during the in-situ pre-epitaxial bake at 900 C. HREM images show ellipsoid-shaped inclusions lying along the homoepitaxial interface for silicon growth conduced with no dichlorosilane (DCS) flow during the prebake in H2. SIMS analysis indicates a large oxygen, fluorine, and carbon concentration at the interface. For structures grown with a small DCS flow in addition to H2 during the prebake, the homoepitaxial structural defects and the oxygen, fluorine, and carbon peaks are removed. DOE

N93-11996 Newcastle-upon-Tyne Univ. (England).
ELECTRONIC AND OPTICAL PROPERTIES OF PERFECT AND IMPERFECT 2 TO 6 SUPERLATTICES Ph.D. Thesis
A. W. Beavis 1990 106 p
Avail: Univ. Microfilms Order No. BRDX96304

The calculation of the electronic and optical properties of mercury telluride-cadmium telluride, HgTe-CdTe, superlattices are presented. An empirical pseudopotential method is employed, which fully accounts for the (large differences in) microscopic potentials and relativistic corrections. We consider superlattices in which the interfaces between the constituent materials are spatially abrupt, the model usually invoked in the literature. We also consider the effect of superlattices with microscopically imperfect interface geometry. These are the first calculations in which such a realistic model is considered. The effect of removing this bulk like translational symmetry at the interfaces is investigated and new states localized at the interfaces are discussed. Experimental data are discussed (transport and photoluminescence results) which may provide evidence for the results found by our calculations. The possibilities and scope of structures available via band structure engineering with II-VI materials is considered. Calculations performed on mercury telluride-zinc cadmium telluride, HgTe-ZnCdTe structures are presented which are examples of how the HgTe-CdTe structures may be engineered. The structures discussed are compared to the equivalent HgTe-CdTe structures. The design of a superlattice comprising of HgCdTe-CdTe is discussed in the context of the enhancement of optical non-linearities. How the HgTe-CdTe superlattice may be tailored to suite the requirements of the mechanism to provide such enhancements is shown. Dissert. Abstr.

N93-12065# Lawrence Livermore National Lab., CA.
SUPERCONDUCTING MULTILAYER STRUCTURES GROWN BY ALL-MBE
I. Bozovic, J. N. Eckstein, M. E. Klausmeier-Brown, G. F. Virshup, and K. S. Ralls 21 May 1992 9 p Presented at the Material Research Society Spring Meeting, San Francisco, CA, 27 Apr. - 2 May 1992
(Contract W-7405-eng-48)
(DE92-018011; UCRL-JC-110726; CONF-920402-46) Avail: CASI HC A02/MF A01

Thin films of various Bi-Sr-Ca-Cu-O (2201, 2212,...,2-2-11-12) compounds have been synthesized using atomic-layer-by-layer molecular beam epitaxy (ALL-MBE). Signal-crystal films with excellent transport properties, smooth surfaces and atomically sharp interfaces in multilayer structures have been obtained. That made it possible to deposit virtually perfect ultrathin layers and superlattices, and fabricate hysteretic Josephson junctions from SIS multilayers. DOE

N93-12073# EG and G Rocky Flats, Inc., Golden, CO.
THE EFFECT OF PRECIPITATE FORMING ELEMENTS IN Al 4.5 PERCENT Mg ALLOYS ON THE MEASURED ACOUSTIC EMISSION AND ON LUEDERS BAND DEFORMATION
D. L. Armentrout and S. H. Carpenter 1992 8 p Presented at the 11th International Acoustic Emission Symposium, Fukuoka (Japan), 26-29 Oct. 1992
(Contract DE-AC34-90DP-62349)
(DE92-016864; RFP-4581; CONF-9210150-1) Avail: CASI HC A02/MF A01

Acoustic emission (AE) was measured in Al 4.5 percent Mg alloys with varying amounts of additional elements which form precipitates in this system. During tensile testing, the samples deformed inhomogeneously with multiple yield points - often called Lueders bands. Calculated strain rates during Lueders deformation were greater than 10/s. Three distinct regions could be observed in close examination of the drop in stress associated with the yield points. The AE signal peak was found to occur during the region of steepest decrease in the stress. The magnitude of the stress drops which is proportional to the amount of plastic deformation in the individual yield points correlated well with the height of the corresponding rms voltage bursts. DOE

N93-12090# Argonne National Lab., IL.
ULTRAFAST PHOTOINDUCED ELECTRON TRANSFER REACTIONS IN SUPRAMOLECULAR ARRAYS: FROM CHARGE SEPARATION AND STORAGE TO MOLECULAR SWITCHES
M. R. Wasielewski 1992 3 p Presented at the 14th IUPAC Symposium on Photochemistry, Leuven (Belgium), 19-25 Jul. 1992
(Contract W-31-109-eng-38)
(DE92-016186; ANL/CP-75590; CONF-9207104-1) Avail: CASI HC A01/MF A01

Photoinduced charge separation reactions form the basis for energy storage processes in both natural and artificial photosynthesis. Moreover, rapid reversible photoinduced electron transfer reactions are a class of photophysical phenomena that can be exploited to develop schemes for optical switching. Examples from each of these fields are discussed. DOE

N93-12093# Lawrence Livermore National Lab., CA.
THE ADSORPTION OF C60 AND THE CO-ADSORPTION OF C60 AND H2O ON (ALPHA)-Al2O3 (1 -1 0 2)-(2X1)
A. V. Hamza and M. Balooch May 1992 16 p Presented at the 14th Combustion Research Meeting, Tahoe City, CA, 14-17 Jun. 1992
(Contract W-7405-eng-48)
(DE92-018002; UCRL-JC-110655; CONF-9206180-4) Avail: CASI HC A03/MF A01

The adsorption of C60 and the co-adsorption of C60 and H20 on (alpha)-Al2O3 (1 -1 0 2)(2x1) has been investigated by temperature-programmed desorption (TPD) spectroscopy. C60 is adsorbed on a clean and well-characterized sapphire surface at room temperature by evaporation from a thin C60 film previously vacuum deposited on a stainless steel substrate or from C60 powder enclosed in gold foil. Multilayer desorption of C60 (detected as a doubly ionized particle, m/e=360, with a quadrupole mass spectrometer) is observed with a peak temperature for desorption increasing from 520 to 570 K with increasing coverage. The peak shape is characteristic of zero-order desorption kinetics with an activation energy of 32.4 +/- 0.4 kcal/mol and a pre-exponential factor of 4.3 x 10(sup 12) monolayer/s. At submonolayer coverages (less than 0.5 monolayer, where one monolayer equals 1.21 x 10(sup 14) molecules/cm(sup 2)) the bonding of the C60 to the substrate is observed with a peak temperature for desorption between 430 and 460 K. Activation energy and pre-exponential factor calculated based on first-order desorption kinetics are 25 +/- 6 kcal/mol and 6.3 x 10(sup 11) s(sup -1) respectively. Exposure of C60 to a water predosed surface at room temperature did not displace the adsorbed surface hydroxyls. Concomitant desorption of C60 and some water is observed from a water predosed surface subsequently exposed to C60 multilayers. Whereas, water post-dosed onto a C60-covered surface has a reduced sticking probability. DOE

N93-12099# California Univ., Berkeley. Lawrence Berkeley Lab.

GROWTH OF 2-6 THIN-FILMS FROM SINGLE-SOURCE PRECURSORS BASED ON STERICALLY ENCUMBERED SITEL LIGANDS

J. Arnold, A. L. Seligson, J. M. Walker, E. D. Bourret, and P. J. Bonasia Apr. 1992 17 p Presented at the 6th International Conference on Metalorganic Vapor Phase Epitaxy, Cambridge, MA, 8-11 Jun. 1992
(Contract DE-AC03-76SF-00098)
(DE92-017077; LBL-31740; CONF-920660-1) Avail: CASI HC A03/MF A01

We have developed a new route to MOCVD of 2-6 compounds based on the use of novel single-source precursors in which the 2-6 elements are combined at the molecular level in a single covalent compound. We have prepared and fully characterized a number of new derivatives of zinc, cadmium, and mercury incorporating large, sterically demanding tellurolate ligands of general formula: M(sitel)(sub 2) where sitel = -TeSi(SiMe)(sub 3). The crystalline compounds are relatively volatile and are easily manipulated under nitrogen. Several of these compounds have been tested for their suitability as precursors in the MOCVD process. Clean pyrolysis reactions and deposition of thin films were achieved. The stoichiometry of the pyrolysis reaction has been determined by analysis of the reaction by-products. DOE

N93-12109# California Univ., Berkeley. Lawrence Berkeley Lab.

INFRARED PHONON STRUCTURE IN EPITAXIAL FILMS OF Tl2Ca2Ba2Cu3O10 AT LOW TEMPERATURES

D. Miller, P. L. Richards, W. Y. Lee (IBM Research Lab., San Jose, CA.), N. Newman (Conductus, Inc., Sunnyvale, CA.), S. M. Garrison (Conductus, Inc., Sunnyvale, CA.), and J. S. Martens (Sandia National Labs., Albuquerque, NM.) Feb. 1992 6 p
(Contract DE-AC03-76SF-00098)
(DE92-017078; LBL-32010) Avail: CASI HC A02/MF A01

We have used both bolometric and cavity techniques to obtain accurate submillimeter and microwave loss data for epitaxial thin films of Tl2Ca2Ba2Cu3O10 at low temperatures. These films have T(c)=121.5 K, are c-axis oriented, contain some volume fraction of the 2:1:2:2 phase, and are characterized by excellent in-plane epitaxy. The absorptivity of these films at 100 cm(sup -1) is a factor of five lower than that obtained by others from a reflectivity measurement on a ceramic sample. We observe strong phonon structure for frequencies between 70 and 600 cm(sup -1), which are in agreement with a lattice dynamical calculation. Our results show remarkably similar phonon structure to that observed in the ceramic sample. This is in strong contrast to the case for other high T(c) superconductors such as YBa2Cu3O7, where phonon structure observed in ceramic samples in absent in epitaxial oriented films and crystals because of the electronic screening due to the high conductivity of the a-b planes. At microwave frequencies the absorptivity follows a frequency squared dependence, and is consistent with the submillimeter results. DOE

N93-12124# California Univ., Berkeley. Lawrence Berkeley Lab.

IMAGE POTENTIAL STATES AT METAL-DIELECTRIC INTERFACES Ph.D. Thesis

W. R. Merry, Jr. Apr. 1992 232 p
(Contract DE-AC03-76SF-00098)
(DE92-017019; LBL-32352) Avail: CASI HC A11/MF A03

Angle-resolved two-photon laser photoemission was used to observe the image potential electronic states on the (111) face of a silver single crystal. The transient image potential states were excited from the occupied bulk bands with photons whose energy was tunable around 4 eV. Photoemission of the image potential states was accomplished with photons of energy tunable around 2 eV. Image potential states were found to persist in the presence of physisorbed adlayers of xenon and cyclohexane. On clean Ag(111), the effective mass of the n=1 image potential state was found to be 1.4 +/- 0.1 times the mass of a free electron (m(sub e)). A binding energy of 0.77 eV, measured by earlier workers, was assumed in analysis of the data for the clean surface. On Ag(111), at 75 K covered by one monolayer of xenon, the binding energy of the n = 1 image potential state was unchanged relative to its value on the clean surface. An effective mass of (1.00 +/- 0.05) (dot) m(sub e) was obtained. On Ag(111) at 167 K, covered by one monolayer of cyclohexane, the binding energy of the n = 2 member of the image potential series was 0.30 +/- 0.05 eV. The energy of the n=1 state was again unchanged by deposition of the adsorbate. The effective masses of both states were (0.90 +/- 0.1) (dot) m(sub e). DOE

N93-12125# California Univ., Berkeley. Lawrence Berkeley Lab.

SUBMILLIMETER AND MICROWAVE RESIDUAL LOSSES IN EPITAXIAL FILMS OF Y-Ba-Cu-O AND Bl-Ca-Ca-Cu-O

D. Miller, P. L. Richards, S. M. Garrison (Conductus, Inc., Sunnyvale, CA.), N. Newman (Conductus, Inc., Sunnyvale, CA.), C. B. Eom (Stanford Univ., CA.), T. H. Geballe (Stanford Univ., CA.), and S. Etemad (Bell Communications Research, Inc., Red Bank, NJ.) Mar. 1992 31 p Presented at the 2nd Symposium on High Temperature Superconductors in High Frequency Fields, Santa Fe, NM, 1-3 Apr. 1992
(Contract DE-AC03-76SF-00098)
(DE92-017075; LBL-32148; CONF-9204169-1) Avail: CASI HC A03/MF A01

We have used a novel bolometric technique and a resonant technique to obtain accurate submillimeter and microwave residual loss data for epitaxial thin films of YBa2Cu3O7, Tl2Ca2Ba2Cu3O10, and Tl2CaBa2Cu2O8. For all films we obtain good agreement between the submillimeter and microwave data, with the residual losses in both the Y-Ba-Cu-O and Tl-Ca-Ba-Cu-O films scaling approximately as frequency squared below approximately 1 THz. We are able to fit the losses in the Y-Ba-Cu-O films to a weakly coupled grain model for the a-b plane conductivity, in good agreement with results from a Kramers-Kronig analysis of the loss data. We observe strong phonon structure in the Tl-Ca-Ba-Cu-O films for frequencies between 2 and 21 THz, and are unable to fit these losses to the simple weakly coupled grain model. This is in strong contrast to the case for other high T(sub c)superconductors such as YBa2Cu3O7, where phonon structure observed in ceramic samples is absent in epitaxial oriented films and crystals because of the electronic screening due to the high conductivity of the a-b planes. DOE

N93-12127# California Univ., Berkeley. Lawrence Berkeley Lab.

FORMATION OF BURIED EPITAXIAL Si-Ge ALLOY LAYERS IN Si (100) CRYSTAL BY HIGH DOSE Ge ION IMPLANTATION

Kin Man Yu, I. G. Brown, and S. Im Nov. 1991 6 p Presented at the Annual Fall Meeting of the Materials Research Society, Boston, MA, 2-6 Dec. 1991

(Contract DE-AC03-76SF-00098)
(DE92-017114; LBL-30989; CONF-911202-82) Avail: CASI HC A02/MF A01

We have synthesized single crystal Si(1-x)Ge(x) alloy layers in Si group of zone axis (100) crystals by high dose Ge ion implantation and solid phase epitaxy. The implantation was performed using the metal vapor vacuum arc (Mevva) ion source. Ge ions at mean energies of 70 and 1000 keV and with doses ranging from 1(10)(exp 16) to 7(10)(exp 16) ions/sq cm were implanted into Si group of zone axes (100) crystals at room temperature, resulting in the formation of Si(1-x)Ge(x) alloy layers with peak Ge concentrations of 4 to 13 atomic percent. Epitaxial regrowth of the amorphous layers were initiated by thermal annealing at temperatures higher than 500 C. The solid phase epitaxy process, the crystal quality, microstructures, interface morphology, and defect structures were characterized by ion channeling and transmission electron microscopy. Compositionally graded single crystal Si(1-x)Ge(x) layers with full width at half maximum approximately 100nm were formed under a approximately 30nm Si layer after annealing at 600 C for 15 min. A high density of defects was found in the layers as well as in the substrate Si just below the original amorphous/crystalline interface. The concentration of these defects was significantly reduced after annealing at 900 C. The kinetics of the regrowth process, the crystalline quality of the alloy layers, the annealing characteristics of the defects, and the strains due to the lattice mismatch between the alloy and the substrate are discussed. DOE

N93-12134# Sandia National Labs., Albuquerque, NM.
THE DEPOSITION CHARACTERISTICS OF COPPER(I) COMPOUNDS FOR CVD BY FT-IR SPECTROSCOPY
F. D. Hardcastle, C. H. F. Peden, T. R. Omstead, R. S. Blewer, J. Farkas (New Mexico Univ., Albuquerque.), M. J. Hampden-Smith (New Mexico Univ., Albuquerque.), and T. T. Kodas (New Mexico Univ., Albuquerque.) 1991 4 p Presented at the Materials Research Society (MRS) Symposium on Advanced Metallization for Very Large Scale Integration (VLSI) Applications, Murray Hill, NJ, 8-10 Oct. 1992
(Contract DE-AC04-76DP-00789)
(DE92-010778; SAND-91-2311C; CONF-921054-1) Avail: CASI HC A01/MF A01

Fourier transform-infrared spectroscopy (FT-IR) was used to investigate the adsorption and thermally-induced decomposition of copper(I) beta-diketonate precursors of the type (hfac)CuL, where hfac is the hexafluoroacetylacetonate bidentate ligand and L is trimethylphosphine or 1,5-cyclooctadiene. The (hfac)CuPMe(sub 3) precursor desorbs from the surface at very low temperatures whereas the (hfac)Cu(1,5-COD) dissociates on adsorption, liberating 1,5-COD and leaving a surface(hfac)Cu complex which can subsequently disproportionate. Evidence is provided for hydrogen-bonding between the hfac ligand and the surface silanols for (hfac)CuPMe(sub 3), but not for (hfac)Cu(1,5-COD). These results are consistent with the selective behavior of these precursors for copper deposition and suggest that the selectivity of the (hfac)CuPMe(sub 3) and (hfac)Cu(1,5-COD) precursors may be due to the ability of the hfac ligand to hydrogen bond to the surface silanol groups. DOE

N93-12169# Sierra Monolithics, Inc., Redondo Beach, CA.
JOSEPHSON JUNCTION DIGITAL WAVEFORM GENERATION FOR VERY WIDEBAND RADARS Final Report, 1 Aug. 1991 - 31 Jan. 1992
Dave Rowe 31 Jan. 1992 39 p
(Contract F49620-91-C-0066)
(AD-A253668; AFOSR-92-0722TR) Avail: CASI HC A03/MF A01

The design, fabrication, and testing of an ultra-wideband DDS, based upon superconducting JJ logic technology, which has direct insertion applications in present and future DOD Radar, Communication, or ECM systems is discussed. The phase 1 objectives are to define the DDS system parameters, develop the DDS architecture for the identified system, and perform detailed circuit designs and a system performance appraisal. In addition, a teaming arrangement with a superconducting foundry will be evaluated for Phase 2 device evaluation. GRA

N93-12175# Duke Univ., Durham, NC. Dept. of Chemistry.
SYNTHESIS AND CHARACTERIZATION OF NOVEL ALUMINUM-ARSENIC COMPOUNDS 2. CRYSTAL STRUCTURES OF (R2AlAs (SiMe3)2)2 (R = i-Bu, Me) AND i-Bu2 (Cl)Al*As (SiMe3)3
R. L. Wells, A. T. McPhail, and T. M. Speer 12 Mar. 1992 20 p
(Contract N00014-89-J-1545)
(AD-A248001; DU/DC/TR-26) Avail: CASI HC A03/MF A01

The feasibility of utilizing dehalosilylation and lithium chloride elimination reactions for the preparation of compounds that may serve as precursors to aluminum-arsenic containing semiconducting materials has been further investigated. The novel aluminum-arsenic dimers (i-Bu2AlAs(SiMe3)2)2 (1) and (Me2AlAs(SiMe3)2)2 (2) were prepared by coupling reactions between LiAs(SiMe3)2 and R2AlCl (R = i-Bu and Me, respectively). Reactions between As(SiMe3)3 and R2AlCl (R = i-Bu, Me) in 1:1 and 1:2 mole ratio at ambient temperature have failed to give expected dehalosilylation products, but have instead yielded the adducts R2(Cl)Al-As(SiMe3)3 (R = i-Bu (3) and Me (4)). All compounds were characterized by partial elemental analysis and H-1, C-13(H-1), and Al-27(H-1) NMR spectroscopy. Compounds 1, 2 and 3 were fully characterized by single-crystal x-ray analysis. Crystal data are as follows: 1, monoclinic, space group C2(sub 1)/c(C(sub 2h)(sup 6)), a = 19.202(2) A, b = 12.601(1) A, c = 19.278(2) A, b = 106.86(1) deg; 2, triclinic, space group P1(C(sub i)(sup 1)) a = 9.723(1) A, b = 9.968(1) A, c = 9.246(1) A, a 99.18(1) deg, b = 115.70(1) deg, g = 77.13(1) deg; 3, monoclinic, space group P2(sub 1)/c(C(sub 2h5)), a = 15.105(1) A, b 11.574(1) A, c = 18.655(1) A, b = 119.25(1) deg. GRA

N93-12178# Argonne National Lab., IL.
FLUX DYNAMICS AND IRREVERSIBILITY IN YBa2Cu3O7 WITH Y2BaCuO5 INCLUSIONS AND IN SINGLE CRYSTAL YBa2Cu3O7
K. Fossheim (Norges Tekniske Hoegskole, Trondheim.), M. G. Karkut (Norges Tekniske Hoegskole, Trondheim.), L. K. Heill (Norges Tekniske Hoegskole, Trondheim.), M. Slaski (Norges Tekniske Hoegskole, Trondheim.), L. T. Sagdahl (Norges Tekniske Hoegskole, Trondheim.), and V. Vinokur Jan. 1992 15 p Presented at the Nobel Jubliee Symposium on Low Dimensional Properties of Solids, Gothenburg, Sweden, 4-7 Dec. 1991
(Contract W-31-109-eng-38)
(DE92-009712; ANL/CP-75450; CONF-9112107-1) Avail: CASI HC A03/MF A01

We have measured the ac magnetic permeability response function mu = mu' +(i)mu'' in melt-processed melt grown (MPMG) YBa2Cu3O7 with Y2BaCuO5 inclusions and in single crystal (SC) YBa2Cu3O7 in applied magnetic fields up to 8 Tesla oriented either parallel or perpendicular to the crystalline c-axis. The ac response of the two samples has been mapped out as a function of temperature, frequency, ac field amplitude, dc applied field, and field orientation. The peak in the lossy part of the susceptibility mu'' is used to probe the flux dynamics in the vicinity of the irreversibility line. The data are interpreted by comparison with expectations of an anisotropic vortex glass-to-liquid transition. The inferred melting lines, as well as the frequency dependence and non-linear response, are in overall agreement with the expected behavior. In the range of available parameters and variables we find the system to be in the solid vortex phase for H(perpendicular)c since there is a strong H(sub ac) dependence and only a weak frequency dependence on the temperature position of the loss peak. For H(parallel)c, the situation is reversed, and the loss peak depends only weakly on H(sub ac) and strongly on the frequency. DOE

N93-12183# TRW Electronic Systems Group, Redondo Beach, CA.
GaAs HETEROJUNCTION DEVICE BASED A/D CONVERTER DEVELOPMENT Final Report, Aug. 1987 - Mar. 1992
Ken DeGraaf, Clark Custer, and Stacey Bui Apr. 1992 59 p
(Contract N00014-87-C-0315)
(AD-A252644) Avail: CASI HC A04/MF A01

This final report summarizes the technical work performed on the development of a GaAs Heterojunction analog-to-digital converter. The program goal was to develop a 12 bit 20 Msps, less than 1 Watt/20 Msps ADC implemented as a single monolithic chip or at most 2 chips. The part developed on this program is a single chip monolithic GaAs Heterojunction Bipolar Transistor (HBT) ADC that includes a sample-and-hold (S/H) and all of the active circuitry required for stand alone operation. The ADC development was taken to the point of fabricating one lot of 3 wafers, wafer probing, and packaging a few of the best candidate ADCS. Yield on the first (and only) lot was 18 percent for 4 MBE wafers. Three MOCVD wafers had low beta and were not finished. Several parts were packaged. Electrical trimming was accomplished on the first 5 most significant bits (msbs) and triangle and sine waveforms processed through the ADC. The chip demonstrated the highest reported SNR of 49.7 dB for a GaAs ADC (8 bit theoretical SNR = 49.9dB). GRA

N93-12218# Pennsylvania State Univ., University Park.
HYDROGEN ASSISTED HEAT TRANSFER DURING DIAMOND GROWTH USING CARBON AND TANTALUM FILAMENTS
W. A. Yarbrough, K. Tankala, M. Mecray, and T. DebRoy 11 Mar. 1992 14 p
(Contract N00014-92-J-1125)
(AD-A247944; TR-2) Avail: CASI HC A03/MF A01

Much of the previous work on the role of atomic hydrogen in diamond has been focussed on its formation on various refractory metal filaments, its reaction in the gas phase, and its role in the growth mechanism. In contrast, the effect of atomic hydrogen recombination on substrate heating is addressed in this paper. Experiments were conducted in vacuum, helium, and hydrogen environments. Tantalum and carbon filaments were used to vary atomic hydrogen generation rates. Furthermore, methane was added in some experiments to determine its effect on hydrogen assisted chemical heating of the substrate. The results indicate that when substantial amounts of atomic hydrogen are generated at the filament, reactions of atomic hydrogen at the diamond growth surface have a pronounced effect on the substrate temperature. Use of carbon filaments lead to significantly diminished atomic hydrogen generation rates and much lower substrate temperatures. Additions of small amounts of methane to hydrogen also resulted in reduced atomic hydrogen generation rates and consequently, lower substrate temperatures. GRA

N93-12228# Florida Univ., Gainesville. Dept. of Electrical Engineering.
DEVELOPMENT OF ULTRA-LOW NOISE, HIGH SENSITIVITY PLANAR METAL GRATING COUPLED AlGaAs/GaAs MULTIQUANTUM WELL IR DETECTORS FOR FOCAL PLANE ARRAY STARING IR SENSOR SYSTEMS Quarterly Progress Report No. 4, 1 May - 31 Jul. 1992
Sheng S. Li 7 Aug. 1992 48 p
(Contract N00014-91-J-1976)
(AD-A254697) Avail: CASI HC A03/MF A01

Project objectives include the following: (1) to develop low dark current and high detectivity planar metal grating coupled bound-to-miniband 3-5 multiquantum well infrared photodetectors (QWIP's) for 8 to 12 microns FPA and IR sensor applications; (2) to develop other new types of 3-5 multicolor QWIP's with broad and multicolor infrared spectral response (5 to 18 microns); (3) to conduct theoretical and experimental studies of the planar metal grating-coupled structures for normal incident illumination on the QWIP's (different metal grating coupler structures using 1-D line-grating and 2-D cross-grating for the QWIP's will be studied in order to achieve high coupling efficiency under normal front- and back-illuminations); and (4) to perform theoretical and experimental studies of dark current, photocurrent, optical absorption, spectral responsivity, noise, and detectivity in different types of QWIP's. GRA

N93-12231# Cornell Univ., Ithaca, NY. Dept. of Chemistry.
SYNTHESIS AND REACTIVITY OF SILOXIDE AND SILAMIDE COMPLEXES PERTAINING TO BOND BREAKING AND AGGREGATION PHENOMENA Final Report, 1 Feb. 1987 - 31 Oct. 1991
Peter T. Wolczanski Jul. 1992 29 p
(Grant AF-AFOSR-0103-87)
(AD-A254703; AFOSR-92-0768TR) Avail: CASI HC A03/MF A01

The synthesis of siloxide and silamide complexes of tantalum has been carried out and their reactivity with respect to bond breaking and aggregation phenomena has been studied. Types of reactions include carbon monoxide cleavage to dicarbides and ketenylidene, carbon monoxide reduction, ketyl formation, ether cleavage, ligation of pyridine and related adducts, hydrocarbon activations, routes to early metal nitrides, and formation of cubic tantalum nitride. GRA

N93-12249# Argonne National Lab., IL.
INFLUENCE OF OXYGEN PARTIAL PRESSURE AND SILVER ADDITIONS ON MICROSTRUCTURE AND RELATED PROPERTIES OF YBCO SUPERCONDUCTORS
J. P. Singh, J. Joo, R. Guttschow, and R. B. Poeppel Feb. 1992 10 p Presented at the High TcSUH Workshop on High Temperature Superconductivity Materials, Bulk Processing, and Bulk Applications, Houston, TX, 27-28 Feb. 1992
(Contract W-31-109-eng-38)
(DE92-011145; ANL/CP-75374; CONF-920240-3) Avail: CASI HC A02/MF A01

Microstructure has a great influence on the mechanical and superconducting properties of YBCO. Mechanical properties of YBCO can be improved by both modifying the monolithic microstructure and developing composites of YBCO with silver (Ag). When monolithic YBCO was sintered to high densities (approximately 91 percent) at a relatively low temperature (approximately 910 C) by controlling oxygen partial pressure during sintering, the result was a small-grain microstructure (average grain size approximately 5 micron) and hence a high strength of 191 +/- 7 MPa. Addition of Ag as a second phase further improved the strength of YBCO. Composites of YBCO with 10 to 15 vol percent Ag has a strength of 225 +/- 6 MPa and a fracture toughness of 3.3 +/- 0.2 MPa the square root of m. These improvements are believed to be due to compressive stresses in the YBCO matrix as a result of thermal mismatch between the YBCO and Ag phases. Furthermore, the Ag particles may provide increased resistance to crack propagation by pinning the crack. On the other hand, addition of Ag as a dopant to substitute for Cu sites in YBCO has a profound but nonmonotonic effect on grain microstructure and the resulting critical current density. DOE

N93-12271# Naval Research Lab., Washington, DC.
ELECTRON TERMS AND RADIATION FROM CRYSTALS Interim Report
K. H. Hellwege and W. L. Faust 13 Aug. 1992 41 p Transl. into ENGLISH from Annalen der Physik (Germany), v. 4, no. 95, 1948
(AD-A254353; NRL/MR/6542-92-7101) Avail: CASI HC A03/MF A01

This paper describes the effect of a crystal field, according to site symmetry, upon the magnetic quantum-level structure of an atomic ion, as expressed in electric dipole transitions. For all 27 noncubic symmetry classes the following are determined: (1) the electron function; (2) the number and degeneracy of the components into which one term of the supposed angular momentum quantum number of a free atom splits; and (3) selection rules for the crystal quantum numbers. GRA

N93-12283# Army Lab. Command, Fort Monmouth, NJ. Electronics Technology and Devices Lab.
QUARTZ CRYSTAL RESONATORS AND OSCILLATORS FOR FREQUENCY CONTROL AND TIMING APPLICATIONS: A TUTORIAL, REVISION 5.2
John R. Vig Jul. 1992 272 p
(AD-A254892; SLCET-TR-88-1-Rev-5.2) Avail: CASI HC A12/MF A03

Subjects covered include: applications of frequency standards; types of oscillators (quartz and atomic); quartz resonator properties; quartz growing, sweeping, and material characteristics; Q and its significance; resonator and oscillator stability, including aging, short-term instability, frequency vs. temperature characteristics, oscillator circuit caused instabilities, frequency vs. drive level effects, acceleration effects, the effect of shock, and radiation effects; emerging technologies; atomic frequency standards; comparison of the major oscillator types; oscillator specifications and selection guidelines; time and timekeeping; clock errors; relativistic time; time transfer; time and frequency subsystem; and other applications of quartz resonators. The goal of this document is to assist in presenting to the nonspecialist the most frequently encountered concepts in frequency control and timing. The document originated as a set of hard copies of presentation visuals (i.e., vugraphs). GRA

N93-12286# Army Lab. Command, Watertown, MA. Material Technology Lab.
SURFACE ANALYSIS OF Ln(2-x)Ce(x)CuO4 (Ln = Pr AND Nd) SINGLE CRYSTALS GROWN BY THE TOP SEEDED SOLUTION METHOD Final Report
Louise C. Sengupta, Somnath Sengupta, Wendy E. Kosik, and J. D. Demaree May 1992 19 p
(AD-A254905; MTL-TR-92-34) Avail: CASI HC A03/MF A01

Large single crystals of Ln(2-x)Ce(x)CU04 (Ln = Pr and Nd), the average size is approximately 5 mm x 5 mm x 1 mm, were grown by the Top Seeded Solution Growth (TSSG) technique. The optical constants of the crystals were determined by Variable Angle Spectroscopic Ellipsometry (VASE) and the results seem to indicate that a 1.5 eV absorption peak appears in the undoped material and is weakened and shifted downward in energy upon annealing. The compositions and crystal structure were examined using Rutherford Backscattering Spectroscopy (RBS) with ion beam channeling. Also, the effect of annealing on the crystalline structure was probed by ion beam channeling. The orientation and lattice parameters of the crystals were determined by x-ray diffraction and the superconductivity of the specimens was monitored using a SQUID magnetometer. The results indicate that the crystals grown by the TSSG method are very uniform in composition and well-oriented; however, analysis of the RBS data indicated up to 1 percent Pt inclusion in the crystals from contact with the Pt crucibles. The inclusion of Pt acted to quench the superconducting transition temperatures and Pt was found to substitute for Cu. GRA

N93-12310# Argonne National Lab., IL.
ION BEAMS AS A MEANS OF DEPOSITION AND IN-SITU CHARACTERIZATION OF THIN FILMS AND THIN FILM LAYERED STRUCTURES
A. R. Krauss, M. Rangaswamy, D. M. Gruen, Y. P. Lin (Northwestern Univ., Evanston, IL.), and J. A. Schultz (Ionwerks, Houston, TX.) 1992 27 p Presented at the 7th Annual Congress of the Brazilian Microelectronics Society, Sao Paolo (Brazil), 6-10 Jul. 1992
(Contract W-31-109-eng-38)
(DE92-016397; ANL/CP-76359; CONF-9207103-1) Avail: CASI HC A03/MF A01

Ion beam-surface interactions produce many effects in thin film deposition which are similar to those encountered in plasma deposition processes. However, because of the lower pressures and higher directionality associated with the ion beam process, it is easier to avoid some sources of film contamination and to provide better control of ion energies and fluxes. Additional effects occur in the ion beam process because of the relatively small degree of thermalization resulting from gas phase collisions with both the ion beam and atoms sputtered from the target. These effects may be either beneficial or detrimental to the film properties, depending on the material and deposition conditions. Ion beam deposition is particularly suited to the deposition of multi-component films and layered structures, and can in principle be extended to a complete device fabrication process. However, complex phenomena occur in the deposition of many materials of high technical interest which make it desirable to monitor the film growth at the monolayer level. It is possible to make use of ion-surface interactions to provide a full suite of surface analytical capabilities in one instrument, and this data may be obtained at ambient pressures which are far too high for conventional surface analysis techniques. Such an instrument is under development and its current performance characteristics and anticipated capabilities are described. DOE

N93-12316# California Univ., Berkeley. Lawrence Berkeley Lab.
DETERMINATION OF Fe(SUP 2+) AND Fe(SUP 3+) CONCENTRATIONS OF SEMI-INSULATING InP:Fe
F. X. Zach, E. D. Bourret, D. Bliss (Rome Air Development Center, Hanscom AFB, MA.), E. R. Weber, and E. E. Haller Jan. 1992 4 p Presented at the 4th International Conference on Indium Phosphide and Related Materials, Newport, RI, 20-24 Apr. 1992
(Contract DE-AC03-76SF-00098)
(DE92-017119; LBL-31578; CONF-9204168-1) Avail: CASI HC A01/MF A01

Semi-insulating InP is most commonly obtained by doping with the deep acceptor iron to compensate the shallow donors which otherwise render the material n-type conducting. As the Fermi level in semi-insulating InP is closed to the iron acceptor level, both charge states - Fe(sup 2+) as well as Fe(sup 3+) corresponding to the acceptor level occupied unoccupied by an electron - are present. Mayor et al.(1) presented a method based on absorption measurements in the nearbandgap region of InP to determine the concentration of both charge states separately. In this paper we compare iron concentrations obtained by this method with the results from intracenter absorption, DLTS, EPR, Hall effect measurements and glow discharge mass spectroscopy. We present a new calibration for the optical absorption cross sections. DOE

N93-12325*# National Aeronautics and Space Administration. Lewis Research Center, Cleveland, OH.
CONDUCTOR-BACKED COPLANAR WAVEGUIDE RESONATORS OF Y-Ba-Cu-O AND Tl-Ba-Ca-Cu-O ON LaAlO3
F. A. Miranda, K. B. Bhasin, M. A. Stan (Kent State Univ., OH.), K. S. Kong (TRW, Inc., Redondo Beach, CA.), and T. Itoh (California Univ., Los Angeles.) Oct. 1992 6 p Presented at the 1992 Applied Superconductivity Conference, Chicago, IL, 23-28 Aug. 1992; sponsored by IEEE
(RTOP 506-72-1B)
(NASA-TM-105890; E-7356; NAS 1.15:105890) Avail: CASI HC A02/MF A01

Conductor-backed coplanar waveguide (CBCPW) resonators operating at 10.8 GHz have been fabricated from Tl-Ba-Ca-O (TBCCO) and Y-Ba-Cu-O (YBCO) thin films on LaAlO3. The resonators consist of a coplanar waveguide (CPW) patterned on the superconducting film side of the LaAlO3 substrate with a gold ground plane coated on the opposite side. These resonators were tested in the temperature range from 14 to 106 K. At 77 K, the best of our TBCCO and YBCO resonators have an unloaded quality factor (Qo) 7 and 4 times, respectively, larger than that of a similar all-gold resonator. In this study, the Qo's of the TBCCO resonators were larger than those of their YBCO counterparts throughout the aforementioned temperature range. Author

N93-12338# Washington State Univ., Pullman.
PHOTOINDUCED ELECTRON TRANSFER COUNTER TO THE BIAS FIELD IN COUPLED QUANTUM WELLS Interim Report
Mark I. Stockman, Leonid S. Muratov, Lakshmi N. Pandey, and Thomas F. George Aug. 1992 8 p

(Contract N00014-90-J-1193)
(AD-A254719; WSU-92/91) Avail: CASI HC A02/MF A01

Optical excitation of electrons in an asymmetric double quantum well is theoretically examined. The well is biased to align the excited levels and permit resonant electron tunneling. Emphasis is made on the photoinduced transfer of electrons counter to the bias electric field force. A density-matrix approach is developed to describe optical excitations in the presence of an arbitrary dephasing. The excitation profiles obtained for cases of different dephasing reveal the full range of tunneling coupling between the wells from completely coherent to incoherent (stepwise). GRA

N93-12396*# Alabama Univ., Huntsville.
HIGH TEMPERATURE SUPERCONDUCTOR MATERIALS AND APPLICATIONS Final Technical Report, 11 Dec. 1989 - 10 Jul. 1990
George B. Doane, III., Curtis Banks, and John Golben 10 Jul. 1990 27 p
(Contract NAS8-36955)
(NASA-CR-184426; NAS 1.26:184426; UAH-5-32313) Avail: CASI HC A03/MF A01

Research on processing methods leading to a significant enhancement in the critical current densities (Jc) and the critical temperature (Tc) of high temperature superconducting in thin bulk and thin film forms. The fabrication of important devices for NASA unique applications (sensors) is investigated. Author

N93-12464# Syracuse Univ., NY. Office of Sponsored Programs.
MMIC GaAs BONDING INVESTIGATION Final Report, Aug. 1990 - Dec. 1991
H. Brumberger, J. Chaiken, P. A. Dowben, J. A. Schwarz, and J. T. Spencer Jun. 1992 81 p
(Contract F30602-89-C-0113)
(AD-A254773; RL-TR-92-124) Avail: CASI HC A05/MF A01

Results of an investigation into methods of applying thin film technology to improve Gallium Arsenide (GaAs) Monolithic Microwave Integrated Circuit (MMIC) fabrication and packaging technologies are discussed. Progress in parallel research efforts to better understand the bonding of III-V compounds to substrates, to develop novel thin film deposition methods, and to design and synthesize new source compounds for III-V materials are reported. Techniques investigated include graphoepitaxy, upside-down structures, Ti bonding layers between metal and ceramic, and metal-organic chemical vapor deposition. The resulting interfaces of thin films and bulk materials were characterized in situ, where possible, by spectroscopic and diffraction analysis. A number of significant Rama spectra are provided. GRA

N93-12499# Rice Univ., Houston, TX.
APPLICATION OF SPIN-SENSITIVE ELECTRON SPECTROSCOPIES TO INVESTIGATIONS OF ELECTRONIC AND MAGNETIC PROPERTIES OF SOLID SURFACES AND EPITAXIAL SYSTEMS Progress Report, 1 Nov. 1991 - 31 Oct. 1992
G. K. Walters and F. B. Dunning Jun. 1992 8 p
(Contract DE-FG05-86ER-45233)
(DE92-018597; DOE/ER-45233/7) Avail: CASI HC A02/MF A01

The Research in this paper focuses on: Investigation of probing depths in electron scattering from epitaxially grown paramagnetic films by means of Spin-Polarized Electron Energy Loss Spectrometry (SPEELS); and Studies of the dynamics of metastable He(2(sup 3)S) deexcitation at surfaces utilizing Spin-Polarized Metasta DOE

77 THERMODYNAMICS AND STATISTICAL PHYSICS

Includes quantum mechanics; theoretical physics; and Bose and Fermi statistics.

For related information see also *25 Inorganic and Physical Chemistry* and *34 Fluid Mechanics and Heat Transfer.*

N93-11276# Washington Univ., Saint Louis, MO. Dept. of Physics.
STUDIES IN QUANTUM FIELD THEORY Progress Report, 1 Apr. 1991 - 31 Mar. 1992
C. M. Bender 1992 70 p
(Contract DE-FG02-91ER-40628)
(DE92-011035; DOE/ER-40628/1) Avail: CASI HC A04/MF A01

Professors Bender, Bernard, and Shrauner, Assistant Professors Ogilvie and Goltermann, Research Assistant Professors Visser and Petcher, and Research Associate Rivas are currently conducting research in many areas of high energy theoretical and mathematical physics. These areas include: lattice gauge calculations of masses and weak matrix elements; strong-coupling approximation; low-energy effective field theories; classical solutions of non-Abelian gauge theories; mean-field approximation in quantum field theory; path integral and coherent state representations in quantum field theory; the nature of perturbation theory in large order; quark condensation in QCD; chiral fermion theories on the lattice; the 1/N expansion in quantum field theory; effective potential and action in quantum field theories, including QCD; studies of the early universe and inflation; and quantum gravity. This work is described in detail in the body of this proposal. DOE

N93-11469# Notre Dame Univ., IN.
HEAT TRANSFER ENHANCEMENT BY CHAOTIC MIXING Annual Report, Jul. 1990 - Aug. 1991
M. Sen and H. C. Chang Nov. 1991 103 p
(Contract GRI-5090-260-1971; Proj. A-90-11-00038)
(PB92-190305; GRI-91/0310) Avail: CASI HC A06/MF A02

The feasibility of using chaotic mixing to enhance heat transfer is studied theoretically and experimentally. The study begins by an examination of the role of chaotic dynamics in transport enhancement in a counter-rotating eccentric annulus. Significant enhancement is seen to be attainable over that of regular mixing for a suitable choice of system parameters. Chaotic advection is then studied in a coiled pipe where the coiling geometry is suitably modified. Numerical investigation in the Dean's limit is used to explore the role of chaotic mixing in furthering heat transfer. These qualitative trends are tested on two coil geometries and an enhancement of between 6-8 percent is experimentally obtained. GRA

N93-11518# California Univ., Berkeley. Lawrence Berkeley Lab.
INDUCED GAUGE THEORIES AND W GRAVITY
K. Schoutens (State Univ. of New York, Stony Brook.), A. Sevrin, and P. VanNieuwenhuizen (European Organization for Nuclear Research, Geneva, Switzerland) Nov. 1991 33 p Presented at the Strings and Symmetries Conference, Stony Brook, NY, 20-25 May 1991
(Contract DE-AC03-76SF-00098)
(DE92-011218; LBL-31381; CONF-9105113-4; ITP-SB-91-54; CERN-TH-6330/91; UCB-PTH-91/51) Avail: CASI HC A03/MF A01

We review some aspects of induced gauge theories in two dimensions. We focus on W(sub 3) gravity, paying particular attention to the treatment of the non-linearities inherent to W gravity. We show that the induced action Gamma(sub ind)(h,b) for chiral W(sub 3) in the c approaches +/- infinity limit is obtained from the induced action of a gauged Sl(3,R) Wess-Zumino-Witten model by imposing constraints on some of the affine currents. Subsequently we investigate the effective action, which is obtained by integrating the induced action over the gauge fields. We show perturbatively that certain subleading terms which appear in the induced action for finite c (and which are related to nonlocal terms in the Ward identifies) get canceled by similar terms due to loop corrections, and we propose an all-order result for the effective action. DOE

N93-11656# Superconducting Super Collider Lab., Dallas, TX.

TABLES OF THERMODYNAMIC PROPERTIES OF HELIUM MAGNET COOLANT, REVISION A

M. McAshan Jul. 1992 104 p
(Contract DE-AC35-89ER-40486)
(DE92-019098; SSCL-131-Rev-A; SSC-Cryo-Note-92-7) Avail: CASI HC A06/MF A02

The most complete treatment of the thermodynamic properties of helium at the present time is the monograph by McCarty: 'Thermodynamic Properties of Helium 4 from 2 to 1500 K at Pressures to 10(exp 8) Pa', Robert D. McCarty, Journal of Physical and Chemical Reference Data, Vol. 2, page 923-1040 (1973). In this work the complete range of data on helium is examined and the P-V-T surface is described by an equation of state consisting of three functions P(r,T) covering different regions together with rules for making the transition from one region to another. From this thermodynamic compilation together with correlations of the transport properties of helium was published the well-known NBS Technical Note: 'Thermophysical Properties of Helium 4 from 2 to 1500 K with pressures to 1000 Atmospheres', Robert D. McCarty, US Department of Commerce, National Bureau of Standards Technical Note 631 (1972). This is the standard reference for helium cryogenics. The NBS 631 tables cover a wide range of temperature and pressure, and as a consequence, the number of points tabulated in the region of the single phase coolant for the SSC magnets are relatively few. The present work sets out to cover the range of interest in more detail in a way that is consistent with NBS 631. This new table is essentially identical to the older one and can be used as an auxiliary to it. DOE

N93-11780# Weizmann Inst. of Science, Rehovoth (Israel).

SEMICLASSICAL ANALYSIS SPECTRAL CORRELATIONS IN MESOSCOPIC SYSTEMS

N. Argaman, Y. Imry, and U. Smilansky Jul. 1991 59 p
(DE92-634887; WIS-PH-91-38) Avail: CASI HC A04/MF A01

We consider the recently developed semiclassical analysis of the quantum mechanical spectral form factor, which may be expressed in terms of classically defiable properties. When applied to electrons whose classical behavior is diffusive, the results of earlier quantum mechanical perturbative derivations, which were developed under a different set of assumptions, are reproduced. The comparison between the two derivations shows that the results depend not on their specific details, but to a large extent on the principle of quantum coherent superposition, and on the generality of the notion of diffusion. The connection with classical properties facilitates application to many physical situations. DOE

N93-12058# EG and G Energy Measurements, Inc., Idaho Falls.

OVERVIEW OF PROPERTY FORMULATIONS FOR HELIUM, NITROGEN, LITHIUM, AND LITHIUM-LEAD IN ATHENA/MOD1 WITH COMPARISON OF CALCULATED PROPERTIES TO MEASURED PROPERTIES

J. Tolli Apr. 1992 48 p
(Contract DE-AC07-76ID-01570)
(DE92-017995; EGG-FSP-10245) Avail: CASI HC A03/MF A01

Formulation for the thermodynamic and transport properties of the fluids used by the ATHENA/MOD1 computer program for fusion safety research have been obtained from various sources, including published documents and empirical curve-fitting to data. The sources and/or formulations are stated. Comparison plots of ATHENA calculated thermodynamic properties and transport properties with measured data ate included as part of the verification and validation effort for the ATHENA fusion fluids. DOE

N93-12102# Brown Univ., Providence, RI. Div. of Engineering.

INTERNAL VARIABLES IN THE LOCAL-EQUILIBRIUM APPROXIMATION

J. Kestin May 1992 31 p Presented at the Symposium on Thermodynamic Fundamentals, Berlin (Germany), 11-12 Jun. 1992
(Contract DE-FG02-87ER-13687)
(DE92-016854; DOE/ER-13687/10; CONF-9206208-1) Avail: CASI HC A03/MF A01

We explore the basis and consequences of the formalism known in the literature as the method of local equilibrium. Contemporary controversies regarding the foundations of thermodynamics are rooted not only in different sets of concepts and principles, but also in semantics. An attempt is made here to use a consistent group of terms, each of whose dictionary meaning corresponds to its physical nature as closely as possible. Since the intention is to study irreversible processes in systems in which even locally there prevails a state of nonequilibrium, the term local equilibrium is abandoned in favor of the phrase principle of local state. In defining the thermodynamic state of system, a distinction is made between the intensive parameters which appear in the physical space and those which describe states of constrained equilibrium in the Gibbsian phase space. The principle of local state is applied by association with every nonequilibrium state n and accompanying equilibrium state e of equal values of U, a, alpha, and by asserting that the entropy (bar-S) assignable in physical space and temperature (bar-T) measured in it can be approximated by the values S and T calculated in the Gibbsian phase space by standard, classical methods. A continuous sequence of accompanying equilibrium states is called an accompanying reversible process, it is conceived as an adiabatic projection of the continuous sequence of nonequilibrium states. The essential part of the method consists in the formulation of the Gibbs equation for the accompanying reversible process in the phase space. It is noted that the local-state approximation, made explicit in this paper, has been used and tested in fluid mechanics though its validity is contested in contemporary continuum mechanics and mechanics of solids. DOE

N93-12490# United Technologies Research Center, East Hartford, CT.

INVESTIGATION OF HOT STREAK MIGRATION AND FILM COOLING EFFECTS ON HEAT TRANSFER IN ROTOR/STATOR INTERACTING FLOWS, REPORT 1 Final Report, 1 Nov. 1988 - 1 Apr. 1992

Daniel J. Dorney, Roger L. Davis, and David E. Edwards 1 Apr. 1992 221 p
(Contract N00140-88-C-0677)
(AD-A250688; UTRC-91-29-Rept-1) Avail: CASI HC A10/MF A03

Experimental data taken from turbine engines has shown that hot streaks exiting combustors can have a significant impact upon the secondary flow and wall temperature of the first stage turbine rotor. Understanding the secondary flow and heat transfer effects due to combustor hot streaks is essential to turbine designers attempting to optimize turbine cooling systems. A numerical investigation has been performed which addresses the issues of multi-blade count ratio and three-dimensionality effects on the prediction of combustor hot streak migration in a turbine stage. The two- and three-dimensional Navier-Stokes analyses are used to predict unsteady viscous rotor-stator interacting flow in the presence of a combustor hot streak with heat transfer and film cooling. Predicted results are presented for a two-dimensional 3-stator/4-rotor and a three-dimensional 1-stator/1-rotor simulations of streak migration through a turbine stage. Comparison of these results with experimental data demonstrates the capability of the three-dimensional procedure to capture most of the flow physics associated with hot streak migration including the effects of combustor hot streaks on turbine rotor surface temperatures. GRA

N93-12530 California Univ., Santa Barbara.
SPACETIME SINGULARITIES IN STRING THEORY Ph.D. Thesis
Alan Robert Steif 1991 111 p
Avail: Univ. Microfilms Order No. DA9218487

We investigate exact classical solutions to string theory which contain spacetime singularities. The first class of solutions which we discuss take the form of singular plane waves. We show that string propagation exhibits singular behavior in these backgrounds. The second class of string solutions contain singularities to the future of a nonsingular initial surface and are similar to the Friedmann solutions. These solutions have conical singularities near which strings display singular behavior. The third class of solutions which we consider are two dimensional charged black holes. These are constructed from a gauged Wess-Zumino-Witten model. Finally, we discuss the implications of spacetime duality for conserved quantities. We show that spacetime duality leads to an equivalence between ADM momentum and axionic charge. Dissert. Abstr.

80 SOCIAL SCIENCES (GENERAL)

Includes educational matters.

No abstracts in this category.

81 ADMINISTRATION AND MANAGEMENT

Includes management planning and research.

N93-10976# Royal Signals and Radar Establishment, Malvern (England).
POST-WAR REGIONAL PLANNING: THE FRENCH SILICON VALLEY
S. L. Holeman (Wolverhampton Polytechnic, England) Aug. 1989 37 p
(RSRE-Memo-4282; BR112080) Copyright Avail: CASI HC A03/MF A01

This dissertation is a study of French regional planning policies with specific reference to the Rhone-Alpes region. In particular, it studies Grenoble and her science-based industries and research laboratories. A critical analysis of the development of this region and of the factors behind its emergence as the French 'silicon valley' is presented. Ever closer ties to Europe with increasing pressure for Anglo-French collaboration plus the impending impact of 1992 lead to the need for a closer awareness of French technical strategy and history. The Royal Signals and Radar Establishment has significant links with the Grenoble area, and this memorandum has been made available to provide useful and relevant background. Author

N93-11163# Euroconsult, Paris (France).
THE EUROPEAN SPACE INDUSTRY. OVERALL SITUATION: SITUATION AND PROSPECTS FOR THE 23 LEADING COMPANIES CONCERNED
1991 29 p
Avail: CASI HC A03/MF A01

The first comprehensive strategic and financial analysis of the European space industry as a whole, with a breakdown for the 23 leading space companies, is studied in the following two parts. Part 1 presents a summary analysis of the overall situation of the European space industry in the areas of employment, sales, statistics by country, and market distribution by type of contracts and customers. It also discusses the relative importance of space production and employment in the companies concerned, especially involving corporate restructuring. Part 2 is a detailed industrial and financial analysis of the 23 European companies with space sales of over ECU 10 million, comprising: (1) an analysis of the overall financial condition of the companies; (2) a roundup of development in all their lines of business; (3) analysis of those companies' space activity and their industrial and financial impact; and (4) a general summary of their space programs. I.I.C.

N93-12212*# Cornell Univ., Ithaca, NY. Dept. of Computer Science.
TRADEOFFS IN IMPLEMENTING PRIMARY-BACKUP PROTOCOLS
Navin Budhiraja and Keith Marzullo Oct. 1992 18 p
(Grant NAG2-593)
(NASA-CR-190970; NAS 1.26:190970; TR-92-1307) Avail: CASI HC A03/MF A01

One way to implement a fault-tolerant service is by using multiple servers that fail independently. The state of the service is replicated and distributed among these servers, and updates are coordinated so that even when a subset of the servers fail, the service remains available. A common approach to structuring such replicated services is to designate one server as the primary and all the others as backups. Clients make requests by sending messages only to the primary. If the primary fails, then a failover occurs and one of the backups takes over. This service architecture is commonly called the primary-backup or the primary-copy approach. In most such primary-backup protocols, when the primary receives a client request, it informs the backups about the request, and then responds to the client. Informally, this primary-backup protocol is non-blocking if the primary does not wait for an acknowledgement from the backups before it sends the response; otherwise, it is blocking. Most of the existing protocols are blocking as non-blocking protocols cannot be constructed for some kinds of failures. However, it is shown that non-blocking protocols can be constructed for most of the process and communication failures that are expected to occur in the primary-backup systems of the future. Since non-blocking protocols can theoretically achieve the smallest possible response time, this paper analyzes these protocols under various system parameters. Two kinds of non-blocking protocols are analyzed: one in which the processes use point-to-point communication to exchange messages, and the other in which processes use hardware broadcasts. L.R.R.

N93-12223# Department of Energy, Washington, DC.
DOE GUIDELINE: GUIDE TO GOOD PRACTICES FOR INCORPORATING OPERATING EXPERIENCES
Jul. 1992 112 p
(DE92-017684; DOE-STD-1010-92) Avail: CASI HC A06/MF A02

This guide contains methods for incorporating operating experiences into facility programs. These experiences from facilities or the industry should be incorporated in a manner that is systematic and timely in conveying useful information. This guide describes the elements of an Operating Experience Review Program that includes the following: (1) selecting and analyzing events appropriate for the facility or facility operation; (2) ensuring those event reports and the subsequent analysis performed are distributed to the appropriate organizations; (3) incorporating the information from the reports into new or existing facility programs and training; (4) tracking the action plans to ensure actions related to the operating experience report are completed; and (5) assessing the effectiveness of changes made as a result of using the information gained from the operating experience. DOE

N93-12273# Institute for Defense Analyses, Alexandria, VA.
RESEARCH AND DEVELOPMENT STRATEGIES FOR HUMAN CENTERED AND GROUP SUPPORT TECHNOLOGIES
Karen J. Richter, D. S. Barnett, and Earl A. Alluisi May 1992 226 p
(Contract MDA903-89-C-0003)
(AD-A254366; IDA-P-2630; IDA/HQ-92-41177; AD-E501558)
Avail: CASI HC A11/MF A03

The Armstrong Laboratory's Acquisition Logistics Research and Development Activity at Wright Patterson Air Force Base, Ohio, is actively investigating both human centered technology and group support technology. In order to ensure the development of these technologies with a focus on customer needs and the use of relevant technological developments, the laboratory has been involved in a strategic planning process for future R and D activities. This paper reports the results of research performed by an Institute for Defense Analyses study team whose immediate goal was to help refine and sharpen the focus of the Acquisition Logistics R and D Activity's strategy for human centered technology and group support technology by providing information about, and analysis of, potential customers, relevant technological developments, and probable alternative strategies. GRA

N93-12542*# Alabama Univ., Huntsville. Dept. of Industrial and Systems Engineering.
DEVELOPMENT OF A MODEL FOR PREDICTING NASA/MSFC PROGRAM SUCCESS Final Monthly Report, 1-30 May 1990
Jeffrey Riggs, Tracy Miller, and Rosemary Finley 30 May 1990 184 p
(Contract NAS8-36955)
(NASA-CR-184423; NAS 1.26:184423) Avail: CASI HC A09/MF A02

Research conducted during the execution of a previous contract (NAS8-36955/0039) firmly established the feasibility of developing a tool to aid decision makers in predicting the potential success of proposed projects. The final report from that investigation contains an outline of the method to be applied in developing this Project Success Predictor Model. As a follow-on to the previous study, this report describes in detail the development of this model and includes full explanation of the data-gathering techniques used to poll expert opinion. The report includes the presentation of the model code itself. Author

N93-11942*# Loral Space and Range Systems, Sunnyvale, CA. Artificial Intelligence Group.
MISSION CONTROL CENTER ENHANCEMENT OPPORTUNITIES IN THE 1990'S
Wayne Hartman *In* NASA. Lyndon B. Johnson Space Center, Fifth Annual Workshop on Space Operations Applications and Research (SOAR 1991), Volume 1 Jan. 1992 p 142-149 (For primary document see N93-11921 02-59)
Avail: CASI HC A02/MF A04

82 DOCUMENTATION AND INFORMATION SCIENCE

Includes information management; information storage and retrieval technology; technical writing; graphic arts; and micrography.

For computer documentation see *61 Computer Programming and Software.*

N93-10990# Oak Ridge National Lab., TN. Carbon Dioxide Information Analysis Center.
CATALOG OF DATA BASES AND REPORTS
M. D. Burtis, comp. Apr. 1992 144 p
(Contract DE-AC05-84OR-21400)
(DE92-018586; ORNL/CDIAC-34/R2) Avail: CASI HC A07/MF A02

The Catalog of Data Bases and Reports provides information about the many reports and other materials made available by the US Department of Energy's Global Change Research Program (GCRP). It is divided into six sections plus an author and a title index: (1) Research plans and budget summaries; (2) technical reports; (3) workshops, proceedings, and reports; (4) other reports; (5) USDA reports on response of vegetation to carbon dioxide; and (6) numeric data packages and computer model packages. DOE

N93-11012# Rolls-Royce Ltd., Derby (England).
EXPERIENCE OF DESIGNING A RELATIONAL MATERIALS DATABASE
Roger J. Bamkin and Sanders C. F. MacRae 1 Sep. 1991 39 p
(PNR-90893; ETN-92-92195) Copyright Avail: CASI HC A03/MF A01

The design of a database for engineering and manufacturing materials data in a tabular (relational) format is described. The freedom permitted by a relational (rather than hierarchical) structure allows better use of the computer's ability to handle n dimensional and complex networks of information. The following features are described: the use of information engineering; the separation of independent variables from property identifiers, to allow extensive scope for storage, interpolation and presentation of complex data; the use of 'inheritance' to allow storage and maintenance of generic information (in a similar manner to that used in knowledge based systems); the capability of holding data of varying quality and for differing applications (design and specification data) within the same database; the use of direct document publishing; and the integration with company wide systems referencing materials information. It is noted that these features are based on the study of the structure of the materials information and are believed to be generic solutions to the modeling of materials property data. ESA

N93-11104# Argonne National Lab., IL.
DATA ARCHIVING AND ANALYSIS FOR CWDD
T. A. Coleman, A. H. Novick, C. C. Meystrik, and J. R. Marselle 1992 8 p Presented at the Neutral Particle Beam Technical Symposium and Scientific Exchange, Argonne, IL, 28 Apr. - 1 May 1992
(Contract W-31-109-eng-38)
(DE92-017064; ANL/CP-76577; CONF-9204170-1) Avail: CASI HC A02/MF A01

A computer system has been developed to handle archiving and analysis of data acquired during operations of the Continuous Wave Deuterium Demonstrator (CWDD). Data files generated by the CWDD Instrumentation and Control system are transferred across a local area network to the CWDD Archive system where they are enlisted into the archive and stored on removeable media optical disk drives. A relational database management system maintains an on-line database catalog of all archived files. This database contains information about file contents and formats, and holds signal parameter configuration tables needed to extract and interpret data from the files. Software has been developed to assist the selection and retrieval of data on demand based upon references in the catalog. Data retrieved from the archive is transferred to commercial data visualization applications for viewing, plotting, and analysis. DOE

N93-11151# California Univ., Berkeley. Lawrence Berkeley Lab.
A PROBABILISTIC APPROACH TO INFORMATION RETRIEVAL IN HETEROGENEOUS DATABASES
A. Chatterjee and A. Segev Aug. 1991 17 p Presented at the Workshop on Information Technologies and Systems, Cambridge, MA, 14-15 Dec. 1991
(Contract DE-AC03-76SF-00098)
(DE92-016993; LBL-31117; CONF-9112126-1) Avail: CASI HC A03/MF A01

During the post decade, organizations have increased their scope and operations beyond their traditional geographic boundaries. At the same time, they have adopted heterogeneous and incompatible information systems independent of each other without a careful consideration that one day they may need to be integrated. As a result of this diversity, many important business applications today require access to data stored in multiple autonomous databases. This paper examines a problem of inter-database information retrieval in a heterogeneous environment, where conventional techniques are no longer efficient. To solve the problem, broader definitions for join, union, intersection, and selection operators are proposed. Also, a probabilistic method to specify the selectivity of these operators is discussed. An algorithm to compute these probabilities is provided in pseudocode. DOE

N93-11215# National Inst. of Standards and Technology, Gaithersburg, MD.
MANAGING DATA: FROM VISION TO REALITY
J. J. Newton, M. L. Melley, and H. Higgins May 1992 165 p
Presented at the 4th Proceedings of the Annual DAMA Symposium, Gaithersburg, MD, 14-15 May 1991 Sponsored in part by Data Administration Management Association, Washington, DC
(PB92-191212; NISTIR-4843) Avail: CASI HC A08/MF A02

The following topics are covered: achieving the data management reality; the road map for CASI implementation; the impact of implementing a new information architecture; data planning; data modeling: the data administrator perspective vs. the traditional application development point of view; data management and information proficiency: a vision for the future; information reengineering; managing information across multiple CASE tools; the atomic database: building the perfect beast; data management and customer satisfaction; data administration, the IBM repository, and CASE technology at Depository Trust Company; status and application of standards for data administration; future vision; and an essential prerequisite for a data management program. GRA

N93-11255 Maryland Univ., College Park.
AN ITERATIVE METHOD FOR DISTRIBUTED DATABASE DESIGN Ph.D. Thesis
Rex Blankinship 1991 212 p
Avail: Univ. Microfilms Order No. DA9222659

Increasingly, organizations are interconnecting computers for cooperative processing, and utilizing Database Management Systems (DBMS) to control access to their information resources. Effective design of distributed DBMS requires solutions to many complex and interrelated design issues. Data allocation and query optimization are two important distributed DBMS design issues. Query optimization depends on how the data are allocated, because transaction processing schedules often include operations on different sites and transmissions between them. However, the optimal method of allocating data depends on the processing strategies used for transactions. In general, researchers studying data allocation have assumed a known set of queries and processing schedules; researchers on query optimization have assumed a known data allocation. By assuming a solution to one problem and solving the other, researchers control the complexity of these two problems, but fail to integrate their solutions. We present an Iterative Method which provides an integrated solution for the combined data allocation and query optimization design problem. The optimization heuristic iterates between finding minimum cost data allocations and minimum cost query strategies until a local minimum for the combined problem is found. A search from convergence efficiency scans the optimization search space for lower cost solutions, and can repeatedly move beyond local optimum solutions. We first apply the Iterative Method within the simple query environment. Using our findings on simple queries, we extend the approach to a general query environment. In both environments, we consider a set of methods minimizing total transmission time, and another minimizing response time. A sophisticated problem generator is implemented, allowing tests on several independent variables. Parametric studies within a simple query environment demonstrate near-optimal performance for the Iterative Method when minimizing total transmission time and response time cost of queries. Test results in the general query environment show the Iterative Method provides significant performance improvements over alternative design methods from the literature. Furthermore, performance improvements appear to increase as environmental assumptions are relaxed, and individual design problems become more complex. These results indicate that the Iterative Method is a powerful and practical tool for design of distributed database systems. Dissert. Abstr.

N93-11274# General Accounting Office, Washington, DC. Information Management and Technology Div.
INFORMATION DISSEMINATION: CASE STUDIES ON ELECTRONIC DISSEMINATION AT FOUR AGENCIES. FACT SHEET FOR THE CHAIRMAN, COMMITTEE ON GOVERNMENTAL AFFAIRS, US SENATE
22 Jul. 1992 46 p
(GAO/IMTEC-92-6FS; B-248094) Avail: CASI HC A03/MF A01; GAO, PO Box 6015, Gaithersburg, MD 20877 HC

This Government Accounting Office (GAO) review examines electronic information dissemination at four government agencies. The review focused on the Department of Agriculture's Computerized Information Delivery Service, the National Technical Information Service's Bibliographic Database, the Bureau of the Census' general information dissemination programs, and the National Library of Medicine's Medical Literature Analysis and Retrieval System (MEDLARS). Each of the agencies' dissemination practices is highlighted in appendices 1 through 4. Appendix 5 focuses on the individual databases comprising the MEDLARS system. GAO describes for each agency: uses of the data, agency planning activities, data integrity practices and controls, agency costs for information dissemination, and prices paid by information users. R.L.B.

N93-11333# Royal Signals and Radar Establishment, Malvern (England).
LIES, DAMNED LIES, AND DATABASES
Simon R. Wiseman Apr. 1992 23 p
(RSRE-Memo-4503-Issue-2; BR311447; ETN-92-92317)
Copyright Avail: CASI HC A03/MF A01

A data base is expected to give correct and complete answers to queries. However, some applications take confidentiality to an extreme and require the database to deceive some users by supplying incorrect answers. Some requirements for databases which are intended to deceive some users are examined. The effectiveness of three secure database implementation techniques are compared. Example requirements for deceptive databases and security models for three implementation techniques are presented. The suitability of the three techniques is examined with respect to applications which deceive with integrity. Of the three techniques for achieving security in databases described, polyinstantiation is the most widely known technique, but view based classifications and the insert low approach are viable alternatives. Any of these three techniques could be used in a data base management system which supports databases that deceive their users. However, the requirement is not simply for a database that deceives, but for one where the deception is controllable. This is where polyinstantiation is weakest. Its inability to enforce even relatively simple integrity constraints means that cover stories can occur unintentionally. The resulting confusion could have serious consequences. Polyinstantiation is not the only technique for achieving security in databases and the alternatives merit further attention. ESA

N93-11353# Carnegie-Mellon Univ., Pittsburgh, PA. Dept. of Psychology.
A COGNITIVE APPROACH TO THE DESIGN OF INFORMATION GRAPHICS Technical Report, 15 Sep. 1986 - 14 Sep. 1991
Stephen Casner 14 Sep. 1991 44 p
(Contract N00014-86-K-0678)
(AD-A252692; AIP-143) Avail: CASI HC A03/MF A01

Graphical representations popularly thought to be useful for communicating and processing information yield mixed results when tested with real users. Cognitive research suggests that current design methodologies fail to exploit the potentials of graphics for expediting human performance of information-processing tasks: (1) allowing users to substitute less effortful visual procedures in place of more demanding non-visual procedures; and (2) streamlining users' search for information by supporting visual search heuristics. BOZ is a design algorithm that constructively applies cognitive principles of the efficiencies that graphical displays can offer to the problem of discovering novel displays to support specific user tasks. BOZ analyzes formal task descriptions and proposes visual displays and procedures that can help streamline performance of a task. BOZ is used to generate graphical alternatives to a standard tabular display of airline schedule information to support a set of common airline reservation tasks. Reaction time studies done with real users are reported that show that the BOZ-designed displays significantly reduce users' performance time to the task. Regression analyses link the observed efficiency savings to visual procedure substitutions and pruning of research. BOZ is also shown to be useful for analyzing existing displays to discover clever design features that can then be subsequently incorporated into BOZ's design algorithm. GRA

N93-11355# Department of Energy, Washington, DC.
RESERVES INFORMATION GATHERING SYSTEM USER'S GUIDE
15 Jan. 1992 73 p
(DE92-018357; DOE/EIA-M042(91)) Avail: CASI HC A04/MF A01

The Reserves Information Gathering System, hereafter referred to as RIGS, is an advanced electronic data entry product developed by the Department of Energy as a more efficient, accurate, and timely alternative for submission of Form EIA-23, 'Annual Survey of Domestic Oil and Gas Reserves' to the Energy Information Administration (EIA). The benefits of filing Form EIA-23 using RIGS software are multiple. RIGS will significantly reduce your reporting burden by: eliminating paperwork; providing on-line correction and edit features; automatically prompting for field footnotes; reducing follow-up calls; and establishing an historical database for future filings. Error messages are designed to prevent inadvertent entries, and help screens and messages answer most on-line questions that may arise. Company and state/subdivision totals can be automatically generated, and print functions are available to produce hard copy of an individual group, and/or total fields reported. DOE

N93-11404# Royal Signals and Radar Establishment, Malvern (England).
A FRONT END IMPLEMENTATION OF THE POLLYANNA SECURE DBMS
G. R. Hutchinson Nov. 1991 14 p
(RSRE-Memo-4540; BR306616; ETN-92-92324) Copyright Avail: CASI HC A03/MF A01

Pollyanna is a simple secure Data Base Management System (DBMS) which utilizes polyinstantiation. It was designed and implemented to illustrate the problems which may be encountered when applications are built on top of a polyinstantiating DBMS. The implementation comprises a front end to a standard commercial relational DBMS. The front end performs query modification and result filtering to achieve security. Pollyanna, the front end software, and some of the problems which arose during the design of the system are described. The design of Pollyanna highlighted some problems with the effects of polyinstantiation on the meaning of update queries. In Pollyanna it was decided to reject update queries that result in duplicate keys. Other solutions are possible, including only updating the most highly classified version of a row. Future work could provide these alternatives as an option and allow further evaluation and comparison of the different approaches. ESA

N93-11441# Martin Marietta Energy Systems, Inc., Oak Ridge, TN.
INFORMATION SYSTEMS PLANNING LEADING TO PERFORMANCE SUPPORT SYSTEMS
H. Pfuderer 1992 3 p Presented at the American Society of Information Science (ASIS) Annual Meeting, Pittsburgh, PA, 26-29 Oct. 1992
(Contract DE-AC05-84OR-21400)
(DE92-018745; CONF-9210136-1) Avail: CASI HC A01/MF A01

Until recently, the typical approach to information system applications was to design and implement independent systems. The result has often been redundant data and insufficient return on the information system investment as many important organizational needs have not been met. However, many decision makers are recognizing that information is a resource like money, materials, facilities, and personnel, and that an information systems plan is needed that makes the information systems available not just to a given functional area, but to the entire organization. A structured approach to analysis of the goals and objectives of the organization characterizes the organization's business processes and the information needed to support those goals, objectives, and processes. The study of the organization and its information needs results in an information architecture or a model depicting the relationship between the business processes and the information systems. Utilizing the information architecture in structuring the systems increases the coordination of information sharing, minimizes the maintenance of systems, and ensures that the data needed by the organization is available when needed in the correct format. DOE

N93-11465# IIT Research Inst., Lanham, MD.
STUDY AND RECOMMENDATION OF AVAILABLE SOURCES OF SCIENTIFIC AND TECHNICAL NUMERIC DATABASES IN THE GOVERNMENT AND PRIVATE SECTOR Final Report
Donna E. Grimes 3 Feb. 1992 34 p
(Contract MDA903-90-D-0022)
(AD-A247266) Avail: CASI HC A03/MF A01

The Defense Technical Information Center's (DTIC) mission for the scientific and technical numeric database project is to provide DoD scientists and engineers, the end users, with access to scientific and technical information and data. Until now, DTIC has been providing its users, who are primarily librarians and technical information specialists, access to bibliographic database or pointers to possible resources of numeric data for end users. In an effort to be more responsive to the DoD community, DTIC has been investigating new services to provide resources directly to the end users. One of these resources is scientific and technical databases. This report focuses on the methodology used to identify and recommend scientific and technical databases that should be accessed or distributed through DTIC. The methodology described is broken into three tasks: (1) Determine which databases from DTIC SCITECH Directory meet specified criteria as to users' needs and investigate them further to determine if the data source is a candidate to make available through DTIC. (2) Contact data source distributors to elicit information and provide a comparative view of the selected databases. (3) Recommend which of the selected databases could be made available through DTIC based on the comparison of the selected databases. GRA

N93-11506# Jackson State Univ., MS.
AN ICONIC QUERY INTERFACE FOR AN IMAGE DATABASE Interim Technical Report, Jul. 1990 - Sep. 1991
V. N. Gudivada and V. V. Raghavan 30 Apr. 1992 15 p
(Contract DAAL03-89-G-0118)
(AD-A253571; TR-91-2; ARO-27247.4-MA-SAH) Avail: CASI HC A03/MF A01

Recently, there has been widespread interest in various kinds of database management systems for managing formatted information. Powerful and flexible querying mechanisms are provided as an integral part of any of the conventional database management systems for formatted data so that they can be highly useful to a casual database user. Querying schemes assume even more critical prominence in systems used for image data management. Most of the existing schemes for querying image databases are variations of either Query-by-Example (QBE) or Structured Query Language (SQL). We feel that this approach to querying image databases is very unsatisfactory in terms of their expressive power and also being not natural to the image data. In this report, we propose a unified multi-layered framework for retrieval in image databases. This framework is expected to be highly flexible enough so that it can be useful across several application areas. The system is implemented using Smalltalk/V Windows which runs under a Graphical User Interface (GUI) known as Microsoft Windows. The system enables a user to interactively sketch an iconic query and then computes its spatial similarity with each and every image in the collection. The images in the collection are then shown in the decreasing order of their similarity for a specified query. GRA

N93-11508# Honeywell, Inc., Minneapolis, MN. Systems and Research Center.
ENGINEERING INFORMATION SYSTEM (EIS) Final Report, Sep. 1987 - Jul. 1991
Raj Kant and Jon Krueger 31 Jan. 1992 79 p
(Contract F33615-87-C-1401)
(AD-A254013; C920049; WL-TR-91-8048) Avail: CASI HC A05/MF A01

The Engineering Information System (EIS) was created in response to increasing concerns about the exchange of engineering information between contractors and the government, contractors on a single team, and contractors on different teams who share technical data and diverse tools. The EIS specifications provide a means for managing heterogeneity among hardware and software platforms, data formats, tools, site-specific policies and methodologies, and interfaces to create multiple-domain, multiple-life-cycle environments. An Engineering Information Model (EIM) and the EIS framework comprise the EIS. The EIM is a semantic model of information found in an EIS. An EIM realization, called the reference schema, is a set of object types that form a specific logical organization of data and operations. The EIS framework contains automated services embodied in software to support the use of the EIM to manage and control the data and activities of the engineering process. Current computer networking gateways require significant enhancement to meet the needs of cost-effective and concurrent engineering information access. The use of integration information gateways is the key to achieving the levels of technical interchange needed between organizations and various engineering environments. The EIS technologies can provide the Integration necessary to allow transparent information access across the information exchange networks. GRA

N93-11583# European Space Agency, Paris (France).
USING SGML IN A LARGE ORGANIZATION
Jordi Farres (European Space Agency. ESRIN, Frascati, Italy) and W. R. Burke, ed. Apr. 1992 25 p
(ESA-STR-234; ISBN-92-9092-164-1; ETN-92-92344) Copyright Avail: CASI HC A03/MF A01

The problem of adopting Standard Generalized Marking Language (SGML) for structured documents in a large organization is discussed. The research work carried out at the European Space Agency led to the definition of Document Type Definition (DTD) nets. These nets visualize the refinement relations between several DTD's (SGML document types) in a documentation environment. Bottom-up DTD design proposes the design of a DTD from several actual documents and does not address organizational matters. Topdown DTD design proposes the successive refinement of DTD's starting from processable DTD's. The results are appropriate for the organized creation of DTD's and for the reuse of user applications to documents of several related DTD's. DTD nets provide a coherent framework for creating and updating DTD's in large organizations, in such a way that application programs can be reused and marked documents can be exchanged. ESA

N93-11689 Politecnico di Milano (Italy). Dipartimento di Elettronica.
THE ESSE PROJECT: SUPPORTING OBJECT-ORIENTED DATABASE SCHEMA ANALYSIS AND EVOLUTION: OVERVIEW Progress Report
Alberto CoenPorisini, Luigi A. Lavazza (Master School CEFRIEL, Milan, Italy), and Roberto Zicari (Johann-Wolfgang-Goethe-Univ., Frankfurt am Main, Germany) Apr. 1992 19 p
(Rept-92-026; ETN-92-92424) Avail: Politecnico di Milano, Piazza Leonardo da Vinci 32, 20133 Milan, Italy

The ESSE research project for the development of an environment supporting database design, schema modification and verification for the O2 (Object Oriented) database system is presented. A tool which verifies type safeness of a given O2 schema is detailed and the architecture of the ESSE system with first implementation is presented. The behavior consistency problem is shown with an example. An overview of the Verify Data Flow (VDF) technique is given. VDF is a tool for verifying behavioral consistency. ESA

N93-11690 Politecnico di Milano (Italy). Dipartimento di Elettronica.
AN OBJECT-ORIENTED APPROACH TO SPATIAL DATABASES
Cristiano Sacchi May 1992 25 p
(Rept-92-034; ETN-92-92425) Avail: Politecnico di Milano, Piazza Leonardo da Vinci 32, 20133 Milan, Italy

An object oriented approach to spatial data management is presented. A class hierarchy is presented with a detailed description of its classes. The idea behind this work is that any shape can be seen as a point set in Euclidean space. Following this idea it is possible to build a system which emphasizes point set operators, and exploiting the object oriented paradigm allows the use of geometric objects at their very basic level. An architecture for a possible implementation is presented in the context of an object oriented Data Base Management System (DBMS). It is noted that the driving force of current research activities are geographical information systems which have the problem of dealing with geometric and alphanumerical information. ESA

N93-11700# Maryland Univ., College Park. Dept. of Civil Engineering.
GEOGRAPHIC INFORMATION SYSTEM TO SUPPORT STATE-WIDE HYDROLOGIC MODELING WITH THE SCS-TR-20 Final Report
Robert M. Ragan 1 Aug. 1991 284 p Sponsored by FAA
(PB92-185768; FHWA/MD-91/02) Avail: CASI HC A13/MF A03

A geographic information system (GIS) that is structured for hydrologic analysis was developed and installed in the Maryland State Highway Administration's (MSHA) Division of Bridge Design in Baltimore. The system is called GISHYDRO. The objective of GISHYDRO is to improve the efficiency and quality of hydraulic design by providing the MSHA engineer with a GIS workstation built around the IBM compatible PC. The workstation allows the engineer to quickly assemble the landuse, soil, and slope data for any watershed in the state and then make the necessary interfaces to define required input parameters and run the SCS-TR-20 hydrologic model for existing or proposed watershed conditions. The same files are used to run a non-point pollution model that estimates BOD, nitrate, phosphate, and other loadings in terms of the watershed landuse and soil types. The databases for GISHYDRO cover 9840 square miles and are stored in 23 county subdirectories. The landuse, hydrologic soil groups, and slope categories are stored in raster format with the cell size of 400 ft x 500 ft GISHYDRO also includes modules for updating existing databases or developing high resolution databases for use on very small watersheds. Author

N93-11710# Advisory Group for Aerospace Research and Development, Neuilly-Sur-Seine (France). Technical Information Panel.
DIRECTORY OF FACTUAL AND NUMERIC DATABASES OF RELEVANCE TO AEROSPACE AND DEFENCE R AND D [REPERTOIRE DE BASES DE DONNEES FACTUELLES OU NUMERIQUES D'INTERET POUR LA R ET D]
Jul. 1992 110 p
(AGARD-R-777; ISBN-92-835-0680-4) Copyright Avail: CASI HC A06/MF A02

Information is presented on nearly 100 unclassified factual or numeric databases of potential interest to aerospace and defense research and development. Information given in this directory includes the name of the organization and a point of contact, the title of the databank and the type of data included, a description of its coverage, information on the form of output available, and details of software used. The directory is listed in order by NASA subject category. This publication was sponsored by the Technical Information Panel of AGARD. Author

N93-11732# Institute for Defense Analyses, Alexandria, VA.
INTEGRITY IN AUTOMATED INFORMATION SYSTEMS Final Report
Terry Mayfield, J. E. Roskos, Stephen R. Welke, John M. Boone, and Catherine W. McDonald Sep. 1991 160 p
(Contract MDA903-89-C-0003)
(AD-A253990; IDA-P-2316; IDA/HQ-89-034883; AD-E501550)
Avail: CASI HC A08/MF A02

For many years, the security research community has focused on the confidentiality aspect of security, and a solid analytical foundation for addressing confidentiality issues has evolved. Now it is recognized that integrity is at least as important as confidentiality in many computer systems; it is also apparent that integrity is not well understood. The purpose of this paper is to lay a foundation for understanding integrity and investigate how it can be promoted and preserved in computer systems. The paper begins by exploring what is meant by integrity. It identifies three primary subgoals of integrity: (1) prevent unauthorized users from accessing system resources or modifying data, (2) maintain traditional data consistency, as well as the consistency of a system with respect to its environment, and (3) prevent authorized users from improperly accessing system resources or modifying data. Having articulated a vision of integrity, the paper discusses principles underlying the preservation of integrity, analyzes manual and automated integrity-preserving mechanisms, and examines integrity models and proposed implementation of the models. The paper concludes that although some gaps in understanding still exist, it is possible to begin to standardize integrity properties of systems. GRA

N93-11741# Army Engineer Topographic Labs., Fort Belvoir, VA.
SPATIAL DATA TRANSFORMATION: FEATURE ATTRIBUTE CONVERSION ISSUES AND PRACTICAL EXPERIENCE
Mark A. Sither 1991 10 p
(AD-A254238; TEC-R-181) Avail: CASI HC A02/MF A01

The need exists for continued development of spatial data transformation tools to provide increase capabilities for conversion of both format and content of locational coordinates, feature attributes, and ancillary information. Although individual geographic information systems (GIS) often provide a means of data import from and export to various other systems, such capabilities typically only permit transformation of the spatial data structure and format from one system to another. Existing feature attribute information is essentially transferred intact, subject to the constraints of the conversion software and other characteristics of each of the conversion software and other characteristics of each particular GIS; thus, reconciliation of differences due to variations in data description are left to the user. The tremendous growth in spatial data holdings constructed using a broad range of evolving systems, techniques and specifications has intensified the demand for enhanced data transformation capabilities to facilitate the integration of numerous existing data bases. GRA

N93-11748# Army Engineer Topographic Labs., Fort Belvoir, VA.
PHOTOGRAMMETRIC GIS TECHNOLOGY: FEATURE MAPPING ON DIGITAL STEREO IMAGERY
Roger O. Brown 12 Aug. 1991 10 p
(AD-A254255; TEC-R-166) Avail: CASI HC A02/MF A01

Geographic Information Systems (GIS) contain functions to process the spatial and attribute data of a map. Digital Photogrammetric systems contain functions to aero-triangulate and visualize digital stereo imagery, rectify imagery, and create Digital Terrain Matrixes (DTM). Integration of GIS and Digital-Photogrammetric systems allows digital feature data processing on the most current stereo imagery. Such photogrammetric GIS technology enables more reliable imagery measurements than two-dimensional GIS technology which only allows horizontal feature extraction from a single image. The single image usually retains geometric distortions from its original exposure complicating the mensuration and delineation of the objects in the map. The U.S. Army Topographic Engineering Center (TEC) has assembled a fully integrated digital image-based mapping system called the Terrain Information Extraction System (TIES). This paper evaluates the photogrammetric GIS technology on the TIES. GRA

N93-11749# SRI International Corp., Menlo Park, CA.
DISTRIBUTED DATABASE INTEGRITY Final Report, Oct. 1989 - Oct. 1990
Ira B. Greenberg and Peter K. Rathman Mar. 1992 59 p
(Contract F30602-89-C-0055)
(AD-A253272; RL-TR-92-36) Avail: CASI HC A04/MF A01

The Distribution Database Integrity (DDBI) project is a research effort funded by Rome Laboratory and conducted at the Computer Science Laboratory of SRI International. The main goal of this effort was to improve data integrity and consistency management techniques for C3 database application environments. The objective of this effort was to examine data integrity, consistency and concurrency control techniques for distributed object-oriented (0-0) database management systems. Specific areas that were investigated include: (1) rule-based concurrency control techniques for dynamic C3 processing, (2) adaptive concurrency techniques for dealing with consistency versus availability of data, (3) temporal database mechanisms for retaining multiple versions of database objects, (4) rules, constraints, and application-specific knowledge-bases for integrity maintenance, (5) active triggers for automatically enforcing integrity rules based upon local or remote updates, and (6) the effect of incrementally mutable objects (IMO's) on distributed database integrity. The contribution is flexible, robust, data integrity techniques for distributed object-oriented database management systems. GRA

N93-11769# Executive Office of the President, Washington, DC. Office of Administration.
PUBLICATIONS OF THE EXECUTIVE OFFICE OF THE PRESIDENT, 20 JANUARY 1989 - 31 MARCH 1992
1992 14 p
(PB92-154913) Avail: CASI HC A03/MF A01

The report lists publications of the Executive Office of the President for the period January 20, 1989 through March 31, 1992 for the Bush Administration. Author

N93-11770# Sandia National Labs., Albuquerque, NM.
REAL-TIME DATA COMPRESSION USING A FFT DIGITAL SIGNAL PROCESSOR
E. Brady Jun. 1992 117 p
(Contract DE-AC04-76DP-00789)
(DE92-017744; SAND-92-1014) Avail: CASI HC A06/MF A02

This report describes a hardware implementation of a fast fourier transform (FFT)-based real-time data compression system. The system is currently configured to compress and analyze airborne vehicle vibration data but it can be utilized for compressing any one- dimensional data stream. The algorithm uses a two-stage process to compress successive stationary time periods of input data. The first stage compresses data by transforming continuous blocks of 2048 points to the frequency domain using Welch's method. The second stage provides further compression by logarithmically averaging adjacent frequency bins of the transformed signal. These compression techniques result in a bandwidth savings from 8:1 to 64:1 per channel compared to strictly analog or digital transmission techniques. The complete technique as well as the hardware used to implement it is described in detail in this report. DOE

N93-11789# Zambia Univ., Lusaka. Dept. of Surveying.
PROCEEDINGS OF THE FIRST SEMINAR ON GEOGRAPHIC INFORMATION SYSTEMS IN ZAMBIA
1992 98 p Seminar held in Lusaka, Zambia, 9 Jan. 1991
Prepared in cooperation with Ministry of Water, Lands and Natural Resources, Lusaka, Zambia
(PB92-207125; ISBN-90-5271-009-0) Avail: CASI HC A05/MF A02

Contents: Concepts of GIS; Data Sources for Geographic Information Systems; Data Processing and Presentation; The Role of GIS in Decision Support Systems - A Management Perspective; Implementation of GIS in Zambia; The Landeval Geographical Information System (LGIS); International Cooperation in GIS, Photogrammetry and Remote Sensing. Author

N93-11796# Oak Ridge Y-12 Plant, TN.
LABORATORY INFORMATION MANAGEMENT SYSTEM PROPOSAL
Bridget Brown, Seth Schweitzer, Cathy Adams, and Steve White
1992 24 p
(Contract DE-AC05-84OS-21400)
(DE92-018243; Y/DK-888/P1) Avail: CASI HC A03/MF A01

The objective is to design a user friendly information management system using a relational database in order to accomplish the following: allow customers direct access to the system; provide customers with direct sample tracking capabilities; provide customers with more timely, consistent reporting; better allocate costs for analyses to appropriate customers; eliminate cumbersome and costly papertrails; and enhance facility utilization by laboratory personnel. The resultant savings through increased efficiency provided by this system should more than offset its cost in the long-term. DOE

N93-11840# Naval Postgraduate School, Monterey, CA.
EVALUATION OF A USER INFORMATION SATISFACTION SHORT-FORM INSTRUMENT M.S. Thesis
Mark S. Lockhart Mar. 1992 126 p
(AD-A250702) Avail: CASI HC A07/MF A02

The objectives of this thesis were to validate and evaluate the Baroudi and Orlikowski (2) short-form UIS instrument as a surrogate measurement of effectiveness of the Department of Defense's Composite Health Care System (CHCS). Hurd (1), using the short-form UIS instrument at the Naval Hospital Charleston, suggested that a fundamental change in the instrument's structure due to significant impact of contractor's services with the CHCS. The three Navy CHCS operational testing and evaluation hospitals were used in this study. The short-form UIS instrument was found to be inadequate for evaluation of overall UIS of the CHCS. Limitations found were: a fundamental change in the factor structure; unevenly distributed variables in a couple of factors; low reliability in one factor; no assessment of user interface with the system; and inconsistent convergent validity findings. A proposed re-design is presented. Statistically significant differences in UIS between groups and sites were found for the four factor solution. Participants were divided into three functional user groups: Physicians, Medical Support, and Administrative Support. All three groups were satisfied with the local Management Information Department staff and services and the system's output. All three groups were dissatisfied with the contractor services. Physicians were significantly less satisfied in three out of the four factors. No significant correlation between time of use of the system and UIS was found, except for the Administrative group's positive correlation with the system's output. GRA

N93-11858 Rutgers - The State Univ., Newark, NJ.
HYPERTEXT FUNCTIONALITY: A THEORETICAL FRAMEWORK Ph.D. Thesis
Usha Rao 1991 281 p
Avail: Univ. Microfilms Order No. DA9201569

Design metaphors for Hypertext systems are quite diverse. On the one hand, we have Hypertext systems that utilize general and unspecific metaphors, resulting in problems due to the ambiguity of the human language. On the other hand, the majority of Hypertext systems are application-dependent and have been tailored to very specific situations. With this latter approach, individuals and organizations will find themselves in a position of having to utilize different Hypertext systems to accomplish different tasks. Hypertext should be treated as a general-purpose tool with approaches to handling nodes, link and retrieval, that fits within the context of any application and conveys common meanings to the users. To accomplish this we need a comprehensive framework for Hypertext based on a cognitive model that allows for the representation of the complete range of human intellectual abilities. A theoretical framework useful for understanding the functionality of Hypertext systems in terms of their ability to satisfy congnitive requirements is proposed. This framework, derived from a re-interpretation of Guilford's Structure of Intellect model, consists of six generic node types and twelve generic link types. Sixteen diverse Hypertext systems were reviewed to test whether the current range of applications could be classified within the proposed framework. The results obtained support our claim that the node and link types in any current or proposed Hypertext system can be mapped into this morphology. The six node and twelve link types were tested for both exhaustiveness and consistency. Node testing consisted of subjects classifying a given node into its appropriate category. Link testing consisted of subjects classifying a link type between a given pair of node types. In both cases the exhaustiveness hypothesis was upheld. In most cases the consistency hypothesis was upheld. In situations giving rise to confusion in the classification scheme, rules and procedures were developed to resolve the confusion. While usability was not a direct objective, the results of the experiment give every indication that the morphology is directly usable. Dissert. Abstr.

N93-11911*# National Aeronautics and Space Administration. Goddard Space Flight Center, Greenbelt, MD.
DIRECTORY INTERCHANGE FORMAT MANUAL, VERSION 4.0
Dec. 1991 85 p
(NASA-TM-107991; NAS 1.15:107991;
NSSDC/WDC-A-R/S-91-32) Avail: CASI HC A05/MF A01

The Directory Interchange Format (DIF) is a data structure used to exchange directory-level information about data sets among information systems. In general the format consists of a number of fields that describe the attributes of a directory entry and text blocks that contain a descriptive summary of and references for the directory entry. All fields and the summary are preceded by labels identifying their contents. All values are ASCII character strings. The structure is intended to be flexible, allowing for future changes in the contents of directory entries. The manual is structured as follows: section 1 is a general description of what constitutes a directory entry; section 2 describes the content of the individual fields within the data structure, together with some examples. Also included in the six appendices is a description of the syntax used within the examples; samples of the directory interchange format applied to different data sets; the allowable discipline keywords; a current list of valid location keywords; a list of allowable parameter keywords; a list of acronyns and a glossary of terms used; and a description of the Standard Formatted Data Unit header, which may be added to the front of a DIF file to identify the file as a registered standard format. L.R.R.

N93-12007*# National Aeronautics and Space Administration. Langley Research Center, Hampton, VA.
NASA/DOD AEROSPACE KNOWLEDGE DIFFUSION RESEARCH PROJECT. PAPER 23: INFORMATION TECHNOLOGY AND AEROSPACE KNOWLEDGE DIFFUSION: EXPLORING THE INTERMEDIARY-END USER INTERFACE IN A POLICY FRAMEWORK
Thomas E. Pinelli, Rebecca O. Barclay (Rensselaer Polytechnic Inst., Troy, NY.), Ann P. Bishop (Illinois Univ., Urbana-Champaign.), and John M. Kennedy (Indiana Univ., Bloomington.) 1992 20 p
Repr. from Electronic Networking: Research, Applications and Policy, v. 2, no. 2, 1992 p 31-49
(Grant NAGw-1682)
(NASA-TM-108077; NAS 1.15:108077) Avail: CASI HC A03/MF A01

Federal attempts to stimulate technological innovation have been unsuccessful because of the application of an inappropriate policy framework that lacks conceptual and empirical knowledge of the process of technological innovation and fails to acknowledge the relationship between knowled reproduction, transfer, and use as equally important components of the process of knowledge diffusion. It is argued that the potential contributions of high-speed computing and networking systems will be diminished unless empirically derived knowledge about the information-seeking behavior of the members of the social system is incorporated into a new policy framework. Findings from the NASA/DoD Aerospace Knowledge Diffusion Research Project are presented in support of this assertion. Author

N93-12068# Los Alamos National Lab., NM.
PERFORMING A SUCCESSFUL AUDIENCE ANALYSIS: HOW TO IMPROVE YOUR PROPOSAL-WRITING SKILLS
O. Ramos, Jr. 1992 11 p Presented at the IEE International Professional Communications Conference: Crossing Frontiers, Santa Fe, NM, 30 Sep. 1992
(Contract W-7405-eng-36)
(DE92-018978; LA-UR-92-2139; CONF-9209142-3) Avail: CASI HC A03/MF A01

Proposal teams conduct an audience analysis in much the same way as they write proposals: they search for characteristics (features) and attempt to conform to such characteristics (benefits). For example, based on experience, the proposal team knows that a specific proposal review board has short attention spans and is graphics-oriented. The team also knew that the evaluators will have to score more then thirty proposals in one weekend. Based on these characteristics, the team decides to use more photos and less text and establish many heads and subheads. The team then begins to write the proposal. DOE

N93-12143# Lawrence Livermore National Lab., CA.
LINK USER MANUAL
21 May 1992 85 p
(Contract W-7405-eng-48)
(DE92-017987; UCRL-CR-110713) Avail: CASI HC A05/MF A01

This section describes the scope of this manual and includes an overview of the Logistics Information Network (LINK), a document overview and the conventions used in this manual. The Logistics Information Network System, or LINK as it is known, provides the capability to access multiple computer systems for information on material in place and material in transportation in a timely manner. LINK provides a solution that satisfies the mission requirement to fulfill insufficiencies in times of war, crisis or peacetime. LINK operates in times of both war and peace to obtain logistics information from existing computer systems and to present this information to decision makers in an understandable format. LM provides a set of customized Gateway applications. Gateway (sometimes referred to as the Intelligent Gateway) provides the necessary capabilities for automated access and data retrieval from remote computer systems. The LINK applications make it easy for users to access remote computers and to retrieve information from databases and other applications running on remote computer systems. DOE

N93-12150*# National Aeronautics and Space Administration. Goddard Space Flight Center, Greenbelt, MD.
NATIONAL SPACE SCIENCE DATA CENTER DATA ARCHIVE AND DISTRIBUTION SERVICE (NDADS) AUTOMATED RETRIEVAL MAIL SYSTEM USER'S GUIDE
Charleen M. Perry (Hughes STX, Inc., Greenbelt, MD.) and Michael E. VanSteenberg 1 Apr. 1992 34 p
(NASA-TM-107990; NAS 1.15:107990; NSSDCA/WDC-A-R/S-92-03) Avail: CASI HC A03/MF A01

The National Space Science Data Center (NSSDC) has developed an automated data retrieval request service utilizing our Data Archive and Distribution Service (NDADS) computer system. NDADS currently has selected project data written to optical disk platters with the disks residing in a robotic 'jukebox' near-line environment. This allows for rapid and automated access to the data with no staff intervention required. There are also automated help information and user services available that can be accessed. The request system permits an average-size data request to be completed within minutes of the request being sent to NSSDC. A mail message, in the format described in this document, retrieves the data and can send it to a remote site. Also listed in this document are the data currently available. Author

N93-12287# Jackson State Univ., MS.
APPLICATION OF MACHINE LEARNING TECHNIQUES FOR EFFECTIVE RETRIEVAL IN IMAGE DATABASE Final Report
V. N. Gudivada and V. V. Raghavan 30 Apr. 1992 14 p
(Contract DAAL03-89-G-0118)
(AD-A254907; ARO-27247.5-MA-SAH) Avail: CASI HC A03/MF A01

Recently, there has been widespread interest in various kinds of database management systems for managing formatted information. Depending upon the domain and the nature of formatted data, these systems are variously referred to as Multimedia Information Systems, Spatial Databases, Pictorial Information Systems, and Image Database Systems. However, the image data models employed in these systems are not based on any general framework. The model is rather extracted often from the implemented system and hence these data models are shaped by the idiosyncratic characteristics of the domains. Similar kinds of problems plague the query language design. By studying the application requirements and the limitations of the proposed approaches, we envision a multi-layered structure for retrieval. The various layers in the scheme are: Physical Layer, Spatial and Shape Layer, Iconic and Attribute Layer, and Conceptual Layer. These layers are not designed to operate in isolation but rather work in cooperation. To avoid redundancy in representation the layers are structured to form a lattice. The layers can also be viewed as multiple representations for the same object. This framework is expected to be highly flexible enough so that it can be useful across several application areas. GRA

N93-12381# Naval Postgraduate School, Monterey, CA.
EXPLOITING CAPTIONS IN RETRIEVAL OF MULTIMEDIA DATA Report, Oct. 1991 - Sep. 1992
Neil C. Rowe and Eugene J. Guglielmo Jul. 1992 24 p
(AD-A255184; NPSCS-92-011) Avail: CASI HC A03/MF A01

Descriptive natural-language captions can help organize multimedia data. We described our MARIE system that interprets English queries directing the fetch of media objects. It is novel in the extent to which it exploits previously interpreted and indexed English captions for the media objects. Our routine filtering of queries through descriptively-complex captions (as opposed to keyword lists) before retrieving data can actually improve retrieval speed, as media data are often bulky and time consuming to retrieve, difficult upon which to perform content analysis, and even small improvements to query prevision can often pay off. Handling the English of captions and queries about them is not as difficult as it might seem, as the matching does not require deep understanding, just a comprehensive type hierarchy for caption concepts. An important innovation of MARIE is supercaptions describing sets of captions, which can minimize caption redundancy. GRA

N93-12404# European Space Agency. European Space Research and Technology Center, ESTEC, Noordwijk (Netherlands). Publications Div.
ESIS: AN INTRODUCTION TO THE EUROPEAN SPACE INFORMATION SYSTEM. A MODERN TOOL FOR SPACE SCIENTISTS
Alessandro Ciarlo and Norman Longdon, ed. Feb. 1992 16 p
LIMITED REPRODUCIBILITY: More than 20% of this document may be affected by color photographs Original contains color illustrations
(ESA-INT-2) Avail: CASI HC A03/MF A01

This pamphlet describes the European Space Information System (ESIS) in a user friendly way. ESIS is being developed to provide simple access to space data archives as well as data processing services to support scientific data analysis. The three main components of the system are the Query Environment (QE), the Correlation Environment (CE) and electronic communication facilities such as electronic mail, conferencing, directories, etc. Two disciplines within the field of space sciences are covered: astronomy & astrophysics and space physics. In addition to archives in place such as the SIMBAD data base at the Strasbourg Stellar Data Center, the International Ultraviolet Explorer (IUE), the

European X-ray Observatory Satellite (EXOSAT), the Garching Space Telescope and the Geophysical Data Facility, ESIS will include access to bibliographic databases from ESA-IRS (Information Retieval Service) - ESRIN (European Space Research Institute). Color imagery will be available for appropriate data.
R.L.B.

N93-12438# Pennsylvania Univ., Philadelphia. Dept. of Chemistry.
ERASABLE OPTICAL INFORMATION STORAGE IN THE POLYANILINES Technical Report, 31 May 1991 - 30 Jun. 1992
R. P. McCall, J. M. Ginder, and A. J. Epstein 5 Jun. 1992 12 p
(Contract N00014-90-J-1559)
(AD-A254873; Rept-1992-7) Avail: CASI HC A03/MF A01

The polyaniline family of polymers exhibits properties that allow for the storage of optical information. Photoexcitation of several forms of polyaniline results in long-lived changes in the absorption spectra, associated with trapped charged defect states. These new absorptions exhibit long lifetimes at low temperature (below approximately 250 K), with erasure occurring upon warming the sample. Use in erasable optical information storage devices and related technologies is discussed. GRA

N93-12495# Westinghouse Idaho Nuclear Co., Inc., Idaho Falls.
RADIOLOGICAL INFORMATION MANAGEMENT SYSTEM (RADIMS)
R. G. Oesterling, S. A. Marko, and A. N. Tschaeche 19 Aug. 1991 20 p Presented at the Westinghouse Computer Symposium, Monroeville, PA, 21-22 Oct. 1991
(Contract DE-AC07-84ID-12435)
(DE92-017221; WINCO-11733; CONF-9110344-10) Avail: CASI HC A03/MF A01

Westinghouse Idaho Nuclear Company, Inc. (WINCO) is developing and implementing an information management system, known as RadIMS, to track and record personnel exposure to ionizing radiation. RadIMS has been designed to fulfill all the requirements of US Department of Energy (USDOE) Order 5480.11, 'Radiation Protection for Occupational Workers.' This Order requires the contractor to maintain detailed radiation exposure records on all individuals who work at the facility. These records must be retrievable for the entire working life of the individual and be available to other USDOE contractors on request. To meet these general needs, RadIMS provides for retrieval of detailed, comprehensive individual exposure histories as well as the usual online interactions to accomplish day-today radiation protection operations. These two extremes of functionality require different approaches in the WINCO computing environment. The exposure histories include database text, paper, microfilm, and electronic bitmaps. DOE

N93-12528# Environmental Protection Agency, Washington, DC. Office of Wetlands, Oceans, and Watersheds.
OFFICE OF WETLANDS, OCEANS, AND WATERSHEDS PUBLICATIONS
Jun. 1992 27 p
(PB92-224310; EPA/840/B-92/001) Avail: CASI HC A03/MF A01

EPA's Office of Wetlands, Oceans, and Watersheds (OWOW) was created in April 1991. OWOW combines EPA's responsibilities for addressing nonpoint source pollution, restoring and protecting wetlands, lakes, rivers, coastal and marine environments, and coordinating surface water monitoring and water quality assessment activities. The publications in this list are divided into seven topic areas. Each topic, except Bulletins, has two sections: General and Technical. General publications can be easily understood by the lay reader. Technical publications are scientific or regulatory in nature and require an understanding of the program area.
GRA

83 ECONOMICS AND COST ANALYSIS

Includes cost effectiveness studies.

N93-12472# Naval Postgraduate School, Monterey, CA.
COST ESTIMATION OF SOFTWARE DEVELOPMENT AND THE IMPLICATIONS FOR THE PROGRAM MANAGER M.S. Thesis
Glenn C. Doyle Jun. 1992 147 p
(AD-A255167) Avail: CASI HC A07/MF A02

Cost estimation of computer software development is a critical problem for the Department of Defense. The acquisition of major weapons or hardware has been impacted by cost overruns and schedule slippage in software development. Program Managers are responsible for estimating a program's cost using the information provided by the contractor and the cost analysis divisions within the System Commands. This study first analyzes why variance exists between the different estimates for the same software project that are provided to the Program Manager as input to the budget estimate. The study then examines four methods that are used to understand and reduce the variance between the estimates to give the Program Manager more control over the software development cost estimation process. A set of five specific decision rules is developed for the Program Manager to implement in the cost estimation process. The intent of the study is to improve the accuracy of the cost estimate by reducing the variance between the independently generated estimates submitted to the Program Manager. GRA

N93-12473# Naval Postgraduate School, Monterey, CA.
THE USE OF LIFE CYCLE COSTING FOR THE ACQUISITION OF NON-MAJOR SYSTEMS AT THE NAVAL REGIONAL CONTRACTING CENTER DETACHMENT M.S. Thesis
R. F. Tucker Jun. 1992 146 p
(AD-A255170) Avail: CASI HC A07/MF A02

The use of Life Cycle Costing (LCC) has many potential benefits for the Government. These benefits range from reduced total ownership costs to increased reliability to improved maintainability. However, prior to applying the LCC technique, an analysis should be conducted to determine its usefulness. Consequently, the purpose of this thesis is to assess the applicability of the LCC concept to the purchase of non-major systems at the Naval Regional Contracting Center (NRCC), Long Beach. The primary method of achieving this objective was through modifying the Graham LCC Decision Model for Spare Parts so that the Model could evaluate the usefulness of LCC for the purchase of a particular non-major system. Through the use of the Modified Graham LCC Decision Model, telephone and personal interviews, and a thorough literature review, the researcher found the usefulness of Life Cycle Costing for the acquisition of non-major system at NRCC to be very limited. GRA

84 LAW, POLITICAL SCIENCE AND SPACE POLICY

Includes NASA appropriation hearings; aviation law; space law and policy; international law; international cooperation; and patent policy.

No abstracts in this category.

85 URBAN TECHNOLOGY AND TRANSPORTATION

Includes applications of space technology to urban problems; technology transfer; technology assessment; and surface and mass transportation.

For related information see also *03 Air Transportation and Safety, 16 Space Transportation,* and *44 Energy Production and Conversion.*

N93-12067# Pacific Northwest Lab., Richland, WA.
SELECTED CASE STUDIES OF TECHNOLOGY TRANSFER FROM MISSION-ORIENTED APPLIED RESEARCH
K. K. Daellenbach, R. L. Watts, J. K. Young, and R. B. Abarcar (Energetics, Inc., Columbia, MD.) Jul. 1992 54 p
(Contract DE-AC06-76RL-01830)
(DE92-018957; PNL-8084) Avail: CASI HC A04/MF A01

The US Department of Energy (DOE) Advanced Industrial Concepts Division (AICD) under the Office of Industrial Technologies (OIT) supports interdisciplinary applied research and exploratory development that will expand the knowledge base to enable industry to improve its energy efficiency and its capability to use alternative energy resources. AICD capitalizes on scientific and technical advances from the United States and abroad, applying them to address critical technical needs of American industry. As a result, AICD research and development products are many and varied, and the effective transfer of these products to diverse targeted users requires different strategies as well. This paper describes the products of AICD research, how they are transferred to potential users, and how actual transfer is determined. DOE

88 SPACE SCIENCES (GENERAL)

No abstracts in this category.

89 ASTRONOMY

Includes radio, gamma-ray, and infrared astronomy, and astrometry.

N93-11073*# Washington Univ., Seattle.
ULTRAVIOLET STUDIES OF CEPHEIDS
Erika Boehm-Vitense 1992 9 p
(Grant NsG-5398)
(NASA-CR-190857; NAS 1.26:190857) Avail: CASI HC A02/MF A01

We discuss whether with new evolutionary tracks we still have a problem fitting the Cepheids and their evolved companions on the appropriate evolutionary tracks. We find that with the Bertelli et al. tracks with convective overshoot by one pressure scale height the problem is essentially removed, though somewhat more mixing would give a better fit. By using the results of recent nonlinear hydrodynamic calculations, we find that we also have no problem matching the observed pulsation periods of the Cepheids with those expected from their new evolutionary masses, provided that Cepheids with periods less than 9 days are overtone pulsators. We investigate possible mass loss of Cepheids from UV studies of the companion spectrum of S Mus and from the ultraviolet spectra of the long period Cepheid l Carinae. For S Mus with a period of 9.6 days we derive an upper limit for the mass loss of M less than 10(exp -9) solar mass, if a standard velocity law is assumed for the wind. For l Carinae with a period of 35.5 days we find a probable mass loss of M is approximately 10(exp -5+/-2) solar mass. Author

N93-11075*# Washington Univ., Seattle.
DETECTION OF A WHITE DWARF IN A VISUAL BINARY SYSTEM
Erika Boehm-Vitense 1980 14 p
(Grant NsG-5398)
(NASA-CR-190856; NAS 1.26:190856) Avail: CASI HC A03/MF A01

The F6 giant HD 160365 was detected to have a white dwarf companion about 8 arcsec south of the star. The UV energy distribution observed with International Ultraviolet Explorer (IUE) shows that the white dwarf has an effective temperature of 23,000 +/- 2,000 K. If log g = 8 the Ly(alpha) profile indicates an effective temperature around 24,500 K. Using the theoretical models, one finds a visual magnitude of m(sub v) is approximately 16.5. For T(sub eff) = 24,500 K one expects for a white dwarf a luminosity of log L/solar luminosity is approximately -1.3 and M(sub V) is approximately 10.67. This gives a distance modulus for the system of m(sub v) - M(sub V) = 5.83 and an absolute magnitude M(sub v) = 0.3 for the giant. Author

N93-11198 California Univ., Berkeley.
A CRYOGENIC PHONON DETECTOR TO SEARCH FOR DARK MATTER PARTICLES Ph.D. Thesis
Ning Wang 1991 220 p
Avail: Univ. Microfilms Order No. DA9203754

The systematic investigation of the thermal and electrical properties of neutron transmutation doped (NTD) Ge at low temperatures and the development of a detector to search for weakly interacting massive particles (WIMP's), predicted by some theories to make up to 90 percent of the matter in the universe, is presented. We have fabricated NTD Ge phonon sensors operated on a dilution refrigerator near 20 mK. The thermal and electrical properties of NTD Ge were investigated first. The zero bias resistance was found to be governed by variable range hopping, but the nonlinearity of the current-voltage characteristics indicated significant hot electron effects near 20 mK. A detailed investigation of hot-electron effects in NTD Ge is described. NTD Ge sensors were found to be very sensitive to high energy phonons generated by interactions of Ge with alpha-particles and photons. The mean absorption length of the high energy phonons in NTD Ge was found to be about 500 microns. In order to use these phonon sensors in conjunction with a target crystal, we developed a bonding technique using a Au-Ge eutectic. The bonds were found to be mechanically strong, thermally cyclable, and more transparent to high energy phonons than conventional silver-filled epoxies. The eutectic bonding technique was also found to leave the thermal and electrical properties of NTD Ge unchanged. We describe ionization signals observed in pure Ge target crystals, generated by the interaction of Ge with alpha-particles and photons; these ionization signals were observed simultaneously with phonon signals from the NTD Ge sensors. Such simultaneous signals can be used to reject unwanted background events, which is an important requirement for a WIMP detector. Finally, we describe the design and testing of a 60 g Ge detector to which six phonon sensors were attached. Simultaneous phonon and ionization signals were observed when irradiating the crystal with photons from Am-241. The energy resolution was found to be about 4 keV for both the phonon and ionization signals, and was limited by microphonic noise. With this prototype detector, we have demonstrated the key aspects necessary for a WIMP detector. Dissert. Abstr.

N93-11248 Council for National Academic Awards (England).
NEAR-INFRARED IMAGING POLARIMETRY OF BIPOLAR NEBULAE Ph.D. Thesis
Nigel Robert Minchin 1990 225 p
Avail: Univ. Microfilms Order No. BRDX96096

High spatial resolution near-infrared (1-5 micrometers) polarization and surface brightness images of the reflection nebulosity around several famous bipolar outflow sources are presented. The images were made in the broad band at J (1.25 micrometers), H (1.65 micrometers), and K (2.2 micrometers), in a narrow band at L (3.6 micrometers), and in the v = 1 approaches

0 S(1) emission line of molecular hydrogen (2.1218 micrometers). Observations were made using one of the new generation of array cameras, sensitive to near-infrared radiation. The observing and data reduction techniques developed and subsequently employed to produce the final reduced and calibrated images are discussed. The images reveal detailed structure in both the polarization vector patterns and surface brightness distributions around several bipolar outflow sources not previously observable. The implications of this structure for the production of the bipolar nebulae are discussed. Both the polarization and surface brightness images provide evidence that each of the outflow sources are surrounded by a disk of material, with the long axis of the disk orthogonal to the direction of mass outflow. The polarization observed from the reflection nebulosity around three of the outflow sources increases markedly with increasing wavelength. This is interpreted as evidence for the presence of grains with a size distribution substantially larger than that normally associated with the diffuse interstellar medium. The spatial distribution of polarization observed from three of the reflection nebulae are compared with those predicted using models of different scattering geometries. The results of the modelling suggests that the outflow scattering geometries are basically parabolic or conical, with scattering taking place mainly from the walls of the outflow geometry.
Dissert. Abstr.

N93-11373 Colorado Univ., Boulder.
FAR ULTRAVIOLET SPECTROPHOTOMETRY OF HOT STARS AND CALIBRATION STANDARDS IN THE FAR ULTRAVIOLET Ph.D. Thesis
Timothy Allan Cook 1991 121 p
Avail: Univ. Microfilms Order No. DA9220401

The purpose of this study is to establish a spectrophotometric calibration standard at far ultraviolet wavelengths between 912 and 1216 A. Previous work has been hampered by the marked disagreement between the results of the Voyager UVS and other experiments. In order to address this issue, I use a far ultraviolet spectroscopic sounding rocket to obtain a photometrically calibrated spectrum of the star BD +28 4211. In contrast to a previous spectrum of alpha Virginis taken with the same instrument, this spectrum is in reasonably good agreement with the Voyager results. I investigate the source of this inconsistency and find that the calibration sources and procedures of the Voyager UVS are neither consistent nor quantitative and that Voyager should not be considered a trustworthy photometric instrument. I will also discuss the spectrum of BD +28 4211 as well as the spectrum of alpha Andromeda which was obtained during a payload attitude update maneuver.
Dissert. Abstr.

N93-11473 Max-Planck-Inst. fuer Physik und Astrophysik, Garching (Germany). Inst. fuer Extraterrestrische Physik.
CONTRIBUTIONS TO THE JOINT DISCUSSION 3: RESULTS FROM ROSAT AND GRO AND OTHER RECENT HIGH ENERGY ASTROPHYSICS MISSIONS OF THE MAX-PLANCK-INSTITUT FUER EXTRATERRESTRISCHE PHYSIK
J. Truemper, ed. Jan. 1992 26 p The 21st International Astronomical Union's General Assembly, Buenos Aires, Argentina, 23 Jul. - 1 Aug. 1991
(MPE-Preprint-215; ETN-92-92172) Copyright Avail: Max-Planck-Inst. fuer Physik und Extraterrestrische Physik, 8046 Garching bei Muenchen, Germany

Contributions concerning results and analysis of the Roentgen satellite (ROSAT) all sky survey are presented. In particular the following are reported: deep imaging studies of the X-ray background; X-ray morpohology of galactic clusters; morphology and physics of supernova remnants; and stellar content of the ROSAT all sky survey. For individual titles, see N93-11474 through N93-11477.

N93-11474 Max-Planck-Inst. fuer Physik und Astrophysik, Garching (Germany). Inst. fuer Extraterrestrische Physik.
ROSAT DEEP SURVEYS
Guenther Hasinger *In its* Contributions to the Joint Discussion 3: Results from Rosat and GRO and Other Recent High Energy Astrophysics Missions of the Max-Planck Institut fuer Extraterrestrische Physik Jan. 1992 p 1-6 (For primary document see N93-11473 02-89)
Copyright Avail: Max-Planck-Inst. fuer Physik und Extraterrestrische Physik, 8046 Garching bei Muenchen, Germany

A series of 20 deep pointed observations with the ROSAT PSPC (Position Sensitive Proportional Counter) is discussed. Exactly 530 X-ray sources with 0.5 to 2 keV fluxes down to 3(10)(exp -15) erg cm(exp -2)s(exp -1) were discovered in 5.9 deg(exp 2). The N(greater than S) relation of the sources selected in the 0.5 to 2 keV band shows a density in excess of 200 deg(exp -2) at the faintest fluxes and a flattening below 2(10)(exp -14) erg cm(exp -2)s(exp -1). The average spectrum of those sources is a power law with energy index 1.2 +/- 0.1. The absorption column densities are consistent with the galactic HI columns. More than 50 percent of the 1 to 2 keV background was resolved into discrete sources in the deepest field. The total background spectrum shows an emission line feature around 0.65 keV, most probably due to to O7-O8 from a 2,000,000 K plasma. Above approximately 1 keV the background is dominated by a power law spectrum with a normalization of 13.4 +/- 0.2 keV cm(exp -2) s (exp -1) sr(exp -1) keV(exp -1) and a slope 1.2 +/- 0.1, i.e., considerably steeper than the extrapolation from higher energies.
ESA

N93-11475 Max-Planck-Inst. fuer Physik und Astrophysik, Garching (Germany). Inst. fuer Extraterrestrische Physik.
X RAY MORPHOLOGY OF CLUSTERS OF GALAXIES
H. Boehringer, R. A. Schwarz, U. G. Briel, H. Ebeling, and W. Voges *In its* Contributions to the Joint Discussion 3: Results from Rosar and GRO and Other Recent High Energy Astrophysics Missions of the Max-Planck-Institut fuer Extraterrestrische Physik Jan. 1992 p 7-11 Sponsored by DFG (For primary document see N93-11473 02-89)
Copyright Avail: Max-Planck-Inst. fuer Physik und Extraterrestrische Physik, 8046 Garching bei Muenchen, Germany

The ROSAT observatory with its high spatial resolution X-ray telescope is an ideal instrument for the study of clusters of galaxies. In the first part of the mission an all sky X-ray survey was conducted with ROSAT. First results of observations of Virgo, Perseus, and some other clusters of galaxies from the all sky survey, are presented. These data illustrate the capabilities of the ROSAT observatory for studies of the morphological structure and physical properties of galaxy clusters.
ESA

N93-11476 Max-Planck-Inst. fuer Physik und Astrophysik, Garching (Germany). Inst. fuer Extraterrestrische Physik.
MORPHOLOGY AND PHYSICS OF SUPERNOVA REMNANTS
B. Aschenbach *In its* Contributions to the Joint Discussion 3: Results from Rosar and GRO and Other Recent High Energy Astrophysics Missions of the Max-Planck-Institut fuer Extraterrestrische Physik Jan. 1992 p 12-17 (For primary document see N93-11473 02-89)
Copyright Avail: Max-Planck-Inst. fuer Physik und Extraterrestrische Physik, 8046 Garching bei Muenchen, Germany

Spectrally resolved X-ray images of the Cygnus Loop and the Vela supernova remnant obtained during the ROSAT all sky survey are discussed. The remnants show highly filamentary brightness distributions. Temperatures between 1,000,000 and 10,000,000 K were measured. Both remnants show significant deviation from thermal pressure equilibrium. The highest pressure excursions of up to a factor of 50 are associated with the X-ray brightest filaments. Pressure variations are expected for very recently shocked clouds, on a smaller scale though. In a limited search of the all sky survey data 14 extended objects were found, tentatively identified as previously unknown supernova remnants. A total number of approximately 60 new remnants are expected from the analysis of the full sky.
ESA

N93-11477 Max-Planck-Inst. fuer Physik und Astrophysik, Garching (Germany). Inst. fuer Extraterrestrische Physik.
STARS IN THE ROSAT ALL-SKY SURVEY
J. H. M. M. Schmitt *In its* Contributions to the Joint Discussion

3: Results from Rosat and GRO and Other Recent High Energy Astrophysics Missions of the Max-Planck-Institut fuer Extraterrestrische Physik Jan. 1992 p 18-22 (For primary document see N93-11473 02-89)
Copyright Avail: Max-Planck-Inst. fuer Physik und Extraterrestrische Physik, 8046 Garching bei Muenchen, Germany

The stellar content of the ROSAT all sky survey and the analysis of the data are addressed. The total number of X-ray sources is expected to be around 60,000. Preliminary results are discussed. The X-ray emitting late type stars are commonly referred to as 'active' stars, and the ROSAT catalog will comprise the most extensive list of such objects. The scatter of active and inactive stars, X-ray observations of young galactic clusters, PSPC (Position Sensitive Proportional Counter) pulse height spectra of active stars, and all sky survey lightcurves of stellar coronae, are discussed. ESA

N93-11750# Arizona Univ., Tucson. Lunar and Planetary Lab.
A SEARCH FOR LOW-LUMINOSITY OBJECTS Final Report, 1 Nov. 1988 - 31 Oct. 1991
Tom Gehrels 31 Oct. 1991 6 p
(Grant AF-AFOSR-0027-89)
(AD-A253301; AFOSR-92-0699TR) Avail: CASI HC A02/MF A01

During this grant, the 2048x2048 Tektronix CCD detector was installed and put into operation on the Spacewatch Telescope at Kitt Peak in Arizona. The CCD was installed in its dewar during the fall of 1988 and tested in January 1989. Scanning for near-Earth asteroids was started in the visual mode awaiting the arrival of the computer system. The first near-Earth asteroid was discovered in the fall of 1989. The Solbourne-Sun computer system was installed and a major effort involved the programming for the computerized discovery of moving objects. The computerized discovery of moving objects was operational in September 1990 and led to the discovery of the asteroid 1990ss. Work has involved the discovery of objects, verification of heliocentric orbit and astrometric determination of orbital parameters. Improvement was made in the observing programs, hardware, and software. Refinements were made in the installation of the Guide Star Catalog of the Hubble Space Telescope. Positions can now be determined in real time with an accuracy of about 0.4 arcseconds. GRA

N93-12244# Tektronix, Inc., Beaverton, OR.
FINAL REPORT, JANUARY 1991 - JULY 1992
Jon Ferrara Jul. 1992 115 p
(Contract N00014-91-C-2052)
(AD-A254659) Avail: CASI HC A06/MF A02

This report covers final schedules, expenses and billings, monthly reports, testing, and deliveries for this contract. The goal of the detector development program for the Solar and Heliospheric Spacecraft (SOHO) EUV Imaging Telescope (EIT) is an Extreme UltraViolet (EUV) CCD (Change Collecting Device) camera. As a part of the CCD screening effort, the quantum efficiency (QE) of a prototype CCD has been measured in the NRL EUV laboratory over the wavelength range of 256 to 735 Angstroms. A simplified model has been applied to these QE measurements to illustrate the relevant physical processes that determine the performance of the detector. The charge transfer efficiency (CTE) characteristics of the Tektronix 1024 X 1024 CCD being developed for STIS/SOHO space imaging applications have been characterized at different signal levels, operating conditions, and temperatures using a variety of test methods. A number of CCD's have been manufactured using processing techniques developed to improve CTE, and test results on these devices will be used in determining the final chip design. In this paper, we discuss the CTE test methods used and present the results and conclusions of these tests. GRA

N93-12336 Stanford Univ., CA.
TEMPORAL AND SPECTRAL VARIABILITY IN LUMINOUS X RAY BINARIES Ph.D. Thesis
Brian Alexander Vaughan 1992 177 p
Avail: Univ. Microfilms Order No. DA9217892

A variety of timing analyses have been applied to data from recent Ginga observations of Galactic Black Hole Candidates (BHC) and Low Mass X-ray Binaries (LMXB) to probe spectral and temporal variability. (1) A cross spectral analysis of Cyg X-1 and GX 339-4. The cross spectral coherence function is used to study temporal correlations between hard and soft photons from Cyg X-1 and GX 339-4. A technique is developed to correct for counting noise and applied to Cyg X-1 to estimate the extent of the Compton scattering region. The region size is found to be of order .014 light seconds. (2) Correlation between QPO and LFN in GX 5-1. Statistical tests are developed to probe correlations between the QPO and LFN in GX 5-1 on the horizontal branch. At long time scales, QPO and LFN amplitudes are found to be correlated, but below 8 seconds the correlation disappears. Tests are calibrated through extensive simulations. We place severe constraints on the Beat Frequency model. (3) X-ray variability of Sco X-1 during a multiwavelength campaign. We present results of a March 1989 Ginga observation of Sco X-1 as part of a simultaneous worldwide multiwavelength campaign. We see both normal and flaring branch QPO. To test Z-diagram position as a state variable, we probe for correlation between velocity along the diagram and measurable quantities. Finally, we perform a search for coherent oscillation and find none, with an upper limit of 0.2 percent. (4) Search for coherent oscillations in Low Mass X-ray Binaries. Using Ginga and HEAO-1 data, we have performed the most sensitive search to date for coherent oscillations in LMXB. We describe a technique to compensate for Doppler smearing by source orbital motion with a single correction parameter, and obtain modulation depth limits for Sco X-1, GX 5-1, Cyg X-2, GX 340 + 0, GX 9 + 1 and 1820-30. Dissert. Abstr.

N93-12348*# Alabama Univ., Huntsville. Dept. of Physics.
GAMMA RAY ASTRONOMY Final Report, 13 Apr. 1991 - 12 Apr. 1992
William S. Paciesas Apr. 1992 28 p
(Contract NAS8-36955)
(NASA-CR-184447; NAS 1.26:184447) Avail: CASI HC A03/MF A01

Miscellaneous tasks related to mission operations and data analysis for the Burst and Transient Source Experiment on the Gamma Ray Observatory, to collection, analysis, and interpretation of data from the Marshall Space Flight Center Very Low Frequency transient monitoring program, and to compilation and analysis of induced radioactivity data were performed. The results are summarized and relevant references are included. Author

90 ASTROPHYSICS

Includes cosmology; celestial mechanics; space plasmas; and interstellar and interplanetary gases and dust.

For related information see also *75 Plasma Physics.*

N93-10993# Los Alamos National Lab., NM.
A LINEAR AND NONLINEAR STUDY OF MIRA
A. N. Cox and D. A. Ostlie 1991 16 p Presented at the International Astronomical Union (IAU) Conference on Nonlinear Phenomena in Stellar Variability, Buenos Aires, Argentina, 23 Jul. - 1 Aug. 1991
(Contract W-7405-eng-36)
(DE92-011265; LA-UR-92-845; CONF-9107218-1) Avail: CASI HC A03/MF A01

Both linear and nonlinear calculations of the 331 day, long period variable star Mira have been undertaken to see what radial pulsation mode is naturally selected. Models are similar to those considered in the linear nonadiabatic stellar pulsation study of Ostlie and Cox. Models are considered with masses near one solar mass, luminosities between 4000 and 5000 solar luminosities, and effective temperatures of approximately 3000 K. These models have fundamental mode periods that closely match the pulsation period of Mira. The equation of state for the stellar material is given by Stellingwerf procedure, and the opacity is obtained from a fit by Cahn that matches the low temperature molecular absorption data for the Population I Ross-Aller 1 mixture calculated from the Los Alamos Astrophysical Opacity Library. For the linear study, the Cox, Brownlee, and Eilers approximation is used for the linear theory variation of the convection luminosity. For the nonlinear work, the method described by Ostlie and Cox is followed. Results showing internal details of the radial fundamental and first overtone modes behavior in linear theory are presented. Preliminary radial fundamental mode nonlinear calculations are discussed. The very tentative conclusion is that neither the fundamental or first overtone mode is excluded from being the actual observed one. DOE

N93-11230 Oklahoma Univ., Norman.

PERIODICITIES IN PULSAR MICROSTRUCTURE Ph.D. Thesis

Jeffrey Foster Friedman 1992 182 p
Avail: Univ. Microfilms Order No. DA9217975

An extensive set of simultaneous dual frequency (196 and 318 MHz) observations of Pulsars, PSR2016 + 28, 1133 + 16 and 0950 + 08 has been examined by computing their cross spectral densities (CSD's) and cross correlation functions (CCF's). Significant periodicities were detected in various subsets of the data from a few tens to several thousand pulses. The signals are not consistent throughout the entire data set and are not seen in every pulse within each subset. Some of the signal can be attributed to 60 Hz harmonics but there exists a residual signal that cannot be attributed to any known source other than the pulsar and its environs. It is suggested that these 'lines' are due, following Boriakoff (1976), to pulsar body oscillations. The ephemeral nature of their existence is not attributed to low Q signals, beating of adjacent modes, mode switching, or masking, but as a result of being on the threshold of detectibility in addition to having an intermittent source. The persistence of a signal over 2000 pulsar periods, and well over 50,000 oscillations, implies a high Q. Three linear calculations of 1/e decays in excess of 60,000 oscillation periods were carried out assuming no driving. These constrain the oscillation types and provide information that could constrain the models of the internal constitution of the neutron stars. Dissert. Abstr.

N93-11243*# Jet Propulsion Lab., California Inst. of Tech., Pasadena.

THE COMET HALLEY ARCHIVE: SUMMARY VOLUME

Zdenek Sekanina, ed. and Lori Fry, ed. Aug. 1991 337 p
Sponsored by NASA, Washington, DC
(NASA-CR-190358; NAS 1.26:190358; PB92-156959) Avail: CASI HC A15/MF A03

The contents are as follows: The Organizational History of the International Halley Watch; Operations of the International Halley Watch from a Lead Center Perspective; The Steering Group; Astrometry Network; Infrared Studies Network; Large-Scale Phenomena Network; Meteor Studies Network; Near-Nucleus Studies Network; Photometry and Polarimetry Network; Radio Science Network; Spectroscopy and Spectrophotometry Network; Amateur Observation Network; Use of the CD-ROM Archive; The 1986 Passage of Comet Halley; and Recent Observations of Comet Halley. GRA

N93-11260 Arizona Univ., Tucson.

A SUBMILLIMETER-MILLIMETERWAVE STUDY OF THE MOLECULAR GAS IN THE NUCLEAR REGIONS OF THREE NEARBY STARBURST GALAXIES Ph.D. Thesis

Constance Elaine Walker 1991 272 p
Avail: Univ. Microfilms Order No. DA9210341

We have used millimeter and submillimeter molecular line observations to probe the interstellar medium in the central region of three nearby starburst galaxies, M82, IC342, and M83. These galaxies were mapped in the CO J = 3 to 2 and CS J = 2 to 1 transitions and, in one case, the CO J = 2 to 1 line. By combining our observations with those of other workers, we were able to characterize the gas morphology, temperature, velocity field, column density, and mass in each galaxy. In addition, high angular resolution 60 and 100 micrometer IRAS images were generated using the Richardson-Lucy algorithm and used to study the distribution and temperature of the dust in IC342 and M83 compared with the gas. The results of our analysis are used to compare the molecular cloud properties in the central regions of these galaxies with those found in the central 1 kpc of the Milky Way. We discuss the cloud stability in the central regions of the three starbursts, the resulting star-formation efficiencies and gas depletion times, and the relationship of star-formation efficiency to cloud diameter. Dissert. Abstr.

N93-11338 Max-Planck-Inst. fuer Physik und Astrophysik, Garching (Germany). Inst. fuer Extraterrestrische Physik.

NON-SELF-SIMILAR CLUSTERING OF GALAXIES

Mirt Gramann (Tartu Astronoomia Observatooriumi, USSR) Nov. 1991 25 p Submitted for publication Sponsored in part by European Southern Observatory
(MPE-Preprint-212; ETN-92-92285) Copyright Avail: Fachinformationszentrum Karslruhe, 7514 Eggenstein-Leopoldshafen 2, Germany

The evolution of an initially Gaussian field in two dimensional n body simulations is examined, in order to detect how the large scale density fluctuations influence the development of small scale clustering. The power spectra of the initial density fluctuations are assumed to have a power law form P(k) proportional to k(sup n) with n = -1 and a different cutoff on large scales. The numerical results show that the evolution of small scale structures is not self similar, but strongly depends on the long wavelength cutoff scale. The scale in which density fluctuations go nonlinear is determined by the value square root of (lambda(sub l) x lambda(sub delta)), where lambda(sub l) is the cutoff scale in the power spectrum, and lambda (sub delta) is the length scale in which the mean square amplitude of the density fluctuations becomes equal to unity. The variance of the power spectrum and potential field in different subsamples and its dependence on lambda(sub l) is analyzed. To investigate the gravitational potential field from observational data, the sample size must be at least of the order of the cutoff scale in the power spectrum. To determine the break of the spectrum of galaxy clustering, the size of the sample must be two times larger than this scale. ESA

N93-11347 Max-Planck-Inst. fuer Physik und Astrophysik, Garching (Germany). Inst. fuer Extraterrestrische Physik.

A MULTI-LINE STUDY OF THE MOLECULAR INTERSTELLAR MEDIUM ON M82'S STARBURST NUCLEUS

W. Wild (European Southern Observatory, Santiago, Chile), A. I. Harris, A. Eckart, R. Genzel, U. U. Graf (Texas Univ., Austin.), J. M. Jackson (Boston Univ., MA.), A. P. G. Russell, and J. Stutzki (Cologne Univ., Germany) Jan. 1992 51 p Submitted for publication
(MPE-Preprint-213; ETN-92-92286) Copyright Avail: MPI fuer Physik und Astrophysik, 8046 Garching bei Muenchen, Germany

The excitation and morphology of the molecular gas in the nucleus of the starburst galaxy was studied using CO and HCN molecular line emissions. Observations and results are presented. Information on cloud structure, based on interpretation of optically thick emission lines from M82's nucleus, is discussed. Column densities and mass distributions derived from optically thin lines are discussed. Optical depth effects in the low excitation lines are large enough to mark a vigorous star formation region near the nucleus. The argumentation supporting this picture is presented. ESA

N93-11379# Los Alamos National Lab., NM.

ARE SOME OF THE LUMINOUS HIGH-LATITUDE STARS ACCRETION-POWERED RUNAWAYS?

P. J. T. Leonard, J. G. Hills, and R. J. Dewey (Jet Propulsion Lab., California Inst. of Tech., Pasadena.) 1992 5 p Presented at the Conference on Luminous High-Latitude Stars, Boston, MA, 28-30 May 1992
(Contract W-7405-eng-36)
(DE92-018853; LA-UR-92-2138; CONF-9205226-3) Avail: CASI HC A01/MF A01

It is well known that (1) runaway stars can be produced via supernova explosions in close binary systems, (2) most of such runaways should possess neutron star companions, and (3) neutron stars receive randomly oriented kicks of approximately 100 to 200 km s(sup -1) at birth. We find that this kick sometimes has the right amplitude and direction to make the neutron star fall into the runaway. Accretion onto a neutron star is a source of energy that is roughly an order of magnitude more mass efficient than nuclear burning. Thus, runaways containing neutron stars may live much longer than would normally be expected, which would allow them to travel great distances from their birthplaces during their lifetimes. Some of the early B-type stars far from the Galactic plane and the high-latitude F and G-type supergiants may be accretion-powered runaway stars. DOE

N93-11546*# McCrone Associates, Inc., Westmont, IL.
THIN-SECTIONING AND ANALYSIS OF FINE-GRAINED METEORITIC MATERIALS Final Report, 2 Jan. 1987 - 30 Apr. 1992
Donald A. Brooks, ed. and John P. Bradley 5 Jun. 1992 93 p
(Contract NAS9-17749)
(NASA-CR-185693; NAS 1.26:185693; MA-15750FR) Avail: CASI HC A05/MF A01

The overall theme of the work was the identification of the sources and formation/aggregation mechanisms of the various classes of interplanetary dust particles (IDP's) and to clarify the relationship between IDP's and conventional meteorites. IDP's are believed to be derived from a much broader range of parent bodies than conventional meteorites. Some of these parent bodies (e.g., comets) have escaped that post accretional processing that has affected the parent bodies of meteorites. Therefore, IDP's are likely to preserve a record of early solar system and possibly presolar grain forming reactions. Using analytical electron microscopy (AEM) and more recently micro-infrared (IR) microspectroscopy to examine ultramicrotomed thin sections, we have addressed the questions of IDP formation mechanisms, sources, and their relationship to conventional meteorites. The following sections describe specific findings resulting from these studies. Author

N93-11695# Los Alamos National Lab., NM.
MONTE CARLO SIMULATIONS OF THE SUPERNOVA EJECTION MECHANISM FOR THE RUNAWAY STARS
P. J. T. Leonard and R. J. Dewey (Jet Propulsion Lab., California Inst. of Tech., Pasadena.) 1992 5 p Presented at the Conference on Luminous High-Latitude Stars, Boston, MA, 28-30 May 1992
(Contract W-7405-eng-36)
(DE92-018367; LA-UR-92-2218; CONF-9205226-2) Avail: CASI HC A01/MF A01

Monte Carlo simulations of supernova explosions in a realistic population of binary systems have been carried out for the purpose of studying the production of runaway stars. Contrary to previous studies, we find that the lowest mass runaways attain the highest velocities, and that there is no low-mass cutoff in the mass spectrum of the runaways. The vast majority of runaways with masses (greater than or =) 5 M have velocities less than 200 km/s. An asymmetric kick during the explosion of 100 to 200 km/s is not enough to disrupt most of the binary systems; thus the majority of the runaways are expected to possess neutron star companions. For runaways with velocities greater than 50 km/s, most of these companions will be in eccentric orbits with periods less than 10 days. Only approx. 1 pct. of the supernova-ejected runaways should be normal binaries consisting of main-sequence stars. Such binaries are produced when the distant component of a dose triple system is the first star to explode. Finally, only one O-type runaway with a velocity (greater than or =) 50 km/s is produced by every 10 to 15 binaries with O-type primaries, and thus the supernova ejection mechanism predicts that less than 10 pct. of all O-type stars should be runaways. DOE

N93-11697# Los Alamos National Lab., NM.
MECHANISM FOR EJECTING STARS FROM THE GALACTIC PLANE
P. J. T. Leonard 1992 4 p Presented at the Conference on Luminous High-Latitude Stars, Boston, MA, 28-30 May 1992
(Contract W-7405-eng-36)
(DE92-018375; LA-UR-92-2219; CONF-9205226-1) Avail: CASI HC A01/MF A01

The two most popular mechanisms for ejecting stars from the plane of the Galaxy are the supernova ejection and dynamical (or cluster) ejection scenarios. These two processes make definite predictions regarding the properties of the runaway stars (e.g., mass-velocity diagram and binary characteristics). The relations between mass and velocity predicted by the two theories are more similar to each other than had been previously believed. The binary properties of the runaways provide the best means of discriminating between the two scenarios. Supernova ejection predicts a high frequency of neutron star companions (approx. or greater than 50 pct.) and a very low frequency of runaway binaries consisting of two normal stars (approx. or = 1 pct.), while dynamical ejection predicts modest frequencies of both normal (approx. or = 10 pct.) and neutron starcompanions (approx. or less than 10 pct.). The observed binary characteristics of runaway stars are more consistent with dynamical rather than supernova ejection. The normality of the runaways and the production rate per unit surface area of the Galactic disk may be two other areas where the predictions of the two theories differ. DOE

N93-11807# Onsala Space Observatory (Sweden).
A CLOSER LOOK AT ACTIVE GALACTIC NUCLEI: THE GREAT ENGINES OF THE UNIVERSE
Lars B. Baath 6 Feb. 1992 21 p
(PB92-184464) Avail: CASI HC A03/MF A01

The intensive radio emission from powerful radio galaxies and quasars make these attractive candidates to become 'standard candles' to probe the Universe. The physics of these radio sources are discussed. Author

N93-11879 Glasgow Univ. (Scotland).
APPLICATIONS OF STAR COMPLEXES IN GROUP THEORY Ph.D. Thesis
Mohamed Soliman Hass El-Mosalamy 1987 148 p
Avail: Univ. Microfilms Order No. BRDX96260

The free subgroups of C(4), T(4) groups are discussed. Collins has investigated the free subgroups of groups with presentations satisfying the C(4), T(4) conditions. He has shown that such groups contain a free subgroup of rank 2 except in some cases which he lists explicitly. The exceptions are all two generator groups. A simple proof is given using star complexes, that if G is a C(4), T(4) group, and if G cannot be generated by fewer than three elements, than G contains a free subgroup of rank 2. Much work has been done for C(4)-T(4), and C(6)-complexes. However T(6)-complexes have not so far been studied very much. For that reason the thesis studied T(6)-complexes. Examples of T(6)-complexes and examples of related complexes called hyperbolic complexes are given. New solutions to the word and conjugacy problems for T(6)-complex are obtained and the dependence problems in general are discussed. The idea of the degree of a presentation and also property-ST(m) and property-st(m) are introduced. These concepts are related to valences of vertices in star-complexes. The question of whether having a presentation of degree m, property-ST(m) or property-st(m) (m is greater than 2) puts any restrictions on the group defined by the presentation was examined. The answer was shown to be no. Dissert. Abstr.

N93-12120# Washington Univ., Seattle. Dept. of Physics.
THE NEUTRINO PROCESS AND NEUTRINO r-PROCESS
W. C. Haxton 1991 6 p Presented at the International Workshop on Unstable Nuclei in Astrophysics, Tokyo (Japan), 7-8 Jun. 1991
(Contract DE-FG06-90ER-40561)
(DE92-014304; DOE/ER-40561/47; CONF-9106226-2) Avail: CASI HC A02/MF A01

Almost all of the 3(10)(exp 53) ergs released in a core-collapse supernova are carried off by the neutrinos emitted from the cooling neutron star. These neutrinos can excite nuclei in the mantle of the star by their neutral and charged current reactions, leading to the spallation of nucleons and (alpha)-particles and the production of new daughter nuclei. I will describe rather detailed network calculations that suggest this 'neutrino process' is an important nucleosynthesis mechanisms that may be responsible for the galactic abundances of Li-7, B-11, F-19, La-138, Ta-180, and a number of other nuclei. I also discuss the possibility of an r-process in the He zone of a low-Z progenitor that could be driven, in part, by neutrinos. DOE

N93-12164 New Mexico Inst. of Mining and Technology, Socorro.

MAGNETIC FIELDS IN THE CLUSTERS OF GALAXIES WITH EXTREME COOLING FLOWS Ph.D. Thesis

Jing Ping Ge 1991 180 p

Avail: Univ. Microfilms Order No. DA9128048

To search for magnetic fields in intra-cluster medium, the VLA has been used to obtain high resolution, high dynamic range, multi-frequency polarization images of extended weak radio sources at the centers of extreme cooling flow clusters. From high quality images of four sources A1795, A2199, A2052 and A2151, we find high Faraday rotation measures (few thousand radians m(exp -2)) in three sources. A2151 does not show large Faraday rotation measures, but it turns out that the radio source (NGC 6047) is not in the center of the cooling flow of A2151. Rotation measures fit a lambda(exp 2) dependence very well, implying that they result from a screen in front of the radio sources. In A2199, rotation measures are both positive and negative implying the reversal of the magnetic field. To account for observed high rotation measures, the cluster magnetic field must be on a scale of a hundred kpc and at least ten macro Gauss near radio sources. High rotation measures are a general phenomena in those with a very dense environment. The magnetic fields may relate to the cluster medium indirectly (through pressure balance) or directly (such as a magnetic field produced and maintained by the turbulence in cluster media). In A1795, the regions of high Faraday rotation measures seem to avoid the H-alpha line emission regions seen by van Breugel, Heckman, and Miley (1984). We argue that this optical line emitting nebulae actually is causing the depolarization in the central 2 kpc. With our new optical spectrum imaging with 4 m telescope at Kitt Peak, we believe the magnetic pressure in the line emitting nebulae dominates the thermal pressure. We modeled the hot x-ray gas distributions in A9175, from the HRI and IPC data. If the density fitted from the x-ray intensity profiles is appropriate for the Faraday screen and the thickness of the screen is similar to the distance of the rotating clouds from the nucleus, then the magnetic field must be about 20 micro-G and the magnetic pressure would be about the same as the thermal pressure.

Dissert. Abstr.

N93-12330 Wisconsin Univ., Milwaukee.

RELATIVISTIC CONDENSATE AND COSMOLOGY Ph.D. Thesis

Yang Zhang 1991 206 p

Avail: Univ. Microfilms Order No. DA9207919

This thesis presents a systematic study of relativistic condensate system and its implications in cosmology. The properties of boson condensate of interest, which constitute the main topics of the thesis, are: (1) the ground state of the condensed charged boson system and the ground state expectation values of the field operators; (2) excitation spectra in the condensate when temperature is nonvanishing; (3) the ground state energy density and pressure and therefore the energy conditions associated with the boson condensate; (4) the transition processes when the condensate is changing with time; and (5) implications in cosmology. We demonstrate that the Bose-Einstein condensation of a charged boson system is a spontaneous symmetry breaking phenomenon. By the Bogolubov quasi-averaged method, we show that the ground state expectation values of the field operators are nonvanishing even when the external symmetry-breaking source is turned off. Then we explicitly construct the ground state as a charge coherent consisting of infinitely many states of different charges. We first study an uncharged scalar boson system. The total energy of the system consists of the ground state energy plus the bosonic excitation contributions. We derive the energy spectrum of bosonic excitation. We obtain the finite quantum corrections to the energy density up to the order lambda(exp 2). The amplitudes of fluctuations in the condensate are derived. Then we discuss the occurrence and implications of negative pressure of the relativistic coherent condensate. Finally we study a charged boson system. We study the energy conditions of high density many-particle systems. Three systems are investigated; all of them contain a charged scalar boson subsystem in condensate. We study the transition amplitudes of a weakly-interacting relativistic condensate from an initial state of a given density to a final state different density. The model is reduced to an ensemble of infinite harmonic oscillators with frequencies decreasing with time. Then we use the coherent-state functional integral technique to calculate the transition amplitudes between these states. Finally we discuss the implications of the relativistic condensate in cosmology. A cosmological model is suggested with relativistic condensate as the dominant matter content in the universe. Dissert. Abstr.

N93-12380# Mitre Corp., McLean, VA.

GLOBAL CHANGE AND THE DARK OF THE MOON Final Report

S. Flatte, S. Koonin, and G. MacDonald 30 Jun. 1992 55 p

(AD-A255181; JSR-91-315) Avail: CASI HC A04/MF A01

We have considered the possibility of using earthshine to measure the reflectance properties of the earth (albedo and phase function). Measurements of earthshine carried out by Danjon in 1926-33 show that even then the average albedo could be determined with a precision of +/- 0.01 and that both synoptic and seasonal variations could be observed clearly. We show that, after correction for wavelength dependence and the opposition effect in the lunar reflectance properties, Danjon's visual albedo of 0.40 can be reconciled with the ERBE satellite Bond albedo of 0.30. We recommend a modern earthshine monitoring program (advantages include global integration, continuous coverage, ground basing, and low cost) as a complement to present and planned satellite measurements. GRA

91 LUNAR AND PLANETARY EXPLORATION

Includes planetology; and manned and unmanned flights.
For spacecraft design or space stations see *18 Spacecraft Design, Testing and Performance.*

N93-11164*# Southwest Research Inst., San Antonio, TX. Instrumentation and Space Research Div.

MODELING THE JOVIAN AURORA Final Report

J. Hunter Waite, Jr. 1 Aug. 1992 65 p Original contains color illustrations

(Grant NAGw-1684; SwRI Proj. 15-2762)

(NASA-CR-190696; NAS 1.26:190696) Avail: CASI HC A04/MF A01; 4 functional color pages

The Jovian aurora is the most powerful aurora in the solar system, over 100 times more powerful than the Earth's aurora. These magnificent visual displays can provide important information about the planetary magnetosphere which is responsible for the acceleration of energetic particles that produce aurora at any planet. Similarities and differences in planetary auroral emissions are thus a viable means of classifying and studying both comparative atmospheric and magnetospheric processes. For instance, at Earth the solar wind is the primary source of auroral power while at Jupiter it is conjectured that the rotation of the planet is the major source of magnetospheric and auroral power. The purpose of this IR project was to develop a model: (1) for use in interpreting the existing set of multispectral observations of Jupiter's aurora; and (2) to design new experiments based on the findings to improve understanding of the underlying auroral processes. For individual titles, see N93-11165 through N93-11167.

N93-11165*# Southwest Research Inst., San Antonio, TX.
THE ROLE OF PROTON PRECIPITATION IN JOVIAN AURORA: THEORY AND OBSERVATION
J. H. Waite, Jr., *D. B. Curran, T. E. Cravens* (Kansas Univ., Lawrence.), and J. T. Clarke (Michigan Univ., Ann Arbor.) *In its* Modeling the Jovian Aurora 1 Aug. 1992 14 p (For primary document see N93-11164 02-91)
Avail: CASI HC A03/MF A01; 4 functional color pages

It was proposed that the Jovian auroral emissions observed by Voyager spacecraft could be explained by energetic protons precipitating into the upper atmosphere of Jupiter. Such precipitation of energetic protons results in Doppler-shifted Lyman alpha emission that can be quantitatively analyzed to determine the energy flux and energy distribution of the incoming particle beam. Modeling of the expected emission from a reasonably chosen Voyager energetic proton spectrum can be used in conjunction with International Ultraviolet Explorer (IUE) observations, which show a relative lack of red-shifted Lyman alpha emission, to set upper limits on the amount of proton precipitation taking place in the Jovian aurora. Such calculations indicate that less than 10 percent of the ultraviolet auroral emissions at Jupiter can be explained by proton precipitation. Author

N93-11166*# Southwest Research Inst., San Antonio, TX.
LYMAN ALPHA LINE SHAPES FROM ELECTRON IMPACT H2 DISSOCIATIVE PROCESSES IN THE JOVIAN AURORAL ZONE
J. H. Waite, Jr. and G. R. Gladstone (California Univ., Berkeley.) *In its* Modeling the Jovian Aurora 1 Aug. 1992 7 p (For primary document see N93-11164 02-91)
Avail: CASI HC A02/MF A01; 4 functional color pages

Over the past two years several Lyman alpha line profile spectra of Jupiter were obtained using the International Ultraviolet Explorer (IUE) telescope. Several different regions of the planet were observed including the auroral zone, the low and mid latitudes, and the equatorial region which includes the Lyman alpha bulge region. These results have presented a very interesting picture of atomic hydrogen on Jupiter with explanations that range from ion outflow in the auroral zone to large thermospheric winds at low and mid latitudes. New data are needed to address the outstanding questions. Almost certainly, high resolution spectra from the Hubble Space Telescope will play a role in new observations. Better data also require better models, and better models require new laboratory data as inputs. The purpose of this program is two-fold: (1) to introduce a method by which new laboratory electron impact measurements of H2 dissociation can be used to calculate both the slow and fast H(S-2) and H(P-2) fragments in an H2 atmosphere; and (2) to determine the predicted Lyman alpha line shape that would result from electron impact production of these dissociative fragments in the Jovian auroral zone. Author

N93-11167*# Southwest Research Inst., San Antonio, TX.
MULTISPECTRAL OBSERVATIONS OF THE JOVIAN AURORA
In its Modeling the Jovian Aurora 1 Aug. 1992 24 p Original contains color illustrations (For primary document see N93-11164 02-91)
Avail: CASI HC A03/MF A01; 4 functional color pages

The upper atmospheres of the Earth and the outer planets form a screen on which precipitating charged particles, like the electron beam in a television, trace fleeting, but revealing patterns of visible, ultraviolet, infrared, and x ray emissions that offer valuable clues to processes occurring within the planetary magnetospheres. At Earth, years of in situ measurements, as well as ground based observations, have yielded a picture (still fuzzy) where the interaction of the solar wind with the magnetosphere of the Earth provides a complex path for the storage and release of energy during magnetic substorms; the ultimate manifestation of terrestrial auroral processes. More recent global imaging of substorm events from high above the Earth (greater than 3.5 R(sub e)) by Dynamics Explorer have made a unique contribution towards understanding the global and temporal evolution of such auroral events by providing a morphological perspective and by providing the crucial observational link that allows the separation of spatial and temporal variations inherent in the interpretation of in situ data. A similar role was played by the Hubble Space Telescope (HST) during the recent encounter of Ulysses with Jupiter in helping to define a new paradigm in Jovian auroral physics. The old paradigm portrayed Jupiter's magnetosphere as totally dominated by internal processes (i.e. Io related tori, heavy ions, etc.) where energetic heavy ion precipitation in the inner magnetosphere was solely responsible for the observed auroral phenomena. Ulysses and HST portray a more Earth-like paradigm where electron acceleration in the outer magnetosphere near the boundary with the solar wind plays a distinct role in the formation of auroral hot spots, yet energetic heavy ions also enter into the picture (similar to the role of the energetic ions from the terrestrial ring current during magnetic substorms). These heavy ions as a result of excitation during their transit through the atmosphere produce the x ray emissions observed in Roentgensatellit (ROSAT) x ray energy spectra. Author

N93-11502# Sandia National Labs., Albuquerque, NM.
RATLER: ROBOTIC ALL-TERRAIN LUNAR EXPLORATION ROVER
J. W. Purvis and P. R. Klarer 1992 8 p Presented at the 1992 Space Operations, Applications and Research Conference, Houston, TX, 5-7 Aug. 1992
(Contract DE-AC04-76DP-00789)
(DE92-019295; SAND-92-1821C; CONF-9208120-1) Avail: CASI HC A02/MF A01

A robotic rover vehicle designed for use in the exploration of the Lunar surface is described. The Robotic All-Terrain Lunar Exploration Rover (RATLER) is a four wheeled all-wheel-drive dual-body vehicle. A uniquely simple method of chassis articulation is employed which allows all four wheels to remain in contact with the ground, even while climbing over step-like obstacles as large as 1.3 wheel diameters. Skid steering and modular construction are used to produce a simple, rugged, highly agile mobility chassis with a reduction in the number of parts required when compared to current designs being considered for planetary exploration missions. The design configuration, mobility parameters, and performance of several existing RATLER prototypes are discussed. DOE

N93-11603*# National Academy of Sciences - National Research Council, Washington, DC. Commission on Physical Sciences, Mathematics, and Applications.
THE SEARCH FOR LIFE'S ORIGINS: PROGRESS AND FUTURE DIRECTIONS IN PLANETARY BIOLOGY AND CHEMICAL EVOLUTION
1990 159 p
(Contract NASw-4102)
(NASA-CR-190929; NAS 1.26:190929; ISBN-0-309-04246-1; LC-90-36899) Copyright Avail: CASI HC A08/MF A02

The current state is reviewed of the study of chemical evolution and planetary biology and the probable future is discussed of the field, at least for the near term. To this end, the report lists the goals and objectives of future research and makes detailed, comprehensive recommendations for accomplishing them, emphasizing those issues that were inadequately discussed in earlier Space Studies Board reports. Author

92 SOLAR PHYSICS

Includes solar activity, solar flares, solar radiation and sunspots.

For related information see *93 Space Radiation.*

N93-11264 Indiana Univ., Bloomington.
A POLYTROPIC SOLAR MODEL Ph.D. Thesis
Jongni Tsai 1991 143 p
Avail: Univ. Microfilms Order No. DA9212331

We develop a composite polytropic solar model characterized by three ploytropic indices. This phenomenological model can represent some of the main features of the standard solar model (SSM). It is used to study neutrino production and various solar properties. Three solar models with lower core temperatures than that predicted by the SSM are considered. We find that lowering the core temperature by 3 percent requires changes of the opacity of the middle layer by 32-35 percent, a factor of three larger than the current uncertainty. Thus, one does not expect that the solar neutrino puzzle can be solved within the framework of the SSM. The calculation of the asymptotic p-mode frequencies reveal the need to modify the polytropic solar model. We also find that the p-mode frequencies are not sensitive to the changes of the central temperature. Finally, the Mikheyev-Smirnov-Wolfenstein effect is studied and considered as a solution to the solar neutrino problem. Dissert. Abstr.

N93-11351 Max-Planck-Inst. fuer Physik und Astrophysik, Garching (Germany). Inst. fuer Extraterrestrische Physik.
TORI AND CHAOS IN A NONLINEAR DYNAMO MODEL FOR SOLAR ACTIVITY
Ulrike Feudel (Max-Planck-Gesellschaft zuer Foerderung der Wissenschaft e.V., Garching, Germany), Wolfgang Jansen (Max-Planck-Gesellschaft zuer Foerderung der Wissenschaft e.V., Garching, Germany), and Juergen Kurths (Max-Planck-Gesellschaft zuer Foerderung der Wissenschaft e.V., Garching, Germany) Feb. 1992 28 p Submitted for publication
(MPE-Preprint-218; ETN-92-92288) Copyright Avail: Fachinformationszentrum Karslruhe, 7514 Eggenstein-Leopoldshafen 2, Germany

A nonlinear dynamo model for solar activity which includes the feedback of the helicity upon the mean magnetic field was investigated. The qualitative behavior of a seven dimensional system of ordinary differential equations obtained by truncation of that model was studied numerically. It was compared with results from a sixth order system derived from the seventh order system by a special polar coordinate transformation. In dependence on characteristic parameters, the seven dimensional model exhibits periodic, quasiperiodic (on T(sup 2) and T(sup 3)) and chaotic behavior where a route to chaos via the transition T(sup 2) to T(sup 3) to T(sup 2) to chaos was found to be typical. In contrast to that, no chaotic state occurs in the reduced system due to a nonregularity of the coordinate transformation. ESA

N93-11374*# National Aeronautics and Space Administration. Lyndon B. Johnson Space Center, Houston, TX.
COMPOSITIONAL ANALYSIS AND CLASSIFICATION OF PROJECTILE RESIDUES IN LDEF IMPACT CRATERS
Friedrich Horz and Ronald P. Bernhard (Lockheed Engineering and Sciences Co., Houston, TX.) Jun. 1992 209 p
(NASA-TM-104750; S-678; NAS 1.15:104750) Avail: CASI HC A10/MF A03

This catalog contains preliminary analyses of residues of hypervelocity projectiles that encountered gold substrates exposed by instrument A0187-1 on the Long Duration Exposure Facility (LDEF). This instrument was on LDEF's trailing edge where relative encounter speeds should be lowest for any non-spinning platform in low Earth orbit (LEO). Approximately 0.6 m(exp 2) of Au substrates yielded 198 impact craters greater than 20 micrometers in diameter. Some 30 percent of the craters were made by natural cosmic dust particles and some 15 percent by man-made objects. Some 50 percent of all features, however, have residues, if any, that are beyond the detection threshold of the SEM-EDXA method used. The purpose of this catalog is to provide detailed evidence and criteria that may be used to arrive at specific particle types on a case-by-case basis and to group such particles into compositional classes. Clearly this is a somewhat interpretative undertaking. For that reason, we encourage and solicit critique and comments from those interested in the systematic analysis of all impact features on LDEF. Author

N93-11696# Los Alamos National Lab., NM.
STATISTICS OF IMF B(z) EVENTS
X. P. Zhao (Stanford Univ., CA.), J. T. Hoeksema (Stanford Univ., CA.), J. T. Gosling, and J. L. Phillips 1991 9 p Presented at the Solar-Terrestrial Predictions Workshop, Ottawa, Ontario, 18-22 May 1991
(Contract W-7405-eng-36)
(DE92-018372; LA-UR-92-2271; CONF-9105361-1) Avail: CASI HC A02/MF A01

From August 1978 to September 1982, 58 intervals with B sub z greater than or = 10 nT and duration of 3 hours or greater were detected. Using detected shocks, magnetic clouds and bidirectional solar wind electron heat flux events (BDE's) to identify the interplanetary counterparts of coronal mass ejections (ICME's), it is found that more than half of the 59 strong B sub z events are ICME-associated: i.e., their strong B sub z occurred at least partially within an ICME, where the field orientation is most likely determined in the corona. Magnetic clouds form a small subset of ICME's and are responsible for one third of the ICME-associated B sub z events. Analysis of 12 major geomagnetic storms with maximum K sub p of 8(sub -) or greater in the same period shows that 7 of 9 storms for which the data was conclusive took place when the Earth encountered both an ICME having strong southward component and a shock sheath in which the ambient magnetic field polarity was expected to produce a southward B sub z component. DOE

N93-11738# National Geophysical Data Center, Boulder, CO.
SOLAR-GEOPHYSICAL DATA NUMBER 569, JANUARY 1992. PART 2: (COMPREHENSIVE REPORTS). DATA FOR JULY 1991 AND MISCELLANEOUS
Helen E. Coffey, ed. Jan. 1992 107 p
(PB92-158898; SGD-569-Pt-2) Avail: CASI HC A06/MF A02

The Solar-Geophysical Data comprehensive reports for July 1991 are provided. Data, in tables, for observations of solar flares, solar radio bursts at fixed frequencies, solar x-ray radiation from GOES satellite, mass ejections from the sun and active prominences and filaments are given. GRA

N93-11877 Alabama Univ., Huntsville.
DIAGNOSTICS OF ELECTRON-HEATED SOLAR FLARES Ph.D. Thesis
Peng Li 1991 222 p
Avail: Univ. Microfilms Order No. DA9203822

Hydrodynamical simulations of nonthermal electron heated solar atmospheres are carried out. The results are presented. In a loop with uniform cross-sectional area and low pressure, an ablation of material from the chromosphere with an associated upward velocity of the order of the local sound speed is always present. Due to this chromospheric evaporation, the profiles of soft x-ray lines, such as Ca XIX, produced in the hot (2(10)(exp 7) K) hydrodynamic gas, are typically blueshifted by several mA. By contrast, in a loop with a tapered geometry, we have found that heating due to the electron bombardment is concentrated in the corona, causing the reduction of the electron precipitation level at the chromospheric region. In the case when preheating occurs before the onset of the hard x-ray burst, the blueshift of the Ca XIX line profile is reduced significantly by the high coronal density. It is found that there exists a threshold time at which 'explosive' evaporation starts. In the case when the loop is uniform and initial pressure is low, we have calculated the spectrum, temporal profile, and spatial structure of the emitted hard x-rays, considering both thermal and nonthermal bremsstrahlung. Even when the primary electrons are nonthermal and produce hard x-rays through nonthermal bremsstrahlung, there is an inevitable thermal hard x-ray component, produced by the hot coronal plasma energized by the same electron beam. The temporal relationship between broadband soft x-rays (1 to approximately 8 A) and hard x-rays (greater than 30 keV) in our models was investigated. It is found that in the model which has a high beam energy flux of 10(exp 11) ergs cm(exp -2) s(exp -1) and a low initial upper pressure of 2.55 dyn cm(exp -2), the soft x-ray time derivative matches the hard x-ray time profile. In the case of a converging magnetic field (i.e., the flare loop is tapered), the role that the beam neutralizing return current plays is significantly reduced from the case when the flare loop has a uniform cross-sectional area. Dissert. Abstr.

N93-12303*# TRW, Inc., Redondo Beach, CA. Space and Technology Group.
FLANK SOLAR WIND INTERACTION Annual Report, Jun. 1991 - Jul. 1992
Stewart L. Moses and Eugene W. Greenstadt 21 Aug. 1992 7 p
(Contract NAS5-31216)
(NASA-CR-189285; NAS 1.26:189285) Avail: CASI HC A02/MF A01

This report summarizes the results of the first 12 months of our program to study the interaction of the Earth's magnetosphere with the solar wind on the far flanks of the bow shock. This study employs data from the ISEE-3 spacecraft during its traversals of the Earth's magnetotail and correlative data from spacecraft monitoring the solar wind upstream. Our main effort to date has involved assembling data sets and developing new plotting programs. Two talks were given at the Spring Meeting of the American Geophysical Union describing our initial results from analyzing data from the far flank foreshock and magnetosheath. The following sections summarize our results. Author

N93-12342 Brandeis Univ., Waltham, MA.
PLASMA PROPERTIES OF SOLAR CORONAL ACTIVE REGIONS Ph.D. Thesis
Katrina Marie Hester Waljeski 1992 133 p
Avail: Univ. Microfilms Order No. DA9217505

The plasma properties of active region loops in the solar corona were investigated using simultaneous broadband and spectroscopic soft x-ray observations. Coordinated observations of an active region were obtained with the American Science and Engineering (AS&E) High Resolution Soft X-ray Imaging Sounding Rocket Payload and the X-Ray Polychromator Flat Crystal Spectrometer (FCS) onboard the Solar Maximum Mission spacecraft. By requiring consistency between the two types of plasma diagnostics, the following problems were investigated: (1) the relative abundances of iron, oxygen, magnesium, and neon in the solar corona; (2) the sensitivity of these observations to different models of differential emission measure; and (3) the relative calibration of the FCS and the AS&E instruments and the mutual consistency of plasma diagnostics from broadband and spectroscopic measurements. The elemental abundances of oxygen, iron, magnesium, and neon in the solar corona were found to be consistent with the 'adopted coronal' abundances tabulated by Meyer (1985, Astrophysical Journal Supplement 57), if the Fe XVII line at 15.01 Angstroms was not considered. The temperatures and emission measures calculated from the Fe XVII line observation were inconsistent with the plasma properties from the broadband observations and the observations of the other FCS lines. The elemental abundances derived from these observations were not consistent with the Allen (1973, Astrophysical Quantities, London: Atholone Press) photospheric abundances, which have been widely used in previous investigations of coronal plasma properties. It was found to be impossible to distinguish a distribution of differential emission measured implied by a simplified steady-state loop model (e.g., Rosner, Tucker, and Vaiana, 1978, Astrophysical Journal 220) from an isothermal distribution of emission measure by means of the lines that may be observed by the FCS in a quiet active region or by means of a combination of these lines and broadband observations. In contrast to previous investigations of this type (e.g., Pye et al., 1978, Astronomy and Astrophysics 65), the temperature and emission measure derived from these broadband and spectroscopic soft x-ray observations are mutually consistent. Dissert. Abstr.

N93-12506# Phillips Lab., Hanscom AFB, MA.
THE SEMIANNUAL VARIATION OF GREAT GEOMAGNETIC STORMS AND THE POSTSHOCK RUSSELL-MCPHERRON EFFECT PRECEDING CORONAL MASS EJECTA
N. U. Crooker, E. W. Cliver, and B. T. Tsurutani 3 Mar. 1992 5 p Previously announced in IAA as A92-27687
(AF Proj. 2311)
(AD-A254955; AD-E201142; PL-TR-92-2182) Avail: CASI HC A01/MF A01

The occurrence rate of great geomagnetic storms displays a pronounced semiannual variation. Of the forty-two great storms during the period 1940-1990, none occurred during the solstitial months of June and December, and 40 percent (17) occurred during the equinoctial months of March and September. This suggests that the semiannual variation found by averaging indices is not the result of some statistical effect superposed on the effects of random storm occurrence but rather is dominated by the storms themselves. Recent results indicate that the intense southward interplanetary magnetic fields (IMF's) responsible for great storms can reside in the postshock plasma preceding the driver gas of coronal mass ejections (CMEs) as well as in the driver gas itself. Here we propose that strong southward fields in the postshock flow result from a major increase in the Russell-McPherron polarity effect through a systematic pattern of compression and draping with the ecliptic plane. Differential compression at the shock increases the Parker spiral angle and, consequently, the azimuthal field component that projects as a southward component onto Earth's dipole axis. The resulting prediction is that southward fields in the postshock plasma maximize at the spring (fall) equinox in CME's emerging from toward (away) sectors. This pattern produces a strong semiannual variation in postshock IMF orientation and may account at least in part for the observed semiannual variation of the occurrence of great geomagnetic storms. GRA

93 SPACE RADIATION

Includes cosmic radiation; and inner and outer earth's radiation belts.

For biological effects of radiation see *52 Aerospace Medicine*. For theory see *73 Nuclear and High-Energy Physics*.

N93-11815# Air Force Inst. of Tech., Wright-Patterson AFB, OH.
A MODEL TO ESTIMATE THE FLUX OF BACKGROUND PARTICLES EXPECTED TO ACCUMULATE ON THE COLLECTOR FOILS OF THE INTERSTELLAR GAS EXPERIMENT ON THE LONG DURATION EXPOSURE FACILITY SPACECRAFT M.S. Thesis
Paul Anthony Gehred 1992 89 p
(AD-A254265; AFIT/CI/CIA-92-069) Avail: CASI HC A05/MF A01

The Interstellar Gas Experiment (IGE) on board the Long Duration Exposure Facility (LDEF) exposed metallic foils to the interstellar wind to collect noble gas particles from outside of the solar system. The terrestrial helium present in the atmosphere at low Earth orbit altitudes was also collected on the foils, along with the interstellar helium particles. In order to discriminate between the desired interstellar helium and the background terrestrial helium particles, an analysis of the expected distribution of atmospheric helium on the foils was conducted. This analysis used the principles of the kinetic theory of gases to simulate the state of the thermosphere for the entire 69-month flight of LDEF. The key parameters needed to apply the kinetic theory of gases were the temperature and density of the helium at LDEF altitude. This information was calculated using the Mass Spectrometer and Incoherent Scatter (MSIS) model. The entire duration of the flight was split into 70 month-long intervals. For each of these intervals, mean values for the kinetic temperature and helium density were calculated. Author (GRA)

99 GENERAL

N93-11078# California Univ., Berkeley. Lawrence Berkeley Lab.
EXPLORATORY RESEARCH AND DEVELOPMENT FUND, FY 1990

May 1992 96 p
(Contract DE-AC03-76SF-00098)
(DE92-017002; LBL-Pub-5346) Avail: CASI HC A05/MF A01

The Lawrence Berkeley Laboratory Exploratory R&D Fund FY 1990 report is compiled from annual reports submitted by principal investigators following the close of the fiscal year. This report describes the projects supported and summarizes their accomplishments. It constitutes a part of an Exploratory R&D Fund (ERF) planning and documentation process that includes an annual planning cycle, projection selection, implementation, and review. The research areas covered in this report are as follows: accelerator and fusion research; applied science; cell and molecular biology; chemical biodynamics; chemical sciences; earth sciences; engineering; information and computing sciences; materials sciences; nuclear science; physics and research medicine and radiation biophysics. DOE

N93-11100* National Aeronautics and Space Administration. Langley Research Center, Hampton, VA.
WINDS OF CHANGE: EXPANDING THE FRONTIERS OF FLIGHT. LANGLEY RESEARCH CENTER'S 75 YEARS OF ACCOMPLISHMENT, 1917-1992
James Schultz 1992 146 p LIMITED REPRODUCIBILITY: More than 20 percent of this document may be affected by color photographs original contains color illustrations
(NASA-NP-130; NAS 1.83:130; ISBN-0-16-037924-5) Avail: CASI HC A07; SOD HC; 52 functional color pages

This commemorative volume highlights in pictures and text seventy five years of accomplishments of the Langley Research Center. The introductory matter features wind tunnels and their contribution to the development of aeronautics. A chronological survey details four different periods in Langley's history. The first period, 1917-1939, is subtitled 'Perfecting the Plane' which details Langley's contribution to early aeronautics with examples from specific aircraft. The second period, 1940-1957, focuses on the development of military aircraft during and after World War II. The third period, 1958-1969, tells the story of Langley's involvement with NASA and the satellite and Apollo era. The fourth period, entitled 'Charting New Courses: 1970-1992 and Beyond', treats various new topics from aerospace planes to Mars landing, as well as older topics such as the Space Shuttle and research spinoffs. R.L.B.

N93-12470# Office of Naval Research, San Francisco, CA. Asian Office.
ONRASIA SCIENTIFIC INFORMATION BULLETIN, VOLUME 17, NUMBER 3 Quarterly Report, Jul. - Sep. 1992
Sachio Yamamoto and Sandy Kawano Sep. 1992 249 p
(AD-A255073; NAVSO-P-3580-V17-N3) Avail: CASI HC A11/MF A03

This is a quarterly publication presenting articles covering recent developments in Far Eastern (particularly Japanese) scientific research. It is hoped that these reports (which do not constitute part of the scientific literature) will prove to be of value to scientists by providing items of interest well in advance of the usual scientific publications. The articles are written primarily by members of the staff of ONRASIA, with certain reports also being contributed by visiting stateside scientists. Occasionally, a regional scientist will be invited to submit an article covering his own work, considered to be of special interest. This publication is approved for official dissemination of technical and scientific information of interest to the Defense research community and the scientific community at large. It is available free of charge to approved members of the DOD scientific community. GRA

N93-12477# Massachusetts Inst. of Tech., Cambridge.
THE COLLABORATIVE PROGRAM OF RESEARCH IN ENGINEERING SCIENCES
Sep. 1991 42 p Prepared in cooperation with Idaho National Engineering Lab., Idaho Falls
(Contract DE-FG02-85ER-13331)
(DE92-016838; DOE/ER-13331/T3) Avail: CASI HC A03/MF A01

In 1985, the Energy Laboratory of the Massachusetts Institute of Technology (MIT) and the Idaho National Engineering Laboratory (INEL) began a collaborative program of energy-related engineering research. This program was extended for another three years starting January 1991. The program continues to pursue three broad goals: to perform quality research on energy-related technologies involved in industrial processes and productivity; to demonstrate the potential of collaborative programs between universities and the national laboratories; and to encourage the transfer of the technology developed to the industrial sector. This annual report describes progress at MIT under the MIT/INEL program during the past year. Highlights of research activities and accomplishments during the past year include the following: Modeling and Control of Droplet Based Thermal Processes: Multivariable Control of GMAW; Metal Transfer Control in Gas-Metal Arc Welding; Fundamentals of Elastic-Plastic Fracture; Three-Dimensional and Mechanistic Modelling Comminution of Energy Materials; Synthesis and Optimization of Integrated Chemical Processes; and Mathematical Modelling of Plasma Systems. DOE

SUBJECT INDEX

SCIENTIFIC AND TECHNICAL AEROSPACE REPORTS VOLUME 31 NUMBER 2

Typical Subject Index Listing

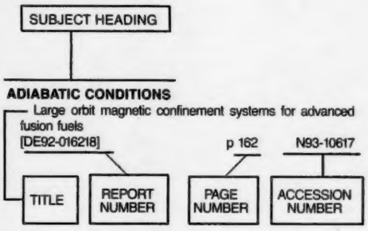

The subject heading is a key to the subject content of the document. Titles, report numbers, and accession numbers of pertinent documents are provided under each subject heading. When the title is insufficiently descriptive of the document content, a title extension has been added, separated from the title by three hyphens. The report number helps to indicate the type of document cited (e.g., NASA report, NASA translation, NASA contractor report). The accession number is the number by which the document abstracts are arranged in this journal and by which the document is sold or requested. The page number helps you locate the the citation in the abstract section. The titles, with title extensions if present, are arranged under each subject heading in ascending accession number order. The subject headings have been selected from the latest revision of the *NASA Thesaurus.*

A

A-7 AIRCRAFT
Evaluation of alternatives for increasing A-7D rearward visibility
[AD-A255071] p 208 N93-12488

ABLATION
Results from the US/USSR exchange for heat load material studies of simulated tokamak disruptions
[DE92-018285] p 453 N93-11694
Carbon/carbon composition ablation effects on ionized boundary layers
[AD-A254465] p 242 N93-12235

ABLATIVE MATERIALS
Laser-ablation processes
[DE92-011226] p 322 N93-12250

ABORT APPARATUS
Booster rocket range safety system
[AD-D015363] p 221 N93-11428

ABRASION RESISTANCE
Sealing characteristics of a carbon segmented circumferential seal for a liquid oxygen turbopump
[NAL-TR-1130] p 329 N93-12364

ABSORBENTS
Comparisons of molecular sieve oxygen concentrators for potential medical use aboard commercial aircraft
[AD-A253648] p 387 N93-11279

ABSORBERS (MATERIALS)
Evaluation of acoustic impedance models for a perforated plate
[NAL-TR-1133] p 435 N93-12375

ABSORPTION
Measurement of absorbed dose to water for medium energy x rays
[NPL-RSA(EXT)-33] p 436 N93-11412

ABSORPTION CROSS SECTIONS
Hypersonic flow diagnostic development
[AD-A255045] p 202 N93-12466

ABSORPTION SPECTRA
Near-IR absorption spectra for the C70 fullerene anions
[AD-A253658] p 246 N93-11280
Optical properties of composite membranes containing arrays of nanoscopic gold cylinders
[AD-A253659] p 238 N93-11281
Exciton kinetics in poly(di-n-hexylsilane)
[DE92-018278] p 283 N93-11800
X pulse radiation around the critical surface
p 318 N93-12027
Absorption spectroscopy of L(alpha, beta) transitions in a laser germanium plasma p 320 N93-12041
Saturation effects in absorption spectroscopy of the K(alpha) rays of aluminum p 254 N93-12042
Erasable optical information storage in the polyanilines
[AD-A254873] p 480 N93-12438

ABSORPTION SPECTROSCOPY
Computer simulation and experimental investigation of the absorption cell for the rocketborne diode-laser experiment MASERATI
[BONN-IR-91-62] p 357 N93-11083
Absorption spectroscopy of L(alpha, beta) transitions in a laser germanium plasma p 320 N93-12041
Saturation effects in absorption spectroscopy of the K(alpha) rays of aluminum p 254 N93-12042
Research at and operation of the material science x ray absorption beamline (X-11) at the National Synchrotron Light source
[DE92-018598] p 251 N93-12172

ABSORPTIVITY
Infrared phonon structure in epitaxial films of Tl2Ca2Ba2Cu3O10 at low temperatures
[DE92-017078] p 466 N93-12109

ABSTRACTS
JPRS report: Science and technology. Central Eurasia: Engineering and equipment
[JPRS-UEQ-92-009] p 220 N93-11169

AC GENERATORS
A theoretical study of the performance of a small permanent magnet, three-phase alternator when driving a purely resistive load via a full-wave rectification circuit
[RAE-TR-84009] p 289 N93-11434

ACCELERATION (PHYSICS)
Evaluation of CKU-5/A ejection seat catapults under varied acceleration levels
[AD-A248021] p 204 N93-12489

ACCELERATION TOLERANCE
The effect of variable seat back angles on human response to +Gz impact accelerations
[AD-A250673] p 387 N93-11559
Physiologically constrained aerocapture for manned Mars missions p 226 N93-12185

ACCELEROMETERS
Residual acceleration data on IML-1: Development of a data reduction and dissemination plan
[NASA-CR-190807] p 223 N93-11101
Accuracy improvement of linear estimated motion using differential type sensors
[NAL-TR-1135] p 314 N93-12365

ACCEPTOR MATERIALS
Preconversion catalytic deoxygenation of phenolic functional groups
[DE92-018304] p 244 N93-10986
Determination of Fe(sup 2+) and Fe(sup 3+) concentrations of semi-insulating InP:Fe
[DE92-017119] p 469 N93-12316

ACCESS CONTROL
A simple, effective media access protocol system for integrated, high data rate networks p 279 N93-11119
Data distribution satellite
[NASA-TM-105778] p 287 N93-12481

ACCUMULATORS (COMPUTERS)
A fast pipelined inner product unit
[REPT-92-025] p 411 N93-11594

ACCURACY
Construction of a geodesic strapdown inertial navigation system for point determination
[SER-C-367] p 205 N93-11344
Evaluation of advanced pressure sensor technology
[DE92-011004] p 312 N93-11806
A comparison of radar rainfall estimates and rain gage measurements during two Denver thunderstorms
[AD-A254267] p 369 N93-11817

ACETATES
Organometallic NLO polymers. 3. Copolymerization of bridged bis(ferrocenyl) and bis(cyanoacetate) monomers via the knoevenagel condensation
[AD-A250214] p 265 N93-11192

ACETYLENE
Chemical reactions and properties of organosilicon compounds related to new materials
[AD-A253233] p 246 N93-11218
Controlled synthesis of polyenes by catalytic methods
[DE92-015286] p 271 N93-12165
Positive ion chemistry of acetylene and methylacetylene clusters. Formation of benzene and C(sub 2n)H(sub 2n)(+) ions via intracluster polymerization reactions
[AD-A250931] p 236 N93-12177
State-resolved collisional energy transfer in highly vibrationally excited polyatomic molecules
[AD-A253299] p 441 N93-12323

ACID BASE EQUILIBRIUM
The relative importance of sulfur and nitrogen compounds in the acidification of freshwater
[DE92-016899] p 354 N93-11680

ACID RAIN
A comprehensive mission to planet Earth: Woods Hole Space Science and Applications Advisory Committee Planning Workshop
[NASA-TM-108011] p 343 N93-11878
Allowance system: Proposed acid rain rule
[PB92-226174] p 356 N93-12524

ACIDS
Acid copper sulfate plating bath: Control of chloride and copper
[DE92-019473] p 249 N93-11644

ACOUSTIC ATTENUATION
Evaluation of acoustic impedance models for a perforated plate
[NAL-TR-1133] p 435 N93-12375

ACOUSTIC COUPLING
Active control of aeroacoustic couplings by means of adaptive systems
[ECL-91-18] p 214 N93-11576

ACOUSTIC EMISSION
Acoustic emission monitoring of HFIR vessel during hydrostatic testing
[DE92-019316] p 332 N93-11601
The effect of precipitate forming elements in Al 4.5 percent Mg alloys on the measured acoustic emission and on Lueders band deformation
[DE92-016864] p 465 N93-12073

ACOUSTIC EXCITATION
An experimental investigation into flow induced acoustic resonances in an annular cascade
[PNR-90959] p 433 N93-11322

ACOUSTIC FREQUENCIES
The effects of plate spacing and downstream plate length on the acoustic resonance excited by flow past two plates in tandem in a duct
[PNR-90958] p 433 N93-11321
Wavefront reconstruction using a least squares approach
[ISVR-TR-203] p 435 N93-12324

ACOUSTIC IMPEDANCE
Sound propagation over rigid porous layers
p 432 N93-11179
Evaluation of acoustic impedance models for a perforated plate
[NAL-TR-1133] p 435 N93-12375

ACOUSTIC MEASUREMENT
A survey of European calibration facilities for underwater acoustics
[NPL-RSA(EXT)-32] p 433 N93-11328
Acoustic emission monitoring of HFIR vessel during hydrostatic testing
[DE92-019316] p 332 N93-11601
Acoustic measurement of the mechanical properties of thin material specimens
[AD-A253538] p 434 N93-11752

The effect of precipitate forming elements in Al 4.5 percent Mg alloys on the measured acoustic emission and on Lueders band deformation
[DE92-016864] p 465 N93-12073

ACOUSTIC PROPAGATION
Sound propagation over rigid porous layers
p 432 N93-11179

ACOUSTIC PROPERTIES
Acoustic measurement of the mechanical properties of thin material specimens
[AD-A253538] p 434 N93-11752
Acoustical evaluation of the NASA Lewis 9 by 15 foot low speed wind tunnel
[NASA-TP-3274] p 218 N93-12016

ACOUSTIC SCATTERING
On the inverse scattering problem for the Helmholtz equation in one dimension
[AD-A253130] p 434 N93-11526
Interaction of sound with sound by novel mechanisms: Ultrasonic four-wave mixing mediated by a suspension and ultrasonic three-wave mixing at a free surface
[AD-A254657] p 435 N93-12097

ACOUSTIC STREAMING
A general introduction to aeroacoustics and atmospheric sound
[NASA-CR-189717] p 435 N93-12021

ACOUSTICS
Recent advances in multidisciplinary optimization of rotorcraft
[NASA-TM-107665] p 206 N93-10968
Feasibility assessment of a transient sound sensor based on the silicon retina architecture
[AD-A252288] p 432 N93-10999
Numerical and experimental results in vibroacoustical active control of structural elements with piezoelectric materials
[DILC-EST-TN-224] p 334 N93-11158
Publications on acoustics research at the Langley Research Center, January 1987 - September 1992
[NASA-TM-107674] p 435 N93-12080

ACOUSTO-OPTICS
A study of the CO2 laser near threshold
p 316 N93-11720

ACQUIRED IMMUNODEFICIENCY SYNDROME
HIV infection in the nineties p 377 N93-11290
AIDS/HIV in the US Military p 377 N93-11291
HIV variability and perspectives of a vaccine
p 378 N93-11294
Analysis of disease progression from clinical observations of US Air Force active duty members infected with the Human Immunodeficiency Virus: Distribution of AIDS survival time from interval censored observations
p 379 N93-11297

ACRYLATES
High energy cast explosives based on dinitropropylacrylate
[AD-D015340] p 273 N93-11045

ACTINIDE SERIES
Chronopotentiometry of refractory metals, actinides and oxyanions in molten salts: A review
[NASA-TM-105862] p 249 N93-11545
Calculation of binary phase diagrams between the actinide elements, rare earth elements, and transition metal elements
[DE92-019119] p 249 N93-11801
Summaries of FY 1991 research in the chemical sciences
[DE92-011920] p 251 N93-12135

ACTINIDE SERIES COMPOUNDS
Chemistry of lower valent actinide halides
[DE92-017031] p 251 N93-12105

ACTIVATION
Catalytic hydrogenation of carbon monoxide
[DE92-014729] p 253 N93-12428

ACTIVATION ENERGY
Pulsed-field-gradient NMR investigations of hydrogen diffusion in ZrH(x)
[DE92-014393] p 459 N93-11238
Studies in nonlinear problems of energy
[DE92-018551] p 345 N93-11733

ACTIVE CONTROL
Numerical and experimental results in vibroacoustical active control of structural elements with piezoelectric materials
[DILC-EST-TN-224] p 334 N93-11158
Intelligent fault management for the Space Station active thermal control system p 391 N93-11930
Active control of complex systems via dynamic (recurrent) neural networks
[AD-A254878] p 422 N93-12439

ACTIVE GALACTIC NUCLEI
Publications of the Executive Office of the President, 20 January 1989 - 31 March 1992
[PB92-154913] p 477 N93-11769
A closer look at active galactic nuclei: The great engines of the Universe
[PB92-184464] p 485 N93-11807

ACTUATOR DISKS
Nondestructive inspection and life determination of disc material
[PNR-90911] p 331 N93-11016

ACTUATORS
Open-loop characteristics of magnetic suspension systems using electromagnets mounted in a planar array
[NASA-TP-3229] p 277 N93-11613
Studies in control for vibration suppression of the UWAA 20-bay planar truss
[AD-A250193] p 341 N93-12253

ADA (PROGRAMMING LANGUAGE)
An embedded rule-based diagnostic expert system in Ada p 392 N93-11928
Design of an Ada expert system shell for the VHSIC avionic modular flight processor p 397 N93-11947
COMPASS: An Ada based scheduler
p 397 N93-11950

ADAPTIVE CONTROL
Active control of aeroacoustic couplings by means of adaptive systems
[ECL-91-18] p 214 N93-11576
Advanced control for the design of STT missile autopilot
[REPT-921-320-102] p 215 N93-11585
Self-tuning PI-PID regulators for stable systems with varying delay
[REPT-92-023] p 421 N93-11593
A PID auto-tuning algorithm based on relay feedback
[REPT-92-019] p 421 N93-11667
Self mobile space manipulator project
p 331 N93-11973
Adaptive neural network models for intelligent computations
[AD-A254689] p 421 N93-12226
Composite tasking for sensor arrays
[AD-A254997] p 287 N93-12512

ADAPTIVE FILTERS
QR decomposition based algorithms and architectures for least-squares adaptive filtering
[RSRE-MEMO-4562] p 408 N93-11390
The design and implementation of radar clutter modelling and adaptive target detection techniques
p 283 N93-11913

ADDITIVES
INAS hole-immobilized doping superlattice long-wave-infrared detector
[NASA-CASE-NPO-17880-1-CU] p 458 N93-11056
Overcharge and overdischarge protection of ambient temperature secondary lithium cells
[NASA-CASE-NPO-18343-1-CU] p 290 N93-11456
The effect of silicon, tin, and chromium on the corrosion and mechanical properties of zirconium - molybdenum - niobium
[AD-A254102] p 258 N93-11787
The mechanical and microstructural stability of austenitic stainless steels strengthened by MC-forming elements
[DE91-015314] p 259 N93-11857
Friction of self-lubricating surfaces by ion beam techniques
[DE92-016069] p 328 N93-12122
Modified epoxy adhesives and primers
[AD-A253857] p 272 N93-12297
Determination of Fe(sup 2+) and Fe(sup 3+) concentrations of semi-insulating InP:Fe
[DE92-017119] p 469 N93-12316

ADHESION
Workshop on Surface Science and Technology
[AD-A253566] p 264 N93-11149
Workshop on Adhesion and Intermolecular Forces
[AD-A255191] p 272 N93-12276

ADHESION TESTS
Study of metal-ceramic interfaces of Co-Cr-Mo alloys: Role of tungsten (W) and manganese (Mn) additions
[ECL-92-01] p 267 N93-11580

ADHESIVE BONDING
Analysis of plasma-treated wire insulation
[DE92-019471] p 291 N93-11643
Modified epoxy adhesives and primers
[AD-A253857] p 272 N93-12297

ADHESIVES
Acoustic measurement of the mechanical properties of thin material specimens
[AD-A253538] p 434 N93-11752

ADJOINTS
Constrained KP hierarchy and bi-Hamiltonian structures
[MATHS-REPT-A-168] p 424 N93-11123
Surface reconstruction of a three-dimensional ultrasonic flaw
[DE92-018029] p 332 N93-11154

ADSORPTION
Molecular mobility of the interface in a model composite: A NMR study
[AD-A253311] p 265 N93-11194
Computer simulations for the adsorption of polymers onto surfaces
[DE92-018942] p 267 N93-11628
Oxidation, nitridation, and fluorine etching of Si
[AD-A253559] p 249 N93-11755
The role of backbond strain in silicon surfaces on the decomposition of NH3 and PH3
[AD-A253771] p 250 N93-12062
The adsorption of C60 and the co-adsorption of C60 and H2O on (alpha)-Al2O3 (1 -1 0 2)-(2x1)
[DE92-018002] p 465 N93-12093
The deposition characteristics of copper(I) compounds for CVD by FT-IR spectroscopy
[DE92-010778] p 467 N93-12134

ADVANCED LAUNCH SYSTEM (STS)
Space Transportation Booster Engine Configuration Study. Volume 3: Program Cost estimates and work breakdown structure and WBS dictionary
[NASA-CR-184458] p 233 N93-12088
Space transportation booster engine configuration study. Volume 2: Design definition document and environmental analysis
[NASA-CR-184459] p 234 N93-12441
Space transportation booster engine configuration study. Volume 1: Executive Summary
[NASA-CR-184457] p 235 N93-12523

ADVANCED SOLID ROCKET MOTOR (STS)
The Space Station Freedom and space launch issues
[S-HRG-102-762] p 225 N93-11908

ADVECTION
Heat transfer enhancement by chaotic mixing
[PB92-190305] p 470 N93-11469

AERIAL PHOTOGRAPHY
Land use/land cover classification using digitally merged spot panchromatic and Landsat thematic mapper imagery
[PB92-188416] p 343 N93-11701

AEROACOUSTICS
Active control of aeroacoustic couplings by means of adaptive systems
[ECL-91-18] p 214 N93-11576
A general introduction to aeroacoustics and atmospheric sound
[NASA-CR-189717] p 435 N93-12021

AEROASSIST
Manned Mars System Study (MMSS): Mars transportation and facility infrastructure study. Volume 2: Technical report
[NASA-CR-184474] p 227 N93-12443

AEROBRAKING
Physiologically constrained aerocapture for manned Mars missions p 226 N93-12185
Thermal protection systems manned spacecraft flight experience p 227 N93-12449

AEROCAPTURE
Physiologically constrained aerocapture for manned Mars missions p 226 N93-12185

AERODYNAMIC CHARACTERISTICS
Flight test results from a supercritical mission adaptive wing with smooth variable camber
[NASA-TM-4415] p 207 N93-11863
Numerical study of advanced rotor blades
p 199 N93-11899
Measured data for the Sandia 34-meter vertical axis wind turbine
[DE92-019807] p 348 N93-12075
An experimental investigation of the flow in a diffusing S-duct
[NASA-TM-105809] p 213 N93-12077
Modeling and model simplification of aeroelastic vehicles: An overview
[NASA-TM-107691] p 215 N93-12216
An approach to constrained aerodynamic design with application to airfoils
[NASA-TP-3260] p 201 N93-12321
A summary of the forebody high-angle-of-attack aerodynamics research on the F-18 and the X-29A aircraft
[NASA-TM-104261] p 202 N93-12353
Wind tunnel investigation of a twin-engine jet transport semi-span model with upper surface blown jet flap
[NAL-TR-1134] p 203 N93-12503

AERODYNAMIC COEFFICIENTS
Lift coefficient of a randomly oscillating hydroplane
[DRA/MAR-TM(MTH)-91320] p 197 N93-11377
A wall interference assessment/correction system
[NASA-CR-190617] p 218 N93-11910
An experimental study of the relationship between forces and moments and vortex breakdown on a pitching delta wing p 208 N93-12206

AERODYNAMIC CONFIGURATIONS
A European collaborative NLF nacelle flight demonstrator
[PNR-90992] p 196 N93-11113
Artificial intelligence and CFD: Expert systems for the design of airfoils and for grid generation
[DIGE-EST-TN-016] p 206 N93-11161
Low-speed longitudinal and lateral-directional aerodynamic characteristics of the X-31 configuration
[NASA-TM-4351] p 198 N93-11622
A preliminary study associated with the experimental measurement of the aero-optic characteristics of hypersonic configurations
[AD-A253792] p 200 N93-12063

AERODYNAMIC DRAG
Application of laminar flow to aero engine nacelles
[PNR-90916] p 195 N93-11020
Numerical investigations into the base drag of various wedges using the base flow model developed by Mauri Tanner
[REPT-B-36] p 202 N93-12414

AERODYNAMIC HEAT TRANSFER
Leading edge film cooking heat transfer including the effect of mainstream turbulence p 199 N93-11886

AERODYNAMIC HEATING
Physiologically constrained aerocapture for manned Mars missions p 226 N93-12185
Active cooling from the sixties to NASP
p 208 N93-12458

AERODYNAMIC INTERFERENCE
A wall interference assessment/correction system
[NASA-CR-190617] p 218 N93-11910

AERODYNAMIC LOADS
Design of a high-temperature experiment for evaluating advanced structural materials
[NASA-TM-105833] p 337 N93-11624

AERODYNAMIC NOISE
A concept for a counterrotating fan with reduced tone noise
[NASA-TM-105736] p 433 N93-11370

AERODYNAMIC STABILITY
Active control of aeroacoustic couplings by means of adaptive systems
[ECL-91-18] p 214 N93-11576
Low-speed longitudinal and lateral-directional aerodynamic characteristics of the X-31 configuration
[NASA-TM-4351] p 198 N93-11622

AERODYNAMIC STALLING
The convection speed of the dynamic stall vortex
[AD-A247258] p 197 N93-11464

AERODYNAMICS
The engine design engine. A clustered computer platform for the aerodynamic inverse design and analysis of a full engine
[NASA-TM-105838] p 196 N93-11223

AEROELASTICITY
Modeling and model simplification of aeroelastic vehicles: An overview
[NASA-TM-107691] p 215 N93-12216
Stochastic sensitivity measure for mistuned high-performance turbines
[NASA-TM-105821] p 341 N93-12277
The Fourth Workshop on Dynamics and Aeroelastic Stability Modeling of Rotorcraft Systems
[AD-A255065] p 208 N93-12485

AERONAUTICAL ENGINEERING
The first meeting of the Advisory Committee on the Future of the US Space Program (C-FUSSP)
[NASA-CR-190995] p 219 N93-11754

AERONAUTICS
Winds of change: Expanding the frontiers of flight. Langley Research Center's 75 years of accomplishment, 1917-1992
[NASA-NP-130] p 490 N93-11100
Directory of factual and numeric databases of relevance to aerospace and defence R and D
[AGARD-R-777] p 476 N93-11710

AEROSOLS
International Conference on the Role of the Polar Regions in Global Change: Proceedings, volume 1
[DE92-013652] p 353 N93-11232
International Conference on the Role of the Polar Regions in Global Change: Proceedings, volume 2
[DE92-013653] p 353 N93-11233
The design, development, and test of balloonborne and groundbased lidar systems. Volume 3: Groundbased lidar systems
[AD-A247552] p 317 N93-11805
Electronic transport and lasing in microstructures
[DE92-018725] p 441 N93-12115
The design, development, and test of balloonborne and groundbased lidar systems. Volume 1: Balloonborne coherent CO2 lidar system
[AD-A247551] p 322 N93-12262

AEROSPACE ENGINEERING
Neutron diffraction residual stress studies for aero-engine component applications
[PNR-90908] p 334 N93-11014
Japanese style total quality control: A first hand experience
[PNR-90909] p 331 N93-11015
Rotational CARS measurements in a rotating cavity with axial throughflow of cooling air: Oxygen concentration measurements
[PNR-90935] p 244 N93-11035
Innovation in engineering
[PNR-90889] p 212 N93-11207
Simultaneous engineering in aero gas turbine design and manufacture
[PNR-90890] p 212 N93-11208
The changing nature of design
[PNR-91011] p 206 N93-11334
Microstructure and mechanical properties of reactive hot isostatic pressed TiAl powder material
[GKSS-91/E/60] p 256 N93-11336
Directory of factual and numeric databases of relevance to aerospace and defence R and D
[AGARD-R-777] p 476 N93-11710
NASA/DOD Aerospace Knowledge Diffusion Research Project. Paper 23: Information technology and aerospace knowledge diffusion: Exploring the intermediary-end user interface in a policy framework
[NASA-TM-108077] p 478 N93-12007

AEROSPACE ENVIRONMENTS
The effects of aluminum oxide on inertial welding of aluminum in space applications
[AD-A255100] p 329 N93-12274

AEROSPACE INDUSTRY
The European space industry. Overall situation: Situation and prospects for the 23 leading companies concerned
p 472 N93-11163

AEROSPACE MEDICINE
Allergic, Immunological and Infectious Disease Problems in Aerospace Medicine
[AGARD-CP-518] p 376 N93-11283
Space flight and immune system p 376 N93-11284
Relating cognitive function to military aviator performance in early HIV infection p 379 N93-11298
Epidemiologic view of allergic diseases in North America: Implications for aerospace medicine
p 382 N93-11311
In vivo and in vitro diagnosis of allergic respiratory disease during screening procedures in the Italian Navy: Comparative evaluation of a recent quantitative automatized enzyme immunoassay method to dose specific IgE p 383 N93-11314
Asthma in aircrew: Assessment, treatment and disposition p 383 N93-11315
Allergy screening and follow-up in student pilots of the Belgian Air Force (BAF) p 383 N93-11316
Allergic and nonallergic rhinitis in Greek pilots
p 383 N93-11317
Fifth Annual Workshop on Space Operations Applications and Research (SOAR 1991), volume 1
[NASA-CP-3127-VOL-1] p 391 N93-11921

AEROSPACE PLANES
Rocket Based Combined Cycle (RBCC) Propulsion Technology Workshop. Volume 1: Executive summary
[NASA-CR-184382] p 231 N93-11042
Simulation analysis of a cable-mount system used for dynamic wind tunnel tests
[NAL-TR-1127] p 219 N93-12359
On stability and control of SSTO spaceplane in super- and hypersonic ascending phase
[NAL-TR-1128T] p 216 N93-12361
Current Technology for Thermal Protection Systems
[NASA-CP-3157] p 227 N93-12447
Current research in oxidation-resistant carbon-carbon composites at NASA. Langley Research Center
p 229 N93-12456
Thermal control/oxidation resistant coatings for titanium-based alloys p 229 N93-12457
Active cooling from the sixties to NASP
p 208 N93-12458

AEROSPACE SCIENCES
Winds of change: Expanding the frontiers of flight. Langley Research Center's 75 years of accomplishment, 1917-1992
[NASA-NP-130] p 490 N93-11100

AEROSPACE SYSTEMS
The Space Station Freedom and space launch issues
[S-HRG-102-762] p 225 N93-11908
An approach to integrating and creating flexible software environments p 396 N93-11946
Ceramic TBS/porous metal compliant layer
p 228 N93-12453

AEROSPACE TECHNOLOGY TRANSFER
NASA/DOD Aerospace Knowledge Diffusion Research Project. Paper 23: Information technology and aerospace knowledge diffusion: Exploring the intermediary-end user interface in a policy framework
[NASA-TM-108077] p 478 N93-12007

AEROSPACE VEHICLES
Predicted and tested performance of durable TPS
p 228 N93-12454
Advanced two-phase heat transfer systems
p 229 N93-12459
Thermostructural applications of heat pipes for cooling leading edges of high-speed aerospace vehicles
p 229 N93-12460
Experiments and analysis concerning the use of external burning to reduce aerospace vehicle transonic drag
p 235 N93-12537

AEROTHERMOCHEMISTRY
Thermokinetic modelling and hypersonic flow
[DILC-EST-TN-218] p 196 N93-11157

AEROTHERMODYNAMICS
Aerothermal test results from the second flight of the Pegasus booster
[NASA-TM-4391] p 296 N93-10969
Design of a high-temperature experiment for evaluating advanced structural materials
[NASA-TM-105833] p 337 N93-11624
Leading edge film cooking heat transfer including the effect of mainstream turbulence p 199 N93-11886
Thermostructural applications of heat pipes for cooling leading edges of high-speed aerospace vehicles
p 229 N93-12460

AFTERBODIES
Calculation of nozzle/aftbody flowfield interactions
p 302 N93-11722

AFTERGLOWS
State-resolved dynamics of ion-molecule collisions in a flowing afterglow
[AD-A247288] p 436 N93-11467

AGGREGATES
Grain boundary transport and related processes in natural fine grained aggregates
[DE92-018239] p 461 N93-11682
The physics of pattern formation at liquid interfaces
[DE92-016971] p 462 N93-11747

AGING (MATERIALS)
Evaluation of epoxy cured with Ethacure 100 curing agent for use in headers for thermal batteries
[DE92-019326] p 267 N93-11552
The degradation of parachutes: Age and mechanical wear
[AD-A252243] p 200 N93-12179

AIR
Thermomechanical fatigue behavior of SiC/Ti-24Al-11Nb in air and argon environments
[NASA-TM-105723] p 238 N93-11399
Particle-fluid two-phase flow modeling
[DE92-017847] p 301 N93-11637
Theoretical study of the radiative and kinetic properties of selected metal oxides and air molecules
[AD-A251090] p 438 N93-11804

AIR BREATHING ENGINES
Rocket Based Combined Cycle (RBCC) Propulsion Technology Workshop. Volume 1: Executive summary
[NASA-CR-184382] p 231 N93-11042
Rocket Based Combined Cycle (RBCC) Propulsion Workshop, volume 2
[NASA-CR-184383] p 231 N93-11043
Predicted aircraft effects on stratospheric ozone
p 352 N93-11096
Air-breathing hypersonic vehicle guidance and control studies: An integrated trajectory/control analysis methodology, phase 2
[NASA-CR-189703] p 216 N93-12413
Experiments and analysis concerning the use of external burning to reduce aerospace vehicle transonic drag
p 235 N93-12537

AIR CONDITIONING
Low cost humidity sensor
[PB92-205772] p 312 N93-11757

AIR COOLING
Rotational CARS measurements in a rotating cavity with axial throughflow of cooling air: Oxygen concentration measurements
[PNR-90935] p 244 N93-11035
Mach 4 testing of scramjet inlet models
[NAL-TR-1137] p 202 N93-12369
Effects of cooling-air injection on secondary flows and losses in a turbine cascade
[NAL-TR-1121T] p 307 N93-12382

AIR FILTERS
Microbiological analysis of debris from STS-42 IML-1 by direct plating of rinse waters
[NASA-TM-108375] p 375 N93-12174

AIR FLOW
Rotational CARS measurements in a rotating cavity with axial throughflow of cooling air: Oxygen concentration measurements
[PNR-90935] p 244 N93-11035
A general introduction to aeroacoustics and atmospheric sound
[NASA-CR-189717] p 435 N93-12021
Hypersonic flow diagnostic development
[AD-A255045] p 202 N93-12466
AIR INTAKES
The combustion time lag and its role in ramjet combustion instability p 245 N93-11137
Wind tunnel investigation of a twin-engine jet transport semi-span model with upper surface blown jet flap
[NAL-TR-1134] p 203 N93-12503
AIR JETS
Numerical investigation of three-dimensionally evolving jets p 303 N93-11870
AIR NAVIGATION
Future FAA telecommunications plan
[AD-A249133] p 283 N93-11760
AIR POLLUTION
Direct catalytic decomposition of nitric oxide
[DE92-018759] p 247 N93-11444
Key wintertime meteorological features of the Grand Canyon and the Colorado Plateaus Basin
[DE92-019134] p 369 N93-11657
Atmospheric reactive nitrogen: A model study of natural and anthropogenic sources and the role of microbial soil emissions
[DE92-010717] p 354 N93-11744
Advanced heat pump for the recovery of volatile organic compounds
[DE92-011592] p 303 N93-11774
Stratospheric aircraft: Impact on the stratosphere?
[DE92-016997] p 355 N93-12104
Stratospheric aircraft exhaust plume and wake chemistry studies
[NASA-CR-189688] p 366 N93-12299
Reduction in global warming due to fuel economy improvements and emissions control of criteria pollutants: New US light-duty vehicles (1968-1991)
[DE92-016636] p 356 N93-12314
Allowance system: Proposed acid rain rule
[PB92-226174] p 356 N93-12524
United States/Canada Air Quality Agreement
[PB92-228030] p 356 N93-12525
AIR QUALITY
Comparison of passive-remote and conventional Fourier transform infrared systems for continuously monitoring incinerator emissions
[DE92-015225] p 355 N93-12098
United States/Canada Air Quality Agreement
[PB92-228030] p 356 N93-12525
AIR SEA ICE INTERACTIONS
International Conference on the Role of the Polar Regions in Global Change: Proceedings, volume 1
[DE92-013652] p 353 N93-11232
International Conference on the Role of the Polar Regions in Global Change: Proceedings, volume 2
[DE92-013653] p 353 N93-11233
AIR TRAFFIC
Upgrade Precision Runway Monitor (PRM) Operational Test and Evaluation (OT/E) test plan
[DOT/FAA/CT-TN92/13] p 217 N93-11616
AIR TRAFFIC CONTROL
Methods and principles for determining task dependent interface content
[NASA-CR-190837] p 204 N93-10961
Design of an air traffic computer simulation system to support investigation of civil tiltrotor aircraft operations
[NASA-CR-190811] p 204 N93-11139
Activities report of the German Institute for Flight Safety
[ETN-92-92272] p 203 N93-11375
High Capacity Voice Recorder (HCVR) Operational Test and Evaluation (OT/E) integration test report
[DOT/FAA/CT-TN92/30] p 310 N93-11460
Upgrade Precision Runway Monitor (PRM) Operational Test and Evaluation (OT/E) test plan
[DOT/FAA/CT-TN92/13] p 217 N93-11616
Controller evaluation of initial data link terminal air traffic control services: Mini study 2, volume 1
[DOT/FAA/CT-92/2-VOL-1] p 205 N93-11704
Controller evaluation of initial data link terminal air traffic control services: Mini study 2, volume 2
[DOT/FAA/CT-92/2-VOL-2] p 205 N93-11705
Implementing system simulation of C3 systems using autonomous objects
[NASA-CR-190845] p 283 N93-11716
Airport stand assignment model
[TT-9104] p 218 N93-11728
Future FAA telecommunications plan
[AD-A249133] p 283 N93-11760
AIR WATER INTERACTIONS
Studies of the role of clouds in CO2-induced climate change
[DE92-018648] p 353 N93-11569
Studies of ocean predictability at decade to century time scales using a global ocean general circulation model in a parallel competing environment
[DE92-019457] p 373 N93-11642
Proceedings of the Sixteenth Annual Climate Diagnostics Workshop
[PB92-198803] p 370 N93-11896
AIRBORNE EQUIPMENT
Embedded training capabilities for the LAMPS MK 3 system
[AD-A250697] p 207 N93-11838
AIRCRAFT
Winds of change: Expanding the frontiers of flight. Langley Research Center's 75 years of accomplishment, 1917-1992
[NASA-NP-130] p 490 N93-11100
AIRCRAFT ACCIDENT INVESTIGATION
Aircraft accident report: Atlantic Southeast Airlines, Inc. Flight 2311, uncontrolled collision with terrain, an Embraer EMB-120, N270AS, Brunswick, Georgia, 5 April 1991
[PB92-910403] p 203 N93-11471
Aircraft accident report: Explosive decompression-loss of cargo door in flight, United Airlines Flight 811, Boeing 747-122, N4713U, Honolulu, HI, 24 February 1989
[PB92-910402] p 204 N93-12193
Evaluation of CKU-5/A ejection seat catapults under varied acceleration levels
[AD-A248021] p 204 N93-12489
AIRCRAFT ACCIDENTS
UK airmisses involving commercial air transport, May-August 1991
[ETN-92-92260] p 203 N93-11357
UK airmisses involving commercial air transport, January-April 1991
[ETN-92-92261] p 298 N93-11358
Aircraft accident report: Atlantic Southeast Airlines, Inc. Flight 2311, uncontrolled collision with terrain, an Embraer EMB-120, N270AS, Brunswick, Georgia, 5 April 1991
[PB92-910403] p 203 N93-11471
Aircraft accident report: Explosive decompression-loss of cargo door in flight, United Airlines Flight 811, Boeing 747-122, N4713U, Honolulu, HI, 24 February 1989
[PB92-910402] p 204 N93-12193
AIRCRAFT CARRIERS
The future of carrier aviation
[AD-A254043] p 430 N93-12260
AIRCRAFT COMMUNICATION
The development of the speaker independent ARM continuous speech recognition system
[RSRE-MEMO-4473] p 260 N93-11383
Controller evaluation of initial data link terminal air traffic control services: Mini study 2, volume 1
[DOT/FAA/CT-92/2-VOL-1] p 205 N93-11704
Controller evaluation of initial data link terminal air traffic control services: Mini study 2, volume 2
[DOT/FAA/CT-92/2-VOL-2] p 205 N93-11705
AIRCRAFT CONSTRUCTION MATERIALS
Nondestructive evaluation of ceramic and metal matrix composites for NASA's HITEMP and enabling propulsion materials programs
[NASA-TM-105807] p 331 N93-10963
Materials: Toward the non-metallic engine
[PNR-90915] p 209 N93-11019
Corrosion protection of materials for aircraft using ion beam processes. Corrosion and bonding strength examinations. Physical analysis of laser composition
[MBB-Z-0405-91-PUB] p 255 N93-11026
Surface protection in the aircraft industry
[MBB-Z-0432-92-PUB] p 255 N93-11027
Aero engine ceramics: The vision, the reality, and the progress
[PNR-90983] p 264 N93-11066
Advanced materials in gas turbine engines: An assessment
[PNR-90946] p 211 N93-11105
Present and future trends in turbine blade material and manufacture technology
[PNR-90960] p 255 N93-11111
Fatigue in single crystal nickel superalloys
[AD-A254603] p 260 N93-12237
Thermal protection systems manned spacecraft flight experience p 227 N93-12449
Thermal protection using very high temperature ceramics p 228 N93-12451
AIRCRAFT CONTROL
Flight-determined stability analysis of multiple-input-multiple-output control systems
[NASA-TM-4416] p 214 N93-11178
Application of eigenstructure assignment to the control of powered lift combat aircraft p 215 N93-11871
Development of a 1/7-scale F/A-18 UAV for supermaneuverability research --- unmanned air vehicle
[AD-A247261] p 208 N93-12053
Neural network models of air combat maneuvering
[AD-A254653] p 421 N93-12096
Modeling and model simplification of aeroelastic vehicles: An overview
[NASA-TM-107691] p 215 N93-12216
Computational nonlinear control
[AD-A253547] p 422 N93-12258
A monitor for the laboratory evaluation of control integrity in digital control systems operating in harsh electromagnetic environments
[NASA-TM-4402] p 215 N93-12304
Analysis of fault-tolerant neurocontrol architectures
[NASA-TM-105898] p 215 N93-12305
DYNAC: A computer program for analyzing the dynamical stability of aircraft
[REPT-B-31] p 216 N93-12415
AIRCRAFT DESIGN
Overview of supersonic laminar flow control research on the F-16XL ships 1 and 2
[NASA-TM-104257] p 196 N93-11221
The changing nature of design
[PNR-91011] p 206 N93-11334
An approach to constrained aerodynamic design with application to airfoils
[NASA-TP-3260] p 201 N93-12321
Concurrent optimization of airframe and engine design parameters
[NASA-TM-105908] p 213 N93-12402
AIRCRAFT DETECTION
Ultra wide band 3-D cross section (RCS) holography
[DE92-019133] p 312 N93-11802
AIRCRAFT ENGINES
Nondestructive evaluation of ceramic and metal matrix composites for NASA's HITEMP and enabling propulsion materials programs
[NASA-TM-105807] p 331 N93-10963
Materials: Toward the non-metallic engine
[PNR-90915] p 209 N93-11019
Application of laminar flow to aero engine nacelles
[PNR-90916] p 195 N93-11020
An experimental evaluation of prediction methods for contrafans
[PNR-90924] p 209 N93-11023
On the basis of experience: Built in product reliability
[PNR-90932] p 331 N93-11034
Rolls-Royce civil engine technology
[PNR-90936] p 210 N93-11036
The Trent: Towards greater thrust
[PNR-90937] p 210 N93-11037
From RB211 to Trent: An ongoing development strategy
[PNR-90938] p 210 N93-11038
Introduction to the Rolls-Royce design process
[PNR-90939] p 210 N93-11039
The application of manufacturing systems engineering for aero engine gears
[PNR-90944] p 324 N93-11054
Simultaneous engineering in the design of aero engines
[PNR-90973] p 211 N93-11062
Aero engine ceramics: The vision, the reality, and the progress
[PNR-90983] p 264 N93-11066
Advanced three-shaft engines: Configured for reliability, efficiency, and growth
[PNR-90986] p 211 N93-11068
Maintainability of large gas turbine aero engines
[PNR-90987] p 211 N93-11069
A combined experimental and theoretical study of laminar flow control with particular relevance to aero engine nacelles
[PNR-90991] p 195 N93-11070
Civil aircraft engines: The next generation
[PNR-90962] p 211 N93-11085
The development of the Rolls-Royce Trent aero gas turbine
[PNR-90949] p 212 N93-11108
Overview of high performance aircraft propulsion research
[NASA-TM-105839] p 213 N93-11530
Evaluation of acoustic impedance models for a perforated plate
[NAL-TR-1133] p 435 N93-12375
AIRCRAFT EQUIPMENT
Simulator, Tactical Use, Flare (STUF) project report
[AD-A254890] p 276 N93-12281
AIRCRAFT GUIDANCE
Hybrid guidance for maneuvering flight vehicles
[AD-A254110] p 225 N93-11798

AIRCRAFT ICING

Developments in icing test techniques for aerospace applications in the RAE Pyestock (England) altitude test facility
[RAE-TM-P-1214] p 207 N93-11485

AIRCRAFT INDUSTRY

Surface protection in the aircraft industry
[MBB-Z-0432-92-PUB] p 255 N93-11027

The application of manufacturing systems engineering for aero engine gears
[PNR-90944] p 324 N93-11054

Activities report of Lufthansa
[ETN-92-92100] p 203 N93-11319

AIRCRAFT INSTRUMENTS

Flight simulator evaluation of D-size liquid crystal flat panel displays
[NAL-TR-1136] p 209 N93-12367

Liquid crystal flat panel display evaluation tests using a flight simulator
[NAL-TR-1122] p 209 N93-12383

AIRCRAFT LANDING

Summary of findings from the PIREP-based analyses conducted during the 1988 to 1990 evaluations of TDWR-based and TDWR/LLWAS-based alert services provided to landing/departing pilots
[AD-A253859] p 367 N93-11144

A problem formulation for glideslope tracking in wind shear using advanced robust control techniques
[NASA-TM-104164] p 214 N93-11176

AIRCRAFT MAINTENANCE

Maintainability of large gas turbine aero engines
[PNR-90987] p 211 N93-11069

Rotorcraft health and usage monitoring systems: A literature survey
[DOT/FAA/RD-91/6] p 206 N93-11461

Using NDT techniques in the maintenance of aeronautical products
[REPT-921-430-102] p 332 N93-11587

AIRCRAFT MANEUVERS

Hybrid guidance for maneuvering flight vehicles
[AD-A254110] p 225 N93-11798

Neural network models of air combat maneuvering
[AD-A254653] p 421 N93-12096

AIRCRAFT MODELS

Application of eigenstructure assignment to the control of powered lift combat aircraft p 215 N93-11871

Introduction of electronic pressure scanning at the Royal Aerospace Establishment
[RAE-TM-AERO-2222] p 199 N93-11882

Study of optical techniques for the Ames unitary wind tunnels. Part 4: Model deformation
[NASA-CR-190980] p 219 N93-12349

Simulation analysis of a cable-mount system used for dynamic wind tunnel tests
[NAL-TR-1127] p 219 N93-12359

AIRCRAFT NOISE

Publications on acoustics research at the Langley Research Center, January 1987 - September 1992
[NASA-TM-107674] p 435 N93-12080

AIRCRAFT PERFORMANCE

Concurrent optimization of airframe and engine design parameters
[NASA-TM-105908] p 213 N93-12402

AIRCRAFT PILOTS

Relating cognitive function to military aviator performance in early HIV infection p 379 N93-11298

The screening of inhalant allergic diseases in the selection of candidates for aircraft piloting
p 382 N93-11312

In vivo and in vitro diagnosis of allergic respiratory disease during screening procedures in the Italian Navy: Comparative evaluation of a recent quantitative automatized enzyme immunoassay method to dose specific IgE p 383 N93-11314

Allergy screening and follow-up in student pilots of the Belgian Air Force (BAF) p 383 N93-11316

Allergic and nonallergic rhinitis in Greek pilots
p 383 N93-11317

Selective factors affecting rotary wing aviator performance with symbology superimposed on night vision goggles
[AD-A254983] p 390 N93-12508

AIRCRAFT RELIABILITY

Advanced three-shaft engines: Configured for reliability, efficiency, and growth
[PNR-90986] p 211 N93-11068

Rotorcraft health and usage monitoring systems: A literature survey
[DOT/FAA/RD-91/6] p 206 N93-11461

Aircraft accident report: Explosive decompression-loss of cargo door in flight, United Airlines Flight 811, Boeing 747-122, N4713U, Honolulu, HI, 24 February 1989
[PB92-910402] p 204 N93-12193

AIRCRAFT SAFETY

Activities report of the German Institute for Flight Safety
[ETN-92-92272] p 203 N93-11375

Aircraft accident report: Atlantic Southeast Airlines, Inc. Flight 2311, uncontrolled collision with terrain, an Embraer EMB-120, N270AS, Brunswick, Georgia, 5 April 1991
[PB92-910403] p 203 N93-11471

Aircraft accident report: Explosive decompression-loss of cargo door in flight, United Airlines Flight 811, Boeing 747-122, N4713U, Honolulu, HI, 24 February 1989
[PB92-910402] p 204 N93-12193

AIRCRAFT STABILITY

Correlation of forebody pressures and aircraft yawing moments on the X-29A aircraft at high angles of attack
[NASA-TM-4417] p 197 N93-11532

Rigid body mode identification of the PAH-2 helicopter using the eigensystem realization algorithm
[NASA-TM-107690] p 336 N93-11544

The 13 ft by 9 ft low speed wind tunnel facility at DRA (Aerospace Division) Bedford (England)
[RAE-TM-AERO-2228] p 199 N93-11883

DYNAC: A computer program for analyzing the dynamical stability of aircraft
[REPT-B-31] p 216 N93-12415

AIRCRAFT STRUCTURES

Magneto-optic imaging inspection of selected corrosion specimens
[DOT/FAA/CT-TN92/20] p 332 N93-11617

DYNAC: A computer program for analyzing the dynamical stability of aircraft
[REPT-B-31] p 216 N93-12415

AIRFOIL OSCILLATIONS

New acceleration potential method for supersonic unsteady aerodynamics of lifting surfaces, further extension of the nonplanar supersonic doublet point method, and nonlinear, nongradient optimized rational function approximations for supersonic, transient response unsteady aerodynamics p 201 N93-12344

AIRFOIL PROFILES

The convection speed of the dynamic stall vortex
[AD-A247258] p 197 N93-11464

Further buffeting tests in a cryogenic wind tunnel
[NASA-TM-107621] p 198 N93-11610

AIRFOILS

Boundary layer relaminarization device
[NASA-CASE-LAR-14470-1] p 199 N93-11876

Dynamic analysis of a pre-and-post ice impacted blade
[NASA-TM-105829] p 276 N93-12197

Fatigue in single crystal nickel superalloys
[AD-A254603] p 260 N93-12237

An approach to constrained aerodynamic design with application to airfoils
[NASA-TP-3260] p 201 N93-12321

AIRFRAMES

Recent advances in multidisciplinary optimization of rotorcraft
[NASA-TM-107665] p 206 N93-10968

Concurrent optimization of airframe and engine design parameters
[NASA-TM-105908] p 213 N93-12402

AIRGLOW

An inversion technique to recover lower thermospheric winds from space-borne remote measurements of (OI) 5577 A p 369 N93-11839

AIRLINE OPERATIONS

An investigation of ground access mode choice for departing passengers
[TT-9201] p 217 N93-11224

Aircraft accident report: Atlantic Southeast Airlines, Inc. Flight 2311, uncontrolled collision with terrain, an Embraer EMB-120, N270AS, Brunswick, Georgia, 5 April 1991
[PB92-910403] p 203 N93-11471

Airport stand assignment model
[TT-9104] p 218 N93-11728

AIRPORT PLANNING

Airport stand assignment model
[TT-9104] p 218 N93-11728

AIRPORTS

An investigation of ground access mode choice for departing passengers
[TT-9201] p 217 N93-11224

AIRSPACE

A simplified numerical procedure to compute the optimal trajectory of an aircraft p 207 N93-11719

ALBEDO

Atlas of albedo and absorbed solar radiation derived from Nimbus 7 earth radiation budget data set, November 1985 to October 1987
[NASA-RP-1281] p 367 N93-11168

ALCOHOLS

Smoking status and body composition, exercise, dietary intake, and alcohol/caffeine consumption
[AD-A250648] p 385 N93-11893

ALDOSTERONE

Effect of hemorrhage on cardiac output, vasopressin, aldosterone, and diuresis during immersion in men
[NASA-TM-103949] p 374 N93-12014

ALGEBRA

Applying algebraic techniques to microcode compilation
[RSRE-MEMO-4568] p 409 N93-11392

ScaLAPACK: A scalable linear algebra library for distributed memory concurrent computers
[DE92-017823] p 426 N93-11636

Formal mechanization of device interactions with a process algebra
[NASA-CR-189644] p 405 N93-12347

Selecting reusable components using algebraic specifications p 415 N93-12387

ALGORITHMS

Matching and vertex packing: How hard are they?
[AD-A245928] p 423 N93-10991

An evidential reasoning approach to the classification of satellite images
[DLR-FB-91-29] p 342 N93-11140

Stochastic control and nonlinear estimation
[AD-A253543] p 420 N93-11147

Terminal slider control of nonlinear robotic systems
[NASA-CASE-NPO-18584-1-CU] p 324 N93-11177

Implicit parallelism in genetic algorithms
[REPT-92-012] p 418 N93-11180

Parallel genetic algorithms: Introduction and overview of current research
[REPT-92-015] p 418 N93-11181

An adaptive differencing scheme for elliptic flows
p 297 N93-11197

Numerical solution of inverse problems in mechanics using the boundary element method
p 424 N93-11199

Optimized software for a generalized Polak-Ribiere algorithm in unconstrained optimization
[MATHS-REPT-A-156] p 406 N93-11210

Preconditioned low-order Newton methods
[MATHS-REPT-A-159] p 425 N93-11211

Boundary condition methods in the numerical solution of the Navier-Stokes equations with the application to free surface problems
[ISBN-0-315-64278-5] p 298 N93-11241

Domain decomposition: A bridge between nature and parallel computers
[NASA-CR-189709] p 425 N93-11246

Object based multi-image matching
[SER-C-375] p 309 N93-11330

Detection of cloud-top height from backscattered radiances within the oxygen A band. Part 1: Theoretical study
[GKSS-91/E/76-PT-1] p 368 N93-11349

Authentication algorithm for the universal Authenticated Item Monitoring Systems (AIMS)
[DE92-018826] p 408 N93-11378

QR decomposition based algorithms and architectures for least-squares adaptive filtering
[RSRE-MEMO-4562] p 408 N93-11390

Ten15 developments to support parallelism
[RSRE-MEMO-4545] p 409 N93-11406

The efficient parallel iterative solution of large sparse linear systems
[DE92-018769] p 425 N93-11446

Object recognition with a robot hand
p 420 N93-11457

Dynamic programming and image processing on distributed memory parallel machines
[ETN-92-92174] p 409 N93-11478

Path planning on a ring of processors
p 410 N93-11480

Symmetric matrix-vector product on a ring of processors p 410 N93-11481

Scattering on a ring of processors
p 410 N93-11482

Z-buffer on a transputer-based machine
p 410 N93-11483

Reduction operations on a distributed memory machine with a reconfigurable interconnection network
p 410 N93-11484

On the inverse scattering problem for the Helmholtz equation in one dimension
[AD-A253130] p 434 N93-11526

Optimization of expressions involving array classes
[DE92-019421] p 411 N93-11536

Design of a PCM data compressor --- pulse code modulation
[DE92-019469] p 404 N93-11539

Rigid body mode identification of the PAH-2 helicopter using the eigensystem realization algorithm
[NASA-TM-107690] p 336 N93-11544

A computer algorithm for automatic beam steering
[DE92-019338] p 411 N93-11555

Computational aspects of Gaussian beam migration
[DE92-018641] p 431 N93-11567

ScaLAPACK: A scalable linear algebra library for distributed memory concurrent computers
[DE92-017823] p 426 N93-11636
A PID auto-tuning algorithm based on relay feedback
[REPT-92-019] p 421 N93-11667
The ESSE project: Supporting object-oriented database schema analysis and evolution: Overview
[REPT-92-026] p 476 N93-11689
Automated extraction of aircraft runway patterns from radar imagery
[AD-A254258] p 218 N93-11751
The sensitivity of the receiver coherence diameter and modulation transfer function to variations of a damp unstable atmosphere
[AD-A253269] p 363 N93-11785
Differential equation-based seismic data filtering
[DE92-016282] p 363 N93-11791
An expert system for diagnosing environmentally induced spacecraft anomalies p 230 N93-11927
Spacecraft attitude control using a smart control system p 230 N93-11932
Design development of a neural network-based telemetry monitor p 394 N93-11933
Methodologies for building robust schedules
p 397 N93-11949
Model-based vision for space applications
p 398 N93-11955
Fault detection and fault tolerance in robotics
p 330 N93-11961
Interactive collision detection p 400 N93-11963
Exoskeleton master controller with force-reflecting telepresence p 330 N93-11970
The order n simulation of tether motions based on a rigid body tether model p 225 N93-11999
Lunar PMAD technology assessment
[NASA-CR-189225] p 347 N93-12017
New methods for nonlinear tracking and nonlinear chaotic signal processing
[AD-A254320] p 284 N93-12095
Polynomial dual network simplex algorithms
[AD-A254340] p 413 N93-12131
Multifractal analysis at negative q
[AD-A254370] p 413 N93-12159
Dynamic multimodal function optimization using genetic algorithms
[DE92-019602] p 414 N93-12234
Assembling polyhedra with single translations
[AD-A254623] p 419 N93-12239
Algorithms for sensor fusion: Decentralized Bayesian hypothesis testing with feedback, volume 1
[AD-A254633] p 414 N93-12242
Computational nonlinear control
[AD-A253547] p 422 N93-12258
A genetic algorithm for search route planning
[AD-A254894] p 414 N93-12284
Oscillations and concentrations in compressible and incompressible fluids
[AD-A254706] p 307 N93-12333
An advancing front Delaunay triangulation algorithm designed for robustness
[NASA-CR-189719] p 416 N93-12400
Active control of complex systems via dynamic (recurrent) neural networks
[AD-A254878] p 422 N93-12439
A vision-based end-point control for a two-link flexible manipulator
[NASA-CR-190967] p 330 N93-12521

ALIGNMENT
A single beam laser tracker as an alignment tool
[DE92-017746] p 316 N93-11691
Mirror alignment techniques for point-focus solar concentrators
[DE92-019643] p 348 N93-12074
Growth, characterization, and device development in monocrystalline diamond films
[AD-A252648] p 271 N93-12184
Method and apparatus for gripping test specimens
[NASA-CASE-LEW-15345-1] p 329 N93-12327

ALKYL COMPOUNDS
Ignition delays, heats of combustion, and reaction rates of aluminum alkyl derivatives as used as ignition and combustion enhancers for supersonic combustors
p 244 N93-11134
Molecular mobility of the interface in a model composite: A NMR study
[AD-A253311] p 265 N93-11194

ALKYLIDENE
Controlled synthesis of polyenes by catalytic methods
[DE92-015286] p 271 N93-12165

ALLERGIC DISEASES
Allergic, Immunological and Infectious Disease Problems in Aerospace Medicine
[AGARD-CP-518] p 376 N93-11283
Immunological parameters in current and former US Air Force personnel p 378 N93-11295
Epidemiologic view of allergic diseases in North America: Implications for aerospace medicine
p 382 N93-11311
The screening of inhalant allergic diseases in the selection of candidates for aircraft piloting
p 382 N93-11312
Phadiatop: A screening test for inhalant allergy
p 383 N93-11313
In vivo and in vitro diagnosis of allergic respiratory disease during screening procedures in the Italian Navy: Comparative evaluation of a recent quantitative automatized enzyme immunoassay method to dose specific IgE p 383 N93-11314
Allergy screening and follow-up in student pilots of the Belgian Air Force (BAF) p 383 N93-11316
Allergic and nonallergic rhinitis in Greek pilots
p 383 N93-11317

ALLOYING
The effect of silicon, tin, and chromium on the corrosion and mechanical properties of zirconium - molybdenum - niobium
[AD-A254102] p 258 N93-11787
Oxidation-sulfidation behavior of iron alloys containing 16 to 40 atomic percent aluminum
[DE92-017824] p 259 N93-11830

ALLOYS
Optimization of film synthesized rare earth transition metal permanent magnet systems
[DE92-018726] p 432 N93-12116

ALPHA PARTICLES
Lyman alpha line shapes from electron impact H2 dissociative processes in the Jovian auroral zone
p 487 N93-11166

ALTERNATING CURRENT
Flux dynamics and irreversibility in YBa2Cu3O7 with Y2BaCuO5 inclusions and in single crystal YBa2Cu3O7
[DE92-009712] p 467 N93-12178
Energy efficient drivepower: An overview
[PB92-199173] p 294 N93-12191

ALTERNATIVES
Evaluation of alternatives for increasing A-7D rearward visibility
[AD-A255071] p 208 N93-12488

ALTIMETRY
Experimental measurement and theoretical modeling of microwave scattering and the structure of the sea surface influencing radar observations from space
[NASA-CR-190998] p 343 N93-12006

ALTITUDE CONTROL
A state-based approach to trend recognition and failure prediction for the Space Station Freedom
p 230 N93-11925

ALUMINIDES
Titanium-aluminides by hot isostatic pressing of cold extruded titanium-aluminium powder mixtures
[GKSS-91/E/67] p 256 N93-11337
Thermomechanical fatigue behavior of SiC/Ti-24Al-11Nb in air and argon environments
[NASA-TM-105723] p 238 N93-11399

ALUMINUM
Development of stable metallization systems
[AD-A253569] p 264 N93-11079
Ignition delays, heats of combustion, and reaction rates of aluminum alkyl derivatives as used as ignition and combustion enhancers for supersonic combustors
p 244 N93-11134
Feasibility of using neutron radiography to inspect the Space Shuttle solid rocket booster aft skirt, forward skirt and frustum. Part 1: Summary report
[NASA-CR-184357] p 231 N93-11173
Preparation, optical and laser properties of Nd-doped sol-gel silica
[DE92-019378] p 461 N93-11602
Interpretation of experiments measuring the back face of thin aluminum strips by comparison with numerical simulations p 318 N93-12029
Study of the dynamic degradation under the action of a shock wave induced by pulsed laser
p 319 N93-12037
Saturation effects in absorption spectroscopy of the K(alpha) rays of aluminum p 254 N93-12042
Gain in a confined aluminum plasma
p 320 N93-12043
Experimental study of x ray laser in lithumoid aluminum p 321 N93-12045

ALUMINUM ALLOYS
Microstructure and mechanical properties of reactive hot isostatic pressed TiAl powder material
[GKSS-91/E/60] p 256 N93-11336
Titanium-aluminides by hot isostatic pressing of cold extruded titanium-aluminium powder mixtures
[GKSS-91/E/67] p 256 N93-11337
Corrosion resistant chromate conversion coatings for heat-treated aluminum alloys
[AD-D015366] p 266 N93-11425
Review of phonon behavior and microstructural development leading to martensitic transformations in Ni(x)Al(100-x) alloys
[DE92-014782] p 256 N93-11519
Environment-induced embrittlement: Stress corrosion cracking and metal-induced embrittlement; environmental embrittlement of iron aluminide alloys
[DE92-018714] p 256 N93-11524
The influence of processing atmosphere on twin-roll melt-spinning of aluminum alloys
[DE92-017895] p 257 N93-11595
Review of the physical and mechanical properties and potential applications of the B2 compound NiAl: Unabridged version of a paper published in International materials review
[NASA-TM-105598] p 258 N93-11635
Mechanical properties of semiconductors and their alloys
[AD-A253908] p 462 N93-11727
Acoustic measurement of the mechanical properties of thin material specimens
[AD-A253538] p 434 N93-11752
Infiltration kinetics and interfacial bond strength of metal matrix composites
[AD-A254002] p 240 N93-11795
Oxidation-sulfidation behavior of iron alloys containing 16 to 40 atomic percent aluminum
[DE92-017824] p 259 N93-11830
Micromechanisms of deformation and fracture in aluminum based MMC's: Interface effects
[AD-A253560] p 259 N93-11850
The effect of precipitate forming elements in Al 4.5 percent Mg alloys on the measured acoustic emission and on Lueders band deformation
[DE92-016864] p 465 N93-12073
Effect of microstructure on passive film formation and breakdown on Al alloys
[AD-A245863] p 260 N93-12118
Nature of the beta-phase of nickel-aluminum system
[AD-A254101] p 261 N93-12269
The effects of aluminum oxide on inertial welding of aluminum in space applications
[AD-A255100] p 329 N93-12274
Shear joint capability versus bolt clearance
[NASA-TM-108378] p 342 N93-12419
Processing and properties of NbTi based alloys
[DE92-016692] p 261 N93-12445
Spectrum fatigue behaviour of powder metallurgy aluminum alloys
[AD-A255060] p 262 N93-12468

ALUMINUM ARSENIDES
Excitons in semiconducting superlattices, quantum wells, and ternary alloys
[DE92-015178] p 464 N93-11894
Synthesis and characterization of novel aluminum-arsenic compounds 2. Crystal structures of (R2AlAs (SiMe3)2)2 (R = i-Bu, Me) and i-Bu2 (Cl)Al*As (SiMe3)3
[AD-A248001] p 467 N93-12175

ALUMINUM COATINGS
Polyethylene-terephthalate/aluminum adhesion
[ECL-91-33] p 257 N93-11578
A Taguchi experimental design study of twin-wire electric arc sprayed aluminum coatings
[DE92-018022] p 262 N93-12494

ALUMINUM GALLIUM ARSENIDES
Investigation of high efficiency monolithic multibandgap solar cells
[AD-A254326] p 348 N93-12144
Development of ultra-low noise, high sensitivity planar metal grating coupled AlGaAs/GaAs multiquantum well IR detectors for focal plane array staring IR sensor systems
[AD-A254697] p 468 N93-12228

ALUMINUM NITRIDES
CVD of AlN and SiC using cyclic organometallic precursors
[AD-A246910] p 266 N93-11413
High temperature oxidation protection of carbon/carbon composites
[REPT-921-430-105] p 239 N93-11589
Growth of solid solutions of aluminum nitride and silicon carbide by metalorganic chemical vapor deposition
[AD-A255000] p 254 N93-12518

ALUMINUM OXIDES
Silicon carbide fiber reinforced strontium aluminosilicate glass-ceramic matrix composite
[NASA-CASE-LEW-15263-1] p 239 N93-11543
Intermediate temperature electrolytes for SOFC
[DE92-018786] p 345 N93-11571
Study and characterization of ceramic-metal bonds manufactured by solid state bonding techniques. Application to Ag/Al2O3
[ECL-91-19] p 267 N93-11577

High temperature oxidation protection of carbon/carbon composites
[REPT-921-430-105] p 239 N93-11589
Proceedings of the DOE/Advanced Heat Exchangers Program Review
[DE92-014385] p 305 N93-12070
Numerical simulation of alumina spraying in argon-helium plasma jet
[DE92-017859] p 455 N93-12092
The effects of aluminum oxide on inertial welding of aluminum in space applications
[AD-A255100] p 329 N93-12274

ALUMINUM-LITHIUM ALLOYS
Long cycle life rechargeable lithium batteries
[NASA-CR-190937] p 291 N93-11604
Mechanisms of localized aqueous corrosion in aluminum-lithium-copper alloys p 259 N93-11895

AMIDES
Synthesis and reactivity of siloxide and silamide complexes pertaining to bond breaking and aggregation phenomena
[AD-A254703] p 468 N93-12231

AMMONIA
State-resolved reaction dynamics
[AD-A254291] p 436 N93-11196
The role of backbond strain in silicon surfaces on the decomposition of NH3 and PH3
[AD-A253771] p 250 N93-12062

AMMUNITION
Numerical computation of the lightning response of an earth-covered munitions storage bunker and comparison with experiments
[DE92-014268] p 367 N93-11236
Characterization of deflagrating munitions by rotating prism high speed photography
[MRL-TR-91-43] p 311 N93-11648
Rocket-triggered lightning test of an earth-covered munitions storage bunker
[DE92-016790] p 369 N93-11678

AMORPHOUS MATERIALS
Development of stable metallization systems
[AD-A253569] p 264 N93-11079
Synthesis and side chain liquid crystal polymers by living ring opening metathesis polymerization. 5: Influence of mesogenic group and interconnecting group on the thermotropic behavior of the resulting polymers
[AD-A253568] p 264 N93-11150
Recrystallization of amorphous or nanocrystalline NdBa2Cu3O(7-x) and GdBa2Cu3O(7-x)
[DE92-016302] p 462 N93-11706
Orientation, stress, and density distributions in injection-moulded amorphous polymers determined by optical techniques
[ETN-92-92271] p 269 N93-11983
Formation of buried epitaxial Si-Ge alloy layers in Si (100) crystal by high dose Ge ion implantation
[DE92-017114] p 466 N93-12127

AMORPHOUS SILICON
Microscopic origins of metastable effects in a-Si:H and deep defect characterization in a-Si,Ge:H alloys
[DE92-010588] p 463 N93-11813
Recombination and metastability in amorphous silicon and silicon germanium alloys
[DE92-010593] p 463 N93-11816
Research on stable, high-efficiency, amorphous silicon multijunction modules
[DE92-010599] p 464 N93-11818

AMPLIFICATION
Scaling of gain with energy spread and energy in the PEP FEL
[DE92-019248] p 316 N93-11500
Chinese Journal of Lasers (selected articles)
[AD-A254100] p 317 N93-11786
The diagnostics system for the multiple heavy ion beams induction linac experiment, MBE-4
[DE92-017109] p 445 N93-12126
Deployable reflector antenna performance optimization using automated surface correction and array-feed compensation
[NASA-TP-3228] p 222 N93-12543

AMPLITUDES
Application of the theory of wave propagation through random media to phase and amplitude fluctuations of seismic P-waves
[AD-A253274] p 363 N93-11788

ANAEROBES
Formic acid: Development of an analytical method and use as process indicator in anaerobic systems
[AD-A250668] p 253 N93-12267

ANALOG CIRCUITS
The adaptive neuron model: An architecture for the rapid learning of nonlinear topological transformations
[NASA-CASE-NPO-18579-1-CU] p 420 N93-11174
Analysis of fault-tolerant neurocontrol architectures
[NASA-TM-105898] p 215 N93-12305

ANALOG DATA
Fiber optic delay line signal processors
[AD-A254691] p 448 N93-12227

ANALOG SIMULATION
An analog macromodel of the SG1525A PWM for use with SPICE2G.6 simulators
[DE92-019423] p 291 N93-11639

ANALOG TO DIGITAL CONVERTERS
GaAs heterojunction device based A/D converter development
[AD-A252644] p 468 N93-12183
Curve fitting and error modeling for the digitization process near the Nyquist rate
[DE92-018189] p 286 N93-12417

ANALYSIS (MATHEMATICS)
Topics on RF beam control of a synchrotron
[DE92-019217] p 443 N93-11498

ANALYSIS OF VARIANCE
Change analysis and Fisher-Score change processes
[AD-A254707] p 429 N93-12334

ANALYTIC FUNCTIONS
Performance of the h-p version of the finite element method with various elements
[AD-A250689] p 427 N93-11837
Fixed points of expansive analytic maps (2)
[AD-A254737] p 344 N93-12357

ANALYTICAL CHEMISTRY
Formic acid: Development of an analytical method and use as process indicator in anaerobic systems
[AD-A250668] p 253 N93-12267

ANELASTICITY
Study of seismic coda generation in crust with non-uniform scattering and anelastic properties
[AD-A254350] p 366 N93-12270

ANGLE OF ATTACK
The hemisphere-cylinder at an angle of attack
p 196 N93-11250
The convection speed of the dynamic stall vortex
[AD-A247258] p 197 N93-11464
Correlation of forebody pressures and aircraft yawing moments on the X-29A aircraft at high angles of attack
[NASA-TM-4417] p 197 N93-11532
An experimental study of the relationship between forces and moments and vortex breakdown on a pitching delta wing p 208 N93-12206

ANGLES (GEOMETRY)
The effect of variable seat back angles on human response to +Gz impact accelerations
[AD-A250673] p 387 N93-11559

ANGULAR DISTRIBUTION
Foil optimization for low energy neutral atom imaging
[DE92-013435] p 365 N93-12263

ANGULAR VELOCITY
Methodology issues concerning the accuracy of kinematic data collection and analysis using the ariel performance analysis system
[NASA-CR-185689] p 389 N93-12211

ANILINE
Erasable optical information storage in the polyanilines
[AD-A254873] p 480 N93-12438

ANIMALS
Physiological analyses of the afferents controlling brain neurochemical systems
[AD-A253185] p 375 N93-11146
Scaling issues for biodiversity protection
[DE92-016689] p 375 N93-12315
An overview of gravitational physiology
[NASA-TM-102849] p 391 N93-12319

ANIONS
Near-IR absorption spectra for the C70 fullerene anions
[AD-A253658] p 246 N93-11280
Chronopotentiometry of refractory metals, actinides and oxyanions in molten salts: A review
[NASA-TM-105862] p 249 N93-11545
Threshold photodetachment spectroscopy of negative ions
[DE92-017090] p 440 N93-12100

ANISOTROPY
New singularity and existence of solutions in anisotropic, time-dependent, maximally Gauss-Bonnet extended gravity p 357 N93-11183
A new pitch angle diagnostic for electron cyclotron resonance plasma p 450 N93-11185
Methods of analysis for thick-section composite structures p 237 N93-11262

ANNEALING
Development of stable metallization systems
[AD-A253569] p 264 N93-11079
Formation of buried epitaxial Si-Ge alloy layers in Si (100) crystal by high dose Ge ion implantation
[DE92-017114] p 466 N93-12127
Processing and properties of NbTi based alloys
[DE92-016692] p 261 N93-12445

ANNIHILATION REACTIONS
Exciton kinetics in poly(di-n-hexylsilane)
[DE92-018278] p 283 N93-11800
High energy hadron-hadron collisions
[DE92-018253] p 441 N93-12224

ANNUAL VARIATIONS
Reinterpretation of ozone data from Base Roi Baudouin (Antarctica)
[AERONOMICA-ACTA-A-365] p 352 N93-11127
Lidar studies of gravity waves in the mesopause region p 358 N93-11222
The effects of magnetic storm phases on F-layer irregularities from auroral to equatorial latitudes
[AD-A253905] p 361 N93-11282
Surface wind speed distributions
[AD-A253268] p 368 N93-11505
The semiannual variation of great geomagnetic storms and the postshock Russell-McPherron effect preceding coronal mass ejecta
[AD-A254955] p 489 N93-12506

ANNULAR FLOW
An experimental investigation into flow induced acoustic resonances in an annular cascade
[PNR-90959] p 433 N93-11322

ANOMALIES
Effect of assembly anomalies on the strain response of composites in the sphere joint region of the DARPA man-rated demonstration article
[AD-A254204] p 240 N93-11739

ANTARCTIC REGIONS
Reinterpretation of ozone data from Base Roi Baudouin (Antarctica)
[AERONOMICA-ACTA-A-365] p 352 N93-11127

ANTENNA ARRAYS
Method of steering the gain of a multiple antenna global positioning system receiver
[AD-D015367] p 281 N93-11426
Optical generation, control and sensing of millimeter waves
[AD-A254700] p 285 N93-12230
Optical beamformer
[AD-A254354] p 448 N93-12272
Composite tasking for sensor arrays
[AD-A254997] p 287 N93-12512
Deployable reflector antenna performance optimization using automated surface correction and array-feed compensation
[NASA-TP-3228] p 222 N93-12543

ANTENNA COMPONENTS
Real-time adaptive sidelobe canceller architectures and implementations
[AD-A254842] p 286 N93-12433

ANTENNA DESIGN
Project and test of a reconfigurable multiple feed system in C-band
[MBB-UK-0162-92-PUB] p 278 N93-11009
Method of steering the gain of a multiple antenna global positioning system receiver
[AD-D015367] p 281 N93-11426
Method of moments analysis of symmetric dual reflector antennas with feeds
[AD-A255171] p 286 N93-12407

ANTENNA FEEDS
Project and test of a reconfigurable multiple feed system in C-band
[MBB-UK-0162-92-PUB] p 278 N93-11009
Method of moments analysis of symmetric dual reflector antennas with feeds
[AD-A255171] p 286 N93-12407

ANTENNA RADIATION PATTERNS
Antenna pattern measurement facilities
[AD-A250219] p 283 N93-11764
Extension of fresnel near-field region by single-cycle sinusoidal pulses
[AD-A254736] p 285 N93-12356
Deployable reflector antenna performance optimization using automated surface correction and array-feed compensation
[NASA-TP-3228] p 222 N93-12543

ANTENNAS
Antenna pattern measurement facilities
[AD-A250219] p 283 N93-11764
Extension of fresnel near-field region by single-cycle sinusoidal pulses
[AD-A254736] p 285 N93-12356

ANTHROPOMETRY
Astronaut candidate strength measurement using the Cybex 2 and the LIDO Multi-Joint 2 dynamometers
[NASA-CR-185679] p 389 N93-12195
Methodology issues concerning the accuracy of kinematic data collection and analysis using the ariel performance analysis system
[NASA-CR-185689] p 389 N93-12211

ANTIBODIES
Estimates of Human Immunodeficiency Virus (HIV) incidence and trends in the US Air Force p 377 N93-11292
Silent HIV infection p 378 N93-11293
Analysis of disease progression from clinical observations of US Air Force active duty members infected with the Human Immunodeficiency Virus: Distribution of AIDS survival time from interval censored observations p 379 N93-11297
Susceptibility in USAF recruits to vaccine preventable diseases p 380 N93-11301

ANTIDIURETICS
Effect of hemorrhage on cardiac output, vasopressin, aldosterone, and diuresis during immersion in men [NASA-TM-103949] p 374 N93-12014

ANTIGENS
Silent HIV infection p 378 N93-11293
Immunological parameters in current and former US Air Force personnel p 378 N93-11295
Early markers of HIV infection and subclinical disease progression p 379 N93-11296
Use of novel adjuvants and delivery systems to improve the humoral and cellular immune response to malaria vaccine candidate antigens p 381 N93-11308
Cytokines as vaccine adjuvants: Interleukin 1 and its synthetic peptide 163-171 p 382 N93-11309

ANTIINFECTIVES AND ANTIBACTERIALS
Clinical and immunological response to vaccination with parenteral or oral vaccines in two groups of 30 recruits p 381 N93-11305

ANTIKNOCK ADDITIVES
The intensity of knock in an internal combustion engine: An experimental and modeling study [DE92-019504] p 326 N93-11540

ANTIMISSILE DEFENSE
Lightweight Exoatmospheric Projectile (LEAP) test program. Supplemental environmental assessment [AD-A252286] p 231 N93-10998
Simulator, Tactical Use, Flare (STUF) project report [AD-A254890] p 276 N93-12281
Theory for a high power free electron laser and tactical applications [AD-A255161] p 323 N93-12405

APERTURES
Three-dimensional image structure in in-line Fraunhofer holography p 311 N93-11723

APEXES
Matching and vertex packing: How hard are they? [AD-A245928] p 423 N93-10991

APPLICATION SPECIFIC INTEGRATED CIRCUITS
An investigation of error correcting techniques for OMV and AXAF [NASA-CR-190950] p 416 N93-12515

APPLICATIONS PROGRAMS (COMPUTERS)
An interactive preprocessor for the NASA engine performance program [NASA-TM-105786] p 209 N93-10983
LV software support for supersonic flow analysis [NASA-CR-190209] p 297 N93-11074
Proceedings of the 14th International Conference on the Numerical Simulation of Plasmas [AD-A249095] p 451 N93-11275
Reserves information gathering system user's guide [DE92-018357] p 475 N93-11355
Operator's guide for VAXGAP, a gamma-ray spectrum analysis package [DE92-019096] p 407 N93-11356
An iconic query interface for an image database [AD-A253571] p 475 N93-11506
Concurrent file operations in a high performance FORTRAN [NASA-CR-189711] p 412 N93-11618
A rule-based system for real-time analysis of control systems [NASA-TM-104258] p 277 N93-11619
Numerical analysis of the flow fields in a RQL gas turbine combustor [DE92-017509] p 302 N93-11767
An embedded rule-based diagnostic expert system in Ada p 392 N93-11928
Space Communication Artificial Intelligence for Link Evaluation Terminal (SCAILET) p 395 N93-11940
The development and technology transfer of software engineering technology at NASA. Johnson Space Center p 396 N93-11943
Micromechanical combined stress analysis: MICSTRAN, a user manual [NASA-CR-189694] p 243 N93-12306

APPROXIMATION
Stochastic control and nonlinear estimation [AD-A253543] p 420 N93-11147
An approximate solution of the fixed gravimetric boundary value problem in the interior and the exterior of the Earth's body [SER-C-379] p 361 N93-11331
Some numerical results on best uniform polynomial approximation of chi(sup alpha) on interval (0,1) [DE92-014859] p 426 N93-11520

AQUEOUS SOLUTIONS
Synthesis of nanocrystalline powders for oxide ceramics by microwave plasma pyrolysis [DE92-017410] p 268 N93-11861

ARABSAT
Lessons drawn from 2 existing satellite networks: ARABSAT and EUTELSAT. Application to the Pacific basin projects [REPT-921-440-101] p 282 N93-11591

ARC JET ENGINES
Numerical modeling of a vortex stabilized arcjet p 232 N93-11889
The 10 kW power electronics for hydrogen arcjets [NASA-TM-105614] p 235 N93-12484

ARC SPRAYING
Comprehensive computational model for thermal plasma processing [DE92-018015] p 454 N93-12066
Numerical simulation of alumina spraying in argon-helium plasma jet [DE92-017859] p 455 N93-12092
A Taguchi experimental design study of twin-wire electric arc sprayed aluminum coatings [DE92-018022] p 262 N93-12494

ARC WELDING
Development of an intelligent system for cooling rate and fill control in GMAW [DE92-017849] p 326 N93-11548
Ultrasonic sensing of GMAW: Laser/EMAT defect detection system [DE92-017916] p 333 N93-12055
Study of residual stresses and microcracks in high strength steel weldments: An investigation of microcrack formation and stressed growth using laser microscopy [AD-A255059] p 342 N93-12467
The collaborative program of research in engineering sciences [DE92-016838] p 490 N93-12477

ARCHITECTURE (COMPUTERS)
QR decomposition based algorithms and architectures for least-squares adaptive filtering [RSRE-MEMO-4562] p 408 N93-11390
Geometrical concepts about learning rules in networks with binary and ternary output functions [REPT-92-020] p 411 N93-11592
A VMEbus ultrasonic sensor controller for mapping and servo control in robotic systems [DE92-013661] p 421 N93-12138
Complex cognitive information processing: A computational architecture with a connectionist implementation [AD-A254041] p 422 N93-12259
Analysis of fault-tolerant neurocontrol architectures [NASA-TM-105898] p 215 N93-12305
Design of a lattice-based faceted classification system p 415 N93-12385
Formal specification of the VIPER microprocessor in HOL [RSRE-90009] p 405 N93-12430

ARGON
Thermomechanical fatigue behavior of SiC/Ti-24Al-11Nb in air and argon environments [NASA-TM-105723] p 238 N93-11399
Experimental study of interactions of highly charged ions with atoms at keV energies [DE92-019512] p 436 N93-11541
Nonlinear behavior of resonant absorption in a plasma at microwave frequency p 319 N93-12032
Numerical simulation of alumina spraying in argon-helium plasma jet [DE92-017859] p 455 N93-12092
The effects of aluminum oxide on inertial welding of aluminum in space applications [AD-A255100] p 329 N93-12274

ARITHMETIC
Reduction operations on a distributed memory machine with a reconfigurable interconnection network p 410 N93-11484

ARIZONA
Key wintertime meteorological features of the Grand Canyon and the Colorado Plateaus Basin [DE92-019134] p 369 N93-11657

ARMATURES
Railgun armature velocity improvement, SBIR phase 2 [AD-A254749] p 222 N93-12505

ARMED FORCES (FOREIGN)
Dramatic reduction of meningococcal meningitis among military recruits in Italy after introduction of specific vaccination p 380 N93-11303

ARMED FORCES (UNITED STATES)
Viral hepatitis in the US Air Force, 1980 - 1989 p 377 N93-11287
Estimates of Human Immunodeficiency Virus (HIV) incidence and trends in the US Air Force p 377 N93-11292
Immunological parameters in current and former US Air Force personnel p 378 N93-11295
Neuropsychiatric morbidity in early HIV disease: Implications for military occupational function p 379 N93-11299
Susceptibility in USAF recruits to vaccine preventable diseases p 380 N93-11301
Introduction to training decisions modeling technologies: The training decisions system [AD-A249862] p 387 N93-12252

ARMOR
Studies of a laser/nuclear thermal hardened body armor [AD-A255128] p 390 N93-12423

AROUSAL
Physiological analyses of the afferents controlling brain neurochemical systems [AD-A253185] p 375 N93-11146

ARTIFICIAL INTELLIGENCE
On understanding in communicating systems and the error in the Chinese Room thought-experiment [RSRE-MEMO-4391] p 278 N93-10977
Ontology of mind, subjective ontology, and the example of temporal expressions [REPT-92-018] p 386 N93-11212
ALECSYS and the AutonoMouse: Learning to control a real robot by distributed classifier systems [REPT-92-011] p 420 N93-11227
From pilot's associate to satellite controller's associate p 390 N93-11922
A model-based reasoning approach to sensor placement for monitorability p 391 N93-11923
Integration of task level planning and diagnosis for an intelligent robot p 393 N93-11929
Intelligent diagnostics systems p 393 N93-11931
Design development of a neural network-based telemetry monitor p 394 N93-11933
Intelligent data management for real-time spacecraft monitoring p 394 N93-11936
Operator assistant to support deep space network link monitor and control p 288 N93-11939
Space Communication Artificial Intelligence for Link Evaluation Terminal (SCAILET) p 395 N93-11940
System diagnostic builder p 396 N93-11944
An integrated dexterous robotic testbed for space applications p 330 N93-11972
Automation and robotics for COLUMBUS: An implementation concept for the free flying laboratory (MTFF) p 331 N93-11974
A smart end-effector for assembly of space truss structures p 230 N93-11982
Real-time classification of signals from three-component seismic sensors using neural nets [DE92-014886] p 364 N93-12155
Adaptive neural network models for intelligent computations [AD-A254689] p 421 N93-12226

ARTIFICIAL SATELLITES
Orbital perturbations due to the albedo effect [GKSS-91/E/59] p 220 N93-11348
Forecasting the relativistic electron flux at geosynchronous orbit [AD-A254016] p 226 N93-12064

ASCENT TRAJECTORIES
Effect of inert propellant injection on Mars ascent vehicle performance [NASA-CR-189238] p 226 N93-12152
On stability and control of SSTO spaceplane in super- and hypersonic ascending phase [NAL-TR-1128T] p 216 N93-12361

ASIA
Crustal and upper mantle velocity gradients in the vicinity of the East Kazakh test site [AD-A246889] p 362 N93-11740
ONRASIA scientific information bulletin, volume 17, number 3 [AD-A255073] p 490 N93-12470

ASPHERICITY
Laser surface profilometer with sub-Angstrom resolution [DE92-018926] p 317 N93-12011

ASSEMBLER ROUTINES
The VISTA structured assembler [RSRE-91034] p 407 N93-11341

ASSEMBLIES
Temperature tracking SPICE macro-model for laser and LED driven opto-coupler assemblies [DE92-019296] p 411 N93-11599

ASSEMBLING
Effect of assembly anomalies on the strain response of composites in the sphere joint region of the DARPA man-rated demonstration article [AD-A254204] p 240 N93-11739

Backward assembly planning with DFA analysis
[NASA-CASE-NPO-18817-1-CU] p 278 N93-12202

Assembling polyhedra with single translations
[AD-A254623] p 419 N93-12239

ASSESSMENTS

Advanced materials in gas turbine engines: An assessment
[PNR-90946] p 211 N93-11105

ASSIMILATION

Validation test report for the first-generation dart Gulf Stream forecasting system
[AD-A254286] p 373 N93-11821

ASTHMA

Epidemiologic view of allergic diseases in North America: Implications for aerospace medicine
p 382 N93-11311

The screening of inhalant allergic diseases in the selection of candidates for aircraft piloting
p 382 N93-11312

Phadiatop: A screening test for inhalant allergy
p 383 N93-11313

In vivo and in vitro diagnosis of allergic respiratory disease during screening procedures in the Italian Navy: Comparative evaluation of a recent quantitative automatized enzyme immunoassay method to dose specific IgE p 383 N93-11314

Asthma in aircrew: Assessment, treatment and disposition p 383 N93-11315

Allergic and nonallergic rhinitis in Greek pilots
p 383 N93-11317

ASTRONAUTS

Residual acceleration data on IML-1: Development of a data reduction and dissemination plan
[NASA-CR-190807] p 223 N93-11101

ASTRONOMICAL CATALOGS

National Space Science Data Center data archive and distribution service (NDADS) automated retrieval mail system user's guide
[NASA-TM-107990] p 479 N93-12150

ASTRONOMICAL PHOTOMETRY

Far ultraviolet spectrophotometry of hot stars and calibration standards in the far ultraviolet
p 482 N93-11373

ASTRONOMICAL POLARIMETRY

Near-infrared imaging polarimetry of bipolar nebulae
p 481 N93-11248

ASTRONOMICAL SPECTROSCOPY

A search for low-luminosity objects
[AD-A253301] p 483 N93-11750

ASTRONOMY

ESIS: An introduction to the European space information system. A modern tool for space scientists
[ESA-INT-2] p 479 N93-12404

ASTROPHYSICS

Morphology and physics of supernova remnants
p 482 N93-11476

Publications of the Executive Office of the President, 20 January 1989 - 31 March 1992
[PB92-154913] p 477 N93-11769

Controls Astrophysics and Structures Experiment in Space (CASES) advanced studies and planning
[NASA-CR-184410] p 220 N93-12213

ESIS: An introduction to the European space information system. A modern tool for space scientists
[ESA-INT-2] p 479 N93-12404

ASYMPTOTIC METHODS

Stochastic control and nonlinear estimation
[AD-A253543] p 420 N93-11147

Asymptotic analysis of reacting materials with saturated explosion. 2: High-frequency waves
[AD-A254473] p 275 N93-12236

Fluid-structure interaction using retarded potential and ABAQUS
[AD-A254735] p 307 N93-12355

ASYMPTOTIC SERIES

Limit theorems for Fisher-score change processes
p 427 N93-12328

ATMOSPHERIC BOUNDARY LAYER

The use of ARM data to test an improved parameterization of upper tropospheric clouds for use in climate models
[DE92-014353] p 367 N93-11237

Structure of the nocturnal boundary layer over a complex terrain
[DE92-018141] p 362 N93-11669

Atmospheric dispersion in mountain valleys and basins
p 355 N93-11920

ATMOSPHERIC CHEMISTRY

Lunar and Martian environmental interactions with nuclear power system radiators
[NASA-TM-105747] p 230 N93-10965

Scientific assessment of ozone depletion: 1991
[NASA-TM-107976] p 350 N93-11087

Tropospheric processes: Observations and interpretation p 351 N93-11092

Future chlorine-bromine loading and ozone depletion
p 352 N93-11095

The relative importance of sulfur and nitrogen compounds in the acidification of freshwater
[DE92-016899] p 354 N93-11680

Atmospheric reactive nitrogen: A model study of natural and anthropogenic sources and the role of microbial soil emissions
[DE92-010717] p 354 N93-11744

Theoretical study of the radiative and kinetic properties of selected metal oxides and air molecules
[AD-A251090] p 438 N93-11804

Proceedings of the Sixteenth Annual Climate Diagnostics Workshop
[PB92-198803] p 370 N93-11896

Laser spectroscopy and dynamics of transient species formed in pyrolysis reactions
[DE92-016206] p 251 N93-12091

Stratospheric aircraft: Impact on the stratosphere?
[DE92-016997] p 355 N93-12104

Multiangle lidar performance in the presence of horizontal inhomogeneities in atmospheric extinction and scattering
[AD-A252882] p 371 N93-12167

Stratospheric aircraft exhaust plume and wake chemistry studies
[NASA-CR-189688] p 366 N93-12299

ATMOSPHERIC CIRCULATION

Radiative forcing of climate p 351 N93-11094

The forcing of a mid-latitude upper-tropospheric jet streak by a simulated mesoscale convective system
p 358 N93-11184

The use of ARM data to test an improved parameterization of upper tropospheric clouds for use in climate models
[DE92-014353] p 367 N93-11237

Studies of the role of clouds in CO2-induced climate change
[DE92-018648] p 353 N93-11569

Studies of ocean predictability at decade to century time scales using a global ocean general circulation model in a parallel competing environment
[DE92-019457] p 373 N93-11642

Key wintertime meteorological features of the Grand Canyon and the Colorado Plateaus Basin
[DE92-019134] p 369 N93-11657

Modeling the dispersion of tracer plumes in the Colorado front range boundary layer during night- and day-time conditions
[DE92-019384] p 354 N93-11676

An inversion technique to recover lower thermospheric winds from space-borne remote measurements of (OI) 5577 A p 369 N93-11839

Dynamics of planetary waves in the atmosphere
p 363 N93-11898

Atmospheric dispersion in mountain valleys and basins
p 355 N93-11920

ATMOSPHERIC COMPOSITION

Scientific assessment of ozone depletion: 1991
[NASA-TM-107976] p 350 N93-11087

Source gases: Concentrations, emissions, and trends
p 350 N93-11088

Ozone and temperature trends p 350 N93-11089

Heterogeneous processes: Laboratory, field, and modeling studies p 350 N93-11090

Stratospheric processes: Observations and interpretation p 351 N93-11091

Future chlorine-bromine loading and ozone depletion
p 352 N93-11095

Predicted aircraft effects on stratospheric ozone
p 352 N93-11096

Predicted rocket and shuttle effects on stratospheric ozone p 352 N93-11097

International Conference on the Role of the Polar Regions in Global Change: Proceedings, volume 1
[DE92-013652] p 353 N93-11232

International Conference on the Role of the Polar Regions in Global Change: Proceedings, volume 2
[DE92-013653] p 353 N93-11233

Studies of the role of clouds in CO2-induced climate change
[DE92-018648] p 353 N93-11569

The potential effects of concurrent increases in temperature, CO2 and O3 on net photosynthesis, as mediated by rubisCO
[DE92-019411] p 374 N93-11630

Tenth International Symposium on Environmental Biogeochemistry
[DE92-016200] p 355 N93-11864

A comprehensive mission to planet Earth: Woods Hole Space Science and Applications Advisory Committee Planning Workshop
[NASA-TM-108011] p 343 N93-11878

Research on stimulated Raman scattering with applications to atmospheric lidar p 322 N93-12163

ATMOSPHERIC DENSITY

Lidar studies of gravity waves in the mesopause region p 358 N93-11222

ATMOSPHERIC EFFECTS

The sensitivity of the receiver coherence diameter and modulation transfer function to variations of a damp unstable atmosphere
[AD-A253269] p 363 N93-11785

Dynamics of space debris p 219 N93-11904

ATMOSPHERIC ELECTRICITY

Numerical computation of the lightning response of an earth-covered munitions storage bunker and comparison with experiments
[DE92-014268] p 367 N93-11236

Temporal monitoring of VHF and LF atmospherics and their relation to lightning
[AD-A252617] p 371 N93-12180

ATMOSPHERIC ENTRY

Erosion mechanisms in ceramic structures
[MBB-UK-0171-92-PUB] p 263 N93-11011

ATMOSPHERIC GENERAL CIRCULATION MODELS

Studies of ocean predictability at decade to century time scales using a global ocean general circulation model in a parallel competing environment
[DE92-019457] p 373 N93-11642

An inversion technique to recover lower thermospheric winds from space-borne remote measurements of (OI) 5577 A p 369 N93-11839

ATMOSPHERIC HEAT BUDGET

A composite study of the Madden-Julian oscillation
[AD-A254269] p 369 N93-11819

ATMOSPHERIC HEATING

The forcing of a mid-latitude upper-tropospheric jet streak by a simulated mesoscale convective system
p 358 N93-11184

ATMOSPHERIC MODELS

Stratospheric processes: Observations and interpretation p 351 N93-11091

Radiative forcing of climate p 351 N93-11094

Future chlorine-bromine loading and ozone depletion
p 352 N93-11095

Numerical and observational investigations of long-lived, MCS-induced, severe surface wind events: The derecho
p 367 N93-11159

Modeling the Jovian aurora
[NASA-CR-190696] p 486 N93-11164

A problem formulation for glideslope tracking in wind shear using advanced robust control techniques
[NASA-TM-104164] p 214 N93-11176

The use of ARM data to test an improved parameterization of upper tropospheric clouds for use in climate models
[DE92-014353] p 367 N93-11237

The Kalman filter for two-dimensional stable and unstable atmospheres p 359 N93-11249

Studies of the role of clouds in CO2-induced climate change
[DE92-018648] p 353 N93-11569

Studies of ocean predictability at decade to century time scales using a global ocean general circulation model in a parallel competing environment
[DE92-019457] p 373 N93-11642

Atmospheric dispersion in mountain valleys and basins
p 355 N93-11920

Visualizing wind velocities by advecting cloud textures
[DE92-014717] p 371 N93-12154

The vertical distribution of heating in the tropical atmosphere
[AD-A254982] p 372 N93-12507

ATMOSPHERIC MOISTURE

Time scales characterizing the processing of water and cloud condensation nuclei by clouds
[CM-80] p 368 N93-11340

A composite study of the Madden-Julian oscillation
[AD-A254269] p 369 N93-11819

ATMOSPHERIC PHYSICS

Proceedings of the Sixteenth Annual Climate Diagnostics Workshop
[PB92-198803] p 370 N93-11896

ESIS: An introduction to the European space information system. A modern tool for space scientists
[ESA-INT-2] p 479 N93-12404

ATMOSPHERIC RADIATION

Atlas of albedo and absorbed solar radiation derived from Nimbus 7 earth radiation budget data set, November 1985 to October 1987
[NASA-RP-1281] p 367 N93-11168

ATMOSPHERIC SCATTERING

The design, development, and test of balloonborne and groundbased lidar systems. Volume 3: Groundbased lidar systems
[AD-A247552] p 317 N93-11805

Research on stimulated Raman scattering with applications to atmospheric lidar p 322 N93-12163

The design, development, and test of balloonborne and groundbased lidar systems. Volume 1: Balloonborne coherent CO2 lidar system
[AD-A247551] p 322 N93-12262
Foil optimization for low energy neutral atom imaging
[DE92-013435] p 365 N93-12263
Low energy neutral atom imaging
[DE92-013531] p 365 N93-12264
Gamma ray astronomy
[NASA-CR-184447] p 483 N93-12348
Global change and the dark of the moon
[AD-A255181] p 486 N93-12380

ATMOSPHERIC SOUNDING
The Transall campaign. A contribution to the German ozone research program
[REPT-37/91] p 349 N93-11082

ATMOSPHERIC TEMPERATURE
Sodium-lidar mesosphere examinations: Selected elements of the experimental construction of a mobile instrument and evaluation of the data acquired with a stationary Na-lidar during the DYANA campaign
[BONN-IR-91-78] p 357 N93-11006
Ozone and temperature trends p 350 N93-11089
An inversion technique to recover lower thermospheric winds from space-borne remote measurements of (OI) 5577 A p 369 N93-11839
Analysis of air and sea physical properties and surface fluxes using a combination of in situ and SEASAT data
p 365 N93-12182
The vertical distribution of heating in the tropical atmosphere
[AD-A254982] p 372 N93-12507

ATMOSPHERIC TURBULENCE
A problem formulation for glideslope tracking in wind shear using advanced robust control techniques
[NASA-TM-104164] p 214 N93-11176
Electron energization in the topside auroral ionosphere: On the importance of ion-acoustic turbulence
p 360 N93-11269
A theory for the analysis of rotorcraft operating in atmospheric turbulence p 207 N93-11725
Atmospheric dispersion in mountain valleys and basins
p 355 N93-11920

ATMOSPHERIC WINDOWS
CO2 laser frequency doubling
[AD-A251060] p 314 N93-10997

ATOMIC BEAMS
Investigation of a cesium Raman time/frequency standard
[AD-A252677] p 310 N93-11562
Matter-wave interferometry with laser cooled atoms
[AD-A253999] p 316 N93-11737

ATOMIC CLOCKS
Investigation of a cesium Raman time/frequency standard
[AD-A252677] p 310 N93-11562

ATOMIC ENERGY LEVELS
Theory of small metal clusters, films, and wires
[AD-A253120] p 256 N93-11240
Electron terms and radiation from crystals
[AD-A254353] p 468 N93-12271

ATOMIC EXCITATIONS
Connected triple excitations in coupled-cluster calculations of hyperpolarizabilities: Neon
p 439 N93-11854

ATOMIC PHYSICS
Matter-wave interferometry with laser cooled atoms
[AD-A253999] p 316 N93-11737
The 1989 Scientific Report of the Laboratory for the Use of High Power Lasers
[ETN-92-92175] p 317 N93-12023
Modeling for the study of an X laser in a recombination plasma; gain calculations at 105.7 and 154.6 A
p 321 N93-12046
Summaries of FY 1991 research in the chemical sciences
[DE92-011920] p 251 N93-12135

ATOMIC RECOMBINATION
Direct radiative recombination of atomic ions
p 321 N93-12048

ATOMIC STRUCTURE
Theory of small metal clusters, films, and wires
[AD-A253120] p 256 N93-11240
Electronic structure and reactivities of transition metal clusters
[DE92-016623] p 258 N93-11762
Atomic structure of Ni-like soft x ray lasing ions
[DE92-019273] p 438 N93-11778
Theoretical studies of high-temperature superconductors and highly compressed hydrogen
p 292 N93-11833
Atomic structure and spectral perturbations in dense and hot plasmas p 321 N93-12049
Workshop on Adhesion and Intermolecular Forces
[AD-A255191] p 272 N93-12276

ATOMIZING
Physical processes involved in injection and atomization of liquid propellants p 248 N93-11453

ATTITUDE (INCLINATION)
Development of a tactile perceived attitude transducer
[AD-A253724] p 385 N93-11081

ATTITUDE CONTROL
Spacecraft attitude control using a smart control system p 230 N93-11932
Fuzzy logic control for camera tracking system
p 314 N93-11935

AUDIO EQUIPMENT
High Capacity Voice Recorder (HCVR) Operational Test and Evaluation (OT/E) integration test report
[DOT/FAA/CT-TN92/30] p 310 N93-11460

AUDIO FREQUENCIES
Feasibility assessment of a transient sound sensor based on the silicon retina architecture
[AD-A252288] p 432 N93-10999

AUDITORY PERCEPTION
Auditory perception
[AD-A255061] p 385 N93-12469

AUDITORY SIGNALS
Super auditory localization for improved human-machine interfaces
[AD-A254699] p 389 N93-12229

AUGER EFFECT
Electron emission during multicharged ion-metal surface interactions
[DE92-017134] p 439 N93-11849

AUGER SPECTROSCOPY
Signal-to-noise assessment and measurement in spectroscopies with particular reference to Auger and x ray photoelectron spectroscopies
[NPL-DMM(A)-45] p 247 N93-11396

AUGMENTATION
Heat transfer enhancement by chaotic mixing
[PB92-190305] p 470 N93-11469

AURORAL ARCS
EISCAT observations of strong ion outflows from the F-region ionosphere during auroral activity: Preliminary results p 360 N93-11267

AURORAL IONIZATION
Ionospheric response to particle precipitation within aurora
[IRF-SR-208] p 359 N93-11265
Observations of thin auroral ionization layers by EISCAT in connection with pulsating aurora p 359 N93-11266
EISCAT observations of strong ion outflows from the F-region ionosphere during auroral activity: Preliminary results p 360 N93-11267
EISCAT observations of topside ionospheric ion outflows during auroral activity: Revisited p 360 N93-11268
On the origin of ion acoustic turbulence in the auroral topside ionosphere p 361 N93-11273

AURORAL SPECTROSCOPY
Modeling the Jovian aurora
[NASA-CR-190696] p 486 N93-11164
The role of proton precipitation in Jovian aurora: Theory and observation p 487 N93-11165

AURORAL ZONES
Lyman alpha line shapes from electron impact H2 dissociative processes in the Jovian auroral zone
p 487 N93-11166
Ionospheric response to particle precipitation within aurora
[IRF-SR-208] p 359 N93-11265
Comment on 'EISCAT Radar Observations of Enhanced Incoherent Scatter Spectra and Their Relation to Auroral Luminosity and Field-Aligned Currents' by P. N. Collis et al. p 360 N93-11271
Scattering of electromagnetic waves from a plasma: Enhanced ion acoustic fluctuations due to ion-ion two-stream instabilities p 361 N93-11272
On the origin of ion acoustic turbulence in the auroral topside ionosphere p 361 N93-11273
The effects of magnetic storm phases on F-layer irregularities from auroral to equatorial latitudes
[AD-A253905] p 361 N93-11282

AURORAS
Diffusion of Echo 7 electron beams during bounce motion
[DE92-018288] p 357 N93-10985
Modeling the Jovian aurora
[NASA-CR-190696] p 486 N93-11164
The role of proton precipitation in Jovian aurora: Theory and observation p 487 N93-11165
Multispectral observations of the Jovian aurora
p 487 N93-11167
Ionospheric response to particle precipitation within aurora
[IRF-SR-208] p 359 N93-11265
EISCAT observations of strong ion outflows from the F-region ionosphere during auroral activity: Preliminary results p 360 N93-11267
EISCAT observations of topside ionospheric ion outflows during auroral activity: Revisited p 360 N93-11268
Electron energization in the topside auroral ionosphere: On the importance of ion-acoustic turbulence
p 360 N93-11269
Publication of papers presented at URSI 23rd General Assembly as a special section of radio science
[AD-A253561] p 283 N93-11811

AUSTENITE
Heat-affected zone cracking of nitronic 60 stainless steel
[DE92-018286] p 254 N93-10984

AUSTENITIC STAINLESS STEELS
The mechanical and microstructural stability of austenitic stainless steels strengthened by MC-forming elements
[DE91-015314] p 259 N93-11857

AUTOIONIZATION
Progress toward x ray lasing between autoionizing transitions
[DE92-017428] p 317 N93-11765
Multiphoton ionization and ion-pair formation in molecular hydrogen
[DE92-019026] p 438 N93-11829

AUTOMATIC CONTROL
Description of the SSF PMAD DC testbed control system data acquisition function
[NASA-TM-105843] p 417 N93-11005
An autonomous vehicle: Constrained test and evaluation
[PB92-205608] p 325 N93-11427
Integrity in automated information systems
[AD-A253990] p 477 N93-11732
Direct manipulation and intermittent automation in advanced cockpits
[AD-A253814] p 388 N93-11784
Integrity-oriented control objectives: Proposed revisions to the Trusted Computer System Evaluation Criteria (TCSEC), DOD 5200.28-STD
[AD-A253989] p 404 N93-11809
Automatic Attenuation/Phase Calibration System (AAPCS)
[DE92-017354] p 284 N93-11917
Requirements and opportunities for satellite autonomy
p 230 N93-11926
Intelligent fault management for the Space Station active thermal control system p 391 N93-11930
Autoguidance video sensor for docking
p 230 N93-11954
Automation and robotics for COLUMBUS: An implementation concept for the free flying laboratory (MTFF) p 331 N93-11974
Habitat automation p 391 N93-11976

AUTOMATIC FLIGHT CONTROL
Automatic control laws for aircraft in parabolic flight
[DILC-EST-TR-211] p 214 N93-11160

AUTOMATIC FREQUENCY CONTROL
Self-tuning PI-PID regulators for stable systems with varying delay
[REPT-92-023] p 421 N93-11593
A PID auto-tuning algorithm based on relay feedback
[REPT-92-019] p 421 N93-11667

AUTOMATIC PILOTS
Advanced control for the design of STT missile autopilot
[REPT-921-320-102] p 215 N93-11585

AUTOMATION
Human performance in complex task environments: A basis for the application of adaptive automation
[AD-A255067] p 390 N93-12486

AUTOMOBILE FUELS
The intensity of knock in an internal combustion engine: An experimental and modeling study
[DE92-019504] p 326 N93-11540
Federal Alternative Fuel Program light duty vehicle operation
[DE92-018124] p 274 N93-11794
Alternative Fuel Evaluation Program: Alternative Fuel Light Duty Vehicle Project. Data collection responsibilities, techniques, and test procedures
[DE92-010598] p 275 N93-12171

AUTOMOBILES
Modeling and identification of flexible joints in vehicle structures p 324 N93-11261
An autonomous vehicle: Constrained test and evaluation
[PB92-205608] p 325 N93-11427
Reduction in global warming due to fuel economy improvements and emissions control of criteria pollutants: New US light-duty vehicles (1968-1991)
[DE92-016636] p 356 N93-12314

AUTONOMY
ALECSYS and the AutonoMouse: Learning to control a real robot by distributed classifier systems
[REPT-92-011] p 420 N93-11227

Implementing system simulation of C3 systems using autonomous objects
[NASA-CR-190845] p 283 N93-11716
Research on a reconfigurable modular manipulator system
[DE92-018943] p 327 N93-11865
Role of automation in the ACRV operations
p 230 N93-11977

AVIATION METEOROLOGY
Proceedings of the National Weather Service Aviation Workshop: Postprint volume
[PB92-176148] p 369 N93-11803

AVIATION PSYCHOLOGY
Human performance in complex task environments: A basis for the application of adaptive automation
[AD-A255067] p 390 N93-12486

AVIONICS
The future of carrier aviation
[AD-A254043] p 430 N93-12260
Integration of radar altimeter, precision navigation, and digital terrain data for low-altitude flight
[NASA-TM-103958] p 205 N93-12320

AXIAL FLOW TURBINES
Three-dimensional turbopump flowfield analysis
[NASA-CR-190978] p 308 N93-12539

AXISYMMETRIC BODIES
Fourier continuum finite elements for nonlinear structural analysis p 340 N93-12210

AXISYMMETRIC FLOW
Numerical calculations of an axisymmetric laminar diffusion flame with detailed and reduced reaction mechanisms p 246 N93-11259

B

BACKGROUND NOISE
A model to estimate the flux of background particles expected to accumulate on the collector foils of the interstellar gas experiment on the long duration exposure facility spacecraft
[AD-A254265] p 489 N93-11815

BACKGROUND RADIATION
Contributions to the Joint Discussion 3: Results from Rosat and GRO and Other Recent High Energy Astrophysics Missions of the Max-Planck-Institut fuer Extraterrestrische Physik
[MPE-PREPRINT-215] p 482 N93-11473
Rosat deep surveys p 482 N93-11474

BACKSCATTERING
Detection of cloud-top height from backscattered radiances within the oxygen A band. Part 1: Theoretical study
[GKSS-91/E/76-PT-1] p 368 N93-11349
Detection of cloud-top height from backscattered radiances within the oxygen A band. Part 2: Measurements
[GKSS-91/E/77-PT-2] p 368 N93-11350
The design, development, and test of balloonborne and groundbased lidar systems. Volume 3: Groundbased lidar systems
[AD-A247552] p 317 N93-11805
Stimulated Brillouin backscattering instability in the case of a high power laser: Application to wave pulsation particle acceleration experiments p 317 N93-12024
Observation and analysis of the Stokes and anti-Stokes components of stimulated Raman backscattering
p 318 N93-12025
Multiangle lidar performance in the presence of horizontal inhomogeneities in atmospheric extinction and scattering
[AD-A252882] p 371 N93-12167
The design, development, and test of balloonborne and groundbased lidar systems. Volume 1: Balloonborne coherent CO2 lidar system
[AD-A247551] p 322 N93-12262

BACTERIA
Ultrafast photoinduced electron transfer reactions in supramolecular arrays: From charge separation and storage to molecular switches
[DE92-016186] p 465 N93-12090
Microbiological analysis of debris from STS-42 IML-1 by direct plating of rinse waters
[NASA-TM-108375] p 375 N93-12174

BAINITE
Relationship of bainitic microstructure to impact toughness in Cr-Mo and Cr-W steels
[DE92-017828] p 258 N93-11773

BALLISTICS
AGARD flight test techniques series. Volume 10: Weapon delivery analysis and ballistic flight testing
[AGARD-AG-300-VOL-10] p 430 N93-11711

BALLOON-BORNE INSTRUMENTS
The design, development, and test of balloonborne and groundbased lidar systems. Volume 3: Groundbased lidar systems
[AD-A247552] p 317 N93-11805
The design, development, and test of balloonborne and groundbased lidar systems. Volume 1: Balloonborne coherent CO2 lidar system
[AD-A247551] p 322 N93-12262

BAND STRUCTURE OF SOLIDS
Image potential states at metal-dielectric interfaces
[DE92-017019] p 466 N93-12124

BANDWIDTH
10 kW L-band amplifier tubes for efficient and reliable troposcatter communication transmitter systems
[AD-A253246] p 290 N93-11504
Real-time data compression using a FFT digital signal processor
[DE92-017744] p 477 N93-11770
Impact of finite frequency deviation on the performance of dual-filter heterodyne FSK lightwave systems
[AD-A247611] p 448 N93-11892
Josephson Junction digital waveform generation for very wideband radars
[AD-A253668] p 467 N93-12169
Real-time adaptive sidelobe canceller architectures and implementations
[AD-A254842] p 286 N93-12433

BARIUM OXIDES
Recrystallization of amorphous or nanocrystalline NdBa2Cu3O(7-x) and GdBa2Cu3O(7-x)
[DE92-016302] p 462 N93-11706
Infrared phonon structure in epitaxial films of Tl2Ca2Ba2Cu3O10 at low temperatures
[DE92-017078] p 466 N93-12109

BARIUM TITANATES
Nanostructure, defect chemistry and properties of relaxor ferroelectrics
[AD-A247294] p 431 N93-11468

BAROCLINIC INSTABILITY
The Kalman filter for two-dimensional stable and unstable atmospheres p 359 N93-11249

BAROCLINITY
The Kalman filter for two-dimensional stable and unstable atmospheres p 359 N93-11249

BAROTROPISM
The Kalman filter for two-dimensional stable and unstable atmospheres p 359 N93-11249

BARRIER LAYERS
Multi-layer light-weight protective coating and method for application
[NASA-CASE-LAR-14448-1] p 269 N93-11912

BARS
A consistent cracked bar vibration theory
p 339 N93-12000

BASE FLOW
Numerical investigations into the base drag of various wedges using the base flow model developed by Mauri Tanner
[REPT-B-36] p 202 N93-12414

BASES (CHEMICAL)
Basicity and optical basicities of slags
[NPL-DMM(A)-48] p 447 N93-11408

BATTERY CHARGERS
Laboratory testing of the electrosource traction battery
[DE92-017993] p 292 N93-12057

BAYES THEOREM
Incorporating prior probabilities and misclassification costs into network training: An example from medical prognosis
[RSRE-MEMO-4343] p 428 N93-10980
Algorithms for sensor fusion: Decentralized Bayesian hypothesis testing with feedback, volume 1
[AD-A254633] p 414 N93-12242
Automatic cloud classification from multi-spectral satellite data
[AD-A255125] p 372 N93-12420

BEAM CURRENTS
Higher-order-mode damping and microwave absorption at 2 K
[DE92-016960] p 442 N93-11077
Static and transient beam loading of a synchrotron
[DE92-019244] p 445 N93-11776
The diagnostics system for the multiple heavy ion beams induction linac experiment, MBE-4
[DE92-017109] p 445 N93-12126

BEAM INJECTION
Analysis of periodic transient beam loading of the AGS
[DE92-019243] p 443 N93-11499
Propagation of relativistic high current electron beams across the geomagnetic field
[DE92-018276] p 362 N93-11564
RF beam loading in the Brookhaven AGS with booster injection
[DE92-019452] p 444 N93-11641
Beam-plasma interactions and radiation generation during the ejection of electron and ion beams in space
[AD-A253993] p 224 N93-11736
Static and transient beam loading of a synchrotron
[DE92-019244] p 445 N93-11776

BEAM INTERACTIONS
Using the 16 viewscreens during commissioning of AmPS
[NIKHEF-K/AMPS/92-01] p 442 N93-11131
Topics on RF beam control of a synchrotron
[DE92-019217] p 443 N93-11498
Alternating-phase focusing: A model to study nonlinear dynamics
[DE92-019027] p 431 N93-11511

BEAM NEUTRALIZATION
Divergence in intense ion beams caused by incomplete charge neutralization
[DE92-016891] p 445 N93-12103

BEAM SPLITTERS
CO2 laser frequency doubling using AgGaSe2
[RSRE-MEMO-4528] p 315 N93-11388

BEAM WAVEGUIDES
High frame-rate, large field wavefront sensor
[DE92-019547] p 310 N93-11542
A single beam laser tracker as an alignment tool
[DE92-017746] p 316 N93-11691

BEAMFORMING
Optical beamformer
[AD-A254354] p 448 N93-12272
Pre-compression of bunch length in the SLC damping rings
[DE92-018154] p 446 N93-12497

BEAMS (RADIATION)
Using the 16 viewscreens during commissioning of AmPS
[NIKHEF-K/AMPS/92-01] p 442 N93-11131
Topics on RF beam control of a synchrotron
[DE92-019217] p 443 N93-11498
Scaling of gain with energy spread and energy in the PEP FEL
[DE92-019248] p 316 N93-11500
Beam-loading stability in synchrotrons with a higher RF harmonic
[DE92-018982] p 443 N93-11510
Computational aspects of Gaussian beam migration
[DE92-018641] p 431 N93-11567
RF beam loading in the Brookhaven AGS with booster injection
[DE92-019452] p 444 N93-11641
A single beam laser tracker as an alignment tool
[DE92-017746] p 316 N93-11691

BEAMS (SUPPORTS)
Analysis of precracking parameters and fracture toughness for ceramic single-edge-precracked-beam specimens
[NASA-TM-105568] p 263 N93-10962
Structural dynamics of large space structures having parametric uncertainties p 225 N93-11836
A consistent cracked bar vibration theory
p 339 N93-12000
The effect of contact stresses in four-point bend testing of graphite/epoxy and graphite/PMR-15 composite beams
[NASA-TM-105891] p 241 N93-12076

BEARINGS
Maximum life spiral bevel reduction design
[NASA-TM-105790] p 323 N93-10982
Optimal output feedback vibration control of rotor-bearing systems p 324 N93-11220

BEND TESTS
Mixed mode bending test of the interlaminar fracture toughness of carbon/epoxy
[FFA-TN-1992-04] p 237 N93-11128
The effect of contact stresses in four-point bend testing of graphite/epoxy and graphite/PMR-15 composite beams
[NASA-TM-105891] p 241 N93-12076
Study of residual stresses and microcracks in high strength steel weldments: An investigation of microcrack formation and stressed growth using laser microscopy
[AD-A255059] p 342 N93-12467

BENDING VIBRATION
Studies in control for vibration suppression of the UWAA 20-bay planar truss
[AD-A250193] p 341 N93-12253

BENZENE
Positive ion chemistry of acetylene and methylacetylene clusters. Formation of benzene and C(sub 2n)H(sub 2n)(+) ions via intracluster polymerization reactions
[AD-A250931] p 236 N93-12177

BERNSTEIN ENERGY PRINCIPLE
Nonlinear effects of ICRF power on drift wave stability and transport in tokamaks, task 1
[DE92-018488] p 453 N93-11729

BETA PARTICLES
High beta and confinement studies on TFTR
[DE92-018647] p 452 N93-11568
BETATRONS
A synopsis of resistive wall effects in very short wavelength free electron lasers
[DE92-018065] p 315 N93-11155
BIAS
Back-gate bias generator
[AD-A255126] p 295 N93-12421
BIBLIOGRAPHIES
Catalog of data bases and reports
[DE92-018586] p 473 N93-10990
Bibliography of publications from the Texas A and M Sea Grant College Program, 1968-1992
[PB92-205517] p 372 N93-11253
Information dissemination: Case studies on electronic dissemination at four agencies. Fact sheet for the Chairman, Committee on Governmental Affairs, US Senate
[GAO/IMTEC-92-6FS] p 474 N93-11274
Materials science and engineering at the Naval Research Laboratory: Research programs and 1990 publications
[PB92-199488] p 238 N93-11422
Climate change and water supply, management and use: A literature review
[DE92-019069] p 353 N93-11655
Publications on acoustics research at the Langley Research Center, January 1987 - September 1992
[NASA-TM-107674] p 435 N93-12080
Energy efficient drivepower: Literature reference list: Culled references
[PB92-199181] p 294 N93-12192
Energy efficient drivepower: Literature reference list. Volume 1: General user's supplement
[PB92-199157] p 294 N93-12294
Energy efficient drivepower: Literature reference list. Volume 2: Design engineer's supplement
[PB92-199165] p 295 N93-12295
BICRYSTALS
High frequency response from YBa2Cu3O(7-x) Josephson devices on SrTiO3 bicrystal substrates
[NPL-DES-118] p 459 N93-11394
Elastic stresses, twin boundaries, and fatigue cracking
p 338 N93-11890
BINARY ALLOYS
Determination of parameters of a new method for predicting alloy properties
[NASA-TM-105895] p 257 N93-11609
Calculation of binary phase diagrams between the actinide elements, rare earth elements, and transition metal elements
[DE92-019119] p 249 N93-11801
BINARY MIXTURES
Liquid-liquid equilibria in binary systems: Monte-Carlo simulation for calculating the effect of nonrandom mixing
[DE92-017020] p 263 N93-10972
Computer simulations for the adsorption of polymers onto surfaces
[DE92-018942] p 267 N93-11628
BINARY STARS
Detection of a white dwarf in a visual binary system
[NASA-CR-190856] p 481 N93-11075
BIOASTRONAUTICS
Residual acceleration data on IML-1: Development of a data reduction and dissemination plan
[NASA-CR-190807] p 223 N93-11101
Space flight and immune system p 376 N93-11284
An overview of gravitational physiology
[NASA-TM-102849] p 391 N93-12319
BIOCHEMICAL OXYGEN DEMAND
Geographic information system to support state-wide hydrologic modeling with the SCS-TR-20
[PB92-185768] p 476 N93-11700
BIOCHEMISTRY
Physiological analyses of the afferents controlling brain neurochemical systems
[AD-A253185] p 375 N93-11146
Magnetic resonance elucidation of molecule/macromolecule interaction stereochemistry
[AD-A253030] p 437 N93-11709
Advanced methods for structural characterization of large multiply charged ions: Obtaining charge state determination and improved sensitivity
[DE91-015264] p 441 N93-12117
BIOCONVERSION
Biological conversion of synthesis gas culture development
[DE92-001279] p 375 N93-12482
BIODEGRADATION
Formic acid: Development of an analytical method and use as process indicator in anaerobic systems
[AD-A250668] p 253 N93-12267
Biological conversion of synthesis gas culture development
[DE92-001279] p 375 N93-12482
BIODYNAMICS
Exploratory Research and Development Fund, FY 1990
[DE92-017002] p 489 N93-11078
The effect of variable seat back angles on human response to +Gz impact accelerations
[AD-A250673] p 387 N93-11559
Astronaut candidate strength measurement using the Cybex 2 and the LIDO Multi-Joint 2 dynamometers
[NASA-CR-185679] p 389 N93-12195
Methodology issues concerning the accuracy of kinematic data collection and analysis using the ariel performance analysis system
[NASA-CR-185689] p 389 N93-12211
BIOELECTRICITY
An introduction to the information processing components of the brain
[RSRE-MEMO-4350] p 385 N93-10979
Cellular and molecular pathways of extremely-low-frequency electromagnetic field interactions with living systems
[DE92-019084] p 282 N93-11515
BIOFEEDBACK
Effects of spatially displaced feedback on remote manipulation tasks p 400 N93-11966
The development of system components to provide proprioceptive and tactile information to the human for future telepresence systems p 330 N93-11968
BIOGEOCHEMISTRY
Tenth International Symposium on Environmental Biogeochemistry
[DE92-016200] p 355 N93-11864
BIOINSTRUMENTATION
Radio pill antenna range test
[DE92-019903] p 282 N93-11661
BIOLOGICAL EFFECTS
Ultraviolet radiation changes p 352 N93-11098
Cellular and molecular pathways of extremely-low-frequency electromagnetic field interactions with living systems
[DE92-019084] p 282 N93-11515
The potential effects of concurrent increases in temperature, CO2 and O3 on net photosynthesis, as mediated by rubisCO
[DE92-019411] p 374 N93-11630
Radiation physics, biophysics, and radiation biology
[DE92-013673] p 375 N93-12266
BIOLOGICAL EVOLUTION
The search for life's origins: Progress and future directions in planetary biology and chemical evolution
[NASA-CR-190929] p 487 N93-11603
BIOLOGICAL MODELS (MATHEMATICS)
Bionics and problems of instrument manufacture
[AD-A254461] p 314 N93-12517
BIOLUMINESCENCE
Parameters for predicting red tides of bioluminescent dinoflagellates: Meteorological events and frontal water circulation patterns
[AD-A254835] p 374 N93-12431
BIOMASS
Estimation of photosynthetic capacity using MODIS polarization: 1988 proposal to NASA Headquarters
[NASA-TM-103945] p 344 N93-12351
BIOMASS ENERGY PRODUCTION
Electricity from biomass: A development strategy
[DE92-010590] p 346 N93-11814
BIOMEDICAL DATA
Fifth Annual Workshop on Space Operations Applications and Research (SOAR 1991), volume 1
[NASA-CP-3127-VOL-1] p 391 N93-11921
BIONICS
Bionics and problems of instrument manufacture
[AD-A254461] p 314 N93-12517
BIOPHYSICS
Exploratory Research and Development Fund, FY 1990
[DE92-017002] p 489 N93-11078
Radiation physics, biophysics, and radiation biology
[DE92-013673] p 375 N93-12266
BIOREACTORS
Formic acid: Development of an analytical method and use as process indicator in anaerobic systems
[AD-A250668] p 253 N93-12267
Biological conversion of synthesis gas culture development
[DE92-001279] p 375 N93-12482
BIOSPHERE
Ultraviolet radiation changes p 352 N93-11098
Global Climate Change (GCC) issues and their impacts on the US Army Corps of Engineers
[AD-A247279] p 353 N93-11466
BIOSYNTHESIS
Formic acid: Development of an analytical method and use as process indicator in anaerobic systems
[AD-A250668] p 253 N93-12267
BIOTELEMETRY
Radio pill antenna range test
[DE92-019903] p 282 N93-11661
BIPOLAR TRANSISTORS
GaAs heterojunction device based A/D converter development
[AD-A252644] p 468 N93-12183
BIPOLARITY
Near-infrared imaging polarimetry of bipolar nebulae
p 481 N93-11248
BIREFRINGENCE
Orientation, stress, and density distributions in injection-moulded amorphous polymers determined by optical techniques
[ETN-92-92271] p 269 N93-11983
The peculiar rheo-optical behaviour of bisphenol-A-polycarbonate and polymethylmethacrylate
p 269 N93-11984
The time-dependent stress-optical behaviour of polycarbonate in the glass transition region
p 269 N93-11985
The measurement and calculation of birefringence in quenched polycarbonate specimens
p 269 N93-11986
Molecular orientation induced by cooling stresses in polycarbonate. 1: Free quenching p 269 N93-11987
Molecular orientation induced by cooling stresses in polycarbonate. 2: Constrained quench and injection moulding p 270 N93-11988
Measurement of the density distributions in quenched polycarbonate specimens by a quantitative Schlieren-optical technique p 270 N93-11989
Analysis of the birefringence distributions in compact discs of polycarbonate p 270 N93-11991
BISMALEIMIDE
Generation of thermal strains in carbon fibre-reinforced bismaleimide (PMR-15) composites, part 1, 2 and 3
[PNR-90976-PT-1-2-3] p 236 N93-11065
Curing and mechanical properties of T800-V398 graphite/bismaleimide at different temperatures
[DLR-FB-92-02] p 237 N93-11143
Molecular mobility of the interface in a model composite: A NMR study
[AD-A253311] p 265 N93-11194
BISMUTH OXIDES
Properties of hot isostatically pressed Bi(2)Sr(1.7)CaCu(2)O(x)
[DE92-016394] p 460 N93-11522
Intermediate temperature electrolytes for SOFC
[DE92-018786] p 345 N93-11571
A study of parameters that influence growth and stability of the (Bi(1-x)Pb(x))2 Sr2Ca2Cu3O(y) phase
[DE92-015187] p 462 N93-11703
Superconducting multilayer structures grown by ALL-MBE
[DE92-018011] p 465 N93-12065
BISPHENOLS
The peculiar rheo-optical behaviour of bisphenol-A-polycarbonate and polymethylmethacrylate
p 269 N93-11984
The time-dependent stress-optical behaviour of polycarbonate in the glass transition region
p 269 N93-11985
BIT ERROR RATE
SITE project. Phase 1: Continuous data bit-error-rate testing
[NASA-TP-3279] p 224 N93-11001
BIVARIATE ANALYSIS
Interactive analysis of gappy bivariate time series using AGSS
[AD-A255160] p 429 N93-12426
BLACK HOLES (ASTRONOMY)
Temporal and spectral variability in luminous x ray binaries p 483 N93-12336
BLADE TIPS
A concept for a counterrotating fan with reduced tone noise
[NASA-TM-105736] p 433 N93-11370
Effects of cooling-air injection on secondary flows and losses in a turbine cascade
[NAL-TR-1121T] p 307 N93-12382
BLADE-VORTEX INTERACTION
A study of the wall-pressure fluctuations downstream of a blade-wall junction
[ECL-91-07] p 299 N93-11363
Unsteady propeller/wing aerodynamic interactions
p 201 N93-12190
BLASIUS FLOW
Nonlinear stability of flows over rigid and flexible boundaries p 198 N93-11874

BLOCK COPOLYMERS
Synthesis and side chain liquid crystal polymers by living ring opening metathesis polymerization. 5: Influence of mesogenic group and interconnecting group on the thermotropic behavior of the resulting polymers [AD-A253568] p 264 N93-11150
BLOCKING
CFD modeling of turbulent flows around the SSME main injector assembly using porosity formulation [NASA-CR-184359] p 297 N93-11171
An experimental study of flow patterns and endwall heat transfer upstream of a surface-mounted rectangular obstruction in a turbulent boundary layer p 302 N93-11698
Tradeoffs in implementing primary-backup protocols [NASA-CR-190970] p 472 N93-12212
BLOOD
Early markers of HIV infection and subclinical disease progression p 379 N93-11296
BLOOD CELLS
Freeze-dried human red blood cells [AD-A253295] p 376 N93-11193
BLOOD CIRCULATION
Freeze-dried human red blood cells [AD-A253295] p 376 N93-11193
BLOOD PLASMA
Silent HIV infection p 378 N93-11293
Carboxyalkylated hemoglobin as a potential blood substitute [AD-A252329] p 384 N93-11561
BLOOD VOLUME
Effect of hemorrhage on cardiac output, vasopressin, aldosterone, and diuresis during immersion in men [NASA-TM-103949] p 374 N93-12014
BLOWING
Experimental investigation of the effects of aft blowing with various nozzle exit geometries on a 3.0 caliber tangent ogive at high angles of attack: Forebody pressure distributions [NASA-CR-190935] p 197 N93-11605
Leading edge film cooking heat transfer including the effect of mainstream turbulence p 199 N93-11886
An investigation of the effects of aft blowing on a 3.0 caliber tangent ogive body at high angles of attack [NASA-CR-190934] p 200 N93-12004
BLUNT LEADING EDGES
Leading edge film cooking heat transfer including the effect of mainstream turbulence p 199 N93-11886
BODY CENTERED CUBIC LATTICES
Development of strength and conductivity in deformation processed copper base alloys [DE92-018807] p 257 N93-11572
Determination of parameters of a new method for predicting alloy properties [NASA-TM-105895] p 257 N93-11609
BODY KINEMATICS
Methodology issues concerning the accuracy of kinematic data collection and analysis using the ariel performance analysis system [NASA-CR-185689] p 389 N93-12211
BODY SIZE (BIOLOGY)
Astronaut candidate strength measurement using the Cybex 2 and the LIDO Multi-Joint 2 dynamometers [NASA-CR-185679] p 389 N93-12195
BODY TEMPERATURE
Effectiveness of NASA 1032 and 1035 and Air Force 1030 and 1034 units in protection against cold water hypothermia [AD-A255120] p 389 N93-12291
BODY-WING CONFIGURATIONS
Aerothermal test results from the second flight of the Pegasus booster [NASA-TM-4391] p 296 N93-10969
Low-speed longitudinal and lateral-directional aerodynamic characteristics of the X-31 configuration [NASA-TM-4351] p 198 N93-11622
BOLOMETERS
Submillimeter and microwave residual losses in epitaxial films of Y-Ba-Cu-O and Bl-Ca-Ca-Cu-O [DE92-017075] p 466 N93-12125
High temperature superconductor materials and applications [NASA-CR-184426] p 470 N93-12396
BOLTS
The technical background to standards for eyebolts [NPL-DMM(A)-52] p 325 N93-11327
The mechanism of bolt loading [NASA-TM-108377] p 342 N93-12412
Shear joint capability versus bolt clearance [NASA-TM-108378] p 342 N93-12419
BOLTZMANN TRANSPORT EQUATION
Using NEKTON to solve systems of discrete Boltzmann equations [DE92-018272] p 303 N93-11799
BONDING
Preconversion catalytic deoxygenation of phenolic functional groups [DE92-018304] p 244 N93-10986
Corrosion protection of materials for aircraft using ion beam processes. Corrosion and bonding strength examinations. Physical analysis of laser composition [MBB-Z-0405-91-PUB] p 255 N93-11026
An interlayer shear slip theory for composite laminates with nonrigid bonding p 237 N93-11229
Infiltration kinetics and interfacial bond strength of metal matrix composites [AD-A254002] p 240 N93-11795
MMIC GaAs bonding investigation [AD-A254773] p 470 N93-12464
BOOSTER ROCKET ENGINES
Feasibility of using neutron radiography to inspect the Space Shuttle solid rocket booster aft skirt, forward skirt and frustum. Part 1: Summary report [NASA-CR-184357] p 231 N93-11173
Booster rocket range safety system [AD-D015363] p 221 N93-11428
Space Transportation Booster Engine Configuration Study. Volume 3: Program Cost estimates and work breakdown structure and WBS dictionary [NASA-CR-184458] p 233 N93-12088
Space transportation booster engine configuration study. Volume 2: Design definition document and environmental analysis [NASA-CR-184459] p 234 N93-12441
Space transportation booster engine configuration study. Volume 1: Executive Summary [NASA-CR-184457] p 235 N93-12523
BORN APPROXIMATION
Surface reconstruction of a three-dimensional ultrasonic flaw [DE92-018029] p 332 N93-11154
Seismic wave propagation in thinly-layered media with steep reflectors [DE92-015619] p 364 N93-12142
BORON CARBIDES
The effects of bypass air on boron carbide combustion in a solid fuel ramjet p 245 N93-11136
Implanted He retention and release from boronized layers [DE92-013983] p 464 N93-11842
BOSONS
Survey of composite particle models of electroweak interaction [DE92-017110] p 441 N93-12111
Relativistic condensate and cosmology p 486 N93-12330
BOUNDARIES
Elastic stresses, twin boundaries, and fatigue cracking p 338 N93-11890
BOUNDARY CONDITIONS
An adaptive differencing scheme for elliptic flows p 297 N93-11197
Boundary condition methods in the numerical solution of the Navier-Stokes equations with the application to free surface problems [ISBN-0-315-64278-5] p 298 N93-11241
The generalized Goursat-Riemann problem for plane waves in isotropic elastic solids p 340 N93-12199
Light scattering from a sphere on or near an interface p 448 N93-12531
BOUNDARY ELEMENT METHOD
Experimental validation of boundary element methods for noise prediction [NASA-TM-105729] p 323 N93-10966
Numerical study for the study of medium speed internal noise problems [DILC-EST-TN-200] p 432 N93-11156
Numerical solution of inverse problems in mechanics using the boundary element method p 424 N93-11199
Application of the boundary element method to elastic wave scattering problems in ultrasonic nondestructive evaluation p 332 N93-11209
Fundamental solutions and boundary element formulations for convective fluid flow p 298 N93-11217
Numerical simulation for the coaxial electromagnetic launcher using hybrid potentials with FE-BE method p 222 N93-11726
Fluid-structure interaction using retarded potential and ABAQUS [AD-A254735] p 307 N93-12355
BOUNDARY INTEGRAL METHOD
Quasigeostrophic vortices in zonal shear p 358 N93-11226
BOUNDARY LAYER CONTROL
Overview of supersonic laminar flow control research on the F-16XL ships 1 and 2 [NASA-TM-104257] p 196 N93-11221
A wind tunnel investigation to determine buffet countermeasures for STOL aircraft alpha-sweep flight testing [NAL-TR-1129] p 216 N93-12362
BOUNDARY LAYER EQUATIONS
On the instability of hypersonic flow past a pointed cone: Comparison of theoretical and experimental results of Mach 18 [DLR-FB-92-02] p 196 N93-11141
Thermokinetic modelling and hypersonic flow [DILC-EST-TN-218] p 196 N93-11157
Carbon/carbon composition ablation effects on ionized boundary layers [AD-A254465] p 242 N93-12235
BOUNDARY LAYER FLOW
Increase of energy use on cooled high temperature turbine, phase 3 [MTUM-B91EW-0029-PHASE-3] p 213 N93-11339
Boundary layer relaminarization device [NASA-CASE-LAR-14470-1] p 199 N93-11876
Application of a two-layer near wall model to fully developed and rotating channel turbulent flows [NASA-CR-184441] p 305 N93-12082
BOUNDARY LAYER SEPARATION
The hemisphere-cylinder at an angle of attack p 196 N93-11250
Effects of sweep on the physics of unsteady shock-induced turbulent separated flows [AD-A247035] p 198 N93-11742
The aerodynamics of curved jets and breakaway in Coanda flares, volumes 1 and 2 p 304 N93-11881
BOUNDARY LAYER STABILITY
Laminar boundary-layer breakdown [AD-A254489] p 306 N93-12162
BOUNDARY LAYER TRANSITION
Progress in developing a transition model for high-speed flows p 301 N93-11615
Studies in nonlinear problems of energy [DE92-018551] p 345 N93-11733
On the Goertler instability of boundary layers [NAL-TR-1120T] p 307 N93-12374
BOUNDARY LAYERS
Turbulence modeling in shock wave/turbulent boundary layer interactions [NASA-CR-190933] p 301 N93-11606
Flight test results from a supercritical mission adaptive wing with smooth variable camber [NASA-TM-4415] p 207 N93-11863
Boundary layer relaminarization device [NASA-CASE-LAR-14470-1] p 199 N93-11876
Laboratory and numerical studies of dynamical processes related to thermal convection in the Earth's mantle p 364 N93-11900
An engineering method for interactive inviscid-boundary layers in three-dimensional hypersonic flows p 203 N93-12529
Light scattering from a sphere on or near an interface p 448 N93-12531
BOUNDARY VALUE PROBLEMS
Quasigeostrophic vortices in zonal shear p 358 N93-11226
An approximate solution of the fixed gravimetric boundary value problem in the interior and the exterior of the Earth's body [SER-C-379] p 361 N93-11331
On the definition and calculation of effective impedances and averaged boundary conditions with application to the analysis of high complexity frequency selective surfaces [RSRE-MEMO-4518] p 281 N93-11387
Resolution of the pressure equation by the boundary element method. Application to multistage turbomachines [ECL-91-16] p 301 N93-11575
The generalized Goursat-Riemann problem for plane waves in isotropic elastic solids p 340 N93-12199
BOW WAVES
Theoretical research program to study chemical reactions in AOTV bow shock tubes [NASA-CR-188927] p 439 N93-11851
BRAGG ANGLE
Interaction of sound with sound by novel mechanisms: Ultrasonic four-wave mixing mediated by a suspension and ultrasonic three-wave mixing at a free surface [AD-A254657] p 435 N93-12097
BRAIN
Physiological analyses of the afferents controlling brain neurochemical systems [AD-A253185] p 375 N93-11146
BRAKES (FOR ARRESTING MOTION)
Payout tension control system for reel mounted cable [AD-D015362] p 325 N93-11423
BRAYTON CYCLE
A gas-cooled cermet reactor system for planetary base power [DE92-018017] p 443 N93-11433

Advanced heat pump for the recovery of volatile organic compounds
[DE92-011592] p 303 N93-11774

BRAZIL
The structure and transport of the Brazil current between 27 deg and 36 deg south
[AD-A247635] p 374 N93-12247

BREADBOARD MODELS
Advanced mechanisms for robotics
p 330 N93-11969

BREMSSTRAHLUNG
Application of the Moyer method to transverse shielding of linear Bremsstrahlung sources
[DE92-017027] p 443 N93-11493
Bremsstrahlung absorption in plasmas
p 321 N93-12047

BRIGHTNESS DISTRIBUTION
Near-infrared imaging polarimetry of bipolar nebulae
p 481 N93-11248

BRILLOUIN EFFECT
Stimulated Brillouin backscattering instability in the case of a high power laser: Application to wave pulsation particle acceleration experiments p 317 N93-12024

BRITTLE MATERIALS
Deep penetration into frictional ductile and brittle materials
[PB92-205566] p 338 N93-11903

BRITTLENESS
Deep penetration into frictional ductile and brittle materials
[PB92-205566] p 338 N93-11903

BROADBAND
Broadband EMP transient measurement preemphasis filter
[AD-A254414] p 284 N93-12160
Josephson Junction digital waveform generation for very wideband radars
[AD-A253668] p 467 N93-12169
Fiber optic delay line signal processors
[AD-A254691] p 448 N93-12227

BROADCASTING
Direct Broadcast Satellite: Radio Program
[NASA-TM-105910] p 224 N93-11430

BROKEN SYMMETRY
Relativistic condensate and cosmology
p 486 N93-12330

BROMIDES
Chemistry of lower valent actinide halides
[DE92-017031] p 251 N93-12105

BROMINE COMPOUNDS
Ozone depletion and chlorine loading potentials
p 351 N93-11093

BUBBLES
Modelling the behaviour of gas bubbles in epoxy resin
[PNR-90961] p 264 N93-11084
Pressure and noise induced by a cavitating marine screw propeller
[VTT-PUBS-87] p 299 N93-11360
Particle-fluid two-phase flow modeling
[DE92-017847] p 301 N93-11637
An analytic description of thick-wall bubbles
[DE92-016465] p 432 N93-11759
Bubble dissolving in turbulent pipe flow
[AD-A252927] p 308 N93-12462

BUCKLING
On the stability of confined shells under external pressure p 335 N93-11202
Crashworthy characteristics of circular tubes in axisymmetric buckling p 337 N93-11721

BUCKMINSTERFULLERENE
The adsorption of C60 and the co-adsorption of C60 and H2O on (alpha)-Al2O3 (1 -1 0 2)-(2x1)
[DE92-018002] p 465 N93-12093

BUFFER STORAGE
Deriving and manipulating module interfaces
[AD-A253869] p 406 N93-11145
Simulation and analysis of support hardware for multiple instruction rollback
[NASA-CR-190972] p 406 N93-12541

BUFFETING
Further buffeting tests in a cryogenic wind tunnel
[NASA-TM-107621] p 198 N93-11610
Flight test results from a supercritical mission adaptive wing with smooth variable camber
[NASA-TM-4415] p 207 N93-11863
A wind tunnel investigation to determine buffet countermeasures for STOL aircraft alpha-sweep flight testing
[NAL-TR-1129] p 216 N93-12362

BUILDINGS
Data report 92-1. Brorfelde Geomagnetic Observatory magnetic results, 1990 p 362 N93-11699

BULK MODULUS
Acoustic measurement of the mechanical properties of thin material specimens
[AD-A253538] p 434 N93-11752

BUNCHING
Topics on RF beam control of a synchrotron
[DE92-019217] p 443 N93-11498
Analysis of periodic transient beam loading of the AGS
[DE92-019243] p 443 N93-11499
Beam-loading stability in synchrotrons with a higher RF harmonic
[DE92-018982] p 443 N93-11510
Analysis of the prebuncher for the KEK 40-MeV proton linac
[DE92-514988] p 444 N93-11525
RF beam loading in the Brookhaven AGS with booster injection
[DE92-019452] p 444 N93-11641
Pre-compression of bunch length in the SLC damping rings
[DE92-018154] p 446 N93-12497

BUOYS
Dredging research program: Feasibility of a kinematic differential Global Positioning System
[AD-A248953] p 205 N93-11419
Translating wedge heat sink
[AD-D015357] p 293 N93-12133

BURNS (INJURIES)
Mechanisms of immune failure in burn injury
p 376 N93-11285

BURSTS
Pressure vessel burst test program
[AD-A253708] p 334 N93-11080

BUS CONDUCTORS
An optical fiber multi-terminal data bus system for aircraft
[NAL-TR-1125] p 209 N93-12370

BYPASS RATIO
The effects of bypass air on boron carbide combustion in a solid fuel ramjet p 245 N93-11136

BYPASSES
The effects of bypass air on boron carbide combustion in a solid fuel ramjet p 245 N93-11136

C

C (PROGRAMMING LANGUAGE)
Optimization of expressions involving array classes
[DE92-019421] p 411 N93-11536
Reengineering using a data abstraction based specification language
[AD-A254726] p 414 N93-12341

C BAND
Project and test of a reconfigurable multiple feed system in C-band
[MBB-UK-0162-92-PUB] p 278 N93-11009

C-160 AIRCRAFT
The Transall campaign. A contribution to the German ozone research program
[REPT-37/91] p 349 N93-11082

CABLES (ROPES)
The theoretical background to BS7167: 1990 - specification for Bordeaux connections
[NPL-DMM(A)-50] p 325 N93-11324
Payout tension control system for reel mounted cable
[AD-D015362] p 325 N93-11423

CADMIUM
VUV and UV sources and spectroscopic applications
[AD-A247293] p 291 N93-11758

CADMIUM TELLURIDES
Excitons in semiconducting superlattices, quantum wells, and ternary alloys
[DE92-015178] p 464 N93-11894
Electronic and optical properties of perfect and imperfect 2 to 6 superlattices p 465 N93-11996

CAFFEINE
Smoking status and body composition, exercise, dietary intake, and alcohol/caffeine consumption
[AD-A250648] p 385 N93-11893

CALCIUM
The structures, binding energies and vibrational frequencies of Ca3 and Ca4: An application of the CCSD(T) method p 439 N93-11852

CALCIUM OXIDES
Properties of hot isostatically pressed Bi(2)Sr(1.7)CaCu(2)O(x)
[DE92-016394] p 460 N93-11522
A study of parameters that influence growth and stability of the (Bi(1-x)Pb(x))2 Sr2Ca2Cu3O(y) phase
[DE92-015187] p 462 N93-11703
Superconducting multilayer structures grown by ALL-MBE
[DE92-018011] p 465 N93-12065
Infrared phonon structure in epitaxial films of Tl2Ca2Ba2Cu3O10 at low temperatures
[DE92-017078] p 466 N93-12109
Submillimeter and microwave residual losses in epitaxial films of Y-Ba-Cu-O and Bi-Ca-Ca-Cu-O
[DE92-017075] p 466 N93-12125

CALIBRATING
Kinetics of diffusional droplet growth in a liquid/liquid two-phase system
[NASA-CR-190805] p 297 N93-11142
A survey of European calibration facilities for underwater acoustics
[NPL-RSA(EXT)-32] p 433 N93-11328
Far ultraviolet spectrophotometry of hot stars and calibration standards in the far ultraviolet
p 482 N93-11373
Acoustic emission monitoring of HFIR vessel during hydrostatic testing
[DE92-019316] p 332 N93-11601
EUROMET project no. 231: Uncertainties in mass measurement. NPL's analysis of data from the calibration of weight set NPLW43
[NPL-MOM-107] p 432 N93-11666
Calibration techniques for high flux x ray detectors
[DE92-017513] p 312 N93-11768
Evaluation of advanced pressure sensor technology
[DE92-011004] p 312 N93-11806
Automatic Attenuation/Phase Calibration System (AAPCS)
[DE92-017354] p 284 N93-11917
Operator assistant to support deep space network link monitor and control p 288 N93-11939

CALIFORNIA
Modeling regional seismic waves
[AD-A246894] p 361 N93-11421

CALORIMETERS
The electron-beam water calorimeter project at the National Physical Laboratory
[NPL-RSA(EXT)-30] p 310 N93-11410
Development of a scintillating optical fiber ionization calorimeter
[NASA-CR-184415] p 311 N93-11662
Operating experience using venturi flow meters at liquid helium temperature
[DE92-014693] p 313 N93-12140

CAMERA SHUTTERS
Shutter apparatus
[AD-D015350] p 309 N93-11049

CAMERAS
An autonomous vehicle: Constrained test and evaluation
[PB92-205608] p 325 N93-11427
Fuzzy logic control for camera tracking system
p 314 N93-11935
Autoguidance video sensor for docking
p 230 N93-11954
Final Report, January 1991 - July 1992
[AD-A254659] p 483 N93-12244

CAMS
Thermal non-Newtonian elastohydrodynamic lubrication of line contacts under sliding-rolling and simple sliding conditions p 324 N93-11263

CANADA
United States/Canada Air Quality Agreement
[PB92-228030] p 356 N93-12525

CANCELLATION
System and method for cancelling expansion waves in a wave rotor
[NASA-CASE-LEW-15218-1] p 297 N93-11172

CANCER
Clinical types of Hepatitis B p 376 N93-11286

CANOPIES
Evaluation of alternatives for increasing A-7D rearward visibility
[AD-A255071] p 208 N93-12488

CANTILEVER BEAMS
The use of high-frequency dynamic information for the evaluation of damage in fiber reinforced composite materials p 241 N93-11998

CAPACITANCE
Measurement of AC electrical characteristics of SSC superconducting dipole magnets
[DE92-018888] p 431 N93-11625
Microscopic origins of metastable effects in a-Si:H and deep defect characterization in a-Si,Ge:H alloys
[DE92-010588] p 463 N93-11813

CAPACITORS
Microwave sintering of multilayer ceramic capacitors
[DE92-018772] p 267 N93-11570
Effects of physical properties and geometry on shapes and stability of polarizable drops in external fields
[DE92-018865] p 301 N93-11638

CAPILLARY FLOW
Advanced two-phase heat transfer systems
p 229 N93-12459

CARBIDES
Synthesis of single phase (alpha)-Fe, Fe3C and Fe7C3 nano-particles by CO2 laser pyrolysis technique
[DE92-015654] p 250 N93-11847

CARBON
An NMR study of the occupation of C(sub 60) interstitial sites by oxygen molecules
[DE92-019436] p 437 N93-11640
Studies on the reactive melt infiltration of silicon and silicon-molybdenum alloys in porous carbon
[NASA-TM-105860] p 273 N93-12398
CARBON COMPOUNDS
Near-IR absorption spectra for the C70 fullerene anions
[AD-A253658] p 246 N93-11280
CARBON CYCLE
The flux and recycling of bioactive substances in the surface sediments of the deep basins off southern California
[DE92-019172] p 373 N93-11734
CARBON DIOXIDE
Lunar and Martian environmental interactions with nuclear power system radiators
[NASA-TM-105747] p 230 N93-10965
Catalog of data bases and reports
[DE92-018586] p 473 N93-10990
Studies of the role of clouds in CO2-induced climate change
[DE92-018648] p 353 N93-11569
The potential effects of concurrent increases in temperature, CO2 and O3 on net photosynthesis, as mediated by rubisCO
[DE92-019411] p 374 N93-11630
Submarine Advanced Integrated Life Support system (SAILS) program
[AD-A253564] p 388 N93-11812
CARBON DIOXIDE CONCENTRATION
Studies of the role of clouds in CO2-induced climate change
[DE92-018648] p 353 N93-11569
The potential effects of concurrent increases in temperature, CO2 and O3 on net photosynthesis, as mediated by rubisCO
[DE92-019411] p 374 N93-11630
CARBON DIOXIDE LASERS
CO2 laser frequency doubling
[AD-A251060] p 314 N93-10997
CO2 laser frequency doubling using AgGaSe2
[RSRE-MEMO-4528] p 315 N93-11388
A study of the CO2 laser near threshold
p 316 N93-11720
The design, development, and test of balloonborne and groundbased lidar systems. Volume 3: Groundbased lidar systems
[AD-A247552] p 317 N93-11805
Synthesis of single phase (alpha)-Fe, Fe3C and Fe7C3 nano-particles by CO2 laser pyrolysis technique
[DE92-015654] p 250 N93-11847
The design, development, and test of balloonborne and groundbased lidar systems. Volume 1: Balloonborne coherent CO2 lidar system
[AD-A247551] p 322 N93-12262
Development summary of a sympathetic discharge CO2 laser for lidar use
[NASA-CR-184433] p 323 N93-12516
CARBON FIBER REINFORCED PLASTICS
Scanning electron microscopy of the effects of moisture and elevated temperature on the fibre/matrix bond in CFRP
[RAE-TM-MAT-STR-1183] p 240 N93-11905
Impact test of carbon, Kevlar, and glass fibre hybrid FRP plates
[NAL-TR-1100] p 243 N93-12371
CARBON FIBERS
Generation of thermal strains in carbon fibre-reinforced bismaleimide (PMR-15) composites, part 1, 2 and 3
[PNR-90976-PT-1-2-3] p 236 N93-11065
VAMAS round robin project on polymer composite delamination in mode 1 and mode 2: Cyclic loading
[NPL-DMM(A)-47] p 266 N93-11397
Recent advances in carbon-carbon substrate technology at NASA. Langley Research Center p 228 N93-12455
CARBON MONOXIDE
Preconversion catalytic deoxygenation of phenolic functional groups
[DE92-018304] p 244 N93-10986
Inhibition of moist carbon monoxide oxidation by trace amounts of hydrocarbons
[DE92-008736] p 253 N93-12257
Catalytic hydrogenation of carbon monoxide
[DE92-014729] p 253 N93-12428
CARBON 13
Molecular mobility of the interface in a model composite: A NMR study
[AD-A253311] p 265 N93-11194
An NMR study of the occupation of C(sub 60) interstitial sites by oxygen molecules
[DE92-019436] p 437 N93-11640
CARBON-CARBON COMPOSITES
Development of advanced carbon-carbon annular flameholders for gas turbines
[PNR-90947] p 211 N93-11106
Small particle impact damage in carbon-carbon composites
[PNR-90948] p 236 N93-11107
High temperature oxidation protection of carbon/carbon composites
[REPT-921-430-105] p 239 N93-11589
Aerospatiale processes for three dimensional preforms
[REPT-921-430-147] p 239 N93-11590
Carbon/carbon composition ablation effects on ionized boundary layers
[AD-A254465] p 242 N93-12235
Predicted and tested performance of durable TPS
p 228 N93-12454
Recent advances in carbon-carbon substrate technology at NASA. Langley Research Center p 228 N93-12455
Current research in oxidation-resistant carbon-carbon composites at NASA. Langley Research Center
p 229 N93-12456
CARBONACEOUS MATERIALS
Composite failure analysis handbook. Volume 2: Technical handbook. Part 3: Case histories
[AD-A249131] p 241 N93-12054
CARBONYL COMPOUNDS
Exploration of the ionizable metal cluster-electrode surface analogy: Infrared spectroelectrochemistry of (Pt24(CO)30)(sup n), (Pt26(CO)32)(sup n), and (Pt38(CO)44)(sup n) (n = 0 to -10), and comparisons with potential-dependent spectra of CO adlayers on platinum surfaces
[AD-A252544] p 250 N93-11808
Biological conversion of synthesis gas culture development
[DE92-001279] p 375 N93-12482
CARBOXYHEMOGLOBIN
Carboxyalkylated hemoglobin as a potential blood substitute
[AD-A252329] p 384 N93-11561
CARDIAC OUTPUT
Effect of hemorrhage on cardiac output, vasopressin, aldosterone, and diuresis during immersion in men
[NASA-TM-103949] p 374 N93-12014
CARGO
Aircraft accident report: Explosive decompression-loss of cargo door in flight, United Airlines Flight 811, Boeing 747-122, N4713U, Honolulu, HI, 24 February 1989
[PB92-910402] p 204 N93-12193
CASCADE FLOW
An experimental investigation into flow induced acoustic resonances in an annular cascade
[PNR-90959] p 433 N93-11322
Increase of energy use on cooled high temperature turbine, phase 3
[MTUM-B91EW-0029-PHASE-3] p 213 N93-11339
CASE BONDED PROPELLANTS
Thermal fracture service life analysis of a case bonded visco-elastic cylinder p 339 N93-12008
CASE HISTORIES
Selected case studies of technology transfer from mission-oriented applied research
[DE92-018957] p 481 N93-12067
CAST ALLOYS
Design and development of Ni-base superalloy and Ti alloys
[NRIM-SR-92-01] p 261 N93-12322
CASTING
Present and future trends in turbine blade material and manufacture technology
[PNR-90960] p 255 N93-11111
Silicon carbide fiber reinforced strontium aluminosilicate glass-ceramic matrix composite
[NASA-CASE-LEW-15263-1] p 239 N93-11543
Development of strength and conductivity in deformation processed copper base alloys
[DE92-018807] p 257 N93-11572
CATALOGS
Computer security training and awareness course compendium
[PB92-205442] p 404 N93-11258
CATALOGS (PUBLICATIONS)
Catalog of data bases and reports
[DE92-018586] p 473 N93-10990
Compositional analysis and classification of projectile residues in LDEF impact craters
[NASA-TM-104750] p 488 N93-11374
CATALYSIS
Preconversion catalytic deoxygenation of phenolic functional groups
[DE92-018304] p 244 N93-10986
Selective carbon oxygen bond scission during reactions of oxygenates on single crystal catalysts
[DE92-018687] p 247 N93-11439
Direct catalytic decomposition of nitric oxide
[DE92-018759] p 247 N93-11444
Synthesis of single phase (alpha)-Fe, Fe3C and Fe7C3 nano-particles by CO2 laser pyrolysis technique
[DE92-015654] p 250 N93-11847
Phase transfer catalytic nucleophilic addition reactions: Synthesis of polymers and acetylenic terminated resins
[AD-A254717] p 272 N93-12337
Catalytic hydrogenation of carbon monoxide
[DE92-014729] p 253 N93-12428
CATALYSTS
Controlled synthesis of polyenes by catalytic methods
[DE92-015286] p 271 N93-12165
CATALYTIC ACTIVITY
Reformers for the production of hydrogen from methanol and alternative fuels for fuel cell powered vehicles
[DE92-019300] p 274 N93-11550
CATHODE RAY TUBES
The locator system for wandering individuals
[NASA-TM-104754] p 388 N93-11649
CATHODES
Submarine Advanced Integrated Life Support system (SAILS) program
[AD-A253564] p 388 N93-11812
CAUCHY PROBLEM
A three dimensional high resolution upwind finite volume Euler solver
[VKI-TN-180] p 198 N93-11686
CAUCHY-RIEMANN EQUATIONS
Difference approximations for hyperbolic conservation laws and consistency with characteristics
[NAL-TR-1098T] p 428 N93-12350
CAVITATION FLOW
Pressure and noise induced by a cavitating marine screw propeller
[VTT-PUBS-87] p 299 N93-11360
CAVITIES
A creep cavity growth model for creep-fatigue life prediction of a unidirectional W/Cu composite
[NASA-TM-105780] p 333 N93-10967
Boundary condition methods in the numerical solution of the Navier-Stokes equations with the application to free surface problems
[ISBN-0-315-64278-5] p 298 N93-11241
10 kW L-band amplifier tubes for efficient and reliable troposcatter communication transmitter systems
[AD-A253246] p 290 N93-11504
CAVITY RESONATORS
Higher-order-mode damping and microwave absorption at 2 K
[DE92-016960] p 442 N93-11077
The foxhole accelerating structure
[DE92-019052] p 443 N93-11429
Alternating-phase focusing: A model to study nonlinear dynamics
[DE92-019027] p 431 N93-11511
Research and development of superconducting linear accelerators for neutral particle beam applications
[DE92-019043] p 444 N93-11652
On some practical consideration of the electron beam breakup transit time oscillator
[DE92-017406] p 445 N93-11919
CELESTIAL MECHANICS
Ephemeris calculation and orbit determination of geostationary satellites, using Taylor series integration
[SER-C-384] p 220 N93-11335
CELL CATHODES
Overcharge and overdischarge protection of ambient temperature secondary lithium cells
[NASA-CASE-NPO-18343-1-CU] p 290 N93-11456
CELL MEMBRANES (BIOLOGY)
Cellular and molecular pathways of extremely-low-frequency electromagnetic field interactions with living systems
[DE92-019084] p 282 N93-11515
CELLS (BIOLOGY)
Physiological analyses of the afferents controlling brain neurochemical systems
[AD-A253185] p 375 N93-11146
CENTRAL PROCESSING UNITS
Parallel architecture for image processing with optic fiber guided missile
[REPT-921-320-101] p 418 N93-11584
Algorithms for sensor fusion: Decentralized Bayesian hypothesis testing with feedback, volume 1
[AD-A254633] p 414 N93-12242
CENTRIFUGAL CASTING
Mechanical properties of centrifugally cast metal matrix composites
[AD-A254321] p 243 N93-12483
CENTRIFUGAL FORCE
On the Goertler instability of boundary layers
[NAL-TR-1120T] p 307 N93-12374
CEPHEID VARIABLES
Ultraviolet studies of Cepheids
[NASA-CR-190857] p 481 N93-11073

CERAMIC BONDING
Study and characterization of ceramic-metal-bonds manufactured by solid state bonding techniques. Application to Ag/Al2O3
[ECL-91-19] p 267 N93-11577
Study of metal-ceramic interfaces of Co-Cr-Mo alloys: Role of tungsten (W) and manganese (Mn) additions
[ECL-92-01] p 267 N93-11580
CERAMIC COATINGS
Ceramic Technology Project
[DE92-018748] p 266 N93-11442
High temperature oxidation protection of carbon/carbon composites
[REPT-921-430-105] p 239 N93-11589
Development of wear resistant ceramic coatings for diesel engine components
[DE92-019068] p 268 N93-11654
Advanced ceramic matrix composites for TPS
p 228 N93-12450
Thermal protection using very high temperature ceramics p 228 N93-12451
CERAMIC FIBERS
Relative sliding durability of candidate high temperature fiber seal materials
[NASA-TM-105806] p 236 N93-10978
Materials: Toward the non-metallic engine
[PNR-90915] p 209 N93-11019
CERAMIC MATRIX COMPOSITES
Nondestructive evaluation of ceramic and metal matrix composites for NASA's HITEMP and enabling propulsion materials programs
[NASA-TM-105807] p 331 N93-10963
Processing of ceramic matrix composites
[PNR-90914] p 263 N93-11018
Aero engine ceramics: The vision, the reality, and the progress
[PNR-90983] p 264 N93-11066
Industrial applications and markets for ceramic matrix composites
[PNR-90884] p 266 N93-11205
Optical properties of composite membranes containing arrays of nanoscopic gold cylinders
[AD-A253659] p 238 N93-11281
Ceramic Technology Project
[DE92-018748] p 266 N93-11442
Silicon carbide fiber reinforced strontium aluminosilicate glass-ceramic matrix composite
[NASA-CASE-LEW-15263-1] p 239 N93-11543
Toughness of Si3N4-SiC whisker composites
[REPT-921-430-101] p 239 N93-11586
Silicon carbide matrix composites
[REPT-921-430-103] p 239 N93-11588
Study of the behavior of titanium and ceramic fiber matrix composite alloy
[ETN-92-92087] p 240 N93-11708
Development of nondestructive evaluation methods and prediction of effects of flaws on the fracture behavior of structural ceramics
[DE92-016395] p 271 N93-12123
Mechanical properties for advanced engine materials
[AD-A252632] p 242 N93-12181
Advanced ceramic matrix composites for TPS
p 228 N93-12450
Superplastic forming of ceramic insulation
p 228 N93-12452
Ceramic TBS/porous metal compliant layer
p 228 N93-12453
CERAMICS
Analysis of precracking parameters and fracture toughness for ceramic single-edge-precracked-beam specimens
[NASA-TM-105568] p 263 N93-10962
Ceramic component reliability with the restructured NASA/CARES computer program
[NASA-TM-105856] p 334 N93-11004
Erosion mechanisms in ceramic structures
[MBB-UK-0171-92-PUB] p 263 N93-11011
Higher-order-mode damping and microwave absorption at 2 K
[DE92-016960] p 442 N93-11077
The dressing of resin bonded diamond grinding wheels
[PNR-90965] p 264 N93-11086
Silver lined ceramic vessel and method of preparation
[AD-D015360] p 266 N93-11400
Ceramic Technology Project
[DE92-018748] p 266 N93-11442
Microwave sintering of multilayer ceramic capacitors
[DE92-018772] p 267 N93-11570
Engine testing of ceramic cam-roller followers
[DE92-019188] p 268 N93-11735
Synthesis of nanocrystalline powders for oxide ceramics by microwave plasma pyrolysis
[DE92-017410] p 268 N93-11861
Proceedings of the DOE/Advanced Heat Exchangers Program Review
[DE92-014385] p 305 N93-12070
Infrared phonon structure in epitaxial films of Tl2Ca2Ba2Cu3O10 at low temperatures
[DE92-017078] p 466 N93-12109
Friction of self-lubricating surfaces by ion beam techniques
[DE92-016069] p 328 N93-12122
Method and apparatus for evaluating multilayer objects for imperfections
[NASA-CASE-LAR-14581-1-SB] p 333 N93-12204
Nanophase ceramics
[AD-A254661] p 272 N93-12246
Thermal protection systems manned spacecraft flight experience p 227 N93-12449
Advanced ceramic matrix composites for TPS
p 228 N93-12450
Thermal protection using very high temperature ceramics p 228 N93-12451
Superplastic forming of ceramic insulation
p 228 N93-12452
Ceramic TBS/porous metal compliant layer
p 228 N93-12453
Atomic bonding at ceramic interfaces using scanning tunneling microscopy
[DE92-018706] p 273 N93-12479
CERMETS
A gas-cooled cermet reactor system for planetary base power
[DE92-018017] p 443 N93-11433
CERTIFICATION
Aircraft accident report: Atlantic Southeast Airlines, Inc. Flight 2311, uncontrolled collision with terrain, an Embraer EMB-120, N270AS, Brunswick, Georgia, 5 April 1991
[PB92-910403] p 203 N93-11471
Automatic Attenuation/Phase Calibration System (AAPCS)
[DE92-017354] p 284 N93-11917
Aircraft accident report: Explosive decompression-loss of cargo door in flight, United Airlines Flight 811, Boeing 747-122, N4713U, Honolulu, HI, 24 February 1989
[PB92-910402] p 204 N93-12193
CESIUM
Investigation of a cesium Raman time/frequency standard
[AD-A252677] p 310 N93-11562
CHAINS
Synthesis and side chain liquid crystal polymers by living ring opening metathesis polymerization. 5: Influence of mesogenic group and interconnecting group on the thermotropic behavior of the resulting polymers
[AD-A253568] p 264 N93-11150
CHALCOGENIDES
Fast electrochromic switching for optical hardening applications
[AD-A248174] p 447 N93-11186
CHANGE DETECTION
Auditory perception
[AD-A255061] p 385 N93-12469
CHANNEL FLOW
Cryostabilization of high-temperature superconducting magnets with subcooled flow in microchannels
[DE92-018174] p 431 N93-11598
Application of a two-layer near wall model to fully developed and rotating channel turbulent flows
[NASA-CR-184441] p 305 N93-12082
Probability density functions in turbulent channel flow
[NASA-CR-4454] p 202 N93-12399
CHANNEL NOISE
Self-supervision in multilayer adaptive networks
[RSRE-MEMO-4467] p 420 N93-11343
CHANNELS (DATA TRANSMISSION)
Scalable parallel communications p 279 N93-11117
A simple, effective media access protocol system for integrated, high data rate networks p 279 N93-11119
Self-supervision in multilayer adaptive networks
[RSRE-MEMO-4467] p 420 N93-11343
Formal design specification of a Processor Interface Unit
[NASA-CR-189698] p 406 N93-12538
CHAOS
Tori and chaos in a nonlinear dynamo model for solar activity
[MPE-PREPRINT-218] p 488 N93-11351
Heat transfer enhancement by chaotic mixing
[PB92-190305] p 470 N93-11469
New methods for nonlinear tracking and nonlinear chaotic signal processing
[AD-A254320] p 284 N93-12095
Laminar boundary-layer breakdown
[AD-A254489] p 306 N93-12162
Singularities of the Euler equation and hydrodynamic stability
[NASA-CR-189720] p 306 N93-12173
CHARGE CARRIERS
Exciton kinetics in poly(di-n-hexylsilane)
[DE92-018278] p 283 N93-11800
CHARGE COUPLED DEVICES
Development of a scintillating optical fiber ionization calorimeter
[NASA-CR-184415] p 311 N93-11662
A search for low-luminosity objects
[AD-A253301] p 483 N93-11750
High-speed test station for solid-state imagers
[DE92-018990] p 312 N93-11822
Final Report, January 1991 - July 1992
[AD-A254659] p 483 N93-12244
Video camera as a visual sensor
[NAL-TR-1132] p 314 N93-12373
Design and evaluation of ion source for satellite charge control
[AD-A255172] p 227 N93-12408
CHARGE EXCHANGE
Advanced electric propulsion research, 1991
[NASA-CR-190761] p 232 N93-11608
Foil optimization for low energy neutral atom imaging
[DE92-013435] p 365 N93-12263
Low energy neutral atom imaging
[DE92-013531] p 365 N93-12264
Helium transport studies on D3-D
[DE92-016251] p 455 N93-12307
CHARGE TRANSFER
Electron transfer rates at semiconductor/liquid interfaces
[DE92-018559] p 289 N93-11438
Advanced electric propulsion research, 1991
[NASA-CR-190761] p 232 N93-11608
Workshop on Adhesion and Intermolecular Forces
[AD-A255191] p 272 N93-12276
CHARGED PARTICLES
The NASA/National Space Science Data Center trapped radiation environment model program, 1964 - 1991
[NASA-TM-107993] p 349 N93-11003
Emittance measuring device for charged particle beams
[AD-D015371] p 442 N93-11060
Multispectral observations of the Jovian aurora
p 487 N93-11167
Advanced methods for structural characterization of large multiply charged ions: Obtaining charge state determination and improved sensitivity
[DE91-015264] p 441 N93-12117
CHARM (PARTICLE PHYSICS)
High energy physics at Tufts University
[DE92-018081] p 444 N93-11668
CHARTS
Design of instrument approach procedure charts: Comprehension speed of missed approach instructions coded in text or icons
[PB92-205673] p 204 N93-11252
CHEMICAL ANALYSIS
Summaries of FY 1991 research in the chemical sciences
[DE92-011920] p 251 N93-12135
Alternative Fuel Evaluation Program: Alternative Fuel Light Duty Vehicle Project. Data collection responsibilities, techniques, and test procedures
[DE92-010598] p 275 N93-12171
CHEMICAL BONDS
Preconversion catalytic deoxygenation of phenolic functional groups
[DE92-018304] p 244 N93-10986
Studies of the 3 to 5 compounds in the megabar regime
[DE92-019517] p 461 N93-11646
The role of backbond strain in silicon surfaces on the decomposition of NH3 and PH3
[AD-A253771] p 250 N93-12062
Synthesis and reactivity of siloxide and silamide complexes pertaining to bond breaking and aggregation phenomena
[AD-A254703] p 468 N93-12231
Atomic bonding at ceramic interfaces using scanning tunneling microscopy
[DE92-018706] p 273 N93-12479
CHEMICAL COMPOSITION
Laser glasses
[DE92-018061] p 267 N93-11549
CHEMICAL ENERGY
Determination of parameters of a new method for predicting alloy properties
[NASA-TM-105895] p 257 N93-11609
CHEMICAL ENGINEERING
Summaries of FY 1991 research in the chemical sciences
[DE92-011920] p 251 N93-12135
CHEMICAL EQUILIBRIUM
Effect of inert propellant injection on Mars ascent vehicle performance
[NASA-CR-189238] p 226 N93-12152

CHEMICAL EVOLUTION

The search for life's origins: Progress and future directions in planetary biology and chemical evolution [NASA-CR-190929] p 487 N93-11603

CHEMICAL EXPLOSIONS

Detonation reactions frozen by free expansion and analyzed by mass spectrometry [DE92-018605] p 274 N93-11566

Asymptotic analysis of reacting materials with saturated explosion. 2: High-frequency waves [AD-A254473] p 275 N93-12236

CHEMICAL PROPERTIES

Chemical reactions and properties of organosilicon compounds related to new materials [AD-A253233] p 246 N93-11218

Tetrahedral atom zincophosphate structures: Synthesis, crystal structure, and spectroscopic studies of (Zn(PO2(OC2H5)2)2)x, a one-dimensional inorganic polymer [AD-A251051] p 437 N93-11560

CHEMICAL REACTIONS

Erosion mechanisms in ceramic structures [MBB-UK-0171-92-PUB] p 263 N93-11011

Tropospheric processes: Observations and interpretation p 351 N93-11092

Effects of reacting flows with turbulence and shock waves on efficiency of scramjet combustors p 235 N93-11133

Synthesis and side chain liquid crystal polymers by living ring opening metathesis polymerization. 5: Influence of mesogenic group and interconnecting group on the thermotropic behavior of the resulting polymers [AD-A253568] p 264 N93-11150

Chemical reactions and properties of organosilicon compounds related to new materials [AD-A253233] p 246 N93-11218

Theoretical research program to study chemical reactions in AOTV bow shock tubes [NASA-CR-188927] p 439 N93-11851

Design and synthesis of molecular systems capable of supporting intracavity chemical reactions [AD-A251024] p 440 N93-11872

Threshold photodetachment spectroscopy of negative ions [DE92-017090] p 440 N93-12100

Asymptotic analysis of reacting materials with saturated explosion. 2: High-frequency waves [AD-A254473] p 275 N93-12236

Inhibition of moist carbon monoxide oxidation by trace amounts of hydrocarbons [DE92-008736] p 253 N93-12257

Biological conversion of synthesis gas culture development [DE92-001279] p 375 N93-12482

CHEMICAL REACTORS

Measuring and modelling of particle-fluid flow in a riser reactor [VTT-PUBS-88] p 299 N93-11359

Reformers for the production of hydrogen from methanol and alternative fuels for fuel cell powered vehicles [DE92-019300] p 274 N93-11550

CHEMICAL WARFARE

The effects of wearing protective chemical warfare combat clothing on human performance [AD-A250716] p 390 N93-12491

CHEMISORPTION

Electronic structure and reactivities of transition metal clusters [DE92-016623] p 258 N93-11762

CHEMOTHERAPY

Allergic, Immunological and Infectious Disease Problems in Aerospace Medicine [AGARD-CP-518] p 376 N93-11283

Early markers of HIV infection and subclinical disease progression p 379 N93-11296

Communicable diseases: A major burden of morbidity and mortality p 380 N93-11300

Recent lessons on the safety and effectiveness of malaria chemoprophylaxis in a non-immune population p 381 N93-11307

Future approaches to vaccine development single-dose vaccines using controlled-release delivery systems p 382 N93-11310

Epidemiologic view of allergic diseases in North America: Implications for aerospace medicine p 382 N93-11311

The screening of inhalant allergic diseases in the selection of candidates for aircraft piloting p 382 N93-11312

Asthma in aircrew: Assessment, treatment and disposition p 383 N93-11315

CHINA

On understanding in communicating systems and the error in the Chinese Room thought-experiment [RSRE-MEMO-4391] p 278 N93-10977

Chinese Journal of Lasers (selected articles) [AD-A254100] p 317 N93-11786

CHIPS (ELECTRONICS)

The VISTA structured assembler [RSRE-91034] p 407 N93-11341

RF vacuum microelectronics [AD-A253910] p 290 N93-11491

An evaluation of the blind lap joint for the surface mount attachment of chip components [DE92-017045] p 277 N93-12106

Analysis of fault-tolerant neurocontrol architectures [NASA-TM-105898] p 215 N93-12305

Natural convection heat transfer studies of simulated and actual electronic components using dielectric liquids for immersion cooling [AD-A255173] p 341 N93-12376

An investigation of error correcting techniques for OMV and AXAF [NASA-CR-190950] p 416 N93-12515

CHIPS (MEMORY DEVICES)

Ultra-dense magnetoresistive mass memory [NASA-CR-190955] p 405 N93-12520

Formal design specification of a Processor Interface Unit [NASA-CR-189698] p 406 N93-12538

CHIRAL DYNAMICS

Nucleon axial coupling constants and QCD sum rules [DE92-014227] p 439 N93-11844

CHLORIDES

Acid copper sulfate plating bath: Control of chloride and copper [DE92-019473] p 249 N93-11644

Chemistry of lower valent actinide halides [DE92-017031] p 251 N93-12105

Synthesis and conductivity of copolymer of 4,4'-diaminodiphenylamine and terephthaloyl chloride [AD-A254880] p 273 N93-12440

CHLORINE COMPOUNDS

Ozone depletion and chlorine loading potentials p 351 N93-11093

Synthesis and characterization of novel organogallium-phosphorus compounds: X ray crystal structures of Ph2GaP (SiMe3)2Ga (Ph2Cl, Ph2 (Cl)Ga.P (SiMe3)3, and Ph3Ga.P (SiMe3)3 [AD-A253841] p 462 N93-11724

CHLOROCARBONS

The role of refrigerants in climate change [DE92-019385] p 354 N93-11677

CHLOROFLUOROCARBONS

The role of refrigerants in climate change [DE92-019385] p 354 N93-11677

CHLOROPHYLLS

Ultrafast photoinduced electron transfer reactions in supramolecular arrays: From charge separation and storage to molecular switches [DE92-016186] p 465 N93-12090

CHOLERA

Immunization of personnel traveling to a destination in tropical countries: French position p 380 N93-11304

CHROMATES

Corrosion resistant chromate conversion coatings for heat-treated aluminum alloys [AD-D015366] p 266 N93-11425

CHROMIUM ALLOYS

Isotopic tailoring with 59-Ni to study the effect of helium on microstructural evolution and mechanical properties of neutron-irradiated Fe-Cr-Ni alloys [DE92-019372] p 257 N93-11557

Study of metal-ceramic interfaces of Co-Cr-Mo alloys: Role of tungsten (W) and manganese (Mn) additions [ECL-92-01] p 267 N93-11580

Oxidation-sulfidation behavior of iron alloys containing 16 to 40 atomic percent aluminum [DE92-017824] p 259 N93-11830

Processing and properties of NbTi based alloys [DE92-016692] p 261 N93-12445

CHROMIUM ISOTOPES

Freeze-dried human red blood cells [AD-A253295] p 376 N93-11193

CHROMIUM OXIDES

Development of wear resistant ceramic coatings for diesel engine components [DE92-019068] p 268 N93-11654

CHROMIUM STEELS

Thermal stress and strain analysis in traveling autogenous welds [DE92-019363] p 326 N93-11556

Relationship of bainitic microstructure to impact toughness in Cr-Mo and Cr-W steels [DE92-017828] p 258 N93-11773

Mechanical properties of 1950's vintage 304 stainless steel weldment components after low temperature neutron irradiation [DE92-017059] p 259 N93-12107

Reactor materials program: Mechanical properties of irradiated types 304 and 304L stainless steel weldment components [DE92-018105] p 260 N93-12158

CHROMOSOMES

Molecular cytogenetics: A novel approach for measuring chromosome translocations in individuals years after exposure to low levels of ionizing radiation [DE92-018066] p 374 N93-10974

CHROMOSPHERE

Diagnostics of electron-heated solar flares p 488 N93-11877

CHRONOLOGY

The NASA/National Space Science Data Center trapped radiation environment model program, 1964 - 1991 [NASA-TM-107993] p 349 N93-11003

CIRCUIT BOARDS

High speed parallel backplane [AD-D015372] p 288 N93-11053

An evaluation of the blind lap joint for the surface mount attachment of chip components [DE92-017045] p 277 N93-12106

An investigation of error correcting techniques for OMV and AXAF [NASA-CR-190950] p 416 N93-12515

CIRCUIT RELIABILITY

Reliability of small geometry VLSI devices for microelectronics [AD-A247355] p 289 N93-11414

VLSI design for reliability [AD-A253207] p 292 N93-11781

VLSI reliability research [AD-A254883] p 295 N93-12360

CIRCUITS

Testability design rating system. Volume 2: Analytical procedure [AD-A254333] p 413 N93-12146

CIRCULAR CYLINDERS

Numerical analysis of oscillating flow about a circular cylinder [AD-A255164] p 307 N93-12406

CIRCULAR PLATES

Inflatable device for excluding sea water from a rocket motor [AD-D015365] p 232 N93-11424

CIRCULAR SHELLS

Linear and geometrically nonlinear p-version three dimensional curved shell element for isotropic, generally orthotropic and laminated composite materials p 339 N93-12194

CIRCULAR TUBES

Crushing behavior of tubular structures in multi-materials [ECL-91-37] p 336 N93-11579

Crashworthy characteristics of circular tubes in axisymmetric buckling p 337 N93-11721

CIRCULATION DISTRIBUTION

The structure and transport of the Brazil current between 27 deg and 36 deg south [AD-A247635] p 374 N93-12247

CIVIL AVIATION

Design of an air traffic computer simulation system to support investigation of civil tiltrotor aircraft operations [NASA-CR-190811] p 204 N93-11139

Activities report of Lufthansa [ETN-92-92100] p 203 N93-11319

UK airmisses involving commercial air transport, May-August 1991 [ETN-92-92260] p 203 N93-11357

UK airmisses involving commercial air transport, January-April 1991 [ETN-92-92261] p 296 N93-11358

Formal representation of the requirements for an Advanced Subsonic Civil Transport (ASCT) flight control system [NASA-CR-189699] p 405 N93-12346

CLADDING

Fiber optic polishing system [AD-D015353] p 446 N93-11052

CLAMPS

Automatic system for installation and replacement of Space Station components [NASA-CASE-LEW-14906-1] p 329 N93-12203

CLASSIFICATIONS

An evidential reasoning approach to the classification of satellite images [DLR-FB-91-29] p 342 N93-11140

Land use/land cover classification using digitally merged spot panchromatic and Landsat thematic mapper imagery [PB92-188416] p 343 N93-11701

Automatic cloud classification from multi-spectral satellite data [AD-A255125] p 372 N93-12420

CLASSIFIERS
Parallel genetic algorithms: Introduction and overview of current research
[REPT-92-015] p 418 N93-11181
ALECSYS and the AutonoMouse: Learning to control a real robot by distributed classifier systems
[REPT-92-011] p 420 N93-11227
CLEAN ROOMS
Analysis of materials from MSFC LDEF experiments
[NASA-CR-184425] p 252 N93-12215
CLEARANCES
Shear joint capability versus bolt clearance
[NASA-TM-108378] p 342 N93-12419
CLIMATE
Global Climate Change (GCC) issues and their impacts on the US Army Corps of Engineers
[AD-A247279] p 353 N93-11466
CCL working group on climate data
[WCDMP-18] p 370 N93-11897
CLIMATE CHANGE
Catalog of data bases and reports
[DE92-018586] p 473 N93-10990
Scientific assessment of ozone depletion: 1991
[NASA-TM-107976] p 350 N93-11087
Source gases: Concentrations, emissions, and trends
p 350 N93-11088
Tropospheric processes: Observations and interpretation p 351 N93-11092
Radiative forcing of climate p 351 N93-11094
International Conference on the Role of the Polar Regions in Global Change: Proceedings, volume 1
[DE92-013652] p 353 N93-11232
International Conference on the Role of the Polar Regions in Global Change: Proceedings, volume 2
[DE92-013653] p 353 N93-11233
Global Climate Change (GCC) issues and their impacts on the US Army Corps of Engineers
[AD-A247279] p 353 N93-11466
Studies of the role of clouds in CO2-induced climate change
[DE92-018648] p 353 N93-11569
Climate change and water supply, management and use: A literature review
[DE92-019069] p 353 N93-11655
The role of refrigerants in climate change
[DE92-019385] p 354 N93-11677
Reports to the Nation on our changing planet. Winter 1991 No. 1: The climate system
[NASA-CR-190954] p 370 N93-11880
The uses and limits of economic models as a climate change policy tool
[DE92-015792] p 356 N93-12474
CLIMATOLOGY
Source gases: Concentrations, emissions, and trends
p 350 N93-11088
Radiative forcing of climate p 351 N93-11094
The use of ARM data to test an improved parameterization of upper tropospheric clouds for use in climate models
[DE92-014353] p 367 N93-11237
Reports to the Nation on our changing planet. Winter 1991 No. 1: The climate system
[NASA-CR-190954] p 370 N93-11880
Proceedings of the Sixteenth Annual Climate Diagnostics Workshop
[PB92-198803] p 370 N93-11896
CCL working group on climate data
[WCDMP-18] p 370 N93-11897
Atmospheric dispersion in mountain valleys and basins
p 355 N93-11920
Parameters for predicting red tides of bioluminescent dinoflagellates: Meteorological events and frontal water circulation patterns
[AD-A254835] p 374 N93-12431
CLINICAL MEDICINE
Clinical types of Hepatitis B p 376 N93-11286
Viral hepatitis in the US Air Force, 1980 - 1989
p 377 N93-11287
Hepatitis A and Hepatitis B: Risks compared to other vaccine preventable diseases and immunization recommendations p 377 N93-11288
Silent HIV infection p 378 N93-11293
Early markers of HIV infection and subclinical disease progression p 379 N93-11296
Analysis of disease progression from clinical observations of US Air Force active duty members infected with the Human Immunodeficiency Virus: Distribution of AIDS survival time from interval censored observations
p 379 N93-11297
Clinical and immunological response to vaccination with parenteral or oral vaccines in two groups of 30 recruits
p 381 N93-11305
Studies of safety, infectivity, and immunogenicity of a new Temperature Sensitive (TS) 51-1 strain of S. typhi as a new live oral typhoid fever vaccine candidate
p 381 N93-11306
Phadiatop: A screening test for inhalant allergy
p 383 N93-11313
CLOSED ECOLOGICAL SYSTEMS
Techniques for optimal crop selection in a controlled ecological life support system
[NASA-TM-103950] p 388 N93-12018
ECLSS medical support activities
[NASA-CR-184429] p 385 N93-12427
CLOUD COVER
Automatic cloud classification from multi-spectral satellite data
[AD-A255125] p 372 N93-12420
CLOUD HEIGHT INDICATORS
Detection of cloud-top height from backscattered radiances within the oxygen A band. Part 1: Theoretical study
[GKSS-91/E/76-PT-1] p 368 N93-11349
Detection of cloud-top height from backscattered radiances within the oxygen A band. Part 2: Measurements
[GKSS-91/E/77-PT-2] p 368 N93-11350
CLOUD PHYSICS
Time scales characterizing the processing of water and cloud condensation nuclei by clouds
[CM-80] p 368 N93-11340
CLOUDS (METEOROLOGY)
The millimeter wave Cloud Profiling Radar System (CPRS)
[DE92-016970] p 366 N93-10971
Time scales characterizing the processing of water and cloud condensation nuclei by clouds
[CM-80] p 368 N93-11340
Global Climate Change (GCC) issues and their impacts on the US Army Corps of Engineers
[AD-A247279] p 353 N93-11466
Studies of the role of clouds in CO2-induced climate change
[DE92-018648] p 353 N93-11569
The design, development, and test of balloonborne and groundbased lidar systems. Volume 3: Groundbased lidar systems
[AD-A247552] p 317 N93-11805
Visualizing wind velocities by advecting cloud textures
[DE92-014717] p 371 N93-12154
Automatic cloud classification from multi-spectral satellite data
[AD-A255125] p 372 N93-12420
CLUSTER ANALYSIS
Positive ion chemistry of acetylene and methylacetylene clusters. Formation of benzene and C(sub 2n)H(sub 2n)(+) ions via intracluster polymerization reactions
[AD-A250931] p 236 N93-12177
CLUSTERS
Theory of small metal clusters, films, and wires
[AD-A253120] p 256 N93-11240
Electronic structure and reactivities of transition metal clusters
[DE92-016623] p 258 N93-11762
The structures, binding energies and vibrational frequencies of Ca3 and Ca4: An application of the CCSD(T) method p 439 N93-11852
CLUTTER
The design and implementation of radar clutter modelling and adaptive target detection techniques
p 283 N93-11913
CMOS
VLSI design for reliability
[AD-A253207] p 292 N93-11781
COAL
3-D turbulent particle dispersion submodel development
[DE92-018212] p 301 N93-11670
3-D turbulent particle dispersion submodel development
[DE92-018228] p 302 N93-11671
Advanced coal-fueled gas turbine systems
[DE92-018939] p 327 N93-11832
COAL UTILIZATION
Advanced coal-fueled gas turbine systems
[DE92-018939] p 327 N93-11832
COANDA EFFECT
The aerodynamics of curved jets and breakaway in Coanda flares, volumes 1 and 2 p 304 N93-11881
COASTS
Physical effects of vegetation on wind-blown sand in the coastal environments of Florida
[PB92-188424] p 354 N93-11702
The Wave Information Studies (WIS) wave model, version 2.0 (user's guide)
[AD-A254313] p 374 N93-12094
COATING
Silver lined ceramic vessel and method of preparation
[AD-D015360] p 266 N93-11400
Corrosion resistant chromate conversion coatings for heat-treated aluminum alloys
[AD-D015366] p 266 N93-11425
Advanced heat pump for the recovery of volatile organic compounds
[DE92-011592] p 303 N93-11774
COATINGS
Workshop on Surface Science and Technology
[AD-A253566] p 264 N93-11149
COAXIAL CABLES
Robust solder joint attachment of coaxial cable leads to piezoelectric ceramic electrodes
[DE92-017042] p 276 N93-11494
Transmission/reflection and short-circuit line methods for measuring permittivity and permeability
[PB92-205376] p 293 N93-12084
COBALT ALLOYS
Study of metal-ceramic interfaces of Co-Cr-Mo alloys: Role of tungsten (W) and manganese (Mn) additions
[ECL-92-01] p 267 N93-11580
Erosion predictions and measurements of high-temperature coatings and superalloys used in turbomachines p 272 N93-12189
COCKPITS
Direct manipulation and intermittent automation in advanced cockpits
[AD-A253814] p 388 N93-11784
Human performance in complex task environments: A basis for the application of adaptive automation
[AD-A255067] p 390 N93-12486
CODERS
An investigation of error correcting techniques for OMV and AXAF
[NASA-CR-190950] p 416 N93-12515
CODING
Self-supervision in multilayer adaptive networks
[RSRE-MEMO-4467] p 420 N93-11343
Digital signal processing
[AD-A254870] p 287 N93-12436
An investigation of error correcting techniques for OMV and AXAF
[NASA-CR-190950] p 416 N93-12515
COEFFICIENTS
Mass energy-transfer and mass energy-absorption coefficients, including in-flight positron annihilation for photon energies 1 keV to 100 MeV, 1992
[PB92-181106] p 438 N93-11715
COGNITION
Ontology of mind, subjective ontology, and the example of temporal expressions
[REPT-92-018] p 386 N93-11212
Complex cognitive information processing: A computational architecture with a connectionist implementation
[AD-A254041] p 422 N93-12259
COGNITIVE PSYCHOLOGY
Ontology of mind, subjective ontology, and the example of temporal expressions
[REPT-92-018] p 386 N93-11212
Relating cognitive function to military aviator performance in early HIV infection p 379 N93-11298
COHERENT ELECTROMAGNETIC RADIATION
Proposal for the experimental demonstration of the coherent radiation
[DE92-017695] p 284 N93-12132
COHERENT LIGHT
The sensitivity of the receiver coherence diameter and modulation transfer function to variations of a damp unstable atmosphere
[AD-A253269] p 363 N93-11785
COHERENT RADAR
The design, development, and test of balloonborne and groundbased lidar systems. Volume 1: Balloonborne coherent CO2 lidar system
[AD-A247551] p 322 N93-12262
COHERENT RADIATION
Organization of the Optical Society of America Photonic Science Topical Meeting Series. Volume 14: Photorefractive materials effects, and devices
[AD-A253001] p 446 N93-11071
Theory for a high power free electron laser and tactical applications
[AD-A255161] p 323 N93-12405
COHERENT SCATTERING
Limitations of multiple feeds in a polarimetric-radar compact range
[DE92-017526] p 284 N93-12101
COLD ROLLING
Processing and properties of NbTi based alloys
[DE92-016692] p 261 N93-12445
COLD WATER
Effectiveness of NASA 1032 and 1035 and Air Force 1030 and 1034 units in protection against cold water hypothermia
[AD-A255120] p 389 N93-12291

COLD WEATHER
Sustaining health and performance in the cold: Environmental medicine guidance for cold-weather operation [AD-A254328] p 385 N93-12145

COLLAPSE
On the stability of confined shells under external pressure p 335 N93-11202
Crashworthy characteristics of circular tubes in axisymmetric buckling p 337 N93-11721

COLLECTION
A model to estimate the flux of background particles expected to accumulate on the collector foils of the interstellar gas experiment on the long duration exposure facility spacecraft [AD-A254265] p 489 N93-11815

COLLIMATORS
System design and radiation field characteristics of the High Flux Neutron Radiography Facility (HFNRF) at Sandia National Laboratories [DE92-013984] p 219 N93-12268

COLLINEARITY
Colliding plane gravitational waves with colinear polarization [MATHS-REPT-A-160] p 357 N93-11120

COLLISION AVOIDANCE
An autonomous vehicle: Constrained test and evaluation [PB92-205608] p 325 N93-11427
A neuro-collision avoidance strategy for robot manipulators p 400 N93-11962
Interactive collision detection p 400 N93-11963
Advanced mechanisms for robotics p 330 N93-11969

COLLISION PARAMETERS
Scattering of polarized electrons by oriented deuterons [DE92-624834] p 440 N93-11914

COLLISIONAL PLASMAS
Diagnostics and modeling of H(-) ion sources [AD-A250664] p 440 N93-11867

COLLISIONS
Colliding plane gravitational waves with colinear polarization [MATHS-REPT-A-160] p 357 N93-11120

COLLOCATION
Spurious modes in spectral collocation methods with two non-periodic directions [NASA-CR-189713] p 427 N93-12298

COLLOIDING
Freeze-dried human red blood cells [AD-A253295] p 376 N93-11193

COLOR
The effects of luminance boundaries on color perception [AD-A250705] p 384 N93-11841

COLOR INFRARED PHOTOGRAPHY
Land use/land cover classification using digitally merged spot panchromatic and Landsat thematic mapper imagery [PB92-188416] p 343 N93-11701

COLOR TELEVISION
Initial laboratory evaluation of color video cameras [DE92-018274] p 311 N93-11673
Guide to synchronization of video systems to IRIG timing [AD-A254626] p 285 N93-12240

COLOR VISION
The effects of luminance boundaries on color perception [AD-A250705] p 384 N93-11841

COLORADO PLATEAU (US)
Key wintertime meteorological features of the Grand Canyon and the Colorado Plateaus Basin [DE92-019134] p 369 N93-11657

COLUMBUS SPACE STATION
Automation and robotics for COLUMBUS: An implementation concept for the free flying laboratory (MTFF) p 331 N93-11974

COMBAT
Neural network models of air combat maneuvering [AD-A254653] p 421 N93-12096
The effects of wearing protective chemical warfare combat clothing on human performance [AD-A250716] p 390 N93-12491

COMBINATORIAL ANALYSIS
Polynomial dual network simplex algorithms [AD-A254340] p 413 N93-12131
Decomposition of balanced matrices. Part 5: Goggles [AD-A247462] p 430 N93-12217

COMBINED STRESS
Micromechanical combined stress analysis: MICSTRAN, a user manual [NASA-CR-189694] p 243 N93-12306

COMBUSTION
Ignition delays, heats of combustion, and reaction rates of aluminum alkyl derivatives as used as ignition and combustion enhancers for supersonic combustors p 244 N93-11134
3-D turbulent particle dispersion submodel development [DE92-018212] p 301 N93-11670
3-D turbulent particle dispersion submodel development [DE92-018228] p 302 N93-11671
Effect of inert propellant injection on Mars ascent vehicle performance [NASA-CR-189238] p 226 N93-12152
Studies in premixed combustion [DE92-018646] p 254 N93-12478

COMBUSTION CHAMBERS
An advanced combustion research facility for validating computational fluid dynamics codes [PNR-90913] p 296 N93-11017
Effects of reacting flows with turbulence and shock waves on efficiency of scramjet combustors p 235 N93-11133
Ignition delays, heats of combustion, and reaction rates of aluminum alkyl derivatives as used as ignition and combustion enhancers for supersonic combustors p 244 N93-11134
The combustion time lag and its role in ramjet combustion instability p 245 N93-11137
CFD modeling of turbulent flows around the SSME main injector assembly using porosity formulation [NASA-CR-184359] p 297 N93-11171
Test program to provide validation data for the Rocket Combustor Interactive Design (ROCCID) code p 247 N93-11450
Hot fire test results of subscale tubular combustion chambers [NASA-TP-3222] p 232 N93-11614
Numerical analysis of the flow fields in a RQL gas turbine combustor [DE92-017509] p 302 N93-11767
Advanced coal-fueled gas turbine systems [DE92-018939] p 327 N93-11832
Flow visualization of supersonic flow through a combustor section p 200 N93-12001
Hypervelocity scramjet combustor-nozzle analysis and design [NASA-CR-190965] p 213 N93-12214
Combustion characteristics of the LO2/GCH4 fuel-rich preburners for staged combustion cycle rocket engines [NAL-TR-1124] p 234 N93-12368
Characteristics of heat transfer to nickel plated chamber walls of high pressure rocket combustors [NAL-TR-1126T] p 234 N93-12372
Investigation of hot streak migration and film cooling effects on heat transfer in rotor/stator interacting flows, report 1 [AD-A250688] p 471 N93-12490

COMBUSTION CHEMISTRY
Probing flame chemistry with MBMS, theory, and modeling [DE92-011433] p 251 N93-12119

COMBUSTION CONTROL
Numerical analysis of the flow fields in a RQL gas turbine combustor [DE92-017509] p 302 N93-11767

COMBUSTION EFFICIENCY
Employment of radicals and excited state species for supersonic combustion photochemical ignition of premixed hydrogen/oxygen mixtures with ArF laser p 245 N93-11135
The effects of bypass air on boron carbide combustion in a solid fuel ramjet p 245 N93-11136
Combustion characteristics of the LO2/GCH4 fuel-rich preburners for staged combustion cycle rocket engines [NAL-TR-1124] p 234 N93-12368

COMBUSTION PHYSICS
Employment of radicals and excited state species for supersonic combustion photochemical ignition of premixed hydrogen/oxygen mixtures with ArF laser p 245 N93-11135
The combustion time lag and its role in ramjet combustion instability p 245 N93-11137
CFD modeling of turbulent flows around the SSME main injector assembly using porosity formulation [NASA-CR-184359] p 297 N93-11171
Studies in nonlinear problems of energy [DE92-018551] p 345 N93-11733

COMBUSTION PRODUCTS
Simplified modelling of soot inception and growth [ETN-92-92266] p 246 N93-11361
Laser spectroscopy and dynamics of transient species formed in pyrolysis reactions [DE92-016206] p 251 N93-12091
OH rotational temperature and concentration measurements in a supersonic jet [DE92-006700] p 252 N93-12255

COMBUSTION STABILITY
Ignition delays, heats of combustion, and reaction rates of aluminum alkyl derivatives as used as ignition and combustion enhancers for supersonic combustors p 244 N93-11134
The combustion time lag and its role in ramjet combustion instability p 245 N93-11137
Test program to provide validation data for the Rocket Combustor Interactive Design (ROCCID) code p 247 N93-11450
A summary of the JANNAF workshop on diagnostics p 248 N93-11451
Studies in nonlinear problems of energy [DE92-018551] p 345 N93-11733
Studies in premixed combustion [DE92-018646] p 254 N93-12478

COMBUSTION TEMPERATURE
Combustion characteristics of the LO2/GCH4 fuel-rich preburners for staged combustion cycle rocket engines [NAL-TR-1124] p 234 N93-12368

COMMAND AND CONTROL
Implementing system simulation of C3 systems using autonomous objects [NASA-CR-190845] p 283 N93-11716
Distributed database integrity [AD-A253272] p 477 N93-11749
From pilot's associate to satellite controller's associate p 390 N93-11922

COMMAND LANGUAGES
The effect of task complexity on user interfaces: A comparison of command language interface and direct manipulation interface [AD-A246061] p 412 N93-11859

COMMERCE
The European space industry. Overall situation: Situation and prospects for the 23 leading companies concerned p 472 N93-11163
Activities report of Lufthansa [ETN-92-92100] p 203 N93-11319
Advanced heat pump for the recovery of volatile organic compounds [DE92-011592] p 303 N93-11774

COMMERCIAL AIRCRAFT
Civil aircraft engines: The next generation [PNR-90962] p 211 N93-11085
Predicted aircraft effects on stratospheric ozone p 352 N93-11096
Comparisons of molecular sieve oxygen concentrators for potential medical use aboard commercial aircraft [AD-A253648] p 387 N93-11279
Activities report of Lufthansa [ETN-92-92100] p 203 N93-11319
UK airmisses involving commercial air transport, May-August 1991 [ETN-92-92260] p 203 N93-11357
UK airmisses involving commercial air transport, January-April 1991 [ETN-92-92261] p 298 N93-11358
Aircraft accident report: Atlantic Southeast Airlines, Inc. Flight 2311, uncontrolled collision with terrain, an Embraer EMB-120, N270AS, Brunswick, Georgia, 5 April 1991 [PB92-910403] p 203 N93-11471
Aircraft accident report: Explosive decompression-loss of cargo door in flight, United Airlines Flight 811, Boeing 747-122, N4713U, Honolulu, HI, 24 February 1989 [PB92-910402] p 204 N93-12193
Flight simulator evaluation of D-size liquid crystal flat panel displays [NAL-TR-1136] p 209 N93-12367
Liquid crystal flat panel display evaluation tests using a flight simulator [NAL-TR-1122] p 209 N93-12383

COMMERCIAL ENERGY
Prospects for the commercial development of hot dry rock geothermal energy in New Mexico [DE92-018999] p 346 N93-11825

COMMERCIAL SPACECRAFT
Direct Broadcast Satellite: Radio Program [NASA-TM-105910] p 224 N93-11430

COMMINUTION
The collaborative program of research in engineering sciences [DE92-016838] p 490 N93-12477

COMMONALITY
Power system commonality study [NASA-CR-190765] p 347 N93-12019

COMMUNICATING
On understanding in communicating systems and the error in the Chinese Room thought-experiment [RSRE-MEMO-4391] p 278 N93-10977
Questioning mechanisms during complex learning [AD-A247382] p 386 N93-11415

COMMUNICATION
An EVACS simulation with nested transactions [NASA-CR-190636] p 412 N93-11717
COMMUNICATION EQUIPMENT
Translating wedge heat sink [AD-D015357] p 293 N93-12133
Formal mechanization of device interactions with a process algebra [NASA-CR-189644] p 405 N93-12347
COMMUNICATION NETWORKS
Photonics and other approaches to high speed communications [NASA-CR-190362] p 279 N93-11116
Scalable parallel communications p 279 N93-11117
High performance interconnection between high data rate networks p 279 N93-11118
Self-supervision in multilayer adaptive networks [RSRE-MEMO-4467] p 420 N93-11343
Controller evaluation of initial data link terminal air traffic control services: Mini study 2, volume 1 [DOT/FAA/CT-92/2-VOL-1] p 205 N93-11704
Controller evaluation of initial data link terminal air traffic control services: Mini study 2, volume 2 [DOT/FAA/CT-92/2-VOL-2] p 205 N93-11705
Integrated services digital network conformance testing. Layer 1, physical layer. Part 2: Basic rate U interface, user side [PB92-181114] p 418 N93-11714
Space Communication Artificial Intelligence for Link Evaluation Terminal (SCAILET) p 395 N93-11940
Low Density Radio Communications Link (LDRCL) Operational Test and Evaluation (OT/E) integration and operation test plan [DOT/FAA/CT-TN92/4] p 285 N93-12331
ISDN at NASA Lewis Research Center [NASA-TM-105911] p 419 N93-12410
COMMUNICATION SATELLITES
Spacecraft flight control system design selection process for a geostationary communication satellite [NASA-TP-3289] p 222 N93-11002
Direct Broadcast Satellite: Radio Program [NASA-TM-105910] p 224 N93-11430
COMMUNITIES
Matching and vertex packing: How hard are they? [AD-A245928] p 423 N93-10991
COMPATIBILITY
Power system commonality study [NASA-CR-190765] p 347 N93-12019
COMPENSATORS
Computational nonlinear control [AD-A253547] p 422 N93-12258
COMPILERS
The VISTA structured assembler [RSRE-91034] p 407 N93-11341
Applying algebraic techniques to microcode compilation [RSRE-MEMO-4568] p 409 N93-11392
A formal definition of the static semantics of ELLA's core [RSRE-91024] p 409 N93-11436
Automatic data partitioning on distributed memory multicomputers [NASA-CR-190976] p 418 N93-11651
Simulation and analysis of support hardware for multiple instruction rollback [NASA-CR-190972] p 406 N93-12541
COMPLETENESS
The complexity of some multicriteria arborescence problems [REPT-92-016] p 424 N93-11182
COMPLEX COMPOUNDS
Theory of small metal clusters, films, and wires [AD-A253120] p 256 N93-11240
Controlled synthesis of polyenes by catalytic methods [DE92-015286] p 271 N93-12165
COMPLEX SYSTEMS
Krylov subspace methods for complex non-Hermitian linear systems [NASA-CR-190931] p 409 N93-11458
A methodology for systems requirements specification and traceability for large real time complex systems [AD-A254738] p 419 N93-12358
Active control of complex systems via dynamic (recurrent) neural networks [AD-A254878] p 422 N93-12439
COMPLEXITY
The complexity of some multicriteria arborescence problems [REPT-92-016] p 424 N93-11182
COMPONENT RELIABILITY
Ceramic component reliability with the restructured NASA/CARES computer program [NASA-TM-105856] p 334 N93-11004
Submarine Advanced Integrated Life Support system (SAILS) program [AD-A253564] p 388 N93-11812
Fault detection and fault tolerance in robotics p 330 N93-11961
COMPOSITE MATERIALS
Advanced materials in gas turbine engines: An assessment [PNR-90946] p 211 N93-11105
An interlayer shear slip theory for composite laminates with nonrigid bonding p 237 N93-11229
Analytical method of calculating the thermoelastic constants of a multi-phase unidirectional composite [NPL-DMM(A)-57] p 238 N93-11409
Design of a high-temperature experiment for evaluating advanced structural materials [NASA-TM-105833] p 337 N93-11624
Linear and geometrically nonlinear p-version three dimensional curved shell element for isotropic, generally orthotropic and laminated composite materials p 339 N93-12194
Current Technology for Thermal Protection Systems [NASA-CP-3157] p 227 N93-12447
Thermostructural applications of heat pipes for cooling leading edges of high-speed aerospace vehicles p 229 N93-12460
Analysis of delamination in composite laminates under low-velocity impact p 243 N93-12532
COMPOSITE PROPELLANTS
Energetic composites of cyclodextrin nitrate esters and nitrate ester plasticizers [AD-D015364] p 274 N93-11665
COMPOSITE STRUCTURES
Industrial applications and markets for ceramic matrix composites [PNR-90884] p 266 N93-11205
Methods of analysis for thick-section composite structures p 237 N93-11262
Study of compression-loaded and impact-damaged structurally efficient graphite-thermoplastic trapezoidal-corrugation sandwich and semisandwich panels [NASA-TP-3264] p 239 N93-11623
Global-local finite element analysis of composite structures [DE92-019138] p 240 N93-11658
Penetration mechanics of composites [AD-A249230] p 240 N93-11835
Computer aided design and manufacturing of composite propfan blades for a cruise missile wind tunnel model [NASA-TM-105269] p 413 N93-12022
The effect of contact stresses in four-point bend testing of graphite/epoxy and graphite/PMR-15 composite beams [NASA-TM-105891] p 241 N93-12076
Thermostructural tailoring of fiber composite structures [NASA-TM-105882] p 242 N93-12078
Linear and geometrically nonlinear p-version three dimensional curved shell element for isotropic, generally orthotropic and laminated composite materials p 339 N93-12194
Current Technology for Thermal Protection Systems [NASA-CP-3157] p 227 N93-12447
Advanced ceramic matrix composites for TPS p 228 N93-12450
Ceramic TBS/porous metal compliant layer p 228 N93-12453
Evaluation of alternatives for increasing A-7D rearward visibility [AD-A255071] p 208 N93-12488
COMPRESSED GAS
Comparisons of molecular sieve oxygen concentrators for potential medical use aboard commercial aircraft [AD-A253648] p 387 N93-11279
COMPRESSIBILITY
Influence of oxygen partial pressure and silver additions on microstructure and related properties of YBCO superconductors [DE92-011145] p 468 N93-12249
Compressible mixing layers with and without particles [AD-A254854] p 308 N93-12435
COMPRESSIBILITY EFFECTS
Compressible mixing layers with and without particles [AD-A254854] p 308 N93-12435
COMPRESSIBLE BOUNDARY LAYER
Effects of sweep on the physics of unsteady shock-induced turbulent separated flows [AD-A247035] p 198 N93-11742
COMPRESSIBLE FLOW
Fundamental solutions and boundary element formulations for convective fluid flow p 298 N93-11217
Simulation of compressible turbulent flows by a mixed finite element/finite volume method [ETN-92-92267] p 299 N93-11362
An experimental investigation of the flow in a diffusing S-duct [NASA-TM-105809] p 213 N93-12077
COMPRESSIBLE FLUIDS
Fundamental solutions and boundary element formulations for convective fluid flow p 298 N93-11217
Review of preconditioning methods for fluid dynamics [NASA-CR-189712] p 198 N93-11607
Oscillations and concentrations in compressible and incompressible fluids [AD-A254706] p 307 N93-12333
COMPRESSION LOADS
Tension and compression fatigue response of unnotched 3D braided composites [NASA-CR-189678] p 239 N93-11611
Study of compression-loaded and impact-damaged structurally efficient graphite-thermoplastic trapezoidal-corrugation sandwich and semisandwich panels [NASA-TP-3264] p 239 N93-11623
COMPRESSIVE STRENGTH
Analysis of delamination in composite laminates under low-velocity impact p 243 N93-12532
COMPRESSORS
Development of the neutron diffraction technique for the determination of near surface residual stresses in critical gas turbine components [PNR-90984] p 212 N93-11112
COMPUTATION
Flow field calculations around the Hermes spaceplane during reentry phase [MBB-UK-0148-91-PUB] p 195 N93-11008
Polynomial dual network simplex algorithms [AD-A254340] p 413 N93-12131
COMPUTATIONAL CHEMISTRY
Theoretical research program to study chemical reactions in AOTV bow shock tubes [NASA-CR-188927] p 439 N93-11851
The structures, binding energies and vibrational frequencies of Ca3 and Ca4: An application of the CCSD(T) method p 439 N93-11852
On the evaluation of derivatives of Gaussian integrals p 439 N93-11853
Connected triple excitations in coupled-cluster calculations of hyperpolarizabilities: Neon p 439 N93-11854
Concerted hydrogen atom exchange between three HF molecules p 439 N93-11855
COMPUTATIONAL FLUID DYNAMICS
An advanced combustion research facility for validating computational fluid dynamics codes [PNR-90913] p 296 N93-11017
Front tracking and the interaction of nonlinear waves [AD-A253544] p 297 N93-11148
Artificial intelligence and CFD: Expert systems for the design of airfoils and for grid generation [DIGE-EST-TN-016] p 206 N93-11161
Fundamental solutions and boundary element formulations for convective fluid flow p 298 N93-11217
Domain decomposition: A bridge between nature and parallel computers [NASA-CR-189709] p 425 N93-11246
Increase of energy use on cooled high temperature turbine, phase 3 [MTUM-B91EW-0029-PHASE-3] p 213 N93-11339
Simplified modelling of soot inception and growth [ETN-92-92266] p 246 N93-11361
Simulation of compressible turbulent flows by a mixed finite element/finite volume method [ETN-92-92267] p 299 N93-11362
A study of the wall-pressure fluctuations downstream of a blade-wall junction [ECL-91-07] p 299 N93-11363
Computation of single solid particle impact on the target of ductile material to study the rebound characteristics of particle p 336 N93-11372
Overview of high performance aircraft propulsion research [NASA-TM-105839] p 213 N93-11530
Comparison of truncation error of finite-difference and finite-volume formulations of convection terms [NASA-TM-105861] p 426 N93-11531
Resolution of the pressure equation by the boundary element method. Application to multistage turbomachines [ECL-91-16] p 301 N93-11575
Progress in developing a transition model for high-speed flows p 301 N93-11615
A three dimensional high resolution upwind finite volume Euler solver [VKI-TN-180] p 198 N93-11686
Mixing regimes in a spatially confined, two-dimensional, supersonic shear layer [AD-A254302] p 302 N93-11756
Numerical analysis of the flow fields in a RQL gas turbine combustor [DE92-017509] p 302 N93-11767

Using NEKTON to solve systems of discrete Boltzmann equations
[DE92-018272] p 303 N93-11799

Mode interaction models in near-wall turbulence p 303 N93-11856

The aerodynamics of curved jets and breakaway in Coanda flares, volumes 1 and 2 p 304 N93-11881

Numerical study of advanced rotor blades p 199 N93-11899

A wall interference assessment/correction system
[NASA-CR-190617] p 218 N93-11910

A comparison of velocity profile measurements in the CDIF diffuser with flow field model calculations
[DE92-015367] p 304 N93-11995

Application of a two-layer near wall model to fully developed and rotating channel turbulent flows
[NASA-CR-184441] p 305 N93-12082

Hypervelocity scramjet combustor-nozzle analysis and design
[NASA-CR-190965] p 213 N93-12214

Spurious modes in spectral collocation methods with two non-periodic directions
[NASA-CR-189713] p 427 N93-12298

Oscillations and concentrations in compressible and incompressible fluids
[AD-A254706] p 307 N93-12333

FNAS computational fluid dynamics
[NASA-CR-184394] p 307 N93-12397

An improved numerical model for wave rotor design and analysis
[NASA-TM-105915] p 214 N93-12418

An engineering method for interactive inviscid-boundary layers in three-dimensional hypersonic flows p 203 N93-12529

Three-dimensional turbopump flowfield analysis
[NASA-CR-190978] p 308 N93-12539

COMPUTATIONAL GRIDS

An adaptive differencing scheme for elliptic flows p 297 N93-11197

Numerical calculations of an axisymmetric laminar diffusion flame with detailed and reduced reaction mechanisms p 246 N93-11259

FNAS computational fluid dynamics
[NASA-CR-184394] p 307 N93-12397

An advancing front Delaunay triangulation algorithm designed for robustness
[NASA-CR-189719] p 416 N93-12400

COMPUTER AIDED DESIGN

An interactive preprocessor for the NASA engine performance program
[NASA-TM-105786] p 209 N93-10983

Simultaneous engineering in aero gas turbine design and manufacture
[PNR-90890] p 212 N93-11208

The engine design engine. A clustered computer platform for the aerodynamic inverse design and analysis of a full engine
[NASA-TM-105838] p 196 N93-11223

Numerical computation of the lightning response of an earth-covered munitions storage bunker and comparison with experiments
[DE92-014268] p 367 N93-11236

Using ELLA for high level design: Modelling the Motorola 6800 microprocessor
[RSRE-MEMO-4515] p 408 N93-11386

A formal definition of the static semantics of ELLA's core
[RSRE-91024] p 409 N93-11436

Test program to provide validation data for the Rocket Combustor Interactive Design (ROCCID) code p 247 N93-11450

Modified optimal control pilot model for computer-aided design and analysis
[NASA-TM-4384] p 214 N93-11459

Temperature tracking SPICE macro-model for laser and LED driven opto-coupler assemblies
[DE92-019296] p 411 N93-11599

VLSI design for reliability
[AD-A253207] p 292 N93-11781

Structural integrity of a confinement vessel for testing nuclear fuels for space propulsion
[DE92-016796] p 232 N93-11824

Distributed environmental control p 391 N93-11924

Computer aided design and manufacturing of composite propfan blades for a cruise missile wind tunnel model
[NASA-TM-105269] p 413 N93-12022

Thermostructural tailoring of fiber composite structures
[NASA-TM-105882] p 242 N93-12078

Users manual for program NYQUIST: Liquid rocket nyquist plots developed for use on a PC computer
[NASA-CR-184451] p 235 N93-12522

COMPUTER AIDED MANUFACTURING

Computer aided design and manufacturing of composite propfan blades for a cruise missile wind tunnel model
[NASA-TM-105269] p 413 N93-12022

COMPUTER AIDED MAPPING

Photogrammetric GIS technology: Feature mapping on digital stereo imagery
[AD-A254255] p 477 N93-11748

A VMEbus ultrasonic sensor controller for mapping and servo control in robotic systems
[DE92-013661] p 421 N93-12138

COMPUTER AIDED TOMOGRAPHY

Trip report: Marshall Space Center computed tomography
[DE92-018139] p 437 N93-11597

High resolution tomographic instrument development
[DE92-017314] p 313 N93-11828

New techniques for positron emission tomography in the study of human neurological disorders
[DE92-015353] p 384 N93-11873

COMPUTER ASSISTED INSTRUCTION

Direct manipulation and intermittent automation in advanced cockpits
[AD-A253814] p 388 N93-11784

Evaluation of a user information satisfaction short-form instrument
[AD-A250702] p 478 N93-11840

COMPUTER COMPATIBLE TAPES

Nimbus-7 Scanning Multichannel Microwave Radiometer (SMMR) PARM tape user's guide
[NASA-RP-1284] p 373 N93-11718

COMPUTER DESIGN

A formal definition of the static semantics of ELLA's core
[RSRE-91024] p 409 N93-11436

COMPUTER GRAPHICS

A cognitive approach to the design of information graphics
[AD-A252692] p 474 N93-11353

An iconic query interface for an image database
[AD-A253571] p 475 N93-11506

System for generating dynamic video imagery for human factors research
[AD-A248675] p 388 N93-11743

Advanced technology for portable personal visualization
[AD-A253808] p 388 N93-11783

A methodology to emulate and evaluate a productive virtual workstation p 395 N93-11938

Interactive collision detection p 400 N93-11963

COMPUTER INFORMATION SECURITY

Computer security training and awareness course compendium
[PB92-205442] p 404 N93-11258

Lies, damned lies, and databases
[RSRE-MEMO-4503-ISSUE-2] p 474 N93-11333

Integrity in automated information systems
[AD-A253990] p 477 N93-11732

Distributed database integrity
[AD-A253272] p 477 N93-11749

Integrity-oriented control objectives: Proposed revisions to the Trusted Computer System Evaluation Criteria (TCSEC), DOD 5200.28-STD
[AD-A253989] p 404 N93-11809

COMPUTER NETWORKS

Incorporating prior probabilities and misclassification costs into network training: An example from medical prognosis
[RSRE-MEMO-4343] p 428 N93-10980

Scalable parallel communications p 279 N93-11117

High performance interconnection between high data rate networks p 279 N93-11118

Computer security training and awareness course compendium
[PB92-205442] p 404 N93-11258

A real-time diagnostic and performance monitor for UNIX
[NASA-CR-190975] p 404 N93-11462

Scattering on a ring of processors p 410 N93-11482

Z-buffer on a transputer-based machine p 410 N93-11483

Reduction operations on a distributed memory machine with a reconfigurable interconnection network p 410 N93-11484

Engineering Information System (EIS)
[AD-A254013] p 476 N93-11508

Integrity in automated information systems
[AD-A253990] p 477 N93-11732

Hypertext functionality: A theoretical framework p 478 N93-11858

Design development of a neural network-based telemetry monitor p 394 N93-11933

A methodology to emulate and evaluate a productive virtual workstation p 395 N93-11938

Advanced satellite workstation: An integrated workstation environment for operational support of satellite system planning and analysis p 391 N93-11941

An approach to integrating and creating flexible software environments p 396 N93-11946

Design of an Ada expert system shell for the VHSIC avionic modular flight processor p 397 N93-11947

LINK user manual
[DE92-017987] p 479 N93-12143

National Space Science Data Center data archive and distribution service (NDADS) automated retrieval mail system user's guide
[NASA-TM-107990] p 479 N93-12150

A neural net-based approach to software metrics p 415 N93-12392

COMPUTER PROGRAMMING

Deriving and manipulating module interfaces
[AD-A253869] p 406 N93-11145

Magnetic resonance elucidation of molecule/macromolecule interaction stereochemistry
[AD-A253030] p 437 N93-11709

Knowledge-based system V and V in the Space Station Freedom program p 396 N93-11945

Higher-order generic functions for CLOS
[DE92-013447] p 413 N93-12137

Computational nonlinear control
[AD-A253547] p 422 N93-12258

Reengineering using a data abstraction based specification language
[AD-A254726] p 414 N93-12341

COMPUTER PROGRAMS

On understanding in communicating systems and the error in the Chinese Room thought-experiment
[RSRE-MEMO-4391] p 278 N93-10977

Maximum life spiral bevel reduction design
[NASA-TM-105790] p 323 N93-10982

Ceramic component reliability with the restructured NASA/CARES computer program
[NASA-TM-105856] p 334 N93-11004

An advanced combustion research facility for validating computational fluid dynamics codes
[PNR-90913] p 296 N93-11017

Automated fringe analysis for moire interferometry
[PNR-90918] p 334 N93-11021

Quality management of finite element analysis
[PNR-90951] p 331 N93-11110

The engine design engine. A clustered computer platform for the aerodynamic inverse design and analysis of a full engine
[NASA-TM-105838] p 196 N93-11223

Evaluation of a Cray performance tool using a large hydrodynamics code
[DE92-013239] p 407 N93-11231

Proceedings of the 14th International Conference on the Numerical Simulation of Plasmas
[AD-A249095] p 451 N93-11275

Software quality methodology integration study results
[AD-A253891] p 408 N93-11371

Use of the program ANISN to calculate response functions for a Bonner sphere set with a He-3 detector
[NPL-RSA(EXT)-31] p 316 N93-11411

A formal definition of the static semantics of ELLA's core
[RSRE-91024] p 409 N93-11436

Diagnostic rhyme test statistical analysis programs
[RSRE-91026] p 281 N93-11487

Engineering Information System (EIS)
[AD-A254013] p 476 N93-11508

Three dimensional and 2D simulation of an expanding plasma using a Darwin hybrid particle code
[DE92-019095] p 451 N93-11516

Optimization of expressions involving array classes
[DE92-019421] p 411 N93-11536

A computer algorithm for automatic beam steering
[DE92-019338] p 411 N93-11555

Temperature tracking SPICE macro-model for laser and LED driven opto-coupler assemblies
[DE92-019296] p 411 N93-11599

Temporal scattering and response software users' manual, version 2 and 3
[DE92-040934] p 282 N93-11632

ScaLAPACK: A scalable linear algebra library for distributed memory concurrent computers
[DE92-017823] p 426 N93-11636

Particle-fluid two-phase flow modeling
[DE92-017847] p 301 N93-11637

Interfacing Matlab and software written in other languages
[NPL-DITC-200/92] p 412 N93-11688

Physical effects of vegetation on wind-blown sand in the coastal environments of Florida
[PB92-188424] p 354 N93-11702

A search for low-luminosity objects
[AD-A253301] p 463 N93-11750

Some remarks on shell element analysis with DYNA3D and NIKE3D
[DE92-018784] p 337 N93-11775

Development of the Personnel-based System Evaluation Aid (PER-SEVAL) performance shaping functions
[AD-A252820] p 386 N93-11779

The effect of task complexity on user interfaces: A comparison of command language interface and direct manipulation interface
[AD-A246061] p 412 N93-11859
An expert system for diagnosing environmentally induced spacecraft anomalies p 230 N93-11927
Spacecraft attitude control using a smart control system p 230 N93-11932
On the acquisition and representation of procedural knowledge p 394 N93-11937
A methodology to emulate and evaluate a productive virtual workstation p 395 N93-11938
Methodologies for building robust schedules
p 397 N93-11949
Fuzzy logic control of telerobot manipulators
p 399 N93-11959
Exoskeleton master controller with force-reflecting telepresence p 330 N93-11970
A smart end-effector for assembly of space truss structures p 230 N93-11982
The measurement and calculation of birefringence in quenched polycarbonate specimens
p 269 N93-11986
Overview of property formulations for helium, nitrogen, lithium, and lithium-lead in ATHENA/MOD1 with comparison of calculated properties to measured properties
[DE92-017995] p 471 N93-12058
A preliminary study associated with the experimental measurement of the aero-optic characteristics of hypersonic configurations
[AD-A253792] p 200 N93-12063
Comprehensive computational model for thermal plasma processing
[DE92-018015] p 454 N93-12066
Mirror alignment techniques for point-focus solar concentrators
[DE92-019643] p 348 N93-12074
Program for implementing software quality metrics
[DE92-018617] p 413 N93-12187
Dynamic analysis of a pre-and-post ice impacted blade
[NASA-TM-105829] p 276 N93-12197
Solution of nonlinear flow equations for complex aerodynamic shapes
[NASA-CR-190979] p 307 N93-12329
Studies of a flat wake rotor theory
[NASA-CR-190936] p 201 N93-12343
Fluid-structure interaction using retarded potential and ABAQUS
[AD-A254735] p 307 N93-12355
Design of a lattice-based faceted classification system
p 415 N93-12385
Supporting multiple domains in a single reuse repository p 415 N93-12390
A neural net-based approach to software metrics
p 415 N93-12392
DYNAC: A computer program for analyzing the dynamical stability of aircraft
[REPT-B-31] p 216 N93-12415
Cost estimation of software development and the implications for the program manager
[AD-A255167] p 480 N93-12472
Users manual for program NYQUIST: Liquid rocket nyquist plots developed for use on a PC computer
[NASA-CR-184451] p 235 N93-12522
Measurement and analysis of operating system fault tolerance
[NASA-CR-190973] p 406 N93-12540

COMPUTER STORAGE DEVICES
Ferroelectric memory devices and a proposed standardized test system design
[AD-A255159] p 405 N93-12425
Ultra-dense magnetoresistive mass memory
[NASA-CR-190955] p 405 N93-12520

COMPUTER SYSTEMS DESIGN
Data archiving and analysis for CWDD
[DE92-017064] p 473 N93-11104
An iterative method for distributed database design
p 474 N93-11255
Automatic data partitioning on distributed memory multicomputers
[NASA-CR-190976] p 418 N93-11651
Requirements and applications for robotic servicing of military space systems p 230 N93-11953
A methodology for systems requirements specification and traceability for large real time complex systems
[AD-A254738] p 419 N93-12358

COMPUTER SYSTEMS PERFORMANCE
High performance interconnection between high data rate networks p 279 N93-11118
A simple, effective media access protocol system for integrated, high data rate networks p 279 N93-11119
A process monitor for the transputer
[RSRE-MEMO-4554] p 408 N93-11389
A real-time diagnostic and performance monitor for UNIX
[NASA-CR-190975] p 404 N93-11462
Automatic data partitioning on distributed memory multicomputers
[NASA-CR-190976] p 418 N93-11651
An expert system for diagnosing environmentally induced spacecraft anomalies p 230 N93-11927
An approach to integrating and creating flexible software environments p 396 N93-11946
Autonomous power system: Integrated scheduling
p 235 N93-11948
Balancing generality and specificity in component-based reuse p 416 N93-12393
Performance evaluation and modeling techniques for parallel processors
[NASA-CR-190974] p 419 N93-12395

COMPUTER SYSTEMS PROGRAMS
Deriving and manipulating module interfaces
[AD-A253869] p 406 N93-11145
Advanced satellite workstation: An integrated workstation environment for operational support of satellite system planning and analysis p 391 N93-11941
A hybrid approach to software repository retrieval: Blending faceted classification and type signatures
p 415 N93-12386

COMPUTER TECHNIQUES
Front tracking and the interaction of nonlinear waves
[AD-A253544] p 297 N93-11148
Visual perception of structure from motion
[AD-A253235] p 386 N93-11503
Integrity in automated information systems
[AD-A253990] p 477 N93-11732
Computer Science and Telecommunications Board summary of activities
[DE92-016467] p 404 N93-11761
Methodologies for building robust schedules
p 397 N93-11949
Operator vision aids for space teleoperation assembly and servicing p 391 N93-11981
A summer program in mathematics and computer science for academically oriented students, June 24 - July 26, 1991, Washington, DC
[AD-A249139] p 427 N93-12061

COMPUTER VISION
Statistical process for the automatic image analysis and its evaluation for object recognition and measurements
[SER-C-370] p 407 N93-11345
Object recognition with a robot hand
p 420 N93-11457
Automated extraction of aircraft runway patterns from radar imagery
[AD-A254258] p 218 N93-11751
Model-based vision for space applications
p 398 N93-11955
An integrated dexterous robotic testbed for space applications p 330 N93-11972
Self mobile space manipulator project
p 331 N93-11973
A vision-based end-point control for a two-link flexible manipulator
[NASA-CR-190967] p 330 N93-12521

COMPUTERIZED SIMULATION
Computer simulation and experimental investigation of the absorption cell for the rocketborne diode-laser experiment MASERATI
[BONN-IR-91-62] p 357 N93-11083
Design of an air traffic computer simulation system to support investigation of civil tiltrotor aircraft operations
[NASA-CR-190811] p 204 N93-11139
Numerical and observational investigations of long-lived, MCS-induced, severe surface wind events: The derecho
p 367 N93-11159
Evaluation of a Cray performance tool using a large hydrodynamics code
[DE92-013239] p 407 N93-11231
Proceedings of the 14th International Conference on the Numerical Simulation of Plasmas
[AD-A249095] p 451 N93-11275
The foxhole accelerating structure
[DE92-019052] p 443 N93-11429
Three dimensional and 2D simulation of an expanding plasma using a Darwin hybrid particle code
[DE92-019095] p 451 N93-11516
Analysis of the prebuncher for the KEK 40-MeV proton linac
[DE92-514988] p 444 N93-11525
Simulation of liquid drop breakup behavior in a flow field using discrete element techniques
[DE92-019435] p 300 N93-11537
Thermal stress and strain analysis in traveling autogenous welds
[DE92-019363] p 326 N93-11556
Computer simulations for the adsorption of polymers onto surfaces
[DE92-018942] p 267 N93-11628
Monte Carlo simulations of the supernova ejection mechanism for the runaway stars
[DE92-018367] p 485 N93-11695
Magnetic resonance elucidation of molecule/macromolecule interaction stereochemistry
[AD-A253030] p 437 N93-11709
Implementing system simulation of C3 systems using autonomous objects
[NASA-CR-190845] p 283 N93-11716
An EVACS simulation with nested transactions
[NASA-CR-190636] p 412 N93-11717
Airport stand assignment model
[TT-9104] p 218 N93-11728
System for generating dynamic video imagery for human factors research
[AD-A248675] p 388 N93-11743
VLSI design for reliability
[AD-A253207] p 292 N93-11781
Application of the theory of wave propagation through random media to phase and amplitude fluctuations of seismic P-waves
[AD-A253274] p 363 N93-11788
Dynamic vacuum analysis for APS high heat flux beamline front ends using optical ray-tracing simulation methods
[DE92-019032] p 445 N93-11831
Diagnostics and modeling of H(-) ion sources
[AD-A250664] p 440 N93-11867
New techniques for positron emission tomography in the study of human neurological disorders
[DE92-015353] p 384 N93-11873
Studies of transition states and radicals by negative ion photodetachment
[DE92-017011] p 440 N93-11875
Distributed environmental control p 391 N93-11924
Spacecraft attitude control using a smart control system p 230 N93-11932
A model for analytical performance prediction of hypervapotron
[DE92-018885] p 305 N93-12010
Development of a hydrodynamic code: MINNIE
p 318 N93-12031
Electron acceleration in a relativistic electron plasma wave p 319 N93-12033
Laser material interaction in confined medium
p 319 N93-12035
Shock waves induced by pulsed laser in confined interaction: Numerical simulation p 319 N93-12038
A preliminary study associated with the experimental measurement of the aero-optic characteristics of hypersonic configurations
[AD-A253792] p 200 N93-12063
Comprehensive computational model for thermal plasma processing
[DE92-018015] p 454 N93-12066
Final Technical Report
[AD-A253529] p 284 N93-12083
Numerical simulation of alumina spraying in argon-helium plasma jet
[DE92-017859] p 455 N93-12092
Super auditory localization for improved human-machine interfaces
[AD-A254699] p 389 N93-12229
The effect of temperature dependent thermal properties on parametric weld size predictions
[DE92-018816] p 260 N93-12232
Fluid-structure interaction using retarded potential and ABAQUS
[AD-A254735] p 307 N93-12355
Computer modeling of tactical high frequency antennas
[AD-A255176] p 286 N93-12377
FNAS computational fluid dynamics
[NASA-CR-184394] p 307 N93-12397
Space Station communications and tracking systems modeling and RF link simulation
[NASA-CR-185684] p 288 N93-12519
Simulation and analysis of support hardware for multiple instruction rollback
[NASA-CR-190972] p 406 N93-12541

CONCATENATED CODES
An investigation of error correcting techniques for OMV and AXAF
[NASA-CR-190950] p 416 N93-12515

CONCENTRATION (COMPOSITION)
Rotational CARS measurements in a rotating cavity with axial throughflow of cooling air: Oxygen concentration measurements
[PNR-90935] p 244 N93-11035
Predicted aircraft effects on stratospheric ozone
p 352 N93-11096
Kinetics of diffusional droplet growth in a liquid/liquid two-phase system
[NASA-CR-190805] p 297 N93-11142

OH rotational temperature and concentration measurements in a supersonic jet
[DE92-006700] p 252 N93-12255

CONCENTRATORS

The 1992 DOE/Sandia crystalline photovoltaic technology project review meeting
[DE92-018544] p 344 N93-10989

Comparisons of molecular sieve oxygen concentrators for potential medical use aboard commercial aircraft
[AD-A253648] p 387 N93-11279

Evaluation tests for photovoltaic concentrator receiver sections and modules
[DE92-017745] p 346 N93-11771

Participation in multilateral effort to develop high performance integrated CPC evacuated collectors
[DE92-015946] p 346 N93-11823

Mirror alignment techniques for point-focus solar concentrators
[DE92-019643] p 348 N93-12074

Photovoltaic systems based on spectrally selective holographic concentrators, phase 1
[AD-A252811] p 348 N93-12166

CONCENTRIC CYLINDERS

On the stability of confined shells under external pressure p 335 N93-11202

Analytical method of calculating the thermoelastic constants of a multi-phase unidirectional composite
[NPL-DMM(A)-57] p 238 N93-11409

CONCORDE AIRCRAFT

Concorde propulsion: Did we get it right? The Rolls-Royce/SNECMA Olympus 593 engine reviewed
[PNR-90970] p 210 N93-11061

CONCRETE STRUCTURES

An evaluation of repair techniques used for uncontrolled longitudinal cracking and failed longitudinal joints
[PB92-205616] p 277 N93-12072

CONCURRENT PROCESSING

Concurrent file operations in a high performance FORTRAN
[NASA-CR-189711] p 412 N93-11618

ScaLAPACK: A scalable linear algebra library for distributed memory concurrent computers
[DE92-017823] p 426 N93-11636

CONDENSATION

Organometallic NLO polymers. 3. Copolymerization of bridged bis(ferrocenyl) and bis(cyanoacetate) monomers via the knoevenagel condensation
[AD-A250214] p 265 N93-11192

CONDENSATION NUCLEI

Time scales characterizing the processing of water and cloud condensation nuclei by clouds
[CM-80] p 368 N93-11340

CONDENSED MATTER PHYSICS

Materials science and engineering at the Naval Research Laboratory: Research programs and 1990 publications
[PB92-199488] p 238 N93-11422

CONDENSERS (LIQUEFIERS)

Proceedings of the DOE/Advanced Heat Exchangers Program Review
[DE92-014385] p 305 N93-12070

CONDITIONS

On a certain McMillan degree condition appearing in control
[MATHS-REPT-A-170] p 424 N93-11125

CONDUCTING POLYMERS

The Peierls ground state, solitons and polarons in ring-containing polymers
[AD-A254914] p 272 N93-12289

Mixed ionic and electronic conductivity in polymers
[DE92-018723] p 273 N93-12500

CONDUCTIVE HEAT TRANSFER

Frequency response in short thermocouple wires
[NASA-CR-190943] p 310 N93-11612

CONDUCTORS

High speed parallel backplane
[AD-D015372] p 288 N93-11053

Optical properties of composite membranes containing arrays of nanoscopic gold cylinders
[AD-A253659] p 238 N93-11281

CONFERENCES

The 1992 DOE/Sandia crystalline photovoltaic technology project review meeting
[DE92-018544] p 344 N93-10989

Rocket Based Combined Cycle (RBCC) Propulsion Workshop, volume 2
[NASA-CR-184383] p 231 N93-11043

The fourth OSA Topical Meeting Proceedings on Picosecond Electronics and Optoelectronics, volume 9
[AD-A253472] p 447 N93-11099

The 28th JANNAF Combustion Subcommittee Meeting, volume 1
[CPIA-PUBL-573-VOL-1] p 244 N93-11132

International Conference on the Role of the Polar Regions in Global Change: Proceedings, volume 1
[DE92-013652] p 353 N93-11232

International Conference on the Role of the Polar Regions in Global Change: Proceedings, volume 2
[DE92-013653] p 353 N93-11233

Allergic, Immunological and Infectious Disease Problems in Aerospace Medicine
[AGARD-CP-518] p 376 N93-11283

The Third Potsdam-5 Kiev International Workshop on Nonlinear Processes in Physics
[AD-A249140] p 430 N93-11420

The 28th JANNAF Combustion Subcommittee Meeting, volume 2
[CPIA-PUBL-573-VOL-2] p 247 N93-11448

ICCG-10: Tenth International Conference on Crystal Growth. Poster presentation abstracts
[NASA-CR-190920] p 461 N93-11683

ICCG-10: Tenth International Conference on Crystal Growth. Oral presentation abstracts
[NASA-CR-190919] p 461 N93-11684

Proceedings of the First Seminar on Geographic Information Systems in Zambia
[PB92-207125] p 477 N93-11789

Proceedings of the National Weather Service Aviation Workshop: Postprint volume
[PB92-176148] p 369 N93-11803

Publication of papers presented at URSI 23rd General Assembly as a special section of radio science
[AD-A253561] p 283 N93-11811

Environmental problems and trends of international responses, 2
[DE92-531118] p 355 N93-11846

Tenth International Symposium on Environmental Biogeochemistry
[DE92-016200] p 355 N93-11864

Proceedings of the Sixteenth Annual Climate Diagnostics Workshop
[PB92-198803] p 370 N93-11896

Workshop on Adhesion and Intermolecular Forces
[AD-A255191] p 272 N93-12276

The 44th Annual Gaseous Electronics Conference
[AD-A254872] p 295 N93-12437

CONFIDENCE LIMITS

Operating characteristic analysis for reliability growth programs
[AD-A254993] p 333 N93-12510

CONFIGURATION INTERACTION

Oxidation, nitridation, and fluorine etching of Si
[AD-A253559] p 249 N93-11755

The structures, binding energies and vibrational frequencies of Ca3 and Ca4: An application of the CCSD(T) method p 439 N93-11852

CONFIGURATION MANAGEMENT

Integrity in automated information systems
[AD-A253990] p 477 N93-11732

Environmental restoration project configuration control
[DE92-017223] p 356 N93-12496

CONFINEMENT

Laser material interaction in confined medium
p 319 N93-12035

Study of the effects of a plastic wave induced by laser pulse in a metallic material. Application to the improvement of fatigue strength p 319 N93-12036

Shock waves induced by pulsed laser in confined interaction: Numerical simulation p 319 N93-12038

Railgun armature velocity improvement, SBIR phase 2
[AD-A254749] p 222 N93-12505

CONFORMAL MAPPING

Orthogonal functions over the oceans and applications to the determination of orbit error, geoid and sea surface topography from satellite altimetry p 373 N93-12002

Fixed points of expansive analytic maps (2)
[AD-A254737] p 344 N93-12357

CONGRESSIONAL REPORTS

The Space Station Freedom and space launch issues
[S-HRG-102-762] p 225 N93-11908

CONICAL BODIES

On the instability of hypersonic flow past a pointed cone: Comparison of theoretical and experimental results of Mach 18
[DLR-FB-92-02] p 196 N93-11141

CONJUGATE GRADIENT METHOD

The efficient parallel iterative solution of large sparse linear systems
[DE92-018769] p 425 N93-11446

Krylov subspace methods for complex non-Hermitian linear systems
[NASA-CR-190931] p 409 N93-11458

Design development of a neural network-based telemetry monitor p 394 N93-11933

CONSERVATION EQUATIONS

Difference approximations for hyperbolic conservation laws and consistency with characteristics
[NAL-TR-1098T] p 428 N93-12350

CONSERVATION LAWS

The basic equations for a four component magnetoplasma flow with non equilibrium ionization
[IPF-91-1] p 449 N93-11102

On an origin of numerical diffusion: Violation of invariance under space-time inversion
[NASA-TM-105776] p 425 N93-11254

Particle-fluid two-phase flow modeling
[DE92-017847] p 301 N93-11637

Difference approximations for hyperbolic conservation laws and consistency with characteristics
[NAL-TR-1098T] p 428 N93-12350

CONSISTENCY

Distributed database integrity
[AD-A253272] p 477 N93-11749

An investigation of electromagnetic launcher repeatability
[AD-A254339] p 222 N93-12130

Some consistency requirements on hardening-recovery evolution equations for welding, part 1
[DE92-015992] p 329 N93-12220

CONSTRAINTS

Constrained KP hierarchy and bi-Hamiltonian structures
[MATHS-REPT-A-168] p 424 N93-11123

Design and synthesis of molecular systems capable of supporting intracavity chemical reactions
[AD-A251024] p 440 N93-11872

CONSUMABLES (SPACECRAFT)

Automated resupply of consumables: Enhancement of space commercialization opportunities
p 403 N93-11980

CONSUMABLES (SPACECREW SUPPLIES)

Automated resupply of consumables: Enhancement of space commercialization opportunities
p 403 N93-11980

CONTACT LOADS

Contact detection and contact motion for error recovery in the presence of uncertainties p 398 N93-11956

The effect of contact stresses in four-point bend testing of graphite/epoxy and graphite/PMR-15 composite beams
[NASA-TM-105891] p 241 N93-12076

CONTACTORS

High-frequency LSI contactor
[DE92-017285] p 292 N93-11916

CONTAINERS

Silver lined ceramic vessel and method of preparation
[AD-D015360] p 266 N93-11400

CONTAMINANTS

Technology evaluation report of Retech, Inc., Plasma Centrifugal Furnace, volume 1
[PB92-216035] p 456 N93-12526

CONTINUITY EQUATION

Analytical and numerical principles for the scaling of plasma focus experiments, with regard to electrical resistance
[IPF-91-2] p 450 N93-11103

Particle-fluid two-phase flow modeling
[DE92-017847] p 301 N93-11637

An observational study of a prefrontal convective rainband using TAMEX single- and dual-Doppler data
[AD-A249839] p 371 N93-12251

CONTINUOUS RADIATION

SITE project. Phase 1: Continuous data bit-error-rate testing
[NASA-TP-3279] p 224 N93-11001

Data archiving and analysis for CWDD
[DE92-017064] p 473 N93-11104

CONTINUOUS WAVE LASERS

High-precision thorium RIMS for geochemistry
[DE92-017405] p 250 N93-11918

CONTINUOUS WAVE RADAR

Short-range radar system
[AD-D015339] p 278 N93-11044

CONTINUUM MECHANICS

Systems of evolution equations in thermochemical equations
[AD-A254891] p 253 N93-12282

CONTINUUM MODELING

Fourier continuum finite elements for nonlinear structural analysis p 340 N93-12210

CONTOURS

Nonnormal multivariate distributions: Inference based on elliptically contoured distributions
[AD-A254999] p 429 N93-12513

CONTRACT MANAGEMENT

Final Report, January 1991 - July 1992
[AD-A254659] p 483 N93-12244

CONTRACTION

Mach 4 testing of scramjet inlet models
[NAL-TR-1137] p 202 N93-12369

CONTRAROTATING PROPELLERS

An experimental evaluation of prediction methods for contrafans
[PNR-90924] p 209 N93-11023

CONTROL EQUIPMENT

Droppable jet vane TVC
[AD-D015341] p 214 N93-11046

Design and evaluation of ion source for satellite charge control
[AD-A255172] p 227 N93-12408

CONTROL SIMULATION

Optimal output feedback vibration control of rotor-bearing systems p 324 N93-11220

CONTROL STABILITY

Advanced control for the design of STT missile autopilot
[REPT-921-320-102] p 215 N93-11585

A monitor for the laboratory evaluation of control integrity in digital control systems operating in harsh electromagnetic environments
[NASA-TM-4402] p 215 N93-12304

CONTROL SYSTEMS DESIGN

Spacecraft flight control system design selection process for a geostationary communication satellite
[NASA-TP-3289] p 222 N93-11002

Description of the SSF PMAD DC testbed control system data acquisition function
[NASA-TM-105843] p 417 N93-11005

Concorde propulsion: Did we get it right? The Rolls-Royce/SNECMA Olympus 593 engine reviewed
[PNR-90970] p 210 N93-11061

A problem formulation for glideslope tracking in wind shear using advanced robust control techniques
[NASA-TM-104164] p 214 N93-11176

Optimal output feedback vibration control of rotor-bearing systems p 324 N93-11220

Payout tension control system for reel mounted cable
[AD-D015362] p 325 N93-11423

Modified optimal control pilot model for computer-aided design and analysis
[NASA-TM-4384] p 214 N93-11459

A rule-based system for real-time analysis of control systems
[NASA-TM-104258] p 277 N93-11619

Distributed database integrity
[AD-A253272] p 477 N93-11749

Integrity-oriented control objectives: Proposed revisions to the Trusted Computer System Evaluation Criteria (TCSEC), DOD 5200.28-STD
[AD-A253989] p 404 N93-11809

Rapid maneuvering of large flexible orbiting systems
p 225 N93-11885

Distributed environmental control p 391 N93-11924

A state-based approach to trend recognition and failure prediction for the Space Station Freedom
p 230 N93-11925

Fuzzy control system for a remote focusing microscope p 314 N93-11934

Decentralized control of large flexible structures by joint decoupling
[NASA-TM-107694] p 339 N93-12020

Modeling and model simplification of aeroelastic vehicles: An overview
[NASA-TM-107691] p 215 N93-12216

Formal representation of the requirements for an Advanced Subsonic Civil Transport (ASCT) flight control system
[NASA-CR-189699] p 405 N93-12346

Air-breathing hypersonic vehicle guidance and control studies: An integrated trajectory/control analysis methodology, phase 2
[NASA-CR-189703] p 216 N93-12413

Ultra-dense magnetoresistive mass memory
[NASA-CR-190955] p 405 N93-12520

A vision-based end-point control for a two-link flexible manipulator
[NASA-CR-190967] p 330 N93-12521

CONTROL THEORY

On a certain McMillan degree condition appearing in control
[MATHS-REPT-A-170] p 424 N93-11125

Stochastic control and nonlinear estimation
[AD-A253543] p 420 N93-11147

Automatic control laws for aircraft in parabolic flight
[DILC-EST-TR-211] p 214 N93-11160

Terminal slider control of nonlinear robotic systems
[NASA-CASE-NPO-18584-1-CU] p 324 N93-11177

Application of eigenstructure assignment to the control of powered lift combat aircraft p 215 N93-11871

Spacecraft attitude control using a smart control system p 230 N93-11932

CONTROLLERS

Phase-stepping fiber-optic projected fringe system for surface topography measurements
[NASA-CASE-LEW-14996-1] p 446 N93-11058

EXOS research on master controllers for robotic devices p 399 N93-11957

Fuzzy logic control of telerobot manipulators
p 399 N93-11959

A new scheme of force reflecting control
p 399 N93-11960

Effects of spatially displaced feedback on remote manipulation tasks p 400 N93-11966

Exoskeleton master controller with force-reflecting telepresence p 330 N93-11970

Decentralized control of large flexible structures by joint decoupling
[NASA-TM-107694] p 339 N93-12020

A VMEbus ultrasonic sensor controller for mapping and servo control in robotic systems
[DE92-013661] p 421 N93-12138

Electromagnetic launcher control using finite state machines
[AD-A254433] p 222 N93-12161

Vacuum chamber translation/positioning mechanism and welding power supply controller
[NASA-CR-184465] p 328 N93-12196

A vision-based end-point control for a two-link flexible manipulator
[NASA-CR-190967] p 330 N93-12521

CONVECTION

Numerical and observational investigations of long-lived, MCS-induced, severe surface wind events: The derecho
p 367 N93-11159

The convection speed of the dynamic stall vortex
[AD-A247258] p 197 N93-11464

A composite study of the Madden-Julian oscillation
[AD-A254269] p 369 N93-11819

Enhanced convective and film boiling heat transfer by surface gas injection
[DE92-016755] p 306 N93-12221

An observational study of a prefrontal convective rainband using TAMEX single- and dual-Doppler data
[AD-A249839] p 371 N93-12251

CONVECTION CURRENTS

The forcing of a mid-latitude upper-tropospheric jet streak by a simulated mesoscale convective system
p 358 N93-11184

CONVECTION-DIFFUSION EQUATION

On an origin of numerical diffusion: Violation of invariance under space-time inversion
[NASA-TM-105776] p 425 N93-11254

CONVECTIVE FLOW

Fundamental solutions and boundary element formulations for convective fluid flow
p 298 N93-11217

CONVECTIVE HEAT TRANSFER

The prediction of convective heat transfer in rotating square ducts
[PNR-90929] p 296 N93-11025

The prediction of convective heat transfer in rotating square ducts
[PNR-90985] p 296 N93-11067

Enhanced convective and film boiling heat transfer by surface gas injection
[DE92-016755] p 306 N93-12221

Inert gas electric heater for elevated temperature testing of small propulsion components
[DE92-017434] p 221 N93-12317

Natural convection heat transfer studies of simulated and actual electronic components using dielectric liquids for immersion cooling
[AD-A255173] p 341 N93-12376

Active cooling from the sixties to NASP
p 208 N93-12458

CONVERGENT-DIVERGENT NOZZLES

Numerical modeling of a vortex stabilized arcjet
p 232 N93-11889

CONVERSION

A metric America: A decision whose time has come - for real
[PB92-205459] p 277 N93-11902

COOLANTS

Tables of thermodynamic properties of helium magnet coolant, revision A
[DE92-019098] p 471 N93-11656

COOLING

Development of an intelligent system for cooling rate and fill control in GMAW
[DE92-017849] p 326 N93-11548

Matter-wave interferometry with laser cooled atoms
[AD-A253999] p 316 N93-11737

Translating wedge heat sink
[AD-D015357] p 293 N93-12133

Natural convection heat transfer studies of simulated and actual electronic components using dielectric liquids for immersion cooling
[AD-A255173] p 341 N93-12376

Active cooling from the sixties to NASP
p 208 N93-12458

COOLING FLOWS (ASTROPHYSICS)

Magnetic fields in the clusters of galaxies with extreme cooling flows p 486 N93-12164

COOLING SYSTEMS

A gas-cooled cermet reactor system for planetary base power
[DE92-018017] p 443 N93-11433

Microtube strip heat exchanger
[DE92-018709] p 300 N93-11440

Overview of property formulations for helium, nitrogen, lithium, and lithium-lead in ATHENA/MOD1 with comparison of calculated properties to measured properties
[DE92-017995] p 471 N93-12058

Advanced two-phase heat transfer systems
p 229 N93-12459

Thermostructural applications of heat pipes for cooling leading edges of high-speed aerospace vehicles
p 229 N93-12460

MHD integrated topping cycle project
[DE92-018087] p 456 N93-12504

COORDINATION

An evaluation of crew coordination and performance during a simulated UH-60 helicopter mission
[AD-A254984] p 390 N93-12509

COPOLYMERIZATION

Organometallic NLO polymers. 3. Copolymerization of bridged bis(ferrocenyl) and bis(cyanoacetate) monomers via the knoevenagel condensation
[AD-A250214] p 265 N93-11192

COPOLYMERS

Chemical reactions and properties of organosilicon compounds related to new materials
[AD-A253233] p 246 N93-11218

Computer simulations for the adsorption of polymers onto surfaces
[DE92-018942] p 267 N93-11628

Comparative effects of drag-reducing polymers. An experimental report
[AD-A254001] p 268 N93-11793

Progress on polymer degradation by photoelectron transfer
[AD-A246276] p 268 N93-11862

Synthesis and conductivity of copolymer of 4,4'-diaminodiphenylamine and terephthaloyl chloride
[AD-A254880] p 273 N93-12440

COPPER

Development of stable metallization systems
[AD-A253569] p 264 N93-11079

COPPER ALLOYS

Development of strength and conductivity in deformation processed copper base alloys
[DE92-018807] p 257 N93-11572

Mechanisms of localized aqueous corrosion in aluminum-lithium-copper alloys p 259 N93-11895

COPPER COMPOUNDS

Acid copper sulfate plating bath: Control of chloride and copper
[DE92-019473] p 249 N93-11644

The deposition characteristics of copper(I) compounds for CVD by FT-IR spectroscopy
[DE92-010778] p 467 N93-12134

COPPER OXIDES

Properties of hot isostatically pressed Bi(2)Sr(1.7)CaCu(2)O(x)
[DE92-016394] p 460 N93-11522

A study of parameters that influence growth and stability of the (Bi(1-x)Pb(x))2 Sr2Ca2Cu3O(y) phase
[DE92-015187] p 462 N93-11703

Recrystallization of amorphous or nanocrystalline NdBa2Cu3O(7-x) and GdBa2Cu3O(7-x)
[DE92-016302] p 462 N93-11706

Infrared phonon structure in epitaxial films of Tl2Ca2Ba2Cu3O10 at low temperatures
[DE92-017078] p 466 N93-12109

COPPER SELENIDES

Admittance spectroscopy of copper indium diselenide/cadmium sulfide solar cells
p 344 N93-11214

CORONAL LOOPS

Plasma properties of solar coronal active regions
p 489 N93-12342

CORRECTION

Correction techniques for depth errors with stereo three-dimensional graphic displays
[NASA-TP-3244] p 206 N93-11170

CORRELATION

Correlation of serum alpha sub 1 antitrypsin with cigarette smoking and pulmonary function status in Greek pilots, for a ten year period p 384 N93-11318

Dynamic test/analysis correlation using reduced analytical models
[NASA-TM-107671] p 341 N93-12300

CORRELATION COEFFICIENTS

Statistical methods for the comparison of spatial patterns in meteorological variables p 370 N93-11997

CORROSION

Workshop on Surface Science and Technology
[AD-A253566] p 264 N93-11149

Magneto-optic imaging inspection of selected corrosion specimens
[DOT/FAA/CT-TN92/20] p 332 N93-11617

Mechanisms of localized aqueous corrosion in aluminum-lithium-copper alloys p 259 N93-11895

Analysis of surfaces from the LDEF A0114, phase 2
[NASA-CR-190596] p 270 N93-11993

CORROSION PREVENTION
Corrosion protection of materials for aircraft using ion beam processes. Corrosion and bonding strength examinations. Physical analysis of laser composition
[MBB-Z-0405-91-PUB] p 255 N93-11026

CORROSION RESISTANCE
Corrosion resistant chromate conversion coatings for heat-treated aluminum alloys
[AD-D015366] p 266 N93-11425
The effect of silicon, tin, and chromium on the corrosion and mechanical properties of zirconium - molybdenum - niobium
[AD-A254102] p 258 N93-11787
Oxidation-sulfidation behavior of iron alloys containing 16 to 40 atomic percent aluminum
[DE92-017824] p 259 N93-11830
Improved corrosion resistance of Hastelloy G-30 in nitric/hydrofluoric acid solutions by welding with Inconel 72 weld wire
[DE92-017233] p 262 N93-12487

CORROSION TESTS
Magneto-optic imaging inspection of selected corrosion specimens
[DOT/FAA/CT-TN92/20] p 332 N93-11617
Oxidation-sulfidation behavior of iron alloys containing 16 to 40 atomic percent aluminum
[DE92-017824] p 259 N93-11830

COSMIC DUST
A submillimeter-millimeterwave study of the molecular gas in the nuclear regions of three nearby starburst galaxies p 484 N93-11260
Compositional analysis and classification of projectile residues in LDEF impact craters
[NASA-TM-104750] p 488 N93-11374

COSMIC RAYS
Development of a scintillating optical fiber ionization calorimeter
[NASA-CR-184415] p 311 N93-11662

COSMOLOGY
New singularity and existence of solutions in anisotropic, time-dependent, maximally Gauss-Bonnet extended gravity p 357 N93-11183
Relativistic condensate and cosmology
p 486 N93-12330

COST ANALYSIS
Incorporating prior probabilities and misclassification costs into network training: An example from medical prognosis
[RSRE-MEMO-4343] p 428 N93-10980
Susceptibility in USAF recruits to vaccine preventable diseases p 380 N93-11301
A development approach for nuclear thermal propulsion
[DE92-018020] p 232 N93-11596
Backward assembly planning with DFA analysis
[NASA-CASE-NPO-18817-1-CU] p 278 N93-12202
Introduction to training decisions modeling technologies: The training decisions system
[AD-A249862] p 387 N93-12252
The hydrogen technology assessment, phase 1
[NASA-CR-190969] p 349 N93-12394
Cost estimation of software development and the implications for the program manager
[AD-A255167] p 480 N93-12472

COST EFFECTIVENESS
An iterative method for distributed database design
p 474 N93-11255
Introduction to training decisions modeling technologies: The training decisions system
[AD-A249862] p 387 N93-12252

COST ESTIMATES
Space Transportation Booster Engine Configuration Study. Volume 3: Program Cost estimates and work breakdown structure and WBS dictionary
[NASA-CR-184458] p 233 N93-12088
Cost estimation of software development and the implications for the program manager
[AD-A255167] p 480 N93-12472
The use of life cycle costing for the acquisition of non-major systems at the Naval Regional Contracting Center Detachment
[AD-A255170] p 480 N93-12473
The uses and limits of economic models as a climate change policy tool
[DE92-015792] p 356 N93-12474

COST REDUCTION
The use of life cycle costing for the acquisition of non-major systems at the Naval Regional Contracting Center Detachment
[AD-A255170] p 480 N93-12473

COUETTE FLOW
Hydrodynamic particle migration in small-amplitude, oscillatory, circular couette flow: The limits of reversibility
[DE92-008480] p 303 N93-11843

COULOMB POTENTIAL
Theory of small metal clusters, films, and wires
[AD-A253120] p 256 N93-11240

COUNTER ROTATION
A concept for a counterrotating fan with reduced tone noise
[NASA-TM-105736] p 433 N93-11370

COUPLERS
Test program, helium II orbital resupply coupling
[NASA-CR-185681] p 326 N93-11650

COUPLING CIRCUITS
Temperature tracking SPICE macro-model for laser and LED driven opto-coupler assemblies
[DE92-019296] p 411 N93-11599
Optical beamformer
[AD-A254354] p 448 N93-12272

COUPLING COEFFICIENTS
Determination of loose spline coupling coefficients of rotor bearing systems in turbomachinery
p 327 N93-11887

COUPLINGS
Synthesis and characterization of novel aluminum-arsenic compounds 2. Crystal structures of (R2AlAs (SiMe3)2)2 (R = i-Bu, Me) and i-Bu2 (Cl)Al*As (SiMe3)3
[AD-A248001] p 467 N93-12175

COVALENT BONDS
Positive ion chemistry of acetylene and methylacetylene clusters. Formation of benzene and C(sub 2n)H(sub 2n)(+) ions via intracluster polymerization reactions
[AD-A250931] p 236 N93-12177

COVARIANCE
Identification and estimation of sources of transmitted variation
[DE92-015246] p 429 N93-11820
Composite tasking for sensor arrays
[AD-A254997] p 287 N93-12512
Nonnormal multivariate distributions: Inference based on elliptically contoured distributions
[AD-A254999] p 429 N93-12513

CRACK CLOSURE
Fatigue crack closure: A review
[RAE-TR-90046] p 335 N93-11369

CRACK GEOMETRY
Analysis of precracking parameters and fracture toughness for ceramic single-edge-precracked-beam specimens
[NASA-TM-105568] p 263 N93-10962

CRACK INITIATION
Application of polyimides to aeroengine components
[PNR-90907] p 334 N93-11013
Short fatigue crack growth in a nickel-base superalloy at room and elevated temperature
[PNR-90892] p 255 N93-11031
Fracture mechanics of model fiber composites
p 237 N93-11247
Tension and compression fatigue response of unnotched 3D braided composites
[NASA-CR-189678] p 239 N93-11611

CRACK PROPAGATION
Short fatigue crack growth in a nickel-base superalloy at room and elevated temperature
[PNR-90892] p 255 N93-11031
Modelling short crack growth behaviour in nickel-base superalloys
[PNR-90912] p 255 N93-11033
Elevated temperature fatigue crack growth in a nickel base superalloy under dwell conditions
[PNR-90997] p 255 N93-11115
Fracture behavior of polymers at cryogenic temperatures
[KFK-4969] p 265 N93-11203
Fracture mechanics of model fiber composites
p 237 N93-11247
Environment-induced embrittlement: Stress corrosion cracking and metal-induced embrittlement; environmental embrittlement of iron aluminide alloys
[DE92-018714] p 256 N93-11524
Acoustic emission monitoring of HFIR vessel during hydrostatic testing
[DE92-019316] p 332 N93-11601
Tension and compression fatigue response of unnotched 3D braided composites
[NASA-CR-189678] p 239 N93-11611
The conversion of plastic work to heat around a dynamically propagating crack in metals
[AD-A253801] p 258 N93-11782
Elastic stresses, twin boundaries, and fatigue cracking
p 338 N93-11890
Slow crack growth in vacuum p 338 N93-11909
Thermal fracture service life analysis of a case bonded visco-elastic cylinder p 339 N93-12008
Mechanical properties for advanced engine materials
[AD-A252632] p 242 N93-12181
Microstructure-based fatigue life prediction methods for naval steel structures
[AD-A254628] p 260 N93-12241
Fatigue crack growth in AerMet 100 steel
[AD-A249068] p 261 N93-12248
Influence of oxygen partial pressure and silver additions on microstructure and related properties of YBCO superconductors
[DE92-011145] p 468 N93-12249
Study of residual stresses and microcracks in high strength steel weldments: An investigation of microcrack formation and stressed growth using laser microscopy
[AD-A255059] p 342 N93-12467
Spectrum fatigue behaviour of powder metallurgy aluminum alloys
[AD-A255060] p 262 N93-12468

CRACK TIPS
On the dependence of the dynamic crack tip temperature fields in metal upon crack tip velocity and material parameters
[AD-A253657] p 335 N93-11219
The conversion of plastic work to heat around a dynamically propagating crack in metals
[AD-A253801] p 258 N93-11782
Slow crack growth in vacuum p 338 N93-11909

CRACKING (CHEMICAL ENGINEERING)
Measuring and modelling of particle-fluid flow in a riser reactor
[VTT-PUBS-88] p 299 N93-11359

CRACKING (FRACTURING)
Short fatigue crack growth in a nickel-base superalloy at room and elevated temperature
[PNR-90892] p 255 N93-11031
On the dependence of the dynamic crack tip temperature fields in metal upon crack tip velocity and material parameters
[AD-A253657] p 335 N93-11219
Thermomechanical fatigue behavior of SiC/Ti-24Al-11Nb in air and argon environments
[NASA-TM-105723] p 238 N93-11399
An evaluation of repair techniques used for uncontrolled longitudinal cracking and failed longitudinal joints
[PB92-205616] p 277 N93-12072
The effect of contact stresses in four-point bend testing of graphite/epoxy and graphite/PMR-15 composite beams
[NASA-TM-105891] p 241 N93-12076
Study of residual stresses and microcracks in high strength steel weldments: An investigation of microcrack formation and stressed growth using laser microscopy
[AD-A255059] p 342 N93-12467

CRACKS
Analysis of precracking parameters and fracture toughness for ceramic single-edge-precracked-beam specimens
[NASA-TM-105568] p 263 N93-10962
Nondestructive evaluation of ceramic and metal matrix composites for NASA's HITEMP and enabling propulsion materials programs
[NASA-TM-105807] p 331 N93-10963
Nondestructive inspection and life determination of disc material
[PNR-90911] p 331 N93-11016
The conversion of plastic work to heat around a dynamically propagating crack in metals
[AD-A253801] p 258 N93-11782
Elastic stresses, twin boundaries, and fatigue cracking
p 338 N93-11890
A consistent cracked bar vibration theory
p 339 N93-12000

CRASHWORTHINESS
Crashworthy characteristics of circular tubes in axisymmetric buckling p 337 N93-11721

CRATERS
Compositional analysis and classification of projectile residues in LDEF impact craters
[NASA-TM-104750] p 488 N93-11374

CRAY COMPUTERS
Evaluation of a Cray performance tool using a large hydrodynamics code
[DE92-013239] p 407 N93-11231

CREEP PROPERTIES
A creep cavity growth model for creep-fatigue life prediction of a unidirectional W/Cu composite
[NASA-TM-105780] p 333 N93-10967
Creep failure in linear and nonlinear viscoelastic materials p 342 N93-12536

CREEP STRENGTH
The mechanical and microstructural stability of austenitic stainless steels strengthened by MC-forming elements
[DE91-015314] p 259 N93-11857

CREEP TESTS
The mechanical and microstructural stability of austenitic stainless steels strengthened by MC-forming elements
[DE91-015314] p 259 N93-11857

Mechanical properties for advanced engine materials
[AD-A252632] p 242 N93-12181

CREW PROCEDURES (INFLIGHT)
An evaluation of crew coordination and performance during a simulated UH-60 helicopter mission
[AD-A254984] p 390 N93-12509

CRITERIA
The complexity of some multicriteria arborescence problems
[REPT-92-016] p 424 N93-11182

CRITICAL FLOW
FNAS computational fluid dynamics
[NASA-CR-184394] p 307 N93-12397

CRITICAL LOADING
Study of compression-loaded and impact-damaged structurally efficient graphite-thermoplastic trapezoidal-corrugation sandwich and semisandwich panels
[NASA-TP-3264] p 239 N93-11623
The relative importance of sulfur and nitrogen compounds in the acidification of freshwater
[DE92-016899] p 354 N93-11680

CRITICAL PATH METHOD
Path planning on a ring of processors
p 410 N93-11480

CRITICAL TEMPERATURE
High temperature superconductor materials and applications
[NASA-CR-184426] p 470 N93-12396

CROSS CORRELATION
Periodicities in pulsar microstructure
p 484 N93-11230

CROSSLINKING
Semi-interpenetrating polymer network for tougher and more microcracking resistant high temperature polymers
[NASA-CASE-LAR-13925-2] p 264 N93-11059
Molecular mobility of the interface in a model composite: A NMR study
[AD-A253311] p 265 N93-11194

CRUISE MISSILES
Computer aided design and manufacturing of composite propfan blades for a cruise missile wind tunnel model
[NASA-TM-105269] p 413 N93-12022

CRUSHING
Crushing behavior of tubular structures in multi-materials
[ECL-91-37] p 336 N93-11579
Crashworthy characteristics of circular tubes in axisymmetric buckling p 337 N93-11721

CRUSTS
Study of seismic coda generation in crust with non-uniform scattering and anelastic properties
[AD-A254350] p 366 N93-12270

CRYOCHEMISTRY
Tables of thermodynamic properties of helium magnet coolant, revision A
[DE92-019098] p 471 N93-11656

CRYOGENIC COOLING
Microtube strip heat exchanger
[DE92-018709] p 300 N93-11440
Cryostabilization of high-temperature superconducting magnets with subcooled flow in microchannels
[DE92-018174] p 431 N93-11598
Operating experience using venturi flow meters at liquid helium temperature
[DE92-014693] p 313 N93-12140
Thermostructural applications of heat pipes for cooling leading edges of high-speed aerospace vehicles
p 229 N93-12460

CRYOGENIC EQUIPMENT
A cryogenic phonon detector to search for dark matter particles p 481 N93-11198
Test program, helium II orbital resupply coupling
[NASA-CR-185681] p 326 N93-11650
Operating experience using venturi flow meters at liquid helium temperature
[DE92-014693] p 313 N93-12140

CRYOGENIC FLUIDS
Cryostabilization of high-temperature superconducting magnets with subcooled flow in microchannels
[DE92-018174] p 431 N93-11598

CRYOGENIC ROCKET PROPELLANTS
Small experiments for the maturation of orbital cryogenic transfer technologies
[NASA-TM-105849] p 296 N93-10981

CRYOGENIC TEMPERATURE
Fracture behavior of polymers at cryogenic temperatures
[KFK-4969] p 265 N93-11203

CRYOGENIC WIND TUNNELS
Further buffeting tests in a cryogenic wind tunnel
[NASA-TM-107621] p 198 N93-11610
Strain-gauge balance performance and internal temperature gradients measured in a cryogenic environment
[RAE-TM-AERO-2232] p 218 N93-11906

CRYOGENICS
A cryogenic enrichment technique for gas chromatographic detection of S2F10 in SF6 discharges
[DE92-011045] p 252 N93-12219

CRYSTAL DEFECTS
Nanostructure, defect chemistry and properties of relaxor ferroelectrics
[AD-A247294] p 431 N93-11468
Oxidation, nitridation, and fluorine etching of Si
[AD-A253559] p 249 N93-11755
Microscopic origins of metastable effects in a-Si:H and deep defect characterization in a-Si,Ge:H alloys
[DE92-010588] p 463 N93-11813
Silicon on insulator structures in selective epitaxial growth
[DE92-017118] p 465 N93-11915
Effect of microstructure on passive film formation and breakdown on Al alloys
[AD-A245863] p 260 N93-12118
Atomic bonding at ceramic interfaces using scanning tunneling microscopy
[DE92-018706] p 273 N93-12479

CRYSTAL DISLOCATIONS
Growth, characterization, and device development in monocrystalline diamond films
[AD-A252648] p 271 N93-12184

CRYSTAL GROWTH
Growth mechanisms of layered superconductors
[DE92-018492] p 458 N93-10987
Fast electrochromic switching for optical hardening applications
[AD-A248174] p 447 N93-11186
ICCG-10: Tenth International Conference on Crystal Growth. Poster presentation abstracts
[NASA-CR-190920] p 461 N93-11683
ICCG-10: Tenth International Conference on Crystal Growth. Oral presentation abstracts
[NASA-CR-190919] p 461 N93-11684
Step-driven surface segregation and ordering during Si-Ge MBE growth
[DE92-017827] p 463 N93-11772
Effect of microstructure on passive film formation and breakdown on Al alloys
[AD-A245863] p 260 N93-12118
Formation of buried epitaxial Si-Ge alloy layers in Si (100) crystal by high dose Ge ion implantation
[DE92-017114] p 466 N93-12127
Hydrogen assisted heat transfer during diamond growth using carbon and tantalum filaments
[AD-A247944] p 468 N93-12218
Surface analysis of Ln(2-x)Ce(x)CuO4 (Ln = Pr and Nd) single crystals grown by the top seeded solution method
[AD-A254905] p 469 N93-12286

CRYSTAL LATTICES
Nature of the beta-phase of nickel-aluminum system
[AD-A254101] p 261 N93-12269
Surface analysis of Ln(2-x)Ce(x)CuO4 (Ln = Pr and Nd) single crystals grown by the top seeded solution method
[AD-A254905] p 469 N93-12286

CRYSTAL OPTICS
Electronic and optical properties of perfect and imperfect 2 to 6 superlattices p 465 N93-11996

CRYSTAL OSCILLATORS
Quartz crystal resonators and oscillators for frequency control and timing applications: A tutorial, revision 5.2
[AD-A254892] p 469 N93-12283

CRYSTAL STRUCTURE
The synthesis and crystal structure of LaHSe2O6, a layered, anhydrous selenite
[AD-A251050] p 458 N93-10996
Review of phonon behavior and microstructural development leading to martensitic transformations in Ni(x)Al(100-x) alloys
[DE92-014782] p 256 N93-11519
Tetrahedral atom zincophosphate structures: Synthesis, crystal structure, and spectroscopic studies of (Zn(PO2(OC2H5)2)2)x, a one-dimensional inorganic polymer
[AD-A251051] p 437 N93-11560
Structure and property of heteroepitaxial TiO2/VO2 multilayers
[DE92-018181] p 460 N93-11563
Determination of parameters of a new method for predicting alloy properties
[NASA-TM-105895] p 257 N93-11609
Studies of the 3 to 5 compounds in the megabar regime
[DE92-019517] p 461 N93-11646
Recrystallization of amorphous or nanocrystalline NdBa2Cu3O(7-x) and GdBa2Cu3O(7-x)
[DE92-016302] p 462 N93-11706
Synthesis and characterization of novel organogallium-phosphorus compounds: X ray crystal structures of Ph2GaP (SiMe3)2Ga (Ph2Cl, Ph2 (Cl)Ga.P (SiMe3)3, and Ph3Ga.P (SiMe3)3
[AD-A253841] p 462 N93-11724
Slow crack growth in vacuum p 338 N93-11909
Electronic and optical properties of perfect and imperfect 2 to 6 superlattices p 465 N93-11996
Synthesis and characterization of novel aluminum-arsenic compounds 2. Crystal structures of (R2AlAs (SiMe3)2)2 (R = i-Bu, Me) and i-Bu2 (Cl)Al*As (SiMe3)3
[AD-A248001] p 467 N93-12175

CRYSTAL SURFACES
Basic principles of organometallic vapor phase epitaxy
[AD-A250665] p 464 N93-11868
Triisopropylindium: Decomposition study and use for low temperature growth
[AD-A250666] p 464 N93-11869
The role of backbond strain in silicon surfaces on the decomposition of NH3 and PH3
[AD-A253771] p 250 N93-12062

CRYSTALLINITY
The 1992 DOE/Sandia crystalline photovoltaic technology project review meeting
[DE92-018544] p 344 N93-10989
The domain structure features of epitaxial PbTiO3 thin films prepared by MOCVD
[DE92-010907] p 459 N93-11190
Growth of 2-6 thin-films from single-source precursors based on sterically encumbered sitel ligands
[DE92-017077] p 466 N93-12099

CRYSTALLIZATION
Synthesis and side chain liquid crystal polymers by living ring opening metathesis polymerization. 5: Influence of mesogenic group and interconnecting group on the thermotropic behavior of the resulting polymers
[AD-A253568] p 264 N93-11150
Synthesis of side chain liquid crystal polymers by living ring opening metathesis polymerization. Report 2: Influence of molecular weight, polydispersity, and flexible spacer length (n=9-12) on the thermotropic behavior of the resulting plymers
[AD-A248700] p 265 N93-11188

CRYSTALLOGRAPHY
The synthesis and crystal structure of LaHSe2O6, a layered, anhydrous selenite
[AD-A251050] p 458 N93-10996
Nature of the beta-phase of nickel-aluminum system
[AD-A254101] p 261 N93-12269

CUES
Correction techniques for depth errors with stereo three-dimensional graphic displays
[NASA-TP-3244] p 206 N93-11170

CULTURE TECHNIQUES
Biological conversion of synthesis gas culture development
[DE92-001279] p 375 N93-12482

CURIE TEMPERATURE
The domain structure features of epitaxial PbTiO3 thin films prepared by MOCVD
[DE92-010907] p 459 N93-11190

CURIE-WEISS LAW
An NMR study of the occupation of C(sub 60) interstitial sites by oxygen molecules
[DE92-019436] p 437 N93-11640

CURING
Curing and mechanical properties of T800-V398 graphite/bismaleimide at different temperatures
[DLR-FB-92-02] p 237 N93-11143
Evaluation of epoxy cured with Ethacure 100 curing agent for use in headers for thermal batteries
[DE92-019326] p 267 N93-11552

CURRENT DENSITY
Critical currents in polycrystalline YBa2Cu3O(7-x): Self-field and grain size dependence
[DE92-617540] p 459 N93-11076
Properties of hot isostatically pressed Bi(2)Sr(1.7)CaCu(2)O(x)
[DE92-016394] p 460 N93-11522
Characteristics of current filamentation in high gain photoconductive semiconductor switching
[DE92-018277] p 291 N93-11693
VLSI design for reliability
[AD-A253207] p 292 N93-11781
High temperature superconductor materials and applications
[NASA-CR-184426] p 470 N93-12396

CURVATURE
An approach to constrained aerodynamic design with application to airfoils
[NASA-TP-3260] p 201 N93-12321

CURVE FITTING
An approach to constrained aerodynamic design with application to airfoils
[NASA-TP-3260] p 201 N93-12321
Curve fitting and error modeling for the digitization process near the Nyquist rate
[DE92-018189] p 286 N93-12417

CURVED BEAMS
Methods of analysis for thick-section composite structures p 237 N93-11262

CYBERNETICS
Bionics and problems of instrument manufacture [AD-A254461] p 314 N93-12517

CYCLES
Interactive analysis of gappy bivariate time series using AGSS [AD-A255160] p 429 N93-12426

CYCLIC COMPOUNDS
Synthesis of side chain liquid crystal polymers by living ring opening metathesis polymerization. Report 3: Influence of molecular weight, interconnecting unit and substituent on the mesomorphic behavior of polymers with laterally attached mesogens [AD-A248698] p 265 N93-11187
Synthesis of side chain liquid crystal polymers by living ring opening metathesis polymerization. Report 2: Influence of molecular weight, polydispersity, and flexible spacer length (n=9-12) on the thermotropic behavior of the resulting plymers [AD-A248700] p 265 N93-11188
Synthesis and characterization of novel organogallium-phosphorus compounds: X ray crystal structures of Ph2GaP (SiMe3)2Ga (Ph2Cl, Ph2 (Cl)Ga.P (SiMe3)3, and Ph3Ga.P (SiMe3)3 [AD-A253841] p 462 N93-11724
Controlled synthesis of polyenes by catalytic methods [DE92-015286] p 271 N93-12165

CYCLIC LOADS
Elevated temperature fatigue crack growth in a nickel base superalloy under dwell conditions [PNR-90997] p 255 N93-11115
Nonlinear response of thin steel plate structures subjected to static, cyclic, and dynamic loads p 335 N93-11200
VAMAS round robin project on polymer composite delamination in mode 1 and mode 2: Cyclic loading [NPL-DMM(A)-47] p 266 N93-11397
A comparison of high cycle fatigue methodologies [NASA-TM-103601] p 233 N93-12148
Verification of rain-flow reconstructions of a variable amplitude load history [NASA-CR-189670] p 341 N93-12411

CYCLONES
Hurricane Research Division fiscal year 1991 programs: Fiscal year 1992 projections [PB92-138320] p 367 N93-11242
Operations plan for the Tropical Cyclone Motion (TCM-92) mini-field experiment [AD-A254723] p 372 N93-12339
A real time sharpening of NOGAPS predictions of mid-latitude Central Pacific cyclones [AD-A255157] p 372 N93-12424

CYCLOTRON RADIATION
A new pitch angle diagnostic for electron cyclotron resonance plasma p 450 N93-11185
Fast cooling phenomena with ice pellet injection in the JIPP T-IIU tokamak [DE92-782105] p 454 N93-11834

CYCLOTRON RESONANCE
A new pitch angle diagnostic for electron cyclotron resonance plasma p 450 N93-11185

CYGNUS CONSTELLATION
Morphology and physics of supernova remnants p 482 N93-11476

CYLINDRICAL BODIES
High speed parallel backplane [AD-D015372] p 288 N93-11053
Optical properties of composite membranes containing arrays of nanoscopic gold cylinders [AD-A253659] p 238 N93-11281
Evaluation of an analytical model for predicting light scattering from cylindrically-shaped objects in the ocean [AD-A248414] p 447 N93-11489
Drag on an oscillating rod in a non-Newtonian fluid [DE92-014746] p 308 N93-12492

CYTOLOGY
Molecular cytogenetics: A novel approach for measuring chromosome translocations in individuals years after exposure to low levels of ionizing radiation [DE92-018066] p 374 N93-10974
Clinical and immunological response to vaccination with parenteral or oral vaccines in two groups of 30 recruits p 381 N93-11305
Use of novel adjuvants and delivery systems to improve the humoral and cellular immune response to malaria vaccine candidate antigens p 381 N93-11308

CYTOMETRY
Early markers of HIV infection and subclinical disease progression p 379 N93-11296

D

DAMAGE
The use of high-frequency dynamic information for the evaluation of damage in fiber reinforced composite materials p 241 N93-11998

DAMAGE ASSESSMENT
Radiation damage by high energy electrons in GaAs: A DLTS (deep level transient spectroscopy) examination [HMI-B-494] p 442 N93-11028
Using NDT techniques in the maintenance of aeronautical products [REPT-921-430-102] p 332 N93-11587
Heat load material studies: Simulated tokamak disruptions [DE92-018275] p 452 N93-11674
Microstructure-based fatigue life prediction methods for naval steel structures [AD-A254628] p 260 N93-12241

DAMPING
Higher-order-mode damping and microwave absorption at 2 K [DE92-016960] p 442 N93-11077
Determination of loose spline coupling coefficients of rotor bearing systems in turbomachinery p 327 N93-11887
ICAN/DAMP-integrated composite analyzer with damping analysis capabilities: User's manual [NASA-TP-3292] p 241 N93-12015
Damping and scattering of electromagnetic waves by small ferrite spheres suspended in an insulator [NASA-TM-105837] p 286 N93-12366

DARK MATTER
A cryogenic phonon detector to search for dark matter particles p 481 N93-11198

DATA ACQUISITION
The millimeter wave Cloud Profiling Radar System (CPRS) [DE92-016970] p 366 N93-10971
Description of the SSF PMAD DC testbed control system data acquisition function [NASA-TM-105843] p 417 N93-11005
Experimental heat transfer results in turbine stators and rotors and a comparison with theory [PNR-90945] p 210 N93-11055
LV software support for supersonic flow analysis [NASA-CR-190209] p 297 N93-11074
Wind tunnel operator aimed comparison between two electronic pressure scanner systems [DLAS-EST-TR-040] p 217 N93-11225
A summary of the JANNAF workshop on diagnostics p 248 N93-11451
Design of a PCM data compressor --- pulse code modulation [DE92-019469] p 404 N93-11539
Trip report: Marshall Space Center computed tomography [DE92-018139] p 437 N93-11597
AGARD flight test techniques series. Volume 10: Weapon delivery analysis and ballistic flight testing [AGARD-AG-300-VOL-10] p 430 N93-11711
High-speed test station for solid-state imagers [DE92-018990] p 312 N93-11822
A distributed data acquisition and centralized data reduction system for flexible and efficient measurements [DE92-019021] p 312 N93-11827
On the acquisition and representation of procedural knowledge p 394 N93-11937
Ultrasonic sensing of GMAW: Laser/EMAT defect detection system [DE92-017916] p 333 N93-12055
The diagnostics system for the multiple heavy ion beams induction linac experiment, MBE-4 [DE92-017109] p 445 N93-12126
Alternative Fuel Evaluation Program: Alternative Fuel Light Duty Vehicle Project. Data collection responsibilities, techniques, and test procedures [DE92-010598] p 275 N93-12171
Methodology issues concerning the accuracy of kinematic data collection and analysis using the ariel performance analysis system [NASA-CR-185689] p 389 N93-12211
Operations plan for the Tropical Cyclone Motion (TCM-92) mini-field experiment [AD-A254723] p 372 N93-12339

DATA BASE MANAGEMENT SYSTEMS
Data archiving and analysis for CWDD [DE92-017064] p 473 N93-11104
A probabilistic approach to information retrieval in heterogeneous databases [DE92-016993] p 473 N93-11151
An iterative method for distributed database design p 474 N93-11255
Lies, damned lies, and databases [RSRE-MEMO-4503-ISSUE-2] p 474 N93-11333
A front end implementation of the Pollyanna secure DBMS [RSRE-MEMO-4540] p 475 N93-11404
An iconic query interface for an image database [AD-A253571] p 475 N93-11506
The ESSE project: Supporting object-oriented database schema analysis and evolution: Overview [REPT-92-026] p 476 N93-11689
Distributed database integrity [AD-A253272] p 477 N93-11749
Laboratory information management system proposal [DE92-018243] p 478 N93-11796
Application of machine learning techniques for effective retrieval in image database [AD-A254907] p 479 N93-12287

DATA BASES
Catalog of data bases and reports [DE92-018586] p 473 N93-10990
Experience of designing a relational materials database [PNR-90893] p 473 N93-11012
Data archiving and analysis for CWDD [DE92-017064] p 473 N93-11104
A probabilistic approach to information retrieval in heterogeneous databases [DE92-016993] p 473 N93-11151
Managing data: From vision to reality [PB92-191212] p 474 N93-11215
An iterative method for distributed database design p 474 N93-11255
Information dissemination: Case studies on electronic dissemination at four agencies. Fact sheet for the Chairman, Committee on Governmental Affairs, US Senate [GAO/IMTEC-92-6FS] p 474 N93-11274
Study and recommendation of available sources of scientific and technical numeric databases in the government and private sector [AD-A247266] p 475 N93-11465
An iconic query interface for an image database [AD-A253571] p 475 N93-11506
Acoustic fill factors for a 120 inch diameter fairing [NASA-CR-189284] p 434 N93-11634
The ESSE project: Supporting object-oriented database schema analysis and evolution: Overview [REPT-92-026] p 476 N93-11689
An object-oriented approach to spatial databases [REPT-92-034] p 476 N93-11690
Directory of factual and numeric databases of relevance to aerospace and defence R and D [AGARD-R-777] p 476 N93-11710
Spatial data transformation: Feature attribute conversion issues and practical experience [AD-A254238] p 477 N93-11741
Distributed database integrity [AD-A253272] p 477 N93-11749
Development of the Personnel-based System Evaluation Aid (PER-SEVAL) performance shaping functions [AD-A252820] p 386 N93-11779
LINK user manual [DE92-017987] p 479 N93-12143
National Space Science Data Center data archive and distribution service (NDADS) automated retrieval mail system user's guide [NASA-TM-107990] p 479 N93-12150
Meta-analysis of integrity tests: A critical examination of validity generalization and moderator variables [AD-A254681] p 386 N93-12225
Application of machine learning techniques for effective retrieval in image database [AD-A254907] p 479 N93-12287
Exploiting captions in retrieval of multimedia data [AD-A255184] p 479 N93-12381
ESIS: An introduction to the European space information system. A modern tool for space scientists [ESA-INT-2] p 479 N93-12404

DATA COMPRESSION
Non-linear data conversion system for dynamic range digital signal processing [AD-D015347] p 278 N93-11047
Design of a PCM data compressor --- pulse code modulation [DE92-019469] p 404 N93-11539
Real-time data compression using a FFT digital signal processor [DE92-017744] p 477 N93-11770
Transient Reduction Analysis using Neural Networks (TRANN) [DE92-012150] p 421 N93-12153

DATA CONVERSION ROUTINES
Non-linear data conversion system for dynamic range digital signal processing [AD-D015347] p 278 N93-11047

DATA FLOW ANALYSIS
Analysis of methods --- information systems evolution environment
[NASA-CR-190278] p 407 N93-11368
The ESSE project: Supporting object-oriented database schema analysis and evolution: Overview
[REPT-92-026] p 476 N93-11689
Nimbus-7 Scanning Multichannel Microwave Radiometer (SMMR) PARM tape user's guide
[NASA-RP-1284] p 373 N93-11718
DATA INTEGRATION
The Kalman filter for two-dimensional stable and unstable atmospheres p 359 N93-11249
DATA LINKS
Controller evaluation of initial data link terminal air traffic control services: Mini study 2, volume 1
[DOT/FAA/CT-92/2-VOL-1] p 205 N93-11704
Controller evaluation of initial data link terminal air traffic control services: Mini study 2, volume 2
[DOT/FAA/CT-92/2-VOL-2] p 205 N93-11705
Space Communication Artificial Intelligence for Link Evaluation Terminal (SCAILET) p 395 N93-11940
Low Density Radio Communications Link (LDRCL) Operational Test and Evaluation (OT/E) integration and operation test plan
[DOT/FAA/CT-TN92/4] p 285 N93-12331
Data distribution satellite
[NASA-TM-105778] p 287 N93-12481
DATA MANAGEMENT
Experience of designing a relational materials database
[PNR-90893] p 473 N93-11012
Managing data: From vision to reality
[PB92-191212] p 474 N93-11215
An object-oriented approach to spatial databases
[REPT-92-034] p 476 N93-11690
Spatial data transformation: Feature attribute conversion issues and practical experience
[AD-A254238] p 477 N93-11741
Distributed database integrity
[AD-A253272] p 477 N93-11749
Intelligent data management for real-time spacecraft monitoring p 394 N93-11936
DATA PROCESSING
Sodium-lidar mesosphere examinations: Selected elements of the experimental construction of a mobile instrument and evaluation of the data acquired with a stationary Na-lidar during the DYANA campaign
[BONN-IR-91-78] p 357 N93-11006
The evolution of Ten15
[RSRE-MEMO-4543] p 409 N93-11405
EUROMET project no. 231: Uncertainties in mass measurement. NPL's analysis of data from the calibration of weight set NPLW43
[NPL-MOM-107] p 432 N93-11666
Nimbus-7 Scanning Multichannel Microwave Radiometer (SMMR) PARM tape user's guide
[NASA-RP-1284] p 373 N93-11718
Spatial data transformation: Feature attribute conversion issues and practical experience
[AD-A254238] p 477 N93-11741
Differential equation-based seismic data filtering
[DE92-016282] p 363 N93-11791
Real-time classification of signals from three-component seismic sensors using neural nets
[DE92-014886] p 364 N93-12155
Alternative Fuel Evaluation Program: Alternative Fuel Light Duty Vehicle Project. Data collection responsibilities, techniques, and test procedures
[DE92-010598] p 275 N93-12171
ESIS: An introduction to the European space information system. A modern tool for space scientists
[ESA-INT-2] p 479 N93-12404
DATA PROCESSING EQUIPMENT
Non-linear data conversion system for dynamic range digital signal processing
[AD-D015347] p 278 N93-11047
High speed parallel backplane
[AD-D015372] p 288 N93-11053
DATA RECORDERS
High Capacity Voice Recorder (HCVR) Operational Test and Evaluation (OT/E) integration test report
[DOT/FAA/CT-TN92/30] p 310 N93-11460
DATA REDUCTION
LV software support for supersonic flow analysis
[NASA-CR-190209] p 297 N93-11074
Residual acceleration data on IML-1: Development of a data reduction and dissemination plan
[NASA-CR-190807] p 223 N93-11101
Reduction operations on a distributed memory machine with a reconfigurable interconnection network
p 410 N93-11484
Computational aspects of Gaussian beam migration
[DE92-018641] p 431 N93-11567
A distributed data acquisition and centralized data reduction system for flexible and efficient measurements
[DE92-019021] p 312 N93-11827
The diagnostics system for the multiple heavy ion beams induction linac experiment, MBE-4
[DE92-017109] p 445 N93-12126
Alternative Fuel Evaluation Program: Alternative Fuel Light Duty Vehicle Project. Data collection responsibilities, techniques, and test procedures
[DE92-010598] p 275 N93-12171
Dynamic multimodal function optimization using genetic algorithms
[DE92-019602] p 414 N93-12234
DATA RETRIEVAL
Lies, damned lies, and databases
[RSRE-MEMO-4503-ISSUE-2] p 474 N93-11333
National Space Science Data Center data archive and distribution service (NDADS) automated retrieval mail system user's guide
[NASA-TM-107990] p 479 N93-12150
DATA STORAGE
Deriving and manipulating module interfaces
[AD-A253869] p 406 N93-11145
Erasable optical information storage in the polyanilines
[AD-A254873] p 480 N93-12438
DATA STRUCTURES
Deriving and manipulating module interfaces
[AD-A253869] p 406 N93-11145
A formal definition of the static semantics of ELLA's core
[RSRE-91024] p 409 N93-11436
Directory interchange format manual, version 4.0
[NASA-TM-107991] p 478 N93-11911
DATA SYSTEMS
An object-oriented approach to spatial databases
[REPT-92-034] p 476 N93-11690
Photogrammetric GIS technology: Feature mapping on digital stereo imagery
[AD-A254255] p 477 N93-11748
A composite study of the Madden-Julian oscillation
[AD-A254269] p 369 N93-11819
Validation test report for the first-generation dart Gulf Stream forecasting system
[AD-A254286] p 373 N93-11821
Directory interchange format manual, version 4.0
[NASA-TM-107991] p 478 N93-11911
National Space Science Data Center data archive and distribution service (NDADS) automated retrieval mail system user's guide
[NASA-TM-107990] p 479 N93-12150
Program for implementing software quality metrics
[DE92-018617] p 413 N93-12187
DATA TRANSFER (COMPUTERS)
Spatial data transformation: Feature attribute conversion issues and practical experience
[AD-A254238] p 477 N93-11741
DATA TRANSMISSION
Controller evaluation of initial data link terminal air traffic control services: Mini study 2, volume 1
[DOT/FAA/CT-92/2-VOL-1] p 205 N93-11704
Controller evaluation of initial data link terminal air traffic control services: Mini study 2, volume 2
[DOT/FAA/CT-92/2-VOL-2] p 205 N93-11705
Identification and estimation of sources of transmitted variation
[DE92-015246] p 429 N93-11820
An optical fiber multi-terminal data bus system for aircraft
[NAL-TR-1125] p 209 N93-12370
Computer modeling of tactical high frequency antennas
[AD-A255176] p 286 N93-12377
DEATH
Smoking status and body composition, exercise, dietary intake, and alcohol/caffeine consumption
[AD-A250648] p 385 N93-11893
DEBRIS
Debris/ice/TPS assessment and integrated photographic analysis for Shuttle Mission STS-46
[NASA-TM-107552] p 223 N93-12151
Microbiological analysis of debris from STS-42 IML-1 by direct plating of rinse waters
[NASA-TM-108375] p 375 N93-12174
DECELERATION
The effect of variable seat back angles on human response to +Gz impact accelerations
[AD-A250673] p 387 N93-11559
DECISION MAKING
Intelligent TDA systems using neural networks, phase 1
[AD-A252556] p 420 N93-11000
Implementing system simulation of C3 systems using autonomous objects
[NASA-CR-190845] p 283 N93-11716
Backward assembly planning with DFA analysis
[NASA-CASE-NPO-18817-1-CU] p 278 N93-12202
Mathematical methods in operations research and computer science
[AD-A254782] p 428 N93-12465
Selective factors affecting rotary wing aviator performance with symbology superimposed on night vision goggles
[AD-A254983] p 390 N93-12508
Development of a model for predicting NASA/MSFC program success
[NASA-CR-184423] p 473 N93-12542
DECISION THEORY
A rule-based system for real-time analysis of control systems
[NASA-TM-104258] p 277 N93-11619
Intelligent data management for real-time spacecraft monitoring p 394 N93-11936
Mathematical methods in operations research and computer science
[AD-A254782] p 428 N93-12465
DECODERS
An investigation of error correcting techniques for OMV and AXAF
[NASA-CR-190950] p 416 N93-12515
DECODING
An investigation of error correcting techniques for OMV and AXAF
[NASA-CR-190950] p 416 N93-12515
DECOMPOSITION
Domain decomposition: A bridge between nature and parallel computers
[NASA-CR-189709] p 425 N93-11246
Selective carbon oxygen bond scission during reactions of oxygenates on single crystal catalysts
[DE92-018687] p 247 N93-11439
Direct catalytic decomposition of nitric oxide
[DE92-018759] p 247 N93-11444
Triisopropylindium: A new precursor for OMVPE growth
[AD-A250672] p 460 N93-11558
Backward assembly planning with DFA analysis
[NASA-CASE-NPO-18817-1-CU] p 278 N93-12202
DECOUPLING
Application of eigenstructure assignment to the control of powered lift combat aircraft p 215 N93-11871
Research and development at ORNL/CESAR towards cooperating robotic systems for hazardous environments
p 331 N93-11979
Decentralized control of large flexible structures by joint decoupling
[NASA-TM-107694] p 339 N93-12020
DECOYS
Simulator, Tactical Use, Flare (STUF) project report
[AD-A254890] p 276 N93-12281
DEEP SPACE NETWORK
Operator assistant to support deep space network link monitor and control p 288 N93-11939
DEFECTS
Nondestructive evaluation of ceramic and metal matrix composites for NASA's HITEMP and enabling propulsion materials programs
[NASA-TM-105807] p 331 N93-10963
A comparison of the achieved and predicted defect rates of some continuously operating electronic equipment
[RTP/909/10-ISSUE-2] p 288 N93-11364
Development of nondestructive evaluation methods and prediction of effects of flaws on the fracture behavior of structural ceramics
[DE92-016395] p 271 N93-12123
Method and apparatus for evaluating multilayer objects for imperfections
[NASA-CASE-LAR-14581-1-SB] p 333 N93-12204
Influence of strain rate on the structure/property behavior of the alpha-2 alloy Ti-24.5Al-10.5Nb-1.5Mo
[DE92-008490] p 261 N93-12256
DEFENDER PROJECT
Lightweight Exoatmospheric Projectile (LEAP) test program. Supplemental environmental assessment
[AD-A252286] p 231 N93-10998
DEFENSE PROGRAM
Integrity-oriented control objectives: Proposed revisions to the Trusted Computer System Evaluation Criteria (TCSEC), DOD 5200.28-STD
[AD-A253989] p 404 N93-11809
Research and development strategies for human centered and group support technologies
[AD-A254366] p 472 N93-12273
ONRASIA scientific information bulletin, volume 17, number 3
[AD-A255073] p 490 N93-12470
Cost estimation of software development and the implications for the program manager
[AD-A255167] p 480 N93-12472
DEFLAGRATION
Characterization of deflagrating munitions by rotating prism high speed photography
[MRL-TR-91-43] p 311 N93-11648

DEFORESTATION
A comprehensive mission to planet Earth: Woods Hole Space Science and Applications Advisory Committee Planning Workshop
[NASA-TM-108011] p 343 N93-11878
DEFORMATION
Development of strength and conductivity in deformation processed copper base alloys
[DE92-018807] p 257 N93-11572
Some exact solutions of the equations of finite elasticity p 337 N93-11713
Fourier continuum finite elements for nonlinear structural analysis p 340 N93-12210
Some consistency requirements on hardening-recovery evolution equations for welding, part 1
[DE92-015992] p 329 N93-12220
Influence of strain rate on the structure/property behavior of the alpha-2 alloy Ti-24.5Al-10.5Nb-1.5Mo
[DE92-008490] p 261 N93-12256
Study of optical techniques for the Ames unitary wind tunnels. Part 4: Model deformation
[NASA-CR-190980] p 219 N93-12349
DEGRADATION
Workshop on Surface Science and Technology
[AD-A253566] p 264 N93-11149
A preliminary investigation of the degradation and stabilisation of the energetic oxetane binder polyNIMMO
[RARDE-7/91] p 273 N93-11376
Progress on polymer degradation by photoelectron transfer
[AD-A246276] p 268 N93-11862
The degradation of parachutes: Age and mechanical wear
[AD-A252243] p 200 N93-12179
Energetics solids degradation in high temperature water
[AD-A254900] p 276 N93-12285
VLSI reliability research
[AD-A254883] p 295 N93-12360
The effects of wearing protective chemical warfare combat clothing on human performance
[AD-A250716] p 390 N93-12491
DEGREES OF FREEDOM
Importance of numerosity and distribution of articulations within the digits, wrists, and arms of telemanipulators confronted with dextrous assembly tasks
p 330 N93-11967
Remote systems development p 330 N93-11971
The order n simulation of tether motions based on a rigid body tether model p 225 N93-11999
Real-time adaptive sidelobe canceller architectures and implementations
[AD-A254842] p 286 N93-12433
DEIONIZATION
Comparative effects of drag-reducing polymers. An experimental report
[AD-A254001] p 268 N93-11793
DELAMINATING
Mixed mode bending test of the interlaminar fracture toughness of carbon/epoxy
[FFA-TN-1992-04] p 237 N93-11128
An interlayer shear slip theory for composite laminates with nonrigid bonding p 237 N93-11229
VAMAS round robin project on polymer composite delamination in mode 1 and mode 2: Cyclic loading
[NPL-DMM(A)-47] p 266 N93-11397
The use of high-frequency dynamic information for the evaluation of damage in fiber reinforced composite materials p 241 N93-11998
Method and apparatus for evaluating multilayer objects for imperfections
[NASA-CASE-LAR-14581-1-SB] p 333 N93-12204
Fracture toughness testing of polymer matrix composites
[NASA-TP-3199] p 243 N93-12302
DELAY
Self-tuning PI-PID regulators for stable systems with varying delay
[REPT-92-023] p 421 N93-11593
DELAY LINES
Fiber optic delay line signal processors
[AD-A254691] p 448 N93-12227
Nonlinear delay line phase shifters for terahertz superconductive electronic circuits
[AD-A255119] p 294 N93-12290
DELPHI METHOD (FORECASTING)
Development of a model for predicting NASA/MSFC program success
[NASA-CR-184423] p 473 N93-12542
DELTA WINGS
Further buffeting tests in a cryogenic wind tunnel
[NASA-TM-107621] p 198 N93-11610
An experimental study of the relationship between forces and moments and vortex breakdown on a pitching delta wing p 208 N93-12206
DEMODULATION
The tomographic formulation of spotlight mode synthetic aperture radar extended to three dimensional targets
[DE92-013666] p 280 N93-11234
All-digital multicarrier demodulators for on-board processing satellites in mobile communication systems
p 285 N93-12207
DEMODULATORS
All-digital multicarrier demodulators for on-board processing satellites in mobile communication systems
p 285 N93-12207
DEMOGRAPHY
Density equalizing map projections: A new algorithm
[DE92-017088] p 413 N93-12110
DENSE PLASMAS
Contributions to plasma focus physics since 1970 from the Institute of Plasma Research, Stuttgart (Fed. Republic of Germany)
[IPF-91-4] p 450 N93-11201
Bremsstrahlung absorption in plasmas
p 321 N93-12047
Atomic structure and spectral perturbations in dense and hot plasmas p 321 N93-12049
DENSITY DISTRIBUTION
Sodium-lidar mesosphere examinations: Selected elements of the experimental construction of a mobile instrument and evaluation of the data acquired with a stationary Na-lidar during the DYANA campaign
[BONN-IR-91-78] p 357 N93-11006
Microscopic origins of metastable effects in a-Si:H and deep defect characterization in a-Si,Ge:H alloys
[DE92-010588] p 463 N93-11813
Orientation, stress, and density distributions in injection-moulded amorphous polymers determined by optical techniques
[ETN-92-92271] p 269 N93-11983
Measurement of the density distributions in quenched polycarbonate specimens by a quantitative Schlieren-optical technique p 270 N93-11989
Gapwise density distributions in injection-moulded polymethylmethacrylate p 270 N93-11990
Nonlinear behavior of resonant absorption in a plasma at microwave frequency p 319 N93-12032
Preliminary study of the homogeneity of the density and temperature of long plasmas used for X laser studies
p 320 N93-12044
DENSITY MEASUREMENT
Sodium-lidar mesosphere examinations: Selected elements of the experimental construction of a mobile instrument and evaluation of the data acquired with a stationary Na-lidar during the DYANA campaign
[BONN-IR-91-78] p 357 N93-11006
Measurement of the density distributions in quenched polycarbonate specimens by a quantitative Schlieren-optical technique p 270 N93-11989
Overview of recent diagnostic measurements at the USA MHD facilities
[DE92-015365] p 454 N93-12087
Hypersonic flow diagnostic development
[AD-A255045] p 202 N93-12466
DEOXYGENATION
Preconversion catalytic deoxygenation of phenolic functional groups
[DE92-018304] p 244 N93-10986
DEPENDENT VARIABLES
A surface integral approach to the motion planning of nonholonomic systems
[AD-A254844] p 329 N93-12434
DEPOSITION
Resonant membrane spatial light modulators
[AD-A253893] p 252 N93-12186
Ion beams as a means of deposition and in-situ characterization of thin films and thin film layered structures
[DE92-016397] p 469 N93-12310
DEPTH
Correction techniques for depth errors with stereo three-dimensional graphic displays
[NASA-TP-3244] p 206 N93-11170
DERIVATION
Probability density functions in turbulent channel flow
[NASA-CR-4454] p 202 N93-12399
DESIGN ANALYSIS
Maximum life spiral bevel reduction design
[NASA-TM-105790] p 323 N93-10982
On the basis of experience: Built in product reliability
[PNR-90932] p 331 N93-11034
Rolls-Royce civil engine technology
[PNR-90936] p 210 N93-11036
The Trent: Towards greater thrust
[PNR-90937] p 210 N93-11037
Introduction to the Rolls-Royce design process
[PNR-90939] p 210 N93-11039
The design and commissioning of an acoustic liner for propeller noise testing in the ARA transonic wind tunnel
[PNR-90880] p 433 N93-11204
The use of simultaneous engineering for the design and manufacture of the low pressure turbine for the Rolls-Royce Trent engine
[PNR-90887] p 212 N93-11206
An iterative method for distributed database design
p 474 N93-11255
The technical background to standards for shackles
[NPL-DMM(A)-51] p 325 N93-11325
10 kW L-band amplifier tubes for efficient and reliable troposcatter communication transmitter systems
[AD-A253246] p 290 N93-11504
Advanced control for the design of STT missile autopilot
[REPT-921-320-102] p 215 N93-11585
Hypervelocity scramjet combustor-nozzle analysis and design
[NASA-CR-190965] p 213 N93-12214
System design and radiation field characteristics of the High Flux Neutron Radiography Facility (HFNRF) at Sandia National Laboratories
[DE92-013984] p 219 N93-12268
An improved numerical model for wave rotor design and analysis
[NASA-TM-105915] p 214 N93-12418
Shear joint capability versus bolt clearance
[NASA-TM-108378] p 342 N93-12419
Laser Doppler experiments
[AD-A252883] p 287 N93-12461
The Fourth Workshop on Dynamics and Aeroelastic Stability Modeling of Rotorcraft Systems
[AD-A255065] p 208 N93-12485
DESORPTION
Oxidation, nitridation, and fluorine etching of Si
[AD-A253559] p 249 N93-11755
Characterization of underivatized pterins by laser desorption Fourier transform mass spectrometry
[DE92-016785] p 323 N93-12514
DESTRUCTION
Destruction of explosives and rocket fuels by supercritical water oxidation
[DE92-018874] p 274 N93-11380
DESTRUCTIVE TESTS
Pressure vessel burst test program
[AD-A253708] p 334 N93-11080
Crushing behavior of tubular structures in multi-materials
[ECL-91-37] p 336 N93-11579
DETERMINANTS
Darboux theorems and Wronskian formulas for integrable systems. 1: Constrained KP flows
[MATHS-REPT-A-172] p 424 N93-11126
A primer on polynomial resultants
[AD-A246883] p 426 N93-11463
DETONATION
Loads from the detonation of hydrogen-air-steam mixtures
[DE92-019318] p 249 N93-11551
Detonation reactions frozen by free expansion and analyzed by mass spectrometry
[DE92-018605] p 274 N93-11566
Characterization of deflagrating munitions by rotating prism high speed photography
[MRL-TR-91-43] p 311 N93-11648
DETONATION WAVES
Detonation reactions frozen by free expansion and analyzed by mass spectrometry
[DE92-018605] p 274 N93-11566
Asymptotic analysis of reacting materials with saturated explosion. 2: High-frequency waves
[AD-A254473] p 275 N93-12236
DETONATORS
Booster rocket range safety system
[AD-D015363] p 221 N93-11428
Hot-wire vs laser, is there a difference?
[DE92-019337] p 310 N93-11554
Analysis of plasma-treated wire insulation
[DE92-019471] p 291 N93-11643
DEUTERIUM
Data archiving and analysis for CWDD
[DE92-017064] p 473 N93-11104
Low energy helium implantation in evaporated nickel surfaces
[DE92-019297] p 257 N93-11600
High bandwidth second-harmonic generation in partially deuterated KDP
[DE92-019505] p 452 N93-11645
DEUTERIUM COMPOUNDS
Molecular mobility of the interface in a model composite: A NMR study
[AD-A253311] p 265 N93-11194
High bandwidth second-harmonic generation in partially deuterated KDP
[DE92-019505] p 452 N93-11645
DEUTERIUM PLASMA
Diagnostics and modeling of H(-) ion sources
[AD-A250664] p 440 N93-11867

DEUTERONS
Photodisintegration of the deuteron at high energy
[DE92-017066] p 445 N93-12108
DEVELOPING NATIONS
Communicable diseases: A major burden of morbidity and mortality p 380 N93-11300
DIAGNOSIS
Phadiatop: A screening test for inhalant allergy
p 383 N93-11313
In vivo and in vitro diagnosis of allergic respiratory disease during screening procedures in the Italian Navy: Comparative evaluation of a recent quantitative automatized enzyme immunoassay method to dose specific IgE p 383 N93-11314
Allergy screening and follow-up in student pilots of the Belgian Air Force (BAF) p 383 N93-11316
Allergic and nonallergic rhinitis in Greek pilots
p 383 N93-11317
DIAMOND FILMS
Workshop on Characterizing Diamond Films
[PB92-205426] p 271 N93-12086
Growth, characterization, and device development in monocrystalline diamond films
[AD-A252648] p 271 N93-12184
DIAMONDS
Workshop on Characterizing Diamond Films
[PB92-205426] p 271 N93-12086
Hydrogen assisted heat transfer during diamond growth using carbon and tantalum filaments
[AD-A247944] p 468 N93-12218
DIAPHRAGMS (MECHANICS)
Kinetics of diffusional droplet growth in a liquid/liquid two-phase system
[NASA-CR-190805] p 297 N93-11142
DIATOMIC GASES
An NMR study of the occupation of C(sub 60) interstitial sites by oxygen molecules
[DE92-019436] p 437 N93-11640
DIELECTRIC PROPERTIES
Nanostructure, defect chemistry and properties of relaxor ferroelectrics
[AD-A247294] p 431 N93-11468
DIELECTRICS
High Temperature Superconductivity Space Experiment (HTSSE)
[AD-A253119] p 288 N93-11239
Natural convection heat transfer studies of simulated and actual electronic components using dielectric liquids for immersion cooling
[AD-A255173] p 341 N93-12376
DIESEL ENGINES
Development of wear resistant ceramic coatings for diesel engine components
[DE92-019068] p 268 N93-11654
Engine testing of ceramic cam-roller followers
[DE92-019188] p 268 N93-11735
DIETS
Smoking status and body composition, exercise, dietary intake, and alcohol/caffeine consumption
[AD-A250648] p 385 N93-11893
DIFFERENTIAL ABSORPTION LIDAR
Research on stimulated Raman scattering with applications to atmospheric lidar p 322 N93-12163
DIFFERENTIAL EQUATIONS
Differential equation-based seismic data filtering
[DE92-016282] p 363 N93-11791
Singularities of the Euler equation and hydrodynamic stability
[NASA-CR-189720] p 306 N93-12173
DIFFERENTIAL PRESSURE
Sealing characteristics of a carbon segmented circumferential seal for a liquid oxygen turbopump
[NAL-TR-1130] p 329 N93-12364
DIFFRACTION
High resolution image processing of geophysical data with diffraction tomography
[DE92-014134] p 359 N93-11235
DIFFRACTION PATTERNS
Fringe analysis of in-plane displacements on high speed rotating components
[PNR-90920] p 334 N93-11022
In-plane ESPI measurements in hostile environments
[PNR-90919] p 309 N93-11320
DIFFUSERS
Air ejector experiments using the two-dimensional supersonic cascade tunnel: Relationship between ejector performance and throat area ratio, part 1
[NAL-TM-642-PT-1] p 202 N93-12352
MHD integrated topping cycle project
[DE92-018087] p 456 N93-12504
DIFFUSION
Diffusion of Echo 7 electron beams during bounce motion
[DE92-018288] p 357 N93-10985
Pulsed-field-gradient NMR investigations of hydrogen diffusion in ZrH(x)
[DE92-014393] p 459 N93-11238
Grain boundary transport and related processes in natural fine grained aggregates
[DE92-018239] p 461 N93-11682
Oxidation, nitridation, and fluorine etching of Si
[AD-A253559] p 249 N93-11755
Multi-layer light-weight protective coating and method for application
[NASA-CASE-LAR-14448-1] p 269 N93-11912
DIFFUSION COEFFICIENT
Modelling the behaviour of gas bubbles in epoxy resin
[PNR-90961] p 264 N93-11084
Kinetics of diffusional droplet growth in a liquid/liquid two-phase system
[NASA-CR-190805] p 297 N93-11142
DIFFUSION FLAMES
Numerical calculations of an axisymmetric laminar diffusion flame with detailed and reduced reaction mechanisms p 246 N93-11259
Studies in nonlinear problems of energy
[DE92-018551] p 345 N93-11733
DIFFUSION LENGTH
Investigation of high efficiency monolithic multibandgap solar cells
[AD-A254326] p 348 N93-12144
DIFFUSION THEORY
On an origin of numerical diffusion: Violation of invariance under space-time inversion
[NASA-TM-105776] p 425 N93-11254
DIFFUSIVITY
Grain boundary transport and related processes in natural fine grained aggregates
[DE92-018239] p 461 N93-11682
DIGITAL COMPUTERS
Non-linear data conversion system for dynamic range digital signal processing
[AD-D015347] p 278 N93-11047
DIGITAL DATA
Computing optimum routes across terrain using DAP
[RSRE-MEMO-4299] p 412 N93-11712
Photogrammetric GIS technology: Feature mapping on digital stereo imagery
[AD-A254255] p 477 N93-11748
Integration of radar altimeter, precision navigation, and digital terrain data for low-altitude flight
[NASA-TM-103958] p 205 N93-12320
DIGITAL SIMULATION
Hybrid guidance for maneuvering flight vehicles
[AD-A254110] p 225 N93-11798
On the Goertler instability of boundary layers
[NAL-TR-1120T] p 307 N93-12374
DIGITAL SYSTEMS
Non-linear data conversion system for dynamic range digital signal processing
[AD-D015347] p 278 N93-11047
Photogrammetric point determination using digital imagery of three-line scanner systems
[SER-C-372] p 309 N93-11346
Spatial data transformation: Feature attribute conversion issues and practical experience
[AD-A254238] p 477 N93-11741
Real-time data compression using a FFT digital signal processor
[DE92-017744] p 477 N93-11770
Systems engineering and technical assistance in support of digital gallium arsenide insertion projects
[AD-A253751] p 463 N93-11790
Advanced one-dimensional optical strain measurement system, phase 4
[NASA-CR-190760] p 314 N93-12279
A monitor for the laboratory evaluation of control integrity in digital control systems operating in harsh electromagnetic environments
[NASA-TM-4402] p 215 N93-12304
ISDN at NASA Lewis Research Center
[NASA-TM-105911] p 419 N93-12410
DIGITAL TECHNIQUES
Self-supervision in multilayer adaptive networks
[RSRE-MEMO-4467] p 420 N93-11343
Photogrammetric point determination using digital imagery of three-line scanner systems
[SER-C-372] p 309 N93-11346
High-speed test station for solid-state imagers
[DE92-018990] p 312 N93-11822
DIGITAL TO ANALOG CONVERTERS
Arbitrary waveform generator
[AD-D015346] p 280 N93-11354
DIHYDRIDES
Pulsed-field-gradient NMR investigations of hydrogen diffusion in ZrH(x)
[DE92-014393] p 459 N93-11238
DIMENSIONAL ANALYSIS
Three dimensional and 2D simulation of an expanding plasma using a Darwin hybrid particle code
[DE92-019095] p 451 N93-11516
DIMERIZATION
Synthesis and characterization of novel aluminum-arsenic compounds 2. Crystal structures of (R2AlAs (SiMe3)2)2 (R = i-Bu, Me) and i-Bu2 (Cl)Al*As (SiMe3)3
[AD-A248001] p 467 N93-12175
DIMERS
VUV and UV sources and spectroscopic applications
[AD-A247293] p 291 N93-11758
DIODES
The development of a one microsecond pulse length, repetitively pulsed, high power modulator, and a long-pulse electron beam diode for the production of intense microwaves
[DE92-015974] p 293 N93-12089
DIPHTHERIA
Absence of protective immunity against diphtheria in a large proportion of young adults p 380 N93-11302
Immunization of personnel traveling to a destination in tropical countries: French position p 380 N93-11304
DIPLEXERS
Unequal stub length diplexing microwave frequency discriminator circuit
[AD-D015352] p 288 N93-11051
DIPOLE ANTENNAS
Computer modeling of tactical high frequency antennas
[AD-A255176] p 286 N93-12377
DIRECT BROADCAST SATELLITES
Direct Broadcast Satellite: Radio Program
[NASA-TM-105910] p 224 N93-11430
DIRECT CURRENT
Flux dynamics and irreversibility in YBa2Cu3O7 with Y2BaCuO5 inclusions and in single crystal YBa2Cu3O7
[DE92-009712] p 467 N93-12178
DIRECTIONAL STABILITY
Correlation of forebody pressures and aircraft yawing moments on the X-29A aircraft at high angles of attack
[NASA-TM-4417] p 197 N93-11532
DIRECTORIES
Directory of factual and numeric databases of relevance to aerospace and defence R and D
[AGARD-R-777] p 476 N93-11710
Directory interchange format manual, version 4.0
[NASA-TM-107991] p 478 N93-11911
DISCRIMINANT ANALYSIS (STATISTICS)
Preliminary results on the use of linear discriminant analysis in the ARM continuous speech recognition system
[RSRE-MEMO-4511] p 280 N93-11384
The use of linear discriminant analysis in the ARM continuous speech recognition system
[RSRE-MEMO-4512] p 280 N93-11385
DISEASES
Density equalizing map projections: A new algorithm
[DE92-017088] p 413 N93-12110
DISINTEGRATION
Photodisintegration of the deuteron at high energy
[DE92-017066] p 445 N93-12108
DISORDERS
Semiclassical analysis spectral correlations in mesoscopic systems
[DE92-634887] p 471 N93-11780
New techniques for positron emission tomography in the study of human neurological disorders
[DE92-015353] p 384 N93-11873
DISPERSION
An experimental study of droplet dispersion in turbulent flows p 248 N93-11455
Analysis of advanced optical glass and systems
[NASA-CR-184434] p 448 N93-12201
DISPERSIONS
3-D turbulent particle dispersion submodel development
[DE92-018212] p 301 N93-11670
3-D turbulent particle dispersion submodel development
[DE92-018228] p 302 N93-11671
DISPLACEMENT
An interlayer shear slip theory for composite laminates with nonrigid bonding p 237 N93-11229
DISPLAY DEVICES
Methods and principles for determining task dependent interface content
[NASA-CR-190837] p 204 N93-10961
Correction techniques for depth errors with stereo three-dimensional graphic displays
[NASA-TP-3244] p 206 N93-11170
Advanced technology for portable personal visualization
[AD-A253808] p 388 N93-11783

Direct manipulation and intermittent automation in advanced cockpits
[AD-A253814] p 388 N93-11784

Advanced satellite workstation: An integrated workstation environment for operational support of satellite system planning and analysis p 391 N93-11941

Guide to synchronization of video systems to IRIG timing
[AD-A254626] p 285 N93-12240

DISSOCIATION

Lyman alpha line shapes from electron impact H2 dissociative processes in the Jovian auroral zone
p 487 N93-11166

The role of backbond strain in silicon surfaces on the decomposition of NH3 and PH3
[AD-A253771] p 250 N93-12062

DISSOLVING

Bubble dissolving in turbulent pipe flow
[AD-A252927] p 308 N93-12462

DISTORTION

Evaluation of alternatives for increasing A-7D rearward visibility
[AD-A255071] p 208 N93-12488

DISTRIBUTED PARAMETER SYSTEMS

Distributed environmental control p 391 N93-11924

DISTRIBUTED PROCESSING

Photonics and other approaches to high speed communications
[NASA-CR-190362] p 279 N93-11116

Scalable parallel communications p 279 N93-11117

An iterative method for distributed database design
p 474 N93-11255

Dynamic programming and image processing on distributed memory parallel machines
[ETN-92-92174] p 409 N93-11478

Z-buffer on a transputer-based machine
p 410 N93-11483

Reduction operations on a distributed memory machine with a reconfigurable interconnection network
p 410 N93-11484

ScaLAPACK: A scalable linear algebra library for distributed memory concurrent computers
[DE92-017823] p 426 N93-11636

Measurement and analysis of operating system fault tolerance
[NASA-CR-190973] p 406 N93-12540

DISTRIBUTION FUNCTIONS

Nucleon structure functions from deep inelastic muon scattering
[NIKHEF-H+K/92-01] p 442 N93-11130

Statistical methods for the comparison of spatial patterns in meteorological variables p 370 N93-11997

DIURESIS

Effect of hemorrhage on cardiac output, vasopressin, aldosterone, and diuresis during immersion in men
[NASA-TM-103949] p 374 N93-12014

DIURNAL VARIATIONS

Lidar studies of gravity waves in the mesopause region p 358 N93-11222

Surface wind speed distributions
[AD-A253268] p 368 N93-11505

DOCUMENTS

Using SGML in a large organization
[ESA-STR-234] p 476 N93-11583

DOMAINS

Domain decomposition: A bridge between nature and parallel computers
[NASA-CR-189709] p 425 N93-11246

Supporting multiple domains in a single reuse repository p 415 N93-12390

DOORS

Aircraft accident report: Explosive decompression-loss of cargo door in flight, United Airlines Flight 811, Boeing 747-122, N4713U, Honolulu, HI, 24 February 1989
[PB92-910402] p 204 N93-12193

DOPED CRYSTALS

A cryogenic phonon detector to search for dark matter particles p 481 N93-11198

Preparation, optical and laser properties of Nd-doped sol-gel silica
[DE92-019378] p 461 N93-11602

Magnetic properties and critical behavior of the conductivity near the M-I transition
[DE92-018948] p 461 N93-11629

DOPPLER RADAR

Summary of findings from the PIREP-based analyses conducted during the 1988 to 1990 evaluations of TDWR-based and TDWR/LLWAS-based alert services provided to landing/departing pilots
[AD-A253859] p 367 N93-11144

DOSAGE

Future approaches to vaccine development single-dose vaccines using controlled-release delivery systems
p 382 N93-11310

Formation of buried epitaxial Si-Ge alloy layers in Si (100) crystal by high dose Ge ion implantation
[DE92-017114] p 466 N93-12127

DOSIMETERS

Development and use of data analysis procedures for the CRRES payloads AFGL-701-2/Dosimeter and AFGL-701-4/Fluxmeter and application of the data analysis results to improve the static and dynamic models of the Earth's radiation belts
[AD-A253287] p 363 N93-11810

Radiation physics, biophysics, and radiation biology
[DE92-013673] p 375 N93-12266

DOUBLE BASE ROCKET PROPELLANTS

Propellant removal from rocket motors containing double-base compositions
[DE92-013567] p 275 N93-12265

DRAG

Drag on an oscillating rod in a non-Newtonian fluid
[DE92-014746] p 308 N93-12492

DRAG REDUCTION

Comparative effects of drag-reducing polymers. An experimental report
[AD-A254001] p 268 N93-11793

Turbulence structure and polymer drag reduction in adverse pressure gradient boundary layers
p 304 N93-12003

Experiments and analysis concerning the use of external burning to reduce aerospace vehicle transonic drag
p 235 N93-12537

DREDGING

Dredging research program: Feasibility of a kinematic differential Global Positioning System
[AD-A248953] p 205 N93-11419

DROP SIZE

The combustion time lag and its role in ramjet combustion instability p 245 N93-11137

Coaxial injector spray characterization using water/air as simulants p 248 N93-11452

Physical processes involved in injection and atomization of liquid propellants p 248 N93-11453

Experimental investigation of rocket injector atomization p 248 N93-11454

DROP TESTS

Materials processing in low gravity
[NASA-CR-184421] p 276 N93-12401

DROPS (LIQUIDS)

Metal slurry droplet and spray combustion
p 245 N93-11138

An experimental study of droplet dispersion in turbulent flows p 248 N93-11455

Simulation of liquid drop breakup behavior in a flow field using discrete element techniques
[DE92-019435] p 300 N93-11537

Effects of physical properties and geometry on shapes and stability of polarizable drops in external fields
[DE92-018865] p 301 N93-11638

DRUGS

Recent lessons on the safety and effectiveness of malaria chemoprophylaxis in a non-immune population
p 381 N93-11307

Future approaches to vaccine development single-dose vaccines using controlled-release delivery systems
p 382 N93-11310

Epidemiologic view of allergic diseases in North America: Implications for aerospace medicine
p 382 N93-11311

The screening of inhalant allergic diseases in the selection of candidates for aircraft piloting
p 382 N93-11312

The OMPAT level 1 Neurophysiological Performance Assessment Battery: NPPAB
[AD-A254840] p 387 N93-12432

DRY HEAT

Status and prospects for Hot Dry Rock (HDR) in the US
[DE92-018876] p 345 N93-11381

DUCT GEOMETRY

Flow in curved ducts of varying cross-section
[AD-A254660] p 306 N93-12245

DUCTED BODIES

The prediction of convective heat transfer in rotating square ducts
[PNR-90985] p 296 N93-11067

DUCTED FLOW

The effects of plate spacing and downstream plate length on the acoustic resonance excited by flow past two plates in tandem in a duct
[PNR-90958] p 433 N93-11321

Flow visualization of supersonic flow through a combustor section p 200 N93-12001

An experimental investigation of the flow in a diffusing S-duct
[NASA-TM-105809] p 213 N93-12077

Flow in curved ducts of varying cross-section
[AD-A254660] p 306 N93-12245

DUCTILITY

International ADI-Seminar: Austempered Ductile Iron
[PB92-180660] p 256 N93-11244

Micromechanisms of deformation and fracture in aluminum based MMC's: Interface effects
[AD-A253560] p 259 N93-11850

Deep penetration into frictional ductile and brittle materials
[PB92-205566] p 338 N93-11903

DUCTS

The prediction of convective heat transfer in rotating square ducts
[PNR-90929] p 296 N93-11025

The combustion time lag and its role in ramjet combustion instability p 245 N93-11137

Flow in curved ducts of varying cross-section
[AD-A254660] p 306 N93-12245

Evaluation of acoustic impedance models for a perforated plate
[NAL-TR-1133] p 435 N93-12375

DUPLEXERS

Superplastic forming of ceramic insulation
p 228 N93-12452

DURABILITY

Relative sliding durability of candidate high temperature fiber seal materials
[NASA-TM-105806] p 236 N93-10978

Research on stable, high-efficiency, amorphous silicon multijunction modules
[DE92-010599] p 464 N93-11818

DUST STORMS

Lunar and Martian environmental interactions with nuclear power system radiators
[NASA-TM-105747] p 230 N93-10965

DWELL

Elevated temperature fatigue crack growth in a nickel base superalloy under dwell conditions
[PNR-90997] p 255 N93-11115

DYE LASERS

Laser spectroscopy and dynamics of transient species formed in pyrolysis reactions
[DE92-016206] p 251 N93-12091

Image potential states at metal-dielectric interfaces
[DE92-017019] p 466 N93-12124

DYES

Optical limiting
[AD-A254620] p 322 N93-12238

DYNAMIC CHARACTERISTICS

Experiments on low aspect ratio hydroplanes to measure lift under static and dynamic conditions
[ARE-TM(UHR)-90306] p 197 N93-11365

State-resolved dynamics of ion-molecule collisions in a flowing afterglow
[AD-A247288] p 436 N93-11467

Vehicle/guideway interaction in maglev systems
[DE92-019051] p 326 N93-11653

Dynamics of space debris p 219 N93-11904

The use of high-frequency dynamic information for the evaluation of damage in fiber reinforced composite materials p 241 N93-11998

Laser spectroscopy and dynamics of transient species formed in pyrolysis reactions
[DE92-016206] p 251 N93-12091

Dynamic multimodal function optimization using genetic algorithms
[DE92-019602] p 414 N93-12234

DYNAMIC CONTROL

Decentralized control of large flexible structures by joint decoupling
[NASA-TM-107694] p 339 N93-12020

DYNAMIC LOADS

Nonlinear response of thin steel plate structures subjected to static, cyclic, and dynamic loads
p 335 N93-11200

An experimental study of the relationship between forces and moments and vortex breakdown on a pitching delta wing p 208 N93-12206

DYNAMIC MODELS

Numerical and experimental results in vibroacoustical active control of structural elements with piezoelectric materials
[DILC-EST-TN-224] p 334 N93-11158

Automatic control laws for aircraft in parabolic flight
[DILC-EST-TR-211] p 214 N93-11160

Semiclassical analysis spectral correlations in mesoscopic systems
[DE92-634887] p 471 N93-11780

Development and use of data analysis procedures for the CRRES payloads AFGL-701-2/Dosimeter and AFGL-701-4/Fluxmeter and application of the data analysis results to improve the static and dynamic models of the Earth's radiation belts
[AD-A253287] p 363 N93-11810

Mode interaction models in near-wall turbulence
p 303 N93-11856

Computational dynamics of high-speed flexible multibody systems p 338 N93-11891
Modeling and model simplification of aeroelastic vehicles: An overview
[NASA-TM-107691] p 215 N93-12216

DYNAMIC PRESSURE
On stability and control of SSTO spaceplane in super- and hypersonic ascending phase
[NAL-TR-1128T] p 216 N93-12361

DYNAMIC PROGRAMMING
Stochastic control and nonlinear estimation
[AD-A253543] p 420 N93-11147
Dynamic programming and image processing on distributed memory parallel machines
[ETN-92-92174] p 409 N93-11478
Dynamic programming on a ring of processors
p 410 N93-11479
Path planning on a ring of processors
p 410 N93-11480
Computing optimum routes across terrain using DAP
[RSRE-MEMO-4299] p 412 N93-11712

DYNAMIC RANGE
Non-linear data conversion system for dynamic range digital signal processing
[AD-D015347] p 278 N93-11047

DYNAMIC RESPONSE
Dynamics and response of polymer-coated acoustic devices
[DE92-014289] p 433 N93-11523
Description of the structural responses in the medium-frequency range by an energetic formulation
[ECL-92-16] p 336 N93-11582
Structural dynamics of large space structures having parametric uncertainties p 225 N93-11836
Computational dynamics of high-speed flexible multibody systems p 338 N93-11891
Studies in control for vibration suppression of the UWAA 20-bay planar truss
[AD-A250193] p 341 N93-12253
Stochastic sensitivity measure for mistuned high-performance turbines
[NASA-TM-105821] p 341 N93-12277

DYNAMIC STABILITY
Beam-loading stability in synchrotrons with a higher RF harmonic
[DE92-018982] p 443 N93-11510
On stability and control of SSTO spaceplane in super- and hypersonic ascending phase
[NAL-TR-1128T] p 216 N93-12361
DYNAC: A computer program for analyzing the dynamical stability of aircraft
[REPT-B-31] p 216 N93-12415

DYNAMIC STRUCTURAL ANALYSIS
An interlayer shear slip theory for composite laminates with nonrigid bonding p 237 N93-11229
Structural dynamics of large space structures having parametric uncertainties p 225 N93-11836
Near-field and far-field sound radiation from a line-driven fluid-loaded infinite flat plate having periodic and non-periodic attached rib stiffeners p 434 N93-11884
Computational dynamics of high-speed flexible multibody systems p 338 N93-11891
The use of high-frequency dynamic information for the evaluation of damage in fiber reinforced composite materials p 241 N93-11998
Development of a 1/7-scale F/A-18 UAV for supermaneuverability research --- unmanned air vehicle
[AD-A247261] p 208 N93-12053
Measured data for the Sandia 34-meter vertical axis wind turbine
[DE92-019807] p 348 N93-12075
Modeling and model simplification of aeroelastic vehicles: An overview
[NASA-TM-107691] p 215 N93-12216
Dynamic test/analysis correlation using reduced analytical models
[NASA-TM-107671] p 341 N93-12300
Fluid-structure interaction using retarded potential and ABAQUS
[AD-A254735] p 307 N93-12355
The mechanism of bolt loading
[NASA-TM-108377] p 342 N93-12412
DYNAC: A computer program for analyzing the dynamical stability of aircraft
[REPT-B-31] p 216 N93-12415

DYNAMICAL SYSTEMS
Computational dynamics of high-speed flexible multibody systems p 338 N93-11891
The order n simulation of tether motions based on a rigid body tether model p 225 N93-11999
Laminar boundary-layer breakdown
[AD-A254489] p 306 N93-12162
Singularities of the Euler equation and hydrodynamic stability
[NASA-CR-189720] p 306 N93-12173
A game theoretic approach to linear dynamic estimation p 340 N93-12200

DYNAMO THEORY
Tori and chaos in a nonlinear dynamo model for solar activity
[MPE-PREPRINT-218] p 488 N93-11351

DYNAMOMETERS
Astronaut candidate strength measurement using the Cybex 2 and the LIDO Multi-Joint 2 dynamometers
[NASA-CR-185679] p 389 N93-12195

E

EARTH (PLANET)
A comprehensive mission to planet Earth: Woods Hole Space Science and Applications Advisory Committee Planning Workshop
[NASA-TM-108011] p 343 N93-11878

EARTH ALBEDO
Orbital perturbations due to the albedo effect
[GKSS-91/E/59] p 220 N93-11348
Global change and the dark of the moon
[AD-A255181] p 486 N93-12380

EARTH ATMOSPHERE
Environmental problems and trends of international responses, 2
[DE92-531118] p 355 N93-11846

EARTH CRUST
Crustal and upper mantle velocity gradients in the vicinity of the East Kazakh test site
[AD-A246889] p 362 N93-11740
Study of seismic coda generation in crust with non-uniform scattering and anelastic properties
[AD-A254350] p 366 N93-12270

EARTH GRAVITATION
An approximate solution of the fixed gravimetric boundary value problem in the interior and the exterior of the Earth's body
[SER-C-379] p 361 N93-11331

EARTH IONOSPHERE
Interpretation of measurements from the suprathermal electron spectrometer on the NEED-2 rocket
[FFI-92/7009] p 357 N93-11129
Propagation of relativistic high current electron beams across the geomagnetic field
[DE92-018276] p 362 N93-11564
Beam-plasma interactions and radiation generation during the ejection of electron and ion beams in space
[AD-A253993] p 224 N93-11736
Publication of papers presented at URSI 23rd General Assembly as a special section of radio science
[AD-A253561] p 283 N93-11811
Fundamental analysis of the tomographic imaging system for reconstructing ionospheric distributions
p 365 N93-12209

EARTH MAGNETOSPHERE
Studies of interactive plasma processes in the polar cusp
[NASA-CR-190892] p 357 N93-10964
Diffusion of Echo 7 electron beams during bounce motion
[DE92-018288] p 357 N93-10985
Plasma measurements in magnetospheric tail
[MPE-233] p 361 N93-11352
Beam-plasma interactions and radiation generation during the ejection of electron and ion beams in space
[AD-A253993] p 224 N93-11736
Publication of papers presented at URSI 23rd General Assembly as a special section of radio science
[AD-A253561] p 283 N93-11811
Foil optimization for low energy neutral atom imaging
[DE92-013435] p 365 N93-12263
Low energy neutral atom imaging
[DE92-013531] p 365 N93-12264
Flank solar wind interaction
[NASA-CR-189285] p 489 N93-12303

EARTH MANTLE
Crustal and upper mantle velocity gradients in the vicinity of the East Kazakh test site
[AD-A246889] p 362 N93-11740
Laboratory and numerical studies of dynamical processes related to thermal convection in the Earth's mantle p 364 N93-11900

EARTH MOVEMENTS
Study of seismic coda generation in crust with non-uniform scattering and anelastic properties
[AD-A254350] p 366 N93-12270

EARTH OBSERVATIONS (FROM SPACE)
Payload advisory panel recommendations
[NASA-TM-108012] p 219 N93-11528
A comprehensive mission to planet Earth: Woods Hole Space Science and Applications Advisory Committee Planning Workshop
[NASA-TM-108011] p 343 N93-11878

EARTH OBSERVING SYSTEM (EOS)
The Kalman filter for two-dimensional stable and unstable atmospheres p 359 N93-11249
Payload advisory panel recommendations
[NASA-TM-108012] p 219 N93-11528
The early Earth Observing System reference handbook: Earth Science and Applications Division missions, 1990-1997
[NASA-TM-107963] p 343 N93-11663
Estimation of photosynthetic capacity using MODIS polarization: 1988 proposal to NASA Headquarters
[NASA-TM-103945] p 344 N93-12351

EARTH ORBITAL ENVIRONMENTS
Compositional analysis and classification of projectile residues in LDEF impact craters
[NASA-TM-104750] p 488 N93-11374
An accurate and efficient method to calculate the rate of single event upsets from the LET spectrum and SEU cross section test results
[AD-A253917] p 290 N93-11492
A model to estimate the flux of background particles expected to accumulate on the collector foils of the interstellar gas experiment on the long duration exposure facility spacecraft
[AD-A254265] p 489 N93-11815
Analysis of surfaces from the LDEF A0114, phase 2
[NASA-CR-190596] p 270 N93-11993
Erosion rates for polymers measured on LDEF
p 270 N93-11994
Forecasting the relativistic electron flux at geosynchronous orbit
[AD-A254016] p 226 N93-12064

EARTH RADIATION BUDGET
Atlas of albedo and absorbed solar radiation derived from Nimbus 7 earth radiation budget data set, November 1985 to October 1987
[NASA-RP-1281] p 367 N93-11168

EARTH RADIATION BUDGET EXPERIMENT
Global change and the dark of the moon
[AD-A255181] p 486 N93-12380

EARTH RESOURCES
Reserves information gathering system user's guide
[DE92-018357] p 475 N93-11355
A comprehensive mission to planet Earth: Woods Hole Space Science and Applications Advisory Committee Planning Workshop
[NASA-TM-108011] p 343 N93-11878

EARTH SCIENCES
Exploratory Research and Development Fund, FY 1990
[DE92-017002] p 489 N93-11078
Payload advisory panel recommendations
[NASA-TM-108012] p 219 N93-11528
The early Earth Observing System reference handbook: Earth Science and Applications Division missions, 1990-1997
[NASA-TM-107963] p 343 N93-11663

EARTH SURFACE
An approximate solution of the fixed gravimetric boundary value problem in the interior and the exterior of the Earth's body
[SER-C-379] p 361 N93-11331

EARTH-IONOSPHERE WAVEGUIDE
Publication of papers presented at URSI 23rd General Assembly as a special section of radio science
[AD-A253561] p 283 N93-11811

EARTH-MOON SYSTEM
Analysis of lunar laser ranging in the framework of a post-Newtonian theory
[SER-C-383] p 315 N93-11332

EARTHQUAKES
Propagation of regional phases: Observations and theory
[AD-A246891] p 359 N93-11228
Modeling regional seismic waves
[AD-A246894] p 361 N93-11421

ECCENTRICITY
Dynamics of space debris p 219 N93-11904

ECOLOGY
Estimation of photosynthetic capacity using MODIS polarization: 1988 proposal to NASA Headquarters
[NASA-TM-103945] p 344 N93-12351

ECONOMIC ANALYSIS
The hydrogen technology assessment, phase 1
[NASA-CR-190969] p 349 N93-12394
The uses and limits of economic models as a climate change policy tool
[DE92-015792] p 356 N93-12474

ECONOMIC IMPACT
The uses and limits of economic models as a climate change policy tool
[DE92-015792] p 356 N93-12474

ECONOMICS
Advanced materials and processing: The Federal program in materials science and technology. A report by the FCCSET Committee on Industry and Technology to supplement the President's fiscal year 1993 budget
[PB92-199108] p 238 N93-11470
ECOSYSTEMS
The relative importance of sulfur and nitrogen compounds in the acidification of freshwater
[DE92-016899] p 354 N93-11680
Scaling issues for biodiversity protection
[DE92-016689] p 375 N93-12315
EDDY CURRENTS
Eddy current characterization of magnetic treatment of materials
[NASA-TM-104573] p 258 N93-11621
Measurement of AC electrical characteristics of SSC superconducting dipole magnets
[DE92-018888] p 431 N93-11625
EDDY VISCOSITY
Application of a two-layer near wall model to fully developed and rotating channel turbulent flows
[NASA-CR-184441] p 305 N93-12082
EDGE DETECTION
Automated extraction of aircraft runway patterns from radar imagery
[AD-A254258] p 218 N93-11751
Model-based vision for space applications
p 398 N93-11955
EDGES
Step-driven surface segregation and ordering during Si-Ge MBE growth
[DE92-017827] p 463 N93-11772
EDITING ROUTINES (COMPUTERS)
Deriving and manipulating module interfaces
[AD-A253869] p 406 N93-11145
EDUCATION
Computer security training and awareness course compendium
[PB92-205442] p 404 N93-11258
Questioning mechanisms during complex learning
[AD-A247382] p 386 N93-11415
Embedded training capabilities for the LAMPS MK 3 system
[AD-A250697] p 207 N93-11838
A summer program in mathematics and computer science for academically oriented students, June 24 - July 26, 1991, Washington, DC
[AD-A249139] p 427 N93-12061
Introduction to training decisions modeling technologies: The training decisions system
[AD-A249862] p 387 N93-12252
EFFERENT NERVOUS SYSTEMS
Physiological analyses of the afferents controlling brain neurochemical systems
[AD-A253185] p 375 N93-11146
EFFICIENCY
10 kW L-band amplifier tubes for efficient and reliable troposcatter communication transmitter systems
[AD-A253246] p 290 N93-11504
Method of moments analysis of symmetric dual reflector antennas with feeds
[AD-A255171] p 286 N93-12407
EFFLUENTS
Predicted rocket and shuttle effects on stratospheric ozone p 352 N93-11097
EIGENVALUES
Remarks on the Robinson-Trautman solutions
[MATHS-REPT-A-167] p 423 N93-11122
EIGENVECTORS
Constrained KP hierarchy and bi-Hamiltonian structures
[MATHS-REPT-A-168] p 424 N93-11123
Darboux theorems and Wronskian formulas for integrable systems. 1: Constrained KP flows
[MATHS-REPT-A-172] p 424 N93-11126
Application of eigenstructure assignment to the control of powered lift combat aircraft p 215 N93-11871
EINSTEIN EQUATIONS
New singularity and existence of solutions in anisotropic, time-dependent, maximally Gauss-Bonnet extended gravity p 357 N93-11183
EISCAT RADAR SYSTEM (EUROPE)
Ionospheric response to particle precipitation within aurora
[IRF-SR-208] p 359 N93-11265
Observations of thin auroral ionization layers by EISCAT in connection with pulsating aurora p 359 N93-11266
EISCAT observations of strong ion outflows from the F-region ionosphere during auroral activity: Preliminary results p 360 N93-11267
EISCAT observations of topside ionospheric ion outflows during auroral activity: Revisited p 360 N93-11268
Electron energization in the topside auroral ionosphere: On the importance of ion-acoustic turbulence
p 360 N93-11269
EJECTION INJURIES
Evaluation of CKU-5/A ejection seat catapults under varied acceleration levels
[AD-A248021] p 204 N93-12489
EJECTION SEATS
The effect of variable seat back angles on human response to +Gz impact accelerations
[AD-A250673] p 387 N93-11559
Evaluation of CKU-5/A ejection seat catapults under varied acceleration levels
[AD-A248021] p 204 N93-12489
EJECTORS
Air ejector experiments using the two-dimensional supersonic cascade tunnel: Relationship between ejector performance and throat area ratio, part 1
[NAL-TM-642-PT-1] p 202 N93-12352
ELASTIC DEFORMATION
Computational dynamics of high-speed flexible multibody systems p 338 N93-11891
ELASTIC MEDIA
The generalized Goursat-Riemann problem for plane waves in isotropic elastic solids p 340 N93-12199
ELASTIC PLATES
Near-field and far-field sound radiation from a line-driven fluid-loaded infinite flat plate having periodic and non-periodic attached rib stiffeners p 434 N93-11884
ELASTIC PROPERTIES
Some exact solutions of the equations of finite elasticity p 337 N93-11713
Physical characterization of magmatic liquids
[DE92-015931] p 363 N93-11848
Elastic stresses, twin boundaries, and fatigue cracking
p 338 N93-11890
Ceramic TBS/porous metal compliant layer
p 228 N93-12453
ELASTIC SCATTERING
Scattering of polarized electrons by oriented deuterons
[DE92-624834] p 440 N93-11914
High energy hadron-hadron collisions
[DE92-018253] p 441 N93-12224
ELASTIC WAVES
System and method for cancelling expansion waves in a wave rotor
[NASA-CASE-LEW-15218-1] p 297 N93-11172
Application of the boundary element method to elastic wave scattering problems in ultrasonic nondestructive evaluation p 332 N93-11209
ELECTRIC ARCS
A Taguchi experimental design study of twin-wire electric arc sprayed aluminum coatings
[DE92-018022] p 262 N93-12494
ELECTRIC BATTERIES
Results of advanced battery technology evaluations for electric vehicle applications
[DE92-018766] p 289 N93-11432
Long cycle life rechargeable lithium batteries
[NASA-CR-190937] p 291 N93-11604
Electron emission during multicharged ion-metal surface interactions
[DE92-017134] p 439 N93-11849
ELECTRIC CHARGE
Overcharge and overdischarge protection of ambient temperature secondary lithium cells
[NASA-CASE-NPO-18343-1-CU] p 290 N93-11456
Electron emission during multicharged ion-metal surface interactions
[DE92-017134] p 439 N93-11849
ELECTRIC CONNECTORS
High speed parallel backplane
[AD-D015372] p 288 N93-11053
ELECTRIC CONTACTS
Robust solder joint attachment of coaxial cable leads to piezoelectric ceramic electrodes
[DE92-017042] p 276 N93-11494
Characteristics of current filamentation in high gain photoconductive semiconductor switching
[DE92-018277] p 291 N93-11693
Research on stable, high-efficiency, amorphous silicon multijunction modules
[DE92-010599] p 464 N93-11818
ELECTRIC CONTROL
The Trent family of engines
[PNR-90974] p 211 N93-11063
ELECTRIC CORONA
A cryogenic enrichment technique for gas chromatographic detection of S2F10 in SF6 discharges
[DE92-011045] p 252 N93-12219
ELECTRIC CURRENT
Current scaling of plasma focus devices
[IPF-90-1] p 449 N93-11029
Critical currents in polycrystalline YBa2Cu3O(7-x): Self-field and grain size dependence
[DE92-617540] p 459 N93-11076
Rocket-triggered lightning test of an earth-covered munitions storage bunker
[DE92-016790] p 369 N93-11678
Characteristics of current filamentation in high gain photoconductive semiconductor switching
[DE92-018277] p 291 N93-11693
Microscopic origins of metastable effects in a-Si:H and deep defect characterization in a-Si,Ge:H alloys
[DE92-010588] p 463 N93-11813
ELECTRIC DIPOLES
On the definition and calculation of effective impedances and averaged boundary conditions with application to the analysis of high complexity frequency selective surfaces
[RSRE-MEMO-4518] p 281 N93-11387
Electron terms and radiation from crystals
[AD-A254353] p 468 N93-12271
ELECTRIC DISCHARGES
Self-generated stochastic heating in an RF discharge
[DE92-018558] p 452 N93-11565
A cryogenic enrichment technique for gas chromatographic detection of S2F10 in SF6 discharges
[DE92-011045] p 252 N93-12219
ELECTRIC EQUIPMENT TESTS
Numerical computation of the lightning response of an earth-covered munitions storage bunker and comparison with experiments
[DE92-014268] p 367 N93-11236
Results of advanced battery technology evaluations for electric vehicle applications
[DE92-018766] p 289 N93-11432
An analog macromodel of the SG1525A PWM for use with SPICE2G.6 simulators
[DE92-019423] p 291 N93-11639
Rocket-triggered lightning test of an earth-covered munitions storage bunker
[DE92-016790] p 369 N93-11678
High-frequency LSI contactor
[DE92-017285] p 292 N93-11916
ELECTRIC FIELDS
On the origin of ion acoustic turbulence in the auroral topside ionosphere p 361 N93-11273
Effects of physical properties and geometry on shapes and stability of polarizable drops in external fields
[DE92-018865] p 301 N93-11638
Flux dynamics and irreversibility in YBa2Cu3O7 with Y2BaCuO5 inclusions and in single crystal YBa2Cu3O7
[DE92-009712] p 467 N93-12178
A monitor for the laboratory evaluation of control integrity in digital control systems operating in harsh electromagnetic environments
[NASA-TM-4402] p 215 N93-12304
ELECTRIC GENERATORS
Electricity from biomass: A development strategy
[DE92-010590] p 346 N93-11814
ELECTRIC MOTOR VEHICLES
Results of advanced battery technology evaluations for electric vehicle applications
[DE92-018766] p 289 N93-11432
Electric and hybrid vehicle program, site operator program
[DE92-018055] p 328 N93-12114
ELECTRIC MOTORS
Energy efficient motors reference guide
[DE92-019073] p 290 N93-11514
Energy efficient drivepower: An overview
[PB92-199173] p 294 N93-12191
Energy efficient drivepower: Literature reference list: Culled references
[PB92-199181] p 294 N93-12192
Energy efficient drivepower: Literature reference list. Volume 1: General user's supplement
[PB92-199157] p 294 N93-12294
Energy efficient drivepower: Literature reference list. Volume 2: Design engineer's supplement
[PB92-199165] p 295 N93-12295
ELECTRIC POTENTIAL
Rocket-triggered lightning test of an earth-covered munitions storage bunker
[DE92-016790] p 369 N93-11678
BANSHEE: High-voltage repetitively pulsed electron-beam driver
[DE92-017413] p 444 N93-11763
Energy efficient drivepower: An overview
[PB92-199173] p 294 N93-12191
Back-gate bias generator
[AD-A255126] p 295 N93-12421
ELECTRIC POWER PLANTS
Evaluation of advanced pressure sensor technology
[DE92-011004] p 312 N93-11806
Models of volcanic eruption hazards
[DE92-013432] p 364 N93-12136
Reliability analysis of a utility-scale solar power plant
[DE92-016550] p 348 N93-12312
ELECTRIC POWER SUPPLIES
Power system commonality study
[NASA-CR-190765] p 347 N93-12019

ELECTRIC PROPULSION
Preliminary characterization of a water vaporizer for resistojet applications
[NASA-TM-105877] p 231 N93-11402
ELECTRIC SWITCHES
Prediction of electromagnetic pulse generation by picosecond avalanches in high-pressure air
[DE92-019382] p 282 N93-11675
Ultra-wideband generators
[DE92-018026] p 293 N93-12113
ELECTRIC WELDING
Vacuum chamber translation/positioning mechanism and welding power supply controller
[NASA-CR-184465] p 328 N93-12196
ELECTRIC WIRE
Payout tension control system for reel mounted cable
[AD-D015362] p 325 N93-11423
Analysis of plasma-treated wire insulation
[DE92-019471] p 291 N93-11643
ELECTRICAL ENGINEERING
Energy efficient drivepower: An overview
[PB92-199173] p 294 N93-12191
Energy efficient drivepower: Literature reference list. Volume 1: General user's supplement
[PB92-199157] p 294 N93-12294
Energy efficient drivepower: Literature reference list. Volume 2: Design engineer's supplement
[PB92-199165] p 295 N93-12295
ELECTRICAL IMPEDANCE
Admittance spectroscopy of copper indium diselenide/cadmium sulfide solar cells
p 344 N93-11214
An uncertainty budget for VHF and UHF reflectometers
[NPL-DES-120] p 281 N93-11395
Analysis of periodic transient beam loading of the AGS
[DE92-019243] p 443 N93-11499
ELECTRICAL INSULATION
Analysis of plasma-treated wire insulation
[DE92-019471] p 291 N93-11643
Damping and scattering of electromagnetic waves by small ferrite spheres suspended in an insulator
[NASA-TM-105837] p 286 N93-12366
ELECTRICAL MEASUREMENT
An uncertainty budget for VHF and UHF reflectometers
[NPL-DES-120] p 281 N93-11395
Transmission/reflection and short-circuit line methods for measuring permittivity and permeability
[PB92-205376] p 293 N93-12084
Two-fluid measurements on thin films
[PB92-205350] p 308 N93-12475
ELECTRICAL PROPERTIES
A cryogenic phonon detector to search for dark matter particles p 481 N93-11198
Dynamics and response of polymer-coated acoustic devices
[DE92-014289] p 433 N93-11523
Application of spin-sensitive electron spectroscopies to investigations of electronic and magnetic properties of solid surfaces and epitaxial systems
[DE92-018597] p 470 N93-12499
ELECTRICAL RESISTANCE
Analytical and numerical principles for the scaling of plasma focus experiments, with regard to electrical resistance
[IPF-91-2] p 450 N93-11103
ELECTRICAL RESISTIVITY
A synopsis of resistive wall effects in very short wavelength free electron lasers
[DE92-018065] p 315 N93-11155
Magnetic properties and critical behavior of the conductivity near the M-I transition
[DE92-018948] p 461 N93-11629
Mixed ionic and electronic conductivity in polymers
[DE92-018723] p 273 N93-12500
ELECTRO-OPTICS
Organization of the Optical Society of America Photonic Science Topical Meeting Series. Volume 14: Photorefractive materials effects, and devices
[AD-A253001] p 446 N93-11071
The fourth OSA Topical Meeting Proceedings on Picosecond Electronics and Optoelectronics, volume 9
[AD-A253472] p 447 N93-11099
Photonics and other approaches to high speed communications
[NASA-CR-190362] p 279 N93-11116
Materials science and engineering at the Naval Research Laboratory: Research programs and 1990 publications
[PB92-199488] p 238 N93-11422
Optoelectronics Research Center
[AD-A253132] p 447 N93-11527
ELECTROACOUSTIC TRANSDUCERS
Ultrasonic sensing of GMAW: Laser/EMAT defect detection system
[DE92-017916] p 333 N93-12055
ELECTROCHEMICAL CELLS
Electron transfer rates at semiconductor/liquid interfaces
[DE92-018559] p 289 N93-11438
NEDO Fuel/Storage Technology Subcommittee
[DE92-526262] p 346 N93-11777
ELECTROCHEMISTRY
Exploration of the ionizable metal cluster-electrode surface analogy: Infrared spectroelectrochemistry of (Pt24(CO)30)(sup n), (Pt26(CO)32)(sup n), and (Pt38(CO)44)(sup n) (n = 0 to -10), and comparisons with potential-dependent spectra of CO adlayers on platinum surfaces
[AD-A252544] p 250 N93-11808
ELECTRODE MATERIALS
Overcharge and overdischarge protection of ambient temperature secondary lithium cells
[NASA-CASE-NPO-18343-1-CU] p 290 N93-11456
ELECTRODEPOSITION
Chronopotentiometry of refractory metals, actinides and oxyanions in molten salts: A review
[NASA-TM-105862] p 249 N93-11545
ELECTRODES
Robust solder joint attachment of coaxial cable leads to piezoelectric ceramic electrodes
[DE92-017042] p 276 N93-11494
Long cycle life rechargeable lithium batteries
[NASA-CR-190937] p 291 N93-11604
ELECTROENCEPHALOGRAPHY
The OMPAT level 1 Neurophysiological Performance Assessment Battery: NPPAB
[AD-A254840] p 387 N93-12432
ELECTROLYSIS
Submarine Advanced Integrated Life Support system (SAILS) program
[AD-A253564] p 388 N93-11812
ELECTROLYTES
Sealant research for solid oxide fuel cells
[DE92-019044] p 345 N93-11513
NEDO Fuel/Storage Technology Subcommittee
[DE92-526262] p 346 N93-11777
ELECTROLYTIC CELLS
Submarine Advanced Integrated Life Support system (SAILS) program
[AD-A253564] p 388 N93-11812
ELECTROMAGNETIC ABSORPTION
Development of ultra-low noise, high sensitivity planar metal grating coupled AlGaAs/GaAs multiquantum well IR detectors for focal plane array staring IR sensor systems
[AD-A254697] p 468 N93-12228
ELECTROMAGNETIC ACCELERATION
An investigation of electromagnetic launcher repeatability
[AD-A254339] p 222 N93-12130
Electromagnetic launcher control using finite state machines
[AD-A254433] p 222 N93-12161
Railgun armature velocity improvement, SBIR phase 2
[AD-A254749] p 222 N93-12505
ELECTROMAGNETIC FIELDS
Cellular and molecular pathways of extremely-low-frequency electromagnetic field interactions with living systems
[DE92-019084] p 282 N93-11515
Analysis of the prebuncher for the KEK 40-MeV proton linac
[DE92-514988] p 444 N93-11525
Rocket-triggered lightning test of an earth-covered munitions storage bunker
[DE92-016790] p 369 N93-11678
ELECTROMAGNETIC INTERACTIONS
Survey of composite particle models of electroweak interaction
[DE92-017110] p 441 N93-12111
ELECTROMAGNETIC PROPULSION
Numerical simulation for the coaxial electromagnetic launcher using hybrid potentials with FE-BE method
p 222 N93-11726
Railgun armature velocity improvement, SBIR phase 2
[AD-A254749] p 222 N93-12505
ELECTROMAGNETIC PULSES
CO2 laser frequency doubling
[AD-A251060] p 314 N93-10997
Prediction of electromagnetic pulse generation by picosecond avalanches in high-pressure air
[DE92-019382] p 282 N93-11675
Broadband EMP transient measurement preemphasis filter
[AD-A254414] p 284 N93-12160
A monitor for the laboratory evaluation of control integrity in digital control systems operating in harsh electromagnetic environments
[NASA-TM-4402] p 215 N93-12304
ELECTROMAGNETIC PUMPS
Results from a large-scale MHD propulsion experiment
[DE92-018177] p 456 N93-12416
ELECTROMAGNETIC RADIATION
Optical generation, control and sensing of millimeter waves
[AD-A254700] p 285 N93-12230
ELECTROMAGNETIC SCATTERING
Temporal scattering and response software users' manual, version 2 and 3
[DE92-040934] p 282 N93-11632
Publication of papers presented at URSI 23rd General Assembly as a special section of radio science
[AD-A253561] p 283 N93-11811
Final Technical Report
[AD-A253529] p 284 N93-12083
Damping and scattering of electromagnetic waves by small ferrite spheres suspended in an insulator
[NASA-TM-105837] p 286 N93-12366
ELECTROMAGNETIC SPECTRA
Optical properties of composite membranes containing arrays of nanoscopic gold cylinders
[AD-A253659] p 238 N93-11281
Microwave guidance technology and its applications
[AD-A254107] p 281 N93-11509
ELECTROMAGNETIC SURFACE WAVES
Nonlinear behavior of resonant absorption in a plasma at microwave frequency p 319 N93-12032
ELECTROMAGNETS
Open-loop characteristics of magnetic suspension systems using electromagnets mounted in a planar array
[NASA-TP-3229] p 277 N93-11613
Electromagnetic launcher control using finite state machines
[AD-A254433] p 222 N93-12161
ELECTROMIGRATION
VLSI design for reliability
[AD-A253207] p 292 N93-11781
VLSI reliability research
[AD-A254883] p 295 N93-12360
ELECTRON ACCELERATION
Electron acceleration in a relativistic electron plasma wave p 319 N93-12033
ELECTRON BEAMS
Diffusion of Echo 7 electron beams during bounce motion
[DE92-018288] p 357 N93-10985
A synopsis of resistive wall effects in very short wavelength free electron lasers
[DE92-018065] p 315 N93-11155
Tunable, short pulse hard x rays from a compact laser synchrotron source
[AD-A254288] p 315 N93-11195
The electron-beam water calorimeter project at the National Physical Laboratory
[NPL-RSA(EXT)-30] p 310 N93-11410
The foxhole accelerating structure
[DE92-019052] p 443 N93-11429
10 kW L-band amplifier tubes for efficient and reliable troposcatter communication transmitter systems
[AD-A253246] p 290 N93-11504
Experimental study of interactions of highly charged ions with atoms at keV energies
[DE92-019512] p 436 N93-11541
Beam-plasma interactions and radiation generation during the ejection of electron and ion beams in space
[AD-A253993] p 224 N93-11736
Scattering of polarized electrons by oriented deuterons
[DE92-624834] p 440 N93-11914
On some practical consideration of the electron beam breakup transit time oscillator
[DE92-017406] p 445 N93-11919
Proposal for the experimental demonstration of the coherent radiation
[DE92-017695] p 284 N93-12132
ELECTRON BOMBARDMENT
Diagnostics of electron-heated solar flares
p 488 N93-11877
The relationship between electrostatic discharges on spacecraft P78-2 and the electron environment
[AD-A255179] p 226 N93-12379
ELECTRON BUNCHING
Proposal for the experimental demonstration of the coherent radiation
[DE92-017695] p 284 N93-12132
ELECTRON COUNTERS
Research at and operation of the material science x ray absorption beamline (X-11) at the National Synchrotron Light source
[DE92-018598] p 251 N93-12172

ELECTRON CYCLOTRON HEATING
A new pitch angle diagnostic for electron cyclotron resonance plasma p 450 N93-11185
Thermal analysis and design of polarizer mirrors for waveguides in the D3-D tokamak [DE92-018884] p 451 N93-11382
ELECTRON DENSITY (CONCENTRATION)
Fundamental analysis of the tomographic imaging system for reconstructing ionospheric distributions p 365 N93-12209
ELECTRON DENSITY PROFILES
Observations of thin auroral ionization layers by EISCAT in connection with pulsating aurora p 359 N93-11266
Fundamental analysis of the tomographic imaging system for reconstructing ionospheric distributions p 365 N93-12209
ELECTRON DISTRIBUTION
Direct electron absorption of fast waves on the D3-D tokamak [DE92-016254] p 449 N93-11041
ELECTRON EMISSION
Electron emission during multicharged ion-metal surface interactions [DE92-017134] p 439 N93-11849
ELECTRON ENERGY
Scaling of lower hybrid current drive with temperature [DE92-018541] p 449 N93-10988
Interpretation of measurements from the suprathermal electron spectrometer on the NEED-2 rocket [FFI-92/7009] p 357 N93-11129
Ionospheric response to particle precipitation within aurora [IRF-SR-208] p 359 N93-11265
Effects of current driven instabilities on the ion and electron temperatures in the topside ionosphere p 360 N93-11270
Comment on 'EISCAT Radar Observations of Enhanced Incoherent Scatter Spectra and Their Relation to Auroral Luminosity and Field-Aligned Currents' by P. N. Collis et al. p 360 N93-11271
Development of a new plasma diagnostic of the critical surface and studies of the ion acoustic decay instability using collective Thomson scattering [DE92-018526] p 453 N93-11731
BANSHEE: High-voltage repetitively pulsed electron-beam driver [DE92-017413] p 444 N93-11763
Diagnostics of electron-heated solar flares p 488 N93-11877
Proposal for the experimental demonstration of the coherent radiation [DE92-017695] p 284 N93-12132
State-resolved collisional energy transfer in highly vibrationally excited polyatomic molecules [AD-A253299] p 441 N93-12323
Ion temperature measurements on field reversed configuration plasmas p 457 N93-12535
ELECTRON FLUX DENSITY
Forecasting the relativistic electron flux at geosynchronous orbit [AD-A254016] p 226 N93-12064
ELECTRON GAS
Hydrodynamic fluctuations and light scattering in hot electron gas of semiconductors [DE92-622800] p 458 N93-10992
ELECTRON GUNS
Experimental and theoretical investigation of high gradient acceleration [DE92-015299] p 315 N93-11278
High-speed FPS vidicon camera [DE92-018989] p 313 N93-12069
The development of a one microsecond pulse length, repetitively pulsed, high power modulator, and a long-pulse electron beam diode for the production of intense microwaves [DE92-015974] p 293 N93-12089
ELECTRON IMPACT
Lyman alpha line shapes from electron impact H2 dissociative processes in the Jovian auroral zone p 487 N93-11166
Advanced electric propulsion research, 1991 [NASA-CR-190761] p 232 N93-11608
ELECTRON MICROSCOPY
Thin-sectioning and analysis of fine-grained meteoritic materials [NASA-CR-185693] p 485 N93-11546
Structure and property of heteroepitaxial TiO2/VO2 multilayers [DE92-018181] p 460 N93-11563
Micromechanisms of deformation and fracture in aluminum based MMC's: Interface effects [AD-A253560] p 259 N93-11850
Scanning electron microscopy of the effects of moisture and elevated temperature on the fibre/matrix bond in CFRP [RAE-TM-MAT-STR-1183] p 240 N93-11905
Atomic bonding at ceramic interfaces using scanning tunneling microscopy [DE92-018706] p 273 N93-12479
ELECTRON MOBILITY
Electronic transport and lasing in microstructures [DE92-018725] p 441 N93-12115
ELECTRON ORBITALS
Mechanical properties of semiconductors and their alloys [AD-A253908] p 462 N93-11727
The structures, binding energies and vibrational frequencies of Ca3 and Ca4: An application of the CCSD(T) method p 439 N93-11852
Theory of normal metals [DE92-016828] p 262 N93-12476
ELECTRON OSCILLATIONS
Proposal for the experimental demonstration of the coherent radiation [DE92-017695] p 284 N93-12132
ELECTRON PLASMA
Atomic structure and spectral perturbations in dense and hot plasmas p 321 N93-12049
ELECTRON PRECIPITATION
Ionospheric response to particle precipitation within aurora [IRF-SR-208] p 359 N93-11265
Observations of thin auroral ionization layers by EISCAT in connection with pulsating aurora p 359 N93-11266
Electron energization in the topside auroral ionosphere: On the importance of ion-acoustic turbulence p 360 N93-11269
Diagnostics of electron-heated solar flares p 488 N93-11877
ELECTRON PRESSURE
Introduction of electronic pressure scanning at the Royal Aerospace Establishment [RAE-TM-AERO-2222] p 199 N93-11882
ELECTRON RADIATION
Electron terms and radiation from crystals [AD-A254353] p 468 N93-12271
ELECTRON SCATTERING
The 44th Annual Gaseous Electronics Conference [AD-A254872] p 295 N93-12437
ELECTRON SOURCES
Design and evaluation of ion source for satellite charge control [AD-A255172] p 227 N93-12408
ELECTRON SPECTROSCOPY
Interpretation of measurements from the suprathermal electron spectrometer on the NEED-2 rocket [FFI-92/7009] p 357 N93-11129
Application of spin-sensitive electron spectroscopies to investigations of electronic and magnetic properties of solid surfaces and epitaxial systems [DE92-018597] p 470 N93-12499
ELECTRON STATES
Theory of small metal clusters, films, and wires [AD-A253120] p 256 N93-11240
Theoretical study of the radiative and kinetic properties of selected metal oxides and air molecules [AD-A251090] p 438 N93-11804
Image potential states at metal-dielectric interfaces [DE92-017019] p 466 N93-12124
The Peierls ground state, solitons and polarons in ring-containing polymers [AD-A254914] p 272 N93-12289
ELECTRON TRANSFER
Electron transfer rates at semiconductor/liquid interfaces [DE92-018559] p 289 N93-11438
Experimental study of interactions of highly charged ions with atoms at keV energies [DE92-019512] p 436 N93-11541
Ultrafast photoinduced electron transfer reactions in supramolecular arrays: From charge separation and storage to molecular switches [DE92-016186] p 465 N93-12090
Electronic transport and lasing in microstructures [DE92-018725] p 441 N93-12115
Electron terms and radiation from crystals [AD-A254353] p 468 N93-12271
Photoinduced electron transfer counter to the bias field in coupled quantum wells [AD-A254719] p 469 N93-12338
ELECTRON TRANSITIONS
Near-IR absorption spectra for the C70 fullerene anions [AD-A253658] p 246 N93-11280
Absorption spectroscopy of L(alpha, beta) transitions in a laser germanium plasma p 320 N93-12041
Saturation effects in absorption spectroscopy of the K(alpha) rays of aluminum p 254 N93-12042
Experimental study of x ray laser in lithumoid aluminum p 321 N93-12045
ELECTRONIC EQUIPMENT
Wind tunnel operator aimed comparison between two electronic pressure scanner systems [DLAS-EST-TR-040] p 217 N93-11225
A comparison of the achieved and predicted defect rates of some continuously operating electronic equipment [RTP/909/10-ISSUE-2] p 288 N93-11364
Data report 92-1. Brorfelde Geomagnetic Observatory magnetic results, 1990 p 362 N93-11699
ELECTRONIC EQUIPMENT TESTS
A comparison of the achieved and predicted defect rates of some continuously operating electronic equipment [RTP/909/10-ISSUE-2] p 288 N93-11364
Testability design rating system. Volume 2: Analytical procedure [AD-A254333] p 413 N93-12146
ELECTRONIC MAIL
ESIS: An introduction to the European space information system. A modern tool for space scientists [ESA-INT-2] p 479 N93-12404
ELECTRONIC PACKAGING
MMIC GaAs bonding investigation [AD-A254773] p 470 N93-12464
ELECTRONIC SPECTRA
Experimental study of interactions of highly charged ions with atoms at keV energies [DE92-019512] p 436 N93-11541
ELECTRONS
Direct electron absorption of fast waves on the D3-D tokamak [DE92-016254] p 449 N93-11041
Semiclassical analysis spectral correlations in mesoscopic systems [DE92-634887] p 471 N93-11780
ELECTROPLATING
Surface protection in the aircraft industry [MBB-Z-0432-92-PUB] p 255 N93-11027
Acid copper sulfate plating bath: Control of chloride and copper [DE92-019473] p 249 N93-11644
ELECTRORHEOLOGICAL FLUIDS
Mechanisms associated with electrorheology p 294 N93-12198
ELECTROSTATIC PROPULSION
Evaluation of transportation systems for advanced space flight missions [ESA-TT-1256] p 223 N93-11685
ELECTROSTATIC WAVES
The extremely low frequency wave analyzer [AD-A255178] p 366 N93-12378
ELECTROSTATICS
Mechanisms associated with electrorheology p 294 N93-12198
The relationship between electrostatic discharges on spacecraft P78-2 and the electron environment [AD-A255179] p 226 N93-12379
ELEMENTARY PARTICLES
Research in elementary particles and interactions [DE92-018089] p 437 N93-11681
Medium energy nuclear physics research [DE92-016972] p 442 N93-12444
ELIMINATION
Synthesis and characterization of novel aluminum-arsenic compounds 2. Crystal structures of (R2AlAs (SiMe3)2)2 (R = i-Bu, Me) and i-Bu2 (Cl)Al*As (SiMe3)3 [AD-A248001] p 467 N93-12175
ELLIPSES
A real time sharpening of NOGAPS predictions of mid-latitude Central Pacific cyclones [AD-A255157] p 372 N93-12424
ELLIPTIC DIFFERENTIAL EQUATIONS
Numerical calculations of an axisymmetric laminar diffusion flame with detailed and reduced reaction mechanisms p 246 N93-11259
EMBEDDED COMPUTER SYSTEMS
Design of an Ada expert system shell for the VHSIC avionic modular flight processor p 397 N93-11947
Formal design specification of a Processor Interface Unit [NASA-CR-189698] p 406 N93-12538
EMBRITTLEMENT
Environment-induced embrittlement: Stress corrosion cracking and metal-induced embrittlement; environmental embrittlement of iron aluminide alloys [DE92-018714] p 256 N93-11524
EMISSION SPECTRA
Modeling the Jovian aurora [NASA-CR-190696] p 486 N93-11164
The role of proton precipitation in Jovian aurora: Theory and observation p 487 N93-11165
A multi-line study of the molecular interstellar medium on M82's starburst nucleus [MPE-PREPRINT-213] p 484 N93-11347
Rosat deep surveys p 482 N93-11474

Potassium D-line fitting for investigation of MHD boundary layers
[DE92-019020] p 454 N93-11826
Analysis of the instrument operation of a focal circle spectrograph and numerical reconstitution of the spectrum emitted by a plasma column p 321 N93-12051

EMITTANCE
Emittance measuring device for charged particle beams
[AD-D015371] p 442 N93-11060

EMPHYSEMA
Correlation of serum alpha sub 1 antitrypsin with cigarette smoking and pulmonary function status in Greek pilots, for a ten year period p 384 N93-11318

ENCEPHALITIS
Immunization of personnel traveling to a destination in tropical countries: French position p 380 N93-11304

END EFFECTORS
EXOS research on master controllers for robotic devices p 399 N93-11957
A new scheme of force reflecting control
p 399 N93-11960
An 8-DOF dual-arm system for advanced teleoperation performance experiments p 400 N93-11964
Performance experiments with alternative advanced teleoperator control modes for a simulated solar maximum satellite repair p 400 N93-11965
The development of system components to provide proprioceptive and tactile information to the human for future telepresence systems p 330 N93-11968
Advanced mechanisms for robotics
p 330 N93-11969
Operator vision aids for space teleoperation assembly and servicing p 391 N93-11981
A smart end-effector for assembly of space truss structures p 230 N93-11982
A vision-based end-point control for a two-link flexible manipulator
[NASA-CR-190967] p 330 N93-12521

END-TO-END DATA SYSTEMS
Description of the SSF PMAD DC testbed control system data acquisition function
[NASA-TM-105843] p 417 N93-11005

ENERGY ABSORPTION
Mass energy-transfer and mass energy-absorption coefficients, including in-flight positron annihilation for photon energies 1 keV to 100 MeV, 1992
[PB92-181106] p 438 N93-11715

ENERGY CONSERVATION
Energy efficient motors reference guide
[DE92-019073] p 290 N93-11514
Advanced heat pump for the recovery of volatile organic compounds
[DE92-011592] p 303 N93-11774
Synthesis of nanocrystalline powders for oxide ceramics by microwave plasma pyrolysis
[DE92-017410] p 268 N93-11861
Proceedings of the DOE/Advanced Heat Exchangers Program Review
[DE92-014385] p 305 N93-12070
Energy efficient drivepower: An overview
[PB92-199173] p 294 N93-12191
Energy efficient drivepower: Literature reference list. Volume 1: General user's supplement
[PB92-199157] p 294 N93-12294
Energy efficient drivepower: Literature reference list. Volume 2: Design engineer's supplement
[PB92-199165] p 295 N93-12295

ENERGY CONSUMPTION
Electric and hybrid vehicle program, site operator program
[DE92-018055] p 328 N93-12114

ENERGY CONVERSION
LIEKKI and JALO: Combustion and fuel conversion
[DE92-540921] p 349 N93-12446

ENERGY CONVERSION EFFICIENCY
The 1992 DOE/Sandia crystalline photovoltaic technology project review meeting
[DE92-018544] p 344 N93-10989
Energy efficient motors reference guide
[DE92-019073] p 290 N93-11514
Participation in multilateral effort to develop high performance integrated CPC evacuated collectors
[DE92-015946] p 346 N93-11823
Selected case studies of technology transfer from mission-oriented applied research
[DE92-018957] p 481 N93-12067
Parameterization of solar cells
[NASA-TM-105885] p 295 N93-12301

ENERGY DISSIPATION
A synopsis of resistive wall effects in very short wavelength free electron lasers
[DE92-018065] p 315 N93-11155
Application of the Moyer method to transverse shielding of linear Bremsstrahlung sources
[DE92-017027] p 443 N93-11493
Effects of cooling-air injection on secondary flows and losses in a turbine cascade
[NAL-TR-1121T] p 307 N93-12382

ENERGY DISTRIBUTION
Scaling of gain with energy spread and energy in the PEP FEL
[DE92-019248] p 316 N93-11500

ENERGY GAPS (SOLID STATE)
Investigation of high efficiency monolithic multibandgap solar cells
[AD-A254326] p 348 N93-12144

ENERGY LEVELS
Landau level quantization and superconductivity
[DE92-019028] p 460 N93-11512
Semiclassical analysis spectral correlations in mesoscopic systems
[DE92-634887] p 471 N93-11780

ENERGY METHODS
Numerical study for the study of medium speed internal noise problems
[DILC-EST-TN-200] p 432 N93-11156

ENERGY POLICY
Selected case studies of technology transfer from mission-oriented applied research
[DE92-018957] p 481 N93-12067
Alternative Fuel Evaluation Program: Alternative Fuel Light Duty Vehicle Project. Data collection responsibilities, techniques, and test procedures
[DE92-010598] p 275 N93-12171
LIEKKI and JALO: Combustion and fuel conversion
[DE92-540921] p 349 N93-12446
The uses and limits of economic models as a climate change policy tool
[DE92-015792] p 356 N93-12474

ENERGY REQUIREMENTS
Design of small Stirling dynamic isotope power system for robotic space missions
[NASA-TM-105919] p 275 N93-12085

ENERGY STORAGE
NEDO Fuel/Storage Technology Subcommittee
[DE92-526262] p 346 N93-11777
NEDO Solar Technology Subcommittee
[DE92-526256] p 347 N93-11845
Ultrafast photoinduced electron transfer reactions in supramolecular arrays: From charge separation and storage to molecular switches
[DE92-016186] p 465 N93-12090

ENERGY TECHNOLOGY
Electricity from biomass: A development strategy
[DE92-010590] p 346 N93-11814
Participation in multilateral effort to develop high performance integrated CPC evacuated collectors
[DE92-015946] p 346 N93-11823
Energy efficient drivepower: Literature reference list: Culled references
[PB92-199181] p 294 N93-12192
The hydrogen technology assessment, phase 1
[NASA-CR-190969] p 349 N93-12394
Medium energy nuclear physics research
[DE92-016972] p 442 N93-12444
The collaborative program of research in engineering sciences
[DE92-016838] p 490 N93-12477

ENERGY TRANSFER
Determination of stepsize parameters for intermolecular vibrational energy transfer
[DE92-010770] p 435 N93-11189
Mass energy-transfer and mass energy-absorption coefficients, including in-flight positron annihilation for photon energies 1 keV to 100 MeV, 1992
[PB92-181106] p 438 N93-11715
Development of a new plasma diagnostic of the critical surface and studies of the ion acoustic decay instability using collective Thomson scattering
[DE92-018508] p 453 N93-11730
State-resolved collisional energy transfer in highly vibrationally excited polyatomic molecules
[AD-A253299] p 441 N93-12323

ENGINE AIRFRAME INTEGRATION
Concurrent optimization of airframe and engine design parameters
[NASA-TM-105908] p 213 N93-12402

ENGINE CONTROL
Concorde propulsion: Did we get it right? The Rolls-Royce/SNECMA Olympus 593 engine reviewed
[PNR-90970] p 210 N93-11061

ENGINE DESIGN
An interactive preprocessor for the NASA engine performance program
[NASA-TM-105786] p 209 N93-10983
Application of polyimides to aeroengine components
[PNR-90907] p 334 N93-11013
Nondestructive inspection and life determination of disc material
[PNR-90911] p 331 N93-11016
An experimental evaluation of prediction methods for contrafans
[PNR-90924] p 209 N93-11023
The prediction of convective heat transfer in rotating square ducts
[PNR-90929] p 296 N93-11025
A test facility for the thermofluid-dynamics of gas bearing lubrication films
[PNR-90897] p 263 N93-11032
On the basis of experience: Built in product reliability
[PNR-90932] p 331 N93-11034
Rolls-Royce civil engine technology
[PNR-90936] p 210 N93-11036
The Trent: Towards greater thrust
[PNR-90937] p 210 N93-11037
From RB211 to Trent: An ongoing development strategy
[PNR-90938] p 210 N93-11038
Introduction to the Rolls-Royce design process
[PNR-90939] p 210 N93-11039
Concorde propulsion: Did we get it right? The Rolls-Royce/SNECMA Olympus 593 engine reviewed
[PNR-90970] p 210 N93-11061
Simultaneous engineering in the design of aero engines
[PNR-90973] p 211 N93-11062
The Trent family of engines
[PNR-90974] p 211 N93-11063
Advanced three-shaft engines: Configured for reliability, efficiency, and growth
[PNR-90986] p 211 N93-11068
The development of the Rolls-Royce Trent aero gas turbine
[PNR-90949] p 212 N93-11108
A European collaborative NLF nacelle flight demonstrator
[PNR-90992] p 196 N93-11113
The use of simultaneous engineering for the design and manufacture of the low pressure turbine for the Rolls-Royce Trent engine
[PNR-90887] p 212 N93-11206
Simultaneous engineering in aero gas turbine design and manufacture
[PNR-90890] p 212 N93-11208
The engine design engine. A clustered computer platform for the aerodynamic inverse design and analysis of a full engine
[NASA-TM-105838] p 196 N93-11223
A concept for a counterrotating fan with reduced tone noise
[NASA-TM-105736] p 433 N93-11370
Design of small Stirling dynamic isotope power system for robotic space missions
[NASA-TM-105919] p 275 N93-12085
Space Transportation Booster Engine Configuration Study. Volume 3: Program Cost estimates and work breakdown structure and WBS dictionary
[NASA-CR-184458] p 233 N93-12088
Concurrent optimization of airframe and engine design parameters
[NASA-TM-105908] p 213 N93-12402

ENGINE FAILURE
Implementation of a model based fault detection and diagnosis for actuation faults of the Space Shuttle main engine
[NASA-TM-105781] p 221 N93-11401

ENGINE INLETS
Application of laminar flow to aero engine nacelles
[PNR-90916] p 195 N93-11020
Mach 4 testing of scramjet inlet models
[NAL-TR-1137] p 202 N93-12369

ENGINE MONITORING INSTRUMENTS
Implementation of a model based fault detection and diagnosis for actuation faults of the Space Shuttle main engine
[NASA-TM-105781] p 221 N93-11401

ENGINE NOISE
An experimental evaluation of prediction methods for contrafans
[PNR-90924] p 209 N93-11023
A concept for a counterrotating fan with reduced tone noise
[NASA-TM-105736] p 433 N93-11370
Publications on acoustics research at the Langley Research Center, January 1987 - September 1992
[NASA-TM-107674] p 435 N93-12080
Evaluation of acoustic impedance models for a perforated plate
[NAL-TR-1133] p 435 N93-12375

ENGINE PARTS
Neutron diffraction residual stress studies for aero-engine component applications
[PNR-90908] p 334 N93-11014
Testing for integrity
[PNR-90927] p 210 N93-11024

The application of manufacturing systems engineering for aero engine gears
[PNR-90944] p 324 N93-11054
The Trent family of engines
[PNR-90974] p 211 N93-11063
Small particle impact damage in carbon-carbon composites
[PNR-90948] p 236 N93-11107
Ceramic Technology Project
[DE92-018748] p 266 N93-11442
Development of wear resistant ceramic coatings for diesel engine components
[DE92-019068] p 268 N93-11654
Engine testing of ceramic cam-roller followers
[DE92-019188] p 268 N93-11735
High temperature rectifiers and MOS devices in 6H-silicon carbide
[AD-A254725] p 295 N93-12340

ENGINE TESTING LABORATORIES
Ground test facility for SEI nuclear rocket engines
[DE92-017418] p 217 N93-11367

ENGINE TESTS
Ground test facilities for evaluating nuclear thermal propulsion engines and fuel elements
[DE92-017039] p 231 N93-10973
An experimental evaluation of prediction methods for contrafans
[PNR-90924] p 209 N93-11023
Testing for integrity
[PNR-90927] p 210 N93-11024
The development of the Rolls-Royce Trent aero gas turbine
[PNR-90949] p 212 N93-11108
Test program to provide validation data for the Rocket Combustor Interactive Design (ROCCID) code
p 247 N93-11450
A summary of the JANNAF workshop on diagnostics
p 248 N93-11451
Design of a high-temperature experiment for evaluating advanced structural materials
[NASA-TM-105833] p 337 N93-11624
Engine testing of ceramic cam-roller followers
[DE92-019188] p 268 N93-11735

ENGINEERING MANAGEMENT
Japanese style total quality control: A first hand experience
[PNR-90909] p 331 N93-11015
Simultaneous engineering in the design of aero engines
[PNR-90973] p 211 N93-11062
The use of simultaneous engineering for the design and manufacture of the low pressure turbine for the Rolls-Royce Trent engine
[PNR-90887] p 212 N93-11206
Innovation in engineering
[PNR-90889] p 212 N93-11207
Simultaneous engineering in aero gas turbine design and manufacture
[PNR-90890] p 212 N93-11208

ENTHALPY
Thermokinetic modelling and hypersonic flow
[DILC-EST-TN-218] p 196 N93-11157

ENVIRONMENT EFFECTS
Activities report of Lufthansa
[ETN-92-92100] p 203 N93-11319
Studies of the role of clouds in CO2-induced climate change
[DE92-018648] p 353 N93-11569
The potential effects of concurrent increases in temperature, CO2 and O3 on net photosynthesis, as mediated by rubisCO
[DE92-019411] p 374 N93-11630
Climate change and water supply, management and use: A literature review
[DE92-019069] p 353 N93-11655
The role of refrigerants in climate change
[DE92-019385] p 354 N93-11677
Atmospheric reactive nitrogen: A model study of natural and anthropogenic sources and the role of microbial soil emissions
[DE92-010717] p 354 N93-11744
Advanced heat pump for the recovery of volatile organic compounds
[DE92-011592] p 303 N93-11774
Tenth International Symposium on Environmental Biogeochemistry
[DE92-016200] p 355 N93-11864
Stratospheric aircraft: Impact on the stratosphere?
[DE92-016997] p 355 N93-12104
Reduction in global warming due to fuel economy improvements and emissions control of criteria pollutants: New US light-duty vehicles (1968-1991)
[DE92-016636] p 356 N93-12314

ENVIRONMENT MANAGEMENT
Payload advisory panel recommendations
[NASA-TM-108012] p 219 N93-11528

ENVIRONMENT MODELS
Geographic information system to support state-wide hydrologic modeling with the SCS-TR-20
[PB92-185768] p 476 N93-11700
The uses and limits of economic models as a climate change policy tool
[DE92-015792] p 356 N93-12474

ENVIRONMENT PROTECTION
Payload advisory panel recommendations
[NASA-TM-108012] p 219 N93-11528
Scaling issues for biodiversity protection
[DE92-016689] p 375 N93-12315
Environmental restoration project configuration control
[DE92-017223] p 356 N93-12496
Allowance system: Proposed acid rain rule
[PB92-226174] p 356 N93-12524

ENVIRONMENT SIMULATORS
Development of a tactile perceived attitude transducer
[AD-A253724] p 385 N93-11081

ENVIRONMENTAL CONTROL
Distributed environmental control p 391 N93-11924
An expert system for diagnosing environmentally induced spacecraft anomalies p 230 N93-11927

ENVIRONMENTAL TESTS
Thermomechanical fatigue behavior of SiC/Ti-24Al-11Nb in air and argon environments
[NASA-TM-105723] p 238 N93-11399
Evaluation tests for photovoltaic concentrator receiver sections and modules
[DE92-017745] p 346 N93-11771
Analysis of surfaces from the LDEF A0114, phase 2
[NASA-CR-190596] p 270 N93-11993
Erosion rates for polymers measured on LDEF
p 270 N93-11994

EOSINOPHILS
Allergic and nonallergic rhinitis in Greek pilots
p 383 N93-11317

EPHEMERIS TIME
Ephemeris calculation and orbit determination of geostationary satellites, using Taylor series integration
[SER-C-384] p 220 N93-11335

EPIDEMIOLOGY
Allergic, Immunological and Infectious Disease Problems in Aerospace Medicine
[AGARD-CP-518] p 376 N93-11283
Viral hepatitis in the US Air Force, 1980 - 1989
p 377 N93-11287
Hepatitis A and Hepatitis B: Risks compared to other vaccine preventable diseases and immunization recommendations p 377 N93-11288
Vaccination against Hepatitis B: The Italian strategy
p 377 N93-11289
HIV infection in the nineties p 377 N93-11290
AIDS/HIV in the US Military p 377 N93-11291
HIV variability and perspectives of a vaccine
p 378 N93-11294
Communicable diseases: A major burden of morbidity and mortality p 380 N93-11300
Dramatic reduction of meningococcal meningitis among military recruits in Italy after introduction of specific vaccination p 380 N93-11303
Epidemiologic view of allergic diseases in North America: Implications for aerospace medicine
p 382 N93-11311
In vivo and in vitro diagnosis of allergic respiratory disease during screening procedures in the Italian Navy: Comparative evaluation of a recent quantitative automatized enzyme immunoassay method to dose specific IgE p 383 N93-11314
Density equalizing map projections: A new algorithm
[DE92-017088] p 413 N93-12110

EPITAXY
The domain structure features of epitaxial PbTiO3 thin films prepared by MOCVD
[DE92-010907] p 459 N93-11190
Triisopropylindium: A new precursor for OMVPE growth
[AD-A250672] p 460 N93-11558
Structure and property of heteroepitaxial TiO2/VO2 multilayers
[DE92-018181] p 460 N93-11563
Silicon on insulator structures in selective epitaxial growth
[DE92-017118] p 465 N93-11915
Infrared phonon structure in epitaxial films of Tl2Ca2Ba2Cu3O10 at low temperatures
[DE92-017078] p 466 N93-12109
Submillimeter and microwave residual losses in epitaxial films of Y-Ba-Cu-O and Bl-Ca-Ca-Cu-O
[DE92-017075] p 466 N93-12125
Formation of buried epitaxial Si-Ge alloy layers in Si (100) crystal by high dose Ge ion implantation
[DE92-017114] p 466 N93-12127
Growth, characterization, and device development in monocrystalline diamond films
[AD-A252648] p 271 N93-12184

EPOXY COMPOUNDS
Evaluation of epoxy cured with Ethacure 100 curing agent for use in headers for thermal batteries
[DE92-019326] p 267 N93-11552

EPOXY MATRIX COMPOSITES
The use of high-frequency dynamic information for the evaluation of damage in fiber reinforced composite materials p 241 N93-11998
Computer aided design and manufacturing of composite propfan blades for a cruise missile wind tunnel model
[NASA-TM-105269] p 413 N93-12022
Composite failure analysis handbook. Volume 2: Technical handbook. Part 3: Case histories
[AD-A249131] p 241 N93-12054

EPOXY RESINS
Modelling the behaviour of gas bubbles in epoxy resin
[PNR-90961] p 264 N93-11084
Modified epoxy adhesives and primers
[AD-A253857] p 272 N93-12297

EQUATIONS
A consistent cracked bar vibration theory
p 339 N93-12000

EQUATIONS OF MOTION
Alternating-phase focusing: A model to study nonlinear dynamics
[DE92-019027] p 431 N93-11511
Some exact solutions of the equations of finite elasticity p 337 N93-11713
Computational dynamics of high-speed flexible multibody systems p 338 N93-11891

EQUATIONS OF STATE
The basic equations for a four component magnetoplasma flow with non equilibrium ionization
[IPF-91-1] p 449 N93-11102

EQUATORIAL REGIONS
The effects of magnetic storm phases on F-layer irregularities from auroral to equatorial latitudes
[AD-A253905] p 361 N93-11282

EQUILIBRIUM EQUATIONS
The basic equations for a four component magnetoplasma flow with non equilibrium ionization
[IPF-91-1] p 449 N93-11102

EQUILIBRIUM METHODS
Structural design using equilibrium programming
[NASA-TM-107593] p 339 N93-12005

EQUIVALENCE
Equivalence transformations of rational matrices
[MATHS-REPT-A-163] p 423 N93-11121
Equivalence transformations of rational matrices and applications
[MATHS-REPT-A-169] p 424 N93-11124
On a certain McMillan degree condition appearing in control
[MATHS-REPT-A-170] p 424 N93-11125

EQUIVALENT CIRCUITS
Measurement of AC electrical characteristics of SSC superconducting dipole magnets
[DE92-018888] p 431 N93-11625
Parameterization of solar cells
[NASA-TM-105885] p 295 N93-12301

EROSION
Erosion mechanisms in ceramic structures
[MBB-UK-0171-92-PUB] p 263 N93-11011
Advanced electric propulsion research, 1991
[NASA-CR-190761] p 232 N93-11608
Analysis of surfaces from the LDEF A0114, phase 2
[NASA-CR-190596] p 270 N93-11993
Erosion rates for polymers measured on LDEF
p 270 N93-11994
Erosion predictions and measurements of high-temperature coatings and superalloys used in turbomachines p 272 N93-12189

ERROR ANALYSIS
Implementation of a model based fault detection and diagnosis for actuation faults of the Space Shuttle main engine
[NASA-TM-105781] p 221 N93-11401
A real-time diagnostic and performance monitor for UNIX
[NASA-CR-190975] p 404 N93-11462
Identification and estimation of sources of transmitted variation
[DE92-015246] p 429 N93-11820
Dynamics of space debris p 219 N93-11904
Orthogonal functions over the oceans and applications to the determination of orbit error, geoid and sea surface topography from satellite altimetry p 373 N93-12002
Transmission/reflection and short-circuit line methods for measuring permittivity and permeability
[PB92-205376] p 293 N93-12084
Curve fitting and error modeling for the digitization process near the Nyquist rate
[DE92-018189] p 286 N93-12417
Two-fluid measurements on thin films
[PB92-205350] p 308 N93-12475

Measurement and analysis of operating system fault tolerance
[NASA-CR-190973] p 406 N93-12540

ERROR CORRECTING CODES
Mappings between codewords of two distinct (N,K) Reed-Solomon codes over GF(2 sup J)
[NASA-CASE-NPO-18771-1-CU] p 412 N93-11664

ERROR DETECTION CODES
A fast pipelined inner product unit
[REPT-92-025] p 411 N93-11594

ERRORS
Correction techniques for depth errors with stereo three-dimensional graphic displays
[NASA-TP-3244] p 206 N93-11170
A monitor for the laboratory evaluation of control integrity in digital control systems operating in harsh electromagnetic environments
[NASA-TM-4402] p 215 N93-12304

ERS-1 (ESA SATELLITE)
ERS-1 user handbook
[ESA-SP-1148] p 344 N93-12280

ERYTHROCYTES
Freeze-dried human red blood cells
[AD-A253295] p 376 N93-11193

ESTERS
Synthesis and side chain liquid crystal polymers by living ring opening metathesis polymerization. 5: Influence of mesogenic group and interconnecting group on the thermotropic behavior of the resulting polymers
[AD-A253568] p 264 N93-11150

ESTIMATES
A comparison of radar rainfall estimates and rain gage measurements during two Denver thunderstorms
[AD-A254267] p 369 N93-11817

ESTIMATING
Identification and estimation of sources of transmitted variation
[DE92-015246] p 429 N93-11820
A game theoretic approach to linear dynamic estimation p 340 N93-12200
Estimation of photosynthetic capacity using MODIS polarization: 1988 proposal to NASA Headquarters
[NASA-TM-103945] p 344 N93-12351

ETCHING
Oxidation, nitridation, and fluorine etching of Si
[AD-A253559] p 249 N93-11755
Resonant membrane spatial light modulators
[AD-A253893] p 252 N93-12186

ETHERS
Synthesis and side chain liquid crystal polymers by living ring opening metathesis polymerization. 5: Influence of mesogenic group and interconnecting group on the thermotropic behavior of the resulting polymers
[AD-A253568] p 264 N93-11150

ETHYL ALCOHOL
Alternative Fuel Evaluation Program: Alternative Fuel Light Duty Vehicle Project. Data collection responsibilities, techniques, and test procedures
[DE92-010598] p 275 N93-12171

ETIOLOGY
The screening of inhalant allergic diseases in the selection of candidates for aircraft piloting
p 382 N93-11312
In vivo and in vitro diagnosis of allergic respiratory disease during screening procedures in the Italian Navy: Comparative evaluation of a recent quantitative automatized enzyme immunoassay method to dose specific IgE p 383 N93-11314

EUCLIDEAN GEOMETRY
An object-oriented approach to spatial databases
[REPT-92-034] p 476 N93-11690

EULER EQUATIONS OF MOTION
Increase of energy use on cooled high temperature turbine, phase 3
[MTUM-B91EW-0029-PHASE-3] p 213 N93-11339
Review of preconditioning methods for fluid dynamics
[NASA-CR-189712] p 198 N93-11607
A three dimensional high resolution upwind finite volume Euler solver
[VKI-TN-180] p 198 N93-11686
Singularities of the Euler equation and hydrodynamic stability
[NASA-CR-189720] p 306 N93-12173
Oscillations and concentrations in compressible and incompressible fluids
[AD-A254706] p 307 N93-12333

EUROPE
A survey of European calibration facilities for underwater acoustics
[NPL-RSA(EXT)-32] p 433 N93-11328

EUROPEAN COMMUNICATIONS SATELLITE
Lessons drawn from 2 existing satellite networks: ARABSAT and EUTELSAT. Application to the Pacific basin projects
[REPT-921-440-101] p 282 N93-11591

EUROPEAN SPACE PROGRAMS
The European space industry. Overall situation: Situation and prospects for the 23 leading companies concerned
p 472 N93-11163

EVALUATION
An experimental evaluation of prediction methods for contrafans
[PNR-90924] p 209 N93-11023
Statistical process for the automatic image analysis and its evaluation for object recognition and measurements
[SER-C-370] p 407 N93-11345
High Capacity Voice Recorder (HCVR) Operational Test and Evaluation (OT/E) integration test report
[DOT/FAA/CT-TN92/30] p 310 N93-11460

EVAPORATIVE COOLING
A model for analytical performance prediction of hypervapotron
[DE92-018885] p 305 N93-12010

EVOKED RESPONSE (PSYCHOPHYSIOLOGY)
The OMPAT level 1 Neurophysiological Performance Assessment Battery: NPPAB
[AD-A254840] p 387 N93-12432

EXCITATION
Employment of radicals and excited state species for supersonic combustion photochemical ignition of premixed hydrogen/oxygen mixtures with ArF laser
p 245 N93-11135
Electron acceleration in a relativistic electron plasma wave p 319 N93-12033
Photoinduced electron transfer counter to the bias field in coupled quantum wells
[AD-A254719] p 469 N93-12338

EXCITONS
Exciton kinetics in poly(di-n-hexylsilane)
[DE92-018278] p 283 N93-11800
Excitons in semiconducting superlattices, quantum wells, and ternary alloys
[DE92-015178] p 464 N93-11894

EXHAUST DIFFUSERS
Aero engine ceramics: The vision, the reality, and the progress
[PNR-90983] p 264 N93-11066

EXHAUST EMISSION
Federal Alternative Fuel Program light duty vehicle operation
[DE92-018124] p 274 N93-11794
Stratospheric aircraft exhaust plume and wake chemistry studies
[NASA-CR-189688] p 366 N93-12299

EXHAUST GASES
Federal Alternative Fuel Program light duty vehicle operation
[DE92-018124] p 274 N93-11794
Stratospheric aircraft: Impact on the stratosphere?
[DE92-016997] p 355 N93-12104
Stratospheric aircraft exhaust plume and wake chemistry studies
[NASA-CR-189688] p 366 N93-12299
Reduction in global warming due to fuel economy improvements and emissions control of criteria pollutants: New US light-duty vehicles (1968-1991)
[DE92-016636] p 356 N93-12314

EXOSAT SATELLITE
ESIS: An introduction to the European space information system. A modern tool for space scientists
[ESA-INT-2] p 479 N93-12404

EXOSKELETONS
Exoskeleton master controller with force-reflecting telepresence p 330 N93-11970

EXOTHERMIC REACTIONS
Oxidation, nitridation, and fluorine etching of Si
[AD-A253559] p 249 N93-11755

EXPANSION
Three dimensional and 2D simulation of an expanding plasma using a Darwin hybrid particle code
[DE92-019095] p 451 N93-11516

EXPENDABLE STAGES (SPACECRAFT)
Space transportation booster engine configuration study. Volume 2: Design definition document and environmental analysis
[NASA-CR-184459] p 234 N93-12441
Space transportation booster engine configuration study. Volume 1: Executive Summary
[NASA-CR-184457] p 235 N93-12523

EXPERIENCE
Thermal protection systems manned spacecraft flight experience p 227 N93-12449

EXPERIMENT DESIGN
A combined experimental and theoretical study of laminar flow control with particular relevance to aero engine nacelles
[PNR-90991] p 195 N93-11070
High beta and confinement studies on TFTR
[DE92-018647] p 452 N93-11568
A design of experiment study of plasma sprayed alumina-titania coatings
[DE92-017877] p 271 N93-12168
A Taguchi experimental design study of twin-wire electric arc sprayed aluminum coatings
[DE92-018022] p 262 N93-12494

EXPERIMENTATION
Hydrodynamic efficiencies in implosion experiments
p 308 N93-12030

EXPERT SYSTEMS
Intelligent TDA systems using neural networks, phase 1
[AD-A252556] p 420 N93-11000
A knowledge-based blackboard system to interpret graphical data from vibration tests of gas turbines
[PNR-90993] p 212 N93-11114
Artificial intelligence and CFD: Expert systems for the design of airfoils and for grid generation
[DIGE-EST-TN-016] p 206 N93-11161
Development of an intelligent system for cooling rate and fill control in GMAW
[DE92-017849] p 326 N93-11548
Hypertext functionality: A theoretical framework
p 478 N93-11858
A state-based approach to trend recognition and failure prediction for the Space Station Freedom
p 230 N93-11925
An expert system for diagnosing environmentally induced spacecraft anomalies p 230 N93-11927
An embedded rule-based diagnostic expert system in Ada p 392 N93-11928
Intelligent fault management for the Space Station active thermal control system p 391 N93-11930
Spacecraft attitude control using a smart control system p 230 N93-11932
On the acquisition and representation of procedural knowledge p 394 N93-11937
A methodology to emulate and evaluate a productive virtual workstation p 395 N93-11938
Advanced satellite workstation: An integrated workstation environment for operational support of satellite system planning and analysis p 391 N93-11941
The development and technology transfer of software engineering technology at NASA. Johnson Space Center
p 396 N93-11943
Knowledge-based system V and V in the Space Station Freedom program p 396 N93-11945
Design of an Ada expert system shell for the VHSIC avionic modular flight processor p 397 N93-11947
Autonomous power system: Integrated scheduling
p 235 N93-11948
Manager's assistant systems for space system planning p 398 N93-11952
Oceanographic expert system: Potential for TESS(3) applications
[AD-A254908] p 374 N93-12288
Automatic cloud classification from multi-spectral satellite data
[AD-A255125] p 372 N93-12420
Formal specification of the VIPER microprocessor in HOL
[RSRE-90009] p 405 N93-12430

EXPLOSIONS
Pressure vessel burst test program
[AD-A253708] p 334 N93-11080

EXPLOSIVE DECOMPRESSION
Aircraft accident report: Explosive decompression-loss of cargo door in flight, United Airlines Flight 811, Boeing 747-122, N4713U, Honolulu, HI, 24 February 1989
[PB92-910402] p 204 N93-12193

EXPLOSIVE DEVICES
Droppable jet vane TVC
[AD-D015341] p 214 N93-11046

EXPLOSIVES
High energy cast explosives based on dinitropropylacrylate
[AD-D015340] p 273 N93-11045
Destruction of explosives and rocket fuels by supercritical water oxidation
[DE92-018874] p 274 N93-11380
Detonation reactions frozen by free expansion and analyzed by mass spectrometry
[DE92-018605] p 274 N93-11566
Characterization of deflagrating munitions by rotating prism high speed photography
[MRL-TR-91-43] p 311 N93-11648
Asymptotic analysis of reacting materials with saturated explosion. 2: High-frequency waves
[AD-A254473] p 275 N93-12236
Energetics solids degradation in high temperature water
[AD-A254900] p 276 N93-12285

EXPOSURE
Effectiveness of NASA 1032 and 1035 and Air Force 1030 and 1034 units in protection against cold water hypothermia
[AD-A255120] p 389 N93-12291
Radiological information management system (RadIMS)
[DE92-017221] p 480 N93-12495

EXTENSIONS
Two extendability in two classes of claw-free graphs
[AD-A254639] p 427 N93-12243

EXTERNAL STORE SEPARATION
AGARD flight test techniques series. Volume 10: Weapon delivery analysis and ballistic flight testing
[AGARD-AG-300-VOL-10] p 430 N93-11711

EXTERNAL STORES
AGARD flight test techniques series. Volume 10: Weapon delivery analysis and ballistic flight testing
[AGARD-AG-300-VOL-10] p 430 N93-11711

EXTINCTION
Multiangle lidar performance in the presence of horizontal inhomogeneities in atmospheric extinction and scattering
[AD-A252882] p 371 N93-12167

EXTRAVEHICULAR ACTIVITY
Tests of an alternate mobile transporter and extravehicular activity assembly procedure for the Space Station Freedom truss
[NASA-TP-3245] p 224 N93-10970
An EVACS simulation with nested transactions
[NASA-CR-190636] p 412 N93-11717
Decision rules for spaceborne operations planning
p 403 N93-11978

EXTREMELY LOW FREQUENCIES
Cellular and molecular pathways of extremely-low-frequency electromagnetic field interactions with living systems
[DE92-019084] p 282 N93-11515
The extremely low frequency wave analyzer
[AD-A255178] p 366 N93-12378

EXTREMELY LOW RADIO FREQUENCIES
The extremely low frequency wave analyzer
[AD-A255178] p 366 N93-12378

EXTRUDING
Titanium-aluminides by hot isostatic pressing of cold extruded titanium-aluminium powder mixtures
[GKSS-91/E/67] p 256 N93-11337

EYE MOVEMENTS
Visual psychophysics of egomotion
[AD-A248349] p 386 N93-11488

F

F REGION
EISCAT observations of strong ion outflows from the F-region ionosphere during auroral activity: Preliminary results p 360 N93-11267
EISCAT observations of topside ionospheric ion outflows during auroral activity: Revisited p 360 N93-11268
The effects of magnetic storm phases on F-layer irregularities from auroral to equatorial latitudes
[AD-A253905] p 361 N93-11282

F-16 AIRCRAFT
Overview of supersonic laminar flow control research on the F-16XL ships 1 and 2
[NASA-TM-104257] p 196 N93-11221
Evaluation of CKU-5/A ejection seat catapults under varied acceleration levels
[AD-A248021] p 204 N93-12489

F-18 AIRCRAFT
A summary of the forebody high-angle-of-attack aerodynamics research on the F-18 and the X-29A aircraft
[NASA-TM-104261] p 202 N93-12353

FABRICATION
Heat-affected zone cracking of nitronic 60 stainless steel
[DE92-018286] p 254 N93-10984
Interfacial and thin film chemistry in electron device fabrication
[AD-A253579] p 288 N93-11257
Silicon carbide fiber reinforced strontium aluminosilicate glass-ceramic matrix composite
[NASA-CASE-LEW-15263-1] p 239 N93-11543
Matter-wave interferometry with laser cooled atoms
[AD-A253999] p 316 N93-11737
Reflection masks for soft x ray projection lithography
[DE92-014779] p 293 N93-12121
A design of experiment study of plasma sprayed alumina-titania coatings
[DE92-017877] p 271 N93-12168
Resonant membrane spatial light modulators
[AD-A253893] p 252 N93-12186
Development of contractor cells, phase 1
[DE92-017343] p 348 N93-12222
Ferroelectric memory devices and a proposed standardized test system design
[AD-A255159] p 405 N93-12425
Ceramic TBS/porous metal compliant layer
p 228 N93-12453
MMIC GaAs bonding investigation
[AD-A254773] p 470 N93-12464

FACE CENTERED CUBIC LATTICES
An NMR study of the occupation of C(sub 60) interstitial sites by oxygen molecules
[DE92-019436] p 437 N93-11640

FACTOR ANALYSIS
Development of the Personnel-based System Evaluation Aid (PER-SEVAL) performance shaping functions
[AD-A252820] p 386 N93-11779

FAILURE
A contribution to fatigue failure morphologies in fiber reinforced plastics
[MBB-Z-0212-91-PUB] p 263 N93-11010
Evaluation tests for photovoltaic concentrator receiver sections and modules
[DE92-017745] p 346 N93-11771
VLSI reliability research
[AD-A254883] p 295 N93-12360
Creep failure in linear and nonlinear viscoelastic materials p 342 N93-12536

FAILURE ANALYSIS
Ceramic component reliability with the restructured NASA/CARES computer program
[NASA-TM-105856] p 334 N93-11004
A contribution to fatigue failure morphologies in fiber reinforced plastics
[MBB-Z-0212-91-PUB] p 263 N93-11010
Pressure vessel burst test program
[AD-A253708] p 334 N93-11080
Fracture mechanics of model fiber composites
p 237 N93-11247
Implementation of a model based fault detection and diagnosis for actuation faults of the Space Shuttle main engine
[NASA-TM-105781] p 221 N93-11401
Penetration mechanics of composites
[AD-A249230] p 240 N93-11835
Thermal fracture service life analysis of a case bonded visco-elastic cylinder p 339 N93-12008
Composite failure analysis handbook. Volume 2: Technical handbook. Part 3: Case histories
[AD-A249131] p 241 N93-12054

FAILURE MODES
A study of the effects of tolerances on rigging screws, turnbuckles, and associated components in BS4429: 1987
[NPL-DMM(A)-53] p 325 N93-11326

FAINT OBJECTS
A search for low-luminosity objects
[AD-A253301] p 483 N93-11750

FAIRINGS
Acoustic fill factors for a 120 inch diameter fairing
[NASA-CR-189284] p 434 N93-11634

FAN BLADES
A concept for a counterrotating fan with reduced tone noise
[NASA-TM-105736] p 433 N93-11370

FAR FIELDS
Antenna pattern measurement facilities
[AD-A250219] p 283 N93-11764
Near-field and far-field sound radiation from a line-driven fluid-loaded infinite flat plate having periodic and non-periodic attached rib stiffeners p 434 N93-11884
Limitations of multiple feeds in a polarimetric-radar compact range
[DE92-017526] p 284 N93-12101

FAR INFRARED RADIATION
UCSB FEL user mode adaption project
[AD-A248734] p 316 N93-11418

FAR ULTRAVIOLET RADIATION
Far ultraviolet spectrophotometry of hot stars and calibration standards in the far ultraviolet
p 482 N93-11373
VUV and UV sources and spectroscopic applications
[AD-A247293] p 291 N93-11758

FARM CROPS
Techniques for optimal crop selection in a controlled ecological life support system
[NASA-TM-103950] p 388 N93-12018

FAST FOURIER TRANSFORMATIONS
Real-time data compression using a FFT digital signal processor
[DE92-017744] p 477 N93-11770

FASTENERS
The mechanism of bolt loading
[NASA-TM-108377] p 342 N93-12412
Shear joint capability versus bolt clearance
[NASA-TM-108378] p 342 N93-12419

FATIGUE (MATERIALS)
A contribution to fatigue failure morphologies in fiber reinforced plastics
[MBB-Z-0212-91-PUB] p 263 N93-11010
Development of the neutron diffraction technique for the determination of near surface residual stresses in critical gas turbine components
[PNR-90984] p 212 N93-11112
Fatigue crack closure: A review
[RAE-TR-90046] p 335 N93-11369
Elastic stresses, twin boundaries, and fatigue cracking
p 338 N93-11890

FATIGUE LIFE
Nondestructive inspection and life determination of disc material
[PNR-90911] p 331 N93-11016
Elevated temperature fatigue crack growth in a nickel base superalloy under dwell conditions
[PNR-90997] p 255 N93-11115
Thermomechanical fatigue behavior of SiC/Ti-24Al-11Nb in air and argon environments
[NASA-TM-105723] p 238 N93-11399
Tension and compression fatigue response of unnotched 3D braided composites
[NASA-CR-189678] p 239 N93-11611
Hot fire test results of subscale tubular combustion chambers
[NASA-TP-3222] p 232 N93-11614
A comparison of high cycle fatigue methodologies
[NASA-TM-103601] p 233 N93-12148
Microstructure-based fatigue life prediction methods for naval steel structures
[AD-A254628] p 260 N93-12241
Verification of rain-flow reconstructions of a variable amplitude load history
[NASA-CR-189670] p 341 N93-12411

FATIGUE TESTS
Short fatigue crack growth in a nickel-base superalloy at room and elevated temperature
[PNR-90892] p 255 N93-11031
VAMAS round robin project on polymer composite delamination in mode 1 and mode 2: Cyclic loading
[NPL-DMM(A)-47] p 266 N93-11397
Thermomechanical fatigue behavior of SiC/Ti-24Al-11Nb in air and argon environments
[NASA-TM-105723] p 238 N93-11399
Measured data for the Sandia 34-meter vertical axis wind turbine
[DE92-019807] p 348 N93-12075
Mechanical properties for advanced engine materials
[AD-A252632] p 242 N93-12181
Fatigue crack growth in AerMet 100 steel
[AD-A249068] p 261 N93-12248
Spectrum fatigue behaviour of powder metallurgy aluminum alloys
[AD-A255060] p 262 N93-12468

FAULT TOLERANCE
Reliability of small geometry VLSI devices for microelectronics
[AD-A247355] p 289 N93-11414
Integration of task level planning and diagnosis for an intelligent robot p 393 N93-11929
Intelligent diagnostics systems p 393 N93-11931
Design development of a neural network-based telemetry monitor p 394 N93-11933
Fault detection and fault tolerance in robotics
p 330 N93-11961
Tradeoffs in implementing primary-backup protocols
[NASA-CR-190970] p 472 N93-12212
A monitor for the laboratory evaluation of control integrity in digital control systems operating in harsh electromagnetic environments
[NASA-TM-4402] p 215 N93-12304
Analysis of fault-tolerant neurocontrol architectures
[NASA-TM-105898] p 215 N93-12305
Formal design specification of a Processor Interface Unit
[NASA-CR-189698] p 406 N93-12538
Measurement and analysis of operating system fault tolerance
[NASA-CR-190973] p 406 N93-12540
Simulation and analysis of support hardware for multiple instruction rollback
[NASA-CR-190972] p 406 N93-12541

FAULT TREES
Fault detection and fault tolerance in robotics
p 330 N93-11961

FEASIBILITY
Feasibility of using neutron radiography to inspect the Space Shuttle solid rocket booster aft skirt, forward skirt and frustum. Part 1: Summary report
[NASA-CR-184357] p 231 N93-11173

FEASIBILITY ANALYSIS
Feasibility assessment of a transient sound sensor based on the silicon retina architecture
[AD-A252288] p 432 N93-10999

FEATHERING
Numerical study of advanced rotor blades p 199 N93-11899

FEED SYSTEMS
Limitations of multiple feeds in a polarimetric-radar compact range [DE92-017526] p 284 N93-12101
Method of moments analysis of symmetric dual reflector antennas with feeds [AD-A255171] p 286 N93-12407

FEEDBACK CONTROL
Coordinated action in 3-D space [AD-A249830] p 387 N93-10994
Phase-stepping fiber-optic projected fringe system for surface topography measurements [NASA-CASE-LEW-14996-1] p 446 N93-11058
Automatic control laws for aircraft in parabolic flight [DILC-EST-TR-211] p 214 N93-11160
Terminal slider control of nonlinear robotic systems [NASA-CASE-NPO-18584-1-CU] p 324 N93-11177
Optimal output feedback vibration control of rotor-bearing systems p 324 N93-11220
Topics on RF beam control of a synchrotron [DE92-019217] p 443 N93-11498
Self-tuning PI-PID regulators for stable systems with varying delay [REPT-92-023] p 421 N93-11593
A PID auto-tuning algorithm based on relay feedback [REPT-92-019] p 421 N93-11667
Embedded training capabilities for the LAMPS MK 3 system [AD-A250697] p 207 N93-11838
A new scheme of force reflecting control p 399 N93-11960
Decentralized control of large flexible structures by joint decoupling [NASA-TM-107694] p 339 N93-12020
Computational nonlinear control [AD-A253547] p 422 N93-12258
On stability and control of SSTO spaceplane in super- and hypersonic ascending phase [NAL-TR-1128T] p 216 N93-12361
Air-breathing hypersonic vehicle guidance and control studies: An integrated trajectory/control analysis methodology, phase 2 [NASA-CR-189703] p 216 N93-12413
Active control of complex systems via dynamic (recurrent) neural networks [AD-A254878] p 422 N93-12439
A vision-based end-point control for a two-link flexible manipulator [NASA-CR-190967] p 330 N93-12521

FEEDFORWARD CONTROL
Incorporating prior probabilities and misclassification costs into network training: An example from medical prognosis [RSRE-MEMO-4343] p 428 N93-10980
A comparison of feed-forward networks and maximum likelihood on a point-source location problem [RSRE-MEMO-4567] p 281 N93-11391
Application of artificial neural networks in nonlinear analysis of trusses [NASA-TM-105319] p 336 N93-11403
Adaptive neural network models for intelligent computations [AD-A254689] p 421 N93-12226
Active control of complex systems via dynamic (recurrent) neural networks [AD-A254878] p 422 N93-12439

FERRITES
Damping and scattering of electromagnetic waves by small ferrite spheres suspended in an insulator [NASA-TM-105837] p 286 N93-12366

FERROCENES
Organometallic NLO polymers. 3. Copolymerization of bridged bis(ferrocenyl) and bis(cyanoacetate) monomers via the knoevenagel condensation [AD-A250214] p 265 N93-11192

FERROELECTRICITY
Nanostructure, defect chemistry and properties of relaxor ferroelectrics [AD-A247294] p 431 N93-11468
Ferroelectric memory devices and a proposed standardized test system design [AD-A255159] p 405 N93-12425

FEVER
Studies of safety, infectivity, and immunogenicity of a new Temperature Sensitive (TS) 51-1 strain of S. typhi as a new live oral typhoid fever vaccine candidate p 381 N93-11306

FIBER COMPOSITES
A creep cavity growth model for creep-fatigue life prediction of a unidirectional W/Cu composite [NASA-TM-105780] p 333 N93-10967
A contribution to fatigue failure morphologies in fiber reinforced plastics [MBB-Z-0212-91-PUB] p 263 N93-11010
Processing of ceramic matrix composites [PNR-90914] p 263 N93-11018
Materials: Toward the non-metallic engine [PNR-90915] p 209 N93-11019
Aero engine ceramics: The vision, the reality, and the progress [PNR-90983] p 264 N93-11066
Fracture mechanics of model fiber composites p 237 N93-11247
Thermomechanical fatigue behavior of SiC/Ti-24Al-11Nb in air and argon environments [NASA-TM-105723] p 238 N93-11399
Silicon carbide fiber reinforced strontium aluminosilicate glass-ceramic matrix composite [NASA-CASE-LEW-15263-1] p 239 N93-11543
Study of the behavior of titanium and ceramic fiber matrix composite alloy [ETN-92-92087] p 240 N93-11708
The use of high-frequency dynamic information for the evaluation of damage in fiber reinforced composite materials p 241 N93-11998
Computer aided design and manufacturing of composite propfan blades for a cruise missile wind tunnel model [NASA-TM-105269] p 413 N93-12022
Composite failure analysis handbook. Volume 2: Technical handbook. Part 3: Case histories [AD-A249131] p 241 N93-12054
Thermostructural tailoring of fiber composite structures [NASA-TM-105882] p 242 N93-12078
Development of nondestructive evaluation methods and prediction of effects of flaws on the fracture behavior of structural ceramics [DE92-016395] p 271 N93-12123
Mechanical properties for advanced engine materials [AD-A252632] p 242 N93-12181
High-performance synthetic fibers for composites [AD-A252645] p 242 N93-12292
Fracture toughness testing of polymer matrix composites [NASA-TP-3199] p 243 N93-12302
Micromechanical combined stress analysis: MICSTRAN, a user manual [NASA-CR-189694] p 243 N93-12306
Ceramic TBS/porous metal compliant layer p 228 N93-12453
Recent advances in carbon-carbon substrate technology at NASA. Langley Research Center p 228 N93-12455

FIBER OPTICS
Fiber optic polishing system [AD-D015353] p 446 N93-11052
Phase-stepping fiber-optic projected fringe system for surface topography measurements [NASA-CASE-LEW-14996-1] p 446 N93-11058
In-plane strain measurement on high speed rotating components using pulsed laser ESPI [PNR-90975] p 315 N93-11064
Photonics and other approaches to high speed communications [NASA-CR-190362] p 279 N93-11116
Contactless optoelectronic integrated circuits for remote fiber optic communication and sensing applications [AD-A253573] p 290 N93-11507
An 8-DOF dual-arm system for advanced teleoperation performance experiments p 400 N93-11964
An integrated dexterous robotic testbed for space applications p 330 N93-11972
Fiber optic delay line signal processors [AD-A254691] p 448 N93-12227

FIBER ORIENTATION
Development of nondestructive evaluation methods and prediction of effects of flaws on the fracture behavior of structural ceramics [DE92-016395] p 271 N93-12123

FIBER STRENGTH
Relative sliding durability of candidate high temperature fiber seal materials [NASA-TM-105806] p 236 N93-10978

FIBER VOLUME FRACTION
Thermal residual stresses in silicon-carbide/titanium (0/90) laminate [NASA-TM-107649] p 236 N93-11072

FIELD ALIGNED CURRENTS
Ionospheric response to particle precipitation within aurora [IRF-SR-208] p 359 N93-11265
EISCAT observations of strong ion outflows from the F-region ionosphere during auroral activity: Preliminary results p 360 N93-11267
EISCAT observations of topside ionospheric ion outflows during auroral activity: Revisited p 360 N93-11268
Effects of current driven instabilities on the ion and electron temperatures in the topside ionosphere p 360 N93-11270
Comment on 'EISCAT Radar Observations of Enhanced Incoherent Scatter Spectra and Their Relation to Auroral Luminosity and Field-Aligned Currents' by P. N. Collis et al. p 360 N93-11271
On the origin of ion acoustic turbulence in the auroral topside ionosphere p 361 N93-11273

FIELD EFFECT TRANSISTORS
Reliability of small geometry VLSI devices for microelectronics [AD-A247355] p 289 N93-11414
Preparation of silicon oxynitride thin films by plasma chemical vapor deposition for chemical implantation. Application to a pH ISFET [ECL-91-12] p 291 N93-11574
An analog macromodel of the SG1525A PWM for use with SPICE2G.6 simulators [DE92-019423] p 291 N93-11639
High temperature rectifiers and MOS devices in 6H-silicon carbide [AD-A254725] p 295 N93-12340
Back-gate bias generator [AD-A255126] p 295 N93-12421
The 10 kW power electronics for hydrogen arcjets [NASA-TM-105614] p 235 N93-12484

FIELD THEORY (ALGEBRA)
Remarks on the Robinson-Trautman solutions [MATHS-REPT-A-167] p 423 N93-11122

FIELD THEORY (PHYSICS)
Studies in quantum field theory [DE92-011035] p 470 N93-11276
Landau level quantization and superconductivity [DE92-019028] p 460 N93-11512

FIGHTER AIRCRAFT
Lightweight Exoatmospheric Projectile (LEAP) test program. Supplemental environmental assessment [AD-A252286] p 231 N93-10998
Overview of high performance aircraft propulsion research [NASA-TM-105839] p 213 N93-11530
Application of eigenstructure assignment to the control of powered lift combat aircraft p 215 N93-11871
The future of carrier aviation [AD-A254043] p 430 N93-12260

FILE MAINTENANCE (COMPUTERS)
Concurrent file operations in a high performance FORTRAN [NASA-CR-189711] p 412 N93-11618

FILM BOILING
Enhanced convective and film boiling heat transfer by surface gas injection [DE92-016755] p 306 N93-12221

FILM COOLING
Leading edge film cooking heat transfer including the effect of mainstream turbulence p 199 N93-11886
Investigation of hot streak migration and film cooling effects on heat transfer in rotor/stator interacting flows, report 1 [AD-A250688] p 471 N93-12490

FILM THICKNESS
Two-fluid measurements on thin films [PB92-205350] p 308 N93-12475

FINANCE
The European space industry. Overall situation: Situation and prospects for the 23 leading companies concerned p 472 N93-11163

FINANCIAL MANAGEMENT
Final Report, January 1991 - July 1992 [AD-A254659] p 483 N93-12244

FINGERS
Importance of numerosity and distribution of articulations within the digits, wrists, and arms of telemanipulators confronted with dextrous assembly tasks p 330 N93-11967

FINITE DIFFERENCE THEORY
An adaptive differencing scheme for elliptic flows p 297 N93-11197
Numerical computation of the lightning response of an earth-covered munitions storage bunker and comparison with experiments [DE92-014268] p 367 N93-11236
On an origin of numerical diffusion: Violation of invariance under space-time inversion [NASA-TM-105776] p 425 N93-11254
Comparison of truncation error of finite-difference and finite-volume formulations of convection terms [NASA-TM-105861] p 426 N93-11531
Temporal scattering and response software users' manual, version 2 and 3 [DE92-040934] p 282 N93-11632
Numerical study of advanced rotor blades p 199 N93-11899
Seismic wave propagation in thinly-layered media with steep reflectors [DE92-015619] p 364 N93-12142

Oscillations and concentrations in compressible and incompressible fluids
[AD-A254706] p 307 N93-12333
New acceleration potential method for supersonic unsteady aerodynamics of lifting surfaces, further extension of the nonplanar supersonic doublet point method, and nonlinear, nongradient optimized rational function approximations for supersonic, transient response unsteady aerodynamics p 201 N93-12344
Numerical analysis of oscillating flow about a circular cylinder
[AD-A255164] p 307 N93-12406

FINITE ELEMENT METHOD
Experimental validation of boundary element methods for noise prediction
[NASA-TM-105729] p 323 N93-10966
Quality management of finite element analysis
[PNR-90951] p 331 N93-11110
Numerical study for the study of medium speed internal noise problems
[DILC-EST-TN-200] p 432 N93-11156
Numerical and experimental results in vibroacoustical active control of structural elements with piezoelectric materials
[DILC-EST-TN-224] p 334 N93-11158
Nonlinear response of thin steel plate structures subjected to static, cyclic, and dynamic loads
p 335 N93-11200
Fracture mechanics of model fiber composites
p 237 N93-11247
Proceedings of the 14th International Conference on the Numerical Simulation of Plasmas
[AD-A249095] p 451 N93-11275
Simulation of compressible turbulent flows by a mixed finite element/finite volume method
[ETN-92-92267] p 299 N93-11362
Global-local finite element analysis of composite structures
[DE92-019138] p 240 N93-11658
Numerical simulation for the coaxial electromagnetic launcher using hybrid potentials with FE-BE method
p 222 N93-11726
Effect of assembly anomalies on the strain response of composites in the sphere joint region of the DARPA man-rated demonstration article
[AD-A254204] p 240 N93-11739
Some remarks on shell element analysis with DYNA3D and NIKE3D
[DE92-018784] p 337 N93-11775
Structural integrity of a confinement vessel for testing nuclear fuels for space propulsion
[DE92-016796] p 232 N93-11824
Performance of the h-p version of the finite element method with various elements
[AD-A250689] p 427 N93-11837
Elastic stresses, twin boundaries, and fatigue cracking
p 338 N93-11890
Computational dynamics of high-speed flexible multibody systems p 338 N93-11891
Fourier continuum finite elements for nonlinear structural analysis p 340 N93-12210
Studies in control for vibration suppression of the UWAA 20-bay planar truss
[AD-A250193] p 341 N93-12253
Advanced modeling and optimization of piezoelectric composites
[AD-A253800] p 242 N93-12296
Dynamic test/analysis correlation using reduced analytical models
[NASA-TM-107671] p 341 N93-12300
Fluid-structure interaction using retarded potential and ABAQUS
[AD-A254735] p 307 N93-12355
Thermostructural applications of heat pipes for cooling leading edges of high-speed aerospace vehicles
p 229 N93-12460
The Fourth Workshop on Dynamics and Aeroelastic Stability Modeling of Rotorcraft Systems
[AD-A255065] p 208 N93-12485
Analysis of delamination in composite laminates under low-velocity impact p 243 N93-12532

FINITE VOLUME METHOD
Simulation of compressible turbulent flows by a mixed finite element/finite volume method
[ETN-92-92267] p 299 N93-11362
Comparison of truncation error of finite-difference and finite-volume formulations of convection terms
[NASA-TM-105861] p 426 N93-11531
Resolution of the pressure equation by the boundary element method. Application to multistage turbomachines
[ECL-91-16] p 301 N93-11575
A three dimensional high resolution upwind finite volume Euler solver
[VKI-TN-180] p 198 N93-11686

FINLAND
LIEKKI and JALO: Combustion and fuel conversion
[DE92-540921] p 349 N93-12446

FISCHER-TROPSCH PROCESS
Synthesis of single phase (alpha)-Fe, Fe3C and Fe7C3 nano-particles by CO2 laser pyrolysis technique
[DE92-015654] p 250 N93-11847

FIXTURES
Test program, helium II orbital resupply coupling
[NASA-CR-185681] p 326 N93-11650

FLAME HOLDERS
Development of advanced carbon-carbon annular flameholders for gas turbines
[PNR-90947] p 211 N93-11106

FLAME PROPAGATION
Studies in nonlinear problems of energy
[DE92-018551] p 345 N93-11733
Freely propagating open premixed turbulent flames stabilized by swirl
[DE92-017116] p 251 N93-12112
Studies in premixed combustion
[DE92-018646] p 254 N93-12478

FLAME STABILITY
Freely propagating open premixed turbulent flames stabilized by swirl
[DE92-017116] p 251 N93-12112

FLAMES
The twenty-third International Symposium on combustion
[AD-A250377] p 250 N93-11866
Probing flame chemistry with MBMS, theory, and modeling
[DE92-011433] p 251 N93-12119

FLAPPING
Numerical study of advanced rotor blades
p 199 N93-11899

FLAT PLATES
The effects of plate spacing and downstream plate length on the acoustic resonance excited by flow past two plates in tandem in a duct
[PNR-90958] p 433 N93-11321
An experimental investigation into flow induced acoustic resonances in an annular cascade
[PNR-90959] p 433 N93-11322
Near-field and far-field sound radiation from a line-driven fluid-loaded infinite flat plate having periodic and non-periodic attached rib stiffeners p 434 N93-11884
Impact test of carbon, Kevlar, and glass fibre hybrid FRP plates
[NAL-TR-1100] p 243 N93-12371

FLAT SURFACES
Direct numerical simulation of instabilities in parallel flow with spherical roughness elements
[NASA-TM-105847] p 300 N93-11529

FLAVOR (PARTICLE PHYSICS)
Nucleon structure functions from deep inelastic muon scattering
[NIKHEF-H+K/92-01] p 442 N93-11130
High energy physics at Tufts University
[DE92-018081] p 444 N93-11668

FLEXIBILITY
Numerical analysis of right-half plane zeros for a single-link manipulator
[NASA-CR-190966] p 426 N93-11547

FLEXIBLE BODIES
Modeling and identification of flexible joints in vehicle structures p 324 N93-11261
Computational dynamics of high-speed flexible multibody systems p 338 N93-11891
KC-135 materials handling robotics
[NASA-CR-184430] p 328 N93-11992
Decentralized control of large flexible structures by joint decoupling
[NASA-TM-107694] p 339 N93-12020

FLEXIBLE SPACECRAFT
Rapid maneuvering of large flexible orbiting systems
p 225 N93-11885

FLIGHT ALTITUDE
Comparisons of molecular sieve oxygen concentrators for potential medical use aboard commercial aircraft
[AD-A253648] p 387 N93-11279

FLIGHT CHARACTERISTICS
Application of eigenstructure assignment to the control of powered lift combat aircraft p 215 N93-11871
Neural network models of air combat maneuvering
[AD-A254653] p 421 N93-12096

FLIGHT CONTROL
Spacecraft flight control system design selection process for a geostationary communication satellite
[NASA-TP-3289] p 222 N93-11002
Flight-determined stability analysis of multiple-input-multiple-output control systems
[NASA-TM-4416] p 214 N93-11178
Development of a 1/7-scale F/A-18 UAV for supermaneuverability research --- unmanned air vehicle
[AD-A247261] p 208 N93-12053
Modeling and model simplification of aeroelastic vehicles: An overview
[NASA-TM-107691] p 215 N93-12216
Formal representation of the requirements for an Advanced Subsonic Civil Transport (ASCT) flight control system
[NASA-CR-189699] p 405 N93-12346
On stability and control of SSTO spaceplane in super- and hypersonic ascending phase
[NAL-TR-1128T] p 216 N93-12361
An optical fiber multi-terminal data bus system for aircraft
[NAL-TR-1125] p 209 N93-12370

FLIGHT CREWS
Asthma in aircrew: Assessment, treatment and disposition p 383 N93-11315
An evaluation of crew coordination and performance during a simulated UH-60 helicopter mission
[AD-A254984] p 390 N93-12509

FLIGHT INSTRUMENTS
Flight simulator evaluation of D-size liquid crystal flat panel displays
[NAL-TR-1136] p 209 N93-12367
Liquid crystal flat panel display evaluation tests using a flight simulator
[NAL-TR-1122] p 209 N93-12383

FLIGHT MECHANICS
Automatic control laws for aircraft in parabolic flight
[DILC-EST-TR-211] p 214 N93-11160

FLIGHT OPERATIONS
Design of an air traffic computer simulation system to support investigation of civil tiltrotor aircraft operations
[NASA-CR-190811] p 204 N93-11139
The first meeting of the Advisory Committee on the Future of the US Space Program (C-FUSSP)
[NASA-CR-190995] p 219 N93-11754

FLIGHT PATHS
A simplified numerical procedure to compute the optimal trajectory of an aircraft p 207 N93-11719
A genetic algorithm for search route planning
[AD-A254894] p 414 N93-12284
Accuracy improvement of linear estimated motion using differential type sensors
[NAL-TR-1135] p 314 N93-12365

FLIGHT PLANS
Future FAA telecommunications plan
[AD-A249133] p 283 N93-11760

FLIGHT SAFETY
UK airmisses involving commercial air transport, May-August 1991
[ETN-92-92260] p 203 N93-11357
UK airmisses involving commercial air transport, January-April 1991
[ETN-92-92261] p 298 N93-11358
Activities report of the German Institute for Flight Safety
[ETN-92-92272] p 203 N93-11375
Proceedings of the National Weather Service Aviation Workshop: Postprint volume
[PB92-176148] p 369 N93-11803

FLIGHT SIMULATION
Design of an air traffic computer simulation system to support investigation of civil tiltrotor aircraft operations
[NASA-CR-190811] p 204 N93-11139
Neural network models of air combat maneuvering
[AD-A254653] p 421 N93-12096
Simulation analysis of a cable-mount system used for dynamic wind tunnel tests
[NAL-TR-1127] p 219 N93-12359
Accuracy improvement of linear estimated motion using differential type sensors
[NAL-TR-1135] p 314 N93-12365
Flight simulator evaluation of D-size liquid crystal flat panel displays
[NAL-TR-1136] p 209 N93-12367

FLIGHT SIMULATORS
Neural network models of air combat maneuvering
[AD-A254653] p 421 N93-12096
Flight simulator evaluation of D-size liquid crystal flat panel displays
[NAL-TR-1136] p 209 N93-12367
Liquid crystal flat panel display evaluation tests using a flight simulator
[NAL-TR-1122] p 209 N93-12383

FLIGHT STABILITY TESTS
Flight-determined stability analysis of multiple-input-multiple-output control systems
[NASA-TM-4416] p 214 N93-11178

FLIGHT TEST INSTRUMENTS
A European collaborative NLF nacelle flight demonstrator
[PNR-90992] p 196 N93-11113

FLIGHT TESTS
Lightweight Exoatmospheric Projectile (LEAP) test program. Supplemental environmental assessment
[AD-A252286] p 231 N93-10998

A European collaborative NLF nacelle flight demonstrator
[PNR-90992] p 196 N93-11113
Correlation of forebody pressures and aircraft yawing moments on the X-29A aircraft at high angles of attack
[NASA-TM-4417] p 197 N93-11532
AGARD flight test techniques series. Volume 10: Weapon delivery analysis and ballistic flight testing
[AGARD-AG-300-VOL-10] p 430 N93-11711
Hybrid guidance for maneuvering flight vehicles
[AD-A254110] p 225 N93-11798
Flight test results from a supercritical mission adaptive wing with smooth variable camber
[NASA-TM-4415] p 207 N93-11863
Flight test progress of the STOL research aircraft ASKA
[NAL-TM-643] p 208 N93-12354

FLIGHT TRAINING
An evaluation of crew coordination and performance during a simulated UH-60 helicopter mission
[AD-A254984] p 390 N93-12509

FLOTATION
Evaluation of flotation for purification of pyrite for use in thermal batteries
[DE92-019330] p 290 N93-11553

FLOW CHARACTERISTICS
Dynamical effects of suction/heating on turbulent boundary layers
[AD-A248459] p 299 N93-11416
Flight test results from a supercritical mission adaptive wing with smooth variable camber
[NASA-TM-4415] p 207 N93-11863
Freely propagating open premixed turbulent flames stabilized by swirl
[DE92-017116] p 251 N93-12112
The influence of the Prandtl number on the thermal performance of tubes with the separation and reattachment enhancement mechanism
[DE92-016601] p 306 N93-12313

FLOW CHARTS
Diagnostic rhyme test statistical analysis programs
[RSRE-91026] p 281 N93-11487

FLOW DISTORTION
The role of turbomachinery testing for stability in distorted flow
[PNR-90943] p 210 N93-11040

FLOW DISTRIBUTION
Flow field calculations around the Hermes spaceplane during reentry phase
[MBB-UK-0148-91-PUB] p 195 N93-11008
The hemisphere-cylinder at an angle of attack
p 196 N93-11250
An evaluation of field-flow fractionation for molecular weight characterization of polymeric materials
[DE92-019192] p 267 N93-11497
Direct numerical simulation of instabilities in parallel flow with spherical roughness elements
[NASA-TM-105847] p 300 N93-11529
Simulation of liquid drop breakup behavior in a flow field using discrete element techniques
[DE92-019435] p 300 N93-11537
Interfacial area and two-phase flow structure development measured by a double-sensor probe
[DE92-019459] p 300 N93-11538
Resolution of the pressure equation by the boundary element method. Application to multistage turbomachines
[ECL-91-16] p 301 N93-11575
Experimental investigation of the effects of aft blowing with various nozzle exit geometries on a 3.0 caliber tangent ogive at high angles of attack: Forebody pressure distributions
[NASA-CR-190935] p 197 N93-11605
Turbulence modeling in shock wave/turbulent boundary layer interactions
[NASA-CR-190933] p 301 N93-11606
Progress in developing a transition model for high-speed flows p 301 N93-11615
Reactant gas flow fields in advanced PEM (Proton Exchange Membrane) fuel cell designs
[DE92-018897] p 345 N93-11626
Fully nonlinear development of the most unstable goertler vortex in a three dimensional boundary layer
[NASA-CR-189710] p 301 N93-11633
An experimental study of flow patterns and endwall heat transfer upstream of a surface-mounted rectangular obstruction in a turbulent boundary layer
p 302 N93-11698
Calculation of nozzle/aftbody flowfield interactions
p 302 N93-11722
Effects of sweep on the physics of unsteady shock-induced turbulent separated flows
[AD-A247035] p 198 N93-11742
Numerical analysis of the flow fields in a RQL gas turbine combustor
[DE92-017509] p 302 N93-11767
Numerical modeling of a vortex stabilized arcjet
p 232 N93-11889
A wall interference assessment/correction system
[NASA-CR-190617] p 218 N93-11910
A comparison of velocity profile measurements in the CDIF diffuser with flow field model calculations
[DE92-015367] p 304 N93-11995
Flow visualization of supersonic flow through a combustor section p 200 N93-12001
An investigation of the effects of aft blowing on a 3.0 caliber tangent ogive body at high angles of attack
[NASA-CR-190934] p 200 N93-12004
A general introduction to aeroacoustics and atmospheric sound
[NASA-CR-189717] p 435 N93-12021
Unsteady propeller/wing aerodynamic interactions
p 201 N93-12190
Solution of nonlinear flow equations for complex aerodynamic shapes
[NASA-CR-190979] p 307 N93-12329
Studies of a flat wake rotor theory
[NASA-CR-190936] p 201 N93-12343
A summary of the forebody high-angle-of-attack aerodynamics research on the F-18 and the X-29A aircraft
[NASA-TM-104261] p 202 N93-12353
Experiments and analysis concerning the use of external burning to reduce aerospace vehicle transonic drag
p 235 N93-12537
Three-dimensional turbopump flowfield analysis
[NASA-CR-190978] p 308 N93-12539

FLOW EQUATIONS
The prediction of convective heat transfer in rotating square ducts
[PNR-90929] p 296 N93-11025
Thermokinetic modelling and hypersonic flow
[DILC-EST-TN-218] p 196 N93-11157
Solution of nonlinear flow equations for complex aerodynamic shapes
[NASA-CR-190979] p 307 N93-12329

FLOW MEASUREMENT
Method of remotely characterizing thermal properties of a sample
[NASA-CASE-LAR-13508-3-CU] p 216 N93-11057
Measuring and modelling of particle-fluid flow in a riser reactor
[VTT-PUBS-88] p 299 N93-11359
Overview of recent diagnostic measurements at the USA MHD facilities
[DE92-015365] p 454 N93-12087
Operating experience using venturi flow meters at liquid helium temperature
[DE92-014693] p 313 N93-12140

FLOW STABILITY
On the instability of hypersonic flow past a pointed cone: Comparison of theoretical and experimental results of Mach 18
[DLR-FB-92-02] p 196 N93-11141
Quasigeostrophic vortices in zonal shear
p 358 N93-11226
Fully nonlinear development of the most unstable goertler vortex in a three dimensional boundary layer
[NASA-CR-189710] p 301 N93-11633
Nonlinear stability of flows over rigid and flexible boundaries p 198 N93-11874
Singularities of the Euler equation and hydrodynamic stability
[NASA-CR-189720] p 306 N93-12173
On the Goertler instability of boundary layers
[NAL-TR-1120T] p 307 N93-12374

FLOW THEORY
A combined experimental and theoretical study of laminar flow control with particular relevance to aero engine nacelles
[PNR-90991] p 195 N93-11070
Numerical investigations into the base drag of various wedges using the base flow model developed by Mauri Tanner
[REPT-B-36] p 202 N93-12414

FLOW VELOCITY
EISCAT observations of topside ionospheric ion outflows during auroral activity: Revisited p 360 N93-11268
The measurement of the velocity field induced by a gust generator in a closed-circuit subsonic wind-tunnel
[RAE-TM-MAT-STR-1102] p 217 N93-11435
Physical processes involved in injection and atomization of liquid propellants p 248 N93-11453
The convection speed of the dynamic stall vortex
[AD-A247258] p 197 N93-11464
Interfacial area and two-phase flow structure development measured by a double-sensor probe
[DE92-019459] p 300 N93-11538
A distributed data acquisition and centralized data reduction system for flexible and efficient measurements
[DE92-019021] p 312 N93-11827
Turbulence structure and polymer drag reduction in adverse pressure gradient boundary layers
p 304 N93-12003
Operating experience using venturi flow meters at liquid helium temperature
[DE92-014693] p 313 N93-12140
Studies of a flat wake rotor theory
[NASA-CR-190936] p 201 N93-12343
An experimental study of a small high speed LH2 rocket pump: Fundamental mechanical design
[NAL-TR-1123] p 330 N93-12463

FLOW VISUALIZATION
An experimental study of flow patterns and endwall heat transfer upstream of a surface-mounted rectangular obstruction in a turbulent boundary layer
p 302 N93-11698
The 13 ft by 9 ft low speed wind tunnel facility at DRA (Aerospace Division) Bedford (England)
[RAE-TM-AERO-2228] p 199 N93-11883
Flow visualization of supersonic flow through a combustor section p 200 N93-12001
An investigation of the effects of aft blowing on a 3.0 caliber tangent ogive body at high angles of attack
[NASA-CR-190934] p 200 N93-12004
Unsteady propeller/wing aerodynamic interactions
p 201 N93-12190
An experimental study of the relationship between forces and moments and vortex breakdown on a pitching delta wing p 208 N93-12206
A summary of the forebody high-angle-of-attack aerodynamics research on the F-18 and the X-29A aircraft
[NASA-TM-104261] p 202 N93-12353

FLOWMETERS
Operating experience using venturi flow meters at liquid helium temperature
[DE92-014693] p 313 N93-12140

FLUE GASES
Direct catalytic decomposition of nitric oxide
[DE92-018759] p 247 N93-11444

FLUENCE
System design and radiation field characteristics of the High Flux Neutron Radiography Facility (HFNRF) at Sandia National Laboratories
[DE92-013984] p 219 N93-12268
The relationship between electrostatic discharges on spacecraft P78-2 and the electron environment
[AD-A255179] p 226 N93-12379

FLUID DYNAMICS
Front tracking and the interaction of nonlinear waves
[AD-A253544] p 297 N93-11148
The Third Potsdam-5 Kiev International Workshop on Nonlinear Processes in Physics
[AD-A249140] p 430 N93-11420

FLUID FILMS
A test facility for the thermofluid-dynamics of gas bearing lubrication films
[PNR-90897] p 263 N93-11032

FLUID FILTERS
Kinetics of diffusional droplet growth in a liquid/liquid two-phase system
[NASA-CR-190805] p 297 N93-11142

FLUID FLOW
Boundary condition methods in the numerical solution of the Navier-Stokes equations with the application to free surface problems
[ISBN-0-315-64278-5] p 298 N93-11241
Measuring and modelling of particle-fluid flow in a riser reactor
[VTT-PUBS-88] p 299 N93-11359
An evaluation of field-flow fractionation for molecular weight characterization of polymeric materials
[DE92-019192] p 267 N93-11497
Cryostabilization of high-temperature superconducting magnets with subcooled flow in microchannels
[DE92-018174] p 431 N93-11598
The effects of chemistry on weld profiles in partial and full penetration welds
[DE92-016865] p 327 N93-11679
Physical effects of vegetation on wind-blown sand in the coastal environments of Florida
[PB92-188424] p 354 N93-11702
Calculation of nozzle/aftbody flowfield interactions
p 302 N93-11722
Overview of property formulations for helium, nitrogen, lithium, and lithium-lead in ATHENA/MOD1 with comparison of calculated properties to measured properties
[DE92-017995] p 471 N93-12058
Regular and chaotic mixing of viscous fluids in eccentric rotating cylinders p 305 N93-12157

FLUID MECHANICS
Comparative effects of drag-reducing polymers. An experimental report
[AD-A254001] p 268 N93-11793

Disruption shape effects on the performance of enhanced tubes with the separation and reattachment mechanism
[DE92-016602] p 305 N93-12128

FLUID PRESSURE
Near-field and far-field sound radiation from a line-driven fluid-loaded infinite flat plate having periodic and non-periodic attached rib stiffeners p 434 N93-11884
Study of sound propagation in a wedge-shaped ocean and comparison with other methods
[AD-A255165] p 435 N93-12471

FLUORIDES
Chemistry of lower valent actinide halides
[DE92-017031] p 251 N93-12105

FLUORINE
Oxidation, nitridation, and fluorine etching of Si
[AD-A253559] p 249 N93-11755

FLUX (RATE)
EISCAT observations of topside ionospheric ion outflows during auroral activity: Revisited p 360 N93-11268
The relationship between electrostatic discharges on spacecraft P78-2 and the electron environment
[AD-A255179] p 226 N93-12379

FLUX DENSITY
The role of proton precipitation in Jovian aurora: Theory and observation p 487 N93-11165
A model to estimate the flux of background particles expected to accumulate on the collector foils of the interstellar gas experiment on the long duration exposure facility spacecraft
[AD-A254265] p 489 N93-11815

FLUX PINNING
Flux pinning in oxygen-depleted YBa2Cu3O(7-y) single crystals
[DE92-019548] p 461 N93-11647

FLUX VECTOR SPLITTING
A three dimensional high resolution upwind finite volume Euler solver
[VKI-TN-180] p 198 N93-11686

FLYING PERSONNEL
Epidemiologic view of allergic diseases in North America: Implications for aerospace medicine
p 382 N93-11311

FOCAL PLANE DEVICES
INAS hole-immobilized doping superlattice long-wave-infrared detector
[NASA-CASE-NPO-17880-1-CU] p 458 N93-11056
Development of ultra-low noise, high sensitivity planar metal grating coupled AlGaAs/GaAs multiquantum well IR detectors for focal plane array staring IR sensor systems
[AD-A254697] p 468 N93-12228

FOCUSING
Using the 16 viewscreens during commissioning of AmPS
[NIKHEF-K/AMPS/92-01] p 442 N93-11131
Alternating-phase focusing: A model to study nonlinear dynamics
[DE92-019027] p 431 N93-11511
Fuzzy control system for a remote focusing microscope p 314 N93-11934
Mirror alignment techniques for point-focus solar concentrators
[DE92-019643] p 348 N93-12074
Divergence in intense ion beams caused by incomplete charge neutralization
[DE92-016891] p 445 N93-12103
Video camera as a visual sensor
[NAL-TR-1132] p 314 N93-12373

FOILS (MATERIALS)
Foil optimization for low energy neutral atom imaging
[DE92-013435] p 365 N93-12263

FOKKER-PLANCK EQUATION
Scaling of lower hybrid current drive with temperature
[DE92-018541] p 449 N93-10988

FORCE DISTRIBUTION
EXOS research on master controllers for robotic devices p 399 N93-11957

FORCED CONVECTION
Metal slurry droplet and spray combustion
p 245 N93-11138

FORCED VIBRATION
Structural dynamics of large space structures having parametric uncertainties p 225 N93-11836

FOREBODIES
Correlation of forebody pressures and aircraft yawing moments on the X-29A aircraft at high angles of attack
[NASA-TM-4417] p 197 N93-11532
A summary of the forebody high-angle-of-attack aerodynamics research on the F-18 and the X-29A aircraft
[NASA-TM-104261] p 202 N93-12353

FORECASTING
Validation test report for the first-generation dart Gulf Stream forecasting system
[AD-A254286] p 373 N93-11821
Forecasting the relativistic electron flux at geosynchronous orbit
[AD-A254016] p 226 N93-12064

FORMAT
Directory interchange format manual, version 4.0
[NASA-TM-107991] p 478 N93-11911

FORMIC ACID
Formic acid: Development of an analytical method and use as process indicator in anaerobic systems
[AD-A250668] p 253 N93-12267

FORMING TECHNIQUES
Superplastic forming of ceramic insulation
p 228 N93-12452

FORTRAN
Concurrent file operations in a high performance FORTRAN
[NASA-CR-189711] p 412 N93-11618
Interfacing Matlab and software written in other languages
[NPL-DITC-200/92] p 412 N93-11688

FOUR-WAVE MIXING
Interaction of sound with sound by novel mechanisms: Ultrasonic four-wave mixing mediated by a suspension and ultrasonic three-wave mixing at a free surface
[AD-A254657] p 435 N93-12097

FOURIER TRANSFORMATION
Fringe analysis of in-plane displacements on high speed rotating components
[PNR-90920] p 334 N93-11022
The tomographic formulation of spotlight mode synthetic aperture radar extended to three dimensional targets
[DE92-013666] p 280 N93-11234
Comparison of passive-remote and conventional Fourier transform infrared systems for continuously monitoring incinerator emissions
[DE92-015225] p 355 N93-12098

FRACTALS
Multifractal analysis at negative q
[AD-A254370] p 413 N93-12159

FRACTIONATION
An evaluation of field-flow fractionation for molecular weight characterization of polymeric materials
[DE92-019192] p 267 N93-11497

FRACTOGRAPHY
Composite failure analysis handbook. Volume 2: Technical handbook. Part 3: Case histories
[AD-A249131] p 241 N93-12054

FRACTURE MECHANICS
Fracture mechanics of model fiber composites
p 237 N93-11247
Fatigue crack closure: A review
[RAE-TR-90046] p 335 N93-11369
A consistent cracked bar vibration theory
p 339 N93-12000
Study of the dynamic degradation under the action of a shock wave induced by pulsed laser
p 319 N93-12037
Development of nondestructive evaluation methods and prediction of effects of flaws on the fracture behavior of structural ceramics
[DE92-016395] p 271 N93-12123
Fatigue in single crystal nickel superalloys
[AD-A254603] p 260 N93-12237
Verification of rain-flow reconstructions of a variable amplitude load history
[NASA-CR-189670] p 341 N93-12411
Analysis of delamination in composite laminates under low-velocity impact p 243 N93-12532

FRACTURE STRENGTH
Analysis of precracking parameters and fracture toughness for ceramic single-edge-precracked-beam specimens
[NASA-TM-105568] p 263 N93-10962
Pressure vessel burst test program
[AD-A253708] p 334 N93-11080
Mixed mode bending test of the interlaminar fracture toughness of carbon/epoxy
[FFA-TN-1992-04] p 237 N93-11128
Microstructure and mechanical properties of reactive hot isostatic pressed TiAl powder material
[GKSS-91/E/60] p 256 N93-11336
Micromechanisms of deformation and fracture in aluminum based MMC's: Interface effects
[AD-A253560] p 259 N93-11850
Slow crack growth in vacuum p 338 N93-11909
Thermal fracture service life analysis of a case bonded visco-elastic cylinder p 339 N93-12008
Mechanical properties of 1950's vintage 304 stainless steel weldment components after low temperature neutron irradiation
[DE92-017059] p 259 N93-12107
Fatigue crack growth in AerMet 100 steel
[AD-A249068] p 261 N93-12248
Influence of oxygen partial pressure and silver additions on microstructure and related properties of YBCO superconductors
[DE92-011145] p 468 N93-12249
Fracture toughness testing of polymer matrix composites
[NASA-TP-3199] p 243 N93-12302
Spectrum fatigue behaviour of powder metallurgy aluminum alloys
[AD-A255060] p 262 N93-12468

FRACTURES (MATERIALS)
Nondestructive evaluation of ceramic and metal matrix composites for NASA's HITEMP and enabling propulsion materials programs
[NASA-TM-105807] p 331 N93-10963
Fracture behavior of polymers at cryogenic temperatures
[KFK-4969] p 265 N93-11203

FRACTURING
A creep cavity growth model for creep-fatigue life prediction of a unidirectional W/Cu composite
[NASA-TM-105780] p 333 N93-10967
Ceramic component reliability with the restructured NASA/CARES computer program
[NASA-TM-105856] p 334 N93-11004
Micromechanisms of deformation and fracture in aluminum based MMC's: Interface effects
[AD-A253560] p 259 N93-11850
Slow crack growth in vacuum p 338 N93-11909
Development of nondestructive evaluation methods and prediction of effects of flaws on the fracture behavior of structural ceramics
[DE92-016395] p 271 N93-12123

FRANCE
Post-war regional planning: The French silicon valley
[RSRE-MEMO-4282] p 472 N93-10976

FRAUNHOFER LINES
Three-dimensional image structure in in-line Fraunhofer holography p 311 N93-11723

FREE BOUNDARIES
Boundary condition methods in the numerical solution of the Navier-Stokes equations with the application to free surface problems
[ISBN-0-315-64276-5] p 298 N93-11241

FREE CONVECTION
Laboratory and numerical studies of dynamical processes related to thermal convection in the Earth's mantle p 364 N93-11900

FREE ELECTRON LASERS
A synopsis of resistive wall effects in very short wavelength free electron lasers
[DE92-018065] p 315 N93-11155
Experimental and theoretical investigation of high gradient acceleration
[DE92-015299] p 315 N93-11278
UCSB FEL user mode adaption project
[AD-A248734] p 316 N93-11418
Scaling of gain with energy spread and energy in the PEP FEL
[DE92-019248] p 316 N93-11500
Theory for a high power free electron laser and tactical applications
[AD-A255161] p 323 N93-12405

FREE FLIGHT
Simulation analysis of a cable-mount system used for dynamic wind tunnel tests
[NAL-TR-1127] p 219 N93-12359

FREE JETS
OH rotational temperature and concentration measurements in a supersonic jet
[DE92-006700] p 252 N93-12255

FREE MOLECULAR FLOW
Using NEKTON to solve systems of discrete Boltzmann equations
[DE92-018272] p 303 N93-11799

FREE RADICALS
Studies of transition states and radicals by negative ion photodetachment
[DE92-017011] p 440 N93-11875
Probing flame chemistry with MBMS, theory, and modeling
[DE92-011433] p 251 N93-12119

FREE VIBRATION
Structural dynamics of large space structures having parametric uncertainties p 225 N93-11836
Dynamic analysis of a pre-and-post ice impacted blade
[NASA-TM-105829] p 276 N93-12197

FREEZE DRYING
Freeze-dried human red blood cells
[AD-A253295] p 376 N93-11193

FREEZING
Developments in icing test techniques for aerospace applications in the RAE Pyestock (England) altitude test facility
[RAE-TM-P-1214] p 207 N93-11485

FREQUENCIES
An EVACS simulation with nested transactions
[NASA-CR-190636] p 412 N93-11717
Impact of finite frequency deviation on the performance of dual-filter heterodyne FSK lightwave systems
[AD-A247611] p 448 N93-11892
FREQUENCY ANALYZERS
The extremely low frequency wave analyzer
[AD-A255178] p 366 N93-12378
FREQUENCY CONTROL
Quartz crystal resonators and oscillators for frequency control and timing applications: A tutorial, revision 5.2
[AD-A254892] p 469 N93-12283
FREQUENCY DISCRIMINATORS
Unequal stub length diplexing microwave frequency discriminator circuit
[AD-D015352] p 288 N93-11051
On the definition and calculation of effective impedances and averaged boundary conditions with application to the analysis of high complexity frequency selective surfaces
[RSRE-MEMO-4518] p 281 N93-11387
FREQUENCY DISTRIBUTION
CO2 laser frequency doubling using AgGaSe2
[RSRE-MEMO-4528] p 315 N93-11388
FREQUENCY DIVISION MULTIPLE ACCESS
All-digital multicarrier demodulators for on-board processing satellites in mobile communication systems
p 285 N93-12207
Space Station communications and tracking systems modeling and RF link simulation
[NASA-CR-185684] p 288 N93-12519
FREQUENCY MEASUREMENT
Auditory perception
[AD-A255061] p 385 N93-12469
FREQUENCY MODULATION
Short-range radar system
[AD-D015339] p 278 N93-11044
A study of the CO2 laser near threshold
p 316 N93-11720
FREQUENCY MULTIPLIERS
CO2 laser frequency doubling
[AD-A251060] p 314 N93-10997
FREQUENCY RESPONSE
High frequency response from YBa2Cu3O(7-x) Josephson devices on SrTiO3 bicrystal substrates
[NPL-DES-118] p 459 N93-11394
Description of the structural responses in the medium-frequency range by an energetic formulation
[ECL-92-16] p 336 N93-11582
FREQUENCY SHIFT
Impact of finite frequency deviation on the performance of dual-filter heterodyne FSK lightwave systems
[AD-A247611] p 448 N93-11892
FRESH WATER
The relative importance of sulfur and nitrogen compounds in the acidification of freshwater
[DE92-016899] p 354 N93-11680
FRESNEL REGION
Extension of fresnel near-field region by single-cycle sinusoidal pulses
[AD-A254736] p 285 N93-12356
FRICTION FACTOR
Deep penetration into frictional ductile and brittle materials
[PB92-205566] p 338 N93-11903
FRICTION WELDING
The effects of aluminum oxide on inertial welding of aluminum in space applications
[AD-A255100] p 329 N93-12274
FRONTS (METEOROLOGY)
Structure of the nocturnal boundary layer over a complex terrain
[DE92-018141] p 362 N93-11669
An observational study of a prefrontal convective rainband using TAMEX single- and dual-Doppler data
[AD-A249839] p 371 N93-12251
FUEL CELL POWER PLANTS
NEDO Fuel/Storage Technology Subcommittee
[DE92-526262] p 346 N93-11777
FUEL CELLS
Sealant research for solid oxide fuel cells
[DE92-019044] p 345 N93-11513
Reformers for the production of hydrogen from methanol and alternative fuels for fuel cell powered vehicles
[DE92-019300] p 274 N93-11550
Intermediate temperature electrolytes for SOFC
[DE92-018786] p 345 N93-11571
Reactant gas flow fields in advanced PEM (Proton Exchange Membrane) fuel cell designs
[DE92-018897] p 345 N93-11626
NEDO Fuel/Storage Technology Subcommittee
[DE92-526262] p 346 N93-11777
FUEL COMBUSTION
The intensity of knock in an internal combustion engine: An experimental and modeling study
[DE92-019504] p 326 N93-11540
The twenty-third International Symposium on combustion
[AD-A250377] p 250 N93-11866
Asymptotic analysis of reacting materials with saturated explosion. 2: High-frequency waves
[AD-A254473] p 275 N93-12236
LIEKKI and JALO: Combustion and fuel conversion
[DE92-540921] p 349 N93-12446
FUEL CONSUMPTION
Civil aircraft engines: The next generation
[PNR-90962] p 211 N93-11085
Federal Alternative Fuel Program light duty vehicle operation
[DE92-018124] p 274 N93-11794
Reduction in global warming due to fuel economy improvements and emissions control of criteria pollutants: New US light-duty vehicles (1968-1991)
[DE92-016636] p 356 N93-12314
FUEL FLOW
Solution of two-phase reacting flow in liquid thrust chambers p 235 N93-11449
FUEL INJECTION
Coaxial injector spray characterization using water/air as simulants p 248 N93-11452
Physical processes involved in injection and atomization of liquid propellants p 248 N93-11453
Experimental investigation of rocket injector atomization p 248 N93-11454
Combustion characteristics of the LO2/GCH4 fuel-rich preburners for staged combustion cycle rocket engines
[NAL-TR-1124] p 234 N93-12368
FUEL PUMPS
An experimental study of a small high speed LH2 rocket pump: Fundamental mechanical design
[NAL-TR-1123] p 330 N93-12463
FUEL-AIR RATIO
Experiments and analysis concerning the use of external burning to reduce aerospace vehicle transonic drag
p 235 N93-12537
FUELS
NEDO Fuel/Storage Technology Subcommittee
[DE92-526262] p 346 N93-11777
The twenty-third International Symposium on combustion
[AD-A250377] p 250 N93-11866
LIEKKI and JALO: Combustion and fuel conversion
[DE92-540921] p 349 N93-12446
FULL SCALE TESTS
Flight test progress of the STOL research aircraft ASKA
[NAL-TM-643] p 208 N93-12354
FULLERENES
Near-IR absorption spectra for the C70 fullerene anions
[AD-A253658] p 246 N93-11280
FUNCTION GENERATORS
Automatic Attenuation/Phase Calibration System (AAPCS)
[DE92-017354] p 284 N93-11917
FUNCTION SPACE
Domain decomposition: A bridge between nature and parallel computers
[NASA-CR-189709] p 425 N93-11246
FUNCTIONAL DESIGN SPECIFICATIONS
10 kW L-band amplifier tubes for efficient and reliable troposcatter communication transmitter systems
[AD-A253246] p 290 N93-11504
Formal design specification of a Processor Interface Unit
[NASA-CR-189698] p 406 N93-12538
FUNCTIONS (MATHEMATICS)
Dynamic multimodal function optimization using genetic algorithms
[DE92-019602] p 414 N93-12234
FUNGI
A trainable image pattern classification system for detection of damaged soybean seeds
p 201 N93-12208
FURNACES
Technology evaluation report of Retech, Inc., Plasma Centrifugal Furnace, volume 1
[PB92-216035] p 456 N93-12526
Technology evaluation report of Retech, Inc., Plasma Centrifugal Furnace, volume 2
[PB92-216043] p 457 N93-12527
FUSELAGES
Correlation of forebody pressures and aircraft yawing moments on the X-29A aircraft at high angles of attack
[NASA-TM-4417] p 197 N93-11532
Evaluation of alternatives for increasing A-7D rearward visibility
[AD-A255071] p 208 N93-12488
FUSION REACTORS
Nova Upgrade: A proposed ICF facility to demonstrate ignition and gain, revision 1
[DE92-018960] p 451 N93-11534
Plasma properties
[DE92-018635] p 455 N93-12188
FUSION WELDING
Some consistency requirements on hardening-recovery evolution equations for welding, part 1
[DE92-015992] p 329 N93-12220
FUZZY SETS
Fuzzy logic control for camera tracking system
p 314 N93-11935
System diagnostic builder p 396 N93-11944
Fuzzy logic control of telerobot manipulators
p 399 N93-11959

G

GADOLINIUM
Recrystallization of amorphous or nanocrystalline NdBa2Cu3O(7-x) and GdBa2Cu3O(7-x)
[DE92-016302] p 462 N93-11706
GALACTIC CLUSTERS
Non-self-similar clustering of galaxies
[MPE-PREPRINT-212] p 484 N93-11338
X ray morphology of clusters of galaxies
p 482 N93-11475
Magnetic fields in the clusters of galaxies with extreme cooling flows p 486 N93-12164
GALACTIC EVOLUTION
Non-self-similar clustering of galaxies
[MPE-PREPRINT-212] p 484 N93-11338
Mechanism for ejecting stars from the Galactic plane
[DE92-018375] p 485 N93-11697
GALACTIC NUCLEI
A multi-line study of the molecular interstellar medium on M82's starburst nucleus
[MPE-PREPRINT-213] p 484 N93-11347
GALACTIC RADIATION
Contributions to the Joint Discussion 3: Results from Rosat and GRO and Other Recent High Energy Astrophysics Missions of the Max-Planck-Institut fuer Extraterrestrische Physik
[MPE-PREPRINT-215] p 482 N93-11473
GALLIUM ARSENIDES
Radiation damage by high energy electrons in GaAs: A DLTS (deep level transient spectroscopy) examination
[HMI-B-494] p 442 N93-11028
Development of stable metallization systems
[AD-A253569] p 264 N93-11079
Electron transfer rates at semiconductor/liquid interfaces
[DE92-018559] p 289 N93-11438
VUV and UV sources and spectroscopic applications
[AD-A247293] p 291 N93-11758
Systems engineering and technical assistance in support of digital gallium arsenide insertion projects
[AD-A253751] p 463 N93-11790
Excitons in semiconducting superlattices, quantum wells, and ternary alloys
[DE92-015178] p 464 N93-11894
GaAs heterojunction device based A/D converter development
[AD-A252644] p 468 N93-12183
Development of ultra-low noise, high sensitivity planar metal grating coupled AlGaAs/GaAs multiquantum well IR detectors for focal plane array staring IR sensor systems
[AD-A254697] p 468 N93-12228
MMIC GaAs bonding investigation
[AD-A254773] p 470 N93-12464
GALLIUM COMPOUNDS
Synthesis and characterization of novel organogallium-phosphorus compounds: X ray crystal structures of Ph2GaP (SiMe3)2Ga (Ph2Cl, Ph2 (Cl)Ga.P (SiMe3)3, and Ph3Ga.P (SiMe3)3
[AD-A253841] p 462 N93-11724
GALLIUM NITRIDES
VUV and UV sources and spectroscopic applications
[AD-A247293] p 291 N93-11758
GALLIUM SELENIDES
CO2 laser frequency doubling using AgGaSe2
[RSRE-MEMO-4528] p 315 N93-11388
GAME THEORY
A game theoretic approach to linear dynamic estimation p 340 N93-12200
GAMMA RAY ASTRONOMY
Gamma ray astronomy
[NASA-CR-184447] p 483 N93-12348
GAMMA RAY BURSTS
Gamma ray astronomy
[NASA-CR-184447] p 483 N93-12348
GAMMA RAY OBSERVATORY
Gamma ray astronomy
[NASA-CR-184447] p 483 N93-12348

GAMMA RAY SPECTRA
Operator's guide for VAXGAP, a gamma-ray spectrum analysis package
[DE92-019096] p 407 N93-11356

GAMMA RAY SPECTROMETERS
Operator's guide for VAXGAP, a gamma-ray spectrum analysis package
[DE92-019096] p 407 N93-11356

GAMMA RAYS
Development of a scintillating optical fiber ionization calorimeter
[NASA-CR-184415] p 311 N93-11662

GAS BAGS
Inflatable device for excluding sea water from a rocket motor
[AD-D015365] p 232 N93-11424

GAS BEARINGS
A test facility for the thermofluid-dynamics of gas bearing lubrication films
[PNR-90897] p 263 N93-11032

GAS CHROMATOGRAPHY
A cryogenic enrichment technique for gas chromatographic detection of S2F10 in SF6 discharges
[DE92-011045] p 252 N93-12219

GAS COMPOSITION
Predicted aircraft effects on stratospheric ozone
p 352 N93-11096
Comparisons of molecular sieve oxygen concentrators for potential medical use aboard commercial aircraft
[AD-A253648] p 387 N93-11279
Silicon on insulator structures in selective epitaxial growth
[DE92-017118] p 465 N93-11915

GAS COOLED REACTORS
A gas-cooled cermet reactor system for planetary base power
[DE92-018017] p 443 N93-11433

GAS DENSITY
Potassium D-line fitting for investigation of MHD boundary layers
[DE92-019020] p 454 N93-11826
Hypersonic flow diagnostic development
[AD-A255045] p 202 N93-12466

GAS FLOW
CFD modeling of turbulent flows around the SSME main injector assembly using porosity formulation
[NASA-CR-184359] p 297 N93-11171
Reactant gas flow fields in advanced PEM (Proton Exchange Membrane) fuel cell designs
[DE92-018897] p 345 N93-11626
Space Station Freedom seal leakage rate analysis and testing summary: Air leaks in ambient versus vacuum exit conditions
[NASA-TM-103604] p 328 N93-12149
An improved numerical model for wave rotor design and analysis
[NASA-TM-105915] p 214 N93-12418
Studies in premixed combustion
[DE92-018646] p 254 N93-12478

GAS GENERATORS
An improved numerical model for wave rotor design and analysis
[NASA-TM-105915] p 214 N93-12418

GAS HEATING
Inert gas electric heater for elevated temperature testing of small propulsion components
[DE92-017434] p 221 N93-12317

GAS INJECTION
Effect of inert propellant injection on Mars ascent vehicle performance
[NASA-CR-189238] p 226 N93-12152
Enhanced convective and film boiling heat transfer by surface gas injection
[DE92-016755] p 306 N93-12221

GAS IONIZATION
Low pressure gas multiphotoionization for wave packet experiments p 319 N93-12034

GAS MIXTURES
Loads from the detonation of hydrogen-air-steam mixtures
[DE92-019318] p 249 N93-11551

GAS STREAMS
Mixing regimes in a spatially confined, two-dimensional, supersonic shear layer
[AD-A254302] p 302 N93-11756

GAS TEMPERATURE
Frequency response in short thermocouple wires
[NASA-CR-190943] p 310 N93-11612
A distributed data acquisition and centralized data reduction system for flexible and efficient measurements
[DE92-019021] p 312 N93-11827

GAS TUNGSTEN ARC WELDING
Heat-affected zone cracking of nitronic 60 stainless steel
[DE92-018286] p 254 N93-10984

GAS TURBINE ENGINES
An interactive preprocessor for the NASA engine performance program
[NASA-TM-105786] p 209 N93-10983
Materials: Toward the non-metallic engine
[PNR-90915] p 209 N93-11019
Testing for integrity
[PNR-90927] p 210 N93-11024
The prediction of convective heat transfer in rotating square ducts
[PNR-90929] p 296 N93-11025
A test facility for the thermofluid-dynamics of gas bearing lubrication films
[PNR-90897] p 263 N93-11032
On the basis of experience: Built in product reliability
[PNR-90932] p 331 N93-11034
Simultaneous engineering in the design of aero engines
[PNR-90973] p 211 N93-11062
Maintainability of large gas turbine aero engines
[PNR-90987] p 211 N93-11069
Advanced materials in gas turbine engines: An assessment
[PNR-90946] p 211 N93-11105
Development of advanced carbon-carbon annular flameholders for gas turbines
[PNR-90947] p 211 N93-11106
Small particle impact damage in carbon-carbon composites
[PNR-90948] p 236 N93-11107
The development of the Rolls-Royce Trent aero gas turbine
[PNR-90949] p 212 N93-11108
Development of the neutron diffraction technique for the determination of near surface residual stresses in critical gas turbine components
[PNR-90984] p 212 N93-11112
Simultaneous engineering in aero gas turbine design and manufacture
[PNR-90890] p 212 N93-11208
Numerical analysis of the flow fields in a RQL gas turbine combustor
[DE92-017509] p 302 N93-11767
Erosion predictions and measurements of high-temperature coatings and superalloys used in turbomachines p 272 N93-12189
An improved numerical model for wave rotor design and analysis
[NASA-TM-105915] p 214 N93-12418
Investigation of hot streak migration and film cooling effects on heat transfer in rotor/stator interacting flows, report 1
[AD-A250688] p 471 N93-12490

GAS TURBINES
A knowledge-based blackboard system to interpret graphical data from vibration tests of gas turbines
[PNR-90993] p 212 N93-11114
NEDO Fuel/Storage Technology Subcommittee
[DE92-526262] p 346 N93-11777
Advanced coal-fueled gas turbine systems
[DE92-018939] p 327 N93-11832

GAS-ION INTERACTIONS
State-resolved dynamics of ion-molecule collisions in a flowing afterglow
[AD-A247288] p 436 N93-11467

GAS-SOLID INTERACTIONS
Interfacial and thin film chemistry in electron device fabrication
[AD-A253579] p 288 N93-11257
Hydrogen assisted heat transfer during diamond growth using carbon and tantalum filaments
[AD-A247944] p 468 N93-12218
Gas-surface interactions near dissociation threshold
[AD-A250205] p 252 N93-12254

GASDYNAMIC LASERS
Atomic structure of Ni-like soft x ray lasing ions
[DE92-019273] p 438 N93-11778

GASEOUS DIFFUSION
Modelling the behaviour of gas bubbles in epoxy resin
[PNR-90961] p 264 N93-11084
An NMR study of the occupation of C(sub 60) interstitial sites by oxygen molecules
[DE92-019436] p 437 N93-11640

GASIFICATION
Metal slurry droplet and spray combustion
p 245 N93-11138
LIEKKI and JALO: Combustion and fuel conversion
[DE92-540921] p 349 N93-12446

GASTROINTESTINAL SYSTEM
Epidemiologic view of allergic diseases in North America: Implications for aerospace medicine
p 382 N93-11311

GAUGE INVARIANCE
Constrained KP hierarchy and bi-Hamiltonian structures
[MATHS-REPT-A-168] p 424 N93-11123
Darboux theorems and Wronskian formulas for integrable systems. 1: Constrained KP flows
[MATHS-REPT-A-172] p 424 N93-11126

GAUGE THEORY
Studies in quantum field theory
[DE92-011035] p 470 N93-11276
Induced gauge theories and W gravity
[DE92-011218] p 470 N93-11518

GAUSS EQUATION
Migration by the Kirchhoff, slant stack, and Gaussian beam methods
[DE92-018640] p 366 N93-12318

GEAR TEETH
Maximum life spiral bevel reduction design
[NASA-TM-105790] p 323 N93-10982

GEARS
Experimental validation of boundary element methods for noise prediction
[NASA-TM-105729] p 323 N93-10966
Maximum life spiral bevel reduction design
[NASA-TM-105790] p 323 N93-10982
The application of manufacturing systems engineering for aero engine gears
[PNR-90944] p 324 N93-11054
Thermal non-Newtonian elastohydrodynamic lubrication of line contacts under sliding-rolling and simple sliding conditions p 324 N93-11263
Time-frequency domain analysis of vibration signals for machinery diagnostics. 3: The present power spectral density
[OUEL-1911/92] p 337 N93-11707

GENETICS
Molecular cytogenetics: A novel approach for measuring chromosome translocations in individuals years after exposure to low levels of ionizing radiation
[DE92-018066] p 374 N93-10974
Implicit parallelism in genetic algorithms
[REPT-92-012] p 418 N93-11180
Parallel genetic algorithms: Introduction and overview of current research
[REPT-92-015] p 418 N93-11181

GEOCHEMISTRY
High-precision thorium RIMS for geochemistry
[DE92-017405] p 250 N93-11918

GEODESY
Construction of a geodesic strapdown inertial navigation system for point determination
[SER-C-367] p 205 N93-11344

GEOGRAPHIC INFORMATION SYSTEMS
Geographic information system to support state-wide hydrologic modeling with the SCS-TR-20
[PB92-185768] p 476 N93-11700
Land use/land cover classification using digitally merged spot panchromatic and Landsat thematic mapper imagery
[PB92-188416] p 343 N93-11701
Spatial data transformation: Feature attribute conversion issues and practical experience
[AD-A254238] p 477 N93-11741
Photogrammetric GIS technology: Feature mapping on digital stereo imagery
[AD-A254255] p 477 N93-11748
Proceedings of the First Seminar on Geographic Information Systems in Zambia
[PB92-207125] p 477 N93-11789

GEOIDS
An approximate solution of the fixed gravimetric boundary value problem in the interior and the exterior of the Earth's body
[SER-C-379] p 361 N93-11331
Orthogonal functions over the oceans and applications to the determination of orbit error, geoid and sea surface topography from satellite altimetry p 373 N93-12002

GEOLOGY
Quaternary volcanism, tectonics, and sedimentation in the Idaho National Engineering Laboratory area
[DE92-017851] p 362 N93-11692

GEOMAGNETIC LATITUDE
The effects of magnetic storm phases on F-layer irregularities from auroral to equatorial latitudes
[AD-A253905] p 361 N93-11282

GEOMAGNETIC TAIL
Plasma measurements in magnetospheric tail
[MPE-233] p 361 N93-11352

GEOMAGNETISM
Diffusion of Echo 7 electron beams during bounce motion
[DE92-018288] p 357 N93-10985
The effects of magnetic storm phases on F-layer irregularities from auroral to equatorial latitudes
[AD-A253905] p 361 N93-11282
Propagation of relativistic high current electron beams across the geomagnetic field
[DE92-018276] p 362 N93-11564
Data report 92-1. Brorfelde Geomagnetic Observatory magnetic results, 1990 p 362 N93-11699

The relationship between electrostatic discharges on spacecraft P78-2 and the electron environment
[AD-A255179] p 226 N93-12379
GEOMETRY
Plasma measurements in magnetospheric tail
[MPE-233] p 361 N93-11352
Effects of physical properties and geometry on shapes and stability of polarizable drops in external fields
[DE92-018865] p 301 N93-11638
GEOPHYSICAL OBSERVATORIES
Data report 92-1. Brorfelde Geomagnetic Observatory magnetic results, 1990 p 362 N93-11699
GEOPHYSICS
High resolution image processing of geophysical data with diffraction tomography
[DE92-014134] p 359 N93-11235
Nimbus-7 Scanning Multichannel Microwave Radiometer (SMMR) PARM tape user's guide
[NASA-RP-1284] p 373 N93-11718
Solar-geophysical data number 569, January 1992. Part 2: (Comprehensive reports). Data for July 1991 and miscellaneous
[PB92-158898] p 488 N93-11738
ESIS: An introduction to the European space information system. A modern tool for space scientists
[ESA-INT-2] p 479 N93-12404
GEOSYNCHRONOUS ORBITS
Spacecraft flight control system design selection process for a geostationary communication satellite
[NASA-TP-3289] p 222 N93-11002
A comprehensive mission to planet Earth: Woods Hole Space Science and Applications Advisory Committee Planning Workshop
[NASA-TM-108011] p 343 N93-11878
Forecasting the relativistic electron flux at geosynchronous orbit
[AD-A254016] p 226 N93-12064
Data distribution satellite
[NASA-TM-105778] p 287 N93-12481
GEOTHERMAL ENERGY CONVERSION
Models of volcanic eruption hazards
[DE92-013432] p 364 N93-12136
GEOTHERMAL ENERGY EXTRACTION
Prospects for the commercial development of hot dry rock geothermal energy in New Mexico
[DE92-018999] p 346 N93-11825
GEOTHERMAL ENERGY UTILIZATION
Status and prospects for Hot Dry Rock (HDR) in the US
[DE92-018876] p 345 N93-11381
Prospects for the commercial development of hot dry rock geothermal energy in New Mexico
[DE92-018999] p 346 N93-11825
GEOTHERMAL RESOURCES
Status and prospects for Hot Dry Rock (HDR) in the US
[DE92-018876] p 345 N93-11381
Prospects for the commercial development of hot dry rock geothermal energy in New Mexico
[DE92-018999] p 346 N93-11825
GEOTHERMAL TECHNOLOGY
Status and prospects for Hot Dry Rock (HDR) in the US
[DE92-018876] p 345 N93-11381
GEOTROPISM
Quasigeostrophic vortices in zonal shear
p 358 N93-11226
GERMANIUM
Atomistic processes of surface segregation during Si-Ge MBE growth
[DE92-019180] p 459 N93-11496
Oxidation, nitridation, and fluorine etching of Si
[AD-A253559] p 249 N93-11755
Absorption spectroscopy of L(alpha, beta) transitions in a laser germanium plasma p 320 N93-12041
GERMANIUM ALLOYS
Step-driven surface segregation and ordering during Si-Ge MBE growth
[DE92-017827] p 463 N93-11772
Microscopic origins of metastable effects in a-Si:H and deep defect characterization in a-Si,Ge:H alloys
[DE92-010588] p 463 N93-11813
Recombination and metastability in amorphous silicon and silicon germanium alloys
[DE92-010593] p 463 N93-11816
GERMANIUM COMPOUNDS
Research at and operation of the material science x ray absorption beamline (X-11) at the National Synchrotron Light source
[DE92-018598] p 251 N93-12172
GERMANY
Activities report of Lufthansa
[ETN-92-92100] p 203 N93-11319
Activities report of the German Institute for Flight Safety
[ETN-92-92272] p 203 N93-11375
GIBBS-HELMHOLTZ EQUATIONS
Liquid-liquid equilibria in binary systems: Monte-Carlo simulation for calculating the effect of nonrandom mixing
[DE92-017020] p 263 N93-10972
GIMBALS
Development of a GPS-aided motion measurement, pointing, and stabilization system for a synthetic aperture radar
[DE92-017053] p 204 N93-11152
GLASS
Laser glasses
[DE92-018061] p 267 N93-11549
Slow crack growth in vacuum p 338 N93-11909
Analysis of advanced optical glass and systems
[NASA-CR-184434] p 448 N93-12201
GLASS FIBER REINFORCED PLASTICS
Penetration mechanics of composites
[AD-A249230] p 240 N93-11835
Impact test of carbon, Kevlar, and glass fibre hybrid FRP plates
[NAL-TR-1100] p 243 N93-12371
GLASS FIBERS
Fiber peel force measuring apparatus
[AD-D015349] p 309 N93-11048
Fiber optic polishing system
[AD-D015353] p 446 N93-11052
VAMAS round robin project on polymer composite delamination in mode 1 and mode 2: Cyclic loading
[NPL-DMM(A)-47] p 266 N93-11397
GLASS LASERS
Laser glasses
[DE92-018061] p 267 N93-11549
GLASS TRANSITION TEMPERATURE
The time-dependent stress-optical behaviour of polycarbonate in the glass transition region
p 269 N93-11985
The measurement and calculation of birefringence in quenched polycarbonate specimens
p 269 N93-11986
GLOBAL POSITIONING SYSTEM
Development of a GPS-aided motion measurement, pointing, and stabilization system for a synthetic aperture radar
[DE92-017053] p 204 N93-11152
Dredging research program: Feasibility of a kinematic differential Global Positioning System
[AD-A248953] p 205 N93-11419
Method of steering the gain of a multiple antenna global positioning system receiver
[AD-D015367] p 281 N93-11426
GLOBAL WARMING
Radiative forcing of climate p 351 N93-11094
Global Climate Change (GCC) issues and their impacts on the US Army Corps of Engineers
[AD-A247279] p 353 N93-11466
Environmental problems and trends of international responses, 2
[DE92-531118] p 355 N93-11846
Tenth International Symposium on Environmental Biogeochemistry
[DE92-016200] p 355 N93-11864
Reports to the Nation on our changing planet. Winter 1991 No. 1: The climate system
[NASA-CR-190954] p 370 N93-11880
Reduction in global warming due to fuel economy improvements and emissions control of criteria pollutants: New US light-duty vehicles (1968-1991)
[DE92-016636] p 356 N93-12314
The uses and limits of economic models as a climate change policy tool
[DE92-015792] p 356 N93-12474
GLUONS
Strange quark matter
[DE92-016949] p 438 N93-11746
GLUTAMATES
Physiological analyses of the afferents controlling brain neurochemical systems
[AD-A253185] p 375 N93-11146
GOERTLER INSTABILITY
Fully nonlinear development of the most unstable goertler vortex in a three dimensional boundary layer
[NASA-CR-189710] p 301 N93-11633
On the Goertler instability of boundary layers
[NAL-TR-1120T] p 307 N93-12374
GOGGLES
Selective factors affecting rotary wing aviator performance with symbology superimposed on night vision goggles
[AD-A254983] p 390 N93-12508
GOLD
Development of stable metallization systems
[AD-A253569] p 264 N93-11079
Optical properties of composite membranes containing arrays of nanoscopic gold cylinders
[AD-A253659] p 238 N93-11281
GOVERNMENT/INDUSTRY RELATIONS
Advanced materials and processing: The Federal program in materials science and technology. A report by the FCCSET Committee on Industry and Technology to supplement the President's fiscal year 1993 budget
[PB92-199108] p 238 N93-11470
GOVERNMENTS
Information dissemination: Case studies on electronic dissemination at four agencies. Fact sheet for the Chairman, Committee on Governmental Affairs, US Senate
[GAO/IMTEC-92-6FS] p 474 N93-11274
GRADIENTS
Experimental and theoretical investigation of high gradient acceleration
[DE92-015299] p 315 N93-11278
GRAIN BOUNDARIES
Grain boundary transport and related processes in natural fine grained aggregates
[DE92-018239] p 461 N93-11682
GRAIN SIZE
Critical currents in polycrystalline YBa2Cu3O(7-x): Self-field and grain size dependence
[DE92-617540] p 459 N93-11076
GRAND CANYON (AZ)
Key wintertime meteorological features of the Grand Canyon and the Colorado Plateaus Basin
[DE92-019134] p 369 N93-11657
GRANULAR MATERIALS
Stochastic models of wavefront propagation in random granular media
[AD-A255127] p 286 N93-12422
GRAPH THEORY
The network destruction problem (extended abstract)
[DE92-016171] p 419 N93-11860
Decomposition of balanced matrices. Part 5: Goggles
[AD-A247462] p 430 N93-12217
Two extendability in two classes of claw-free graphs
[AD-A254639] p 427 N93-12243
GRAPHIC ARTS
A cognitive approach to the design of information graphics
[AD-A252692] p 474 N93-11353
GRAPHITE
Curing and mechanical properties of T800-V398 graphite/bismaleimide at different temperatures
[DLR-FB-92-02] p 237 N93-11143
Results from the US/USSR exchange for heat load material studies of simulated tokamak disruptions
[DE92-018285] p 453 N93-11694
GRAPHITE-EPOXY COMPOSITES
Mixed mode bending test of the interlaminar fracture toughness of carbon/epoxy
[FFA-TN-1992-04] p 237 N93-11128
Composite failure analysis handbook. Volume 2: Technical handbook. Part 3: Case histories
[AD-A249131] p 241 N93-12054
The effect of contact stresses in four-point bend testing of graphite/epoxy and graphite/PMR-15 composite beams
[NASA-TM-105891] p 241 N93-12076
GRAPHITE-POLYIMIDE COMPOSITES
The effect of contact stresses in four-point bend testing of graphite/epoxy and graphite/PMR-15 composite beams
[NASA-TM-105891] p 241 N93-12076
GRAPHS (CHARTS)
Matching and vertex packing: How hard are they?
[AD-A245928] p 423 N93-10991
The complexity of some multicriteria arborescence problems
[REPT-92-016] p 424 N93-11182
Two extendability in two classes of claw-free graphs
[AD-A254639] p 427 N93-12243
GRATINGS (SPECTRA)
Matter-wave interferometry with laser cooled atoms
[AD-A253999] p 316 N93-11737
Photovoltaic systems based on spectrally selective holographic concentrators, phase 1
[AD-A252811] p 348 N93-12166
Development of ultra-low noise, high sensitivity planar metal grating coupled AlGaAs/GaAs multiquantum well IR detectors for focal plane array staring IR sensor systems
[AD-A254697] p 468 N93-12228
GRAVIMETRY
An approximate solution of the fixed gravimetric boundary value problem in the interior and the exterior of the Earth's body
[SER-C-379] p 361 N93-11331
GRAVITATION
Residual acceleration data on IML-1: Development of a data reduction and dissemination plan
[NASA-CR-190807] p 223 N93-11101

GRAVITATION THEORY
New singularity and existence of solutions in anisotropic, time-dependent, maximally Gauss-Bonnet extended gravity p 357 N93-11183
An approximate solution of the fixed gravimetric boundary value problem in the interior and the exterior of the Earth's body
[SER-C-379] p 361 N93-11331
Induced gauge theories and W gravity
[DE92-011218] p 470 N93-11518

GRAVITATIONAL EFFECTS
An overview of gravitational physiology
[NASA-TM-102849] p 391 N93-12319

GRAVITATIONAL FIELDS
Remarks on the Robinson-Trautman solutions
[MATHS-REPT-A-167] p 423 N93-11122
New singularity and existence of solutions in anisotropic, time-dependent, maximally Gauss-Bonnet extended gravity p 357 N93-11183

GRAVITATIONAL PHYSIOLOGY
Space flight and immune system p 376 N93-11284
Asthma in aircrew: Assessment, treatment and disposition p 383 N93-11315
An overview of gravitational physiology
[NASA-TM-102849] p 391 N93-12319

GRAVITATIONAL WAVES
Colliding plane gravitational waves with colinear polarization
[MATHS-REPT-A-160] p 357 N93-11120

GRAVITY WAVES
Lidar studies of gravity waves in the mesopause region p 358 N93-11222

GREENHOUSE EFFECT
Global Climate Change (GCC) issues and their impacts on the US Army Corps of Engineers
[AD-A247279] p 353 N93-11466
The role of refrigerants in climate change
[DE92-019385] p 354 N93-11677
Environmental problems and trends of international responses, 2
[DE92-531118] p 355 N93-11846
A comprehensive mission to planet Earth: Woods Hole Space Science and Applications Advisory Committee Planning Workshop
[NASA-TM-108011] p 343 N93-11878

GRID GENERATION (MATHEMATICS)
Artificial intelligence and CFD: Expert systems for the design of airfoils and for grid generation
[DIGE-EST-TN-016] p 206 N93-11161
FNAS computational fluid dynamics
[NASA-CR-184394] p 307 N93-12397
An advancing front Delaunay triangulation algorithm designed for robustness
[NASA-CR-189719] p 416 N93-12400

GRINDING (MATERIAL REMOVAL)
The dressing of resin bonded diamond grinding wheels
[PNR-90965] p 264 N93-11086

GROOVING
An evaluation of repair techniques used for uncontrolled longitudinal cracking and failed longitudinal joints
[PB92-205616] p 277 N93-12072

GROUND BASED CONTROL
Airport stand assignment model
[TT-9104] p 218 N93-11728
Operator assistant to support deep space network link monitor and control p 288 N93-11939
Mission Control Center enhancement opportunities in the 1990's p 396 N93-11942

GROUND RESONANCE
Rigid body mode identification of the PAH-2 helicopter using the eigensystem realization algorithm
[NASA-TM-107690] p 336 N93-11544

GROUND STATE
Theory of small metal clusters, films, and wires
[AD-A253120] p 256 N93-11240
The Peierls ground state, solitons and polarons in ring-containing polymers
[AD-A254914] p 272 N93-12289

GROUND TESTS
Tests of an alternate mobile transporter and extravehicular activity assembly procedure for the Space Station Freedom truss
[NASA-TP-3245] p 224 N93-10970
Ground test facilities for evaluating nuclear thermal propulsion engines and fuel elements
[DE92-017039] p 231 N93-10973
Lightweight Exoatmospheric Projectile (LEAP) test program. Supplemental environmental assessment
[AD-A252286] p 231 N93-10998
Ground test facility for SEI nuclear rocket engines
[DE92-017418] p 217 N93-11367
A preliminary study associated with the experimental measurement of the aero-optic characteristics of hypersonic configurations
[AD-A253792] p 200 N93-12063
Dynamic test/analysis correlation using reduced analytical models
[NASA-TM-107671] p 341 N93-12300
Advanced two-phase heat transfer systems p 229 N93-12459

GROUND WATER
A new two-phase flow and transport model with interphase mass exchange
[PB92-206564] p 298 N93-11251
Models of volcanic eruption hazards
[DE92-013432] p 364 N93-12136

GROUND WAVE PROPAGATION
LORAN and the effects of terrestrial propagation
[PB92-197219] p 205 N93-11472

GROUND WIND
Numerical and observational investigations of long-lived, MCS-induced, severe surface wind events: The derecho p 367 N93-11159
Surface wind speed distributions
[AD-A253268] p 368 N93-11505

GROUP DYNAMICS
An evaluation of crew coordination and performance during a simulated UH-60 helicopter mission
[AD-A254984] p 390 N93-12509

GROUP THEORY
Applications of star complexes in group theory p 485 N93-11879
An isomorphism for algebra of distributions with compact support on Lie groups
[DE92-603605] p 427 N93-12176

GUIDANCE (MOTION)
Microwave guidance technology and its applications
[AD-A254107] p 281 N93-11509

GULF STREAM
Validation test report for the first-generation dart Gulf Stream forecasting system
[AD-A254286] p 373 N93-11821
Oceanographic expert system: Potential for TESS(3) applications
[AD-A254908] p 374 N93-12288

GUN PROPELLANTS
The 28th JANNAF Combustion Subcommittee Meeting, volume 1
[CPIA-PUBL-573-VOL-1] p 244 N93-11132
Energetic composites of cyclodextrin nitrate esters and nitrate ester plasticizers
[AD-D015364] p 274 N93-11665

GUSTS
The measurement of the velocity field induced by a gust generator in a closed-circuit subsonic wind-tunnel
[RAE-TM-MAT-STR-1102] p 217 N93-11435

H

H-INFINITY CONTROL
A problem formulation for glideslope tracking in wind shear using advanced robust control techniques
[NASA-TM-104164] p 214 N93-11176

HABITATS
Habitat automation p 391 N93-11976
Scaling issues for biodiversity protection
[DE92-016689] p 375 N93-12315

HADRONS
High energy hadron-hadron collisions
[DE92-018253] p 441 N93-12224

HALL EFFECT
Magnetic properties and critical behavior of the conductivity near the M-I transition
[DE92-018948] p 461 N93-11629

HALLEY'S COMET
The Comet Halley archive: Summary volume
[NASA-CR-190358] p 484 N93-11243

HALOCARBONS
Scientific assessment of ozone depletion: 1991
[NASA-TM-107976] p 350 N93-11087
Future chlorine-bromine loading and ozone depletion p 352 N93-11095

HALOGEN COMPOUNDS
Studies of transition states and radicals by negative ion photodetachment
[DE92-017011] p 440 N93-11875

HAMILTONIAN FUNCTIONS
Constrained KP hierarchy and bi-Hamiltonian structures
[MATHS-REPT-A-168] p 424 N93-11123
Theory of normal metals
[DE92-016828] p 262 N93-12476

HANDBOOKS
The early Earth Observing System reference handbook: Earth Science and Applications Division missions, 1990-1997
[NASA-TM-107963] p 343 N93-11663
Testability design rating system. Volume 2: Analytical procedure
[AD-A254333] p 413 N93-12146

HARDENING
Some consistency requirements on hardening-recovery evolution equations for welding, part 1
[DE92-015992] p 329 N93-12220

HARDENING (MATERIALS)
Fast electrochromic switching for optical hardening applications
[AD-A248174] p 447 N93-11186

HARDENING (SYSTEMS)
Studies of a laser/nuclear thermal hardened body armor
[AD-A255128] p 390 N93-12423

HARDNESS
Microstructure and mechanical properties of reactive hot isostatic pressed TiAl powder material
[GKSS-91/E/60] p 256 N93-11336

HARDWARE
Using ELLA for high level design: Modelling the Motorola 6800 microprocessor
[RSRE-MEMO-4515] p 408 N93-11386

HARMONIC GENERATIONS
High bandwidth second-harmonic generation in partially deuterated KDP
[DE92-019505] p 452 N93-11645

HARMONIC OSCILLATION
Numerical analysis of oscillating flow about a circular cylinder
[AD-A255164] p 307 N93-12406

HARMONICS
Beam-loading stability in synchrotrons with a higher RF harmonic
[DE92-018982] p 443 N93-11510

HASTELLOY (TRADEMARK)
Improved corrosion resistance of Hastelloy G-30 in nitric/hydrofluoric acid solutions by welding with Inconel 72 weld wire
[DE92-017233] p 262 N93-12487

HAZARDS
Models of volcanic eruption hazards
[DE92-013432] p 364 N93-12136

HEAD MOVEMENT
Correction techniques for depth errors with stereo three-dimensional graphic displays
[NASA-TP-3244] p 206 N93-11170

HEAD-UP DISPLAYS
Selective factors affecting rotary wing aviator performance with symbology superimposed on night vision goggles
[AD-A254983] p 390 N93-12508

HEALTH
Sustaining health and performance in the cold: Environmental medicine guidance for cold-weather operation
[AD-A254328] p 385 N93-12145

HEARING
Feasibility assessment of a transient sound sensor based on the silicon retina architecture
[AD-A252288] p 432 N93-10999

HEAT AFFECTED ZONE
Heat-affected zone cracking of nitronic 60 stainless steel
[DE92-018286] p 254 N93-10984

HEAT ENGINES
Stirling heat pump external heat systems: An appliance perspective
[DE92-018251] p 349 N93-12498

HEAT EXCHANGERS
Preliminary characterization of a water vaporizer for resistojet applications
[NASA-TM-105877] p 231 N93-11402
Microtube strip heat exchanger
[DE92-018709] p 300 N93-11440
Proceedings of the DOE/Advanced Heat Exchangers Program Review
[DE92-014385] p 305 N93-12070
Disruption shape effects on the performance of enhanced tubes with the separation and reattachment mechanism
[DE92-016602] p 305 N93-12128
The influence of the Prandtl number on the thermal performance of tubes with the separation and reattachment enhancement mechanism
[DE92-016601] p 306 N93-12313
Inert gas electric heater for elevated temperature testing of small propulsion components
[DE92-017434] p 221 N93-12317
Natural convection heat transfer studies of simulated and actual electronic components using dielectric liquids for immersion cooling
[AD-A255173] p 341 N93-12376

HEAT FLUX
Aerothermal test results from the second flight of the Pegasus booster
[NASA-TM-4391] p 296 N93-10969

Heat load material studies: Simulated tokamak disruptions
[DE92-018275] p 452 N93-11674
Results from the US/USSR exchange for heat load material studies of simulated tokamak disruptions
[DE92-018285] p 453 N93-11694
Enhanced convective and film boiling heat transfer by surface gas injection
[DE92-016755] p 306 N93-12221
The structure and transport of the Brazil current between 27 deg and 36 deg south
[AD-A247635] p 374 N93-12247
The vertical distribution of heating in the tropical atmosphere
[AD-A254982] p 372 N93-12507

HEAT OF FORMATION
Determination of parameters of a new method for predicting alloy properties
[NASA-TM-105895] p 257 N93-11609

HEAT PIPES
Participation in multilateral effort to develop high performance integrated CPC evacuated collectors
[DE92-015946] p 346 N93-11823
Thermostructural applications of heat pipes for cooling leading edges of high-speed aerospace vehicles
p 229 N93-12460

HEAT PUMPS
Advanced heat pump for the recovery of volatile organic compounds
[DE92-011592] p 303 N93-11774
NEDO Fuel/Storage Technology Subcommittee
[DE92-526262] p 346 N93-11777
Stirling heat pump external heat systems: An appliance perspective
[DE92-018251] p 349 N93-12498

HEAT RESISTANT ALLOYS
Modelling short crack growth behaviour in nickel-base superalloys
[PNR-90912] p 255 N93-11033
Sigma phase in nickel based superalloys
[PNR-90950] p 255 N93-11109
Present and future trends in turbine blade material and manufacture technology
[PNR-90960] p 255 N93-11111
Friction of self-lubricating surfaces by ion beam techniques
[DE92-016069] p 328 N93-12122
Erosion predictions and measurements of high-temperature coatings and superalloys used in turbomachines p 272 N93-12189
Fatigue in single crystal nickel superalloys
[AD-A254603] p 260 N93-12237
Design and development of Ni-base superalloy and Ti alloys
[NRIM-SR-92-01] p 261 N93-12322

HEAT SINKS
Translating wedge heat sink
[AD-D015357] p 293 N93-12133

HEAT SOURCES
Design of small Stirling dynamic isotope power system for robotic space missions
[NASA-TM-105919] p 275 N93-12085
Milliwatt Generator Project
[DE92-015348] p 294 N93-12156

HEAT STORAGE
Sodium reflux pool-boiler solar receiver on-sun test results
[DE92-018932] p 347 N93-12012

HEAT TOLERANCE
The effects of wearing protective chemical warfare combat clothing on human performance
[AD-A250716] p 390 N93-12491

HEAT TRANSFER
Experimental heat transfer results in turbine stators and rotors and a comparison with theory
[PNR-90945] p 210 N93-11055
An adaptive differencing scheme for elliptic flows
p 297 N93-11197
Heat transfer enhancement by chaotic mixing
[PB92-190305] p 470 N93-11469
Development of an intelligent system for cooling rate and fill control in GMAW
[DE92-017849] p 326 N93-11548
Turbulence modeling in shock wave/turbulent boundary layer interactions
[NASA-CR-190933] p 301 N93-11606
An experimental study of flow patterns and endwall heat transfer upstream of a surface-mounted rectangular obstruction in a turbulent boundary layer
p 302 N93-11698
Development of a new plasma diagnostic of the critical surface and studies of the ion acoustic decay instability using collective Thomson scattering
[DE92-018508] p 453 N93-11730
A model for analytical performance prediction of hypervapotron
[DE92-018885] p 305 N93-12010
Superconducting applications in propulsion systems. Magnetic insulation for plasma propulsion devices
[NASA-CR-184401] p 233 N93-12013
Overview of property formulations for helium, nitrogen, lithium, and lithium-lead in ATHENA/MOD1 with comparison of calculated properties to measured properties
[DE92-017995] p 471 N93-12058
Disruption shape effects on the performance of enhanced tubes with the separation and reattachment mechanism
[DE92-016602] p 305 N93-12128
Translating wedge heat sink
[AD-D015357] p 293 N93-12133
Hydrogen assisted heat transfer during diamond growth using carbon and tantalum filaments
[AD-A247944] p 468 N93-12218
Enhanced convective and film boiling heat transfer by surface gas injection
[DE92-016755] p 306 N93-12221
The influence of the Prandtl number on the thermal performance of tubes with the separation and reattachment enhancement mechanism
[DE92-016601] p 306 N93-12313
Characteristics of heat transfer to nickel plated chamber walls of high pressure rocket combustors
[NAL-TR-1126T] p 234 N93-12372
On the Goertler instability of boundary layers
[NAL-TR-1120T] p 307 N93-12374
Advanced two-phase heat transfer systems
p 229 N93-12459
Investigation of hot streak migration and film cooling effects on heat transfer in rotor/stator interacting flows, report 1
[AD-A250688] p 471 N93-12490

HEAT TRANSFER COEFFICIENTS
Leading edge film cooking heat transfer including the effect of mainstream turbulence p 199 N93-11886

HEAT TRANSMISSION
The effects of chemistry on weld profiles in partial and full penetration welds
[DE92-016865] p 327 N93-11679

HEAT TREATMENT
International ADI-Seminar: Austempered Ductile Iron
[PB92-180660] p 256 N93-11244

HEATERS
Inert gas electric heater for elevated temperature testing of small propulsion components
[DE92-017434] p 221 N93-12317

HEAVY IONS
Research in heavy-ion nuclear physics
[DE92-015099] p 443 N93-11521
Research in elementary particles and interactions
[DE92-018089] p 437 N93-11681
The diagnostics system for the multiple heavy ion beams induction linac experiment, MBE-4
[DE92-017109] p 445 N93-12126

HELICOPTER WAKES
Studies of a flat wake rotor theory
[NASA-CR-190936] p 201 N93-12343

HELICOPTERS
Rotorcraft health and usage monitoring systems: A literature survey
[DOT/FAA/RD-91/6] p 206 N93-11461
Time-frequency domain analysis of vibration signals for machinery diagnostics. 3: The present power spectral density
[OUEL-1911/92] p 337 N93-11707
Embedded training capabilities for the LAMPS MK 3 system
[AD-A250697] p 207 N93-11838
Integration of radar altimeter, precision navigation, and digital terrain data for low-altitude flight
[NASA-TM-103958] p 205 N93-12320
Verification of rain-flow reconstructions of a variable amplitude load history
[NASA-CR-189670] p 341 N93-12411
Selective factors affecting rotary wing aviator performance with symbology superimposed on night vision goggles
[AD-A254983] p 390 N93-12508

HELIOTRONS
Shafranov shift in low-aspect-ratio heliotron/torsatron CHS
[DE92-782100] p 451 N93-11277

HELIUM
Low energy helium implantation in evaporated nickel surfaces
[DE92-019297] p 257 N93-11600
Tables of thermodynamic properties of helium magnet coolant, revision A
[DE92-019098] p 471 N93-11656
A model to estimate the flux of background particles expected to accumulate on the collector foils of the interstellar gas experiment on the long duration exposure facility spacecraft
[AD-A254265] p 489 N93-11815
Numerical simulation of alumina spraying in argon-helium plasma jet
[DE92-017859] p 455 N93-12092
Hydrogen assisted heat transfer during diamond growth using carbon and tantalum filaments
[AD-A247944] p 468 N93-12218
Helium transport studies on D3-D
[DE92-016251] p 455 N93-12307
Inert gas electric heater for elevated temperature testing of small propulsion components
[DE92-017434] p 221 N93-12317

HELIUM ISOTOPES
Implanted He retention and release from boronized layers
[DE92-013983] p 464 N93-11842

HELIUM-NEON LASERS
A single beam laser tracker as an alignment tool
[DE92-017746] p 316 N93-11691

HELMET MOUNTED DISPLAYS
Advanced technology for portable personal visualization
[AD-A253808] p 388 N93-11783
Selective factors affecting rotary wing aviator performance with symbology superimposed on night vision goggles
[AD-A254983] p 390 N93-12508

HELMHOLTZ EQUATIONS
On the inverse scattering problem for the Helmholtz equation in one dimension
[AD-A253130] p 434 N93-11526
Orthogonal functions over the oceans and applications to the determination of orbit error, geoid and sea surface topography from satellite altimetry p 373 N93-12002

HEMISPHERE CYLINDER BODIES
The hemisphere-cylinder at an angle of attack
p 196 N93-11250

HEMORRHAGES
Effect of hemorrhage on cardiac output, vasopressin, aldosterone, and diuresis during immersion in men
[NASA-TM-103949] p 374 N93-12014

HEPATITIS
Clinical types of Hepatitis B p 376 N93-11286
Viral hepatitis in the US Air Force, 1980 - 1989
p 377 N93-11287
Hepatitis A and Hepatitis B: Risks compared to other vaccine preventable diseases and immunization recommendations p 377 N93-11288
Vaccination against Hepatitis B: The Italian strategy
p 377 N93-11289
Communicable diseases: A major burden of morbidity and mortality p 380 N93-11300
Immunization of personnel traveling to a destination in tropical countries: French position p 380 N93-11304

HERMES MANNED SPACEPLANE
Development trends in space transportation systems: From Hermes to Saenger
[MBB-UK-0146-91-PUB] p 223 N93-11007
Flow field calculations around the Hermes spaceplane during reentry phase
[MBB-UK-0148-91-PUB] p 195 N93-11008

HETEROGENEITY
Heterogeneous processes: Laboratory, field, and modeling studies p 350 N93-11090
Stratospheric processes: Observations and interpretation p 351 N93-11091
Predicted rocket and shuttle effects on stratospheric ozone p 352 N93-11097
Application of the theory of wave propagation through random media to phase and amplitude fluctuations of seismic P-waves
[AD-A253274] p 363 N93-11788

HETEROJUNCTION DEVICES
GaAs heterojunction device based A/D converter development
[AD-A252644] p 468 N93-12183

HETEROJUNCTIONS
Contactless optoelectronic integrated circuits for remote fiber optic communication and sensing applications
[AD-A253573] p 290 N93-11507

HEURISTIC METHODS
An iterative method for distributed database design
p 474 N93-11255
The efficient parallel iterative solution of large sparse linear systems
[DE92-018769] p 425 N93-11446
An expert system for diagnosing environmentally induced spacecraft anomalies p 230 N93-11927
Autonomous power system: Integrated scheduling
p 235 N93-11948
Manager's assistant systems for space system planning p 398 N93-11952

Backward assembly planning with DFA analysis
[NASA-CASE-NPO-18817-1-CU] p 278 N93-12202

HIERARCHIES

Constrained KP hierarchy and bi-Hamiltonian structures
[MATHS-REPT-A-168] p 424 N93-11123
Darboux theorems and Wronskian formulas for integrable systems. 1: Constrained KP flows
[MATHS-REPT-A-172] p 424 N93-11126
Exploiting captions in retrieval of multimedia data
[AD-A255184] p 479 N93-12381

HIGH ACCELERATION

Experimental and theoretical investigation of high gradient acceleration
[DE92-015299] p 315 N93-11278
KC-135 materials handling robotics
[NASA-CR-184430] p 328 N93-11992
Evaluation of CKU-5/A ejection seat catapults under varied acceleration levels
[AD-A248021] p 204 N93-12489

HIGH DEFINITION TELEVISION

High-speed FPS vidicon camera
[DE92-018989] p 313 N93-12069

HIGH ELECTRON MOBILITY TRANSISTORS

Programme and abstracts. Workshop on Expert Evaluation and Control of Compound Semiconductor Materials and Technologies No. 1: (EXAMTEC 199)
[AD-A254023] p 292 N93-12071

HIGH ENERGY ELECTRONS

Radiation damage by high energy electrons in GaAs: A DLTS (deep level transient spectroscopy) examination
[HMI-B-494] p 442 N93-11028
Tunable, short pulse hard x rays from a compact laser synchrotron source
[AD-A254288] p 315 N93-11195
Development and use of data analysis procedures for the CRRES payloads AFGL-701-2/Dosimeter and AFGL-701-4/Fluxmeter and application of the data analysis results to improve the static and dynamic models of the Earth's radiation belts
[AD-A253287] p 363 N93-11810
Forecasting the relativistic electron flux at geosynchronous orbit
[AD-A254016] p 226 N93-12064

HIGH ENERGY INTERACTIONS

Particle physics experiments, 1991
[RAL-92-001] p 444 N93-11687
Strange quark matter
[DE92-016949] p 438 N93-11746
Scattering of polarized electrons by oriented deuterons
[DE92-624834] p 440 N93-11914
High energy hadron-hadron collisions
[DE92-018253] p 441 N93-12224

HIGH ENERGY PROPELLANTS

High energy cast explosives based on dinitropropylacrylate
[AD-D015340] p 273 N93-11045

HIGH FLUX ISOTOPE REACTORS

Acoustic emission monitoring of HFIR vessel during hydrostatic testing
[DE92-019316] p 332 N93-11601

HIGH FREQUENCIES

High frequency response from YBa2Cu3O(7-x) Josephson devices on SrTiO3 bicrystal substrates
[NPL-DES-118] p 459 N93-11394
10 kW L-band amplifier tubes for efficient and reliable troposcatter communication transmitter systems
[AD-A253246] p 290 N93-11504
Asymptotic analysis of reacting materials with saturated explosion. 2: High-frequency waves
[AD-A254473] p 275 N93-12236
Computer modeling of tactical high frequency antennas
[AD-A255176] p 286 N93-12377

HIGH PASS FILTERS

Broadband EMP transient measurement preemphasis filter
[AD-A254414] p 284 N93-12160

HIGH POLYMERS

Fracture behavior of polymers at cryogenic temperatures
[KFK-4969] p 265 N93-11203

HIGH POWER LASERS

Topics in high-intensity laser plasma interaction
p 450 N93-11191
Tunable, short pulse hard x rays from a compact laser synchrotron source
[AD-A254288] p 315 N93-11195
The 1989 Scientific Report of the Laboratory for the Use of High Power Lasers
[ETN-92-92175] p 317 N93-12023
Stimulated Brillouin backscattering instability in the case of a high power laser: Application to wave pulsation particle acceleration experiments p 317 N93-12024
Preliminary study of the homogeneity of the density and temperature of long plasmas used for X laser studies
p 320 N93-12044
Experimental study of x ray laser in lithumoid aluminum p 321 N93-12045
Activity of the technical groups (LULI Palaiseau, France) p 322 N93-12052
Optical limiting
[AD-A254620] p 322 N93-12238
Theory for a high power free electron laser and tactical applications
[AD-A255161] p 323 N93-12405

HIGH PRESSURE

Sigma phase in nickel based superalloys
[PNR-90950] p 255 N93-11109
Studies of the 3 to 5 compounds in the megabar regime
[DE92-019517] p 461 N93-11646
Theoretical studies of high-temperature superconductors and highly compressed hydrogen
p 292 N93-11833
An experimental study of a small high speed LH2 rocket pump: Fundamental mechanical design
[NAL-TR-1123] p 330 N93-12463

HIGH RESOLUTION

State-resolved reaction dynamics
[AD-A254291] p 436 N93-11196
High resolution image processing of geophysical data with diffraction tomography
[DE92-014134] p 359 N93-11235
High resolution tomographic instrument development
[DE92-017314] p 313 N93-11828
Laser surface profilometer with sub-Angstrom resolution
[DE92-018926] p 317 N93-12011
A ring coded-aperture microscope for high-resolution imaging of high-energy x rays
[DE92-018004] p 454 N93-12059

HIGH REYNOLDS NUMBER

Compressible mixing layers with and without particles
[AD-A254854] p 308 N93-12435

HIGH SPEED PHOTOGRAPHY

Characterization of deflagrating munitions by rotating prism high speed photography
[MRL-TR-91-43] p 311 N93-11648
Debris/ice/TPS assessment and integrated photographic analysis for Shuttle Mission STS-46
[NASA-TM-107552] p 223 N93-12151

HIGH STRENGTH STEELS

Shear joint capability versus bolt clearance
[NASA-TM-108378] p 342 N93-12419
Study of residual stresses and microcracks in high strength steel weldments: An investigation of microcrack formation and stressed growth using laser microscopy
[AD-A255059] p 342 N93-12467

HIGH TEMPERATURE

Application of polyimides to aeroengine components
[PNR-90907] p 334 N93-11013
Semi-interpenetrating polymer network for tougher and more microcracking resistant high temperature polymers
[NASA-CASE-LAR-13925-2] p 264 N93-11059
Elevated temperature fatigue crack growth in a nickel base superalloy under dwell conditions
[PNR-90997] p 255 N93-11115
Theoretical studies of high-temperature superconductors and highly compressed hydrogen
p 292 N93-11833
Nuclear fuels for very high temperature applications
[DE92-018021] p 446 N93-12129
Energetics solids degradation in high temperature water
[AD-A254900] p 276 N93-12285

HIGH TEMPERATURE ENVIRONMENTS

Materials: Toward the non-metallic engine
[PNR-90915] p 209 N93-11019
Sigma phase in nickel based superalloys
[PNR-90950] p 255 N93-11109
Design of a high-temperature experiment for evaluating advanced structural materials
[NASA-TM-105833] p 337 N93-11624
Multi-layer light-weight protective coating and method for application
[NASA-CASE-LAR-14448-1] p 269 N93-11912
Compensated high temperature strain gage
[NASA-CASE-LAR-14776-1] p 313 N93-12205
High temperature rectifiers and MOS devices in 6H-silicon carbide
[AD-A254725] p 295 N93-12340

HIGH TEMPERATURE GASES

Potassium D-line fitting for investigation of MHD boundary layers
[DE92-019020] p 454 N93-11826

HIGH TEMPERATURE PLASMAS

Diagnostics of electron-heated solar flares
p 488 N93-11877
Atomic structure and spectral perturbations in dense and hot plasmas p 321 N93-12049
Anomalous ion thermal transport in hot ion plasmas by the ion temperature gradient mode
[DE92-016686] p 456 N93-12493

HIGH TEMPERATURE RESEARCH

Current research in oxidation-resistant carbon-carbon composites at NASA. Langley Research Center
p 229 N93-12456

HIGH TEMPERATURE SUPERCONDUCTORS

High Temperature Superconductivity Space Experiment (HTSSE)
[AD-A253119] p 288 N93-11239
A mutual inductance technique for contact-free T(sub c) measurement of high temperature superconductors
[NPL-DES-116] p 289 N93-11393
Landau level quantization and superconductivity
[DE92-019028] p 460 N93-11512
Properties of hot isostatically pressed Bi(2)Sr(1.7)CaCu(2)O(x)
[DE92-016394] p 460 N93-11522
Cryostabilization of high-temperature superconducting magnets with subcooled flow in microchannels
[DE92-018174] p 431 N93-11598
Recrystallization of amorphous or nanocrystalline NdBa2Cu3O(7-x) and GdBa2Cu3O(7-x)
[DE92-016302] p 462 N93-11706
Theoretical studies of high-temperature superconductors and highly compressed hydrogen
p 292 N93-11833
Infrared phonon structure in epitaxial films of Tl2Ca2Ba2Cu3O10 at low temperatures
[DE92-017078] p 466 N93-12109
High temperature superconductor materials and applications
[NASA-CR-184426] p 470 N93-12396

HIGH TEMPERATURE TESTS

Relative sliding durability of candidate high temperature fiber seal materials
[NASA-TM-105806] p 236 N93-10978
Scanning electron microscopy of the effects of moisture and elevated temperature on the fibre/matrix bond in CFRP
[RAE-TM-MAT-STR-1183] p 240 N93-11905
Erosion predictions and measurements of high-temperature coatings and superalloys used in turbomachines p 272 N93-12189

HIGH THRUST

From RB211 to Trent: An ongoing development strategy
[PNR-90938] p 210 N93-11038

HIGH VOLTAGES

BANSHEE: High-voltage repetitively pulsed electron-beam driver
[DE92-017413] p 444 N93-11763
The development of a one microsecond pulse length, repetitively pulsed, high power modulator, and a long-pulse electron beam diode for the production of intense microwaves
[DE92-015974] p 293 N93-12089
Ultra-wideband generators
[DE92-018026] p 293 N93-12113

HINGES

Modeling and identification of flexible joints in vehicle structures p 324 N93-11261

HISTORIES

The NASA/National Space Science Data Center trapped radiation environment model program, 1964 - 1991
[NASA-TM-107993] p 349 N93-11003
Winds of change: Expanding the frontiers of flight. Langley Research Center's 75 years of accomplishment, 1917-1992
[NASA-NP-130] p 490 N93-11100

HMX

High energy cast explosives based on dinitropropylacrylate
[AD-D015340] p 273 N93-11045

HOLLOW CATHODES

Extended-testing of xenon ion thruster hollow cathodes
[NASA-CR-189227] p 234 N93-12409

HOLOGRAPHY

Three-dimensional image structure in in-line Fraunhofer holography p 311 N93-11723
Ultra wide band 3-D cross section (RCS) holography
[DE92-019133] p 312 N93-11802
Photovoltaic systems based on spectrally selective holographic concentrators, phase 1
[AD-A252811] p 348 N93-12166

HOMOGENEITY

Preliminary study of the homogeneity of the density and temperature of long plasmas used for X laser studies
p 320 N93-12044

HOMOMORPHISMS
An isomorphism for algebra of distributions with compact support on Lie groups
[DE92-603605] p 427 N93-12176
HOOP COLUMN ANTENNAS
Deployable reflector antenna performance optimization using automated surface correction and array-feed compensation
[NASA-TP-3228] p 222 N93-12543
HORSESHOE VORTICES
A study of the wall-pressure fluctuations downstream of a blade-wall junction
[ECL-91-07] p 299 N93-11363
HOT ELECTRONS
Hydrodynamic fluctuations and light scattering in hot electron gas of semiconductors
[DE92-622800] p 458 N93-10992
A cryogenic phonon detector to search for dark matter particles p 481 N93-11196
HOT ISOSTATIC PRESSING
Microstructure and mechanical properties of reactive hot isostatic pressed TiAl powder material
[GKSS-91/E/60] p 256 N93-11336
Titanium-aluminides by hot isostatic pressing of cold extruded titanium-aluminium powder mixtures
[GKSS-91/E/67] p 256 N93-11337
Properties of hot isostatically pressed Bi(2)Sr(1.7)CaCu(2)O(x)
[DE92-016394] p 460 N93-11522
HOT PRESSING
Silicon carbide fiber reinforced strontium aluminosilicate glass-ceramic matrix composite
[NASA-CASE-LEW-15263-1] p 239 N93-11543
HOT STARS
Far ultraviolet spectrophotometry of hot stars and calibration standards in the far ultraviolet
p 482 N93-11373
HOT-WIRE ANEMOMETERS
An experimental study of flow patterns and endwall heat transfer upstream of a surface-mounted rectangular obstruction in a turbulent boundary layer
p 302 N93-11698
HUBBLE SPACE TELESCOPE
A search for low-luminosity objects
[AD-A253301] p 483 N93-11750
HUMAN BEHAVIOR
The locator system for wandering individuals
[NASA-TM-104754] p 388 N93-11649
HUMAN BEINGS
Molecular cytogenetics: A novel approach for measuring chromosome translocations in individuals years after exposure to low levels of ionizing radiation
[DE92-018066] p 374 N93-10974
Absence of protective immunity against diphtheria in a large proportion of young adults p 380 N93-11302
Effect of hemorrhage on cardiac output, vasopressin, aldosterone, and diuresis during immersion in men
[NASA-TM-103949] p 374 N93-12014
HUMAN BODY
New techniques for positron emission tomography in the study of human neurological disorders
[DE92-015353] p 384 N93-11873
Methodology issues concerning the accuracy of kinematic data collection and analysis using the ariel performance analysis system
[NASA-CR-185689] p 389 N93-12211
Studies of a laser/nuclear thermal hardened body armor
[AD-A255128] p 390 N93-12423
HUMAN CENTRIFUGES
Development of a tactile perceived attitude transducer
[AD-A253724] p 385 N93-11081
HUMAN FACTORS ENGINEERING
Methods and principles for determining task dependent interface content
[NASA-CR-190837] p 204 N93-10961
Coordinated action in 3-D space
[AD-A249830] p 387 N93-10994
Design of instrument approach procedure charts: Comprehension speed of missed approach instructions coded in text or icons
[PB92-205673] p 204 N93-11252
A cognitive approach to the design of information graphics
[AD-A252692] p 474 N93-11353
The effect of variable seat back angles on human response to +Gz impact accelerations
[AD-A250673] p 387 N93-11559
System for generating dynamic video imagery for human factors research
[AD-A248675] p 388 N93-11743
Development of the Personnel-based System Evaluation Aid (PER-SEVAL) performance shaping functions
[AD-A252820] p 386 N93-11779
Direct manipulation and intermittent automation in advanced cockpits
[AD-A253814] p 388 N93-11784
Evaluation of multilayer mask concept for RESPO 21
[AD-A253392] p 389 N93-12079
Research and development strategies for human centered and group support technologies
[AD-A254366] p 472 N93-12273
Human performance in complex task environments: A basis for the application of adaptive automation
[AD-A255067] p 390 N93-12486
HUMAN IMMUNODEFICIENCY VIRUS
HIV infection in the nineties p 377 N93-11290
AIDS/HIV in the US Military p 377 N93-11291
Estimates of Human Immunodeficiency Virus (HIV) incidence and trends in the US Air Force
p 377 N93-11292
Silent HIV infection p 378 N93-11293
HIV variability and perspectives of a vaccine
p 378 N93-11294
Immunological parameters in current and former US Air Force personnel p 378 N93-11295
Early markers of HIV infection and subclinical disease progression p 379 N93-11296
Analysis of disease progression from clinical observations of US Air Force active duty members infected with the Human Immunodeficiency Virus: Distribution of AIDS survival time from interval censored observations
p 379 N93-11297
Relating cognitive function to military aviator performance in early HIV infection p 379 N93-11298
Neuropsychiatric morbidity in early HIV disease: Implications for military occupational function
p 379 N93-11299
HUMAN PATHOLOGY
Allergic, Immunological and Infectious Disease Problems in Aerospace Medicine
[AGARD-CP-518] p 376 N93-11283
HUMAN PERFORMANCE
Development of a tactile perceived attitude transducer
[AD-A253724] p 385 N93-11081
Neuropsychiatric morbidity in early HIV disease: Implications for military occupational function
p 379 N93-11299
A cognitive approach to the design of information graphics
[AD-A252692] p 474 N93-11353
System for generating dynamic video imagery for human factors research
[AD-A248675] p 388 N93-11743
Development of the Personnel-based System Evaluation Aid (PER-SEVAL) performance shaping functions
[AD-A252820] p 386 N93-11779
Direct manipulation and intermittent automation in advanced cockpits
[AD-A253814] p 388 N93-11784
Mission Control Center enhancement opportunities in the 1990's p 396 N93-11942
Effects of spatially displaced feedback on remote manipulation tasks p 400 N93-11966
Meta-analysis of integrity tests: A critical examination of validity generalization and moderator variables
[AD-A254681] p 386 N93-12225
The OMPAT level 1 Neurophysiological Performance Assessment Battery: NPPAB
[AD-A254840] p 387 N93-12432
Human performance in complex task environments: A basis for the application of adaptive automation
[AD-A255067] p 390 N93-12486
The effects of wearing protective chemical warfare combat clothing on human performance
[AD-A250716] p 390 N93-12491
An evaluation of crew coordination and performance during a simulated UH-60 helicopter mission
[AD-A254984] p 390 N93-12509
HUMIDITY
Low cost humidity sensor
[PB92-205772] p 312 N93-11757
Analysis of air and sea physical properties and surface fluxes using a combination of in situ and SEASAT data
p 365 N93-12182
Modified epoxy adhesives and primers
[AD-A253857] p 272 N93-12297
HUMIDITY MEASUREMENT
Low cost humidity sensor
[PB92-205772] p 312 N93-11757
HURRICANES
Hurricane Research Division fiscal year 1991 programs: Fiscal year 1992 projections
[PB92-138320] p 367 N93-11242
Diagnostic report of the National Hurricane Center: October and November 1990, volume 3, number 3
[PB91-242297] p 370 N93-11888
Mariners Weather Log, volume 36, number 2, Spring 1992
[PB92-204213] p 371 N93-12293
HYDRAZINES
Occupational safety considerations with hydrazine fuels p 276 N93-11951
HYDROCARBONS
Simplified modelling of soot inception and growth
[ETN-92-92266] p 246 N93-11361
Inhibition of moist carbon monoxide oxidation by trace amounts of hydrocarbons
[DE92-008736] p 253 N93-12257
HYDROCHLORIC ACID
Heterogeneous processes: Laboratory, field, and modeling studies p 350 N93-11090
HYDRODYNAMIC RAM EFFECT
Ribless ram air parachute
[AD-D015351] p 195 N93-11050
HYDRODYNAMICS
Hydrodynamic fluctuations and light scattering in hot electron gas of semiconductors
[DE92-622800] p 458 N93-10992
Evaluation of a Cray performance tool using a large hydrodynamics code
[DE92-013239] p 407 N93-11231
Hydrodynamic particle migration in small-amplitude, oscillatory, circular couette flow: The limits of reversibility
[DE92-008480] p 303 N93-11843
Hydrodynamic efficiencies in implosion experiments
p 308 N93-12030
Development of a hydrodynamic code: MINNIE
p 318 N93-12031
Modeling for the study of an X laser in a recombination plasma; gain calculations at 105.7 and 154.6 A
p 321 N93-12046
Hydrodynamic study of multilayer targets by spatial and temporal resolution shadow spectroscopy
p 254 N93-12050
X ray laser program, FY 1991
[AD-A255190] p 322 N93-12275
HYDROFLUORIC ACID
Concerted hydrogen atom exchange between three HF molecules p 439 N93-11855
Improved corrosion resistance of Hastelloy G-30 in nitric/hydrofluoric acid solutions by welding with Inconel 72 weld wire
[DE92-017233] p 262 N93-12487
HYDROGEN
Internal friction peaks due to oxygen, nitrogen, and hydrogen in V-Nb alloys
[DE92-012155] p 254 N93-10995
Lyman alpha line shapes from electron impact H2 dissociative processes in the Jovian auroral zone
p 487 N93-11166
Pulsed-field-gradient NMR investigations of hydrogen diffusion in ZrH(x)
[DE92-014393] p 459 N93-11238
Mixing regimes in a spatially confined, two-dimensional, supersonic shear layer
[AD-A254302] p 302 N93-11756
Hydrogen assisted heat transfer during diamond growth using carbon and tantalum filaments
[AD-A247944] p 468 N93-12218
The hydrogen technology assessment, phase 1
[NASA-CR-190969] p 349 N93-12394
The 10 kW power electronics for hydrogen arcjets
[NASA-TM-105614] p 235 N93-12484
Experiments and analysis concerning the use of external burning to reduce aerospace vehicle transonic drag
p 235 N93-12537
HYDROGEN ATOMS
Concerted hydrogen atom exchange between three HF molecules p 439 N93-11855
HYDROGEN BONDS
The synthesis and crystal structure of LaHSe2O6, a layered, anhydrous selenite
[AD-A251050] p 458 N93-10996
Design and synthesis of molecular systems capable of supporting intracavity chemical reactions
[AD-A251024] p 440 N93-11872
HYDROGEN COMPOUNDS
The synthesis and crystal structure of LaHSe2O6, a layered, anhydrous selenite
[AD-A251050] p 458 N93-10996
HYDROGEN FUELS
The hydrogen technology assessment, phase 1
[NASA-CR-190969] p 349 N93-12394
HYDROGEN IONS
Multiphoton ionization and ion-pair formation in molecular hydrogen
[DE92-019026] p 438 N93-11829
Diagnostics and modeling of H(-) ion sources
[AD-A250664] p 440 N93-11867
Low energy neutral atom imaging
[DE92-013531] p 365 N93-12264
HYDROGEN OXYGEN ENGINES
Hot fire test results of subscale tubular combustion chambers
[NASA-TP-3222] p 232 N93-11614

HYDROGEN PRODUCTION
Reformers for the production of hydrogen from methanol and alternative fuels for fuel cell powered vehicles
[DE92-019300] p 274 N93-11550

HYDROGEN SULFIDE
Biological conversion of synthesis gas culture development
[DE92-001279] p 375 N93-12482

HYDROGENATION
Catalytic hydrogenation of carbon monoxide
[DE92-014729] p 253 N93-12428

HYDROGRAPHY
Dredging research program: Feasibility of a kinematic differential Global Positioning System
[AD-A248953] p 205 N93-11419

HYDROLOGICAL CYCLE
Time scales characterizing the processing of water and cloud condensation nuclei by clouds
[CM-80] p 368 N93-11340

HYDROLOGY
Climate change and water supply, management and use: A literature review
[DE92-019069] p 353 N93-11655
Reports to the Nation on our changing planet. Winter 1991 No. 1: The climate system
[NASA-CR-190954] p 370 N93-11860

HYDROLOGY MODELS
A new two-phase flow and transport model with interphase mass exchange
[PB92-206564] p 298 N93-11251
Geographic information system to support state-wide hydrologic modeling with the SCS-TR-20
[PB92-185768] p 476 N93-11700

HYDROPLANES (SURFACES)
Experiments on low aspect ratio hydroplanes to measure lift under static and dynamic conditions
[ARE-TM(UHR)-90306] p 197 N93-11365
Lift coefficient of a randomly oscillating hydroplane
[DRA/MAR-TM(MTH)-91320] p 197 N93-11377

HYDROXYL RADICALS
Tropospheric processes: Observations and interpretation p 351 N93-11092

HYPERNUCLEI
Strange quark matter
[DE92-016949] p 438 N93-11746

HYPERONS
Strange quark matter
[DE92-016949] p 438 N93-11746

HYPERSONIC FLIGHT
Rocket Based Combined Cycle (RBCC) Propulsion Workshop, volume 2
[NASA-CR-184383] p 231 N93-11043
On stability and control of SSTO spaceplane in super- and hypersonic ascending phase
[NAL-TR-1128T] p 216 N93-12361

HYPERSONIC FLOW
Employment of radicals and excited state species for supersonic combustion photochemical ignition of premixed hydrogen/oxygen mixtures with ArF laser
p 245 N93-11135
On the instability of hypersonic flow past a pointed cone: Comparison of theoretical and experimental results of Mach 18
[DLR-FB-92-02] p 196 N93-11141
Thermokinetic modelling and hypersonic flow
[DILC-EST-TN-218] p 196 N93-11157
Progress in developing a transition model for high-speed flows p 301 N93-11615
A preliminary study associated with the experimental measurement of the aero-optic characteristics of hypersonic configurations
[AD-A253792] p 200 N93-12063
Hypersonic flow diagnostic development
[AD-A255045] p 202 N93-12466
An engineering method for interactive inviscid-boundary layers in three-dimensional hypersonic flows
p 203 N93-12529

HYPERSONIC NOZZLES
Hypervelocity scramjet combustor-nozzle analysis and design
[NASA-CR-190965] p 213 N93-12214

HYPERSONIC VEHICLES
Mixing regimes in a spatially confined, two-dimensional, supersonic shear layer
[AD-A254302] p 302 N93-11756
Air-breathing hypersonic vehicle guidance and control studies: An integrated trajectory/control analysis methodology, phase 2
[NASA-CR-189703] p 216 N93-12413
Current research in oxidation-resistant carbon-carbon composites at NASA. Langley Research Center
p 229 N93-12456
Thermal control/oxidation resistant coatings for titanium-based alloys p 229 N93-12457

HYPERVELOCITY
Hypervelocity scramjet combustor-nozzle analysis and design
[NASA-CR-190965] p 213 N93-12214

HYPERVELOCITY LAUNCHERS
An investigation of electromagnetic launcher repeatability
[AD-A254339] p 222 N93-12130
Electromagnetic launcher control using finite state machines
[AD-A254433] p 222 N93-12161
Railgun armature velocity improvement, SBIR phase 2
[AD-A254749] p 222 N93-12505

HYPERVELOCITY PROJECTILES
Compositional analysis and classification of projectile residues in LDEF impact craters
[NASA-TM-104750] p 488 N93-11374

HYPERVOLEMIA
Effect of hemorrhage on cardiac output, vasopressin, aldosterone, and diuresis during immersion in men
[NASA-TM-103949] p 374 N93-12014

HYPOTHERMIA
Effectiveness of NASA 1032 and 1035 and Air Force 1030 and 1034 units in protection against cold water hypothermia
[AD-A255120] p 389 N93-12291

HYPOTHESES
Operations plan for the Tropical Cyclone Motion (TCM-92) mini-field experiment
[AD-A254723] p 372 N93-12339

HYSTERESIS
Stress dependence of the magnetic properties of steels
[DE92-018804] p 261 N93-12261

I

ICE
Fast cooling phenomena with ice pellet injection in the JIPP T-IIU tokamak
[DE92-782105] p 454 N93-11834
Dynamic analysis of a pre-and-post ice impacted blade
[NASA-TM-105829] p 276 N93-12197

ICE FORMATION
Developments in icing test techniques for aerospace applications in the RAE Pyestock (England) altitude test facility
[RAE-TM-P-1214] p 207 N93-11485

IDAHO
Quaternary volcanism, tectonics, and sedimentation in the Idaho National Engineering Laboratory area
[DE92-017851] p 362 N93-11692

IDEAL GAS
Comprehensive computational model for thermal plasma processing
[DE92-018015] p 454 N93-12066
An improved numerical model for wave rotor design and analysis
[NASA-TM-105915] p 214 N93-12418

IDENTIFYING
A trainable image pattern classification system for detection of damaged soybean seeds
p 201 N93-12208

IGNITION
Ignition delays, heats of combustion, and reaction rates of aluminum alkyl derivatives as used as ignition and combustion enhancers for supersonic combustors
p 244 N93-11134
The effects of bypass air on boron carbide combustion in a solid fuel ramjet p 245 N93-11136
Metal slurry droplet and spray combustion
p 245 N93-11138
Impact ignition of liquid propellants
[AD-A252299] p 249 N93-11490
Nova Upgrade: A proposed ICF facility to demonstrate ignition and gain, revision 1
[DE92-018960] p 451 N93-11534
Loads from the detonation of hydrogen-air-steam mixtures
[DE92-019318] p 249 N93-11551
Hot-wire vs laser, is there a difference?
[DE92-019337] p 310 N93-11554

IGNITION SYSTEMS
Hot-wire vs laser, is there a difference?
[DE92-019337] p 310 N93-11554

IGNITION TEMPERATURE
Employment of radicals and excited state species for supersonic combustion photochemical ignition of premixed hydrogen/oxygen mixtures with ArF laser
p 245 N93-11135

ILLUMINATING
Video camera as a visual sensor
[NAL-TR-1132] p 314 N93-12373

ILLUMINATION
Shutter apparatus
[AD-D015350] p 309 N93-11049

IMAGE ANALYSIS
Statistical process for the automatic image analysis and its evaluation for object recognition and measurements
[SER-C-370] p 407 N93-11345
Visual perception of structure from motion
[AD-A253235] p 386 N93-11503
Automated extraction of aircraft runway patterns from radar imagery
[AD-A254258] p 218 N93-11751
Oceanographic expert system: Potential for TESS(3) applications
[AD-A254908] p 374 N93-12288
Nonlinear resistive grid wavelet transformations for texture feature extraction
[AD-A254705] p 285 N93-12332

IMAGE CONTRAST
Nuclear magnetic resonance microscopy: New theoretical and technical developments
p 313 N93-11907

IMAGE CORRELATORS
A trainable image pattern classification system for detection of damaged soybean seeds
p 201 N93-12208

IMAGE INTENSIFIERS
High frame-rate, large field wavefront sensor
[DE92-019547] p 310 N93-11542

IMAGE PROCESSING
X ray diagnostic techniques in ICF
[DE92-018069] p 449 N93-10975
Fringe analysis of in-plane displacements on high speed rotating components
[PNR-90920] p 334 N93-11022
An evidential reasoning approach to the classification of satellite images
[DLR-FB-91-29] p 342 N93-11140
Surface reconstruction of a three-dimensional ultrasonic flaw
[DE92-018029] p 332 N93-11154
High resolution image processing of geophysical data with diffraction tomography
[DE92-014134] p 359 N93-11235
Object based multi-image matching
[SER-C-375] p 309 N93-11330
Statistical process for the automatic image analysis and its evaluation for object recognition and measurements
[SER-C-370] p 407 N93-11345
Dynamic programming and image processing on distributed memory parallel machines
[ETN-92-92174] p 409 N93-11478
High energy x ray imaging diagnostic on Nova
[DE92-018067] p 451 N93-11495
Computational aspects of Gaussian beam migration
[DE92-018641] p 431 N93-11567
Parallel architecture for image processing with optic fiber guided missile
[REPT-921-320-101] p 418 N93-11584
System for generating dynamic video imagery for human factors research
[AD-A248675] p 388 N93-11743
Photogrammetric GIS technology: Feature mapping on digital stereo imagery
[AD-A254255] p 477 N93-11748
Automated extraction of aircraft runway patterns from radar imagery
[AD-A254258] p 218 N93-11751
Ultra wide band 3-D cross section (RCS) holography
[DE92-019133] p 312 N93-11802
High resolution tomographic instrument development
[DE92-017314] p 313 N93-11828
Operator vision aids for space teleoperation assembly and servicing p 391 N93-11981
A ring coded-aperture microscope for high-resolution imaging of high-energy x rays
[DE92-018004] p 454 N93-12059
Foil optimization for low energy neutral atom imaging
[DE92-013435] p 365 N93-12263
Low energy neutral atom imaging
[DE92-013531] p 365 N93-12264
A dip-dependent divergence correction
[DE92-016283] p 366 N93-12308
Digital signal processing
[AD-A254870] p 287 N93-12436

IMAGE RECONSTRUCTION
Object based multi-image matching
[SER-C-375] p 309 N93-11330
Nuclear magnetic resonance microscopy: New theoretical and technical developments
p 313 N93-11907
Fundamental analysis of the tomographic imaging system for reconstructing ionospheric distributions
p 365 N93-12209

IMAGE RESOLUTION
Extraction of shape information from predicted irradiance profiles in infrared images [RSRE-MEMO-4464] p 447 N93-11342
Three-dimensional image structure in in-line Fraunhofer holography p 311 N93-11723
Fuzzy control system for a remote focusing microscope p 314 N93-11934
Fundamental analysis of the tomographic imaging system for reconstructing ionospheric distributions p 365 N93-12209
Video camera as a visual sensor [NAL-TR-1132] p 314 N93-12373
IMAGERY
Photogrammetric point determination using digital imagery of three-line scanner systems [SER-C-372] p 309 N93-11346
Application of machine learning techniques for effective retrieval in image database [AD-A254907] p 479 N93-12287
IMAGES
Object based multi-image matching [SER-C-375] p 309 N93-11330
An iconic query interface for an image database [AD-A253571] p 475 N93-11506
IMAGING SPECTROMETERS
Estimation of photosynthetic capacity using MODIS polarization: 1988 proposal to NASA Headquarters [NASA-TM-103945] p 344 N93-12351
IMAGING TECHNIQUES
Method of remotely characterizing thermal properties of a sample [NASA-CASE-LAR-13508-3-CU] p 216 N93-11057
The tomographic formulation of spotlight mode synthetic aperture radar extended to three dimensional targets [DE92-013666] p 280 N93-11234
High resolution image processing of geophysical data with diffraction tomography [DE92-014134] p 359 N93-11235
Photogrammetric point determination using digital imagery of three-line scanner systems [SER-C-372] p 309 N93-11346
High energy x ray imaging diagnostic on Nova [DE92-018067] p 451 N93-11495
Magneto-optic imaging inspection of selected corrosion specimens [DOT/FAA/CT-TN92/20] p 332 N93-11617
System for generating dynamic video imagery for human factors research [AD-A248675] p 388 N93-11743
Advanced technology for portable personal visualization [AD-A253808] p 388 N93-11783
High-speed test station for solid-state imagers [DE92-018990] p 312 N93-11822
Fuzzy control system for a remote focusing microscope p 314 N93-11934
Model-based vision for space applications p 398 N93-11955
Effect of microstructure on passive film formation and breakdown on Al alloys [AD-A245863] p 260 N93-12118
Reflection masks for soft x ray projection lithography [DE92-014779] p 293 N93-12121
Fundamental analysis of the tomographic imaging system for reconstructing ionospheric distributions p 365 N93-12209
Final Report, January 1991 - July 1992 [AD-A254659] p 483 N93-12244
Foil optimization for low energy neutral atom imaging [DE92-013435] p 365 N93-12263
Low energy neutral atom imaging [DE92-013531] p 365 N93-12264
Laser Doppler experiments [AD-A252883] p 287 N93-12461
IMMUNE SYSTEMS
Use of novel adjuvants and delivery systems to improve the humoral and cellular immune response to malaria vaccine candidate antigens p 381 N93-11308
IMMUNITY
Mechanisms of immune failure in burn injury p 376 N93-11285
Silent HIV infection p 378 N93-11293
Immunological parameters in current and former US Air Force personnel p 378 N93-11295
Susceptibility in USAF recruits to vaccine preventable diseases p 380 N93-11301
Absence of protective immunity against diphtheria in a large proportion of young adults p 380 N93-11302
Studies of safety, infectivity, and immunogenicity of a new Temperature Sensitive (TS) 51-1 strain of S. typhi as a new live oral typhoid fever vaccine candidate p 381 N93-11306
Recent lessons on the safety and effectiveness of malaria chemoprophylaxis in a non-immune population p 381 N93-11307
Use of novel adjuvants and delivery systems to improve the humoral and cellular immune response to malaria vaccine candidate antigens p 381 N93-11308
Cytokines as vaccine adjuvants: Interleukin 1 and its synthetic peptide 163-171 p 382 N93-11309
IMMUNOASSAY
Early markers of HIV infection and subclinical disease progression p 379 N93-11296
Absence of protective immunity against diphtheria in a large proportion of young adults p 380 N93-11302
The screening of inhalant allergic diseases in the selection of candidates for aircraft piloting p 382 N93-11312
Phadiatop: A screening test for inhalant allergy p 383 N93-11313
In vivo and in vitro diagnosis of allergic respiratory disease during screening procedures in the Italian Navy: Comparative evaluation of a recent quantitative automatized enzyme immunoassay method to dose specific IgE p 383 N93-11314
Allergy screening and follow-up in student pilots of the Belgian Air Force (BAF) p 383 N93-11316
IMMUNOLOGY
Allergic, Immunological and Infectious Disease Problems in Aerospace Medicine [AGARD-CP-518] p 376 N93-11283
Space flight and immune system p 376 N93-11284
Mechanisms of immune failure in burn injury p 376 N93-11285
Clinical types of Hepatitis B p 376 N93-11286
Hepatitis A and Hepatitis B: Risks compared to other vaccine preventable diseases and immunization recommendations p 377 N93-11288
Vaccination against Hepatitis B: The Italian strategy p 377 N93-11289
Silent HIV infection p 378 N93-11293
Immunological parameters in current and former US Air Force personnel p 378 N93-11295
Early markers of HIV infection and subclinical disease progression p 379 N93-11296
Analysis of disease progression from clinical observations of US Air Force active duty members infected with the Human Immunodeficiency Virus: Distribution of AIDS survival time from interval censored observations p 379 N93-11297
Dramatic reduction of meningococcal meningitis among military recruits in Italy after introduction of specific vaccination p 380 N93-11303
Immunization of personnel traveling to a destination in tropical countries: French position p 380 N93-11304
Clinical and immunological response to vaccination with parenteral or oral vaccines in two groups of 30 recruits p 381 N93-11305
Studies of safety, infectivity, and immunogenicity of a new Temperature Sensitive (TS) 51-1 strain of S. typhi as a new live oral typhoid fever vaccine candidate p 381 N93-11306
Recent lessons on the safety and effectiveness of malaria chemoprophylaxis in a non-immune population p 381 N93-11307
Use of novel adjuvants and delivery systems to improve the humoral and cellular immune response to malaria vaccine candidate antigens p 381 N93-11308
Future approaches to vaccine development single-dose vaccines using controlled-release delivery systems p 382 N93-11310
IMPACT
Computation of single solid particle impact on the target of ductile material to study the rebound characteristics of particle p 336 N93-11372
IMPACT ACCELERATION
The effect of variable seat back angles on human response to +Gz impact accelerations [AD-A250673] p 387 N93-11559
IMPACT DAMAGE
Small particle impact damage in carbon-carbon composites [PNR-90948] p 236 N93-11107
Study of compression-loaded and impact-damaged structurally efficient graphite-thermoplastic trapezoidal-corrugation sandwich and semisandwich panels [NASA-TP-3264] p 239 N93-11623
Dynamic analysis of a pre-and-post ice impacted blade [NASA-TM-105829] p 276 N93-12197
IMPACT LOADS
Impact ignition of liquid propellants [AD-A252299] p 249 N93-11490
IMPACT STRENGTH
Penetration mechanics of composites [AD-A249230] p 240 N93-11835
Impact test of carbon, Kevlar, and glass fibre hybrid FRP plates [NAL-TR-1100] p 243 N93-12371
IMPACT TESTS
The effect of variable seat back angles on human response to +Gz impact accelerations [AD-A250673] p 387 N93-11559
Determination of loose spline coupling coefficients of rotor bearing systems in turbomachinery p 327 N93-11887
Impact test of carbon, Kevlar, and glass fibre hybrid FRP plates [NAL-TR-1100] p 243 N93-12371
IMPEDANCE
Eddy current characterization of magnetic treatment of materials [NASA-TM-104573] p 258 N93-11621
IMPEDANCE MEASUREMENT
Sound propagation over rigid porous layers p 432 N93-11179
IMPELLERS
Three-dimensional turbopump flowfield analysis [NASA-CR-190978] p 308 N93-12539
IMPLANTATION
Low energy helium implantation in evaporated nickel surfaces [DE92-019297] p 257 N93-11600
IMPLOSIONS
Hydrodynamic efficiencies in implosion experiments p 308 N93-12030
IMPURITIES
Instabilities in the rundown phase of the plasma focus [IPF-90-3] p 449 N93-11030
Atomistic processes of surface segregation during Si-Ge MBE growth [DE92-019180] p 459 N93-11496
Mechanisms of localized aqueous corrosion in aluminum-lithium-copper alloys p 259 N93-11895
IN SITU MEASUREMENT
Analysis of air and sea physical properties and surface fluxes using a combination of in situ and SEASAT data p 365 N93-12182
Stress dependence of the magnetic properties of steels [DE92-018804] p 261 N93-12261
IN-FLIGHT MONITORING
Flight test progress of the STOL research aircraft ASKA [NAL-TM-643] p 208 N93-12354
INCINERATORS
Technology evaluation report of Retech, Inc., Plasma Centrifugal Furnace, volume 2 [PB92-216043] p 457 N93-12527
INCLUSIONS
Silicon on insulator structures in selective epitaxial growth [DE92-017118] p 465 N93-11915
Flux dynamics and irreversibility in YBa2Cu3O7 with Y2BaCuO5 inclusions and in single crystal YBa2Cu3O7 [DE92-009712] p 467 N93-12178
INCOMPRESSIBLE FLOW
Direct numerical simulation of instabilities in parallel flow with spherical roughness elements [NASA-TM-105847] p 300 N93-11529
Application of a two-layer near wall model to fully developed and rotating channel turbulent flows [NASA-CR-184441] p 305 N93-12082
Flow in curved ducts of varying cross-section [AD-A254660] p 306 N93-12245
INCOMPRESSIBLE FLUIDS
Fundamental solutions and boundary element formulations for convective fluid flow p 298 N93-11217
Review of preconditioning methods for fluid dynamics [NASA-CR-189712] p 198 N93-11607
Oscillations and concentrations in compressible and incompressible fluids [AD-A254706] p 307 N93-12333
INCONEL (TRADEMARK)
Improved corrosion resistance of Hastelloy G-30 in nitric/hydrofluoric acid solutions by welding with Inconel 72 weld wire [DE92-017233] p 262 N93-12487
INDEPENDENT VARIABLES
A surface integral approach to the motion planning of nonholonomic systems [AD-A254844] p 329 N93-12434
INDIUM COMPOUNDS
Admittance spectroscopy of copper indium diselenide/cadmium sulfide solar cells p 344 N93-11214
Triisopropylindium: A new precursor for OMVPE growth [AD-A250672] p 460 N93-11558
Triisopropylindium: Decomposition study and use for low temperature growth [AD-A250666] p 464 N93-11869

INDIUM GALLIUM ARSENIDES
Contactless optoelectronic integrated circuits for remote fiber optic communication and sensing applications
[AD-A253573] p 290 N93-11507
INDIUM PHOSPHIDES
Contactless optoelectronic integrated circuits for remote fiber optic communication and sensing applications
[AD-A253573] p 290 N93-11507
Determination of Fe(sup 2+) and Fe(sup 3+) concentrations of semi-insulating InP:Fe
[DE92-017119] p 469 N93-12316
INDOOR AIR POLLUTION
Comparison of passive-remote and conventional Fourier transform infrared systems for continuously monitoring incinerator emissions
[DE92-015225] p 355 N93-12098
INDUCTANCE
A mutual inductance technique for contact-free T(sub c) measurement of high temperature superconductors
[NPL-DES-116] p 289 N93-11393
Nonlinear delay line phase shifters for terahertz superconductive electronic circuits
[AD-A255119] p 294 N93-12290
INDUSTRIAL MANAGEMENT
Activities report of Lufthansa
[ETN-92-92100] p 203 N93-11319
INDUSTRIAL WASTES
Trip report: Marshall Space Center computed tomography
[DE92-018139] p 437 N93-11597
Environmental restoration project configuration control
[DE92-017223] p 356 N93-12496
Technology evaluation report of Retech, Inc., Plasma Centrifugal Furnace, volume 1
[PB92-216035] p 456 N93-12526
Technology evaluation report of Retech, Inc., Plasma Centrifugal Furnace, volume 2
[PB92-216043] p 457 N93-12527
INDUSTRIES
Industrial applications and markets for ceramic matrix composites
[PNR-90884] p 266 N93-11205
Energy efficient drivepower: An overview
[PB92-199173] p 294 N93-12191
INELASTIC SCATTERING
Nucleon structure functions from deep inelastic muon scattering
[NIKHEF-H+K/92-01] p 442 N93-11130
High energy hadron-hadron collisions
[DE92-018253] p 441 N93-12224
INERTIAL CONFINEMENT FUSION
Development of a geometry-compensated neutron time-of-flight detector for ICF applications with approximately 200 ps time response
[DE92-018024] p 450 N93-11153
Nova Upgrade: A proposed ICF facility to demonstrate ignition and gain, revision 1
[DE92-018960] p 451 N93-11534
A ring coded-aperture microscope for high-resolution imaging of high-energy x rays
[DE92-018004] p 454 N93-12059
Plasma temperatures from first-hit neutron time-of-flight spectra
[DE92-018006] p 454 N93-12060
The 44th Annual Gaseous Electronics Conference
[AD-A254872] p 295 N93-12437
INERTIAL GUIDANCE
Hybrid guidance for maneuvering flight vehicles
[AD-A254110] p 225 N93-11798
INERTIAL NAVIGATION
Development of a GPS-aided motion measurement, pointing, and stabilization system for a synthetic aperture radar
[DE92-017053] p 204 N93-11152
INERTIAL PLATFORMS
Development of a GPS-aided motion measurement, pointing, and stabilization system for a synthetic aperture radar
[DE92-017053] p 204 N93-11152
INFECTIOUS DISEASES
Allergic, Immunological and Infectious Disease Problems in Aerospace Medicine
[AGARD-CP-518] p 376 N93-11283
Communicable diseases: A major burden of morbidity and mortality p 380 N93-11300
Susceptibility in USAF recruits to vaccine preventable diseases p 380 N93-11301
Absence of protective immunity against diphtheria in a large proportion of young adults p 380 N93-11302
Cytokines as vaccine adjuvants: Interleukin 1 and its synthetic peptide 163-171 p 382 N93-11309
Allergic and nonallergic rhinitis in Greek pilots
p 383 N93-11317
INFERENCE
A model-based reasoning approach to sensor placement for monitorability p 391 N93-11923
Design of an Ada expert system shell for the VHSIC avionic modular flight processor p 397 N93-11947
Research in statistical inference
[AD-A252928] p 429 N93-12429
Nonnormal multivariate distributions: Inference based on elliptically contoured distributions
[AD-A254999] p 429 N93-12513
INFILTRATION
Processing of ceramic matrix composites
[PNR-90914] p 263 N93-11018
Infiltration kinetics and interfacial bond strength of metal matrix composites
[AD-A254002] p 240 N93-11795
Studies on the reactive melt infiltration of silicon and silicon-molybdenum alloys in porous carbon
[NASA-TM-105860] p 273 N93-12398
INFORMATION DISSEMINATION
Information dissemination: Case studies on electronic dissemination at four agencies. Fact sheet for the Chairman, Committee on Governmental Affairs, US Senate
[GAO/IMTEC-92-6FS] p 474 N93-11274
NASA/DOD Aerospace Knowledge Diffusion Research Project. Paper 23: Information technology and aerospace knowledge diffusion: Exploring the intermediary-end user interface in a policy framework
[NASA-TM-108077] p 478 N93-12007
ONRASIA scientific information bulletin, volume 17, number 3
[AD-A255073] p 490 N93-12470
INFORMATION FLOW
Self-supervision in multilayer adaptive networks
[RSRE-MEMO-4467] p 420 N93-11343
INFORMATION MANAGEMENT
Methods and principles for determining task dependent interface content
[NASA-CR-190837] p 204 N93-10961
Experience of designing a relational materials database
[PNR-90893] p 473 N93-11012
Managing data: From vision to reality
[PB92-191212] p 474 N93-11215
An iterative method for distributed database design
p 474 N93-11255
Analysis of methods — information systems evolution environment
[NASA-CR-190278] p 407 N93-11368
Using SGML in a large organization
[ESA-STR-234] p 476 N93-11583
Computer Science and Telecommunications Board summary of activities
[DE92-016467] p 404 N93-11761
Laboratory information management system proposal
[DE92-018243] p 478 N93-11796
NASA/DOD Aerospace Knowledge Diffusion Research Project. Paper 23: Information technology and aerospace knowledge diffusion: Exploring the intermediary-end user interface in a policy framework
[NASA-TM-108077] p 478 N93-12007
Radiological information management system (RadIMS)
[DE92-017221] p 480 N93-12495
INFORMATION PROCESSING (BIOLOGY)
An introduction to the information processing components of the brain
[RSRE-MEMO-4350] p 385 N93-10979
Complex cognitive information processing: A computational architecture with a connectionist implementation
[AD-A254041] p 422 N93-12259
INFORMATION RETRIEVAL
Data archiving and analysis for CWDD
[DE92-017064] p 473 N93-11104
A probabilistic approach to information retrieval in heterogeneous databases
[DE92-016993] p 473 N93-11151
Study and recommendation of available sources of scientific and technical numeric databases in the government and private sector
[AD-A247266] p 475 N93-11465
An iconic query interface for an image database
[AD-A253571] p 475 N93-11506
Using SGML in a large organization
[ESA-STR-234] p 476 N93-11583
The effect of task complexity on user interfaces: A comparison of command language interface and direct manipulation interface
[AD-A246061] p 412 N93-11859
LINK user manual
[DE92-017987] p 479 N93-12143
ERS-1 user handbook
[ESA-SP-1148] p 344 N93-12280
Application of machine learning techniques for effective retrieval in image database
[AD-A254907] p 479 N93-12287
Exploiting captions in retrieval of multimedia data
[AD-A255184] p 479 N93-12381
Assessing repository technology: Where do we go from here? p 415 N93-12391
INFORMATION SYSTEMS
Methods and principles for determining task dependent interface content
[NASA-CR-190837] p 204 N93-10961
Data archiving and analysis for CWDD
[DE92-017064] p 473 N93-11104
Information dissemination: Case studies on electronic dissemination at four agencies. Fact sheet for the Chairman, Committee on Governmental Affairs, US Senate
[GAO/IMTEC-92-6FS] p 474 N93-11274
Reserves information gathering system user's guide
[DE92-018357] p 475 N93-11355
Information systems planning leading to performance support systems
[DE92-018745] p 475 N93-11441
Engineering Information System (EIS)
[AD-A254013] p 476 N93-11508
Integrity in automated information systems
[AD-A253990] p 477 N93-11732
Spatial data transformation: Feature attribute conversion issues and practical experience
[AD-A254238] p 477 N93-11741
Photogrammetric GIS technology: Feature mapping on digital stereo imagery
[AD-A254255] p 477 N93-11748
Proceedings of the First Seminar on Geographic Information Systems in Zambia
[PB92-207125] p 477 N93-11789
Integrity-oriented control objectives: Proposed revisions to the Trusted Computer System Evaluation Criteria (TCSEC), DOD 5200.28-STD
[AD-A253989] p 404 N93-11809
Directory interchange format manual, version 4.0
[NASA-TM-107991] p 478 N93-11911
NASA/DOD Aerospace Knowledge Diffusion Research Project. Paper 23: Information technology and aerospace knowledge diffusion: Exploring the intermediary-end user interface in a policy framework
[NASA-TM-108077] p 478 N93-12007
LINK user manual
[DE92-017987] p 479 N93-12143
Application of machine learning techniques for effective retrieval in image database
[AD-A254907] p 479 N93-12287
Assessing repository technology: Where do we go from here? p 415 N93-12391
The hydrogen technology assessment, phase 1
[NASA-CR-190969] p 349 N93-12394
ESIS: An introduction to the European space information system. A modern tool for space scientists
[ESA-INT-2] p 479 N93-12404
ONRASIA scientific information bulletin, volume 17, number 3
[AD-A255073] p 490 N93-12470
Data distribution satellite
[NASA-TM-105778] p 287 N93-12481
Radiological information management system (RadIMS)
[DE92-017221] p 480 N93-12495
INFORMATION THEORY
Digital signal processing
[AD-A254870] p 287 N93-12436
INFORMATION TRANSFER
Reserves information gathering system user's guide
[DE92-018357] p 475 N93-11355
Directory interchange format manual, version 4.0
[NASA-TM-107991] p 478 N93-11911
NASA/DOD Aerospace Knowledge Diffusion Research Project. Paper 23: Information technology and aerospace knowledge diffusion: Exploring the intermediary-end user interface in a policy framework
[NASA-TM-108077] p 478 N93-12007
INFRARED ASTRONOMY
The Comet Halley archive: Summary volume
[NASA-CR-190358] p 484 N93-11243
INFRARED DETECTORS
INAS hole-immobilized doping superlattice long-wave-infrared detector
[NASA-CASE-NPO-17880-1-CU] p 458 N93-11056
On the dependence of the dynamic crack tip temperature fields in metal upon crack tip velocity and material parameters
[AD-A253657] p 335 N93-11219
Development of ultra-low noise, high sensitivity planar metal grating coupled AlGaAs/GaAs multiquantum well IR detectors for focal plane array staring IR sensor systems
[AD-A254697] p 468 N93-12228
INFRARED IMAGERY
Volcanology from space: Applications of infrared remote sensing p 343 N93-11213

Near-infrared imaging polarimetry of bipolar nebulae
p 481 N93-11248
Extraction of shape information from predicted irradiance profiles in infrared images
[RSRE-MEMO-4464] p 447 N93-11342

INFRARED INSTRUMENTS
Comparison of passive-remote and conventional Fourier transform infrared systems for continuously monitoring incinerator emissions
[DE92-015225] p 355 N93-12098

INFRARED LASERS
CO2 laser frequency doubling
[AD-A251060] p 314 N93-10997
UCSB FEL user mode adaption project
[AD-A248734] p 316 N93-11418
Research on stimulated Raman scattering with applications to atmospheric lidar p 322 N93-12163

INFRARED RADIATION
Multispectral observations of the Jovian aurora
p 487 N93-11167
Microwave guidance technology and its applications
[AD-A254107] p 281 N93-11509
Development of ultra-low noise, high sensitivity planar metal grating coupled AlGaAs/GaAs multiquantum well IR detectors for focal plane array staring IR sensor systems
[AD-A254697] p 468 N93-12228

INFRARED SCANNERS
Debris/ice/TPS assessment and integrated photographic analysis for Shuttle Mission STS-46
[NASA-TM-107552] p 223 N93-12151

INFRARED SPECTRA
Near-IR absorption spectra for the C70 fullerene anions
[AD-A253658] p 246 N93-11280
Comparison of passive-remote and conventional Fourier transform infrared systems for continuously monitoring incinerator emissions
[DE92-015225] p 355 N93-12098

INFRARED SPECTROMETERS
On-line analysis of chemical composition using an FT-Raman spectrometer in the near-IR
[DE92-016503] p 253 N93-12311

INFRARED SPECTROSCOPY
Tetrahedral atom zincophosphate structures: Synthesis, crystal structure, and spectroscopic studies of (Zn(PO2(OC2H5)2)2)x, a one-dimensional inorganic polymer
[AD-A251051] p 437 N93-11560
Exploration of the ionizable metal cluster-electrode surface analogy: Infrared spectroelectrochemistry of (Pt24(CO)30)(sup n), (Pt26(CO)32)(sup n), and (Pt38(CO)44)(sup n) (n = 0 to -10), and comparisons with potential-dependent spectra of CO adlayers on platinum surfaces
[AD-A252544] p 250 N93-11808
Comparison of passive-remote and conventional Fourier transform infrared systems for continuously monitoring incinerator emissions
[DE92-015225] p 355 N93-12098
The deposition characteristics of copper(I) compounds for CVD by FT-IR spectroscopy
[DE92-010778] p 467 N93-12134
Energetics solids degradation in high temperature water
[AD-A254900] p 276 N93-12285

INGESTION (BIOLOGY)
Smoking status and body composition, exercise, dietary intake, and alcohol/caffeine consumption
[AD-A250648] p 385 N93-11893

INHIBITORS
Inhibition of moist carbon monoxide oxidation by trace amounts of hydrocarbons
[DE92-008736] p 253 N93-12257

INJECTION
Fast cooling phenomena with ice pellet injection in the JIPP T-IIU tokamak
[DE92-782105] p 454 N93-11834

INJECTION MOLDING
Orientation, stress, and density distributions in injection-moulded amorphous polymers determined by optical techniques
[ETN-92-92271] p 269 N93-11983
Molecular orientation induced by cooling stresses in polycarbonate. 2: Constrained quench and injection moulding p 270 N93-11988
Gapwise density distributions in injection-moulded polymethylmethacrylate p 270 N93-11990
Analysis of the birefringence distributions in compact discs of polycarbonate p 270 N93-11991

INJECTORS
Higher-order-mode damping and microwave absorption at 2 K
[DE92-016960] p 442 N93-11077
CFD modeling of turbulent flows around the SSME main injector assembly using porosity formulation
[NASA-CR-184359] p 297 N93-11171
Coaxial injector spray characterization using water/air as simulants p 248 N93-11452
Experimental investigation of rocket injector atomization p 248 N93-11454

INLET FLOW
An experimental investigation of the flow in a diffusing S-duct
[NASA-TM-105809] p 213 N93-12077

INPUT/OUTPUT ROUTINES
Using ELLA for high level design: Modelling the Motorola 6800 microprocessor
[RSRE-MEMO-4515] p 408 N93-11386
Concurrent file operations in a high performance FORTRAN
[NASA-CR-189711] p 412 N93-11618

INSERTION
Systems engineering and technical assistance in support of digital gallium arsenide insertion projects
[AD-A253751] p 463 N93-11790

INSERTION LOSS
High Temperature Superconductivity Space Experiment (HTSSE)
[AD-A253119] p 288 N93-11239

INSPECTION
Nondestructive inspection and life determination of disc material
[PNR-90911] p 331 N93-11016
Feasibility of using neutron radiography to inspect the Space Shuttle solid rocket booster aft skirt, forward skirt and frustum. Part 1: Summary report
[NASA-CR-184357] p 231 N93-11173
Aircraft accident report: Atlantic Southeast Airlines, Inc. Flight 2311, uncontrolled collision with terrain, an Embraer EMB-120, N270AS, Brunswick, Georgia, 5 April 1991
[PB92-910403] p 203 N93-11471
Debris/ice/TPS assessment and integrated photographic analysis for Shuttle Mission STS-46
[NASA-TM-107552] p 223 N93-12151

INSTALLING
Acoustic emission monitoring of HFIR vessel during hydrostatic testing
[DE92-019316] p 332 N93-11601
Automatic system for installation and replacement of Space Station components
[NASA-CASE-LEW-14906-1] p 329 N93-12203

INSTRUCTION SETS (COMPUTERS)
The VISTA structured assembler
[RSRE-91034] p 407 N93-11341
Using ELLA for high level design: Modelling the Motorola 6800 microprocessor
[RSRE-MEMO-4515] p 408 N93-11386
Applying algebraic techniques to microcode compilation
[RSRE-MEMO-4568] p 409 N93-11392
The WEB approach to ELLA
[RSRE-MEMO-4549] p 409 N93-11407
A formal definition of the static semantics of ELLA's core
[RSRE-91024] p 409 N93-11436

INSTRUMENT APPROACH
Design of instrument approach procedure charts: Comprehension speed of missed approach instructions coded in text or icons
[PB92-205673] p 204 N93-11252

INSTRUMENT COMPENSATION
Deployable reflector antenna performance optimization using automated surface correction and array-feed compensation
[NASA-TP-3228] p 222 N93-12543

INSTRUMENTS
High resolution tomographic instrument development
[DE92-017314] p 313 N93-11828

INSULATION
Thermal protection systems manned spacecraft flight experience p 227 N93-12449
Superplastic forming of ceramic insulation
p 228 N93-12452

INSULATORS
Silicon on insulator structures in selective epitaxial growth
[DE92-017118] p 465 N93-11915
Gas-surface interactions near dissociation threshold
[AD-A250205] p 252 N93-12254
Damping and scattering of electromagnetic waves by small ferrite spheres suspended in an insulator
[NASA-TM-105837] p 286 N93-12366

INTEGRAL TRANSFORMATIONS
Inverse spectral transform for the 2 + 1-dimensional Gardner equation
[MATHS-REPT-A-138] p 425 N93-11323

INTEGRALS
On the evaluation of derivatives of Gaussian integrals
p 439 N93-11853

INTEGRATED CIRCUITS
Contactless optoelectronic integrated circuits for remote fiber optic communication and sensing applications
[AD-A253573] p 290 N93-11507
An analog macromodel of the SG1525A PWM for use with SPICE2G.6 simulators
[DE92-019423] p 291 N93-11639
High-frequency LSI contactor
[DE92-017285] p 292 N93-11916
Reflection masks for soft x ray projection lithography
[DE92-014779] p 293 N93-12121
MMIC GaAs bonding investigation
[AD-A254773] p 470 N93-12464

INTEGRATED MISSION CONTROL CENTER
Mission Control Center enhancement opportunities in the 1990's p 396 N93-11942

INTEGRITY
Testing for integrity
[PNR-90927] p 210 N93-11024
Integrity in automated information systems
[AD-A253990] p 477 N93-11732
Distributed database integrity
[AD-A253272] p 477 N93-11749
Integrity-oriented control objectives: Proposed revisions to the Trusted Computer System Evaluation Criteria (TCSEC), DOD 5200.28-STD
[AD-A253989] p 404 N93-11809

INTERACTIONAL AERODYNAMICS
Unsteady propeller/wing aerodynamic interactions
p 201 N93-12190

INTERACTIVE CONTROL
An interactive preprocessor for the NASA engine performance program
[NASA-TM-105786] p 209 N93-10983

INTERCALATION
Fast electrochromic switching for optical hardening applications
[AD-A248174] p 447 N93-11186

INTERFACIAL ENERGY
Slow crack growth in vacuum p 338 N93-11909
Growth, characterization, and device development in monocrystalline diamond films
[AD-A252648] p 271 N93-12184

INTERFACIAL TENSION
The effects of chemistry on weld profiles in partial and full penetration welds
[DE92-016865] p 327 N93-11679

INTERFEROMETERS
Phase-stepping fiber-optic projected fringe system for surface topography measurements
[NASA-CASE-LEW-14996-1] p 446 N93-11058
Matter-wave interferometry with laser cooled atoms
[AD-A253999] p 316 N93-11737

INTERFEROMETRY
Geostationary-satellite beacon-receiver array for studies of ionospheric irregularities
[DE92-018979] p 362 N93-11535
Matter-wave interferometry with laser cooled atoms
[AD-A253999] p 316 N93-11737

INTERLAMINAR STRESS
An interlayer shear slip theory for composite laminates with nonrigid bonding p 237 N93-11229

INTERLAYERS
An interlayer shear slip theory for composite laminates with nonrigid bonding p 237 N93-11229

INTERMETALLICS
Mechanical properties of semiconductors and their alloys
[AD-A253908] p 462 N93-11727

INTERMITTENCY
Mode interaction models in near-wall turbulence
p 303 N93-11856

INTERMOLECULAR FORCES
Workshop on Adhesion and Intermolecular Forces
[AD-A255191] p 272 N93-12276

INTERNAL COMBUSTION ENGINES
The intensity of knock in an internal combustion engine: An experimental and modeling study
[DE92-019504] p 326 N93-11540

INTERNAL ENERGY
The chemistry of Si3N4 and Si deposition studied using molecular beam techniques
[DE92-018268] p 463 N93-11797

INTERNAL FRICTION
Internal friction peaks due to oxygen, nitrogen, and hydrogen in V-Nb alloys
[DE92-012155] p 254 N93-10995

INTERNATIONAL COOPERATION
Civil aircraft engines: The next generation
[PNR-90962] p 211 N93-11085
Lessons drawn from 2 existing satellite networks: ARABSAT and EUTELSAT. Application to the Pacific basin projects
[REPT-921-440-101] p 282 N93-11591

Environmental problems and trends of international responses, 2
[DE92-531118] p 355 N93-11846
United States/Canada Air Quality Agreement
[PB92-228030] p 356 N93-12525

INTERNATIONAL SYSTEM OF UNITS
Recommended agency procedures for implementing federal metric policy
[PB92-205467] p 277 N93-11901
A metric America: A decision whose time has come - for real
[PB92-205459] p 277 N93-11902

INTERPLANETARY DUST
Thin-sectioning and analysis of fine-grained meteoritic materials
[NASA-CR-185693] p 485 N93-11546

INTERPLANETARY FLIGHT
Closed form low-thrust trajectories for Mars missions
[DE92-017431] p 232 N93-11766

INTERPLANETARY MAGNETIC FIELDS
Statistics of IMF B(z) events
[DE92-018372] p 488 N93-11696
The semiannual variation of great geomagnetic storms and the postshock Russell-McPherron effect preceding coronal mass ejecta
[AD-A254955] p 489 N93-12506

INTERPLANETARY TRAJECTORIES
Closed form low-thrust trajectories for Mars missions
[DE92-017431] p 232 N93-11766

INTERPOLATION
Interactive analysis of gappy bivariate time series using AGSS
[AD-A255160] p 429 N93-12426

INTERPROCESSOR COMMUNICATION
Photonics and other approaches to high speed communications
[NASA-CR-190362] p 279 N93-11116
High performance interconnection between high data rate networks p 279 N93-11118
Dynamic programming on a ring of processors
p 410 N93-11479
Path planning on a ring of processors
p 410 N93-11480
Symmetric matrix-vector product on a ring of processors p 410 N93-11481
Scattering on a ring of processors
p 410 N93-11482
Reduction operations on a distributed memory machine with a reconfigurable interconnection network
p 410 N93-11484
Advanced satellite workstation: An integrated workstation environment for operational support of satellite system planning and analysis p 391 N93-11941
Formal design specification of a Processor Interface Unit
[NASA-CR-189698] p 406 N93-12538

INTERSECTIONS
A study of the wall-pressure fluctuations downstream of a blade-wall junction
[ECL-91-07] p 299 N93-11363

INTERSTELLAR GAS
A model to estimate the flux of background particles expected to accumulate on the collector foils of the interstellar gas experiment on the long duration exposure facility spacecraft
[AD-A254265] p 489 N93-11815

INTERSTELLAR MATTER
A submillimeter-millimeterwave study of the molecular gas in the nuclear regions of three nearby starburst galaxies p 484 N93-11260
A multi-line study of the molecular interstellar medium on M82's starburst nucleus
[MPE-PREPRINT-213] p 484 N93-11347

INTERSTITIALS
Internal friction peaks due to oxygen, nitrogen, and hydrogen in V-Nb alloys
[DE92-012155] p 254 N93-10995
An NMR study of the occupation of C(sub 60) interstitial sites by oxygen molecules
[DE92-019436] p 437 N93-11640

INVARIANCE
On an origin of numerical diffusion: Violation of invariance under space-time inversion
[NASA-TM-105776] p 425 N93-11254

INVERSE KINEMATICS
The adaptive neuron model: An architecture for the rapid learning of nonlinear topological transformations
[NASA-CASE-NPO-18579-1-CU] p 420 N93-11174
Numerical analysis of right-half plane zeros for a single-link manipulator
[NASA-CR-190966] p 426 N93-11547

INVERSE SCATTERING
On the inverse scattering problem for the Helmholtz equation in one dimension
[AD-A253130] p 434 N93-11526

INVERSIONS
On an origin of numerical diffusion: Violation of invariance under space-time inversion
[NASA-TM-105776] p 425 N93-11254
On the inverse scattering problem for the Helmholtz equation in one dimension
[AD-A253130] p 434 N93-11526

INVISCID FLOW
Fundamental solutions and boundary element formulations for convective fluid flow
p 298 N93-11217
Review of preconditioning methods for fluid dynamics
[NASA-CR-189712] p 198 N93-11607
Numerical investigation of three-dimensionally evolving jets p 303 N93-11870
Nonlinear stability of flows over rigid and flexible boundaries p 198 N93-11874
On the Goertler instability of boundary layers
[NAL-TR-1120T] p 307 N93-12374
An engineering method for interactive inviscid-boundary layers in three-dimensional hypersonic flows
p 203 N93-12529

ION ACCELERATORS
The diagnostics system for the multiple heavy ion beams induction linac experiment, MBE-4
[DE92-017109] p 445 N93-12126

ION ACOUSTIC WAVES
Development of a new plasma diagnostic of the critical surface and studies of the ion acoustic decay instability using collective Thomson scattering
[DE92-018508] p 453 N93-11730
Development of a new plasma diagnostic of the critical surface and studies of the ion acoustic decay instability using collective Thomson scattering
[DE92-018526] p 453 N93-11731

ION ATOM INTERACTIONS
Experimental study of interactions of highly charged ions with atoms at keV energies
[DE92-019512] p 436 N93-11541
Electron emission during multicharged ion-metal surface interactions
[DE92-017134] p 439 N93-11849

ION BEAMS
Corrosion protection of materials for aircraft using ion beam processes. Corrosion and bonding strength examinations. Physical analysis of laser composition
[MBB-Z-0405-91-PUB] p 255 N93-11026
North American radioactive beam initiatives
[DE92-019185] p 443 N93-11517
Beam-plasma interactions and radiation generation during the ejection of electron and ion beams in space
[AD-A253993] p 224 N93-11736
Divergence in intense ion beams caused by incomplete charge neutralization
[DE92-016891] p 445 N93-12103
Friction of self-lubricating surfaces by ion beam techniques
[DE92-016069] p 328 N93-12122
The diagnostics system for the multiple heavy ion beams induction linac experiment, MBE-4
[DE92-017109] p 445 N93-12126
Ion beams as a means of deposition and in-situ characterization of thin films and thin film layered structures
[DE92-016397] p 469 N93-12310
The 44th Annual Gaseous Electronics Conference
[AD-A254872] p 295 N93-12437

ION CURRENTS
Mixed ionic and electronic conductivity in polymers
[DE92-018723] p 273 N93-12500

ION ENGINES
Extended-testing of xenon ion thruster hollow cathodes
[NASA-CR-189227] p 234 N93-12409

ION EXCHANGE MEMBRANE ELECTROLYTES
Reactant gas flow fields in advanced PEM (Proton Exchange Membrane) fuel cell designs
[DE92-018897] p 345 N93-11626

ION IMPLANTATION
Preparation of silicon oxynitride thin films by plasma chemical vapor deposition for chemical implantation. Application to a pH ISFET
[ECL-91-12] p 291 N93-11574
Implanted He retention and release from boronized layers
[DE92-013983] p 464 N93-11842
Friction of self-lubricating surfaces by ion beam techniques
[DE92-016069] p 328 N93-12122
Formation of buried epitaxial Si-Ge alloy layers in Si (100) crystal by high dose Ge ion implantation
[DE92-017114] p 466 N93-12127

ION MOTION
Mixed ionic and electronic conductivity in polymers
[DE92-018723] p 273 N93-12500

ION PRODUCTION RATES
Advanced electric propulsion research, 1991
[NASA-CR-190761] p 232 N93-11608
Diagnostics and modeling of H(-) ion sources
[AD-A250664] p 440 N93-11867

ION PROPULSION
Advanced electric propulsion research, 1991
[NASA-CR-190761] p 232 N93-11608
Extended-testing of xenon ion thruster hollow cathodes
[NASA-CR-189227] p 234 N93-12409

ION RECOMBINATION
Modeling for the study of an X laser in a recombination plasma; gain calculations at 105.7 and 154.6 A
p 321 N93-12046

ION SCATTERING
Ion temperature measurements in tokamak plasmas by Rutherford scattering
[PB92-184738] p 451 N93-11245

ION SELECTIVE ELECTRODES
Acid copper sulfate plating bath: Control of chloride and copper
[DE92-019473] p 249 N93-11644

ION SOURCES
North American radioactive beam initiatives
[DE92-019185] p 443 N93-11517
Electron emission during multicharged ion-metal surface interactions
[DE92-017134] p 439 N93-11849
Divergence in intense ion beams caused by incomplete charge neutralization
[DE92-016891] p 445 N93-12103
Design and evaluation of ion source for satellite charge control
[AD-A255172] p 227 N93-12408

ION TEMPERATURE
A new pitch angle diagnostic for electron cyclotron resonance plasma p 450 N93-11185
Ion temperature measurements in tokamak plasmas by Rutherford scattering
[PB92-184738] p 451 N93-11245
Diagnostics and modeling of H(-) ion sources
[AD-A250664] p 440 N93-11867
Plasma temperatures from first-hit neutron time-of-flight spectra
[DE92-018006] p 454 N93-12060
Anomalous ion thermal transport in hot ion plasmas by the ion temperature gradient mode
[DE92-016686] p 456 N93-12493
Ion temperature measurements on field reversed configuration plasmas p 457 N93-12535

IONIC COLLISIONS
Strange quark matter
[DE92-016949] p 438 N93-11746
Electron emission during multicharged ion-metal surface interactions
[DE92-017134] p 439 N93-11849

IONIC CRYSTALS
Electron terms and radiation from crystals
[AD-A254353] p 468 N93-12271

IONIC MOBILITY
State-resolved dynamics of ion-molecule collisions in a flowing afterglow
[AD-A247288] p 436 N93-11467

IONIC REACTIONS
State-resolved reaction dynamics
[AD-A254291] p 436 N93-11196
Positive ion chemistry of acetylene and methylacetylene clusters. Formation of benzene and C(sub 2n)H(sub 2n)(+) ions via intracluster polymerization reactions
[AD-A250931] p 236 N93-12177

IONIZATION
Atomic structure of Ni-like soft x ray lasing ions
[DE92-019273] p 438 N93-11778
High-precision thorium RIMS for geochemistry
[DE92-017405] p 250 N93-11918
Advanced methods for structural characterization of large multiply charged ions: Obtaining charge state determination and improved sensitivity
[DE91-015264] p 441 N93-12117
Positive ion chemistry of acetylene and methylacetylene clusters. Formation of benzene and C(sub 2n)H(sub 2n)(+) ions via intracluster polymerization reactions
[AD-A250931] p 236 N93-12177
Carbon/carbon composition ablation effects on ionized boundary layers
[AD-A254465] p 242 N93-12235
Characterization of underivatized pterins by laser desorption Fourier transform mass spectrometry
[DE92-016785] p 323 N93-12514

IONIZATION CHAMBERS
Measurement of absorbed dose to water for medium energy x rays
[NPL-RSA(EXT)-33] p 436 N93-11412

IONIZED GASES
The 44th Annual Gaseous Electronics Conference
[AD-A254872] p 295 N93-12437
IONIZING RADIATION
Molecular cytogenetics: A novel approach for measuring chromosome translocations in individuals years after exposure to low levels of ionizing radiation
[DE92-018066] p 374 N93-10974
IONOSONDES
Geostationary-satellite beacon-receiver array for studies of ionospheric irregularities
[DE92-018979] p 362 N93-11535
IONOSPHERIC DISTURBANCES
The extremely low frequency wave analyzer
[AD-A255178] p 366 N93-12378
IONOSPHERIC ELECTRON DENSITY
Electron energization in the topside auroral ionosphere: On the importance of ion-acoustic turbulence
p 360 N93-11269
Fundamental analysis of the tomographic imaging system for reconstructing ionospheric distributions
p 365 N93-12209
IONOSPHERIC HEATING
Electron energization in the topside auroral ionosphere: On the importance of ion-acoustic turbulence
p 360 N93-11269
IONOSPHERIC PROPAGATION
Publication of papers presented at URSI 23rd General Assembly as a special section of radio science
[AD-A253561] p 283 N93-11811
IONS
Advanced methods for structural characterization of large multiply charged ions: Obtaining charge state determination and improved sensitivity
[DE91-015264] p 441 N93-12117
IRISES (MECHANICAL APERTURES)
Video camera as a visual sensor
[NAL-TR-1132] p 314 N93-12373
IRON
Determination of Fe(sup 2+) and Fe(sup 3+) concentrations of semi-insulating InP:Fe
[DE92-017119] p 469 N93-12316
IRON ALLOYS
International ADI-Seminar: Austempered Ductile Iron
[PB92-180660] p 256 N93-11244
Environment-induced embrittlement: Stress corrosion cracking and metal-induced embrittlement; environmental embrittlement of iron aluminide alloys
[DE92-018714] p 256 N93-11524
Isotopic tailoring with 59-Ni to study the effect of helium on microstructural evolution and mechanical properties of neutron-irradiated Fe-Cr-Ni alloys
[DE92-019372] p 257 N93-11557
Oxidation-sulfidation behavior of iron alloys containing 16 to 40 atomic percent aluminum
[DE92-017824] p 259 N93-11830
Optimization of film synthesized rare earth transition metal permanent magnet systems
[DE92-018726] p 432 N93-12116
IRON COMPOUNDS
Synthesis of single phase (alpha)-Fe, Fe3C and Fe7C3 nano-particles by CO2 laser pyrolysis technique
[DE92-015654] p 250 N93-11847
IRREGULARITIES
The effects of magnetic storm phases on F-layer irregularities from auroral to equatorial latitudes
[AD-A253905] p 361 N93-11282
ISOELECTRONIC SEQUENCE
Direct radiative recombination of atomic ions
p 321 N93-12048
ISOMERS
Synthesis of side chain liquid crystal polymers by living ring opening metathesis polymerization. Report 3: Influence of molecular weight, interconnecting unit and substituent on the mesomorphic behavior of polymers with laterally attached mesogens
[AD-A248698] p 265 N93-11187
Organometallic NLO polymers. 3. Copolymerization of bridged bis(ferrocenyl) and bis(cyanoacetate) monomers via the knoevenagel condensation
[AD-A250214] p 265 N93-11192
ISOMORPHISM
An isomorphism for algebra of distributions with compact support on Lie groups
[DE92-603605] p 427 N93-12176
ISOPARAMETRIC FINITE ELEMENTS
Fourier continuum finite elements for nonlinear structural analysis p 340 N93-12210
ISOTHERMAL FLOW
Using NEKTON to solve systems of discrete Boltzmann equations
[DE92-018272] p 303 N93-11799
ISOTOPIC LABELING
Freeze-dried human red blood cells
[AD-A253295] p 376 N93-11193
Molecular mobility of the interface in a model composite: A NMR study
[AD-A253311] p 265 N93-11194
New techniques for positron emission tomography in the study of human neurological disorders
[DE92-015353] p 384 N93-11873
ISOTROPIC MEDIA
Linear and geometrically nonlinear p-version three dimensional curved shell element for isotropic, generally orthotropic and laminated composite materials
p 339 N93-12194
The generalized Goursat-Riemann problem for plane waves in isotropic elastic solids p 340 N93-12199
ITALY
Vaccination against Hepatitis B: The Italian strategy
p 377 N93-11289
Dramatic reduction of meningococcal meningitis among military recruits in Italy after introduction of specific vaccination p 380 N93-11303
ITERATION
An approach to constrained aerodynamic design with application to airfoils
[NASA-TP-3260] p 201 N93-12321
ITERATIVE SOLUTION
Preconditioned low-order Newton methods
[MATHS-REPT-A-159] p 425 N93-11211
An iterative method for distributed database design
p 474 N93-11255
The efficient parallel iterative solution of large sparse linear systems
[DE92-018769] p 425 N93-11446
IUE
ESIS: An introduction to the European space information system. A modern tool for space scientists
[ESA-INT-2] p 479 N93-12404

J

JAPAN
Japanese style total quality control: A first hand experience
[PNR-90909] p 331 N93-11015
JET AIRCRAFT NOISE
A concept for a counterrotating fan with reduced tone noise
[NASA-TM-105736] p 433 N93-11370
JET ENGINES
The Trent family of engines
[PNR-90974] p 211 N93-11063
A concept for a counterrotating fan with reduced tone noise
[NASA-TM-105736] p 433 N93-11370
JET FLAPS
Wind tunnel investigation of a twin-engine jet transport semi-span model with upper surface blown jet flap
[NAL-TR-1134] p 203 N93-12503
JET FLOW
Numerical investigation of three-dimensionally evolving jets p 303 N93-11870
The aerodynamics of curved jets and breakaway in Coanda flares, volumes 1 and 2 p 304 N93-11881
JET PROPULSION
Concorde propulsion: Did we get it right? The Rolls-Royce/SNECMA Olympus 593 engine reviewed
[PNR-90970] p 210 N93-11061
JET STREAMS (METEOROLOGY)
The forcing of a mid-latitude upper-tropospheric jet streak by a simulated mesoscale convective system
p 358 N93-11184
JET THRUST
Results from a large-scale MHD propulsion experiment
[DE92-018177] p 456 N93-12416
JET VANES
Droppable jet vane TVC
[AD-D015341] p 214 N93-11046
JOINING
Effect of assembly anomalies on the strain response of composites in the sphere joint region of the DARPA man-rated demonstration article
[AD-A254204] p 240 N93-11739
JOINTS (JUNCTIONS)
Modeling and identification of flexible joints in vehicle structures p 324 N93-11261
The theoretical background to BS7167: 1990 - specification for Bordeaux connections
[NPL-DMM(A)-50] p 325 N93-11324
The technical background to standards for shackles
[NPL-DMM(A)-51] p 325 N93-11325
An evaluation of repair techniques used for uncontrolled longitudinal cracking and failed longitudinal joints
[PB92-205616] p 277 N93-12072
The mechanism of bolt loading
[NASA-TM-108377] p 342 N93-12412
Shear joint capability versus bolt clearance
[NASA-TM-108378] p 342 N93-12419
JOSEPHSON JUNCTIONS
High frequency response from YBa2Cu3O(7-x) Josephson devices on SrTiO3 bicrystal substrates
[NPL-DES-118] p 459 N93-11394
Superconducting multilayer structures grown by ALL-MBE
[DE92-018011] p 465 N93-12065
Josephson Junction digital waveform generation for very wideband radars
[AD-A253668] p 467 N93-12169
Nonlinear delay line phase shifters for terahertz superconductive electronic circuits
[AD-A255119] p 294 N93-12290
JUNCTION DIODES
Development of stable metallization systems
[AD-A253569] p 264 N93-11079
JUPITER (PLANET)
Modeling the Jovian aurora
[NASA-CR-190696] p 486 N93-11164
Multispectral observations of the Jovian aurora
p 487 N93-11167
JUPITER ATMOSPHERE
Modeling the Jovian aurora
[NASA-CR-190696] p 486 N93-11164
The role of proton precipitation in Jovian aurora: Theory and observation p 487 N93-11165
Multispectral observations of the Jovian aurora
p 487 N93-11167

K

K-EPSILON TURBULENCE MODEL
Simulation of compressible turbulent flows by a mixed finite element/finite volume method
[ETN-92-92267] p 299 N93-11362
Progress in developing a transition model for high-speed flows p 301 N93-11615
A comparison of velocity profile measurements in the CDIF diffuser with flow field model calculations
[DE92-015367] p 304 N93-11995
Application of a two-layer near wall model to fully developed and rotating channel turbulent flows
[NASA-CR-184441] p 305 N93-12082
Flow in curved ducts of varying cross-section
[AD-A254660] p 306 N93-12245
KALMAN FILTERS
The Kalman filter for two-dimensional stable and unstable atmospheres p 359 N93-11249
A monitor for the laboratory evaluation of control integrity in digital control systems operating in harsh electromagnetic environments
[NASA-TM-4402] p 215 N93-12304
Integration of radar altimeter, precision navigation, and digital terrain data for low-altitude flight
[NASA-TM-103958] p 205 N93-12320
Accuracy improvement of linear estimated motion using differential type sensors
[NAL-TR-1135] p 314 N93-12365
KENYA
Recent lessons on the safety and effectiveness of malaria chemoprophylaxis in a non-immune population
p 381 N93-11307
KETONES
Synthesis and conductivity of copolymer of 4,4'-diaminodiphenylamine and terephthaloyl chloride
[AD-A254880] p 273 N93-12440
KINEMATICS
A composite study of the Madden-Julian oscillation
[AD-A254269] p 369 N93-11819
Importance of numerosity and distribution of articulations within the digits, wrists, and arms of telemanipulators confronted with dextrous assembly tasks
p 330 N93-11967
KINETICS
Thermokinetic modelling and hypersonic flow
[DILC-EST-TN-218] p 196 N93-11157
KLYSTRONS
10 kW L-band amplifier tubes for efficient and reliable troposcatter communication transmitter systems
[AD-A253246] p 290 N93-11504
The development of a one microsecond pulse length, repetitively pulsed, high power modulator, and a long-pulse electron beam diode for the production of intense microwaves
[DE92-015974] p 293 N93-12089
KNOWLEDGE BASES (ARTIFICIAL INTELLIGENCE)
A knowledge-based blackboard system to interpret graphical data from vibration tests of gas turbines
[PNR-90993] p 212 N93-11114
Artificial intelligence and CFD: Expert systems for the design of airfoils and for grid generation
[DIGE-EST-TN-016] p 206 N93-11161

A rule-based system for real-time analysis of control systems
[NASA-TM-104258] p 277 N93-11619
Hypertext functionality: A theoretical framework
p 478 N93-11858
An expert system for diagnosing environmentally induced spacecraft anomalies p 230 N93-11927
An embedded rule-based diagnostic expert system in Ada p 392 N93-11928
Intelligent fault management for the Space Station active thermal control system p 391 N93-11930
Fuzzy control system for a remote focusing microscope p 314 N93-11934
Fuzzy logic control for camera tracking system
p 314 N93-11935
Intelligent data management for real-time spacecraft monitoring p 394 N93-11936
The development and technology transfer of software engineering technology at NASA. Johnson Space Center
p 396 N93-11943
System diagnostic builder p 396 N93-11944
Knowledge-based system V and V in the Space Station Freedom program p 396 N93-11945
Manager's assistant systems for space system planning p 398 N93-11952

KNOWLEDGE REPRESENTATION
Hypertext functionality: A theoretical framework
p 478 N93-11858
On the acquisition and representation of procedural knowledge p 394 N93-11937
Methodologies for building robust schedules
p 397 N93-11949
COMPASS: An Ada based scheduler
p 397 N93-11950

KORTEWEG-DEVRIES EQUATION
Inverse spectral transform for the 2 + 1-dimensional Gardner equation
[MATHS-REPT-A-138] p 425 N93-11323

L

LABORATORIES
Laboratory information management system proposal
[DE92-018243] p 478 N93-11796
Activity of the technical groups (LULI Palaiseau, France) p 322 N93-12052
X ray laser program, FY 1991
[AD-A255190] p 322 N93-12275

LAGRANGE COORDINATES
New singularity and existence of solutions in anisotropic, time-dependent, maximally Gauss-Bonnet extended gravity p 357 N93-11183

LAMINAR BOUNDARY LAYER
Overview of supersonic laminar flow control research on the F-16XL ships 1 and 2
[NASA-TM-104257] p 196 N93-11221
The hemisphere-cylinder at an angle of attack
p 196 N93-11250
Laminar boundary-layer breakdown
[AD-A254489] p 306 N93-12162
Carbon/carbon composition ablation effects on ionized boundary layers
[AD-A254465] p 242 N93-12235

LAMINAR FLOW
Application of laminar flow to aero engine nacelles
[PNR-90916] p 195 N93-11020
A combined experimental and theoretical study of laminar flow control with particular relevance to aero engine nacelles
[PNR-90991] p 195 N93-11070
A European collaborative NLF nacelle flight demonstrator
[PNR-90992] p 196 N93-11113
Overview of supersonic laminar flow control research on the F-16XL ships 1 and 2
[NASA-TM-104257] p 196 N93-11221
Numerical calculations of an axisymmetric laminar diffusion flame with detailed and reduced reaction mechanisms p 246 N93-11259
Direct numerical simulation of instabilities in parallel flow with spherical roughness elements
[NASA-TM-105847] p 300 N93-11529
Experimental investigation of the effects of aft blowing with various nozzle exit geometries on a 3.0 caliber tangent ogive at high angles of attack: Forebody pressure distributions
[NASA-CR-190935] p 197 N93-11605
Studies in nonlinear problems of energy
[DE92-018551] p 345 N93-11733
The twenty-third International Symposium on combustion
[AD-A250377] p 250 N93-11866
Boundary layer relaminarization device
[NASA-CASE-LAR-14470-1] p 199 N93-11876

LAMINATES
Generation of thermal strains in carbon fibre-reinforced bismaleimide (PMR-15) composites, part 1, 2 and 3
[PNR-90976-PT-1-2-3] p 236 N93-11065
Thermal residual stresses in silicon-carbide/titanium (0/90) laminate
[NASA-TM-107649] p 236 N93-11072
Mixed mode bending test of the interlaminar fracture toughness of carbon/epoxy
[FFA-TN-1992-04] p 237 N93-11128
Curing and mechanical properties of T800-V398 graphite/bismaleimide at different temperatures
[DLR-FB-92-02] p 237 N93-11143
An interlayer shear slip theory for composite laminates with nonrigid bonding p 237 N93-11229
Methods of analysis for thick-section composite structures p 237 N93-11262
Aerospatiale processes for three dimensional preforms
[REPT-921-430-147] p 239 N93-11590
Global-local finite element analysis of composite structures
[DE92-019138] p 240 N93-11658
Effect of assembly anomalies on the strain response of composites in the sphere joint region of the DARPA man-rated demonstration article
[AD-A254204] p 240 N93-11739
Micromechanisms of deformation and fracture in aluminum based MMC's: Interface effects
[AD-A253560] p 259 N93-11850
ICAN/DAMP-integrated composite analyzer with damping analysis capabilities: User's manual
[NASA-TP-3292] p 241 N93-12015
Composite failure analysis handbook. Volume 2: Technical handbook. Part 3: Case histories
[AD-A249131] p 241 N93-12054
Superconducting multilayer structures grown by ALL-MBE
[DE92-018011] p 465 N93-12065
Linear and geometrically nonlinear p-version three dimensional curved shell element for isotropic, generally orthotropic and laminated composite materials
p 339 N93-12194
Fracture toughness testing of polymer matrix composites
[NASA-TP-3199] p 243 N93-12302

LANDAU DAMPING
Direct electron absorption of fast waves on the D3-D tokamak
[DE92-016254] p 449 N93-11041

LANDFORMS
Seismic wave propagation in thinly-layered media with steep reflectors
[DE92-015619] p 364 N93-12142

LANDING GEAR
Fatigue crack growth in AerMet 100 steel
[AD-A249068] p 261 N93-12248

LANDSAT SATELLITES
Land use/land cover classification using digitally merged spot panchromatic and Landsat thematic mapper imagery
[PB92-188416] p 343 N93-11701

LANGUAGE PROGRAMMING
Optimization of expressions involving array classes
[DE92-019421] p 411 N93-11536
Interfacing Matlab and software written in other languages
[NPL-DITC-200/92] p 412 N93-11668
Syntax and lexis of the specification language Z
[RSRE-MEMO-4367] p 414 N93-12326

LANGUAGES
On understanding in communicating systems and the error in the Chinese Room thought-experiment
[RSRE-MEMO-4391] p 278 N93-10977

LANTHANUM COMPOUNDS
The synthesis and crystal structure of LaHSe2O6, a layered, anhydrous selenite
[AD-A251050] p 458 N93-10996

LANTHANUM OXIDES
Intermediate temperature electrolytes for SOFC
[DE92-018786] p 345 N93-11571

LAP JOINTS
An evaluation of the blind lap joint for the surface mount attachment of chip components
[DE92-017045] p 277 N93-12106

LAPLACE EQUATION
An approximate solution of the fixed gravimetric boundary value problem in the interior and the exterior of the Earth's body
[SER-C-379] p 361 N93-11331

LARGE SCALE INTEGRATION
High-frequency LSI contactor
[DE92-017285] p 292 N93-11916

LARGE SPACE STRUCTURES
Tests of an alternate mobile transporter and extravehicular activity assembly procedure for the Space Station Freedom truss
[NASA-TP-3245] p 224 N93-10970
Structural dynamics of large space structures having parametric uncertainties p 225 N93-11836
Dynamic test/analysis correlation using reduced analytical models
[NASA-TM-107671] p 341 N93-12300
Advanced two-phase heat transfer systems
p 229 N93-12459

LASER ABLATION
Interpretation of experiments measuring the back face of thin aluminum strips by comparison with numerical simulations p 318 N93-12029
Laser-ablation processes
[DE92-011226] p 322 N93-12250

LASER APPLICATIONS
Method of remotely characterizing thermal properties of a sample
[NASA-CASE-LAR-13508-3-CU] p 216 N93-11057
UCSB FEL user mode adaption project
[AD-A248734] p 316 N93-11418
Center of Excellence in laser medicine
[DE92-018760] p 384 N93-11445
Laser glasses
[DE92-018061] p 267 N93-11549
Temperature tracking SPICE macro-model for laser and LED driven opto-coupler assemblies
[DE92-019296] p 411 N93-11599
Diagnostics and modeling of H(-) ion sources
[AD-A250664] p 440 N93-11867
Novel nonlinear laser diagnostic techniques
[AD-A254709] p 323 N93-12335
Development summary of a sympathetic discharge CO2 laser for lidar use
[NASA-CR-184433] p 323 N93-12516

LASER BEAMS
High frame-rate, large field wavefront sensor
[DE92-019547] p 310 N93-11542
A single beam laser tracker as an alignment tool
[DE92-017746] p 316 N93-11691
Matter-wave interferometry with laser cooled atoms
[AD-A253999] p 316 N93-11737

LASER CAVITIES
A study of the CO2 laser near threshold
p 316 N93-11720

LASER DAMAGE
Optical limiting
[AD-A254620] p 322 N93-12238

LASER DOPPLER VELOCIMETERS
LV software support for supersonic flow analysis
[NASA-CR-190209] p 297 N93-11074
An experimental study of flow patterns and endwall heat transfer upstream of a surface-mounted rectangular obstruction in a turbulent boundary layer
p 302 N93-11698
Laser Doppler experiments
[AD-A252883] p 287 N93-12461

LASER GYROSCOPES
Development of a GPS-aided motion measurement, pointing, and stabilization system for a synthetic aperture radar
[DE92-017053] p 204 N93-11152

LASER INDUCED FLUORESCENCE
State-resolved dynamics of ion-molecule collisions in a flowing afterglow
[AD-A247288] p 436 N93-11467
Novel nonlinear laser diagnostic techniques
[AD-A254709] p 323 N93-12335
Hypersonic flow diagnostic development
[AD-A255045] p 202 N93-12466

LASER MATERIALS
Preparation, optical and laser properties of Nd-doped sol-gel silica
[DE92-019378] p 461 N93-11602
High bandwidth second-harmonic generation in partially deuterated KDP
[DE92-019505] p 452 N93-11645
Development of a hydrodynamic code: MINNIE
p 318 N93-12031
Studies of a laser/nuclear thermal hardened body armor
[AD-A255128] p 390 N93-12423

LASER MICROSCOPY
Study of residual stresses and microcracks in high strength steel weldments: An investigation of microcrack formation and stressed growth using laser microscopy
[AD-A255059] p 342 N93-12467

LASER MODE LOCKING
CO2 laser frequency doubling
[AD-A251060] p 314 N93-10997

LASER OUTPUTS
CO2 laser frequency doubling
[AD-A251060] p 314 N93-10997

UCSB FEL user mode adaption project
[AD-A248734] p 316 N93-11418

Experimental studies of x ray laser spectral profiles: Observation of gain narrowing and saturation behavior
[DE92-019603] p 316 N93-11659

Prediction of electromagnetic pulse generation by picosecond avalanches in high-pressure air
[DE92-019382] p 282 N93-11675

Preliminary study of the homogeneity of the density and temperature of long plasmas used for X laser studies
p 320 N93-12044

Experimental study of x ray laser in lithumoid aluminum p 321 N93-12045

Research on stimulated Raman scattering with applications to atmospheric lidar p 322 N93-12163

LASER PLASMA INTERACTIONS

Topics in high-intensity laser plasma interaction
p 450 N93-11191

The 1989 Scientific Report of the Laboratory for the Use of High Power Lasers
[ETN-92-92175] p 317 N93-12023

Study of filamentation in subdense plasma interaction experiments p 318 N93-12026

X pulse radiation around the critical surface
p 318 N93-12027

Interpretation of experiments measuring the back face of thin aluminum strips by comparison with numerical simulations p 318 N93-12029

Development of a hydrodynamic code: MINNIE
p 318 N93-12031

Laser material interaction in confined medium
p 319 N93-12035

LASER PLASMAS

X ray diagnostic techniques in ICF
[DE92-018069] p 449 N93-10975

Topics in high-intensity laser plasma interaction
p 450 N93-11191

High energy x ray imaging diagnostic on Nova
[DE92-018067] p 451 N93-11495

Development of a new plasma diagnostic of the critical surface and studies of the ion acoustic decay instability using collective Thomson scattering
[DE92-018526] p 453 N93-11731

The 1989 Scientific Report of the Laboratory for the Use of High Power Lasers
[ETN-92-92175] p 317 N93-12023

Stimulated Brillouin backscattering instability in the case of a high power laser: Application to wave pulsation particle acceleration experiments p 317 N93-12024

Observation and analysis of the Stokes and anti-Stokes components of stimulated Raman backscattering
p 318 N93-12025

Study of filamentation in subdense plasma interaction experiments p 318 N93-12026

X-UV spectroscopy temporal resolution
p 318 N93-12028

Development of a hydrodynamic code: MINNIE
p 318 N93-12031

Nonlinear behavior of resonant absorption in a plasma at microwave frequency p 319 N93-12032

Low pressure gas multiphotoionization for wave packet experiments p 319 N93-12034

Absorption spectroscopy of L(alpha, beta) transitions in a laser germanium plasma p 320 N93-12041

Saturation effects in absorption spectroscopy of the K(alpha) rays of aluminum p 254 N93-12042

Preliminary study of the homogeneity of the density and temperature of long plasmas used for X laser studies
p 320 N93-12044

Modeling for the study of an X laser in a recombination plasma; gain calculations at 105.7 and 154.6 A
p 321 N93-12046

Hydrodynamic study of multilayer targets by spatial and temporal resolution shadow spectroscopy
p 254 N93-12050

A ring coded-aperture microscope for high-resolution imaging of high-energy x rays
[DE92-018004] p 454 N93-12059

Plasma temperatures from first-hit neutron time-of-flight spectra
[DE92-018006] p 454 N93-12060

LASER PUMPING

CO2 laser frequency doubling
[AD-A251060] p 314 N93-10997

Preparation, optical and laser properties of Nd-doped sol-gel silica
[DE92-019378] p 461 N93-11602

LASER RANGER/TRACKER

Analysis of lunar laser ranging in the framework of a post-Newtonian theory
[SER-C-383] p 315 N93-11332

A single beam laser tracker as an alignment tool
[DE92-017746] p 316 N93-11691

LASER SPECTROSCOPY

Laser spectroscopy and dynamics of transient species formed in pyrolysis reactions
[DE92-016206] p 251 N93-12091

On-line analysis of chemical composition using an FT-Raman spectrometer in the near-IR
[DE92-016503] p 253 N93-12311

Novel nonlinear laser diagnostic techniques
[AD-A254709] p 323 N93-12335

Characterization of underivatized pterins by laser desorption Fourier transform mass spectrometry
[DE92-016785] p 323 N93-12514

LASER STABILITY

Stimulated Brillouin backscattering instability in the case of a high power laser: Application to wave pulsation particle acceleration experiments p 317 N93-12024

LASER TARGET INTERACTIONS

Laser material interaction in confined medium
p 319 N93-12035

Study of the dynamic degradation under the action of a shock wave induced by pulsed laser
p 319 N93-12037

Shock waves induced by pulsed laser in confined interaction: Numerical simulation p 319 N93-12038

Laser-ablation processes
[DE92-011226] p 322 N93-12250

LASER TARGETS

X ray diagnostic techniques in ICF
[DE92-018069] p 449 N93-10975

Nova Upgrade: A proposed ICF facility to demonstrate ignition and gain, revision 1
[DE92-018960] p 451 N93-11534

Hydrodynamic efficiencies in implosion experiments
p 308 N93-12030

LASER WEAPONS

Computation of small scale velocity turbulence and its effect on optical scintillations and stimulated thermal Rayleigh scattering
[DE92-018934] p 448 N93-11627

Studies of a laser/nuclear thermal hardened body armor
[AD-A255128] p 390 N93-12423

LASERS

Hot-wire vs laser, is there a difference?
[DE92-019337] p 310 N93-11554

Laser surface profilometer with sub-Angstrom resolution
[DE92-018926] p 317 N93-12011

LASING

Progress toward x ray lasing between autoionizing transitions
[DE92-017428] p 317 N93-11765

Atomic structure of Ni-like soft x ray lasing ions
[DE92-019273] p 438 N93-11778

LATE STARS

Stars in the Rosat all-sky survey p 482 N93-11477

LATERAL CONTROL

Optimal output feedback vibration control of rotor-bearing systems p 324 N93-11220

LATTICES (MATHEMATICS)

Design of a lattice-based faceted classification system
p 415 N93-12385

LAUNCH VEHICLES

Lightweight Exoatmospheric Projectile (LEAP) test program. Supplemental environmental assessment
[AD-A252286] p 231 N93-10998

Rocket Based Combined Cycle (RBCC) Propulsion Workshop, volume 2
[NASA-CR-184383] p 231 N93-11043

LAUNCHERS

Numerical simulation for the coaxial electromagnetic launcher using hybrid potentials with FE-BE method
p 222 N93-11726

LAVA

Physical characterization of magmatic liquids
[DE92-015931] p 363 N93-11848

LAYERS

The synthesis and crystal structure of LaHSe2O6, a layered, anhydrous selenite
[AD-A251050] p 458 N93-10996

Evaluation of multilayer mask concept for RESPO 21
[AD-A253392] p 389 N93-12079

LAYOUTS

VLSI design for reliability
[AD-A253207] p 292 N93-11781

LEAD ACID BATTERIES

Results of advanced battery technology evaluations for electric vehicle applications
[DE92-018766] p 289 N93-11432

Laboratory testing of the electrosource traction battery
[DE92-017993] p 292 N93-12057

LEAD OXIDES

A study of parameters that influence growth and stability of the (Bi(1-x)Pb(x))2 Sr2Ca2Cu3O(y) phase
[DE92-015187] p 462 N93-11703

LEAD TITANATES

The domain structure features of epitaxial PbTiO3 thin films prepared by MOCVD
[DE92-010907] p 459 N93-11190

LEADING EDGES

The convection speed of the dynamic stall vortex
[AD-A247258] p 197 N93-11464

Flight test results from a supercritical mission adaptive wing with smooth variable camber
[NASA-TM-4415] p 207 N93-11863

Boundary layer relaminarization device
[NASA-CASE-LAR-14470-1] p 199 N93-11876

An approach to constrained aerodynamic design with application to airfoils
[NASA-TP-3260] p 201 N93-12321

Thermostructural applications of heat pipes for cooling leading edges of high-speed aerospace vehicles
p 229 N93-12460

LEAKAGE

Test program, helium II orbital resupply coupling
[NASA-CR-185681] p 326 N93-11650

Space Station Freedom seal leakage rate analysis and testing summary: Air leaks in ambient versus vacuum exit conditions
[NASA-TM-103604] p 328 N93-12149

Sealing characteristics of a carbon segmented circumferential seal for a liquid oxygen turbopump
[NAL-TR-1130] p 329 N93-12364

An experimental study of a small high speed LH2 rocket pump: Fundamental mechanical design
[NAL-TR-1123] p 330 N93-12463

Railgun armature velocity improvement, SBIR phase 2
[AD-A254749] p 222 N93-12505

LEARNING

Questioning mechanisms during complex learning
[AD-A247382] p 386 N93-11415

LEAST SQUARES METHOD

QR decomposition based algorithms and architectures for least-squares adaptive filtering
[RSRE-MEMO-4562] p 408 N93-11390

EUROMET project no. 231: Uncertainties in mass measurement. NPL's analysis of data from the calibration of weight set NPLW43
[NPL-MOM-107] p 432 N93-11666

LEGENDRE FUNCTIONS

Orthogonal functions over the oceans and applications to the determination of orbit error, geoid and sea surface topography from satellite altimetry p 373 N93-12002

LENS DESIGN

Analysis of advanced optical glass and systems
[NASA-CR-184434] p 448 N93-12201

LENSES

A preliminary study associated with the experimental measurement of the aero-optic characteristics of hypersonic configurations
[AD-A253792] p 200 N93-12063

Analysis of advanced optical glass and systems
[NASA-CR-184434] p 448 N93-12201

LIE GROUPS

An isomorphism for algebra of distributions with compact support on Lie groups
[DE92-603605] p 427 N93-12176

LIFE (DURABILITY)

A creep cavity growth model for creep-fatigue life prediction of a unidirectional W/Cu composite
[NASA-TM-105780] p 333 N93-10967

The use of life cycle costing for the acquisition of non-major systems at the Naval Regional Contracting Center Detachment
[AD-A255170] p 480 N93-12473

LIFE CYCLE COSTS

Role of automation in the ACRV operations
p 230 N93-11977

The use of life cycle costing for the acquisition of non-major systems at the Naval Regional Contracting Center Detachment
[AD-A255170] p 480 N93-12473

LIFE SCIENCES

Fifth Annual Workshop on Space Operations Applications and Research (SOAR 1991), volume 1
[NASA-CP-3127-VOL-1] p 391 N93-11921

LIFE SUPPORT SYSTEMS

Submarine Advanced Integrated Life Support system (SAILS) program
[AD-A253564] p 388 N93-11812

LIFT

Experiments on low aspect ratio hydroplanes to measure lift under static and dynamic conditions
[ARE-TM(UHR)-90306] p 197 N93-11365

Lift coefficient of a randomly oscillating hydroplane
[DRA/MAR-TM(MTH)-91320] p 197 N93-11377

A wind tunnel investigation to determine buffet countermeasures for STOL aircraft alpha-sweep flight testing
[NAL-TR-1129] p 216 N93-12362

LIFT DEVICES
The theoretical background to BS7167: 1990 - specification for Bordeaux connections
[NPL-DMM(A)-50] p 325 N93-11324
A study of the effects of tolerances on rigging screws, turnbuckles, and associated components in BS4429: 1987
[NPL-DMM(A)-53] p 325 N93-11326
LIFT DRAG RATIO
Physiologically constrained aerocapture for manned Mars missions p 226 N93-12185
LIFTING BODIES
New acceleration potential method for supersonic unsteady aerodynamics of lifting surfaces, further extension of the nonplanar supersonic doublet point method, and nonlinear, nongradient optimized rational function approximations for supersonic, transient response unsteady aerodynamics p 201 N93-12344
LIFTING ROTORS
Studies of a flat wake rotor theory
[NASA-CR-190936] p 201 N93-12343
LIGANDS
Growth of 2-6 thin-films from single-source precursors based on sterically encumbered sitel ligands
[DE92-017077] p 466 N93-12099
LIGHT (VISIBLE RADIATION)
CO2 laser frequency doubling
[AD-A251060] p 314 N93-10997
Near-IR absorption spectra for the C70 fullerene anions
[AD-A253658] p 246 N93-11280
Observation of pulses propagating at supraluminous speed in an optical fiber p 320 N93-12040
LIGHT AMPLIFIERS
Organization of the Optical Society of America Photonic Science Topical Meeting Series. Volume 14: Photorefractive materials effects, and devices
[AD-A253001] p 446 N93-11071
Chinese Journal of Lasers (selected articles)
[AD-A254100] p 317 N93-11786
LIGHT BEAMS
High frame-rate, large field wavefront sensor
[DE92-019547] p 310 N93-11542
A computer algorithm for automatic beam steering
[DE92-019338] p 411 N93-11555
Dynamic vacuum analysis for APS high heat flux beamline front ends using optical ray-tracing simulation methods
[DE92-019032] p 445 N93-11831
LIGHT EMITTING DIODES
Radiation damage by high energy electrons in GaAs: A DLTS (deep level transient spectroscopy) examination
[HMI-B-494] p 442 N93-11028
Temperature tracking SPICE macro-model for laser and LED driven opto-coupler assemblies
[DE92-019296] p 411 N93-11599
LIGHT GAS GUNS
Operating characteristics of a 7.6 mm (0.30 inch) diameter two-stage light-gas gun
[DE92-018783] p 217 N93-11447
LIGHT MODULATION
Resonant membrane spatial light modulators
[AD-A253893] p 252 N93-12186
LIGHT SCATTERING
Hydrodynamic fluctuations and light scattering in hot electron gas of semiconductors
[DE92-622800] p 458 N93-10992
Evaluation of an analytical model for predicting light scattering from cylindrically-shaped objects in the ocean
[AD-A248414] p 447 N93-11489
Electronic transport and lasing in microstructures
[DE92-018725] p 441 N93-12115
Studies of a laser/nuclear thermal hardened body armor
[AD-A255128] p 390 N93-12423
Light scattering from a sphere on or near an interface p 448 N93-12531
LIGHT SOURCES
Generation of 3-D surface maps in waste storage silos using a structured light source p 399 N93-11958
LIGHT TRANSMISSION
Evaluation of an analytical model for predicting light scattering from cylindrically-shaped objects in the ocean
[AD-A248414] p 447 N93-11489
Research on stable, high-efficiency, amorphous silicon multijunction modules
[DE92-010599] p 464 N93-11818
Development of ultra-low noise, high sensitivity planar metal grating coupled AlGaAs/GaAs multiquantum well IR detectors for focal plane array staring IR sensor systems
[AD-A254697] p 468 N93-12228
LIGHTNING
Numerical computation of the lightning response of an earth-covered munitions storage bunker and comparison with experiments
[DE92-014268] p 367 N93-11236
Lightning threat warning system at the Tonopah Test Range
[DE92-040444] p 221 N93-11631
Rocket-triggered lightning test of an earth-covered munitions storage bunker
[DE92-016790] p 369 N93-11678
Weather impacts on space operations
[AD-A253720] p 371 N93-12170
Temporal monitoring of VHF and LF atmospherics and their relation to lightning
[AD-A252617] p 371 N93-12180
A monitor for the laboratory evaluation of control integrity in digital control systems operating in harsh electromagnetic environments
[NASA-TM-4402] p 215 N93-12304
LIMITS (MATHEMATICS)
Implicit parallelism in genetic algorithms
[REPT-92-012] p 418 N93-11180
LINE SHAPE
Lyman alpha line shapes from electron impact H2 dissociative processes in the Jovian auroral zone
p 487 N93-11166
LINE SPECTRA
Lyman alpha line shapes from electron impact H2 dissociative processes in the Jovian auroral zone
p 487 N93-11166
Scattering of electromagnetic waves from a plasma: Enhanced ion acoustic fluctuations due to ion-ion two-stream instabilities p 361 N93-11272
On the origin of ion acoustic turbulence in the auroral topside ionosphere p 361 N93-11273
A multi-line study of the molecular interstellar medium on M82's starburst nucleus
[MPE-PREPRINT-213] p 484 N93-11347
Potassium D-line fitting for investigation of MHD boundary layers
[DE92-019020] p 454 N93-11826
LINEAR ACCELERATORS
Higher-order-mode damping and microwave absorption at 2 K
[DE92-016960] p 442 N93-11077
Experimental and theoretical investigation of high gradient acceleration
[DE92-015299] p 315 N93-11278
The foxhole accelerating structure
[DE92-019052] p 443 N93-11429
Application of the Moyer method to transverse shielding of linear Bremsstrahlung sources
[DE92-017027] p 443 N93-11493
Alternating-phase focusing: A model to study nonlinear dynamics
[DE92-019027] p 431 N93-11511
Analysis of the prebuncher for the KEK 40-MeV proton linac
[DE92-514988] p 444 N93-11525
Research and development of superconducting linear accelerators for neutral particle beam applications
[DE92-019043] p 444 N93-11652
The diagnostics system for the multiple heavy ion beams induction linac experiment, MBE-4
[DE92-017109] p 445 N93-12126
Pre-compression of bunch length in the SLC damping rings
[DE92-018154] p 446 N93-12497
LINEAR ENERGY TRANSFER (LET)
An accurate and efficient method to calculate the rate of single event upsets from the LET spectrum and SEU cross section test results
[AD-A253917] p 290 N93-11492
LINEAR EQUATIONS
Perturbation theory for the solution of systems of linear equations
[AD-A254994] p 428 N93-12511
LINEAR POLARIZATION
Colliding plane gravitational waves with colinear polarization
[MATHS-REPT-A-160] p 357 N93-11120
LINEAR QUADRATIC REGULATOR
Optimal output feedback vibration control of rotor-bearing systems p 324 N93-11220
LINEAR SYSTEMS
On a certain McMillan degree condition appearing in control
[MATHS-REPT-A-170] p 424 N93-11125
The efficient parallel iterative solution of large sparse linear systems
[DE92-018769] p 425 N93-11446
Krylov subspace methods for complex non-Hermitian linear systems
[NASA-CR-190931] p 409 N93-11458
A game theoretic approach to linear dynamic estimation p 340 N93-12200
Perturbation theory for the solution of systems of linear equations
[AD-A254994] p 428 N93-12511
LINEARIZATION
The basic equations for a four component magnetoplasma flow with non equilibrium ionization
[IPF-91-1] p 449 N93-11102
Remarks on the Robinson-Trautman solutions
[MATHS-REPT-A-167] p 423 N93-11122
Computational nonlinear control
[AD-A253547] p 422 N93-12258
LINGUISTICS
Ontology of mind, subjective ontology, and the example of temporal expressions
[REPT-92-018] p 386 N93-11212
LININGS
On the stability of confined shells under external pressure p 335 N93-11202
The design and commissioning of an acoustic liner for propeller noise testing in the ARA transonic wind tunnel
[PNR-90880] p 433 N93-11204
LINKAGES
Synthesis and side chain liquid crystal polymers by living ring opening metathesis polymerization. 5: Influence of mesogenic group and interconnecting group on the thermotropic behavior of the resulting polymers
[AD-A253568] p 264 N93-11150
The theoretical background to BS7167: 1990 - specification for Bordeaux connections
[NPL-DMM(A)-50] p 325 N93-11324
LIQUID ATOMIZATION
Coaxial injector spray characterization using water/air as simulants p 248 N93-11452
Experimental investigation of rocket injector atomization p 248 N93-11454
LIQUID CHROMATOGRAPHY
An evaluation of field-flow fractionation for molecular weight characterization of polymeric materials
[DE92-019192] p 267 N93-11497
LIQUID CRYSTALS
Synthesis and side chain liquid crystal polymers by living ring opening metathesis polymerization. 5: Influence of mesogenic group and interconnecting group on the thermotropic behavior of the resulting polymers
[AD-A253568] p 264 N93-11150
Synthesis of side chain liquid crystal polymers by living ring opening metathesis polymerization. Report 3: Influence of molecular weight, interconnecting unit and substituent on the mesomorphic behavior of polymers with laterally attached mesogens
[AD-A248698] p 265 N93-11187
Synthesis of side chain liquid crystal polymers by living ring opening metathesis polymerization. Report 2: Influence of molecular weight, polydispersity, and flexible spacer length (n=9-12) on the thermotropic behavior of the resulting plymers
[AD-A248700] p 265 N93-11188
Chemical reactions and properties of organosilicon compounds related to new materials
[AD-A253233] p 246 N93-11218
LIQUID FLOW
Operating experience using venturi flow meters at liquid helium temperature
[DE92-014693] p 313 N93-12140
LIQUID FUELS
Metal slurry droplet and spray combustion
p 245 N93-11138
LIQUID HELIUM
Tables of thermodynamic properties of helium magnet coolant, revision A
[DE92-019098] p 471 N93-11656
Operating experience using venturi flow meters at liquid helium temperature
[DE92-014693] p 313 N93-12140
LIQUID HELIUM 2
Test program, helium II orbital resupply coupling
[NASA-CR-185681] p 326 N93-11650
LIQUID METALS
Infiltration kinetics and interfacial bond strength of metal matrix composites
[AD-A254002] p 240 N93-11795
LIQUID NITROGEN
Experimental investigation of rocket injector atomization p 248 N93-11454
Test program, helium II orbital resupply coupling
[NASA-CR-185681] p 326 N93-11650
LIQUID OXYGEN
CFD modeling of turbulent flows around the SSME main injector assembly using porosity formulation
[NASA-CR-184359] p 297 N93-11171
LIQUID PROPELLANT ROCKET ENGINES
Solution of two-phase reacting flow in liquid thrust chambers p 235 N93-11449

A summary of the JANNAF workshop on diagnostics p 248 N93-11451
Coaxial injector spray characterization using water/air as simulants p 248 N93-11452
Combustion characteristics of the LO2/GCH4 fuel-rich preburners for staged combustion cycle rocket engines [NAL-TR-1124] p 234 N93-12368
Characteristics of heat transfer to nickel plated chamber walls of high pressure rocket combustors [NAL-TR-1126T] p 234 N93-12372
Users manual for program NYQUIST: Liquid rocket nyquist plots developed for use on a PC computer [NASA-CR-184451] p 235 N93-12522

LIQUID ROCKET PROPELLANTS
The 28th JANNAF Combustion Subcommittee Meeting, volume 1 [CPIA-PUBL-573-VOL-1] p 244 N93-11132
The 28th JANNAF Combustion Subcommittee Meeting, volume 2 [CPIA-PUBL-573-VOL-2] p 247 N93-11448
Solution of two-phase reacting flow in liquid thrust chambers p 235 N93-11449
Physical processes involved in injection and atomization of liquid propellants p 248 N93-11453
Experimental investigation of rocket injector atomization p 248 N93-11454
An experimental study of droplet dispersion in turbulent flows p 248 N93-11455
Impact ignition of liquid propellants [AD-A252299] p 249 N93-11490
Soviet chemical propellant research and development [PB92-195577] p 275 N93-12147

LIQUID-LIQUID INTERFACES
Liquid-liquid equilibria in binary systems: Monte-Carlo simulation for calculating the effect of nonrandom mixing [DE92-017020] p 263 N93-10972
The physics of pattern formation at liquid interfaces [DE92-016971] p 462 N93-11747

LIQUID-SOLID INTERFACES
Electron transfer rates at semiconductor/liquid interfaces [DE92-018559] p 289 N93-11438

LIQUID-VAPOR INTERFACES
Interfacial area and two-phase flow structure development measured by a double-sensor probe [DE92-019459] p 300 N93-11538

LIQUIDS
Liquid-liquid equilibria in binary systems: Monte-Carlo simulation for calculating the effect of nonrandom mixing [DE92-017020] p 263 N93-10972
Natural convection heat transfer studies of simulated and actual electronic components using dielectric liquids for immersion cooling [AD-A255173] p 341 N93-12376

LISP (PROGRAMMING LANGUAGE)
Higher-order generic functions for CLOS [DE92-013447] p 413 N93-12137

LITHIUM ALLOYS
Evaluation of flotation for purification of pyrite for use in thermal batteries [DE92-019330] p 290 N93-11553

LITHIUM CHLORIDES
Synthesis and characterization of novel aluminum-arsenic compounds 2. Crystal structures of (R2AlAs (SiMe3)2)2 (R = i-Bu, Me) and i-Bu2 (Cl)Al*As (SiMe3)3 [AD-A248001] p 467 N93-12175

LITHIUM OXIDES
Overcharge and overdischarge protection of ambient temperature secondary lithium cells [NASA-CASE-NPO-18343-1-CU] p 290 N93-11456

LITHOGRAPHY
Organization of the Optical Society of America Photonic Science Topical Meeting Series. Volume 14: Photorefractive materials effects, and devices [AD-A253001] p 446 N93-11071

LOAD DISTRIBUTION (FORCES)
The dressing of resin bonded diamond grinding wheels [PNR-90965] p 264 N93-11086
Crashworthy characteristics of circular tubes in axisymmetric buckling p 337 N93-11721

LOAD TESTING MACHINES
Method and apparatus for gripping test specimens [NASA-CASE-LEW-15345-1] p 329 N93-12327

LOAD TESTS
Testing for integrity [PNR-90927] p 210 N93-11024
Mixed mode bending test of the interlaminar fracture toughness of carbon/epoxy [FFA-TN-1992-04] p 237 N93-11128
Engine testing of ceramic cam-roller followers [DE92-019188] p 268 N93-11735
An evaluation of the blind lap joint for the surface mount attachment of chip components [DE92-017045] p 277 N93-12106
Fracture toughness testing of polymer matrix composites [NASA-TP-3199] p 243 N93-12302
Verification of rain-flow reconstructions of a variable amplitude load history [NASA-CR-189670] p 341 N93-12411

LOADS (FORCES)
Fiber peel force measuring apparatus [AD-D015349] p 309 N93-11048
The technical background to standards for eyebolts [NPL-DMM(A)-52] p 325 N93-11327
Loads from the detonation of hydrogen-air-steam mixtures [DE92-019318] p 249 N93-11551
Computational dynamics of high-speed flexible multibody systems p 338 N93-11891
Self mobile space manipulator project p 331 N93-11973
The mechanism of bolt loading [NASA-TM-108377] p 342 N93-12412
Shear joint capability versus bolt clearance [NASA-TM-108378] p 342 N93-12419

LOCAL AREA NETWORKS
Data archiving and analysis for CWDD [DE92-017064] p 473 N93-11104
Photonics and other approaches to high speed communications [NASA-CR-190362] p 279 N93-11116
A simple, effective media access protocol system for integrated, high data rate networks p 279 N93-11119
The engine design engine. A clustered computer platform for the aerodynamic inverse design and analysis of a full engine [NASA-TM-105838] p 196 N93-11223

LOCAL THERMODYNAMIC EQUILIBRIUM
Internal variables in the local-equilibrium approximation [DE92-016854] p 471 N93-12102

LOCOMOTION
Self mobile space manipulator project p 331 N93-11973

LOGIC CIRCUITS
A formal definition of the static semantics of ELLA's core [RSRE-91024] p 409 N93-11436
High-frequency LSI contactor [DE92-017285] p 292 N93-11916
Electromagnetic launcher control using finite state machines [AD-A254433] p 222 N93-12161
Formal specification of the VIPER microprocessor in HOL [RSRE-90009] p 405 N93-12430

LOGISTICS
Research and development strategies for human centered and group support technologies [AD-A254366] p 472 N93-12273

LOGISTICS MANAGEMENT
LINK user manual [DE92-017987] p 479 N93-12143
Research and development strategies for human centered and group support technologies [AD-A254366] p 472 N93-12273

LONG DURATION EXPOSURE FACILITY
Compositional analysis and classification of projectile residues in LDEF impact craters [NASA-TM-104750] p 488 N93-11374
A model to estimate the flux of background particles expected to accumulate on the collector foils of the interstellar gas experiment on the long duration exposure facility spacecraft [AD-A254265] p 489 N93-11815
Analysis of surfaces from the LDEF A0114, phase 2 [NASA-CR-190596] p 270 N93-11993
Erosion rates for polymers measured on LDEF p 270 N93-11994
Analysis of materials from MSFC LDEF experiments [NASA-CR-184425] p 252 N93-12215

LONG TERM EFFECTS
Orbit perturbations due to an axi-symmetric gravitational field, analyzed over extended periods of time [RAE-TM-SPACE-386] p 220 N93-11486

LONG WAVE RADIATION
INAS hole-immobilized doping superlattice long-wave-infrared detector [NASA-CASE-NPO-17880-1-CU] p 458 N93-11056
A composite study of the Madden-Julian oscillation [AD-A254269] p 369 N93-11819

LOOP ANTENNAS
Radio pill antenna range test [DE92-019903] p 282 N93-11661

LORAN
LORAN and the effects of terrestrial propagation [PB92-197219] p 205 N93-11472

LOUDNESS
Laboratory study of effects of sonic boom shaping on subjective loudness and acceptability [NASA-TP-3269] p 434 N93-11620

LOW ALTITUDE
The design, development, and test of balloonborne and groundbased lidar systems. Volume 3: Groundbased lidar systems [AD-A247552] p 317 N93-11805
Integration of radar altimeter, precision navigation, and digital terrain data for low-altitude flight [NASA-TM-103958] p 205 N93-12320

LOW ASPECT RATIO
Shafranov shift in low-aspect-ratio heliotron/torsatron CHS [DE92-782100] p 451 N93-11277
Experiments on low aspect ratio hydroplanes to measure lift under static and dynamic conditions [ARE-TM(UHR)-90306] p 197 N93-11365

LOW CARBON STEELS
Relationship of bainitic microstructure to impact toughness in Cr-Mo and Cr-W steels [DE92-017828] p 258 N93-11773

LOW COST
Electromagnetic launcher control using finite state machines [AD-A254433] p 222 N93-12161

LOW FREQUENCIES
Temporal monitoring of VHF and LF atmospherics and their relation to lightning [AD-A252617] p 371 N93-12180

LOW LEVEL TURBULENCE
Summary of findings from the PIREP-based analyses conducted during the 1988 to 1990 evaluations of TDWR-based and TDWR/LLWAS-based alert services provided to landing/departing pilots [AD-A253859] p 367 N93-11144

LOW PASS FILTERS
Broadband EMP transient measurement preemphasis filter [AD-A254414] p 284 N93-12160

LOW PRESSURE
Low pressure gas multiphotoionization for wave packet experiments p 319 N93-12034

LOW SPEED WIND TUNNELS
The 13 ft by 9 ft low speed wind tunnel facility at DRA (Aerospace Division) Bedford (England) [RAE-TM-AERO-2228] p 199 N93-11883
Acoustical evaluation of the NASA Lewis 9 by 15 foot low speed wind tunnel [NASA-TP-3274] p 218 N93-12016
Simulation analysis of a cable-mount system used for dynamic wind tunnel tests [NAL-TR-1127] p 219 N93-12359

LOW TEMPERATURE
Triisopropylindium: Decomposition study and use for low temperature growth [AD-A250666] p 464 N93-11869
Nanophase ceramics [AD-A254661] p 272 N93-12246
Effectiveness of NASA 1032 and 1035 and Air Force 1030 and 1034 units in protection against cold water hypothermia [AD-A255120] p 389 N93-12291
Erasable optical information storage in the polyanilines [AD-A254873] p 480 N93-12438

LOW THRUST PROPULSION
Closed form low-thrust trajectories for Mars missions [DE92-017431] p 232 N93-11766

LUBRICANTS
A test facility for the thermofluid-dynamics of gas bearing lubrication films [PNR-90897] p 263 N93-11032
Thermal non-Newtonian elastohydrodynamic lubrication of line contacts under sliding-rolling and simple sliding conditions p 324 N93-11263

LUBRICATION
Thermal non-Newtonian elastohydrodynamic lubrication of line contacts under sliding-rolling and simple sliding conditions p 324 N93-11263

LUMINANCE
The effects of luminance boundaries on color perception [AD-A250705] p 384 N93-11841

LUMINOSITY
Detection of a white dwarf in a visual binary system [NASA-CR-190856] p 481 N93-11075
A search for low-luminosity objects [AD-A253301] p 483 N93-11750

LUNAR BASED EQUIPMENT
Power system commonality study [NASA-CR-190765] p 347 N93-12019

LUNAR BASES
Lunar and Martian environmental interactions with nuclear power system radiators [NASA-TM-105747] p 230 N93-10965

Habitat automation p 391 N93-11976

LUNAR ENVIRONMENT

Lunar and Martian environmental interactions with nuclear power system radiators [NASA-TM-105747] p 230 N93-10965

LUNAR EXPLORATION

Nuclear thermal propulsion transportation systems for lunar/Mars exploration [NASA-TM-105870] p 233 N93-12363

Manned Mars System Study (MMSS): Mars transportation and facility study. Volume 1: Executive Summary [NASA-CR-184473] p 227 N93-12442

LUNAR LUMINESCENCE

Global change and the dark of the moon [AD-A255181] p 486 N93-12380

LUNAR PROGRAMS

JPRS report: Science and technology. Central Eurasia: Space. Development of Soviet spacecraft for manned missions [JPRS-USP-92-003] p 224 N93-11162

LUNAR RANGEFINDING

Analysis of lunar laser ranging in the framework of a post-Newtonian theory [SER-C-383] p 315 N93-11332

LUNAR ROVING VEHICLES

RATLER: Robotic All-Terrain Lunar Exploration Rover [DE92-019295] p 487 N93-11502

LUNGS

Correlation of serum alpha sub 1 antitrypsin with cigarette smoking and pulmonary function status in Greek pilots, for a ten year period p 384 N93-11318

LYMAN ALPHA RADIATION

The role of proton precipitation in Jovian aurora: Theory and observation p 487 N93-11165

Lyman alpha line shapes from electron impact H2 dissociative processes in the Jovian auroral zone p 487 N93-11166

LYMPHOCYTES

Space flight and immune system p 376 N93-11284

Mechanisms of immune failure in burn injury p 376 N93-11285

Immunological parameters in current and former US Air Force personnel p 378 N93-11295

M

MACH NUMBER

OH rotational temperature and concentration measurements in a supersonic jet [DE92-006700] p 252 N93-12255

MACHINE LEARNING

Incorporating prior probabilities and misclassification costs into network training: An example from medical prognosis [RSRE-MEMO-4343] p 428 N93-10980

The adaptive neuron model: An architecture for the rapid learning of nonlinear topological transformations [NASA-CASE-NPO-18579-1-CU] p 420 N93-11174

Parallel genetic algorithms: Introduction and overview of current research [REPT-92-015] p 418 N93-11181

ALECSYS and the AutonoMouse: Learning to control a real robot by distributed classifier systems [REPT-92-011] p 420 N93-11227

Geometrical concepts about learning rules in networks with binary and ternary output functions [REPT-92-020] p 411 N93-11592

Application of machine learning techniques for effective retrieval in image database [AD-A254907] p 479 N93-12287

MACHINE TOOLS

Eddy current characterization of magnetic treatment of materials [NASA-TM-104573] p 258 N93-11621

MACHINE TRANSLATION

The evolution of Ten15 [RSRE-MEMO-4543] p 409 N93-11405

MACHINING

Superplastic forming of ceramic insulation p 228 N93-12452

MAGMA

Physical characterization of magmatic liquids [DE92-015931] p 363 N93-11848

MAGNESIUM ALLOYS

The effect of precipitate forming elements in Al 4.5 percent Mg alloys on the measured acoustic emission and on Lueders band deformation [DE92-016864] p 465 N93-12073

MAGNETIC CLOUDS

Statistics of IMF B(z) events [DE92-018372] p 488 N93-11696

MAGNETIC COILS

Open-loop characteristics of magnetic suspension systems using electromagnets mounted in a planar array [NASA-TP-3229] p 277 N93-11613

MAGNETIC DIPOLES

Electron terms and radiation from crystals [AD-A254353] p 468 N93-12271

MAGNETIC FIELD CONFIGURATIONS

Shafranov shift in low-aspect-ratio heliotron/torsatron CHS [DE92-782100] p 451 N93-11277

Ion temperature measurements on field reversed configuration plasmas p 457 N93-12535

MAGNETIC FIELDS

Direct electron absorption of fast waves on the D3-D tokamak [DE92-016254] p 449 N93-11041

Landau level quantization and superconductivity [DE92-019028] p 460 N93-11512

Three dimensional and 2D simulation of an expanding plasma using a Darwin hybrid particle code [DE92-019095] p 451 N93-11516

Effects of physical properties and geometry on shapes and stability of polarizable drops in external fields [DE92-018865] p 301 N93-11638

Semiclassical analysis spectral correlations in mesoscopic systems [DE92-634887] p 471 N93-11780

A comprehensive mission to planet Earth: Woods Hole Space Science and Applications Advisory Committee Planning Workshop [NASA-TM-108011] p 343 N93-11878

Nuclear magnetic resonance microscopy: New theoretical and technical developments p 313 N93-11907

Superconducting applications in propulsion systems. Magnetic insulation for plasma propulsion devices [NASA-CR-184401] p 233 N93-12013

Magnetic fields in the clusters of galaxies with extreme cooling flows p 486 N93-12164

Flux dynamics and irreversibility in YBa2Cu3O7 with Y2BaCuO5 inclusions and in single crystal YBa2Cu3O7 [DE92-009712] p 467 N93-12178

MAGNETIC FILMS

Optimization of film synthesized rare earth transition metal permanent magnet systems [DE92-018726] p 432 N93-12116

MAGNETIC LEVITATION VEHICLES

Vehicle/guideway interaction in maglev systems [DE92-019051] p 326 N93-11653

MAGNETIC MATERIALS

Eddy current characterization of magnetic treatment of materials [NASA-TM-104573] p 258 N93-11621

Superconducting applications in propulsion systems. Magnetic insulation for plasma propulsion devices [NASA-CR-184401] p 233 N93-12013

MAGNETIC MEASUREMENT

Data report 92-1. Brorfelde Geomagnetic Observatory magnetic results, 1990 p 362 N93-11699

Stress dependence of the magnetic properties of steels [DE92-018804] p 261 N93-12261

MAGNETIC MOMENTS

Research in elementary particles and interactions [DE92-018089] p 437 N93-11681

MAGNETIC PERMEABILITY

Flux dynamics and irreversibility in YBa2Cu3O7 with Y2BaCuO5 inclusions and in single crystal YBa2Cu3O7 [DE92-009712] p 467 N93-12178

MAGNETIC PROPERTIES

Magnetic properties of high-T(c) superconductors [DE92-018809] p 460 N93-11533

Magnetic properties and critical behavior of the conductivity near the M-I transition [DE92-018948] p 461 N93-11629

Stress dependence of the magnetic properties of steels [DE92-018804] p 261 N93-12261

Damping and scattering of electromagnetic waves by small ferrite spheres suspended in an insulator [NASA-TM-105837] p 286 N93-12366

Application of spin-sensitive electron spectroscopies to investigations of electronic and magnetic properties of solid surfaces and epitaxial systems [DE92-018597] p 470 N93-12499

MAGNETIC RESONANCE

Magnetic resonance elucidation of molecule/macromolecule interaction stereochemistry [AD-A253030] p 437 N93-11709

MAGNETIC STORMS

The effects of magnetic storm phases on F-layer irregularities from auroral to equatorial latitudes [AD-A253905] p 361 N93-11282

Statistics of IMF B(z) events [DE92-018372] p 488 N93-11696

The semiannual variation of great geomagnetic storms and the postshock Russell-McPherron effect preceding coronal mass ejecta [AD-A254955] p 489 N93-12506

MAGNETIC SUSPENSION

Open-loop characteristics of magnetic suspension systems using electromagnets mounted in a planar array [NASA-TP-3229] p 277 N93-11613

Vehicle/guideway interaction in maglev systems [DE92-019051] p 326 N93-11653

MAGNETIC VARIATIONS

The semiannual variation of great geomagnetic storms and the postshock Russell-McPherron effect preceding coronal mass ejecta [AD-A254955] p 489 N93-12506

MAGNETIZATION

Magnetic properties of high-T(c) superconductors [DE92-018809] p 460 N93-11533

MAGNETO-OPTICS

Magneto-optic imaging inspection of selected corrosion specimens [DOT/FAA/CT-TN92/20] p 332 N93-11617

MAGNETOHYDRODYNAMIC FLOW

The basic equations for a four component magnetoplasma flow with non equilibrium ionization [IPF-91-1] p 449 N93-11102

Plasma measurements in magnetospheric tail [MPE-233] p 361 N93-11352

Nonlinear evolution of resistive tearing mode instability with shear flow and viscosity [DE92-012138] p 453 N93-11745

Potassium D-line fitting for investigation of MHD boundary layers [DE92-019020] p 454 N93-11826

A comparison of velocity profile measurements in the CDIF diffuser with flow field model calculations [DE92-015367] p 304 N93-11995

MAGNETOHYDRODYNAMIC GENERATORS

Potassium D-line fitting for investigation of MHD boundary layers [DE92-019020] p 454 N93-11826

A distributed data acquisition and centralized data reduction system for flexible and efficient measurements [DE92-019021] p 312 N93-11827

Overview of recent diagnostic measurements at the USA MHD facilities [DE92-015365] p 454 N93-12087

Transient phenomena in MHD experiments [DE92-014496] p 455 N93-12139

The role of advanced optical diagnostics in monitoring and controlling an MHD power plant. Part 2: 50 MW(t), POC topping cycle [DE92-015368] p 455 N93-12141

Particle-jet interactions in an MHD second stage combustor [DE92-016390] p 455 N93-12309

MHD integrated topping cycle project [DE92-018087] p 456 N93-12504

MAGNETOHYDRODYNAMIC STABILITY

Instabilities in the rundown phase of the plasma focus [IPF-90-3] p 449 N93-11030

Effects of current driven instabilities on the ion and electron temperatures in the topside ionosphere p 360 N93-11270

Scattering of electromagnetic waves from a plasma: Enhanced ion acoustic fluctuations due to ion-ion two-stream instabilities p 361 N93-11272

On the origin of ion acoustic turbulence in the auroral topside ionosphere p 361 N93-11273

Shafranov shift in low-aspect-ratio heliotron/torsatron CHS [DE92-782100] p 451 N93-11277

Heat load material studies: Simulated tokamak disruptions [DE92-018275] p 452 N93-11674

Results from the US/USSR exchange for heat load material studies of simulated tokamak disruptions [DE92-018285] p 453 N93-11694

Nonlinear effects of ICRF power on drift wave stability and transport in tokamaks, task 1 [DE92-018488] p 453 N93-11729

Development of a new plasma diagnostic of the critical surface and studies of the ion acoustic decay instability using collective Thomson scattering [DE92-018508] p 453 N93-11730

Development of a new plasma diagnostic of the critical surface and studies of the ion acoustic decay instability using collective Thomson scattering [DE92-018526] p 453 N93-11731

Nonlinear evolution of resistive tearing mode instability with shear flow and viscosity [DE92-012138] p 453 N93-11745

Stimulated Brillouin backscattering instability in the case of a high power laser: Application to wave pulsation particle acceleration experiments p 317 N93-12024

Observation and analysis of the Stokes and anti-Stokes components of stimulated Raman backscattering
p 318 N93-12025

Plasma properties
[DE92-018635] p 455 N93-12188

Anomalous ion thermal transport in hot ion plasmas by the ion temperature gradient mode
[DE92-016686] p 456 N93-12493

Transport mechanisms acting in toroidal devices: A theoretician's view
[DE92-018738] p 456 N93-12501

MAGNETOHYDRODYNAMIC WAVES

Direct electron absorption of fast waves on the D3-D tokamak
[DE92-016254] p 449 N93-11041

MAGNETOHYDRODYNAMICS

Analytical and numerical principles for the scaling of plasma focus experiments, with regard to electrical resistance
[IPF-91-2] p 450 N93-11103

Proceedings of the 14th International Conference on the Numerical Simulation of Plasmas
[AD-A249095] p 451 N93-11275

Low pressure gas multiphotoionization for wave packet experiments p 319 N93-12034

Transient phenomena in MHD experiments
[DE92-014496] p 455 N93-12139

The role of advanced optical diagnostics in monitoring and controlling an MHD power plant. Part 2: 50 MW(t), POC topping cycle
[DE92-015368] p 455 N93-12141

Results from a large-scale MHD propulsion experiment
[DE92-018177] p 456 N93-12416

MAGNETORESISTIVITY

Magnetic properties and critical behavior of the conductivity near the M-I transition
[DE92-018948] p 461 N93-11629

Ultra-dense magnetoresistive mass memory
[NASA-CR-190955] p 405 N93-12520

MAGNETOSHEATH

Flank solar wind interaction
[NASA-CR-189285] p 489 N93-12303

MAGNETOSPHERIC INSTABILITY

Ionospheric response to particle precipitation within aurora
[IRF-SR-208] p 359 N93-11265

Effects of current driven instabilities on the ion and electron temperatures in the topside ionosphere
p 360 N93-11270

Comment on 'EISCAT Radar Observations of Enhanced Incoherent Scatter Spectra and Their Relation to Auroral Luminosity and Field-Aligned Currents' by P. N. Collis et al. p 360 N93-11271

Scattering of electromagnetic waves from a plasma: Enhanced ion acoustic fluctuations due to ion-ion two-stream instabilities p 361 N93-11272

On the origin of ion acoustic turbulence in the auroral topside ionosphere p 361 N93-11273

MAGNETOSPHERIC ION DENSITY

Studies of interactive plasma processes in the polar cusp
[NASA-CR-190892] p 357 N93-10964

MAGNETOSTRICTION

Advanced mechanisms for robotics
p 330 N93-11969

MAGNETRON SPUTTERING

Friction of self-lubricating surfaces by ion beam techniques
[DE92-016069] p 328 N93-12122

MAINTAINABILITY

On the basis of experience: Built in product reliability
[PNR-90932] p 331 N93-11034

Maintainability of large gas turbine aero engines
[PNR-90987] p 211 N93-11069

MAINTENANCE

An interactive preprocessor for the NASA engine performance program
[NASA-TM-105786] p 209 N93-10983

An evaluation of repair techniques used for uncontrolled longitudinal cracking and failed longitudinal joints
[PB92-205616] p 277 N93-12072

MALES

Clinical and immunological response to vaccination with parenteral or oral vaccines in two groups of 30 recruits
p 381 N93-11305

MAMMALS

Feasibility assessment of a transient sound sensor based on the silicon retina architecture
[AD-A252288] p 432 N93-10999

MAN ENVIRONMENT INTERACTIONS

Cellular and molecular pathways of extremely-low-frequency electromagnetic field interactions with living systems
[DE92-019084] p 282 N93-11515

Reports to the Nation on our changing planet. Winter 1991 No. 1: The climate system
[NASA-CR-190954] p 370 N93-11880

Scaling issues for biodiversity protection
[DE92-016689] p 375 N93-12315

MAN MACHINE SYSTEMS

Advanced technology for portable personal visualization
[AD-A253808] p 388 N93-11783

From pilot's associate to satellite controller's associate p 390 N93-11922

Intelligent diagnostics systems p 393 N93-11931

Super auditory localization for improved human-machine interfaces
[AD-A254699] p 389 N93-12229

MAN TENDED FREE FLYERS

Automation and robotics for COLUMBUS: An implementation concept for the free flying laboratory (MTFF) p 331 N93-11974

MAN-COMPUTER INTERFACE

Methods and principles for determining task dependent interface content
[NASA-CR-190837] p 204 N93-10961

A cognitive approach to the design of information graphics
[AD-A252692] p 474 N93-11353

Direct manipulation and intermittent automation in advanced cockpits
[AD-A253814] p 388 N93-11784

The effect of task complexity on user interfaces: A comparison of command language interface and direct manipulation interface
[AD-A246061] p 412 N93-11859

An embedded rule-based diagnostic expert system in Ada p 392 N93-11928

Integration of task level planning and diagnosis for an intelligent robot p 393 N93-11929

Space Communication Artificial Intelligence for Link Evaluation Terminal (SCAILET) p 395 N93-11940

Super auditory localization for improved human-machine interfaces
[AD-A254699] p 389 N93-12229

A hybrid approach to software repository retrieval: Blending faceted classification and type signatures
p 415 N93-12386

MANAGEMENT INFORMATION SYSTEMS

Managing data: From vision to reality
[PB92-191212] p 474 N93-11215

Analysis of methods --- information systems evolution environment
[NASA-CR-190278] p 407 N93-11368

An iconic query interface for an image database
[AD-A253571] p 475 N93-11506

Engineering Information System (EIS)
[AD-A254013] p 476 N93-11508

Integrity-oriented control objectives: Proposed revisions to the Trusted Computer System Evaluation Criteria (TCSEC), DOD 5200.28-STD
[AD-A253989] p 404 N93-11809

Evaluation of a user information satisfaction short-form instrument
[AD-A250702] p 478 N93-11840

Intelligent diagnostics systems p 393 N93-11931

MANAGEMENT METHODS

Distributed database integrity
[AD-A253272] p 477 N93-11749

DOE guideline: Guide to good practices for incorporating operating experiences
[DE92-017684] p 472 N93-12223

MANAGEMENT PLANNING

Japanese style total quality control: A first hand experience
[PNR-90909] p 331 N93-11015

Exploratory Research and Development Fund, FY 1990
[DE92-017002] p 489 N93-11078

Innovation in engineering
[PNR-90889] p 212 N93-11207

Airport stand assignment model
[TT-9104] p 218 N93-11728

Research and development strategies for human centered and group support technologies
[AD-A254366] p 472 N93-12273

Operating characteristic analysis for reliability growth programs
[AD-A254993] p 333 N93-12510

MANAGEMENT SYSTEMS

Quality management of finite element analysis
[PNR-90951] p 331 N93-11110

MANEUVERABILITY

Overview of high performance aircraft propulsion research
[NASA-TM-105839] p 213 N93-11530

Development of a 1/7-scale F/A-18 UAV for supermaneuverability research --- unmanned air vehicle
[AD-A247261] p 208 N93-12053

MANGANESE

Study of metal-ceramic interfaces of Co-Cr-Mo alloys: Role of tungsten (W) and manganese (Mn) additions
[ECL-92-01] p 267 N93-11580

MANIPULATORS

Numerical analysis of right-half plane zeros for a single-link manipulator
[NASA-CR-190966] p 426 N93-11547

Research on a reconfigurable modular manipulator system
[DE92-018943] p 327 N93-11865

Fuzzy logic control of telerobot manipulators
p 399 N93-11959

A neuro-collision avoidance strategy for robot manipulators p 400 N93-11962

An 8-DOF dual-arm system for advanced teleoperation performance experiments p 400 N93-11964

The development of system components to provide proprioceptive and tactile information to the human for future telepresence systems p 330 N93-11968

Exoskeleton master controller with force-reflecting telepresence p 330 N93-11970

Self mobile space manipulator project
p 331 N93-11973

Research and development at ORNL/CESAR towards cooperating robotic systems for hazardous environments
p 331 N93-11979

KC-135 materials handling robotics
[NASA-CR-184430] p 328 N93-11992

A vision-based end-point control for a two-link flexible manipulator
[NASA-CR-190967] p 330 N93-12521

MANNED MARS MISSIONS

Lunar and Martian environmental interactions with nuclear power system radiators
[NASA-TM-105747] p 230 N93-10965

Tutorial on nuclear thermal propulsion safety for Mars
[DE92-017946] p 233 N93-12056

Physiologically constrained aerocapture for manned Mars missions p 226 N93-12185

Manned Mars System Study (MMSS): Mars transportation and facility study. Volume 1: Executive Summary
[NASA-CR-184473] p 227 N93-12442

Manned Mars System Study (MMSS): Mars transportation and facility infrastructure study. Volume 2: Technical report
[NASA-CR-184474] p 227 N93-12443

MANNED REENTRY

Physiologically constrained aerocapture for manned Mars missions p 226 N93-12185

MANNED SPACE FLIGHT

JPRS report: Science and technology. Central Eurasia: Space. Development of Soviet spacecraft for manned missions
[JPRS-USP-92-003] p 224 N93-11162

MANNED SPACECRAFT

Manned Mars System Study (MMSS): Mars transportation and facility study. Volume 1: Executive Summary
[NASA-CR-184473] p 227 N93-12442

Manned Mars System Study (MMSS): Mars transportation and facility infrastructure study. Volume 2: Technical report
[NASA-CR-184474] p 227 N93-12443

Thermal protection systems manned spacecraft flight experience p 227 N93-12449

MANUAL CONTROL

Coordinated action in 3-D space
[AD-A249830] p 387 N93-10994

Modified optimal control pilot model for computer-aided design and analysis
[NASA-TM-4384] p 214 N93-11459

MANUALS

An interactive preprocessor for the NASA engine performance program
[NASA-TM-105786] p 209 N93-10983

Directory interchange format manual, version 4.0
[NASA-TM-107991] p 478 N93-11911

MANUFACTURING

Processing of ceramic matrix composites
[PNR-90914] p 263 N93-11018

The application of manufacturing systems engineering for aero engine gears
[PNR-90944] p 324 N93-11054

Present and future trends in turbine blade material and manufacture technology
[PNR-90960] p 255 N93-11111

The use of simultaneous engineering for the design and manufacture of the low pressure turbine for the Rolls-Royce Trent engine
[PNR-90887] p 212 N93-11206

Simultaneous engineering in aero gas turbine design and manufacture
[PNR-90890] p 212 N93-11208

Silicon carbide matrix composites
[REPT-921-430-103] p 239 N93-11588
Aerospatiale processes for three dimensional preforms
[REPT-921-430-147] p 239 N93-11590
Effect of assembly anomalies on the strain response of composites in the sphere joint region of the DARPA man-rated demonstration article
[AD-A254204] p 240 N93-11739
Assembling polyhedra with single translations
[AD-A254623] p 419 N93-12239

MANY BODY PROBLEM
Diagnostics and modeling of H(-) ion sources
[AD-A250664] p 440 N93-11867

MAP MATCHING GUIDANCE
Hybrid guidance for maneuvering flight vehicles
[AD-A254110] p 225 N93-11798

MAPPING
Density equalizing map projections: A new algorithm
[DE92-017088] p 413 N93-12110

MAPS
Computing optimum routes across terrain using DAP
[RSRE-MEMO-4299] p 412 N93-11712

MARINE ENVIRONMENTS
Bibliography of publications from the Texas A and M Sea Grant College Program, 1968-1992
[PB92-205517] p 372 N93-11253
Comparative effects of drag-reducing polymers. An experimental report
[AD-A254001] p 268 N93-11793
Office of Wetlands, Oceans, and Watersheds publications
[PB92-224310] p 480 N93-12528

MARINE METEOROLOGY
Mariners Weather Log, volume 36, number 1, Winter 1992
[PB92-161025] p 368 N93-11256
Mariners Weather Log, volume 36, number 2, Spring 1992
[PB92-204213] p 371 N93-12293

MARINE PROPULSION
Pressure and noise induced by a cavitating marine screw propeller
[VTT-PUBS-87] p 299 N93-11360
Results from a large-scale MHD propulsion experiment
[DE92-018177] p 456 N93-12416

MARINE RESOURCES
Bibliography of publications from the Texas A and M Sea Grant College Program, 1968-1992
[PB92-205517] p 372 N93-11253

MARINE TECHNOLOGY
Bibliography of publications from the Texas A and M Sea Grant College Program, 1968-1992
[PB92-205517] p 372 N93-11253

MARINE TRANSPORTATION
Mariners Weather Log, volume 36, number 2, Spring 1992
[PB92-204213] p 371 N93-12293

MARKET RESEARCH
The European space industry. *Overall situation:* Situation and prospects for the 23 leading companies concerned
p 472 N93-11163

MARKETING
The European space industry. Overall situation: Situation and prospects for the 23 leading companies concerned
p 472 N93-11163
Industrial applications and markets for ceramic matrix composites
[PNR-90884] p 266 N93-11205

MARKOV PROCESSES
The development of the speaker independent ARM continuous speech recognition system
[RSRE-MEMO-4473] p 280 N93-11383
Preliminary results on the use of linear discriminant analysis in the ARM continuous speech recognition system
[RSRE-MEMO-4511] p 280 N93-11384
The use of linear discriminant analysis in the ARM continuous speech recognition system
[RSRE-MEMO-4512] p 280 N93-11385
Fatigue in single crystal nickel superalloys
[AD-A254603] p 260 N93-12237
Stochastic models of wavefront propagation in random granular media
[AD-A255127] p 286 N93-12422

MARS (PLANET)
Closed form low-thrust trajectories for Mars missions
[DE92-017431] p 232 N93-11766
Nuclear thermal propulsion transportation systems for lunar/Mars exploration
[NASA-TM-105870] p 233 N93-12363

MARS ATMOSPHERE
Effect of inert propellant injection on Mars ascent vehicle performance
[NASA-CR-189238] p 226 N93-12152

MARS ENVIRONMENT
Lunar and Martian environmental interactions with nuclear power system radiators
[NASA-TM-105747] p 230 N93-10965

MARTENSITIC TRANSFORMATION
Review of phonon behavior and microstructural development leading to martensitic transformations in Ni(x)Al(100-x) alloys
[DE92-014782] p 256 N93-11519

MASKING
Auditory perception
[AD-A255061] p 385 N93-12469

MASKS
Evaluation of multilayer mask concept for RESPO 21
[AD-A253392] p 389 N93-12079
Reflection masks for soft x ray projection lithography
[DE92-014779] p 293 N93-12121

MASS
EUROMET project no. 231: Uncertainties in mass measurement. NPL's analysis of data from the calibration of weight set NPLW43
[NPL-MOM-107] p 432 N93-11666

MASS FLOW
System and method for cancelling expansion waves in a wave rotor
[NASA-CASE-LEW-15218-1] p 297 N93-11172
Numerical analysis of the flow fields in a RQL gas turbine combustor
[DE92-017509] p 302 N93-11767

MASS SPECTROMETERS
Thermochemistry of transition metal clusters
[DE92-018713] p 262 N93-12480

MASS SPECTROSCOPY
Detonation reactions frozen by free expansion and analyzed by mass spectrometry
[DE92-018605] p 274 N93-11566
High-precision thorium RIMS for geochemistry
[DE92-017405] p 250 N93-11918
Advanced methods for structural characterization of large multiply charged ions: Obtaining charge state determination and improved sensitivity
[DE91-015264] p 441 N93-12117
Probing flame chemistry with MBMS, theory, and modeling
[DE92-011433] p 251 N93-12119
Characterization of underivatized pterins by laser desorption Fourier transform mass spectrometry
[DE92-016785] p 323 N93-12514

MASS TRANSFER
Kinetics of diffusional droplet growth in a liquid/liquid two-phase system
[NASA-CR-190805] p 297 N93-11142
A new two-phase flow and transport model with interphase mass exchange
[PB92-206564] p 298 N93-11251
Development of an intelligent system for cooling rate and fill control in GMAW
[DE92-017849] p 326 N93-11548

MASSIVELY PARALLEL PROCESSORS
Current state and future direction of computer systems at NASA Langley Research Center
[NASA-TM-107685] p 414 N93-12278
Performance evaluation and modeling techniques for parallel processors
[NASA-CR-190974] p 419 N93-12395

MATCHING
Matching and vertex packing: How hard are they?
[AD-A245928] p 423 N93-10991
Object based multi-image matching
[SER-C-375] p 309 N93-11330

MATERIAL ABSORPTION
Research at and operation of the material science x ray absorption beamline (X-11) at the National Synchrotron Light source
[DE92-018598] p 251 N93-12172

MATERIALS
Experience of designing a relational materials database
[PNR-90893] p 473 N93-11012

MATERIALS HANDLING
Automated resupply of consumables: Enhancement of space commercialization opportunities
p 403 N93-11980
Analysis of materials from MSFC LDEF experiments
[NASA-CR-184425] p 252 N93-12215

MATERIALS RECOVERY
Advanced heat pump for the recovery of volatile organic compounds
[DE92-011592] p 303 N93-11774

MATERIALS SCIENCE
Materials science and engineering at the Naval Research Laboratory: Research programs and 1990 publications
[PB92-199488] p 238 N93-11422
Advanced materials and processing: The Federal program in materials science and technology. A report by the FCCSET Committee on Industry and Technology to supplement the President's fiscal year 1993 budget
[PB92-199108] p 238 N93-11470
Solid state sciences committee forum
[AD-A253556] p 463 N93-11753
Materials processing in low gravity
[NASA-CR-184421] p 276 N93-12401

MATERIALS TESTS
Analysis of surfaces from the LDEF A0114, phase 2
[NASA-CR-190596] p 270 N93-11993
Erosion rates for polymers measured on LDEF
p 270 N93-11994
Analysis of materials from MSFC LDEF experiments
[NASA-CR-184425] p 252 N93-12215

MATHEMATICAL LOGIC
On recursive free types in Z
[RSRE-91028] p 425 N93-11437

MATHEMATICAL MODELS
A creep cavity growth model for creep-fatigue life prediction of a unidirectional W/Cu composite
[NASA-TM-105780] p 333 N93-10967
Ground test facilities for evaluating nuclear thermal propulsion engines and fuel elements
[DE92-017039] p 231 N93-10973
The prediction of convective heat transfer in rotating square ducts
[PNR-90929] p 296 N93-11025
Current scaling of plasma focus devices
[IPF-90-1] p 449 N93-11029
Modelling short crack growth behaviour in nickel-base superalloys
[PNR-90912] p 255 N93-11033
The role of turbomachinery testing for stability in distorted flow
[PNR-90943] p 210 N93-11040
The prediction of convective heat transfer in rotating square ducts
[PNR-90985] p 296 N93-11067
Modelling the behaviour of gas bubbles in epoxy resin
[PNR-90961] p 264 N93-11084
Front tracking and the interaction of nonlinear waves
[AD-A253544] p 297 N93-11148
Development of a geometry-compensated neutron time-of-flight detector for ICF applications with approximately 200 ps time response
[DE92-018024] p 450 N93-11153
Thermokinetic modelling and hypersonic flow
[DILC-EST-TN-218] p 196 N93-11157
Micromechanics of metal matrix composites using the Generalized Method of Cells model (GMC) user's guide
[NASA-CR-190756] p 335 N93-11175
Nonlinear response of thin steel plate structures subjected to static, cyclic, and dynamic loads
p 335 N93-11200
An interlayer shear slip theory for composite laminates with nonrigid bonding p 237 N93-11229
A new two-phase flow and transport model with interphase mass exchange
[PB92-206564] p 298 N93-11251
Modeling and identification of flexible joints in vehicle structures p 324 N93-11261
Effects of current driven instabilities on the ion and electron temperatures in the topside ionosphere
p 360 N93-11270
Simplified modelling of soot inception and growth
[ETN-92-92266] p 246 N93-11361
Experiments on low aspect ratio hydroplanes to measure lift under static and dynamic conditions
[ARE-TM(UHR)-90306] p 197 N93-11365
Implementation of a model based fault detection and diagnosis for actuation faults of the Space Shuttle main engine
[NASA-TM-105781] p 221 N93-11401
Application of artificial neural networks in nonlinear analysis of trusses
[NASA-TM-105319] p 336 N93-11403
Analytical method of calculating the thermoelastic constants of a multi-phase unidirectional composite
[NPL-DMM(A)-57] p 238 N93-11409
Modeling regional seismic waves
[AD-A246894] p 361 N93-11421
Stationary time series analysis using information and spectral analysis p 425 N93-11431
A theoretical study of the performance of a small permanent magnet, three-phase alternator when driving a purely resistive load via a full-wave rectification circuit
[RAE-TR-84009] p 289 N93-11434
Evaluation of an analytical model for predicting light scattering from cylindrically-shaped objects in the ocean
[AD-A248414] p 447 N93-11489
Visual perception of structure from motion
[AD-A253235] p 386 N93-11503

The intensity of knock in an internal combustion engine: An experimental and modeling study
[DE92-019504] p 326 N93-11540

Thermal stress and strain analysis in traveling autogenous welds
[DE92-019363] p 326 N93-11556

Temperature tracking SPICE macro-model for laser and LED driven opto-coupler assemblies
[DE92-019296] p 411 N93-11599

Measurement of AC electrical characteristics of SSC superconducting dipole magnets
[DE92-018888] p 431 N93-11625

Reactant gas flow fields in advanced PEM (Proton Exchange Membrane) fuel cell designs
[DE92-018897] p 345 N93-11626

Computer simulations for the adsorption of polymers onto surfaces
[DE92-018942] p 267 N93-11628

Particle-fluid two-phase flow modeling
[DE92-017847] p 301 N93-11637

An analog macromodel of the SG1525A PWM for use with SPICE2G.6 simulators
[DE92-019423] p 291 N93-11639

Modeling the dispersion of tracer plumes in the Colorado front range boundary layer during night- and day-time conditions
[DE92-019384] p 354 N93-11676

A three dimensional high resolution upwind finite volume Euler solver
[VKI-TN-180] p 198 N93-11686

Three-dimensional image structure in in-line Fraunhofer holography p 311 N93-11723

Crustal and upper mantle velocity gradients in the vicinity of the East Kazakh test site
[AD-A246889] p 362 N93-11740

Atmospheric reactive nitrogen: A model study of natural and anthropogenic sources and the role of microbial soil emissions
[DE92-010717] p 354 N93-11744

An analytic description of thick-wall bubbles
[DE92-016465] p 432 N93-11759

Semiclassical analysis spectral correlations in mesoscopic systems
[DE92-634887] p 471 N93-11780

Application of the theory of wave propagation through random media to phase and amplitude fluctuations of seismic P-waves
[AD-A253274] p 363 N93-11788

Identification and estimation of sources of transmitted variation
[DE92-015246] p 429 N93-11820

Numerical modeling of a vortex stabilized arcjet
p 232 N93-11889

Laboratory and numerical studies of dynamical processes related to thermal convection in the Earth's mantle p 364 N93-11900

Dynamics of space debris p 219 N93-11904

Experimental measurement and theoretical modeling of microwave scattering and the structure of the sea surface influencing radar observations from space
[NASA-CR-190996] p 343 N93-12006

Lunar PMAD technology assessment
[NASA-CR-189225] p 347 N93-12017

Laser material interaction in confined medium
p 319 N93-12035

Modeling for the study of an X laser in a recombination plasma; gain calculations at 105.7 and 154.6 A
p 321 N93-12046

Comprehensive computational model for thermal plasma processing
[DE92-018015] p 454 N93-12066

Numerical simulation of alumina spraying in argon-helium plasma jet
[DE92-017859] p 455 N93-12092

Models of volcanic eruption hazards
[DE92-013432] p 364 N93-12136

Seismic wave propagation in thinly-layered media with steep reflectors
[DE92-015619] p 364 N93-12142

Mechanisms associated with electrorheology
p 294 N93-12198

The generalized Goursat-Riemann problem for plane waves in isotropic elastic solids p 340 N93-12199

Analysis of advanced optical glass and systems
[NASA-CR-184434] p 448 N93-12201

Modeling and model simplification of aeroelastic vehicles: An overview
[NASA-TM-107691] p 215 N93-12216

Asymptotic analysis of reacting materials with saturated explosion. 2: High-frequency waves
[AD-A254473] p 275 N93-12236

Advanced modeling and optimization of piezoelectric composites
[AD-A253800] p 242 N93-12296

Dynamic test/analysis correlation using reduced analytical models
[NASA-TM-107671] p 341 N93-12300

Static assignment of complex stochastic tasks using stochastic majorization
[NASA-CR-189716] p 416 N93-12403

The mechanism of bolt loading
[NASA-TM-108377] p 342 N93-12412

Numerical investigations into the base drag of various wedges using the base flow model developed by Mauri Tanner
[REPT-B-36] p 202 N93-12414

An improved numerical model for wave rotor design and analysis
[NASA-TM-105915] p 214 N93-12418

Superplastic forming of ceramic insulation
p 228 N93-12452

Thermostructural applications of heat pipes for cooling leading edges of high-speed aerospace vehicles
p 229 N93-12460

The uses and limits of economic models as a climate change policy tool
[DE92-015792] p 356 N93-12474

Space Station communications and tracking systems modeling and RF link simulation
[NASA-CR-185684] p 288 N93-12519

Development of a model for predicting NASA/MSFC program success
[NASA-CR-184423] p 473 N93-12542

MATHEMATICS

Solid state sciences committee forum
[AD-A253556] p 463 N93-11753

A summer program in mathematics and computer science for academically oriented students, June 24 - July 26, 1991, Washington, DC
[AD-A249139] p 427 N93-12061

MATRICES (MATHEMATICS)

Equivalence transformations of rational matrices
[MATHS-REPT-A-163] p 423 N93-11121

Equivalence transformations of rational matrices and applications
[MATHS-REPT-A-169] p 424 N93-11124

On a certain McMillan degree condition appearing in control
[MATHS-REPT-A-170] p 424 N93-11125

Preconditioned low-order Newton methods
[MATHS-REPT-A-159] p 425 N93-11211

Krylov subspace methods for complex non-Hermitian linear systems
[NASA-CR-190931] p 409 N93-11458

Optimization of expressions involving array classes
[DE92-019421] p 411 N93-11536

Decomposition of balanced matrices. Part 5: Goggles
[AD-A247462] p 430 N93-12217

Perturbation theory for the solution of systems of linear equations
[AD-A254994] p 428 N93-12511

MATRIX MATERIALS

Fracture mechanics of model fiber composites
p 237 N93-11247

ICAN/DAMP-integrated composite analyzer with damping analysis capabilities: User's manual
[NASA-TP-3292] p 241 N93-12015

MATRIX THEORY

Symmetric matrix-vector product on a ring of processors p 410 N93-11481

Perturbation theory for the solution of systems of linear equations
[AD-A254994] p 428 N93-12511

MATTER (PHYSICS)

Matter-wave interferometry with laser cooled atoms
[AD-A253999] p 316 N93-11737

MAXIMUM LIKELIHOOD ESTIMATES

A comparison of feed-forward networks and maximum likelihood on a point-source location problem
[RSRE-MEMO-4567] p 281 N93-11391

Identification and estimation of sources of transmitted variation
[DE92-015246] p 429 N93-11820

Nonnormal multivariate distributions: Inference based on elliptically contoured distributions
[AD-A254999] p 429 N93-12513

MAXWELL EQUATION

Alternating-phase focusing: A model to study nonlinear dynamics
[DE92-019027] p 431 N93-11511

Effects of physical properties and geometry on shapes and stability of polarizable drops in external fields
[DE92-018865] p 301 N93-11638

MEASURING INSTRUMENTS

Fiber peel force measuring apparatus
[AD-D015349] p 309 N93-11048

Low cost humidity sensor
[PB92-205772] p 312 N93-11757

Repeatable sensitivity of optical-time-domain-reflectometry-based strain measurement
[DE92-016910] p 338 N93-11792

The role of advanced optical diagnostics in monitoring and controlling an MHD power plant. Part 2: 50 MW(t), POC topping cycle
[DE92-015368] p 455 N93-12141

Compensated high temperature strain gage
[NASA-CASE-LAR-14776-1] p 313 N93-12205

Analysis of materials from MSFC LDEF experiments
[NASA-CR-184425] p 252 N93-12215

MECHANICAL DRIVES

Energy efficient drivepower: An overview
[PB92-199173] p 294 N93-12191

MECHANICAL ENGINEERING

Energy efficient drivepower: An overview
[PB92-199173] p 294 N93-12191

MECHANICAL PROPERTIES

Experience of designing a relational materials database
[PNR-90893] p 473 N93-11012

Corrosion protection of materials for aircraft using ion beam processes. Corrosion and bonding strength examinations. Physical analysis of laser composition
[MBB-Z-0405-91-PUB] p 255 N93-11026

Advanced materials in gas turbine engines: An assessment
[PNR-90946] p 211 N93-11105

Development of advanced carbon-carbon annular flameholders for gas turbines
[PNR-90947] p 211 N93-11106

Curing and mechanical properties of T800-V398 graphite/bismaleimide at different temperatures
[DLR-FB-92-02] p 237 N93-11143

International ADI-Seminar: Austempered Ductile Iron
[PB92-180660] p 256 N93-11244

Review of the physical and mechanical properties and potential applications of the B2 compound NiAl: Unabridged version of a paper published in International materials review
[NASA-TM-105598] p 258 N93-11635

Analysis of plasma-treated wire insulation
[DE92-019471] p 291 N93-11643

Mechanical properties of semiconductors and their alloys
[AD-A253908] p 462 N93-11727

Acoustic measurement of the mechanical properties of thin material specimens
[AD-A253538] p 434 N93-11752

The effect of silicon, tin, and chromium on the corrosion and mechanical properties of zirconium - molybdenum - niobium
[AD-A254102] p 258 N93-11787

Workshop on Characterizing Diamond Films
[PB92-205426] p 271 N93-12086

Reactor materials program: Mechanical properties of irradiated types 304 and 304L stainless steel weldment components
[DE92-018105] p 260 N93-12158

Mechanisms associated with electrorheology
p 294 N93-12198

Mechanical properties of centrifugally cast metal matrix composites
[AD-A254321] p 243 N93-12483

MECHANIZATION

Formal mechanization of device interactions with a process algebra
[NASA-CR-189644] p 405 N93-12347

MEDICAL EQUIPMENT

Comparisons of molecular sieve oxygen concentrators for potential medical use aboard commercial aircraft
[AD-A253648] p 387 N93-11279

High resolution tomographic instrument development
[DE92-017314] p 313 N93-11828

Evaluation of a user information satisfaction short-form instrument
[AD-A250702] p 478 N93-11840

MEDICAL SCIENCE

Incorporating prior probabilities and misclassification costs into network training: An example from medical prognosis
[RSRE-MEMO-4343] p 428 N93-10980

Center of Excellence in laser medicine
[DE92-018760] p 384 N93-11445

MEDICAL SERVICES

Mechanisms of immune failure in burn injury
p 376 N93-11285

Evaluation of a user information satisfaction short-form instrument
[AD-A250702] p 478 N93-11840

MELT SPINNING

The influence of processing atmosphere on twin-roll melt-spinning of aluminum alloys
[DE92-017895] p 257 N93-11595

MELTS (CRYSTAL GROWTH)

Studies on the reactive melt infiltration of silicon and silicon-molybdenum alloys in porous carbon
[NASA-TM-105860] p 273 N93-12398

MEMBRANES

Optical properties of composite membranes containing arrays of nanoscopic gold cylinders
[AD-A253659] p 238 N93-11281

Resonant membrane spatial light modulators
[AD-A253893] p 252 N93-12186

MEMORY (COMPUTERS)

Concurrent file operations in a high performance FORTRAN
[NASA-CR-189711] p 412 N93-11618

Automatic data partitioning on distributed memory multicomputers
[NASA-CR-190976] p 418 N93-11651

Ferroelectric memory devices and a proposed standardized test system design
[AD-A255159] p 405 N93-12425

MENINGITIS

Dramatic reduction of meningococcal meningitis among military recruits in Italy after introduction of specific vaccination p 380 N93-11303

Immunization of personnel traveling to a destination in tropical countries: French position p 380 N93-11304

MENTAL HEALTH

Neuropsychiatric morbidity in early HIV disease: Implications for military occupational function
p 379 N93-11299

MENTAL PERFORMANCE

Relating cognitive function to military aviator performance in early HIV infection p 379 N93-11298

The development of system components to provide proprioceptive and tactile information to the human for future telepresence systems p 330 N93-11968

Complex cognitive information processing: A computational architecture with a connectionist implementation
[AD-A254041] p 422 N93-12259

MERCURY TELLURIDES

Electronic and optical properties of perfect and imperfect 2 to 6 superlattices p 465 N93-11996

MERIDIONAL FLOW

The structure and transport of the Brazil current between 27 deg and 36 deg south
[AD-A247635] p 374 N93-12247

MESOPAUSE

Lidar studies of gravity waves in the mesopause region p 358 N93-11222

MESOSCALE PHENOMENA

Numerical and observational investigations of long-lived, MCS-induced, severe surface wind events: The derecho
p 367 N93-11159

The forcing of a mid-latitude upper-tropospheric jet streak by a simulated mesoscale convective system
p 358 N93-11184

Validation test report for the first-generation dart Gulf Stream forecasting system
[AD-A254286] p 373 N93-11821

Oceanographic expert system: Potential for TESS(3) applications
[AD-A254908] p 374 N93-12288

Operations plan for the Tropical Cyclone Motion (TCM-92) mini-field experiment
[AD-A254723] p 372 N93-12339

MESOSPHERE

Sodium-lidar mesosphere examinations: Selected elements of the experimental construction of a mobile instrument and evaluation of the data acquired with a stationary Na-lidar during the DYANA campaign
[BONN-IR-91-78] p 357 N93-11006

MESSAGE PROCESSING

High performance interconnection between high data rate networks p 279 N93-11118

Operator assistant to support deep space network link monitor and control p 288 N93-11939

Tradeoffs in implementing primary-backup protocols
[NASA-CR-190970] p 472 N93-12212

METABOLISM

Allergic and nonallergic rhinitis in Greek pilots
p 383 N93-11317

METABOLITES

New techniques for positron emission tomography in the study of human neurological disorders
[DE92-015353] p 384 N93-11873

METAL BONDING

Study and characterization of ceramic-metal bonds manufactured by solid state bonding techniques. Application to Ag/Al2O3
[ECL-91-19] p 267 N93-11577

Study of metal-ceramic interfaces of Co-Cr-Mo alloys: Role of tungsten (W) and manganese (Mn) additions
[ECL-92-01] p 267 N93-11580

METAL COATINGS

Silver lined ceramic vessel and method of preparation
[AD-D015360] p 266 N93-11400

Chronopotentiometry of refractory metals, actinides and oxyanions in molten salts: A review
[NASA-TM-105862] p 249 N93-11545

Characteristics of heat transfer to nickel plated chamber walls of high pressure rocket combustors
[NAL-TR-1126T] p 234 N93-12372

METAL COMBUSTION

Metal slurry droplet and spray combustion
p 245 N93-11138

METAL CRYSTALS

Fast electrochromic switching for optical hardening applications
[AD-A248174] p 447 N93-11186

METAL FATIGUE

Fatigue in single crystal nickel superalloys
[AD-A254603] p 260 N93-12237

Microstructure-based fatigue life prediction methods for naval steel structures
[AD-A254628] p 260 N93-12241

Fatigue crack growth in AerMet 100 steel
[AD-A249068] p 261 N93-12248

Spectrum fatigue behaviour of powder metallurgy aluminum alloys
[AD-A255060] p 262 N93-12468

Creep failure in linear and nonlinear viscoelastic materials p 342 N93-12536

METAL FIBERS

Ceramic TBS/porous metal compliant layer
p 228 N93-12453

METAL FILMS

Theory of small metal clusters, films, and wires
[AD-A253120] p 256 N93-11240

Analysis of surfaces from the LDEF A0114, phase 2
[NASA-CR-190596] p 270 N93-11993

METAL FOILS

A model to estimate the flux of background particles expected to accumulate on the collector foils of the interstellar gas experiment on the long duration exposure facility spacecraft
[AD-A254265] p 489 N93-11815

METAL IONS

Acid copper sulfate plating bath: Control of chloride and copper
[DE92-019473] p 249 N93-11644

Electronic structure and reactivities of transition metal clusters
[DE92-016623] p 258 N93-11762

Atomic structure of Ni-like soft x ray lasing ions
[DE92-019273] p 438 N93-11778

Design and evaluation of ion source for satellite charge control
[AD-A255172] p 227 N93-12408

METAL MATRIX COMPOSITES

Nondestructive evaluation of ceramic and metal matrix composites for NASA's HITEMP and enabling propulsion materials programs
[NASA-TM-105807] p 331 N93-10963

A creep cavity growth model for creep-fatigue life prediction of a unidirectional W/Cu composite
[NASA-TM-105780] p 333 N93-10967

Thermal residual stresses in silicon-carbide/titanium (0/90) laminate
[NASA-TM-107649] p 236 N93-11072

Micromechanics of metal matrix composites using the Generalized Method of Cells model (GMC) user's guide
[NASA-CR-190756] p 335 N93-11175

Thermomechanical fatigue behavior of SiC/Ti-24Al-11Nb in air and argon environments
[NASA-TM-105723] p 238 N93-11399

Study of the behavior of titanium and ceramic fiber matrix composite alloy
[ETN-92-92087] p 240 N93-11708

Infiltration kinetics and interfacial bond strength of metal matrix composites
[AD-A254002] p 240 N93-11795

Micromechanisms of deformation and fracture in aluminum based MMC's: Interface effects
[AD-A253560] p 259 N93-11850

Mechanical properties for advanced engine materials
[AD-A252632] p 242 N93-12181

Mechanical properties of centrifugally cast metal matrix composites
[AD-A254321] p 243 N93-12483

METAL OXIDE SEMICONDUCTORS

Reliability of small geometry VLSI devices for microelectronics
[AD-A247355] p 289 N93-11414

An analog macromodel of the SG1525A PWM for use with SPICE2G.6 simulators
[DE92-019423] p 291 N93-11639

High temperature rectifiers and MOS devices in 6H-silicon carbide
[AD-A254725] p 295 N93-12340

METAL PARTICLES

Metal slurry droplet and spray combustion
p 245 N93-11138

Optical properties of composite membranes containing arrays of nanoscopic gold cylinders
[AD-A253659] p 238 N93-11281

METAL PLATES

Nonlinear response of thin steel plate structures subjected to static, cyclic, and dynamic loads
p 335 N93-11200

The effects of aluminum oxide on inertial welding of aluminum in space applications
[AD-A255100] p 329 N93-12274

METAL SHEETS

Ceramic TBS/porous metal compliant layer
p 228 N93-12453

METAL SURFACES

Low energy helium implantation in evaporated nickel surfaces
[DE92-019297] p 257 N93-11600

Exploration of the ionizable metal cluster-electrode surface analogy: Infrared spectroelectrochemistry of (Pt24(CO)30)(sup n), (Pt26(CO)32)(sup n), and (Pt38(CO)44)(sup n) (n = 0 to -10), and comparisons with potential-dependent spectra of CO adlayers on platinum surfaces
[AD-A252544] p 250 N93-11808

Application of spin-sensitive electron spectroscopies to investigations of electronic and magnetic properties of solid surfaces and epitaxial systems
[DE92-018597] p 470 N93-12499

METAL VAPOR LASERS

Chinese Journal of Lasers (selected articles)
[AD-A254100] p 317 N93-11786

METAL-GAS SYSTEMS

Internal friction peaks due to oxygen, nitrogen, and hydrogen in V-Nb alloys
[DE92-012155] p 254 N93-10995

METAL-METAL BONDING

The role of backbond strain in silicon surfaces on the decomposition of NH3 and PH3
[AD-A253771] p 250 N93-12062

METALLIC HYDROGEN

Theoretical studies of high-temperature superconductors and highly compressed hydrogen
p 292 N93-11833

METALLIC PLASMAS

Laser material interaction in confined medium
p 319 N93-12035

Study of the effects of a plastic wave induced by laser pulse in a metallic material. Application to the improvement of fatigue strength p 319 N93-12036

Gain in a confined aluminum plasma
p 320 N93-12043

Preliminary study of the homogeneity of the density and temperature of long plasmas used for X laser studies
p 320 N93-12044

METALLIZING

Development of stable metallization systems
[AD-A253569] p 264 N93-11079

METALLOIDS

Development of stable metallization systems
[AD-A253569] p 264 N93-11079

METALORGANIC CHEMICAL VAPOR DEPOSITION

The domain structure features of epitaxial PbTiO3 thin films prepared by MOCVD
[DE92-010907] p 459 N93-11190

CVD of AlN and SiC using cyclic organometallic precursors
[AD-A246910] p 266 N93-11413

Triisopropylindium: A new precursor for OMVPE growth
[AD-A250672] p 460 N93-11558

VUV and UV sources and spectroscopic applications
[AD-A247293] p 291 N93-11758

Basic principles of organometallic vapor phase epitaxy
[AD-A250665] p 464 N93-11868

Triisopropylindium: Decomposition study and use for low temperature growth
[AD-A250666] p 464 N93-11869

Growth of 2-6 thin-films from single-source precursors based on sterically encumbered sitel ligands
[DE92-017077] p 466 N93-12099

Growth of solid solutions of aluminum nitride and silicon carbide by metalorganic chemical vapor deposition
[AD-A255000] p 254 N93-12518

METALS

Electron emission during multicharged ion-metal surface interactions
[DE92-017134] p 439 N93-11849

Summaries of FY 1991 research in the chemical sciences
[DE92-011920] p 251 N93-12135

Theory of normal metals
[DE92-016828] p 262 N93-12476

METASTABLE STATE
Recombination and metastability in amorphous silicon and silicon germanium alloys
[DE92-010593] p 463 N93-11816

METATHESIS
Synthesis and side chain liquid crystal polymers by living ring opening metathesis polymerization. 5: Influence of mesogenic group and interconnecting group on the thermotropic behavior of the resulting polymers
[AD-A253568] p 264 N93-11150
Synthesis of side chain liquid crystal polymers by living ring opening metathesis polymerization. Report 3: Influence of molecular weight, interconnecting unit and substituent on the mesomorphic behavior of polymers with laterally attached mesogens
[AD-A248698] p 265 N93-11187
Synthesis of side chain liquid crystal polymers by living ring opening metathesis polymerization. Report 2: Influence of molecular weight, polydispersity, and flexible spacer length (n=9-12) on the thermotropic behavior of the resulting plymers
[AD-A248700] p 265 N93-11188

METEORITES
Thin-sectioning and analysis of fine-grained meteoritic materials
[NASA-CR-185693] p 485 N93-11546

METEOROLOGICAL CHARTS
Mariners Weather Log, volume 36, number 2, Spring 1992
[PB92-204213] p 371 N93-12293

METEOROLOGICAL PARAMETERS
The use of ARM data to test an improved parameterization of upper tropospheric clouds for use in climate models
[DE92-014353] p 367 N93-11237
The sensitivity of the receiver coherence diameter and modulation transfer function to variations of a damp unstable atmosphere
[AD-A253269] p 363 N93-11785
Proceedings of the National Weather Service Aviation Workshop: Postprint volume
[PB92-176148] p 369 N93-11803
Statistical methods for the comparison of spatial patterns in meteorological variables p 370 N93-11997
Analysis of air and sea physical properties and surface fluxes using a combination of in situ and SEASAT data
p 365 N93-12182
Interactive analysis of gappy bivariate time series using AGSS
[AD-A255160] p 429 N93-12426
Parameters for predicting red tides of bioluminescent dinoflagellates: Meteorological events and frontal water circulation patterns
[AD-A254835] p 374 N93-12431
The vertical distribution of heating in the tropical atmosphere
[AD-A254982] p 372 N93-12507
Interannual variabilities of the East Asian summer monsoon and tropical sea surface temperatures
p 372 N93-12534

METEOROLOGICAL RADAR
The millimeter wave Cloud Profiling Radar System (CPRS)
[DE92-016970] p 366 N93-10971
Summary of findings from the PIREP-based analyses conducted during the 1988 to 1990 evaluations of TDWR-based and TDWR/LLWAS-based alert services provided to landing/departing pilots
[AD-A253859] p 367 N93-11144
A comparison of radar rainfall estimates and rain gage measurements during two Denver thunderstorms
[AD-A254267] p 369 N93-11817
An observational study of a prefrontal convective rainband using TAMEX single- and dual-Doppler data
[AD-A249839] p 371 N93-12251

METEOROLOGICAL SERVICES
Proceedings of the National Weather Service Aviation Workshop: Postprint volume
[PB92-176148] p 369 N93-11803
Weather impacts on space operations
[AD-A253720] p 371 N93-12170

METEOROLOGY
Key wintertime meteorological features of the Grand Canyon and the Colorado Plateaus Basin
[DE92-019134] p 369 N93-11657
Data report 92-1. Brorfelde Geomagnetic Observatory magnetic results, 1990 p 362 N93-11699
A comparison of radar rainfall estimates and rain gage measurements during two Denver thunderstorms
[AD-A254267] p 369 N93-11817
Proceedings of the Sixteenth Annual Climate Diagnostics Workshop
[PB92-198803] p 370 N93-11896
CCL working group on climate data
[WCDMP-18] p 370 N93-11897
Weather impacts on space operations
[AD-A253720] p 371 N93-12170
Interactive analysis of gappy bivariate time series using AGSS
[AD-A255160] p 429 N93-12426

METHANE
Formic acid: Development of an analytical method and use as process indicator in anaerobic systems
[AD-A250668] p 253 N93-12267

METHOD OF CHARACTERISTICS
Difference approximations for hyperbolic conservation laws and consistency with characteristics
[NAL-TR-1098T] p 428 N93-12350

METHOD OF MOMENTS
Method of moments analysis of symmetric dual reflector antennas with feeds
[AD-A255171] p 286 N93-12407

METHODOLOGY
Analysis of methods — information systems evolution environment
[NASA-CR-190278] p 407 N93-11368
Software quality methodology integration study results
[AD-A253891] p 408 N93-11371
Methodology issues concerning the accuracy of kinematic data collection and analysis using the ariel performance analysis system
[NASA-CR-185689] p 389 N93-12211

METHYL ALCOHOL
Selective carbon oxygen bond scission during reactions of oxygenates on single crystal catalysts
[DE92-018687] p 247 N93-11439
Reformers for the production of hydrogen from methanol and alternative fuels for fuel cell powered vehicles
[DE92-019300] p 274 N93-11550
Alternative Fuel Evaluation Program: Alternative Fuel Light Duty Vehicle Project. Data collection responsibilities, techniques, and test procedures
[DE92-010598] p 275 N93-12171

METHYL COMPOUNDS
Positive ion chemistry of acetylene and methylacetylene clusters. Formation of benzene and C(sub 2n)H(sub 2n)(+) ions via intracluster polymerization reactions
[AD-A250931] p 236 N93-12177

METHYLENE
Synthesis and side chain liquid crystal polymers by living ring opening metathesis polymerization. 5: Influence of mesogenic group and interconnecting group on the thermotropic behavior of the resulting polymers
[AD-A253568] p 264 N93-11150

METRICATION
A metric America: A decision whose time has come - for real
[PB92-205459] p 277 N93-11902

MICROANALYSIS
Thin-sectioning and analysis of fine-grained meteoritic materials
[NASA-CR-185693] p 485 N93-11546
Interfacial microchemical characterization needs in surface processing
[DE92-018269] p 277 N93-11672

MICROBIOLOGY
Microbiological analysis of debris from STS-42 IML-1 by direct plating of rinse waters
[NASA-TM-108375] p 375 N93-12174
ECLSS medical support activities
[NASA-CR-184429] p 385 N93-12427

MICROCHANNELS
Cryostabilization of high-temperature superconducting magnets with subcooled flow in microchannels
[DE92-018174] p 431 N93-11598

MICROCRACKS
Application of polyimides to aeroengine components
[PNR-90907] p 334 N93-11013
Semi-interpenetrating polymer network for tougher and more microcracking resistant high temperature polymers
[NASA-CASE-LAR-13925-2] p 264 N93-11059
Titanium-aluminides by hot isostatic pressing of cold extruded titanium-aluminium powder mixtures
[GKSS-91/E/67] p 256 N93-11337
Method and apparatus for evaluating multilayer objects for imperfections
[NASA-CASE-LAR-14581-1-SB] p 333 N93-12204
Microstructure-based fatigue life prediction methods for naval steel structures
[AD-A254628] p 260 N93-12241
Characteristics of heat transfer to nickel plated chamber walls of high pressure rocket combustors
[NAL-TR-1126T] p 234 N93-12372
Study of residual stresses and microcracks in high strength steel weldments: An investigation of microcrack formation and stressed growth using laser microscopy
[AD-A255059] p 342 N93-12467

MICROELECTRONICS
Materials science and engineering at the Naval Research Laboratory: Research programs and 1990 publications
[PB92-199488] p 238 N93-11422
RF vacuum microelectronics
[AD-A253910] p 290 N93-11491
An accurate and efficient method to calculate the rate of single event upsets from the LET spectrum and SEU cross section test results
[AD-A253917] p 290 N93-11492
Current state and future direction of computer systems at NASA Langley Research Center
[NASA-TM-107685] p 414 N93-12278
Mesoscopic effects in electronic microstructures
[AD-A254889] p 295 N93-12502

MICROMECHANICS
Thermal residual stresses in silicon-carbide/titanium (0/90) laminate
[NASA-TM-107649] p 236 N93-11072
Micromechanics of metal matrix composites using the Generalized Method of Cells model (GMC) user's guide
[NASA-CR-190756] p 335 N93-11175
Micromechanisms of deformation and fracture in aluminum based MMC's: Interface effects
[AD-A253560] p 259 N93-11850
Scanning electron microscopy of the effects of moisture and elevated temperature on the fibre/matrix bond in CFRP
[RAE-TM-MAT-STR-1183] p 240 N93-11905
ICAN/DAMP-integrated composite analyzer with damping analysis capabilities: User's manual
[NASA-TP-3292] p 241 N93-12015
Fatigue in single crystal nickel superalloys
[AD-A254603] p 260 N93-12237
Micromechanical combined stress analysis: MICSTRAN, a user manual
[NASA-CR-189694] p 243 N93-12306

MICROMETEORITES
Thin-sectioning and analysis of fine-grained meteoritic materials
[NASA-CR-185693] p 485 N93-11546

MICROMINIATURIZED ELECTRONIC DEVICES
Mesoscopic effects in electronic microstructures
[AD-A254889] p 295 N93-12502

MICROORGANISMS
Evaluation of an analytical model for predicting light scattering from cylindrically-shaped objects in the ocean
[AD-A248414] p 447 N93-11489
Microbiological analysis of debris from STS-42 IML-1 by direct plating of rinse waters
[NASA-TM-108375] p 375 N93-12174
ECLSS medical support activities
[NASA-CR-184429] p 385 N93-12427

MICROPOROSITY
Optical properties of composite membranes containing arrays of nanoscopic gold cylinders
[AD-A253659] p 238 N93-11281
Influence of strain rate on the structure/property behavior of the alpha-2 alloy Ti-24.5Al-10.5Nb-1.5Mo
[DE92-008490] p 261 N93-12256

MICROPROCESSORS
The VISTA structured assembler
[RSRE-91034] p 407 N93-11341
Using ELLA for high level design: Modelling the Motorola 6800 microprocessor
[RSRE-MEMO-4515] p 408 N93-11386
A smart end-effector for assembly of space truss structures p 230 N93-11982
Current state and future direction of computer systems at NASA Langley Research Center
[NASA-TM-107685] p 414 N93-12278
Formal specification of the VIPER microprocessor in HOL
[RSRE-90009] p 405 N93-12430
Formal design specification of a Processor Interface Unit
[NASA-CR-189698] p 406 N93-12538

MICROPROGRAMMING
Applying algebraic techniques to microcode compilation
[RSRE-MEMO-4568] p 409 N93-11392

MICROSCOPES
Fuzzy control system for a remote focusing microscope p 314 N93-11934

MICROSCOPY
Microwave sintering of multilayer ceramic capacitors
[DE92-018772] p 267 N93-11570
Studies of the 3 to 5 compounds in the megabar regime
[DE92-019517] p 461 N93-11646
Nuclear magnetic resonance microscopy: New theoretical and technical developments
p 313 N93-11907

A ring coded-aperture microscope for high-resolution imaging of high-energy x rays [DE92-018004] p 454 N93-12059

MICROSTRIP TRANSMISSION LINES

Unequal stub length diplexing microwave frequency discriminator circuit [AD-D015352] p 288 N93-11051

MICROSTRUCTURE

A creep cavity growth model for creep-fatigue life prediction of a unidirectional W/Cu composite [NASA-TM-105780] p 333 N93-10967

Critical currents in polycrystalline YBa2Cu3O(7-x): Self-field and grain size dependence [DE92-617540] p 459 N93-11076

Microstructure and mechanical properties of reactive hot isostatic pressed TiAl powder material [GKSS-91/E/60] p 256 N93-11336

Review of phonon behavior and microstructural development leading to martensitic transformations in Ni(x)Al(100-x) alloys [DE92-014782] p 256 N93-11519

Thin-sectioning and analysis of fine-grained meteoritic materials [NASA-CR-185693] p 485 N93-11546

Isotopic tailoring with 59-Ni to study the effect of helium on microstructural evolution and mechanical properties of neutron-irradiated Fe-Cr-Ni alloys [DE92-019372] p 257 N93-11557

Review of the physical and mechanical properties and potential applications of the B2 compound NiAl: Unabridged version of a paper published in International materials review [NASA-TM-105598] p 258 N93-11635

Grain boundary transport and related processes in natural fine grained aggregates [DE92-018239] p 461 N93-11682

The physics of pattern formation at liquid interfaces [DE92-016971] p 462 N93-11747

Step-driven surface segregation and ordering during Si-Ge MBE growth [DE92-017827] p 463 N93-11772

Relationship of bainitic microstructure to impact toughness in Cr-Mo and Cr-W steels [DE92-017828] p 258 N93-11773

Micromechanisms of deformation and fracture in aluminum based MMC's: Interface effects [AD-A253560] p 259 N93-11850

The mechanical and microstructural stability of austenitic stainless steels strengthened by MC-forming elements [DE91-015314] p 259 N93-11857

Mechanisms of localized aqueous corrosion in aluminum-lithium-copper alloys p 259 N93-11895

Effect of microstructure on passive film formation and breakdown on Al alloys [AD-A245863] p 260 N93-12118

Microstructure-based fatigue life prediction methods for naval steel structures [AD-A254628] p 260 N93-12241

Influence of oxygen partial pressure and silver additions on microstructure and related properties of YBCO superconductors [DE92-011145] p 468 N93-12249

Influence of strain rate on the structure/property behavior of the alpha-2 alloy Ti-24.5Al-10.5Nb-1.5Mo [DE92-008490] p 261 N93-12256

MICROWAVE ABSORPTION

Higher-order-mode damping and microwave absorption at 2 K [DE92-016960] p 442 N93-11077

MICROWAVE AMPLIFIERS

On some practical consideration of the electron beam breakup transit time oscillator [DE92-017406] p 445 N93-11919

The development of a one microsecond pulse length, repetitively pulsed, high power modulator, and a long-pulse electron beam diode for the production of intense microwaves [DE92-015974] p 293 N93-12089

MICROWAVE ANTENNAS

The millimeter wave Cloud Profiling Radar System (CPRS) [DE92-016970] p 366 N93-10971

MICROWAVE CIRCUITS

Unequal stub length diplexing microwave frequency discriminator circuit [AD-D015352] p 288 N93-11051

The fourth OSA Topical Meeting Proceedings on Picosecond Electronics and Optoelectronics, volume 9 [AD-A253472] p 447 N93-11099

MMIC GaAs bonding investigation [AD-A254773] p 470 N93-12464

MICROWAVE EQUIPMENT

SITE project. Phase 1: Continuous data bit-error-rate testing [NASA-TP-3279] p 224 N93-11001

The fourth OSA Topical Meeting Proceedings on Picosecond Electronics and Optoelectronics, volume 9 [AD-A253472] p 447 N93-11099

Microwave guidance technology and its applications [AD-A254107] p 281 N93-11509

Automatic Attenuation/Phase Calibration System (AAPCS) [DE92-017354] p 284 N93-11917

MICROWAVE FREQUENCIES

Unequal stub length diplexing microwave frequency discriminator circuit [AD-D015352] p 288 N93-11051

MICROWAVE RADIOMETERS

Nimbus-7 Scanning Multichannel Microwave Radiometer (SMMR) PARM tape user's guide [NASA-RP-1284] p 373 N93-11718

MICROWAVE REFLECTOMETERS

An uncertainty budget for VHF and UHF reflectometers [NPL-DES-120] p 281 N93-11395

MICROWAVE SCATTERING

Experimental measurement and theoretical modeling of microwave scattering and the structure of the sea surface influencing radar observations from space [NASA-CR-190998] p 343 N93-12006

MICROWAVE SWITCHING

Data distribution satellite [NASA-TM-105778] p 287 N93-12481

MICROWAVE TRANSMISSION

Josephson Junction digital waveform generation for very wideband radars [AD-A253668] p 467 N93-12169

MICROWAVES

Microwave sintering of multilayer ceramic capacitors [DE92-018772] p 267 N93-11570

Synthesis of nanocrystalline powders for oxide ceramics by microwave plasma pyrolysis [DE92-017410] p 268 N93-11861

Electronic transport and lasing in microstructures [DE92-018725] p 441 N93-12115

Submillimeter and microwave residual losses in epitaxial films of Y-Ba-Cu-O and Bl-Ca-Ca-Cu-O [DE92-017075] p 466 N93-12125

MIDDLE ATMOSPHERE

Computer simulation and experimental investigation of the absorption cell for the rocketborne diode-laser experiment MASERATI [BONN-IR-91-62] p 357 N93-11083

MIDLATITUDE ATMOSPHERE

The forcing of a mid-latitude upper-tropospheric jet streak by a simulated mesoscale convective system p 358 N93-11184

MIE SCATTERING

Light scattering from a sphere on or near an interface p 448 N93-12531

MIGRATION

Hydrodynamic particle migration in small-amplitude, oscillatory, circular couette flow: The limits of reversibility [DE92-008480] p 303 N93-11843

MILITARY AIRCRAFT

Winds of change: Expanding the frontiers of flight. Langley Research Center's 75 years of accomplishment, 1917-1992 [NASA-NP-130] p 490 N93-11100

MILITARY HELICOPTERS

Rigid body mode identification of the PAH-2 helicopter using the eigensystem realization algorithm [NASA-TM-107690] p 336 N93-11544

The Fourth Workshop on Dynamics and Aeroelastic Stability Modeling of Rotorcraft Systems [AD-A255065] p 208 N93-12485

An evaluation of crew coordination and performance during a simulated UH-60 helicopter mission [AD-A254984] p 390 N93-12509

MILITARY OPERATIONS

Mechanisms of immune failure in burn injury p 376 N93-11285

AIDS/HIV in the US Military p 377 N93-11291

Estimates of Human Immunodeficiency Virus (HIV) incidence and trends in the US Air Force p 377 N93-11292

Global Climate Change (GCC) issues and their impacts on the US Army Corps of Engineers [AD-A247279] p 353 N93-11466

Integrity-oriented control objectives: Proposed revisions to the Trusted Computer System Evaluation Criteria (TCSEC), DOD 5200.28-STD [AD-A253989] p 404 N93-11809

LINK user manual [DE92-017987] p 479 N93-12143

Sustaining health and performance in the cold: Environmental medicine guidance for cold-weather operation [AD-A254328] p 385 N93-12145

The future of carrier aviation [AD-A254043] p 430 N93-12260

MILITARY PSYCHOLOGY

Relating cognitive function to military aviator performance in early HIV infection p 379 N93-11298

Neuropsychiatric morbidity in early HIV disease: Implications for military occupational function p 379 N93-11299

MILITARY SPACECRAFT

Requirements and applications for robotic servicing of military space systems p 230 N93-11953

MILITARY TECHNOLOGY

Speech recognition systems and their military applications [BR91882] p 280 N93-11366

Solid state sciences committee forum [AD-A253556] p 463 N93-11753

MILLIMETER WAVES

The millimeter wave Cloud Profiling Radar System (CPRS) [DE92-016970] p 366 N93-10971

A submillimeter-millimeterwave study of the molecular gas in the nuclear regions of three nearby starburst galaxies p 484 N93-11260

Microwave guidance technology and its applications [AD-A254107] p 281 N93-11509

MIMD (COMPUTERS)

An implementation of a parallel MOL solver on the Intel Gamma parallel computer [DE92-018947] p 419 N93-12233

MIMO (CONTROL SYSTEMS)

Flight-determined stability analysis of multiple-input-multiple-output control systems [NASA-TM-4416] p 214 N93-11178

MINIATURIZATION

Microtube strip heat exchanger [DE92-018709] p 300 N93-11440

MINORITY CARRIERS

Investigation of high efficiency monolithic multibandgap solar cells [AD-A254326] p 348 N93-12144

MIRA VARIABLES

A linear and nonlinear study of Mira [DE92-011265] p 483 N93-10993

MIRRORS

Thermal analysis and design of polarizer mirrors for waveguides in the D3-D tokamak [DE92-018884] p 451 N93-11382

High frame-rate, large field wavefront sensor [DE92-019547] p 310 N93-11542

Laser surface profilometer with sub-Angstrom resolution [DE92-018926] p 317 N93-12011

Mirror alignment techniques for point-focus solar concentrators [DE92-019643] p 348 N93-12074

Fiber optic delay line signal processors [AD-A254691] p 448 N93-12227

MIS (SEMICONDUCTORS)

Magnetic properties and critical behavior of the conductivity near the M-I transition [DE92-018948] p 461 N93-11629

MISSILE COMPONENTS

Droppable jet vane TVC [AD-D015341] p 214 N93-11046

Inflatable device for excluding sea water from a rocket motor [AD-D015365] p 232 N93-11424

Booster rocket range safety system [AD-D015363] p 221 N93-11428

MISSILE CONTROL

Droppable jet vane TVC [AD-D015341] p 214 N93-11046

Parallel architecture for image processing with optic fiber guided missile [REPT-921-320-101] p 418 N93-11584

Advanced control for the design of STT missile autopilot [REPT-921-320-102] p 215 N93-11585

MISSILES

Inflatable device for excluding sea water from a rocket motor [AD-D015365] p 232 N93-11424

Booster rocket range safety system [AD-D015363] p 221 N93-11428

Translating wedge heat sink [AD-D015357] p 293 N93-12133

MISSION ADAPTIVE WINGS

Flight test results from a supercritical mission adaptive wing with smooth variable camber [NASA-TM-4415] p 207 N93-11863

MISSION PLANNING

Payload advisory panel recommendations [NASA-TM-108012] p 219 N93-11528

Evaluation of transportation systems for advanced space flight missions [ESA-TT-1256] p 223 N93-11685

Manager's assistant systems for space system planning p 398 N93-11952
Manned Mars System Study (MMSS): Mars transportation and facility study. Volume 1: Executive Summary
[NASA-CR-184473] p 227 N93-12442
Development of a model for predicting NASA/MSFC program success
[NASA-CR-184423] p 473 N93-12542

MIXED OXIDES
Recrystallization of amorphous or nanocrystalline NdBa2Cu3O(7-x) and GdBa2Cu3O(7-x)
[DE92-016302] p 462 N93-11706
Infrared phonon structure in epitaxial films of Tl2Ca2Ba2Cu3O10 at low temperatures
[DE92-017078] p 466 N93-12109

MIXING
Liquid-liquid equilibria in binary systems: Monte-Carlo simulation for calculating the effect of nonrandom mixing
[DE92-017020] p 263 N93-10972
Front tracking and the interaction of nonlinear waves
[AD-A253544] p 297 N93-11148
Heat transfer enhancement by chaotic mixing
[PB92-190305] p 470 N93-11469
Regular and chaotic mixing of viscous fluids in eccentric rotating cylinders p 305 N93-12157

MIXING LAYERS (FLUIDS)
Front tracking and the interaction of nonlinear waves
[AD-A253544] p 297 N93-11148
Mixing regimes in a spatially confined, two-dimensional, supersonic shear layer
[AD-A254302] p 302 N93-11756
Flow visualization of supersonic flow through a combustor section p 200 N93-12001
Compressible mixing layers with and without particles
[AD-A254854] p 308 N93-12435

MIXING LENGTH FLOW THEORY
Anomalous ion thermal transport in hot ion plasmas by the ion temperature gradient mode
[DE92-016686] p 456 N93-12493

MOBILE COMMUNICATION SYSTEMS
Direct Broadcast Satellite: Radio Program
[NASA-TM-105910] p 224 N93-11430
All-digital multicarrier demodulators for on-board processing satellites in mobile communication systems
p 285 N93-12207

MOBILITY
Molecular mobility of the interface in a model composite: A NMR study
[AD-A253311] p 265 N93-11194

MODELS
The use of statistical measures to validate system dynamics models
[AD-A248569] p 428 N93-11417
Modified optimal control pilot model for computer-aided design and analysis
[NASA-TM-4384] p 214 N93-11459

MODERATORS
Meta-analysis of integrity tests: A critical examination of validity generalization and moderator variables
[AD-A254681] p 386 N93-12225

MODFETS
Programme and abstracts. Workshop on Expert Evaluation and Control of Compound Semiconductor Materials and Technologies No. 1: (EXAMTEC 199)
[AD-A254023] p 292 N93-12071

MODULARITY
Research on a reconfigurable modular manipulator system
[DE92-018943] p 327 N93-11865

MODULATION TRANSFER FUNCTION
The sensitivity of the receiver coherence diameter and modulation transfer function to variations of a damp unstable atmosphere
[AD-A253269] p 363 N93-11785

MODULATORS
BANSHEE: High-voltage repetitively pulsed electron-beam driver
[DE92-017413] p 444 N93-11763

MODULES
Evaluation tests for photovoltaic concentrator receiver sections and modules
[DE92-017745] p 346 N93-11771

MODULUS OF ELASTICITY
Advanced one-dimensional optical strain measurement system, phase 4
[NASA-CR-190760] p 314 N93-12279
Modified epoxy adhesives and primers
[AD-A253857] p 272 N93-12297

MOIRE FRINGES
Automated fringe analysis for moire interferometry
[PNR-90918] p 334 N93-11021

MOIRE INTERFEROMETRY
Automated fringe analysis for moire interferometry
[PNR-90918] p 334 N93-11021

MOLECULAR BEAM EPITAXY
INAS hole-immobilized doping superlattice long-wave-infrared detector
[NASA-CASE-NPO-17880-1-CU] p 458 N93-11056
Interfacial and thin film chemistry in electron device fabrication
[AD-A253579] p 288 N93-11257
Atomistic processes of surface segregation during Si-Ge MBE growth
[DE92-019180] p 459 N93-11496
Step-driven surface segregation and ordering during Si-Ge MBE growth
[DE92-017827] p 463 N93-11772
Superconducting multilayer structures grown by ALL-MBE
[DE92-018011] p 465 N93-12065

MOLECULAR BEAMS
The chemistry of Si3N4 and Si deposition studied using molecular beam techniques
[DE92-018268] p 463 N93-11797

MOLECULAR BIOLOGY
Molecular cytogenetics: A novel approach for measuring chromosome translocations in individuals years after exposure to low levels of ionizing radiation
[DE92-018066] p 374 N93-10974
Exploratory Research and Development Fund, FY 1990
[DE92-017002] p 489 N93-11078
Radiation physics, biophysics, and radiation biology
[DE92-013673] p 375 N93-12266

MOLECULAR CHAINS
Synthesis of side chain liquid crystal polymers by living ring opening metathesis polymerization. Report 3: Influence of molecular weight, interconnecting unit and substituent on the mesomorphic behavior of polymers with laterally attached mesogens
[AD-A248698] p 265 N93-11187
Synthesis of side chain liquid crystal polymers by living ring opening metathesis polymerization. Report 2: Influence of molecular weight, polydispersity, and flexible spacer length (n=9-12) on the thermotropic behavior of the resulting plymers
[AD-A248700] p 265 N93-11188

MOLECULAR CLOUDS
A submillimeter-millimeterwave study of the molecular gas in the nuclear regions of three nearby starburst galaxies p 484 N93-11260

MOLECULAR COLLISIONS
Determination of stepsize parameters for intermolecular vibrational energy transfer
[DE92-010770] p 435 N93-11189
State-resolved dynamics of ion-molecule collisions in a flowing afterglow
[AD-A247288] p 436 N93-11467
State-resolved collisional energy transfer in highly vibrationally excited polyatomic molecules
[AD-A253299] p 441 N93-12323

MOLECULAR ENERGY LEVELS
Determination of stepsize parameters for intermolecular vibrational energy transfer
[DE92-010770] p 435 N93-11189
State-resolved collisional energy transfer in highly vibrationally excited polyatomic molecules
[AD-A253299] p 441 N93-12323

MOLECULAR EXCITATION
Determination of stepsize parameters for intermolecular vibrational energy transfer
[DE92-010770] p 435 N93-11189
State-resolved reaction dynamics
[AD-A254291] p 436 N93-11196
A multi-line study of the molecular interstellar medium on M82's starburst nucleus
[MPE-PREPRINT-213] p 484 N93-11347
State-resolved dynamics of ion-molecule collisions in a flowing afterglow
[AD-A247288] p 436 N93-11467
Investigation of a cesium Raman time/frequency standard
[AD-A252677] p 310 N93-11562
Multiphoton ionization and ion-pair formation in molecular hydrogen
[DE92-019026] p 438 N93-11829
Studies of transition states and radicals by negative ion photodetachment
[DE92-017011] p 440 N93-11875
Laser spectroscopy and dynamics of transient species formed in pyrolysis reactions
[DE92-016206] p 251 N93-12091
State-resolved collisional energy transfer in highly vibrationally excited polyatomic molecules
[AD-A253299] p 441 N93-12323

MOLECULAR GASES
A submillimeter-millimeterwave study of the molecular gas in the nuclear regions of three nearby starburst galaxies p 484 N93-11260
A multi-line study of the molecular interstellar medium on M82's starburst nucleus
[MPE-PREPRINT-213] p 484 N93-11347
Multiphoton ionization and ion-pair formation in molecular hydrogen
[DE92-019026] p 438 N93-11829

MOLECULAR INTERACTIONS
State-resolved reaction dynamics
[AD-A254291] p 436 N93-11196
Cellular and molecular pathways of extremely-low-frequency electromagnetic field interactions with living systems
[DE92-019084] p 282 N93-11515
Comparative effects of drag-reducing polymers. An experimental report
[AD-A254001] p 268 N93-11793

MOLECULAR OSCILLATIONS
Determination of stepsize parameters for intermolecular vibrational energy transfer
[DE92-010770] p 435 N93-11189

MOLECULAR RELAXATION
Determination of stepsize parameters for intermolecular vibrational energy transfer
[DE92-010770] p 435 N93-11189
State-resolved collisional energy transfer in highly vibrationally excited polyatomic molecules
[AD-A253299] p 441 N93-12323

MOLECULAR ROTATION
State-resolved reaction dynamics
[AD-A254291] p 436 N93-11196

MOLECULAR SPECTRA
A multi-line study of the molecular interstellar medium on M82's starburst nucleus
[MPE-PREPRINT-213] p 484 N93-11347

MOLECULAR STRUCTURE
Detonation reactions frozen by free expansion and analyzed by mass spectrometry
[DE92-018605] p 274 N93-11566
Magnetic resonance elucidation of molecule/macromolecule interaction stereochemistry
[AD-A253030] p 437 N93-11709
Theoretical studies of high-temperature superconductors and highly compressed hydrogen
p 292 N93-11833
Concerted hydrogen atom exchange between three HF molecules p 439 N93-11855
Advanced methods for structural characterization of large multiply charged ions: Obtaining charge state determination and improved sensitivity
[DE91-015264] p 441 N93-12117

MOLECULAR WEIGHT
Synthesis of side chain liquid crystal polymers by living ring opening metathesis polymerization. Report 2: Influence of molecular weight, polydispersity, and flexible spacer length (n=9-12) on the thermotropic behavior of the resulting plymers
[AD-A248700] p 265 N93-11188
An evaluation of field-flow fractionation for molecular weight characterization of polymeric materials
[DE92-019192] p 267 N93-11497
Progress on polymer degradation by photoelectron transfer
[AD-A246276] p 268 N93-11862
Advanced methods for structural characterization of large multiply charged ions: Obtaining charge state determination and improved sensitivity
[DE91-015264] p 441 N93-12117
Probing flame chemistry with MBMS, theory, and modeling
[DE92-011433] p 251 N93-12119

MOLECULES
Gas-surface interactions near dissociation threshold
[AD-A250205] p 252 N93-12254

MOLTEN SALTS
Chronopotentiometry of refractory metals, actinides and oxyanions in molten salts: A review
[NASA-TM-105862] p 249 N93-11545

MOLYBDENUM ALLOYS
Study of metal-ceramic interfaces of Co-Cr-Mo alloys: Role of tungsten (W) and manganese (Mn) additions
[ECL-92-01] p 267 N93-11580
Mechanical properties for advanced engine materials
[AD-A252632] p 242 N93-12181
Studies on the reactive melt infiltration of silicon and silicon-molybdenum alloys in porous carbon
[NASA-TM-105860] p 273 N93-12398

MOLYBDENUM COMPOUNDS
Synthesis and side chain liquid crystal polymers by living ring opening metathesis polymerization. 5: Influence of mesogenic group and interconnecting group on the thermotropic behavior of the resulting polymers
[AD-A253568] p 264 N93-11150

MOMENTUM
Particle-fluid two-phase flow modeling
[DE92-017847] p 301 N93-11637

MONITORS
Authentication algorithm for the universal Authenticated Item Monitoring Systems (AIMS)
[DE92-018826] p 408 N93-11378
Rotorcraft health and usage monitoring systems: A literature survey
[DOT/FAA/RD-91/6] p 206 N93-11461
Acoustic emission monitoring of HFIR vessel during hydrostatic testing
[DE92-019316] p 332 N93-11601
A model-based reasoning approach to sensor placement for monitorability p 391 N93-11923
MONKEYS
Freeze-dried human red blood cells
[AD-A253295] p 376 N93-11193
MONOMERS
Organometallic NLO polymers. 3. Copolymerization of bridged bis(ferrocenyl) and bis(cyanoacetate) monomers via the knoevenagel condensation
[AD-A250214] p 265 N93-11192
MONSOONS
Interannual variabilities of the East Asian summer monsoon and tropical sea surface temperatures
p 372 N93-12534
MONTE CARLO METHOD
Liquid-liquid equilibria in binary systems: Monte-Carlo simulation for calculating the effect of nonrandom mixing
[DE92-017020] p 263 N93-10972
Stochastic control and nonlinear estimation
[AD-A253543] p 420 N93-11147
Monte Carlo simulations of the supernova ejection mechanism for the runaway stars
[DE92-018367] p 485 N93-11695
Oxidation, nitridation, and fluorine etching of Si
[AD-A253559] p 249 N93-11755
Curve fitting and error modeling for the digitization process near the Nyquist rate
[DE92-018189] p 286 N93-12417
Mixed ionic and electronic conductivity in polymers
[DE92-018723] p 273 N93-12500
MOORING
Deep penetration into frictional ductile and brittle materials
[PB92-205566] p 338 N93-11903
MORPHOLOGY
A contribution to fatigue failure morphologies in fiber reinforced plastics
[MBB-Z-0212-91-PUB] p 263 N93-11010
X ray morphology of clusters of galaxies
p 482 N93-11475
Morphology and physics of supernova remnants
p 482 N93-11476
MORTALITY
Communicable diseases: A major burden of morbidity and mortality p 380 N93-11300
MOTION PERCEPTION
Visual psychophysics of egomotion
[AD-A248349] p 386 N93-11488
Visual perception of structure from motion
[AD-A253235] p 386 N93-11503
MOUNTAINS
Crustal and upper mantle velocity gradients in the vicinity of the East Kazakh test site
[AD-A246889] p 362 N93-11740
Atmospheric dispersion in mountain valleys and basins
p 355 N93-11920
MTBF
Operating characteristic analysis for reliability growth programs
[AD-A254993] p 333 N93-12510
MULTIBEAM ANTENNAS
Project and test of a reconfigurable multiple feed system in C-band
[MBB-UK-0162-92-PUB] p 278 N93-11009
MULTIGRID METHODS
An adaptive differencing scheme for elliptic flows
p 297 N93-11197
MULTIPHASE FLOW
3-D turbulent particle dispersion submodel development
[DE92-018212] p 301 N93-11670
MULTIPHOTON ABSORPTION
Propagation of relativistic high current electron beams across the geomagnetic field
[DE92-018276] p 362 N93-11564
Multiphoton ionization and ion-pair formation in molecular hydrogen
[DE92-019026] p 438 N93-11829
Image potential states at metal-dielectric interfaces
[DE92-017019] p 466 N93-12124
MULTIPLE ACCESS
A simple, effective media access protocol system for integrated, high data rate networks p 279 N93-11119
MULTIPLEXING
Digital signal processing
[AD-A254870] p 287 N93-12436
MULTIPLIERS
A fast pipelined inner product unit
[REPT-92-025] p 411 N93-11594
MULTIPOLAR FIELDS
Nonlinear behavior of resonant absorption in a plasma at microwave frequency p 319 N93-12032
MULTIPROCESSING (COMPUTERS)
Scalable parallel communications p 279 N93-11117
Scattering on a ring of processors
p 410 N93-11482
ScaLAPACK: A scalable linear algebra library for distributed memory concurrent computers
[DE92-017823] p 426 N93-11636
Automatic data partitioning on distributed memory multicomputers
[NASA-CR-190976] p 418 N93-11651
Model-based vision for space applications
p 398 N93-11955
An integrated dexterous robotic testbed for space applications p 330 N93-11972
An implementation of a parallel MOL solver on the Intel Gamma parallel computer
[DE92-018947] p 419 N93-12233
Performance evaluation and modeling techniques for parallel processors
[NASA-CR-190974] p 419 N93-12395
Measurement and analysis of operating system fault tolerance
[NASA-CR-190973] p 406 N93-12540
MULTIPROGRAMMING
Performance evaluation and modeling techniques for parallel processors
[NASA-CR-190974] p 419 N93-12395
MULTISENSOR APPLICATIONS
Algorithms for sensor fusion: Decentralized Bayesian hypothesis testing with feedback, volume 1
[AD-A254633] p 414 N93-12242
MULTISPECTRAL RADAR
Detection of cloud-top height from backscattered radiances within the oxygen A band. Part 2: Measurements
[GKSS-91/E/77-PT-2] p 368 N93-11350
MUONS
Nucleon structure functions from deep inelastic muon scattering
[NIKHEF-H+K/92-01] p 442 N93-11130
Research in elementary particles and interactions
[DE92-018089] p 437 N93-11681

N

NACELLES
Application of laminar flow to aero engine nacelles
[PNR-90916] p 195 N93-11020
A combined experimental and theoretical study of laminar flow control with particular relevance to aero engine nacelles
[PNR-90991] p 195 N93-11070
A European collaborative NLF nacelle flight demonstrator
[PNR-90992] p 196 N93-11113
A wind tunnel investigation to determine buffet countermeasures for STOL aircraft alpha-sweep flight testing
[NAL-TR-1129] p 216 N93-12362
NAP-OF-THE-EARTH NAVIGATION
Integration of radar altimeter, precision navigation, and digital terrain data for low-altitude flight
[NASA-TM-103958] p 205 N93-12320
NASA PROGRAMS
Winds of change: Expanding the frontiers of flight. Langley Research Center's 75 years of accomplishment, 1917-1992
[NASA-NP-130] p 490 N93-11100
The NASA CSTI high capacity power project
[NASA-TM-105813] p 221 N93-11398
The early Earth Observing System reference handbook: Earth Science and Applications Division missions, 1990-1997
[NASA-TM-107963] p 343 N93-11663
ISDN at NASA Lewis Research Center
[NASA-TM-105911] p 419 N93-12410
Development of a model for predicting NASA/MSFC program success
[NASA-CR-184423] p 473 N93-12542
NASA SPACE PROGRAMS
The first meeting of the Advisory Committee on the Future of the US Space Program (C-FUSSP)
[NASA-CR-190995] p 219 N93-11754
NATIONAL AIRSPACE SYSTEM
Methods and principles for determining task dependent interface content
[NASA-CR-190837] p 204 N93-10961
Low Density Radio Communications Link (LDRCL) Operational Test and Evaluation (OT/E) integration and operation test plan
[DOT/FAA/CT-TN92/4] p 285 N93-12331
NATURAL GAS
Biological conversion of synthesis gas culture development
[DE92-001279] p 375 N93-12482
NATURAL LANGUAGE (COMPUTERS)
Exploiting captions in retrieval of multimedia data
[AD-A255184] p 479 N93-12381
Selecting reusable components using algebraic specifications p 415 N93-12387
NAVIER-STOKES EQUATION
On the instability of hypersonic flow past a pointed cone: Comparison of theoretical and experimental results of Mach 18
[DLR-FB-92-02] p 196 N93-11141
Boundary condition methods in the numerical solution of the Navier-Stokes equations with the application to free surface problems
[ISBN-0-315-64278-5] p 298 N93-11241
Increase of energy use on cooled high temperature turbine, phase 3
[MTUM-B91EW-0029-PHASE-3] p 213 N93-11339
Solution of two-phase reacting flow in liquid thrust chambers p 235 N93-11449
A three dimensional high resolution upwind finite volume Euler solver
[VKI-TN-180] p 198 N93-11686
Numerical study of advanced rotor blades
p 199 N93-11899
Application of a two-layer near wall model to fully developed and rotating channel turbulent flows
[NASA-CR-184441] p 305 N93-12082
Flow in curved ducts of varying cross-section
[AD-A254660] p 306 N93-12245
Spurious modes in spectral collocation methods with two non-periodic directions
[NASA-CR-189713] p 427 N93-12298
NAVIGATION AIDS
Development of a GPS-aided motion measurement, pointing, and stabilization system for a synthetic aperture radar
[DE92-017053] p 204 N93-11152
LORAN and the effects of terrestrial propagation
[PB92-197219] p 205 N93-11472
Flight simulator evaluation of D-size liquid crystal flat panel displays
[NAL-TR-1136] p 209 N93-12367
Liquid crystal flat panel display evaluation tests using a flight simulator
[NAL-TR-1122] p 209 N93-12383
NAVIGATION TECHNOLOGY SATELLITES
Integrated services digital network conformance testing. Layer 1, physical layer. Part 2: Basic rate U interface, user side
[PB92-181114] p 418 N93-11714
NAVY
The future of carrier aviation
[AD-A254043] p 430 N93-12260
NEAR FIELDS
Antenna pattern measurement facilities
[AD-A250219] p 283 N93-11764
Ultra wide band 3-D cross section (RCS) holography
[DE92-019133] p 312 N93-11802
Near-field and far-field sound radiation from a line-driven fluid-loaded infinite flat plate having periodic and non-periodic attached rib stiffeners p 434 N93-11884
Extension of fresnel near-field region by single-cycle sinusoidal pulses
[AD-A254736] p 285 N93-12356
NEAR INFRARED RADIATION
Near-infrared imaging polarimetry of bipolar nebulae
p 481 N93-11248
Near-IR absorption spectra for the C70 fullerene anions
[AD-A253658] p 246 N93-11280
NEGATIVE IONS
Studies of transition states and radicals by negative ion photodetachment
[DE92-017011] p 440 N93-11875
Threshold photodetachment spectroscopy of negative ions
[DE92-017090] p 440 N93-12100
Characterization of underivatized pterins by laser desorption Fourier transform mass spectrometry
[DE92-016785] p 323 N93-12514
NEODYMIUM
Preparation, optical and laser properties of Nd-doped sol-gel silica
[DE92-019378] p 461 N93-11602
NEODYMIUM COMPOUNDS
Recrystallization of amorphous or nanocrystalline NdBa2Cu3O(7-x) and GdBa2Cu3O(7-x)
[DE92-016302] p 462 N93-11706

NEODYMIUM LASERS
Nova Upgrade: A proposed ICF facility to demonstrate ignition and gain, revision 1
[DE92-018960] p 451 N93-11534
High bandwidth second-harmonic generation in partially deuterated KDP
[DE92-019505] p 452 N93-11645

NEON
VUV and UV sources and spectroscopic applications
[AD-A247293] p 291 N93-11758
Connected triple excitations in coupled-cluster calculations of hyperpolarizabilities: Neon
p 439 N93-11854

NERVOUS SYSTEM
Physiological analyses of the afferents controlling brain neurochemical systems
[AD-A253185] p 375 N93-11146
New techniques for positron emission tomography in the study of human neurological disorders
[DE92-015353] p 384 N93-11873

NETWORK ANALYSIS
The network destruction problem (extended abstract)
[DE92-016171] p 419 N93-11860
Polynomial dual network simplex algorithms
[AD-A254340] p 413 N93-12131
Data distribution satellite
[NASA-TM-105778] p 287 N93-12481

NETWORK CONTROL
High performance interconnection between high data rate networks p 279 N93-11118
A simple, effective media access protocol system for integrated, high data rate networks p 279 N93-11119
A comparison of feed-forward networks and maximum likelihood on a point-source location problem
[RSRE-MEMO-4567] p 281 N93-11391
Application of artificial neural networks in nonlinear analysis of trusses
[NASA-TM-105319] p 336 N93-11403

NEUMANN PROBLEM
On an origin of numerical diffusion: Violation of invariance under space-time inversion
[NASA-TM-105776] p 425 N93-11254

NEURAL NETS
An introduction to the information processing components of the brain
[RSRE-MEMO-4350] p 385 N93-10979
Intelligent TDA systems using neural networks, phase 1
[AD-A252556] p 420 N93-11000
The adaptive neuron model: An architecture for the rapid learning of nonlinear topological transformations
[NASA-CASE-NPO-18579-1-CU] p 420 N93-11174
A comparison of feed-forward networks and maximum likelihood on a point-source location problem
[RSRE-MEMO-4567] p 281 N93-11391
Application of artificial neural networks in nonlinear analysis of trusses
[NASA-TM-105319] p 336 N93-11403
Geometrical concepts about learning rules in networks with binary and ternary output functions
[REPT-92-020] p 411 N93-11592
Design development of a neural network-based telemetry monitor p 394 N93-11933
A neuro-collision avoidance strategy for robot manipulators p 400 N93-11962
Self mobile space manipulator project
p 331 N93-11973
Forecasting the relativistic electron flux at geosynchronous orbit
[AD-A254016] p 226 N93-12064
Neural network models of air combat maneuvering
[AD-A254653] p 421 N93-12096
Transient Reduction Analysis using Neural Networks (TRANN)
[DE92-012150] p 421 N93-12153
Real-time classification of signals from three-component seismic sensors using neural nets
[DE92-014886] p 364 N93-12155
Adaptive neural network models for intelligent computations
[AD-A254689] p 421 N93-12226
Complex cognitive information processing: A computational architecture with a connectionist implementation
[AD-A254041] p 422 N93-12259
Analysis of fault-tolerant neurocontrol architectures
[NASA-TM-105898] p 215 N93-12305
Neural network-based retrieval from software reuse repositories p 415 N93-12388
A neural net-based approach to software metrics
p 415 N93-12392
Active control of complex systems via dynamic (recurrent) neural networks
[AD-A254878] p 422 N93-12439
Ultrasonic flaw classification and sizing
p 333 N93-12533

NEUROLOGY
An introduction to the information processing components of the brain
[RSRE-MEMO-4350] p 385 N93-10979
Physiological analyses of the afferents controlling brain neurochemical systems
[AD-A253185] p 375 N93-11146

NEURONS
An introduction to the information processing components of the brain
[RSRE-MEMO-4350] p 385 N93-10979
Physiological analyses of the afferents controlling brain neurochemical systems
[AD-A253185] p 375 N93-11146
The adaptive neuron model: An architecture for the rapid learning of nonlinear topological transformations
[NASA-CASE-NPO-18579-1-CU] p 420 N93-11174

NEUROPHYSIOLOGY
An introduction to the information processing components of the brain
[RSRE-MEMO-4350] p 385 N93-10979
Physiological analyses of the afferents controlling brain neurochemical systems
[AD-A253185] p 375 N93-11146
Neuropsychiatric morbidity in early HIV disease: Implications for military occupational function
p 379 N93-11299
The OMPAT level 1 Neurophysiological Performance Assessment Battery: NPPAB
[AD-A254840] p 387 N93-12432

NEUTRAL ATMOSPHERES
An inversion technique to recover lower thermospheric winds from space-borne remote measurements of (OI) 5577 A p 369 N93-11839

NEUTRAL ATOMS
Foil optimization for low energy neutral atom imaging
[DE92-013435] p 365 N93-12263
Low energy neutral atom imaging
[DE92-013531] p 365 N93-12264

NEUTRAL BEAMS
Shafranov shift in low-aspect-ratio heliotron/torsatron CHS
[DE92-782100] p 451 N93-11277

NEUTRAL PARTICLES
Instabilities in the rundown phase of the plasma focus
[IPF-90-3] p 449 N93-11030
Research and development of superconducting linear accelerators for neutral particle beam applications
[DE92-019043] p 444 N93-11652

NEUTRINOS
The neutrino process and neutrino r-process
[DE92-014304] p 485 N93-12120

NEUTRON COUNTERS
Development of a geometry-compensated neutron time-of-flight detector for ICF applications with approximately 200 ps time response
[DE92-018024] p 450 N93-11153

NEUTRON DIFFRACTION
Neutron diffraction residual stress studies for aero-engine component applications
[PNR-90908] p 334 N93-11014
Development of the neutron diffraction technique for the determination of near surface residual stresses in critical gas turbine components
[PNR-90984] p 212 N93-11112

NEUTRON FLUX DENSITY
System design and radiation field characteristics of the High Flux Neutron Radiography Facility (HFNRF) at Sandia National Laboratories
[DE92-013984] p 219 N93-12268

NEUTRON IRRADIATION
Mechanical properties of 1950's vintage 304 stainless steel weldment components after low temperature neutron irradiation
[DE92-017059] p 259 N93-12107

NEUTRON RADIOGRAPHY
Feasibility of using neutron radiography to inspect the Space Shuttle solid rocket booster aft skirt, forward skirt and frustum. Part 1: Summary report
[NASA-CR-184357] p 231 N93-11173
System design and radiation field characteristics of the High Flux Neutron Radiography Facility (HFNRF) at Sandia National Laboratories
[DE92-013984] p 219 N93-12268

NEUTRON SOURCES
System design and radiation field characteristics of the High Flux Neutron Radiography Facility (HFNRF) at Sandia National Laboratories
[DE92-013984] p 219 N93-12268

NEUTRON SPECTROMETERS
Use of the program ANISN to calculate response functions for a Bonner sphere set with a He-3 detector
[NPL-RSA(EXT)-31] p 316 N93-11411

NEUTRON STARS
Are some of the luminous high-latitude stars accretion-powered runaways?
[DE92-018853] p 484 N93-11379
The neutrino process and neutrino r-process
[DE92-014304] p 485 N93-12120

NEUTRONS
Development of a geometry-compensated neutron time-of-flight detector for ICF applications with approximately 200 ps time response
[DE92-018024] p 450 N93-11153
Contributions to plasma focus physics since 1970 from the Institute of Plasma Research, Stuttgart (Fed. Republic of Germany)
[IPF-91-4] p 450 N93-11201

NEW MEXICO
Prospects for the commercial development of hot dry rock geothermal energy in New Mexico
[DE92-018999] p 346 N93-11825

NEWTON METHODS
Preconditioned low-order Newton methods
[MATHS-REPT-A-159] p 425 N93-11211

NEWTON THEORY
Analysis of lunar laser ranging in the framework of a post-Newtonian theory
[SER-C-383] p 315 N93-11332

NEWTONIAN FLUIDS
Fundamental solutions and boundary element formulations for convective fluid flow
p 298 N93-11217
Hydrodynamic particle migration in small-amplitude, oscillatory, circular couette flow: The limits of reversibility
[DE92-008480] p 303 N93-11843
Turbulence structure and polymer drag reduction in adverse pressure gradient boundary layers
p 304 N93-12003
Drag on an oscillating rod in a non-Newtonian fluid
[DE92-014746] p 308 N93-12492

NICKEL
Heat-affected zone cracking of nitronic 60 stainless steel
[DE92-018286] p 254 N93-10984
Low energy helium implantation in evaporated nickel surfaces
[DE92-019297] p 257 N93-11600
Atomic structure of Ni-like soft x ray lasing ions
[DE92-019273] p 438 N93-11778
Characteristics of heat transfer to nickel plated chamber walls of high pressure rocket combustors
[NAL-TR-1126T] p 234 N93-12372

NICKEL ALLOYS
Short fatigue crack growth in a nickel-base superalloy at room and elevated temperature
[PNR-90892] p 255 N93-11031
Modelling short crack growth behaviour in nickel-base superalloys
[PNR-90912] p 255 N93-11033
Sigma phase in nickel based superalloys
[PNR-90950] p 255 N93-11109
Present and future trends in turbine blade material and manufacture technology
[PNR-90960] p 255 N93-11111
Review of phonon behavior and microstructural development leading to martensitic transformations in Ni(x)Al(100-x) alloys
[DE92-014782] p 256 N93-11519
Isotopic tailoring with 59-Ni to study the effect of helium on microstructural evolution and mechanical properties of neutron-irradiated Fe-Cr-Ni alloys
[DE92-019372] p 257 N93-11557
Eddy current characterization of magnetic treatment of materials
[NASA-TM-104573] p 258 N93-11621
Review of the physical and mechanical properties and potential applications of the B2 compound NiAl: Unabridged version of a paper published in International materials review
[NASA-TM-105598] p 258 N93-11635
Mechanical properties of semiconductors and their alloys
[AD-A253908] p 462 N93-11727
Erosion predictions and measurements of high-temperature coatings and superalloys used in turbomachines p 272 N93-12189
Fatigue in single crystal nickel superalloys
[AD-A254603] p 260 N93-12237
Nature of the beta-phase of nickel-aluminum system
[AD-A254101] p 261 N93-12269
Design and development of Ni-base superalloy and Ti alloys
[NRIM-SR-92-01] p 261 N93-12322

NICKEL CADMIUM BATTERIES
Results of advanced battery technology evaluations for electric vehicle applications
[DE92-018766] p 289 N93-11432

NICKEL IRON BATTERIES
Results of advanced battery technology evaluations for electric vehicle applications
[DE92-018766] p 289 N93-11432

NICKEL ISOTOPES
Isotopic tailoring with 59-Ni to study the effect of helium on microstructural evolution and mechanical properties of neutron-irradiated Fe-Cr-Ni alloys
[DE92-019372] p 257 N93-11557

NICKEL ZINC BATTERIES
Results of advanced battery technology evaluations for electric vehicle applications
[DE92-018766] p 289 N93-11432

NIGHT
Structure of the nocturnal boundary layer over a complex terrain
[DE92-018141] p 362 N93-11669

NIGHT VISION
Selective factors affecting rotary wing aviator performance with symbology superimposed on night vision goggles
[AD-A254983] p 390 N93-12508

NIMBUS 7 SATELLITE
Atlas of albedo and absorbed solar radiation derived from Nimbus 7 earth radiation budget data set, November 1985 to October 1987
[NASA-RP-1281] p 367 N93-11168
Nimbus-7 Scanning Multichannel Microwave Radiometer (SMMR) PARM tape user's guide
[NASA-RP-1284] p 373 N93-11718

NIOBATES
Nanostructure, defect chemistry and properties of relaxor ferroelectrics
[AD-A247294] p 431 N93-11468

NIOBIUM ALLOYS
Internal friction peaks due to oxygen, nitrogen, and hydrogen in V-Nb alloys
[DE92-012155] p 254 N93-10995
Processing and properties of NbTi based alloys
[DE92-016692] p 261 N93-12445

NITRAMINE PROPELLANTS
The 28th JANNAF Combustion Subcommittee Meeting, volume 1
[CPIA-PUBL-573-VOL-1] p 244 N93-11132

NITRATE ESTERS
A preliminary investigation of the degradation and stabilisation of the energetic oxetane binder polyNIMMO
[RARDE-7/91] p 273 N93-11376
Energetic composites of cyclodextrin nitrate esters and nitrate ester plasticizers
[AD-D015364] p 274 N93-11665

NITRIC ACID
Atmospheric reactive nitrogen: A model study of natural and anthropogenic sources and the role of microbial soil emissions
[DE92-010717] p 354 N93-11744
Improved corrosion resistance of Hastelloy G-30 in nitric/hydrofluoric acid solutions by welding with Inconel 72 weld wire
[DE92-017233] p 262 N93-12487

NITRIC OXIDE
State-resolved reaction dynamics
[AD-A254291] p 436 N93-11196
Direct catalytic decomposition of nitric oxide
[DE92-018759] p 247 N93-11444

NITRO COMPOUNDS
Studies of transition states and radicals by negative ion photodetachment
[DE92-017011] p 440 N93-11875

NITROGEN
Internal friction peaks due to oxygen, nitrogen, and hydrogen in V-Nb alloys
[DE92-012155] p 254 N93-10995
Impact test of carbon, Kevlar, and glass fibre hybrid FRP plates
[NAL-TR-1100] p 243 N93-12371

NITROGEN COMPOUNDS
The relative importance of sulfur and nitrogen compounds in the acidification of freshwater
[DE92-016899] p 354 N93-11680

NITROGEN IONS
Electron emission during multicharged ion-metal surface interactions
[DE92-017134] p 439 N93-11849

NITROGEN OXIDES
Atmospheric reactive nitrogen: A model study of natural and anthropogenic sources and the role of microbial soil emissions
[DE92-010717] p 354 N93-11744
Stratospheric aircraft: Impact on the stratosphere?
[DE92-016997] p 355 N93-12104
Allowance system: Proposed acid rain rule
[PB92-226174] p 356 N93-12524

NOISE INTENSITY
Laboratory study of effects of sonic boom shaping on subjective loudness and acceptability
[NASA-TP-3269] p 434 N93-11620

NOISE MEASUREMENT
The design and commissioning of an acoustic liner for propeller noise testing in the ARA transonic wind tunnel
[PNR-90880] p 433 N93-11204

NOISE POLLUTION
Laboratory study of effects of sonic boom shaping on subjective loudness and acceptability
[NASA-TP-3269] p 434 N93-11620

NOISE PREDICTION
Experimental validation of boundary element methods for noise prediction
[NASA-TM-105729] p 323 N93-10966
Numerical study for the study of medium speed internal noise problems
[DILC-EST-TN-200] p 432 N93-11156

NOISE PROPAGATION
Laboratory study of effects of sonic boom shaping on subjective loudness and acceptability
[NASA-TP-3269] p 434 N93-11620

NOISE REDUCTION
Civil aircraft engines: The next generation
[PNR-90962] p 211 N93-11085
Numerical and experimental results in vibroacoustical active control of structural elements with piezoelectric materials
[DILC-EST-TN-224] p 334 N93-11158
A concept for a counterrotating fan with reduced tone noise
[NASA-TM-105736] p 433 N93-11370
Publications on acoustics research at the Langley Research Center, January 1987 - September 1992
[NASA-TM-107674] p 435 N93-12080
Evaluation of acoustic impedance models for a perforated plate
[NAL-TR-1133] p 435 N93-12375
Composite tasking for sensor arrays
[AD-A254997] p 287 N93-12512

NOISE SPECTRA
Auditory perception
[AD-A255061] p 385 N93-12469

NOMOGRAPHS
Debris/ice/TPS assessment and integrated photographic analysis for Shuttle Mission STS-46
[NASA-TM-107552] p 223 N93-12151

NONDESTRUCTIVE TESTS
Nondestructive evaluation of ceramic and metal matrix composites for NASA's HITEMP and enabling propulsion materials programs
[NASA-TM-105807] p 331 N93-10963
Nondestructive inspection and life determination of disc material
[PNR-90911] p 331 N93-11016
Feasibility of using neutron radiography to inspect the Space Shuttle solid rocket booster aft skirt, forward skirt and frustum. Part 1: Summary report
[NASA-CR-184357] p 231 N93-11173
Application of the boundary element method to elastic wave scattering problems in ultrasonic nondestructive evaluation p 332 N93-11209
Using NDT techniques in the maintenance of aeronautical products
[REPT-921-430-102] p 332 N93-11587
Acoustic emission monitoring of HFIR vessel during hydrostatic testing
[DE92-019316] p 332 N93-11601
Magneto-optic imaging inspection of selected corrosion specimens
[DOT/FAA/CT-TN92/20] p 332 N93-11617
The use of high-frequency dynamic information for the evaluation of damage in fiber reinforced composite materials p 241 N93-11998
Effect of microstructure on passive film formation and breakdown on Al alloys
[AD-A245863] p 260 N93-12118
Development of nondestructive evaluation methods and prediction of effects of flaws on the fracture behavior of structural ceramics
[DE92-016395] p 271 N93-12123
Method and apparatus for evaluating multilayer objects for imperfections
[NASA-CASE-LAR-14581-1-SB] p 333 N93-12204
Ultrasonic flaw classification and sizing
p 333 N93-12533

NONEQUILIBRIUM FLOW
Thermokinetic modelling and hypersonic flow
[DILC-EST-TN-218] p 196 N93-11157

NONEQUILIBRIUM IONIZATION
The basic equations for a four component magnetoplasma flow with non equilibrium ionization
[IPF-91-1] p 449 N93-11102

NONHOLONOMIC EQUATIONS
A surface integral approach to the motion planning of nonholonomic systems
[AD-A254844] p 329 N93-12434

NONINTRUSIVE MEASUREMENT
Hypersonic flow diagnostic development
[AD-A255045] p 202 N93-12466

NONLINEAR EQUATIONS
A primer on polynomial resultants
[AD-A246883] p 426 N93-11463
Solution of nonlinear flow equations for complex aerodynamic shapes
[NASA-CR-190979] p 307 N93-12329

NONLINEAR EVOLUTION EQUATIONS
Systems of evolution equations in thermochemical equations
[AD-A254891] p 253 N93-12282

NONLINEAR FEEDBACK
Terminal slider control of nonlinear robotic systems
[NASA-CASE-NPO-18584-1-CU] p 324 N93-11177

NONLINEAR FILTERS
Stochastic control and nonlinear estimation
[AD-A253543] p 420 N93-11147
The Kalman filter for two-dimensional stable and unstable atmospheres p 359 N93-11249

NONLINEAR OPTICS
The Third Potsdam-5 Kiev International Workshop on Nonlinear Processes in Physics
[AD-A249140] p 430 N93-11420
Electronic and optical properties of perfect and imperfect 2 to 6 superlattices p 465 N93-11996
Optical limiting
[AD-A254620] p 322 N93-12238

NONLINEAR PROGRAMMING
Structural design using equilibrium programming
[NASA-TM-107593] p 339 N93-12005

NONLINEAR SYSTEMS
Non-linear data conversion system for dynamic range digital signal processing
[AD-D015347] p 278 N93-11047
Front tracking and the interaction of nonlinear waves
[AD-A253544] p 297 N93-11148
Terminal slider control of nonlinear robotic systems
[NASA-CASE-NPO-18584-1-CU] p 324 N93-11177
Optimized software for a generalized Polak-Ribiere algorithm in unconstrained optimization
[MATHS-REPT-A-156] p 406 N93-11210
Application of artificial neural networks in nonlinear analysis of trusses
[NASA-TM-105319] p 336 N93-11403
The Third Potsdam-5 Kiev International Workshop on Nonlinear Processes in Physics
[AD-A249140] p 430 N93-11420
A primer on polynomial resultants
[AD-A246883] p 426 N93-11463
Alternating-phase focusing: A model to study nonlinear dynamics
[DE92-019027] p 431 N93-11511
On the inverse scattering problem for the Helmholtz equation in one dimension
[AD-A253130] p 434 N93-11526
Nonlinear evolution of resistive tearing mode instability with shear flow and viscosity
[DE92-012138] p 453 N93-11745
Structural dynamics of large space structures having parametric uncertainties p 225 N93-11836
Laminar boundary-layer breakdown
[AD-A254489] p 306 N93-12162
Computational nonlinear control
[AD-A253547] p 422 N93-12258
Nonlinear delay line phase shifters for terahertz superconductive electronic circuits
[AD-A255119] p 294 N93-12290

NONLINEARITY
Stochastic control and nonlinear estimation
[AD-A253543] p 420 N93-11147
Front tracking and the interaction of nonlinear waves
[AD-A253544] p 297 N93-11148
The adaptive neuron model: An architecture for the rapid learning of nonlinear topological transformations
[NASA-CASE-NPO-18579-1-CU] p 420 N93-11174
Nonlinear response of thin steel plate structures subjected to static, cyclic, and dynamic loads
p 335 N93-11200
Optimized software for a generalized Polak-Ribiere algorithm in unconstrained optimization
[MATHS-REPT-A-156] p 406 N93-11210
Tori and chaos in a nonlinear dynamo model for solar activity
[MPE-PREPRINT-218] p 488 N93-11351
Fully nonlinear development of the most unstable goertler vortex in a three dimensional boundary layer
[NASA-CR-189710] p 301 N93-11633
Application of eigenstructure assignment to the control of powered lift combat aircraft p 215 N93-11871

Nonlinear stability of flows over rigid and flexible boundaries p 198 N93-11674
New methods for nonlinear tracking and nonlinear chaotic signal processing
[AD-A254320] p 284 N93-12095
Interaction of sound with sound by novel mechanisms: Ultrasonic four-wave mixing mediated by a suspension and ultrasonic three-wave mixing at a free surface
[AD-A254657] p 435 N93-12097
Studies in control for vibration suppression of the UWAA 20-bay planar truss
[AD-A250193] p 341 N93-12253
Computational nonlinear control
[AD-A253547] p 422 N93-12258
Stochastic models of wavefront propagation in random granular media
[AD-A255127] p 286 N93-12422
Active control of complex systems via dynamic (recurrent) neural networks
[AD-A254878] p 422 N93-12439
The Fourth Workshop on Dynamics and Aeroelastic Stability Modeling of Rotorcraft Systems
[AD-A255065] p 208 N93-12485

NONPOINT SOURCES
Office of Wetlands, Oceans, and Watersheds publications
[PB92-224310] p 480 N93-12528

NONTHERMAL RADIATION
Diagnostics of electron-heated solar flares
p 488 N93-11877

NONUNIFORMITY
Study of seismic coda generation in crust with non-uniform scattering and anelastic properties
[AD-A254350] p 366 N93-12270

NOREPINEPHRINE
Physiological analyses of the afferents controlling brain neurochemical systems
[AD-A253185] p 375 N93-11146

NORMAL DENSITY FUNCTIONS
Computational aspects of Gaussian beam migration
[DE92-018641] p 431 N93-11567
Time-frequency domain analysis of vibration signals for machinery diagnostics. 3: The present power spectral density
[OUEL-1911/92] p 337 N93-11707
Nonnormal multivariate distributions: Inference based on elliptically contoured distributions
[AD-A254999] p 429 N93-12513

NORTHERN HEMISPHERE
A composite study of the Madden-Julian oscillation
[AD-A254269] p 369 N93-11819

NOSE (ANATOMY)
Allergic and nonallergic rhinitis in Greek pilots
p 383 N93-11317

NOZZLE DESIGN
Hypervelocity scramjet combustor-nozzle analysis and design
[NASA-CR-190965] p 213 N93-12214

NOZZLE EFFICIENCY
Developments in icing test techniques for aerospace applications in the RAE Pyestock (England) altitude test facility
[RAE-TM-P-1214] p 207 N93-11485

NOZZLE FLOW
Hypervelocity scramjet combustor-nozzle analysis and design
[NASA-CR-190965] p 213 N93-12214

NOZZLE GEOMETRY
Experimental investigation of the effects of aft blowing with various nozzle exit geometries on a 3.0 caliber tangent ogive at high angles of attack: Forebody pressure distributions
[NASA-CR-190935] p 197 N93-11605
An investigation of the effects of aft blowing on a 3.0 caliber tangent ogive body at high angles of attack
[NASA-CR-190934] p 200 N93-12004

NOZZLE WALLS
Numerical modeling of a vortex stabilized arcjet
p 232 N93-11889

NUCLEAR BINDING ENERGY
The structures, binding energies and vibrational frequencies of Ca3 and Ca4: An application of the CCSD(T) method p 439 N93-11852
Image potential states at metal-dielectric interfaces
[DE92-017019] p 466 N93-12124

NUCLEAR CAPTURE
Particle physics experiments, 1991
[RAL-92-001] p 444 N93-11687

NUCLEAR DEVICES
Shafranov shift in low-aspect-ratio heliotron/torsatron CHS
[DE92-782100] p 451 N93-11277

NUCLEAR ENGINE FOR ROCKET VEHICLES
Nuclear thermal propulsion transportation systems for lunar/Mars exploration
[NASA-TM-105870] p 233 N93-12363

NUCLEAR EXPLOSIONS
Propagation of regional phases: Observations and theory
[AD-A246891] p 359 N93-11228

NUCLEAR FISSION
Research in heavy-ion nuclear physics
[DE92-015099] p 443 N93-11521

NUCLEAR FUEL ELEMENTS
Ground test facilities for evaluating nuclear thermal propulsion engines and fuel elements
[DE92-017039] p 231 N93-10973
A gas-cooled cermet reactor system for planetary base power
[DE92-018017] p 443 N93-11433

NUCLEAR FUELS
Nuclear fuels for very high temperature applications
[DE92-018021] p 446 N93-12129
A design of experiment study of plasma sprayed alumina-titania coatings
[DE92-017877] p 271 N93-12168
A Taguchi experimental design study of twin-wire electric arc sprayed aluminum coatings
[DE92-018022] p 262 N93-12494

NUCLEAR FUSION
Fusion programs in applied plasma physics
[DE92-019639] p 452 N93-11660
Overview of property formulations for helium, nitrogen, lithium, and lithium-lead in ATHENA/MOD1 with comparison of calculated properties to measured properties
[DE92-017995] p 471 N93-12058
The neutrino process and neutrino r-process
[DE92-014304] p 485 N93-12120
Plasma properties
[DE92-018635] p 455 N93-12188

NUCLEAR INTERACTIONS
Particle physics experiments, 1991
[RAL-92-001] p 444 N93-11687

NUCLEAR MAGNETIC RESONANCE
Molecular mobility of the interface in a model composite: A NMR study
[AD-A253311] p 265 N93-11194
Pulsed-field-gradient NMR investigations of hydrogen diffusion in ZrH(x)
[DE92-014393] p 459 N93-11238
Tetrahedral atom zincophosphate structures: Synthesis, crystal structure, and spectroscopic studies of (Zn(PO2(OC2H5)2)2)x, a one-dimensional inorganic polymer
[AD-A251051] p 437 N93-11560
An NMR study of the occupation of C(sub 60) interstitial sites by oxygen molecules
[DE92-019436] p 437 N93-11640
Magnetic resonance elucidation of molecule/macromolecule interaction stereochemistry
[AD-A253030] p 437 N93-11709
Nuclear magnetic resonance microscopy: New theoretical and technical developments
p 313 N93-11907

NUCLEAR MODELS
Nuclear structure models: Applications and development
[DE92-018758] p 436 N93-11443
Survey of composite particle models of electroweak interaction
[DE92-017110] p 441 N93-12111

NUCLEAR PHYSICS
North American radioactive beam initiatives
[DE92-019185] p 443 N93-11517
Research in heavy-ion nuclear physics
[DE92-015099] p 443 N93-11521
Medium energy nuclear physics research
[DE92-016972] p 442 N93-12444

NUCLEAR POTENTIAL
High energy physics at Tufts University
[DE92-018081] p 444 N93-11668

NUCLEAR POWER PLANTS
Overview of property formulations for helium, nitrogen, lithium, and lithium-lead in ATHENA/MOD1 with comparison of calculated properties to measured properties
[DE92-017995] p 471 N93-12058

NUCLEAR PROPULSION
Ground test facilities for evaluating nuclear thermal propulsion engines and fuel elements
[DE92-017039] p 231 N93-10973
Ground test facility for SEI nuclear rocket engines
[DE92-017418] p 217 N93-11367
A development approach for nuclear thermal propulsion
[DE92-018020] p 232 N93-11596
Evaluation of transportation systems for advanced space flight missions
[ESA-TT-1256] p 223 N93-11685
Structural integrity of a confinement vessel for testing nuclear fuels for space propulsion
[DE92-016796] p 232 N93-11824
Tutorial on nuclear thermal propulsion safety for Mars
[DE92-017946] p 233 N93-12056
Nuclear thermal propulsion transportation systems for lunar/Mars exploration
[NASA-TM-105870] p 233 N93-12363

NUCLEAR REACTIONS
A cryogenic phonon detector to search for dark matter particles p 481 N93-11198
Research in heavy-ion nuclear physics
[DE92-015099] p 443 N93-11521
Scattering of polarized electrons by oriented deuterons
[DE92-624834] p 440 N93-11914
System design and radiation field characteristics of the High Flux Neutron Radiography Facility (HFNRF) at Sandia National Laboratories
[DE92-013984] p 219 N93-12268

NUCLEAR REACTORS
A model for analytical performance prediction of hypervapotron
[DE92-018885] p 305 N93-12010
Tutorial on nuclear thermal propulsion safety for Mars
[DE92-017946] p 233 N93-12056
Reactor materials program: Mechanical properties of irradiated types 304 and 304L stainless steel weldment components
[DE92-018105] p 260 N93-12158

NUCLEAR ROCKET ENGINES
Ground test facility for SEI nuclear rocket engines
[DE92-017418] p 217 N93-11367
Nuclear thermal propulsion transportation systems for lunar/Mars exploration
[NASA-TM-105870] p 233 N93-12363

NUCLEAR SPIN
Nuclear structure models: Applications and development
[DE92-018758] p 436 N93-11443

NUCLEAR STRUCTURE
Nuclear structure models: Applications and development
[DE92-018758] p 436 N93-11443

NUCLEATION
Growth mechanisms of layered superconductors
[DE92-018492] p 458 N93-10987
Review of phonon behavior and microstructural development leading to martensitic transformations in Ni(x)Al(100-x) alloys
[DE92-014782] p 256 N93-11519
Growth, characterization, and device development in monocrystalline diamond films
[AD-A252648] p 271 N93-12184

NUCLEONS
Nucleon axial coupling constants and QCD sum rules
[DE92-014227] p 439 N93-11844
The neutrino process and neutrino r-process
[DE92-014304] p 485 N93-12120

NULL HYPOTHESIS
Limit theorems for Fisher-score change processes
p 427 N93-12328

NUMERICAL ANALYSIS
Analytical and numerical principles for the scaling of plasma focus experiments, with regard to electrical resistance
[IPF-91-2] p 450 N93-11103
Stochastic control and nonlinear estimation
[AD-A253543] p 420 N93-11147
Sound propagation over rigid porous layers
p 432 N93-11179
Some exact solutions of the equations of finite elasticity p 337 N93-11713
Numerical analysis of the flow fields in a RQL gas turbine combustor
[DE92-017509] p 302 N93-11767
A consistent cracked bar vibration theory
p 339 N93-12000
Numerical analysis of oscillating flow about a circular cylinder
[AD-A255164] p 307 N93-12406

NUMERICAL CONTROL
Topics on RF beam control of a synchrotron
[DE92-019217] p 443 N93-11498
A search for low-luminosity objects
[AD-A253301] p 483 N93-11750
Automatic Attenuation/Phase Calibration System (AAPCS)
[DE92-017354] p 284 N93-11917
Ultrasonic sensing of GMAW: Laser/EMAT defect detection system
[DE92-017916] p 333 N93-12055
A VMEbus ultrasonic sensor controller for mapping and servo control in robotic systems
[DE92-013661] p 421 N93-12138

Vacuum chamber translation/positioning mechanism and welding power supply controller
[NASA-CR-184465] p 328 N93-12196

A monitor for the laboratory evaluation of control integrity in digital control systems operating in harsh electromagnetic environments
[NASA-TM-4402] p 215 N93-12304

NUMERICAL DATA BASES

Study and recommendation of available sources of scientific and technical numeric databases in the government and private sector
[AD-A247266] p 475 N93-11465

NUMERICAL FLOW VISUALIZATION

Flow field calculations around the Hermes spaceplane during reentry phase
[MBB-UK-0148-91-PUB] p 195 N93-11008

The hemisphere-cylinder at an angle of attack
p 196 N93-11250

Direct numerical simulation of instabilities in parallel flow with spherical roughness elements
[NASA-TM-105847] p 300 N93-11529

NUMERICAL STABILITY

Numerical calculations of an axisymmetric laminar diffusion flame with detailed and reduced reaction mechanisms p 246 N93-11259

On the inverse scattering problem for the Helmholtz equation in one dimension
[AD-A253130] p 434 N93-11526

NUMERICAL WEATHER FORECASTING

The forcing of a mid-latitude upper-tropospheric jet streak by a simulated mesoscale convective system
p 358 N93-11184

The Kalman filter for two-dimensional stable and unstable atmospheres p 359 N93-11249

NYLON (TRADEMARK)

The degradation of parachutes: Age and mechanical wear
[AD-A252243] p 200 N93-12179

NYQUIST DIAGRAM

Users manual for program NYQUIST: Liquid rocket nyquist plots developed for use on a PC computer
[NASA-CR-184451] p 235 N93-12522

O

OBJECT-ORIENTED PROGRAMMING

Software quality methodology integration study results
[AD-A253891] p 408 N93-11371

The ESSE project: Supporting object-oriented database schema analysis and evolution: Overview
[REPT-92-026] p 476 N93-11689

An object-oriented approach to spatial databases
[REPT-92-034] p 476 N93-11690

Higher-order generic functions for CLOS
[DE92-013447] p 413 N93-12137

Inheritance for software reuse: The good, the bad, and the ugly p 415 N93-12389

OBSERVATORIES

ESIS: An introduction to the European space information system. A modern tool for space scientists
[ESA-INT-2] p 479 N93-12404

OCEAN BOTTOM

The flux and recycling of bioactive substances in the surface sediments of the deep basins off southern California
[DE92-019172] p 373 N93-11734

Study of sound propagation in a wedge-shaped ocean and comparison with other methods
[AD-A255165] p 435 N93-12471

OCEAN CURRENTS

Studies of ocean predictability at decade to century time scales using a global ocean general circulation model in a parallel competing environment
[DE92-019457] p 373 N93-11642

The structure and transport of the Brazil current between 27 deg and 36 deg south
[AD-A247635] p 374 N93-12247

Oceanographic expert system: Potential for TESS(3) applications
[AD-A254908] p 374 N93-12288

OCEAN DYNAMICS

Studies of ocean predictability at decade to century time scales using a global ocean general circulation model in a parallel competing environment
[DE92-019457] p 373 N93-11642

Validation test report for the first-generation dart Gulf Stream forecasting system
[AD-A254286] p 373 N93-11821

The structure and transport of the Brazil current between 27 deg and 36 deg south
[AD-A247635] p 374 N93-12247

OCEAN MODELS

LAM and NEDWAM statistics over the period October 1990 - April 1991
[KNMI-TR-137] p 368 N93-11329

Studies of ocean predictability at decade to century time scales using a global ocean general circulation model in a parallel competing environment
[DE92-019457] p 373 N93-11642

Validation test report for the first-generation dart Gulf Stream forecasting system
[AD-A254286] p 373 N93-11821

The Wave Information Studies (WIS) wave model, version 2.0 (user's guide)
[AD-A254313] p 374 N93-12094

OCEAN SURFACE

Orthogonal functions over the oceans and applications to the determination of orbit error, geoid and sea surface topography from satellite altimetry p 373 N93-12002

Experimental measurement and theoretical modeling of microwave scattering and the structure of the sea surface influencing radar observations from space
[NASA-CR-190998] p 343 N93-12006

The Wave Information Studies (WIS) wave model, version 2.0 (user's guide)
[AD-A254313] p 374 N93-12094

OCEANOGRAPHIC PARAMETERS

Analysis of air and sea physical properties and surface fluxes using a combination of in situ and SEASAT data
p 365 N93-12182

OCEANOGRAPHY

Bibliography of publications from the Texas A and M Sea Grant College Program, 1968-1992
[PB92-205517] p 372 N93-11253

Validation test report for the first-generation dart Gulf Stream forecasting system
[AD-A254286] p 373 N93-11821

Reports to the Nation on our changing planet. Winter 1991 No. 1: The climate system
[NASA-CR-190954] p 370 N93-11880

Oceanographic expert system: Potential for TESS(3) applications
[AD-A254908] p 374 N93-12288

Interactive analysis of gappy bivariate time series using AGSS
[AD-A255160] p 429 N93-12426

OCEANS

Office of Wetlands, Oceans, and Watersheds publications
[PB92-224310] p 480 N93-12528

OFFSHORE PLATFORMS

Deep penetration into frictional ductile and brittle materials
[PB92-205566] p 338 N93-11903

OGIVES

An investigation of the effects of aft blowing on a 3.0 caliber tangent ogive body at high angles of attack
[NASA-CR-190934] p 200 N93-12004

OLIGOMERS

Chemical reactions and properties of organosilicon compounds related to new materials
[AD-A253233] p 246 N93-11218

ON-LINE SYSTEMS

Data archiving and analysis for CWDD
[DE92-017064] p 473 N93-11104

Reserves information gathering system user's guide
[DE92-018357] p 475 N93-11355

Directory of factual and numeric databases of relevance to aerospace and defence R and D
[AGARD-R-777] p 476 N93-11710

Interactive collision detection p 400 N93-11963

On-line analysis of chemical composition using an FT-Raman spectrometer in the near-IR
[DE92-016503] p 253 N93-12311

ONBOARD DATA PROCESSING

Intelligent fault management for the Space Station active thermal control system p 391 N93-11930

Autonomous power system: Integrated scheduling
p 235 N93-11948

All-digital multicarrier demodulators for on-board processing satellites in mobile communication systems
p 285 N93-12207

Data distribution satellite
[NASA-TM-105778] p 287 N93-12481

OPERATING SYSTEMS (COMPUTERS)

Measurement and analysis of operating system fault tolerance
[NASA-CR-190973] p 406 N93-12540

OPERATING TEMPERATURE

Application of polyimides to aeroengine components
[PNR-90907] p 334 N93-11013

OPERATIONS RESEARCH

Structural design using equilibrium programming
[NASA-TM-107593] p 339 N93-12005

Mathematical methods in operations research and computer science
[AD-A254782] p 428 N93-12465

OPERATOR PERFORMANCE

From pilot's associate to satellite controller's associate p 390 N93-11922

Performance experiments with alternative advanced teleoperator control modes for a simulated solar maximum satellite repair p 400 N93-11965

OPERATORS (MATHEMATICS)

An isomorphism for algebra of distributions with compact support on Lie groups
[DE92-603605] p 427 N93-12176

Dynamic multimodal function optimization using genetic algorithms
[DE92-019602] p 414 N93-12234

OPTICAL COMMUNICATION

Contactless optoelectronic integrated circuits for remote fiber optic communication and sensing applications
[AD-A253573] p 290 N93-11507

Optical generation, control and sensing of millimeter waves
[AD-A254700] p 285 N93-12230

OPTICAL COUPLING

Temperature tracking SPICE macro-model for laser and LED driven opto-coupler assemblies
[DE92-019296] p 411 N93-11599

An optical fiber multi-terminal data bus system for aircraft
[NAL-TR-1125] p 209 N93-12370

OPTICAL DATA STORAGE MATERIALS

Erasable optical information storage in the polyanilines
[AD-A254873] p 480 N93-12438

OPTICAL DENSITY

Saturation effects in absorption spectroscopy of the K(alpha) rays of aluminum p 254 N93-12042

OPTICAL DISKS

Analysis of the birefringence distributions in compact discs of polycarbonate p 270 N93-11991

National Space Science Data Center data archive and distribution service (NDADS) automated retrieval mail system user's guide
[NASA-TM-107990] p 479 N93-12150

OPTICAL EQUIPMENT

Reflection masks for soft x ray projection lithography
[DE92-014779] p 293 N93-12121

The role of advanced optical diagnostics in monitoring and controlling an MHD power plant. Part 2: 50 MW(t), POC topping cycle
[DE92-015368] p 455 N93-12141

OPTICAL FIBERS

Fiber peel force measuring apparatus
[AD-D015349] p 309 N93-11048

Fiber optic polishing system
[AD-D015353] p 446 N93-11052

Laser glasses
[DE92-018061] p 267 N93-11549

Parallel architecture for image processing with optic fiber guided missile
[REPT-921-320-101] p 418 N93-11584

Development of a scintillating optical fiber ionization calorimeter
[NASA-CR-184415] p 311 N93-11662

Repeatable sensitivity of optical-time-domain-reflectometry-based strain measurement
[DE92-016910] p 338 N93-11792

Observation of pulses propagating at supraluminous speed in an optical fiber p 320 N93-12040

Fiber optic delay line signal processors
[AD-A254691] p 448 N93-12227

An optical fiber multi-terminal data bus system for aircraft
[NAL-TR-1125] p 209 N93-12370

OPTICAL MATERIALS

Organization of the Optical Society of America Photonic Science Topical Meeting Series. Volume 14: Photorefractive materials effects, and devices
[AD-A253001] p 446 N93-11071

Analysis of advanced optical glass and systems
[NASA-CR-184434] p 448 N93-12201

Optical limiting
[AD-A254620] p 322 N93-12238

OPTICAL MEASUREMENT

The effects of magnetic storm phases on F-layer irregularities from auroral to equatorial latitudes
[AD-A253905] p 361 N93-11282

A distributed data acquisition and centralized data reduction system for flexible and efficient measurements
[DE92-019021] p 312 N93-11827

Orientation, stress, and density distributions in injection-moulded amorphous polymers determined by optical techniques
[ETN-92-92271] p 269 N93-11983

The peculiar rheo-optical behaviour of bisphenol-A-polycarbonate and polymethylmethacrylate
p 269 N93-11984

The time-dependent stress-optical behaviour of polycarbonate in the glass transition region
p 269 N93-11985

The measurement and calculation of birefringence in quenched polycarbonate specimens p 269 N93-11986
Molecular orientation induced by cooling stresses in polycarbonate. 1: Free quenching p 269 N93-11987
Measurement of the density distributions in quenched polycarbonate specimens by a quantitative Schlieren-optical technique p 270 N93-11989
Gapwise density distributions in injection-moulded polymethylmethacrylate p 270 N93-11990
Overview of recent diagnostic measurements at the USA MHD facilities
[DE92-015365] p 454 N93-12087
Advanced one-dimensional optical strain measurement system, phase 4
[NASA-CR-190760] p 314 N93-12279

OPTICAL MEASURING INSTRUMENTS
Laser surface profilometer with sub-Angstrom resolution
[DE92-018926] p 317 N93-12011
Advanced one-dimensional optical strain measurement system, phase 4
[NASA-CR-190760] p 314 N93-12279

OPTICAL POLARIZATION
Orientation, stress, and density distributions in injection-moulded amorphous polymers determined by optical techniques
[ETN-92-92271] p 269 N93-11983
Molecular orientation induced by cooling stresses in polycarbonate. 1: Free quenching p 269 N93-11987
Molecular orientation induced by cooling stresses in polycarbonate. 2: Constrained quench and injection moulding p 270 N93-11988

OPTICAL PROPERTIES
Basicity and optical basicities of slags
[NPL-DMM(A)-48] p 447 N93-11408
Preparation, optical and laser properties of Nd-doped sol-gel silica
[DE92-019378] p 461 N93-11602
The peculiar rheo-optical behaviour of bisphenol-A-polycarbonate and polymethylmethacrylate p 269 N93-11984
Electronic and optical properties of perfect and imperfect 2 to 6 superlattices p 465 N93-11996
A preliminary study associated with the experimental measurement of the aero-optic characteristics of hypersonic configurations
[AD-A253792] p 200 N93-12063
Analysis of advanced optical glass and systems
[NASA-CR-184434] p 448 N93-12201
A trainable image pattern classification system for detection of damaged soybean seeds p 201 N93-12208
Surface analysis of Ln(2-x)Ce(x)CuO4 (Ln = Pr and Nd) single crystals grown by the top seeded solution method
[AD-A254905] p 469 N93-12286

OPTICAL PUMPING
Progress toward x ray lasing between autoionizing transitions
[DE92-017428] p 317 N93-11765

OPTICAL RADAR
The millimeter wave Cloud Profiling Radar System (CPRS)
[DE92-016970] p 366 N93-10971
Sodium-lidar mesosphere examinations: Selected elements of the experimental construction of a mobile instrument and evaluation of the data acquired with a stationary Na-lidar during the DYANA campaign
[BONN-IR-91-78] p 357 N93-11006
Lidar studies of gravity waves in the mesopause region p 358 N93-11222
Detection of cloud-top height from backscattered radiances within the oxygen A band. Part 2: Measurements
[GKSS-91/E/77-PT-2] p 368 N93-11350
The design, development, and test of balloonborne and groundbased lidar systems. Volume 3: Groundbased lidar systems
[AD-A247552] p 317 N93-11805
Research on stimulated Raman scattering with applications to atmospheric lidar p 322 N93-12163
Multiangle lidar performance in the presence of horizontal inhomogeneities in atmospheric extinction and scattering
[AD-A252882] p 371 N93-12167
Fiber optic delay line signal processors
[AD-A254691] p 448 N93-12227
Guide to synchronization of video systems to IRIG timing
[AD-A254626] p 285 N93-12240
The design, development, and test of balloonborne and groundbased lidar systems. Volume 1: Balloonborne coherent CO2 lidar system
[AD-A247551] p 322 N93-12262
Development summary of a sympathetic discharge CO2 laser for lidar use
[NASA-CR-184433] p 323 N93-12516

OPTICAL RELAY SYSTEMS
Optical beamformer
[AD-A254354] p 448 N93-12272

OPTICAL RESONANCE
Investigation of a cesium Raman time/frequency standard
[AD-A252677] p 310 N93-11562

OPTICAL SWITCHING
Organization of the Optical Society of America Photonic Science Topical Meeting Series. Volume 14: Photorefractive materials effects, and devices
[AD-A253001] p 446 N93-11071
Fast electrochromic switching for optical hardening applications
[AD-A248174] p 447 N93-11186

OPTICAL THICKNESS
Detection of cloud-top height from backscattered radiances within the oxygen A band. Part 1: Theoretical study
[GKSS-91/E/76-PT-1] p 368 N93-11349
Detection of cloud-top height from backscattered radiances within the oxygen A band. Part 2: Measurements
[GKSS-91/E/77-PT-2] p 368 N93-11350
Saturation effects in absorption spectroscopy of the K(alpha) rays of aluminum p 254 N93-12042

OPTICAL TRACKING
Shutter apparatus
[AD-D015350] p 309 N93-11049
Laser Doppler experiments
[AD-A252883] p 287 N93-12461

OPTICAL TRANSITION
Emittance measuring device for charged particle beams
[AD-D015371] p 442 N93-11060

OPTICAL WAVEGUIDES
Chinese Journal of Lasers (selected articles)
[AD-A254100] p 317 N93-11786

OPTIMAL CONTROL
Stochastic control and nonlinear estimation
[AD-A253543] p 420 N93-11147
Optimal output feedback vibration control of rotor-bearing systems p 324 N93-11220
Modified optimal control pilot model for computer-aided design and analysis
[NASA-TM-4384] p 214 N93-11459
Rapid maneuvering of large flexible orbiting systems p 225 N93-11885

OPTIMIZATION
Recent advances in multidisciplinary optimization of rotorcraft
[NASA-TM-107665] p 206 N93-10968
Maximum life spiral bevel reduction design
[NASA-TM-105790] p 323 N93-10982
The complexity of some multicriteria arborescence problems
[REPT-92-016] p 424 N93-11182
Innovation in engineering
[PNR-90889] p 212 N93-11207
Optimized software for a generalized Polak-Ribiere algorithm in unconstrained optimization
[MATHS-REPT-A-156] p 406 N93-11210
Preconditioned low-order Newton methods
[MATHS-REPT-A-159] p 425 N93-11211
Dynamic programming on a ring of processors p 410 N93-11479
Path planning on a ring of processors p 410 N93-11480
Symmetric matrix-vector product on a ring of processors p 410 N93-11481
Dynamic multimodal function optimization using genetic algorithms
[DE92-019602] p 414 N93-12234
Foil optimization for low energy neutral atom imaging
[DE92-013435] p 365 N93-12263
A genetic algorithm for search route planning
[AD-A254894] p 414 N93-12284

OPTOELECTRONIC DEVICES
Contactless optoelectronic integrated circuits for remote fiber optic communication and sensing applications
[AD-A253573] p 290 N93-11507
Optoelectronics Research Center
[AD-A253132] p 447 N93-11527
Programme and abstracts. Workshop on Expert Evaluation and Control of Compound Semiconductor Materials and Technologies No. 1: (EXAMTEC 199)
[AD-A254023] p 292 N93-12071
Optical limiting
[AD-A254620] p 322 N93-12238

ORBIT CALCULATION
Ephemeris calculation and orbit determination of geostationary satellites, using Taylor series integration
[SER-C-384] p 220 N93-11335

ORBIT PERTURBATION
Orbit perturbations due to an axi-symmetric gravitational field, analyzed over extended periods of time
[RAE-TM-SPACE-386] p 220 N93-11486
Dynamics of space debris p 219 N93-11904

ORBIT TRANSFER VEHICLES
Theoretical research program to study chemical reactions in AOTV bow shock tubes
[NASA-CR-188927] p 439 N93-11851
An experimental study of a small high speed LH2 rocket pump: Fundamental mechanical design
[NAL-TR-1123] p 330 N93-12463

ORBITAL ASSEMBLY
Tests of an alternate mobile transporter and extravehicular activity assembly procedure for the Space Station Freedom truss
[NASA-TP-3245] p 224 N93-10970
Contact detection and contact motion for error recovery in the presence of uncertainties p 398 N93-11956
Operator vision aids for space teleoperation assembly and servicing p 391 N93-11981
A smart end-effector for assembly of space truss structures p 230 N93-11982
Manned Mars System Study (MMSS): Mars transportation and facility infrastructure study. Volume 2: Technical report
[NASA-CR-184474] p 227 N93-12443

ORBITAL ELEMENTS
Dynamics of space debris p 219 N93-11904

ORBITAL MANEUVERING VEHICLES
An investigation of error correcting techniques for OMV and AXAF
[NASA-CR-190950] p 416 N93-12515

ORBITAL MANEUVERS
Rapid maneuvering of large flexible orbiting systems p 225 N93-11885
Numerical modeling of a vortex stabilized arcjet p 232 N93-11889

ORBITAL MECHANICS
Orbit perturbations due to an axi-symmetric gravitational field, analyzed over extended periods of time
[RAE-TM-SPACE-386] p 220 N93-11486

ORBITAL RENDEZVOUS
Autoguidance video sensor for docking p 230 N93-11954

ORBITAL SERVICING
Small experiments for the maturation of orbital cryogenic transfer technologies
[NASA-TM-105849] p 296 N93-10981
Requirements and applications for robotic servicing of military space systems p 230 N93-11953
Performance experiments with alternative advanced teleoperator control modes for a simulated solar maximum satellite repair p 400 N93-11965
Automation and robotics for COLUMBUS: An implementation concept for the free flying laboratory (MTFF) p 331 N93-11974
Automatic system for installation and replacement of Space Station components
[NASA-CASE-LEW-14906-1] p 329 N93-12203

ORDNANCE
High resolution image processing of geophysical data with diffraction tomography
[DE92-014134] p 359 N93-11235
Hot-wire vs laser, is there a difference?
[DE92-019337] p 310 N93-11554

ORGANIC COMPOUNDS
Advanced heat pump for the recovery of volatile organic compounds
[DE92-011592] p 303 N93-11774
Laser spectroscopy and dynamics of transient species formed in pyrolysis reactions
[DE92-016206] p 251 N93-12091
Characterization of underivatized pterins by laser desorption Fourier transform mass spectrometry
[DE92-016785] p 323 N93-12514

ORGANIC LIQUIDS
Synthesis of side chain liquid crystal polymers by living ring opening metathesis polymerization. Report 2: Influence of molecular weight, polydispersity, and flexible spacer length (n=9-12) on the thermotropic behavior of the resulting plymers
[AD-A248700] p 265 N93-11188

ORGANIC MATERIALS
The flux and recycling of bioactive substances in the surface sediments of the deep basins off southern California
[DE92-019172] p 373 N93-11734

ORGANIC NITRATES
Energetic composites of cyclodextrin nitrate esters and nitrate ester plasticizers
[AD-D015364] p 274 N93-11665

ORGANIC SEMICONDUCTORS
The Peierls ground state, solitons and polarons in ring-containing polymers
[AD-A254914] p 272 N93-12289

ORGANIC SILICON COMPOUNDS

Chemical reactions and properties of organosilicon compounds related to new materials

[AD-A253233] p 246 N93-11218

Synthesis and characterization of novel organogallium-phosphorus compounds: X ray crystal structures of Ph2GaP (SiMe3)2Ga (Ph2Cl, Ph2 (Cl)Ga.P (SiMe3)3, and Ph3Ga.P (SiMe3)3

[AD-A253841] p 462 N93-11724

Exciton kinetics in poly(di-n-hexylsilane)

[DE92-018278] p 283 N93-11800

Synthesis and reactivity of siloxide and silamide complexes pertaining to bond breaking and aggregation phenomena

[AD-A254703] p 468 N93-12231

ORGANOMETALLIC COMPOUNDS

Synthesis and side chain liquid crystal polymers by living ring opening metathesis polymerization. 5: Influence of mesogenic group and interconnecting group on the thermotropic behavior of the resulting polymers

[AD-A253568] p 264 N93-11150

CVD of AlN and SiC using cyclic organometallic precursors

[AD-A246910] p 266 N93-11413

Triisopropylindium: A new precursor for OMVPE growth

[AD-A250672] p 460 N93-11558

Synthesis and characterization of novel organogallium-phosphorus compounds: X ray crystal structures of Ph2GaP (SiMe3)2Ga (Ph2Cl, Ph2 (Cl)Ga.P (SiMe3)3, and Ph3Ga.P (SiMe3)3

[AD-A253841] p 462 N93-11724

Submarine Advanced Integrated Life Support system (SAILS) program

[AD-A253564] p 388 N93-11812

The deposition characteristics of copper(I) compounds for CVD by FT-IR spectroscopy

[DE92-010778] p 467 N93-12134

Synthesis and characterization of novel aluminum-arsenic compounds 2. Crystal structures of (R2AlAs (SiMe3)2)2 (R = i-Bu, Me) and i-Bu2 (Cl)Al*As (SiMe3)3

[AD-A248001] p 467 N93-12175

Catalytic hydrogenation of carbon monoxide

[DE92-014729] p 253 N93-12428

ORGANOMETALLIC POLYMERS

Synthesis of side chain liquid crystal polymers by living ring opening metathesis polymerization. Report 2: Influence of molecular weight, polydispersity, and flexible spacer length (n=9-12) on the thermotropic behavior of the resulting plymers

[AD-A248700] p 265 N93-11188

Organometallic NLO polymers. 3. Copolymerization of bridged bis(ferrocenyl) and bis(cyanoacetate) monomers via the knoevenagel condensation

[AD-A250214] p 265 N93-11192

Tetrahedral atom zincophosphate structures: Synthesis, crystal structure, and spectroscopic studies of (Zn(PO2(OC2H5)2)2)x, a one-dimensional inorganic polymer

[AD-A251051] p 437 N93-11560

ORIFICE FLOW

An experimental study of a small high speed LH2 rocket pump: Fundamental mechanical design

[NAL-TR-1123] p 330 N93-12463

ORTHOGONAL FUNCTIONS

Orthogonal functions over the oceans and applications to the determination of orbit error, geoid and sea surface topography from satellite altimetry p 373 N93-12002

ORTHOGONALITY

Preconditioned low-order Newton methods

[MATHS-REPT-A-159] p 425 N93-11211

ORTHONORMAL FUNCTIONS

Orthogonal functions over the oceans and applications to the determination of orbit error, geoid and sea surface topography from satellite altimetry p 373 N93-12002

ORTHOTROPIC SHELLS

Linear and geometrically nonlinear p-version three dimensional curved shell element for isotropic, generally orthotropic and laminated composite materials

p 339 N93-12194

OSCILLATING FLOW

Oscillations and concentrations in compressible and incompressible fluids

[AD-A254706] p 307 N93-12333

Numerical analysis of oscillating flow about a circular cylinder

[AD-A255164] p 307 N93-12406

OSCILLATIONS

A synopsis of resistive wall effects in very short wavelength free electron lasers

[DE92-018065] p 315 N93-11155

Experiments on low aspect ratio hydroplanes to measure lift under static and dynamic conditions

[ARE-TM(UHR)-90306] p 197 N93-11365

Lift coefficient of a randomly oscillating hydroplane

[DRA/MAR-TM(MTH)-91320] p 197 N93-11377

A composite study of the Madden-Julian oscillation

[AD-A254269] p 369 N93-11819

Dynamics of planetary waves in the atmosphere

p 363 N93-11898

Drag on an oscillating rod in a non-Newtonian fluid

[DE92-014746] p 308 N93-12492

OSCILLATORS

On some practical consideration of the electron beam breakup transit time oscillator

[DE92-017406] p 445 N93-11919

Theory for a high power free electron laser and tactical applications

[AD-A255161] p 323 N93-12405

OUTER RADIATION BELT

Forecasting the relativistic electron flux at geosynchronous orbit

[AD-A254016] p 226 N93-12064

OUTLET FLOW

Effects of cooling-air injection on secondary flows and losses in a turbine cascade

[NAL-TR-1121T] p 307 N93-12382

OXIDATION

Near-IR absorption spectra for the C70 fullerene anions

[AD-A253658] p 246 N93-11280

Destruction of explosives and rocket fuels by supercritical water oxidation

[DE92-018874] p 274 N93-11380

Oxidation, nitridation, and fluorine etching of Si

[AD-A253559] p 249 N93-11755

Oxidation-sulfidation behavior of iron alloys containing 16 to 40 atomic percent aluminum

[DE92-017824] p 259 N93-11830

Inhibition of moist carbon monoxide oxidation by trace amounts of hydrocarbons

[DE92-008736] p 253 N93-12257

Processing and properties of NbTi based alloys

[DE92-016692] p 261 N93-12445

Current research in oxidation-resistant carbon-carbon composites at NASA. Langley Research Center

p 229 N93-12456

Thermal control/oxidation resistant coatings for titanium-based alloys p 229 N93-12457

OXIDATION RESISTANCE

Small particle impact damage in carbon-carbon composites

[PNR-90948] p 236 N93-11107

High temperature oxidation protection of carbon/carbon composites

[REPT-921-430-105] p 239 N93-11589

Processing and properties of NbTi based alloys

[DE92-016692] p 261 N93-12445

Current research in oxidation-resistant carbon-carbon composites at NASA. Langley Research Center

p 229 N93-12456

Thermal control/oxidation resistant coatings for titanium-based alloys p 229 N93-12457

OXIDATION-REDUCTION REACTIONS

Chronopotentiometry of refractory metals, actinides and oxyanions in molten salts: A review

[NASA-TM-105862] p 249 N93-11545

Mixing regimes in a spatially confined, two-dimensional, supersonic shear layer

[AD-A254302] p 302 N93-11756

OXIDE FILMS

Chronopotentiometry of refractory metals, actinides and oxyanions in molten salts: A review

[NASA-TM-105862] p 249 N93-11545

Development of contractor cells, phase 1

[DE92-017343] p 348 N93-12222

OXIDES

Sealant research for solid oxide fuel cells

[DE92-019044] p 345 N93-11513

Intermediate temperature electrolytes for SOFC

[DE92-018786] p 345 N93-11571

OXYFLUORIDES

Chemistry of lower valent actinide halides

[DE92-017031] p 251 N93-12105

OXYGEN

Internal friction peaks due to oxygen, nitrogen, and hydrogen in V-Nb alloys

[DE92-012155] p 254 N93-10995

Rotational CARS measurements in a rotating cavity with axial throughflow of cooling air: Oxygen concentration measurements

[PNR-90935] p 244 N93-11035

Comparisons of molecular sieve oxygen concentrators for potential medical use aboard commercial aircraft

[AD-A253648] p 387 N93-11279

Selective carbon oxygen bond scission during reactions of oxygenates on single crystal catalysts

[DE92-018687] p 247 N93-11439

An NMR study of the occupation of C(sub 60) interstitial sites by oxygen molecules

[DE92-019436] p 437 N93-11640

Mixing regimes in a spatially confined, two-dimensional, supersonic shear layer

[AD-A254302] p 302 N93-11756

Influence of oxygen partial pressure and silver additions on microstructure and related properties of YBCO superconductors

[DE92-011145] p 468 N93-12249

OXYGEN ATOMS

Preconversion catalytic deoxygenation of phenolic functional groups

[DE92-018304] p 244 N93-10986

Analysis of surfaces from the LDEF A0114, phase 2

[NASA-CR-190596] p 270 N93-11993

OXYGEN COMPOUNDS

Laser spectroscopy and dynamics of transient species formed in pyrolysis reactions

[DE92-016206] p 251 N93-12091

OXYGEN PLASMA

Resonant membrane spatial light modulators

[AD-A253893] p 252 N93-12186

OXYGEN PRODUCTION

Submarine Advanced Integrated Life Support system (SAILS) program

[AD-A253564] p 388 N93-11812

OXYGEN-HYDROCARBON ROCKET ENGINES

Test program to provide validation data for the Rocket Combustor Interactive Design (ROCCID) code

p 247 N93-11450

Space transportation booster engine configuration study. Volume 2: Design definition document and environmental analysis

[NASA-CR-184459] p 234 N93-12441

Space transportation booster engine configuration study. Volume 1: Executive Summary

[NASA-CR-184457] p 235 N93-12523

OZONE

The Transall campaign. A contribution to the German ozone research program

[REPT-37/91] p 349 N93-11082

Scientific assessment of ozone depletion: 1991

[NASA-TM-107976] p 350 N93-11087

Source gases: Concentrations, emissions, and trends

p 350 N93-11088

Ozone and temperature trends p 350 N93-11089

Heterogeneous processes: Laboratory, field, and modeling studies p 350 N93-11090

Stratospheric processes: Observations and interpretation p 351 N93-11091

Tropospheric processes: Observations and interpretation p 351 N93-11092

Ozone depletion and chlorine loading potentials

p 351 N93-11093

Future chlorine-bromine loading and ozone depletion

p 352 N93-11095

Predicted aircraft effects on stratospheric ozone

p 352 N93-11096

Predicted rocket and shuttle effects on stratospheric ozone p 352 N93-11097

Reinterpretation of ozone data from Base Roi Baudouin (Antarctica)

[AERONOMICA-ACTA-A-365] p 352 N93-11127

The potential effects of concurrent increases in temperature, CO2 and O3 on net photosynthesis, as mediated by rubisCO

[DE92-019411] p 374 N93-11630

The role of refrigerants in climate change

[DE92-019385] p 354 N93-11677

Atmospheric reactive nitrogen: A model study of natural and anthropogenic sources and the role of microbial soil emissions

[DE92-010717] p 354 N93-11744

A comprehensive mission to planet Earth: Woods Hole Space Science and Applications Advisory Committee Planning Workshop

[NASA-TM-108011] p 343 N93-11878

OZONE DEPLETION

Scientific assessment of ozone depletion: 1991

[NASA-TM-107976] p 350 N93-11087

Source gases: Concentrations, emissions, and trends

p 350 N93-11088

Heterogeneous processes: Laboratory, field, and modeling studies p 350 N93-11090

Stratospheric processes: Observations and interpretation p 351 N93-11091

Tropospheric processes: Observations and interpretation p 351 N93-11092

Ozone depletion and chlorine loading potentials

p 351 N93-11093

Radiative forcing of climate p 351 N93-11094

Future chlorine-bromine loading and ozone depletion

p 352 N93-11095

Predicted rocket and shuttle effects on stratospheric ozone p 352 N93-11097

Ultraviolet radiation changes p 352 N93-11098
Stratospheric aircraft: Impact on the stratosphere?
[DE92-016997] p 355 N93-12104

OZONOMETRY
The Transall campaign. A contribution to the German ozone research program
[REPT-37/91] p 349 N93-11082

OZONOSPHERE
Ozone depletion and chlorine loading potentials
p 351 N93-11093

P

P WAVES
Application of the theory of wave propagation through random media to phase and amplitude fluctuations of seismic P-waves
[AD-A253274] p 363 N93-11788

P-N JUNCTIONS
Development of stable metallization systems
[AD-A253569] p 264 N93-11079

PACIFIC OCEAN
Lessons drawn from 2 existing satellite networks: ARABSAT and EUTELSAT. Application to the Pacific basin projects
[REPT-921-440-101] p 282 N93-11591

PACKET TRANSMISSION
High performance interconnection between high data rate networks p 279 N93-11118
A simple, effective media access protocol system for integrated, high data rate networks p 279 N93-11119

PACKING
Matching and vertex packing: How hard are they?
[AD-A245928] p 423 N93-10991

PACKING DENSITY
Theoretical studies of high-temperature superconductors and highly compressed hydrogen
p 292 N93-11833

PAIR PRODUCTION
Mass energy-transfer and mass energy-absorption coefficients, including in-flight positron annihilation for photon energies 1 keV to 100 MeV, 1992
[PB92-181106] p 438 N93-11715

PANEL METHOD (FLUID DYNAMICS)
Numerical investigations into the base drag of various wedges using the base flow model developed by Mauri Tanner
[REPT-B-36] p 202 N93-12414

PARABOLIC FLIGHT
Automatic control laws for aircraft in parabolic flight
[DILC-EST-TR-211] p 214 N93-11160

PARACHUTE FABRICS
Ribless ram air parachute
[AD-D015351] p 195 N93-11050

PARACHUTES
Ribless ram air parachute
[AD-D015351] p 195 N93-11050
The degradation of parachutes: Age and mechanical wear
[AD-A252243] p 200 N93-12179

PARALLEL COMPUTERS
Scalable parallel communications p 279 N93-11117
Front tracking and the interaction of nonlinear waves
[AD-A253544] p 297 N93-11148
Parallel genetic algorithms: Introduction and overview of current research
[REPT-92-015] p 418 N93-11181
Domain decomposition: A bridge between nature and parallel computers
[NASA-CR-189709] p 425 N93-11246
Dynamic programming and image processing on distributed memory parallel machines
[ETN-92-92174] p 409 N93-11478

PARALLEL FLOW
Direct numerical simulation of instabilities in parallel flow with spherical roughness elements
[NASA-TM-105847] p 300 N93-11529

PARALLEL PROCESSING (COMPUTERS)
High speed parallel backplane
[AD-D015372] p 288 N93-11053
Photonics and other approaches to high speed communications
[NASA-CR-190362] p 279 N93-11116
Scalable parallel communications p 279 N93-11117
Implicit parallelism in genetic algorithms
[REPT-92-012] p 418 N93-11180
Parallel genetic algorithms: Introduction and overview of current research
[REPT-92-015] p 418 N93-11181
The engine design engine. A clustered computer platform for the aerodynamic inverse design and analysis of a full engine
[NASA-TM-105838] p 196 N93-11223
ALECSYS and the AutonoMouse: Learning to control a real robot by distributed classifier systems
[REPT-92-011] p 420 N93-11227
Domain decomposition: A bridge between nature and parallel computers
[NASA-CR-189709] p 425 N93-11246
A process monitor for the transputer
[RSRE-MEMO-4554] p 408 N93-11389
Ten15 developments to support parallelism
[RSRE-MEMO-4545] p 409 N93-11406
The efficient parallel iterative solution of large sparse linear systems
[DE92-018769] p 425 N93-11446
Parallel architecture for image processing with optic fiber guided missile
[REPT-921-320-101] p 418 N93-11584
ScaLAPACK: A scalable linear algebra library for distributed memory concurrent computers
[DE92-017823] p 426 N93-11636
Studies of ocean predictability at decade to century time scales using a global ocean general circulation model in a parallel competing environment
[DE92-019457] p 373 N93-11642
Automatic data partitioning on distributed memory multicomputers
[NASA-CR-190976] p 418 N93-11651
Operator assistant to support deep space network link monitor and control p 288 N93-11939
An implementation of a parallel MOL solver on the Intel Gamma parallel computer
[DE92-018947] p 419 N93-12233
Analysis of fault-tolerant neurocontrol architectures
[NASA-TM-105898] p 215 N93-12305
Performance evaluation and modeling techniques for parallel processors
[NASA-CR-190974] p 419 N93-12395
Static assignment of complex stochastic tasks using stochastic majorization
[NASA-CR-189716] p 416 N93-12403

PARALLEL PROGRAMMING
An adaptive differencing scheme for elliptic flows
p 297 N93-11197
Evaluation of a Cray performance tool using a large hydrodynamics code
[DE92-013239] p 407 N93-11231
Dynamic programming on a ring of processors
p 410 N93-11479
Path planning on a ring of processors
p 410 N93-11480
Symmetric matrix-vector product on a ring of processors p 410 N93-11481
Z-buffer on a transputer-based machine
p 410 N93-11483
Current state and future direction of computer systems at NASA Langley Research Center
[NASA-TM-107685] p 414 N93-12278

PARAMAGNETIC RESONANCE
X pulse radiation around the critical surface
p 318 N93-12027
Nonlinear behavior of resonant absorption in a plasma at microwave frequency p 319 N93-12032

PARAMETER IDENTIFICATION
Symmetric matrix-vector product on a ring of processors p 410 N93-11481
Self-tuning PI-PID regulators for stable systems with varying delay
[REPT-92-023] p 421 N93-11593

PARAMETERIZATION
The use of ARM data to test an improved parameterization of upper tropospheric clouds for use in climate models
[DE92-014353] p 367 N93-11237
Parameterization of solar cells
[NASA-TM-105885] p 295 N93-12301

PARASITIC DISEASES
Allergic, Immunological and Infectious Disease Problems in Aerospace Medicine
[AGARD-CP-518] p 376 N93-11283
Communicable diseases: A major burden of morbidity and mortality p 380 N93-11300
Immunization of personnel traveling to a destination in tropical countries: French position p 380 N93-11304
Recent lessons on the safety and effectiveness of malaria chemoprophylaxis in a non-immune population
p 381 N93-11307
Use of novel adjuvants and delivery systems to improve the humoral and cellular immune response to malaria vaccine candidate antigens p 381 N93-11308

PARTIAL DIFFERENTIAL EQUATIONS
Stochastic control and nonlinear estimation
[AD-A253543] p 420 N93-11147
Domain decomposition: A bridge between nature and parallel computers
[NASA-CR-189709] p 425 N93-11246
Krylov subspace methods for complex non-Hermitian linear systems
[NASA-CR-190931] p 409 N93-11458

PARTIAL PRESSURE
Influence of oxygen partial pressure and silver additions on microstructure and related properties of YBCO superconductors
[DE92-011145] p 468 N93-12249

PARTICLE ACCELERATION
Research and development of superconducting linear accelerators for neutral particle beam applications
[DE92-019043] p 444 N93-11652
Stimulated Brillouin backscattering instability in the case of a high power laser: Application to wave pulsation particle acceleration experiments p 317 N93-12024

PARTICLE ACCELERATOR TARGETS
Surface reconstruction of a three-dimensional ultrasonic flaw
[DE92-018029] p 332 N93-11154
Scattering of polarized electrons by oriented deuterons
[DE92-624834] p 440 N93-11914

PARTICLE ACCELERATORS
The foxhole accelerating structure
[DE92-019052] p 443 N93-11429
North American radioactive beam initiatives
[DE92-019185] p 443 N93-11517
Propagation of relativistic high current electron beams across the geomagnetic field
[DE92-018276] p 362 N93-11564
Radiation physics, biophysics, and radiation biology
[DE92-013673] p 375 N93-12266

PARTICLE BEAMS
Emittance measuring device for charged particle beams
[AD-D015371] p 442 N93-11060
Analysis of periodic transient beam loading of the AGS
[DE92-019243] p 443 N93-11499
Research and development of superconducting linear accelerators for neutral particle beam applications
[DE92-019043] p 444 N93-11652
A single beam laser tracker as an alignment tool
[DE92-017746] p 316 N93-11691

PARTICLE COLLISIONS
Research in elementary particles and interactions
[DE92-018089] p 437 N93-11681
High energy hadron-hadron collisions
[DE92-018253] p 441 N93-12224

PARTICLE INTERACTIONS
High energy physics at Tufts University
[DE92-018081] p 444 N93-11668

PARTICLE LADEN JETS
Particle-jet interactions in an MHD second stage combustor
[DE92-016390] p 455 N93-12309

PARTICLE MOTION
Self-generated stochastic heating in an RF discharge
[DE92-018558] p 452 N93-11565

PARTICLE PRODUCTION
A Polytropic solar model p 487 N93-11264
High energy physics at Tufts University
[DE92-018081] p 444 N93-11668
Strange quark matter
[DE92-016949] p 438 N93-11746

PARTICLE SIZE DISTRIBUTION
Experimental investigation of rocket injector atomization p 248 N93-11454
Development of strength and conductivity in deformation processed copper base alloys
[DE92-018807] p 257 N93-11572

PARTICLE THEORY
Nucleon structure functions from deep inelastic muon scattering
[NIKHEF-H+K/92-01] p 442 N93-11130
Studies in quantum field theory
[DE92-011035] p 470 N93-11276
Research in elementary particles and interactions
[DE92-018089] p 437 N93-11681
Medium energy nuclear physics research
[DE92-016972] p 442 N93-12444

PARTICLE TRAJECTORIES
Computation of single solid particle impact on the target of ductile material to study the rebound characteristics of particle p 336 N93-11372

PARTICLES
Measuring and modelling of particle-fluid flow in a riser reactor
[VTT-PUBS-88] p 299 N93-11359

PARTICULATES
3-D turbulent particle dispersion submodel development
[DE92-018212] p 301 N93-11670
3-D turbulent particle dispersion submodel development
[DE92-018228] p 302 N93-11671

PARTITIONS (MATHEMATICS)
Assembling polyhedra with single translations
[AD-A254623] p 419 N93-12239

PASSENGER AIRCRAFT
Rolls-Royce civil engine technology
[PNR-90936] p 210 N93-11036
The Trent: Towards greater thrust
[PNR-90937] p 210 N93-11037

PASSENGERS
An investigation of ground access mode choice for departing passengers
[TT-9201] p 217 N93-11224

PASSIVITY
Development of contractor cells, phase 1
[DE92-017343] p 348 N93-12222

PATHOGENESIS
Viral hepatitis in the US Air Force, 1980 - 1989
p 377 N93-11287
HIV variability and perspectives of a vaccine
p 378 N93-11294
Analysis of disease progression from clinical observations of US Air Force active duty members infected with the Human Immunodeficiency Virus: Distribution of AIDS survival time from interval censored observations
p 379 N93-11297
In vivo and in vitro diagnosis of allergic respiratory disease during screening procedures in the Italian Navy: Comparative evaluation of a recent quantitative automatized enzyme immunoassay method to dose specific IgE p 383 N93-11314

PATHOLOGICAL EFFECTS
Carboxyalkylated hemoglobin as a potential blood substitute
[AD-A252329] p 384 N93-11561

PATTERN RECOGNITION
Incorporating prior probabilities and misclassification costs into network training: An example from medical prognosis
[RSRE-MEMO-4343] p 428 N93-10980
Extraction of shape information from predicted irradiance profiles in infrared images
[RSRE-MEMO-4464] p 447 N93-11342
Statistical process for the automatic image analysis and its evaluation for object recognition and measurements
[SER-C-370] p 407 N93-11345
Application of artificial neural networks in nonlinear analysis of trusses
[NASA-TM-105319] p 336 N93-11403
The physics of pattern formation at liquid interfaces
[DE92-016971] p 462 N93-11747
Automated extraction of aircraft runway patterns from radar imagery
[AD-A254258] p 218 N93-11751
Transient Reduction Analysis using Neural Networks (TRANN)
[DE92-012150] p 421 N93-12153
A trainable image pattern classification system for detection of damaged soybean seeds
p 201 N93-12208
Nonlinear resistive grid wavelet transformations for texture feature extraction
[AD-A254705] p 285 N93-12332
Video camera as a visual sensor
[NAL-TR-1132] p 314 N93-12373

PAVEMENTS
An evaluation of repair techniques used for uncontrolled longitudinal cracking and failed longitudinal joints
[PB92-205616] p 277 N93-12072

PAYLOADS
Payload advisory panel recommendations
[NASA-TM-108012] p 219 N93-11528
Acoustic fill factors for a 120 inch diameter fairing
[NASA-CR-189284] p 434 N93-11634
Development and use of data analysis procedures for the CRRES payloads AFGL-701-2/Dosimeter and AFGL-701-4/Fluxmeter and application of the data analysis results to improve the static and dynamic models of the Earth's radiation belts
[AD-A253287] p 363 N93-11810

PCM TELEMETRY
Design of a PCM data compressor --- pulse code modulation
[DE92-019469] p 404 N93-11539

PEEK
Phase transfer catalytic nucleophilic addition reactions: Synthesis of polymers and acetylenic terminated resins
[AD-A254717] p 272 N93-12337

PEGASUS AIR-LAUNCHED BOOSTER
Aerothermal test results from the second flight of the Pegasus booster
[NASA-TM-4391] p 296 N93-10969

PELLETS
Fast cooling phenomena with ice pellet injection in the JIPP T-IIU tokamak
[DE92-782105] p 454 N93-11834

PENETRATION
The effects of chemistry on weld profiles in partial and full penetration welds
[DE92-016865] p 327 N93-11679
Deep penetration into frictional ductile and brittle materials
[PB92-205566] p 338 N93-11903

PEPTIDES
Cytokines as vaccine adjuvants: Interleukin 1 and its synthetic peptide 163-171 p 382 N93-11309

PERCEPTION
Object recognition with a robot hand
p 420 N93-11457

PERFORATED PLATES
Evaluation of acoustic impedance models for a perforated plate
[NAL-TR-1133] p 435 N93-12375

PERFORMANCE PREDICTION
An interactive preprocessor for the NASA engine performance program
[NASA-TM-105786] p 209 N93-10983
A comparison of the achieved and predicted defect rates of some continuously operating electronic equipment
[RTP/909/10-ISSUE-2] p 288 N93-11364
A model for analytical performance prediction of hypervapotron
[DE92-018885] p 305 N93-12010
Analysis of advanced optical glass and systems
[NASA-CR-184434] p 448 N93-12201
Meta-analysis of integrity tests: A critical examination of validity generalization and moderator variables
[AD-A254681] p 386 N93-12225
Parameterization of solar cells
[NASA-TM-105885] p 295 N93-12301
Predicted and tested performance of durable TPS
p 228 N93-12454

PERFORMANCE TESTS
Lightweight Exoatmospheric Projectile (LEAP) test program. Supplemental environmental assessment
[AD-A252286] p 231 N93-10998
A test facility for the thermofluid-dynamics of gas bearing lubrication films
[PNR-90897] p 263 N93-11032
The role of turbomachinery testing for stability in distorted flow
[PNR-90943] p 210 N93-11040
The development of the Rolls-Royce Trent aero gas turbine
[PNR-90949] p 212 N93-11108
Evaluation of a Cray performance tool using a large hydrodynamics code
[DE92-013239] p 407 N93-11231
High Temperature Superconductivity Space Experiment (HTSSE)
[AD-A253119] p 288 N93-11239
The technical background to standards for shackles
[NPL-DMM(A)-51] p 325 N93-11325
The electron-beam water calorimeter project at the National Physical Laboratory
[NPL-RSA(EXT)-30] p 310 N93-11410
Operating characteristics of a 7.6 mm (0.30 inch) diameter two-stage light-gas gun
[DE92-018783] p 217 N93-11447
High Capacity Voice Recorder (HCVR) Operational Test and Evaluation (OT/E) integration test report
[DOT/FAA/CT-TN92/30] p 310 N93-11460
Antenna pattern measurement facilities
[AD-A250219] p 283 N93-11764
Development of the Personnel-based System Evaluation Aid (PER-SEVAL) performance shaping functions
[AD-A252820] p 386 N93-11779
Validation test report for the first-generation dart Gulf Stream forecasting system
[AD-A254286] p 373 N93-11821
Embedded training capabilities for the LAMPS MK 3 system
[AD-A250697] p 207 N93-11838
Sodium reflux pool-boiler solar receiver on-sun test results
[DE92-018932] p 347 N93-12012
Laboratory testing of the electrosource traction battery
[DE92-017993] p 292 N93-12057
Measured data for the Sandia 34-meter vertical axis wind turbine
[DE92-019807] p 348 N93-12075
An investigation of electromagnetic launcher repeatability
[AD-A254339] p 222 N93-12130
Evaluation of CKU-5/A ejection seat catapults under varied acceleration levels
[AD-A248021] p 204 N93-12489
MHD integrated topping cycle project
[DE92-018087] p 456 N93-12504

PERIODIC VARIATIONS
Atlas of albedo and absorbed solar radiation derived from Nimbus 7 earth radiation budget data set, November 1985 to October 1987
[NASA-RP-1281] p 367 N93-11168
Periodicities in pulsar microstructure
p 484 N93-11230

PERMANENT MAGNETS
A theoretical study of the performance of a small permanent magnet, three-phase alternator when driving a purely resistive load via a full-wave rectification circuit
[RAE-TR-84009] p 289 N93-11434
Open-loop characteristics of magnetic suspension systems using electromagnets mounted in a planar array
[NASA-TP-3229] p 277 N93-11613
Optimization of film synthesized rare earth transition metal permanent magnet systems
[DE92-018726] p 432 N93-12116

PERMEABILITY
Occupational safety considerations with hydrazine fuels p 276 N93-11951
Transmission/reflection and short-circuit line methods for measuring permittivity and permeability
[PB92-205376] p 293 N93-12084

PERMITTIVITY
High Temperature Superconductivity Space Experiment (HTSSE)
[AD-A253119] p 288 N93-11239
Transmission/reflection and short-circuit line methods for measuring permittivity and permeability
[PB92-205376] p 293 N93-12084
Two-fluid measurements on thin films
[PB92-205350] p 308 N93-12475

PEROVSKITES
Nanostructure, defect chemistry and properties of relaxor ferroelectrics
[AD-A247294] p 431 N93-11468

PERSONAL COMPUTERS
Geographic information system to support state-wide hydrologic modeling with the SCS-TR-20
[PB92-185768] p 476 N93-11700

PERSONNEL
The NASA/National Space Science Data Center trapped radiation environment model program, 1964 - 1991
[NASA-TM-107993] p 349 N93-11003
Viral hepatitis in the US Air Force, 1980 - 1989
p 377 N93-11287
Estimates of Human Immunodeficiency Virus (HIV) incidence and trends in the US Air Force
p 377 N93-11292
Immunological parameters in current and former US Air Force personnel p 378 N93-11295
Neuropsychiatric morbidity in early HIV disease: Implications for military occupational function
p 379 N93-11299
Susceptibility in USAF recruits to vaccine preventable diseases p 380 N93-11301
Development of the Personnel-based System Evaluation Aid (PER-SEVAL) performance shaping functions
[AD-A252820] p 386 N93-11779
Sustaining health and performance in the cold: Environmental medicine guidance for cold-weather operation
[AD-A254328] p 385 N93-12145

PERSONNEL DEVELOPMENT
Meta-analysis of integrity tests: A critical examination of validity generalization and moderator variables
[AD-A254681] p 386 N93-12225
Introduction to training decisions modeling technologies: The training decisions system
[AD-A249862] p 387 N93-12252

PERSONNEL SELECTION
Astronaut candidate strength measurement using the Cybex 2 and the LIDO Multi-Joint 2 dynamometers
[NASA-CR-185679] p 389 N93-12195
Meta-analysis of integrity tests: A critical examination of validity generalization and moderator variables
[AD-A254681] p 386 N93-12225

PERTURBATION
Lidar studies of gravity waves in the mesopause region p 358 N93-11222
Atomic structure and spectral perturbations in dense and hot plasmas p 321 N93-12049
Difference approximations for hyperbolic conservation laws and consistency with characteristics
[NAL-TR-1098T] p 428 N93-12350

PERTURBATION THEORY
Boundary condition methods in the numerical solution of the Navier-Stokes equations with the application to free surface problems
[ISBN-0-315-64278-5] p 298 N93-11241
Studies in quantum field theory
[DE92-011035] p 470 N93-11276
Orbit perturbations due to an axi-symmetric gravitational field, analyzed over extended periods of time
[RAE-TM-SPACE-386] p 220 N93-11486

Perturbation theory for the solution of systems of linear equations
[AD-A254994] p 428 N93-12511

PETN
Detonation reactions frozen by free expansion and analyzed by mass spectrometry
[DE92-018605] p 274 N93-11566

PETROGRAPHY
Thin-sectioning and analysis of fine-grained meteoritic materials
[NASA-CR-185693] p 485 N93-11546

PH FACTOR
Preparation of silicon oxynitride thin films by plasma chemical vapor deposition for chemical implantation. Application to a pH ISFET
[ECL-91-12] p 291 N93-11574

PHASE DIAGRAMS
Magnetic properties of high-T(c) superconductors
[DE92-018809] p 460 N93-11533
Calculation of binary phase diagrams between the actinide elements, rare earth elements, and transition metal elements
[DE92-019119] p 249 N93-11801

PHASE SEPARATION (MATERIALS)
Frustrated phase separation and high temperature superconductivity
[DE92-019249] p 459 N93-11501

PHASE SHIFT
Phase-stepping fiber-optic projected fringe system for surface topography measurements
[NASA-CASE-LEW-14996-1] p 446 N93-11058
Frequency response in short thermocouple wires
[NASA-CR-190943] p 310 N93-11612

PHASE SHIFT CIRCUITS
Nonlinear delay line phase shifters for terahertz superconductive electronic circuits
[AD-A255119] p 294 N93-12290

PHASE TRANSFORMATIONS
Sigma phase in nickel based superalloys
[PNR-90950] p 255 N93-11109
Frustrated phase separation and high temperature superconductivity
[DE92-019249] p 459 N93-11501
An analytic description of thick-wall bubbles
[DE92-016465] p 432 N93-11759
Research at and operation of the material science x ray absorption beamline (X-11) at the National Synchrotron Light source
[DE92-018598] p 251 N93-12172

PHASES
Nature of the beta-phase of nickel-aluminum system
[AD-A254101] p 261 N93-12269

PHENOLS
Preconversion catalytic deoxygenation of phenolic functional groups
[DE92-018304] p 244 N93-10986

PHILOSOPHY
Ontology of mind, subjective ontology, and the example of temporal expressions
[REPT-92-018] p 386 N93-11212

PHONONS
A cryogenic phonon detector to search for dark matter particles p 481 N93-11198
Review of phonon behavior and microstructural development leading to martensitic transformations in Ni(x)Al(100-x) alloys
[DE92-014782] p 256 N93-11519
Infrared phonon structure in epitaxial films of Tl2Ca2Ba2Cu3O10 at low temperatures
[DE92-017078] p 466 N93-12109
Electronic transport and lasing in microstructures
[DE92-018725] p 441 N93-12115
Theory of normal metals
[DE92-016828] p 262 N93-12476

PHOSPHATES
Tetrahedral atom zincophosphate structures: Synthesis, crystal structure, and spectroscopic studies of (Zn(PO2(OC2H5)2)2)x, a one-dimensional inorganic polymer
[AD-A251051] p 437 N93-11560

PHOSPHINES
The role of backbond strain in silicon surfaces on the decomposition of NH3 and PH3
[AD-A253771] p 250 N93-12062

PHOSPHORUS COMPOUNDS
Synthesis and characterization of novel organogallium-phosphorus compounds: X ray crystal structures of Ph2GaP (SiMe3)2Ga (Ph2Cl, Ph2 (Cl)Ga.P (SiMe3)3, and Ph3Ga.P (SiMe3)3
[AD-A253841] p 462 N93-11724

PHOTOCATHODES
Experimental and theoretical investigation of high gradient acceleration
[DE92-015299] p 315 N93-11278

PHOTOCHEMICAL REACTIONS
Heterogeneous processes: Laboratory, field, and modeling studies p 350 N93-11090
Employment of radicals and excited state species for supersonic combustion photochemical ignition of premixed hydrogen/oxygen mixtures with ArF laser
p 245 N93-11135
Determination of stepsize parameters for intermolecular vibrational energy transfer
[DE92-010770] p 435 N93-11189
Interfacial and thin film chemistry in electron device fabrication
[AD-A253579] p 288 N93-11257
Electron transfer rates at semiconductor/liquid interfaces
[DE92-018559] p 289 N93-11438
Summaries of FY 1991 research in the chemical sciences
[DE92-011920] p 251 N93-12135

PHOTOCONDUCTIVITY
Microscopic origins of metastable effects in a-Si:H and deep defect characterization in a-Si,Ge:H alloys
[DE92-010588] p 463 N93-11813

PHOTOCONDUCTORS
Characteristics of current filamentation in high gain photoconductive semiconductor switching
[DE92-018277] p 291 N93-11693

PHOTODETACHMENT
Diagnostics and modeling of H(-) ion sources
[AD-A250664] p 440 N93-11867
Studies of transition states and radicals by negative ion photodetachment
[DE92-017011] p 440 N93-11875
Threshold photodetachment spectroscopy of negative ions
[DE92-017090] p 440 N93-12100

PHOTODISSOCIATION
Gas-surface interactions near dissociation threshold
[AD-A250205] p 252 N93-12254
Thermochemistry of transition metal clusters
[DE92-018713] p 262 N93-12480

PHOTOELECTRIC EMISSION
Image potential states at metal-dielectric interfaces
[DE92-017019] p 466 N93-12124

PHOTOELECTRICITY
Electron transfer rates at semiconductor/liquid interfaces
[DE92-018559] p 289 N93-11438
Microscopic origins of metastable effects in a-Si:H and deep defect characterization in a-Si,Ge:H alloys
[DE92-010588] p 463 N93-11813

PHOTOELECTRON SPECTROSCOPY
State-resolved reaction dynamics
[AD-A254291] p 436 N93-11196
Signal-to-noise assessment and measurement in spectroscopies with particular reference to Auger and x ray photoelectron spectroscopies
[NPL-DMM(A)-45] p 247 N93-11396
Threshold photodetachment spectroscopy of negative ions
[DE92-017090] p 440 N93-12100

PHOTOELECTRONS
State-resolved reaction dynamics
[AD-A254291] p 436 N93-11196
Progress on polymer degradation by photoelectron transfer
[AD-A246276] p 268 N93-11862

PHOTOEXCITATION
Erasable optical information storage in the polyanilines
[AD-A254873] p 480 N93-12438

PHOTOGRAMMETRY
Object based multi-image matching
[SER-C-375] p 309 N93-11330
Photogrammetric point determination using digital imagery of three-line scanner systems
[SER-C-372] p 309 N93-11346
Photogrammetric GIS technology: Feature mapping on digital stereo imagery
[AD-A254255] p 477 N93-11748
Proceedings of the First Seminar on Geographic Information Systems in Zambia
[PB92-207125] p 477 N93-11789

PHOTOIONIZATION
State-resolved reaction dynamics
[AD-A254291] p 436 N93-11196
Multiphoton ionization and ion-pair formation in molecular hydrogen
[DE92-019026] p 438 N93-11829
Low pressure gas multiphotoionization for wave packet experiments p 319 N93-12034

PHOTOLITHOGRAPHY
Reflection masks for soft x ray projection lithography
[DE92-014779] p 293 N93-12121
Development of contractor cells, phase 1
[DE92-017343] p 348 N93-12222

PHOTOLUMINESCENCE
Characteristics of current filamentation in high gain photoconductive semiconductor switching
[DE92-018277] p 291 N93-11693
Programme and abstracts. Workshop on Expert Evaluation and Control of Compound Semiconductor Materials and Technologies No. 1: (EXAMTEC 199)
[AD-A254023] p 292 N93-12071

PHOTOLYSIS
Progress on polymer degradation by photoelectron transfer
[AD-A246276] p 268 N93-11862

PHOTOMAPPING
Photogrammetric GIS technology: Feature mapping on digital stereo imagery
[AD-A254255] p 477 N93-11748

PHOTOMETERS
Phase-stepping fiber-optic projected fringe system for surface topography measurements
[NASA-CASE-LEW-14996-1] p 446 N93-11058

PHOTON BEAMS
Computation of small scale velocity turbulence and its effect on optical scintillations and stimulated thermal Rayleigh scattering
[DE92-018934] p 448 N93-11627
Dynamic vacuum analysis for APS high heat flux beamline front ends using optical ray-tracing simulation methods
[DE92-019032] p 445 N93-11831

PHOTONICS
Organization of the Optical Society of America Photonic Science Topical Meeting Series. Volume 14: Photorefractive materials effects, and devices
[AD-A253001] p 446 N93-11071
The fourth OSA Topical Meeting Proceedings on Picosecond Electronics and Optoelectronics, volume 9
[AD-A253472] p 447 N93-11099
Photonics and other approaches to high speed communications
[NASA-CR-190362] p 279 N93-11116

PHOTONS
High energy x ray imaging diagnostic on Nova
[DE92-018067] p 451 N93-11495
Mass energy-transfer and mass energy-absorption coefficients, including in-flight positron annihilation for photon energies 1 keV to 100 MeV, 1992
[PB92-181106] p 438 N93-11715
Exciton kinetics in poly(di-n-hexylsilane)
[DE92-018278] p 283 N93-11800
Bremsstrahlung absorption in plasmas
p 321 N93-12047
Image potential states at metal-dielectric interfaces
[DE92-017019] p 466 N93-12124

PHOTONUCLEAR REACTIONS
Photodisintegration of the deuteron at high energy
[DE92-017066] p 445 N93-12108

PHOTOSYNTHESIS
The potential effects of concurrent increases in temperature, CO2 and O3 on net photosynthesis, as mediated by rubisCO
[DE92-019411] p 374 N93-11630
Ultrafast photoinduced electron transfer reactions in supramolecular arrays: From charge separation and storage to molecular switches
[DE92-016186] p 465 N93-12090
Estimation of photosynthetic capacity using MODIS polarization: 1988 proposal to NASA Headquarters
[NASA-TM-103945] p 344 N93-12351

PHOTOVOLTAIC CELLS
Contactless optoelectronic integrated circuits for remote fiber optic communication and sensing applications
[AD-A253573] p 290 N93-11507

PHOTOVOLTAIC CONVERSION
The 1992 DOE/Sandia crystalline photovoltaic technology project review meeting
[DE92-018544] p 344 N93-10989
NEDO Solar Technology Subcommittee
[DE92-526256] p 347 N93-11845

PHYSICAL EXAMINATIONS
Estimates of Human Immunodeficiency Virus (HIV) incidence and trends in the US Air Force
p 377 N93-11292

PHYSICAL EXERCISE
Smoking status and body composition, exercise, dietary intake, and alcohol/caffeine consumption
[AD-A250648] p 385 N93-11893

PHYSICAL FITNESS
Smoking status and body composition, exercise, dietary intake, and alcohol/caffeine consumption
[AD-A250648] p 385 N93-11893

PHYSICAL OPTICS
High frame-rate, large field wavefront sensor
[DE92-019547] p 310 N93-11542

Experimental measurement and theoretical modeling of microwave scattering and the structure of the sea surface influencing radar observations from space
[NASA-CR-190998] p 343 N93-12006

PHYSICAL PROPERTIES
Effects of physical properties and geometry on shapes and stability of polarizable drops in external fields
[DE92-018865] p 301 N93-11638

PHYSIOLOGICAL ACCELERATION
Physiologically constrained aerocapture for manned Mars missions p 226 N93-12185

PHYSIOLOGICAL EFFECTS
An overview of gravitational physiology
[NASA-TM-102849] p 391 N93-12319

PHYSIOLOGICAL RESPONSES
Physiological analyses of the afferents controlling brain neurochemical systems
[AD-A253185] p 375 N93-11146
Mechanisms of immune failure in burn injury
p 376 N93-11285
Use of novel adjuvants and delivery systems to improve the humoral and cellular immune response to malaria vaccine candidate antigens p 381 N93-11308
Effect of hemorrhage on cardiac output, vasopressin, aldosterone, and diuresis during immersion in men
[NASA-TM-103949] p 374 N93-12014
An overview of gravitational physiology
[NASA-TM-102849] p 391 N93-12319

PHYSIOLOGY
Mechanisms of immune failure in burn injury
p 376 N93-11285

PIEZOELECTRIC CERAMICS
Robust solder joint attachment of coaxial cable leads to piezoelectric ceramic electrodes
[DE92-017042] p 276 N93-11494

PIEZOELECTRIC CRYSTALS
Numerical and experimental results in vibroacoustical active control of structural elements with piezoelectric materials
[DILC-EST-TN-224] p 334 N93-11158

PIEZOELECTRIC GAGES
Numerical and experimental results in vibroacoustical active control of structural elements with piezoelectric materials
[DILC-EST-TN-224] p 334 N93-11158

PIEZOELECTRIC TRANSDUCERS
Advanced modeling and optimization of piezoelectric composites
[AD-A253800] p 242 N93-12296

PIEZOELECTRICITY
Advanced modeling and optimization of piezoelectric composites
[AD-A253800] p 242 N93-12296

PILOT PERFORMANCE
Design of instrument approach procedure charts: Comprehension speed of missed approach instructions coded in text or icons
[PB92-205673] p 204 N93-11252
Relating cognitive function to military aviator performance in early HIV infection p 379 N93-11298
Modified optimal control pilot model for computer-aided design and analysis
[NASA-TM-4384] p 214 N93-11459
Selective factors affecting rotary wing aviator performance with symbology superimposed on night vision goggles
[AD-A254983] p 390 N93-12508

PILOT SELECTION
The screening of inhalant allergic diseases in the selection of candidates for aircraft piloting
p 382 N93-11312
Asthma in aircrew: Assessment, treatment and disposition p 383 N93-11315

PILOT TRAINING
An evaluation of crew coordination and performance during a simulated UH-60 helicopter mission
[AD-A254984] p 390 N93-12509

PILOTLESS AIRCRAFT
Development of a 1/7-scale F/A-18 UAV for supermaneuverability research --- unmanned air vehicle
[AD-A247261] p 208 N93-12053

PINHOLE OCCULTER FACILITY
Controls Astrophysics and Structures Experiment in Space (CASES) advanced studies and planning
[NASA-CR-184410] p 220 N93-12213

PIPE FLOW
Interfacial area and two-phase flow structure development measured by a double-sensor probe
[DE92-019459] p 300 N93-11538
Bubble dissolving in turbulent pipe flow
[AD-A252927] p 308 N93-12462

PIPELINING (COMPUTERS)
A fast pipelined inner product unit
[REPT-92-025] p 411 N93-11594

PIPES (TUBES)
Methods of analysis for thick-section composite structures p 237 N93-11262
Heat transfer enhancement by chaotic mixing
[PB92-190305] p 470 N93-11469
Users manual for program NYQUIST: Liquid rocket nyquist plots developed for use on a PC computer
[NASA-CR-184451] p 235 N93-12522

PISTON ENGINES
Design of small Stirling dynamic isotope power system for robotic space missions
[NASA-TM-105919] p 275 N93-12085

PITCH (INCLINATION)
A new pitch angle diagnostic for electron cyclotron resonance plasma p 450 N93-11185

PIVOTS
Polynomial dual network simplex algorithms
[AD-A254340] p 413 N93-12131

PLAINS
Quaternary volcanism, tectonics, and sedimentation in the Idaho National Engineering Laboratory area
[DE92-017851] p 362 N93-11692

PLANAR STRUCTURES
Three-dimensional image structure in in-line Fraunhofer holography p 311 N93-11723
Optical generation, control and sensing of millimeter waves
[AD-A254700] p 285 N93-12230
Studies in control for vibration suppression of the UWAA 20-bay planar truss
[AD-A250193] p 341 N93-12253
Conductor-backed coplanar waveguide resonators of Y-Ba-Cu-O and Tl-Ba-Ca-Cu-O on LaAlO3
[NASA-TM-105890] p 469 N93-12325

PLANE STRAIN
Analysis of delamination in composite laminates under low-velocity impact p 243 N93-12532

PLANE WAVES
Colliding plane gravitational waves with colinear polarization
[MATHS-REPT-A-160] p 357 N93-11120
Methods of analysis for thick-section composite structures p 237 N93-11262
Final Technical Report
[AD-A253529] p 284 N93-12083
The generalized Goursat-Riemann problem for plane waves in isotropic elastic solids p 340 N93-12199
Wavefront reconstruction using a least squares approach
[ISVR-TR-203] p 435 N93-12324
Spacetime singularities in string theory
p 472 N93-12530

PLANETARY BASES
A gas-cooled cermet reactor system for planetary base power
[DE92-018017] p 443 N93-11433

PLANETARY EVOLUTION
The search for life's origins: Progress and future directions in planetary biology and chemical evolution
[NASA-CR-190929] p 487 N93-11603

PLANETARY MAGNETOSPHERES
Modeling the Jovian aurora
[NASA-CR-190696] p 486 N93-11164
Multispectral observations of the Jovian aurora
p 487 N93-11167

PLANETARY WAVES
Dynamics of planetary waves in the atmosphere
p 363 N93-11898

PLANFORMS
Laboratory and numerical studies of dynamical processes related to thermal convection in the Earth's mantle p 364 N93-11900

PLANNING
Information systems planning leading to performance support systems
[DE92-018745] p 475 N93-11441

PLANTS (BOTANY)
Techniques for optimal crop selection in a controlled ecological life support system
[NASA-TM-103950] p 388 N93-12018
Scaling issues for biodiversity protection
[DE92-016689] p 375 N93-12315

PLASMA COMPOSITION
Plasma properties of solar coronal active regions
p 489 N93-12342

PLASMA CONTROL
X ray diagnostic techniques in ICF
[DE92-018069] p 449 N93-10975
Development of a geometry-compensated neutron time-of-flight detector for ICF applications with approximately 200 ps time response
[DE92-018024] p 450 N93-11153
High beta and confinement studies on TFTR
[DE92-018647] p 452 N93-11568
Gain in a confined aluminum plasma
p 320 N93-12043

Plasma temperatures from first-hit neutron time-of-flight spectra
[DE92-018006] p 454 N93-12060
Transport mechanisms acting in toroidal devices: A theoretician's view
[DE92-018738] p 456 N93-12501
Ion temperature measurements on field reversed configuration plasmas p 457 N93-12535

PLASMA CURRENTS
Scaling of lower hybrid current drive with temperature
[DE92-018541] p 449 N93-10988
Effects of current driven instabilities on the ion and electron temperatures in the topside ionosphere
p 360 N93-11270

PLASMA DECAY
Development of a new plasma diagnostic of the critical surface and studies of the ion acoustic decay instability using collective Thomson scattering
[DE92-018508] p 453 N93-11730
Development of a new plasma diagnostic of the critical surface and studies of the ion acoustic decay instability using collective Thomson scattering
[DE92-018526] p 453 N93-11731

PLASMA DENSITY
Nonlinear behavior of resonant absorption in a plasma at microwave frequency p 319 N93-12032
Helium transport studies on D3-D
[DE92-016251] p 455 N93-12307

PLASMA DIAGNOSTICS
X ray diagnostic techniques in ICF
[DE92-018069] p 449 N93-10975
Analytical and numerical principles for the scaling of plasma focus experiments, with regard to electrical resistance
[IPF-91-2] p 450 N93-11103
A new pitch angle diagnostic for electron cyclotron resonance plasma p 450 N93-11185
Ion temperature measurements in tokamak plasmas by Rutherford scattering
[PB92-184738] p 451 N93-11245
Plasma measurements in magnetospheric tail
[MPE-233] p 361 N93-11352
High energy x ray imaging diagnostic on Nova
[DE92-018067] p 451 N93-11495
Fusion programs in applied plasma physics
[DE92-019639] p 452 N93-11660
Development of a new plasma diagnostic of the critical surface and studies of the ion acoustic decay instability using collective Thomson scattering
[DE92-018508] p 453 N93-11730
Development of a new plasma diagnostic of the critical surface and studies of the ion acoustic decay instability using collective Thomson scattering
[DE92-018526] p 453 N93-11731
A distributed data acquisition and centralized data reduction system for flexible and efficient measurements
[DE92-019021] p 312 N93-11827
Diagnostics of electron-heated solar flares
p 488 N93-11877
The 1989 Scientific Report of the Laboratory for the Use of High Power Lasers
[ETN-92-92175] p 317 N93-12023
A ring coded-aperture microscope for high-resolution imaging of high-energy x rays
[DE92-018004] p 454 N93-12059
Plasma temperatures from first-hit neutron time-of-flight spectra
[DE92-018006] p 454 N93-12060
The role of advanced optical diagnostics in monitoring and controlling an MHD power plant. Part 2: 50 MW(t), POC topping cycle
[DE92-015368] p 455 N93-12141

PLASMA DIFFUSION
Anomalous ion thermal transport in hot ion plasmas by the ion temperature gradient mode
[DE92-016686] p 456 N93-12493

PLASMA DYNAMICS
Contributions to plasma focus physics since 1970 from the Institute of Plasma Research, Stuttgart (Fed. Republic of Germany)
[IPF-91-4] p 450 N93-11201
Low pressure gas multiphotoionization for wave packet experiments p 319 N93-12034
Transient phenomena in MHD experiments
[DE92-014496] p 455 N93-12139
Transport mechanisms acting in toroidal devices: A theoretician's view
[DE92-018738] p 456 N93-12501

PLASMA EQUILIBRIUM
Hydrodynamic fluctuations and light scattering in hot electron gas of semiconductors
[DE92-622800] p 458 N93-10992
Shafranov shift in low-aspect-ratio heliotron/torsatron CHS
[DE92-782100] p 451 N93-11277

Nonlinear evolution of resistive tearing mode instability with shear flow and viscosity
[DE92-012138] p 453 N93-11745
PLASMA ETCHING
A new pitch angle diagnostic for electron cyclotron resonance plasma p 450 N93-11185
PLASMA FLUX MEASUREMENT
Laser material interaction in confined medium
p 319 N93-12035
PLASMA FOCUS
Current scaling of plasma focus devices
[IPF-90-1] p 449 N93-11029
Instabilities in the rundown phase of the plasma focus
[IPF-90-3] p 449 N93-11030
Analytical and numerical principles for the scaling of plasma focus experiments, with regard to electrical resistance
[IPF-91-2] p 450 N93-11103
Contributions to plasma focus physics since 1970 from the Institute of Plasma Research, Stuttgart (Fed. Republic of Germany)
[IPF-91-4] p 450 N93-11201
PLASMA HEATING
Scaling of lower hybrid current drive with temperature
[DE92-018541] p 449 N93-10988
Direct electron absorption of fast waves on the D3-D tokamak
[DE92-016254] p 449 N93-11041
Thermal analysis and design of polarizer mirrors for waveguides in the D3-D tokamak
[DE92-018884] p 451 N93-11382
Self-generated stochastic heating in an RF discharge
[DE92-018558] p 452 N93-11565
Nonlinear effects of ICRF power on drift wave stability and transport in tokamaks, task 1
[DE92-018488] p 453 N93-11729
Diagnostics of electron-heated solar flares
p 488 N93-11877
PLASMA INTERACTION EXPERIMENT
Beam-plasma interactions and radiation generation during the ejection of electron and ion beams in space
[AD-A253993] p 224 N93-11736
PLASMA INTERACTIONS
Interpretation of measurements from the suprathermal electron spectrometer on the NEED-2 rocket
[FFI-92/7009] p 357 N93-11129
Flank solar wind interaction
[NASA-CR-189285] p 489 N93-12303
PLASMA JETS
Numerical simulation of alumina spraying in argon-helium plasma jet
[DE92-017859] p 455 N93-12092
PLASMA LAYERS
Plasma measurements in magnetospheric tail
[MPE-233] p 361 N93-11352
PLASMA PHYSICS
Contributions to plasma focus physics since 1970 from the Institute of Plasma Research, Stuttgart (Fed. Republic of Germany)
[IPF-91-4] p 450 N93-11201
Three dimensional and 2D simulation of an expanding plasma using a Darwin hybrid particle code
[DE92-019095] p 451 N93-11516
Fusion programs in applied plasma physics
[DE92-019639] p 452 N93-11660
Activity of the technical groups (LULI Palaiseau, France) p 322 N93-12052
Plasma properties
[DE92-018635] p 455 N93-12188
The 44th Annual Gaseous Electronics Conference
[AD-A254872] p 295 N93-12437
PLASMA PINCH
Analytical and numerical principles for the scaling of plasma focus experiments, with regard to electrical resistance
[IPF-91-2] p 450 N93-11103
PLASMA PRESSURE
Laser material interaction in confined medium
p 319 N93-12035
Study of the effects of a plastic wave induced by laser pulse in a metallic material. Application to the improvement of fatigue strength p 319 N93-12036
PLASMA PROPULSION
Superconducting applications in propulsion systems. Magnetic insulation for plasma propulsion devices
[NASA-CR-184401] p 233 N93-12013
PLASMA RADIATION
Analysis of the instrument operation of a focal circle spectrograph and numerical reconstitution of the spectrum emitted by a plasma column p 321 N93-12051
Plasma properties of solar coronal active regions
p 489 N93-12342
PLASMA SHEATHS
Self-generated stochastic heating in an RF discharge
[DE92-018558] p 452 N93-11565
PLASMA SPECTRA
Plasma temperatures from first-hit neutron time-of-flight spectra
[DE92-018006] p 454 N93-12060
PLASMA SPRAYING
Analysis of plasma-treated wire insulation
[DE92-019471] p 291 N93-11643
Development of wear resistant ceramic coatings for diesel engine components
[DE92-019068] p 268 N93-11654
Comprehensive computational model for thermal plasma processing
[DE92-018015] p 454 N93-12066
A design of experiment study of plasma sprayed alumina-titania coatings
[DE92-017877] p 271 N93-12168
Thermal protection using very high temperature ceramics p 228 N93-12451
A Taguchi experimental design study of twin-wire electric arc sprayed aluminum coatings
[DE92-018022] p 262 N93-12494
PLASMA TEMPERATURE
Effects of current driven instabilities on the ion and electron temperatures in the topside ionosphere
p 360 N93-11270
Comment on 'EISCAT Radar Observations of Enhanced Incoherent Scatter Spectra and Their Relation to Auroral Luminosity and Field-Aligned Currents' by P. N. Collis et al. p 360 N93-11271
Plasma measurements in magnetospheric tail
[MPE-233] p 361 N93-11352
Plasma temperatures from first-hit neutron time-of-flight spectra
[DE92-018006] p 454 N93-12060
Plasma properties of solar coronal active regions
p 489 N93-12342
PLASMA TORCHES
Comprehensive computational model for thermal plasma processing
[DE92-018015] p 454 N93-12066
Technology evaluation report of Retech, Inc., Plasma Centrifugal Furnace, volume 1
[PB92-216035] p 456 N93-12526
Technology evaluation report of Retech, Inc., Plasma Centrifugal Furnace, volume 2
[PB92-216043] p 457 N93-12527
PLASMA TURBULENCE
The role of advanced optical diagnostics in monitoring and controlling an MHD power plant. Part 2: 50 MW(t), POC topping cycle
[DE92-015368] p 455 N93-12141
Transport mechanisms acting in toroidal devices: A theoretician's view
[DE92-018738] p 456 N93-12501
PLASMA WAVES
Topics in high-intensity laser plasma interaction
p 450 N93-11191
Observations of thin auroral ionization layers by EISCAT in connection with pulsating aurora p 359 N93-11266
Scattering of electromagnetic waves from a plasma: Enhanced ion acoustic fluctuations due to ion-ion two-stream instabilities p 361 N93-11272
Nonlinear effects of ICRF power on drift wave stability and transport in tokamaks, task 1
[DE92-018488] p 453 N93-11729
Observation and analysis of the Stokes and anti-Stokes components of stimulated Raman backscattering
p 318 N93-12025
X pulse radiation around the critical surface
p 318 N93-12027
Electron acceleration in a relativistic electron plasma wave p 319 N93-12033
Low pressure gas multiphotoionization for wave packet experiments p 319 N93-12034
Study of the effects of a plastic wave induced by laser pulse in a metallic material. Application to the improvement of fatigue strength p 319 N93-12036
Experimental study of x ray laser in lithumoid aluminum p 321 N93-12045
PLASMA-PARTICLE INTERACTIONS
Beam-plasma interactions and radiation generation during the ejection of electron and ion beams in space
[AD-A253993] p 224 N93-11736
PLASMAS (PHYSICS)
The basic equations for a four component magnetoplasma flow with non equilibrium ionization
[IPF-91-1] p 449 N93-11102
Proceedings of the 14th International Conference on the Numerical Simulation of Plasmas
[AD-A249095] p 451 N93-11275
Three dimensional and 2D simulation of an expanding plasma using a Darwin hybrid particle code
[DE92-019095] p 451 N93-11516
Fast cooling phenomena with ice pellet injection in the JIPP T-IIU tokamak
[DE92-782105] p 454 N93-11834
Synthesis of nanocrystalline powders for oxide ceramics by microwave plasma pyrolysis
[DE92-017410] p 268 N93-11861
Direct radiative recombination of atomic ions
p 321 N93-12048
The 44th Annual Gaseous Electronics Conference
[AD-A254872] p 295 N93-12437
Railgun armature velocity improvement, SBIR phase 2
[AD-A254749] p 222 N93-12505
PLASTIC ANISOTROPY
Contribution to the monocrystal behavior study during large plastic strains
[ECL-92-13] p 461 N93-11581
PLASTIC DEFORMATION
On the dependence of the dynamic crack tip temperature fields in metal upon crack tip velocity and material parameters
[AD-A253657] p 335 N93-11219
Contribution to the study of the anisotropic viscoelasticity of large strains: The case of the monocrystal
[ECL-90-29] p 460 N93-11573
Crushing behavior of tubular structures in multi-materials
[ECL-91-37] p 336 N93-11579
Contribution to the monocrystal behavior study during large plastic strains
[ECL-92-13] p 461 N93-11581
The conversion of plastic work to heat around a dynamically propagating crack in metals
[AD-A253801] p 258 N93-11782
Micromechanisms of deformation and fracture in aluminum based MMC's: Interface effects
[AD-A253560] p 259 N93-11850
Study of the effects of a plastic wave induced by laser pulse in a metallic material. Application to the improvement of fatigue strength p 319 N93-12036
Nanophase ceramics
[AD-A254661] p 272 N93-12246
Systems of evolution equations in thermochemical equations
[AD-A254891] p 253 N93-12282
PLASTIC PROPERTIES
Mechanical properties of semiconductors and their alloys
[AD-A253908] p 462 N93-11727
PLASTICIZERS
Energetic composites of cyclodextrin nitrate esters and nitrate ester plasticizers
[AD-D015364] p 274 N93-11665
PLASTICS
An evaluation of field-flow fractionation for molecular weight characterization of polymeric materials
[DE92-019192] p 267 N93-11497
Phase transfer catalytic nucleophilic addition reactions: Synthesis of polymers and acetylenic terminated resins
[AD-A254717] p 272 N93-12337
PLATES (STRUCTURAL MEMBERS)
Methods of analysis for thick-section composite structures p 237 N93-11262
PLATING
Characteristics of heat transfer to nickel plated chamber walls of high pressure rocket combustors
[NAL-TR-1126T] p 234 N93-12372
PLATINUM
Selective carbon oxygen bond scission during reactions of oxygenates on single crystal catalysts
[DE92-018687] p 247 N93-11439
Intermediate temperature electrolytes for SOFC
[DE92-018786] p 345 N93-11571
PLATINUM COMPOUNDS
Exploration of the ionizable metal cluster-electrode surface analogy: Infrared spectroelectrochemistry of (Pt24(CO)30)(sup n), (Pt26(CO)32)(sup n), and (Pt38(CO)44)(sup n) (n = 0 to -10), and comparisons with potential-dependent spectra of CO adlayers on platinum surfaces
[AD-A252544] p 250 N93-11808
PLUMES
Modeling the dispersion of tracer plumes in the Colorado front range boundary layer during night- and day-time conditions
[DE92-019384] p 354 N93-11676
Stratospheric aircraft exhaust plume and wake chemistry studies
[NASA-CR-189688] p 366 N93-12299
PLY ORIENTATION
Thermal residual stresses in silicon-carbide/titanium (0/90) laminate
[NASA-TM-107649] p 236 N93-11072
PNEUMATIC EQUIPMENT
Pressure vessel burst test program
[AD-A253708] p 334 N93-11080
POINT DEFECTS
Slow crack growth in vacuum p 338 N93-11909

POINT SOURCES
A comparison of feed-forward networks and maximum likelihood on a point-source location problem
[RSRE-MEMO-4567] p 281 N93-11391

POISSON EQUATION
An approximate solution of the fixed gravimetric boundary value problem in the interior and the exterior of the Earth's body
[SER-C-379] p 361 N93-11331

POLAR CUSPS
Studies of interactive plasma processes in the polar cusp
[NASA-CR-190892] p 357 N93-10964

POLAR ORBITS
A comprehensive mission to planet Earth: Woods Hole Space Science and Applications Advisory Committee Planning Workshop
[NASA-TM-108011] p 343 N93-11878

POLAR REGIONS
International Conference on the Role of the Polar Regions in Global Change: Proceedings, volume 1
[DE92-013652] p 353 N93-11232

International Conference on the Role of the Polar Regions in Global Change: Proceedings, volume 2
[DE92-013653] p 353 N93-11233

The effects of magnetic storm phases on F-layer irregularities from auroral to equatorial latitudes
[AD-A253905] p 361 N93-11282

POLARIMETERS
The millimeter wave Cloud Profiling Radar System (CPRS)
[DE92-016970] p 366 N93-10971

POLARIMETRY
The millimeter wave Cloud Profiling Radar System (CPRS)
[DE92-016970] p 366 N93-10971

Limitations of multiple feeds in a polarimetric-radar compact range
[DE92-017526] p 284 N93-12101

POLARIZATION
Near-infrared imaging polarimetry of bipolar nebulae
p 481 N93-11248

Effects of physical properties and geometry on shapes and stability of polarizable drops in external fields
[DE92-018865] p 301 N93-11638

Estimation of photosynthetic capacity using MODIS polarization: 1988 proposal to NASA Headquarters
[NASA-TM-103945] p 344 N93-12351

POLARIZATION (CHARGE SEPARATION)
Ultrafast photoinduced electron transfer reactions in supramolecular arrays: From charge separation and storage to molecular switches
[DE92-016186] p 465 N93-12090

POLARIZATION (WAVES)
CO2 laser frequency doubling using AgGaSe2
[RSRE-MEMO-4528] p 315 N93-11388

POLARIZATION CHARACTERISTICS
Connected triple excitations in coupled-cluster calculations of hyperpolarizabilities: Neon
p 439 N93-11854

Scattering of polarized electrons by oriented deuterons
[DE92-624834] p 440 N93-11914

POLARIZED LIGHT
Evaluation of an analytical model for predicting light scattering from cylindrically-shaped objects in the ocean
[AD-A248414] p 447 N93-11489

POLARIZED RADIATION
Scattering of polarized electrons by oriented deuterons
[DE92-624834] p 440 N93-11914

POLARIZERS
Thermal analysis and design of polarizer mirrors for waveguides in the D3-D tokamak
[DE92-018884] p 451 N93-11382

POLARONS
The Peierls ground state, solitons and polarons in ring-containing polymers
[AD-A254914] p 272 N93-12289

POLICIES
Integrity in automated information systems
[AD-A253990] p 477 N93-11732

Solid state sciences committee forum
[AD-A253556] p 463 N93-11753

Computer Science and Telecommunications Board summary of activities
[DE92-016467] p 404 N93-11761

Environmental problems and trends of international responses, 2
[DE92-531118] p 355 N93-11846

Recommended agency procedures for implementing federal metric policy
[PB92-205467] p 277 N93-11901

NASA/DOD Aerospace Knowledge Diffusion Research Project. Paper 23: Information technology and aerospace knowledge diffusion: Exploring the intermediary-end user interface in a policy framework
[NASA-TM-108077] p 478 N93-12007

High-performance synthetic fibers for composites
[AD-A252645] p 242 N93-12292

POLIOMYELITIS
Immunization of personnel traveling to a destination in tropical countries: French position p 380 N93-11304

POLISHING
Fiber optic polishing system
[AD-D015353] p 446 N93-11052

POLLUTION CONTROL
Civil aircraft engines: The next generation
[PNR-90962] p 211 N93-11085

Activities report of Lufthansa
[ETN-92-92100] p 203 N93-11319

Direct catalytic decomposition of nitric oxide
[DE92-018759] p 247 N93-11444

Advanced heat pump for the recovery of volatile organic compounds
[DE92-011592] p 303 N93-11774

Reduction in global warming due to fuel economy improvements and emissions control of criteria pollutants: New US light-duty vehicles (1968-1991)
[DE92-016636] p 356 N93-12314

POLLUTION MONITORING
Allowance system: Proposed acid rain rule
[PB92-226174] p 356 N93-12524

POLLUTION TRANSPORT
Modeling the dispersion of tracer plumes in the Colorado front range boundary layer during night- and day-time conditions
[DE92-019384] p 354 N93-11676

POLYACETYLENE
The Peierls ground state, solitons and polarons in ring-containing polymers
[AD-A254914] p 272 N93-12289

POLYAMIDE RESINS
Synthesis and conductivity of copolymer of 4,4'-diaminodiphenylamine and terephthaloyl chloride
[AD-A254880] p 273 N93-12440

POLYATOMIC MOLECULES
Determination of stepsize parameters for intermolecular vibrational energy transfer
[DE92-010770] p 435 N93-11189

State-resolved collisional energy transfer in highly vibrationally excited polyatomic molecules
[AD-A253299] p 441 N93-12323

POLYCARBONATES
Fracture behavior of polymers at cryogenic temperatures
[KFK-4969] p 265 N93-11203

An evaluation of field-flow fractionation for molecular weight characterization of polymeric materials
[DE92-019192] p 267 N93-11497

Orientation, stress, and density distributions in injection-moulded amorphous polymers determined by optical techniques
[ETN-92-92271] p 269 N93-11983

The peculiar rheo-optical behaviour of bisphenol-A-polycarbonate and polymethylmethacrylate
p 269 N93-11984

The time-dependent stress-optical behaviour of polycarbonate in the glass transition region
p 269 N93-11985

The measurement and calculation of birefringence in quenched polycarbonate specimens
p 269 N93-11986

Molecular orientation induced by cooling stresses in polycarbonate. 1: Free quenching p 269 N93-11987

Molecular orientation induced by cooling stresses in polycarbonate. 2: Constrained quench and injection moulding p 270 N93-11988

Measurement of the density distributions in quenched polycarbonate specimens by a quantitative Schlieren-optical technique p 270 N93-11989

Analysis of the birefringence distributions in compact discs of polycarbonate p 270 N93-11991

POLYCRYSTALS
Critical currents in polycrystalline YBa2Cu3O(7-x): Self-field and grain size dependence
[DE92-617540] p 459 N93-11076

Grain boundary transport and related processes in natural fine grained aggregates
[DE92-018239] p 461 N93-11682

Superplastic forming of ceramic insulation
p 228 N93-12452

POLYETHER RESINS
Mixed ionic and electronic conductivity in polymers
[DE92-018723] p 273 N93-12500

POLYETHYLENES
Use of the program ANISN to calculate response functions for a Bonner sphere set with a He-3 detector
[NPL-RSA(EXT)-31] p 316 N93-11411

Analysis of plasma-treated wire insulation
[DE92-019471] p 291 N93-11643

Comparative effects of drag-reducing polymers. An experimental report
[AD-A254001] p 268 N93-11793

POLYHEDRONS
Assembling polyhedra with single translations
[AD-A254623] p 419 N93-12239

POLYIMIDE RESINS
Semi-interpenetrating polymer network for tougher and more microcracking resistant high temperature polymers
[NASA-CASE-LAR-13925-2] p 264 N93-11059

Modified epoxy adhesives and primers
[AD-A253857] p 272 N93-12297

POLYIMIDES
Application of polyimides to aeroengine components
[PNR-90907] p 334 N93-11013

Modified epoxy adhesives and primers
[AD-A253857] p 272 N93-12297

POLYMER MATRIX COMPOSITES
Application of polyimides to aeroengine components
[PNR-90907] p 334 N93-11013

Semi-interpenetrating polymer network for tougher and more microcracking resistant high temperature polymers
[NASA-CASE-LAR-13925-2] p 264 N93-11059

Curing and mechanical properties of T800-V398 graphite/bismaleimide at different temperatures
[DLR-FB-92-02] p 237 N93-11143

Molecular mobility of the interface in a model composite: A NMR study
[AD-A253311] p 265 N93-11194

VAMAS round robin project on polymer composite delamination in mode 1 and mode 2: Cyclic loading
[NPL-DMM(A)-47] p 266 N93-11397

ICAN/DAMP-integrated composite analyzer with damping analysis capabilities: User's manual
[NASA-TP-3292] p 241 N93-12015

Advanced modeling and optimization of piezoelectric composites
[AD-A253800] p 242 N93-12296

Fracture toughness testing of polymer matrix composites
[NASA-TP-3199] p 243 N93-12302

POLYMER PHYSICS
Comparative effects of drag-reducing polymers. An experimental report
[AD-A254001] p 268 N93-11793

POLYMERIC FILMS
Dynamics and response of polymer-coated acoustic devices
[DE92-014289] p 433 N93-11523

Low cost humidity sensor
[PB92-205772] p 312 N93-11757

Two-fluid measurements on thin films
[PB92-205350] p 308 N93-12475

POLYMERIZATION
Application of polyimides to aeroengine components
[PNR-90907] p 334 N93-11013

Synthesis and side chain liquid crystal polymers by living ring opening metathesis polymerization. 5: Influence of mesogenic group and interconnecting group on the thermotropic behavior of the resulting polymers
[AD-A253568] p 264 N93-11150

Synthesis of side chain liquid crystal polymers by living ring opening metathesis polymerization. Report 3: Influence of molecular weight, interconnecting unit and substituent on the mesomorphic behavior of polymers with laterally attached mesogens
[AD-A248698] p 265 N93-11187

Synthesis of side chain liquid crystal polymers by living ring opening metathesis polymerization. Report 2: Influence of molecular weight, polydispersity, and flexible spacer length (n=9-12) on the thermotropic behavior of the resulting plymers
[AD-A248700] p 265 N93-11188

Progress on polymer degradation by photoelectron transfer
[AD-A246276] p 268 N93-11862

Controlled synthesis of polyenes by catalytic methods
[DE92-015286] p 271 N93-12165

Phase transfer catalytic nucleophilic addition reactions: Synthesis of polymers and acetylenic terminated resins
[AD-A254717] p 272 N93-12337

POLYMERS
Analysis of surfaces from the LDEF A0114, phase 2
[NASA-CR-190596] p 270 N93-11993

Erosion rates for polymers measured on LDEF
p 270 N93-11994

Turbulence structure and polymer drag reduction in adverse pressure gradient boundary layers
p 304 N93-12003

POLYMETHYL METHACRYLATE
The peculiar rheo-optical behaviour of bisphenol-A-polycarbonate and polymethylmethacrylate
p 269 N93-11984

Gapwise density distributions in injection-moulded polymethylmethacrylate p 270 N93-11990

POLYNOMIALS
Matching and vertex packing: How hard are they?
[AD-A245928] p 423 N93-10991
Equivalence transformations of rational matrices
[MATHS-REPT-A-163] p 423 N93-11121
Equivalence transformations of rational matrices and applications
[MATHS-REPT-A-169] p 424 N93-11124
A primer on polynomial resultants
[AD-A246883] p 426 N93-11463
Some numerical results on best uniform polynomial approximation of chi(sup alpha) on interval (0,1)
[DE92-014859] p 426 N93-11520
Polynomial dual network simplex algorithms
[AD-A254340] p 413 N93-12131
Assembling polyhedra with single translations
[AD-A254623] p 419 N93-12239

POLYSACCHARIDES
Comparative effects of drag-reducing polymers. An experimental report
[AD-A254001] p 268 N93-11793

POLYSILANES
Chemical reactions and properties of organosilicon compounds related to new materials
[AD-A253233] p 246 N93-11218

POLYSTYRENE
Fracture behavior of polymers at cryogenic temperatures
[KFK-4969] p 265 N93-11203
An evaluation of field-flow fractionation for molecular weight characterization of polymeric materials
[DE92-019192] p 267 N93-11497

POLYTROPIC PROCESSES
A Polytropic solar model p 487 N93-11264

POLYURETHANE RESINS
An evaluation of field-flow fractionation for molecular weight characterization of polymeric materials
[DE92-019192] p 267 N93-11497

PONDEROMOTIVE FORCES
Study of filamentation in subdense plasma interaction experiments p 318 N93-12026

POPULATION INVERSION
Modeling for the study of an X laser in a recombination plasma; gain calculations at 105.7 and 154.6 A
p 321 N93-12046
X ray laser program, FY 1991
[AD-A255190] p 322 N93-12275

POPULATIONS
Density equalizing map projections: A new algorithm
[DE92-017088] p 413 N93-12110

POROSITY
Nondestructive evaluation of ceramic and metal matrix composites for NASA's HITEMP and enabling propulsion materials programs
[NASA-TM-105807] p 331 N93-10963
Modelling the behaviour of gas bubbles in epoxy resin
[PNR-90961] p 264 N93-11084
CFD modeling of turbulent flows around the SSME main injector assembly using porosity formulation
[NASA-CR-184359] p 297 N93-11171

POROUS MATERIALS
Sound propagation over rigid porous layers
p 432 N93-11179
Silver lined ceramic vessel and method of preparation
[AD-D015360] p 266 N93-11400
Studies on the reactive melt infiltration of silicon and silicon-molybdenum alloys in porous carbon
[NASA-TM-105860] p 273 N93-12398

PORPHYRINS
Catalytic hydrogenation of carbon monoxide
[DE92-014729] p 253 N93-12428

PORTABLE EQUIPMENT
Direct Broadcast Satellite: Radio Program
[NASA-TM-105910] p 224 N93-11430

POSITION (LOCATION)
High resolution image processing of geophysical data with diffraction tomography
[DE92-014134] p 359 N93-11235
The locator system for wandering individuals
[NASA-TM-104754] p 388 N93-11649
A single beam laser tracker as an alignment tool
[DE92-017746] p 316 N93-11691

POSITION ERRORS
Construction of a geodesic strapdown inertial navigation system for point determination
[SER-C-367] p 205 N93-11344
Methodology issues concerning the accuracy of kinematic data collection and analysis using the ariel performance analysis system
[NASA-CR-185689] p 389 N93-12211

POSITION INDICATORS
Construction of a geodesic strapdown inertial navigation system for point determination
[SER-C-367] p 205 N93-11344
Photogrammetric point determination using digital imagery of three-line scanner systems
[SER-C-372] p 309 N93-11346

POSITION SENSING
Development of a GPS-aided motion measurement, pointing, and stabilization system for a synthetic aperture radar
[DE92-017053] p 204 N93-11152
A comparison of feed-forward networks and maximum likelihood on a point-source location problem
[RSRE-MEMO-4567] p 281 N93-11391
Accuracy improvement of linear estimated motion using differential type sensors
[NAL-TR-1135] p 314 N93-12365

POSITIONING
Dredging research program: Feasibility of a kinematic differential Global Positioning System
[AD-A248953] p 205 N93-11419
Numerical analysis of right-half plane zeros for a single-link manipulator
[NASA-CR-190966] p 426 N93-11547
Importance of numerosity and distribution of articulations within the digits, wrists, and arms of telemanipulators confronted with dextrous assembly tasks
p 330 N93-11967
A vision-based end-point control for a two-link flexible manipulator
[NASA-CR-190967] p 330 N93-12521

POSITIONING DEVICES (MACHINERY)
Vacuum chamber translation/positioning mechanism and welding power supply controller
[NASA-CR-184465] p 328 N93-12196

POSITIVE IONS
Positive ion chemistry of acetylene and methylacetylene clusters. Formation of benzene and C(sub 2n)H(sub 2n)(+) ions via intracluster polymerization reactions
[AD-A250931] p 236 N93-12177
Design and evaluation of ion source for satellite charge control
[AD-A255172] p 227 N93-12408

POSITRON ANNIHILATION
Mass energy-transfer and mass energy-absorption coefficients, including in-flight positron annihilation for photon energies 1 keV to 100 MeV, 1992
[PB92-181106] p 438 N93-11715

POSITRONS
High resolution tomographic instrument development
[DE92-017314] p 313 N93-11828
New techniques for positron emission tomography in the study of human neurological disorders
[DE92-015353] p 384 N93-11873

POTASSIUM
Potassium D-line fitting for investigation of MHD boundary layers
[DE92-019020] p 454 N93-11826

POTASSIUM HYDRIDES
High bandwidth second-harmonic generation in partially deuterated KDP
[DE92-019505] p 452 N93-11645

POTENTIAL ENERGY
Simulation of liquid drop breakup behavior in a flow field using discrete element techniques
[DE92-019435] p 300 N93-11537
Theoretical study of the radiative and kinetic properties of selected metal oxides and air molecules
[AD-A251090] p 438 N93-11804
Studies of transition states and radicals by negative ion photodetachment
[DE92-017011] p 440 N93-11875

POTENTIAL FLOW
Quasigeostrophic vortices in zonal shear
p 358 N93-11226
Numerical investigations into the base drag of various wedges using the base flow model developed by Mauri Tanner
[REPT-B-36] p 202 N93-12414

POTENTIOMETRIC ANALYSIS
Chronopotentiometry of refractory metals, actinides and oxyanions in molten salts: A review
[NASA-TM-105862] p 249 N93-11545

POWDER (PARTICLES)
Synthesis of nanocrystalline powders for oxide ceramics by microwave plasma pyrolysis
[DE92-017410] p 268 N93-11861
A design of experiment study of plasma sprayed alumina-titania coatings
[DE92-017877] p 271 N93-12168

POWDER METALLURGY
Microstructure and mechanical properties of reactive hot isostatic pressed TiAl powder material
[GKSS-91/E/60] p 256 N93-11336
Titanium-aluminides by hot isostatic pressing of cold extruded titanium-aluminium powder mixtures
[GKSS-91/E/67] p 256 N93-11337
Spectrum fatigue behaviour of powder metallurgy aluminum alloys
[AD-A255060] p 262 N93-12468

POWER AMPLIFIERS
Analysis of periodic transient beam loading of the AGS
[DE92-019243] p 443 N93-11499
RF beam loading in the Brookhaven AGS with booster injection
[DE92-019452] p 444 N93-11641

POWER CONDITIONING
Autonomous power system: Integrated scheduling
p 235 N93-11948
Lunar PMAD technology assessment
[NASA-CR-189225] p 347 N93-12017
MHD integrated topping cycle project
[DE92-018087] p 456 N93-12504

POWER EFFICIENCY
The 10 kW power electronics for hydrogen arcjets
[NASA-TM-105614] p 235 N93-12484

POWER GAIN
RF beam loading in the Brookhaven AGS with booster injection
[DE92-019452] p 444 N93-11641

POWER SPECTRA
Lidar studies of gravity waves in the mesopause region p 358 N93-11222
Non-self-similar clustering of galaxies
[MPE-PREPRINT-212] p 484 N93-11338
Time-frequency domain analysis of vibration signals for machinery diagnostics. 3: The present power spectral density
[OUEL-1911/92] p 337 N93-11707

POWER SUPPLIES
Vacuum chamber translation/positioning mechanism and welding power supply controller
[NASA-CR-184465] p 328 N93-12196

POWERED LIFT AIRCRAFT
Application of eigenstructure assignment to the control of powered lift combat aircraft p 215 N93-11871

PRANDTL NUMBER
The influence of the Prandtl number on the thermal performance of tubes with the separation and reattachment enhancement mechanism
[DE92-016601] p 306 N93-12313

PRASEODYMIUM COMPOUNDS
The synthesis and crystal structure of LaHSe2O6, a layered, anhydrous selenite
[AD-A251050] p 458 N93-10996

PREBURNERS
Combustion characteristics of the LO2/GCH4 fuel-rich preburners for staged combustion cycle rocket engines
[NAL-TR-1124] p 234 N93-12368

PRECIPITATES
The effect of precipitate forming elements in Al 4.5 percent Mg alloys on the measured acoustic emission and on Lueders band deformation
[DE92-016864] p 465 N93-12073
Effect of microstructure on passive film formation and breakdown on Al alloys
[AD-A245863] p 260 N93-12118

PRECIPITATION (METEOROLOGY)
Interannual variabilities of the East Asian summer monsoon and tropical sea surface temperatures
p 372 N93-12534

PRECONDITIONING
Preconditioned low-order Newton methods
[MATHS-REPT-A-159] p 425 N93-11211
Review of preconditioning methods for fluid dynamics
[NASA-CR-189712] p 198 N93-11607

PRECOOLING
Fast cooling phenomena with ice pellet injection in the JIPP T-IIU tokamak
[DE92-782105] p 454 N93-11834

PREDICTION ANALYSIS TECHNIQUES
Micromechanics of metal matrix composites using the Generalized Method of Cells model (GMC) user's guide
[NASA-CR-190756] p 335 N93-11175
Fracture mechanics of model fiber composites
p 237 N93-11247
LAM and NEDWAM statistics over the period October 1990 - April 1991
[KNMI-TR-137] p 368 N93-11329
Reactant gas flow fields in advanced PEM (Proton Exchange Membrane) fuel cell designs
[DE92-018897] p 345 N93-11626
Statistical methods for the comparison of spatial patterns in meteorological variables p 370 N93-11997
The order n simulation of tether motions based on a rigid body tether model p 225 N93-11999
The effect of temperature dependent thermal properties on parametric weld size predictions
[DE92-018816] p 260 N93-12232
Microstructure-based fatigue life prediction methods for naval steel structures
[AD-A254628] p 260 N93-12241

Verification of rain-flow reconstructions of a variable amplitude load history
[NASA-CR-189670] p 341 N93-12411
The Fourth Workshop on Dynamics and Aeroelastic Stability Modeling of Rotorcraft Systems
[AD-A255065] p 208 N93-12485
Three-dimensional turbopump flowfield analysis
[NASA-CR-190978] p 308 N93-12539
Development of a model for predicting NASA/MSFC program success
[NASA-CR-184423] p 473 N93-12542

PREDICTIONS
LAM and NEDWAM statistics over the period October 1990 - April 1991
[KNMI-TR-137] p 368 N93-11329
Parameters for predicting red tides of bioluminescent dinoflagellates: Meteorological events and frontal water circulation patterns
[AD-A254835] p 374 N93-12431

PREDICTOR-CORRECTOR METHODS
An experimental evaluation of prediction methods for contrafans
[PNR-90924] p 209 N93-11023

PREFORMS
Aerospatiale processes for three dimensional preforms
[REPT-921-430-147] p 239 N93-11590
Studies on the reactive melt infiltration of silicon and silicon-molybdenum alloys in porous carbon
[NASA-TM-105860] p 273 N93-12398

PREMIXED FLAMES
Freely propagating open premixed turbulent flames stabilized by swirl
[DE92-017116] p 251 N93-12112
Studies in premixed combustion
[DE92-018646] p 254 N93-12478

PREMIXING
Employment of radicals and excited state species for supersonic combustion photochemical ignition of premixed hydrogen/oxygen mixtures with ArF laser
p 245 N93-11135

PREPREGS
Curing and mechanical properties of T800-V398 graphite/bismaleimide at different temperatures
[DLR-FB-92-02] p 237 N93-11143

PREPROCESSING
An interactive preprocessor for the NASA engine performance program
[NASA-TM-105786] p 209 N93-10983

PRESENTATION
Performing a successful audience analysis: How to improve your proposal-writing skills
[DE92-018978] p 479 N93-12068

PRESSURE
Plasma measurements in magnetospheric tail
[MPE-233] p 361 N93-11352

PRESSURE DISTRIBUTION
A combined experimental and theoretical study of laminar flow control with particular relevance to aero engine nacelles
[PNR-90991] p 195 N93-11070
Pressure and noise induced by a cavitating marine screw propeller
[VTT-PUBS-87] p 299 N93-11360
Correlation of forebody pressures and aircraft yawing moments on the X-29A aircraft at high angles of attack
[NASA-TM-4417] p 197 N93-11532
Experimental investigation of the effects of aft blowing with various nozzle exit geometries on a 3.0 caliber tangent ogive at high angles of attack: Forebody pressure distributions
[NASA-CR-190935] p 197 N93-11605
Effects of sweep on the physics of unsteady shock-induced turbulent separated flows
[AD-A247035] p 198 N93-11742
Flight test results from a supercritical mission adaptive wing with smooth variable camber
[NASA-TM-4415] p 207 N93-11863
Near-field and far-field sound radiation from a line-driven fluid-loaded infinite flat plate having periodic and non-periodic attached rib stiffeners p 434 N93-11884
A wall interference assessment/correction system
[NASA-CR-190617] p 218 N93-11910
An investigation of the effects of aft blowing on a 3.0 caliber tangent ogive body at high angles of attack
[NASA-CR-190934] p 200 N93-12004
Unsteady propeller/wing aerodynamic interactions
p 201 N93-12190
An approach to constrained aerodynamic design with application to airfoils
[NASA-TP-3260] p 201 N93-12321

PRESSURE DROP
Disruption shape effects on the performance of enhanced tubes with the separation and reattachment mechanism
[DE92-016602] p 305 N93-12128

PRESSURE EFFECTS
Studies of the 3 to 5 compounds in the megabar regime
[DE92-019517] p 461 N93-11646
Gapwise density distributions in injection-moulded polymethylmethacrylate p 270 N93-11990
Influence of oxygen partial pressure and silver additions on microstructure and related properties of YBCO superconductors
[DE92-011145] p 468 N93-12249

PRESSURE GRADIENTS
Turbulence structure and polymer drag reduction in adverse pressure gradient boundary layers
p 304 N93-12003
Numerical simulation of a pressure gradient in a multilayer target: Temperature evolution
p 309 N93-12039
Wavefront reconstruction using a least squares approach
[ISVR-TR-203] p 435 N93-12324

PRESSURE MEASUREMENT
Aerothermal test results from the second flight of the Pegasus booster
[NASA-TM-4391] p 296 N93-10969
The hemisphere-cylinder at an angle of attack
p 196 N93-11250
An experimental study of flow patterns and endwall heat transfer upstream of a surface-mounted rectangular obstruction in a turbulent boundary layer
p 302 N93-11698
Evaluation of advanced pressure sensor technology
[DE92-011004] p 312 N93-11806
Operating experience using venturi flow meters at liquid helium temperature
[DE92-014693] p 313 N93-12140

PRESSURE OSCILLATIONS
The combustion time lag and its role in ramjet combustion instability p 245 N93-11137

PRESSURE RECOVERY
Mach 4 testing of scramjet inlet models
[NAL-TR-1137] p 202 N93-12369

PRESSURE SENSORS
Wind tunnel operator aimed comparison between two electronic pressure scanner systems
[DLAS-EST-TR-040] p 217 N93-11225
Evaluation of advanced pressure sensor technology
[DE92-011004] p 312 N93-11806

PRESSURE VESSEL DESIGN
Structural integrity of a confinement vessel for testing nuclear fuels for space propulsion
[DE92-016796] p 232 N93-11824

PRESSURE VESSELS
Pressure vessel burst test program
[AD-A253708] p 334 N93-11080
Development of an intelligent system for cooling rate and fill control in GMAW
[DE92-017849] p 326 N93-11548
Acoustic emission monitoring of HFIR vessel during hydrostatic testing
[DE92-019316] p 332 N93-11601
Structural integrity of a confinement vessel for testing nuclear fuels for space propulsion
[DE92-016796] p 232 N93-11824
Reactor materials program: Mechanical properties of irradiated types 304 and 304L stainless steel weldment components
[DE92-018105] p 260 N93-12158

PRESTRESSING
The mechanism of bolt loading
[NASA-TM-108377] p 342 N93-12412

PRIMERS
Modified epoxy adhesives and primers
[AD-A253857] p 272 N93-12297

PRINTED CIRCUITS
High speed parallel backplane
[AD-D015372] p 288 N93-11053

PRISMS
Characterization of deflagrating munitions by rotating prism high speed photography
[MRL-TR-91-43] p 311 N93-11648

PROBABILITY DENSITY FUNCTIONS
Probability density functions in turbulent channel flow
[NASA-CR-4454] p 202 N93-12399

PROBABILITY DISTRIBUTION FUNCTIONS
Limit theorems for Fisher-score change processes
p 427 N93-12328
Digital signal processing
[AD-A254870] p 287 N93-12436

PROBABILITY THEORY
Incorporating prior probabilities and misclassification costs into network training: An example from medical prognosis
[RSRE-MEMO-4343] p 428 N93-10980
A probabilistic approach to information retrieval in heterogeneous databases
[DE92-016993] p 473 N93-11151
Limit theorems for Fisher-score change processes
p 427 N93-12328
Static assignment of complex stochastic tasks using stochastic majorization
[NASA-CR-189716] p 416 N93-12403
A real time sharpening of NOGAPS predictions of mid-latitude Central Pacific cyclones
[AD-A255157] p 372 N93-12424
Digital signal processing
[AD-A254870] p 287 N93-12436
Mathematical methods in operations research and computer science
[AD-A254782] p 428 N93-12465

PROBLEM SOLVING
Remarks on the Robinson-Trautman solutions
[MATHS-REPT-A-167] p 423 N93-11122
Ontology of mind, subjective ontology, and the example of temporal expressions
[REPT-92-018] p 386 N93-11212
The network destruction problem (extended abstract)
[DE92-016171] p 419 N93-11860

PROCEDURES
On the acquisition and representation of procedural knowledge p 394 N93-11937

PROCESS CONTROL (INDUSTRY)
Optimization of film synthesized rare earth transition metal permanent magnet systems
[DE92-018726] p 432 N93-12116

PROCESSING
Advanced materials and processing: The Federal program in materials science and technology. A report by the FCCSET Committee on Industry and Technology to supplement the President's fiscal year 1993 budget
[PB92-199108] p 238 N93-11470

PROCUREMENT
The use of life cycle costing for the acquisition of non-major systems at the Naval Regional Contracting Center Detachment
[AD-A255170] p 480 N93-12473

PRODUCT DEVELOPMENT
Rolls-Royce civil engine technology
[PNR-90936] p 210 N93-11036
The Trent: Towards greater thrust
[PNR-90937] p 210 N93-11037
Introduction to the Rolls-Royce design process
[PNR-90939] p 210 N93-11039
Simultaneous engineering in the design of aero engines
[PNR-90973] p 211 N93-11062
The Trent family of engines
[PNR-90974] p 211 N93-11063
Advanced materials in gas turbine engines: An assessment
[PNR-90946] p 211 N93-11105
The development of the Rolls-Royce Trent aero gas turbine
[PNR-90949] p 212 N93-11108
Industrial applications and markets for ceramic matrix composites
[PNR-90884] p 266 N93-11205
The use of simultaneous engineering for the design and manufacture of the low pressure turbine for the Rolls-Royce Trent engine
[PNR-90887] p 212 N93-11206
Innovation in engineering
[PNR-90889] p 212 N93-11207
Simultaneous engineering in aero gas turbine design and manufacture
[PNR-90890] p 212 N93-11208
The changing nature of design
[PNR-91011] p 206 N93-11334

PRODUCTION ENGINEERING
Introduction to the Rolls-Royce design process
[PNR-90939] p 210 N93-11039
Simultaneous engineering in the design of aero engines
[PNR-90973] p 211 N93-11062
The use of simultaneous engineering for the design and manufacture of the low pressure turbine for the Rolls-Royce Trent engine
[PNR-90887] p 212 N93-11206
Innovation in engineering
[PNR-90889] p 212 N93-11207

PRODUCTION MANAGEMENT
Introduction to the Rolls-Royce design process
[PNR-90939] p 210 N93-11039

PRODUCTION PLANNING
Assembling polyhedra with single translations
[AD-A254623] p 419 N93-12239

PRODUCTIVITY
Advanced materials and processing: The Federal program in materials science and technology. A report by the FCCSET Committee on Industry and Technology to supplement the President's fiscal year 1993 budget
[PB92-199108] p 238 N93-11470

PROFILOMETERS
Laser surface profilometer with sub-Angstrom resolution
[DE92-018926] p 317 N93-12011
PROGNOSIS
Incorporating prior probabilities and misclassification costs into network training: An example from medical prognosis
[RSRE-MEMO-4343] p 428 N93-10980
PROGRAM VERIFICATION (COMPUTERS)
An advanced combustion research facility for validating computational fluid dynamics codes
[PNR-90913] p 296 N93-11017
Software quality methodology integration study results
[AD-A253891] p 408 N93-11371
Intelligent fault management for the Space Station active thermal control system p 391 N93-11930
System diagnostic builder p 396 N93-11944
Knowledge-based system V and V in the Space Station Freedom program p 396 N93-11945
An integrated dexterous robotic testbed for space applications p 330 N93-11972
PROGRAMMING LANGUAGES
The VISTA structured assembler
[RSRE-91034] p 407 N93-11341
Using ELLA for high level design: Modelling the Motorola 6800 microprocessor
[RSRE-MEMO-4515] p 408 N93-11386
The evolution of Ten15
[RSRE-MEMO-4543] p 409 N93-11405
Ten15 developments to support parallelism
[RSRE-MEMO-4545] p 409 N93-11406
The WEB approach to ELLA
[RSRE-MEMO-4549] p 409 N93-11407
Using SGML in a large organization
[ESA-STR-234] p 476 N93-11583
Syntax and lexis of the specification language Z
[RSRE-MEMO-4367] p 414 N93-12326
Requirements Specification Language (RSL) and supporting tools
[NASA-CR-189700] p 405 N93-12345
Formal representation of the requirements for an Advanced Subsonic Civil Transport (ASCT) flight control system
[NASA-CR-189699] p 405 N93-12346
Inheritance for software reuse: The good, the bad, and the ugly p 415 N93-12389
PROGRAMS
Fusion programs in applied plasma physics
[DE92-019639] p 452 N93-11660
Electric and hybrid vehicle program, site operator program
[DE92-018055] p 328 N93-12114
The collaborative program of research in engineering sciences
[DE92-016838] p 490 N93-12477
PROJECT MANAGEMENT
A development approach for nuclear thermal propulsion
[DE92-018020] p 232 N93-11596
Systems engineering and technical assistance in support of digital gallium arsenide insertion projects
[AD-A253751] p 463 N93-11790
DOE guideline: Guide to good practices for incorporating operating experiences
[DE92-017684] p 472 N93-12223
Environmental restoration project configuration control
[DE92-017223] p 356 N93-12496
PROJECT PLANNING
DOE guideline: Guide to good practices for incorporating operating experiences
[DE92-017684] p 472 N93-12223
Environmental restoration project configuration control
[DE92-017223] p 356 N93-12496
Development of a model for predicting NASA/MSFC program success
[NASA-CR-184423] p 473 N93-12542
PROJECTILES
Lightweight Exoatmospheric Projectile (LEAP) test program. Supplemental environmental assessment
[AD-A252286] p 231 N93-10998
Railgun armature velocity improvement, SBIR phase 2
[AD-A254749] p 222 N93-12505
PROP-FAN TECHNOLOGY
Computer aided design and manufacturing of composite propfan blades for a cruise missile wind tunnel model
[NASA-TM-105269] p 413 N93-12022
PROPELLANT BINDERS
High energy cast explosives based on dinitropropylacrylate
[AD-D015340] p 273 N93-11045
PROPELLANT COMBUSTION
The 28th JANNAF Combustion Subcommittee Meeting, volume 1
[CPIA-PUBL-573-VOL-1] p 244 N93-11132
Metal slurry droplet and spray combustion
p 245 N93-11138
The 28th JANNAF Combustion Subcommittee Meeting, volume 2
[CPIA-PUBL-573-VOL-2] p 247 N93-11448
Experiments and analysis concerning the use of external burning to reduce aerospace vehicle transonic drag
p 235 N93-12537
PROPELLANT EXPLOSIONS
Impact ignition of liquid propellants
[AD-A252299] p 249 N93-11490
PROPELLANT SPRAYS
Solution of two-phase reacting flow in liquid thrust chambers p 235 N93-11449
Coaxial injector spray characterization using water/air as simulants p 248 N93-11452
Physical processes involved in injection and atomization of liquid propellants p 248 N93-11453
Experimental investigation of rocket injector atomization p 248 N93-11454
An experimental study of droplet dispersion in turbulent flows p 248 N93-11455
PROPELLANT TESTS
A summary of the JANNAF workshop on diagnostics
p 248 N93-11451
PROPELLANT TRANSFER
Small experiments for the maturation of orbital cryogenic transfer technologies
[NASA-TM-105849] p 296 N93-10981
Propellant removal from rocket motors containing double-base compositions
[DE92-013567] p 275 N93-12265
PROPELLANTS
Effect of inert propellant injection on Mars ascent vehicle performance
[NASA-CR-189238] p 226 N93-12152
PROPELLER BLADES
Pressure and noise induced by a cavitating marine screw propeller
[VTT-PUBS-87] p 299 N93-11360
PROPELLER FANS
Computer aided design and manufacturing of composite propfan blades for a cruise missile wind tunnel model
[NASA-TM-105269] p 413 N93-12022
PROPELLER NOISE
The design and commissioning of an acoustic liner for propeller noise testing in the ARA transonic wind tunnel
[PNR-90880] p 433 N93-11204
Pressure and noise induced by a cavitating marine screw propeller
[VTT-PUBS-87] p 299 N93-11360
PROPELLER SLIPSTREAMS
Unsteady propeller/wing aerodynamic interactions
p 201 N93-12190
PROPELLERS
Aircraft accident report: Atlantic Southeast Airlines, Inc. Flight 2311, uncontrolled collision with terrain, an Embraer EMB-120, N270AS, Brunswick, Georgia, 5 April 1991
[PB92-910403] p 203 N93-11471
Unsteady propeller/wing aerodynamic interactions
p 201 N93-12190
PROPHYLAXIS
Recent lessons on the safety and effectiveness of malaria chemoprophylaxis in a non-immune population
p 381 N93-11307
PROPORTIONAL COUNTERS
Contributions to the Joint Discussion 3: Results from Rosat and GRO and Other Recent High Energy Astrophysics Missions of the Max-Planck-Institut fuer Extraterrestrische Physik
[MPE-PREPRINT-215] p 482 N93-11473
Rosat deep surveys p 482 N93-11474
PROPOSALS
Performing a successful audience analysis: How to improve your proposal-writing skills
[DE92-018978] p 479 N93-12068
PROPRIOCEPTION
The development of system components to provide proprioceptive and tactile information to the human for future telepresence systems p 330 N93-11968
PROPULSION SYSTEM CONFIGURATIONS
Rocket Based Combined Cycle (RBCC) Propulsion Technology Workshop. Volume 1: Executive summary
[NASA-CR-184382] p 231 N93-11042
Rocket Based Combined Cycle (RBCC) Propulsion Workshop, volume 2
[NASA-CR-184383] p 231 N93-11043
Preliminary characterization of a water vaporizer for resistojet applications
[NASA-TM-105877] p 231 N93-11402
Overview of high performance aircraft propulsion research
[NASA-TM-105839] p 213 N93-11530
Closed form low-thrust trajectories for Mars missions
[DE92-017431] p 232 N93-11766
Tutorial on nuclear thermal propulsion safety for Mars
[DE92-017946] p 233 N93-12056
Nuclear thermal propulsion transportation systems for lunar/Mars exploration
[NASA-TM-105870] p 233 N93-12363
Space transportation booster engine configuration study. Volume 2: Design definition document and environmental analysis
[NASA-CR-184459] p 234 N93-12441
The 10 kW power electronics for hydrogen arcjets
[NASA-TM-105614] p 235 N93-12484
Space transportation booster engine configuration study. Volume 1: Executive Summary
[NASA-CR-184457] p 235 N93-12523
PROPULSION SYSTEM PERFORMANCE
An interactive preprocessor for the NASA engine performance program
[NASA-TM-105786] p 209 N93-10983
Rocket Based Combined Cycle (RBCC) Propulsion Technology Workshop. Volume 1: Executive summary
[NASA-CR-184382] p 231 N93-11042
Rocket Based Combined Cycle (RBCC) Propulsion Workshop, volume 2
[NASA-CR-184383] p 231 N93-11043
Preliminary characterization of a water vaporizer for resistojet applications
[NASA-TM-105877] p 231 N93-11402
Overview of high performance aircraft propulsion research
[NASA-TM-105839] p 213 N93-11530
Reformers for the production of hydrogen from methanol and alternative fuels for fuel cell powered vehicles
[DE92-019300] p 274 N93-11550
Hot fire test results of subscale tubular combustion chambers
[NASA-TP-3222] p 232 N93-11614
Tutorial on nuclear thermal propulsion safety for Mars
[DE92-017946] p 233 N93-12056
Nuclear thermal propulsion transportation systems for lunar/Mars exploration
[NASA-TM-105870] p 233 N93-12363
Concurrent optimization of airframe and engine design parameters
[NASA-TM-105908] p 213 N93-12402
Extended-testing of xenon ion thruster hollow cathodes
[NASA-CR-189227] p 234 N93-12409
Results from a large-scale MHD propulsion experiment
[DE92-018177] p 456 N93-12416
The 10 kW power electronics for hydrogen arcjets
[NASA-TM-105614] p 235 N93-12484
PROTECTION
Inflatable device for excluding sea water from a rocket motor
[AD-D015365] p 232 N93-11424
Rocket-triggered lightning test of an earth-covered munitions storage bunker
[DE92-016790] p 369 N93-11678
PROTECTIVE CLOTHING
Evaluation of multilayer mask concept for RESPO 21
[AD-A253392] p 389 N93-12079
Sustaining health and performance in the cold: Environmental medicine guidance for cold-weather operation
[AD-A254328] p 385 N93-12145
Effectiveness of NASA 1032 and 1035 and Air Force 1030 and 1034 units in protection against cold water hypothermia
[AD-A255120] p 389 N93-12291
The effects of wearing protective chemical warfare combat clothing on human performance
[AD-A250716] p 390 N93-12491
PROTECTIVE COATINGS
Surface protection in the aircraft industry
[MBB-Z-0432-92-PUB] p 255 N93-11027
Development of advanced carbon-carbon annular flameholders for gas turbines
[PNR-90947] p 211 N93-11106
Small particle impact damage in carbon-carbon composites
[PNR-90948] p 236 N93-11107
Corrosion resistant chromate conversion coatings for heat-treated aluminum alloys
[AD-D015366] p 266 N93-11425
Multi-layer light-weight protective coating and method for application
[NASA-CASE-LAR-14448-1] p 269 N93-11912
Erosion predictions and measurements of high-temperature coatings and superalloys used in turbomachines p 272 N93-12189
Studies of a laser/nuclear thermal hardened body armor
[AD-A255128] p 390 N93-12423

Current research in oxidation-resistant carbon-carbon composites at NASA. Langley Research Center
p 229 N93-12456

PROTOCOL (COMPUTERS)
Photonics and other approaches to high speed communications
[NASA-CR-190362] p 279 N93-11116
Scalable parallel communications p 279 N93-11117
A simple, effective media access protocol system for integrated, high data rate networks p 279 N93-11119
The engine design engine. A clustered computer platform for the aerodynamic inverse design and analysis of a full engine
[NASA-TM-105838] p 196 N93-11223
Higher-order generic functions for CLOS
[DE92-013447] p 413 N93-12137
Tradeoffs in implementing primary-backup protocols
[NASA-CR-190970] p 472 N93-12212

PROTON BEAMS
Analysis of the prebuncher for the KEK 40-MeV proton linac
[DE92-514988] p 444 N93-11525

PROTON PRECIPITATION
The role of proton precipitation in Jovian aurora: Theory and observation p 487 N93-11165

PROTONS
Reactant gas flow fields in advanced PEM (Proton Exchange Membrane) fuel cell designs
[DE92-018897] p 345 N93-11626

PROTOTYPES
The changing nature of design
[PNR-91011] p 206 N93-11334

PROTOZOA
Parameters for predicting red tides of bioluminescent dinoflagellates: Meteorological events and frontal water circulation patterns
[AD-A254835] p 374 N93-12431

PROVING
Dynamic test/analysis correlation using reduced analytical models
[NASA-TM-107671] p 341 N93-12300
Predicted and tested performance of durable TPS
p 228 N93-12454

PROXIMITY
Interactive collision detection p 400 N93-11963

PSYCHOLOGICAL TESTS
Visual perception of structure from motion
[AD-A253235] p 386 N93-11503
Meta-analysis of integrity tests: A critical examination of validity generalization and moderator variables
[AD-A254681] p 386 N93-12225

PSYCHOLOGY
Performing a successful audience analysis: How to improve your proposal-writing skills
[DE92-018978] p 479 N93-12068

PSYCHOPHYSICS
Visual psychophysics of egomotion
[AD-A248349] p 386 N93-11488

PSYCHOPHYSIOLOGY
Neuropsychiatric morbidity in early HIV disease: Implications for military occupational function
p 379 N93-11299
The OMPAT level 1 Neurophysiological Performance Assessment Battery: NPPAB
[AD-A254840] p 387 N93-12432

PUBLIC HEALTH
Vaccination against Hepatitis B: The Italian strategy
p 377 N93-11289
Evaluation of a user information satisfaction short-form instrument
[AD-A250702] p 478 N93-11840
Smoking status and body composition, exercise, dietary intake, and alcohol/caffeine consumption
[AD-A250648] p 385 N93-11893

PUBLIC SPEAKING
Performing a successful audience analysis: How to improve your proposal-writing skills
[DE92-018978] p 479 N93-12068

PULLEYS
Payout tension control system for reel mounted cable
[AD-D015362] p 325 N93-11423

PULMONARY FUNCTIONS
Asthma in aircrew: Assessment, treatment and disposition p 383 N93-11315
Correlation of serum alpha sub 1 antitrypsin with cigarette smoking and pulmonary function status in Greek pilots, for a ten year period p 384 N93-11318

PULSARS
Periodicities in pulsar microstructure
p 484 N93-11230

PULSE AMPLITUDE
Observations of thin auroral ionization layers by EISCAT in connection with pulsating aurora p 359 N93-11266

PULSE CODE MODULATION
Design of a PCM data compressor --- pulse code modulation
[DE92-019469] p 404 N93-11539

PULSE DURATION
Chinese Journal of Lasers (selected articles)
[AD-A254100] p 317 N93-11786

PULSE DURATION MODULATION
An analog macromodel of the SG1525A PWM for use with SPICE2G.6 simulators
[DE92-019423] p 291 N93-11639
The 10 kW power electronics for hydrogen arcjets
[NASA-TM-105614] p 235 N93-12484

PULSE GENERATORS
BANSHEE: High-voltage repetitively pulsed electron-beam driver
[DE92-017413] p 444 N93-11763
The development of a one microsecond pulse length, repetitively pulsed, high power modulator, and a long-pulse electron beam diode for the production of intense microwaves
[DE92-015974] p 293 N93-12089
Ultra-wideband generators
[DE92-018026] p 293 N93-12113

PULSED LASERS
In-plane strain measurement on high speed rotating components using pulsed laser ESPI
[PNR-90975] p 315 N93-11064
Tunable, short pulse hard x rays from a compact laser synchrotron source
[AD-A254288] p 315 N93-11195
Chinese Journal of Lasers (selected articles)
[AD-A254100] p 317 N93-11786
Study of the dynamic degradation under the action of a shock wave induced by pulsed laser
p 319 N93-12037
Shock waves induced by pulsed laser in confined interaction: Numerical simulation p 319 N93-12038
Observation of pulses propagating at supraluminous speed in an optical fiber p 320 N93-12040
X ray laser program, FY 1991
[AD-A255190] p 322 N93-12275
Development summary of a sympathetic discharge CO2 laser for lidar use
[NASA-CR-184433] p 323 N93-12516

PUMP IMPELLERS
An experimental study of a small high speed LH2 rocket pump: Fundamental mechanical design
[NAL-TR-1123] p 330 N93-12463

PUMP SEALS
Sealing characteristics of a carbon segmented circumferential seal for a liquid oxygen turbopump
[NAL-TR-1130] p 329 N93-12364

PUMPING
Implanted He retention and release from boronized layers
[DE92-013983] p 464 N93-11842

PURIFICATION
Evaluation of flotation for purification of pyrite for use in thermal batteries
[DE92-019330] p 290 N93-11553

PYRITES
Evaluation of flotation for purification of pyrite for use in thermal batteries
[DE92-019330] p 290 N93-11553

PYROLYSIS
Synthesis of single phase (alpha)-Fe, Fe3C and Fe7C3 nano-particles by CO2 laser pyrolysis technique
[DE92-015654] p 250 N93-11847
Synthesis of nanocrystalline powders for oxide ceramics by microwave plasma pyrolysis
[DE92-017410] p 268 N93-11861
Laser spectroscopy and dynamics of transient species formed in pyrolysis reactions
[DE92-016206] p 251 N93-12091
Growth of 2-6 thin-films from single-source precursors based on sterically encumbered sitel ligands
[DE92-017077] p 466 N93-12099

PYROTECHNICS
Destruction of explosives and rocket fuels by supercritical water oxidation
[DE92-018874] p 274 N93-11380

PYRROLES
Mixed ionic and electronic conductivity in polymers
[DE92-018723] p 273 N93-12500

Q

Q FACTORS
High Temperature Superconductivity Space Experiment (HTSSE)
[AD-A253119] p 288 N93-11239

Q VALUES
Multifractal analysis at negative q
[AD-A254370] p 413 N93-12159

QUALITY CONTROL
Japanese style total quality control: A first hand experience
[PNR-90909] p 331 N93-11015
Quality management of finite element analysis
[PNR-90951] p 331 N93-11110
Software quality methodology integration study results
[AD-A253891] p 408 N93-11371
Integrated services digital network conformance testing. Layer 1, physical layer. Part 2: Basic rate U interface, user side
[PB92-181114] p 418 N93-11714
History of statistics in real time: Hammers and nails
[AD-A253521] p 429 N93-12081
Program for implementing software quality metrics
[DE92-018617] p 413 N93-12187
Research and development strategies for human centered and group support technologies
[AD-A254366] p 472 N93-12273

QUANTILES
History of statistics in real time: Hammers and nails
[AD-A253521] p 429 N93-12081

QUANTITATIVE ANALYSIS
Measurement of the density distributions in quenched polycarbonate specimens by a quantitative Schlieren-optical technique p 270 N93-11989

QUANTUM CHEMISTRY
Mechanical properties of semiconductors and their alloys
[AD-A253908] p 462 N93-11727
Oxidation, nitridation, and fluorine etching of Si
[AD-A253559] p 249 N93-11755
Theoretical study of the radiative and kinetic properties of selected metal oxides and air molecules
[AD-A251090] p 438 N93-11804
Theoretical research program to study chemical reactions in AOTV bow shock tubes
[NASA-CR-188927] p 439 N93-11851
The structures, binding energies and vibrational frequencies of Ca3 and Ca4: An application of the CCSD(T) method p 439 N93-11852
On the evaluation of derivatives of Gaussian integrals
p 439 N93-11853
Connected triple excitations in coupled-cluster calculations of hyperpolarizabilities: Neon
p 439 N93-11854
Concerted hydrogen atom exchange between three HF molecules p 439 N93-11855

QUANTUM CHROMODYNAMICS
Studies in quantum field theory
[DE92-011035] p 470 N93-11276
Nucleon axial coupling constants and QCD sum rules
[DE92-014227] p 439 N93-11844

QUANTUM EFFICIENCY
Progress toward x ray lasing between autoionizing transitions
[DE92-017428] p 317 N93-11765

QUANTUM ELECTRONICS
The fourth OSA Topical Meeting Proceedings on Picosecond Electronics and Optoelectronics, volume 9
[AD-A253472] p 447 N93-11099
Development of ultra-low noise, high sensitivity planar metal grating coupled AlGaAs/GaAs multiquantum well IR detectors for focal plane array staring IR sensor systems
[AD-A254697] p 468 N93-12228
Mesoscopic effects in electronic microstructures
[AD-A254889] p 295 N93-12502

QUANTUM MECHANICS
Semiclassical analysis spectral correlations in mesoscopic systems
[DE92-634887] p 471 N93-11780
Final Technical Report
[AD-A253529] p 284 N93-12083

QUANTUM NUMBERS
Electron terms and radiation from crystals
[AD-A254353] p 468 N93-12271

QUANTUM OPTICS
Matter-wave interferometry with laser cooled atoms
[AD-A253999] p 316 N93-11737

QUANTUM THEORY
Studies in quantum field theory
[DE92-011035] p 470 N93-11276
Landau level quantization and superconductivity
[DE92-019028] p 460 N93-11512
Transport mechanisms acting in toroidal devices: A theoretician's view
[DE92-018738] p 456 N93-12501

QUANTUM WELLS
Excitons in semiconducting superlattices, quantum wells, and ternary alloys
[DE92-015178] p 464 N93-11894

Development of ultra-low noise, high sensitivity planar metal grating coupled AlGaAs/GaAs multiquantum well IR detectors for focal plane array staring IR sensor systems
[AD-A254697] p 468 N93-12228
Photoinduced electron transfer counter to the bias field in coupled quantum wells
[AD-A254719] p 469 N93-12338

QUARKS
High energy physics at Tufts University
[DE92-018081] p 444 N93-11668
Research in elementary particles and interactions
[DE92-018089] p 437 N93-11681
Strange quark matter
[DE92-016949] p 438 N93-11746
Nucleon axial coupling constants and QCD sum rules
[DE92-014227] p 439 N93-11844
Survey of composite particle models of electroweak interaction
[DE92-017110] p 441 N93-12111

QUARTZ CRYSTALS
Quartz crystal resonators and oscillators for frequency control and timing applications: A tutorial, revision 5.2
[AD-A254892] p 469 N93-12283

QUASARS
Publications of the Executive Office of the President, 20 January 1989 - 31 March 1992
[PB92-154913] p 477 N93-11769
A closer look at active galactic nuclei: The great engines of the Universe
[PB92-184464] p 485 N93-11807

QUENCHING (COOLING)
The measurement and calculation of birefringence in quenched polycarbonate specimens
p 269 N93-11986
Molecular orientation induced by cooling stresses in polycarbonate. 1: Free quenching p 269 N93-11987
Molecular orientation induced by cooling stresses in polycarbonate. 2: Constrained quench and injection moulding p 270 N93-11988
Measurement of the density distributions in quenched polycarbonate specimens by a quantitative Schlieren-optical technique p 270 N93-11989

QUERY LANGUAGES
A front end implementation of the Pollyanna secure DBMS
[RSRE-MEMO-4540] p 475 N93-11404
An iconic query interface for an image database
[AD-A253571] p 475 N93-11506
Application of machine learning techniques for effective retrieval in image database
[AD-A254907] p 479 N93-12287

R

RADAR
Microwave guidance technology and its applications
[AD-A254107] p 281 N93-11509
Automatic Attenuation/Phase Calibration System (AAPCS)
[DE92-017354] p 264 N93-11917

RADAR BEACONS
Geostationary-satellite beacon-receiver array for studies of ionospheric irregularities
[DE92-018979] p 362 N93-11535

RADAR CROSS SECTIONS
Ultra wide band 3-D cross section (RCS) holography
[DE92-019133] p 312 N93-11802

RADAR DETECTION
Short-range radar system
[AD-D015339] p 278 N93-11044
The design and implementation of radar clutter modelling and adaptive target detection techniques
p 283 N93-11913

RADAR EQUIPMENT
Sodium-lidar mesosphere examinations: Selected elements of the experimental construction of a mobile instrument and evaluation of the data acquired with a stationary Na-lidar during the DYANA campaign
[BONN-IR-91-78] p 357 N93-11006
Josephson Junction digital waveform generation for very wideband radars
[AD-A253668] p 467 N93-12169

RADAR IMAGERY
Automated extraction of aircraft runway patterns from radar imagery
[AD-A254258] p 218 N93-11751
Ultra wide band 3-D cross section (RCS) holography
[DE92-019133] p 312 N93-11802

RADAR MEASUREMENT
Sodium-lidar mesosphere examinations: Selected elements of the experimental construction of a mobile instrument and evaluation of the data acquired with a stationary Na-lidar during the DYANA campaign
[BONN-IR-91-78] p 357 N93-11006
A comparison of radar rainfall estimates and rain gage measurements during two Denver thunderstorms
[AD-A254267] p 369 N93-11817
Multiangle lidar performance in the presence of horizontal inhomogeneities in atmospheric extinction and scattering
[AD-A252882] p 371 N93-12167

RADAR NETWORKS
Embedded training capabilities for the LAMPS MK 3 system
[AD-A250697] p 207 N93-11838

RADAR RECEIVERS
Geostationary-satellite beacon-receiver array for studies of ionospheric irregularities
[DE92-018979] p 362 N93-11535
Limitations of multiple feeds in a polarimetric-radar compact range
[DE92-017526] p 284 N93-12101

RADAR TARGETS
Short-range radar system
[AD-D015339] p 278 N93-11044
The design and implementation of radar clutter modelling and adaptive target detection techniques
p 283 N93-11913

RADAR TRANSMISSION
Short-range radar system
[AD-D015339] p 278 N93-11044

RADAR TRANSMITTERS
Limitations of multiple feeds in a polarimetric-radar compact range
[DE92-017526] p 284 N93-12101

RADIANT FLUX DENSITY
Proposal for the experimental demonstration of the coherent radiation
[DE92-017695] p 284 N93-12132

RADIANT HEATING
Microwave sintering of multilayer ceramic capacitors
[DE92-018772] p 267 N93-11570

RADIATION ABSORPTION
Hydrodynamic efficiencies in implosion experiments
p 308 N93-12030
Bremsstrahlung absorption in plasmas
p 321 N93-12047
Hydrodynamic study of multilayer targets by spatial and temporal resolution shadow spectroscopy
p 254 N93-12050
Optical limiting
[AD-A254620] p 322 N93-12238

RADIATION BELTS
Development and use of data analysis procedures for the CRRES payloads AFGL-701-2/Dosimeter and AFGL-701-4/Fluxmeter and application of the data analysis results to improve the static and dynamic models of the Earth's radiation belts
[AD-A253287] p 363 N93-11810

RADIATION CHEMISTRY
Summaries of FY 1991 research in the chemical sciences
[DE92-011920] p 251 N93-12135

RADIATION COUNTERS
A cryogenic phonon detector to search for dark matter particles p 481 N93-11198

RADIATION DAMAGE
Radiation damage by high energy electrons in GaAs: A DLTS (deep level transient spectroscopy) examination
[HMI-B-494] p 442 N93-11028
Isotopic tailoring with 59-Ni to study the effect of helium on microstructural evolution and mechanical properties of neutron-irradiated Fe-Cr-Ni alloys
[DE92-019372] p 257 N93-11557

RADIATION DETECTORS
High energy x ray imaging diagnostic on Nova
[DE92-018067] p 451 N93-11495
Particle physics experiments, 1991
[RAL-92-001] p 444 N93-11687
A ring coded-aperture microscope for high-resolution imaging of high-energy x rays
[DE92-018004] p 454 N93-12059

RADIATION DISTRIBUTION
System design and radiation field characteristics of the High Flux Neutron Radiography Facility (HFNRF) at Sandia National Laboratories
[DE92-013984] p 219 N93-12268

RADIATION DOSAGE
Molecular cytogenetics: A novel approach for measuring chromosome translocations in individuals years after exposure to low levels of ionizing radiation
[DE92-018066] p 374 N93-10974
Freeze-dried human red blood cells
[AD-A253295] p 376 N93-11193
The electron-beam water calorimeter project at the National Physical Laboratory
[NPL-RSA(EXT)-30] p 310 N93-11410
Measurement of absorbed dose to water for medium energy x rays
[NPL-RSA(EXT)-33] p 436 N93-11412
Development and use of data analysis procedures for the CRRES payloads AFGL-701-2/Dosimeter and AFGL-701-4/Fluxmeter and application of the data analysis results to improve the static and dynamic models of the Earth's radiation belts
[AD-A253287] p 363 N93-11810

RADIATION EFFECTS
Molecular cytogenetics: A novel approach for measuring chromosome translocations in individuals years after exposure to low levels of ionizing radiation
[DE92-018066] p 374 N93-10974
An accurate and efficient method to calculate the rate of single event upsets from the LET spectrum and SEU cross section test results
[AD-A253917] p 290 N93-11492
Fifth Annual Workshop on Space Operations Applications and Research (SOAR 1991), volume 1
[NASA-CP-3127-VOL-1] p 391 N93-11921
Mechanical properties of 1950's vintage 304 stainless steel weldment components after low temperature neutron irradiation
[DE92-017059] p 259 N93-12107
Reactor materials program: Mechanical properties of irradiated types 304 and 304L stainless steel weldment components
[DE92-018105] p 260 N93-12158
Radiation physics, biophysics, and radiation biology
[DE92-013673] p 375 N93-12266
A monitor for the laboratory evaluation of control integrity in digital control systems operating in harsh electromagnetic environments
[NASA-TM-4402] p 215 N93-12304
Photoinduced electron transfer counter to the bias field in coupled quantum wells
[AD-A254719] p 469 N93-12338
VLSI reliability research
[AD-A254883] p 295 N93-12360
Back-gate bias generator
[AD-A255126] p 295 N93-12421

RADIATION HARDENING
Reliability of small geometry VLSI devices for microelectronics
[AD-A247355] p 289 N93-11414

RADIATION HAZARDS
Radiological information management system (RadIMS)
[DE92-017221] p 480 N93-12495

RADIATION MEASUREMENT
Molecular cytogenetics: A novel approach for measuring chromosome translocations in individuals years after exposure to low levels of ionizing radiation
[DE92-018066] p 374 N93-10974
Emittance measuring device for charged particle beams
[AD-D015371] p 442 N93-11060
Development of a geometry-compensated neutron time-of-flight detector for ICF applications with approximately 200 ps time response
[DE92-018024] p 450 N93-11153
Detection of cloud-top height from backscattered radiances within the oxygen A band. Part 2: Measurements
[GKSS-91/E/77-PT-2] p 368 N93-11350
Proposal for the experimental demonstration of the coherent radiation
[DE92-017695] p 284 N93-12132
System design and radiation field characteristics of the High Flux Neutron Radiography Facility (HFNRF) at Sandia National Laboratories
[DE92-013984] p 219 N93-12268

RADIATION MEASURING INSTRUMENTS
Shutter apparatus
[AD-D015350] p 309 N93-11049

RADIATION PRESSURE
Interaction of sound with sound by novel mechanisms: Ultrasonic four-wave mixing mediated by a suspension and ultrasonic three-wave mixing at a free surface
[AD-A254657] p 435 N93-12097

RADIATION PROTECTION
Shutter apparatus
[AD-D015350] p 309 N93-11049
Optical limiting
[AD-A254620] p 322 N93-12238

RADIATION SHIELDING
Application of the Moyer method to transverse shielding of linear Bremsstrahlung sources
[DE92-017027] p 443 N93-11493

RADIATION SOURCES
Application of the Moyer method to transverse shielding of linear Bremsstrahlung sources
[DE92-017027] p 443 N93-11493

RADIATION SPECTRA
Lyman alpha line shapes from electron impact H2 dissociative processes in the Jovian auroral zone
p 487 N93-11166
Rosat deep surveys p 482 N93-11474

RADIATION TOLERANCE
Reliability of small geometry VLSI devices for microelectronics
[AD-A247355] p 289 N93-11414

RADIATION TRANSPORT
X-UV spectroscopy temporal resolution
p 318 N93-12028
X ray laser program, FY 1991
[AD-A255190] p 322 N93-12275

RADIATION TRAPPING
The NASA/National Space Science Data Center trapped radiation environment model program, 1964 - 1991
[NASA-TM-107993] p 349 N93-11003

RADIATIVE RECOMBINATION
Recombination and metastability in amorphous silicon and silicon germanium alloys
[DE92-010593] p 463 N93-11816
Direct radiative recombination of atomic ions
p 321 N93-12048

RADIATIVE TRANSFER
Radiative forcing of climate p 351 N93-11094
Detection of cloud-top height from backscattered radiances within the oxygen A band. Part 1: Theoretical study
[GKSS-91/E/76-PT-1] p 368 N93-11349
Interpretation of experiments measuring the back face of thin aluminum strips by comparison with numerical simulations p 318 N93-12029
Development of a hydrodynamic code: MINNIE
p 318 N93-12031

RADIATORS
Theoretical study of the radiative and kinetic properties of selected metal oxides and air molecules
[AD-A251090] p 438 N93-11804

RADICALS
Employment of radicals and excited state species for supersonic combustion photochemical ignition of premixed hydrogen/oxygen mixtures with ArF laser
p 245 N93-11135

RADIO ALTIMETERS
Integration of radar altimeter, precision navigation, and digital terrain data for low-altitude flight
[NASA-TM-103958] p 205 N93-12320

RADIO ANTENNAS
Radio pill antenna range test
[DE92-019903] p 282 N93-11661

RADIO ASTRONOMY
The Comet Halley archive: Summary volume
[NASA-CR-190358] p 484 N93-11243

RADIO BEACONS
Radio pill antenna range test
[DE92-019903] p 282 N93-11661

RADIO COMMUNICATION
Summary of findings from the PIREP-based analyses conducted during the 1988 to 1990 evaluations of TDWR-based and TDWR/LLWAS-based alert services provided to landing/departing pilots
[AD-A253859] p 367 N93-11144
Embedded training capabilities for the LAMPS MK 3 system
[AD-A250697] p 207 N93-11838
Low Density Radio Communications Link (LDRCL) Operational Test and Evaluation (OT/E) integration and operation test plan
[DOT/FAA/CT-TN92/4] p 285 N93-12331

RADIO EMISSION
Publications of the Executive Office of the President, 20 January 1989 - 31 March 1992
[PB92-154913] p 477 N93-11769
A closer look at active galactic nuclei: The great engines of the Universe
[PB92-184464] p 485 N93-11807

RADIO FREQUENCIES
Topics on RF beam control of a synchrotron
[DE92-019217] p 443 N93-11498
Beam-loading stability in synchrotrons with a higher RF harmonic
[DE92-018982] p 443 N93-11510
Self-generated stochastic heating in an RF discharge
[DE92-018558] p 452 N93-11565
RF beam loading in the Brookhaven AGS with booster injection
[DE92-019452] p 444 N93-11641
The locator system for wandering individuals
[NASA-TM-104754] p 388 N93-11649
Antenna pattern measurement facilities
[AD-A250219] p 283 N93-11764
Space Station communications and tracking systems modeling and RF link simulation
[NASA-CR-185684] p 288 N93-12519

RADIO FREQUENCY HEATING
Self-generated stochastic heating in an RF discharge
[DE92-018558] p 452 N93-11565

RADIO FREQUENCY INTERFERENCE
LORAN and the effects of terrestrial propagation
[PB92-197219] p 205 N93-11472

RADIO GALAXIES
Publications of the Executive Office of the President, 20 January 1989 - 31 March 1992
[PB92-154913] p 477 N93-11769
A closer look at active galactic nuclei: The great engines of the Universe
[PB92-184464] p 485 N93-11807

RADIO METEOROLOGY
An observational study of a prefrontal convective rainband using TAMEX single- and dual-Doppler data
[AD-A249839] p 371 N93-12251

RADIO NAVIGATION
LORAN and the effects of terrestrial propagation
[PB92-197219] p 205 N93-11472

RADIO RECEIVERS
Direct Broadcast Satellite: Radio Program
[NASA-TM-105910] p 224 N93-11430

RADIO SOURCES (ASTRONOMY)
Periodicities in pulsar microstructure
p 484 N93-11230
Publications of the Executive Office of the President, 20 January 1989 - 31 March 1992
[PB92-154913] p 477 N93-11769

RADIO SPECTRA
Periodicities in pulsar microstructure
p 484 N93-11230

RADIO TRANSMISSION
Publication of papers presented at URSI 23rd General Assembly as a special section of radio science
[AD-A253561] p 283 N93-11811

RADIOACTIVE DECAY
High energy physics at Tufts University
[DE92-018081] p 444 N93-11668

RADIOACTIVE WASTES
Trip report: Marshall Space Center computed tomography
[DE92-018139] p 437 N93-11597

RADIOACTIVITY
North American radioactive beam initiatives
[DE92-019185] p 443 N93-11517
Gamma ray astronomy
[NASA-CR-184447] p 483 N93-12348

RADIOCHEMISTRY
Summaries of FY 1991 research in the chemical sciences
[DE92-011920] p 251 N93-12135

RADIOGRAPHY
System design and radiation field characteristics of the High Flux Neutron Radiography Facility (HFNRF) at Sandia National Laboratories
[DE92-013984] p 219 N93-12268

RADIOIMMUNOASSAY
Phadiatop: A screening test for inhalant allergy
p 383 N93-11313

RADIOISOTOPE BATTERIES
Milliwatt Generator Project
[DE92-015348] p 294 N93-12156

RADIOLOGY
Radiological information management system (RadIMS)
[DE92-017221] p 480 N93-12495

RAIL TRANSPORTATION
Vehicle/guideway interaction in maglev systems
[DE92-019051] p 326 N93-11653

RAILGUN ACCELERATORS
An investigation of electromagnetic launcher repeatability
[AD-A254339] p 222 N93-12130
Electromagnetic launcher control using finite state machines
[AD-A254433] p 222 N93-12161
Railgun armature velocity improvement, SBIR phase 2
[AD-A254749] p 222 N93-12505

RAIN
A comparison of radar rainfall estimates and rain gage measurements during two Denver thunderstorms
[AD-A254267] p 369 N93-11817
An observational study of a prefrontal convective rainband using TAMEX single- and dual-Doppler data
[AD-A249839] p 371 N93-12251
Verification of rain-flow reconstructions of a variable amplitude load history
[NASA-CR-189670] p 341 N93-12411

RAMAN LASERS
Research on stimulated Raman scattering with applications to atmospheric lidar p 322 N93-12163

RAMAN SPECTRA
Observation and analysis of the Stokes and anti-Stokes components of stimulated Raman backscattering
p 318 N93-12025
Workshop on Characterizing Diamond Films
[PB92-205426] p 271 N93-12086
Research on stimulated Raman scattering with applications to atmospheric lidar p 322 N93-12163

RAMAN SPECTROSCOPY
Rotational CARS measurements in a rotating cavity with axial throughflow of cooling air: Oxygen concentration measurements
[PNR-90935] p 244 N93-11035
Energetics solids degradation in high temperature water
[AD-A254900] p 276 N93-12285
On-line analysis of chemical composition using an FT-Raman spectrometer in the near-IR
[DE92-016503] p 253 N93-12311

RAMJET ENGINES
The effects of bypass air on boron carbide combustion in a solid fuel ramjet p 245 N93-11136
The combustion time lag and its role in ramjet combustion instability p 245 N93-11137

RANGE SAFETY
Booster rocket range safety system
[AD-D015363] p 221 N93-11428

RANKINE CYCLE
A gas-cooled cermet reactor system for planetary base power
[DE92-018017] p 443 N93-11433

RAPID TRANSIT SYSTEMS
Vehicle/guideway interaction in maglev systems
[DE92-019051] p 326 N93-11653

RARE EARTH ALLOYS
Optimization of film synthesized rare earth transition metal permanent magnet systems
[DE92-018726] p 432 N93-12116

RARE EARTH COMPOUNDS
Recrystallization of amorphous or nanocrystalline NdBa2Cu3O(7-x) and GdBa2Cu3O(7-x)
[DE92-016302] p 462 N93-11706

RARE EARTH ELEMENTS
Calculation of binary phase diagrams between the actinide elements, rare earth elements, and transition metal elements
[DE92-019119] p 249 N93-11801

RARE GASES
VUV and UV sources and spectroscopic applications
[AD-A247293] p 291 N93-11758
Inert gas electric heater for elevated temperature testing of small propulsion components
[DE92-017434] p 221 N93-12317

RAREFIED GAS DYNAMICS
Using NEKTON to solve systems of discrete Boltzmann equations
[DE92-018272] p 303 N93-11799

RATES (PER TIME)
An investigation of electromagnetic launcher repeatability
[AD-A254339] p 222 N93-12130

RATINGS
Testability design rating system. Volume 2: Analytical procedure
[AD-A254333] p 413 N93-12146

RAY TRACING
Dynamic vacuum analysis for APS high heat flux beamline front ends using optical ray-tracing simulation methods
[DE92-019032] p 445 N93-11831
Mirror alignment techniques for point-focus solar concentrators
[DE92-019643] p 348 N93-12074

RAYLEIGH EQUATIONS
Sealing characteristics of a carbon segmented circumferential seal for a liquid oxygen turbopump
[NAL-TR-1130] p 329 N93-12364

RAYLEIGH SCATTERING
Computation of small scale velocity turbulence and its effect on optical scintillations and stimulated thermal Rayleigh scattering
[DE92-018934] p 448 N93-11627

REACTING FLOW
Effects of reacting flows with turbulence and shock waves on efficiency of scramjet combustors
p 235 N93-11133
Numerical calculations of an axisymmetric laminar diffusion flame with detailed and reduced reaction mechanisms p 246 N93-11259
Solution of two-phase reacting flow in liquid thrust chambers p 235 N93-11449
Flow visualization of supersonic flow through a combustor section p 200 N93-12001
Carbon/carbon composition ablation effects on ionized boundary layers
[AD-A254465] p 242 N93-12235

REACTION KINETICS
Heterogeneous processes: Laboratory, field, and modeling studies p 350 N93-11090
Ignition delays, heats of combustion, and reaction rates of aluminum alkyl derivatives as used as ignition and combustion enhancers for supersonic combustors
p 244 N93-11134

Numerical calculations of an axisymmetric laminar diffusion flame with detailed and reduced reaction mechanisms p 246 N93-11259
The intensity of knock in an internal combustion engine: An experimental and modeling study
[DE92-019504] p 326 N93-11540
Electronic structure and reactivities of transition metal clusters
[DE92-016623] p 258 N93-11762
Exciton kinetics in poly(di-n-hexylsilane)
[DE92-018278] p 283 N93-11800
The twenty-third International Symposium on combustion
[AD-A250377] p 250 N93-11866
Laser spectroscopy and dynamics of transient species formed in pyrolysis reactions
[DE92-016206] p 251 N93-12091
Probing flame chemistry with MBMS, theory, and modeling
[DE92-011433] p 251 N93-12119
Asymptotic analysis of reacting materials with saturated explosion. 2: High-frequency waves
[AD-A254473] p 275 N93-12236
Inhibition of moist carbon monoxide oxidation by trace amounts of hydrocarbons
[DE92-008736] p 253 N93-12257
Catalytic hydrogenation of carbon monoxide
[DE92-014729] p 253 N93-12428

REACTION PRODUCTS
Scattering of polarized electrons by oriented deuterons
[DE92-624834] p 440 N93-11914

REACTIVITY
Heterogeneous processes: Laboratory, field, and modeling studies p 350 N93-11090
Electronic structure and reactivities of transition metal clusters
[DE92-016623] p 258 N93-11762
The chemistry of Si3N4 and Si deposition studied using molecular beam techniques
[DE92-018268] p 463 N93-11797
Threshold photodetachment spectroscopy of negative ions
[DE92-017090] p 440 N93-12100
Synthesis and reactivity of siloxide and silamide complexes pertaining to bond breaking and aggregation phenomena
[AD-A254703] p 468 N93-12231
Studies on the reactive melt infiltration of silicon and silicon-molybdenum alloys in porous carbon
[NASA-TM-105860] p 273 N93-12398

REACTOR DESIGN
A gas-cooled cermet reactor system for planetary base power
[DE92-018017] p 443 N93-11433

REACTOR MATERIALS
Heat load material studies: Simulated tokamak disruptions
[DE92-018275] p 452 N93-11674
Results from the US/USSR exchange for heat load material studies of simulated tokamak disruptions
[DE92-018285] p 453 N93-11694
Mechanical properties of 1950's vintage 304 stainless steel weldment components after low temperature neutron irradiation
[DE92-017059] p 259 N93-12107
Reactor materials program: Mechanical properties of irradiated types 304 and 304L stainless steel weldment components
[DE92-018105] p 260 N93-12158

REACTOR SAFETY
Ground test facility for SEI nuclear rocket engines
[DE92-017418] p 217 N93-11367
A gas-cooled cermet reactor system for planetary base power
[DE92-018017] p 443 N93-11433
A development approach for nuclear thermal propulsion
[DE92-018020] p 232 N93-11596
Tutorial on nuclear thermal propulsion safety for Mars
[DE92-017946] p 233 N93-12056
Overview of property formulations for helium, nitrogen, lithium, and lithium-lead in ATHENA/MOD1 with comparison of calculated properties to measured properties
[DE92-017995] p 471 N93-12058

REACTOR STARTUP TESTS
Nova Upgrade: A proposed ICF facility to demonstrate ignition and gain, revision 1
[DE92-018960] p 451 N93-11534

READING
Coordinated action in 3-D space
[AD-A249830] p 387 N93-10994

REAL TIME OPERATION
Intelligent TDA systems using neural networks, phase 1
[AD-A252556] p 420 N93-11000
Implementation of a model based fault detection and diagnosis for actuation faults of the Space Shuttle main engine
[NASA-TM-105781] p 221 N93-11401
A real-time diagnostic and performance monitor for UNIX
[NASA-CR-190975] p 404 N93-11462
A rule-based system for real-time analysis of control systems
[NASA-TM-104258] p 277 N93-11619
A search for low-luminosity objects
[AD-A253301] p 483 N93-11750
Real-time data compression using a FFT digital signal processor
[DE92-017744] p 477 N93-11770
Intelligent data management for real-time spacecraft monitoring p 394 N93-11936
Model-based vision for space applications
p 398 N93-11955
Real-time classification of signals from three-component seismic sensors using neural nets
[DE92-014886] p 364 N93-12155
A methodology for systems requirements specification and traceability for large real time complex systems
[AD-A254738] p 419 N93-12358
A real time sharpening of NOGAPS predictions of mid-latitude Central Pacific cyclones
[AD-A255157] p 372 N93-12424
Real-time adaptive sidelobe canceller architectures and implementations
[AD-A254842] p 286 N93-12433

RECEIVERS
Method of steering the gain of a multiple antenna global positioning system receiver
[AD-D015367] p 281 N93-11426
Evaluation tests for photovoltaic concentrator receiver sections and modules
[DE92-017745] p 346 N93-11771
The sensitivity of the receiver coherence diameter and modulation transfer function to variations of a damp unstable atmosphere
[AD-A253269] p 363 N93-11785

RECHARGING
Long cycle life rechargeable lithium batteries
[NASA-CR-190937] p 291 N93-11604

RECOGNITION
Object recognition with a robot hand
p 420 N93-11457
Research on a reconfigurable modular manipulator system
[DE92-018943] p 327 N93-11865

RECOIL IONS
Experimental study of interactions of highly charged ions with atoms at keV energies
[DE92-019512] p 436 N93-11541

RECOMMENDATIONS
Study and recommendation of available sources of scientific and technical numeric databases in the government and private sector
[AD-A247266] p 475 N93-11465

RECORDS MANAGEMENT
Radiological information management system (RadIMS)
[DE92-017221] p 480 N93-12495

RECOVERABLE LAUNCH VEHICLES
Development trends in space transportation systems: From Hermes to Saenger
[MBB-UK-0146-91-PUB] p 223 N93-11007

RECOVERY
Some consistency requirements on hardening-recovery evolution equations for welding, part 1
[DE92-015992] p 329 N93-12220

RECRYSTALLIZATION
Titanium-aluminides by hot isostatic pressing of cold extruded titanium-aluminium powder mixtures
[GKSS-91/E/67] p 256 N93-11337
Recrystallization of amorphous or nanocrystalline NdBa2Cu3O(7-x) and GdBa2Cu3O(7-x)
[DE92-016302] p 462 N93-11706

RECTIFIERS
High temperature rectifiers and MOS devices in 6H-silicon carbide
[AD-A254725] p 295 N93-12340

RECURSIVE FUNCTIONS
On recursive free types in Z
[RSRE-91028] p 425 N93-11437
Backward assembly planning with DFA analysis
[NASA-CASE-NPO-18817-1-CU] p 278 N93-12202

RECYCLING
The flux and recycling of bioactive substances in the surface sediments of the deep basins off southern California
[DE92-019172] p 373 N93-11734

RED TIDE
Parameters for predicting red tides of bioluminescent dinoflagellates: Meteorological events and frontal water circulation patterns
[AD-A254835] p 374 N93-12431

REDUCED GRAVITY
Small experiments for the maturation of orbital cryogenic transfer technologies
[NASA-TM-105849] p 296 N93-10981
Residual acceleration data on IML-1: Development of a data reduction and dissemination plan
[NASA-CR-190807] p 223 N93-11101
Space flight and immune system p 376 N93-11284
KC-135 materials handling robotics
[NASA-CR-184430] p 328 N93-11992
Materials processing in low gravity
[NASA-CR-184421] p 276 N93-12401

REDUCTION
Near-IR absorption spectra for the C70 fullerene anions
[AD-A253658] p 246 N93-11280

REDUNDANCY ENCODING
Fault detection and fault tolerance in robotics
p 330 N93-11961
Simulation and analysis of support hardware for multiple instruction rollback
[NASA-CR-190972] p 406 N93-12541

REED-SOLOMON CODES
Mappings between codewords of two distinct (N,K) Reed-Solomon codes over GF(2 sup J)
[NASA-CASE-NPO-18771-1-CU] p 412 N93-11664
An investigation of error correcting techniques for OMV and AXAF
[NASA-CR-190950] p 416 N93-12515

REELS
Fiber peel force measuring apparatus
[AD-D015349] p 309 N93-11048
Payout tension control system for reel mounted cable
[AD-D015362] p 325 N93-11423

REENTRY
Flow field calculations around the Hermes spaceplane during reentry phase
[MBB-UK-0148-91-PUB] p 195 N93-11008
Hybrid guidance for maneuvering flight vehicles
[AD-A254110] p 225 N93-11798

REENTRY EFFECTS
Erosion mechanisms in ceramic structures
[MBB-UK-0171-92-PUB] p 263 N93-11011

REENTRY PHYSICS
Erosion mechanisms in ceramic structures
[MBB-UK-0171-92-PUB] p 263 N93-11011

REENTRY SHIELDING
Erosion mechanisms in ceramic structures
[MBB-UK-0171-92-PUB] p 263 N93-11011

REENTRY VEHICLES
Hybrid guidance for maneuvering flight vehicles
[AD-A254110] p 225 N93-11798

REFLECTANCE
Fast electrochromic switching for optical hardening applications
[AD-A248174] p 447 N93-11186
Detection of cloud-top height from backscattered radiances within the oxygen A band. Part 2: Measurements
[GKSS-91/E/77-PT-2] p 368 N93-11350
On the definition and calculation of effective impedances and averaged boundary conditions with application to the analysis of high complexity frequency selective surfaces
[RSRE-MEMO-4518] p 281 N93-11387
A comparison of radar rainfall estimates and rain gage measurements during two Denver thunderstorms
[AD-A254267] p 369 N93-11817
Erosion rates for polymers measured on LDEF
p 270 N93-11994
An observational study of a prefrontal convective rainband using TAMEX single- and dual-Doppler data
[AD-A249839] p 371 N93-12251
Global change and the dark of the moon
[AD-A255181] p 486 N93-12380
Study of sound propagation in a wedge-shaped ocean and comparison with other methods
[AD-A255165] p 435 N93-12471

REFLECTED WAVES
System and method for cancelling expansion waves in a wave rotor
[NASA-CASE-LEW-15218-1] p 297 N93-11172

REFLECTION
The synthesis and crystal structure of LaHSe2O6, a layered, anhydrous selenite
[AD-A251050] p 458 N93-10996

Light scattering from a sphere on or near an interface
p 448 N93-12531

REFLECTION NEBULAE
Near-infrared imaging polarimetry of bipolar nebulae
p 481 N93-11248

REFLECTOR ANTENNAS
Project and test of a reconfigurable multiple feed system in C-band
[MBB-UK-0162-92-PUB] p 278 N93-11009
Method of moments analysis of symmetric dual reflector antennas with feeds
[AD-A255171] p 286 N93-12407
Deployable reflector antenna performance optimization using automated surface correction and array-feed compensation
[NASA-TP-3228] p 222 N93-12543

REFLECTORS
Antenna pattern measurement facilities
[AD-A250219] p 283 N93-11764
Seismic wave propagation in thinly-layered media with steep reflectors
[DE92-015619] p 364 N93-12142

REFRACTION
Laser glasses
[DE92-018061] p 267 N93-11549
Study of filamentation in subdense plasma interaction experiments p 318 N93-12026

REFRACTIVITY
Analysis of advanced optical glass and systems
[NASA-CR-184434] p 448 N93-12201

REFRACTORY COATINGS
Chronopotentiometry of refractory metals, actinides and oxyanions in molten salts: A review
[NASA-TM-105862] p 249 N93-11545
Current Technology for Thermal Protection Systems
[NASA-CP-3157] p 227 N93-12447

REFRACTORY MATERIALS
Current Technology for Thermal Protection Systems
[NASA-CP-3157] p 227 N93-12447
Thermal protection using very high temperature ceramics p 228 N93-12451
Recent advances in carbon-carbon substrate technology at NASA. Langley Research Center p 228 N93-12455
Thermostructural applications of heat pipes for cooling leading edges of high-speed aerospace vehicles
p 229 N93-12460

REFRACTORY METALS
A gas-cooled cermet reactor system for planetary base power
[DE92-018017] p 443 N93-11433
Chronopotentiometry of refractory metals, actinides and oxyanions in molten salts: A review
[NASA-TM-105862] p 249 N93-11545
Hydrogen assisted heat transfer during diamond growth using carbon and tantalum filaments
[AD-A247944] p 468 N93-12218

REFRIGERANTS
The role of refrigerants in climate change
[DE92-019385] p 354 N93-11677

REFUELING
Small experiments for the maturation of orbital cryogenic transfer technologies
[NASA-TM-105849] p 296 N93-10981

REGIONAL PLANNING
Post-war regional planning: The French silicon valley
[RSRE-MEMO-4282] p 472 N93-10976

REGRESSION ANALYSIS
Development of the Personnel-based System Evaluation Aid (PER-SEVAL) performance shaping functions
[AD-A252820] p 386 N93-11779
Research in statistical inference
[AD-A252928] p 429 N93-12429

REGULATIONS
Comparison of passive-remote and conventional Fourier transform infrared systems for continuously monitoring incinerator emissions
[DE92-015225] p 355 N93-12098
DOE guideline: Guide to good practices for incorporating operating experiences
[DE92-017684] p 472 N93-12223

REINFORCED PLASTICS
A contribution to fatigue failure morphologies in fiber reinforced plastics
[MBB-Z-0212-91-PUB] p 263 N93-11010

REINFORCING FIBERS
A contribution to fatigue failure morphologies in fiber reinforced plastics
[MBB-Z-0212-91-PUB] p 263 N93-11010
Toughness of Si3N4-SiC whisker composites
[REPT-921-430-101] p 239 N93-11586
High-performance synthetic fibers for composites
[AD-A252645] p 242 N93-12292

RELATIVISTIC EFFECTS
Relativistic condensate and cosmology
p 486 N93-12330

RELATIVISTIC ELECTRON BEAMS
Propagation of relativistic high current electron beams across the geomagnetic field
[DE92-018276] p 362 N93-11564
BANSHEE: High-voltage repetitively pulsed electron-beam driver
[DE92-017413] p 444 N93-11763
Electron acceleration in a relativistic electron plasma wave p 319 N93-12033
Forecasting the relativistic electron flux at geosynchronous orbit
[AD-A254016] p 226 N93-12064

RELATIVISTIC PARTICLES
Strange quark matter
[DE92-016949] p 438 N93-11746

RELATIVISTIC PLASMAS
Topics in high-intensity laser plasma interaction
p 450 N93-11191
Electron acceleration in a relativistic electron plasma wave p 319 N93-12033

RELATIVISTIC VELOCITY
Observation of pulses propagating at supraluminous speed in an optical fiber p 320 N93-12040

RELAXATION (MECHANICS)
Growth mechanisms of layered superconductors
[DE92-018492] p 458 N93-10987

RELIABILITY
On the basis of experience: Built in product reliability
[PNR-90932] p 331 N93-11034
Civil aircraft engines: The next generation
[PNR-90962] p 211 N93-11085
Evaluation tests for photovoltaic concentrator receiver sections and modules
[DE92-017745] p 346 N93-11771
Operating characteristic analysis for reliability growth programs
[AD-A254993] p 333 N93-12510

RELIABILITY ANALYSIS
Ceramic component reliability with the restructured NASA/CARES computer program
[NASA-TM-105856] p 334 N93-11004
On the basis of experience: Built in product reliability
[PNR-90932] p 331 N93-11034
Advanced three-shaft engines: Configured for reliability, efficiency, and growth
[PNR-90986] p 211 N93-11068
VLSI design for reliability
[AD-A253207] p 292 N93-11781
Algorithms for sensor fusion: Decentralized Bayesian hypothesis testing with feedback, volume 1
[AD-A254633] p 414 N93-12242
Reliability analysis of a utility-scale solar power plant
[DE92-016550] p 348 N93-12312
VLSI reliability research
[AD-A254883] p 295 N93-12360

RELIABILITY ENGINEERING
Ceramic component reliability with the restructured NASA/CARES computer program
[NASA-TM-105856] p 334 N93-11004
Role of automation in the ACRV operations
p 230 N93-11977
Ultrasonic flaw classification and sizing
p 333 N93-12533

RELIEF MAPS
Generation of 3-D surface maps in waste storage silos using a structured light source p 399 N93-11958

REMOTE CONTROL
Effects of spatially displaced feedback on remote manipulation tasks p 400 N93-11966
Remote systems development p 330 N93-11971

REMOTE SENSING
The millimeter wave Cloud Profiling Radar System (CPRS)
[DE92-016970] p 366 N93-10971
The Transall campaign. A contribution to the German ozone research program
[REPT-37/91] p 349 N93-11082
An evidential reasoning approach to the classification of satellite images
[DLR-FB-91-29] p 342 N93-11140
Volcanology from space: Applications of infrared remote sensing p 343 N93-11213
Payload advisory panel recommendations
[NASA-TM-108012] p 219 N93-11528
The early Earth Observing System reference handbook: Earth Science and Applications Division missions, 1990-1997
[NASA-TM-107963] p 343 N93-11663
Nimbus-7 Scanning Multichannel Microwave Radiometer (SMMR) PARM tape user's guide
[NASA-RP-1284] p 373 N93-11718
Proceedings of the First Seminar on Geographic Information Systems in Zambia
[PB92-207125] p 477 N93-11789
Foil optimization for low energy neutral atom imaging
[DE92-013435] p 365 N93-12263
Low energy neutral atom imaging
[DE92-013531] p 365 N93-12264
ERS-1 user handbook
[ESA-SP-1148] p 344 N93-12280
Estimation of photosynthetic capacity using MODIS polarization: 1988 proposal to NASA Headquarters
[NASA-TM-103945] p 344 N93-12351

REPRODUCTION (COPYING)
Using SGML in a large organization
[ESA-STR-234] p 476 N93-11583

REQUIREMENTS
Advanced materials in gas turbine engines: An assessment
[PNR-90946] p 211 N93-11105
Integrity-oriented control objectives: Proposed revisions to the Trusted Computer System Evaluation Criteria (TCSEC), DOD 5200.28-STD
[AD-A253989] p 404 N93-11809
Requirements Specification Language (RSL) and supporting tools
[NASA-CR-189700] p 405 N93-12345

RESEARCH AIRCRAFT
Flight test progress of the STOL research aircraft ASKA
[NAL-TM-643] p 208 N93-12354

RESEARCH AND DEVELOPMENT
From RB211 to Trent: An ongoing development strategy
[PNR-90938] p 210 N93-11038
Exploratory Research and Development Fund, FY 1990
[DE92-017002] p 489 N93-11078
Workshop on Surface Science and Technology
[AD-A253566] p 264 N93-11149
JPRS report: Science and technology. Central Eurasia: Engineering and equipment
[JPRS-UEQ-92-009] p 220 N93-11169
The NASA CSTI high capacity power project
[NASA-TM-105813] p 221 N93-11398
Materials science and engineering at the Naval Research Laboratory: Research programs and 1990 publications
[PB92-199488] p 238 N93-11422
Advanced materials and processing: The Federal program in materials science and technology. A report by the FCCSET Committee on Industry and Technology to supplement the President's fiscal year 1993 budget
[PB92-199108] p 238 N93-11470
Solid state sciences committee forum
[AD-A253556] p 463 N93-11753
The first meeting of the Advisory Committee on the Future of the US Space Program (C-FUSSP)
[NASA-CR-190995] p 219 N93-11754
Evaluation of advanced pressure sensor technology
[DE92-011004] p 312 N93-11806
Electricity from biomass: A development strategy
[DE92-010590] p 346 N93-11814
NASA/DOD Aerospace Knowledge Diffusion Research Project. Paper 23: Information technology and aerospace knowledge diffusion: Exploring the intermediary-end user interface in a policy framework
[NASA-TM-108077] p 478 N93-12007
Activity of the technical groups (LULI Palaiseau, France) p 322 N93-12052
Soviet chemical propellant research and development
[PB92-195577] p 275 N93-12147
Final Report, January 1991 - July 1992
[AD-A254659] p 483 N93-12244
Research and development strategies for human centered and group support technologies
[AD-A254366] p 472 N93-12273
High-performance synthetic fibers for composites
[AD-A252645] p 242 N93-12292
Laser Doppler experiments
[AD-A252883] p 287 N93-12461
The collaborative program of research in engineering sciences
[DE92-016838] p 490 N93-12477

RESEARCH FACILITIES
An advanced combustion research facility for validating computational fluid dynamics codes
[PNR-90913] p 296 N93-11017
North American radioactive beam initiatives
[DE92-019185] p 443 N93-11517
Data report 92-1. Brorfelde Geomagnetic Observatory magnetic results, 1990 p 362 N93-11699
Radiation physics, biophysics, and radiation biology
[DE92-013673] p 375 N93-12266
System design and radiation field characteristics of the High Flux Neutron Radiography Facility (HFNRF) at Sandia National Laboratories
[DE92-013984] p 219 N93-12268

RESEARCH MANAGEMENT
Japanese style total quality control: A first hand experience
[PNR-90909] p 331 N93-11015

Exploratory Research and Development Fund, FY 1990
[DE92-017002] p 489 N93-11078
A development approach for nuclear thermal propulsion
[DE92-018020] p 232 N93-11596
Interfacial microchemical characterization needs in surface processing
[DE92-018269] p 277 N93-11672
Solid state sciences committee forum
[AD-A253556] p 463 N93-11753
Computer Science and Telecommunications Board summary of activities
[DE92-016467] p 404 N93-11761
Selected case studies of technology transfer from mission-oriented applied research
[DE92-018957] p 481 N93-12067
Plasma properties
[DE92-018635] p 455 N93-12188
Radiation physics, biophysics, and radiation biology
[DE92-013673] p 375 N93-12266
Medium energy nuclear physics research
[DE92-016972] p 442 N93-12444

RESEARCH PROJECTS
Hurricane Research Division fiscal year 1991 programs: Fiscal year 1992 projections
[PB92-138320] p 367 N93-11242
Ceramic Technology Project
[DE92-018748] p 266 N93-11442
Research in heavy-ion nuclear physics
[DE92-015099] p 443 N93-11521
Fusion programs in applied plasma physics
[DE92-019639] p 452 N93-11660
Electric and hybrid vehicle program, site operator program
[DE92-018055] p 328 N93-12114
Radiation physics, biophysics, and radiation biology
[DE92-013673] p 375 N93-12266
Medium energy nuclear physics research
[DE92-016972] p 442 N93-12444
LIEKKI and JALO: Combustion and fuel conversion
[DE92-540921] p 349 N93-12446

RESEARCH VEHICLES
A summary of the forebody high-angle-of-attack aerodynamics research on the F-18 and the X-29A aircraft
[NASA-TM-104261] p 202 N93-12353

RESERVES
Reserves information gathering system user's guide
[DE92-018357] p 475 N93-11355

RESIDUAL STRENGTH
Study of the effects of a plastic wave induced by laser pulse in a metallic material. Application to the improvement of fatigue strength p 319 N93-12036
Creep failure in linear and nonlinear viscoelastic materials p 342 N93-12536

RESIDUAL STRESS
Neutron diffraction residual stress studies for aero-engine component applications
[PNR-90908] p 334 N93-11014
Generation of thermal strains in carbon fibre-reinforced bismaleimide (PMR-15) composites, part 1, 2 and 3
[PNR-90976-PT-1-2-3] p 236 N93-11065
Thermal residual stresses in silicon-carbide/titanium (0/90) laminate
[NASA-TM-107649] p 236 N93-11072
The dressing of resin bonded diamond grinding wheels
[PNR-90965] p 264 N93-11086
Development of the neutron diffraction technique for the determination of near surface residual stresses in critical gas turbine components
[PNR-90984] p 212 N93-11112
Orientation, stress, and density distributions in injection-moulded amorphous polymers determined by optical techniques
[ETN-92-92271] p 269 N93-11983
Molecular orientation induced by cooling stresses in polycarbonate. 1: Free quenching p 269 N93-11987
Study of residual stresses and microcracks in high strength steel weldments: An investigation of microcrack formation and stressed growth using laser microscopy
[AD-A255059] p 342 N93-12467

RESIDUES
Compositional analysis and classification of projectile residues in LDEF impact craters
[NASA-TM-104750] p 488 N93-11374

RESIN MATRIX COMPOSITES
Semi-interpenetrating polymer network for tougher and more microcracking resistant high temperature polymers
[NASA-CASE-LAR-13925-2] p 264 N93-11059

RESINS
Phase transfer catalytic nucleophilic addition reactions: Synthesis of polymers and acetylenic terminated resins
[AD-A254717] p 272 N93-12337

RESISTOJET ENGINES
Preliminary characterization of a water vaporizer for resistojet applications
[NASA-TM-105877] p 231 N93-11402

RESISTORS
High-frequency LSI contactor
[DE92-017285] p 292 N93-11916

RESONANCE
State-resolved reaction dynamics
[AD-A254291] p 436 N93-11196
The effects of plate spacing and downstream plate length on the acoustic resonance excited by flow past two plates in tandem in a duct
[PNR-90958] p 433 N93-11321
High-precision thorium RIMS for geochemistry
[DE92-017405] p 250 N93-11918

RESONANT FREQUENCIES
Experimental validation of boundary element methods for noise prediction
[NASA-TM-105729] p 323 N93-10966
An experimental investigation into flow induced acoustic resonances in an annular cascade
[PNR-90959] p 433 N93-11322
Dynamic analysis of a pre-and-post ice impacted blade
[NASA-TM-105829] p 276 N93-12197

RESONATORS
High Temperature Superconductivity Space Experiment (HTSSE)
[AD-A253119] p 288 N93-11239
Dynamics and response of polymer-coated acoustic devices
[DE92-014289] p 433 N93-11523
Quartz crystal resonators and oscillators for frequency control and timing applications: A tutorial, revision 5.2
[AD-A254892] p 469 N93-12283
Conductor-backed coplanar waveguide resonators of Y-Ba-Cu-O and Tl-Ba-Ca-Cu-O on LaAlO3
[NASA-TM-105890] p 469 N93-12325

RESOURCES
Study and recommendation of available sources of scientific and technical numeric databases in the government and private sector
[AD-A247266] p 475 N93-11465

RESPIRATION
Occupational safety considerations with hydrazine fuels p 276 N93-11951

RESPIRATORY DISEASES
Allergic, Immunological and Infectious Disease Problems in Aerospace Medicine
[AGARD-CP-518] p 376 N93-11283
Communicable diseases: A major burden of morbidity and mortality p 380 N93-11300
Epidemiologic view of allergic diseases in North America: Implications for aerospace medicine
p 382 N93-11311
The screening of inhalant allergic diseases in the selection of candidates for aircraft piloting
p 382 N93-11312
Phadiatop: A screening test for inhalant allergy
p 383 N93-11313
In vivo and in vitro diagnosis of allergic respiratory disease during screening procedures in the Italian Navy: Comparative evaluation of a recent quantitative automatized enzyme immunoassay method to dose specific IgE p 383 N93-11314
Asthma in aircrew: Assessment, treatment and disposition p 383 N93-11315
Allergic and nonallergic rhinitis in Greek pilots
p 383 N93-11317

RESPIRATORY PHYSIOLOGY
Asthma in aircrew: Assessment, treatment and disposition p 383 N93-11315

RESPONSE BIAS
Super auditory localization for improved human-machine interfaces
[AD-A254699] p 389 N93-12229

RESPONSE TIME (COMPUTERS)
Intelligent data management for real-time spacecraft monitoring p 394 N93-11936

RESPONSES
Use of the program ANISN to calculate response functions for a Bonner sphere set with a He-3 detector
[NPL-RSA(EXT)-31] p 316 N93-11411

RESTORATION
Environmental restoration project configuration control
[DE92-017223] p 356 N93-12496

RETAINING
Implanted He retention and release from boronized layers
[DE92-013983] p 464 N93-11842

RETINA
Feasibility assessment of a transient sound sensor based on the silicon retina architecture
[AD-A252288] p 432 N93-10999

RETURN TO EARTH SPACE FLIGHT
Physiologically constrained aerocapture for manned Mars missions p 226 N93-12185

REUSABLE HEAT SHIELDING
Reusable thermal protection system development: A prospective p 227 N93-12448
Predicted and tested performance of durable TPS
p 228 N93-12454

REUSABLE ROCKET ENGINES
Space Transportation Booster Engine Configuration Study. Volume 3: Program Cost estimates and work breakdown structure and WBS dictionary
[NASA-CR-184458] p 233 N93-12088
Space transportation booster engine configuration study. Volume 2: Design definition document and environmental analysis
[NASA-CR-184459] p 234 N93-12441
Space transportation booster engine configuration study. Volume 1: Executive Summary
[NASA-CR-184457] p 235 N93-12523

REUSABLE SPACECRAFT
Development trends in space transportation systems: From Hermes to Saenger
[MBB-UK-0146-91-PUB] p 223 N93-11007
Reusable thermal protection system development: A prospective p 227 N93-12448

REVERSE ENGINEERING
Reengineering using a data abstraction based specification language
[AD-A254726] p 414 N93-12341

REVERSE FIELD PINCH
Ion temperature measurements on field reversed configuration plasmas p 457 N93-12535

REVERSING
Hydrodynamic particle migration in small-amplitude, oscillatory, circular couette flow: The limits of reversibility
[DE92-008480] p 303 N93-11843

REYNOLDS EQUATION
Application of a two-layer near wall model to fully developed and rotating channel turbulent flows
[NASA-CR-184441] p 305 N93-12082

REYNOLDS NUMBER
The hemisphere-cylinder at an angle of attack
p 196 N93-11250
Direct numerical simulation of instabilities in parallel flow with spherical roughness elements
[NASA-TM-105847] p 300 N93-11529
Leading edge film cooking heat transfer including the effect of mainstream turbulence p 199 N93-11886
Compressible mixing layers with and without particles
[AD-A254854] p 308 N93-12435
Bubble dissolving in turbulent pipe flow
[AD-A252927] p 308 N93-12462

RHEOLOGY
The peculiar rheo-optical behaviour of bisphenol-A-polycarbonate and polymethylmethacrylate
p 269 N93-11984

RHODIUM COMPOUNDS
Catalytic hydrogenation of carbon monoxide
[DE92-014729] p 253 N93-12428

RIBS (SUPPORTS)
Near-field and far-field sound radiation from a line-driven fluid-loaded infinite flat plate having periodic and non-periodic attached rib stiffeners p 434 N93-11884

RICCATI EQUATION
On the inverse scattering problem for the Helmholtz equation in one dimension
[AD-A253130] p 434 N93-11526

RIGGING
A study of the effects of tolerances on rigging screws, turnbuckles, and associated components in BS4429: 1987
[NPL-DMM(A)-53] p 325 N93-11326

RIGID STRUCTURES
Sound propagation over rigid porous layers
p 432 N93-11179
Rigid body mode identification of the PAH-2 helicopter using the eigensystem realization algorithm
[NASA-TM-107690] p 336 N93-11544
Numerical study of advanced rotor blades
p 199 N93-11899
The order n simulation of tether motions based on a rigid body tether model p 225 N93-11999
Advanced one-dimensional optical strain measurement system, phase 4
[NASA-CR-190760] p 314 N93-12279

RING LASERS
Development of a GPS-aided motion measurement, pointing, and stabilization system for a synthetic aperture radar
[DE92-017053] p 204 N93-11152

RING STRUCTURES
Synthesis and characterization of novel aluminum-arsenic compounds 2. Crystal structures of (R2AlAs (SiMe3)2)2 (R = i-Bu, Me) and i-Bu2 (Cl)Al*As (SiMe3)3 [AD-A248001] p 467 N93-12175

RISERS
Measuring and modelling of particle-fluid flow in a riser reactor [VTT-PUBS-88] p 299 N93-11359

RISK
Operating characteristic analysis for reliability growth programs [AD-A254993] p 333 N93-12510

ROADS
Computing optimum routes across terrain using DAP [RSRE-MEMO-4299] p 412 N93-11712

ROBOT ARMS
EXOS research on master controllers for robotic devices p 399 N93-11957
A new scheme of force reflecting control p 399 N93-11960
A neuro-collision avoidance strategy for robot manipulators p 400 N93-11962
An 8-DOF dual-arm system for advanced teleoperation performance experiments p 400 N93-11964
An integrated dexterous robotic testbed for space applications p 330 N93-11972
Research and development at ORNL/CESAR towards cooperating robotic systems for hazardous environments p 331 N93-11979

ROBOT CONTROL
The adaptive neuron model: An architecture for the rapid learning of nonlinear topological transformations [NASA-CASE-NPO-18579-1-CU] p 420 N93-11174
Terminal slider control of nonlinear robotic systems [NASA-CASE-NPO-18584-1-CU] p 324 N93-11177
Numerical analysis of right-half plane zeros for a single-link manipulator [NASA-CR-190966] p 426 N93-11547
Integration of task level planning and diagnosis for an intelligent robot p 393 N93-11929
Contact detection and contact motion for error recovery in the presence of uncertainties p 398 N93-11956
EXOS research on master controllers for robotic devices p 399 N93-11957
A new scheme of force reflecting control p 399 N93-11960
An 8-DOF dual-arm system for advanced teleoperation performance experiments p 400 N93-11964
Performance experiments with alternative advanced teleoperator control modes for a simulated solar maximum satellite repair p 400 N93-11965
Importance of numerosity and distribution of articulations within the digits, wrists, and arms of telemanipulators confronted with dextrous assembly tasks p 330 N93-11967
Advanced mechanisms for robotics p 330 N93-11969
An integrated dexterous robotic testbed for space applications p 330 N93-11972
Space Station robotics planning tools p 331 N93-11975
Research and development at ORNL/CESAR towards cooperating robotic systems for hazardous environments p 331 N93-11979
KC-135 materials handling robotics [NASA-CR-184430] p 328 N93-11992
A VMEbus ultrasonic sensor controller for mapping and servo control in robotic systems [DE92-013661] p 421 N93-12138
A vision-based end-point control for a two-link flexible manipulator [NASA-CR-190967] p 330 N93-12521

ROBOT DYNAMICS
Numerical analysis of right-half plane zeros for a single-link manipulator [NASA-CR-190966] p 426 N93-11547
Contact detection and contact motion for error recovery in the presence of uncertainties p 398 N93-11956
EXOS research on master controllers for robotic devices p 399 N93-11957
KC-135 materials handling robotics [NASA-CR-184430] p 328 N93-11992

ROBOTICS
Object recognition with a robot hand p 420 N93-11457
RATLER: Robotic All-Terrain Lunar Exploration Rover [DE92-019295] p 487 N93-11502
Generation of 3-D surface maps in waste storage silos using a structured light source p 399 N93-11958
A neuro-collision avoidance strategy for robot manipulators p 400 N93-11962
An 8-DOF dual-arm system for advanced teleoperation performance experiments p 400 N93-11964
Automation and robotics for COLUMBUS: An implementation concept for the free flying laboratory (MTFF) p 331 N93-11974
Space Station robotics planning tools p 331 N93-11975
Role of automation in the ACRV operations p 230 N93-11977
Decision rules for spaceborne operations planning p 403 N93-11978
Research and development at ORNL/CESAR towards cooperating robotic systems for hazardous environments p 331 N93-11979
Automated resupply of consumables: Enhancement of space commercialization opportunities p 403 N93-11980
A smart end-effector for assembly of space truss structures p 230 N93-11982
KC-135 materials handling robotics [NASA-CR-184430] p 328 N93-11992
A VMEbus ultrasonic sensor controller for mapping and servo control in robotic systems [DE92-013661] p 421 N93-12138

ROBOTS
Terminal slider control of nonlinear robotic systems [NASA-CASE-NPO-18584-1-CU] p 324 N93-11177
ALECSYS and the AutonoMouse: Learning to control a real robot by distributed classifier systems [REPT-92-011] p 420 N93-11227
RATLER: Robotic All-Terrain Lunar Exploration Rover [DE92-019295] p 487 N93-11502
Numerical analysis of right-half plane zeros for a single-link manipulator [NASA-CR-190966] p 426 N93-11547
Research on a reconfigurable modular manipulator system [DE92-018943] p 327 N93-11865
Fuzzy logic control of telerobot manipulators p 399 N93-11959
Fault detection and fault tolerance in robotics p 330 N93-11961
Advanced mechanisms for robotics p 330 N93-11969
Remote systems development p 330 N93-11971
Decision rules for spaceborne operations planning p 403 N93-11978
Computational nonlinear control [AD-A253547] p 422 N93-12258
A vision-based end-point control for a two-link flexible manipulator [NASA-CR-190967] p 330 N93-12521

ROBUSTNESS (MATHEMATICS)
A problem formulation for glideslope tracking in wind shear using advanced robust control techniques [NASA-TM-104164] p 214 N93-11176
An advancing front Delaunay triangulation algorithm designed for robustness [NASA-CR-189719] p 416 N93-12400
Research in statistical inference [AD-A252928] p 429 N93-12429

ROCKET ENGINE DESIGN
Rocket Based Combined Cycle (RBCC) Propulsion Technology Workshop. Volume 1: Executive summary [NASA-CR-184382] p 231 N93-11042
Test program to provide validation data for the Rocket Combustor Interactive Design (ROCCID) code p 247 N93-11450
Space transportation booster engine configuration study. Volume 2: Design definition document and environmental analysis [NASA-CR-184459] p 234 N93-12441
Users manual for program NYQUIST: Liquid rocket nyquist plots developed for use on a PC computer [NASA-CR-184451] p 235 N93-12522
Space transportation booster engine configuration study. Volume 1: Executive Summary [NASA-CR-184457] p 235 N93-12523

ROCKET ENGINES
Thermal fracture service life analysis of a case bonded visco-elastic cylinder p 339 N93-12008
Effect of inert propellant injection on Mars ascent vehicle performance [NASA-CR-189238] p 226 N93-12152

ROCKET EXHAUST
Predicted rocket and shuttle effects on stratospheric ozone p 352 N93-11097

ROCKET FLIGHT
Lightweight Exoatmospheric Projectile (LEAP) test program. Supplemental environmental assessment [AD-A252286] p 231 N93-10998
Computer simulation and experimental investigation of the absorption cell for the rocketborne diode-laser experiment MASERATI [BONN-IR-91-62] p 357 N93-11083

ROCKET LAUNCHING
Lightweight Exoatmospheric Projectile (LEAP) test program. Supplemental environmental assessment [AD-A252286] p 231 N93-10998
Laser Doppler experiments [AD-A252883] p 287 N93-12461

ROCKET LININGS
Hot fire test results of subscale tubular combustion chambers [NASA-TP-3222] p 232 N93-11614

ROCKET NOZZLES
Calculation of nozzle/aftbody flowfield interactions p 302 N93-11722

ROCKET PROPELLANTS
Destruction of explosives and rocket fuels by supercritical water oxidation [DE92-018874] p 274 N93-11380
Occupational safety considerations with hydrazine fuels p 276 N93-11951

ROCKET TEST FACILITIES
Ground test facility for SEI nuclear rocket engines [DE92-017418] p 217 N93-11367

ROCKET THRUST
Examination of various turbulence models for application in liquid rocket thrust chambers [NASA-CR-184406] p 233 N93-12009

ROCKET VEHICLES
Development trends in space transportation systems: From Hermes to Saenger [MBB-UK-0146-91-PUB] p 223 N93-11007

ROCKET-BORNE INSTRUMENTS
Computer simulation and experimental investigation of the absorption cell for the rocketborne diode-laser experiment MASERATI [BONN-IR-91-62] p 357 N93-11083

ROCKS
Physical characterization of magmatic liquids [DE92-015931] p 363 N93-11848
Deep penetration into frictional ductile and brittle materials [PB92-205566] p 338 N93-11903

RODS
Drag on an oscillating rod in a non-Newtonian fluid [DE92-014746] p 308 N93-12492

ROLLER BEARINGS
Thermal non-Newtonian elastohydrodynamic lubrication of line contacts under sliding-rolling and simple sliding conditions p 324 N93-11263

ROOM TEMPERATURE
Influence of strain rate on the structure/property behavior of the alpha-2 alloy Ti-24.5Al-10.5Nb-1.5Mo [DE92-008490] p 261 N93-12256

ROOT-MEAN-SQUARE ERRORS
Statistical methods for the comparison of spatial patterns in meteorological variables p 370 N93-11997

ROSAT MISSION
Contributions to the Joint Discussion 3: Results from Rosat and GRO and Other Recent High Energy Astrophysics Missions of the Max-Planck-Institut fuer Extraterrestrische Physik [MPE-PREPRINT-215] p 482 N93-11473
Rosat deep surveys p 482 N93-11474
X ray morphology of clusters of galaxies p 482 N93-11475
Morphology and physics of supernova remnants p 482 N93-11476
Stars in the Rosat all-sky survey p 482 N93-11477

ROTARY WING AIRCRAFT
Rotorcraft health and usage monitoring systems: A literature survey [DOT/FAA/RD-91/6] p 206 N93-11461
A theory for the analysis of rotorcraft operating in atmospheric turbulence p 207 N93-11725
The Fourth Workshop on Dynamics and Aeroelastic Stability Modeling of Rotorcraft Systems [AD-A255065] p 208 N93-12485

ROTARY WINGS
Numerical study of advanced rotor blades p 199 N93-11899
Studies of a flat wake rotor theory [NASA-CR-190936] p 201 N93-12343

ROTATING BODIES
In-plane strain measurement on high speed rotating components using pulsed laser ESPI [PNR-90975] p 315 N93-11064
The prediction of convective heat transfer in rotating square ducts [PNR-90985] p 296 N93-11067
In-plane ESPI measurements in hostile environments [PNR-90919] p 309 N93-11320

ROTATING CYLINDERS
Hydrodynamic particle migration in small-amplitude, oscillatory, circular couette flow: The limits of reversibility [DE92-008480] p 303 N93-11843
Regular and chaotic mixing of viscous fluids in eccentric rotating cylinders p 305 N93-12157

ROTATING DISKS
Rotational CARS measurements in a rotating cavity with axial throughflow of cooling air: Oxygen concentration measurements
[PNR-90935] p 244 N93-11035
ROTATING FLUIDS
Application of a two-layer near wall model to fully developed and rotating channel turbulent flows
[NASA-CR-184441] p 305 N93-12082
ROTATING SHAFTS
Optimal output feedback vibration control of rotor-bearing systems p 324 N93-11220
An experimental study of a small high speed LH2 rocket pump: Fundamental mechanical design
[NAL-TR-1123] p 330 N93-12463
ROTATING SPHERES
Hydrodynamic particle migration in small-amplitude, oscillatory, circular couette flow: The limits of reversibility
[DE92-008480] p 303 N93-11843
ROTATION
The prediction of convective heat transfer in rotating square ducts
[PNR-90929] p 296 N93-11025
ROTOR AERODYNAMICS
Recent advances in multidisciplinary optimization of rotorcraft
[NASA-TM-107665] p 206 N93-10968
ROTOR BLADES
Recent advances in multidisciplinary optimization of rotorcraft
[NASA-TM-107665] p 206 N93-10968
Numerical study of advanced rotor blades
p 199 N93-11899
ROTOR DYNAMICS
Recent advances in multidisciplinary optimization of rotorcraft
[NASA-TM-107665] p 206 N93-10968
Optimal output feedback vibration control of rotor-bearing systems p 324 N93-11220
Determination of loose spline coupling coefficients of rotor bearing systems in turbomachinery
p 327 N93-11887
ROTORCRAFT AIRCRAFT
Recent advances in multidisciplinary optimization of rotorcraft
[NASA-TM-107665] p 206 N93-10968
ROTORS
Experimental heat transfer results in turbine stators and rotors and a comparison with theory
[PNR-90945] p 210 N93-11055
System and method for cancelling expansion waves in a wave rotor
[NASA-CASE-LEW-15218-1] p 297 N93-11172
Optimal output feedback vibration control of rotor-bearing systems p 324 N93-11220
Stochastic sensitivity measure for mistuned high-performance turbines
[NASA-TM-105821] p 341 N93-12277
An improved numerical model for wave rotor design and analysis
[NASA-TM-105915] p 214 N93-12418
Investigation of hot streak migration and film cooling effects on heat transfer in rotor/stator interacting flows, report 1
[AD-A250688] p 471 N93-12490
ROUTES
Computing optimum routes across terrain using DAP
[RSRE-MEMO-4299] p 412 N93-11712
A genetic algorithm for search route planning
[AD-A254894] p 414 N93-12284
RUBIDIUM
Matter-wave interferometry with laser cooled atoms
[AD-A253999] p 316 N93-11737
RULES
Geometrical concepts about learning rules in networks with binary and ternary output functions
[REPT-92-020] p 411 N93-11592
RUN TIME (COMPUTERS)
An adaptive differencing scheme for elliptic flows
p 297 N93-11197
Dynamic programming on a ring of processors
p 410 N93-11479
RUNGE-KUTTA METHOD
Beam-loading stability in synchrotrons with a higher RF harmonic
[DE92-018982] p 443 N93-11510
RUNWAYS
Upgrade Precision Runway Monitor (PRM) Operational Test and Evaluation (OT/E) test plan
[DOT/FAA/CT-TN92/13] p 217 N93-11616
Automated extraction of aircraft runway patterns from radar imagery
[AD-A254258] p 218 N93-11751
RUPTURING
Pressure vessel burst test program
[AD-A253708] p 334 N93-11080

S

S MATRIX THEORY
Limitations of multiple feeds in a polarimetric-radar compact range
[DE92-017526] p 284 N93-12101
SACCADIC EYE MOVEMENTS
Coordinated action in 3-D space
[AD-A249830] p 387 N93-10994
SAFETY DEVICES
An autonomous vehicle: Constrained test and evaluation
[PB92-205608] p 325 N93-11427
SAFETY FACTORS
Studies of safety, infectivity, and immunogenicity of a new Temperature Sensitive (TS) 51-1 strain of S. typhi as a new live oral typhoid fever vaccine candidate
p 381 N93-11306
Recent lessons on the safety and effectiveness of malaria chemoprophylaxis in a non-immune population
p 381 N93-11307
Epidemiologic view of allergic diseases in North America: Implications for aerospace medicine
p 382 N93-11311
SAFETY MANAGEMENT
Introduction to the Rolls-Royce design process
[PNR-90939] p 210 N93-11039
Lightning threat warning system at the Tonopah Test Range
[DE92-040444] p 221 N93-11631
Radiological information management system (RadIMS)
[DE92-017221] p 480 N93-12495
SAGE SATELLITE
Ozone and temperature trends p 350 N93-11089
SAMARIUM
Optimization of film synthesized rare earth transition metal permanent magnet systems
[DE92-018726] p 432 N93-12116
SAMPLED DATA SYSTEMS
LV software support for supersonic flow analysis
[NASA-CR-190209] p 297 N93-11074
Self-tuning PI-PID regulators for stable systems with varying delay
[REPT-92-023] p 421 N93-11593
SAMPLING
A fast pipelined inner product unit
[REPT-92-025] p 411 N93-11594
Curve fitting and error modeling for the digitization process near the Nyquist rate
[DE92-018189] p 286 N93-12417
SANDS
Physical effects of vegetation on wind-blown sand in the coastal environments of Florida
[PB92-188424] p 354 N93-11702
SANDWICH STRUCTURES
Study of compression-loaded and impact-damaged structurally efficient graphite-thermoplastic trapezoidal-corrugation sandwich and semisandwich panels
[NASA-TP-3264] p 239 N93-11623
SAPPHIRE
High Temperature Superconductivity Space Experiment (HTSSE)
[AD-A253119] p 288 N93-11239
The adsorption of C60 and the co-adsorption of C60 and H2O on (alpha)-Al2O3 (1 -1 0 2)-(2x1)
[DE92-018002] p 465 N93-12093
SATELLITE ANTENNAS
Method of steering the gain of a multiple antenna global positioning system receiver
[AD-D015367] p 281 N93-11426
SATELLITE COMMUNICATION
SITE project. Phase 1: Continuous data bit-error-rate testing
[NASA-TP-3279] p 224 N93-11001
Space Communication Artificial Intelligence for Link Evaluation Terminal (SCAILET) p 395 N93-11940
All-digital multicarrier demodulators for on-board processing satellites in mobile communication systems
p 285 N93-12207
SATELLITE CONTROL
From pilot's associate to satellite controller's associate p 390 N93-11922
SATELLITE IMAGERY
An evidential reasoning approach to the classification of satellite images
[DLR-FB-91-29] p 342 N93-11140
Land use/land cover classification using digitally merged spot panchromatic and Landsat thematic mapper imagery
[PB92-188416] p 343 N93-11701
Oceanographic expert system: Potential for TESS(3) applications
[AD-A254908] p 374 N93-12288
Automatic cloud classification from multi-spectral satellite data
[AD-A255125] p 372 N93-12420
SATELLITE NETWORKS
Lessons drawn from 2 existing satellite networks: ARABSAT and EUTELSAT. Application to the Pacific basin projects
[REPT-921-440-101] p 282 N93-11591
All-digital multicarrier demodulators for on-board processing satellites in mobile communication systems
p 285 N93-12207
ISDN at NASA Lewis Research Center
[NASA-TM-105911] p 419 N93-12410
SATELLITE OBSERVATION
The early Earth Observing System reference handbook: Earth Science and Applications Division missions, 1990-1997
[NASA-TM-107963] p 343 N93-11663
Nimbus-7 Scanning Multichannel Microwave Radiometer (SMMR) PARM tape user's guide
[NASA-RP-1284] p 373 N93-11718
Proceedings of the National Weather Service Aviation Workshop: Postprint volume
[PB92-176148] p 369 N93-11803
Analysis of air and sea physical properties and surface fluxes using a combination of in situ and SEASAT data
p 365 N93-12182
ERS-1 user handbook
[ESA-SP-1148] p 344 N93-12280
SATELLITE ORBITS
Ephemeris calculation and orbit determination of geostationary satellites, using Taylor series integration
[SER-C-384] p 220 N93-11335
Orbital perturbations due to the albedo effect
[GKSS-91/E/59] p 220 N93-11348
SATELLITE PERTURBATION
Orbital perturbations due to the albedo effect
[GKSS-91/E/59] p 220 N93-11348
SATELLITE-BORNE INSTRUMENTS
The early Earth Observing System reference handbook: Earth Science and Applications Division missions, 1990-1997
[NASA-TM-107963] p 343 N93-11663
SAWTOOTH WAVEFORMS
Fast cooling phenomena with ice pellet injection in the JIPP T-IIU tokamak
[DE92-782105] p 454 N93-11834
SCALE EFFECT
Computation of small scale velocity turbulence and its effect on optical scintillations and stimulated thermal Rayleigh scattering
[DE92-018934] p 448 N93-11627
SCALE MODELS
Low-speed longitudinal and lateral-directional aerodynamic characteristics of the X-31 configuration
[NASA-TM-4351] p 198 N93-11622
Development of a 1/7-scale F/A-18 UAV for supermaneuverability research --- unmanned air vehicle
[AD-A247261] p 208 N93-12053
SCALING LAWS
Scaling of lower hybrid current drive with temperature
[DE92-018541] p 449 N93-10988
Current scaling of plasma focus devices
[IPF-90-1] p 449 N93-11029
Analytical and numerical principles for the scaling of plasma focus experiments, with regard to electrical resistance
[IPF-91-2] p 450 N93-11103
Scaling of gain with energy spread and energy in the PEP FEL
[DE92-019248] p 316 N93-11500
SCANNERS
Wind tunnel operator aimed comparison between two electronic pressure scanner systems
[DLAS-EST-TR-040] p 217 N93-11225
Photogrammetric point determination using digital imagery of three-line scanner systems
[SER-C-372] p 309 N93-11346
SCANNING
Introduction of electronic pressure scanning at the Royal Aerospace Establishment
[RAE-TM-AERO-2222] p 199 N93-11882
SCANNING ELECTRON MICROSCOPY
Effect of microstructure on passive film formation and breakdown on Al alloys
[AD-A245863] p 260 N93-12118
SCANNING TUNNELING MICROSCOPY
Atomic bonding at ceramic interfaces using scanning tunneling microscopy
[DE92-018706] p 273 N93-12479
SCATHA SATELLITE
The relationship between electrostatic discharges on spacecraft P78-2 and the electron environment
[AD-A255179] p 226 N93-12379

SCATTERING

Diffusion of Echo 7 electron beams during bounce motion
[DE92-018288] p 357 N93-10985

Study of seismic coda generation in crust with non-uniform scattering and anelastic properties
[AD-A254350] p 366 N93-12270

SCATTERING AMPLITUDE

Scattering of polarized electrons by oriented deuterons
[DE92-624834] p 440 N93-11914

SCATTERING CROSS SECTIONS

Ion temperature measurements in tokamak plasmas by *Rutherford scattering*
[PB92-184738] p 451 N93-11245

SCAVENGING

Time scales characterizing the processing of water and cloud condensation nuclei by clouds
[CM-80] p 368 N93-11340

SCENE ANALYSIS

Extraction of shape information from predicted irradiance profiles in infrared images
[RSRE-MEMO-4464] p 447 N93-11342

A comparison of feed-forward networks and maximum likelihood on a point-source location problem
[RSRE-MEMO-4567] p 281 N93-11391

SCHEDULES

A development approach for nuclear thermal propulsion
[DE92-018020] p 232 N93-11596

Methodologies for building robust schedules
p 397 N93-11949

Final Report, January 1991 - July 1992
[AD-A254659] p 483 N93-12244

SCHEDULING

Autonomous power system: Integrated scheduling
p 235 N93-11948

Methodologies for building robust schedules
p 397 N93-11949

COMPASS: An Ada based scheduler
p 397 N93-11950

SCHLIEREN PHOTOGRAPHY

Detonation reactions frozen by free expansion and analyzed by mass spectrometry
[DE92-018605] p 274 N93-11566

Measurement of the density distributions in quenched polycarbonate specimens by a quantitative Schlieren-optical technique p 270 N93-11989

Study of filamentation in subdense plasma interaction experiments p 318 N93-12026

SCINTILLATION

Computation of small scale velocity turbulence and its effect on optical scintillations and stimulated thermal Rayleigh scattering
[DE92-018934] p 448 N93-11627

Development of a scintillating optical fiber ionization calorimeter
[NASA-CR-184415] p 311 N93-11662

SCINTILLATION COUNTERS

Development of a geometry-compensated neutron time-of-flight detector for ICF applications with approximately 200 ps time response
[DE92-018024] p 450 N93-11153

SCREWS

A study of the effects of tolerances on rigging screws, turnbuckles, and associated components in BS4429: 1987
[NPL-DMM(A)-53] p 325 N93-11326

SCRUBBERS

Technology evaluation report of Retech, Inc., Plasma Centrifugal Furnace, volume 1
[PB92-216035] p 456 N93-12526

SEA LAUNCHING

Inflatable device for excluding sea water from a rocket motor
[AD-D015365] p 232 N93-11424

SEA SURFACE TEMPERATURE

Orthogonal functions over the oceans and applications to the determination of orbit error, geoid and sea surface topography from satellite altimetry p 373 N93-12002

Analysis of air and sea physical properties and surface fluxes using a combination of in situ and SEASAT data
p 365 N93-12182

Interannual variabilities of the East Asian summer monsoon and tropical sea surface temperatures
p 372 N93-12534

SEA WATER

Inflatable device for excluding sea water from a rocket motor
[AD-D015365] p 232 N93-11424

Evaluation of an analytical model for predicting light scattering from cylindrically-shaped objects in the ocean
[AD-A248414] p 447 N93-11489

Comparative effects of drag-reducing polymers. An experimental report
[AD-A254001] p 268 N93-11793

SEALERS

Sealant research for solid oxide fuel cells
[DE92-019044] p 345 N93-11513

SEALING

Sealing characteristics of a carbon segmented circumferential seal for a liquid oxygen turbopump
[NAL-TR-1130] p 329 N93-12364

SEALS (STOPPERS)

Relative sliding durability of candidate high temperature fiber seal materials
[NASA-TM-105806] p 236 N93-10978

Test program, helium II orbital resupply coupling
[NASA-CR-185681] p 326 N93-11650

Space Station Freedom seal leakage rate analysis and testing summary: Air leaks in ambient versus vacuum exit conditions
[NASA-TM-103604] p 328 N93-12149

SEAS

The design and implementation of radar clutter modelling and adaptive target detection techniques
p 283 N93-11913

SECONDARY FLOW

Increase of energy use on cooled high temperature turbine, phase 3
[MTUM-B91EW-0029-PHASE-3] p 213 N93-11339

Air ejector experiments using the two-dimensional supersonic cascade tunnel: Relationship between ejector performance and throat area ratio, part 1
[NAL-TM-642-PT-1] p 202 N93-12352

Effects of cooling-air injection on secondary flows and losses in a turbine cascade
[NAL-TR-1121T] p 307 N93-12382

Investigation of hot streak migration and film cooling effects on heat transfer in rotor/stator interacting flows, report 1
[AD-A250688] p 471 N93-12490

SECURITY

Authentication algorithm for the universal Authenticated Item Monitoring Systems (AIMS)
[DE92-018826] p 408 N93-11378

SEDIMENT TRANSPORT

The flux and recycling of bioactive substances in the surface sediments of the deep basins off southern California
[DE92-019172] p 373 N93-11734

SEDIMENTS

Quaternary volcanism, tectonics, and sedimentation in the Idaho National Engineering Laboratory area
[DE92-017851] p 362 N93-11692

The flux and recycling of bioactive substances in the surface sediments of the deep basins off southern California
[DE92-019172] p 373 N93-11734

SEEDS

A trainable image pattern classification system for detection of damaged soybean seeds
p 201 N93-12208

SEISMIC WAVES

Propagation of regional phases: Observations and theory
[AD-A246891] p 359 N93-11228

Modeling regional seismic waves
[AD-A246894] p 361 N93-11421

Application of the theory of wave propagation through random media to phase and amplitude fluctuations of seismic P-waves
[AD-A253274] p 363 N93-11788

Differential equation-based seismic data filtering
[DE92-016282] p 363 N93-11791

Physical characterization of magmatic liquids
[DE92-015931] p 363 N93-11848

Seismic wave propagation in thinly-layered media with steep reflectors
[DE92-015619] p 364 N93-12142

A dip-dependent divergence correction
[DE92-016283] p 366 N93-12308

Migration by the Kirchhoff, slant stack, and Gaussian beam methods
[DE92-018640] p 366 N93-12318

SEISMOGRAPHS

Propagation of regional phases: Observations and theory
[AD-A246891] p 359 N93-11228

SEISMOLOGY

Differential equation-based seismic data filtering
[DE92-016282] p 363 N93-11791

Real-time classification of signals from three-component seismic sensors using neural nets
[DE92-014886] p 364 N93-12155

Study of seismic coda generation in crust with non-uniform scattering and anelastic properties
[AD-A254350] p 366 N93-12270

A dip-dependent divergence correction
[DE92-016283] p 366 N93-12308

Migration by the Kirchhoff, slant stack, and Gaussian beam methods
[DE92-018640] p 366 N93-12318

SELECTIVE DISSEMINATION OF INFORMATION

Lies, damned lies, and databases
[RSRE-MEMO-4503-ISSUE-2] p 474 N93-11333

SELECTIVE SURFACES

On the definition and calculation of effective impedances and averaged boundary conditions with application to the analysis of high complexity frequency selective surfaces
[RSRE-MEMO-4518] p 281 N93-11387

SELENIUM

Experimental studies of x ray laser spectral profiles: *Observation of gain narrowing and saturation behavior*
[DE92-019603] p 316 N93-11659

SELF CONSISTENT FIELDS

Theoretical research program to study chemical reactions in AOTV bow shock tubes
[NASA-CR-188927] p 439 N93-11851

SEMANTICS

A formal definition of the static semantics of ELLA's core
[RSRE-91024] p 409 N93-11436

Selecting reusable components using algebraic specifications p 415 N93-12387

Neural network-based retrieval from software reuse repositories p 415 N93-12388

SEMICONDUCTING FILMS

Ion beams as a means of deposition and in-situ characterization of thin films and thin film layered structures
[DE92-016397] p 469 N93-12310

SEMICONDUCTOR DEVICES

Interfacial and thin film chemistry in electron device fabrication
[AD-A253579] p 288 N93-11257

An accurate and efficient method to calculate the rate of single event upsets from the LET spectrum and SEU cross section test results
[AD-A253917] p 290 N93-11492

Characteristics of current filamentation in high gain photoconductive semiconductor switching
[DE92-018277] p 291 N93-11693

Mesoscopic effects in electronic microstructures
[AD-A254889] p 295 N93-12502

SEMICONDUCTOR JUNCTIONS

Electron transfer rates at semiconductor/liquid interfaces
[DE92-018559] p 289 N93-11438

Recombination and metastability in amorphous silicon and silicon germanium alloys
[DE92-010593] p 463 N93-11816

Research on stable, high-efficiency, amorphous silicon multijunction modules
[DE92-010599] p 464 N93-11818

SEMICONDUCTOR LASERS

In-plane strain measurement on high speed rotating components using pulsed laser ESPI
[PNR-90975] p 315 N93-11064

Investigation of a cesium Raman time/frequency standard
[AD-A252677] p 310 N93-11562

Electronic transport and lasing in microstructures
[DE92-018725] p 441 N93-12115

SEMICONDUCTORS (MATERIALS)

Hydrodynamic fluctuations and light scattering in hot electron gas of semiconductors
[DE92-622800] p 458 N93-10992

INAS hole-immobilized doping superlattice long-wave-infrared detector
[NASA-CASE-NPO-17880-1-CU] p 458 N93-11056

Triisopropylindium: A new precursor for OMVPE growth
[AD-A250672] p 460 N93-11558

Magnetic properties and critical behavior of the conductivity near the M-I transition
[DE92-018948] p 461 N93-11629

Mechanical properties of semiconductors and their alloys
[AD-A253908] p 462 N93-11727

Basic principles of organometallic vapor phase epitaxy
[AD-A250665] p 464 N93-11868

Triisopropylindium: Decomposition study and use for low temperature growth
[AD-A250666] p 464 N93-11869

Excitons in semiconducting superlattices, quantum wells, and ternary alloys
[DE92-015178] p 464 N93-11894

Programme and abstracts. Workshop on Expert Evaluation and Control of Compound Semiconductor Materials and Technologies No. 1: (EXAMTEC 199)
[AD-A254023] p 292 N93-12071

Electronic transport and lasing in microstructures
[DE92-018725] p 441 N93-12115

Investigation of high efficiency monolithic multibandgap solar cells
[AD-A254326] p 348 N93-12144
Synthesis and characterization of novel aluminum-arsenic compounds 2. Crystal structures of (R2AlAs (SiMe3)2)2 (R = i-Bu, Me) and i-Bu2 (Cl)Al*As (SiMe3)3
[AD-A248001] p 467 N93-12175
Gas-surface interactions near dissociation threshold
[AD-A250205] p 252 N93-12254
Determination of Fe(sup 2+) and Fe(sup 3+) concentrations of semi-insulating InP:Fe
[DE92-017119] p 469 N93-12316

SENSITIVITY
Studies of safety, infectivity, and immunogenicity of a new Temperature Sensitive (TS) 51-1 strain of S. typhi as a new live oral typhoid fever vaccine candidate
p 381 N93-11306
Surface wind speed distributions
[AD-A253268] p 368 N93-11505
Initial laboratory evaluation of color video cameras
[DE92-018274] p 311 N93-11673
The sensitivity of the receiver coherence diameter and modulation transfer function to variations of a damp unstable atmosphere
[AD-A253269] p 363 N93-11785
Repeatable sensitivity of optical-time-domain-reflectometry-based strain measurement
[DE92-016910] p 338 N93-11792
Development of ultra-low noise, high sensitivity planar metal grating coupled AlGaAs/GaAs multiquantum well IR detectors for focal plane array staring IR sensor systems
[AD-A254697] p 468 N93-12228

SENSORS
Feasibility assessment of a transient sound sensor based on the silicon retina architecture
[AD-A252288] p 432 N93-10999
Shutter apparatus
[AD-D015350] p 309 N93-11049
Low cost humidity sensor
[PB92-205772] p 312 N93-11757
High-speed test station for solid-state imagers
[DE92-018990] p 312 N93-11822
A model-based reasoning approach to sensor placement for monitorability p 391 N93-11923
High temperature superconductor materials and applications
[NASA-CR-184426] p 470 N93-12396

SENSORY FEEDBACK
The development of system components to provide proprioceptive and tactile information to the human for future telepresence systems p 330 N93-11968

SENSORY PERCEPTION
Development of a tactile perceived attitude transducer
[AD-A253724] p 385 N93-11081
The OMPAT level 1 Neurophysiological Performance Assessment Battery: NPPAB
[AD-A254840] p 387 N93-12432

SEPARATED FLOW
An investigation of the effects of aft blowing on a 3.0 caliber tangent ogive body at high angles of attack
[NASA-CR-190934] p 200 N93-12004
Numerical investigations into the base drag of various wedges using the base flow model developed by Mauri Tanner
[REPT-B-36] p 202 N93-12414

SEQUENCING
Parallel genetic algorithms: Introduction and overview of current research
[REPT-92-015] p 418 N93-11181

SEROTONIN
Physiological analyses of the afferents controlling brain neurochemical systems
[AD-A253185] p 375 N93-11146

SERUMS
Correlation of serum alpha sub 1 antitrypsin with cigarette smoking and pulmonary function status in Greek pilots, for a ten year period p 384 N93-11318

SERVICE LIFE
Maximum life spiral bevel reduction design
[NASA-TM-105790] p 323 N93-10982
Results of advanced battery technology evaluations for electric vehicle applications
[DE92-018766] p 289 N93-11432
Long cycle life rechargeable lithium batteries
[NASA-CR-190937] p 291 N93-11604
Eddy current characterization of magnetic treatment of materials
[NASA-TM-104573] p 258 N93-11621
Thermal fracture service life analysis of a case bonded visco-elastic cylinder p 339 N93-12008
Verification of rain-flow reconstructions of a variable amplitude load history
[NASA-CR-189670] p 341 N93-12411

SERVICES
An investigation of ground access mode choice for departing passengers
[TT-9201] p 217 N93-11224

SERVOCONTROL
A VMEbus ultrasonic sensor controller for mapping and servo control in robotic systems
[DE92-013661] p 421 N93-12138

SET THEORY
Decomposition of balanced matrices. Part 5: Goggles
[AD-A247462] p 430 N93-12217

SHAFTS (MACHINE ELEMENTS)
Maximum life spiral bevel reduction design
[NASA-TM-105790] p 323 N93-10982
Payout tension control system for reel mounted cable
[AD-D015362] p 325 N93-11423
A consistent cracked bar vibration theory
p 339 N93-12000

SHALLOW WATER
The Wave Information Studies (WIS) wave model, version 2.0 (user's guide)
[AD-A254313] p 374 N93-12094

SHAPE FUNCTIONS
Performance of the h-p version of the finite element method with various elements
[AD-A250689] p 427 N93-11837

SHAPES
Disruption shape effects on the performance of enhanced tubes with the separation and reattachment mechanism
[DE92-016602] p 305 N93-12128

SHARP LEADING EDGES
Further buffeting tests in a cryogenic wind tunnel
[NASA-TM-107621] p 198 N93-11610

SHEAR CREEP
The time-dependent stress-optical behaviour of polycarbonate in the glass transition region
p 269 N93-11985

SHEAR FLOW
Quasigeostrophic vortices in zonal shear
p 358 N93-11226
Nonlinear evolution of resistive tearing mode instability with shear flow and viscosity
[DE92-012138] p 453 N93-11745

SHEAR LAYERS
Mixing regimes in a spatially confined, two-dimensional, supersonic shear layer
[AD-A254302] p 302 N93-11756
Numerical investigation of three-dimensionally evolving jets p 303 N93-11870
The structure and transport of the Brazil current between 27 deg and 36 deg south
[AD-A247635] p 374 N93-12247

SHEAR PROPERTIES
Studies of the 3 to 5 compounds in the megabar regime
[DE92-019517] p 461 N93-11646
Study of the behavior of titanium and ceramic fiber matrix composite alloy
[ETN-92-92087] p 240 N93-11708

SHEAR STRENGTH
An evaluation of the blind lap joint for the surface mount attachment of chip components
[DE92-017045] p 277 N93-12106
Shear joint capability versus bolt clearance
[NASA-TM-108378] p 342 N93-12419

SHEAR STRESS
An interlayer shear slip theory for composite laminates with nonrigid bonding p 237 N93-11229
Analytical method of calculating the thermoelastic constants of a multi-phase unidirectional composite
[NPL-DMM(A)-57] p 238 N93-11409
Contribution to the monocrystal behavior study during large plastic strains
[ECL-92-13] p 461 N93-11581
The peculiar rheo-optical behaviour of bisphenol-A-polycarbonate and polymethylmethacrylate
p 269 N93-11984
Turbulence structure and polymer drag reduction in adverse pressure gradient boundary layers
p 304 N93-12003
Drag on an oscillating rod in a non-Newtonian fluid
[DE92-014746] p 308 N93-12492

SHEARING
Some exact solutions of the equations of finite elasticity p 337 N93-11713

SHELL STABILITY
On the stability of confined shells under external pressure p 335 N93-11202

SHELL THEORY
Linear and geometrically nonlinear p-version three dimensional curved shell element for isotropic, generally orthotropic and laminated composite materials
p 339 N93-12194

SHELLS (STRUCTURAL FORMS)
Some remarks on shell element analysis with DYNA3D and NIKE3D
[DE92-018784] p 337 N93-11775

SHIPS
Dredging research program: Feasibility of a kinematic differential Global Positioning System
[AD-A248953] p 205 N93-11419
Mariners Weather Log, volume 36, number 2, Spring 1992
[PB92-204213] p 371 N93-12293
Results from a large-scale MHD propulsion experiment
[DE92-018177] p 456 N93-12416

SHOCK LAYERS
Increase of energy use on cooled high temperature turbine, phase 3
[MTUM-B91EW-0029-PHASE-3] p 213 N93-11339
Turbulence modeling in shock wave/turbulent boundary layer interactions
[NASA-CR-190933] p 301 N93-11606

SHOCK LOADS
Penetration mechanics of composites
[AD-A249230] p 240 N93-11835

SHOCK TUBES
Theoretical research program to study chemical reactions in AOTV bow shock tubes
[NASA-CR-188927] p 439 N93-11851

SHOCK WAVE INTERACTION
Increase of energy use on cooled high temperature turbine, phase 3
[MTUM-B91EW-0029-PHASE-3] p 213 N93-11339
Turbulence modeling in shock wave/turbulent boundary layer interactions
[NASA-CR-190933] p 301 N93-11606
Effects of sweep on the physics of unsteady shock-induced turbulent separated flows
[AD-A247035] p 198 N93-11742
Numerical simulation of a pressure gradient in a multilayer target: Temperature evolution
p 309 N93-12039

SHOCK WAVE PROPAGATION
Interpretation of experiments measuring the back face of thin aluminum strips by comparison with numerical simulations p 318 N93-12029
Shock waves induced by pulsed laser in confined interaction: Numerical simulation p 319 N93-12038

SHOCK WAVES
Effects of reacting flows with turbulence and shock waves on efficiency of scramjet combustors
p 235 N93-11133
Study of the dynamic degradation under the action of a shock wave induced by pulsed laser
p 319 N93-12037
Numerical simulation of a pressure gradient in a multilayer target: Temperature evolution
p 309 N93-12039
A preliminary study associated with the experimental measurement of the aero-optic characteristics of hypersonic configurations
[AD-A253792] p 200 N93-12063
The generalized Goursat-Riemann problem for plane waves in isotropic elastic solids p 340 N93-12199
Mach 4 testing of scramjet inlet models
[NAL-TR-1137] p 202 N93-12369
Stochastic models of wavefront propagation in random granular media
[AD-A255127] p 286 N93-12422

SHORT CIRCUITS
Transmission/reflection and short-circuit line methods for measuring permittivity and permeability
[PB92-205376] p 293 N93-12084

SHORT TAKEOFF AIRCRAFT
A wind tunnel investigation to determine buffet countermeasures for STOL aircraft alpha-sweep flight testing
[NAL-TR-1129] p 216 N93-12362

SHORT WAVE RADIATION
VUV and UV sources and spectroscopic applications
[AD-A247293] p 291 N93-11758

SHOT NOISE
Investigation of a cesium Raman time/frequency standard
[AD-A252677] p 310 N93-11562
Multiangle lidar performance in the presence of horizontal inhomogeneities in atmospheric extinction and scattering
[AD-A252882] p 371 N93-12167

SHOT PEENING
Development of the neutron diffraction technique for the determination of near surface residual stresses in critical gas turbine components
[PNR-90984] p 212 N93-11112

SIDELOBE REDUCTION
Real-time adaptive sidelobe canceller architectures and implementations
[AD-A254842] p 286 N93-12433
SIGNAL ANALYSIS
Time-frequency domain analysis of vibration signals for machinery diagnostics. 3: The present power spectral density
[OUEL-1911/92] p 337 N93-11707
SIGNAL ANALYZERS
Fiber optic delay line signal processors
[AD-A254691] p 448 N93-12227
SIGNAL DETECTION
Algorithms for sensor fusion: Decentralized Bayesian hypothesis testing with feedback, volume 1
[AD-A254633] p 414 N93-12242
Auditory perception
[AD-A255061] p 385 N93-12469
SIGNAL DETECTORS
Feasibility assessment of a transient sound sensor based on the silicon retina architecture
[AD-A252288] p 432 N93-10999
SIGNAL GENERATORS
Arbitrary waveform generator
[AD-D015346] p 280 N93-11354
SIGNAL PROCESSING
Short-range radar system
[AD-D015339] p 278 N93-11044
Non-linear data conversion system for dynamic range digital signal processing
[AD-D015347] p 278 N93-11047
A comparison of feed-forward networks and maximum likelihood on a point-source location problem
[RSRE-MEMO-4567] p 281 N93-11391
Stationary time series analysis using information and spectral analysis p 425 N93-11431
Real-time data compression using a FFT digital signal processor
[DE92-017744] p 477 N93-11770
New methods for nonlinear tracking and nonlinear chaotic signal processing
[AD-A254320] p 284 N93-12095
Transient Reduction Analysis using Neural Networks (TRANN)
[DE92-012150] p 421 N93-12153
Real-time classification of signals from three-component seismic sensors using neural nets
[DE92-014886] p 364 N93-12155
All-digital multicarrier demodulators for on-board processing satellites in mobile communication systems
p 285 N93-12207
Fiber optic delay line signal processors
[AD-A254691] p 448 N93-12227
Algorithms for sensor fusion: Decentralized Bayesian hypothesis testing with feedback, volume 1
[AD-A254633] p 414 N93-12242
Advanced one-dimensional optical strain measurement system, phase 4
[NASA-CR-190760] p 314 N93-12279
Real-time adaptive sidelobe canceller architectures and implementations
[AD-A254842] p 286 N93-12433
Digital signal processing
[AD-A254870] p 287 N93-12436
Laser Doppler experiments
[AD-A252883] p 287 N93-12461
Composite tasking for sensor arrays
[AD-A254997] p 287 N93-12512
SIGNAL TO NOISE RATIOS
Signal-to-noise assessment and measurement in spectroscopies with particular reference to Auger and x ray photoelectron spectroscopies
[NPL-DMM(A)-45] p 247 N93-11396
Investigation of a cesium Raman time/frequency standard
[AD-A252677] p 310 N93-11562
New methods for nonlinear tracking and nonlinear chaotic signal processing
[AD-A254320] p 284 N93-12095
Broadband EMP transient measurement preemphasis filter
[AD-A254414] p 284 N93-12160
Composite tasking for sensor arrays
[AD-A254997] p 287 N93-12512
SIGNATURE ANALYSIS
A wall interference assessment/correction system
[NASA-CR-190617] p 218 N93-11910
SIGNATURES
Laser Doppler experiments
[AD-A252883] p 287 N93-12461
SIGNS AND SYMPTOMS
Early markers of HIV infection and subclinical disease progression p 379 N93-11296
The screening of inhalant allergic diseases in the selection of candidates for aircraft piloting
p 382 N93-11312
Phadiatop: A screening test for inhalant allergy
p 383 N93-11313
Allergic and nonallergic rhinitis in Greek pilots
p 383 N93-11317
SILANES
Molecular mobility of the interface in a model composite: A NMR study
[AD-A253311] p 265 N93-11194
SILICON
The 1992 DOE/Sandia crystalline photovoltaic technology project review meeting
[DE92-018544] p 344 N93-10989
Development of stable metallization systems
[AD-A253569] p 264 N93-11079
Atomistic processes of surface segregation during Si-Ge MBE growth
[DE92-019180] p 459 N93-11496
Oxidation, nitridation, and fluorine etching of Si
[AD-A253559] p 249 N93-11755
Silicon on insulator structures in selective epitaxial growth
[DE92-017118] p 465 N93-11915
The role of backbond strain in silicon surfaces on the decomposition of NH3 and PH3
[AD-A253771] p 250 N93-12062
SILICON ALLOYS
Step-driven surface segregation and ordering during Si-Ge MBE growth
[DE92-017827] p 463 N93-11772
Recombination and metastability in amorphous silicon and silicon germanium alloys
[DE92-010593] p 463 N93-11816
Studies on the reactive melt infiltration of silicon and silicon-molybdenum alloys in porous carbon
[NASA-TM-105860] p 273 N93-12398
SILICON CARBIDES
Thermal residual stresses in silicon-carbide/titanium (0/90) laminate
[NASA-TM-107649] p 236 N93-11072
Thermomechanical fatigue behavior of SiC/Ti-24Al-11Nb in air and argon environments
[NASA-TM-105723] p 238 N93-11399
CVD of AlN and SiC using cyclic organometallic precursors
[AD-A246910] p 266 N93-11413
Silicon carbide fiber reinforced strontium aluminosilicate glass-ceramic matrix composite
[NASA-CASE-LEW-15263-1] p 239 N93-11543
Silicon carbide matrix composites
[REPT-921-430-103] p 239 N93-11588
Infiltration kinetics and interfacial bond strength of metal matrix composites
[AD-A254002] p 240 N93-11795
Research on stable, high-efficiency, amorphous silicon multijunction modules
[DE92-010599] p 464 N93-11818
Proceedings of the DOE/Advanced Heat Exchangers Program Review
[DE92-014385] p 305 N93-12070
Growth, characterization, and device development in monocrystalline diamond films
[AD-A252648] p 271 N93-12184
High temperature rectifiers and MOS devices in 6H-silicon carbide
[AD-A254725] p 295 N93-12340
Growth of solid solutions of aluminum nitride and silicon carbide by metalorganic chemical vapor deposition
[AD-A255000] p 254 N93-12518
SILICON COMPOUNDS
Oxidation, nitridation, and fluorine etching of Si
[AD-A253559] p 249 N93-11755
SILICON DIOXIDE
Preparation, optical and laser properties of Nd-doped sol-gel silica
[DE92-019378] p 461 N93-11602
SILICON NITRIDES
Development of stable metallization systems
[AD-A253569] p 264 N93-11079
The dressing of resin bonded diamond grinding wheels
[PNR-90965] p 264 N93-11086
Engine testing of ceramic cam-roller followers
[DE92-019188] p 268 N93-11735
The chemistry of Si3N4 and Si deposition studied using molecular beam techniques
[DE92-018268] p 463 N93-11797
Synthesis and reactivity of siloxide and silamide complexes pertaining to bond breaking and aggregation phenomena
[AD-A254703] p 468 N93-12231
Superplastic forming of ceramic insulation
p 228 N93-12452
SILICON OXIDES
Development of contractor cells, phase 1
[DE92-017343] p 348 N93-12222
Synthesis and reactivity of siloxide and silamide complexes pertaining to bond breaking and aggregation phenomena
[AD-A254703] p 468 N93-12231
SILICONES
An evaluation of field-flow fractionation for molecular weight characterization of polymeric materials
[DE92-019192] p 267 N93-11497
SILVER
Silver lined ceramic vessel and method of preparation
[AD-D015360] p 266 N93-11400
Study and characterization of ceramic-metal bonds manufactured by solid state bonding techniques. Application to Ag/Al2O3
[ECL-91-19] p 267 N93-11577
Influence of oxygen partial pressure and silver additions on microstructure and related properties of YBCO superconductors
[DE92-011145] p 468 N93-12249
SILVER COMPOUNDS
CO2 laser frequency doubling using AgGaSe2
[RSRE-MEMO-4528] p 315 N93-11388
SIMD (COMPUTERS)
Computing optimum routes across terrain using DAP
[RSRE-MEMO-4299] p 412 N93-11712
SIMPLEX METHOD
Polynomial dual network simplex algorithms
[AD-A254340] p 413 N93-12131
SIMULATION
Numerical investigation of three-dimensionally evolving jets p 303 N93-11870
A wall interference assessment/correction system
[NASA-CR-190617] p 218 N93-11910
The order n simulation of tether motions based on a rigid body tether model p 225 N93-11999
Advanced ceramic matrix composites for TPS
p 228 N93-12450
SIMULATORS
An analog macromodel of the SG1525A PWM for use with SPICE2G.6 simulators
[DE92-019423] p 291 N93-11639
Simulator, Tactical Use, Flare (STUF) project report
[AD-A254890] p 276 N93-12281
SINE WAVES
Extension of fresnel near-field region by single-cycle sinusoidal pulses
[AD-A254736] p 285 N93-12356
Numerical analysis of oscillating flow about a circular cylinder
[AD-A255164] p 307 N93-12406
SINGLE CHANNEL PER CARRIER TRANSMISSION
All-digital multicarrier demodulators for on-board processing satellites in mobile communication systems
p 285 N93-12207
SINGLE CRYSTALS
The synthesis and crystal structure of LaHSe2O6, a layered, anhydrous selenite
[AD-A251050] p 458 N93-10996
Present and future trends in turbine blade material and manufacture technology
[PNR-90960] p 255 N93-11111
CO2 laser frequency doubling using AgGaSe2
[RSRE-MEMO-4528] p 315 N93-11388
Contribution to the study of the anisotropic viscoelasticity of large strains: The case of the monocrystal
[ECL-90-29] p 460 N93-11573
Contribution to the monocrystal behavior study during large plastic strains
[ECL-92-13] p 461 N93-11581
Flux pinning in oxygen-depleted YBa2Cu3O(7-y) single crystals
[DE92-019548] p 461 N93-11647
Slow crack growth in vacuum p 338 N93-11909
Image potential states at metal-dielectric interfaces
[DE92-017019] p 466 N93-12124
Formation of buried epitaxial Si-Ge alloy layers in Si (100) crystal by high dose Ge ion implantation
[DE92-017114] p 466 N93-12127
Flux dynamics and irreversibility in YBa2Cu3O7 with Y2BaCuO5 inclusions and in single crystal YBa2Cu3O7
[DE92-009712] p 467 N93-12178
Growth, characterization, and device development in monocrystalline diamond films
[AD-A252648] p 271 N93-12184
Fatigue in single crystal nickel superalloys
[AD-A254603] p 260 N93-12237
Surface analysis of Ln(2-x)Ce(x)CuO4 (Ln = Pr and Nd) single crystals grown by the top seeded solution method
[AD-A254905] p 469 N93-12286
SINGLE EVENT UPSETS
An accurate and efficient method to calculate the rate of single event upsets from the LET spectrum and SEU cross section test results
[AD-A253917] p 290 N93-11492

SINGLE STAGE TO ORBIT VEHICLES
Rocket Based Combined Cycle (RBCC) Propulsion Technology Workshop. Volume 1: Executive summary [NASA-CR-184382] p 231 N93-11042
Rocket Based Combined Cycle (RBCC) Propulsion Workshop, volume 2 [NASA-CR-184383] p 231 N93-11043
On stability and control of SSTO spaceplane in super- and hypersonic ascending phase [NAL-TR-1128T] p 216 N93-12361
Air-breathing hypersonic vehicle guidance and control studies: An integrated trajectory/control analysis methodology, phase 2 [NASA-CR-189703] p 216 N93-12413
SINGULARITY (MATHEMATICS)
New singularity and existence of solutions in anisotropic, time-dependent, maximally Gauss-Bonnet extended gravity p 357 N93-11183
Singularities of the Euler equation and hydrodynamic stability [NASA-CR-189720] p 306 N93-12173
Spacetime singularities in string theory p 472 N93-12530
SINTERING
Microwave sintering of multilayer ceramic capacitors [DE92-018772] p 267 N93-11570
Nanophase ceramics [AD-A254661] p 272 N93-12246
Ceramic TBS/porous metal compliant layer p 228 N93-12453
SKIN (ANATOMY)
Occupational safety considerations with hydrazine fuels p 276 N93-11951
SKIRTS
Feasibility of using neutron radiography to inspect the Space Shuttle solid rocket booster aft skirt, forward skirt and frustum. Part 1: Summary report [NASA-CR-184357] p 231 N93-11173
SKY SURVEYS (ASTRONOMY)
Contributions to the Joint Discussion 3: Results from Rosat and GRO and Other Recent High Energy Astrophysics Missions of the Max-Planck-Institut fuer Extraterrestrische Physik [MPE-PREPRINT-215] p 482 N93-11473
Rosat deep surveys p 482 N93-11474
X ray morphology of clusters of galaxies p 482 N93-11475
Morphology and physics of supernova remnants p 482 N93-11476
Stars in the Rosat all-sky survey p 482 N93-11477
SLAGS
Basicity and optical basicities of slags [NPL-DMM(A)-48] p 447 N93-11408
SLENDER WINGS
Further buffeting tests in a cryogenic wind tunnel [NASA-TM-107621] p 198 N93-11610
SLEWING
Rapid maneuvering of large flexible orbiting systems p 225 N93-11885
SLIDING
Terminal slider control of nonlinear robotic systems [NASA-CASE-NPO-18584-1-CU] p 324 N93-11177
SLIDING FRICTION
Relative sliding durability of candidate high temperature fiber seal materials [NASA-TM-105806] p 236 N93-10978
Thermal non-Newtonian elastohydrodynamic lubrication of line contacts under sliding-rolling and simple sliding conditions p 324 N93-11263
Friction of self-lubricating surfaces by ion beam techniques [DE92-016069] p 328 N93-12122
SLIP
An interlayer shear slip theory for composite laminates with nonrigid bonding p 237 N93-11229
SLURRY PROPELLANTS
Metal slurry droplet and spray combustion p 245 N93-11138
SMOKE
Correlation of serum alpha sub 1 antitrypsin with cigarette smoking and pulmonary function status in Greek pilots, for a ten year period p 384 N93-11318
SOCIAL FACTORS
Neuropsychiatric morbidity in early HIV disease: Implications for military occupational function p 379 N93-11299
Communicable diseases: A major burden of morbidity and mortality p 380 N93-11300
SODIUM
Sodium-lidar mesosphere examinations: Selected elements of the experimental construction of a mobile instrument and evaluation of the data acquired with a stationary Na-lidar during the DYANA campaign [BONN-IR-91-78] p 357 N93-11006
Sodium reflux pool-boiler solar receiver on-sun test results [DE92-018932] p 347 N93-12012
SODIUM SULFUR BATTERIES
Results of advanced battery technology evaluations for electric vehicle applications [DE92-018766] p 289 N93-11432
SOFTWARE ENGINEERING
Intelligent TDA systems using neural networks, phase 1 [AD-A252556] p 420 N93-11000
LV software support for supersonic flow analysis [NASA-CR-190209] p 297 N93-11074
Optimized software for a generalized Polak-Ribiere algorithm in unconstrained optimization [MATHS-REPT-A-156] p 406 N93-11210
Software quality methodology integration study results [AD-A253891] p 408 N93-11371
The WEB approach to ELLA [RSRE-MEMO-4549] p 409 N93-11407
The use of statistical measures to validate system dynamics models [AD-A248569] p 428 N93-11417
The development and technology transfer of software engineering technology at NASA. Johnson Space Center p 396 N93-11943
System diagnostic builder p 396 N93-11944
An approach to integrating and creating flexible software environments p 396 N93-11946
COMPASS: An Ada based scheduler p 397 N93-11950
Program for implementing software quality metrics [DE92-018617] p 413 N93-12187
Current state and future direction of computer systems at NASA Langley Research Center [NASA-TM-107685] p 414 N93-12278
The SoRReL papers: Recent publications of the Software Reuse Repository Lab [NASA-CR-190894] p 414 N93-12384
A hybrid approach to software repository retrieval: Blending faceted classification and type signatures p 415 N93-12386
Neural network-based retrieval from software reuse repositories p 415 N93-12388
Supporting multiple domains in a single reuse repository p 415 N93-12390
Assessing repository technology: Where do we go from here? p 415 N93-12391
A neural net-based approach to software metrics p 415 N93-12392
Balancing generality and specificity in component-based reuse p 416 N93-12393
Cost estimation of software development and the implications for the program manager [AD-A255167] p 480 N93-12472
SOFTWARE REUSE
The SoRReL papers: Recent publications of the Software Reuse Repository Lab [NASA-CR-190894] p 414 N93-12384
Design of a lattice-based faceted classification system p 415 N93-12385
A hybrid approach to software repository retrieval: Blending faceted classification and type signatures p 415 N93-12386
Selecting reusable components using algebraic specifications p 415 N93-12387
Neural network-based retrieval from software reuse repositories p 415 N93-12388
Inheritance for software reuse: The good, the bad, and the ugly p 415 N93-12389
Supporting multiple domains in a single reuse repository p 415 N93-12390
Assessing repository technology: Where do we go from here? p 415 N93-12391
Balancing generality and specificity in component-based reuse p 416 N93-12393
SOFTWARE TOOLS
Deriving and manipulating module interfaces [AD-A253869] p 406 N93-11145
Managing data: From vision to reality [PB92-191212] p 474 N93-11215
Evaluation of a Cray performance tool using a large hydrodynamics code [DE92-013239] p 407 N93-11231
A process monitor for the transputer [RSRE-MEMO-4554] p 408 N93-11389
A front end implementation of the Pollyanna secure DBMS [RSRE-MEMO-4540] p 475 N93-11404
Ten15 developments to support parallelism [RSRE-MEMO-4545] p 409 N93-11406
The ESSE project: Supporting object-oriented database schema analysis and evolution: Overview [REPT-92-026] p 476 N93-11689
Hypertext functionality: A theoretical framework p 478 N93-11858
Distributed environmental control p 391 N93-11924
An embedded rule-based diagnostic expert system in Ada p 392 N93-11928
Intelligent diagnostics systems p 393 N93-11931
On the acquisition and representation of procedural knowledge p 394 N93-11937
System diagnostic builder p 396 N93-11944
COMPASS: An Ada based scheduler p 397 N93-11950
Manager's assistant systems for space system planning p 398 N93-11952
Habitat automation p 391 N93-11976
The SoRReL papers: Recent publications of the Software Reuse Repository Lab [NASA-CR-190894] p 414 N93-12384
Selecting reusable components using algebraic specifications p 415 N93-12387
Assessing repository technology: Where do we go from here? p 415 N93-12391
Balancing generality and specificity in component-based reuse p 416 N93-12393
SOHO MISSION
Final Report, January 1991 - July 1992 [AD-A254659] p 483 N93-12244
SOI (SEMICONDUCTORS)
Silicon on insulator structures in selective epitaxial growth [DE92-017118] p 465 N93-11915
Back-gate bias generator [AD-A255126] p 295 N93-12421
SOL-GEL PROCESSES
Preparation, optical and laser properties of Nd-doped sol-gel silica [DE92-019378] p 461 N93-11602
SOLAR ACTIVITY
The effects of magnetic storm phases on F-layer irregularities from auroral to equatorial latitudes [AD-A253905] p 361 N93-11282
Tori and chaos in a nonlinear dynamo model for solar activity [MPE-PREPRINT-218] p 488 N93-11351
Solar-geophysical data number 569, January 1992. Part 2: (Comprehensive reports). Data for July 1991 and miscellaneous [PB92-158898] p 488 N93-11738
SOLAR ARRAYS
Parameterization of solar cells [NASA-TM-105885] p 295 N93-12301
SOLAR CELLS
The 1992 DOE/Sandia crystalline photovoltaic technology project review meeting [DE92-018544] p 344 N93-10989
Admittance spectroscopy of copper indium diselenide/cadmium sulfide solar cells p 344 N93-11214
Evaluation tests for photovoltaic concentrator receiver sections and modules [DE92-017745] p 346 N93-11771
NEDO Solar Technology Subcommittee [DE92-526256] p 347 N93-11845
Investigation of high efficiency monolithic multibandgap solar cells [AD-A254326] p 348 N93-12144
Photovoltaic systems based on spectrally selective holographic concentrators, phase 1 [AD-A252811] p 348 N93-12166
Development of contractor cells, phase 1 [DE92-017343] p 348 N93-12222
Parameterization of solar cells [NASA-TM-105885] p 295 N93-12301
SOLAR COLLECTORS
The 1992 DOE/Sandia crystalline photovoltaic technology project review meeting [DE92-018544] p 344 N93-10989
Evaluation tests for photovoltaic concentrator receiver sections and modules [DE92-017745] p 346 N93-11771
Participation in multilateral effort to develop high performance integrated CPC evacuated collectors [DE92-015946] p 346 N93-11823
NEDO Solar Technology Subcommittee [DE92-526256] p 347 N93-11845
Sodium reflux pool-boiler solar receiver on-sun test results [DE92-018932] p 347 N93-12012
Mirror alignment techniques for point-focus solar concentrators [DE92-019643] p 348 N93-12074
Reliability analysis of a utility-scale solar power plant [DE92-016550] p 348 N93-12312
SOLAR CORONA
Plasma properties of solar coronal active regions p 489 N93-12342

The semiannual variation of great geomagnetic storms and the postshock Russell-McPherron effect preceding coronal mass ejecta
[AD-A254955] p 489 N93-12506

SOLAR ELECTRIC PROPULSION
The 10 kW power electronics for hydrogen arcjets
[NASA-TM-105614] p 235 N93-12484

SOLAR ENERGY
NEDO Solar Technology Subcommittee
[DE92-526256] p 347 N93-11845

SOLAR ENERGY CONVERSION
Participation in multilateral effort to develop high performance integrated CPC evacuated collectors
[DE92-015946] p 346 N93-11823
Sodium reflux pool-boiler solar receiver on-sun test results
[DE92-018932] p 347 N93-12012
Photovoltaic systems based on spectrally selective holographic concentrators, phase 1
[AD-A252811] p 348 N93-12166
Reliability analysis of a utility-scale solar power plant
[DE92-016550] p 348 N93-12312

SOLAR FLARES
Solar-geophysical data number 569, January 1992. Part 2: (Comprehensive reports). Data for July 1991 and miscellaneous
[PB92-158898] p 488 N93-11738
Diagnostics of electron-heated solar flares
p 488 N93-11877

SOLAR FLUX
Lunar and Martian environmental interactions with nuclear power system radiators
[NASA-TM-105747] p 230 N93-10965

SOLAR GENERATORS
NEDO Solar Technology Subcommittee
[DE92-526256] p 347 N93-11845
Reliability analysis of a utility-scale solar power plant
[DE92-016550] p 348 N93-12312

SOLAR HEATING
NEDO Solar Technology Subcommittee
[DE92-526256] p 347 N93-11845
Sodium reflux pool-boiler solar receiver on-sun test results
[DE92-018932] p 347 N93-12012

SOLAR MAGNETIC FIELD
Tori and chaos in a nonlinear dynamo model for solar activity
[MPE-PREPRINT-218] p 488 N93-11351

SOLAR NEUTRINOS
A Polytropic solar model p 487 N93-11264

SOLAR PHYSICS
Solar-geophysical data number 569, January 1992. Part 2: (Comprehensive reports). Data for July 1991 and miscellaneous
[PB92-158898] p 488 N93-11738

SOLAR RADIATION
Ultraviolet radiation changes p 352 N93-11098
Atlas of albedo and absorbed solar radiation derived from Nimbus 7 earth radiation budget data set, November 1985 to October 1987
[NASA-RP-1281] p 367 N93-11168
Detection of cloud-top height from backscattered radiances within the oxygen A band. Part 1: Theoretical study
[GKSS-91/E/76-PT-1] p 368 N93-11349
Detection of cloud-top height from backscattered radiances within the oxygen A band. Part 2: Measurements
[GKSS-91/E/77-PT-2] p 368 N93-11350
Global change and the dark of the moon
[AD-A255181] p 486 N93-12380

SOLAR RADIO BURSTS
Solar-geophysical data number 569, January 1992. Part 2: (Comprehensive reports). Data for July 1991 and miscellaneous
[PB92-158898] p 488 N93-11738

SOLAR SPECTRA
Photovoltaic systems based on spectrally selective holographic concentrators, phase 1
[AD-A252811] p 348 N93-12166

SOLAR SYSTEM
Modeling the Jovian aurora
[NASA-CR-190696] p 486 N93-11164

SOLAR TERRESTRIAL INTERACTIONS
Flank solar wind interaction
[NASA-CR-189285] p 489 N93-12303
The semiannual variation of great geomagnetic storms and the postshock Russell-McPherron effect preceding coronal mass ejecta
[AD-A254955] p 489 N93-12506

SOLAR THERMAL PROPULSION
Evaluation of transportation systems for advanced space flight missions
[ESA-TT-1256] p 223 N93-11685

SOLAR WIND
Statistics of IMF B(z) events
[DE92-018372] p 488 N93-11696
Flank solar wind interaction
[NASA-CR-189285] p 489 N93-12303

SOLAR X-RAYS
Solar-geophysical data number 569, January 1992. Part 2: (Comprehensive reports). Data for July 1991 and miscellaneous
[PB92-158898] p 488 N93-11738

SOLDERED JOINTS
Robust solder joint attachment of coaxial cable leads to piezoelectric ceramic electrodes
[DE92-017042] p 276 N93-11494
An evaluation of the blind lap joint for the surface mount attachment of chip components
[DE92-017045] p 277 N93-12106

SOLDERING
Robust solder joint attachment of coaxial cable leads to piezoelectric ceramic electrodes
[DE92-017042] p 276 N93-11494
An evaluation of the blind lap joint for the surface mount attachment of chip components
[DE92-017045] p 277 N93-12106

SOLDERS
An evaluation of the blind lap joint for the surface mount attachment of chip components
[DE92-017045] p 277 N93-12106

SOLENOIDS
Stress dependence of the magnetic properties of steels
[DE92-018804] p 261 N93-12261

SOLID ELECTROLYTES
Intermediate temperature electrolytes for SOFC
[DE92-018786] p 345 N93-11571

SOLID LUBRICANTS
Friction of self-lubricating surfaces by ion beam techniques
[DE92-016069] p 328 N93-12122

SOLID PHASES
Synthesis of single phase (alpha)-Fe, Fe3C and Fe7C3 nano-particles by CO2 laser pyrolysis technique
[DE92-015654] p 250 N93-11847
Formation of buried epitaxial Si-Ge alloy layers in Si (100) crystal by high dose Ge ion implantation
[DE92-017114] p 466 N93-12127

SOLID PROPELLANT COMBUSTION
The effects of bypass air on boron carbide combustion in a solid fuel ramjet p 245 N93-11136
The twenty-third International Symposium on combustion
[AD-A250377] p 250 N93-11866

SOLID PROPELLANT ROCKET ENGINES
Inflatable device for excluding sea water from a rocket motor
[AD-D015365] p 232 N93-11424

SOLID ROCKET BINDERS
A preliminary investigation of the degradation and stabilisation of the energetic oxetane binder polyNIMMO
[RARDE-7/91] p 273 N93-11376

SOLID ROCKET PROPELLANTS
The 28th JANNAF Combustion Subcommittee Meeting, volume 2
[CPIA-PUBL-573-VOL-2] p 247 N93-11448
Soviet chemical propellant research and development
[PB92-195577] p 275 N93-12147

SOLID SOLUTIONS
Nature of the beta-phase of nickel-aluminum system
[AD-A254101] p 261 N93-12269
Growth of solid solutions of aluminum nitride and silicon carbide by metalorganic chemical vapor deposition
[AD-A255000] p 254 N93-12518

SOLID STATE
Study and characterization of ceramic-metal bonds manufactured by solid state bonding techniques. Application to Ag/Al2O3
[ECL-91-19] p 267 N93-11577

SOLID STATE DEVICES
High-speed test station for solid-state imagers
[DE92-018990] p 312 N93-11822

SOLID STATE PHYSICS
Materials science and engineering at the Naval Research Laboratory: Research programs and 1990 publications
[PB92-199488] p 238 N93-11422
Solid state sciences committee forum
[AD-A253556] p 463 N93-11753

SOLID SURFACES
Drag on an oscillating rod in a non-Newtonian fluid
[DE92-014746] p 308 N93-12492
Application of spin-sensitive electron spectroscopies to investigations of electronic and magnetic properties of solid surfaces and epitaxial systems
[DE92-018597] p 470 N93-12499

SOLID WASTES
Technology evaluation report of Retech, Inc., Plasma Centrifugal Furnace, volume 2
[PB92-216043] p 457 N93-12527

SOLID-SOLID INTERFACES
Study and characterization of ceramic-metal bonds manufactured by solid state bonding techniques. Application to Ag/Al2O3
[ECL-91-19] p 267 N93-11577
Polyethylene-terephthalate/aluminum adhesion
[ECL-91-33] p 257 N93-11578
Study of metal-ceramic interfaces of Co-Cr-Mo alloys: Role of tungsten (W) and manganese (Mn) additions
[ECL-92-01] p 267 N93-11580
Infiltration kinetics and interfacial bond strength of metal matrix composites
[AD-A254002] p 240 N93-11795

SOLIDIFICATION
Atomistic processes of surface segregation during Si-Ge MBE growth
[DE92-019180] p 459 N93-11496
The physics of pattern formation at liquid interfaces
[DE92-016971] p 462 N93-11747

SOLIDS
Sealant research for solid oxide fuel cells
[DE92-019044] p 345 N93-11513
Energetics solids degradation in high temperature water
[AD-A254900] p 276 N93-12285

SOLITARY WAVES
The Third Potsdam-5 Kiev International Workshop on Nonlinear Processes in Physics
[AD-A249140] p 430 N93-11420
The Peierls ground state, solitons and polarons in ring-containing polymers
[AD-A254914] p 272 N93-12289

SOLUBILITY
Basicity and optical basicities of slags
[NPL-DMM(A)-48] p 447 N93-11408

SONIC BOOMS
Laboratory study of effects of sonic boom shaping on subjective loudness and acceptability
[NASA-TP-3269] p 434 N93-11620
A general introduction to aeroacoustics and atmospheric sound
[NASA-CR-189717] p 435 N93-12021

SONOBUOYS
Embedded training capabilities for the LAMPS MK 3 system
[AD-A250697] p 207 N93-11838
Translating wedge heat sink
[AD-D015357] p 293 N93-12133

SOOT
Simplified modelling of soot inception and growth
[ETN-92-92266] p 246 N93-11361

SOUND FIELDS
Wavefront reconstruction using a least squares approach
[ISVR-TR-203] p 435 N93-12324

SOUND GENERATORS
Arbitrary waveform generator
[AD-D015346] p 280 N93-11354
Dynamics and response of polymer-coated acoustic devices
[DE92-014289] p 433 N93-11523

SOUND LOCALIZATION
Super auditory localization for improved human-machine interfaces
[AD-A254699] p 389 N93-12229

SOUND PRESSURE
Acoustic fill factors for a 120 inch diameter fairing
[NASA-CR-189284] p 434 N93-11634
Near-field and far-field sound radiation from a line-driven fluid-loaded infinite flat plate having periodic and non-periodic attached rib stiffeners p 434 N93-11884
Wavefront reconstruction using a least squares approach
[ISVR-TR-203] p 435 N93-12324
Study of sound propagation in a wedge-shaped ocean and comparison with other methods
[AD-A255165] p 435 N93-12471

SOUND PROPAGATION
Sound propagation over rigid porous layers
p 432 N93-11179
A general introduction to aeroacoustics and atmospheric sound
[NASA-CR-189717] p 435 N93-12021
Study of sound propagation in a wedge-shaped ocean and comparison with other methods
[AD-A255165] p 435 N93-12471

SOUND TRANSMISSION
Study of sound propagation in a wedge-shaped ocean and comparison with other methods
[AD-A255165] p 435 N93-12471

SOUND WAVES

Numerical study for the study of medium speed internal noise problems
[DILC-EST-TN-200] p 432 N93-11156

Sound propagation over rigid porous layers
p 432 N93-11179

Near-field and far-field sound radiation from a line-driven fluid-loaded infinite flat plate having periodic and non-periodic attached rib stiffeners p 434 N93-11884

Interaction of sound with sound by novel mechanisms: Ultrasonic four-wave mixing mediated by a suspension and ultrasonic three-wave mixing at a free surface
[AD-A254657] p 435 N93-12097

Method and apparatus for evaluating multilayer objects for imperfections
[NASA-CASE-LAR-14581-1-SB] p 333 N93-12204

Wavefront reconstruction using a least squares approach
[ISVR-TR-203] p 435 N93-12324

SOVIET SPACECRAFT

JPRS report: Science and technology. Central Eurasia: Space. Development of Soviet spacecraft for manned missions
[JPRS-USP-92-003] p 224 N93-11162

SOYBEANS

A trainable image pattern classification system for detection of damaged soybean seeds
p 201 N93-12208

SPACE CHARGE

Analysis of the prebuncher for the KEK 40-MeV proton linac
[DE92-514988] p 444 N93-11525

On some practical consideration of the electron beam breakup transit time oscillator
[DE92-017406] p 445 N93-11919

Divergence in intense ion beams caused by incomplete charge neutralization
[DE92-016891] p 445 N93-12103

Atomic bonding at ceramic interfaces using scanning tunneling microscopy
[DE92-018706] p 273 N93-12479

SPACE COLONIES

Habitat automation p 391 N93-11976

SPACE COMMERCIALIZATION

The Space Station Freedom and space launch issues
[S-HRG-102-762] p 225 N93-11908

SPACE DEBRIS

Contributions to CD Space Committee, 1991: Summary and analysis
[PB92-195312] p 219 N93-11216

Compositional analysis and classification of projectile residues in LDEF impact craters
[NASA-TM-104750] p 488 N93-11374

Dynamics of space debris p 219 N93-11904

SPACE ENVIRONMENT SIMULATION

KC-135 materials handling robotics
[NASA-CR-184430] p 328 N93-11992

SPACE ERECTABLE STRUCTURES

Tests of an alternate mobile transporter and extravehicular activity assembly procedure for the Space Station Freedom truss
[NASA-TP-3245] p 224 N93-10970

SPACE EXPLORATION

The search for life's origins: Progress and future directions in planetary biology and chemical evolution
[NASA-CR-190929] p 487 N93-11603

The first meeting of the Advisory Committee on the Future of the US Space Program (C-FUSSP)
[NASA-CR-190995] p 219 N93-11754

Remote systems development p 330 N93-11971

Effect of inert propellant injection on Mars ascent vehicle performance
[NASA-CR-189238] p 226 N93-12152

Nuclear thermal propulsion transportation systems for lunar/Mars exploration
[NASA-TM-105870] p 233 N93-12363

SPACE FLIGHT STRESS

Space flight and immune system p 376 N93-11284

SPACE HABITATS

Manned Mars System Study (MMSS): Mars transportation and facility infrastructure study. Volume 2: Technical report
[NASA-CR-184474] p 227 N93-12443

SPACE HEATING (BUILDINGS)

Low cost humidity sensor
[PB92-205772] p 312 N93-11757

SPACE LOGISTICS

Habitat automation p 391 N93-11976

Automated resupply of consumables: Enhancement of space commercialization opportunities
p 403 N93-11980

SPACE MAINTENANCE

Performance experiments with alternative advanced teleoperator control modes for a simulated solar maximum satellite repair p 400 N93-11965

Decision rules for spaceborne operations planning
p 403 N93-11978

Automatic system for installation and replacement of Space Station components
[NASA-CASE-LEW-14906-1] p 329 N93-12203

SPACE MISSIONS

The early Earth Observing System reference handbook: Earth Science and Applications Division missions, 1990-1997
[NASA-TM-107963] p 343 N93-11663

The development and technology transfer of software engineering technology at NASA. Johnson Space Center
p 396 N93-11943

Design of small Stirling dynamic isotope power system for robotic space missions
[NASA-TM-105919] p 275 N93-12085

Manned Mars System Study (MMSS): Mars transportation and facility infrastructure study. Volume 2: Technical report
[NASA-CR-184474] p 227 N93-12443

SPACE PLASMAS

Studies of interactive plasma processes in the polar cusp
[NASA-CR-190892] p 357 N93-10964

Plasma properties
[DE92-018635] p 455 N93-12188

SPACE POWER REACTORS

Lunar and Martian environmental interactions with nuclear power system radiators
[NASA-TM-105747] p 230 N93-10965

Ground test facilities for evaluating nuclear thermal propulsion engines and fuel elements
[DE92-017039] p 231 N93-10973

Ground test facility for SEI nuclear rocket engines
[DE92-017418] p 217 N93-11367

The NASA CSTI high capacity power project
[NASA-TM-105813] p 221 N93-11398

A gas-cooled cermet reactor system for planetary base power
[DE92-018017] p 443 N93-11433

A development approach for nuclear thermal propulsion
[DE92-018020] p 232 N93-11596

Nuclear fuels for very high temperature applications
[DE92-018021] p 446 N93-12129

SPACE PROBES

Spacecraft flight control system design selection process for a geostationary communication satellite
[NASA-TP-3289] p 222 N93-11002

SPACE PROCESSING

Materials processing in low gravity
[NASA-CR-184421] p 276 N93-12401

SPACE PROGRAMS

The first meeting of the Advisory Committee on the Future of the US Space Program (C-FUSSP)
[NASA-CR-190995] p 219 N93-11754

SPACE SHUTTLE BOOSTERS

Feasibility of using neutron radiography to inspect the Space Shuttle solid rocket booster aft skirt, forward skirt and frustum. Part 1: Summary report
[NASA-CR-184357] p 231 N93-11173

SPACE SHUTTLE MAIN ENGINE

CFD modeling of turbulent flows around the SSME main injector assembly using porosity formulation
[NASA-CR-184359] p 297 N93-11171

Implementation of a model based fault detection and diagnosis for actuation faults of the Space Shuttle main engine
[NASA-TM-105781] p 221 N93-11401

A comparison of high cycle fatigue methodologies
[NASA-TM-103601] p 233 N93-12148

SPACE SHUTTLE MISSIONS

Fifth Annual Workshop on Space Operations Applications and Research (SOAR 1991), volume 1
[NASA-CP-3127-VOL-1] p 391 N93-11921

SPACE SHUTTLE ORBITERS

Reusable thermal protection system development: A prospective p 227 N93-12448

Thermal protection systems manned spacecraft flight experience p 227 N93-12449

Predicted and tested performance of durable TPS
p 228 N93-12454

SPACE SHUTTLES

Role of automation in the ACRV operations
p 230 N93-11977

Current Technology for Thermal Protection Systems
[NASA-CP-3157] p 227 N93-12447

SPACE SIMULATORS

Analysis of materials from MSFC LDEF experiments
[NASA-CR-184425] p 252 N93-12215

SPACE STATION FREEDOM

Tests of an alternate mobile transporter and extravehicular activity assembly procedure for the Space Station Freedom truss
[NASA-TP-3245] p 224 N93-10970

Description of the SSF PMAD DC testbed control system data acquisition function
[NASA-TM-105843] p 417 N93-11005

The Space Station Freedom and space launch issues
[S-HRG-102-762] p 225 N93-11908

Fifth Annual Workshop on Space Operations Applications and Research (SOAR 1991), volume 1
[NASA-CP-3127-VOL-1] p 391 N93-11921

A state-based approach to trend recognition and failure prediction for the Space Station Freedom
p 230 N93-11925

Intelligent fault management for the Space Station active thermal control system p 391 N93-11930

Space Station robotics planning tools
p 331 N93-11975

Role of automation in the ACRV operations
p 230 N93-11977

Decision rules for spaceborne operations planning
p 403 N93-11978

Space Station Freedom seal leakage rate analysis and testing summary: Air leaks in ambient versus vacuum exit conditions
[NASA-TM-103604] p 328 N93-12149

SPACE STATION POWER SUPPLIES

Description of the SSF PMAD DC testbed control system data acquisition function
[NASA-TM-105843] p 417 N93-11005

SPACE STATIONS

Preliminary characterization of a water vaporizer for resistojet applications
[NASA-TM-105877] p 231 N93-11402

Automatic system for installation and replacement of Space Station components
[NASA-CASE-LEW-14906-1] p 329 N93-12203

Space Station communications and tracking systems modeling and RF link simulation
[NASA-CR-185684] p 288 N93-12519

SPACE TECHNOLOGY EXPERIMENTS

Contributions to CD Space Committee, 1991: Summary and analysis
[PB92-195312] p 219 N93-11216

SPACE TRANSPORTATION

The Space Station Freedom and space launch issues
[S-HRG-102-762] p 225 N93-11908

Manned Mars System Study (MMSS): Mars transportation and facility study. Volume 1: Executive Summary
[NASA-CR-184473] p 227 N93-12442

Manned Mars System Study (MMSS): Mars transportation and facility infrastructure study. Volume 2: Technical report
[NASA-CR-184474] p 227 N93-12443

SPACE TRANSPORTATION SYSTEM

Development trends in space transportation systems: From Hermes to Saenger
[MBB-UK-0146-91-PUB] p 223 N93-11007

Nuclear thermal propulsion transportation systems for lunar/Mars exploration
[NASA-TM-105870] p 233 N93-12363

Space transportation booster engine configuration study. Volume 2: Design definition document and environmental analysis
[NASA-CR-184459] p 234 N93-12441

Predicted and tested performance of durable TPS
p 228 N93-12454

Space transportation booster engine configuration study. Volume 1: Executive Summary
[NASA-CR-184457] p 235 N93-12523

SPACE TRANSPORTATION SYSTEM FLIGHTS

Debris/ice/TPS assessment and integrated photographic analysis for Shuttle Mission STS-46
[NASA-TM-107552] p 223 N93-12151

SPACE-TIME FUNCTIONS

New singularity and existence of solutions in anisotropic, time-dependent, maximally Gauss-Bonnet extended gravity p 357 N93-11183

On an origin of numerical diffusion: Violation of invariance under space-time inversion
[NASA-TM-105776] p 425 N93-11254

Spacetime singularities in string theory
p 472 N93-12530

SPACEBORNE ASTRONOMY

Contributions to the Joint Discussion 3: Results from Rosat and GRO and Other Recent High Energy Astrophysics Missions of the Max-Planck-Institut fuer Extraterrestrische Physik
[MPE-PREPRINT-215] p 482 N93-11473

Rosat deep surveys p 482 N93-11474

Stars in the Rosat all-sky survey p 482 N93-11477

SPACEBORNE EXPERIMENTS

Small experiments for the maturation of orbital cryogenic transfer technologies
[NASA-TM-105849] p 296 N93-10981

Computer simulation and experimental investigation of the absorption cell for the rocketborne diode-laser experiment MASERATI [BONN-IR-91-62] p 357 N93-11083
Residual acceleration data on IML-1: Development of a data reduction and dissemination plan [NASA-CR-190807] p 223 N93-11101
High Temperature Superconductivity Space Experiment (HTSSE) [AD-A253119] p 288 N93-11239
A model to estimate the flux of background particles expected to accumulate on the collector foils of the interstellar gas experiment on the long duration exposure facility spacecraft [AD-A254265] p 489 N93-11815
Controls Astrophysics and Structures Experiment in Space (CASES) advanced studies and planning [NASA-CR-184410] p 220 N93-12213

SPACECRAFT CHARGING
Beam-plasma interactions and radiation generation during the ejection of electron and ion beams in space [AD-A253993] p 224 N93-11736
Design and evaluation of ion source for satellite charge control [AD-A255172] p 227 N93-12408

SPACECRAFT COMMUNICATION
Space Station communications and tracking systems modeling and RF link simulation [NASA-CR-185684] p 288 N93-12519

SPACECRAFT COMPONENTS
Shear joint capability versus bolt clearance [NASA-TM-108378] p 342 N93-12419

SPACECRAFT CONFIGURATIONS
Manned Mars System Study (MMSS): Mars transportation and facility study. Volume 1: Executive Summary [NASA-CR-184473] p 227 N93-12442
Manned Mars System Study (MMSS): Mars transportation and facility infrastructure study. Volume 2: Technical report [NASA-CR-184474] p 227 N93-12443

SPACECRAFT CONSTRUCTION MATERIALS
Erosion mechanisms in ceramic structures [MBB-UK-0171-92-PUB] p 263 N93-11011
Thermal protection using very high temperature ceramics p 228 N93-12451
Predicted and tested performance of durable TPS p 228 N93-12454
Recent advances in carbon-carbon substrate technology at NASA. Langley Research Center p 228 N93-12455

SPACECRAFT CONTROL
Spacecraft flight control system design selection process for a geostationary communication satellite [NASA-TP-3289] p 222 N93-11002
Rapid maneuvering of large flexible orbiting systems p 225 N93-11885
A state-based approach to trend recognition and failure prediction for the Space Station Freedom p 230 N93-11925
Requirements and opportunities for satellite autonomy p 230 N93-11926
Spacecraft attitude control using a smart control system p 230 N93-11932
Interactive collision detection p 400 N93-11963
Space Station robotics planning tools p 331 N93-11975
Design and evaluation of ion source for satellite charge control [AD-A255172] p 227 N93-12408
Air-breathing hypersonic vehicle guidance and control studies: An integrated trajectory/control analysis methodology, phase 2 [NASA-CR-189703] p 216 N93-12413

SPACECRAFT DESIGN
JPRS report: Science and technology. Central Eurasia: Space. Development of Soviet spacecraft for manned missions [JPRS-USP-92-003] p 224 N93-11162
Requirements and applications for robotic servicing of military space systems p 230 N93-11953
Air-breathing hypersonic vehicle guidance and control studies: An integrated trajectory/control analysis methodology, phase 2 [NASA-CR-189703] p 216 N93-12413
Shear joint capability versus bolt clearance [NASA-TM-108378] p 342 N93-12419
Predicted and tested performance of durable TPS p 228 N93-12454
Space transportation booster engine configuration study. Volume 1: Executive Summary [NASA-CR-184457] p 235 N93-12523

SPACECRAFT DOCKING
Autoguidance video sensor for docking p 230 N93-11954

SPACECRAFT GUIDANCE
Autoguidance video sensor for docking p 230 N93-11954
Air-breathing hypersonic vehicle guidance and control studies: An integrated trajectory/control analysis methodology, phase 2 [NASA-CR-189703] p 216 N93-12413

SPACECRAFT INSTRUMENTS
Development and use of data analysis procedures for the CRRES payloads AFGL-701-2/Dosimeter and AFGL-701-4/Fluxmeter and application of the data analysis results to improve the static and dynamic models of the Earth's radiation belts [AD-A253287] p 363 N93-11810
Controls Astrophysics and Structures Experiment in Space (CASES) advanced studies and planning [NASA-CR-184410] p 220 N93-12213
The extremely low frequency wave analyzer [AD-A255178] p 366 N93-12378

SPACECRAFT LAUNCHING
The Space Station Freedom and space launch issues [S-HRG-102-762] p 225 N93-11908
Debris/ice/TPS assessment and integrated photographic analysis for Shuttle Mission STS-46 [NASA-TM-107552] p 223 N93-12151
Weather impacts on space operations [AD-A253720] p 371 N93-12170
Advanced two-phase heat transfer systems p 229 N93-12459

SPACECRAFT MAINTENANCE
A state-based approach to trend recognition and failure prediction for the Space Station Freedom p 230 N93-11925
Requirements and opportunities for satellite autonomy p 230 N93-11926
Integration of task level planning and diagnosis for an intelligent robot p 393 N93-11929
Intelligent diagnostics systems p 393 N93-11931

SPACECRAFT MANEUVERS
Rapid maneuvering of large flexible orbiting systems p 225 N93-11885

SPACECRAFT POWER SUPPLIES
The NASA CSTI high capacity power project [NASA-TM-105813] p 221 N93-11398
Autonomous power system: Integrated scheduling p 235 N93-11948
Lunar PMAD technology assessment [NASA-CR-189225] p 347 N93-12017
Design of small Stirling dynamic isotope power system for robotic space missions [NASA-TM-105919] p 275 N93-12085
Nuclear fuels for very high temperature applications [DE92-018021] p 446 N93-12129

SPACECRAFT PROPULSION
Ground test facilities for evaluating nuclear thermal propulsion engines and fuel elements [DE92-017039] p 231 N93-10973
Preliminary characterization of a water vaporizer for resistojet applications [NASA-TM-105877] p 231 N93-11402
Theoretical research program to study chemical reactions in AOTV bow shock tubes [NASA-CR-188927] p 439 N93-11851
Tutorial on nuclear thermal propulsion safety for Mars [DE92-017946] p 233 N93-12056
Nuclear thermal propulsion transportation systems for lunar/Mars exploration [NASA-TM-105870] p 233 N93-12363
Manned Mars System Study (MMSS): Mars transportation and facility infrastructure study. Volume 2: Technical report [NASA-CR-184474] p 227 N93-12443
The 10 kW power electronics for hydrogen arcjets [NASA-TM-105614] p 235 N93-12484

SPACECRAFT REENTRY
Physiologically constrained aerocapture for manned Mars missions p 226 N93-12185

SPACECRAFT SHIELDING
Predicted and tested performance of durable TPS p 228 N93-12454

SPACECRAFT STABILITY
Spacecraft flight control system design selection process for a geostationary communication satellite [NASA-TP-3289] p 222 N93-11002

SPACECRAFT STRUCTURES
Structural dynamics of large space structures having parametric uncertainties p 225 N93-11836
A smart end-effector for assembly of space truss structures p 230 N93-11982

SPACECRAFT TRACKING
Space Station communications and tracking systems modeling and RF link simulation [NASA-CR-185684] p 288 N93-12519

SPACECRAFT TRAJECTORIES
Closed form low-thrust trajectories for Mars missions [DE92-017431] p 232 N93-11766
Air-breathing hypersonic vehicle guidance and control studies: An integrated trajectory/control analysis methodology, phase 2 [NASA-CR-189703] p 216 N93-12413

SPACELAB
Residual acceleration data on IML-1: Development of a data reduction and dissemination plan [NASA-CR-190807] p 223 N93-11101
Microbiological analysis of debris from STS-42 IML-1 by direct plating of rinse waters [NASA-TM-108375] p 375 N93-12174

SPACING
The effects of plate spacing and downstream plate length on the acoustic resonance excited by flow past two plates in tandem in a duct [PNR-90958] p 433 N93-11321
An experimental investigation into flow induced acoustic resonances in an annular cascade [PNR-90959] p 433 N93-11322

SPALLATION
The neutrino process and neutrino r-process [DE92-014304] p 485 N93-12120
Laser-ablation processes [DE92-011226] p 322 N93-12250

SPALLING
Study of the dynamic degradation under the action of a shock wave induced by pulsed laser p 319 N93-12037

SPATIAL DISTRIBUTION
Development of a tactile perceived attitude transducer [AD-A253724] p 385 N93-11081
Implementing system simulation of C3 systems using autonomous objects [NASA-CR-190845] p 283 N93-11716
Beam-plasma interactions and radiation generation during the ejection of electron and ion beams in space [AD-A253993] p 224 N93-11736
Measurement of the density distributions in quenched polycarbonate specimens by a quantitative Schlieren-optical technique p 270 N93-11989
Statistical methods for the comparison of spatial patterns in meteorological variables p 370 N93-11997
Gain in a confined aluminum plasma p 320 N93-12043

SPATIAL RESOLUTION
Initial laboratory evaluation of color video cameras [DE92-018274] p 311 N93-11673
Nuclear magnetic resonance microscopy: New theoretical and technical developments p 313 N93-11907
Effects of spatially displaced feedback on remote manipulation tasks p 400 N93-11966
Laser surface profilometer with sub-Angstrom resolution [DE92-018926] p 317 N93-12011
Hydrodynamic study of multilayer targets by spatial and temporal resolution shadow spectroscopy p 254 N93-12050

SPECIFIC HEAT
On the dependence of the dynamic crack tip temperature fields in metal upon crack tip velocity and material parameters [AD-A253657] p 335 N93-11219
Evaluation of epoxy cured with Ethacure 100 curing agent for use in headers for thermal batteries [DE92-019326] p 267 N93-11552

SPECIFIC IMPULSE
Experiments and analysis concerning the use of external burning to reduce aerospace vehicle transonic drag p 235 N93-12537

SPECIFICATIONS
The theoretical background to BS7167: 1990 - specification for Bordeaux connections [NPL-DMM(A)-50] p 325 N93-11324
A study of the effects of tolerances on rigging screws, turnbuckles, and associated components in BS4429: 1987 [NPL-DMM(A)-53] p 325 N93-11326
Integrated services digital network conformance testing. Layer 1, physical layer. Part 2: Basic rate U interface, user side [PB92-181114] p 418 N93-11714
Requirements Specification Language (RSL) and supporting tools [NASA-CR-189700] p 405 N93-12345
A methodology for systems requirements specification and traceability for large real time complex systems [AD-A254738] p 419 N93-12358
Formal specification of the VIPER microprocessor in HOL [RSRE-90009] p 405 N93-12430

SPECIMEN GEOMETRY
Fracture toughness testing of polymer matrix composites [NASA-TP-3199] p 243 N93-12302

SPECIMENS
In-plane ESPI measurements in hostile environments [PNR-90919] p 309 N93-11320
Impact test of carbon, Kevlar, and glass fibre hybrid FRP plates [NAL-TR-1100] p 243 N93-12371
SPECKLE INTERFEROMETRY
Fringe analysis of in-plane displacements on high speed rotating components [PNR-90920] p 334 N93-11022
In-plane strain measurement on high speed rotating components using pulsed laser ESPI [PNR-90975] p 315 N93-11064
In-plane ESPI measurements in hostile environments [PNR-90919] p 309 N93-11320
SPECKLE PATTERNS
In-plane ESPI measurements in hostile environments [PNR-90919] p 309 N93-11320
SPECTRA
Magnetic resonance elucidation of molecule/macromolecule interaction stereochemistry [AD-A253030] p 437 N93-11709
SPECTRAL CORRELATION
Periodicities in pulsar microstructure p 484 N93-11230
Semiclassical analysis spectral correlations in mesoscopic systems [DE92-634887] p 471 N93-11780
SPECTRAL ENERGY DISTRIBUTION
Periodicities in pulsar microstructure p 484 N93-11230
Scattering of electromagnetic waves from a plasma: Enhanced ion acoustic fluctuations due to ion-ion two-stream instabilities p 361 N93-11272
Time-frequency domain analysis of vibration signals for machinery diagnostics. 3: The present power spectral density [OUEL-1911/92] p 337 N93-11707
SPECTRAL LINE WIDTH
Experimental studies of x ray laser spectral profiles: Observation of gain narrowing and saturation behavior [DE92-019603] p 316 N93-11659
SPECTRAL METHODS
Inverse spectral transform for the 2 + 1-dimensional Gardner equation [MATHS-REPT-A-138] p 425 N93-11323
Spurious modes in spectral collocation methods with two non-periodic directions [NASA-CR-189713] p 427 N93-12298
SPECTRAL RESOLUTION
Morphology and physics of supernova remnants p 482 N93-11476
SPECTROGRAPHS
X-UV spectroscopy temporal resolution p 318 N93-12028
Analysis of the instrument operation of a focal circle spectrograph and numerical reconstitution of the spectrum emitted by a plasma column p 321 N93-12051
SPECTROMETERS
Interpretation of measurements from the suprathermal electron spectrometer on the NEED-2 rocket [FFI-92/7009] p 357 N93-11129
Comparison of passive-remote and conventional Fourier transform infrared systems for continuously monitoring incinerator emissions [DE92-015225] p 355 N93-12098
SPECTRORADIOMETERS
A trainable image pattern classification system for detection of damaged soybean seeds p 201 N93-12208
SPECTROSCOPIC ANALYSIS
Radiation damage by high energy electrons in GaAs: A DLTS (deep level transient spectroscopy) examination [HMI-B-494] p 442 N93-11028
Signal-to-noise assessment and measurement in spectroscopies with particular reference to Auger and x ray photoelectron spectroscopies [NPL-DMM(A)-45] p 247 N93-11396
Energetics solids degradation in high temperature water [AD-A254900] p 276 N93-12265
On-line analysis of chemical composition using an FT-Raman spectrometer in the near-IR [DE92-016503] p 253 N93-12311
Characterization of underivatized pterins by laser desorption Fourier transform mass spectrometry [DE92-016785] p 323 N93-12514
SPECTROSCOPY
Radiation damage by high energy electrons in GaAs: A DLTS (deep level transient spectroscopy) examination [HMI-B-494] p 442 N93-11028
The fourth OSA Topical Meeting Proceedings on Picosecond Electronics and Optoelectronics, volume 9 [AD-A253472] p 447 N93-11099
Admittance spectroscopy of copper indium diselenide/cadmium sulfide solar cells p 344 N93-11214
Plasma properties of solar coronal active regions p 489 N93-12342
SPECTRUM ANALYSIS
Non-self-similar clustering of galaxies [MPE-PREPRINT-212] p 484 N93-11338
Operator's guide for VAXGAP, a gamma-ray spectrum analysis package [DE92-019096] p 407 N93-11356
Stationary time series analysis using information and spectral analysis p 425 N93-11431
X-UV spectroscopy temporal resolution p 318 N93-12028
Analysis of the instrument operation of a focal circle spectrograph and numerical reconstitution of the spectrum emitted by a plasma column p 321 N93-12051
Interactive analysis of gappy bivariate time series using AGSS [AD-A255160] p 429 N93-12426
SPECULAR REFLECTION
Estimation of photosynthetic capacity using MODIS polarization: 1988 proposal to NASA Headquarters [NASA-TM-103945] p 344 N93-12351
SPEECH RECOGNITION
Speech recognition systems and their military applications [BR91882] p 280 N93-11366
The development of the speaker independent ARM continuous speech recognition system [RSRE-MEMO-4473] p 280 N93-11383
Preliminary results on the use of linear discriminant analysis in the ARM continuous speech recognition system [RSRE-MEMO-4511] p 280 N93-11384
The use of linear discriminant analysis in the ARM continuous speech recognition system [RSRE-MEMO-4512] p 280 N93-11385
SPHERES
Effect of assembly anomalies on the strain response of composites in the sphere joint region of the DARPA man-rated demonstration article [AD-A254204] p 240 N93-11739
Damping and scattering of electromagnetic waves by small ferrite spheres suspended in an insulator [NASA-TM-105837] p 286 N93-12366
Light scattering from a sphere on or near an interface p 448 N93-12531
SPIN STABILIZATION
Spacecraft flight control system design selection process for a geostationary communication satellite [NASA-TP-3289] p 222 N93-11002
SPIN-LATTICE RELAXATION
Pulsed-field-gradient NMR investigations of hydrogen diffusion in ZrH(x) [DE92-014393] p 459 N93-11238
SPINE
The effect of variable seat back angles on human response to +Gz impact accelerations [AD-A250673] p 387 N93-11559
Evaluation of CKU-5/A ejection seat catapults under varied acceleration levels [AD-A248021] p 204 N93-12489
SPIRALS
Maximum life spiral bevel reduction design [NASA-TM-105790] p 323 N93-10982
SPLINES
Determination of loose spline coupling coefficients of rotor bearing systems in turbomachinery p 327 N93-11887
SPONTANEOUS EMISSION
Novel nonlinear laser diagnostic techniques [AD-A254709] p 323 N93-12335
SPRAYED COATINGS
Development of wear resistant ceramic coatings for diesel engine components [DE92-019068] p 268 N93-11654
A design of experiment study of plasma sprayed alumina-titania coatings [DE92-017877] p 271 N93-12168
A Taguchi experimental design study of twin-wire electric arc sprayed aluminum coatings [DE92-018022] p 262 N93-12494
SPRAYERS
Coaxial injector spray characterization using water/air as simulants p 248 N93-11452
Experimental investigation of rocket injector atomization p 248 N93-11454
SPUTTERING
High temperature superconductor materials and applications [NASA-CR-184426] p 470 N93-12396
STABILITY DERIVATIVES
An experimental study of the relationship between forces and moments and vortex breakdown on a pitching delta wing p 208 N93-12206
STABILITY TESTS
The role of turbomachinery testing for stability in distorted flow [PNR-90943] p 210 N93-11040
STABILIZATION
Development of a GPS-aided motion measurement, pointing, and stabilization system for a synthetic aperture radar [DE92-017053] p 204 N93-11152
A preliminary investigation of the degradation and stabilisation of the energetic oxetane binder polyNIMMO [RARDE-7/91] p 273 N93-11376
Cryostabilization of high-temperature superconducting magnets with subcooled flow in microchannels [DE92-018174] p 431 N93-11598
STABLE OSCILLATIONS
Beam-loading stability in synchrotrons with a higher RF harmonic [DE92-018982] p 443 N93-11510
STAGNATION TEMPERATURE
Flow visualization of supersonic flow through a combustor section p 200 N93-12001
STAINLESS STEELS
Heat-affected zone cracking of nitronic 60 stainless steel [DE92-018286] p 254 N93-10984
Thermal stress and strain analysis in traveling autogenous welds [DE92-019363] p 326 N93-11556
Mechanical properties of 1950's vintage 304 stainless steel weldment components after low temperature neutron irradiation [DE92-017059] p 259 N93-12107
Reactor materials program: Mechanical properties of irradiated types 304 and 304L stainless steel weldment components [DE92-018105] p 260 N93-12158
STANDARDIZATION
Workshop on Characterizing Diamond Films [PB92-205426] p 271 N93-12086
Syntax and lexis of the specification language Z [RSRE-MEMO-4367] p 414 N93-12326
Ferroelectric memory devices and a proposed standardized test system design [AD-A255159] p 405 N93-12425
STANDARDS
The technical background to standards for shackles [NPL-DMM(A)-51] p 325 N93-11325
The technical background to standards for eyebolts [NPL-DMM(A)-52] p 325 N93-11327
Far ultraviolet spectrophotometry of hot stars and calibration standards in the far ultraviolet p 482 N93-11373
Integrated services digital network conformance testing. Layer 1, physical layer. Part 2: Basic rate U interface, user side [PB92-181114] p 418 N93-11714
Workshop on Characterizing Diamond Films [PB92-205426] p 271 N93-12086
Allowance system: Proposed acid rain rule [PB92-226174] p 356 N93-12524
STANDING WAVE RATIOS
Computer modeling of tactical high frequency antennas [AD-A255176] p 286 N93-12377
STANDING WAVES
Computer modeling of tactical high frequency antennas [AD-A255176] p 286 N93-12377
STAR DISTRIBUTION
Stars in the Rosat all-sky survey p 482 N93-11477
STAR FORMATION
A submillimeter-millimeterwave study of the molecular gas in the nuclear regions of three nearby starburst galaxies p 484 N93-11260
STAR FORMATION RATE
A submillimeter-millimeterwave study of the molecular gas in the nuclear regions of three nearby starburst galaxies p 484 N93-11260
STARBURST GALAXIES
A submillimeter-millimeterwave study of the molecular gas in the nuclear regions of three nearby starburst galaxies p 484 N93-11260
A multi-line study of the molecular interstellar medium on M82's starburst nucleus [MPE-PREPRINT-213] p 484 N93-11347
STARS
ESIS: An introduction to the European space information system. A modern tool for space scientists [ESA-INT-2] p 479 N93-12404

STATE ESTIMATION

A game theoretic approach to linear dynamic estimation p 340 N93-12200

STATIC AERODYNAMIC CHARACTERISTICS

Low-speed longitudinal and lateral-directional aerodynamic characteristics of the X-31 configuration [NASA-TM-4351] p 198 N93-11622

STATIC LOADS

Nonlinear response of thin steel plate structures subjected to static, cyclic, and dynamic loads p 335 N93-11200

An experimental study of the relationship between forces and moments and vortex breakdown on a pitching delta wing p 208 N93-12206

STATIC MODELS

Development and use of data analysis procedures for the CRRES payloads AFGL-701-2/Dosimeter and AFGL-701-4/Fluxmeter and application of the data analysis results to improve the static and dynamic models of the Earth's radiation belts [AD-A253287] p 363 N93-11810

STATIC PRESSURE

The hemisphere-cylinder at an angle of attack p 196 N93-11250

STATISTICAL ANALYSIS

Numerical study for the study of medium speed internal noise problems [DILC-EST-TN-200] p 432 N93-11156

Analysis of disease progression from clinical observations of US Air Force active duty members infected with the Human Immunodeficiency Virus: Distribution of AIDS survival time from interval censored observations p 379 N93-11297

LAM and NEDWAM statistics over the period October 1990 - April 1991 [KNMI-TR-137] p 368 N93-11329

Statistical process for the automatic image analysis and its evaluation for object recognition and measurements [SER-C-370] p 407 N93-11345

The use of statistical measures to validate system dynamics models [AD-A248569] p 428 N93-11417

Stationary time series analysis using information and spectral analysis p 425 N93-11431

Diagnostic rhyme test statistical analysis programs [RSRE-91026] p 281 N93-11487

Application of the theory of wave propagation through random media to phase and amplitude fluctuations of seismic P-waves [AD-A253274] p 363 N93-11788

Dynamics of space debris p 219 N93-11904

Statistical methods for the comparison of spatial patterns in meteorological variables p 370 N93-11997

History of statistics in real time: Hammers and nails [AD-A253521] p 429 N93-12081

Change analysis and Fisher-Score change processes [AD-A254707] p 429 N93-12334

Static assignment of complex stochastic tasks using stochastic majorization [NASA-CR-189716] p 416 N93-12403

Research in statistical inference [AD-A252928] p 429 N93-12429

Active control of complex systems via dynamic (recurrent) neural networks [AD-A254878] p 422 N93-12439

Operating characteristic analysis for reliability growth programs [AD-A254993] p 333 N93-12510

STATISTICAL CORRELATION

Multifractal analysis at negative q [AD-A254370] p 413 N93-12159

STATISTICAL DISTRIBUTIONS

Nonnormal multivariate distributions: Inference based on elliptically contoured distributions [AD-A254999] p 429 N93-12513

STATISTICAL TESTS

Modeling and identification of flexible joints in vehicle structures p 324 N93-11261

History of statistics in real time: Hammers and nails [AD-A253521] p 429 N93-12081

STATISTICAL WEATHER FORECASTING

Statistical methods for the comparison of spatial patterns in meteorological variables p 370 N93-11997

STATISTICS

History of statistics in real time: Hammers and nails [AD-A253521] p 429 N93-12081

STATORS

Experimental heat transfer results in turbine stators and rotors and a comparison with theory [PNR-90945] p 210 N93-11055

Investigation of hot streak migration and film cooling effects on heat transfer in rotor/stator interacting flows, report 1 [AD-A250688] p 471 N93-12490

STEAM

Reformers for the production of hydrogen from methanol and alternative fuels for fuel cell powered vehicles [DE92-019300] p 274 N93-11550

Proceedings of the DOE/Advanced Heat Exchangers Program Review [DE92-014385] p 305 N93-12070

STEEL STRUCTURES

Nonlinear response of thin steel plate structures subjected to static, cyclic, and dynamic loads p 335 N93-11200

An evaluation of repair techniques used for uncontrolled longitudinal cracking and failed longitudinal joints [PB92-205616] p 277 N93-12072

Microstructure-based fatigue life prediction methods for naval steel structures [AD-A254628] p 260 N93-12241

STEELS

On the dependence of the dynamic crack tip temperature fields in metal upon crack tip velocity and material parameters [AD-A253657] p 335 N93-11219

The conversion of plastic work to heat around a dynamically propagating crack in metals [AD-A253801] p 258 N93-11782

Microstructure-based fatigue life prediction methods for naval steel structures [AD-A254628] p 260 N93-12241

Fatigue crack growth in AerMet 100 steel [AD-A249068] p 261 N93-12248

Stress dependence of the magnetic properties of steels [DE92-018804] p 261 N93-12261

STEERABLE ANTENNAS

Method of steering the gain of a multiple antenna global positioning system receiver [AD-D015367] p 281 N93-11426

STEERING

Method of steering the gain of a multiple antenna global positioning system receiver [AD-D015367] p 281 N93-11426

A computer algorithm for automatic beam steering [DE92-019338] p 411 N93-11555

STELLAR CONVECTION

A linear and nonlinear study of Mira [DE92-011265] p 483 N93-10993

STELLAR EVOLUTION

Ultraviolet studies of Cepheids [NASA-CR-190857] p 481 N93-11073

STELLAR LUMINOSITY

A linear and nonlinear study of Mira [DE92-011265] p 483 N93-10993

STELLAR MAGNITUDE

Detection of a white dwarf in a visual binary system [NASA-CR-190856] p 481 N93-11075

STELLAR MASS

Ultraviolet studies of Cepheids [NASA-CR-190857] p 481 N93-11073

Monte Carlo simulations of the supernova ejection mechanism for the runaway stars [DE92-018367] p 485 N93-11695

Mechanism for ejecting stars from the Galactic plane [DE92-018375] p 485 N93-11697

STELLAR MASS ACCRETION

Are some of the luminous high-latitude stars accretion-powered runaways? [DE92-018853] p 484 N93-11379

STELLAR MASS EJECTION

Monte Carlo simulations of the supernova ejection mechanism for the runaway stars [DE92-018367] p 485 N93-11695

Statistics of IMF B(z) events [DE92-018372] p 488 N93-11696

Mechanism for ejecting stars from the Galactic plane [DE92-018375] p 485 N93-11697

The semiannual variation of great geomagnetic storms and the postshock Russell-McPherron effect preceding coronal mass ejecta [AD-A254955] p 489 N93-12506

STELLAR MODELS

A linear and nonlinear study of Mira [DE92-011265] p 483 N93-10993

Ultraviolet studies of Cepheids [NASA-CR-190857] p 481 N93-11073

Detection of a white dwarf in a visual binary system [NASA-CR-190856] p 481 N93-11075

A Polytropic solar model p 487 N93-11264

Monte Carlo simulations of the supernova ejection mechanism for the runaway stars [DE92-018367] p 485 N93-11695

Mechanism for ejecting stars from the Galactic plane [DE92-018375] p 485 N93-11697

STELLAR MOTIONS

Are some of the luminous high-latitude stars accretion-powered runaways? [DE92-018853] p 484 N93-11379

A search for low-luminosity objects [AD-A253301] p 483 N93-11750

STELLAR OSCILLATIONS

A linear and nonlinear study of Mira [DE92-011265] p 483 N93-10993

Periodicities in pulsar microstructure p 484 N93-11230

STELLAR RADIATION

A linear and nonlinear study of Mira [DE92-011265] p 483 N93-10993

Stars in the Rosat all-sky survey p 482 N93-11477

STELLAR SPECTRA

Detection of a white dwarf in a visual binary system [NASA-CR-190856] p 481 N93-11075

Periodicities in pulsar microstructure p 484 N93-11230

Stars in the Rosat all-sky survey p 482 N93-11477

Temporal and spectral variability in luminous x ray binaries p 483 N93-12336

STELLAR SPECTROPHOTOMETRY

Far ultraviolet spectrophotometry of hot stars and calibration standards in the far ultraviolet p 482 N93-11373

STELLAR STRUCTURE

Periodicities in pulsar microstructure p 484 N93-11230

STELLAR TEMPERATURE

Detection of a white dwarf in a visual binary system [NASA-CR-190856] p 481 N93-11075

STELLARATORS

Shafranov shift in low-aspect-ratio heliotron/torsatron CHS [DE92-782100] p 451 N93-11277

STEREOCHEMISTRY

Magnetic resonance elucidation of molecule/macromolecule interaction stereochemistry [AD-A253030] p 437 N93-11709

Design and synthesis of molecular systems capable of supporting intracavity chemical reactions [AD-A251024] p 440 N93-11672

STEREOSCOPIC VISION

Correction techniques for depth errors with stereo three-dimensional graphic displays [NASA-TP-3244] p 206 N93-11170

STIFFNESS

Determination of loose spline coupling coefficients of rotor bearing systems in turbomachinery p 327 N93-11887

The mechanism of bolt loading [NASA-TM-108377] p 342 N93-12412

STIFFNESS MATRIX

Application of artificial neural networks in nonlinear analysis of trusses [NASA-TM-105319] p 336 N93-11403

Computational dynamics of high-speed flexible multibody systems p 338 N93-11891

STIMULATED EMISSION

Bremsstrahlung absorption in plasmas p 321 N93-12047

Hydrodynamic study of multilayer targets by spatial and temporal resolution shadow spectroscopy p 254 N93-12050

STIRLING ENGINES

Sodium reflux pool-boiler solar receiver on-sun test results [DE92-018932] p 347 N93-12012

Design of small Stirling dynamic isotope power system for robotic space missions [NASA-TM-105919] p 275 N93-12085

Stirling heat pump external heat systems: An appliance perspective [DE92-018251] p 349 N93-12498

STOCHASTIC PROCESSES

Hydrodynamic fluctuations and light scattering in hot electron gas of semiconductors [DE92-622800] p 458 N93-10992

Stochastic control and nonlinear estimation [AD-A253543] p 420 N93-11147

Self-generated stochastic heating in an RF discharge [DE92-018558] p 452 N93-11565

A theory for the analysis of rotorcraft operating in atmospheric turbulence p 207 N93-11725

A game theoretic approach to linear dynamic estimation p 340 N93-12200

Stochastic sensitivity measure for mistuned high-performance turbines [NASA-TM-105821] p 341 N93-12277

Static assignment of complex stochastic tasks using stochastic majorization [NASA-CR-189716] p 416 N93-12403

Stochastic models of wavefront propagation in random granular media [AD-A255127] p 286 N93-12422

Mathematical methods in operations research and computer science [AD-A254782] p 428 N93-12465

STOKES LAW OF RADIATION
Observation and analysis of the Stokes and anti-Stokes components of stimulated Raman backscattering
p 318 N93-12025
STORAGE BATTERIES
Overcharge and overdischarge protection of ambient temperature secondary lithium cells
[NASA-CASE-NPO-18343-1-CU] p 290 N93-11456
STORAGE RINGS (PARTICLE ACCELERATORS)
Using the 16 viewscreens during commissioning of AmPS
[NIKHEF-K/AMPS/92-01] p 442 N93-11131
Tunable, short pulse hard x rays from a compact laser synchrotron source
[AD-A254288] p 315 N93-11195
Scaling of gain with energy spread and energy in the PEP FEL
[DE92-019248] p 316 N93-11500
Beam-loading stability in synchrotrons with a higher RF harmonic
[DE92-018982] p 443 N93-11510
STORAGE STABILITY
The degradation of parachutes: Age and mechanical wear
[AD-A252243] p 200 N93-12179
STORMS
Lightning threat warning system at the Tonopah Test Range
[DE92-040444] p 221 N93-11631
STOVL AIRCRAFT
Overview of high performance aircraft propulsion research
[NASA-TM-105839] p 213 N93-11530
STRAIN DISTRIBUTION
Systems of evolution equations in thermochemical equations
[AD-A254891] p 253 N93-12282
STRAIN ENERGY METHODS
Some exact solutions of the equations of finite elasticity p 337 N93-11713
STRAIN ENERGY RELEASE RATE
Fracture mechanics of model fiber composites
p 237 N93-11247
VAMAS round robin project on polymer composite delamination in mode 1 and mode 2: Cyclic loading
[NPL-DMM(A)-47] p 266 N93-11397
STRAIN GAGE BALANCES
Strain-gauge balance performance and internal temperature gradients measured in a cryogenic environment
[RAE-TM-AERO-2232] p 218 N93-11906
STRAIN GAGES
Repeatable sensitivity of optical-time-domain-reflectometry-based strain measurement
[DE92-016910] p 338 N93-11792
Compensated high temperature strain gage
[NASA-CASE-LAR-14776-1] p 313 N93-12205
STRAIN HARDENING
Influence of strain rate on the structure/property behavior of the alpha-2 alloy Ti-24.5Al-10.5Nb-1.5Mo
[DE92-008490] p 261 N93-12256
STRAIN MEASUREMENT
In-plane strain measurement on high speed rotating components using pulsed laser ESPI
[PNR-90975] p 315 N93-11064
Repeatable sensitivity of optical-time-domain-reflectometry-based strain measurement
[DE92-016910] p 338 N93-11792
Advanced one-dimensional optical strain measurement system, phase 4
[NASA-CR-190760] p 314 N93-12279
STRAIN RATE
On the dependence of the dynamic crack tip temperature fields in metal upon crack tip velocity and material parameters
[AD-A253657] p 335 N93-11219
Influence of strain rate on the structure/property behavior of the alpha-2 alloy Ti-24.5Al-10.5Nb-1.5Mo
[DE92-008490] p 261 N93-12256
STRANGENESS
Strange quark matter
[DE92-016949] p 438 N93-11746
STRAPDOWN INERTIAL GUIDANCE
Construction of a geodesic strapdown inertial navigation system for point determination
[SER-C-367] p 205 N93-11344
STRATOSPHERE
The Transall campaign. A contribution to the German ozone research program
[REPT-37/91] p 349 N93-11082
Scientific assessment of ozone depletion: 1991
[NASA-TM-107976] p 350 N93-11087
Source gases: Concentrations, emissions, and trends
p 350 N93-11088
Heterogeneous processes: Laboratory, field, and modeling studies p 350 N93-11090
Stratospheric processes: Observations and interpretation p 351 N93-11091
Tropospheric processes: Observations and interpretation p 351 N93-11092
Ozone depletion and chlorine loading potentials
p 351 N93-11093
Radiative forcing of climate p 351 N93-11094
Future chlorine-bromine loading and ozone depletion
p 352 N93-11095
Predicted aircraft effects on stratospheric ozone
p 352 N93-11096
Predicted rocket and shuttle effects on stratospheric ozone p 352 N93-11097
Proceedings of the Sixteenth Annual Climate Diagnostics Workshop
[PB92-198803] p 370 N93-11896
Dynamics of planetary waves in the atmosphere
p 363 N93-11898
Stratospheric aircraft: Impact on the stratosphere?
[DE92-016997] p 355 N93-12104
Stratospheric aircraft exhaust plume and wake chemistry studies
[NASA-CR-189688] p 366 N93-12299
STREAK CAMERAS
High energy x ray imaging diagnostic on Nova
[DE92-018067] p 451 N93-11495
Laser material interaction in confined medium
p 319 N93-12035
STRESS (PHYSIOLOGY)
Space flight and immune system p 376 N93-11284
STRESS (PSYCHOLOGY)
Space flight and immune system p 376 N93-11284
STRESS ANALYSIS
Automated fringe analysis for moire interferometry
[PNR-90918] p 334 N93-11021
Fiber peel force measuring apparatus
[AD-D015349] p 309 N93-11048
Methods of analysis for thick-section composite structures p 237 N93-11262
The technical background to standards for shackles
[NPL-DMM(A)-51] p 325 N93-11325
The effect of precipitate forming elements in Al 4.5 percent Mg alloys on the measured acoustic emission and on Lueders band deformation
[DE92-016864] p 465 N93-12073
The effect of contact stresses in four-point bend testing of graphite/epoxy and graphite/PMR-15 composite beams
[NASA-TM-105891] p 241 N93-12076
Stress dependence of the magnetic properties of steels
[DE92-018804] p 261 N93-12261
Micromechanical combined stress analysis: MICSTRAN, a user manual
[NASA-CR-189694] p 243 N93-12306
Verification of rain-flow reconstructions of a variable amplitude load history
[NASA-CR-189670] p 341 N93-12411
An experimental study of a small high speed LH2 rocket pump: Fundamental mechanical design
[NAL-TR-1123] p 330 N93-12463
STRESS CORROSION
Creep failure in linear and nonlinear viscoelastic materials p 342 N93-12536
STRESS CORROSION CRACKING
Environment-induced embrittlement: Stress corrosion cracking and metal-induced embrittlement; environmental embrittlement of iron aluminide alloys
[DE92-018714] p 256 N93-11524
Mechanisms of localized aqueous corrosion in aluminum-lithium-copper alloys p 259 N93-11895
Spectrum fatigue behaviour of powder metallurgy aluminum alloys
[AD-A255060] p 262 N93-12468
STRESS DISTRIBUTION
Analysis of precracking parameters and fracture toughness for ceramic single-edge-precracked-beam specimens
[NASA-TM-105568] p 263 N93-10962
Elastic stresses, twin boundaries, and fatigue cracking
p 338 N93-11890
STRESS INTENSITY FACTORS
Analysis of precracking parameters and fracture toughness for ceramic single-edge-precracked-beam specimens
[NASA-TM-105568] p 263 N93-10962
Fatigue crack growth in AerMet 100 steel
[AD-A249068] p 261 N93-12248
STRESS MEASUREMENT
Development of the neutron diffraction technique for the determination of near surface residual stresses in critical gas turbine components
[PNR-90984] p 212 N93-11112
Stress dependence of the magnetic properties of steels
[DE92-018804] p 261 N93-12261
STRESS RATIO
Fatigue crack growth in AerMet 100 steel
[AD-A249068] p 261 N93-12248
STRESS TENSORS
Some exact solutions of the equations of finite elasticity p 337 N93-11713
STRESS-STRAIN DIAGRAMS
Effect of assembly anomalies on the strain response of composites in the sphere joint region of the DARPA man-rated demonstration article
[AD-A254204] p 240 N93-11739
STRESS-STRAIN RELATIONSHIPS
Contribution to the monocrystal behavior study during large plastic strains
[ECL-92-13] p 461 N93-11581
Verification of rain-flow reconstructions of a variable amplitude load history
[NASA-CR-189670] p 341 N93-12411
STRING THEORY
New singularity and existence of solutions in anisotropic, time-dependent, maximally Gauss-Bonnet extended gravity p 357 N93-11183
Studies in quantum field theory
[DE92-011035] p 470 N93-11276
Research in elementary particles and interactions
[DE92-018089] p 437 N93-11681
Spacetime singularities in string theory
p 472 N93-12530
STRIP TRANSMISSION LINES
Optical generation, control and sensing of millimeter waves
[AD-A254700] p 285 N93-12230
STRONTIUM COMPOUNDS
Superconducting multilayer structures grown by ALL-MBE
[DE92-018011] p 465 N93-12065
STRONTIUM OXIDES
Properties of hot isostatically pressed Bi(2)Sr(1.7)CaCu(2)O(x)
[DE92-016394] p 460 N93-11522
Silicon carbide fiber reinforced strontium aluminosilicate glass-ceramic matrix composite
[NASA-CASE-LEW-15263-1] p 239 N93-11543
STRONTIUM TITANATES
High frequency response from YBa2Cu3O(7-x) Josephson devices on SrTiO3 bicrystal substrates
[NPL-DES-118] p 459 N93-11394
Atomic bonding at ceramic interfaces using scanning tunneling microscopy
[DE92-018706] p 273 N93-12479
STRUCTURAL ANALYSIS
Modeling and identification of flexible joints in vehicle structures p 324 N93-11261
Application of artificial neural networks in nonlinear analysis of trusses
[NASA-TM-105319] p 336 N93-11403
Structure and property of heteroepitaxial TiO2/VO2 multilayers
[DE92-018181] p 460 N93-11563
Global-local finite element analysis of composite structures
[DE92-019138] p 240 N93-11658
VUV and UV sources and spectroscopic applications
[AD-A247293] p 291 N93-11758
Some remarks on shell element analysis with DYNA3D and NIKE3D
[DE92-018784] p 337 N93-11775
Structural design using equilibrium programming
[NASA-TM-107593] p 339 N93-12005
Thermostructural tailoring of fiber composite structures
[NASA-TM-105882] p 242 N93-12078
Advanced methods for structural characterization of large multiply charged ions: Obtaining charge state determination and improved sensitivity
[DE91-015264] p 441 N93-12117
Fourier continuum finite elements for nonlinear structural analysis p 340 N93-12210
Studies in control for vibration suppression of the UWAA 20-bay planar truss
[AD-A250193] p 341 N93-12253
Stress dependence of the magnetic properties of steels
[DE92-018804] p 261 N93-12261
STRUCTURAL BASINS
Atmospheric dispersion in mountain valleys and basins
p 355 N93-11920
STRUCTURAL DESIGN
Structural design using equilibrium programming
[NASA-TM-107593] p 339 N93-12005
Current research in oxidation-resistant carbon-carbon composites at NASA. Langley Research Center
p 229 N93-12456

STRUCTURAL PROPERTIES (GEOLOGY)
Quaternary volcanism, tectonics, and sedimentation in the Idaho National Engineering Laboratory area
[DE92-017851] p 362 N93-11692

STRUCTURAL STABILITY
Nonlinear response of thin steel plate structures subjected to static, cyclic, and dynamic loads
p 335 N93-11200
The mechanical and microstructural stability of austenitic stainless steels strengthened by MC-forming elements
[DE91-015314] p 259 N93-11857
DYNAC: A computer program for analyzing the dynamical stability of aircraft
[REPT-B-31] p 216 N93-12415

STRUCTURAL VIBRATION
Numerical and experimental results in vibroacoustical active control of structural elements with piezoelectric materials
[DILC-EST-TN-224] p 334 N93-11158
Rigid body mode identification of the PAH-2 helicopter using the eigensystem realization algorithm
[NASA-TM-107690] p 336 N93-11544
Description of the structural responses in the medium-frequency range by an energetic formulation
[ECL-92-16] p 336 N93-11582
A consistent cracked bar vibration theory
p 339 N93-12000

STRUCTURAL WEIGHT
Lunar PMAD technology assessment
[NASA-CR-189225] p 347 N93-12017

STRUCTURED PROGRAMMING
The WEB approach to ELLA
[RSRE-MEMO-4549] p 409 N93-11407
Using SGML in a large organization
[ESA-STR-234] p 476 N93-11583

STUDENTS
Questioning mechanisms during complex learning
[AD-A247382] p 386 N93-11415
A summer program in mathematics and computer science for academically oriented students, June 24 - July 26, 1991, Washington, DC
[AD-A249139] p 427 N93-12061

SUBASSEMBLIES
Backward assembly planning with DFA analysis
[NASA-CASE-NPO-18817-1-CU] p 278 N93-12202
Assembling polyhedra with single translations
[AD-A254623] p 419 N93-12239

SUBDUCTION (GEOLOGY)
Laboratory and numerical studies of dynamical processes related to thermal convection in the Earth's mantle p 364 N93-11900

SUBGROUPS
Applications of star complexes in group theory
p 485 N93-11879

SUBLIMATION
Erosion mechanisms in ceramic structures
[MBB-UK-0171-92-PUB] p 263 N93-11011

SUBMARINES
Submarine Advanced Integrated Life Support system (SAILS) program
[AD-A253564] p 388 N93-11812

SUBMERGED BODIES
Fluid-structure interaction using retarded potential and ABAQUS
[AD-A254735] p 307 N93-12355

SUBMERGING
Effect of hemorrhage on cardiac output, vasopressin, aldosterone, and diuresis during immersion in men
[NASA-TM-103949] p 374 N93-12014

SUBMILLIMETER WAVES
A submillimeter-millimeterwave study of the molecular gas in the nuclear regions of three nearby starburst galaxies p 484 N93-11260
Submillimeter and microwave residual losses in epitaxial films of Y-Ba-Cu-O and BI-Ca-Ca-Cu-O
[DE92-017075] p 466 N93-12125

SUBREFLECTORS
Method of moments analysis of symmetric dual reflector antennas with feeds
[AD-A255171] p 286 N93-12407

SUBSONIC FLOW
Experimental investigation of the effects of aft blowing with various nozzle exit geometries on a 3.0 caliber tangent ogive at high angles of attack: Forebody pressure distributions
[NASA-CR-190935] p 197 N93-11605
An experimental investigation of the flow in a diffusing S-duct
[NASA-TM-105809] p 213 N93-12077

SUBSONIC SPEED
A concept for a counterrotating fan with reduced tone noise
[NASA-TM-105736] p 433 N93-11370
Formal representation of the requirements for an Advanced Subsonic Civil Transport (ASCT) flight control system
[NASA-CR-189699] p 405 N93-12346

SUBSONIC WIND TUNNELS
The measurement of the velocity field induced by a gust generator in a closed-circuit subsonic wind-tunnel
[RAE-TM-MAT-STR-1102] p 217 N93-11435

SUBSTITUTES
Synthesis of side chain liquid crystal polymers by living ring opening metathesis polymerization. Report 3: Influence of molecular weight, interconnecting unit and substituent on the mesomorphic behavior of polymers with laterally attached mesogens
[AD-A248698] p 265 N93-11187
Carboxyalkylated hemoglobin as a potential blood substitute
[AD-A252329] p 384 N93-11561
Nature of the beta-phase of nickel-aluminum system
[AD-A254101] p 261 N93-12269

SUBSTRATES
Growth mechanisms of layered superconductors
[DE92-018492] p 458 N93-10987
High frequency response from YBa2Cu3O(7-x) Josephson devices on SrTiO3 bicrystal substrates
[NPL-DES-118] p 459 N93-11394
Multi-layer light-weight protective coating and method for application
[NASA-CASE-LAR-14448-1] p 269 N93-11912
Reflection masks for soft x ray projection lithography
[DE92-014779] p 293 N93-12121
Friction of self-lubricating surfaces by ion beam techniques
[DE92-016069] p 328 N93-12122
Formation of buried epitaxial Si-Ge alloy layers in Si (100) crystal by high dose Ge ion implantation
[DE92-017114] p 466 N93-12127
Compensated high temperature strain gage
[NASA-CASE-LAR-14776-1] p 313 N93-12205
Natural convection heat transfer studies of simulated and actual electronic components using dielectric liquids for immersion cooling
[AD-A255173] p 341 N93-12376
Recent advances in carbon-carbon substrate technology at NASA. Langley Research Center p 228 N93-12455
MMIC GaAs bonding investigation
[AD-A254773] p 470 N93-12464
Growth of solid solutions of aluminum nitride and silicon carbide by metalorganic chemical vapor deposition
[AD-A255000] p 254 N93-12518

SUBSTRUCTURES
Complex cognitive information processing: A computational architecture with a connectionist implementation
[AD-A254041] p 422 N93-12259

SUCTION
Dynamical effects of suction/heating on turbulent boundary layers
[AD-A248459] p 299 N93-11416

SULFATES
Acid copper sulfate plating bath: Control of chloride and copper
[DE92-019473] p 249 N93-11644
Synthesis and conductivity of copolymer of 4,4'-diaminodiphenylamine and terephthaloyl chloride
[AD-A254880] p 273 N93-12440

SULFIDATION
Oxidation-sulfidation behavior of iron alloys containing 16 to 40 atomic percent aluminum
[DE92-017824] p 259 N93-11830

SULFIDES
Biological conversion of synthesis gas culture development
[DE92-001279] p 375 N93-12482

SULFONES
Phase transfer catalytic nucleophilic addition reactions: Synthesis of polymers and acetylenic terminated resins
[AD-A254717] p 272 N93-12337

SULFONIC ACID
Carboxyalkylated hemoglobin as a potential blood substitute
[AD-A252329] p 384 N93-11561

SULFUR COMPOUNDS
The relative importance of sulfur and nitrogen compounds in the acidification of freshwater
[DE92-016899] p 354 N93-11680

SULFUR DIOXIDES
Allowance system: Proposed acid rain rule
[PB92-226174] p 356 N93-12524

SULFUR FLUORIDES
A cryogenic enrichment technique for gas chromatographic detection of S2F10 in SF6 discharges
[DE92-011045] p 252 N93-12219

SUM RULES
Nucleon axial coupling constants and QCD sum rules
[DE92-014227] p 439 N93-11844

SUPERCOMPUTERS
The engine design engine. A clustered computer platform for the aerodynamic inverse design and analysis of a full engine
[NASA-TM-105838] p 196 N93-11223
Studies of ocean predictability at decade to century time scales using a global ocean general circulation model in a parallel competing environment
[DE92-019457] p 373 N93-11642
Current state and future direction of computer systems at NASA Langley Research Center
[NASA-TM-107685] p 414 N93-12278
Performance evaluation and modeling techniques for parallel processors
[NASA-CR-190974] p 419 N93-12395

SUPERCONDUCTING FILMS
A mutual inductance technique for contact-free T(sub c) measurement of high temperature superconductors
[NPL-DES-116] p 289 N93-11393
High frequency response from YBa2Cu3O(7-x) Josephson devices on SrTiO3 bicrystal substrates
[NPL-DES-118] p 459 N93-11394
Superconducting multilayer structures grown by ALL-MBE
[DE92-018011] p 465 N93-12065
Submillimeter and microwave residual losses in epitaxial films of Y-Ba-Cu-O and BI-Ca-Ca-Cu-O
[DE92-017075] p 466 N93-12125
Ion beams as a means of deposition and in-situ characterization of thin films and thin film layered structures
[DE92-016397] p 469 N93-12310
Conductor-backed coplanar waveguide resonators of Y-Ba-Cu-O and Tl-Ba-Ca-Cu-O on LaAlO3
[NASA-TM-105890] p 469 N93-12325
High temperature superconductor materials and applications
[NASA-CR-184426] p 470 N93-12396

SUPERCONDUCTING MAGNETS
Cryostabilization of high-temperature superconducting magnets with subcooled flow in microchannels
[DE92-018174] p 431 N93-11598
Measurement of AC electrical characteristics of SSC superconducting dipole magnets
[DE92-018888] p 431 N93-11625
Research and development of superconducting linear accelerators for neutral particle beam applications
[DE92-019043] p 444 N93-11652
Tables of thermodynamic properties of helium magnet coolant, revision A
[DE92-019098] p 471 N93-11656
Operating experience using venturi flow meters at liquid helium temperature
[DE92-014693] p 313 N93-12140
Results from a large-scale MHD propulsion experiment
[DE92-018177] p 456 N93-12416

SUPERCONDUCTING SUPER COLLIDER
Measurement of AC electrical characteristics of SSC superconducting dipole magnets
[DE92-018888] p 431 N93-11625
Tables of thermodynamic properties of helium magnet coolant, revision A
[DE92-019098] p 471 N93-11656
High energy physics at Tufts University
[DE92-018081] p 444 N93-11668

SUPERCONDUCTIVITY
Frustrated phase separation and high temperature superconductivity
[DE92-019249] p 459 N93-11501
Landau level quantization and superconductivity
[DE92-019028] p 460 N93-11512
Theoretical studies of high-temperature superconductors and highly compressed hydrogen
p 292 N93-11833
Superconducting applications in propulsion systems. Magnetic insulation for plasma propulsion devices
[NASA-CR-184401] p 233 N93-12013
Electronic transport and lasing in microstructures
[DE92-018725] p 441 N93-12115
Josephson Junction digital waveform generation for very wideband radars
[AD-A253668] p 467 N93-12169
Theory of normal metals
[DE92-016828] p 262 N93-12476

SUPERCONDUCTORS
Growth mechanisms of layered superconductors
[DE92-018492] p 458 N93-10987
Higher-order-mode damping and microwave absorption at 2 K
[DE92-016960] p 442 N93-11077
A study of parameters that influence growth and stability of the (Bi(1-x)Pb(x))2 Sr2Ca2Cu3O(y) phase
[DE92-015187] p 462 N93-11703
NEDO Fuel/Storage Technology Subcommittee
[DE92-526262] p 346 N93-11777

Superconducting multilayer structures grown by ALL-MBE
[DE92-018011] p 465 N93-12065
Surface analysis of Ln(2-x)Ce(x)CuO4 (Ln = Pr and Nd) single crystals grown by the top seeded solution method
[AD-A254905] p 469 N93-12286
Nonlinear delay line phase shifters for terahertz superconductive electronic circuits
[AD-A255119] p 294 N93-12290

SUPERCRITICAL PRESSURES
Destruction of explosives and rocket fuels by supercritical water oxidation
[DE92-018874] p 274 N93-11380

SUPERCRITICAL WINGS
Flight test results from a supercritical mission adaptive wing with smooth variable camber
[NASA-TM-4415] p 207 N93-11863

SUPERGIANT STARS
Are some of the luminous high-latitude stars accretion-powered runaways?
[DE92-018853] p 484 N93-11379

SUPERLATTICES
Growth mechanisms of layered superconductors
[DE92-018492] p 458 N93-10987
INAS hole-immobilized doping superlattice long-wave-infrared detector
[NASA-CASE-NPO-17880-1-CU] p 458 N93-11056
Atomistic processes of surface segregation during Si-Ge MBE growth
[DE92-019180] p 459 N93-11496
Step-driven surface segregation and ordering during Si-Ge MBE growth
[DE92-017827] p 463 N93-11772
Excitons in semiconducting superlattices, quantum wells, and ternary alloys
[DE92-015178] p 464 N93-11894
Electronic and optical properties of perfect and imperfect 2 to 6 superlattices p 465 N93-11996
Superconducting multilayer structures grown by ALL-MBE
[DE92-018011] p 465 N93-12065

SUPERNOVA REMNANTS
Morphology and physics of supernova remnants
p 482 N93-11476

SUPERNOVAE
Monte Carlo simulations of the supernova ejection mechanism for the runaway stars
[DE92-018367] p 485 N93-11695
Mechanism for ejecting stars from the Galactic plane
[DE92-018375] p 485 N93-11697
The neutrino process and neutrino r-process
[DE92-014304] p 485 N93-12120

SUPERPLASTICITY
Nanophase ceramics
[AD-A254661] p 272 N93-12246
Design and development of Ni-base superalloy and Ti alloys
[NRIM-SR-92-01] p 261 N93-12322
Superplastic forming of ceramic insulation
p 228 N93-12452

SUPERSONIC AIRCRAFT
Predicted aircraft effects on stratospheric ozone
p 352 N93-11096
Overview of high performance aircraft propulsion research
[NASA-TM-105839] p 213 N93-11530

SUPERSONIC BOUNDARY LAYERS
Overview of supersonic laminar flow control research on the F-16XL ships 1 and 2
[NASA-TM-104257] p 196 N93-11221

SUPERSONIC COMBUSTION
Employment of radicals and excited state species for supersonic combustion photochemical ignition of premixed hydrogen/oxygen mixtures with ArF laser
p 245 N93-11135

SUPERSONIC COMBUSTION RAMJET ENGINES
Effects of reacting flows with turbulence and shock waves on efficiency of scramjet combustors
p 235 N93-11133
Hypervelocity scramjet combustor-nozzle analysis and design
[NASA-CR-190965] p 213 N93-12214
Mach 4 testing of scramjet inlet models
[NAL-TR-1137] p 202 N93-12369

SUPERSONIC FLIGHT
Concorde propulsion: Did we get it right? The Rolls-Royce/SNECMA Olympus 593 engine reviewed
[PNR-90970] p 210 N93-11061
Overview of high performance aircraft propulsion research
[NASA-TM-105839] p 213 N93-11530
On stability and control of SSTO spaceplane in super- and hypersonic ascending phase
[NAL-TR-1128T] p 216 N93-12361

SUPERSONIC FLOW
LV software support for supersonic flow analysis
[NASA-CR-190209] p 297 N93-11074
Overview of supersonic laminar flow control research on the F-16XL ships 1 and 2
[NASA-TM-104257] p 196 N93-11221
Turbulence modeling in shock wave/turbulent boundary layer interactions
[NASA-CR-190933] p 301 N93-11606
Boundary layer relaminarization device
[NASA-CASE-LAR-14470-1] p 199 N93-11876
A comparison of velocity profile measurements in the CDiF diffuser with flow field model calculations
[DE92-015367] p 304 N93-11995
Flow visualization of supersonic flow through a combustor section p 200 N93-12001
Air ejector experiments using the two-dimensional supersonic cascade tunnel: Relationship between ejector performance and throat area ratio, part 1
[NAL-TM-642-PT-1] p 202 N93-12352

SUPERSONIC JET FLOW
OH rotational temperature and concentration measurements in a supersonic jet
[DE92-006700] p 252 N93-12255

SUPERSONIC TRANSPORTS
Overview of supersonic laminar flow control research on the F-16XL ships 1 and 2
[NASA-TM-104257] p 196 N93-11221
Stratospheric aircraft: Impact on the stratosphere?
[DE92-016997] p 355 N93-12104
Stratospheric aircraft exhaust plume and wake chemistry studies
[NASA-CR-189688] p 366 N93-12299
Current Technology for Thermal Protection Systems
[NASA-CP-3157] p 227 N93-12447

SUPERSONIC TURBINES
Increase of energy use on cooled high temperature turbine, phase 3
[MTUM-B91EW-0029-PHASE-3] p 213 N93-11339

SUPERSONIC WIND TUNNELS
Air ejector experiments using the two-dimensional supersonic cascade tunnel: Relationship between ejector performance and throat area ratio, part 1
[NAL-TM-642-PT-1] p 202 N93-12352

SUPERSONICS
New acceleration potential method for supersonic unsteady aerodynamics of lifting surfaces, further extension of the nonplanar supersonic doublet point method, and nonlinear, nongradient optimized rational function approximations for supersonic, transient response unsteady aerodynamics p 201 N93-12344

SUPERSYMMETRY
Studies in quantum field theory
[DE92-011035] p 470 N93-11276
Induced gauge theories and W gravity
[DE92-011218] p 470 N93-11518

SUPPORT SYSTEMS
Information systems planning leading to performance support systems
[DE92-018745] p 475 N93-11441
Introduction to training decisions modeling technologies: The training decisions system
[AD-A249862] p 387 N93-12252
Research and development strategies for human centered and group support technologies
[AD-A254366] p 472 N93-12273

SURFACE CRACKS
An evaluation of repair techniques used for uncontrolled longitudinal cracking and failed longitudinal joints
[PB92-205616] p 277 N93-12072

SURFACE DEFECTS
Surface reconstruction of a three-dimensional ultrasonic flaw
[DE92-018029] p 332 N93-11154
Oxidation, nitridation, and fluorine etching of Si
[AD-A253559] p 249 N93-11755

SURFACE DISTORTION
Deployable reflector antenna performance optimization using automated surface correction and array-feed compensation
[NASA-TP-3228] p 222 N93-12543

SURFACE ENERGY
Growth mechanisms of layered superconductors
[DE92-018492] p 458 N93-10987
Infiltration kinetics and interfacial bond strength of metal matrix composites
[AD-A254002] p 240 N93-11795

SURFACE FINISHING
Surface protection in the aircraft industry
[MBB-Z-0432-92-PUB] p 255 N93-11027
Interfacial microchemical characterization needs in surface processing
[DE92-018269] p 277 N93-11672

SURFACE LAYERS
The structure and transport of the Brazil current between 27 deg and 36 deg south
[AD-A247635] p 374 N93-12247
Light scattering from a sphere on or near an interface
p 448 N93-12531

SURFACE PROPERTIES
Atomistic processes of surface segregation during Si-Ge MBE growth
[DE92-019180] p 459 N93-11496
Study of the effects of a plastic wave induced by laser pulse in a metallic material. Application to the improvement of fatigue strength p 319 N93-12036
Laser-ablation processes
[DE92-011226] p 322 N93-12250

SURFACE REACTIONS
Interfacial and thin film chemistry in electron device fabrication
[AD-A253579] p 288 N93-11257
Computer simulations for the adsorption of polymers onto surfaces
[DE92-018942] p 267 N93-11628
The chemistry of Si3N4 and Si deposition studied using molecular beam techniques
[DE92-018268] p 463 N93-11797
Electron emission during multicharged ion-metal surface interactions
[DE92-017134] p 439 N93-11849
Analysis of surfaces from the LDEF A0114, phase 2
[NASA-CR-190596] p 270 N93-11993
Erosion rates for polymers measured on LDEF
p 270 N93-11994
The role of backbond strain in silicon surfaces on the decomposition of NH3 and PH3
[AD-A253771] p 250 N93-12062
The adsorption of C60 and the co-adsorption of C60 and H2O on (alpha)-Al2O3 (1 -1 0 2)-(2x1)
[DE92-018002] p 465 N93-12093
Hydrogen assisted heat transfer during diamond growth using carbon and tantalum filaments
[AD-A247944] p 468 N93-12218
Gas-surface interactions near dissociation threshold
[AD-A250205] p 252 N93-12254
Workshop on Adhesion and Intermolecular Forces
[AD-A255191] p 272 N93-12276

SURFACE ROUGHNESS
Direct numerical simulation of instabilities in parallel flow with spherical roughness elements
[NASA-TM-105847] p 300 N93-11529
Deployable reflector antenna performance optimization using automated surface correction and array-feed compensation
[NASA-TP-3228] p 222 N93-12543

SURFACE TEMPERATURE
Gas-surface interactions near dissociation threshold
[AD-A250205] p 252 N93-12254

SURFACE TREATMENT
Analysis of plasma-treated wire insulation
[DE92-019471] p 291 N93-11643

SURFACE WAVES
Sound propagation over rigid porous layers
p 432 N93-11179

SURFACES
Workshop on Surface Science and Technology
[AD-A253566] p 264 N93-11149

SURFACTANTS
Computer simulations for the adsorption of polymers onto surfaces
[DE92-018942] p 267 N93-11628

SURVEYS
Aerothermal test results from the second flight of the Pegasus booster
[NASA-TM-4391] p 296 N93-10969
A survey of European calibration facilities for underwater acoustics
[NPL-RSA(EXT)-32] p 433 N93-11328
Environmental problems and trends of international responses, 2
[DE92-531118] p 355 N93-11846
Smoking status and body composition, exercise, dietary intake, and alcohol/caffeine consumption
[AD-A250648] p 385 N93-11893

SURVIVAL
Mechanisms of immune failure in burn injury
p 376 N93-11285

SUSPENDING (MIXING)
Hydrodynamic particle migration in small-amplitude, oscillatory, circular couette flow: The limits of reversibility
[DE92-008480] p 303 N93-11843
Interaction of sound with sound by novel mechanisms: Ultrasonic four-wave mixing mediated by a suspension and ultrasonic three-wave mixing at a free surface
[AD-A254657] p 435 N93-12097

SUSPENSIONS
The degradation of parachutes: Age and mechanical wear
[AD-A252243] p 200 N93-12179
SWEAT COOLING
A preliminary study associated with the experimental measurement of the aero-optic characteristics of hypersonic configurations
[AD-A253792] p 200 N93-12063
SWEEP ANGLE
Effects of sweep on the physics of unsteady shock-induced turbulent separated flows
[AD-A247035] p 198 N93-11742
SWEPT WINGS
Overview of supersonic laminar flow control research on the F-16XL ships 1 and 2
[NASA-TM-104257] p 196 N93-11221
Boundary layer relaminarization device
[NASA-CASE-LAR-14470-1] p 199 N93-11876
SWEPTBACK WINGS
Mach 4 testing of scramjet inlet models
[NAL-TR-1137] p 202 N93-12369
SWITCHES
Characteristics of current filamentation in high gain photoconductive semiconductor switching
[DE92-018277] p 291 N93-11693
SWITCHING CIRCUITS
Characteristics of current filamentation in high gain photoconductive semiconductor switching
[DE92-018277] p 291 N93-11693
SYMBOLIC PROGRAMMING
A primer on polynomial resultants
[AD-A246883] p 426 N93-11463
SYMBOLS
Design of instrument approach procedure charts: Comprehension speed of missed approach instructions coded in text or icons
[PB92-205673] p 204 N93-11252
Syntax and lexis of the specification language Z
[RSRE-MEMO-4367] p 414 N93-12326
SYMMETRY
Nucleon axial coupling constants and QCD sum rules
[DE92-014227] p 439 N93-11844
SYNCHRONISM
Guide to synchronization of video systems to IRIG timing
[AD-A254626] p 285 N93-12240
Formal mechanization of device interactions with a process algebra
[NASA-CR-189644] p 405 N93-12347
SYNCHRONOUS SATELLITES
Ephemeris calculation and orbit determination of geostationary satellites, using Taylor series integration
[SER-C-384] p 220 N93-11335
SYNCHROTRON RADIATION
Tunable, short pulse hard x rays from a compact laser synchrotron source
[AD-A254288] p 315 N93-11195
Calibration techniques for high flux x ray detectors
[DE92-017513] p 312 N93-11768
Dynamic vacuum analysis for APS high heat flux beamline front ends using optical ray-tracing simulation methods
[DE92-019032] p 445 N93-11831
SYNCHROTRONS
Topics on RF beam control of a synchrotron
[DE92-019217] p 443 N93-11498
Analysis of periodic transient beam loading of the AGS
[DE92-019243] p 443 N93-11499
Beam-loading stability in synchrotrons with a higher RF harmonic
[DE92-018982] p 443 N93-11510
RF beam loading in the Brookhaven AGS with booster injection
[DE92-019452] p 444 N93-11641
Calibration techniques for high flux x ray detectors
[DE92-017513] p 312 N93-11768
Static and transient beam loading of a synchrotron
[DE92-019244] p 445 N93-11776
SYNTAX
Syntax and lexis of the specification language Z
[RSRE-MEMO-4367] p 414 N93-12326
Requirements Specification Language (RSL) and supporting tools
[NASA-CR-189700] p 405 N93-12345
SYNTHESIS (CHEMISTRY)
The synthesis and crystal structure of LaHSe2O6, a layered, anhydrous selenite
[AD-A251050] p 458 N93-10996
Chemical reactions and properties of organosilicon compounds related to new materials
[AD-A253233] p 246 N93-11218
Synthesis and characterization of novel organogallium-phosphorus compounds: X ray crystal structures of Ph2GaP (SiMe3)2Ga (Ph2Cl, Ph2 (Cl)Ga.P (SiMe3)3, and Ph3Ga.P (SiMe3)3
[AD-A253841] p 462 N93-11724
Synthesis of single phase (alpha)-Fe, Fe3C and Fe7C3 nano-particles by CO2 laser pyrolysis technique
[DE92-015654] p 250 N93-11847
Design and synthesis of molecular systems capable of supporting intracavity chemical reactions
[AD-A251024] p 440 N93-11872
Synthesis and reactivity of siloxide and silamide complexes pertaining to bond breaking and aggregation phenomena
[AD-A254703] p 468 N93-12231
High-performance synthetic fibers for composites
[AD-A252645] p 242 N93-12292
Biological conversion of synthesis gas culture development
[DE92-001279] p 375 N93-12482
SYNTHETIC APERTURE RADAR
Development of a GPS-aided motion measurement, pointing, and stabilization system for a synthetic aperture radar
[DE92-017053] p 204 N93-11152
The tomographic formulation of spotlight mode synthetic aperture radar extended to three dimensional targets
[DE92-013666] p 280 N93-11234
A comprehensive mission to planet Earth: Woods Hole Space Science and Applications Advisory Committee Planning Workshop
[NASA-TM-108011] p 343 N93-11878
SYNTHETIC FIBERS
High-performance synthetic fibers for composites
[AD-A252645] p 242 N93-12292
SYSTEM EFFECTIVENESS
Evaluation of a user information satisfaction short-form instrument
[AD-A250702] p 478 N93-11840
SYSTEM FAILURES
Tradeoffs in implementing primary-backup protocols
[NASA-CR-190970] p 472 N93-12212
SYSTEMS ANALYSIS
Flight-determined stability analysis of multiple-input-multiple-output control systems
[NASA-TM-4416] p 214 N93-11178
Analysis of methods — information systems evolution environment
[NASA-CR-190278] p 407 N93-11368
Information systems planning leading to performance support systems
[DE92-018745] p 475 N93-11441
Development of the Personnel-based System Evaluation Aid (PER-SEVAL) performance shaping functions
[AD-A252820] p 386 N93-11779
Systems engineering and technical assistance in support of digital gallium arsenide insertion projects
[AD-A253751] p 463 N93-11790
Integrity-oriented control objectives: Proposed revisions to the Trusted Computer System Evaluation Criteria (TCSEC), DOD 5200.28-STD
[AD-A253989] p 404 N93-11809
An approach to integrating and creating flexible software environments p 396 N93-11946
SYSTEMS ENGINEERING
Experience of designing a relational materials database
[PNR-90893] p 473 N93-11012
Introduction to the Rolls-Royce design process
[PNR-90939] p 210 N93-11039
The application of manufacturing systems engineering for aero engine gears
[PNR-90944] p 324 N93-11054
Artificial intelligence and CFD: Expert systems for the design of airfoils and for grid generation
[DIGE-EST-TN-016] p 206 N93-11161
Engineering Information System (EIS)
[AD-A254013] p 476 N93-11508
Systems engineering and technical assistance in support of digital gallium arsenide insertion projects
[AD-A253751] p 463 N93-11790
Power system commonality study
[NASA-CR-190765] p 347 N93-12019
Reengineering using a data abstraction based specification language
[AD-A254726] p 414 N93-12341
A methodology for systems requirements specification and traceability for large real time complex systems
[AD-A254738] p 419 N93-12358
SYSTEMS INTEGRATION
SITE project. Phase 1: Continuous data bit-error-rate testing
[NASA-TP-3279] p 224 N93-11001
Deriving and manipulating module interfaces
[AD-A253869] p 406 N93-11145
Formal mechanization of device interactions with a process algebra
[NASA-CR-189644] p 405 N93-12347
SYSTEMS MANAGEMENT
Description of the SSF PMAD DC testbed control system data acquisition function
[NASA-TM-105843] p 417 N93-11005
Integrity in automated information systems
[AD-A253990] p 477 N93-11732

T

TACTICS
Intelligent TDA systems using neural networks, phase 1
[AD-A252556] p 420 N93-11000
TACTILE SENSORS (ROBOTICS)
Object recognition with a robot hand
p 420 N93-11457
Contact detection and contact motion for error recovery in the presence of uncertainties p 398 N93-11956
TAKEOFF
Summary of findings from the PIREP-based analyses conducted during the 1988 to 1990 evaluations of TDWR-based and TDWR/LLWAS-based alert services provided to landing/departing pilots
[AD-A253859] p 367 N93-11144
TANKS (CONTAINERS)
Mechanical properties of 1950's vintage 304 stainless steel weldment components after low temperature neutron irradiation
[DE92-017059] p 259 N93-12107
TANTALUM ALLOYS
Development of stable metallization systems
[AD-A253569] p 264 N93-11079
Effect of microstructure on passive film formation and breakdown on Al alloys
[AD-A245863] p 260 N93-12118
TANTALUM COMPOUNDS
Synthesis and reactivity of siloxide and silamide complexes pertaining to bond breaking and aggregation phenomena
[AD-A254703] p 468 N93-12231
TANTALUM NITRIDES
Synthesis and reactivity of siloxide and silamide complexes pertaining to bond breaking and aggregation phenomena
[AD-A254703] p 468 N93-12231
TARGET ACQUISITION
Short-range radar system
[AD-D015339] p 278 N93-11044
The design and implementation of radar clutter modelling and adaptive target detection techniques
p 283 N93-11913
TARGET RECOGNITION
Nonlinear resistive grid wavelet transformations for texture feature extraction
[AD-A254705] p 285 N93-12332
TARGETS
Laser material interaction in confined medium
p 319 N93-12035
Study of the dynamic degradation under the action of a shock wave induced by pulsed laser
p 319 N93-12037
Numerical simulation of a pressure gradient in a multilayer target: Temperature evolution
p 309 N93-12039
TASK COMPLEXITY
The effect of task complexity on user interfaces: A comparison of command language interface and direct manipulation interface
[AD-A246061] p 412 N93-11859
Mission Control Center enhancement opportunities in the 1990's p 396 N93-11942
Human performance in complex task environments: A basis for the application of adaptive automation
[AD-A255067] p 390 N93-12486
TASKS
The effects of wearing protective chemical warfare combat clothing on human performance
[AD-A250716] p 390 N93-12491
TAYLOR INSTABILITY
Front tracking and the interaction of nonlinear waves
[AD-A253544] p 297 N93-11148
TAYLOR SERIES
Ephemeris calculation and orbit determination of geostationary satellites, using Taylor series integration
[SER-C-384] p 220 N93-11335
Comparison of truncation error of finite-difference and finite-volume formulations of convection terms
[NASA-TM-105861] p 426 N93-11531
TEA LASERS
CO2 laser frequency doubling
[AD-A251060] p 314 N93-10997

TEARING MODES (PLASMAS)
Heat load material studies: Simulated tokamak disruptions
[DE92-018275] p 452 N93-11674
Results from the US/USSR exchange for heat load material studies of simulated tokamak disruptions
[DE92-018285] p 453 N93-11694
Nonlinear evolution of resistive tearing mode instability with shear flow and viscosity
[DE92-012138] p 453 N93-11745

TECHNOLOGIES
Workshop on Surface Science and Technology
[AD-A253566] p 264 N93-11149
JPRS report: Science and technology. Central Eurasia: Engineering and equipment
[JPRS-UEQ-92-009] p 220 N93-11169

TECHNOLOGY ASSESSMENT
Rolls-Royce civil engine technology
[PNR-90936] p 210 N93-11036
The Trent: Towards greater thrust
[PNR-90937] p 210 N93-11037
Introduction to the Rolls-Royce design process
[PNR-90939] p 210 N93-11039
Development of advanced carbon-carbon annular flameholders for gas turbines
[PNR-90947] p 211 N93-11106
Present and future trends in turbine blade material and manufacture technology
[PNR-90960] p 255 N93-11111
Contributions to CD Space Committee, 1991: Summary and analysis
[PB92-195312] p 219 N93-11216
The technical background to standards for eyebolts
[NPL-DMM(A)-52] p 325 N93-11327
Speech recognition systems and their military applications
[BR91882] p 280 N93-11366
Solid state sciences committee forum
[AD-A253556] p 463 N93-11753
Systems engineering and technical assistance in support of digital gallium arsenide insertion projects
[AD-A253751] p 463 N93-11790
Evaluation of advanced pressure sensor technology
[DE92-011004] p 312 N93-11806
Electricity from biomass: A development strategy
[DE92-010590] p 346 N93-11814
The hydrogen technology assessment, phase 1
[NASA-CR-190969] p 349 N93-12394

TECHNOLOGY TRANSFER
Advanced materials and processing: The Federal program in materials science and technology. A report by the FCCSET Committee on Industry and Technology to supplement the President's fiscal year 1993 budget
[PB92-199108] p 238 N93-11470
Computer Science and Telecommunications Board summary of activities
[DE92-016467] p 404 N93-11761
The development and technology transfer of software engineering technology at NASA. Johnson Space Center
p 396 N93-11943
Selected case studies of technology transfer from mission-oriented applied research
[DE92-018957] p 481 N93-12067
FNAS computational fluid dynamics
[NASA-CR-184394] p 307 N93-12397
ONRASIA scientific information bulletin, volume 17, number 3
[AD-A255073] p 490 N93-12470

TECHNOLOGY UTILIZATION
Speech recognition systems and their military applications
[BR91882] p 280 N93-11366
Systems engineering and technical assistance in support of digital gallium arsenide insertion projects
[AD-A253751] p 463 N93-11790
ONRASIA scientific information bulletin, volume 17, number 3
[AD-A255073] p 490 N93-12470

TECTONICS
Quaternary volcanism, tectonics, and sedimentation in the Idaho National Engineering Laboratory area
[DE92-017851] p 362 N93-11692

TELECOMMUNICATION
On understanding in communicating systems and the error in the Chinese Room thought-experiment
[RSRE-MEMO-4391] p 278 N93-10977
10 kW L-band amplifier tubes for efficient and reliable troposcatter communication transmitter systems
[AD-A253246] p 290 N93-11504
Integrated services digital network conformance testing. Layer 1, physical layer. Part 2: Basic rate U interface, user side
[PB92-181114] p 418 N93-11714
Implementing system simulation of C3 systems using autonomous objects
[NASA-CR-190845] p 283 N93-11716
Future FAA telecommunications plan
[AD-A249133] p 283 N93-11760
Computer Science and Telecommunications Board summary of activities
[DE92-016467] p 404 N93-11761

TELEMETRY
Design development of a neural network-based telemetry monitor p 394 N93-11933
Transient Reduction Analysis using Neural Networks (TRANN)
[DE92-012150] p 421 N93-12153

TELEOPERATORS
A new scheme of force reflecting control
p 399 N93-11960
An 8-DOF dual-arm system for advanced teleoperation performance experiments p 400 N93-11964
Performance experiments with alternative advanced teleoperator control modes for a simulated solar maximum satellite repair p 400 N93-11965
The development of system components to provide proprioceptive and tactile information to the human for future telepresence systems p 330 N93-11968
Exoskeleton master controller with force-reflecting telepresence p 330 N93-11970
Remote systems development p 330 N93-11971
Operator vision aids for space teleoperation assembly and servicing p 391 N93-11981

TELEROBOTICS
Integration of task level planning and diagnosis for an intelligent robot p 393 N93-11929
Fuzzy control system for a remote focusing microscope p 314 N93-11934
Requirements and applications for robotic servicing of military space systems p 230 N93-11953
Effects of spatially displaced feedback on remote manipulation tasks p 400 N93-11966
Remote systems development p 330 N93-11971
Self mobile space manipulator project
p 331 N93-11973
Operator vision aids for space teleoperation assembly and servicing p 391 N93-11981

TELESCOPES
Final Report, January 1991 - July 1992
[AD-A254659] p 483 N93-12244

TELEVISION CAMERAS
Initial laboratory evaluation of color video cameras
[DE92-018274] p 311 N93-11673
High-speed FPS vidicon camera
[DE92-018989] p 313 N93-12069
Video camera as a visual sensor
[NAL-TR-1132] p 314 N93-12373

TEMPERATE REGIONS
A real time sharpening of NOGAPS predictions of mid-latitude Central Pacific cyclones
[AD-A255157] p 372 N93-12424

TEMPERATURE CONTROL
Intelligent fault management for the Space Station active thermal control system p 391 N93-11930
Lunar PMAD technology assessment
[NASA-CR-189225] p 347 N93-12017
Current Technology for Thermal Protection Systems
[NASA-CP-3157] p 227 N93-12447
Thermal control/oxidation resistant coatings for titanium-based alloys p 229 N93-12457
Advanced two-phase heat transfer systems
p 229 N93-12459

TEMPERATURE DEPENDENCE
Magnetic properties and critical behavior of the conductivity near the M-I transition
[DE92-018948] p 461 N93-11629
The effect of temperature dependent thermal properties on parametric weld size predictions
[DE92-018816] p 260 N93-12232
OH rotational temperature and concentration measurements in a supersonic jet
[DE92-006700] p 252 N93-12255
Combustion characteristics of the LO2/GCH4 fuel-rich preburners for staged combustion cycle rocket engines
[NAL-TR-1124] p 234 N93-12368

TEMPERATURE DISTRIBUTION
Sodium-lidar mesosphere examinations: Selected elements of the experimental construction of a mobile instrument and evaluation of the data acquired with a stationary Na-lidar during the DYANA campaign
[BONN-IR-91-78] p 357 N93-11006
Method of remotely characterizing thermal properties of a sample
[NASA-CASE-LAR-13508-3-CU] p 216 N93-11057
On the dependence of the dynamic crack tip temperature fields in metal upon crack tip velocity and material parameters
[AD-A253657] p 335 N93-11219
Frequency response in short thermocouple wires
[NASA-CR-190943] p 310 N93-11612
Review of the physical and mechanical properties and potential applications of the B2 compound NiAl: Unabridged version of a paper published in International materials review
[NASA-TM-105598] p 258 N93-11635
Potassium D-line fitting for investigation of MHD boundary layers
[DE92-019020] p 454 N93-11826
Numerical simulation of a pressure gradient in a multilayer target: Temperature evolution
p 309 N93-12039
Preliminary study of the homogeneity of the density and temperature of long plasmas used for X laser studies
p 320 N93-12044
Hydrogen assisted heat transfer during diamond growth using carbon and tantalum filaments
[AD-A247944] p 468 N93-12218

TEMPERATURE EFFECTS
Elevated temperature fatigue crack growth in a nickel base superalloy under dwell conditions
[PNR-90997] p 255 N93-11115
Curing and mechanical properties of T800-V398 graphite/bismaleimide at different temperatures
[DLR-FB-92-02] p 237 N93-11143
Synthesis and side chain liquid crystal polymers by living ring opening metathesis polymerization. 5: Influence of mesogenic group and interconnecting group on the thermotropic behavior of the resulting polymers
[AD-A253568] p 264 N93-11150
The domain structure features of epitaxial PbTiO3 thin films prepared by MOCVD
[DE92-010907] p 459 N93-11190
On the dependence of the dynamic crack tip temperature fields in metal upon crack tip velocity and material parameters
[AD-A253657] p 335 N93-11219
Thermal non-Newtonian elastohydrodynamic lubrication of line contacts under sliding-rolling and simple sliding conditions p 324 N93-11263
Studies of safety, infectivity, and immunogenicity of a new Temperature Sensitive (TS) 51-1 strain of S. typhi as a new live oral typhoid fever vaccine candidate
p 381 N93-11306
Evaluation of epoxy cured with Ethacure 100 curing agent for use in headers for thermal batteries
[DE92-019326] p 267 N93-11552
Development of strength and conductivity in deformation processed copper base alloys
[DE92-018807] p 257 N93-11572
Design of a high-temperature experiment for evaluating advanced structural materials
[NASA-TM-105833] p 337 N93-11624
The potential effects of concurrent increases in temperature, CO2 and O3 on net photosynthesis, as mediated by rubisCO
[DE92-019411] p 374 N93-11630
Review of the physical and mechanical properties and potential applications of the B2 compound NiAl: Unabridged version of a paper published in International materials review
[NASA-TM-105598] p 258 N93-11635
Heat load material studies: Simulated tokamak disruptions
[DE92-018275] p 452 N93-11674
Numerical simulation for the coaxial electromagnetic launcher using hybrid potentials with FE-BE method
p 222 N93-11726
The mechanical and microstructural stability of austenitic stainless steels strengthened by MC-forming elements
[DE91-015314] p 259 N93-11857
Laboratory and numerical studies of dynamical processes related to thermal convection in the Earth's mantle p 364 N93-11900
Compensated high temperature strain gage
[NASA-CASE-LAR-14776-1] p 313 N93-12205
The effect of temperature dependent thermal properties on parametric weld size predictions
[DE92-018816] p 260 N93-12232
Influence of strain rate on the structure/property behavior of the alpha-2 alloy Ti-24.5Al-10.5Nb-1.5Mo
[DE92-008490] p 261 N93-12256

TEMPERATURE GRADIENTS
Design of a high-temperature experiment for evaluating advanced structural materials
[NASA-TM-105833] p 337 N93-11624
Anomalous ion thermal transport in hot ion plasmas by the ion temperature gradient mode
[DE92-016686] p 456 N93-12493

TEMPERATURE MEASUREMENT
Aerothermal test results from the second flight of the Pegasus booster
[NASA-TM-4391] p 296 N93-10969

Sodium-lidar mesosphere examinations: Selected elements of the experimental construction of a mobile instrument and evaluation of the data acquired with a stationary Na-lidar during the DYANA campaign
[BONN-IR-91-78] p 357 N93-11006
Experimental heat transfer results in turbine stators and rotors and a comparison with theory
[PNR-90945] p 210 N93-11055
Method of remotely characterizing thermal properties of a sample
[NASA-CASE-LAR-13508-3-CU] p 216 N93-11057
Ion temperature measurements in tokamak plasmas by Rutherford scattering
[PB92-184738] p 451 N93-11245
A mutual inductance technique for contact-free T(sub c) measurement of high temperature superconductors
[NPL-DES-116] p 289 N93-11393
A distributed data acquisition and centralized data reduction system for flexible and efficient measurements
[DE92-019021] p 312 N93-11827
Numerical simulation of a pressure gradient in a multilayer target: Temperature evolution
p 309 N93-12039
Plasma temperatures from first-hit neutron time-of-flight spectra
[DE92-018006] p 454 N93-12060
Operating experience using venturi flow meters at liquid helium temperature
[DE92-014693] p 313 N93-12140
The role of advanced optical diagnostics in monitoring and controlling an MHD power plant. Part 2: 50 MW(t), POC topping cycle
[DE92-015368] p 455 N93-12141
Ion temperature measurements on field reversed configuration plasmas p 457 N93-12535

TEMPERATURE MEASURING INSTRUMENTS
A cryogenic phonon detector to search for dark matter particles p 481 N93-11198

TEMPERATURE PROFILES
Strain-gauge balance performance and internal temperature gradients measured in a cryogenic environment
[RAE-TM-AERO-2232] p 218 N93-11906

TEMPERATURE SENSORS
Natural convection heat transfer studies of simulated and actual electronic components using dielectric liquids for immersion cooling
[AD-A255173] p 341 N93-12376

TEMPERING
International ADI-Seminar: Austempered Ductile Iron
[PB92-180660] p 256 N93-11244

TEMPORAL DISTRIBUTION
Temporal scattering and response software users' manual, version 2 and 3
[DE92-040934] p 282 N93-11632
Experimental study of x ray laser in lithumoid aluminum p 321 N93-12045

TEMPORAL RESOLUTION
Emittance measuring device for charged particle beams
[AD-D015371] p 442 N93-11060
X-UV spectroscopy temporal resolution
p 318 N93-12028
Hydrodynamic study of multilayer targets by spatial and temporal resolution shadow spectroscopy
p 254 N93-12050

TENSILE CREEP
The time-dependent stress-optical behaviour of polycarbonate in the glass transition region
p 269 N93-11985

TENSILE DEFORMATION
Fracture mechanics of model fiber composites
p 237 N93-11247
The effect of precipitate forming elements in Al 4.5 percent Mg alloys on the measured acoustic emission and on Lueders band deformation
[DE92-016864] p 465 N93-12073

TENSILE PROPERTIES
Micromechanisms of deformation and fracture in aluminum based MMC's: Interface effects
[AD-A253560] p 259 N93-11850
Processing and properties of NbTi based alloys
[DE92-016692] p 261 N93-12445
Spectrum fatigue behaviour of powder metallurgy aluminum alloys
[AD-A255060] p 262 N93-12468
Mechanical properties of centrifugally cast metal matrix composites
[AD-A254321] p 243 N93-12483

TENSILE STRENGTH
Relative sliding durability of candidate high temperature fiber seal materials
[NASA-TM-105806] p 236 N93-10978
Curing and mechanical properties of T800-V398 graphite/bismaleimide at different temperatures
[DLR-FB-92-02] p 237 N93-11143
Microstructure and mechanical properties of reactive hot isostatic pressed TiAl powder material
[GKSS-91/E/60] p 256 N93-11336
Penetration mechanics of composites
[AD-A249230] p 240 N93-11835
Mechanical properties of 1950's vintage 304 stainless steel weldment components after low temperature neutron irradiation
[DE92-017059] p 259 N93-12107

TENSILE STRESS
Analytical method of calculating the thermoelastic constants of a multi-phase unidirectional composite
[NPL-DMM(A)-57] p 238 N93-11409
Tension and compression fatigue response of unnotched 3D braided composites
[NASA-CR-189678] p 239 N93-11611
The measurement and calculation of birefringence in quenched polycarbonate specimens
p 269 N93-11986

TENSILE TESTS
Isotopic tailoring with 59-Ni to study the effect of helium on microstructural evolution and mechanical properties of neutron-irradiated Fe-Cr-Ni alloys
[DE92-019372] p 257 N93-11557
The time-dependent stress-optical behaviour of polycarbonate in the glass transition region
p 269 N93-11985
Mechanical properties for advanced engine materials
[AD-A252632] p 242 N93-12181
Method and apparatus for gripping test specimens
[NASA-CASE-LEW-15345-1] p 329 N93-12327

TENSION
Payout tension control system for reel mounted cable
[AD-D015362] p 325 N93-11423

TERMINAL BALLISTICS
Penetration mechanics of composites
[AD-A249230] p 240 N93-11835

TERMINAL GUIDANCE
Controller evaluation of initial data link terminal air traffic control services: Mini study 2, volume 1
[DOT/FAA/CT-92/2-VOL-1] p 205 N93-11704
Controller evaluation of initial data link terminal air traffic control services: Mini study 2, volume 2
[DOT/FAA/CT-92/2-VOL-2] p 205 N93-11705

TERNARY ALLOYS
Development of stable metallization systems
[AD-A253569] p 264 N93-11079
The effect of silicon, tin, and chromium on the corrosion and mechanical properties of zirconium - molybdenum - niobium
[AD-A254102] p 258 N93-11787
Excitons in semiconducting superlattices, quantum wells, and ternary alloys
[DE92-015178] p 464 N93-11894

TERRAIN
Structure of the nocturnal boundary layer over a complex terrain
[DE92-018141] p 362 N93-11669
Computing optimum routes across terrain using DAP
[RSRE-MEMO-4299] p 412 N93-11712
Photogrammetric GIS technology: Feature mapping on digital stereo imagery
[AD-A254255] p 477 N93-11748
Automated extraction of aircraft runway patterns from radar imagery
[AD-A254258] p 218 N93-11751
Integration of radar altimeter, precision navigation, and digital terrain data for low-altitude flight
[NASA-TM-103958] p 205 N93-12320

TERRAIN ANALYSIS
Generation of 3-D surface maps in waste storage silos using a structured light source p 399 N93-11958

TERRAIN FOLLOWING AIRCRAFT
Integration of radar altimeter, precision navigation, and digital terrain data for low-altitude flight
[NASA-TM-103958] p 205 N93-12320

TERRESTRIAL RADIATION
Global change and the dark of the moon
[AD-A255181] p 486 N93-12380

TEST CHAMBERS
Acoustical evaluation of the NASA Lewis 9 by 15 foot low speed wind tunnel
[NASA-TP-3274] p 218 N93-12016

TEST EQUIPMENT
Method and apparatus for gripping test specimens
[NASA-CASE-LEW-15345-1] p 329 N93-12327

TEST FACILITIES
Ground test facilities for evaluating nuclear thermal propulsion engines and fuel elements
[DE92-017039] p 231 N93-10973
Testing for integrity
[PNR-90927] p 210 N93-11024
A test facility for the thermofluid-dynamics of gas bearing lubrication films
[PNR-90897] p 263 N93-11032
Rotational CARS measurements in a rotating cavity with axial throughflow of cooling air: Oxygen concentration measurements
[PNR-90935] p 244 N93-11035
A survey of European calibration facilities for underwater acoustics
[NPL-RSA(EXT)-32] p 433 N93-11328
Developments in icing test techniques for aerospace applications in the RAE Pyestock (England) altitude test facility
[RAE-TM-P-1214] p 207 N93-11485
A development approach for nuclear thermal propulsion
[DE92-018020] p 232 N93-11596

TEST FIRING
Hot fire test results of subscale tubular combustion chambers
[NASA-TP-3222] p 232 N93-11614

TEST RANGES
Lightning threat warning system at the Tonopah Test Range
[DE92-040444] p 221 N93-11631

TEST STANDS
A summary of the JANNAF workshop on diagnostics
p 248 N93-11451
Measured data for the Sandia 34-meter vertical axis wind turbine
[DE92-019807] p 348 N93-12075

TETHERED SATELLITES
The order n simulation of tether motions based on a rigid body tether model p 225 N93-11999

TETHERING
The order n simulation of tether motions based on a rigid body tether model p 225 N93-11999

TETHERLINES
The order n simulation of tether motions based on a rigid body tether model p 225 N93-11999

TEXTURES
Visualizing wind velocities by advecting cloud textures
[DE92-014717] p 371 N93-12154
Nonlinear resistive grid wavelet transformations for texture feature extraction
[AD-A254705] p 285 N93-12332

THALLIUM COMPOUNDS
Infrared phonon structure in epitaxial films of Tl2Ca2Ba2Cu3O10 at low temperatures
[DE92-017078] p 466 N93-12109
Submillimeter and microwave residual losses in epitaxial films of Y-Ba-Cu-O and Bl-Ca-Ca-Cu-O
[DE92-017075] p 466 N93-12125

THEMATIC MAPPERS (LANDSAT)
Land use/land cover classification using digitally merged spot panchromatic and Landsat thematic mapper imagery
[PB92-188416] p 343 N93-11701

THEOREM PROVING
Implicit parallelism in genetic algorithms
[REPT-92-012] p 418 N93-11180
Formal mechanization of device interactions with a process algebra
[NASA-CR-189644] p 405 N93-12347

THEOREMS
Matching and vertex packing: How hard are they?
[AD-A245928] p 423 N93-10991
Implicit parallelism in genetic algorithms
[REPT-92-012] p 418 N93-11180
Geometrical concepts about learning rules in networks with binary and ternary output functions
[REPT-92-020] p 411 N93-11592
Limit theorems for Fisher-score change processes
p 427 N93-12328

THERAPY
Center of Excellence in laser medicine
[DE92-018760] p 384 N93-11445

THERMAL ANALYSIS
Studies of interactive plasma processes in the polar cusp
[NASA-CR-190892] p 357 N93-10964
Method of remotely characterizing thermal properties of a sample
[NASA-CASE-LAR-13508-3-CU] p 216 N93-11057
Thermal analysis and design of polarizer mirrors for waveguides in the D3-D tokamak
[DE92-018884] p 451 N93-11382
Thermal stress and strain analysis in traveling autogenous welds
[DE92-019363] p 326 N93-11556
Thermal fracture service life analysis of a case bonded visco-elastic cylinder p 339 N93-12008
Thermostructural tailoring of fiber composite structures
[NASA-TM-105882] p 242 N93-12078

THERMAL BATTERIES
Evaluation of epoxy cured with Ethacure 100 curing agent for use in headers for thermal batteries
[DE92-019326] p 267 N93-11552

Evaluation of flotation for purification of pyrite for use in thermal batteries
[DE92-019330] p 290 N93-11553

THERMAL BOUNDARY LAYER
Potassium D-line fitting for investigation of MHD boundary layers
[DE92-019020] p 454 N93-11826

THERMAL CONDUCTIVITY
CO2 laser frequency doubling
[AD-A251060] p 314 N93-10997
On the dependence of the dynamic crack tip temperature fields in metal upon crack tip velocity and material parameters
[AD-A253657] p 335 N93-11219
Thermal non-Newtonian elastohydrodynamic lubrication of line contacts under sliding-rolling and simple sliding conditions p 324 N93-11263
Development of strength and conductivity in deformation processed copper base alloys
[DE92-018807] p 257 N93-11572
The conversion of plastic work to heat around a dynamically propagating crack in metals
[AD-A253801] p 258 N93-11782
Workshop on Characterizing Diamond Films
[PB92-205426] p 271 N93-12086

THERMAL CONTROL COATINGS
Thermal control/oxidation resistant coatings for titanium-based alloys p 229 N93-12457

THERMAL CYCLING TESTS
Application of polyimides to aeroengine components
[PNR-90907] p 334 N93-11013
Generation of thermal strains in carbon fibre-reinforced bismaleimide (PMR-15) composites, part 1, 2 and 3
[PNR-90976-PT-1-2-3] p 236 N93-11065
An evaluation of the blind lap joint for the surface mount attachment of chip components
[DE92-017045] p 277 N93-12106

THERMAL ENERGY
On the dependence of the dynamic crack tip temperature fields in metal upon crack tip velocity and material parameters
[AD-A253657] p 335 N93-11219

THERMAL ENVIRONMENTS
Physiologically constrained aerocapture for manned Mars missions p 226 N93-12185

THERMAL FATIGUE
A creep cavity growth model for creep-fatigue life prediction of a unidirectional W/Cu composite
[NASA-TM-105780] p 333 N93-10967
Short fatigue crack growth in a nickel-base superalloy at room and elevated temperature
[PNR-90892] p 255 N93-11031
Elevated temperature fatigue crack growth in a nickel base superalloy under dwell conditions
[PNR-90997] p 255 N93-11115
Thermomechanical fatigue behavior of SiC/Ti-24Al-11Nb in air and argon environments
[NASA-TM-105723] p 238 N93-11399

THERMAL INSULATION
Superconducting applications in propulsion systems. Magnetic insulation for plasma propulsion devices
[NASA-CR-184401] p 233 N93-12013
Current Technology for Thermal Protection Systems
[NASA-CP-3157] p 227 N93-12447

THERMAL PLASMAS
Comprehensive computational model for thermal plasma processing
[DE92-018015] p 454 N93-12066
The collaborative program of research in engineering sciences
[DE92-016838] p 490 N93-12477

THERMAL PROTECTION
Current Technology for Thermal Protection Systems
[NASA-CP-3157] p 227 N93-12447
Reusable thermal protection system development: A prospective p 227 N93-12448
Thermal protection systems manned spacecraft flight experience p 227 N93-12449
Advanced ceramic matrix composites for TPS
p 228 N93-12450
Thermal protection using very high temperature ceramics p 228 N93-12451
Predicted and tested performance of durable TPS
p 228 N93-12454
Current research in oxidation-resistant carbon-carbon composites at NASA. Langley Research Center
p 229 N93-12456
Active cooling from the sixties to NASP
p 208 N93-12458

THERMAL RESISTANCE
The effect of silicon, tin, and chromium on the corrosion and mechanical properties of zirconium - molybdenum - niobium
[AD-A254102] p 258 N93-11787
Characteristics of heat transfer to nickel plated chamber walls of high pressure rocket combustors
[NAL-TR-1126T] p 234 N93-12372

THERMAL STABILITY
Triisopropylindium: Decomposition study and use for low temperature growth
[AD-A250666] p 464 N93-11869
Nuclear fuels for very high temperature applications
[DE92-018021] p 446 N93-12129
Energetics solids degradation in high temperature water
[AD-A254900] p 276 N93-12285
Thermal control/oxidation resistant coatings for titanium-based alloys p 229 N93-12457

THERMAL STRESSES
Generation of thermal strains in carbon fibre-reinforced bismaleimide (PMR-15) composites, part 1, 2 and 3
[PNR-90976-PT-1-2-3] p 236 N93-11065
Thermal residual stresses in silicon-carbide/titanium (0/90) laminate
[NASA-TM-107649] p 236 N93-11072
Thermal stress and strain analysis in traveling autogenous welds
[DE92-019363] p 326 N93-11556
Design of a high-temperature experiment for evaluating advanced structural materials
[NASA-TM-105833] p 337 N93-11624
Molecular orientation induced by cooling stresses in polycarbonate. 1: Free quenching p 269 N93-11987
Molecular orientation induced by cooling stresses in polycarbonate. 2: Constrained quench and injection moulding p 270 N93-11988
Thermal fracture service life analysis of a case bonded visco-elastic cylinder p 339 N93-12008
Analysis of delamination in composite laminates under low-velocity impact p 243 N93-12532

THERMIONIC POWER GENERATION
Nuclear fuels for very high temperature applications
[DE92-018021] p 446 N93-12129

THERMOCHEMISTRY
Probing flame chemistry with MBMS, theory, and modeling
[DE92-011433] p 251 N93-12119
Carbon/carbon composition ablation effects on ionized boundary layers
[AD-A254465] p 242 N93-12235
Systems of evolution equations in thermochemical equations
[AD-A254891] p 253 N93-12282
Thermochemistry of transition metal clusters
[DE92-018713] p 262 N93-12480

THERMOCOUPLES
Aerothermal test results from the second flight of the Pegasus booster
[NASA-TM-4391] p 296 N93-10969
Frequency response in short thermocouple wires
[NASA-CR-190943] p 310 N93-11612

THERMODYNAMIC EFFICIENCY
Hydrodynamic efficiencies in implosion experiments
p 308 N93-12030

THERMODYNAMIC EQUILIBRIUM
Liquid-liquid equilibria in binary systems: Monte-Carlo simulation for calculating the effect of nonrandom mixing
[DE92-017020] p 263 N93-10972

THERMODYNAMIC PROPERTIES
Method of remotely characterizing thermal properties of a sample
[NASA-CASE-LAR-13508-3-CU] p 216 N93-11057
Basicity and optical basicities of slags
[NPL-DMM(A)-48] p 447 N93-11408
Tables of thermodynamic properties of helium magnet coolant, revision A
[DE92-019098] p 471 N93-11656
Physical characterization of magmatic liquids
[DE92-015931] p 363 N93-11848
Overview of property formulations for helium, nitrogen, lithium, and lithium-lead in ATHENA/MOD1 with comparison of calculated properties to measured properties
[DE92-017995] p 471 N93-12058
The effect of temperature dependent thermal properties on parametric weld size predictions
[DE92-018816] p 260 N93-12232
Mesoscopic effects in electronic microstructures
[AD-A254889] p 295 N93-12502

THERMODYNAMICS
Numerical and observational investigations of long-lived, MCS-induced, severe surface wind events: The derecho
p 367 N93-11159
A composite study of the Madden-Julian oscillation
[AD-A254269] p 369 N93-11819
Internal variables in the local-equilibrium approximation
[DE92-016854] p 471 N93-12102

THERMOELASTICITY
Analytical method of calculating the thermoelastic constants of a multi-phase unidirectional composite
[NPL-DMM(A)-57] p 238 N93-11409

THERMOELECTRIC GENERATORS
Milliwatt Generator Project
[DE92-015348] p 294 N93-12156

THERMOELECTRIC POWER GENERATION
The NASA CSTI high capacity power project
[NASA-TM-105813] p 221 N93-11398

THERMOGRAVIMETRY
Thermal control/oxidation resistant coatings for titanium-based alloys p 229 N93-12457

THERMOPLASTICITY
Semi-interpenetrating polymer network for tougher and more microcracking resistant high temperature polymers
[NASA-CASE-LAR-13925-2] p 264 N93-11059

THERMOSPHERE
An inversion technique to recover lower thermospheric winds from space-borne remote measurements of (OI) 5577 A p 369 N93-11839

THICK WALLS
An analytic description of thick-wall bubbles
[DE92-016465] p 432 N93-11759

THICKNESS
Plasma measurements in magnetospheric tail
[MPE-233] p 361 N93-11352

THIN FILMS
The domain structure features of epitaxial PbTiO3 thin films prepared by MOCVD
[DE92-010907] p 459 N93-11190
Interfacial and thin film chemistry in electron device fabrication
[AD-A253579] p 288 N93-11257
A mutual inductance technique for contact-free T(sub c) measurement of high temperature superconductors
[NPL-DES-116] p 289 N93-11393
High frequency response from YBa2Cu3O(7-x) Josephson devices on SrTiO3 bicrystal substrates
[NPL-DES-118] p 459 N93-11394
Low cost humidity sensor
[PB92-205772] p 312 N93-11757
Analysis of surfaces from the LDEF A0114, phase 2
[NASA-CR-190596] p 270 N93-11993
Numerical simulation of a pressure gradient in a multilayer target: Temperature evolution
p 309 N93-12039
Superconducting multilayer structures grown by ALL-MBE
[DE92-018011] p 465 N93-12065
Growth of 2-6 thin-films from single-source precursors based on sterically encumbered sitel ligands
[DE92-017077] p 466 N93-12099
Infrared phonon structure in epitaxial films of Tl2Ca2Ba2Cu3O10 at low temperatures
[DE92-017078] p 466 N93-12109
Effect of microstructure on passive film formation and breakdown on Al alloys
[AD-A245863] p 260 N93-12118
Submillimeter and microwave residual losses in epitaxial films of Y-Ba-Cu-O and Bl-Ca-Ca-Cu-O
[DE92-017075] p 466 N93-12125
Investigation of high efficiency monolithic multibandgap solar cells
[AD-A254326] p 348 N93-12144
Growth, characterization, and device development in monocrystalline diamond films
[AD-A252648] p 271 N93-12184
Development of contractor cells, phase 1
[DE92-017343] p 348 N93-12222
Workshop on Adhesion and Intermolecular Forces
[AD-A255191] p 272 N93-12276
Ion beams as a means of deposition and in-situ characterization of thin films and thin film layered structures
[DE92-016397] p 469 N93-12310
Conductor-backed coplanar waveguide resonators of Y-Ba-Cu-O and Tl-Ba-Ca-Cu-O on LaAlO3
[NASA-TM-105890] p 469 N93-12325
High temperature superconductor materials and applications
[NASA-CR-184426] p 470 N93-12396
Ferroelectric memory devices and a proposed standardized test system design
[AD-A255159] p 405 N93-12425
MMIC GaAs bonding investigation
[AD-A254773] p 470 N93-12464
Two-fluid measurements on thin films
[PB92-205350] p 308 N93-12475

THIN PLATES
Nonlinear response of thin steel plate structures subjected to static, cyclic, and dynamic loads
p 335 N93-11200
Acoustic measurement of the mechanical properties of thin material specimens
[AD-A253538] p 434 N93-11752

THIN WALLED SHELLS
On the stability of confined shells under external pressure p 335 N93-11202

THIN WALLS
Design and evaluation of ion source for satellite charge control
[AD-A255172] p 227 N93-12408

THOMSON SCATTERING
Tunable, short pulse hard x rays from a compact laser synchrotron source
[AD-A254288] p 315 N93-11195
Development of a new plasma diagnostic of the critical surface and studies of the ion acoustic decay instability using collective Thomson scattering
[DE92-018508] p 453 N93-11730
Development of a new plasma diagnostic of the critical surface and studies of the ion acoustic decay instability using collective Thomson scattering
[DE92-018526] p 453 N93-11731

THORIUM
High-precision thorium RIMS for geochemistry
[DE92-017405] p 250 N93-11918

THORIUM COMPOUNDS
Chemistry of lower valent actinide halides
[DE92-017031] p 251 N93-12105

THREADS
A study of the effects of tolerances on rigging screws, turnbuckles, and associated components in BS4429: 1987
[NPL-DMM(A)-53] p 325 N93-11326

THREE DIMENSIONAL BOUNDARY LAYER
Fully nonlinear development of the most unstable goertler vortex in a three dimensional boundary layer
[NASA-CR-189710] p 301 N93-11633

THREE DIMENSIONAL COMPOSITES
Tension and compression fatigue response of unnotched 3D braided composites
[NASA-CR-189678] p 239 N93-11611

THREE DIMENSIONAL FLOW
A study of the wall-pressure fluctuations downstream of a blade-wall junction
[ECL-91-07] p 299 N93-11363
The effects of chemistry on weld profiles in partial and full penetration welds
[DE92-016865] p 327 N93-11679
An experimental study of a small high speed LH2 rocket pump: Fundamental mechanical design
[NAL-TR-1123] p 330 N93-12463
An engineering method for interactive inviscid-boundary layers in three-dimensional hypersonic flows
p 203 N93-12529

THREE DIMENSIONAL MODELS
Coordinated action in 3-D space
[AD-A249830] p 387 N93-10994
Crustal and upper mantle velocity gradients in the vicinity of the East Kazakh test site
[AD-A246889] p 362 N93-11740
Numerical investigation of three-dimensionally evolving jets p 303 N93-11870
Generation of 3-D surface maps in waste storage silos using a structured light source p 399 N93-11958
Linear and geometrically nonlinear p-version three dimensional curved shell element for isotropic, generally orthotropic and laminated composite materials
p 339 N93-12194

THRESHOLD VOLTAGE
Back-gate bias generator
[AD-A255126] p 295 N93-12421

THRUST
Introduction to the Rolls-Royce design process
[PNR-90939] p 210 N93-11039
Civil aircraft engines: The next generation
[PNR-90962] p 211 N93-11085

THRUST BEARINGS
A test facility for the thermofluid-dynamics of gas bearing lubrication films
[PNR-90897] p 263 N93-11032

THRUST CHAMBERS
Solution of two-phase reacting flow in liquid thrust chambers p 235 N93-11449
Examination of various turbulence models for application in liquid rocket thrust chambers
[NASA-CR-184406] p 233 N93-12009
Characteristics of heat transfer to nickel plated chamber walls of high pressure rocket combustors
[NAL-TR-1126T] p 234 N93-12372

THRUST CONTROL
An experimental study of a small high speed LH2 rocket pump: Fundamental mechanical design
[NAL-TR-1123] p 330 N93-12463

THRUST VECTOR CONTROL
Droppable jet vane TVC
[AD-D015341] p 214 N93-11046

THRUST-WEIGHT RATIO
Aero engine ceramics: The vision, the reality, and the progress
[PNR-90983] p 264 N93-11066

THRUSTORS
Preliminary characterization of a water vaporizer for resistojet applications
[NASA-TM-105877] p 231 N93-11402

THUNDERSTORMS
A comparison of radar rainfall estimates and rain gage measurements during two Denver thunderstorms
[AD-A254267] p 369 N93-11817
Weather impacts on space operations
[AD-A253720] p 371 N93-12170
Temporal monitoring of VHF and LF atmospherics and their relation to lightning
[AD-A252617] p 371 N93-12180

TIBET
Modeling regional seismic waves
[AD-A246894] p 361 N93-11421

TILT ROTOR AIRCRAFT
Design of an air traffic computer simulation system to support investigation of civil tiltrotor aircraft operations
[NASA-CR-190811] p 204 N93-11139
The Fourth Workshop on Dynamics and Aeroelastic Stability Modeling of Rotorcraft Systems
[AD-A255065] p 208 N93-12485

TIME DEPENDENCE
New singularity and existence of solutions in anisotropic, time-dependent, maximally Gauss-Bonnet extended gravity p 357 N93-11183
Beam-plasma interactions and radiation generation during the ejection of electron and ion beams in space
[AD-A253993] p 224 N93-11736
Mixing regimes in a spatially confined, two-dimensional, supersonic shear layer
[AD-A254302] p 302 N93-11756
The time-dependent stress-optical behaviour of polycarbonate in the glass transition region
p 269 N93-11985

TIME DIVISION MULTIPLE ACCESS
All-digital multicarrier demodulators for on-board processing satellites in mobile communication systems
p 285 N93-12207

TIME FUNCTIONS
New singularity and existence of solutions in anisotropic, time-dependent, maximally Gauss-Bonnet extended gravity p 357 N93-11183

TIME LAG
The combustion time lag and its role in ramjet combustion instability p 245 N93-11137

TIME OF FLIGHT SPECTROMETERS
Development of a geometry-compensated neutron time-of-flight detector for ICF applications with approximately 200 ps time response
[DE92-018024] p 450 N93-11153
Plasma temperatures from first-hit neutron time-of-flight spectra
[DE92-018006] p 454 N93-12060

TIME SERIES ANALYSIS
Stationary time series analysis using information and spectral analysis p 425 N93-11431
Interactive analysis of gappy bivariate time series using AGSS
[AD-A255160] p 429 N93-12426

TIME SHARING
Performance evaluation and modeling techniques for parallel processors
[NASA-CR-190974] p 419 N93-12395

TIME TEMPERATURE PARAMETER
Thermal fracture service life analysis of a case bonded visco-elastic cylinder p 339 N93-12008

TIMING DEVICES
Quartz crystal resonators and oscillators for frequency control and timing applications: A tutorial, revision 5.2
[AD-A254892] p 469 N93-12283

TIP SPEED
A concept for a counterrotating fan with reduced tone noise
[NASA-TM-105736] p 433 N93-11370

TITANIUM
On the dependence of the dynamic crack tip temperature fields in metal upon crack tip velocity and material parameters
[AD-A253657] p 335 N93-11219

TITANIUM ALLOYS
Thermal residual stresses in silicon-carbide/titanium (0/90) laminate
[NASA-TM-107649] p 236 N93-11072
Microstructure and mechanical properties of reactive hot isostatic pressed TiAl powder material
[GKSS-91/E/60] p 256 N93-11336
Titanium-aluminides by hot isostatic pressing of cold extruded titanium-aluminium powder mixtures
[GKSS-91/E/67] p 256 N93-11337
Thermomechanical fatigue behavior of SiC/Ti-24Al-11Nb in air and argon environments
[NASA-TM-105723] p 238 N93-11399
The conversion of plastic work to heat around a dynamically propagating crack in metals
[AD-A253801] p 258 N93-11782
Multi-layer light-weight protective coating and method for application
[NASA-CASE-LAR-14448-1] p 269 N93-11912
Optimization of film synthesized rare earth transition metal permanent magnet systems
[DE92-018726] p 432 N93-12116
Design and development of Ni-base superalloy and Ti alloys
[NRIM-SR-92-01] p 261 N93-12322
Processing and properties of NbTi based alloys
[DE92-016692] p 261 N93-12445
Thermal control/oxidation resistant coatings for titanium-based alloys p 229 N93-12457

TITANIUM OXIDES
Structure and property of heteroepitaxial TiO2/VO2 multilayers
[DE92-018181] p 460 N93-11563

TOBACCO
Correlation of serum alpha sub 1 antitrypsin with cigarette smoking and pulmonary function status in Greek pilots, for a ten year period p 384 N93-11318
Smoking status and body composition, exercise, dietary intake, and alcohol/caffeine consumption
[AD-A250648] p 385 N93-11893

TOKAMAK DEVICES
Scaling of lower hybrid current drive with temperature
[DE92-018541] p 449 N93-10988
Direct electron absorption of fast waves on the D3-D tokamak
[DE92-016254] p 449 N93-11041
Ion temperature measurements in tokamak plasmas by Rutherford scattering
[PB92-184738] p 451 N93-11245
Thermal analysis and design of polarizer mirrors for waveguides in the D3-D tokamak
[DE92-018884] p 451 N93-11382
High beta and confinement studies on TFTR
[DE92-018647] p 452 N93-11568
Low energy helium implantation in evaporated nickel surfaces
[DE92-019297] p 257 N93-11600
Heat load material studies: Simulated tokamak disruptions
[DE92-018275] p 452 N93-11674
Results from the US/USSR exchange for heat load material studies of simulated tokamak disruptions
[DE92-018285] p 453 N93-11694
Nonlinear effects of ICRF power on drift wave stability and transport in tokamaks, task 1
[DE92-018488] p 453 N93-11729
Fast cooling phenomena with ice pellet injection in the JIPP T-IIU tokamak
[DE92-782105] p 454 N93-11834
Helium transport studies on D3-D
[DE92-016251] p 455 N93-12307
Anomalous ion thermal transport in hot ion plasmas by the ion temperature gradient mode
[DE92-016686] p 456 N93-12493
Transport mechanisms acting in toroidal devices: A theoretician's view
[DE92-018738] p 456 N93-12501

TOLERANCES (MECHANICS)
A study of the effects of tolerances on rigging screws, turnbuckles, and associated components in BS4429: 1987
[NPL-DMM(A)-53] p 325 N93-11326
Using NDT techniques in the maintenance of aeronautical products
[REPT-921-430-102] p 332 N93-11587
Study of compression-loaded and impact-damaged structurally efficient graphite-thermoplastic trapezoidal-corrugation sandwich and semisandwich panels
[NASA-TP-3264] p 239 N93-11623

TOMOGRAPHY
Surface reconstruction of a three-dimensional ultrasonic flaw
[DE92-018029] p 332 N93-11154
The tomographic formulation of spotlight mode synthetic aperture radar extended to three dimensional targets
[DE92-013666] p 280 N93-11234
High resolution image processing of geophysical data with diffraction tomography
[DE92-014134] p 359 N93-11235
Fundamental analysis of the tomographic imaging system for reconstructing ionospheric distributions
p 365 N93-12209

TOPOGRAPHY
Phase-stepping fiber-optic projected fringe system for surface topography measurements
[NASA-CASE-LEW-14996-1] p 446 N93-11058
Spatial data transformation: Feature attribute conversion issues and practical experience
[AD-A254238] p 477 N93-11741
Generation of 3-D surface maps in waste storage silos using a structured light source p 399 N93-11958

TOROIDAL PLASMAS
High beta and confinement studies on TFTR
[DE92-018647] p 452 N93-11568

TOROIDS
Tori and chaos in a nonlinear dynamo model for solar activity
[MPE-PREPRINT-218] p 488 N93-11351

TORSIONAL VIBRATION
A consistent cracked bar vibration theory
p 339 N93-12000

TORUSES
Tori and chaos in a nonlinear dynamo model for solar activity
[MPE-PREPRINT-218] p 488 N93-11351

TOTAL OZONE MAPPING SPECTROMETER
Ozone and temperature trends p 350 N93-11089
A comprehensive mission to planet Earth: Woods Hole Space Science and Applications Advisory Committee Planning Workshop
[NASA-TM-108011] p 343 N93-11878

TOTAL QUALITY MANAGEMENT
The application of manufacturing systems engineering for aero engine gears
[PNR-90944] p 324 N93-11054

TOUGHNESS
Analysis of precracking parameters and fracture toughness for ceramic single-edge-precracked-beam specimens
[NASA-TM-105568] p 263 N93-10962
Semi-interpenetrating polymer network for tougher and more microcracking resistant high temperature polymers
[NASA-CASE-LAR-13925-2] p 264 N93-11059
Toughness of Si3N4-SiC whisker composites
[REPT-921-430-101] p 239 N93-11586
Relationship of bainitic microstructure to impact toughness in Cr-Mo and Cr-W steels
[DE92-017828] p 258 N93-11773
Micromechanisms of deformation and fracture in aluminum based MMC's: Interface effects
[AD-A253560] p 259 N93-11850
Fracture toughness testing of polymer matrix composites
[NASA-TP-3199] p 243 N93-12302

TOWNSEND AVALANCHE
Prediction of electromagnetic pulse generation by picosecond avalanches in high-pressure air
[DE92-019382] p 282 N93-11675

TOXICITY
Absence of protective immunity against diphtheria in a large proportion of young adults p 380 N93-11302
Clinical and immunological response to vaccination with parenteral or oral vaccines in two groups of 30 recruits
p 381 N93-11305

TOXICOLOGY
ECLSS medical support activities
[NASA-CR-184429] p 385 N93-12427

TOXINS AND ANTITOXINS
Absence of protective immunity against diphtheria in a large proportion of young adults p 380 N93-11302

TRACE CONTAMINANTS
Modeling the dispersion of tracer plumes in the Colorado front range boundary layer during night- and day-time conditions
[DE92-019384] p 354 N93-11676

TRACE ELEMENTS
Computer simulation and experimental investigation of the absorption cell for the rocketborne diode-laser experiment MASERATI
[BONN-IR-91-62] p 357 N93-11083
Source gases: Concentrations, emissions, and trends
p 350 N93-11088
Stratospheric processes: Observations and interpretation p 351 N93-11091
Future chlorine-bromine loading and ozone depletion
p 352 N93-11095
International Conference on the Role of the Polar Regions in Global Change: Proceedings, volume 1
[DE92-013652] p 353 N93-11232
International Conference on the Role of the Polar Regions in Global Change: Proceedings, volume 2
[DE92-013653] p 353 N93-11233

TRACKING (POSITION)
A problem formulation for glideslope tracking in wind shear using advanced robust control techniques
[NASA-TM-104164] p 214 N93-11176
Radio pill antenna range test
[DE92-019903] p 282 N93-11661
Fuzzy logic control for camera tracking system
p 314 N93-11935
Model-based vision for space applications
p 398 N93-11955

TRACTION
Thermal non-Newtonian elastohydrodynamic lubrication of line contacts under sliding-rolling and simple sliding conditions p 324 N93-11263

TRAFFIC CONTROL
Future FAA telecommunications plan
[AD-A249133] p 283 N93-11760
Fuzzy logic control for camera tracking system
p 314 N93-11935

TRAILING EDGES
Flight test results from a supercritical mission adaptive wing with smooth variable camber
[NASA-TM-4415] p 207 N93-11863

TRAINING ANALYSIS
Questioning mechanisms during complex learning
[AD-A247382] p 386 N93-11415

TRAINING EVALUATION
An evaluation of crew coordination and performance during a simulated UH-60 helicopter mission
[AD-A254984] p 390 N93-12509

TRAJECTORIES
Lightweight Exoatmospheric Projectile (LEAP) test program. Supplemental environmental assessment
[AD-A252286] p 231 N93-10998
Hybrid guidance for maneuvering flight vehicles
[AD-A254110] p 225 N93-11798

TRAJECTORY ANALYSIS
Air-breathing hypersonic vehicle guidance and control studies: An integrated trajectory/control analysis methodology, phase 2
[NASA-CR-189703] p 216 N93-12413

TRAJECTORY CONTROL
Terminal slider control of nonlinear robotic systems
[NASA-CASE-NPO-18584-1-CU] p 324 N93-11177
Air-breathing hypersonic vehicle guidance and control studies: An integrated trajectory/control analysis methodology, phase 2
[NASA-CR-189703] p 216 N93-12413
A surface integral approach to the motion planning of nonholonomic systems
[AD-A254844] p 329 N93-12434

TRAJECTORY OPTIMIZATION
Computing optimum routes across terrain using DAP
[RSRE-MEMO-4299] p 412 N93-11712
A simplified numerical procedure to compute the optimal trajectory of an aircraft p 207 N93-11719
Closed form low-thrust trajectories for Mars missions
[DE92-017431] p 232 N93-11766

TRAJECTORY PLANNING
Path planning on a ring of processors
p 410 N93-11480
A simplified numerical procedure to compute the optimal trajectory of an aircraft p 207 N93-11719
Integration of task level planning and diagnosis for an intelligent robot p 393 N93-11929
Fuzzy logic control of telerobot manipulators
p 399 N93-11959
A neuro-collision avoidance strategy for robot manipulators p 400 N93-11962
A surface integral approach to the motion planning of nonholonomic systems
[AD-A254844] p 329 N93-12434

TRANSDUCERS
Development of a tactile perceived attitude transducer
[AD-A253724] p 385 N93-11081

TRANSFERRING
Progress on polymer degradation by photoelectron transfer
[AD-A246276] p 268 N93-11862

TRANSFORMATIONS (MATHEMATICS)
Equivalence transformations of rational matrices
[MATHS-REPT-A-163] p 423 N93-11121
Constrained KP hierarchy and bi-Hamiltonian structures
[MATHS-REPT-A-168] p 424 N93-11123
Equivalence transformations of rational matrices and applications
[MATHS-REPT-A-169] p 424 N93-11124
On a certain McMillan degree condition appearing in control
[MATHS-REPT-A-170] p 424 N93-11125
Darboux theorems and Wronskian formulas for integrable systems. 1: Constrained KP flows
[MATHS-REPT-A-172] p 424 N93-11126
Differential equation-based seismic data filtering
[DE92-016282] p 363 N93-11791

TRANSGRANULAR CORROSION
Environment-induced embrittlement: Stress corrosion cracking and metal-induced embrittlement; environmental embrittlement of iron aluminide alloys
[DE92-018714] p 256 N93-11524

TRANSIENT RESPONSE
Feasibility assessment of a transient sound sensor based on the silicon retina architecture
[AD-A252288] p 432 N93-10999
Structural dynamics of large space structures having parametric uncertainties p 225 N93-11836
Broadband EMP transient measurement preemphasis filter
[AD-A254414] p 284 N93-12160
New acceleration potential method for supersonic unsteady aerodynamics of lifting surfaces, further extension of the nonplanar supersonic doublet point method, and nonlinear, nongradient optimized rational function approximations for supersonic, transient response unsteady aerodynamics p 201 N93-12344

TRANSISTOR CIRCUITS
VLSI design for reliability
[AD-A253207] p 292 N93-11781

TRANSISTORS
The fourth OSA Topical Meeting Proceedings on Picosecond Electronics and Optoelectronics, volume 9
[AD-A253472] p 447 N93-11099
Natural convection heat transfer studies of simulated and actual electronic components using dielectric liquids for immersion cooling
[AD-A255173] p 341 N93-12376

TRANSIT TIME
On some practical consideration of the electron beam breakup transit time oscillator
[DE92-017406] p 445 N93-11919

TRANSITION METALS
Theory of small metal clusters, films, and wires
[AD-A253120] p 256 N93-11240
Studies of the 3 to 5 compounds in the megabar regime
[DE92-019517] p 461 N93-11646
Electronic structure and reactivities of transition metal clusters
[DE92-016623] p 258 N93-11762
Calculation of binary phase diagrams between the actinide elements, rare earth elements, and transition metal elements
[DE92-019119] p 249 N93-11801
Optimization of film synthesized rare earth transition metal permanent magnet systems
[DE92-018726] p 432 N93-12116
Thermochemistry of transition metal clusters
[DE92-018713] p 262 N93-12480

TRANSITION POINTS
Relationship of bainitic microstructure to impact toughness in Cr-Mo and Cr-W steels
[DE92-017828] p 258 N93-11773

TRANSITION PROBABILITIES
Absorption spectroscopy of L(alpha, beta) transitions in a laser germanium plasma p 320 N93-12041

TRANSITION TEMPERATURE
A mutual inductance technique for contact-free T(sub c) measurement of high temperature superconductors
[NPL-DES-116] p 289 N93-11393
Relationship of bainitic microstructure to impact toughness in Cr-Mo and Cr-W steels
[DE92-017828] p 258 N93-11773
Theoretical studies of high-temperature superconductors and highly compressed hydrogen
p 292 N93-11833

TRANSLATING
Assembling polyhedra with single translations
[AD-A254623] p 419 N93-12239

TRANSLATIONAL MOTION
Vacuum chamber translation/positioning mechanism and welding power supply controller
[NASA-CR-184465] p 328 N93-12196

TRANSMITTANCE
Erosion rates for polymers measured on LDEF
p 270 N93-11994

TRANSOCEANIC COMMUNICATION
Translating wedge heat sink
[AD-D015357] p 293 N93-12133

TRANSONIC WIND TUNNELS
The design and commissioning of an acoustic liner for propeller noise testing in the ARA transonic wind tunnel
[PNR-90880] p 433 N93-11204

TRANSPARENCE
Optical properties of composite membranes containing arrays of nanoscopic gold cylinders
[AD-A253659] p 238 N93-11281

TRANSPONDERS
SITE project. Phase 1: Continuous data bit-error-rate testing
[NASA-TP-3279] p 224 N93-11001

TRANSPORT AIRCRAFT
Formal representation of the requirements for an Advanced Subsonic Civil Transport (ASCT) flight control system
[NASA-CR-189699] p 405 N93-12346

TRANSPORT PROPERTIES
Electronic transport and lasing in microstructures
[DE92-018725] p 441 N93-12115
The structure and transport of the Brazil current between 27 deg and 36 deg south
[AD-A247635] p 374 N93-12247
Helium transport studies on D3-D
[DE92-016251] p 455 N93-12307
Anomalous ion thermal transport in hot ion plasmas by the ion temperature gradient mode
[DE92-016686] p 456 N93-12493
Mesoscopic effects in electronic microstructures
[AD-A254889] p 295 N93-12502
TRANSPORT THEORY
Overview of property formulations for helium, nitrogen, lithium, and lithium-lead in ATHENA/MOD1 with comparison of calculated properties to measured properties
[DE92-017995] p 471 N93-12058
Transport mechanisms acting in toroidal devices: A theoretician's view
[DE92-018738] p 456 N93-12501
TRANSPORTATION
An investigation of ground access mode choice for departing passengers
[TT-9201] p 217 N93-11224
Interfacial microchemical characterization needs in surface processing
[DE92-018269] p 277 N93-11672
TRANSPORTATION NETWORKS
Land use/land cover classification using digitally merged spot panchromatic and Landsat thematic mapper imagery
[PB92-188416] p 343 N93-11701
TRANSPORTER
Tests of an alternate mobile transporter and extravehicular activity assembly procedure for the Space Station Freedom truss
[NASA-TP-3245] p 224 N93-10970
TRANSPUTERS
A process monitor for the transputer
[RSRE-MEMO-4554] p 408 N93-11389
Z-buffer on a transputer-based machine
p 410 N93-11483
TRANSURANIUM ELEMENTS
Summaries of FY 1991 research in the chemical sciences
[DE92-011920] p 251 N93-12135
TRANSVERSE OSCILLATION
Simulation analysis of a cable-mount system used for dynamic wind tunnel tests
[NAL-TR-1127] p 219 N93-12359
TRAPPING
Implanted He retention and release from boronized layers
[DE92-013983] p 464 N93-11842
TRAVELING IONOSPHERIC DISTURBANCES
Geostationary-satellite beacon-receiver array for studies of ionospheric irregularities
[DE92-018979] p 362 N93-11535
TRAVELING WAVES
Alternating-phase focusing: A model to study nonlinear dynamics
[DE92-019027] p 431 N93-11511
Application of the theory of wave propagation through random media to phase and amplitude fluctuations of seismic P-waves
[AD-A253274] p 363 N93-11788
TREES (MATHEMATICS)
The complexity of some multicriteria arborescence problems
[REPT-92-016] p 424 N93-11182
TRENDS
From RB211 to Trent: An ongoing development strategy
[PNR-90938] p 210 N93-11038
Ozone and temperature trends p 350 N93-11089
Stratospheric processes: Observations and interpretation p 351 N93-11091
Present and future trends in turbine blade material and manufacture technology
[PNR-90960] p 255 N93-11111
TRIANGULATION
QR decomposition based algorithms and architectures for least-squares adaptive filtering
[RSRE-MEMO-4562] p 408 N93-11390
An advancing front Delaunay triangulation algorithm designed for robustness
[NASA-CR-189719] p 416 N93-12400
TRIMERS
Concerted hydrogen atom exchange between three HF molecules p 439 N93-11855
TRIMETHYL COMPOUNDS
Triisopropylindium: Decomposition study and use for low temperature growth
[AD-A250666] p 464 N93-11869
TRINITRO COMPOUNDS
Detonation reactions frozen by free expansion and analyzed by mass spectrometry
[DE92-018605] p 274 N93-11566
TRIODES
RF vacuum micrcelectronics
[AD-A253910] p 290 N93-11491
TRITIUM
Use of the program ANISN to calculate response functions for a Bonner sphere set with a He-3 detector
[NPL-RSA(EXT)-31] p 316 N93-11411
TROPICAL METEOROLOGY
Atlas of albedo and absorbed solar radiation derived from Nimbus 7 earth radiation budget data set, November 1985 to October 1987
[NASA-RP-1281] p 367 N93-11168
Hurricane Research Division fiscal year 1991 programs: Fiscal year 1992 projections
[PB92-138320] p 367 N93-11242
Diagnostic report of the National Hurricane Center: October and November 1990, volume 3, number 3
[PB91-242297] p 370 N93-11888
The vertical distribution of heating in the tropical atmosphere
[AD-A254982] p 372 N93-12507
TROPICAL REGIONS
Immunization of personnel traveling to a destination in tropical countries: French position p 380 N93-11304
Dynamics of planetary waves in the atmosphere
p 363 N93-11898
Interannual variabilities of the East Asian summer monsoon and tropical sea surface temperatures
p 372 N93-12534
TROPICAL STORMS
Diagnostic report of the National Hurricane Center: October and November 1990, volume 3, number 3
[PB91-242297] p 370 N93-11888
Operations plan for the Tropical Cyclone Motion (TCM-92) mini-field experiment
[AD-A254723] p 372 N93-12339
TROPOSPHERE
Source gases: Concentrations, emissions, and trends
p 350 N93-11088
Tropospheric processes: Observations and interpretation p 351 N93-11092
Predicted aircraft effects on stratospheric ozone
p 352 N93-11096
Numerical and observational investigations of long-lived, MCS-induced, severe surface wind events: The derecho
p 367 N93-11159
The forcing of a mid-latitude upper-tropospheric jet streak by a simulated mesoscale convective system
p 358 N93-11184
The use of ARM data to test an improved parameterization of upper tropospheric clouds for use in climate models
[DE92-014353] p 367 N93-11237
Dynamics of planetary waves in the atmosphere
p 363 N93-11898
TROPOSPHERIC SCATTERING
10 kW L-band amplifier tubes for efficient and reliable troposcatter communication transmitter systems
[AD-A253246] p 290 N93-11504
TRUCKS
Federal Alternative Fuel Program light duty vehicle operation
[DE92-018124] p 274 N93-11794
Reduction in global warming due to fuel economy improvements and emissions control of criteria pollutants: New US light-duty vehicles (1968-1991)
[DE92-016636] p 356 N93-12314
TRUNCATION ERRORS
Comparison of truncation error of finite-difference and finite-volume formulations of convection terms
[NASA-TM-105861] p 426 N93-11531
TRUSSES
Tests of an alternate mobile transporter and extravehicular activity assembly procedure for the Space Station Freedom truss
[NASA-TP-3245] p 224 N93-10970
Application of artificial neural networks in nonlinear analysis of trusses
[NASA-TM-105319] p 336 N93-11403
Structural dynamics of large space structures having parametric uncertainties p 225 N93-11836
A smart end-effector for assembly of space truss structures p 230 N93-11982
Studies in control for vibration suppression of the UWAA 20-bay planar truss
[AD-A250193] p 341 N93-12253
TUBERCULOSIS
Immunological parameters in current and former US Air Force personnel p 378 N93-11295
Communicable diseases: A major burden of morbidity and mortality p 380 N93-11300
TUNABLE LASERS
Tunable, short pulse hard x rays from a compact laser synchrotron source
[AD-A254288] p 315 N93-11195
UCSB FEL user mode adaption project
[AD-A248734] p 316 N93-11418
Research on stimulated Raman scattering with applications to atmospheric lidar p 322 N93-12163
TUNGSTEN
Study of metal-ceramic interfaces of Co-Cr-Mo alloys: Role of tungsten (W) and manganese (Mn) additions
[ECL-92-01] p 267 N93-11580
TUNGSTEN ALLOYS
Development of strength and conductivity in deformation processed copper base alloys
[DE92-018807] p 257 N93-11572
TUNING
Self-tuning PI-PID regulators for stable systems with varying delay
[REPT-92-023] p 421 N93-11593
A PID auto-tuning algorithm based on relay feedback
[REPT-92-019] p 421 N93-11667
TURBINE BLADES
Present and future trends in turbine blade material and manufacture technology
[PNR-90960] p 255 N93-11111
Erosion predictions and measurements of high-temperature coatings and superalloys used in turbomachines p 272 N93-12189
Stochastic sensitivity measure for mistuned high-performance turbines
[NASA-TM-105821] p 341 N93-12277
Effects of cooling-air injection on secondary flows and losses in a turbine cascade
[NAL-TR-1121T] p 307 N93-12382
TURBINE PUMPS
A comparison of high cycle fatigue methodologies
[NASA-TM-103601] p 233 N93-12148
Stochastic sensitivity measure for mistuned high-performance turbines
[NASA-TM-105821] p 341 N93-12277
Sealing characteristics of a carbon segmented circumferential seal for a liquid oxygen turbopump
[NAL-TR-1130] p 329 N93-12364
An experimental study of a small high speed LH2 rocket pump: Fundamental mechanical design
[NAL-TR-1123] p 330 N93-12463
Three-dimensional turbopump flowfield analysis
[NASA-CR-190978] p 308 N93-12539
TURBINES
Experimental heat transfer results in turbine stators and rotors and a comparison with theory
[PNR-90945] p 210 N93-11055
The use of simultaneous engineering for the design and manufacture of the low pressure turbine for the Rolls-Royce Trent engine
[PNR-90887] p 212 N93-11206
Increase of energy use on cooled high temperature turbine, phase 3
[MTUM-B91EW-0029-PHASE-3] p 213 N93-11339
TURBOFAN ENGINES
From RB211 to Trent: An ongoing development strategy
[PNR-90938] p 210 N93-11038
TURBOMACHINERY
The role of turbomachinery testing for stability in distorted flow
[PNR-90943] p 210 N93-11040
Resolution of the pressure equation by the boundary element method. Application to multistage turbomachines
[ECL-91-16] p 301 N93-11575
Active control of aeroacoustic couplings by means of adaptive systems
[ECL-91-18] p 214 N93-11576
Determination of loose spline coupling coefficients of rotor bearing systems in turbomachinery
p 327 N93-11887
Erosion predictions and measurements of high-temperature coatings and superalloys used in turbomachines p 272 N93-12189
Stochastic sensitivity measure for mistuned high-performance turbines
[NASA-TM-105821] p 341 N93-12277
Three-dimensional turbopump flowfield analysis
[NASA-CR-190978] p 308 N93-12539
TURBOSHAFTS
Advanced three-shaft engines: Configured for reliability, efficiency, and growth
[PNR-90986] p 211 N93-11068
Determination of loose spline coupling coefficients of rotor bearing systems in turbomachinery
p 327 N93-11887

TURBULENCE
Effects of reacting flows with turbulence and shock waves on efficiency of scramjet combustors
p 235 N93-11133
Structure of the nocturnal boundary layer over a complex terrain
[DE92-018141] p 362 N93-11669
An experimental study of flow patterns and endwall heat transfer upstream of a surface-mounted rectangular obstruction in a turbulent boundary layer
p 302 N93-11698
Freely propagating open premixed turbulent flames stabilized by swirl
[DE92-017116] p 251 N93-12112
Flow in curved ducts of varying cross-section
[AD-A254660] p 306 N93-12245

TURBULENCE EFFECTS
Computation of small scale velocity turbulence and its effect on optical scintillations and stimulated thermal Rayleigh scattering
[DE92-018934] p 448 N93-11627
3-D turbulent particle dispersion submodel development
[DE92-018212] p 301 N93-11670
3-D turbulent particle dispersion submodel development
[DE92-018228] p 302 N93-11671
Leading edge film cooking heat transfer including the effect of mainstream turbulence p 199 N93-11886
Examination of various turbulence models for application in liquid rocket thrust chambers
[NASA-CR-184406] p 233 N93-12009
A general introduction to aeroacoustics and atmospheric sound
[NASA-CR-189717] p 435 N93-12021

TURBULENCE MODELS
The prediction of convective heat transfer in rotating square ducts
[PNR-90929] p 296 N93-11025
The prediction of convective heat transfer in rotating square ducts
[PNR-90985] p 296 N93-11067
A problem formulation for glideslope tracking in wind shear using advanced robust control techniques
[NASA-TM-104164] p 214 N93-11176
Turbulence modeling in shock wave/turbulent boundary layer interactions
[NASA-CR-190933] p 301 N93-11606
Physical effects of vegetation on wind-blown sand in the coastal environments of Florida
[PB92-188424] p 354 N93-11702
Calculation of nozzle/aftbody flowfield interactions
p 302 N93-11722
A theory for the analysis of rotorcraft operating in atmospheric turbulence p 207 N93-11725
Mode interaction models in near-wall turbulence
p 303 N93-11856
Examination of various turbulence models for application in liquid rocket thrust chambers
[NASA-CR-184406] p 233 N93-12009
Disruption shape effects on the performance of enhanced tubes with the separation and reattachment mechanism
[DE92-016602] p 305 N93-12128
Three-dimensional turbopump flowfield analysis
[NASA-CR-190978] p 308 N93-12539

TURBULENT BOUNDARY LAYER
Dynamical effects of suction/heating on turbulent boundary layers
[AD-A248459] p 299 N93-11416
Progress in developing a transition model for high-speed flows p 301 N93-11615
An experimental study of flow patterns and endwall heat transfer upstream of a surface-mounted rectangular obstruction in a turbulent boundary layer
p 302 N93-11698
Mode interaction models in near-wall turbulence
p 303 N93-11856
Turbulence structure and polymer drag reduction in adverse pressure gradient boundary layers
p 304 N93-12003
Laminar boundary-layer breakdown
[AD-A254489] p 306 N93-12162
Carbon/carbon composition ablation effects on ionized boundary layers
[AD-A254465] p 242 N93-12235
On the Goertler instability of boundary layers
[NAL-TR-1120T] p 307 N93-12374

TURBULENT COMBUSTION
Simplified modelling of soot inception and growth
[ETN-92-92266] p 246 N93-11361
The twenty-third International Symposium on combustion
[AD-A250377] p 250 N93-11866

TURBULENT DIFFUSION
Computation of small scale velocity turbulence and its effect on optical scintillations and stimulated thermal Rayleigh scattering
[DE92-018934] p 448 N93-11627
Atmospheric dispersion in mountain valleys and basins
p 355 N93-11920
Bubble dissolving in turbulent pipe flow
[AD-A252927] p 308 N93-12462

TURBULENT FLOW
CFD modeling of turbulent flows around the SSME main injector assembly using porosity formulation
[NASA-CR-184359] p 297 N93-11171
Simulation of compressible turbulent flows by a mixed finite element/finite volume method
[ETN-92-92267] p 299 N93-11362
An experimental study of droplet dispersion in turbulent flows p 248 N93-11455
Effects of sweep on the physics of unsteady shock-induced turbulent separated flows
[AD-A247035] p 198 N93-11742
Mode interaction models in near-wall turbulence
p 303 N93-11856
Turbulence structure and polymer drag reduction in adverse pressure gradient boundary layers
p 304 N93-12003
Application of a two-layer near wall model to fully developed and rotating channel turbulent flows
[NASA-CR-184441] p 305 N93-12082
Disruption shape effects on the performance of enhanced tubes with the separation and reattachment mechanism
[DE92-016602] p 305 N93-12128
Flow in curved ducts of varying cross-section
[AD-A254660] p 306 N93-12245
Particle-jet interactions in an MHD second stage combustor
[DE92-016390] p 455 N93-12309
Probability density functions in turbulent channel flow
[NASA-CR-4454] p 202 N93-12399
Bubble dissolving in turbulent pipe flow
[AD-A252927] p 308 N93-12462
Studies in premixed combustion
[DE92-018646] p 254 N93-12478

TURBULENT HEAT TRANSFER
Leading edge film cooking heat transfer including the effect of mainstream turbulence p 199 N93-11886

TURBULENT MIXING
Compressible mixing layers with and without particles
[AD-A254854] p 308 N93-12435

TVD SCHEMES
Difference approximations for hyperbolic conservation laws and consistency with characteristics
[NAL-TR-1098T] p 428 N93-12350

TWO DIMENSIONAL BOUNDARY LAYER
Fully nonlinear development of the most unstable goertler vortex in a three dimensional boundary layer
[NASA-CR-189710] p 301 N93-11633

TWO DIMENSIONAL FLOW
An adaptive differencing scheme for elliptic flows
p 297 N93-11197
Using NEKTON to solve systems of discrete Boltzmann equations
[DE92-018272] p 303 N93-11799
Air ejector experiments using the two-dimensional supersonic cascade tunnel: Relationship between ejector performance and throat area ratio, part 1
[NAL-TM-642-PT-1] p 202 N93-12352

TWO DIMENSIONAL MODELS
Ceramic component reliability with the restructured NASA/CARES computer program
[NASA-TM-105856] p 334 N93-11004
Application of laminar flow to aero engine nacelles
[PNR-90916] p 195 N93-11020
The Kalman filter for two-dimensional stable and unstable atmospheres p 359 N93-11249
Mixing regimes in a spatially confined, two-dimensional, supersonic shear layer
[AD-A254302] p 302 N93-11756

TWO PHASE FLOW
Front tracking and the interaction of nonlinear waves
[AD-A253544] p 297 N93-11148
A new two-phase flow and transport model with interphase mass exchange
[PB92-206564] p 298 N93-11251
Measuring and modelling of particle-fluid flow in a riser reactor
[VTT-PUBS-88] p 299 N93-11359
Solution of two-phase reacting flow in liquid thrust chambers p 235 N93-11449
Interfacial area and two-phase flow structure development measured by a double-sensor probe
[DE92-019459] p 300 N93-11538
Reactant gas flow fields in advanced PEM (Proton Exchange Membrane) fuel cell designs
[DE92-018897] p 345 N93-11626
Particle-fluid two-phase flow modeling
[DE92-017847] p 301 N93-11637
3-D turbulent particle dispersion submodel development
[DE92-018228] p 302 N93-11671
Current Technology for Thermal Protection Systems
[NASA-CP-3157] p 227 N93-12447
Bubble dissolving in turbulent pipe flow
[AD-A252927] p 308 N93-12462

TYPHOID
Immunization of personnel traveling to a destination in tropical countries: French position p 380 N93-11304
Clinical and immunological response to vaccination with parenteral or oral vaccines in two groups of 30 recruits
p 381 N93-11305
Studies of safety, infectivity, and immunogenicity of a new Temperature Sensitive (TS) 51-1 strain of S. typhi as a new live oral typhoid fever vaccine candidate
p 381 N93-11306

U

U.S.S.R.
JPRS report: Science and technology. Central Eurasia: Engineering and equipment
[JPRS-UEQ-92-009] p 220 N93-11169
Soviet chemical propellant research and development
[PB92-195577] p 275 N93-12147

U.S.S.R. SPACE PROGRAM
JPRS report: Science and technology. Central Eurasia: Space. Development of Soviet spacecraft for manned missions
[JPRS-USP-92-003] p 224 N93-11162

ULTRAHIGH FREQUENCIES
An uncertainty budget for VHF and UHF reflectometers
[NPL-DES-120] p 281 N93-11395

ULTRASONIC FLAW DETECTION
Application of the boundary element method to elastic wave scattering problems in ultrasonic nondestructive evaluation p 332 N93-11209
Ultrasonic sensing of GMAW: Laser/EMAT defect detection system
[DE92-017916] p 333 N93-12055
Ultrasonic flaw classification and sizing
p 333 N93-12533

ULTRASONIC RADIATION
Interaction of sound with sound by novel mechanisms: Ultrasonic four-wave mixing mediated by a suspension and ultrasonic three-wave mixing at a free surface
[AD-A254657] p 435 N93-12097

ULTRASONIC TESTS
Surface reconstruction of a three-dimensional ultrasonic flaw
[DE92-018029] p 332 N93-11154
Application of the boundary element method to elastic wave scattering problems in ultrasonic nondestructive evaluation p 332 N93-11209
Ultrasonic sensing of GMAW: Laser/EMAT defect detection system
[DE92-017916] p 333 N93-12055
A VMEbus ultrasonic sensor controller for mapping and servo control in robotic systems
[DE92-013661] p 421 N93-12138
Impact test of carbon, Kevlar, and glass fibre hybrid FRP plates
[NAL-TR-1100] p 243 N93-12371

ULTRASONICS
Dynamics and response of polymer-coated acoustic devices
[DE92-014289] p 433 N93-11523

ULTRAVIOLET ASTRONOMY
Far ultraviolet spectrophotometry of hot stars and calibration standards in the far ultraviolet
p 482 N93-11373

ULTRAVIOLET DETECTORS
Final Report, January 1991 - July 1992
[AD-A254659] p 483 N93-12244

ULTRAVIOLET EMISSION
The role of proton precipitation in Jovian aurora: Theory and observation p 487 N93-11165
Lyman alpha line shapes from electron impact H2 dissociative processes in the Jovian auroral zone
p 487 N93-11166

ULTRAVIOLET LASERS
VUV and UV sources and spectroscopic applications
[AD-A247293] p 291 N93-11758
Interpretation of experiments measuring the back face of thin aluminum strips by comparison with numerical simulations p 318 N93-12029
Novel nonlinear laser diagnostic techniques
[AD-A254709] p 323 N93-12335

ULTRAVIOLET RADIATION
Ultraviolet radiation changes p 352 N93-11098

Evaluation tests for photovoltaic concentrator receiver sections and modules
[DE92-017745] p 346 N93-11771

ULTRAVIOLET SPECTRA
Ultraviolet studies of Cepheids
[NASA-CR-190857] p 481 N93-11073

ULTRAVIOLET SPECTROSCOPY
X-UV spectroscopy temporal resolution
p 318 N93-12028

ULYSSES MISSION
Studies of interactive plasma processes in the polar cusp
[NASA-CR-190892] p 357 N93-10964

UNDERGROUND EXPLOSIONS
Propagation of regional phases: Observations and theory
[AD-A246891] p 359 N93-11228
Study of seismic coda generation in crust with non-uniform scattering and anelastic properties
[AD-A254350] p 366 N93-12270

UNDERWATER ACOUSTICS
A survey of European calibration facilities for underwater acoustics
[NPL-RSA(EXT)-32] p 433 N93-11328
Study of sound propagation in a wedge-shaped ocean and comparison with other methods
[AD-A255165] p 435 N93-12471

UNIFIED FIELD THEORY
New singularity and existence of solutions in anisotropic, time-dependent, maximally Gauss-Bonnet extended gravity p 357 N93-11183

UNITED KINGDOM
UK airmisses involving commercial air transport, May-August 1991
[ETN-92-92260] p 203 N93-11357
UK airmisses involving commercial air transport, January-April 1991
[ETN-92-92261] p 298 N93-11358

UNITED STATES
Recommended agency procedures for implementing federal metric policy
[PB92-205467] p 277 N93-11901
A metric America: A decision whose time has come - for real
[PB92-205459] p 277 N93-11902
United States/Canada Air Quality Agreement
[PB92-228030] p 356 N93-12525

UNITS OF MEASUREMENT
A metric America: A decision whose time has come - for real
[PB92-205459] p 277 N93-11902

UNIVERSE
Publications of the Executive Office of the President, 20 January 1989 - 31 March 1992
[PB92-154913] p 477 N93-11769

UNIVERSITY PROGRAM
Optoelectronics Research Center
[AD-A253132] p 447 N93-11527

UNIX (OPERATING SYSTEM)
A real-time diagnostic and performance monitor for UNIX
[NASA-CR-190975] p 404 N93-11462

UNSTEADY AERODYNAMICS
The aerodynamics of curved jets and breakaway in Coanda flares, volumes 1 and 2 p 304 N93-11881
Unsteady propeller/wing aerodynamic interactions
p 201 N93-12190
New acceleration potential method for supersonic unsteady aerodynamics of lifting surfaces, further extension of the nonplanar supersonic doublet point method, and nonlinear, nongradient optimized rational function approximations for supersonic, transient response unsteady aerodynamics p 201 N93-12344

UNSTEADY FLOW
System and method for cancelling expansion waves in a wave rotor
[NASA-CASE-LEW-15218-1] p 297 N93-11172
Effects of sweep on the physics of unsteady shock-induced turbulent separated flows
[AD-A247035] p 198 N93-11742
Unsteady propeller/wing aerodynamic interactions
p 201 N93-12190
An improved numerical model for wave rotor design and analysis
[NASA-TM-105915] p 214 N93-12418
Investigation of hot streak migration and film cooling effects on heat transfer in rotor/stator interacting flows, report 1
[AD-A250688] p 471 N93-12490

UPPER ATMOSPHERE
Multispectral observations of the Jovian aurora
p 487 N93-11167

UPPER STAGE ROCKET ENGINES
An experimental study of a small high speed LH2 rocket pump: Fundamental mechanical design
[NAL-TR-1123] p 330 N93-12463

UPPER SURFACE BLOWING
A wind tunnel investigation to determine buffet countermeasures for STOL aircraft alpha-sweep flight testing
[NAL-TR-1129] p 216 N93-12362
Wind tunnel investigation of a twin-engine jet transport semi-span model with upper surface blown jet flap
[NAL-TR-1134] p 203 N93-12503

URANIUM
Theoretical study of the radiative and kinetic properties of selected metal oxides and air molecules
[AD-A251090] p 438 N93-11804

URANIUM CARBIDES
Nuclear fuels for very high temperature applications
[DE92-018021] p 446 N93-12129

URANIUM COMPOUNDS
Chemistry of lower valent actinide halides
[DE92-017031] p 251 N93-12105

URANIUM OXIDES
Theoretical study of the radiative and kinetic properties of selected metal oxides and air molecules
[AD-A251090] p 438 N93-11804
Nuclear fuels for very high temperature applications
[DE92-018021] p 446 N93-12129

URBAN DEVELOPMENT
Post-war regional planning: The French silicon valley
[RSRE-MEMO-4282] p 472 N93-10976

USER MANUALS (COMPUTER PROGRAMS)
An interactive preprocessor for the NASA engine performance program
[NASA-TM-105786] p 209 N93-10983
Micromechanics of metal matrix composites using the Generalized Method of Cells model (GMC) user's guide
[NASA-CR-190756] p 335 N93-11175
Reserves information gathering system user's guide
[DE92-018357] p 475 N93-11355
Operator's guide for VAXGAP, a gamma-ray spectrum analysis package
[DE92-019096] p 407 N93-11356
Temporal scattering and response software users' manual, version 2 and 3
[DE92-040934] p 282 N93-11632
ICAN/DAMP-integrated composite analyzer with damping analysis capabilities: User's manual
[NASA-TP-3292] p 241 N93-12015
The Wave Information Studies (WIS) wave model, version 2.0 (user's guide)
[AD-A254313] p 374 N93-12094
LINK user manual
[DE92-017987] p 479 N93-12143
Testability design rating system. Volume 2: Analytical procedure
[AD-A254333] p 413 N93-12146
Micromechanical combined stress analysis: MICSTRAN, a user manual
[NASA-CR-189694] p 243 N93-12306
Space Station communications and tracking systems modeling and RF link simulation
[NASA-CR-185684] p 288 N93-12519
Users manual for program NYQUIST: Liquid rocket nyquist plots developed for use on a PC computer
[NASA-CR-184451] p 235 N93-12522

USER REQUIREMENTS
Quality management of finite element analysis
[PNR-90951] p 331 N93-11110
Optimized software for a generalized Polak-Ribiere algorithm in unconstrained optimization
[MATHS-REPT-A-156] p 406 N93-11210
Study and recommendation of available sources of scientific and technical numeric databases in the government and private sector
[AD-A247266] p 475 N93-11465
The effect of task complexity on user interfaces: A comparison of command language interface and direct manipulation interface
[AD-A246061] p 412 N93-11859
Formal representation of the requirements for an Advanced Subsonic Civil Transport (ASCT) flight control system
[NASA-CR-189699] p 405 N93-12346

UTILIZATION
Workshop on Surface Science and Technology
[AD-A253566] p 264 N93-11149
Industrial applications and markets for ceramic matrix composites
[PNR-90884] p 266 N93-11205

V

VACANCIES (CRYSTAL DEFECTS)
Atomic bonding at ceramic interfaces using scanning tunneling microscopy
[DE92-018706] p 273 N93-12479

VACCINES
Allergic, Immunological and Infectious Disease Problems in Aerospace Medicine
[AGARD-CP-518] p 376 N93-11283
Vaccination against Hepatitis B: The Italian strategy
p 377 N93-11289
HIV variability and perspectives of a vaccine
p 378 N93-11294
Communicable diseases: A major burden of morbidity and mortality p 380 N93-11300
Susceptibility in USAF recruits to vaccine preventable diseases p 380 N93-11301
Absence of protective immunity against diphtheria in a large proportion of young adults p 380 N93-11302
Dramatic reduction of meningococcal meningitis among military recruits in Italy after introduction of specific vaccination p 380 N93-11303
Immunization of personnel traveling to a destination in tropical countries: French position p 380 N93-11304
Clinical and immunological response to vaccination with parenteral or oral vaccines in two groups of 30 recruits
p 381 N93-11305
Studies of safety, infectivity, and immunogenicity of a new Temperature Sensitive (TS) 51-1 strain of S. typhi as a new live oral typhoid fever vaccine candidate
p 381 N93-11306
Use of novel adjuvants and delivery systems to improve the humoral and cellular immune response to malaria vaccine candidate antigens p 381 N93-11308
Cytokines as vaccine adjuvants: Interleukin 1 and its synthetic peptide 163-171 p 382 N93-11309
Future approaches to vaccine development single-dose vaccines using controlled-release delivery systems
p 382 N93-11310

VACUUM
Remarks on the Robinson-Trautman solutions
[MATHS-REPT-A-167] p 423 N93-11122
Slow crack growth in vacuum p 338 N93-11909
Space Station Freedom seal leakage rate analysis and testing summary: Air leaks in ambient versus vacuum exit conditions
[NASA-TM-103604] p 328 N93-12149

VACUUM CHAMBERS
Vacuum chamber translation/positioning mechanism and welding power supply controller
[NASA-CR-184465] p 328 N93-12196

VACUUM SYSTEMS
Dynamic vacuum analysis for APS high heat flux beamline front ends using optical ray-tracing simulation methods
[DE92-019032] p 445 N93-11831

VACUUM TESTS
Development of stable metallization systems
[AD-A253569] p 264 N93-11079

VALLEYS
Atmospheric dispersion in mountain valleys and basins
p 355 N93-11920

VALUE ENGINEERING
On the basis of experience: Built in product reliability
[PNR-90932] p 331 N93-11034
Research and development strategies for human centered and group support technologies
[AD-A254366] p 472 N93-12273

VAN DE GRAAFF ACCELERATORS
Radiation physics, biophysics, and radiation biology
[DE92-013673] p 375 N93-12266

VANADIUM ALLOYS
Internal friction peaks due to oxygen, nitrogen, and hydrogen in V-Nb alloys
[DE92-012155] p 254 N93-10995
Optimization of film synthesized rare earth transition metal permanent magnet systems
[DE92-018726] p 432 N93-12116

VANADIUM OXIDES
Structure and property of heteroepitaxial TiO2/VO2 multilayers
[DE92-018181] p 460 N93-11563

VAPOR DEPOSITION
Structure and property of heteroepitaxial TiO2/VO2 multilayers
[DE92-018181] p 460 N93-11563
Preparation of silicon oxynitride thin films by plasma chemical vapor deposition for chemical implantation. Application to a pH ISFET
[ECL-91-12] p 291 N93-11574
Polyethylene-terephthalate/aluminum adhesion
[ECL-91-33] p 257 N93-11578
Development of wear resistant ceramic coatings for diesel engine components
[DE92-019068] p 268 N93-11654
The chemistry of Si3N4 and Si deposition studied using molecular beam techniques
[DE92-018268] p 463 N93-11797
Silicon on insulator structures in selective epitaxial growth
[DE92-017118] p 465 N93-11915

Workshop on Characterizing Diamond Films
[PB92-205426] p 271 N93-12086
The deposition characteristics of copper(I) compounds for CVD by FT-IR spectroscopy
[DE92-010778] p 467 N93-12134
VAPOR PHASE EPITAXY
Basic principles of organometallic vapor phase epitaxy
[AD-A250665] p 464 N93-11868
Triisopropylindium: Decomposition study and use for low temperature growth
[AD-A250666] p 464 N93-11869
VAPOR PHASES
Heterogeneous processes: Laboratory, field, and modeling studies p 350 N93-11090
VAPORIZERS
Preliminary characterization of a water vaporizer for resistojet applications
[NASA-TM-105877] p 231 N93-11402
VAPORIZING
Laser-ablation processes
[DE92-011226] p 322 N93-12250
VAPORS
Occupational safety considerations with hydrazine fuels p 276 N93-11951
VARIABLE STARS
Ultraviolet studies of Cepheids
[NASA-CR-190857] p 481 N93-11073
VARIATIONS
Hydrodynamic fluctuations and light scattering in hot electron gas of semiconductors
[DE92-622800] p 458 N93-10992
VECTOR QUANTIZATION
Self-supervision in multilayer adaptive networks
[RSRE-MEMO-4467] p 420 N93-11343
VEGETATION
Catalog of data bases and reports
[DE92-018586] p 473 N93-10990
Physical effects of vegetation on wind-blown sand in the coastal environments of Florida
[PB92-188424] p 354 N93-11702
Estimation of photosynthetic capacity using MODIS polarization: 1988 proposal to NASA Headquarters
[NASA-TM-103945] p 344 N93-12351
VEGETATIVE INDEX
Estimation of photosynthetic capacity using MODIS polarization: 1988 proposal to NASA Headquarters
[NASA-TM-103945] p 344 N93-12351
VELOCITY
Computation of small scale velocity turbulence and its effect on optical scintillations and stimulated thermal Rayleigh scattering
[DE92-018934] p 448 N93-11627
VELOCITY DISTRIBUTION
Quasigeostrophic vortices in zonal shear
p 358 N93-11226
The measurement of the velocity field induced by a gust generator in a closed-circuit subsonic wind-tunnel
[RAE-TM-MAT-STR-1102] p 217 N93-11435
Coaxial injector spray characterization using water/air as simulants p 248 N93-11452
Surface wind speed distributions
[AD-A253268] p 368 N93-11505
Direct numerical simulation of instabilities in parallel flow with spherical roughness elements
[NASA-TM-105847] p 300 N93-11529
A theory for the analysis of rotorcraft operating in atmospheric turbulence p 207 N93-11725
Crustal and upper mantle velocity gradients in the vicinity of the East Kazakh test site
[AD-A246889] p 362 N93-11740
A comparison of velocity profile measurements in the CDIF diffuser with flow field model calculations
[DE92-015367] p 304 N93-11995
Turbulence structure and polymer drag reduction in adverse pressure gradient boundary layers
p 304 N93-12003
On the Goertler instability of boundary layers
[NAL-TR-1120T] p 307 N93-12374
VELOCITY ERRORS
Methodology issues concerning the accuracy of kinematic data collection and analysis using the ariel performance analysis system
[NASA-CR-185689] p 389 N93-12211
VELOCITY MEASUREMENT
An experimental study of flow patterns and endwall heat transfer upstream of a surface-mounted rectangular obstruction in a turbulent boundary layer
p 302 N93-11698
Physical characterization of magmatic liquids
[DE92-015931] p 363 N93-11848
A comparison of velocity profile measurements in the CDIF diffuser with flow field model calculations
[DE92-015367] p 304 N93-11995
VENTILATION
Low cost humidity sensor
[PB92-205772] p 312 N93-11757
VENTING
Small experiments for the maturation of orbital cryogenic transfer technologies
[NASA-TM-105849] p 296 N93-10981
VENTURI TUBES
Operating experience using venturi flow meters at liquid helium temperature
[DE92-014693] p 313 N93-12140
VERTICAL AIR CURRENTS
Numerical and observational investigations of long-lived, MCS-induced, severe surface wind events: The derecho
p 367 N93-11159
Lidar studies of gravity waves in the mesopause region p 358 N93-11222
VERTICAL DISTRIBUTION
The vertical distribution of heating in the tropical atmosphere
[AD-A254982] p 372 N93-12507
VERTICAL TAKEOFF AIRCRAFT
Flight test progress of the STOL research aircraft ASKA
[NAL-TM-643] p 208 N93-12354
VERY HIGH FREQUENCIES
An uncertainty budget for VHF and UHF reflectometers
[NPL-DES-120] p 281 N93-11395
RF vacuum microelectronics
[AD-A253910] p 290 N93-11491
High-frequency LSI contactor
[DE92-017285] p 292 N93-11916
Temporal monitoring of VHF and LF atmospherics and their relation to lightning
[AD-A252617] p 371 N93-12180
VERY LARGE SCALE INTEGRATION
Reliability of small geometry VLSI devices for microelectronics
[AD-A247355] p 289 N93-11414
VLSI design for reliability
[AD-A253207] p 292 N93-11781
Analysis of fault-tolerant neurocontrol architectures
[NASA-TM-105898] p 215 N93-12305
VLSI reliability research
[AD-A254883] p 295 N93-12360
VHSIC (CIRCUITS)
Design of an Ada expert system shell for the VHSIC avionic modular flight processor p 397 N93-11947
VIBRATION
Experimental validation of boundary element methods for noise prediction
[NASA-TM-105729] p 323 N93-10966
Residual acceleration data on IML-1: Development of a data reduction and dissemination plan
[NASA-CR-190807] p 223 N93-11101
Thermokinetic modelling and hypersonic flow
[DILC-EST-TN-218] p 196 N93-11157
Determination of stepsize parameters for intermolecular vibrational energy transfer
[DE92-010770] p 435 N93-11189
State-resolved collisional energy transfer in highly vibrationally excited polyatomic molecules
[AD-A253299] p 441 N93-12323
VIBRATION DAMPING
Numerical and experimental results in vibroacoustical active control of structural elements with piezoelectric materials
[DILC-EST-TN-224] p 334 N93-11158
Optimal output feedback vibration control of rotor-bearing systems p 324 N93-11220
Studies in control for vibration suppression of the UWAA 20-bay planar truss
[AD-A250193] p 341 N93-12253
VIBRATION MODE
Rigid body mode identification of the PAH-2 helicopter using the eigensystem realization algorithm
[NASA-TM-107690] p 336 N93-11544
Description of the structural responses in the medium-frequency range by an energetic formulation
[ECL-92-16] p 336 N93-11582
The use of high-frequency dynamic information for the evaluation of damage in fiber reinforced composite materials p 241 N93-11998
Dynamic analysis of a pre-and-post ice impacted blade
[NASA-TM-105829] p 276 N93-12197
VIBRATION TESTS
A contribution to fatigue failure morphologies in fiber reinforced plastics
[MBB-Z-0212-91-PUB] p 263 N93-11010
Testing for integrity
[PNR-90927] p 210 N93-11024
A knowledge-based blackboard system to interpret graphical data from vibration tests of gas turbines
[PNR-90993] p 212 N93-11114
Dynamic test/analysis correlation using reduced analytical models
[NASA-TM-107671] p 341 N93-12300
VIBRATIONAL SPECTRA
Time-frequency domain analysis of vibration signals for machinery diagnostics. 3: The present power spectral density
[OUEL-1911/92] p 337 N93-11707
Exploration of the ionizable metal cluster-electrode surface analogy: Infrared spectroelectrochemistry of (Pt24(CO)30)(sup n), (Pt26(CO)32)(sup n), and (Pt38(CO)44)(sup n) (n = 0 to -10), and comparisons with potential-dependent spectra of CO adlayers on platinum surfaces
[AD-A252544] p 250 N93-11808
The structures, binding energies and vibrational frequencies of Ca3 and Ca4: An application of the CCSD(T) method p 439 N93-11852
VIDEO EQUIPMENT
System for generating dynamic video imagery for human factors research
[AD-A248675] p 388 N93-11743
High-speed test station for solid-state imagers
[DE92-018990] p 312 N93-11822
Guide to synchronization of video systems to IRIG timing
[AD-A254626] p 285 N93-12240
VIDICONS
High-speed FPS vidicon camera
[DE92-018989] p 313 N93-12069
VIEWING
Visual perception of structure from motion
[AD-A253235] p 386 N93-11503
VIRAL DISEASES
Clinical types of Hepatitis B p 376 N93-11286
Viral hepatitis in the US Air Force, 1980 - 1989
p 377 N93-11287
Hepatitis A and Hepatitis B: Risks compared to other vaccine preventable diseases and immunization recommendations p 377 N93-11288
Vaccination against Hepatitis B: The Italian strategy
p 377 N93-11289
VIRTUAL REALITY
Advanced technology for portable personal visualization
[AD-A253808] p 388 N93-11783
A methodology to emulate and evaluate a productive virtual workstation p 395 N93-11938
VIRUSES
Immunization of personnel traveling to a destination in tropical countries: French position p 380 N93-11304
VISCOELASTICITY
Contribution to the study of the anisotropic viscoelasticity of large strains: The case of the monocrystal
[ECL-90-29] p 460 N93-11573
Creep failure in linear and nonlinear viscoelastic materials p 342 N93-12536
VISCOPLASTICITY
Contribution to the study of the anisotropic viscoelasticity of large strains: The case of the monocrystal
[ECL-90-29] p 460 N93-11573
Contribution to the monocrystal behavior study during large plastic strains
[ECL-92-13] p 461 N93-11581
VISCOSITY
Stochastic control and nonlinear estimation
[AD-A253543] p 420 N93-11147
Nonlinear evolution of resistive tearing mode instability with shear flow and viscosity
[DE92-012138] p 453 N93-11745
VISCOUS FLOW
Fundamental solutions and boundary element formulations for convective fluid flow
p 298 N93-11217
Review of preconditioning methods for fluid dynamics
[NASA-CR-189712] p 198 N93-11607
Numerical modeling of a vortex stabilized arcjet
p 232 N93-11889
Flow in curved ducts of varying cross-section
[AD-A254660] p 306 N93-12245
VISCOUS FLUIDS
Regular and chaotic mixing of viscous fluids in eccentric rotating cylinders p 305 N93-12157
VISIBILITY
Video camera as a visual sensor
[NAL-TR-1132] p 314 N93-12373
Evaluation of alternatives for increasing A-7D rearward visibility
[AD-A255071] p 208 N93-12488
VISUAL AIDS
Operator vision aids for space teleoperation assembly and servicing p 391 N93-11981
Performing a successful audience analysis: How to improve your proposal-writing skills
[DE92-018978] p 479 N93-12068
VISUAL PERCEPTION
Coordinated action in 3-D space
[AD-A249830] p 387 N93-10994

Visual psychophysics of egomotion
[AD-A248349] p 386 N93-11488
Visual perception of structure from motion
[AD-A253235] p 386 N93-11503
The effects of luminance boundaries on color perception
[AD-A250705] p 384 N93-11841
Effects of spatially displaced feedback on remote manipulation tasks p 400 N93-11966

VISUAL SIGNALS
Super auditory localization for improved human-machine interfaces
[AD-A254699] p 389 N93-12229

VISUAL STIMULI
The effects of luminance boundaries on color perception
[AD-A250705] p 384 N93-11841

VOICE COMMUNICATION
The development of the speaker independent ARM continuous speech recognition system
[RSRE-MEMO-4473] p 280 N93-11383
Preliminary results on the use of linear discriminant analysis in the ARM continuous speech recognition system
[RSRE-MEMO-4511] p 280 N93-11384
The use of linear discriminant analysis in the ARM continuous speech recognition system
[RSRE-MEMO-4512] p 280 N93-11385
Diagnostic rhyme test statistical analysis programs
[RSRE-91026] p 281 N93-11487

VOICE DATA PROCESSING
Speech recognition systems and their military applications
[BR91882] p 280 N93-11366
Preliminary results on the use of linear discriminant analysis in the ARM continuous speech recognition system
[RSRE-MEMO-4511] p 280 N93-11384
High Capacity Voice Recorder (HCVR) Operational Test and Evaluation (OT/E) integration test report
[DOT/FAA/CT-TN92/30] p 310 N93-11460
Diagnostic rhyme test statistical analysis programs
[RSRE-91026] p 281 N93-11487

VOICE OF AMERICA
Direct Broadcast Satellite: Radio Program
[NASA-TM-105910] p 224 N93-11430

VOIDS
Method and apparatus for evaluating multilayer objects for imperfections
[NASA-CASE-LAR-14581-1-SB] p 333 N93-12204

VOLATILITY
Advanced heat pump for the recovery of volatile organic compounds
[DE92-011592] p 303 N93-11774

VOLCANOES
Volcanology from space: Applications of infrared remote sensing p 343 N93-11213
Models of volcanic eruption hazards
[DE92-013432] p 364 N93-12136

VOLCANOLOGY
Volcanology from space: Applications of infrared remote sensing p 343 N93-11213
Quaternary volcanism, tectonics, and sedimentation in the Idaho National Engineering Laboratory area
[DE92-017851] p 362 N93-11692
Models of volcanic eruption hazards
[DE92-013432] p 364 N93-12136

VORTEX FILAMENTS
Study of filamentation in subdense plasma interaction experiments p 318 N93-12026

VORTEX RINGS
Numerical investigation of three-dimensionally evolving jets p 303 N93-11870

VORTEX SHEDDING
The effects of plate spacing and downstream plate length on the acoustic resonance excited by flow past two plates in tandem in a duct
[PNR-90958] p 433 N93-11321
An investigation of the effects of aft blowing on a 3.0 caliber tangent ogive body at high angles of attack
[NASA-CR-190934] p 200 N93-12004

VORTICES
Quasigeostrophic vortices in zonal shear
p 358 N93-11226
Dynamical effects of suction/heating on turbulent boundary layers
[AD-A248459] p 299 N93-11416
The convection speed of the dynamic stall vortex
[AD-A247258] p 197 N93-11464
Experimental investigation of the effects of aft blowing with various nozzle exit geometries on a 3.0 caliber tangent ogive at high angles of attack: Forebody pressure distributions
[NASA-CR-190935] p 197 N93-11605
An experimental study of flow patterns and endwall heat transfer upstream of a surface-mounted rectangular obstruction in a turbulent boundary layer
p 302 N93-11698
Numerical investigation of three-dimensionally evolving jets p 303 N93-11870
An investigation of the effects of aft blowing on a 3.0 caliber tangent ogive body at high angles of attack
[NASA-CR-190934] p 200 N93-12004
Examination of various turbulence models for application in liquid rocket thrust chambers
[NASA-CR-184406] p 233 N93-12009
Unsteady propeller/wing aerodynamic interactions
p 201 N93-12190
Oscillations and concentrations in compressible and incompressible fluids
[AD-A254706] p 307 N93-12333

VORTICITY
Quasigeostrophic vortices in zonal shear
p 358 N93-11226
Boundary condition methods in the numerical solution of the Navier-Stokes equations with the application to free surface problems
[ISBN-0-315-64278-5] p 298 N93-11241
Mode interaction models in near-wall turbulence
p 303 N93-11856
Numerical investigation of three-dimensionally evolving jets p 303 N93-11870
Flow visualization of supersonic flow through a combustor section p 200 N93-12001
Compressible mixing layers with and without particles
[AD-A254854] p 308 N93-12435

VORTICITY EQUATIONS
Boundary condition methods in the numerical solution of the Navier-Stokes equations with the application to free surface problems
[ISBN-0-315-64278-5] p 298 N93-11241

W

WAFERS
Investigation of high efficiency monolithic multibandgap solar cells
[AD-A254326] p 348 N93-12144
Ultra-dense magnetoresistive mass memory
[NASA-CR-190955] p 405 N93-12520

WAKES
Stratospheric aircraft exhaust plume and wake chemistry studies
[NASA-CR-189688] p 366 N93-12299

WALL FLOW
Nonlinear stability of flows over rigid and flexible boundaries p 198 N93-11874
On the Goertler instability of boundary layers
[NAL-TR-1120T] p 307 N93-12374

WALL JETS
The aerodynamics of curved jets and breakaway in Coanda flares, volumes 1 and 2 p 304 N93-11881

WALL PRESSURE
A study of the wall-pressure fluctuations downstream of a blade-wall junction
[ECL-91-07] p 299 N93-11363

WALL TEMPERATURE
Investigation of hot streak migration and film cooling effects on heat transfer in rotor/stator interacting flows, report 1
[AD-A250688] p 471 N93-12490

WALLS
A synopsis of resistive wall effects in very short wavelength free electron lasers
[DE92-018065] p 315 N93-11155
Nonlinear response of thin steel plate structures subjected to static, cyclic, and dynamic loads
p 335 N93-11200

WARNING SYSTEMS
Summary of findings from the PIREP-based analyses conducted during the 1988 to 1990 evaluations of TDWR-based and TDWR/LLWAS-based alert services provided to landing/departing pilots
[AD-A253859] p 367 N93-11144
Lightning threat warning system at the Tonopah Test Range
[DE92-040444] p 221 N93-11631

WASPALOY
Short fatigue crack growth in a nickel-base superalloy at room and elevated temperature
[PNR-90892] p 255 N93-11031
Elevated temperature fatigue crack growth in a nickel base superalloy under dwell conditions
[PNR-90997] p 255 N93-11115

WASTE DISPOSAL
Destruction of explosives and rocket fuels by supercritical water oxidation
[DE92-018874] p 274 N93-11380
Trip report: Marshall Space Center computed tomography
[DE92-018139] p 437 N93-11597
Technology evaluation report of Retech, Inc., Plasma Centrifugal Furnace, volume 1
[PB92-216035] p 456 N93-12526
Technology evaluation report of Retech, Inc., Plasma Centrifugal Furnace, volume 2
[PB92-216043] p 457 N93-12527

WASTE TREATMENT
Technology evaluation report of Retech, Inc., Plasma Centrifugal Furnace, volume 1
[PB92-216035] p 456 N93-12526
Technology evaluation report of Retech, Inc., Plasma Centrifugal Furnace, volume 2
[PB92-216043] p 457 N93-12527

WATER
Destruction of explosives and rocket fuels by supercritical water oxidation
[DE92-018874] p 274 N93-11380
The electron-beam water calorimeter project at the National Physical Laboratory
[NPL-RSA(EXT)-30] p 310 N93-11410
Particle-fluid two-phase flow modeling
[DE92-017847] p 301 N93-11637
Comparative effects of drag-reducing polymers. An experimental report
[AD-A254001] p 268 N93-11793
Submarine Advanced Integrated Life Support system (SAILS) program
[AD-A253564] p 388 N93-11812
The adsorption of C60 and the co-adsorption of C60 and H2O on (alpha)-Al2O3 (1 -1 0 2)-(2x1)
[DE92-018002] p 465 N93-12093
Enhanced convective and film boiling heat transfer by surface gas injection
[DE92-016755] p 306 N93-12221
Energetics solids degradation in high temperature water
[AD-A254900] p 276 N93-12285

WATER CIRCULATION
Parameters for predicting red tides of bioluminescent dinoflagellates: Meteorological events and frontal water circulation patterns
[AD-A254835] p 374 N93-12431

WATER DEPTH
The Wave Information Studies (WIS) wave model, version 2.0 (user's guide)
[AD-A254313] p 374 N93-12094

WATER FLOW
Turbulence structure and polymer drag reduction in adverse pressure gradient boundary layers
p 304 N93-12003
Bubble dissolving in turbulent pipe flow
[AD-A252927] p 308 N93-12462

WATER MANAGEMENT
Climate change and water supply, management and use: A literature review
[DE92-019069] p 353 N93-11655

WATER POLLUTION
Office of Wetlands, Oceans, and Watersheds publications
[PB92-224310] p 480 N93-12528

WATER QUALITY
Climate change and water supply, management and use: A literature review
[DE92-019069] p 353 N93-11655
Office of Wetlands, Oceans, and Watersheds publications
[PB92-224310] p 480 N93-12528

WATER RECLAMATION
ECLSS medical support activities
[NASA-CR-184429] p 385 N93-12427

WATER RESOURCES
Climate change and water supply, management and use: A literature review
[DE92-019069] p 353 N93-11655

WATER TREATMENT
ECLSS medical support activities
[NASA-CR-184429] p 385 N93-12427

WATER TUNNEL TESTS
Experiments on low aspect ratio hydroplanes to measure lift under static and dynamic conditions
[ARE-TM(UHR)-90306] p 197 N93-11365
Lift coefficient of a randomly oscillating hydroplane
[DRA/MAR-TM(MTH)-91320] p 197 N93-11377

WATER VAPOR
Time scales characterizing the processing of water and cloud condensation nuclei by clouds
[CM-80] p 368 N93-11340
Detection of cloud-top height from backscattered radiances within the oxygen A band. Part 1: Theoretical study
[GKSS-91/E/76-PT-1] p 368 N93-11349

Preliminary characterization of a water vaporizer for resistojet applications
[NASA-TM-105877] p 231 N93-11402
WATER WAVES
LAM and NEDWAM statistics over the period October 1990 - April 1991
[KNMI-TR-137] p 368 N93-11329
The Wave Information Studies (WIS) wave model, version 2.0 (user's guide)
[AD-A254313] p 374 N93-12094
WATERPROOFING
Inflatable device for excluding sea water from a rocket motor
[AD-D015365] p 232 N93-11424
WATERSHEDS
Geographic information system to support state-wide hydrologic modeling with the SCS-TR-20
[PB92-185768] p 476 N93-11700
Office of Wetlands, Oceans, and Watersheds publications
[PB92-224310] p 480 N93-12528
WAVE AMPLIFICATION
Chinese Journal of Lasers (selected articles)
[AD-A254100] p 317 N93-11786
Gain in a confined aluminum plasma
p 320 N93-12043
WAVE ATTENUATION
Crustal and upper mantle velocity gradients in the vicinity of the East Kazakh test site
[AD-A246889] p 362 N93-11740
Physical characterization of magmatic liquids
[DE92-015931] p 363 N93-11848
WAVE DEGRADATION
Impact of finite frequency deviation on the performance of dual-filter heterodyne FSK lightwave systems
[AD-A247611] p 448 N93-11892
Study of the dynamic degradation under the action of a shock wave induced by pulsed laser
p 319 N93-12037
WAVE DISPERSION
Nonlinear stability of flows over rigid and flexible boundaries p 198 N93-11874
WAVE EQUATIONS
Colliding plane gravitational waves with colinear polarization
[MATHS-REPT-A-160] p 357 N93-11120
WAVE FRONT RECONSTRUCTION
Wavefront reconstruction using a least squares approach
[ISVR-TR-203] p 435 N93-12324
WAVE FRONTS
Colliding plane gravitational waves with colinear polarization
[MATHS-REPT-A-160] p 357 N93-11120
High frame-rate, large field wavefront sensor
[DE92-019547] p 310 N93-11542
The generalized Goursat-Riemann problem for plane waves in isotropic elastic solids p 340 N93-12199
Theory for a high power free electron laser and tactical applications
[AD-A255161] p 323 N93-12405
Stochastic models of wavefront propagation in random granular media
[AD-A255127] p 286 N93-12422
WAVE FUNCTIONS
Description of the structural responses in the medium-frequency range by an energetic formulation
[ECL-92-16] p 336 N93-11582
On the evaluation of derivatives of Gaussian integrals
p 439 N93-11853
WAVE INTERACTION
Front tracking and the interaction of nonlinear waves
[AD-A253544] p 297 N93-11148
Asymptotic analysis of reacting materials with saturated explosion. 2: High-frequency waves
[AD-A254473] p 275 N93-12236
WAVE PACKETS
Publication of papers presented at URSI 23rd General Assembly as a special section of radio science
[AD-A253561] p 283 N93-11811
Low pressure gas multiphotoionization for wave packet experiments p 319 N93-12034
WAVE PROPAGATION
Propagation of regional phases: Observations and theory
[AD-A246891] p 359 N93-11228
Methods of analysis for thick-section composite structures p 237 N93-11262
Modeling regional seismic waves
[AD-A246894] p 361 N93-11421
Propagation of relativistic high current electron beams across the geomagnetic field
[DE92-018276] p 362 N93-11564
Computational aspects of Gaussian beam migration
[DE92-018641] p 431 N93-11567
Computation of small scale velocity turbulence and its effect on optical scintillations and stimulated thermal Rayleigh scattering
[DE92-018934] p 448 N93-11627
Prediction of electromagnetic pulse generation by picosecond avalanches in high-pressure air
[DE92-019382] p 282 N93-11675
Crustal and upper mantle velocity gradients in the vicinity of the East Kazakh test site
[AD-A246889] p 362 N93-11740
Application of the theory of wave propagation through random media to phase and amplitude fluctuations of seismic P-waves
[AD-A253274] p 363 N93-11788
Dynamics of planetary waves in the atmosphere
p 363 N93-11898
Observation of pulses propagating at supraluminous speed in an optical fiber p 320 N93-12040
Final Technical Report
[AD-A253529] p 284 N93-12083
The Wave Information Studies (WIS) wave model, version 2.0 (user's guide)
[AD-A254313] p 374 N93-12094
Seismic wave propagation in thinly-layered media with steep reflectors
[DE92-015619] p 364 N93-12142
The generalized Goursat-Riemann problem for plane waves in isotropic elastic solids p 340 N93-12199
Study of seismic coda generation in crust with non-uniform scattering and anelastic properties
[AD-A254350] p 366 N93-12270
Migration by the Kirchhoff, slant stack, and Gaussian beam methods
[DE92-018640] p 366 N93-12318
Stochastic models of wavefront propagation in random granular media
[AD-A255127] p 286 N93-12422
WAVE REFLECTION
Experimental measurement and theoretical modeling of microwave scattering and the structure of the sea surface influencing radar observations from space
[NASA-CR-190998] p 343 N93-12006
WAVE SCATTERING
Application of the boundary element method to elastic wave scattering problems in ultrasonic nondestructive evaluation p 332 N93-11209
WAVEFORMS
Arbitrary waveform generator
[AD-D015346] p 280 N93-11354
Modeling regional seismic waves
[AD-A246894] p 361 N93-11421
Chinese Journal of Lasers (selected articles)
[AD-A254100] p 317 N93-11786
Josephson Junction digital waveform generation for very wideband radars
[AD-A253668] p 467 N93-12169
GaAs heterojunction device based A/D converter development
[AD-A252644] p 468 N93-12183
WAVEGUIDES
Thermal analysis and design of polarizer mirrors for waveguides in the D3-D tokamak
[DE92-018884] p 451 N93-11382
Final Technical Report
[AD-A253529] p 284 N93-12083
Transmission/reflection and short-circuit line methods for measuring permittivity and permeability
[PB92-205376] p 293 N93-12084
Conductor-backed coplanar waveguide resonators of Y-Ba-Cu-O and Tl-Ba-Ca-Cu-O on LaAlO3
[NASA-TM-105890] p 469 N93-12325
WEAK INTERACTIONS (FIELD THEORY)
Survey of composite particle models of electroweak interaction
[DE92-017110] p 441 N93-12111
WEAPON SYSTEMS
Surface wind speed distributions
[AD-A253268] p 368 N93-11505
WEAPONS DELIVERY
AGARD flight test techniques series. Volume 10: Weapon delivery analysis and ballistic flight testing
[AGARD-AG-300-VOL-10] p 430 N93-11711
WEAR
Workshop on Surface Science and Technology
[AD-A253566] p 264 N93-11149
Friction of self-lubricating surfaces by ion beam techniques
[DE92-016069] p 328 N93-12122
The degradation of parachutes: Age and mechanical wear
[AD-A252243] p 200 N93-12179
WEAR RESISTANCE
Heat-affected zone cracking of nitronic 60 stainless steel
[DE92-018286] p 254 N93-10984
Development of wear resistant ceramic coatings for diesel engine components
[DE92-019068] p 268 N93-11654
WEAR TESTS
Relative sliding durability of candidate high temperature fiber seal materials
[NASA-TM-105806] p 236 N93-10978
Extended-testing of xenon ion thruster hollow cathodes
[NASA-CR-189227] p 234 N93-12409
WEATHER
Mariners Weather Log, volume 36, number 1, Winter 1992
[PB92-161025] p 368 N93-11256
Proceedings of the National Weather Service Aviation Workshop: Postprint volume
[PB92-176148] p 369 N93-11803
Weather impacts on space operations
[AD-A253720] p 371 N93-12170
Mariners Weather Log, volume 36, number 2, Spring 1992
[PB92-204213] p 371 N93-12293
WEATHER FORECASTING
Summary of findings from the PIREP-based analyses conducted during the 1988 to 1990 evaluations of TDWR-based and TDWR/LLWAS-based alert services provided to landing/departing pilots
[AD-A253859] p 367 N93-11144
Weather impacts on space operations
[AD-A253720] p 371 N93-12170
A real time sharpening of NOGAPS predictions of mid-latitude Central Pacific cyclones
[AD-A255157] p 372 N93-12424
WEATHER RECONNAISSANCE AIRCRAFT
Operations plan for the Tropical Cyclone Motion (TCM-92) mini-field experiment
[AD-A254723] p 372 N93-12339
WEDGES
Translating wedge heat sink
[AD-D015357] p 293 N93-12133
Method and apparatus for gripping test specimens
[NASA-CASE-LEW-15345-1] p 329 N93-12327
Numerical investigations into the base drag of various wedges using the base flow model developed by Mauri Tanner
[REPT-B-36] p 202 N93-12414
WEIBULL DENSITY FUNCTIONS
Surface wind speed distributions
[AD-A253268] p 368 N93-11505
WEIGHTING FUNCTIONS
Acoustic fill factors for a 120 inch diameter fairing
[NASA-CR-189284] p 434 N93-11634
Limit theorems for Fisher-score change processes
p 427 N93-12328
WEIGHTLESSNESS
An overview of gravitational physiology
[NASA-TM-102849] p 391 N93-12319
WELD STRENGTH
Mechanical properties of 1950's vintage 304 stainless steel weldment components after low temperature neutron irradiation
[DE92-017059] p 259 N93-12107
The effects of aluminum oxide on inertial welding of aluminum in space applications
[AD-A255100] p 329 N93-12274
WELD TESTS
Ultrasonic sensing of GMAW: Laser/EMAT defect detection system
[DE92-017916] p 333 N93-12055
WELDABILITY
Heat-affected zone cracking of nitronic 60 stainless steel
[DE92-018286] p 254 N93-10984
WELDED JOINTS
The effects of chemistry on weld profiles in partial and full penetration welds
[DE92-016865] p 327 N93-11679
Mechanical properties of 1950's vintage 304 stainless steel weldment components after low temperature neutron irradiation
[DE92-017059] p 259 N93-12107
Reactor materials program: Mechanical properties of irradiated types 304 and 304L stainless steel weldment components
[DE92-018105] p 260 N93-12158
Some consistency requirements on hardening-recovery evolution equations for welding, part 1
[DE92-015992] p 329 N93-12220
The effect of temperature dependent thermal properties on parametric weld size predictions
[DE92-018816] p 260 N93-12232
The effects of aluminum oxide on inertial welding of aluminum in space applications
[AD-A255100] p 329 N93-12274

Study of residual stresses and microcracks in high strength steel weldments: An investigation of microcrack formation and stressed growth using laser microscopy
[AD-A255059] p 342 N93-12467
Improved corrosion resistance of Hastelloy G-30 in nitric/hydrofluoric acid solutions by welding with Inconel 72 weld wire
[DE92-017233] p 262 N93-12487
Ultrasonic flaw classification and sizing
p 333 N93-12533

WELDING MACHINES
Development of an intelligent system for cooling rate and fill control in GMAW
[DE92-017849] p 326 N93-11548

WEST GERMANY
The Transall campaign. A contribution to the German ozone research program
[REPT-37/91] p 349 N93-11082

WETLANDS
Office of Wetlands, Oceans, and Watersheds publications
[PB92-224310] p 480 N93-12528

WETTABILITY
Infiltration kinetics and interfacial bond strength of metal matrix composites
[AD-A254002] p 240 N93-11795

WHISKER COMPOSITES
Toughness of Si3N4-SiC whisker composites
[REPT-921-430-101] p 239 N93-11586

WHISTLERS
Temporal monitoring of VHF and LF atmospherics and their relation to lightning
[AD-A252617] p 371 N93-12180

WHITE DWARF STARS
Detection of a white dwarf in a visual binary system
[NASA-CR-190856] p 481 N93-11075

WHITE NOISE
Development of ultra-low noise, high sensitivity planar metal grating coupled AlGaAs/GaAs multiquantum well IR detectors for focal plane array staring IR sensor systems
[AD-A254697] p 468 N93-12228

WIGGLER MAGNETS
A synopsis of resistive wall effects in very short wavelength free electron lasers
[DE92-018065] p 315 N93-11155
Scaling of gain with energy spread and energy in the PEP FEL
[DE92-019248] p 316 N93-11500
Dynamic vacuum analysis for APS high heat flux beamline front ends using optical ray-tracing simulation methods
[DE92-019032] p 445 N93-11831

WIND (METEOROLOGY)
Lidar studies of gravity waves in the mesopause region p 358 N93-11222
LAM and NEDWAM statistics over the period October 1990 - April 1991
[KNMI-TR-137] p 368 N93-11329
Structure of the nocturnal boundary layer over a complex terrain
[DE92-018141] p 362 N93-11669
Physical effects of vegetation on wind-blown sand in the coastal environments of Florida
[PB92-188424] p 354 N93-11702
The design, development, and test of balloonborne and groundbased lidar systems. Volume 3: Groundbased lidar systems
[AD-A247552] p 317 N93-11805

WIND EFFECTS
Physical effects of vegetation on wind-blown sand in the coastal environments of Florida
[PB92-188424] p 354 N93-11702

WIND PROFILES
An inversion technique to recover lower thermospheric winds from space-borne remote measurements of (OI) 5577 A p 369 N93-11839

WIND SHEAR
Summary of findings from the PIREP-based analyses conducted during the 1988 to 1990 evaluations of TDWR-based and TDWR/LLWAS-based alert services provided to landing/departing pilots
[AD-A253859] p 367 N93-11144
Numerical and observational investigations of long-lived, MCS-induced, severe surface wind events: The derecho
p 367 N93-11159
A problem formulation for glideslope tracking in wind shear using advanced robust control techniques
[NASA-TM-104164] p 214 N93-11176
Lidar studies of gravity waves in the mesopause region p 358 N93-11222

WIND TUNNEL APPARATUS
Hypersonic flow diagnostic development
[AD-A255045] p 202 N93-12466

WIND TUNNEL MODELS
Computer aided design and manufacturing of composite propfan blades for a cruise missile wind tunnel model
[NASA-TM-105269] p 413 N93-12022
Study of optical techniques for the Ames unitary wind tunnels. Part 4: Model deformation
[NASA-CR-190980] p 219 N93-12349
Mach 4 testing of scramjet inlet models
[NAL-TR-1137] p 202 N93-12369

WIND TUNNEL TESTS
Application of laminar flow to aero engine nacelles
[PNR-90916] p 195 N93-11020
An experimental evaluation of prediction methods for contrafans
[PNR-90924] p 209 N93-11023
Method of remotely characterizing thermal properties of a sample
[NASA-CASE-LAR-13508-3-CU] p 216 N93-11057
The effects of plate spacing and downstream plate length on the acoustic resonance excited by flow past two plates in tandem in a duct
[PNR-90958] p 433 N93-11321
The measurement of the velocity field induced by a gust generator in a closed-circuit subsonic wind-tunnel
[RAE-TM-MAT-STR-1102] p 217 N93-11435
The convection speed of the dynamic stall vortex
[AD-A247258] p 197 N93-11464
Experimental investigation of the effects of aft blowing with various nozzle exit geometries on a 3.0 caliber tangent ogive at high angles of attack: Forebody pressure distributions
[NASA-CR-190935] p 197 N93-11605
Further buffeting tests in a cryogenic wind tunnel
[NASA-TM-107621] p 198 N93-11610
Low-speed longitudinal and lateral-directional aerodynamic characteristics of the X-31 configuration
[NASA-TM-4351] p 198 N93-11622
Introduction of electronic pressure scanning at the Royal Aerospace Establishment
[RAE-TM-AERO-2222] p 199 N93-11882
The 13 ft by 9 ft low speed wind tunnel facility at DRA (Aerospace Division) Bedford (England)
[RAE-TM-AERO-2228] p 199 N93-11883
Strain-gauge balance performance and internal temperature gradients measured in a cryogenic environment
[RAE-TM-AERO-2232] p 218 N93-11906
A wall interference assessment/correction system
[NASA-CR-190617] p 218 N93-11910
An investigation of the effects of aft blowing on a 3.0 caliber tangent ogive body at high angles of attack
[NASA-CR-190934] p 200 N93-12004
Computer aided design and manufacturing of composite propfan blades for a cruise missile wind tunnel model
[NASA-TM-105269] p 413 N93-12022
A preliminary study associated with the experimental measurement of the aero-optic characteristics of hypersonic configurations
[AD-A253792] p 200 N93-12063
An experimental study of the relationship between forces and moments and vortex breakdown on a pitching delta wing p 208 N93-12206
Solution of nonlinear flow equations for complex aerodynamic shapes
[NASA-CR-190979] p 307 N93-12329
Study of optical techniques for the Ames unitary wind tunnels. Part 4: Model deformation
[NASA-CR-190980] p 219 N93-12349
Simulation analysis of a cable-mount system used for dynamic wind tunnel tests
[NAL-TR-1127] p 219 N93-12359
A wind tunnel investigation to determine buffet countermeasures for STOL aircraft alpha-sweep flight testing
[NAL-TR-1129] p 216 N93-12362
Mach 4 testing of scramjet inlet models
[NAL-TR-1137] p 202 N93-12369
Wind tunnel investigation of a twin-engine jet transport semi-span model with upper surface blown jet flap
[NAL-TR-1134] p 203 N93-12503

WIND TUNNEL WALLS
Dynamical effects of suction/heating on turbulent boundary layers
[AD-A248459] p 299 N93-11416
A wall interference assessment/correction system
[NASA-CR-190617] p 218 N93-11910

WIND TUNNELS
Winds of change: Expanding the frontiers of flight. Langley Research Center's 75 years of accomplishment, 1917-1992
[NASA-NP-130] p 490 N93-11100
An experimental study of flow patterns and endwall heat transfer upstream of a surface-mounted rectangular obstruction in a turbulent boundary layer
p 302 N93-11698
A wall interference assessment/correction system
[NASA-CR-190617] p 218 N93-11910

WIND TURBINES
Measured data for the Sandia 34-meter vertical axis wind turbine
[DE92-019807] p 348 N93-12075

WIND VELOCITY
Surface wind speed distributions
[AD-A253268] p 368 N93-11505
An inversion technique to recover lower thermospheric winds from space-borne remote measurements of (OI) 5577 A p 369 N93-11839
Visualizing wind velocities by advecting cloud textures
[DE92-014717] p 371 N93-12154
Analysis of air and sea physical properties and surface fluxes using a combination of in situ and SEASAT data
p 365 N93-12182

WINDPOWER UTILIZATION
NEDO Solar Technology Subcommittee
[DE92-526256] p 347 N93-11845

WINDS ALOFT
An inversion technique to recover lower thermospheric winds from space-borne remote measurements of (OI) 5577 A p 369 N93-11839

WING CAMBER
Flight test results from a supercritical mission adaptive wing with smooth variable camber
[NASA-TM-4415] p 207 N93-11863

WING LOADING
An experimental study of the relationship between forces and moments and vortex breakdown on a pitching delta wing p 208 N93-12206

WING PROFILES
Wind tunnel investigation of a twin-engine jet transport semi-span model with upper surface blown jet flap
[NAL-TR-1134] p 203 N93-12503

WINGS
Unsteady propeller/wing aerodynamic interactions
p 201 N93-12190
The future of carrier aviation
[AD-A254043] p 430 N93-12260

WINTER
Key wintertime meteorological features of the Grand Canyon and the Colorado Plateaus Basin
[DE92-019134] p 369 N93-11657
A composite study of the Madden-Julian oscillation
[AD-A254269] p 369 N93-11819
Sustaining health and performance in the cold: Environmental medicine guidance for cold-weather operation
[AD-A254328] p 385 N93-12145

WIRE
Theory of small metal clusters, films, and wires
[AD-A253120] p 256 N93-11240
The theoretical background to BS7167: 1990 - specification for Bordeaux connections
[NPL-DMM(A)-50] p 325 N93-11324
Frequency response in short thermocouple wires
[NASA-CR-190943] p 310 N93-11612

WIRELESS COMMUNICATION
The locator system for wandering individuals
[NASA-TM-104754] p 388 N93-11649

WORKING FLUIDS
System and method for cancelling expansion waves in a wave rotor
[NASA-CASE-LEW-15218-1] p 297 N93-11172

WORKLOADS (PSYCHOPHYSIOLOGY)
From pilot's associate to satellite controller's associate p 390 N93-11922
Human performance in complex task environments: A basis for the application of adaptive automation
[AD-A255067] p 390 N93-12486

WORKSTATIONS
Geographic information system to support state-wide hydrologic modeling with the SCS-TR-20
[PB92-185768] p 476 N93-11700
A methodology to emulate and evaluate a productive virtual workstation p 395 N93-11938
Advanced satellite workstation: An integrated workstation environment for operational support of satellite system planning and analysis p 391 N93-11941

WORLD METEOROLOGICAL ORGANIZATION
CCL working group on climate data
[WCDMP-18] p 370 N93-11897

WOVEN COMPOSITES
Aerospatiale processes for three dimensional preforms
[REPT-921-430-147] p 239 N93-11590

WRIST
Importance of numerosity and distribution of articulations within the digits, wrists, and arms of telemanipulators confronted with dextrous assembly tasks
p 330 N93-11967

X

X RAY ABSORPTION
X pulse radiation around the critical surface p 318 N93-12027
Research at and operation of the material science x ray absorption beamline (X-11) at the National Synchrotron Light source [DE92-018598] p 251 N93-12172
X RAY ANALYSIS
X ray diagnostic techniques in ICF [DE92-018069] p 449 N93-10975
X RAY APPARATUS
A ring coded-aperture microscope for high-resolution imaging of high-energy x rays [DE92-018004] p 454 N93-12059
X RAY ASTRONOMY
Contributions to the Joint Discussion 3: Results from Rosat and GRO and Other Recent High Energy Astrophysics Missions of the Max-Planck-Institut fuer Extraterrestrische Physik [MPE-PREPRINT-215] p 482 N93-11473
X ray morphology of clusters of galaxies p 482 N93-11475
Stars in the Rosat all-sky survey p 482 N93-11477
Controls Astrophysics and Structures Experiment in Space (CASES) advanced studies and planning [NASA-CR-184410] p 220 N93-12213
Temporal and spectral variability in luminous x ray binaries p 483 N93-12336
X RAY ASTROPHYSICS FACILITY
An investigation of error correcting techniques for OMV and AXAF [NASA-CR-190950] p 416 N93-12515
X RAY BINARIES
Temporal and spectral variability in luminous x ray binaries p 483 N93-12336
X RAY DENSITY MEASUREMENT
Measurement of absorbed dose to water for medium energy x rays [NPL-RSA(EXT)-33] p 436 N93-11412
X RAY DETECTORS
Calibration techniques for high flux x ray detectors [DE92-017513] p 312 N93-11768
X RAY DIFFRACTION
The synthesis and crystal structure of LaHSe2O6, a layered, anhydrous selenite [AD-A251050] p 458 N93-10996
Sigma phase in nickel based superalloys [PNR-90950] p 255 N93-11109
The domain structure features of epitaxial PbTiO3 thin films prepared by MOCVD [DE92-010907] p 459 N93-11190
Structure and property of heteroepitaxial TiO2/VO2 multilayers [DE92-018181] p 460 N93-11563
Studies of the 3 to 5 compounds in the megabar regime [DE92-019517] p 461 N93-11646
Synthesis and characterization of novel organogallium-phosphorus compounds: X ray crystal structures of Ph2GaP (SiMe3)2Ga (Ph2Cl, Ph2 (Cl)Ga.P (SiMe3)3, and Ph3Ga.P (SiMe3)3 [AD-A253841] p 462 N93-11724
Nature of the beta-phase of nickel-aluminum system [AD-A254101] p 261 N93-12269
X RAY IMAGERY
High energy x ray imaging diagnostic on Nova [DE92-018067] p 451 N93-11495
A ring coded-aperture microscope for high-resolution imaging of high-energy x rays [DE92-018004] p 454 N93-12059
Controls Astrophysics and Structures Experiment in Space (CASES) advanced studies and planning [NASA-CR-184410] p 220 N93-12213
X RAY IRRADIATION
X pulse radiation around the critical surface p 318 N93-12027
X RAY LASERS
Experimental studies of x ray laser spectral profiles: Observation of gain narrowing and saturation behavior [DE92-019603] p 316 N93-11659
Progress toward x ray lasing between autoionizing transitions [DE92-017428] p 317 N93-11765
Experimental study of x ray laser in lithumoid aluminum p 321 N93-12045
Modeling for the study of an X laser in a recombination plasma; gain calculations at 105.7 and 154.6 A p 321 N93-12046
X ray laser program, FY 1991 [AD-A255190] p 322 N93-12275
X RAY SOURCES
Calibration techniques for high flux x ray detectors [DE92-017513] p 312 N93-11768
X RAY SPECTRA
Sigma phase in nickel based superalloys [PNR-90950] p 255 N93-11109
Multispectral observations of the Jovian aurora p 487 N93-11167
Temporal and spectral variability in luminous x ray binaries p 483 N93-12336
X RAY SPECTROSCOPY
Signal-to-noise assessment and measurement in spectroscopies with particular reference to Auger and x ray photoelectron spectroscopies [NPL-DMM(A)-45] p 247 N93-11396
Polyethylene-terephthalate/aluminum adhesion [ECL-91-33] p 257 N93-11578
X-UV spectroscopy temporal resolution p 318 N93-12028
Hydrodynamic study of multilayer targets by spatial and temporal resolution shadow spectroscopy p 254 N93-12050
X RAY STARS
Contributions to the Joint Discussion 3: Results from Rosat and GRO and Other Recent High Energy Astrophysics Missions of the Max-Planck-Institut fuer Extraterrestrische Physik [MPE-PREPRINT-215] p 482 N93-11473
Stars in the Rosat all-sky survey p 482 N93-11477
X RAY TELESCOPES
X ray morphology of clusters of galaxies p 482 N93-11475
X RAYS
Tunable, short pulse hard x rays from a compact laser synchrotron source [AD-A254288] p 315 N93-11195
Measurement of absorbed dose to water for medium energy x rays [NPL-RSA(EXT)-33] p 436 N93-11412
Progress toward x ray lasing between autoionizing transitions [DE92-017428] p 317 N93-11765
Calibration techniques for high flux x ray detectors [DE92-017513] p 312 N93-11768
Reflection masks for soft x ray projection lithography [DE92-014779] p 293 N93-12121
ESIS: An introduction to the European space information system. A modern tool for space scientists [ESA-INT-2] p 479 N93-12404
X-29 AIRCRAFT
Flight-determined stability analysis of multiple-input-multiple-output control systems [NASA-TM-4416] p 214 N93-11178
Correlation of forebody pressures and aircraft yawing moments on the X-29A aircraft at high angles of attack [NASA-TM-4417] p 197 N93-11532
A summary of the forebody high-angle-of-attack aerodynamics research on the F-18 and the X-29A aircraft [NASA-TM-104261] p 202 N93-12353
XENON
Extended-testing of xenon ion thruster hollow cathodes [NASA-CR-189227] p 234 N93-12409

Y

YAWING MOMENTS
Correlation of forebody pressures and aircraft yawing moments on the X-29A aircraft at high angles of attack [NASA-TM-4417] p 197 N93-11532
YBCO SUPERCONDUCTORS
Critical currents in polycrystalline YBa2Cu3O(7-x): Self-field and grain size dependence [DE92-617540] p 459 N93-11076
High frequency response from YBa2Cu3O(7-x) Josephson devices on SrTiO3 bicrystal substrates [NPL-DES-118] p 459 N93-11394
Frustrated phase separation and high temperature superconductivity [DE92-019249] p 459 N93-11501
Magnetic properties of high-T(c) superconductors [DE92-018809] p 460 N93-11533
Flux pinning in oxygen-depleted YBa2Cu3O(7-y) single crystals [DE92-019548] p 461 N93-11647
Submillimeter and microwave residual losses in epitaxial films of Y-Ba-Cu-O and Bl-Ca-Ca-Cu-O [DE92-017075] p 466 N93-12125
Flux dynamics and irreversibility in YBa2Cu3O7 with Y2BaCuO5 inclusions and in single crystal YBa2Cu3O7 [DE92-009712] p 467 N93-12178
Influence of oxygen partial pressure and silver additions on microstructure and related properties of YBCO superconductors [DE92-011145] p 468 N93-12249
Conductor-backed coplanar waveguide resonators of Y-Ba-Cu-O and Tl-Ba-Ca-Cu-O on LaAlO3 [NASA-TM-105890] p 469 N93-12325
YIELD
Synthesis of side chain liquid crystal polymers by living ring opening metathesis polymerization. Report 2: Influence of molecular weight, polydispersity, and flexible spacer length (n=9-12) on the thermotropic behavior of the resulting plymers [AD-A248700] p 265 N93-11188
YIELD STRENGTH
Mechanical properties of 1950's vintage 304 stainless steel weldment components after low temperature neutron irradiation [DE92-017059] p 259 N93-12107
Processing and properties of NbTi based alloys [DE92-016692] p 261 N93-12445
YTTRIUM OXIDES
Magnetic properties of high-T(c) superconductors [DE92-018809] p 460 N93-11533
Intermediate temperature electrolytes for SOFC [DE92-018786] p 345 N93-11571

Z

ZAMBIA
Proceedings of the First Seminar on Geographic Information Systems in Zambia [PB92-207125] p 477 N93-11789
ZINC
VUV and UV sources and spectroscopic applications [AD-A247293] p 291 N93-11758
ZINC COMPOUNDS
Tetrahedral atom zincophosphate structures: Synthesis, crystal structure, and spectroscopic studies of (Zn(PO2(OC2H5)2)2)x, a one-dimensional inorganic polymer [AD-A251051] p 437 N93-11560
ZINC OXIDES
Nanostructure, defect chemistry and properties of relaxor ferroelectrics [AD-A247294] p 431 N93-11468
Research on stable, high-efficiency, amorphous silicon multijunction modules [DE92-010599] p 464 N93-11818
ZINC TELLURIDES
Excitons in semiconducting superlattices, quantum wells, and ternary alloys [DE92-015178] p 464 N93-11894
Electronic and optical properties of perfect and imperfect 2 to 6 superlattices p 465 N93-11996
ZIRCONIUM
Pulsed-field-gradient NMR investigations of hydrogen diffusion in ZrH(x) [DE92-014393] p 459 N93-11238
ZIRCONIUM ALLOYS
The effect of silicon, tin, and chromium on the corrosion and mechanical properties of zirconium - molybdenum - niobium [AD-A254102] p 258 N93-11787
Optimization of film synthesized rare earth transition metal permanent magnet systems [DE92-018726] p 432 N93-12116
ZIRCONIUM OXIDES
Intermediate temperature electrolytes for SOFC [DE92-018786] p 345 N93-11571
Development of wear resistant ceramic coatings for diesel engine components [DE92-019068] p 268 N93-11654
Synthesis of nanocrystalline powders for oxide ceramics by microwave plasma pyrolysis [DE92-017410] p 268 N93-11861
Superplastic forming of ceramic insulation p 228 N93-12452
ZONAL FLOW (METEOROLOGY)
Quasigeostrophic vortices in zonal shear p 358 N93-11226

PERSONAL AUTHOR INDEX

SCIENTIFIC AND TECHNICAL AEROSPACE REPORTS VOLUME 31 NUMBER 2

Typical Personal Author Index Listing

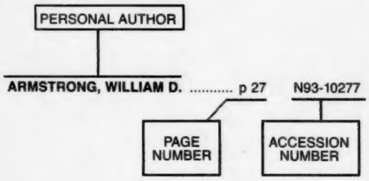

Listings in this index are arranged alphabetically by personal author. The page number helps you locate the citation in the abstract section. The accession number denotes the number by which the citation is identified.

A

AARONS, JULES p 361 N93-11282
ABARCAR, R. B. p 481 N93-12067
ABBITT, JOHN DAVID, III p 200 N93-12001
ABBOTT, J. R. p 303 N93-11843
ABDELATIF, GAILILA p 320 N93-12044
ABDY, GHASEM L. p 199 N93-11899
ABEDIN, M. N. p 333 N93-12204
ABO, EIICHI p 208 N93-12354
ABOOD, DORIS A. p 385 N93-11893
ABOUDI, JACOB p 335 N93-11175
ABRAHAM, K. M. p 291 N93-11604
ABRAMSON, BRUCE p 394 N93-11936
ABUMERI, G. H. p 276 N93-12197
ACKLEY, KEITH A. p 407 N93-11368
ACQUAVIVA, THOMAS H. p 242 N93-12078
ADAIR, R. p 437 N93-11681
ADAMCZYK, GEORGE R. p 228 N93-12451
ADAMOVA, A. S. p 258 N93-11787
ADAMS, CATHY p 478 N93-11796
ADELMAN, HOWARD M. p 206 N93-10968
AGELIDIS, A. p 383 N93-11317
AGUADO, M. T. p 382 N93-11310
AHMED, S. p 274 N93-11550
AINSWORTH, R. W. p 210 N93-11055
AIRENTI, GABRIELLA p 386 N93-11212
AISO, HIDEAKI p 428 N93-12350
AIUTI, FERNANDO p 378 N93-11293
AKERA, H. p 460 N93-11512
AL-HAKEEM, SAMAWAL p 414 N93-12242
ALABRABA, M. p 255 N93-11115
ALAM, J. p 336 N93-11403
ALBRIGHT, K. L. p 312 N93-11822
ALDRICH, K. S. p 257 N93-11595
ALEWINE, NEIL J. p 406 N93-12541
ALEXANDER, D. J. p 258 N93-11773
ALEXANDER, J. IWAN D. p 223 N93-11101
ALI, MOHAMMED HUSSAIN p 283 N93-11913
ALLAN, W. D. E. p 210 N93-11055
ALLEN, G. C. p 231 N93-10973
ALLUISI, EARL A. p 472 N93-12273
ALLWINE, K. J. p 369 N93-11657
ALLWINE, K. JERRY p 355 N93-11920
ALLWOOD, R. J. p 212 N93-11114
ALMGREN, ROBERT F. p 275 N93-12236
ALMLOEF, JAN p 439 N93-11854
ALTOBELLI, S. A. p 303 N93-11843
ALYEA, FRED N. p 350 N93-11088
AMATO, C. p 266 N93-11413
AMIRANOFF, FRANCOIS p 319 N93-12034
AN, BEN p 399 N93-11957
ANDERSEN, M. E. p 276 N93-11951
ANDERSEN, NIELS H. p 437 N93-11709
ANDERSON, BIANCA T. p 196 N93-11221
ANDERSON, D. V. p 451 N93-11516
ANDERSON, HAROLD M. p 295 N93-12437
ANDERSON, R. J. p 277 N93-11672
ANDERSON, T. W. p 429 N93-12513
ANDRAKA, C. E. p 347 N93-12012
ANDREWS, M. K. p 437 N93-11597
ANGELUCCI, A. FILIPPO p 341 N93-12300
ANGUS, JAMES P. p 264 N93-11066
ANNIS, CHARLES p 260 N93-12237
ANTHONY, G. T. p 325 N93-11325
ANZALONE, G. p 383 N93-11314
APPELBAUM, J. p 295 N93-12301
ARAGON, JORGE p 379 N93-11297
ARGAMAN, N. p 471 N93-11780
ARMAN, B. p 305 N93-12128
p 306 N93-12313
ARMENGAUD, M. p 318 N93-12027
ARMENTROUT, D. L. p 465 N93-12073
ARMENTROUT, P. B. p 262 N93-12480
ARMISTEAD, MAURICE F. p 230 N93-11982
ARMSTRONG, WILBUR C. p 235 N93-12522
ARNAS, CECILE p 318 N93-12027
ARNEFTE, S. A. p 308 N93-12435
ARNOLD, DAVID p 343 N93-12006
ARNOLD, J. p 466 N93-12099
ARNOLD, R. J. p 430 N93-11711
ARRANZ, JEAN-PIERRE p 321 N93-12049
ARTHEY, R. P. p 211 N93-11085
ASCHENBACH, B. p 482 N93-11476
ASHBAUGH, N. E. p 242 N93-12181
ASHBY, P. C. p 357 N93-11120
ASHENBERG, JOSHUA p 219 N93-11904
ASHFORD, N. J. p 218 N93-11728
ASHFORD, NORMAN p 217 N93-11224
ASHOUR-ABDALLA, M. p 224 N93-11736
ASHWILL, T. D. p 348 N93-12075
ASKEW, GREGORY K. p 389 N93-12291
ASSINK, R. A. p 437 N93-11640
ASTILLERO, RICARDO p 217 N93-11616
ATENCIO, J. H. p 274 N93-11380
ATHERTON, C. S. p 354 N93-11744
ATKINS, JOHN p 415 N93-12385
ATKINSON, COLLIN p 412 N93-11717
ATKINSON, ROGER p 351 N93-11092
ATTIA, ALAN I. p 290 N93-11456
ATTIX, F. H. p 438 N93-11715
AUBUCHON, STEVEN R. p 462 N93-11724
AUDEBERT, PATRICK p 254 N93-12050
AULD, BERT A. p 242 N93-12296
AULUCK, S. K. H. p 449 N93-11029
AURILIO, G. p 317 N93-11805
p 322 N93-12262
AUSTON, D. p 288 N93-11257
AUTY, DAVID p 412 N93-11717
AVARA, ELTON P. p 368 N93-11505
AVERBACK, ROBERT S. p 272 N93-12246
AVICOLA, K. p 310 N93-11542
AZZI, B. p 240 N93-11835

B

BAATH, LARS B. p 485 N93-11807
BABA, SHIGERU p 216 N93-12362
BABIC, E. p 459 N93-11076
BABUSKA, I. p 427 N93-11837
BACAL, MARTHE p 440 N93-11867
BACHALO, W. D. p 248 N93-11454
BADER, J. W. p 231 N93-11173
BADER, MICHAEL G. p 264 N93-11084
BAEZ, ANASTACIO N. p 417 N93-11005
BAI, G. R. p 459 N93-11190
BAI, SHUZHEN p 237 N93-11143
BAILEY, M. C. p 222 N93-12543
BAIN, ADDISON p 349 N93-12394
BAIN, R. p 281 N93-11487
BAIRD, JAMES K. p 297 N93-11142
BAIRD, R. J. p 277 N93-11672
BAKER-JARVIS, JAMES p 293 N93-12084
BAKES, CATHERINE MURPHY p 419 N93-12410
BALACHANDAR, S. p 427 N93-12298
BALAZS, A. C. p 267 N93-11628
BALCH, K. S. p 310 N93-11542
BALDIS, H. A. p 318 N93-12025
p 318 N93-12026
BALIN, LIONEL J. p 266 N93-11425
BALLARD, PATRICK p 319 N93-12035
p 319 N93-12036
BALLAS, JAMES A. p 388 N93-11784
BALOOCH, M. p 465 N93-12093
BAMKIN, ROGER J. p 473 N93-11012
BANAVAR, RAVI N. p 340 N93-12200
BANKS, CURTIS p 470 N93-12396
BANKS, DANIEL W. p 198 N93-11622
BANSAL, NAROTTAM p 239 N93-11543
BANSAL, NAROTTAM P. p 249 N93-11545
BARABAS, N. J. p 221 N93-12317
BARBEE, TROY WALTER, III p 292 N93-11833
BARBIER, PIERRE p 332 N93-11587
BARCLAY, REBECCA O. p 478 N93-12007
BARIBEAU, J. M. p 459 N93-11496
p 463 N93-11772
BARLETTA, W. A. p 315 N93-11155
BARLOW, JOHN p 331 N93-11110
BARNDEN, JOHN A. p 422 N93-12259
BARNES, BERNIS p 427 N93-12061
BARNES, R. G. p 459 N93-11238
BARNETT, D. S. p 472 N93-12273
BARON, MILES HUNT p 457 N93-12535
BARRACLOUGH, B. L. p 365 N93-12263
BARRET, C. p 222 N93-11002
BARRETT, DAVID M. p 229 N93-12456
BARRON, MICHAEL H. p 313 N93-12069
BARRON, ROGER L. p 422 N93-12439
BARTHOLET, STEPHEN J. p 330 N93-11970
BARTOLOTTA, PAUL A. p 238 N93-11399
BARTON, J. P. p 231 N93-11173
BASARAN, O. A. p 301 N93-11638
BASELEY, H. M. p 211 N93-11068
BASSOM, ANDREW P. p 301 N93-11633
BASU, R. p 375 N93-12482
BATON, SOPHIE p 318 N93-12025
p 318 N93-12026
BATSON, P. J. p 316 N93-11659
BATTRICK, BRUCE p 344 N93-12280
BAUCHE-ARNOULT, C. p 320 N93-12041
BAUCHE, J. p 320 N93-12041
BAUER, DAVID P. p 222 N93-12505
BAUM, KURT p 275 N93-12147
BAUMAN, L. E. p 454 N93-11826
p 454 N93-12087
BAUMAN, W. H. p 371 N93-12170
BAUMGART, C. W. p 286 N93-12417
BAUMJOHANN, WOLFGANG p 361 N93-11352
BAXI, C. B. p 451 N93-11382
p 305 N93-12010
BEASLEY, MALCOM R. p 294 N93-12290
BEAVIS, A. W. p 465 N93-11996
BECK, D. F. p 231 N93-10973
BECK, JON p 416 N93-12393
BECKMAN, T. M. p 310 N93-11554
BECKSTEAD, MERRILL W. p 275 N93-12147
BEESON, MICHAEL R. p 371 N93-12251
BEETZ, CHARLES P. p 271 N93-12086
BEEVERS, C. J. p 255 N93-11031
BEGLEY, J. A. p 259 N93-12107
BEHEIM, GLENN p 446 N93-11058
BEHRENDT, D. R. p 273 N93-12398
BEJCZY, A. K. p 400 N93-11965
BEJCZY, ANTAL K. p 400 N93-11964
BEKEFI, G. p 315 N93-11278
BELCASTRO, CELESTE M. p 215 N93-12304
BELCASTRO, CHRISTINE M. p 214 N93-11176
BELFORD, K. A. p 308 N93-12539
BELL, BRAD p 400 N93-11963
BELL, P. M. p 454 N93-12059
BELL, WAYNE p 310 N93-11460
BELL, WAYNE E. p 285 N93-12331
BELL, WILLIAM A. p 297 N93-11074
BELLANTI, J. A. p 381 N93-11306
p 382 N93-11311
BELLMAN, KIRSTIE L. p 396 N93-11946
BELOT, CHRISTOPHE p 246 N93-11361
BELYAVIN, A. J. p 281 N93-11487
BENATTAR, RENE p 318 N93-12028
p 318 N93-12029
BENDER, C. M. p 470 N93-11276
BENDOTTI, P. p 215 N93-11585
BENKHEIRI, P. p 319 N93-12034

BENNETT, M. p 464 N93-11818
BENNETT, RODNEY G. p 230 N93-11953
BENNETT, THEODORE J., JR. p 373 N93-11821
BENNETT, WINSTON R. p 387 N93-12252
BENSON, ALAN E. p 421 N93-12096
BENTON, R. D. p 312 N93-11827
p 454 N93-12087
BENTS, D. J. p 275 N93-12085
BERDING, M. A. p 462 N93-11727
BERGER, M. J. p 438 N93-11715
BERGIN, A. L. p 195 N93-11020
BERGMANN, V. L. p 232 N93-11824
BERKE, L. p 336 N93-11403
BERLAND, M. p 320 N93-12044
BERMAN, D. H. p 284 N93-12083
BERNAUER, E. M. p 374 N93-12014
BERNHARD, RONALD P. p 488 N93-11374
BERNIK, S. p 459 N93-11076
BERS, A. p 449 N93-10988
BERTON, JEFFREY J. p 209 N93-10983
BERTONI, ALBERTO p 418 N93-11180
BERTRAM, L. A. p 329 N93-12220
BESS, T. DALE p 367 N93-11168
BESSON, J. L. p 239 N93-11586
BEWLEY, WILLIAM L. p 398 N93-11952
BHASIN, K. B. p 469 N93-12325
BHATIA, R. p 245 N93-11138
BHATTACHARJEE, A. p 452 N93-11568
BHATTACHARYA, R. S. p 328 N93-12122
BI, X. X. p 250 N93-11847
BIERBAUM, VERONICA M. p 436 N93-11467
BIERSCHWALE, JOHN M. p 400 N93-11966
BIESIADNY, THOMAS J. p 213 N93-11530
BIGBEE, LARRY R. p 377 N93-11292
BIGELOW, C. A. p 236 N93-11072
BILELLO, JOHN C. p 264 N93-11149
BINIENDA, WIESLAW K. p 241 N93-12076
BIONDO, A. C. p 460 N93-11522
BIRCH, J. R. p 459 N93-11394
BIRCH, N. T. p 196 N93-11113
BIRNBAUM, LARRY E. p 294 N93-12191
p 294 N93-12294
p 295 N93-12295
BISELLI, R. p 380 N93-11303
p 382 N93-11312
BISELLI, ROBERTO p 381 N93-11305
BISHOP, ANN P. p 478 N93-12007
BISHOP, LANE p 350 N93-11089
BITSAKTSIS, A. p 384 N93-11318
BJARKE, LISA J. p 202 N93-12353
BLACK, JOHN D. p 244 N93-11035
BLACKMON, FLETCHER A. p 280 N93-11354
BLACKWELDER, RON p 299 N93-11416
BLAIS, N. C. p 274 N93-11566
BLAKE, DON p 350 N93-11088
BLANKINSHIP, REX p 474 N93-11255
BLEWER, R. S. p 467 N93-12134
BLINN, THOMAS M. p 407 N93-11368
BLISS, D. p 469 N93-12316
BLOCH, JEAN-JACQUES p 282 N93-11591
BLONDET, PASCAL p 332 N93-11587
BLOOM, I. p 345 N93-11513
p 345 N93-11571
BLOSSER, MAX L. p 208 N93-12458
BLUM, FRANK D. p 265 N93-11194
BLUMENBERG, J. p 263 N93-11011
BLUMENTHAL, M. S. p 404 N93-11761
BLUMTHALER, M. p 352 N93-11098
BO, T. p 296 N93-11025
p 296 N93-11067
BOBO, STEPHEN N. p 332 N93-11617
BODENMILLER, CHARLES A. p 407 N93-11368
BOEHM-VITENSE, ERIKA p 481 N93-11073
p 481 N93-11075
BOEHM, T. F. p 292 N93-11916
BOEHRINGER, H. p 482 N93-11475
BOETTICHER, G. p 415 N93-12392
BOHLMANN, R. E. p 240 N93-11739
BOHN-MEYER, MARTA p 196 N93-11221
BOHN, C. L. p 444 N93-11652
BOJANCZYK, A. p 287 N93-12512
BOJKOV, RUMEN D. p 350 N93-11089
BOLLAND, SARA LOUISE p 217 N93-11224
BONASIA, P. J. p 466 N93-12099
BONETTI, DENA M. p 387 N93-11559
BONNELL, D. A. p 273 N93-12479
BONOLI, P. T. p 449 N93-11041
BOOK, MICHAEL L. p 230 N93-11954
BOONE, JOHN M. p 477 N93-11732
p 404 N93-11809
BORHANI, K. J. p 249 N93-11644
BORKOWSKI, JEFFREY A. p 443 N93-11433
BOROWSKI, STANLEY K. p 233 N93-12363
BORRELLI, SALVATORE p 196 N93-11157
BOSWELL, R. N. p 379 N93-11296
BOTINEAU, JEAN p 320 N93-12040
BOTJE, M. A. J. p 442 N93-11130
BOU, MADELEINE p 257 N93-11578
BOUDENNE, JEAN-MICHEL p 308 N93-12030
BOUILLARD, J. X. p 456 N93-12416
BOUKADIA, JOSEPH AIME MICHEL
p 460 N93-11573
BOURNE, N. K. p 249 N93-11490
BOURRET, E. D. p 466 N93-12099
p 469 N93-12316
BOURSERAU, F. p 239 N93-11589
BOUSQUET, CLAIRE p 321 N93-12049
BOUSTIE, MICHEL p 319 N93-12037
BOWEN, P. R. p 217 N93-11447
BOWMAN, B. C. p 364 N93-12155
BOWMAN, RANDY R. p 258 N93-11635
BOX, G. E. P. p 429 N93-11820
BOYACK, K. W. p 249 N93-11551
BOYD, BILLIE F. p 371 N93-12170
BOYDEN, R. P. p 198 N93-11610
BOZOVIC, I. p 465 N93-12065
BOZZOLO, GUILLERMO p 257 N93-11609
BRADLEY, JOHN P. p 485 N93-11546
BRADY, E. p 477 N93-11770
BRALEY, D. M. p 396 N93-11943
BRAMSON, MICHAEL p 446 N93-11052
BRANDT, R. G. p 272 N93-12276
BRAR, N. S. p 240 N93-11835
BRASCHE, L. J. H. p 254 N93-10995
BRASE, J. p 310 N93-11542
BRASSEUR, GUY P. p 351 N93-11091
BRATTON, THOMAS p 217 N93-11616
BREILAND, W. G. p 463 N93-11797
BRENADELAROSA, A. p 248 N93-11454
BRENIZER, J. S. p 231 N93-11173
BRENNER, DOUGLAS p 287 N93-12461
BRENNER, H. p 303 N93-11843
BREZANY, PETER p 412 N93-11618
BRIAND, JACQUES p 318 N93-12027
BRIEL, U. G. p 482 N93-11475
BRILL, THOMAS B. p 276 N93-12285
BRINKLEY, JAMES W. p 387 N93-11559
p 204 N93-12489
BRISARD, M. p 321 N93-12049
BRITCHER, COLIN P. p 277 N93-11613
BROCK, B. C. p 284 N93-12101
BROMLEY, DAVID WILSON p 316 N93-11720
BROOKS, DONALD A. p 485 N93-11546
BROOKS, FREDERICK P., JR. p 388 N93-11783
BROOKS, J. N. p 257 N93-11600
BROOKS, THURSTON L. p 391 N93-11981
BROUGHTON, T. p 212 N93-11207
p 212 N93-11208
BROUGHTON, W. R. p 266 N93-11397
BROWN, BRIDGET p 478 N93-11796
BROWN, CLARE p 343 N93-11701
BROWN, D. p 345 N93-11381
BROWN, GEORGE R. p 379 N93-11299
BROWN, H. BEN p 331 N93-11973
BROWN, I. G. p 466 N93-12127
BROWN, J. p 405 N93-12520
BROWN, JERE L. p 222 N93-12130
BROWN, PAUL R. p 276 N93-12281
BROWN, R. C. p 366 N93-12299
BROWN, ROGER O. p 477 N93-11748
BROWNELL, JOHN B. p 334 N93-11021
BROWNING, R. p 293 N93-12121
BRUCE, D. I. p 409 N93-11405
p 409 N93-11406
BRUECK, S. R. p 447 N93-11527
BRUMBERGER, H. p 470 N93-12464
BRUNE, WILLIAM H. p 351 N93-11091
p 351 N93-11092
BRUNEAU, J. p 320 N93-12041
BRYAN, THOMAS C. p 230 N93-11954
BUCHER, HANS p 313 N93-12069
BUCHHEIT, RUDOLPH G., JR. p 259 N93-11895
BUCK, O. p 254 N93-10995
BUCKLEY, BRIAN p 230 N93-11932
BUCKLEY, JAMES A. p 195 N93-11050
BUCKNAM, R. D. p 317 N93-11805
p 322 N93-12262
BUDEN, D. p 232 N93-11596
p 233 N93-12056
BUDGE, K. G. p 411 N93-11536
BUDHIRAJA, NAVIN p 472 N93-12212
BUELOW, S. J. p 274 N93-11380
BUI, STACEY p 468 N93-12183
BULLARD, J. B. p 296 N93-11017
BUNYAN, P. p 273 N93-11376
BURCH, RICHARD p 292 N93-11781
BURGARDT, P. p 327 N93-11679
BURKE, DONALD S. p 377 N93-11291
BURKE, JAMES B. p 330 N93-11970
BURKE, ROGER p 396 N93-11944
BURKE, W. R. p 476 N93-11583
BURKEN, JOHN J. p 214 N93-11178
BURKS, B. L. p 399 N93-11958
BURLATON, J. P. p 380 N93-11304
BURNARD, ROBERT p 398 N93-11952
BURRELL, K. H. p 455 N93-12307
BURTIS, M. D. p 473 N93-10990
BUSH, HAROLD G. p 224 N93-10970
BUSS, R. J. p 463 N93-11797
BUSSELL, TIM J. p 311 N93-11648
BUTCHER, M. C. p 212 N93-11206
BUTLER, B. P. p 412 N93-11688
BUTLER, DANIEL H. p 463 N93-11790
BUTTO, S. p 378 N93-11294
BUTTRILL, CAREY S. p 215 N93-12216
BYRNE, J. p 255 N93-11115

C

CABLE, M. D. p 454 N93-12060
CACHEIRO, R. A. p 252 N93-12219
CADIEU, F. J. p 432 N93-12116
CAHUZAC, GEORGES p 239 N93-11590
CAI, Y. p 326 N93-11653
CAIN, MAURICE R. p 334 N93-11080
CALDARELLA, GERALD J. p 390 N93-12423
CALVERT, JACK G. p 350 N93-11090
CAMARDA, CHARLES J. p 229 N93-12460
CAMPBELL, R. D. p 327 N93-11679
CAMPBELL, RICHARD L. p 201 N93-12321
CAMPBELL, W. SPENCER p 230 N93-11926
CAMPISI, I. E. p 442 N93-11077
CAMPONESCHI, E. T., JR. p 240 N93-11739
CANT, C. J. p 409 N93-11392
CARILLON, ANTOINE p 320 N93-12043
p 320 N93-12044
p 321 N93-12045
p 321 N93-12051
CARLOS, R. C. p 362 N93-11535
CARLSON, N. M. p 333 N93-12055
CARLSON, O. N. p 254 N93-10995
CARLUCCI, F. p 411 N93-11592
CAROLLO, SALVATORE L. p 448 N93-12272
CARPENTER, A. J. p 426 N93-11520
CARPENTER, S. H. p 465 N93-12073
CARR, T. T. p 240 N93-11739
CARRERAS, B. A. p 456 N93-12501
CARROLL, AMY E. p 389 N93-12195
p 389 N93-12211
CARROLL, RAYMOND J. p 429 N93-12429
CARTER, C. H., JR. p 295 N93-12340
CARTER, EMILY A. p 249 N93-11755
CARTER, W. L. p 462 N93-11703
CARVER, GARY P. p 277 N93-11901
p 277 N93-11902
CASADY, WILLIAM WALTER p 201 N93-12208
CASHON, JOHN L. p 328 N93-12196
CASKEY, G. R., JR. p 259 N93-12107
p 260 N93-12158
CASNER, STEPHEN p 474 N93-11353
CASTRO-CEDENO, MARIO p 337 N93-11624
CATALANO, A. p 464 N93-11818
CATTOLICA, R. J. p 252 N93-12255
CAVALLARO, JOSEPH R. p 330 N93-11961
CE, WANG p 242 N93-12235
CEBULA, R. P. p 373 N93-11718
CEDENO, W. p 414 N93-12234
CEGLIO, N. M. p 293 N93-12121
CHA, HUNGSE p 292 N93-11781
CHA, Y. S. p 431 N93-11598
CHACONAS, KAREN p 398 N93-11955
CHAIKEN, J. p 470 N93-12464
CHAIT, A. p 295 N93-12301
CHAMBERS, D. H. p 448 N93-11627
CHAMBERS, JOHN G. p 211 N93-11069
CHAMIS, C. C. p 276 N93-12197
CHAMPION, E. p 239 N93-11586
CHAN, AMY W. p 393 N93-11929
CHAN, C. K. p 251 N93-12112
CHAN, K. S. p 260 N93-12241
CHANDRASEKARAN, SHIVKUMAR
p 428 N93-12511
CHANG, B.-C. p 214 N93-11176
CHANG, C. A. p 388 N93-11743
CHANG, C. H. p 454 N93-12066
p 455 N93-12092
CHANG, H. C. p 470 N93-11469
CHANG, H. L. M. p 459 N93-11190
p 460 N93-11563
CHANG, JUI-HUNG p 222 N93-11726
CHANG, L. H. p 353 N93-11655
CHANG, S. L. p 455 N93-12309
CHANG, SIN-CHUNG p 425 N93-11254
CHANIN, MARIE-LISE p 350 N93-11089
CHAPARRO, A. p 384 N93-11841
CHASE, MIKE p 290 N93-11504
CHATO, DAVID J. p 296 N93-10981

CHATTERJEE, A. p 473 N93-11151
CHAUHAN, H. p 356 N93-12314
CHEETHAM, ANTHONY K. p 458 N93-10996
CHELETTE, TAMARA L. p 385 N93-11081
CHEN, A.-B. p 462 N93-11727
CHEN, C. p 315 N93-11278
CHEN, C. H. p 460 N93-11558
p 464 N93-11869
CHEN, C. P. p 305 N93-12082
CHEN, H. H. p 421 N93-12226
CHEN, L. p 464 N93-11818
CHEN, N. p 254 N93-12518
CHEN, P. J. p 250 N93-12062
CHEN, PI-FUAY p 218 N93-11751
CHEN, PING p 363 N93-11898
CHEN, QUAN p 302 N93-11698
CHEN, S. p 315 N93-11278
CHEN, S. S. p 326 N93-11653
CHEN, Y. S. p 297 N93-11171
CHEN, YING p 294 N93-12198
CHEN, YU p 434 N93-11526
CHENAIS-POPOVICS, CLAUDE p 320 N93-12041
p 254 N93-12042
p 254 N93-12050
CHENAOUI, AHMED p 461 N93-11581
CHENETTE, D. L. p 290 N93-11492
CHENG, GARY C. p 297 N93-11171
CHENG, R. K. p 251 N93-12112
CHERN, E. JAMES p 258 N93-11621
CHICK, MICHAEL C. p 311 N93-11648
CHIE, CHAK M. p 288 N93-12519
CHIEN, STEVE p 391 N93-11923
CHIGIER, NORMAN p 248 N93-11453
CHIMONAS, E. p 383 N93-11317
CHIN, KERIC B. O. p 387 N93-12252
CHIN, W. K. p 251 N93-12112
CHINZEI, NOBUO p 202 N93-12369
CHIRON, ARNAUD p 319 N93-12032
CHISHOLM, M. F. p 458 N93-10987
CHIU, C. T. p 460 N93-11558
CHIU, S. C. p 449 N93-11041
CHODA, L. p 408 N93-11389
CHOI, JAEYOUNG p 426 N93-11636
CHOI, SUNG R. p 263 N93-10962
CHOI, U. S. p 431 N93-11598
CHOJNACKI, KENT T. p 231 N93-11042
p 231 N93-11043
CHOKANI, NDAONA p 197 N93-11605
CHOPRA, INDERJIT p 208 N93-12485
CHOU, T. T. p 441 N93-12224
CHOVELON, JEAN-MARC p 291 N93-11574
CHRISTE, KARL O. p 275 N93-12147
CHRISTENSEN, B. p 399 N93-11958
CHU, WILLIAM p 350 N93-11089
CHU, ZHIPING p 322 N93-12163
CHULYA, ABHISAK p 263 N93-10962
CHUNG, T. J. p 235 N93-11133
CIARLO, ALESSANDRO p 479 N93-12404
CIARLO, D. R. p 454 N93-12059
CLARDY, W. F. p 377 N93-11287
CLARDY, WILLIAM F. p 380 N93-11301
CLARK, JOHN S. p 233 N93-12363
CLARK, RONALD K. p 269 N93-11912
p 229 N93-12457
CLARKE, DAVID A. p 263 N93-11018
p 266 N93-11205
CLARKE, J. T. p 487 N93-11165
CLAUS, J. p 443 N93-11429
CLAUSEN, E. C. p 375 N93-12482
CLAY, K. p 334 N93-11014
p 255 N93-11109
CLEVELAND, GARY A. p 391 N93-11924
CLEWELL, H. J. p 276 N93-11951
CLINE, MICHAEL C. p 302 N93-11767
CLIVER, E. W. p 489 N93-12506
CLOTHIAUX, JOHN D. p 341 N93-12411
CLOUTHIER, D. J. p 251 N93-12091
CODUTI, P. L. p 277 N93-11672
COE, H. H. p 323 N93-10982
COENPORISINI, ALBERTO p 476 N93-11689
COFFEY, HELEN E. p 488 N93-11738
COGAN, STUART F. p 447 N93-11186
COGOLI, A. p 376 N93-11284
COHEN, GERALD C. p 405 N93-12345
p 405 N93-12346
p 405 N93-12347
p 406 N93-12538
COHEN, J. D. p 463 N93-11813
COHEN, MARION F. p 385 N93-12469
COKER, D. p 242 N93-12181
COLAIANNI, M. L. p 250 N93-12062
COLELLA, PHILLIP p 307 N93-12333
COLEMAN, MICHAEL D. p 334 N93-11080
COLEMAN, T. A. p 473 N93-11104
COLINGE, J. P. p 295 N93-12421
COLLIGNON, STEVEN L. p 274 N93-11665
COLLINS, H. D. p 312 N93-11802
COLLINS, S. p 385 N93-10979
COLOMBETTI, MARCO p 386 N93-11212
COLON, ANDY p 310 N93-11460
COLTON, R. J. p 272 N93-12276
COLVIN, JAMES E. p 226 N93-12152
CONCILIO, ANTONIO p 334 N93-11158
CONFORTI, MICHELE p 430 N93-12217
CONNELL, PETER p 351 N93-11093
CONSAGA, JOHN P. p 274 N93-11665
CONWAY, TERRY L. p 385 N93-11893
COOK, J. E. p 385 N93-12145
COOK, R. L. p 304 N93-11995
p 454 N93-12087
p 455 N93-12141
COOK, S. C. p 331 N93-11015
COOK, TIMOTHY ALLAN p 482 N93-11373
COOLBAUGH, M. T. p 236 N93-12177
COOPER, LYNNE P. p 288 N93-11939
COOPER, P. J. p 219 N93-12268
COPPI, B. p 456 N93-12493
CORDA, ALBERT J. p 288 N93-11053
CORDES, W. p 368 N93-11350
CORMIER, VERNON F. p 362 N93-11740
CORNETTE, JAMES B. p 222 N93-12130
p 222 N93-12161
CORNUEJOLS, GERARD p 430 N93-12217
CORSICO, A. p 383 N93-11314
CORTEZ, M. M. p 257 N93-11595
COSTELLO, MARK FRANCIS p 207 N93-11725
COTTET, FRANCOIS p 319 N93-12037
COTTLE, RICHARD W. p 428 N93-12465
COUEFFIN, R. E. p 280 N93-11366
COVELLI, JAVIER M. p 405 N93-12425
COVINO-HRBACEK, JOSEPHINE p 309 N93-11048
COWART, J. S. p 326 N93-11540
COX, A. N. p 483 N93-10993
COX, J. W. R. p 289 N93-11434
COX, R. ANTHONY p 351 N93-11091
CRAIG, HUGH K. p 331 N93-11016
CRAVENS, T. E. p 487 N93-11165
CRAWFIS, R. p 371 N93-12154
CRAWFORD, J. F. p 453 N93-11694
CRAY, BENJAMIN ADAMS p 434 N93-11884
CREEL, THEODORE R. p 199 N93-11876
CRIM, F. F. p 441 N93-12323
CRIPPS, M. N. p 199 N93-11883
CROOKER, N. U. p 489 N93-12506
CROS, BRIGITTE p 319 N93-12032
CRUMP, J. WESLEY p 407 N93-11368
CRUMP, WILLIAM J. p 385 N93-12427
CULBERT, CHRIS p 396 N93-11945
p 397 N93-11950
CULLEN, JOHN W. p 268 N93-11862
CUMMINS, W. F. p 282 N93-11661
CUMPSON, P. J. p 247 N93-11396
CUNLIFFE, A. V. p 273 N93-11376
CUNNINGTON, GEORGE R. p 229 N93-12457
CUNNOLD, DEREK M. p 350 N93-11088
CURRAN, D. B. p 487 N93-11165
CURRY, DONALD M. p 227 N93-12449
CURTIS, J. p 288 N93-11239
CURTISS, H. C., JR. p 201 N93-12343
CUSTER, CLARK p 468 N93-12183

D

DABNEY, RICHARD W. p 230 N93-11954
DADDA, LUIGI p 411 N93-11594
DAELLENBACH, K. K. p 481 N93-12067
DAHL, L. F. p 250 N93-11808
DAHL, MILO D. p 218 N93-12016
DAHMS, M. p 256 N93-11336
p 256 N93-11337
DAIELLO, R. p 464 N93-11818
DALLMANN, UWE p 196 N93-11141
DALPORTO, J. F. p 277 N93-12106
DAMELIO, R. p 380 N93-11303
p 382 N93-11312
DAMELIO, RAFFAELE p 381 N93-11305
DAMKROGER, B. K. p 254 N93-10984
DANG, ANTHONY p 235 N93-11449
DANIELSON, KENT THOMAS p 340 N93-12210
DANLY, B. p 315 N93-11278
DANTZIG, GEORGE B. p 428 N93-12465
DARQUEY, PATRICK p 319 N93-12038
DAS, H. p 400 N93-11965
DAS, SHUVRA p 424 N93-11199
DASILVA, L. B. p 316 N93-11659
DASKALOPOULOS, CH. p 384 N93-11318
DAUGHTON, J. M. p 405 N93-12520
DAVIDSON, D. L. p 260 N93-12241
DAVIDSON, JOHN B. p 214 N93-11459
DAVIDSON, SHAYLA p 388 N93-11649
DAVIDSON, STUART p 432 N93-11666
DAVIS, A. p 273 N93-11376
DAVIS, G. C. p 326 N93-11540
DAVIS, J. p 408 N93-11378
DAVIS, J. BRADLEY p 223 N93-12151
DAVIS, ROBERT F. p 271 N93-12184
DAVIS, ROGER L. p 471 N93-12490
DAWSON, J. F. p 332 N93-11601
DEAN, JOHN H. p 397 N93-11949
DEANGELIS, C. p 382 N93-11312
DEANGELIS, RICHARD M. p 368 N93-11256
p 371 N93-12293
DEANNA, R. G. p 300 N93-11529
DEATON, JOHN E. p 390 N93-12486
DEBROY, T. p 468 N93-12218
DEBRUIN, J. G. p 270 N93-11989
p 270 N93-11990
DEBUTTS, EDWARD H. p 275 N93-12147
DECKER, F. J. p 446 N93-12497
DECKER, LOUIS P. p 407 N93-11368
DEFONZO, ALFRED P. p 285 N93-12230
DEGRAAF, KEN p 468 N93-12183
DEGRASSIE, J. S. p 449 N93-11041
DEGROOT, J. S. p 453 N93-11730
p 453 N93-11731
DEHMER, J. L. p 438 N93-11829
DEHMER, P. M. p 438 N93-11829
DEHOFF, RONALD L. p 393 N93-11931
DEIBLER, J. E. p 240 N93-11658
DELAYEN, J. R. p 431 N93-11511
p 444 N93-11652
DELFRATE, JOHN H. p 202 N93-12353
DELGATTO, SAVERIO F. p 334 N93-11158
DELLACORTE, CHRISTOPHER p 236 N93-10978
DELLORCO, P. C. p 274 N93-11380
DELTRECCO, M. p 383 N93-11314
DELUCA, DANIEL P. p 260 N93-12237
DELUCA, W. H. p 289 N93-11432
DEMAREE, J. D. p 469 N93-12286
DEMIRGIAN, J. C. p 355 N93-12098
DENG, H. L. p 364 N93-12142
DENISON, G. J. p 291 N93-11693
DENNIS, K. W. p 462 N93-11706
DEROSA, S. p 432 N93-11156
DESAI, RAJIV p 288 N93-11939
DESENNE, D. p 320 N93-12041
DETAT, BRIGITTE p 321 N93-12049
DEVAN, J. H. p 259 N93-11830
DEVAUX, DAVID p 319 N93-12035
p 319 N93-12036
DEVENEY, M. F. p 411 N93-11599
DEVINE, M. K. p 261 N93-12261
DEWALT, KEVIN p 205 N93-11472
DEWEY, R. J. p 484 N93-11379
p 485 N93-11695
DHAOUADI, ZOUBEIDA p 321 N93-12049
DHEZ, P. p 320 N93-12044
DIBBLE, JOHN G. p 309 N93-11049
DICHTER, BRONISLAW K. p 363 N93-11810
DIDELOT, F. p 380 N93-11304
DIECKMAN, S. L. p 271 N93-12123
DIEKMANN, ANDREAS p 216 N93-12361
DIETRICHS, HANS-JUERGEN p 213 N93-11339
DIGNON, J. p 354 N93-11744
DIMPSEY, ROBERT TOD p 419 N93-12395
DINAVAHI, SURYA P. G. p 202 N93-12399
DING, M. p 351 N93-11094
DINGUIRARD, JEAN-PIERRE p 318 N93-12031
DINGUS, R. S. p 322 N93-12250
DINKINS, M. A. p 399 N93-11958
DIRLING, R. p 211 N93-11106
DITTMAR, JAMES H. p 433 N93-11370
DIVECHA, AMARNATH P. p 266 N93-11400
DIVER, R. B. p 347 N93-12012
p 348 N93-12074
DIXON, DAVID A. p 439 N93-11855
DJOMEHRI, M. JAHED p 307 N93-12329
DMITRIEV, V. p 254 N93-12518
DOANE, GEORGE B., III. p 470 N93-12396
DOANE, J. L. p 451 N93-11382
DOBRAC, D. p 459 N93-11076
DODD, A. G. p 212 N93-11206
DOGGETT, WILLIAM R. p 230 N93-11982
DOLAN, M. J. p 379 N93-11296
DOLCE, JAMES L. p 329 N93-12203
DOLLING, DAVID S. p 198 N93-11742
DONG, HONGCHAO p 404 N93-11462
DONGARRA, J. J. p 426 N93-11636
DORHOUT, PETER K. p 246 N93-11280
DORIGO, MARCO p 418 N93-11180
p 418 N93-11181
p 420 N93-11227
DORNEY, DANIEL J. p 471 N93-12490
DORRIS, S. E. p 345 N93-11513
DOTY, F. D. p 300 N93-11440
DOUGLASS, ANNE p 351 N93-11091
DOVER, C. B. p 438 N93-11746

DOWBEN, P. A. p 470 N93-12464
DOWLA, F. p 364 N93-12155
DOWLING, NORMAN E. p 341 N93-12411
DOWNEY, J. W. p 461 N93-11647
DOWNEY, KEVIN M. p 413 N93-12022
DOYLE, B. L. p 257 N93-11600
p 464 N93-11842
DOYLE, GLENN C. p 480 N93-12472
DOYLE, RICHARD p 391 N93-11923
DRAGE, R. G. T. p 207 N93-11485
DRAKE, R. P. p 453 N93-11731
DRAVES, J. D. p 353 N93-11655
DRENNAN, E. p 411 N93-11555
DREW, ANNETTE C. p 389 N93-12291
DRISCOLL, DAVID INFANTE p 302 N93-11722
DRORY, MICHAEL p 271 N93-12086
DROTNING, W. D. p 421 N93-12138
DRYER, F. L. p 253 N93-12257
DU, CHANGQING p 335 N93-11200
DUBACH, J. F. p 442 N93-12444
DUCHANE, D. p 345 N93-11381
DUCHANE, D. V. p 346 N93-11825
DUDAS, CHARLES p 217 N93-11616
DUDENHOEFER, J. p 221 N93-11398
DUFFIE, NELL p 330 N93-11967
DUIGNAN, M. R. p 306 N93-12221
DUNHAM, M. E. p 286 N93-12417
DUNNAVAN, GEORGE M. p 372 N93-12339
DUNNING, F. B. p 470 N93-12499
DUNSKY, BETSY p 388 N93-12018
DUPUIS, T. p 405 N93-12520
DURAN, RANDALL E. p 414 N93-12341
DURLACH, NATHANIEL p 389 N93-12229
DUYAR, A. p 221 N93-11401
DYER, R. B. p 274 N93-11380
DYKA, C. T. p 307 N93-12355
DYSON, ANTHONY p 319 N93-12034

E

EASTMAN, WILLARD L. p 286 N93-12433
EBELING, H. p 482 N93-11475
EBERMAN, BRIAN p 399 N93-11957
ECCLES, N. C. p 296 N93-11017
ECKART, A. p 484 N93-11347
ECKSTEIN, J. N. p 465 N93-12065
ECONOMOU, N. p 293 N93-12121
EDEN, J. G. p 291 N93-11758
EDMOND, J. A. p 295 N93-12340
EDMONDS, JAE A. p 351 N93-11094
EDWARDS, DAVID E. p 471 N93-12490
EDWARDS, GARY E. p 398 N93-11952
EDWARDS, GLEN R. p 240 N93-11795
EDWARDS, MICHAEL p 419 N93-12358
EDWARDS, P. W. p 409 N93-11406
EGERLAND, WALTER O. p 344 N93-12357
EHRLICH, H. L. p 355 N93-11864
EICHMANN, DAVID A. p 414 N93-12384
p 415 N93-12385
p 415 N93-12386
p 415 N93-12387
p 415 N93-12388
p 415 N93-12389
p 415 N93-12390
p 415 N93-12391
p 415 N93-12392
p 416 N93-12393
EIMERL, D. p 452 N93-11645
EINERSON, C. J. p 326 N93-11548
EINSTEIN, H. H. p 338 N93-11903
EISEN, EDWARD L. p 290 N93-11504
EKBLAD, U. p 219 N93-11216
EKLUND, P. C. p 250 N93-11847
EL-BALAWY, KHALED MAHMOUD p 342 N93-12536
EL-GENK, M. S. p 300 N93-11537
EL-HUSSEIN, K. p 427 N93-12176
EL-MOSALAMY, MOHAMED SOLIMAN HASSAN
p 485 N93-11879
ELBAUM, MAREK p 287 N93-12461
ELLINGSON, W. A. p 271 N93-12123
ELLIOTT, C. M. p 246 N93-11280
ELLIOTT, G. S. p 308 N93-12435
ELLNER, PAUL M. p 333 N93-12510
ELMAN, H. C. p 427 N93-11837
ELSBERRY, RUSSELL L. p 372 N93-12339
ELSNER, MICHAEL p 263 N93-11011
ELTOM, A. H. p 290 N93-11514
EMERY, V. J. p 459 N93-11501
ENGELMANN, B. E. p 337 N93-11775
ENGELS, JOHANNES p 361 N93-11331
ENGLAND, HARVEY M., JR. p 387 N93-11279
ENGLERT, GERALD W. p 286 N93-12366
ENSOLI, FABRIZIO p 378 N93-11293
EOM, C. B. p 466 N93-12125
EPSTEIN, A. J. p 272 N93-12289
p 480 N93-12438
p 273 N93-12440
ERB, D. M. p 396 N93-11943
ERICKSON, A. p 293 N93-12089
EROGLU, H. p 248 N93-11453
ESAREY, ERIC p 315 N93-11195
ESKEW, R. T., JR. p 384 N93-11841
ETEMAD, S. p 466 N93-12125
EUBANKS, STEVEN W. p 419 N93-12410
EVANS, ALAN G. p 281 N93-11426
EVANS, M. C. p 221 N93-12317
EVERHART, KATHIE p 404 N93-11258
EYLON, S. p 445 N93-12126
EZEILO, A. N. p 212 N93-11112
EZEKIEL, SHAOUL p 310 N93-11562

F

FABBRO, REMY p 319 N93-12035
p 319 N93-12036
FABRE, EDOUARD p 308 N93-12030
FAEHL, R. J. p 293 N93-12089
FALTER, H. p 305 N93-12010
FALTISCO, ROBERT M. p 391 N93-11930
FALVEY, ROBERT J. p 369 N93-11819
FAN, GUANGWUU WILLIAM p 324 N93-11220
FANNING, F. JESSE p 397 N93-11947
FARIS, GREGORY W. p 323 N93-12335
FARKAS, J. p 467 N93-12134
FARMER, RICHARD C. p 297 N93-11171
FARRES, JORDI p 476 N93-11583
FARVER, J. R. p 461 N93-11682
FATTOROSSI, A. p 380 N93-11303
FATTOROSSI, ANDREA p 381 N93-11305
FAUST, W. L. p 468 N93-12271
FAZIO, M. V. p 293 N93-12089
FAZZARI, F. p 366 N93-12308
FEAREY, B. L. p 250 N93-11918
FEDERICO, M. p 378 N93-11294
FEENSTRA, R. p 458 N93-10987
FELDHEIM, DANIEL L. p 246 N93-11280
FELDMAN, ALBERT p 271 N93-12086
FELLERHOFF, J. R. p 204 N93-11152
FEMEC, D. A. p 407 N93-11356
FENG, CHEN p 448 N93-12201
FERGUSON, D. p 221 N93-11398
FERNOW, R. C. p 443 N93-11429
FERRANDO, WILLIAM A. p 266 N93-11400
FERRANTE, JOHN p 257 N93-11609
FERRARA, JON p 483 N93-12244
FEUDEL, ULRIKE p 488 N93-11351
FEWS, P. p 308 N93-12030
FIEDZIUSKO, J. p 288 N93-11239
FIELD-RICHARDS, H. S. p 409 N93-11407
FIELD, J. E. p 249 N93-11490
FIESELMANN, B. p 464 N93-11818
FIEVET, CHRISTIAN p 254 N93-12042
FILIPPONE, E. p 214 N93-11160
FILYUSHKIN, V. p 352 N93-11098
FINGER, K. E. p 442 N93-11077
FINKENTHAL, D. F. p 455 N93-12307
FINLEY, ROSEMARY p 473 N93-12542
FINN, CORY p 388 N93-12018
FIOLETOV, VITALI p 350 N93-11089
FIORELLI, VALERIA p 378 N93-11293
FIORITO, RALPH B. p 442 N93-11060
FISCHER, J. p 368 N93-11349
p 368 N93-11350
FISCHL, ROBERT p 214 N93-11176
p 215 N93-12304
FISHER, A. S. p 316 N93-11500
FISHER, AMNON p 315 N93-11195
FISHER, DAVID F. p 197 N93-11532
p 202 N93-12353
FISHER, DONALD A. p 351 N93-11093
FISHER, GENE p 405 N93-12345
p 405 N93-12346
FISHER, R. J. p 369 N93-11678
FLATTE, S. p 486 N93-12380
FLATTE, STANLEY M. p 363 N93-11788
FLEMING, WENDELL H. p 420 N93-11147
FLORYAN, J. M. p 307 N93-12374
FLYNN, G. p 288 N93-11257
FLYTZANI-STEPHANOPOULOS, M.
p 247 N93-11444
FOECKERSPERGER, S. p 263 N93-11011
FOERSTNER, WOLFGANG p 407 N93-11345
FOKAS, A. S. p 430 N93-11420
FOLKERTS, T. J. p 462 N93-11706
FORD, D. A. p 255 N93-11111
p 206 N93-11334
FORME, F. R. E. p 360 N93-11269
p 360 N93-11270
p 361 N93-11272
p 361 N93-11273
FORNEY, L. J. p 310 N93-11612
FORREST, STEPHEN R. p 290 N93-11507
FORTUNKO, C. M. p 333 N93-12055
FOSS, COLBY A. p 246 N93-11280
FOSS, COLBY A., JR. p 238 N93-11281
FOSSHEIM, K. p 467 N93-12178
FOSTER, C. M. p 459 N93-11190
FOUDRIAT, E. C. p 279 N93-11117
p 279 N93-11118
p 279 N93-11119
FOULKES, P. W. p 447 N93-11342
FOURNIER, JEAN p 319 N93-12035
p 319 N93-12036
FOWLER, DAVID W. p 277 N93-12072
FOX, L. p 408 N93-11378
FOY, B. R. p 274 N93-11380
FRAIGNIAUD, PIERRE p 410 N93-11482
FRALICK, G. C. p 310 N93-11612
FRANCOLINI, P. p 380 N93-11302
FRANK, G. J. p 208 N93-12488
FRANK, WILLIAM M. p 372 N93-12507
FRANKE, ERNEST A. p 399 N93-11959
FRANZ, HORST E. p 263 N93-11010
FRASER, PAUL J. p 350 N93-11088
FREDERICK, JOHN E. p 352 N93-11098
FRENSTER, JEFF p 206 N93-11461
FREUND, ROLAND W. p 409 N93-11458
FRIDGE, E. M., III p 396 N93-11943
FRIED, A. p 350 N93-11090
FRIEDMAN, JEFFREY FOSTER p 484 N93-11230
FRIEDMAN, MARK p 331 N93-11973
FRIEND, EDWARD L. p 207 N93-11863
FRIESEL, M. A. p 332 N93-11601
FRINCKE, DEBORAH p 405 N93-12345
p 405 N93-12346
FRITZ, R. H. p 314 N93-11935
FROST, DAVID J. p 323 N93-12405
FRY, H. A. p 274 N93-11566
FRY, LORI p 484 N93-11243
FRYE, G. C. p 433 N93-11523
FRYER, JOHN p 416 N93-12515
FU, C. C. p 373 N93-11718
FU, LYONG ZUEN p 440 N93-11914
FUCHS, HENRY p 388 N93-11783
FUCHS, V. p 449 N93-10988
FUGLESTVEDT, J. A. p 351 N93-11092
FUHAN, WANG p 242 N93-12235
FUJIEDA, HIROTOSHI p 203 N93-12503
FUJIKAWA, GENE p 224 N93-11001
FUJIMURA, K. p 331 N93-11979
FUJITA, TOSHIMI p 203 N93-12503
FULLER, E. N. p 267 N93-11497
FUNK, K. A. p 274 N93-11380
FUNSTEN, H. O. p 365 N93-12263
p 365 N93-12264
FURA, DAVID A. p 406 N93-12538
FURSAEV, A. V. p 440 N93-11914
FUSCO, F. p 217 N93-11225

G

GAARENSTROOM, S. W. p 277 N93-11672
GADDY, J. L. p 375 N93-12482
GAHL, J. M. p 452 N93-11674
p 453 N93-11694
GAIER, JAMES R. p 230 N93-10965
GAINES, D. P. p 293 N93-12121
GALBRAITH, R. A. p 197 N93-11464
GALLAGHER, J. G. p 281 N93-11387
GALLEGOS, ROBERT A. p 313 N93-12069
GAMBOGI, JOAN E. p 265 N93-11194
GAMES, RICHARD A. p 286 N93-12433
GAMMEL, FRANZ JOSEF p 255 N93-11027
GANLEY, G. A. p 210 N93-11061
GANNAWAY, MARY T. p 244 N93-11132
p 247 N93-11448
GAO, Y. p 460 N93-11563
GARCIA, P. p 421 N93-12138
GARDNER, R. H. p 375 N93-12315
GARNER, F. A. p 257 N93-11557
GAROUM, MOHAMMED p 299 N93-11363
GARRATT, V. E. W. p 207 N93-11485
GARRETT, J. D. p 443 N93-11517
GARRISON, A. A. p 253 N93-12311
GARRISON, S. M. p 466 N93-12109
p 466 N93-12125
GARSIDE, T. p 210 N93-11055
GARTON, ANDREW p 272 N93-12297
GARVEY, JAMES F. p 236 N93-12177
GASSER, LES p 394 N93-11936
GATLIN, GREGORY M. p 198 N93-11622
GAUTHE, BERNARD p 320 N93-12043
GAUTHIER, JEAN-CLAUDE p 320 N93-12041
p 254 N93-12042
p 254 N93-12050
GAUTIER, CATHERINE p 372 N93-12420

GAY, JEFFREY M. p 222 N93-12161
GAYDOSH, M. p 316 N93-11691
GDANSKI, CHRIS p 230 N93-11926
GE, JING PING p 486 N93-12164
GEBALLE, T. H. p 466 N93-12125
GEDDES, NORMAN D. p 204 N93-10961
GEHRED, PAUL ANTHONY p 489 N93-11815
GEHRELS, TOM p 483 N93-11750
GEINDRE, JEAN-PAUL p 320 N93-12041
p 254 N93-12042
p 254 N93-12050
GENERAZIO, EDWARD R. p 331 N93-10963
GENZEL, R. p 484 N93-11347
GEORGE, M. E. p 276 N93-11951
GEORGE, THOMAS F. p 469 N93-12338
GERMAINE, J. T. p 338 N93-11903
GERNDT, MICHAEL p 412 N93-11618
GEYER, RICHARD G. p 293 N93-12084
GIARRATANO, J. p 314 N93-11935
GIER, THURMAN E. p 437 N93-11560
GIESS, S. C. p 278 N93-10977
GILLIE, K. R. p 289 N93-11432
GINDER, J. M. p 480 N93-12438
GIOVANNONI, F. p 380 N93-11302
GIRVIN, DOUGLAS LYNN p 426 N93-11547
GITTNER, N. M. p 197 N93-11605
GITTNER, NATHAN M. p 200 N93-12004
GIUDICELLI, C. P. p 380 N93-11304
GIULIETTI, D. p 318 N93-12026
GLADDEN, HERBERT J. p 337 N93-11624
GLADSTONE, G. R. p 487 N93-11166
GLASS, DAVID E. p 229 N93-12460
GLAWE, D. D. p 308 N93-12435
GLEESON, RONALD F. p 426 N93-11463
GLIMM, JAMES p 297 N93-11148
GLOERSEN, P. p 373 N93-11718
GLUCKMAN, JONATHAN P. p 390 N93-12486
GODIN, SOPHIE p 350 N93-11089
GODIOT, JACQUES p 319 N93-12032
GOELZ, G. p 331 N93-11974
GOFF, F. p 346 N93-11825
GOFFE, DOMINIQUE p 246 N93-11361
GOHNG, JUNHO p 460 N93-11533
GOLBEN, JOHN p 470 N93-12396
GOLDBERG, FREDRIC p 419 N93-12410
GOLDSMITH, TIMOTHY E. p 421 N93-12096
GOLDSTEIN, HOWARD p 227 N93-12448
GOMES, ALAIN p 318 N93-12027
GOMI, HIROMI p 314 N93-12373
GONZALEZ, ARMANDO CARLOS p 338 N93-11909
GONZALEZ, DORA E. p 233 N93-12013
GOODING, R. H. p 220 N93-11486
GOODSELL, B. H. p 288 N93-11364
GOPALAN, PERIYA p 338 N93-11890
GORDAN, ANDREW L. p 329 N93-12203
GORDON, D. M. p 381 N93-11308
GORDON, G. p 273 N93-12440
GORETTA, K. C. p 460 N93-11522
GORHAM, E. D. p 300 N93-11537
GORLEY, T. A. E. p 325 N93-11324
p 325 N93-11325
p 325 N93-11326
p 325 N93-11327
GORNEY, D. J. p 226 N93-12379
GORNEY, DAVID p 230 N93-11927
GORNEY, DAVID J. p 226 N93-12064
GORTON, E. K. p 315 N93-11388
GOSLING, J. T. p 488 N93-11696
p 365 N93-12264
GOSS, DANIEL A. p 278 N93-11044
GOULETTE, M. p 211 N93-11105
GOURBAT, J. P. p 380 N93-11304
GOURSAT, P. p 239 N93-11586
GOWING, SCOTT p 308 N93-12462
GRABOWSKI, L. p 255 N93-11031
p 255 N93-11033
p 255 N93-11115
GRACE, KEVIN H. p 286 N93-12433
GRACE, THOMAS M. p 349 N93-12446
GRADY, JOSEPH E. p 243 N93-12302
GRAESSER, ARTHUR C. p 386 N93-11415
GRAF, U. U. p 484 N93-11347
GRAHAM, A. L. p 303 N93-11843
GRAMANN, MIRT p 484 N93-11338
GRAPPASONNI, J. p 377 N93-11289
GRASS, ROLF-DIETER p 203 N93-11319
GRASSL, H. p 368 N93-11349
GRAY, G. T., III p 261 N93-12256
GRAY, GARY W. p 383 N93-11315
GRAY, ROBERT A. p 238 N93-11422
GRECI, ANTHONY M. p 448 N93-12272
GREEN, R. B. p 197 N93-11464
GREENBERG, IRA B. p 477 N93-11749
GREENE, G. A. p 306 N93-12221
GREENEBAUM, MICHAEL p 287 N93-12461
GREENLEAF, J. E. p 374 N93-12014
GREENSTADT, EUGENE W. p 489 N93-12303
GREENWOOD, D. W. p 217 N93-11447
GREENWOOD, L. R. p 257 N93-11557
GREGORY, BOBBY G., JR. p 286 N93-12377
GREGORY, C. p 319 N93-12034
GREGORY, JOHN C. p 270 N93-11993
p 270 N93-11994
GREINER, N. R. p 274 N93-11566
GRIFFITHS, S. p 275 N93-12265
GRIFFTHS, J. B. p 357 N93-11120
GRIGG, KEN p 410 N93-11481
GRIGOREAS, C. p 383 N93-11317
GRIMES, DONNA E. p 475 N93-11465
GRISWOLD, NORMAN C. p 325 N93-11427
GRONSKY, R. p 465 N93-11915
GROOM, NELSON J. p 277 N93-11613
GROSS, KLAUS W. p 235 N93-11449
GROSVENOR, JOHN H, JR. p 293 N93-12084
GROUSET, DIDIER p 246 N93-11361
GROVE, JOHN W. p 297 N93-11148
GRUBB, MONTY G. p 390 N93-12508
GRUEN, D. M. p 462 N93-11703
p 469 N93-12310
GRUMBERG, JEANNE p 321 N93-12049
GRUZDEVA, N. M. p 258 N93-11787
GUARNACCIA, J. F. p 298 N93-11251
GUDIVADA, V. N. p 475 N93-11506
p 479 N93-12287
GUENNOU, HELENE p 321 N93-12046
GUERRA, EMMA p 378 N93-11293
GUGLIELMO, EUGENE J. p 479 N93-12381
GUIDOTTI, R. A. p 267 N93-11552
p 290 N93-11553
GULATI, SANDEEP p 324 N93-11177
GULATI, SURESH K. p 245 N93-11135
GUMINA, STEPHANIE p 236 N93-12177
GUO, K. L. p 305 N93-12082
GUO, T.-H. p 221 N93-11401
GUPTA, MANISH p 418 N93-11651
GUPTA, S. p 211 N93-11105
p 211 N93-11106
p 236 N93-11107
GUSEVA, L. N. p 261 N93-12269
GUTKOWICZ-KRUSIN, DINA p 371 N93-12167
GUTTSCHOW, R. p 468 N93-12249
GYEKENYESI, JOHN P. p 334 N93-11004

H

HABERMAN, DAVID p 395 N93-11938
HACKETT, W. R. p 362 N93-11692
HADDAD, T. S. p 276 N93-11951
HADDEN, GEORGE D. p 230 N93-11925
HAEGGSTROEM, I. p 360 N93-11268
p 360 N93-11269
p 361 N93-11273
HAERING, EDWARD A., JR. p 296 N93-10969
HAGHGOOIE, M. p 326 N93-11540
HAHN, M. T. p 262 N93-12468
HAJJ, IBRAHIM N. p 292 N93-11781
HALE, D. p 431 N93-11567
HALE, DAVE p 366 N93-12318
HALFORD, GARY R. p 333 N93-10967
HALL, E. J. p 375 N93-12266
HALL, J. p 240 N93-11739
HALL, R. p 255 N93-11115
HALL, T. E. p 312 N93-11802
HALLER, E. E. p 469 N93-12316
HALPERT, GERALD p 290 N93-11456
HAMBY, C. p 267 N93-11570
HAMILTON, DAVID p 396 N93-11945
HAMILTON, DAVID B. p 390 N93-12508
HAMILTON, M. L. p 257 N93-11557
HAMLEY, JOHN A. p 235 N93-12484
HAMMEL, B. A. p 451 N93-11495
HAMMER, C. L. p 355 N93-12098
HAMMOND, JAMES H. p 207 N93-11838
HAMPDEN-SMITH, M. J. p 467 N93-12134
HAMPSON, ROBERT F. p 350 N93-11090
HAMZA, A. V. p 465 N93-12093
HAN, D. p 373 N93-11718
HANCOCK, H. A. R. p 280 N93-11366
HANSEN, CHARLES E. p 344 N93-12357
HANSER, FREDERICK A. p 363 N93-11810
HARBOUR, J. R. p 437 N93-11597
HARBRIDGE, W. B. p 366 N93-12378
HARDCASTLE, F. D. p 467 N93-12134
HARDIN, J. E. p 292 N93-12057
HARKRIDER, DAVID G. p 361 N93-11421
HARLOWE, W. W. p 244 N93-11134
HARMER, M. P. p 431 N93-11468
HARMON, C. D. p 231 N93-10973
p 217 N93-11367
HARPER, F. T. p 300 N93-11537
HARRADINE, D. M. p 274 N93-11380
HARRINGTON, EDWARD J. p 372 N93-12424
HARRIS, A. I. p 484 N93-11347
HARRISON, WALTER A. p 256 N93-11240
HARRISON, WILLIAM T. p 458 N93-10996
p 437 N93-11560
HARRISS, ROBERT p 350 N93-11088
HARTMAN, G. A. p 242 N93-12181
HARTMAN, KENNETH O. p 275 N93-12147
HARTMAN, WAYNE p 396 N93-11942
HARTMANN, GERHARD p 195 N93-11008
HARVEY, N. W. p 210 N93-11055
HARVEY, R. W. p 449 N93-10988
HARWOOD, ROBERT S. p 352 N93-11097
HASELKORN, M. H. p 268 N93-11654
HASH, M. C. p 345 N93-11513
p 345 N93-11571
HASHIDATE, MASATAKA p 216 N93-12362
HASHIMOTO, RYOSAKU p 243 N93-12371
HASINGER, GUENTHER p 482 N93-11474
HATCHETT, S. P. p 454 N93-12060
HATTIS, PHILIP D. p 216 N93-12413
HAVENER, C. C. p 439 N93-11849
HAWKE, R. S. p 217 N93-11447
HAWRYLUK, A. M. p 293 N93-12121
HAWTHORNE, J. R. p 259 N93-12107
HAXTON, W. C. p 485 N93-12120
HAYASHI, YOSHIO p 216 N93-12362
HAYNES, R. p 412 N93-11712
HAYTON, G. E. p 424 N93-11125
HEALY, J. C. p 255 N93-11031
HEARD, WALTER L., JR. p 224 N93-10970
HEATH, D. MICHELE p 216 N93-11057
HEDLIN, M. A. p 359 N93-11228
HEILL, L. K. p 467 N93-12178
HEITMEYER, CONSTANCE L. p 388 N93-11784
HELDT, L. A. p 256 N93-11524
HELGAKER, TRYGVE p 439 N93-11853
HELGESON, W. D. p 291 N93-11693
HELLWEGE, K. H. p 468 N93-12271
HELMBERGER, DONALD V. p 361 N93-11421
HENDRIX, C. W. p 379 N93-11296
HENDRIX, CRAIG W. p 377 N93-11292
HENKE, ANDREA L. p 420 N93-11000
HENLEY, E. M. p 439 N93-11844
HENSHAW, DAVID GEOFFREY p 209 N93-11023
HERDA, D. A. p 233 N93-12148
HERMAN, I. p 288 N93-11257
HERMANN, BRUCE R. p 281 N93-11426
HERNANDEZ, J. E. p 413 N93-12137
HERNING, R. I. p 387 N93-12432
HEROLD, H. p 449 N93-11029
p 450 N93-11103
HERON, ANNE p 319 N93-12032
HESTER, M. p 291 N93-11643
HETTICH, R. L. p 323 N93-12514
HEVENOR, RICHARD A. p 218 N93-11751
HEYMAN, JOSEPH S. p 216 N93-11057
p 333 N93-12204
HEYSE, MARK W. p 222 N93-12130
p 222 N93-12161
HICKS, R. S. p 442 N93-12444
HIGGINBOTHAM, G. J. S. p 255 N93-11111
HIGGINBOTHAM, SCOTT A. p 223 N93-12151
HIGGINS, H. p 474 N93-11215
HIGGINS, P. D. p 438 N93-11715
HILDENBRAND, D. L. p 251 N93-12105
HILL, D. p 456 N93-12416
HILL, GERALD M. p 235 N93-12484
HILL, M. G. p 409 N93-11436
HILL, R. J. p 211 N93-11062
p 211 N93-11063
HILL, S. W. p 334 N93-11013
HILL, TIM p 391 N93-11930
HILLIS, D. L. p 455 N93-12307
HILLS, J. G. p 484 N93-11379
HISER, A. L. p 259 N93-12107
HO, P. p 463 N93-11797
HOANG, NGOC THAI p 196 N93-11250
HOBBINS, R. R. p 446 N93-12129
HOCKADAY, R. G. p 312 N93-11768
HOEBERLING, R. F. p 293 N93-12089
HOEKSEMA, J. T. p 488 N93-11696
HOENSELAERS, C. p 423 N93-11122
HOENSELAERS, C. A. p 357 N93-11120
HOFFMAN, JOE D. p 213 N93-12214
HOGAN, J. T. p 455 N93-12307
HOGG, S. I. p 263 N93-11032
HOLCOMBE, C. E. p 267 N93-11570
HOLDEN, ANTHONY p 206 N93-11170
HOLDEN, MICHAEL S. p 200 N93-12063
HOLEMAN, S. L. p 472 N93-10976
HOLLANSWORTH, JAMES E. p 224 N93-11430
HOLLOWAY, D. L. p 271 N93-12123
HOLLY, F. F. p 388 N93-11743
HOLLY, SANDOR p 271 N93-12086
HOLMES, J. W. p 199 N93-11882

HOLT, R. J. p 445 N93-12108
HOMEMDEMELLO, LUIZ p 391 N93-11923
HONG, JOOYOO p 432 N93-11759
HONG, SUN IG p 261 N93-12256
HOOKE, A. M. p 381 N93-11306
HORNBLOWER, C. p 210 N93-11036
p 210 N93-11037
p 210 N93-11038
HORNYAK, GABOR L. p 238 N93-11281
HORSLEY, J. p 210 N93-11024
HORSTMANN, K. H. p 196 N93-11113
HORTON, W. p 456 N93-12493
HORVATH, LAJOS p 427 N93-12328
HORZ, FRIEDRICH p 488 N93-11374
HOSHINO, HIDEO p 216 N93-12362
HOSKINS, BROCK E. p 277 N93-12072
HOSSACK, JOHN A. p 242 N93-12296
HOSTICKA, B. p 231 N93-11173
HOUGHTON, D. C. p 459 N93-11496
p 463 N93-11772
HOWARD, G. D. p 240 N93-11905
HOWARD, RICHARD T. p 230 N93-11954
HOWELL, STEVEN L. p 419 N93-12358
HOWORTH, CRAIG p 432 N93-11179
HRUBY, J. p 275 N93-12265
HU, CHENMING p 295 N93-12360
HU, Y. F. p 425 N93-11211
HUANG, CHEN-KUO p 290 N93-11456
HUBBELL, J. H. p 438 N93-11715
HUBERTZ, J. M. p 374 N93-12094
HUBLER, D. p 196 N93-11223
HUESTIS, DAVID L. p 323 N93-12335
HUGGETT, A. R. p 408 N93-11386
HUGHES, I. G. p 439 N93-11849
HUGHES, S. J. p 263 N93-11032
HULL, J. R. p 431 N93-11598
HULL, JONATHAN P. p 284 N93-12160
HULL, PATRICIA G. p 447 N93-11489
HUNG, R. J. p 233 N93-12009
HUNSAKER, C. T. p 353 N93-11655
HUNTLEY, JACK E. p 353 N93-11466
HUNTLEY, M. STEPHEN p 204 N93-11252
HURD, A. G. p 317 N93-11805
p 322 N93-12262
HURLEY, C. D. p 296 N93-11017
HUSSEY, I. W. p 255 N93-11115
HUSSEY, J. p 330 N93-11971
HUTCHINSON, G. R. p 475 N93-11404
HUTTERMAN, L. L. p 356 N93-12496
HUXHOLD, RUSSELL J. p 276 N93-12281
HWANG, CHEINWAY p 373 N93-12002
HWANG, ELLEN Y. p 400 N93-11966
HWANG, W. Y. P. p 439 N93-11844
HYATT, WILLIAM S. p 326 N93-11650
HYNES, T. P. p 210 N93-11040

I

IACONO, R. p 452 N93-11568
IACOVIDES, H. p 296 N93-11025
IBRAHIM, ABDEL MONEIM p 352 N93-11095
IDA, K. p 451 N93-11277
IDZOREK, G. C. p 312 N93-11768
IGUCHI, H. p 451 N93-11277
ILYAS, MOHAMMAD p 352 N93-11098
IM, S. p 466 N93-12127
IMRY, Y. p 471 N93-11780
INCE, ILHAN p 391 N93-11981
INDRAWIRAWAN, H. p 254 N93-10995
INGELS, FRANK p 416 N93-12515
INOUE, TAKASHI p 216 N93-12362
INSOO, M. p 257 N93-11572
INTERRANTE, L. V. p 266 N93-11413
IPSEN, ILSE p 428 N93-12511
IRONS, G. p 262 N93-12494
IRVINE, K. G. p 254 N93-12518
IRVINE, T. F., JR. p 306 N93-12221
ISAKOVIC, A. p 248 N93-11454
ISAKSEN, IVAR S. A. p 351 N93-11092
ISHII, MAMORU p 300 N93-11538
ISHII, YOSHIHIKO p 300 N93-11538
ITOH, T. p 469 N93-12325
IWANOWICZ, STEPHEN EDWARD p 342 N93-12467
IWASAKI, AKIHITO p 203 N93-12503
IYER, R. K. p 406 N93-12540
IZYGON, M. E. p 396 N93-11943

J

JACCARINO, VINCENT p 316 N93-11418
JACKMAN, CHARLES H. p 352 N93-11097
JACKSON, A. J. B. p 210 N93-11039
JACKSON, J. M. p 484 N93-11347
JACOBOSKI, D. p 399 N93-11958
JACOBS, BARRY L. p 375 N93-11146
JACOBS, P. M. p 236 N93-11065
JACOBSON, A. R. p 362 N93-11535
JACOBSON, K. B. p 323 N93-12514
JACOBSON, MICHAEL D. p 214 N93-11046
JACQUET, F. p 319 N93-12034
JAEGLE, PIERRE p 320 N93-12043
p 321 N93-12045
p 321 N93-12051
JAENISCH, HOLGER M. p 323 N93-12516
JAFFE, RICHARD p 245 N93-11135
JAFFRE, ALAIN p 246 N93-11361
JAHNKE, R. A. p 373 N93-11734
JAHSHAN, SALIM N. p 443 N93-11433
JAKOWATZ, C. V., JR. p 280 N93-11234
JAMELOT, G. p 321 N93-12045
JAMELOT, GERARD p 320 N93-12043
p 321 N93-12051
JANEZIC, MICHAEL D. p 293 N93-12084
JANG, PING-REY p 312 N93-11827
JANI, YASHVANT p 314 N93-11935
JANKOVSKY, ROBERT S. p 232 N93-11614
JANSEN, WOLFGANG p 488 N93-11351
JARRABET, G. P. p 228 N93-12453
JARVIS, A. F. p 211 N93-11106
JASINSKI, JERRY P. p 462 N93-11724
JAVEED, MEHZAD p 341 N93-12300
JEFFREY, WILLIAM A. p 275 N93-12147
JEFFRIES, JAY B. p 323 N93-12335
JEGLEY, DAWN C. p 239 N93-11623
JENG, FU SHU p 338 N93-11903
JENKINS, C. p 408 N93-11378
JENKINS, I. p 254 N93-12518
JENKINS, RICHARD A. p 379 N93-11299
JENSEN, J. KERMIT p 224 N93-10970
JESSON, D. E. p 458 N93-10987
p 459 N93-11496
p 463 N93-11772
JIANG, X. p 250 N93-11808
JIH, CHAN-JIUN p 243 N93-12532
JOHNSON, A. M. p 442 N93-11077
JOHNSON, COLIN p 351 N93-11092
p 352 N93-11096
JOHNSON, E. C. p 434 N93-11752
JOHNSON, E. R. p 375 N93-12482
JOHNSON, J. A. p 326 N93-11548
p 333 N93-12055
JOHNSON, MARK p 413 N93-12159
JOHNSON, R. BARRY p 448 N93-12201
p 252 N93-12215
p 323 N93-12516
JOHNSON, R. W. p 262 N93-12494
JOHNSON, W. G., JR. p 198 N93-11610
JOHNSTON, H. p 355 N93-12104
JOHNSTON, ROBERT THOMAS p 201 N93-12190
JONES, F. R. p 236 N93-11065
JONES, G. O. L. p 360 N93-11268
JONES, M. T. p 425 N93-11446
JONES, R. T. p 217 N93-11435
JONES, ROBERT E. p 392 N93-11928
JONES, ROCHELLE B. p 447 N93-11186
JONES, ROD L. p 350 N93-11090
JONES, T. V. p 263 N93-11032
p 210 N93-11055
JOO, J. p 468 N93-12249
JORDAN, DON p 294 N93-12191
JORDAN, DON L. p 294 N93-12294
p 295 N93-12295
JUANG, JER-NAN p 339 N93-12020
JUHASZ, A. p 221 N93-11398

K

KAEMPF, GEORGE L p 390 N93-12509
KAEPPELER, H. J. p 449 N93-11029
p 449 N93-11030
p 449 N93-11102
p 450 N93-11103
p 450 N93-11201
KALISH, Y. p 268 N93-11735
KALLINGS, LARS O. p 377 N93-11290
KALMBACH, MICHAEL D. p 362 N93-11740
KAM, MOSHE p 215 N93-12304
KAMIJO, KENJIRO p 330 N93-12463
KANADE, T. p 327 N93-11865
KANADE, TAKEO p 331 N93-11973
KANDA, TAKESHI p 202 N93-12369
KANE, R. J. p 282 N93-11661
KANIA, D. R. p 454 N93-12059
KANT, RAJ p 476 N93-11508
KAR, R. J. p 241 N93-12054
KARAMPETAKIS, N. P. p 423 N93-11121
p 424 N93-11124
p 424 N93-11125
KARKUT, M. G. p 467 N93-12178
KAROL, IGOR L. p 352 N93-11097
KARR, GERALD R. p 233 N93-12013
KARR, T. J. p 448 N93-11627
KATNIK, GREGORY N. p 223 N93-12151
KATO, TAKAO p 444 N93-11525
KATZAN, CYNTHIA M. p 230 N93-10965
KAUFMAN, ALBERT p 337 N93-11624
KAUFMAN, JONATHAN W. p 389 N93-12291
KAUP, D. J. p 430 N93-11420
KAWAHARA, HIROYASU p 209 N93-12367
p 209 N93-12383
KAWANO, SANDY p 490 N93-12470
KAY, G. G. p 379 N93-11298
KAYABA, SHIGEO p 216 N93-12362
KAZAROFF, JOHN M. p 232 N93-11614
KAZOVSKY, LEONID G. p 448 N93-11892
KEIL, L. C. p 374 N93-12014
KELDER, H. p 352 N93-11127
KELLER, DIETER p 205 N93-11344
KELLER, MICHAEL E. p 413 N93-12146
KELLEY, KEITH p 396 N93-11945
KELLMAN, RAY p 272 N93-12337
KELLY, H. NEALE p 208 N93-12458
KELLY, J. G. p 219 N93-12268
KEMP, R. M. J. p 335 N93-11369
KENDALL, SARAH N. p 379 N93-11299
KENNEDY, JOHN M. p 478 N93-12007
KENNEDY, W. L. p 444 N93-11652
KEPLER, R. G. p 283 N93-11800
KERCEL, S. W. p 338 N93-11792
KERCZEWSKI, ROBERT J. p 224 N93-11001
KERR, JAMES p 266 N93-11400
KERSHAW, J. p 407 N93-11341
KESNER, J. p 452 N93-11568
KESTIN, J. p 471 N93-12102
KEY, M. p 321 N93-12045
KEYES, DAVID E. p 425 N93-11246
KHANNA, S. p 279 N93-11117
p 279 N93-11119
KHOBAIB, M. p 242 N93-12181
KHODA, K. M. p 406 N93-11210
KHOSLA, P. K. p 327 N93-11865
KIKUCHI, MASATAKA p 330 N93-12463
KIKUCTI, MASATAKA p 329 N93-12364
KILGORE, MELVIN V., JR. p 385 N93-12427
KILKENNY, J. D. p 449 N93-10975
KILLIAN, E. W. p 407 N93-11356
KIM, J. Y. p 456 N93-12493
KIM, S. T. p 373 N93-11718
KIM, W. S. p 400 N93-11965
KIM, WON S. p 399 N93-11960
KIM, YOUNG-SUK p 333 N93-10967
KIMBLE, M. C. p 345 N93-11626
KING, J. E. p 255 N93-11033
KING, S. P. p 212 N93-11114
KING, W. C. p 359 N93-11235
KINGCOMBE, R. C. p 210 N93-11055
KINSEY, TREVOR J. p 311 N93-11648
KIRBY, F. A. p 273 N93-11376
KIRCHHOFF, VOLKER p 350 N93-11089
KIRKEBY, O. p 435 N93-12324
KISSLINGER, L. S. p 439 N93-11844
KITAURA, TAKAYUKI p 357 N93-11183
KITSOPOULOS, T. N. p 440 N93-12100
KIVELSON, S. A. p 459 N93-11501
KLAPISCH, M. p 320 N93-12041
KLAPPROTT, DAVID K. p 272 N93-12337
KLARER, P. R. p 487 N93-11502
KLASSON, K. T. p 375 N93-12482
KLAUSMEIER-BROWN, M. E. p 465 N93-12065
KLEM, MARK D. p 247 N93-11450
p 248 N93-11452
KLEPPER, C. C. p 455 N93-12307
KLEUSBERG, ALFRED p 205 N93-11419
KLEY, DIETER p 352 N93-11096
KLISNICK, ANNIE p 321 N93-12045
p 321 N93-12046
KLUEH, R. L. p 258 N93-11773
KLUTE, GLENN K. p 389 N93-12211
KNIGHT, J. B. p 430 N93-11711
KNOROVSKY, G. A. p 260 N93-12232
KO, M. K. W. p 366 N93-12299
KO, MALCOLM K. W. p 351 N93-11093
p 352 N93-11096
KOCH, J. A. p 316 N93-11659
KOCH, LILY E. p 273 N93-11045
KOCH, ROBERT MICHAEL p 225 N93-11836
KOCH, URSULA p 255 N93-11026
KOCHELAP, V. A. p 458 N93-10992
KODAS, T. T. p 467 N93-12134
KOELLE, DIETRICH E. p 223 N93-11007
KOENIG, MICHEL p 308 N93-12030
KOERNER, STEVE J. p 278 N93-11047
KOHLER, S. M. p 204 N93-11152
KOLB, C. E. p 366 N93-12299
KOLB, G. J. p 348 N93-12312

KOLODZIEJ, PAUL p 296 N93-10969
KOMIYA, ZEN p 264 N93-11150
p 265 N93-11188
KOMORNICKI, ANDREW p 439 N93-11855
KOMURO, TOMOYUKI p 202 N93-12369
KONDO, YASUHIRO p 307 N93-12382
KONG, J. A. p 343 N93-12006
KONG, K. S. p 469 N93-12325
KONOPELCHENKO, B. G. p 425 N93-11323
KOO, LAT S. p 332 N93-11154
KOONIN, S. p 486 N93-12380
KOONS, H. C. p 366 N93-12378
p 226 N93-12379
KOONS, HARRY C. p 230 N93-11927
p 226 N93-12064
KOSIK, WENDY E. p 469 N93-12286
KOSKIE, JOHN EDWARD p 304 N93-12003
KOSTINKO, WASH p 266 N93-11425
KOSTROUN, V. O. p 436 N93-11541
KRAMER, D. P. p 310 N93-11554
KRAMER, M. J. p 462 N93-11706
KRATOCHVIL, W. R. p 262 N93-12494
KRAUSS, A. p 257 N93-11600
KRAUSS, A. R. p 469 N93-12310
KRENER, A. J. p 422 N93-12258
KRISHEN, KUMAR p 391 N93-11921
KRISHNAMURTHY, S. p 462 N93-11727
KRONAUER, R. E. p 384 N93-11841
KROUPA, J. L. p 242 N93-12181
KROUTIL, R. T. p 355 N93-12098
KRUBSACK, DAVID p 395 N93-11938
KRUEGER, JON p 476 N93-11508
KRUGER, J. p 260 N93-12118
KRUMPELT, M. p 345 N93-11513
p 274 N93-11550
p 345 N93-11571
KUBIAK, CLIFFORD P. p 244 N93-10986
KUDO, KENJI p 202 N93-12369
KUHL, D. E. p 384 N93-11873
KULAGA, J. E. p 289 N93-11432
KUMAKAWA, AKINAGA p 234 N93-12372
KUMAR, R. p 274 N93-11550
KUMAR, R. A. p 455 N93-12141
KURSTJENS, A. V. p 270 N93-11989
KURTHS, JUERGEN p 488 N93-11351
KURYLO, MICHAEL J. p 350 N93-11090
KUSHNER, HAROLD J. p 420 N93-11147
KWAN, T. J. T. p 445 N93-11919
p 293 N93-12089
KYRIAKOS, K. p 384 N93-11318

L

LABAUNE, CHRISTINE p 317 N93-12023
p 318 N93-12025
p 318 N93-12026
LACOVIDES, H. p 296 N93-11067
LAINE, SEPPO p 202 N93-12414
LAKE, MARK S. p 224 N93-10970
LAM, D. J. p 459 N93-11190
p 460 N93-11563
LAM, SHU WAI p 450 N93-11185
LAMANTHE, G. p 240 N93-11708
LAMB, THEODORE A. p 387 N93-12252
LAMBERT, B. p 369 N93-11803
LAMBERT, S. M. p 263 N93-10972
LAMOUREUX, MICHELE p 321 N93-12047
LAN, M. D. p 461 N93-11647
LANDEN, O. L. p 451 N93-11495
LANDERS, STEPHEN p 197 N93-11532
LANDIS, GEOFFREY A. p 226 N93-12152
LANGE, R. p 354 N93-11676
LANNING, R. K. p 221 N93-12317
LANT, CHRISTIAN T. p 314 N93-12279
LARKIN, D. J. p 266 N93-11413
LARNER, K. p 363 N93-11791
LARREY, ERIC p 301 N93-11575
LARSEN, E. D. p 333 N93-12055
LARSON, P. T. p 421 N93-12153
LARSON, R. p 275 N93-12265
LARSON, RICHARD R. p 277 N93-11619
LASE, YUSKAR p 336 N93-11582
LASKY, JEFFREY A. p 408 N93-11371
LATIMER, T. W. p 294 N93-12156
LAU, K. H. p 251 N93-12105
LAU, K. S. p 251 N93-12112
LAUF, R. J. p 267 N93-11570
LAUNDER, B. E. p 296 N93-11025
p 296 N93-11067
LAURIENTE, MICHAEL p 230 N93-11927
LAVAL, GUY p 317 N93-12024
LAVALLEE, D. p 372 N93-12420
LAVAZZA, LUIGI A. p 476 N93-11689
LAVELLE, THOMAS M. p 213 N93-12402
LAVID, MOSHE p 245 N93-11135
LAW, R. D. p 218 N93-11906
LAWKINS, W. F. p 419 N93-12233
LAWSON, DEL R. p 246 N93-11280
LAX, M. p 441 N93-12115
LEA, ROBERT N. p 314 N93-11935
LEATHERWOOD, JACK D. p 434 N93-11620
LEBOUCHER-DALIMIER, ELISABETH
p 321 N93-12049
LECCE, L. p 432 N93-11156
LECCE, LEONARDO p 334 N93-11158
LECOCQ, C. p 316 N93-11691
LEDFORD, OTTO C., JR. p 230 N93-11953
LEE, EUN U. p 261 N93-12248
LEE, GEORGE p 219 N93-12349
LEE, GREG p 391 N93-11981
LEE, H. M. p 342 N93-12412
p 342 N93-12419
LEE, I. p 406 N93-12540
LEE, KWANGJU p 324 N93-11261
LEE, SUKHAN p 278 N93-12202
LEE, TIMOTHY J. p 439 N93-11852
p 439 N93-11854
LEE, W. Y. p 466 N93-12109
LEE, Y. ALBERT p 434 N93-11634
LEE, Y. C. p 421 N93-12226
LEE, YUAN-PERN p 351 N93-11092
LEEMANS, WIM PIETER p 450 N93-11191
LEGENDRE, A. J. p 400 N93-11966
LEGERTON, M. L. p 433 N93-11321
p 433 N93-11322
LEGLER, DAVID M. p 365 N93-12182
LEGRAND, OLIVIER p 320 N93-12040
LEHMANN, BERTEL p 442 N93-11028
LELIEVELD, JOSEPH p 351 N93-11092
p 351 N93-11094
LEMBECK, MICHAEL F. p 394 N93-11933
LEONARD, B. P. p 426 N93-11531
LEONARD, P. J. T. p 484 N93-11379
p 485 N93-11695
p 485 N93-11697
LEONE, GIUSEPPE p 196 N93-11157
LEONE, STEPHEN R. p 436 N93-11467
LEOVY, CONWAY p 351 N93-11094
LEPIE, ALBERT H. p 309 N93-11048
LERCHE, R. A. p 450 N93-11153
p 454 N93-12060
LERIBAULT, CATHERINE p 299 N93-11362
LESPADE, P. p 239 N93-11586
p 239 N93-11588
LEU, M.-T. p 350 N93-11090
LEUNG, WAIHUNG p 300 N93-11538
LEVA, A. p 421 N93-11593
LEVA, ALBERTO p 421 N93-11667
LEVITT, KARL p 405 N93-12347
LEWANDOWSKI, JOHN J. p 259 N93-11850
LEWIS, C. p 321 N93-12045
LEWIS, G. J. p 250 N93-11808
LEWIS, N. S. p 289 N93-11438
LEWIS, PETER A. p 429 N93-12426
LEWIS, SYLVIA p 432 N93-11666
LEYCURAS, CLAUDE p 320 N93-12040
LI, FEIYUE p 225 N93-11885
LI, FENGSHOU p 335 N93-11202
LI, JIAN-JIN p 410 N93-11483
LI, JIANCHAO p 363 N93-11791
LI, LARRY C. p 330 N93-11972
LI, PENG p 488 N93-11877
LI, SHENG S. p 468 N93-12228
LI, Y. p 464 N93-11818
LIBBY, S. B. p 317 N93-11765
LIBERA, J. p 456 N93-12416
LIBERMAN, EUGENE M. p 392 N93-11928
LICHTENBERG, A. p 452 N93-11565
LIEHR, MICHAEL p 277 N93-11672
LIENERT, T. J. p 254 N93-10984
LIGHTHILL, JAMES p 435 N93-12021
LILENSTEN, J. p 360 N93-11269
LILLARD, R. S. p 260 N93-12118
LIMBERG, T. p 446 N93-12497
LIN, Y. P. p 469 N93-12310
LIND, D. J. p 334 N93-11013
LIND, EDWARD p 310 N93-11460
LIND, GEORGE p 287 N93-12461
LINDNER, J. S. p 454 N93-12087
LINDSEY, WILLIAM C. p 288 N93-12519
LINEBERRY, J. T. p 455 N93-12139
LING, DEHAI p 225 N93-11798
LIPKIN, J. p 275 N93-12265
LITTMAN, FRANKLIN D. p 347 N93-12019
LIU, BEDE p 287 N93-12436
LIU, J. Z. p 461 N93-11647
LIU, LU p 281 N93-11509
LIU, Y. p 406 N93-11210
LIVINGS, JEFFREY p 217 N93-11616
LIZZA, CARL p 390 N93-11922
LJUNG, KAARE p 237 N93-11128
LLOYD, A. R. J. M. p 197 N93-11365
LO, CHING F. p 218 N93-11910
LOCKHART, MARK S. p 478 N93-11840
LOFTIN, R. B. p 394 N93-11937
LOGE, G. W. p 250 N93-11918
LOHMANN, GABRIELE p 342 N93-11140
LOHR, J. p 449 N93-11041
LOKOS, WILLIAM A. p 207 N93-11863
LONG, B. p 275 N93-12265
LONG, CHRISTOPHER A. p 244 N93-11035
LONG, MAUREEN p 238 N93-11422
LONG, S. p 374 N93-11630
LONGDON, NORMAN p 479 N93-12404
LONGUET, B. p 418 N93-11584
LORD, KENNETH M. p 407 N93-11231
LORIA, EDWARD A. p 261 N93-12445
LOTSHAW, JOHN E. p 307 N93-12406
LOTT, R. A. p 259 N93-12107
LOTTES, S. A. p 455 N93-12309
LOU, J. p 465 N93-11915
LOUBRIEL, G. M. p 291 N93-11693
LOUIS-JACQUET, M. p 320 N93-12041
LOWE, DAVID p 428 N93-10980
LOWNDES, D. H. p 458 N93-10987
LOY, D. A. p 437 N93-11640
LU, XIANQIANG p 237 N93-11229
LUCAS, JOE NATHAN p 374 N93-10974
LUCCIOLI, S. p 381 N93-11306
LUCE, T. C. p 449 N93-11041
LUCEY, D. R. p 379 N93-11296
LUCEY, DANIEL R. p 377 N93-11292
LUDMAN, JACQUES E. p 348 N93-12166
LUECKING, P. p 198 N93-11113
LUMIA, RONALD p 398 N93-11955
LUNDBERG, L. B. p 446 N93-12129
LUO, J. S. p 462 N93-11703
LUO, JIAYI p 237 N93-11262
LUTTRELL, STEPHEN P. p 420 N93-11343
LUTZ, MICHAEL J. p 408 N93-11371
LUZI, GIUSEPPE p 378 N93-11293
LYBANON, M. p 374 N93-12288
LYNE, JAMES EVANS p 226 N93-12185

M

MA, J. p 310 N93-11612
MAAHS, HOWARD G. p 228 N93-12455
MAAS, R. p 442 N93-11131
MABEY, D. G. p 198 N93-11610
MACDONALD, A. H. p 460 N93-11512
MACDONALD, G. p 486 N93-12380
MACGOWAN, B. J. p 316 N93-11659
MACKAY, A. J. p 281 N93-11387
MACKAY, REBECCA A. p 329 N93-12327
MACKIN, MICHAEL p 417 N93-11005
MACLAUNCHLAN, ROBERT A. p 400 N93-11962
MACMILLAN, D. p 373 N93-11718
MACOMBER, BENNIE E. p 278 N93-11044
MACRAE, SANDERS C. F. p 473 N93-11012
MADABHUSHI, RAVI K. p 427 N93-12298
MADIGOU, V. p 239 N93-11586
MADRONICH, SASHA p 352 N93-11098
MADURA, J. T. p 371 N93-12170
MAFFEZZONI, C. p 421 N93-11593
MAFFIOLI, FRANCESCO p 424 N93-11182
MAGUIRE, GREGORY J. p 413 N93-12146
MAGUIRE, M. C. p 254 N93-10984
MAHAN, G. D. p 262 N93-12476
MAHER, J. V. p 462 N93-11747
MAHON, D. R. p 377 N93-11287
MAISH, ALEXANDER p 344 N93-10989
MAJDA, ANDREW p 275 N93-12236
MAJER, G. p 459 N93-11238
MAKER, B. N. p 337 N93-11775
MAKIDE, YOSHIHIRO p 350 N93-11088
MAKSOUD, T. M. A. p 264 N93-11086
MALAVASIC, M. J. p 381 N93-11306
MALCHOW, HARVEY L. p 216 N93-12413
MALKA, VICTOR p 318 N93-12029
MALNOULT, PHILIPPE p 321 N93-12049
MALTBY, J. D. p 243 N93-12483
MALY, K. p 279 N93-11117
p 279 N93-11118
p 279 N93-11119
MALY, KURT p 279 N93-11116
MANAHAN, MEERA K. p 400 N93-11966
MANESCHY, C. E. p 308 N93-12492
MANGHNANI, M. H. p 363 N93-11848
MANIEZZO, VITTORIO p 418 N93-11181
MANN, R. C. p 331 N93-11979
MANNA, M. p 198 N93-11686
MANNING, JAMES M. p 384 N93-11561
MANOUCHEHRI, DAVOUD p 403 N93-11980
MANOYLOV, V. Y. p 314 N93-12517
MANSUR, D. J. p 317 N93-12011

MAPOU, R. L. p 379 N93-11298
MARAWA, A. p 218 N93-11728
MARCEROU, PASCAL p 318 N93-12031
MARCUS, BETH A. p 399 N93-11957
MARKO, S. A. p 480 N93-12495
MARKOVITCH, R. p 328 N93-12149
MARKUS, R. p 399 N93-11958
MAROHNIC, Z. p 459 N93-11076
MARONI, V. A. p 462 N93-11703
MARQUARDT, B. J. p 261 N93-12256
MARQUES, JEAN-RAPHAEL p 319 N93-12034
MARSELLE, J. R. p 473 N93-11104
MARSHALL, F. R. p 217 N93-11447
MARTENS, J. S. p 466 N93-12109
MARTIN, CHARLES R. p 238 N93-11281
MARTIN, JAMES E. p 303 N93-11870
MARTIN, S. J. p 433 N93-11523
MARTINEZ-SANCHEZ, M. p 366 N93-12299
MARTINEZ, ELMAIN p 288 N93-11939
MARTINEZ, S. p 289 N93-11393
MARULO, F. p 432 N93-11156
MARZULLO, KEITH p 472 N93-12212
MASERJIAN, JOSEPH p 458 N93-11056
MASON, J. J. p 258 N93-11782
MASON, JAMES J. p 335 N93-11219
MASON, P. D. p 315 N93-11388
MASSOUDI, M. p 308 N93-12492
MASUYA, GORO p 202 N93-12369
MATACOTTA, F. C. p 459 N93-11076
MATAGA, T. G. p 252 N93-12255
MATHIS, ROBERT E. p 377 N93-11292
MATKOWSKY, B. J. p 345 N93-11733
MATRICARDI, P. M. p 380 N93-11303
p 382 N93-11312
MATRICARDI, PAOLO M. p 381 N93-11305
MATSUSHIMA, ISAO p 254 N93-12042
p 254 N93-12050
MATSUSHIMA, KOICHI p 216 N93-12361
MATTHEWS, D. L. p 316 N93-11659
MATTHEWS, W. ANDREW p 351 N93-11091
MATTHIEUSSENT, GILLES p 319 N93-12032
MATUSIAK, JERZY p 299 N93-11360
MAUCERI, A. J. p 403 N93-11980
MAUEL, M. E. p 452 N93-11568
MAVRIPLIS, D. J. p 416 N93-12400
MAX, N. p 371 N93-12154
MAYANAGI, MITSUYOSHI p 209 N93-12370
MAYBERRY, M. J. p 449 N93-11041
MAYER, PAULA S. D. p 407 N93-11368
MAYER, RICHARD J. p 407 N93-11368
MAYFIELD, TERRY p 477 N93-11732
p 404 N93-11809
MAYHALL, D. J. p 282 N93-11675
MAYS, M. Z. p 385 N93-12145
MAZIASZ, P. J. p 259 N93-11857
MAZURCZAK, J. p 388 N93-11743
MCADIE, C. J. p 370 N93-11888
MCANUALTY, D. M. p 390 N93-12509
MCASHAN, M. p 471 N93-11656
MCBRIDE, J. B. p 453 N93-11729
MCCALL, R. P. p 480 N93-12438
MCCALLUM, R. W. p 462 N93-11706
MCCARTNEY, L. N. p 238 N93-11409
MCCLUNG, R. C. p 260 N93-12241
MCCOMAS, D. J. p 365 N93-12263
p 365 N93-12264
MCCORMACK, ANN p 388 N93-12018
MCCORMACK, E. F. p 438 N93-11829
MCCORMICK, M. PATRICK p 351 N93-11094
MCCOY, M. G. p 449 N93-10988
MCCRACKEN, JAMES B. p 277 N93-11901
MCCRORY, F. M. p 219 N93-12268
MCCULLOUGH, B. FRANK p 277 N93-12072
MCDONALD, CATHERINE W. p 477 N93-11732
MCDONALD, J. M. p 452 N93-11674
p 453 N93-11694
MCDOUGAL, J. N. p 276 N93-11951
MCEWEN, M. R. p 310 N93-11410
MCFADDEN, P. D. p 337 N93-11707
MCGOWAN, PAUL E. p 341 N93-12300
MCGRATH, R. T. p 453 N93-11694
MCILWAIN, MELVIN C. p 233 N93-12363
MCINROY, R. E. p 274 N93-11380
MCINTOSH, R. E. p 366 N93-10971
MCINTYRE, DAVID p 316 N93-11737
MCKENZIE, RICHARD L. p 352 N93-11098
MCKILLIP, R. M., JR. p 201 N93-12343
MCKINLEY, ERIC J. p 372 N93-12339
MCKISSOCK, B. I. p 275 N93-12085
MCLAUGHLIN, D. L. p 291 N93-11693
MCLEAN, GARNET A. p 387 N93-11279
MCLEES, R. E. p 405 N93-12346
MCLEOD, R. R. p 282 N93-11632
MCMAHON, MARY BETH p 397 N93-11950
MCMANIS, SUSAN E. p 379 N93-11299
MCPHAIL, A. T. p 467 N93-12175
MCQUISTON, BARBARA p 206 N93-11461
MCQUISTON, BARBARA M. p 393 N93-11931
MCWHIRTER, J. G. p 408 N93-11390
MECRAY, M. p 468 N93-12218
MEDLEY, C. J. p 281 N93-11395
MEEKS, E. L. p 310 N93-11612
MEHROTRA, PIYUSH p 412 N93-11618
MEISEL, L. V. p 413 N93-12159
MELCHER, G. P. p 379 N93-11296
MELILLO, MICHAEL R. p 285 N93-12331
MELLEY, M. L. p 474 N93-11215
MELVIN, MICHAEL E. p 227 N93-12408
MENDILLO, MICHAEL p 361 N93-11282
MENZEL, CHRISTOPHER P. p 407 N93-11368
MERCER, CAROLYN R. p 446 N93-11058
MERCHANT, N. p 462 N93-11703
MEREWETHER, K. O. p 367 N93-11236
MERKEL, PHILIP A. p 390 N93-11922
MERRILL, D. W. p 413 N93-12110
MERRILL, W. p 221 N93-11401
p 215 N93-12305
MERRY, W. R., JR. p 466 N93-12124
METCALF, KENNETH J. p 347 N93-12017
METWALLY, METWALLY ANWAR p 272 N93-12189
METZ, R. B. p 440 N93-11875
MEYER, F. W. p 439 N93-11849
MEYER, MEINHARD p 255 N93-11026
MEYSTRIK, C. C. p 473 N93-11104
MEZZAROMA, IVANO p 378 N93-11293
MIAKE-LYE, R. C. p 366 N93-12299
MICHALEK, JOEL E. p 378 N93-11295
MICHALOPOULOU, S. p 384 N93-11318
MICHARD, ALAIN p 308 N93-12030
MICHELS, H. H. p 438 N93-11804
MICKLOW, GERALD J. p 302 N93-11767
MIERS, BRUCE T. p 368 N93-11505
MIGUET, SERGE p 409 N93-11478
p 410 N93-11479
p 410 N93-11480
p 410 N93-11481
p 410 N93-11482
p 410 N93-11483
p 410 N93-11484
MIKESELL, BRIAN G. p 204 N93-10961
MILES, MARK W. p 252 N93-12186
MILLARD, D. EDWARD p 277 N93-11619
MILLER, C. M. p 250 N93-11918
MILLER, D. p 466 N93-12109
p 466 N93-12125
MILLER, D. J. p 460 N93-11522
MILLER, LARRY p 206 N93-11461
MILLER, TRACY p 473 N93-12542
MILLER, WILLIAM E. p 216 N93-11057
MILLIGAN, W. W. p 256 N93-11524
MILLS, K. C. p 447 N93-11408
MILNER, K. R. p 408 N93-11389
MINCHIN, NIGEL ROBERT p 481 N93-11248
MINE, P. p 319 N93-12034
MINER, JUDSON C. p 378 N93-11295
MINTMIRE, J. W. p 272 N93-12276
MIODUSKI, ROBERT E. p 333 N93-12510
MIODUSZEWSKI, P. K. p 455 N93-12307
MIQUEL, JAIME p 391 N93-12319
MIRANDA, F. A. p 469 N93-12325
MISCONI, N. Y. p 390 N93-12423
MISHIN, E. V. p 360 N93-11270
p 360 N93-11271
p 361 N93-11272
MISKIMEN, R. A. p 442 N93-12444
MITCHELL, JOHN L. p 222 N93-12543
MIZUNO, K. p 453 N93-11730
p 453 N93-11731
MOCKLER, THEODORE T. p 337 N93-11624
MOERL, P. p 368 N93-11350
MOES, TIMOTHY R. p 296 N93-10969
MOHR, M. S. p 413 N93-12110
MOLINA, MARIO J. p 350 N93-11090
MOLLER, C. p 321 N93-12046
MONHEISER, JEFFERY M. p 232 N93-11608
MONTENBRUCK, OLIVER p 220 N93-11335
MONTES, B. p 319 N93-12034
MONTES, CARLOS p 320 N93-12040
MONTHIOUX, M. p 239 N93-11586
MONTS, D. L. p 454 N93-12087
MOORE, BERRIEN, III p 219 N93-11528
MOORE, K. L. p 326 N93-11548
MOORE, K. R. p 365 N93-12264
MOORE, THOMAS C., SR. p 313 N93-12205
MOPSIK, FREDERICK I. p 308 N93-12475
MORA, PATRICK p 319 N93-12033
MORAN, P. J. p 260 N93-12118
MORENO, J. B. p 347 N93-12012
MORGAN, J. E. p 264 N93-11086
MORISON, J. D. p 409 N93-11436
MOROSIN, B. p 437 N93-11640
MORREN, W. EARL p 231 N93-11402
MORRIS, M. E. p 367 N93-11236
MORRIS, RUSSELL E. p 458 N93-10996
MORRISON, J. J. p 293 N93-12113
MORRISON, JEFFREY G. p 390 N93-12486
MORRISON, P. J. p 453 N93-11745
MORTENSEN, G. A. p 301 N93-11637
MORTIER, N. p 383 N93-11316
MOSES, J. D. p 286 N93-12417
MOSES, STEWART L. p 489 N93-12303
MOSS, T. A. p 347 N93-12012
MOUNAIX, PHILIPPE p 317 N93-12024
MROWKA, S. p 316 N93-11659
MSAAD, M. p 215 N93-11585
MUELLER, FRANZ p 309 N93-11346
MUELLER, JUERGEN p 315 N93-11332
MUHS, J. D. p 338 N93-11792
MUKHERJEE, RANJAN p 329 N93-12434
MUKKAMALA, R. p 279 N93-11117
MULLENDER, A. J. p 195 N93-11020
p 195 N93-11070
MULLER, C. p 352 N93-11127
MUNGER, A. C. p 310 N93-11554
MURAKAMI, ATSUO p 202 N93-12369
MURAO, RINICHI p 307 N93-12382
MURATOV, LEONID S. p 469 N93-12338
MURPHREE, G. p 268 N93-11793
MURPHY, JEREMIAH GERARD p 337 N93-11713
MURPHY, T. J. p 450 N93-11153
p 454 N93-12060
MURRELL, M. T. p 250 N93-11918
MURTHY, DURBHA V. p 341 N93-12277
MURTHY, P. L. N. p 276 N93-12197
MUSGRAVE, J. p 221 N93-11401
MUTHUSUBRAMANIAN, P. p 352 N93-11098
MYLES, K. M. p 274 N93-11550

N

NA, HELEN RU-LIN p 365 N93-12209
NACCACHE, D. p 320 N93-12041
NACHSHON, YEHUDA p 245 N93-11135
NAGAYASU, MASAHIKO p 219 N93-12359
p 314 N93-12365
NAHORY, R. E. p 464 N93-11894
NAIK, R. A. p 243 N93-12306
NAKAYA, TERUOMI p 216 N93-12362
NARDI, BRUNO p 369 N93-11839
NASH, S. p 460 N93-11522
NASHMAN, MARILYN p 398 N93-11955
NASSAOPOULOS, GEORGE p 435 N93-12471
NATAN, BENVENISTE p 245 N93-11136
NATHAL, MICHAEL V. p 258 N93-11635
p 329 N93-12327
NATHRATH, NORBERT p 278 N93-11009
NATUMURA, TADASI p 243 N93-12371
NAVAZ, HOMAYUN K. p 235 N93-11449
NAVICKAS, T. A. p 404 N93-11539
NAVRATIL, G. A. p 452 N93-11568
NAYFEH, ALI H. p 306 N93-12162
NAZAR, P. p 459 N93-11076
NDOH, PATRICK N. p 217 N93-11224
NEANDER, JOHN E. p 353 N93-11466
NEDELEC, G. p 380 N93-11304
NEDUNGADI, ASHOK p 399 N93-11959
NEELY, D. p 321 N93-12045
NELSON, DAVID K. p 330 N93-11970
NELSON, G. C. p 277 N93-11672
NELSON, KYLE S. p 230 N93-11925
NELSON, M. B. p 454 N93-12060
NELSON, P. A. p 435 N93-12324
NEMZEK, R. J. p 357 N93-10985
NENCIONI, L. p 380 N93-11302
p 381 N93-11306
NENOFF, TINA M. p 437 N93-11560
NETZER, DAVID W. p 245 N93-11136
NEUMAN, D. A. p 433 N93-11204
NEWELL, A. C. p 430 N93-11420
NEWMAN, C. E. p 326 N93-11540
NEWMAN, N. p 466 N93-12109
p 466 N93-12125
NEWTON, J. p 464 N93-11818
NEWTON, J. J. p 474 N93-11215
NEYLAND, DAVID L. p 390 N93-11922
NGUYEN, H. L. p 302 N93-11767
NGUYEN, HAI p 330 N93-11972
NGUYEN, HOE p 321 N93-12049
NGUYEN, THONG V. p 247 N93-11450
NGUYEN, TRUNG H. p 447 N93-11186
NI, R. H. p 308 N93-12539
NICHOLLS, G. L. p 444 N93-11652
NICOL, DAVID p 416 N93-12403
NICOLET, MARC-A. p 264 N93-11079
NIEDORODA, A. W. p 354 N93-11702
NIEH, T. G. p 228 N93-12452
NIELSEN, R. W. p 445 N93-11831

NIETEN, JOSEPH L. p 396 N93-11944
NISINI, R. p 380 N93-11303
p 382 N93-11312
NISINI, ROBERTO p 376 N93-11286
p 381 N93-11305
NITTI, F. p 217 N93-11225
NITZE, W. A. p 356 N93-12474
NIVEN, A. J. p 197 N93-11464
NODA, Y. p 256 N93-11519
NOEBE, RONALD D. p 258 N93-11635
NOFFZ, GREGORY K. p 296 N93-10969
NOGUCHI, MASAYOSHI p 216 N93-12362
NOKES, JAMES PHILLIP p 241 N93-11998
NONAKA, ISAMU p 216 N93-12362
NORBY, B. C. p 262 N93-12487
NORD, ROBERT L. p 406 N93-11145
NORMAN, M. R. p 460 N93-11512
NORTON, O. P. p 304 N93-11995
p 454 N93-12087
NOSAKA, MASATAKA p 329 N93-12364
p 330 N93-12463
NOVICK, A. H. p 473 N93-11104
NYGREN, R. E. p 257 N93-11600

O

OBERGFELL, KLAUS p 330 N93-12521
OBRIEN, LAWRENCE H. p 386 N93-11779
OESTERLING, R. G. p 480 N93-12495
OEVEL, W. p 424 N93-11123
p 424 N93-11126
OFMAN, L. p 453 N93-11745
OGALLAGHER, J. J. p 346 N93-11823
OGAWA, AKINORI p 243 N93-12371
OGAWA, Y. p 454 N93-11834
OHLHORST, CRAIG W. p 229 N93-12456
OHOTAKE, KUNIHIKO p 243 N93-12371
OIKE, MAMORU p 329 N93-12364
OKEEFE, ANTHONY p 202 N93-12466
OKIISHI, THEODORE H. p 213 N93-12077
OKUDA, H. p 224 N93-11736
OLDHAM, W. p 465 N93-11915
OLIVARES, J. A. p 250 N93-11918
OLIVER, B. M. p 257 N93-11557
OLSEN, LARRY p 348 N93-12144
OLSEN, R. p 330 N93-11971
OLSON, C. L. p 445 N93-12103
OLSON, DAVID L. p 240 N93-11795
OMALLEY, M. W. p 291 N93-11693
OMSTEAD, T. R. p 467 N93-12134
ONEILL, R. V. p 375 N93-12315
ONEMA, JOEL P. p 400 N93-11962
ONES, D. S. p 386 N93-12225
ONO, FUMIEI p 234 N93-12368
p 234 N93-12372
OPGENOORTH, H. J. p 359 N93-11266
p 360 N93-11267
p 360 N93-11268
p 360 N93-11269
p 360 N93-11270
p 360 N93-11271
p 361 N93-11272
p 361 N93-11273
OPPENHEIMER, CLIVE p 343 N93-11213
OPPENHEIMER, MICHAEL p 351 N93-11092
ORAN, E. S. p 302 N93-11756
ORCUTT, J. A. p 359 N93-11228
ORDONEZ, MANUEL V. p 286 N93-12407
ORHAUG, T. p 219 N93-11216
ORLANSKY, JESSE p 390 N93-12491
ORLIN, JAMES B. p 413 N93-12131
ORTIZ, C. p 394 N93-11937
OSBORN, A. R. p 207 N93-11485
OSBORN, D. p 326 N93-11556
OSBORNE, DAVID W. p 204 N93-11252
OSGOOD, R. p 288 N93-11257
OSTERHELD, A. L. p 317 N93-11765
OSTLIE, D. A. p 483 N93-10993
OSTOJA-STARZEWSKI, MARTIN p 286 N93-12422
OSWALD, FRED B. p 323 N93-10966
OTTENBERGER, W. p 257 N93-11600
OTTINGER, C. A. p 217 N93-11367
OTTO, S. R. p 301 N93-11633
OU, SHICHUAN p 199 N93-11886
OVERBURY, S. H. p 439 N93-11849
OVERSTREET, C. M. p 279 N93-11117
p 279 N93-11118
p 279 N93-11119

P

PACIESAS, WILLIAM S. p 483 N93-12348
PACKER, C. p 412 N93-11712
PALERMOS, J. p 384 N93-11318
PALMOUR, J. W. p 295 N93-12340
PANDEY, LAKSHMI N. p 469 N93-12238
PAONESSA, A. p 432 N93-11156
PAPADOPOULOS, DEMETRIOS S. p 241 N93-12076
PAPPA, RICHARD S. p 336 N93-11544
PAPPAS, D. p 383 N93-11317
PARK, SANG KYU p 327 N93-11887
PARKER, B. E., JR. p 422 N93-12439
PARKER, M. J. p 362 N93-11669
PARKER, R. p 433 N93-11321
p 433 N93-11322
PARKER, RIC J. p 334 N93-11021
PARKINSON, M. D. p 377 N93-11287
PARLIER, M. p 239 N93-11588
PARRISH, J. A. p 384 N93-11445
PARRISH, RUSSELL V. p 206 N93-11170
PARZEN, EMANUEL p 425 N93-11431
p 429 N93-12081
p 427 N93-12328
p 429 N93-12334
PASHA, R. A. p 451 N93-11495
PASQUARIELLO, D. M. p 291 N93-11604
PATEL, V. C. p 306 N93-12245
PATER, RUTH H. p 264 N93-11059
PATTERSON, R. p 221 N93-11398
PAULSON, JOHN W., JR. p 198 N93-11622
PAVLI, ALBERT J. p 232 N93-11614
PAWLAS, GARY EDWARD p 232 N93-11889
PAXSON, DANIEL E. p 297 N93-11172
p 214 N93-12418
PAXTON, A. T. p 462 N93-11727
PAYNE, J. S. p 419 N93-12233
PAYNE, S. A. p 461 N93-11602
PAZMANY, A. L. p 366 N93-10971
PEARSON, S. M. p 375 N93-12315
PEASE, R. F. p 293 N93-12121
PEDEN, C. H. F. p 467 N93-12134
PEELING, S. M. p 280 N93-11384
p 280 N93-11385
PELLACCIO, DENNIS G. p 233 N93-12363
PELLETT, G. L. p 244 N93-11134
PENKETT, STUART A. p 350 N93-11088
PENNER, J. E. p 354 N93-11744
PENNYCOOK, S. J. p 458 N93-10987
p 459 N93-11496
p 463 N93-11772
PERAGALLO, M. p 380 N93-11302
PEREZ-DAVIS, MARLA E. p 230 N93-10965
PEREZ, MANUEL A. p 388 N93-11784
PERJES, Z. p 423 N93-11122
PERKINS, SHARON L. p 253 N93-12267
PERLMAN, MARVIN p 412 N93-11664
PERNOT, P. p 239 N93-11588
PERRY, CHARLEEN M. p 479 N93-12150
PERRY, CHRIS E. p 387 N93-11559
PERSSON, M. A. L. p 360 N93-11269
p 360 N93-11270
p 361 N93-11272
p 361 N93-11273
PESME, DENIS p 317 N93-12024
p 318 N93-12025
PETERS, PIET W. M. p 237 N93-11143
PETERSON, BENJAMIN B. p 205 N93-11472
PETERSON, D. T. p 254 N93-10995
PETERSON, G. A. p 442 N93-12444
PETERSON, P. p 372 N93-12420
PETRELLI, G. p 382 N93-11312
PETRICK, M. p 456 N93-12416
PETRIK, EDWARD J. p 395 N93-11940
PETTENSKI, T. A. p 389 N93-12079
PETTY, C. C. p 449 N93-11041
PEWSEY, STEPHEN M. S. p 324 N93-11054
PEZZULLO, G. p 432 N93-11156
PFUDERER, H. p 475 N93-11441
PHELPS, JAMES E. p 224 N93-10970
PHILLION, D. W. p 293 N93-12121
PHILLIP, T. p 312 N93-11827
PHILLIPS, C. A. p 419 N93-11860
PHILLIPS, J. L. p 488 N93-11696
PHILLIPSON, M. p 289 N93-11393
PICHOLLE, ERIC p 320 N93-12040
PICKWORTH, W. p 387 N93-12432
PIERRE, CHRISTOPHE p 341 N93-12277
PIERSON, E. S. p 456 N93-12416
PINCOSY, P. A. p 293 N93-12113
PINDER, G. F. p 298 N93-11251
PINDERA, MAREK-JERZY p 335 N93-11175
PINELLI, THOMAS E. p 478 N93-12007
PINERO, LUIS R. p 235 N93-12484
PINSKER, R. I. p 449 N93-11041
PINTER, ELENA p 378 N93-11293
PISCHEL, K. p 196 N93-11223
PITMAN, C. L. p 396 N93-11943
PITSTICK, M. E. p 356 N93-12314
PITTS, M. C. p 350 N93-11090
PITTS, N. J. p 212 N93-11114
PITZ, W. J. p 326 N93-11540
PLASSMANN, P. E. p 425 N93-11446
PLENCNER, ROBERT M. p 209 N93-10983
p 213 N93-12402
PLOTKIN, SERGE A. p 413 N93-12131
PLUMMER, MICHAEL D. p 423 N93-10991
p 427 N93-12243
PODDA, A. p 380 N93-11302
PODLESNY, R. p 464 N93-11818
POEPPEL, R. B. p 460 N93-11522
p 468 N93-12249
POILLEUX, P. p 319 N93-12034
POLINER, JEFF p 389 N93-12211
POLL, D. I. A. p 195 N93-11020
p 195 N93-11070
POLLCHIK, J. D. p 434 N93-11752
PONTING, K. M. p 280 N93-11384
p 280 N93-11385
POOLE, LAMONT R. p 350 N93-11090
POQUERUSSE, ALAIN p 321 N93-12048
PORKOLAB, M. p 449 N93-11041
PORTANOVA, M. A. p 239 N93-11611
POSTANS, P. J. p 209 N93-11019
POTTS, JACQUELINE MARY p 370 N93-11997
POUKEY, J. W. p 445 N93-12103
POULSEN, P. p 293 N93-12113
POWERS, LYNN M. p 334 N93-11004
POWERS, SHERYLL GOECKE p 207 N93-11863
POZO, R. p 426 N93-11636
PRASANNA, M. G. p 323 N93-10982
PRAST, G. p 270 N93-11989
PRATER, R. p 449 N93-11041
PRATHER, MICHAEL J. p 352 N93-11095
p 352 N93-11096
p 352 N93-11097
PRATT, R. L. p 281 N93-11487
PRATT, S. T. p 438 N93-11829
PRAUSNITZ, J. M. p 263 N93-10972
PREATER, RICHARD W. T. p 334 N93-11022
p 315 N93-11064
p 309 N93-11320
PRENDEZ, MARGARITA p 351 N93-11091
PRESS, RONALD E. p 413 N93-12146
PRESTA, R. p 310 N93-11542
PRESTER, M. p 459 N93-11076
PRESTON, ROY C. p 433 N93-11328
PRIEBE, CAREY E. p 285 N93-12332
PRIEST, DON p 290 N93-11504
PRITCHARD, JOCELYN I. p 206 N93-10968
PRITCHETT, P. L. p 224 N93-11736
PROSSER, F. W. p 443 N93-11521
PROUD, LOIS p 344 N93-12280
PROUDLER, I. K. p 408 N93-11390
PUGH, A. C. p 423 N93-11121
p 424 N93-11124
p 424 N93-11125
PUGH, COLEEN p 265 N93-11187
p 265 N93-11188
PUNG, Y.-H. p 381 N93-11306
PURSER, MICHAEL J. p 232 N93-11424
PURVIS, J. W. p 487 N93-11502
p 232 N93-11766
PUSATCIOGLU, SELAMI Y. p 312 N93-11757
PYGOTT, C. H. p 405 N93-12430
PYLE, JOHN A. p 351 N93-11093
p 352 N93-11097

Q

QIAN, CATHY X. p 218 N93-11910
QIU, LIAN-XIONG p 352 N93-11097
QUAGLIARELLA, DOMENICO p 206 N93-11161
QUEMENER, YVES p 318 N93-12027
QUINCEY, P. G. p 289 N93-11393
p 459 N93-11394
QUINN, JARUS W. p 446 N93-11071
p 447 N93-11099

R

RABAS, T. J. p 305 N93-12128
p 306 N93-12313
RACHELE, HENRY p 363 N93-11785
RADOUSKY, H. B. p 461 N93-11647
RAGAN, ROBERT M. p 476 N93-11700
RAGHAVAN, V. V. p 475 N93-11506
p 479 N93-12287
RAHEMI, HOSSEIN p 339 N93-12008
RAI, A. K. p 328 N93-12122
RAJULU, SUDHAKAR p 389 N93-12211
RAKA, E. p 444 N93-11641
RALLS, K. S. p 465 N93-12065
RAM, A. K. p 449 N93-10988
RAMAN, S. p 362 N93-11669

RAMANSWAMY, V. p 351 N93-11094
RAMOS, O., JR. p 479 N93-12068
RAMSDEN, S. p 321 N93-12045
RANDALL, CHARLIE p 412 N93-11717
RANDALL, D. A. p 367 N93-11237
p 353 N93-11569
RANEY, C. W. p 291 N93-11639
RANGASWAMY, M. p 469 N93-12310
RANSONE, PHILIP O. p 228 N93-12455
RAO, M. R. p 430 N93-12217
RAO, USHA p 478 N93-11858
RAO, VASANT B. p 292 N93-11781
RAOUF, ABDUL p 311 N93-11723
RAPPAPORT, E. N. p 370 N93-11888
RAPPAPORT, S. A. p 322 N93-12262
RAPPUOLI, R. p 380 N93-11302
RASHIDIAN, BIJAN p 207 N93-11719
RASKY, DANIEL J. p 228 N93-12450
RATHMAN, PETER K. p 477 N93-11749
RATNER, M. A. p 273 N93-12500
RAUCOURT, JEAN-PIERRE p 320 N93-12043
p 320 N93-12044
p 321 N93-12045
p 321 N93-12051
RAUH, R. D. p 447 N93-11186
RAVICHANDRAN, G. p 258 N93-11782
RAY, BONNIE p 429 N93-12426
READER, J. p 438 N93-11778
REARDON, FREDERICK H. p 245 N93-11137
REBSCHER, DOROTHEE p 357 N93-11083
REBUFFAT, DENIS p 246 N93-11361
REDDY, E. S. p 276 N93-12197
REEBER, ROBERT R. p 264 N93-11149
REEDER, M. F. p 308 N93-12435
REEVES, D. L. p 387 N93-12432
REICHERT, BRUCE A. p 213 N93-12077
REINHARD, NANCY A. p 412 N93-11859
REINHARDT, F. W. p 290 N93-11553
REINHOLDT, R. D. p 292 N93-11916
REISLER, HANNA p 252 N93-12254
REMINGTON, B. A. p 451 N93-11495
REMY, DAVID E. p 268 N93-11862
RENDELL, ALISTAIR P. p 439 N93-11852
RENGER, W. p 368 N93-11350
RENKO, KARI p 216 N93-12415
RENZ, ULRICH p 349 N93-12446
RENZ, W. p 459 N93-11238
RENZI, JOHN R. p 221 N93-11428
RESS, D. p 454 N93-12059
REVANKAR, S. T. p 300 N93-11538
REX, J. p 288 N93-11364
RHODES, MARVIN D. p 230 N93-11982
RHODES, ROBERT C. p 373 N93-11821
RHODES, THERESE ESTELLE p 297 N93-11197
RICE, JULIA E. p 439 N93-11854
RICHARDS, P. L. p 466 N93-12109
p 466 N93-12125
RICHTER, KAREN J. p 472 N93-12273
RICHWINE, DAVID M. p 197 N93-11532
RICKEL, D. G. p 293 N93-12089
RIDLER, N. M. p 281 N93-11395
RIEDEL, H. p 196 N93-11113
RIEMER, C. A. p 413 N93-12187
RIGGS, JEFFREY p 473 N93-12542
RIGGS, W. L. II p 262 N93-12494
RIGGS, W. L., II p 271 N93-12168
RILEY, CHRISTOPHER J. p 203 N93-12529
RILEY, G. N., JR. p 462 N93-11703
RINEHART, G. H. p 294 N93-12156
RINGER, MARK J. p 235 N93-11948
RIZZETTO, MARIO p 376 N93-11286
ROACH, JOSEPH F. p 390 N93-12423
ROBERT, YVES p 410 N93-11479
p 410 N93-11480
p 410 N93-11481
p 410 N93-11482
p 410 N93-11484
ROBERTIE, N. F. p 317 N93-11805
ROBERTS, B. A. p 444 N93-11687
ROBERTS, D. E. p 385 N93-12145
ROBERTS, GARY D. p 241 N93-12076
ROBERTS, J. B. G. p 412 N93-11712
ROBERTS, K. M. p 418 N93-11714
ROBERTS, KENNETH STANLEY p 420 N93-11457
ROBINO, C. V. p 254 N93-10984
ROBINSON, G. N. p 366 N93-12299
ROBINSON, J. M. p 274 N93-11380
ROBINSON, M. T. p 439 N93-11849
ROBINSON, STEPHEN P. p 433 N93-11328
ROCHE, C. T. p 444 N93-11652
ROCKWOOD, A. L. p 441 N93-12117
RODHE, HENNING p 351 N93-11094
p 368 N93-11340
RODRIGUEZ, J. M. p 366 N93-12299
RODRIGUEZ, JOSE M. p 351 N93-11091
RODRIGUEZ, P. I. p 328 N93-12149
ROEDER, J. L. p 366 N93-12378
ROFER, C. K. p 274 N93-11380
ROGERS, GEORGE W. p 285 N93-12332
ROGERS, JAMES L. p 414 N93-12278
ROGERS, MELISSA J. B. p 223 N93-11101
ROGERS, RALPH V. p 204 N93-11139
p 283 N93-11716
ROLAND, HEIKE p 255 N93-11026
ROLINCIK, MARK p 230 N93-11927
ROMAIN, JEAN-PIERRE p 319 N93-12038
p 309 N93-12039
ROMALEWSKI, ROBERT S. p 207 N93-11838
ROMANO, L. p 377 N93-11289
ROPER, J. R. p 326 N93-11556
RORABAUGH, TERRY L. p 286 N93-12433
ROSAKIS, A. J. p 258 N93-11782
ROSAKIS, ARES J. p 335 N93-11219
ROSALES, RODOLFO R. p 275 N93-12236
ROSKOS, J. E. p 477 N93-11732
ROSSEG, HERBERT p 278 N93-11009
ROSSER, K. E. p 436 N93-11412
ROSSI, G. B. p 378 N93-11294
ROTE, D. M. p 326 N93-11653
ROTH, J. D. p 250 N93-11808
ROTHWELL, P. p 359 N93-11266
ROUSH, G. B. p 396 N93-11943
ROUSSEAU, G. p 239 N93-11589
ROWE, DAVE p 467 N93-12169
ROWE, J. C. p 399 N93-11958
ROWE, NEIL C. p 479 N93-12381
ROWLAND, F. SHERWOOD p 350 N93-11088
ROY, COLIN E. p 352 N93-11098
ROZSNYAI, B. p 321 N93-12047
RUFFNER, JOHN W. p 390 N93-12508
RUGGIERO, A. G. p 284 N93-12132
RULAND, R. E. p 316 N93-11691
RULE, DONALD W. p 442 N93-11060
RUNDELL, JAMES R. p 379 N93-11298
p 379 N93-11299
RUOFF, A. L. p 461 N93-11646
RUSSELL, A. P. G. p 484 N93-11347
RUSSELL, M. J. p 280 N93-11383
RUST, K. p 293 N93-12089
RUTAN, DAVID p 367 N93-11168
RYAN, T. W., III p 244 N93-11134
RYU, JEHA p 338 N93-11891

S

SAATKAMP, THOMAS p 265 N93-11203
SABBAGH, S. A. p 452 N93-11568
SACCHI, CRISTIANO p 476 N93-11690
SADANANDAN, N. D. p 290 N93-11514
SAFFORD, L. K. p 250 N93-11808
SAGALOVSKY, L. p 431 N93-11511
p 444 N93-11652
SAGDAHL, L. T. p 467 N93-12178
SAITO, MASAKI p 203 N93-12503
SAITO, T. p 394 N93-11937
SAKAGUCHI, HAJIME p 202 N93-12352
SAKAMOTO, HIROSHI p 234 N93-12368
p 234 N93-12372
SAKAMOTO, M. p 454 N93-11834
SALEM, JONATHAN A. p 263 N93-10962
SALMINEN, ESA p 202 N93-12414
SALMON, J. T. p 310 N93-11542
SAMADDAR, S. N. p 285 N93-12356
SAMIMY, M. p 308 N93-12435
SANCHEZ, L. C. p 217 N93-11367
SANDERS, S. J. p 443 N93-11521
SANDERS, TOMMY J. p 276 N93-12281
SANDHAGE, K. H. p 462 N93-11703
SANDWEISS, J. p 437 N93-11681
SANFELIZ, JOSE G. p 241 N93-12015
SANGHI, SANJEEV p 303 N93-11856
SANHUEZA, EUGENIO p 350 N93-11088
SANKAR, SUBRA V. p 248 N93-11454
SANTAVICCA, D. A. p 248 N93-11455
SANTINI, D. J. p 356 N93-12314
SANTORO, ROBERT J. p 248 N93-11451
SANZ, J. p 196 N93-11223
SARACHIK, M. p 461 N93-11629
SARAVANOS, DIMITRIOUS A. p 241 N93-12015
SAROFIM, A. F. p 247 N93-11444
SAROFIM, ADEL F. p 349 N93-12446
SARVER-VERHEY, TIMOTHY R. p 234 N93-12409
SASA, SHUICHI p 219 N93-12359
p 314 N93-12365
SASAKI, MASAKI p 234 N93-12368
p 234 N93-12372
SASAKI, TORU p 350 N93-11088
p 352 N93-11095
SATO, K. N. p 454 N93-11834
SATO, KAZUO p 234 N93-12372
SAUER, EDWARD p 330 N93-11972
SAUERS, I. p 252 N93-12219
SAUGNAC, F. p 239 N93-11589
SAVAGE, M. p 323 N93-10982
SAVELY, R. T. p 396 N93-11943
SCATTOLINI, R. p 421 N93-11593
SCHAEDLA, W. H. p 284 N93-12101
SCHAEFER, O. p 330 N93-11971
SCHAFBUCH, PAUL JAY p 332 N93-11209
SCHAPS, S. R. p 333 N93-12055
SCHENK, AXEL p 336 N93-11544
SCHENKER, P. S. p 400 N93-11965
SCHETTINO, ANTONIO p 196 N93-11157
SCHIFANO, E. p 318 N93-12026
SCHIPANI, S. P. p 388 N93-11743
SCHIRBER, J. E. p 437 N93-11640
SCHIUMA, C. p 449 N93-11029
SCHIUMA, CARLO p 450 N93-11103
SCHLEGELMILCH, RICHARD F. p 395 N93-11940
SCHLEINITZ, JUERGEN P. p 223 N93-11685
SCHMIDT, DAVID K. p 214 N93-11459
p 215 N93-12216
SCHMIDT, F. p 386 N93-12225
SCHMIDT, JEROME MICHAEL p 367 N93-11159
SCHMIDT, M. p 437 N93-11681
SCHMIDT, P. P. p 272 N93-12276
SCHMITT, J. H. M. M. p 482 N93-11477
SCHMITZ-PFEIFFER, A. p 368 N93-11350
SCHMITZ, P. p 221 N93-11398
SCHMITZ, P. C. p 275 N93-12085
SCHMITZ, STEFAN p 357 N93-11006
SCHNEIDER, CARL-THOMAS p 309 N93-11330
SCHNETZER, G. H. p 369 N93-11678
SCHOENEMAN, L. p 408 N93-11378
SCHOENFELDER, C. p 275 N93-12265
SCHOUTENS, K. p 470 N93-11518
SCHRADER, MERRALD p 290 N93-11504
SCHREIBER, J. G. p 275 N93-12085
SCHRIVER, D. p 224 N93-11736
SCHROCK, R. R. p 271 N93-12165
SCHROCK, RICHARD R. p 264 N93-11150
p 265 N93-11187
p 265 N93-11188
SCHROEDER, LYLE C. p 222 N93-12543
SCHRYVERS, D. p 256 N93-11519
SCHUBERT, E. THOMAS p 405 N93-12347
SCHULTZ, J. A. p 469 N93-12310
SCHULTZ, JAMES p 490 N93-11100
SCHUMAKER, T. L. p 290 N93-11492
SCHURR, J. N. p 434 N93-11752
SCHVANEVELDT, ROGER W. p 421 N93-12096
SCHWAB, STUART T. p 244 N93-11134
SCHWARZ, J. A. p 470 N93-12464
SCHWARZ, R. A. p 482 N93-11475
SCHWARZE, G. p 221 N93-11398
SCHWEIKARD, ACHIM p 419 N93-12239
SCHWEITZER, SETH p 478 N93-11796
SCHWEIZER, D. p 372 N93-12420
SCHWUTTKE, URSULA M. p 394 N93-11936
SCOTT, BARBARA A. p 273 N93-11045
SCOTT, D. P. p 385 N93-12145
SCOTT, J. A. p 264 N93-11086
SCOTTI, STEPHEN J. p 339 N93-12005
p 227 N93-12447
SCUSERIA, GUSTAVO E. p 439 N93-11854
SEAH, M. P. p 247 N93-11396
SEARICH, G. V. p 262 N93-12468
SEBBANI, MOHAMMED p 214 N93-11576
SEEGER, A. p 459 N93-11238
SEEGER, J. p 256 N93-11337
SEGARS, RONALD A. p 200 N93-12179
SEGEV, A. p 473 N93-11151
SEHNAL, L. p 220 N93-11348
SEIDEL, JONATHAN A. p 213 N93-12402
SEIGNEURIC, A. p 380 N93-11304
SEKA, W. p 453 N93-11730
p 453 N93-11731
SEKANINA, ZDENEK p 484 N93-11243
SEKELSKY, S. M. p 366 N93-10971
SEKHAR, Y. S. p 279 N93-11117
SELF, MARK F. p 462 N93-11724
SELIGER, HOWARD H. p 374 N93-12431
SELIGSON, A. L. p 466 N93-12099
SELLE, J. E. p 249 N93-11801
SELLECK, C. p 399 N93-11958
SELLERS, C. H. p 257 N93-11595
SELTZER, S. M. p 438 N93-11715
SELVIN, S. p 413 N93-12110
SEMMES, P. B. p 436 N93-11443
SEN, M. p 470 N93-11469
SENFT, DANIEL CHARLES p 358 N93-11222
SENGUPTA, LOUISE C. p 469 N93-12286
SENGUPTA, S. p 460 N93-11522
SENGUPTA, SOMNATH p 469 N93-12286
SENIOR, PETER p 304 N93-11881
SENNETT, C. T. p 414 N93-12326
SEPAHBAN, S. F. p 230 N93-11977

SERAYDARIAN, R. P. p 455 N93-12307
SERIER, BOUALEM p 267 N93-11577
SEROTA, ROSTISLAV p 295 N93-12502
SEVERIN, B. A. B. p 353 N93-11232
p 353 N93-11233
SEVIER, D. L. p 451 N93-11382
SEVRIN, A. p 470 N93-11518
SEWELL, MARK W. p 293 N93-12133
SEYBERT, A. F. p 323 N93-10966
SEZEN, AYBARS p 318 N93-12028
SHAFER, R. E. p 431 N93-11625
SHAHIDI, ANOOSH K. p 395 N93-11940
SHAKHATRE, M. p 449 N93-11029
SHALIN, VALERIE L. p 204 N93-10961
SHAPIRO, S. M. p 256 N93-11519
SHARMA, O. P. p 308 N93-12539
SHARP, DOUGLAS E. p 334 N93-11080
SHAVIT, U. p 248 N93-11453
SHEAFFER, D. A. p 421 N93-12153
SHEEN, S. H. p 271 N93-12123
SHELTON, MICHAEL S. p 208 N93-12053
SHELTON, R. N. p 461 N93-11647
SHEN, SUHUNG p 372 N93-12534
SHEPARD, R. L. p 312 N93-11806
SHEPARD, W. S. p 454 N93-12087
SHEPHERD, MICHAEL J. p 341 N93-12253
SHEPHERD, O. p 317 N93-11805
p 322 N93-12262
SHEPPARD, D. M. p 354 N93-11702
SHER, A. p 462 N93-11727
SHI, D. p 460 N93-11522
SHI, YIFEI p 298 N93-11217
SHIA, R-L. p 366 N93-12299
SHIDELER, JOHN L. p 228 N93-12454
SHIMOMURA, TAKASHI p 219 N93-12359
p 314 N93-12365
SHIMURA, TAKASHI p 330 N93-12463
SHINE, KEITH p 351 N93-11094
SHIPERS, L. R. p 231 N93-10973
p 217 N93-11367
SHIPLEY, P. P. p 196 N93-11113
SHIRES, D. R. p 388 N93-11743
SHOGAN, R. P. p 259 N93-12107
SHOOP, JAMES p 398 N93-11952
SHRIVER, D. F. p 273 N93-12500
SHULTZ, THOMAS p 287 N93-12461
SHUMAKER, D. E. p 451 N93-11516
SHURU, WEI p 242 N93-12235
SICKAFUS, K. E. p 268 N93-11861
SICKLES, W. L. p 218 N93-11910
SIDEBOTTOM, HOWARD p 351 N93-11092
SIGMAN, MATTHEW S. p 265 N93-11192
SIKKA, VINOD K. p 261 N93-12445
SILVER, M. p 463 N93-11816
SIM, A. p 281 N93-11487
SIMANONOK, K. p 374 N93-12014
SIMEN, MARTIN p 196 N93-11141
SIMHA, RAHUL p 416 N93-12403
SIMMONS, MARGARET L. p 407 N93-11231
SIMON, ROBERT p 386 N93-11779
SIMONSON, G. F. p 451 N93-11516
SIMPSON, HARRY J. p 435 N93-12097
SIMPSON, M. p 236 N93-11065
SIMPSON, P. p 412 N93-11712
SINCLAIR, R. p 405 N93-12520
SINDELAR, R. L. p 259 N93-12107
p 260 N93-12158
SINGH, D. p 271 N93-12123
SINGH, J. P. p 454 N93-12087
p 271 N93-12123
p 468 N93-12249
SINGH, M. p 273 N93-12398
SIRIGNANO, W. A. p 245 N93-11138
SITARAMAN, MURALI p 415 N93-12389
SITHER, MARK A. p 477 N93-11741
SIVASHINSKY, G. I. p 254 N93-12478
SIVERS, E. A. p 271 N93-12123
SLASKI, M. p 467 N93-12178
SMADJA, DANIELLE p 317 N93-12023
SMAGA, J. A. p 289 N93-11432
SMALL, C. p 334 N93-11014
p 255 N93-11109
SMARSLY, W. p 256 N93-11337
SMARSLY, W. G. p 256 N93-11336
SMARTT, H. B. p 326 N93-11548
SMEDLEY, K. M. p 431 N93-11625
SMEYS, P. p 295 N93-12421
SMILANSKY, U. p 471 N93-11780
SMITH, A. p 425 N93-11437
SMITH, G. LOUIS p 367 N93-11168
SMITH, J. P. p 301 N93-11670
SMITH, JAMES E., JR. p 328 N93-12196
SMITH, JEFFREY H. p 403 N93-11978
SMITH, M. J. p 197 N93-11377
SMITH, MICHAEL H. p 329 N93-12274
SMITH, P. J. p 302 N93-11671
SMITH, PHILIP p 463 N93-11753
SMITH, PHILLIP RAYMOND p 215 N93-11871
SMITH, R. p 221 N93-11631
SMITH, R. D. p 441 N93-12117
SMITH, R. P. p 362 N93-11692
SMITH, RICHARD N. p 448 N93-12272
SMITH, SCOT E. p 343 N93-11701
SMITHERS, G. A. p 375 N93-12174
SMITS, A. J. p 301 N93-11606
SMYTH, D. M. p 431 N93-11468
SNORTLAND, HOWARD J. p 294 N93-12290
SOANE, D. S. p 263 N93-10972
SOEGIJONO, BAMBANG p 267 N93-11580
SOLKA, JEFFREY L. p 285 N93-12332
SOLOMON, SUSAN p 351 N93-11093
SOLTANI, MOHAMMAD REZA p 208 N93-12206
SOMMER, B. p 331 N93-11974
SOMMER, ERNST p 278 N93-11009
SONG, SUNG-JIN p 333 N93-12533
SONG, Y.-H. p 248 N93-11455
SOOS, Z. G. p 283 N93-11800
SOREM, ROBERT MICHAEL p 339 N93-12194
SORENSEN, K. W. p 284 N93-12101
SOTIROPOULOS, F. p 306 N93-12245
SOUZA, KENNETH A. p 391 N93-12319
SPARKES, BRIAN G. p 376 N93-11285
SPEER, T. M. p 467 N93-12175
SPELCE, T. E. p 337 N93-11775
SPELTZ, DAVID J. p 369 N93-11817
SPENCER, G. A. p 379 N93-11296
SPENCER, J. T. p 470 N93-12464
SPENCER, M. A. p 212 N93-11108
SPENCER, M. G. p 254 N93-12518
SPEZIALE, CHARLES G. p 306 N93-12173
SPRANGLE, PHILLIP p 315 N93-11195
SRINIVAS, KANKANAHALLI p 415 N93-12388
p 415 N93-12392
STAMNES, K. p 352 N93-11098
STAMPS, D. W. p 249 N93-11551
STAN, M. A. p 469 N93-12325
STANNY, R. R. p 387 N93-12432
STANUSH, JULIE p 389 N93-12211
STARLINGER, ALOIS p 334 N93-11004
STASIEWICZ, K. p 361 N93-11273
STASTNY, P. p 459 N93-11076
STEEPER, T. J. p 271 N93-12168
p 262 N93-12494
STEFFEN, R. p 377 N93-11288
p 381 N93-11307
STEIF, ALAN ROBERT p 472 N93-12530
STEIGLITZ, KEN p 287 N93-12436
STEINETZ, BRUCE M. p 236 N93-10978
STEINHARDT, A. p 287 N93-12512
STEINOLFSON, R. S. p 453 N93-11745
STENGER, G. J. p 208 N93-12488
STENZ, CHRISTIAN p 319 N93-12034
STEPHAN, TODD D. p 428 N93-11417
STEPHENS, THOMAS S. p 309 N93-11048
STEVENS, GRADY H. p 287 N93-12481
STEVENS, JOHN G. p 245 N93-11135
STEVENSON, LLOYD p 367 N93-11144
STEWART, D. p 293 N93-12121
STEWART, J. E. p 454 N93-12059
STEWART, M. p 459 N93-11394
STILL, C. J. p 284 N93-11917
STINMAN, ROBERT M. p 387 N93-10994
STOCKERT, JON A. p 238 N93-11281
STOCKMAN, MARK I. p 469 N93-12338
STOKESBERRY, D. P. p 418 N93-11714
STOLARSKI, RICHARD S. p 350 N93-11089
STONEMAN, S. A. T. p 433 N93-11321
p 433 N93-11322
STORDAL, FRODE p 351 N93-11093
p 352 N93-11095
STOREY, C. p 406 N93-11210
p 425 N93-11211
STORTIGAJANI, G. p 411 N93-11592
STOTTLER, RICHARD H. p 420 N93-11000
STOUT, R. W. p 377 N93-11287
STRAKA, J. p 220 N93-11348
STRAMPP, W. p 424 N93-11123
STRAUME, TORE p 374 N93-10974
STREINZ, C. C. p 260 N93-12118
STRIFLER, WALTER A. p 344 N93-11214
STRINGFELLOW, G. B. p 460 N93-11558
p 464 N93-11868
p 464 N93-11869
STRINGFIELD, R. M. p 293 N93-12089
STROFFOLINI, T. p 380 N93-11303
STROMEYER, C. F., III p 384 N93-11841
STUART, MARK A. p 400 N93-11966
p 389 N93-12211
STUBBINS, J. F. p 257 N93-11557
STUBERT, BERTRAM p 213 N93-11339
STUCKY, GALEN D. p 458 N93-10996
p 437 N93-11560
STURGE, M. D. p 464 N93-11894
STUTZKI, J. p 484 N93-11347
SU, TZU-JENG p 339 N93-12020
SULLIVAN, BRENDA M. p 434 N93-11620
SUMMERS, L. K. p 442 N93-11077
SUN, G. Z. p 421 N93-12226
SUN, R. K. p 443 N93-11493
SUN, W. p 279 N93-11118
SURAMPUDI, SUBBARAO p 290 N93-11456
SUREAU, ALAIN p 321 N93-12046
SUSOEFF, A. R. p 217 N93-11447
SUTHERLAND, LINDA W. p 435 N93-12080
SUTTON, STEWART A. p 391 N93-11941
SUZUKI, MAHIKO p 441 N93-12111
SUZUKI, MINEO p 330 N93-12463
SVENES, KNUT p 357 N93-11129
SWAB, RODNEY E. p 391 N93-11976
SWAIN, ROBIN C. p 334 N93-11022
p 315 N93-11064
p 309 N93-11320
SWAMINATHAN, HARIHARAN p 386 N93-11779
SWANSON, PAUL DAVID p 305 N93-12157
SWANSON, THEODORE D. p 229 N93-12459
SWANSON, W. P. p 443 N93-11493
SWINDEMAN, R. W. p 259 N93-11857
SZAKALY, ZOLTAN F. p 400 N93-11964
SZOKE, A. p 317 N93-11765

T

TADDEO, B. p 378 N93-11294
TAGLIABUE, ALDO p 382 N93-11309
TAKAHASHI, HITOSHI p 216 N93-12362
p 203 N93-12503
TAKAHASHI, Y. p 311 N93-11662
TAKAMORI, SUSUMU p 202 N93-12352
TAKIZAWA, MINORU p 209 N93-12370
TALOTTA, NICHOLAS J. p 205 N93-11704
p 205 N93-11705
TAMARGO, M. C. p 464 N93-11894
TAMM, M. A. p 307 N93-12355
TAMURA, HIROSHI p 234 N93-12368
TANG, D. p 406 N93-12540
TANI, B. S. p 462 N93-11703
TANI, KOUICHIRO p 202 N93-12369
TANKALA, K. p 468 N93-12218
TANNER, L. E. p 256 N93-11519
TANRIKULU, M. O. p 448 N93-11892
TANVEER, S. p 306 N93-12173
TANZI, E. p 377 N93-11289
TARDOS, EVA p 413 N93-12131
TARDY, D. C. p 435 N93-11189
TARTAKOVSKIJ, V. K. p 440 N93-11914
TAWEL, RAOUL p 420 N93-11174
TAYLOR, HENRY F. p 448 N93-12227
TAYLOR, HENRY L. p 390 N93-12491
TAYLOR, P. L. p 326 N93-11548
TAYLOR, PATRICK J. p 269 N93-11912
TAYLOR, PETER p 439 N93-11851
TAYLOR, PETER R. p 439 N93-11852
p 439 N93-11853
p 439 N93-11854
p 439 N93-11855
TAYLOR, WILLIAM J. p 296 N93-10981
TEMKIN, R. J. p 315 N93-11278
TENFORDE, T. S. p 282 N93-11515
TERRY, P. L. p 311 N93-11673
TESTA, BRIDGET MINTZ p 331 N93-11975
TEWARI, ASHISH p 201 N93-12344
THOMAS, D. J. p 316 N93-11411
THOMAS, I. M. p 461 N93-11602
THOMAS, J. F. p 349 N93-12498
THOMAS, J. K. p 259 N93-12107
THOMAS, MICHAEL DOMINIC p 198 N93-11874
THOMAS, R. H. p 443 N93-11493
THOMPSON, ANNE p 351 N93-11092
THOMPSON, D. p 295 N93-12301
THOMPSON, H. DOYLE p 213 N93-12214
THOMPSON, P. A. p 280 N93-11234
THOMPSON, RONALD G., JR p 341 N93-12376
THOMSEN, M. F. p 365 N93-12264
THORNE, J. R. G. p 283 N93-11800
THORNTON, R. C. p 390 N93-12509
THORP, SCOTT A. p 413 N93-12022
THURMOND, LEO E. p 222 N93-12505
TIESZEN, S. R. p 249 N93-11551
TING, ANTONIO p 315 N93-11195
TISSUE, B. M. p 250 N93-11918
TITRAN, R. p 221 N93-11398
TODD, JAMES T. p 386 N93-11503
TODLING, RICARDO p 359 N93-11249
TOLAND, JOEL A. p 407 N93-11368
TOLER, CARL G. p 204 N93-12489
TOLLI, J. p 471 N93-12058
TOLOKAN, ROBERT P. p 228 N93-12453

TOMBS, D. J. p 409 N93-11405
p 409 N93-11406
TONGUZ, OZAN K. p 448 N93-11892
TORCZYNSKI, J. R. p 303 N93-11799
TORRIGIANI, G. p 380 N93-11300
TORTORELLI, P. F. p 259 N93-11830
TOWSLEY, DON p 416 N93-12403
TRAMONT, E. C. p 379 N93-11298
TRAMONT, EDMUND C. p 377 N93-11291
TRAN, LUC P. p 314 N93-11934
TRAN, TUAN A. p 285 N93-12331
TRAPP, J. A. p 301 N93-11637
TREFNY, CHARLES JOSEPH p 235 N93-12537
TRESSELT, CARL P. p 288 N93-11051
TROEIM, JAN p 357 N93-11129
TROTTER, THOMAS W. p 430 N93-12260
TROUDET, T. p 215 N93-12305
TRUEMPER, J. p 482 N93-11473
TSAI, JONGNI p 487 N93-11264
TSANG, CHIT-SANG p 288 N93-12519
TSCHAECHE, A. N. p 480 N93-12495
TSEREVITINOV, S. p 452 N93-11674
TSURUTANI, B. T. p 489 N93-12506
TUCKER, JERRY H. p 414 N93-12278
TUCKER, R. F. p 480 N93-12473
TUMMILLO, A. F. p 289 N93-11432
TUNICK, ARNOLD p 363 N93-11785
TURANO, KATHLEEN p 386 N93-11488
TURCO, RICHARD p 351 N93-11091
TURKEL, ELI p 198 N93-11607
TURKO, B. T. p 312 N93-11822
TURNER, J. p 446 N93-12497
TURNER, M. G. p 375 N93-12315
TURRO, N. p 288 N93-11257
TZAVARAS, ATHANASSIOS p 253 N93-12282

U

UBERTINI, T. R. p 381 N93-11306
UDSETH, H. R. p 441 N93-12117
UHOMOIBHI, J. p 321 N93-12045
ULA, SADRUL p 294 N93-12191
p 294 N93-12294
p 295 N93-12295
ULBRICH, N. p 218 N93-11910
UNDERWOOD, J. H. p 316 N93-11659
UNSEREN, M. A. p 331 N93-11979
URBANI, L. p 382 N93-11312
URSIC, J. R. p 359 N93-11235

V

VACCARO, JOHN J. p 286 N93-12433
VAIDYANATHAN, GOPAL p 236 N93-12177
VANBLOKLAND, A. A. E. p 451 N93-11245
VANBUSKIRK, ROBERT DANIEL p 358 N93-11226
VANCLARK, A., JR. p 333 N93-12055
VANCUTSEM, C. p 383 N93-11316
VANDENBOSCH, P. p 383 N93-11316
VANDERBILT, VERN C. p 344 N93-12351
VANDERBORGH, N. E. p 345 N93-11626
VANDERSANDE, J. p 221 N93-11398
VANEMMICHOVEN, P. A. ZEIJLMANS
p 439 N93-11849
VANHAAFTEN, F. p 444 N93-11763
p 293 N93-12089
VANMIEGROET, H. p 354 N93-11680
VANMOERKERKEN, R. A. p 368 N93-11329
VANNI, R. p 381 N93-11306
VANNIEUWENHUIZEN, P. p 470 N93-11518
VANSTEENBERG, MICHAEL E. p 479 N93-12150
VANSTRYLAND, ERIC W. p 322 N93-12238
VANZANDT, JAMES R. p 414 N93-12284
VARACALLE, D. J., JR. p 271 N93-12168
p 262 N93-12494
VARDULAKIS, A. I. p 424 N93-11124
VARDULAKIS, A. I. G. p 423 N93-11121
p 424 N93-11125
VARGA, R. S. p 426 N93-11520
VARMA, R. p 268 N93-11861
VARSHNEY, PRAMOD K. p 414 N93-12242
VASILAKIS, A. D. p 349 N93-12498
VAUGHAN, BRIAN ALEXANDER p 483 N93-12336
VAUGHAN, DAVID S. p 387 N93-12252
VAUGHN, WALLACE L. p 229 N93-12456
VEAL, B. W. p 461 N93-11647
VELSKO, S. P. p 452 N93-11645
VEMURI, V. p 414 N93-12234
VENKATARAMAN, SUBARAMANIAN T.
p 324 N93-11177
VERANI, P. p 378 N93-11294
VERDE, L. p 214 N93-11160
VERRILLI, MICHAEL J. p 333 N93-10967
p 238 N93-11399
VETRO, S. p 381 N93-11306
VETTE, JAMES I. p 349 N93-11003
VIANCO, P. T. p 276 N93-11494
p 277 N93-12106
VIDALE, JOHN E. p 366 N93-12270
VIDEEN, GORDEN WAYNE p 448 N93-12531
VIECELLI, J. A. p 448 N93-11627
VIG, JOHN R. p 469 N93-12283
VIITANEN, PEKKA p 299 N93-11359
VINOKUR, V. p 467 N93-12178
VIRMONT, JEAN p 319 N93-12035
p 321 N93-12046
VIRSHUP, G. F. p 465 N93-12065
VISCONTI, GUIDO p 352 N93-11095
VISINSKY, MONICA p 330 N93-11961
VISWANATHAN, SRINATH p 261 N93-12445
VISWESVARN, C. p 386 N93-12225
VIZZACCARO, A. p 383 N93-11314
VOGES, W. p 482 N93-11475
VOKROUHLICKY, D. p 220 N93-11348
VOLLATH, D. p 268 N93-11861
VOLOKITIN, A. S. p 361 N93-11272
VONTEIN, VOLKER p 223 N93-11007
VOORHES, D. W. p 317 N93-12011
VOSSLER, J. p 326 N93-11556
VRANISH, JOHN M. p 330 N93-11969
VUILLERMOZ, P. p 302 N93-11756

W

WAAG, WAYNE L. p 421 N93-12096
WADE, C. E. p 374 N93-12014
WADE, M. R. p 455 N93-12307
WADSWORTH, J. p 228 N93-12452
WAGNER, J. S. p 362 N93-11564
WAGNER, J. W. p 260 N93-12118
WAHLUND, JAN-ERIK p 359 N93-11265
p 359 N93-11266
p 360 N93-11267
p 360 N93-11268
p 360 N93-11269
p 360 N93-11270
p 360 N93-11271
p 361 N93-11272
p 361 N93-11273
WAHNER, ANDREAS p 350 N93-11090
p 352 N93-11098
WAITE, J. H., JR. p 487 N93-11165
p 487 N93-11166
WAITE, J. HUNTER, JR. p 357 N93-10964
p 486 N93-11164
WAKAIRO, KAORU p 209 N93-12367
p 209 N93-12370
p 209 N93-12383
WAKAMATSU, YOSHIO p 202 N93-12369
WALJESKI, KATRINA MARIE HESTER
p 489 N93-12342
WALKER, CONSTANCE ELAINE p 484 N93-11260
WALKER, D. W. p 426 N93-11636
WALKER, IAN D. p 330 N93-11961
WALKER, J. M. p 466 N93-12099
WALKER, R. E. p 247 N93-11450
WALLACE, TERRYL A. p 229 N93-12457
WALLEY, S. M. p 249 N93-11490
WALLING, R. S. p 317 N93-11765
WALLSOM, RICHARD E. p 224 N93-10970
WALSH, D. S. p 257 N93-11600
p 464 N93-11842
WALSH, JOANNE L. p 206 N93-10968
WALTERS, G. K. p 470 N93-12499
WALTERS, JERRY L. p 395 N93-11940
WALTJEN, K. p 310 N93-11542
WALTON, J. J. p 354 N93-11744
WAMPLER, W. R. p 464 N93-11842
WAND, B. T. p 316 N93-11691
WANG, CHI p 237 N93-11247
WANG, NING p 481 N93-11198
WANG, SHAO p 324 N93-11263
WANG, TAI-SEN F. p 443 N93-11510
WANG, TANKIN p 340 N93-12199
WANG, W. J. p 337 N93-11707
WANG, WEI-CHYUNG p 351 N93-11094
WANG, XUGUANG p 336 N93-11579
WARASHINA, SHOUGO p 330 N93-12463
WARD, B. p 197 N93-11365
WARD, DAVID G. p 422 N93-12439
WARNER, R. W. p 377 N93-11287
WARNER, RONALD p 379 N93-11297
WARNER, RONALD D. p 377 N93-11292
WARREN, J. F. p 328 N93-12114
WARREN, JOHN p 285 N93-12331
WASIELEWSKI, M. R. p 465 N93-12090
WASIERSKI, R. F. p 293 N93-12089
WASZAK, MARTIN R. p 215 N93-12216
WATANABE, AKIRA p 209 N93-12367
p 209 N93-12370
p 209 N93-12383
WATANABE, MINORU p 435 N93-12375
WATANABE, MITSUO p 330 N93-12463
WATANABE, YOSHIAKI p 329 N93-12364
WATSON, JUDITH J. p 224 N93-10970
WATTS, R. L. p 481 N93-12067
WAYLAND, B. B. p 253 N93-12428
WEBB, ANDREW R. p 428 N93-10980
p 281 N93-11391
WEBB, LANNIE D. p 207 N93-11863
WEBB, M. S. p 452 N93-11645
WEBER, E. R. p 469 N93-12316
WEBER, M. J. p 267 N93-11549
WEBSTER, C. E. p 289 N93-11432
WEBSTER, G. A. p 212 N93-11112
WEBSTER, P. J. p 212 N93-11112
WEBSTER, P. S. p 212 N93-11112
WEILAND, CLAUS p 195 N93-11008
WEININGER, STEPHEN J. p 268 N93-11862
WEINSTEIN, STUART ALAN p 364 N93-11900
WEISENSTEIN, DEBRA p 351 N93-11093
p 352 N93-11096
WEISS, J. M. p 312 N93-11806
WEISS, JONATHAN J. p 314 N93-11934
WEITZNER, HAROLD p 455 N93-12188
WELCH, CHRISTOPHER p 216 N93-11057
WELKE, STEPHEN R. p 477 N93-11732
p 404 N93-11809
WELLBORN, STEVEN R. p 213 N93-12077
WELLER, G. p 353 N93-11232
p 353 N93-11233
WELLS, B. J. p 267 N93-11552
WELLS, DAVID E. p 205 N93-11419
WELLS, M. SUE p 407 N93-11368
WELLS, R. L. p 467 N93-12175
WELLS, RICHARD L. p 462 N93-11724
WENDELBERGER, J. R. p 429 N93-11820
WENG, W. T. p 443 N93-11498
p 443 N93-11499
p 444 N93-11641
p 445 N93-11776
WENG, Z. p 465 N93-11915
WEST, ROBERT p 246 N93-11218
WEST, W. P. p 455 N93-12307
WESTBROOK, C. K. p 326 N93-11540
WESTMORELAND, P. R. p 251 N93-12119
WESTON, M. E. p 377 N93-11287
WESTON, MARY p 379 N93-11297
WESTON, MARY E. p 377 N93-11292
WESTPHAL, W. p 211 N93-11106
p 236 N93-11107
WESTWOOD, JOHN D. p 447 N93-11186
WEVER, A. M. J. p 383 N93-11313
WHEATCRAFT, LOUIS p 230 N93-11932
WHEELER, M. J. p 271 N93-12123
WHINNERY, L. p 275 N93-12265
WHIPPLE, M. L. p 346 N93-11771
WHIRLEY, R. G. p 337 N93-11775
WHITE, C. L. p 256 N93-11524
WHITE, MARVIN H. p 289 N93-11414
WHITE, STEVE p 478 N93-11796
WHITE, T. A. D. p 278 N93-10977
WHITEHEAD, J. C. p 221 N93-12317
WHITEMAN, C. D. p 369 N93-11657
WHITLOCK, HOWARD W., JR. p 440 N93-11872
WHITTLE, A. J. p 338 N93-11903
WICKS, M. C. p 459 N93-11394
WIEDEMANN, KARL E. p 269 N93-11912
p 229 N93-12457
WIKER, STEVEN F. p 330 N93-11967
WILCOX, BRUCE C., JR. p 387 N93-11279
WILCOX, DAVID C. p 301 N93-11615
WILD, W. p 484 N93-11347
WILDHAGEN, B. p 256 N93-11337
WILKE, G. D. p 461 N93-11602
WILLEMSEN, JORGE F. p 432 N93-10999
WILLIAMS, D. p 371 N93-12154
WILLIAMS, D. D. p 210 N93-11040
WILLIAMS, ROBERT M. p 426 N93-11463
WILLIAMS, STEVEN P. p 206 N93-11170
WILLIAMSON, A. E. p 290 N93-11492
WILLSTAEDT, E. B. p 291 N93-11604
WILMINGTON, R. P. p 389 N93-12211
WILMINGTON, ROBERT P. p 389 N93-12195
WILSON, C. L. p 353 N93-11232
p 353 N93-11233
WILSON, G. C. p 271 N93-12168
p 262 N93-12494
WILSON, G. F. p 387 N93-12432
WILSON, JACK p 214 N93-12418
WILSON, RANDALL H. p 419 N93-12239
WILSON, W. W. p 304 N93-11995
p 454 N93-12087
WIMBERGER-FRIEDL, REINHOLD p 269 N93-11983
p 269 N93-11984
p 269 N93-11985
p 269 N93-11986

p 269 N93-11987
p 270 N93-11988
p 270 N93-11989
p 270 N93-11990
p 270 N93-11991
WINDLEY, PHILLIP J. .... p 406 N93-12538
WINFREE, WILLIAM P. .... p 216 N93-11057
WINKLEMAN, B. C. .... p 455 N93-12139
WINKLER, GERHARD B. .... p 325 N93-11423
WINSER, K. J. .... p 360 N93-11268
WINSTON, R. .... p 346 N93-11823
WINTER, J. .... p 221 N93-11398
WISE, MARION A. .... p 230 N93-11982
WISEMAN, SIMON R. .... p 474 N93-11333
WITHROW, C. A. .... p 275 N93-12085
WITTEN, A. J. .... p 359 N93-11235
WITTENAUER, J. P. .... p 228 N93-12452
WITTIG, CURT .... p 252 N93-12254
WOFSY, STEVE .... p 352 N93-11096
WOHLER, DIANE .... p 206 N93-11461
WOHLETZ, K. H. .... p 364 N93-12136
WOHLHUTER, F. K. .... p 301 N93-11638
WOLBER, DAVE .... p 405 N93-12345
p 405 N93-12346
WOLCZANSKI, PETER T. .... p 468 N93-12231
WOLF, BART JOSEPH .... p 358 N93-11184
WOLF, HELMUT .... p 278 N93-11009
WOLF, RANDY .... p 223 N93-11101
WOLFE, W. H. .... p 377 N93-11287
WOLFE, WILLIAM H. .... p 378 N93-11295
WOOD, JONATHAN R. .... p 264 N93-11084
WOOD, M. E. .... p 433 N93-11204
WOODWARD, GREGORY SCOTT p 225 N93-11999
WOODWARD, RICHARD P. .... p 218 N93-12016
WOODWORTH, J. R. .... p 346 N93-11771
WORKMAN, GARY L. .... p 328 N93-11992
p 276 N93-12401
WORSNOP, D. R. .... p 366 N93-12299
WOUDENBERG, RICHARD C. .... p 462 N93-11724
WRIGHT, AMMON K. .... p 330 N93-11968
WRIGHT, JON A. .... p 284 N93-12095
WRIGHT, MICHAEL E. .... p 265 N93-11192
WRIGHT, R. N. .... p 257 N93-11595
WRIGHT, THEODORE .... p 417 N93-11005
WU, GUANGHUI .... p 362 N93-11535
WU, K. C. .... p 313 N93-12140
WU, S. T. .... p 220 N93-12213
WUEBBLES, D. J. .... p 354 N93-11677
WUEBBLES, DONALD J. .... p 351 N93-11093
p 351 N93-11094
p 352 N93-11096
WURTELE, J. S. .... p 315 N93-11278
WYNTJES, G. .... p 317 N93-12011

X

XIAO, JING .... p 398 N93-11956
XU, M. .... p 248 N93-11453
XU, S. .... p 445 N93-11831
XU, YANGSHENG .... p 331 N93-11973
XU, YOUWEN .... p 462 N93-11706
XU, YUENONG .... p 246 N93-11259

Y

YAMADA, H. .... p 451 N93-11277
YAMAKI, Y. ROBERT .... p 228 N93-12455
YAMAMOTO, ATSUMASA .... p 307 N93-12382
YAMAMOTO, SACHIO .... p 490 N93-12470
YAMAZAKI, MICHIO .... p 261 N93-12322
YANAGIHARA, MASAAKI .... p 219 N93-12359
p 314 N93-12365
YANG, HUA .... p 298 N93-11241
YANG, L. .... p 464 N93-11818
YANG, PING .... p 292 N93-11781
YANG, S. L. .... p 302 N93-11767
YAO, JONATHAN YI .... p 339 N93-12000
YARBROUGH, W. A. .... p 468 N93-12218
YATES, G. J. .... p 312 N93-11822
YATES, GEORGE J. .... p 313 N93-12069
YATES, J. T., JR. .... p 250 N93-12062
YATSUYANAGI, NOBUYUKI .... p 234 N93-12372
YEE, J. H. .... p 282 N93-11675
YEH, K. C. .... p 283 N93-11811
YEN, THOMAS .... p 330 N93-11967
YETTER, R. A. .... p 253 N93-12257
YEUAN, JIAN JONG .... p 336 N93-11372
YIM, WAN HUNG .... p 285 N93-12207
YOO, S. I. .... p 462 N93-11706
YOON, W. S. .... p 235 N93-11133
YOUNG, A. J. .... p 385 N93-12145
YOUNG, B. K. F. .... p 317 N93-11765
YOUNG, J. K. .... p 481 N93-12067
YU, KIN MAN .... p 466 N93-12127
YUAN, YONG-BIN .... p 337 N93-11721
YUE, J. .... p 273 N93-12440
YUEH, F. Y. .... p 454 N93-12087
YULE, H. P. .... p 413 N93-12187
YUND, R. A. .... p 461 N93-11682

Z

ZACH, F. X. .... p 469 N93-12316
ZAHNISER, M. S. .... p 366 N93-12299
ZAK, H. .... p 400 N93-11965
ZAKHAROV, A. .... p 452 N93-11674
p 453 N93-11694
ZAKHAROV, V. E. .... p 430 N93-11420
ZAKHLENIUK, N. A. .... p 458 N93-10992
ZALLER, MICHELLE M. .... p 248 N93-11452
ZALUZEC, M. J. .... p 277 N93-11672
ZANDER, RUDI J. .... p 351 N93-11091
ZANETTI, A. R. .... p 377 N93-11289
ZARE, RICHARD N. .... p 436 N93-11196
ZAWODNY, JOSEPH M. .... p 350 N93-11089
ZEBROWSKI, J. P. .... p 345 N93-11571
ZEHNER, D. M. .... p 439 N93-11849
ZELENKA, RICHARD E. .... p 205 N93-12320
ZELIGS, B. J. .... p 381 N93-11306
ZELLER, JOSEPH L., JR. .... p 390 N93-12509
ZEMBA, JAN C. .... p 374 N93-12247
ZEMKE, ARTHUR E. .... p 371 N93-12180
ZEREFOS, CHRISTOS S. .... p 350 N93-11089
ZHADIN, EVGENY A. .... p 352 N93-11096
ZHANG, L. .... p 279 N93-11118
p 279 N93-11119
ZHANG, S. Y. .... p 443 N93-11498
p 443 N93-11499
p 444 N93-11641
p 445 N93-11776
ZHANG, T. J. .... p 460 N93-11563
ZHANG, Y. .... p 247 N93-11444
ZHANG, YANG .... p 486 N93-12330
ZHAO, X. P. .... p 488 N93-11696
ZHOU, XIAOHONG .... p 313 N93-11907
ZHOU, XIUJI .... p 351 N93-11091
ZHU, S. .... p 458 N93-10987
ZICARI, ROBERTO .... p 476 N93-11689
ZIEBARTH, JOHN P. .... p 307 N93-12397
ZIMA, HANS .... p 412 N93-11618
ZIMMERMAN, M. B. .... p 356 N93-12474
ZOERNER, W. .... p 263 N93-11011
ZUBAIR, M. .... p 279 N93-11117
ZUERCHER, JOE C. .... p 312 N93-11757
ZURAWSKI, D. .... p 345 N93-11571
ZUTAVERN, F. J. .... p 291 N93-11693
ZVENIGORODSKY, SERGEI .... p 351 N93-11093

CORPORATE SOURCE INDEX

SCIENTIFIC AND TECHNICAL AEROSPACE REPORTS VOLUME 31 NUMBER 2

Typical Corporate Source Index Listing

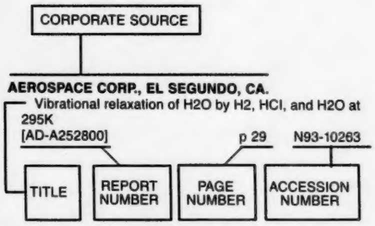
CORPORATE SOURCE
AEROSPACE CORP., EL SEGUNDO, CA.
Vibrational relaxation of H2O by H2, HCl, and H2O at 295K
[AD-A252800]
p 29
N93-10263
TITLE
REPORT NUMBER
PAGE NUMBER
ACCESSION NUMBER

Listings in this index are arranged alphabetically by corporate source. The title of the document provides the user with a brief description of the subject matter. The report number helps to indicate the type of document cited (e.g., NASA report, translation, NASA contractor report). The accession number denotes the number by which the citation is identified. The page number helps you locate the citation in the abstract section. The titles are arranged under each corporate source in ascending accession number order.

A

ACADEMY OF SCIENCES OF THE UKRAINIAN SSR, KIEV.

Scattering of polarized electrons by oriented deuterons
[DE92-624834] p 440 N93-11914

ADMIRALTY RESEARCH ESTABLISHMENT, GOSPORT (ENGLAND).

Experiments on low aspect ratio hydroplanes to measure lift under static and dynamic conditions
[ARE-TM(UHR)-90306] p 197 N93-11365

Lift coefficient of a randomly oscillating hydroplane
[DRA/MAR-TM(MTH)-91320] p 197 N93-11377

ADVISORY COMMITTEE ON THE FUTURE OF THE US SPACE PROGRAM, WASHINGTON, DC.

The first meeting of the Advisory Committee on the Future of the US Space Program (C-FUSSP)
[NASA-CR-190995] p 219 N93-11754

ADVISORY GROUP FOR AEROSPACE RESEARCH AND DEVELOPMENT, NEUILLY-SUR-SEINE (FRANCE).

Allergic, Immunological and Infectious Disease Problems in Aerospace Medicine
[AGARD-CP-518] p 376 N93-11283

Directory of factual and numeric databases of relevance to aerospace and defence R and D
[AGARD-R-777] p 476 N93-11710

AGARD flight test techniques series. Volume 10: Weapon delivery analysis and ballistic flight testing
[AGARD-AG-300-VOL-10] p 430 N93-11711

AERODYNE RESEARCH, INC., BILLERICA, MA.

Stratospheric aircraft exhaust plume and wake chemistry studies
[NASA-CR-189688] p 366 N93-12299

AEROMETRICS, INC., SUNNYVALE, CA.

Experimental investigation of rocket injector atomization p 248 N93-11454

AERONAUTICAL RESEARCH INST. OF SWEDEN, STOCKHOLM.

Mixed mode bending test of the interlaminar fracture toughness of carbon/epoxy
[FFA-TN-1992-04] p 237 N93-11128

AEROSPACE CORP., ALBUQUERQUE, NM.

Requirements and opportunities for satellite autonomy
p 230 N93-11926

AEROSPACE CORP., EL SEGUNDO, CA.

Acoustic measurement of the mechanical properties of thin material specimens
[AD-A253538] p 434 N93-11752

An approach to integrating and creating flexible software environments p 396 N93-11946

Forecasting the relativistic electron flux at geosynchronous orbit
[AD-A254016] p 226 N93-12064

The extremely low frequency wave analyzer
[AD-A255178] p 366 N93-12378

The relationship between electrostatic discharges on spacecraft P78-2 and the electron environment
[AD-A255179] p 226 N93-12379

AEROSPACE CORP., LOS ANGELES, CA.

Advanced satellite workstation: An integrated workstation environment for operational support of satellite system planning and analysis p 391 N93-11941

AEROSPACE MEDICAL RESEARCH LABS., BROOKS AFB, TX.

Viral hepatitis in the US Air Force, 1980 - 1989
p 377 N93-11287

Estimates of Human Immunodeficiency Virus (HIV) incidence and trends in the US Air Force
p 377 N93-11292

Immunological parameters in current and former US Air Force personnel p 378 N93-11295

Susceptibility in USAF recruits to vaccine preventable diseases p 380 N93-11301

AEROSPACE MEDICAL RESEARCH LABS., WRIGHT-PATTERSON AFB, OH.

Development of a tactile perceived attitude transducer
[AD-A253724] p 385 N93-11081

The effect of variable seat back angles on human response to +Gz impact accelerations
[AD-A250673] p 387 N93-11559

Occupational safety considerations with hydrazine fuels p 276 N93-11951

The development of system components to provide proprioceptive and tactile information to the human for future telepresence systems p 330 N93-11968

AEROSPATIALE, CANNES (FRANCE).

Lessons drawn from 2 existing satellite networks: ARABSAT and EUTELSAT. Application to the Pacific basin projects
[REPT-921-440-101] p 282 N93-11591

AEROSPATIALE, CHATILLON (FRANCE).

Parallel architecture for image processing with optic fiber guided missile
[REPT-921-320-101] p 418 N93-11584

Advanced control for the design of STT missile autopilot
[REPT-921-320-102] p 215 N93-11585

AEROSPATIALE AQUITAINE, SAINT-MEDARD EN JALLES (FRANCE).

Toughness of Si3N4-SiC whisker composites
[REPT-921-430-101] p 239 N93-11586

Using NDT techniques in the maintenance of aeronautical products
[REPT-921-430-102] p 332 N93-11587

Silicon carbide matrix composites
[REPT-921-430-103] p 239 N93-11588

High temperature oxidation protection of carbon/carbon composites
[REPT-921-430-105] p 239 N93-11589

Aerospatiale processes for three dimensional preforms
[REPT-921-430-147] p 239 N93-11590

AIR FORCE INST. OF TECH., WRIGHT-PATTERSON AFB, OH.

Microwave guidance technology and its applications
[AD-A254107] p 281 N93-11509

Chinese Journal of Lasers (selected articles)
[AD-A254100] p 317 N93-11786

The effect of silicon, tin, and chromium on the corrosion and mechanical properties of zirconium - molybdenum - niobium
[AD-A254102] p 258 N93-11787

Hybrid guidance for maneuvering flight vehicles
[AD-A254110] p 225 N93-11798

A model to estimate the flux of background particles expected to accumulate on the collector foils of the interstellar gas experiment on the long duration exposure facility spacecraft
[AD-A254265] p 489 N93-11815

A comparison of radar rainfall estimates and rain gage measurements during two Denver thunderstorms
[AD-A254267] p 369 N93-11817

A composite study of the Madden-Julian oscillation
[AD-A254269] p 369 N93-11819

Design of an Ada expert system shell for the VHSIC avionic modular flight processor p 397 N93-11947

Temporal monitoring of VHF and LF atmospherics and their relation to lightning
[AD-A252617] p 371 N93-12180

Carbon/carbon composition ablation effects on ionized boundary layers
[AD-A254465] p 242 N93-12235

An observational study of a prefrontal convective rainband using TAMEX single- and dual-Doppler data
[AD-A249839] p 371 N93-12251

Studies in control for vibration suppression of the UWAA 20-bay planar truss
[AD-A250193] p 341 N93-12253

Nature of the beta-phase of nickel-aluminum system
[AD-A254101] p 261 N93-12269

Bionics and problems of instrument manufacture
[AD-A254461] p 314 N93-12517

AIR FORCE MEDICAL CENTER, LACKLAND AFB, TX.

Early markers of HIV infection and subclinical disease progression p 379 N93-11296

Neuropsychiatric morbidity in early HIV disease: Implications for military occupational function
p 379 N93-11299

AIR FORCE SYSTEMS COMMAND, BROOKS AFB, TX.

Introduction to training decisions modeling technologies: The training decisions system
[AD-A249862] p 387 N93-12252

AIR FORCE SYSTEMS COMMAND, WRIGHT-PATTERSON AFB, OH.

Evaluation of CKU-5/A ejection seat catapults under varied acceleration levels
[AD-A248021] p 204 N93-12489

AKRON UNIV., OH.

Fracture mechanics of model fiber composites
p 237 N93-11247

ALABAMA UNIV., HUNTSVILLE.

Rocket Based Combined Cycle (RBCC) Propulsion Technology Workshop. Volume 1: Executive summary
[NASA-CR-184382] p 231 N93-11042

Rocket Based Combined Cycle (RBCC) Propulsion Workshop, volume 2
[NASA-CR-184383] p 231 N93-11043

Residual acceleration data on IML-1: Development of a data reduction and dissemination plan
[NASA-CR-190807] p 223 N93-11101

Effects of reacting flows with turbulence and shock waves on efficiency of scramjet combustors
p 235 N93-11133

Kinetics of diffusional droplet growth in a liquid/liquid two-phase system
[NASA-CR-190805] p 297 N93-11142

Development of a scintillating optical fiber ionization calorimeter
[NASA-CR-184415] p 311 N93-11662

Diagnostics of electron-heated solar flares
p 488 N93-11877

KC-135 materials handling robotics
[NASA-CR-184430] p 328 N93-11992

Analysis of surfaces from the LDEF A0114, phase 2
[NASA-CR-190596] p 270 N93-11993

Erosion rates for polymers measured on LDEF
p 270 N93-11994

Examination of various turbulence models for application in liquid rocket thrust chambers
[NASA-CR-184406] p 233 N93-12009

Superconducting applications in propulsion systems. Magnetic insulation for plasma propulsion devices
[NASA-CR-184401] p 233 N93-12013
Application of a two-layer near wall model to fully developed and rotating channel turbulent flows
[NASA-CR-184441] p 305 N93-12082
Vacuum chamber translation/positioning mechanism and welding power supply controller
[NASA-CR-184465] p 328 N93-12196
Analysis of advanced optical glass and systems
[NASA-CR-184434] p 448 N93-12201
Controls Astrophysics and Structures Experiment in Space (CASES) advanced studies and planning
[NASA-CR-184410] p 220 N93-12213
Analysis of materials from MSFC LDEF experiments
[NASA-CR-184425] p 252 N93-12215
Gamma ray astronomy
[NASA-CR-184447] p 483 N93-12348
High temperature superconductor materials and applications
[NASA-CR-184426] p 470 N93-12396
FNAS computational fluid dynamics
[NASA-CR-184394] p 307 N93-12397
Materials processing in low gravity
[NASA-CR-184421] p 276 N93-12401
ECLSS medical support activities
[NASA-CR-184429] p 385 N93-12427
Development summary of a sympathetic discharge CO2 laser for lidar use
[NASA-CR-184433] p 323 N93-12516
Users manual for program NYQUIST: Liquid rocket nyquist plots developed for use on a PC computer
[NASA-CR-184451] p 235 N93-12522
Development of a model for predicting NASA/MSFC program success
[NASA-CR-184423] p 473 N93-12542

ALASKA UNIV., FAIRBANKS.
International Conference on the Role of the Polar Regions in Global Change: Proceedings, volume 1
[DE92-013652] p 353 N93-11232
International Conference on the Role of the Polar Regions in Global Change: Proceedings, volume 2
[DE92-013653] p 353 N93-11233

ALLIANCE TO SAVE ENERGY, WASHINGTON, DC.
The uses and limits of economic models as a climate change policy tool
[DE92-015792] p 356 N93-12474

ALLIED-SIGNAL AEROSPACE CO., KANSAS CITY, MO.
An evaluation of field-flow fractionation for molecular weight characterization of polymeric materials
[DE92-019192] p 267 N93-11497
Design of a PCM data compressor
[DE92-019469] p 404 N93-11539
Analysis of plasma-treated wire insulation
[DE92-019471] p 291 N93-11643
Acid copper sulfate plating bath: Control of chloride and copper
[DE92-019473] p 249 N93-11644
High-frequency LSI contactor
[DE92-017285] p 292 N93-11916

AMES LAB., IA.
Internal friction peaks due to oxygen, nitrogen, and hydrogen in V-Nb alloys
[DE92-012155] p 254 N93-10995
Pulsed-field-gradient NMR investigations of hydrogen diffusion in ZrH(x)
[DE92-014393] p 459 N93-11238
Magnetic properties of high-T(c) superconductors
[DE92-018809] p 460 N93-11533
Development of strength and conductivity in deformation processed copper base alloys
[DE92-018807] p 257 N93-11572
Recrystallization of amorphous or nanocrystalline NdBa2Cu3O(7-x) and GdBa2Cu3O(7-x)
[DE92-016302] p 462 N93-11706
Stress dependence of the magnetic properties of steels
[DE92-018804] p 261 N93-12261

ANACAPA SCIENCES, INC., FORT RUCKER, AL.
Selective factors affecting rotary wing aviator performance with symbology superimposed on night vision goggles
[AD-A254983] p 390 N93-12508
An evaluation of crew coordination and performance during a simulated UH-60 helicopter mission
[AD-A254984] p 390 N93-12509

ANALYTICAL SERVICES AND MATERIALS, INC., HAMPTON, VA.
Micromechanical combined stress analysis: MICSTRAN, a user manual
[NASA-CR-189694] p 243 N93-12306
Probability density functions in turbulent channel flow
[NASA-CR-4454] p 202 N93-12399

ARGONNE NATIONAL LAB., IL.
Data archiving and analysis for CWDD
[DE92-017064] p 473 N93-11104
The domain structure features of epitaxial PbTiO3 thin films prepared by MOCVD
[DE92-010907] p 459 N93-11190
Results of advanced battery technology evaluations for electric vehicle applications
[DE92-018766] p 289 N93-11432
The efficient parallel iterative solution of large sparse linear systems
[DE92-018769] p 425 N93-11446
Alternating-phase focusing: A model to study nonlinear dynamics
[DE92-019027] p 431 N93-11511
Landau level quantization and superconductivity
[DE92-019028] p 460 N93-11512
Sealant research for solid oxide fuel cells
[DE92-019044] p 345 N93-11513
Some numerical results on best uniform polynomial approximation of chi(sup alpha) on interval (0,1)
[DE92-014859] p 426 N93-11520
Properties of hot isostatically pressed Bi(2)Sr(1.7)CaCu(2)O(x)
[DE92-016394] p 460 N93-11522
Reformers for the production of hydrogen from methanol and alternative fuels for fuel cell powered vehicles
[DE92-019300] p 274 N93-11550
Structure and property of heteroepitaxial TiO2/VO2 multilayers
[DE92-018181] p 460 N93-11563
Intermediate temperature electrolytes for SOFC
[DE92-018786] p 345 N93-11571
Cryostabilization of high-temperature superconducting magnets with subcooled flow in microchannels
[DE92-018174] p 431 N93-11598
Research and development of superconducting linear accelerators for neutral particle beam applications
[DE92-019043] p 444 N93-11652
Vehicle/guideway interaction in maglev systems
[DE92-019051] p 326 N93-11653
A study of parameters that influence growth and stability of the (Bi(1-x)Pb(x))2 Sr2Ca2Cu3O(y) phase
[DE92-015187] p 462 N93-11703
Multiphoton ionization and ion-pair formation in molecular hydrogen
[DE92-019026] p 438 N93-11829
Dynamic vacuum analysis for APS high heat flux beamline front ends using optical ray-tracing simulation methods
[DE92-019032] p 445 N93-11831
Ultrafast photoinduced electron transfer reactions in supramolecular arrays: From charge separation and storage to molecular switches
[DE92-016186] p 465 N93-12090
Comparison of passive-remote and conventional Fourier transform infrared systems for continuously monitoring incinerator emissions
[DE92-015225] p 355 N93-12098
Photodisintegration of the deuteron at high energy
[DE92-017066] p 445 N93-12108
Development of nondestructive evaluation methods and prediction of effects of flaws on the fracture behavior of structural ceramics
[DE92-016395] p 271 N93-12123
Disruption shape effects on the performance of enhanced tubes with the separation and reattachment mechanism
[DE92-016602] p 305 N93-12128
Flux dynamics and irreversibility in YBa2Cu3O7 with Y2BaCuO5 inclusions and in single crystal YBa2Cu3O7
[DE92-009712] p 467 N93-12178
Program for implementing software quality metrics
[DE92-018617] p 413 N93-12187
Influence of oxygen partial pressure and silver additions on microstructure and related properties of YBCO superconductors
[DE92-011145] p 468 N93-12249
Particle-jet interactions in an MHD second stage combustor
[DE92-016390] p 455 N93-12309
Ion beams as a means of deposition and in-situ characterization of thin films and thin film layered structures
[DE92-016397] p 469 N93-12310
The influence of the Prandtl number on the thermal performance of tubes with the separation and reattachment enhancement mechanism
[DE92-016601] p 306 N93-12313
Reduction in global warming due to fuel economy improvements and emissions control of criteria pollutants: New US light-duty vehicles (1968-1991)
[DE92-016636] p 356 N93-12314
Results from a large-scale MHD propulsion experiment
[DE92-018177] p 456 N93-12416

ARIZONA STATE UNIV., TEMPE.
Optimal output feedback vibration control of rotor-bearing systems p 324 N93-11220
Electronic structure and reactivities of transition metal clusters
[DE92-016623] p 258 N93-11762
Numerical study of advanced rotor blades
p 199 N93-11899

ARIZONA UNIV., TUCSON.
A submillimeter-millimeterwave study of the molecular gas in the nuclear regions of three nearby starburst galaxies p 484 N93-11260
A search for low-luminosity objects
[AD-A253301] p 483 N93-11750
Light scattering from a sphere on or near an interface
p 448 N93-12531

ARKANSAS UNIV., FAYETTEVILLE.
Biological conversion of synthesis gas culture development
[DE92-001279] p 375 N93-12482

ARMY ARMAMENT RESEARCH, DEVELOPMENT AND ENGINEERING CENTER, WATERVLIET, NY.
Multifractal analysis at negative q
[AD-A254370] p 413 N93-12159

ARMY CHEMICAL RESEARCH AND DEVELOPMENT CENTER, ABERDEEN PROVING GROUND, MD.
Fixed points of expansive analytic maps (2)
[AD-A254737] p 344 N93-12357

ARMY ELECTRONIC PROVING GROUND, FORT HUACHUCA, AZ.
Antenna pattern measurement facilities
[AD-A250219] p 283 N93-11764

ARMY ENGINEER TOPOGRAPHIC LABS., FORT BELVOIR, VA.
Global Climate Change (GCC) issues and their impacts on the US Army Corps of Engineers
[AD-A247279] p 353 N93-11466
Spatial data transformation: Feature attribute conversion issues and practical experience
[AD-A254238] p 477 N93-11741
Photogrammetric GIS technology: Feature mapping on digital stereo imagery
[AD-A254255] p 477 N93-11748
Automated extraction of aircraft runway patterns from radar imagery
[AD-A254258] p 218 N93-11751

ARMY LAB. COMMAND, FORT MONMOUTH, NJ.
Quartz crystal resonators and oscillators for frequency control and timing applications: A tutorial, revision 5.2
[AD-A254892] p 469 N93-12283

ARMY LAB. COMMAND, WATERTOWN, MA.
Surface analysis of Ln(2-x)Ce(x)CuO4 (Ln = Pr and Nd) single crystals grown by the top seeded solution method
[AD-A254905] p 469 N93-12286

ARMY LAB. COMMAND, WHITE SANDS MISSILE RANGE, NM.
Surface wind speed distributions
[AD-A253268] p 368 N93-11505
The sensitivity of the receiver coherence diameter and modulation transfer function to variations of a damp unstable atmosphere
[AD-A253269] p 363 N93-11785

ARMY MATERIEL SYSTEMS ANALYSIS ACTIVITY, ABERDEEN PROVING GROUND, MD.
Operating characteristic analysis for reliability growth programs
[AD-A254993] p 333 N93-12510

ARMY NATICK LABS., MA.
Progress on polymer degradation by photoelectron transfer
[AD-A246276] p 268 N93-11862

ARMY NATICK RESEARCH AND DEVELOPMENT COMMAND, MA.
The degradation of parachutes: Age and mechanical wear
[AD-A252243] p 200 N93-12179

ARMY RESEARCH INST. OF ENVIRONMENTAL MEDICINE, NATICK, MA.
Sustaining health and performance in the cold: Environmental medicine guidance for cold-weather operation
[AD-A254328] p 385 N93-12145

ASTRONAUTICS CORP. OF AMERICA, MILWAUKEE, WI.
A methodology to emulate and evaluate a productive virtual workstation p 395 N93-11938

AUBURN UNIV., AL.
Ion temperature measurements on field reversed configuration plasmas p 457 N93-12535

B

BALL CORP., BOULDER, CO.
Test program, helium II orbital resupply coupling
[NASA-CR-185681] p 326 N93-11650

BARRIOS TECHNOLOGY, INC., HOUSTON, TX.
Interactive collision detection p 400 N93-11963

Space Station robotics planning tools
p 331 N93-11975
BARRON ASSOCIATES, INC., STANDARDSVILLE, VA.
Active control of complex systems via dynamic (recurrent) neural networks
[AD-A254878] p 422 N93-12439
BATTELLE COLUMBUS LABS., OH.
Evaluation of multilayer mask concept for RESPO 21
[AD-A253392] p 389 N93-12079
BELGIAN AIR FORCE, BRUSSELS.
Allergy screening and follow-up in student pilots of the Belgian Air Force (BAF) p 383 N93-11316
BERTIN ET CIE, TARNOS (FRANCE).
Simplified modelling of soot inception and growth
[ETN-92-92266] p 246 N93-11361
BOEING CO., SEATTLE, WA.
Requirements Specification Language (RSL) and supporting tools
[NASA-CR-189700] p 405 N93-12345
Formal representation of the requirements for an Advanced Subsonic Civil Transport (ASCT) flight control system
[NASA-CR-189699] p 405 N93-12346
BOEING MILITARY AIRPLANE DEVELOPMENT, SEATTLE, WA.
Formal mechanization of device interactions with a process algebra
[NASA-CR-189644] p 405 N93-12347
Formal design specification of a Processor Interface Unit
[NASA-CR-189698] p 406 N93-12538
BONN UNIV. (GERMANY).
Sodium-lidar mesosphere examinations: Selected elements of the experimental construction of a mobile instrument and evaluation of the data acquired with a stationary Na-lidar during the DYANA campaign
[BONN-IR-91-78] p 357 N93-11006
Computer simulation and experimental investigation of the absorption cell for the rocketborne diode-laser experiment MASERATI
[BONN-IR-91-62] p 357 N93-11083
BOOZ-ALLEN AND HAMILTON, INC., ARLINGTON, VA.
Systems engineering and technical assistance in support of digital gallium arsenide insertion projects
[AD-A253751] p 463 N93-11790
BOSTON UNIV., MA.
The effects of magnetic storm phases on F-layer irregularities from auroral to equatorial latitudes
[AD-A253905] p 361 N93-11282
Visual perception of structure from motion
[AD-A253235] p 386 N93-11503
BRANDEIS UNIV., WALTHAM, MA.
Plasma properties of solar coronal active regions
p 489 N93-12342
BROOKHAVEN NATIONAL LAB., UPTON, NY.
The foxhole accelerating structure
[DE92-019052] p 443 N93-11429
Topics on RF beam control of a synchrotron
[DE92-019217] p 443 N93-11498
Analysis of periodic transient beam loading of the AGS
[DE92-019243] p 443 N93-11499
Scaling of gain with energy spread and energy in the PEP FEL
[DE92-019248] p 316 N93-11500
Frustrated phase separation and high temperature superconductivity
[DE92-019249] p 459 N93-11501
The potential effects of concurrent increases in temperature, CO2 and O3 on net photosynthesis, as mediated by rubisCO
[DE92-019411] p 374 N93-11630
RF beam loading in the Brookhaven AGS with booster injection
[DE92-019452] p 444 N93-11641
Strange quark matter
[DE92-016949] p 438 N93-11746
Static and transient beam loading of a synchrotron
[DE92-019244] p 445 N93-11776
Proposal for the experimental demonstration of the coherent radiation
[DE92-017695] p 284 N93-12132
Operating experience using venturi flow meters at liquid helium temperature
[DE92-014693] p 313 N93-12140
Enhanced convective and film boiling heat transfer by surface gas injection
[DE92-016755] p 306 N93-12221
BROWN UNIV., PROVIDENCE, RI.
Stochastic control and nonlinear estimation
[AD-A253543] p 420 N93-11147
Grain boundary transport and related processes in natural fine grained aggregates
[DE92-018239] p 461 N93-11682
Numerical investigation of three-dimensionally evolving jets p 303 N93-11870
Internal variables in the local-equilibrium approximation
[DE92-016854] p 471 N93-12102
BRUNEL UNIV., UXBRIDGE (ENGLAND).
Three-dimensional image structure in in-line Fraunhofer holography p 311 N93-11723
BUNDESANSTALT FUER FLUGSICHERUNG, FRANKFURT AM MAIN (GERMANY).
Activities report of the German Institute for Flight Safety
[ETN-92-92272] p 203 N93-11375
BUNDESMINISTERIUM FUER FORSCHUNG UND TECHNOLOGIE, BONN (GERMANY).
The Transall campaign. A contribution to the German ozone research program
[REPT-37/91] p 349 N93-11062

C

CALIFORNIA INST. OF TECH., PASADENA.
Development of stable metallization systems
[AD-A253569] p 264 N93-11079
On the dependence of the dynamic crack tip temperature fields in metal upon crack tip velocity and material parameters
[AD-A253657] p 335 N93-11219
Modeling regional seismic waves
[AD-A246894] p 361 N93-11421
Electron transfer rates at semiconductor/liquid interfaces
[DE92-018559] p 289 N93-11438
The conversion of plastic work to heat around a dynamically propagating crack in metals
[AD-A253801] p 258 N93-11782
CALIFORNIA STATE UNIV., SACRAMENTO.
The combustion time lag and its role in ramjet combustion instability p 245 N93-11137
CALIFORNIA STATE UNIV., SAN DIEGO.
Automatic cloud classification from multi-spectral satellite data
[AD-A255125] p 372 N93-12420
CALIFORNIA UNIV., BERKELEY.
A cryogenic phonon detector to search for dark matter particles p 481 N93-11198
Self-generated stochastic heating in an RF discharge
[DE92-018558] p 452 N93-11565
Some exact solutions of the equations of finite elasticity p 337 N93-11713
Theoretical studies of high-temperature superconductors and highly compressed hydrogen
p 292 N93-11833
Oscillations and concentrations in compressible and incompressible fluids
[AD-A254706] p 307 N93-12333
VLSI reliability research
[AD-A254883] p 295 N93-12360
CALIFORNIA UNIV., BERKELEY. LAWRENCE BERKELEY LAB.
Liquid-liquid equilibria in binary systems: Monte-Carlo simulation for calculating the effect of nonrandom mixing
[DE92-017020] p 263 N93-10972
Exploratory Research and Development Fund, FY 1990
[DE92-017002] p 489 N93-11078
A probabilistic approach to information retrieval in heterogeneous databases
[DE92-016993] p 473 N93-11151
Application of the Moyer method to transverse shielding of linear Bremsstrahlung sources
[DE92-017027] p 443 N93-11493
Induced gauge theories and W gravity
[DE92-011218] p 470 N93-11518
Studies of transition states and radicals by negative ion photodetachment
[DE92-017011] p 440 N93-11875
Silicon on insulator structures in selective epitaxial growth
[DE92-017118] p 465 N93-11915
Growth of 2-6 thin-films from single-source precursors based on sterically encumbered sitel ligands
[DE92-017077] p 466 N93-12099
Threshold photodetachment spectroscopy of negative ions
[DE92-017090] p 440 N93-12100
Stratospheric aircraft: Impact on the stratosphere?
[DE92-016997] p 355 N93-12104
Infrared phonon structure in epitaxial films of Tl2Ca2Ba2Cu3O10 at low temperatures
[DE92-017078] p 466 N93-12109
Density equalizing map projections: A new algorithm
[DE92-017088] p 413 N93-12110
Survey of composite particle models of electroweak interaction
[DE92-017110] p 441 N93-12111
Freely propagating open premixed turbulent flames stabilized by swirl
[DE92-017116] p 251 N93-12112
Image potential states at metal-dielectric interfaces
[DE92-017019] p 466 N93-12124
Submillimeter and microwave residual losses in epitaxial films of Y-Ba-Cu-O and BI-Ca-Ca-Cu-O
[DE92-017075] p 466 N93-12125
The diagnostics system for the multiple heavy ion beams induction linac experiment, MBE-4
[DE92-017109] p 445 N93-12126
Formation of buried epitaxial Si-Ge alloy layers in Si (100) crystal by high dose Ge ion implantation
[DE92-017114] p 466 N93-12127
Determination of Fe(sup 2+) and Fe(sup 3+) concentrations of semi-insulating InP:Fe
[DE92-017119] p 469 N93-12316
CALIFORNIA UNIV., DAVIS.
Development of a new plasma diagnostic of the critical surface and studies of the ion acoustic decay instability using collective Thomson scattering
[DE92-018508] p 453 N93-11730
Development of a new plasma diagnostic of the critical surface and studies of the ion acoustic decay instability using collective Thomson scattering
[DE92-018526] p 453 N93-11731
Computational nonlinear control
[AD-A253547] p 422 N93-12258
CALIFORNIA UNIV., IRVINE.
Metal slurry droplet and spray combustion
p 245 N93-11138
CALIFORNIA UNIV., LOS ANGELES.
Topics in high-intensity laser plasma interaction
p 450 N93-11191
The Kalman filter for two-dimensional stable and unstable atmospheres p 359 N93-11249
Beam-plasma interactions and radiation generation during the ejection of electron and ion beams in space
[AD-A253993] p 224 N93-11736
Oxidation, nitridation, and fluorine etching of Si
[AD-A253559] p 249 N93-11755
CALIFORNIA UNIV., SAN DIEGO, LA JOLLA.
Studies of ocean predictability at decade to century time scales using a global ocean general circulation model in a parallel competing environment
[DE92-019457] p 373 N93-11642
CALIFORNIA UNIV., SANTA BARBARA.
The synthesis and crystal structure of LaHSe2O6, a layered, anhydrous selenite
[AD-A251050] p 458 N93-10996
UCSB FEL user mode adaption project
[AD-A248734] p 316 N93-11418
Tetrahedral atom zincophosphate structures: Synthesis, crystal structure, and spectroscopic studies of (Zn(PO2(OC2H5)2)2)x, a one-dimensional inorganic polymer
[AD-A251051] p 437 N93-11560
Spacetime singularities in string theory
p 472 N93-12530
CALIFORNIA UNIV., SANTA CRUZ.
Application of the theory of wave propagation through random media to phase and amplitude fluctuations of seismic P-waves
[AD-A253274] p 363 N93-11788
Study of seismic coda generation in crust with non-uniform scattering and anelastic properties
[AD-A254350] p 366 N93-12270
CALSPAN-BUFFALO UNIV. RESEARCH CENTER, NY.
A preliminary study associated with the experimental measurement of the aero-optic characteristics of hypersonic configurations
[AD-A253792] p 200 N93-12063
CAMBRIDGE UNIV. (ENGLAND).
Ozone depletion and chlorine loading potentials
p 351 N93-11093
Impact ignition of liquid propellants
[AD-A252299] p 249 N93-11490
CAMERINO UNIV. (ITALY).
Vaccination against Hepatitis B: The Italian strategy
p 377 N93-11289
CARNEGIE-MELLON UNIV., PITTSBURGH, PA.
Deriving and manipulating module interfaces
[AD-A253869] p 406 N93-11145
A cognitive approach to the design of information graphics
[AD-A252692] p 474 N93-11353
Physical processes involved in injection and atomization of liquid propellants p 248 N93-11453
Research on a reconfigurable modular manipulator system
[DE92-018943] p 327 N93-11865
Self mobile space manipulator project
p 331 N93-11973
Decomposition of balanced matrices. Part 5: Goggles
[AD-A247462] p 430 N93-12217

CASE WESTERN RESERVE UNIV., CLEVELAND, OH.
Micromechanisms of deformation and fracture in aluminum based MMC's: Interface effects
[AD-A253560] p 259 N93-11850
CATERPILLAR TRACTOR CO., PEORIA, IL.
Development of wear resistant ceramic coatings for diesel engine components
[DE92-019068] p 268 N93-11654
CENTRO ITALIANO RICERCHE AEROSPAZIALI, NAPLES.
Numerical study for the study of medium speed internal noise problems
[DILC-EST-TN-200] p 432 N93-11156
Thermokinetic modelling and hypersonic flow
[DILC-EST-TN-218] p 196 N93-11157
Numerical and experimental results in vibroacoustical active control of structural elements with piezoelectric materials
[DILC-EST-TN-224] p 334 N93-11158
Automatic control laws for aircraft in parabolic flight
[DILC-EST-TR-211] p 214 N93-11160
Artificial intelligence and CFD: Expert systems for the design of airfoils and for grid generation
[DIGE-EST-TN-016] p 206 N93-11161
Wind tunnel operator aimed comparison between two electronic pressure scanner systems
[DLAS-EST-TR-040] p 217 N93-11225
CHICAGO UNIV., IL.
Participation in multilateral effort to develop high performance integrated CPC evacuated collectors
[DE92-015946] p 346 N93-11823
CINCINNATI UNIV., OH.
Computation of single solid particle impact on the target of ductile material to study the rebound characteristics of particle p 336 N93-11372
Erosion predictions and measurements of high-temperature coatings and superalloys used in turbomachines p 272 N93-12189
Mesoscopic effects in electronic microstructures
[AD-A254889] p 295 N93-12502
CITY COLL. OF THE CITY UNIV. OF NEW YORK, NY.
Magnetic properties and critical behavior of the conductivity near the M-I transition
[DE92-018948] p 461 N93-11629
Electronic transport and lasing in microstructures
[DE92-018725] p 441 N93-12115
Studies in premixed combustion
[DE92-018646] p 254 N93-12478
CITY UNIV. OF NEW YORK, NY.
Mode interaction models in near-wall turbulence
p 303 N93-11856
CIVIL AVIATION AUTHORITY, LONDON (ENGLAND).
UK airmisses involving commercial air transport, May-August 1991
[ETN-92-92260] p 203 N93-11357
UK airmisses involving commercial air transport, January-April 1991
[ETN-92-92261] p 298 N93-11358
CLARKSON UNIV., POTSDAM, NY.
The Third Potsdam-5 Kiev International Workshop on Nonlinear Processes in Physics
[AD-A249140] p 430 N93-11420
An experimental study of flow patterns and endwall heat transfer upstream of a surface-mounted rectangular obstruction in a turbulent boundary layer
p 302 N93-11698
CLEVELAND CLINIC FOUNDATION, OH.
Mass energy-transfer and mass energy-absorption coefficients, including in-flight positron annihilation for photon energies 1 keV to 100 MeV, 1992
[PB92-181106] p 438 N93-11715
CLIMATE ANALYSIS CENTER, WASHINGTON, DC.
Proceedings of the Sixteenth Annual Climate Diagnostics Workshop
[PB92-198803] p 370 N93-11896
COAST GUARD ACADEMY, NEW LONDON, CT.
LORAN and the effects of terrestrial propagation
[PB92-197219] p 205 N93-11472
COASTAL ENGINEERING RESEARCH CENTER, VICKSBURG, MS.
The Wave Information Studies (WIS) wave model, version 2.0 (user's guide)
[AD-A254313] p 374 N93-12094
COLORADO SCHOOL OF MINES, GOLDEN.
Computational aspects of Gaussian beam migration
[DE92-018641] p 431 N93-11567
Differential equation-based seismic data filtering
[DE92-016282] p 363 N93-11791
Infiltration kinetics and interfacial bond strength of metal matrix composites
[AD-A254002] p 240 N93-11795
Seismic wave propagation in thinly-layered media with steep reflectors
[DE92-015819] p 364 N93-12142
A dip-dependent divergence correction
[DE92-016283] p 366 N93-12308
Migration by the Kirchhoff, slant stack, and Gaussian beam methods
[DE92-018640] p 366 N93-12318
COLORADO STATE UNIV., FORT COLLINS.
Numerical and observational investigations of long-lived, MCS-induced, severe surface wind events: The derecho
p 367 N93-11159
The use of ARM data to test an improved parameterization of upper tropospheric clouds for use in climate models
[DE92-014353] p 367 N93-11237
Near-IR absorption spectra for the C70 fullerene anions
[AD-A253658] p 246 N93-11280
Optical properties of composite membranes containing arrays of nanoscopic gold cylinders
[AD-A253659] p 238 N93-11281
Studies of the role of clouds in CO2-induced climate change
[DE92-018648] p 353 N93-11569
Advanced electric propulsion research, 1991
[NASA-CR-190761] p 232 N93-11608
COLORADO UNIV., BOULDER.
Far ultraviolet spectrophotometry of hot stars and calibration standards in the far ultraviolet
p 482 N93-11373
COLUMBIA UNIV., NEW YORK, NY.
Interfacial and thin film chemistry in electron device fabrication
[AD-A253579] p 288 N93-11257
Object recognition with a robot hand
p 420 N93-11457
High beta and confinement studies on TFTR
[DE92-018647] p 452 N93-11568
Radiation physics, biophysics, and radiation biology
[DE92-013673] p 375 N93-12266
COMBUSTION INST., PITTSBURGH, PA.
The twenty-third International Symposium on combustion
[AD-A250377] p 250 N93-11866
COMMITTEE ON COMMERCE, SCIENCE, AND TRANSPORTATION (U.S. SENATE).
The Space Station Freedom and space launch issues
[S-HRG-102-762] p 225 N93-11908
CONNECTICUT UNIV., STORRS.
Crustal and upper mantle velocity gradients in the vicinity of the East Kazakh test site
[AD-A246889] p 362 N93-11740
Modified epoxy adhesives and primers
[AD-A253857] p 272 N93-12297
Auditory perception
[AD-A255061] p 385 N93-12465
CONTINUOUS ELECTRON BEAM ACCELERATOR FACILITY, NEWPORT NEW, VA.
Higher-order-mode damping and microwave absorption at 2 K
[DE92-016960] p 442 N93-11077
CORNELL UNIV., ITHACA, NY.
Experimental study of interactions of highly charged ions with atoms at keV energies
[DE92-019512] p 436 N93-11541
Studies of the 3 to 5 compounds in the megabar regime
[DE92-019517] p 461 N93-11646
Tradeoffs in implementing primary-backup protocols
[NASA-CR-190970] p 472 N93-12212
Synthesis and reactivity of siloxide and silamide complexes pertaining to bond breaking and aggregation phenomena
[AD-A254703] p 468 N93-12231
Composite tasking for sensor arrays
[AD-A254997] p 287 N93-12512
CORTANA CORP., FALLS CHURCH, VA.
Comparative effects of drag-reducing polymers. An experimental report
[AD-A254001] p 268 N93-11793
COUNCIL FOR NATIONAL ACADEMIC AWARDS (ENGLAND).
Near-infrared imaging polarimetry of bipolar nebulae
p 481 N93-11248
CRANFIELD INST. OF TECH., BEDFORD (ENGLAND).
The design and implementation of radar clutter modelling and adaptive target detection techniques
p 283 N93-11913
CREE RESEARCH, INC., DURHAM, NC.
High temperature rectifiers and MOS devices in 6H-silicon carbide
[AD-A254725] p 295 N93-12340
CRYOPHARM CORP., PASADENA, CA.
Freeze-dried human red blood cells
[AD-A253295] p 376 N93-11193

D

DANISH METEOROLOGICAL INST., COPENHAGEN.
Data report 92-1. Brorfelde Geomagnetic Observatory magnetic results, 1990 p 362 N93-11699
DARTMOUTH COLL., HANOVER, NH.
Excitons in semiconducting superlattices, quantum wells, and ternary alloys
[DE92-015178] p 464 N93-11894
DAYTON UNIV., OH.
Mechanical properties for advanced engine materials
[AD-A252632] p 242 N93-12181
Evaluation of alternatives for increasing A-7D rearward visibility
[AD-A255071] p 208 N93-12488
DAYTON UNIV. RESEARCH INST., OH.
Penetration mechanics of composites
[AD-A249230] p 240 N93-11835
DCW INDUSTRIES, LA CANADA, CA.
Progress in developing a transition model for high-speed flows p 301 N93-11615
DEACON RESEARCH, PALO ALTO, CA.
Hypersonic flow diagnostic development
[AD-A255045] p 202 N93-12466
DEFENCE AND CIVIL INST. OF ENVIRONMENTAL MEDICINE, NORTH YORK (ONTARIO).
Mechanisms of immune failure in burn injury
p 376 N93-11285
Asthma in aircrew: Assessment, treatment and disposition p 383 N93-11315
DEFENSE ADVANCED RESEARCH PROJECTS AGENCY, ARLINGTON, VA.
From pilot's associate to satellite controller's associate p 390 N93-11922
DELAWARE UNIV., NEWARK.
Energetics solids degradation in high temperature water
[AD-A254900] p 276 N93-12285
DEPARTMENT OF ENERGY, OAK RIDGE, TN.
Summaries of FY 1991 research in the chemical sciences
[DE92-011920] p 251 N93-12135
DEPARTMENT OF ENERGY, WASHINGTON, DC.
Reserves information gathering system user's guide
[DE92-018357] p 475 N93-11355
Federal Alternative Fuel Program light duty vehicle operation
[DE92-018124] p 274 N93-11794
DOE guideline: Guide to good practices for incorporating operating experiences
[DE92-017684] p 472 N93-12223
DEPARTMENT OF SCIENTIFIC AND INDUSTRIAL RESEARCH, LAUDER (NEW ZEALAND).
Ultraviolet radiation changes p 352 N93-11098
DEPARTMENT OF THE ENVIRONMENT, LONDON (ENGLAND).
Scientific assessment of ozone depletion: 1991
[NASA-TM-107976] p 350 N93-11087
DEPARTMENT OF THE NAVY, WASHINGTON, DC.
Short-range radar system
[AD-D015339] p 278 N93-11044
High energy cast explosives based on dinitropropylacrylate
[AD-D015340] p 273 N93-11045
Droppable jet vane TVC
[AD-D015341] p 214 N93-11046
Non-linear data conversion system for dynamic range digital signal processing
[AD-D015347] p 278 N93-11047
Fiber peel force measuring apparatus
[AD-D015349] p 309 N93-11048
Shutter apparatus
[AD-D015350] p 309 N93-11049
Ribless ram air parachute
[AD-D015351] p 195 N93-11050
Unequal stub length diplexing microwave frequency discriminator circuit
[AD-D015352] p 288 N93-11051
Fiber optic polishing system
[AD-D015353] p 446 N93-11052
High speed parallel backplane
[AD-D015372] p 288 N93-11053
Emittance measuring device for charged particle beams
[AD-D015371] p 442 N93-11060
Arbitrary waveform generator
[AD-D015346] p 280 N93-11354
Silver lined ceramic vessel and method of preparation
[AD-D015360] p 266 N93-11400
Payout tension control system for reel mounted cable
[AD-D015362] p 325 N93-11423
Inflatable device for excluding sea water from a rocket motor
[AD-D015365] p 232 N93-11424

Corrosion resistant chromate conversion coatings for heat-treated aluminum alloys
[AD-D015366] p 266 N93-11425
Method of steering the gain of a multiple antenna global positioning system receiver
[AD-D015367] p 281 N93-11426
Booster rocket range safety system
[AD-D015363] p 221 N93-11428
Energetic composites of cyclodextrin nitrate esters and nitrate ester plasticizers
[AD-D015364] p 274 N93-11665
Translating wedge heat sink
[AD-D015357] p 293 N93-12133

DETROIT DIESEL ALLISON, MI.
Engine testing of ceramic cam-roller followers
[DE92-019188] p 268 N93-11735

DEUTSCHE AGENTUR FUER RAUMFAHRTANGELEGENHEITEN G.M.B.H., BONN (GERMANY).
Automation and robotics for COLUMBUS: An implementation concept for the free flying laboratory (MTFF) p 331 N93-11974

DEUTSCHE FORSCHUNGSANSTALT FUER LUFT- UND RAUMFAHRT, COLOGNE (GERMANY).
Curing and mechanical properties of T800-V398 graphite/bismaleimide at different temperatures
[DLR-FB-92-02] p 237 N93-11143

DEUTSCHE FORSCHUNGSANSTALT FUER LUFT- UND RAUMFAHRT, GOETTINGEN (GERMANY).
On the instability of hypersonic flow past a pointed cone: Comparison of theoretical and experimental results of Mach 18
[DLR-FB-92-02] p 196 N93-11141

DEUTSCHE FORSCHUNGSANSTALT FUER LUFT- UND RAUMFAHRT, OBERPFAFFENHOFEN (GERMANY).
An evidential reasoning approach to the classification of satellite images
[DLR-FB-91-29] p 342 N93-11140

DEUTSCHE GEODAETISCHE KOMMISSION, MUNICH (GERMANY).
Object based multi-image matching
[SER-C-375] p 309 N93-11330
An approximate solution of the fixed gravimetric boundary value problem in the interior and the exterior of the Earth's body
[SER-C-379] p 361 N93-11331
Analysis of lunar laser ranging in the framework of a post-Newtonian theory
[SER-C-383] p 315 N93-11332
Ephemeris calculation and orbit determination of geostationary satellites, using Taylor series integration
[SER-C-384] p 220 N93-11335
Construction of a geodesic strapdown inertial navigation system for point determination
[SER-C-367] p 205 N93-11344
Statistical process for the automatic image analysis and its evaluation for object recognition and measurements
[SER-C-370] p 407 N93-11345
Photogrammetric point determination using digital imagery of three-line scanner systems
[SER-C-372] p 309 N93-11346

DEUTSCHE LUFTHANSA A.G., COLOGNE (GERMANY).
Activities report of Lufthansa
[ETN-92-92100] p 203 N93-11319

DEXTER CORP., PITTSBURGH, CA.
Phase transfer catalytic nucleophilic addition reactions: Synthesis of polymers and acetylenic terminated resins
[AD-A254717] p 272 N93-12337

DISTRICT OF COLUMBIA UNIV., WASHINGTON, DC.
A summer program in mathematics and computer science for academically oriented students, June 24 - July 26, 1991, Washington, DC
[AD-A249139] p 427 N93-12061

DIVISIONE AEREA STUDI RICERCHE E SPERIMENTAZIONI, PRATICA DI MARE (ITALY).
Dramatic reduction of meningococcal meningitis among military recruits in Italy after introduction of specific vaccination p 380 N93-11303
Clinical and immunological response to vaccination with parenteral or oral vaccines in two groups of 30 recruits
p 381 N93-11305
The screening of inhalant allergic diseases in the selection of candidates for aircraft piloting
p 382 N93-11312

DOMPE S.P.A., L'AQUILA (ITALY).
Cytokines as vaccine adjuvants: Interleukin 1 and its synthetic peptide 163-171 p 382 N93-11309

DOTY SCIENTIFIC, INC., COLUMBIA, SC.
Microtube strip heat exchanger
[DE92-018709] p 300 N93-11440

DRAPER (CHARLES STARK) LAB., INC., CAMBRIDGE, MA.
Air-breathing hypersonic vehicle guidance and control studies: An integrated trajectory/control analysis methodology, phase 2
[NASA-CR-189703] p 216 N93-12413

DREXEL UNIV., PHILADELPHIA, PA.
A study of the CO2 laser near threshold
p 316 N93-11720

DUKE UNIV., DURHAM, NC.
Synthesis and characterization of novel organogallium-phosphorus compounds: X ray crystal structures of Ph2GaP (SiMe3)2Ga (Ph2Cl, Ph2 (Cl)Ga.P (SiMe3)3, and Ph3Ga.P (SiMe3)3
[AD-A253841] p 462 N93-11724
Synthesis and characterization of novel aluminum-arsenic compounds 2. Crystal structures of (R2AlAs (SiMe3)2)2 (R = i-Bu, Me) and i-Bu2 (Cl)Al*As (SiMe3)3
[AD-A248001] p 467 N93-12175

DURHAM UNIV. (ENGLAND).
The aerodynamics of curved jets and breakaway in Coanda flares, volumes 1 and 2 p 304 N93-11881

DYNAMICS RESEARCH CORP., WILMINGTON, MA.
Development of the Personnel-based System Evaluation Aid (PER-SEVAL) performance shaping functions
[AD-A252820] p 386 N93-11779

E

EATON CORP., MILWAUKEE, WI.
Low cost humidity sensor
[PB92-205772] p 312 N93-11757

ECOLE CENTRALE DE LYON (FRANCE).
Simulation of compressible turbulent flows by a mixed finite element/finite volume method
[ETN-92-92267] p 299 N93-11362
A study of the wall-pressure fluctuations downstream of a blade-wall junction
[ECL-91-07] p 299 N93-11363
Contribution to the study of the anisotropic viscoelasticity of large strains: The case of the monocrystal
[ECL-90-29] p 460 N93-11573
Preparation of silicon oxynitride thin films by plasma chemical vapor deposition for chemical implantation. Application to a pH ISFET
[ECL-91-12] p 291 N93-11574
Resolution of the pressure equation by the boundary element method. Application to multistage turbomachines
[ECL-91-16] p 301 N93-11575
Active control of aeroacoustic couplings by means of adaptive systems
[ECL-91-18] p 214 N93-11576
Study and characterization of ceramic-metal bonds manufactured by solid state bonding techniques. Application to Ag/Al2O3
[ECL-91-19] p 267 N93-11577
Polyethylene-terephthalate/aluminum adhesion
[ECL-91-33] p 257 N93-11578
Crushing behavior of tubular structures in multi-materials
[ECL-91-37] p 336 N93-11579
Study of metal-ceramic interfaces of Co-Cr-Mo alloys: Role of tungsten (W) and manganese (Mn) additions
[ECL-92-01] p 267 N93-11580
Contribution to the monocrystal behavior study during large plastic strains
[ECL-92-13] p 461 N93-11581
Description of the structural responses in the medium-frequency range by an energetic formulation
[ECL-92-16] p 336 N93-11582
Programme and abstracts. Workshop on Expert Evaluation and Control of Compound Semiconductor Materials and Technologies No. 1: (EXAMTEC 199)
[AD-A254023] p 292 N93-12071

ECOLE NATIONALE SUPERIEURE DE MECANIQUE ET D'AEROTECHNIQUE, POITIERS (FRANCE).
Study of the dynamic degradation under the action of a shock wave induced by pulsed laser
p 319 N93-12037
Shock waves induced by pulsed laser in confined interaction: Numerical simulation p 319 N93-12038
Numerical simulation of a pressure gradient in a multilayer target: Temperature evolution
p 309 N93-12039

ECOLE NORMALE SUPERIEURE, LYON (FRANCE).
Dynamic programming on a ring of processors
p 410 N93-11479
Path planning on a ring of processors
p 410 N93-11480
Symmetric matrix-vector product on a ring of processors p 410 N93-11481
Scattering on a ring of processors
p 410 N93-11482
Z-buffer on a transputer-based machine
p 410 N93-11483
Reduction operations on a distributed memory machine with a reconfigurable interconnection network
p 410 N93-11484

ECOLE POLYTECHNIQUE, PALAISEAU (FRANCE).
Diagnostics and modeling of H(-) ion sources
[AD-A250664] p 440 N93-11867
The 1989 Scientific Report of the Laboratory for the Use of High Power Lasers
[ETN-92-92175] p 317 N93-12023
Stimulated Brillouin backscattering instability in the case of a high power laser: Application to wave pulsation particle acceleration experiments p 317 N93-12024
Observation and analysis of the Stokes and anti-Stokes components of stimulated Raman backscattering
p 318 N93-12025
Study of filamentation in subdense plasma interaction experiments p 318 N93-12026
X-UV spectroscopy temporal resolution
p 318 N93-12028
Interpretation of experiments measuring the back face of thin aluminum strips by comparison with numerical simulations p 318 N93-12029
Hydrodynamic efficiencies in implosion experiments
p 308 N93-12030
Electron acceleration in a relativistic electron plasma wave p 319 N93-12033
Low pressure gas multiphotoionization for wave packet experiments p 319 N93-12034
Laser material interaction in confined medium
p 319 N93-12035
Absorption spectroscopy of L(alpha, beta) transitions in a laser germanium plasma p 320 N93-12041
Saturation effects in absorption spectroscopy of the K(alpha) rays of aluminum p 254 N93-12042
Modeling for the study of an X laser in a recombination plasma; gain calculations at 105.7 and 154.6 A
p 321 N93-12046
Direct radiative recombination of atomic ions
p 321 N93-12048
Hydrodynamic study of multilayer targets by spatial and temporal resolution shadow spectroscopy
p 254 N93-12050
Activity of the technical groups (LULI Palaiseau, France) p 322 N93-12052

EDGERTON, GERMESHAUSEN AND GRIER, INC., IDAHO FALLS, ID.
Development of an intelligent system for cooling rate and fill control in GMAW
[DE92-017849] p 326 N93-11548
The influence of processing atmosphere on twin-roll melt-spinning of aluminum alloys
[DE92-017895] p 257 N93-11595
A development approach for nuclear thermal propulsion
[DE92-018020] p 232 N93-11596
Particle-fluid two-phase flow modeling
[DE92-017847] p 301 N93-11637
Quaternary volcanism, tectonics, and sedimentation in the Idaho National Engineering Laboratory area
[DE92-017851] p 362 N93-11692

EG AND G ENERGY MEASUREMENTS, INC., IDAHO FALLS.
Surface reconstruction of a three-dimensional ultrasonic flaw
[DE92-018029] p 332 N93-11154
Operator's guide for VAXGAP, a gamma-ray spectrum analysis package
[DE92-019096] p 407 N93-11356
A gas-cooled cermet reactor system for planetary base power
[DE92-018017] p 443 N93-11433
Ultrasonic sensing of GMAW: Laser/EMAT defect detection system
[DE92-017916] p 333 N93-12055
Tutorial on nuclear thermal propulsion safety for Mars
[DE92-017946] p 233 N93-12056
Laboratory testing of the electrosource traction battery
[DE92-017993] p 292 N93-12057
Overview of property formulations for helium, nitrogen, lithium, and lithium-lead in ATHENA/MOD1 with comparison of calculated properties to measured properties
[DE92-017995] p 471 N93-12058
Comprehensive computational model for thermal plasma processing
[DE92-018015] p 454 N93-12066
Numerical simulation of alumina spraying in argon-helium plasma jet
[DE92-017859] p 455 N93-12092
Electric and hybrid vehicle program, site operator program
[DE92-018055] p 328 N93-12114
Nuclear fuels for very high temperature applications
[DE92-018021] p 446 N93-12129
A design of experiment study of plasma sprayed alumina-titania coatings
[DE92-017877] p 271 N93-12168

A Taguchi experimental design study of twin-wire electric arc sprayed aluminum coatings
[DE92-018022] p 262 N93-12494

EG AND G ENERGY MEASUREMENTS, INC., LAS VEGAS, NV.
Curve fitting and error modeling for the digitization process near the Nyquist rate
[DE92-018189] p 286 N93-12417

EG AND G ROCKY FLATS, INC., GOLDEN, CO.
Thermal stress and strain analysis in traveling autogenous welds
[DE92-019363] p 326 N93-11556
The effects of chemistry on weld profiles in partial and full penetration welds
[DE92-016865] p 327 N93-11679
Calculation of binary phase diagrams between the actinide elements, rare earth elements, and transition metal elements
[DE92-019119] p 249 N93-11801
The effect of precipitate forming elements in Al 4.5 percent Mg alloys on the measured acoustic emission and on Lueders band deformation
[DE92-016864] p 465 N93-12073

EIC, INC., NORWOOD, MA.
Fast electrochromic switching for optical hardening applications
[AD-A248174] p 447 N93-11186
Long cycle life rechargeable lithium batteries
[NASA-CR-190937] p 291 N93-11604

EIDGENOESSISCHE TECHNISCHE HOCHSCHULE, ZURICH (SWITZERLAND).
Space flight and immune system p 376 N93-11284

ELECTRO-OPTICAL SCIENCES, INC., IRVINGTON, NY.
Multiangle lidar performance in the presence of horizontal inhomogeneities in atmospheric extinction and scattering
[AD-A252882] p 371 N93-12167
Laser Doppler experiments
[AD-A252883] p 287 N93-12461

ELORET CORP., PALO ALTO, CA.
Solution of nonlinear flow equations for complex aerodynamic shapes
[NASA-CR-190979] p 307 N93-12329

ELORET CORP., SUNNYVALE, CA.
Theoretical research program to study chemical reactions in AOTV bow shock tubes
[NASA-CR-188927] p 439 N93-11851

ENERGETICS, INC., COLUMBIA, MD.
Proceedings of the DOE/Advanced Heat Exchangers Program Review
[DE92-014385] p 305 N93-12070

ENVIRONMENTAL PROTECTION AGENCY, WASHINGTON, DC.
Allowance system: Proposed acid rain rule
[PB92-226174] p 356 N93-12524
United States/Canada Air Quality Agreement
[PB92-228030] p 356 N93-12525
Office of Wetlands, Oceans, and Watersheds publications
[PB92-224310] p 480 N93-12528

ENVIRONMENTAL SCIENCE AND ENGINEERING, INC., GAINESVILLE, FL.
Physical effects of vegetation on wind-blown sand in the coastal environments of Florida
[PB92-188424] p 354 N93-11702

ETALON, INC., BOSTON, MA.
Resonant membrane spatial light modulators
[AD-A253893] p 252 N93-12186

EUROCONSULT, PARIS (FRANCE).
The European space industry. Overall situation: Situation and prospects for the 23 leading companies concerned
p 472 N93-11163

EUROPEAN SPACE AGENCY, PARIS (FRANCE).
Using SGML in a large organization
[ESA-STR-234] p 476 N93-11583
Evaluation of transportation systems for advanced space flight missions
[ESA-TT-1256] p 223 N93-11685

EUROPEAN SPACE AGENCY. ESRIN, FRASCATI (ITALY).
ERS-1 user handbook
[ESA-SP-1148] p 344 N93-12280

EUROPEAN SPACE AGENCY. EUROPEAN SPACE RESEARCH AND TECHNOLOGY CENTER, ESTEC, NOORDWIJK (NETHERLANDS).
ESIS: An introduction to the European space information system. A modern tool for space scientists
[ESA-INT-2] p 479 N93-12404

EXECUTIVE OFFICE OF THE PRESIDENT, WASHINGTON, DC.
Publications of the Executive Office of the President, 20 January 1989 - 31 March 1992
[PB92-154913] p 477 N93-11769

EXOS, INC., BURLINGTON, MA.
EXOS research on master controllers for robotic devices p 399 N93-11957

F

FEDERAL AVIATION ADMINISTRATION, ATLANTIC CITY, NJ.
High Capacity Voice Recorder (HCVR) Operational Test and Evaluation (OT/E) integration test report
[DOT/FAA/CT-TN92/30] p 310 N93-11460
Upgrade Precision Runway Monitor (PRM) Operational Test and Evaluation (OT/E) test plan
[DOT/FAA/CT-TN92/13] p 217 N93-11616
Controller evaluation of initial data link terminal air traffic control services: Mini study 2, volume 1
[DOT/FAA/CT-92/2-VOL-1] p 205 N93-11704
Controller evaluation of initial data link terminal air traffic control services: Mini study 2, volume 2
[DOT/FAA/CT-92/2-VOL-2] p 205 N93-11705
Low Density Radio Communications Link (LDRCL) Operational Test and Evaluation (OT/E) integration and operation test plan
[DOT/FAA/CT-TN92/4] p 285 N93-12331

FEDERAL AVIATION ADMINISTRATION, CAMBRIDGE, MA.
Design of instrument approach procedure charts: Comprehension speed of missed approach instructions coded in text or icons
[PB92-205673] p 204 N93-11252
Magneto-optic imaging inspection of selected corrosion specimens
[DOT/FAA/CT-TN92/20] p 332 N93-11617

FEDERAL AVIATION ADMINISTRATION, WASHINGTON, DC.
Summary of findings from the PIREP-based analyses conducted during the 1988 to 1990 evaluations of TDWR-based and TDWR/LLWAS-based alert services provided to landing/departing pilots
[AD-A253859] p 367 N93-11144
Comparisons of molecular sieve oxygen concentrators for potential medical use aboard commercial aircraft
[AD-A253648] p 387 N93-11279
Future FAA telecommunications plan
[AD-A249133] p 283 N93-11760

FEDERAL COORDINATING COUNCIL FOR SCIENCE, ENGINEERING AND TECHNOLOGY, WASHINGTON, DC.
Advanced materials and processing: The Federal program in materials science and technology. A report by the FCCSET Committee on Industry and Technology to supplement the President's fiscal year 1993 budget
[PB92-199108] p 238 N93-11470

FERMI NATIONAL ACCELERATOR LAB., BATAVIA, IL.
A computer algorithm for automatic beam steering
[DE92-019338] p 411 N93-11555

FLORIDA INST. OF TECH., MELBOURNE.
Studies of a laser/nuclear thermal hardened body armor
[AD-A255128] p 390 N93-12423

FLORIDA STATE UNIV., TALLAHASSEE.
Analysis of air and sea physical properties and surface fluxes using a combination of in situ and SEASAT data
p 365 N93-12182

FLORIDA UNIV., GAINESVILLE.
Land use/land cover classification using digitally merged spot panchromatic and Landsat thematic mapper imagery
[PB92-188416] p 343 N93-11701
Physical effects of vegetation on wind-blown sand in the coastal environments of Florida
[PB92-188424] p 354 N93-11702
An analytic description of thick-wall bubbles
[DE92-016465] p 432 N93-11759
Development of ultra-low noise, high sensitivity planar metal grating coupled AlGaAs/GaAs multiquantum well IR detectors for focal plane array staring IR sensor systems
[AD-A254697] p 468 N93-12228

G

GENERAL ACCOUNTING OFFICE, WASHINGTON, DC.
Information dissemination: Case studies on electronic dissemination at four agencies. Fact sheet for the Chairman, Committee on Governmental Affairs, US Senate
[GAO/IMTEC-92-6FS] p 474 N93-11274

GENERAL ATOMIC CO., SAN DIEGO, CA.
Scaling of lower hybrid current drive with temperature
[DE92-016541] p 449 N93-10988
Direct electron absorption of fast waves on the D3-D tokamak
[DE92-016254] p 449 N93-11041
Thermal analysis and design of polarizer mirrors for waveguides in the D3-D tokamak
[DE92-018884] p 451 N93-11382
Fusion programs in applied plasma physics
[DE92-019639] p 452 N93-11660
A model for analytical performance prediction of hypervapotron
[DE92-018885] p 305 N93-12010
Helium transport studies on D3-D
[DE92-016251] p 455 N93-12307

GENERAL PHYSICS CORP., CAPE CANAVERAL AFS, FL.
Pressure vessel burst test program
[AD-A253708] p 334 N93-11080

GEORGETOWN UNIV., WASHINGTON, DC.
Studies of safety, infectivity, and immunogenicity of a new Temperature Sensitive (TS) 51-1 strain of S. typhi as a new live oral typhoid fever vaccine candidate
p 381 N93-11306
Epidemiologic view of allergic diseases in North America: Implications for aerospace medicine
p 382 N93-11311

GEORGIA INST. OF TECH., ATLANTA.
Numerical analysis of right-half plane zeros for a single-link manipulator
[NASA-CR-190966] p 426 N93-11547
Frequency response in short thermocouple wires
[NASA-CR-190943] p 310 N93-11612
A theory for the analysis of rotorcraft operating in atmospheric turbulence p 207 N93-11725
Formic acid: Development of an analytical method and use as process indicator in anaerobic systems
[AD-A250668] p 253 N93-12267
A vision-based end-point control for a two-link flexible manipulator
[NASA-CR-190967] p 330 N93-12521

GEORGIA TECH RESEARCH INST., ATLANTA.
LV software support for supersonic flow analysis
[NASA-CR-190209] p 297 N93-11074

GEORGIA UNIV., ATHENS.
High energy hadron-hadron collisions
[DE92-018253] p 441 N93-12224

GKSS-FORSCHUNGSZENTRUM GEESTHACHT (GERMANY).
Microstructure and mechanical properties of reactive hot isostatic pressed TiAl powder material
[GKSS-91/E/60] p 256 N93-11336
Titanium-aluminides by hot isostatic pressing of cold extruded titanium-aluminium powder mixtures
[GKSS-91/E/67] p 256 N93-11337
Orbital perturbations due to the albedo effect
[GKSS-91/E/59] p 220 N93-11348
Detection of cloud-top height from backscattered radiances within the oxygen A band. Part 1: Theoretical study
[GKSS-91/E/76-PT-1] p 368 N93-11349
Detection of cloud-top height from backscattered radiances within the oxygen A band. Part 2: Measurements
[GKSS-91/E/77-PT-2] p 368 N93-11350

GLASGOW UNIV. (SCOTLAND).
The convection speed of the dynamic stall vortex
[AD-A247258] p 197 N93-11464
Applications of star complexes in group theory
p 485 N93-11879

GRUMMAN AEROSPACE CORP., BETHPAGE, NY.
Remote systems development p 330 N93-11971

H

HAHN-MEITNER-INST. FUER KERNFORSCHUNG, BERLIN (GERMANY).
Radiation damage by high energy electrons in GaAs: A DLTS (deep level transient spectroscopy) examination
[HMI-B-494] p 442 N93-11028

HAMILTON STANDARD DIV., UNITED AIRCRAFT CORP., WINDSOR LOCKS, CT.
Submarine Advanced Integrated Life Support system (SAILS) program
[AD-A253564] p 388 N93-11812

HARVARD SCHOOL OF PUBLIC HEALTH, BOSTON, MA.
Analysis of disease progression from clinical observations of US Air Force active duty members infected with the Human Immunodeficiency Virus: Distribution of AIDS survival time from interval censored observations
p 379 N93-11297

HARVARD UNIV., CAMBRIDGE, MA.
Quasigeostrophic vortices in zonal shear
p 358 N93-11226
The effects of luminance boundaries on color perception
[AD-A250705] p 384 N93-11841

HAWAII UNIV., HONOLULU.
Physical characterization of magmatic liquids
[DE92-015931] p 363 N93-11848

HELLENIC AIR FORCE GENERAL HOSPITAL, ATHENS (GREECE).
Allergic and nonallergic rhinitis in Greek pilots p 383 N93-11317
Correlation of serum alpha sub 1 antitrypsin with cigarette smoking and pulmonary function status in Greek pilots, for a ten year period p 384 N93-11318

HELSINKI UNIV. OF TECHNOLOGY, ESPOO (FINLAND).
International ADI-Seminar: Austempered Ductile Iron [PB92-180660] p 256 N93-11244

HELSINKI UNIV. OF TECHNOLOGY, OTANIEMI (FINLAND).
Numerical investigations into the base drag of various wedges using the base flow model developed by Mauri Tanner [REPT-B-36] p 202 N93-12414
DYNAC: A computer program for analyzing the dynamical stability of aircraft [REPT-B-31] p 216 N93-12415

HONEYWELL, INC., MINNEAPOLIS, MN.
Engineering Information System (EIS) [AD-A254013] p 476 N93-11508
A state-based approach to trend recognition and failure prediction for the Space Station Freedom p 230 N93-11925

HOPITAL D'INSTRUCTION DES ARMEES, PARIS (FRANCE).
Immunization of personnel traveling to a destination in tropical countries: French position p 380 N93-11304

HOWARD UNIV., WASHINGTON, DC.
Rapid maneuvering of large flexible orbiting systems p 225 N93-11885
Growth of solid solutions of aluminum nitride and silicon carbide by metalorganic chemical vapor deposition [AD-A255000] p 254 N93-12518

HUMAN ENGINEERING LABS., ABERDEEN PROVING GROUND, MD.
System for generating dynamic video imagery for human factors research [AD-A248675] p 388 N93-11743

I

IAP RESEARCH, INC., DAYTON, OH.
Railgun armature velocity improvement, SBIR phase 2 [AD-A254749] p 222 N93-12505

IDAHO NATIONAL ENGINEERING LAB., IDAHO FALLS.
The collaborative program of research in engineering sciences [DE92-016838] p 490 N93-12477

IIT RESEARCH INST., LANHAM, MD.
Study and recommendation of available sources of scientific and technical numeric databases in the government and private sector [AD-A247266] p 475 N93-11465

ILLINOIS UNIV., CHICAGO.
The generalized Goursat-Riemann problem for plane waves in isotropic elastic solids p 340 N93-12199

ILLINOIS UNIV., URBANA.
Selective carbon oxygen bond scission during reactions of oxygenates on single crystal catalysts [DE92-018687] p 247 N93-11439
VUV and UV sources and spectroscopic applications [AD-A247293] p 291 N93-11758
VLSI design for reliability [AD-A253207] p 292 N93-11781
Publication of papers presented at URSI 23rd General Assembly as a special section of radio science [AD-A253561] p 283 N93-11811
Nanophase ceramics [AD-A254661] p 272 N93-12246

ILLINOIS UNIV., URBANA-CHAMPAIGN.
A real-time diagnostic and performance monitor for UNIX [NASA-CR-190975] p 404 N93-11462
Automatic data partitioning on distributed memory multicomputers [NASA-CR-190976] p 418 N93-11651
Performance evaluation and modeling techniques for parallel processors [NASA-CR-190974] p 419 N93-12395
Measurement and analysis of operating system fault tolerance [NASA-CR-190973] p 406 N93-12540
Simulation and analysis of support hardware for multiple instruction rollback [NASA-CR-190972] p 406 N93-12541

ILLINOIS UNIV. AT URBANA-CHAMPAIGN, SAVOY.
Lidar studies of gravity waves in the mesopause region p 358 N93-11222
Thermal non-Newtonian elastohydrodynamic lubrication of line contacts under sliding-rolling and simple sliding conditions p 324 N93-11263
Dynamics of planetary waves in the atmosphere p 363 N93-11898
Nuclear magnetic resonance microscopy: New theoretical and technical developments p 313 N93-11907
An experimental study of the relationship between forces and moments and vortex breakdown on a pitching delta wing p 208 N93-12206
A trainable image pattern classification system for detection of damaged soybean seeds p 201 N93-12208
Fundamental analysis of the tomographic imaging system for reconstructing ionospheric distributions p 365 N93-12209

INDIANA UNIV., BLOOMINGTON.
A Polytropic solar model p 487 N93-11264

INSTITUT D'AERONOMIE SPATIALE DE BELGIQUE, BRUSSELS.
Reinterpretation of ozone data from Base Roi Baudouin (Antarctica) [AERONOMICA-ACTA-A-365] p 352 N93-11127

INSTITUT NATIONAL POLYTECHNIQUE, GRENOBLE (FRANCE).
Dynamic programming and image processing on distributed memory parallel machines [ETN-92-92174] p 409 N93-11478

INSTITUTE FOR COMPUTER APPLICATIONS IN SCIENCE AND ENGINEERING, HAMPTON, VA.
Domain decomposition: A bridge between nature and parallel computers [NASA-CR-189709] p 425 N93-11246
Review of preconditioning methods for fluid dynamics [NASA-CR-189712] p 198 N93-11607
Concurrent file operations in a high performance FORTRAN [NASA-CR-189711] p 412 N93-11618
Fully nonlinear development of the most unstable goertler vortex in a three dimensional boundary layer [NASA-CR-189710] p 301 N93-11633
A general introduction to aeroacoustics and atmospheric sound [NASA-CR-189717] p 435 N93-12021
Singularities of the Euler equation and hydrodynamic stability [NASA-CR-189720] p 306 N93-12173
Spurious modes in spectral collocation methods with two non-periodic directions [NASA-CR-189713] p 427 N93-12298
An advancing front Delaunay triangulation algorithm designed for robustness [NASA-CR-189719] p 416 N93-12400
Static assignment of complex stochastic tasks using stochastic majorization [NASA-CR-189716] p 416 N93-12403

INSTITUTE FOR DEFENSE ANALYSES, ALEXANDRIA, VA.
Integrity in automated information systems [AD-A253990] p 477 N93-11732
Integrity-oriented control objectives: Proposed revisions to the Trusted Computer System Evaluation Criteria (TCSEC), DOD 5200.28-STD [AD-A253989] p 404 N93-11809
Research and development strategies for human centered and group support technologies [AD-A254366] p 472 N93-12273
The effects of wearing protective chemical warfare combat clothing on human performance [AD-A250716] p 390 N93-12491

INSTITUTE OF ENERGY ECONOMICS OF JAPAN.
Environmental problems and trends of international responses, 2 [DE92-531118] p 355 N93-11846

INSTITUTE OF SOUND AND VIBRATION RESEARCH, SOUTHAMPTON (ENGLAND).
Wavefront reconstruction using a least squares approach [ISVR-TR-203] p 435 N93-12324

INTERFACE AND CONTROL SYSTEMS, WEST MELBOURNE, FL.
Spacecraft attitude control using a smart control system p 230 N93-11932

INTERNATIONAL CENTRE FOR THEORETICAL PHYSICS, TRIESTE (ITALY).
Hydrodynamic fluctuations and light scattering in hot electron gas of semiconductors [DE92-622800] p 458 N93-10992
Critical currents in polycrystalline YBa2Cu3O(7-x): Self-field and grain size dependence [DE92-617540] p 459 N93-11076
An isomorphism for algebra of distributions with compact support on Lie groups [DE92-603605] p 427 N93-12176

INTERUNIVERSITY MICRO-ELECTRONICS CENTER, LEUVEN (BELGIUM).
Back-gate bias generator [AD-A255126] p 295 N93-12421

IOWA STATE UNIV. OF SCIENCE AND TECHNOLOGY, AMES.
Numerical solution of inverse problems in mechanics using the boundary element method p 424 N93-11199
Application of the boundary element method to elastic wave scattering problems in ultrasonic nondestructive evaluation p 332 N93-11209
Ultrasonic flaw classification and sizing p 333 N93-12533

IOWA UNIV., IOWA CITY.
Determination of stepsize parameters for intermolecular vibrational energy transfer [DE92-010770] p 435 N93-11189
Computational dynamics of high-speed flexible multibody systems p 338 N93-11891
Final Technical Report [AD-A253529] p 284 N93-12083
Meta-analysis of integrity tests: A critical examination of validity generalization and moderator variables [AD-A254681] p 386 N93-12225
Flow in curved ducts of varying cross-section [AD-A254660] p 306 N93-12245

ISTITUTO SUPERIORE DI SANITA, ROME (ITALY).
HIV variability and perspectives of a vaccine p 378 N93-11294

ISX CORP., WESTLAKE VILLAGE, CA.
Manager's assistant systems for space system planning p 398 N93-11952

J

JACKSON (HENRY M.) FOUNDATION, WASHINGTON, DC.
Relating cognitive function to military aviator performance in early HIV infection p 379 N93-11298

JACKSON STATE UNIV., MS.
An iconic query interface for an image database [AD-A253571] p 475 N93-11506
Application of machine learning techniques for effective retrieval in image database [AD-A254907] p 479 N93-12287

JET PROPULSION LAB., CALIFORNIA INST. OF TECH., PASADENA.
INAS hole-immobilized doping superlattice long-wave-infrared detector [NASA-CASE-NPO-17880-1-CU] p 458 N93-11056
The adaptive neuron model: An architecture for the rapid learning of nonlinear topological transformations [NASA-CASE-NPO-18579-1-CU] p 420 N93-11174
Terminal slider control of nonlinear robotic systems [NASA-CASE-NPO-18584-1-CU] p 324 N93-11177
The Comet Halley archive: Summary volume [NASA-CR-190358] p 484 N93-11243
Overcharge and overdischarge protection of ambient temperature secondary lithium cells [NASA-CASE-NPO-18343-1-CU] p 290 N93-11456
Mappings between codewords of two distinct (N,K) Reed-Solomon codes over GF(2 sup J) [NASA-CASE-NPO-18771-1-CU] p 412 N93-11664
A model-based reasoning approach to sensor placement for monitorability p 391 N93-11923
Intelligent data management for real-time spacecraft monitoring p 394 N93-11936
Operator assistant to support deep space network link monitor and control p 268 N93-11939
A new scheme of force reflecting control p 399 N93-11960
An 8-DOF dual-arm system for advanced teleoperation performance experiments p 400 N93-11964
Performance experiments with alternative advanced teleoperator control modes for a simulated solar maximum satellite repair p 400 N93-11965
Decision rules for spaceborne operations planning p 403 N93-11978
Backward assembly planning with DFA analysis [NASA-CASE-NPO-18817-1-CU] p 278 N93-12202

JOHNS HOPKINS UNIV., BALTIMORE, MD.
Laboratory and numerical studies of dynamical processes related to thermal convection in the Earth's mantle p 364 N93-11900
Effect of microstructure on passive film formation and breakdown on Al alloys [AD-A245863] p 260 N93-12118
Parameters for predicting red tides of bioluminescent dinoflagellates: Meteorological events and frontal water circulation patterns [AD-A254835] p 374 N93-12431

JOHNS HOPKINS UNIV., COLUMBIA, MD.
The 28th JANNAF Combustion Subcommittee Meeting, volume 1 [CPIA-PUBL-573-VOL-1] p 244 N93-11132
The 28th JANNAF Combustion Subcommittee Meeting, volume 2 [CPIA-PUBL-573-VOL-2] p 247 N93-11448

JOINT INST. FOR LAB. ASTROPHYSICS, BOULDER, CO.
State-resolved dynamics of ion-molecule collisions in a flowing afterglow
[AD-A247288] p 436 N93-11467

JOINT PUBLICATIONS RESEARCH SERVICE, ARLINGTON, VA.
JPRS report: Science and technology. Central Eurasia: *Space. Development of Soviet spacecraft for manned missions*
[JPRS-USP-92-003] p 224 N93-11162
JPRS report: Science and technology. Central Eurasia: Engineering and equipment
[JPRS-UEQ-92-009] p 220 N93-11169

K

KAMAN SCIENCES CORP., COLORADO SPRINGS, CO.
Algorithms for sensor fusion: Decentralized Bayesian hypothesis testing with feedback, volume 1
[AD-A254633] p 414 N93-12242

KANSAS UNIV., LAWRENCE.
Research in heavy-ion nuclear physics
[DE92-015099] p 443 N93-11521
Linear and geometrically nonlinear p-version three dimensional curved shell element for isotropic, generally orthotropic and laminated composite materials
p 339 N93-12194

KAUPPA-JA TEOLLISUUSMINISTERIO, HELSINKI (FINLAND).
LIEKKI and JALO: Combustion and fuel conversion
[DE92-540921] p 349 N93-12446

KENT UNIV., CANTERBURY (ENGLAND).
Statistical methods for the comparison of spatial patterns in meteorological variables p 370 N93-11997

KENTUCKY UNIV., LEXINGTON.
Synthesis of single phase (alpha)-Fe, Fe3C and Fe7C3 nano-particles by CO2 laser pyrolysis technique
[DE92-015654] p 250 N93-11847
Laser spectroscopy and dynamics of transient species formed in pyrolysis reactions
[DE92-016206] p 251 N93-12091

KERNFORSCHUNGSZENTRUM G.M.B.H., KARLSRUHE (GERMANY).
Fracture behavior of polymers at cryogenic temperatures
[KFK-4969] p 265 N93-11203

L

LAWRENCE LIVERMORE NATIONAL LAB., CA.
Molecular cytogenetics: A novel approach for measuring chromosome translocations in individuals years after exposure to low levels of ionizing radiation
[DE92-018066] p 374 N93-10974
X ray diagnostic techniques in ICF
[DE92-018069] p 449 N93-10975
Development of a geometry-compensated neutron time-of-flight detector for ICF applications with approximately 200 ps time response
[DE92-018024] p 450 N93-11153
A synopsis of resistive wall effects in very short wavelength free electron lasers
[DE92-018065] p 315 N93-11155
Operating characteristics of a 7.6 mm (0.30 inch) diameter two-stage light-gas gun
[DE92-018783] p 217 N93-11447
High energy x ray imaging diagnostic on Nova
[DE92-018067] p 451 N93-11495
Three dimensional and 2D simulation of an expanding plasma using a Darwin hybrid particle code
[DE92-019095] p 451 N93-11516
Review of phonon behavior and microstructural development leading to martensitic transformations in Ni(x)Al(100-x) alloys
[DE92-014782] p 256 N93-11519
Nova Upgrade: A proposed ICF facility to demonstrate ignition and gain, revision 1
[DE92-018960] p 451 N93-11534
The intensity of knock in an internal combustion engine: An experimental and modeling study
[DE92-019504] p 326 N93-11540
High frame-rate, large field wavefront sensor
[DE92-019547] p 310 N93-11542
Laser glasses
[DE92-018061] p 267 N93-11549
Preparation, optical and laser properties of Nd-doped sol-gel silica
[DE92-019378] p 461 N93-11602
Computation of small scale velocity turbulence and its effect on optical scintillations and stimulated thermal Rayleigh scattering
[DE92-018934] p 448 N93-11627
Temporal scattering and response software users' manual, version 2 and 3
[DE92-040934] p 282 N93-11632
High bandwidth second-harmonic generation in partially deuterated KDP
[DE92-019505] p 452 N93-11645
Flux pinning in oxygen-depleted YBa2Cu3O(7-y) single crystals
[DE92-019548] p 461 N93-11647
Experimental studies of x ray laser spectral profiles: Observation of gain narrowing and saturation behavior
[DE92-019603] p 316 N93-11659
Radio pill antenna range test
[DE92-019903] p 282 N93-11661
Prediction of electromagnetic pulse generation by picosecond avalanches in high-pressure air
[DE92-019382] p 282 N93-11675
Modeling the dispersion of tracer plumes in the Colorado front range boundary layer during night- and day-time conditions
[DE92-019384] p 354 N93-11676
The role of refrigerants in climate change
[DE92-019385] p 354 N93-11677
Atmospheric reactive nitrogen: A model study of natural and anthropogenic sources and the role of microbial soil emissions
[DE92-010717] p 354 N93-11744
Progress toward x ray lasing between autoionizing transitions
[DE92-017428] p 317 N93-11765
Some remarks on shell element analysis with DYNA3D and NIKE3D
[DE92-018784] p 337 N93-11775
Bremsstrahlung absorption in plasmas
p 321 N93-12047
A ring coded-aperture microscope for high-resolution imaging of high-energy x rays
[DE92-018004] p 454 N93-12059
Plasma temperatures from first-hit neutron time-of-flight spectra
[DE92-018006] p 454 N93-12060
Superconducting multilayer structures grown by ALL-MBE
[DE92-018011] p 465 N93-12065
The adsorption of C60 and the co-adsorption of C60 and H2O on (alpha)-Al2O3 (1 -1 0 2)-(2x1)
[DE92-018002] p 465 N93-12093
Ultra-wideband generators
[DE92-018026] p 293 N93-12113
Reflection masks for soft x ray projection lithography
[DE92-014779] p 293 N93-12121
Higher-order generic functions for CLOS
[DE92-013447] p 413 N93-12137
LINK user manual
[DE92-017987] p 479 N93-12143
Visualizing wind velocities by advecting cloud textures
[DE92-014717] p 371 N93-12154
Real-time classification of signals from three-component seismic sensors using neural nets
[DE92-014886] p 364 N93-12155
Dynamic multimodal function optimization using genetic algorithms
[DE92-019602] p 414 N93-12234
Inert gas electric heater for elevated temperature testing of small propulsion components
[DE92-017434] p 221 N93-12317

LEHIGH UNIV., BETHLEHEM, PA.
Reliability of small geometry VLSI devices for microelectronics
[AD-A247355] p 289 N93-11414
Nanostructure, defect chemistry and properties of relaxor ferroelectrics
[AD-A247294] p 431 N93-11468

LINCOM CORP., LOS ANGELES, CA.
Space Station communications and tracking systems modeling and RF link simulation
[NASA-CR-185684] p 288 N93-12519

LOCKHEED ENGINEERING AND SCIENCES CO., HAMPTON, VA.
Tension and compression fatigue response of unnotched 3D braided composites
[NASA-CR-189678] p 239 N93-11611

LOCKHEED ENGINEERING AND SCIENCES CO., HOUSTON, TX.
Astronaut candidate strength measurement using the Cybex 2 and the LIDO Multi-Joint 2 dynamometers
[NASA-CR-185679] p 389 N93-12195
Methodology issues concerning the accuracy of kinematic data collection and analysis using the ariel performance analysis system
[NASA-CR-185689] p 389 N93-12211

LOCKHEED MISSILES AND SPACE CO., PALO ALTO, CA.
An accurate and efficient method to calculate the rate of single event upsets from the LET spectrum and SEU cross section test results
[AD-A253917] p 290 N93-11492
Superplastic forming of ceramic insulation
p 228 N93-12452

LOCKHEED MISSILES AND SPACE CO., SUNNYVALE, CA.
Acoustic fill factors for a 120 inch diameter fairing
[NASA-CR-189284] p 434 N93-11634

LORAL SPACE AND RANGE SYSTEMS, SUNNYVALE, CA.
Mission Control Center enhancement opportunities in the 1990's p 396 N93-11942

LOS ALAMOS NATIONAL LAB., NM.
Diffusion of Echo 7 electron beams during bounce motion
[DE92-018288] p 357 N93-10985
A linear and nonlinear study of Mira
[DE92-011265] p 483 N93-10993
Evaluation of a Cray performance tool using a large hydrodynamics code
[DE92-013239] p 407 N93-11231
Are some of the luminous high-latitude stars accretion-powered runaways?
[DE92-018853] p 484 N93-11379
Destruction of explosives and rocket fuels by supercritical water oxidation
[DE92-018874] p 274 N93-11380
Status and prospects for Hot Dry Rock (HDR) in the US
[DE92-018876] p 345 N93-11381
Beam-loading stability in synchrotrons with a higher RF harmonic
[DE92-018982] p 443 N93-11510
Geostationary-satellite beacon-receiver array for studies of ionospheric irregularities
[DE92-018979] p 362 N93-11535
Detonation reactions frozen by free expansion and analyzed by mass spectrometry
[DE92-018605] p 274 N93-11566
Measurement of AC electrical characteristics of SSC superconducting dipole magnets
[DE92-018888] p 431 N93-11625
Reactant gas flow fields in advanced PEM (Proton Exchange Membrane) fuel cell designs
[DE92-018897] p 345 N93-11626
Monte Carlo simulations of the supernova ejection mechanism for the runaway stars
[DE92-018367] p 485 N93-11695
Statistics of IMF B(z) events
[DE92-018372] p 488 N93-11696
Mechanism for ejecting stars from the Galactic plane
[DE92-018375] p 485 N93-11697
BANSHEE: High-voltage repetitively pulsed electron-beam driver
[DE92-017413] p 444 N93-11763
Numerical analysis of the flow fields in a RQL gas turbine combustor
[DE92-017509] p 302 N93-11767
Calibration techniques for high flux x ray detectors
[DE92-017513] p 312 N93-11768
Identification and estimation of sources of transmitted variation
[DE92-015246] p 429 N93-11820
High-speed test station for solid-state imagers
[DE92-018990] p 312 N93-11822
Prospects for the commercial development of hot dry rock geothermal energy in New Mexico
[DE92-018999] p 346 N93-11825
Hydrodynamic particle migration in small-amplitude, oscillatory, circular couette flow: The limits of reversibility
[DE92-008480] p 303 N93-11843
Synthesis of nanocrystalline powders for oxide ceramics by microwave plasma pyrolysis
[DE92-017410] p 268 N93-11861
High-precision thorium RIMS for geochemistry
[DE92-017405] p 250 N93-11918
On some practical consideration of the electron beam breakup transit time oscillator
[DE92-017406] p 445 N93-11919
Performing a successful audience analysis: How to improve your proposal-writing skills
[DE92-018978] p 479 N93-12068
High-speed FPS vidicon camera
[DE92-018989] p 313 N93-12069
The development of a one microsecond pulse length, repetitively pulsed, high power modulator, and a long-pulse electron beam diode for the production of intense microwaves
[DE92-015974] p 293 N93-12089
Models of volcanic eruption hazards
[DE92-013432] p 364 N93-12136

Milliwatt Generator Project
[DE92-015348] p 294 N93-12156
Laser-ablation processes
[DE92-011226] p 322 N93-12250
Influence of strain rate on the structure/property behavior of the alpha-2 alloy Ti-24.5Al-10.5Nb-1.5Mo
[DE92-008490] p 261 N93-12256
Foil optimization for low energy neutral atom imaging
[DE92-013435] p 365 N93-12263
Low energy neutral atom imaging
[DE92-013531] p 365 N93-12264

LOUGHBOROUGH UNIV. OF TECHNOLOGY (ENGLAND).
Colliding plane gravitational waves with colinear polarization
[MATHS-REPT-A-160] p 357 N93-11120
Equivalence transformations of rational matrices
[MATHS-REPT-A-163] p 423 N93-11121
Remarks on the Robinson-Trautman solutions
[MATHS-REPT-A-167] p 423 N93-11122
Constrained KP hierarchy and bi-Hamiltonian structures
[MATHS-REPT-A-168] p 424 N93-11123
Equivalence transformations of rational matrices and applications
[MATHS-REPT-A-169] p 424 N93-11124
On a certain McMillan degree condition appearing in control
[MATHS-REPT-A-170] p 424 N93-11125
Darboux theorems and Wronskian formulas for integrable systems. 1: Constrained KP flows
[MATHS-REPT-A-172] p 424 N93-11126
Optimized software for a generalized Polak-Ribiere algorithm in unconstrained optimization
[MATHS-REPT-A-156] p 406 N93-11210
Preconditioned low-order Newton methods
[MATHS-REPT-A-159] p 425 N93-11211
An investigation of ground access mode choice for departing passengers
[TT-9201] p 217 N93-11224
Inverse spectral transform for the 2 + 1-dimensional Gardner equation
[MATHS-REPT-A-138] p 425 N93-11323
Airport stand assignment model
[TT-9104] p 218 N93-11728

LOUISIANA STATE UNIV., BATON ROUGE.
An adaptive differencing scheme for elliptic flows
p 297 N93-11197

M

MAINE UNIV., ORONO.
Nonlinear response of thin steel plate structures subjected to static, cyclic, and dynamic loads
p 335 N93-11200

MARQUETTE UNIV., MILWAUKEE, WI.
A methodology to emulate and evaluate a productive virtual workstation p 395 N93-11938

MARTIN MARIETTA ENERGY SYSTEMS, INC., OAK RIDGE, TN.
Information systems planning leading to performance support systems
[DE92-018745] p 475 N93-11441
Microwave sintering of multilayer ceramic capacitors
[DE92-018772] p 267 N93-11570

MARTIN MARIETTA SPACE SYSTEMS, INC., DENVER, CO.
Manned Mars System Study (MMSS): Mars transportation and facility study. Volume 1: Executive Summary
[NASA-CR-184473] p 227 N93-12442
Manned Mars System Study (MMSS): Mars transportation and facility infrastructure study. Volume 2: Technical report
[NASA-CR-184474] p 227 N93-12443

MARYLAND UNIV., COLLEGE PARK.
Coordinated action in 3-D space
[AD-A249830] p 387 N93-10994
An iterative method for distributed database design
p 474 N93-11255
Geographic information system to support state-wide hydrologic modeling with the SCS-TR-20
[PB92-185768] p 476 N93-11700
Performance of the h-p version of the finite element method with various elements
[AD-A250689] p 427 N93-11837
Research on stimulated Raman scattering with applications to atmospheric lidar p 322 N93-12163
Adaptive neural network models for intelligent computations
[AD-A254689] p 421 N93-12226
The Fourth Workshop on Dynamics and Aeroelastic Stability Modeling of Rotorcraft Systems
[AD-A255065] p 208 N93-12485
Interannual variabilities of the East Asian summer monsoon and tropical sea surface temperatures
p 372 N93-12534
Experiments and analysis concerning the use of external burning to reduce aerospace vehicle transonic drag
p 235 N93-12537

MASSACHUSETTS GENERAL HOSPITAL, BOSTON.
Center of Excellence in laser medicine
[DE92-018760] p 384 N93-11445
High resolution tomographic instrument development
[DE92-017314] p 313 N93-11828

MASSACHUSETTS INST. OF TECH., CAMBRIDGE.
Synthesis and side chain liquid crystal polymers by living ring opening metathesis polymerization. 5: Influence of mesogenic group and interconnecting group on the thermotropic behavior of the resulting polymers
[AD-A253568] p 264 N93-11150
Synthesis of side chain liquid crystal polymers by living ring opening metathesis polymerization. Report 3: Influence of molecular weight, interconnecting unit and substituent on the mesomorphic behavior of polymers with laterally attached mesogens
[AD-A248698] p 265 N93-11187
Synthesis of side chain liquid crystal polymers by living ring opening metathesis polymerization. Report 2: Influence of molecular weight, polydispersity, and flexible spacer length (n=9-12) on the thermotropic behavior of the resulting plymers
[AD-A248700] p 265 N93-11188
Experimental and theoretical investigation of high gradient acceleration
[DE92-015299] p 315 N93-11278
Direct catalytic decomposition of nitric oxide
[DE92-018759] p 247 N93-11444
Investigation of a cesium Raman time/frequency standard
[AD-A252677] p 310 N93-11562
Deep penetration into frictional ductile and brittle materials
[PB92-205566] p 338 N93-11903
Experimental measurement and theoretical modeling of microwave scattering and the structure of the sea surface influencing radar observations from space
[NASA-CR-190998] p 343 N93-12006
Controlled synthesis of polyenes by catalytic methods
[DE92-015286] p 271 N93-12165
Super auditory localization for improved human-machine interfaces
[AD-A254699] p 389 N93-12229
The effects of aluminum oxide on inertial welding of aluminum in space applications
[AD-A255100] p 329 N93-12274
Study of residual stresses and microcracks in high strength steel weldments: An investigation of microcrack formation and stressed growth using laser microscopy
[AD-A255059] p 342 N93-12467
The collaborative program of research in engineering sciences
[DE92-016838] p 490 N93-12477

MASSACHUSETTS UNIV., AMHERST.
The millimeter wave Cloud Profiling Radar System (CPRS)
[DE92-016970] p 366 N93-10971
Probing flame chemistry with MBMS, theory, and modeling
[DE92-011433] p 251 N93-12119
Regular and chaotic mixing of viscous fluids in eccentric rotating cylinders p 305 N93-12157
Optical generation, control and sensing of millimeter waves
[AD-A254700] p 285 N93-12230
Medium energy nuclear physics research
[DE92-016972] p 442 N93-12444

MATERIALS RESEARCH LABS., MELBOURNE (AUSTRALIA).
Characterization of deflagrating munitions by rotating prism high speed photography
[MRL-TR-91-43] p 311 N93-11648

MAX-PLANCK-INST. FUER PHYSIK UND ASTROPHYSIK, GARCHING (GERMANY).
Non-self-similar clustering of galaxies
[MPE-PREPRINT-212] p 484 N93-11338
A multi-line study of the molecular interstellar medium on M82's starburst nucleus
[MPE-PREPRINT-213] p 484 N93-11347
Tori and chaos in a nonlinear dynamo model for solar activity
[MPE-PREPRINT-218] p 488 N93-11351
Plasma measurements in magnetospheric tail
[MPE-233] p 361 N93-11352
Contributions to the Joint Discussion 3: Results from Rosat and GRO and Other Recent High Energy Astrophysics Missions of the Max-Planck-Institut fuer Extraterrestrische Physik
[MPE-PREPRINT-215] p 482 N93-11473
Rosat deep surveys p 482 N93-11474
X ray morphology of clusters of galaxies
p 482 N93-11475
Morphology and physics of supernova remnants
p 482 N93-11476
Stars in the Rosat all-sky survey p 482 N93-11477

MCAT INST., SAN JOSE, CA.
Study of optical techniques for the Ames unitary wind tunnels. Part 4: Model deformation
[NASA-CR-190980] p 219 N93-12349

MCCRONE ASSOCIATES, INC., WESTMONT, IL.
Thin-sectioning and analysis of fine-grained meteoritic materials
[NASA-CR-185693] p 485 N93-11546

MCDONNELL-DOUGLAS SPACE SYSTEMS CO., HOUSTON, TX.
Intelligent fault management for the Space Station active thermal control system p 391 N93-11930
Fuzzy control system for a remote focusing microscope p 314 N93-11934
Methodologies for building robust schedules
p 397 N93-11949

MCDONNELL-DOUGLAS SPACE SYSTEMS CO., HUNTINGTON BEACH, CA.
Distributed environmental control p 391 N93-11924

MEMPHIS STATE UNIV., TN.
Questioning mechanisms during complex learning
[AD-A247382] p 386 N93-11415

MESSERSCHMITT-BOELKOW-BLOHM G.M.B.H., MUNICH (GERMANY).
Flow field calculations around the Hermes spaceplane during reentry phase
[MBB-UK-0148-91-PUB] p 195 N93-11008
Project and test of a reconfigurable multiple feed system in C-band
[MBB-UK-0162-92-PUB] p 278 N93-11009
Erosion mechanisms in ceramic structures
[MBB-UK-0171-92-PUB] p 263 N93-11011
Corrosion protection of materials for aircraft using ion beam processes. Corrosion and bonding strength examinations. Physical analysis of laser composition
[MBB-Z-0405-91-PUB] p 255 N93-11026
Surface protection in the aircraft industry
[MBB-Z-0432-92-PUB] p 255 N93-11027

MESSERSCHMITT-BOELKOW-BLOHM G.M.B.H., OTTOBRUNN (GERMANY).
Development trends in space transportation systems: From Hermes to Saenger
[MBB-UK-0146-91-PUB] p 223 N93-11007
A contribution to fatigue failure morphologies in fiber reinforced plastics
[MBB-Z-0212-91-PUB] p 263 N93-11010

MIAMI UNIV., FL.
Feasibility assessment of a transient sound sensor based on the silicon retina architecture
[AD-A252288] p 432 N93-10999

MICHIGAN STATE UNIV., EAST LANSING.
An interlayer shear slip theory for composite laminates with nonrigid bonding p 237 N93-11229
The use of high-frequency dynamic information for the evaluation of damage in fiber reinforced composite materials p 241 N93-11998
Stochastic models of wavefront propagation in random granular media
[AD-A255127] p 286 N93-12422

MICHIGAN TECHNOLOGICAL UNIV., HOUGHTON.
Environment-induced embrittlement: Stress corrosion cracking and metal-induced embrittlement; environmental embrittlement of iron aluminide alloys
[DE92-018714] p 256 N93-11524
Crashworthy characteristics of circular tubes in axisymmetric buckling p 337 N93-11721

MICHIGAN UNIV., ANN ARBOR.
Workshop on Surface Science and Technology
[AD-A253566] p 264 N93-11149
An inversion technique to recover lower thermospheric winds from space-borne remote measurements of (OI) 5577 A p 369 N93-11839
New techniques for positron emission tomography in the study of human neurological disorders
[DE92-015353] p 384 N93-11673

MIDWEST RESEARCH INST., GOLDEN, CO.
Microscopic origins of metastable effects in a-Si:H and deep defect characterization in a-Si,Ge:H alloys
[DE92-010588] p 463 N93-11813
Electricity from biomass: A development strategy
[DE92-010590] p 346 N93-11814
Recombination and metastability in amorphous silicon and silicon germanium alloys
[DE92-010593] p 463 N93-11816
Research on stable, high-efficiency, amorphous silicon multijunction modules
[DE92-010599] p 464 N93-11818
Alternative Fuel Evaluation Program: Alternative Fuel Light Duty Vehicle Project. Data collection responsibilities, techniques, and test procedures
[DE92-010598] p 275 N93-12171

MINISTRY OF WATER, LANDS AND NATURAL RESOURCES, LUSAKA (ZAMBIA).
Proceedings of the First Seminar on Geographic Information Systems in Zambia
[PB92-207125] p 477 N93-11789

MINNESOTA MINING AND MFG. CO., SAINT PAUL.
Advanced heat pump for the recovery of volatile organic compounds
[DE92-011592] p 303 N93-11774

MISSISSIPPI STATE UNIV., MISSISSIPPI STATE.
Potassium D-line fitting for investigation of MHD boundary layers
[DE92-019020] p 454 N93-11826
A distributed data acquisition and centralized data reduction system for flexible and efficient measurements
[DE92-019021] p 312 N93-11827
A comparison of velocity profile measurements in the CDIF diffuser with flow field model calculations
[DE92-015367] p 304 N93-11995
Overview of recent diagnostic measurements at the USA MHD facilities
[DE92-015365] p 454 N93-12087
The role of advanced optical diagnostics in monitoring and controlling an MHD power plant. Part 2: 50 MW(t), POC topping cycle
[DE92-015368] p 455 N93-12141
An investigation of error correcting techniques for OMV and AXAF
[NASA-CR-190950] p 416 N93-12515

MISSOURI UNIV., ROLLA.
Molecular mobility of the interface in a model composite: A NMR study
[AD-A253311] p 265 N93-11194
New acceleration potential method for supersonic unsteady aerodynamics of lifting surfaces, further extension of the nonplanar supersonic doublet point method, and nonlinear, nongradient optimized rational function approximations for supersonic, transient response unsteady aerodynamics p 201 N93-12344

MITRE CORP., BEDFORD, MA.
A genetic algorithm for search route planning
[AD-A254894] p 414 N93-12284
Real-time adaptive sidelobe canceller architectures and implementations
[AD-A254842] p 286 N93-12433

MITRE CORP., MCLEAN, VA.
Global change and the dark of the moon
[AD-A255181] p 486 N93-12380

MOTOREN- UND TURBINEN-UNION MUENCHEN G.M.B.H. (GERMANY).
Increase of energy use on cooled high temperature turbine, phase 3
[MTUM-B91EW-0029-PHASE-3] p 213 N93-11339

MOUND LAB., MIAMISBURG, OH.
Hot-wire vs laser, is there a difference?
[DE92-019337] p 310 N93-11554

N

N RAY ENGINEERING CO., INC., SAN DIEGO, CA.
Feasibility of using neutron radiography to inspect the Space Shuttle solid rocket booster aft skirt, forward skirt and frustum. Part 1: Summary report
[NASA-CR-184357] p 231 N93-11173

NATIONAAL INST. VOOR KERNFYSICA EN HOGE ENERGIEFYSICA, AMSTERDAM (NETHERLANDS).
Nucleon structure functions from deep inelastic muon scattering
[NIKHEF-H+K/92-01] p 442 N93-11130
Using the 16 viewscreens during commissioning of AmPS
[NIKHEF-K/AMPS/92-01] p 442 N93-11131

NATIONAL ACADEMY OF SCIENCES - NATIONAL RESEARCH COUNCIL, WASHINGTON, DC.
The search for life's origins: Progress and future directions in planetary biology and chemical evolution
[NASA-CR-190929] p 487 N93-11603
Solid state sciences committee forum
[AD-A253556] p 463 N93-11753
Computer Science and Telecommunications Board summary of activities
[DE92-016467] p 404 N93-11761

NATIONAL AERONAUTICS AND SPACE ADMINISTRATION, WASHINGTON, DC.
Scientific assessment of ozone depletion: 1991
[NASA-TM-107976] p 350 N93-11087
Payload advisory panel recommendations
[NASA-TM-108012] p 219 N93-11528
ICCG-10: Tenth International Conference on Crystal Growth. Poster presentation abstracts
[NASA-CR-190920] p 461 N93-11683
ICCG-10: Tenth International Conference on Crystal Growth. Oral presentation abstracts
[NASA-CR-190919] p 461 N93-11684
A comprehensive mission to planet Earth: Woods Hole Space Science and Applications Advisory Committee Planning Workshop
[NASA-TM-108011] p 343 N93-11878

NATIONAL AERONAUTICS AND SPACE ADMINISTRATION. AMES RESEARCH CENTER, MOFFETT FIELD, CA.
Employment of radicals and excited state species for supersonic combustion photochemical ignition of premixed hydrogen/oxygen mixtures with ArF laser
p 245 N93-11135
The structures, binding energies and vibrational frequencies of Ca3 and Ca4: An application of the CCSD(T) method p 439 N93-11852
Connected triple excitations in coupled-cluster calculations of hyperpolarizabilities: Neon
p 439 N93-11854
Habitat automation p 391 N93-11976
Effect of hemorrhage on cardiac output, vasopressin, aldosterone, and diuresis during immersion in men
[NASA-TM-103949] p 374 N93-12014
Techniques for optimal crop selection in a controlled ecological life support system
[NASA-TM-103950] p 388 N93-12018
An overview of gravitational physiology
[NASA-TM-102849] p 391 N93-12319
Integration of radar altimeter, precision navigation, and digital terrain data for low-altitude flight
[NASA-TM-103958] p 205 N93-12320
Estimation of photosynthetic capacity using MODIS polarization: 1988 proposal to NASA Headquarters
[NASA-TM-103945] p 344 N93-12351
Reusable thermal protection system development: A prospective p 227 N93-12448
Advanced ceramic matrix composites for TPS
p 228 N93-12450

NATIONAL AERONAUTICS AND SPACE ADMINISTRATION. GODDARD SPACE FLIGHT CENTER, GREENBELT, MD.
The NASA/National Space Science Data Center trapped radiation environment model program, 1964 - 1991
[NASA-TM-107993] p 349 N93-11003
Ozone and temperature trends p 350 N93-11089
Stratospheric processes: Observations and interpretation p 351 N93-11091
Tropospheric processes: Observations and interpretation p 351 N93-11092
Future chlorine-bromine loading and ozone depletion
p 352 N93-11095
Predicted aircraft effects on stratospheric ozone
p 352 N93-11096
Predicted rocket and shuttle effects on stratospheric ozone p 352 N93-11097
Eddy current characterization of magnetic treatment of materials
[NASA-TM-104573] p 258 N93-11621
The early Earth Observing System reference handbook: Earth Science and Applications Division missions, 1990-1997
[NASA-TM-107963] p 343 N93-11663
Nimbus-7 Scanning Multichannel Microwave Radiometer (SMMR) PARM tape user's guide
[NASA-RP-1284] p 373 N93-11718
Directory interchange format manual, version 4.0
[NASA-TM-107991] p 478 N93-11911
An expert system for diagnosing environmentally induced spacecraft anomalies p 230 N93-11927
Advanced mechanisms for robotics
p 330 N93-11969
National Space Science Data Center data archive and distribution service (NDADS) automated retrieval mail system user's guide
[NASA-TM-107990] p 479 N93-12150
Advanced two-phase heat transfer systems
p 229 N93-12459

NATIONAL AERONAUTICS AND SPACE ADMINISTRATION. HUGH L. DRYDEN FLIGHT RESEARCH FACILITY, EDWARDS, CA.
Aerothermal test results from the second flight of the Pegasus booster
[NASA-TM-4391] p 296 N93-10969
Flight-determined stability analysis of multiple-input-multiple-output control systems
[NASA-TM-4416] p 214 N93-11178
Overview of supersonic laminar flow control research on the F-16XL ships 1 and 2
[NASA-TM-104257] p 196 N93-11221
Correlation of forebody pressures and aircraft yawing moments on the X-29A aircraft at high angles of attack
[NASA-TM-4417] p 197 N93-11532
A rule-based system for real-time analysis of control systems
[NASA-TM-104258] p 277 N93-11619
Flight test results from a supercritical mission adaptive wing with smooth variable camber
[NASA-TM-4415] p 207 N93-11863
A summary of the forebody high-angle-of-attack aerodynamics research on the F-18 and the X-29A aircraft
[NASA-TM-104261] p 202 N93-12353

NATIONAL AERONAUTICS AND SPACE ADMINISTRATION. JOHN F. KENNEDY SPACE CENTER, COCOA BEACH, FL.
Debris/ice/TPS assessment and integrated photographic analysis for Shuttle Mission STS-46
[NASA-TM-107552] p 223 N93-12151

NATIONAL AERONAUTICS AND SPACE ADMINISTRATION. LYNDON B. JOHNSON SPACE CENTER, HOUSTON, TX.
Compositional analysis and classification of projectile residues in LDEF impact craters
[NASA-TM-104750] p 488 N93-11374
The locator system for wandering individuals
[NASA-TM-104754] p 388 N93-11649
Fifth Annual Workshop on Space Operations Applications and Research (SOAR 1991), volume 1
[NASA-CP-3127-VOL-1] p 391 N93-11921
Fuzzy logic control for camera tracking system
p 314 N93-11935
On the acquisition and representation of procedural knowledge p 394 N93-11937
The development and technology transfer of software engineering technology at NASA. Johnson Space Center
p 396 N93-11943
System diagnostic builder p 396 N93-11944
Knowledge-based system V and V in the Space Station Freedom program p 396 N93-11945
COMPASS: An Ada based scheduler
p 397 N93-11950
Effects of spatially displaced feedback on remote manipulation tasks p 400 N93-11966
An integrated dexterous robotic testbed for space applications p 330 N93-11972
Role of automation in the ACRV operations
p 230 N93-11977
Thermal protection systems manned spacecraft flight experience p 227 N93-12449

NATIONAL AERONAUTICS AND SPACE ADMINISTRATION. LANGLEY RESEARCH CENTER, HAMPTON, VA.
Recent advances in multidisciplinary optimization of rotorcraft
[NASA-TM-107665] p 206 N93-10968
Tests of an alternate mobile transporter and extravehicular activity assembly procedure for the Space Station Freedom truss
[NASA-TP-3245] p 224 N93-10970
Method of remotely characterizing thermal properties of a sample
[NASA-CASE-LAR-13508-3-CU] p 216 N93-11057
Semi-interpenetrating polymer network for tougher and more microcracking resistant high temperature polymers
[NASA-CASE-LAR-13925-2] p 264 N93-11059
Thermal residual stresses in silicon-carbide/titanium (0/90) laminate
[NASA-TM-107649] p 236 N93-11072
Source gases: Concentrations, emissions, and trends
p 350 N93-11088
Heterogeneous processes: Laboratory, field, and modeling studies p 350 N93-11090
Radiative forcing of climate p 351 N93-11094
Winds of change: Expanding the frontiers of flight. Langley Research Center's 75 years of accomplishment, 1917-1992
[NASA-NP-130] p 490 N93-11100
Ignition delays, heats of combustion, and reaction rates of aluminum alkyl derivatives as used as ignition and combustion enhancers for supersonic combustors
p 244 N93-11134
Atlas of albedo and absorbed solar radiation derived from Nimbus 7 earth radiation budget data set, November 1985 to October 1987
[NASA-RP-1281] p 367 N93-11168
Correction techniques for depth errors with stereo three-dimensional graphic displays
[NASA-TP-3244] p 206 N93-11170
A problem formulation for glideslope tracking in wind shear using advanced robust control techniques
[NASA-TM-104164] p 214 N93-11176
Modified optimal control pilot model for computer-aided design and analysis
[NASA-TM-4384] p 214 N93-11459
Rigid body mode identification of the PAH-2 helicopter using the eigensystem realization algorithm
[NASA-TM-107690] p 336 N93-11544
Further buffeting tests in a cryogenic wind tunnel
[NASA-TM-107621] p 198 N93-11610
Open-loop characteristics of magnetic suspension systems using electromagnets mounted in a planar array
[NASA-TP-3229] p 277 N93-11613

Laboratory study of effects of sonic boom shaping on subjective loudness and acceptability
[NASA-TP-3269] p 434 N93-11620

Low-speed longitudinal and lateral-directional aerodynamic characteristics of the X-31 configuration
[NASA-TM-4351] p 198 N93-11622

Study of compression-loaded and impact-damaged structurally efficient graphite-thermoplastic trapezoidal-corrugation sandwich and semisandwich panels
[NASA-TP-3264] p 239 N93-11623

Boundary layer relaminarization device
[NASA-CASE-LAR-14470-1] p 199 N93-11876

Multi-layer light-weight protective coating and method for application
[NASA-CASE-LAR-14448-1] p 269 N93-11912

A smart end-effector for assembly of space truss structures p 230 N93-11982

Structural design using equilibrium programming
[NASA-TM-107593] p 339 N93-12005

NASA/DOD Aerospace Knowledge Diffusion Research Project. Paper 23: Information technology and aerospace knowledge diffusion: Exploring the intermediary-end user interface in a policy framework
[NASA-TM-108077] p 478 N93-12007

Decentralized control of large flexible structures by joint decoupling
[NASA-TM-107694] p 339 N93-12020

Publications on acoustics research at the Langley Research Center, January 1987 - September 1992
[NASA-TM-107674] p 435 N93-12080

Method and apparatus for evaluating multilayer objects for imperfections
[NASA-CASE-LAR-14581-1-SB] p 333 N93-12204

Compensated high temperature strain gage
[NASA-CASE-LAR-14776-1] p 313 N93-12205

Modeling and model simplification of aeroelastic vehicles: An overview
[NASA-TM-107691] p 215 N93-12216

Current state and future direction of computer systems at NASA Langley Research Center
[NASA-TM-107685] p 414 N93-12278

Dynamic test/analysis correlation using reduced analytical models
[NASA-TM-107671] p 341 N93-12300

A monitor for the laboratory evaluation of control integrity in digital control systems operating in harsh electromagnetic environments
[NASA-TM-4402] p 215 N93-12304

An approach to constrained aerodynamic design with application to airfoils
[NASA-TP-3260] p 201 N93-12321

Current Technology for Thermal Protection Systems
[NASA-CP-3157] p 227 N93-12447

Predicted and tested performance of durable TPS
p 228 N93-12454

Recent advances in carbon-carbon substrate technology at NASA. Langley Research Center p 228 N93-12455

Current research in oxidation-resistant carbon-carbon composites at NASA. Langley Research Center
p 229 N93-12456

Thermal control/oxidation resistant coatings for titanium-based alloys p 229 N93-12457

Active cooling from the sixties to NASP
p 208 N93-12458

Thermostructural applications of heat pipes for cooling leading edges of high-speed aerospace vehicles
p 229 N93-12460

Deployable reflector antenna performance optimization using automated surface correction and array-feed compensation
[NASA-TP-3228] p 222 N93-12543

NATIONAL AERONAUTICS AND SPACE ADMINISTRATION. LEWIS RESEARCH CENTER, CLEVELAND, OH.

Analysis of precracking parameters and fracture toughness for ceramic single-edge-precracked-beam specimens
[NASA-TM-105568] p 263 N93-10962

Nondestructive evaluation of ceramic and metal matrix composites for NASA's HITEMP and enabling propulsion materials programs
[NASA-TM-105807] p 331 N93-10963

Lunar and Martian environmental interactions with nuclear power system radiators
[NASA-TM-105747] p 230 N93-10965

Experimental validation of boundary element methods for noise prediction
[NASA-TM-105729] p 323 N93-10966

A creep cavity growth model for creep-fatigue life prediction of a unidirectional W/Cu composite
[NASA-TM-105780] p 333 N93-10967

Relative sliding durability of candidate high temperature fiber seal materials
[NASA-TM-105806] p 236 N93-10978

Small experiments for the maturation of orbital cryogenic transfer technologies
[NASA-TM-105849] p 296 N93-10981

Maximum life spiral bevel reduction design
[NASA-TM-105790] p 323 N93-10982

An interactive preprocessor for the NASA engine performance program
[NASA-TM-105786] p 209 N93-10983

SITE project. Phase 1: Continuous data bit-error-rate testing
[NASA-TP-3279] p 224 N93-11001

Ceramic component reliability with the restructured NASA/CARES computer program
[NASA-TM-105856] p 334 N93-11004

Description of the SSF PMAD DC testbed control system data acquisition function
[NASA-TM-105843] p 417 N93-11005

Phase-stepping fiber-optic projected fringe system for surface topography measurements
[NASA-CASE-LEW-14996-1] p 446 N93-11058

System and method for cancelling expansion waves in a wave rotor
[NASA-CASE-LEW-15218-1] p 297 N93-11172

The engine design engine. A clustered computer platform for the aerodynamic inverse design and analysis of a full engine
[NASA-TM-105838] p 196 N93-11223

On an origin of numerical diffusion: Violation of invariance under space-time inversion
[NASA-TM-105776] p 425 N93-11254

A concept for a counterrotating fan with reduced tone noise
[NASA-TM-105736] p 433 N93-11370

The NASA CSTI high capacity power project
[NASA-TM-105813] p 221 N93-11398

Thermomechanical fatigue behavior of SiC/Ti-24Al-11Nb in air and argon environments
[NASA-TM-105723] p 238 N93-11399

Implementation of a model based fault detection and diagnosis for actuation faults of the Space Shuttle main engine
[NASA-TM-105781] p 221 N93-11401

Preliminary characterization of a water vaporizer for resistojet applications
[NASA-TM-105877] p 231 N93-11402

Application of artificial neural networks in nonlinear analysis of trusses
[NASA-TM-105319] p 336 N93-11403

Direct Broadcast Satellite: Radio Program
[NASA-TM-105910] p 224 N93-11430

Test program to provide validation data for the Rocket Combustor Interactive Design (ROCCID) code
p 247 N93-11450

Coaxial injector spray characterization using water/air as simulants p 248 N93-11452

Direct numerical simulation of instabilities in parallel flow with spherical roughness elements
[NASA-TM-105847] p 300 N93-11529

Overview of high performance aircraft propulsion research
[NASA-TM-105839] p 213 N93-11530

Comparison of truncation error of finite-difference and finite-volume formulations of convection terms
[NASA-TM-105861] p 426 N93-11531

Silicon carbide fiber reinforced strontium aluminosilicate glass-ceramic matrix composite
[NASA-CASE-LEW-15263-1] p 239 N93-11543

Chronopotentiometry of refractory metals, actinides and oxyanions in molten salts: A review
[NASA-TM-105862] p 249 N93-11545

Determination of parameters of a new method for predicting alloy properties
[NASA-TM-105895] p 257 N93-11609

Hot fire test results of subscale tubular combustion chambers
[NASA-TP-3222] p 232 N93-11614

Design of a high-temperature experiment for evaluating advanced structural materials
[NASA-TM-105833] p 337 N93-11624

Review of the physical and mechanical properties and potential applications of the B2 compound NiAl: Unabridged version of a paper published in International materials review
[NASA-TM-105598] p 258 N93-11635

An embedded rule-based diagnostic expert system in Ada p 392 N93-11928

Space Communication Artificial Intelligence for Link Evaluation Terminal (SCAILET) p 395 N93-11940

ICAN/DAMP-integrated composite analyzer with damping analysis capabilities: User's manual
[NASA-TP-3292] p 241 N93-12015

Acoustical evaluation of the NASA Lewis 9 by 15 foot low speed wind tunnel
[NASA-TP-3274] p 218 N93-12016

Computer aided design and manufacturing of composite propfan blades for a cruise missile wind tunnel model
[NASA-TM-105269] p 413 N93-12022

The effect of contact stresses in four-point bend testing of graphite/epoxy and graphite/PMR-15 composite beams
[NASA-TM-105891] p 241 N93-12076

An experimental investigation of the flow in a diffusing S-duct
[NASA-TM-105809] p 213 N93-12077

Thermostructural tailoring of fiber composite structures
[NASA-TM-105882] p 242 N93-12078

Design of small Stirling dynamic isotope power system for robotic space missions
[NASA-TM-105919] p 275 N93-12085

Dynamic analysis of a pre-and-post ice impacted blade
[NASA-TM-105829] p 276 N93-12197

Automatic system for installation and replacement of Space Station components
[NASA-CASE-LEW-14906-1] p 329 N93-12203

Stochastic sensitivity measure for mistuned high-performance turbines
[NASA-TM-105821] p 341 N93-12277

Parameterization of solar cells
[NASA-TM-105885] p 295 N93-12301

Fracture toughness testing of polymer matrix composites
[NASA-TP-3199] p 243 N93-12302

Analysis of fault-tolerant neurocontrol architectures
[NASA-TM-105898] p 215 N93-12305

Conductor-backed coplanar waveguide resonators of Y-Ba-Cu-O and Tl-Ba-Ca-Cu-O on LaAlO3
[NASA-TM-105890] p 469 N93-12325

Method and apparatus for gripping test specimens
[NASA-CASE-LEW-15345-1] p 329 N93-12327

Nuclear thermal propulsion transportation systems for lunar/Mars exploration
[NASA-TM-105870] p 233 N93-12363

Damping and scattering of electromagnetic waves by small ferrite spheres suspended in an insulator
[NASA-TM-105837] p 286 N93-12366

Studies on the reactive melt infiltration of silicon and silicon-molybdenum alloys in porous carbon
[NASA-TM-105860] p 273 N93-12398

Concurrent optimization of airframe and engine design parameters
[NASA-TM-105908] p 213 N93-12402

ISDN at NASA Lewis Research Center
[NASA-TM-105911] p 419 N93-12410

An improved numerical model for wave rotor design and analysis
[NASA-TM-105915] p 214 N93-12418

Data distribution satellite
[NASA-TM-105778] p 287 N93-12481

The 10 kW power electronics for hydrogen arcjets
[NASA-TM-105614] p 235 N93-12484

NATIONAL AERONAUTICS AND SPACE ADMINISTRATION. MARSHALL SPACE FLIGHT CENTER, HUNTSVILLE, AL.

Spacecraft flight control system design selection process for a geostationary communication satellite
[NASA-TP-3289] p 222 N93-11002

Solution of two-phase reacting flow in liquid thrust chambers p 235 N93-11449

Autoguidance video sensor for docking
p 230 N93-11954

A comparison of high cycle fatigue methodologies
[NASA-TM-103601] p 233 N93-12148

Space Station Freedom seal leakage rate analysis and testing summary: Air leaks in ambient versus vacuum exit conditions
[NASA-TM-103604] p 328 N93-12149

Microbiological analysis of debris from STS-42 IML-1 by direct plating of rinse waters
[NASA-TM-108375] p 375 N93-12174

The mechanism of bolt loading
[NASA-TM-108377] p 342 N93-12412

Shear joint capability versus bolt clearance
[NASA-TM-108378] p 342 N93-12419

NATIONAL AERONAUTICS AND SPACE ADMINISTRATION. PASADENA OFFICE, CA.

INAS hole-immobilized doping superlattice long-wave-infrared detector
[NASA-CASE-NPO-17880-1-CU] p 458 N93-11056

The adaptive neuron model: An architecture for the rapid learning of nonlinear topological transformations
[NASA-CASE-NPO-18579-1-CU] p 420 N93-11174

Terminal slider control of nonlinear robotic systems
[NASA-CASE-NPO-18584-1-CU] p 324 N93-11177

Overcharge and overdischarge protection of ambient temperature secondary lithium cells
[NASA-CASE-NPO-18343-1-CU] p 290 N93-11456

Mappings between codewords of two distinct (N,K) Reed-Solomon codes over GF(2 sup J)
[NASA-CASE-NPO-18771-1-CU] p 412 N93-11664

Backward assembly planning with DFA analysis
[NASA-CASE-NPO-18817-1-CU] p 278 N93-12202

NATIONAL AEROSPACE LAB., KAKUDA (JAPAN).
Sealing characteristics of a carbon segmented circumferential seal for a liquid oxygen turbopump
[NAL-TR-1130] p 329 N93-12364
Combustion characteristics of the LO2/GCH4 fuel-rich preburners for staged combustion cycle rocket engines
[NAL-TR-1124] p 234 N93-12368
Mach 4 testing of scramjet inlet models
[NAL-TR-1137] p 202 N93-12369
Characteristics of heat transfer to nickel plated chamber walls of high pressure rocket combustors
[NAL-TR-1126T] p 234 N93-12372
An experimental study of a small high speed LH2 rocket pump: Fundamental mechanical design
[NAL-TR-1123] p 330 N93-12463

NATIONAL AEROSPACE LAB., TOKYO (JAPAN).
Difference approximations for hyperbolic conservation laws and consistency with characteristics
[NAL-TR-1098T] p 428 N93-12350
Air ejector experiments using the two-dimensional supersonic cascade tunnel: Relationship between ejector performance and throat area ratio, part 1
[NAL-TM-642-PT-1] p 202 N93-12352
Flight test progress of the STOL research aircraft ASKA
[NAL-TM-643] p 208 N93-12354
Simulation analysis of a cable-mount system used for dynamic wind tunnel tests
[NAL-TR-1127] p 219 N93-12359
On stability and control of SSTO spaceplane in super- and hypersonic ascending phase
[NAL-TR-1128T] p 216 N93-12361
A wind tunnel investigation to determine buffet countermeasures for STOL aircraft alpha-sweep flight testing
[NAL-TR-1129] p 216 N93-12362
Accuracy improvement of linear estimated motion using differential type sensors
[NAL-TR-1135] p 314 N93-12365
Flight simulator evaluation of D-size liquid crystal flat panel displays
[NAL-TR-1136] p 209 N93-12367
An optical fiber multi-terminal data bus system for aircraft
[NAL-TR-1125] p 209 N93-12370
Impact test of carbon, Kevlar, and glass fibre hybrid FRP plates
[NAL-TR-1100] p 243 N93-12371
Video camera as a visual sensor
[NAL-TR-1132] p 314 N93-12373
On the Goertler instability of boundary layers
[NAL-TR-1120T] p 307 N93-12374
Evaluation of acoustic impedance models for a perforated plate
[NAL-TR-1133] p 435 N93-12375
Effects of cooling-air injection on secondary flows and losses in a turbine cascade
[NAL-TR-1121T] p 307 N93-12382
Liquid crystal flat panel display evaluation tests using a flight simulator
[NAL-TR-1122] p 209 N93-12383
Wind tunnel investigation of a twin-engine jet transport semi-span model with upper surface blown jet flap
[NAL-TR-1134] p 203 N93-12503

NATIONAL GEOPHYSICAL DATA CENTER, BOULDER, CO.
Solar-geophysical data number 569, January 1992. Part 2: (Comprehensive reports). Data for July 1991 and miscellaneous
[PB92-158898] p 488 N93-11738

NATIONAL HURRICANE CENTER, CORAL GABLES, FL.
Diagnostic report of the National Hurricane Center: October and November 1990, volume 3, number 3
[PB91-242297] p 370 N93-11888

NATIONAL HYDROGEN ASSOCIATION, WASHINGTON, DC.
The hydrogen technology assessment, phase 1
[NASA-CR-190969] p 349 N93-12394

NATIONAL INST. FOR FUSION SCIENCE, NAGOYA (JAPAN).
Shafranov shift in low-aspect-ratio heliotron/torsatron CHS
[DE92-782100] p 451 N93-11277
Fast cooling phenomena with ice pellet injection in the JIPP T-IIU tokamak
[DE92-782105] p 454 N93-11834

NATIONAL INST. OF STANDARDS AND TECHNOLOGY, BOULDER, CO.
Transmission/reflection and short-circuit line methods for measuring permittivity and permeability
[PB92-205376] p 293 N93-12084

NATIONAL INST. OF STANDARDS AND TECHNOLOGY, GAITHERSBURG, MD.
Managing data: From vision to reality
[PB92-191212] p 474 N93-11215
Computer security training and awareness course compendium
[PB92-205442] p 404 N93-11258
Integrated services digital network conformance testing. Layer 1, physical layer. Part 2: Basic rate U interface, user side
[PB92-181114] p 418 N93-11714
Mass energy-transfer and mass energy-absorption coefficients, including in-flight positron annihilation for photon energies 1 keV to 100 MeV, 1992
[PB92-181106] p 438 N93-11715
Atomic structure of Ni-like soft x ray lasing ions
[DE92-019273] p 438 N93-11778
Recommended agency procedures for implementing federal metric policy
[PB92-205467] p 277 N93-11901
A metric America: A decision whose time has come - for real
[PB92-205459] p 277 N93-11902
Model-based vision for space applications
p 398 N93-11955
Workshop on Characterizing Diamond Films
[PB92-205426] p 271 N93-12086
Two-fluid measurements on thin films
[PB92-205350] p 308 N93-12475

NATIONAL LAB. FOR HIGH ENERGY PHYSICS, TSUKUBA (JAPAN).
Analysis of the prebuncher for the KEK 40-MeV proton linac
[DE92-514988] p 444 N93-11525

NATIONAL MATERIALS ADVISORY BOARD, WASHINGTON, DC.
High-performance synthetic fibers for composites
[AD-A252645] p 242 N93-12292

NATIONAL OCEANIC AND ATMOSPHERIC ADMINISTRATION, BOULDER, CO.
Reports to the Nation on our changing planet. Winter 1991 No. 1: The climate system
[NASA-CR-190954] p 370 N93-11880

NATIONAL OCEANIC AND ATMOSPHERIC ADMINISTRATION, MIAMI, FL.
Hurricane Research Division fiscal year 1991 programs: Fiscal year 1992 projections
[PB92-138320] p 367 N93-11242

NATIONAL OCEANIC AND ATMOSPHERIC ADMINISTRATION, WASHINGTON, DC.
Scientific assessment of ozone depletion: 1991
[NASA-TM-107976] p 350 N93-11087

NATIONAL OCEANOGRAPHIC DATA CENTER, WASHINGTON, DC.
Mariners Weather Log, volume 36, number 1, Winter 1992
[PB92-161025] p 368 N93-11256
Mariners Weather Log, volume 36, number 2, Spring 1992
[PB92-204213] p 371 N93-12293

NATIONAL PHYSICAL LAB., TEDDINGTON (ENGLAND).
The theoretical background to BS7167: 1990 - specification for Bordeaux connections
[NPL-DMM(A)-50] p 325 N93-11324
The technical background to standards for shackles
[NPL-DMM(A)-51] p 325 N93-11325
A study of the effects of tolerances on rigging screws, turnbuckles, and associated components in BS4429: 1987
[NPL-DMM(A)-53] p 325 N93-11326
The technical background to standards for eyebolts
[NPL-DMM(A)-52] p 325 N93-11327
A survey of European calibration facilities for underwater acoustics
[NPL-RSA(EXT)-32] p 433 N93-11328
A mutual inductance technique for contact-free T(sub c) measurement of high temperature superconductors
[NPL-DES-116] p 289 N93-11393
High frequency response from YBa2Cu3O(7-x) Josephson devices on SrTiO3 bicrystal substrates
[NPL-DES-118] p 459 N93-11394
An uncertainty budget for VHF and UHF reflectometers
[NPL-DES-120] p 281 N93-11395
Signal-to-noise assessment and measurement in spectroscopies with particular reference to Auger and x ray photoelectron spectroscopies
[NPL-DMM(A)-45] p 247 N93-11396
VAMAS round robin project on polymer composite delamination in mode 1 and mode 2: Cyclic loading
[NPL-DMM(A)-47] p 266 N93-11397
Basicity and optical basicities of slags
[NPL-DMM(A)-48] p 447 N93-11408
Analytical method of calculating the thermoelastic constants of a multi-phase unidirectional composite
[NPL-DMM(A)-57] p 238 N93-11409
The electron-beam water calorimeter project at the National Physical Laboratory
[NPL-RSA(EXT)-30] p 310 N93-11410
Use of the program ANISN to calculate response functions for a Bonner sphere set with a He-3 detector
[NPL-RSA(EXT)-31] p 316 N93-11411
Measurement of absorbed dose to water for medium energy x rays
[NPL-RSA(EXT)-33] p 436 N93-11412
EUROMET project no. 231: Uncertainties in mass measurement. NPL's analysis of data from the calibration of weight set NPLW43
[NPL-MOM-107] p 432 N93-11666
Interfacing Matlab and software written in other languages
[NPL-DITC-200/92] p 412 N93-11688

NATIONAL RESEARCH INST. FOR METALS, TOKYO (JAPAN).
Design and development of Ni-base superalloy and Ti alloys
[NRIM-SR-92-01] p 261 N93-12322

NATIONAL TRANSPORTATION SAFETY BOARD, WASHINGTON, DC.
Aircraft accident report: Atlantic Southeast Airlines, Inc. Flight 2311, uncontrolled collision with terrain, an Embraer EMB-120, N270AS, Brunswick, Georgia, 5 April 1991
[PB92-910403] p 203 N93-11471
Aircraft accident report: Explosive decompression-loss of cargo door in flight, United Airlines Flight 811, Boeing 747-122, N4713U, Honolulu, HI, 24 February 1989
[PB92-910402] p 204 N93-12193

NATIONAL WEATHER SERVICE, KANSAS CITY, MO.
Proceedings of the National Weather Service Aviation Workshop: Postprint volume
[PB92-176148] p 369 N93-11803

NAVAL AEROSPACE MEDICAL RESEARCH LAB., PENSACOLA, FL.
The OMPAT level 1 Neurophysiological Performance Assessment Battery: NPPAB
[AD-A254840] p 387 N93-12432

NAVAL AIR DEVELOPMENT CENTER, WARMINSTER, PA.
A primer on polynomial resultants
[AD-A246883] p 426 N93-11463
Fatigue crack growth in AerMet 100 steel
[AD-A249068] p 261 N93-12248

NAVAL AIR WARFARE CENTER, WARMINSTER, PA.
Effectiveness of NASA 1032 and 1035 and Air Force 1030 and 1034 units in protection against cold water hypothermia
[AD-A255120] p 389 N93-12291
Human performance in complex task environments: A basis for the application of adaptive automation
[AD-A255067] p 390 N93-12486

NAVAL COMMAND, CONTROL AND OCEAN SURVEILLANCE CENTER, SAN DIEGO, CA.
Mechanical properties of centrifugally cast metal matrix composites
[AD-A254321] p 243 N93-12483

NAVAL HEALTH RESEARCH CENTER, SAN DIEGO, CA.
Smoking status and body composition, exercise, dietary intake, and alcohol/caffeine consumption
[AD-A250648] p 385 N93-11893

NAVAL OCEANOGRAPHIC AND ATMOSPHERIC RESEARCH LAB., BAY SAINT LOUIS, MS.
Validation test report for the first-generation dart Gulf Stream forecasting system
[AD-A254286] p 373 N93-11821
Embedded training capabilities for the LAMPS MK 3 system
[AD-A250697] p 207 N93-11838
Oceanographic expert system: Potential for TESS(3) applications
[AD-A254908] p 374 N93-12288

NAVAL POSTGRADUATE SCHOOL, MONTEREY, CA.
The effects of bypass air on boron carbide combustion in a solid fuel ramjet p 245 N93-11136
The use of statistical measures to validate system dynamics models
[AD-A248569] p 428 N93-11417
Evaluation of a user information satisfaction short-form instrument
[AD-A250702] p 478 N93-11840
The effect of task complexity on user interfaces: A comparison of command language interface and direct manipulation interface
[AD-A246061] p 412 N93-11859
Development of a 1/7-scale F/A-18 UAV for supermaneuverability research
[AD-A247261] p 208 N93-12053
Operations plan for the Tropical Cyclone Motion (TCM-92) mini-field experiment
[AD-A254723] p 372 N93-12339

Natural convection heat transfer studies of simulated and actual electronic components using dielectric liquids for immersion cooling
[AD-A255173] p 341 N93-12376
Computer modeling of tactical high frequency antennas
[AD-A255176] p 286 N93-12377
Exploiting captions in retrieval of multimedia data
[AD-A255184] p 479 N93-12381
Theory for a high power free electron laser and tactical applications
[AD-A255161] p 323 N93-12405
Numerical analysis of oscillating flow about a circular cylinder
[AD-A255164] p 307 N93-12406
Method of moments analysis of symmetric dual reflector antennas with feeds
[AD-A255171] p 286 N93-12407
Design and evaluation of ion source for satellite charge control
[AD-A255172] p 227 N93-12408
A real time sharpening of NOGAPS predictions of mid-latitude Central Pacific cyclones
[AD-A255157] p 372 N93-12424
Ferroelectric memory devices and a proposed standardized test system design
[AD-A255159] p 405 N93-12425
Interactive analysis of gappy bivariate time series using AGSS
[AD-A255160] p 429 N93-12426
A surface integral approach to the motion planning of nonholonomic systems
[AD-A254844] p 329 N93-12434
Study of sound propagation in a wedge-shaped ocean and comparison with other methods
[AD-A255165] p 435 N93-12471
Cost estimation of software development and the implications for the program manager
[AD-A255167] p 480 N93-12472
The use of life cycle costing for the acquisition of non-major systems at the Naval Regional Contracting Center Detachment
[AD-A255170] p 480 N93-12473

NAVAL RESEARCH LAB., WASHINGTON, DC.
Tunable, short pulse hard x rays from a compact laser synchrotron source
[AD-A254288] p 315 N93-11195
Proceedings of the 14th International Conference on the Numerical Simulation of Plasmas
[AD-A249095] p 451 N93-11275
Materials science and engineering at the Naval Research Laboratory: Research programs and 1990 publications
[PB92-199488] p 238 N93-11422
Mixing regimes in a spatially confined, two-dimensional, supersonic shear layer
[AD-A254302] p 302 N93-11756
Direct manipulation and intermittent automation in advanced cockpits
[AD-A253814] p 388 N93-11784
Electron terms and radiation from crystals
[AD-A254353] p 468 N93-12271
X ray laser program, FY 1991
[AD-A255190] p 322 N93-12275
Workshop on Adhesion and Intermolecular Forces
[AD-A255191] p 272 N93-12276
Fluid-structure interaction using retarded potential and ABAQUS
[AD-A254735] p 307 N93-12355
Extension of fresnel near-field region by single-cycle sinusoidal pulses
[AD-A254736] p 285 N93-12356

NAVAL SURFACE WARFARE CENTER, BETHESDA, MD.
Effect of assembly anomalies on the strain response of composites in the sphere joint region of the DARPA man-rated demonstration article
[AD-A254204] p 240 N93-11739
Bubble dissolving in turbulent pipe flow
[AD-A252927] p 308 N93-12462

NAVAL SURFACE WARFARE CENTER, CRANE, IN.
Simulator, Tactical Use, Flare (STUF) project report
[AD-A254890] p 276 N93-12281

NAVAL SURFACE WARFARE CENTER, SILVER SPRING, MD.
Reengineering using a data abstraction based specification language
[AD-A254726] p 414 N93-12341
A methodology for systems requirements specification and traceability for large real time complex systems
[AD-A254738] p 419 N93-12358

NAVAL SURFACE WEAPONS CENTER, DAHLGREN, VA.
Nonlinear resistive grid wavelet transformations for texture feature extraction
[AD-A254705] p 285 N93-12332

NAVAL WAR COLL., NEWPORT, RI.
The future of carrier aviation
[AD-A254043] p 430 N93-12260

NAVY HOSPITAL, LA SPEZIA (ITALY).
In vivo and in vitro diagnosis of allergic respiratory disease during screening procedures in the Italian Navy: Comparative evaluation of a recent quantitative automatized enzyme immunoassay method to dose specific IgE p 383 N93-11314

NEW BRUNSWICK UNIV., FREDERICTON.
Dredging research program: Feasibility of a kinematic differential Global Positioning System
[AD-A248953] p 205 N93-11419

NEW ENERGY DEVELOPMENT ORGANIZATION, TOKYO (JAPAN).
NEDO Fuel/Storage Technology Subcommittee
[DE92-526262] p 346 N93-11777
NEDO Solar Technology Subcommittee
[DE92-526256] p 347 N93-11845

NEW MEXICO INST. OF MINING AND TECHNOLOGY, SOCORRO.
Magnetic fields in the clusters of galaxies with extreme cooling flows p 486 N93-12164

NEW MEXICO STATE UNIV., LAS CRUCES.
Neural network models of air combat maneuvering
[AD-A254653] p 421 N93-12096
Complex cognitive information processing: A computational architecture with a connectionist implementation
[AD-A254041] p 422 N93-12259

NEW MEXICO UNIV., ALBUQUERQUE.
Optoelectronics Research Center
[AD-A253132] p 447 N93-11527
The 44th Annual Gaseous Electronics Conference
[AD-A254872] p 295 N93-12437

NEW YORK UNIV., NEW YORK.
Plasma properties
[DE92-018635] p 455 N93-12188

NEWCASTLE-UPON-TYNE UNIV. (ENGLAND).
Electronic and optical properties of perfect and imperfect 2 to 6 superlattices p 465 N93-11996

NICE UNIV. (FRANCE).
Observation of pulses propagating at supraluminous speed in an optical fiber p 320 N93-12040

NONVOLATILE ELECTRONICS, INC., PLYMOUTH, MN.
Ultra-dense magnetoresistive mass memory
[NASA-CR-190955] p 405 N93-12520

NORTH CAROLINA STATE UNIV., RALEIGH.
Experimental investigation of the effects of aft blowing with various nozzle exit geometries on a 3.0 caliber tangent ogive at high angles of attack: Forebody pressure distributions
[NASA-CR-190935] p 197 N93-11605
Near-field and far-field sound radiation from a line-driven fluid-loaded infinite flat plate having periodic and non-periodic attached rib stiffeners p 434 N93-11884
An investigation of the effects of aft blowing on a 3.0 caliber tangent ogive body at high angles of attack
[NASA-CR-190934] p 200 N93-12004
Research at and operation of the material science x ray absorption beamline (X-11) at the National Synchrotron Light source
[DE92-018598] p 251 N93-12172
Growth, characterization, and device development in monocrystalline diamond films
[AD-A252648] p 271 N93-12184
Physiologically constrained aerocapture for manned Mars missions p 226 N93-12185
Mechanisms associated with electrorheology
p 294 N93-12198
An engineering method for interactive inviscid-boundary layers in three-dimensional hypersonic flows
p 203 N93-12529

NORTH CAROLINA UNIV., CHAPEL HILL.
Advanced technology for portable personal visualization
[AD-A253808] p 388 N93-11783

NORTH CAROLINA UNIV., CHARLOTTE.
Contact detection and contact motion for error recovery in the presence of uncertainties p 398 N93-11956

NORTHEAST PHOTOSCIENCES, HOLLIS, NH.
Photovoltaic systems based on spectrally selective holographic concentrators, phase 1
[AD-A252811] p 348 N93-12166

NORTHROP CORP., HAWTHORNE, CA.
Composite failure analysis handbook. Volume 2: Technical handbook. Part 3: Case histories
[AD-A249131] p 241 N93-12054
Spectrum fatigue behaviour of powder metallurgy aluminum alloys
[AD-A255060] p 262 N93-12468

NORTHWEST RESEARCH ASSOCIATES, INC., BELLEVUE, WA.
New methods for nonlinear tracking and nonlinear chaotic signal processing
[AD-A254320] p 284 N93-12095

NORTHWESTERN UNIV., EVANSTON, IL.
Studies in nonlinear problems of energy
[DE92-018551] p 345 N93-11733
Mixed ionic and electronic conductivity in polymers
[DE92-018723] p 273 N93-12500

NORWEGIAN DEFENCE RESEARCH ESTABLISHMENT, KJELLER.
Interpretation of measurements from the suprathermal electron spectrometer on the NEED-2 rocket
[FFI-92/7009] p 357 N93-11129

NOTRE DAME UNIV., IN.
Heat transfer enhancement by chaotic mixing
[PB92-190305] p 470 N93-11469

O

OAK RIDGE NATIONAL LAB., TN.
Growth mechanisms of layered superconductors
[DE92-018492] p 458 N93-10987
Catalog of data bases and reports
[DE92-018586] p 473 N93-10990
High resolution image processing of geophysical data with diffraction tomography
[DE92-014134] p 359 N93-11235
Ceramic Technology Project
[DE92-018748] p 266 N93-11442
Atomistic processes of surface segregation during Si-Ge MBE growth
[DE92-019180] p 459 N93-11496
North American radioactive beam initiatives
[DE92-019185] p 443 N93-11517
ScaLAPACK: A scalable linear algebra library for distributed memory concurrent computers
[DE92-017823] p 426 N93-11636
Effects of physical properties and geometry on shapes and stability of polarizable drops in external fields
[DE92-018865] p 301 N93-11638
Development of wear resistant ceramic coatings for diesel engine components
[DE92-019068] p 268 N93-11654
Climate change and water supply, management and use: A literature review
[DE92-019069] p 353 N93-11655
The relative importance of sulfur and nitrogen compounds in the acidification of freshwater
[DE92-016899] p 354 N93-11680
Engine testing of ceramic cam-roller followers
[DE92-019188] p 268 N93-11735
Step-driven surface segregation and ordering during Si-Ge MBE growth
[DE92-017827] p 463 N93-11772
Relationship of bainitic microstructure to impact toughness in Cr-Mo and Cr-W steels
[DE92-017828] p 258 N93-11773
Repeatable sensitivity of optical-time-domain-reflectometry-based strain measurement
[DE92-016910] p 338 N93-11792
Evaluation of advanced pressure sensor technology
[DE92-011004] p 312 N93-11806
Oxidation-sulfidation behavior of iron alloys containing 16 to 40 atomic percent aluminum
[DE92-017824] p 259 N93-11830
Electron emission during multicharged ion-metal surface interactions
[DE92-017134] p 439 N93-11849
The mechanical and microstructural stability of austenitic stainless steels strengthened by MC-forming elements
[DE91-015314] p 259 N93-11857
Generation of 3-D surface maps in waste storage silos using a structured light source p 399 N93-11958
Research and development at ORNL/CESAR towards cooperating robotic systems for hazardous environments
p 331 N93-11979
A cryogenic enrichment technique for gas chromatographic detection of S2F10 in SF6 discharges
[DE92-011045] p 252 N93-12219
An implementation of a parallel MOL solver on the Intel Gamma parallel computer
[DE92-018947] p 419 N93-12233
Scaling issues for biodiversity protection
[DE92-016689] p 375 N93-12315
Processing and properties of NbTi based alloys
[DE92-016692] p 261 N93-12445
Theory of normal metals
[DE92-016828] p 262 N93-12476
Stirling heat pump external heat systems: An appliance perspective
[DE92-018251] p 349 N93-12498
Transport mechanisms acting in toroidal devices: A theoretician's view
[DE92-018738] p 456 N93-12501
Characterization of underivatized pterins by laser desorption Fourier transform mass spectrometry
[DE92-016785] p 323 N93-12514

OAK RIDGE Y-12 PLANT, TN.
Laboratory information management system proposal [DE92-018243] p 478 N93-11796

ODETICS, INC., ANAHEIM, CA.
Exoskeleton master controller with force-reflecting telepresence p 330 N93-11970

OFFICE OF NAVAL RESEARCH, SAN FRANCISCO, CA.
ONRASIA scientific information bulletin, volume 17, number 3 [AD-A255073] p 490 N93-12470

OHIO STATE UNIV., COLUMBUS.
Orthogonal functions over the oceans and applications to the determination of orbit error, geoid and sea surface topography from satellite altimetry p 373 N93-12002
Compressible mixing layers with and without particles [AD-A254854] p 308 N93-12435

OKLAHOMA UNIV., NORMAN.
Periodicities in pulsar microstructure p 484 N93-11230

OLD DOMINION UNIV., NORFOLK, VA.
Photonics and other approaches to high speed communications [NASA-CR-190362] p 279 N93-11116
Scalable parallel communications p 279 N93-11117
High performance interconnection between high data rate networks p 279 N93-11118
A simple, effective media access protocol system for integrated, high data rate networks p 279 N93-11119

ONSALA SPACE OBSERVATORY (SWEDEN).
A closer look at active galactic nuclei: The great engines of the Universe [PB92-184464] p 485 N93-11807

OPEN UNIV., OXFORD (ENGLAND).
Sound propagation over rigid porous layers p 432 N93-11179
Volcanology from space: Applications of infrared remote sensing p 343 N93-11213

OPTICAL SOCIETY OF AMERICA, WASHINGTON, DC.
Organization of the Optical Society of America Photonic Science Topical Meeting Series. Volume 14: Photorefractive materials effects, and devices [AD-A253001] p 446 N93-11071
The fourth OSA Topical Meeting Proceedings on Picosecond Electronics and Optoelectronics, volume 9 [AD-A253472] p 447 N93-11099

OPTRA, INC., BEVERLY, MA.
Laser surface profilometer with sub-Angstrom resolution [DE92-018926] p 317 N93-12011

OREGON STATE UNIV., CORVALLIS.
Matter-wave interferometry with laser cooled atoms [AD-A253999] p 316 N93-11737

OSLO UNIV. (NORWAY).
On the evaluation of derivatives of Gaussian integrals p 439 N93-11853

OXFORD UNIV. (ENGLAND).
Time-frequency domain analysis of vibration signals for machinery diagnostics. 3: The present power spectral density [OUEL-1911/92] p 337 N93-11707

P

PACIFIC NORTHWEST LAB., RICHLAND, WA.
Cellular and molecular pathways of extremely-low-frequency electromagnetic field interactions with living systems [DE92-019084] p 282 N93-11515
Isotopic tailoring with 59-Ni to study the effect of helium on microstructural evolution and mechanical properties of neutron-irradiated Fe-Cr-Ni alloys [DE92-019372] p 257 N93-11557
Acoustic emission monitoring of HFIR vessel during hydrostatic testing [DE92-019316] p 332 N93-11601
Key wintertime meteorological features of the Grand Canyon and the Colorado Plateaus Basin [DE92-019134] p 369 N93-11657
Global-local finite element analysis of composite structures [DE92-019138] p 240 N93-11658
Ultra wide band 3-D cross section (RCS) holography [DE92-019133] p 312 N93-11802
Selected case studies of technology transfer from mission-oriented applied research [DE92-018957] p 481 N93-12067
Advanced methods for structural characterization of large multiply charged ions: Obtaining charge state determination and improved sensitivity [DE91-015264] p 441 N93-12117

PANAMETRICS, INC., WALTHAM, MA.
Development and use of data analysis procedures for the CRRES payloads AFGL-701-2/Dosimeter and AFGL-701-4/Fluxmeter and application of the data analysis results to improve the static and dynamic models of the Earth's radiation belts [AD-A253287] p 363 N93-11810

PARIS-SUD UNIV., ORSAY (FRANCE).
Gain in a confined aluminum plasma p 320 N93-12043
Preliminary study of the homogeneity of the density and temperature of long plasmas used for X laser studies p 320 N93-12044
Experimental study of x ray laser in lithumoid aluminum p 321 N93-12045
Modeling for the study of an X laser in a recombination plasma; gain calculations at 105.7 and 154.6 A p 321 N93-12046
Analysis of the instrument operation of a focal circle spectrograph and numerical reconstitution of the spectrum emitted by a plasma column p 321 N93-12051

PARIS VI UNIV. (FRANCE).
Atomic structure and spectral perturbations in dense and hot plasmas p 321 N93-12049

PARIS XI UNIV., ORSAY (FRANCE).
Nonlinear behavior of resonant absorption in a plasma at microwave frequency p 319 N93-12032

PENNSYLVANIA STATE UNIV., UNIVERSITY PARK.
A summary of the JANNAF workshop on diagnostics p 248 N93-11451
An experimental study of droplet dispersion in turbulent flows p 248 N93-11455
Slow crack growth in vacuum p 338 N93-11909
Hydrogen assisted heat transfer during diamond growth using carbon and tantalum filaments [AD-A247944] p 468 N93-12218
The vertical distribution of heating in the tropical atmosphere [AD-A254982] p 372 N93-12507

PENNSYLVANIA UNIV., PHILADELPHIA.
The Peierls ground state, solitons and polarons in ring-containing polymers [AD-A254914] p 272 N93-12289
Catalytic hydrogenation of carbon monoxide [DE92-014729] p 253 N93-12428
Erasable optical information storage in the polyanilines [AD-A254873] p 480 N93-12438
Synthesis and conductivity of copolymer of 4,4'-diaminodiphenylamine and terephthaloyl chloride [AD-A254880] p 273 N93-12440
Atomic bonding at ceramic interfaces using scanning tunneling microscopy [DE92-018706] p 273 N93-12479

PEUGEOT S.A., VELIZY (FRANCE).
Study of the effects of a plastic wave induced by laser pulse in a metallic material. Application to the improvement of fatigue strength p 319 N93-12036

PHILLIPS LAB., HANSCOM AFB, MA.
The semiannual variation of great geomagnetic storms and the postshock Russell-McPherron effect preceding coronal mass ejecta [AD-A254955] p 489 N93-12506

PHILLIPS LAB., KIRTLAND AFB, NM.
Broadband EMP transient measurement preemphasis filter [AD-A254414] p 284 N93-12160

PITTSBURGH ENERGY TECHNOLOGY CENTER, PA.
Drag on an oscillating rod in a non-Newtonian fluid [DE92-014746] p 308 N93-12492

PITTSBURGH UNIV., PA.
Computer simulations for the adsorption of polymers onto surfaces [DE92-018942] p 267 N93-11628
The physics of pattern formation at liquid interfaces [DE92-016971] p 462 N93-11747
The role of backbond strain in silicon surfaces on the decomposition of NH3 and PH3 [AD-A253771] p 250 N93-12062

PLANNING RESEARCH CORP., EL SEGUNDO, CA.
Requirements and applications for robotic servicing of military space systems p 230 N93-11953

POLITECNICO DI MILANO (ITALY).
Implicit parallelism in genetic algorithms [REPT-92-012] p 418 N93-11180
Parallel genetic algorithms: Introduction and overview of current research [REPT-92-015] p 418 N93-11181
The complexity of some multicriteria arborescence problems [REPT-92-016] p 424 N93-11182
Ontology of mind, subjective ontology, and the example of temporal expressions [REPT-92-018] p 386 N93-11212
ALECSYS and the AutonoMouse: Learning to control a real robot by distributed classifier systems [REPT-92-011] p 420 N93-11227
Geometrical concepts about learning rules in networks with binary and ternary output functions [REPT-92-020] p 411 N93-11592
Self-tuning PI-PID regulators for stable systems with varying delay [REPT-92-023] p 421 N93-11593
A fast pipelined inner product unit [REPT-92-025] p 411 N93-11594
A PID auto-tuning algorithm based on relay feedback [REPT-92-019] p 421 N93-11667
The ESSE project: Supporting object-oriented database schema analysis and evolution: Overview [REPT-92-026] p 476 N93-11689
An object-oriented approach to spatial databases [REPT-92-034] p 476 N93-11690

POLYATOMICS RESEARCH, INC., MOUNTAIN VIEW, CA.
Concerted hydrogen atom exchange between three HF molecules p 439 N93-11855

POLYTECHNIC UNIV., BROOKLYN, NY.
Structural dynamics of large space structures having parametric uncertainties p 225 N93-11836
Elastic stresses, twin boundaries, and fatigue cracking p 338 N93-11890

PRATT AND WHITNEY AIRCRAFT, EAST HARTFORD, CT.
Three-dimensional turbopump flowfield analysis [NASA-CR-190978] p 308 N93-12539

PRATT AND WHITNEY AIRCRAFT, WEST PALM BEACH, FL.
Space Transportation Booster Engine Configuration Study. Volume 3: Program Cost estimates and work breakdown structure and WBS dictionary [NASA-CR-184458] p 233 N93-12088
Fatigue in single crystal nickel superalloys [AD-A254603] p 260 N93-12237
Space transportation booster engine configuration study. Volume 2: Design definition document and environmental analysis [NASA-CR-184459] p 234 N93-12441
Space transportation booster engine configuration study. Volume 1: Executive Summary [NASA-CR-184457] p 235 N93-12523

PRINCETON UNIV., NJ.
Physiological analyses of the afferents controlling brain neurochemical systems [AD-A253185] p 375 N93-11146
Turbulence modeling in shock wave/turbulent boundary layer interactions [NASA-CR-190933] p 301 N93-11606
Asymptotic analysis of reacting materials with saturated explosion. 2: High-frequency waves [AD-A254473] p 275 N93-12236
Inhibition of moist carbon monoxide oxidation by trace amounts of hydrocarbons [DE92-008736] p 253 N93-12257
Studies of a flat wake rotor theory [NASA-CR-190936] p 201 N93-12343
Digital signal processing [AD-A254870] p 287 N93-12436

PURDUE UNIV., INDIANAPOLIS, IN.
Calculation of nozzle/aftbody flowfield interactions p 302 N93-11722

PURDUE UNIV., WEST LAFAYETTE, IN.
Preconversion catalytic deoxygenation of phenolic functional groups [DE92-018304] p 244 N93-10986
Methods of analysis for thick-section composite structures p 237 N93-11262
Visual psychophysics of egomotion [AD-A248349] p 386 N93-11488
Interfacial area and two-phase flow structure development measured by a double-sensor probe [DE92-019459] p 300 N93-11538
Exploration of the ionizable metal cluster-electrode surface analogy: Infrared spectroelectrochemistry of (Pt24(CO)30)(sup n), (Pt26(CO)32)(sup n), and (Pt38(CO)44)(sup n) (n = 0 to -10), and comparisons with potential-dependent spectra of CO adlayers on platinum surfaces [AD-A252544] p 250 N93-11808
Turbulence structure and polymer drag reduction in adverse pressure gradient boundary layers p 304 N93-12003
Unsteady propeller/wing aerodynamic interactions p 201 N93-12190
Hypervelocity scramjet combustor-nozzle analysis and design [NASA-CR-190965] p 213 N93-12214
Analysis of delamination in composite laminates under low-velocity impact p 243 N93-12532

Q

QUEENS COLL., FLUSHING, NY.
Optimization of film synthesized rare earth transition metal permanent magnet systems
[DE92-018726] p 432 N93-12116

R

RANGE COMMANDERS COUNCIL, WHITE SANDS MISSILE RANGE, NM.
Guide to synchronization of video systems to IRIG timing
[AD-A254626] p 285 N93-12240

RAYTHEON CO., LEXINGTON, MA.
RF vacuum microelectronics
[AD-A253910] p 290 N93-11491

RAYTHEON CO., MARLBOROUGH, MA.
Testability design rating system. Volume 2: Analytical procedure
[AD-A254333] p 413 N93-12146

RED CROSS HOSPITAL, THE HAGUE (NETHERLANDS)
Phadiatop: A screening test for inhalant allergy
p 383 N93-11313

RENSSELAER POLYTECHNIC INST., TROY, NY.
CVD of AIN and SiC using cyclic organometallic precursors
[AD-A246910] p 266 N93-11413
Tenth International Symposium on Environmental Biogeochemistry
[DE92-016200] p 355 N93-11864

RESEARCH INST. FOR ADVANCED COMPUTER SCIENCE, MOFFETT FIELD, CA.
Krylov subspace methods for complex non-Hermitian linear systems
[NASA-CR-190931] p 409 N93-11458

RESEARCH INST. FOR COMPUTING AND INFORMATION SYSTEMS, HOUSTON, TX.
Analysis of methods
[NASA-CR-190278] p 407 N93-11368
An EVACS simulation with nested transactions
[NASA-CR-190636] p 412 N93-11717
The SoRReL papers: Recent publications of the Software Reuse Repository Lab
[NASA-CR-190894] p 414 N93-12384

RESEARCH INST. OF NATIONAL DEFENCE, LINKOEPING (SWEDEN).
Contributions to CD Space Committee, 1991: Summary and analysis
[PB92-195312] p 219 N93-11216

REX, THOMPSON AND PARTNERS, FARNHAM (ENGLAND).
A comparison of the achieved and predicted defect rates of some continuously operating electronic equipment
[RTP/909/10-ISSUE-2] p 288 N93-11364

RICE UNIV., HOUSTON, TX.
Fault detection and fault tolerance in robotics
p 330 N93-11961
Application of spin-sensitive electron spectroscopies to investigations of electronic and magnetic properties of solid surfaces and epitaxial systems
[DE92-018597] p 470 N93-12499

ROCHESTER INST. OF TECH., NY.
Software quality methodology integration study results
[AD-A253891] p 408 N93-11371

ROCKEFELLER UNIV., NEW YORK, NY.
Carboxyalkylated hemoglobin as a potential blood substitute
[AD-A252329] p 384 N93-11561

ROCKWELL INTERNATIONAL CORP., CANOGA PARK, CA.
Lunar PMAD technology assessment
[NASA-CR-189225] p 347 N93-12017
Power system commonality study
[NASA-CR-190765] p 347 N93-12019

ROCKWELL INTERNATIONAL CORP., DOWNEY, CA.
Automated resupply of consumables: Enhancement of space commercialization opportunities
p 403 N93-11980

ROLLS-ROYCE, INC., ATLANTA, GA.
Advanced materials in gas turbine engines: An assessment
[PNR-90946] p 211 N93-11105
Development of advanced carbon-carbon annular flameholders for gas turbines
[PNR-90947] p 211 N93-11106
Small particle impact damage in carbon-carbon composites
[PNR-90948] p 236 N93-11107

ROLLS-ROYCE LTD., DERBY (ENGLAND).
Experience of designing a relational materials database
[PNR-90893] p 473 N93-11012
Application of polyimides to aeroengine components
[PNR-90907] p 334 N93-11013
Neutron diffraction residual stress studies for aero-engine component applications
[PNR-90908] p 334 N93-11014
Japanese style total quality control: A first hand experience
[PNR-90909] p 331 N93-11015
Nondestructive inspection and life determination of disc material
[PNR-90911] p 331 N93-11016
An advanced combustion research facility for validating computational fluid dynamics codes
[PNR-90913] p 296 N93-11017
Processing of ceramic matrix composites
[PNR-90914] p 263 N93-11018
Materials: Toward the non-metallic engine
[PNR-90915] p 209 N93-11019
Application of laminar flow to aero engine nacelles
[PNR-90916] p 195 N93-11020
Automated fringe analysis for moire interferometry
[PNR-90918] p 334 N93-11021
Fringe analysis of in-plane displacements on high speed rotating components
[PNR-90920] p 334 N93-11022
An experimental evaluation of prediction methods for contrafans
[PNR-90924] p 209 N93-11023
Testing for integrity
[PNR-90927] p 210 N93-11024
The prediction of convective heat transfer in rotating square ducts
[PNR-90929] p 296 N93-11025
Short fatigue crack growth in a nickel-base superalloy at room and elevated temperature
[PNR-90892] p 255 N93-11031
A test facility for the thermofluid-dynamics of gas bearing lubrication films
[PNR-90897] p 263 N93-11032
Modelling short crack growth behaviour in nickel-base superalloys
[PNR-90912] p 255 N93-11033
On the basis of experience: Built in product reliability
[PNR-90932] p 331 N93-11034
Rotational CARS measurements in a rotating cavity with axial throughflow of cooling air: Oxygen concentration measurements
[PNR-90935] p 244 N93-11035
Rolls-Royce civil engine technology
[PNR-90936] p 210 N93-11036
The Trent: Towards greater thrust
[PNR-90937] p 210 N93-11037
From RB211 to Trent: An ongoing development strategy
[PNR-90938] p 210 N93-11038
Introduction to the Rolls-Royce design process
[PNR-90939] p 210 N93-11039
The role of turbomachinery testing for stability in distorted flow
[PNR-90943] p 210 N93-11040
The application of manufacturing systems engineering for aero engine gears
[PNR-90944] p 324 N93-11054
Experimental heat transfer results in turbine stators and rotors and a comparison with theory
[PNR-90945] p 210 N93-11055
Concorde propulsion: Did we get it right? The Rolls-Royce/SNECMA Olympus 593 engine reviewed
[PNR-90970] p 210 N93-11061
Simultaneous engineering in the design of aero engines
[PNR-90973] p 211 N93-11062
The Trent family of engines
[PNR-90974] p 211 N93-11063
In-plane strain measurement on high speed rotating components using pulsed laser ESPI
[PNR-90975] p 315 N93-11064
Generation of thermal strains in carbon fibre-reinforced bismaleimide (PMR-15) composites, part 1, 2 and 3
[PNR-90976-PT-1-2-3] p 236 N93-11065
Aero engine ceramics: The vision, the reality, and the progress
[PNR-90983] p 264 N93-11066
The prediction of convective heat transfer in rotating square ducts
[PNR-90985] p 296 N93-11067
Advanced three-shaft engines: Configured for reliability, efficiency, and growth
[PNR-90986] p 211 N93-11068
Maintainability of large gas turbine aero engines
[PNR-90987] p 211 N93-11069
A combined experimental and theoretical study of laminar flow control with particular relevance to aero engine nacelles
[PNR-90991] p 195 N93-11070
Modelling the behaviour of gas bubbles in epoxy resin
[PNR-90961] p 264 N93-11084
Civil aircraft engines: The next generation
[PNR-90962] p 211 N93-11085
The dressing of resin bonded diamond grinding wheels
[PNR-90965] p 264 N93-11086
The development of the Rolls-Royce Trent aero gas turbine
[PNR-90949] p 212 N93-11108
Sigma phase in nickel based superalloys
[PNR-90950] p 255 N93-11109
Quality management of finite element analysis
[PNR-90951] p 331 N93-11110
Present and future trends in turbine blade material and manufacture technology
[PNR-90960] p 255 N93-11111
Development of the neutron diffraction technique for the determination of near surface residual stresses in critical gas turbine components
[PNR-90984] p 212 N93-11112
A European collaborative NLF nacelle flight demonstrator
[PNR-90992] p 196 N93-11113
A knowledge-based blackboard system to interpret graphical data from vibration tests of gas turbines
[PNR-90993] p 212 N93-11114
Elevated temperature fatigue crack growth in a nickel base superalloy under dwell conditions
[PNR-90997] p 255 N93-11115
The design and commissioning of an acoustic liner for propeller noise testing in the ARA transonic wind tunnel
[PNR-90880] p 433 N93-11204
Industrial applications and markets for ceramic matrix composites
[PNR-90884] p 266 N93-11205
The use of simultaneous engineering for the design and manufacture of the low pressure turbine for the Rolls-Royce Trent engine
[PNR-90887] p 212 N93-11206
Innovation in engineering
[PNR-90889] p 212 N93-11207
Simultaneous engineering in aero gas turbine design and manufacture
[PNR-90890] p 212 N93-11208
In-plane ESPI measurements in hostile environments
[PNR-90919] p 309 N93-11320
The effects of plate spacing and downstream plate length on the acoustic resonance excited by flow past two plates in tandem in a duct
[PNR-90958] p 433 N93-11321
An experimental investigation into flow induced acoustic resonances in an annular cascade
[PNR-90959] p 433 N93-11322
The changing nature of design
[PNR-91011] p 206 N93-11334

ROME LAB., GRIFFISS AFB, NY.
Optical beamformer
[AD-A254354] p 448 N93-12272

ROME UNIV. (ITALY).
Silent HIV infection p 378 N93-11293

ROYAL AEROSPACE ESTABLISHMENT, BEDFORD (ENGLAND).
Introduction of electronic pressure scanning at the Royal Aerospace Establishment
[RAE-TM-AERO-2222] p 199 N93-11882
The 13 ft by 9 ft low speed wind tunnel facility at DRA (Aerospace Division) Bedford (England)
[RAE-TM-AERO-2226] p 199 N93-11883
Strain-gauge balance performance and internal temperature gradients measured in a cryogenic environment
[RAE-TM-AERO-2232] p 218 N93-11906

ROYAL AEROSPACE ESTABLISHMENT, FARNBOROUGH (ENGLAND).
A theoretical study of the performance of a small permanent magnet, three-phase alternator when driving a purely resistive load via a full-wave rectification circuit
[RAE-TR-84009] p 289 N93-11434
The measurement of the velocity field induced by a gust generator in a closed-circuit subsonic wind-tunnel
[RAE-TM-MAT-STR-1102] p 217 N93-11435
Developments in icing test techniques for aerospace applications in the RAE Pyestock (England) altitude test facility
[RAE-TM-P-1214] p 207 N93-11485
Orbit perturbations due to an axi-symmetric gravitational field, analyzed over extended periods of time
[RAE-TM-SPACE-386] p 220 N93-11486
Scanning electron microscopy of the effects of moisture and elevated temperature on the fibre/matrix bond in CFRP
[RAE-TM-MAT-STR-1183] p 240 N93-11905

ROYAL AIRCRAFT ESTABLISHMENT, FARNBOROUGH (ENGLAND).
Fatigue crack closure: A review
[RAE-TR-90046] p 335 N93-11369

ROYAL ARMAMENT RESEARCH AND DEVELOPMENT ESTABLISHMENT, FORT HALSTEAD (ENGLAND).
A preliminary investigation of the degradation and stabilisation of the energetic oxetane binder polyNIMMO
[RARDE-7/91] p 273 N93-11376

ROYAL MILITARY COLL. OF SCIENCE, SHRIVENHAM (ENGLAND).
Speech recognition systems and their military applications
[BR91882] p 280 N93-11366

ROYAL NETHERLANDS METEOROLOGICAL INST., DE BILT.
LAM and NEDWAM statistics over the period October 1990 - April 1991
[KNMI-TR-137] p 368 N93-11329

ROYAL SIGNALS AND RADAR ESTABLISHMENT, MALVERN (ENGLAND).
Post-war regional planning: The French silicon valley
[RSRE-MEMO-4282] p 472 N93-10976
On understanding in communicating systems and the error in the Chinese Room thought-experiment
[RSRE-MEMO-4391] p 278 N93-10977
An introduction to the information processing components of the brain
[RSRE-MEMO-4350] p 385 N93-10979
Incorporating prior probabilities and misclassification costs into network training: An example from medical prognosis
[RSRE-MEMO-4343] p 428 N93-10980
Lies, damned lies, and databases
[RSRE-MEMO-4503-ISSUE-2] p 474 N93-11333
The VISTA structured assembler
[RSRE-91034] p 407 N93-11341
Extraction of shape information from predicted irradiance profiles in infrared images
[RSRE-MEMO-4464] p 447 N93-11342
Self-supervision in multilayer adaptive networks
[RSRE-MEMO-4467] p 420 N93-11343
The development of the speaker independent ARM continuous speech recognition system
[RSRE-MEMO-4473] p 280 N93-11383
Preliminary results on the use of linear discriminant analysis in the ARM continuous speech recognition system
[RSRE-MEMO-4511] p 280 N93-11384
The use of linear discriminant analysis in the ARM continuous speech recognition system
[RSRE-MEMO-4512] p 280 N93-11385
Using ELLA for high level design: Modelling the Motorola 6800 microprocessor
[RSRE-MEMO-4515] p 408 N93-11386
On the definition and calculation of effective impedances and averaged boundary conditions with application to the analysis of high complexity frequency selective surfaces
[RSRE-MEMO-4518] p 281 N93-11387
CO2 laser frequency doubling using AgGaSe2
[RSRE-MEMO-4528] p 315 N93-11388
A process monitor for the transputer
[RSRE-MEMO-4554] p 408 N93-11389
QR decomposition based algorithms and architectures for least-squares adaptive filtering
[RSRE-MEMO-4562] p 408 N93-11390
A comparison of feed-forward networks and maximum likelihood on a point-source location problem
[RSRE-MEMO-4567] p 281 N93-11391
Applying algebraic techniques to microcode compilation
[RSRE-MEMO-4568] p 409 N93-11392
A front end implementation of the Pollyanna secure DBMS
[RSRE-MEMO-4540] p 475 N93-11404
The evolution of Ten15
[RSRE-MEMO-4543] p 409 N93-11405
Ten15 developments to support parallelism
[RSRE-MEMO-4545] p 409 N93-11406
The WEB approach to ELLA
[RSRE-MEMO-4549] p 409 N93-11407
A formal definition of the static semantics of ELLA's core
[RSRE-91024] p 409 N93-11436
On recursive free types in Z
[RSRE-91028] p 425 N93-11437
Diagnostic rhyme test statistical analysis programs
[RSRE-91026] p 281 N93-11487
Computing optimum routes across terrain using DAP
[RSRE-MEMO-4299] p 412 N93-11712
Syntax and lexis of the specification language Z
[RSRE-MEMO-4367] p 414 N93-12326
Formal specification of the VIPER microprocessor in HOL
[RSRE-90009] p 405 N93-12430

RUTGERS - THE STATE UNIV., NEWARK, NJ.
Hypertext functionality: A theoretical framework
p 478 N93-11858

RUTHERFORD APPLETON LAB., CHILTON (ENGLAND).
Particle physics experiments, 1991
[RAL-92-001] p 444 N93-11687

S

SAINT ANDREW'S UNIV. (SCOTLAND).
Nonlinear stability of flows over rigid and flexible boundaries p 198 N93-11874

SANDIA NATIONAL LABS., ALBUQUERQUE, NM.
Ground test facilities for evaluating nuclear thermal propulsion engines and fuel elements
[DE92-017039] p 231 N93-10973
Heat-affected zone cracking of nitronic 60 stainless steel
[DE92-018286] p 254 N93-10984
The 1992 DOE/Sandia crystalline photovoltaic technology project review meeting
[DE92-018544] p 344 N93-10989
Development of a GPS-aided motion measurement, pointing, and stabilization system for a synthetic aperture radar
[DE92-017053] p 204 N93-11152
The tomographic formulation of spotlight mode synthetic aperture radar extended to three dimensional targets
[DE92-013666] p 280 N93-11234
Numerical computation of the lightning response of an earth-covered munitions storage bunker and comparison with experiments
[DE92-014268] p 367 N93-11236
Ground test facility for SEI nuclear rocket engines
[DE92-017418] p 217 N93-11367
Authentication algorithm for the universal Authenticated Item Monitoring Systems (AIMS)
[DE92-018826] p 408 N93-11378
Robust solder joint attachment of coaxial cable leads to piezoelectric ceramic electrodes
[DE92-017042] p 276 N93-11494
RATLER: Robotic All-Terrain Lunar Exploration Rover
[DE92-019295] p 487 N93-11502
Dynamics and response of polymer-coated acoustic devices
[DE92-014289] p 433 N93-11523
Optimization of expressions involving array classes
[DE92-019421] p 411 N93-11536
Simulation of liquid drop breakup behavior in a flow field using discrete element techniques
[DE92-019435] p 300 N93-11537
Loads from the detonation of hydrogen-air-steam mixtures
[DE92-019318] p 249 N93-11551
Evaluation of epoxy cured with Ethacure 100 curing agent for use in headers for thermal batteries
[DE92-019326] p 267 N93-11552
Evaluation of flotation for purification of pyrite for use in thermal batteries
[DE92-019330] p 290 N93-11553
Propagation of relativistic high current electron beams across the geomagnetic field
[DE92-018276] p 362 N93-11564
Temperature tracking SPICE macro-model for laser and LED driven opto-coupler assemblies
[DE92-019296] p 411 N93-11599
Low energy helium implantation in evaporated nickel surfaces
[DE92-019297] p 257 N93-11600
Lightning threat warning system at the Tonopah Test Range
[DE92-040444] p 221 N93-11631
An analog macromodel of the SG1525A PWM for use with SPICE2G.6 simulators
[DE92-019423] p 291 N93-11639
An NMR study of the occupation of C(sub 60) interstitial sites by oxygen molecules
[DE92-019436] p 437 N93-11640
Interfacial microchemical characterization needs in surface processing
[DE92-018269] p 277 N93-11672
Initial laboratory evaluation of color video cameras
[DE92-018274] p 311 N93-11673
Heat load material studies: Simulated tokamak disruptions
[DE92-018275] p 452 N93-11674
Rocket-triggered lightning test of an earth-covered munitions storage bunker
[DE92-016790] p 369 N93-11678
Characteristics of current filamentation in high gain photoconductive semiconductor switching
[DE92-018277] p 291 N93-11693
Results from the US/USSR exchange for heat load material studies of simulated tokamak disruptions
[DE92-018285] p 453 N93-11694
Closed form low-thrust trajectories for Mars missions
[DE92-017431] p 232 N93-11766
Real-time data compression using a FFT digital signal processor
[DE92-017744] p 477 N93-11770
Evaluation tests for photovoltaic concentrator receiver sections and modules
[DE92-017745] p 346 N93-11771
The chemistry of Si3N4 and Si deposition studied using molecular beam techniques
[DE92-018268] p 463 N93-11797
Using NEKTON to solve systems of discrete Boltzmann equations
[DE92-018272] p 303 N93-11799
Exciton kinetics in poly(di-n-hexylsilane)
[DE92-018278] p 283 N93-11800
Structural integrity of a confinement vessel for testing nuclear fuels for space propulsion
[DE92-016796] p 232 N93-11824
Implanted He retention and release from boronized layers
[DE92-013983] p 464 N93-11842
The network destruction problem (extended abstract)
[DE92-016171] p 419 N93-11860
Automatic Attenuation/Phase Calibration System (AAPCS)
[DE92-017354] p 284 N93-11917
Sodium reflux pool-boiler solar receiver on-sun test results
[DE92-018932] p 347 N93-12012
Mirror alignment techniques for point-focus solar concentrators
[DE92-019643] p 348 N93-12074
Measured data for the Sandia 34-meter vertical axis wind turbine
[DE92-019807] p 348 N93-12075
Limitations of multiple feeds in a polarimetric-radar compact range
[DE92-017526] p 284 N93-12101
Divergence in intense ion beams caused by incomplete charge neutralization
[DE92-016891] p 445 N93-12103
An evaluation of the blind lap joint for the surface mount attachment of chip components
[DE92-017045] p 277 N93-12106
The deposition characteristics of copper(I) compounds for CVD by FT-IR spectroscopy
[DE92-010778] p 467 N93-12134
A VMEbus ultrasonic sensor controller for mapping and servo control in robotic systems
[DE92-013661] p 421 N93-12138
Development of contractor cells, phase 1
[DE92-017343] p 348 N93-12222
The effect of temperature dependent thermal properties on parametric weld size predictions
[DE92-018816] p 260 N93-12232
System design and radiation field characteristics of the High Flux Neutron Radiography Facility (HFNRF) at Sandia National Laboratories
[DE92-013984] p 219 N93-12268
Reliability analysis of a utility-scale solar power plant
[DE92-016550] p 346 N93-12312

SANDIA NATIONAL LABS., LIVERMORE, CA.
Transient Reduction Analysis using Neural Networks (TRANN)
[DE92-012150] p 421 N93-12153
Some consistency requirements on hardening-recovery evolution equations for welding, part 1
[DE92-015992] p 329 N93-12220
OH rotational temperature and concentration measurements in a supersonic jet
[DE92-006700] p 252 N93-12255
Propellant removal from rocket motors containing double-base compositions
[DE92-013567] p 275 N93-12265

SCIENCE APPLICATIONS INTERNATIONAL CORP., SAN DIEGO, CA.
Nonlinear effects of ICRF power on drift wave stability and transport in tokamaks, task 1
[DE92-018488] p 453 N93-11729
Soviet chemical propellant research and development
[PB92-195577] p 275 N93-12147
Technology evaluation report of Retech, Inc., Plasma Centrifugal Furnace, volume 1
[PB92-216035] p 456 N93-12526
Technology evaluation report of Retech, Inc., Plasma Centrifugal Furnace, volume 2
[PB92-216043] p 457 N93-12527

SCLAVO RESEARCH CENTER, ROME (ITALY).
Absence of protective immunity against diphtheria in a large proportion of young adults p 380 N93-11302

SCLAVO S.P.A., SIENNA (ITALY).
Studies of safety, infectivity, and immunogenicity of a new Temperature Sensitive (TS) 51-1 strain of S. typhi as a new live oral typhoid fever vaccine candidate
p 381 N93-11306

SCRIPPS INSTITUTION OF OCEANOGRAPHY, LA JOLLA, CA.
Propagation of regional phases: Observations and theory
[AD-A246891] p 359 N93-11228

SECA, INC., HUNTSVILLE, AL.
CFD modeling of turbulent flows around the SSME main injector assembly using porosity formulation
[NASA-CR-184359] p 297 N93-11171

SIERRA MONOLITHICS, INC., REDONDO BEACH, CA.
Josephson Junction digital waveform generation for very wideband radars
[AD-A253668] p 467 N93-12169

SKIDAWAY INST. OF OCEANOGRAPHY, SAVANNAH, GA.
The flux and recycling of bioactive substances in the surface sediments of the deep basins off southern California
[DE92-019172] p 373 N93-11734

SOCIETE NATIONALE D'ETUDE ET DE CONSTRUCTION DE MOTEURS D'AVIATION, PARIS (FRANCE).
Study of the behavior of titanium and ceramic fiber matrix composite alloy
[ETN-92-92087] p 240 N93-11708

SOUTHAMPTON UNIV. (ENGLAND).
Application of eigenstructure assignment to the control of powered lift combat aircraft p 215 N93-11871

SOUTHWEST RESEARCH INST., SAN ANTONIO, TX.
Studies of interactive plasma processes in the polar cusp
[NASA-CR-190892] p 357 N93-10964
Modeling the Jovian aurora
[NASA-CR-190696] p 486 N93-11164
The role of proton precipitation in Jovian aurora: Theory and observation p 487 N93-11165
Lyman alpha line shapes from electron impact H2 dissociative processes in the Jovian auroral zone
p 487 N93-11166
Multispectral observations of the Jovian aurora
p 487 N93-11167
Fuzzy logic control of telerobot manipulators
p 399 N93-11959
Microstructure-based fatigue life prediction methods for naval steel structures
[AD-A254628] p 260 N93-12241

SPACE INDUSTRIES, INC., WEBSTER, TX.
Design development of a neural network-based telemetry monitor p 394 N93-11933

SPACE SYSTEMS/LORAL, PALO ALTO, CA.
High Temperature Superconductivity Space Experiment (HTSSE)
[AD-A253119] p 288 N93-11239

SRI INTERNATIONAL CORP., MENLO PARK, CA.
Mechanical properties of semiconductors and their alloys
[AD-A253908] p 462 N93-11727
Distributed database integrity
[AD-A253272] p 477 N93-11749
Chemistry of lower valent actinide halides
[DE92-017031] p 251 N93-12105
Novel nonlinear laser diagnostic techniques
[AD-A254709] p 323 N93-12335

ST SYSTEMS CORP., LANHAM, MD.
Operator vision aids for space teleoperation assembly and servicing p 391 N93-11981

STANFORD LINEAR ACCELERATOR CENTER, CA.
A single beam laser tracker as an alignment tool
[DE92-017746] p 316 N93-11691
Pre-compression of bunch length in the SLC damping rings
[DE92-018154] p 446 N93-12497

STANFORD UNIV., CA.
State-resolved reaction dynamics
[AD-A254291] p 436 N93-11196
Admittance spectroscopy of copper indium diselenide/cadmium sulfide solar cells
p 344 N93-11214
Theory of small metal clusters, films, and wires
[AD-A253120] p 256 N93-11240
The order n simulation of tether motions based on a rigid body tether model p 225 N93-11999
Polynomial dual network simplex algorithms
[AD-A254340] p 413 N93-12131
Assembling polyhedra with single translations
[AD-A254623] p 419 N93-12239
Nonlinear delay line phase shifters for terahertz superconductive electronic circuits
[AD-A255119] p 294 N93-12290
Advanced modeling and optimization of piezoelectric composites
[AD-A253800] p 242 N93-12296
Temporal and spectral variability in luminous x ray binaries p 483 N93-12336
Mathematical methods in operations research and computer science
[AD-A254782] p 428 N93-12465
Nonnormal multivariate distributions: Inference based on elliptically contoured distributions
[AD-A254999] p 429 N93-12513

STATE UNIV. OF NEW YORK, BUFFALO.
Methods and principles for determining task dependent interface content
[NASA-CR-190837] p 204 N93-10961
Impact of finite frequency deviation on the performance of dual-filter heterodyne FSK lightwave systems
[AD-A247611] p 448 N93-11892
Positive ion chemistry of acetylene and methylacetylene clusters. Formation of benzene and C(sub 2n)H(sub 2n)(+) ions via intracluster polymerization reactions
[AD-A250931] p 236 N93-12177

STATE UNIV. OF NEW YORK, STONY BROOK.
Front tracking and the interaction of nonlinear waves
[AD-A253544] p 297 N93-11148

STATE UNIV. OF NEW YORK AT BUFFALO, AMHERST.
Fundamental solutions and boundary element formulations for convective fluid flow
p 298 N93-11217

STOCKHOLM UNIV. (SWEDEN).
Time scales characterizing the processing of water and cloud condensation nuclei by clouds
[CM-80] p 368 N93-11340

STOTTLER HENKE ASSOCIATES, INC., BELMONT, CA.
Intelligent TDA systems using neural networks, phase 1
[AD-A252556] p 420 N93-11000

STRATEGIC DEFENSE INITIATIVE ORGANIZATION, WASHINGTON, DC.
Lightweight Exoatmospheric Projectile (LEAP) test program. Supplemental environmental assessment
[AD-A252286] p 231 N93-10998

STUTTGART UNIV. (GERMANY).
Current scaling of plasma focus devices
[IPF-90-1] p 449 N93-11029
Instabilities in the rundown phase of the plasma focus
[IPF-90-3] p 449 N93-11030
The basic equations for a four component magnetoplasma flow with non equilibrium ionization
[IPF-91-1] p 449 N93-11102
Analytical and numerical principles for the scaling of plasma focus experiments, with regard to electrical resistance
[IPF-91-2] p 450 N93-11103
Contributions to plasma focus physics since 1970 from the Institute of Plasma Research, Stuttgart (Fed. Republic of Germany)
[IPF-91-4] p 450 N93-11201

SUPERCONDUCTING SUPER COLLIDER LAB., DALLAS, TX.
Tables of thermodynamic properties of helium magnet coolant, revision A
[DE92-019098] p 471 N93-11656

SUPERMATERIALS RESEARCH AND DEVELOPMENT CORP., CLEVELAND, OH.
Thermal protection using very high temperature ceramics p 228 N93-12451

SURREY UNIV., LONDON (ENGLAND).
All-digital multicarrier demodulators for on-board processing satellites in mobile communication systems
p 285 N93-12207

SVERDRUP TECHNOLOGY, INC., BROOK PARK, OH.
Autonomous power system: Integrated scheduling
p 235 N93-11948
Effect of inert propellant injection on Mars ascent vehicle performance
[NASA-CR-189238] p 226 N93-12152
Advanced one-dimensional optical strain measurement system, phase 4
[NASA-CR-190760] p 314 N93-12279
Extended-testing of xenon ion thruster hollow cathodes
[NASA-CR-189227] p 234 N93-12409

SWALES AND ASSOCIATES, BELTSVILLE, MD.
Acoustic fill factors for a 120 inch diameter fairing
[NASA-CR-189284] p 434 N93-11634

SWEDISH INST. OF SPACE PHYSICS, UPPSALA.
Ionospheric response to particle precipitation within aurora
[IRF-SR-208] p 359 N93-11265
Observations of thin auroral ionization layers by EISCAT in connection with pulsating aurora p 359 N93-11266
EISCAT observations of strong ion outflows from the F-region ionosphere during auroral activity: Preliminary results p 360 N93-11267
EISCAT observations of topside ionospheric ion outflows during auroral activity: Revisited p 360 N93-11268
Electron energization in the topside auroral ionosphere: On the importance of ion-acoustic turbulence
p 360 N93-11269
Effects of current driven instabilities on the ion and electron temperatures in the topside ionosphere
p 360 N93-11270
Comment on 'EISCAT Radar Observations of Enhanced Incoherent Scatter Spectra and Their Relation to Auroral Luminosity and Field-Aligned Currents' by P. N. Collis et al. p 360 N93-11271
Scattering of electromagnetic waves from a plasma: Enhanced ion acoustic fluctuations due to ion-ion two-stream instabilities p 361 N93-11272
On the origin of ion acoustic turbulence in the auroral topside ionosphere p 361 N93-11273

SYRACUSE UNIV., NY.
MMIC GaAs bonding investigation
[AD-A254773] p 470 N93-12464

SYSTEMS CONTROL TECHNOLOGY, INC., ARLINGTON, VA.
Rotorcraft health and usage monitoring systems: A literature survey
[DOT/FAA/RD-91/6] p 206 N93-11461

SYSTEMS CONTROL TECHNOLOGY, INC., PALO ALTO, CA.
Intelligent diagnostics systems p 393 N93-11931

T

TECHNETICS, INC., DELAND, FL.
Ceramic TBS/porous metal compliant layer
p 228 N93-12453

TECHNICAL RESEARCH CENTRE OF FINLAND, ESPOO.
Measuring and modelling of particle-fluid flow in a riser reactor
[VTT-PUBS-88] p 299 N93-11359
Pressure and noise induced by a cavitating marine screw propeller
[VTT-PUBS-87] p 299 N93-11360

TECHNISCHE UNIV., EINDHOVEN (NETHERLANDS).
Orientation, stress, and density distributions in injection-moulded amorphous polymers determined by optical techniques
[ETN-92-92271] p 269 N93-11983
The peculiar rheo-optical behaviour of bisphenol-A-polycarbonate and polymethylmethacrylate
p 269 N93-11984
The time-dependent stress-optical behaviour of polycarbonate in the glass transition region
p 269 N93-11985
The measurement and calculation of birefringence in quenched polycarbonate specimens
p 269 N93-11986
Molecular orientation induced by cooling stresses in polycarbonate. 1: Free quenching p 269 N93-11987
Molecular orientation induced by cooling stresses in polycarbonate. 2: Constrained quench and injection moulding p 270 N93-11988
Measurement of the density distributions in quenched polycarbonate specimens by a quantitative Schlieren-optical technique p 270 N93-11989
Gapwise density distributions in injection-moulded polymethylmethacrylate p 270 N93-11990
Analysis of the birefringence distributions in compact discs of polycarbonate p 270 N93-11991

TEKTRONIX, INC., BEAVERTON, OR.
Final Report, January 1991 - July 1992
[AD-A254659] p 483 N93-12244

TENNESSEE STATE UNIV., NASHVILLE.
Evaluation of an analytical model for predicting light scattering from cylindrically-shaped objects in the ocean
[AD-A248414] p 447 N93-11489

TENNESSEE TECHNOLOGICAL UNIV., COOKEVILLE.
Nuclear structure models: Applications and development
[DE92-018758] p 436 N93-11443

TENNESSEE UNIV., KNOXVILLE.
On-line analysis of chemical composition using an FT-Raman spectrometer in the near-IR
[DE92-016503] p 253 N93-12311

TENNESSEE UNIV., TULLAHOMA.
Transient phenomena in MHD experiments
[DE92-014496] p 455 N93-12139

TENNESSEE UNIV. SPACE INST., TULLAHOMA.
A wall interference assessment/correction system
[NASA-CR-190617] p 218 N93-11910

TENNESSEE VALLEY AUTHORITY, CHATTANOOGA.
Energy efficient motors reference guide
[DE92-019073] p 290 N93-11514

TEXAS A&I UNIV., KINGSVILLE.
A neuro-collision avoidance strategy for robot manipulators p 400 N93-11962

TEXAS A&M UNIV., COLLEGE STATION.
An autonomous vehicle: Constrained test and evaluation
[PB92-205608] p 325 N93-11427

Stationary time series analysis using information and spectral analysis p 425 N93-11431

Leading edge film cooking heat transfer including the effect of mainstream turbulence p 199 N93-11886

Determination of loose spline coupling coefficients of rotor bearing systems in turbomachinery
p 327 N93-11887

History of statistics in real time: Hammers and nails
[AD-A253521] p 429 N93-12081

Fourier continuum finite elements for nonlinear structural analysis p 340 N93-12210

Fiber optic delay line signal processors
[AD-A254691] p 448 N93-12227

Limit theorems for Fisher-score change processes
p 427 N93-12328

Change analysis and Fisher-Score change processes
[AD-A254707] p 429 N93-12334

Research in statistical inference
[AD-A252928] p 429 N93-12429

TEXAS A&M UNIV., GALVESTON.

Bibliography of publications from the Texas A and M Sea Grant College Program, 1968-1992
[PB92-205517] p 372 N93-11253

TEXAS STATE DEPT. OF HIGHWAYS AND PUBLIC TRANSPORTATION, AUSTIN.

An evaluation of repair techniques used for uncontrolled longitudinal cracking and failed longitudinal joints
[PB92-205616] p 277 N93-12072

TEXAS UNIV., AUSTIN.

On the stability of confined shells under external pressure p 335 N93-11202

Numerical simulation for the coaxial electromagnetic launcher using hybrid potentials with FE-BE method
p 222 N93-11726

Effects of sweep on the physics of unsteady shock-induced turbulent separated flows
[AD-A247035] p 198 N93-11742

Nonlinear evolution of resistive tearing mode instability with shear flow and viscosity
[DE92-012138] p 453 N93-11745

Dynamics of space debris p 219 N93-11904

An evaluation of repair techniques used for uncontrolled longitudinal cracking and failed longitudinal joints
[PB92-205616] p 277 N93-12072

A game theoretic approach to linear dynamic estimation p 340 N93-12200

Anomalous ion thermal transport in hot ion plasmas by the ion temperature gradient mode
[DE92-016686] p 456 N93-12493

TEXTRON DEFENSE SYSTEMS, EVERETT, MA.

CO2 laser frequency doubling
[AD-A251060] p 314 N93-10997

TOLEDO UNIV., OH.

Numerical modeling of a vortex stabilized arcjet
p 232 N93-11889

TOULOUSE UNIV. (FRANCE).

X pulse radiation around the critical surface
p 318 N93-12027

Development of a hydrodynamic code: MINNIE
p 318 N93-12031

TRW, INC., REDONDO BEACH, CA.

Flank solar wind interaction
[NASA-CR-189285] p 489 N93-12303

TRW ELECTRONIC SYSTEMS GROUP, REDONDO BEACH, CA.

GaAs heterojunction device based A/D converter development
[AD-A252644] p 468 N93-12183

TRW SPACE TECHNOLOGY LABS., REDONDO BEACH, CA.

MHD integrated topping cycle project
[DE92-018087] p 456 N93-12504

TUFTS UNIV., MEDFORD, MA.

High energy physics at Tufts University
[DE92-018081] p 444 N93-11668

TURIN UNIV. (ITALY).

Clinical types of Hepatitis B p 376 N93-11286

U

UFA, INC., NEWTON, MA.

Integration of task level planning and diagnosis for an intelligent robot p 393 N93-11929

UNITED NATIONS ENVIRONMENT PROGRAMME, NAIROBI (KENYA).

Scientific assessment of ozone depletion: 1991
[NASA-TM-107976] p 350 N93-11087

UNITED TECHNOLOGIES RESEARCH CENTER, EAST HARTFORD, CT.

Theoretical study of the radiative and kinetic properties of selected metal oxides and air molecules
[AD-A251090] p 438 N93-11804

Investigation of hot streak migration and film cooling effects on heat transfer in rotor/stator interacting flows, report 1
[AD-A250688] p 471 N93-12490

UNIVERSAL ENERGY SYSTEMS, INC., DAYTON, OH.

Friction of self-lubricating surfaces by ion beam techniques
[DE92-016069] p 328 N93-12122

UNIVERSITY OF CENTRAL FLORIDA, ORLANDO.

Design of an air traffic computer simulation system to support investigation of civil tiltrotor aircraft operations
[NASA-CR-190811] p 204 N93-11139

Implementing system simulation of C3 systems using autonomous objects
[NASA-CR-190845] p 283 N93-11716

Optical limiting
[AD-A254620] p 322 N93-12238

UNIVERSITY OF SOUTHERN CALIFORNIA, LOS ANGELES.

Dynamical effects of suction/heating on turbulent boundary layers
[AD-A248459] p 299 N93-11416

Contactless optoelectronic integrated circuits for remote fiber optic communication and sensing applications
[AD-A253573] p 290 N93-11507

Gas-surface interactions near dissociation threshold
[AD-A250205] p 252 N93-12254

UNIVERSITY OF WESTERN ONTARIO, LONDON.

Boundary condition methods in the numerical solution of the Navier-Stokes equations with the application to free surface problems
[ISBN-0-315-64278-5] p 298 N93-11241

UTAH STATE UNIV., LOGAN.

New singularity and existence of solutions in anisotropic, time-dependent, maximally Gauss-Bonnet extended gravity p 357 N93-11183

Organometallic NLO polymers. 3. Copolymerization of bridged bis(ferrocenyl) and bis(cyanoacetate) monomers via the knoevenagel condensation
[AD-A250214] p 265 N93-11192

UTAH UNIV., SALT LAKE CITY.

Triisopropylindium: A new precursor for OMVPE growth
[AD-A250672] p 460 N93-11558

3-D turbulent particle dispersion submodel development
[DE92-018212] p 301 N93-11670

3-D turbulent particle dispersion submodel development
[DE92-018228] p 302 N93-11671

Basic principles of organometallic vapor phase epitaxy
[AD-A250665] p 464 N93-11868

Triisopropylindium: Decomposition study and use for low temperature growth
[AD-A250666] p 464 N93-11869

Thermochemistry of transition metal clusters
[DE92-018713] p 262 N93-12480

UTRECHT STATE UNIV. (NETHERLANDS).

Ion temperature measurements in tokamak plasmas by Rutherford scattering
[PB92-184738] p 451 N93-11245

V

VANDERBILT UNIV., NASHVILLE, TN.

Matching and vertex packing: How hard are they?
[AD-A245928] p 423 N93-10991

Two extendability in two classes of claw-free graphs
[AD-A254639] p 427 N93-12243

VARIAN ASSOCIATES, PALO ALTO, CA.

10 kW L-band amplifier tubes for efficient and reliable troposcatter communication transmitter systems
[AD-A253246] p 290 N93-11504

VERMONT UNIV., BURLINGTON.

A new two-phase flow and transport model with interphase mass exchange
[PB92-206564] p 298 N93-11251

VIRGINIA POLYTECHNIC INST. AND STATE UNIV., BLACKSBURG.

The hemisphere-cylinder at an angle of attack
p 196 N93-11250

Modeling and identification of flexible joints in vehicle structures p 324 N93-11261

Thermal fracture service life analysis of a case bonded visco-elastic cylinder p 339 N93-12008

Laminar boundary-layer breakdown
[AD-A254489] p 306 N93-12162

Verification of rain-flow reconstructions of a variable amplitude load history
[NASA-CR-189670] p 341 N93-12411

VIRGINIA UNIV., CHARLOTTESVILLE.

Micromechanics of metal matrix composites using the Generalized Method of Cells model (GMC) user's guide
[NASA-CR-190756] p 335 N93-11175

Mechanisms of localized aqueous corrosion in aluminum-lithium-copper alloys p 259 N93-11895

Flow visualization of supersonic flow through a combustor section p 200 N93-12001

VISIDYNE, INC., BURLINGTON, MA.

The design, development, and test of balloonborne and groundbased lidar systems. Volume 3: Groundbased lidar systems
[AD-A247552] p 317 N93-11805

The design, development, and test of balloonborne and groundbased lidar systems. Volume 1: Balloonborne coherent CO2 lidar system
[AD-A247551] p 322 N93-12262

VON KARMAN INST. FOR FLUID DYNAMICS, RHODE-SAINT-GENESE (BELGIUM).

A three dimensional high resolution upwind finite volume Euler solver
[VKI-TN-180] p 198 N93-11686

W

WALTER REED ARMY MEDICAL CENTER, WASHINGTON, DC.

AIDS/HIV in the US Military p 377 N93-11291

Use of novel adjuvants and delivery systems to improve the humoral and cellular immune response to malaria vaccine candidate antigens p 381 N93-11308

WASHINGTON STATE UNIV., PULLMAN.

Atmospheric dispersion in mountain valleys and basins
p 355 N93-11920

Interaction of sound with sound by novel mechanisms: Ultrasonic four-wave mixing mediated by a suspension and ultrasonic three-wave mixing at a free surface
[AD-A254657] p 435 N93-12097

Photoinduced electron transfer counter to the bias field in coupled quantum wells
[AD-A254719] p 469 N93-12338

WASHINGTON UNIV., SAINT LOUIS, MO.

Studies in quantum field theory
[DE92-011035] p 470 N93-11276

WASHINGTON UNIV., SEATTLE.

Ultraviolet studies of Cepheids
[NASA-CR-190857] p 481 N93-11073

Detection of a white dwarf in a visual binary system
[NASA-CR-190856] p 481 N93-11075

Magnetic resonance elucidation of molecule/macromolecule interaction stereochemistry
[AD-A253030] p 437 N93-11709

Nucleon axial coupling constants and QCD sum rules
[DE92-014227] p 439 N93-11844

A consistent cracked bar vibration theory
p 339 N93-12000

The neutrino process and neutrino r-process
[DE92-014304] p 485 N93-12120

Investigation of high efficiency monolithic multibandgap solar cells
[AD-A254326] p 348 N93-12144

WEATHER SQUADRON (45TH), PATRICK AFB, FL.

Weather impacts on space operations
[AD-A253720] p 371 N93-12170

WEIZMANN INST. OF SCIENCE, REHOVOTH (ISRAEL).

Semiclassical analysis spectral correlations in mesoscopic systems
[DE92-634887] p 471 N93-11780

WEST VIRGINIA UNIV., MORGANTOWN.

Design of a lattice-based faceted classification system
p 415 N93-12385

A hybrid approach to software repository retrieval: Blending faceted classification and type signatures
p 415 N93-12386

Selecting reusable components using algebraic specifications p 415 N93-12387

Neural network-based retrieval from software reuse repositories p 415 N93-12388

Inheritance for software reuse: The good, the bad, and the ugly p 415 N93-12389

Supporting multiple domains in a single reuse repository p 415 N93-12390

Assessing repository technology: Where do we go from here? p 415 N93-12391

A neural net-based approach to software metrics
p 415 N93-12392

Balancing generality and specificity in component-based reuse p 416 N93-12393

WESTINGHOUSE ELECTRIC CORP., ORLANDO, FL.

Advanced coal-fueled gas turbine systems
[DE92-018939] p 327 N93-11832

WESTINGHOUSE IDAHO NUCLEAR CO., INC., IDAHO FALLS.

Improved corrosion resistance of Hastelloy G-30 in nitric/hydrofluoric acid solutions by welding with Inconel 72 weld wire
[DE92-017233] p 262 N93-12487

Radiological information management system (RadIMS)
[DE92-017221] p 480 N93-12495

Environmental restoration project configuration control
[DE92-017223] p 356 N93-12496

WESTINGHOUSE SAVANNAH RIVER CO., AIKEN, SC.

Trip report: Marshall Space Center computed tomography
[DE92-018139] p 437 N93-11597

Structure of the nocturnal boundary layer over a complex terrain
[DE92-018141] p 362 N93-11669

Mechanical properties of 1950's vintage 304 stainless steel weldment components after low temperature neutron irradiation
[DE92-017059] p 259 N93-12107

Reactor materials program: Mechanical properties of irradiated types 304 and 304L stainless steel weldment components
[DE92-018105] p 260 N93-12158

WICHITA STATE UNIV., KS.

A simplified numerical procedure to compute the optimal trajectory of an aircraft p 207 N93-11719

WISCONSIN UNIV., MADISON.

The forcing of a mid-latitude upper-tropospheric jet streak by a simulated mesoscale convective system
p 358 N93-11184

A new pitch angle diagnostic for electron cyclotron resonance plasma p 450 N93-11185

Chemical reactions and properties of organosilicon compounds related to new materials
[AD-A253233] p 246 N93-11218

Mass energy-transfer and mass energy-absorption coefficients, including in-flight positron annihilation for photon energies 1 keV to 100 MeV, 1992
[PB92-181106] p 438 N93-11715

Design and synthesis of molecular systems capable of supporting intracavity chemical reactions
[AD-A251024] p 440 N93-11872

Importance of numerosity and distribution of articulations within the digits, wrists, and arms of telemanipulators confronted with dextrous assembly tasks
p 330 N93-11967

Systems of evolution equations in thermochemical equations
[AD-A254891] p 253 N93-12282

State-resolved collisional energy transfer in highly vibrationally excited polyatomic molecules
[AD-A253299] p 441 N93-12323

WISCONSIN UNIV., MILWAUKEE.

Relativistic condensate and cosmology
p 486 N93-12330

Creep failure in linear and nonlinear viscoelastic materials p 342 N93-12536

WOODS HOLE OCEANOGRAPHIC INST., MA.

The structure and transport of the Brazil current between 27 deg and 36 deg south
[AD-A247635] p 374 N93-12247

WORLD HEALTH ORGANIZATION, GENEVA (SWITZERLAND).

HIV infection in the nineties p 377 N93-11290

Communicable diseases: A major burden of morbidity and mortality p 380 N93-11300

Future approaches to vaccine development single-dose vaccines using controlled-release delivery systems
p 382 N93-11310

WORLD METEOROLOGICAL ORGANIZATION, GENEVA (SWITZERLAND).

Scientific assessment of ozone depletion: 1991
[NASA-TM-107976] p 350 N93-11087

CCL working group on climate data
[WCDMP-18] p 370 N93-11897

WRIGHT LAB., EGLIN AFB, FL.

Electromagnetic launcher control using finite state machines
[AD-A254433] p 222 N93-12161

WRIGHT LAB., WRIGHT-PATTERSON AFB, OH.

An investigation of electromagnetic launcher repeatability
[AD-A254339] p 222 N93-12130

WYOMING UNIV., LARAMIE.

Energy efficient drivepower: An overview
[PB92-199173] p 294 N93-12191

Energy efficient drivepower: Literature reference list: Culled references
[PB92-199181] p 294 N93-12192

Energy efficient drivepower: Literature reference list. Volume 1: General user's supplement
[PB92-199157] p 294 N93-12294

Energy efficient drivepower: Literature reference list. Volume 2: Design engineer's supplement
[PB92-199165] p 295 N93-12295

Y

YALE UNIV., NEW HAVEN, CT.

Numerical calculations of an axisymmetric laminar diffusion flame with detailed and reduced reaction mechanisms p 246 N93-11259

On the inverse scattering problem for the Helmholtz equation in one dimension
[AD-A253130] p 434 N93-11526

Research in elementary particles and interactions
[DE92-018089] p 437 N93-11681

Perturbation theory for the solution of systems of linear equations
[AD-A254994] p 428 N93-12511

Z

ZAMBIA UNIV., LUSAKA.

Proceedings of the First Seminar on Geographic Information Systems in Zambia
[PB92-207125] p 477 N93-11789

ZURICH UNIV. (SWITZERLAND).

Hepatitis A and Hepatitis B: Risks compared to other vaccine preventable diseases and immunization recommendations p 377 N93-11288

Recent lessons on the safety and effectiveness of malaria chemoprophylaxis in a non-immune population
p 381 N93-11307

CONTRACT NUMBER INDEX

Typical Contract Number Index Listing

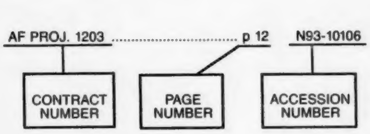

Listings in this index are arranged alphanumerically by contract number. Under each contract number the accession numbers denoting documents that have been produced as a result of research done under that contract are arranged in ascending order. The page number helps to locate the citation in the abstract section. The accession number denotes the number by which the citation is identified.

AF PROJ. 1121 .... p 387 N93-12252
AF PROJ. 1203 .... p 222 N93-12130
AF PROJ. 1209 .... p 284 N93-12160
AF PROJ. 2311 .... p 489 N93-12506
AF PROJ. 4519 .... p 448 N93-12272
AF PROJ. 7231 .... p 387 N93-11559
p 204 N93-12489
AF-AFOSR-0004-89 .... p 246 N93-11218
AF-AFOSR-0008-89 .... p 385 N93-12469
AF-AFOSR-0015-89 .... p 420 N93-11147
AF-AFOSR-0016-89 .... p 386 N93-11503
AF-AFOSR-0027-89 .... p 483 N93-11750
AF-AFOSR-0028-89 .... p 441 N93-12323
AF-AFOSR-0038-89 .... p 291 N93-11758
AF-AFOSR-0057-89 .... p 252 N93-12254
AF-AFOSR-0095-91 .... p 348 N93-12144
AF-AFOSR-0103-87 .... p 468 N93-12231
AF-AFOSR-0106-88 .... p 285 N93-12230
AF-AFOSR-0108-89 .... p 249 N93-11755
AF-AFOSR-0112-86 .... p 198 N93-11742
AF-AFOSR-0124-91 .... p 387 N93-10994
AF-AFOSR-0154-91 .... p 386 N93-11488
AF-AFOSR-0176-91 .... p 446 N93-11071
p 447 N93-11099
AF-AFOSR-0185-91 .... p 463 N93-11753
AF-AFOSR-0200-90 .... p 389 N93-12229
AF-AFOSR-0209-90 .... p 372 N93-12420
AF-AFOSR-0215-88 .... p 422 N93-12259
AF-AFOSR-0228-91 .... p 422 N93-12258
AF-AFOSR-0240-89 .... p 429 N93-12429
AF-AFOSR-0264-89 .... p 436 N93-11196
AF-AFOSR-0294-90 .... p 375 N93-11146
AF-AFOSR-0304-89 .... p 384 N93-11841
AF-AFOSR-0332-90 .... p 250 N93-11866
AF-AFOSR-0360-90 .... p 295 N93-12421
AF-AFOSR-0397-89 .... p 197 N93-11464
AF-AFOSR-0492-89 .... p 421 N93-12226
AF-AFOSR-0538-89 .... p 440 N93-11867
AF-AFOSR-0783-89 .... p 436 N93-11467
ARPA ORDER 5404 .... p 406 N93-11145
ARPA ORDER 81-62 .... p 290 N93-11491
BMFT-LVT-8701-1 .... p 213 N93-11339
CEC-B16-003-UK .... p 316 N93-11411
CIT-596045 .... p 279 N93-11117
p 279 N93-11119
DA PROJ. 1L1-61102-AH-45 .... p 206 N93-11170
p 300 N93-11529
DA PROJ. 1L1-61102-AH-52 .... p 268 N93-11862
DA PROJ. 1L1-61102-BH-57 .... p 249 N93-11490
DA PROJ. 1L1-62211-A-47-A .... p 323 N93-10966
p 206 N93-10968
p 323 N93-10982
DA PROJ. 1L1-62786-AH-98 .... p 390 N93-12423
DA PROJ. 1L1-62786-D-283 .... p 200 N93-12179
DA PROJ. 2Q1-62785-A-791 .... p 386 N93-11779
DAAL03-86-D-0001 .... p 205 N93-11419
DAAL03-88-K-0090 .... p 272 N93-12297
DAAL03-88-K-0094 .... p 272 N93-12246
DAAL03-88-K-0185 .... p 253 N93-12282
DAAL03-88-K-0197 .... p 307 N93-12333
DAAL03-89-C-0028 .... p 228 N93-12452
DAAL03-89-G-0118 .... p 475 N93-11506
p 479 N93-12287
DAAL03-89-K-0013 .... p 275 N93-12236
DAAL03-89-K-0017 .... p 297 N93-11148
DAAL03-89-K-0021 .... p 290 N93-11507
DAAL03-89-K-0031 .... p 240 N93-11835
DAAL03-89-K-0033 .... p 429 N93-12513
DAAL03-89-K-0049 .... p 264 N93-11079
DAAL03-89-K-0068 .... p 259 N93-11850
DAAL03-89-K-0074 .... p 287 N93-12436
DAAL03-89-K-0096 .... p 276 N93-12285
DAAL03-89-K-0108 .... p 295 N93-12502
DAAL03-90-G-0069 .... p 425 N93-11431
p 429 N93-12081
p 427 N93-12328
p 429 N93-12334
DAAL03-90-G-0089 .... p 322 N93-12238
DAAL03-90-G-0092 .... p 287 N93-12512
DAAL03-90-G-0135 .... p 264 N93-11149
DAAL03-91-C-0028 .... p 252 N93-12186
DAAL03-91-C-0046 .... p 295 N93-12340
DAAL03-91-G-0137 .... p 248 N93-11455
DAAL03-91-G-0159 .... p 208 N93-12485
DAAL03-91-G-0326 .... p 295 N93-12437
DAAL03-91-M-0149 .... p 283 N93-11811
DACA39-90-M-2528 .... p 286 N93-12422
DACA76-91-C-0026 .... p 420 N93-11000
DAEA18-90-C-0044 .... p 388 N93-11783
DAJA45-91-M-0061 .... p 249 N93-11490
DAJS45-92-M-0190 .... p 292 N93-12071
DAMD17-88-C-8169 .... p 384 N93-11561
DE-AC02-76CH-00016 .... p 443 N93-11429
p 443 N93-11498
p 443 N93-11499
p 316 N93-11500
p 459 N93-11501
p 256 N93-11519
p 374 N93-11630
p 444 N93-11641
p 438 N93-11746
p 445 N93-11776
p 284 N93-12132
p 313 N93-12140
p 306 N93-12221
DE-AC02-76CH-03000 .... p 411 N93-11555
DE-AC02-76CH-03073 .... p 449 N93-11041
DE-AC02-78ET-51013 .... p 449 N93-11041
DE-AC02-79ET-10815 .... p 455 N93-12139
DE-AC02-80ET-15601 .... p 454 N93-11826
p 312 N93-11827
p 304 N93-11995
p 454 N93-12087
p 455 N93-12141
DE-AC02-83CH-10093 .... p 463 N93-11813
p 346 N93-11814
p 463 N93-11816
p 464 N93-11818
p 275 N93-12171
DE-AC02-88CE-90026 .... p 328 N93-12122
DE-AC02-88ER-80585 .... p 317 N93-12011
DE-AC03-76SF-00098 .... p 263 N93-10972
p 489 N93-11078
p 473 N93-11151
p 443 N93-11493
p 470 N93-11518
p 316 N93-11659
p 312 N93-11822
p 440 N93-11875
p 465 N93-11915
p 466 N93-12099
p 440 N93-12100
p 355 N93-12104
p 466 N93-12109
p 413 N93-12110
p 441 N93-12111
p 251 N93-12112
p 466 N93-12124
p 466 N93-12125
p 445 N93-12126
p 466 N93-12127
p 469 N93-12316
DE-AC03-76SF-00515 .... p 316 N93-11691
p 446 N93-12497
DE-AC03-88ER-53270 .... p 453 N93-11729
DE-AC03-89ER-51114 .... p 449 N93-10988
p 449 N93-11041
p 451 N93-11382
p 305 N93-12010
p 455 N93-12307
DE-AC03-89ER-53277 .... p 452 N93-11660
DE-AC04-76DP-00613 .... p 267 N93-11497
p 404 N93-11539
p 291 N93-11643
p 249 N93-11644
p 292 N93-11916
DE-AC04-76DP-00789 .... p 231 N93-10973
p 254 N93-10984
p 344 N93-10989
p 204 N93-11152
p 280 N93-11234
p 367 N93-11236
p 217 N93-11367
p 408 N93-11378
p 276 N93-11494
p 487 N93-11502
p 433 N93-11523
p 411 N93-11536
p 300 N93-11537
p 249 N93-11551
p 267 N93-11552
p 290 N93-11553
p 362 N93-11564
p 411 N93-11599
p 257 N93-11600
p 221 N93-11631
p 291 N93-11639
p 437 N93-11640
p 277 N93-11672
p 311 N93-11673
p 452 N93-11674
p 369 N93-11678
p 291 N93-11693
p 453 N93-11694
p 232 N93-11766
p 477 N93-11770
p 346 N93-11771
p 463 N93-11797
p 303 N93-11799
p 283 N93-11800
p 232 N93-11824
p 464 N93-11842
p 303 N93-11843
p 419 N93-11860
p 284 N93-11917
p 347 N93-12012
p 348 N93-12074
p 348 N93-12075
p 284 N93-12101
p 445 N93-12103
p 277 N93-12106
p 467 N93-12134
p 421 N93-12138
p 329 N93-12220
p 348 N93-12222
p 260 N93-12232
p 219 N93-12268
p 348 N93-12312
DE-AC04-76DR-00789 .... p 421 N93-12153
p 252 N93-12255
p 275 N93-12265
DE-AC04-88DP-43495 .... p 310 N93-11554
DE-AC05-84ER-40150 .... p 442 N93-11077
DE-AC05-84OR-21400 .... p 458 N93-10987
p 473 N93-10990
p 449 N93-11041
p 359 N93-11235
p 475 N93-11441
p 266 N93-11442
p 459 N93-11496
p 443 N93-11517
p 267 N93-11570
p 426 N93-11636
p 301 N93-11638
p 268 N93-11654
p 353 N93-11655
p 354 N93-11680

p 268 N93-11735
p 463 N93-11772
p 258 N93-11773
p 338 N93-11792
p 312 N93-11806
p 259 N93-11830
p 439 N93-11849
p 259 N93-11857
p 399 N93-11958
p 252 N93-12219
p 419 N93-12233
p 375 N93-12315
p 261 N93-12445
p 262 N93-12476
p 349 N93-12498
p 456 N93-12501
p 323 N93-12514
DE-AC05-84OS-21400 .... p 478 N93-11796
DE-AC06-76RL-01830 .... p 282 N93-11515
p 257 N93-11557
p 332 N93-11601
p 369 N93-11657
p 240 N93-11658
p 312 N93-11802
p 481 N93-12067
p 441 N93-12117
DE-AC07-76ID-01570 .... p 332 N93-11154
p 407 N93-11356
p 443 N93-11433
p 326 N93-11548
p 257 N93-11595
p 232 N93-11596
p 301 N93-11637
p 362 N93-11692
p 333 N93-12055
p 233 N93-12056
p 292 N93-12057
p 471 N93-12058
p 454 N93-12066
p 455 N93-12092
p 328 N93-12114
p 446 N93-12129
p 271 N93-12168
p 262 N93-12494
DE-AC07-84ID-12435 .... p 262 N93-12487
p 480 N93-12495
p 356 N93-12496
DE-AC08-88NV-10617 .... p 286 N93-12417
DE-AC09-89SR-18035 .... p 437 N93-11597
p 362 N93-11669
p 259 N93-12107
p 260 N93-12158
DE-AC21-86MC-23167 .... p 327 N93-11832
DE-AC22-87PC-90274 .... p 456 N93-12504
DE-AC22-91PC-90056 .... p 250 N93-11847
DE-AC34-90DP-62349 .... p 326 N93-11556
p 327 N93-11679
p 249 N93-11801
p 465 N93-12073
DE-AC35-89ER-40486 .... p 471 N93-11656
DE-AI05-87OR-21749 .... p 263 N93-10962
DE-FC07-88ID-12691 .... p 253 N93-12311
DE-FC07-88ID-12707 .... p 303 N93-11774
DE-FG01-90CE-15440 .... p 300 N93-11440
DE-FG01-91PE-10015 .... p 356 N93-12474
DE-FG02-84ER-45058 .... p 441 N93-12115
DE-FG02-84ER-45131 .... p 462 N93-11747
DE-FG02-84ER-45153 .... p 461 N93-11629
DE-FG02-85ER-13331 .... p 490 N93-12477
DE-FG02-85ER-45220 .... p 273 N93-12500
DE-FG02-86ER-13503 .... p 253 N93-12257
DE-FG02-86ER-13519 .... p 436 N93-11541
DE-FG02-86ER-13558 .... p 258 N93-11762
DE-FG02-86ER-13564 .... p 271 N93-12165
DE-FG02-86ER-13615 .... p 253 N93-12428
DE-FG02-86ER-45247 .... p 460 N93-11512
DE-FG02-86ER-45255 .... p 256 N93-11524
DE-FG02-86ER-45265 .... p 432 N93-12116
DE-FG02-86ER-53223 .... p 455 N93-12188
DE-FG02-87ER-13687 .... p 471 N93-12102
DE-FG02-87ER-13700 .... p 435 N93-11189
DE-FG02-87ER-25027 .... p 345 N93-11733
DE-FG02-87ER-45320 .... p 461 N93-11646
DE-FG02-87ER-45330 .... p 464 N93-11894
DE-FG02-87ER-60519 .... p 313 N93-11828
DE-FG02-87ER-60561 .... p 384 N93-11873
DE-FG02-88ER-13822 .... p 254 N93-12478
DE-FG02-88ER-40415 .... p 442 N93-12444
DE-FG02-88ER-60631 .... p 375 N93-12266
DE-FG02-89ER-14042 .... p 327 N93-11865
DE-FG02-89ER-14079 .... p 431 N93-11567
p 363 N93-11791
p 364 N93-12142
p 366 N93-12308
p 366 N93-12318
DE-FG02-89ER-40506 .... p 443 N93-11521
DE-FG02-89ER-53297 .... p 452 N93-11568
DE-FG02-89ER-69027 .... p 353 N93-11569
DE-FG02-90ER-14144 .... p 461 N93-11682
DE-FG02-90ER-14147 .... p 300 N93-11538
DE-FG02-90ER-45427 .... p 462 N93-11706
DE-FG02-90ER-45428 .... p 273 N93-12479
DE-FG02-90ER-45438 .... p 267 N93-11628
DE-FG02-90ER-54084 .... p 449 N93-10988
DE-FG02-90ER-61060 .... p 366 N93-10971
DE-FG02-91ER-14178 .... p 247 N93-11439
DE-FG02-91ER-14192 .... p 251 N93-12119
DE-FG02-91ER-14193 .... p 262 N93-12480
DE-FG02-91ER-40628 .... p 470 N93-11276
DE-FG02-91ER-40648 .... p 315 N93-11278
DE-FG02-91ER-61228 .... p 384 N93-11445
DE-FG02-92ER-14270 .... p 306 N93-12173
DE-FG02-92ER-40702 .... p 444 N93-11668
DE-FG02-92ER-40704 .... p 437 N93-11681
DE-FG02-92ER-61363 .... p 367 N93-11237
DE-FG03-85ER-13418 .... p 363 N93-11848
DE-FG03-86SF-16592 .... p 346 N93-11823
DE-FG03-87ER-13727 .... p 452 N93-11565
DE-FG03-88ER-13932 .... p 289 N93-11438
DE-FG03-89ER-13986 .... p 251 N93-12105
DE-FG03-89ER-51116 .... p 455 N93-12307
DE-FG03-91ER-61215 .... p 373 N93-11642
DE-FG03-91SF-18861 .... p 453 N93-11730
p 453 N93-11731
DE-FG03-91SF-18865 .... p 438 N93-11778
DE-FG05-80ET-53088 .... p 453 N93-11745
p 456 N93-12493
DE-FG05-86ER-13544 .... p 251 N93-12091
DE-FG05-86ER-40272 .... p 432 N93-11759
DE-FG05-86ER-45233 .... p 470 N93-12499
DE-FG05-87ER-25029 .... p 404 N93-11761
DE-FG05-89ER-45384 .... p 251 N93-12172
DE-FG05-91ER-61105 .... p 355 N93-11864
DE-FG05-92ER-40694 .... p 436 N93-11443
DE-FG06-88ER-40427 .... p 439 N93-11844
DE-FG06-90ER-40561 .... p 485 N93-12120
DE-FG06-90ER-60949 .... p 353 N93-11232
p 353 N93-11233
DE-FG09-84ER-40160 .... p 441 N93-12224
DE-FG09-88ER-60627 .... p 373 N93-11734
DE-FG21-90MC-27225 .... p 375 N93-12482
DE-FG22-89PC-89770 .... p 244 N93-10986
DE-FG22-90PC-90094 .... p 301 N93-11670
p 302 N93-11671
DE-FG22-91PC-91293 .... p 247 N93-11444
DLA900-86-C-2045 .... p 389 N93-12079
DNA001-88-C-0032 .... p 438 N93-11804
DNA001-88-C-0102 .... p 447 N93-11186
DNA001-90-C-0024 .... p 222 N93-12505
DRET/DS/SR-90150 .... p 240 N93-11708
DTFA01-87-C-00014 .... p 206 N93-11461
EPA-R-818955 .... p 298 N93-11251
EPA-68-CO-0048 .... p 456 N93-12526
p 457 N93-12527
FAA-T2001-B .... p 205 N93-11704
p 205 N93-11705
F04701-88-C-0089 .... p 434 N93-11752
p 230 N93-11927
p 226 N93-12064
p 366 N93-12378
p 226 N93-12379
F19628-86-C-0105 .... p 317 N93-11805
p 322 N93-12262
F19628-86-K-0002 .... p 310 N93-11562
F19628-87-C-0169 .... p 363 N93-11810
F19628-87-K-0050 .... p 294 N93-12290
F19628-88-K-0022 .... p 224 N93-11736
F19628-88-K-0053 .... p 448 N93-12227
F19628-89-C-0001 .... p 414 N93-12284
p 286 N93-12433
F19628-89-K-0018 .... p 359 N93-11228
F19628-89-K-0027 .... p 363 N93-11788
F19628-89-K-0028 .... p 361 N93-11421
F19628-89-K-0048 .... p 366 N93-12270
F19628-90-C-0101 .... p 290 N93-11492
F19628-90-K-0043 .... p 362 N93-11740
F30602-83-C-0149 .... p 290 N93-11504
F30602-88-D-0026 .... p 408 N93-11371
F30602-88-D-0028 .... p 292 N93-11781
F30602-89-C-0055 .... p 477 N93-11749
F30602-89-C-0082 .... p 414 N93-12242
F30602-89-C-0113 .... p 470 N93-12464
F30602-89-C-0121 .... p 413 N93-12146
F33615-C-5041 .... p 262 N93-12468
F33615-84-C-3404 .... p 208 N93-12488
F33615-87-C-1401 .... p 476 N93-11508
F33615-87-C-5243 .... p 242 N93-12181
F33615-88-C-0010 .... p 421 N93-12096
F33615-90-C-3000 .... p 202 N93-12466
F33615-91-C-2136 .... p 348 N93-12166
F33616-87-C-5212 .... p 241 N93-12054
F49620-88-K-0009 .... p 462 N93-11727
F49620-89-C-0028 .... p 447 N93-11527
F49620-90-C-0044 .... p 323 N93-12335
F49620-91-C-0026 .... p 200 N93-12063
F49620-91-C-0052 .... p 272 N93-12337
F49620-91-C-0066 .... p 467 N93-12169
GRI-5087-245-1518 .... p 312 N93-11757
GRI-5090-260-1971 .... p 470 N93-11469
HSE-1533 .... p 325 N93-11324
p 325 N93-11325
p 325 N93-11326
p 325 N93-11327
IED-RA-6/25/01 .... p 238 N93-11409
INF-89-002-01 .... p 279 N93-11118
K/MGW11A/334 .... p 288 N93-11364
MDA903-86-C-0412 .... p 386 N93-11779
MDA903-87-C-0523 .... p 390 N93-12508
p 390 N93-12509
MDA903-89-C-0003 .... p 477 N93-11732
p 404 N93-11809
p 472 N93-12273
p 390 N93-12491
MDA903-89-K-0078 .... p 242 N93-12292
MDA903-90-D-0022 .... p 475 N93-11465
MDA972-88-C-0064 .... p 268 N93-11793
MDA972-89-C-0035 .... p 463 N93-11790
MDA972-91-C-0032 .... p 290 N93-11491
MDA972-92-C-0028 .... p 242 N93-12292
MIPR-FQ8671-9001535 .... p 250 N93-11866
MT-CWR-092-028 .... p 240 N93-11795
NAGW-1272 .... p 343 N93-12006
NAGW-1356 .... p 248 N93-11451
NAGW-1657 .... p 357 N93-10964
NAGW-1682 .... p 478 N93-12007
NAGW-1684 .... p 486 N93-11164
NAGW-3079 .... p 461 N93-11683
p 461 N93-11684
NAG1-1038 .... p 201 N93-12343
NAG1-1228 .... p 270 N93-11993
NAG1-1342 .... p 204 N93-10961
NAG1-613 .... p 404 N93-11462
p 418 N93-11651
p 419 N93-12395
p 406 N93-12540
p 406 N93-12541
NAG1-623 .... p 426 N93-11547
p 330 N93-12521
NAG1-822 .... p 341 N93-12411
NAG1-854 .... p 213 N93-12214
NAG1-87263 .... p 279 N93-11117
p 279 N93-11119
NAG1-908 .... p 279 N93-11116
p 279 N93-11118
NAG2-593 .... p 472 N93-12212
NAG2-625 .... p 204 N93-11139
p 283 N93-11716
NAG2-733 .... p 218 N93-11910
NAG3-1032 .... p 301 N93-11606
NAG3-1163 .... p 341 N93-12277
NAG3-1215 .... p 297 N93-11074
NAG3-742 .... p 341 N93-12277
NAG8-104 .... p 416 N93-12515
NAG8-126 .... p 248 N93-11453
NAG8-160 .... p 248 N93-11455
NAG8-759 .... p 223 N93-11101
NAG8-816 .... p 297 N93-11142
NASW-4102 .... p 487 N93-11603
NAS1-18565 .... p 216 N93-12413
NAS1-18586 .... p 405 N93-12345
p 405 N93-12346
p 405 N93-12347
p 406 N93-12538
NAS1-18599 .... p 202 N93-12399
NAS1-18605 .... p 425 N93-11246
p 412 N93-11618
p 301 N93-11633
p 435 N93-12021
p 306 N93-12173
p 416 N93-12400
p 416 N93-12403
NAS1-19000 .... p 239 N93-11611
NAS1-19161 .... p 366 N93-12299
NAS1-19399 .... p 243 N93-12306
NAS1-19480 .... p 425 N93-11246
p 198 N93-11607
p 412 N93-11618
p 301 N93-11633
p 306 N93-12173
p 427 N93-12298
p 416 N93-12400
p 416 N93-12403
NAS2-13187 .... p 245 N93-11135
NAS3-25266 .... p 248 N93-11452
p 235 N93-11948
p 234 N93-12409
NAS3-25556 .... p 247 N93-11450
NAS3-25808 .... p 347 N93-12017

p 347 N93-12019
NAS5-29386 p 373 N93-11718
NAS5-30375 p 434 N93-11634
NAS5-31216 p 489 N93-12303
NAS7-1100 p 291 N93-11604
NAS7-1152 p 405 N93-12520
NAS7-918 p 420 N93-11174
p 324 N93-11177
p 290 N93-11456
p 412 N93-11664
p 278 N93-12202
NAS8-36857 p 233 N93-12088
p 234 N93-12441
p 235 N93-12523
NAS8-36950 p 308 N93-12539
NAS8-36955 p 311 N93-11662
p 328 N93-11992
p 233 N93-12009
p 233 N93-12013
p 305 N93-12082
p 328 N93-12196
p 448 N93-12201
p 220 N93-12213
p 252 N93-12215
p 483 N93-12348
p 470 N93-12396
p 307 N93-12397
p 276 N93-12401
p 385 N93-12427
p 323 N93-12516
p 235 N93-12522
p 473 N93-12542
NAS8-37126 p 227 N93-12442
p 227 N93-12443
NAS8-37403 p 248 N93-11454
NAS8-38420 p 393 N93-11929
NAS8-38609 p 231 N93-11042
p 231 N93-11043
NAS8-38681 p 231 N93-11173
NAS8-38798 p 235 N93-11449
NAS8-38871 p 297 N93-11171
NAS8-38910 p 399 N93-11957
NAS9-17332 p 288 N93-12519
NAS9-17749 p 485 N93-11546
NAS9-17885 p 397 N93-11949
p 397 N93-11950
NAS9-17900 p 389 N93-12195
p 389 N93-12211
NAS9-18021 p 326 N93-11650
NAS9-18452 p 399 N93-11957
NA16RG0457-01 p 372 N93-11253
NA86AA-D-SG089 p 338 N93-11903
NA90AA-H-CZ-809 p 343 N93-11701
NCC1-46 p 197 N93-11605
p 200 N93-12004
NCC10-0006 p 349 N93-12394
NCC2-371 p 439 N93-11851
p 439 N93-11852
p 439 N93-11853
NCC2-387 p 409 N93-11458
NCC2-689 p 307 N93-12329
NCC2-716 p 219 N93-12349
NCC3-135 p 310 N93-11612
NCC3-233 p 426 N93-11531
NCC5-42 p 370 N93-11880
NCC9-16 p 407 N93-11368
p 412 N93-11717
p 414 N93-12384
NGR-06-002-112 p 232 N93-11608
NOAA PROJECT RO-33 p 338 N93-11903
NR PROJ. RR0-330 p 372 N93-12339
NSF ASC-88-19393 p 416 N93-12403
NSF CCR-88-20279 p 427 N93-11837
NSF CCR-90-08226 p 413 N93-12131
NSF CCR-91-02853 p 428 N93-12511
NSF DCR-84-12314 p 409 N93-11458
NSF DDM-88-00281 p 430 N93-12217
NSF DDM-89-01495 p 430 N93-12217
NSF DDM-90-01705 p 430 N93-12217
NSF DMS-90-12751 p 434 N93-11526
NSF DMS-91-07608 p 306 N93-12173
NSF ECS-89-57475 p 425 N93-11246
NSF MIP-86-57563 p 418 N93-11651
NSF MIP-89-09498 p 330 N93-11961
NSF MSS-90-24391 p 330 N93-11961
NSF NCR-89-07909 p 416 N93-12403
NSF OCE-86-14486 p 374 N93-12247
NSG-5398 p 481 N93-11073
p 481 N93-11075
N00014-82-C-0019 p 374 N93-12247
N00014-82-C-0280 p 250 N93-12062
N00014-82-K-0190 p 431 N93-11468
N00014-82-K-0612 p 246 N93-11280
p 238 N93-11281
N00014-84-K-0415 p 406 N93-11145
N00014-85-K-0488 p 423 N93-10991
N00014-85-K-0803 p 295 N93-12360
N00014-86-K-0110 p 316 N93-11418
N00014-86-K-0411 p 289 N93-11414
N00014-86-K-0678 p 474 N93-11353
N00014-86-K-0694 p 288 N93-11257
N00014-87-C-0315 p 468 N93-12183
N00014-87-C-0790 p 388 N93-11812
N00014-87-K-0169 p 308 N93-12435
N00014-88-K-0166 p 413 N93-12131
N00014-88-K-0202 p 437 N93-11709
N00014-88-K-0358 p 440 N93-11872
N00014-88-K-0483 p 236 N93-12177
N00014-88-K-0500 p 240 N93-11795
N00014-88-K-0573 p 428 N93-12511
N00014-88-K-0620 p 419 N93-12239
N00014-89-C-0137 p 422 N93-12439
N00014-89-J-1135 p 245 N93-11138
N00014-89-J-1180 p 260 N93-12118
N00014-89-J-1527 p 434 N93-11526
N00014-89-J-1542 p 265 N93-11187
p 265 N93-11188
N00014-89-J-1545 p 462 N93-11724
p 467 N93-12175
N00014-89-J-1659 p 428 N93-12465
N00014-89-J-1754 p 361 N93-11282
N00014-89-J-2042 p 284 N93-12083
N00014-89-J-3800 p 435 N93-12097
N00014-90-C-0053 p 376 N93-11193
N00014-90-C-0215 p 371 N93-12167
p 287 N93-12461
N00014-90-J-1030 p 427 N93-11837
N00014-90-J-1159 p 458 N93-10996
p 437 N93-11560
N00014-90-J-1193 p 469 N93-12338
N00014-90-J-1270 p 418 N93-11651
N00014-90-J-1340 p 335 N93-11219
p 258 N93-11782
N00014-90-J-1492 p 386 N93-11415
N00014-90-J-1559 p 272 N93-12289
p 480 N93-12438
p 273 N93-12440
N00014-90-J-1588 p 447 N93-11489
N00014-90-J-1604 p 271 N93-12184
N00014-90-J-1670 p 256 N93-11240
N00014-90-J-1730 p 308 N93-12435
N00014-90-J-1924 p 242 N93-12296
N00014-91-C-0001 p 244 N93-11132
p 247 N93-11448
N00014-91-C-0124 p 260 N93-12237
N00014-91-C-0214 p 260 N93-12241
N00014-91-C-2052 p 483 N93-12244
N00014-91-C-2056 p 288 N93-11239
N00014-91-C-2279 p 314 N93-10997
N00014-91-J-1116 p 419 N93-12395
p 406 N93-12540
N00014-91-J-1142 p 423 N93-10991
p 427 N93-12243
N00014-91-J-1198 p 316 N93-11737
N00014-91-J-1274 p 265 N93-11194
N00014-91-J-1309 p 306 N93-12162
N00014-91-J-1393 p 437 N93-11709
N00014-91-J-1409 p 250 N93-11808
N00014-91-J-1447 p 460 N93-11558
p 464 N93-11868
p 464 N93-11869
N00014-91-J-1625 p 265 N93-11192
N00014-91-J-1857 p 448 N93-11892
N00014-91-J-1917 p 266 N93-11413
N00014-91-J-1976 p 468 N93-12228
N00014-91-J-4168 p 386 N93-12225
N00014-92-C-0043 p 284 N93-12095
N00014-92-J-1062 p 299 N93-11416
N00014-92-J-1069 p 372 N93-12507
N00014-92-J-1094 p 374 N93-12431
N00014-92-J-1125 p 468 N93-12218
N00014-92-J-1136 p 254 N93-12518
N00014-92-J-1192 p 432 N93-10999
N00014-92-J-1433 p 264 N93-11150
N00123-89-G-0573 p 253 N93-12267
N00140-88-C-0677 p 471 N93-12490
N00174-C-91-0119 p 279 N93-11117
p 279 N93-11119
PROJ. A-90-11-00038 p 470 N93-11469
PROJ. 6547 p 425 N93-11431
p 427 N93-12328
RF-596044 p 279 N93-11118
RICIS PROJ. IM-06 p 407 N93-11368
RICIS PROJ. SE-16 p 412 N93-11717
RICIS PROJ. SE-43 p 414 N93-12384
RRO-4106 p 437 N93-11709
RTOP 107-30-31 p 391 N93-12319
RTOP 144-10-2A p 224 N93-11430
RTOP 144-50-50 p 287 N93-12481
RTOP 199-18-12-07 p 374 N93-12014
RTOP 199-61-12-42 p 388 N93-12018
RTOP 307-50-00 p 336 N93-11403
RTOP 462-61-04-10 p 344 N93-12351
RTOP 469-01-11-02 p 339 N93-12020
RTOP 474-42-10 p 417 N93-11005
RTOP 505-01-50 p 249 N93-11545
RTOP 505-59-10-03 p 201 N93-12321
RTOP 505-59-30-01 p 198 N93-11610
RTOP 505-59-40 p 296 N93-10969
RTOP 505-62-OK p 300 N93-11529
RTOP 505-62-10 p 214 N93-12418
RTOP 505-62-21 p 426 N93-11531
p 218 N93-12016
p 341 N93-12277
RTOP 505-62-50 p 215 N93-12305
RTOP 505-62-52 p 196 N93-11223
p 425 N93-11254
p 213 N93-12077
p 286 N93-12366
RTOP 505-63-M p 263 N93-10962
RTOP 505-63-1A p 236 N93-10978
RTOP 505-63-1B p 243 N93-12302
RTOP 505-63-36-06 p 206 N93-10968
RTOP 505-63-36 p 323 N93-10966
p 323 N93-10982
RTOP 505-63-5A p 258 N93-11635
p 241 N93-12076
RTOP 505-63-5B p 334 N93-11004
RTOP 505-63-50-04 p 239 N93-11611
p 243 N93-12306
p 341 N93-12411
RTOP 505-63-50-08 p 239 N93-11623
RTOP 505-63-53 p 241 N93-12015
RTOP 505-64-10-06 p 405 N93-12345
RTOP 505-64-10-07 p 405 N93-12346
p 405 N93-12347
p 406 N93-12538
RTOP 505-64-10-10 p 215 N93-12304
RTOP 505-64-13-32 p 206 N93-11170
RTOP 505-64-13 p 205 N93-12320
RTOP 505-64-30-01 p 214 N93-11459
RTOP 505-64-30 p 277 N93-11619
RTOP 505-64-52-01 p 214 N93-11176
RTOP 505-64-52-03 p 215 N93-12216
RTOP 505-68-1C p 276 N93-12197
RTOP 505-68-30-04 p 198 N93-11622
RTOP 505-68-32 p 213 N93-11530
RTOP 505-68-71 p 202 N93-12353
RTOP 505-69-50 p 209 N93-10983
p 213 N93-12402
RTOP 505-70-64-01 p 216 N93-12413
RTOP 505-90-52-01 p 425 N93-11246
p 198 N93-11607
p 412 N93-11618
p 301 N93-11633
p 435 N93-12021
p 306 N93-12173
p 427 N93-12298
p 416 N93-12400
RTOP 505-90-52 p 242 N93-12078
RTOP 505-90-53 p 257 N93-11609
RTOP 506-41-11 p 226 N93-12152
p 295 N93-12301
RTOP 506-41-41 p 230 N93-10965
RTOP 506-42-31 p 231 N93-11402
p 234 N93-12409
p 235 N93-12484
RTOP 506-42-73 p 296 N93-10981
RTOP 506-43-31-04 p 227 N93-12447
RTOP 506-43-41-02 p 224 N93-10970
RTOP 506-43-71-04 p 339 N93-12005
RTOP 506-72-1B p 469 N93-12325
RTOP 509-10-11-04 p 414 N93-12278
RTOP 510-01-50 p 331 N93-10963
p 333 N93-10967
p 335 N93-11175
p 238 N93-11399
p 337 N93-11624
RTOP 533-02-11 p 207 N93-11863
RTOP 533-02-38 p 214 N93-11178
p 197 N93-11532
p 202 N93-12353
RTOP 533-02-39 p 196 N93-11221
RTOP 535-03-0B p 413 N93-12022
RTOP 535-03-10 p 433 N93-11370
RTOP 535-03-11-03 p 435 N93-12080
RTOP 537-01-20-01 p 366 N93-12299
RTOP 537-03-21-03 p 434 N93-11620
RTOP 537-04-10 p 273 N93-12398
RTOP 578-12-26-70 p 367 N93-11168
RTOP 582-01-41 p 221 N93-11401
RTOP 590-13-00 p 221 N93-11398
RTOP 590-13-11 p 275 N93-12085
RTOP 590-14-11-02 p 277 N93-11613
RTOP 590-14-21-01 p 341 N93-12300
RTOP 590-14-41-03 p 222 N93-12543
RTOP 590-14-61-01 p 336 N93-11544
RTOP 590-21-11 p 314 N93-12279

RTOP 593-12-21 .... p 232 N93-11614
RTOP 593-71-00 .... p 233 N93-12363
RTOP 650-60-23 .... p 224 N93-11001
RTOP 763-22-28 .... p 236 N93-10978
RTOP 763-23-35-19 .... p 202 N93-12399
RTOP 763-23-41-85 .... p 236 N93-11072
SUN-596044 .... p 279 N93-11117
SWRI PROJ. 15-2762 .... p 486 N93-11164
SWRI PROJ. 15-2783 .... p 357 N93-10964
UF PROJ. 4910451123312 .... p 354 N93-11702
UHCL-102 .... p 412 N93-11717
W-31-109-ENG-38 .... p 473 N93-11104
p 459 N93-11190
p 289 N93-11432
p 425 N93-11446
p 431 N93-11511
p 460 N93-11512
p 345 N93-11513
p 426 N93-11520
p 460 N93-11522
p 274 N93-11550
p 460 N93-11563
p 345 N93-11571
p 431 N93-11598
p 444 N93-11652
p 326 N93-11653
p 462 N93-11703
p 438 N93-11829
p 445 N93-11831
p 465 N93-12090
p 355 N93-12098
p 445 N93-12108
p 271 N93-12123
p 305 N93-12128
p 467 N93-12178
p 413 N93-12187
p 468 N93-12249
p 455 N93-12309
p 469 N93-12310
p 306 N93-12313
p 356 N93-12314
p 456 N93-12416
W-7405-ENG-36 .... p 357 N93-10985
p 483 N93-10993
p 407 N93-11231
p 484 N93-11379
p 274 N93-11380
p 345 N93-11381
p 443 N93-11510
p 362 N93-11535
p 274 N93-11566
p 431 N93-11625
p 345 N93-11626
p 485 N93-11695
p 488 N93-11696
p 485 N93-11697
p 444 N93-11763
p 302 N93-11767
p 312 N93-11768
p 429 N93-11820
p 312 N93-11822
p 346 N93-11825
p 303 N93-11843
p 268 N93-11861
p 250 N93-11918
p 445 N93-11919
p 479 N93-12068
p 313 N93-12069
p 293 N93-12089
p 364 N93-12136
p 294 N93-12156
p 322 N93-12250
p 261 N93-12256
p 365 N93-12263
p 365 N93-12264
W-7405-ENG-48 .... p 374 N93-10974
p 449 N93-10975
p 449 N93-10988
p 450 N93-11153
p 315 N93-11155
p 217 N93-11447
p 451 N93-11495
p 451 N93-11516
p 256 N93-11519
p 451 N93-11534
p 326 N93-11540
p 310 N93-11542
p 267 N93-11549
p 461 N93-11602
p 448 N93-11627
p 282 N93-11632
p 452 N93-11645
p 461 N93-11647
p 316 N93-11659
p 282 N93-11661
p 282 N93-11675
p 354 N93-11676
p 354 N93-11677
p 354 N93-11744
p 317 N93-11765
p 337 N93-11775
p 454 N93-12059
p 454 N93-12060
p 465 N93-12065
p 465 N93-12093
p 293 N93-12113
p 293 N93-12121
p 413 N93-12137
p 479 N93-12143
p 371 N93-12154
p 364 N93-12155
p 414 N93-12234
p 221 N93-12317
W-7405-ENG-82 .... p 254 N93-10995
p 332 N93-11154
p 459 N93-11238
p 460 N93-11533
p 257 N93-11572
p 462 N93-11706
p 261 N93-12261

REPORT NUMBER INDEX

Typical Report Number Index Listing

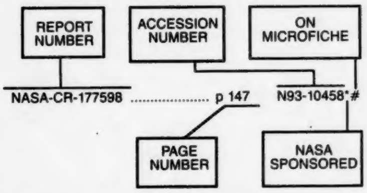

Listings in this index are arranged alphanumerically by report number. The accession number denotes the number by which the citation is identified. The page number helps to locate the citation in the abstract section. An asterisk (*) indicates that the item is a NASA report. A pound sign (#) indicates that the item is available on microfiche.

A-90237 .... p 391 N93-12319 * #
A-92141 .... p 374 N93-12014 * #
A-92142 .... p 388 N93-12018 * #
A-92145 .... p 344 N93-12351 * #
A-92158 .... p 205 N93-12320 * #

AD-A242147 .... p 405 N93-12430 #
AD-A245863 .... p 260 N93-12118 #
AD-A245928 .... p 423 N93-10991 #
AD-A246061 .... p 412 N93-11859 #
AD-A246276 .... p 268 N93-11862 #
AD-A246883 .... p 426 N93-11463 #
AD-A246889 .... p 362 N93-11740 #
AD-A246891 .... p 359 N93-11228 #
AD-A246894 .... p 361 N93-11421 #
AD-A246910 .... p 266 N93-11413 #
AD-A247035 .... p 198 N93-11742 #
AD-A247258 .... p 197 N93-11464 #
AD-A247261 .... p 208 N93-12053 #
AD-A247266 .... p 475 N93-11465 #
AD-A247279 .... p 353 N93-11466 #
AD-A247288 .... p 436 N93-11467 #
AD-A247293 .... p 291 N93-11758 #
AD-A247294 .... p 431 N93-11468 #
AD-A247355 .... p 289 N93-11414 #
AD-A247382 .... p 386 N93-11415 #
AD-A247462 .... p 430 N93-12217 #
AD-A247551 .... p 322 N93-12262 #
AD-A247552 .... p 317 N93-11805 #
AD-A247611 .... p 448 N93-11892 #
AD-A247635 .... p 374 N93-12247 #
AD-A247944 .... p 468 N93-12218 #
AD-A248001 .... p 467 N93-12175 #
AD-A248021 .... p 204 N93-12489 #
AD-A248174 .... p 447 N93-11186 #
AD-A248349 .... p 386 N93-11488 #
AD-A248414 .... p 447 N93-11489 #
AD-A248459 .... p 299 N93-11416 #
AD-A248569 .... p 428 N93-11417 #
AD-A248675 .... p 388 N93-11743 #
AD-A248698 .... p 265 N93-11187 #
AD-A248700 .... p 265 N93-11188 #
AD-A248734 .... p 316 N93-11418 #
AD-A248953 .... p 205 N93-11419 #
AD-A249068 .... p 261 N93-12248 #
AD-A249095 .... p 451 N93-11275 #
AD-A249131 .... p 241 N93-12054 #
AD-A249133 .... p 283 N93-11760 #
AD-A249139 .... p 427 N93-12061 #
AD-A249140 .... p 430 N93-11420 #
AD-A249230 .... p 240 N93-11835 #
AD-A249830 .... p 387 N93-10994 #
AD-A249839 .... p 371 N93-12251 #
AD-A249862 .... p 387 N93-12252 #
AD-A250193 .... p 341 N93-12253 #
AD-A250205 .... p 252 N93-12254 #
AD-A250214 .... p 265 N93-11192 #
AD-A250219 .... p 283 N93-11764 #
AD-A250377 .... p 250 N93-11866 #
AD-A250648 .... p 385 N93-11893 #
AD-A250664 .... p 440 N93-11867 #
AD-A250665 .... p 464 N93-11868 #
AD-A250666 .... p 464 N93-11869 #
AD-A250668 .... p 253 N93-12267 #
AD-A250672 .... p 460 N93-11558 #
AD-A250673 .... p 387 N93-11559 #
AD-A250688 .... p 471 N93-12490 #
AD-A250689 .... p 427 N93-11837 #
AD-A250697 .... p 207 N93-11838 #
AD-A250702 .... p 478 N93-11840 #
AD-A250705 .... p 384 N93-11841 #
AD-A250716 .... p 390 N93-12491 #
AD-A250931 .... p 236 N93-12177 #
AD-A251024 .... p 440 N93-11872 #
AD-A251050 .... p 458 N93-10996 #
AD-A251051 .... p 437 N93-11560 #
AD-A251060 .... p 314 N93-10997 #
AD-A251090 .... p 438 N93-11804 #
AD-A252243 .... p 200 N93-12179 #
AD-A252286 .... p 231 N93-10998 #
AD-A252288 .... p 432 N93-10999 #
AD-A252299 .... p 249 N93-11490 #
AD-A252329 .... p 384 N93-11561 #
AD-A252544 .... p 250 N93-11808 #
AD-A252556 .... p 420 N93-11000 #
AD-A252617 .... p 371 N93-12180 #
AD-A252632 .... p 242 N93-12181 #
AD-A252644 .... p 468 N93-12183 #
AD-A252645 .... p 242 N93-12292 #
AD-A252648 .... p 271 N93-12184 #
AD-A252677 .... p 310 N93-11562 #
AD-A252692 .... p 474 N93-11353 #
AD-A252811 .... p 348 N93-12166 #
AD-A252820 .... p 386 N93-11779 #
AD-A252882 .... p 371 N93-12167 #
AD-A252883 .... p 287 N93-12461 #
AD-A252927 .... p 308 N93-12462 #
AD-A252928 .... p 429 N93-12429 #
AD-A253001 .... p 446 N93-11071 #
AD-A253030 .... p 437 N93-11709 #
AD-A253119 .... p 288 N93-11239 #
AD-A253120 .... p 256 N93-11240 #
AD-A253130 .... p 434 N93-11526 #
AD-A253132 .... p 447 N93-11527 #
AD-A253185 .... p 375 N93-11146 #
AD-A253207 .... p 292 N93-11781 #
AD-A253233 .... p 246 N93-11218 #
AD-A253235 .... p 386 N93-11503 #
AD-A253246 .... p 290 N93-11504 #
AD-A253268 .... p 368 N93-11505 #
AD-A253269 .... p 363 N93-11785 #
AD-A253272 .... p 477 N93-11749 #
AD-A253274 .... p 363 N93-11788 #
AD-A253287 .... p 363 N93-11810 #
AD-A253295 .... p 376 N93-11193 #
AD-A253299 .... p 441 N93-12323 #
AD-A253301 .... p 483 N93-11750 #
AD-A253311 .... p 265 N93-11194 #
AD-A253392 .... p 389 N93-12079 #
AD-A253472 .... p 447 N93-11099 #
AD-A253521 .... p 429 N93-12081 #
AD-A253529 .... p 284 N93-12083 #
AD-A253538 .... p 434 N93-11752 #
AD-A253543 .... p 420 N93-11147 #
AD-A253544 .... p 297 N93-11148 #
AD-A253547 .... p 422 N93-12258 #
AD-A253556 .... p 463 N93-11753 #
AD-A253559 .... p 249 N93-11755 #
AD-A253560 .... p 259 N93-11850 #
AD-A253561 .... p 283 N93-11811 #
AD-A253564 .... p 388 N93-11812 #
AD-A253566 .... p 264 N93-11149 #
AD-A253568 .... p 264 N93-11150 #
AD-A253569 .... p 264 N93-11079 #
AD-A253571 .... p 475 N93-11506 #
AD-A253573 .... p 290 N93-11507 #
AD-A253579 .... p 288 N93-11257 #
AD-A253648 .... p 387 N93-11279 #
AD-A253657 .... p 335 N93-11219 #
AD-A253658 .... p 246 N93-11280 #
AD-A253659 .... p 238 N93-11281 #
AD-A253668 .... p 467 N93-12169 #
AD-A253708 .... p 334 N93-11080 #
AD-A253720 .... p 371 N93-12170 #
AD-A253724 .... p 385 N93-11081 #
AD-A253751 .... p 463 N93-11790 #
AD-A253771 .... p 250 N93-12062 #
AD-A253792 .... p 200 N93-12063 #
AD-A253800 .... p 242 N93-12296 #
AD-A253801 .... p 258 N93-11782 #
AD-A253808 .... p 388 N93-11783 #
AD-A253814 .... p 388 N93-11784 #
AD-A253841 .... p 462 N93-11724 #
AD-A253857 .... p 272 N93-12297 #
AD-A253859 .... p 367 N93-11144 #
AD-A253869 .... p 406 N93-11145 #
AD-A253891 .... p 408 N93-11371 #
AD-A253893 .... p 252 N93-12186 #
AD-A253905 .... p 361 N93-11282 #
AD-A253908 .... p 462 N93-11727 #
AD-A253910 .... p 290 N93-11491 #
AD-A253917 .... p 290 N93-11492 #
AD-A253989 .... p 404 N93-11809 #
AD-A253990 .... p 477 N93-11732 #
AD-A253993 .... p 224 N93-11736 #
AD-A253999 .... p 316 N93-11737 #
AD-A254001 .... p 268 N93-11793 #
AD-A254002 .... p 240 N93-11795 #
AD-A254013 .... p 476 N93-11508 #
AD-A254016 .... p 226 N93-12064 #
AD-A254023 .... p 292 N93-12071 #
AD-A254041 .... p 422 N93-12259 #
AD-A254043 .... p 430 N93-12260 #
AD-A254100 .... p 317 N93-11786 #
AD-A254101 .... p 261 N93-12269 #
AD-A254102 .... p 258 N93-11787 #
AD-A254107 .... p 281 N93-11509 #
AD-A254110 .... p 225 N93-11798 #
AD-A254204 .... p 240 N93-11739 #
AD-A254238 .... p 477 N93-11741 #
AD-A254255 .... p 477 N93-11748 #
AD-A254258 .... p 218 N93-11751 #
AD-A254265 .... p 489 N93-11815 #
AD-A254267 .... p 369 N93-11817 #
AD-A254269 .... p 369 N93-11819 #
AD-A254286 .... p 373 N93-11821 #
AD-A254288 .... p 315 N93-11195 #
AD-A254291 .... p 436 N93-11196 #
AD-A254302 .... p 302 N93-11756 #
AD-A254313 .... p 374 N93-12094 #
AD-A254320 .... p 284 N93-12095 #
AD-A254321 .... p 243 N93-12483 #
AD-A254326 .... p 348 N93-12144 #
AD-A254328 .... p 385 N93-12145 #
AD-A254333 .... p 413 N93-12146 #
AD-A254339 .... p 222 N93-12130 #
AD-A254340 .... p 413 N93-12131 #
AD-A254350 .... p 366 N93-12270 #
AD-A254353 .... p 468 N93-12271 #
AD-A254354 .... p 448 N93-12272 #
AD-A254366 .... p 472 N93-12273 #
AD-A254370 .... p 413 N93-12159 #
AD-A254414 .... p 284 N93-12160 #
AD-A254433 .... p 222 N93-12161 #
AD-A254461 .... p 314 N93-12517 #
AD-A254465 .... p 242 N93-12235 #
AD-A254473 .... p 275 N93-12236 #
AD-A254489 .... p 306 N93-12162 #
AD-A254603 .... p 260 N93-12237 #
AD-A254620 .... p 322 N93-12238 #
AD-A254623 .... p 419 N93-12239 #
AD-A254626 .... p 285 N93-12240 #
AD-A254628 .... p 260 N93-12241 #
AD-A254633 .... p 414 N93-12242 #
AD-A254639 .... p 427 N93-12243 #
AD-A254653 .... p 421 N93-12096 #
AD-A254657 .... p 435 N93-12097 #
AD-A254659 .... p 483 N93-12244 #
AD-A254660 .... p 306 N93-12245 #
AD-A254661 .... p 272 N93-12246 #
AD-A254681 .... p 386 N93-12225 #

AD-A254689 p 421 N93-12226 #
AD-A254691 p 448 N93-12227 #
AD-A254697 p 468 N93-12228 #
AD-A254699 p 389 N93-12229 #
AD-A254700 p 285 N93-12230 #
AD-A254703 p 468 N93-12231 #
AD-A254705 p 285 N93-12332 #
AD-A254706 p 307 N93-12333 #
AD-A254707 p 429 N93-12334 #
AD-A254709 p 323 N93-12335 #
AD-A254717 p 272 N93-12337 #
AD-A254719 p 469 N93-12338 #
AD-A254723 p 372 N93-12339 #
AD-A254725 p 295 N93-12340 #
AD-A254726 p 414 N93-12341 #
AD-A254735 p 307 N93-12355 #
AD-A254736 p 285 N93-12356 #
AD-A254737 p 344 N93-12357 #
AD-A254738 p 419 N93-12358 #
AD-A254749 p 222 N93-12505 #
AD-A254773 p 470 N93-12464 #
AD-A254782 p 428 N93-12465 #
AD-A254835 p 374 N93-12431 #
AD-A254840 p 387 N93-12432 #
AD-A254842 p 286 N93-12433 #
AD-A254844 p 329 N93-12434 #
AD-A254854 p 308 N93-12435 #
AD-A254870 p 287 N93-12436 #
AD-A254872 p 295 N93-12437 #
AD-A254873 p 480 N93-12438 #
AD-A254878 p 422 N93-12439 #
AD-A254880 p 273 N93-12440 #
AD-A254883 p 295 N93-12360 #
AD-A254889 p 295 N93-12502 #
AD-A254890 p 276 N93-12281 #
AD-A254891 p 253 N93-12282 #
AD-A254892 p 469 N93-12283 #
AD-A254894 p 414 N93-12284 #
AD-A254900 p 276 N93-12285 #
AD-A254905 p 469 N93-12286 #
AD-A254907 p 479 N93-12287 #
AD-A254908 p 374 N93-12288 #
AD-A254914 p 272 N93-12289 #
AD-A254955 p 489 N93-12506 #
AD-A254982 p 372 N93-12507 #
AD-A254983 p 390 N93-12508 #
AD-A254984 p 390 N93-12509 #
AD-A254993 p 333 N93-12510 #
AD-A254994 p 428 N93-12511 #
AD-A254997 p 287 N93-12512 #
AD-A254999 p 429 N93-12513 #
AD-A255000 p 254 N93-12518 #
AD-A255045 p 202 N93-12466 #
AD-A255059 p 342 N93-12467 #
AD-A255060 p 262 N93-12468 #
AD-A255061 p 385 N93-12469 #
AD-A255065 p 208 N93-12485 #
AD-A255067 p 390 N93-12486 #
AD-A255071 p 208 N93-12488 #
AD-A255073 p 490 N93-12470 #
AD-A255100 p 329 N93-12274 #
AD-A255119 p 294 N93-12290 #
AD-A255120 p 389 N93-12291 #
AD-A255125 p 372 N93-12420 #
AD-A255126 p 295 N93-12421 #
AD-A255127 p 286 N93-12422 #
AD-A255128 p 390 N93-12423 #
AD-A255157 p 372 N93-12424 #
AD-A255159 p 405 N93-12425 #
AD-A255160 p 429 N93-12426 #
AD-A255161 p 323 N93-12405 #
AD-A255164 p 307 N93-12406 #
AD-A255165 p 435 N93-12471 #
AD-A255167 p 480 N93-12472 #
AD-A255170 p 480 N93-12473 #
AD-A255171 p 286 N93-12407 #
AD-A255172 p 227 N93-12408 #
AD-A255173 p 341 N93-12376 #
AD-A255176 p 286 N93-12377 #
AD-A255178 p 366 N93-12378 #
AD-A255179 p 226 N93-12379 #
AD-A255181 p 486 N93-12380 #
AD-A255184 p 479 N93-12381 #
AD-A255190 p 322 N93-12275 #
AD-A255191 p 272 N93-12276 #

AD-D015339 p 278 N93-11044
AD-D015340 p 273 N93-11045
AD-D015341 p 214 N93-11046
AD-D015346 p 280 N93-11354 #
AD-D015347 p 278 N93-11047 #
AD-D015349 p 309 N93-11048
AD-D015350 p 309 N93-11049
AD-D015351 p 195 N93-11050
AD-D015352 p 268 N93-11051
AD-D015353 p 446 N93-11052 #
AD-D015357 p 293 N93-12133 #
AD-D015360 p 266 N93-11400
AD-D015362 p 325 N93-11423
AD-D015363 p 221 N93-11428
AD-D015364 p 274 N93-11665
AD-D015365 p 232 N93-11424
AD-D015366 p 266 N93-11425
AD-D015367 p 281 N93-11426
AD-D015371 p 442 N93-11060
AD-D015372 p 288 N93-11053

AD-E200865 p 359 N93-11228 #
AD-E200867 p 361 N93-11421 #
AD-E200868 p 362 N93-11740 #
AD-E200874 p 317 N93-11805 #
AD-E200880 p 322 N93-12262 #
AD-E201028 p 363 N93-11788 #
AD-E201097 p 363 N93-11810 #
AD-E201115 p 290 N93-11492 #
AD-E201120 p 284 N93-12160 #
AD-E201132 p 366 N93-12270 #
AD-E201142 p 489 N93-12506 #
AD-E501518 p 390 N93-12491 #
AD-E501549 p 404 N93-11809 #
AD-E501550 p 477 N93-11732 #
AD-E501558 p 472 N93-12273 #

AERONOMICA-ACTA-A-365 p 352 N93-11127

AFIT/CI/CIA-91-122 p 371 N93-12251 #
AFIT/CI/CIA-91-133 p 341 N93-12253 #
AFIT/CI/CIA-92-026 p 371 N93-12180 #
AFIT/CI/CIA-92-068 p 369 N93-11819 #
AFIT/CI/CIA-92-069 p 489 N93-11815 #
AFIT/CI/CIA-92-070 p 369 N93-11817 #

AFOSR-92-0114TR p 291 N93-11758 #
AFOSR-92-0151TR p 436 N93-11467 #
AFOSR-92-0154TR p 198 N93-11742 #
AFOSR-92-0202TR p 386 N93-11488 #
AFOSR-92-0233TR p 387 N93-10994 #
AFOSR-92-0273TR p 440 N93-11867 #
AFOSR-92-0306TR p 252 N93-12254 #
AFOSR-92-0375TR p 384 N93-11841 #
AFOSR-92-0511TR-VOL-14 p 446 N93-11071 #
AFOSR-92-0520TR-VOL-9 p 447 N93-11099 #
AFOSR-92-0672TR p 447 N93-11527 #
AFOSR-92-0679TR p 441 N93-12323 #
AFOSR-92-0680TR p 429 N93-12429 #
AFOSR-92-0690TR p 462 N93-11727 #
AFOSR-92-0692TR p 200 N93-12063 #
AFOSR-92-0698TR p 246 N93-11218 #
AFOSR-92-0699TR p 483 N93-11750 #
AFOSR-92-0703TR p 386 N93-11503 #
AFOSR-92-0715TR p 420 N93-11147 #
AFOSR-92-0717TR p 249 N93-11755 #
AFOSR-92-0722TR p 467 N93-12169 #
AFOSR-92-0723TR p 463 N93-11753 #
AFOSR-92-0727TR p 372 N93-12420 #
AFOSR-92-0728TR p 422 N93-12258 #
AFOSR-92-0734TR p 375 N93-11146 #
AFOSR-92-0762TR p 389 N93-12229 #
AFOSR-92-0768TR p 468 N93-12231 #
AFOSR-92-0781TR p 285 N93-12230 #
AFOSR-92-0784TR p 348 N93-12144 #
AFOSR-92-0792TR p 436 N93-11196 #
AFOSR-92-0795TR p 422 N93-12259 #
AFOSR-92-0825TR p 272 N93-12337 #
AFOSR-92-0826TR p 421 N93-12226 #
AFOSR-92-0850TR p 385 N93-12469 #

AGARD-AG-300-VOL-10 p 430 N93-11711 #

AGARD-CP-518 p 376 N93-11283 #

AGARD-R-777 p 476 N93-11710 #

AGS/AD-92-1 p 445 N93-11776 #
AGS/AD-92-2 p 443 N93-11499 #
AGS/AD-92-3 p 443 N93-11498 #

AIAA PAPER 92-3204 p 234 N93-12409 * #
AIAA PAPER 92-3447 p 226 N93-12152 * #
AIAA PAPER 92-3533 p 231 N93-11402 * #
AIAA PAPER 92-3608 p 334 N93-11080 #
AIAA PAPER 92-3622 p 213 N93-12077 * #
AIAA PAPER 92-3696 p 233 N93-12056 #
AIAA PAPER 92-4101 p 207 N93-11863 * #
AIAA PAPER 92-4105 p 197 N93-11532 * #
AIAA PAPER 92-4396 p 214 N93-11178 * #
AIAA PAPER 92-4713 p 213 N93-12402 * #
AIAA PAPER 92-4777 p 206 N93-10968 * #
AIAA PAPER 93-0482 p 214 N93-12418 * #

AIP-143 p 474 N93-11353 #

AL-SR-91-0002 p 385 N93-11081 #

AL-TP-1992-0014 p 387 N93-12252 #

AL-TR-1991-0110 p 387 N93-11559 #
AL-TR-1991-0111 p 204 N93-12489 #
AL-TR-1992-0037 p 421 N93-12096 #

AMSAA-TR-524 p 333 N93-12510 #

ANL-92/19 p 326 N93-11653 #
ANL-92/31 p 274 N93-11550 #

ANL/CP-72465 p 271 N93-12123 #
ANL/CP-73655 p 462 N93-11703 #
ANL/CP-74716 p 355 N93-12098 #
ANL/CP-74842 p 460 N93-11522 #
ANL/CP-75268 p 356 N93-12314 #
ANL/CP-75351 p 305 N93-12128 #
ANL/CP-75374 p 468 N93-12249 #
ANL/CP-75446 p 455 N93-12309 #
ANL/CP-75450 p 467 N93-12178 #
ANL/CP-75523 p 431 N93-11598 #
ANL/CP-75590 p 465 N93-12090 #
ANL/CP-75722 p 459 N93-11190 #
ANL/CP-75751 p 460 N93-11563 #
ANL/CP-75917 p 426 N93-11520 #
ANL/CP-76052 p 306 N93-12313 #
ANL/CP-76280 p 438 N93-11829 #
ANL/CP-76343 p 345 N93-11571 #
ANL/CP-76359 p 469 N93-12310 #
ANL/CP-76387 p 345 N93-11513 #
ANL/CP-76530 p 445 N93-12108 #
ANL/CP-76577 p 473 N93-11104 #
ANL/CP-76578 p 444 N93-11652 #
ANL/CP-76633 p 456 N93-12416 #
ANL/CP-76653 p 460 N93-11512 #
ANL/CP-76665 p 431 N93-11511 #
ANL/CP-76687 p 289 N93-11432 #
ANL/CP-76700 p 445 N93-11831 #
ANL/CP-76726 p 425 N93-11446 #

ANL/EAIS/TM-71 p 413 N93-12187 #

AR-006-842 p 311 N93-11648 #

ARCCB-TR-92037 p 413 N93-12159 #

ARE-TM(UHR)-90306 p 197 N93-11365 #

ARI-RN-92-50 p 386 N93-11779 #
ARI-RN-92-63 p 390 N93-12509 #

ARI-RR-1622 p 390 N93-12508 #
ARI-RR-902 p 366 N93-12299 * #

ARO-24102.3-MS p 240 N93-11835 #
ARO-25390.9-MS p 259 N93-11850 #
ARO-25526.10-MS p 272 N93-12246 #
ARO-25760.6-MS p 272 N93-12297 #
ARO-26113.15-MA p 275 N93-12236 #
ARO-26118.1-EL p 287 N93-12436 #
ARO-26147.3-EL p 290 N93-11507 #
ARO-26218.6-MA p 253 N93-12282 #
ARO-26272.8-MA p 307 N93-12333 #
ARO-26287.29-MS p 264 N93-11079 #
ARO-26616.26-MA p 297 N93-11148 #
ARO-26887.1-CH p 276 N93-12285 #
ARO-26941.7-EL p 295 N93-12502 #
ARO-26945.8-MA-SDI p 287 N93-12512 #
ARO-27247.4-MA-SAH p 475 N93-11506 #
ARO-27247.5-MA-SAH p 479 N93-12287 #
ARO-27574.6-MA p 429 N93-12081 #
ARO-27574.7-MA p 429 N93-12334 #
ARO-27838.4-PH p 322 N93-12238 #
ARO-28216.1-MS-CF p 264 N93-11149 #
ARO-28787.1-GS p 283 N93-11811 #
ARO-28860.1-EG-CF p 208 N93-12485 #
ARO-28901.1-PH-CF p 295 N93-12437 #
ARO-29024.1-EL-SBI p 252 N93-12186 #

ASI690-344-91 p 390 N93-12509 #
ASI690-349-91 p 390 N93-12508 #

ASL-TR-0313 p 368 N93-11505 #
ASL-TR-0314 p 363 N93-11785 #

ATCOM-TR-92-B-011 p 206 N93-11170 * #

AVSCOM-TR-92-B-012 p 206 N93-10968 * #
AVSCOM-TR-92-C-004 p 323 N93-10982 * #
AVSCOM-TR-92-C-013 p 323 N93-10966 * #
AVSCOM-TR-92-C-023 p 300 N93-11529 * #

B-248094 p 474 N93-11274 #

BD-92-02 .... p 388 N93-11812 #

BDX-613-3417 .... p 249 N93-11644 #

BN-1128 .... p 427 N93-11837 #

BNL-47149 .... p 444 N93-11641 #
BNL-47507 .... p 313 N93-12140 #
BNL-47599 .... p 284 N93-12132 #
BNL-47624 .... p 374 N93-11630 #
BNL-47670 .... p 438 N93-11746 #
BNL-47771 .... p 443 N93-11499 #
BNL-47773 .... p 445 N93-11776 #
BNL-47796 .... p 459 N93-11501 #
BNL-47803 .... p 316 N93-11500 #
BNL-47813 .... p 443 N93-11498 #
BNL-52326 .... p 306 N93-12221 #
BNL-52336 .... p 443 N93-11429 #

BONN-IR-91-62 .... p 357 N93-11083 #
BONN-IR-91-78 .... p 357 N93-11006 #

BRL-TR-3394 .... p 344 N93-12357 #

BR106727 .... p 217 N93-11435 #
BR111965 .... p 412 N93-11712 #
BR112080 .... p 472 N93-10976 #
BR113093 .... p 428 N93-10980 #
BR113301 .... p 385 N93-10979 #
BR113378 .... p 414 N93-12326 #
BR114028 .... p 197 N93-11365 #
BR115853 .... p 278 N93-10977 #
BR300216 .... p 335 N93-11369 #
BR301923 .... p 447 N93-11342 #
BR304494-5 .... p 405 N93-12430 #
BR305095-16 .... p 240 N93-11905 #
BR305232 .... p 408 N93-11386 #
BR305233 .... p 409 N93-11436 #
BR305563 .... p 197 N93-11377 #
BR305818 .... p 199 N93-11882 #
BR305835 .... p 281 N93-11487 #
BR306616 .... p 475 N93-11404 #
BR307520 .... p 409 N93-11407 #
BR307617 .... p 409 N93-11406 #
BR308061 .... p 420 N93-11343 #
BR308887 .... p 281 N93-11391 #
BR308888 .... p 408 N93-11390 #
BR308889 .... p 407 N93-11341 #
BR308890 .... p 280 N93-11383 #
BR308891 .... p 315 N93-11388 #
BR308892 .... p 409 N93-11405 #
BR308893 .... p 408 N93-11389 #
BR308896 .... p 199 N93-11883 #
BR308899 .... p 280 N93-11384 #
BR308900 .... p 280 N93-11385 #
BR308904 .... p 273 N93-11376 #
BR309561 .... p 409 N93-11392 #
BR309781 .... p 220 N93-11486 #
BR309937 .... p 218 N93-11906 #
BR311447 .... p 474 N93-11333 #
BR86833 .... p 288 N93-11364 #
BR91882 .... p 280 N93-11366 #
BR92327 .... p 289 N93-11434 #

CAP-85-92R .... p 316 N93-11500 #
CAP-86-92R .... p 443 N93-11429 #

CARDEROCKDIV-SME-92/22 .... p 240 N93-11739 #

CDNSWC/SHD-1348-01 .... p 308 N93-12462 #

CEBAF-PR-92-010 .... p 442 N93-11077 #

CERC-WIS-27 .... p 374 N93-12094 #

CERN-TH-6330/91 .... p 470 N93-11518 #

CM-303 .... p 343 N93-11701 #
CM-80 .... p 368 N93-11340 #

CMS-CS-92-126 .... p 406 N93-11145 #

CONF-9006128-VOL-1 .... p 353 N93-11232 #
CONF-9006128-VOL-2 .... p 353 N93-11233 #
CONF-9102177-SUMM .... p 356 N93-12474 #
CONF-910374-2 .... p 254 N93-10995 #
CONF-9105113-4 .... p 470 N93-11518 #
CONF-9105181-30 .... p 441 N93-12117 #
CONF-9105344-1 .... p 426 N93-11520 #
CONF-9105361-1 .... p 488 N93-11696 #
CONF-9106226-2 .... p 485 N93-12120 #
CONF-9107115-76 .... p 293 N93-12121 #
CONF-9107218-1 .... p 483 N93-10993 #
CONF-9107232-1 .... p 362 N93-11564 #
CONF-9108209-ABSTS .... p 355 N93-11864 #
CONF-910981-66 .... p 356 N93-12496 #
CONF-9110118-7 .... p 445 N93-12126 #
CONF-9110188-1 .... p 357 N93-10985 #
CONF-9110344-10 .... p 480 N93-12495 #
CONF-9110382-1 .... p 439 N93-11844 #
CONF-9110404-1 .... p 425 N93-11446 #
CONF-911111-41 .... p 452 N93-11674 #
CONF-911202-80 .... p 256 N93-11519 #
CONF-911202-82 .... p 466 N93-12127 #
CONF-911202-83 .... p 465 N93-11915 #
CONF-9112107-1 .... p 467 N93-12178 #
CONF-911212-1 .... p 354 N93-11744 #
CONF-911212-2 .... p 355 N93-12104 #
CONF-9112126-1 .... p 473 N93-11151 #
CONF-9112129-1 .... p 312 N93-11827 #
CONF-911281-2 .... p 277 N93-11672 #
CONF-920124-19 .... p 322 N93-12250 #
CONF-920124-25 .... p 293 N93-12113 #
CONF-920124-26 .... p 452 N93-11645 #
CONF-9202108-SUMM .... p 305 N93-12070 #
CONF-9202111-5 .... p 315 N93-11155 #
CONF-9202120-1 .... p 449 N93-10975 #
CONF-920240-3 .... p 468 N93-12249 #
CONF-920305-13 .... p 257 N93-11595 #
CONF-920311-22 .... p 453 N93-11694 #
CONF-920311-23 .... p 257 N93-11600 #
CONF-920311-9 .... p 464 N93-11842 #
CONF-9203110-3 .... p 459 N93-11190 #
CONF-9203139-2 .... p 310 N93-11542 #
CONF-9203140-3 .... p 251 N93-12112 #
CONF-920315-41 .... p 442 N93-11077 #
CONF-9203164-2 .... p 443 N93-11517 #
CONF-9203165-1 .... p 253 N93-12311 #
CONF-9203168-1 .... p 441 N93-12111 #
CONF-9203173-1 .... p 317 N93-12011 #
CONF-9203174-1 .... p 431 N93-11511 #
CONF-920362-35 .... p 454 N93-12060 #
CONF-920362-37 .... p 454 N93-12059 #
CONF-920362-38 .... p 451 N93-11495 #
CONF-920362-39 .... p 450 N93-11153 #
CONF-920402-23 .... p 462 N93-11703 #
CONF-920402-33 .... p 462 N93-11706 #
CONF-920402-35 .... p 460 N93-11522 #
CONF-920402-43 .... p 268 N93-11861 #
CONF-920402-44 .... p 463 N93-11772 #
CONF-920402-46 .... p 465 N93-12065 #
CONF-920402-48 .... p 458 N93-10987 #
CONF-920402-49 .... p 267 N93-11570 #
CONF-920402-50 .... p 437 N93-11640 #
CONF-920402-51 .... p 461 N93-11647 #
CONF-9204144-3 .... p 439 N93-11849 #
CONF-9204167-1 .... p 262 N93-12476 #
CONF-9204168-1 .... p 469 N93-12316 #
CONF-9204169-1 .... p 466 N93-12125 #
CONF-9204170-1 .... p 473 N93-11104 #
CONF-9204170-3 .... p 444 N93-11652 #
CONF-9204174-1 .... p 254 N93-10984 #
CONF-9204174-2-EXTD-ABST .... p 260 N93-12232 #
CONF-920458-10 .... p 262 N93-12487 #
CONF-920505-3 .... p 259 N93-11857 #
CONF-9205118-1 .... p 374 N93-10974 #
CONF-9205123-10 .... p 271 N93-12123 #
CONF-9205147-2 .... p 454 N93-12066 #
CONF-920515-18 .... p 293 N93-12089 #
CONF-920515-27 .... p 445 N93-12103 #
CONF-920515-29 .... p 445 N93-11919 #
CONF-920515-32 .... p 282 N93-11675 #
CONF-9205157-1 .... p 219 N93-12268 #
CONF-9205222-1 .... p 276 N93-11494 #
CONF-9205226-1 .... p 485 N93-11697 #
CONF-9205226-2 .... p 485 N93-11695 #
CONF-9205226-3 .... p 484 N93-11379 #
CONF-9205227-1 .... p 362 N93-11692 #
CONF-920523-1 .... p 317 N93-11765 #
CONF-9205236-1 .... p 459 N93-11501 #
CONF-920527-7 .... p 355 N93-12098 #
CONF-920538-6 .... p 312 N93-11806 #
CONF-920550-1 .... p 332 N93-11154 #
CONF-920574-14 .... p 250 N93-11918 #
CONF-920604-1 .... p 261 N93-12256 #
CONF-920610-13 .... p 456 N93-12501 #
CONF-920610-9 .... p 455 N93-12307 #
CONF-9206130-2 .... p 354 N93-11677 #
CONF-9206135-3 .... p 455 N93-12092 #
CONF-9206135-4 .... p 262 N93-12494 #
CONF-9206135-5 .... p 271 N93-12168 #
CONF-9206140-1 .... p 252 N93-12219 #
CONF-9206141-2 .... p 267 N93-11549 #
CONF-920617-7 .... p 443 N93-11493 #
CONF-9206171-1 .... p 359 N93-11235 #
CONF-9206172-1 .... p 433 N93-11523 #
CONF-9206173-5 .... p 327 N93-11679 #
CONF-9206173-6 .... p 326 N93-11548 #
CONF-9206173-8 .... p 333 N93-12055 #
CONF-9206175-1 .... p 459 N93-11238 #
CONF-9206180-4 .... p 465 N93-12093 #
CONF-9206185-8 .... p 419 N93-12233 #
CONF-9206193-2 .... p 284 N93-12132 #
CONF-9206206-1 .... p 232 N93-11824 #
CONF-9206207-1 .... p 323 N93-12514 #
CONF-9206208-1 .... p 471 N93-12102 #
CONF-9206212-1 .... p 204 N93-11152 #
CONF-9206213-1 .... p 413 N93-12110 #
CONF-9206221-1 .... p 460 N93-11563 #
CONF-9206226-1 .... p 274 N93-11566 #
CONF-9206231-1 .... p 274 N93-11380 #
CONF-9206234-1 .... p 259 N93-11830 #
CONF-9206253-1 .... p 240 N93-11658 #
CONF-9206254-1 .... p 374 N93-11630 #
CONF-9206255-1 .... p 316 N93-11659 #
CONF-9206256-1 .... p 369 N93-11657 #
CONF-920630-1 .... p 282 N93-11515 #
CONF-920637-1 .... p 438 N93-11746 #
CONF-920637-2 .... p 445 N93-12108 #
CONF-920647-1 .... p 275 N93-12265 #
CONF-920660-1 .... p 466 N93-12099 #
CONF-920671-3 .... p 444 N93-11763 #
CONF-920671-7 .... p 291 N93-11693 #
CONF-920673-10 .... p 257 N93-11557 #
CONF-920673-7 .... p 259 N93-12107 #
CONF-920677-11 .... p 304 N93-11995 #
CONF-920677-14 .... p 455 N93-12309 #
CONF-920677-16 .... p 456 N93-12416 #
CONF-920694-1 .... p 283 N93-11800 #
CONF-920694-2 .... p 459 N93-11496 #
CONF-920706-10 .... p 431 N93-11625 #
CONF-920706-11 .... p 443 N93-11510 #
CONF-920706-24 .... p 444 N93-11641 #
CONF-920706-7 .... p 446 N93-12497 #
CONF-920707-10 .... p 252 N93-12255 #
CONF-920707-21 .... p 253 N93-12257 #
CONF-9207102-39 .... p 408 N93-11378 #
CONF-9207102-8 .... p 311 N93-11673 #
CONF-9207103-1 .... p 469 N93-12310 #
CONF-9207104-1 .... p 465 N93-12090 #
CONF-9207105-2 .... p 263 N93-10972 #
CONF-9207106-1 .... p 375 N93-12315 #
CONF-9207110 .... p 344 N93-10989 #
CONF-9207111-2 .... p 454 N93-11826 #
CONF-9207115-1 .... p 301 N93-11637 #
CONF-9207117-1 .... p 301 N93-11638 #
CONF-9207118-1 .... p 362 N93-11535 #
CONF-9207136-1 .... p 411 N93-11536 #
CONF-920717-2 .... p 449 N93-11041 #
CONF-920717-4 .... p 449 N93-10988 #
CONF-920722-3 .... p 258 N93-11773 #
CONF-920735-2 .... p 438 N93-11829 #
CONF-920747-5 .... p 221 N93-12317 #
CONF-920747-6 .... p 232 N93-11766 #
CONF-920747-7 .... p 302 N93-11767 #
CONF-920747-8 .... p 217 N93-11367 #
CONF-920747-9 .... p 233 N93-12056 #
CONF-920748-2 .... p 345 N93-11571 #
CONF-920748-3 .... p 345 N93-11513 #
CONF-920750-6 .... p 284 N93-12101 #
CONF-920768-5 .... p 445 N93-11831 #
CONF-920792-14 .... p 312 N93-11768 #
CONF-920792-19 .... p 312 N93-11822 #
CONF-920792-20 .... p 313 N93-12069 #
CONF-920792-21 .... p 451 N93-11382 #
CONF-920792-25 .... p 461 N93-11602 #
CONF-920792-2 .... p 365 N93-12264 #
CONF-920792-6 .... p 338 N93-11792 #
CONF-920793-1 .... p 365 N93-12263 #
CONF-920796-8 .... p 310 N93-11554 #
CONF-920799-1 .... p 312 N93-11802 #
CONF-920801-11 .... p 356 N93-12314 #
CONF-920801-18 .... p 446 N93-12129 #
CONF-920801-19 .... p 349 N93-12498 #
CONF-920801-20 .... p 345 N93-11626 #
CONF-920802-1 .... p 431 N93-11598 #
CONF-920803-14 .... p 231 N93-10973 #
CONF-920803-16 .... p 443 N93-11433 #
CONF-920804-15 .... p 306 N93-12313 #
CONF-920804-16 .... p 305 N93-12128 #
CONF-9208103-1 .... p 348 N93-12312 #
CONF-9208104-1 .... p 277 N93-12106 #
CONF-9208110-1 .... p 460 N93-11512 #
CONF-9208113-1 .... p 289 N93-11432 #
CONF-9208114-1 .... p 232 N93-11596 #
CONF-9208118-1 .... p 414 N93-12234 #
CONF-9208119-1 .... p 411 N93-11599 #
CONF-9208119-2 .... p 291 N93-11639 #
CONF-9208120-1 .... p 487 N93-11502 #
CONF-920852-1 .... p 303 N93-11843 #
CONF-920892-2 .... p 316 N93-11691 #
CONF-920893-1 .... p 429 N93-11820 #
CONF-920903-10 .... p 305 N93-12010 #
CONF-920903-11 .... p 300 N93-11537 #
CONF-9209107-3 .... p 367 N93-11236 #
CONF-9209109-1 .... p 407 N93-11231 #
CONF-9209113-1 .... p 421 N93-12138 #
CONF-9209114-1 .... p 280 N93-11234 #

CONF-9209142-3 .... p 479 N93-12068 #
CONF-9209156-1 .... p 354 N93-11680 #
CONF-9209158-1 .... p 362 N93-11669 #
CONF-9209158-4 .... p 354 N93-11676 #
CONF-9209164-3 .... p 346 N93-11825 #
CONF-9209170-1 .... p 326 N93-11556 #
CONF-920932-1 .... p 261 N93-12445 #
CONF-9210113-1 .... p 369 N93-11678 #
CONF-9210128-1-EXTD-ABST ..... p 419 N93-11860 #
CONF-9210135-1 .... p 303 N93-11799 #
CONF-9210136-1 .... p 475 N93-11441 #
CONF-9210148-1 .... p 426 N93-11636 #
CONF-9210150-1 .... p 465 N93-12073 #
CONF-9210152-1 .... p 326 N93-11540 #
CONF-921036-4 .... p 463 N93-11797 #
CONF-921038-1 .... p 455 N93-12139 #
CONF-921038-2 .... p 454 N93-12087 #
CONF-921038-3-PT-2 .... p 455 N93-12141 #
CONF-921054-1 .... p 467 N93-12134 #
CONF-921055-2 .... p 313 N93-12140 #
CONF-921065-1 .... p 421 N93-12153 #
CONF-921079-2 .... p 371 N93-12154 #
CONF-921083-2 .... p 364 N93-12136 #
CONF-921083-6 .... p 345 N93-11381 #
CONF-921084-1 .... p 413 N93-12137 #
CONF-921098-1 .... p 364 N93-12155 #

CPIA-PUBL-573-VOL-1 .... p 244 N93-11132
CPIA-PUBL-573-VOL-2 .... p 247 N93-11448

CRHC-92-17 .... p 404 N93-11462 * #
CRHC-92-18 .... p 419 N93-12395 * #
CRHC-92-19 .... p 418 N93-11651 * #
CRHC-92-21 .... p 406 N93-12541 * #
CRHC-92-22 .... p 406 N93-12540 * #

CTR-3-12D-84-920-4 .... p 277 N93-12072 #

CWP-114 .... p 364 N93-12142 #
CWP-116 .... p 366 N93-12308 #
CWP-124 .... p 363 N93-11791 #
CWP-126 .... p 366 N93-12318 #
CWP-127 .... p 431 N93-11567 #

C920049 .... p 476 N93-11508 #
C946F .... p 447 N93-11186 #

DE91-015264 .... p 441 N93-12117 #
DE91-015314 .... p 259 N93-11857 #
DE92-001279 .... p 375 N93-12482 #
DE92-006700 .... p 252 N93-12255 #
DE92-008480 .... p 303 N93-11843 #
DE92-008490 .... p 261 N93-12256 #
DE92-008736 .... p 253 N93-12257 #
DE92-009712 .... p 467 N93-12178 #
DE92-010588 .... p 463 N93-11813 #
DE92-010590 .... p 346 N93-11814 #
DE92-010593 .... p 463 N93-11816 #
DE92-010598 .... p 275 N93-12171 #
DE92-010599 .... p 464 N93-11818 #
DE92-010717 .... p 354 N93-11744 #
DE92-010770 .... p 435 N93-11189 #
DE92-010778 .... p 467 N93-12134 #
DE92-010907 .... p 459 N93-11190 #
DE92-011004 .... p 312 N93-11806 #
DE92-011035 .... p 470 N93-11276 #
DE92-011045 .... p 252 N93-12219 #
DE92-011145 .... p 468 N93-12249 #
DE92-011218 .... p 470 N93-11518 #
DE92-011226 .... p 322 N93-12250 #
DE92-011265 .... p 483 N93-10993 #
DE92-011433 .... p 251 N93-12119 #
DE92-011592 .... p 303 N93-11774 #
DE92-011920 .... p 251 N93-12135 #
DE92-012138 .... p 453 N93-11745 #
DE92-012150 .... p 421 N93-12153 #
DE92-012155 .... p 254 N93-10995 #
DE92-013239 .... p 407 N93-11231 #
DE92-013432 .... p 364 N93-12136 #
DE92-013435 .... p 365 N93-12263 #
DE92-013447 .... p 413 N93-12137 #
DE92-013531 .... p 365 N93-12264 #
DE92-013567 .... p 275 N93-12265 #
DE92-013652 .... p 353 N93-11232 #
DE92-013653 .... p 353 N93-11233 #
DE92-013661 .... p 421 N93-12138 #
DE92-013666 .... p 280 N93-11234 #
DE92-013673 .... p 375 N93-12266 #
DE92-013983 .... p 464 N93-11842 #
DE92-013984 .... p 219 N93-12268 #
DE92-014134 .... p 359 N93-11235 #
DE92-014227 .... p 439 N93-11844 #
DE92-014268 .... p 367 N93-11236 #
DE92-014289 .... p 433 N93-11523 #
DE92-014304 .... p 485 N93-12120 #
DE92-014353 .... p 367 N93-11237 #
DE92-014385 .... p 305 N93-12070 #
DE92-014393 .... p 459 N93-11238 #
DE92-014496 .... p 455 N93-12139 #
DE92-014693 .... p 313 N93-12140 #
DE92-014717 .... p 371 N93-12154 #
DE92-014729 .... p 253 N93-12428 #
DE92-014746 .... p 308 N93-12492 #
DE92-014779 .... p 293 N93-12121 #
DE92-014782 .... p 256 N93-11519 #
DE92-014859 .... p 426 N93-11520 #
DE92-014886 .... p 364 N93-12155 #
DE92-015099 .... p 443 N93-11521 #
DE92-015178 .... p 464 N93-11894 #
DE92-015187 .... p 462 N93-11703 #
DE92-015225 .... p 355 N93-12098 #
DE92-015246 .... p 429 N93-11820 #
DE92-015286 .... p 271 N93-12165 #
DE92-015299 .... p 315 N93-11278 #
DE92-015348 .... p 294 N93-12156 #
DE92-015353 .... p 384 N93-11873 #
DE92-015365 .... p 454 N93-12087 #
DE92-015367 .... p 304 N93-11995 #
DE92-015368 .... p 455 N93-12141 #
DE92-015619 .... p 364 N93-12142 #
DE92-015654 .... p 250 N93-11847 #
DE92-015792 .... p 356 N93-12474 #
DE92-015931 .... p 363 N93-11848 #
DE92-015946 .... p 346 N93-11823 #
DE92-015974 .... p 293 N93-12089 #
DE92-015992 .... p 329 N93-12220 #
DE92-016069 .... p 328 N93-12122 #
DE92-016171 .... p 419 N93-11860 #
DE92-016186 .... p 465 N93-12090 #
DE92-016200 .... p 355 N93-11864 #
DE92-016206 .... p 251 N93-12091 #
DE92-016251 .... p 455 N93-12307 #
DE92-016254 .... p 449 N93-11041 #
DE92-016282 .... p 363 N93-11791 #
DE92-016283 .... p 366 N93-12308 #
DE92-016302 .... p 462 N93-11706 #
DE92-016390 .... p 455 N93-12309 #
DE92-016394 .... p 460 N93-11522 #
DE92-016395 .... p 271 N93-12123 #
DE92-016397 .... p 469 N93-12310 #
DE92-016465 .... p 432 N93-11759 #
DE92-016467 .... p 404 N93-11761 #
DE92-016503 .... p 253 N93-12311 #
DE92-016550 .... p 348 N93-12312 #
DE92-016601 .... p 306 N93-12313 #
DE92-016602 .... p 305 N93-12128 #
DE92-016623 .... p 258 N93-11762 #
DE92-016636 .... p 356 N93-12314 #
DE92-016686 .... p 456 N93-12493 #
DE92-016689 .... p 375 N93-12315 #
DE92-016692 .... p 261 N93-12445 #
DE92-016755 .... p 306 N93-12221 #
DE92-016785 .... p 323 N93-12514 #
DE92-016790 .... p 369 N93-11678 #
DE92-016796 .... p 232 N93-11824 #
DE92-016828 .... p 262 N93-12476 #
DE92-016838 .... p 490 N93-12477 #
DE92-016854 .... p 471 N93-12102 #
DE92-016864 .... p 465 N93-12073 #
DE92-016865 .... p 327 N93-11679 #
DE92-016891 .... p 445 N93-12103 #
DE92-016899 .... p 354 N93-11680 #
DE92-016910 .... p 338 N93-11792 #
DE92-016919 .... p 438 N93-11746 #
DE92-016960 .... p 442 N93-11077 #
DE92-016970 .... p 366 N93-10971 #
DE92-016971 .... p 462 N93-11747 #
DE92-016972 .... p 442 N93-12444 #
DE92-016993 .... p 473 N93-11151 #
DE92-016997 .... p 355 N93-12104 #
DE92-017002 .... p 489 N93-11078 #
DE92-017011 .... p 440 N93-11875 #
DE92-017019 .... p 466 N93-12124 #
DE92-017020 .... p 263 N93-10972 #
DE92-017027 .... p 443 N93-11493 #
DE92-017031 .... p 251 N93-12105 #
DE92-017039 .... p 231 N93-10973 #
DE92-017042 .... p 276 N93-11494 #
DE92-017045 .... p 277 N93-12106 #
DE92-017053 .... p 204 N93-11152 #
DE92-017059 .... p 259 N93-12107 #
DE92-017064 .... p 473 N93-11104 #
DE92-017066 .... p 445 N93-12108 #
DE92-017075 .... p 466 N93-12125 #
DE92-017077 .... p 466 N93-12099 #
DE92-017078 .... p 466 N93-12109 #
DE92-017088 .... p 413 N93-12110 #
DE92-017090 .... p 440 N93-12100 #
DE92-017109 .... p 445 N93-12126 #
DE92-017110 .... p 441 N93-12111 #
DE92-017114 .... p 466 N93-12127 #
DE92-017116 .... p 251 N93-12112 #
DE92-017118 .... p 465 N93-11915 #
DE92-017119 .... p 469 N93-12316 #
DE92-017134 .... p 439 N93-11849 #
DE92-017221 .... p 480 N93-12495 #
DE92-017223 .... p 356 N93-12496 #
DE92-017233 .... p 262 N93-12487 #
DE92-017285 .... p 292 N93-11916 #
DE92-017314 .... p 313 N93-11828 #
DE92-017343 .... p 348 N93-12222 #
DE92-017354 .... p 284 N93-11917 #
DE92-017405 .... p 250 N93-11918 #
DE92-017406 .... p 445 N93-11919 #
DE92-017410 .... p 268 N93-11861 #
DE92-017413 .... p 444 N93-11763 #
DE92-017418 .... p 217 N93-11367 #
DE92-017428 .... p 317 N93-11765 #
DE92-017431 .... p 232 N93-11766 #
DE92-017434 .... p 221 N93-12317 #
DE92-017509 .... p 302 N93-11767 #
DE92-017513 .... p 312 N93-11768 #
DE92-017526 .... p 284 N93-12101 #
DE92-017684 .... p 472 N93-12223 #
DE92-017695 .... p 284 N93-12132 #
DE92-017744 .... p 477 N93-11770 #
DE92-017745 .... p 346 N93-11771 #
DE92-017746 .... p 316 N93-11691 #
DE92-017823 .... p 426 N93-11636 #
DE92-017824 .... p 259 N93-11830 #
DE92-017827 .... p 463 N93-11772 #
DE92-017828 .... p 258 N93-11773 #
DE92-017847 .... p 301 N93-11637 #
DE92-017849 .... p 326 N93-11548 #
DE92-017851 .... p 362 N93-11692 #
DE92-017859 .... p 455 N93-12092 #
DE92-017877 .... p 271 N93-12168 #
DE92-017895 .... p 257 N93-11595 #
DE92-017916 .... p 333 N93-12055 #
DE92-017946 .... p 233 N93-12056 #
DE92-017987 .... p 479 N93-12143 #
DE92-017993 .... p 292 N93-12057 #
DE92-017995 .... p 471 N93-12058 #
DE92-018002 .... p 465 N93-12093 #
DE92-018004 .... p 454 N93-12059 #
DE92-018006 .... p 454 N93-12060 #
DE92-018011 .... p 465 N93-12065 #
DE92-018015 .... p 454 N93-12066 #
DE92-018017 .... p 443 N93-11433 #
DE92-018020 .... p 232 N93-11596 #
DE92-018021 .... p 446 N93-12129 #
DE92-018022 .... p 262 N93-12494 #
DE92-018024 .... p 450 N93-11153 #
DE92-018026 .... p 293 N93-12113 #
DE92-018029 .... p 332 N93-11154 #
DE92-018055 .... p 328 N93-12114 #
DE92-018061 .... p 267 N93-11549 #
DE92-018065 .... p 315 N93-11155 #
DE92-018066 .... p 374 N93-10974 #
DE92-018067 .... p 451 N93-11495 #
DE92-018069 .... p 449 N93-10975 #
DE92-018081 .... p 444 N93-11668 #
DE92-018087 .... p 456 N93-12504 #
DE92-018089 .... p 437 N93-11681 #
DE92-018105 .... p 260 N93-12158 #
DE92-018124 .... p 274 N93-11794 #
DE92-018139 .... p 437 N93-11597 #
DE92-018141 .... p 362 N93-11669 #
DE92-018154 .... p 446 N93-12497 #
DE92-018174 .... p 431 N93-11598 #
DE92-018177 .... p 456 N93-12416 #
DE92-018181 .... p 460 N93-11563 #
DE92-018189 .... p 286 N93-12417 #
DE92-018212 .... p 301 N93-11670 #
DE92-018228 .... p 302 N93-11671 #
DE92-018239 .... p 461 N93-11682 #
DE92-018243 .... p 478 N93-11796 #
DE92-018251 .... p 349 N93-12498 #
DE92-018253 .... p 441 N93-12224 #
DE92-018268 .... p 463 N93-11797 #
DE92-018269 .... p 277 N93-11672 #
DE92-018272 .... p 303 N93-11799 #
DE92-018274 .... p 311 N93-11673 #
DE92-018275 .... p 452 N93-11674 #
DE92-018276 .... p 362 N93-11564 #
DE92-018277 .... p 291 N93-11693 #
DE92-018278 .... p 283 N93-11800 #
DE92-018285 .... p 453 N93-11694 #
DE92-018286 .... p 254 N93-10984 #
DE92-018288 .... p 357 N93-10985 #
DE92-018304 .... p 244 N93-10986 #
DE92-018357 .... p 475 N93-11355 #
DE92-018367 .... p 485 N93-11695 #
DE92-018372 .... p 488 N93-11696 #
DE92-018375 .... p 485 N93-11697 #
DE92-018488 .... p 453 N93-11729 #
DE92-018492 .... p 458 N93-10987 #
DE92-018508 .... p 453 N93-11730 #

DE92-018526 p 453 N93-11731 #
DE92-018541 p 449 N93-10988 #
DE92-018544 p 344 N93-10989 #
DE92-018551 p 345 N93-11733 #
DE92-018558 p 452 N93-11565 #
DE92-018559 p 289 N93-11438 #
DE92-018586 p 473 N93-10990 #
DE92-018597 p 470 N93-12499 #
DE92-018598 p 251 N93-12172 #
DE92-018605 p 274 N93-11566 #
DE92-018617 p 413 N93-12187 #
DE92-018635 p 455 N93-12188 #
DE92-018640 p 366 N93-12318 #
DE92-018641 p 431 N93-11567 #
DE92-018646 p 254 N93-12478 #
DE92-018647 p 452 N93-11568 #
DE92-018648 p 353 N93-11569 #
DE92-018687 p 247 N93-11439 #
DE92-018706 p 273 N93-12479 #
DE92-018709 p 300 N93-11440 #
DE92-018713 p 262 N93-12480 #
DE92-018714 p 256 N93-11524 #
DE92-018723 p 273 N93-12500 #
DE92-018725 p 441 N93-12115 #
DE92-018726 p 432 N93-12116 #
DE92-018738 p 456 N93-12501 #
DE92-018745 p 475 N93-11441 #
DE92-018748 p 266 N93-11442 #
DE92-018758 p 436 N93-11443 #
DE92-018759 p 247 N93-11444 #
DE92-018760 p 384 N93-11445 #
DE92-018766 p 289 N93-11432 #
DE92-018769 p 425 N93-11446 #
DE92-018772 p 267 N93-11570 #
DE92-018783 p 217 N93-11447 #
DE92-018784 p 337 N93-11775 #
DE92-018786 p 345 N93-11571 #
DE92-018804 p 261 N93-12261 #
DE92-018807 p 257 N93-11572 #
DE92-018809 p 460 N93-11533 #
DE92-018816 p 260 N93-12232 #
DE92-018826 p 408 N93-11378 #
DE92-018853 p 484 N93-11379 #
DE92-018865 p 301 N93-11638 #
DE92-018874 p 274 N93-11380 #
DE92-018876 p 345 N93-11381 #
DE92-018884 p 451 N93-11382 #
DE92-018885 p 305 N93-12010 #
DE92-018888 p 431 N93-11625 #
DE92-018897 p 345 N93-11626 #
DE92-018926 p 317 N93-12011 #
DE92-018932 p 347 N93-12012 #
DE92-018934 p 448 N93-11627 #
DE92-018939 p 327 N93-11832 #
DE92-018942 p 267 N93-11628 #
DE92-018943 p 327 N93-11865 #
DE92-018947 p 419 N93-12233 #
DE92-018948 p 461 N93-11629 #
DE92-018957 p 481 N93-12067 #
DE92-018960 p 451 N93-11534 #
DE92-018978 p 479 N93-12068 #
DE92-018979 p 362 N93-11535 #
DE92-018982 p 443 N93-11510 #
DE92-018989 p 313 N93-12069 #
DE92-018990 p 312 N93-11822 #
DE92-018999 p 346 N93-11825 #
DE92-019020 p 454 N93-11826 #
DE92-019021 p 312 N93-11827 #
DE92-019026 p 438 N93-11829 #
DE92-019027 p 431 N93-11511 #
DE92-019028 p 460 N93-11512 #
DE92-019032 p 445 N93-11831 #
DE92-019043 p 444 N93-11652 #
DE92-019044 p 345 N93-11513 #
DE92-019051 p 326 N93-11653 #
DE92-019052 p 443 N93-11429 #
DE92-019068 p 268 N93-11654 #
DE92-019069 p 353 N93-11655 #
DE92-019073 p 290 N93-11514 #
DE92-019084 p 282 N93-11515 #
DE92-019095 p 451 N93-11516 #
DE92-019096 p 407 N93-11356 #
DE92-019098 p 471 N93-11656 #
DE92-019119 p 249 N93-11801 #
DE92-019133 p 312 N93-11802 #
DE92-019134 p 369 N93-11657 #
DE92-019138 p 240 N93-11658 #
DE92-019172 p 373 N93-11734 #
DE92-019180 p 459 N93-11496 #
DE92-019185 p 443 N93-11517 #
DE92-019188 p 268 N93-11735 #
DE92-019192 p 267 N93-11497 #
DE92-019217 p 443 N93-11498 #
DE92-019243 p 443 N93-11499 #
DE92-019244 p 445 N93-11776 #
DE92-019248 p 316 N93-11500 #
DE92-019249 p 459 N93-11501 #
DE92-019273 p 438 N93-11778 #
DE92-019295 p 487 N93-11502 #
DE92-019296 p 411 N93-11599 #
DE92-019297 p 257 N93-11600 #
DE92-019300 p 274 N93-11550 #
DE92-019316 p 332 N93-11601 #
DE92-019318 p 249 N93-11551 #
DE92-019326 p 267 N93-11552 #
DE92-019330 p 290 N93-11553 #
DE92-019337 p 310 N93-11554 #
DE92-019338 p 411 N93-11555 #
DE92-019363 p 326 N93-11556 #
DE92-019372 p 257 N93-11557 #
DE92-019378 p 461 N93-11602 #
DE92-019382 p 282 N93-11675 #
DE92-019384 p 354 N93-11676 #
DE92-019385 p 354 N93-11677 #
DE92-019411 p 374 N93-11630 #
DE92-019421 p 411 N93-11536 #
DE92-019423 p 291 N93-11639 #
DE92-019435 p 300 N93-11537 #
DE92-019436 p 437 N93-11640 #
DE92-019452 p 444 N93-11641 #
DE92-019457 p 373 N93-11642 #
DE92-019459 p 300 N93-11538 #
DE92-019469 p 404 N93-11539 #
DE92-019471 p 291 N93-11643 #
DE92-019473 p 249 N93-11644 #
DE92-019504 p 326 N93-11540 #
DE92-019505 p 452 N93-11645 #
DE92-019512 p 436 N93-11541 #
DE92-019517 p 461 N93-11646 #
DE92-019547 p 310 N93-11542 #
DE92-019548 p 461 N93-11647 #
DE92-019602 p 414 N93-12234 #
DE92-019603 p 316 N93-11659 #
DE92-019639 p 452 N93-11660 #
DE92-019643 p 348 N93-12074 #
DE92-019807 p 348 N93-12075 #
DE92-019903 p 282 N93-11661 #
DE92-040444 p 221 N93-11631 #
DE92-040934 p 282 N93-11632 #
DE92-514988 p 444 N93-11525 #
DE92-526256 p 347 N93-11845 #
DE92-526262 p 346 N93-11777 #
DE92-531118 p 355 N93-11846 #
DE92-540921 p 349 N93-12446 #
DE92-603605 p 427 N93-12176 #
DE92-617540 p 459 N93-11076 #
DE92-622800 p 458 N93-10992 #
DE92-624834 p 440 N93-11914 #
DE92-634887 p 471 N93-11780 #
DE92-782100 p 451 N93-11277 #
DE92-782105 p 454 N93-11834 #

DIGE-EST-TN-016 p 206 N93-11161 #

DILC-EST-TN-200 p 432 N93-11156 #
DILC-EST-TN-218 p 196 N93-11157 #
DILC-EST-TN-224 p 334 N93-11158 #

DILC-EST-TR-211 p 214 N93-11160 #

DLAS-EST-TR-040 p 217 N93-11225 #

DLR-FB-90-39 p 223 N93-11685 #
DLR-FB-91-29 p 342 N93-11140 #
DLR-FB-92-02 p 196 N93-11141 #
DLR-FB-92-02 p 237 N93-11143 #

DLR-IB-232-91/J07 p 336 N93-11544 * #

DNA-TR-91-189 p 438 N93-11804 #
DNA-TR-91-99 p 447 N93-11186 #
DNA-TR-92-10 p 222 N93-12505 #

DOE-STD-1010-92 p 472 N93-12223 #

DOE/CE-0351 p 274 N93-11794 #
DOE/CE-15440/T5 p 300 N93-11440 #
DOE/CE-90026/3 p 328 N93-12122 #

DOE/CH-10093/152 p 346 N93-11814 #

DOE/EIA-M042(91) p 475 N93-11355 #

DOE/ER-0144-10 p 251 N93-12135 #
DOE/ER-13331/T3 p 490 N93-12477 #
DOE/ER-13418/T2 p 363 N93-11848 #
DOE/ER-13519/6 p 436 N93-11541 #
DOE/ER-13544/5 p 251 N93-12091 #
DOE/ER-13558/6 p 258 N93-11762 #
DOE/ER-13564/11 p 271 N93-12165 #
DOE/ER-13615/6 p 253 N93-12428 #
DOE/ER-13687/10 p 471 N93-12102 #
DOE/ER-13700/T2 p 435 N93-11189 #
DOE/ER-13727/T2 p 452 N93-11565 #
DOE/ER-13822/5 p 254 N93-12478 #
DOE/ER-13932/T2 p 289 N93-11438 #
DOE/ER-13986/T1 p 251 N93-12105 #
DOE/ER-14042/3 p 327 N93-11865 #
DOE/ER-14079/12 p 364 N93-12142 #
DOE/ER-14079/14 p 363 N93-11791 #
DOE/ER-14079/15 p 366 N93-12308 #
DOE/ER-14079/16 p 366 N93-12318 #
DOE/ER-14079/17 p 431 N93-11567 #
DOE/ER-14144/3 p 461 N93-11682 #
DOE/ER-14147/2 p 300 N93-11538 #
DOE/ER-14178/T1 p 247 N93-11439 #
DOE/ER-14192/1 p 251 N93-12119 #
DOE/ER-14193/1 p 262 N93-12480 #
DOE/ER-25027/6 p 345 N93-11733 #
DOE/ER-25029/3 p 404 N93-11761 #
DOE/ER-40150/188 p 442 N93-11077 #
DOE/ER-40160/8 p 441 N93-12224 #
DOE/ER-40272/161 p 432 N93-11759 #
DOE/ER-40415/19 p 442 N93-12444 #
DOE/ER-40427/35-N91 p 439 N93-11844 #
DOE/ER-40506/5 p 443 N93-11521 #
DOE/ER-40561/47 p 485 N93-12120 #
DOE/ER-40628/1 p 470 N93-11276 #
DOE/ER-40648/1 p 315 N93-11278 #
DOE/ER-40694/1 p 436 N93-11443 #
DOE/ER-40702/2 p 444 N93-11668 #
DOE/ER-40704/1 p 437 N93-11681 #
DOE/ER-45058/8 p 441 N93-12115 #
DOE/ER-45131/10 p 462 N93-11747 #
DOE/ER-45153/9 p 461 N93-11629 #
DOE/ER-45220/7 p 273 N93-12500 #
DOE/ER-45233/7 p 470 N93-12499 #
DOE/ER-45255/4 p 256 N93-11524 #
DOE/ER-45265/6 p 432 N93-12116 #
DOE/ER-45320/5 p 461 N93-11646 #
DOE/ER-45330/5 p 464 N93-11894 #
DOE/ER-45384/T1 p 251 N93-12172 #
DOE/ER-45428/1 p 273 N93-12479 #
DOE/ER-45438/2 p 267 N93-11628 #
DOE/ER-53223/178 p 455 N93-12188 #
DOE/ER-53270/T2 p 453 N93-11729 #
DOE/ER-53297/4 p 452 N93-11568 #
DOE/ER-60519/T4 p 313 N93-11828 #
DOE/ER-60561/6 p 384 N93-11873 #
DOE/ER-60627/4 p 373 N93-11734 #
DOE/ER-60631/10 p 375 N93-12266 #
DOE/ER-61060/2 p 366 N93-10971 #
DOE/ER-61215/1 p 373 N93-11642 #
DOE/ER-61228/3 p 384 N93-11445 #
DOE/ER-61363/T1 p 367 N93-11237 #
DOE/ER-69027/3 p 353 N93-11569 #

DOE/ET-10815/192 p 455 N93-12139 #
DOE/ET-53088/530 p 453 N93-11745 #
DOE/ET-53088/553 p 456 N93-12493 #

DOE/ID-12707/T1 p 303 N93-11774 #

DOE/MC-23167/3099 p 327 N93-11832 #
DOE/MC-27225/3091 p 375 N93-12482 #

DOE/PC-89770/T12 p 244 N93-10986 #
DOE/PC-90056/T4 p 250 N93-11847 #
DOE/PC-90094/T1 p 302 N93-11671 #
DOE/PC-90094/T2 p 301 N93-11670 #
DOE/PC-90274/T18 p 456 N93-12504 #
DOE/PC-91293/2 p 247 N93-11444 #

DOE/PETC-TR/92/8 p 308 N93-12492 #

DOE/SF-16592/T1 p 346 N93-11823 #
DOE/SF-18861/T1 p 453 N93-11730 #
DOE/SF-18861/T2 p 453 N93-11731 #
DOE/SF-18865/T1 p 438 N93-11778 #

DOT-VNTSC-FAA-91-15 p 367 N93-11144 #
DOT-VNTSC-FAA-92-3 p 204 N93-11252 #

DOT-VNTSC-FA1H2-92 p 332 N93-11617 #

DOT/FAA/AM-92/22 p 387 N93-11279 #

DOT/FAA/CT-TN92/13 p 217 N93-11616 #
DOT/FAA/CT-TN92/20 p 332 N93-11617 #
DOT/FAA/CT-TN92/30 p 310 N93-11460 #
DOT/FAA/CT-TN92/4 p 285 N93-12331 #

DOT/FAA/CT-91-23-VOL-2-PT-3 p 241 N93-12054 #
DOT/FAA/CT-92/2-VOL-1 p 205 N93-11704 #
DOT/FAA/CT-92/2-VOL-2 p 205 N93-11705 #

DOT/FAA/NR/92-6 p 367 N93-11144 #

DOT/FAA/RD-91/6 .... p 206 N93-11461 #
DOT/FAA/RD-92/3 .... p 204 N93-11252 #

DRA/MAR-TM(MTH)-91320 .... p 197 N93-11377 #

DU/DC/TR-26 .... p 467 N93-12175 #
DU/DC/TR-28 .... p 462 N93-11724 #

E-6137 .... p 218 N93-12016 * #
E-6287 .... p 337 N93-11624 * #
E-6363-1 .... p 286 N93-12366 * #
E-6455 .... p 243 N93-12302 * #
E-6497 .... p 413 N93-12022 * #
E-6513 .... p 224 N93-11001 * #
E-6676 .... p 336 N93-11403 * #
E-6797 .... p 334 N93-11004 * #
E-6849 .... p 232 N93-11614 * #
E-6893 .... p 263 N93-10962 * #
E-6898 .... p 241 N93-12015 * #
E-6925 .... p 258 N93-11635 * #
E-6951 .... p 235 N93-12484 * #
E-7045-1 .... p 230 N93-10965 * #
E-7066 .... p 425 N93-11254 * #
E-7122 .... p 238 N93-11399 * #
E-7132 .... p 323 N93-10966 * #
E-7138 .... p 433 N93-11370 * #
E-7188 .... p 295 N93-12301 * #
E-7205 .... p 287 N93-12481 * #
E-7207 .... p 333 N93-10967 * #
E-7208 .... p 221 N93-11401 * #
E-7210 .... p 215 N93-12305 * #
E-7216 .... p 209 N93-10983 * #
E-7220 .... p 323 N93-10982 * #
E-7236 .... p 236 N93-10978 * #
E-7238 .... p 331 N93-10963 * #
E-7240 .... p 213 N93-12077 * #
E-7244 .... p 221 N93-11398 * #
E-7252 .... p 341 N93-12277 * #
E-7264 .... p 276 N93-12197 * #
E-7278 .... p 196 N93-11223 * #
E-7279 .... p 234 N93-12409 * #
E-7280 .... p 213 N93-11530 * #
E-7286 .... p 417 N93-11005 * #
E-7291 .... p 300 N93-11529 * #
E-7295 .... p 296 N93-10981 * #
E-7312 .... p 226 N93-12152 * #
E-7320 .... p 273 N93-12398 * #
E-7321 .... p 426 N93-11531 * #
E-7322 .... p 249 N93-11545 * #
E-7334 .... p 233 N93-12363 * #
E-7342 .... p 231 N93-11402 * #
E-7349 .... p 242 N93-12078 * #
E-7354 .... p 335 N93-11175 * #
E-7355 .... p 224 N93-11430 * #
E-7356 .... p 469 N93-12325 * #
E-7358 .... p 241 N93-12076 * #
E-7361 .... p 257 N93-11609 * #
E-7382 .... p 213 N93-12402 * #
E-7388 .... p 419 N93-12410 * #
E-7390 .... p 314 N93-12279 * #
E-7395 .... p 275 N93-12085 * #
E-7398 .... p 214 N93-12418 * #

ECL-90-29 .... p 460 N93-11573 #
ECL-91-07 .... p 299 N93-11363 #
ECL-91-12 .... p 291 N93-11574 #
ECL-91-16 .... p 301 N93-11575 #
ECL-91-18 .... p 214 N93-11576 #
ECL-91-19 .... p 267 N93-11577 #
ECL-91-33 .... p 257 N93-11578 #
ECL-91-37 .... p 336 N93-11579 #
ECL-92-01 .... p 267 N93-11580 #
ECL-92-13 .... p 461 N93-11581 #
ECL-92-16 .... p 336 N93-11582 #

EGG-EP-10152 .... p 328 N93-12114 #
EGG-EP-9701 .... p 292 N93-12057 #

EGG-FSP-10245 .... p 471 N93-12058 #

EGG-M-91298 .... p 262 N93-12494 #
EGG-M-91307 .... p 455 N93-12092 #
EGG-M-91349 .... p 257 N93-11595 #
EGG-M-91626 .... p 443 N93-11433 #
EGG-M-91631 .... p 332 N93-11154 #
EGG-M-92006 .... p 271 N93-12168 #
EGG-M-92067 .... p 446 N93-12129 #
EGG-M-92071 .... p 362 N93-11692 #
EGG-M-92264 .... p 454 N93-12066 #
EGG-M-92274 .... p 233 N93-12056 #
EGG-M-92287 .... p 333 N93-12055 #
EGG-M-92359 .... p 232 N93-11596 #
EGG-M-92378 .... p 301 N93-11637 #
EGG-M-92381 .... p 326 N93-11548 #

EGG-10617-5101 .... p 286 N93-12417 #

EGG-2672 .... p 407 N93-11356 #

EOS/FR-0214 .... p 287 N93-12461 #
EOS/FR-0215 .... p 371 N93-12167 #

EPA/400/1-91/034 .... p 356 N93-12524 #
EPA/400/1-92/002 .... p 356 N93-12525 #
EPA/540/5-91/007A-VOL-1 .... p 456 N93-12526 #
EPA/540/5-91/007B-VOL-2 .... p 457 N93-12527 #
EPA/600/A-92/156 .... p 298 N93-11251 #
EPA/840/B-92/001 .... p 480 N93-12528 #

ESA-INT-2 .... p 479 N93-12404 #

ESA-SP-1148 .... p 344 N93-12280 #

ESA-STR-234 .... p 476 N93-11583 #

ESA-TT-1256 .... p 223 N93-11685 #

ESD-TR-92-262 .... p 414 N93-12284 #

ETDE/JP-MF-92526256 .... p 347 N93-11845 #
ETDE/JP-MF-92526262 .... p 346 N93-11777 #

ETN-92-92063 .... p 337 N93-11707 #
ETN-92-92087 .... p 240 N93-11708 #
ETN-92-92100 .... p 203 N93-11319 #
ETN-92-92101 .... p 349 N93-11082 #
ETN-92-92106 .... p 357 N93-11083 #
ETN-92-92107 .... p 357 N93-11006 #
ETN-92-92112 .... p 223 N93-11007 #
ETN-92-92113 .... p 195 N93-11008 #
ETN-92-92114 .... p 278 N93-11009 #
ETN-92-92115 .... p 263 N93-11011 #
ETN-92-92116 .... p 263 N93-11010 #
ETN-92-92122 .... p 255 N93-11026 #
ETN-92-92126 .... p 255 N93-11027 #
ETN-92-92146 .... p 442 N93-11028 #
ETN-92-92148 .... p 449 N93-11029 #
ETN-92-92149 .... p 449 N93-11030 #
ETN-92-92151 .... p 449 N93-11102 #
ETN-92-92152 .... p 450 N93-11103 #
ETN-92-92154 .... p 450 N93-11201 #
ETN-92-92158 .... p 265 N93-11203 #
ETN-92-92170 .... p 359 N93-11265 #
ETN-92-92172 .... p 482 N93-11473
ETN-92-92174 .... p 409 N93-11478 #
ETN-92-92175 .... p 317 N93-12023 #
ETN-92-92188 .... p 433 N93-11204 #
ETN-92-92189 .... p 266 N93-11205 #
ETN-92-92191 .... p 212 N93-11206 #
ETN-92-92192 .... p 212 N93-11207 #
ETN-92-92193 .... p 212 N93-11208 #
ETN-92-92194 .... p 255 N93-11031 #
ETN-92-92195 .... p 473 N93-11012 #
ETN-92-92196 .... p 263 N93-11032 #
ETN-92-92197 .... p 334 N93-11013 #
ETN-92-92198 .... p 334 N93-11014 #
ETN-92-92199 .... p 331 N93-11015 #
ETN-92-92200 .... p 331 N93-11016 #
ETN-92-92201 .... p 255 N93-11033 #
ETN-92-92202 .... p 296 N93-11017 #
ETN-92-92203 .... p 263 N93-11018 #
ETN-92-92204 .... p 209 N93-11019 #
ETN-92-92205 .... p 195 N93-11020 #
ETN-92-92206 .... p 334 N93-11021 #
ETN-92-92207 .... p 309 N93-11320 #
ETN-92-92208 .... p 334 N93-11022 #
ETN-92-92209 .... p 209 N93-11023 #
ETN-92-92210 .... p 210 N93-11024 #
ETN-92-92211 .... p 296 N93-11025 #
ETN-92-92212 .... p 331 N93-11034 #
ETN-92-92215 .... p 244 N93-11035 #
ETN-92-92216 .... p 210 N93-11036 #
ETN-92-92217 .... p 210 N93-11037 #
ETN-92-92218 .... p 210 N93-11038 #
ETN-92-92219 .... p 210 N93-11039 #
ETN-92-92220 .... p 210 N93-11040 #
ETN-92-92221 .... p 324 N93-11054 #
ETN-92-92222 .... p 210 N93-11055 #
ETN-92-92223 .... p 211 N93-11105 #
ETN-92-92224 .... p 211 N93-11106 #
ETN-92-92225 .... p 236 N93-11107 #
ETN-92-92226 .... p 212 N93-11108 #
ETN-92-92227 .... p 255 N93-11109 #
ETN-92-92228 .... p 331 N93-11110 #
ETN-92-92231 .... p 433 N93-11321 #
ETN-92-92232 .... p 433 N93-11322 #
ETN-92-92233 .... p 255 N93-11111 #
ETN-92-92234 .... p 264 N93-11084 #
ETN-92-92235 .... p 211 N93-11085 #
ETN-92-92236 .... p 264 N93-11086 #
ETN-92-92237 .... p 210 N93-11061 #
ETN-92-92238 .... p 211 N93-11062 #
ETN-92-92239 .... p 211 N93-11063 #
ETN-92-92240 .... p 315 N93-11064 #
ETN-92-92241 .... p 236 N93-11065 #
ETN-92-92242 .... p 264 N93-11066 #
ETN-92-92243 .... p 212 N93-11112 #
ETN-92-92244 .... p 296 N93-11067 #
ETN-92-92245 .... p 211 N93-11068 #
ETN-92-92246 .... p 211 N93-11069 #
ETN-92-92247 .... p 195 N93-11070 #
ETN-92-92248 .... p 196 N93-11113 #
ETN-92-92249 .... p 212 N93-11114 #
ETN-92-92251 .... p 255 N93-11115 #
ETN-92-92253 .... p 206 N93-11334 #
ETN-92-92254 .... p 425 N93-11323 #
ETN-92-92255 .... p 325 N93-11324
ETN-92-92256 .... p 325 N93-11325
ETN-92-92257 .... p 325 N93-11326
ETN-92-92258 .... p 325 N93-11327
ETN-92-92259 .... p 433 N93-11328
ETN-92-92260 .... p 203 N93-11357
ETN-92-92261 .... p 298 N93-11358
ETN-92-92262 .... p 299 N93-11359 #
ETN-92-92263 .... p 299 N93-11360 #
ETN-92-92266 .... p 246 N93-11361 #
ETN-92-92267 .... p 299 N93-11362 #
ETN-92-92268 .... p 299 N93-11363 #
ETN-92-92270 .... p 368 N93-11329
ETN-92-92271 .... p 269 N93-11983 #
ETN-92-92272 .... p 203 N93-11375
ETN-92-92273 .... p 205 N93-11344
ETN-92-92274 .... p 407 N93-11345
ETN-92-92275 .... p 309 N93-11346
ETN-92-92276 .... p 309 N93-11330
ETN-92-92277 .... p 361 N93-11331
ETN-92-92278 .... p 315 N93-11332
ETN-92-92279 .... p 220 N93-11335
ETN-92-92280 .... p 220 N93-11348
ETN-92-92281 .... p 256 N93-11336
ETN-92-92282 .... p 256 N93-11337
ETN-92-92283 .... p 368 N93-11349
ETN-92-92284 .... p 368 N93-11350
ETN-92-92285 .... p 484 N93-11338
ETN-92-92286 .... p 484 N93-11347
ETN-92-92288 .... p 488 N93-11351
ETN-92-92290 .... p 361 N93-11352
ETN-92-92291 .... p 213 N93-11339
ETN-92-92292 .... p 368 N93-11340 #
ETN-92-92293 .... p 273 N93-11376 #
ETN-92-92294 .... p 197 N93-11377 #
ETN-92-92295 .... p 288 N93-11364 #
ETN-92-92296 .... p 197 N93-11365 #
ETN-92-92297 .... p 280 N93-11366 #
ETN-92-92298 .... p 289 N93-11434 #
ETN-92-92299 .... p 217 N93-11435 #
ETN-92-92300 .... p 207 N93-11485 #
ETN-92-92302 .... p 220 N93-11486 #
ETN-92-92303 .... p 240 N93-11905 #
ETN-92-92304 .... p 199 N93-11882 #
ETN-92-92305 .... p 199 N93-11883 #
ETN-92-92306 .... p 218 N93-11906 #
ETN-92-92308 .... p 405 N93-12430 #
ETN-92-92309 .... p 409 N93-11436 #
ETN-92-92310 .... p 281 N93-11487 #
ETN-92-92311 .... p 425 N93-11437 #
ETN-92-92312 .... p 407 N93-11341 #
ETN-92-92314 .... p 447 N93-11342 #
ETN-92-92315 .... p 420 N93-11343 #
ETN-92-92316 .... p 280 N93-11383 #
ETN-92-92317 .... p 474 N93-11333 #
ETN-92-92318 .... p 280 N93-11384 #
ETN-92-92319 .... p 280 N93-11385 #
ETN-92-92320 .... p 408 N93-11386 #
ETN-92-92321 .... p 281 N93-11387 #
ETN-92-92322 .... p 315 N93-11388 #
ETN-92-92324 .... p 475 N93-11404 #
ETN-92-92325 .... p 409 N93-11405 #
ETN-92-92326 .... p 409 N93-11406 #
ETN-92-92327 .... p 409 N93-11407 #
ETN-92-92328 .... p 408 N93-11389 #
ETN-92-92330 .... p 408 N93-11390 #
ETN-92-92332 .... p 281 N93-11391 #
ETN-92-92333 .... p 409 N93-11392 #
ETN-92-92334 .... p 460 N93-11573 #
ETN-92-92335 .... p 291 N93-11574 #
ETN-92-92336 .... p 301 N93-11575 #
ETN-92-92337 .... p 214 N93-11576 #
ETN-92-92338 .... p 267 N93-11577 #
ETN-92-92339 .... p 257 N93-11578 #
ETN-92-92340 .... p 336 N93-11579 #
ETN-92-92341 .... p 267 N93-11580 #
ETN-92-92342 .... p 461 N93-11581 #
ETN-92-92343 .... p 336 N93-11582 #
ETN-92-92344 .... p 476 N93-11583 #
ETN-92-92345 .... p 344 N93-12280 #
ETN-92-92346 .... p 223 N93-11685 #
ETN-92-92347 .... p 418 N93-11584 #
ETN-92-92348 .... p 215 N93-11585 #

ETN-92-92349 .... p 239 N93-11586 #
ETN-92-92350 .... p 332 N93-11587 #
ETN-92-92351 .... p 239 N93-11588 #
ETN-92-92353 .... p 239 N93-11589 #
ETN-92-92354 .... p 239 N93-11590 #
ETN-92-92355 .... p 282 N93-11591 #
ETN-92-92363 .... p 198 N93-11686 #
ETN-92-92364 .... p 444 N93-11687 #
ETN-92-92365 .... p 289 N93-11393
ETN-92-92366 .... p 459 N93-11394
ETN-92-92367 .... p 281 N93-11395
ETN-92-92368 .... p 247 N93-11396
ETN-92-92369 .... p 266 N93-11397
ETN-92-92370 .... p 447 N93-11408
ETN-92-92371 .... p 238 N93-11409
ETN-92-92372 .... p 310 N93-11410
ETN-92-92373 .... p 316 N93-11411
ETN-92-92374 .... p 436 N93-11412
ETN-92-92375 .... p 432 N93-11666
ETN-92-92377 .... p 412 N93-11688
ETN-92-92378 .... p 218 N93-11728 #
ETN-92-92379 .... p 217 N93-11224 #
ETN-92-92380 .... p 406 N93-11210 #
ETN-92-92382 .... p 425 N93-11211 #
ETN-92-92383 .... p 357 N93-11120 #
ETN-92-92384 .... p 423 N93-11121 #
ETN-92-92385 .... p 423 N93-11122 #
ETN-92-92386 .... p 424 N93-11123 #
ETN-92-92387 .... p 424 N93-11124 #
ETN-92-92388 .... p 424 N93-11125 #
ETN-92-92389 .... p 424 N93-11126 #
ETN-92-92390 .... p 352 N93-11127
ETN-92-92391 .... p 237 N93-11128 #
ETN-92-9239337 .... p 357 N93-11129 #
ETN-92-92395 .... p 442 N93-11130 #
ETN-92-92396 .... p 442 N93-11131 #
ETN-92-92398 .... p 342 N93-11140 #
ETN-92-92400 .... p 196 N93-11141 #
ETN-92-92404 .... p 237 N93-11143 #
ETN-92-92409 .... p 432 N93-11156 #
ETN-92-92410 .... p 196 N93-11157 #
ETN-92-92411 .... p 334 N93-11158 #
ETN-92-92412 .... p 214 N93-11160 #
ETN-92-92413 .... p 206 N93-11161 #
ETN-92-92414 .... p 217 N93-11225 #
ETN-92-92415 .... p 420 N93-11227
ETN-92-92416 .... p 418 N93-11180
ETN-92-92417 .... p 418 N93-11181
ETN-92-92418 .... p 424 N93-11182
ETN-92-92419 .... p 386 N93-11212
ETN-92-92420 .... p 421 N93-11667
ETN-92-92421 .... p 411 N93-11592
ETN-92-92422 .... p 421 N93-11593
ETN-92-92423 .... p 411 N93-11594
ETN-92-92424 .... p 476 N93-11689
ETN-92-92425 .... p 476 N93-11690

E19-666-4 .... p 310 N93-11612 * #

FASTC-ID(RS)T-0785-91 .... p 242 N93-12235 #
FASTC-ID(RS)T-0787-91 .... p 225 N93-11798 #
FASTC-ID(RS)T-1064-91 .... p 281 N93-11509 #
FASTC-ID(RS)T-1237-91 .... p 314 N93-12517 #

FFA-TN-1992-04 .... p 237 N93-11128 #

FFI-92/7009 .... p 357 N93-11129 #

FHWA/MD-91/02 .... p 476 N93-11700 #

FHWA/TX-91/920-4 .... p 277 N93-12072 #
FHWA/TX-92/1245-1 .... p 325 N93-11427 #

FNAL-TM-1787 .... p 411 N93-11555 #

FOA-A-30061-9.4 .... p 219 N93-11216 #

FR-19691-4-VOL-1 .... p 235 N93-12523 * #
FR-19691-4-VOL-2 .... p 234 N93-12441 * #
FR-19691-4-VOL-3 .... p 233 N93-12088 * #

FTD-ID(RS)T-0785-91 .... p 242 N93-12235 #
FTD-ID(RS)T-0921-91 .... p 258 N93-11787 #
FTD-ID(RS)T-1199-91 .... p 261 N93-12269 #
FTD-ID(RS)T-1474-90 .... p 317 N93-11786 #

FY1455-91-08827-RPT-1-PHASE 1 p 348 N93-12166 #

GA-A-20933 .... p 455 N93-12307 #
GA-A-20934 .... p 449 N93-11041 #
GA-A-20945 .... p 449 N93-10988 #
GA-A-20959 .... p 305 N93-12010 #
GA-A-20972 .... p 451 N93-11382 #
GA-A-21007 .... p 452 N93-11660 #

GALCIT-SM-92-17 .... p 258 N93-11782 #

GALCIT-SM-92-3 .... p 335 N93-11219 #

GAO/IMTEC-92-6FS .... p 474 N93-11274 #

GKSS-91/E/59 .... p 220 N93-11348
GKSS-91/E/60 .... p 256 N93-11336
GKSS-91/E/67 .... p 256 N93-11337
GKSS-91/E/76-PT-1 .... p 368 N93-11349
GKSS-91/E/77-PT-2 .... p 368 N93-11350

GMR-7661 .... p 277 N93-11672 #

GORMP-25 .... p 350 N93-11087 * #

GPO-57-213CC .... p 225 N93-11908 #

GRI-91/0310 .... p 470 N93-11469 #
GRI-92/0142 .... p 312 N93-11757 #

GU-AERO-9202 .... p 197 N93-11464 #

H-1827 .... p 296 N93-10969 * #
H-1837 .... p 214 N93-11178 * #
H-1851 .... p 197 N93-11532 * #
H-1855 .... p 207 N93-11863 * #
H-1858 .... p 196 N93-11221 * #
H-1859 .... p 277 N93-11619 * #
H-1862 .... p 202 N93-12353 * #

HEL-TN-3-92 .... p 388 N93-11743 #

HMI-B-494 .... p 442 N93-11028 #

IAP-TR-91-09 .... p 222 N93-12505 #

IC-91/235 .... p 427 N93-12176 #
IC-91/301 .... p 458 N93-10992 #
IC-91/345 .... p 459 N93-11076 #

ICAF-1776 .... p 335 N93-11369 #

ICASE-92-44 .... p 425 N93-11246 * #
ICASE-92-45 .... p 301 N93-11633 * #
ICASE-92-46 .... p 412 N93-11618 * #
ICASE-92-47 .... p 198 N93-11607 * #
ICASE-92-48 .... p 427 N93-12298 * #
ICASE-92-49 .... p 416 N93-12400 * #
ICASE-92-51 .... p 416 N93-12403 * #
ICASE-92-52 .... p 435 N93-12021 * #
ICASE-92-54 .... p 306 N93-12173 * #

ICOMP-92-13 .... p 341 N93-12277 * #
ICOMP-92-19 .... p 426 N93-11531 * #

IDA-D-967 .... p 404 N93-11809 #

IDA-P-2316 .... p 477 N93-11732 #
IDA-P-2433 .... p 390 N93-12491 #
IDA-P-2630 .... p 472 N93-12273 #

IDA/HQ-89-034883 .... p 477 N93-11732 #
IDA/HQ-90-36732 .... p 390 N93-12491 #
IDA/HQ-91-038812 .... p 404 N93-11809 #
IDA/HQ-92-41177 .... p 472 N93-12273 #

IEE-SR-228 .... p 355 N93-11846 #

IFSR-530 .... p 453 N93-11745 #
IFSR-553 .... p 456 N93-12493 #

IIHR-358 .... p 306 N93-12245 #

INT-PATENT-CLASS-C08L-79/08 p 264 N93-11059 *

INT-PATENT-CLASS-G01B-11/02 p 446 N93-11058 *
INT-PATENT-CLASS-G01N-25/72 p 216 N93-11057 *

INT-PATENT-CLASS-H01L-29/205 p 458 N93-11056 *
INT-PATENT-CLASS-H01L-31/10 p 458 N93-11056 *

IPF-90-1 .... p 449 N93-11029 #
IPF-90-3 .... p 449 N93-11030 #
IPF-91-1 .... p 449 N93-11102 #
IPF-91-2 .... p 450 N93-11103 #
IPF-91-4 .... p 450 N93-11201 #

IRF-SR-208 .... p 359 N93-11265 #

IS-M-683 .... p 254 N93-10995 #
IS-M-712 .... p 459 N93-11238 #
IS-M-716 .... p 462 N93-11706 #

IS-T-1539 .... p 261 N93-12261 #
IS-T-1576 .... p 257 N93-11572 #
IS-T-1625 .... p 460 N93-11533 #

ISBN-0-16-037924-5 .... p 490 N93-11100 *
ISBN-0-16-039175-X .... p 225 N93-11908 #
ISBN-0-309-04246-1 .... p 487 N93-11603 * #
ISBN-0-315-64278-5 .... p 298 N93-11241
ISBN-0-904747-36-X .... p 217 N93-11224 #
ISBN-0-904947-31-9 .... p 218 N93-11728 #
ISBN-3-7696-9415-5 .... p 205 N93-11344
ISBN-3-7696-9417-1 .... p 407 N93-11345
ISBN-3-7696-9419-7 .... p 309 N93-11346
ISBN-3-7696-9422-8 .... p 309 N93-11330
ISBN-3-7696-9425-2 .... p 361 N93-11331
ISBN-3-7696-9429-5 .... p 315 N93-11332
ISBN-3-7696-9430-9 .... p 220 N93-11335
ISBN-90-369-2004-3 .... p 368 N93-11329
ISBN-90-5271-009-0 .... p 477 N93-11789 #
ISBN-92-835-0664-2 .... p 376 N93-11283 #
ISBN-92-835-0677-4 .... p 430 N93-11711 #
ISBN-92-835-0680-4 .... p 476 N93-11710 #
ISBN-92-9092-029-7 .... p 344 N93-12280 #
ISBN-92-9092-164-1 .... p 476 N93-11583 #
ISBN-951-22-0519-X .... p 216 N93-12415 #
ISBN-951-22-0920-9 .... p 256 N93-11244 #
ISBN-951-22-1042-8 .... p 202 N93-12414 #
ISBN-951-38-4065-4 .... p 299 N93-11360 #
ISBN-951-38-4066-2 .... p 299 N93-11359 #
ISBN-951-47-4473-X .... p 349 N93-12446 #

ISVR-TR-203 .... p 435 N93-12324

ITF-91-2 .... p 440 N93-11914 #

ITP-SB-91-54 .... p 470 N93-11518 #

JPB-014NA .... p 231 N93-11173 * #

JPRS-UEQ-92-009 .... p 220 N93-11169 #

JPRS-USP-92-003 .... p 224 N93-11162 #

JSR-91-315 .... p 486 N93-12380 #

JTN-92-80391 .... p 428 N93-12350 #
JTN-92-80392 .... p 234 N93-12368 #
JTN-92-80393 .... p 209 N93-12370 #
JTN-92-80394 .... p 234 N93-12372 #
JTN-92-80395 .... p 219 N93-12359 #
JTN-92-80396 .... p 216 N93-12361 #
JTN-92-80397 .... p 216 N93-12362 #
JTN-92-80398 .... p 329 N93-12364 #
JTN-92-80400 .... p 314 N93-12373 #
JTN-92-80401 .... p 435 N93-12375 #
JTN-92-80402 .... p 203 N93-12503 #
JTN-92-80403 .... p 314 N93-12365 #
JTN-92-80404 .... p 209 N93-12367 #
JTN-92-80405 .... p 202 N93-12369 #
JTN-92-80406 .... p 243 N93-12371 #
JTN-92-80407 .... p 307 N93-12374 #
JTN-92-80408 .... p 307 N93-12382 #
JTN-92-80409 .... p 209 N93-12383 #
JTN-92-80410 .... p 330 N93-12463 #
JTN-92-80411 .... p 202 N93-12352 #
JTN-92-80412 .... p 208 N93-12354 #

KBSL-89-1001 .... p 407 N93-11368 *

KCP-613-4800 .... p 292 N93-11916 #
KCP-613-4802 .... p 267 N93-11497 #
KCP-613-4810 .... p 291 N93-11643 #
KCP-613-4972 .... p 404 N93-11539 #

KEK-91-10 .... p 444 N93-11525 #

KFK-4969 .... p 265 N93-11203 #

KNMI-TR-137 .... p 368 N93-11329

KTM/E-B-106 .... p 349 N93-12446 #

L-16921 .... p 198 N93-11622 * #
L-16979 .... p 214 N93-11459 * #
L-17045 .... p 206 N93-11170 * #
L-17050 .... p 434 N93-11620 * #
L-17051 .... p 224 N93-10970 * #
L-17055 .... p 277 N93-11613 * #
L-17057 .... p 215 N93-12304 * #
L-17065 .... p 222 N93-12543 * #
L-17107 .... p 367 N93-11168 * #
L-17108 .... p 201 N93-12321 * #
L-17118 .... p 227 N93-12447 * #
L-17129 .... p 239 N93-11623 * #

LA-UR-92-1329 .... p 365 N93-12264 #
LA-UR-92-1360 .... p 365 N93-12263 #
LA-UR-92-1372 .... p 364 N93-12136 #
LA-UR-92-1453 .... p 407 N93-11231 #
LA-UR-92-1695 .... p 293 N93-12089 #

LA-UR-92-1707 p 429 N93-11820 #
LA-UR-92-1716 p 444 N93-11763 #
LA-UR-92-1779 p 268 N93-11861 #
LA-UR-92-1828 p 445 N93-11919 #
LA-UR-92-1841 p 250 N93-11918 #
LA-UR-92-1942 p 312 N93-11768 #
LA-UR-92-1964 p 302 N93-11767 #
LA-UR-92-2086 p 443 N93-11510 #
LA-UR-92-2125 p 362 N93-11535 #
LA-UR-92-2138 p 484 N93-11379 #
LA-UR-92-2139 p 479 N93-12068 #
LA-UR-92-2155 p 345 N93-11626 #
LA-UR-92-2179 p 431 N93-11625 #
LA-UR-92-2189 p 345 N93-11381 #
LA-UR-92-2218 p 485 N93-11695 #
LA-UR-92-2219 p 485 N93-11697 #
LA-UR-92-2271 p 488 N93-11696 #
LA-UR-92-2284 p 357 N93-10985 #
LA-UR-92-2351 p 313 N93-12069 #
LA-UR-92-2352 p 312 N93-11822 #
LA-UR-92-2378 p 274 N93-11380 #
LA-UR-92-2388 p 274 N93-11566 #
LA-UR-92-2489 p 346 N93-11825 #
LA-UR-92-633 p 303 N93-11843 #
LA-UR-92-659 p 261 N93-12256 #
LA-UR-92-845 p 483 N93-10993 #
LA-UR-92-989 p 322 N93-12250 #

LA-12236-PR p 294 N93-12156 #

LBL-PUB-5346 p 489 N93-11078 #

LBL-30989 p 466 N93-12127 #
LBL-31117 p 473 N93-11151 #
LBL-31381 p 470 N93-11518 #
LBL-31427 p 445 N93-12126 #
LBL-31578 p 469 N93-12316 #
LBL-31581 p 251 N93-12112 #
LBL-31609 p 465 N93-11915 #
LBL-31653 p 443 N93-11493 #
LBL-31740 p 466 N93-12099 #
LBL-31876 p 440 N93-12100 #
LBL-31878 p 440 N93-11875 #
LBL-31884 p 355 N93-12104 #
LBL-31984 p 413 N93-12110 #
LBL-32010 p 466 N93-12109 #
LBL-32148 p 466 N93-12125 #
LBL-32295 p 263 N93-10972 #
LBL-32352 p 466 N93-12124 #
LBL-32363 p 441 N93-12111 #

LC-90-36899 p 487 N93-11603 * #

LESC-30277 p 389 N93-12195 * #
LESC-30302 p 389 N93-12211 * #

M-700 p 222 N93-11002 * #

MA-15750FR p 485 N93-11546 * #

MAE-T1960 p 201 N93-12343 * #

MATHS-REPT-A-138 p 425 N93-11323 #
MATHS-REPT-A-156 p 406 N93-11210 #
MATHS-REPT-A-159 p 425 N93-11211 #
MATHS-REPT-A-160 p 357 N93-11120 #
MATHS-REPT-A-163 p 423 N93-11121 #
MATHS-REPT-A-167 p 423 N93-11122 #
MATHS-REPT-A-168 p 424 N93-11123 #
MATHS-REPT-A-169 p 424 N93-11124 #
MATHS-REPT-A-170 p 424 N93-11125 #
MATHS-REPT-A-172 p 424 N93-11126 #

MBB-UK-0146-91-PUB p 223 N93-11007 #
MBB-UK-0148-91-PUB p 195 N93-11008 #
MBB-UK-0162-92-PUB p 278 N93-11009 #
MBB-UK-0171-92-PUB p 263 N93-11011 #

MBB-Z-0212-91-PUB p 263 N93-11010 #
MBB-Z-0405-91-PUB p 255 N93-11026 #
MBB-Z-0432-92-PUB p 255 N93-11027 #

MCAT-92-016 p 219 N93-12349 * #

MCR-90-537-VOL-1 p 227 N93-12442 * #
MCR-90-537-VOL-2 p 227 N93-12443 * #

MD91-33-IBHR p 427 N93-11837 #

MHD-ITC-92-001 p 456 N93-12504 #

MITSG-92-7 p 338 N93-11903 #

MLM-3758(OP) p 310 N93-11554 #

MP-92-142 p 323 N93-12335 #

MPE-PREPRINT-212 p 484 N93-11338
MPE-PREPRINT-213 p 484 N93-11347
MPE-PREPRINT-215 p 482 N93-11473
MPE-PREPRINT-218 p 488 N93-11351

MPE-233 p 361 N93-11352

MRL-TR-91-43 p 311 N93-11648 #

MSRR-573 p 430 N93-12217 #

MTL-TR-92-34 p 469 N93-12286 #

MTR-11177 p 414 N93-12284 #

MTUM-B91EW-0029-PHASE-3 p 213 N93-11339

M91-60 p 286 N93-12433 #

NADC-91111-60 p 261 N93-12248 #
NADC-91112-50 p 426 N93-11463 #

NAL-TM-642-PT-1 p 202 N93-12352 #
NAL-TM-643 p 208 N93-12354 #

NAL-TR-1098T p 428 N93-12350 #
NAL-TR-1100 p 243 N93-12371 #
NAL-TR-1120T p 307 N93-12374 #
NAL-TR-1121T p 307 N93-12382 #
NAL-TR-1122 p 209 N93-12383 #
NAL-TR-1123 p 330 N93-12463 #
NAL-TR-1124 p 234 N93-12368 #
NAL-TR-1125 p 209 N93-12370 #
NAL-TR-1126T p 234 N93-12372 #
NAL-TR-1127 p 219 N93-12359 #
NAL-TR-1128T p 216 N93-12361 #
NAL-TR-1129 p 216 N93-12362 #
NAL-TR-1130 p 329 N93-12364 #
NAL-TR-1132 p 314 N93-12373 #
NAL-TR-1133 p 435 N93-12375 #
NAL-TR-1134 p 203 N93-12503 #
NAL-TR-1135 p 314 N93-12365 #
NAL-TR-1136 p 209 N93-12367 #
NAL-TR-1137 p 202 N93-12369 #

NAMRL-MONO-43 p 387 N93-12432 #

NAS 1.15:102849 p 391 N93-12319 * #
NAS 1.15:103601 p 233 N93-12148 * #
NAS 1.15:103604 p 328 N93-12149 * #
NAS 1.15:103945 p 344 N93-12351 * #
NAS 1.15:103949 p 374 N93-12014 * #
NAS 1.15:103950 p 388 N93-12018 * #
NAS 1.15:103958 p 205 N93-12320 * #
NAS 1.15:104164 p 214 N93-11176 * #
NAS 1.15:104257 p 196 N93-11221 * #
NAS 1.15:104258 p 277 N93-11619 * #
NAS 1.15:104261 p 202 N93-12353 * #
NAS 1.15:104573 p 258 N93-11621 * #
NAS 1.15:104750 p 488 N93-11374 * #
NAS 1.15:104754 p 388 N93-11649 * #
NAS 1.15:105269 p 413 N93-12022 * #
NAS 1.15:105319 p 336 N93-11403 * #
NAS 1.15:105568 p 263 N93-10962 * #
NAS 1.15:105598 p 258 N93-11635 * #
NAS 1.15:105614 p 235 N93-12484 * #
NAS 1.15:105723 p 238 N93-11399 * #
NAS 1.15:105729 p 323 N93-10966 * #
NAS 1.15:105736 p 433 N93-11370 * #
NAS 1.15:105747 p 230 N93-10965 * #
NAS 1.15:105776 p 425 N93-11254 * #
NAS 1.15:105778 p 287 N93-12481 * #
NAS 1.15:105780 p 333 N93-10967 * #
NAS 1.15:105781 p 221 N93-11401 * #
NAS 1.15:105786 p 209 N93-10983 * #
NAS 1.15:105790 p 323 N93-10982 * #
NAS 1.15:105806 p 236 N93-10978 * #
NAS 1.15:105807 p 331 N93-10963 * #
NAS 1.15:105809 p 213 N93-12077 * #
NAS 1.15:105813 p 221 N93-11398 * #
NAS 1.15:105821 p 341 N93-12277 * #
NAS 1.15:105829 p 276 N93-12197 * #
NAS 1.15:105833 p 337 N93-11624 * #
NAS 1.15:105837 p 286 N93-12366 * #
NAS 1.15:105838 p 196 N93-11223 * #
NAS 1.15:105839 p 213 N93-11530 * #
NAS 1.15:105843 p 417 N93-11005 * #
NAS 1.15:105847 p 300 N93-11529 * #
NAS 1.15:105849 p 296 N93-10981 * #
NAS 1.15:105856 p 334 N93-11004 * #
NAS 1.15:105860 p 273 N93-12398 * #
NAS 1.15:105861 p 426 N93-11531 * #
NAS 1.15:105862 p 249 N93-11545 * #
NAS 1.15:105870 p 233 N93-12363 * #
NAS 1.15:105877 p 231 N93-11402 * #
NAS 1.15:105882 p 242 N93-12078 * #
NAS 1.15:105885 p 295 N93-12301 * #
NAS 1.15:105890 p 469 N93-12325 * #
NAS 1.15:105891 p 241 N93-12076 * #
NAS 1.15:105895 p 257 N93-11609 * #
NAS 1.15:105898 p 215 N93-12305 * #
NAS 1.15:105908 p 213 N93-12402 * #
NAS 1.15:105910 p 224 N93-11430 * #
NAS 1.15:105911 p 419 N93-12410 * #
NAS 1.15:105915 p 214 N93-12418 * #
NAS 1.15:105919 p 275 N93-12085 * #
NAS 1.15:107552 p 223 N93-12151 * #
NAS 1.15:107593 p 339 N93-12005 * #
NAS 1.15:107621 p 198 N93-11610 * #
NAS 1.15:107649 p 236 N93-11072 * #
NAS 1.15:107665 p 206 N93-10968 * #
NAS 1.15:107671 p 341 N93-12300 * #
NAS 1.15:107674 p 435 N93-12080 * #
NAS 1.15:107685 p 414 N93-12278 * #
NAS 1.15:107690 p 336 N93-11544 * #
NAS 1.15:107691 p 215 N93-12216 * #
NAS 1.15:107694 p 339 N93-12020 * #
NAS 1.15:107963 p 343 N93-11663 * #
NAS 1.15:107976 p 350 N93-11087 * #
NAS 1.15:107990 p 479 N93-12150 * #
NAS 1.15:107991 p 478 N93-11911 * #
NAS 1.15:107993 p 349 N93-11003 * #
NAS 1.15:108011 p 343 N93-11878 * #
NAS 1.15:108012 p 219 N93-11528 * #
NAS 1.15:108077 p 478 N93-12007 * #
NAS 1.15:108375 p 375 N93-12174 * #
NAS 1.15:108377 p 342 N93-12412 * #
NAS 1.15:108378 p 342 N93-12419 * #
NAS 1.15:4351 p 198 N93-11622 * #
NAS 1.15:4384 p 214 N93-11459 * #
NAS 1.15:4391 p 296 N93-10969 * #
NAS 1.15:4402 p 215 N93-12304 * #
NAS 1.15:4415 p 207 N93-11863 * #
NAS 1.15:4416 p 214 N93-11178 * #
NAS 1.15:4417 p 197 N93-11532 * #
NAS 1.26:184357 p 231 N93-11173 * #
NAS 1.26:184359 p 297 N93-11171 * #
NAS 1.26:184382 p 231 N93-11042 * #
NAS 1.26:184383 p 231 N93-11043 * #
NAS 1.26:184394 p 307 N93-12397 * #
NAS 1.26:184401 p 233 N93-12013 * #
NAS 1.26:184406 p 233 N93-12009 * #
NAS 1.26:184410 p 220 N93-12213 * #
NAS 1.26:184415 p 311 N93-11662 * #
NAS 1.26:184421 p 276 N93-12401 * #
NAS 1.26:184423 p 473 N93-12542 * #
NAS 1.26:184425 p 252 N93-12215 * #
NAS 1.26:184426 p 470 N93-12396 * #
NAS 1.26:184429 p 385 N93-12427 * #
NAS 1.26:184430 p 328 N93-11992 * #
NAS 1.26:184433 p 323 N93-12516 * #
NAS 1.26:184434 p 448 N93-12201 * #
NAS 1.26:184441 p 305 N93-12082 * #
NAS 1.26:184447 p 483 N93-12348 * #
NAS 1.26:184451 p 235 N93-12522 * #
NAS 1.26:184457 p 235 N93-12523 * #
NAS 1.26:184458 p 233 N93-12088 * #
NAS 1.26:184459 p 234 N93-12441 * #
NAS 1.26:184465 p 328 N93-12196 * #
NAS 1.26:184473 p 227 N93-12442 * #
NAS 1.26:184474 p 227 N93-12443 * #
NAS 1.26:185679 p 389 N93-12195 * #
NAS 1.26:185681 p 326 N93-11650 * #
NAS 1.26:185684 p 288 N93-12519 * #
NAS 1.26:185689 p 389 N93-12211 * #
NAS 1.26:185693 p 485 N93-11546 * #
NAS 1.26:188927 p 439 N93-11851 * #
NAS 1.26:189225 p 347 N93-12017 * #
NAS 1.26:189227 p 234 N93-12409 * #
NAS 1.26:189238 p 226 N93-12152 * #
NAS 1.26:189284 p 434 N93-11634 * #
NAS 1.26:189285 p 489 N93-12303 * #
NAS 1.26:189644 p 405 N93-12347 * #
NAS 1.26:189670 p 341 N93-12411 * #
NAS 1.26:189678 p 239 N93-11611 * #
NAS 1.26:189688 p 366 N93-12299 * #
NAS 1.26:189694 p 243 N93-12306 * #
NAS 1.26:189698 p 406 N93-12538 * #
NAS 1.26:189699 p 405 N93-12346 * #
NAS 1.26:189700 p 405 N93-12345 * #
NAS 1.26:189703 p 216 N93-12413 * #
NAS 1.26:189709 p 425 N93-11246 * #
NAS 1.26:189710 p 301 N93-11633 * #
NAS 1.26:189711 p 412 N93-11618 * #
NAS 1.26:189712 p 198 N93-11607 * #
NAS 1.26:189713 p 427 N93-12298 * #
NAS 1.26:189716 p 416 N93-12403 * #
NAS 1.26:189717 p 435 N93-12021 * #
NAS 1.26:189719 p 416 N93-12400 * #
NAS 1.26:189720 p 306 N93-12173 * #
NAS 1.26:190209 p 297 N93-11074 * #
NAS 1.26:190278 p 407 N93-11368 *

NAS 1.26:190358 .... p 484 N93-11243 * #
NAS 1.26:190362 .... p 279 N93-11116 * #
NAS 1.26:190596 .... p 270 N93-11993 * #
NAS 1.26:190617 .... p 218 N93-11910 * #
NAS 1.26:190636 .... p 412 N93-11717 * #
NAS 1.26:190696 .... p 486 N93-11164 * #
NAS 1.26:190756 .... p 335 N93-11175 * #
NAS 1.26:190760 .... p 314 N93-12279 * #
NAS 1.26:190761 .... p 232 N93-11608 * #
NAS 1.26:190765 .... p 347 N93-12019 * #
NAS 1.26:190805 .... p 297 N93-11142 * #
NAS 1.26:190807 .... p 223 N93-11101 * #
NAS 1.26:190811 .... p 204 N93-11139 * #
NAS 1.26:190837 .... p 204 N93-10961 * #
NAS 1.26:190845 .... p 283 N93-11716 * #
NAS 1.26:190856 .... p 481 N93-11075 * #
NAS 1.26:190857 .... p 481 N93-11073 * #
NAS 1.26:190892 .... p 357 N93-10964 * #
NAS 1.26:190894 .... p 414 N93-12384 * #
NAS 1.26:190919 .... p 461 N93-11684 * #
NAS 1.26:190920 .... p 461 N93-11683 * #
NAS 1.26:190929 .... p 487 N93-11603 * #
NAS 1.26:190931 .... p 409 N93-11458 * #
NAS 1.26:190933 .... p 301 N93-11606 * #
NAS 1.26:190934 .... p 200 N93-12004 * #
NAS 1.26:190935 .... p 197 N93-11605 * #
NAS 1.26:190936 .... p 201 N93-12343 * #
NAS 1.26:190937 .... p 291 N93-11604 * #
NAS 1.26:190943 .... p 310 N93-11612 * #
NAS 1.26:190950 .... p 416 N93-12515 * #
NAS 1.26:190954 .... p 370 N93-11880 * #
NAS 1.26:190955 .... p 405 N93-12520 * #
NAS 1.26:190965 .... p 213 N93-12214 * #
NAS 1.26:190966 .... p 426 N93-11547 * #
NAS 1.26:190967 .... p 330 N93-12521 * #
NAS 1.26:190969 .... p 349 N93-12394 * #
NAS 1.26:190970 .... p 472 N93-12212 * #
NAS 1.26:190972 .... p 406 N93-12541 * #
NAS 1.26:190973 .... p 406 N93-12540 * #
NAS 1.26:190974 .... p 419 N93-12395 * #
NAS 1.26:190975 .... p 404 N93-11462 * #
NAS 1.26:190976 .... p 418 N93-11651 * #
NAS 1.26:190978 .... p 308 N93-12539 * #
NAS 1.26:190979 .... p 307 N93-12329 * #
NAS 1.26:190980 .... p 219 N93-12349 * #
NAS 1.26:190995 .... p 219 N93-11754 * #
NAS 1.26:190998 .... p 343 N93-12006 * #
NAS 1.26:4454 .... p 202 N93-12399 * #
NAS 1.55:3127-VOL-1 .... p 391 N93-11921 * #
NAS 1.55:3157 .... p 227 N93-12447 * #
NAS 1.60:3199 .... p 243 N93-12302 * #
NAS 1.60:3222 .... p 232 N93-11614 * #
NAS 1.60:3228 .... p 222 N93-12543 * #
NAS 1.60:3229 .... p 277 N93-11613 * #
NAS 1.60:3244 .... p 206 N93-11170 * #
NAS 1.60:3245 .... p 224 N93-10970 * #
NAS 1.60:3260 .... p 201 N93-12321 * #
NAS 1.60:3264 .... p 239 N93-11623 * #
NAS 1.60:3269 .... p 434 N93-11620 * #
NAS 1.60:3274 .... p 218 N93-12016 * #
NAS 1.60:3279 .... p 224 N93-11001 * #
NAS 1.60:3289 .... p 222 N93-11002 * #
NAS 1.60:3292 .... p 241 N93-12015 * #
NAS 1.61:1281 .... p 367 N93-11168 * #
NAS 1.61:1284 .... p 373 N93-11718 * #
NAS 1.71:LAR-14448-1 .... p 269 N93-11912 * #
NAS 1.71:LAR-14470-1 .... p 199 N93-11876 * #
NAS 1.71:LAR-14581-1-SB .... p 333 N93-12204 * #
NAS 1.71:LAR-14776-1 .... p 313 N93-12205 * #
NAS 1.71:LEW-14906-1 .... p 329 N93-12203 * #
NAS 1.71:LEW-15218-1 .... p 297 N93-11172 * #
NAS 1.71:LEW-15263-1 .... p 239 N93-11543 * #
NAS 1.71:LEW-15345-1 .... p 329 N93-12327 * #
NAS 1.71:NPO-18343-1-CU .... p 290 N93-11456 * #
NAS 1.71:NPO-18579-1-CU .... p 420 N93-11174 * #
NAS 1.71:NPO-18584-1-CU .... p 324 N93-11177 * #
NAS 1.71:NPO-18771-1-CU .... p 412 N93-11664 * #
NAS 1.71:NPO-18817-1-CU .... p 278 N93-12202 * #
NAS 1.83:130 .... p 490 N93-11100 *

NASA-CASE-LAR-13508-3-CU .... p 216 N93-11057 *
NASA-CASE-LAR-13925-2 .... p 264 N93-11059 *
NASA-CASE-LAR-14448-1 .... p 269 N93-11912 * #
NASA-CASE-LAR-14470-1 .... p 199 N93-11876 * #
NASA-CASE-LAR-14581-1-SB .... p 333 N93-12204 * #
NASA-CASE-LAR-14776-1 .... p 313 N93-12205 * #

NASA-CASE-LEW-14906-1 .... p 329 N93-12203 * #
NASA-CASE-LEW-14996-1 .... p 446 N93-11058 *
NASA-CASE-LEW-15218-1 .... p 297 N93-11172 * #
NASA-CASE-LEW-15263-1 .... p 239 N93-11543 * #
NASA-CASE-LEW-15345-1 .... p 329 N93-12327 * #

NASA-CASE-NPO-17880-1-CU .... p 458 N93-11056 *
NASA-CASE-NPO-18343-1-CU .... p 290 N93-11456 * #
NASA-CASE-NPO-18579-1-CU .... p 420 N93-11174 * #
NASA-CASE-NPO-18584-1-CU .... p 324 N93-11177 * #
NASA-CASE-NPO-18771-1-CU .... p 412 N93-11664 * #
NASA-CASE-NPO-18817-1-CU .... p 278 N93-12202 * #

NASA-CP-3127-VOL-1 .... p 391 N93-11921 * #
NASA-CP-3157 .... p 227 N93-12447 * #

NASA-CR-184357 .... p 231 N93-11173 * #
NASA-CR-184359 .... p 297 N93-11171 * #
NASA-CR-184382 .... p 231 N93-11042 * #
NASA-CR-184383 .... p 231 N93-11043 * #
NASA-CR-184394 .... p 307 N93-12397 * #
NASA-CR-184401 .... p 233 N93-12013 * #
NASA-CR-184406 .... p 233 N93-12009 * #
NASA-CR-184410 .... p 220 N93-12213 * #
NASA-CR-184415 .... p 311 N93-11662 * #
NASA-CR-184421 .... p 276 N93-12401 * #
NASA-CR-184423 .... p 473 N93-12542 * #
NASA-CR-184425 .... p 252 N93-12215 * #
NASA-CR-184426 .... p 470 N93-12396 * #
NASA-CR-184429 .... p 385 N93-12427 * #
NASA-CR-184430 .... p 328 N93-11992 * #
NASA-CR-184433 .... p 323 N93-12516 * #
NASA-CR-184434 .... p 448 N93-12201 * #
NASA-CR-184441 .... p 305 N93-12082 * #
NASA-CR-184447 .... p 483 N93-12348 * #
NASA-CR-184451 .... p 235 N93-12522 * #
NASA-CR-184457 .... p 235 N93-12523 * #
NASA-CR-184458 .... p 233 N93-12088 * #
NASA-CR-184459 .... p 234 N93-12441 * #
NASA-CR-184465 .... p 328 N93-12196 * #
NASA-CR-184473 .... p 227 N93-12442 * #
NASA-CR-184474 .... p 227 N93-12443 * #
NASA-CR-185679 .... p 389 N93-12195 * #
NASA-CR-185681 .... p 326 N93-11650 * #
NASA-CR-185684 .... p 288 N93-12519 * #
NASA-CR-185689 .... p 389 N93-12211 * #
NASA-CR-185693 .... p 485 N93-11546 * #
NASA-CR-188927 .... p 439 N93-11851 * #
NASA-CR-189225 .... p 347 N93-12017 * #
NASA-CR-189227 .... p 234 N93-12409 * #
NASA-CR-189238 .... p 226 N93-12152 * #
NASA-CR-189284 .... p 434 N93-11634 * #
NASA-CR-189285 .... p 489 N93-12303 * #
NASA-CR-189644 .... p 405 N93-12347 * #
NASA-CR-189670 .... p 341 N93-12411 * #
NASA-CR-189678 .... p 239 N93-11611 * #
NASA-CR-189688 .... p 366 N93-12299 * #
NASA-CR-189694 .... p 243 N93-12306 * #
NASA-CR-189698 .... p 406 N93-12538 * #
NASA-CR-189699 .... p 405 N93-12346 * #
NASA-CR-189700 .... p 405 N93-12345 * #
NASA-CR-189703 .... p 216 N93-12413 * #
NASA-CR-189709 .... p 425 N93-11246 * #
NASA-CR-189710 .... p 301 N93-11633 * #
NASA-CR-189711 .... p 412 N93-11618 * #
NASA-CR-189712 .... p 198 N93-11607 * #
NASA-CR-189713 .... p 427 N93-12298 * #
NASA-CR-189716 .... p 416 N93-12403 * #
NASA-CR-189717 .... p 435 N93-12021 * #
NASA-CR-189719 .... p 416 N93-12400 * #
NASA-CR-189720 .... p 306 N93-12173 * #
NASA-CR-190209 .... p 297 N93-11074 * #
NASA-CR-190278 .... p 407 N93-11368 *
NASA-CR-190358 .... p 484 N93-11243 * #
NASA-CR-190362 .... p 279 N93-11116 * #
NASA-CR-190596 .... p 270 N93-11993 * #
NASA-CR-190617 .... p 218 N93-11910 * #
NASA-CR-190636 .... p 412 N93-11717 * #
NASA-CR-190696 .... p 486 N93-11164 * #
NASA-CR-190756 .... p 335 N93-11175 * #
NASA-CR-190760 .... p 314 N93-12279 * #
NASA-CR-190761 .... p 232 N93-11608 * #
NASA-CR-190765 .... p 347 N93-12019 * #
NASA-CR-190805 .... p 297 N93-11142 * #
NASA-CR-190807 .... p 223 N93-11101 * #
NASA-CR-190811 .... p 204 N93-11139 * #
NASA-CR-190837 .... p 204 N93-10961 * #
NASA-CR-190845 .... p 283 N93-11716 * #
NASA-CR-190856 .... p 481 N93-11075 * #
NASA-CR-190857 .... p 481 N93-11073 * #
NASA-CR-190892 .... p 357 N93-10964 * #
NASA-CR-190894 .... p 414 N93-12384 * #
NASA-CR-190919 .... p 461 N93-11684 * #
NASA-CR-190920 .... p 461 N93-11683 * #
NASA-CR-190929 .... p 487 N93-11603 * #
NASA-CR-190931 .... p 409 N93-11458 * #
NASA-CR-190933 .... p 301 N93-11606 * #
NASA-CR-190934 .... p 200 N93-12004 * #
NASA-CR-190935 .... p 197 N93-11605 * #
NASA-CR-190936 .... p 201 N93-12343 * #
NASA-CR-190937 .... p 291 N93-11604 * #
NASA-CR-190943 .... p 310 N93-11612 * #
NASA-CR-190950 .... p 416 N93-12515 * #
NASA-CR-190954 .... p 370 N93-11880 * #
NASA-CR-190955 .... p 405 N93-12520 * #
NASA-CR-190965 .... p 213 N93-12214 * #
NASA-CR-190966 .... p 426 N93-11547 * #
NASA-CR-190967 .... p 330 N93-12521 * #
NASA-CR-190969 .... p 349 N93-12394 * #
NASA-CR-190970 .... p 472 N93-12212 * #
NASA-CR-190972 .... p 406 N93-12541 * #
NASA-CR-190973 .... p 406 N93-12540 * #
NASA-CR-190974 .... p 419 N93-12395 * #
NASA-CR-190975 .... p 404 N93-11462 * #
NASA-CR-190976 .... p 418 N93-11651 * #
NASA-CR-190978 .... p 308 N93-12539 * #
NASA-CR-190979 .... p 307 N93-12329 * #
NASA-CR-190980 .... p 219 N93-12349 * #
NASA-CR-190995 .... p 219 N93-11754 * #
NASA-CR-190998 .... p 343 N93-12006 * #
NASA-CR-4454 .... p 202 N93-12399 * #

NASA-NP-130 .... p 490 N93-11100 *

NASA-RP-1281 .... p 367 N93-11168 * #
NASA-RP-1284 .... p 373 N93-11718 * #

NASA-TM-102849 .... p 391 N93-12319 * #
NASA-TM-103601 .... p 233 N93-12148 * #
NASA-TM-103604 .... p 328 N93-12149 * #
NASA-TM-103945 .... p 344 N93-12351 * #
NASA-TM-103949 .... p 374 N93-12014 * #
NASA-TM-103950 .... p 388 N93-12018 * #
NASA-TM-103958 .... p 205 N93-12320 * #
NASA-TM-104164 .... p 214 N93-11176 * #
NASA-TM-104257 .... p 196 N93-11221 * #
NASA-TM-104258 .... p 277 N93-11619 * #
NASA-TM-104261 .... p 202 N93-12353 * #
NASA-TM-104573 .... p 258 N93-11621 * #
NASA-TM-104750 .... p 488 N93-11374 * #
NASA-TM-104754 .... p 388 N93-11649 * #
NASA-TM-105269 .... p 413 N93-12022 * #
NASA-TM-105319 .... p 336 N93-11403 * #
NASA-TM-105568 .... p 263 N93-10962 * #
NASA-TM-105598 .... p 258 N93-11635 * #
NASA-TM-105614 .... p 235 N93-12484 * #
NASA-TM-105723 .... p 238 N93-11399 * #
NASA-TM-105729 .... p 323 N93-10966 * #
NASA-TM-105736 .... p 433 N93-11370 * #
NASA-TM-105747 .... p 230 N93-10965 * #
NASA-TM-105776 .... p 425 N93-11254 * #
NASA-TM-105778 .... p 287 N93-12481 * #
NASA-TM-105780 .... p 333 N93-10967 * #
NASA-TM-105781 .... p 221 N93-11401 * #
NASA-TM-105786 .... p 209 N93-10983 * #
NASA-TM-105790 .... p 323 N93-10982 * #
NASA-TM-105806 .... p 236 N93-10978 * #
NASA-TM-105807 .... p 331 N93-10963 * #
NASA-TM-105809 .... p 213 N93-12077 * #
NASA-TM-105813 .... p 221 N93-11398 * #
NASA-TM-105821 .... p 341 N93-12277 * #
NASA-TM-105829 .... p 276 N93-12197 * #
NASA-TM-105833 .... p 337 N93-11624 * #
NASA-TM-105837 .... p 286 N93-12366 * #
NASA-TM-105838 .... p 196 N93-11223 * #
NASA-TM-105839 .... p 213 N93-11530 * #
NASA-TM-105843 .... p 417 N93-11005 * #
NASA-TM-105847 .... p 300 N93-11529 * #
NASA-TM-105849 .... p 296 N93-10981 * #
NASA-TM-105856 .... p 334 N93-11004 * #
NASA-TM-105860 .... p 273 N93-12398 * #
NASA-TM-105861 .... p 426 N93-11531 * #
NASA-TM-105862 .... p 249 N93-11545 * #
NASA-TM-105870 .... p 233 N93-12363 * #
NASA-TM-105877 .... p 231 N93-11402 * #
NASA-TM-105882 .... p 242 N93-12078 * #
NASA-TM-105885 .... p 295 N93-12301 * #
NASA-TM-105890 .... p 469 N93-12325 * #
NASA-TM-105891 .... p 241 N93-12076 * #
NASA-TM-105895 .... p 257 N93-11609 * #
NASA-TM-105898 .... p 215 N93-12305 * #
NASA-TM-105908 .... p 213 N93-12402 * #
NASA-TM-105910 .... p 224 N93-11430 * #
NASA-TM-105911 .... p 419 N93-12410 * #
NASA-TM-105915 .... p 214 N93-12418 * #
NASA-TM-105919 .... p 275 N93-12085 * #
NASA-TM-107552 .... p 223 N93-12151 * #
NASA-TM-107593 .... p 339 N93-12005 * #
NASA-TM-107621 .... p 198 N93-11610 * #
NASA-TM-107649 .... p 236 N93-11072 * #
NASA-TM-107665 .... p 206 N93-10968 * #
NASA-TM-107671 .... p 341 N93-12300 * #
NASA-TM-107674 .... p 435 N93-12080 * #
NASA-TM-107685 .... p 414 N93-12278 * #
NASA-TM-107690 .... p 336 N93-11544 * #
NASA-TM-107691 .... p 215 N93-12216 * #
NASA-TM-107694 .... p 339 N93-12020 * #
NASA-TM-107963 .... p 343 N93-11663 * #
NASA-TM-107976 .... p 350 N93-11087 * #
NASA-TM-107990 .... p 479 N93-12150 * #
NASA-TM-107991 .... p 478 N93-11911 * #

NASA-TM-107993 p 349 N93-11003 * #
NASA-TM-108011 p 343 N93-11878 * #
NASA-TM-108012 p 219 N93-11528 * #
NASA-TM-108077 p 478 N93-12007 * #
NASA-TM-108375 p 375 N93-12174 * #
NASA-TM-108377 p 342 N93-12412 * #
NASA-TM-108378 p 342 N93-12419 * #
NASA-TM-4351 p 198 N93-11622 * #
NASA-TM-4384 p 214 N93-11459 * #
NASA-TM-4391 p 296 N93-10969 * #
NASA-TM-4402 p 215 N93-12304 * #
NASA-TM-4415 p 207 N93-11863 * #
NASA-TM-4416 p 214 N93-11178 * #
NASA-TM-4417 p 197 N93-11532 * #

NASA-TP-3199 p 243 N93-12302 * #
NASA-TP-3222 p 232 N93-11614 * #
NASA-TP-3228 p 222 N93-12543 * #
NASA-TP-3229 p 277 N93-11613 * #
NASA-TP-3244 p 206 N93-11170 * #
NASA-TP-3245 p 224 N93-10970 * #
NASA-TP-3260 p 201 N93-12321 * #
NASA-TP-3264 p 239 N93-11623 * #
NASA-TP-3269 p 434 N93-11620 * #
NASA-TP-3274 p 218 N93-12016 * #
NASA-TP-3279 p 224 N93-11001 * #
NASA-TP-3289 p 222 N93-11002 * #
NASA-TP-3292 p 241 N93-12015 * #

NATICK-TR-92/130 p 390 N93-12423 #

NATICK/TR-92/010 p 268 N93-11862 #
NATICK/TR-92/035 p 200 N93-12179 #

NAVSO-P-3580-V17-N3 p 490 N93-12470 #

NAVSWC-TR-91-388 p 414 N93-12341 #
NAVSWC-TR-91-584 p 419 N93-12358 #

NAVY-CASE-73624 p 280 N93-11354 #
NAVY-CASE-74029 p 293 N93-12133 #

NAWCADWAR-92032-60 p 390 N93-12486 #
NAWCADWAR-92056-60 p 389 N93-12291 #

NHRC-91-22 p 385 N93-11893 #

NIFS-110 p 451 N93-11277 #
NIFS-116 p 454 N93-11834 #

NIKHEF-H+K/92-01 p 442 N93-11130 #

NIKHEF-K/AMPS/92-01 p 442 N93-11131 #

NIST/SP-823/2 p 418 N93-11714 #

NIST/TN-1284 p 308 N93-12475 #
NIST/TN-1355 p 293 N93-12084 #

NISTIR-4812 p 438 N93-11715 #
NISTIR-4843 p 474 N93-11215 #
NISTIR-4846 p 404 N93-11258 #
NISTIR-4849 p 271 N93-12086 #
NISTIR-4855 p 277 N93-11901 #
NISTIR-4858 p 277 N93-11902 #

NMAB-458 p 242 N93-12292 #

NOAA-TM-NWS-CR-102 p 369 N93-11803 #

NOARL-PR-92-020-252 p 207 N93-11838 #

NOARL-TN-286 p 374 N93-12288 #

NOARL-20 p 373 N93-11821 #

NOR-91-49 p 262 N93-12468 #

NPL-DES-116 p 289 N93-11393
NPL-DES-118 p 459 N93-11394
NPL-DES-120 p 281 N93-11395

NPL-DITC-200/92 p 412 N93-11688

NPL-DMM(A)-45 p 247 N93-11396
NPL-DMM(A)-47 p 266 N93-11397
NPL-DMM(A)-48 p 447 N93-11408
NPL-DMM(A)-50 p 325 N93-11324
NPL-DMM(A)-51 p 325 N93-11325
NPL-DMM(A)-52 p 325 N93-11327
NPL-DMM(A)-53 p 325 N93-11326
NPL-DMM(A)-57 p 238 N93-11409

NPL-MOM-107 p 432 N93-11666

NPL-RSA(EXT)-30 p 310 N93-11410
NPL-RSA(EXT)-31 p 316 N93-11411
NPL-RSA(EXT)-32 p 433 N93-11328
NPL-RSA(EXT)-33 p 436 N93-11412

NPS-ME-92-003 p 329 N93-12434 #

NPS-MR-92-002 p 372 N93-12339 #

NPSCS-92-011 p 479 N93-12381 #

NPSOR-92-013 p 429 N93-12426 #

NRAD-TR-1517 p 243 N93-12483 #

NRE-052992 p 231 N93-11173 * #

NREL/TP-411-4995 p 464 N93-11818 #
NREL/TP-420-4894 p 275 N93-12171 #
NREL/TP-451-4938 p 463 N93-11813 #
NREL/TP-451-4962 p 463 N93-11816 #

NRIM-SR-92-01 p 261 N93-12322 #

NRL-PUB-183-6000 p 238 N93-11422 #

NRL/FR/5534-92-9375 p 388 N93-11784 #

NRL/MR/4404-92-7106 p 302 N93-11756 #
NRL/MR/4721-92-6980 p 322 N93-12275 #
NRL/MR/4790-92-6973 p 315 N93-11195 #
NRL/MR/5313-92-7111 p 285 N93-12356 #
NRL/MR/6179-92-7143 p 272 N93-12276 #
NRL/MR/6386-92-7104 p 307 N93-12355 #
NRL/MR/6542-92-7101 p 468 N93-12271 #

NSSDC/WDC-A-R/S-91-29 p 349 N93-11003 * #
NSSDC/WDC-A-R/S-91-32 p 478 N93-11911 * #

NSSDCA/WDC-A-R/S-92-03 p 479 N93-12150 * #

NSWCCR/RDTR-92/0006 p 276 N93-12281 #

NSWCDD-TR-92/237 p 285 N93-12332 #

NTSB/AAR-92/02 p 204 N93-12193 #
NTSB/AAR-92/03 p 203 N93-11471 #

ORNL/CDIAC-34/R2 p 473 N93-10990 #
ORNL/CDIAC-52 p 353 N93-11655 #

ORNL/SUB-87-SA582/1 p 268 N93-11654 #
ORNL/SUB-90-SF985/1 p 268 N93-11735 #

ORNL/TM-11984 p 266 N93-11442 #

OUEL-1911/92 p 337 N93-11707 #

PB91-242297 p 370 N93-11888 #
PB92-138320 p 367 N93-11242 #
PB92-154913 p 477 N93-11769 #
PB92-156959 p 484 N93-11243 * #
PB92-158898 p 488 N93-11738 #
PB92-161025 p 368 N93-11256 #
PB92-176148 p 369 N93-11803 #
PB92-180660 p 256 N93-11244 #
PB92-181106 p 438 N93-11715 #
PB92-181114 p 418 N93-11714 #
PB92-184464 p 485 N93-11807 #
PB92-184738 p 451 N93-11245 #
PB92-185768 p 476 N93-11700 #
PB92-188416 p 343 N93-11701 #
PB92-188424 p 354 N93-11702 #
PB92-190305 p 470 N93-11469 #
PB92-191212 p 474 N93-11215 #
PB92-195312 p 219 N93-11216 #
PB92-195577 p 275 N93-12147 #
PB92-197219 p 205 N93-11472 #
PB92-198803 p 370 N93-11896 #
PB92-199108 p 238 N93-11470 #
PB92-199157 p 294 N93-12294 #
PB92-199165 p 295 N93-12295 #
PB92-199173 p 294 N93-12191 #
PB92-199181 p 294 N93-12192 #
PB92-199488 p 238 N93-11422 #
PB92-204213 p 371 N93-12293 #
PB92-205350 p 308 N93-12475 #
PB92-205376 p 293 N93-12084 #
PB92-205426 p 271 N93-12086 #
PB92-205442 p 404 N93-11258 #
PB92-205459 p 277 N93-11902 #
PB92-205467 p 277 N93-11901 #
PB92-205517 p 372 N93-11253 #
PB92-205566 p 338 N93-11903 #
PB92-205608 p 325 N93-11427 #
PB92-205616 p 277 N93-12072 #
PB92-205673 p 204 N93-11252 #
PB92-205772 p 312 N93-11757 #
PB92-206564 p 298 N93-11251 #
PB92-207125 p 477 N93-11789 #
PB92-216035 p 456 N93-12526 #
PB92-216043 p 457 N93-12527 #
PB92-224310 p 480 N93-12528 #
PB92-226174 p 356 N93-12524 #
PB92-228030 p 356 N93-12525 #
PB92-910402 p 204 N93-12193 #
PB92-910403 p 203 N93-11471 #

PL-TR-91-1083 p 284 N93-12160 #
PL-TR-91-2160 p 359 N93-11228 #
PL-TR-91-2191-VOL-1 p 322 N93-12262 #
PL-TR-91-2191-VOL-3 p 317 N93-11805 #
PL-TR-91-2192 p 361 N93-11421 #
PL-TR-91-2215 p 362 N93-11740 #
PL-TR-92-2036 p 363 N93-11788 #
PL-TR-92-2038 p 366 N93-12270 #
PL-TR-92-2066 p 363 N93-11810 #
PL-TR-92-2084 p 290 N93-11492 #
PL-TR-92-2182 p 489 N93-12506 #

PNL-SA-19123 p 441 N93-12117 #
PNL-SA-19945 p 257 N93-11557 #
PNL-SA-20368 p 282 N93-11515 #
PNL-SA-20809 p 369 N93-11657 #
PNL-SA-20954 p 312 N93-11802 #
PNL-SA-21006 p 240 N93-11658 #

PNL-8084 p 481 N93-12067 #
PNL-8277 p 332 N93-11601 #

PNR-90880 p 433 N93-11204 #
PNR-90884 p 266 N93-11205 #
PNR-90887 p 212 N93-11206 #
PNR-90889 p 212 N93-11207 #
PNR-90890 p 212 N93-11208 #
PNR-90892 p 255 N93-11031 #
PNR-90893 p 473 N93-11012 #
PNR-90897 p 263 N93-11032 #
PNR-90907 p 334 N93-11013 #
PNR-90908 p 334 N93-11014 #
PNR-90909 p 331 N93-11015 #
PNR-90911 p 331 N93-11016 #
PNR-90912 p 255 N93-11033 #
PNR-90913 p 296 N93-11017 #
PNR-90914 p 263 N93-11018 #
PNR-90915 p 209 N93-11019 #
PNR-90916 p 195 N93-11020 #
PNR-90918 p 334 N93-11021 #
PNR-90919 p 309 N93-11320 #
PNR-90920 p 334 N93-11022 #
PNR-90924 p 209 N93-11023 #
PNR-90927 p 210 N93-11024 #
PNR-90929 p 296 N93-11025 #
PNR-90932 p 331 N93-11034 #
PNR-90935 p 244 N93-11035 #
PNR-90936 p 210 N93-11036 #
PNR-90937 p 210 N93-11037 #
PNR-90938 p 210 N93-11038 #
PNR-90939 p 210 N93-11039 #
PNR-90943 p 210 N93-11040 #
PNR-90944 p 324 N93-11054 #
PNR-90945 p 210 N93-11055 #
PNR-90946 p 211 N93-11105 #
PNR-90947 p 211 N93-11106 #
PNR-90948 p 236 N93-11107 #
PNR-90949 p 212 N93-11108 #
PNR-90950 p 255 N93-11109 #
PNR-90951 p 331 N93-11110 #
PNR-90958 p 433 N93-11321 #
PNR-90959 p 433 N93-11322 #
PNR-90960 p 255 N93-11111 #
PNR-90961 p 264 N93-11084 #
PNR-90962 p 211 N93-11085 #
PNR-90965 p 264 N93-11086 #
PNR-90970 p 210 N93-11061 #
PNR-90973 p 211 N93-11062 #
PNR-90974 p 211 N93-11063 #
PNR-90975 p 315 N93-11064 #
PNR-90976-PT-1-2-3 p 236 N93-11065 #
PNR-90983 p 264 N93-11066 #
PNR-90984 p 212 N93-11112 #
PNR-90985 p 296 N93-11067 #
PNR-90986 p 211 N93-11068 #
PNR-90987 p 211 N93-11069 #
PNR-90991 p 195 N93-11070 #
PNR-90992 p 196 N93-11113 #
PNR-90993 p 212 N93-11114 #
PNR-90997 p 255 N93-11115 #
PNR-91011 p 206 N93-11334 #

PU-NE-92/1 p 300 N93-11538 #

PW-FR-21998-10 p 260 N93-12237 #

PWA-6142-43 p 308 N93-12539 * #

P304769-42 p 281 N93-11387 #
P304797-47 p 425 N93-11437 #
P305695-04 p 207 N93-11485 #

R/D-6541-AN-09 p 249 N93-11490 #
R/D-6901-EE-03 p 292 N93-12071 #

RAE-RAD-NAV-130 p 289 N93-11434 #

RAE-TM-AERO-2222 p 199 N93-11882 #
RAE-TM-AERO-2228 p 199 N93-11883 #
RAE-TM-AERO-2231 p 198 N93-11610 * #
RAE-TM-AERO-2232 p 218 N93-11906 #

RAE-TM-MAT-STR-1102 p 217 N93-11435 #
RAE-TM-MAT-STR-1183 p 240 N93-11905 #

RAE-TM-P-1214 p 207 N93-11485 #

RAE-TM-SPACE-386 p 220 N93-11486 #

RAE-TR-84009 p 289 N93-11434 #
RAE-TR-90046 p 335 N93-11369 #

RAL-92-001 p 444 N93-11687 #

RARDE-7/91 p 273 N93-11376 #

RCC-456-92 p 285 N93-12240 #

REPT-B-31 p 216 N93-12415 #
REPT-B-36 p 202 N93-12414 #

REPT-141-02/03-F p 422 N93-12439 #
REPT-1992-12 p 273 N93-12440 #
REPT-1992-7 p 480 N93-12438 #
REPT-3-448724-22529 p 422 N93-12258 #
REPT-37/91 p 349 N93-11082 #
REPT-45SPW-TR-92-1 p 334 N93-11080 #
REPT-45SPW-TR-92-2 p 371 N93-12170 #
REPT-533614 p 431 N93-11468 #
REPT-6871 p 436 N93-11196 #
REPT-89063 p 291 N93-11604 * #
REPT-92-011 p 420 N93-11227
REPT-92-012 p 418 N93-11180
REPT-92-015 p 418 N93-11181
REPT-92-016 p 424 N93-11182
REPT-92-018 p 386 N93-11212
REPT-92-019 p 421 N93-11667
REPT-92-020 p 411 N93-11592
REPT-92-023 p 421 N93-11593
REPT-92-025 p 411 N93-11594
REPT-92-026 p 476 N93-11689
REPT-92-034 p 476 N93-11690
REPT-92B00104 p 373 N93-11718 * #
REPT-92E02736 p 258 N93-11621 * #
REPT-921-320-101 p 418 N93-11584 #
REPT-921-320-102 p 215 N93-11585 #
REPT-921-430-101 p 239 N93-11586 #
REPT-921-430-102 p 332 N93-11587 #
REPT-921-430-103 p 239 N93-11588 #
REPT-921-430-105 p 239 N93-11589 #
REPT-921-430-147 p 239 N93-11590 #
REPT-921-440-101 p 282 N93-11591 #

RFP-4450 p 249 N93-11801 #
RFP-4522 p 327 N93-11679 #
RFP-4581 p 465 N93-12073 #
RFP-4608 p 326 N93-11556 #

RHD-03 p 295 N93-12421 #

RIACS-TR-91.11 p 409 N93-11458 * #

RL-TR-91-413 p 310 N93-11562 #
RL-TR-91-423-VOL-1 p 414 N93-12242 #
RL-TR-91-429 p 292 N93-11781 #
RL-TR-92-12-VOL-2 p 413 N93-12146 #
RL-TR-92-124 p 470 N93-12464 #
RL-TR-92-135 p 448 N93-12227 #
RL-TR-92-156 p 294 N93-12290 #
RL-TR-92-23 p 224 N93-11736 #
RL-TR-92-36 p 477 N93-11749 #
RL-TR-92-5 p 290 N93-11504 #
RL-TR-92-74 p 448 N93-12272 #
RL-TR-92-79 p 408 N93-11371 #

RR-1245-1 p 325 N93-11427 #
RR-920-4 p 277 N93-12072 #

RSRE-MEMO-4282 p 472 N93-10976 #
RSRE-MEMO-4299 p 412 N93-11712 #
RSRE-MEMO-4343 p 428 N93-10980 #
RSRE-MEMO-4350 p 385 N93-10979 #
RSRE-MEMO-4367 p 414 N93-12326 #
RSRE-MEMO-4391 p 278 N93-10977 #
RSRE-MEMO-4464 p 447 N93-11342 #
RSRE-MEMO-4467 p 420 N93-11343 #
RSRE-MEMO-4473 p 280 N93-11383 #
RSRE-MEMO-4503-ISSUE-2 p 474 N93-11333 #
RSRE-MEMO-4511 p 280 N93-11384 #
RSRE-MEMO-4512 p 280 N93-11385 #
RSRE-MEMO-4515 p 408 N93-11386 #
RSRE-MEMO-4518 p 281 N93-11387 #
RSRE-MEMO-4528 p 315 N93-11388 #
RSRE-MEMO-4540 p 475 N93-11404 #
RSRE-MEMO-4543 p 409 N93-11405 #
RSRE-MEMO-4545 p 409 N93-11406 #
RSRE-MEMO-4549 p 409 N93-11407 #
RSRE-MEMO-4554 p 408 N93-11389 #
RSRE-MEMO-4562 p 408 N93-11390 #
RSRE-MEMO-4567 p 281 N93-11391 #
RSRE-MEMO-4568 p 409 N93-11392 #

RSRE-90009 p 405 N93-12430 #
RSRE-91024 p 409 N93-11436 #
RSRE-91026 p 281 N93-11487 #
RSRE-91028 p 425 N93-11437 #
RSRE-91034 p 407 N93-11341 #

RTP/909/10-ISSUE-2 p 288 N93-11364 #

R91-927893 p 438 N93-11804 #

S-HRG-102-762 p 225 N93-11908 #

S-650-VOL-1 p 391 N93-11921 * #
S-678 p 488 N93-11374 * #
S-688 p 388 N93-11649 * #

SAE PAPER 92-1994 p 196 N93-11221 * #

SAE-92-1996 p 202 N93-12353 * #

SAIC-92/1160 p 453 N93-11729 #

SAND-89-2773 p 347 N93-12012 #
SAND-90-0351 p 221 N93-11631 #
SAND-91-1492C p 362 N93-11564 #
SAND-91-1613C p 452 N93-11674 #
SAND-91-1743 p 284 N93-11917 #
SAND-91-2228 p 348 N93-12075 #
SAND-91-2273C p 303 N93-11843 #
SAND-91-2303C p 204 N93-11152 #
SAND-91-2311C p 467 N93-12134 #
SAND-91-2484C p 464 N93-11842 #
SAND-91-2579C p 311 N93-11673 #
SAND-91-2592C p 437 N93-11640 #
SAND-91-2654C p 369 N93-11678 #
SAND-91-2689C p 219 N93-12268 #
SAND-91-2744C p 445 N93-12103 #
SAND-91-2899C p 284 N93-12101 #
SAND-91-8733 p 252 N93-12255 #
SAND-92-0003C p 276 N93-11494 #
SAND-92-0102C p 433 N93-11523 #
SAND-92-0186C p 419 N93-11860 #
SAND-92-0212C p 277 N93-12106 #
SAND-92-0254C p 291 N93-11693 #
SAND-92-0315C p 232 N93-11824 #
SAND-92-0370C p 257 N93-11600 #
SAND-92-0374C p 421 N93-12138 #
SAND-92-0541 p 249 N93-11551 #
SAND-92-0660C p 291 N93-11639 #
SAND-92-0661C p 411 N93-11599 #
SAND-92-0668 p 348 N93-12074 #
SAND-92-0722C p 463 N93-11797 #
SAND-92-0763 p 267 N93-11552 #
SAND-92-0777C p 303 N93-11799 #
SAND-92-0797C p 453 N93-11694 #
SAND-92-0874 p 290 N93-11553 #
SAND-92-0958 p 346 N93-11771 #
SAND-92-1009C p 367 N93-11236 #
SAND-92-1014 p 477 N93-11770 #
SAND-92-1045C p 280 N93-11234 #
SAND-92-1099C p 231 N93-10973 #
SAND-92-1252C p 348 N93-12312 #
SAND-92-1357C p 283 N93-11800 #
SAND-92-1454 p 344 N93-10989 #
SAND-92-1518C p 277 N93-11672 #
SAND-92-1566C p 217 N93-11367 #
SAND-92-1598C p 232 N93-11766 #
SAND-92-1646C p 408 N93-11378 #
SAND-92-1655C p 411 N93-11536 #
SAND-92-1795C p 300 N93-11537 #
SAND-92-1799C p 260 N93-12232 #
SAND-92-1803C p 254 N93-10984 #
SAND-92-1821C p 487 N93-11502 #
SAND-92-7006 p 348 N93-12222 #
SAND-92-8447-PT-1 p 329 N93-12220 #
SAND-92-8494C p 421 N93-12153 #
SAND-92-8503C p 275 N93-12265 #

SCR-91RR-5 p 206 N93-11461 #

SER-C-367 p 205 N93-11344
SER-C-370 p 407 N93-11345
SER-C-372 p 309 N93-11346
SER-C-375 p 309 N93-11330
SER-C-379 p 361 N93-11331
SER-C-383 p 315 N93-11332
SER-C-384 p 220 N93-11335

SGD-569-PT-2 p 488 N93-11738 #

SLCET-TR-88-1-REV-5.2 p 469 N93-12283 #

SMC-TR-92-35 p 226 N93-12379 #

SR-1 p 362 N93-11740 #
SR-4 p 363 N93-11810 #

SS-1666-7750 p 434 N93-11634 * #

SSC-CRYO-NOTE-92-7 p 471 N93-11656 #

SSCL-131-REV-A p 471 N93-11656 #

SSD-TR-92-XX p 366 N93-12378 #
SSD-TR-92-17 p 434 N93-11752 #
SSD-TR-92-29 p 226 N93-12064 #

SSV-2197 p 434 N93-11634 * #

SU-SLAC-PUB-5847 p 316 N93-11691 #
SU-SLAC-PUB-5871 p 446 N93-12497 #

SU-STAN-CS-91-1374 p 413 N93-12131 #
SU-STAN-CS-91-1387 p 419 N93-12239 #

SU-TR-28 p 429 N93-12513 #

TAMU-SG-92-603 p 372 N93-11253 #

TEC-R-166 p 477 N93-11748 #
TEC-R-168 p 218 N93-11751 #
TEC-R-181 p 477 N93-11741 #

TEC-SR-1 p 353 N93-11466 #

TEC-0007 p 420 N93-11000 #

TOP-6-2-604 p 283 N93-11764 #

TR-MEMS-92-101 p 308 N93-12435 #

TR-0091(6935-08)-1 p 434 N93-11752 #
TR-0091(6940-06)-2 p 226 N93-12379 #
TR-0091(6940-06)-6 p 366 N93-12378 #
TR-123 p 250 N93-11808 #
TR-14-REPT-2 p 265 N93-11188 #
TR-15-REPT-3 p 265 N93-11187 #
TR-170 p 429 N93-12081 #
TR-171 p 429 N93-12334 #
TR-18 p 264 N93-11150 #
TR-1992-13 p 272 N93-12289 #
TR-19 p 460 N93-11558 #
TR-20 p 464 N93-11869 #
TR-2 p 468 N93-12218 #
TR-30 p 236 N93-12177 #
TR-33 p 464 N93-11868 #
TR-49 p 250 N93-12062 #
TR-74-ONR p 238 N93-11281 #
TR-75-ONR p 246 N93-11280 #
TR-8513-03 p 288 N93-12519 * #
TR-91-2 p 475 N93-11506 #
TR-92(2508)-1 p 226 N93-12064 #
TR-92-1-ONR p 386 N93-11415 #
TR-92-1307 p 472 N93-12212 * #

TR91-33 p 427 N93-11837 #

TT-9104 p 218 N93-11728 #
TT-9201 p 217 N93-11224 #

TTI-2-1-90/1-1245 p 325 N93-11427 #

TVA-92019073 p 290 N93-11514 #

UAH-TR-91/001-VOL-2 p 231 N93-11043 * #
UAH-TR-92/001-VOL-1 p 231 N93-11042 * #

UAH-5-32274 p 311 N93-11662 * #
UAH-5-32313 p 470 N93-12396 * #
UAH-5-32354 p 252 N93-12215 * #
UAH-5-32389 p 448 N93-12201 * #
UAH-5-32439 p 323 N93-12516 * #

UCB-PTH-91/51 ..... p 470 N93-11518 #
UCB-PTH-92/17 ..... p 441 N93-12111 #

UCID-21771-REV-1 ..... p 448 N93-11627 #

UCRL-CR-110713 ..... p 479 N93-12143 #

UCRL-ID-109852 ..... p 451 N93-11516 #
UCRL-ID-110111 ..... p 337 N93-11775 #
UCRL-ID-110629 ..... p 282 N93-11661 #
UCRL-ID-111473 ..... p 217 N93-11447 #

UCRL-JC-107332 ..... p 449 N93-10975 #
UCRL-JC-107393 ..... p 354 N93-11744 #
UCRL-JC-107579 ..... p 293 N93-12113 #
UCRL-JC-107924 ..... p 256 N93-11519 #
UCRL-JC-108669 ..... p 293 N93-12121 #
UCRL-JC-108748 ..... p 282 N93-11675 #
UCRL-JC-109256 ..... p 461 N93-11602 #
UCRL-JC-109356 ..... p 450 N93-11153 #
UCRL-JC-109357 ..... p 454 N93-12060 #
UCRL-JC-109368 ..... p 454 N93-12059 #
UCRL-JC-109410 ..... p 364 N93-12155 #
UCRL-JC-109473 ..... p 451 N93-11495 #
UCRL-JC-109552 ..... p 310 N93-11542 #
UCRL-JC-109555 ..... p 452 N93-11645 #
UCRL-JC-109776 ..... p 413 N93-12137 #
UCRL-JC-109842 ..... p 317 N93-11765 #
UCRL-JC-109874 ..... p 374 N93-10974 #
UCRL-JC-109922 ..... p 267 N93-11549 #
UCRL-JC-110069 ..... p 326 N93-11540 #
UCRL-JC-110209 ..... p 316 N93-11659 #
UCRL-JC-110242 ..... p 371 N93-12154 #
UCRL-JC-110298 ..... p 315 N93-11155 #
UCRL-JC-110481 ..... p 461 N93-11647 #
UCRL-JC-110559 ..... p 354 N93-11676 #
UCRL-JC-110655 ..... p 465 N93-12093 #
UCRL-JC-110726 ..... p 465 N93-12065 #
UCRL-JC-110859 ..... p 354 N93-11677 #
UCRL-JC-110950 ..... p 221 N93-12317 #
UCRL-JC-111089 ..... p 414 N93-12234 #

UCRL-LR-106736-REV-1 ..... p 451 N93-11534 #

UCRL-MA-104861-VER-2-3 ..... p 282 N93-11632 #

UCSC-1992001 ..... p 363 N93-11788 #
UCSC-1992002 ..... p 366 N93-12270 #

UDR-TR-90-121 ..... p 208 N93-12488 #
UDR-TR-91-149 ..... p 242 N93-12181 #
UDR-TR-92-45 ..... p 240 N93-11835 #

UFIFT-HEP-92-15 ..... p 432 N93-11759 #

UILU-ENG-92-2232 ..... p 404 N93-11462 * #
UILU-ENG-92-2234 ..... p 419 N93-12395 * #
UILU-ENG-92-2237 ..... p 418 N93-11651 * #
UILU-ENG-92-2239 ..... p 406 N93-12541 * #
UILU-ENG-92-2240 ..... p 406 N93-12540 * #

UMR-FDB-26 ..... p 265 N93-11194 #

UPN-90100411 ..... p 354 N93-11702 #

US-PATENT-APPL-SN-146939 ..... p 216 N93-11057 *
US-PATENT-APPL-SN-301925 ..... p 264 N93-11059 *
US-PATENT-APPL-SN-412248 ..... p 278 N93-11047 #
US-PATENT-APPL-SN-471314 ..... p 288 N93-11053
US-PATENT-APPL-SN-519626 ..... p 195 N93-11050
US-PATENT-APPL-SN-524108 ..... p 216 N93-11057 *
US-PATENT-APPL-SN-529294 ..... p 325 N93-11423
US-PATENT-APPL-SN-537640 ..... p 214 N93-11046
US-PATENT-APPL-SN-548652 ..... p 442 N93-11060
US-PATENT-APPL-SN-591208 ..... p 446 N93-11052 #
US-PATENT-APPL-SN-621685 ..... p 281 N93-11426
US-PATENT-APPL-SN-644363 ..... p 288 N93-11051
US-PATENT-APPL-SN-651882 ..... p 458 N93-11056 *
US-PATENT-APPL-SN-664897 ..... p 309 N93-11049
US-PATENT-APPL-SN-665371 ..... p 264 N93-11059 *
US-PATENT-APPL-SN-671592 ..... p 266 N93-11425
US-PATENT-APPL-SN-677193 ..... p 278 N93-11044
US-PATENT-APPL-SN-682937 ..... p 273 N93-11045
US-PATENT-APPL-SN-697351 ..... p 309 N93-11048
US-PATENT-APPL-SN-700375 ..... p 266 N93-11400
US-PATENT-APPL-SN-703435 ..... p 446 N93-11058 *
US-PATENT-APPL-SN-728918 ..... p 274 N93-11665
US-PATENT-APPL-SN-765618 ..... p 221 N93-11428
US-PATENT-APPL-SN-768094 ..... p 216 N93-11057 *
US-PATENT-APPL-SN-805594 ..... p 232 N93-11424
US-PATENT-APPL-SN-807577 ..... p 280 N93-11354 #
US-PATENT-APPL-SN-823809 ..... p 199 N93-11876 * #
US-PATENT-APPL-SN-873407 ..... p 333 N93-12204 * #
US-PATENT-APPL-SN-884976 ..... p 293 N93-12133 #
US-PATENT-APPL-SN-884980 ..... p 329 N93-12327 * #
US-PATENT-APPL-SN-889003 ..... p 297 N93-11172 * #
US-PATENT-APPL-SN-889572 ..... p 329 N93-12203 * #
US-PATENT-APPL-SN-892054 ..... p 239 N93-11543 * #
US-PATENT-APPL-SN-912960 ..... p 269 N93-11912 * #
US-PATENT-APPL-SN-921192 ..... p 324 N93-11177 * #
US-PATENT-APPL-SN-928865 ..... p 313 N93-12205 * #
US-PATENT-APPL-SN-937335 ..... p 420 N93-11174 * #
US-PATENT-APPL-SN-942491 ..... p 290 N93-11456 * #
US-PATENT-APPL-SN-942499 ..... p 278 N93-12202 * #
US-PATENT-APPL-SN-942500 ..... p 412 N93-11664 * #

US-PATENT-CLASS-102-378 ..... p 221 N93-11428
US-PATENT-CLASS-148-247 ..... p 266 N93-11425
US-PATENT-CLASS-149-19.3 ..... p 273 N93-11045
US-PATENT-CLASS-149-88 ..... p 274 N93-11665
US-PATENT-CLASS-244-145 ..... p 195 N93-11050
US-PATENT-CLASS-244-322 ..... p 214 N93-11046
US-PATENT-CLASS-250-214 ..... p 309 N93-11049
US-PATENT-CLASS-254-391 ..... p 325 N93-11423
US-PATENT-CLASS-329-322 ..... p 288 N93-11051
US-PATENT-CLASS-341-138 ..... p 278 N93-11047 #
US-PATENT-CLASS-342-128 ..... p 278 N93-11044
US-PATENT-CLASS-342-423 ..... p 281 N93-11426
US-PATENT-CLASS-356-356 ..... p 446 N93-11058 *
US-PATENT-CLASS-356-360 ..... p 446 N93-11058 *
US-PATENT-CLASS-356-376 ..... p 446 N93-11058 *
US-PATENT-CLASS-357-16 ..... p 458 N93-11056 *
US-PATENT-CLASS-357-30 ..... p 458 N93-11056 *
US-PATENT-CLASS-357-4 ..... p 458 N93-11056 *
US-PATENT-CLASS-361-413 ..... p 288 N93-11053
US-PATENT-CLASS-364-575 ..... p 446 N93-11058 *
US-PATENT-CLASS-374-4 ..... p 216 N93-11057 *
US-PATENT-CLASS-374-57 ..... p 216 N93-11057 *
US-PATENT-CLASS-374-5 ..... p 216 N93-11057 *
US-PATENT-CLASS-382-26 ..... p 446 N93-11058 *
US-PATENT-CLASS-427-229 ..... p 266 N93-11400
US-PATENT-CLASS-51-309 ..... p 446 N93-11052 #
US-PATENT-CLASS-525-422 ..... p 264 N93-11059 *
US-PATENT-CLASS-525-432 ..... p 264 N93-11059 *
US-PATENT-CLASS-525-903 ..... p 264 N93-11059 *
US-PATENT-CLASS-73-147 ..... p 216 N93-11057 *
US-PATENT-CLASS-73-828 ..... p 309 N93-11048
US-PATENT-CLASS-89-109 ..... p 232 N93-11424

US-PATENT-5,061,933 ..... p 278 N93-11044
US-PATENT-5,066,952 ..... p 278 N93-11047 #
US-PATENT-5,078,344 ..... p 195 N93-11050
US-PATENT-5,081,424 ..... p 288 N93-11051
US-PATENT-5,082,202 ..... p 214 N93-11046
US-PATENT-5,092,944 ..... p 273 N93-11045
US-PATENT-5,103,678 ..... p 309 N93-11048
US-PATENT-5,106,394 ..... p 446 N93-11052 #
US-PATENT-5,111,036 ..... p 309 N93-11049
US-PATENT-5,114,506 ..... p 274 N93-11665
US-PATENT-5,117,758 ..... p 221 N93-11428
US-PATENT-5,119,103 ..... p 281 N93-11426
US-PATENT-5,119,273 ..... p 288 N93-11053
US-PATENT-5,120,024 ..... p 325 N93-11423
US-PATENT-5,120,575 ..... p 266 N93-11400
US-PATENT-5,120,968 ..... p 442 N93-11060
US-PATENT-5,123,978 ..... p 266 N93-11425
US-PATENT-5,125,318 ..... p 232 N93-11424
US-PATENT-5,131,758 ..... p 216 N93-11057 *
US-PATENT-5,132,763 ..... p 458 N93-11056 *
US-PATENT-5,146,293 ..... p 446 N93-11058 *
US-PATENT-5,149,746 ..... p 264 N93-11059 *

USARIEM-TN-92-2 ..... p 385 N93-12145 #

USCGA-07-92 ..... p 205 N93-11472 #

UTRC-91-29-REPT-1 ..... p 471 N93-12490 #

VAL-7/1991 ..... p 256 N93-11244 #

VI-1707-A-VOL-1 ..... p 322 N93-12262 #
VI-1707-C-VOL-3 ..... p 317 N93-11805 #

VKI-TN-180 ..... p 198 N93-11686 #

VTT-PUBS-87 ..... p 299 N93-11360 #
VTT-PUBS-88 ..... p 299 N93-11359 #

WCDMP-18 ..... p 370 N93-11897 #

WES/CR/SL-92-5 ..... p 286 N93-12422 #

WES/TR/DRP-92-1 ..... p 205 N93-11419 #

WHOI-91-37 ..... p 374 N93-12247 #

WINCO-11733 ..... p 480 N93-12495 #
WINCO-11735 ..... p 356 N93-12496 #
WINCO-11787 ..... p 262 N93-12487 #

WIS-PH-91-38 ..... p 471 N93-11780 #

WL-TP-92-009 ..... p 222 N93-12130 #

WL-TR-91-4032-VOL-2-PT-3 ..... p 241 N93-12054 #
WL-TR-91-4064 ..... p 262 N93-12468 #
WL-TR-91-4149 ..... p 242 N93-12181 #
WL-TR-91-8048 ..... p 476 N93-11508 #
WL-TR-92-2041-PHASE-1 ..... p 348 N93-12166 #
WL-TR-92-3009 ..... p 208 N93-12488 #
WL-TR-92-3034 ..... p 202 N93-12466 #

WL/MN-TR-92-008 ..... p 222 N93-12161 #

WMO/TD-488 ..... p 370 N93-11897 #

WSRC-MS-91-293 ..... p 259 N93-12107 #
WSRC-MS-92-236 ..... p 362 N93-11669 #

WSRC-RD-91-25 ..... p 437 N93-11597 #

WSRC-TR-91-11 ..... p 260 N93-12158 #

WSU-92/91 ..... p 469 N93-12338 #

Y/DK-888/P1 ..... p 478 N93-11796 #

YALEU/DCS/RR-866 ..... p 428 N93-12511 #

Appendix

NASA SCIENTIFIC AND TECHNICAL INFORMATION PROGRAM PRODUCTS AND SERVICES

The NASA Scientific and Technical Information (STI) Program provides for the collection and announcement of aerospace-related reports and literature obtained worldwide through agreements and exchanges. The result of the collection is the comprehensive NASA STI Database that covers aeronautics, space, and supporting disciplines.

The STI Database, documents generated or obtained by NASA, and products and services derived from or supporting the database are made available to the NASA research community and to the public. Descriptions and sources of these items are presented in the following pages.

Scientific and Technical Aerospace Reports (*STAR*) is an abstract journal, listing citations with abstracts for aerospace-related reports obtained from worldwide sources. *STAR* is issued on the first of each month, and announces current documents that have been entered into the NASA STI Database during the previous month. The reports are of the following types:

- NASA, NASA contractor, and NASA grantee reports;
- Reports issued by other U.S. Government agencies, domestic and foreign institutions, universities, and private firms;
- Translations in report form;
- NASA-owned patents and patent applications;
- Other U.S. Government agency and foreign patents and patent applications;
- Domestic and foreign dissertations and theses.

Journal, book, and conference literature, journal translations, and certain foreign dissertations having the same subject scope as *STAR* are announced in a companion journal, *International Aerospace Abstracts* (*IAA*). *IAA* is issued on the 1st and 15th of each month and is available from the American Institute of Aeronautics and Astronautics, Technical Information Service, 555 West 57th Street, 12th Floor, New York, NY 10019.

ELIGIBILITY AND REGISTRATION FOR NASA STI PRODUCTS AND SERVICES

Organizations of the type listed below that have registered with NASA can receive products and services.

- NASA offices and installations, contractors, subcontractors, grantees, and consultants;
- Other U.S. Government agencies and their contractors;
- Libraries in the United States that have arrangements with NASA to maintain collections of NASA documents for public reference;
- Other organizations in the United States having a need for NASA documents in work related to aeronautics and space research;
- Organizations abroad that have established reciprocal documents exchange arrangements with NASA.

The central service points — central points of document acquisition and control within qualified organizations — or individuals are eligible to register for NASA STI products and services. Domestic organizations or individuals may be eligible to receive various classes of NASA publications and services and should address their requests for registration or further information to:

NASA Center for AeroSpace Information
ATTN: Registration Services
P.O. Box 8757
Baltimore, MD 21240-0757
301-621-0390

Organizations abroad should direct requests to:

National Aeronautics and Space Administration
Scientific and Technical Information Program (JTT)
International STI Program
Washington, DC 20546-0001
USA
703-271-5640

SUBJECT SCOPE

The subject scope of *STAR* and *IAA* includes all aspects of aeronautics and space research and development, supporting basic and applied research, and applications. Aerospace aspects of Earth resources, energy development, conservation, oceanography, environmental protection, urban transportation, and other topics of high national priority are also covered.

HOW TO USE *STAR* SUBJECT CATEGORIES

Abstracts in *STAR* are categorized by 10 major subject divisions that are divided further into 76 specific subject categories. The subject divisions and categories are listed in the Table of Contents together with a note for each that defines its scope and provides any cross-references. For example:

> **16 SPACE TRANSPORTATION**
> Includes passenger and cargo space transportation, e.g., shuttle operations; and space rescue techniques. For related information see also *03 Air Transportation and Safety* and *18 Spacecraft Design, Testing and Performance.* For space suits see *54 Man/System Technology and Life Support.*

CROSS-REFERENCES

Individual *STAR* abstracts are not ordinarily cross-referenced, except for certain conference reports or book translations that have had separate abstracts written for their component papers or chapters. Citations and abstracts of the components follow immediately after those of the parent document. When the subject content of a component differs sufficiently from the general content of the parent, a cross-reference citation also is printed at the end of the category to which it normally would have been assigned if it were independent.

DOCUMENTS ON MICROFICHE

Documents available on microfiche are designated by a pound sign (#) following the accession number.

LIMITED REPRODUCIBILITY

A note of limited reproducibility appears in the citation, if there are factors affecting the reproducibility of more than 20% of the document. These factors include faint or broken type, color photographs, black and white photographs, foldouts, dot matrix print, or some other factor that limits the reproducibility of the document. This notation also appears on the microfiche header.

COLOR COPIES

An increasing number of NASA scientific and technical reports are being produced with color graphs, charts, illustrations, and photographs. An indication that a document has color pages follows the source and pricing (SAP) information in the *STAR* citation.

Registered users of the NASA Scientific and Technical Information Program will receive ordered documents with color at no additional cost, as long as stock copies of the document are available. Otherwise, an additional fee of $2.00 per color page will be charged. The NASA Center for AeroSpace Information staff will contact registered users to determine individual user's needs.

NASA PATENTS AND PATENT APPLICATIONS

Patents and patent applications owned by NASA are announced in *STAR* under appropriate subject categories and are referenced in the *STAR* indexes. In the Report/Accession Number Index, patents are indexed by the NASA Case Number, and the U.S. Patent Class. Patent applications are indexed by the NASA Case Number and the U.S. Patent Application Serial Number.

Printed copies of patents (which are not microfiched) are available for purchase from the U.S. Patent and Trademark Office.

When ordering patents, the U.S. Patent Number should be used, and payment must be remitted in advance, by money order or check payable to the Commissioner of Patents and Trademarks. Prepaid purchase coupons for ordering are also available from the U.S. Patent and Trademark Office.

NASA patent application specifications are sold in both paper copy and microfiche by the NASA Center for AeroSpace Information (CASI). The N accession number should be used in ordering either paper copy or microfiche from CASI.

The patents and patent applications announced in *STAR* are owned by NASA and are available for royalty-free licensing. Requests for licensing terms and further information should be addressed to:

National Aeronautics and Space Administration
Associate General Counsel for Intellectual Property
Code GP
Washington, DC 20546-0001

SOURCES FOR DOCUMENTS

One or more sources from which a document announced in *STAR* is available to the public is given in each citation. The most commonly indicated sources and their acronyms or abbreviations are listed below, and their addresses are listed on page A-6. If the publication is available from a source other than those listed, the publisher and address will be displayed on the availability line or in combination with the corporate source line.

Avail: CASI. Sold by the NASA Center for AeroSpace Information. Prices for hard copy (HC) and microfiche (MF) are indicated by a price code following the letters HC or MF in the *STAR* citation. Current values for the price codes are given in the tables on page A-7.

NOTE ON ORDERING DOCUMENTS: When ordering publications from CASI, use the N accession number or other report number. It is also advisable to cite the title and other bibliographic identification.

Avail: SOD (or GPO). Sold by the Superintendent of Documents, U.S. Government Printing Office, in hard copy.

Avail: BLL (formerly NLL): British Library Lending Division, Boston Spa, Wetherby, Yorkshire, England. Photocopies available from this organization at the price shown. (If none is given, address inquiry to the BLL.)

Avail: DOE Depository Libraries. Organizations in U.S. cities and abroad that maintain collections of Department of Energy reports, usually in microfiche form, are listed in *Energy Research Abstracts.* Services available from the DOE and its depositories are described in a booklet, *DOE Technical Information Center - Its Functions and Services* (TID-4660), which may be obtained without charge from the DOE Technical Information Center.

Avail: ESDU. Pricing information on specific data, computer programs, and details on Engineering Sciences Data Unit (ESDU) topic categories can be obtained from ESDU International Ltd. Requesters in North America should use the Virginia address while all other requesters should use the London address, both of which are on page A-6.

Avail: Fachinformationszentrum, Karlsruhe. Gesellschaft fur wissenschaftlich-technische Information mbH 7514 Eggenstein-Leopoldshafen 2, Germany.

Avail: HMSO. Publications of Her Majesty's Stationery Office are sold in the U.S. by Pendragon House, Inc. (PHI), Redwood City, CA. The U.S. price (including a service and mailing charge) is given, or a conversion table may be obtained from PHI.

Avail: Issuing Activity, or Corporate Author, or no indication of availability. Inquiries as to the availability of these documents should be addressed to the organization shown in the citation as the corporate author of the document.

Avail: NASA Public Document Rooms. Documents so indicated may be examined at or purchased from the National Aeronautics and Space Administration (JBD-4), Public Documents Room (Room 1H23), Washington, DC 20546-0001, or public document rooms located at NASA installations, and the NASA Pasadena Office at the Jet Propulsion Laboratory.

Avail: NTIS. Sold by the National Technical Information Service. Initially distributed microfiche under the NTIS SRIM (Selected Research in Microfiche) are available. For information concerning this service, consult the NTIS Subscription Section, Springfield, VA 22161.

Avail: Univ. Microfilms. Documents so indicated are dissertations selected from *Dissertation Abstracts* and are sold by University Microfilms as xerographic copy (HC) and microfilm. All requests should cite the author and the Order Number as they appear in the citation.

Avail: US Patent and Trademark Office. Sold by Commissioner of Patents and Trademarks, U.S. Patent and Trademark Office, at the standard price of $1.50 each, postage free. (See discussion of NASA patents and patent applications on page A-3.)

Avail: (US Sales Only). These foreign documents are available to users within the United States from the National Technical Information Service (NTIS). They are available to users outside the United States through the International Nuclear Information Service (INIS) representative in their country, or by applying directly to the issuing organization.

Avail: USGS. Originals of many reports from the U.S. Geological Survey, which may contain color illustrations, or otherwise may not have the quality of illustrations preserved in the microfiche or facsimile reproduction, may be examined by the public at the libraries of the USGS field offices whose addresses are listed on page A-6. The libraries may be queried concerning the availability of specific documents and the possible utilization of local copying services, such as color reproduction.

FEDERAL DEPOSITORY LIBRARIES: To provide the general public with greater access to U.S. Government publications, Congress established the Federal Depository Library Program under the Government Printing Office (GPO), with 53 regional depositories responsible for permanent retention of material, inter-library loan, and reference services. (These libraries are not sales outlets.) At least one copy of nearly every NASA and NASA-sponsored publication, either in printed or microfiche format, is received and retained by the 53 regional depositories. A list of the regional GPO libraries, appears on page A-8. A local library can contact a regional depository library to help locate specific reports, or direct contact may be made by an individual.

PUBLIC COLLECTION OF NASA DOCUMENTS

An extensive collection of NASA and NASA-sponsored publications is maintianed by the British Library Lending Divison, Boston Spa, Wetherby, Yorkshire, England, for public access. The British Library Lending Division also has available many of the non-NASA publications cited in *STAR*.

European requesters may purchase facsimile copy or microfiche of NASA and NASA-sponsored documents, those identified by both the symbols # and * from ESA—Information Retrieval Service, European Space Agency, 8-10 rue Mario-Nikis, 75738 Paris CEDEX 15, France.

SUBMITTING DOCUMENTS

All users of this abstract service are urged to forward reports to be considered for announcement in *STAR*. This will aid NASA in its efforts to provide the fullest possible coverage of all scientific and technical publications that might support aeronautics and space research and development. If you have prepared relevant reports (other than those you will transmit to NASA, DOD, or DOE through the usual contract- or grant-reporting channels), please send them for consideration to the NASA Center for AeroSpace Information, P.O. Box 8757, Baltimore, MD 21240-0757.

Reprints of journal articles, book chapters, and conference papers are also welcome. These will be considered for announcement in *STAR*'s companion journal, *IAA*.

You may specify a particular source to be included in a report announcement if you wish; otherwise the report will be placed on a public sale at the NASA Center for AeroSpace Information. Copyrighted publications will be announced but not distributed or sold.

PURCHASE OF *STAR*

STAR is publicly available on annual subscription from the NASA Center for AeroSpace Information (CASI) at $114.00.

STAR is available to registered users on annual subscription from the NASA Center for AeroSpace Information, ATTN: Registration Services, P.O. Box 8757, Baltimore, MD 21240-0757.

Microfiche of the abstract sections of *STAR* are available, on annual subscription, from CASI. Annual subscription rates are $216.00 North America; $432.00 foreign.

ADDRESSES OF ORGANIZATIONS

American Institute of Aeronautics and Astronautics
Technical Information Service
555 West 57th Street, 12th Floor
New York, New York 10019

British Library Lending Division,
Boston Spa, Wetherby, Yorkshire,
England

Commissioner of Patents and Trademarks
U.S. Patent and Trademark Office
Washington, DC 20231

Department of Energy
Technical Information Center
P.O. Box 62
Oak Ridge, Tennessee 37830

European Space Agency-Information Retrieval Service
ESRIN
Via Galileo Galilei
00044 Frascati (Rome) Italy

Engineering Sciences Data Unit International
P.O. Box 1633
Manassas, Virginia 22110

Engineering Sciences Data Unit International, Ltd.
251-259 Regent Street
London, W1R 7AD, England

Fachinformationszentrum Karlsruhe
Gesellschaft fur wissenschaftlich-technische
Information mbH
7514 Eggenstein-Leopoldshafen 2, Germany

Her Majesty's Stationery Office
P.O. Box 569, S.E. 1
London, England

NASA Center for AeroSpace Information
P.O. Box 8757
Baltimore, Maryland 21240-0757

National Aeronautics and Space Administration
Scientific and Technical Information Program (JTT)
Washington, DC 20546-0001

National Technical Information Service
5285 Port Royal Road
Springfield, Virginia 22161

Pendragon House, Inc.
899 Broadway Avenue
Redwood City, California 94063

Superintendent of Documents
U.S. Government Printing Office
Washington, DC 20402

University Microfilms
A Xerox Company
300 North Zeeb Road
Ann Arbor, Michigan 48106

University Microfilms, Ltd.
Tylers Green
London, England

U.S. Geological Survey Library National Center
MS 950
12201 Sunrise Valley Drive
Reston, Virginia 22092

U.S. Geological Survey Library
2255 North Gemini Drive
Flagstaff, Arizona 86001

U.S. Geological Survey
345 Middlefield Road
Menlo Park, California 94025

U.S. Geological Survey Library
Box 25046
Denver Federal Center, MS914
Denver, Colorado 80225

CASI PRICE TABLES

(Effective October 1, 1992)

STANDARD PRICE DOCUMENTS

PRICE CODE	NORTH AMERICAN PRICE	FOREIGN PRICE
A01	$ 9.00	$ 18.00
A02	12.50	25.00
A03	17.00	34.00
A04-A05	19.00	38.00
A06-A09	26.00	52.00
A10-A13	35.00	70.00
A14-A17	43.00	86.00
A18-A21	50.00	100.00
A22-A25	59.00	118.00
A99	69.00	138.00

MICROFICHE

PRICE CODE	NORTH AMERICAN PRICE	FOREIGN PRICE
A01	$ 9.00	$ 18.00
A02	12.50	25.00
A03	17.00	34.00
A04	19.00	38.00
A06	26.00	52.00
A10	35.00	70.00

IMPORTANT NOTICE

CASI Shipping and Handling Charges
U.S. — ADD $3.00 per TOTAL ORDER
Canada and Mexico — ADD $3.50 per TOTAL ORDER
All Other Countries — ADD $7.50 per TOTAL ORDER
Does NOT apply to orders
requesting CASI RUSH HANDLING.
Contact CASI for charge.

FEDERAL REGIONAL DEPOSITORY LIBRARIES

ALABAMA

AUBURN UNIV. AT MONTGOMERY LIBRARY
Documents Dept.
7300 University Drive
Montgomery, AL 36117-3596
(205) 244-3650 FAX: (205) 244-0678

UNIV. OF ALABAMA
Amelia Gayle Gorgas Library
Govt. Documents
Box 870266
Tuscaloosa, AL 35487-0266
(205) 348-6046 FAX: (205) 348-8833

ARIZONA

DEPT. OF LIBRARY, ARCHIVES, AND PUBLIC RECORDS
Federal Documents
Third Floor State Capitol
1700 West Washington
Phoenix, AZ 85007
(602) 542-4121 FAX: (602) 542-4400; 542-4500

ARKANSAS

ARKANSAS STATE LIBRARY
State Library Services
One Capitol Mall
Little Rock, AR 72201
(501) 682-2869

CALIFORNIA

CALIFORNIA STATE LIBRARY
Govt. Publications Section
914 Capitol Mall - P.O. Box 942837
Sacramento, CA 94237-0001
(916) 322-4572 FAX: (916) 324-8120

COLORADO

UNIV. OF COLORADO - BOULDER
Norlin Library
Govt. Publications
Campus Box 184
Boulder, CO 80309-0184
(303) 492-8834 FAX: (303) 492-2185

DENVER PUBLIC LIBRARY
Govt. Publications Dept. BS/GPD
1357 Broadway
Denver, CO 80203
(303) 571-2135

CONNECTICUT

CONNECTICUT STATE LIBRARY
231 Capitol Avenue
Hartford, CT 06106
(203) 566-4971 FAX: (203) 566-3322

FLORIDA

UNIV. OF FLORIDA LIBRARIES
Documents Dept.
Library West
Gainesville, FL 32611-2048
(904) 392-0366 FAX: (904) 392-7251

GEORGIA

UNIV. OF GEORGIA LIBRARIES
Govt. Documents Dept.
Jackson Street
Athens, GA 30602
(404) 542-8949 FAX: (404) 542-6522

HAWAII

UNIV. OF HAWAII
Hamilton Library
Govt. Documents Collection
2550 The Mall
Honolulu, HI 96822
(808) 948-8230 FAX: (808) 956-5968

IDAHO

UNIV. OF IDAHO LIBRARY
Documents Section
Moscow, ID 83843
(208) 885-6344 FAX: (208) 885-6817

ILLINOIS

ILLINOIS STATE LIBRARY
Reference Dept.
300 South Second
Springfield, IL 62701-1796
(217) 782-7596 FAX: (217) 524-0041

INDIANA

INDIANA STATE LIBRARY
Serials/Documents Section
140 North Senate Avenue
Indianapolis, IN 46204
(317) 232-3678 FAX: (317) 232-3728

IOWA

UNIV. OF IOWA LIBRARIES
Govt. Publications Dept.
Washington & Madison Streets
Iowa City, IA 52242
(319) 335-5926 FAX: (319) 335-5830

KANSAS

UNIV. OF KANSAS
Govt. Documents & Map Library
6001 Malatt Hall
Lawrence, KS 66045-2800
(913) 864-4660 FAX: (913) 864-5380

KENTUCKY

UNIV. OF KENTUCKY LIBRARIES
Govt. Publications/Maps Dept.
Lexington, KY 40506-0039
(606) 257-3139 FAX: (606) 257-1563; 257-8379

LOUISIANA

LOUISIANA STATE UNIV.
Middleton Library
Govt. Documents Dept.
Baton Rouge, LA 70803
(504) 388-2570 FAX: (504) 388-6992

LOUISIANA TECHNICAL UNIV.
Prescott Memorial Library
Govt. Documents Dept.
305 Wisteria Street
Ruston, LA 71270-9985
(318) 257-4962 FAX: (318) 257-2447

MAINE

TRI-STATE DOCUMENTS DEPOSITORY
Raymond H. Fogler Library
Govt. Documents & Microforms Dept.
Univ. of Maine
Orono, ME 04469
(207) 581-1680

MARYLAND

UNIV. OF MARYLAND
Hornbake Library
Govt. Documents/Maps Unit
College Park, MD 20742
(301) 454-3034 FAX: (301) 454-4985

MASSACHUSETTS

BOSTON PUBLIC LIBRARY
Govt. Documents Dept.
666 Boylston Street
Boston, MA 02117
(617) 536-5400 ext. 226
FAX: (617) 267-8273; 267-8248

MICHIGAN

DETROIT PUBLIC LIBRARY
5201 Woodward Avenue
Detroit, MI 48202-4093
(313) 833-1440; 833-1409
FAX: (313) 833-5039

LIBRARY OF MICHIGAN
Govt. Documents Unit
P.O. Box 30007
Lansing, MI 48909
(517) 373-0640 FAX: (517) 373-3381

MINNESOTA

UNIV. OF MINNESOTA
Wilson Library
Govt. Publications Library
309 19th Avenue South
Minneapolis, MN 55455
(612) 624-5073 FAX: (612) 626-9353

MISSISSIPPI

UNIV. OF MISSISSIPPI
J.D. Williams Library
Federal Documents Dept.
106 Old Gym Bldg.
University, MS 38677
(601) 232-5857 FAX: (601) 232-5453

MISSOURI

UNIV. OF MISSOURI - COLUMBIA
Ellis Library
Govt. Documents
Columbia, MO 65201
(314) 882-6733 FAX: (314) 882-8044

MONTANA

UNIV. OF MONTANA
Maureen & Mike Mansfield Library
Documents Div.
Missoula, MT 59812-1195
(406) 243-6700 FAX: (406) 243-2060

NEBRASKA

UNIV. OF NEBRASKA - LINCOLN
D.L. Love Memorial Library
Documents Dept.
Lincoln, NE 68588
(402) 472-2562

NEVADA

UNIV. OF NEVADA
Reno Library
Govt. Publications Dept.
Reno, NV 89557
(702) 784-6579 FAX: (702) 784-1751

NEW JERSEY

NEWARK PUBLIC LIBRARY
U.S. Documents Div.
5 Washington Street - P.O. Box 630
Newark, NJ 07101-0630
(201) 733-7812 FAX: (201) 733-5648

NEW MEXICO

UNIV. OF NEW MEXICO
General Library
Govt. Publications Dept.
Albuquerque, NM 87131-1466
(505) 277-5441 FAX: (505) 277-6019

NEW MEXICO STATE LIBRARY
325 Don Gaspar Avenue
Santa Fe, NM 87503
(505) 827-3826 FAX: (505) 827-3820

NEW YORK

NEW YORK STATE LIBRARY
Documents/Gift & Exchange Section
Federal Depository Program
Cultural Education Center
Albany, NY 12230
(518) 474-5563 FAX: (518) 474-5786

NORTH CAROLINA

UNIV. OF NORTH CAROLINA - CHAPEL HILL
CB#3912, Davis Library
BA/SS Dept.—Documents
Chapel Hill, NC 27599
(919) 962-1151 FAX: (919) 962-0484

NORTH DAKOTA

NORTH DAKOTA STATE UNIV. LIBRARY
Documents Office
Fargo, ND 58105
(701) 237-8886 FAX: (701) 237-7138
In cooperation with Univ. of North Dakota, Chester Fritz Library Grand Forks

OHIO

STATE LIBRARY OF OHIO
Documents Dept.
65 South Front Street
Columbus, OH 43266
(614) 644-7051 FAX: (614) 752-9178

OKLAHOMA

OKLAHOMA DEPT. OF LIBRARIES
U.S. Govt. Information Div.
200 NE 18th Street
Oklahoma City, OK 73105-3298
(405) 521-2502, ext. 252, 253
FAX: (405) 525-7804

OKLAHOMA STATE UNIV.
Edmon Low Library
Documents Dept.
Stillwater, OK 74078
(405) 744-6546 FAX: (405) 744-5183

OREGON

PORTLAND STATE UNIV.
Millar Library
934 SW Harrison - P.O. Box 1151
Portland, OR 97207
(503) 725-3673 FAX: (503) 725-4527

PENNSYLVANIA

STATE LIBRARY OF PENN.
Govt. Publications Section
Walnut St. & Commonwealth Ave. - P.O. Box 1601
Harrisburg, PA 17105
(717) 787-3752

SOUTH CAROLINA

CLEMSON UNIV.
Cooper Library
Public Documents Unit
Clemson, SC 29634-3001
(803) 656-5174 FAX: (803) 656-3025
In cooperation with Univ. of South Carolina, Thomas Cooper Library, Columbia

TENNESSEE

MEMPHIS STATE UNIV. LIBRARIES
Govt. Documents
Memphis, TN 38152
(901) 678-2586 FAX: (901) 678-2511

TEXAS

TEXAS STATE LIBRARY
United States Documents
P.O. Box 12927 - 1201 Brazos
Austin, TX 78711
(512) 463-5455 FAX: (512) 463-5436

TEXAS TECH. UNIV. LIBRARY
Documents Dept.
Lubbock, TX 79409
(806) 742-2268 FAX: (806) 742-1920

UTAH

UTAH STATE UNIV.
Merrill Library & Learning Resources Center, UMC-3000
Documents Dept.
Logan, UT 84322-3000
(801) 750-2684 FAX: (801) 750-2677

VIRGINIA

UNIV. OF VIRGINIA
Alderman Library
Govt. Documents
Charlottesville, VA 22903-2498
(804) 924-3133 FAX: (804) 924-4337

WASHINGTON

WASHINGTON STATE LIBRARY
Document Section
MS AJ-11
Olympia, WA 98504-0111
(206) 753-4027 FAX: (206) 753-3546

WEST VIRGINIA

WEST VIRGINIA UNIV. LIBRARY
Govt. Documents Section
P.O. Box 6069
Morgantown, WV 26506
(304) 293-3640

WISCONSIN

ST. HIST. SOC. OF WISCONSIN LIBRARY
Govt. Publications Section
816 State Street
Madison, WI 53706
(608) 262-2781 FAX: (608) 262-4711
In cooperation with Univ. of Wisconsin-Madison, Memorial Library

MILWAUKEE PUBLIC LIBRARY
Documents Div.
814 West Wisconsin Avenue
Milwaukee, WI 53233
(414) 278-2167 FAX: (414) 278-2137

*U.S. G.P.O.:1993-342-599:60026

National Aeronautics and
Space Administration
Code JTT
Washington, D.C.
20546-0001

Official Business
Penalty for Private Use, $300

SPECIAL FOURTH-CLASS RATE
POSTAGE & FEES PAID
NASA
PERMIT No. G27

NASA

POSTMASTER: If Undeliverable (Section 158
Postal Manual) Do Not Return